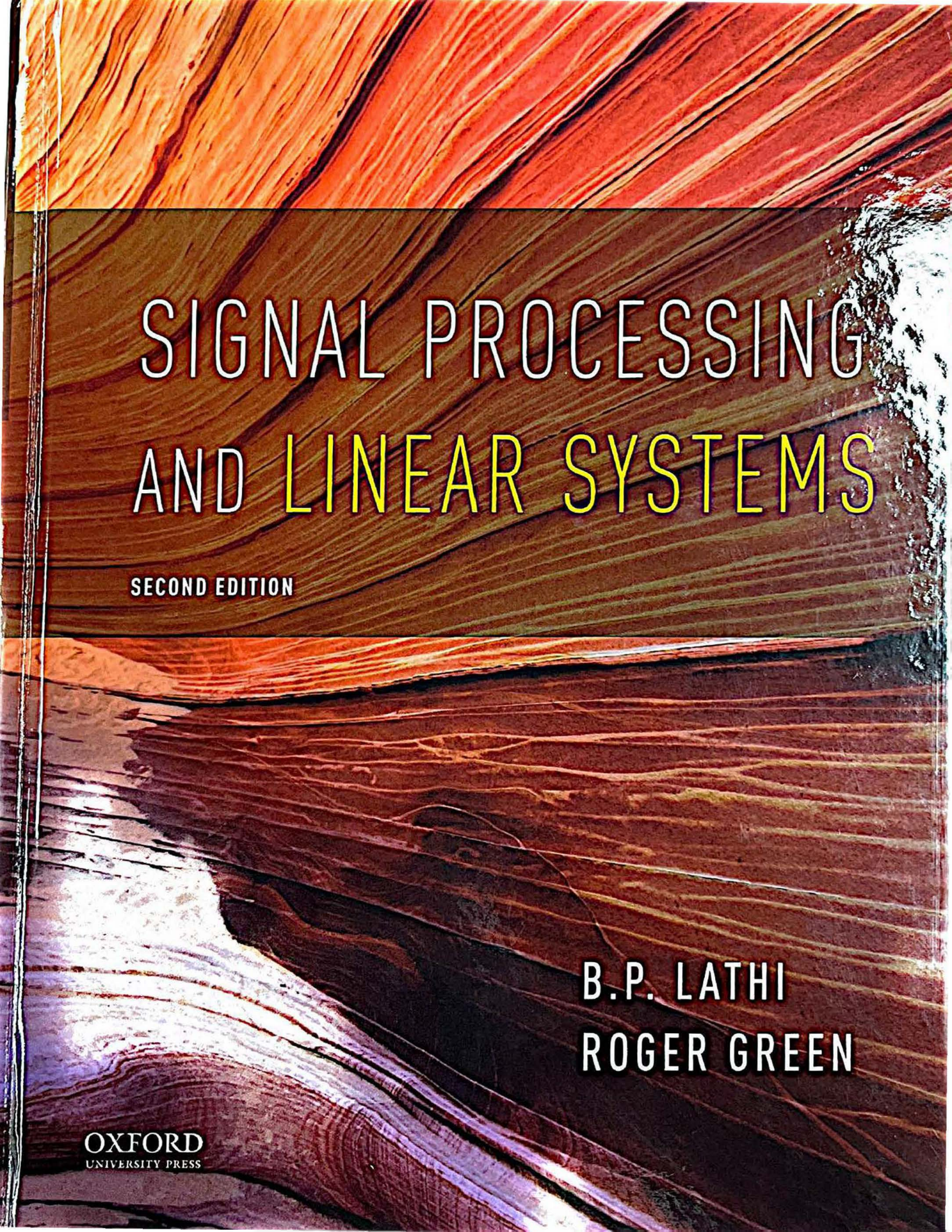
SIGNAL PROCESSING
AND LINEAR SYSTEMS
SECOND EDITION
B.P. LATHI
ROGER GREEN
OXFORD
UNIVERSITY PRESS

Not for Profit. All for Education.

Oxford University Press USA is a not-for-profit publisher dedicated to offering the highest quality textbooks at the best possible prices. We believe that it is important to provide everyone with access to superior textbooks at affordable prices. Oxford University Press textbooks are 30%–70% less expensive than comparable books from commercial publishers.

The press is a department of the University of Oxford, and our publishing proudly serves the university's mission: promoting excellence in research, scholarship, and education around the globe. We do not publish in order to generate revenue: we generate revenue in order to publish and also to fund scholarships, provide start-up grants to early-stage researchers, and refurbish libraries.

What does this mean to you?
It means that Oxford University Press USA published this book to best support your studies while also being mindful of your wallet.

***Not* for Profit. *All* for Education.**
As a not-for-profit publisher, Oxford University Press USA is uniquely situated to offer the highest quality scholarship at the best possible prices.

OXFORD
UNIVERSITY PRESS

SIGNAL PROCESSING AND LINEAR SYSTEMS

THE OXFORD SERIES IN ELECTRICAL AND COMPUTER ENGINEERING

Adel S. Sedra, Series Editor

Allen and Holberg, *CMOS Analog Circuit Design, 3rd edition*
Bobrow, *Elementary Linear Circuit Analysis, 2nd edition*
Bobrow, *Fundamentals of Electrical Engineering, 2nd edition*
Campbell, *Fabrication Engineering at the Micro- and Nanoscale, 4th edition*
Chen, *Digital Signal Processing*
Chen, *Linear System Theory and Design, 4th edition*
Chen, *Signals and Systems, 3rd edition*
Comer, *Digital Logic and State Machine Design, 3rd edition*
Comer, *Microprocessor-Based System Design*
Cooper and McGillem, *Probabilistic Methods of Signal and System Analysis, 3rd edition*
Dimitrijev, *Principles of Semiconductor Device, 2nd edition*
Dimitrijev, *Understanding Semiconductor Devices*
Fortney, *Principles of Electronics: Analog & Digital*
Franco, *Electric Circuits Fundamentals*
Ghausi, *Electronic Devices and Circuits: Discrete and Integrated*
Guru and Hiziroğlu, *Electric Machinery and Transformers, 3rd edition*
Houts, *Signal Analysis in Linear Systems*
Jones, *Introduction to Optical Fiber Communication Systems*
Krein, *Elements of Power Electronics, 2nd edition*
Kuo, *Digital Control Systems, 3rd edition*
Lathi and Green, *Linear Systems and Signals, 3rd edition*
Lathi and Ding, *Modern Digital and Analog Communication Systems, 5th edition*
Lathi, *Signal Processing and Linear Systems, 2nd edition*
Martin, *Digital Integrated Circuit Design*
Miner, *Lines and Electromagnetic Fields for Engineers*
Mitra, *Signals and Systems*
Parhami, *Computer Architecture*
Parhami, *Computer Arithmetic, 2nd edition*
Roberts and Sedra, *SPICE, 2nd edition*
Roberts, Taenzler, and Burns, *An Introduction to Mixed-Signal IC Test and Measurement, 2nd edition*
Roulston, *An Introduction to the Physics of Semiconductor Devices*
Sadiku, *Elements of Electromagnetics, 7th edition*
Santina, Stubberud, and Hostetter, *Digital Control System Design, 2nd edition*
Sarma, *Introduction to Electrical Engineering*
Schaumann, Xiao, and Van Valkenburg, *Design of Analog Filters, 3rd edition*
Schwarz and Oldham, *Electrical Engineering: An Introduction, 2nd edition*
Sedra and Smith, *Microelectronic Circuits, 8th edition*
Stefani, Shahian, Savant, and Hostetter, *Design of Feedback Control Systems, 4th edition*
Tsividis, *Operation and Modeling of the MOS Transistor, 3rd edition*
Van Valkenburg, *Analog Filter Design*
Warner and Grung, *Semiconductor Device Electronics*
Wolovich, *Automatic Control Systems*
Yariv and Yeh, *Photonics: Optical Electronics in Modern Communications, 6th edition*
Żak, *Systems and Control*

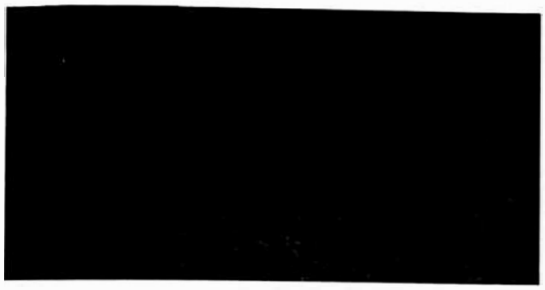

SIGNAL PROCESSING AND LINEAR SYSTEMS

SECOND EDITION

B. P. Lathi and R. A. Green

New York Oxford
OXFORD UNIVERSITY PRESS
2018

Oxford University Press is a department of the University of Oxford.
It furthers the University's objective of excellence in research, scholarship,
and education by publishing worldwide. Oxford is a registered trademark
of Oxford University Press in the UK and certain other countries.

Published in the United States of America by Oxford University Press
198 Madison Avenue, New York, NY 10016, United States of America.

© 2021 by Oxford University Press

For titles covered by Section 112 of the US Higher Education Opportunity Act, please visit www.oup.com/us/he for the latest information about pricing and alternate formats.

All rights reserved. No part of this publication may be reproduced, stored
in a retrieval system, or transmitted, in any form or by any means, without
the prior permission in writing of Oxford University Press, or as expressly
permitted by law, by license, or under terms agreed with the appropriate
reproduction rights organization. Inquiries concerning reproduction outside
the scope of the above should be sent to the Rights Department, Oxford
University Press, at the address above.

You must not circulate this work in any other form
and you must impose this same condition on any acquirer.

Library of Congress Cataloging-in-Publication Data
Names: Lathi, B. P. (Bhagwandas Pannalal), author. | Green, R. A. (Roger A.), author.
Title: Signal processing and linear systems / B.P. Lathi and R.A. Green.
Description: Second edition. | New York: Oxford University Press, 2021. |
Series: The Oxford series in electrical and computer engineering |
Includes index. |
[redacted]
Subjects: LCSH: Signal processing. | Linear systems. | System analysis.
[redacted]

[redacted]
Printed by LSC Communications, United States of America

CONTENTS

PREFACE x

B BACKGROUND

B.1 Complex Numbers 1
B.2 Sinusoids 16
B.3 Sketching Signals 20
B.4 Cramer's Rule 22
B.5 Partial Fraction Expansion 25
B.6 Vectors and Matrices 35
B.7 MATLAB: Elementary Operations 42
B.8 Appendix: Useful Mathematical Formulas 54
References 58
Problems 59

1 SIGNALS AND SYSTEMS

1.1 Size of a Signal 64
1.2 Some Useful Signal Operations 71
1.3 Classification of Signals 78
1.4 Some Useful Signal Models 82
1.5 Even and Odd Functions 92
1.6 Systems 95
1.7 Classification of Systems 97
1.8 System Model: Input–Output Description 111
1.9 Internal and External Descriptions of a System 119
1.10 Internal Description: The State-Space Description 121
1.11 MATLAB: Working with Functions 126
1.12 Summary 133
References 135
Problems 136

2 TIME-DOMAIN ANALYSIS OF CONTINUOUS-TIME SYSTEMS

2.1 Introduction 150
2.2 System Response to Internal Conditions: The Zero-Input Response 151
2.3 The Unit Impulse Response $h(t)$ 163
2.4 System Response to External Input: The Zero-State Response 168
2.5 System Stability 196
2.6 Intuitive Insights into System Behavior 203
2.7 MATLAB: M-Files 212
2.8 Appendix: Determining the Impulse Response 220
2.9 Summary 221
References 223
Problems 223

3 SIGNAL REPRESENTATION BY FOURIER SERIES

3.1 Signals as Vectors 237
3.2 Signal Comparison: Correlation 243
3.3 Signal Representation by an Orthogonal Signal Set 250
3.4 Trigonometric Fourier Series 261
3.5 Existence and Convergence of the Fourier Series 277
3.6 Exponential Fourier Series 286
3.7 LTIC System Response to Periodic Inputs 303
3.8 Numerical Computation of D_n 307
3.9 MATLAB: Fourier Series Applications 309
3.10 Summary 316
References 317
Problems 318

4 CONTINUOUS-TIME SIGNAL ANALYSIS: THE FOURIER TRANSFORM

4.1 Aperiodic Signal Representation by the Fourier Integral 330
4.2 Transforms of Some Useful Functions 340
4.3 Some Properties of the Fourier Transform 352
4.4 Signal Transmission Through LTIC Systems 372
4.5 Ideal and Practical Filters 381
4.6 Signal Energy 384
4.7 Application to Communications: Amplitude Modulation 388
4.8 Angle Modulation 401
4.9 Data Truncation: Window Functions 414
4.10 MATLAB: Fourier Transform Topics 420
4.11 Summary 425

References 427
Problems 427

5 SAMPLING

5.1 The Sampling Theorem 440
5.2 Signal Reconstruction 449
5.3 Analog-to-Digital (A/D) Conversion 463
5.4 Dual of Time Sampling: Spectral Sampling 466
5.5 Numerical Computation of the Fourier Transform: The Discrete Fourier Transform 469
5.6 The Fast Fourier Transform (FFT) 488
5.7 MATLAB: The Discrete Fourier Transform 491
5.8 Summary 498
References 499
Problems 499

6 CONTINUOUS-TIME SYSTEM ANALYSIS USING THE LAPLACE TRANSFORM

6.1 The Laplace Transform 509
6.2 Some Properties of the Laplace Transform 532
6.3 Solution of Differential and Integro-Differential Equations 544
6.4 Analysis of Electrical Networks: The Transformed Network 557
6.5 Block Diagrams 570
6.6 System Realization 572
6.7 Application to Feedback and Controls 588
6.8 The Bilateral Laplace Transform 612
6.9 Summary 622
References 624
Problems 624

7 FREQUENCY RESPONSE AND ANALOG FILTERS

7.1 Frequency Response of an LTIC System 638
7.2 Bode Plots 646
7.3 Control System Design Using Frequency Response 662
7.4 Filter Design by Placement of Poles and Zeros of $H(s)$ 667
7.5 Butterworth Filters 677
7.6 Chebyshev Filters 688
7.7 Frequency Transformations 700
7.8 Filters to Satisfy Distortionless Transmission Conditions 714
7.9 MATLAB: Continuous-Time Filters 716

7.10 Summary 721
References 722
Problems 722

8 DISCRETE-TIME SIGNALS AND SYSTEMS

8.1 Introduction 730
8.2 Useful Signal Operations 733
8.3 Some Useful Discrete-Time Signal Models 738
8.4 Aliasing and Sampling Rate 753
8.5 Examples of Discrete-Time Systems 756
8.6 MATLAB: Representing, Manipulating, and Plotting Discrete-Time Signals 765
8.7 Summary 766
Problems 768

9 TIME-DOMAIN ANALYSIS OF DISCRETE-TIME SYSTEMS

9.1 Classification of Discrete-Time Systems 774
9.2 Discrete-Time System Equations 777
9.3 System Response to Internal Conditions: The Zero-Input Response 782
9.4 The Unit Impulse Response $h[n]$ 789
9.5 System Response to External Input: The Zero-State Response 793
9.6 System Stability 811
9.7 Intuitive Insights into System Behavior 817
9.8 MATLAB: Discrete-Time Systems 819
9.9 Appendix: Impulse Response for a Special Case 823
9.10 Summary 824
Problems 825

10 FOURIER ANALYSIS OF DISCRETE-TIME SIGNALS

10.1 Periodic Signal Representation by Discrete-Time Fourier Series 838
10.2 Aperiodic Signal Representation by Fourier Integral 847
10.3 Properties of the DTFT 859
10.4 DTFT Connection with the CTFT 869
10.5 LTI Discrete-Time System Analysis by DTFT 872
10.6 Signal Processing by the DFT and FFT 877
10.7 Generalization of the DTFT to the z-Transform 899
10.8 MATLAB: Working with the DTFS and the DTFT 902
10.9 Summary 905
Reference 906
Problems 906

11 DISCRETE-TIME SYSTEM ANALYSIS USING THE z-TRANSFORM

11.1 The z-Transform 918
11.2 Some Properties of the z-Transform 931
11.3 z-Transform Solution of Linear Difference Equations 939
11.4 System Realization 950
11.5 Connecting the Laplace and z-Transforms 956
11.6 Sampled-Data (Hybrid) Systems 959
11.7 The Bilateral z-Transform 966
11.8 Summary 975
Reference 975
Problems 976

12 FREQUENCY RESPONSE AND DIGITAL FILTERS

12.1 Frequency Response of Discrete-Time Systems 986
12.2 Frequency Response from Pole-Zero Locations 993
12.3 Digital Filters 1001
12.4 Filter Design Criteria 1003
12.5 Recursive Filter Design by the Time-Domain Criterion: The Impulse Invariance Method 1006
12.6 Recursive Filter Design by the Frequency-Domain Criterion: The Bilinear Transformation Method 1012
12.7 Nonrecursive Filters 1027
12.8 Nonrecursive Filter Design 1031
12.9 MATLAB: Designing High-Order Filters 1047
12.10 Summary 1053
Reference 1054
Problems 1054

13 STATE-SPACE ANALYSIS

13.1 Mathematical Preliminaries 1065
13.2 Introduction to State Space 1069
13.3 A Systematic Procedure to Determine State Equations 1072
13.4 Solution of State Equations 1082
13.5 Linear Transformation of a State Vector 1095
13.6 Controllability and Observability 1103
13.7 State-Space Analysis of Discrete-Time Systems 1109
13.8 MATLAB: Toolboxes and State-Space Analysis 1117
13.9 Summary 1125
References 1125
Problems 1126

INDEX 1130

PREFACE

This book, *Signal Processing and Linear Systems*, presents a comprehensive treatment of signals and linear systems at an introductory level, most suitable for junior and senior college/university students in electrical engineering. This second edition contains most of the material from the third edition of our book *Linear Systems and Signals* (2018), with added chapters on analog and digital filters and digital signal processing. Additional applications to communications and controls are also included. The sequence of topics in this book are somewhat different from those in the *Linear Systems and Signals* book. Here, the Laplace transform follows Fourier, whereas in the 2018 book, the sequence is the exact opposite. This book, like its 2018 sibling, contains enough material on discrete-time systems so that it can be used not only for a traditional course in Signals and Systems, but also for an introductory course in Digital Signal Processing.

One perceptive author has said: "The function of a teacher is not so much to cover the topics of study as to uncover them for students." The same can be said of a textbook. It is in this spirit that our textbooks emphasize a physical appreciation of concepts through *heuristic reasoning*[†] and the use of metaphors, analogies, and creative explanations. Such an approach is much different from a purely deductive technique that uses mere mathematical manipulation of symbols. There is a temptation to treat engineering subjects as a branch of applied mathematics. Such an approach is a perfect match to the public image of engineering as a dry and dull discipline. It ignores the physical meaning behind various derivations and deprives a student of not only an intuitive understanding but also the enjoyable experience of logically uncovering the subject matter. In this book, we use mathematics not so much to prove axiomatic theory as to support and enhance physical and intuitive understanding. Wherever possible, theoretical results are interpreted heuristically and enhanced by carefully chosen examples and analogies.

This second edition, which closely follows the organization of the first edition, has been refined in many ways. Discussions are streamlined, with material added or trimmed as needed. Equation, example, and section labeling is simplified and improved. Computer examples are fully updated to reflect the most current version of MATLAB, and new sections are included throughout the text that illustrate the use of MATLAB as a useful tool to investigate concepts and solve problems. Hundreds of additional problems provide new opportunities to learn and understand topics.

[†] Heuristic (from the Greek *heuriskein*, meaning "to invent, discover"): a method of education in which students are trained to find out things for themselves. The word "eureka" (I have found it) is the first-person singular perfect active indicative of *heuriskein*. We hope that this book provides every reader with many opportunities for their own *eureka* moments.

NOTABLE FEATURES

The notable features of this book include the following:

1. Intuitive and heuristic understanding of the concepts and physical meaning of mathematical results are emphasized throughout. Such an approach not only leads to deeper appreciation and easier comprehension of the concepts, but also makes learning enjoyable for students.
2. Often, students lack an adequate background in basic material such as complex numbers, sinusoids, quick sketching of functions, Cramer's rule, partial fraction expansion, and matrix algebra. We include a background chapter that addresses these basic and pervasive topics in electrical engineering. The response by students has been unanimously enthusiastic.
3. There are hundreds of worked out examples in addition to exercises (usually with answers) for students to test their understanding. Also, there are over 900 end-of-chapter problems of varying difficulty.
4. Modern electrical engineering practice requires the use of computer calculation and simulation, most often the software package MATLAB. Thus, we integrate MATLAB into many of the worked examples throughout the book. Additionally, most chapters conclude with a section devoted to learning and using MATLAB in the context and support of book topics. Problem sets also contain numerous computer problems.
5. The discrete-time and continuous-time systems may be treated in sequence, or they may be integrated by using a parallel approach.
6. The summary at the end of each chapter will prove helpful to students in summing up essential developments in the chapter.
7. There are several historical notes to enhance students' interest in the subject. This information introduces students to the historical background that influenced the development of electrical engineering.
8. Unlike *Linear Signals and Systems*, this book provides extensive applications in the areas of communication, controls, and filtering.

ORGANIZATION AND USE

The book opens with a chapter titled "Background," which deals with the mathematical background material that the reader is expected to have already mastered. It includes topics such as complex numbers, sinusoids, sketching signals, Cramer's rule, partial fraction expansion, and matrix algebra. The next seven chapters address continuous-time signals and systems, followed by five chapters treating discrete-time signals and systems. The last chapter introduces state-space analysis. There are MATLAB examples dispersed throughout the book. The book can be readily tailored for a variety of courses of 30 to 90 lecture hours. It can also be used as a text for a first undergraduate course in Digital Signal Processing (DSP).

The organization of the book permits a great deal of flexibility in teaching continuous-time and discrete-time concepts. The natural sequence of chapters is meant for a sequential approach in which continuous-time analysis is covered first, followed by discrete-time analysis. It is also possible to integrate (interweave) continuous-time and discrete-time analysis by using an appropriate sequence of chapters.

MATLAB

MATLAB is a sophisticated language that serves as a powerful tool to better understand engineering topics, including control theory, filter design, and, of course, linear systems and signals. MATLAB's flexible programming structure promotes rapid development and analysis. Outstanding visualization capabilities provide unique insight into system behavior and signal character.

As with any language, learning MATLAB is incremental and requires practice. This book provides two levels of exposure to MATLAB. First, MATLAB is integrated into many examples throughout the text to reinforce concepts and perform various computations. These examples utilize standard MATLAB functions as well as functions from the control system, signal-processing, and symbolic math toolboxes. MATLAB has many more toolboxes available, but these three are commonly available in most engineering departments.

A second and deeper level of exposure to MATLAB is achieved by concluding most chapters with a separate MATLAB section. Taken together, these sections provide a self-contained introduction to the MATLAB environment that allows even novice users to quickly gain MATLAB proficiency and competence. These sessions provide detailed instruction on how to use MATLAB to solve problems in linear systems and signals. Except for the very last chapter, care has been taken to generally avoid the use of toolbox functions in the MATLAB sessions. Rather, readers are shown the process of developing their own code. In this way, those readers without toolbox access are not at a disadvantage. All of this book's MATLAB code is available for download at the OUP Companion Website.

CREDITS AND ACKNOWLEDGMENTS

Portrait of Gerolamo Cardano, courtesy of Wellcome Collection. Portrait of Karl Friedrich Gauss, courtesy of Gauß-Gesellschaft Göttingen e.V. (Foto: A. Wittmann). Photo of Albert Michelson, courtesy of Smithsonian Institution Libraries. Portrait of Josiah Willard Gibbs, courtesy of F. B. Carpenter. Portrait of Jean-Baptiste-Joseph Fourier, courtesy of Smithsonian Institution Libraries. Portrait of Napoleon, © iStock/GeorgiosArt. Portrait of Pierre-Simon de Laplace, courtesy of Wellcome Collection. CC BY. Photo of Oliver Heaviside, courtesy of Smithsonian Institution Libraries.

Many individuals have helped us in the preparation of this book, as well as its earlier editions. We are grateful to each and every one of them for their helpful suggestions and comments. Book writing is an obsessively time-consuming activity, which causes much hardship for an author's family. We both are grateful to our families for their enormous but invisible sacrifices.

B. P. Lathi
R. A. Green

BACKGROUND

The topics discussed in this chapter are not entirely new to students taking this course. You have already studied many of these topics in earlier courses or are expected to know them from your previous training. Even so, this background material deserves a review because it is so pervasive in the area of signals and systems. Investing a little time in such a review will pay big dividends later. Furthermore, this material is useful not only for this course but also for several courses that follow. It will also be helpful later, as reference material in your professional career.

B.1 COMPLEX NUMBERS

Complex numbers are an extension of ordinary numbers and are an integral part of the modern number system. Complex numbers, particularly *imaginary numbers*, sometimes seem mysterious and unreal. This feeling of unreality derives from their unfamiliarity and novelty rather than their supposed nonexistence! Mathematicians blundered in calling these numbers "imaginary," for the term immediately prejudices perception. Had these numbers been called by some other name, they would have become demystified long ago, just as irrational numbers or negative numbers were. Many futile attempts have been made to ascribe some physical meaning to imaginary numbers. However, this effort is needless. In mathematics we assign symbols and operations any meaning we wish as long as internal consistency is maintained. The history of mathematics is full of entities that were unfamiliar and held in abhorrence until familiarity made them acceptable. This fact will become clear from the following historical note.

B.1.1 A Historical Note

Among early people the number system consisted only of natural numbers (positive integers) needed to express the number of children, cattle, and quivers of arrows. These people had no need for fractions. Whoever heard of two and one-half children or three and one-fourth cows!

However, with the advent of agriculture, people needed to measure continuously varying quantities, such as the length of a field and the weight of a quantity of butter. The number system, therefore, was extended to include fractions. The ancient Egyptians and Babylonians knew how

to handle fractions, but *Pythagoras* discovered that some numbers (like the diagonal of a unit square) could not be expressed as a whole number or a fraction. Pythagoras, a number mystic, who regarded numbers as the essence and principle of all things in the universe, was so appalled at his discovery that he swore his followers to secrecy and imposed a death penalty for divulging this secret [1]. These numbers, however, were included in the number system by the time of Descartes, and they are now known as *irrational numbers*.

Until recently, *negative numbers* were not a part of the number system. The concept of negative numbers must have appeared absurd to early man. However, the medieval Hindus had a clear understanding of the significance of positive and negative numbers [2, 3]. They were also the first to recognize the existence of absolute negative quantities [4]. The works of *Bhaskar* (1114–1185) on arithmetic (*Līlāvatī*) and algebra (*Bījaganit*) not only use the decimal system but also give rules for dealing with negative quantities. Bhaskar recognized that positive numbers have two square roots [5]. Much later, in Europe, the men who developed the banking system that arose in Florence and Venice during the late Renaissance (fifteenth century) are credited with introducing a crude form of negative numbers. The seemingly absurd subtraction of 7 from 5 seemed reasonable when bankers began to allow their clients to draw seven gold ducats while their deposit stood at five. All that was necessary for this purpose was to write the difference, 2, on the debit side of a ledger [6].

Thus, the number system was once again broadened (generalized) to include negative numbers. The acceptance of negative numbers made it possible to solve equations such as $x+5=0$, which had no solution before. Yet for equations such as $x^2+1=0$, leading to $x^2=-1$, the solution could not be found in the real number system. It was therefore necessary to define a completely new kind of number with its square equal to -1. During the time of Descartes and Newton, imaginary (or complex) numbers came to be accepted as part of the number system, but they were still regarded as algebraic fiction. The Swiss mathematician *Leonhard Euler* introduced the notation i (for *imaginary*) around 1777 to represent $\sqrt{-1}$. Electrical engineers use the notation j instead of i to avoid confusion with the notation i often used for electrical current. Thus,

$$j^2=-1 \qquad \text{and} \qquad \sqrt{-1}=\pm j$$

This notation allows us to determine the square root of any negative number. For example,

$$\sqrt{-4}=\sqrt{4}\times\sqrt{-1}=\pm 2j$$

When imaginary numbers are included in the number system, the resulting numbers are called *complex numbers*.

Origins of Complex Numbers

Ironically (and contrary to popular belief), it was not the solution of a quadratic equation, such as $x^2+1=0$, but a cubic equation with real roots that made imaginary numbers plausible and acceptable to early mathematicians. They could dismiss $\sqrt{-1}$ as pure nonsense when it appeared as a solution to $x^2+1=0$ because this equation has no real solution. But in 1545, *Gerolamo Cardano* of Milan published *Ars Magna* (The Great Art), the most important algebraic work of the Renaissance. In this book, he gave a method of solving a general cubic equation in which a root

of a negative number appeared in an intermediate step. According to his method, the solution to a third-order equation†

$$x^3 + ax + b = 0$$

is given by

$$x = \sqrt[3]{-\frac{b}{2} + \sqrt{\frac{b^2}{4} + \frac{a^3}{27}}} + \sqrt[3]{-\frac{b}{2} - \sqrt{\frac{b^2}{4} + \frac{a^3}{27}}}$$

For example, to find a solution of $x^3 + 6x - 20 = 0$, we substitute $a = 6, b = -20$ in the foregoing equation to obtain

$$x = \sqrt[3]{10 + \sqrt{108}} + \sqrt[3]{10 - \sqrt{108}} = \sqrt[3]{20.392} - \sqrt[3]{0.392} = 2$$

We can readily verify that 2 is indeed a solution of $x^3 + 6x - 20 = 0$. But when Cardano tried to solve the equation $x^3 - 15x - 4 = 0$ by this formula, his solution was

$$x = \sqrt[3]{2 + \sqrt{-121}} + \sqrt[3]{2 - \sqrt{-121}}$$

What was Cardano to make of this equation in the year 1545? In those days, negative numbers were themselves suspect, and a square root of a negative number was doubly preposterous! Today, we know that

$$(2 \pm j)^3 = 2 \pm j11 = 2 \pm \sqrt{-121}$$

Therefore, Cardano's formula gives

$$x = (2 + j) + (2 - j) = 4$$

We can readily verify that $x = 4$ is indeed a solution of $x^3 - 15x - 4 = 0$. Cardano tried to explain halfheartedly the presence of $\sqrt{-121}$ but ultimately dismissed the whole enterprise as being "as subtle as it is useless." A generation later, however, *Raphael Bombelli* (1526–1573), after examining Cardano's results, proposed acceptance of imaginary numbers as a necessary vehicle that would transport the mathematician from the *real* cubic equation to its *real* solution. In other words, although we begin and end with real numbers, we seem compelled to move into an unfamiliar world of imaginaries to complete our journey. To mathematicians of the day, this proposal seemed incredibly strange [7]. Yet they could not dismiss the idea of imaginary numbers so easily because this concept yielded the real solution of an equation. It took two more centuries

† This equation is known as the *depressed cubic* equation. A general cubic equation

$$y^3 + py^2 + qy + r = 0$$

can always be reduced to a depressed cubic form by substituting $y = x - (p/3)$. Therefore, any general cubic equation can be solved if we know the solution to the depressed cubic. The depressed cubic was independently solved, first by *Scipione del Ferro* (1465–1526) and then by *Niccolo Fontana* (1499–1557). The latter is better known in the history of mathematics as *Tartaglia* ("Stammerer"). Cardano learned the secret of the depressed cubic solution from Tartaglia. He then showed that by using the substitution $y = x - (p/3)$, a general cubic is reduced to a depressed cubic.

for the full importance of complex numbers to become evident in the works of Euler, Gauss, and Cauchy. Still, Bombelli deserves credit for recognizing that such numbers have a role to play in algebra [7].

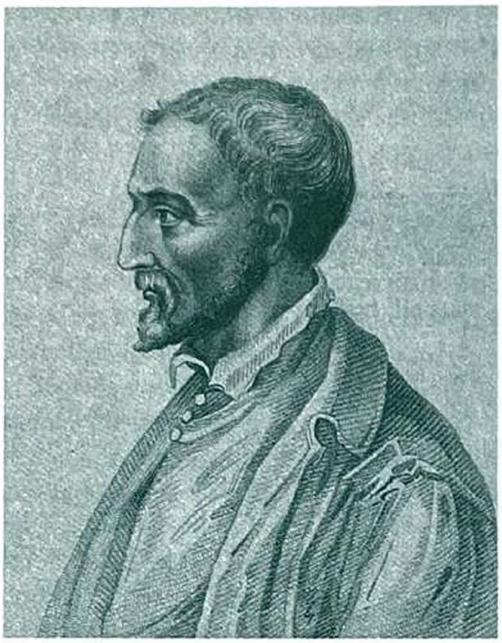

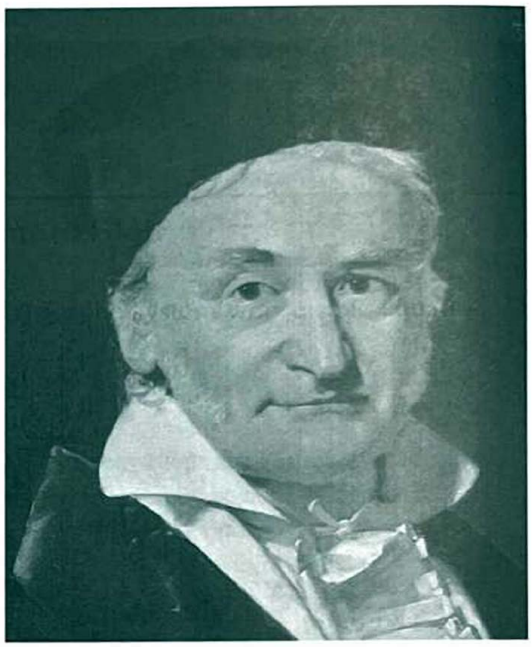

Gerolamo Cardano and Karl Friedrich Gauss

In 1799 the German mathematician *Karl Friedrich Gauss*, at the ripe age of 22, proved the fundamental theorem of algebra, namely that every algebraic equation in one unknown has a root in the form of a complex number. He showed that every equation of the nth order has exactly n solutions (roots), no more and no less. Gauss was also one of the first to give a coherent account of complex numbers and to interpret them as points in a complex plane. It is he who introduced the term *complex numbers* and paved the way for their general and systematic use. The number system was once again broadened or generalized to include imaginary numbers. Ordinary (or real) numbers became a special case of generalized (or complex) numbers.

The utility of complex numbers can be understood readily by an analogy with two neighboring countries X and Y, as illustrated in Fig. B.1. If we want to travel from City a to City b (both in Country X), the shortest route is through Country Y, although the journey begins and ends in Country X. We may, if we desire, perform this journey by an alternate route that lies exclusively in X, but this alternate route is longer. In mathematics we have a similar situation with real numbers (Country X) and complex numbers (Country Y). Most real-world problems start with real numbers, and the final results must also be in real numbers. But the derivation of results is considerably simplified by using complex numbers as an intermediary. It is also possible to solve any real-world problem by an alternate method, using real numbers exclusively, but such procedures would increase the work needlessly.

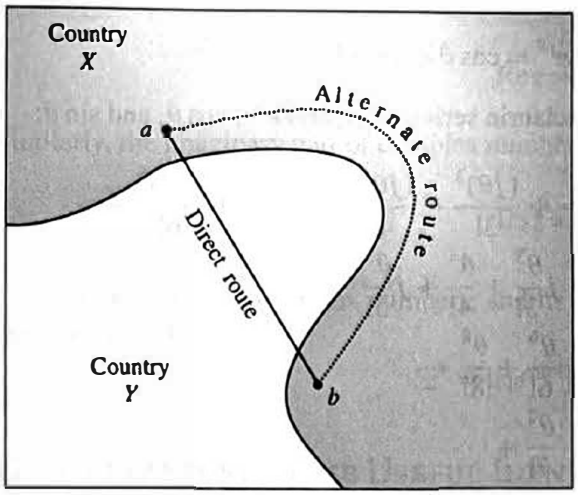

Figure B.1 Use of complex numbers can reduce the work.

B.1.2 Algebra of Complex Numbers

A complex number (a,b) or $a+jb$ can be represented graphically by a point whose Cartesian coordinates are (a,b) in a complex plane (Fig. B.2). Let us denote this complex number by z so that

$$z = a + jb \tag{B.1}$$

This representation is the Cartesian (or rectangular) form of complex number z. The numbers a and b (the abscissa and the ordinate) of z are the *real part* and the *imaginary part*, respectively, of z. They are also expressed as

$$\text{Re}\, z = a \qquad \text{and} \qquad \text{Im}\, z = b$$

Note that in this plane all real numbers lie on the horizontal axis, and all imaginary numbers lie on the vertical axis.

Complex numbers may also be expressed in terms of polar coordinates. If (r,θ) are the polar coordinates of a point $z = a + jb$ (see Fig. B.2), then

$$a = r\cos\theta \qquad \text{and} \qquad b = r\sin\theta$$

Consequently,

$$z = a + jb = r\cos\theta + jr\sin\theta = r(\cos\theta + j\sin\theta) \tag{B.2}$$

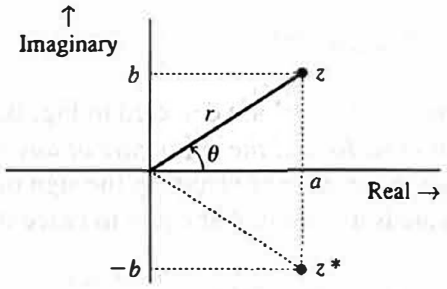

Figure B.2 Representation of a number in the complex plane.

Euler's formula states that

$$e^{j\theta} = \cos\theta + j\sin\theta \tag{B.3}$$

To prove Euler's formula, we use a Maclaurin series to expand $e^{j\theta}$, $\cos\theta$, and $\sin\theta$:

$$\begin{aligned} e^{j\theta} &= 1 + j\theta + \frac{(j\theta)^2}{2!} + \frac{(j\theta)^3}{3!} + \frac{(j\theta)^4}{4!} + \frac{(j\theta)^5}{5!} + \frac{(j\theta)^6}{6!} + \cdots \\ &= 1 + j\theta - \frac{\theta^2}{2!} - j\frac{\theta^3}{3!} + \frac{\theta^4}{4!} + j\frac{\theta^5}{5!} - \frac{\theta^6}{6!} - \cdots \\ \cos\theta &= 1 - \frac{\theta^2}{2!} + \frac{\theta^4}{4!} - \frac{\theta^6}{6!} + \frac{\theta^8}{8!} \cdots \\ \sin\theta &= \theta - \frac{\theta^3}{3!} + \frac{\theta^5}{5!} - \frac{\theta^7}{7!} + \cdots \end{aligned}$$

Clearly, it follows that $e^{j\theta} = \cos\theta + j\sin\theta$. Using Eq. (B.3) in Eq. (B.2) yields

$$z = re^{j\theta} \tag{B.4}$$

This representation is the polar form of complex number z.

Summarizing, a complex number can be expressed in rectangular form $a + jb$ or polar form $re^{j\theta}$ with

$$\begin{aligned} a &= r\cos\theta \\ b &= r\sin\theta \end{aligned} \qquad \text{and} \qquad \begin{aligned} r &= \sqrt{a^2 + b^2} \\ \theta &= \tan^{-1}\left(\tfrac{b}{a}\right) \end{aligned} \tag{B.5}$$

Observe that r is the distance of the point z from the origin. For this reason, r is also called the *magnitude* (or *absolute value*) of z and is denoted by $|z|$. Similarly, θ is called the angle of z and is denoted by $\angle z$. Therefore, we can also write polar form of Eq. (B.4) as

$$z = |z|e^{j\angle z} \qquad \text{where } |z| = r \text{ and } \angle z = \theta$$

Using polar form, we see that the reciprocal of a complex number is given by

$$\frac{1}{z} = \frac{1}{re^{j\theta}} = \frac{1}{r}e^{-j\theta} = \frac{1}{|z|}e^{-j\angle z}$$

Conjugate of a Complex Number

We define z^*, the *conjugate* of $z = a + jb$, as

$$z^* = a - jb = re^{-j\theta} = |z|e^{-j\angle z} \tag{B.6}$$

The graphical representations of a number z and its conjugate z^* are depicted in Fig. B.2. Observe that z^* is a mirror image of z about the horizontal axis. *To find the conjugate of any number, we need only replace j with $-j$ in that number* (which is the same as changing the sign of its angle).

The sum of a complex number and its conjugate is a real number equal to twice the real part of the number:

$$z + z^* = (a + jb) + (a - jb) = 2a = 2\,\mathrm{Re}\,z$$

Thus, we see that the real part of complex number z can be computed as

$$\mathrm{Re}z = \frac{z+z^*}{2} \tag{B.7}$$

Similarly, the imaginary part of complex number z can be computed as

$$\mathrm{Im}z = \frac{z-z^*}{2j} \tag{B.8}$$

The product of a complex number z and its conjugate is a real number $|z|^2$, the square of the magnitude of the number:

$$zz^* = |z|e^{j\angle z}|z|e^{-j\angle z} = |z|^2 \tag{B.9}$$

Understanding Some Useful Identities

In a complex plane, $re^{j\theta}$ represents a point at a distance r from the origin and at an angle θ with the horizontal axis, as shown in Fig. B.3a. For example, the number -1 is at a unit distance from the origin and has an angle π or $-\pi$ (more generally, π plus any integer multiple of 2π), as seen from Fig. B.3b. Therefore,

$$-1 = e^{j(\pi+2\pi n)} \qquad n \text{ integer}$$

The number 1, on the other hand, is also at a unit distance from the origin, but has an angle 0 (more generally, 0 plus any integer multiple of 2π). Therefore,

$$1 = e^{j2\pi n} \qquad n \text{ integer} \tag{B.10}$$

The number j is at a unit distance from the origin and its angle is $\frac{\pi}{2}$ (more generally, $\frac{\pi}{2}$ plus any integer multiple of 2π), as seen from Fig. B.3b. Therefore,

$$j = e^{j(\frac{\pi}{2}+2\pi n)} \qquad n \text{ integer}$$

Similarly,

$$-j = e^{j(-\frac{\pi}{2}+2\pi n)} \qquad n \text{ integer}$$

Notice that the angle of any complex number is only known within an integer multiple of 2π.

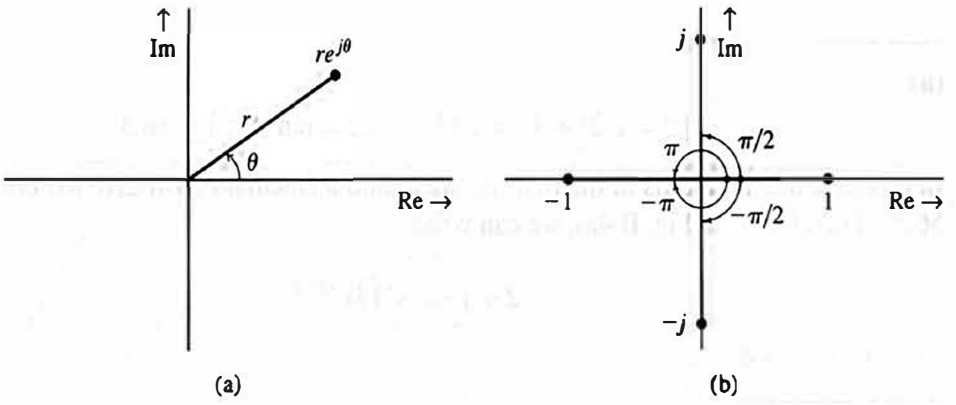

Figure B.3 Understanding some useful identities in terms of $re^{j\theta}$.

This discussion shows the usefulness of the graphic picture of $re^{j\theta}$. This picture is also helpful in several other applications. For example, to determine the limit of $e^{(\alpha+j\omega)t}$ as $t \to \infty$, we note that

$$e^{(\alpha+j\omega)t} = e^{\alpha t}e^{j\omega t}$$

Now the magnitude of $e^{j\omega t}$ is unity regardless of the value of ω or t because $e^{j\omega t} = re^{j\theta}$ with $r = 1$. Therefore, $e^{\alpha t}$ determines the behavior of $e^{(\alpha+j\omega)t}$ as $t \to \infty$ and

$$\lim_{t\to\infty} e^{(\alpha+j\omega)t} = \lim_{t\to\infty} e^{\alpha t}e^{j\omega t} = \begin{cases} 0 & \alpha < 0 \\ \infty & \alpha > 0 \end{cases}$$

In future discussions, you will find it very useful to remember $re^{j\theta}$ as a number at a distance r from the origin and at an angle θ with the horizontal axis of the complex plane.

A Warning About Computing Angles with Calculators

From the Cartesian form $a + jb$, we can readily compute the polar form $re^{j\theta}$ [see Eq. (B.5)]. Calculators provide ready conversion of rectangular into polar and vice versa. However, if a calculator computes an angle of a complex number by using an inverse tangent function $\theta = \tan^{-1}(b/a)$, proper attention must be paid to the quadrant in which the number is located. For instance, θ corresponding to the number $-2 - j3$ is $\tan^{-1}(-3/-2)$. This result is not the same as $\tan^{-1}(3/2)$. The former is $-123.7°$, whereas the latter is $56.3°$. A calculator cannot make this distinction and can give a correct answer only for angles in the first and fourth quadrants.† A calculator will read $\tan^{-1}(-3/-2)$ as $\tan^{-1}(3/2)$, which is clearly wrong. When you are computing inverse trigonometric functions, if the angle appears in the second or third quadrant, the answer of the calculator is off by 180°. The correct answer is obtained by adding or subtracting 180° to the value found with the calculator (either adding or subtracting yields the correct answer). For this reason, it is advisable to draw the point in the complex plane and determine the quadrant in which the point lies. This issue will be clarified by the following examples.

EXAMPLE B.1 Cartesian to Polar Form

Express the following numbers in polar form: **(a)** $2 + j3$, **(b)** $-2 + j1$, **(c)** $-2 - j3$, and **(d)** $1 - j3$.

(a)

$$|z| = \sqrt{2^2 + 3^2} = \sqrt{13} \qquad \angle z = \tan^{-1}\left(\tfrac{3}{2}\right) = 56.3°$$

In this case the number is in the first quadrant, and a calculator will give the correct value of 56.3°. Therefore (see Fig. B.4a), we can write

$$2 + j3 = \sqrt{13}e^{j56.3°}$$

---

† Calculators with two-argument inverse tangent functions will correctly compute angles.

(b)

$$|z| = \sqrt{(-2)^2 + 1^2} = \sqrt{5} \qquad \angle z = \tan^{-1}\left(\frac{1}{-2}\right) = 153.4°$$

In this case the angle is in the second quadrant (see Fig. B.4b), and therefore the answer given by the calculator, $\tan^{-1}(1/-2) = -26.6°$, is off by 180°. The correct answer is $(-26.6 \pm 180)° = 153.4°$ or $-206.6°$. Both values are correct because they represent the same angle. It is a common practice to choose an angle whose numerical value is less than 180°. Such a value is called the *principal value* of the angle, which in this case is 153.4°. Therefore,

$$-2 + j1 = \sqrt{5}e^{j153.4°}$$

(c)

$$|z| = \sqrt{(-2)^2 + (-3)^2} = \sqrt{13} \qquad \angle z = \tan^{-1}\left(\frac{-3}{-2}\right) = -123.7°$$

In this case the angle appears in the third quadrant (see Fig. B.4c), and therefore the answer obtained by the calculator ($\tan^{-1}(-3/-2) = 56.3°$) is off by 180°. The correct answer is $(56.3 \pm 180)° = 236.3°$ or $-123.7°$. We choose the principal value $-123.7°$ so that (see Fig. B.4c)

$$-2 - j3 = \sqrt{13}e^{-j123.7°}$$

(d)

$$|z| = \sqrt{1^2 + (-3)^2} = \sqrt{10} \qquad \angle z = \tan^{-1}\left(\frac{-3}{1}\right) = -71.6°$$

In this case the angle appears in the fourth quadrant (see Fig. B.4d), and therefore the answer given by the calculator, $\tan^{-1}(-3/1) = -71.6°$, is correct (see Fig. B.4d):

$$1 - j3 = \sqrt{10}e^{-j71.6°}$$

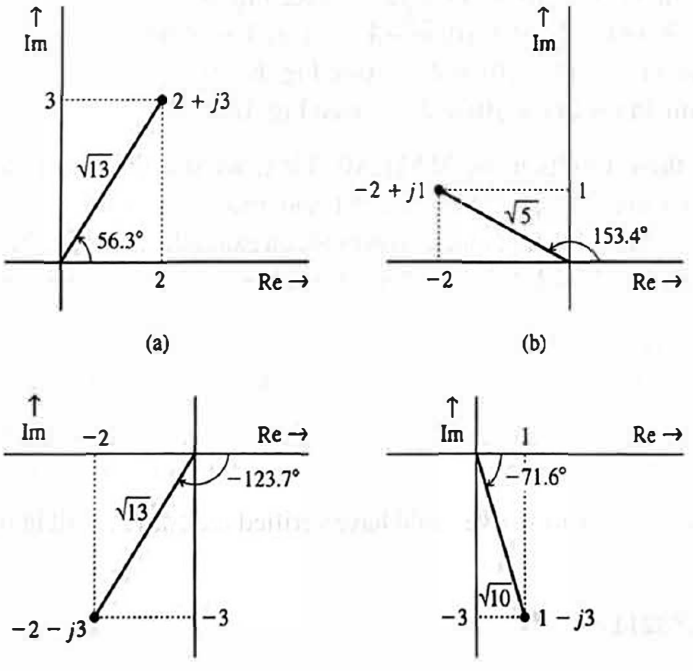

Figure B.4 From Cartesian to polar form.

We can easily verify these results using the MATLAB `abs` and `angle` commands. To obtain units of degrees, we must multiply the radian result of the `angle` command by $\frac{180}{\pi}$. Furthermore, the `angle` command correctly computes angles for all four quadrants of the complex plane. To provide an example, let us use MATLAB to verify that $-2 + j1 = \sqrt{5}e^{j153.4^\circ} = 2.2361e^{j153.4^\circ}$.

```
>> abs(-2+1j)
   ans = 2.2361
>> angle(-2+1j)*180/pi
   ans = 153.4349
```

One can also use the `cart2pol` command to convert Cartesian to polar coordinates. Readers, particularly those who are unfamiliar with MATLAB, will benefit by reading the overview in Sec. B.7.

EXAMPLE B.2 Polar to Cartesian Form

Represent the following numbers in the complex plane and express them in Cartesian form: **(a)** $2e^{j\pi/3}$, **(b)** $4e^{-j3\pi/4}$, **(c)** $2e^{j\pi/2}$, **(d)** $3e^{-j3\pi}$, **(e)** $2e^{j4\pi}$, and **(f)** $2e^{-j4\pi}$.

(a) $2e^{j\pi/3} = 2(\cos\pi/3 + j\sin\pi/3) = 1 + j\sqrt{3}$ (see Fig. B.5a)
(b) $4e^{-j3\pi/4} = 4(\cos 3\pi/4 - j\sin 3\pi/4) = -2\sqrt{2} - j2\sqrt{2}$ (see Fig. B.5b)
(c) $2e^{j\pi/2} = 2(\cos\pi/2 + j\sin\pi/2) = 2(0 + j1) = j2$ (see Fig. B.5c)
(d) $3e^{-j3\pi} = 3(\cos 3\pi - j\sin 3\pi) = 3(-1 + j0) = -3$ (see Fig. B.5d)
(e) $2e^{j4\pi} = 2(\cos 4\pi + j\sin 4\pi) = 2(1 + j0) = 2$ (see Fig. B.5e)
(f) $2e^{-j4\pi} = 2(\cos 4\pi - j\sin 4\pi) = 2(1 - j0) = 2$ (see Fig. B.5f)

We can readily verify these results using MATLAB. First, we use the `exp` function to represent a number in polar form. Next, we use the `real` and `imag` commands to determine the real and imaginary components of that number. To provide an example, let us use MATLAB to verify the result of part (a): $2e^{j\pi/3} = 1 + j\sqrt{3} = 1 + j1.7321$.

```
>> real(2*exp(1j*pi/3))
   ans = 1.0000
>> imag(2*exp(1j*pi/3))
   ans = 1.7321
```

Since MATLAB defaults to Cartesian form, we could have verified the entire result in one step.

```
>> 2*exp(1j*pi/3)
   ans = 1.0000 + 1.7321i
```

One can also use the `pol2cart` command to convert polar to Cartesian coordinates.

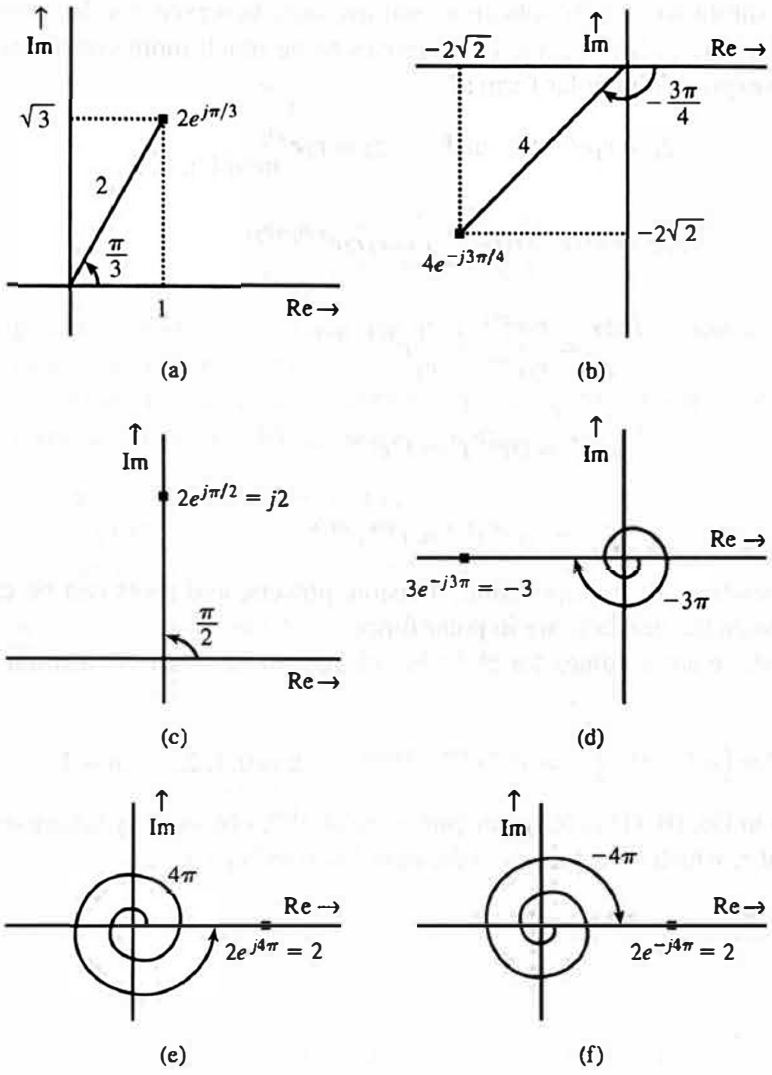

Figure B.5 From polar to Cartesian form.

Arithmetical Operations, Powers, and Roots of Complex Numbers

To conveniently perform addition and subtraction, complex numbers should be expressed in Cartesian form. Thus, if

$$z_1 = 3 + j4 = 5e^{j53.1°}$$

and

$$z_2 = 2 + j3 = \sqrt{13}e^{j56.3°}$$

then

$$z_1 + z_2 = (3 + j4) + (2 + j3) = 5 + j7$$

If z_1 and z_2 are given in polar form, we would need to convert them into Cartesian form for the purpose of adding (or subtracting). Multiplication and division, however, can be carried out in either Cartesian or polar form, although the latter proves to be much more convenient. This is because if z_1 and z_2 are expressed in polar form as

$$z_1 = r_1 e^{j\theta_1} \quad \text{and} \quad z_2 = r_2 e^{j\theta_2}$$

then

$$z_1 z_2 = (r_1 e^{j\theta_1})(r_2 e^{j\theta_2}) = r_1 r_2 e^{j(\theta_1+\theta_2)}$$

and

$$\frac{z_1}{z_2} = \frac{r_1 e^{j\theta_1}}{r_2 e^{j\theta_2}} = \frac{r_1}{r_2} e^{j(\theta_1-\theta_2)}$$

Moreover,

$$z^n = (re^{j\theta})^n = r^n e^{jn\theta}$$

and

$$z^{1/n} = (re^{j\theta})^{1/n} = r^{1/n} e^{j\theta/n} \tag{B.11}$$

This shows that the operations of multiplication, division, powers, and roots can be carried out with remarkable ease when the numbers are in polar form.

Strictly speaking, there are n values for $z^{1/n}$ (the nth root of z). To find all the n roots, we reexamine Eq. (B.11):

$$z^{1/n} = [re^{j\theta}]^{1/n} = \left[re^{j(\theta+2\pi k)}\right]^{1/n} = r^{1/n} e^{j(\theta+2\pi k)/n} \qquad k = 0, 1, 2, \ldots, n-1 \tag{B.12}$$

The value of $z^{1/n}$ given in Eq. (B.11) is the *principal value* of $z^{1/n}$, obtained by taking the nth root of the principal value of z, which corresponds to the case $k = 0$ in Eq. (B.12).

EXAMPLE B.3 Multiplication and Division of Complex Numbers

Using both polar and Cartesian forms, determine $z_1 z_2$ and z_1/z_2 for the numbers

$$z_1 = 3 + j4 = 5e^{j53.1^\circ} \quad \text{and} \quad z_2 = 2 + j3 = \sqrt{13}e^{j56.3^\circ}$$

Multiplication: Cartesian Form

$$z_1 z_2 = (3 + j4)(2 + j3) = (6 - 12) + j(8 + 9) = -6 + j17$$

Multiplication: Polar Form

$$z_1 z_2 = (5e^{j53.1^\circ})\left(\sqrt{13}e^{j56.3^\circ}\right) = 5\sqrt{13}e^{j109.4^\circ}$$

Division: Cartesian Form

$$\frac{z_1}{z_2} = \frac{3 + j4}{2 + j3}$$

To eliminate the complex number in the denominator, we multiply both the numerator and the denominator of the right-hand side by $2 - j3$, the denominator's conjugate. This yields

$$\frac{z_1}{z_2} = \frac{(3+j4)(2-j3)}{(2+j3)(2-j3)} = \frac{18-j1}{2^2+3^2} = \frac{18-j1}{13} = \frac{18}{13} - j\frac{1}{13}$$

Division: Polar Form

$$\frac{z_1}{z_2} = \frac{5e^{j53.1°}}{\sqrt{13}e^{j56.3°}} = \frac{5}{\sqrt{13}}e^{j(53.1°-56.3°)} = \frac{5}{\sqrt{13}}e^{-j3.2°}$$

It is clear from this example that multiplication and division are easier to accomplish in polar form than in Cartesian form.

These results are also easily verified using MATLAB. To provide one example, let us use Cartesian forms in MATLAB to verify that $z_1 z_2 = -6 + j17$.

```
>> z1 = 3+4j; z2 = 2+3j;
>> z1*z2
   ans = -6.0000 + 17.0000i
```

As a second example, let us use polar forms in MATLAB to verify that $z_1/z_2 = 1.3868e^{-j3.2°}$. Since MATLAB generally expects angles to be represented in the natural units of radians, we must use appropriate conversion factors in moving between degrees and radians (and vice versa).

```
>> z1 = 5*exp(1j*53.1*pi/180); z2 = sqrt(13)*exp(1j*56.3*pi/180);
>> abs(z1/z2)
   ans = 1.3868
>> angle(z1/z2)*180/pi
   ans = -3.2000
```

EXAMPLE B.4 Working with Complex Numbers

For $z_1 = 2e^{j\pi/4}$ and $z_2 = 8e^{j\pi/3}$, find the following: **(a)** $2z_1 - z_2$, **(b)** $1/z_1$, **(c)** z_1/z_2^2, and **(d)** $\sqrt[3]{z_2}$.

(a) Since subtraction cannot be performed directly in polar form, we convert z_1 and z_2 to Cartesian form:

$$z_1 = 2e^{j\pi/4} = 2\left(\cos\frac{\pi}{4} + j\sin\frac{\pi}{4}\right) = \sqrt{2} + j\sqrt{2}$$

$$z_2 = 8e^{j\pi/3} = 8\left(\cos\frac{\pi}{3} + j\sin\frac{\pi}{3}\right) = 4 + j4\sqrt{3}$$

Therefore,

$$2z_1 - z_2 = 2(\sqrt{2} + j\sqrt{2}) - (4 + j4\sqrt{3}) = (2\sqrt{2} - 4) + j(2\sqrt{2} - 4\sqrt{3}) = -1.17 - j4.1$$

(b)

$$\frac{1}{z_1} = \frac{1}{2e^{j\pi/4}} = \frac{1}{2}e^{-j\pi/4}$$

(c)

$$\frac{z_1}{z_2^2} = \frac{2e^{j\pi/4}}{(8e^{j\pi/3})^2} = \frac{2e^{j\pi/4}}{64e^{j2\pi/3}} = \frac{1}{32}e^{j(\pi/4 - 2\pi/3)} = \frac{1}{32}e^{-j(5\pi/12)}$$

(d) There are three cube roots of $8e^{j(\pi/3)} = 8e^{j(\pi/3 + 2\pi k)}$, $k = 0, 1, 2$.

$$\sqrt[3]{z_2} = z_2^{1/3} = \left[8e^{j(\pi/3 + 2\pi k)}\right]^{1/3} = 8^{1/3}\left(e^{j[(6\pi k + \pi)/3]}\right)^{1/3} = \begin{cases} 2e^{j\pi/9} & k = 0 \\ 2e^{j7\pi/9} & k = 1 \\ 2e^{j13\pi/9} & k = 2 \end{cases}$$

The value corresponding to $k = 0$ is termed the *principal value*.

EXAMPLE B.5 Standard Forms of Complex Numbers

Consider $X(\omega)$, a complex function of a real variable ω:

$$X(\omega) = \frac{2 + j\omega}{3 + j4\omega}$$

(a) Express $X(\omega)$ in Cartesian form, and find its real and imaginary parts.

(b) Express $X(\omega)$ in polar form, and find its magnitude $|X(\omega)|$ and angle $\angle X(\omega)$.

(a) To obtain the real and imaginary parts of $X(\omega)$, we must eliminate imaginary terms in the denominator of $X(\omega)$. This is readily done by multiplying both the numerator and the denominator of $X(\omega)$ by $3 - j4\omega$, the conjugate of the denominator $3 + j4\omega$ so that

$$X(\omega) = \frac{(2 + j\omega)(3 - j4\omega)}{(3 + j4\omega)(3 - j4\omega)} = \frac{(6 + 4\omega^2) - j5\omega}{9 + 16\omega^2} = \frac{6 + 4\omega^2}{9 + 16\omega^2} - j\frac{5\omega}{9 + 16\omega^2}$$

This is the Cartesian form of $X(\omega)$. Clearly, the real and imaginary parts $X_r(\omega)$ and $X_i(\omega)$ are given by

$$X_r(\omega) = \frac{6 + 4\omega^2}{9 + 16\omega^2} \quad \text{and} \quad X_i(\omega) = \frac{-5\omega}{9 + 16\omega^2}$$

(b)

$$X(\omega)=\frac{2+j\omega}{3+j4\omega}=\frac{\sqrt{4+\omega^2}\,e^{j\tan^{-1}(\omega/2)}}{\sqrt{9+16\omega^2}\,e^{j\tan^{-1}(4\omega/3)}}=\sqrt{\frac{4+\omega^2}{9+16\omega^2}}\,e^{j[\tan^{-1}(\omega/2)-\tan^{-1}(4\omega/3)]}$$

This is the polar representation of $X(\omega)$. Observe that

$$|X(\omega)|=\sqrt{\frac{4+\omega^2}{9+16\omega^2}}\qquad\text{and}\qquad \angle X(\omega)=\tan^{-1}\left(\frac{\omega}{2}\right)-\tan^{-1}\left(\frac{4\omega}{3}\right)$$

Logarithms of Complex Numbers

To take the natural logarithm of a complex number z, we first express z in general polar form as

$$z=re^{j\theta}=re^{j(\theta\pm 2\pi k)}\qquad k=0,1,2,3,\ldots$$

Taking the natural logarithm, we see that

$$\ln z=\ln\left(re^{j(\theta\pm 2\pi k)}\right)=\ln r\pm j(\theta+2\pi k)\qquad k=0,1,2,3,\ldots$$

The value of $\ln z$ for $k=0$ is called the *principal value* of $\ln z$ and is denoted by $\operatorname{Ln} z$. In this way, we see that

$$\ln 1=\ln(1e^{\pm j2\pi k})=\pm j2\pi k\qquad k=0,1,2,3,\ldots$$

$$\ln(-1)=\ln[1e^{\pm j\pi(2k+1)}]=\pm j(2k+1)\pi\qquad k=0,1,2,3,\ldots$$

$$\ln j=\ln\left(e^{j\pi(1\pm 4k)/2}\right)=j\frac{\pi(1\pm 4k)}{2}\qquad k=0,1,2,3,\ldots$$

$$j^j=e^{j\ln j}=e^{-\pi(1\pm 4k)/2}\qquad k=0,1,2,3,\ldots$$

In all of these cases, setting $k=0$ yields the principal value of the expression.

We can further our logarithm skills by noting that the familiar properties of logarithms hold for complex arguments. Therefore, we have

$$\log(z_1z_2)=\log z_1+\log z_2$$

$$\log(z_1/z_2)=\log z_1-\log z_2$$

$$a^{(z_1+z_2)}=a^{z_1}\times a^{z_2}$$

$$z^c=e^{c\ln z}$$

$$a^z=e^{z\ln a}$$

B.2 SINUSOIDS

Consider the sinusoid

$$x(t) = C\cos(2\pi f_0 t + \theta) \tag{B.13}$$

We know that

$$\cos\varphi = \cos(\varphi + 2n\pi) \qquad n = 0, \pm 1, \pm 2, \pm 3, \ldots$$

Therefore, $\cos\varphi$ repeats itself for every change of 2π in the angle φ. For the sinusoid in Eq. (B.13), the angle $2\pi f_0 t + \theta$ changes by 2π when t changes by $1/f_0$. Clearly, this sinusoid repeats every $1/f_0$ seconds. As a result, there are f_0 repetitions per second. This is the *frequency* of the sinusoid, and the repetition interval T_0 given by

$$T_0 = \frac{1}{f_0} \tag{B.14}$$

is the *period*. For the sinusoid in Eq. (B.13), C is the *amplitude*, f_0 is the *frequency* (in hertz), and θ is the phase. Let us consider two special cases of this sinusoid when $\theta = 0$ and $\theta = -\pi/2$ as follows:

$$x(t) = C\cos 2\pi f_0 t \qquad (\theta = 0)$$

and

$$x(t) = C\cos(2\pi f_0 t - \pi/2) = C\sin 2\pi f_0 t \qquad (\theta = -\pi/2)$$

The angle or phase can be expressed in units of degrees or radians. Although the radian is the proper unit, in this book we shall often use the degree unit because students generally have a better feel for the relative magnitudes of angles expressed in degrees rather than in radians. For example, we relate better to the angle 24° than to 0.419 radian. Remember, however, when in doubt, use the radian unit and, above all, be consistent. In other words, in a given problem or an expression, do not mix the two units.

It is convenient to use the variable ω_0 (*radian frequency*) to express $2\pi f_0$:

$$\omega_0 = 2\pi f_0 \tag{B.15}$$

With this notation, the sinusoid in Eq. (B.13) can be expressed as

$$x(t) = C\cos(\omega_0 t + \theta)$$

in which the period T_0 and frequency ω_0 are given by [see Eqs. (B.14) and (B.15)]

$$T_0 = \frac{1}{\omega_0/2\pi} = \frac{2\pi}{\omega_0} \qquad \text{and} \qquad \omega_0 = \frac{2\pi}{T_0}$$

Although we shall often refer to ω_0 as the frequency of the signal $\cos(\omega_0 t + \theta)$, it should be clearly understood that ω_0 is the *radian frequency*; the *hertzian frequency* of this sinusoid is $f_0 = \omega_0/2\pi$.

The signals $C\cos\omega_0 t$ and $C\sin\omega_0 t$ are illustrated in Figs. B.6a and B.6b, respectively. A general sinusoid $C\cos(\omega_0 t + \theta)$ can be readily sketched by shifting the signal $C\cos\omega_0 t$ in Fig. B.6a by the appropriate amount. Consider, for example,

$$x(t) = C\cos(\omega_0 t - 60°)$$

This signal can be obtained by shifting (delaying) the signal $C\cos\omega_0 t$ (Fig. B.6a) to the right by a phase (angle) of 60°. We know that a sinusoid undergoes a 360° change of phase (or angle) in one

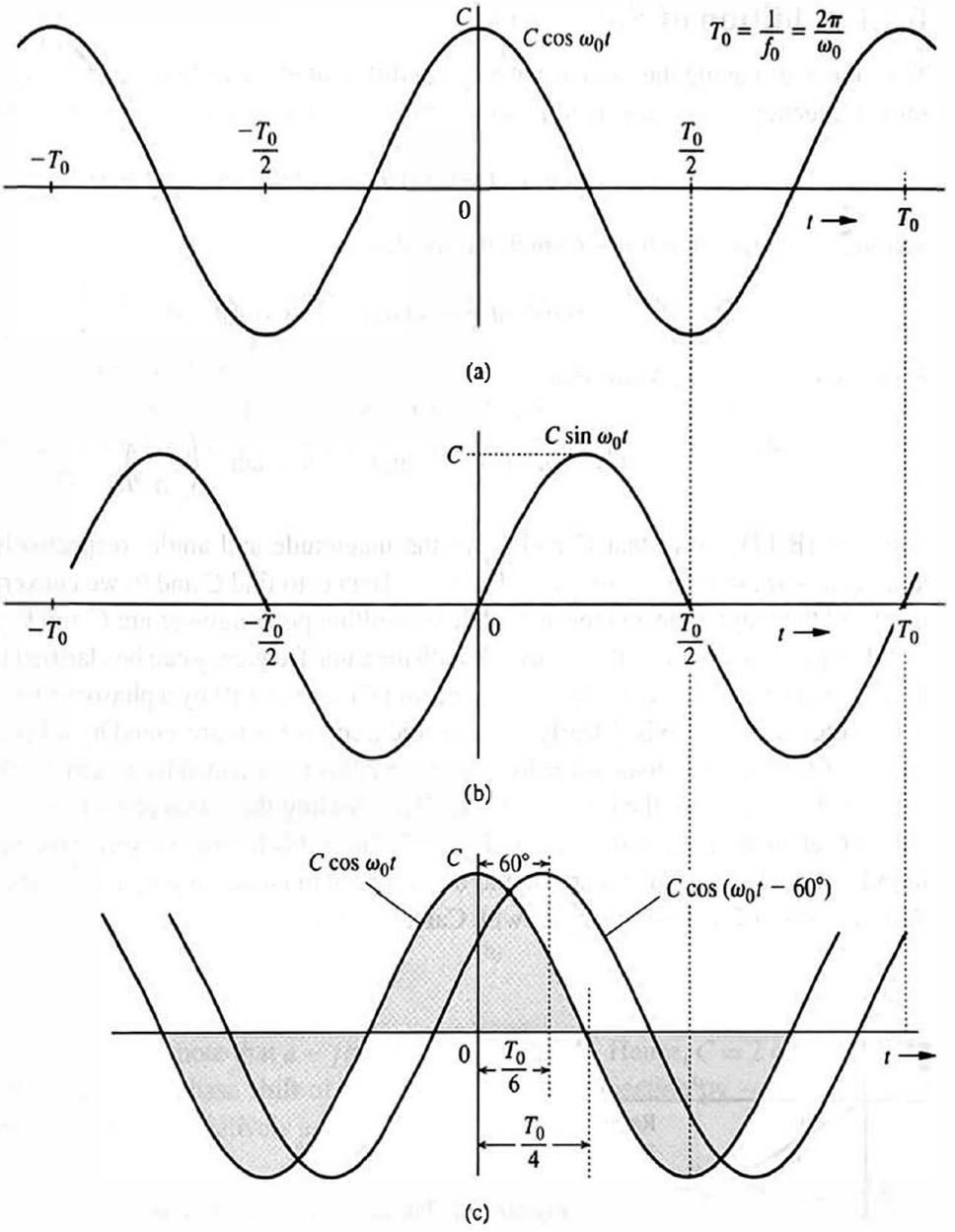

Figure B.6 Sketching a sinusoid.

cycle. A quarter-cycle segment corresponds to a 90° change of angle. We therefore shift (delay) the signal in Fig. B.6a by two-thirds of a quarter-cycle segment to obtain $C\cos(\omega_0 t - 60°)$, as shown in Fig. B.6c.

Observe that if we delay $C\cos\omega_0 t$ in Fig. B.6a by a quarter-cycle (angle of 90° or $\pi/2$ radians), we obtain the signal $C\sin\omega_0 t$, depicted in Fig. B.6b. This verifies the well-known trigonometric identity

$$C\cos(\omega_0 t - \pi/2) = C\sin\omega_0 t$$

Alternatively, if we advance $C\sin\omega_0 t$ by a quarter-cycle, we obtain $C\cos\omega_0 t$. Therefore,

$$C\sin(\omega_0 t + \pi/2) = C\cos\omega_0 t$$

These observations mean that $\sin\omega_0 t$ lags $\cos\omega_0 t$ by 90°($\pi/2$ radians) and that $\cos\omega_0 t$ leads $\sin\omega_0 t$ by 90°.

B.2.1 Addition of Sinusoids

Two sinusoids having the same frequency but different phases add to form a single sinusoid of the same frequency. This fact is readily seen from the well-known trigonometric identity

$$C\cos\theta\cos\omega_0 t - C\sin\theta\sin\omega_0 t = C\cos(\omega_0 t + \theta)$$

Setting $a = C\cos\theta$ and $b = -C\sin\theta$, we see that

$$a\cos\omega_0 t + b\sin\omega_0 t = C\cos(\omega_0 t + \theta) \tag{B.16}$$

From trigonometry, we know that

$$C = \sqrt{a^2 + b^2} \quad \text{and} \quad \theta = \tan^{-1}\left(\frac{-b}{a}\right) \tag{B.17}$$

Equation (B.17) shows that C and θ are the magnitude and angle, respectively, of a complex number $a - jb$. In other words, $a - jb = Ce^{j\theta}$. Hence, to find C and θ, we convert $a - jb$ to polar form and the magnitude and the angle of the resulting polar number are C and θ, respectively.

The process of adding two sinusoids with the same frequency can be clarified by using *phasors* to represent sinusoids. We represent the sinusoid $C\cos(\omega_0 t + \theta)$ by a phasor of length C at an angle θ with the horizontal axis. Clearly, the sinusoid $a\cos\omega_0 t$ is represented by a horizontal phasor of length a ($\theta = 0$), while $b\sin\omega_0 t = b\cos(\omega_0 t - \pi/2)$ is represented by a vertical phasor of length b at an angle $-\pi/2$ with the horizontal (Fig. B.7). Adding these two phasors results in a phasor of length C at an angle θ, as depicted in Fig. B.7. From this figure, we verify the values of C and θ found in Eq. (B.17). Proper care should be exercised in computing θ, as explained on page 8 ("A Warning About Computing Angles with Calculators").

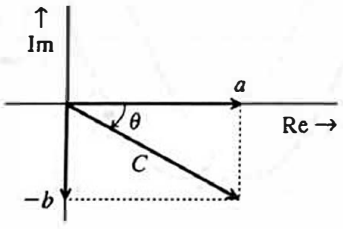

Figure B.7 Phasor addition of sinusoids.

EXAMPLE B.6 Addition of Sinusoids

In the following cases, express $x(t)$ as a single sinusoid:

(a) $x(t) = \cos\omega_0 t - \sqrt{3}\sin\omega_0 t$

(b) $x(t) = -3\cos\omega_0 t + 4\sin\omega_0 t$

(a) In this case, $a = 1$ and $b = -\sqrt{3}$. Using Eq. (B.17) yields

$$C = \sqrt{1^2 + (-\sqrt{3})^2} = 2 \quad \text{and} \quad \theta = \tan^{-1}\left(\frac{\sqrt{3}}{1}\right) = 60°$$

Therefore,

$$x(t) = 2\cos(\omega_0 t + 60°)$$

We can verify this result by drawing phasors corresponding to the two sinusoids. The sinusoid $\cos \omega_0 t$ is represented by a phasor of unit length at a zero angle with the horizontal. The phasor $\sin \omega_0 t$ is represented by a unit phasor at an angle of $-90°$ with the horizontal. Therefore, $-\sqrt{3}\sin \omega_0 t$ is represented by a phasor of length $\sqrt{3}$ at 90° with the horizontal, as depicted in Fig. B.8a. The two phasors added yield a phasor of length 2 at 60° with the horizontal (also shown in Fig. B.8a).

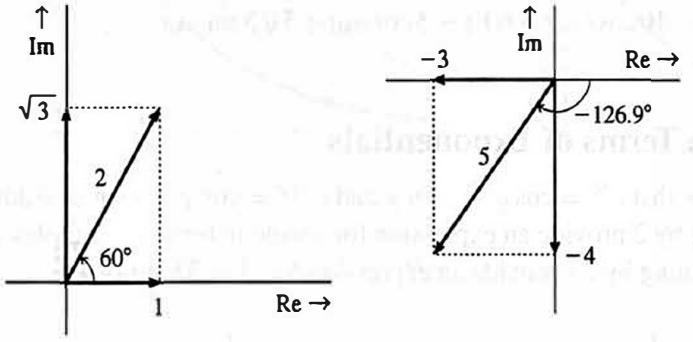

Figure B.8 Phasor addition of sinusoids.

Alternately, we note that $a - jb = 1 + j\sqrt{3} = 2e^{j\pi/3}$. Hence, $C = 2$ and $\theta = \pi/3$.

Observe that a phase shift of $\pm\pi$ amounts to multiplication by -1. Therefore, $x(t)$ can also be expressed alternatively as

$$x(t) = -2\cos(\omega_0 t + 60° \pm 180°) = -2\cos(\omega_0 t - 120°) = -2\cos(\omega_0 t + 240°)$$

In practice, the principal value, that is, $-120°$, is preferred.

(b) In this case, $a = -3$ and $b = 4$. Using Eq. (B.17) yields

$$C = \sqrt{(-3)^2 + 4^2} = 5 \quad \text{and} \quad \theta = \tan^{-1}\left(\frac{-4}{-3}\right) = -126.9°$$

Observe that

$$\tan^{-1}\left(\frac{-4}{-3}\right) \neq \tan^{-1}\left(\frac{4}{3}\right) = 53.1°$$

Therefore,

$$x(t) = 5\cos(\omega_0 t - 126.9°)$$

This result is readily verified in the phasor diagram in Fig. B.8b. Alternately, $a - jb = -3 - j4 = 5e^{-j126.9°}$, a fact readily confirmed using MATLAB.

```
>> C = abs(-3+4j)
   C = 5
>> theta = angle(-3+4j)*180/pi
   theta = 126.8699
```

Hence, $C = 5$ and $\theta = -126.8699°$.

We can also perform the reverse operation, expressing $C\cos(\omega_0 t + \theta)$ in terms of $\cos \omega_0 t$ and $\sin \omega_0 t$ by again using the trigonometric identity

$$C\cos(\omega_0 t + \theta) = C\cos\theta\cos\omega_0 t - C\sin\theta\sin\omega_0 t$$

For example,

$$10\cos(\omega_0 t - 60°) = 5\cos\omega_0 t + 5\sqrt{3}\sin\omega_0 t$$

B.2.2 Sinusoids in Terms of Exponentials

From Eq. (B.3), we know that $e^{j\varphi} = \cos\varphi + j\sin\varphi$ and $e^{-j\varphi} = \cos\varphi - j\sin\varphi$. Adding these two expressions and dividing by 2 provide an expression for cosine in terms of complex exponentials, while subtracting and scaling by $2j$ provide an expression for sine. That is,

$$\cos\varphi = \frac{1}{2}(e^{j\varphi} + e^{-j\varphi}) \qquad \text{and} \qquad \sin\varphi = \frac{1}{2j}(e^{j\varphi} - e^{-j\varphi}) \tag{B.18}$$

B.3 SKETCHING SIGNALS

In this section, we discuss the sketching of a few useful signals, starting with exponentials.

B.3.1 Monotonic Exponentials

The signal e^{-at} decays monotonically, and the signal e^{at} grows monotonically with t (assuming $a > 0$), as depicted in Fig. B.9. For the sake of simplicity, we shall consider an exponential e^{-at} starting at $t = 0$, as shown in Fig. B.10a.

The signal e^{-at} has a unit value at $t = 0$. At $t = 1/a$, the value drops to $1/e$ (about 37% of its initial value), as illustrated in Fig. B.10a. This time interval over which the exponential reduces by a factor e (i.e., drops to about 37% of its value) is known as the *time constant* of the exponential. Therefore, the time constant of e^{-at} is $1/a$. Observe that the exponential is reduced to 37% of its initial value over any time interval of duration $1/a$. This can be shown by considering any set of instants t_1 and t_2 separated by one time constant so that

$$t_2 - t_1 = \frac{1}{a}$$

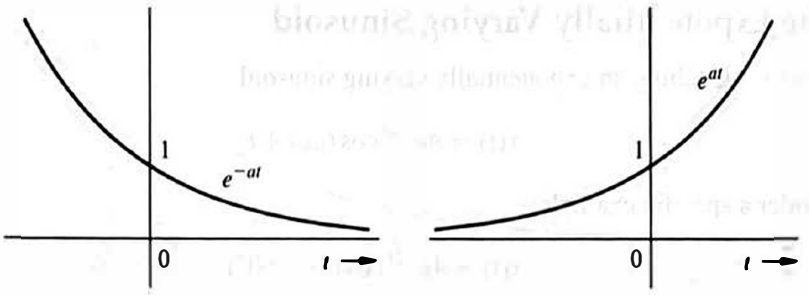

Figure B.9 Monotonic exponentials.

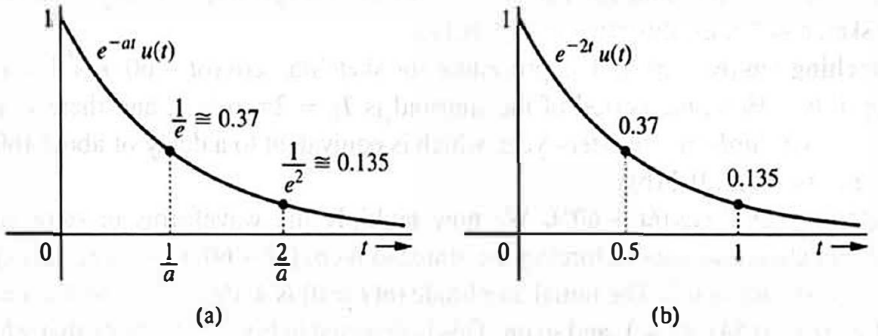

Figure B.10 (a) Sketching e^{-at}. (b) Sketching e^{-2t}.

Now the ratio of e^{-at_2} to e^{-at_1} is given by

$$\frac{e^{-at_2}}{e^{-at_1}} = e^{-a(t_2-t_1)} = \frac{1}{e} \approx 0.37$$

We can use this fact to sketch an exponential quickly. For example, consider

$$x(t) = e^{-2t}$$

The time constant in this case is 0.5. The value of $x(t)$ at $t = 0$ is 1. At $t = 0.5$ (one time constant), it is $1/e$ (about 0.37). The value of $x(t)$ continues to drop further by the factor $1/e$ (37%) over the next half-second interval (one time constant). Thus, $x(t)$ at $t = 1$ is $(1/e)^2$. Continuing in this manner, we see that $x(t) = (1/e)^3$ at $t = 1.5$, and so on. A knowledge of the values of $x(t)$ at $t = 0$, 0.5, 1, and 1.5 allows us to sketch the desired signal, as shown in Fig. B.10b.[†]

For a monotonically growing exponential e^{at}, the waveform increases by a factor e over each interval of $1/a$ seconds.

[†] If we wish to refine the sketch further, we could consider intervals of half the time constant over which the signal decays by a factor $1/\sqrt{e}$. Thus, at $t = 0.25$, $x(t) = 1/\sqrt{e}$, and at $t = 0.75$, $x(t) = 1/e\sqrt{e}$, and so on.

B.3.2 The Exponentially Varying Sinusoid

We now discuss sketching an exponentially varying sinusoid

$$x(t) = Ae^{-at}\cos(\omega_0 t + \theta)$$

Let us consider a specific example:

$$x(t) = 4e^{-2t}\cos(6t - 60°)$$

We shall sketch $4e^{-2t}$ and $\cos(6t - 60°)$ separately and then multiply them:

(a) **Sketching $4e^{-2t}$.** This monotonically decaying exponential has a time constant of 0.5 second and an initial value of 4 at $t = 0$. Therefore, its values at $t = 0.5$, 1, 1.5, and 2 are $4/e$, $4/e^2$, $4/e^3$, and $4/e^4$, or about 1.47, 0.54, 0.2, and 0.07, respectively. Using these values as a guide, we sketch $4e^{-2t}$, as illustrated in Fig. B.11a.

(b) **Sketching $\cos(6t - 60°)$.** The procedure for sketching $\cos(6t - 60°)$ is discussed in Sec. B.2 (Fig. B.6c). Here, the period of the sinusoid is $T_0 = 2\pi/6 \approx 1$, and there is a phase delay of 60°, or two-thirds of a quarter-cycle, which is equivalent to a delay of about $(60/360)(1) \approx 1/6$ seconds (see Fig. B.11b).

(c) **Sketching $4e^{-2t}\cos(6t - 60°)$.** We now multiply the waveforms in steps (a) and (b). This multiplication amounts to forcing the sinusoid $4\cos(6t - 60°)$ to decrease exponentially with a time constant of 0.5. The initial amplitude (at $t = 0$) is 4, decreasing to $4/e$ (=1.47) at $t = 0.5$, to $1.47/e$ (=0.54) at $t = 1$, and so on. This is depicted in Fig. B.11c. Note that when $\cos(6t - 60°)$ has a value of unity (peak amplitude),

$$4e^{-2t}\cos(6t - 60°) = 4e^{-2t}$$

Therefore, $4e^{-2t}\cos(6t - 60°)$ touches $4e^{-2t}$ at the instants at which the sinusoid $\cos(6t - 60°)$ is at its positive peaks. Clearly, $4e^{-2t}$ is an envelope for positive amplitudes of $4e^{-2t}\cos(6t - 60°)$. Similar argument shows that $4e^{-2t}\cos(6t - 60°)$ touches $-4e^{-2t}$ at its negative peaks. Therefore, $-4e^{-2t}$ is an envelope for negative amplitudes of $4e^{-2t}\cos(6t - 60°)$. Thus, to sketch $4e^{-2t}\cos(6t - 60°)$, we first draw the envelopes $4e^{-2t}$ and $-4e^{-2t}$ (the mirror image of $4e^{-2t}$ about the horizontal axis), and then sketch the sinusoid $\cos(6t - 60°)$, with these envelopes acting as constraints on the sinusoid's amplitude (see Fig. B.11c).

In general, $Ke^{-at}\cos(\omega_0 t + \theta)$ can be sketched in this manner, with Ke^{-at} and $-Ke^{-at}$ constraining the amplitude of $\cos(\omega_0 t + \theta)$.

B.4 CRAMER'S RULE

Cramer's rule offers a very convenient way to solve simultaneous linear equations. Consider a set of n linear simultaneous equations in n unknowns $x_1, x_2, \ldots, x_n$:

$$\begin{aligned} a_{11}x_1 + a_{12}x_2 + \cdots + a_{1n}x_n &= y_1 \\ a_{21}x_1 + a_{22}x_2 + \cdots + a_{2n}x_n &= y_2 \\ &\vdots \\ a_{n1}x_1 + a_{n2}x_2 + \cdots + a_{nn}x_n &= y_n \end{aligned} \tag{B.19}$$

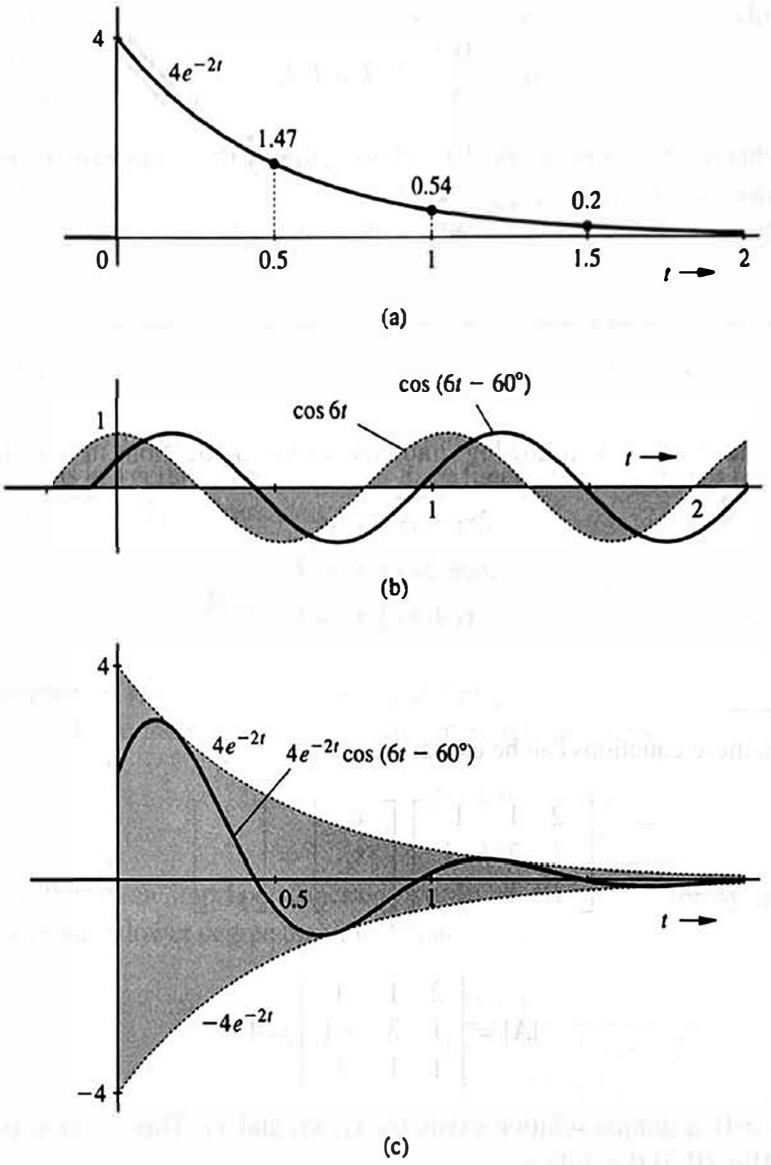

Figure B.11 Sketching an exponentially varying sinusoid.

These equations can be expressed in matrix form as

$$\begin{bmatrix} a_{11} & a_{12} & \cdots & a_{1n} \\ a_{21} & a_{22} & \cdots & a_{2n} \\ \vdots & \vdots & \cdots & \vdots \\ a_{n1} & a_{n2} & \cdots & a_{nn} \end{bmatrix} \begin{bmatrix} x_1 \\ x_2 \\ \vdots \\ x_n \end{bmatrix} = \begin{bmatrix} y_1 \\ y_2 \\ \vdots \\ y_n \end{bmatrix} \tag{B.20}$$

We denote the matrix on the left-hand side formed by the elements a_{ij} as $\mathbf{A}$. The determinant of $\mathbf{A}$ is denoted by $|\mathbf{A}|$. If the determinant $|\mathbf{A}|$ is not zero, Eq. (B.19) has a unique solution given by

Cramer's formula

$$x_k = \frac{|\mathbf{D}_k|}{|\mathbf{A}|} \qquad k = 1,2,\ldots,n \tag{B.21}$$

where $|\mathbf{D}_k|$ is obtained by replacing the kth column of $\mathbf{A}$ by the column on the right-hand side of Eq. (B.20) (with elements $y_1, y_2, \ldots, y_n$).

We shall demonstrate the use of this rule with an example.

EXAMPLE B.7 Using Cramer's Rule to Solve a System of Equations

Use Cramer's rule to solve the following simultaneous linear equations in three unknowns:

$$\begin{aligned} 2x_1 + x_2 + x_3 &= 3 \\ x_1 + 3x_2 - x_3 &= 7 \\ x_1 + x_2 + x_3 &= 1 \end{aligned}$$

In matrix form, these equations can be expressed as

$$\begin{bmatrix} 2 & 1 & 1 \\ 1 & 3 & -1 \\ 1 & 1 & 1 \end{bmatrix} \begin{bmatrix} x_1 \\ x_2 \\ x_3 \end{bmatrix} = \begin{bmatrix} 3 \\ 7 \\ 1 \end{bmatrix}$$

Here,

$$|\mathbf{A}| = \begin{vmatrix} 2 & 1 & 1 \\ 1 & 3 & -1 \\ 1 & 1 & 1 \end{vmatrix} = 4$$

Since $|\mathbf{A}| = 4 \neq 0$, a unique solution exists for x_1, x_2, and x_3. This solution is provided by Cramer's rule [Eq. (B.21)] as follows:

$$x_1 = \frac{1}{|\mathbf{A}|} \begin{vmatrix} 3 & 1 & 1 \\ 7 & 3 & -1 \\ 1 & 1 & 1 \end{vmatrix} = \frac{8}{4} = 2$$

$$x_2 = \frac{1}{|\mathbf{A}|} \begin{vmatrix} 2 & 3 & 1 \\ 1 & 7 & -1 \\ 1 & 1 & 1 \end{vmatrix} = \frac{4}{4} = 1$$

$$x_3 = \frac{1}{|\mathbf{A}|} \begin{vmatrix} 2 & 1 & 3 \\ 1 & 3 & 7 \\ 1 & 1 & 1 \end{vmatrix} = \frac{-8}{4} = -2$$

MATLAB is well suited to compute Cramer's formula, so these results are easy to verify. To provide an example, let us verify that $x_1 = 2$ using MATLAB's det command to compute the needed matrix determinants.

```
>> x1 = det([3 1 1;7 3 -1;1 1 1])/det([2 1 1;1 3 -1;1 1 1])
   x1 = 2.0000
```

B.5 PARTIAL FRACTION EXPANSION

In the analysis of linear time-invariant systems, we encounter functions that are ratios of two polynomials in a certain variable, say, x. Such functions are known as *rational functions*. A rational function $F(x)$ can be expressed as

$$F(x) = \frac{b_m x^m + b_{m-1}x^{m-1} + \cdots + b_1 x + b_0}{x^n + a_{n-1}x^{n-1} + \cdots + a_1 x + a_0} = \frac{P(x)}{Q(x)} \tag{B.22}$$

The function $F(x)$ is *improper* if $m \geq n$ and *proper* if $m < n$.[†] An improper function can always be separated into the sum of a polynomial in x and a proper function. Consider, for example, the function

$$F(x) = \frac{2x^3 + 9x^2 + 11x + 2}{x^2 + 4x + 3}$$

Because this is an improper function, we divide the numerator by the denominator until the remainder has a lower degree than the denominator.

$$\begin{array}{r} 2x+1 \\ x^2+4x+3 \;\overline{)\;2x^3+9x^2+11x+2} \\ \underline{2x^3+8x^2+6x} \\ x^2+5x+2 \\ \underline{x^2+4x+3} \\ x-1 \end{array}$$

Therefore, $F(x)$ can be expressed as

$$F(x) = \frac{2x^3 + 9x^2 + 11x + 2}{x^2 + 4x + 3} = \underbrace{2x+1}_{\text{polynomial in } x} + \underbrace{\frac{x-1}{x^2+4x+3}}_{\text{proper function}}$$

A proper function can be further expanded into partial fractions. The remaining discussion in this section is concerned with various ways of doing this.

[†] Some sources classify $F(x)$ as strictly proper if $m < n$, proper if $m \leq n$, and improper if $m > n$.

B.5.1 Method of Clearing Fractions

A rational function can be written as a sum of appropriate partial fractions with unknown coefficients, which are determined by clearing fractions and equating the coefficients of similar powers on the two sides. This procedure is demonstrated by the following example.

EXAMPLE B.8 Method of Clearing Fractions

Expand the following rational function $F(x)$ into partial fractions:

$$F(x) = \frac{x^3 + 3x^2 + 4x + 6}{(x+1)(x+2)(x+3)^2}$$

This function can be expressed as a sum of partial fractions with denominators $(x+1)$, $(x+2)$, $(x+3)$, and $(x+3)^2$, as follows:

$$F(x) = \frac{x^3 + 3x^2 + 4x + 6}{(x+1)(x+2)(x+3)^2} = \frac{k_1}{x+1} + \frac{k_2}{x+2} + \frac{k_3}{x+3} + \frac{k_4}{(x+3)^2}$$

To determine the unknowns k_1, k_2, k_3, and k_4, we clear fractions by multiplying both sides by $(x+1)(x+2)(x+3)^2$ to obtain

$$\begin{aligned} x^3 + 3x^2 + 4x + 6 &= k_1(x^3 + 8x^2 + 21x + 18) + k_2(x^3 + 7x^2 + 15x + 9) \\ &\quad + k_3(x^3 + 6x^2 + 11x + 6) + k_4(x^2 + 3x + 2) \\ &= x^3(k_1 + k_2 + k_3) + x^2(8k_1 + 7k_2 + 6k_3 + k_4) \\ &\quad + x(21k_1 + 15k_2 + 11k_3 + 3k_4) + (18k_1 + 9k_2 + 6k_3 + 2k_4) \end{aligned}$$

Equating coefficients of similar powers on both sides yields

$$\begin{aligned} k_1 + k_2 + k_3 &= 1 \\ 8k_1 + 7k_2 + 6k_3 + k_4 &= 3 \\ 21k_1 + 15k_2 + 11k_3 + 3k_4 &= 4 \\ 18k_1 + 9k_2 + 6k_3 + 2k_4 &= 6 \end{aligned}$$

Solution of these four simultaneous equations yields

$$k_1 = 1, \qquad k_2 = -2, \qquad k_3 = 2, \qquad k_4 = -3$$

Therefore,

$$F(x) = \frac{1}{x+1} - \frac{2}{x+2} + \frac{2}{x+3} - \frac{3}{(x+3)^2}$$

Although this method is straightforward and applicable to all situations, it is not necessarily the most efficient. We now discuss other methods that can reduce numerical work considerably.

B.5.2 The Heaviside "Cover-Up" Method

Distinct Factors of $Q(x)$

We shall first consider the partial fraction expansion of $F(x) = P(x)/Q(x)$, in which all the factors of $Q(x)$ are distinct (not repeated). Consider the proper function

$$F(x) = \frac{b_m x^m + b_{m-1}x^{m-1} + \cdots + b_1 x + b_0}{x^n + a_{n-1}x^{n-1} + \cdots + a_1 x + a_0} \qquad m < n$$
$$= \frac{P(x)}{(x-\lambda_1)(x-\lambda_2)\cdots(x-\lambda_n)}$$

As seen in Ex. B.8, $F(x)$ can be expressed as the sum of partial fractions

$$F(x) = \frac{k_1}{x-\lambda_1} + \frac{k_2}{x-\lambda_2} + \cdots + \frac{k_n}{x-\lambda_n} \tag{B.23}$$

To determine the coefficient k_1, we multiply both sides of Eq. (B.23) by $x-\lambda_1$ and then let $x = \lambda_1$. This yields

$$(x-\lambda_1)F(x)|_{x=\lambda_1} = k_1 + \frac{k_2(x-\lambda_1)}{(x-\lambda_2)} + \frac{k_3(x-\lambda_1)}{(x-\lambda_3)} + \cdots + \frac{k_n(x-\lambda_1)}{(x-\lambda_n)}\bigg|_{x=\lambda_1}$$

On the right-hand side, all the terms except k_1 vanish. Therefore,

$$k_1 = (x-\lambda_1)F(x)|_{x=\lambda_1}$$

Similarly, we can show that

$$k_r = (x-\lambda_r)F(x)|_{x=\lambda_r} \qquad r = 1,2,\ldots,n \tag{B.24}$$

This procedure also goes under the name *method of residues*.

EXAMPLE B.9 Heaviside "Cover-Up" Method

Expand the following rational function $F(x)$ into partial fractions:

$$F(x) = \frac{2x^2 + 9x - 11}{(x+1)(x-2)(x+3)} = \frac{k_1}{x+1} + \frac{k_2}{x-2} + \frac{k_3}{x+3}$$

To determine k_1, we let $x = -1$ in $(x+1)F(x)$. Note that $(x+1)F(x)$ is obtained from $F(x)$ by omitting the term $(x+1)$ from its denominator. Therefore, to compute k_1 corresponding to

the factor $(x+1)$, we cover up the term $(x+1)$ in the denominator of $F(x)$ and then substitute $x=-1$ in the remaining expression. [Mentally conceal the term $(x+1)$ in $F(x)$ with a finger and then let $x=-1$ in the remaining expression.] The steps in covering up the function

$$F(x)=\frac{2x^2+9x-11}{(x+1)(x-2)(x+3)}$$

are as follows.

Step 1. Cover up (conceal) the factor $(x+1)$ from $F(x)$:

$$\frac{2x^2+9x-11}{(x+1)(x-2)(x+3)}$$

Step 2. Substitute $x=-1$ in the remaining expression to obtain k_1:

$$k_1=\frac{2-9-11}{(-1-2)(-1+3)}=\frac{-18}{-6}=3$$

Similarly, to compute k_2, we cover up the factor $(x-2)$ in $F(x)$ and let $x=2$ in the remaining function, as follows:

$$k_2=\left.\frac{2x^2+9x-11}{(x+1)(x-2)(x+3)}\right|_{x=2}=\frac{8+18-11}{(2+1)(2+3)}=\frac{15}{15}=1$$

and

$$k_3=\left.\frac{2x^2+9x-11}{(x+1)(x-2)(x+3)}\right|_{x=-3}=\frac{18-27-11}{(-3+1)(-3-2)}=\frac{-20}{10}=-2$$

Therefore,

$$F(x)=\frac{2x^2+9x-11}{(x+1)(x-2)(x+3)}=\frac{3}{x+1}+\frac{1}{x-2}-\frac{2}{x+3}$$

Complex Factors of $Q(x)$

The procedure just given works regardless of whether the factors of $Q(x)$ are real or complex. Consider, for example,

$$F(x)=\frac{4x^2+2x+18}{(x+1)(x^2+4x+13)}=\frac{4x^2+2x+18}{(x+1)(x+2-j3)(x+2+j3)}$$
$$=\frac{k_1}{x+1}+\frac{k_2}{x+2-j3}+\frac{k_3}{x+2+j3} \tag{B.25}$$

where

$$k_1=\left[\frac{4x^2+2x+18}{(x+1)\,(x^2+4x+13)}\right]_{x=-1}=2$$

Similarly,

$$k_2 = \left[\frac{4x^2+2x+18}{(x+1)(x+2-j3)(x+2+j3)}\right]_{x=-2+j3} = 1+j2 = \sqrt{5}e^{j63.43^\circ}$$

$$k_3 = \left[\frac{4x^2+2x+18}{(x+1)(x+2-j3)(x+2+j3)}\right]_{x=-2-j3} = 1-j2 = \sqrt{5}e^{-j63.43^\circ}$$

Therefore,

$$F(x) = \frac{2}{x+1} + \frac{\sqrt{5}e^{j63.43^\circ}}{x+2-j3} + \frac{\sqrt{5}e^{-j63.43^\circ}}{x+2+j3}$$

The coefficients k_2 and k_3 corresponding to the complex-conjugate factors are also conjugates of each other. This is generally true when the coefficients of a rational function are real. In such a case, we need to compute only one of the coefficients.

Quadratic Factors

Often we are required to combine the two terms arising from complex-conjugate factors into one quadratic factor. For example, $F(x)$ in Eq. (B.25) can be expressed as

$$F(x) = \frac{4x^2+2x+18}{(x+1)(x^2+4x+13)} = \frac{k_1}{x+1} + \frac{c_1x+c_2}{x^2+4x+13}$$

The coefficient k_1 is found by the Heaviside method to be 2. Therefore,

$$\frac{4x^2+2x+18}{(x+1)(x^2+4x+13)} = \frac{2}{x+1} + \frac{c_1x+c_2}{x^2+4x+13} \tag{B.26}$$

The values of c_1 and c_2 are determined by clearing fractions and equating the coefficients of similar powers of x on both sides of the resulting equation. Clearing fractions on both sides of Eq. (B.26) yields

$$\begin{aligned} 4x^2+2x+18 &= 2(x^2+4x+13)+(c_1x+c_2)(x+1) \\ &= (2+c_1)x^2+(8+c_1+c_2)x+(26+c_2) \end{aligned}$$

Equating terms of similar powers yields $c_1 = 2$, $c_2 = -8$, and

$$\frac{4x^2+2x+18}{(x+1)(x^2+4x+13)} = \frac{2}{x+1} + \frac{2x-8}{x^2+4x+13}$$

Shortcuts

The values of c_1 and c_2 in Eq. (B.26) can also be determined by using shortcuts. After computing $k_1 = 2$ by the Heaviside method as before, we let $x = 0$ on both sides of Eq. (B.26) to eliminate c_1. This gives us

$$\frac{18}{13} = 2 + \frac{c_2}{13} \quad \Rightarrow \quad c_2 = -8$$

To determine c_1, we multiply both sides of Eq. (B.26) by x and then let $x \to \infty$. Remember that when $x \to \infty$, only the terms of the highest power are significant. Therefore,

$$4 = 2 + c_1 \qquad \Rightarrow \qquad c_1 = 2$$

In the procedure discussed here, we let $x = 0$ to determine c_2 and then multiply both sides by x and let $x \to \infty$ to determine c_1. However, nothing is sacred about these values ($x = 0$ or $x = \infty$). We use them because they reduce the number of computations involved. We could just as well use other convenient values for x, such as $x = 1$. Consider the case

$$F(x) = \frac{2x^2 + 4x + 5}{x(x^2 + 2x + 5)} = \frac{k}{x} + \frac{c_1 x + c_2}{x^2 + 2x + 5}$$

We find $k = 1$ by the Heaviside method in the usual manner. As a result,

$$\frac{2x^2 + 4x + 5}{x(x^2 + 2x + 5)} = \frac{1}{x} + \frac{c_1 x + c_2}{x^2 + 2x + 5} \tag{B.27}$$

If we try letting $x = 0$ to determine c_1 and c_2, we obtain ∞ on both sides. So let us choose $x = 1$. This yields

$$\frac{11}{8} = 1 + \frac{c_1 + c_2}{8} \qquad \text{or} \qquad c_1 + c_2 = 3$$

We can now choose some other value for x, such as $x = 2$, to obtain one more relationship to use in determining c_1 and c_2. In this case, however, a simple method is to multiply both sides of Eq. (B.27) by x and then let $x \to \infty$. This yields

$$2 = 1 + c_1 \qquad \Rightarrow \qquad c_1 = 1$$

Since $c_1 + c_2 = 3$, we see that $c_2 = 2$ and therefore,

$$F(x) = \frac{1}{x} + \frac{x + 2}{x^2 + 2x + 5}$$

B.5.3 Repeated Factors of $Q(x)$

If a function $F(x)$ has a repeated factor in its denominator, it has the form

$$F(x) = \frac{P(x)}{(x - \lambda)^r (x - \alpha_1)(x - \alpha_2) \cdots (x - \alpha_j)}$$

Its partial fraction expansion is given by

$$F(x) = \frac{a_0}{(x - \lambda)^r} + \frac{a_1}{(x - \lambda)^{r-1}} + \cdots + \frac{a_{r-1}}{(x - \lambda)} + \frac{k_1}{x - \alpha_1} + \frac{k_2}{x - \alpha_2} + \cdots + \frac{k_j}{x - \alpha_j} \tag{B.28}$$

The coefficients $k_1, k_2, \ldots, k_j$ corresponding to the unrepeated factors in this equation are determined by the Heaviside method, as before [Eq. (B.24)]. To find the coefficients a_0, a_1, $a_2, \ldots, a_{r-1}$, we multiply both sides of Eq. (B.28) by $(x-\lambda)^r$. This gives us

$$(x-\lambda)^r F(x) = a_0 + a_1(x-\lambda) + a_2(x-\lambda)^2 + \cdots + a_{r-1}(x-\lambda)^{r-1} + k_1\frac{(x-\lambda)^r}{x-\alpha_1} + k_2\frac{(x-\lambda)^r}{x-\alpha_2} + \cdots + k_n\frac{(x-\lambda)^r}{x-\alpha_n} \tag{B.29}$$

If we let $x = \lambda$ on both sides of Eq. (B.29), we obtain

$$(x-\lambda)^r F(x)|_{x=\lambda} = a_0$$

Therefore, a_0 is obtained by concealing the factor $(x-\lambda)^r$ in $F(x)$ and letting $x=\lambda$ in the remaining expression (the Heaviside "cover-up" method). If we take the derivative (with respect to x) of both sides of Eq. (B.29), the right-hand side is a_1 + terms containing a factor $(x-\lambda)$ in their numerators. Letting $x = \lambda$ on both sides of this equation, we obtain

$$\frac{d}{dx}\left[(x-\lambda)^r F(x)\right]\Big|_{x=\lambda} = a_1$$

Thus, a_1 is obtained by concealing the factor $(x-\lambda)^r$ in $F(x)$, taking the derivative of the remaining expression, and then letting $x = \lambda$. Continuing in this manner, we find

$$a_j = \frac{1}{j!}\frac{d^j}{dx^j}\left[(x-\lambda)^r F(x)\right]\Big|_{x=\lambda} \tag{B.30}$$

Observe that $(x-\lambda)^r F(x)$ is obtained from $F(x)$ by omitting the factor $(x-\lambda)^r$ from its denominator. Therefore, the coefficient a_j is obtained by concealing the factor $(x-\lambda)^r$ in $F(x)$, taking the jth derivative of the remaining expression, and then letting $x = \lambda$ (while dividing by $j!$).

EXAMPLE B.10 Partial Fraction Expansion with Repeated Factors

Expand $F(x)$ into partial fractions if

$$F(x) = \frac{4x^3 + 16x^2 + 23x + 13}{(x+1)^3(x+2)}$$

The partial fractions are

$$F(x) = \frac{a_0}{(x+1)^3} + \frac{a_1}{(x+1)^2} + \frac{a_2}{x+1} + \frac{k}{x+2}$$

The coefficient k is obtained by concealing the factor $(x+2)$ in $F(x)$ and then substituting $x=-2$ in the remaining expression:

$$k=\left.\frac{4x^3+16x^2+23x+13}{(x+1)^3(x+2)}\right|_{x=-2}=1$$

To find a_0, we conceal the factor $(x+1)^3$ in $F(x)$ and let $x=-1$ in the remaining expression:

$$a_0=\left.\frac{4x^3+16x^2+23x+13}{(x+1)^3(x+2)}\right|_{x=-1}=2$$

To find a_1, we conceal the factor $(x+1)^3$ in $F(x)$, take the derivative of the remaining expression, and then let $x=-1$:

$$a_1=\frac{d}{dx}\left[\frac{4x^3+16x^2+23x+13}{(x+1)^3(x+2)}\right]\Bigg|_{x=-1}=1$$

Similarly,

$$a_2=\frac{1}{2!}\frac{d^2}{dx^2}\left[\frac{4x^3+16x^2+23x+13}{(x+1)^3(x+2)}\right]\Bigg|_{x=-1}=3$$

Therefore,

$$F(x)=\frac{2}{(x+1)^3}+\frac{1}{(x+1)^2}+\frac{3}{x+1}+\frac{1}{x+2}$$

B.5.4 A Combination of Heaviside "Cover-Up" and Clearing Fractions

For multiple roots, especially of higher order, the Heaviside expansion method, which requires repeated differentiation, can become cumbersome. For a function that contains several repeated and unrepeated roots, a hybrid of the two procedures proves to be the best. The simpler coefficients are determined by the Heaviside method, and the remaining coefficients are found by clearing fractions or shortcuts, thus incorporating the best of the two methods. We demonstrate this procedure by solving Ex. B.10 once again by this method.

In Ex. B.10, coefficients k and a_0 are relatively simple to determine by the Heaviside expansion method. These values were found to be $k_1=1$ and $a_0=2$. Therefore,

$$\frac{4x^3+16x^2+23x+13}{(x+1)^3(x+2)}=\frac{2}{(x+1)^3}+\frac{a_1}{(x+1)^2}+\frac{a_2}{x+1}+\frac{1}{x+2}$$

We now multiply both sides of this equation by $(x+1)^3(x+2)$ to clear the fractions. This yields

$$\begin{aligned}4x^3+16x^2+23x+13&=2(x+2)+a_1(x+1)(x+2)+a_2(x+1)^2(x+2)+(x+1)^3\\&=(1+a_2)x^3+(a_1+4a_2+3)x^2+(5+3a_1+5a_2)x+(4+2a_1+2a_2+1)\end{aligned}$$

Equating coefficients of the third and second powers of x on both sides, we obtain

$$\left.\begin{aligned} 1+a_2 &= 4 \\ a_1+4a_2+3 &= 16 \end{aligned}\right\} \implies \begin{aligned} a_1 &= 1 \\ a_2 &= 3 \end{aligned}$$

We may stop here if we wish because the two desired coefficients, a_1 and a_2, are now determined. However, equating the coefficients of the two remaining powers of x yields a convenient check on the answer. Equating the coefficients of the x^1 and x^0 terms, we obtain

$$\begin{aligned} 23 &= 5+3a_1+5a_2 \\ 13 &= 4+2a_1+2a_2+1 \end{aligned}$$

These equations are satisfied by the values $a_1 = 1$ and $a_2 = 3$, found earlier, providing an additional check for our answers. Therefore,

$$F(x) = \frac{2}{(x+1)^3} + \frac{1}{(x+1)^2} + \frac{3}{x+1} + \frac{1}{x+2}$$

which agrees with the earlier result.

A Combination of Heaviside "Cover-Up" and Shortcuts

In Ex. B.10, after determining the coefficients $a_0 = 2$ and $k = 1$ by the Heaviside method as before, we have

$$\frac{4x^3+16x^2+23x+13}{(x+1)^3(x+2)} = \frac{2}{(x+1)^3} + \frac{a_1}{(x+1)^2} + \frac{a_2}{x+1} + \frac{1}{x+2}$$

There are only two unknown coefficients, a_1 and a_2. If we multiply both sides of this equation by x and then let $x \to \infty$, we can eliminate a_1. This yields

$$4 = a_2 + 1 \implies a_2 = 3$$

Therefore,

$$\frac{4x^3+16x^2+23x+13}{(x+1)^3(x+2)} = \frac{2}{(x+1)^3} + \frac{a_1}{(x+1)^2} + \frac{3}{x+1} + \frac{1}{x+2}$$

There is now only one unknown a_1, which can be readily found by setting x equal to any convenient value, say, $x = 0$. This yields

$$\frac{13}{2} = 2 + a_1 + 3 + \frac{1}{2} \implies a_1 = 1$$

which agrees with our earlier answer.

There are other possible shortcuts. For example, we can compute a_0 (coefficient of the highest power of the repeated root), subtract this term from both sides, and then repeat the procedure.

B.5.5 Improper $F(x)$ with $m = n$

A general method of handling an improper function is indicated in the beginning of this section. However, for the special case of when the numerator and denominator polynomials of $F(x)$ have

the same degree ($m = n$), the procedure is the same as that for a proper function. We can show that for

$$F(x) = \frac{b_n x^n + b_{n-1}x^{n-1} + \cdots + b_1 x + b_0}{x^n + a_{n-1}x^{n-1} + \cdots + a_1 x + a_0} = b_n + \frac{k_1}{x-\lambda_1} + \frac{k_2}{x-\lambda_2} + \cdots + \frac{k_n}{x-\lambda_n}$$

the coefficients $k_1, k_2, \ldots, k_n$ are computed as if $F(x)$ were proper. Thus,

$$k_r = (x-\lambda_r)F(x)|_{x=\lambda_r}$$

For quadratic or repeated factors, the appropriate procedures discussed in Secs. B.5.2 or B.5.3 should be used as if $F(x)$ were proper. In other words, when $m = n$, the only difference between the proper and improper case is the appearance of an extra constant b_n in the latter. Otherwise, the procedure remains the same. The proof is left as an exercise for the reader.

EXAMPLE B.11 Partial Fraction Expansion of Improper Rational Function

Expand $F(x)$ into partial fractions if

$$F(x) = \frac{3x^2+9x-20}{x^2+x-6} = \frac{3x^2+9x-20}{(x-2)(x+3)}$$

Here, $m = n = 2$ with $b_n = b_2 = 3$. Therefore,

$$F(x) = \frac{3x^2+9x-20}{(x-2)(x+3)} = 3 + \frac{k_1}{x-2} + \frac{k_2}{x+3}$$

in which

$$k_1 = \left.\frac{3x^2+9x-20}{(x-2)(x+3)}\right|_{x=2} = \frac{12+18-20}{(2+3)} = \frac{10}{5} = 2$$

and

$$k_2 = \left.\frac{3x^2+9x-20}{(x-2)(x+3)}\right|_{x=-3} = \frac{27-27-20}{(-3-2)} = \frac{-20}{-5} = 4$$

Therefore,

$$F(x) = \frac{3x^2+9x-20}{(x-2)(x+3)} = 3 + \frac{2}{x-2} + \frac{4}{x+3}$$

B.5.6 Modified Partial Fractions

In finding the inverse z-transform (Ch. 11), we require partial fractions of the form $kx/(x-\lambda_i)^r$ rather than $k/(x-\lambda_i)^r$. This can be achieved by expanding $F(x)/x$ into partial fractions. Consider, for example,

$$F(x)=\frac{5x^2+20x+18}{(x+2)(x+3)^2}$$

Dividing both sides by x yields

$$\frac{F(x)}{x}=\frac{5x^2+20x+18}{x(x+2)(x+3)^2}$$

Expansion of the right-hand side into partial fractions as usual yields

$$\frac{F(x)}{x}=\frac{5x^2+20x+18}{x(x+2)(x+3)^2}=\frac{a_1}{x}+\frac{a_2}{x+2}+\frac{a_3}{(x+3)}+\frac{a_4}{(x+3)^2}$$

Using the procedure discussed earlier, we find $a_1=1$, $a_2=1$, $a_3=-2$, and $a_4=1$. Therefore,

$$\frac{F(x)}{x}=\frac{1}{x}+\frac{1}{x+2}-\frac{2}{x+3}+\frac{1}{(x+3)^2}$$

Now multiplying both sides by x yields

$$F(x)=1+\frac{x}{x+2}-\frac{2x}{x+3}+\frac{x}{(x+3)^2}$$

This expresses $F(x)$ as the sum of partial fractions having the form $kx/(x-\lambda_i)^r$.

B.6 VECTORS AND MATRICES

An entity specified by n numbers in a certain order (ordered n-tuple) is an n-dimensional *vector*. Thus, an ordered n-tuple $(x_1, x_2, \ldots, x_n)$ represents an n-dimensional vector $\mathbf{x}$. A vector may be represented as a row (*row vector*):

$$\mathbf{x}=\begin{bmatrix} x_1 & x_2 & \cdots & x_n \end{bmatrix}$$

or as a column (*column vector*):

$$\mathbf{x}=\begin{bmatrix} x_1 \\ x_2 \\ \vdots \\ x_n \end{bmatrix}$$

Simultaneous linear equations can be viewed as the transformation of one vector into another. Consider, for example, the m simultaneous linear equations

$$\begin{aligned} y_1 &= a_{11}x_1 + a_{12}x_2 + \cdots + a_{1n}x_n \\ y_2 &= a_{21}x_1 + a_{22}x_2 + \cdots + a_{2n}x_n \\ &\vdots \\ y_m &= a_{m1}x_1 + a_{m2}x_2 + \cdots + a_{mn}x_n \end{aligned} \tag{B.31}$$

If we define two column vectors $\mathbf{x}$ and $\mathbf{y}$ as

$$\mathbf{x} = \begin{bmatrix} x_1 \\ x_2 \\ \vdots \\ x_n \end{bmatrix} \quad \text{and} \quad \mathbf{y} = \begin{bmatrix} y_1 \\ y_2 \\ \vdots \\ y_m \end{bmatrix}$$

then Eq. (B.31) may be viewed as the relationship or the function that transforms vector $\mathbf{x}$ into vector $\mathbf{y}$. Such a transformation is called a *linear transformation* of vectors. To perform a linear transformation, we need to define the array of coefficients a_{ij} appearing in Eq. (B.31). This array is called a *matrix* and is denoted by $\mathbf{A}$ for convenience:

$$\mathbf{A} = \begin{bmatrix} a_{11} & a_{12} & \cdots & a_{1n} \\ a_{21} & a_{22} & \cdots & a_{2n} \\ \vdots & \vdots & \cdots & \vdots \\ a_{m1} & a_{m2} & \cdots & a_{mn} \end{bmatrix}$$

A matrix with m rows and n columns is called a matrix of order (m,n) or an $(m \times n)$ matrix. For the special case of $m = n$, the matrix is called a *square matrix* of order n.

It should be stressed at this point that a matrix is not a number such as a determinant, but an array of numbers arranged in a particular order. It is convenient to abbreviate the representation of matrix $\mathbf{A}$ with the form $(a_{ij})_{m\times n}$, implying a matrix of order $m \times n$ with a_{ij} as its ijth element. In practice, when the order $m \times n$ is understood or need not be specified, the notation can be abbreviated to (a_{ij}). Note that the first index i of a_{ij} indicates the row and the second index j indicates the column of the element a_{ij} in matrix $\mathbf{A}$.

Equation (B.31) may now be expressed in a matrix form as

$$\begin{bmatrix} y_1 \\ y_2 \\ \vdots \\ y_m \end{bmatrix} = \begin{bmatrix} a_{11} & a_{12} & \cdots & a_{1n} \\ a_{21} & a_{22} & \cdots & a_{2n} \\ \vdots & \vdots & \cdots & \vdots \\ a_{m1} & a_{m2} & \cdots & a_{mn} \end{bmatrix} \begin{bmatrix} x_1 \\ x_2 \\ \vdots \\ x_n \end{bmatrix} \quad \text{or} \quad \mathbf{y} = \mathbf{A}\mathbf{x} \tag{B.32}$$

At this point, we have not defined the multiplication of a matrix by a vector. The quantity $\mathbf{Ax}$ is not meaningful until such an operation has been defined.

B.6.1 Some Definitions and Properties

A square matrix whose elements are zero everywhere except on the main diagonal is a *diagonal matrix*. An example of a diagonal matrix is

$$\begin{bmatrix} 2 & 0 & 0 \\ 0 & 1 & 0 \\ 0 & 0 & 5 \end{bmatrix}$$

A diagonal matrix with unity for all its diagonal elements is called an *identity matrix* or a *unit matrix*, denoted by $\mathbf{I}$. This is a square matrix:

$$\mathbf{I} = \begin{bmatrix} 1 & 0 & 0 & \cdots & 0 \\ 0 & 1 & 0 & \cdots & 0 \\ 0 & 0 & 1 & \cdots & 0 \\ \vdots & \vdots & \vdots & \cdots & \vdots \\ 0 & 0 & 0 & \cdots & 1 \end{bmatrix}$$

The order of the unit matrix is sometimes indicated by a subscript. Thus, $\mathbf{I}_n$ represents the $n \times n$ unit matrix (or identity matrix). However, we shall omit the subscript since order is easily understood by context.

A matrix having all its elements zero is a *zero matrix*.

A square matrix $\mathbf{A}$ is a *symmetric matrix* if $a_{ij} = a_{ji}$ (symmetry about the main diagonal).

Two matrices of the same order are said to be *equal* if they are equal element by element. Thus, if

$$\mathbf{A} = (a_{ij})_{m \times n} \qquad \text{and} \qquad \mathbf{B} = (b_{ij})_{m \times n}$$

then $\mathbf{A} = \mathbf{B}$ only if $a_{ij} = b_{ij}$ for all i and j.

If the rows and columns of an $m \times n$ matrix $\mathbf{A}$ are interchanged so that the elements in the ith row now become the elements of the ith column (for $i = 1, 2, \ldots, m$), the resulting matrix is called the *transpose* of $\mathbf{A}$ and is denoted by $\mathbf{A}^T$. It is evident that $\mathbf{A}^T$ is an $n \times m$ matrix. For example, if

$$\mathbf{A} = \begin{bmatrix} 2 & 1 \\ 3 & 2 \\ 1 & 3 \end{bmatrix}, \qquad \text{then} \qquad \mathbf{A}^T = \begin{bmatrix} 2 & 3 & 1 \\ 1 & 2 & 3 \end{bmatrix}$$

Using the abbreviated notation, if $\mathbf{A} = (a_{ij})_{m \times n}$, then $\mathbf{A}^T = (a_{ji})_{n \times m}$. Intuitively, further notice that $(\mathbf{A}^T)^T = \mathbf{A}$.

B.6.2 Matrix Algebra

We shall now define matrix operations, such as addition, subtraction, multiplication, and division of matrices. The definitions should be formulated so that they are useful in the manipulation of matrices.

Addition of Matrices

For two matrices **A** and **B**, both of the same order ($m \times n$),

$$\mathbf{A} = \begin{bmatrix} a_{11} & a_{12} & \cdots & a_{1n} \\ a_{21} & a_{22} & \cdots & a_{2n} \\ \vdots & \vdots & \cdots & \vdots \\ a_{m1} & a_{m2} & \cdots & a_{mn} \end{bmatrix} \quad \text{and} \quad \mathbf{B} = \begin{bmatrix} b_{11} & b_{12} & \cdots & b_{1n} \\ b_{21} & b_{22} & \cdots & b_{2n} \\ \vdots & \vdots & \cdots & \vdots \\ b_{m1} & b_{m2} & \cdots & b_{mn} \end{bmatrix}$$

we define the sum $\mathbf{A} + \mathbf{B}$ as

$$\mathbf{A}+\mathbf{B} = \begin{bmatrix} (a_{11}+b_{11}) & (a_{12}+b_{12}) & \cdots & (a_{1n}+b_{1n}) \\ (a_{21}+b_{21}) & (a_{22}+b_{22}) & \cdots & (a_{2n}+b_{2n}) \\ \vdots & \vdots & \cdots & \vdots \\ (a_{m1}+b_{m1}) & (a_{m2}+b_{m2}) & \cdots & (a_{mn}+b_{mn}) \end{bmatrix}$$

or

$$\mathbf{A}+\mathbf{B} = (a_{ij}+b_{ij})_{m\times n}$$

Note that two matrices can be added only if they are of the same order.

Multiplication of a Matrix by a Scalar

We multiply a matrix **A** by a scalar c as follows:

$$c\mathbf{A} = c\begin{bmatrix} a_{11} & a_{12} & \cdots & a_{1n} \\ a_{21} & a_{22} & \cdots & a_{2n} \\ \vdots & \vdots & \cdots & \vdots \\ a_{m1} & a_{m2} & \cdots & a_{mn} \end{bmatrix} = \begin{bmatrix} ca_{11} & ca_{12} & \cdots & ca_{1n} \\ ca_{21} & ca_{22} & \cdots & ca_{2n} \\ \vdots & \vdots & \cdots & \vdots \\ ca_{m1} & ca_{m2} & \cdots & ca_{mn} \end{bmatrix} = \mathbf{A}c$$

Thus, we also observe that the scalar c and the matrix **A** commute: $c\mathbf{A} = \mathbf{A}c$.

Matrix Multiplication

We define the product

$$\mathbf{AB} = \mathbf{C}$$

in which c_{ij}, the element of **C** in the ith row and jth column, is found by adding the products of the elements of **A** in the ith row multiplied by the corresponding elements of **B** in the jth column. Thus,

$$c_{ij} = a_{i1}b_{1j} + a_{i2}b_{2j} + \cdots + a_{in}b_{nj} = \sum_{k=1}^{n} a_{ik}b_{kj} \tag{B.33}$$

This result is expressed as follows:

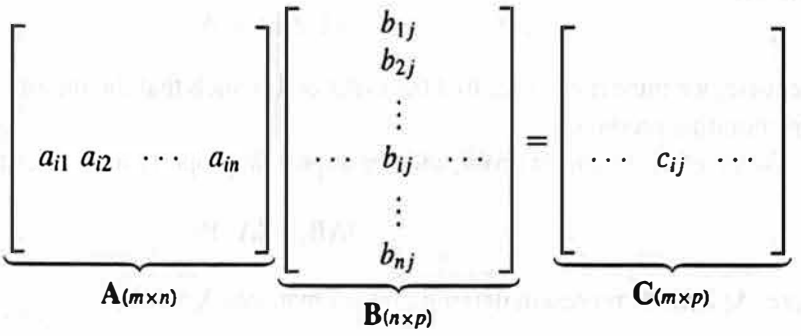

Note carefully that if this procedure is to work, the number of columns of **A** must be equal to the number of rows of **B**. In other words, **AB**, the product of matrices **A** and **B**, is defined only if the number of columns of **A** is equal to the number of rows of **B**. If this condition is not satisfied, the product **AB** is not defined and is meaningless. When the number of columns of **A** is equal to the number of rows of **B**, matrix **A** is said to be *conformable* to matrix **B** for the product **AB**. Observe that if **A** is an $m \times n$ matrix and **B** is an $n \times p$ matrix, **A** and **B** are conformable for the product, and **C** is an $m \times p$ matrix.

We demonstrate the use of the rule in Eq. (B.33) with the following examples:

$$\begin{bmatrix} 2 & 3 \\ 1 & 1 \\ 3 & 1 \end{bmatrix}\begin{bmatrix} 1 & 3 & 1 & 2 \\ 2 & 1 & 1 & 1 \end{bmatrix} = \begin{bmatrix} 8 & 9 & 5 & 7 \\ 3 & 4 & 2 & 3 \\ 5 & 10 & 4 & 7 \end{bmatrix}$$

$$\begin{bmatrix} 2 & 1 & 3 \end{bmatrix}\begin{bmatrix} 2 \\ 1 \\ 1 \end{bmatrix} = 8$$

In both cases, the two matrices are conformable. However, if we interchange the order of the first matrices as follows:

$$\begin{bmatrix} 1 & 3 & 1 & 2 \\ 2 & 1 & 1 & 1 \end{bmatrix}\begin{bmatrix} 2 & 3 \\ 1 & 1 \\ 3 & 1 \end{bmatrix}$$

the matrices are no longer conformable for the product. It is evident that, in general,

$$\mathbf{AB} \neq \mathbf{BA}$$

Indeed, **AB** may exist and **BA** may not exist, or vice versa, as in our examples. We shall see later that for some special matrices, $\mathbf{AB} = \mathbf{BA}$. When this is true, matrices **A** and **B** are said to *commute*. We re-emphasize that, in general, matrices do not commute.

In the matrix product **AB**, matrix **A** is said to be *postmultiplied* by **B** or matrix **B** is said to be *premultiplied* by **A**. We may also verify the following relationships:

$$(\mathbf{A}+\mathbf{B})\mathbf{C} = \mathbf{AC}+\mathbf{BC}$$
$$\mathbf{C}(\mathbf{A}+\mathbf{B}) = \mathbf{CA}+\mathbf{CB}$$

We can verify that any matrix **A** premultiplied or postmultiplied by the identity matrix **I** remains unchanged:

$$\mathbf{AI} = \mathbf{IA} = \mathbf{A}$$

Of course, we must make sure that the order of **I** is such that the matrices are conformable for the corresponding product.

We give here, without proof, another important property of matrices:

$$|\mathbf{AB}| = |\mathbf{A}||\mathbf{B}|$$

where $|\mathbf{A}|$ and $|\mathbf{B}|$ represent determinants of matrices **A** and **B**.

Multiplication of a Matrix by a Vector

Consider Eq. (B.32), which represents Eq. (B.31). The right-hand side of Eq. (B.32) is a product of the $m \times n$ matrix **A** and a vector **x**. If, for the time being, we treat the vector **x** as if it were an $n \times 1$ matrix, then the product **Ax**, according to the matrix multiplication rule, yields the right-hand side of Eq. (B.31). Thus, we may multiply a matrix by a vector by treating the vector as if it were an $n \times 1$ matrix. Note that the constraint of conformability still applies. Thus, in this case, **xA** is not defined and is meaningless.

Matrix Inversion

To define the inverse of a matrix, let us consider the set of equations represented by Eq. (B.32) when $m = n$:

$$\begin{bmatrix} y_1 \\ y_2 \\ \vdots \\ y_n \end{bmatrix} = \begin{bmatrix} a_{11} & a_{12} & \cdots & a_{1n} \\ a_{21} & a_{22} & \cdots & a_{2n} \\ \vdots & \vdots & \cdots & \vdots \\ a_{n1} & a_{n2} & \cdots & a_{nn} \end{bmatrix} \begin{bmatrix} x_1 \\ x_2 \\ \vdots \\ x_n \end{bmatrix} \tag{B.34}$$

We can solve this set of equations for $x_1, x_2, \ldots, x_n$ in terms of $y_1, y_2, \ldots, y_n$ by using Cramer's rule [see Eq. (B.21)]. This yields

$$\begin{bmatrix} x_1 \\ x_2 \\ \vdots \\ x_n \end{bmatrix} = \begin{bmatrix} \dfrac{|\mathbf{D}_{11}|}{|\mathbf{A}|} & \dfrac{|\mathbf{D}_{21}|}{|\mathbf{A}|} & \cdots & \dfrac{|\mathbf{D}_{n1}|}{|\mathbf{A}|} \\ \dfrac{|\mathbf{D}_{12}|}{|\mathbf{A}|} & \dfrac{|\mathbf{D}_{22}|}{|\mathbf{A}|} & \cdots & \dfrac{|\mathbf{D}_{n2}|}{|\mathbf{A}|} \\ \vdots & \vdots & \cdots & \vdots \\ \dfrac{|\mathbf{D}_{1n}|}{|\mathbf{A}|} & \dfrac{|\mathbf{D}_{2n}|}{|\mathbf{A}|} & \cdots & \dfrac{|\mathbf{D}_{nn}|}{|\mathbf{A}|} \end{bmatrix} \begin{bmatrix} y_1 \\ y_2 \\ \vdots \\ y_n \end{bmatrix} \tag{B.35}$$

in which $|\mathbf{A}|$ is the determinant of the matrix **A** and $|\mathbf{D}_{ij}|$ is the *cofactor* of element a_{ij} in the matrix **A**. The cofactor of element a_{ij} is given by $(-1)^{i+j}$ times the determinant of the $(n-1) \times (n-1)$ matrix that is obtained when the ith row and the jth column in matrix **A** are deleted.

We can express Eq. (B.34) in compact matrix form as

$$\mathbf{y} = \mathbf{Ax} \tag{B.36}$$

We now define $\mathbf{A}^{-1}$, the inverse of a square matrix $\mathbf{A}$, with the property

$$\mathbf{A}^{-1}\mathbf{A} = \mathbf{I} \qquad \text{(unit matrix)}$$

Then, premultiplying both sides of Eq. (B.36) by $\mathbf{A}^{-1}$, we obtain

$$\mathbf{A}^{-1}\mathbf{y} = \mathbf{A}^{-1}\mathbf{A}\mathbf{x} = \mathbf{I}\mathbf{x} = \mathbf{x}$$

or

$$\mathbf{x} = \mathbf{A}^{-1}\mathbf{y} \tag{B.37}$$

A comparison of Eq. (B.37) with Eq. (B.35) shows that

$$\mathbf{A}^{-1} = \frac{1}{|\mathbf{A}|}\begin{bmatrix} |\mathbf{D}_{11}| & |\mathbf{D}_{21}| & \cdots & |\mathbf{D}_{n1}| \\ |\mathbf{D}_{12}| & |\mathbf{D}_{22}| & \cdots & |\mathbf{D}_{n2}| \\ \vdots & \vdots & \cdots & \vdots \\ |\mathbf{D}_{1n}| & |\mathbf{D}_{2n}| & \cdots & |\mathbf{D}_{nn}| \end{bmatrix}$$

One of the conditions necessary for a unique solution of Eq. (B.34) is that the number of equations must equal the number of unknowns. This implies that the matrix $\mathbf{A}$ must be a square matrix. In addition, we observe from the solution as given in Eq. (B.35) that if the solution is to exist, $|\mathbf{A}| \neq 0$.[†] Therefore, the inverse exists only for a square matrix and only under the condition that the determinant of the matrix be nonzero. A matrix whose determinant is nonzero is a *nonsingular* matrix. Thus, an inverse exists only for a nonsingular, square matrix. Since $\mathbf{A}^{-1}\mathbf{A} = \mathbf{I} = \mathbf{A}\mathbf{A}^{-1}$, we further note that the matrices $\mathbf{A}$ and $\mathbf{A}^{-1}$ commute.[‡]

The operation of matrix division can be accomplished through matrix inversion.

EXAMPLE B.12 Computing the Inverse of a Matrix

Let us find $\mathbf{A}^{-1}$ if

$$\mathbf{A} = \begin{bmatrix} 2 & 1 & 1 \\ 1 & 2 & 3 \\ 3 & 2 & 1 \end{bmatrix}$$

Here,

$$\begin{aligned} |\mathbf{D}_{11}| &= -4, & |\mathbf{D}_{12}| &= 8, & |\mathbf{D}_{13}| &= -4 \\ |\mathbf{D}_{21}| &= 1, & |\mathbf{D}_{22}| &= -1, & |\mathbf{D}_{23}| &= -1 \\ |\mathbf{D}_{31}| &= 1, & |\mathbf{D}_{32}| &= -5, & |\mathbf{D}_{33}| &= 3 \end{aligned}$$

[†] These two conditions imply that the number of equations is equal to the number of unknowns and that all the equations are independent.

[‡] To prove $\mathbf{A}\mathbf{A}^{-1} = \mathbf{I}$, notice first that we define $\mathbf{A}^{-1}\mathbf{A} = \mathbf{I}$. Thus, $\mathbf{I}\mathbf{A} = \mathbf{A}\mathbf{I} = \mathbf{A}(\mathbf{A}^{-1}\mathbf{A}) = (\mathbf{A}\mathbf{A}^{-1})\mathbf{A}$. Subtracting $(\mathbf{A}\mathbf{A}^{-1})\mathbf{A}$, we see that $\mathbf{I}\mathbf{A} - (\mathbf{A}\mathbf{A}^{-1})\mathbf{A} = 0$ or $(\mathbf{I} - \mathbf{A}\mathbf{A}^{-1})\mathbf{A} = 0$. This requires $\mathbf{A}\mathbf{A}^{-1} = \mathbf{I}$.

and $|\mathbf{A}| = -4$. Therefore,

$$\mathbf{A}^{-1} = -\frac{1}{4}\begin{bmatrix} -4 & 1 & 1 \\ 8 & -1 & -5 \\ -4 & -1 & 3 \end{bmatrix}$$

B.7 MATLAB: ELEMENTARY OPERATIONS

B.7.1 MATLAB Overview

Although MATLAB® (a registered trademark of The MathWorks, Inc.) is easy to use, it can be intimidating to new users. Over the years, MATLAB has evolved into a sophisticated computational package with thousands of functions and thousands of pages of documentation. This section provides a brief introduction to the software environment.

When MATLAB is first launched, its command window appears. When MATLAB is ready to accept an instruction or input, a command prompt (>>) is displayed in the command window. Nearly all MATLAB activity is initiated at the command prompt.

Entering instructions at the command prompt generally results in the creation of an object or objects. Many classes of objects are possible, including functions and strings, but usually objects are just data. Objects are placed in what is called the MATLAB workspace. If not visible, the workspace can be viewed in a separate window by typing `workspace` at the command prompt. The workspace provides important information about each object, including the object's name, size, and class.

Another way to view the workspace is the `whos` command. When `whos` is typed at the command prompt, a summary of the workspace is printed in the command window. The `who` command is a short version of `whos` that reports only the names of workspace objects.

Several functions exist to remove unnecessary data and help free system resources. To remove specific variables from the workspace, the `clear` command is typed, followed by the names of the variables to be removed. Just typing `clear` removes all objects from the workspace. Additionally, the `clc` command clears the command window, and the `clf` command clears the current figure window.

Often, important data and objects created in one session need to be saved for future use. The `save` command, followed by the desired filename, saves the entire workspace to a file, which has the .mat extension. It is also possible to selectively save objects by typing `save` followed by the filename and then the names of the objects to be saved. The `load` command followed by the filename is used to load the data and objects contained in a MATLAB data file (.mat file).

Although MATLAB does not automatically save workspace data from one session to the next, lines entered at the command prompt are recorded in the command history. Previous command lines can be viewed, copied, and executed directly from the command history window. From the command window, pressing the up or down arrow key scrolls through previous commands and redisplays them at the command prompt. Typing the first few characters and then pressing the arrow keys scrolls through the previous commands that start with the same characters. The arrow keys allow command sequences to be repeated without retyping.

Perhaps the most important and useful command for new users is `help`. To learn more about a function, simply type `help` followed by the function name. Helpful text is then displayed in

the command window. The obvious shortcoming of `help` is that the function name must first be known. This is especially limiting for MATLAB beginners. Fortunately, help screens often conclude by referencing related or similar functions. These references are an excellent way to learn new MATLAB commands. Typing `help help`, for example, displays detailed information on the `help` command itself and also provides reference to relevant functions, such as the `lookfor` command. The `lookfor` command helps locate MATLAB functions based on a keyword search. Simply type `lookfor` followed by a single keyword, and MATLAB searches for functions that contain that keyword.

MATLAB also has comprehensive HTML-based help. The HTML help is accessed by using MATLAB's integrated help browser, which also functions as a standard web browser. The HTML help facility includes a function and topic index as well as full text-searching capabilities. Since HTML documents can contain graphics and special characters, HTML help can provide more information than the command-line help. After a little practice, it is easy to find information in MATLAB.

When MATLAB graphics are created, the `print` command can save figures in a common file format such as postscript, encapsulated postscript, JPEG, or TIFF. The format of displayed data, such as the number of digits displayed, is selected by using the `format` command. MATLAB help provides the necessary details for both these functions. When a MATLAB session is complete, the `exit` command terminates MATLAB.

B.7.2 Calculator Operations

MATLAB can function as a simple calculator, working as easily with complex numbers as with real numbers. Scalar addition, subtraction, multiplication, division, and exponentiation are accomplished using the traditional operator symbols `+`, `-`, `*`, `/`, and `^`. Since MATLAB predefines `i = j` $= \sqrt{-1}$, a complex constant is readily created using Cartesian coordinates. For example,

```
>>  z = -3-4j
    z = -3.0000 - 4.0000i
```

assigns the complex constant $-3 - j4$ to the variable z.

The real and imaginary components of z are extracted by using the `real` and `imag` operators. In MATLAB, the input to a function is placed parenthetically following the function name.

```
>>  z_real = real(z); z_imag = imag(z);
```

When a command is terminated with a semicolon, the statement is evaluated but the results are not displayed to the screen. This feature is useful when one is computing intermediate results, and it allows multiple instructions on a single line. Although not displayed, the results `z_real = -3` and `z_imag = -4` are calculated and available for additional operations such as computing $|z|$.

There are many ways to compute the modulus, or magnitude, of a complex quantity. Trigonometry confirms that $z = -3 - j4$, which corresponds to a 3-4-5 triangle, has modulus $|z| = |-3 - j4| = \sqrt{(-3)^2 + (-4)^2} = 5$. The MATLAB `sqrt` command provides one way to compute the required square root.

```
>>  z_mag = sqrt(z_real^2 + z_imag^2)
    z_mag = 5
```

In MATLAB, most commands, including `sqrt`, accept inputs in a variety of forms, including constants, variables, functions, expressions, and combinations thereof.

The same result is also obtained by computing $|z| = \sqrt{zz^*}$. In this case, complex conjugation is performed by using the `conj` command.

```
>> z_mag = sqrt(z*conj(z))
   z_mag = 5
```

More simply, MATLAB computes absolute values directly by using the `abs` command.

```
>> z_mag = abs(z)
   z_mag = 5
```

In addition to magnitude, polar notation requires phase information. The `angle` command provides the angle of a complex number.

```
>> z_rad = angle(z)
   z_rad = -2.2143
```

MATLAB expects and returns angles in a radian measure. Angles expressed in degrees require an appropriate conversion factor.

```
>> z_deg = angle(z)*180/pi
   z_deg = -126.8699
```

Notice, MATLAB predefines the variable `pi` $= \pi$.

It is also possible to obtain the angle of z using a two-argument arc-tangent function, `atan2`.

```
>> z_rad = atan2(z_imag,z_real)
   z_rad = -2.2143
```

Unlike a single-argument arctangent function, the two-argument arctangent function ensures that the angle reflects the proper quadrant. MATLAB supports a full complement of trigonometric functions: standard trigonometric functions `cos`, `sin`, `tan`; reciprocal trigonometric functions `sec`, `csc`, `cot`; inverse trigonometric functions `acos`, `asin`, `atan`, `asec`, `acsc`, `acot`; and hyperbolic variations `cosh`, `sinh`, `tanh`, `sech`, `csch`, `coth`, `acosh`, `asinh`, `atanh`, `asech`, `acsch`, and `acoth`. Of course, MATLAB comfortably supports complex arguments for any trigonometric function. As with the `angle` command, MATLAB trigonometric functions utilize units of radians.

The concept of trigonometric functions with complex-valued arguments is rather intriguing. The results can contradict what is often taught in introductory mathematics courses. For example, a common claim is that $|\cos(x)| \leq 1$. While this is true for real x, it is not necessarily true for complex x. This is readily verified by example using MATLAB and the `cos` function.

```
>> cos(1j)
   ans = 1.5431
```

Problem B.1-19 investigates these ideas further.

Similarly, the claim that it is impossible to take the logarithm of a negative number is false. For example, the principal value of $\ln(-1)$ is $j\pi$, a fact easily verified by means of Euler's

equation. In MATLAB, base-10 and base-e logarithms are computed by using the `log10` and `log` commands, respectively.

```
>> log(-1)
   ans = 0 + 3.1416i
```

B.7.3 Vector Operations

The power of MATLAB becomes apparent when vector arguments replace scalar arguments. Rather than computing one value at a time, a single expression computes many values. Typically, vectors are classified as row vectors or column vectors. For now, we consider the creation of row vectors with evenly spaced, real elements. To create such a vector, the notation `a:b:c` is used, where `a` is the initial value, `b` designates the step size, and `c` is the termination value. For example, `0:2:11` creates the length-6 vector of even-valued integers ranging from 0 to 10.

```
>> k = 0:2:11
   k =  0    2    4    6    8   10
```

In this case, the termination value does not appear as an element of the vector. Negative and noninteger step sizes are also permissible.

```
>> k = 11:-10/3:0
   k = 11.0000    7.6667    4.3333    1.0000
```

If a step size is not specified, a value of 1 is assumed.

```
>> k = 0:11
   k =  0    1    2    3    4    5    6    7    8    9   10   11
```

Vector notation provides the basis for solving a wide variety of problems.

For example, consider finding the three cube roots of minus one, $w^3 = -1 = e^{j(\pi+2\pi k)}$ for integer k. Taking the cube root of each side yields $w = e^{j(\pi/3+2\pi k/3)}$. To find the three unique solutions, use any three consecutive integer values of k and MATLAB's exp function.

```
>> k = 0:2; w = exp(1j*(pi/3 + 2*pi*k/3))
   w = 0.5000 + 0.8660i  -1.0000 + 0.0000i   0.5000 - 0.8660i
```

The solutions, particularly $w = -1$, are easy to verify.

Finding the 100 unique roots of $w^{100} = -1$ is just as simple.

```
>> k = 0:99; w = exp(1j*(pi/100 + 2*pi*k/100));
```

A semicolon concludes the final instruction to suppress the inconvenient display of all 100 solutions. To view a particular solution, the user must use an index to specify desired elements. MATLAB indices are integers that increase from a starting value of 1. For example, the fifth element of w is extracted using an index of 5.†

† Some other programming languages, such as C, begin indexing at 0. Careful attention is warranted.

```
>> w(5)
   ans = 0.9603 + 0.2790i
```

Notice that this solution corresponds to $k = 4$. The independent variable of a function, in this case k, rarely serves as the index. Since k is also a vector, it can likewise be indexed. In this way, we can verify that the fifth value of k is indeed 4.

```
>> k(5)
   ans = 4
```

It is also possible to use a vector index to access multiple values. For example, index vector `98:100` identifies the last three solutions corresponding to $k = [97, 98, 99]$.

```
>> w(98:100)
   ans = 0.9877 - 0.1564i   0.9956 - 0.0941i   0.9995 - 0.0314i
```

Vector representations provide the foundation to rapidly create and explore various signals. Consider the simple 10 Hz sinusoid described by $f(t) = \sin(2\pi 10t + \pi/6)$. Two cycles of this sinusoid are included in the interval $0 \leq t < 0.2$. A vector t is used to uniformly represent 500 points over this interval.

```
>> t = 0:0.2/500:0.2-0.2/500;
```

Next, the function $f(t)$ is evaluated at these points.

```
>> f = sin(2*pi*10*t+pi/6)
```

The value of $f(t)$ at $t = 0$ is the first element of the vector and is thus obtained by using an index of 1.

```
>> f(1)
   ans = 0.5000
```

Unfortunately, MATLAB's indexing syntax conflicts with standard equation notation.† That is, the MATLAB indexing command `f(1)` is not the same as the standard notation $f(1) = f(t)|_{t=1}$. Care must be taken to avoid confusion; remember that the index parameter rarely reflects the independent variable of a function.

B.7.4 Simple Plotting

MATLAB's `plot` command provides a convenient way to visualize data, such as graphing $f(t)$ against the independent variable t.

```
>> plot(t,f);
```

Axis labels are added using the `xlabel` and `ylabel` commands, where the desired string must be enclosed by single quotation marks. The result is shown in Fig. B.12.

† MATLAB anonymous functions, considered in Sec. 1.11, are an important and useful exception.

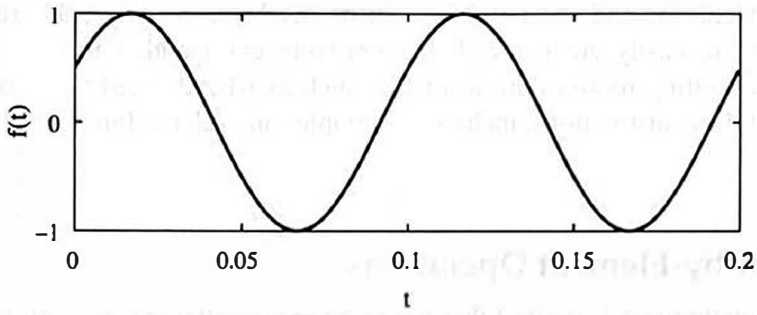

Figure B.12 $f(t) = \sin(2\pi 10t + \pi/6)$.

```
>> xlabel('t'); ylabel('f(t)')
```

The `title` command is used to add a title above the current axis.

By default, MATLAB connects data points with solid lines. Plotting discrete points, such as the 100 unique roots of $w^{100} = -1$, is accommodated by supplying the `plot` command with an additional string argument. For example, the string `'o'` tells MATLAB to mark each data point with a circle rather than connecting points with lines. A full description of the supported plot options is available from MATLAB's help facilities.

```
>> plot(real(w),imag(w),'o');
>> xlabel('Re(w)'); ylabel('Im(w)'); axis equal
```

The `axis equal` command ensures that the scale used for the horizontal axis is equal to the scale used for the vertical axis. Without `axis equal`, the plot would appear elliptical rather than circular. Figure B.13 illustrates that the 100 unique roots of $w^{100} = -1$ lie equally spaced on the unit circle, a fact not easily discerned from the raw numerical data.

MATLAB also includes many specialized plotting functions. For example, MATLAB commands `semilogx`, `semilogy`, and `loglog` operate like the `plot` command but use base-10 logarithmic scales for the horizontal axis, vertical axis, and the horizontal and vertical axes,

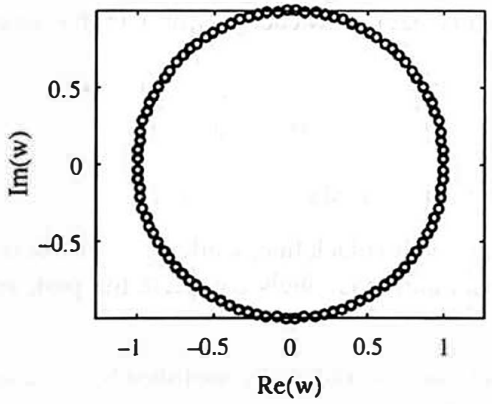

Figure B.13 Unique roots of $w^{100} = -1$.

respectively. Monochrome and color images can be displayed by using the `image` command, and contour plots are easily created with the `contour` command. Furthermore, a variety of three-dimensional plotting routines are available, such as `plot3`, `contour3`, `mesh`, and `surf`. Information about these instructions, including examples and related functions, is available from MATLAB help.

B.7.5 Element-by-Element Operations

Suppose a new function $h(t)$ is desired that forces an exponential envelope on the sinusoid $f(t)$, $h(t) = f(t)g(t)$, where $g(t) = e^{-10t}$. First, row vector $g(t)$ is created.

```
>>  g = exp(-10*t);
```

Given MATLAB's vector representation of $g(t)$ and $f(t)$, computing $h(t)$ requires some form of vector multiplication. There are three standard ways to multiply vectors: inner product, outer product, and element-by-element product. As a matrix-oriented language, MATLAB defines the standard multiplication operator * according to the rules of matrix algebra: the multiplicand must be conformable to the multiplier. A $1 \times N$ row vector times an $N \times 1$ column vector results in the scalar-valued inner product. An $N \times 1$ column vector times a $1 \times M$ row vector results in the outer product, which is an $N \times M$ matrix. Matrix algebra prohibits multiplication of two row vectors or multiplication of two column vectors. Thus, the * operator is not used to perform element-by-element multiplication.[†]

Element-by-element operations require vectors to have the same dimensions. An error occurs if element-by-element operations are attempted between row and column vectors. In such cases, one vector must first be transposed to ensure both vector operands have the same dimensions. In MATLAB, most element-by-element operations are preceded by a period. For example, element-by-element multiplication, division, and exponentiation are accomplished using `.*`, `./`, and `.^`, respectively. Vector addition and subtraction are intrinsically element-by-element operations and require no period. Intuitively, we know $h(t)$ should be the same size as both $g(t)$ and $f(t)$. Thus, $h(t)$ is computed using element-by-element multiplication.

```
>>  h = f.*g;
```

The `plot` command accommodates multiple curves and also allows modification of line properties. This facilitates side-by-side comparison of different functions, such as $h(t)$ and $f(t)$. Line characteristics are specified by using options that follow each vector pair and are enclosed in single quotes.

```
>>  plot(t,f,'-k',t,h,':k');
>>  xlabel('t'); ylabel('Amplitude');
>>  legend('f(t)','h(t)');
```

Here, `'-k'` instructs MATLAB to plot $f(t)$ using a solid black line, while `':k'` instructs MATLAB to use a dotted black line to plot $h(t)$. A legend and axis labels complete the plot, as shown in

[†] While grossly inefficient, element-by-element multiplication can be accomplished by extracting the main diagonal from the outer product of two N-length vectors.

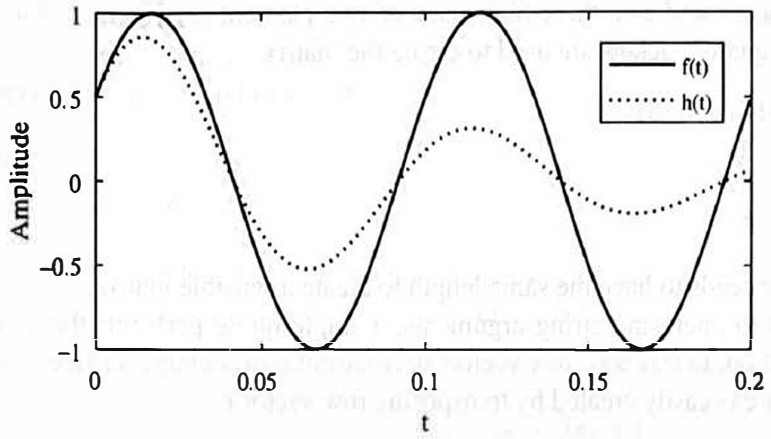

Figure B.14 Graphical comparison of $f(t)$ and $h(t)$.

Fig. B.14. It is also possible, although more cumbersome, to use pull-down menus to modify line properties and to add labels and legends directly in the figure window.

B.7.6 Matrix Operations

Many applications require more than row vectors with evenly spaced elements; row vectors, column vectors, and matrices with arbitrary elements are typically needed.

MATLAB provides several functions to generate common, useful matrices. Given integers `m`, `n`, and vector `x`, the function `eye(m)` creates the $m \times m$ identity matrix; the function `ones(m,n)` creates the $m \times n$ matrix of all ones; the function `zeros(m,n)` creates the $m \times n$ matrix of all zeros; and the function `diag(x)` uses vector `x` to create a diagonal matrix. The creation of general matrices and vectors, however, requires each individual element to be specified.

Vectors and matrices can be input spreadsheet style by using MATLAB's array editor. This graphical approach is rather cumbersome and is not often used. A more direct method is preferable.

Consider a simple row vector **r**,

$$\mathbf{r} = [\,1 \quad 0 \quad 0\,]$$

The MATLAB notation `a:b:c` cannot create this row vector. Rather, square brackets are used to create **r**.

```
>>  r = [1 0 0]
    r = 1    0    0
```

Square brackets enclose elements of the vector, and spaces or commas are used to separate row elements.

Next, consider the 3×2 matrix **A**,

$$\mathbf{A} = \begin{bmatrix} 2 & 3 \\ 4 & 5 \\ 0 & 6 \end{bmatrix}$$

Matrix **A** can be viewed as a three-high stack of two-element row vectors. With a semicolon to separate rows, square brackets are used to create the matrix.

```
>>  A = [2 3;4 5;0 6]
    A = 2    3
        4    5
        0    6
```

Each row vector needs to have the same length to create a sensible matrix.

In addition to enclosing string arguments, a single quote performs the complex conjugate transpose operation. In this way, row vectors become column vectors and vice versa. For example, a column vector **c** is easily created by transposing row vector **r**.

```
>>  c = r'
    c = 1
        0
```

Since vector **r** is real, the complex-conjugate transpose is just the transpose. Had **r** been complex, the simple transpose could have been accomplished by either `r.'` or `(conj(r))'`.

More formally, square brackets are referred to as a concatenation operator. A concatenation combines or connects smaller pieces into a larger whole. Concatenations can involve simple numbers, such as the six-element concatenation used to create the 3×2 matrix **A**. It is also possible to concatenate larger objects, such as vectors and matrices. For example, vector **c** and matrix **A** can be concatenated to form a 3×3 matrix **B**.

```
>>  B = [c A]
    B = 1    2    3
        0    4    5
        0    0    6
```

Errors will occur if the component dimensions do not sensibly match; a 2×2 matrix would not be concatenated with a 3×3 matrix, for example.

Elements of a matrix are indexed much like vectors, except two indices are typically used to specify row and column.† Element (1, 2) of matrix **B**, for example, is 2.

```
>>  B(1,2)
    ans = 2
```

Indices can likewise be vectors. For example, vector indices allow us to extract the elements common to the first two rows and last two columns of matrix **B**.

```
>>  B(1:2,2:3)
    ans = 2    3
          4    5
```

---

†Matrix elements can also be accessed by means of a single index, which enumerates along columns. Formally, the element from row m and column n of an $M \times N$ matrix may be obtained with a single index $(n-1)M+m$. For example, element (1, 2) of matrix **B** is accessed by using the index $(2-1)3+1=4$. That is, `B(4)` yields 2.

One indexing technique is particularly useful and deserves special attention. A colon can be used to specify all elements along a specified dimension. For example, `B(2,:)` selects all column elements along the second row of **B**.

```
>>  B(2,:)
    ans = 0     4     5
```

Now that we understand basic vector and matrix creation, we turn our attention to using these tools on real problems. Consider solving a set of three linear simultaneous equations in three unknowns.

$$\begin{aligned} x_1 - 2x_2 + 3x_3 &= 1 \\ -\sqrt{3}x_1 + x_2 - \sqrt{5}x_3 &= \pi \\ 3x_1 - \sqrt{7}x_2 + x_3 &= e \end{aligned}$$

This system of equations is represented in matrix form according to $\mathbf{Ax} = \mathbf{y}$, where

$$\mathbf{A} = \begin{bmatrix} 1 & -2 & 3 \\ -\sqrt{3} & 1 & -\sqrt{5} \\ 3 & -\sqrt{7} & 1 \end{bmatrix}, \quad \mathbf{x} = \begin{bmatrix} x_1 \\ x_2 \\ x_3 \end{bmatrix}, \text{ and } \quad \mathbf{y} = \begin{bmatrix} 1 \\ \pi \\ e \end{bmatrix}$$

Although Cramer's rule can be used to solve $\mathbf{Ax} = \mathbf{y}$, it is more convenient to solve by multiplying both sides by the matrix inverse of **A**. That is, $\mathbf{x} = \mathbf{A}^{-1}\mathbf{Ax} = \mathbf{A}^{-1}\mathbf{y}$. Solving for **x** by hand or by calculator would be tedious at best, so MATLAB is used. We first create **A** and **y**.

```
>>  A = [1 -2 3;-sqrt(3) 1 -sqrt(5);3 -sqrt(7) 1]; y = [1;pi;exp(1)];
```

The vector solution is found by using MATLAB's `inv` function.

```
>>  x = inv(A)*y
    x = -1.9999
        -3.8998
        -1.5999
```

It is also possible to use MATLAB's left divide operator `x = A\y` to find the same solution. The left divide is generally more computationally efficient than matrix inverses. As with matrix multiplication, left division requires that the two arguments be conformable.

Of course, Cramer's rule can be used to compute individual solutions, such as x_1, by using vector indexing, concatenation, and MATLAB's `det` command to compute determinants.

```
>>  x1 = det([y,A(:,2:3)])/det(A)
    x1 = -1.9999
```

Another nice application of matrices is the simultaneous creation of a family of curves. Consider $h_\alpha(t) = e^{-\alpha t}\sin(2\pi 10t + \pi/6)$ over $0 \le t \le 0.2$. Figure B.14 shows $h_\alpha(t)$ for $\alpha = 0$ and $\alpha = 10$. Let's investigate the family of curves $h_\alpha(t)$ for $\alpha = [0, 1, \ldots, 10]$.

An inefficient way to solve this problem is create $h_\alpha(t)$ for each α of interest. This requires 11 individual cases. Instead, a matrix approach allows all 11 curves to be computed simultaneously. First, a vector is created that contains the desired values of α.

```
>> alpha = (0:10);
```

By using a sampling interval of 1 millisecond, $\Delta t = 0.001$, a time vector is also created.

```
>> t = (0:0.001:0.2)';
```

The result is a length-201 column vector. By replicating the time vector for each of the 11 curves required, a time matrix T is created. This replication can be accomplished by using an outer product between t and a 1×11 vector of ones.†

```
>> T = t*ones(1,11);
```

The result is a 201×11 matrix that has identical columns. Right multiplying T by a diagonal matrix created from α, columns of T can be individually scaled and the final result is computed.

```
>> H = exp(-T*diag(alpha)).*sin(2*pi*10*T+pi/6);
```

Here, H is a 201×11 matrix, where each column corresponds to a different value of α. That is, $\mathbf{H} = [\mathbf{h}_0, \mathbf{h}_1, \ldots, \mathbf{h}_{10}]$, where $\mathbf{h}_\alpha$ are column vectors. As shown in Fig. B.15, the 11 desired curves are simultaneously displayed by using MATLAB's plot command, which allows matrix arguments.

```
>> plot(t,H); xlabel('t'); ylabel('h(t)');
```

This example illustrates an important technique called vectorization, which increases execution efficiency for interpretive languages such as MATLAB. Algorithm vectorization uses matrix and

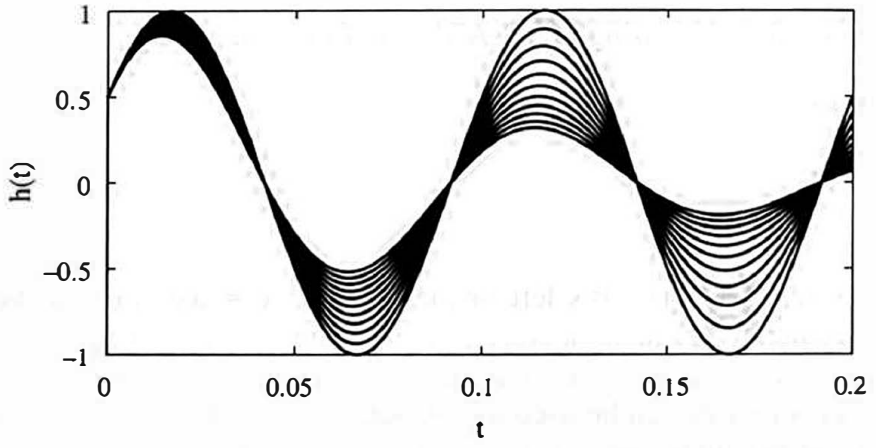

Figure B.15 $h_\alpha(t)$ for $\alpha = [0, 1, \ldots, 10]$.

† The `repmat` command provides a more flexible method to replicate or tile objects. Equivalently, `T = repmat(t,1,11)`.

vector operations to avoid manual repetition and loop structures. It takes practice and effort to become proficient at vectorization, but the worthwhile result is efficient, compact code.[†]

B.7.7 Partial Fraction Expansions

There are a wide variety of techniques and shortcuts to compute the partial fraction expansion of rational function $F(x) = B(x)/A(x)$, but few are more simple than the MATLAB `residue` command. The basic form of this command is

```
>>  [R,P,K] = residue(B,A)
```

The two input vectors `B` and `A` specify the polynomial coefficients of the numerator and denominator, respectively. These vectors are ordered in descending powers of the independent variable. Three vectors are output. The vector `R` contains the coefficients of each partial fraction, and vector `P` contains the corresponding roots of each partial fraction. For a root repeated r times, the r partial fractions are ordered in ascending powers. When the rational function is not proper, the vector `K` contains the direct terms, which are ordered in descending powers of the independent variable.

To demonstrate the power of the `residue` command, consider finding the partial fraction expansion of

$$F(x) = \frac{x^5+\pi}{(x+\sqrt{2})(x-\sqrt{2})^3} = \frac{x^5+\pi}{x^4-\sqrt{8}x^3+\sqrt{32}x-4}$$

By hand, the partial fraction expansion of $F(x)$ is difficult to compute. MATLAB, however, makes short work of the expansion.

```
>>  [R,P,K] = residue([1 0 0 0 0 pi],[1 -sqrt(8) 0 sqrt(32) -4]);
>>  R = R.', P = P.', K
    R = 7.8888    5.9713    3.1107    0.1112
    P = 1.4142    1.4142    1.4142   -1.4142
    K = 1.0000    2.8284
```

Written in standard form, the partial fraction expansion of $F(x)$ is

$$F(x) = x + 2.8284 + \frac{7.8888}{x-\sqrt{2}} + \frac{5.9713}{(x-\sqrt{2})^2} + \frac{3.1107}{(x-\sqrt{2})^3} + \frac{0.1112}{x+\sqrt{2}}$$

The signal-processing toolbox function `residuez` is similar to the `residue` command and offers more convenient expansion of certain rational functions, such as those commonly encountered in the study of discrete-time systems. Additional information about the `residue` and `residuez` commands is available from MATLAB's help facilities.

[†] The benefits of vectorization are less pronounced in recent versions of MATLAB.

B.8 Appendix: Useful Mathematical Formulas

We conclude this chapter with a selection of useful mathematical facts.

B.8.1 Some Useful Constants

$\pi \approx 3.1415926535$

$e \approx 2.7182818284$

$\frac{1}{e} \approx 0.3678794411$

$\log_{10} 2 \approx 0.30103$

$\log_{10} 3 \approx 0.47712$

B.8.2 Complex Numbers

$e^{\pm j\pi/2} = \pm j$

$$e^{\pm jn\pi} = \begin{cases} 1 & n \text{ even} \\ -1 & n \text{ odd} \end{cases}$$

$e^{\pm j\theta} = \cos\theta \pm j \sin\theta$

$a + jb = re^{j\theta} \qquad r = \sqrt{a^2 + b^2},\ \theta = \tan^{-1}\left(\frac{b}{a}\right)$

$(re^{j\theta})^k = r^k e^{jk\theta}$

$(r_1 e^{j\theta_1})(r_2 e^{j\theta_2}) = r_1 r_2 e^{j(\theta_1 + \theta_2)}$

B.8.3 Sums

$$\sum_{k=m}^{n} r^k = \frac{r^{n+1} - r^m}{r - 1} \qquad r \neq 1$$

$$\sum_{k=0}^{n} k = \frac{n(n+1)}{2}$$

$$\sum_{k=0}^{n} k^2 = \frac{n(n+1)(2n+1)}{6}$$

$$\sum_{k=0}^{n} k r^k = \frac{r + [n(r-1) - 1]r^{n+1}}{(r-1)^2} \qquad r \neq 1$$

$$\sum_{k=0}^{n} k^2 r^k = \frac{r[(1+r)(1-r^n) - 2n(1-r)r^n - n^2(1-r)^2 r^n]}{(1-r)^3} \qquad r \neq 1$$

B.8.4 Taylor and Maclaurin Series

$$f(x) = f(a) + \frac{(x-a)}{1!}\dot{f}(a) + \frac{(x-a)^2}{2!}\ddot{f}(a) + \cdots = \sum_{k=0}^{\infty} \frac{(x-a)^k}{k!} f^{(k)}(a)$$

$$f(x) = f(0) + \frac{x}{1!}\dot{f}(0) + \frac{x^2}{2!}\ddot{f}(0) + \cdots = \sum_{k=0}^{\infty} \frac{x^k}{k!} f^{(k)}(0)$$

B.8.5 Power Series

$$e^x = 1 + x + \frac{x^2}{2!} + \frac{x^3}{3!} + \cdots + \frac{x^n}{n!} + \cdots$$

$$\sin x = x - \frac{x^3}{3!} + \frac{x^5}{5!} - \frac{x^7}{7!} + \cdots$$

$$\cos x = 1 - \frac{x^2}{2!} + \frac{x^4}{4!} - \frac{x^6}{6!} + \frac{x^8}{8!} - \cdots$$

$$\tan x = x + \frac{x^3}{3} + \frac{2x^5}{15} + \frac{17x^7}{315} + \cdots \qquad x^2 < \pi^2/4$$

$$\tanh x = x - \frac{x^3}{3} + \frac{2x^5}{15} - \frac{17x^7}{315} + \cdots \qquad x^2 < \pi^2/4$$

$$(1+x)^n = 1 + nx + \frac{n(n-1)}{2!}x^2 + \frac{n(n-1)(n-2)}{3!}x^3 + \cdots + \binom{n}{k}x^k + \cdots + x^n$$

$$(1+x)^n \approx 1 + nx \qquad |x| \ll 1$$

$$\frac{1}{1-x} = 1 + x + x^2 + x^3 + \cdots \qquad |x| < 1$$

B.8.6 Trigonometric Identities

$$e^{\pm jx} = \cos x \pm j \sin x$$

$$\cos x = \tfrac{1}{2}[e^{jx} + e^{-jx}]$$

$$\sin x = \tfrac{1}{2j}[e^{jx} - e^{-jx}]$$

$$\cos(x \pm \tfrac{\pi}{2}) = \mp \sin x$$

$$\sin(x \pm \tfrac{\pi}{2}) = \pm \cos x$$

$$2 \sin x \cos x = \sin 2x$$

$$\sin^2 x + \cos^2 x = 1$$

$$\cos^2 x - \sin^2 x = \cos 2x$$

$$\cos^2 x = \tfrac{1}{2}(1 + \cos 2x)$$

$$\sin^2 x = \tfrac{1}{2}(1 - \cos 2x)$$

$$\cos^3 x = \tfrac{1}{4}(3\cos x + \cos 3x)$$
$$\sin^3 x = \tfrac{1}{4}(3\sin x - \sin 3x)$$
$$\sin(x \pm y) = \sin x \cos y \pm \cos x \sin y$$
$$\cos(x \pm y) = \cos x \cos y \mp \sin x \sin y$$
$$\tan(x \pm y) = \frac{\tan x \pm \tan y}{1 \mp \tan x \tan y}$$
$$\sin x \sin y = \tfrac{1}{2}[\cos(x-y) - \cos(x+y)]$$
$$\cos x \cos y = \tfrac{1}{2}[\cos(x-y) + \cos(x+y)]$$
$$\sin x \cos y = \tfrac{1}{2}[\sin(x-y) + \sin(x+y)]$$
$$a\cos x + b\sin x = C\cos(x+\theta) \qquad C = \sqrt{a^2+b^2},\ \theta = \tan^{-1}\left(\tfrac{-b}{a}\right)$$

B.8.7 Common Derivative Formulas

$$\frac{d}{dx}f(u) = \frac{d}{du}f(u)\frac{du}{dx}$$
$$\frac{d}{dx}(uv) = u\frac{dv}{dx} + v\frac{du}{dx}$$
$$\frac{d}{dx}\left(\frac{u}{v}\right) = \frac{v\frac{du}{dx} - u\frac{dv}{dx}}{v^2}$$
$$\frac{dx^n}{dx} = nx^{n-1}$$
$$\frac{d}{dx}\ln(ax) = \frac{1}{x}$$
$$\frac{d}{dx}\log(ax) = \frac{\log e}{x}$$
$$\frac{d}{dx}e^{bx} = be^{bx}$$
$$\frac{d}{dx}a^{bx} = b(\ln a)a^{bx}$$
$$\frac{d}{dx}\sin ax = a\cos ax$$
$$\frac{d}{dx}\cos ax = -a\sin ax$$
$$\frac{d}{dx}\tan ax = \frac{a}{\cos^2 ax}$$
$$\frac{d}{dx}(\sin^{-1} ax) = \frac{a}{\sqrt{1-a^2x^2}}$$
$$\frac{d}{dx}(\cos^{-1} ax) = \frac{-a}{\sqrt{1-a^2x^2}}$$
$$\frac{d}{dx}(\tan^{-1} ax) = \frac{a}{1+a^2x^2}$$

B.8.8 Indefinite Integrals

$$\int u\,dv = uv - \int v\,du$$

$$\int f(x)\dot{g}(x)\,dx = f(x)g(x) - \int \dot{f}(x)g(x)\,dx$$

$$\int \sin ax\,dx = -\frac{1}{a}\cos ax \qquad \int \cos ax\,dx = \frac{1}{a}\sin ax$$

$$\int \sin^2 ax\,dx = \frac{x}{2} - \frac{\sin 2ax}{4a} \qquad \int \cos^2 ax\,dx = \frac{x}{2} + \frac{\sin 2ax}{4a}$$

$$\int x\sin ax\,dx = \frac{1}{a^2}(\sin ax - ax\cos ax)$$

$$\int x\cos ax\,dx = \frac{1}{a^2}(\cos ax + ax\sin ax)$$

$$\int x^2 \sin ax\,dx = \frac{1}{a^3}(2ax\sin ax + 2\cos ax - a^2x^2\cos ax)$$

$$\int x^2 \cos ax\,dx = \frac{1}{a^3}(2ax\cos ax - 2\sin ax + a^2x^2\sin ax)$$

$$\int \sin ax \sin bx\,dx = \frac{\sin(a-b)x}{2(a-b)} - \frac{\sin(a+b)x}{2(a+b)} \qquad a^2 \neq b^2$$

$$\int \sin ax\cos bx\,dx = -\left[\frac{\cos(a-b)x}{2(a-b)} + \frac{\cos(a+b)x}{2(a+b)}\right] \qquad a^2 \neq b^2$$

$$\int \cos ax\cos bx\,dx = \frac{\sin(a-b)x}{2(a-b)} + \frac{\sin(a+b)x}{2(a+b)} \qquad a^2 \neq b^2$$

$$\int e^{ax}\,dx = \frac{1}{a}e^{ax}$$

$$\int xe^{ax}\,dx = \frac{e^{ax}}{a^2}(ax-1)$$

$$\int x^2e^{ax}\,dx = \frac{e^{ax}}{a^3}(a^2x^2 - 2ax + 2)$$

$$\int e^{ax}\sin bx\,dx = \frac{e^{ax}}{a^2+b^2}(a\sin bx - b\cos bx)$$

$$\int e^{ax}\cos bx\,dx = \frac{e^{ax}}{a^2+b^2}(a\cos bx + b\sin bx)$$

$$\int \frac{1}{x^2+a^2}\,dx = \frac{1}{a}\tan^{-1}\frac{x}{a}$$

$$\int \frac{x}{x^2+a^2}\,dx = \frac{1}{2}\ln(x^2+a^2)$$

B.8.9 L'Hôpital's Rule

If $\lim f(x)/g(x)$ results in the indeterministic form $0/0$ or ∞/∞, then

$$\lim \frac{f(x)}{g(x)} = \lim \frac{\dot{f}(x)}{\dot{g}(x)}$$

B.8.10 Solution of Quadratic and Cubic Equations

Any *quadratic* equation can be reduced to the form

$$ax^2 + bx + c = 0$$

The solution of this equation is provided by

$$x = \frac{-b \pm \sqrt{b^2 - 4ac}}{2a}$$

A general *cubic* equation

$$y^3 + py^2 + qy + r = 0$$

may be reduced to the *depressed cubic* form

$$x^3 + ax + b = 0$$

by substituting

$$y = x - \frac{p}{3}$$

This yields

$$a = \tfrac{1}{3}(3q - p^2) \qquad b = \tfrac{1}{27}(2p^3 - 9pq + 27r)$$

Now let

$$A = \sqrt[3]{-\frac{b}{2} + \sqrt{\frac{b^2}{4} + \frac{a^3}{27}}} \qquad B = \sqrt[3]{-\frac{b}{2} - \sqrt{\frac{b^2}{4} + \frac{a^3}{27}}}$$

The solution of the depressed cubic is

$$x = A + B, \qquad x = -\frac{A+B}{2} + \frac{A-B}{2}\sqrt{-3}, \qquad x = -\frac{A+B}{2} - \frac{A-B}{2}\sqrt{-3}$$

and

$$y = x - \frac{p}{3}$$

REFERENCES

1. Asimov, Isaac, *Asimov on Numbers*, Bell Publishing, New York, 1982.
2. Calinger, R., ed., *Classics of Mathematics*, Moore Publishing, Oak Park, IL, 1982.
3. Hogben, Lancelot, *Mathematics in the Making*, Doubleday, New York, 1960.

4. Cajori, Florian, *A History of Mathematics*, 4th ed., Chelsea, New York, 1985.
5. Encyclopaedia Britannica, *Micropaedia* IV, 15th ed., vol. 11, p. 1043, Chicago, 1982.
6. Singh, Jagjit, *Great Ideas of Modern Mathematics*, Dover, New York, 1959.
7. Dunham, William, *Journey Through Genius*, Wiley, New York, 1990.

PROBLEMS

B.1-1 Given a complex number $w = x + jy$, the complex conjugate of w is defined in rectangular coordinates as $w^* = x - jy$. Use this fact to derive complex conjugation in polar form.

B.1-2 Express the following numbers in polar form:
(a) $w_a = 1 + j$
(b) $w_b = 1 + e^j$
(c) $w_c = -4 + j3$
(d) $w_d = (1 + j)(-4 + j3)$
(e) $w_e = e^{j\pi/4} + 2e^{-j\pi/4}$
(f) $w_f = \frac{1+j}{2j}$
(g) $w_g = (1 + j)/(-4 + j3)$
(h) $w_h = \frac{1-j}{\sin(j)}$

B.1-3 Express the following numbers in Cartesian (rectangular) form:
(a) $w_a = j + e^j$
(b) $w_b = 3e^{j\pi/4}$
(c) $w_c = 1/e^j$
(d) $w_d = (1 + j)(-4 + j3)$
(e) $w_e = e^{j\pi/4} + 2e^{-j\pi/4}$
(f) $w_f = e^j + 1$
(g) $w_g = 1/2^j$
(h) $w_h = j^{j^j}$ (j raised to the j raised to the j)

B.1-4 Showing all work and simplifying your answer, determine the real part of the following numbers:
(a) $w_a = \frac{1}{j}(j - 5e^{2-3j})$
(b) $w_b = (1 + j)\ln(1 + j)$

B.1-5 Showing all work and simplifying your answer, determine the imaginary part of the following numbers:
(a) $w_a = -je^{j\pi/4}$
(b) $w_b = 1 - 2je^{2-4j}$
(c) $w_c = \tan(j)$

B.1-6 For complex constant w, prove:
(a) $\mathrm{Re}(w) = (w + w^*)/2$
(b) $\mathrm{Im}(w) = (w - w^*)/2j$

B.1-7 Given $w = x - jy$, determine:
(a) $\mathrm{Re}(e^w)$
(b) $\mathrm{Im}(e^w)$

B.1-8 For arbitrary complex constants w_1 and w_2, prove or disprove the following:
(a) $\mathrm{Re}(jw_1) = -\mathrm{Im}(w_1)$
(b) $\mathrm{Im}(jw_1) = \mathrm{Re}(w_1)$
(c) $\mathrm{Re}(w_1) + \mathrm{Re}(w_2) = \mathrm{Re}(w_1 + w_2)$
(d) $\mathrm{Im}(w_1) + \mathrm{Im}(w_2) = \mathrm{Im}(w_1 + w_2)$
(e) $\mathrm{Re}(w_1)\mathrm{Re}(w_2) = \mathrm{Re}(w_1 w_2)$
(f) $\mathrm{Im}(w_1)/\mathrm{Im}(w_2) = \mathrm{Im}(w_1/w_2)$

B.1-9 Given $w_1 = 3 + j4$ and $w_2 = 2e^{j\pi/4}$:
(a) Express w_1 in standard polar form.
(b) Express w_2 in standard rectangular form.
(c) Determine $|w_1|^2$ and $|w_2|^2$.
(d) Express $w_1 + w_2$ in standard rectangular form.
(e) Express $w_1 - w_2$ in standard polar form.
(f) Express $w_1 w_2$ in standard rectangular form.
(g) Express w_1/w_2 in standard polar form.

B.1-10 Repeat Prob. B.1-9 using $w_1 = (3 + j4)^2$ and $w_2 = 2.5je^{-j40\pi}$.

B.1-11 Repeat Prob. B.1-9 using $w_1 = j + e^{\pi/4}$ and $w_2 = \cos(j)$.

B.1-12 Using the complex plane:
(a) Evaluate and locate the distinct solutions to $(w)^4 = -1$.
(b) Evaluate and locate the distinct solutions to $(w - (1 + j2))^5 = (32/\sqrt{2})(1 + j)$.
(c) Sketch the solution to $|w - 2j| = 3$.
(d) Graph $w(t) = (1 + t)e^{jt}$ for $(-10 \le t \le 10)$.

B.1-13 The distinct solutions to $(w - w_1)^n = w_2$ lie on a circle in the complex plane, as shown in Fig. PB.1-13. One solution is located on the real axis at $\sqrt{3} + 1 = 2.732$, and one solution is located on the imaginary axis at $\sqrt{3} - 1 = 0.732$. Determine w_1, w_2, and n.

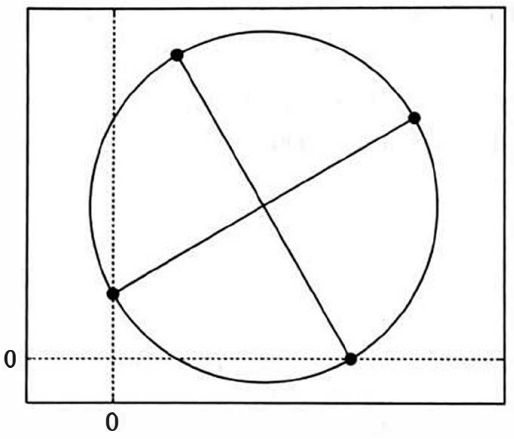

Figure PB.1-13

B.1-14 Find the distinct solutions to each of the following. Use MATLAB to graph each solution set in the complex plane.
(a) $w^3 = -\frac{8}{27}$
(b) $(w+1)^8 = 1$
(c) $w^2 + j = 0$
(d) $16(w-1)^4 + 81 = 0$
(e) $(w+2j)^3 = -8$
(f) $(j-w)^{1.5} = 2 + j2$
(g) $(w-1)^{2.5} = j4\sqrt{2}$

B.1-15 If $j = \sqrt{-1}$, what is $\sqrt{j}$?

B.1-16 Find all the values of $\ln(-e)$, expressing your answer in Cartesian form.

B.1-17 Determine all values of $\log_{10}(-1)$, expressing your answer in Cartesian form. Notice that the logarithm has base 10, not e.

B.1-18 Express the following in standard rectangular coordinates:
(a) $w_a = \ln(1/(1+j))$
(b) $w_b = \cos(1+j)$
(c) $w_c = (1-j)^j$

B.1-19 By constraining w to be purely imaginary, show that the equation $\cos(w) = 2$ can be represented as a standard quadratic equation. Solve this equation for w.

B.1-20 Certain integrals, although expressed in relatively simple form, are quite difficult to solve. For example, $\int e^{-x^2} dx$ cannot be evaluated in terms of elementary functions; most calculators that perform integration cannot handle this indefinite integral. Fortunately, you are smarter than most calculators.
(a) Express e^{-x^2} using a Taylor series expansion.
(b) Using your series expansion for e^{-x^2}, determine $\int e^{-x^2} dx$.
(c) Using a suitably truncated series, evaluate the definite integral $\int_0^1 e^{-x^2} dx$.

B.1-21 Repeat Prob. B.1-20 for $\int e^{-x^3} dx$.

B.1-22 Repeat Prob. B.1-20 for $\int \cos x^2 dx$.

B.1-23 For each function, determine a suitable series expansion.
(a) $f_a(x) = (2-x^2)^{-1}$
(b) $f_b(x) = (0.5)^x$

B.1-24 Consider the function $f(x) = 1+x+x^2+x^3$.
(a) Express $f(x)$ using a Taylor series with an expansion point of $a = 1$. Explicitly write out every term. [*Hint:* See Sec. B.8.4.]
(b) Describe a good reason why you might want to express a function that is already a simple polynomial using such a series.

B.1-25 Determine the Maclaurin series expansion of each of the following. [*Hint:* See Sec. B.8.4.]
(a) $f_a(x) = 2^x$
(b) $f_b(x) = \left(\frac{1}{3}\right)^x$

B.2-1 Determine the fundamental period T_0, frequency f_0, and radian frequency ω_0 for the following sinusoids:
(a) $\cos(5\pi t + 3)$
(b) $7\sin\left(\frac{2t-\pi}{3}\right)$

B.2-2 Determine an expression for a sinusoid that oscillates 15 times per second, that has a value of -1 at $t = 0$, and whose peak amplitude is 3. Use MATLAB to plot the signal over $0 \le t \le 1$.

B.2-3 Let $x_1(t) = 2\cos(3t + 1)$ and $x_2(t) = -3\cos(3t-2)$.
(a) Determine a_1 and b_1 so that $x_1(t) = a_1\cos(3t) + b_1\sin(3t)$.
(b) Determine a_2 and b_2 so that $x_2(t) = a_2\cos(3t) + b_2\sin(3t)$.
(c) Determine C and θ so that $x_1(t) + x_2(t) = C\cos(3t+\theta)$.

B.2-4 In addition to the traditional sine and cosine functions, there are the *hyperbolic* sine and cosine functions, which are defined by $\sinh(w) = (e^w - e^{-w})/2$ and $\cosh(w) = (e^w + e^{-w})/2$. In general, the argument is a complex constant $w = x + jy$.

(a) Show that $\cosh(w) = \cosh(x)\cos(y) + j\sinh(x)\sin(y)$.
(b) Determine a similar expression for $\sinh(w)$ in rectangular form that only uses functions of real arguments, such as $\sin(x)$, $\cosh(y)$, and so on.

B.2-5 Use Euler's identity to solve or prove the following:
(a) Find real, positive constants c and ϕ for all real t such that $2.5\cos(3t) - 1.5\sin(3t + \pi/3) = c\cos(3t + \phi)$. Sketch the resulting sinusoid.
(b) Prove that $\cos(\theta \pm \phi) = \cos(\theta)\cos(\phi) \mp \sin(\theta)\sin(\phi)$.
(c) Given real constants a, b, and α, complex constant w, and the fact that

$$\int_a^b e^{wx}\,dx = \frac{1}{w}(e^{wb} - e^{wa})$$

evaluate the integral

$$\int_a^b e^{wx}\sin(\alpha x)\,dx$$

B.2-6 A particularly boring stretch of interstate highway has a posted speed limit of 70 mph. A highway engineer wants to install "rumble bars" (raised ridges on the side of the road) so that cars traveling the speed limit will produce quarter-second bursts of 1 kHz sound every second, a strategy that is particularly effective at startling sleepy drivers awake. Provide design specifications for the engineer.

B.3-1 By hand, accurately sketch the following signals over $(0 \le t \le 1)$:
(a) $x_a(t) = e^{-t}$
(b) $x_b(t) = \sin(2\pi 5t)$
(c) $x_c(t) = e^{-t}\sin(2\pi 5t)$

B.3-2 In 1950, the human population was approximately 2.5 billion people. Assuming a doubling time of 40 years, formulate an exponential model for human population in the form $p(t) = ae^{bt}$, where t is measured in years. Sketch $p(t)$ over the interval $1950 \le t \le 2100$. According to this model, in what year can we expect the population to reach the estimated 15 billion carrying capacity of the earth?

B.3-3 Determine an expression for an exponentially decaying sinusoid that oscillates three times per second and whose amplitude envelope decreases by 50% every 2 seconds. Use MATLAB to plot the signal over $-2 \le t \le 2$.

B.3-4 By hand, sketch the following against independent variable t:
(a) $x_a(t) = \mathrm{Re}\left(2e^{(-1+j2\pi)t}\right)$
(b) $x_b(t) = \mathrm{Im}\left(3 - e^{(1-j2\pi)t}\right)$
(c) $x_c(t) = 3 - \mathrm{Im}\left(e^{(1-j2\pi)t}\right)$

B.4-1 Consider the following system of equations:

$$\begin{bmatrix} -1 & 2 \\ 3 & -4 \end{bmatrix}\begin{bmatrix} x_1 \\ x_2 \end{bmatrix} = \begin{bmatrix} 3 \\ -1 \end{bmatrix}$$

Expressing all answers in rational form (ratio of integers), use Cramer's rule to determine x_1 and x_2. Perform all calculations by hand, including matrix determinants.

B.4-2 Consider the following system of equations

$$\begin{bmatrix} 1 & 2 & 0 \\ 0 & 3 & 4 \\ 5 & 0 & 6 \end{bmatrix}\begin{bmatrix} x_1 \\ x_2 \\ x_3 \end{bmatrix} = \begin{bmatrix} 7 \\ 8 \\ 9 \end{bmatrix}$$

Expressing all answers in rational form (ratio of integers), use Cramer's rule to determine x_1, x_2, and x_3. Perform all calculations by hand, including matrix determinants.

B.4-3 Consider the following system of equations:

$$\begin{aligned} x_1 + x_2 + x_3 &= 1 \\ x_1 + 2x_2 + 3x_3 &= 3 \\ x_1 - x_2 &= -3 \end{aligned}$$

Use Cramer's rule to determine x_1, x_2, and x_3. Matrix determinants can be computed by using MATLAB's `det` command.

B.5-1 Determine the constants a_0, a_1, and a_2 of the partial fraction expansion

$$\begin{aligned} F(s) &= \frac{s}{(s+1)^3} \\ &= \frac{a_0}{(s+1)^3} + \frac{a_1}{(s+1)^2} + \frac{a_2}{(s+1)} \end{aligned}$$

B.5-2 Compute by hand the partial fraction expansions of the following rational functions:
(a) $H_a(s) = \frac{s^2+5s+6}{s^3+s^2+s+1}$, which has denominator poles at $s = \pm j$ and $s = -1$
(b) $H_b(s) = \frac{1}{H_1(s)} = \frac{s^3+s^2+s+1}{s^2+5s+6}$

(c) $H_c(s) = \frac{1}{(s+1)^2(s^2+1)}$

(d) $H_d(s) = \frac{s^2+5s+6}{3s^2+2s+1}$

B.5-3 Compute by hand the partial fraction expansions of the following rational functions:

(a) $F_a(x) = \frac{(x-1)(x-2)}{(x-3)^2}$

(b) $F_b(x) = \frac{(x-1)^2}{(3x-1)(2x-1)}$

(c) $F_c(x) = \frac{(x-1)^2}{(3x-1)^2(2x-1)}$

(d) $F_d(x) = \frac{x^2-5x+6}{2x^2+8x+6}$

(e) $F_e(x) = \frac{2x^2-3x-11}{x^2-x-2}$

(f) $F_f(x) = \frac{3+2x^2}{-3+2x+x^2}$

(g) $F_g(x) = \frac{x^3+2x^2+3x+4}{x^2+1}$

(h) $F_h(x) = \frac{1+2x+3x^2}{x^2+5x+6}$

(i) $F_i(x) = \frac{3x^3-x^2+14x+4}{x^2+4}$

(j) $F_j(x) = \frac{2x^{-1}-1+2x}{x-5+6x^{-1}}$

(k) $F_k(x) = 3\frac{-5x^2-9x+23}{x^2+x-2}$

B.6-1 A system of equations in terms of unknowns x_1 and x_2 and arbitrary constants a, b, c, d, e, and f is given by

$$ax_1 + bx_2 = c$$
$$dx_1 + ex_2 = f$$

(a) Represent this system of equations in matrix form.

(b) Identify specific constants a, b, c, d, e, and f such that $x_1 = 3$ and $x_2 = -2$. Are the constants you selected unique?

(c) Identify nonzero constants a, b, c, d, e, and f such that no solutions x_1 and x_2 exist.

(d) Identify nonzero constants a, b, c, d, e, and f such that an infinite number of solutions x_1 and x_2 exist.

B.6-2 Using a matrix approach, solve the following system of equations:

$$x_1 + x_2 + x_3 + x_4 = 4$$
$$x_1 + x_2 + x_3 - x_4 = 2$$
$$x_1 + x_2 - x_3 - x_4 = 0$$
$$x_1 - x_2 - x_3 - x_4 = -2$$

B.6-3 Using a matrix approach, solve the following system of equations:

$$x_1 + x_2 + x_3 + x_4 = 1$$
$$x_1 - 2x_2 + 3x_3 = 2$$
$$x_1 - x_3 + 7x_4 = 3$$
$$-2x_2 + 3x_3 - 4x_4 = 4$$

B.6-4 A signal $f(t) = a\cos(3t) + b\sin(3t)$ reaches a peak amplitude of 5 at $t = 1.8799$ and has a zero crossing at $t = 0.3091$. Use a matrix-based approach to determine the constants a and b.

B.6-5 Define

$$\mathbf{x} = \begin{bmatrix} 1 & 3 \\ -2 & 4 \end{bmatrix}, \quad \mathbf{y} = \begin{bmatrix} -5 \\ 2 \end{bmatrix},$$

$$\text{and} \quad \mathbf{z} = \begin{bmatrix} 0 & 1 \\ -1 & 0 \end{bmatrix}$$

By hand, calculate the following:

(a) $\mathbf{f}_a = \mathbf{y}^T\mathbf{y}$

(b) $\mathbf{f}_b = \mathbf{y}\mathbf{y}^T$

(c) $\mathbf{f}_c = \mathbf{x}\mathbf{y}$

(d) $\mathbf{f}_d = \mathbf{x}^T\mathbf{y}$

(e) $\mathbf{f}_e = \mathbf{y}^T\mathbf{x}$

(f) $\mathbf{f}_f = \mathbf{x}\mathbf{z}$

(g) $\mathbf{f}_g = \mathbf{z}\mathbf{x}\mathbf{z}$

(h) $\mathbf{f}_h = \mathbf{x}^T - \mathbf{z}$

B.7-1 Use MATLAB to produce the plots requested in Prob. B.3-4.

B.7-2 Use MATLAB to plot the function $x(t) = t\sin(2\pi t)$ over $0 \le t \le 10$ using 501 equally spaced points. What is the maximum value of $x(t)$ over this range of t?

B.7-3 Use MATLAB to plot $x(t) = \cos(t)\sin(20t)$ over a suitable range of t.

B.7-4 Use MATLAB to plot $x(t) = \sum_{k=1}^{10} \cos(2\pi kt)$ over a suitable range of t. The MATLAB command `sum` may prove useful.

B.7-5 When a bell is struck with a mallet, it produces a ringing sound. Write an equation that approximates the sound produced by a small, light bell. Carefully identify your assumptions. How does your equation change if the bell is large and heavy? You can assess the quality of your models by using the MATLAB `sound` command to listen to your "bell."

B.7-6 You are working on a digital quadrature amplitude modulation (QAM) communication receiver. The QAM receiver requires a pair of quadrature signals: $\cos \Omega n$ and $\sin \Omega n$. These can be simultaneously generated by following a simple procedure: (1) choose a point w on the unit circle, (2) multiply w by itself and store the result, (3) multiply w by the last result and store, and (4) repeat step 3.

(a) Show that this method can generate the desired pair of quadrature sinusoids.

(b) Determine a suitable value of w so that good-quality, periodic, $2\pi \times 100{,}000$ rad/s signals can be generated. How much time is available for the processing unit to compute each sample?

(c) Simulate this procedure by using MATLAB and report your results.

(d) Identify as many assumptions and limitations to this technique as possible. For example, can your system operate correctly for an indefinite period of time?

B.7-7 Using MATLAB's `residue` command,

(a) Verify the results of Prob. B.5-2a.

(b) Verify the results of Prob. B.5-2b.

(c) Verify the results of Prob. B.5-2c.

(d) Verify the results of Prob. B.5-2d.

B.7-8 Using MATLAB's `residue` command,

(a) Verify the results of Prob. B.5-3a.

(b) Verify the results of Prob. B.5-3b.

(c) Verify the results of Prob. B.5-3c.

(d) Verify the results of Prob. B.5-3d.

(e) Verify the results of Prob. B.5-3e.

(f) Verify the results of Prob. B.5-3f.

(g) Verify the results of Prob. B.5-3g.

(h) Verify the results of Prob. B.5-3h.

(i) Verify the results of Prob. B.5-3i.

(j) Verify the results of Prob. B.5-3j.

(k) Verify the results of Prob. B.5-3k.

B.7-9 Determine the original length-3 vectors a and b need to produce the MATLAB output:

```
>> [r,p,k] = residue(b,a)
r =  0 + 2.0000i
     0 - 2.0000i
p =  3
    -3
k =  0 + 1.0000i
```

B.7-10 Let $N = [n_7, n_6, n_5, \ldots, n_2, n_1]$ represent the seven digits of your phone number. Construct a rational function according to

$$H_N(s) = \frac{n_7 s^2 + n_6 s + n_5 + n_4 s^{-1}}{n_3 s^2 + n_2 s + n_1}$$

Use MATLAB's `residue` command to compute the partial fraction expansion of $H_N(s)$.

B.7-11 When plotted in the complex plane for $-\pi \leq \omega \leq \pi$, the function $f(\omega) = \cos(\omega) + j0.1 \sin(2\omega)$ results in a so-called Lissajous figure that resembles a two-bladed propeller.

(a) In MATLAB, create two row vectors `fr` and `fi` corresponding to the real and imaginary portions of $f(\omega)$, respectively, over a suitable number N samples of ω. Plot the real portion against the imaginary portion and verify the figure resembles a propeller.

(b) Let complex constant $w = x + jy$ be represented in vector form

$$\mathbf{w} = \begin{bmatrix} x \\ y \end{bmatrix}$$

Consider the 2×2 rotational matrix $\mathbf{R}$:

$$\mathbf{R} = \begin{bmatrix} \cos\theta & -\sin\theta \\ \sin\theta & \cos\theta \end{bmatrix}$$

Show that $\mathbf{Rw}$ rotates vector $\mathbf{w}$ by θ radians.

(c) Create a rotational matrix R corresponding to 10° and multiply it by the $2 \times N$ matrix `f = [fr;fi];`. Plot the result to verify that the "propeller" has indeed rotated counterclockwise.

(d) Given the matrix R determined in part (c), what is the effect of performing `RRf`? How about `RRRf`? Generalize the result.

(e) Investigate the behavior of multiplying $f(\omega)$ by the function $e^{j\theta}$.

SIGNALS AND SYSTEMS

In this chapter we shall discuss basic aspects of signals. We shall also introduce fundamental concepts and qualitative explanations of the hows and whys of systems theory, thus building a solid foundation for understanding the quantitative analysis in the remainder of the book. For simplicity, the focus of this chapter is on continuous-time signals and systems. Chapter 8 presents the same ideas for discrete-time signals and systems.

SIGNALS

A *signal* is a set of data or information. Examples include a telephone or a television signal, monthly sales of a corporation, or daily closing prices of a stock market (e.g., the Dow Jones averages). In all these examples, the signals are functions of the independent variable *time*. This is not always the case, however. When an electrical charge is distributed over a body, for instance, the signal is the charge density, a function of *space* rather than time. In this book we deal almost exclusively with signals that are functions of time. The discussion, however, applies equally well to other independent variables.

SYSTEMS

Signals may be processed further by *systems,* which may modify them or extract additional information from them. For example, an anti-aircraft gun operator may want to know the future location of a hostile moving target that is being tracked by his radar. Knowing the radar signal, he knows the past location and velocity of the target. By properly processing the radar signal (the input), he can approximately estimate the future location of the target. Thus, a system is an entity that *processes* a set of signals (*inputs*) to yield another set of signals (*outputs*). A system may be made up of physical components, as in electrical, mechanical, or hydraulic systems (hardware realization), or it may be an algorithm that computes an output from an input signal (software realization).

1.1 SIZE OF A SIGNAL

The size of any entity is a number that indicates the largeness or strength of that entity. Generally speaking, the signal amplitude varies with time. How can a signal that exists over a certain time

interval with varying amplitude be measured by one number that will indicate the signal size or signal strength? Such a measure must consider not only the signal amplitude, but also its duration. For instance, if we are to devise a single number V as a measure of the size of a human being, we must consider not only his or her width (girth), but also the height. If we make a simplifying assumption that the shape of a person is a cylinder of variable radius r (which varies with the height h), then one possible measure of the size of a person of height H is the person's volume V, given by

$$V = \pi \int_0^H r^2(h)\, dh$$

1.1.1 Signal Energy

Arguing in this manner, we may consider the area under a signal $x(t)$ as a possible measure of its size, because it takes account not only of the amplitude but also of the duration. However, this will be a defective measure because even for a large signal $x(t)$, its positive and negative areas could cancel each other, indicating a signal of small size. This difficulty can be corrected by defining the signal size as the area under $|x(t)|^2$, which is always positive. We call this measure the *signal energy* E_x, defined as

$$E_x = \int_{-\infty}^{\infty} |x(t)|^2\, dt \tag{1.1}$$

This definition simplifies for a real-valued signal $x(t)$ to $E_x = \int_{-\infty}^{\infty} x^2(t)\, dt$. There are also other possible measures of signal size, such as the area under $|x(t)|$. The energy measure, however, is not only more tractable mathematically but is also more meaningful (as shown later) in the sense that it is indicative of the energy that can be extracted from the signal.

1.1.2 Signal Power

Signal energy must be finite for it to be a meaningful measure of signal size. A necessary condition for the energy to be finite is that the signal amplitude $\to 0$ as $|t| \to \infty$ (Fig. 1.1a). Otherwise, the integral in Eq. (1.1) will not converge.

When the amplitude of $x(t)$ does not $\to 0$ as $|t| \to \infty$ (Fig. 1.1b), the signal energy is infinite. A more meaningful measure of the signal size in such a case would be the time average of the energy, if it exists. This measure is called the *power* of the signal. For a signal $x(t)$, we define its power P_x as

$$P_x = \lim_{T\to\infty} \frac{1}{T} \int_{-T/2}^{T/2} |x(t)|^2\, dt \tag{1.2}$$

This definition simplifies for a real-valued signal $x(t)$ to $P_x = \lim_{T\to\infty} \frac{1}{T} \int_{-T/2}^{T/2} x^2(t)\, dt$. Observe that the signal power P_x is the time average (mean) of the signal magnitude squared, that is, the *mean-square* value of $|x(t)|$. Indeed, the square root of P_x is the familiar *rms* (root-mean-square) value of $x(t)$.

Generally, the mean of an entity averaged over a large time interval approaching infinity exists if the entity either is periodic or has a statistical regularity. If such a condition is not satisfied, the average may not exist. For instance, a ramp signal $x(t) = t$ increases indefinitely as $|t| \to \infty$, and neither the energy nor the power exists for this signal. However, the unit step function, which is not periodic nor has statistical regularity, does have a finite power.

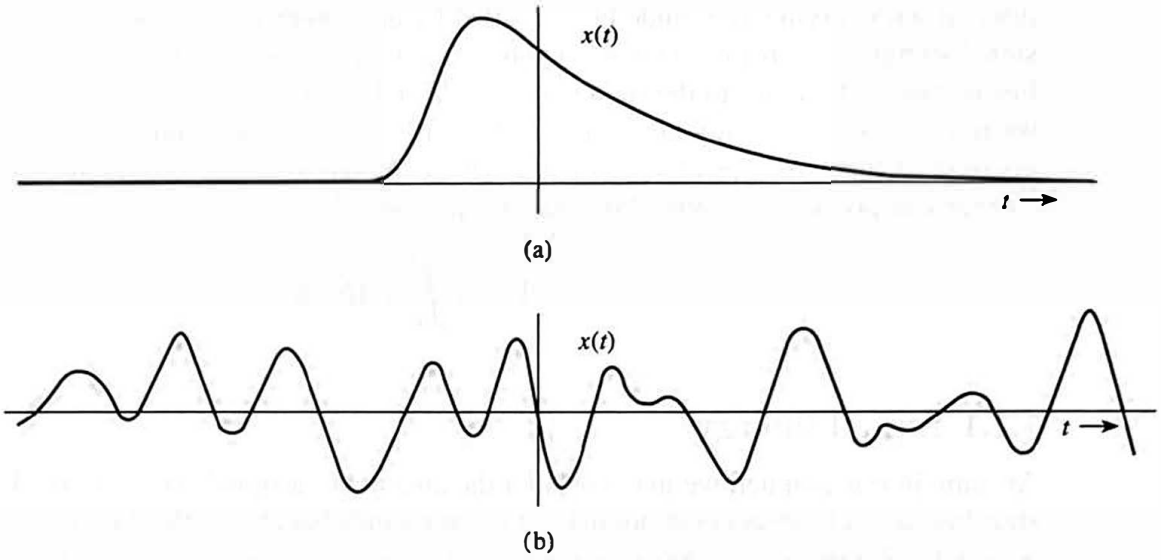

Figure 1.1 Examples of signals: **(a)** a signal with finite energy and **(b)** a signal with finite power.

When $x(t)$ is periodic, $|x(t)|^2$ is also periodic. Hence, the power of $x(t)$ can be computed from Eq. (1.2) by averaging $|x(t)|^2$ over one period.

Comments. The signal energy as defined in Eq. (1.1) does not indicate the actual energy (in the conventional sense) of the signal because the signal energy depends not only on the signal, but also on the load. It can, however, be interpreted as the energy dissipated in a normalized load of a 1 ohm resistor if a voltage $x(t)$ were to be applied across the 1 ohm resistor [or if a current $x(t)$ were to be passed through the 1 ohm resistor]. The measure of "energy" is therefore indicative of the energy capability of the signal, not the actual energy. For this reason the concepts of conservation of energy should not be applied to this "signal energy." Parallel observation applies to "signal power" defined in Eq. (1.2). These measures are but convenient indicators of the signal size, which prove useful in many applications. For instance, if we approximate a signal $x(t)$ by another signal $g(t)$, the error in the approximation is $e(t) = x(t) - g(t)$. The energy (or power) of $e(t)$ is a convenient indicator of the goodness of the approximation. It provides us with a quantitative measure of determining the closeness of the approximation. In communication systems, during transmission over a channel, message signals are corrupted by unwanted signals (noise). The quality of the received signal is judged by the relative sizes of the desired signal and the unwanted signal (noise). In this case the ratio of the message signal and noise signal powers (signal-to-noise power ratio) is a good indication of the received signal quality.

Units of Energy and Power. Equation (1.1) is not correct dimensionally. This is because here we are using the term *energy* not in its conventional sense, but to indicate the signal size. The same observation applies to Eq. (1.2) for power. The units of energy and power, as defined here, depend on the nature of the signal $x(t)$. If $x(t)$ is a voltage signal, its energy E_x has units of volts squared-seconds (V^2 s), and its power P_x has units of volts squared. If $x(t)$ is a current signal, these units will be amperes squared-seconds (A^2 s) and amperes squared, respectively.

EXAMPLE 1.1 Classifying Energy and Power Signals

Determine the suitable measures of the signals in Fig. 1.2.

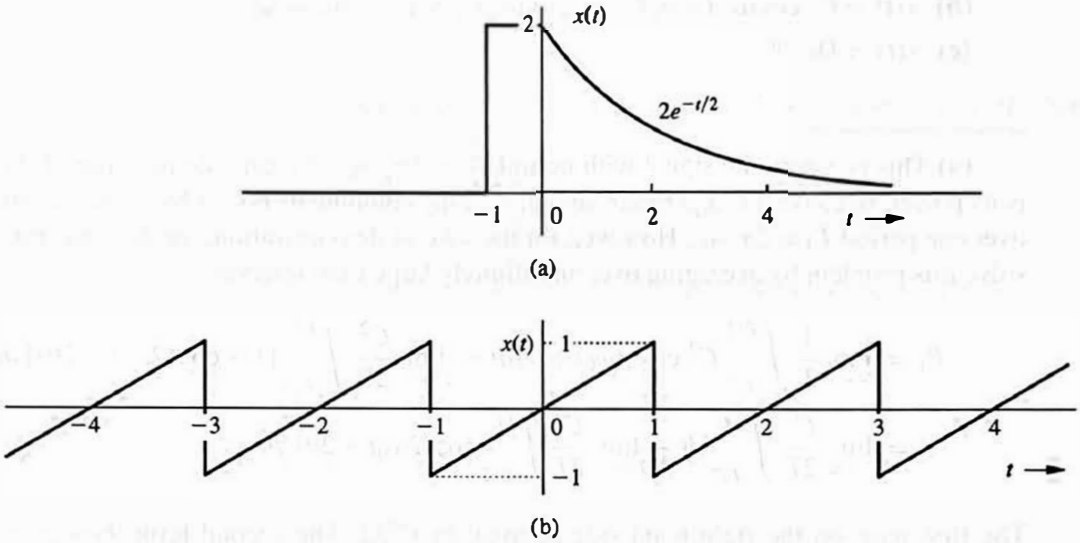

Figure 1.2 Signals for Ex. 1.1.

In Fig. 1.2a, the signal amplitude $\to 0$ as $|t| \to \infty$. Therefore, the suitable measure for this signal is its energy E_x given by

$$E_x = \int_{-\infty}^{\infty} |x(t)|^2\,dt = \int_{-1}^{0} (2)^2\,dt + \int_{0}^{\infty} 4e^{-t}\,dt = 4+4 = 8$$

In Fig. 1.2b, the signal magnitude does not $\to 0$ as $|t| \to \infty$. However, it is periodic, and therefore its power exists. We can use Eq. (1.2) to determine its power. We can simplify the procedure for periodic signals by observing that a periodic signal repeats regularly each period (2 seconds in this case). Therefore, averaging $|x(t)|^2$ over an infinitely large interval is identical to averaging this quantity over one period (2 seconds in this case). Thus,

$$P_x = \tfrac{1}{2}\int_{-1}^{1} |x(t)|^2\,dt = \tfrac{1}{2}\int_{-1}^{1} t^2\,dt = \tfrac{1}{3}$$

Recall that the signal power is the square of its rms value. Therefore, the rms value of this signal is $1/\sqrt{3}$.

EXAMPLE 1.2 Determining Power and RMS Value

Determine the power and the rms value of

(a) $x(t) = C\cos(\omega_0 t + \theta)$

(b) $x(t) = C_1\cos(\omega_1 t + \theta_1) + C_2\cos(\omega_2 t + \theta_2) \qquad \omega_1 \neq \omega_2$

(c) $x(t) = De^{j\omega_0 t}$

(a) This is a periodic signal with period $T_0 = 2\pi/\omega_0$. The suitable measure of this signal is its power. Because it is a periodic signal, we may compute its power by averaging its energy over one period $T_0 = 2\pi/\omega_0$. However, for the sake of demonstration, we shall use Eq. (1.2) to solve this problem by averaging over an infinitely large time interval.

$$P_x = \lim_{T\to\infty}\frac{1}{T}\int_{-T/2}^{T/2} C^2\cos^2(\omega_0 t+\theta)\,dt = \lim_{T\to\infty}\frac{C^2}{2T}\int_{-T/2}^{T/2}[1+\cos(2\omega_0 t+2\theta)]\,dt$$

$$= \lim_{T\to\infty}\frac{C^2}{2T}\int_{-T/2}^{T/2} dt + \lim_{T\to\infty}\frac{C^2}{2T}\int_{-T/2}^{T/2}\cos(2\omega_0 t+2\theta)\,dt$$

The first term on the right-hand side is equal to $C^2/2$. The second term, however, is zero because the integral appearing in this term represents the area under a sinusoid over a very large time interval T with $T\to\infty$. This area is at most equal to the area of half the cycle because of cancellations of the positive and negative areas of a sinusoid. The second term is this area multiplied by $C^2/2T$ with $T\to\infty$. Clearly, this term is zero, and

$$P_x = \frac{C^2}{2}$$

This shows that a sinusoid of amplitude C has a power $C^2/2$ regardless of the value of its frequency ω_0 ($\omega_0 \neq 0$) and phase θ. The rms value is $C/\sqrt{2}$. If the signal frequency is zero (dc or a constant signal of amplitude C), the reader can show that the power is C^2.

(b) In Ch. 3 we shall show that a sum of two sinusoids may or may not be periodic, depending on whether the ratio ω_1/ω_2 is a rational number. Therefore, the period of this signal is not known. Hence, its power will be determined by averaging its energy over T seconds with $T\to\infty$. Thus,

$$P_x = \lim_{T\to\infty}\frac{1}{T}\int_{-T/2}^{T/2}[C_1\cos(\omega_1 t+\theta_1)+C_2\cos(\omega_2 t+\theta_2)]^2\,dt$$

$$= \lim_{T\to\infty}\frac{1}{T}\int_{-T/2}^{T/2} {C_1}^2\cos^2(\omega_1 t+\theta_1)\,dt + \lim_{T\to\infty}\frac{1}{T}\int_{-T/2}^{T/2} {C_2}^2\cos^2(\omega_2 t+\theta_2)\,dt$$

$$+ \lim_{T\to\infty}\frac{2C_1C_2}{T}\int_{-T/2}^{T/2}\cos(\omega_1 t+\theta_1)\cos(\omega_2 t+\theta_2)\,dt$$

The first and second integrals on the right-hand side are the powers of the two sinusoids, which are $C_1^2/2$ and $C_2^2/2$, as found in part (a). The third term, the product of two sinusoids, can be expressed as a sum of two sinusoids $\cos[(\omega_1+\omega_2)t+(\theta_1+\theta_2)]$ and $\cos[(\omega_1-\omega_2)t+(\theta_1-\theta_2)]$, respectively. Now, arguing as in part (a), we see that the third term is zero. Hence, we have[†]

$$P_x = \frac{C_1^2}{2} + \frac{C_2^2}{2}$$

and the rms value is $\sqrt{(C_1^2+C_2^2)/2}$.

We can readily extend this result to a sum of any number of sinusoids with distinct frequencies. Thus, if

$$x(t) = \sum_{n=1}^{\infty} C_n \cos(\omega_n t + \theta_n)$$

assuming that none of the two sinusoids have identical frequencies and $\omega_n \neq 0$, then

$$P_x = \tfrac{1}{2}\sum_{n=1}^{\infty} C_n^2$$

If $x(t)$ also has a dc term, as

$$x(t) = C_0 + \sum_{n=1}^{\infty} C_n \cos(\omega_n t + \theta_n)$$

then

$$P_x = C_0^2 + \tfrac{1}{2}\sum_{n=1}^{\infty} C_n^2 \tag{1.3}$$

(c) In this case the signal is complex, and we use Eq. (1.2) to compute the power.

$$P_x = \lim_{T\to\infty} \frac{1}{T}\int_{-T/2}^{T/2} |De^{j\omega_0 t}|^2$$

Recall that $|e^{j\omega_0 t}| = 1$ so that $|De^{j\omega_0 t}|^2 = |D|^2$, and

$$P_x = |D|^2 \tag{1.4}$$

The rms value is $|D|$.

[†] This is true only if $\omega_1 \neq \omega_2$. If $\omega_1 = \omega_2$, the integrand of the third term contains a constant $\cos(\theta_1 - \theta_2)$, and the third term $\to 2C_1C_2\cos(\theta_1-\theta_2)$ as $T\to\infty$.

Comment. In part (b) of Ex. 1.2, we have shown that the power of the sum of two sinusoids is equal to the sum of the powers of the sinusoids. It may appear that the power of $x_1(t) + x_2(t)$ is $P_{x_1} + P_{x_2}$. Unfortunately, this conclusion is not true in general. It is true only under a certain condition (orthogonality), discussed later (Sec. 3.1.3).

DRILL 1.1 Computing Energy, Power, and RMS Value

Show that the energies of the signals in Figs. 1.3a, 1.3b, 1.3c, and 1.3d are 4, 1, 4/3, and 4/3, respectively. Observe that doubling a signal quadruples the energy, and time shifting a signal has no effect on the energy. Show also that the power of the signal in Fig. 1.3e is 0.4323. What is the rms value of the signal in Fig. 1.3e?

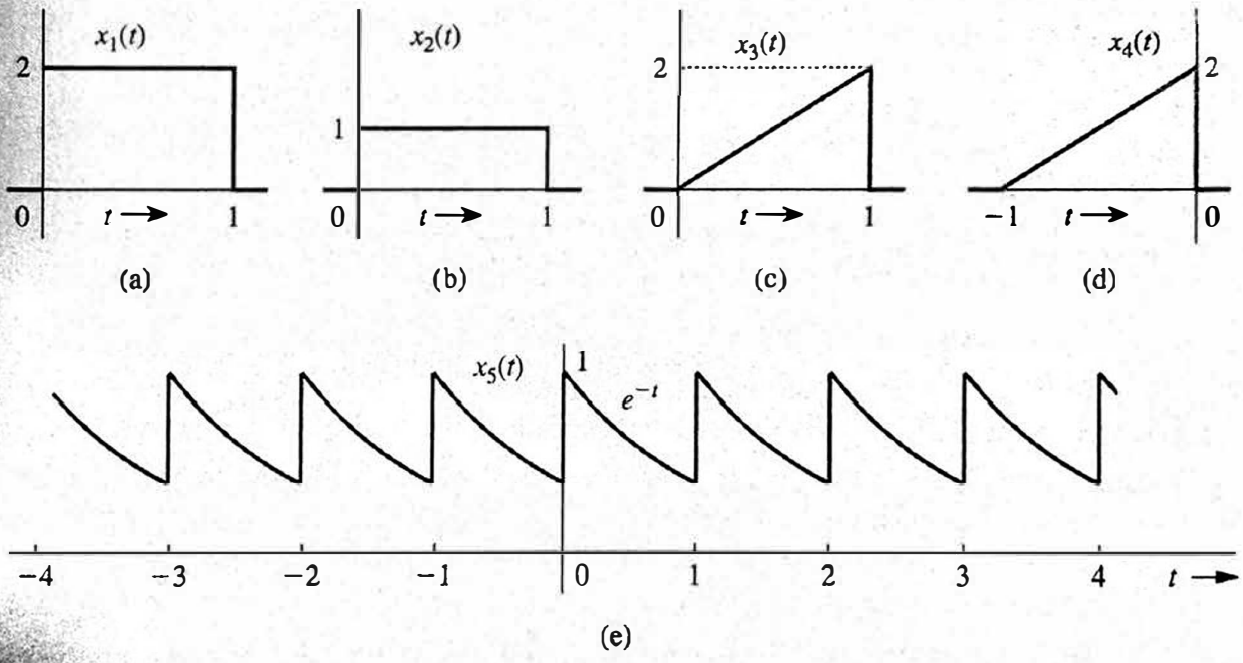

Figure 1.3 Signals for Drill 1.1.

DRILL 1.2 Computing Power over a Period

Redo Ex. 1.1a to find the power of a sinusoid $C\cos(\omega_0 t + \theta)$ by averaging the signal energy over one period $T_0 = 2\pi/\omega_0$ (rather than averaging over the infinitely large interval). Show also that the power of a dc signal $x(t) = C_0$ is C_0^2, and its rms value is C_0.

DRILL 1.3 Power of a Sum of Two Equal-Frequency Sinusoids

Show that if $\omega_1 = \omega_2$, the power of $x(t) = C_1\cos(\omega_1 t + \theta_1) + C_2\cos(\omega_2 t + \theta_2)$ is $[C_1{}^2 + C_2{}^2 + 2C_1C_2\cos(\theta_1 - \theta_2)]/2$, which is not equal to the Ex. 1.2b result of $(C_1{}^2 + C_2{}^2)/2$.

1.2 SOME USEFUL SIGNAL OPERATIONS

We discuss here three useful signal operations: shifting, scaling, and inversion. Since the independent variable in our signal description is time, these operations are discussed as *time shifting*, *time scaling*, and *time reversal* (inversion). However, this discussion is valid for functions having independent variables other than time (e.g., frequency or distance).

1.2.1 Time Shifting

Consider a signal $x(t)$ (Fig. 1.4a) and the same signal delayed by T seconds (Fig. 1.4b), which we shall denote by $\phi(t)$. Whatever happens in $x(t)$ (Fig. 1.4a) at some instant t also happens in $\phi(t)$ (Fig. 1.4b) T seconds later at the instant $t+T$. Therefore,

$$\phi(t+T)=x(t) \qquad \text{and} \qquad \phi(t)=x(t-T)$$

Thus, to time-shift a signal by T, we replace t with $t-T$, so that $x(t-T)$ represents $x(t)$ time-shifted by T seconds. If T is positive, the shift is to the right (delay), as in Fig. 1.4b. If T is negative, the shift is to the left (advance), as in Fig. 1.4c. Clearly, $x(t-2)$ is $x(t)$ delayed (right-shifted) by 2 seconds, and $x(t+2)$ is $x(t)$ advanced (left-shifted) by 2 seconds.

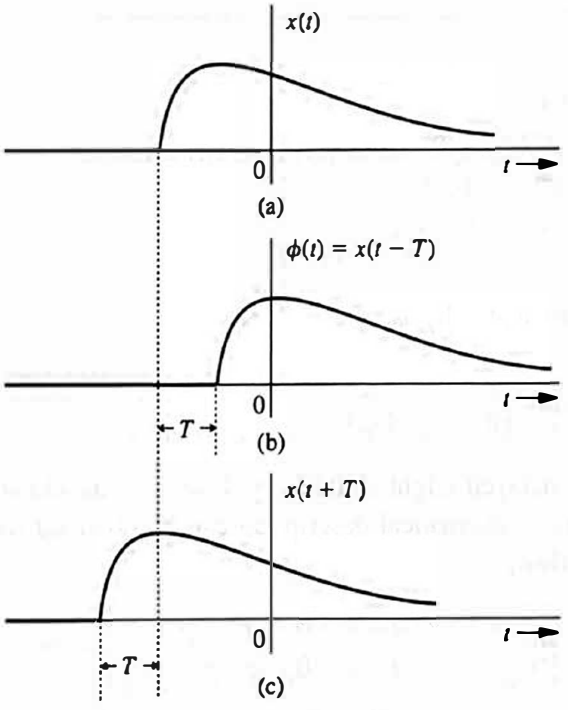

Figure 1.4 Time shifting a signal.

EXAMPLE 1.3 Time Shifting

An exponential function $x(t) = e^{-2t}$ shown in Fig. 1.5a is delayed by 1 second. Sketch and mathematically describe the delayed function. Repeat the problem with $x(t)$ advanced by 1 second.

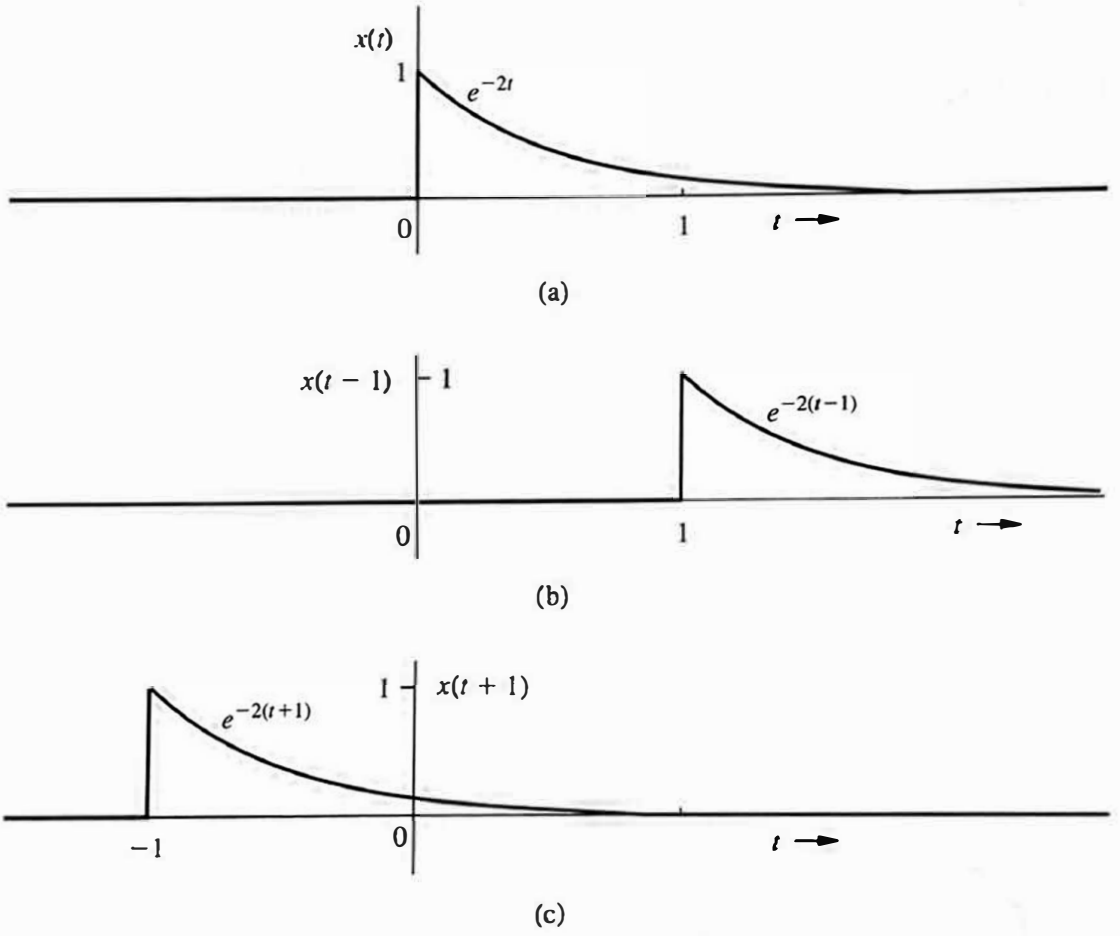

Figure 1.5 **(a)** Signal $x(t)$. **(b)** Signal $x(t)$ delayed by 1 second. **(c)** Signal $x(t)$ advanced by 1 second.

The function $x(t)$ can be described mathematically as

$$x(t) = \begin{cases} e^{-2t} & t \geq 0 \\ 0 & t < 0 \end{cases} \tag{1.5}$$

Let $x_d(t)$ represent the function $x(t)$ delayed (right-shifted) by 1 second, as illustrated in Fig. 1.5b. This function is $x(t-1)$; its mathematical description can be obtained from $x(t)$ by replacing t with $t-1$ in Eq. (1.5). Thus,

$$x_d(t) = x(t-1) = \begin{cases} e^{-2(t-1)} & t-1 \geq 0 \quad \text{or} \quad t \geq 1 \\ 0 & t-1 < 0 \quad \text{or} \quad t < 1 \end{cases}$$

Let $x_a(t)$ represent the function $x(t)$ advanced (left-shifted) by 1 second, as depicted in Fig. 1.5c. This function is $x(t+1)$; its mathematical description can be obtained from $x(t)$ by replacing t with $t+1$ in Eq. (1.5). Thus,

$$x_a(t) = x(t+1) = \begin{cases} e^{-2(t+1)} & t+1 \geq 0 \quad \text{or} \quad t \geq -1 \\ 0 & t+1 < 0 \quad \text{or} \quad t < -1 \end{cases}$$

DRILL 1.4 Working with Time Delay and Time Advance

Write a mathematical description of the signal $x_3(t)$ in Fig. 1.3c. Next, delay this signal by 2 seconds. Sketch the delayed signal. Show that this delayed signal $x_d(t)$ can be described mathematically as $x_d(t) = 2(t-2)$ for $2 \leq t \leq 3$, and equal to 0 otherwise. Now repeat the procedure with the signal advanced (left-shifted) by 1 second. Show that this advanced signal $x_a(t)$ can be described as $x_a(t) = 2(t+1)$ for $-1 \leq t \leq 0$, and 0 otherwise.

1.2.2 Time Scaling

The compression or expansion of a signal in time is known as *time scaling*. Consider the signal $x(t)$ of Fig. 1.6a. The signal $\phi(t)$ in Fig. 1.6b is $x(t)$ compressed in time by a factor of 2. Therefore, whatever happens in $x(t)$ at some instant t also happens to $\phi(t)$ at the instant $t/2$ so that

$$\phi\left(\frac{t}{2}\right) = x(t) \qquad \text{and} \qquad \phi(t) = x(2t)$$

Observe that because $x(t) = 0$ at $t = T_1$ and T_2, we must have $\phi(t) = 0$ at $t = T_1/2$ and $T_2/2$, as shown in Fig. 1.6b. If $x(t)$ were recorded on a tape and played back at twice the normal recording speed, we would obtain $x(2t)$. In general, if $x(t)$ is compressed in time by a factor a ($a > 1$), the resulting signal $\phi(t)$ is given by

$$\phi(t) = x(at)$$

Using a similar argument, we can show that $x(t)$ expanded (slowed down) in time by a factor a ($a > 1$) is given by

$$\phi(t) = x\left(\frac{t}{a}\right)$$

Figure 1.6c shows $x(t/2)$, which is $x(t)$ expanded in time by a factor of 2. Observe that in a time-scaling operation, the origin $t = 0$ is the anchor point, which remains unchanged under the scaling operation because at $t = 0$, $x(t) = x(at) = x(0)$.

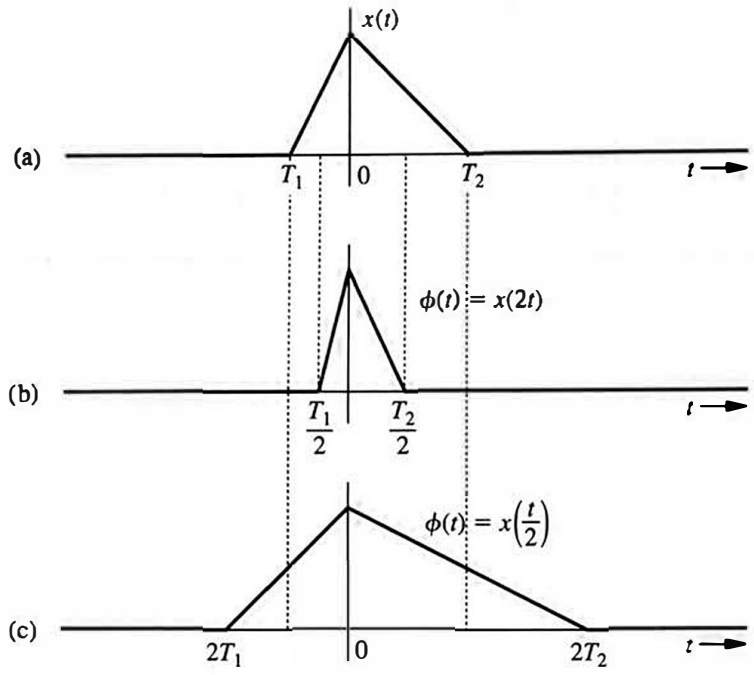

Figure 1.6 Time scaling a signal.

In summary, to time-scale a signal by a factor a, we replace t with at. If $a > 1$, the scaling results in compression, and if $a < 1$, the scaling results in expansion.

EXAMPLE 1.4 Continuous Time-Scaling Operation

Figure 1.7a shows a signal $x(t)$. Sketch and describe mathematically this signal time-compressed by factor 3. Repeat the problem for the same signal time-expanded by factor 2.

The signal $x(t)$ can be described as

$$x(t) = \begin{cases} 2 & -1.5 \le t < 0 \\ 2e^{-t/2} & 0 \le t < 3 \\ 0 & \text{otherwise} \end{cases} \tag{1.6}$$

Figure 1.7b shows $x_c(t)$, which is $x(t)$ time-compressed by factor 3; consequently, it can be described mathematically as $x(3t)$, which is obtained by replacing t with $3t$ in the right-hand side of Eq. (1.6). Thus,

$$x_c(t) = x(3t) = \begin{cases} 2 & -1.5 \le 3t < 0 \quad \text{or} \quad -0.5 \le t < 0 \\ 2e^{-3t/2} & 0 \le 3t < 3 \quad \text{or} \quad 0 \le t < 1 \\ 0 & \text{otherwise} \end{cases}$$

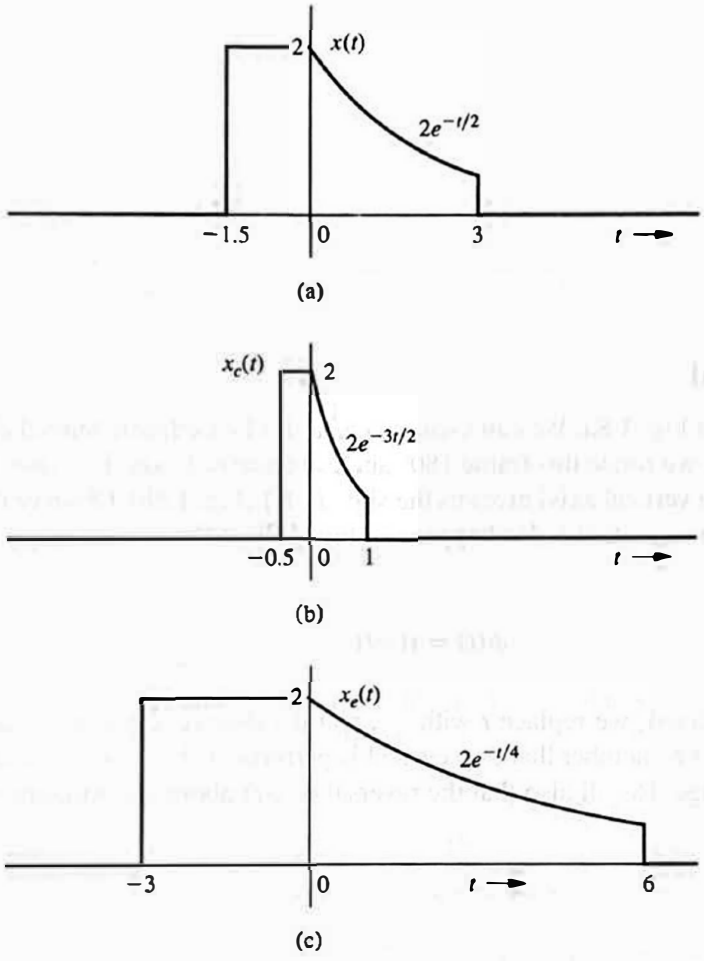

Figure 1.7 **(a)** Signal $x(t)$, **(b)** signal $x(3t)$, and **(c)** signal $x(t/2)$.

Observe that the instants $t = -1.5$ and 3 in $x(t)$ correspond to the instants $t = -0.5$, and 1 in the compressed signal $x(3t)$.

Figure 1.7c shows $x_e(t)$, which is $x(t)$ time-expanded by factor 2; consequently, it can be described mathematically as $x(t/2)$, which is obtained by replacing t with $t/2$ in $x(t)$. Thus,

$$x_e(t) = x\left(\frac{t}{2}\right) = \begin{cases} 2 & -1.5 \le \dfrac{t}{2} < 0 \quad \text{or} \quad -3 \le t < 0 \\ 2e^{-t/4} & 0 \le \dfrac{t}{2} < 3 \quad \text{or} \quad 0 \le t < 6 \\ 0 & \text{otherwise} \end{cases}$$

Observe that the instants $t = -1.5$ and 3 in $x(t)$ correspond to the instants $t = -3$ and 6 in the expanded signal $x(t/2)$.

DRILL 1.5 Compression and Expansion of Sinusoids

Show that the time compression by an integer factor n ($n > 1$) of a sinusoid results in a sinusoid of the same amplitude and phase, but with the frequency increased n-fold. Similarly, the time expansion by an integer factor n ($n > 1$) of a sinusoid results in a sinusoid of the same amplitude and phase, but with the frequency reduced by a factor n. Verify your conclusion by sketching a sinusoid $\sin 2t$ and the same sinusoid compressed by a factor 3 and expanded by a factor 2.

1.2.3 Time Reversal

Consider the signal $x(t)$ in Fig. 1.8a. We can view $x(t)$ as a rigid wire frame hinged at the vertical axis. To time-reverse $x(t)$, we rotate this frame 180° about the vertical axis. This time reversal [the reflection of $x(t)$ about the vertical axis] gives us the signal $\phi(t)$ (Fig. 1.8b). Observe that whatever happens in Fig. 1.8a at some instant t also happens in Fig. 1.8b at the instant $-t$, and vice versa. Therefore,

$$\phi(t) = x(-t)$$

Thus, to time-reverse a signal, we replace t with $-t$, and the time reversal of signal $x(t)$ results in a signal $x(-t)$. We must remember that the reversal is performed about the vertical axis, which acts as an anchor or a hinge. Recall also that the reversal of $x(t)$ about the horizontal axis results in $-x(t)$.

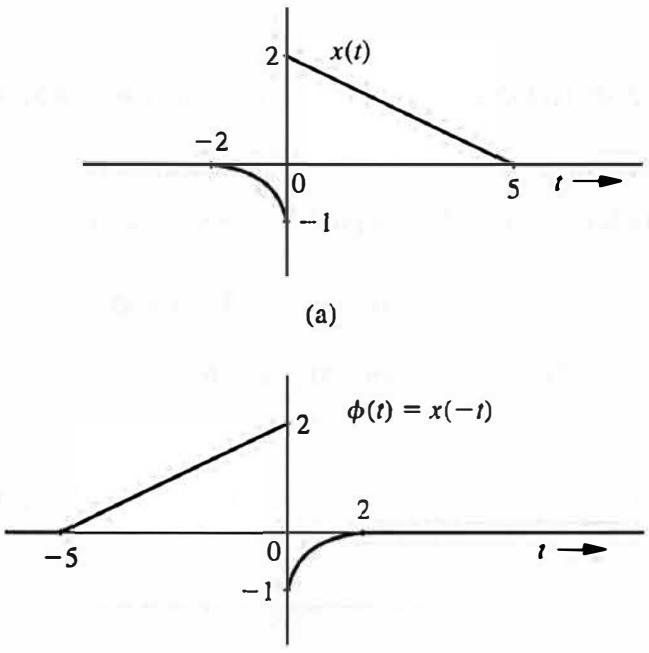

Figure 1.8 Time reversal of a signal.

EXAMPLE 1.5 Time Reversal of a Signal

For the signal $x(t)$ illustrated in Fig. 1.9a, sketch $x(-t)$, which is time-reversed $x(t)$.

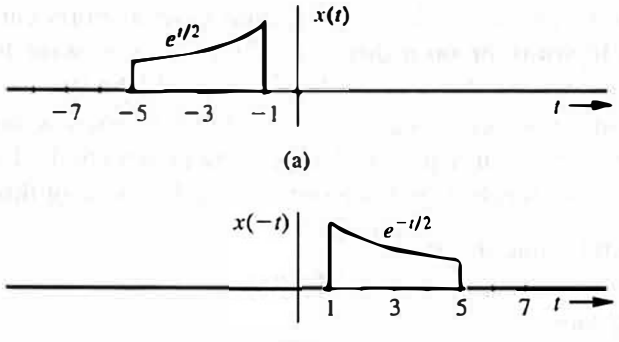

Figure 1.9 Example of time reversal.

The instants -1 and -5 in $x(t)$ are mapped into instants 1 and 5 in $x(-t)$. Because $x(t) = e^{t/2}$, we have $x(-t) = e^{-t/2}$. The signal $x(-t)$ is depicted in Fig. 1.9b. We can describe $x(t)$ and $x(-t)$ as

$$x(t) = \begin{cases} e^{t/2} & -1 \geq t > -5 \\ 0 & \text{otherwise} \end{cases}$$

and its time-reversed version $x(-t)$ is obtained by replacing t with $-t$ in $x(t)$ as

$$x(-t) = \begin{cases} e^{-t/2} & -1 \geq -t > -5 \quad \text{or} \quad 1 \leq t < 5 \\ 0 & \text{otherwise} \end{cases}$$

1.2.4 Combined Operations

Certain complex operations require simultaneous use of more than one of the operations just described. The most general operation involving all three operations is $x(at - b)$, which is realized in two possible sequences of operation:

1. Time-shift $x(t)$ by b to obtain $x(t - b)$. Now time-scale the shifted signal $x(t - b)$ by a [i.e., replace t with at] to obtain $x(at - b)$.
2. Time-scale $x(t)$ by a to obtain $x(at)$. Now time-shift $x(at)$ by b/a [i.e., replace t with $t - (b/a)$] to obtain $x[a(t - b/a)] = x(at - b)$. In either case, if a is negative, time scaling involves time reversal.

For example, the signal $x(2t - 6)$ can be obtained in two ways. We can delay $x(t)$ by 6 to obtain $x(t - 6)$, and then time-compress this signal by factor 2 (replace t with $2t$) to obtain $x(2t - 6)$.

Alternately, we can first time-compress $x(t)$ by factor 2 to obtain $x(2t)$, then delay this signal by 3 (replace t with $t-3$) to obtain $x(2t-6)$.

1.3 CLASSIFICATION OF SIGNALS

Classification helps us better understand and utilize the items around us. Cars, for example, are classified as sports, offroad, family, and so forth. Knowing you have a sports car is useful in deciding whether to drive on a highway or on a dirt road. Knowing you want to drive up a mountain, you would probably choose an offroad vehicle over a family sedan. Similarly, there are several classes of signals. Some signal classes are more suitable for certain applications than others. Further, different signal classes often require different mathematical tools. Here, we shall consider only the following classes of signals, which are suitable for the scope of this book:

1. Continuous-time and discrete-time signals
2. Analog and digital signals
3. Periodic and aperiodic signals
4. Energy and power signals
5. Deterministic and probabilistic signals

1.3.1 Continuous-Time and Discrete-Time Signals

A signal that is specified for every value of time t is a *continuous-time signal*. Since the signal is known for every value of time, precise event localization is possible. The tidal height data displayed in Fig. 1.10a is an example of a continuous-time signal, and signal features such as daily tides as well as the effects of a massive tsunami are easy to locate.

A signal that is specified only at discrete values of time is a *discrete-time signal*. Ordinarily, the independent variable for discrete-time signals is denoted by the integer n. For discrete-time signals, events are localized within the sampling period. The two decades of quarterly United States Gross National Product (GNP) data displayed in Fig. 1.10b is an example of a discrete-time signal, and features such as the modest 2001 and massive 2008 recessions are easily visible.

1.3.2 Analog and Digital Signals

The concept of continuous time is often confused with that of analog. The two are not the same. The same is true of the concepts of discrete time and digital. A signal whose amplitude can take on any value in a continuous range is an *analog signal*. This means that an analog signal amplitude can take on an infinite number of values. A *digital signal*, on the other hand, is one whose amplitude can take on only a finite number of values. Signals associated with a digital computer are digital because they take on only two values (binary signals). A digital signal whose amplitudes can take on M values is an M-ary signal of which binary ($M = 2$) is a special case. The terms *continuous time* and *discrete time* qualify the nature of a signal along the time (horizontal) axis. The terms *analog* and *digital*, on the other hand, qualify the nature of the signal amplitude (vertical axis). Figure 1.11 shows examples of signals of various types. It is clear that analog is not necessarily continuous-time and digital need not be discrete-time. Figure 1.11c shows an example of an analog discrete-time signal. An analog signal can be converted into a digital signal [analog-to-digital (A/D) conversion] through quantization (rounding off), as explained in Sec. 5.3.

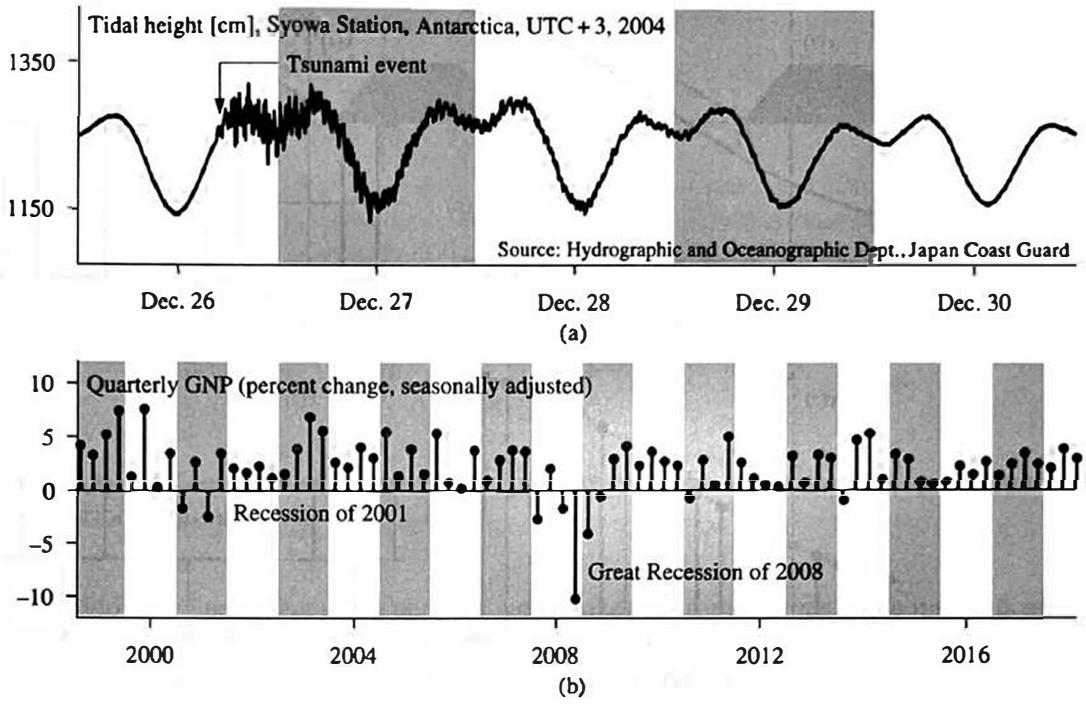

Figure 1.10 **(a)** Continuous-time and **(b)** discrete-time signals.

1.3.3 Periodic and Aperiodic Signals

A signal $x(t)$ is said to be *periodic* if for some positive constant T_0

$$x(t) = x(t + T_0) \qquad \text{for all } t \tag{1.7}$$

The *smallest* value of T_0 that satisfies the periodicity condition of Eq. (1.7) is the *fundamental period* of $x(t)$. The signals in Figs. 1.2b and 1.3e are periodic signals with periods 2 and 1, respectively. A signal is *aperiodic* if it is not periodic. Signals in Figs. 1.2a, 1.3a, 1.3b, 1.3c, and 1.3d are all aperiodic.

By definition, a periodic signal $x(t)$ remains unchanged when time-shifted by one period. For this reason, a periodic signal must start at $t = -\infty$: if it started at some finite instant, say, $t = 0$, the time-shifted signal $x(t + T_0)$ would start at $t = -T_0$ and $x(t + T_0)$ would not be the same as $x(t)$. Therefore, a *periodic signal, by definition, must start at* $t = -\infty$ *and continue forever, as illustrated in Fig. 1.12.*

Another important property of a periodic signal $x(t)$ is that $x(t)$ can be generated by *periodic extension* of any segment of $x(t)$ of duration T_0 (the period). As a result, we can generate $x(t)$ from any segment of $x(t)$ having a duration of one period by placing this segment and the reproduction thereof end to end ad infinitum on either side. Figure 1.13 shows a periodic signal $x(t)$ of period $T_0 = 6$. The shaded portion of Fig. 1.13a shows a segment of $x(t)$ starting at $t = -1$ and having a duration of one period (6 seconds). This segment, when repeated forever in either direction, results in the periodic signal $x(t)$. Figure 1.13b shows another shaded segment of $x(t)$ of duration

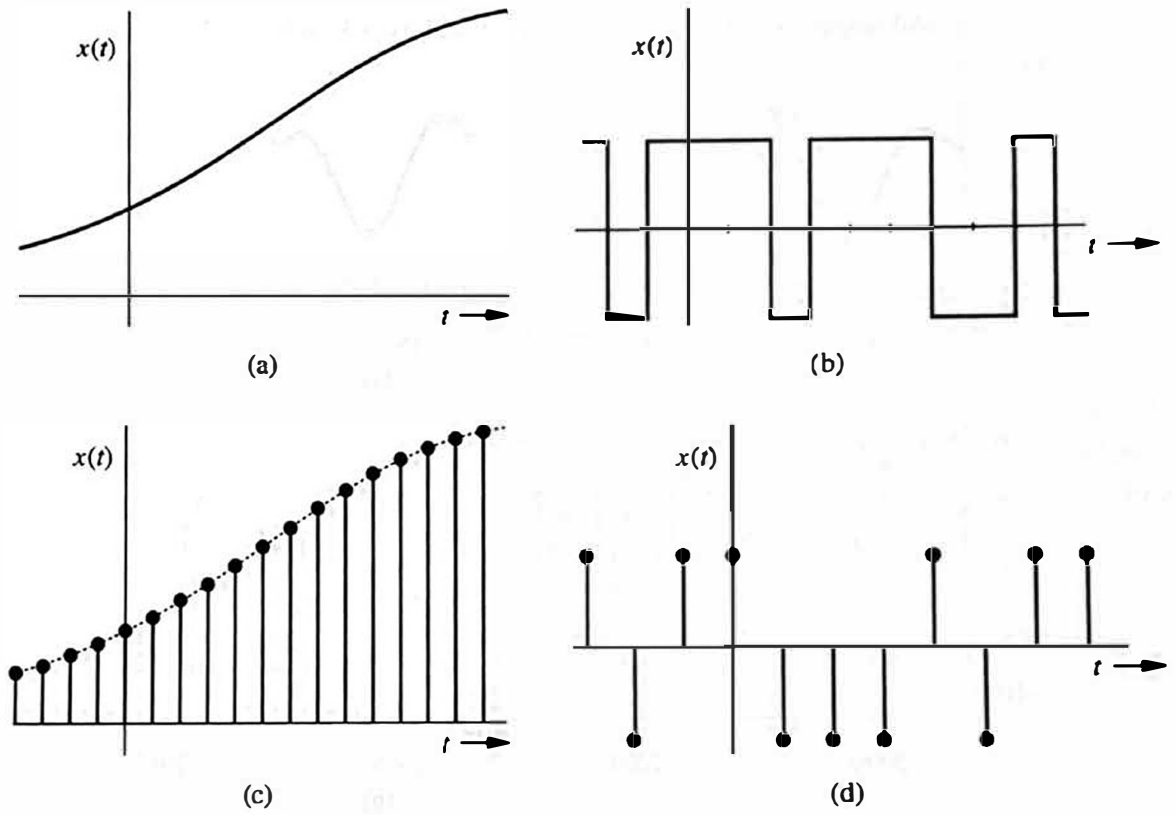

Figure 1.11 Examples of signals: **(a)** analog, continuous-time, **(b)** digital, continuous-time, **(c)** analog, discrete-time, and **(d)** digital, discrete-time.

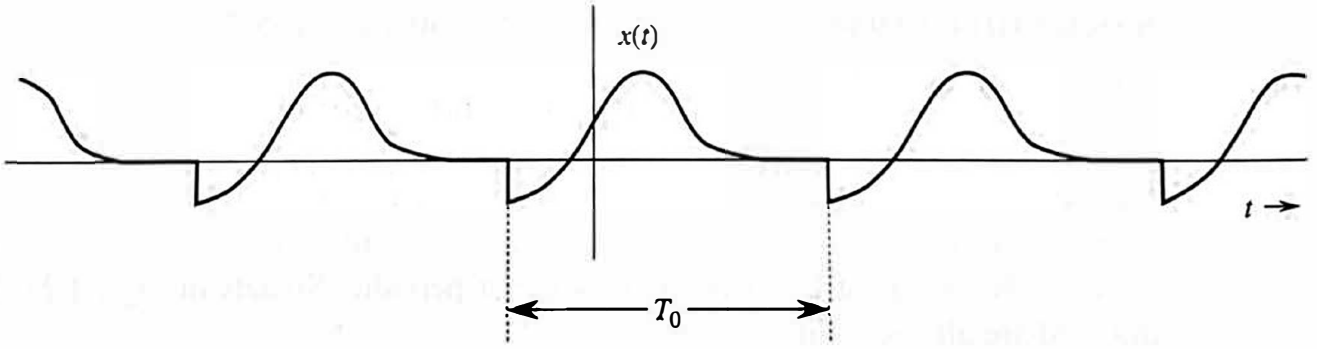

Figure 1.12 A periodic signal of period T_0.

T_0 starting at $t = 0$. Again, we see that this segment, when repeated forever on either side, results in $x(t)$. The reader can verify that this construction is possible with any segment of $x(t)$ starting at any instant as long as the segment duration is one period.

An additional useful property of a periodic signal $x(t)$ of period T_0 is that the area under $x(t)$ over any interval of duration T_0 is the same; that is, for any real numbers a and b,

$$\int_a^{a+T_0} x(t)\,dt = \int_b^{b+T_0} x(t)\,dt$$

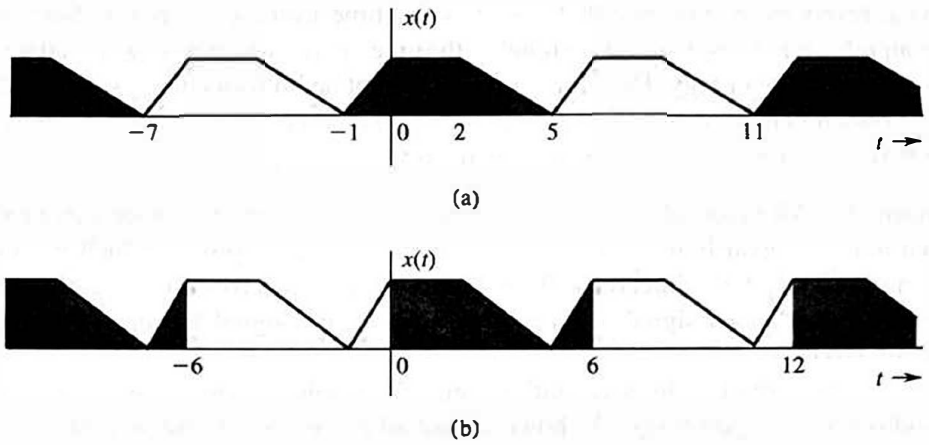

Figure 1.13 Generation of a periodic signal by periodic extension of its segment of one-period duration.

This result follows from the fact that a periodic signal takes the same values at the intervals of T_0. Hence, the values over any segment of duration T_0 are repeated in any other interval of the same duration. For convenience, the area under $x(t)$ over any interval of duration T_0 will be denoted by

$$\int_{T_0} x(t)\,dt$$

It is helpful to label signals that start at $t = -\infty$ and continue forever as *everlasting* signals. Thus, an everlasting signal exists over the entire interval $-\infty < t < \infty$. The signals in Figs. 1.1b and 1.2b are examples of everlasting signals. Clearly, a periodic signal, by definition, is an everlasting signal.

A signal that does not start before $t = 0$ is a *causal* signal. In other words, $x(t)$ is a causal signal if

$$x(t) = 0 \qquad t < 0$$

The signals in Figs. 1.3a–1.3c are causal signals. A signal that starts before $t = 0$ is a *noncausal* signal. All the signals in Figs. 1.1 and 1.2 are noncausal. Observe that an everlasting signal is always noncausal but a noncausal signal is not necessarily everlasting. The everlasting signal in Fig. 1.2b is noncausal; however, the noncausal signal in Fig. 1.2a is not everlasting. A signal that is zero for all $t \geq 0$ is called an *anti-causal* signal.

Comment. A true everlasting signal cannot be generated in practice for obvious reasons. Why should we bother to postulate such a signal? In later chapters we shall see that certain signals (e.g., an impulse and an everlasting sinusoid) that cannot be generated in practice *do* serve a very useful purpose in the study of signals and systems.

1.3.4 Energy and Power Signals

A signal with finite energy is an *energy signal,* and a signal with finite and nonzero power is a *power signal.* The signals in Figs. 1.2a and 1.2b are examples of energy and power

signals, respectively. Observe that power is the time average of energy. Since the averaging is over an infinitely large interval, a signal with finite energy has zero power, and a signal with finite power has infinite energy. Therefore, a signal cannot be both an energy signal and a power signal. If it is one, it cannot be the other. On the other hand, there are signals that are neither energy nor power signals. The ramp signal is one such case.

Comments. All practical signals have finite energies and are therefore energy signals. A power signal must necessarily have infinite duration; otherwise, its power, which is its energy averaged over an infinitely large interval, will not approach a (nonzero) limit. Clearly, it is impossible to generate a true power signal in practice because such a signal has infinite duration and infinite energy.

Also, because of periodic repetition, periodic signals for which the area under $|x(t)|^2$ over one period is finite are power signals; however, not all power signals are periodic.

DRILL 1.6 Neither Energy nor Power

Show that an everlasting exponential e^{-at} is neither an energy nor a power signal for any real value of a. However, if a is imaginary, it is a power signal with power $P_x = 1$ regardless of the value of a.

1.3.5 Deterministic and Random Signals

A signal whose physical description is known completely, in either a mathematical form or a graphical form, is a *deterministic signal*. A signal whose values cannot be predicted precisely but are known only in terms of probabilistic description, such as mean value or mean-squared value, is a *random signal*. In this book we shall exclusively deal with deterministic signals. Random signals are beyond the scope of this study.

1.4 SOME USEFUL SIGNAL MODELS

In the area of signals and systems, the step, the impulse, and the exponential functions play very important roles. Not only do they serve as a basis for representing other signals, but their use can simplify many aspects of the signals and systems.

1.4.1 The Unit Step Function $u(t)$

In much of our discussion, the signals begin at $t = 0$ (causal signals). Such signals can be conveniently described in terms of unit step function $u(t)$ shown in Fig. 1.14a. This function is defined by

$$u(t) = \begin{cases} 1 & t \geq 0 \\ 0 & t < 0 \end{cases} \tag{1.8}$$

If we want a signal to start at $t = 0$ (so that it has a value of zero for $t < 0$), we need only multiply the signal by $u(t)$. For instance, the signal e^{-at} represents an everlasting exponential that starts at $t = -\infty$. The causal form of this exponential (Fig. 1.14b) can be described as $e^{-at}u(t)$.

The unit step function also proves very useful in specifying a function with different mathematical descriptions over different intervals. Examples of such functions appear in Fig. 1.7. These functions have different mathematical descriptions over different segments of time, as seen from Eqs. (1.5) and (1.6). Such a description often proves clumsy and inconvenient in mathematical treatment. We can use the unit step function to describe such functions by a single expression that is valid for all t.

Consider, for example, the rectangular pulse depicted in Fig. 1.15a. We can express such a pulse in terms of familiar step functions by observing that the pulse $x(t)$ can be expressed as the sum of the two delayed unit step functions, as shown in Fig. 1.15b. The unit step function $u(t)$ delayed by T seconds is $u(t-T)$. From Fig. 1.15b, it is clear that

$$x(t) = u(t-2) - u(t-4)$$

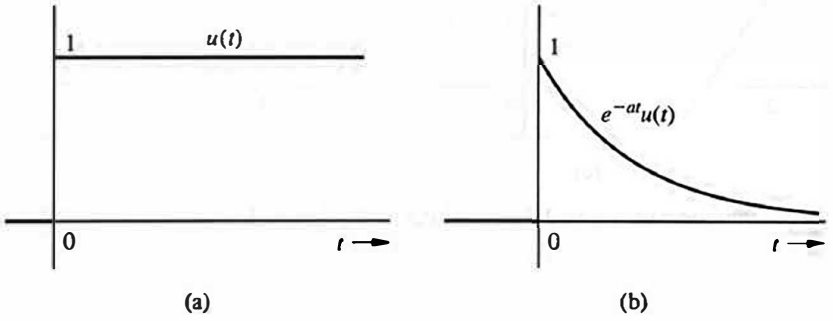

Figure 1.14 (a) Unit step function $u(t)$. (b) Exponential $e^{-at}u(t)$.

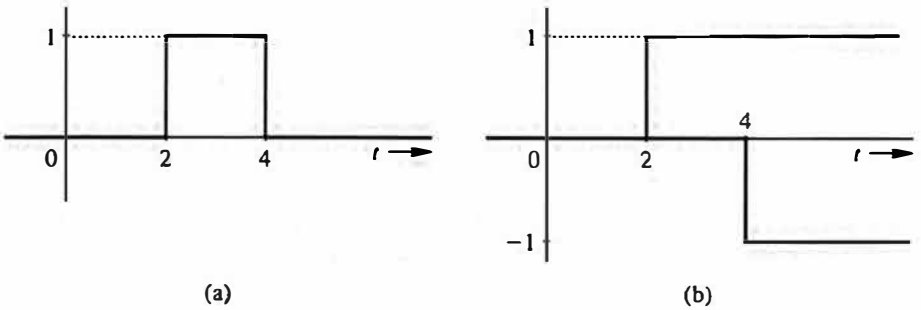

Figure 1.15 Representation of a rectangular pulse by step functions.

EXAMPLE 1.6 Describing a Triangle Function with the Unit Step

Use the unit step function to describe the signal in Fig. 1.16a.

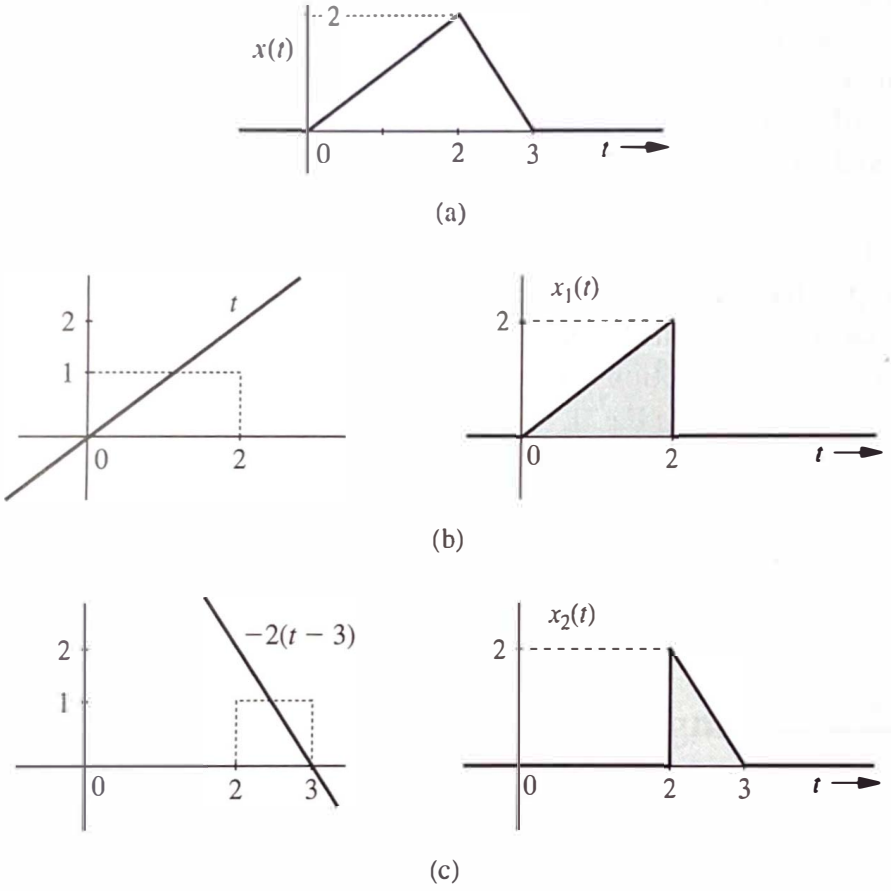

Figure 1.16 Representation of a signal defined interval by interval.

The signal illustrated in Fig. 1.16a can be conveniently handled by breaking it up into the two components $x_1(t)$ and $x_2(t)$, depicted in Figs. 1.16b and 1.16c, respectively. Here, $x_1(t)$ can be obtained by multiplying the ramp t by the gate pulse $u(t) - u(t-2)$, as shown in Fig. 1.16b. Therefore,

$$x_1(t) = t[u(t) - u(t-2)]$$

The signal $x_2(t)$ can be obtained by multiplying another ramp by the gate pulse illustrated in Fig. 1.16c. This ramp has a slope -2; hence it can be described by $-2t + c$. Now, because the ramp has a zero value at $t = 3$, the constant $c = 6$, and the ramp can be described by $-2(t-3)$. Also, the gate pulse in Fig. 1.16c is $u(t-2) - u(t-3)$. Therefore,

$$x_2(t) = -2(t-3)[u(t-2) - u(t-3)]$$

and

$$\begin{aligned} x(t) &= x_1(t) + x_2(t) \\ &= t[u(t) - u(t-2)] - 2(t-3)[u(t-2) - u(t-3)] \\ &= tu(t) - 3(t-2)u(t-2) + 2(t-3)u(t-3) \end{aligned}$$

EXAMPLE 1.7 Describing a Piecewise Function with the Unit Step

Describe the signal in Fig. 1.7a by a single expression valid for all t.

Over the interval from -1.5 to 0, the signal can be described by a constant 2, and over the interval from 0 to 3, it can be described by $2e^{-t/2}$. Therefore,

$$\begin{aligned} x(t) &= \underbrace{2[u(t+1.5) - u(t)]}_{\text{constant part}} + \underbrace{2e^{-t/2}[u(t) - u(t-3)]}_{\text{exponential part}} \\ &= 2u(t+1.5) - 2(1 - e^{-t/2})u(t) - 2e^{-t/2}u(t-3) \end{aligned}$$

Compare this expression with the expression for the same function found in Eq. (1.6).

DRILL 1.7 Using Reflected Unit Step Functions

Show that the signals depicted in Figs. 1.17a and 1.17b can be described as $u(-t)$ and $e^{-at}u(-t)$, respectively.

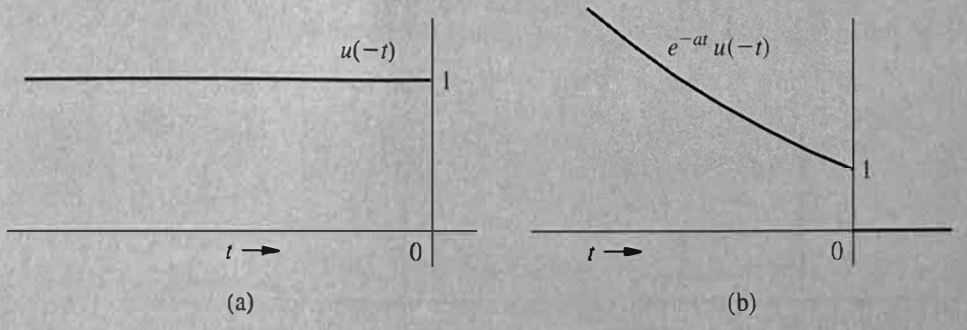

Figure 1.17 Signals for Drill 1.7.

DRILL 1.8 Describing a Piecewise Function with the Unit Step

Show that the signal shown in Fig. 1.18 can be described as

$$x(t) = (t-1)u(t-1) - (t-2)u(t-2) - u(t-4)$$

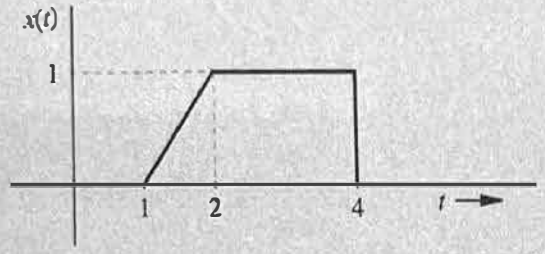

Figure 1.18 Signal for Drill 1.8.

1.4.2 The Unit Impulse Function $\delta(t)$

The unit impulse function $\delta(t)$ is one of the most important functions in the study of signals and systems. This function was first defined in two parts by P. A. M. Dirac as

$$\delta(t) = 0 \quad t \neq 0 \qquad \text{and} \qquad \int_{-\infty}^{\infty} \delta(t)\,dt = 1 \tag{1.9}$$

We can visualize an impulse as a tall, narrow, rectangular pulse of unit area, as illustrated in Fig. 1.19b. The width of this rectangular pulse is a very small value $\epsilon \to 0$. Consequently, its height is a very large value $1/\epsilon \to \infty$. The unit impulse therefore can be regarded as a rectangular pulse with a width that has become infinitesimally small, a height that has become infinitely large, and an overall area that has been maintained at unity. Thus, $\delta(t) = 0$ everywhere except at $t = 0$, where it is undefined. For this reason, a unit impulse is represented by the spearlike symbol in Fig. 1.19a.

Other pulses, such as the exponential, triangular, or Gaussian types, may also be used in impulse approximation. The important feature of the unit impulse function is not its shape but the fact that its effective duration (pulse width) approaches zero while its area remains at unity. For example, the exponential pulse $\alpha e^{-\alpha t}u(t)$ in Fig. 1.20a becomes taller and narrower as α increases. In the limit as $\alpha \to \infty$, the pulse height $\to \infty$, and its width or duration $\to 0$. Yet, the area under the pulse is unity regardless of the value of α because

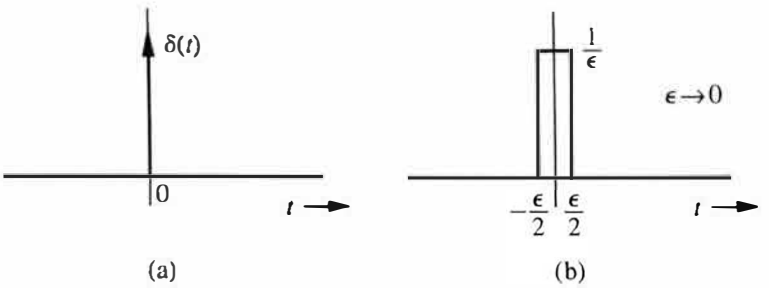

Figure 1.19 A unit impulse and its approximation.

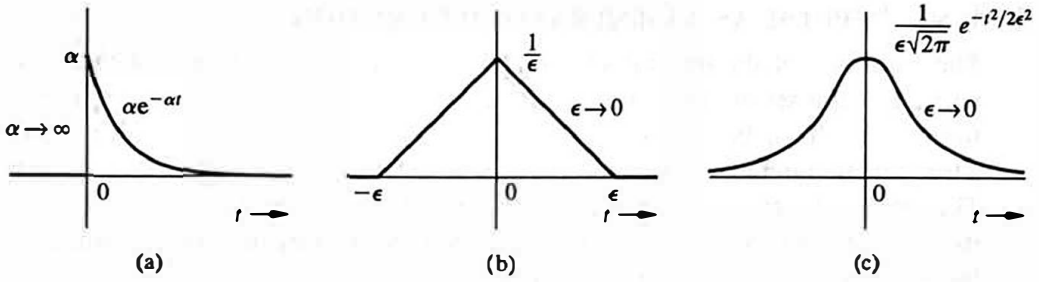

Figure 1.20 Other possible approximations to a unit impulse.

$$\int_0^\infty \alpha e^{-\alpha t}\,dt = 1$$

The pulses in Figs. 1.20b and 1.20c behave in a similar fashion. Clearly, the exact impulse function cannot be generated in practice; it can only be approached.

From Eq. (1.9), it follows that the function $k\delta(t) = 0$ for all $t \neq 0$, and its area is k. Thus, $k\delta(t)$ is an impulse function whose area is k (in contrast to the unit impulse function, whose area is 1).

Multiplication of a Function by an Impulse

Let us now consider what happens when we multiply the unit impulse $\delta(t)$ by a function $\phi(t)$ that is known to be continuous at $t = 0$. Since the impulse has nonzero value only at $t = 0$, and the value of $\phi(t)$ at $t = 0$ is $\phi(0)$, we obtain

$$\phi(t)\delta(t) = \phi(0)\delta(t)$$

Thus, multiplication of a continuous-time function $\phi(t)$ with an unit impulse located at $t = 0$ results in an impulse, which is located at $t = 0$ and has strength $\phi(0)$ [the value of $\phi(t)$ at the location of the impulse]. Use of exactly the same argument leads to the generalization of this result, stating that provided $\phi(t)$ is continuous at $t = T$, $\phi(t)$ multiplied by an impulse $\delta(t - T)$ (impulse located at $t = T$) results in an impulse located at $t = T$ and having strength $\phi(T)$ [the value of $\phi(t)$ at the location of the impulse].

$$\phi(t)\delta(t - T) = \phi(T)\delta(t - T) \tag{1.10}$$

Sampling Property of the Unit Impulse Function

From Eq. (1.10) it follows that

$$\int_{-\infty}^{\infty} \phi(t)\delta(t - T)\,dt = \phi(T)\int_{-\infty}^{\infty} \delta(t)\,dt = \phi(T) \tag{1.11}$$

provided $\phi(t)$ is continuous at $t = T$. This result means that *the area under the product of a function with an impulse $\delta(t - T)$ is equal to the value of that function at the instant at which the unit impulse is located.* This property is very important and useful and is known as the *sampling* or *sifting property* of the unit impulse.

Unit Impulse as a Generalized Function

The definition of the unit impulse function given in Eq. (1.9) is not mathematically rigorous, which leads to serious difficulties. First, the impulse function does not define a unique function: for example, it can be shown that $\delta(t) + \dot{\delta}(t)$ also satisfies Eq. (1.9) [1]. Moreover, $\delta(t)$ is not even a true function in the ordinary sense. An ordinary function is specified by its values for all time t. The impulse function is zero everywhere except at $t = 0$, and at this, the only interesting part of its range, it is undefined. These difficulties are resolved by defining the impulse as a generalized function rather than an ordinary function. A *generalized function* is defined by its effect on other functions instead of by its value at every instant of time.

In this approach the impulse function is defined by the sampling property [Eq. (1.11)]. We say nothing about what the impulse function is or what it looks like. Instead, the impulse function is defined in terms of its effect on a test function $\phi(t)$. We define a unit impulse as a function for which the area under its product with a function $\phi(t)$ is equal to the value of the function $\phi(t)$ at the instant at which the impulse is located. It is assumed that $\phi(t)$ is continuous at the location of the impulse. Recall that the sampling property [Eq. (1.11)] is the consequence of the classical (Dirac) definition of the unit impulse in Eq. (1.9). In contrast, *the sampling property [Eq. (1.11)] defines the impulse function in the generalized function approach.*

We now present an interesting application of the generalized function definition of an impulse. Because the unit step function $u(t)$ is discontinuous at $t = 0$, its derivative du/dt does not exist at $t = 0$ in the ordinary sense. We now show that this derivative *does* exist in the generalized sense, and it is, in fact, $\delta(t)$. As a proof, let us evaluate the integral of $(du/dt)\phi(t)$, using integration by parts:

$$\begin{aligned}\int_{-\infty}^{\infty} \frac{du(t)}{dt}\phi(t)\,dt &= u(t)\phi(t)\Big|_{-\infty}^{\infty} - \int_{-\infty}^{\infty} u(t)\dot{\phi}(t)\,dt \\ &= \phi(\infty) - 0 - \int_{0}^{\infty} \dot{\phi}(t)\,dt \\ &= \phi(\infty) - \phi(t)|_0^{\infty} = \phi(0)\end{aligned}$$

This result shows that du/dt satisfies the sampling property of $\delta(t)$. Therefore, it is an impulse $\delta(t)$ in the generalized sense—that is,

$$\frac{du(t)}{dt} = \delta(t) \tag{1.12}$$

Consequently,

$$\int_{-\infty}^{t} \delta(\tau)\,d\tau = u(t)$$

These results can also be obtained graphically from Fig. 1.19b. We observe that the area from $-\infty$ to t under the limiting form of $\delta(t)$ in Fig. 1.19b is zero if $t < -\epsilon/2$ and unity if $t \geq \epsilon/2$ with $\epsilon \to 0$. Consequently,

$$\begin{aligned}\int_{-\infty}^{t} \delta(\tau)\,d\tau &= \begin{cases} 0 & t < 0 \\ 1 & t \geq 0 \end{cases} \\ &= u(t)\end{aligned}$$

This result shows that the unit step function can be obtained by integrating the unit impulse function. Similarly, the unit ramp function $x(t) = tu(t)$ can be obtained by integrating the unit step function. We may continue with unit parabolic function $t^2/2$ obtained by integrating the unit ramp, and so on. On the other side, we have derivatives of impulse function, which can be defined as generalized functions (see Prob. 1.4-12). All these functions, derived from the unit impulse function (successive derivatives and integrals), are called *singularity functions*.[†]

DRILL 1.9 Simplifying Expressions Containing the Unit Impulse

Show that

(a) $(t^3+3)\delta(t) = 3\delta(t)$

(b) $\left[\sin\left(t^2 - \frac{\pi}{2}\right)\right]\delta(t) = -\delta(t)$

(c) $e^{-2t}\delta(t) = \delta(t)$

(d) $\frac{\omega^2+1}{\omega^2+9}\delta(\omega-1) = \frac{1}{5}\delta(\omega-1)$

DRILL 1.10 Simplifying Integrals Containing the Unit Impulse

Show that

(a) $\int_{-\infty}^{\infty} \delta(t)e^{-j\omega t}\,dt = 1$

(b) $\int_{-\infty}^{\infty} \delta(t-2)\cos\left(\frac{\pi t}{4}\right)dt = 0$

(c) $\int_{-\infty}^{\infty} e^{-2(x-t)}\delta(2-t)\,dt = e^{-2(x-2)}$

1.4.3 The Exponential Function e^{st}

Another important function in the area of signals and systems is the exponential signal e^{st}, where s is complex in general, given by

$$s = \sigma + j\omega$$

Therefore,

$$e^{st} = e^{(\sigma+j\omega)t} = e^{\sigma t}e^{j\omega t} = e^{\sigma t}(\cos\omega t + j\sin\omega t) \tag{1.13}$$

[†] Singularity functions were defined by the late Prof. S. J. Mason as follows. A singularity is a point at which a function does not possess a derivative. Each of the singularity functions (or if not the function itself, then the function differentiated a finite number of times) has a singular point at the origin and is zero elsewhere [2].

Since $s^* = \sigma - j\omega$ (the conjugate of s), then

$$e^{s^*t} = e^{(\sigma - j\omega)t} = e^{\sigma t}e^{-j\omega t} = e^{\sigma t}(\cos \omega t - j \sin \omega t)$$

and

$$e^{\sigma t} \cos \omega t = \tfrac{1}{2}(e^{st} + e^{s^*t}) \tag{1.14}$$

A comparison of Eq. (1.13) with Euler's formula shows that e^{st} is a generalization of the function $e^{j\omega t}$, where the frequency variable $j\omega$ is generalized to a complex variable $s = \sigma + j\omega$. For this reason, we designate the variable s as the *complex frequency*. In fact, function e^{st} encompasses a large class of functions. The following functions are either special cases of or can be expressed in terms of e^{st}:

1. A constant $k = ke^{0t}$ $(s = 0)$
2. A monotonic exponential $e^{\sigma t}$ $(\omega = 0, s = \sigma)$
3. A sinusoid $\cos \omega t$ $(\sigma = 0, s = \pm j\omega)$
4. An exponentially varying sinusoid $e^{\sigma t} \cos \omega t$ $(s = \sigma \pm j\omega)$

These functions are illustrated in Fig. 1.21.

The complex frequency s can be conveniently represented on a *complex frequency plane* (s plane), as depicted in Fig. 1.22. The horizontal axis is the real axis (σ axis), and the vertical axis is the imaginary axis (ω axis). The absolute value of the imaginary part of s is $|\omega|$ (the *radian* frequency), which indicates the frequency of oscillation of e^{st}; the real part σ (the *neper* frequency)

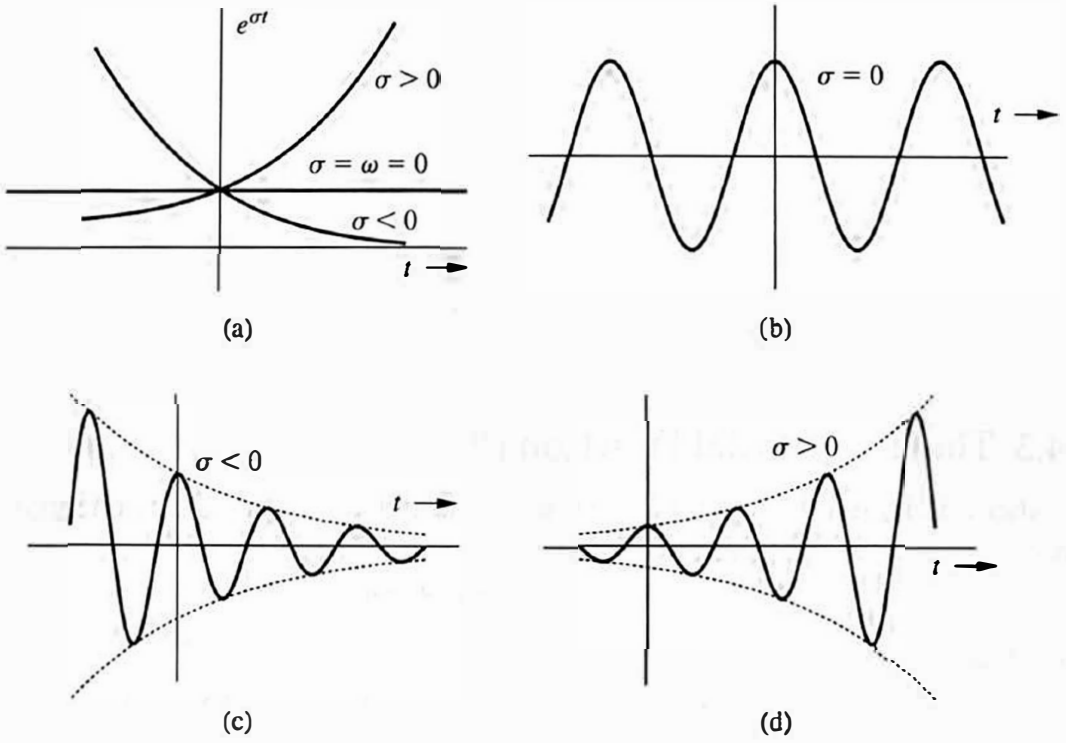

Figure 1.21 Sinusoids of complex frequency $\sigma + j\omega$.

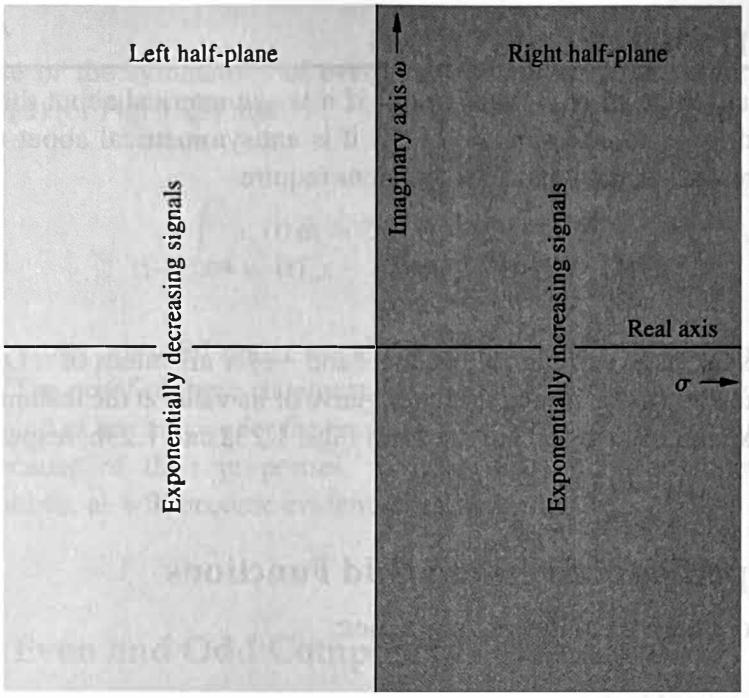

Figure 1.22 Complex frequency plane.

gives information about the rate of increase or decrease of the amplitude of e^{st}. For signals whose complex frequencies lie on the real axis (σ axis, where $\omega = 0$), the frequency of oscillation is zero. Consequently, these signals are monotonically increasing or decreasing exponentials (Fig. 1.21a). For signals whose frequencies lie on the imaginary axis (ω axis, where $\sigma = 0$), $e^{\sigma t} = 1$. Therefore, these signals are conventional sinusoids with constant amplitude (Fig. 1.21b). The case $s = 0$ ($\sigma = \omega = 0$) corresponds to a constant (dc) signal because $e^{0t} = 1$. For the signals illustrated in Figs. 1.21c and 1.21d, both σ and ω are nonzero; the frequency s is complex and does not lie on either axis. The signal in Fig. 1.21c decays exponentially. Therefore, σ is negative, and s lies to the left of the imaginary axis. In contrast, the signal in Fig. 1.21d *grows* exponentially. Therefore, σ is positive, and s lies to the right of the imaginary axis. Thus, the s plane (Fig. 1.21) can be separated into two parts: the *left half-plane* (LHP) corresponding to exponentially decaying signals and the *right half-plane* (RHP) corresponding to exponentially growing signals. The imaginary axis separates the two regions and corresponds to signals of constant amplitude.

An exponentially growing sinusoid $e^{2t}\cos 5t$, for example, can be expressed as a linear combination of exponentials $e^{(2+j5)t}$ and $e^{(2-j5)t}$ with complex frequencies $2 + j5$ and $2 - j5$, respectively, which lie in the RHP. An exponentially decaying sinusoid $e^{-2t}\cos 5t$ can be expressed as a linear combination of exponentials $e^{(-2+j5)t}$ and $e^{(-2-j5)t}$ with complex frequencies $-2 + j5$ and $-2 - j5$, respectively, which lie in the LHP. A constant-amplitude sinusoid $\cos 5t$ can be expressed as a linear combination of exponentials e^{j5t} and e^{-j5t} with complex frequencies $\pm j5$, which lie on the imaginary axis. Observe that the monotonic exponentials $e^{\pm 2t}$ are also generalized sinusoids with complex frequencies ± 2.

1.5 EVEN AND ODD FUNCTIONS

A function $x_e(t)$ is said to be an *even function* of t if it is symmetrical about the vertical axis. A function $x_o(t)$ is said to be an *odd function* of t if it is antisymmetrical about the vertical axis. Mathematically expressed, these symmetry conditions require

$$x_e(t) = x_e(-t) \qquad \text{and} \qquad x_o(t) = -x_o(-t) \tag{1.15}$$

An even function has the same value at the instants t and $-t$ for all values of t. On the other hand, the value of an odd function at the instant t is the negative of its value at the instant $-t$. An example even signal and an example odd signal are shown in Figs. 1.23a and 1.23b, respectively.

1.5.1 Some Properties of Even and Odd Functions

Even and odd functions have the following properties:

$$\text{even function} \times \text{odd function} = \text{odd function}$$
$$\text{odd function} \times \text{odd function} = \text{even function}$$
$$\text{even function} \times \text{even function} = \text{even function}$$

The proofs are trivial and follow directly from the definition of odd and even functions [Eq. (1.15)].

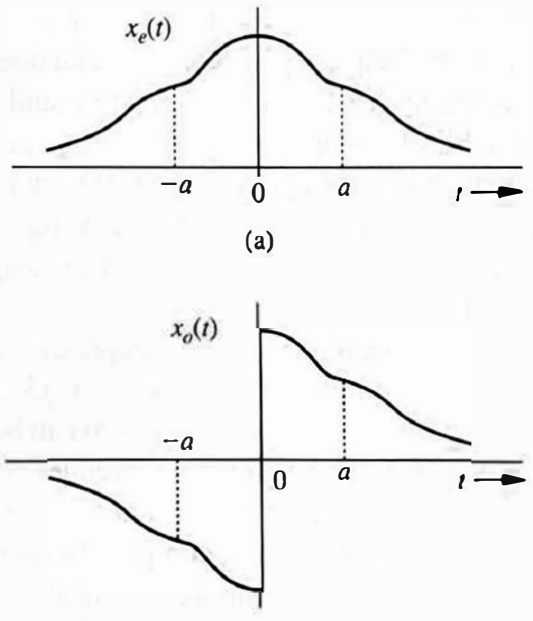

Figure 1.23 Functions of t: **(a)** even and **(b)** odd.

AREA

Because of the symmetries of even and odd functions about the vertical axis, it follows from Eq. (1.15) [or Fig. 1.23] that

$$\int_{-a}^{a} x_e(t)\,dt = 2\int_{0}^{a} x_e(t)\,dt \qquad \text{and} \qquad \int_{-a}^{a} x_o(t)\,dt = 0 \tag{1.16}$$

These results are valid under the assumption that there is no impulse (or its derivatives) at the origin. The proof of these statements is obvious from the plots of even and odd functions. Formal proofs, left as an exercise for the reader, can be accomplished by using the definitions in Eq. (1.15).

Because of their properties, study of odd and even functions proves useful in many applications, as will become evident in later chapters.

1.5.2 Even and Odd Components of a Signal

Every signal $x(t)$ can be expressed as a sum of even and odd components because

$$x(t) = \underbrace{\tfrac{1}{2}[x(t)+x(-t)]}_{\text{even}} + \underbrace{\tfrac{1}{2}[x(t)-x(-t)]}_{\text{odd}} \tag{1.17}$$

From the definitions in Eq. (1.15), we can clearly see that the first component on the right-hand side is an even function, while the second component is odd. This is apparent from the fact that replacing t by $-t$ in the first component yields the same function. The same maneuver in the second component yields the negative of that component.

EXAMPLE 1.8 Finding the Even and Odd Components of a Signal

Find and sketch the even and odd components of $x(t) = e^{-at}u(t)$.

Based on Eq. (1.17), we can express $x(t)$ as a sum of the even component $x_e(t)$ and the odd component $x_o(t)$ as

$$x(t) = x_e(t) + x_o(t)$$

where

$$x_e(t) = \tfrac{1}{2}[e^{-at}u(t) + e^{at}u(-t)] \qquad \text{and} \qquad x_o(t) = \tfrac{1}{2}[e^{-at}u(t) - e^{at}u(-t)]$$

The function $e^{-at}u(t)$ and its even and odd components are illustrated in Fig. 1.24.

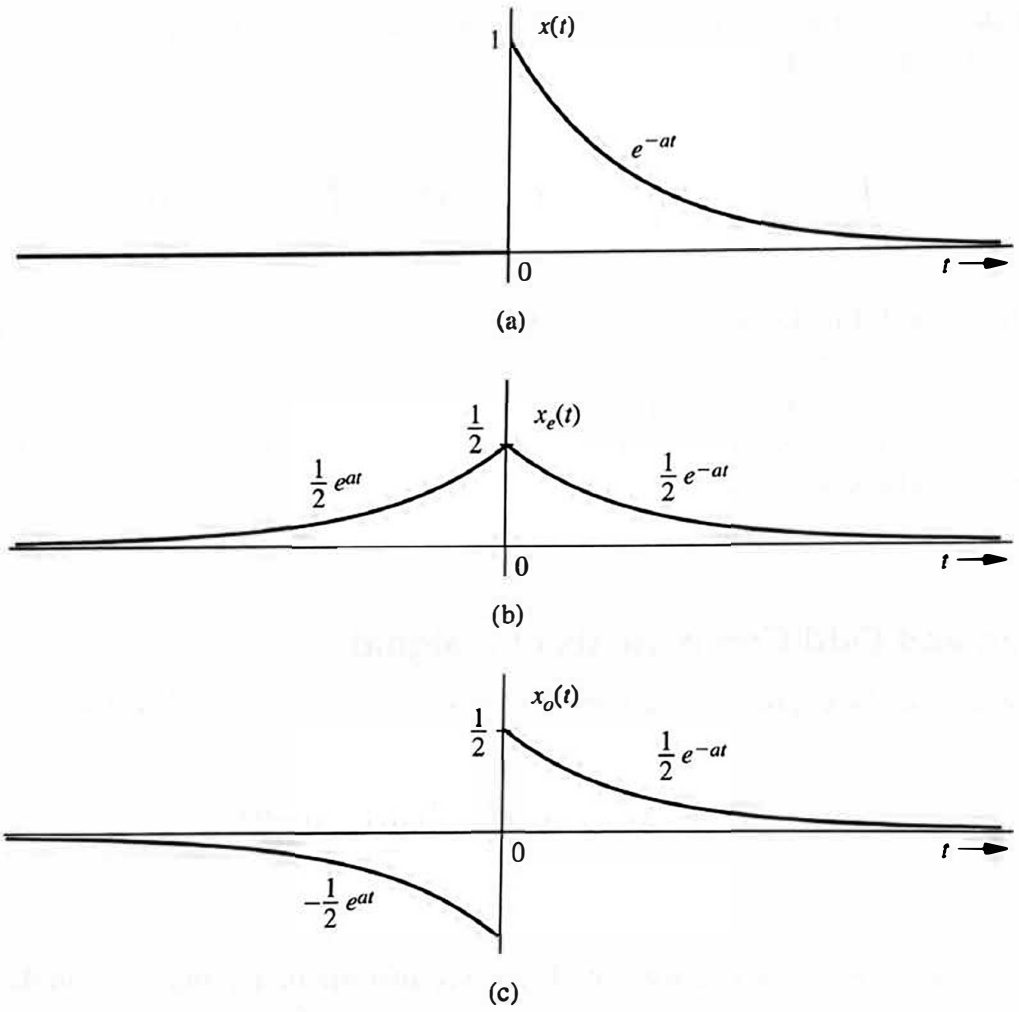

Figure 1.24 Finding even and odd components of a signal.

EXAMPLE 1.9 Finding the Even and Odd Components of a Complex Signal

Find the even and odd components of e^{jt}.

From Eq. (1.17),

$$e^{jt} = x_e(t) + x_o(t)$$

where

$$x_e(t) = \tfrac{1}{2}[e^{jt} + e^{-jt}] = \cos t \qquad \text{and} \qquad x_o(t) = \tfrac{1}{2}[e^{jt} - e^{-jt}] = j \sin t$$

A Modification for Complex Signals

While a complex signal can be decomposed into even and odd components, it is more common to decompose complex signals using conjugate symmetries. A complex signal $x(t)$ is said to be *conjugate-symmetric* if $x(t) = x^*(-t)$. A conjugate-symmetric signal is even in the real part and odd in the imaginary part. Thus, a real conjugate-symmetric signal is an even signal. A signal is *conjugate-antisymmetric* if $x(t) = -x^*(-t)$. A conjugate-antisymmetric signal is odd in the real part and even in the imaginary part. A real conjugate-antisymmetric signal is an odd signal. Any signal $x(t)$ can be decomposed into a conjugate-symmetric portion $x_{cs}(t)$ plus a conjugate-antisymmetric portion $x_{ca}(t)$. That is,

$$x(t) = x_{cs}(t) + x_{ca}(t)$$

where

$$x_{cs}(t) = \frac{x(t) + x^*(-t)}{2} \quad \text{and} \quad x_{ca}(t) = \frac{x(t) - x^*(-t)}{2}$$

The proof is similar to the one for decomposing a signal into even and odd components. As we shall see in later chapters, conjugate symmetries commonly occur in real-world signals and their transforms.

1.6 Systems

As mentioned in Sec. 1.1, systems are used to process signals to allow modification or extraction of additional information from the signals. A system may consist of physical components (hardware realization) or of an algorithm that computes the output signal from the input signal (software realization).

Roughly speaking, a physical system consists of interconnected components, which are characterized by their terminal (input–output) relationships. In addition, a system is governed by laws of interconnection. For example, in electrical systems, the terminal relationships are the familiar voltage-current relationships for the resistors, capacitors, inductors, transformers, transistors, and so on, as well as the laws of interconnection (i.e., Kirchhoff's laws). We use these laws to derive mathematical equations relating the outputs to the inputs. These equations then represent a *mathematical model* of the system.

A system can be conveniently illustrated by a "black box" with one set of accessible terminals where the input variables $x_1(t), x_2(t), \ldots, x_j(t)$ are applied and another set of accessible terminals where the output variables $y_1(t), y_2(t), \ldots, y_k(t)$ are observed (Fig. 1.25).

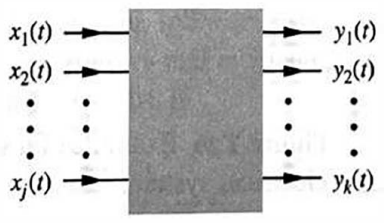

Figure 1.25 Representation of a system.

The study of systems consists of three major areas: mathematical modeling, analysis, and design. Although we shall be dealing with mathematical modeling, our main concern is with analysis and design. The major portion of this book is devoted to the analysis problem—how to determine the system outputs for the given inputs and a given mathematical model of the system (or rules governing the system). To a lesser extent, we will also consider the problem of design or synthesis—how to construct a system that will produce a desired set of outputs for the given inputs.

Data Needed to Compute System Response

To understand what data we need to compute a system response, consider a simple *RC* circuit with a current source $x(t)$ as its input (Fig. 1.26).

The output voltage $y(t)$ is given by

$$y(t) = Rx(t) + \frac{1}{C}\int_{-\infty}^{t} x(\tau)\,d\tau \tag{1.18}$$

The limits of the integral on the right-hand side are from $-\infty$ to t because this integral represents the capacitor charge due to the current $x(t)$ flowing in the capacitor, and this charge is the result of the current flowing in the capacitor from $-\infty$. Now, Eq. (1.18) can be expressed as

$$y(t) = Rx(t) + \frac{1}{C}\int_{-\infty}^{0} x(\tau)\,d\tau + \frac{1}{C}\int_{0}^{t} x(\tau)\,d\tau$$

The middle term on the right-hand side is $v_C(0)$, the capacitor voltage at $t = 0$. Therefore,

$$y(t) = v_C(0) + Rx(t) + \frac{1}{C}\int_{0}^{t} x(\tau)\,d\tau \qquad t \geq 0$$

This equation can be readily generalized as

$$y(t) = v_C(t_0) + Rx(t) + \frac{1}{C}\int_{t_0}^{t} x(\tau)\,d\tau \qquad t \geq t_0 \tag{1.19}$$

From Eq. (1.18), the output voltage $y(t)$ at an instant t can be computed if we know the input current flowing in the capacitor throughout its entire past ($-\infty$ to t). Alternatively, if we know the input current $x(t)$ from some moment t_0 onward, then, using Eq. (1.19), we can still calculate $y(t)$ for $t \geq t_0$ from a knowledge of the input current, provided we know $v_C(t_0)$, the initial capacitor

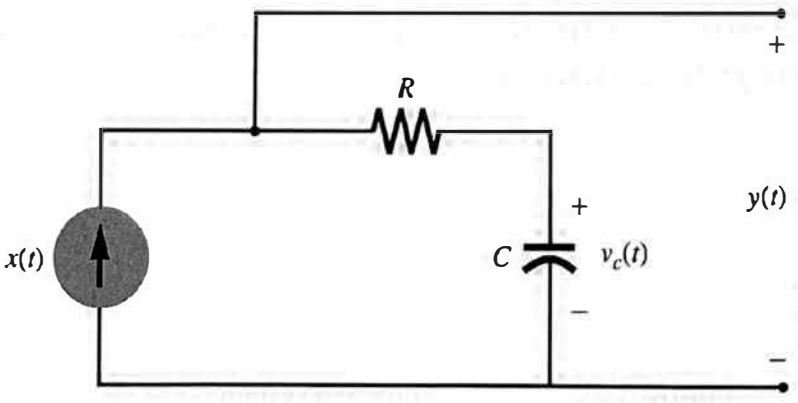

Figure 1.26 Example of a simple electrical system.

voltage (voltage at t_0). Thus, $v_C(t_0)$ contains all the relevant information about the circuit's entire past ($-\infty$ to t_0) that we need to compute $y(t)$ for $t \geq t_0$. Therefore, the response of a system at $t \geq t_0$ can be determined from its input(s) during the interval t_0 to t and from certain *initial conditions* at $t = t_0$.

In the preceding example, we needed only one initial condition. However, in more complex systems, several initial conditions may be necessary. We know, for example, that in passive *RLC* networks, the initial values of all inductor currents and all capacitor voltages[†] are needed to determine the outputs at any instant $t \geq 0$ if the inputs are given over the interval $[0, t]$.

1.7 Classification of Systems

Systems may be classified broadly in the following categories:

1. Linear and nonlinear systems
2. Constant-parameter and time-varying-parameter systems
3. Instantaneous (memoryless) and dynamic (with memory) systems
4. Causal and noncausal systems
5. Continuous-time and discrete-time systems
6. Analog and digital systems
7. Invertible and noninvertible systems
8. Stable and unstable systems

Other classifications, such as deterministic and probabilistic systems, are beyond the scope of this text and are not considered.

1.7.1 Linear and Nonlinear Systems

The Concept of Linearity

A system whose output is proportional to its input is an *example* of a linear system. But linearity implies more than this; it also implies the *additivity property*: that is, if several inputs are acting on a system, then the total effect on the system due to all these inputs can be determined by considering one input at a time while assuming all the other inputs to be zero. The total effect is then the sum of all the component effects. This property may be expressed as follows: for a linear system, if an input x_1 acting alone has an effect y_1, and if another input x_2, also acting alone, has an effect y_2, then, with both inputs acting on the system, the total effect will be $y_1 + y_2$. Thus, if

$$x_1 \longrightarrow y_1 \qquad \text{and} \qquad x_2 \longrightarrow y_2$$

then for all x_1 and x_2

$$x_1 + x_2 \longrightarrow y_1 + y_2 \tag{1.20}$$

In addition, a linear system must satisfy the *homogeneity* or scaling property, which states that for arbitrary real or imaginary number k, if an input is increased k-fold, the effect also increases k-fold. Thus, if

$$x \longrightarrow y$$

[†] Strictly speaking, this means independent inductor currents and capacitor voltages.

then for all real or imaginary k

$$kx \longrightarrow ky \tag{1.21}$$

Thus, linearity implies two properties: homogeneity (scaling) and additivity.† Both these properties can be combined into one property (*superposition*), which is expressed as follows: If

$$x_1 \longrightarrow y_1 \qquad \text{and} \qquad x_2 \longrightarrow y_2$$

then for all inputs x_1 and x_2 and all constants k_1 and k_2,

$$k_1x_1 + k_2x_2 \longrightarrow k_1y_1 + k_2y_2 \tag{1.22}$$

There is another useful way to view the linearity condition described in Eq. (1.22): the response of a linear system is unchanged whether the operations of summing and scaling precede the system (sum and scale act on inputs) or follow the system (sum and scale act on outputs). *Thus, linearity implies commutability between a system and the operations of summing and scaling.* It may appear that additivity implies homogeneity. Unfortunately, homogeneity does not always follow from additivity. Drill 1.11 demonstrates such a case.

DRILL 1.11 Additivity but Not Homogeneity

Show that a system with the input $x(t)$ and the output $y(t)$ related by $y(t) = \text{Re}\{x(t)\}$ satisfies the additivity property but violates the homogeneity property. Hence, such a system is not linear. [*Hint:* Show that Eq. (1.21) is not satisfied when k is complex.]

Response of a Linear System

For the sake of simplicity, we discuss only *single-input, single-output* (*SISO*) systems. But the discussion can be readily extended to *multiple-input, multiple-output* (*MIMO*) systems.

A system's output for $t \geq 0$ is the result of two independent causes: the initial conditions of the system (or the system state) at $t = 0$ and the input $x(t)$ for $t \geq 0$. If a system is to be linear, the output must be the sum of the two components resulting from these two causes: first, the *zero-input response* (ZIR) that results only from the initial conditions at $t = 0$ with the input $x(t) = 0$ for $t \geq 0$, and then the *zero-state response* (ZSR) that results only from the input $x(t)$ for $t \geq 0$ when the initial conditions (at $t = 0$) are assumed to be zero. When all the appropriate initial conditions are zero, the system is said to be in *zero state*. The system output is zero when the input is zero only if the system is in zero state.

In summary, a linear system response can be expressed as the sum of the zero-input and zero-state responses:

$$\text{total response} = \text{zero-input response} + \text{zero-state response}$$

† A linear system must also satisfy the additional condition of *smoothness*, where small changes in the system's inputs must result in small changes in its outputs [3].

This property of linear systems, which permits the separation of an output into components resulting from the initial conditions and from the input, is called the *decomposition property*. For the *RC* circuit of Fig. 1.26, the response $y(t)$ was found to be [see Eq. (1.19) with $t_0 = 0$]

$$y(t) = \underbrace{v_C(0)}_{\text{ZIR}} + \underbrace{Rx(t) + \frac{1}{C}\int_0^t x(\tau)\,d\tau}_{\text{ZSR}} \tag{1.23}$$

From Eq. (1.23), it is clear that if the input $x(t) = 0$ for $t \geq 0$, the output $y(t) = v_C(0)$. Hence $v_C(0)$ is the zero-input response of the response $y(t)$. Similarly, if the system state (the voltage v_C in this case) is zero at $t = 0$, the output is given by the second component on the right-hand side of Eq. (1.23). Clearly, this is the zero-state response of the response $y(t)$.

In addition to the decomposition property, linearity implies that both the zero-input and zero-state components must obey the principle of superposition with respect to each of their respective causes. For example, if we increase the initial condition k-fold, the zero-input response must also increase k-fold. Similarly, if we increase the input k-fold, the zero-state response must also increase k-fold. These facts can be readily verified from Eq. (1.23) for the *RC* circuit in Fig. 1.26. For instance, if we double the initial condition $v_C(0)$, the zero-input response doubles; if we double the input $x(t)$, the zero-state response doubles.

EXAMPLE 1.10 Linearity of Constant-Coefficient Linear Differential Equations

Show that the system described by the equation

$$\frac{dy(t)}{dt} + 3y(t) = x(t) \tag{1.24}$$

is linear.

Let the system response to the inputs $x_1(t)$ and $x_2(t)$ be $y_1(t)$ and $y_2(t)$, respectively. Then

$$\frac{dy_1(t)}{dt} + 3y_1(t) = x_1(t) \qquad \text{and} \qquad \frac{dy_2(t)}{dt} + 3y_2(t) = x_2(t)$$

Multiplying the first equation by k_1, the second by k_2, and adding them yield

$$\frac{d}{dt}[k_1y_1(t) + k_2y_2(t)] + 3[k_1y_1(t) + k_2y_2(t)] = k_1x_1(t) + k_2x_2(t)$$

But this equation is the system equation [Eq. (1.24)] with

$$x(t) = k_1x_1(t) + k_2x_2(t) \qquad \text{and} \qquad y(t) = k_1y_1(t) + k_2y_2(t)$$

Therefore, when the input is $k_1x_1(t) + k_2x_2(t)$, the system response is $k_1y_1(t) + k_2y_2(t)$. Consequently, the system is linear. Using this argument, we can readily generalize the result to

show that a system described by a differential equation of the form

$$a_0\frac{d^N y(t)}{dt^N}+a_1\frac{d^{N-1}y(t)}{dt^{N-1}}+\cdots+a_N y(t)=b_{N-M}\frac{d^M x(t)}{dt^M}+\cdots+b_{N-1}\frac{dx(t)}{dt}+b_N x(t) \quad (1.25)$$

is a linear system. The coefficients a_i and b_i in this equation can be constants or functions of time. Although here we proved only zero-state linearity, it can be shown that such systems are also zero-input linear and have the decomposition property.

DRILL 1.12 Linearity of a Differential Equation with Time-Varying Parameters

Show that the system described by the following equation is linear:

$$\frac{dy(t)}{dt}+t^2y(t)=(2t+3)x(t)$$

DRILL 1.13 A Nonlinear Differential Equation

Show that the system described by the following equation is nonlinear:

$$y(t)\frac{dy(t)}{dt}+3y(t)=x(t)$$

More Comments on Linear Systems

Almost all systems observed in practice become nonlinear when large enough signals are applied to them. However, it is possible to approximate most of the nonlinear systems by linear systems for small-signal analysis. The analysis of nonlinear systems is generally difficult. Nonlinearities can arise in so many ways that describing them with a common mathematical form is impossible. Not only is each system a category in itself, but even for a given system, changes in initial conditions or input amplitudes may change the nature of the problem. On the other hand, the superposition property of linear systems is a powerful unifying principle that allows for a general solution. The superposition property (linearity) greatly simplifies the analysis of linear systems. Because of the decomposition property, we can evaluate separately the two components of the output. The zero-input response can be computed by assuming the input to be zero, and the zero-state response can be computed by assuming zero initial conditions. Moreover, if we express an input $x(t)$ as a sum of simpler functions,

$$x(t)=a_1x_1(t)+a_2x_2(t)+\cdots+a_mx_m(t)$$

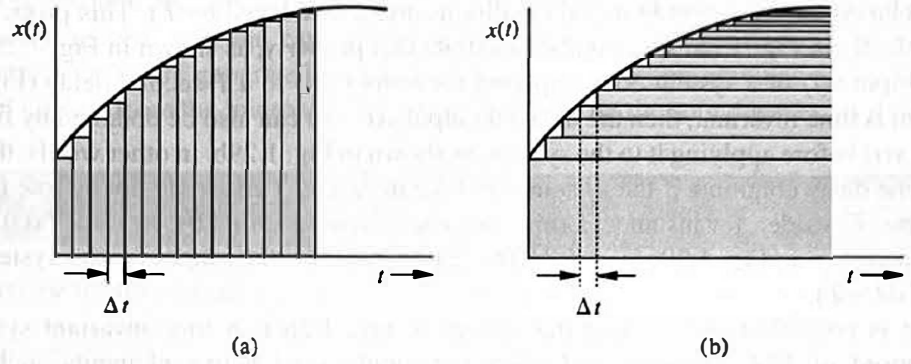

Figure 1.27 Signal representation in terms of impulse and step components.

then, by virtue of linearity, the response $y(t)$ is given by

$$y(t) = a_1 y_1(t) + a_2 y_2(t) + \cdots + a_m y_m(t)$$

where $y_k(t)$ is the zero-state response to an input $x_k(t)$. This apparently trivial observation has profound implications. As we shall see repeatedly in later chapters, it proves extremely useful and opens new avenues for analyzing linear systems.

For example, consider an arbitrary input $x(t)$ such as the one shown in Fig. 1.27a. We can approximate $x(t)$ with a sum of rectangular pulses of width Δt and of varying heights. The approximation improves as $\Delta t \to 0$, when the rectangular pulses become impulses spaced Δt seconds apart (with $\Delta t \to 0$).[†] Thus, an arbitrary input can be replaced by a weighted sum of impulses spaced Δt ($\Delta t \to 0$) seconds apart. Therefore, if we know the system response to a unit impulse, we can immediately determine the system response to an arbitrary input $x(t)$ by adding the system response to each impulse component of $x(t)$. A similar situation is depicted in Fig. 1.27b, where $x(t)$ is approximated by a sum of step functions of varying magnitude and spaced Δt seconds apart. The approximation improves as Δt becomes smaller. Therefore, if we know the system response to a unit step input, we can compute the system response to any arbitrary input $x(t)$ with relative ease. Time-domain analysis of linear systems (discussed in Ch. 2) uses this approach.

Chapters 3, 4, 6, and 11 employ the same approach but instead use sinusoids or exponentials as the basic signal components. We show that any arbitrary input signal can be expressed as a weighted sum of sinusoids (or exponentials) having various frequencies. Thus, a knowledge of the system response to a sinusoid enables us to determine the system response to an arbitrary input $x(t)$.

1.7.2 Time-Invariant and Time-Varying Systems

Systems whose parameters do not change with time are *time-invariant* (also *constant-parameter*) systems. For such a system, if the input is delayed by T seconds, the output is the same as before

[†] Here, the discussion of a rectangular pulse approaching an impulse at $\Delta t \to 0$ is somewhat imprecise. It is explained in Sec. 2.4 with more rigor.

but delayed by T (assuming initial conditions are also delayed by T). This property is expressed graphically in Fig. 1.28. We can also illustrate this property, as shown in Fig. 1.29. We can delay the output $y(t)$ of a system $\mathcal{S}$ by applying the output $y(t)$ to a T second delay (Fig. 1.29a). If the system is time invariant, then the delayed output $y(t-T)$ can also be obtained by first delaying the input $x(t)$ before applying it to the system, as shown in Fig. 1.29b. In other words, the system $\mathcal{S}$ and the time delay commute if the system $\mathcal{S}$ is time invariant. This would not be true for time-varying systems. Consider, for instance, a time-varying system specified by $y(t) = e^{-t}x(t)$. The output for such a system in Fig. 1.29a is $e^{-(t-T)}x(t-T)$. In contrast, the output for the system in Fig. 1.29b is $e^{-t}x(t-T)$.

It is possible to verify that the system in Fig. 1.26 is a time-invariant system. Networks composed of *RLC* elements and other commonly used active elements such as transistors are time-invariant systems. A system with an input–output relationship described by a linear differential equation of the form given in Ex. 1.10 [Eq. (1.25)] is a linear time-invariant (LTI) system when the coefficients a_i and b_i in the equation are constants. If these coefficients are functions of time, then the system is a linear *time-varying* system.

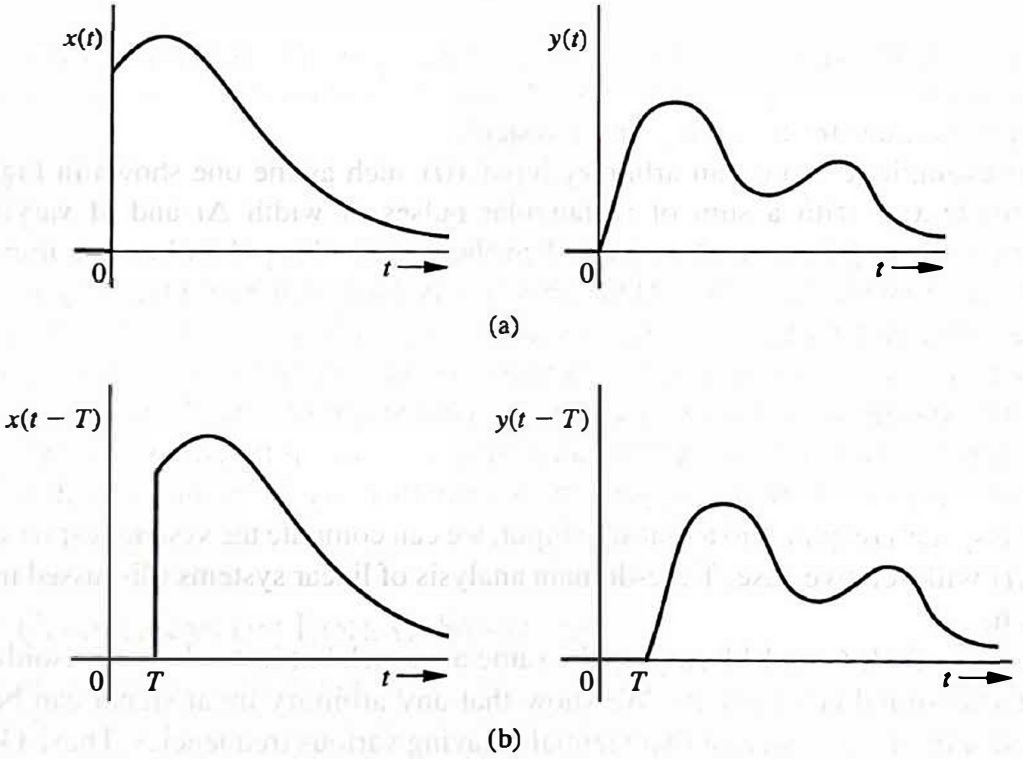

Figure 1.28 Time-invariance property.

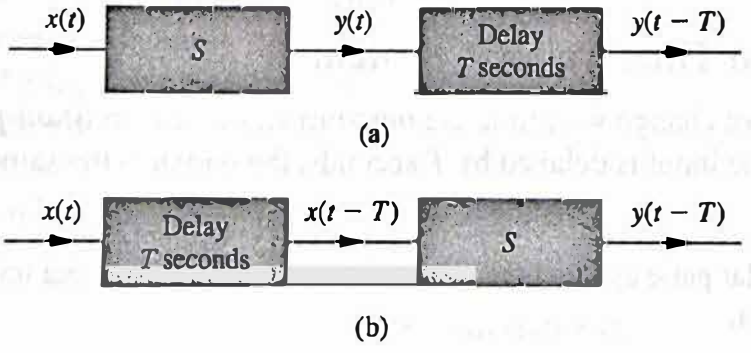

Figure 1.29 Illustration of time-invariance property.

The system described in Drill 1.12 is linear time varying. Another familiar example of a time-varying system is the carbon microphone, in which the resistance R is a function of the mechanical pressure generated by sound waves on the carbon granules of the microphone. The output current from the microphone is thus modulated by the sound waves, as desired.

EXAMPLE 1.11 Assessing System Time Invariance

Determine the time invariance of the following systems: **(a)** $y(t) = x(t)u(t)$ and **(b)** $y(t) = \frac{d}{dt}x(t)$.

(a) In this case, the output equals the input for $t \geq 0$ and is otherwise zero. Clearly, the input is being modified by a time-dependent function, so the system is likely time variant. We can prove that the system is not time invariant through a counterexample. Letting $x_1(t) = \delta(t+1)$, we see that $y_1(t) = 0$. However, $x_2(t) = x_1(t-2) = \delta(t-1)$ produces an output of $y_2(t) = \delta(t-1)$, which does not equal $y_1(t-2) = 0$ as time invariance would require. Thus, $y(t) = x(t)u(t)$ is a time-variant system.

(b) Although it appears that $x(t)$ is being modified by a time-dependent function, this is not the case. The output of this system is simply the slope of the input. If the input is delayed, so too is the output. Applying input $x(t)$ to the system produces output $y(t) = \frac{d}{dt}x(t)$; delaying this output by T produces $y(t-T) = \frac{d}{d(t-T)}x(t-T) = \frac{d}{dt}x(t-T)$. This is just the output of the system to a delayed input $x(t-T)$. Since the T-delayed output of the system to input $x(t)$ equals the output of the system to the T-delayed input $x(t-T)$, the system is time invariant.

DRILL 1.14 A Time-Variant System

Show that a system described by the following equation is a time-varying-parameter system:

$$y(t) = (\sin t)x(t-2)$$

[*Hint:* Show that the system fails to satisfy the time-invariance property.]

1.7.3 Instantaneous and Dynamic Systems

As observed earlier, a system's output at any instant t generally depends on the entire past input. However, in a special class of systems, the output at any instant t depends only on its input at that instant. In resistive networks, for example, any output of the network at some instant t depends only on the input at the instant t. In these systems, past history is irrelevant in determining the response. Such systems are said to be *instantaneous* or *memoryless* systems. More precisely, a system is said to be instantaneous (or memoryless) if its output at any instant t depends, at most, on the strength of its input(s) at the same instant t, and not on any past or future values of the

input(s). Otherwise, the system is said to be *dynamic* (or a system with memory). A system whose response at t is completely determined by the input signals over the past T seconds [interval from $(t-T)$ to t] is a *finite-memory system* with a memory of T seconds. Networks containing inductive and capacitive elements generally have infinite memory because the response of such networks at any instant t is determined by their inputs over the entire past $(-\infty, t)$. This is true for the RC circuit of Fig. 1.26.

EXAMPLE 1.12 Assessing System Memory

Determine whether the following systems are memoryless: **(a)** $y(t-1) = 2x(t-1)$, **(b)** $y(t) = \frac{d}{dt}x(t)$, and **(c)** $y(t) = (t-1)x(t)$.

(a) In this case, the output at time $t-1$ is just twice the input at the same time $t-1$. Since the output at a particular time depends only on the strength of the input at the same time, the system is memoryless.

(b) Although it appears that the output $y(t)$ at time t depends on the input $x(t)$ at the same time t, we know that the slope (derivative) of $x(t)$ cannot be determined solely from a single point. There must be some memory, even if infinitesimally small, involved. This is confirmed by using the fundamental theorem of calculus to express the system as

$$y(t) = \lim_{T \to 0} \frac{x(t) - x(t-T)}{T}$$

Since the output at a particular time depends on more than just the input at the same time, the system is not memoryless.

(c) The output $y(t)$ at time t is just the input $x(t)$ at the same time t multiplied by the (time-dependent) coefficient $t-1$. Since the output at a particular time depends only on the strength of the input at the same time, the system is memoryless.

1.7.4 Causal and Noncausal Systems

A *causal* (also known as a *physical* or *nonanticipative*) system is one for which the output at any instant t_0 depends only on the value of the input $x(t)$ for $t \leq t_0$. In other words, the value of the output at the present instant depends only on the past and present values of the input $x(t)$, not on its future values. To put it simply, in a causal system the output cannot start before the input is applied. If the response starts before the input, it means that the system knows the input in the future and acts on this knowledge before the input is applied. A system that violates the condition of causality is called a *noncausal* (or *anticipative*) system.

Any practical system that operates in real time[†] must necessarily be causal. We do not yet know how to build a system that can respond to future inputs (inputs not yet applied). A noncausal

---

[†] In real-time operations, the response to an input is essentially simultaneous (contemporaneous) with the input itself.

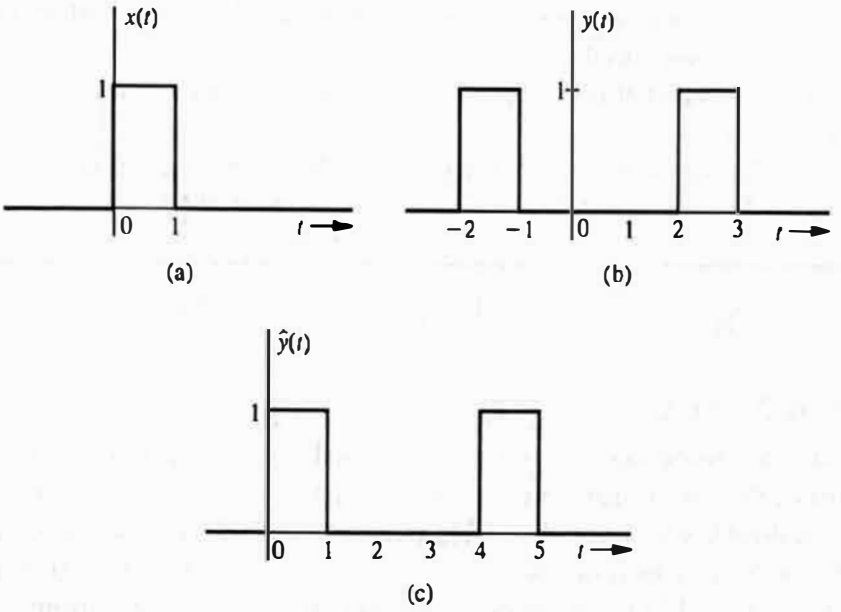

Figure 1.30 Input–output of a noncausal system and the causal output achieved by delay.

system is a prophetic system that knows the future input and acts on it in the present. Thus, if we apply an input starting at $t = 0$ to a noncausal system, the output would begin even before $t = 0$. For example, consider the system specified by

$$y(t) = x(t-2) + x(t+2) \tag{1.26}$$

For the input $x(t)$ illustrated in Fig. 1.30a, the output $y(t)$, as computed from Eq. (1.26) (shown in Fig. 1.30b), starts even before the input is applied. Equation (1.26) shows that $y(t)$, the output at t, is given by the sum of the input values 2 seconds before and 2 seconds after t (at $t-2$ and $t+2$, respectively). But if we are operating the system in real time at t, we do not know what the value of the input will be 2 seconds later. Thus, it is impossible to implement this system in real time. For this reason, noncausal systems are unrealizable in *real time*.

EXAMPLE 1.13 Assessing System Causality

Determine whether the following systems are causal: **(a)** $y(t) = x(-t)$, **(b)** $y(t) = x(t+1)$, and **(c)** $y(t+1) = x(t)$.

(a) Here, the output is a reflection of the input. We can easily use a counterexample to disprove the causality of this system. The input $x(t) = \delta(t-1)$, which is nonzero at $t = 1$, produces an

output $y(t) = \delta(t + 1)$, which is nonzero at $t = -1$, a time 2 seconds earlier than the input! Clearly, the system is not causal.
(b) In this case, the output at time t depends on the input at future time of $t + 1$. Clearly, the system is not causal.
(c) In this case, the output at time $t + 1$ depends on the input 1 second in the past, at time t. Since the output does not depend on future values of the input, the system is causal.

Why Study Noncausal Systems?

The foregoing discussion may suggest that noncausal systems have no practical purpose. This is not the case; they are valuable in the study of systems for several reasons. First, noncausal systems *are* realizable when the independent variable is other than "time" (e.g., *space*). Consider, for example, an electric charge of density $q(x)$ placed along the x axis for $x \geq 0$. This charge density produces an electric field $E(x)$ that is present at every point on the x axis from $x = -\infty$ to ∞. In this case, the input [i.e., the charge density $q(x)$] starts at $x = 0$, but its output [the electric field $E(x)$] begins before $x = 0$. Clearly, this space-charge system is noncausal. This discussion shows that only temporal systems (systems with time as an independent variable) must be causal to be realizable. The terms "before" and "after" have a special connection to causality only when the independent variable is time. This connection is lost for variables other than time. Nontemporal systems, such as those occurring in optics, can be noncausal and still realizable.

Moreover, even for temporal systems, such as those used for signal processing, the study of noncausal systems is important. In such systems, we may have all input data prerecorded. This often happens with speech, geophysical, and meteorological signals, and with space probes. In such cases, the input's future values are available to us. For example, suppose we had a set of input signal records available for the system described by Eq. (1.26). We can then compute $y(t)$ since, for any t, we need only refer to the records to find the input's value 2 seconds before and 2 seconds after t. Thus, noncausal systems can be realized, although not in real time. We may therefore be able to realize a noncausal system, provided we are willing to accept a time delay in the output. Consider a system whose output $\hat{y}(t)$ is the same as $y(t)$ in Eq. (1.26) delayed by 2 seconds (Fig. 1.30c) so that

$$\hat{y}(t) = y(t - 2) = x(t - 4) + x(t)$$

Here, the value of the output $\hat{y}$ at any instant t is the sum of the values of the input x at t and at the instant 4 seconds earlier [at $(t - 4)$]. In this case, the output at any instant t does not depend on future values of the input, and the system is causal. The output of this system, which is $\hat{y}(t)$, is identical to that in Eq. (1.26) or Fig. 1.30b except for a delay of 2 seconds. Thus, a noncausal system may be realized or satisfactorily approximated in real time by using a causal system with a delay.

A third reason for studying noncausal systems is that they provide an upper bound on the performance of causal systems. For example, if we wish to design a filter for separating a signal from noise, then the optimum filter is invariably a noncausal system. Although unrealizable, this

Noncausal systems are realizable with time delay!

noncausal system's performance acts as the upper limit on what can be achieved and gives us a standard for evaluating the performance of causal filters.

At first glance, noncausal systems may seem to be inscrutable. Actually, there is nothing mysterious about these systems and their approximate realization through physical systems with delay. If we want to know what will happen one year from now, we have two choices: go to a prophet (an unrealizable person) who can give the answers instantly, or go to a wise man and allow him a delay of one year to give us the answer! If the wise man is truly wise, he may even be able, by studying trends, to shrewdly guess the future very closely with a delay of less than a year. Such is the case with noncausal systems—nothing more and nothing less.

DRILL 1.15 A Noncausal System

Show that a system described by the following equation is noncausal:

$$y(t) = \int_{t-5}^{t+5} x(\tau)\,d\tau$$

Show that this system can be realized physically if we accept a delay of 5 seconds in the output.

1.7.5 Continuous-Time and Discrete-Time Systems

Signals defined or specified over a continuous range of time are *continuous-time signals*, denoted by symbols $x(t)$, $y(t)$, and so on. Systems whose inputs and outputs are continuous-time signals are *continuous-time systems*. On the other hand, signals defined only at discrete instants of time $t_0, t_1, t_2, \ldots, t_n, \ldots$ are *discrete-time signals*, denoted by the symbols $x(t_n)$, $y(t_n)$, and so on, where n is some integer. Systems whose inputs and outputs are discrete-time signals are *discrete-time systems*. A digital computer is a familiar example of this type of system. In practice, discrete-time signals can arise from sampling continuous-time signals. For example, when the sampling is

uniform, the discrete instants $t_0, t_1, t_2, \ldots$ are uniformly spaced so that

$$t_{k+1} - t_k = T \qquad \text{for all } k$$

In such cases, the discrete-time signals represented by the samples of continuous-time signals $x(t), y(t)$, and so on can be expressed as $x(nT)$, $y(nT)$, and so on; for convenience, we further simplify this notation to $x[n]$, $y[n]$, . . ., where it is understood that $x[n] = x(nT)$ and that n is some integer. A typical discrete-time signal is shown in Fig. 1.31. A discrete-time signal may also be viewed as a sequence of numbers . . ., $x[-1]$, $x[0]$, $x[1]$, $x[2]$, ... Thus, a discrete-time system may be seen as processing a sequence of numbers $x[n]$ and yielding as an output another sequence of numbers $y[n]$.

Discrete-time signals arise naturally in situations that are inherently discrete time, such as population studies, amortization problems, national income models, and radar tracking. They may also arise as a result of sampling continuous-time signals in sampled data systems, digital filtering, and the like. Digital filtering is a particularly interesting application in which continuous-time signals are processed by using discrete-time systems, as shown in Fig. 1.32. A continuous-time signal $x(t)$ is first sampled to convert it into a discrete-time signal $x[n]$, which then is processed by the discrete-time system to yield a discrete-time output $y[n]$. A continuous-time signal $y(t)$ is finally constructed from $y[n]$. In this manner, we can process a continuous-time signal with an appropriate discrete-time system such as a digital computer. Because discrete-time systems have several significant advantages over continuous-time systems, there is an accelerating trend toward processing continuous-time signals with discrete-time systems.

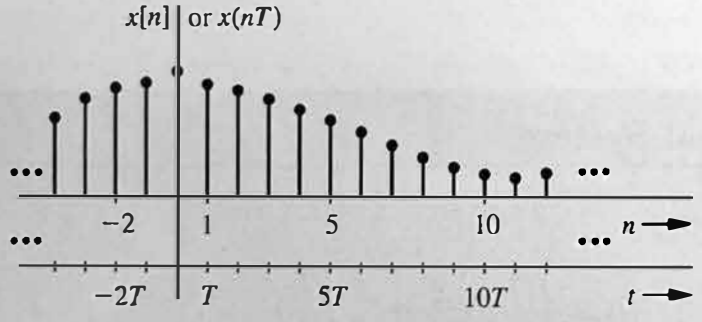

Figure 1.31 A discrete-time signal.

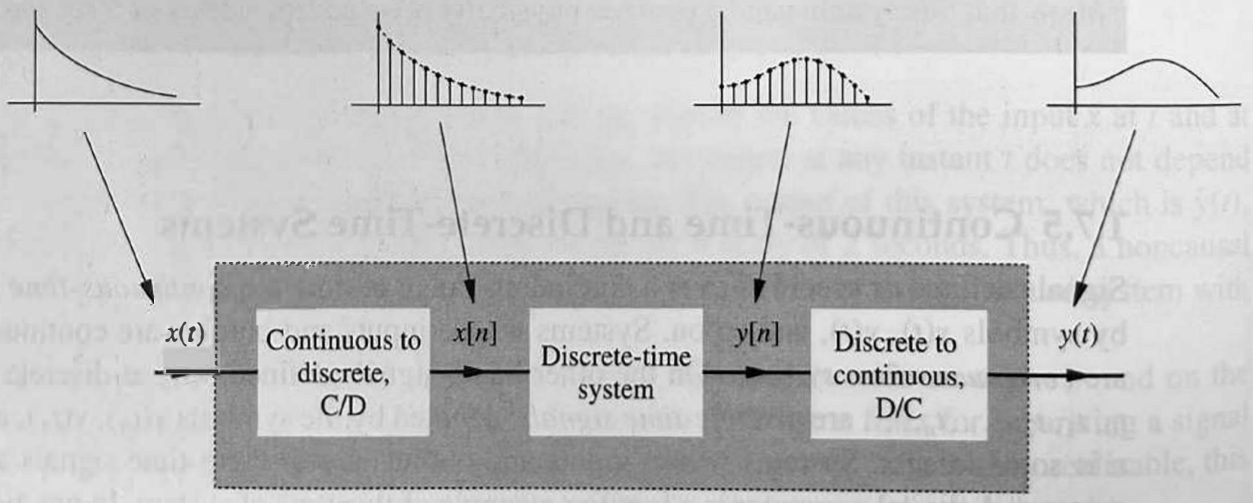

Figure 1.32 Processing continuous-time signals by discrete-time systems.

1.7.6 Analog and Digital Systems

Analog and digital signals are discussed in Sec. 1.3.2. A system whose input and output signals are analog is an *analog system*; a system whose input and output signals are digital is a *digital system*. A digital computer is an example of a digital (binary) system. Observe that a digital computer is a digital as well as a discrete-time system.

1.7.7 Invertible and Noninvertible Systems

A system $\mathcal{S}$ performs certain operation(s) on input signal(s). If we can obtain the input $x(t)$ back from the corresponding output $y(t)$ by some operation, the system $\mathcal{S}$ is said to be *invertible*. When several different inputs result in the same output (as in a rectifier), it is impossible to obtain the input from the output, and the system is *noninvertible*. Therefore, for an invertible system, it is essential that every input have a unique output so that there is a one-to-one mapping between an input and the corresponding output. The system that achieves the inverse operation [of obtaining $x(t)$ from $y(t)$] is the *inverse system* for $\mathcal{S}$. For instance, if $\mathcal{S}$ is an ideal integrator, then its inverse system is an ideal differentiator. Consider a system $\mathcal{S}$ connected in tandem with its inverse $\mathcal{S}_i$, as shown in Fig. 1.33. The input $x(t)$ to this tandem system results in signal $y(t)$ at the output of $\mathcal{S}$, and the signal $y(t)$, which now acts as an input to $\mathcal{S}_i$, yields back the signal $x(t)$ at the output of $\mathcal{S}_i$. Thus, $\mathcal{S}_i$ undoes the operation of $\mathcal{S}$ on $x(t)$, yielding back $x(t)$. A system whose output is equal to the input (for all possible inputs) is an *identity* system. Cascading a system with its inverse system, as shown in Fig. 1.33, results in an identity system.

In contrast, a rectifier, specified by an equation $y(t) = |x(t)|$, is noninvertible because the rectification operation cannot be undone.

Inverse systems are very important in signal processing. In many applications, the signals are distorted during the processing, and it is necessary to undo the distortion. For instance, in transmission of data over a communication channel, the signals are distorted owing to non-ideal frequency response and finite bandwidth of a channel. It is necessary to restore the signal as closely as possible to its original shape. Such equalization is also used in audio systems and photographic systems.

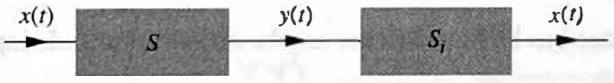

Figure 1.33 A cascade of a system with its inverse results in an identity system.

EXAMPLE 1.14 Assessing System Invertibility

Determine whether the following systems are invertible: **(a)** $y(t) = x(-t)$, **(b)** $y(t) = tx(t)$, and **(c)** $y(t) = \frac{d}{dt}x(t)$.

(a) Here, the output is a reflection of the input, which does not cause any loss to the input. The input can, in fact, be exactly recovered by simply reflecting the output $[x(t) = y(-t)]$, which is to say that a reflecting system is its own inverse. Thus, $y(t) = x(-t)$ is an invertible system.

(b) In this case, one might be tempted to recover the input from the output as $x(t) = \frac{1}{t}y(t)$. This approach works almost everywhere, except at $t = 0$ where the input value $x(0)$ cannot be recovered. Due to this single lost point, the system $y(t) = tx(t)$ is not invertible.

(c) Differentiation eliminates any dc component. For example, the inputs $x_1(t) = 1$ and $x_2(t) = 2$ both produce the same output $y(t) = 0$. Given only $y(t) = 0$, it is impossible to know if the original input was $x_1(t) = 1$, $x_2(t) = 2$, or something else entirely. Since unique inputs do produce unique outputs, we know that $y(t) = \frac{d}{dt}x(t)$ is not an invertible system.

1.7.8 Stable and Unstable Systems

Systems can also be classified as *stable* or *unstable* systems. Stability can be *internal* or *external*. If every *bounded input* applied at the input terminal results in a *bounded output*, the system is said to be stable *externally*. External stability can be ascertained by measurements at the external terminals (input and output) of the system. This type of stability is also known as the stability in the BIBO (bounded-input/bounded-output) sense. The concept of internal stability is postponed to Ch. 2 because it requires some understanding of internal system behavior, introduced in that chapter.

EXAMPLE 1.15 Assessing System BIBO Stability

Determine whether the following systems are BIBO-stable: **(a)** $y(t) = x^2(t)$, **(b)** $y(t) = tx(t)$, and **(c)** $y(t) = \frac{d}{dt}x(t)$.

(a) This system squares an input to produce the output. If the input is bounded, which is to say that $|x(t)| \leq M_x < \infty$ for all t, then we see that

$$|y(t)| = |x^2(t)| = |x(t)|^2 \leq M_x^2 < \infty$$

Since the output amplitude is guaranteed to be bounded for any bounded-amplitude input, the system $y(t) = x^2(t)$ is BIBO-stable.

(b) We can prove that $y(t) = tx(t)$ is not BIBO-stable with a simple example. The bounded-amplitude input $x(t) = u(t)$ produces the output $y(t) = tu(t)$ whose amplitude grows to infinity as $t \to \infty$. Thus, $y(t) = tx(t)$ is a BIBO-unstable system.

(c) We can prove that $y(t) = \frac{d}{dt}x(t)$ is not BIBO-stable with an example. The bounded-amplitude input $x(t) = u(t)$ produces the output $y(t) = \delta(t)$ whose amplitude is infinite at $t = 0$. Thus, $y(t) = \frac{d}{dt}x(t)$ is a BIBO-unstable system.

DRILL 1.16 A Noninvertible BIBO-Stable System

Show that a system described by the equation $y(t) = x^2(t)$ is noninvertible but BIBO-stable.

1.8 System Model: Input–Output Description

A system description in terms of the measurements at the input and output terminals is called the *input–output description*. As mentioned earlier, systems theory encompasses a variety of systems, such as electrical, mechanical, hydraulic, acoustic, electromechanical, and chemical, as well as social, political, economic, and biological. The first step in analyzing any system is the construction of a system model, which is a mathematical expression or a rule that satisfactorily approximates the dynamical behavior of the system. In this chapter, we shall consider only continuous-time systems. Modeling of discrete-time systems is discussed in Ch. 9.

1.8.1 Electrical Systems

To construct a system model, we must study the relationships between different variables in the system. In electrical systems, for example, we must determine a satisfactory model for the voltage-current relationship of each element, such as Ohm's law for a resistor. In addition, we must determine the various constraints on voltages and currents when several electrical elements are interconnected. These are the laws of interconnection—the well-known Kirchhoff laws for voltage and current (KVL and KCL). From all these equations, we eliminate unwanted variables to obtain equation(s) relating the desired output variable(s) to the input(s). The following examples demonstrate the procedure of deriving input–output relationships for some LTI electrical systems.

EXAMPLE 1.16 Input–Output Equation of a Series *RLC* Circuit

For the series *RLC* circuit of Fig. 1.34, find the input–output equation relating the input voltage $x(t)$ to the output current (loop current) $y(t)$.

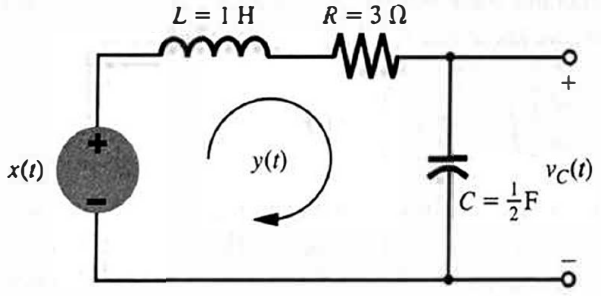

Figure 1.34 Circuit for Ex. 1.16.

Application of Kirchhoff's voltage law around the loop yields

$$v_L(t) + v_R(t) + v_C(t) = x(t)$$

By using the voltage-current laws of each element (inductor, resistor, and capacitor), we can express this equation as

$$\frac{dy(t)}{dt} + 3y(t) + 2\int_{-\infty}^{t} y(\tau)\,d\tau = x(t) \tag{1.27}$$

Differentiating both sides of this equation, we obtain

$$\frac{d^2y(t)}{dt^2} + 3\frac{dy(t)}{dt} + 2y(t) = \frac{dx(t)}{dt} \tag{1.28}$$

This differential equation is the input--output relationship between the output $y(t)$ and the input $x(t)$.

It proves convenient to use a compact notation D for the differential operator d/dt. This notation can be repeatedly applied. Thus,

$$\frac{dy(t)}{dt} \equiv Dy(t), \qquad \frac{d^2y(t)}{dt^2} \equiv D^2y(t), \qquad \ldots, \qquad \frac{d^Ny(t)}{dt^N} \equiv D^Ny(t)$$

With this notation, Eq. (1.28) can be expressed as

$$(D^2 + 3D + 2)y(t) = Dx(t) \tag{1.29}$$

The differential operator is the inverse of the integral operator, so we can use the operator $1/D$ to represent integration.[†]

$$\int_{-\infty}^{t} y(\tau)\,d\tau \equiv \frac{1}{D}y(t)$$

[†] Use of operator $1/D$ for integration generates some subtle mathematical difficulties because the operators D and $1/D$ do not commute. For instance, we know that $D(1/D) = 1$ because

$$\frac{d}{dt}\left[\int_{-\infty}^{t} y(\tau)\,d\tau\right] = y(t)$$

However, $(1/D)D$ is not necessarily unity. Use of Cramer's rule in solving simultaneous integro-differential equations will always result in cancellation of operators $1/D$ and D. This procedure may yield erroneous results when the factor D occurs in the numerator as well as in the denominator. This happens, for instance, in circuits with all-inductor loops or all-capacitor cut sets. To eliminate this problem, avoid the integral operation in system equations so that the resulting equations are differential rather than integro-differential. In electrical circuits, this can be done by using charge (instead of current) variables in loops containing capacitors and choosing current variables for loops without capacitors. In the literature, this problem of commutativity of D and $1/D$ is largely ignored. As mentioned earlier, such a procedure gives erroneous results only in special systems, such as the circuits with all-inductor loops or all-capacitor cut sets. Fortunately, such systems constitute a very small fraction of the systems we deal with. For further discussion of this topic and a correct method of handling problems involving integrals, see [4].

Consequently, Eq. (1.27) can be expressed as

$$\left(D+3+\frac{2}{D}\right)y(t)=x(t)$$

Multiplying both sides by D to differentiate the expression, we obtain

$$(D^2+3D+2)y(t)=Dx(t)$$

which is identical to Eq. (1.29).

Recall that Eq. (1.29) is not an algebraic equation, and D^2+3D+2 is not an algebraic term that multiplies $y(t)$; it is an operator that operates on $y(t)$. It means that we must perform the following operations on $y(t)$: take the second derivative of $y(t)$ and add to it 3 times the first derivative of $y(t)$ and 2 times $y(t)$. Clearly, a polynomial in D multiplied by $y(t)$ represents a certain differential operation on $y(t)$.

EXAMPLE 1.17 Input–Output Equation of a Series *RC* Circuit

Using operator notation, find the equation relating input to output for the series *RC* circuit of Fig. 1.35 if the input is the voltage $x(t)$ and output is

(a) the loop current $i(t)$

(b) the capacitor voltage $y(t)$

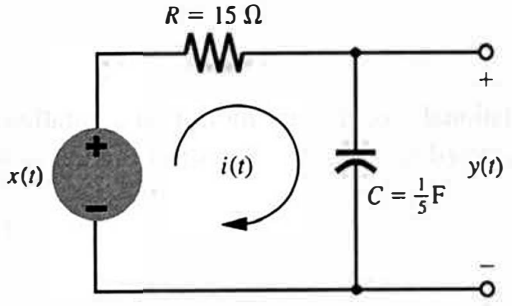

Figure 1.35 Circuit for Ex. 1.17.

(a) The loop equation for the circuit is

$$Ri(t)+\frac{1}{C}\int_{-\infty}^{t} i(\tau)\,d\tau=x(t)$$

or

$$15\,i(t)+5\int_{-\infty}^{t} i(\tau)\,d\tau=x(t)$$

With operator notation, this equation can be expressed as

$$15\,i(t)+\frac{5}{D}i(t)=x(t) \tag{1.30}$$

(b) Multiplying both sides of Eq. (1.30) by D (i.e., differentiating the equation), we obtain

$$(15D+5)\,i(t) = Dx(t)$$

Using the fact that $i(t) = C\frac{dy(t)}{dt} = \frac{1}{5}Dy(t)$, simple substitution yields

$$(3D+1)y(t) = x(t) \tag{1.31}$$

DRILL 1.17 Input–Output Equation of a Series *RLC* Circuit with Inductor Voltage as Output

If the inductor voltage $v_L(t)$ is taken as the output, show that the *RLC* circuit in Fig. 1.34 has an input–output equation of $(D^2+3D+2)v_L(t) = D^2x(t)$.

DRILL 1.18 Input–Output Equation of a Series *RC* Circuit with Capacitor Voltage as Output

If the capacitor voltage $v_C(t)$ is taken as the output, show that the *RLC* circuit in Fig. 1.34 has an input–output equation of $(D^2+3D+2)v_C(t) = 2x(t)$.

1.8.2 Mechanical Systems

Planar motion can be resolved into translational (rectilinear) motion and rotational (torsional) motion. Translational motion will be considered first. We shall restrict ourselves to motions in one dimension.

Translational Systems

The basic elements used in modeling translational systems are ideal masses, linear springs, and dashpots providing viscous damping. The laws of various mechanical elements are now discussed.

For a *mass* M (Fig. 1.36a), a force $x(t)$ causes a motion $y(t)$ and acceleration $\ddot{y}(t)$. From Newton's law of motion,

$$x(t) = M\ddot{y}(t) = M\frac{d^2y(t)}{dt^2} = MD^2y(t)$$

The force $x(t)$ required to stretch (or compress) a *linear spring* (Fig. 1.36b) by an amount $y(t)$ is given by

$$x(t) = Ky(t)$$

where K is the *stiffness* of the spring.

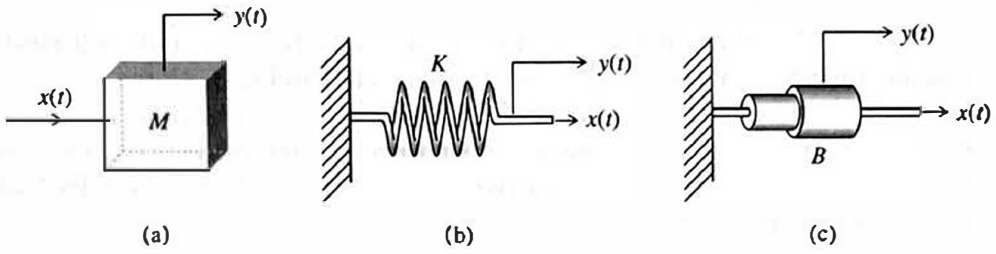

Figure 1.36 Some elements in translational mechanical systems.

For *a linear dashpot* (Fig. 1.36c), which operates by virtue of viscous friction, the force moving the dashpot is proportional to the relative velocity $\dot{y}(t)$ of one surface with respect to the other. Thus,

$$x(t) = B\dot{y}(t) = B\frac{dy(t)}{dt} = BDy(t)$$

where B is the *damping coefficient* of the dashpot or the viscous friction.

EXAMPLE 1.18 Input–Output Equation for a Translational Mechanical System

Find the input–output relationship for the translational mechanical system shown in Fig. 1.37a or its equivalent in Fig. 1.37b. The input is the force $x(t)$, and the output is the mass position $y(t)$.

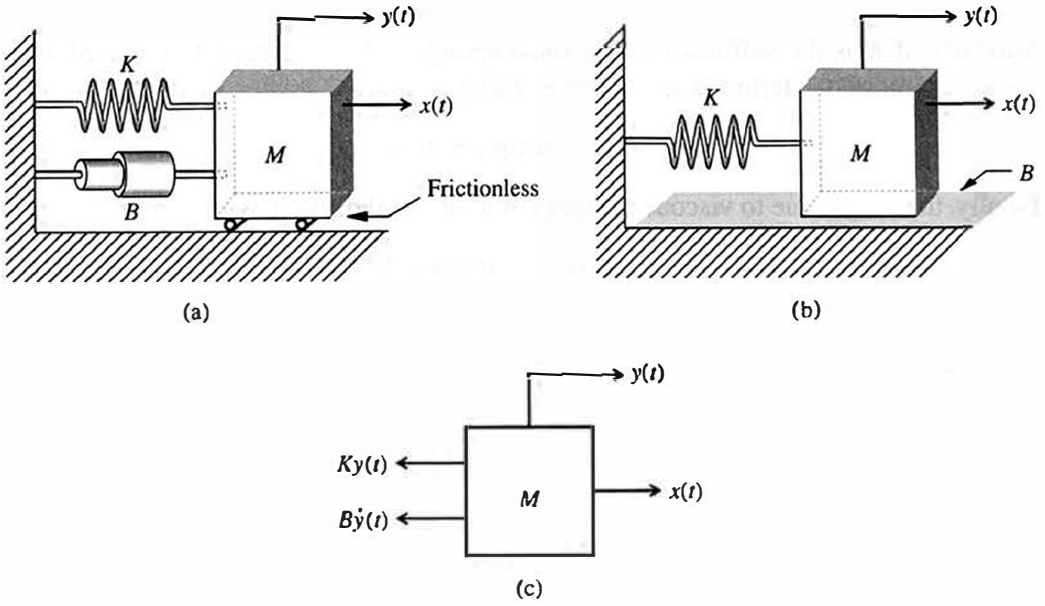

Figure 1.37 Mechanical system for Ex. 1.18.

In mechanical systems, it is helpful to draw a free-body diagram of each junction, which is a point at which two or more elements are connected. In Fig. 1.37, the point representing the mass is a junction. The displacement of the mass is denoted by $y(t)$. The spring is also stretched by the amount $y(t)$, and therefore it exerts a force $-Ky(t)$ on the mass. The dashpot exerts a force $-B\dot{y}(t)$ on the mass, as shown in the free-body diagram (Fig. 1.37c). By Newton's second law, the net force must be $M\ddot{y}(t)$. Therefore,

$$M\ddot{y}(t) = -B\dot{y}(t) - Ky(t) + x(t)$$

or

$$(MD^2 + BD + K)y(t) = x(t)$$

Rotational Systems

In rotational systems, the motion of a body may be defined as its motion about a certain axis. The variables used to describe rotational motion are torque (in place of force), angular position (in place of linear position), angular velocity (in place of linear velocity), and angular acceleration (in place of linear acceleration). The system elements are *rotational mass* or *moment of inertia* (in place of mass) and *torsional springs* and *torsional dashpots* (in place of linear springs and dashpots). The terminal equations for these elements are analogous to the corresponding equations for translational elements. If J is the moment of inertia (or rotational mass) of a rotating body about a certain axis, then the external torque required for this motion is equal to J (rotational mass) times the angular acceleration. If $\theta(t)$ is the angular position of the body, $\ddot{\theta}(t)$ is its angular acceleration, and

$$\text{torque} = J\ddot{\theta}(t) = J\frac{d^2\theta(t)}{dt^2} = JD^2\theta(t)$$

Similarly, if K is the stiffness of a torsional spring (per unit angular twist), and θ is the angular displacement of one terminal of the spring with respect to the other, then

$$\text{torque} = K\theta(t)$$

Finally, the torque due to viscous damping of a torsional dashpot with damping coefficient B is

$$\text{torque} = B\dot{\theta}(t) = BD\theta(t)$$

EXAMPLE 1.19 Input–Output Equation for Aircraft Roll Angle

The attitude of an aircraft can be controlled by three sets of surfaces (shown shaded in Fig. 1.38): elevators, rudder, and ailerons. By manipulating these surfaces, one can set the aircraft on a desired flight path. The roll angle $\varphi(t)$ can be controlled by deflecting in the opposite direction the two aileron surfaces as shown in Fig. 1.38. Assuming only rolling motion, find the equation relating the roll angle $\varphi(t)$ to the input (deflection) $\theta(t)$.

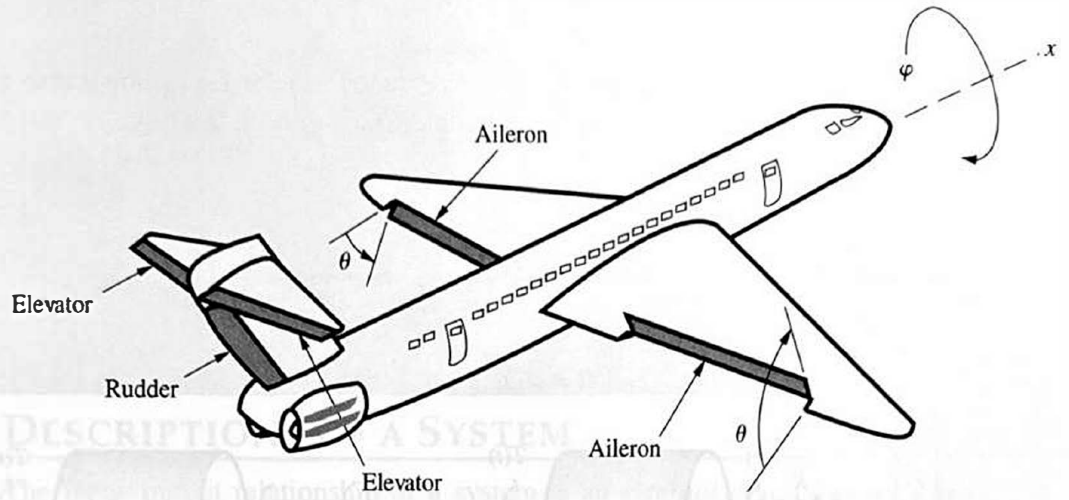

Figure 1.38 Attitude control of an airplane.

The aileron surfaces generate a torque about the roll axis proportional to the aileron deflection angle $\theta(t)$. Let this torque be $c\theta(t)$, where c is the constant of proportionality. Air friction dissipates the torque $B\dot{\varphi}(t)$. The torque available for rolling motion is then $c\theta(t) - B\dot{\varphi}(t)$. If J is the moment of inertia of the plane about the x axis (roll axis), then

$$\text{net torque} = J\ddot{\varphi}(t) = c\theta(t) - B\dot{\varphi}(t)$$

and

$$J\frac{d^2\varphi(t)}{dt^2} + B\frac{d\varphi(t)}{dt} = c\theta(t) \qquad \text{or} \qquad (JD^2 + BD)\varphi(t) = c\theta(t)$$

This is the desired equation relating the output (roll angle $\varphi(t)$) to the input (aileron angle $\theta(t)$).

The roll velocity $\omega(t)$ is $\dot{\varphi}(t)$. If the desired output is the roll velocity $\omega(t)$ rather than the roll angle $\varphi(t)$, then the input–output equation would be

$$J\frac{d\omega(t)}{dt} + B\omega(t) = c\theta(t) \qquad \text{or} \qquad (JD + B)\omega(t) = c\theta(t)$$

DRILL 1.19 Input–Output Equation of a Rotational Mechanical System

Torque $T(t)$ is applied to the rotational mechanical system shown in Fig. 1.39a. The torsional spring stiffness is K; the rotational mass (the cylinder's moment of inertia about the shaft) is J; the viscous damping coefficient between the cylinder and the ground is B. Find the equation

relating the output angle $\theta(t)$ to the input torque $\mathcal{T}(t)$. [*Hint:* A free-body diagram is shown in Fig. 1.39b.]

ANSWERS

$$J\frac{d^2\theta(t)}{dt^2}+B\frac{d\theta(t)}{dt}+K\theta(t)=\mathcal{T}(t)$$

or

$$(JD^2+BD+K)\theta(t)=\mathcal{T}(t)$$

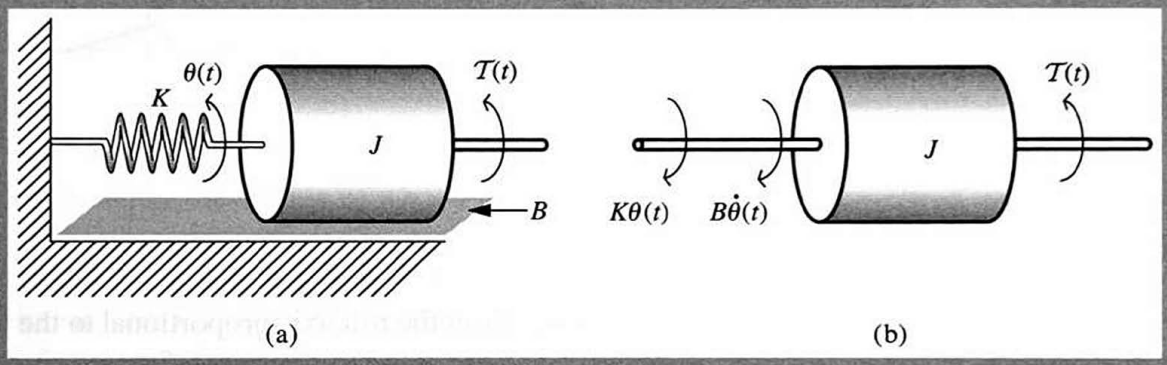

Figure 1.39 Rotational system for Drill 1.19.

1.8.3 Electromechanical Systems

A wide variety of electromechanical systems is used to convert electrical signals into mechanical motion (mechanical energy) and vice versa. Here, we consider a rather simple example of an armature-controlled dc motor driven by a current source $x(t)$, as shown in Fig. 1.40a. The torque $\mathcal{T}(t)$ generated in the motor is proportional to the armature current $x(t)$. Therefore,

$$\mathcal{T}(t)=K_T x(t)$$

where K_T is a constant of the motor. This torque drives a mechanical load whose free-body diagram is shown in Fig. 1.40b. The viscous damping (with coefficient B) dissipates a torque $B\dot{\theta}(t)$. If J is the moment of inertia of the load (including the rotor of the motor), then the net torque $\mathcal{T}(t)-B\dot{\theta}(t)$ must be equal to $J\ddot{\theta}(t)$:

$$J\ddot{\theta}(t)=\mathcal{T}(t)-B\dot{\theta}(t)$$

Thus,

$$(JD^2+BD)\theta(t)=\mathcal{T}(t)=K_T x(t)$$

which in conventional form can be expressed as

$$J\frac{d^2\theta(t)}{dt^2}+B\frac{d\theta(t)}{dt}=K_T x(t) \tag{1.32}$$

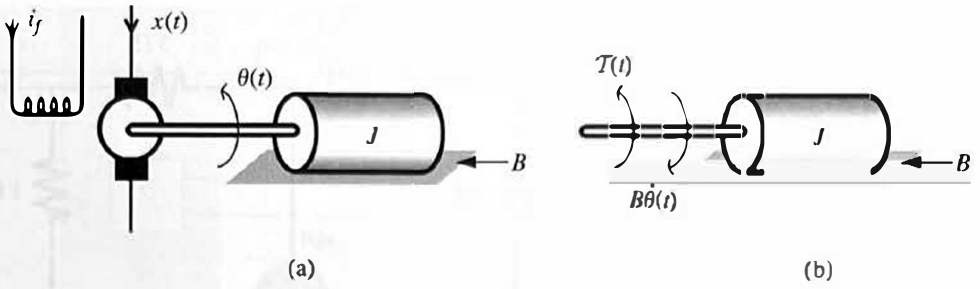

Figure 1.40 Armature-controlled dc motor.

1.9 Internal and External Descriptions of a System

The input–output relationship of a system is an *external description* of that system. We have found an external description (not the *internal description*) of systems in all the examples discussed so far. This may puzzle the reader because in each of these cases, we derived the input–output relationship by analyzing the internal structure of that system. Why is this not an internal description? What makes a description internal? Although it is true that we did find the input--output description by internal analysis of the system, we did so strictly for convenience. We could have obtained the input–output description by making observations at the external (input and output) terminals, for example, by measuring the output for certain inputs, such as an impulse or a sinusoid. A description that can be obtained from measurements at the external terminals (even when the rest of the system is sealed inside an inaccessible black box) is an external description. Clearly, the input–output description is an external description. What, then, is an internal description? An internal description is capable of providing complete information about all possible signals in the system. An external description may not give such complete information. An external description can always be found from an internal description, but the converse is not necessarily true. We shall now give an example to clarify the distinction between an external and an internal description.

Let the circuit in Fig. 1.41a with the input $x(t)$ and the output $y(t)$ be enclosed inside a "black box" with only the input and the output terminals accessible. To determine its external description, let us apply a known voltage $x(t)$ at the input terminals and measure the resulting output voltage $y(t)$.

Let us also assume that there is some initial charge Q_0 present on the capacitor. The output voltage will generally depend on both, the input $x(t)$ and the initial charge Q_0. To compute the output resulting because of the charge Q_0, assume the input $x(t) = 0$ (short across the input). In this case, the currents in the two 2 Ω resistors in the upper and the lower branches at the output terminals are equal and opposite because of the balanced nature of the circuit. Clearly, the capacitor charge results in zero voltage at the output.[†]

Now, to compute the output $y(t)$ resulting from the input voltage $x(t)$, we assume zero initial capacitor charge (short across the capacitor terminals). The current $i(t)$ (Fig. 1.41a), in this case, divides equally between the two parallel branches because the circuit is balanced. Thus, the voltage

[†] The output voltage $y(t)$ resulting because of the capacitor charge [assuming $x(t) = 0$] is the zero-input response, which, as argued above, is zero. The output component due to the input $x(t)$ (assuming zero initial capacitor charge) is the zero-state response. Complete analysis of this problem is given later in Ex. 1.21.

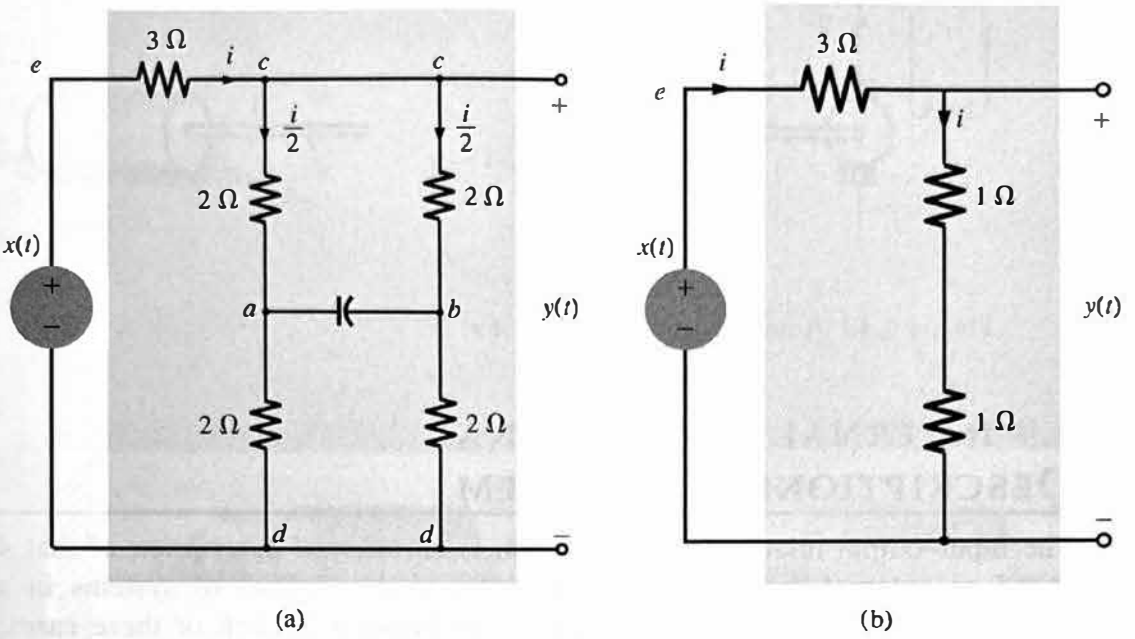

Figure 1.41 A system that cannot be described by external measurements.

across the capacitor continues to remain zero. Therefore, for the purpose of computing the current $i(t)$, the capacitor may be removed or replaced by a short. The resulting circuit is equivalent to that shown in Fig. 1.41b, which shows that the input $x(t)$ sees a load of 5 Ω, and

$$i(t) = \tfrac{1}{5}x(t)$$

Also, because $y(t) = 2i(t)$,

$$y(t) = \tfrac{2}{5}x(t)$$

This is the total response. Clearly, for the external description, the capacitor does not exist. No external measurement or external observation can detect the presence of the capacitor. Furthermore, if the circuit is enclosed inside a "black box" so that only the external terminals are accessible, it is impossible to determine the currents (or voltages) inside the circuit from external measurements or observations. An internal description, however, can provide every possible signal inside the system. In Ex. 1.21, we shall find the internal description of this system and show that it is capable of determining every possible signal in the system.

For most systems, the external and internal descriptions are equivalent, but there are a few exceptions, as in the present case, where the external description gives an inadequate picture of the system. This happens when the system is *uncontrollable* and/or *unobservable*.

Figure 1.42 shows structural representations of simple uncontrollable and unobservable systems. In Fig. 1.42a, we note that part of the system (subsystem $\mathcal{S}_2$) inside the box cannot be controlled by the input $x(t)$. In Fig. 1.42b, some of the system outputs (those in subsystem $\mathcal{S}_2$) cannot be observed from the output terminals. If we try to describe either of these systems by applying an external input $x(t)$ and then measuring the output $y(t)$, the measurement will not characterize the complete system but only the part of the system (here, $\mathcal{S}_1$) that is both controllable and observable (linked to both the input and output). Such systems are undesirable in practice and should be avoided in any system design. The system in Fig. 1.41a can be shown to be neither controllable nor observable. It can be represented structurally as a combination of the systems in Figs. 1.42a and 1.42b.

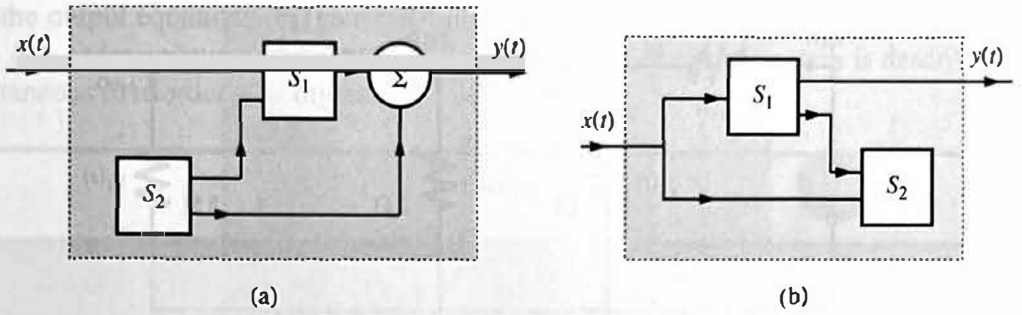

Figure 1.42 Structures of uncontrollable and unobservable systems.

1.10 Internal Description: The State-Space Description

We shall now introduce the *state-space* description of a linear system, which is an internal description of a system. In this approach, we identify certain key variables, called the *state variables*, of the system. These variables have the property that every possible signal in the system can be expressed as a linear combination of these state variables. For example, we can show that every possible signal in a passive *RLC* circuit can be expressed as a linear combination of independent capacitor voltages and inductor currents, which, therefore, are state variables for the circuit.

To illustrate this point, consider the network in Fig. 1.43. We identify two state variables: the capacitor voltage q_1 and the inductor current q_2. If the values of q_1, q_2, and the input $x(t)$ are known at some instant t, we can demonstrate that every possible signal (current or voltage) in the circuit can be determined at t. For example, if $q_1 = 10$, $q_2 = 1$, and the input $x = 20$ at some instant, the remaining voltages and currents at that instant will be

$$\begin{aligned} i_1 &= (x - q_1)/1 = 20 - 10 = 10\,\text{A} \\ v_1 &= x - q_1 = 20 - 10 = 10\,\text{V} \\ v_2 &= q_1 = 10\,\text{V} \\ i_2 &= q_1/2 = 5\,\text{A} \\ i_C &= i_1 - i_2 - q_2 = 10 - 5 - 1 = 4\,\text{A} \\ i_3 &= q_2 = 1\,\text{A} \\ v_3 &= 5q_2 = 5\,\text{V} \\ v_L &= q_1 - v_3 = 10 - 5 = 5\,\text{V} \end{aligned} \tag{1.33}$$

Thus, all signals in this circuit are determined. Clearly, state variables consist of the *key variables* in a system; a knowledge of the state variables allows one to determine every possible output of the system. Note that the *state-variable description is an internal description* of a system because it is capable of describing all possible signals in the system.

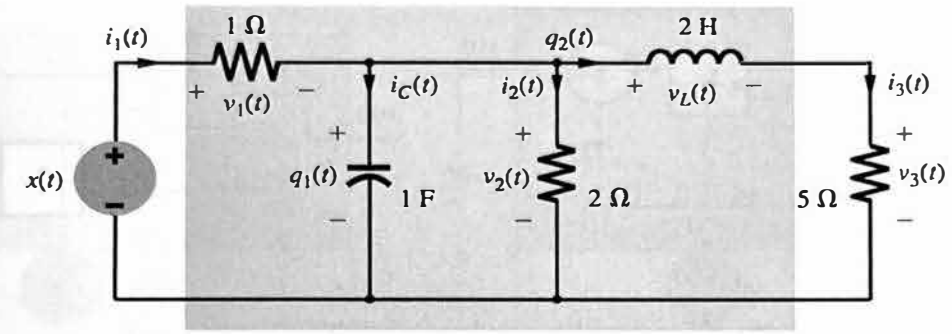

Figure 1.43 Choosing suitable initial conditions in a network.

EXAMPLE 1.20 State-Space Description of a System

This example illustrates how state equations may be natural and easier to determine than other descriptions, such as loop or node equations. Consider again the network in Fig. 1.43 with q_1 and q_2 as the state variables and write the state equations.

This can be done by simple inspection of Fig. 1.43. Since $\dot{q}_1$ is the current through the capacitor,

$$\begin{aligned}\dot{q}_1 &= i_C = i_1 - i_2 - q_2 \\ &= (x - q_1) - 0.5q_1 - q_2 \\ &= -1.5q_1 - q_2 + x\end{aligned}$$

Also $2\dot{q}_2$, the voltage across the inductor, is given by

$$\begin{aligned}2\dot{q}_2 &= q_1 - v_3 \\ &= q_1 - 5q_2\end{aligned}$$

or

$$\dot{q}_2 = 0.5q_1 - 2.5q_2$$

Thus, the state equations are

$$\begin{aligned}\dot{q}_1 &= -1.5q_1 - q_2 + x \\ \dot{q}_2 &= 0.5q_1 - 2.5q_2\end{aligned} \tag{1.34}$$

This is a set of two simultaneous first-order differential equations. This set of equations comprises the *state equations*. Once these equations have been solved for q_1 and q_2, everything else in the circuit can be determined by using Eq. (1.33), which are known as the *output equations*. Thus, in this approach, we have two sets of equations, the state equations and the output equations. Once we have solved the state equations, all possible outputs can be obtained

from the output equations. In the input–output description, an Nth-order system is described by an Nth-order equation. In the state-variable approach, the same system is described by N simultaneous first-order state equations.†

EXAMPLE 1.21 Controllability and Observability

Investigate the nature of state equations and the issue of controllability and observability for the circuit in Fig. 1.41a.

This circuit has only one capacitor and no inductors. Hence, there is only one state variable, the capacitor voltage $q(t)$. Since $C = 1$ F, the capacitor current is $\dot{q}$. There are two sources in this circuit: the input $x(t)$ and the capacitor voltage $q(t)$. The response due to $x(t)$, assuming $q(t) = 0$, is the zero-state response, which can be found from Fig. 1.44a, where we have shorted the capacitor [$q(t) = 0$]. The response due to $q(t)$, assuming $x(t) = 0$, is the zero-input response, which can be found from Fig. 1.44b, where we have shorted $x(t)$ to ensure $x(t) = 0$. It is now trivial to find both the components.

Figure 1.44a shows zero-state currents in every branch. It is clear that the input $x(t)$ sees an effective resistance of 5 Ω, and, hence, the current through $x(t)$ is $x/5$ A, which divides in the two parallel branches, resulting in the current $x/10$ through each branch.

Examining the circuit in Fig. 1.44b for the zero-input response, we note that the capacitor voltage is q and the current is $\dot{q}$. We also observe that the capacitor sees two loops in parallel, each with resistance 4 Ω and current $\dot{q}/2$. Interestingly, the 3 Ω branch is effectively shorted because the circuit is balanced, and thus the voltage across the terminals cd is zero. The total current in any branch is the sum of the currents in that branch in Figs. 1.44a and 1.44b (principle of superposition).

Branch	Current	Voltage
ca	$\frac{x}{10}+\frac{\dot{q}}{2}$	$2\left(\frac{x}{10}+\frac{\dot{q}}{2}\right)$
cb	$\frac{x}{10}-\frac{\dot{q}}{2}$	$2\left(\frac{x}{10}-\frac{\dot{q}}{2}\right)$
ad	$\frac{x}{10}-\frac{\dot{q}}{2}$	$2\left(\frac{x}{10}-\frac{\dot{q}}{2}\right)$
bd	$\frac{x}{10}+\frac{\dot{q}}{2}$	$2\left(\frac{x}{10}+\frac{\dot{q}}{2}\right)$
ec	$\frac{x}{5}$	$3\left(\frac{x}{5}\right)$
ed	$\frac{x}{5}$	x

(1.35)

† This assumes the system to be controllable and observable. If it is not, the input–output description equation will be of an order lower than the corresponding number of state equations.

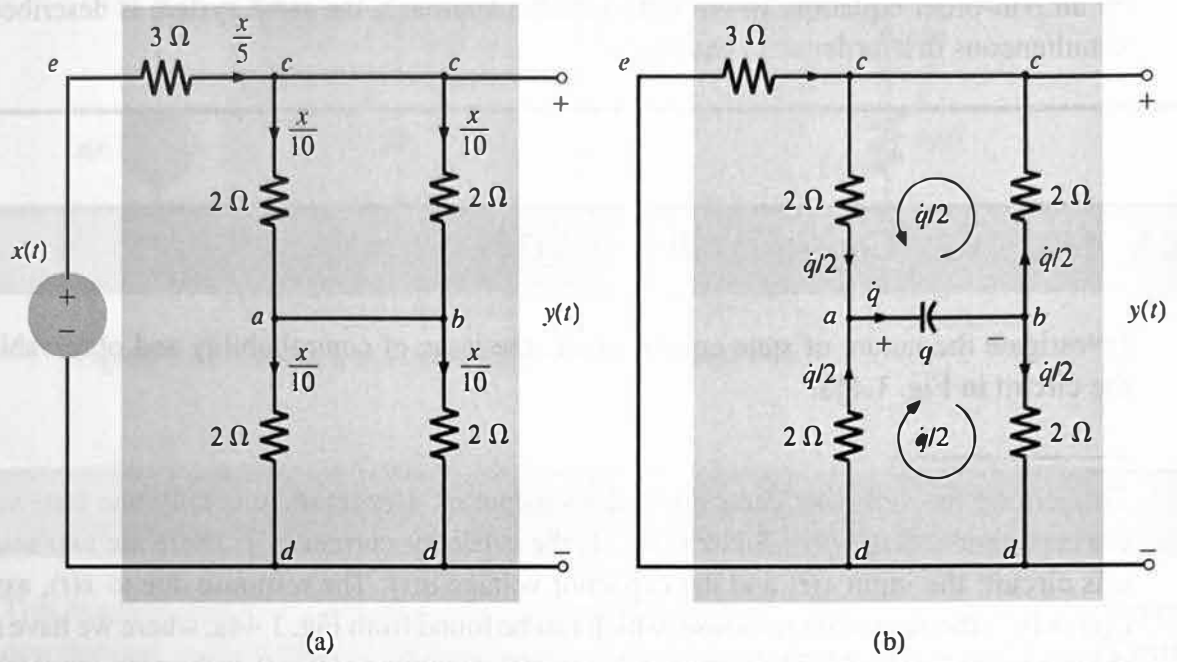

Figure 1.44 Analysis of a system that is neither controllable nor observable.

To find the state equation, we note that the current in branch ca is $(x/10)+\dot{q}/2$ and the current in branch cb is $(x/10)-\dot{q}/2$. Hence, the equation around the loop $acba$ is

$$q=2\left[-\frac{x}{10}-\frac{\dot{q}}{2}\right]+2\left[\frac{x}{10}-\frac{\dot{q}}{2}\right]=-2\dot{q}$$

or

$$\dot{q}=-0.5q \tag{1.36}$$

This is the desired state equation.

Substitution of $\dot{q}=-0.5q$ in Eq. (1.35) shows that every possible current and voltage in the circuit can be expressed in terms of the state variable q and the input x, as desired. Hence, the set of Eq. (1.35) is the output equation for this circuit. Once we have solved the state equation [Eq. (1.36)] for q, we can determine every possible output in the circuit.

The output $y(t)$ is given by

$$y(t)=2\left[\frac{x}{10}-\frac{\dot{q}}{2}\right]+2\left[\frac{x}{10}+\frac{\dot{q}}{2}\right]=\frac{2}{5}x(t) \tag{1.37}$$

A little examination of the state and the output equations indicates the nature of this system. Equation (1.36) shows that the state $q(t)$ is independent of the input $x(t)$; hence, the system state q cannot be controlled by the input. Moreover, Eq. (1.37) shows that the output $y(t)$ does not depend on the state $q(t)$. Thus, the system state cannot be observed from the output terminals. Hence, the system is neither controllable nor observable. Such is not the case with other systems examined earlier. Consider, for example, the circuit in Fig. 1.43. The state equations [Eq. (1.34)] show that the states are influenced by the input directly or indirectly. Hence, the system is controllable. Moreover, as Eq. (1.33) shows, every possible output is expressed in terms of the state variables and the input. Hence, the states are also observable.

State-space techniques are useful not just because of their ability to provide internal system description, but for several other reasons, including the following:

1. State equations of a system provide a mathematical model of great generality that can describe not just linear systems, but also nonlinear systems; not just time-invariant systems, but also time-varying parameter systems; not just SISO (single-input/single-output) systems, but also multiple-input/multiple-output (MIMO) systems. Indeed, state equations are ideally suited for the analysis, synthesis, and optimization of MIMO systems.
2. Compact matrix notation and the powerful techniques of linear algebra greatly facilitate complex manipulations. Without such features, many important results of the modern system theory would have been difficult to obtain. State equations can yield a great deal of information about a system even when they are not solved explicitly.
3. State equations lend themselves readily to digital computer simulation of complex systems of high order, with or without nonlinearities, and with multiple inputs and outputs.
4. For second-order systems ($N = 2$), a graphical method called *phase-plane analysis* can be used on state equations, whether they are linear or nonlinear.

The real benefits of the state-space approach, however, are realized for highly complex systems of large order. Much of this book is devoted to the introduction of the basic concepts of linear systems analysis, which must necessarily begin with simpler systems without using the state-space approach. Chapter 10 deals with the state-space analysis of linear, time-invariant, continuous-time, and discrete-time systems.

DRILL 1.20 State Equations for a Series *RLC* Circuit

Write the state equations for the series *RLC* circuit shown in Fig. 1.45, using the inductor current $q_1(t)$ and the capacitor voltage $q_2(t)$ as state variables. Express every voltage and current in this circuit as a linear combination of q_1, q_2, and x.

ANSWERS

$\dot{q}_1 = -3q_1 - q_2 + x$ and $\dot{q}_2 = 2q_1$.

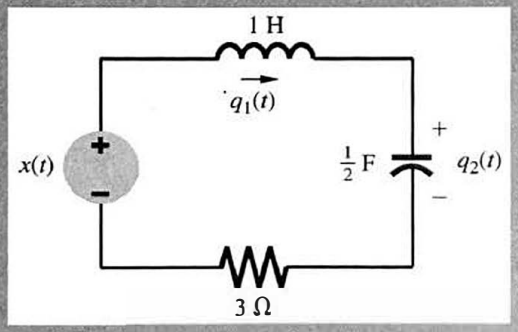

Figure 1.45 Circuit for Drill 1.20.

1.11 MATLAB: WORKING WITH FUNCTIONS

Working with functions is fundamental to signals and systems applications. MATLAB provides several methods of defining and evaluating functions. An understanding and proficient use of these methods are therefore necessary and beneficial.

1.11.1 Anonymous Functions

Many simple functions are most conveniently represented by using MATLAB anonymous functions. An anonymous function provides a symbolic representation of a function defined in terms of MATLAB operators, functions, or other anonymous functions. For example, consider defining the exponentially damped sinusoid $f(t) = e^{-t}\cos(2\pi t)$.

```
>>  f = @(t) exp(-t).*cos(2*pi*t);
```

In this context, the `@` symbol identifies the expression as an anonymous function, which is assigned a name of `f`. Parentheses following the `@` symbol are used to identify the function's independent variables (input arguments), which in this case is the single time variable `t`. Input arguments, such as `t`, are local to the anonymous function and are not related to any workspace variables with the same names.

Once defined, $f(t)$ can be evaluated simply by passing the input values of interest. For example,

```
>>  t = 0; f(t)
    ans = 1
```

evaluates $f(t)$ at $t = 0$, confirming the expected result of unity. The same result is obtained by passing $t = 0$ directly.

```
>>  f(0)
    ans = 1
```

Vector inputs allow the evaluation of multiple values simultaneously. Consider the task of plotting $f(t)$ over the interval $(-2 \leq t \leq 2)$. Gross function behavior is clear: $f(t)$ should oscillate four times with a decaying envelope. Since accurate hand sketches are cumbersome, MATLAB-generated plots are an attractive alternative. As the following example illustrates, care must be taken to ensure reliable results.

Suppose vector `t` is chosen to include only the integers contained in $(-2 \leq t \leq 2)$, namely, $[-2, -1, 0, 1, 2]$.

```
>>  t = (-2:2);
```

This vector input is evaluated to form a vector output.

```
>>  f(t)
    ans = 7.3891    2.7183    1.0000    0.3679    0.1353
```

The `plot` command graphs the result, which is shown in Fig. 1.46.

```
>> plot(t,f(t));
>> xlabel('t'); ylabel('f(t)'); grid;
```

Grid lines, added by using the `grid` command, aid feature identification. Unfortunately, the plot does not illustrate the expected oscillatory behavior. More points are required to adequately represent $f(t)$.

The question, then, is how many points are enough?† If too few points are chosen, information is lost. If too many points are chosen, memory and time are wasted. A balance is needed. For oscillatory functions, plotting 20 to 200 points per oscillation is normally adequate. For the present case, `t` is chosen to give 100 points per oscillation.

```
>> t = (-2:0.01:2);
```

Again, the function is evaluated and plotted.

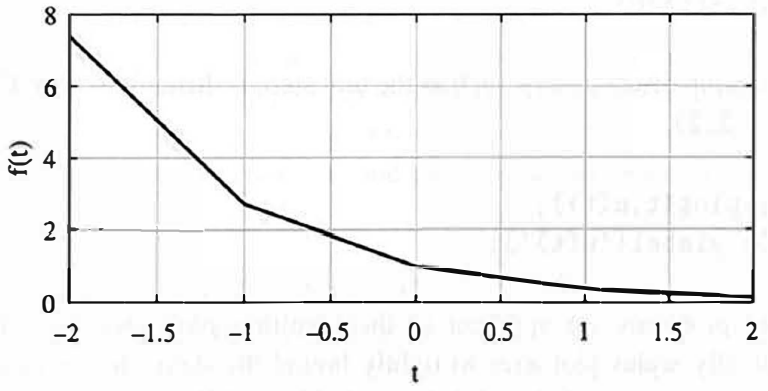

Figure 1.46 $f(t) = e^{-t}\cos(2\pi t)$ for `t = (-2:2)`.

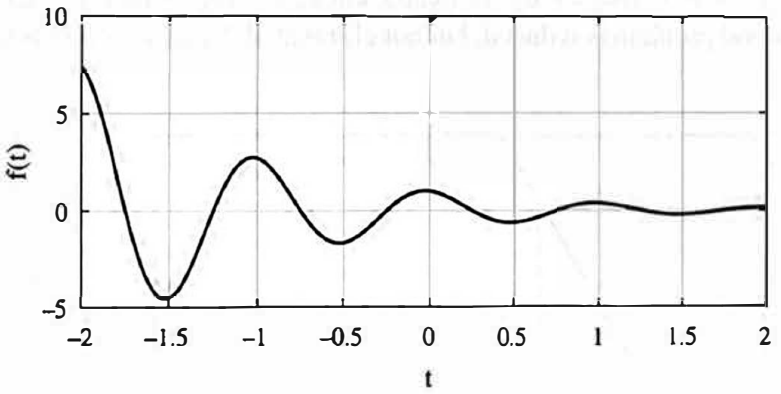

Figure 1.47 $f(t) = e^{-t}\cos(2\pi t)$ for `t = (-2:0.01:2)`.

† Sampling theory, presented later, formally addresses important aspects of this question.

```
>> plot(t,f(t));
>> xlabel('t'); ylabel('f(t)'); grid;
```

The result, shown in Fig. 1.47, is an accurate depiction of $f(t)$.

1.11.2 Relational Operators and the Unit Step Function

The unit step function $u(t)$ arises naturally in many practical situations. For example, a unit step can model the act of turning on a system. With the help of relational operators, anonymous functions can represent the unit step function.

In MATLAB, a relational operator compares two items. If the comparison is true, a logical true (1) is returned. If the comparison is false, a logical false (0) is returned. Sometimes called indicator functions, relational operators indicate whether a condition is true. Six relational operators are available: <, >, <=, >=, ==, and ~=.

The unit step function is readily defined using the >= relational operator.

```
>> u = @(t) 1.0.*(t>=0);
```

Any function with a jump discontinuity, such as the unit step, is difficult to plot. Consider plotting $u(t)$ by using `t = (-2:2)`.

```
>> t = (-2:2); plot(t,u(t));
>> xlabel('t'); ylabel('u(t)');
```

Two significant problems are apparent in the resulting plot, shown in Fig. 1.48. First, MATLAB automatically scales plot axes to tightly bound the data. In this case, this normally desirable feature obscures most of the plot. Second, MATLAB connects plot data with lines, making a true jump discontinuity difficult to achieve. The coarse resolution of vector `t` emphasizes the effect by showing an erroneous sloping line between $t = -1$ and $t = 0$.

The first problem is corrected by vertically enlarging the bounding box with the `axis` command. The second problem is reduced, but not eliminated, by adding points to vector `t`.

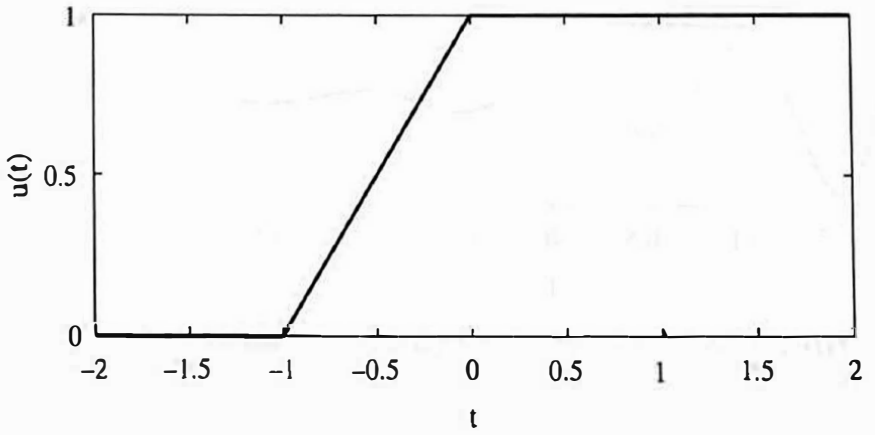

Figure 1.48 $u(t)$ for `t = (-2:2)`.

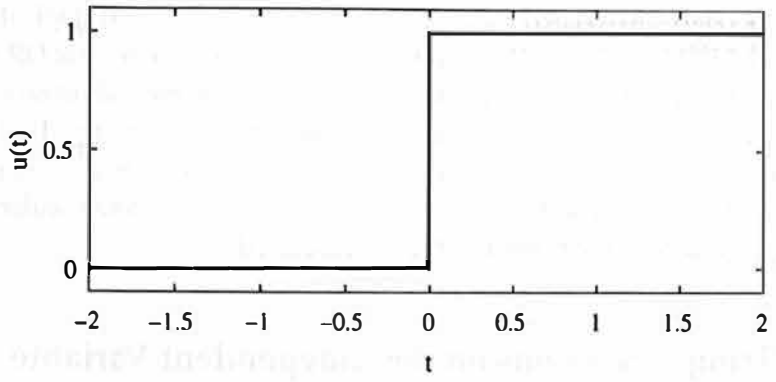

Figure 1.49 $u(t)$ for `t = (-2:0.01:2)` with axis modification.

```
>> t = (-2:0.01:2); plot(t,u(t));
>> xlabel('t'); ylabel('u(t)');
>> axis([-2 2 -0.1 1.1]);
```

The four-element vector argument of `axis` specifies x axis minimum, x axis maximum, y axis minimum, and y axis maximum, respectively. The improved results are shown in Fig. 1.49.

Relational operators can be combined using logical AND, logical OR, and logical negation: `&`, `|`, and `~`, respectively. For example, `(t>0)&(t<1)` and `~((t<=0)|(t>=1))` both test if $0 < t < 1$. To demonstrate, consider defining and plotting the unit pulse $p(t) = u(t) - u(t-1)$, as shown in Fig. 1.50:

```
>> p = @(t) 1.0.*((t>=0)&(t<1));
>> t = (-1:0.01:2); plot(t,p(t));
>> xlabel('t'); ylabel('p(t) = u(t)-u(t-1)');
>> axis([-1 2 -.1 1.1]);
```

Since anonymous functions can be constructed using other anonymous functions, we could have used our previously defined unit step anonymous function to define $p(t)$ as `p = @(t) u(t)-u(t-1);`.

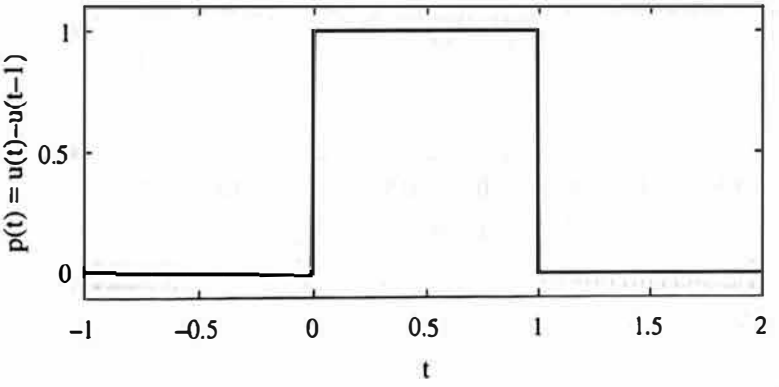

Figure 1.50 $p(t) = u(t) - u(t-1)$ over $(-1 \le t \le 2)$.

For scalar operands, MATLAB also supports two short-circuit logical constructs. A short-circuit logical AND is performed by using `&&`, and a short-circuit logical OR is performed by using `||`. Short-circuit logical operators are often more efficient than traditional logical operators because they test the second portion of the expression only when necessary. That is, when scalar expression `A` is found false in `(A&&B)`, scalar expression `B` is not evaluated, since a false result is already guaranteed. Similarly, scalar expression `B` is not evaluated when scalar expression `A` is found true in `(A||B)`, since a true result is already guaranteed.

1.11.3 Visualizing Operations on the Independent Variable

Two operations on a function's independent variable are commonly encountered: shifting and scaling. Anonymous functions are well suited to investigate both operations.

Consider $g(t) = f(t)u(t) = e^{-t}\cos(2\pi t)u(t)$, a causal version of $f(t)$. MATLAB easily multiplies anonymous functions. Thus, we create $g(t)$ by multiplying our anonymous functions for $f(t)$ and $u(t)$.[†]

```
>> g = @(t) f(t).*u(t);
```

A combined shifting and scaling operation is represented by $g(at + b)$, where a and b are arbitrary real constants. As an example, consider plotting $g(2t + 1)$ over $(-2 \leq t \leq 2)$. With $a = 2$, the function is compressed by a factor of 2, resulting in twice the oscillations per unit t. Adding the condition $b > 0$ shifts the waveform to the left. Given anonymous function g, an accurate plot is nearly trivial to obtain.

```
>> t = (-2:0.01:2);
>> plot(t,g(2*t+1)); xlabel('t'); ylabel('g(2t+1)'); grid;
```

Figure 1.51 confirms the expected waveform compression and left shift. As a final check, realize that function $g(\cdot)$ turns on when the input argument is zero. Therefore, $g(2t + 1)$ should turn on when $2t + 1 = 0$ or at $t = -0.5$, a fact again confirmed by Fig. 1.51.

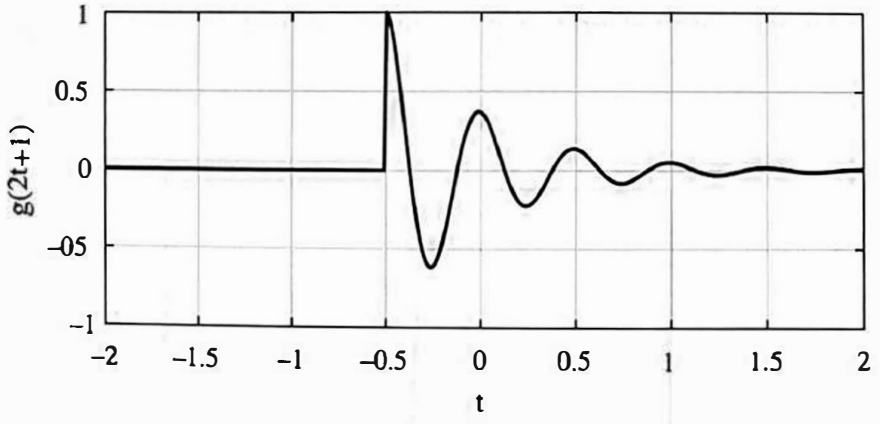

Figure 1.51 $g(2t + 1)$ over $(-2 \leq t \leq 2)$.

[†] Although we define g in terms of `f` and `u`, the function g will not change if we later change either `f` or `u` unless we subsequently redefine g as well.

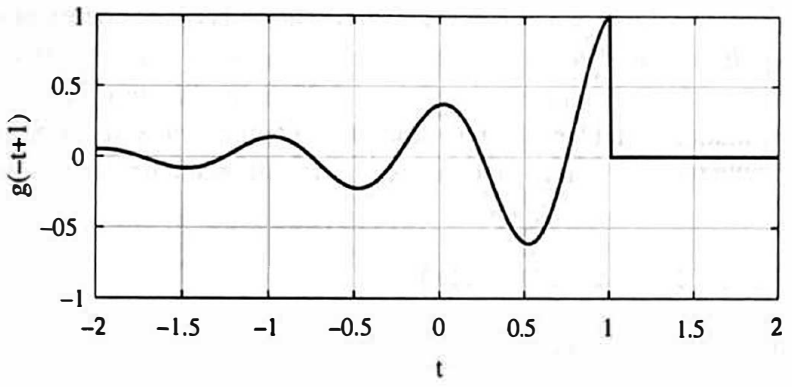

Figure 1.52 $g(-t+1)$ over $(-2 \leq t \leq 2)$.

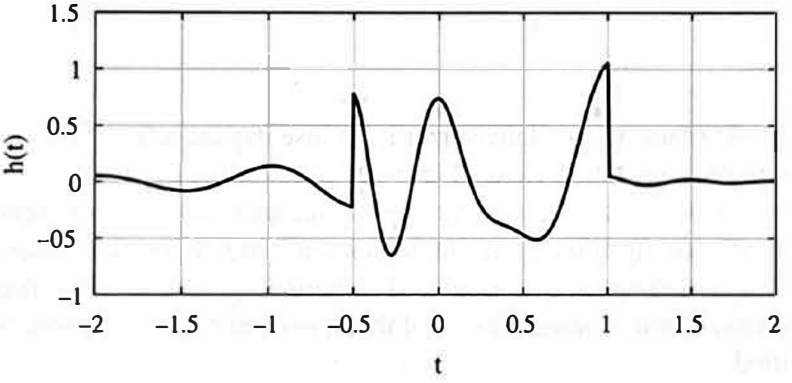

Figure 1.53 $h(t) = g(2t+1) + g(-t+1)$ over $(-2 \leq t \leq 2)$.

Next, consider plotting $g(-t+1)$ over $(-2 \leq t \leq 2)$. Since $a < 0$, the waveform will be reflected. Adding the condition $b > 0$ shifts the final waveform to the right.

```
>> plot(t,g(-t+1)); xlabel('t'); ylabel('g(-t+1)'); grid;
```

Figure 1.52 confirms both the reflection and the right shift.

Up to this point, Figs. 1.51 and 1.52 could be reasonably sketched by hand. Consider plotting the more complicated function $h(t) = g(2t+1) + g(-t+1)$ over $(-2 \leq t \leq 2)$ (Fig. 1.53); an accurate hand sketch would be quite difficult. With MATLAB, the work is much less burdensome.

```
>> plot(t,g(2*t+1)+g(-t+1)); xlabel('t'); ylabel('h(t)'); grid;
```

1.11.4 Numerical Integration and Estimating Signal Energy

Interesting signals often have nontrivial mathematical representations. Computing signal energy, which involves integrating the square of these expressions, can be a daunting task. Fortunately, many difficult integrals can be accurately estimated by means of numerical integration techniques. Even if the integration appears simple, numerical integration provides a good way to verify analytical results.

To start, consider the simple signal $x(t) = e^{-t}(u(t) - u(t-1))$. The energy of $x(t)$ is expressed as $E_x = \int_{-\infty}^{\infty} |x(t)|^2\,dt = \int_0^1 e^{-2t}\,dt$. Integrating yields $E_x = 0.5(1 - e^{-2}) \approx 0.4323$. The energy integral can also be evaluated numerically. Figure 1.27 helps illustrate the simple method of rectangular approximation: evaluate the integrand at points uniformly separated by Δt, multiply each by Δt to compute rectangle areas, and then sum over all rectangles. First, we create function $x(t)$.

```
>> x = @(t) exp(-t).*((t>=0)&(t<1));
```

With $\Delta t = 0.01$, a suitable time vector is created.

```
>> t = (0:0.01:1);
```

The final result is computed by using the `sum` command.

```
>> E_x = sum(x(t).*x(t)*0.01)
   E_x = 0.4367
```

The result is not perfect, but at 1% relative error it is close. By reducing Δt, the approximation is improved. For example, $\Delta t = 0.001$ yields `E_x = 0.4328`, or 0.1% relative error.

Although simple to visualize, rectangular approximation is not the best numerical integration technique. The MATLAB function quad implements a better numerical integration technique called recursive adaptive Simpson quadrature.† To operate, quad requires a function describing the integrand, the lower limit of integration, and the upper limit of integration. Notice that no Δt needs to be specified.

To use quad to estimate E_x, the integrand must first be described.

```
>> x_squared = @(t) x(t).*x(t);
```

Estimating E_x immediately follows.

```
>> E_x = quad(x_squared,0,1)
   E_x = 0.4323
```

In this case, the relative error is -0.0026%.

The same techniques can be used to estimate the energy of more complex signals. Consider $g(t)$, defined previously. Energy is expressed as $E_g = \int_0^{\infty} e^{-2t}\cos^2(2\pi t)\,dt$. A closed-form solution exists, but it takes some effort. MATLAB provides an answer more quickly.

```
>> g_squared = @(t) g(t).*g(t);
```

Although the upper limit of integration is infinity, the exponentially decaying envelope ensures $g(t)$ is effectively zero well before $t = 100$. Thus, an upper limit of $t = 100$ is used along with $\Delta t = 0.001$.

---

† A comprehensive treatment of numerical integration is outside the scope of this text. Details of this particular method are not important for the current discussion; it is sufficient to say that it is better than the rectangular approximation.

```
>>  t = (0:0.001:100);
>>  E_g = sum(g_squared(t)*0.001)
    E_g = 0.2567
```

A slightly better approximation is obtained with the quad function.

```
>>  E_g = quad(g_squared,0,100)
    E_g = 0.2562
```

DRILL 1.21 Computing Signal Energy with MATLAB

Use MATLAB to confirm that the energy of signal $h(t)$, defined previously as $h(t) = g(2t+1) + g(-t+1)$, is $E_h = 0.3768$.

1.12 SUMMARY

A *signal* is a set of data or information. A *system* processes input signals to modify them or extract additional information from them to produce output signals (response). A system may be made up of physical components (hardware realization), or it may be an algorithm that computes an output signal from an input signal (software realization).

A convenient measure of the size of a signal is its energy, if it is finite. If the signal energy is infinite, the appropriate measure is its power, if it exists. The signal power is the time average of its energy (averaged over the entire time interval from $-\infty$ to ∞). For periodic signals, the time averaging need be performed over only one period in view of the periodic repetition of the signal. Signal power is also equal to the mean squared value of the signal (averaged over the entire time interval from $t = -\infty$ to ∞).

Signals can be classified in several ways.

1. A *continuous-time signal* is specified for a continuum of values of the independent variable (such as time t). A *discrete-time signal* is specified only at a finite or a countable set of time instants.
2. An *analog signal* is a signal whose amplitude can take on any value over a continuum. On the other hand, a signal whose amplitudes can take on only a finite number of values is a *digital signal*. The terms *discrete-time* and *continuous-time* qualify the nature of a signal along the time axis (horizontal axis). The terms *analog* and *digital*, on the other hand, qualify the nature of the signal amplitude (vertical axis).
3. A *periodic signal* $x(t)$ is defined by the fact that $x(t) = x(t + T_0)$ for some T_0. The smallest positive value of T_0 for which this relationship is satisfied is called the *fundamental period*. A periodic signal remains unchanged when shifted by an integer multiple of its period. A periodic signal $x(t)$ can be generated by a periodic extension of any contiguous segment of $x(t)$ of duration T_0. Finally, a periodic signal, by definition, must exist over the entire time interval $-\infty < t < \infty$. A signal is *aperiodic* if it is not periodic.
4. An *everlasting signal* starts at $t = -\infty$ and continues forever to $t = \infty$. Hence, periodic signals are everlasting signals. A *causal signal* is a signal that is zero for $t < 0$.

5. A signal with finite energy is an *energy signal*. Similarly, a signal with a finite and nonzero power (mean-square value) is a *power signal*. A signal can be either an energy signal or a power signal, but not both. However, there are signals that are neither energy nor power signals.
6. A signal whose physical description is known completely in a mathematical or graphical form is a *deterministic signal*. A *random signal* is known only in terms of its probabilistic description such as mean value or mean-square value, rather than by its mathematical or graphical form.

A signal $x(t)$ delayed by T seconds (right-shifted) can be expressed as $x(t - T)$; on the other hand, $x(t)$ advanced by T (left-shifted) is $x(t + T)$. A signal $x(t)$ time-compressed by a factor a ($a > 1$) is expressed as $x(at)$; on the other hand, the same signal time-expanded by factor a ($a > 1$) is $x(t/a)$. The signal $x(t)$ when time-reversed can be expressed as $x(-t)$.

The unit step function $u(t)$ is very useful in representing causal signals and signals with different mathematical descriptions over different intervals.

In the classical (Dirac) definition, the unit impulse function $\delta(t)$ is characterized by unit area and is concentrated at a single instant $t = 0$. The impulse function has a sampling (or sifting) property, which states that the area under the product of a function with a unit impulse is equal to the value of that function at the instant at which the impulse is located (assuming the function to be continuous at the impulse location). In the modern approach, the impulse function is viewed as a generalized function and is defined by the sampling property.

The exponential function e^{st}, where s is complex, encompasses a large class of signals that includes a constant, a monotonic exponential, a sinusoid, and an exponentially varying sinusoid.

A real signal that is symmetrical about the vertical axis ($t = 0$) is an *even* function of time, and a real signal that is antisymmetrical about the vertical axis is an *odd* function of time. The product of an even function and an odd function is an odd function. However, the product of an even function and an even function or an odd function and an odd function is an even function. The area under an odd function from $t = -a$ to a is always zero regardless of the value of a. On the other hand, the area under an even function from $t = -a$ to a is two times the area under the same function from $t = 0$ to a (or from $t = -a$ to 0). Every signal can be expressed as a sum of odd and even functions of time.

A system processes input signals to produce output signals (response). The input is the cause, and the output is its effect. In general, the output is affected by two causes: the internal conditions of the system (such as the initial conditions) and the external input.

Systems can be classified in several ways.

1. Linear systems are characterized by the linearity property, which implies superposition; if several causes (such as various inputs and initial conditions) are acting on a linear system, the total output (response) is the sum of the responses from each cause, assuming that all the remaining causes are absent. A system is nonlinear if superposition does not hold.
2. In time-invariant systems, system parameters do not change with time. The parameters of time-varying-parameter systems change with time.
3. For memoryless (or instantaneous) systems, the system response at any instant t depends only on the value of the input at t. For systems with memory (also known as dynamic systems), the system response at any instant t depends not only on the present value of the input, but also on the past values of the input (values before t).

4. In contrast, if a system response at t also depends on the future values of the input (values of input beyond t), the system is noncausal. In causal systems, the response does not depend on the future values of the input. Because of the dependence of the response on the future values of input, the effect (response) of noncausal systems occurs before the cause. When the independent variable is time (temporal systems), the noncausal systems are prophetic systems, and therefore, unrealizable, although close approximation is possible with some time delay in the response. Noncausal systems with independent variables other than time (e.g., space) are realizable.
5. Systems whose inputs and outputs are continuous-time signals are continuous-time systems; systems whose inputs and outputs are discrete-time signals are discrete-time systems. If a continuous-time signal is sampled, the resulting signal is a discrete-time signal. We can process a continuous-time signal by processing the samples of the signal with a discrete-time system.
6. Systems whose inputs and outputs are analog signals are analog systems; those whose inputs and outputs are digital signals are digital systems.
7. If we can obtain the input $x(t)$ back from the output $y(t)$ of a system S by some operation, the system S is said to be invertible. Otherwise, the system is noninvertible.
8. A system is stable if bounded input produces bounded output. This defines external stability because it can be ascertained from measurements at the external terminals of the system. External stability is also known as the stability in the BIBO (bounded-input/bounded-output) sense. Internal stability, discussed later in Ch. 2, is measured in terms of the internal behavior of the system.

The system model derived from a knowledge of the internal structure of the system is its internal description. In contrast, an external description is a representation of a system as seen from its input and output terminals; it can be obtained by applying a known input and measuring the resulting output. In the majority of practical systems, an external description of a system so obtained is equivalent to its internal description. At times, however, the external description fails to describe the system adequately. Such is the case with the so-called uncontrollable or unobservable systems.

A system may also be described in terms of a certain set of key variables called state variables. In this description, an Nth-order system can be characterized by a set of N simultaneous first-order differential equations in N state variables. State equations of a system represent an internal description of that system.

REFERENCES

1. Papoulis, A., *The Fourier Integral and Its Applications,* McGraw-Hill, New York, 1962.
2. Mason, S. J., *Electronic Circuits, Signals, and Systems,* Wiley, New York, 1960.
3. Kailath, T., *Linear Systems,* Prentice-Hall, Englewood Cliffs, NJ, 1980.
4. Lathi, B. P., *Signals and Systems,* Berkeley-Cambridge Press, Carmichael, CA, 1987.

PROBLEMS

1.1-1 Find the energies of the signals illustrated in Fig. P1.1-1. Comment on the effect on energy of sign change, time shifting, or doubling of the signal. What is the effect on the energy if the signal is multiplied by k?

1.1-2 Repeat Prob. 1.1-1 for the signals in Fig. P1.1-2.

1.1-3 (a) Find the energies of the pair of signals $x(t)$ and $y(t)$ depicted in Figs. P1.1-3a and P1.1-3b. Sketch and find the energies of signals $x(t) + y(t)$ and $x(t) - y(t)$. Can you make any observation from these results?

(b) Repeat part (a) for the signal pair illustrated in Fig. P1.1-3c. Is your observation in part (a) still valid?

1.1-4 Find the power of the periodic signal $x(t)$ shown in Fig. P1.1-4. Find also the powers and the rms values of:

(a) $-x(t)$

(b) $2x(t)$

(c) $cx(t)$

Comment.

1.1-5 By original design, a system outputs a 10-volt pulse that is 3 seconds in duration. It is desired to upgrade the square-pulse output with a "soft-start" pulse that steps up to 10 volts in 1-volt increments spaced every 20 milliseconds. Determine the signal duration T so that the "soft-start" pulse has the same signal energy as the original square pulse.

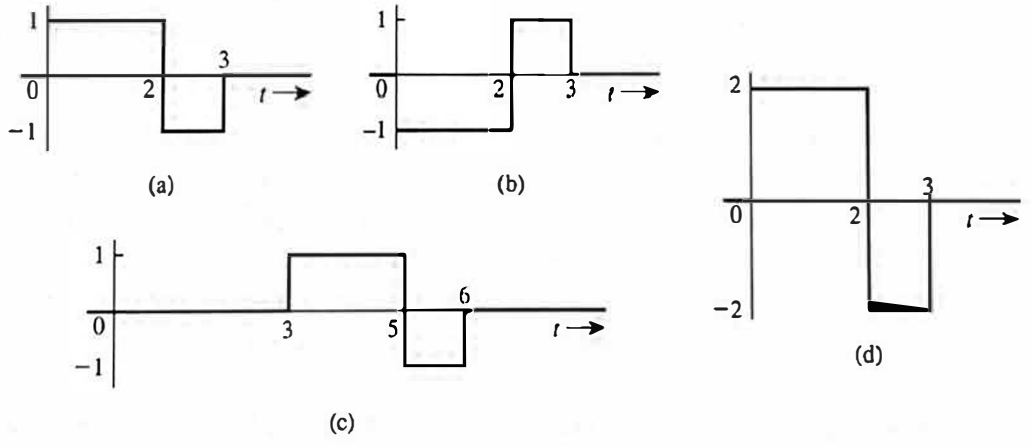

Figure P1.1-1

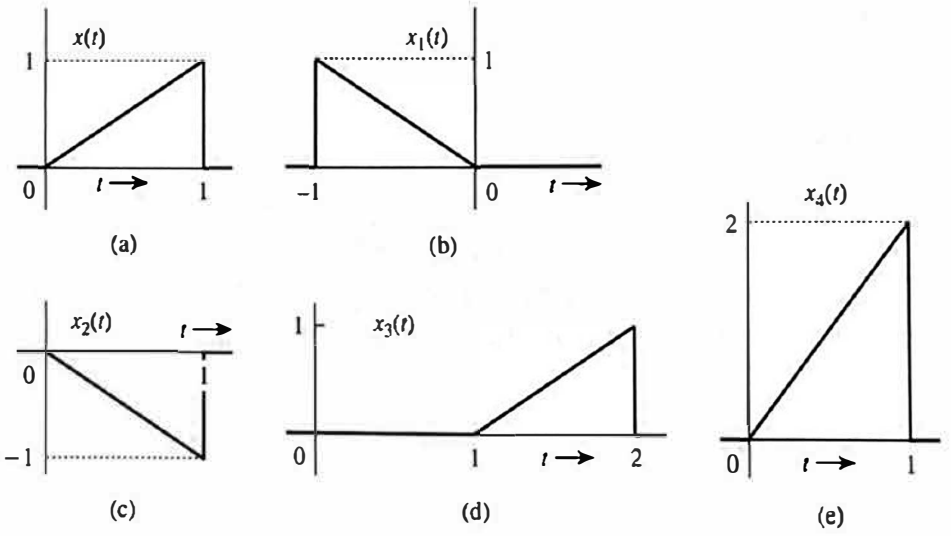

Figure P1.1-2

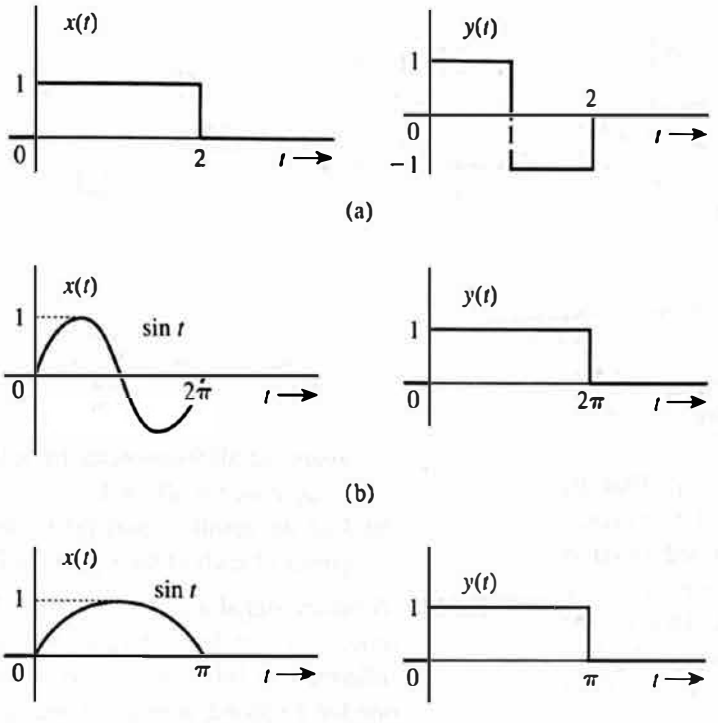

Figure P1.1-3

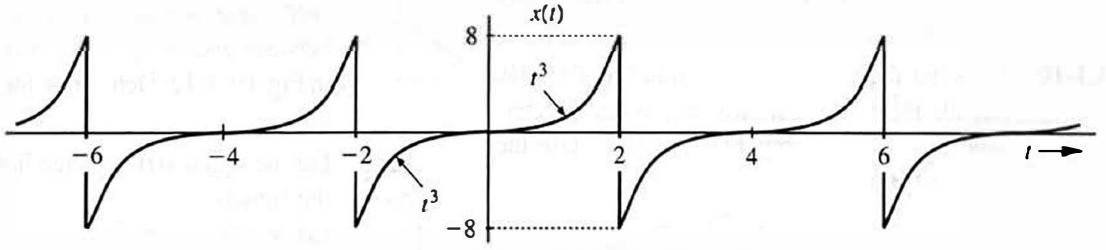

Figure P1.1-4

1.1-6 Determine the power and the rms value for each of the following signals:

(a) $5 + 10\cos(100t + \pi/3)$

(b) $10\cos(100t + \pi/3) + 16\sin(150t + \pi/5)$

(c) $(10 + 2\sin 3t)\cos 10t$

(d) $10\cos 5t \cos 10t$

(e) $10\sin 5t \cos 10t$

(f) $e^{j\alpha t}\cos\omega_0 t$

1.1-7 Figure P1.1-7 shows a periodic 50% duty cycle dc-offset sawtooth wave $x(t)$ with peak amplitude A. Determine the energy and power of $x(t)$.

1.1-8 Two periodic signals that differ only by a 90-degree phase shift are considered to be quadrature signals. For example, $\cos(2\pi t)$ and $\sin(2\pi t)$ are quadrature signals. Another pair of quadrature signals is $x(t) = \text{sgn}[\cos(2\pi t)]$ and $y(t) = \text{sgn}[\sin(2\pi t)]$, where sgn is the sign (or signum) function.

(a) Plot $x(t)$ and determine its power P_x and energy E_x.

(b) Plot $y(t)$ and determine its power P_y and energy E_y.

(c) Consider the complex function $f(t) = x(t) + jy(t)$. Determine the power and energy of $f(t)$.

(d) When real functions $x(t)$ and $y(t)$ are combined as $f(t) = x(t) + jy(t)$, is it generally true that $E_f = E_x + E_y$ and $P_f = P_x + P_y$? Prove your answer.

1.1-9 There are many useful properties related to signal energy. Prove each of the following statements. In each case, let energy signal $x_1(t)$ have energy $E[x_1(t)]$, let energy signal $x_2(t)$ have

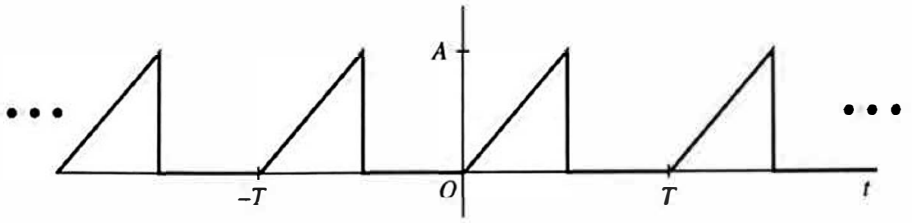

Figure P1.1-7

energy $E[x_2(t)]$, and let T be a nonzero, finite, real-valued constant.

(a) Prove $E[Tx_1(t)] = T^2E[x_1(t)]$. That is, amplitude scaling a signal by constant T scales the signal energy by T^2.

(b) Prove $E[x_1(t)] = E[x_1(t - T)]$. That is, shifting a signal does not affect its energy.

(c) If $(x_1(t) \neq 0) \Rightarrow (x_2(t) = 0)$ and $(x_2(t) \neq 0) \Rightarrow (x_1(t) = 0)$, then prove $E[x_1(t) + x_2(t)] = E[x_1(t)] + E[x_2(t)]$. That is, the energy of the sum of two nonoverlapping signals is the sum of the two individual energies.

(d) Prove $E[x_1(Tt)] = (1/|T|)E[x_1(t)]$. That is, time-scaling a signal by T reciprocally scales the signal energy by $1/|T|$.

1.1-10 Consider the signal $x(t)$ shown in Fig. P1.1-10. Outside the interval shown, $x(t)$ is zero. Determine the signal energy $E[x(t)]$. [*Hint:* Use the results of Prob. 1.1-9.]

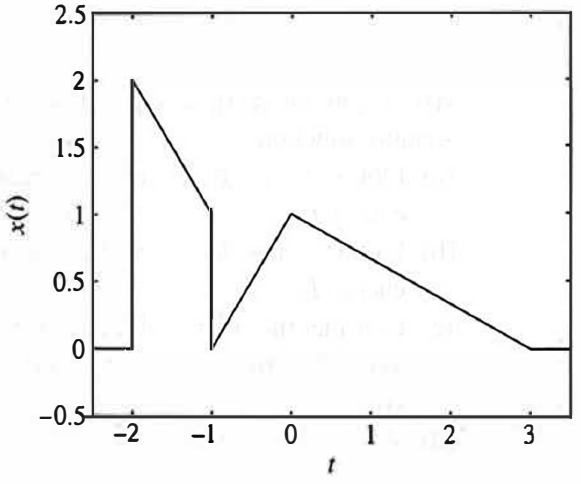

Figure P1.1-10

1.1-11 (a) Show that the power of a signal

$$x(t) = \sum_{k=m}^{n} D_k e^{j\omega_k t}$$

is

$$P_x = \sum_{k=m}^{n} |D_k|^2$$

assuming all frequencies to be distinct, that is, $\omega_i \neq \omega_k$ for all $i \neq k$.

(b) Use the result in part (a) to determine the power of each of the signals in Prob. 1.1-6.

1.1-12 A binary signal $x(t) = 0$ for $t < 0$. For positive time, $x(t)$ toggles between one and zero as follows: one for 1 second, zero for 1 second, one for 1 second, zero for 2 seconds, one for 1 second, zero for 3 seconds, and so forth. That is, the "on" time is always 1 second, but the "off" time successively increases by 1 second between each toggle. A portion of $x(t)$ is shown in Fig. P1.1-12. Determine the energy and power of $x(t)$.

1.2-1 For the signal $x(t)$ depicted in Fig. P1.2-1, sketch the signals

(a) $x(-t)$

(b) $x(t+6)$

(c) $x(3t)$

(d) $x(t/2)$

1.2-2 For the signal $x(t)$ illustrated in Fig. P1.2-2, sketch

(a) $x(t-4)$

(b) $x(t/1.5)$

(c) $x(-t)$

(d) $x(2t-4)$

(e) $x(2-t)$

1.2-3 In Fig. P1.2-3, express signals $x_1(t)$, $x_2(t)$, $x_3(t)$, $x_4(t)$, and $x_5(t)$ in terms of signal $x(t)$ and its time-shifted, time-scaled, or time-reversed versions.

1.2-4 For an energy signal $x(t)$ with energy E_x, show that the energy of any one of the signals $-x(t)$, $x(-t)$, and $x(t - T)$ is E_x. Show also that the energy of $x(at)$ as well as $x(at - b)$ is E_x/a, but the energy of $ax(t)$ is a^2E_x. This shows that time

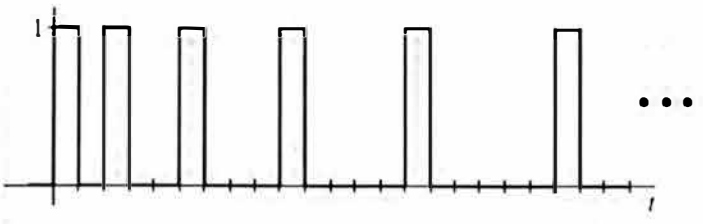

Figure P1.1-12

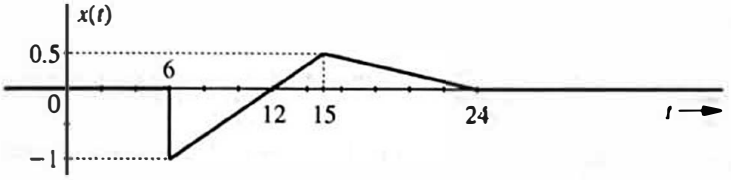

Figure P1.2-1

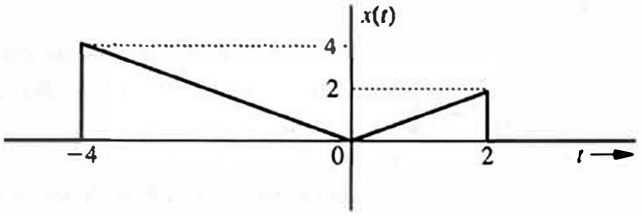

Figure P1.2-2

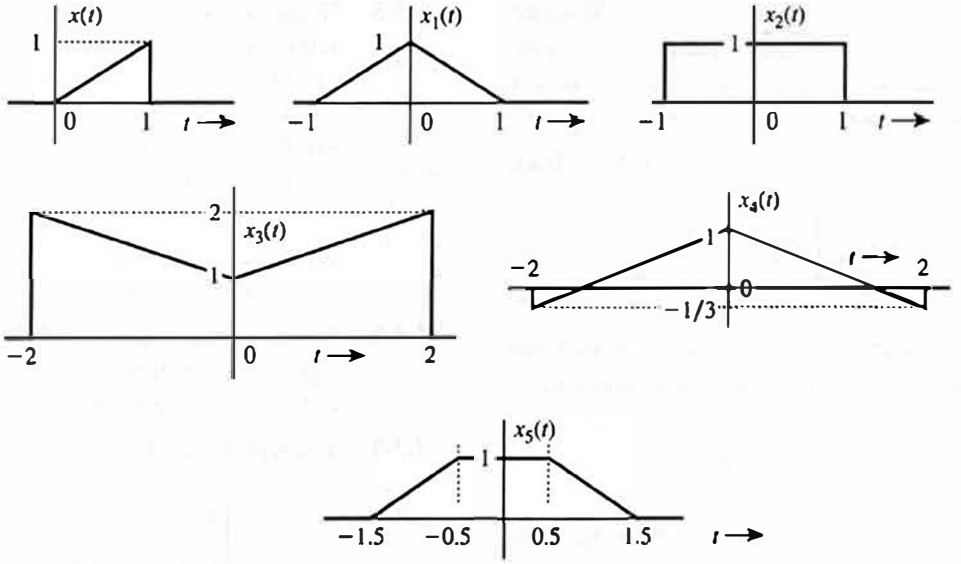

Figure P1.2-3

inversion and time shifting do not affect signal energy. On the other hand, time compression of a signal ($a > 1$) reduces the energy, and time expansion of a signal ($a < 1$) increases the energy. What is the effect on signal energy if the signal is multiplied by a constant a?

1.2-5 Define $2x(-3t+1) = t[u(-t-1) - u(-t+1)]$, where $u(t)$ is the unit step function.

(a) Plot $2x(-3t+1)$ over a suitable range of t.

(b) Plot $x(t)$ over a suitable range of t.

1.2-6 Consider the signal $x(t) = 2^{-tu(t)}$, where $u(t)$ is the unit step function.

(a) Accurately sketch $x(t)$ over $(-1 \leq t \leq 1)$.

(b) Accurately sketch $y(t) = 0.5x(1-2t)$ over $(-1 \leq t \leq 1)$.

1.2-7 Define signals $y(t)$ and $z(t)$ as in Fig. P1.2-7.

(a) Determine constants a, b, and c to produce $z(t) = ax(bt+c)$ in Fig. P1.2-7.

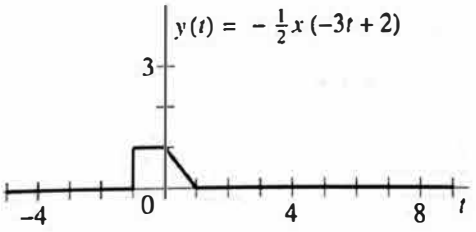

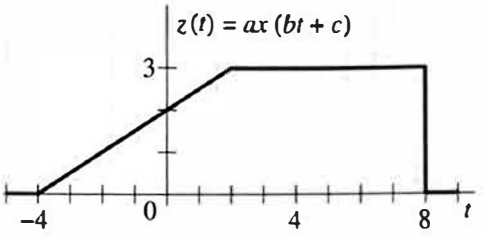

Figure P1.2-7

(b) Determine and sketch a signal $v(t)$ such that $z(t) = \int_{-\infty}^{t} v(\tau)\,d\tau$.

1.3-1 Think of a real-world signal that is personally relevant and interesting. Describe the signal and then classify it according to the six following characteristics:

(a) continuous-time or discrete-time
(b) analog or digital
(c) periodic or aperiodic
(d) energy or power
(e) causal or noncausal
(f) deterministic or random

If possible, think of a second real-world signal that has the opposite six characteristics of your first signal. If such a second signal is not possible, carefully explain why that is the case.

1.3-2 Define signal $y(t) = \sum_{k=-\infty}^{\infty} x(0.5t - 10k)$, where

$$x(t) = \begin{cases} e^{-2t} & t \geq 1 \\ 0 & t < 1 \end{cases}$$

(a) Determine the constant a such that the signal $x(-2t + a)$ is borderline anticausal.
(b) Is the signal $y(t)$ periodic? If so, determine the period T_y. If not, explain why $y(t)$ is not periodic.

1.3-3 Determine whether each of the following statements is true or false. If the statement is false, demonstrate this by proof or example.

(a) Every continuous-time signal is an analog signal.
(b) Every discrete-time signal is a digital signal.
(c) If a signal is not an energy signal, then it must be a power signal and vice versa.
(d) An energy signal must be of finite duration.
(e) A power signal cannot be causal.
(f) A periodic signal cannot be anticausal.

1.3-4 Determine whether each of the following statements is true or false. If the statement is false, demonstrate by proof or example why the statement is false.

(a) Every bounded periodic signal is a power signal.
(b) Every bounded power signal is a periodic signal.
(c) If an energy signal $x(t)$ has energy E, then the energy of $x(at)$ is E/a. Assume a is real and positive.
(d) If a power signal $x(t)$ has power P, then the power of $x(at)$ is P/a. Assume a is real and positive.

1.3-5 Given $x_1(t) = \cos(t)$, $x_2(t) = \sin(\pi t)$, and $x_3(t) = x_1(t) + x_2(t)$.

(a) Determine the fundamental periods T_1 and T_2 of signals $x_1(t)$ and $x_2(t)$.
(b) Show that $x_3(t)$ is not periodic, which requires $T_3 = k_1 T_1 = k_2 T_2$ for some integers k_1 and k_2.
(c) Determine the powers P_{x_1}, P_{x_2}, and P_{x_3} of signals $x_1(t)$, $x_2(t)$, and $x_3(t)$.

1.3-6 For any constant ω, is the function $f(t) = \sin(\omega t)$ a periodic function of the independent variable t? Justify your answer.

1.3-7 The signal shown in Fig. P1.3-7 is defined as

$$x(t) = \begin{cases} t & 0 \leq t < 1 \\ 0.5 + 0.5\cos(2\pi t) & 1 \leq t < 2 \\ 3 - t & 2 \leq t < 3 \\ 0 & \text{otherwise} \end{cases}$$

The energy of $x(t)$ is $E \approx 1.0417$.

(a) What is the energy of $y_1(t) = (1/3)x(2t)$?
(b) A periodic signal $y_2(t)$ is defined as

$$y_2(t) = \begin{cases} x(t) & 0 \leq t < 4 \\ y_2(t+4) & \forall t \end{cases}$$

What is the power of $y_2(t)$?

(c) What is the power of $y_3(t) = (1/3)y_2(2t)$?

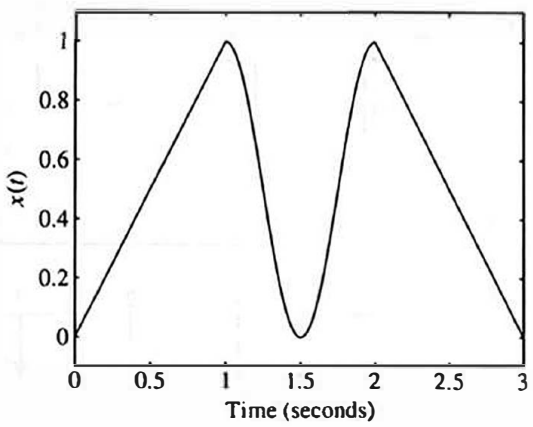

Figure P1.3-7

1.3-8 Let $y_1(t) = y_2(t) = t^2$ over $0 \le t \le 1$. Notice, this statement does not require $y_1(t) = y_2(t)$ for all t.

(a) Define $y_1(t)$ as an even, periodic signal with period $T_1 = 2$. Sketch $y_1(t)$ and determine its power.

(b) Design an odd, periodic signal $y_2(t)$ with period $T_2 = 3$ and power equal to unity. Fully describe $y_2(t)$ and sketch the signal over at least one full period. [*Hint:* There are an infinite number of possible solutions to this problem—you need to find only one of them!]

(c) We can create a complex-valued function $y_3(t) = y_1(t) + jy_2(t)$. Determine whether this signal is periodic. If yes, determine the period T_3. If no, justify why the signal is not periodic.

(d) Determine the power of $y_3(t)$ defined in part (c). The power of a complex-valued function $z(t)$ is

$$P = \lim_{T\to\infty} \frac{1}{T} \int_{-T/2}^{T/2} z(\tau) z^*(\tau)\, d\tau$$

1.4-1 Sketch the following signals:

(a) $u(t-5) - u(t-7)$

(b) $u(t-5) + u(t-7)$

(c) $t^2[u(t-1) - u(t-2)]$

(d) $(t-4)[u(t-2) - u(t-4)]$

1.4-2 Express each of the signals in Fig. P1.4-2 by a single expression valid for all t.

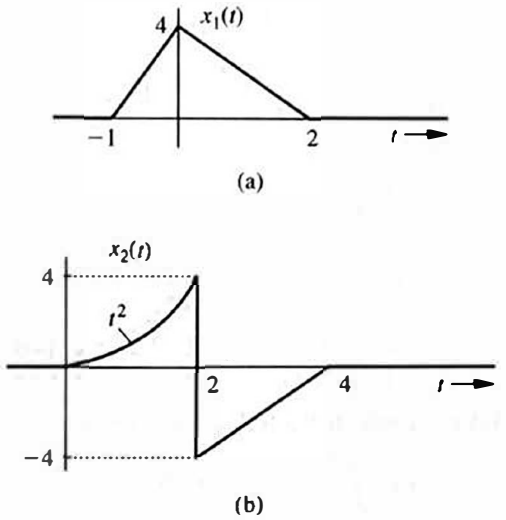

Figure P1.4-2

1.4-3 Letting $w(t) = t[u(t) - u(t-1)]$, define the periodic signal $x(t)$ as

$$x(t) = \sum_{k=-\infty}^{\infty} w(2t+2k) - 0.5w(2t+2k-1)$$

(a) Sketch $w(t)$ and $x(t)$. What is the fundamental period T_0 of signal $x(t)$?

(b) Sketch $y(t) = \frac{d}{dt}x(1-0.5t)$.

(c) Determine the energy E_z and power P_z of the signal $z(t) = x(0.5 - 1.5t)[u(t) - u(t-1)]$. Sketching $z(t)$ should help.

1.4-4 Define signal $x(t) = u(t-1) - u(t-2.5) - 2\delta(t-4) + \delta(t-6)$.

(a) Sketch $y(t) = \int_{-\infty}^{t} x(\tau)\, d\tau$.

(b) Describe a simple change that can be made to the right-most delta function in $x(t)$ so that $y(t) = \int_{-\infty}^{t} x(\tau)\, d\tau$ has finite energy.

(c) Sketch $z(t) = \int_{t}^{\infty} x(\tau)\, d\tau$.

(d) Determine real constants A and B so that $w(t) = x\left(\frac{t-A}{B}\right)$ has a region of support $[-2,2]$.

1.4-5 Simplify the following expressions:

(a) $\left(\frac{\sin t}{t^2+2}\right)\delta(t)$

(b) $\left(\frac{j\omega+2}{\omega^2+9}\right)\delta(\omega)$

(c) $[e^{-t}\cos(3t-60°)]\delta(t)$

(d) $\left(\frac{\sin\left[\frac{\pi}{2}(t-2)\right]}{t^2+4}\right)\delta(1-t)$

(e) $\left(\frac{1}{j\omega+2}\right)\delta(\omega+3)$

(f) $\left(\frac{\sin k\omega}{\omega}\right)\delta(\omega)$

[*Hint:* Use Eq. (1.10). For part (f), use L'Hôpital's rule.]

1.4-6 Evaluate the following integrals:

(a) $\int_{-\infty}^{\infty}\delta(\tau)x(t-\tau)\,d\tau$

(b) $\int_{-\infty}^{\infty}x(\tau)\delta(t-\tau)\,d\tau$

(c) $\int_{-\infty}^{\infty}\delta(t)e^{-j\omega t}\,dt$

(d) $\int_{-\infty}^{\infty}\delta(2t-3)\sin\pi t\,dt$

(e) $\int_{-\infty}^{\infty}\delta(t+3)e^{-t}\,dt$

(f) $\int_{-\infty}^{\infty}(t^3+4)\delta(1-t)\,dt$

(g) $\int_{-\infty}^{\infty}x(2-t)\delta(3-t)\,dt$

(h) $\int_{-\infty}^{\infty}e^{(x-1)}\cos\left[\frac{\pi}{2}(x-5)\right]\delta(x-3)\,dx$

1.4-7 For real and positive constant a, evaluate the following integral:

$$\int_{-\infty}^{\infty}\delta(at)\,dt$$

1.4-8 (a) Find and sketch dx/dt for the signal $x(t)$ shown in Fig. P1.2-2.

(b) Find and sketch d^2x/dt^2 for the signal $x_1(t)$ depicted in Fig. P1.4-2a.

1.4-9 Find and sketch $\int_{-\infty}^{t}x(t)\,dt$ for the signals $x(t)$ illustrated in Fig. P1.4-9.

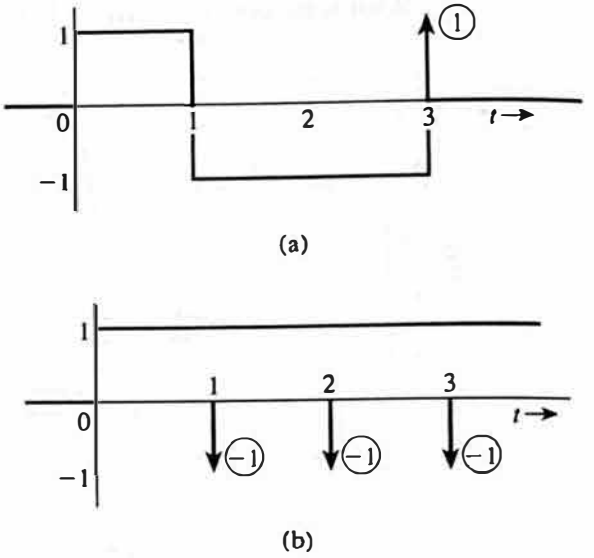

Figure P1.4-9

1.4-10 Using the generalized function definition of impulse [Eq. (1.11) with $T=0$], show that $\delta(t)$ is an even function of t.

1.4-11 Using the generalized function definition of impulse [Eq. (1.11) with $T=0$], show that

$$\delta(at)=\frac{1}{|a|}\delta(t)$$

1.4-12 Show that

$$\int_{-\infty}^{\infty}\dot{\delta}(t)\phi(t)\,dt=-\dot{\phi}(0)$$

where $\phi(t)$ and $\dot{\phi}(t)$ are continuous at $t=0$, and $\phi(t)\to 0$ as $t\to\pm\infty$. This integral defines $\dot{\delta}(t)$ as a generalized function. [*Hint:* Use integration by parts.]

1.4-13 A sinusoid $e^{\sigma t}\cos\omega t$ can be expressed as a sum of exponentials e^{st} and e^{-st} [Eq. (1.14)] with complex frequencies $s=\sigma+j\omega$ and $s=\sigma-j\omega$. Locate in the complex plane the frequencies of the following sinusoids:

(a) $\cos 3t$
(b) $e^{-3t}\cos 3t$
(c) $e^{2t}\cos 3t$
(d) e^{-2t}
(e) e^{2t}
(f) 5

1.5-1 Find and sketch the odd and the even components of the following:

(a) $u(t)$
(b) $tu(t)$
(c) $\sin \omega_0 t$
(d) $\cos \omega_0 t$
(e) $\cos(\omega_0 t + \theta)$
(f) $\sin \omega_0 t u(t)$
(g) $\cos \omega_0 t u(t)$

1.5-2 Define $x(t) = 2u(t+1) - u(t-2) - u(t-3)$.
(a) Letting $x_o(t)$ designate the odd portion of $x(t)$, accurately sketch $x_o(1-2t)$.
(b) Letting $x_e(t)$ designate the even portion of $x(t)$, accurately sketch $x_e(2+t/3)$.

1.5-3 (a) Determine even and odd components of the signal $x(t) = e^{-2t}u(t)$.
(b) Show that the energy of $x(t)$ is the sum of energies of its odd and even components found in part (a).
(c) Generalize the result in part (b) for any finite energy signal.

1.5-4 (a) If $x_e(t)$ and $x_o(t)$ are even and the odd components of a real signal $x(t)$, then show that

$$\int_{-\infty}^{\infty} x_e(t)x_o(t)\,dt = 0$$

(b) Show that

$$\int_{-\infty}^{\infty} x(t)\,dt = \int_{-\infty}^{\infty} x_e(t)\,dt$$

1.5-5 An aperiodic signal is defined as $x(t) = \sin(\pi t)u(t)$, where $u(t)$ is the continuous-time step function. Is the odd portion of this signal, $x_o(t)$, periodic? Justify your answer.

1.5-6 An aperiodic signal is defined as $x(t) = \cos(\pi t)u(t)$, where $u(t)$ is the continuous-time step function. Is the even portion of this signal, $x_e(t)$, periodic? Justify your answer.

1.5-7 Consider the signal $x(t)$ shown in Fig. P1.5-7.

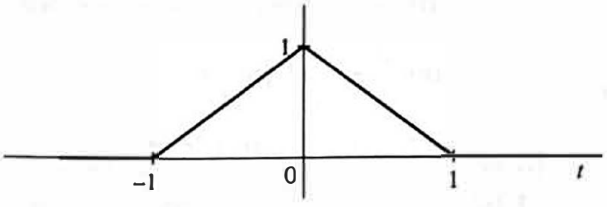

Figure P1.5-7

(a) Determine and carefully sketch $v(t) = 3x(-(1/2)(t+1))$.
(b) Determine the energy and power of $v(t)$.
(c) Determine and carefully sketch the even portion of $v(t)$, $v_e(t)$.
(d) Let $a = 2$ and $b = 3$; sketch $v(at+b)$, $v(at)+b$, $av(t+b)$, and $av(t)+b$.
(e) Let $a = -3$ and $b = -2$; sketch $v(at+b)$, $v(at)+b$, $av(t+b)$, and $av(t)+b$.

1.5-8 Consider the signal $y(t) = (1/5)x(-2t-3)$ shown in Fig. P1.5-8.

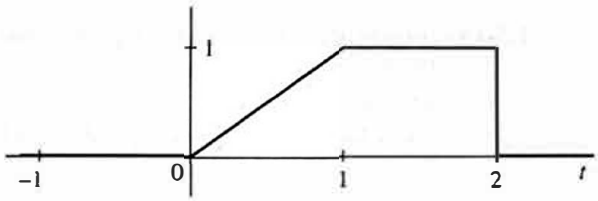

Figure P1.5-8

(a) Does $y(t)$ have an odd portion, $y_o(t)$? If so, determine and carefully sketch $y_o(t)$. Otherwise, explain why no odd portion exists.
(b) Determine and carefully sketch the original signal $x(t)$.

1.5-9 Consider the signal $-(1/2)x(-3t+2)$ shown in Fig. P1.5-9.

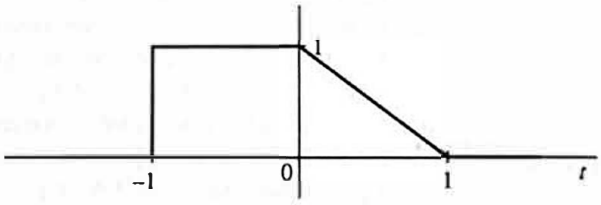

Figure P1.5-9

(a) Determine and carefully sketch the original signal $x(t)$.
(b) Determine and carefully sketch the even portion of the original signal $x(t)$.
(c) Determine and carefully sketch the odd portion of the original signal $x(t)$.

1.5-10 The conjugate symmetric (or Hermitian) portion of a signal is defined as $w_{cs}(t) = (w(t) + w^*(-t))/2$. Show that the real portion of $w_{cs}(t)$ is even and that the imaginary portion of $w_{cs}(t)$ is odd.

1.5-11 The conjugate antisymmetric (or skew-Hermitian) portion of a signal is defined as $w_{ca}(t) = (w(t) - w^*(-t))/2$. Show that the real portion of $w_{ca}(t)$ is odd and that the imaginary portion of $w_{ca}(t)$ is even.

1.5-12 Define $w(t) = e^{j(t+\pi/4)}$.

(a) Referring to the definition in Prob. 1.5-10, determine $w_{cs}(t)$. Express your simplified answer in standard rectangular form.

(b) Referring to the definition in Prob. 1.5-11, determine $w_{ca}(t)$. Express your simplified answer in standard polar form.

1.5-13 Figure P1.5-13 plots a complex signal $w(t)$ in the complex plane over the time range $(0 \leq t \leq 1)$. The time $t = 0$ corresponds with the origin, while the time $t = 1$ corresponds with the point $(2, 1)$.

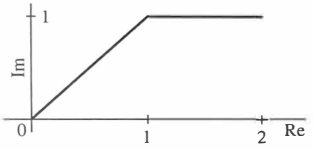

Figure P1.5-13

(a) In the complex plane, plot $w(t)$ over $(-1 \leq t \leq 1)$ if $w(t)$ is an even signal.

(b) In the complex plane, plot $w(t)$ over $(-1 \leq t \leq 1)$ if $w(t)$ is an odd signal.

(c) In the complex plane, plot $w(t)$ over $(-1 \leq t \leq 1)$ if $w(t)$ is a conjugate symmetric signal. [*Hint:* See Prob. 1.5-10.]

(d) In the complex plane, plot $w(t)$ over $(-1 \leq t \leq 1)$ if $w(t)$ is a conjugate antisymmetric signal. [*Hint:* See Prob. 1.5-11.]

(e) In the complex plane, plot as much of $w(3t)$ as possible.

1.5-14 Define complex signal $x(t) = t^2(1 + j)$ over interval $(1 \leq t \leq 2)$. The remaining portion is defined such that $x(t)$ is a minimum-energy, skew-Hermitian signal.

(a) Fully describe $x(t)$ for all t.

(b) Sketch $y(t) = \text{Re}\{x(t)\}$ versus the independent variable t.

(c) Sketch $z(t) = \text{Re}\{jx(-2t + 1)\}$ versus the independent variable t.

(d) Determine the energy and power of $x(t)$.

[*Hint:* See Prob. 1.5-11 for a definition of skew-Hermitian signals.]

1.6-1 Write the input–output relationship for an ideal integrator. Determine the zero-input and zero-state components of the response.

1.6-2 A force $x(t)$ acts on a ball of mass M (Fig. P1.6-2). Show that the velocity $v(t)$ of the ball at any instant $t > 0$ can be determined if we know the force $x(t)$ over the interval from 0 to t and the ball's initial velocity $v(0)$.

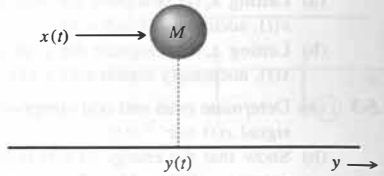

Figure P1.6-2

1.6-3 From your personal experience, provide an example of:

(a) a single-input, single-output (SISO) system

(b) a multiple-input, single-output (MISO) system

(c) a single-input, multiple-output (SIMO) system

(d) a multiple-input, multiple-output (MIMO) system

1.7-1 For the systems described by the following equations, with the input $x(t)$ and output $y(t)$, determine which of the systems are linear and which are nonlinear.

(a) $\dfrac{dy(t)}{dt} + 2y(t) = x^2(t)$

(b) $\dfrac{dy(t)}{dt} + 3ty(t) = t^2x(t)$

(c) $3y(t) + 2 = x(t)$

(d) $\dfrac{dy(t)}{dt} + y^2(t) = x(t)$

(e) $\left(\dfrac{dy(t)}{dt}\right)^2 + 2y(t) = x(t)$

(f) $\dfrac{dy(t)}{dt} + (\sin t)y(t) = \dfrac{dx(t)}{dt} + 2x(t)$

(g) $\dfrac{dy(t)}{dt} + 2y(t) = x(t)\dfrac{dx(t)}{dt}$

(h) $y(t) = \displaystyle\int_{-\infty}^{t} x(\tau)\,d\tau$

1.7-2 For the systems described by the following equations, with the input $x(t)$ and output $y(t)$, explain with reasons which of the systems are

time-invariant parameter systems and which are time-varying-parameter systems.

(a) $y(t) = x(t-2)$
(b) $y(t) = x(-t)$
(c) $y(t) = x(at)$
(d) $y(t) = tx(t-2)$
(e) $y(t) = \int_{-5}^{5} x(\tau)\,d\tau$
(f) $y(t) = \left(\frac{dx(t)}{dt}\right)^2$

1.7-3 Two inputs, temperature $T(t)$ and wind speed $V(t)$, produce an output, wind chill $W(t)$, according to $W(t) = 35.74 + 0.6215T(t) - 35.75\{V(t)\}^{0.16} + 0.4275T(t)\{V(t)\}^{0.16}$. The independent variable here is time, t. Answer the following questions yes or no, and provide mathematical justification for each answer.

(a) Is this system BIBO-stable?
(b) Is the system memoryless?
(c) Is the system causal?
(d) For simplicity, let the wind speed be constant, $V(t) = k_V$. Thus, $W(t) = k_1 + k_2T(t)$ for some constants k_1 and k_2. Is this simplified system linear?
(e) For simplicity, let the temperature be constant, $T(t) = k_T$. Thus, $W(t) = k_3 + k_4\{V(t)\}^{0.16}$ for some constants k_3 and k_4. Is this simplified system linear?

1.7-4 Input voltage $x(t)$ applied to an inverting op-amp follower circuit produces output $y(t)$ according to

$$y(t+t_p) = \begin{cases} -V_{ref} & x(t) > V_{ref} \\ V_{ref} & x(t) < -V_{ref} \\ -x(t) & \text{otherwise} \end{cases}$$

where op-amp reference voltage V_{ref} and propagation delay t_p are both positive constants. Answer the following questions yes or no, and provide mathematical justification for each answer.

(a) Is this system BIBO-stable?
(b) Is the system causal?
(c) Is the system invertible?
(d) Is the system linear?
(e) Is the system memoryless?
(f) Is the system time invariant?

1.7-5 Repeat Prob. 1.7-4 for a system with input $x(t)$ that produces output $y(t)$ according to

$$y(t+1) = \begin{cases} -2x(t) & \text{when } x(t) \geq 0 \\ 0 & \text{otherwise} \end{cases}$$

1.7-6 Repeat Prob. 1.7-4 for a system with input $x(t)$ that produces output $y(t)$ according to

$$y(t-1) = \begin{cases} x(t-1) & \text{when } \frac{d}{dt}x(t) \geq 0 \\ x(t-2) & \text{otherwise} \end{cases}$$

1.7-7 Repeat Prob. 1.7-4 for a system that multiplies a given input by a ramp function, $r(t) = tu(t)$. That is, $y(t) = x(t)r(t)$.

1.7-8 Repeat Prob. 1.7-4 for a system with input $x(t)$ that produces output $y(t)$ according to

$$y(t) = \frac{d}{dt}x(t-1)$$

1.7-9 Repeat Prob. 1.7-4 for a system with input $x(t)$ that produces output $y(t)$ according to

$$y(t) = \begin{cases} x(t) & \text{if } x(t) > 0 \\ 0 & \text{if } x(t) \leq 0 \end{cases}$$

1.7-10 A continuous-time system is given by

$$y(t) = 0.5\int_{-\infty}^{\infty} x(\tau)[\delta(t-\tau) - \delta(t+\tau)]\,d\tau$$

Recall that $\delta(t)$ designates the Dirac delta function.

(a) Explain what this system does.
(b) Is the system BIBO-stable? Justify your answer.
(c) Is the system linear? Justify your answer.
(d) Is the system memoryless? Justify your answer.
(e) Is the system causal? Justify your answer.
(f) Is the system time invariant? Justify your answer.

1.7-11 For a certain LTI system with the input $x(t)$, the output $y(t)$, and the two initial conditions $q_1(0)$ and $q_2(0)$, the following observations were made:

$x(t)$	$q_1(0)$	$q_2(0)$	$y(t)$
0	1	−1	$e^{-t}u(t)$
0	2	1	$e^{-t}(3t+2)u(t)$
$u(t)$	−1	−1	$2u(t)$

Determine $y(t)$ when both the initial conditions are zero and the input $x(t)$ is as shown in Fig. P1.7-11. [*Hint:* There are three causes: the input and each of the two initial conditions. Because of the linearity property, if a cause is increased by a factor k, the response to that cause

also increases by the same factor k. Moreover, if causes are added, the corresponding responses add.]

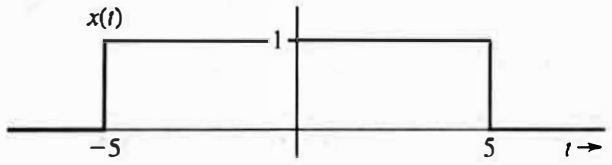

Figure P1.7-11

1.7-12 A system is specified by its input–output relationship as

$$y(t) = \frac{x^2(t)}{dx(t)/dt}$$

Show that the system satisfies the homogeneity property but not the additivity property.

1.7-13 Show that the circuit in Fig. P1.7-13 is zero-state linear but not zero-input linear. Assume all diodes have identical (matched) characteristics. The output is the current $y(t)$.

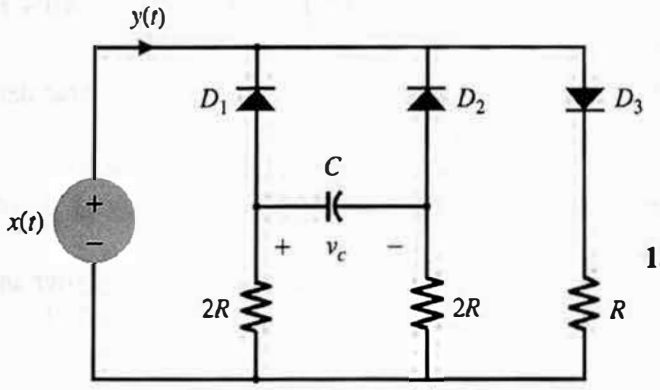

Figure P1.7-13

1.7-14 The inductor L and the capacitor C in Fig. P1.7-14 are nonlinear, which makes the circuit nonlinear. The remaining three elements are linear. Show that the output $y(t)$ of this nonlinear circuit satisfies the linearity conditions with respect to the input $x(t)$ and the initial conditions (all the initial inductor currents and capacitor voltages).

1.7-15 For the systems described by the following equations, with the input $x(t)$ and output $y(t)$, determine which are causal and which are noncausal.

(a) $y(t) = x(t-2)$
(b) $y(t) = x(-t)$
(c) $y(t) = x(at) \qquad a > 1$
(d) $y(t) = x(at) \qquad a < 1$

1.7-16 For the systems described by the following equations, with the input $x(t)$ and output $y(t)$, determine which are invertible and which are noninvertible. For the invertible systems, find the input–output relationship of the inverse system.

(a) $y(t) = \int_{-\infty}^{t} x(\tau)\,d\tau$
(b) $y(t) = x^n(t)$, $x(t)$ real, n integer
(c) $y(t) = \dfrac{dx(t)}{dt}$
(d) $y(t) = x(3t-6)$
(e) $y(t) = \cos[x(t)]$
(f) $y(t) = e^{x(t)}$, $x(t)$ real

1.7-17 Figure P1.7-17 displays an input $x_1(t)$ to a linear time-invariant (LTI) system H, the corresponding output $y_1(t)$, and a second input $x_2(t)$.

(a) Bill suggests that $x_2(t) = 2x_1(3t) - x_1(t-1)$. Is Bill correct? If yes, prove it. If not, correct his error.
(b) Bill wants to know the output $y_2(t)$ in response to the input $x_2(t)$. Provide him with

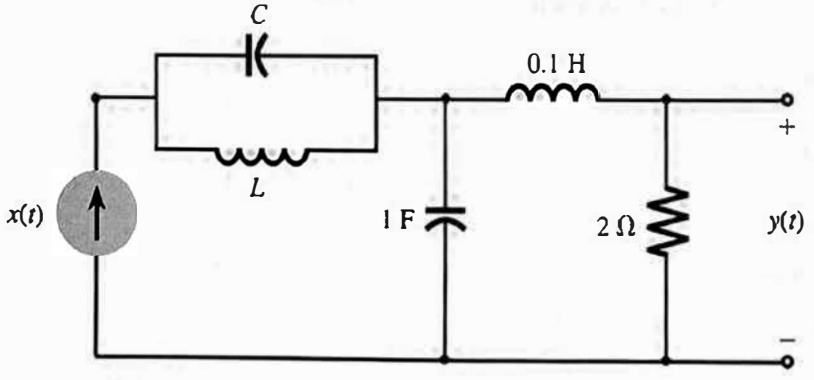

Figure P1.7-14

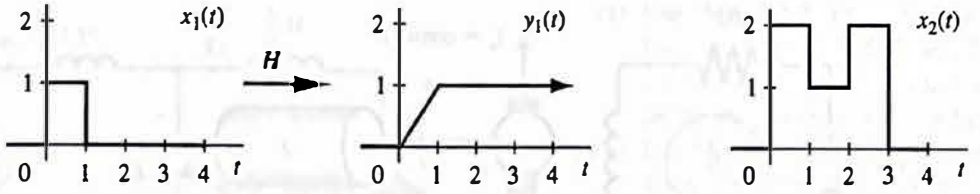

Figure P1.7-17

an expression for $y_2(t)$ in terms of $y_1(t)$. Use MATLAB to plot $y_2(t)$.

1.7-18 A linear time-invariant system H acts on input $x(t) = u(t - 0.5) - u(t - 1.5)$ to produce output $y(t) = H\{x(t)\} = 0.5u(t) + 0.5u(t - 1) - u(t - 2)$.

(a) Is it possible that the system is causal? Explain your answer. If not causal, determine the shift necessary to make the system causal.

(b) Is it possible that the system is memoryless? Explain your answer.

(c) Suppose the output $y(t)$ is applied to an identical system H to produce output

$$z(t) = H\{y(t)\} = H\{H\{x(t)\}\}$$

If possible, determine and sketch $z(t)$. If not possible, explain why $z(t)$ cannot be determined using the information given.

1.8-1 For the circuit depicted in Fig. P1.8-1, find the differential equations relating outputs $y_1(t)$ and $y_2(t)$ to the input $x(t)$.

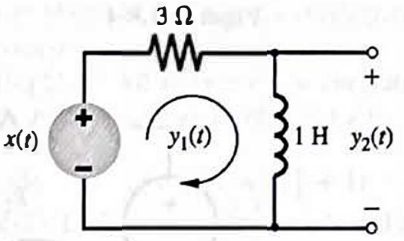

Figure P1.8-1

1.8-2 For the circuit depicted in Fig. P1.8-2, find the differential equations relating outputs $y_1(t)$ and $y_2(t)$ to the input $x(t)$.

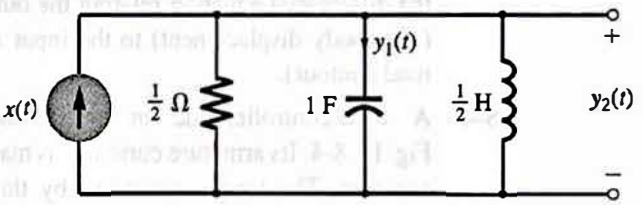

Figure P1.8-2

1.8-3 A simplified (one-dimensional) model of an automobile suspension system is shown in Fig. P1.8-3. In this case, the input is not a force but a displacement $x(t)$ (the road contour). Find

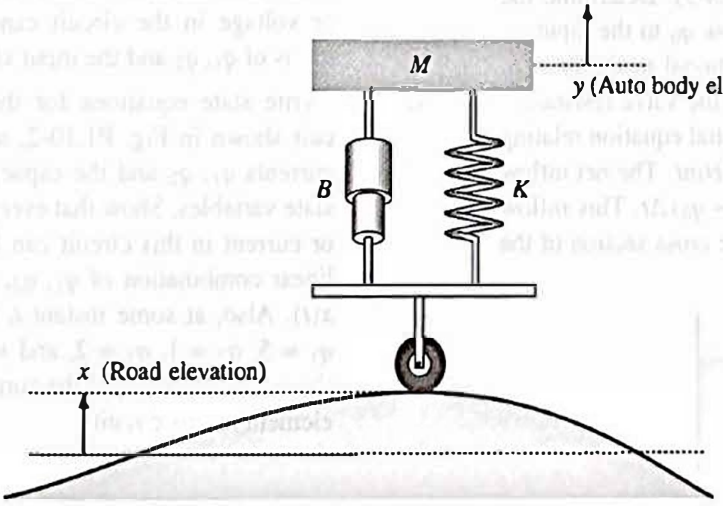

Figure P1.8-3

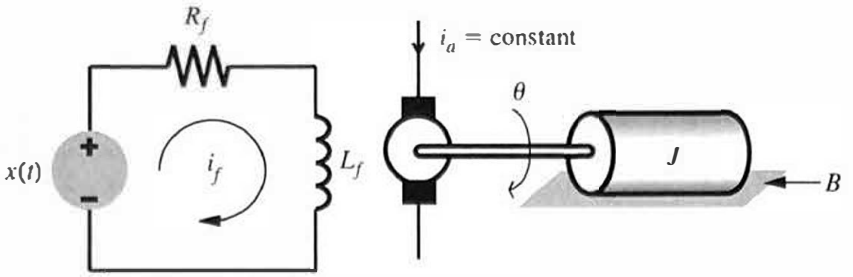

Figure P1.8-4

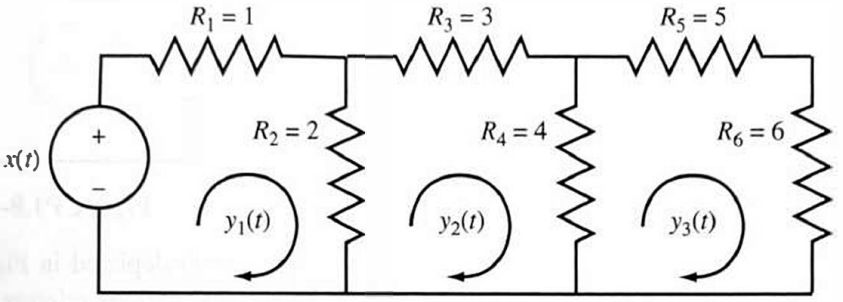

Figure P1.8-6

the differential equation relating the output $y(t)$ (auto body displacement) to the input $x(t)$ (the road contour).

1.8-4 A field-controlled dc motor is shown in Fig. P1.8-4. Its armature current i_a is maintained constant. The torque generated by this motor is proportional to the field current i_f (torque$= K_f i_f$). Find the differential equation relating the output position θ to the input voltage $x(t)$. The motor and load together have a moment of inertia J.

1.8-5 Water flows into a tank at a rate of q_i units/s and flows out through the outflow valve at a rate of q_0 units/s (Fig. P1.8-5). Determine the equation relating the outflow q_0 to the input q_i. The outflow rate is proportional to the head h. Thus, $q_0 = Rh$, where R is the valve resistance. Determine also the differential equation relating the head h to the input q_i. [*Hint:* The net inflow of water in time Δt is $(q_i - q_0)\Delta t$. This inflow is also $A\Delta h$, where A is the cross section of the tank.]

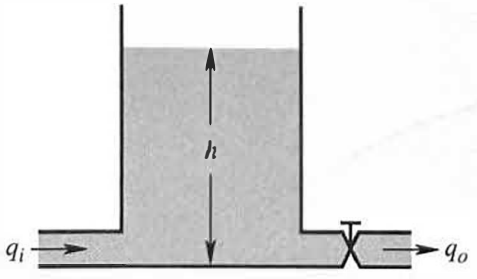

Figure P1.8-5

1.8-6 Consider the circuit shown in Fig. P1.8-6, with input voltage $x(t)$ and output currents $y_1(t)$, $y_2(t)$, and $y_3(t)$.

(a) What is the order of this system? Explain your answer.

(b) Determine the matrix representation for this system.

(c) Use Cramer's rule to determine the output current $y_3(t)$ for the input voltage $x(t) = [2 - |\cos(t)|]u(t-1)$.

1.10-1 Write state equations for the parallel *RLC* circuit in Fig. P1.8-2. Use the capacitor voltage q_1 and the inductor current q_2 as your state variables. Show that every possible current or voltage in the circuit can be expressed in terms of q_1, q_2 and the input $x(t)$.

1.10-2 Write state equations for the third-order circuit shown in Fig. P1.10-2, using the inductor currents q_1, q_2 and the capacitor voltage q_3 as state variables. Show that every possible voltage or current in this circuit can be expressed as a linear combination of q_1, q_2, q_3, and the input $x(t)$. Also, at some instant t, it was found that $q_1 = 5$, $q_2 = 1$, $q_3 = 2$, and $x = 10$. Determine the voltage across and the current through every element in this circuit.

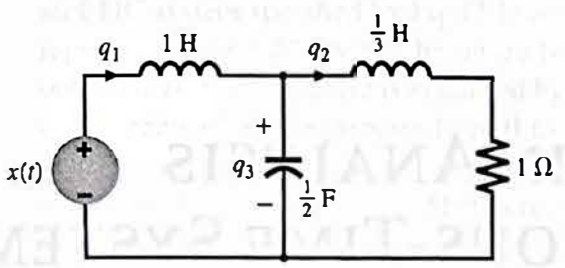

Figure P1.10-2

1.11-1 Provide MATLAB code and output that plots the odd portion $x_o(t)$ of the function $x(t) = 2^{-t}\cos(2\pi t)u(t-\pi)$ over a suitable-length interval using a suitable number of points.

1.11-2 Provide MATLAB code and output that plots the even portion $x_e(t)$ of the function $x(t) = 2^{-t/2}\cos(4\pi t)u(t-0.5)$ over a suitable t using $\Delta t = 0.002$ second between points.

1.11-3 Define $x(t) = e^{t(1+j2\pi)}u(-t)$ and $y(t) = \text{Re}\left\{2x\left(\frac{-5-t}{2}\right)\right\}$.

(a) Use MATLAB to plot $\text{Re}\{x(t)\}$ versus $\text{Im}\{x(at)\}$ for $a = 0.5$, 1, and 2 and $-10 \le t \le 10$. How important is the scale factor a on the shape of the resulting figure?

(b) Use MATLAB to plot $y(t)$ over $-10 \le t \le 10$. Analytically determine the time t_0 where $y(t)$ has a jump discontinuity. Verify your calculation of t_0 using the plot of $y(t)$.

(c) Use MATLAB and numerical integration to compute the energy E_x of signal $x(t)$.

(d) Use MATLAB and numerical integration to compute the energy E_y of signal $y(t)$.

1.11-4 Consider the signal $x(t) = u(\frac{t}{2}+1) - u(t-1) - \delta(\frac{t}{2})$. Define $y(t) = \int_{-\infty}^{t-3} x(\tau)\,d\tau$ and $z(t) = \int_{t}^{\infty} x(\tau)\,d\tau$.

(a) Using MATLAB, accurately plot $y(t)$.

(b) Using MATLAB, accurately plot $z(t)$.

(c) Using MATLAB, accurately plot $w(t) = \frac{d}{dt}[y(t)+z(t)]$.

CHAPTER 2

TIME-DOMAIN ANALYSIS OF CONTINUOUS-TIME SYSTEMS

In this book, we consider two methods of analysis of linear time-invariant (LTI) systems: the time-domain method and the frequency-domain method. In this chapter, we discuss the *time-domain analysis* of linear, time-invariant, continuous-time (LTIC) systems.

2.1 INTRODUCTION

For the purpose of analysis, we shall consider *linear differential systems*. This is the class of LTIC systems introduced in Ch. 1, for which the input $x(t)$ and the output $y(t)$ are related by linear differential equations of the form

$$\frac{d^N y(t)}{dt^N} + a_1 \frac{d^{N-1} y(t)}{dt^{N-1}} + \cdots + a_{N-1} \frac{dy(t)}{dt} + a_N y(t)$$
$$= b_{N-M} \frac{d^M x(t)}{dt^M} + b_{N-M+1} \frac{d^{M-1} x(t)}{dt^{M-1}} + \cdots + b_{N-1} \frac{dx(t)}{dt} + b_N x(t) \tag{2.1}$$

where all the coefficients a_i and b_i are constants. Using operator notation D to represent d/dt, we can express this equation as

$$(D^N + a_1 D^{N-1} + \cdots + a_{N-1} D + a_N) y(t)$$
$$= (b_{N-M} D^M + b_{N-M+1} D^{M-1} + \cdots + b_{N-1} D + b_N) x(t)$$

or

$$Q(D) y(t) = P(D) x(t) \tag{2.2}$$

where the polynomials $Q(D)$ and $P(D)$ are

$$Q(D) = D^N + a_1 D^{N-1} + \cdots + a_{N-1} D + a_N$$
$$P(D) = b_{N-M} D^M + b_{N-M+1} D^{M-1} + \cdots + b_{N-1} D + b_N$$

Theoretically, the powers M and N in the foregoing equations can take on any value. However, practical considerations make $M > N$ undesirable for two reasons. In Sec. 6.3.3, we shall show that

an LTIC system specified by Eq. (2.1) acts as an $(M-N)$th-order differentiator. A differentiator represents an unstable system because a bounded input like the step input results in an unbounded output, $\delta(t)$. Second, noise is enhanced by a differentiator. Noise is a wideband signal containing components of all frequencies from 0 to a very high frequency approaching ∞.[†] Hence, noise contains a significant amount of rapidly varying components. We know that the derivative of any rapidly varying signal is high. Therefore, any system specified by Eq. (2.1) in which $M > N$ will magnify the high-frequency components of noise through differentiation. It is entirely possible for noise to be magnified so much that it swamps the desired system output even if the noise signal at the system's input is tolerably small. Hence, practical systems generally use $M \leq N$. For the rest of this text, we assume implicitly that $M \leq N$. For the sake of generality, we shall assume $M = N$ in Eq. (2.1).

In Ch. 1, we demonstrated that a system described by Eq. (2.2) is linear. Therefore, its response can be expressed as the sum of two components: the zero-input response and the zero-state response (decomposition property).[‡] Therefore,

$$\text{total response} = \text{zero-input response} + \text{zero-state response}$$

The zero-input response is the system output when the input $x(t) = 0$, and thus it is the result of internal system conditions (such as energy storages, initial conditions) alone. It is independent of the external input $x(t)$. In contrast, the zero-state response is the system output to the external input $x(t)$ when the system is in zero state, meaning the absence of all internal energy storages: that is, all initial conditions are zero.

2.2 System Response to Internal Conditions: The Zero-Input Response

The zero-input response $y_0(t)$ is the solution of Eq. (2.2) when the input $x(t) = 0$ so that

$$Q(D)y_0(t) = 0$$

[†] Noise is any undesirable signal, natural or manufactured, that interferes with the desired signals in the system. Some of the sources of noise are the electromagnetic radiation from stars, the random motion of electrons in system components, interference from nearby radio and television stations, transients produced by automobile ignition systems, and fluorescent lighting.

[‡] We can verify readily that the system described by Eq. (2.2) has the decomposition property. If $y_0(t)$ is the zero-input response, then, by definition,

$$Q(D)y_0(t) = 0$$

If $y(t)$ is the zero-state response, then $y(t)$ is the solution of

$$Q(D)y(t) = P(D)x(t)$$

subject to zero initial conditions (zero-state). Adding these two equations, we have

$$Q(D)[y_0(t) + y(t)] = P(D)x(t)$$

Clearly, $y_0(t) + y(t)$ is the general solution of Eq. (2.2).

or

$$(D^N + a_1 D^{N-1} + \cdots + a_{N-1} D + a_N) y_0(t) = 0 \tag{2.3}$$

A solution to this equation can be obtained systematically [1]. However, we will take a shortcut by using heuristic reasoning. Equation (2.3) shows that a linear combination of $y_0(t)$ and its N successive derivatives is zero, not at *some* values of t, but for all t. Such a result is possible *if and only if* $y_0(t)$ and all its N successive derivatives are of the same form. Otherwise, their sum can never add to zero for all values of t. We know that only an exponential function $e^{\lambda t}$ has this property. So, let us assume that

$$y_0(t) = ce^{\lambda t}$$

is a solution to Eq. (2.3). Then

$$Dy_0(t) = \frac{dy_0(t)}{dt} = c\lambda e^{\lambda t}$$

$$D^2 y_0(t) = \frac{d^2 y_0(t)}{dt^2} = c\lambda^2 e^{\lambda t}$$

$$\vdots$$

$$D^N y_0(t) = \frac{d^N y_0(t)}{dt^N} = c\lambda^N e^{\lambda t}$$

Substituting these results in Eq. (2.3), we obtain

$$c(\lambda^N + a_1 \lambda^{N-1} + \cdots + a_{N-1}\lambda + a_N) e^{\lambda t} = 0$$

For a nontrivial solution of this equation,

$$\lambda^N + a_1 \lambda^{N-1} + \cdots + a_{N-1}\lambda + a_N = 0 \tag{2.4}$$

This result means that $ce^{\lambda t}$ is indeed a solution of Eq. (2.3), provided λ satisfies Eq. (2.4). Note that the polynomial in Eq. (2.4) is identical to the polynomial $Q(D)$ in Eq. (2.3), with λ replacing D. Therefore, Eq. (2.4) can be expressed as

$$Q(\lambda) = 0$$

Expressing $Q(\lambda)$ in factorized form, we obtain

$$Q(\lambda) = (\lambda - \lambda_1)(\lambda - \lambda_2) \cdots (\lambda - \lambda_N) = 0 \tag{2.5}$$

Clearly, λ has N solutions: $\lambda_1, \lambda_2, \ldots, \lambda_N$, assuming that all λ_i are distinct. Consequently, Eq. (2.3) has N possible solutions: $c_1 e^{\lambda_1 t}$, $c_2 e^{\lambda_2 t}$, $\ldots$, $c_N e^{\lambda_N t}$, with $c_1, c_2, \ldots, c_N$ as arbitrary constants.

We can readily show that a general solution is given by the sum of these N solutions[†] so that

$$y_0(t) = c_1 e^{\lambda_1 t} + c_2 e^{\lambda_2 t} + \cdots + c_N e^{\lambda_N t} \tag{2.6}$$

where $c_1, c_2, \ldots, c_N$ are arbitrary constants determined by N constraints (the auxiliary conditions) on the solution.

Observe that the polynomial $Q(\lambda)$, which is characteristic of the system, has nothing to do with the input. For this reason the polynomial $Q(\lambda)$ is called the *characteristic polynomial* of the system. The equation

$$Q(\lambda) = 0$$

is called the *characteristic equation* of the system. Equation (2.5) clearly indicates that $\lambda_1, \lambda_2, \ldots, \lambda_N$ are the roots of the characteristic equation; consequently, they are called the *characteristic roots* of the system. The terms *characteristic values, eigenvalues,* and *natural frequencies* are also used for characteristic roots.[‡] The exponentials $e^{\lambda_i t}$ $(i = 1, 2, \ldots, n)$ in the zero-input response are the *characteristic modes* (also known as *natural modes* or simply as *modes*) of the system. There is a characteristic mode for each characteristic root of the system, and the *zero-input response is a linear combination of the characteristic modes of the system.*

An LTIC system's characteristic modes comprise its single most important attribute. Characteristic modes not only determine the zero-input response but also play an important role in determining the zero-state response. In other words, the entire behavior of a system is dictated primarily by its characteristic modes. In the rest of this chapter, we shall see the pervasive presence of characteristic modes in every aspect of system behavior.

Repeated Roots

The solution of Eq. (2.3) as given in Eq. (2.6) assumes that the N characteristic roots $\lambda_1, \lambda_2, \ldots, \lambda_N$ are distinct. If there are repeated roots (same root occurring more than once), the form of the solution is modified slightly. By direct substitution, we can show that the solution of the equation

$$(D - \lambda)^2 y_0(t) = 0$$

is given by

$$y_0(t) = (c_1 + c_2 t) e^{\lambda t}$$

[†] To prove this assertion, assume that $y_1(t), y_2(t), \ldots, y_N(t)$ are all solutions of Eq. (2.3). Then

$$Q(D)y_1(t) = 0$$
$$Q(D)y_2(t) = 0$$
$$\vdots$$
$$Q(D)y_N(t) = 0$$

Multiplying these equations by $c_1, c_2, \ldots, c_N$, respectively, and adding them together yield

$$Q(D)[c_1 y_1(t) + c_2 y_2(t) + \cdots + c_N y_n(t)] = 0$$

This result shows that $c_1 y_1(t) + c_2 y_2(t) + \cdots + c_N y_n(t)$ is also a solution of the homogeneous equation [Eq. (2.3)].

[‡] *Eigenvalue* is German for "characteristic value."

In this case, the root λ repeats twice. Observe that the characteristic modes in this case are $e^{\lambda t}$ and $te^{\lambda t}$. Continuing this pattern, we can show that for the differential equation

$$(D-\lambda)^r y_0(t) = 0$$

the characteristic modes are $e^{\lambda t}, te^{\lambda t}, t^2e^{\lambda t}, \ldots, t^{r-1}e^{\lambda t}$, and that the solution is

$$y_0(t) = (c_1 + c_2 t + \cdots + c_r t^{r-1})e^{\lambda t}$$

Consequently, for a system with the characteristic polynomial

$$Q(\lambda) = (\lambda-\lambda_1)^r(\lambda-\lambda_{r+1})\cdots(\lambda-\lambda_N)$$

the characteristic modes are $e^{\lambda_1 t}, te^{\lambda_1 t}, \ldots, t^{r-1}e^{\lambda_1 t}, e^{\lambda_{r+1} t}, \ldots, e^{\lambda_N t}$ and the solution is

$$y_0(t) = (c_1 + c_2 t + \cdots + c_r t^{r-1})e^{\lambda_1 t} + c_{r+1}e^{\lambda_{r+1} t} + \cdots + c_N e^{\lambda_N t}$$

Complex Roots

The procedure for handling complex roots is the same as that for real roots. For complex roots, the usual procedure leads to complex characteristic modes and the complex form of solution. However, it is possible to avoid the complex form altogether by selecting a real form of solution, as described next.

For a real system, complex roots must occur in pairs of conjugates if the coefficients of the characteristic polynomial $Q(\lambda)$ are to be real. Therefore, if $\alpha + j\beta$ is a characteristic root, $\alpha - j\beta$ must also be a characteristic root. The zero-input response corresponding to this pair of complex conjugate roots is

$$y_0(t) = c_1 e^{(\alpha+j\beta)t} + c_2 e^{(\alpha-j\beta)t} \tag{2.7}$$

For a real system, the response $y_0(t)$ must also be real. This is possible only if c_1 and c_2 are conjugates. Let

$$c_1 = \frac{c}{2}e^{j\theta} \quad \text{and} \quad c_2 = \frac{c}{2}e^{-j\theta}$$

This yields

$$\begin{aligned} y_0(t) &= \frac{c}{2}e^{j\theta}e^{(\alpha+j\beta)t} + \frac{c}{2}e^{-j\theta}e^{(\alpha-j\beta)t} \\ &= \frac{c}{2}e^{\alpha t}\left[e^{j(\beta t+\theta)} + e^{-j(\beta t+\theta)}\right] \\ &= ce^{\alpha t}\cos(\beta t+\theta) \end{aligned} \tag{2.8}$$

Therefore, the zero-input response corresponding to complex conjugate roots $\alpha \pm j\beta$ can be expressed in a complex form [Eq. (2.7)] or a real form [Eq. (2.8)].

EXAMPLE 2.1 Finding the Zero-Input Response

Find $y_0(t)$, the zero-input response of the response for an LTIC system described by

(a) the simple-root system $(D^2 + 3D + 2)y(t) = Dx(t)$ with initial conditions $y_0(0) = 0$ and $\dot{y}_0(0) = -5$.

(b) the repeated-root system $(D^2 + 6D + 9)y(t) = (3D + 5)x(t)$ with initial conditions $y_0(0) = 3$ and $\dot{y}_0(0) = -7$.

(c) the complex-root system $(D^2 + 4D + 40)y(t) = (D + 2)x(t)$ with initial conditions $y_0(0) = 2$ and $\dot{y}_0(0) = 16.78$.

(a) Note that $y_0(t)$, being the zero-input response ($x(t) = 0$), is the solution of $(D^2 + 3D + 2)y_0(t) = 0$. The characteristic polynomial of the system is $\lambda^2 + 3\lambda + 2$. The characteristic equation of the system is therefore $\lambda^2 + 3\lambda + 2 = (\lambda + 1)(\lambda + 2) = 0$. The characteristic roots of the system are $\lambda_1 = -1$ and $\lambda_2 = -2$, and the characteristic modes of the system are e^{-t} and e^{-2t}. Consequently, the zero-input response is

$$y_0(t) = c_1 e^{-t} + c_2 e^{-2t}$$

Differentiating this expression, we obtain

$$\dot{y}_0(t) = -c_1 e^{-t} - 2c_2 e^{-2t}$$

To determine the constants c_1 and c_2, we set $t = 0$ in the equations for $y_0(t)$ and $\dot{y}_0(t)$ and substitute the initial conditions $y_0(0) = 0$ and $\dot{y}_0(0) = -5$, yielding

$$0 = c_1 + c_2$$
$$-5 = -c_1 - 2c_2$$

Solving these two simultaneous equations in two unknowns for c_1 and c_2 yields

$$c_1 = -5 \quad \text{and} \quad c_2 = 5$$

Therefore,

$$y_0(t) = -5e^{-t} + 5e^{-2t} \tag{2.9}$$

This is the zero-input response of $y(t)$. Because $y_0(t)$ is present at $t = 0^-$, we are justified in assuming that it exists for $t \geq 0$.[†]

(b) The characteristic polynomial is $\lambda^2 + 6\lambda + 9 = (\lambda + 3)^2$, and its characteristic roots are $\lambda_1 = -3$, $\lambda_2 = -3$ (repeated roots). Consequently, the characteristic modes of the system are e^{-3t} and te^{-3t}. The zero-input response, being a linear combination of the characteristic modes, is given by

$$y_0(t) = (c_1 + c_2 t)e^{-3t}$$

[†] $y_0(t)$ may be present even before $t = 0^-$. However, we can be sure of its presence only from $t = 0^-$ onward.

We can find the arbitrary constants c_1 and c_2 from the initial conditions $y_0(0) = 3$ and $\dot{y}_0(0) = -7$ following the procedure in part (a). The reader can show that $c_1 = 3$ and $c_2 = 2$. Hence,

$$y_0(t) = (3 + 2t)e^{-3t} \qquad t \geq 0$$

(c) The characteristic polynomial is $\lambda^2 + 4\lambda + 40 = (\lambda + 2 - j6)(\lambda + 2 + j6)$. The characteristic roots are $-2 \pm j6$.† The solution can be written either in the complex form [Eq. (2.7)] or in the real form [Eq. (2.8)]. The complex form is $y_0(t) = c_1 e^{\lambda_1 t} + c_2 e^{\lambda_2 t}$, where $\lambda_1 = -2 + j6$ and $\lambda_2 = -2 - j6$. Since $\alpha = -2$ and $\beta = 6$, the real-form solution is [see Eq. (2.8)]

$$y_0(t) = ce^{-2t}\cos(6t + \theta)$$

Differentiating this expression, we obtain

$$\dot{y}_0(t) = -2ce^{-2t}\cos(6t + \theta) - 6ce^{-2t}\sin(6t + \theta)$$

To determine the constants c and θ, we set $t = 0$ in the equations for $y_0(t)$ and $\dot{y}_0(t)$ and substitute the initial conditions $y_0(0) = 2$ and $\dot{y}_0(0) = 16.78$, yielding

$$2 = c\cos\theta$$

$$16.78 = -2c\cos\theta - 6c\sin\theta$$

Solution of these two simultaneous equations in two unknowns $c\cos\theta$ and $c\sin\theta$ yields

$$c\cos\theta = 2 \qquad \text{and} \qquad c\sin\theta = -3.463$$

Squaring and then adding these two equations yield

$$c^2 = (2)^2 + (-3.464)^2 = 16 \Longrightarrow c = 4$$

Next, dividing $c\sin\theta = -3.463$ by $c\cos\theta = 2$ yields

$$\tan\theta = \frac{-3.463}{2}$$

and

$$\theta = \tan^{-1}\left(\frac{-3.463}{2}\right) = -\frac{\pi}{3}$$

Therefore,

$$y_0(t) = 4e^{-2t}\cos\left(6t - \frac{\pi}{3}\right)$$

For the plot of $y_0(t)$, refer again to Fig. B.11c.

† The complex conjugate roots of a second-order polynomial can be determined by using the formula in Sec. B.8.10 or by expressing the polynomial as a sum of two squares. The latter can be accomplished by completing the square with the first two terms, as follows:

$$\lambda^2 + 4\lambda + 40 = (\lambda^2 + 4\lambda + 4) + 36 = (\lambda + 2)^2 + (6)^2 = (\lambda + 2 - j6)(\lambda + 2 + j6)$$

EXAMPLE 2.2 Using MATLAB to Find Polynomial Roots

Find the roots λ_1 and λ_2 of the polynomial $\lambda^2 + 4\lambda + k$ for three values of k: **(a)** $k = 3$, **(b)** $k = 4$, and **(c)** $k = 40$.

(a)

```
>> r = roots([1 4 3]).'
   r = -3  -1
```

For $k = 3$, the polynomial roots are therefore $\lambda_1 = -3$ and $\lambda_2 = -1$.

(b)

```
>> r = roots([1 4 4]).'
   r = -2  -2
```

For $k = 4$, the polynomial roots are therefore $\lambda_1 = \lambda_2 = -2$.

(c)

```
>> r = roots([1 4 40]).'
   r = -2.00+6.00i  -2.00-6.00i
```

For $k = 40$, the polynomial roots are therefore $\lambda_1 = -2 + j6$ and $\lambda_2 = -2 - j6$.

EXAMPLE 2.3 Using MATLAB to Find the Zero-Input Response

Consider an LTIC system specified by the differential equation

$$(D^2 + 4D + k)y(t) = (3D + 5)x(t)$$

Using initial conditions $y_0(0) = 3$ and $\dot{y}_0(0) = -7$, apply MATLAB's `dsolve` command to determine the zero-input response when **(a)** $k = 3$, **(b)** $k = 4$, and **(c)** $k = 40$.

(a)

```
>> y_0 = dsolve('D2y+4*Dy+3*y=0','y(0)=3','Dy(0)=-7','t')
   y_0 = 1/exp(t) + 2/exp(3*t)
```

For $k = 3$, the zero-input response is therefore $y_0(t) = e^{-t} + 2e^{-3t}$.

(b)

```
>> y_0 = dsolve('D2y+4*Dy+4*y=0','y(0)=3','Dy(0)=-7','t')
   y_0 = 3/exp(2*t) - t/exp(2*t)
```

For $k = 4$, the zero-input response is therefore $y_0(t) = 3e^{-2t} - te^{-2t}$.

(c)

```
>> y_0 = dsolve('D2y+4*Dy+40*y=0','y(0)=3','Dy(0)=-7','t')
   y_0 = (3*cos(6*t))/exp(2*t) - sin(6*t)/(6*exp(2*t))
```

For $k = 40$, the zero-input response is therefore $y_0(t) = 3e^{-2t}\cos(6t) - \frac{1}{6}e^{-2t}\sin(6t)$.

DRILL 2.1 Finding the Zero-Input Response of a First-Order System

Find the zero-input response of an LTIC system described by $(D+5)y(t) = x(t)$ if the initial condition is $y(0) = 5$.

ANSWER

$y_0(t) = 5e^{-5t} \qquad t \geq 0$

DRILL 2.2 Finding the Zero-Input Response of a Second-Order System

Letting $y_0(0) = 1$ and $\dot{y}_0(0) = 4$, solve

$$(D^2 + 2D)y_0(t) = 0$$

ANSWER

$y_0(t) = 3 - 2e^{-2t} \qquad t \geq 0$

Practical Initial Conditions and the Meaning of 0^- and 0^+

In Ex. 2.1, the initial conditions $y_0(0)$ and $\dot{y}_0(0)$ were supplied. In practical problems, we must derive such conditions from the physical situation. For instance, in an *RLC* circuit, we may be given the conditions (initial capacitor voltages, initial inductor currents, etc.).

From this information, we need to derive $y_0(0)$, $\dot{y}_0(0)$, ... for the desired variable as demonstrated in the next example.

In much of our discussion, the input is assumed to start at $t = 0$, unless otherwise mentioned. Hence, $t = 0$ is the reference point. The conditions immediately before $t = 0$ (just before the input is applied) are the conditions at $t = 0^-$, and those immediately after $t = 0$ (just after the input is applied) are the conditions at $t = 0^+$ (compare this with the historical time frames BCE and CE).

In practice, we are likely to know the initial conditions at $t = 0^-$ rather than at $t = 0^+$. The two sets of conditions are generally different, although in some cases they may be identical.

The total response $y(t)$ consists of two components: the zero-input response $y_0(t)$ [response due to the initial conditions alone with $x(t) = 0$] and the zero-state response resulting from the input alone with all initial conditions zero. At $t = 0^-$, the total response $y(t)$ consists solely of the zero-input response $y_0(t)$ because the input has not started yet. Hence, the initial conditions on $y(t)$ are identical to those of $y_0(t)$. Thus, $y(0^-) = y_0(0^-)$, $\dot{y}(0^-) = \dot{y}_0(0^-)$, and so on. Moreover, $y_0(t)$ is the response due to initial conditions alone and does not depend on the input $x(t)$. Hence, application of the input at $t = 0$ does not affect $y_0(t)$. This means the initial conditions on $y_0(t)$ at $t = 0^-$ and 0^+ are identical; that is, $y_0(0^-)$, $\dot{y}_0(0^-)$, . . . are identical to $y_0(0^+)$, $\dot{y}_0(0^+)$, . . ., respectively. It is clear that for $y_0(t)$, there is no distinction between the initial conditions at $t = 0^-$, 0, and 0^+. They are all the same. But this is not the case with the total response $y(t)$, which consists of both the zero-input and zero-state responses. Thus, in general, $y(0^-) \neq y(0^+)$, $\dot{y}(0^-) \neq \dot{y}(0^+)$, and so on.

EXAMPLE 2.4 Consideration of Initial Conditions

A voltage $x(t) = 10e^{-3t}u(t)$ is applied at the input of the *RLC* circuit illustrated in Fig. 2.1a. Find the loop current $y(t)$ for $t \geq 0$ if the initial inductor current is zero [$y(0^-) = 0$] and the initial capacitor voltage is 5 volts [$v_C(0^-) = 5$].

The differential (loop) equation relating $y(t)$ to $x(t)$ was derived in Eq. (1.29) as

$$(D^2 + 3D + 2)y(t) = Dx(t)$$

The zero-state component of $y(t)$ resulting from the input $x(t)$, assuming that all initial conditions are zero, that is, $y(0^-) = v_C(0^-) = 0$, will be obtained later in Ex. 2.9. In this example we shall find the zero-input reponse $y_0(t)$. For this purpose, we need two initial conditions, $y_0(0)$ and $\dot{y}_0(0)$. These conditions can be derived from the given initial conditions, $y(0^-) = 0$ and $v_C(0^-) = 5$, as follows. Recall that $y_0(t)$ is the loop current when the input terminals are shorted so that the input $x(t) = 0$ (zero-input), as depicted in Fig. 2.1b. We now compute $y_0(0)$ and $\dot{y}_0(0)$, the values of the loop current and its derivative at $t = 0$, from the initial values of the inductor current and the capacitor voltage. Remember that the inductor current cannot change instantaneously in the absence of an impulsive voltage. Similarly, the capacitor voltage cannot change instantaneously in the absence of an impulsive current. Therefore, when the input terminals are shorted at $t = 0$, the inductor current is still zero and the capacitor voltage is still 5 volts. Thus,

$$y_0(0) = 0$$

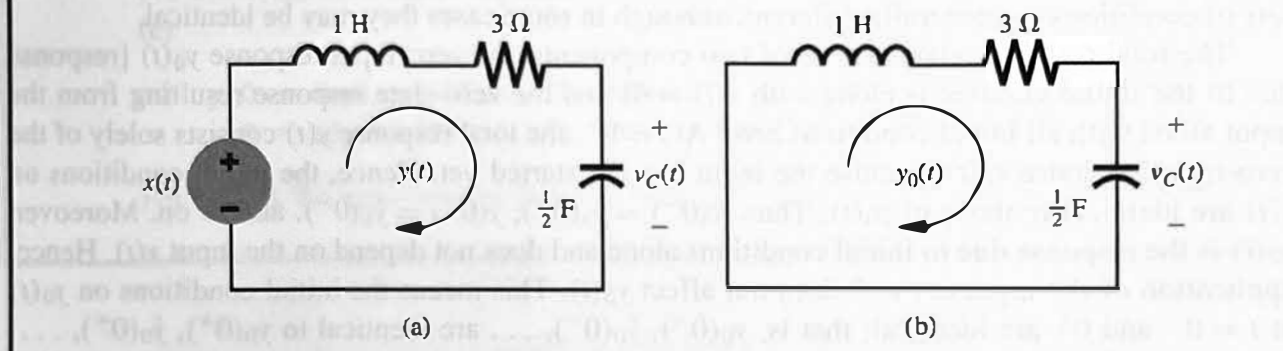

Figure 2.1 Circuits for Ex. 2.4.

To determine $\dot{y}_0(0)$, we use the loop equation for the circuit in Fig. 2.1b. Because the voltage across the inductor is $L(dy_0/dt)$ or $\dot{y}_0(t)$, this equation can be written as follows:

$$\dot{y}_0(t) + 3y_0(t) + v_C(t) = 0$$

Setting $t = 0$, we obtain

$$\dot{y}_0(0) + 3y_0(0) + v_C(0) = 0$$

But $y_0(0) = 0$ and $v_C(0) = 5$. Consequently,

$$\dot{y}_0(0) = -5$$

Therefore, the desired initial conditions are

$$y_0(0) = 0 \qquad \text{and} \qquad \dot{y}_0(0) = -5$$

Thus, the problem reduces to finding $y_0(t)$, the zero-input component of $y(t)$ of the system specified by the equation $(D^2 + 3D + 2)y(t) = Dx(t)$, when the initial conditions are $y_0(0) = 0$ and $\dot{y}_0(0) = -5$. We have already solved this problem in Ex. 2.1a, where we found

$$y_0(t) = -5e^{-t} + 5e^{-2t} \qquad t \geq 0$$

This is the zero-input component of the loop current $y(t)$.

It is interesting to find the initial conditions at $t = 0^-$ and 0^+ for the total response $y(t)$. Let us compare $y(0^-)$ and $\dot{y}(0^-)$ with $y(0^+)$ and $\dot{y}(0^+)$. The two pairs can be compared by writing the loop equation for the circuit in Fig. 2.1a at $t = 0^-$ and $t = 0^+$. The only difference between the two situations is that at $t = 0^-$, the input $x(t) = 0$, whereas at $t = 0^+$, the input $x(t) = 10$ [because $x(t) = 10e^{-3t}$]. Hence, the two loop equations are

$$\dot{y}(0^-) + 3y(0^-) + v_C(0^-) = 0$$
$$\dot{y}(0^+) + 3y(0^+) + v_C(0^+) = 10$$

The loop current $y(0^+) = y(0^-) = 0$ because it cannot change instantaneously in the absence of impulsive voltage. The same is true of the capacitor voltage. Hence, $v_C(0^+) =$

$v_C(0^-) = 5$. Substituting these values in the foregoing equations, we obtain $\dot{y}(0^-) = -5$ and $\dot{y}(0^+) = 5$. Thus,

$$y(0^-) = 0,\ \dot{y}(0^-) = -5 \quad \text{and} \quad y(0^+) = 0,\ \dot{y}(0^+) = 5 \tag{2.10}$$

DRILL 2.3 Zero-Input Response of an *RC* Circuit

In the circuit in Fig. 2.1a, the inductance $L = 0$ and the initial capacitor voltage $v_C(0) = 30$ volts. Show that the zero-input component of the loop current is given by $y_0(t) = -10e^{-2t/3}$ for $t \geq 0$.

Independence of the Zero-Input and Zero-State Responses

In Ex. 2.4, we computed the zero-input component without using the input $x(t)$. The zero-state response can be computed from the knowledge of the input $x(t)$ alone; the initial conditions are assumed to be zero (system in zero state). The two components of the system response (the zero-input and zero-state responses) are independent of each other. *The two worlds of zero-input response and zero-state response coexist side by side, neither one knowing or caring what the other is doing. For each component, the other is totally irrelevant.*

Role of Auxiliary Conditions in Solution of Differential Equations

The solution of a differential equation requires additional pieces of information (the *auxiliary conditions*). Why? We now show heuristically why a differential equation does not, in general, have a unique solution unless some additional constraints (or conditions) on the solution are known.

Differentiation operation is not invertible unless one piece of information about $y(t)$ is given. To get back $y(t)$ from dy/dt, we must know one piece of information, such as $y(0)$. Thus, differentiation is an irreversible (noninvertible) operation during which certain information is lost. To invert this operation, one piece of information about $y(t)$ must be provided to restore the original $y(t)$. Using a similar argument, we can show that, given d^2y/dt^2, we are able to determine $y(t)$ uniquely only if two additional pieces of information (constraints) about $y(t)$ are given. In general, to determine $y(t)$ uniquely from its Nth derivative, we need N additional pieces of information (constraints) about $y(t)$. These constraints are also called *auxiliary conditions*. When these conditions are given at $t = 0$, they are called *initial conditions*.

2.2.1 Some Insights into the Zero-Input Behavior of a System

By definition, the zero-input response is the system response to its internal conditions, assuming that its input is zero. Understanding this phenomenon provides interesting insight into system behavior. If a system is disturbed momentarily from its rest position and if the disturbance is then removed, the system will not come back to rest instantaneously. In general, it will come back to

rest over a period of time and only through a special type of motion that is characteristic of the system.† For example, if we press on an automobile fender momentarily and then release it at $t = 0$, there is no external force on the automobile for $t > 0$.‡ The auto body will eventually come back to its rest (equilibrium) position, but not through any arbitrary motion. It must do so by using only a form of response that is sustainable by the system on its own without any external source, since the input is zero. Only characteristic modes satisfy this condition. *The system uses a proper combination of characteristic modes to come back to the rest position while satisfying appropriate boundary (or initial) conditions.*

If the shock absorbers of the automobile are in good condition (high damping coefficient), the characteristic modes will be monotonically decaying exponentials, and the auto body will come to rest rapidly without oscillation. In contrast, for poor shock absorbers (low damping coefficients), the characteristic modes will be exponentially decaying sinusoids, and the body will come to rest through oscillatory motion. When a series *RC* circuit with an initial charge on the capacitor is shorted, the capacitor will start to discharge exponentially through the resistor. This response of the *RC* circuit is caused entirely by its internal conditions and is sustained by this system without the aid of any external input. The exponential current waveform is therefore the characteristic mode of the *RC* circuit.

Mathematically, we know that *any combination of characteristic modes can be sustained by the system alone without requiring an external input.* This fact can be readily verified for the series *RL* circuit shown in Fig. 2.2. The loop equation for this system is

$$(D+2)y(t) = x(t)$$

It has a single characteristic root $\lambda = -2$, and the characteristic mode is e^{-2t}. We now verify that a loop current $y(t) = ce^{-2t}$ can be sustained through this circuit without any input voltage. The input voltage $x(t)$ required to drive a loop current $y(t) = ce^{-2t}$ is given by

$$\begin{aligned} x(t) &= L\frac{dy(t)}{dt} + Ry(t) \\ &= \frac{d}{dt}(ce^{-2t}) + 2ce^{-2t} \\ &= -2ce^{-2t} + 2ce^{-2t} = 0 \end{aligned}$$

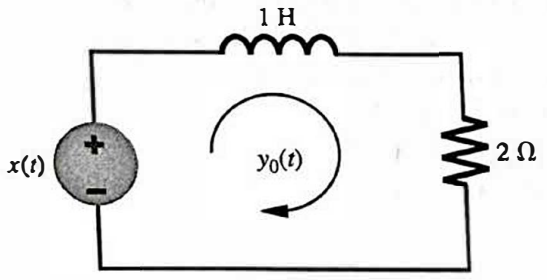

Figure 2.2 Modes always get a free ride.

† This assumes that the system will eventually come back to its original rest (or equilibrium) position.

‡ We ignore the force of gravity, which merely causes a constant displacement of the auto body without affecting the other motion.

Clearly, the loop current $y(t) = ce^{-2t}$ is sustained by the RL circuit on its own, without the necessity of an external input.

The Resonance Phenomenon

We have seen that any signal consisting of a system's characteristic mode is sustained by the system on its own; the system offers no obstacle to such signals. Imagine what would happen if we were to drive the system with an external input that is one of its characteristic modes. This would be like pouring gasoline on a fire in a dry forest or hiring a child to eat ice cream. A child would gladly do the job without pay. Think what would happen if he were paid by the amount of ice cream he ate! He would work overtime. He would work day and night, until he became sick. The same thing happens with a system driven by an input of the form of characteristic mode. The system response grows without limit, until it burns out.[†] We call this behavior the *resonance phenomenon*. An intelligent discussion of this important phenomenon requires an understanding of the zero-state response; for this reason, we postpone this topic until Sec. 2.6.7.

2.3 The Unit Impulse Response $h(t)$

In Ch. 1, we explained how a system response to an input $x(t)$ may be found by breaking this input into narrow rectangular pulses, as illustrated earlier in Fig. 1.27a, and then summing the system response to all the components. The rectangular pulses become impulses in the limit as their widths approach zero. Therefore, the system response is the sum of its responses to various impulse components. This discussion shows that if we know the system response to an impulse input, we can determine the system response to an arbitrary input $x(t)$. We now discuss a method of determining $h(t)$, the unit impulse response of an LTIC system described by the Nth-order differential equation [Eq. (2.1)]:

$$\frac{d^N y(t)}{dt^N} + a_1 \frac{d^{N-1} y(t)}{dt^{N-1}} + \cdots + a_{N-1} \frac{dy(t)}{dt} + a_N y(t)$$
$$= b_{N-M} \frac{d^M x(t)}{dt^M} + b_{N-M+1} \frac{d^{M-1} x(t)}{dt^{M-1}} + \cdots + b_{N-1} \frac{dx(t)}{dt} + b_N x(t)$$

Recall that noise considerations restrict practical systems to $M \leq N$. Under this constraint, the most general case is $M = N$. Therefore, Eq. (2.1) can be expressed as

$$(D^N + a_1 D^{N-1} + \cdots + a_{N-1} D + a_N) y(t) = (b_0 D^N + b_1 D^{N-1} + \cdots + b_{N-1} D + b_N) x(t) \quad (2.11)$$

Before deriving the general expression for the unit impulse response $h(t)$, it is illuminating to understand qualitatively the nature of $h(t)$. The impulse response $h(t)$ is the system response to an impulse input $\delta(t)$ applied at $t = 0$ with all the initial conditions zero at $t = 0^-$. An impulse input $\delta(t)$ is like lightning, which strikes instantaneously and then vanishes. But in its wake, in that single moment, objects that have been struck are rearranged. Similarly, an impulse input $\delta(t)$ appears momentarily at $t = 0$, and then it is gone forever. But in that moment it generates energy storages; that is, it creates nonzero initial conditions instantaneously within the system at

[†] In practice, the system in resonance is more likely to go in saturation because of high amplitude levels.

$t = 0^+$. Although the impulse input $\delta(t)$ vanishes for $t > 0$ so that the system has no input after the impulse has been applied, the system will still have a response generated by these newly created initial conditions. The impulse response $h(t)$, therefore, must consist of the system's characteristic modes for $t \geq 0^+$. As a result,

$$h(t) = \text{characteristic mode terms} \qquad t \geq 0^+$$

This response is valid for $t > 0$. But what happens at $t = 0$? At a single moment $t = 0$, there can at most be an impulse,[†] so the form of the complete response $h(t)$ is

$$h(t) = A_0\delta(t) + \text{characteristic mode terms} \qquad t \geq 0 \tag{2.12}$$

Setting $x(t) = \delta(t)$ and $y(t) = h(t)$ in Eq. (2.11) yields

$$(D^N + a_1D^{N-1} + \cdots + a_{N-1}D + a_N)h(t) = (b_0D^N + b_1D^{N-1} + \cdots + b_{N-1}D + b_N)\delta(t)$$

In this equation, we substitute $h(t)$ from Eq. (2.12) and compare the coefficients of similar impulsive terms on both sides. The highest order of the derivative of impulse on both sides is N, with its coefficient value as A_0 on the left-hand side and b_0 on the right-hand side. The two values must be matched. Therefore, $A_0 = b_0$ and

$$h(t) = b_0\delta(t) + \text{characteristic modes} \tag{2.13}$$

In Eq. (2.11), if $M < N$, $b_0 = 0$. Hence, the impulse term $b_0\delta(t)$ exists only if $M = N$. The unknown coefficients of the N characteristic modes in $h(t)$ in Eq. (2.13) can be determined by using the technique of impulse matching, as explained in the following example.

EXAMPLE 2.5 Impulse Response via Impulse Matching

Find the impulse response $h(t)$ for a system specified by

$$(D^2 + 5D + 6)y(t) = (D + 1)x(t) \tag{2.14}$$

In this case, $b_0 = 0$. Hence, $h(t)$ consists of only the characteristic modes. The characteristic polynomial is $\lambda^2 + 5\lambda + 6 = (\lambda + 2)(\lambda + 3)$. The roots are -2 and -3. Hence, the impulse

---

[†] It might be possible for the derivatives of $\delta(t)$ to appear at the origin. However, if $M \leq N$, it is impossible for $h(t)$ to have any derivatives of $\delta(t)$. This conclusion follows from Eq. (2.11) with $x(t) = \delta(t)$ and $y(t) = h(t)$. The coefficients of the impulse and all its derivatives must be matched on both sides of this equation. If $h(t)$ contains $\delta^{(1)}(t)$, the first derivative of $\delta(t)$, the left-hand side of Eq. (2.11) will contain a term $\delta^{(N+1)}(t)$. But the highest-order derivative term on the right-hand side is $\delta^{(N)}(t)$. Therefore, the two sides cannot match. Similar arguments can be made against the presence of the impulse's higher-order derivatives in $h(t)$.

response $h(t)$ is

$$h(t) = (c_1 e^{-2t} + c_2 e^{-3t})\, u(t) \tag{2.15}$$

Letting $x(t) = \delta(t)$ and $y(t) = h(t)$ in Eq. (2.14), we obtain

$$\ddot{h}(t) + 5\dot{h}(t) + 6h(t) = \dot{\delta}(t) + \delta(t) \tag{2.16}$$

Recall that initial conditions $h(0^-)$ and $\dot{h}(0^-)$ are both zero. But the application of an impulse at $t = 0$ creates new initial conditions at $t = 0^+$. Let $h(0^+) = K_1$ and $\dot{h}(0^+) = K_2$. These jump discontinuities in $h(t)$ and $\dot{h}(t)$ at $t = 0$ result in impulse terms $\dot{h}(0) = K_1\delta(t)$ and $\ddot{h}(0) = K_1\dot{\delta}(t) + K_2\delta(t)$ on the left-hand side. Matching the coefficients of impulse terms on both sides of Eq. (2.16) yields

$$5K_1 + K_2 = 1, \qquad K_1 = 1 \qquad \Longrightarrow \qquad K_1 = 1, K_2 = -4$$

We now use these values $h(0^+) = K_1 = 1$ and $\dot{h}(0^+) = K_2 = -4$ in Eq. (2.15) to find c_1 and c_2. Setting $t = 0^+$ in Eq. (2.15), we obtain $c_1 + c_2 = 1$. Also setting $t = 0^+$ in $\dot{h}(t)$, we obtain $-2c_1 - 3c_1^2 = -4$. These two simultaneous equations yield $c_1 = -1$ and $c_2 = 2$. Therefore,

$$h(t) = (-e^{-2t} + 2e^{-3t})u(t)$$

Although the method used in this example is relatively simple, we can simplify it still further by using a modified version of impulse matching.

Simplified Impulse Matching Method

The alternate technique we present now allows us to reduce the procedure to a simple routine to determine $h(t)$. To avoid the needless distraction, the proof for this procedure is placed in Sec. 2.8. There, we show that for an LTIC system specified by Eq. (2.11), the unit impulse response $h(t)$ is given by

$$h(t) = b_0\delta(t) + [P(D)y_n(t)]u(t) \tag{2.17}$$

where $y_n(t)$ is a linear combination of the characteristic modes of the system subject to the following initial conditions:

$$y_n(0) = \dot{y}_n(0) = \ddot{y}_n(0) = \cdots = y_n^{(N-2)}(0) = 0 \qquad \text{and} \qquad y_n^{(N-1)}(0) = 1 \tag{2.18}$$

where $y_n^{(k)}(0)$ is the value of the kth derivative of $y_n(t)$ at $t = 0$. We can express this set of conditions for various values of N (the system order) as follows:

$$N = 1 : y_n(0) = 1$$
$$N = 2 : y_n(0) = 0, \dot{y}_n(0) = 1$$
$$N = 3 : y_n(0) = \dot{y}_n(0) = 0, \ddot{y}_n(0) = 1$$

and so on.

As stated earlier, if the order of $P(D)$ is less than the order of $Q(D)$, that is, if $M < N$, then $b_0 = 0$, and the impulse term $b_0\delta(t)$ in $h(t)$ is zero.

EXAMPLE 2.6 Impulse Response via Simplified Impulse Matching

Determine the unit impulse response $h(t)$ for a system specified by the equation

$$(D^2+3D+2)y(t)=Dx(t) \tag{2.19}$$

This is a second-order system ($N=2$) having the characteristic polynomial

$$(\lambda^2+3\lambda+2)=(\lambda+1)(\lambda+2)$$

The characteristic roots of this system are $\lambda=-1$ and $\lambda=-2$. Therefore,

$$y_n(t)=c_1e^{-t}+c_2e^{-2t} \tag{2.20}$$

Differentiation of this equation yields

$$\dot{y}_n(t)=-c_1e^{-t}-2c_2e^{-2t} \tag{2.21}$$

The initial conditions are [see Eq. (2.18)]

$$\dot{y}_n(0)=1 \qquad \text{and} \qquad y_n(0)=0$$

Setting $t=0$ in Eqs. (2.20) and (2.21), and substituting the initial conditions just given, we obtain

$$0=c_1+c_2$$
$$1=-c_1-2c_2$$

Solution of these two simultaneous equations yields

$$c_1=1 \qquad \text{and} \qquad c_2=-1$$

Therefore,

$$y_n(t)=e^{-t}-e^{-2t}$$

Moreover, according to Eq. (2.19), $P(D)=D$ so that

$$P(D)y_n(t)=Dy_n(t)=\dot{y}_n(t)=-e^{-t}+2e^{-2t}$$

Also in this case, $b_0=0$ [the second-order term is absent in $P(D)$]. Therefore,

$$h(t)=[P(D)y_n(t)]u(t)=(-e^{-t}+2e^{-2t})u(t)$$

Comment. In the above discussion, we have assumed $M \leq N$, as specified by Eq. (2.11). Section 2.8 shows that the expression for $h(t)$ applicable to all possible values of M and N is given by

$$h(t) = P(D)[y_n(t)u(t)]$$

where $y_n(t)$ is a linear combination of the characteristic modes of the system subject to initial conditions [Eq. (2.18)]. This expression reduces to Eq. (2.17) when $M \leq N$.

Determination of the impulse response $h(t)$ using the procedures in this section is relatively simple. However, in Ch. 6 we shall discuss another, even simpler method using the Laplace transform. As the next example demonstrates, it is also possible to find $h(t)$ using functions from MATLAB's symbolic math toolbox.

EXAMPLE 2.7 Using MATLAB to Find the Impulse Response

Determine the impulse response $h(t)$ for an LTIC system specified by the differential equation

$$(D^2 + 3D + 2)y(t) = Dx(t)$$

This is a second-order system with $b_0 = 0$. First, we find the zero-input component for initial conditions $y(0^-) = 0$ and $\dot{y}(0^-) = 1$. Since $P(D) = D$, the zero-input response is differentiated and the impulse response immediately follows as $h(t) = 0\delta(t) + [Dy_n(t)]u(t)$.

```
>> y_n = dsolve('D2y+3*Dy+2*y=0','y(0)=0','Dy(0)=1','t'); h = diff(y_n)
   h = 2/exp(2*t) - 1/exp(t)
```

Therefore, $h(t) = (2e^{-2t} - e^{-t})u(t)$.

DRILL 2.4 Finding the Impulse Response

Determine the unit impulse response of LTIC systems described by the following equations:

(a) $(D + 2)y(t) = (3D + 5)x(t)$

(b) $D(D + 2)y(t) = (D + 4)x(t)$

(c) $(D^2 + 2D + 1)y(t) = Dx(t)$

ANSWERS

(a) $3\delta(t) - e^{-2t}u(t)$

(b) $(2 - e^{-2t})u(t)$

(c) $(1 - t)e^{-t}u(t)$

System Response to Delayed Impulse

If $h(t)$ is the response of an LTIC system to the input $\delta(t)$, then $h(t-T)$ is the response of this same system to the input $\delta(t-T)$. This conclusion follows from the time-invariance property of LTIC systems. Thus, by knowing the unit impulse response $h(t)$, we can determine the system response to a delayed impulse $\delta(t-T)$. Next, we put this result to good use in finding an LTIC system's zero-state response.

2.4 System Response to External Input: The Zero-State Response

This section is devoted to the determination of the zero-state response of an LTIC system. This is the system response $y(t)$ to an input $x(t)$ when the system is in the zero state, that is, when all initial conditions are zero. *We shall assume that the systems discussed in this section are in the zero state unless mentioned otherwise.* Under these conditions, the zero-state response will be the total response of the system.

We shall use the superposition property for finding the system response to an arbitrary input $x(t)$. Let us define a basic pulse $p(t)$ of unit height and width $\Delta\tau$, starting at $t=0$ as illustrated in Fig. 2.3a. Figure 2.3b shows an input $x(t)$ as a sum of narrow rectangular pulses. The pulse starting at $t=n\Delta\tau$ in Fig. 2.3b has a height $x(n\Delta\tau)$ and can be expressed as $x(n\Delta\tau)p(t-n\Delta\tau)$. Now, $x(t)$ is the sum of all such pulses. Hence,

$$x(t)=\lim_{\Delta\tau\to 0}\sum_{\tau}x(n\Delta\tau)p(t-n\Delta\tau)=\lim_{\Delta\tau\to 0}\sum_{\tau}\left[\frac{x(n\Delta\tau)}{\Delta\tau}\right]p(t-n\Delta\tau)\Delta\tau$$

The term $[x(n\Delta\tau)/\Delta\tau]p(t-n\Delta\tau)$ represents a pulse $p(t-n\Delta\tau)$ with height $\left[x(n\Delta\tau)/\Delta\tau\right]$. As $\Delta\tau\to 0$, the height of this strip $\to\infty$, but its area remains $x(n\Delta\tau)$. Hence, this strip approaches an impulse $x(n\Delta\tau)\delta(t-n\Delta\tau)$ as $\Delta\tau\to 0$ (Fig. 2.3e). Therefore,

$$x(t)=\lim_{\Delta\tau\to 0}\sum_{\tau}x(n\Delta\tau)\delta(t-n\Delta\tau)\,\Delta\tau \tag{2.22}$$

To find the response for this input $x(t)$, we consider the input and the corresponding output pairs, as shown in Figs. 2.3c–2.3f and also shown by directed arrow notation as follows:

$$\begin{aligned}
\text{input} &\Longrightarrow \text{output}\\
\delta(t) &\Longrightarrow h(t)\\
\delta(t-n\Delta\tau) &\Longrightarrow h(t-n\Delta\tau)\\
[x(n\Delta\tau)\Delta\tau]\delta(t-n\Delta\tau) &\Longrightarrow [x(n\Delta\tau)\Delta\tau]h(t-n\Delta\tau)\\
\underbrace{\lim_{\Delta\tau\to 0}\sum_{\tau}x(n\Delta\tau)\delta(t-n\Delta\tau)\,\Delta\tau}_{x(t)\ \text{[see Eq. (2.22)]}} &\Longrightarrow \underbrace{\lim_{\Delta\tau\to 0}\sum_{\tau}x(n\Delta\tau)h(t-n\Delta\tau)\Delta\tau}_{y(t)}
\end{aligned}$$

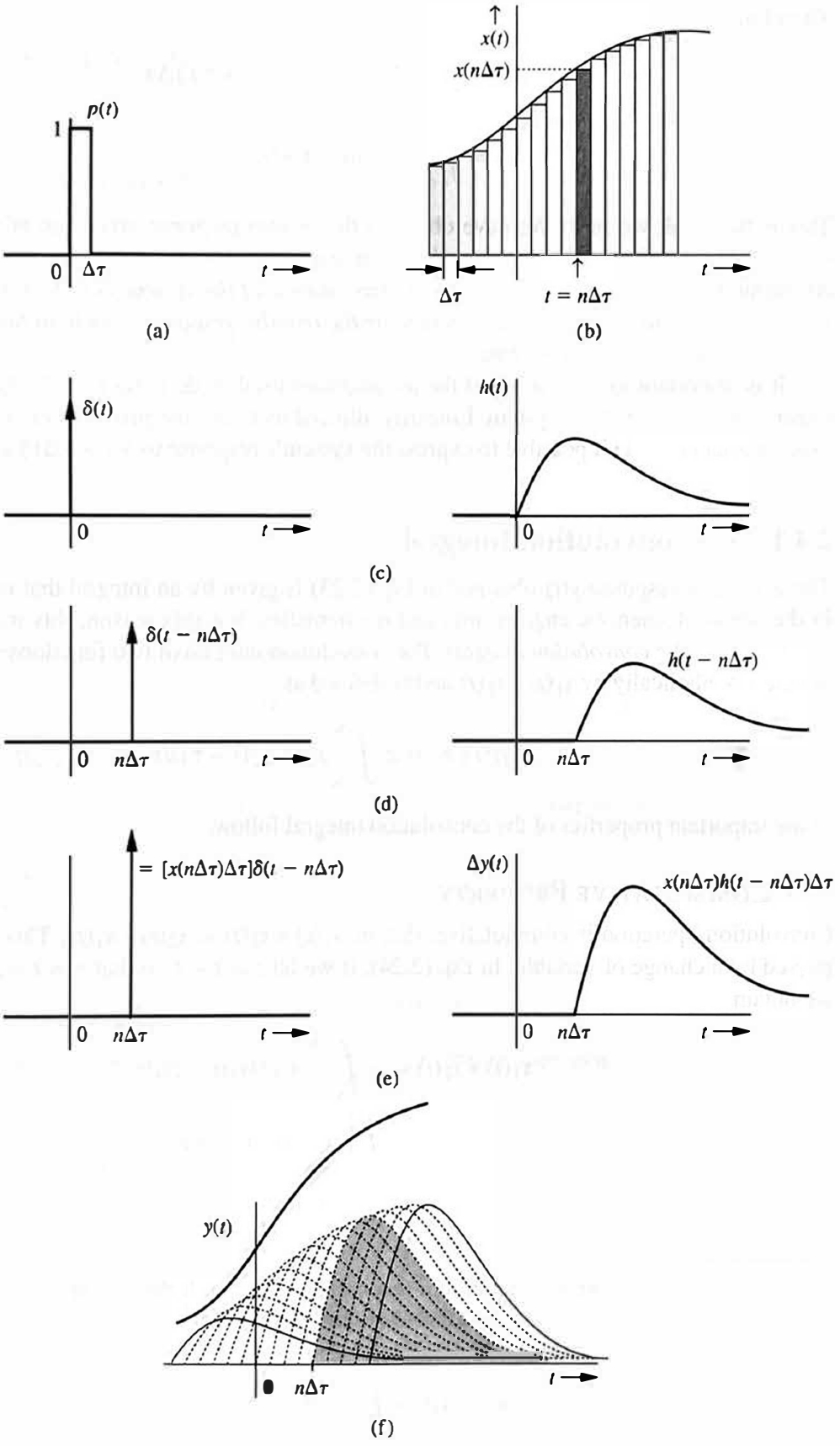

Figure 2.3 Finding the system response to an arbitrary input $x(t)$.

Therefore,[†]

$$y(t) = \lim_{\Delta\tau \to 0} \sum_{\tau} x(n\Delta\tau)h(t-n\Delta\tau)\Delta\tau$$

$$= \int_{-\infty}^{\infty} x(\tau)h(t-\tau)\,d\tau \tag{2.23}$$

This is the result we seek. We have obtained the system response $y(t)$ to an arbitrary input $x(t)$ in terms of the unit impulse response $h(t)$. Knowing $h(t)$, we can determine the response $y(t)$ to any input. *Observe once again the all-pervasive nature of the system's characteristic modes. The system response to any input is determined by the impulse response, which, in turn, is made up of characteristic modes of the system.*

It is important to keep in mind the assumptions used in deriving Eq. (2.23). We assumed a linear time-invariant (LTI) system. Linearity allowed us to use the principle of superposition, and time invariance made it possible to express the system's response to $\delta(t-n\Delta\tau)$ as $h(t-n\Delta\tau)$.

2.4.1 The Convolution Integral

The zero-state response $y(t)$ obtained in Eq. (2.23) is given by an integral that occurs frequently in the physical sciences, engineering, and mathematics. For this reason, this integral is given a special name: the *convolution integral*. The convolution integral of two functions $x_1(t)$ and $x_2(t)$ is denoted symbolically by $x_1(t) * x_2(t)$ and is defined as

$$x_1(t) * x_2(t) \equiv \int_{-\infty}^{\infty} x_1(\tau)x_2(t-\tau)\,d\tau \tag{2.24}$$

Some important properties of the convolution integral follow.

The Commutative Property

Convolution operation is commutative; that is, $x_1(t) * x_2(t) = x_2(t) * x_1(t)$. This property can be proved by a change of variable. In Eq. (2.24), if we let $z = t - \tau$ so that $\tau = t - z$ and $d\tau = -dz$, we obtain

$$x_1(t) * x_2(t) = -\int_{\infty}^{-\infty} x_2(z)x_1(t-z)\,dz$$

$$= \int_{-\infty}^{\infty} x_2(z)x_1(t-z)\,dz$$

$$= x_2(t) * x_1(t) \tag{2.25}$$

[†] In deriving this result, we have assumed a time-invariant system. If the system is time-varying, then the system response to the input $\delta(t-n\Delta\tau)$ cannot be expressed as $h(t-n\Delta\tau)$ but instead has the form $h(t,n\Delta\tau)$. Use of this form modifies Eq. (2.23) to

$$y(t) = \int_{-\infty}^{\infty} x(\tau)h(t,\tau)\,d\tau$$

where $h(t,\tau)$ is the system response at instant t to a unit impulse input located at τ.

The Distributive Property

According to the distributive property,

$$x_1(t) * [x_2(t) + x_3(t)] = x_1(t) * x_2(t) + x_1(t) * x_3(t) \tag{2.26}$$

The Associative Property

According to the associative property,

$$x_1(t) * [x_2(t) * x_3(t)] = [x_1(t) * x_2(t)] * x_3(t) \tag{2.27}$$

The proofs of Eqs. (2.26) and (2.27) follow directly from the definition of the convolution integral. They are left as an exercise for the reader.

The Shift Property

If

$$x_1(t) * x_2(t) = c(t)$$

then

$$x_1(t) * x_2(t-T) = x_1(t-T) * x_2(t) = c(t-T)$$

More generally, we see that

$$x_1(t-T_1) * x_2(t-T_2) = c(t-T_1-T_2) \tag{2.28}$$

Proof. We are given

$$x_1(t) * x_2(t) = \int_{-\infty}^{\infty} x_1(\tau) x_2(t-\tau)\, d\tau = c(t)$$

Therefore,

$$\begin{aligned} x_1(t) * x_2(t-T) &= \int_{-\infty}^{\infty} x_1(\tau) x_2(t-T-\tau)\, d\tau \\ &= c(t-T) \end{aligned}$$

The equally simple proof of Eq. (2.28) follows a similar approach.

Convolution with an Impulse

Convolution of a function $x(t)$ with a unit impulse results in the function $x(t)$ itself. By definition of convolution,

$$x(t) * \delta(t) = \int_{-\infty}^{\infty} x(\tau)\delta(t-\tau)\, d\tau$$

Because $\delta(t-\tau)$ is an impulse located at $\tau = t$, according to the sampling property of the impulse [Eq. (1.11)], the integral here is just the value of $x(\tau)$ at $\tau = t$, that is, $x(t)$. Therefore,

$$x(t) * \delta(t) = x(t)$$

Actually, this result was derived earlier [Eq. (2.22)].

The Width Property

If the durations (widths) of $x_1(t)$ and $x_2(t)$ are finite, given by T_1 and T_2, respectively, then the duration (width) of $x_1(t) * x_2(t)$ is $T_1 + T_2$ (Fig. 2.4). The proof of this property follows readily from the graphical considerations discussed later in Sec. 2.4.2.

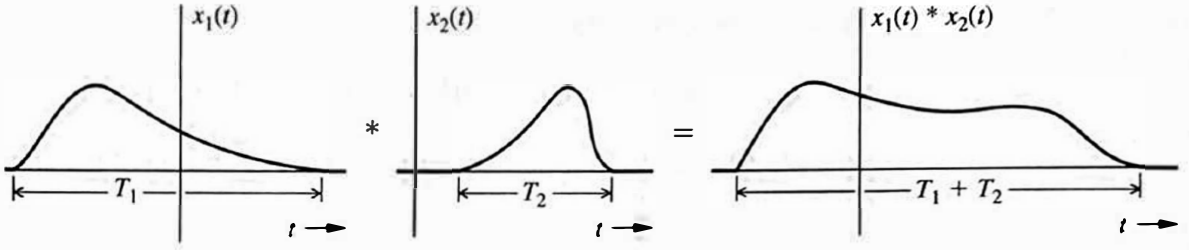

Figure 2.4 Width property of convolution.

Zero-State Response and Causality

The (zero-state) response $y(t)$ of an LTIC system is

$$y(t) = x(t) * h(t) = \int_{-\infty}^{\infty} x(\tau)h(t-\tau)\,d\tau \tag{2.29}$$

In deriving Eq. (2.29), we assumed the system to be linear and time-invariant. There were no other restrictions either on the system or on the input signal $x(t)$. Since, in practice, most systems are causal, their response cannot begin before the input. Furthermore, most inputs are also causal, which means they start at $t = 0$.

Causality restriction on both signals and systems further simplifies the limits of integration in Eq. (2.29). By definition, the response of a causal system cannot begin before its input begins. Consequently, the causal system's response to a unit impulse $\delta(t)$ (which is located at $t = 0$) cannot begin before $t = 0$. Therefore, a *causal system's unit impulse response $h(t)$ is a causal signal.*

It is important to remember that the integration in Eq. (2.29) is performed with respect to τ (not t). If the input $x(t)$ is causal, $x(\tau) = 0$ for $\tau < 0$. Therefore, $x(\tau) = 0$ for $\tau < 0$, as illustrated in Fig. 2.5a. Similarly, if $h(t)$ is causal, $h(t-\tau) = 0$ for $t - \tau < 0$; that is, for $\tau > t$, as depicted in Fig. 2.5a. Therefore, the product $x(\tau)h(t-\tau) = 0$ everywhere except over the nonshaded interval $0 \le \tau \le t$ shown in Fig. 2.5a (assuming $t \ge 0$). Observe that if t is negative, $x(\tau)h(t-\tau) = 0$ for all τ, as shown in Fig. 2.5b. Therefore, Eq. (2.29) reduces to

$$y(t) = x(t) * h(t) = \begin{cases} \int_{0^-}^{t} x(\tau)h(t-\tau)\,d\tau & t \ge 0 \\ 0 & t < 0 \end{cases} \tag{2.30}$$

The lower limit of integration in Eq. (2.30) is taken as 0^- to avoid the difficulty in integration that can arise if $x(t)$ contains an impulse at the origin. This result shows that if $x(t)$ and $h(t)$ are both causal, the response $y(t)$ is also causal.

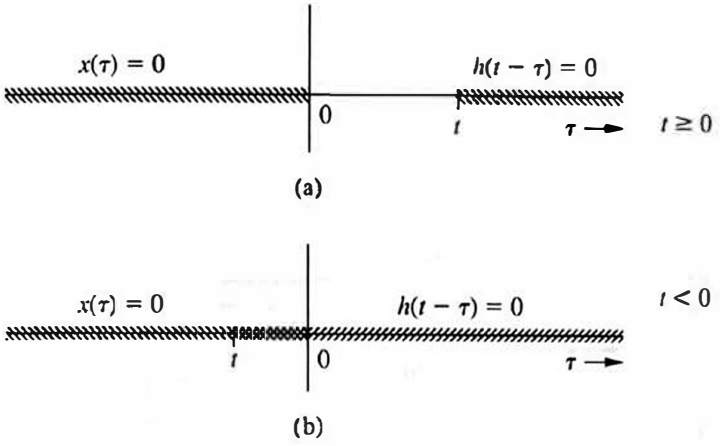

Figure 2.5 Limits of the convolution integral.

Because of the convolution's commutative property [Eq. (2.25)], we can also express Eq. (2.30) as [assuming causal $x(t)$ and $h(t)$]

$$y(t) = \begin{cases} \displaystyle\int_{0^-}^{t} h(\tau)x(t-\tau)\,d\tau & t \geq 0 \\ 0 & t < 0 \end{cases}$$

Hereafter, the lower limit of 0^- will be implied even when we write it as 0. As in Eq. (2.30), this result assumes that both the input and the system are causal.

EXAMPLE 2.8 Computing the Zero-State Response

For an LTIC system with the unit impulse response $h(t) = e^{-2t}u(t)$, determine the response $y(t)$ for the input

$$x(t) = e^{-t}u(t)$$

Here, both $x(t)$ and $h(t)$ are causal (Fig. 2.6). Hence, from Eq. (2.30), we obtain

$$y(t) = \int_0^t x(\tau)h(t-\tau)\,d\tau \qquad t \geq 0$$

Because $x(t) = e^{-t}u(t)$ and $h(t) = e^{-2t}u(t)$,

$$x(\tau) = e^{-\tau}u(\tau) \qquad \text{and} \qquad h(t-\tau) = e^{-2(t-\tau)}u(t-\tau)$$

Remember that the integration is performed with respect to τ (not t), and the region of integration is $0 \leq \tau \leq t$. Hence, $\tau \geq 0$ and $t - \tau \geq 0$. Therefore, $u(\tau) = 1$ and $u(t-\tau) = 1$; consequently,

$$y(t) = \int_0^t e^{-\tau}e^{-2(t-\tau)}\,d\tau \qquad t \geq 0$$

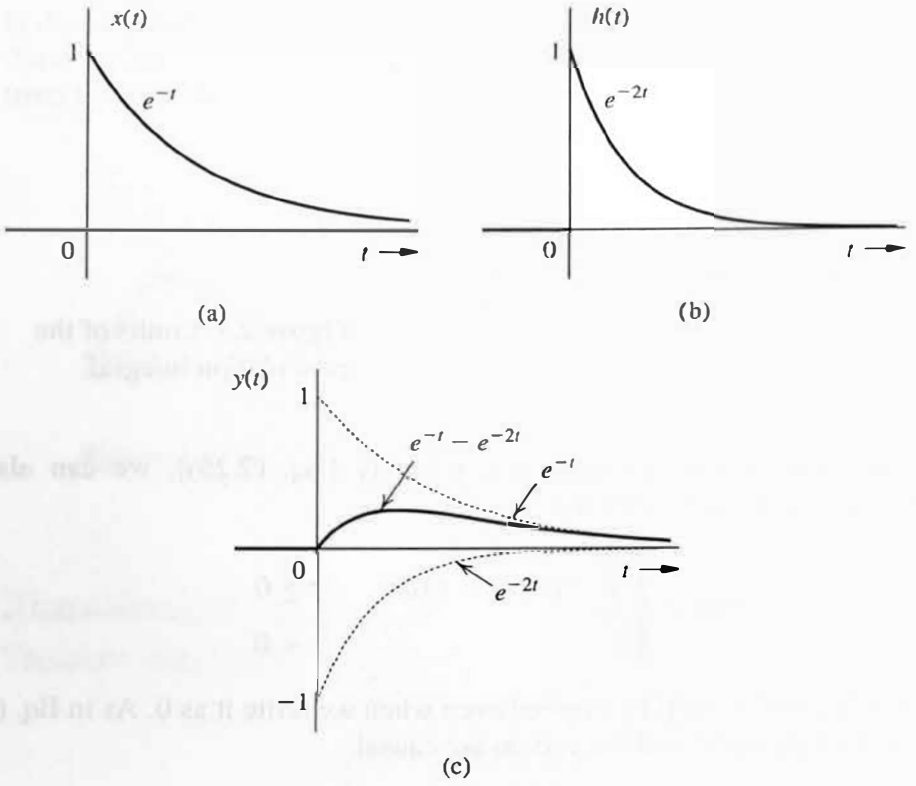

Figure 2.6 Convolution of $x(t)$ and $h(t)$.

Because this integration is with respect to τ, we can pull e^{-2t} outside the integral, giving us

$$y(t) = e^{-2t} \int_0^t e^{\tau}\, d\tau = e^{-2t}(e^t - 1) = e^{-t} - e^{-2t} \qquad t \geq 0$$

Moreover, $y(t) = 0$ when $t < 0$ [see Eq. (2.30)]. Therefore,

$$y(t) = (e^{-t} - e^{-2t})u(t)$$

The response is depicted in Fig. 2.6c.

DRILL 2.5 Computing the Zero-State Response

For an LTIC system with the impulse response $h(t) = 6e^{-t}u(t)$, determine the system response to the input: **(a)** $2u(t)$ and **(b)** $3e^{-3t}u(t)$.

ANSWERS

(a) $12(1 - e^{-t})u(t)$

(b) $9(e^{-t} - e^{-3t})u(t)$

DRILL 2.6 Zero-State Response with Resonance

Repeat Drill 2.5 for the input $x(t) = e^{-t}u(t)$.

ANSWER

$6te^{-t}u(t)$

The Convolution Table

The task of convolution is considerably simplified by a ready-made convolution table (Table 2.1). This table, which lists several pairs of signals and their convolution, can conveniently determine $y(t)$, a system response to an input $x(t)$, without performing the tedious job of integration. For instance, we could have readily found the convolution in Ex. 2.8 by using pair 4 (with $\lambda_1 = -1$ and $\lambda_2 = -2$) to be $(e^{-t} - e^{-2t})u(t)$. The following example demonstrates the utility of this table.

EXAMPLE 2.9 Convolution by Tables

Use Table 2.1 to compute the loop current $y(t)$ of the *RLC* circuit in Ex. 2.4 for the input $x(t) = 10e^{-3t}u(t)$ when all the initial conditions are zero.

The loop equation for this circuit [see Ex. 1.16 or Eq. (1.29)] is

$$(D^2 + 3D + 2)y(t) = Dx(t)$$

The impulse response $h(t)$ for this system, as obtained in Ex. 2.6, is

$$h(t) = (2e^{-2t} - e^{-t})u(t)$$

The input is $x(t) = 10e^{-3t}u(t)$, and the response $y(t)$ is

$$y(t) = x(t) * h(t) = 10e^{-3t}u(t) * [2e^{-2t} - e^{-t}]u(t)$$

Using the distributive property of the convolution [Eq. (2.26)], we obtain

$$\begin{aligned} y(t) &= 10e^{-3t}u(t) * 2e^{-2t}u(t) - 10e^{-3t}u(t) * e^{-t}u(t) \\ &= 20[e^{-3t}u(t) * e^{-2t}u(t)] - 10[e^{-3t}u(t) * e^{-t}u(t)] \end{aligned}$$

Now using pair 4 in Table 2.1 yields

$$\begin{aligned} y(t) &= \frac{20}{-3-(-2)}[e^{-3t} - e^{-2t}]u(t) - \frac{10}{-3-(-1)}[e^{-3t} - e^{-t}]u(t) \\ &= -20(e^{-3t} - e^{-2t})u(t) + 5(e^{-3t} - e^{-t})u(t) \\ &= (-5e^{-t} + 20e^{-2t} - 15e^{-3t})u(t) \end{aligned}$$

TABLE 2.1 Select Convolution Integrals

No.	$x_1(t)$	$x_2(t)$	$x_1(t) * x_2(t) = x_2(t) * x_1(t)$
1	$x(t)$	$\delta(t-T)$	$x(t-T)$
2	$e^{\lambda t}u(t)$	$u(t)$	$\dfrac{1-e^{\lambda t}}{-\lambda}u(t)$
3	$u(t)$	$u(t)$	$tu(t)$
4	$e^{\lambda_1 t}u(t)$	$e^{\lambda_2 t}u(t)$	$\dfrac{e^{\lambda_1 t}-e^{\lambda_2 t}}{\lambda_1-\lambda_2}u(t)$ $\quad \lambda_1 \neq \lambda_2$
5	$e^{\lambda t}u(t)$	$e^{\lambda t}u(t)$	$te^{\lambda t}u(t)$
6	$te^{\lambda t}u(t)$	$e^{\lambda t}u(t)$	$\dfrac{1}{2}t^2e^{\lambda t}u(t)$
7	$t^N u(t)$	$e^{\lambda t}u(t)$	$\dfrac{N!e^{\lambda t}}{\lambda^{N+1}}u(t)-\sum_{k=0}^{N}\dfrac{N!t^{N-k}}{\lambda^{k+1}(N-k)!}u(t)$
8	$t^M u(t)$	$t^N u(t)$	$\dfrac{M!N!}{(M+N+1)!}t^{M+N+1}u(t)$
9	$te^{\lambda_1 t}u(t)$	$e^{\lambda_2 t}u(t)$	$\dfrac{e^{\lambda_2 t}-e^{\lambda_1 t}+(\lambda_1-\lambda_2)te^{\lambda_1 t}}{(\lambda_1-\lambda_2)^2}u(t)$
10	$t^M e^{\lambda t}u(t)$	$t^N e^{\lambda t}u(t)$	$\dfrac{M!N!}{(N+M+1)!}t^{M+N+1}e^{\lambda t}u(t)$
11	$t^M e^{\lambda_1 t}u(t)$	$t^N e^{\lambda_2 t}u(t)$	$\sum_{k=0}^{M}\dfrac{(-1)^k M!(N+k)!t^{M-k}e^{\lambda_1 t}}{k!(M-k)!(\lambda_1-\lambda_2)^{N+k+1}}u(t)$
	$\lambda_1 \neq \lambda_2$		$+\sum_{k=0}^{N}\dfrac{(-1)^k N!(M+k)!t^{N-k}e^{\lambda_2 t}}{k!(N-k)!(\lambda_2-\lambda_1)^{M+k+1}}u(t)$
12	$e^{-\alpha t}\cos(\beta t+\theta)u(t)$	$e^{\lambda t}u(t)$	$\dfrac{\cos(\theta-\phi)e^{\lambda t}-e^{-\alpha t}\cos(\beta t+\theta-\phi)}{\sqrt{(\alpha+\lambda)^2+\beta^2}}u(t)$
			$\phi=\tan^{-1}[-\beta/(\alpha+\lambda)]$
13	$e^{\lambda_1 t}u(t)$	$e^{\lambda_2 t}u(-t)$	$\dfrac{e^{\lambda_1 t}u(t)+e^{\lambda_2 t}u(-t)}{\lambda_2-\lambda_1}$ $\quad \mathrm{Re}\,\lambda_2 > \mathrm{Re}\,\lambda_1$
14	$e^{\lambda_1 t}u(-t)$	$e^{\lambda_2 t}u(-t)$	$\dfrac{e^{\lambda_1 t}-e^{\lambda_2 t}}{\lambda_2-\lambda_1}u(-t)$

DRILL 2.7 Convolution by Tables

Use Table 2.1 to show $e^{-2t}u(t) * (1-e^{-t})u(t) = \left(\frac{1}{2} - e^{-t} + \frac{1}{2}e^{-2t}\right)u(t)$.

DRILL 2.8 Zero-State Response by Convolution Table

Rework Drills 2.5 and 2.6 using Table 2.1.

DRILL 2.9 Another Zero-State Response by Convolution Table

For an LTIC system with the unit impulse response $h(t) = e^{-2t}u(t)$, determine the zero-state response $y(t)$ if the input $x(t) = \sin 3t\,u(t)$. [*Hint:* Use pair 12 from Table 2.1.]

ANSWER

$\frac{1}{13}[3e^{-2t} + \sqrt{13}\cos(3t - 146.32°)]u(t)$ or $\frac{1}{13}[3e^{-2t} - \sqrt{13}\cos(3t + 33.68°)]u(t)$

Response to Complex Inputs

The LTIC system response discussed so far applies to general input signals, real or complex. However, if the system is real, that is, if $h(t)$ is real, then we shall show that the real part of the input generates the real part of the output, and a similar conclusion applies to the imaginary part.

If the input is $x(t) = x_r(t) + jx_i(t)$, where $x_r(t)$ and $x_i(t)$ are the real and imaginary parts of $x(t)$, then for real $h(t)$

$$y(t) = h(t) * [x_r(t) + jx_i(t)] = h(t) * x_r(t) + jh(t) * x_i(t) = y_r(t) + jy_i(t)$$

where $y_r(t)$ and $y_i(t)$ are the real and the imaginary parts of $y(t)$. Using the right-directed-arrow notation to indicate a pair of the input and the corresponding output, the foregoing result can be expressed as follows. If

$$x(t) = x_r(t) + jx_i(t) \implies y(t) = y_r(t) + jy_i(t)$$

then

$$x_r(t) \implies y_r(t) \quad \text{and} \quad x_i(t) \implies y_i(t) \tag{2.31}$$

Multiple Inputs

Multiple inputs to LTI systems can be treated by applying the superposition principle. Each input is considered separately, with all other inputs assumed to be zero. The sum of all these individual system responses constitutes the total system output when all the inputs are applied simultaneously.

2.4.2 Graphical Understanding of Convolution Operation

The convolution operation can be grasped readily through a graphical interpretation of the convolution integral. Such an understanding is helpful in evaluating the convolution integral of more complex signals. In addition, graphical convolution allows us to grasp visually or mentally the convolution integral's result, which can be of great help in sampling, filtering, and many other problems. Finally, many signals have no exact mathematical description, so they can be described only graphically. If two such signals are to be convolved, we have no choice but to perform their convolution graphically.

We shall now explain the convolution operation by convolving the signals $x(t)$ and $g(t)$, illustrated in Figs. 2.7a and 2.7b, respectively. If $c(t)$ is the convolution of $x(t)$ with $g(t)$, then

$$c(t) = \int_{-\infty}^{\infty} x(\tau)g(t-\tau)\,d\tau$$

One of the crucial points to remember here is that this integration is performed with respect to τ so that t is just a parameter (like a constant). This consideration is especially important when we sketch the graphical representations of the functions $x(\tau)$ and $g(t-\tau)$. Both these functions should be sketched as functions of τ, not of t.

The function $x(\tau)$ is identical to $x(t)$, with τ replacing t (Fig. 2.7c). Therefore, $x(t)$ and $x(\tau)$ will have the same graphical representations. Similar remarks apply to $g(t)$ and $g(\tau)$ (Fig. 2.7d).

To appreciate what $g(t-\tau)$ looks like, let us start with the function $g(\tau)$ (Fig. 2.7d). Time reversal of this function (reflection about the vertical axis $\tau = 0$) yields $g(-\tau)$ (Fig. 2.7e). Let us denote this function by $\phi(\tau)$:

$$\phi(\tau) = g(-\tau)$$

Now $\phi(\tau)$ shifted by t seconds is $\phi(\tau - t)$, given by

$$\phi(\tau - t) = g[-(\tau - t)] = g(t - \tau)$$

Therefore, we first time-reverse $g(\tau)$ to obtain $g(-\tau)$ and then time-shift $g(-\tau)$ by t to obtain $g(t-\tau)$. For positive t, the shift is to the right (Fig. 2.7f); for negative t, the shift is to the left (Figs. 2.7g and 2.7h).

The preceding discussion gives us a graphical interpretation of the functions $x(\tau)$ and $g(t-\tau)$. The convolution $c(t)$ is the area under the product of these two functions. Thus, to compute $c(t)$ at some positive instant $t = t_1$, we first obtain $g(-\tau)$ by inverting $g(\tau)$ about the vertical axis. Next, we right-shift or delay $g(-\tau)$ by t_1 to obtain $g(t_1 - \tau)$ (Fig. 2.7f), and then we multiply this function by $x(\tau)$, giving us the product $x(\tau)g(t_1 - \tau)$ (shaded portion in Fig. 2.7f). The area A_1 under this product is $c(t_1)$, the value of $c(t)$ at $t = t_1$. We can therefore plot $c(t_1) = A_1$ on a curve describing $c(t)$, as shown in Fig. 2.7i. The area under the product $x(\tau)g(-\tau)$ in Fig. 2.7e is $c(0)$, the value of the convolution for $t = 0$ (at the origin).

A similar procedure is followed in computing the value of $c(t)$ at $t = t_2$, where t_2 is negative (Fig. 2.7g). In this case, the function $g(-\tau)$ is shifted by a negative amount (that is, left-shifted) to obtain $g(t_2 - \tau)$. Multiplication of this function with $x(\tau)$ yields the product $x(\tau)g(t_2 - \tau)$. The area under this product is $c(t_2) = A_2$, giving us another point on the curve $c(t)$ at $t = t_2$ (Fig. 2.7i). This procedure can be repeated for all values of t, from $-\infty$ to ∞. The result will be a curve describing $c(t)$ for all time t. Note that when $t \leq -3$, $x(\tau)$ and $g(t-\tau)$ do not overlap (see Fig. 2.7h); therefore, $c(t) = 0$ for $t \leq -3$.

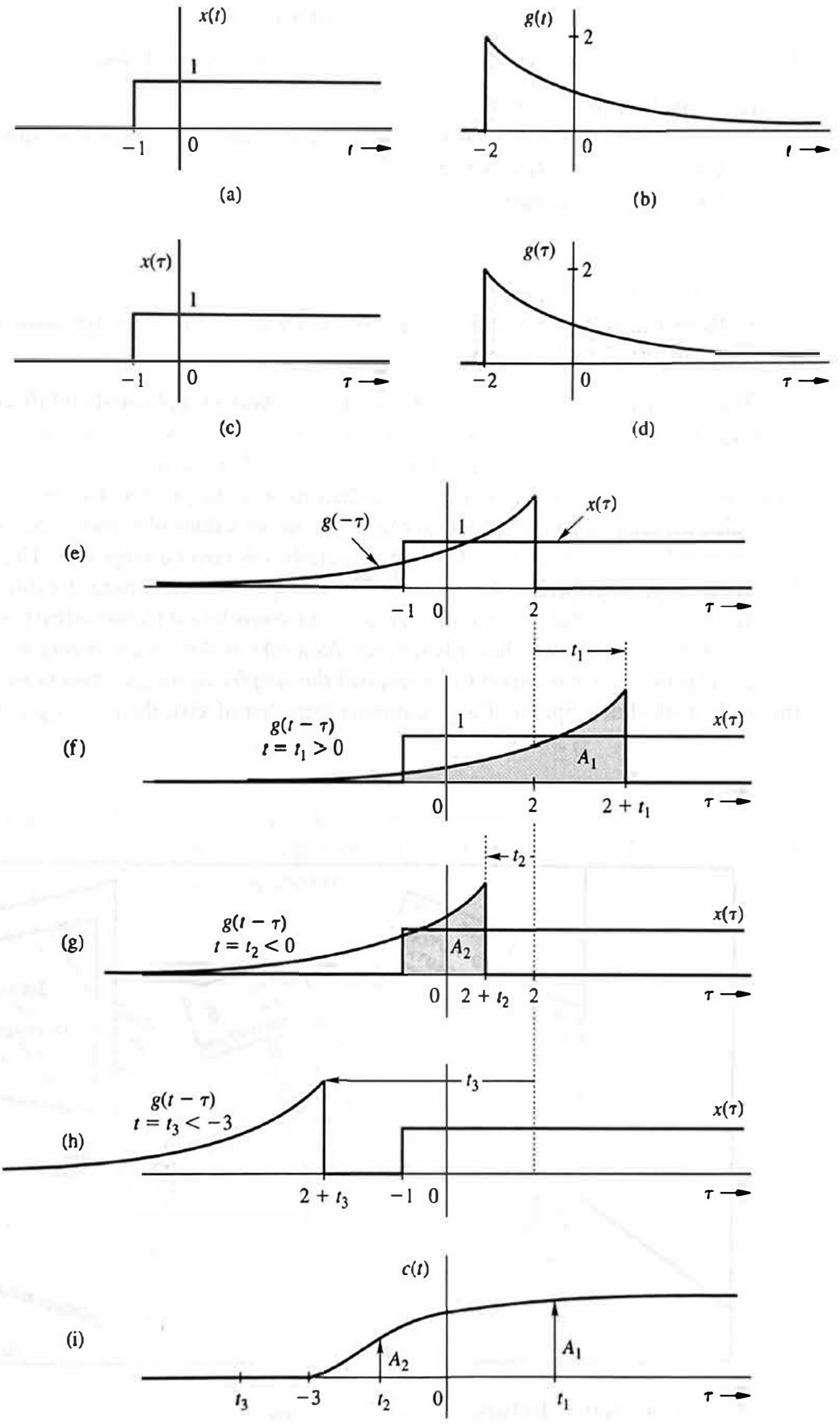

Figure 2.7 Graphical explanation of the convolution operation.

Summary of the Graphical Procedure

The procedure for graphical convolution can be summarized as follows:

1. Keep the function $x(\tau)$ fixed.
2. Visualize the function $g(\tau)$ as a rigid wire frame, and rotate (or invert) this frame about the vertical axis ($\tau = 0$) to obtain $g(-\tau)$.
3. Shift the inverted frame along the τ axis by t_0 seconds. The shifted frame now represents $g(t_0 - \tau)$.
4. The area under the product of $x(\tau)$ and $g(t_0 - \tau)$ (the shifted frame) is $c(t_0)$, the value of the convolution at $t = t_0$.
5. Repeat this procedure, shifting the frame by different values (positive and negative) to obtain $c(t)$ for all values of t.

The graphical procedure discussed here appears very complicated and discouraging at first reading. Indeed, some people claim that convolution has driven many electrical engineering undergraduates to contemplate theology either for salvation or as an alternative career [2]. Actually, the bark of convolution is worse than its bite. In graphical convolution, we need to determine the area under the product $x(\tau)g(t - \tau)$ for all values of t from $-\infty$ to ∞. However, a mathematical description of $x(\tau)g(t - \tau)$ is generally valid over a range of t. Therefore, repeating the procedure for every value of t amounts to repeating it only a few times for different ranges of t.

We can also use the commutative property of convolution to our advantage by computing $x(t) * g(t)$ or $g(t) * x(t)$, whichever is simpler. As a rule of thumb, *convolution computations are simplified if we choose to invert (time-reverse) the simpler of the two functions*. For example, if the mathematical description of $g(t)$ is simpler than that of $x(t)$, then $x(t) * g(t)$ will be easier to

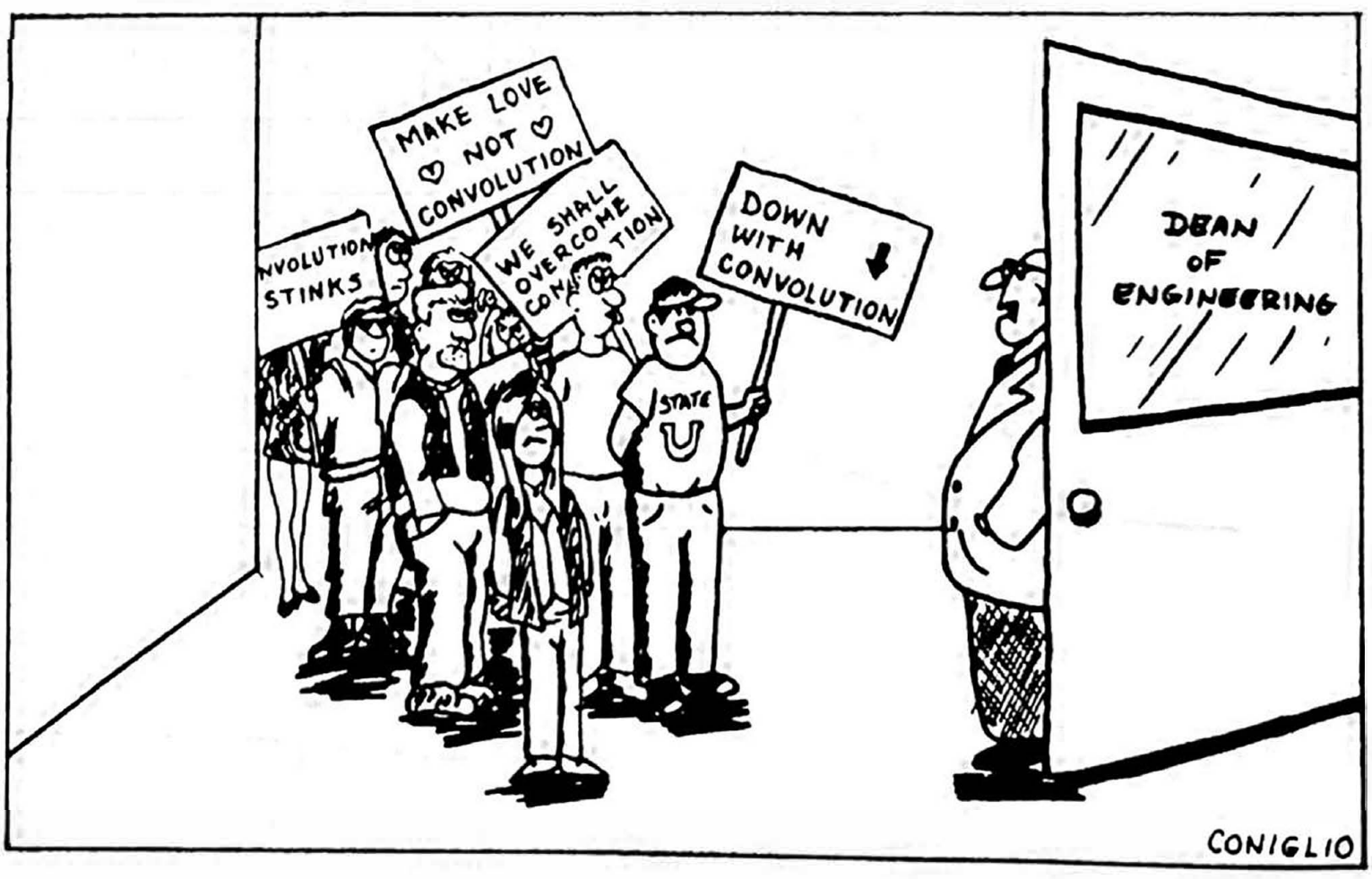

Convolution: Its bark is worse than its bite!

compute than $g(t) * x(t)$. In contrast, if the mathematical description of $x(t)$ is simpler, the reverse will be true.

We shall demonstrate graphical convolution with the following examples. Let us start by using this graphical method to rework Ex. 2.8.

EXAMPLE 2.10 Graphical Convolution of Two Causal Functions

Determine graphically $y(t) = x(t) * h(t)$ for $x(t) = e^{-t}u(t)$ and $h(t) = e^{-2t}u(t)$.

In Figs. 2.8a and 2.8b, we have $x(t)$ and $h(t)$, respectively; and Fig. 2.8c shows $x(\tau)$ and $h(-\tau)$ as functions of τ. The function $h(t-\tau)$ is now obtained by shifting $h(-\tau)$ by t. If t is positive, the shift is to the right (delay); if t is negative, the shift is to the left (advance). Figure 2.8d shows that for negative t, $h(t-\tau)$ [obtained by left-shifting $h(-\tau)$] does not overlap $x(\tau)$, and the product $x(\tau)h(t-\tau) = 0$ so that

$$y(t) = 0 \qquad t < 0$$

Figure 2.8e shows the situation for $t \geq 0$. Here, $x(\tau)$ and $h(t-\tau)$ do overlap, but the product is nonzero only over the interval $0 \leq \tau \leq t$ (shaded interval). Therefore,

$$y(t) = \int_0^t x(\tau)h(t-\tau)\,d\tau \qquad t \geq 0$$

All we need to do now is substitute correct expressions for $x(\tau)$ and $h(t-\tau)$ in this integral. From Figs. 2.8a and 2.8b, it is clear that the segments of $x(t)$ and $g(t)$ to be used in this convolution (Fig. 2.8e) are described by

$$x(t) = e^{-t} \qquad \text{and} \qquad h(t) = e^{-2t}$$

Therefore,

$$x(\tau) = e^{-\tau} \qquad \text{and} \qquad h(t-\tau) = e^{-2(t-\tau)}$$

Consequently,

$$y(t) = \int_0^t e^{-\tau}e^{-2(t-\tau)}\,d\tau = e^{-2t}\int_0^t e^{\tau}\,d\tau = e^{-t} - e^{-2t} \qquad t \geq 0$$

Moreover, $y(t) = 0$ for $t < 0$ so that

$$y(t) = (e^{-t} - e^{-2t})u(t)$$

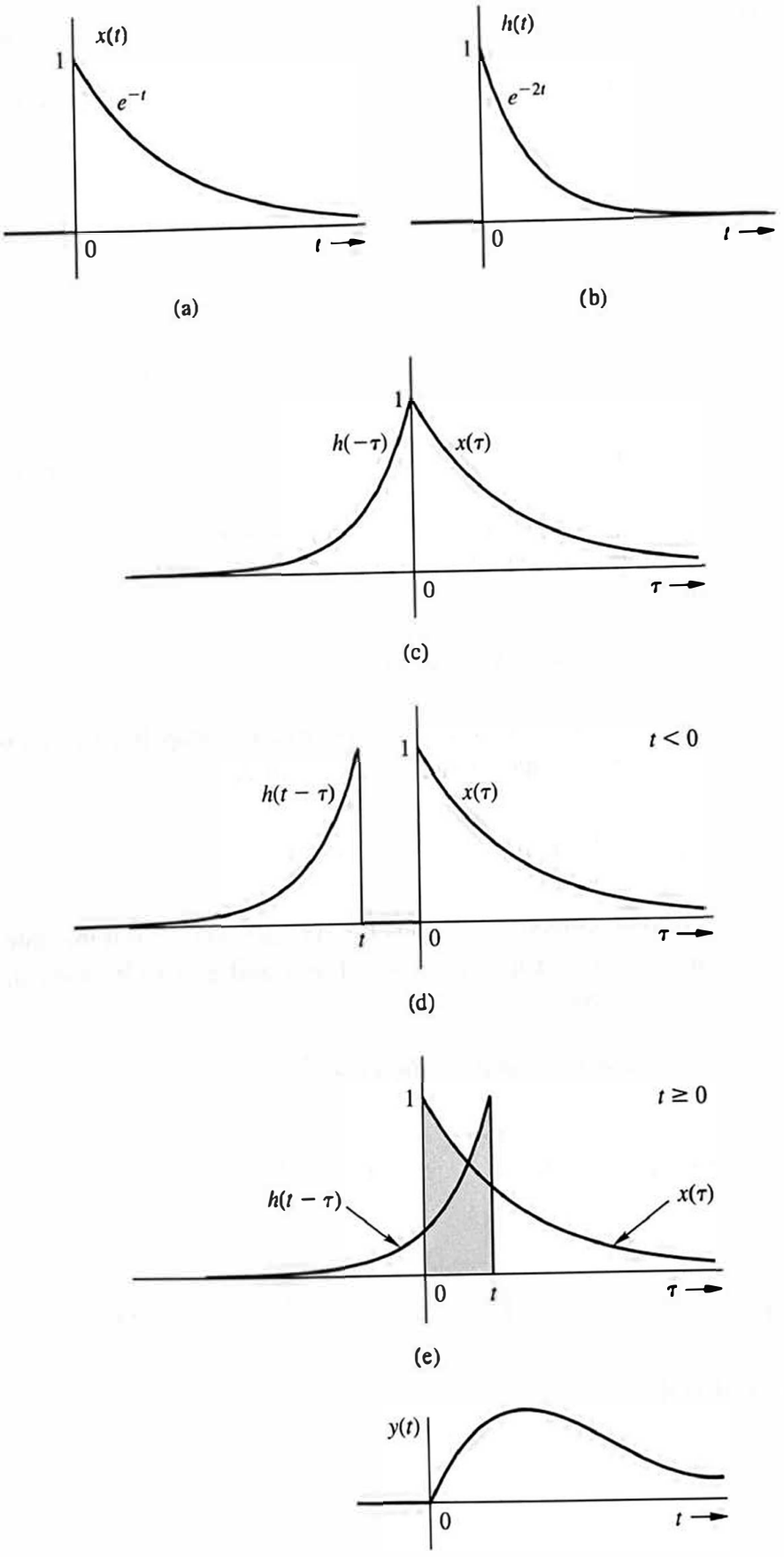

Figure 2.8 Convolution of $x(t)$ and $h(t)$.

EXAMPLE 2.11 Graphical Convolution: Causal Function and Two-Sided Function

Find $c(t) = x(t) * g(t)$ for the signals depicted in Figs. 2.9a and 2.9b.

Since $x(t)$ is simpler than $g(t)$, it is easier to evaluate $g(t) * x(t)$ than $x(t) * g(t)$. However, we shall intentionally take the more difficult route and evaluate $x(t) * g(t)$.

From $x(t)$ and $g(t)$ (Figs. 2.9a and 2.9b, respectively), observe that $g(t)$ is composed of two segments. As a result, it can be described as

$$g(t) = \begin{cases} 2e^{-t} & \text{segment A} \\ -2e^{2t} & \text{segment B} \end{cases}$$

Therefore,

$$g(t-\tau) = \begin{cases} 2e^{-(t-\tau)} & \text{segment A} \\ -2e^{2(t-\tau)} & \text{segment B} \end{cases}$$

The segment of $x(t)$ that is used in convolution is $x(t) = 1$ so that $x(\tau) = 1$. Figure 2.9c shows $x(\tau)$ and $g(-\tau)$.

To compute $c(t)$ for $t \geq 0$, we right-shift $g(-\tau)$ to obtain $g(t-\tau)$, as illustrated in Fig. 2.9d. Clearly, $g(t-\tau)$ overlaps with $x(\tau)$ over the shaded interval, that is, over the range $\tau \geq 0$; segment A overlaps with $x(\tau)$ over the interval $(0, t)$, while segment B overlaps with $x(\tau)$ over (t, ∞). Remembering that $x(\tau) = 1$, we have

$$\begin{aligned} c(t) &= \int_0^\infty x(\tau) g(t-\tau)\, d\tau \\ &= \int_0^t 2e^{-(t-\tau)}\, d\tau + \int_t^\infty -2e^{2(t-\tau)}\, d\tau \\ &= 2(1-e^{-t}) - 1 = 1 - 2e^{-t} \qquad t \geq 0 \end{aligned}$$

Figure 2.9e shows the situation for $t < 0$. Here, the overlap is over the shaded interval, that is, over the range $\tau \geq 0$, where only the segment B of $g(t)$ is involved. Therefore,

$$c(t) = \int_0^\infty x(\tau) g(t-\tau)\, d\tau = \int_0^\infty -2e^{2(t-\tau)}\, d\tau = -e^{2t} \qquad t \leq 0$$

Therefore,

$$c(t) = \begin{cases} 1 - 2e^{-t} & t \geq 0 \\ -e^{2t} & t \leq 0 \end{cases}$$

Figure 2.9f shows a plot of $c(t)$.

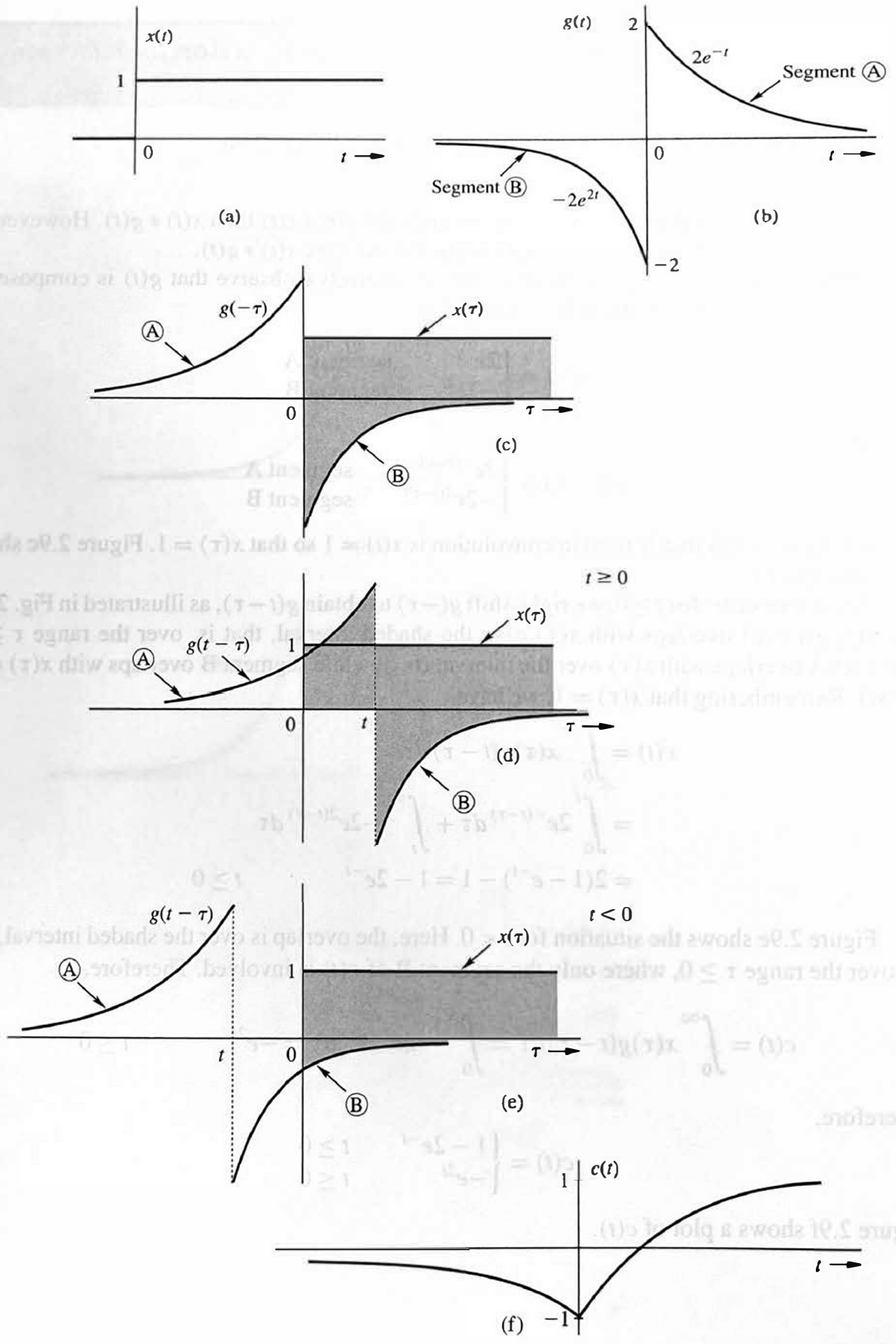

Figure 2.9 Convolution of $x(t)$ and $g(t)$.

EXAMPLE 2.12 Graphical Convolution of Two Finite-Duration Functions

Find $x(t) * g(t)$ for the functions $x(t)$ and $g(t)$ shown in Figs. 2.10a and 2.10b.

Here, $x(t)$ has a simpler mathematical description than that of $g(t)$, so it is preferable to time-reverse $x(t)$. Hence, we shall determine $g(t) * x(t)$ rather than $x(t) * g(t)$. Thus,

$$c(t) = g(t) * x(t) = \int_{-\infty}^{\infty} g(\tau)x(t-\tau)\,d\tau$$

First, we determine the expressions for the segments of $x(t)$ and $g(t)$ used in finding $c(t)$. According to Figs. 2.10a and 2.10b, these segments can be expressed as

$$x(t) = 1 \qquad \text{and} \qquad g(t) = \tfrac{1}{3}t$$

so that

$$x(t-\tau) = 1 \qquad \text{and} \qquad g(\tau) = \tfrac{1}{3}\tau$$

Figure 2.10c shows $g(\tau)$ and $x(-\tau)$, whereas Fig. 2.10d shows $g(\tau)$ and $x(t-\tau)$, which is $x(-\tau)$ shifted by t. Because the edges of $x(-\tau)$ are at $\tau = -1$ and 1, the edges of $x(t-\tau)$ are at $-1+t$ and $1+t$. The two functions overlap over the interval $(0, 1+t)$ (shaded interval) so that

$$c(t) = \int_0^{1+t} g(\tau)x(t-\tau)\,d\tau = \int_0^{1+t} \tfrac{1}{3}\tau\,d\tau = \tfrac{1}{6}(t+1)^2 \qquad -1 \le t \le 1 \qquad (2.32)$$

This situation, depicted in Fig. 2.10d, is valid only for $-1 \le t \le 1$. For $t \ge 1$ but ≤ 2, the situation is as illustrated in Fig. 2.10e. The two functions overlap only over the range $-1+t$ to $1+t$ (shaded interval). Note that the expressions for $g(\tau)$ and $x(t-\tau)$ do not change; only the range of integration changes. Therefore,

$$c(t) = \int_{-1+t}^{1+t} \tfrac{1}{3}\tau\,d\tau = \tfrac{2}{3}t \qquad 1 \le t \le 2 \qquad (2.33)$$

Also note that the expressions in Eqs. (2.32) and (2.33) both apply at $t = 1$, the transition point between their respective ranges. We can readily verify that both expressions yield a value of $2/3$ at $t = 1$ so that $c(1) = 2/3$. The continuity of $c(t)$ at transition points indicates a high probability of a correct answer. Continuity of $c(t)$ at transition points is assured as long as $x(t)$ and $g(t)$ contain no impulse functions.

For $t \ge 2$ but ≤ 4, the situation is as shown in Fig. 2.10f. The functions $g(\tau)$ and $x(t-\tau)$ overlap over the interval from $-1+t$ to 3 (shaded interval) so that

$$c(t) = \int_{-1+t}^{3} \tfrac{1}{3}\tau\,d\tau = -\tfrac{1}{6}(t^2 - 2t - 8) \qquad 2 \le t \le 4 \qquad (2.34)$$

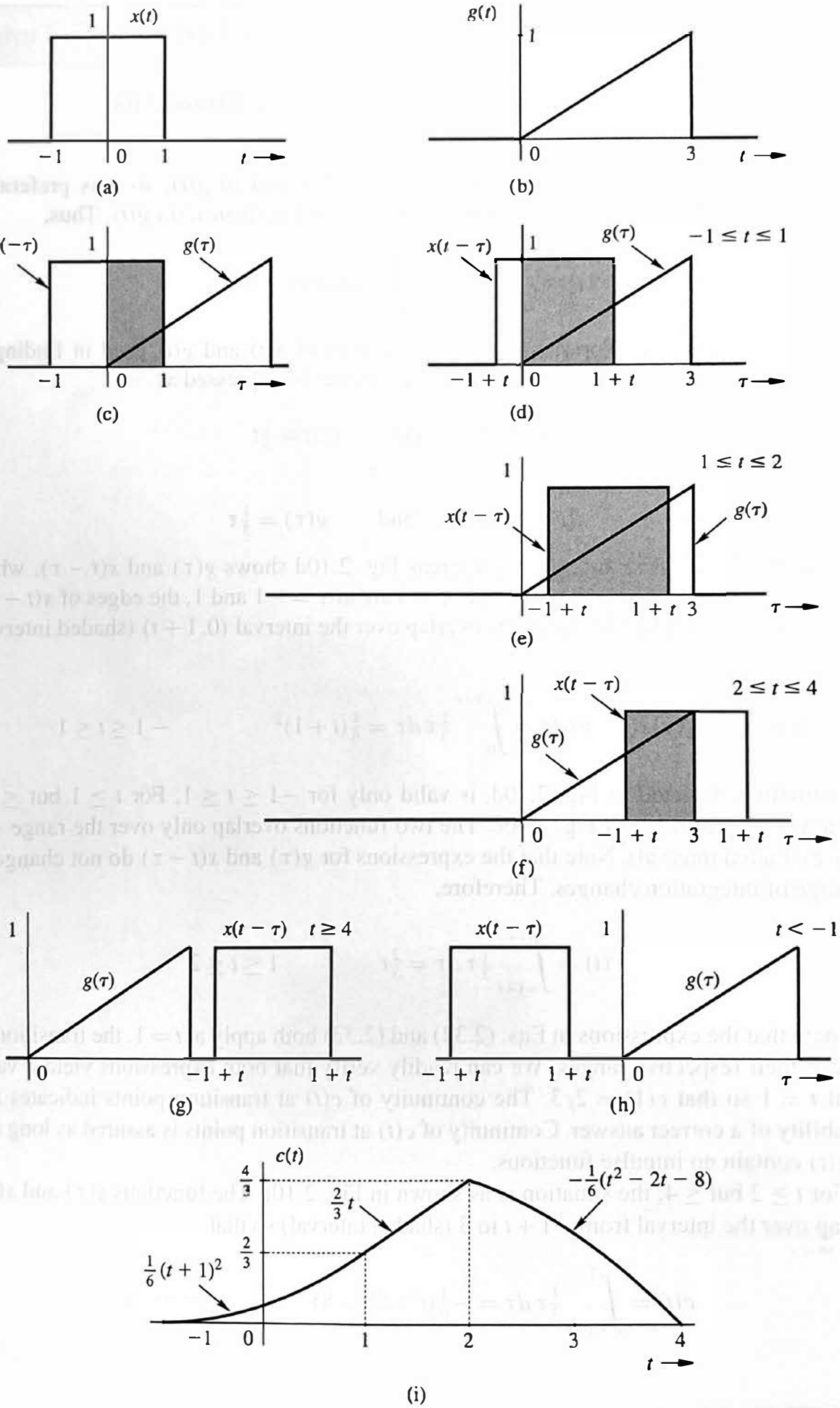

Figure 2.10 Convolution of $x(t)$ and $g(t)$.

Both Eqs. (2.33) and (2.34) apply at the transition point $t = 2$. We can readily verify that $c(2) = 4/3$ when either of these expressions is used.

For $t \geq 4$, $x(t-\tau)$ has been shifted so far to the right that it no longer overlaps with $g(\tau)$ as depicted in Fig. 2.10g. Consequently,

$$c(t) = 0 \qquad t \geq 4$$

We now turn our attention to negative values of t. We have already determined $c(t)$ up to $t = -1$. For $t < -1$, there is no overlap between the two functions, as illustrated in Fig. 2.10h, so that

$$c(t) = 0 \qquad t \leq -1$$

Combining our results, we see that

$$c(t) = \begin{cases} \frac{1}{6}(t+1)^2 & -1 \leq t < 1 \\ \frac{2}{3}t & 1 \leq t < 2 \\ -\frac{1}{6}(t^2 - 2t - 8) & 2 \leq t < 4 \\ 0 & \text{otherwise} \end{cases}$$

Figure 2.10i plots $c(t)$ according to this expression.

The Width of Convolved Functions

The widths (durations) of $x(t)$, $g(t)$, and $c(t)$ in Ex. 2.12 (Fig. 2.10) are 2, 3, and 5, respectively. Note that the width of $c(t)$ in this case is the sum of the widths of $x(t)$ and $g(t)$. This observation is not a coincidence. Using the concept of graphical convolution, we can readily see that if $x(t)$ and $g(t)$ have the finite widths of T_1 and T_2, respectively, then the width of $c(t)$ is equal to $T_1 + T_2$. The reason is that the time it takes for a signal of width (duration) T_1 to completely pass another signal of width (duration) T_2 so that they become non-overlapping is $T_1 + T_2$. When the two signals become non-overlapping, the convolution goes to zero.

DRILL 2.10 Interchanging Convolution Order

Rework Ex. 2.11 by evaluating $g(t) * x(t)$.

DRILL 2.11 Showing Commutability Using Two Causal Signals

Use graphical convolution to show that $x(t) * g(t) = g(t) * x(t) = c(t)$ in Fig. 2.11.

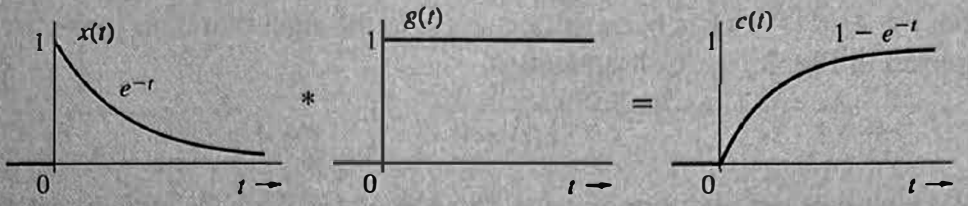

Figure 2.11 Convolution of causal signals $x(t)$ and $g(t)$.

DRILL 2.12 Showing Commutability Using a Causal Signal and an Anticausal Signal

Repeat Drill 2.11 for the functions in Fig. 2.12.

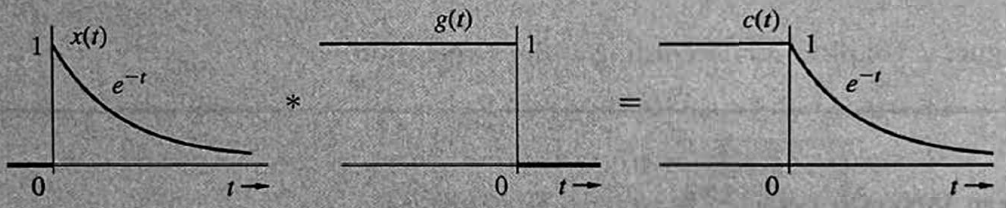

Figure 2.12 Convolution of causal $x(t)$ and anticausal $g(t)$.

DRILL 2.13 Showing Commutability Using Shifted Signals

Repeat Drill 2.11 for the functions in Fig. 2.13.

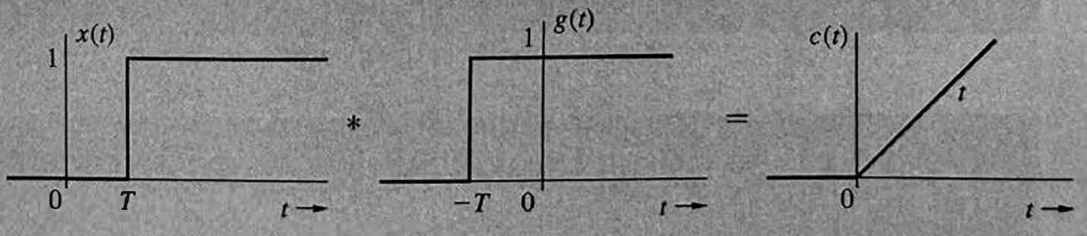

Figure 2.13 Convolution of shifted signals $x(t)$ and $g(t)$.

The Phantom of the Signals and Systems Opera

In the study of signals and systems, we often come across some signals such as an impulse, which cannot be generated in practice and have never been sighted by anyone.† One wonders why we even consider such idealized signals. The answer should be clear from our discussion so far in this chapter. Even if the impulse function has no physical existence, we can compute the system response $h(t)$ to this phantom input according to the procedure in Sec. 2.3, and knowing $h(t)$, we can compute the system response to any arbitrary input. The concept of impulse response, therefore, provides an effective intermediary for computing system response to an arbitrary input. In addition, the impulse response $h(t)$ itself provides a great deal of information and insight about the system behavior. In Sec. 2.6, we show that the knowledge of impulse response provides much valuable information, such as the response time, pulse dispersion, and filtering properties of the system. Many other useful insights about the system behavior can be obtained by inspection of $h(t)$.

Similarly, in frequency-domain analysis (discussed in later chapters), we use an *everlasting exponential* (or *sinusoid)* to determine system response. An everlasting exponential (or sinusoid), too, is a phantom, which nobody has ever seen and which has no physical existence. But it provides another effective intermediary for computing the system response to an arbitrary input. Moreover, the system response to everlasting exponential (or sinusoid) provides valuable information and insight regarding the system's behavior. Clearly, idealized impulses and everlasting sinusoids are friendly and helpful spirits.

Interestingly, the unit impulse and the everlasting exponential (or sinusoid) are the dual of each other in the time-frequency duality, to be studied in Ch. 4. Actually, the time-domain and the frequency-domain methods of analysis are the dual of each other.

Why Convolution? An Intuitive Explanation of System Response

On the surface, it appears rather strange that the response of linear systems (those gentlest of the gentle systems) should be given by such a tortuous operation of convolution, where one signal is fixed and the other is inverted and shifted. To understand this odd behavior, consider a hypothetical impulse response $h(t)$ that decays linearly with time (Fig. 2.14a). This response is strongest at $t = 0$, the moment the impulse is applied, and it decays linearly at future instants so that one second later (at $t = 1$ and beyond), it ceases to exist. This means that the closer the impulse input is to an instant t, the stronger is its response at t.

Now consider the input $x(t)$ shown in Fig. 2.14b. To compute the system response, we break the input into rectangular pulses and approximate these pulses with impulses. Generally, the response of a causal system at some instant t will be determined by all the impulse components of the input before t. Each of these impulse components will have different weight in determining the response at the instant t, depending on its proximity to t. As seen earlier, the closer the impulse is to

† The late Prof. S. J. Mason, the inventor of signal flow graph techniques, used to tell a story of a student frustrated with the impulse function. The student said, "The unit impulse is a thing that is so small you can't see it, except at one place (the origin), where it is so big you can't see it. In other words, you can't see it at all; at least I can't!" [3].

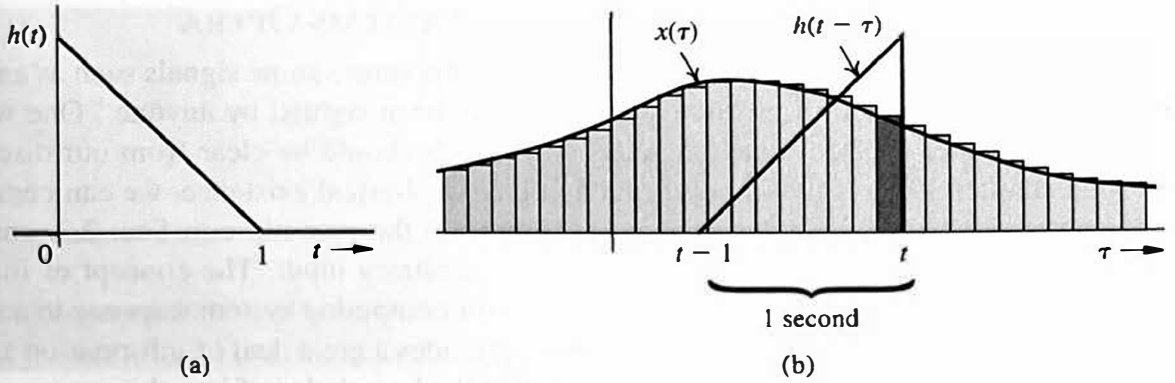

Figure 2.14 Intuitive explanation of convolution.

t, the stronger is its influence at t. The impulse at t has the greatest weight (unity) in determining the response at t. The weight decreases linearly for all impulses before t until the instant $t-1$. The input before $t-1$ has no influence (zero weight). Thus, to determine the system response at t, we must assign a linearly decreasing weight to impulses occurring before t, as shown in Fig. 2.14b. This weighting function is precisely the function $h(t-\tau)$. The system response at t is then determined not by the input $x(\tau)$ but by the weighted input $x(\tau)h(t-\tau)$, and the summation of all these weighted inputs is the convolution integral.

2.4.3 Interconnected Systems

A larger, more complex system can often be viewed as the interconnection of several smaller subsystems, each of which is easier to characterize. Knowing the characterizations of these subsystems, it becomes simpler to analyze such large systems. We shall consider here two basic interconnections, cascade and parallel. Figure 2.15a shows $\mathcal{S}_1$ and $\mathcal{S}_2$, two LTIC subsystems connected in parallel, and Fig. 2.15b shows the same two systems connected in cascade.

In Fig. 2.15a, the device depicted by the symbol Σ inside a circle represents an adder, which adds signals at its inputs. Also the junction from which two (or more) branches radiate out is called the *pickoff node*. Every branch that radiates out from the pickoff node carries the same signal (the signal at the junction). In Fig. 2.15a, for instance, the junction at which the input is applied is a pickoff node from which two branches radiate out, each of which carries the input signal at the node.

Let the impulse response of $\mathcal{S}_1$ and $\mathcal{S}_2$ be $h_1(t)$ and $h_2(t)$, respectively. Further assume that interconnecting these systems, as shown in Fig. 2.15, does not load them. This means that the impulse response of either of these systems remains unchanged whether observed when these systems are unconnected or when they are interconnected.

To find $h_p(t)$, the impulse response of the parallel system $\mathcal{S}_p$ in Fig. 2.15a, we apply an impulse at the input of $\mathcal{S}_p$. This results in the signal $\delta(t)$ at the inputs of $\mathcal{S}_1$ and $\mathcal{S}_2$, leading to their outputs $h_1(t)$ and $h_2(t)$, respectively. These signals are added by the adder to yield $h_1(t)+h_2(t)$ as the output of $\mathcal{S}_p$:

$$h_p(t) = h_1(t) + h_2(t)$$

To find $h_c(t)$, the impulse response of the cascade system $\mathcal{S}_c$ in Fig. 2.15b, we apply the input $\delta(t)$ at the input of $\mathcal{S}_c$, which is also the input to $\mathcal{S}_1$. Hence, the output of $\mathcal{S}_1$ is $h_1(t)$, which now acts

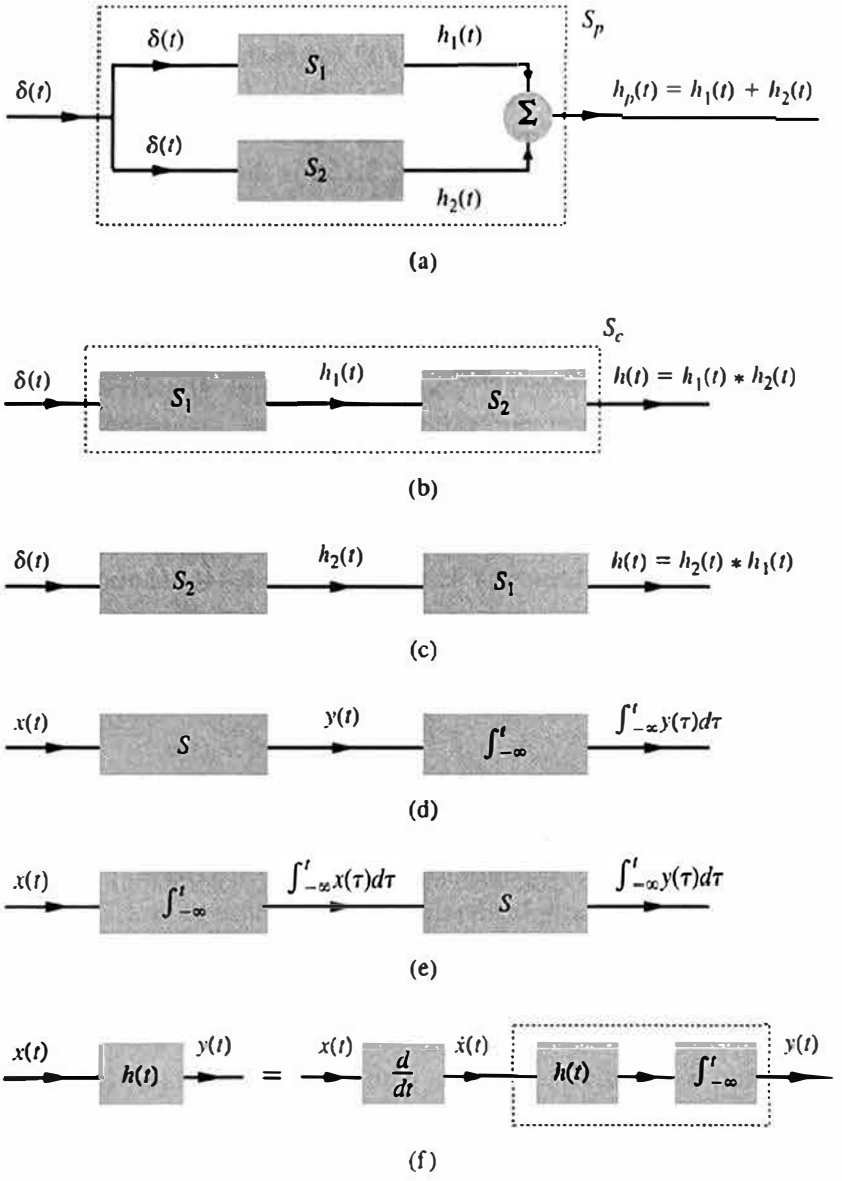

Figure 2.15 Interconnected systems.

as the input to $\mathcal{S}_2$. The response of $\mathcal{S}_2$ to input $h_1(t)$ is $h_1(t) * h_2(t)$. Therefore,

$$h_c(t) = h_1(t) * h_2(t)$$

Because of the commutative property of convolution, it follows that interchanging the systems $\mathcal{S}_1$ and $\mathcal{S}_2$, as shown in Fig. 2.15c, results in the same impulse response $h_1(t) * h_2(t)$. This means that when several LTIC systems are cascaded, the order of systems does not affect the impulse response of the composite system. In other words, linear operations, performed in cascade, commute. The order in which they are performed is not important, at least theoretically.[†]

[†] Change of order, however, could affect performance because of physical limitations and sensitivities to changes in the subsystems involved.

We shall give here another interesting application of the commutative property of LTIC systems. Figure 2.15d shows a cascade of two LTIC systems: a system $\mathcal{S}$ with impulse response $h(t)$, followed by an ideal integrator. Figure 2.15e shows a cascade of the same two systems in reverse order; an ideal integrator followed by $\mathcal{S}$. In Fig. 2.15d, if the input $x(t)$ to $\mathcal{S}$ yields the output $y(t)$, then the output of the system of Fig. 2.15d is the integral of $y(t)$. In Fig. 2.15e, the output of the integrator is the integral of $x(t)$. The output in Fig. 2.15e is identical to the output in Fig. 2.15d. Hence, it follows that if an LTIC system response to input $x(t)$ is $y(t)$, then the response of the same system to the integral of $x(t)$ is the integral of $y(t)$. In other words,

$$\text{if } x(t) \Longrightarrow y(t) \qquad \text{then } \int_{-\infty}^{t} x(\tau)\,d\tau \Longrightarrow \int_{-\infty}^{t} y(\tau)\,d\tau$$

Replacing the ideal integrator with an ideal differentiator in Figs. 2.15d and 2.15e, and following a similar argument, we conclude that

$$\text{if } x(t) \Longrightarrow y(t) \qquad \text{then } \frac{dx(t)}{dt} \Longrightarrow \frac{dy(t)}{dt}$$

If we let $x(t) = \delta(t)$ and $y(t) = h(t)$ in Fig. 2.15e, we find that $g(t)$, the unit step response of an LTIC system with impulse $h(t)$, is given by

$$g(t) = \int_{-\infty}^{t} h(\tau)\,d\tau \tag{2.35}$$

We can also show that the system response to $\dot{\delta}(t)$ is $dh(t)/dt$. These results can be extended to other singularity functions. For example, the unit ramp response of an LTIC system is the integral of its unit step response, and so on.

Inverse Systems

In Fig. 2.15b, if $\mathcal{S}_1$ and $\mathcal{S}_2$ are inverse systems with impulse response $h(t)$ and $h_i(t)$, respectively, then the impulse response of the cascade of these systems is $h(t) * h_i(t)$. But, the cascade of a system with its inverse is an identity system, whose output is the same as the input. In other words, the unit impulse response of the cascade of inverse systems is also an unit impulse $\delta(t)$. Hence,

$$h(t) * h_i(t) = \delta(t) \tag{2.36}$$

We shall give an interesting application of the commutative property. As seen from Eq. (2.36), a cascade of inverse systems is an identity system. Moreover, in a cascade of several LTIC subsystems, changing the order of the subsystems in any manner does not affect the impulse response of the cascade system. Using these facts, we observe that the two systems, shown in Fig. 2.15f, are equivalent. We can compute the response of the cascade system on the right-hand side, by computing the response of the system inside the dotted box to the input $\dot{x}(t)$. The impulse response of the dotted box is $g(t)$, the integral of $h(t)$, as given in Eq. (2.35). Hence, it follows that

$$y(t) = x(t) * h(t) = \dot{x}(t) * g(t) \tag{2.37}$$

Recall that $g(t)$ is the unit step response of the system. Hence, an LTIC response can also be obtained as a convolution of $\dot{x}(t)$ (the derivative of the input) with the unit step response of the

system. This result can be readily extended to higher derivatives of the input. An LTIC system response is the convolution of the nth derivative of the input with the nth integral of the impulse response.

2.4.4 A Very Special Function for LTIC Systems: The Everlasting Exponential e^{st}

There is a very special connection of LTIC systems with the everlasting exponential function e^{st}, where s is a complex variable, in general. We now show that the LTIC system's (zero-state) response to everlasting exponential input e^{st} is also the same everlasting exponential (within a multiplicative constant). Moreover, no other function can make the same claim. Such an input for which the system response is also of the same form is called the *characteristic function* (also *eigenfunction*) of the system. Because a sinusoid is a form of exponential ($s = \pm j\omega$), an everlasting sinusoid is also a characteristic function of an LTIC system. Note that we are talking here of an everlasting exponential (or sinusoid), which starts at $t = -\infty$.

If $h(t)$ is the system's unit impulse response, then system response $y(t)$ to an everlasting exponential e^{st} is given by

$$y(t) = h(t) * e^{st} = \int_{-\infty}^{\infty} h(\tau) e^{s(t-\tau)}\, d\tau = e^{st} \int_{-\infty}^{\infty} h(\tau) e^{-s\tau}\, d\tau$$

The integral on the right-most side is a function of a complex variable s and a constant with respect to t. Let us denote this term by $H(s)$, which is also complex, in general. Thus,

$$y(t) = H(s) e^{st} \tag{2.38}$$

where

$$H(s) = \int_{-\infty}^{\infty} h(\tau) e^{-s\tau}\, d\tau \tag{2.39}$$

Equation (2.38) is valid only for the values of s for which $H(s)$ exists, that is, if $\int_{-\infty}^{\infty} h(\tau) e^{-s\tau}\, d\tau$ exists (or converges). The region in the s plane for which this integral converges is called the *region of convergence* for $H(s)$. Further elaboration of the region of convergence is presented in Ch. 6.

For a given s, note that $H(s)$ is a constant. Thus, the input and the output are the same (within a multiplicative constant) for the everlasting exponential signal.

$H(s)$, which is called the *transfer function* of the system, is a function of complex variable s. An alternate definition of the transfer function $H(s)$ of an LTIC system, as seen from Eq. (2.38), is

$$H(s) = \left. \frac{\text{output signal}}{\text{input signal}} \right|_{\text{input=everlasting exponential } e^{st}} \tag{2.40}$$

The transfer function is defined for, and is meaningful to, LTIC systems only. It does not exist for nonlinear or time-varying systems, in general.

We repeat again that this discussion is about the everlasting exponential, which starts at $t = -\infty$, not the causal exponential $e^{st}u(t)$, which starts at $t = 0$.

For a system specified by Eq. (2.2), the transfer function is given by

$$H(s) = \frac{P(s)}{Q(s)} \tag{2.41}$$

This follows readily by considering an everlasting input $x(t) = e^{st}$. According to Eq. (2.38), the output is $y(t) = H(s)e^{st}$. Substitution of this $x(t)$ and $y(t)$ in Eq. (2.2) yields

$$H(s)[Q(D)e^{st}] = P(D)e^{st}$$

Moreover,

$$D^r e^{st} = \frac{d^r e^{st}}{dt^r} = s^r e^{st}$$

Hence,

$$P(D)e^{st} = P(s)e^{st} \qquad \text{and} \qquad Q(D)e^{st} = Q(s)e^{st}$$

Consequently,

$$H(s) = \frac{P(s)}{Q(s)}$$

DRILL 2.14 Ideal Integrator and Differentiator Transfer Functions

Show that the transfer function of an ideal integrator is $H(s) = 1/s$ and that of an ideal differentiator is $H(s) = s$. Find the answer in two ways: using Eq. (2.39) and using Eq. (2.41). [*Hint:* Find $h(t)$ for the ideal integrator and differentiator. You also may need to use the result in Prob. 1.4-12.]

A Fundamental Property of LTI Systems

We can show that Eq. (2.38) is a fundamental property of LTI systems and it follows directly as a consequence of linearity and time invariance. To show this, let us assume that the response of an LTI system to an everlasting exponential e^{st} is $y(s,t)$. If we define

$$H(s,t) = \frac{y(s,t)}{e^{st}}$$

then

$$y(s,t) = H(s,t)\,e^{st}$$

Because of the time-invariance property, the system response to input $e^{s(t-T)}$ is $H(s,t-T)\,e^{s(t-T)}$, that is,

$$y(s,t-T) = H(s,t-T)\,e^{s(t-T)} \tag{2.42}$$

The delayed input $e^{s(t-T)}$ represents the input e^{st} multiplied by a constant e^{-sT}. Hence, according to the linearity property, the system response to $e^{s(t-T)}$ must be $y(s,t)\,e^{-sT}$. Hence,

$$y(s,t-T) = y(s,t)\,e^{-sT} = H(s,t)\,e^{s(t-T)}$$

Comparison of this result with Eq. (2.42) shows that

$$H(s,t) = H(s,t-T) \qquad \text{for all } T$$

This means $H(s,t)$ is independent of t, and we can express $H(s,t) = H(s)$. Hence,

$$y(s,t) = H(s)\,e^{st}$$

2.4.5 Total Response

Assuming distinct roots, the total response of a linear system can be expressed as the sum of its zero-input response (ZIR) and its zero-state response (ZSR):

$$\text{total response} = \underbrace{\sum_{k=1}^{N} c_k e^{\lambda_k t}}_{\text{ZIR}} + \underbrace{x(t) * h(t)}_{\text{ZSR}}$$

For repeated roots, the zero-input component should be appropriately modified.

For the series *RLC* circuit in Ex. 2.4 with the input $x(t) = 10e^{-3t}u(t)$ and the initial conditions $y(0^-) = 0, v_C(0^-) = 5$, we determined the zero-input response in Ex. 2.1a [Eq. (2.9)]. We found the zero-state response in Ex. 2.9. From the results in Exs. 2.1a and 2.9, we obtain

$$\text{total current} = \underbrace{(-5e^{-t} + 5e^{-2t})}_{\text{zero-input current}} + \underbrace{(-5e^{-t} + 20e^{-2t} - 15e^{-3t})}_{\text{zero-state current}} \qquad t \geq 0 \qquad (2.43)$$

Figure 2.16a shows the zero-input, zero-state, and total responses.

Natural and Forced Response

For the *RLC* circuit in Ex. 2.4, the characteristic modes were found to be e^{-t} and e^{-2t}. As we expected, the zero-input response is composed exclusively of characteristic modes. Note, however,

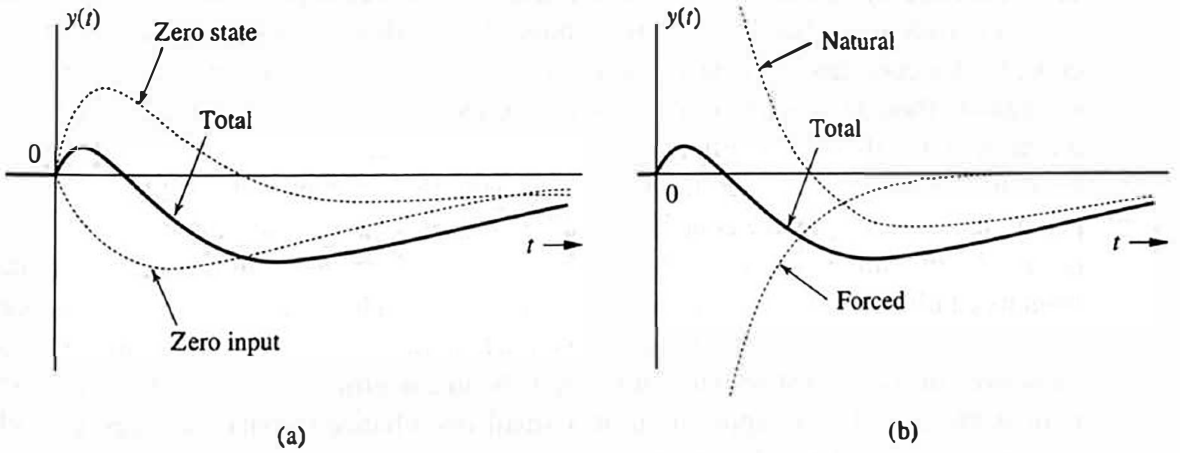

Figure 2.16 Total response and its components.

that even the zero-state response [Eq. (2.43)] contains characteristic mode terms. This observation is generally true of LTIC systems. We can now lump together all the characteristic mode terms in the total response, giving us a component known as the *natural response* $y_n(t)$. The remainder, consisting entirely of noncharacteristic mode terms, is known as the *forced response* $y_\phi(t)$. The total response of the *RLC* circuit in Ex. 2.4 can be expressed in terms of natural and forced components by regrouping the terms in Eq. (2.43) as

$$\text{total current} = \underbrace{(-10e^{-t} + 25e^{-2t})}_{\text{natural response } y_n(t)} + \underbrace{(-15e^{-3t})}_{\text{forced response } y_\phi(t)} \qquad t \geq 0 \tag{2.44}$$

Figure 2.16b shows the natural, forced, and total responses.

The classical solution to a differential equation includes the natural (also called the *homogeneous* or *complementary*) solution and the forced (also known as the *particular*) solution; traditional courses on differential equations provide simplified procedures to determine these components. Unfortunately, the classical solution lacks the engineering intuition and utility afforded by the zero-input and zero-state responses. The classical approach cannot separate the responses arising from internal conditions and external input. While the natural and forced solutions can be obtained from the zero-input and zero-state responses, the converse is not true. Further, the classical method is unable to express the system response to an input $x(t)$ as an explicit function of $x(t)$. In fact, the classical method is restricted to a certain class of inputs and cannot handle arbitrary inputs, as can the method to determine the zero-state response. For these (and other) reasons, we do not further detail the classical solution of differential equations.

2.5 System Stability

Stability is an important system property. Two types of system stability are generally considered: external (BIBO) stability and internal (asymptotic) stability. Let us consider both stability types in turn.

2.5.1 External (BIBO) Stability

To understand the intuitive basis for the BIBO (bounded-input/bounded-output) stability of a system introduced in Sec. 1.7, let us examine the stability concept as applied to a right circular cone. Such a cone can be made to stand forever on its circular base, on its apex, or on its side. For this reason, these three states of the cone are said to be *equilibrium states*. Qualitatively, however, the three states show very different behavior. If the cone, standing on its circular base, were to be disturbed slightly and then left to itself, it would eventually return to its original equilibrium position. In such a case, the cone is said to be in *stable equilibrium*. In contrast, if the cone stands on its apex, then the slightest disturbance will cause the cone to move farther and farther away from its equilibrium state. The cone in this case is said to be in an *unstable equilibrium*. The cone lying on its side, if disturbed, will neither go back to the original state nor continue to move farther away from the original state. Thus, it is said to be in a *neutral equilibrium*. Clearly, when a system is in stable equilibrium, application of a small disturbance (input) produces a small response. In contrast, when the system is in unstable equilibrium, even a minuscule disturbance (input) produces an unbounded response. The BIBO-stability definition can be understood in the light of

this concept. If every bounded input produces bounded output, the system is (BIBO) stable.[†] In contrast, if even one bounded input results in unbounded response, the system is (BIBO) unstable.

For an LTIC system,

$$y(t) = h(t) * x(t) = \int_{-\infty}^{\infty} h(\tau)x(t-\tau)\,d\tau$$

Therefore,

$$|y(t)| \leq \int_{-\infty}^{\infty} |h(\tau)||x(t-\tau)|\,d\tau$$

Moreover, if $x(t)$ is bounded, then $|x(t-\tau)| < K_1 < \infty$, and

$$|y(t)| \leq K_1 \int_{-\infty}^{\infty} |h(\tau)|\,d\tau$$

Hence for BIBO stability,

$$\int_{-\infty}^{\infty} |h(\tau)|\,d\tau < \infty \tag{2.45}$$

This is a sufficient condition for BIBO stability. We can show that this is also a necessary condition (see Prob. 2.5-7). Therefore, for an LTIC system, if its impulse response $h(t)$ is absolutely integrable, the system is (BIBO) stable. Otherwise, it is (BIBO) unstable. In addition, we shall show in Ch. 6 that a necessary (but not sufficient) condition for an LTIC system described by Eq. (2.1) to be BIBO-stable is $M \leq N$. If $M > N$, the system is unstable. This is one of the reasons to avoid systems with $M > N$.

Because the BIBO stability of a system can be ascertained by measurements at the external terminals (input and output), this is an external stability criterion. It is no coincidence that the BIBO criterion in Eq. (2.45) is in terms of the impulse response, which is an external description of the system.

As observed in Sec. 1.9, the internal behavior of a system is not always ascertainable from the external terminals. Therefore, external (BIBO) stability may not be a correct indication of internal stability. Indeed, some systems that appear stable by the BIBO criterion may be internally unstable. This is like a room on fire inside a house: no trace of fire is visible from outside, but the entire house will be burned to ashes.

The BIBO stability is meaningful only for systems in which the internal and the external description are equivalent (controllable and observable systems). Fortunately, most practical systems fall into this category, and whenever we apply this criterion, we implicitly assume that the system, in fact, belongs to this category. Internal stability is all-inclusive, and external stability can always be determined from internal stability. For this reason, we now investigate the internal stability criterion.

[†] The system is assumed to be in zero state.

2.5.2 Internal (Asymptotic) Stability

Because of the great variety of possible system behaviors, there are several definitions of internal stability in the literature. Here, we shall consider a definition that is suitable for causal, linear, time-invariant (LTI) systems.

If, in the absence of an external input, a system remains in a particular state (or condition) indefinitely, then that state is said to be an *equilibrium state* of the system. For an LTI system, zero state, in which all initial conditions are zero, is an equilibrium state. Now suppose an LTI system is in zero state and we change this state by creating small nonzero initial conditions (a small disturbance). These initial conditions will generate signals consisting of characteristic modes in the system. By analogy with the cone, if the system is stable, it should eventually return to zero state. In other words, when left to itself, every mode in a stable system arising as a result of nonzero initial conditions should approach 0 as $t \to \infty$. However, if even one of the modes grows with time, the system will never return to zero state, and the system would be identified as unstable. In the borderline case, some modes neither decay to zero nor grow indefinitely, while all the remaining modes decay to zero. This case is like the neutral equilibrium in the cone. Such a system is said to be *marginally* stable. Internal stability is also called *asymptotic* stability or stability in the sense of *Lyapunov*.

For a system characterized by Eq. (2.1), we can restate the internal stability criterion in terms of the location of the N characteristic roots $\lambda_1, \lambda_2, \ldots, \lambda_N$ of the system in a complex plane. The characteristic modes are of the form $e^{\lambda_k t}$ or $t^r e^{\lambda_k t}$. The locations of various roots in the complex plane and the corresponding modes are shown in Fig. 2.17. These modes $\to 0$ as $t \to \infty$ if Re $\lambda_k < 0$. In contrast, the modes $\to \infty$ as $t \to \infty$ if Re $\lambda_k > 0$.[†]

From Fig. 2.17, we see that a system is (asymptotically) stable if all its characteristic roots lie in the LHP, that is, if Re $\lambda_k < 0$ for all k. If even a single characteristic root lies in the RHP, the system is (asymptotically) unstable. Modes due to roots on the imaginary axis ($\lambda = \pm j\omega_0$) are of the form $e^{\pm j\omega_0 t}$. Hence, if some roots are on the imaginary axis, and all the remaining roots are in the LHP, the system is marginally stable (assuming that the roots on the imaginary axis are not repeated). If the imaginary axis roots are repeated, the characteristic modes are of the form $t^r e^{\pm j\omega_k t}$, which *do* grow with time indefinitely. Hence, the system is unstable. Figure 2.18 shows stability regions in the complex plane.

To summarize:

1. An LTIC system is asymptotically stable if, and only if, all the characteristic roots are in the LHP. The roots may be simple (unrepeated) or repeated.
2. An LTIC system is unstable if, and only if, one or both of the following conditions exist: (i) at least one root is in the RHP; (ii) there are repeated roots on the imaginary axis.
3. An LTIC system is marginally stable if, and only if, there are no roots in the RHP, and there are some unrepeated roots on the imaginary axis.

[†] This may be seen from the fact that if α and β are the real and the imaginary parts of a root λ, then

$$\lim_{t\to\infty} e^{\lambda t} = \lim_{t\to\infty} e^{(\alpha+j\beta)t} = \lim_{t\to\infty} e^{\alpha t} e^{j\beta t} = \begin{cases} 0 & \alpha < 0 \\ \infty & \alpha > 0 \end{cases}$$

This conclusion is also valid for the terms of the form $t^r e^{\lambda t}$.

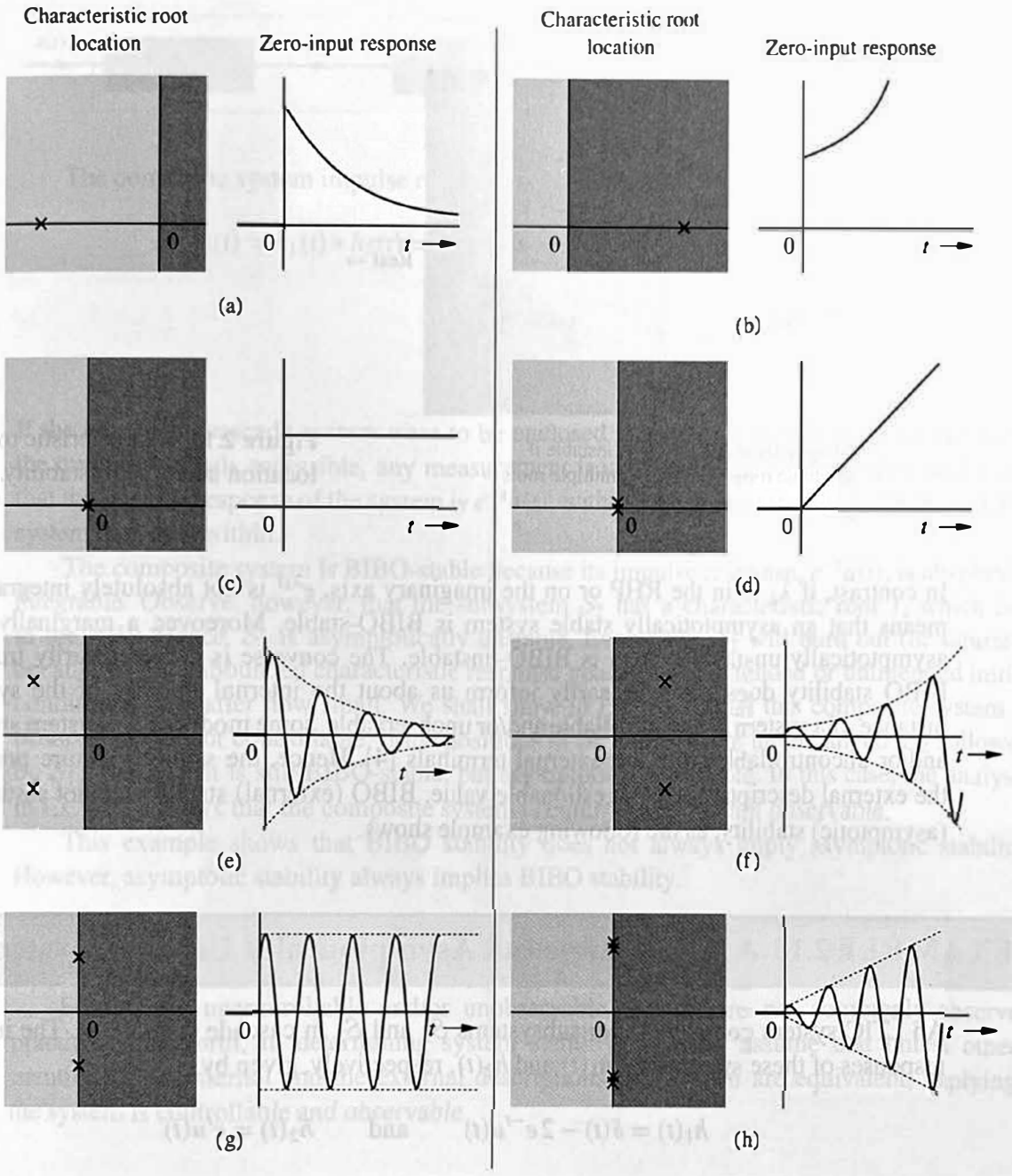

Figure 2.17 Location of characteristic roots and the corresponding characteristic modes.

2.5.3 Relationship Between BIBO and Asymptotic Stability

External stability is determined by applying an external input with zero initial conditions, while internal stability is determined by applying the nonzero initial conditions and no external input. This is why these stabilities are also called the *zero-state stability* and the *zero-input stability*, respectively.

Recall that $h(t)$, the impulse response of an LTIC system, is a linear combination of the system characteristic modes. For an LTIC system, specified by Eq. (2.1), we can readily show that when a characteristic root λ_k is in the LHP, the corresponding mode $e^{\lambda_k t}$ is absolutely integrable.

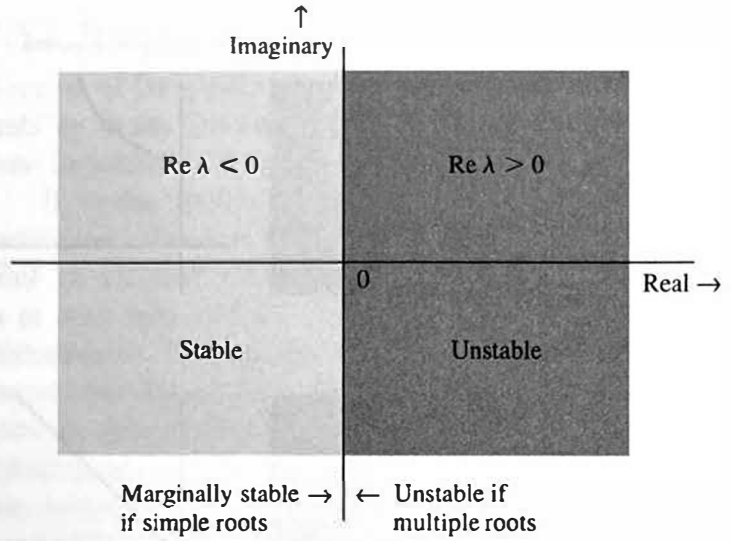

Figure 2.18 Characteristic roots location and system stability.

In contrast, if λ_k is in the RHP or on the imaginary axis, $e^{\lambda_k t}$ is not absolutely integrable.[†] This means that an asymptotically stable system is BIBO-stable. Moreover, a marginally stable or asymptotically unstable system is BIBO-unstable. The converse is not necessarily true; that is, BIBO stability does not necessarily inform us about the internal stability of the system. For instance, if a system is uncontrollable and/or unobservable, some modes of the system are invisible and/or uncontrollable from the external terminals [4]. Hence, the stability picture portrayed by the external description is of questionable value. BIBO (external) stability cannot assure internal (asymptotic) stability, as the following example shows.

EXAMPLE 2.13 A BIBO-Stable but Asymptotically Unstable System

An LTIC system consists of two subsystems $\mathcal{S}_1$ and $\mathcal{S}_2$ in cascade (Fig. 2.19). The impulse responses of these systems are $h_1(t)$ and $h_2(t)$, respectively, given by

$$h_1(t) = \delta(t) - 2e^{-t}u(t) \qquad \text{and} \qquad h_2(t) = e^{t}u(t)$$

Comment on the BIBO and asymptotic stability of the composite system.

[†] Consider a mode of the form $e^{\lambda t}$, where $\lambda = \alpha + j\beta$. Hence, $e^{\lambda t} = e^{\alpha t}e^{j\beta t}$ and $|e^{\lambda t}| = e^{\alpha t}$. Therefore,

$$\int_{-\infty}^{\infty} |e^{\lambda \tau}\, u(\tau)|\, d\tau = \int_{0}^{\infty} e^{\alpha \tau}\, d\tau = \begin{cases} -1/\alpha & \alpha < 0 \\ \infty & \alpha \geq 0 \end{cases}$$

This conclusion is also valid when the integrand is of the form $|t^k e^{\lambda t}u(t)|$.

Figure 2.19 Composite system for Ex. 2.13.

The composite system impulse response $h(t)$ is given by

$$\begin{aligned} h(t) = h_1(t) * h_2(t) = h_2(t) * h_1(t) &= e^t u(t) * [\delta(t) - 2e^{-t}u(t)] \\ &= e^t u(t) - 2\left[\frac{e^t - e^{-t}}{2}\right] u(t) \\ &= e^{-t}u(t) \end{aligned}$$

If the composite cascade system were to be enclosed in a black box with only the input and the output terminals accessible, any measurement from these external terminals would show that the impulse response of the system is $e^{-t}u(t)$, without any hint of the dangerously unstable system harbored within.

The composite system is BIBO-stable because its impulse response, $e^{-t}u(t)$, is absolutely integrable. Observe, however, that the subsystem $\mathcal{S}_2$ has a characteristic root 1, which lies in the RHP. Hence, $\mathcal{S}_2$ is asymptotically unstable. Eventually, $\mathcal{S}_2$ will burn out (or saturate) because of the unbounded characteristic response generated by intended or unintended initial conditions, no matter how small. We shall show in Ex. 13.12 that this composite system is observable, but not controllable. If the positions of $\mathcal{S}_1$ and $\mathcal{S}_2$ were interchanged ($\mathcal{S}_2$ followed by $\mathcal{S}_1$), the system is still BIBO-stable, but asymptotically unstable. In this case, the analysis in Ex. 13.12 shows that the composite system is controllable, but not observable.

This example shows that BIBO stability does not always imply asymptotic stability. However, asymptotic stability always implies BIBO stability.

Fortunately, uncontrollable and/or unobservable systems are not commonly observed in practice. Henceforth, in determining system stability, we shall assume that unless otherwise mentioned, the internal and the external descriptions of a system are equivalent, implying that the system is controllable and observable.

EXAMPLE 2.14 Investigating Asymptotic and BIBO Stability

Investigate the asymptotic and the BIBO stability of LTIC systems described by the following equations, assuming that the equations are internal system descriptions:

(a) $(D+1)(D^2+4D+8)y(t) = (D-3)x(t)$

(b) $(D-1)(D^2+4D+8)y(t) = (D+2)x(t)$

(c) $(D+2)(D^2+4)y(t) = (D^2+D+1)x(t)$

(d) $(D+1)(D^2+4)^2y(t) = (D^2+2D+8)x(t)$

The characteristic polynomials of these systems are

(a) $(\lambda+1)(\lambda^2+4\lambda+8)=(\lambda+1)(\lambda+2-j2)(\lambda+2+j2)$

(b) $(\lambda-1)(\lambda^2+4\lambda+8)=(\lambda-1)(\lambda+2-j2)(\lambda+2+j2)$

(c) $(\lambda+2)(\lambda^2+4)=(\lambda+2)(\lambda-j2)(\lambda+j2)$

(d) $(\lambda+1)(\lambda^2+4)^2=(\lambda+2)(\lambda-j2)^2(\lambda+j2)^2$

Consequently, the characteristic roots of the systems are (see Fig. 2.20)

(a) $-1, -2\pm j2$

(b) $1, -2\pm j2$

(c) $-2, \pm j2$

(d) $-1, \pm j2, \pm j2$

System (a) is asymptotically stable (all roots in LHP), system (b) is unstable (one root in RHP), system (c) is marginally stable (unrepeated roots on imaginary axis) and no roots in RHP, and system (d) is unstable (repeated roots on the imaginary axis). BIBO stability is readily determined from the asymptotic stability. System (a) is BIBO-stable, system (b) is BIBO-unstable, system (c) is BIBO-unstable, and system (d) is BIBO-unstable. We have assumed that these systems are controllable and observable.

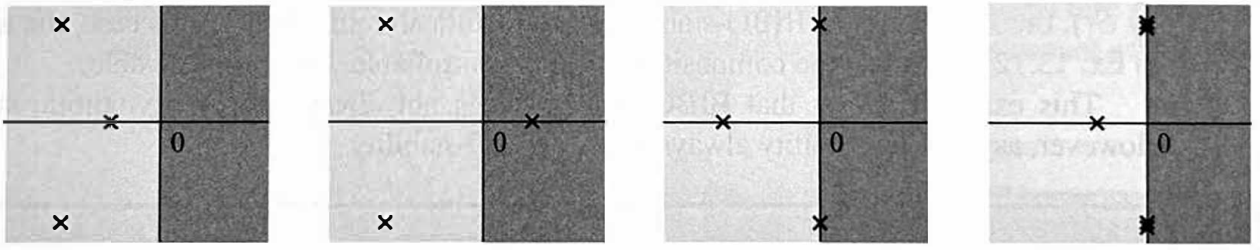

Figure 2.20 Characteristic root locations for the systems of Ex. 2.14.

DRILL 2.15 Assessing Stability by Characteristic Roots

For each case, plot the characteristic roots and determine asymptotic and BIBO stabilities. Assume the equations reflect internal descriptions.

(a) $D(D+2)y(t)=3x(t)$

(b) $D^2(D+3)y(t)=(D+5)x(t)$

(c) $(D+1)(D+2)y(t)=(2D+3)x(t)$

(d) $(D^2+1)(D^2+9)y(t)=(D^2+2D+4)x(t)$

(e) $(D+1)(D^2-4D+9)y(t)=(D+7)x(t)$

ANSWERS

(a) Marginally stable, but BIBO-unstable
(b) Unstable in both senses
(c) Stable in both senses
(d) Marginally stable, but BIBO-unstable
(e) Unstable in both senses.

Implications of Stability

All practical signal-processing systems must be asymptotically stable. Unstable systems are useless from the viewpoint of signal processing because any set of intended or unintended initial conditions leads to an unbounded response that either destroys the system or (more likely) leads it to some saturation conditions that change the nature of the system. Even if the discernible initial conditions are zero, stray voltages or thermal noise signals generated within the system will act as initial conditions. Because of exponential growth of a mode or modes in unstable systems, a stray signal, no matter how small, will eventually cause an unbounded output.

Marginally stable systems, though BIBO unstable, do have one important application in the oscillator, which is a system that generates a signal on its own without the application of an external input. Consequently, the oscillator output is a zero-input response. If such a response is to be a sinusoid of frequency ω_0, the system should be marginally stable with characteristic roots at $\pm j\omega_0$. Thus, to design an oscillator of frequency ω_0, we should pick a system with the characteristic polynomial $(\lambda - j\omega_0)(\lambda + j\omega_0) = \lambda^2 + \omega_0{}^2$. A system described by the differential equation

$$(D^2 + \omega_0{}^2)y(t) = x(t)$$

will do the job. However, practical oscillators are invariably realized using nonlinear systems.

2.6 Intuitive Insights into System Behavior

This section attempts to provide an understanding of what determines system behavior. Because of its intuitive nature, the discussion is more or less qualitative. We shall now show that the most important attributes of a system are its characteristic roots or characteristic modes because they determine not only the zero-input response but also the entire behavior of the system.

2.6.1 Dependence of System Behavior on Characteristic Modes

Recall that the zero-input response of a system consists of the system's characteristic modes. For a stable system, these characteristic modes decay exponentially and eventually vanish. This behavior may give the impression that these modes do not substantially affect system behavior in general and system response in particular. This impression is totally wrong! We shall now see that the system's characteristic modes leave their imprint on every aspect of the system behavior. *We may compare the system's characteristic modes (or roots) to a seed that eventually dissolves in*

the ground; however, the plant that springs from it is totally determined by the seed. The imprint of the seed exists on every cell of the plant.

To understand this interesting phenomenon, recall that the characteristic modes of a system are very special to that system because it can sustain these signals without the application of an external input. In other words, the system offers a free ride and ready access to these signals. Now imagine what would happen if we actually drove the system with an input having the form of a characteristic mode! We would expect the system to respond strongly (this is, in fact, the resonance phenomenon discussed later in this section). If the input is not exactly a characteristic mode but is close to such a mode, we would still expect the system response to be strong. However, if the input is very different from any of the characteristic modes, we would expect the system to respond poorly. We shall now show that these intuitive deductions are indeed true.

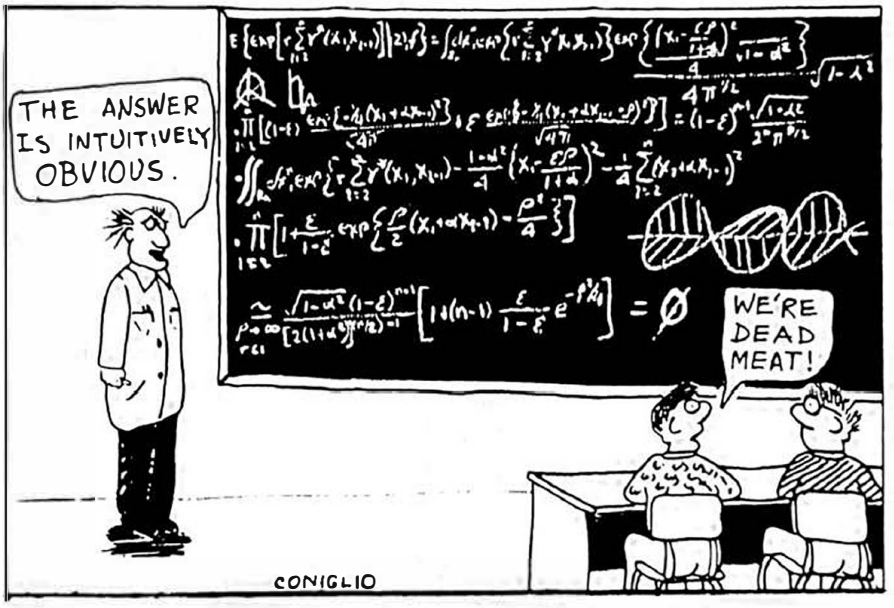

Intuition can cut the math jungle instantly!

We have devised a measure of similarity of signals later (see in Ch. 3). Here, we shall take a simpler approach. Let us restrict the system's inputs to exponentials of the form $e^{\zeta t}$, where ζ is generally a complex number. The similarity of two exponential signals $e^{\zeta t}$ and $e^{\lambda t}$ will then be measured by the closeness of ζ and λ. If the difference $\zeta - \lambda$ is small, the signals are similar; if $\zeta - \lambda$ is large, the signals are dissimilar.

Now consider a first-order system with a single characteristic mode $e^{\lambda t}$ and the input $e^{\zeta t}$. The impulse response of this system is then given by $Ae^{\lambda t}$, where the exact value of A is not important for this qualitative discussion. The system response $y(t)$ is given by

$$y(t) = h(t) * x(t) = Ae^{\lambda t}u(t) * e^{\zeta t}u(t)$$

From the convolution table (Table 2.1), we obtain

$$y(t) = \frac{A}{\zeta - \lambda}[e^{\zeta t} - e^{\lambda t}]u(t) \tag{2.46}$$

Clearly, if the input $e^{\zeta t}$ is similar to $e^{\lambda t}$, $\zeta - \lambda$ is small and the system response is large. *The closer the input $x(t)$ to the characteristic mode, the stronger the system response.* In contrast, if the input is very different from the natural mode, $\zeta - \lambda$ is large and the system responds poorly. This is precisely what we set out to prove.

We have proved the foregoing assertion for a single-mode (first-order) system. It can be generalized to an Nth-order system, which has N characteristic modes. The impulse response $h(t)$ of such a system is a linear combination of its N modes. Therefore, if $x(t)$ is similar to any one of the modes, the corresponding response will be high; if it is similar to none of the modes, the response will be small. Clearly, the characteristic modes are very influential in determining system response to a given input.

It would be tempting to conclude on the basis of Eq. (2.46) that if the input is identical to the characteristic mode, so that $\zeta = \lambda$, then the response goes to infinity. Remember, however, that if $\zeta = \lambda$, the numerator on the right-hand side of Eq. (2.46) also goes to zero. We shall study this interesting behavior (resonance phenomenon) later in this section.

We now show that *mere inspection of the impulse response $h(t)$ (which is composed of characteristic modes) reveals a great deal about the system behavior.*

2.6.2 Response Time of a System: The System Time Constant

Like human beings, systems have a certain response time. In other words, when an input (stimulus) is applied to a system, a certain amount of time elapses before the system fully responds to that input. This time lag or response time is called the system *time constant*. As we shall see, a system's time constant is equal to the width of its impulse response $h(t)$.

An input $\delta(t)$ to a system is instantaneous (zero duration), but its response $h(t)$ has a duration T_h. Therefore, the system requires a time T_h to respond fully to this input, and we are justified in viewing T_h as the system's response time or time constant. We arrive at the same conclusion via another argument. The output is a convolution of the input with $h(t)$. If an input is a pulse of width T_x, then the output pulse width is $T_x + T_h$ according to the width property of convolution. This conclusion shows that the system requires T_h seconds to respond fully to any input. *The system time constant indicates how fast the system is. A system with a smaller time constant is a faster system that responds quickly to an input. A system with a relatively large time constant is a sluggish system that cannot respond well to rapidly varying signals.*

Strictly speaking, the duration of the impulse response $h(t)$ is ∞ because the characteristic modes approach zero asymptotically as $t \to \infty$. However, beyond some value of t, $h(t)$ becomes negligible. It is therefore necessary to use some suitable measure of the impulse response's effective width.

There is no single satisfactory definition of effective signal duration (or width) applicable to every situation. For the situation depicted in Fig. 2.21, a reasonable definition of the duration $h(t)$ would be T_h, the width of the rectangular pulse $\hat{h}(t)$. This rectangular pulse $\hat{h}(t)$ has an area identical to that of $h(t)$ and a height identical to that of $h(t)$ at some suitable instant $t = t_0$. In Fig. 2.21, t_0 is chosen as the instant at which $h(t)$ is maximum. According to this definition,[†]

$$T_h h(t_0) = \int_{-\infty}^{\infty} h(t)\,dt$$

[†]This definition is satisfactory when $h(t)$ is a single, mostly positive (or mostly negative) pulse. Such systems are lowpass systems. This definition should not be applied indiscriminately to all systems.

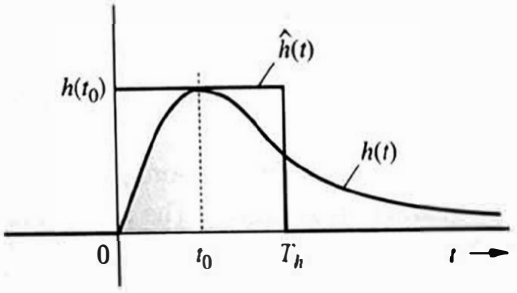

Figure 2.21 Effective duration of an impulse response.

or

$$T_h = \frac{\int_{-\infty}^{\infty} h(t)\,dt}{h(t_0)} \tag{2.47}$$

Now if a system has a single mode

$$h(t) = Ae^{\lambda t}u(t)$$

with λ negative and real, then $h(t)$ is maximum at $t = 0$ with value $h(0) = A$. Therefore, according to Eq. (2.47),

$$T_h = \frac{1}{A}\int_0^{\infty} Ae^{\lambda t}\,dt = -\frac{1}{\lambda}$$

Thus, the time constant in this case is simply the (negative of the) reciprocal of the system's characteristic root. For the multimode case, $h(t)$ is a weighted sum of the system's characteristic modes, and T_h is a weighted average of the time constants associated with the N modes of the system.

2.6.3 Time Constant and Rise Time of a System

Rise time of a system, defined as the time required for the unit step response to rise from 10% to 90% of its steady-state value, is an indication of the speed of response.[†] The system time constant may also be viewed from a perspective of rise time. The unit step response $y(t)$ of a system is the convolution of $u(t)$ with $h(t)$. Let the impulse response $h(t)$ be a rectangular pulse of width T_h, as shown in Fig. 2.22. This assumption simplifies the discussion, yet gives satisfactory results for qualitative discussion. The result of this convolution is illustrated in Fig. 2.22. Note that the output does not rise from zero to a final value instantaneously as the input rises; instead, the output takes T_h seconds to accomplish this. Hence, the rise time T_r of the system is equal to the system time constant

$$T_r = T_h$$

This result and Fig. 2.22 show clearly that a system generally does not respond to an input instantaneously. Instead, it takes time T_h for the system to respond fully.

[†] Because of varying definitions of rise time, the reader may find different results in the literature. The qualitative and intuitive nature of this discussion should always be kept in mind.

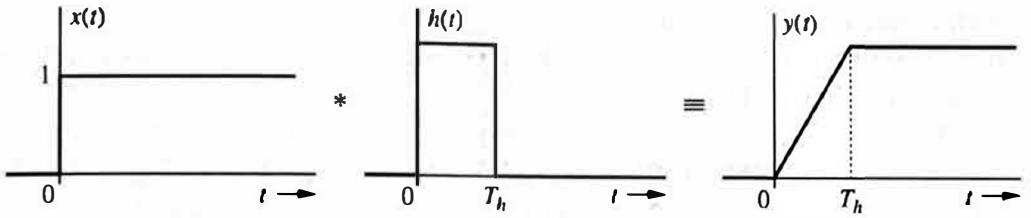

Figure 2.22 Rise time of a system.

2.6.4 Time Constant and Filtering

A larger time constant implies a sluggish system because the system takes longer to respond fully to an input. Such a system cannot respond effectively to rapid variations in the input. In contrast, a smaller time constant indicates that a system is capable of responding to rapid variations in the input. Thus, there is a direct connection between a system's time constant and its filtering properties.

A high-frequency sinusoid varies rapidly with time. A system with a large time constant will not be able to respond well to this input. Therefore, such a system will suppress rapidly varying (high-frequency) sinusoids and other high-frequency signals, thereby acting as a lowpass filter (a filter allowing the transmission of low-frequency signals only). We shall now show that a system

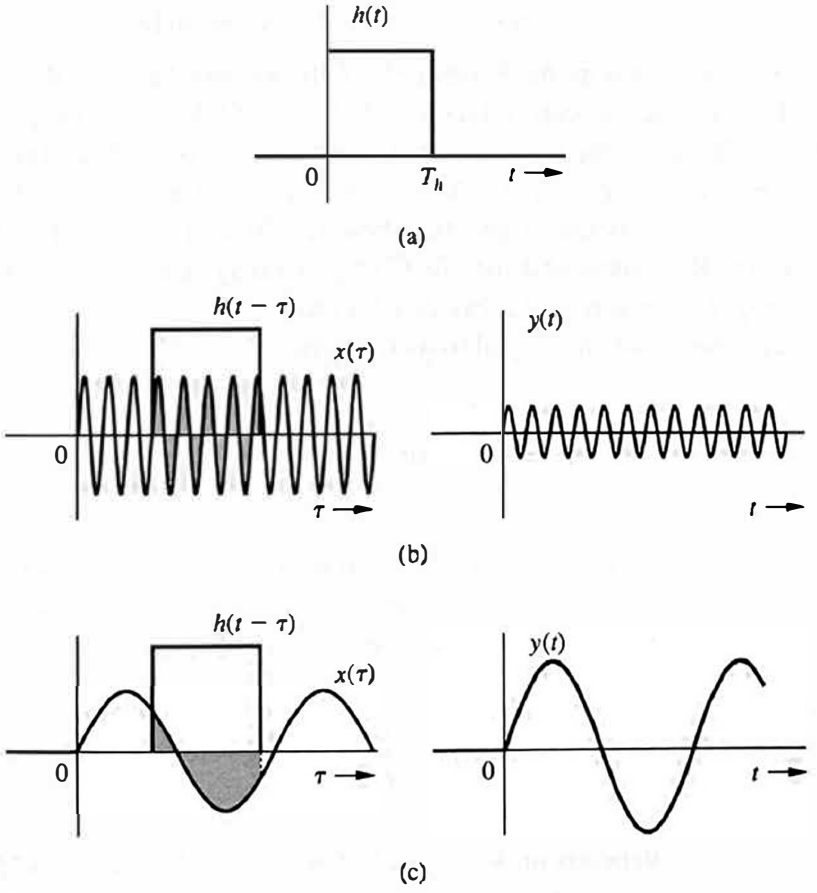

Figure 2.23 Time constant and filtering.

with a time constant T_h acts as a lowpass filter having a cutoff frequency of $f_c = 1/T_h$ hertz so that sinusoids with frequencies below f_c Hz are transmitted reasonably well, while those with frequencies above f_c Hz are suppressed.

To demonstrate this fact, let us determine the system response to a sinusoidal input $x(t)$ by convolving this input with the effective impulse response $h(t)$ in Fig. 2.23a. From Figs. 2.23b and 2.23c, we see the process of convolution of $h(t)$ with the sinusoidal inputs of two different frequencies. The sinusoid in Fig. 2.23b has a relatively high frequency, while the frequency of the sinusoid in Fig. 2.23c is low. Recall that the convolution of $x(t)$ and $h(t)$ is equal to the area under the product $x(\tau)h(t-\tau)$. This area is shown shaded in Figs. 2.23b and 2.23c for the two cases. For the high-frequency sinusoid, it is clear from Fig. 2.23b that the area under $x(\tau)h(t-\tau)$ is very small because its positive and negative areas nearly cancel each other out. In this case the output $y(t)$ remains periodic but has a rather small amplitude. This happens when the period of the sinusoid is much smaller than the system time constant T_h. In contrast, for the low-frequency sinusoid, the period of the sinusoid is larger than T_h, rendering the partial cancellation of area under $x(\tau)h(t-\tau)$ less effective. Consequently, the output $y(t)$ is much larger, as depicted in Fig. 2.23c.

Between these two possible extremes in system behavior, a transition point occurs when the period of the sinusoid is equal to the system time constant T_h. The frequency at which this transition occurs is known as the *cutoff frequency* f_c of the system. Because T_h is the period of cutoff frequency f_c,

$$f_c = \frac{1}{T_h}$$

The frequency f_c is also known as the bandwidth of the system because the system transmits or passes sinusoidal components with frequencies below f_c while attenuating components with frequencies above f_c. Of course, the transition in system behavior is gradual. There is no dramatic change in system behavior at $f_c = 1/T_h$. Moreover, these results are based on an idealized (rectangular pulse) impulse response; in practice these results will vary somewhat, depending on the exact shape of $h(t)$. Remember that the "feel" of general system behavior is more important than exact system response for this qualitative discussion.

Since the system time constant is equal to its rise time, we have

$$T_r = \frac{1}{f_c} \quad \text{or} \quad f_c = \frac{1}{T_r} \tag{2.48}$$

Thus, a system's bandwidth is inversely proportional to its rise time. Although Eq. (2.48) was derived for an idealized (rectangular) impulse response, its implications are valid for lowpass LTIC systems, in general. For a general case, we can show that [1]

$$f_c = \frac{k}{T_r}$$

where the exact value of k depends on the nature of $h(t)$. An experienced engineer often can estimate quickly the bandwidth of an unknown system by simply observing the system response to a step input on an oscilloscope.

2.6.5 Time Constant and Pulse Dispersion (Spreading)

In general, the transmission of a pulse through a system causes pulse dispersion (or spreading). Therefore, the output pulse is generally wider than the input pulse. This system behavior can have serious consequences in communication systems in which information is transmitted by pulse amplitudes. Dispersion (or spreading) causes interference or overlap with neighboring pulses, thereby distorting pulse amplitudes and introducing errors in the received information.

Earlier we saw that if an input $x(t)$ is a pulse of width T_x, then T_y, the width of the output $y(t)$, is

$$T_y = T_x + T_h$$

This result shows that an input pulse spreads out (disperses) as it passes through a system. Since T_h is also the system's time constant or rise time, the amount of spread in the pulse is equal to the time constant (or rise time) of the system.

2.6.6 Time Constant and Rate of Information Transmission

In pulse communications systems, which convey information through pulse amplitudes, the rate of information transmission is proportional to the rate of pulse transmission. We shall demonstrate that to avoid the destruction of information caused by dispersion of pulses during their transmission through the channel (transmission medium), the rate of information transmission should not exceed the bandwidth of the communications channel.

Since an input pulse spreads out by T_h seconds, the consecutive pulses should be spaced T_h seconds apart to avoid interference between pulses. Thus, the rate of pulse transmission should not exceed $1/T_h$ pulses/second. But $1/T_h = f_c$, the channel's bandwidth, so that we can transmit pulses through a communications channel at a rate of f_c pulses per second and still avoid significant interference between the pulses. The rate of information transmission is therefore proportional to the channel's bandwidth (or to the reciprocal of its time constant).[†]

The discussion of Secs. 2.6.2, 2.6.3, 2.6.4, 2.6.5, and 2.6.6 shows that the system time constant determines much of a system's behavior—its filtering characteristics, rise time, pulse dispersion, and so on. In turn, the time constant is determined by the system's characteristic roots. Clearly, the characteristic roots and their relative amounts in the impulse response $h(t)$ determine the behavior of a system.

EXAMPLE 2.15 Intuitive Insights into Lowpass System Behavior

Find the time constant T_h, rise time T_r, and cutoff frequency f_c for a lowpass system that has impulse response $h(t) = te^{-t}u(t)$. Determine the maximum rate that pulses of 1 second

[†] Theoretically, a channel of bandwidth f_c can transmit correctly up to $2f_c$ pulse amplitudes per second [5]. Our derivation here, being very simple and qualitative, yields only half the theoretical limit. In practice it is not easy to attain the upper theoretical limit.

duration can be transmitted through the system so that interference is essentially avoided between adjacent pulses at the system output.

The system impulse response $h(t) = te^{-t}u(t)$, which looks similar to the impulse response of Fig. 2.21, has a peak value of $e^{-1} = 0.3679$ at a time $t_0 = 1$. According to Eq. (2.47) and using integration by parts, the system time constant is therefore

$$T_h = \frac{\int_0^\infty te^{-t}\,dt}{e^{-1}} = e^1\left(-te^{-t}\Big|_0^\infty + \int_0^\infty e^{-t}\,dt\right) = e^1\left(0 - e^{-t}\Big|_0^\infty\right) = e^1(1) = 2.7183$$

Thus,

$$T_h = 2.7183\text{ s}, \qquad T_r = T_h = 2.7183\text{ s}, \qquad \text{and} \qquad f_c = \frac{1}{T_h} = 0.3679\text{ Hz}$$

Due to its lowpass nature, this system will spread an input pulse of 1 second to an output with width

$$T_y = T_x + T_h = 1 + 2.7183 = 3.7183\text{ s}$$

To avoid interference between pulses at the output, the pulse transmission rate should be no more than the reciprocal of the output pulse width. That is,

$$\text{maximum pulse transmission rate} = \tfrac{1}{3.7183} = 0.2689\text{ pulse/s}$$

By narrowing the input pulses, the pulse transmission rate could increase up to $f_c = 0.3679$ pulse/s.

2.6.7 The Resonance Phenomenon

Finally, we come to the fascinating phenomenon of resonance. As we have already mentioned several times, this phenomenon is observed when the input signal is identical or is very close to a characteristic mode of the system. For the sake of simplicity and clarity, we consider a first-order system having only a single mode, $e^{\lambda t}$. Let the impulse response of this system be†

$$h(t) = Ae^{\lambda t}$$

and let the input be

$$x(t) = e^{(\lambda-\epsilon)t}$$

The system response $y(t)$ is then given by

$$y(t) = Ae^{\lambda t} * e^{(\lambda-\epsilon)t}$$

---

† For convenience, we omit multiplying $x(t)$ and $h(t)$ by $u(t)$. Throughout this discussion, we assume that they are causal.

From the convolution table, we obtain

$$y(t) = \frac{A}{\epsilon}\left[e^{\lambda t} - e^{(\lambda-\epsilon)t}\right] = Ae^{\lambda t}\left(\frac{1-e^{-\epsilon t}}{\epsilon}\right) \tag{2.49}$$

Now, as $\epsilon \to 0$, both the numerator and the denominator of the term in the parentheses approach zero. Applying L'Hôpital's rule to this term yields

$$\lim_{\epsilon \to 0} y(t) = Ate^{\lambda t}$$

Clearly, the response does not go to infinity as $\epsilon \to 0$, but it acquires a factor t, which approaches ∞ as $t \to \infty$. If λ has a negative real part (so that it lies in the LHP), $e^{\lambda t}$ decays faster than t and $y(t) \to 0$ as $t \to \infty$. The resonance phenomenon in this case is present, but its manifestation is aborted by the signal's own exponential decay.

This discussion shows that *resonance is a cumulative phenomenon,* not instantaneous. It builds up linearly with t.[†] When the mode decays exponentially, the signal decays too fast for resonance to counteract the decay; as a result, the signal vanishes before resonance has a chance to build it up. However, if the mode were to decay at a rate less than $1/t$, we should see the resonance phenomenon clearly. This specific condition would be possible if Re $\lambda \geq 0$. For instance, when Re $\lambda = 0$ so that λ lies on the imaginary axis of the complex plane ($\lambda = j\omega$), the output becomes

$$y(t) = Ate^{j\omega t}$$

Here, the response does go to infinity linearly with t.

For a real system, if $\lambda = j\omega$ is a root, $\lambda^* = -j\omega$ must also be a root; the impulse response is of the form $Ae^{j\omega t} + Ae^{-j\omega t} = 2A\cos\omega t$. The response of this system to input $A\cos\omega t$ is $2A\cos\omega t * \cos\omega t$. The reader can show that this convolution contains a term of the form $At\cos\omega t$. The resonance phenomenon is clearly visible. The system response to its characteristic mode increases linearly with time, eventually reaching ∞, as indicated in Fig. 2.24.

Recall that when $\lambda = j\omega$, the system is marginally stable. As we have indicated, the full effect of resonance cannot be seen for an asymptotically stable system; only in a marginally stable system does the resonance phenomenon boost the system's response to infinity when the system's input

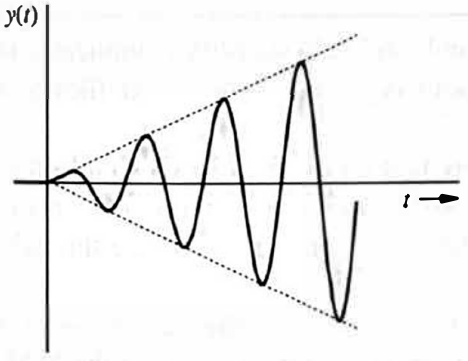

Figure 2.24 Buildup of system response in resonance.

[†] If the characteristic root in question repeats r times, the resonance effect increases as t^{r-1}. However, $t^{r-1}e^{\lambda t} \to 0$ as $t \to \infty$ for any value of r, provided Re $\lambda < 0$ (λ in the LHP).

is a characteristic mode. But even in an asymptotically stable system, we see a manifestation of resonance if its characteristic roots are close to the imaginary axis so that Re λ is a small, negative value. We can show that when the characteristic roots of a system are $\sigma \pm j\omega_0$, then the system response to the input $e^{j\omega_0 t}$ or the sinusoid $\cos \omega_0 t$ is very large for small σ.[†] The system response drops off rapidly as the input signal frequency moves away from ω_0. This frequency-selective behavior can be studied more profitably after an understanding of frequency-domain analysis has been acquired. For this reason we postpone full discussion of this subject until Ch. 6.

Importance of the Resonance Phenomenon

The resonance phenomenon is very important because it allows us to design frequency-selective systems by choosing their characteristic roots properly. Lowpass, bandpass, highpass, and bandstop filters are all examples of frequency-selective networks. In mechanical systems, the inadvertent presence of resonance can cause signals of such tremendous magnitude that the system may fall apart. A musical note (periodic vibrations) of proper frequency can shatter glass if the frequency is matched to the characteristic root of the glass, which acts as a mechanical system. Similarly, a company of soldiers marching in step across a bridge amounts to applying a periodic force to the bridge. If the frequency of this input force happens to be nearer to a characteristic root of the bridge, the bridge may respond (vibrate) violently and collapse, even though it would have been strong enough to carry many soldiers marching out of step. A case in point is the Tacoma Narrows Bridge failure of 1940. This bridge was opened to traffic in July 1940. Within four months of opening (on November 7, 1940), it collapsed in a mild gale, not because of the wind's brute force but because the frequencies of wind-generated vortices, which matched the natural frequencies (characteristic roots) of the bridge, caused resonance.

Because of the great damage that may occur, mechanical resonance is generally to be avoided, especially in structures or vibrating mechanisms. If an engine with periodic force (such as piston motion) is mounted on a platform, the platform with its mass and springs should be designed so that their characteristic roots are not close to the engine's frequency of vibration. Proper design of this platform can not only avoid resonance, but also attenuate vibrations if the system roots are placed far away from the frequency of vibration.

2.7 MATLAB: M-Files

M-files are stored sequences of MATLAB commands and help simplify complicated tasks. There are two types of M-file: script and function. Both types are simple text files and require a `.m` filename extension.

Although M-files can be created by using any text editor, MATLAB's built-in editor is the preferable choice because of its special features. As with any program, comments improve the readability of an M-file. Comments begin with the `%` character and continue through the end of the line.

An M-file is executed by simply typing the filename (without the `.m` extension). To execute, M-files need to be located in the current directory or any other directory in the MATLAB path. New directories are easily added to the MATLAB path by using the `addpath` command.

[†] This follows directly from Eq. (2.49) with $\lambda = \sigma + j\omega_0$ and $\epsilon = \sigma$.

2.7.1 Script M-Files

Script files, the simplest type of M-file, consist of a series of MATLAB commands. Script files record and automate a series of steps, and they are easy to modify. To demonstrate the utility of a script file, consider the operational amplifier circuit shown in Fig. 2.25.

The system's characteristic modes define the circuit's behavior and provide insight regarding system behavior. Using ideal, infinite gain difference amplifier characteristics, we first derive the differential equation that relates output $y(t)$ to input $x(t)$. Kirchhoff's current law (KCL) at the node shared by R_1 and R_3 provides

$$\frac{x(t)-v(t)}{R_3}+\frac{y(t)-v(t)}{R_2}+\frac{0-v(t)}{R_1}-C_2\dot{v}(t)=0$$

KCL at the inverting input of the op amp gives

$$\frac{v(t)}{R_1}+C_1\dot{y}(t)=0$$

Combining and simplifying the KCL equations yield

$$\ddot{y}(t)+\frac{1}{C_2}\left\{\frac{1}{R_1}+\frac{1}{R_2}+\frac{1}{R_3}\right\}\dot{y}(t)+\frac{1}{R_1R_2C_1C_2}y(t)=-\frac{1}{R_1R_3C_1C_2}x(t)$$

which is the desired constant coefficient differential equation. Thus, the characteristic equation is given by

$$\lambda^2+\frac{1}{C_2}\left\{\frac{1}{R_1}+\frac{1}{R_2}+\frac{1}{R_3}\right\}\lambda+\frac{1}{R_1R_2C_1C_2}=(a_0\lambda^2+a_1\lambda+a_2)=0 \tag{2.50}$$

The roots λ_1 and λ_2 of Eq. (2.50) establish the nature of the characteristic modes $e^{\lambda_1 t}$ and $e^{\lambda_2 t}$.

As a first case, assign nominal component values of $R_1 = R_2 = R_3 = 10$ kΩ and $C_1 = C_2 = 1$ μF. A series of MATLAB commands allows convenient computation of the roots $\lambda = [\lambda_1;\lambda_2]$. Although λ can be determined using the quadratic equation, MATLAB's `roots` command is more convenient. The `roots` command requires an input vector that contains the polynomial coefficients in descending order. Even if a coefficient is zero, it must still be included in the vector.

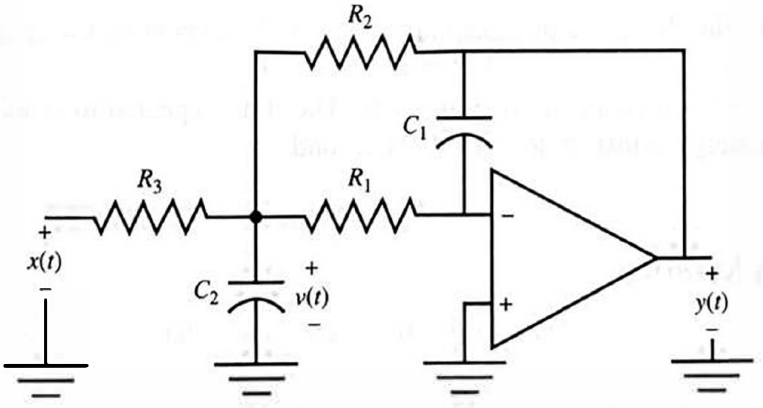

Figure 2.25 Operation amplifier circuit.

```
% CH2MP1.m : Chapter 2, MATLAB Program 1
% Script M-file determines characteristic roots of op-amp circuit.

% Set component values:
R = [1e4, 1e4, 1e4]; C = [1e-6, 1e-6];
% Determine coefficients for characteristic equation:
A = [1, (1/R(1)+1/R(2)+1/R(3))/C(2), 1/(R(1)*R(2)*C(1)*C(2))];
% Determine characteristic roots:
lambda = roots(A);
```

A script file is created by placing these commands in a text file, which in this case is named `CH2MP1.m`. While comment lines improve program clarity, their removal does not affect program functionality. The program is executed by typing

```
>>  CH2MP1
```

After execution, all the resulting variables are available in the workspace. For example, to view the characteristic roots, type

```
>>  lambda
    lambda = -261.8034
             -38.1966
```

Thus, the characteristic modes are simple decaying exponentials: $e^{-261.8034t}$ and $e^{-38.1966t}$.

Script files permit simple or incremental changes, thereby saving significant effort. Consider what happens when capacitor C_1 is changed from 1.0 μF to 1.0 nF. Changing `CH2MP1.m` so that `C = [1e-9, 1e-6]` allows computation of the new characteristic roots:

```
>>  CH2MP1
>>  lambda
    lambda = 1.0e+003 *
             -0.1500 + 3.1587i
             -0.1500 - 3.1587i
```

Perhaps surprisingly, the characteristic modes are now complex exponentials capable of supporting oscillations. The imaginary portion of λ dictates an oscillation rate of 3158.7 rad/s or about 503 Hz. The real portion dictates the rate of decay. The time expected to reduce the amplitude to 25% is approximately $t = \ln 0.25/\mathrm{Re}(\lambda) \approx 0.01$ second.

2.7.2 Function M-Files

It is inconvenient to modify and save a script file each time a change of parameters is desired. Function M-files provide a sensible alternative. Unlike script M-files, function M-files can accept input arguments as well as return outputs. Functions truly extend the MATLAB language in ways that script files cannot.

Syntactically, a function M-file is identical to a script M-file except for the first line. The general form of the first line is

```
function [output1, ..., outputN] = filename(input1, ..., inputM)
```

For example, consider modification of `CH2MP1.m` to make function `CH2MP2.m`. Component values are passed to the function as two separate inputs: a length-3 vector of resistor values and a length-2 vector of capacitor values. The characteristic roots are returned as a 2×1 complex vector.

```
function [lambda] = CH2MP2(R,C)
% CH2MP2.m : Chapter 2, MATLAB Program 2
% Function M-file finds characteristic roots of op-amp circuit.
% INPUTS:   R = length-3 vector of resistances
%           C = length-2 vector of capacitances
% OUTPUTS:  lambda = characteristic roots

% Determine coefficients for characteristic equation:
A = [1, (1/R(1)+1/R(2)+1/R(3))/C(2), 1/(R(1)*R(2)*C(1)*C(2))];
% Determine characteristic roots:
lambda = roots(A);
```

As with script M-files, function M-files execute by typing the name at the command prompt. However, inputs must also be included. For example, `CH2MP2` easily confirms the oscillatory modes of the preceding example.

```
>>  lambda = CH2MP2([1e4, 1e4, 1e4],[1e-9, 1e-6])
    lambda = 1.0e+003 *
             -0.1500 + 3.1587i
             -0.1500 - 3.1587i
```

Although scripts and functions have similarities, they also have distinct differences that are worth pointing out. Scripts operate on workspace data; either functions must be supplied data through inputs or they must create their own data. Unless passed as an output, variables and data created by functions remain local to the function; variables or data generated by scripts are global and are added to the workspace. To emphasize this point, consider polynomial coefficient vector `A`, which is created and used in both `CH2MP1.m` and `CH2MP2.m`. Following execution of function `CH2MP2`, the variable `A` is not added to the workspace. Following execution of script `CH2MP1`, however, `A` is available in the workspace. Recall, the workspace is easily viewed by typing either `who` or `whos`.

2.7.3 For-Loops

Real resistors and capacitors never exactly equal their nominal values. Suppose that the circuit components are measured as $R_1 = 10.322\ \text{k}\Omega$, $R_2 = 9.952\ \text{k}\Omega$, $R_3 = 10.115\ \text{k}\Omega$, $C_1 = 1.120\ \text{nF}$, and $C_2 = 1.320\ \mu\text{F}$. These values are consistent with the 10 and 25% tolerance resistor and capacitor values commonly and readily available. `CH2MP2.m` uses these component values to calculate the new values of λ.

```
>> lambda = CH2MP2([10322,9592,10115],[1.12e-9, 1.32e-6])
   lambda = 1.0e+003 *
            -0.1136 + 2.6113i
            -0.1136 - 2.6113i
```

Now the natural modes oscillate at 2611.3 rad/s or about 416 Hz. Decay to 25% amplitude is expected in $t = \ln 0.25/(-113.6) \approx 0.012$ second. These values, which differ significantly from the nominal values of 503 Hz and $t \approx 0.01$ second, warrant a more formal investigation of the effect of component variations on the locations of the characteristic roots.

It is sensible to look at three values for each component: the nominal value, a low value, and a high value. Low and high values are based on component tolerances. For example, a 10% 1 kΩ resistor could have an expected low value of $1000(1 - 0.1) = 900\ \Omega$ and an expected high value of $1000(1 + 0.1) = 1100\ \Omega$. For the five passive components in the design, $3^5 = 243$ permutations are possible.

Using either `CH2MP1.m` or `CH2MP2.m` to solve each of the 243 cases would be very tedious and boring. For-loops help automate repetitive tasks such as this. In MATLAB, the general structure of a `for` statement is

```
for variable = expression, statement, ..., statement, end
```

Five nested for-loops, one for each passive component, are required for the present example.

```
% CH2MP3.m : Chapter 2, MATLAB Program 3
% Script M-file determines char. roots over a range of component values.

% Pre-allocate memory for all computed roots:
lambda = zeros(2,243);
% Initialize index to identify each permutation:
p=0;
for R1 = 1e4*[0.9,1.0,1.1],
    for R2 = 1e4*[0.9,1.0,1.1],
        for R3 = 1e4*[0.9,1.0,1.1],
            for C1 = 1e-9*[0.75,1.0,1.25],
                for C2 = 1e-6*[0.75,1.0,1.25],
                    p = p+1;
                    lambda(:,p) = CH2MP2([R1 R2 R3],[C1 C2]);
                end
            end
        end
    end
end

plot(real(lambda(:)),imag(lambda(:)),'kx',...
    real(lambda(:,1)),imag(lambda(:,1)),'kv',...
    real(lambda(:,end)),imag(lambda(:,end)),'k^')
xlabel('Real'),ylabel('Imaginary')
legend('Char. Roots','Min. Val. Roots','Max. Val. Roots','Location','West');
```

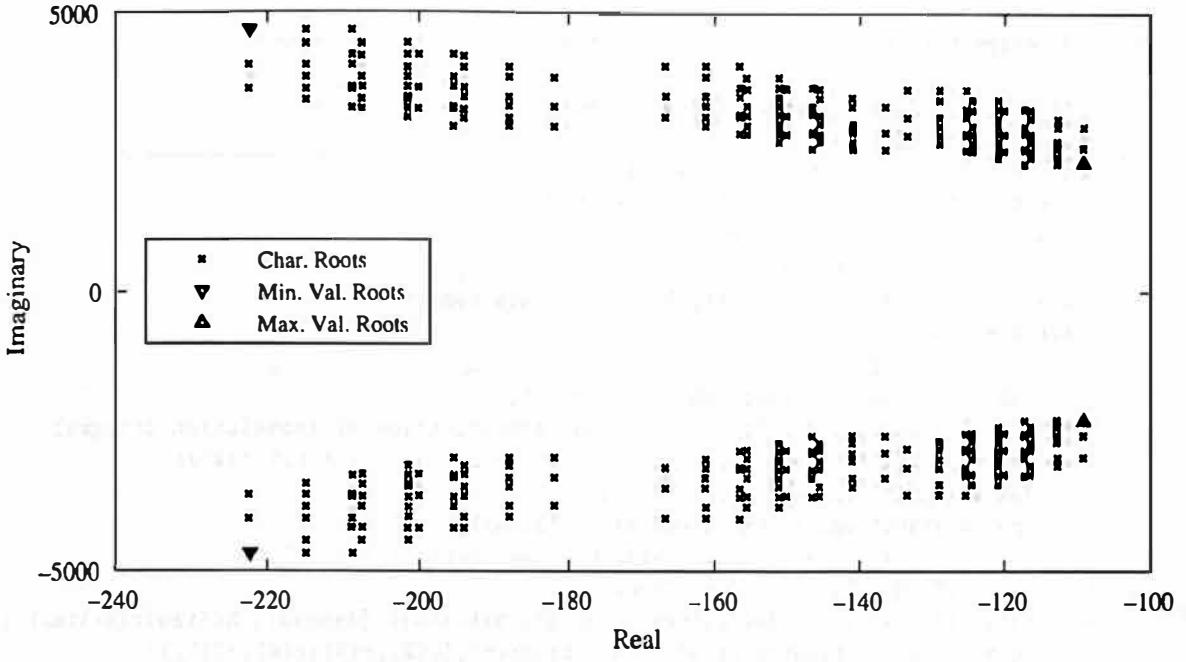

Figure 2.26 Effect of component values on characteristic root locations.

The command `lambda = zeros(2,243)` preallocates a 2×243 array to store the computed roots. When necessary, MATLAB performs dynamic memory allocation, so this command is not strictly necessary. However, preallocation significantly improves script execution speed. Notice also that it would be nearly useless to call script `CH2MP1` from within the nested loop; script file parameters cannot be changed during execution.

The plot instruction is quite long. Long commands can be broken across several lines by terminating intermediate lines with three dots (...). The three dots tell MATLAB to continue the present command to the next line. Black x's locate roots of each permutation. The command `lambda(:)` vectorizes the 2×243 matrix `lambda` into a 486×1 vector. This is necessary in this case to ensure that a proper legend is generated. Because of loop order, permutation $p = 1$ corresponds to the case of all components at the smallest values and permutation $p = 243$ corresponds to the case of all components at the largest values. This information is used to separately highlight the minimum and maximum cases using down-triangles (∇) and up-triangles (Δ), respectively. In addition to terminating each for loop, `end` is used to indicate the final index along a particular dimension, which eliminates the need to remember the particular size of a variable. An overloaded function, such as `end`, serves multiple uses and is typically interpreted based on context.

The graphical results provided by `CH2MP3` are shown in Fig. 2.26. Between extremes, root oscillations vary from 365 to 745 Hz and decay times to 25% amplitude vary from 6.2 to 12.7 ms. Clearly, this circuit's behavior is quite sensitive to ordinary component variations.

2.7.4 Graphical Understanding of Convolution

MATLAB graphics effectively illustrate the convolution process. Consider the case of $y(t) = x(t) * h(t)$, where $x(t) = 1.5 \sin(\pi t)(u(t) - u(t-1))$ and $h(t) = 1.5(u(t) - u(t-1.5)) - u(t-2) + u(t-2.5)$. Program `CH2MP4` steps through the convolution over the time interval $(-0.25 \leq t \leq 3.75)$.

```
% CH2MP4.m : Chapter 2, MATLAB Program 4
% Script M-file graphically demonstrates the convolution process.

figure(1) % Create figure window and make visible on screen
u = @(t) 1.0*(t>=0);
x = @(t) 1.5*sin(pi*t).*(u(t)-u(t-1));
h = @(t) 1.5*(u(t)-u(t-1.5))-u(t-2)+u(t-2.5);
dtau = 0.005; tau = -1:dtau:4;
ti = 0; tvec = -.25:.1:3.75;
y = NaN*zeros(1,length(tvec)); % Pre-allocate memory
for t = tvec,
    ti = ti+1; % Time index
    xh = x(t-tau).*h(tau); lxh = length(xh);
    y(ti) = sum(xh.*dtau); % Trapezoidal approximation of convolution integral
    subplot(2,1,1),plot(tau,h(tau),'k-',tau,x(t-tau),'k--',t,0,'ok');
    axis([tau(1) tau(end) -2.0 2.5]);
    patch([tau(1:end-1);tau(1:end-1);tau(2:end);tau(2:end)],...
        [zeros(1,lxh-1);xh(1:end-1);xh(2:end);zeros(1,lxh-1)],...
        [.8 .8 .8],'edgecolor','none');
    xlabel('\tau'); title('h(\tau) [solid], x(t-\tau) [dashed], h(\tau)x(t-\tau) [gray]');
    c = get(gca,'children'); set(gca,'children',[c(2);c(3);c(4);c(1)]);
    subplot(2,1,2),plot(tvec,y,'k',tvec(ti),y(ti),'ok');
    xlabel('t'); ylabel('y(t) = \int h(\tau)x(t-\tau) d\tau');
    axis([tau(1) tau(end) -1.0 2.0]); grid;
    drawnow;
end
```

At each step, the program plots $h(\tau)$, $x(t-\tau)$, and shades the area $h(\tau)x(t-\tau)$ gray. This gray area, which reflects the integral of $h(\tau)x(t-\tau)$, is also the desired result, $y(t)$. Figures 2.27, 2.28, and 2.29 display the convolution process at times t of 0.75, 2.25, and 2.85 seconds, respectively. These figures help illustrate how the regions of integration change with time. Figure 2.27 has limits of integration from 0 to $(t = 0.75)$. Figure 2.28 has two regions of integration, with limits $(t-1 = 1.25)$ to 1.5 and 2.0 to $(t = 2.25)$. The last plot, Fig. 2.29, has limits from 2.0 to 2.5.

Several comments regarding CH2MP4 are in order. The command `figure(1)` opens the first figure window and, more important, makes sure it is visible. Anonymous functions are used to represent the functions $u(t)$, $x(t)$, and $h(t)$. NaN, standing for not-a-number, usually results from operations such as 0/0 or $\infty - \infty$. MATLAB refuses to plot NaN values, so preallocating $y(t)$ with NaNs ensures that MATLAB displays only values of $y(t)$ that have been computed. As its name suggests, `length` returns the length of the input vector. The `subplot(a,b,c)` command partitions the current figure window into an a-by-b matrix of axes and selects axes c for use. Subplots facilitate graphical comparison by allowing multiple axes in a single figure window. The `patch` command is used to create the gray-shaded area for $h(\tau)x(t-\tau)$. In CH2MP4, the `get` and `set` commands are used to reorder `plot` objects so that the gray area does not obscure other lines. Details of the `patch`, `get`, and `set` commands, as used in CH2MP4, are somewhat advanced and are not pursued here.[†] MATLAB also prints most Greek letters if the Greek name is preceded by a backslash (\) character. For example, `\tau` in the `xlabel` command produces the symbol τ in the plot's axis label. Similarly, an integral sign is produced by `\int`. Finally, the `drawnow`

[†] Interested students should consult the MATLAB help facilities for further information. Actually, the `get` and `set` commands are extremely powerful and can help modify plots in almost any conceivable way.

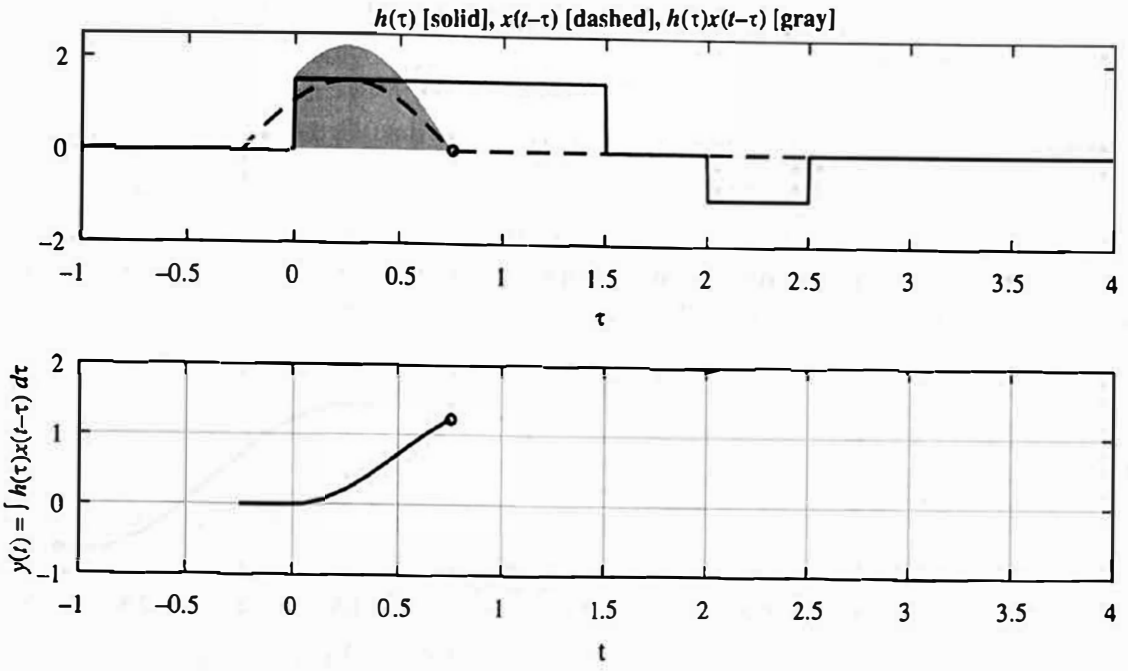

Figure 2.27 Graphical convolution at step $t = 0.75$ second.

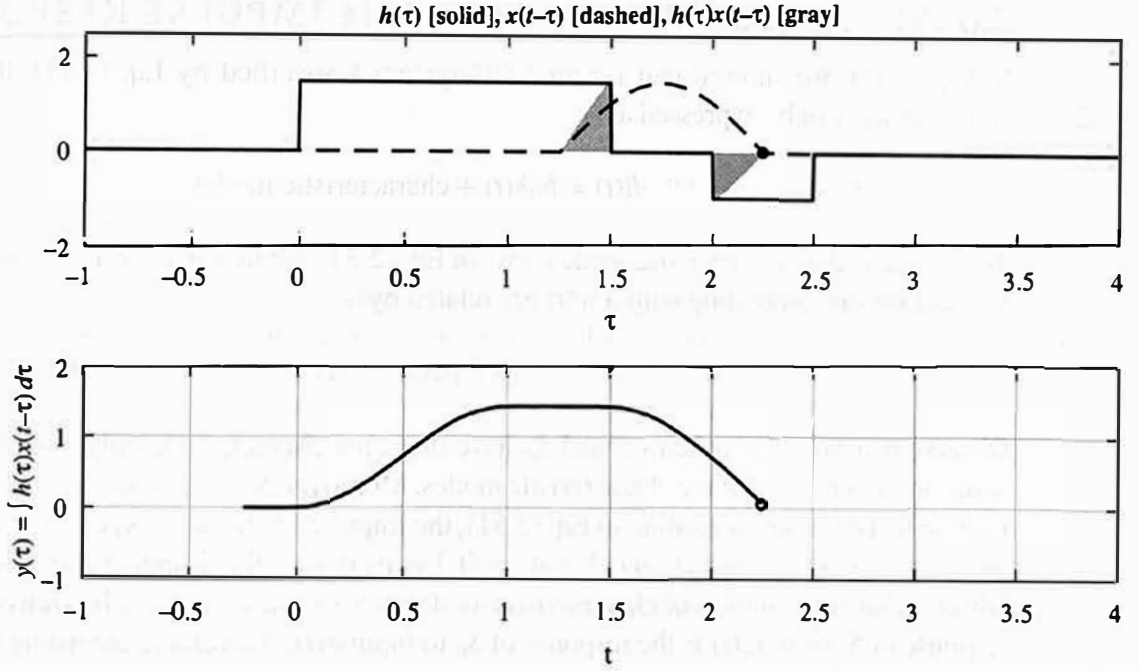

Figure 2.28 Graphical convolution at step $t = 2.25$ seconds.

command forces MATLAB to update the graphics window for each loop iteration. Although slow, this creates an animation-like effect. Replacing `drawnow` with the `pause` command allows users to manually step through the convolution process. The `pause` command still forces the graphics window to update, but the program will not continue until a key is pressed.

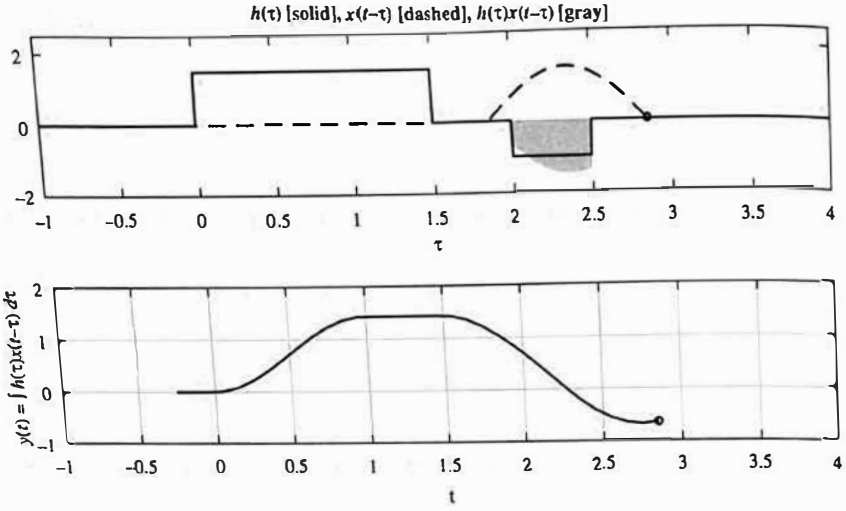

Figure 2.29 Graphical convolution at step $t = 2.85$ seconds.

2.8 APPENDIX: DETERMINING THE IMPULSE RESPONSE

In Eq. (2.13), we showed that for an LTIC system S specified by Eq. (2.11), the unit impulse response $h(t)$ can be expressed as

$$h(t) = b_0\delta(t) + \text{characteristic modes} \tag{2.51}$$

To determine the characteristic mode terms in Eq. (2.51), let us consider a system S_0 whose input $x(t)$ and the corresponding output $w(t)$ are related by

$$Q(D)w(t) = x(t) \tag{2.52}$$

Observe that both the systems S and S_0 have the same characteristic polynomial; namely, $Q(\lambda)$, and, consequently, the same characteristic modes. Moreover, S_0 is the same as S with $P(D) = 1$, that is, $b_0 = 0$. Therefore, according to Eq. (2.51), the impulse response of S_0 consists of characteristic mode terms only without an impulse at $t = 0$. Let us denote this impulse response of S_0 by $y_n(t)$. Observe that $y_n(t)$ consists of characteristic modes of S and therefore may be viewed as a zero-input response of S. Now $y_n(t)$ is the response of S_0 to input $\delta(t)$. Therefore, according to Eq. (2.52),

$$Q(D)y_n(t) = \delta(t)$$

or

$$(D^N + a_1D^{N-1} + \cdots + a_{N1}D + a_N)y_n(t) = \delta(t)$$

or

$$y_n^{(N)}(t) + a_1y_n^{(N-1)}(t) + \cdots + a_{N-1}y_n^{(1)}(t) + a_Ny_n(t) = \delta(t)$$

where $y_n^{(k)}(t)$ represents the kth derivative of $y_n(t)$. The right-hand side contains a single impulse term, $\delta(t)$. This is possible only if $y_n^{(N-1)}(t)$ has a unit jump discontinuity at $t = 0$ so that $y_n^{(N)}(t) = \delta(t)$. Moreover, the lower-order terms cannot have any jump discontinuity because this would mean the presence of the derivatives of $\delta(t)$. Therefore $y_n(0) = y_n^{(1)}(0) = \cdots = y_n^{(N-2)}(0) = 0$ (no discontinuity at $t = 0$), and the N initial conditions on $y_n(t)$ are

$$y_n(0) = y_n^{(1)}(0) = \cdots = y_n^{(N-2)}(0) = 0 \qquad \text{and} \qquad y_n^{(N-1)}(0) = 1 \tag{2.53}$$

This discussion means that $y_n(t)$ is the zero-input response of the system S subject to initial conditions [Eq. (2.53)].

We now show that for the same input $x(t)$ to both systems, S and S_0, their respective outputs $y(t)$ and $w(t)$ are related by

$$y(t) = P(D)w(t) \tag{2.54}$$

To prove this result, we operate on both sides of Eq. (2.52) by $P(D)$ to obtain

$$Q(D)P(D)w(t) = P(D)x(t)$$

Comparison of this equation with Eq. (2.2) leads immediately to Eq. (2.54).

Now if the input $x(t) = \delta(t)$, the output of S_0 is $y_n(t)$, and the output of S, according to Eq. (2.54), is $P(D)y_n(t)$. This output is $h(t)$, the unit impulse response of S. Note, however, that because it is an impulse response of a causal system S_0, the function $y_n(t)$ is causal. To incorporate this fact, we must represent this function as $y_n(t)u(t)$. Now it follows that $h(t)$, the unit impulse response of the system S, is given by

$$h(t) = P(D)[y_n(t)u(t)] \tag{2.55}$$

where $y_n(t)$ is a linear combination of the characteristic modes of the system subject to initial conditions (2.53).

The right-hand side of Eq. (2.55) is a linear combination of the derivatives of $y_n(t)u(t)$. Evaluating these derivatives is clumsy and inconvenient because of the presence of $u(t)$. The derivatives will generate an impulse and its derivatives at the origin. Fortunately when $M \leq N$ [Eq. (2.11)], we can avoid this difficulty by using the observation in Eq. (2.51), which asserts that at $t = 0$ (the origin), $h(t) = b_0\delta(t)$. Therefore, we need not bother to find $h(t)$ at the origin. This simplification means that instead of deriving $P(D)[y_n(t)u(t)]$, we can derive $P(D)y_n(t)$ and add to it the term $b_0\delta(t)$ so that

$$\begin{aligned} h(t) &= b_0\delta(t) + P(D)y_n(t) \qquad t \geq 0 \\ &= b_0\delta(t) + [P(D)y_n(t)]u(t) \end{aligned}$$

This expression is valid when $M \leq N$ [the form given in Eq. (2.11)]. When $M > N$, Eq. (2.55) should be used.

2.9 SUMMARY

This chapter discusses time-domain analysis of LTIC systems. The total response of a linear system is a sum of the zero-input response and zero-state response. The zero-input response is the system

response generated only by the internal conditions (initial conditions) of the system, assuming that the external input is zero; hence the adjective "zero-input." The zero-state response is the system response generated by the external input, assuming that all initial conditions are zero, that is, when the system is in zero state.

Every system can sustain certain forms of response on its own with no external input (zero input). These forms are intrinsic characteristics of the system; that is, they do not depend on any external input. For this reason they are called characteristic modes of the system. Needless to say, the zero-input response is made up of characteristic modes chosen in a combination required to satisfy the initial conditions of the system. For an Nth-order system, there are N distinct modes.

The unit impulse function is an idealized mathematical model of a signal that cannot be generated in practice.[†] Nevertheless, introduction of such a signal as an intermediary is very helpful in analysis of signals and systems. The unit impulse response of a system is a combination of the characteristic modes of the system[‡] because the impulse $\delta(t) = 0$ for $t > 0$. Therefore, the system response for $t > 0$ must necessarily be a zero-input response, which, as seen earlier, is a combination of characteristic modes.

The zero-state response (response due to external input) of a linear system can be obtained by breaking the input into simpler components and then adding the responses to all the components. In this chapter we represent an arbitrary input $x(t)$ as a sum of narrow rectangular pulses [staircase approximation of $x(t)$]. In the limit as the pulse width $\to 0$, the rectangular pulse components approach impulses. Knowing the impulse response of the system, we can find the system response to all the impulse components and add them to yield the system response to the input $x(t)$. The sum of the responses to the impulse components is in the form of an integral, known as the convolution integral. The system response is obtained as the convolution of the input $x(t)$ with the system's impulse response $h(t)$. Therefore, the knowledge of the system's impulse response allows us to determine the system response to any arbitrary input.

LTIC systems have a very special relationship to the everlasting exponential signal e^{st} because the response of an LTIC system to such an input signal is the same signal within a multiplicative constant. The response of an LTIC system to the everlasting exponential input e^{st} is $H(s)e^{st}$, where $H(s)$ is the transfer function of the system.

If every bounded input results in a bounded output, the system is stable in the bounded-input/bounded-output (BIBO) sense. An LTIC system is BIBO-stable if and only if its impulse response is absolutely integrable. Otherwise, it is BIBO-unstable. BIBO stability is a stability seen from external terminals of the system. Hence, it is also called external stability or zero-state stability.

In contrast, internal stability (or the zero-input stability) examines the system stability from inside. When some initial conditions are applied to a system in zero state, then, if the system eventually returns to zero state, the system is said to be stable in the asymptotic or Lyapunov sense. If the system's response increases without bound, it is unstable. If the system does not go to zero state and the response does not increase indefinitely, the system is marginally stable. The internal stability criterion, in terms of the location of a system's characteristic roots, can be summarized as follows:

[†] However, it can be closely approximated by a narrow pulse of unit area and having a width that is much smaller than the time constant of an LTIC system in which it is used.

[‡] There is the possibility of an impulse in addition to the characteristic modes.

1. An LTIC system is asymptotically stable if, and only if, all the characteristic roots are in the LHP. The roots may be repeated or unrepeated.
2. An LTIC system is unstable if, and only if, either one or both of the following conditions exist: (i) at least one root is in the RHP; (ii) there are repeated roots on the imaginary axis.
3. An LTIC system is marginally stable if, and only if, there are no roots in the RHP, and there are some unrepeated roots on the imaginary axis.

It is possible for a system to be externally (BIBO) stable but internally unstable. When a system is controllable and observable, its external and internal descriptions are equivalent. Hence, external (BIBO) and internal (asymptotic) stabilities are equivalent and provide the same information. Such a BIBO-stable system is also asymptotically stable, and vice versa. Similarly, a BIBO-unstable system is either a marginally stable or asymptotically unstable system.

The characteristic behavior of a system is extremely important because it determines not only the system response to internal conditions (zero-input behavior), but also the system response to external inputs (zero-state behavior) and the system stability. The system response to external inputs is determined by the impulse response, which itself is made up of characteristic modes. The width of the impulse response is called the time constant of the system, which indicates how fast the system can respond to an input. The time constant plays an important role in determining such diverse system behaviors as the response time and filtering properties of the system, dispersion of pulses, and the rate of pulse transmission through the system.

REFERENCES

1. Lathi, B. P., *Signals and Systems,* Berkeley-Cambridge Press, Carmichael, CA, 1987.
2. P. J. Nahin, "Behind the Laplace transform," in *IEEE Spectrum*, vol. 28, no. 3, pp. 60, March 1991, doi: 10.1109/6.67288.
3. Mason, S. J., *Electronic Circuits, Signals, and Systems,* Wiley, New York, 1960.
4. Kailath, T., *Linear System,* Prentice-Hall, Englewood Cliffs, NJ, 1980.
5. Lathi, B. P. and Ding, Z., *Modern Digital and Analog Communication Systems,* 4th ed., Oxford University Press, New York, 2009.

PROBLEMS

2.2-1 Determine the constants c_1, c_2, λ_1, and λ_2 for each of the following second-order systems, which have zero-input responses of the form $y_{zir}(t) = c_1 e^{\lambda_1 t} + c_2 e^{\lambda_2 t}$.

(a) $\ddot{y}(t) + 2\dot{y}(t) + 5y(t) = \ddot{x}(t) - 5x(t)$ with $y_{zir}(0) = 2$ and $\dot{y}_{zir}(0) = 0$.

(b) $\ddot{y}(t) + 2\dot{y}(t) + 5y(t) = \ddot{x}(t) - 5x(t)$ with $y_{zir}(0) = 4$ and $\dot{y}_{zir}(0) = -1$.

(c) $\frac{d^2}{dt^2}y(t) + 2\frac{d}{dt}y(t) = x(t)$ with $y_{zir}(0) = 1$ and $\dot{y}_{zir}(0) = 2$.

(d) $(D^2 + 2D + 10)\{y(t)\} = (D^5 - D)\{x(t)\}$ with $y_{zir}(0) = \dot{y}_{zir}(0) = 1$.

(e) $(D^2 + \frac{7}{2}D + \frac{3}{2})\{y(t)\} = (D + 2)\{x(t)\}$ with $y_{zir}(0) = 3$ and $\ddot{y}_{zir}(0) = -8$. [*Caution:* The second IC is given in terms of the second derivative, not the first derivative.]

(f) $13y(t) + 4\frac{d}{dt}y(t) + \frac{d^2}{dt^2}y(t) = 2x(t) - 4\frac{d}{dt}x(t)$ with $y_{zir}(0) = 3$ and $\ddot{y}_{zir}(0) = -15$. [*Caution:* The second IC is given in terms of the second derivative, not the first derivative.]

2.2-2 Consider a linear time-invariant system with input $x(t)$ and output $y(t)$ that is described by the differential equation

$$(D + 1)(D^2 - 1)\{y(t)\} = (D^5 - 1)\{x(t)\}$$

Furthermore, assume $y(0) = \dot{y}(0) = \ddot{y}(0) = 1$.

(a) What is the order of this system?
(b) What are the characteristic roots of this system?
(c) Determine the zero-input response $y_{zir}(t)$. Simplify your answer.

2.2-3 A real LTIC system with input $x(t)$ and output $y(t)$ is described by the following constant-coefficient linear differential equation:

$$(D^3+9D)\{y(t)\} = (2D^3+1)\{x(t)\}$$

(a) What is the characteristic equation of this system?
(b) What are the characteristic modes of this system?
(c) Assuming $y_{zir}(0) = 4$, $\dot{y}_{zir}(0) = -18$, and $\ddot{y}_{zir}(0) = 0$, determine this system's zero-input response $y_{zir}(t)$. Simplify $y_{zir}(t)$ to include only real terms (i.e., no j's should appear in your answer).

2.2-4 An LTIC system is specified by the equation

$$(D^2+5D+6)y(t) = (D+1)x(t)$$

(a) Find the characteristic polynomial, characteristic equation, characteristic roots, and characteristic modes of this system.
(b) Find $y_0(t)$, the zero-input component of the response $y(t)$ for $t \geq 0$, if the initial conditions are $y_0(0^-) = 2$ and $\dot{y}_0(0^-) = -1$.

2.2-5 Repeat Prob. 2.2-4 for

$$(D^2+4D+4)y(t) = Dx(t)$$

and $y_0(0^-) = 3$, $\dot{y}_0(0^-) = -4$.

2.2-6 Repeat Prob. 2.2-4 for

$$D(D+1)y(t) = (D+2)x(t)$$

and $y_0(0^-) = \dot{y}_0(0^-) = 1$.

2.2-7 Repeat Prob. 2.2-4 for

$$(D^2+9)y(t) = (3D+2)x(t)$$

and $y_0(0^-) = 0$, $\dot{y}_0(0^-) = 6$.

2.2-8 Repeat Prob. 2.2-4 for

$$(D^2+4D+13)y(t) = 4(D+2)x(t)$$

with $y_0(0^-) = 5$, $\dot{y}_0(0^-) = 15.98$.

2.2-9 Repeat Prob. 2.2-4 for

$$D^2(D+1)y(t) = (D^2+2)x(t)$$

with $y_0(0^-) = 4$, $\dot{y}_0(0^-) = 3$, and $\ddot{y}_0(0^-) = -1$.

2.2-10 Repeat Prob. 2.2-4 for

$$(D+1)(D^2+5D+6)y(t) = Dx(t)$$

with $y_0(0^-) = 2$, $\dot{y}_0(0^-) = -1$, and $\ddot{y}_0(0^-) = 5$.

2.2-11 A system is described by a constant-coefficient linear differential equation and has zero-input response given by $y_0(t) = 2e^{-t} + 3$.
(a) Is it possible for the system's characteristic equation to be $\lambda + 1 = 0$? Justify your answer.
(b) Is it possible for the system's characteristic equation to be $\sqrt{3}(\lambda^2+\lambda) = 0$? Justify your answer.
(c) Is it possible for the system's characteristic equation to be $\lambda(\lambda+1)^2 = 0$? Justify your answer.

2.2-12 Consider the circuit of Fig. P2.2-12. Using operator notation, this system can be described as $(D+a_1)\{y(t)\} = (b_0D+b_1)\{x(t)\}$.
(a) Determine the constants a_1, b_0, and b_1 in terms of the system components R, R_f, and C.
(b) Assume that $R = 300\ \text{k}\Omega$, $R_f = 1.2\ \text{M}\Omega$, and $C = 5\ \mu\text{F}$. What is the zero-input response $y_0(t)$ of this system, assuming $v_C(0) = 1$ V?

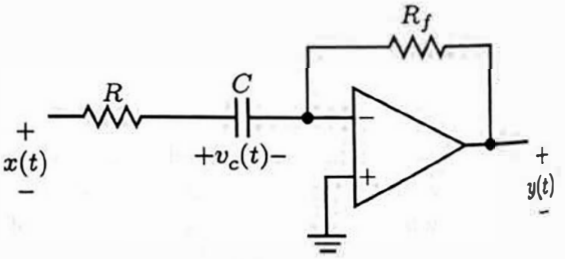

Figure P2.2-12

2.3-1 Determine the characteristic equation, characteristic modes, and impulse response $h(t)$ for each of the following real LTIC systems. Since the systems are real, express each $h(t)$ using only real terms (i.e., no j's should appear in your answers).

(a) $(D^2+1)\{y(t)\} = 2D\{x(t)\}$
(b) $(D^3+D)\{y(t)\} = (2D^3+1)\{x(t)\}$
(c) $\frac{d^2}{dt^2}y(t) + 2\frac{d}{dt}y(t) + 5y(t) = 8x(t)$

2.3-2 Find the unit impulse response of a system specified by the equation

$$(D^2+4D+3)y(t) = (D+5)x(t)$$

2.3-3 Repeat Prob. 2.3-2 for

$$(D^2+5D+6)y(t) = (D^2+7D+11)x(t)$$

2.3-4 Repeat Prob. 2.3-2 for the first-order allpass filter specified by the equation

$$(D+1)y(t) = -(D-1)x(t)$$

2.3-5 Find the unit impulse response of an LTIC system specified by the equation

$$(D^2+6D+9)y(t) = (2D+9)x(t)$$

2.3-6 Determine and plot the unit impulse response $h(t)$ of the op-amp circuit of Fig. P2.2-12, assuming that $R = 300\ \text{k}\Omega$, $R_f = 1.2\ \text{M}\Omega$, and $C = 5\ \mu\text{F}$.

2.3-7 A causal LTIC system with input $x(t)$ and output $y(t)$ is described by the constant coefficient integral equation

$$y(t) + \int 3y(t)\,dt + \iint 2y(t)\,dt = \iint x(t)\,dt - \iiint x(t)\,dt$$

(a) Express this system as a constant coefficient linear differential equation in standard operator form.
(b) Determine the characteristic modes of this system.
(c) Determine the impulse response $h(t)$ of this system.

2.4-1 Let $f(t) = h_1(t) * h_2(t)$, where $h_1(t)$ and $h_2(t)$ are shown in Fig. P2.4-1. In the following, use the graphical convolution procedure where you flip and shift $h_2(t)$.
(a) Plot $h_1(\tau)$ and $h_2(t-\tau)$ as functions of τ. Clearly label the plots, including necessary function parameterizations.
(b) Determine the (piecewise) regions of $f(t)$ and set up the corresponding integrals that describe $f(t)$ in those regions. Do not evaluate the integrals, only set them up!
(c) Determine $f(1)$, which is $f(t)$ evaluated at $t = 1$. Provide a number, not a formula.

2.4-2 Consider signals $h(t) = u(t+3) - 2u(t+1) + u(t-1)$ and $x(t) = \cos(t)\left[u(t-\pi/2) - u(t-3\pi/2)\right]$. Let $y(t) = x(t) * h(t)$.
(a) Determine the last time t_{last} that $y(t)$ is nonzero. That is, find the smallest value t_{last} such that $y(t) = 0$ for all $t > t_{\text{last}}$.
(b) Determine the approximate time t_{max} where $y(t)$ is a maximum.

2.4-3 Consider signals $h(t) = -u(t+2) + 3u(t-1) - 2u(t-\frac{5}{2})$ and $x(t) = \sin(t)[u(t+2\pi) - u(t+\pi)]$. Determine the approximate time t_{min}, where $y(t) = x(t) * h(t)$ is a minimum. Note, the minimum value of $y(t) \neq 0$!

2.4-4 An LTIC system has impulse response $h(t) = 3u(t-2)$. For input $x(t)$ shown in Fig. P2.4-4, use the graphical convolution procedure to determine $y_{\text{zsr}}(t) = h(t) * x(t)$. Accurately sketch $y_{\text{zsr}}(t)$. When solving for $y_{\text{zsr}}(t)$, flip and shift $x(t)$ and explicitly show all integration steps—even if apparently trivial!

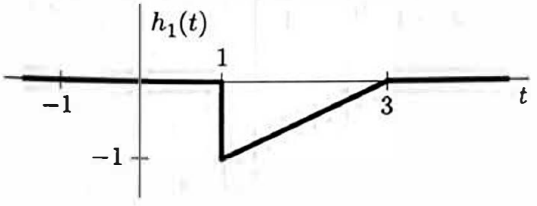

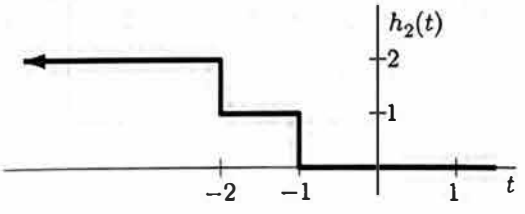

Figure P2.4-1

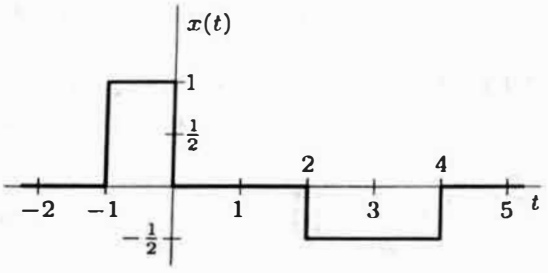

Figure P2.4-4

2.4-5 Suppose an LTIC system has impulse response $h(t)$ and input $x(t) = u(t)$. Figure P2.4-5 shows $x(t)$ and $h(t + 1)$, respectively. Be careful! Figure P2.4-5 shows $h(t + 1)$, not $h(t)$.

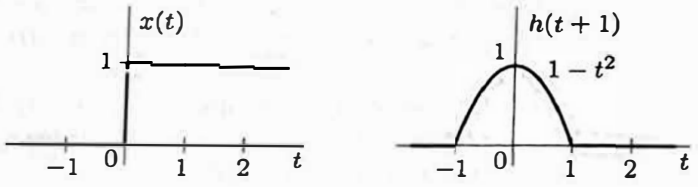

Figure P2.4-5

(a) Is system $h(t)$ causal? Mathematically justify your answer.

(b) Use the graphical convolution procedure to determine $y_{zsr}(t) = x(t) * h(t)$. Accurately sketch $y_{zsr}(t)$. When solving for $y_{zsr}(t)$, flip and shift $x(t)$ and explicitly show all integration steps.

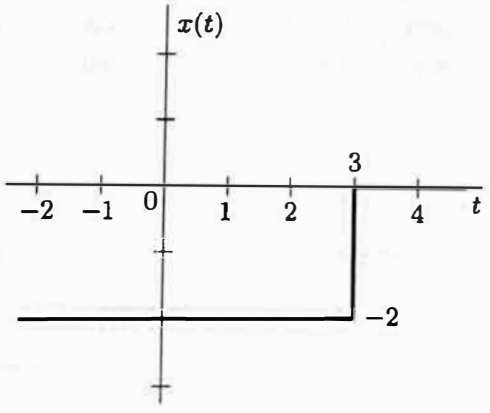

Figure P2.4-7

2.4-6 Repeat Prob. 2.4-5 using the signals of Fig. P2.4-6, rather than those of Fig. P2.4-5. Be careful! Figure P2.4-6 shows $h(t - 1)$, not $h(t)$.

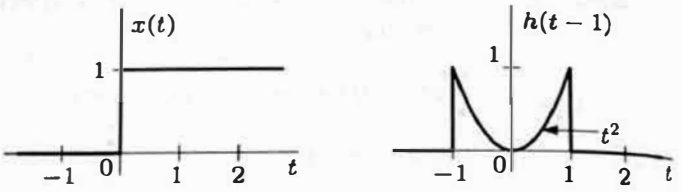

Figure P2.4-6

2.4-7 Suppose an LTIC system has impulse response $h(t)$ and input $x(t)$, both shown in Fig. P2.4-7. Use the graphical convolution procedure to determine $y_{zsr}(t) = x(t) * h(t)$. Accurately sketch $y_{zsr}(t)$. When solving for $y_{zsr}(t)$, flip and shift $x(t)$ and explicitly show all integration steps.

2.4-8 An LTIC system has impulse response $h(t)$, as shown in Fig. P2.4-8. Let t have units of seconds. Let the input be $x(t) = u(-t - 2)$ and designate the output as $y_{zsr}(t) = x(t) * h(t)$.

(a) Use the graphical convolution procedure where $h(t)$ is flipped and shifted to determine $y_{zsr}(t)$. Accurately plot your result.

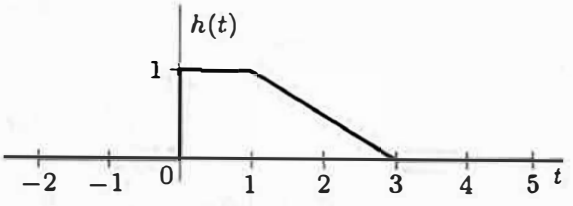

Figure P2.4-8

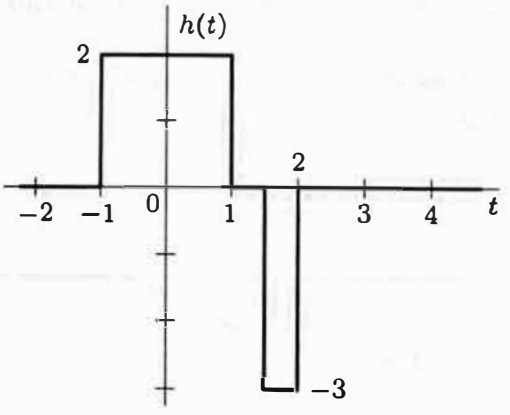

(b) Use the graphical convolution procedure where $x(t)$ is flipped and shifted to determine $y_{zsr}(t)$. Accurately plot your result.

2.4-9 If $c(t) = x(t) * g(t)$, then show that $A_c = A_x A_g$, where A_x, A_g, and A_c are the areas under $x(t)$, $g(t)$, and $c(t)$, respectively. Verify this *area property* of convolution in Exs. 2.10 and 2.12.

2.4-10 If $x(t) * g(t) = c(t)$, then show that $x(at) * g(at) = |1/a|c(at)$. This *time-scaling property* of convolution states that if both $x(t)$ and $g(t)$ are time-scaled by a, their convolution is also time-scaled by a (and multiplied by $|1/a|$).

2.4-11 Show that the convolution of an odd and an even function is an odd function and the convolution of two odd or two even functions is an even function. [*Hint:* Use the time-scaling property of convolution in Prob. 2.4-10.]

2.4-12 Suppose an LTIC system has impulse response $h(t) = (1-t)[u(t) - u(t-1)]$ and input $x(t) = u(-t-1) + u(t-1)$. Use the graphical convolution procedure to determine $y_{zsr}(t) = x(t) * h(t)$. Accurately sketch $y_{zsr}(t)$. When solving for $y_{zsr}(t)$, flip and shift $h(t)$, explicitly show all integration steps, and simplify your answer.

2.4-13 Using direct integration, find $e^{-at}u(t) * e^{-bt}u(t)$.

2.4-14 Using direct integration, find $u(t) * u(t)$, $e^{-at}u(t) * e^{-at}u(t)$, and $tu(t) * u(t)$.

2.4-15 Using direct integration, find $\sin t\,u(t) * u(t)$ and $\cos t\,u(t) * u(t)$.

2.4-16 The unit impulse response of an LTIC system is

$$h(t) = e^{-t}u(t)$$

Find this system's (zero-state) response $y(t)$ if the input $x(t)$ is:
(a) $u(t)$
(b) $e^{-t}u(t)$
(c) $e^{-2t}u(t)$
(d) $\sin 3t\,u(t)$
Use the convolution table (Table 2.1) to find your answers.

2.4-17 Repeat Prob. 2.4-16 for

$$h(t) = [2e^{-3t} - e^{-2t}]u(t)$$

and if the input $x(t)$ is:
(a) $u(t)$
(b) $e^{-t}u(t)$
(c) $e^{-2t}u(t)$

2.4-18 Repeat Prob. 2.4-16 for

$$h(t) = (1-2t)e^{-2t}u(t)$$

and input $x(t) = u(t)$.

2.4-19 Repeat Prob. 2.4-16 for

$$h(t) = 4e^{-2t}\cos 3t\,u(t)$$

and each of the following inputs $x(t)$:
(a) $u(t)$
(b) $e^{-t}u(t)$

2.4-20 Repeat Prob. 2.4-16 for

$$h(t) = e^{-t}u(t)$$

and each of the following inputs $x(t)$:
(a) $e^{-2t}u(t)$
(b) $e^{-2(t-3)}u(t)$
(c) $e^{-2t}u(t-3)$
(d) the gate pulse depicted in Fig. P2.4-20; also provide a sketch of $y(t)$.

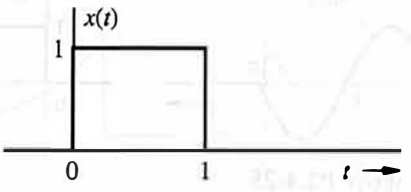

Figure P2.4-20

2.4-21 A first-order allpass filter impulse response is given by

$$h(t) = -\delta(t) + 2e^{-t}u(t)$$

(a) Find the zero-state response of this filter for the input $e^{t}u(-t)$.
(b) Sketch the input and the corresponding zero-state response.

2.4-22 Figure P2.4-22 shows the input $x(t)$ and the impulse response $h(t)$ for an LTIC system. Let the output be $y(t)$.
(a) By inspection of $x(t)$ and $h(t)$, find $y(-1)$, $y(0), y(1), y(2), y(3), y(4), y(5)$, and $y(6)$. Thus, by merely examining $x(t)$ and $h(t)$, you are required to see what the result of convolution yields at $t = -1, 0, 1, 2, 3, 4, 5$, and 6.
(b) Find the system response to the input $x(t)$.

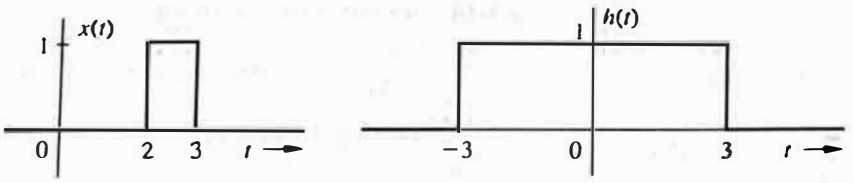

Figure P2.4-22

2.4-23 The zero-state response of an LTIC system to an input $x(t) = 2e^{-2t}u(t)$ is $y(t) = [4e^{-2t} + 6e^{-3t}]u(t)$. Find the impulse response of the system. [*Hint:* We have not yet developed a method of finding $h(t)$ from the knowledge of the input and the corresponding output. Knowing the form of $x(t)$ and $y(t)$, you will have to make the best guess of the general form of $h(t)$.]

2.4-24 Sketch the functions $x(t) = 1/(t^2 + 1)$ and $u(t)$. Now find $x(t) * u(t)$ and sketch the result.

2.4-25 Figure P2.4-25 shows $x(t)$ and $g(t)$. Find and sketch $c(t) = x(t) * g(t)$.

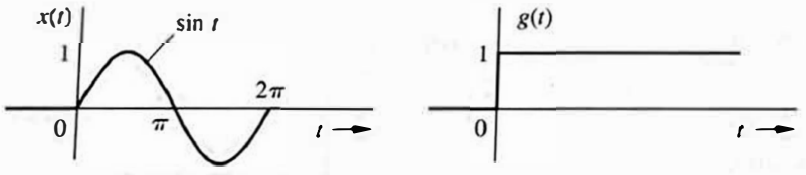

Figure P2.4-25

2.4-26 Find and sketch $c(t) = x(t) * g(t)$ for the functions depicted in Fig. P2.4-26.

2.4-27 Find and sketch $c(t) = x_1(t) * x_2(t)$ for the pairs of functions illustrated in Fig. P2.4-27.

2.4-28 Use Eq. (2.37) to find the convolution of $x(t)$ and $w(t)$, shown in Fig. P2.4-28.

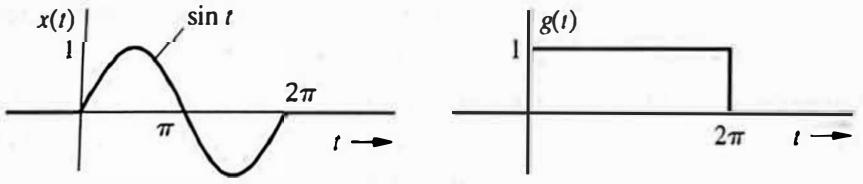

Figure P2.4-26

2.4-29 Determine $H(s)$, the transfer function of an ideal time delay of T seconds. Find your answer by two methods: using Eq. (2.39) and using Eq. (2.40).

2.4-30 Determine $y(t) = x(t) * h(t)$ for the signals depicted in Fig. P2.4-30.

2.4-31 Two linear time-invariant systems, each with impulse response $h(t)$, are connected in cascade. Refer to Fig. P2.4-31. Given input $x(t) = u(t)$, determine $y(1)$. That is, determine the step response at time $t = 1$ for the cascaded system shown.

2.4-32 Consider the electric circuit shown in Fig. P2.4-32.

(a) Determine the differential equation that relates the input $x(t)$ to output $y(t)$. Recall that $i_C(t) = C\frac{dv_C(t)}{dt}$ and $v_L(t) = L\frac{di_L(t)}{dt}$.

(b) Find the characteristic equation for this circuit, and express the root(s) of the characteristic equation in terms of L and C.

(c) Determine the zero-input response given an initial capacitor voltage of 1 volt and an initial inductor current of zero amps. That is, find $y_0(t)$ given $v_C(0) = 1$ V and

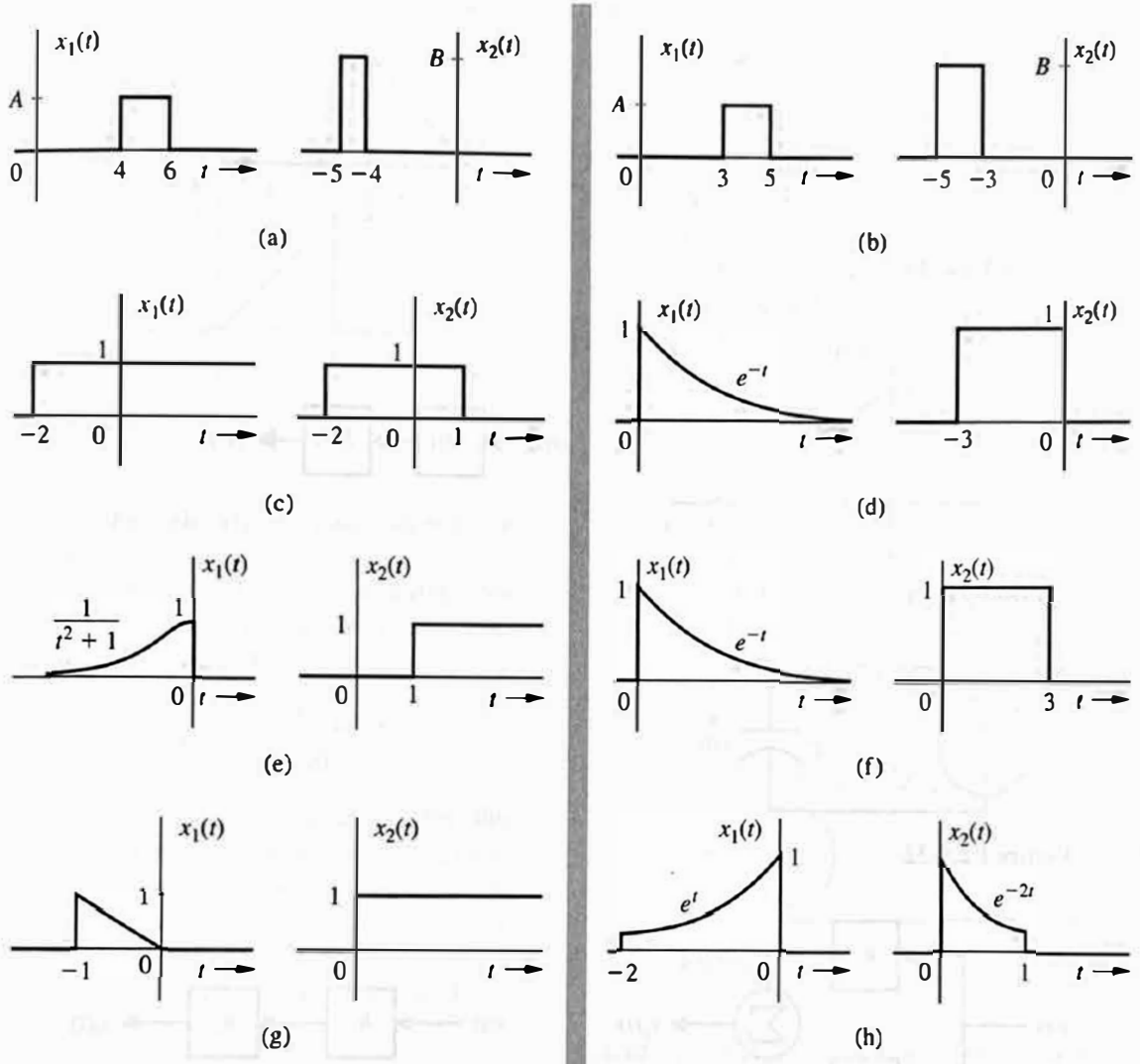

Figure P2.4-27

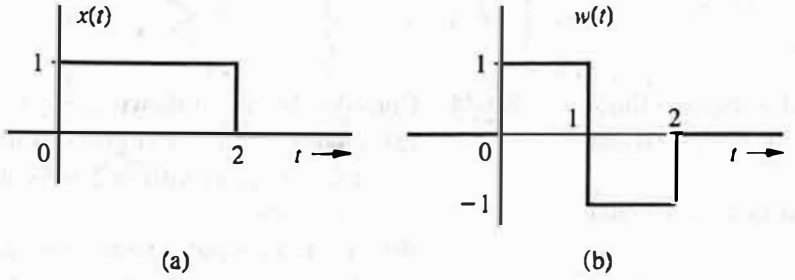

Figure P2.4-28

$i_L(0) = 0$ A. [*Hint:* The coefficient(s) in $y_0(t)$ are independent of L and C.]

(d) Plot $y_0(t)$ for $t \geq 0$. Does the zero-input response, which is caused solely by initial conditions, ever "die out"?

(e) Determine the total response $y(t)$ to the input $x(t) = e^{-t}u(t)$. Assume an initial inductor current of $i_L(0^-) = 0$ A, an initial capacitor voltage of $v_C(0^-) = 1$ V, $L = 1$ H, and $C = 1$ F.

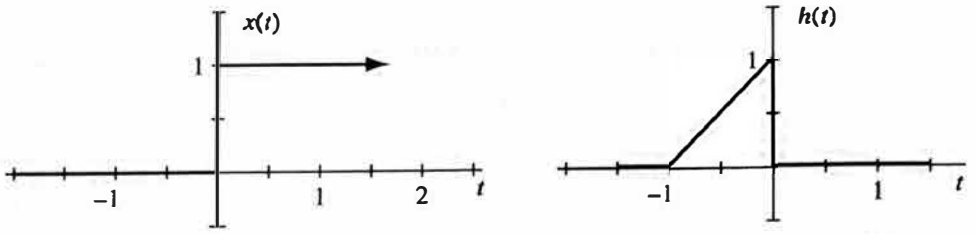

Figure P2.4-30

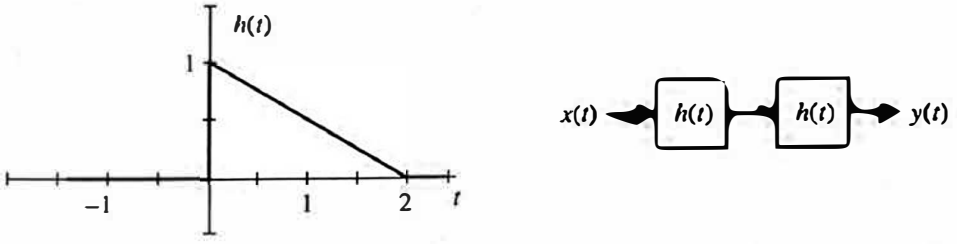

Figure P2.4-31

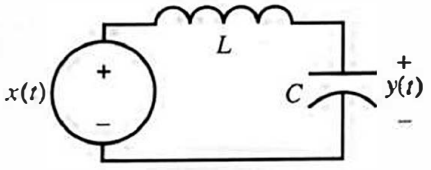

Figure P2.4-32

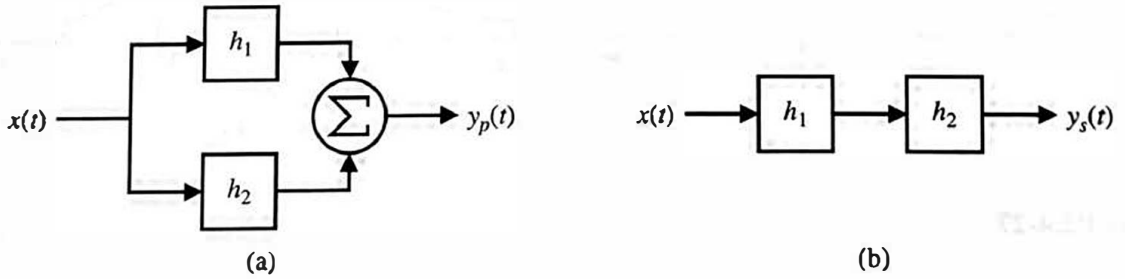

Figure P2.4-33

2.4-33 Two LTIC systems have impulse response functions given by $h_1(t) = (1-t)[u(t) - u(t-1)]$ and $h_2(t) = t[u(t+2) - u(t-2)]$.

(a) Carefully sketch the functions $h_1(t)$ and $h_2(t)$.

(b) Assume that the two systems are connected in parallel, as shown in Fig. P2.4-33a. Carefully plot the equivalent impulse response function, $h_p(t)$.

(c) Assume that the two systems are connected in cascade, as shown in Fig. P2.4-33b. Carefully plot the equivalent impulse response function, $h_s(t)$.

2.4-34 Consider the circuit shown in Fig. P2.4-34.

(a) Find the output $y(t)$ given an initial capacitor voltage of $y(0) = 2$ volts and an input $x(t) = u(t)$.

(b) Given an input $x(t) = u(t-1)$, determine the initial capacitor voltage $y(0)$ so that the output $y(t)$ is 0.5 volt at $t = 2$ seconds.

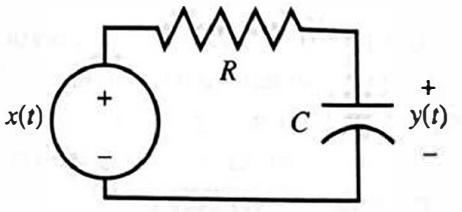

Figure P2.4-34

2.4-35 An analog signal is given by $x(t) = t[u(t) - u(t-1)]$, as shown in Fig. P2.4-35. Determine and plot $y(t) = x(t) * x(2t)$.

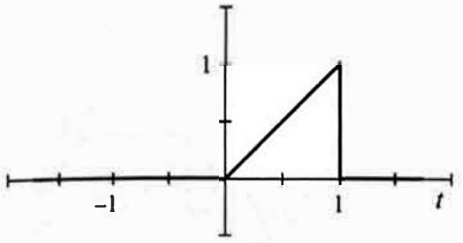

Figure P2.4-35

2.4-36 Consider the electric circuit shown in Fig. P2.4-36.

(a) Determine the differential equation that relates the input current $x(t)$ to output current $y(t)$. Recall that

$$v_L(t) = L\frac{di_L(t)}{dt}$$

(b) Find the characteristic equation for this circuit, and express the root(s) of the characteristic equation in terms of L_1, L_2, and R.

(c) Determine the zero-input response given initial inductor currents of 1 ampere each. That is, find $y_0(t)$ given $i_{L_1}(0) = i_{L_2}(0) = 1$ A.

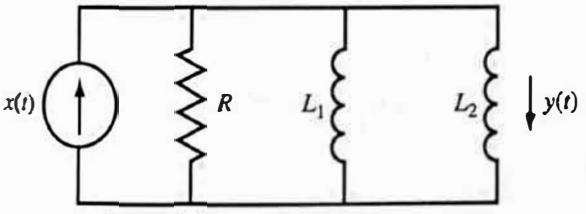

Figure P2.4-36

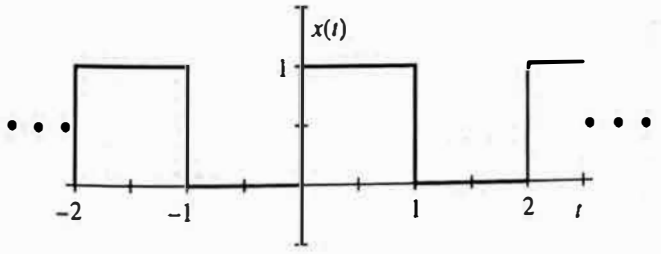

Figure P2.4-38

2.4-37 An LTI system has step response given by $g(t) = e^{-t}u(t) - e^{-2t}u(t)$. Determine the output of this system $y(t)$ given an input $x(t) = \delta(t - \pi) - \cos(\sqrt{3})u(t)$.

2.4-38 The periodic signal $x(t)$ shown in Fig. P2.4-38 is input to a system with impulse response function $h(t) = t[u(t) - u(t-1.5)]$, also shown in Fig. P2.4-38. Use convolution to determine the output $y(t)$ of this system. Plot $y(t)$ over $(-3 \le t \le 3)$.

2.4-39 Consider the electric circuit shown in Fig. P2.4-39.

(a) Determine the differential equation relating input $x(t)$ to output $y(t)$.

(b) Determine the output $y(t)$ in response to the input $x(t) = 4te^{-3t/2}u(t)$. Assume component values of $R = 1\ \Omega$, $C_1 = 1$ F, and $C_2 = 2$ F, and initial capacitor voltages of $V_{C_1} = 2$ V and $V_{C_2} = 1$ V.

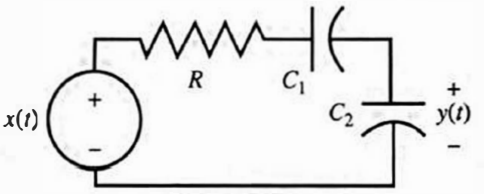

Figure P2.4-39

2.4-40 An LTIC system has impulse response $h(t) = 3e^{-|t|}$.

(a) Is the system causal? Mathematically justify your answer.

(b) Determine the zero-state response of this system if the input is $x(t) = u(2 - t)$.

2.4-41 A cardiovascular researcher is attempting to model the human heart. He has recorded ventricular pressure, which he believes corresponds to the heart's impulse response function $h(t)$, as shown in Fig. P2.4-41. Comment on the function

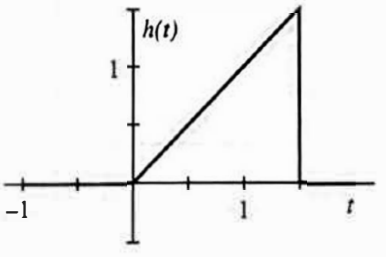

$h(t)$ shown in Fig. P2.4-41. Can you establish any system properties, such as causality or stability? Do the data suggest any reason to suspect that the measurement is not a true impulse response?

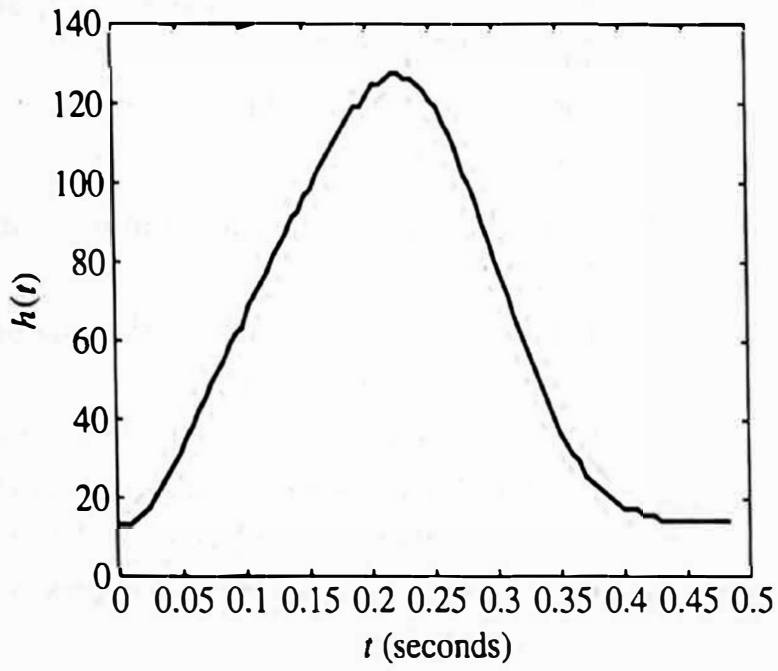

Figure P2.4-41

2.4-42 Consider an integrator system, $y(t) = \int_{-\infty}^{t} x(\tau)d\tau$.

(a) What is the unit impulse response $h_i(t)$ of this system?

(b) If two such integrators are put in parallel, what is the resulting impulse response $h_p(t)$?

(c) If two such integrators are put in series, what is the resulting impulse response $h_s(t)$?

2.4-43 The autocorrelation of a function $x(t)$ is given by $r_{xx}(t) = \int_{-\infty}^{\infty} x(\tau)x(\tau - t)\,d\tau$. This equation is computed in a manner nearly identical to convolution.

(a) Show $r_{xx}(t) = x(t) * x(-t)$.

(b) Determine and plot $r_{xx}(t)$ for the signal $x(t)$ depicted in Fig. P2.4-43. [*Hint:* $r_{xx}(t) = r_{xx}(-t)$.]

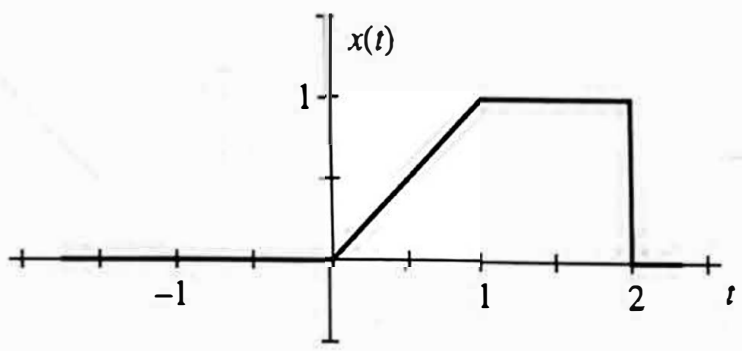

Figure P2.4-43

2.4-44 Consider the circuit shown in Fig. P2.4-44. This circuit functions as an integrator. Assume ideal op-amp behavior and recall that

$$i_C(t) = C\frac{dV_C(t)}{dt}$$

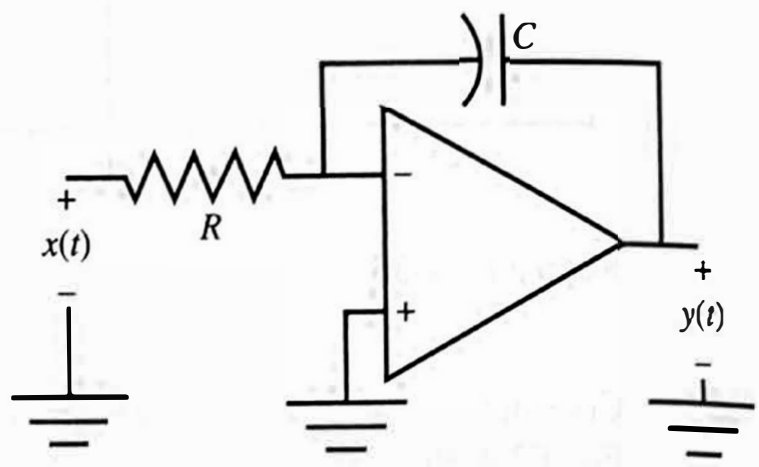

Figure P2.4-44

(a) Determine the differential equation that relates the input $x(t)$ to the output $y(t)$.

(b) This circuit does not behave well at dc. Demonstrate this by computing the zero-state response $y(t)$ for a unit step input $x(t) = u(t)$.

2.4-45 Derive the result in Eq. (2.37) in another way. As mentioned in Ch. 1 (Fig. 1.27b), it is possible to express an input in terms of its step components, as shown in Fig. P2.4-45. Find the system response as a sum of the responses to the step components of the input.

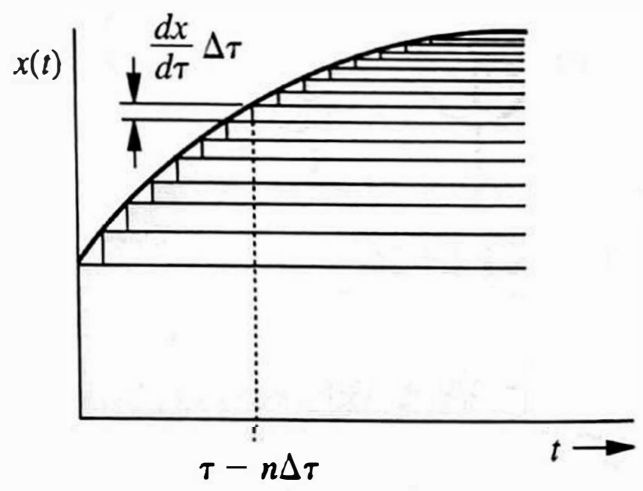

Figure P2.4-45

2.4-46 Show that an LTIC system response to an everlasting sinusoid $\cos \omega_0 t$ is given by

$$y(t) = |H(j\omega_0)| \cos [\omega_0 t + \angle H(j\omega_0)]$$

where

$$H(j\omega) = \int_{-\infty}^{\infty} h(t)e^{-j\omega t}\,dt$$

assuming the integral on the right-hand side exists.

2.4-47 A line charge is located along the x axis with a charge density $Q(x)$ coulombs per meter. Show that the electric field $E(x)$ produced by this line charge at a point x is given by

$$E(x) = Q(x) * h(x)$$

where $h(x) = 1/4\pi\epsilon x^2$. [*Hint:* The charge over an interval $\Delta\tau$ located at $\tau = n\Delta\tau$ is $Q(n\Delta\tau)\Delta\tau$. Also by Coulomb's law, the electric field $E(r)$ at a distance r from a charge q coulombs is given by $E(r) = q/4\pi\epsilon r^2$.]

2.4-48 A system is called complex if a real-valued input can produce a complex-valued output. Suppose a linear time-invariant complex system has impulse response $h(t) = j[u(-t+2) - u(-t)]$.

(a) Is this system causal? Explain.

(b) Use convolution to determine the zero-state response $y_1(t)$ of this system in response to the unit-duration pulse $x_1(t) = u(t) - u(t-1)$.

(c) Using the result from part (a), determine the zero-state response $y_2(t)$ in response to $x_2(t) = 2u(t-1) - u(t-2) - u(t-3)$.

2.5-1 Explain, with reasons, whether the LTIC systems described by the following equations are (i) stable or unstable in the BIBO sense; (ii) asymptotically stable, unstable, or marginally stable. Assume that the systems are controllable and observable.

(a) $(D^2+8D+12)y(t) = (D-1)x(t)$

(b) $D(D^2+3D+2)y(t) = (D+5)x(t)$

(c) $D^2(D^2+2)y(t) = x(t)$

(d) $(D+1)(D^2-6D+5)y(t) = (3D+1)x(t)$

2.5-2 Repeat Prob. 2.5-1 for the following:

(a) $(D+1)(D^2+2D+5)^2y(t) = x(t)$

(b) $(D+1)(D^2+9)y(t) = (2D+9)x(t)$

(c) $(D+1)(D^2+9)^2y(t) = (2D+9)x(t)$

(d) $(D^2+1)(D^2+4)(D^2+9)y(t) = 3Dx(t)$

2.5-3 Consider an LTIC system with unit impulse response $h(t) = e^t\left[\frac{2}{3}\cos(\frac{3}{2}t) + \frac{1}{3}\sin(\pi t)\right]u(123-t)$. Is this system BIBO-stable? Mathematically justify your answer.

2.5-4 Consider an LTIC system with unit impulse response $h(t) = \frac{1}{t}u(t-T)$.

(a) Determine, if possible, the value(s) of T for which this system is causal.

(b) Determine, if possible, the value(s) of T for which this system is BIBO-stable.

Justify all answers mathematically.

2.5-5 You are given the choice of a system that is guaranteed internally stable or a system that is guaranteed externally stable. Which do you choose? Why?

2.5-6 For a certain LTIC system, the impulse response $h(t) = u(t)$.

(a) Determine the characteristic root(s) of this system.

(b) Is this system asymptotically or marginally stable, or is it unstable?

(c) Is this system BIBO-stable?

(d) What can this system be used for?

2.5-7 In Sec. 2.5, we demonstrated that for an LTIC system, the condition of Eq. (2.45) is sufficient for BIBO stability. Show that this is also a necessary condition for BIBO stability in such systems. In other words, show that if Eq. (2.45) is not satisfied, then there exists a bounded input that produces an unbounded output. [*Hint:* Assume that a system exists for which $h(t)$ violates Eq. (2.45) and yet produces an output that is bounded for every bounded input. Establish the contradiction in this statement by considering an input $x(t)$ defined by $x(t_1-\tau) = 1$ when $h(\tau) \geq 0$ and $x(t_1-\tau) = -1$ when $h(\tau) < 0$, where t_1 is some fixed instant.]

2.5-8 An analog LTIC system with impulse response function $h(t) = u(t+2) - u(t-2)$ is presented with an input $x(t) = t(u(t) - u(t-2))$.

(a) Determine and plot the system output $y(t) = x(t) * h(t)$.

(b) Is this system stable? Is this system causal? Justify your answers.

2.5-9 A system has an impulse response function shaped like a rectangular pulse, $h(t) = u(t) - u(t-1)$. Is the system stable? Is the system causal?

2.5-10 A continuous-time LTI system has impulse response function $h(t) = \sum_{i=0}^{\infty}(0.5)^i\delta(t-i)$.

(a) Is the system causal? Prove your answer.
(b) Is the system stable? Prove your answer.

2.6-1 Data at a rate of 1 million pulses per second are to be transmitted over a certain communications channel. The unit step response $g(t)$ for this channel is shown in Fig. P2.6-1.
(a) Can this channel transmit data at the required rate? Explain your answer.
(b) Can an audio signal consisting of components with frequencies up to 15 kHz be transmitted over this channel with reasonable fidelity?

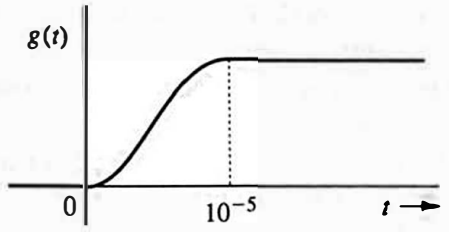

Figure P2.6-1

2.6-2 Determine a frequency ω that will cause the input $x(t) = \cos(\omega t)$ to produce a strong response when applied to the system described by $(D^2 + 2D + 13/4)\{y(t)\} = x(t)$. Carefully explain your choice.

2.6-3 Figure P2.6-3 shows the impulse response $h(t)$ of a lowpass LTIC system. Determine the peak amplitude A and time constant T_h so that rectangular impulse response $\hat{h}(t)$ is an appropriate approximation of $h(t)$. The two graphs of Fig. P2.6-3 are not necessarily drawn to the same scale.

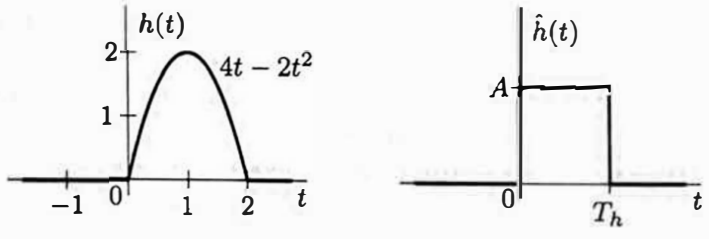

Figure P2.6-3

2.6-4 A certain communication channel has a bandwidth of 10 kHz. A pulse of 0.5 ms duration is transmitted over this channel.
(a) Determine the width (duration) of the received pulse.
(b) Find the maximum rate at which these pulses can be transmitted over this channel without interference between the successive pulses.

2.6-5 A first-order LTIC system has a characteristic root $\lambda = -10^4$.
(a) Determine T_r, the rise time of its unit step input response.
(b) Determine the bandwidth of this system.
(c) Determine the rate at which the information pulses can be transmitted through this system.

2.6-6 A lowpass system with a 6 MHz cutoff frequency needs to transmit data pulses that are $\frac{500}{6}$ ns wide. Determine a suitable transmission rate F_{rate} (pulses/s) for this system.

2.6-7 Sketch an impulse response $h(t)$ of a non-causal LP system that has an approximate cutoff frequency of 5 kHz. Since many solutions are possible, be sure to properly justify your answer.

2.6-8 Two LTIC transmission channels are available: the first has impulse response $h_1(t) = u(t) - u(t-1)$ and the second has impulse response $h_2(t) = \delta(t) + 0.5\delta(t-1) + 0.25\delta(t-2)$. Explain which channel is better suited for the transmission of high-speed digital data (pulses).

2.6-9 Consider a linear time-invariant system with impulse response $h(t)$ shown in Fig. P2.6-9. Outside the interval shown, $h(t) = 0$.
(a) What is the rise time T_r of this system? Remember, rise time is the time between the application of a unit step and the moment at which the system has "fully" responded.
(b) Suppose $h(t)$ represents the response of a communication channel. What conditions might cause the channel to have such an impulse response? What is the maximum average number of pulses per unit time that can be transmitted without causing interference? Justify your answer.
(c) Determine the system output $y(t) = x(t) * h(t)$ for $x(t) = [u(t-2) - u(t)]$. Accurately sketch $y(t)$ over $(0 \le t \le 10)$.

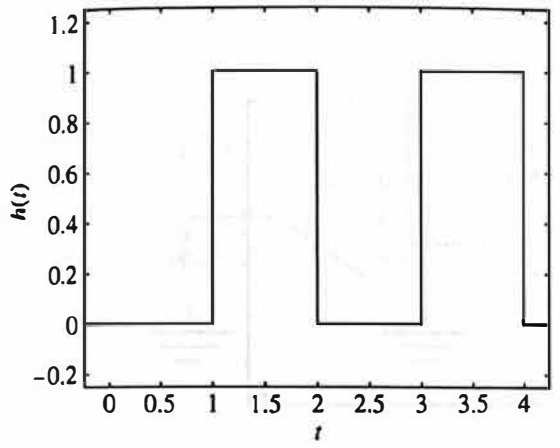

Figure P2.6-9

2.6-10 A lowpass LTIC system has impulse response $h(t) = -te^{-t}u(t)$.

(a) Accurately sketch $h(t)$.

(b) Describe a rectangular impulse response $\hat{h}(t)$ as an appropriate approximation of $h(t)$. What is the approximate cutoff frequency of this system?

2.6-11 A lowpass LTIC system has impulse response $h(t)$, as shown in Fig. P2.4-8.

(a) As discussed in Sec. 2.6.2, determine a rectangular approximation $\hat{h}(t)$ to $h(t)$.

(b) Using $\hat{h}(t)$, what is the time constant T_h of this lowpass system?

(c) Using $\hat{h}(t)$, what is the approximate radian cutoff frequency ω_c of this lowpass system?

(d) Assuming a frequency $\omega_0 \ll \omega_c$, what is the system response $y(t)$ to the input $x(t) = \sin(\omega_0 t + \pi/3)$?

2.6-12 A first CT lowpass system with time constant $T_1 = 4$ μs is put in series with a second CT lowpass system with time constant $T_2 = 2$ μs. Make an educated sketch of the overall impulse response function $h_{\text{series}}(t)$. What is the time constant T_{series} of the overall series-connected system?

2.7-1 An LTIC system with input $x(t)$ and output $y(t)$ is described by the following constant coefficient linear differential equation:

$$(D^4 - 16)\{y(t)\} = (D - 2)\{x(t)\}$$

(a) What are the four characteristic roots of this system (λ_1, λ_2, λ_3, and λ_4)? Determine the roots by hand and then verify your answers using MATLAB's `roots` command.

(b) From Eq. (2.17), computing $h(t)$ requires a signal $\tilde{y}_n(t) = \sum_{k=1}^{4} c_k e^{\lambda_k t}$. First, determine a matrix representation of the system of equations needed to solve for the four coefficients c_k. Second, write MATLAB code that computes the length-4 column vector of coefficients c_k.

2.7-2 Define $x(t) = 2u(t + \frac{2}{3}) - 2u(t)$. Further, define the periodic signal $h_1(t)$ as

$$h_1(t) = \begin{cases} t & 0 \le t < 1 \\ h_1(t+1) & \forall t \end{cases}$$

Lastly, define the aperiodic signal $h_2(t)$ in terms of $h_1(t)$ as

$$h_2(t) = h_1(t)[u(t-1) - u(t-2)]$$

(a) Use MATLAB to plot $x(t)$, $h_1(t)$, and $h_2(t)$ over the interval $-2.5 \le t \le 3.5$.

(b) Using the graphical convolution procedure, compute $y_2(t) = x(t) * h_2(t)$.

(c) Compute by hand and then MATLAB plot $y_1(t) = x(t) * h_1(t)$. Modify program `CH2MP4.m` in Sec. 2.7.4 to validate your analytical result.

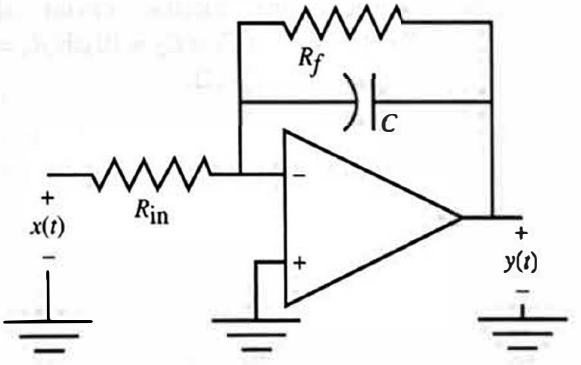

Figure P2.7-3

2.7-3 Consider the circuit shown in Fig. P2.7-3. Assume ideal op-amp behavior and recall that

$$i_C(t) = C\frac{dV_C(t)}{dt}$$

Without a feedback resistor R_f, the circuit functions as an integrator and is unstable, particularly

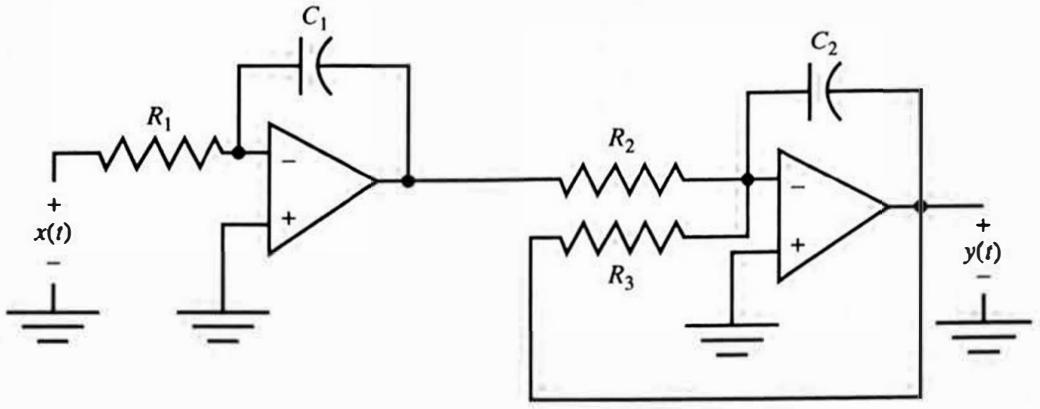

Figure P2.7-4

at dc. A feedback resistor R_f corrects this problem and results in a stable circuit that functions as a "lossy" integrator.

(a) Determine the differential equation that relates the input $x(t)$ to the output $y(t)$. What is the corresponding characteristic equation?

(b) To demonstrate that this "lossy" integrator is well behaved at dc, determine the zero-state response $y(t)$ given a unit step input $x(t) = u(t)$.

(c) Investigate the effect of 10% resistor and 25% capacitor tolerances on the system's characteristic root(s).

2.7-4 Consider the electric circuit shown in Fig. P2.7-4. Let $C_1 = C_2 = 10\ \mu\text{F}$, $R_1 = R_2 = 100\ \text{k}\Omega$, and $R_3 = 50\ \text{k}\Omega$.

(a) Determine the corresponding differential equation describing this circuit. Is the circuit BIBO-stable?

(b) Determine the zero-input response $y_0(t)$ if the output of each op amp initially reads 1 volt.

(c) Determine the zero-state response $y(t)$ to a step input $x(t) = u(t)$.

(d) Investigate the effect of 10% resistor and 25% capacitor tolerances on the system's characteristic roots.

2.7-5 Input $x(t) = 3[u(t) - u(t-1)] + 2[u(t-2) - u(t-3)]$ is applied to a lowpass LTIC system with impulse response $h(t) = (4-t)[u(t) - u(t-2)]$ to produce output $y(t) = x(t) * h(t)$. Modify program `CH2MP4.m` in Sec. 2.7.4 to perform the graphical convolution procedure to produce a plot of $y(t)$.

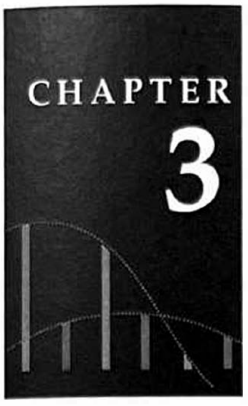

SIGNAL REPRESENTATION BY FOURIER SERIES

This chapter is important for basic understanding of signal representation and signal comparison. In Ch. 2, we expressed an arbitrary input $x(t)$ as a sum of its impulse components. The LTI system (zero-state) response to input $x(t)$ was obtained by summing the system's responses to all these components in the form of the convolution integral. There are infinite possible ways of expressing an input $x(t)$ in terms of other signals. For this reason, the problem of signal representation in terms of a set of signals is very important in the study of signals and systems. This chapter addresses the issue of representing a signal as a sum of its components. The problem is similar to that of representing a vector in terms of its components.

3.1 SIGNALS AS VECTORS

There is a perfect analogy between signals and vectors; the analogy is so strong that the term *analogy* understates the reality. Signals are not just *like* vectors. Signals *are* vectors! A vector can be represented as a sum of its components in a variety of ways, depending on the choice of coordinate system. A signal can also be represented as a sum of its components in a variety of ways. Let us begin with some basic vector concepts and then apply these concepts to signals.

3.1.1 Component of a Vector

A vector is specified by its magnitude and its direction. We shall denote all vectors by boldface. For example, $\mathbf{x}$ is a certain vector with magnitude or length $|\mathbf{x}|$. For the two vectors $\mathbf{x}$ and $\mathbf{y}$ shown in Fig. 3.1, we define their dot (inner or scalar) product as

$$\mathbf{x} \cdot \mathbf{y} = |\mathbf{x}||\mathbf{y}| \cos \theta$$

where θ is the angle between these vectors. Using this definition, we can express $|\mathbf{x}|$, the length of a vector $\mathbf{x}$, as

$$|\mathbf{x}|^2 = \mathbf{x} \cdot \mathbf{x}$$

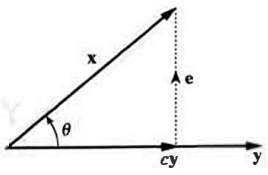

Figure 3.1 Component (projection) of a vector along another vector.

Let the component of $\mathbf{x}$ along $\mathbf{y}$ be $c\mathbf{y}$ as depicted in Fig. 3.1. Geometrically, the component of $\mathbf{x}$ along $\mathbf{y}$ is the projection of $\mathbf{x}$ on $\mathbf{y}$ and is obtained by drawing a perpendicular from the tip of $\mathbf{x}$ on the vector $\mathbf{y}$, as illustrated in Fig. 3.1. What is the mathematical significance of a component of a vector along another vector? As seen from Fig. 3.1, the vector $\mathbf{x}$ can be expressed in terms of vector $\mathbf{y}$ as

$$\mathbf{x} = c\mathbf{y} + \mathbf{e}$$

However, this is not the only way to express $\mathbf{x}$ in terms of $\mathbf{y}$. From Fig. 3.2, which shows two of the infinite other possibilities, we have

$$\mathbf{x} = c_1\mathbf{y} + \mathbf{e}_1 = c_2\mathbf{y} + \mathbf{e}_2$$

In each of these three representations, $\mathbf{x}$ is represented in terms of $\mathbf{y}$ plus another vector called the *error vector*. If we approximate $\mathbf{x}$ by $c\mathbf{y}$,

$$\mathbf{x} \simeq c\mathbf{y}$$

the error in the approximation is the vector $\mathbf{e} = \mathbf{x} - c\mathbf{y}$. Similarly, the errors in approximations in these drawings are $\mathbf{e}_1$ (Fig. 3.2a) and $\mathbf{e}_2$ (Fig. 3.2b). What is unique about the approximation in Fig. 3.1 is that the error vector is the smallest. We can now define mathematically the component of a vector $\mathbf{x}$ along vector $\mathbf{y}$ to be $c\mathbf{y}$, where c is chosen to minimize the length of the error vector $\mathbf{e} = \mathbf{x} - c\mathbf{y}$. Now, the length of the component of $\mathbf{x}$ along $\mathbf{y}$ is $|\mathbf{x}|\cos\theta$. But it is also $c|\mathbf{y}|$, as seen from Fig. 3.1. Therefore,

$$c|\mathbf{y}| = |\mathbf{x}|\cos\theta$$

Multiplying both sides by $|\mathbf{y}|$ yields

$$c|\mathbf{y}|^2 = |\mathbf{x}||\mathbf{y}|\cos\theta = \mathbf{x}\cdot\mathbf{y}$$

Therefore,

$$c = \frac{\mathbf{x}\cdot\mathbf{y}}{\mathbf{y}\cdot\mathbf{y}} = \frac{1}{|\mathbf{y}|^2}\mathbf{x}\cdot\mathbf{y} \tag{3.1}$$

From Fig. 3.1, it is apparent that when $\mathbf{x}$ and $\mathbf{y}$ are perpendicular, or orthogonal, then $\mathbf{x}$ has a zero component along $\mathbf{y}$; consequently, $c = 0$. Keeping an eye on Eq. (3.1), we therefore define $\mathbf{x}$ and $\mathbf{y}$ to be *orthogonal* if the inner (scalar or dot) product of the two vectors is zero, that is, if

$$\mathbf{x}\cdot\mathbf{y} = 0$$

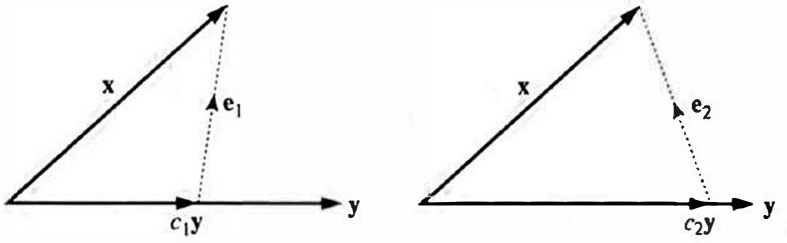

Figure 3.2 Approximation of a vector in terms of another vector.

3.1.2 Component of a Signal

The concept of a vector component and orthogonality can be extended to signals. Consider the problem of approximating a real signal $x(t)$ in terms of another real signal $y(t)$ over an interval (t_1, t_2):

$$x(t) \simeq cy(t) \qquad t_1 < t < t_2$$

The error $e(t)$ in this approximation is

$$e(t) = \begin{cases} x(t) - cy(t) & t_1 < t < t_2 \\ 0 & \text{otherwise} \end{cases}$$

We now select a criterion for the "best approximation." We know that the signal energy is one possible measure of a signal size. For best approximation, we shall use the criterion that minimizes the size or energy of the error signal $e(t)$ over the interval (t_1, t_2). This energy E_e is given by

$$E_e = \int_{t_1}^{t_2} e^2(t)\,dt = \int_{t_1}^{t_2} [x(t) - cy(t)]^2\,dt$$

Note that the right-hand side is a definite integral with t as the dummy variable. Hence, E_e is a function of the parameter c (not t) and E_e is minimum for some choice of c. To minimize E_e, a necessary condition is

$$\frac{dE_e}{dc} = 0$$

or

$$\frac{d}{dc}\left[\int_{t_1}^{t_2} [x(t) - cy(t)]^2\,dt\right] = 0$$

Expanding the squared term inside the integral, we obtain

$$\frac{d}{dc}\left[\int_{t_1}^{t_2} x^2(t)\,dt\right] - \frac{d}{dc}\left[2c\int_{t_1}^{t_2} x(t)y(t)\,dt\right] + \frac{d}{dc}\left[c^2\int_{t_1}^{t_2} y^2(t)\,dt\right] = 0$$

from which we get

$$-2\int_{t_1}^{t_2} x(t)y(t)\,dt + 2c\int_{t_1}^{t_2} y^2(t)\,dt = 0$$

$$c = \frac{\int_{t_1}^{t_2} x(t)y(t)\,dt}{\int_{t_1}^{t_2} y^2(t)\,dt} = \frac{1}{E_y}\int_{t_1}^{t_2} x(t)y(t)\,dt \tag{3.2}$$

We observe a remarkable similarity between the behavior of vectors and signals, as indicated by Eqs. (3.1) and (3.2). It is evident from these two parallel expressions that *the area under the product of two signals corresponds to the inner (scalar or dot) product of two vectors.* In fact, the area under the product of $x(t)$ and $y(t)$ is called the *inner product* of $x(t)$ and $y(t)$, and is denoted by (x, y). The energy of a signal is the inner product of a signal with itself, and corresponds to the vector length square (which is the inner product of the vector with itself).

To summarize our discussion, if a signal $x(t)$ is approximated by another signal $y(t)$ as

$$x(t) \simeq cy(t)$$

then the optimum value of c that minimizes the energy of the error signal in this approximation is given by Eq. (3.2).

Taking our clue from vectors, we say that a signal $x(t)$ contains a component $cy(t)$, where c is given by Eq. (3.2). Note that in vector terminology, $cy(t)$ is the projection of $x(t)$ on $y(t)$. Continuing with the analogy, we say that if the component of a signal $x(t)$ of the form $y(t)$ is zero (i.e., $c = 0$), the signals $x(t)$ and $y(t)$ are orthogonal over the interval (t_1, t_2). Therefore, we define the real signals $x(t)$ and $y(t)$ to be orthogonal over the interval (t_1, t_2) if [†]

$$\int_{t_1}^{t_2} x(t)y(t)\,dt = 0 \tag{3.3}$$

EXAMPLE 3.1 Sine-Wave Approximation of a Square Wave

For the square signal $x(t)$ shown in Fig. 3.3, find the component in $x(t)$ of the form $\sin t$. In other words, approximate $x(t)$ in terms of $\sin t$

$$x(t) \simeq c \sin t \qquad 0 < t < 2\pi$$

so that the energy of the error signal is minimum.

[†] For complex signals, the definition is modified as in Eq. (3.6).

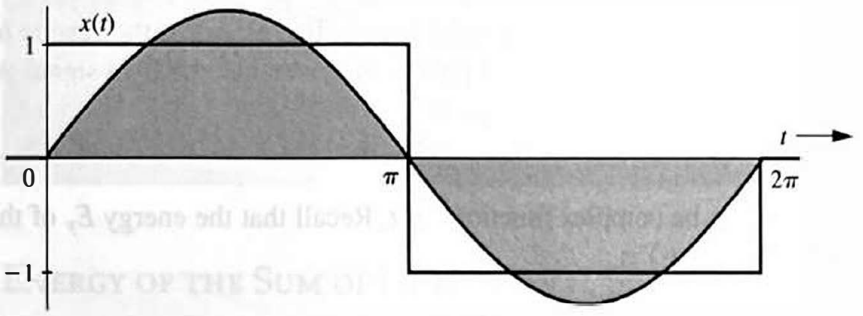

Figure 3.3 Approximation of a square wave in terms of a single sinusoid.

In this case,

$$y(t) = \sin t \qquad \text{and} \qquad E_y = \int_0^{2\pi} \sin^2(t)\, dt = \pi$$

From Eq. (3.2), we find

$$c = \frac{1}{\pi}\int_0^{2\pi} x(t)\sin t\, dt = \frac{1}{\pi}\left[\int_0^{\pi} \sin t\, dt + \int_{\pi}^{2\pi} -\sin t\, dt\right] = \frac{4}{\pi}$$

Thus,

$$x(t) \simeq \frac{4}{\pi}\sin t$$

represents the best approximation of $x(t)$ by the function $\sin t$, which will minimize the error energy. This sinusoidal component of $x(t)$ is shaded in Fig. 3.3. By analogy with vectors, we say that the square function $x(t)$ depicted in Fig. 3.3 has a component of signal $\sin t$ and that the magnitude of this component is $4/\pi$.

DRILL 3.1 Sine Wave Approximation of a Ramp Function

Show that over an interval $(-\pi < t < \pi)$, the "best" approximation of the signal $x(t) = t$ in terms of the function $\sin t$ is $2\sin t$. Verify that the error signal $e(t) = t - 2\sin t$ is orthogonal to the signal $\sin t$ over the interval $-\pi < t < \pi$. Sketch the signals t and $2\sin t$ over the interval $-\pi < t < \pi$.

3.1.3 Extension to Complex Signals

So far we have restricted ourselves to real functions of t. To generalize the results to complex functions of t, consider again the problem of approximating a signal $x(t)$ by a signal $y(t)$ over an interval $(t_1 < t < t_2)$:

$$x(t) \simeq cy(t)$$

where $x(t)$ and $y(t)$ now can be complex functions of t. Recall that the energy E_y of the complex signal $y(t)$ over an interval (t_1, t_2) is

$$E_y = \int_{t_1}^{t_2} |y(t)|^2 \, dt$$

In this case, both the coefficient c and the error

$$e(t) = x(t) - cy(t)$$

are complex (in general). For the "best" approximation, we choose c to minimize the energy E_e of the error signal $e(t)$. Now,

$$E_e = \int_{t_1}^{t_2} |x(t) - cy(t)|^2 \, dt \tag{3.4}$$

Recall also that

$$|u+v|^2 = (u+v)(u^*+v^*) = |u|^2 + |v|^2 + u^*v + uv^* \tag{3.5}$$

After some manipulation, we can use this result to rearrange Eq. (3.4) as

$$E_e = \int_{t_1}^{t_2} |x(t)|^2 \, dt - \left| \frac{1}{\sqrt{E_y}} \int_a^{t_2} x(t) y^*(t) \, dt \right|^2 + \left| c\sqrt{E_y} - \frac{1}{\sqrt{E_y}} \int_{t_1}^{t_2} x(t) y^*(t) \, dt \right|^2$$

Since the first two terms on the right-hand side are independent of c, it is clear that E_e is minimized by choosing c so that the third term on the right-hand side is zero. This yields

$$c = \frac{1}{E_y} \int_{t_1}^{t_2} x(t) y^*(t) \, dt$$

In light of this result, we need to redefine orthogonality for the complex case as follows: two complex functions $x_1(t)$ and $x_2(t)$ are orthogonal over an interval $(t_1 < t < t_2)$ if

$$\int_{t_1}^{t_2} x_1(t) x_2^*(t) \, dt = 0 \qquad \text{or} \qquad \int_{t_1}^{t_2} x_1^*(t) x_2(t) \, dt = 0 \tag{3.6}$$

Either equality suffices. This is a general definition of orthogonality, which reduces to Eq. (3.3) when the functions are real.

DRILL 3.2 Complex Exponential Approximation of a Square Wave

Show that over an interval $(0 < t < 2\pi)$, the "best" approximation of the square signal $x(t)$ in Fig. 3.3 in terms of the signal e^{jt} is given by $(2/j\pi)e^{jt}$. Verify that the error signal $e(t) = x(t) - (2/j\pi)e^{jt}$ is orthogonal to the signal e^{jt}.

Energy of the Sum of Orthogonal Signals

We know that the square of the length of a sum of two orthogonal vectors is equal to the sum of the squares of the lengths of the two vectors. Thus, if vectors $\mathbf{x}$ and $\mathbf{y}$ are orthogonal, and if $\mathbf{z} = \mathbf{x} + \mathbf{y}$, then

$$|\mathbf{z}|^2 = |\mathbf{x}|^2 + |\mathbf{y}|^2$$

We have a similar result for signals. The energy of the sum of two orthogonal signals is equal to the sum of the energies of the two signals. Thus, if signals $x(t)$ and $y(t)$ are orthogonal over an interval (t_1, t_2), and if $z(t) = x(t) + y(t)$, then

$$E_z = E_x + E_y$$

We now prove this result for complex signals, of which real signals are a special case. From Eq. (3.5), it follows that

$$\begin{aligned}\int_{t_1}^{t_2} |x(t) + y(t)|^2\, dt &= \int_{t_1}^{t_2} |x(t)|^2\, dt + \int_{t_1}^{t_2} |y(t)|^2\, dt + \int_{t_1}^{t_2} x(t)y^*(t)\, dt + \int_{t_1}^{t_2} x^*(t)y(t)\, dt \\ &= \int_{t_1}^{t_2} |x(t)|^2\, dt + \int_{t_1}^{t_2} |y(t)|^2\, dt\end{aligned}$$

The last result follows from the fact that because of orthogonality, the two integrals of the products $x(t)y^*(t)$ and $x^*(t)y(t)$ are zero [see Eq. (3.6)]. This result can be extended to the sum of any number of mutually orthogonal signals.

3.2 Signal Comparison: Correlation

Section 3.1 has prepared the foundation for signal comparison. Here again, we can benefit by considering the concept of vector comparison. Two vectors $\mathbf{x}$ and $\mathbf{y}$ are similar if $\mathbf{x}$ has a large component along $\mathbf{y}$. In other words, if c in Eq. (3.1) is large, the vectors $\mathbf{x}$ and $\mathbf{y}$ are similar. We could consider c as a quantitative measure of similarity between $\mathbf{x}$ and $\mathbf{y}$. Such a measure, however, would be defective. The degree of similarity between $\mathbf{x}$ and $\mathbf{y}$ should be independent of the lengths of $\mathbf{x}$ and $\mathbf{y}$. If we double the length of $\mathbf{x}$, for example, the degree of similarity between $\mathbf{x}$ and $\mathbf{y}$ should not change. From Eq. (3.1), however, we see that doubling $\mathbf{x}$ doubles the value of c (whereas doubling $\mathbf{y}$ halves the value of c). Our measure is clearly faulty. Similarity between two vectors is indicated by the angle θ between the vectors. The smaller the θ, the greater the

similarity, and vice versa. The degree of similarity can therefore be conveniently measured by $\cos\theta$. The larger the $\cos\theta$, the greater is the similarity between the two vectors. Thus, a suitable measure would be $\rho = \cos\theta$, which is given by

$$\rho = \cos\theta = \frac{\mathbf{x}\cdot\mathbf{y}}{|\mathbf{x}|\,|\mathbf{y}|} \tag{3.7}$$

We can readily verify that this measure is independent of the lengths of $\mathbf{x}$ and $\mathbf{y}$. This similarity measure ρ is known as the *correlation coefficient*. Observe that

$$-1 \le \rho \le 1$$

Thus, the magnitude of ρ is never greater than unity. If the two vectors are aligned, the similarity is maximum ($\rho = 1$). Two vectors aligned in opposite directions have the maximum dissimilarity ($\rho = -1$). If the two vectors are orthogonal, the similarity is zero.

We use the same argument in defining a similarity index (correlation coefficient) for signals. We shall consider signals over the entire time interval from $-\infty$ to ∞. To make c in Eq. (3.2) independent of energies (sizes) of $x(t)$ and $y(t)$, we must normalize c by using both signal energies. Thus, the appropriate similarity index ρ analogous to Eq. (3.7) is given by

$$\rho = \frac{1}{\sqrt{E_x E_y}} \int_{-\infty}^{\infty} x(t)y(t)\,dt \tag{3.8}$$

Observe that multiplying either $x(t)$ or $y(t)$ by any constant has no effect on this index. It is independent of the size (energies) of $x(t)$ and $y(t)$. Using the Schwarz inequality,[†] we can show that the magnitude of ρ is never greater than 1; that is,

$$-1 \le \rho \le 1$$

Best Friends, Worst Enemies, and Complete Strangers

We can readily verify that if $x(t) = Ky(t)$, then $\rho = 1$ when K is any positive constant, and $\rho = -1$ when K is any negative constant. Also $\rho = 0$ if $x(t)$ and $y(t)$ are orthogonal. Thus, maximum similarity [when $x(t) = Ky(t)$] is indicated by $\rho = 1$, and maximum dissimilarity [when $x(t) = -Ky(t)$] is indicated by $\rho = -1$. When two signals are orthogonal, the similarity is zero. Qualitatively speaking, we may view orthogonal signals as unrelated signals. Note that maximum dissimilarity is qualitatively different from being unrelated. For example, we have best friends ($\rho = 1$), worst enemies ($\rho = -1$), and complete strangers, who do not care whether we exist or not ($\rho = 0$). Enemies are not strangers, but in many ways, people who think like us, only in opposite ways.

[†] For two real energy signals $x(t)$ and $y(t)$, the Schwarz inequality states that

$$\left(\int_{-\infty}^{\infty} x(t)y(t)\,dt\right)^2 \le E_x E_y$$

with equality if and only if $y(t) = Kx(t)$ for some constant K. There is a similar inequality for complex signals.

We can readily extend this discussion to complex signal comparison. We generalize the definition of ρ to include complex signals as

$$\rho = \frac{1}{\sqrt{E_x E_y}} \int_{-\infty}^{\infty} x(t) y^*(t)\, dt$$

EXAMPLE 3.2 Computing the Correlation Coefficient

Compute the correlation coefficient ρ between the pulse $x(t)$ and the signals $y_i(t)$, $i = 1, 2, 3, 4, 5$, and 6 illustrated in Fig. 3.4.

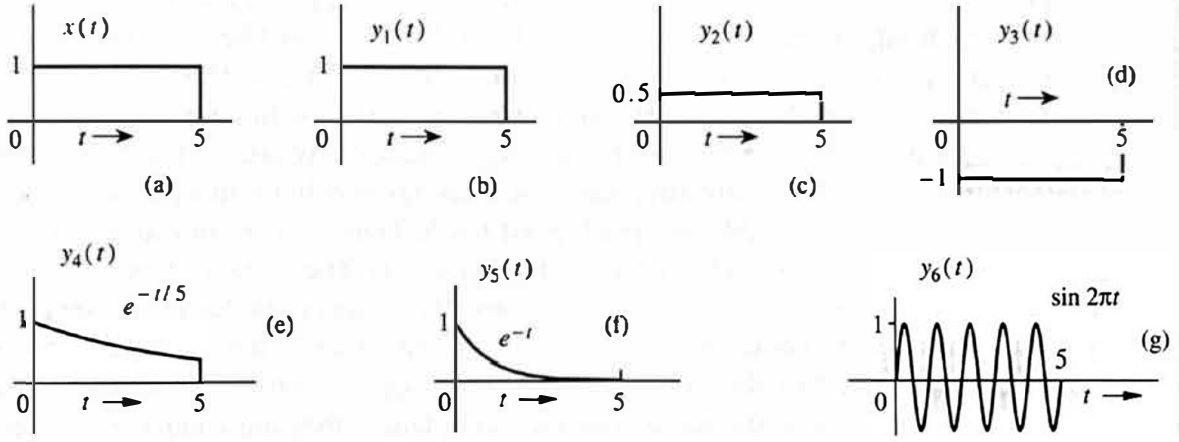

Figure 3.4 Signals for Ex. 3.2.

We shall compute ρ using Eq. (3.8) for each of the six cases. Let us first compute the energies of all the signals.

$$E_x = \int_0^5 x^2(t)\, dt = \int_0^5 dt = 5$$

In the same way, we find $E_{y_1} = 5$, $E_{y_2} = 1.25$, and $E_{y_3} = 5$. To determine E_{y_4} and E_{y_5}, we first determine the energy E of $e^{-at}u(t)$ over the interval $t = 0$ to T:

$$E = \int_0^T \left(e^{-at}\right)^2 dt = \int_0^T e^{-2at}\, dt = \frac{1}{2a}(1 - e^{-2aT})$$

For $y_4(t)$, $a = 1/5$ and $T = 5$. Therefore $E_{y_4} = 2.1617$. For $y_5(t)$, $a = 1$ and $T = \infty$. Therefore, $E_{y_5} = 0.5$. The energy of E_{y_6} is given by

$$E_{y_6} = \int_0^5 \sin^2 2\pi t\, dt = 2.5$$

Using Eq. (3.8), the correlation coefficients for the six cases are found as

$$i=1: \quad \rho = \frac{1}{\sqrt{(5)(5)}} \int_0^5 dt = 1 \qquad i=2: \quad \rho = \frac{1}{\sqrt{(1.25)(5)}} \int_0^5 (0.5)\,dt = 1$$

$$i=3: \quad \rho = \frac{1}{\sqrt{(5)(5)}} \int_0^5 (-1)\,dt = -1 \qquad i=4: \quad \rho = \frac{1}{\sqrt{(2.1617)(5)}} \int_0^5 e^{-t/5}\,dt = 0.961$$

$$i=5: \quad \rho = \frac{1}{\sqrt{(0.5)(5)}} \int_0^5 e^{-t}\,dt = 0.628 \qquad i=6: \quad \rho = \frac{1}{\sqrt{(2.5)(5)}} \int_0^5 \sin 2\pi t\,dt = 0$$

Comments on the results: Because $y_1(t) = x(t)$, the two signals have the maximum possible similarity and $\rho = 1$. However, the signal $y_2(t)$ also shows maximum possible similarity with $\rho = 1$. The reason is that we have defined ρ to measure the similarity of the waveshapes; it is independent of the amplitude (strength) of the signals compared. The signal $y_2(t)$ is identical to $x(t)$ in shape; only the amplitude (strength) is different. Hence, $\rho = 1$. The signal $y_3(t)$, on the other hand, has the maximum possible dissimilarity with $x(t)$ because it is equal to $-x(t)$. For $y_4(t)$, $\rho = 0.961$, implying a high degree of similarity with $x(t)$. This is reasonable because, as visual inspection shows, $y_4(t)$ is very similar to $x(t)$ over the duration of $x(t)$ (for $0 \le t \le 5$). The level of similarity decreases for $y_5(t)$, whose quick decay does not match $x(t)$. However, there is still substantial similarity; both signals always remain positive, show no oscillations, and have zero or negligible strength beyond $t = 5$. Thus, $y_5(t)$ is similar to $x(t)$ but not as similar as is $y_4(t)$. This is reflected in $\rho = 0.628$ for $y_5(t)$. The signal $y_6(t)$ is orthogonal to $x(t)$ so that $\rho = 0$. That is, $x(t)$ and $y_6(t)$ are unrelated. It may seem odd that $y_3(t)$ is more dissimilar to $x(t)$ than is $y_6(t)$. The dissimilarity between $x(t)$ and $y_3(t)$ is of the nature of antipathy (worst enemy): what one does, the other is certain to do the opposite. On the other hand, $x(t)$ and $y_6(t)$ are almost of different species or from different planets; they are complete strangers to one another with nothing in common (not even in opposition).

DRILL 3.3 Computing the Correlation Coefficient

Show that ρ of signals $y_2(t)$ and $y_3(t)$ in Fig. 3.4 is -1, that of $y_2(t)$ and $y_4(t)$ is 0.961, and that of $y_3(t)$ and $y_6(t)$ is zero.

3.2.1 Application to Signal Detection

Correlation is an extremely important concept that measures the degree of similarity (agreement or alignment) between two signals. This concept is widely used for signal processing applications such as GPS systems, radar, sonar, digital communication, electronic warfare, and many others.

One of the most important uses of correlation is for signal detection. To illustrate this concept, consider a radar example where a signal pulse is transmitted in order to detect a suspected target. If a target is present, the pulse will be reflected by it. If a target is not present, there will be no reflected pulse, just noise. The presence or absence of the reflected pulse confirms the presence

or absence of a target. The crucial problem in this procedure is to detect the heavily attenuated, reflected pulse (of known waveform) buried in unwanted noise signal. In this situation, correlation of the received pulse with the transmitted pulse can be of great help. If the correlation coefficient is large, there is a good chance the signal is present. If the correlation coefficient is near zero, there is little evidence to suggest the signal is present. A similar situation exists in digital communication where we are required to detect the presence of one of the two known waveforms in the presence of noise.

We now explain qualitatively how signal detection using correlation is accomplished. Consider the case of binary communication where two known waveforms are received in a random sequence. Each time we receive a pulse, our task is to determine which of the two (known) waveforms is received. To make the detection easier, we must make the two pulses as dissimilar as possible. Therefore, we should select pulse pairs that are negatives of one another. This choice gives the highest dissimilarity ($\rho = -1$). This scheme is sometimes called the *antipodal* scheme. We can also use orthogonal pulses, which result in $\rho = 0$. In practice, both these options are used, although antipodal is the best in terms of distinguishability between the two pulses.

Let us consider the antipodal scheme in which the two pulses are $p(t)$ and $-p(t)$. The correlation coefficient ρ of these pulses is -1. Assume that there is no noise or any other imperfections in the transmission. The receiver consists of a correlator that computes the correlation between $p(t)$ and the received pulse. If the correlation is 1, we decide that $p(t)$ is received, and if the correlation is -1, we decide that $-p(t)$ is received. Detection is made easy because of the maximum possible dissimilarity between the two pulses. The situation is almost like that in a fairy tale where everybody lives happily ever after. In practice, however, several imperfections occur. There is always an unwanted signal (noise) superimposed on the received pulses. Moreover, during transmission, pulses get distorted and dispersed (spread out) in time. Consequently, a received pulse is corrupted by overlapping tails from other pulses. This changes the shape of received pulses, and the correlation coefficient is no longer ± 1 but rather a smaller magnitude, thus reducing the distinguishability of pulses. We use a *threshold detector*, which decides that if the correlation is positive ($\rho > 0$), the received pulse is $p(t)$, and if the correlation is negative ($\rho < 0$), the received pulse is $-p(t)$.

Suppose, for example, that $p(t)$ has been transmitted. In the ideal case, correlation of this pulse at the receiver would be 1, the maximum possible. Now because of noise and other imperfections, the correlation is going to be less than 1. In some extreme situation, the noise and overlapping from other pulses can make this pulse so dissimilar to $p(t)$ that the correlation can be a negative amount. In this case, the threshold detector decides that $-p(t)$ has been received, thus causing a detection error. In the same way, if $-p(t)$ is transmitted, the channel noise, pulse distortion, and the overlapping from other pulses could result in a positive correlation, causing a detection error. Our task is to make sure that the transmitted pulses have sufficient energy to keep the relative damage to the pulse caused by noise within a limit and the error probability below acceptable bounds. In the ideal case, the margin provided by the correlation ρ for distinguishing the two pulses is 2 (from 1 to -1 and vice versa). Noise and other imperfections reduce this margin. That is why it is important to start with as large a margin as possible. For this reason, the antipodal scheme has the best performance in terms of guarding against the channel noise and other imperfections. However, as mentioned earlier, because of some other reasons, different schemes such as an orthogonal scheme, where $\rho = 0$, are also used even when they provide a smaller margin (from 0 to 1 and vice versa) in distinguishing the pulses.

Some aspects of pulse dispersion were discussed in Secs. 2.6.5 and 2.6.6. In Ch. 4, we shall discuss pulse distortion during transmission. Calculation of error probability in the presence of noise and other imperfections are beyond the scope of this work. For a detailed treatment of this subject, the reader may refer to [1].

3.2.2 Correlation Functions

Consider an application of correlation to signal detection in radar, where a signal pulse is transmitted in order to detect a suspected target. If a target is present, the pulse will be reflected by it. In contrast, if the target is not present, there will be no reflected pulse, just noise. By detecting the presence or absence of the reflected pulse, we confirm the presence or absence of the target. By measuring the time delay between the transmitted and received (reflected) pulse, we determine the distance of the target. Let the transmitted and the reflected pulses be denoted by $x(t)$ and $y(t)$, respectively, as shown in Fig. 3.5.

If we use Eq. (3.8) directly to measure the correlation coefficient ρ, we obtain

$$\rho = \frac{1}{\sqrt{E_x E_y}} \int_{-\infty}^{\infty} x(t)y(t)\,dt = 0$$

Even though the pulses themselves are identical, the correlation is zero because the pulses are disjoint (nonoverlapping in time). To avoid this difficulty, we compare the received pulse $y(t)$ with a delayed pulse $x(t)$ for various values of delay. If for some value of delay parameter there is a strong correlation, we not only detect the presence of the pulse but we also detect the relative time shift of $y(t)$ with respect to $x(t)$. For this reason, instead of using the integral on the right-hand side, we use the modified integral $\psi_{yx}(t)$, the *crosscorrelation* function of two real signals $y(t)$ and $x(t)$ defined by†

$$\psi_{yx}(t) \equiv \int_{-\infty}^{\infty} y(\tau)x(\tau - t)\,d\tau \tag{3.9}$$

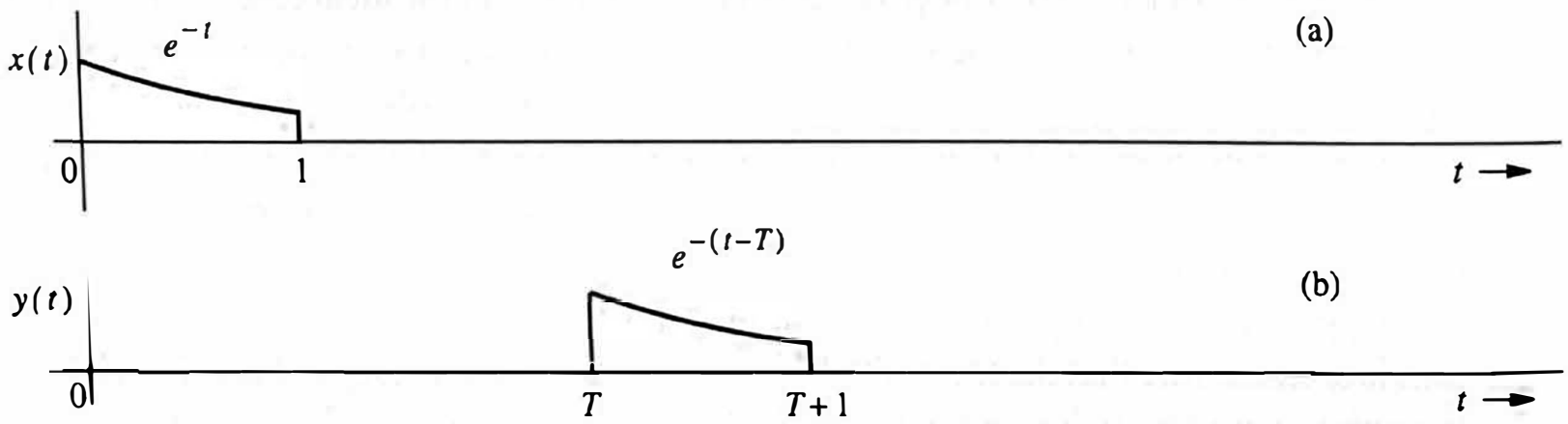

Figure 3.5 Physical explanation of the correlation function.

† For complex signals, we define

$$\psi_{yx}(t) \equiv \int_{-\infty}^{\infty} y(\tau)x^*(\tau - t)\,d\tau$$

Here, τ is a dummy variable of integration, and $x(\tau - t)$ is the signal $x(\tau)$ delayed by t seconds with respect to the $y(\tau)$. Therefore, $\psi_{yx}(t)$ is an indication of similarity (correlation) of $y(t)$ with $x(t)$ delayed by t seconds. By incorporating delay, $\psi_{yx}(t)$ can measure the similarity of pulses even if they are disjoint. For the signals in Fig. 3.5, $\psi_{yx}(t)$ will show significant correlation around $t = T$. This observation allows us not only to detect the presence of the target, but also to calculate its distance.

Convolution and Correlation

We now examine the close connection between the convolution and the crosscorrelation of $y(t)$ and $x(t)$ [given by Eq. (3.9)]. Note that $x(\tau - t)$ is $x(\tau)$ time-shifted by t. Thus, $\psi_{yx}(t)$ is equal to the area under the product of the y signal and the x signal time-shifted by t (without time inversion). In convolution also we follow the same procedure, except that the x signal is time-inverted before it is shifted by t. This observation suggests that $\psi_{yx}(t)$ is equal to $y(t) * x(-t)$ [the convolution of $y(t)$ with time-inverted $x(t)$]. That is,

$$\psi_{yx}(t) = y(t) * x(-t) \tag{3.10}$$

This can be formally proved as follows. Letting $x(-t) = w(t)$,

$$y(t) * x(-t) = y(t) * w(t) = \int_{-\infty}^{\infty} y(\tau) w(t - \tau)\, d\tau = \int_{-\infty}^{\infty} y(\tau) x(\tau - t)\, d\tau = \psi_{yx}(t)$$

Complex signals require the small adjustment $\psi_{yx}(t) = y(t) * x^*(-t)$.

DRILL 3.4 Crosscorrelation by Convolution

(a) Show that $\psi_{xg}(t)$, the crosscorrelation function of $x(t)$ and $g(t)$ in Fig. 2.11, is given by $c(t)$ in Fig. 2.12.

(b) Show that $\psi_{xg}(t)$, the crosscorrelation function of $x(t)$ and $g(t)$ in Fig. 2.12, is given by $c(t)$ in Fig. 2.11.

Autocorrelation Function

The correlation of a signal with itself is called *autocorrelation*. The autocorrelation function $\psi_x(t)$ of a signal $x(t)$ is defined as

$$\psi_x(t) \equiv \int_{-\infty}^{\infty} x(\tau) x^*(\tau - t)\, d\tau \tag{3.11}$$

In Ch. 4, we show that the autocorrelation function provides valuable spectral information about the signal.

3.3 SIGNAL REPRESENTATION BY AN ORTHOGONAL SIGNAL SET

In this section, we show a way of representing a signal as a sum of orthogonal signals. Here again, we can benefit from the insight gained from a similar problem in vectors. We know that a vector can be represented as a sum of orthogonal vectors, which form the coordinate system of a vector space. The problem in signals is analogous, and the results for signals are parallel to those for vectors. So, let us review the case of vector representation.

3.3.1 Orthogonal Vector Space

Let us investigate a three-dimensional Cartesian vector space described by three mutually orthogonal vectors $\mathbf{x}_1$, $\mathbf{x}_2$, and $\mathbf{x}_3$, as illustrated in Fig. 3.6. First, we shall seek to approximate a three-dimensional vector $\mathbf{x}$ in terms of two mutually orthogonal vectors $\mathbf{x}_1$ and $\mathbf{x}_2$:

$$\mathbf{x} \simeq c_1\mathbf{x}_1 + c_2\mathbf{x}_2$$

The error $\mathbf{e}$ in this approximation is

$$\mathbf{e} = \mathbf{x} - (c_1\mathbf{x}_1 + c_2\mathbf{x}_2)$$

or

$$\mathbf{x} = c_1\mathbf{x}_1 + c_2\mathbf{x}_2 + \mathbf{e}$$

As in the earlier geometrical argument, we see from Fig. 3.6 that the length of $\mathbf{e}$ is minimum when $\mathbf{e}$ is perpendicular to the $\mathbf{x}_1$–$\mathbf{x}_2$ plane, and $c_1\mathbf{x}_1$ and $c_2\mathbf{x}_2$ are the projections (components) of $\mathbf{x}$ on $\mathbf{x}_1$ and $\mathbf{x}_2$, respectively. Therefore, the constants c_1 and c_2 are given by Eq. (3.1). Observe that the error vector is orthogonal to both the vectors $\mathbf{x}_1$ and $\mathbf{x}_2$.

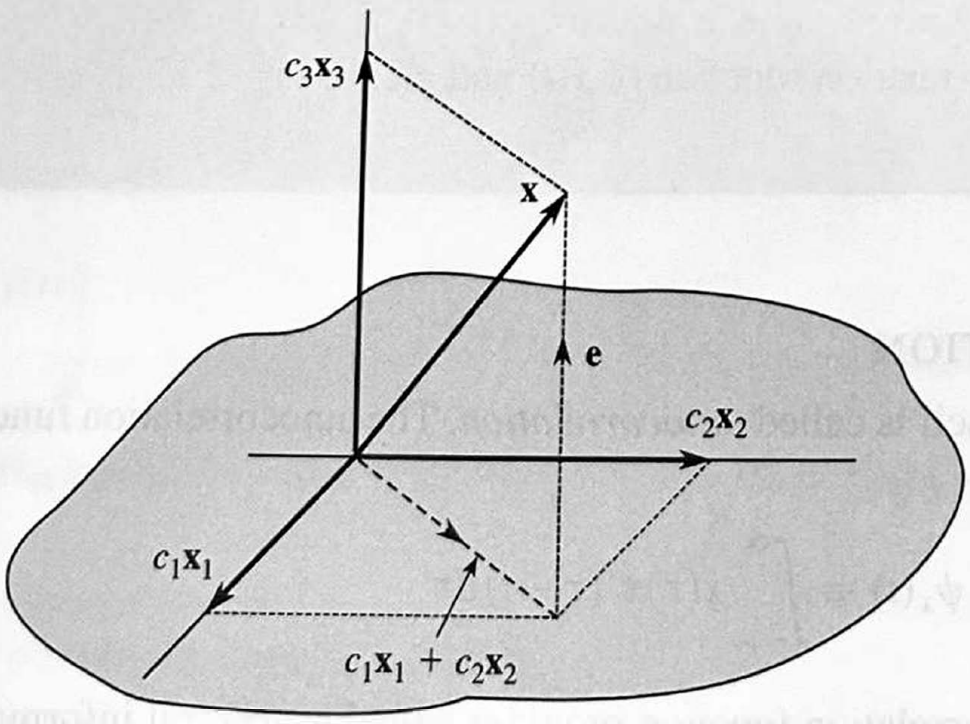

Figure 3.6 Representation of a vector in three-dimensional space.

Now, let us determine the "best" approximation to $\mathbf{x}$ in terms of all three mutually orthogonal vectors $\mathbf{x}_1$, $\mathbf{x}_2$, and $\mathbf{x}_3$:

$$\mathbf{x} \simeq c_1\mathbf{x}_1 + c_2\mathbf{x}_2 + c_3\mathbf{x}_3 \tag{3.12}$$

Figure 3.6 shows that a unique choice of c_1, c_2, and c_3 exists, for which Eq. (3.12) is no longer an approximation but an equality

$$\mathbf{x} = c_1\mathbf{x}_1 + c_2\mathbf{x}_2 + c_3\mathbf{x}_3$$

In this case, $c_1\mathbf{x}_1, c_2\mathbf{x}_2$, and $c_3\mathbf{x}_3$ are the projections (components) of $\mathbf{x}$ on $\mathbf{x}_1, \mathbf{x}_2$, and $\mathbf{x}_3$, respectively; that is,

$$c_i = \frac{\mathbf{x}\cdot\mathbf{x}_i}{\mathbf{x}_i\cdot\mathbf{x}_i} = \frac{1}{|\mathbf{x}_i|^2}\mathbf{x}\cdot\mathbf{x}_i \qquad i = 1,2,3 \tag{3.13}$$

Note that the error in the approximation is zero when $\mathbf{x}$ is approximated in terms of three mutually orthogonal vectors: $\mathbf{x}_1$, $\mathbf{x}_2$, and $\mathbf{x}_3$. The reason is that $\mathbf{x}$ is a three-dimensional vector, and the vectors $\mathbf{x}_1$, $\mathbf{x}_2$, and $\mathbf{x}_3$ represent a *complete set* of orthogonal vectors in three-dimensional space. Completeness here means that it is impossible to find another vector $\mathbf{x}_4$ in this space, which is orthogonal to all three vectors, $\mathbf{x}_1, \mathbf{x}_2$, and $\mathbf{x}_3$. Any vector in this space can then be represented (with zero error) in terms of these three vectors. Such vectors are known as *basis* vectors. If a set of vectors $\{\mathbf{x}_i\}$ is not complete, the error in the approximation will generally not be zero. Thus, in the three-dimensional case discussed earlier, it is generally not possible to represent a vector $\mathbf{x}$ in terms of only two basis vectors without an error.

The choice of basis vectors is not unique. In fact, a set of basis vectors corresponds to a particular choice of coordinate system. Thus, a three-dimensional vector $\mathbf{x}$ may be represented in many different ways, depending on the coordinate system used.

3.3.2 Orthogonal Signal Space

We start with real signals and then extend the discussion to complex signals. We proceed with our signal approximation problem, using clues and insights developed for vector approximation. As before, we define orthogonality of a real signal set $x_1(t), x_2(t), \ldots, x_N(t)$ over interval (t_1, t_2) as

$$\int_{t_1}^{t_2} x_m(t)x_n(t)\,dt = \begin{cases} 0 & m \neq n \\ E_n & m = n \end{cases} \tag{3.14}$$

If the energies $E_n = 1$ for all n, then the set is *normalized* and is called an *orthonormal set*. An orthogonal set can always be normalized by dividing $x_n(t)$ by $\sqrt{E_n}$ for all n.

Now, consider approximating a signal $x(t)$ over the interval (t_1, t_2) by a set of N real, mutually orthogonal signals $x_1(t), x_2(t), \ldots, x_N(t)$ as

$$x(t) \simeq c_1x_1(t) + c_2x_2(t) + \cdots + c_Nx_N(t) \simeq \sum_{n=1}^{N} c_nx_n(t) \tag{3.15}$$

In the approximation of Eq. (3.15), the error $e(t)$ is

$$e(t) = x(t) - \sum_{n=1}^{N} c_nx_n(t)$$

and E_e, the error signal energy, is

$$E_e = \int_{t_1}^{t_2} e^2(t)\,dt = \int_{t_1}^{t_2} \left[x(t) - \sum_{n=1}^{N} c_nx_n(t)\right]^2 dt \tag{3.16}$$

According to our criterion for best approximation, we select the values of c_i that minimize E_e. Hence, the necessary condition is $\partial E_e/dc_i = 0$ for $i = 1, 2, \ldots, N$, that is,

$$\frac{\partial}{\partial c_i}\int_{t_1}^{t_2}\left[x(t) - \sum_{n=1}^{N} c_n x_n(t)\right]^2 dt = 0$$

When we expand the integrand, we find that all the cross-multiplication terms arising from the orthogonal signals are zero by virtue of orthogonality: that is, all terms of the form $\int x_m(t)x_n(t)\,dt$ with $m \neq n$ vanish. Similarly, the derivative with respect to c_i of all terms that do not contain c_i is zero. For each i, this leaves only two nonzero terms:

$$\frac{\partial}{\partial c_i}\int_{t_1}^{t_2}\left[-2c_i x(t)x_i(t) + c_i{}^2 x_i{}^2(t)\right]dt = 0$$

or

$$-2\int_{t_1}^{t_2} x(t)x_i(t)\,dt + 2c_i\int_{t_1}^{t_2} x_i{}^2(t)\,dt = 0 \qquad i = 1, 2, \ldots, N$$

Therefore,

$$c_i = \frac{\displaystyle\int_{t_1}^{t_2} x(t)x_i(t)\,dt}{\displaystyle\int_{t_1}^{t_2} x_i{}^2(t)\,dt} = \frac{1}{E_i}\int_{t_1}^{t_2} x(t)x_i(t)\,dt \qquad i = 1, 2, \ldots, N \tag{3.17}$$

A comparison of Eq. (3.17) with Eq. (3.13) forcefully brings out the analogy of signals with vectors.

Finality Property. Equation (3.17) shows one interesting property of the coefficients of c_1, c_2, $\ldots$, c_N: the optimum value of any coefficient in Eq. (3.15) is independent of the number of terms used in the approximation. For example, if we used only one term ($N = 1$) or two terms ($N = 2$) or any number of terms, the optimum value of the coefficient c_1 would be the same [as given by Eq. (3.17)]. The advantage of this approximation of a signal $x(t)$ by a set of mutually orthogonal signals is that we can continue to add terms to the approximation without disturbing the previous terms. This property of *finality* of the values of the coefficients is very important from a practical point of view.†

---

† Contrast this situation with a polynomial approximation of $x(t)$. Suppose we wish to find a two-point approximation of $x(t)$ by a polynomial in t; that is, the polynomial is to be equal to $x(t)$ at two points t_1 and t_2. This can be done by choosing a first-order polynomial $a_0 + a_1 t$ with

$$x(t_1) = a_0 + a_1 t_1 \qquad \text{and} \qquad x(t_2) = a_0 + a_1 t_2$$

Solution of these equations yields the desired values of a_0 and a_1. For a three-point approximation, we must choose the polynomial $a_0 + a_1 t + a_2 t^2$ with

$$x(t_i) = a_0 + a_1 t_i + a_2 t_i{}^2 \qquad i = 1, 2, \text{ and } 3$$

The approximation improves with a larger number of points (higher-order polynomial), but the coefficients $a_0, a_1, a_2, \ldots$ do not have the finality property. Every time we increase the number of terms in the polynomial, we need to recalculate the coefficients.

Energy of the Error Signal

When the coefficients c_i in Eq. (3.15) are chosen according to Eq. (3.17), the error signal energy is minimized. This minimum value of E_e is given by Eq. (3.16):

$$E_e = \int_{t_1}^{t_2} \left[x(t) - \sum_{n=1}^{N} c_n x_n(t) \right]^2 dt$$

$$= \int_{t_1}^{t_2} x^2(t)\,dt + \sum_{n=1}^{N} c_n^2 \int_{t_1}^{t_2} x_n^2(t)\,dt - 2\sum_{n=1}^{N} c_n \int_{t_1}^{t_2} x(t)x_n(t)\,dt$$

Substitution of Eqs. (3.14) and (3.17) in this equation yields

$$E_e = \int_{t_1}^{t_2} x^2(t)\,dt + \sum_{n=1}^{N} c_n^2 E_n - 2\sum_{n=1}^{N} c_n^2 E_n = \int_{t_1}^{t_2} x^2(t)\,dt - \sum_{n=1}^{N} c_n^2 E_n \tag{3.18}$$

Observe that because the term $c_k^2 E_k$ is nonnegative, the error energy E_e generally decreases as N, the number of terms, is increased. Hence, it is possible that the error energy $\to 0$ as $N \to \infty$. When this happens, the orthogonal signal set is said to be *complete*. In this case, Eq. (3.15) is no more an approximation but an equality

$$x(t) = c_1 x_1(t) + c_2 x_2(t) + \cdots + c_n x_n(t) + \cdots = \sum_{n=1}^{\infty} c_n x_n(t) \qquad t_1 < t < t_2 \tag{3.19}$$

where the coefficients c_n are given by Eq. (3.17). Because the error signal energy approaches zero, it follows that the energy of $x(t)$ is now equal to the sum of the energies of its orthogonal components $c_1 x_1(t)$, $c_2 x_2(t)$, $c_3 x_3(t)$, ...

The series on the right-hand side of Eq. (3.19) is called the *generalized Fourier series* of $x(t)$ with respect to the set $\{x_n(t)\}$. When the set $\{x_n(t)\}$ is such that the error energy $E_e \to 0$ as $N \to \infty$ for every member of some particular class, we say that the set $\{x_n(t)\}$ is complete on (t_1, t_2) for that class of $x(t)$, and the set $\{x_n(t)\}$ is called a set of *basis functions* or *basis signals*. Unless otherwise mentioned, in the future we shall consider only the class of energy signals.

Thus, when the set $\{x_n(t)\}$ is complete, we have the equality of Eq. (3.19). One subtle point that must be understood clearly is the meaning of equality in Eq. (3.19). *The equality here is not an equality in the ordinary sense, but in the sense that the error energy, that is, the energy of the difference between the two sides of Eq. (3.19), approaches zero.* If the equality exists in the ordinary sense, the error energy is always zero, but the converse is not necessarily true. The error energy can approach zero even though $e(t)$, the difference between the two sides, is nonzero at some isolated instants. The reason is that even if $e(t)$ is nonzero at such instants, the area under $e^2(t)$ is still zero; thus, the Fourier series on the right-hand side of Eq. (3.19) may differ from $x(t)$ at a finite number of points.

In Eq. (3.19), the energy of the left-hand side is E_x, and the energy of the right-hand side is the sum of the energies of all the orthogonal components.[†] Thus,

$$\int_{t_1}^{t_2} x^2(t)\,dt = c_1^2 E_1 + c_2^2 E_2 + \cdots = \sum_{n=1}^{\infty} c_n^2 E_n \tag{3.20}$$

[†] Note that the energy of a signal $cx(t)$ is $c^2 E_x$.

This is *Parseval's theorem* expressed for energy signals. Recall that the signal energy (area under the squared value of a signal) is analogous to the square of the length of a vector in the vector-signal analogy. In vector space, we know that the square of the length of a vector is equal to the sum of the squares of the lengths of its orthogonal components. Parseval's theorem of Eq. (3.20) is the statement of this fact as it applies to signals.

Generalization to Complex Signals

The foregoing results can be generalized to complex signals as follows: a set of functions $x_1(t)$, $x_2(t), \ldots, x_N(t)$ is mutually orthogonal over the interval (t_1, t_2) if

$$\int_{t_1}^{t_2} x_m(t)x_n^*(t)\,dt = \begin{cases} 0 & m \neq n \\ E_n & m = n \end{cases}$$

If this set is complete for a certain class of functions, then a function $x(t)$ in this class can be expressed as

$$x(t) = c_1x_1(t) + c_2x_2(t) + \cdots + c_ix_i(t) + \cdots \tag{3.21}$$

where

$$c_n = \frac{1}{E_n}\int_{t_1}^{t_2} x(t)x_n^*(t)\,dt \tag{3.22}$$

EXAMPLE 3.3 Approximating a Square Wave with a Set of Harmonic Sine Waves

In Ex. 3.1, the square signal $x(t)$ in Fig. 3.3 is approximated by a single sinusoid $\sin t$. In this example, we approximate $x(t)$ using the set of harmonic sine waves $\sin t$, $\sin 2t, \ldots, \sin nt, \ldots$, and see how the approximation improves with the number of terms.

To begin, we note that the set of harmonic sine waves $\sin t$, $\sin 2t, \ldots, \sin nt, \ldots$ is orthogonal over any interval of duration 2π.[†] The reader can verify this fact by showing that for any real number a,

$$\int_a^{a+2\pi} \sin mt \sin nt\,dt = \begin{cases} 0 & m \neq n \\ \pi & m = n \end{cases} \tag{3.23}$$

Using this set, we approximate $x(t)$ as

$$x(t) \simeq c_1 \sin t + c_2 \sin 2t + \cdots + c_n \sin Nt$$

where

$$c_n = \frac{\displaystyle\int_0^{2\pi} x(t)\sin nt\,dt}{\displaystyle\int_0^{2\pi} \sin^2 nt\,dt} = \frac{1}{\pi}\left[\int_0^{\pi} \sin nt\,dt + \int_{\pi}^{2\pi} -\sin nt\,dt\right]$$

[†] This sine set, along with the cosine set $\cos 0t, \cos t, \cos 2t, \ldots, \cos nt, \ldots$, forms a complete set. In this case, however, the coefficients c_i corresponding to the cosine terms are zero. For this reason, we have omitted cosine terms in this example. This composite sine and cosine set is the basis set for the trigonometric Fourier series, which is developed in Sec. 3.4.

$$= \begin{cases} \dfrac{4}{\pi n} & n \text{ odd} \\ 0 & n \text{ even} \end{cases}$$

Therefore,

$$x(t) \simeq \frac{4}{\pi}\left(\sin t + \frac{1}{3}\sin 3t + \frac{1}{5}\sin 5t + \cdots + \frac{1}{N}\sin Nt\right) \tag{3.24}$$

Note that coefficients of terms $\sin kt$ are zero for even values of k. Figure 3.7 shows how the approximation improves as we increase the number of terms in the series.

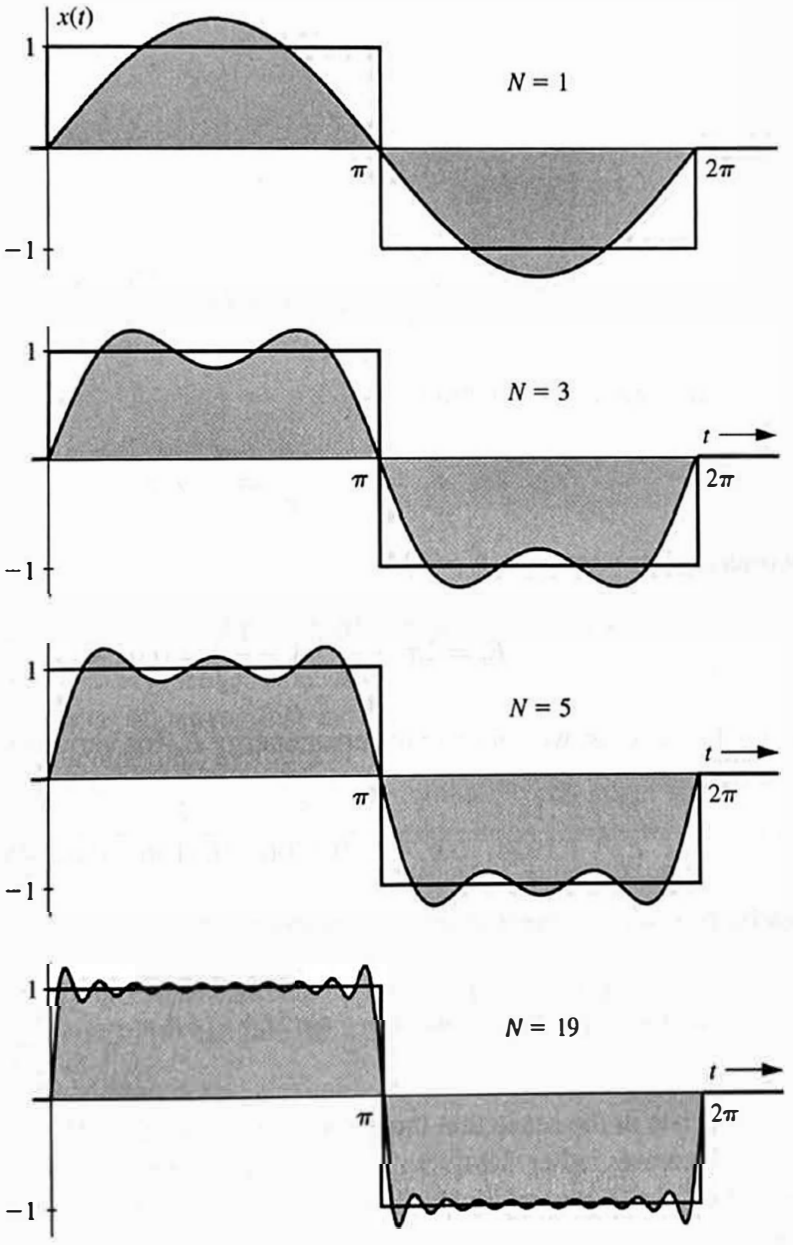

Figure 3.7 Approximation of a square wave by a sum of harmonic sinusoids.

Let us investigate the error signal energy as $N \to \infty$. From Eq. (3.18),

$$E_e = \int_0^{2\pi} x^2(t)\,dt - \sum_{n=1}^{\infty} c_n^2 E_n$$

Note that

$$\int_0^{2\pi} x^2(t)\,dt = \int_0^{\pi} 1^2\,dt + \int_{\pi}^{2\pi} -1^2\,dt = 2\pi$$

$$c_n^2 = \begin{cases} \dfrac{16}{n^2\pi^2} & n \text{ odd} \\ 0 & n \text{ even} \end{cases}$$

and from Eq. (3.23),

$$E_n = \pi$$

Therefore,

$$E_e = 2\pi - \sum_{n=1,3,5,\ldots}^{N} \frac{16}{n^2\pi^2}\pi = 2\pi - \frac{16}{\pi} \sum_{n=1,3,5,\ldots}^{N} \frac{1}{n^2}$$

For a single-term approximation ($N = 1$),

$$E_e = 2\pi - \frac{16}{\pi} = 1.1938$$

For a two-term approximation ($N = 3$),

$$E_e = 2\pi - \frac{16}{\pi}\left(1 + \frac{1}{9}\right) = 0.6243$$

Continuing this process, we compute the error energy E_e for various values of N as

N	1	3	5	7	99	∞
E_e	1.1938	0.6243	0.4206	0.3166	0.02545	0

Clearly, $x(t)$ can be represented by the infinite series

$$x(t) = \frac{4}{\pi}\left(\sin t + \frac{1}{3}\sin 3t + \frac{1}{5}\sin 5t + \cdots\right) = \frac{4}{\pi} \sum_{n=1,3,5,\ldots}^{\infty} \frac{1}{n}\sin nt$$

The equality exists in the sense that the error signal energy $\to 0$ as $N \to \infty$. In this case, the error energy decreases rather slowly with N, indicating that the series converges slowly. As we shall see in Sec. 3.5.2, this relatively slow convergence is a consequence of $x(t)$ having jump discontinuities.

DRILL 3.5 Approximating a Ramp Signal with a Set of Harmonic Sine Waves

Approximate the signal $x(t) = t - \pi$ (Fig. 3.8) over the interval $(0, 2\pi)$ in terms of the set of sinusoids $\{\sin nt\}$, $n = 0, 1, 2, \ldots$, used in Ex. 3.3. Find E_e, the error energy. Show that $E_e \to 0$ as $N \to \infty$.

ANSWERS

$x(t) \simeq -2\sum_{n=1}^{N} \frac{1}{N} \sin nt$ and $E_e = \frac{2}{3}\pi^3 - \sum_{n=1}^{N} \frac{4\pi}{n^2}$

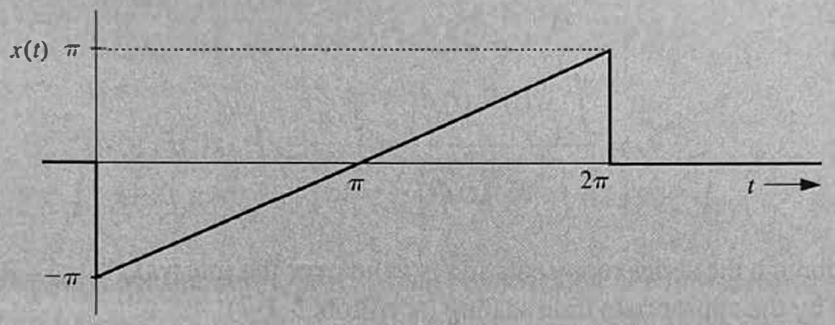

Figure 3.8 Ramp signal for Drill 3.5.

Some Examples of Generalized Fourier Series

Signals are vectors in every sense. Like a vector, a signal can be represented as a sum of its components in a variety of ways. Just as vector coordinate systems are formed by mutually orthogonal vectors (rectangular, cylindrical, spherical), we also have signal coordinate systems (basis signals) formed by a variety of sets of mutually orthogonal signals. There exist a large number of orthogonal signal sets that can be used as basis signals for generalized Fourier series. Some well-known signal sets are trigonometric (sinusoid) functions, exponential functions, Walsh functions, Bessel functions, Legendre polynomials, Laguerre functions, Jacobi polynomials, Hermite polynomials, and Chebyshev polynomials. Although the functions that concern us most in this book are the trigonometric and the exponential sets discussed in the rest of this chapter, we now take a brief moment to investigate the example of the Legendre Fourier series.

Legendre Fourier Series

A set of Legendre polynomials $P_n(t)$ $(n = 0, 1, 2, 3, \ldots)$ forms a complete set of mutually orthogonal functions over an interval $(-1 < t < 1)$. These polynomials can be defined by the Rodrigues formula:

$$P_n(t) = \frac{1}{2^n n!} \frac{d^n}{dt^n}(t^2 - 1)^n \qquad n = 0, 1, 2, \ldots$$

It follows from this equation that

$$P_0(t) = 1, P_1(t) = t, P_2(t) = \left(\tfrac{3}{2}t^2 - \tfrac{1}{2}\right), P_3(t) = \left(\tfrac{5}{2}t^3 - \tfrac{3}{2}t\right), \text{ and so on}$$

We may verify the orthogonality of these polynomials by showing that

$$\int_{-1}^{1} P_m(t)P_n(t)\,dt = \begin{cases} 0 & m \neq n \\ \dfrac{2}{2m+1} & m = n \end{cases}$$

We can express a function $x(t)$ in terms of Legendre polynomials over an interval $(-1 < t < 1)$ as

$$x(t) = c_0P_0(t) + c_1P_1(t) + \cdots + c_rP_r(t) + \cdots \tag{3.25}$$

where

$$c_r = \frac{\int_{-1}^{1} x(t)P_r(t)\,dt}{\int_{-1}^{1} P_r{}^2(t)\,dt} = \frac{2r+1}{2}\int_{-1}^{1} x(t)P_r(t)\,dt \tag{3.26}$$

Note that although the series representation is valid over the interval $(-1, 1)$, it can be extended to any interval by the appropriate time scaling (see Prob. 3.1-7).

EXAMPLE 3.4 Legendre Fourier Series

Determine the Legendre Fourier series of the square signal shown in Fig. 3.9.

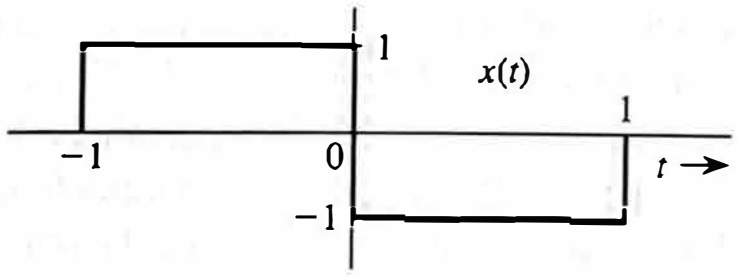

Figure 3.9 Square signal for Ex. 3.4.

From Eq. (3.25), we know that the Legendre Fourier series takes the form

$$x(t) = c_0P_0(t) + c_1P_1(t) + \cdots + c_rP_r(t) + \cdots$$

The coefficients $c_0, c_1, c_2, \ldots, c_r$ may be found from Eq. (3.26). We have

$$x(t) = \begin{cases} 1 & \cdots -1 < t < 0 \\ -1 & \cdots 0 < t < 1 \end{cases}$$

and

$$c_0 = \frac{1}{2}\int_{-1}^{1} x(t)\,dt = 0$$

$$c_1 = \frac{3}{2}\int_{-1}^{1} tx(t)\,dt = \frac{3}{2}\left(\int_{-1}^{0} t\,dt - \int_{0}^{1} t\,dt\right) = -\frac{3}{2}$$

$$c_2 = \frac{5}{2}\int_{-1}^{1} x(t)\left(\frac{3}{2}t^2 - \frac{1}{2}\right)dt = 0$$

This result follows immediately from the fact that the integrand is an odd function of t. In fact, this is true of all c_r for even values of r, that is,

$$c_0 = c_2 = c_4 = c_6 = \cdots = 0$$

Also,

$$c_3 = \frac{7}{2}\int_{-1}^{1} x(t)\left(\frac{5}{2}t^3 - \frac{3}{2}t\right)dt = \frac{7}{2}\left[\int_{-1}^{0}\left(\frac{5}{2}t^3 - \frac{3}{2}t\right)dt - \int_{0}^{1}\left(\frac{5}{2}t^3 - \frac{3}{2}t\right)dt\right] = \frac{7}{8}$$

In a similar way, coefficients $c_5, c_7, \ldots$ can be evaluated. We now have

$$x(t) = -\tfrac{3}{2}t + \tfrac{7}{8}\left(\tfrac{5}{2}t^3 - \tfrac{3}{2}t\right) + \cdots$$

A Historical Note: Baron Jean-Baptiste-Joseph Fourier (1768–1830)

The Fourier series and integral comprise a most beautiful and fruitful development, which serves as an indispensable instrument in the treatment of many problems in mathematics, science, and engineering. Maxwell was so taken by the beauty of the Fourier series that he called it a great mathematical poem. In electrical engineering, it is central to the areas of communication, signal processing, and several other fields, including antennas, but its initial reception by the scientific world was not enthusiastic. In fact, Fourier could not get his results published as a paper.

Fourier, a tailor's son, was orphaned at age 8 and educated at a local military college (run by Benedictine monks), where he excelled in mathematics. The Benedictines prevailed upon the young genius to choose the priesthood as his vocation, but revolution broke out before he could take his vows. Fourier joined the people's party. But in its early days, the French Revolution, like most such upheavals, liquidated a large segment of the intelligentsia, including prominent scientists such as Lavoisier. Observing this trend, many intellectuals decided to leave France to save themselves from a rapidly rising tide of barbarism. Fourier, despite his early enthusiasm for the Revolution, narrowly escaped the guillotine twice. It was to the everlasting credit of Napoleon that he stopped the persecution of the intelligentsia and founded new schools to replenish their ranks. The 26-year-old Fourier was appointed chair of mathematics at the newly created École Normale in 1794 [2].

Napoleon was the first modern ruler with a scientific education, and he was one of the rare persons who are equally comfortable with soldiers and scientists. The age of Napoleon was one of the most fruitful in the history of science. Napoleon liked to sign himself as "member of Institut

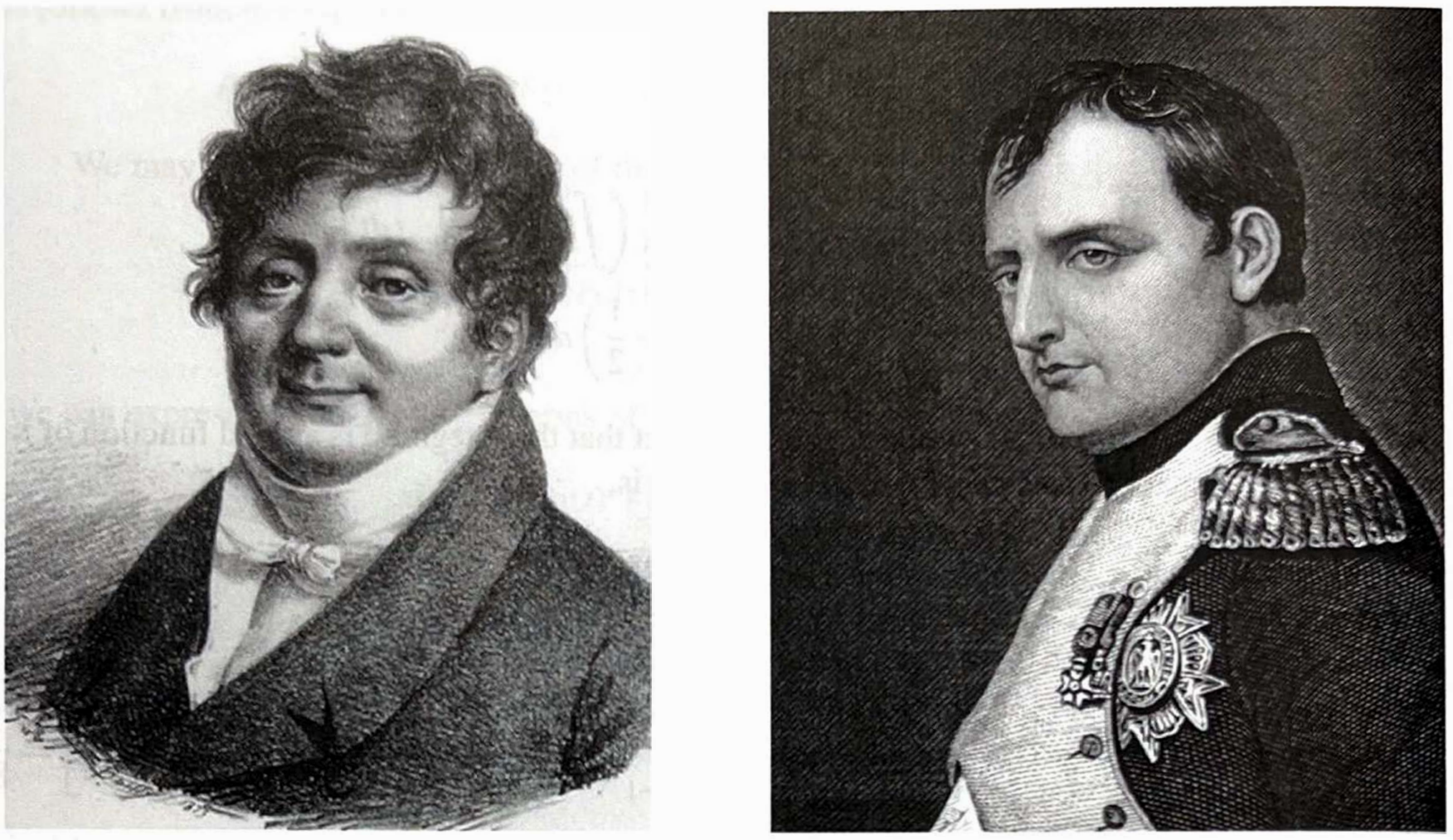

Jean-Baptiste-Joseph Fourier and Napoleon

de France" (a fraternity of scientists), and he once expressed to Laplace his regret that "force of circumstances has led me so far from the career of a scientist" [3]. Many great figures in science and mathematics, including Fourier and Laplace, were honored and promoted by Napoleon. In 1798, he took a group of scientists, artists, and scholars—Fourier among them—on his Egyptian expedition, with the promise of an exciting and historic union of adventure and research. Fourier proved to be a capable administrator of the newly formed Institut d'Égypte, which, incidentally, was responsible for the discovery of the Rosetta Stone. The inscription on this stone in two languages and three scripts (hieroglyphic, demotic, and Greek) enabled Thomas Young and Jean-François Champollion, a protégé of Fourier, to invent a method of translating hieroglyphic writings of ancient Egypt—the only significant result of Napoleon's Egyptian expedition.

Back in France in 1801, Fourier briefly served in his former position as professor of mathematics at the École Polytechnique in Paris. In 1802, Napoleon appointed him the prefect of Isère (with its headquarters in Grenoble), a position in which Fourier served with distinction. Fourier was named Baron of the Empire by Napoleon in 1809. Later, when Napoleon was exiled to Elba, his route was to take him through Grenoble. Fourier had the route changed to avoid meeting Napoleon, which would have displeased Fourier's new master, King Louis XVIII. Within a year, Napoleon escaped from Elba and returned to France. At Grenoble, Fourier was brought before him in chains. Napoleon scolded Fourier for his ungrateful behavior but reappointed him the prefect of Rhône at Lyons. Within four months Napoleon was defeated at Waterloo and was exiled to St. Helena, where he died in 1821. Fourier once again was in disgrace as a Bonapartist and had to pawn his possessions to keep himself alive. But through the intercession of a former student, who was now a prefect of Paris, he was appointed director of the statistical bureau of the Seine, a position that allowed him ample time for scholarly pursuits. Later, in 1827, he was elected to the powerful position of perpetual secretary of the Paris Academy of Science, a section of the Institut de France [4].

While serving as the prefect of Grenoble, Fourier carried on his elaborate investigation of the propagation of heat in solid bodies, which led him to the Fourier series and the Fourier integral. On December 21, 1807, he announced these results in a prize paper on the theory of heat. Fourier claimed that an arbitrary function (continuous or with discontinuities) defined in a finite interval by an arbitrarily capricious graph can always be expressed as a sum of sinusoids (Fourier series). The judges, who included the great French mathematicians Laplace, Lagrange, Legendre, Monge, and LaCroix, admitted the novelty and importance of Fourier's work but criticized it for lack of mathematical rigor and generality. Lagrange thought it incredible that a sum of sines and cosines could add up to anything but an infinitely differentiable function. Moreover, one of the properties of an infinitely differentiable function is that if we know its behavior over an arbitrarily small interval, we can determine its behavior over the entire range (the Taylor–Maclaurin series). Such a function is far from an arbitrary or a capriciously drawn graph [5]. Laplace had additional reason to criticize Fourier's work. Laplace and his students had already approached the problem of heat conduction from a different angle, and Laplace was reluctant to accept the superiority of Fourier's method [6]. Fourier thought the criticism unjustified but was unable to prove his claim because the tools required for operations with infinite series were not available at the time. However, posterity has proved Fourier to be closer to the truth than his critics. This is the classic conflict between pure mathematicians and physicists or engineers, as we shall see again in the life of Oliver Heaviside (p. 530). In 1829, Dirichlet proved Fourier's claim concerning capriciously drawn functions with a few restrictions (the so-called Dirichlet conditions).

Although three of the four judges were in favor of publication, Fourier's paper was rejected because of vehement opposition by Lagrange. Fifteen years later, after several attempts and disappointments, Fourier published the results in expanded form as a text, *Théorie analytique de la chaleur,* which is now a classic.

3.4 Trigonometric Fourier Series

We now turn our attention to the trigonometric Fourier series, which represents a signal using a set of sinusoids:

$$\{1, \cos\omega_0 t, \cos 2\omega_0 t, \ldots, \cos n\omega_0 t, \ldots; \\ \sin\omega_0 t, \sin 2\omega_0 t, \ldots, \sin n\omega_0 t, \ldots\} \tag{3.27}$$

A sinusoid of frequency $n\omega_0$ is called the nth *harmonic* of the sinusoid of frequency ω_0 when n is an integer. In this set, the sinusoid of frequency ω_0, called the *fundamental*, serves as an anchor of which all the remaining terms are harmonics. Note that the constant term 1 is the 0th harmonic in this set because $\cos(0 \times \omega_0 t) = 1$. We next show that it is an orthogonal set over any interval of duration $T_0 = 2\pi/\omega_0$.

Consider an integral I defined by

$$I = \int_{T_0} \cos n\omega_0 t \cos m\omega_0 t \, dt$$

where $\int_{T_0}$ stands for integration over any contiguous interval of T_0 seconds. By using a trigonometric identity (see Sec. B.8.6), this integral can be expressed as

$$I = \frac{1}{2}\left[\int_{T_0} \cos(n+m)\omega_0 t\, dt + \int_{T_0} \cos(n-m)\omega_0 t\, dt\right] \tag{3.28}$$

Because $\cos \omega_0 t$ executes one complete cycle during any interval of duration T_0, $\cos(n+m)\omega_0 t$ executes $(n+m)$ complete cycles during any interval of duration T_0. Therefore, the first integral in Eq. (3.28), which represents the area under $n+m$ complete cycles of a sinusoid, equals zero. The same argument shows that the second integral in Eq. (3.28) is also zero, except when $n = m$. Hence, I in Eq. (3.28) is zero for all $n \neq m$. When $n = m$, the first integral in Eq. (3.28) is still zero, but the second integral yields

$$I = \frac{1}{2}\int_{T_0} dt = \frac{T_0}{2}$$

Thus,

$$\int_{T_0} \cos n\omega_0 t \cos m\omega_0 t\, dt = \begin{cases} 0 & n \neq m \\ \dfrac{T_0}{2} & m = n \neq 0 \end{cases} \tag{3.29}$$

Using similar arguments, we can show that

$$\int_{T_0} \sin n\omega_0 t \sin m\omega_0 t\, dt = \begin{cases} 0 & n \neq m \\ \dfrac{T_0}{2} & n = m \neq 0 \end{cases} \tag{3.30}$$

and

$$\int_{T_0} \sin n\omega_0 t \cos m\omega_0 t\, dt = 0 \qquad \text{for all } n \text{ and } m \tag{3.31}$$

These equations show that the set of sinusoids in Eq. (3.27) is orthogonal over any contiguous interval of duration T_0. This is the *trigonometric set*, which can be shown to be a complete set [7, 8]. Following Eq. (3.19), we can therefore express a signal $x(t)$ by a trigonometric Fourier series over any interval of duration T_0 seconds as

$$\begin{aligned} x(t) = a_0 &+ a_1 \cos \omega_0 t + a_2 \cos 2\omega_0 t + \cdots \\ &+ b_1 \sin \omega_0 t + b_2 \sin 2\omega_0 t + \cdots \end{aligned}$$

or

$$x(t) = a_0 + \sum_{n=1}^{\infty} a_n \cos n\omega_0 t + b_n \sin n\omega_0 t \qquad t_1 < t < t_1 + T_0$$

where

$$\omega_0 = 2\pi f_0 = \frac{2\pi}{T_0}$$

We can use Eq. (3.17) to determine the Fourier coefficients a_0, a_n, and b_n. Thus,

$$a_n = \frac{\int_{t_1}^{t_1+T_0} x(t)\cos n\omega_0 t\,dt}{\int_{t_1}^{t_1+T_0} \cos^2 n\omega_0 t\,dt} \tag{3.32}$$

The integral in the denominator of Eq. (3.32) has already been found to be $T_0/2$ when $n \neq 0$ [Eq. (3.29) with $m = n$]. For $n = 0$, the denominator is T_0. Hence,

$$a_0 = \frac{1}{T_0}\int_{t_1}^{t_1+T_0} x(t)\,dt \quad \text{and} \quad a_n = \frac{2}{T_0}\int_{t_1}^{t_1+T_0} x(t)\cos n\omega_0 t\,dt \qquad n = 1,2,3,\ldots$$

Similarly, we find that

$$b_n = \frac{2}{T_0}\int_{t_1}^{t_1+T_0} x(t)\sin n\omega_0 t\,dt \qquad n = 1,2,3,\ldots$$

To sum up our discussion, the trigonometric Fourier series represents a signal $x(t)$ over an interval of duration T_0 as a sum of a sinusoid of period T_0 and its harmonics as

$$x(t) = a_0 + \sum_{n=1}^{\infty} a_n \cos n\omega_0 t + b_n \sin n\omega_0 t \qquad t_1 < t < t_1 + T_0 \tag{3.33}$$

where $\omega_0 = 2\pi f_0 = \frac{2\pi}{T_0}$ and

$$a_0 = \frac{1}{T_0}\int_{t_1}^{t_1+T_0} x(t)\,dt, \quad a_n = \frac{2}{T_0}\int_{t_1}^{t_1+T_0} x(t)\cos n\omega_0 t\,dt, \quad \text{and} \quad b_n = \frac{2}{T_0}\int_{t_1}^{t_1+T_0} x(t)\sin n\omega_0 t\,dt \tag{3.34}$$

Note that the series in Eq. (3.24) of Ex. 3.3 is indeed the trigonometric Fourier series with $T_0 = 2\pi$ and $\omega_0 = 2\pi/T_0$. In this particular example, it is easy to verify from Eq. (3.32) that $a_n = 0$ for all n, including $n = 0$. Hence, the Fourier series in that example consisted only of sine terms.

Compact Trigonometric Fourier Series

The results derived so far are general and apply whether $x(t)$ is a real or a complex function of t. However, when $x(t)$ is real, coefficients a_n and b_n are real for all n, and the trigonometric Fourier series can be expressed in a *compact form*, using the results in Eq. (B.16):

$$x(t) = C_0 + \sum_{n=1}^{\infty} C_n \cos(n\omega_0 t + \theta_n) \tag{3.35}$$

where C_n and θ_n are related to a_n and b_n, as [see Eq. (B.17)]

$$C_0 = a_0, \quad C_n = \sqrt{a_n{}^2 + b_n{}^2}, \quad \text{and} \quad \theta_n = \tan^{-1}\left(\frac{-b_n}{a_n}\right) \tag{3.36}$$

The compact form in Eq. (3.35) uses the cosine form. We could just as well have used the sine form, with terms $\sin(n\omega_0 t + \theta_n)$ instead of $\cos(n\omega_0 t + \theta_n)$. The literature overwhelmingly favors the cosine form, for no apparent reason except possibly that the cosine phasor is represented by the horizontal axis, which happens to be the reference axis in phasor representation.

Equation (3.34) shows that a_0 (and thus C_0) is the average value of $x(t)$ (averaged over T_0). This value can often be determined by inspection of $x(t)$. Because a_n and b_n are assumed real in this discussion, C_n and θ_n are also real. In the following discussion of trigonometric Fourier series, we shall assume real $x(t)$, unless mentioned otherwise.

The Fourier Spectrum

The compact trigonometric Fourier series in Eq. (3.35) indicates that a periodic signal $x(t)$ can be expressed as a sum of sinusoids of frequencies 0 (dc), ω_0, $2\omega_0$, . . ., $n\omega_0$, . . ., whose amplitudes are C_0, C_1, C_2, . . ., C_n, . . ., and whose phases are 0, θ_1, θ_2, . . ., θ_n, . . ., respectively. We can readily plot amplitude C_n versus n (*the amplitude spectrum*) and θ_n versus n (the *phase spectrum*).† Because n is proportional to the frequency $n\omega_0$, these plots are scaled plots of C_n versus ω and θ_n versus ω. The two plots together are the *frequency spectra* of $x(t)$. These spectra show at a glance the frequency contents of the signal $x(t)$ with their amplitudes and phases. Knowing these spectra, we can reconstruct or synthesize the signal $x(t)$ according to Eq. (3.35). Therefore, frequency spectra, which are an alternative way of describing a periodic signal $x(t)$, are in every way equivalent to the plot of $x(t)$ as a function of t. The frequency spectra of a signal constitute the *frequency-domain description* of $x(t)$, in contrast to the *time-domain description,* where $x(t)$ is specified as a function of time. *A signal, therefore, has a dual identity: the time-domain identity $x(t)$ and the frequency-domain identity (Fourier spectra). The two identities complement each other; taken together, they provide a better understanding of a signal.*

In computing θ_n, the phase of the nth harmonic from Eq. (3.36), the quadrant in which θ_n lies should be determined from the signs of a_n and b_n. For example, if $a_n = -1$ and $b_n = 1$, θ_n lies in the third quadrant, and

$$\theta_n = \tan^{-1}\left(\frac{-1}{-1}\right) = -135^\circ$$

Observe that

$$\tan^{-1}\left(\frac{-1}{-1}\right) \neq \tan^{-1}(1) = 45^\circ$$

Although C_n, the amplitude of the nth harmonic as defined in Eq. (3.36), is positive, we shall find it convenient to allow C_n to take on negative values when $b_n = 0$. This will become clear in later examples.

---

† The amplitude C_n, by definition here, is nonnegative. Some authors define amplitude A_n that can take positive or negative values and magnitude $C_n = |A_n|$ that can only be nonnegative. Thus, what we call amplitude spectrum becomes magnitude spectrum. The distinction between amplitude and magnitude, although useful, is avoided in this book in the interest of keeping definitions of essentially similar entities to a minimum.

EXAMPLE 3.5 Compact Trigonometric Fourier Series of a Decaying Exponential

Find the compact trigonometric Fourier series for the exponential $e^{-t/2}$ depicted in Fig. 3.10a over the shaded interval $0 \le t \le \pi$.

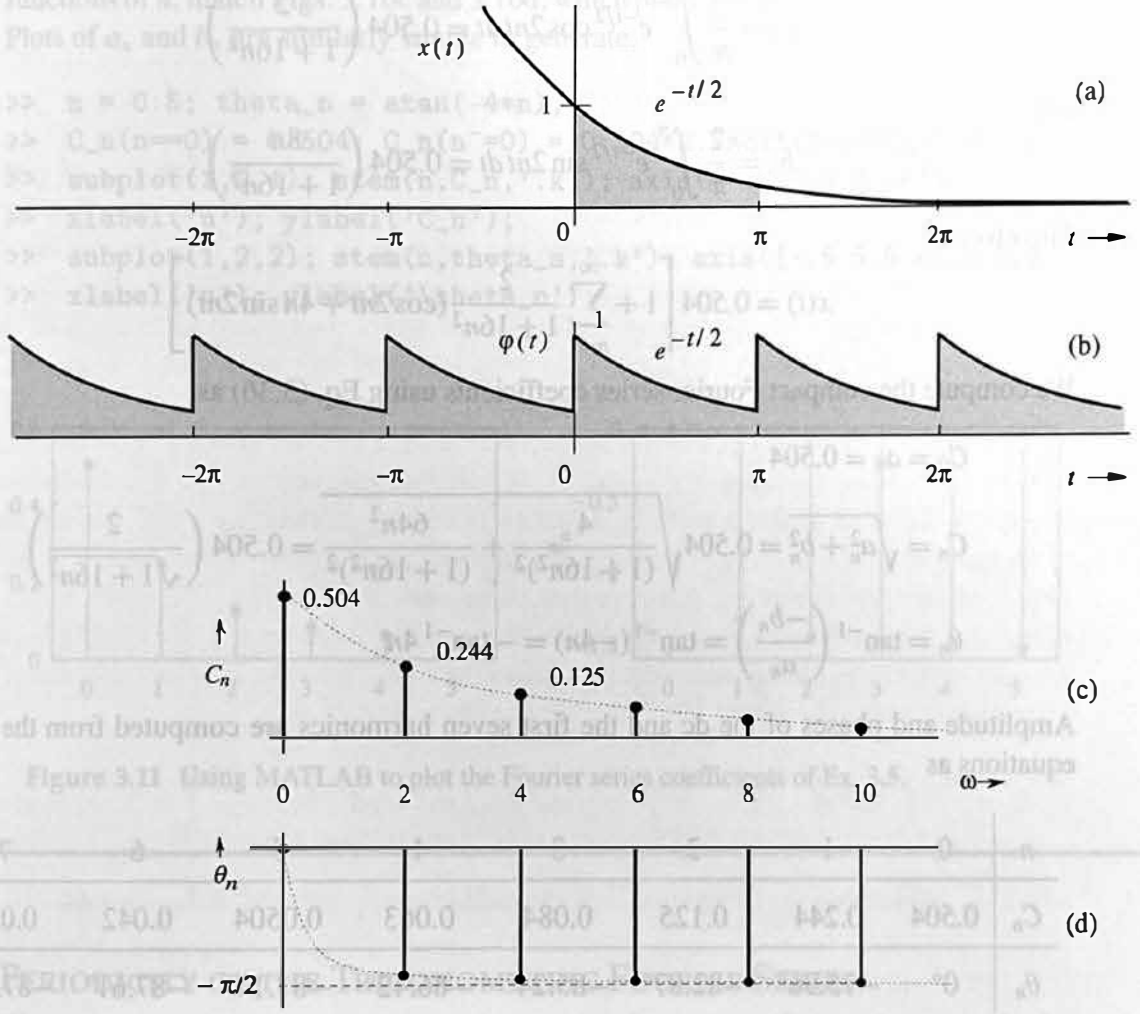

Figure 3.10 An exponential signal and its Fourier spectra.

Because we are required to represent $x(t)$ by the trigonometric Fourier series over the interval $0 \le t \le \pi$ only, $T_0 = \pi$, and the fundamental frequency is

$$\omega_0 = \frac{2\pi}{T_0} = 2 \text{ rad/s}$$

Therefore,

$$x(t) = a_0 + \sum_{n=1}^{\infty} a_n \cos 2nt + b_n \sin 2nt$$

where [from Eq. (3.34)]

$$a_0 = \frac{1}{\pi}\int_0^{\pi} e^{-t/2}\,dt = 0.504$$

$$a_n = \frac{2}{\pi}\int_0^{\pi} e^{-t/2}\cos 2nt\,dt = 0.504\left(\frac{2}{1+16n^2}\right)$$

and

$$b_n = \frac{2}{\pi}\int_0^{\pi} e^{-t/2}\sin 2nt\,dt = 0.504\left(\frac{8n}{1+16n^2}\right)$$

Therefore,

$$x(t) = 0.504\left[1 + \sum_{n=1}^{\infty} \frac{2}{1+16n^2}(\cos 2nt + 4n \sin 2nt)\right]$$

We compute the compact Fourier series coefficients using Eq. (3.36) as

$$C_0 = a_0 = 0.504$$

$$C_n = \sqrt{a_n^2 + b_n^2} = 0.504\sqrt{\frac{4}{(1+16n^2)^2} + \frac{64n^2}{(1+16n^2)^2}} = 0.504\left(\frac{2}{\sqrt{1+16n^2}}\right)$$

$$\theta_n = \tan^{-1}\left(\frac{-b_n}{a_n}\right) = \tan^{-1}(-4n) = -\tan^{-1} 4n$$

Amplitude and phases of the dc and the first seven harmonics are computed from the above equations as

n	0	1	2	3	4	5	6	7
C_n	0.504	0.244	0.125	0.084	0.063	0.0504	0.042	0.036
θ_n	0°	−75.96°	−82.87°	−85.24°	−86.42°	−87.14°	−87.61°	−87.95°

Plots of C_n and θ_n (the amplitude and phase spectra) are shown in Figs. 3.10c and 3.10d, respectively. These spectra provide a snapshot of the frequency composition of $x(t)$. In this case, we see that $x(t)$ is dominated by low-frequency content.

We can use C_n and θ_n to express $x(t)$ as a compact trigonometric Fourier series as

$$\begin{aligned} x(t) &= 0.504 + 0.504\sum_{n=1}^{\infty} \frac{2}{\sqrt{1+16n^2}}\cos(2nt - \tan^{-1} 4n) \\ &= 0.504 + 0.244\cos(2t - 75.96°) + 0.125\cos(4t - 82.87°) \\ &\quad + 0.084\cos(6t - 85.24°) + 0.063\cos(8t - 86.42°) + \cdots \end{aligned} \tag{3.37}$$

Remember that the right-hand side represents $e^{-t/2}$ over the interval 0 to $\pi/2$ only. Outside this interval, the two sides need not be equal.

Plotting Fourier Series Spectra Using MATLAB

MATLAB is well suited to compute and plot Fourier series spectra. Since the spectra are functions of a discrete rather than continuous variable, we use the `stem` command rather than the `plot` command to generate the graphs. The results in Fig. 3.11, which plot C_n and θ_n as functions of n, match Figs. 3.10c and 3.10d, which plot C_n and θ_n as functions of $\omega = n\omega_0 = 2n$. Plots of a_n and b_n are similarly simple to generate.

```
>> n = 0:5; theta_n = atan(-4*n);
>> C_n(n==0) = 0.504; C_n(n~=0) = 0.504*2./sqrt(1+16*n(n~=0).^2);
>> subplot(1,2,1); stem(n,C_n,'.k'); axis([-.5 5.5 0 .6])
>> xlabel('n'); ylabel('C_n');
>> subplot(1,2,2); stem(n,theta_n,'.k'); axis([-.5 5.5 -1.6 0])
>> xlabel('n'); ylabel('\theta_n');
```

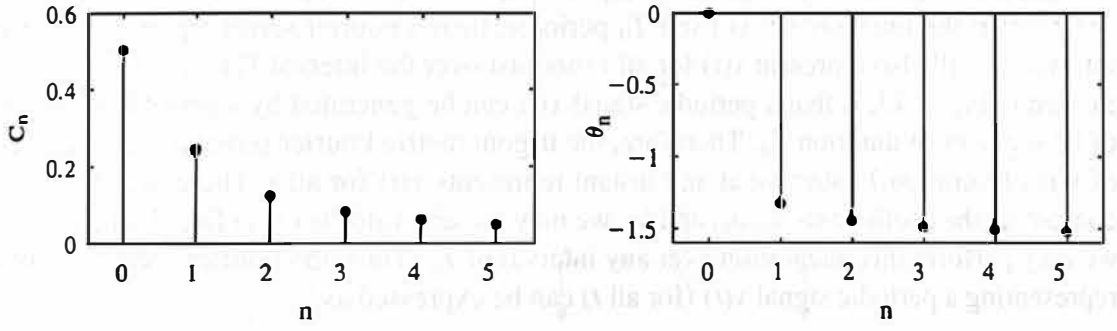

Figure 3.11 Using MATLAB to plot the Fourier series coefficients of Ex. 3.5.

Periodicity of the Trigonometric Fourier Series

We have shown how an arbitrary signal $x(t)$ may be expressed as a trigonometric Fourier series over any interval of T_0 seconds. In Ex. 3.5, for instance, we represented $e^{-t/2}$ over the interval from 0 to $\pi/2$ only. The Fourier series found in Eq. (3.37) is equal to $e^{-t/2}$ over this interval alone. Outside this interval, the series is not necessarily equal to $e^{-t/2}$. It would be interesting to find out what happens to the Fourier series outside this interval. We now show that the trigonometric Fourier series is a periodic function of period T_0 (the period of the fundamental). Let us denote the trigonometric Fourier series on the right-hand side of Eq. (3.35) by $\varphi(t)$. Therefore,

$$\varphi(t) = C_0 + \sum_{n=1}^{\infty} C_n \cos(n\omega_0 t + \theta_n) \qquad \text{for all } t$$

and

$$\begin{aligned}\varphi(t+T_0) &= C_0 + \sum_{n=1}^{\infty} C_n \cos[n\omega_0(t+T_0)+\theta_n] \\ &= C_0 + \sum_{n=1}^{\infty} C_n[\cos(n\omega_0 t + 2n\pi)+\theta_n] \\ &= C_0 + \sum_{n=1}^{\infty} C_n \cos(n\omega_0 t + \theta_n) \\ &= \varphi(t) \qquad \text{for all } t\end{aligned}$$

This result shows that the trigonometric Fourier series is a periodic function of period T_0 (the period of its fundamental). For instance, $\varphi(t)$, the Fourier series on the right-hand side of Eq. (3.37), is a periodic function in which the segment of $x(t)$ in Fig. 3.10a over the interval $(0 \le t \le \pi)$ repeats periodically every π seconds, as illustrated in Fig. 3.10b.[†] Thus, when we represent a signal $x(t)$ by the trigonometric Fourier series over a certain interval of duration T_0, the function $x(t)$ and its Fourier series $\varphi(t)$ need be equal only over that interval of T_0 seconds. Outside this interval, the Fourier series repeats periodically with period T_0.

Now, if the function $x(t)$ is itself T_0-periodic, then a Fourier series representing $x(t)$ over an interval T_0 will also represent $x(t)$ for all t (not just over the interval T_0). Another interesting fact, as seen in Fig. 1.13, is that a periodic signal $x(t)$ can be generated by a periodic repetition of any of its segment of duration T_0. Therefore, the trigonometric Fourier series representing a segment of $x(t)$ of duration T_0 starting at any instant represents $x(t)$ for all t. Therefore, it follows that in computing the coefficients a_0, a_n, and b_n, we may use any value for t_1 in Eq. (3.34). In other words, we may perform this integration over any interval of T_0. Thus, the Fourier coefficients of a series representing a periodic signal $x(t)$ (for all t) can be expressed as

$$a_0 = \frac{1}{T_0}\int_{T_0} x(t)\,dt, \quad a_n = \frac{2}{T_0}\int_{T_0} x(t)\cos n\omega_0 t\,dt, \quad \text{and} \quad b_n = \frac{2}{T_0}\int_{T_0} x(t)\sin n\omega_0 t\,dt \tag{3.38}$$

where $\int_{T_0}$ means that the integration is performed over any interval of T_0 seconds.

Series Convergence at Jump Discontinuities

An interesting aspect of a Fourier series is that whenever there is a jump discontinuity in $x(t)$, the series at the point of discontinuity converges to an average of the left-hand and right-hand limits of $x(t)$ at the instant of discontinuity.[‡] In Fig. 3.10b, for instance, $\varphi(t)$ is discontinuous at $t=0$ with $\varphi(0^+)=1$ and $\varphi(0^-)=e^{-\pi/2}=0.208$. The corresponding Fourier series converges to a value $(1+0.208)/2=0.604$ at $t=0$. This conclusion is easily verified from Eq. (3.37) by setting $t=0$.

[†] In reality, the series convergence at the points of discontinuity shows about 9% overshoot (Gibbs phenomenon, [7]) as discussed later.

[‡] This behavior of the Fourier series is dictated by its error energy minimization property, discussed in Sec. 3.3.

EXAMPLE 3.6 Compact Trigonometric Fourier Series of a Periodic Triangle Wave

Find the compact trigonometric Fourier series for the triangular periodic signal $x(t)$ shown in Fig. 3.12a, and sketch the amplitude and phase spectra for $x(t)$.

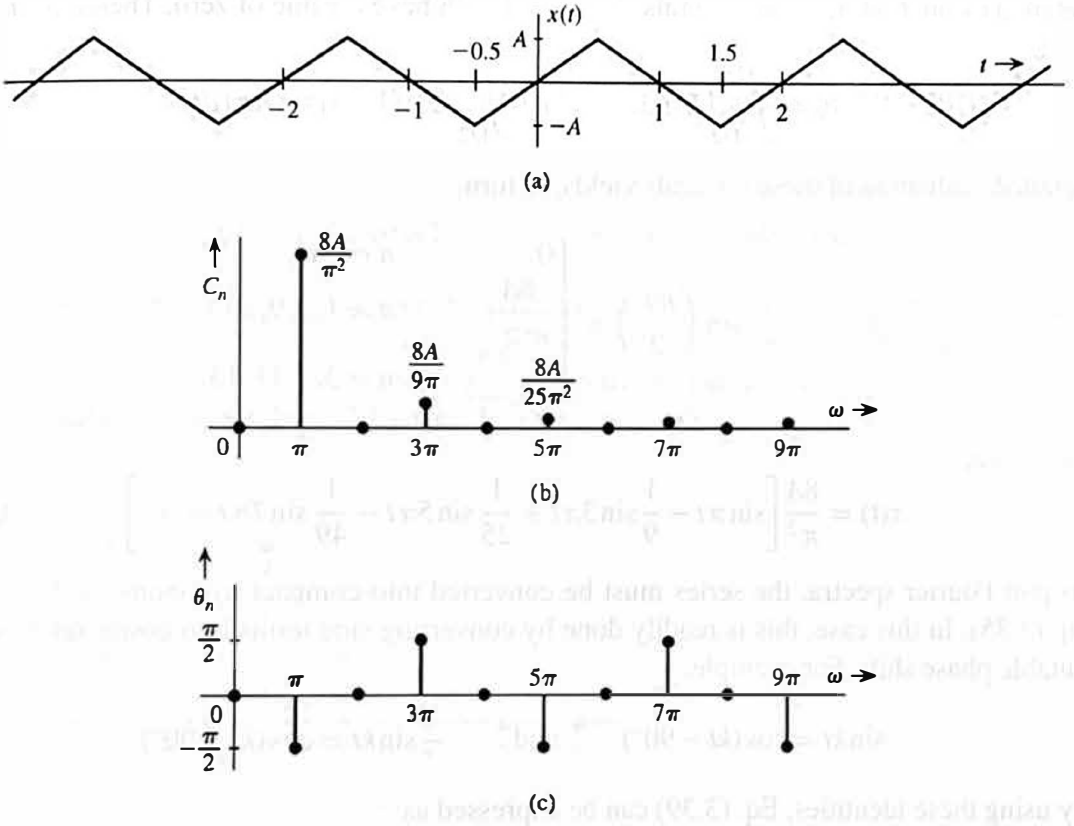

Figure 3.12 (**a**) A triangular periodic signal and (**b, c**) its Fourier spectra.

In this case, the period $T_0 = 2$. Hence,

$$\omega_0 = \frac{2\pi}{2} = \pi$$

and

$$x(t) = a_0 + \sum_{n=1}^{\infty} a_n \cos n\pi t + b_n \sin n\pi t$$

where

$$x(t) = \begin{cases} 2At & |t| < \frac{1}{2} \\ 2A(1-t) & \frac{1}{2} < t < \frac{3}{2} \end{cases}$$

Here, it will be advantageous to choose the interval of integration from $-1/2$ to $3/2$ rather than 0 to 2.

A glance at Fig. 3.12a shows that the average value (dc) of $x(t)$ is zero so that $a_0 = 0$. Also,

$$a_n = \frac{2}{2}\int_{-1/2}^{3/2} x(t)\cos n\pi t\,dt$$
$$= \int_{-1/2}^{1/2} 2At\cos n\pi t\,dt + \int_{1/2}^{3/2} 2A(1-t)\cos n\pi t\,dt$$

Detailed evaluation of these integrals shows that both have a value of zero. Therefore, $a_n = 0$. Next,

$$b_n = \int_{-1/2}^{1/2} 2At\sin n\pi t\,dt + \int_{1/2}^{3/2} 2A(1-t)\sin n\pi t\,dt$$

Detailed evaluation of these integrals yields, in turn,

$$b_n = \frac{8A}{n^2\pi^2}\sin\left(\frac{n\pi}{2}\right) = \begin{cases} 0 & n \text{ even} \\ \dfrac{8A}{n^2\pi^2} & n = 1,5,9,13,\ldots \\ -\dfrac{8A}{n^2\pi^2} & n = 3,7,11,15,\ldots \end{cases}$$

Therefore,

$$x(t) = \frac{8A}{\pi^2}\left[\sin\pi t - \frac{1}{9}\sin 3\pi t + \frac{1}{25}\sin 5\pi t - \frac{1}{49}\sin 7\pi t + \cdots\right] \tag{3.39}$$

To plot Fourier spectra, the series must be converted into compact trigonometric form as in Eq. (3.35). In this case, this is readily done by converting sine terms into cosine terms with a suitable phase shift. For example,

$$\sin kt = \cos(kt - 90°) \qquad \text{and} \qquad -\sin kt = \cos(kt + 90°)$$

By using these identities, Eq. (3.39) can be expressed as

$$x(t) = \frac{8A}{\pi^2}\left[\cos(\pi t - 90°) + \frac{1}{9}\cos(3\pi t + 90°) + \frac{1}{25}\cos(5\pi t - 90°) + \frac{1}{49}\cos(7\pi t + 90°) + \cdots\right]$$

In this series, all the even harmonics are missing. The phases of the odd harmonics alternate from $-90°$ to $90°$. Figures 3.12b and c shows the amplitude and phase spectra for $x(t)$.

EXAMPLE 3.7 Converting a Trigonometric FS to a Compact Trigonometric FS

A periodic signal $x(t)$ is represented by a trigonometric Fourier series

$$x(t) = 2 + 3\cos 2t + 4\sin 2t + 2\sin(3t + 30°) - \cos(7t + 150°)$$

Express this series as a compact trigonometric Fourier series and sketch amplitude and phase spectra for $x(t)$.

In compact trigonometric Fourier series, the sine and cosine terms of the same frequency are combined into a single term and all terms are expressed as cosine terms with positive amplitudes. Using Eqs. (3.35) and (3.36), we have

$$3\cos 2t + 4\sin 2t = 5\cos(2t - 53.13°)$$

Also,

$$\sin(3t + 30°) = \cos(3t + 30° - 90°) = \cos(3t - 60°)$$

and

$$-\cos(7t + 150°) = \cos(7t + 150° - 180°) = \cos(7t - 30°)$$

Therefore,

$$x(t) = 2 + 5\cos(2t - 53.13°) + 2\cos(3t - 60°) + \cos(7t - 30°)$$

In this case, only four components (including dc) are present. The amplitude of dc is 2. The remaining three components are of frequencies $\omega = 2$, 3, and 7 with amplitudes 5, 2, and 1 and phases $-53.13°$, $-60°$, and $-30°$, respectively. The amplitude and phase spectra for this signal are shown in Figs. 3.13a and 3.13b, respectively.

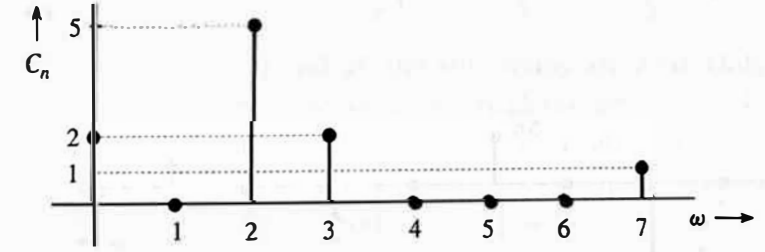

(a)

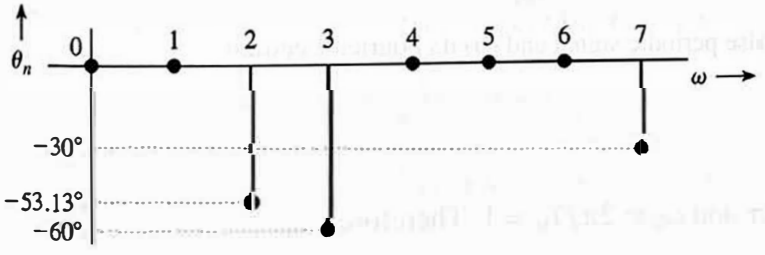

(b)

Figure 3.13 Fourier spectra of the signal.

EXAMPLE 3.8 Compact Trigonometric Fourier Series of a Periodic Square Wave

Find the compact trigonometric Fourier series for the square-pulse periodic signal shown in Fig. 3.14a and sketch its Fourier spectrum.

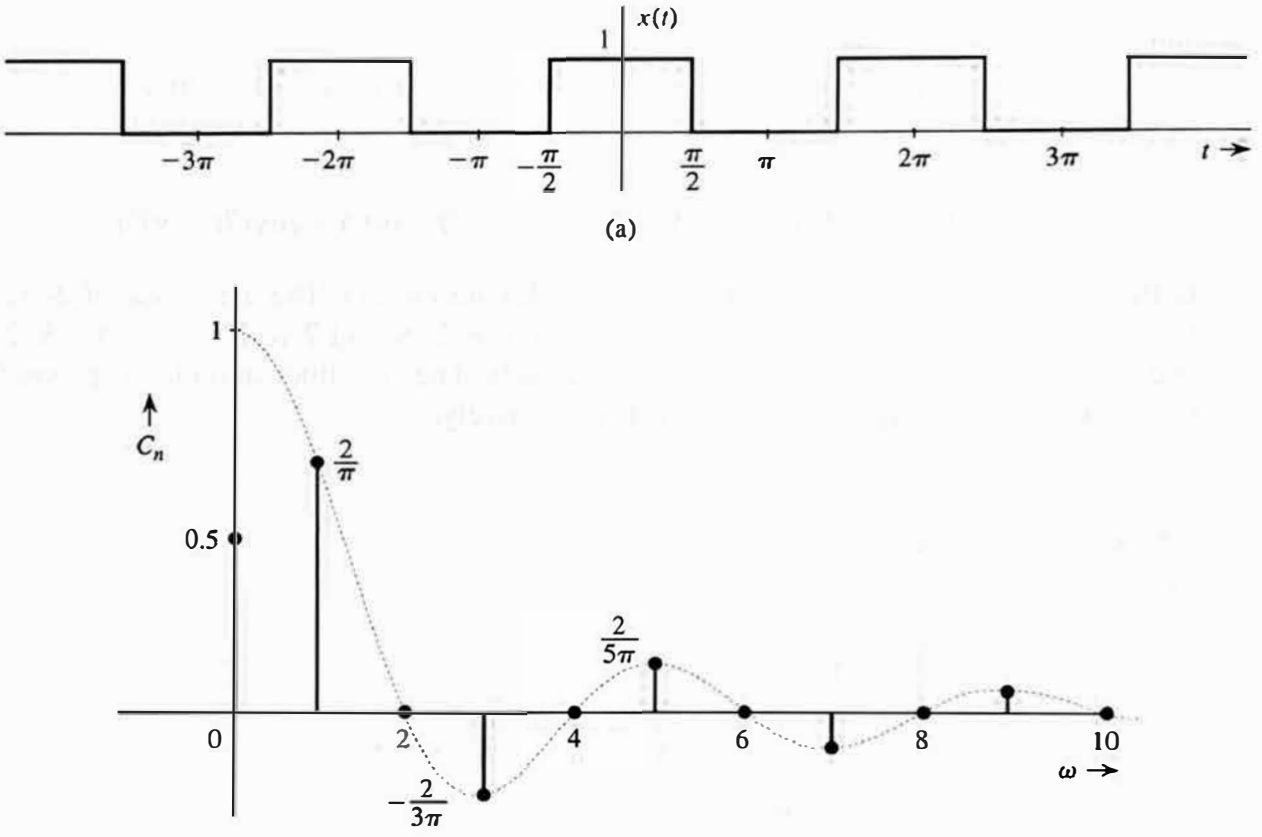

Figure 3.14 **(a)** A square pulse periodic signal and **(b)** its Fourier spectrum.

Here, the period is $T_0 = 2\pi$ and $\omega_0 = 2\pi/T_0 = 1$. Therefore,

$$x(t) = a_0 + \sum_{n=1}^{\infty} a_n \cos nt + b_n \sin nt$$

where

$$a_0 = \frac{1}{T_0} \int_{T_0} x(t)\, dt$$

From Fig. 3.14a, it is clear that a proper choice of region of integration is from $-\pi$ to π. But since $x(t) = 1$ only over $(-\pi/2, \pi/2)$, and $x(t) = 0$ over the remaining segment,

$$a_0 = \frac{1}{2\pi}\int_{-\pi/2}^{\pi/2} dt = \frac{1}{2}$$

We could have found a_0, the average value of $x(t)$, to be $1/2$ merely by inspection of $x(t)$ in Fig. 3.14a. Also,

$$a_n = \frac{1}{\pi}\int_{-\pi/2}^{\pi/2} \cos nt\, dt = \frac{2}{n\pi}\sin\left(\frac{n\pi}{2}\right)$$

$$= \begin{cases} 0 & n \text{ even} \\ \dfrac{2}{\pi n} & n = 1,5,9,13,\ldots \\ -\dfrac{2}{\pi n} & n = 3,7,11,15,\ldots \end{cases}$$

$$b_n = \frac{1}{\pi}\int_{-\pi/2}^{\pi/2} \sin nt\, dt = 0$$

Therefore,

$$x(t) = \frac{1}{2} + \frac{2}{\pi}\left(\cos t - \frac{1}{3}\cos 3t + \frac{1}{5}\cos 5t - \frac{1}{7}\cos 7t + \cdots\right) \tag{3.40}$$

Observe that $b_n = 0$ and all the sine terms are zero. Only the cosine terms appear in the trigonometric series. The series is therefore already in the compact form except that the amplitudes of alternating harmonics are negative. Now by definition, amplitudes C_n are positive [see Eq. (3.36)]. The negative sign can be accommodated by associating a proper phase, as seen from the trigonometric identity†

$$-\cos x = \cos(x - \pi)$$

Using this fact, we can express the series in Eq. (3.40) as

$$x(t) = \frac{1}{2} + \frac{2}{\pi}\left[\cos\omega_0 t + \frac{1}{3}\cos(3\omega_0 t - \pi) + \frac{1}{5}\cos 5\omega_0 t + \frac{1}{7}\cos(7\omega_0 t - \pi) + \frac{1}{9}\cos 9\omega_0 t + \cdots\right]$$

This is the desired form of the compact trigonometric Fourier series. The amplitudes are

$$C_0 = \frac{1}{2} \quad \text{and} \quad C_n = \begin{cases} 0 & n \text{ even} \\ \dfrac{2}{\pi n} & n \text{ odd} \end{cases}$$

† Because $\cos(x \pm \pi) = -\cos x$, we could have chosen the phase π or $-\pi$. In fact, $\cos(x \pm N\pi) = -\cos x$ for any odd integral value of N. Therefore, the phase can be chosen as $\pm N\pi$, where N is any convenient odd integer.

The phases are

$$\theta_n = \begin{cases} 0 & \text{for all } n \neq 3,7,11,15,\ldots \\ -\pi & n = 3,7,11,15,\ldots \end{cases}$$

We might use these values to plot amplitude and phase spectra. However, we can simplify our task in this special case if we allow amplitude C_n to take on negative values. If this is allowed, we do not need a phase of $-\pi$ to account for the sign as seen from Eq. (3.40). This means that the phases of all components are zero, and we can discard the phase spectrum and manage with only the amplitude spectrum, as shown in Fig. 3.14b. Observe that there is no loss of information in doing so and that the amplitude spectrum in Fig. 3.14b has the complete information about the Fourier series in Eq. (3.40). *Therefore, whenever all sine terms vanish ($b_n = 0$), it is convenient to allow C_n to take on negative values.* This permits the spectral information to be conveyed by a single spectrum.†

Let us investigate the behavior of the series at the points of discontinuities. For the discontinuity at $t = \pi/2$, the values of $x(t)$ on either sides of the discontinuity are $x((\pi/2)^-) = 1$ and $x((\pi/2)^+) = 0$. We can verify by setting $t = \pi/2$ in Eq. (3.40) that $x(\pi/2) = 0.5$, which is a value midway between the values of $x(t)$ on either side of the discontinuity at $t = \pi/2$.

† Here, the distinction between amplitude A_n and magnitude $C_n = |A_n|$ would have been useful. But, for the reasons mentioned in the footnote on page 264, we refrain from this distinction formally.

3.4.1 The Effect of Symmetry

The Fourier series for the signal $\varphi(t)$ in Fig. 3.10b (Ex. 3.5) consists of sine and cosine terms, but the series for the signal $x(t)$ in Fig. 3.12a (Ex. 3.6) consists of sine terms only, and the series for the signal $x(t)$ in Fig. 3.14a (Ex. 3.8) consists of cosine terms only. This is no accident. We can show that the Fourier series of any even periodic function $x(t)$ consists of cosine terms only and the series for any odd periodic function $x(t)$ consists of sine terms only. Moreover, because of symmetry (even or odd), the information of one period of $x(t)$ is implicit in only half the period, as seen in Figs. 3.12a and 3.14a. In these cases, knowing the signal over a half-period and knowing the kind of symmetry (even or odd), we can determine the signal waveform over a complete period. For this reason, the Fourier coefficients in these cases can be computed by integrating over only half the period rather than a complete period. To prove this result, recall that

$$a_0 = \frac{1}{T_0}\int_{-T_0/2}^{T_0/2} x(t)\,dt, \quad a_n = \frac{2}{T_0}\int_{-T_0/2}^{T_0/2} x(t)\cos n\omega_0 t\,dt, \quad \text{and} \quad b_n = \frac{2}{T_0}\int_{-T_0/2}^{T_0/2} x(t)\sin n\omega_0 t\,dt$$

Recall also that $\cos n\omega_0 t$ is an even function and $\sin n\omega_0 t$ is an odd function of t. If $x(t)$ is an even function of t, then $x(t)\cos n\omega_0 t$ is also an even function and $x(t)\sin n\omega_0 t$ is an odd function of t (see Sec. 1.5.1). Therefore, following from Eq. (1.16),

$$a_0 = \frac{2}{T_0}\int_0^{T_0/2} x(t)\,dt, \quad a_n = \frac{4}{T_0}\int_0^{T_0/2} x(t)\cos n\omega_0 t\,dt, \quad \text{and} \quad b_n = 0 \tag{3.41}$$

Similarly, if $x(t)$ is an odd function of t, then $x(t)\cos n\omega_0 t$ is an odd function of t and $x(t)\sin n\omega_0 t$ is an even function of t. Therefore,

$$a_n = 0 \quad \text{and} \quad b_n = \frac{4}{T_0}\int_0^{T_0/2} x(t)\sin n\omega_0 t\,dt \tag{3.42}$$

Observe that because of symmetry, the integration required to compute the coefficients need be performed over only half the period.

If a periodic signal $x(t)$ shifted by half the period remains unchanged except for a sign—that is, if

$$x\left(t-\frac{T_0}{2}\right) = -x(t)$$

then the signal is said to have a *half-wave* symmetry. It can be shown that for a signal with a half-wave symmetry, all the even-numbered harmonics vanish (see Prob. 3.4-8). The signal in Fig. 3.12a is an example of such a symmetry. The signal in Fig. 3.14a also has this symmetry, although it is not obvious owing to a dc component. If we subtract the dc component of 0.5 from this signal, the remaining signal has half-wave symmetry. For this reason, this signal has only odd harmonics and a dc component of 0.5.

DRILL 3.6 Compact Trigonometric Fourier Series

Find the compact trigonometric Fourier series for periodic signals shown in Fig. 3.15. Sketch their amplitude and phase spectra. Allow C_n to take on negative values if $b_n = 0$ so that the phase spectrum can be eliminated. [*Hint:* Use Eqs. (3.41) and (3.42) for appropriate symmetry conditions.]

ANSWERS

(a) $$x(t) = \frac{1}{3} - \frac{4}{\pi^2}\left(\cos\pi t - \frac{1}{4}\cos 2\pi t + \frac{1}{9}\cos 3\pi t - \frac{1}{16}\cos 4\pi t + \cdots\right)$$
$$= \frac{1}{3} + \frac{4}{\pi^2}\sum_{n=1}^{\infty}\frac{(-1)^n}{n^2}\cos n\pi t$$

(b) $$x(t) = \frac{2A}{\pi}\left[\sin\pi t - \frac{1}{2}\sin 2\pi t + \frac{1}{3}\sin 3\pi t - \frac{1}{4}\sin 4\pi t + \cdots\right]$$
$$= \frac{2A}{\pi}\left[\cos(\pi t - 90°) + \frac{1}{2}\cos(2\pi t + 90°) + \frac{1}{3}\cos(3\pi t - 90°)\right.$$
$$\left. + \tfrac{1}{4}\cos(4\pi t + 90°) + \cdots\right]$$

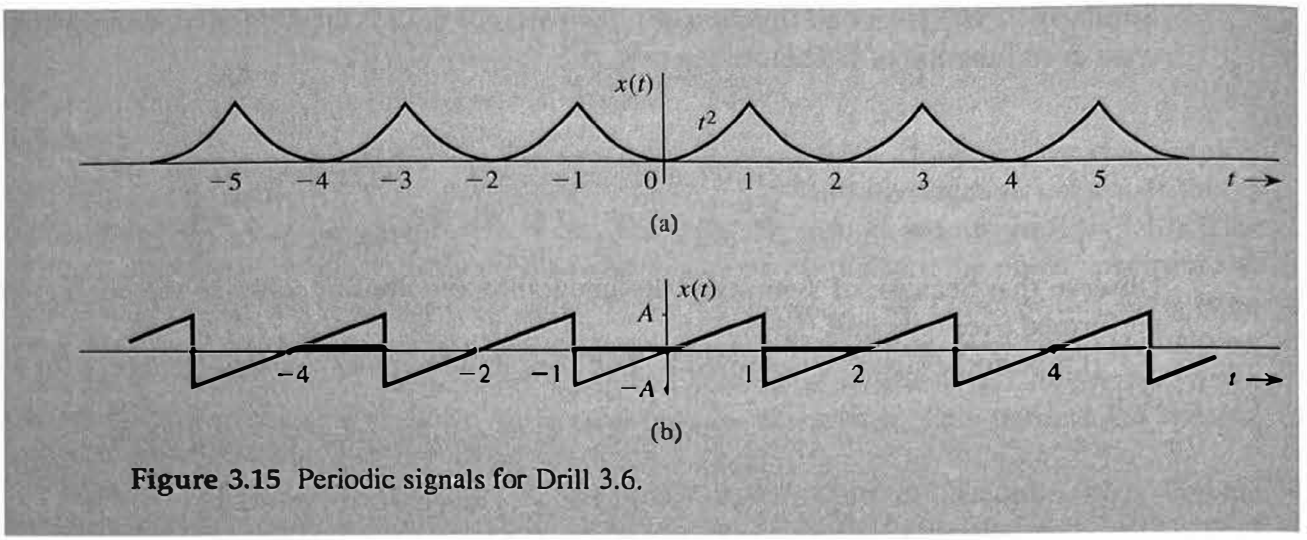

Figure 3.15 Periodic signals for Drill 3.6.

3.4.2 Determining the Fundamental Frequency and Period

We have seen that every periodic signal can be expressed as a sum of sinusoids of a fundamental frequency ω_0 and its harmonics. One may ask whether a sum of sinusoids of *any* frequencies represents a periodic signal. If so, how does one determine the period? Consider the following three functions:

$$x_1(t) = 2 + 7\cos\left(\tfrac{1}{2}t + \theta_1\right) + 3\cos\left(\tfrac{2}{3}t + \theta_2\right) + 5\cos\left(\tfrac{7}{6}t + \theta_3\right)$$

$$x_2(t) = 2\cos(2t + \theta_1) + 5\sin(\pi t + \theta_2)$$

$$x_3(t) = 3\sin\left(3\sqrt{2}t + \theta\right) + 7\cos\left(6\sqrt{2}t + \phi\right)$$

Recall that every frequency in a periodic signal is an integer multiple of the fundamental frequency ω_0. Therefore, the ratio of any two frequencies is of the form m/n, where m and n are integers. This means that the ratio of any two frequencies is a rational number. When the ratio of two frequencies is a rational number, the frequencies are said to be *harmonically* related.

The largest number of which all the frequencies are integer multiples is the fundamental frequency. In other words, the fundamental frequency is the *greatest common factor* (GCF) of all the frequencies in the series. The frequencies in the spectrum of $x_1(t)$ are 1/2, 2/3, and 7/6 (we do not consider dc). The ratios of the successive frequencies are 3:4 and 4:7, respectively. Because both these numbers are rational, all three frequencies in the spectrum are harmonically related, and the signal $x_1(t)$ is periodic. The GCF, that is, the greatest number of which 1/2, 2/3, and 7/6 are integer multiples, is 1/6.† Moreover, 3(1/6) = 1/2, 4(1/6) = 2/3, and 7(1/6) = 7/6. Therefore, the fundamental frequency is 1/6, and the three frequencies in the spectrum are the third, fourth, and seventh harmonics. Observe that the fundamental frequency component is absent in this Fourier series.

---

† The greatest common factor of a_1/b_1, a_2/b_2, . . ., a_m/b_m is the ratio of the GCF of the numerators set $(a_1, a_2, \ldots, a_m)$ to the LCM (least common multiple) of the denominator set $(b_1, b_2, \ldots, b_m)$. For instance, for the set (2/3, 6/7, 2), the GCF of the numerator set (2, 6, 2) is 2; the LCM of the denominator set (3, 7, 1) is 21. Therefore, 2/21 is the largest number of which 2/3, 6/7, and 2 are integer multiples.

The signal $x_2(t)$ is not periodic because the ratio of two frequencies in the spectrum is $2/\pi$, which is not a rational number. The signal $x_3(t)$ is periodic because the ratio of frequencies $3\sqrt{2}$ and $6\sqrt{2}$ is $1/2$, a rational number. The greatest common factor of $3\sqrt{2}$ and $6\sqrt{2}$ is $3\sqrt{2}$. Therefore, the fundamental frequency $\omega_0 = 3\sqrt{2}$, and the period

$$T_0 = \frac{2\pi}{(3\sqrt{2})} = \frac{\sqrt{2}}{3}\pi$$

DRILL 3.7 Determining Periodicity, Fundamental Frequency, and Harmonic Content

Determine whether the signal

$$x(t) = \cos\left(\tfrac{2}{3}t + 30°\right) + \sin\left(\tfrac{4}{5}t + 45°\right)$$

is periodic. If it is periodic, find the fundamental frequency and the period. What harmonics are present in $x(t)$?

ANSWERS

Periodic with $\omega_0 = 2/15$ and period $T_0 = 15\pi$. Signal $x(t)$ contains the fifth and sixth harmonics.

3.5 Existence and Convergence of the Fourier Series

For the existence of the Fourier series, coefficients a_0, a_n, and b_n in Eq. (3.38) must be finite. It follows from Eq. (3.38) that the existence of these coefficients is guaranteed if $x(t)$ is absolutely integrable over one period; that is,

$$\int_{T_0} |x(t)|\,dt < \infty \tag{3.43}$$

However, existence, by itself, does not inform us about the nature and the manner in which the series converges. We shall first discuss the notion of convergence.

3.5.1 Convergence of a Series

The key to many puzzles lies in the nature of the convergence of the Fourier series. Convergence of infinite series is a complex problem. It took mathematicians several decades to understand the convergence aspect of the Fourier series. We shall barely scratch the surface here.

Nothing annoys a student more than the discussion of convergence. "Have we not proved," they ask, "that a periodic signal $x(t)$ can be expressed as a Fourier series?" Then why spoil the fun by this annoying discussion? Although we have developed the Fourier series through our discussion of representing signals using an orthogonal signal space, we have not delved into whether the Fourier series representation can actually exactly match an arbitrary periodic signal (or a signal on some interval T_0). We have hinted that a Fourier series matches a signal not in the ordinary sense, but in the mean-square sense. But what does this mean? Furthermore, the astute reader should have been skeptical of the claims of the Fourier series to represent discontinuous

functions such as in Fig. 3.14a. If $x(t)$ has a jump discontinuity, say, at $t = 0$, then $x(0^+), x(0)$, and $x(0^-)$ are generally different. How could a series consisting of the sum of continuous functions of the smoothest type (sinusoids) add to one value at $t = 0^-$ and a different value at $t = 0$ and yet another value at $t = 0^+$? The demand is impossible to satisfy unless the math involved executes some spectacular acrobatics. How does a Fourier series act under such conditions? Precisely for this reason, the great mathematicians Lagrange and Laplace, two of the judges examining Fourier's paper, were skeptical of Fourier's claims and voted against publication of the paper that later became a classic.

There are also other issues. In any practical application, we can use only a finite number of terms in a series. If, with a fixed number of terms, the series guarantees convergence within an arbitrarily small error at every value of t, such a series is highly desirable and is called a *uniformly convergent* series. If a series converges at every value of t, but to guarantee convergence within a given error requires a different number of terms at different t, then the series is still convergent, but less desirable. It goes under the name *pointwise convergent* series.

Finally, we have the case of a series that refuses to converge at some t, no matter how many terms are added. But the series may *converge in the mean*; that is, the energy of the difference between $x(t)$ and the corresponding finite term series approaches zero as the number of terms approaches infinity.† To explain this concept, let us consider representation of a function $x(t)$ by an infinite series

$$x(t) = \sum_{n=1}^{\infty} z_n(t)$$

Let the partial sum of the first N terms of the series on the right-hand side be denoted by $x_N(t)$, that is,

$$x_N(t) = \sum_{n=1}^{N} z_n(t)$$

If we approximate $x(t)$ by $x_N(t)$ (the partial sum of the first N terms of the series), the *error* in the approximation is the difference $x(t) - x_N(t)$. The series converges *in the mean* to $x(t)$ in the interval $(0, T_0)$ if

$$\int_0^{T_0} |x(t) - x_N(t)|^2 \, dt \to 0 \qquad \text{as} \quad N \to \infty$$

Hence, the energy of the error $x(t) - x_N(t)$ approaches zero as $N \to \infty$. This form of convergence does not require the series to be equal to $x(t)$ for all t. It just requires the energy of the difference (area under $|x(t) - x_N(t)|^2$) to vanish as $N \to \infty$. Superficially, it may appear that if the energy of a signal over an interval is zero, the signal (the error) must be zero everywhere. This is not true. The signal energy can be zero even if there are nonzero values at a finite number of isolated points. This is because although the signal is nonzero at a point (and zero everywhere else), the area under its square is still zero. Thus, a series that converges in the mean to $x(t)$ need not converge to $x(t)$ at a finite number of points. This is precisely what happens to the Fourier series when $x(t)$ has jump discontinuities. This is also what makes Fourier series convergence compatible with the Gibbs phenomenon, to be discussed later in this section.

---

† This behavior is called "convergence in the mean" because minimizing the error energy over a certain interval is equivalent to minimizing the mean-square value of the error over the same interval.

There is a simple criterion for ensuring that a periodic signal $x(t)$ has a Fourier series that converges in the mean. The Fourier series for $x(t)$ converges to $x(t)$ in the mean if $x(t)$ has a finite energy over one period, that is,

$$\int_{T_0} |x(t)|^2 dt < \infty \tag{3.44}$$

Thus, the periodic signal $x(t)$, having a finite energy over one period, guarantees the convergence in the mean of its Fourier series. In all the examples discussed so far, Eq. (3.44) is satisfied; hence the corresponding Fourier series converges in the mean. Equation (3.44), like Eq. (3.43), guarantees that the Fourier coefficients are finite.

We shall now discuss an alternate set of criteria, due to Dirichlet, for convergence of the Fourier series.

Dirichlet Conditions

Dirichlet showed that if $x(t)$ satisfies certain conditions (*Dirichlet conditions*), its Fourier series is guaranteed to converge pointwise at all points where $x(t)$ is continuous. Moreover, at the points of discontinuities, $x(t)$ converges to the value midway between the two values of $x(t)$ on either side of the discontinuity. These conditions are:

1. The function $x(t)$ must be absolutely integrable; that is, it must satisfy Eq. (3.43).
2. The function $x(t)$ must have only a finite number of finite discontinuities in one period.
3. The function $x(t)$ must contain only a finite number of maxima and minima in one period.

All practical signals, including those in Exs. 3.5, 3.6, 3.7, and 3.8, satisfy these conditions.

3.5.2 The Role of Amplitude and Phase Spectra in Waveshaping

The trigonometric Fourier series of a signal $x(t)$ shows explicitly the sinusoidal components of $x(t)$. We can synthesize $x(t)$ by adding the sinusoids in the spectrum of $x(t)$. Let us synthesize the square-pulse periodic signal $x(t)$ of Fig. 3.14a by adding successive harmonics in its spectrum step by step and observing the similarity of the resulting signal to $x(t)$. The Fourier series for this function as found in Eq. (3.40) is

$$x(t) = \frac{1}{2} + \frac{2}{\pi}\left(\cos t - \frac{1}{3}\cos 3t + \frac{1}{5}\cos 5t - \frac{1}{7}\cos 7t + \cdots\right)$$

We start the synthesis with only the first term in the series ($n = 0$), a constant 1/2 (dc); this is a gross approximation of the square wave, as shown in Fig. 3.16a. In the next step, we add the dc ($n = 0$) and the first harmonic (fundamental), which results in a signal shown in Fig. 3.16b. Observe that the synthesized signal somewhat resembles $x(t)$. It is a smoothed-out version of $x(t)$. The sharp corners in $x(t)$ are not reproduced in this signal because sharp corners mean rapid changes, and their reproduction requires rapidly varying (i.e., higher-frequency) components, which are excluded. Figure 3.16c shows the sum of dc, first, and third harmonics (even harmonics are absent). As we increase the number of harmonics progressively, as shown in Figs. 3.16d (sum up to the fifth harmonic) and 3.16e (sum up to the nineteenth harmonic), the edges of the pulses become sharper and the signal resembles $x(t)$ more closely.

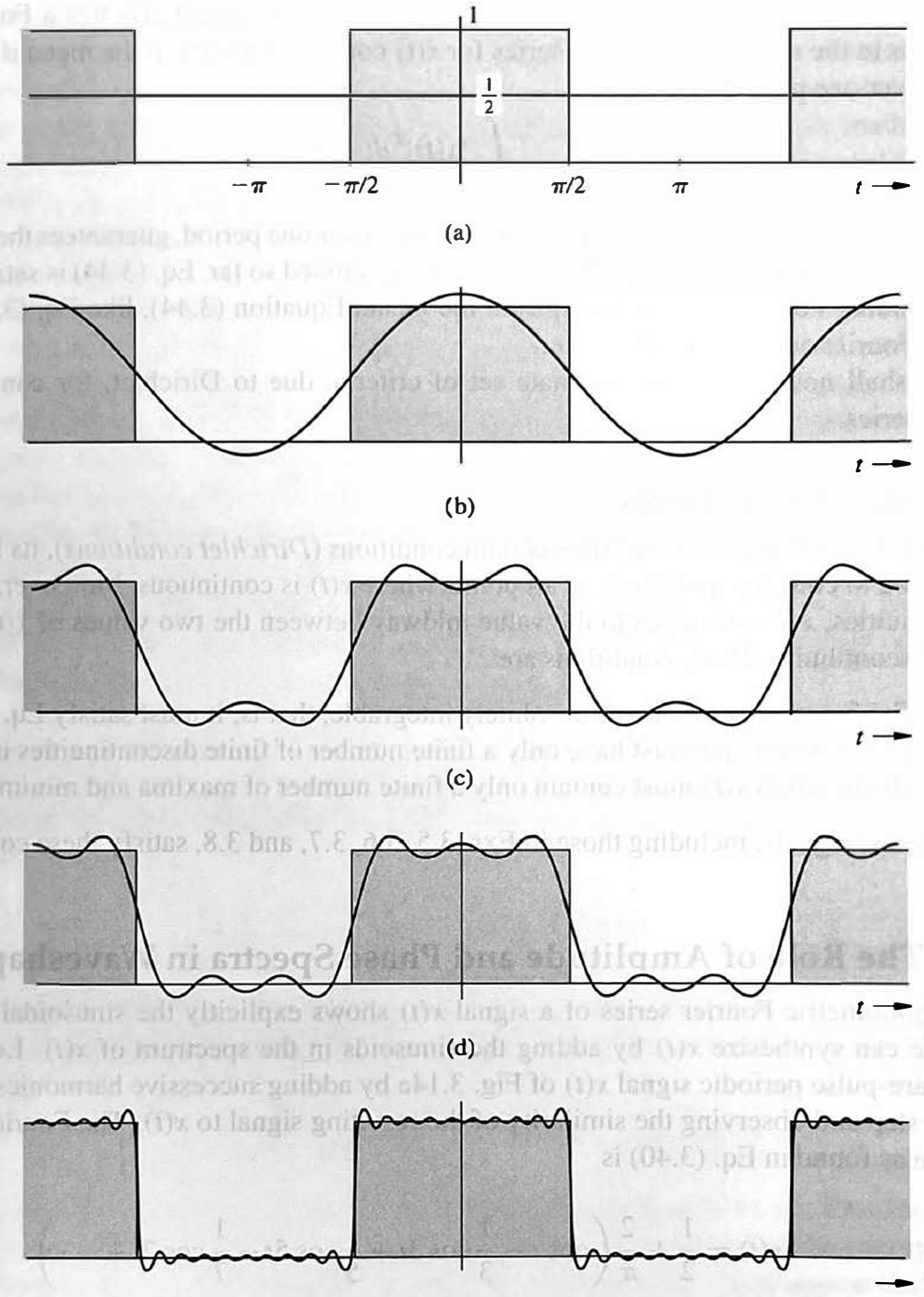

Figure 3.16 Synthesis of a square-pulse periodic signal by successive addition of its harmonics.

Asymptotic Rate of Amplitude Spectrum Decay

Figure 3.16 brings out one interesting aspect of the Fourier series. Lower frequencies in the Fourier series affect the large-scale behavior of $x(t)$, whereas the higher frequencies determine the fine structure such as rapid wiggling. Hence, sharp changes in $x(t)$, being a part of fine structure,

necessitate higher frequencies in the Fourier series. The sharper the change [the higher the time derivative $\dot{x}(t)$], the higher are the frequencies needed in the series.

The amplitude spectrum indicates the amounts (amplitudes) of various frequency components of $x(t)$. If $x(t)$ is a smooth function, its variations are less rapid. Synthesis of such a function requires predominantly lower-frequency sinusoids and relatively small amounts of rapidly varying (higher-frequency) sinusoids. The amplitude spectrum of such a function would decay swiftly with frequency. To synthesize such a function, we require fewer terms in the Fourier series for a good approximation. On the other hand, a signal with sharp changes, such as jump discontinuities, contains rapid variations, and its synthesis requires a relatively large amount of high-frequency components. The amplitude spectrum of such a signal would decay slowly with frequency, and to synthesize such a function, we require many terms in its Fourier series for a good approximation. The square wave $x(t)$ is a discontinuous function with jump discontinuities, and therefore its amplitude spectrum decays rather slowly, as $1/n$ [see Eq. (3.40)]. On the other hand, the triangular-pulse periodic signal in Fig. 3.12a is smoother because it is a continuous function (no jump discontinuities). Its spectrum decays rapidly with frequency as $1/n^2$ [see Eq. (3.39)].

We can show that if the first $k-1$ derivatives of a periodic signal $x(t)$ are continuous and the kth derivative is discontinuous, then its amplitude spectrum C_n decays with frequency at least as rapidly as $1/n^{k+1}$ [9]. This result provides a simple and useful means for predicting the asymptotic rate of convergence of the Fourier series. In the case of the square-wave signal (Fig. 3.14a), the zeroth derivative of the signal (the signal itself) is discontinuous so that $k=0$. For the triangular periodic signal in Fig. 3.12a, the first derivative is discontinuous; that is, $k=1$. For this reason, the spectra of these signals decay as $1/n$ and $1/n^2$, respectively.

EXAMPLE 3.9 Square Wave Synthesis by Truncated Fourier Series Using MATLAB

Use MATLAB to synthesize and plot the square wave of Fig. 3.16a using a Fourier series that is truncated to the 19th harmonic. The result should match Fig. 3.16e.

To synthesize the waveform, we use the Fourier series of Eq. (3.40).

```
>> x = @(t) 1.0*(mod(t+pi/2,2*pi)<=pi);
>> t = linspace(-2*pi,2*pi,10001);
>> x19 = 0.5*ones(size(t));
>> for n=1:19, x19 = x19+2/(pi*n)*sin(pi*n/2)*cos(n*t); end
>> plot(t,x19,'k-'); axis([-2*pi 2*pi -0.2 1.2]);
>> xlabel('t'); ylabel('x_{19}(t)');
```

As expected, the result of Fig. 3.17 matches Fig. 3.16e.

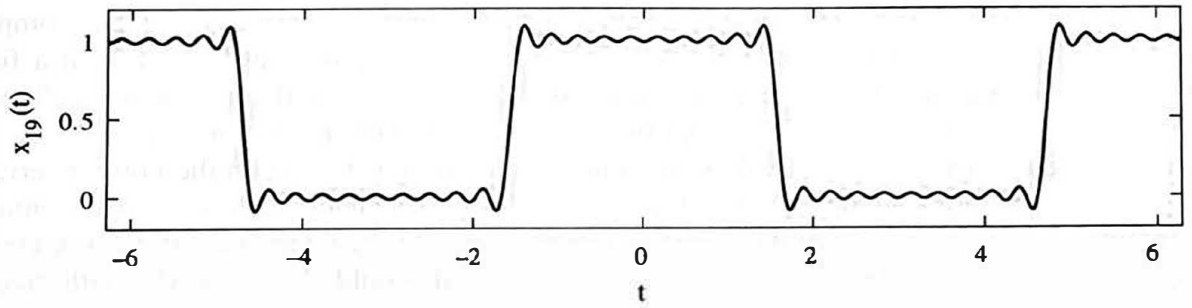

Figure 3.17 Using MATLAB to synthesize a square wave via truncated Fourier series.

Phase Spectrum: Hidden Figures

The role of the amplitude spectrum in shaping the waveform $x(t)$ is quite clear. However, the role of the phase spectrum in shaping this waveform is less obvious. Yet, like the hidden figures of NASA's space program†, the phase spectrum plays a crucial role in waveshaping. We can explain this role by considering a signal $x(t)$ that has rapid changes, such as jump discontinuities. To synthesize an instantaneous change at a jump discontinuity, the phases of the various sinusoidal components in its spectrum must be such that all (or most) of the harmonic components will have one sign before the discontinuity, the phases of the various sinusoidal components in its spectrum must be such that all (or most) of the harmonic components will have one sign before the discontinuity and the opposite sign after the discontinuity. This will result in a sharp change in $x(t)$ at the point of discontinuity. We can verify this fact in any waveform with jump discontinuity. Consider, for example, the sawtooth waveform in Fig. 3.15b. This waveform has a discontinuity at $t = 1$. The Fourier series for this waveform, as given in Drill 3.6b, is

$$x(t) = \frac{2A}{\pi}\left[\cos(\pi t - 90°) + \frac{1}{2}\cos(2\pi t + 90°) + \frac{1}{3}\cos(3\pi t - 90°) + \frac{1}{4}\cos(4\pi t + 90°) + \cdots\right]$$

Figure 3.18 shows the first three components of this series. The phases of all the (infinite) components are such that all the components are positive just before $t = 1$ and turn negative just after $t = 1$, the point of discontinuity. The same behavior is also observed at $t = -1$, where a similar discontinuity occurs. This sign change in all the harmonics adds up to produce very nearly a jump discontinuity. The role of the phase spectrum is crucial in achieving a sharp change in the waveform. If we ignore the phase spectrum when trying to reconstruct this signal, the result will be a smeared and spread-out waveform. In general, the phase spectrum is just as crucial as the amplitude spectrum in determining the waveform. *The synthesis of any signal $x(t)$ is achieved by using a proper combination of amplitudes and phases of various sinusoids. This unique combination is the Fourier spectrum of $x(t)$.*

† See Margot Shetterly's 2016 book "Hidden Figures" or the 2017 movie adaptation.

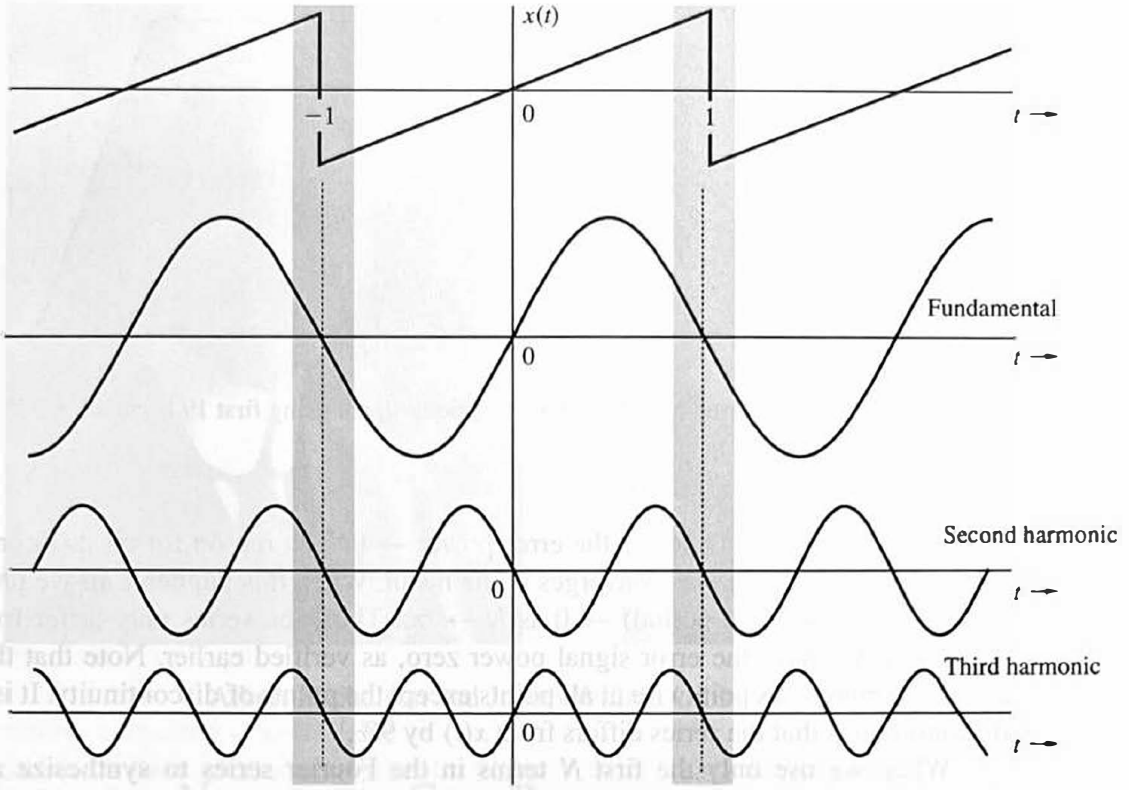

Figure 3.18 Role of the phase spectrum in shaping a periodic signal.

Fourier Synthesis of Discontinuous Functions: The Gibbs Phenomenon

Figure 3.16 showed the square function $x(t)$ and its approximation by a truncated trigonometric Fourier series that includes only the first N harmonics for $N = 1$, 3, 5, and 19. The plot of the truncated series approximates closely the function $x(t)$ as N increases, and we expect that the series will converge exactly to $x(t)$ as $N \to \infty$. Yet the curious fact, as seen from Fig. 3.16, is that even for large N, the truncated series exhibits an oscillatory behavior and an overshoot approaching a value of about 9% in the vicinity of the discontinuity at the nearest peak of oscillation.[†] Regardless of the value of N, the overshoot remains at about 9%. Such strange behavior certainly would undermine anyone's faith in the Fourier series. In fact, this behavior puzzled many scholars at the turn of the century. Josiah Willard Gibbs, an eminent mathematical physicist who was the inventor of vector analysis, gave a mathematical explanation of this behavior (now called the *Gibbs phenomenon*).

We can reconcile the apparent aberration in the behavior of the Fourier series by observing from Fig. 3.16 that the frequency of oscillation of the synthesized signal is Nf_0, so the width of the spike with 9% overshoot is approximately $1/2Nf_0$. As we increase N, the frequency of oscillation increases and the spike width $1/2Nf_0$ diminishes. As $N \to \infty$, the error power $\to 0$ because the error consists mostly of the spikes, whose widths $\to 0$. Therefore, as $N \to \infty$, the corresponding Fourier series differs from $x(t)$ by about 9% at the immediate left and right of the

[†] There is also an undershoot of 9% at the other side [at $t = (\pi/2)^+$] of the discontinuity.

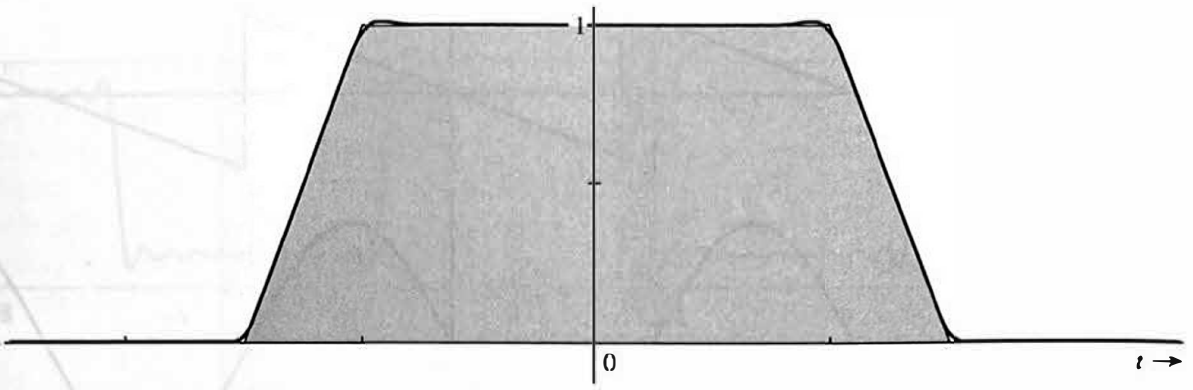

Figure 3.19 Fourier synthesis of a continuous signal using first 19 harmonics.

points of discontinuity, and yet the error power $\to 0$. The reason for all this confusion is that in this case, the Fourier series converges in the mean. When this happens, all we promise is that the error energy (over one period) $\to 0$ as $N \to \infty$. Thus, the series may differ from $x(t)$ at some points and yet have the error signal power zero, as verified earlier. Note that the series, in this case, also converges pointwise at all points except the points of discontinuity. It is precisely at the discontinuities that the series differs from $x(t)$ by 9%.[†]

When we use only the first N terms in the Fourier series to synthesize a signal, we are abruptly terminating the series, giving a unit weight to the first N harmonics and zero weight to all the remaining harmonics beyond N. This abrupt termination of the series causes the Gibbs phenomenon in the synthesis of discontinuous functions. Section 4.9 offers more discussion on the Gibbs phenomenon, its ramifications, and cure.

The Gibbs phenomenon is present only when there is a jump discontinuity in $x(t)$. When a continuous function $x(t)$ is synthesized by using the first N terms of the Fourier series, the synthesized function approaches $x(t)$ for all t as $N \to \infty$. No Gibbs phenomenon appears. This can be seen in Fig. 3.19, which shows one cycle of a continuous periodic signal being synthesized from the first 19 harmonics. Compare the similar situation for a discontinuous signal in Fig. 3.16.

DRILL 3.8 Rate of Spectral Decay

By inspection of signals in Figs. 3.10b, 3.15a, and 3.15b, determine the asymptotic rate of decay of their amplitude spectra.

ANSWERS

$1/n, 1/n^2$, and $1/n$, respectively.

[†] Actually, at discontinuities, the series converges to a value midway between the values on either side of the discontinuity. The 9% overshoot occurs at $t = (\pi/2)^-$ and 9% undershoot occurs at $t = (\pi/2)^+$.

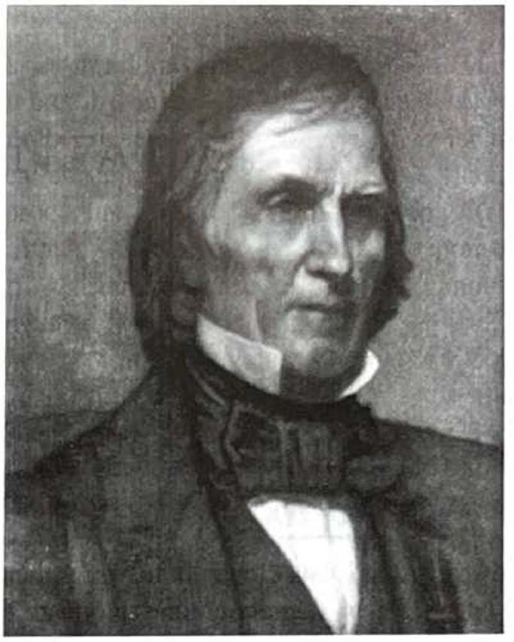

Albert Michelson and Josiah Willard Gibbs

A Historical Note on the Gibbs Phenomenon

Normally speaking, troublesome functions with strange behavior are invented by mathematicians; we rarely see such oddities in practice. In the case of the Gibbs phenomenon, however, the tables were turned. A rather puzzling behavior was observed in a mundane object, a mechanical wave synthesizer, and then well-known mathematicians of the day were dispatched on the scent of it to discover its hideout.

Albert Michelson (of Michelson–Morley fame) was an intense, practical man who developed ingenious physical instruments of extraordinary precision, mostly in the field of optics. His harmonic analyzer, developed in 1898, could compute the first 80 coefficients of the Fourier series of a signal $x(t)$ specified by any graphical description. The instrument could also be used as a harmonic synthesizer, which could plot a function $x(t)$ generated by summing the first 80 harmonics (Fourier components) of arbitrary amplitudes and phases. This analyzer, therefore, had the ability of self-checking its operation by analyzing a signal $x(t)$ and then adding the resulting 80 components to see whether the sum yielded a close approximation of $x(t)$.

Michelson found that the instrument checked very well with most signals analyzed. However, when he tried a discontinuous function, such as a square wave,[†] a curious behavior was observed. The sum of 80 components showed oscillatory behavior (ringing), with an overshoot of 9% in the vicinity of the points of discontinuity. Moreover, this behavior was a constant feature regardless of the number of terms added. A larger number of terms made the oscillations proportionately faster, but regardless of the number of terms added, the overshoot remained 9%. This puzzling behavior caused Michelson to suspect some mechanical defect in his synthesizer. He wrote about his observation in a letter to *Nature* (December 1898). Josiah Willard Gibbs, who was a professor

[†] Actually, it was a periodic sawtooth signal.

at Yale, investigated and clarified this behavior for a sawtooth periodic signal in a letter to *Nature* [10]. Later, in 1906, Bôcher generalized the result for any function with discontinuity [11]. It was Bôcher who gave the name *Gibbs phenomenon* to this behavior. Gibbs showed that the peculiar behavior in the synthesis of a square wave was inherent in the behavior of the Fourier series because of nonuniform convergence at the points of discontinuity.

This, however, is not the end of the story. Both Bôcher and Gibbs were under the impression that this property had remained undiscovered until Gibbs's work published in 1899. It is now known that what is called the Gibbs phenomenon had been observed in 1848 by Wilbraham of Trinity College, Cambridge, who clearly saw the behavior of the sum of the Fourier series components in the periodic sawtooth signal later investigated by Gibbs [12]. Apparently, this work was not known to most people, including Gibbs and Bôcher.

3.6 EXPONENTIAL FOURIER SERIES

By using Euler's equality, we can express $\cos n\omega_0 t$ and $\sin n\omega_0 t$ in terms of exponentials $e^{jn\omega_0 t}$ and $e^{-jn\omega_0 t}$. Clearly, we should be able to express the trigonometric Fourier series in Eq. (3.33) in terms of exponentials of the form $e^{jn\omega_0 t}$ with the index n taking on all integer values from $-\infty$ to ∞, including zero. Derivation of the exponential Fourier series from the results already derived for the trigonometric Fourier series is straightforward, involving conversion of sinusoids to exponentials. We shall, however, derive them here using our foundation of signal representation by an orthogonal signal set.

To begin, we note that the set of exponentials $e^{jn\omega_0 t}$ $(n = 0, \pm 1, \pm 2, \ldots)$ is orthogonal over any interval of duration $T_0 = 2\pi/\omega_0$, that is,[†]

$$\int_{T_0} e^{jn\omega_0 t} e^{-jm\omega_0 t}\, dt = \begin{cases} 0 & m \neq n \\ T_0 & m = n \end{cases} \tag{3.45}$$

Moreover, the exponential set is a complete set [7, 8]. From Eqs. (3.21) and (3.22), it follows that a signal $x(t)$ can be expressed over an interval of duration T_0 seconds as an exponential Fourier series

$$x(t) = \sum_{n=-\infty}^{\infty} D_n e^{jn\omega_0 t} \qquad \text{where} \qquad D_n = \frac{1}{T_0}\int_{T_0} x(t)\, e^{-jn\omega_0 t}\, dt \tag{3.46}$$

The exponential Fourier series is basically another form of the trigonometric Fourier series. Each sinusoid of frequency $n\omega_0$ can be expressed as a sum of two exponentials $e^{jn\omega_0 t}$ and $e^{-jn\omega_0 t}$. This results in the exponential Fourier series consisting of components of the form $e^{jn\omega_0 t}$ with n varying from $-\infty$ to ∞. The exponential Fourier series in Eq. (3.46) is periodic with period T_0.

[†] We can readily prove this property as follows. For the case of $m = n$, the integrand in Eq. (3.45) is unity and the integral is T_0. When $m \neq n$, the integral on the left-hand side of Eq. (3.45) can be expressed as

$$\int_{T_0} e^{j(n-m)\omega_0 t}\, dt = \int_{T_0} \cos(n-m)\omega_0 t\, dt + j\int_{T_0} \sin(n-m)\omega_0 t\, dt$$

Both the integrals on the right-hand side represent area under $n - m$ number of cycles. Because $n - m$ is an integer, both the areas are zero. Hence follows Eq. (3.45).

Observe the compactness of Eq. (3.46) and compare it with the trigonometric Fourier series expression. Such a comparison demonstrates very clearly the principal virtue of the exponential Fourier series. First, the form of the series is most compact. Second, the mathematical expression for deriving the coefficients of the series is also compact. It is much more convenient to handle the exponential series than the trigonometric one. For these reasons, we shall use the exponential (rather than trigonometric) representation of signals in the rest of the book.

We can now relate D_n to trigonometric series coefficients a_n and b_n. Setting $n = 0$ in Eq. (3.46), we obtain

$$D_0 = a_0$$

Moreover, for $n \neq 0$,

$$D_n = \frac{1}{T_0}\int_{T_0} x(t)\cos n\omega_0 t\,dt - \frac{j}{T_0}\int_{T_0} x(t)\sin n\omega_0 t\,dt = \frac{1}{2}(a_n - jb_n) \tag{3.47}$$

and

$$D_{-n} = \frac{1}{T_0}\int_{T_0} x(t)\cos n\omega_0 t\,dt + \frac{j}{T_0}\int_{T_0} x(t)\sin n\omega_0 t\,dt = \frac{1}{2}(a_n + jb_n) \tag{3.48}$$

These results are valid for general $x(t)$, real or complex. When $x(t)$ is real, a_n and b_n are real, and Eqs. (3.47)and (3.48) show that D_n and D_{-n} are conjugates.

$$D_{-n} = D_n^*$$

Moreover, from Eq. (3.36), we observe that

$$a_n - jb_n = \sqrt{a_n^2 + b_n^2}\, e^{j\tan^{-1}\left(\frac{-b_n}{a_n}\right)} = C_n e^{j\theta_n}$$

Hence,

$$D_0 = a_0 = C_0$$

and

$$D_n = \tfrac{1}{2}C_n e^{j\theta_n} \qquad D_{-n} = \tfrac{1}{2}C_n e^{-j\theta_n}$$

Therefore, for $n \neq 0$,

$$|D_n| = |D_{-n}| = \tfrac{1}{2}C_n, \quad \angle D_n = \theta_n, \quad \text{and} \quad \angle D_{-n} = -\theta_n \tag{3.49}$$

Note that $|D_n|$ are the amplitudes and $\angle D_n$ are the angles of various exponential components. From Eq. (3.49), it follows that when $x(t)$ is real, the amplitude spectrum ($|D_n|$ versus ω) is an even function of ω and the angle spectrum ($\angle D_n$ versus ω) is an odd function of ω. For complex $x(t)$, D_n and D_{-n} are generally not conjugates. The various forms of the Fourier series and the equations to convert between these forms are summarized in Table 3.1.

TABLE 3.1 Fourier Series Representation of a Periodic Signal of Period T_0 ($\omega_0 = 2\pi/T_0$)

Series Form	Coefficient Computation	Conversion Formulas
Trigonometric	$a_0 = \frac{1}{T_0}\int_{T_0} f(t)\,dt$	$a_0 = C_0 = D_0$
$f(t) = a_0 + \sum_{n=1}^{\infty} a_n \cos n\omega_0 t + b_n \sin n\omega_0 t$	$a_n = \frac{2}{T_0}\int_{T_0} f(t)\cos n\omega_0 t\,dt$	$a_n - jb_n = C_n e^{j\theta_n} = 2D_n$
	$b_n = \frac{2}{T_0}\int_{T_0} f(t)\sin n\omega_0 t\,dt$	$a_n + jb_n = C_n e^{-j\theta_n} = 2D_{-n}$
Compact trigonometric	$C_0 = a_0$	$C_0 = D_0$
$f(t) = C_0 + \sum_{n=1}^{\infty} C_n \cos(n\omega_0 t + \theta_n)$	$C_n = \sqrt{a_n{}^2 + b_n{}^2}$	$C_n = 2\lvert D_n\rvert \quad n \geq 1$
	$\theta_n = \tan^{-1}\left(\frac{-b_n}{a_n}\right)$	$\theta_n = \angle D_n$
Exponential		
$f(t) = \sum_{n=-\infty}^{\infty} D_n e^{jn\omega_0 t}$	$D_n = \frac{1}{T_0}\int_{T_0} f(t)e^{-jn\omega_0 t}\,dt$	

EXAMPLE 3.10 Exponential Fourier Series of Periodic Exponential Wave

Find the exponential Fourier series for the signal of Fig. 3.10b from Ex. 3.5.

In this case, $T_0 = \pi$, $\omega_0 = 2\pi/T_0 = 2$, and

$$\varphi(t) = \sum_{n=-\infty}^{\infty} D_n e^{j2nt}$$

where

$$D_n = \frac{1}{T_0}\int_{T_0} \varphi(t)e^{-j2nt}\,dt = \frac{1}{\pi}\int_0^{\pi} e^{-t/2}e^{-j2nt}\,dt = \frac{1}{\pi}\int_0^{\pi} e^{-(1/2+j2n)t}\,dt$$
$$= \frac{-1}{\pi\left(\frac{1}{2}+j2n\right)}e^{-(1/2+j2n)t}\Big|_0^{\pi} = \frac{0.504}{1+j4n}$$

and

$$\varphi(t) = 0.504\sum_{n=-\infty}^{\infty}\frac{1}{1+j4n}e^{j2nt}$$
$$= 0.504\left[1 + \frac{1}{1+j4}e^{j2t} + \frac{1}{1+j8}e^{j4t} + \frac{1}{1+j12}e^{j6t} + \cdots\right.$$
$$\left. + \frac{1}{1-j4}e^{-j2t} + \frac{1}{1-j8}e^{-j4t} + \frac{1}{1-j12}e^{-j6t} + \cdots\right]$$

Observe that the coefficients D_n are complex. Moreover, D_n and D_{-n} are conjugates, as expected.

3.6.1 Exponential Fourier Spectra

In exponential spectra, we plot coefficients D_n as a function of ω. But since D_n is complex in general, we need both parts of one of two sets of plots: the real and the imaginary parts of D_n, or the magnitude and the angle of D_n. We prefer the latter because of its close connection to the amplitudes and phases of corresponding components of the trigonometric Fourier series. We therefore plot $|D_n|$ versus ω and $\angle D_n$ versus ω. This requires that the coefficients D_n be expressed in polar form as $|D_n|e^{j\angle D_n}$, where $|D_n|$ are the amplitudes and $\angle D_n$ are the angles of various exponential components. Equation (3.49) shows that for real $x(t)$, the amplitude spectrum ($|D_n|$ versus ω) is an even function of ω and the angle spectrum ($\angle D_n$ versus ω) is an odd function of ω.

For the series in Ex. 3.10, for instance,

$$D_0 = 0.504$$

$$D_1 = \frac{0.504}{1+j4} = 0.122e^{-j75.96^\circ} \implies |D_1| = 0.122,\ \angle D_1 = -75.96^\circ$$

$$D_{-1} = \frac{0.504}{1-j4} = 0.122e^{j75.96^\circ} \implies |D_{-1}| = 0.122,\ \angle D_{-1} = 75.96^\circ$$

and

$$D_2 = \frac{0.504}{1+j8} = 0.0625e^{-j82.87^\circ} \implies |D_2| = 0.0625,\ \angle D_2 = -82.87^\circ$$

$$D_{-2} = \frac{0.504}{1-j8} = 0.0625e^{j82.87^\circ} \implies |D_{-2}| = 0.0625,\ \angle D_{-2} = 82.87^\circ$$

and so on. Note that D_n and D_{-n} are conjugates, as expected [see Eq. (3.49)].

As a second example, Fig. 3.20 shows the frequency spectra (amplitude and angle) of the exponential Fourier series for the periodic signal $\varphi(t)$ in Fig. 3.10b.

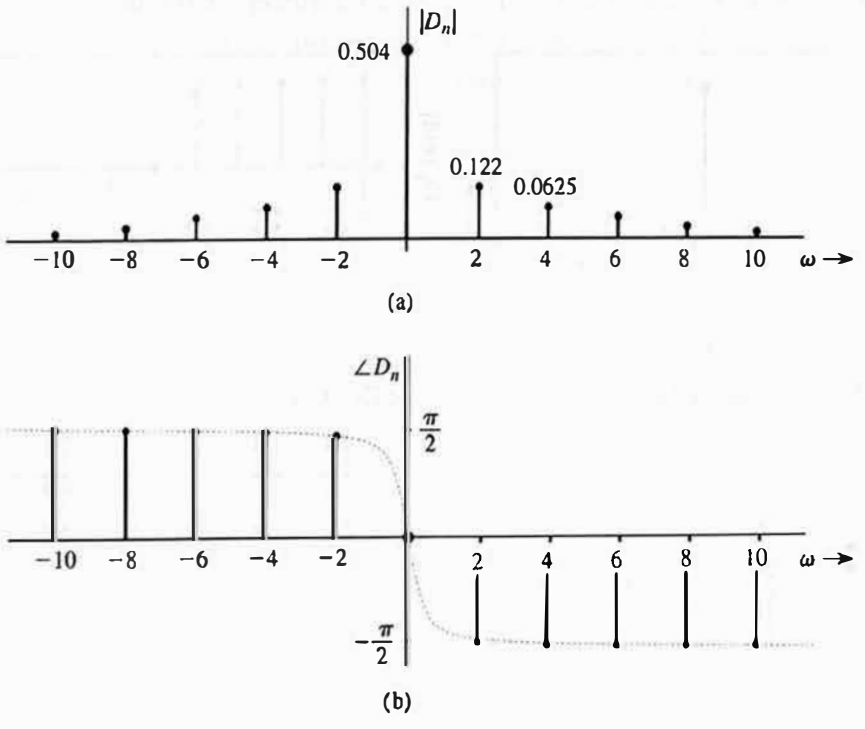

Figure 3.20 Exponential Fourier spectra for the signal in Fig. 3.10b.

Since the time-domain signals are real in these examples, the amplitude spectra are even functions of ω and the angle spectra are odd functions of ω. Unlike the trigonometric Fourier spectra, the exponential Fourier spectra exist for positive as well as negative values of ω (the frequency), a distinction that we will investigate shortly.

At times it may appear that the phase spectrum of a real periodic signal fails to satisfy the odd symmetry: for example, when $D_k = D_{-k} = -10$. In this case, $D_k = 10e^{j\pi}$, and therefore, $D_{-k} = 10e^{-j\pi}$. Recall that $e^{\pm j\pi} = -1$. Here, although $D_k = D_{-k}$, their phases should be taken as π and $-\pi$.

EXAMPLE 3.11 Plotting Fourier Series Spectra with MATLAB

Using MATLAB and the results of Ex. 3.10, compute and plot the exponential Fourier spectra for the periodic signal $\varphi(t)$ shown in Fig. 3.10b. The result should match Fig. 3.20.

The expression for D_n is derived in Ex. 3.10.

```
>> clf; n = (-5:5); D_n = 0.504./(1+4j*n);
>> subplot(1,2,1); stem(n,abs(D_n),'.k');
>> xlabel('n'); ylabel('|D_n|');
>> subplot(1,2,2); stem(n,angle(D_n),'.k');
>> xlabel('n'); ylabel('\angle D_n [rad]');
```

Except that it is plotted as a function of n rather than ω, the result in Fig. 3.21 matches Fig. 3.20.

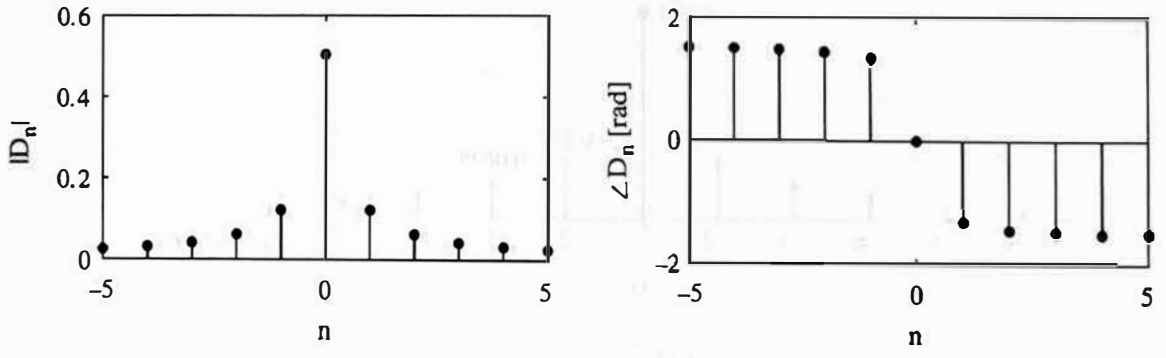

Figure 3.21 Exponential Fourier Series spectra for Ex. 3.11.

What Is a Negative Frequency?

The existence of the spectrum at negative frequencies is somewhat disturbing because, by definition, the frequency (number of repetitions per second) is a positive quantity. How do we interpret a negative frequency? We can use a trigonometric identity to express a sinusoid of a negative frequency $-\omega_0$ as

$$\cos(-\omega_0 t + \theta) = \cos(\omega_0 t - \theta)$$

This equation clearly shows that the frequency of a sinusoid $\cos(\omega_0 t + \theta)$ is $|\omega_0|$, which is a positive quantity. The same conclusion is reached by observing that

$$e^{\pm j\omega_0 t} = \cos \omega_0 t \pm j \sin \omega_0 t$$

Thus, the frequency of exponentials $e^{\pm j\omega_0 t}$ is indeed $|\omega_0|$. How do we then interpret the spectral plots for negative values of ω? A more satisfying way of looking at the situation is to say that *exponential spectra are a graphical representation of coefficients D_n as a function of ω. Existence of the spectrum at $\omega = -n\omega_0$ is merely an indication that an exponential component $e^{-jn\omega_0 t}$ exists in the series.* We know that a sinusoid of frequency $n\omega_0$ can be expressed in terms of a pair of exponentials $e^{jn\omega_0 t}$ and $e^{-jn\omega_0 t}$.

We see a close connection between the exponential spectra in Fig. 3.20 and the spectra of the corresponding trigonometric Fourier series (Figs. 3.10c, 3.10d). Equation (3.49) explains the reason for the close connection, for real time-domain signals, between the trigonometric spectra (C_n and θ_n) with exponential spectra ($|D_n|$ and $\angle D_n$). The dc components D_0 and C_0 are identical in both spectra. Moreover, the exponential amplitude spectrum $|D_n|$ is half the trigonometric amplitude spectrum C_n for $n \geq 1$. The exponential angle spectrum $\angle D_n$ is identical to the trigonometric phase spectrum θ_n for $n \geq 0$. We can therefore produce the exponential spectra merely by inspection of trigonometric spectra, and vice versa. The following example demonstrates this feature.

EXAMPLE 3.12 Relating Exponential to Trigonometric Fourier Series Spectra

The trigonometric Fourier spectra of a certain periodic signal $x(t)$ are shown in Fig. 3.22a. By inspecting these spectra, sketch the corresponding exponential Fourier spectra and verify your results analytically.

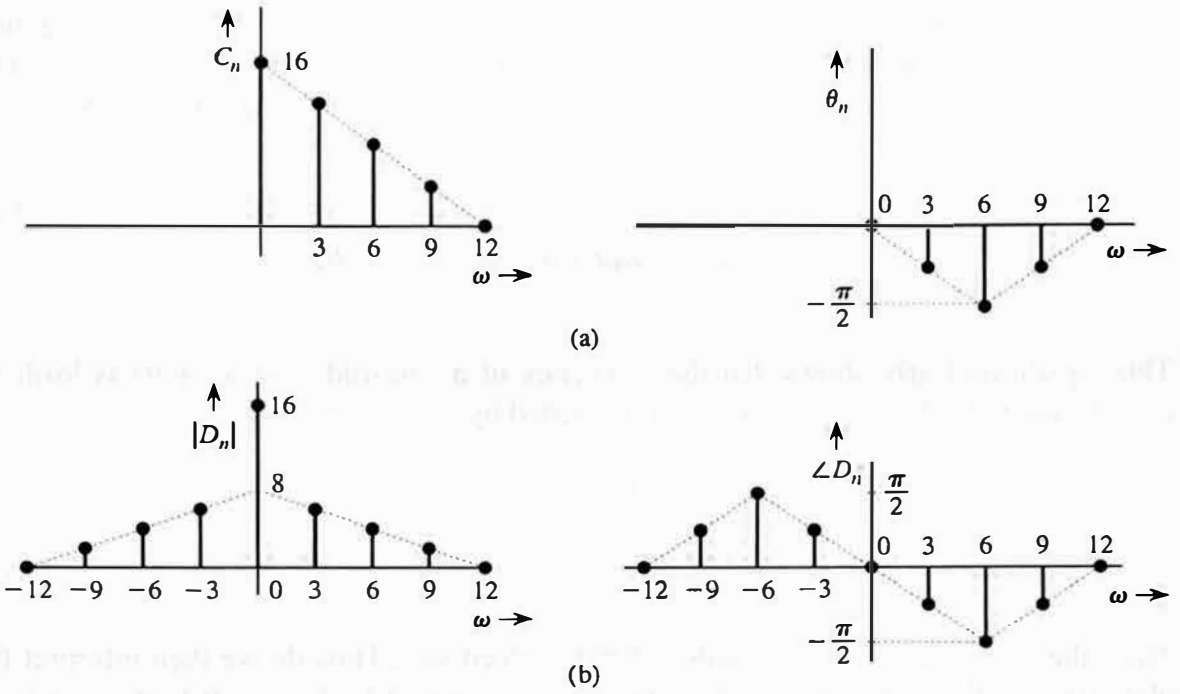

Figure 3.22 Fourier series spectra for Ex. 3.12.

The trigonometric spectral components exist at frequencies 0, 3, 6, and 9. The exponential spectral components exist at 0, 3, 6, 9 and −3, −6, −9. Consider first the amplitude spectrum. The dc component remains unchanged: that is, $D_0 = C_0 = 16$. Now $|D_n|$ is an even function of ω and $|D_n| = |D_{-n}| = C_n/2$. Thus, all the remaining spectrum $|D_n|$ for positive n is half the trigonometric amplitude spectrum C_n, and the spectrum $|D_n|$ for negative n is a reflection about the vertical axis of the spectrum for positive n, as shown in Fig. 3.22b.

The angle spectrum is $\angle D_n = \theta_n$ for positive n and is $-\theta_n$ for negative n, as depicted in Fig. 3.22b. We shall now verify that both sets of spectra represent the same signal.

Signal $x(t)$, whose trigonometric spectra are shown in Fig. 3.22a, has four spectral components of frequencies 0, 3, 6, and 9. The dc component is 16. The amplitude and the phase of the component of frequency 3 are 12 and $-\pi/4$, respectively. Therefore, this component can be expressed as $12\cos(3t - \pi/4)$. Proceeding in this manner, we can write the Fourier series for $x(t)$ as

$$x(t) = 16 + 12\cos\left(3t - \frac{\pi}{4}\right) + 8\cos\left(6t - \frac{\pi}{2}\right) + 4\cos\left(9t - \frac{\pi}{4}\right)$$

Consider now the exponential spectra in Fig. 3.22b. They contain components of frequencies 0 (dc), ±3, ±6, and ±9. The dc component is $D_0 = 16$. The component e^{j3t} (frequency 3) has magnitude 6 and angle $-\pi/4$. Therefore, this component strength is

$6e^{-j\pi/4}$, and it can be expressed as $(6e^{-j\pi/4})e^{j3t}$. Similarly, the component of frequency -3 is $(6e^{j\pi/4})e^{-j3t}$. Proceeding in this manner, $\hat{x}(t)$, the signal corresponding to the spectra in Fig. 3.22b, is

$$\begin{aligned}\hat{x}(t) &= 16+\left[6e^{-j\pi/4}e^{j3t}+6e^{j\pi/4}e^{-j3t}\right]+\left[4e^{-j\pi/2}e^{j6t}+4e^{j\pi/2}e^{-j6t}\right]\\ &\qquad +\left[2e^{-j\pi/4}e^{j9t}+2e^{j\pi/4}e^{-j9t}\right]\\ &= 16+6\left[e^{j(3t-\pi/4)}+e^{-j(3t-\pi/4)}\right]+4\left[e^{j(6t-\pi/2)}+e^{-j(6t-\pi/2)}\right]\\ &\qquad +2\left[e^{j(9t-\pi/4)}+e^{-j(9t-\pi/4)}\right]\\ &= 16+12\cos\left(3t-\frac{\pi}{4}\right)+8\cos\left(6t-\frac{\pi}{2}\right)+4\cos\left(9t-\frac{\pi}{4}\right)\end{aligned}$$

Clearly, both sets of spectra represent the same periodic signal.

Bandwidth of a Signal

The difference between the highest and the lowest frequencies of the spectral components of a signal is the *bandwidth* of the signal. The bandwidth of the signal whose exponential spectra are shown in Fig. 3.22b is 9 (in radians). The highest and lowest frequencies are 9 and 0, respectively. Note that the component of frequency 12 has zero amplitude and is nonexistent. Moreover, the lowest frequency is 0, not -9. Recall that the frequencies (in the conventional sense) of the spectral components at $\omega = -3$, -6, and -9 in reality are 3, 6, and 9.[†] The bandwidth can be more readily seen from the trigonometric spectra in Fig. 3.22a.

EXAMPLE 3.13 Fourier Series Spectra of an Impulse Train

Find the exponential Fourier series and sketch the corresponding spectra for the impulse train $\delta_{T_0}(t)$ depicted in Fig. 3.23a. From this result, sketch the trigonometric spectrum and write the trigonometric Fourier series for $\delta_{T_0}(t)$.

[†] Some authors *do* define bandwidth as the difference between the highest and the lowest (negative) frequency in the exponential spectrum. The bandwidth according to this definition is twice that defined here. In reality, this phrasing defines not the signal bandwidth but the *spectral width* (width of the exponential spectrum of the signal).

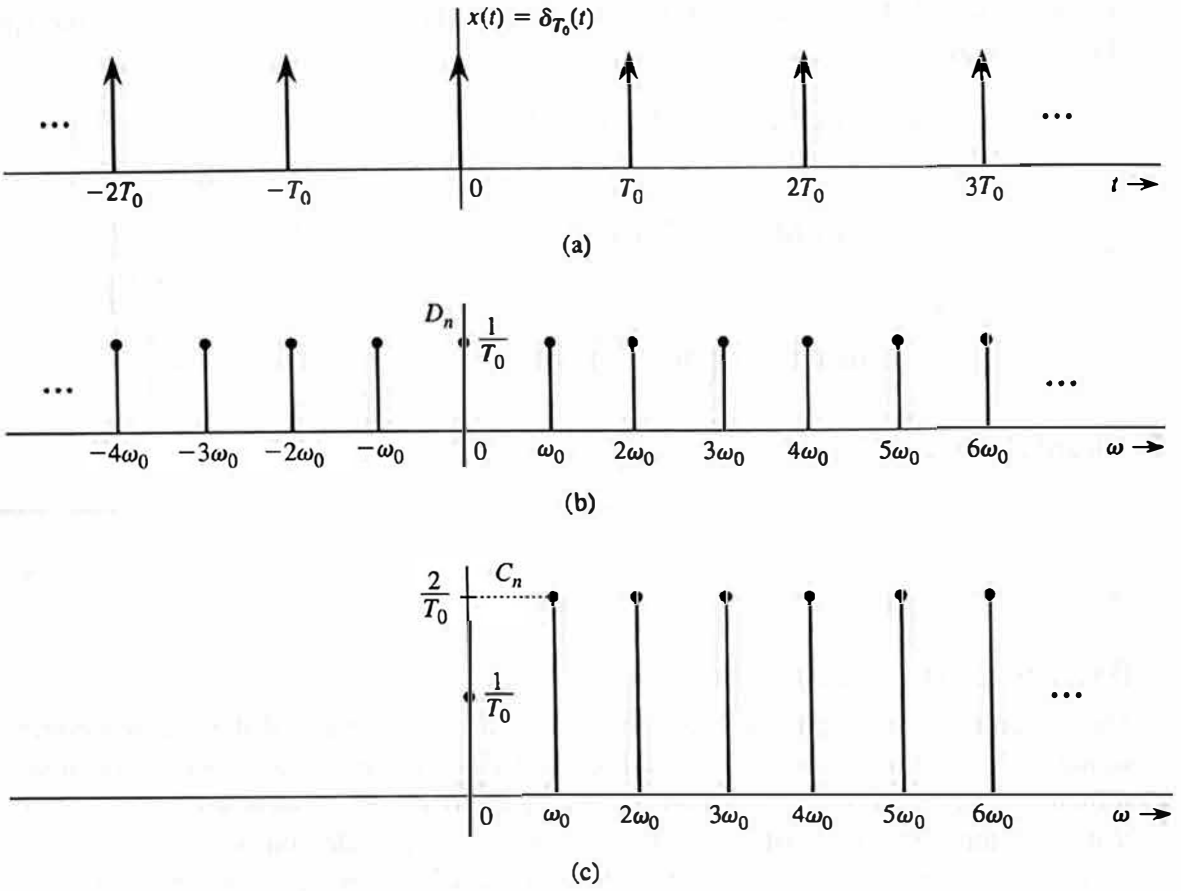

Figure 3.23 **(a)** Impulse train and **(b, c)** its Fourier spectra.

The unit impulse train shown in Fig. 3.23a can be expressed as

$$\sum_{n=-\infty}^{\infty} \delta(t - nT_0)$$

Following Papoulis, we shall denote this function as $\delta_{T_0}(t)$ for the sake of notational brevity.

The exponential Fourier series is given by

$$\delta_{T_0}(t) = \sum_{n=-\infty}^{\infty} D_n e^{jn\omega_0 t} \qquad \omega_0 = \frac{2\pi}{T_0} \tag{3.50}$$

where

$$D_n = \frac{1}{T_0} \int_{T_0} \delta_{T_0}(t) e^{-jn\omega_0 t}\, dt$$

Choosing the interval of integration $(-T_0/2, T_0/2)$ and recognizing that over this interval $\delta_{T_0}(t) = \delta(t)$, we get

$$D_n = \frac{1}{T_0}\int_{-T_0/2}^{T_0/2} \delta(t) e^{-jn\omega_0 t}\, dt$$

In this integral, the impulse is located at $t = 0$. From the sampling property of Eq. (1.11), the integral on the right-hand side is the value of $e^{-jn\omega_0 t}$ at $t = 0$ (where the impulse is located). Therefore,

$$D_n = \frac{1}{T_0} \tag{3.51}$$

From this result, we see that the exponential spectrum is constant for all frequencies, as shown in Fig. 3.23b. The spectrum, being real, requires only the amplitude plot. All phases are zero.

Substituting $D_n = \frac{1}{T_0}$ into Eq. (3.50) yields the desired exponential Fourier series

$$\delta_{T_0}(t) = \frac{1}{T_0}\sum_{n=-\infty}^{\infty} e^{jn\omega_0 t} \qquad \omega_0 = \frac{2\pi}{T_0}$$

To sketch the trigonometric spectrum, we use Eq. (3.49) to obtain

$$C_0 = D_0 = \frac{1}{T_0}$$

$$C_n = 2|D_n| = \frac{2}{T_0} \qquad n = 1, 2, 3, \ldots$$

$$\theta_n = 0$$

Figure 3.23c shows the trigonometric Fourier spectrum. From this spectrum, we can express $\delta_{T_0}(t)$ as

$$\delta_{T_0}(t) = \frac{1}{T_0}[1 + 2(\cos\omega_0 t + \cos 2\omega_0 t + \cos 3\omega_0 t + \cdots)] \qquad \omega_0 = \frac{2\pi}{T_0} \tag{3.52}$$

Effect of Symmetry in Exponential Fourier Series

When $x(t)$ has an even symmetry, $b_n = 0$, and from Eq. (3.47), $D_n = a_n/2$, which is real (positive or negative). Hence, $\angle D_n$ can only be 0 or $\pm\pi$. Moreover, we may compute $D_n = a_n/2$ by using Eq. (3.41), which requires integration over a half-period only. Similarly, when $x(t)$ has an odd symmetry, $a_n = 0$, and $D_n = -jb_n/2$ is imaginary (positive or negative). Hence, $\angle D_n$ can only be 0 or $\pm\pi/2$. Moreover, we may compute $D_n = -jb_n/2$ by using Eq. (3.42), which requires integration over a half-period only. Note, however, that in the exponential case, we are using the symmetry property indirectly by finding the trigonometric coefficients. We cannot apply it directly in finding D_n from Eq. (3.46) since the function $e^{jn\omega_0 t}$ is neither even nor odd.

DRILL 3.9 Relating Trigonometric to Exponential Fourier Series Spectra

The exponential Fourier spectra of a certain periodic signal $x(t)$ are shown in Fig. 3.24. Determine and sketch the trigonometric Fourier spectra of $x(t)$ by inspection of Fig. 3.24. Now write the (compact) trigonometric Fourier series for $x(t)$.

ANSWER

$$x(t) = 4 + 6\cos\left(3t - \frac{\pi}{6}\right) + 2\cos\left(6t - \frac{\pi}{4}\right) + 4\cos\left(9t - \frac{\pi}{2}\right)$$

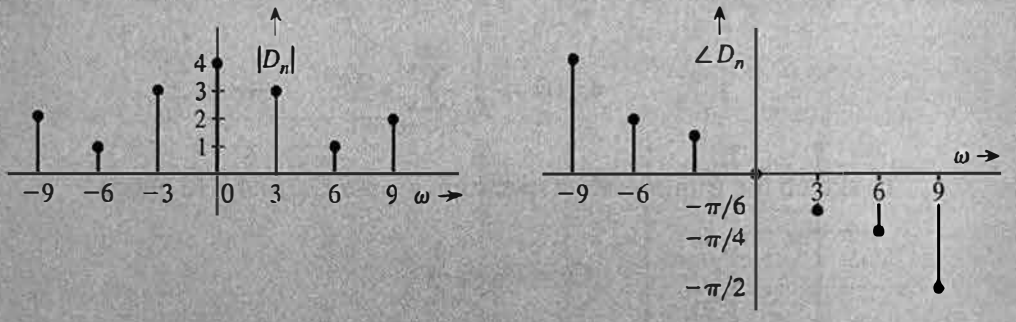

Figure 3.24 Exponential Fourier series spectra for Drill 3.9.

DRILL 3.10 Fourier Series Spectrum of a Full-Wave Rectified Sine Wave

Find the exponential Fourier series and sketch the corresponding Fourier spectrum D_n versus ω for the full-wave rectified sine wave depicted in Fig. 3.25.

ANSWER

$$x(t) = \frac{2}{\pi}\sum_{n=-\infty}^{\infty} \frac{1}{1-4n^2} e^{j2nt}$$

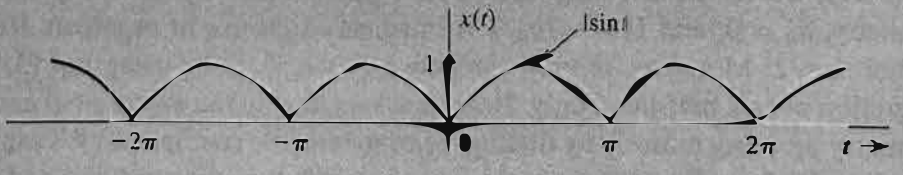

Figure 3.25 Full-wave rectified sine wave for Drill 3.10.

DRILL 3.11 Exponential Fourier Series and Spectra

Find the exponential Fourier series and sketch the corresponding Fourier spectra for the periodic signals shown in Fig. 3.15.

ANSWERS

(a) $x(t) = \frac{1}{3} + \frac{2}{\pi^2} \sum_{n=-\infty (n\neq 0)}^{\infty} \frac{(-1)^n}{n^2} e^{jn\pi t}$

(b) $x(t) = \frac{jA}{\pi} \sum_{n=-\infty (n\neq 0)}^{\infty} \frac{(-1)^n}{n} e^{jn\pi t}$

3.6.2 Parseval's Theorem

The trigonometric Fourier series of a periodic signal $x(t)$ is given by

$$x(t) = C_0 + \sum_{n=1}^{\infty} C_n \cos(n\omega_0 t + \theta_n)$$

Every term on the right-hand side of this equation is a power signal. As shown in Ex. 1.2, Eq. (1.3), the power of $x(t)$ is equal to the sum of the powers of all the sinusoidal components on the right-hand side.

$$P_x = C_0^2 + \frac{1}{2}\sum_{n=1}^{\infty} C_n^2 \tag{3.53}$$

This result is *Parseval's theorem* as applied to power signals.† It states that the power of a periodic signal is equal to the sum of the powers of its Fourier components.

We can apply the same argument to the exponential Fourier series (see Prob. 1.1-11). The power of a periodic signal $x(t)$ can be expressed as a sum of the powers of its exponential components. In Eq. (1.4), we showed that the power of an exponential $De^{j\omega_0 t}$ is $|D^2|$. We can use this result to express the power of a periodic signal $x(t)$ in terms of its exponential Fourier series coefficients as

$$P_x = \sum_{n=-\infty}^{\infty} |D_n|^2 \tag{3.54}$$

For a real $x(t)$, $|D_{-n}| = |D_n|$. Therefore,

$$P_x = D_0^2 + 2\sum_{n=1}^{\infty} |D_n|^2 \tag{3.55}$$

† Recall, Eq. (3.20) provides Parseval's theorem as applied to energy signals.

EXAMPLE 3.14 Harmonic Distortion of Clipped Sinusoid

The input signal to an audio amplifier of gain 100 is given by $x(t) = 0.1\cos\omega_0 t$. Hence, the output is a sinusoid $10\cos\omega_0 t$. However, the amplifier, being nonlinear at higher amplitude levels, clips all amplitudes beyond ± 8 volts as shown in Fig. 3.26a. We shall determine the harmonic distortion incurred in this operation.

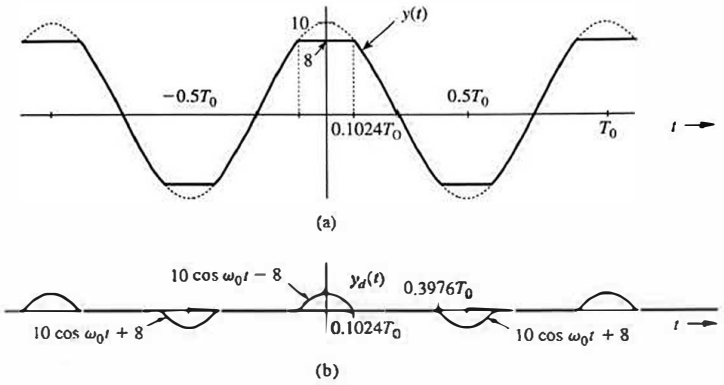

Figure 3.26 **(a)** A clipped sinusoid $\cos\omega_0 t$. **(b)** The distortion component $x_d(t)$ of the signal in (a).

The output $y(t)$ is the clipped signal in Fig. 3.26a. The distortion signal $y_d(t)$, shown in Fig. 3.26b, is the difference between the undistorted sinusoid $10\cos\omega_0 t$ and the output signal $y(t)$. The signal $y_d(t)$, whose period is T_0 [the same as that of $y(t)$], can be described over the first cycle as

$$y_d(t) = \begin{cases} 10\cos\omega_0 t - 8 & |t| \le 0.1024T_0 \\ 10\cos\omega_0 t + 8 & \dfrac{T_0}{2} - 0.1024T_0 \le |t| \le \dfrac{T_0}{2} + 0.1024T_0 \\ 0 & \text{everywhere else} \end{cases}$$

Observe that $y_d(t)$ is an even function of t and its mean value is zero. Hence, $a_0 = C_0 = 0$, and $b_n = 0$. Thus, $C_n = a_n$ and the Fourier series for $y_d(t)$ can be expressed as

$$y_d(t) = \sum_{n=1}^{\infty} C_n \cos n\omega_0 t$$

As usual, we can compute the coefficients C_n (which is equal to a_n) by integrating $y_d(t)\cos n\omega_0 t$ over one cycle (and then dividing by $2/T_0$). Because $y_d(t)$ has even symmetry,

we can find a_n by integrating the expression over a half-cycle only using Eq. (3.41). The straightforward evaluation of the appropriate integral yields†

$$C_n = \begin{cases} \dfrac{20}{\pi}\left[\dfrac{\sin[0.6435(n+1)]}{n+1} + \dfrac{\sin[0.6435(n-1)]}{n-1}\right] - \dfrac{32}{\pi}\left[\dfrac{\sin(0.6435n)}{n}\right] & n \text{ odd} \\ 0 & n \text{ even} \end{cases}$$

Computing the coefficients $C_1, C_2, C_3, \ldots$ from this expression, we can write

$$y_d(t) = 1.04\cos\omega_0 t + 0.733\cos 3\omega_0 t + 0.311\cos 5\omega_0 t + \cdots$$

Computing Harmonic Distortion

We can compute the amount of harmonic distortion in the output signal by computing the power of the distortion component $y_d(t)$. Because $y_d(t)$ is an even function of t and because the energy in the first half-cycle is identical to the energy in the second half-cycle, we can compute the power by averaging the energy over a quarter-cycle. Thus,

$$P_{y_d} = \frac{1}{T_0}\int_{-T_0/2}^{T_0/2} y_d^2(t)\,dt = \frac{1}{T_0/4}\int_0^{T_0/4} y_d^2(t)\,dt$$
$$= \frac{4}{T_0}\int_0^{0.1024T_0} (10\cos\omega_0 t - 8)^2\,dt = 0.865$$

The power of the desired signal $10\cos\omega_0 t$ is $(10)^2/2 = 50$. Hence, the total harmonic distortion is‡

$$D_{\text{tot}} = \frac{0.865}{50} \times 100 = 1.73\%$$

The power of the third harmonic components of $y_d(t)$ is $(0.733)^2/2 = 0.2686$. The third harmonic distortion is

$$D_3 = \frac{0.2686}{50} \times 100 = 0.5372\%$$

---

† In addition, $y_d(t)$ exhibits half-wave symmetry (see Prob. 3.4-8), where the second half-cycle is the negative of the first. Because of this property, all the even harmonics vanish, and the odd harmonics can be computed by integrating the appropriate expressions over the first half-cycle only (from $-T_0/4$ to $T_0/4$) and doubling the resulting values. Moreover, because of even symmetry, we can integrate the appropriate expressions over 0 to $T_0/4$ (instead of from $-T_0/4$ to $T_0/4$) and double the resulting values. In essence, this allows us to compute C_n by integrating the expression over the quarter-cycle only and then quadrupling the resulting values. Thus,

$$C_n = a_n = \frac{8}{T_0}\int_0^{0.1024T_0} [10\cos\omega_0 t - 8]\cos n\omega_0 t\,dt$$

‡ In the literature, the harmonic distortion often refers to the rms distortion rather than the power distortion. The rms values are the square-root values of the corresponding powers. Thus, the third harmonic distortion in this sense is $\sqrt{(0.2686/50)} \times 100 = 7.33\%$. Alternately, we may also compute this value directly from the amplitudes of the third harmonic 0.733 and that of the fundamental as 10. The ratio of the rms values is $(0.733/\sqrt{2}) : (10/\sqrt{2}) = 0.0733$ and the percentage distortion is 7.33%.

3.6.3 Making Life Easier: Fourier Series Properties

Although the Fourier series is undoubtedly a useful signal processing tool, it can be tedious to perform the integration to determine a signal's Fourier series coefficients. Furthermore, the task of integration does not particularly lend insight into a signal and its spectrum. Fortunately, there are a variety of Fourier series properties that can simplify work and provide a more intuitive understanding of signals. Table 3.2 provides the most important properties of the Fourier series for a periodic signal $x(t)$ and its spectrum D_n.[†] Properties that involve two signals require that the two signals have a common fundamental frequency ω_0. While not given here, the proofs of these properties are straightforward. Later chapters on Laplace and z-transforms will spend more time showing how to prove properties.

To demonstrate the utility of Fourier series properties, let us consider an example where we use a selection of properties to simplify the work of finding a piecewise polynomial signal's spectrum.

TABLE 3.2 Selected Fourier Series Properties

Operation	$x(t)$	D_n
Scalar multiplication	$kx(t)$	kD_n
Addition	$x_1(t)+x_2(t)$	$D_{1,n}+D_{2,n}$
	$x_1(t), x_2(t)$ require same ω_0	
Conjugation	$x^*(t)$	D^*_{-n}
Reversal	$x(-t)$	D_{-n}
Time shifting	$x(t-t_0)$	$D_n e^{-jn\omega_0 t_0}$
Frequency shifting	$x(t)e^{jn_0\omega_0 t}$	D_{n-n_0}
Frequency convolution	$x_1(t)x_2(t)$	$D_{1,n} * D_{2,n}$
	$x_1(t), x_2(t)$ require same ω_0	
Time differentiation	$\dfrac{d^k x(t)}{dt^k}$	$(jn\omega_0)^k D_n$

EXAMPLE 3.15 Using Fourier Series Properties

Use properties rather than integration to compute the exponential Fourier series coefficients D_n of the triangular signal $x(t)$ shown in Fig. 3.12. Verify the correctness of D_n for $A = 1$ by synthesizing $x(t)$ with a suitable truncation of Eq. (3.46).

From Fig. 3.12, we see that $x(t)$ is a piecewise linear function that is $T_0 = 2$ periodic. To compute D_n directly using Eq. (3.46) would therefore require tedious integration by parts.

[†] Although we present Fourier series properties in terms of the exponential Fourier series coefficients D_n, the properties can just as easily be cast in terms of trigonometric or compact trigonometric Fourier series coefficients.

Fortunately, we can compute D_n without integration by instead using Fourier series properties. First, however, we must compute the dc component D_0 separately from other D_n. By simple inspection of Fig. 3.12, we see that $x(t)$ has no dc component, so $D_0 = 0$.

To determine the remaining D_n, we begin by noting that $x(t)$ has a constant slope of either $2A$ or $-2A$. Thus, differentiating $x(t)$ once yields a square wave with amplitude $\pm 2A$. Here, differentiation reduces $x(t)$ from a piecewise linear to a piecewise constant function, thereby eliminating the need for integration by parts.† Differentiating $x(t)$ twice yields a pair of shifted impulse trains, weighted by $\pm 4A$. This second differentiation eliminates the need for any integration whatsoever, since the Fourier series coefficients of an impulse train are known to be $\frac{1}{T_0}$ (see Ex. 3.13).

Stated mathematically, we see that

$$\frac{d^2}{dt^2}x(t) = 4A\delta_2(t+\tfrac{1}{2}) - 4A\delta_2(t-\tfrac{1}{2})$$

Transforming this expression and using the Fourier series properties of scalar multiplication, addition, frequency shifting, and time differentiation yield (for $n \neq 0$)

$$(jn\pi)^2 D_n = 4A\frac{e^{jn\omega_0/2}}{2} - 4A\frac{e^{-jn\omega_0/2}}{2}$$

Substituting $\omega_0 = 2\pi/T_0 = \pi$ and solving for D_n yield

$$D_n = 4A\frac{e^{jn\pi/2} - e^{-jn\pi/2}}{-2n^2\pi^2}$$

Combining with the dc component and simplifying expressions, the final result is

$$D_n = \begin{cases} 0 & n = 0 \\ \frac{-A4j\sin(n\pi/2)}{n^2\pi^2} & n \neq 0 \end{cases}$$

Overall, this is a neat way to determine the signal's spectrum. Through the selective use of properties, we have determined D_n without any integration. With a little care, this basic approach can yield the spectrum of *any piecewise polynomial periodic function*. Since all periodic functions of practical interest to engineers can, to an arbitrary level of accuracy, be represented as piecewise polynomial functions, we can always find their spectra without integration except for the dc term D_0.

Using a Truncated Fourier Series to Verify Spectrum Correctness

While a signal's spectrum D_n provides useful insight into signal character, it can be difficult to look at D_n and know that it is correct for a particular signal $x(t)$. For example, is it at all obvious that $D_n = \frac{4Aj\sin(n\pi/2)}{-n^2\pi^2}$ is the spectrum for the triangle wave of Fig. 3.12? Probably not.

† Differentiation also destroys the dc component of the signal, providing further justification as to why the dc component needs to be separately computed.

There is an easy way, however, to verify a signal's spectrum: synthesize $x(t)$ using a suitable truncation of Eq. (3.46). If the synthesized signal closely matches the original, we can be relatively certain that the spectrum D_n is correct. What is a suitable truncation? Well, it depends. All significant D_n terms need to be included, but not so many as to make the reconstruction impractical to compute. Since in the present case D_n decays at a rate $1/n^2$, a good approximation is possible with a relatively few number of terms; a 10-harmonic truncation should be just fine. Let us use MATLAB to synthesize $x(t)$ using a 10-harmonic truncated Fourier series.

To begin, we define A, D_n, T_0, ω_0, and a time vector that spans two periods of the waveform.

```
>> A = 1; D = @(n) -A*4j*sin(n*pi/2)./(n.^2*pi^2);
>> T0 = 2; omega0 = 2*pi/T0; t = (-T0:.001:T0);
```

Next, we set the dc portion of the signal.

```
>> D0 = 0; x10 = D0*ones(size(t));
```

To add the desired 10 harmonics, we enter a loop for $1 \leq n \leq 10$ and add in the D_n and D_{-n} terms. Although $x(t)$ should be real, small round-off errors cause the reconstruction to be complex. These small imaginary parts are removed using the `real` command.

```
>> for n = 1:10,
>>     x10 = x10+real(D(n)*exp(1j*omega0*n*t)+D(-n)*exp(-1j*omega0*n*t));
>> end
```

Lastly, we plot the resulting truncated Fourier series synthesis of $x(t)$.

```
>> plot(t,x10,'k'); xlabel('t'); ylabel('x_{10}(t)');
```

Since the synthesized waveform shown in Fig. 3.27 closely matches the original waveform in Fig. 3.12, we have high confidence that the computed D_n are correct.

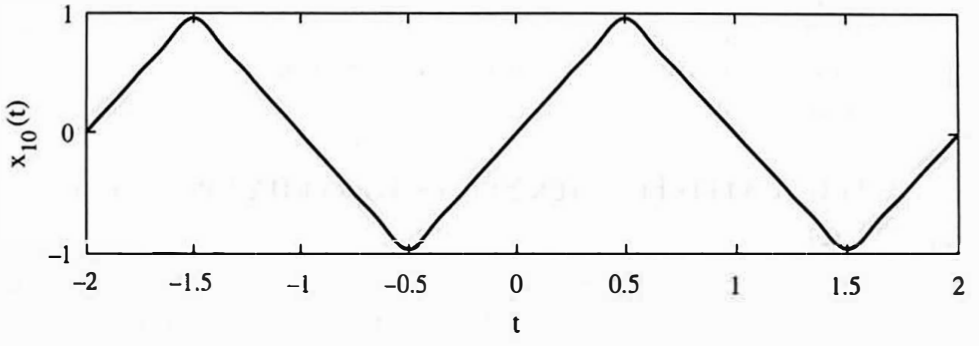

Figure 3.27 A 10-harmonic truncated Fourier series of $x(t)$.

3.7 LTIC System Response to Periodic Inputs

A periodic signal can be expressed as a sum of everlasting exponentials (or sinusoids). We also know how to find the response of an LTIC system to an everlasting exponential. From this information, we can readily determine the response of an LTIC system to periodic inputs. A periodic signal $x(t)$ with period T_0 can be expressed as an exponential Fourier series

$$x(t) = \sum_{n=-\infty}^{\infty} D_n e^{jn\omega_0 t} \qquad \omega_0 = \frac{2\pi}{T_0}$$

In Sec. 2.4.4, we showed that the response of an LTIC system with transfer function $H(s)$ to an everlasting exponential input $e^{j\omega t}$ is an everlasting exponential $H(j\omega)e^{j\omega t}$. This input–output pair can be displayed as[†]

$$\underbrace{e^{j\omega t}}_{\text{input}} \Longrightarrow \underbrace{H(j\omega)e^{j\omega t}}_{\text{output}}$$

Therefore, from the linearity property,

$$\underbrace{\sum_{n=-\infty}^{\infty} D_n e^{jn\omega_0 t}}_{\text{input } x(t)} \Longrightarrow \underbrace{\sum_{n=-\infty}^{\infty} D_n H(jn\omega_0) e^{jn\omega_0 t}}_{\text{response } y(t)} \tag{3.56}$$

The response $y(t)$ is obtained in the form of an exponential Fourier series and is therefore a periodic signal of the same period as that of the input.

We shall demonstrate the utility of these results with the following example.

EXAMPLE 3.16 Full-Wave Rectifier

A full-wave rectifier (Fig. 3.28a) is used to obtain a dc signal from a sinusoid $\sin t$. The rectified signal $x(t)$, depicted in Fig. 3.25, is applied to the input of a lowpass RC filter, which suppresses the time-varying component and yields a dc component with some residual ripple. Find the filter output $y(t)$. Find also the dc output and the rms value of the ripple voltage.

[†]This result applies only to asymptotically stable systems. This is because when $s = j\omega$, the integral on the right-hand side of Eq. (2.39) does not converge for unstable systems. Moreover, for marginally stable systems also, that integral does not converge in the ordinary sense, and $H(j\omega)$ cannot be obtained from $H(s)$ by replacing s with $j\omega$.

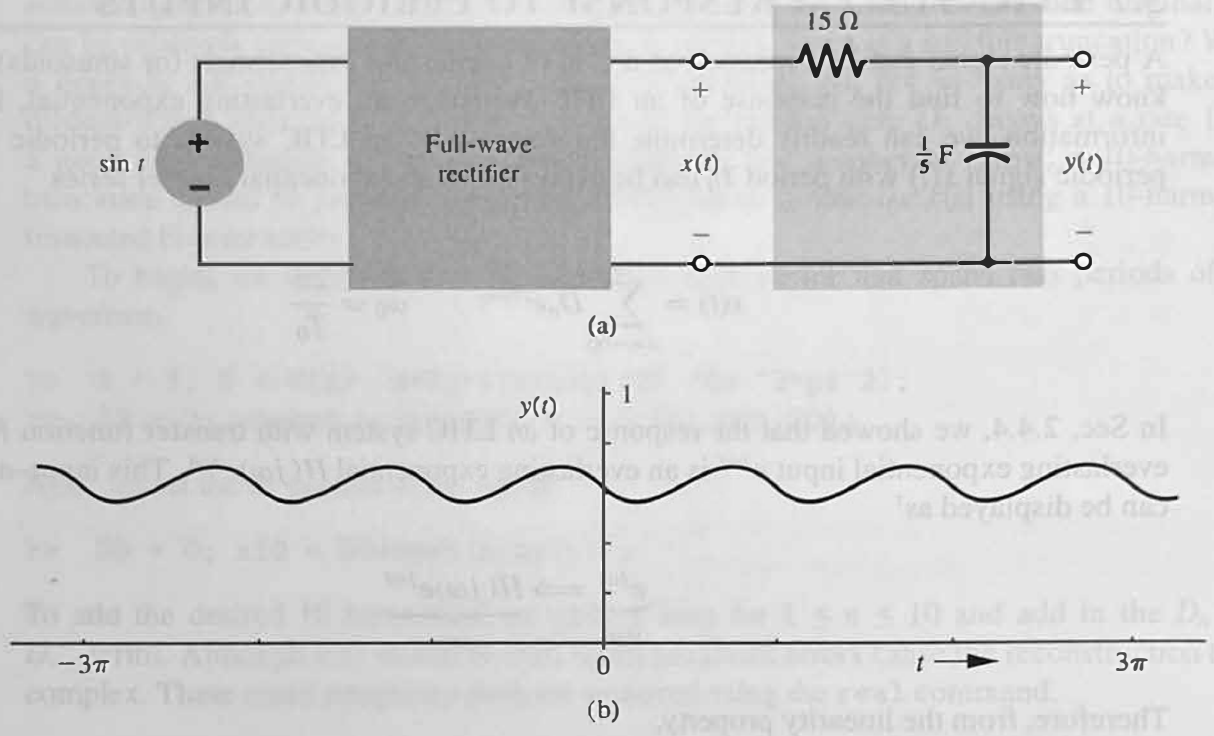

Figure 3.28 **(a)** Full-wave rectifier with a lowpass filter and **(b)** its output.

First, we shall find the Fourier series for the rectified signal $x(t)$, whose period is $T_0 = \pi$. Consequently, $\omega_0 = 2$, and

$$x(t) = \sum_{n=-\infty}^{\infty} D_n e^{j2nt}$$

where

$$D_n = \frac{1}{\pi}\int_0^{\pi} \sin t\, e^{-j2nt}\, dt = \frac{2}{\pi(1-4n^2)} \tag{3.57}$$

Therefore,

$$x(t) = \sum_{n=-\infty}^{\infty} \frac{2}{\pi(1-4n^2)} e^{j2nt}$$

Next, we find the transfer function of the *RC* filter in Fig. 3.28a. This filter is identical to the *RC* circuit in Ex. 1.17 (Fig. 1.35) for which the differential equation relating the output (capacitor voltage) to the input $x(t)$ was found to be [Eq. (1.31)]

$$(3D+1)y(t) = x(t)$$

The transfer function $H(s)$ for this system is found from Eq. (2.41) as

$$H(s) = \frac{1}{3s+1}$$

and

$$H(j\omega) = \frac{1}{3j\omega+1} \tag{3.58}$$

From Eq. (3.56), the filter output $y(t)$ can be expressed as (with $\omega_0 = 2$)

$$y(t) = \sum_{n=-\infty}^{\infty} D_n H(jn\omega_0) e^{jn\omega_0 t} = \sum_{n=-\infty}^{\infty} D_n H(j2n) e^{j2nt}$$

Substituting D_n and $H(j2n)$ from Eqs. (3.57) and (3.58) in the foregoing equation, we obtain

$$y(t) = \sum_{n=-\infty}^{\infty} \frac{2}{\pi(1-4n^2)(j6n+1)} e^{j2nt}$$

Note that the output $y(t)$ is also a periodic signal given by the exponential Fourier series on the right-hand side. The output is shown in Fig. 3.28b.

The output Fourier series coefficient corresponding to $n = 0$ is the dc component of the output, given by $2/\pi$. The remaining terms in the Fourier series constitute the unwanted component called the ripple. We can determine the rms value of the ripple voltage by using Eq. (3.54) to find the power of the ripple component. The power of the ripple is the power of all the components except the dc ($n = 0$). Note that $\hat{D}_n$, the exponential Fourier coefficient for the output $y(t)$, is

$$\hat{D}_n = \frac{2}{\pi(1-4n^2)(j6n+1)}$$

Therefore, from Eq. (3.55), we have

$$P_{\text{ripple}} = 2\sum_{n=1}^{\infty} |D_n|^2 = 2\sum_{n=1}^{\infty} \left| \frac{2}{\pi(1-4n^2)(j6n+1)} \right|^2 = \frac{8}{\pi^2} \sum_{n=1}^{\infty} \frac{1}{(1-4n^2)^2(36n^2+1)}$$

Numerical computation of the right-hand side yields $P_{\text{ripple}} = 0.0025$, and the ripple rms value $= \sqrt{P_{\text{ripple}}} = 0.05$. This shows that the rms ripple voltage is 5% of the amplitude of the input sinusoid.

Why Use Exponentials?

During the development of the Fourier series, it is natural to ask what is so special about exponential signals. If $x(t)$ can be represented in terms of hundreds of different orthogonal sets, why do we exclusively use the exponential (or trigonometric) set for the representation of signals or LTI systems? It so happens that the exponential signal is an eigenfunction of LTI systems.

In other words, for an LTI system, only an exponential input e^{st} yields the response that is also an exponential of the same form, given by $H(s)e^{st}$. The same is true of the trigonometric set. This fact makes the use of exponential signals natural for LTI systems in the sense that the system analysis using exponentials as the basis signals is greatly simplified.

Furthermore, the exponential form is generally preferred over the trigonometric form. The exponential Fourier series is just another way of representing trigonometric Fourier series (or vice versa). The two forms carry identical information—no more, no less. The reasons for preferring the exponential form have already been mentioned: this form is more compact, and the expression for deriving the exponential coefficients is also more compact than those in the trigonometric series. Furthermore, the LTIC system response to exponential signals is also simpler (more compact) than the system response to sinusoids. In addition, the exponential form proves to be much easier than the trigonometric form to manipulate mathematically and otherwise handle in the area of signals as well as systems. Moreover, exponential representation proves much more convenient for analysis of complex $x(t)$. For these reasons, in our future discussion we shall use the exponential form exclusively.

A minor disadvantage of the exponential form is that it cannot be visualized as easily as sinusoids. For intuitive and qualitative understanding, the sinusoids have the edge over exponentials. Fortunately, this difficulty can be overcome readily because of the close connection between exponential and Fourier spectra. For the purpose of mathematical analysis, we shall continue to use exponential signals and spectra; but to understand the physical situation intuitively or qualitatively, we shall speak in terms of sinusoids and trigonometric spectra. Thus, although all mathematical manipulation will be in terms of exponential spectra, we shall now speak of exponential and sinusoids interchangeably when we discuss intuitive and qualitative insights in attempting to arrive at an understanding of physical situations. This is an important point; readers should make an extra effort to familiarize themselves with the two forms of spectra, their relationships, and their convertibility.

Dual Personality of a Signal

The discussion so far has shown that a periodic signal has a dual personality—the time domain and the frequency domain. It can be described by its waveform or by its Fourier spectra. The time- and frequency-domain descriptions provide complementary insights into a signal. For an in-depth perspective, we need to understand both these identities. It is important to learn to think of a signal from both perspectives. In the next chapter, we shall see that aperiodic signals also have this dual personality. Moreover, we shall show that even LTI systems have this dual personality, which offers complementary insights into the system behavior.

Limitations of the Fourier Series Method of Analysis

We have developed here a method of representing a periodic signal as a weighted sum of everlasting exponentials whose frequencies lie along the ω axis in the s plane. This representation (Fourier series) is valuable in many applications. However, as a tool for analyzing linear systems, it has serious limitations and consequently has limited utility for the following reasons:

1. The Fourier series can be used only for periodic inputs. All practical inputs are aperiodic (remember that a periodic signal starts at $t = -\infty$).
2. The Fourier methods can be applied readily to BIBO-stable (or asymptotically stable) systems. It cannot handle unstable or even marginally stable systems.

The first limitation can be overcome by representing aperiodic signals in terms of everlasting exponentials. This representation can be achieved through the Fourier integral, which may be considered to be an extension of the Fourier series. We shall therefore use the Fourier series as a stepping-stone to the Fourier integral developed in the next chapter. The second limitation can be overcome by using exponentials e^{st}, where s is not restricted to the imaginary axis but is free to take on complex values. This generalization leads to the Laplace integral, discussed in Ch. 6 (the Laplace transform).

3.8 Numerical Computation of D_n

We can compute D_n numerically by using the DFT (the discrete Fourier transform discussed in Sec. 5.5), which uses the samples of a periodic signal $x(t)$ over one period. The sampling interval is T seconds. Hence, there are $N_0 = T_0/T$ number of samples in one period T_0. To find the relationship between D_n and the samples of $x(t)$, consider Eq. (3.46) and write

$$\begin{aligned} D_n &= \frac{1}{T_0}\int_{T_0} x(t)e^{-jn\omega_0 t}\,dt \\ &= \lim_{T\to 0}\frac{1}{N_0 T}\sum_{k=0}^{N_0-1} x(kT)e^{-jn\omega_0 kT}\,T \\ &= \lim_{T\to 0}\frac{1}{N_0}\sum_{k=0}^{N_0-1} x(kT)e^{-jn\Omega_0 k} \end{aligned} \tag{3.59}$$

where $x(kT)$ is the kth sample of $x(t)$ and

$$N_0 = \frac{T_0}{T} \qquad \text{and} \qquad \Omega_0 = \omega_0 T = \frac{2\pi}{N_0}$$

In practice, it is impossible to make $T \to 0$ in computing the right-hand side of Eq. (3.59). We can make T small, but not zero, which will cause the data to increase without limit. Thus, we shall ignore the limit on T in Eq. (3.59) with the implicit understanding that T is reasonably small. Nonzero T will result in some computational error, which is inevitable in any numerical evaluation of an integral. The error resulting from nonzero T is called the *aliasing error*, which is discussed in more detail in Ch. 5. Thus, we can express Eq. (3.59) as

$$D_n \approx \frac{1}{N_0}\sum_{k=0}^{N_0-1} x(kT)e^{-jn\Omega_0 k} \tag{3.60}$$

Since $\Omega_0 N_0 = 2\pi$, we know that $e^{jn\Omega_0(k+N_0)} = e^{jn\Omega_0 k}$, and it follows that

$$D_{n+N_0} = D_n$$

The periodicity property $D_{n+N_0} = D_n$ means that beyond $n = N_0/2$, the coefficients represent the values for negative n. For instance, when $N_0 = 32$, $D_{17} = D_{-15}$, $D_{18} = D_{-14}, \ldots, D_{31} = D_{-1}$. The cycle repeats again from $n = 32$ on.

We can use the efficient FFT (the *fast Fourier transform* discussed in Sec. 5.6) to compute the right-hand side of Eq. (3.60). We shall use MATLAB to implement the FFT algorithm. For this purpose, we need samples of $x(t)$ over one period starting at $t = 0$. In this algorithm, it is also preferable (although not necessary) that N_0 be a power of 2 (i.e., $N_0 = 2^m$, where m is an integer).

EXAMPLE 3.17 Numerical Computation of Fourier Spectra

Numerically compute and then plot the exponential Fourier spectra for the periodic signal in Fig. 3.10b (Ex. 3.5).

The samples of $\varphi(t)$ start at $t = 0$ and the last (N_0th) sample is at $t = T_0 - T$. At the points of discontinuity, the sample value is taken as the average of the values of the function on two sides of the discontinuity. Thus, the sample at $t = 0$ is not 1 but $(e^{-\pi/2} + 1)/2 = 0.604$. To determine N_0, we require that D_n for $n \geq N_0/2$ to be negligible. Because $\varphi(t)$ has a jump discontinuity, D_n decays rather slowly as $1/n$. Hence, a choice of $N_0 = 200$ is acceptable because the $(N_0/2)$nd (100th) harmonic is about 1% of the fundamental. However, we also require N_0 to be power of 2. Hence, we shall take $N_0 = 256 = 2^8$.

First, the basic parameters are established.

```
>> T_0 = pi; N_0 = 256; T = T_0/N_0; t = (0:T:T*(N_0-1))';
>> varphi = exp(-t/2); varphi(1) = (exp(-pi/2)+1)/2;
```

Next, the DFT, computed by means of the `fft` function, is used to approximate the exponential Fourier spectra up to $n = N_0/2$. The `fftshift` command shifts the `fft` results to plot over the range $-\frac{N_0}{2}$ to $\frac{N_0}{2} - 1$ rather than the default 0 to $N_0 - 1$ [the details will be given in Sec. 5.7.1]. To facilitate comparison with previous plots of D_n, we only plot the results over $-5 \leq n \leq 5$.

```
>> D_n = fft(varphi)/N_0; n = [-N_0/2:N_0/2-1]';
>> clf; subplot(1,2,1); stem(n,abs(fftshift(D_n)),'.k');
>> axis([-5 5 0 .6]); xlabel('n'); ylabel('|D_n|');
>> subplot(1,2,2); stem(n,angle(fftshift(D_n)),'.k');
>> axis([-5 5 -2 2]); xlabel('n'); ylabel('\angle D_n [rad]');
```

As shown in Fig. 3.29, the resulting approximation is visually indistinguishable from the true Fourier series spectra shown in Fig. 3.20 or Fig. 3.21.

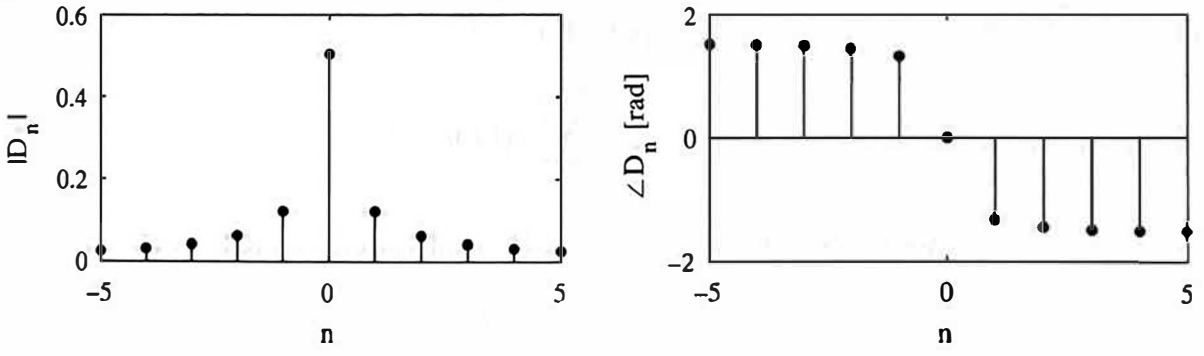

Figure 3.29 Numerical approximation of exponential Fourier series spectra using the DFT.

3.9 MATLAB: Fourier Series Applications

Computational packages such as MATLAB simplify the Fourier-based analysis, design, and synthesis of periodic signals. MATLAB permits rapid and sophisticated calculations, which promote practical application and intuitive understanding of the Fourier series.

3.9.1 Periodic Functions and the Gibbs Phenomenon

It is sufficient to define any T_0-periodic function over the interval $(0 \leq t < T_0)$. For example, consider the 2π-periodic function given by

$$x(t) = \begin{cases} t/A & 0 \leq t < A \\ 1 & A \leq t < \pi \\ 0 & \pi \leq t < 2\pi \\ x(t+2\pi) & \text{otherwise} \end{cases}$$

Although similar to a square wave, $x(t)$ has a linearly rising edge of width A, where $(0 < A < \pi)$. As $A \to 0$, $x(t)$ approaches a square wave; as $A \to \pi$, $x(t)$ approaches a type of sawtooth wave.

In MATLAB, the `mod` command helps represent periodic signals such as $x(t)$.

```
>>  x = @(t,A) mod(t,2*pi)/A.*(mod(t,2*pi)<A)+...
>>      ((mod(t,2*pi)>=A)&(mod(t,2*pi)<pi));
```

Sometimes referred to as the signed remainder after division, `mod(t,2*pi)` returns the value t modulo 2π. Thought of another way, the `mod` operator appropriately shifts t into $[0, T_0)$, where $x(t)$ is conveniently defined. Notice also that an anonymous function can be defined with multiple input variables.

The exponential Fourier series coefficients for $x(t)$ (see Prob. 3.6-2) are given by

$$D_n = \begin{cases} \dfrac{2\pi - A}{4\pi} & n = 0 \\ \dfrac{1}{2\pi n}\left(\dfrac{e^{-jnA} - 1}{nA} + je^{-jn\pi}\right) & \text{otherwise} \end{cases}$$

Since $x(t)$ is real, $D_{-n} = D_n^*$. Truncating the Fourier series at $|n| = N$ yields the approximation

$$x(t) \approx x_N(t) = D_0 + \sum_{n=1}^{N} \left(D_n e^{jnt} + D_n^* e^{-jnt}\right) \tag{3.61}$$

For a user-specified N, program `CH3MP1` uses Eq. (3.61) to compute $x_N(t)$ over $-\pi/4 \leq t < 2\pi + \pi/4$.

```
function [x_N,t] = CH3MP1(A,N);
% CH3MP1.m : Chapter 3, MATLAB Program 1
% Function M-file approximates x(t) using Fourier series truncated at |n|=N
% INPUTS :   A = width of rising edge
%            N = largest harmonic of truncated Fourier series
```

```
% OUTPUTS:  x_N = Nth harmonic truncated Fourier series
%           t = time vector for x_N

% Define FS coefficients for signal x(t)
D = @(n) 1/(2*pi*n)*((exp(-1j*n*A)-1)/(n*A) + 1j*exp(-1j*n*pi));
% Construct truncated FS approximation of x(t) using N harmonics
t = linspace(-pi/4,2*pi+pi/4,10000);    % Time vector exceeds one period.
x_N = (2*pi-A)/(4*pi)*ones(size(t));    % Compute dc term
for n = 1:N,                            % Compute N remaining terms
    x_N = x_N+real(D(n)*exp(1j*n*t) + conj(D(n))*exp(-1j*n*t));
end
```

Although theoretically not required, the `real` command ensures that small computer round-off errors do not cause a complex-valued result.

Using program CH3MP1 with $A = \pi/2$ and $N = 20$, Fig. 3.30 compares $x(t)$ and $x_{20}(t)$.

```
>>  A = pi/2; [x_20,t] = CH6MP1(A,20);
>>  plot(t,x_20,'k',t,x(t,A),'k:'); axis([-pi/4,2*pi+pi/4,-0.1,1.1]);
>>  xlabel('t'); ylabel('x_{20}(t)');
```

As expected, the falling edge is accompanied by the overshoot that is characteristic of the Gibbs phenomenon.

Increasing N to 100, as shown in Fig. 3.31, improves the approximation but does not reduce the overshoot.

```
>>  [x_100,t] = CH3MP1(A,100);
>>  plot(t,x_100,'k',t,x(t,A),'k:'); axis([-pi/4,2*pi+pi/4,-0.1,1.1]);
>>  xlabel('t'); ylabel('x_{100}(t)');
```

Reducing A to $\pi/64$ produces a curious result. For $N = 20$, both the rising and falling edges are accompanied by roughly 9% of overshoot, as shown in Fig. 3.32. As the number of terms is increased, overshoot persists only in the vicinity of jump discontinuities. For $x_N(t)$, increasing N

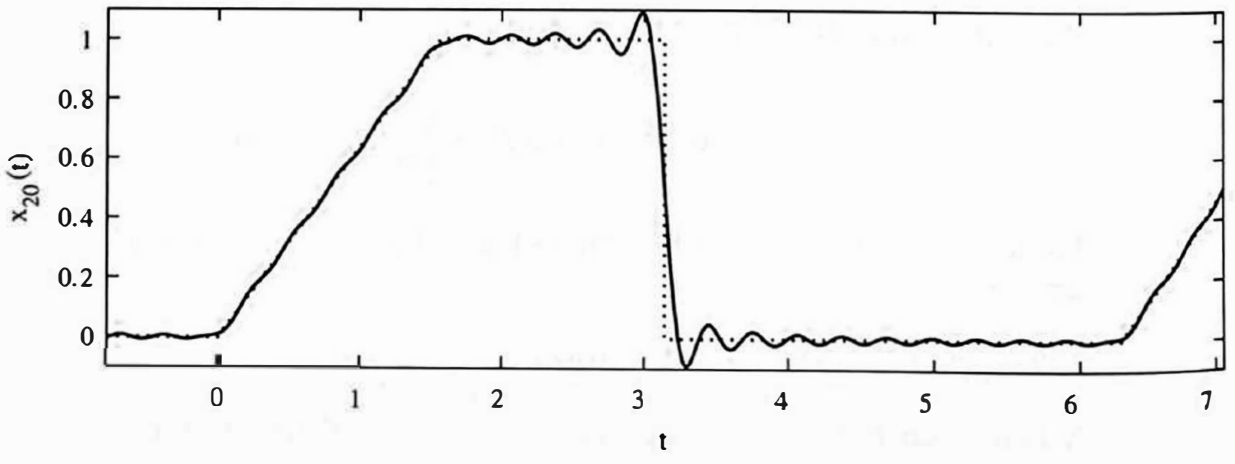

Figure 3.30 Comparison of $x_{20}(t)$ and $x(t)$ when $A = \pi/2$.

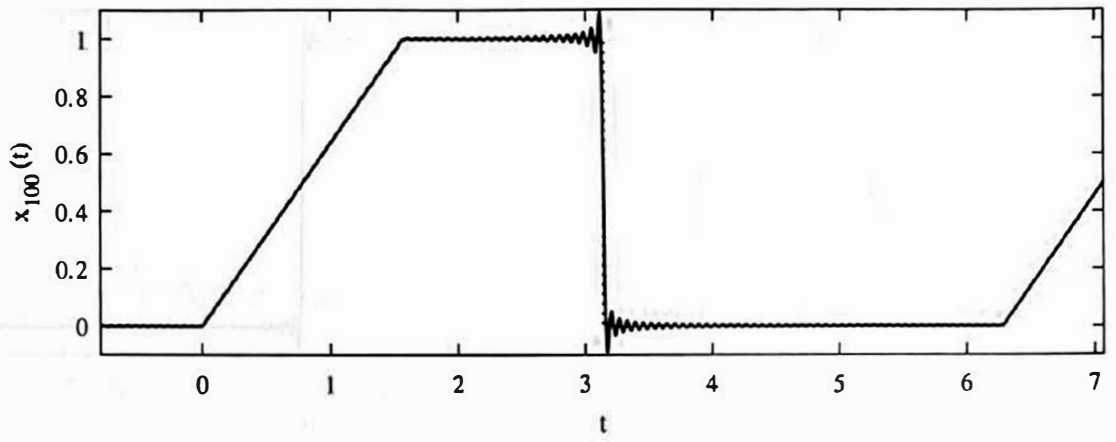

Figure 3.31 Comparison of $x_{100}(t)$ and $x(t)$ when $A = \pi/2$.

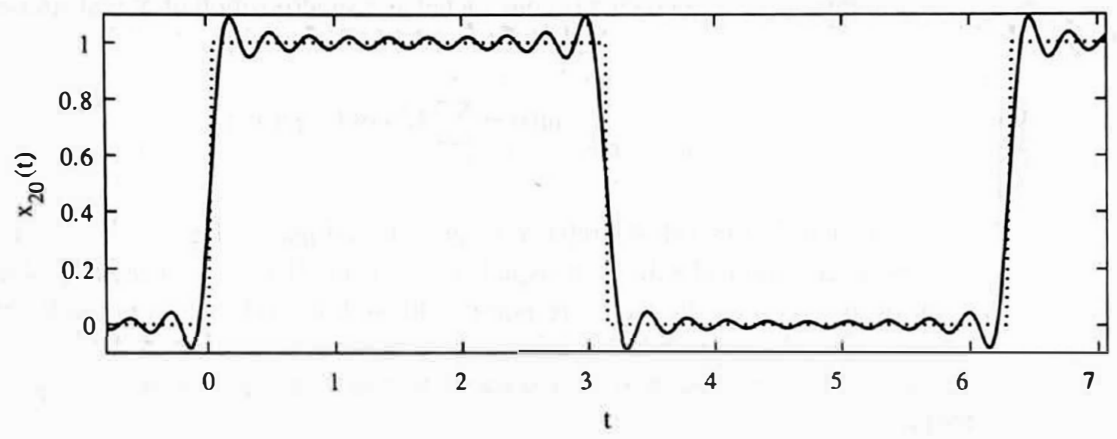

Figure 3.32 Comparison of $x_{20}(t)$ and $x(t)$ when $A = \pi/64$.

decreases the overshoot near the rising edge but not near the falling edge. Remember that it is a true jump discontinuity that causes the Gibbs phenomenon. A continuous signal, no matter how sharply it rises, can always be represented by a Fourier series at every point within any small error by increasing N. This is not the case when a true jump discontinuity is present. Figure 3.33 illustrates this behavior using $N = 100$.

3.9.2 Optimization and Phase Spectra

Although magnitude spectra typically receive the most attention, phase spectra are critically important in some applications. Consider the problem of characterizing the frequency response of an unknown system. By applying sinusoids one at a time, the frequency response is empirically measured one point at a time. This process is tedious at best. Applying a superposition of many sinusoids, however, allows simultaneous measurement of many points of the frequency response. Such measurements can be taken by a spectrum analyzer equipped with a transfer function mode or by applying Fourier analysis techniques, which are discussed in later chapters.

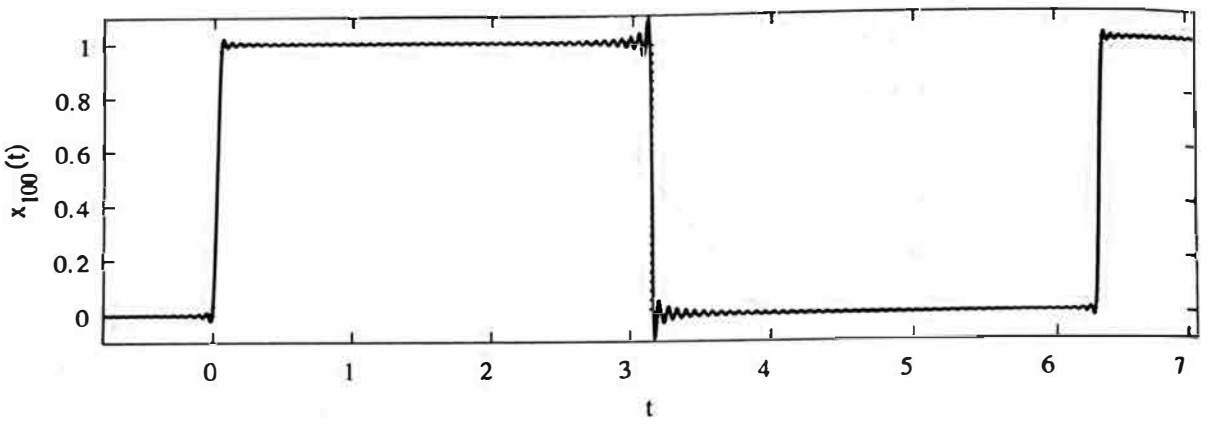

Figure 3.33 Comparison of $x_{100}(t)$ and $x(t)$ when $A = \pi/64$.

A multitone test signal $m(t)$ is constructed as a superposition of N real sinusoids

$$m(t) = \sum_{n=1}^{N} M_n \cos(\omega_n t + \theta_n)$$

where M_n and θ_n establish the relative magnitude and phase of each sinusoidal component. It is sensible to constrain all gains to be equal, $M_n = M$ for all n. This ensures equal treatment at each point of the measured frequency response. Although the value M is normally chosen to set the desired signal power, we set $M = 1$ for convenience.

While not required, it is also sensible to space the sinusoidal components uniformly in frequency.

$$m(t) = \sum_{n=1}^{N} \cos(n\omega_0 t + \theta_n) \tag{3.62}$$

Another sensible alternative, which spaces components logarithmically in frequency, is treated in Prob. 3.9-4.

Equation (3.62) is now a truncated compact-form Fourier series with a flat magnitude spectrum. Frequency resolution and range are set by ω_0 and N, respectively. For example, a 2 kHz range with a resolution of 100 Hz requires $\omega_0 = 2\pi\,100$ and $N = 20$. The only remaining unknowns are the θ_n.

While it is tempting to set $\theta_n = 0$ for all n, the results are quite unsatisfactory. MATLAB helps demonstrate the problem by using $\omega_0 = 2\pi\,100$ and $N = 20$ sinusoids, each with a peak-to-peak voltage of 1 volt.

```
>> m = @(theta,t,omega) sum(cos(omega*t+theta*ones(size(t))));
>> N = 20; omega = 2*pi*100*[1:N]'; theta = zeros(size(omega));
>> t = linspace(-0.01,0.01,10000);
>> plot(t,m(theta,t,omega),'k'); xlabel('t [sec]'); ylabel('m(t) [volts]');
```

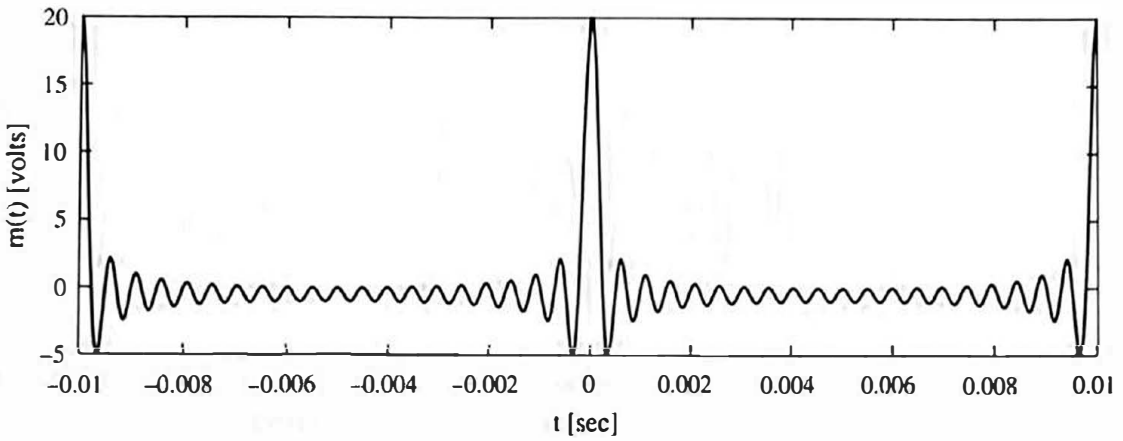

Figure 3.34 Test signal $m(t)$ with $\theta_n = 0$.

As shown in Fig. 3.34, $\theta_n = 0$ causes each sinusoid to constructively add. The resulting 20 volt peak can saturate system components, such as operational amplifiers operating with ± 12 volt rails. To improve signal performance, the maximum amplitude of $m(t)$ over t needs to be reduced.

One way to reduce $\max_t(|m(t)|)$ is to reduce M, the strength of each component. Unfortunately, this approach reduces the system's signal-to-noise ratio and ultimately degrades measurement quality. Therefore, reducing M is not a smart decision. The phases θ_n, however, can be adjusted to reduce $\max_t(|m(t)|)$ while preserving signal power. In fact, since $\theta_n = 0$ maximizes $\max_t(|m(t)|)$, just about any other choice of θ_n will improve the situation. Even a random choice should improve performance.

As with any computer, MATLAB cannot generate truly random numbers. Rather, it generates pseudo-random numbers. Pseudo-random numbers are deterministic sequences that appear to be random. The particular sequence of numbers that is realized depends entirely on the initial state of the pseudo-random number generator. Setting the generator's initial state to a known value allows a "random" experiment with reproducible results. The command `rng(0)` initializes the state of the pseudo-random number generator to a known condition of zero, and the MATLAB command `rand(a,b)` generates an a-by-b matrix of pseudo-random numbers that are uniformly distributed over the interval $(0,1)$. Radian phases occupy the wider interval $(0,2\pi)$, so the results from `rand` need to be appropriately scaled.

```
>> rng(0); theta_rand0 = 2*pi*rand(N,1);
```

Next, we recompute and plot $m(t)$ using the randomly chosen θ_n.

```
>> m_rand0 = m(theta_rand0,t,omega);
>> plot(t,m_rand0,'k'); axis([-0.01,0.01,-10,10]);
>> xlabel('t [sec]'); ylabel('m(t) [volts]');
>> set(gca,'ytick',[min(m_rand0),max(m_rand0)]); grid on;
```

For a vector input, the `min` and `max` commands return the minimum and maximum values of the vector. Using these values to set y-axis tick marks makes it easy to identify the extreme values of $m(t)$. As seen from Fig. 3.35, the maximum amplitude is now 7.6307, which is significantly smaller than the maximum of 20 when $\theta_n = 0$.

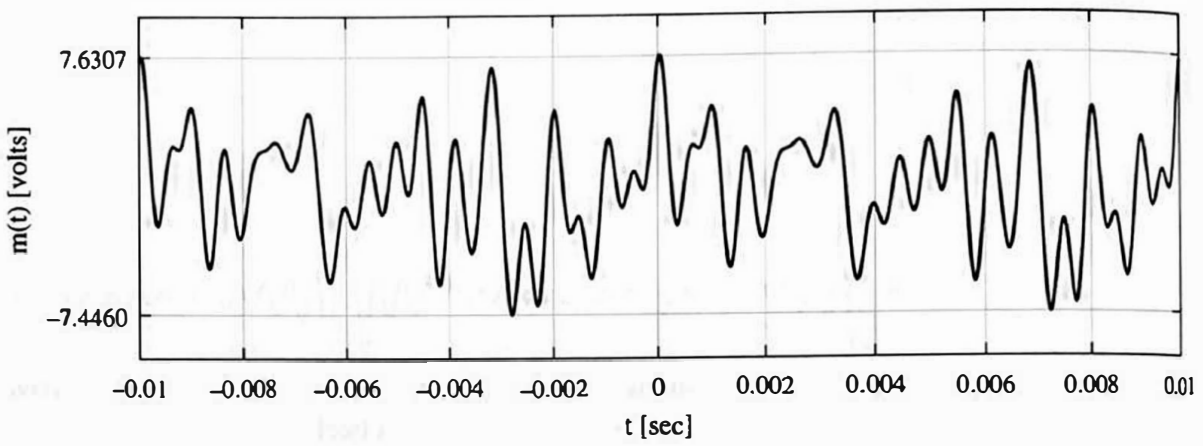

Figure 3.35 Test signal $m(t)$ with random θ_n found by using `rng(0)`.

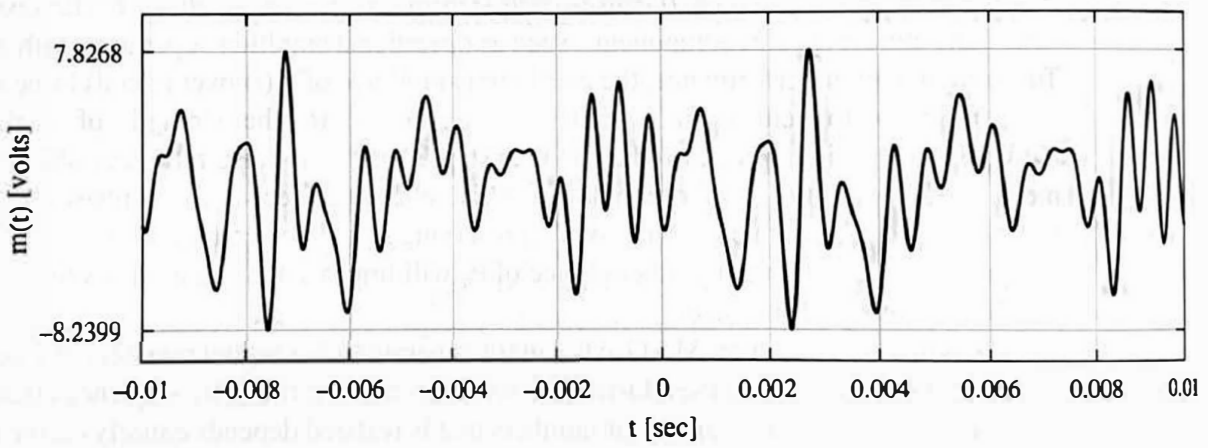

Figure 3.36 Test signal $m(t)$ with random θ_n found by using `rng(5)`.

Randomly chosen phases suffer a fatal fault: there is little guarantee of optimal performance. For example, repeating the experiment with `rng(5)` produces a maximum magnitude of 8.2399 volts, as shown in Fig. 3.36. This value is significantly higher than the previous maximum of 7.6307 volts. Clearly, it is better to replace a random solution with an optimal solution.

What constitutes "optimal"? Many choices exist, but desired signal criteria naturally suggest that optimal phases minimize the maximum magnitude of $m(t)$ over all t. To find these optimal phases, MATLAB's `fminsearch` command is useful. First, the function to be minimized, called the objective function, is defined.

```
>> maxmagm = @(theta,t,omega) max(abs(sum(...
>>       cos(omega*t+theta*ones(size(t))))));
```

The anonymous function argument order is important; `fminsearch` uses the first input argument as the variable of minimization. To minimize over θ, as desired, θ must be the first argument of the objective function `maxmagm`.

Next, the time vector is shortened to include only one period of $m(t)$.

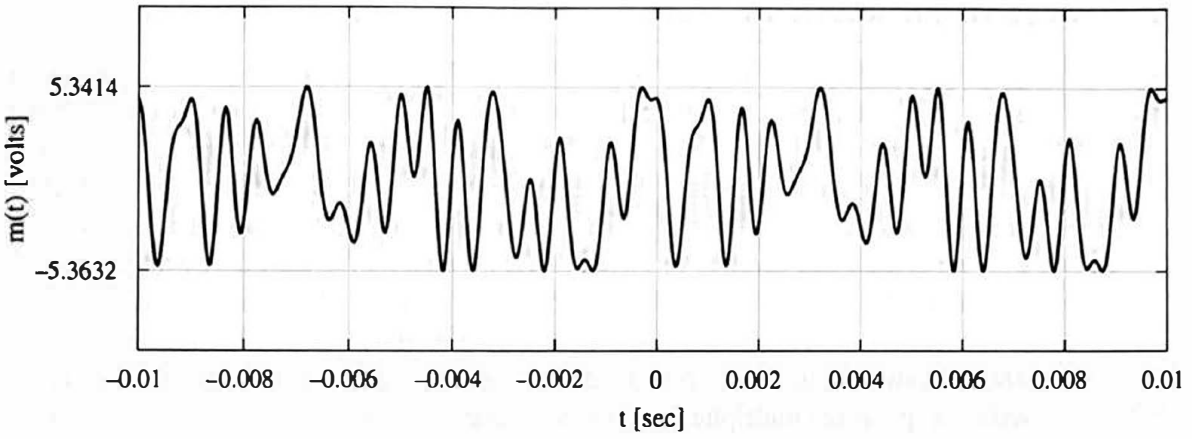

Figure 3.37 Test signal $m(t)$ with optimized phases.

```
>> t = linspace(0,0.01,401);
```

A full period ensures that all values of $m(t)$ are considered; the short length of `t` helps ensure that functions execute quickly. An initial value of θ is randomly chosen to begin the search.

```
>> rng(0); theta_init = 2*pi*rand(N,1);
>> theta_opt = fminsearch(maxmagm,theta_init,[],t,omega);
```

Notice that `fminsearch` finds the minimizer to `maxmagm` over θ by using an initial value `theta_init`. Most numerical minimization techniques are capable of finding only local minima, and `fminsearch` is no exception. As a result, `fminsearch` does not always produce a unique solution. The empty square brackets indicate no special options are requested, and the remaining ordered arguments are secondary inputs for the objective function. Full format details for `fminsearch` are available from MATLAB's help facilities.

Figure 3.37 shows the phase-optimized test signal. The maximum magnitude is reduced to a value of 5.3632 volts, which is a significant improvement over the original peak of 20 volts.

Although the signals shown in Figs. 3.34 through 3.37 look different, they all possess the same magnitude spectra. The signals differ only in phase spectra. It is interesting to investigate the similarities and differences of these signals in ways other than graphs and mathematics. For example, is there an audible difference between the signals? For computers equipped with sound capability, the MATLAB `sound` command can be used to find out.

```
>> Fs = 8000; t = [0:1/Fs:2];       % Two seconds at 8kHz sampling rate
>> sound(m(theta,t,omega)/20,Fs); % Play (scaled) m(t) made with 0 phases
```

Since the `sound` command clips magnitudes that exceed 1, the input vector is scaled by 1/20 to avoid clipping and the resulting sound distortion. The signals using other phase assignments are created and played in a similar fashion. How well does the human ear discern the differences in phase spectra? If you are like most people, you will not be able to discern any differences in how these waveforms sound.

3.10 SUMMARY

This chapter discusses the foundations of signal representation in terms of its components. There is a perfect analogy between vectors and signals; the analogy is so strong that the term *analogy* understates the reality. Signals are not just *like* vectors. Signals *are* vectors. The inner or scalar product of two (real) signals is the area under the product of the two signals. If this inner or scalar product is zero, then the signals are said to be orthogonal. A signal $x(t)$ has a component $cy(t)$, where c is the inner product of $x(t)$ and $y(t)$ divided by E_y, the energy of $y(t)$.

A good measure of similarity of two signals $x(t)$ and $y(t)$ is the correlation coefficient ρ, which is equal to the inner product of $x(t)$ and $y(t)$ divided by $\sqrt{E_x E_y}$. It can be shown that $-1 \leq \rho \leq 1$. The maximum similarity ($\rho = 1$) occurs only when the two signals have the same waveform within a (positive) multiplicative constant, that is, when $x(t) = Ky(t)$. The maximum dissimilarity ($\rho = -1$) occurs only when $x(t) = -Ky(t)$. Zero similarity ($\rho = 0$) occurs when the signals are orthogonal. In binary communication, where we are required to distinguish between two known waveforms in the presence of noise and distortion, selecting the two waveforms with maximum dissimilarity ($\rho = -1$) provides maximum distinguishability.

Just as a vector can be represented by the sum of its orthogonal components in a complete orthogonal vector space, a signal can also be represented by the sum of its orthogonal components in a complete orthogonal signal space. Such a representation is known as the *generalized Fourier series* representation. A vector can be represented by its orthogonal components in many different ways, depending on the coordinate system used. Similarly, a signal can be represented in terms of different orthogonal signal sets, of which the trigonometric and the exponential signal sets are two examples. We have shown that the trigonometric and exponential Fourier series are periodic with a period equal to that of the fundamental in the set. In this chapter, we have shown how a periodic signal can be represented as a sum of (everlasting) sinusoids or exponentials. If the frequency of a periodic signal is ω_0, then it can be expressed as a sum of the sinusoid of frequency ω_0 and its harmonics (trigonometric Fourier series). We can reconstruct the periodic signal from a knowledge of the amplitudes and phases of these sinusoidal components (amplitude and phase spectra).

If a periodic signal $x(t)$ has an even symmetry, its Fourier series contains only cosine terms (including dc). In contrast, if $x(t)$ has an odd symmetry, its Fourier series contains only sine terms. If $x(t)$ has neither type of symmetry, its Fourier series contains both sine and cosine terms.

At points of discontinuity, the Fourier series for $x(t)$ converges to the mean of the values of $x(t)$ on either side of the discontinuity. For signals with discontinuities, the Fourier series converges in the mean and exhibits the Gibbs phenomenon at the points of discontinuity. The amplitude spectrum of the Fourier series for a periodic signal $x(t)$ with jump discontinuities decays slowly (as $1/n$) with frequency. We need a large number of terms in the Fourier series to approximate $x(t)$ within a given error. In contrast, a smoother periodic signal amplitude spectrum decays faster with frequency and we require a fewer number of terms in the series to approximate $x(t)$ within a given error.

A sinusoid can be expressed in terms of exponentials. Therefore, the Fourier series of a periodic signal can also be expressed as a sum of exponentials (the exponential Fourier series). The exponential form of the Fourier series and the expressions for the series coefficients are more compact than those of the trigonometric Fourier series. Also, the response of LTIC systems to an

exponential input is much simpler than that for a sinusoidal input. Moreover, the exponential form of representation lends itself better to mathematical manipulations than does the trigonometric form. This includes the establishment of useful Fourier series properties that simplify work and help provide a more intuitive understanding of signals. For these reasons, the exponential form of the series is preferred in modern practice in the areas of signals and systems.

The plots of amplitudes and angles of various exponential components of the Fourier series as functions of the frequency are the exponential Fourier spectra (amplitude and angle spectra) of the signal. Because a sinusoid $\cos\omega_0 t$ can be represented as a sum of two exponentials, $e^{j\omega_0 t}$ and $e^{-j\omega_0 t}$, the frequencies in the exponential spectra range from $\omega = -\infty$ to ∞. By definition, the frequency of a signal is always a positive quantity. The presence of a spectral component of a negative frequency $-n\omega_0$ merely indicates that the Fourier series contains terms of the form $e^{-jn\omega_0 t}$. The spectra of the trigonometric and exponential Fourier series are closely related, and one can be found by the inspection of the other.

In Sec. 3.7, we discuss a method of finding the response of an LTIC system to a periodic input signal. The periodic input is expressed as an exponential Fourier series, which consists of everlasting exponentials of the form $e^{jn\omega_0 t}$. We also know that the response of an LTIC system to an everlasting exponential $e^{jn\omega_0 t}$ is $H(jn\omega_0)e^{jn\omega_0 t}$. The system response is the sum of the system's responses to all the exponential components in the Fourier series for the input. The response is, therefore, also an exponential Fourier series. Thus, the response is also a periodic signal of the same period as that of the input.

The Fourier series coefficients C_n or D_n may be computed numerically using the discrete Fourier transform (DFT), which can be implemented by an efficient FFT (fast Fourier transform) algorithm. This method uses N_0 uniform samples of $x(t)$ over one period starting at $t = 0$.

REFERENCES

1. Lathi, B. P. and Ding, Z., *Modern Digital and Analog Communication Systems,* 4th ed., Oxford University Press, New York, 2009.
2. Bell, E. T., *Men of Mathematics,* Simon & Schuster, New York, 1937.
3. Durant, W., and Durant, A., *The Age of Napoleon,* Part XI in *The Story of Civilization Series,* Simon & Schuster, New York, 1975.
4. Calinger, R., *Classics of Mathematics,* 4th ed., Moore Publishing, Oak Park, IL, 1982.
5. Lanczos, C., *Discourse on Fourier Series,* Oliver Boyd, London, 1966.
6. Körner, T. W., *Fourier Analysis,* Cambridge University Press, Cambridge, UK, 1989.
7. Walker P. L., *The Theory of Fourier Series and Integrals,* Wiley, New York, 1986.
8. Churchill, R. V., and Brown, J. W., *Fourier Series and Boundary Value Problems,* 3rd ed., McGraw-Hill, New York, 1978.
9. Guillemin, E. A., *Theory of Linear Physical Systems,* Wiley, New York, 1963.
10. Gibbs, W. J., *Nature,* vol. 59, p. 606, April 1899.
11. Bôcher, M., *Annals of Mathematics,* vol. 7, no. 2, 1906.
12. Carslaw, H. S., *Bulletin of the American Mathematical Society,* vol. 31, pp. 420–424, October 1925.

PROBLEMS

3.1-1 Derive Eq. (3.1) in an alternate way by observing that $\mathbf{e} = (\mathbf{x} - c\mathbf{y})$ and $|\mathbf{e}|^2 = (\mathbf{x} - c\mathbf{y}) \cdot (\mathbf{x} - c\mathbf{y}) = |\mathbf{x}|^2 + c^2|\mathbf{y}|^2 - 2c\mathbf{x} \cdot \mathbf{y}$. [*Hint:* Find the value of c to minimize $|\mathbf{e}|^2$.]

3.1-2 A signal $x(t)$ is approximated in terms of a signal $y(t)$ over an interval (t_1, t_2):

$$x(t) \simeq cy(t) \qquad t_1 < t < t_2$$

where c is chosen to minimize the error energy.

(a) Show that $y(t)$ and the error $e(t) = x(t) - cy(t)$ are orthogonal over the interval (t_1, t_2).

(b) If possible, explain the result in terms of a signal-vector analogy.

(c) Verify this result for the square signal $x(t)$ in Fig. 3.3 and its approximation in terms of signal $\sin t$.

3.1-3 (a) For the signals $x(t)$ and $y(t)$ depicted in Fig. P3.1-3, find the component of the form $y(t)$ contained in $x(t)$. In other words, find the optimum value of c in the approximation $x(t) \approx cy(t)$ so that the error signal energy is minimum.

(b) Find the error signal $e(t)$ and its energy E_e. Show that the error signal is orthogonal to $y(t)$, and that $E_x = c^2E_y + E_e$. Explain this result in terms of vectors.

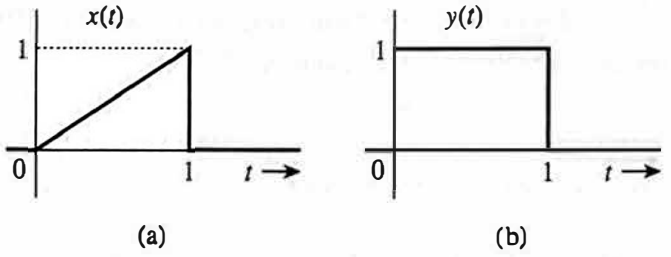

Figure P3.1-3

3.1-4 For the signals $x(t)$ and $y(t)$ shown in Fig. P3.1-3, find the component of the form $x(t)$ contained in $y(t)$. In other words, find the optimum value of c in the approximation $y(t) \approx cx(t)$ so that the error signal energy is minimum. What is the error signal energy?

3.1-5 Repeat Prob. P3.1-3 if $y(t)$ is instead defined as $y(t) = \sin(2\pi t)\,[u(t) - u(t-1)]$.

3.1-6 If $x(t)$ and $y(t)$ are orthogonal, then show that the energy of the signal $x(t) + y(t)$ is identical to the energy of the signal $x(t) - y(t)$ and is given by $E_x + E_y$. Explain this result by using the vector analogy. In general, show that for orthogonal signals $x(t)$ and $y(t)$ and for any pair of arbitrary real constants c_1 and c_2, the energies of $c_1x(t) + c_2y(t)$ and $c_1x(t) - c_2y(t)$ are both given by $c_1^2E_x + c_2^2E_y$.

3.1-7 In Ex. 3.4, we represented the function in Fig. 3.9 by Legendre polynomials.

(a) Use the results in Ex. 3.4 to represent the signal $g(t)$ in Fig. P3.1-7 by Legendre polynomials.

(b) Compute the error energy for the approximations having one and two (nonzero) terms.

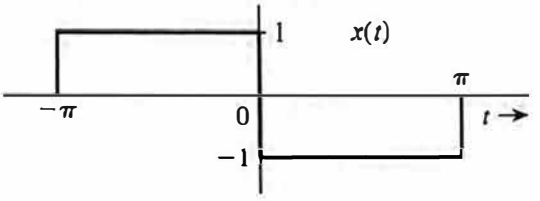

Figure P3.1-7

3.1-8 For the four-dimensional real space $\mathcal{R}^4$, the so-called Walsh basis is given by $\phi_1 = [1,1,1,1]$, $\phi_2 = [1,1,-1,-1]$, $\phi_3 = [1,-1,-1,1]$, and $\phi_4 = [1,-1,1,-1]$. Denoting elements $x = [x_1,x_2,x_3,x_4]$ and $y = [y_1,y_2,y_3,y_4]$ $(x,y \in \mathcal{R}^4)$, we can define orthogonality as $\sum_{k=1}^{4} x_k y_k^* = 0$. In linear algebra terminology, orthogonality here means that the inner product of vectors x and y is zero. Lastly, define a vector $z = [-4,0,1,-7]$.

(a) Show that the Walsh basis functions are mutually orthogonal. This requires a total of six calculations.

(b) Are the Walsh basis functions normal? That is, does the inner product of each Walsh basis function with itself evaluate to 1?

(c) Determine the coefficients $[c_1, c_2, c_3, c_4]$ to represent z using Walsh basis functions as $\hat{z} = \sum_{k=1}^{4} c_k \phi_k$.

(d) Determine the best three-dimensional approximation $\hat{z}_{3D}$ to z in terms of the Walsh basis functions. That is, your estimate can only be a linear combination of three functions from $[\phi_1, \phi_2, \phi_3, \phi_4]$. Evaluate the three-term sum to determine the four elements of vector $\hat{z}_{3D}$.

3.1-9 A function can be expanded in terms of many different types of basis functions, not just the complex exponentials of Fourier analysis. For example, Legendre polynomials are explored in Ex. 3.4. Another possible set of basis functions are *Laguerre* polynomials $L_k(t)$, which have support on the interval $[0, \infty)$. The Laguerre expansion of $x(t)$ is given by $x(t) = \sum_{k=0}^{\infty} c_k L_k(t)$, where $L_0(t) = 1$, $L_1(t) = (1 - t), \ldots, L_k(t) = e^t \frac{d^k}{dt^k}\left(t^k e^{-t}\right)$. As with a Fourier series, we can truncate the expansion using any number of terms we choose. For the Laguerre expansion, we define orthogonality a little differently as

$$\int_0^{\infty} e^{-t} x(t) y(t) dt = 0$$

Notice the presence of the e^{-t} term in the integral. Using this definition, Laguerre polynomials are orthonormal.

(a) Show that $L_0(t)$ is normal. That is, show that

$$\int_0^{\infty} e^{-t} L_0(t) L_0^*(t) dt = 1$$

(b) Show that $L_1(t)$ is normal. That is, show that

$$\int_0^{\infty} e^{-t} L_1(t) L_1^*(t) dt = 1$$

(c) Show that $L_0(t)$ is orthogonal to $L_1(t)$.

(d) Compute the coefficient c_0 that produces the best approximation $\hat{x}_0(t) = c_0 L_0(t)$ of the function $x(t) = e^{-t}u(t)$.

(e) For the best estimate $\hat{x}_1(t) = c_0 L_0(t) + c_1 L_1(t)$ of the function $x(t) = e^{-t}u(t)$, the coefficient c_0 remains unchanged from part (d) and $c_1 = \frac{1}{4}$. Confirm that $c_1 = \frac{1}{4}$ and explain why the coefficient c_0 does not change.

3.2-1 Find the correlation coefficient ρ of signal $y(t)$ and each of the four pulses $x_1(t)$, $x_2(t)$, $x_3(t)$, and $x_4(t)$ depicted in Fig. P3.2-1. Which pair of pulses would you select for a binary communication in order to provide maximum margin against noise along the transmission path?

3.3-1 Let $x_1(t)$ and $x_2(t)$ be two signals that are orthonormal (mutually orthogonal and unit energies) over an interval from $t = t_1$ to t_2.

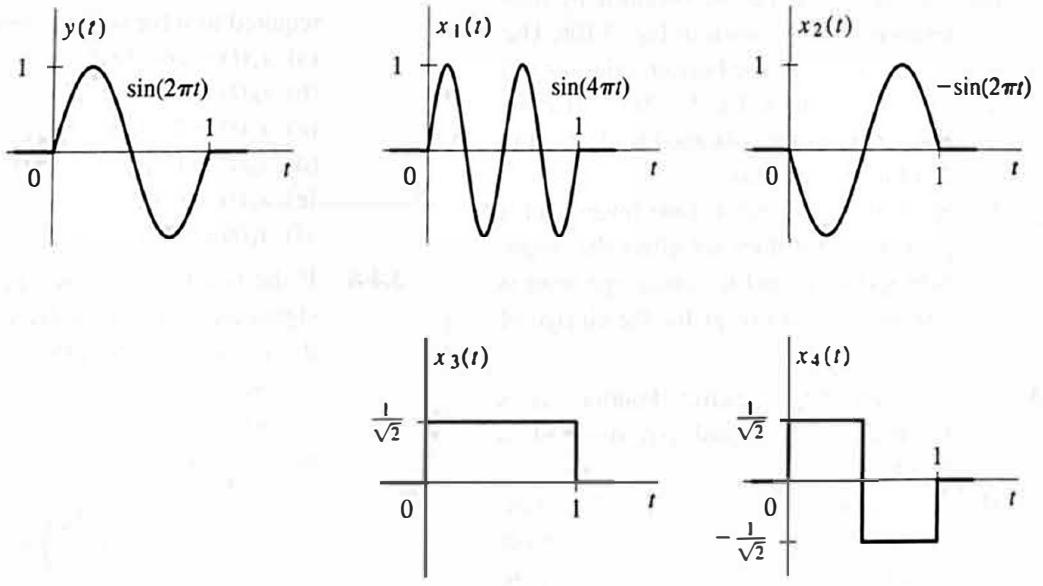

Figure P3.2-1

Consider a signal $f(t)$ where

$$f(t) = c_1 x_1(t) + c_2 x_2(t) \qquad t_1 \le t \le t_2$$

This signal can be represented by a two-dimensional vector $\mathbf{f}(c_1, c_2)$.

(a) Determine the vector representation of the following six signals in the two-dimensional vector space: $f_a(t) = 2x_1(t) - x_2(t)$, $f_b(t) = -x_1(t) + 2x_2(t)$, $f_c(t) = -x_2(t)$, $f_d(t) = x_1(t) + 2x_2(t)$, $f_e(t) = 2x_1(t) + x_2(t)$, and $f_f(t) = 3x_1(t)$.

(b) Point out pairs of mutually orthogonal vectors among these six vectors. Verify that the pairs of signals corresponding to these orthogonal vectors are also orthogonal.

3.4-1 Sketch the signal $x(t) = t^2$ for all t and find the trigonometric Fourier series $\varphi(t)$ to represent $x(t)$ over the interval $(-1, 1)$. Sketch $\varphi(t)$ for all values of t.

3.4-2 Sketch the signal $x(t) = t$ for all t and find the trigonometric Fourier series $\varphi(t)$ to represent $x(t)$ over the interval $(-\pi, \pi)$. Sketch $\varphi(t)$ for all values of t.

3.4-3 For each of the periodic signals shown in Fig. P3.4-3, find the compact trigonometric Fourier series and sketch the amplitude and phase spectra. If either the sine or cosine terms are absent in the Fourier series, explain why.

3.4-4 (a) Find the trigonometric Fourier series for $y(t)$ shown in Fig. P3.4-4.

(b) The signal $y(t)$ can be obtained by time reversal of $\varphi(t)$ shown in Fig. 3.10b. Use this fact to obtain the Fourier series for $y(t)$ from the results in Ex. 3.5. Verify that the Fourier series thus obtained is identical to that found in part (a).

(c) Show that, in general, time reversal of a periodic signal does not affect the amplitude spectrum, and the phase spectrum is also unchanged except for the change of sign.

3.4-5 (a) Find the trigonometric Fourier series for the periodic signal $y(t)$ depicted in Fig. P3.4-5.

(b) The signal $y(t)$ can be obtained by time compression of $\varphi(t)$ shown in Fig. 3.10b by a factor 2. Use this fact to obtain the Fourier series for $y(t)$ from the results in Ex. 3.5. Verify that the Fourier series thus obtained is identical to that found in part (a).

(c) Show that, in general, time compression of a periodic signal by a factor a expands the Fourier spectra along the ω axis by the same factor a. In other words, C_0, C_n, and θ_n remain unchanged, but the fundamental frequency is increased by the factor a, thus expanding the spectrum. Similarly, time expansion of a periodic signal by a factor a compresses its Fourier spectra along the ω axis by the factor a.

3.4-6 (a) Find the trigonometric Fourier series for the periodic signal $g(t)$ in Fig. P3.4-6. Take advantage of the symmetry.

(b) Observe that $g(t)$ is identical to $x(t)$ in Fig. 3.12a left-shifted by 0.5 second. Use this fact to obtain the Fourier series for $g(t)$ from the results in Ex. 3.6. Verify that the Fourier series thus obtained is identical to that found in part (a).

(c) Show that, in general, a time shift of T seconds of a periodic signal does not affect the amplitude spectrum. However, the phase of the nth harmonic is increased or decreased $n\omega_0 T$ depending on whether the signal is advanced or delayed by T seconds.

3.4-7 Determine the trigonometric Fourier series coefficients a_n and b_n for the following signals. In each case, also determine the signals' fundamental radian frequency ω_0. No integration is required to solve this problem.

(a) $x_a(t) = \cos(3\pi t)$

(b) $x_b(t) = \sin(7\pi t)$

(c) $x_c(t) = 2 + 4\cos(3\pi t) - 2j\sin(7\pi t)$

(d) $x_d(t) = (1+j)\sin(3\pi t) + (2-j)\cos(7\pi t)$

(e) $x_e(t) = \sin(3\pi t + 1) + 2\cos(7\pi t - 2)$

(f) $x_f(t) = \sin(6\pi t) + 2\cos(14\pi t)$

3.4-8 If the two halves of one period of a periodic signal are identical in shape except that one is the negative of the other, the periodic signal is said to have a *half-wave symmetry*. If a periodic signal $x(t)$ with a period T_0 satisfies the half-wave symmetry condition, then

$$x\left(t - \frac{T_0}{2}\right) = -x(t)$$

In this case, show that all the even-numbered harmonics vanish and that the odd-numbered harmonic coefficients are given by

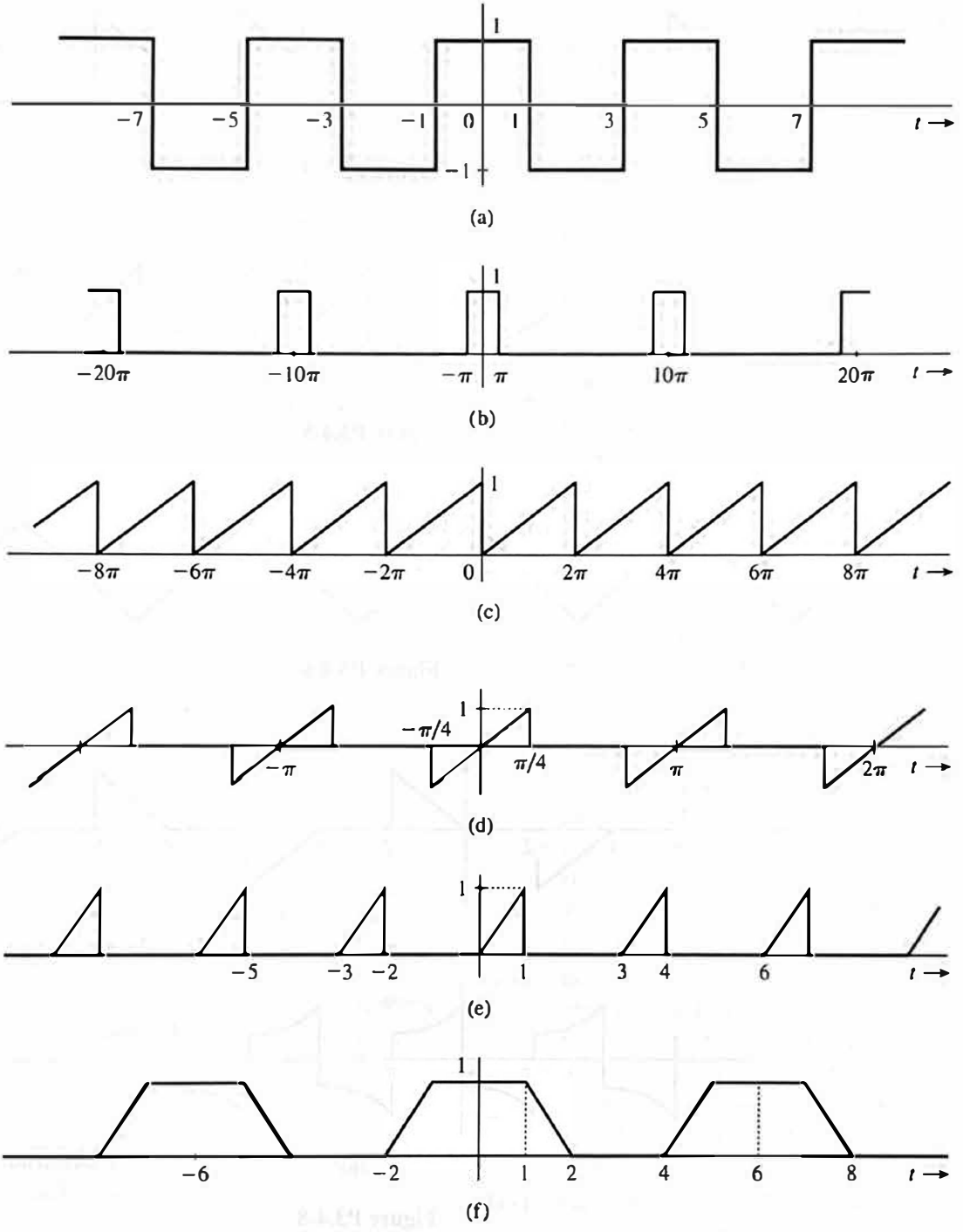

Figure P3.4-3

$$a_n = \frac{4}{T_0}\int_0^{T_0/2} x(t)\cos n\omega_0 t\,dt$$

and

$$b_n = \frac{4}{T_0}\int_0^{T_0/2} x(t)\sin n\omega_0 t\,dt$$

Using these results, find the Fourier series for the periodic signals in Fig. P3.4-8.

3.4-9 Over a finite interval, a signal can be represented by more than one trigonometric (or exponential) Fourier series. For instance, if we wish to represent $x(t) = t$ over an interval

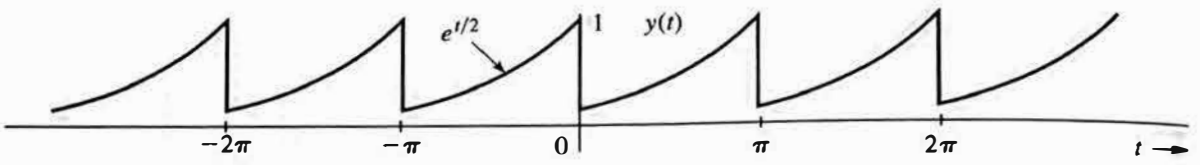

Figure P3.4-4

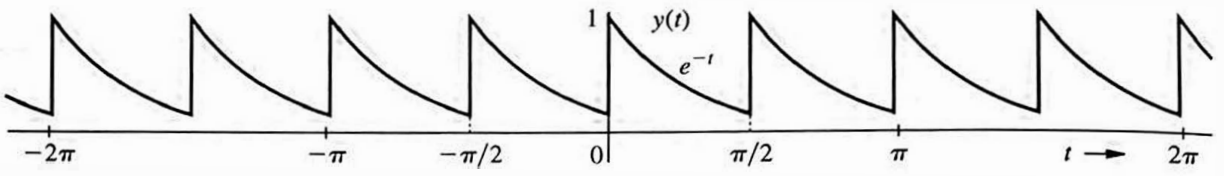

Figure P3.4-5

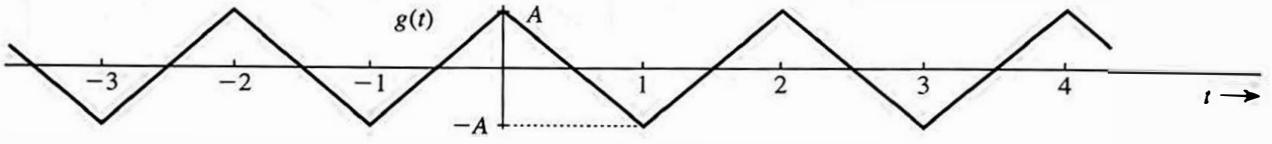

Figure P3.4-6

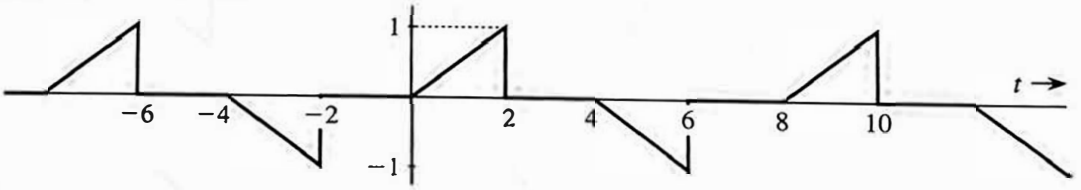

(a)

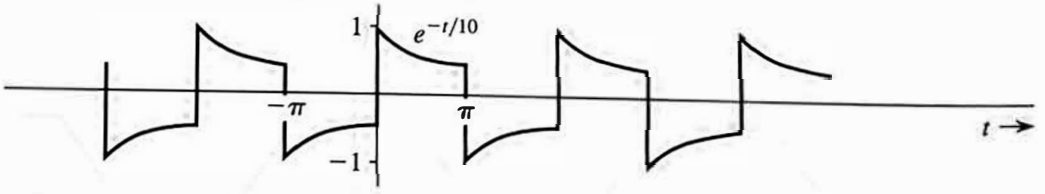

(b)

Figure P3.4-8

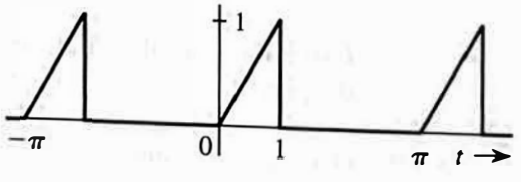

(a)

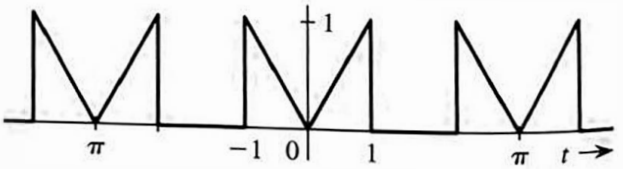

(b)

Figure P3.4-9

$0 < t < 1$ by a Fourier series with fundamental frequency $\omega_0 = 2$, we can draw a pulse $x(t) = t$ over the interval $0 < t < 1$ and repeat the pulse every π seconds so that $T_0 = \pi$ and $\omega_0 = 2$ (Fig. P3.4-9a). If we want the fundamental frequency ω_0 to be 4, we repeat the pulse every $\pi/2$ seconds. If we want the series to contain only cosine terms with $\omega_0 = 2$, we construct a pulse $x(t) = |t|$ over $-1 < t < 1$, and repeat it every π seconds (Fig. P3.4-9b). The resulting signal is an even function with period π. Hence, its Fourier series will have only cosine terms with $\omega_0 = 2$. The resulting Fourier series represents $x(t) = t$ over $0 < t < 1$, as desired. We do not care what it represents outside this interval.

Sketch the periodic signal $x(t)$ such that $x(t) = t$ for $0 < t < 1$ and the Fourier series for $x(t)$ satisfies the following conditions:

(a) $\omega_0 = \pi/2$ and contains all harmonics, but cosine terms only

(b) $\omega_0 = 2$ and contains all harmonics, but sine terms only

(c) $\omega_0 = \pi/2$ and contains all harmonics, which are exclusively neither sine nor cosine

(d) $\omega_0 = 1$ and contains only odd harmonics and cosine terms

(e) $\omega_0 = \pi/2$ and contains only odd harmonics and sine terms

(f) $\omega_0 = 1$ and contains only odd harmonics, which are exclusively neither sine nor cosine.

[*Hint:* For parts (d), (e), and (f), you need to use half-wave symmetry as discussed in Prob. 3.4-8. Cosine terms imply a possible dc component.] You are asked only to sketch the periodic signal $x(t)$ satisfying the given conditions. Do not find the values of the Fourier coefficients.

3.4-10 State with reasons whether the following signals are periodic or aperiodic. For periodic signals, find the period and state which harmonics are present in the series.

(a) $3\sin t + 2\sin 3t$

(b) $2 + 5\sin 4t + 4\cos 7t$

(c) $2\sin 3t + 7\cos \pi t$

(d) $7\cos \pi t + 5\sin 2\pi t$

(e) $3\cos \sqrt{2}t + 5\cos 2t$

(f) $\sin\frac{5t}{2} + 3\cos\frac{6t}{5} + 3\sin\left(\frac{t}{7} + 30°\right)$

(g) $\sin 3t + \cos\frac{15}{4}t$

(h) $(3\sin 2t + \sin 5t)^2$

(i) $(5\sin 2t)^3$

3.4-11 Represent the signal $x(t)$ shown in Fig. P3.1-3a over the interval from 0 to 1 by a trigonometric Fourier series of fundamental frequency $\omega_0 = 2\pi$. Compute the error energy in the representation of $x(t)$ by only the first N terms of this series for $N = 1$, 2, 3, and 4.

3.4-12 Walsh functions, which can take on only two amplitude values, form a complete set of orthonormal functions and are of great practical importance in digital applications because they can be easily generated by logic circuitry and because multiplication with these functions can be implemented by simply using a polarity-reversing switch. Figure P3.4-12 shows the first eight functions in this set. Represent $x(t)$ in Fig. P3.1-3a over the interval (0, 1) by using a Walsh Fourier series with these eight basis functions. Compute the energy of $e(t)$, the error in the approximation, using the first N nonzero terms in the series for N = 1, 2, 3, and 4. In Prob. 3.4-11, we found the trigonometric Fourier series for $x(t)$. How does the Walsh series compare with the trigonometric series in Prob. 3.4-11 from the viewpoint of the error energy for a given N?

3.4-13 Represent $x(t) = t$ over the interval $(0, 1)$ by a trigonometric Fourier series that has

(a) $\omega_0 = 2\pi$ and only sine terms

(b) $\omega_0 = \pi$ and only sine terms

(c) $\omega_0 = \pi$ and only cosine terms

You may use a dc term in these series if necessary.

3.6-1 For each of the periodic signals in Fig. P3.4-3, find the exponential Fourier series and sketch the corresponding spectra.

3.6-2 A 2π-periodic signal $x(t)$ is specified over one period as

$$x(t) = \begin{cases} \frac{1}{A}t & 0 \le t < A \\ 1 & A \le t < \pi \\ 0 & \pi \le t < 2\pi \end{cases}$$

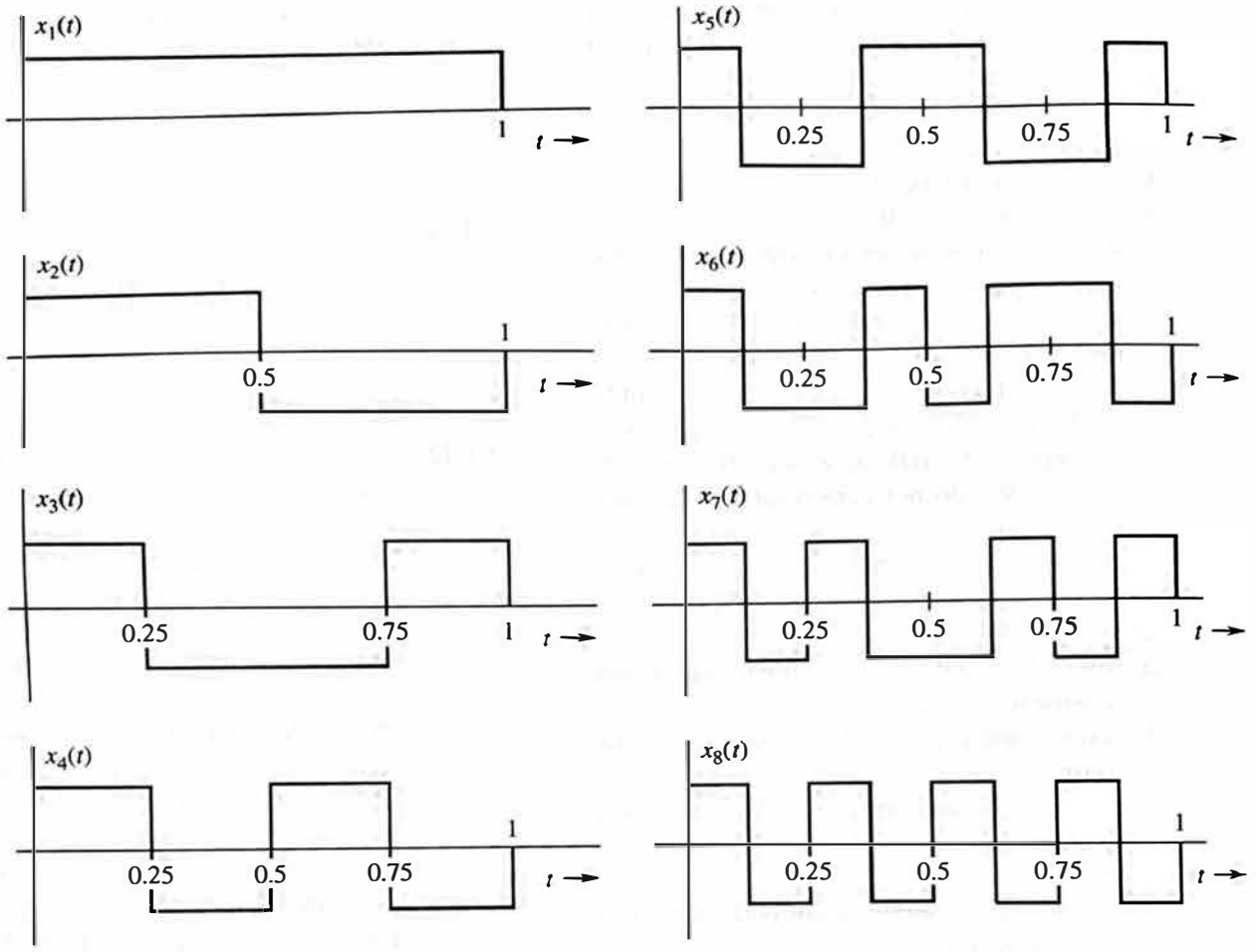

Figure P3.4-12

Sketch $x(t)$ over two periods from $t = 0$ to 4π. Show that the exponential Fourier series coefficients D_n for this series are given by

$$D_n = \begin{cases} \dfrac{2\pi - A}{4\pi} & n = 0 \\ \dfrac{1}{2\pi n}\left(\dfrac{e^{-jAn} - 1}{An} + je^{-jn\pi}\right) & n \neq 0 \end{cases}$$

3.6-3 A periodic signal $x(t)$ is expressed by the following Fourier series:

$$x(t) = 3\cos t + \sin\left(5t - \tfrac{\pi}{6}\right) - 2\cos\left(8t - \tfrac{\pi}{3}\right)$$

(a) Sketch the amplitude and phase spectra for the trigonometric series.
(b) By inspection of spectra in part (a), sketch the exponential Fourier series spectra.
(c) By inspection of spectra in part (b), write the exponential Fourier series for $x(t)$.
(d) Show that the series found in part (c) is equivalent to the trigonometric series for $x(t)$.

3.6-4 The trigonometric Fourier series of a certain periodic signal is given by

$$x(t) = 3 + \sqrt{3}\cos 2t + \sin 2t + \sin 3t - \frac{1}{2}\cos\left(5t + \frac{\pi}{3}\right)$$

(a) Sketch the trigonometric Fourier spectra.
(b) By inspection of spectra in part (a), sketch the exponential Fourier series spectra.
(c) By inspection of spectra in part (b), write the exponential Fourier series for $x(t)$.
(d) Show that the series found in part (c) is equivalent to the trigonometric series for $x(t)$.

3.6-5 The exponential Fourier series of a certain function is given as

$$x(t) = (2 + j2)e^{-j3t} + j2e^{-jt} + 3 - j2e^{jt} + (2 - j2)e^{j3t}$$

(a) Sketch the exponential Fourier spectra.
(b) By inspection of the spectra in part (a), sketch the trigonometric Fourier spectra for $x(t)$. Find the compact trigonometric Fourier series from these spectra.
(c) Show that the trigonometric series found in part (b) is equivalent to the exponential series for $x(t)$.
(d) Find the signal bandwidth.

3.6-6 Figure P3.6-6 shows the trigonometric Fourier spectra of a periodic signal $x(t)$.
(a) By inspection of Fig. P3.6-6, find the trigonometric Fourier series representing $x(t)$.
(b) By inspection of Fig. P3.6-6, sketch the exponential Fourier spectra of $x(t)$.
(c) By inspection of the exponential Fourier spectra obtained in part (b), find the exponential Fourier series for $x(t)$.
(d) Show that the series found in parts (a) and (c) are equivalent.

3.6-7 Figure P3.6-7 shows the exponential Fourier spectra of a periodic signal $x(t)$.
(a) By inspection of Fig. P3.6-7, find the exponential Fourier series representing $x(t)$.
(b) By inspection of Fig. P3.6-7, sketch the trigonometric Fourier spectra for $x(t)$.
(c) By inspection of the trigonometric Fourier spectra found in part (b), find the trigonometric Fourier series for $x(t)$.
(d) Show that the series found in parts (a) and (c) are equivalent.

3.6-8 Let periodic signal $x(t)$ have exponential Fourier series spectrum D_n. Prove the following properties:
(a) If $x(t)$ has even symmetry, then D_n also has even symmetry.

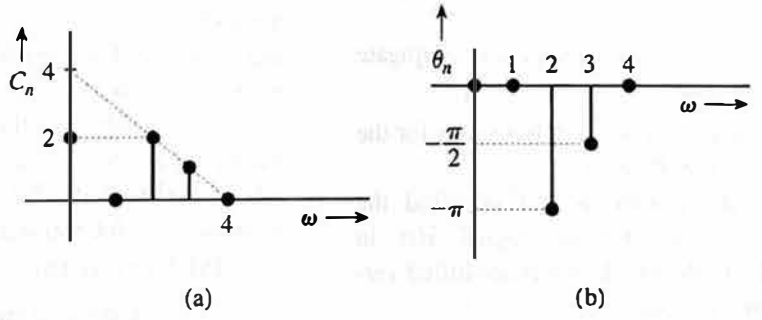

(a) (b)

Figure P3.6-6

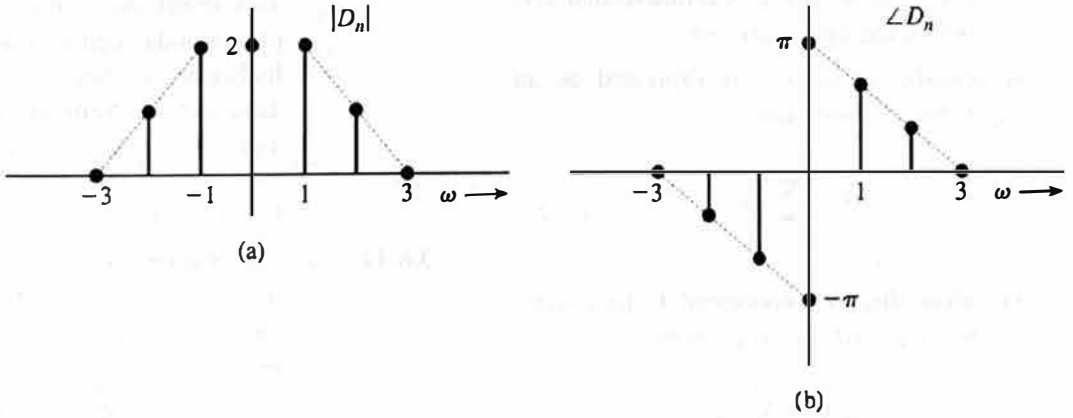

(a) (b)

Figure P3.6-7

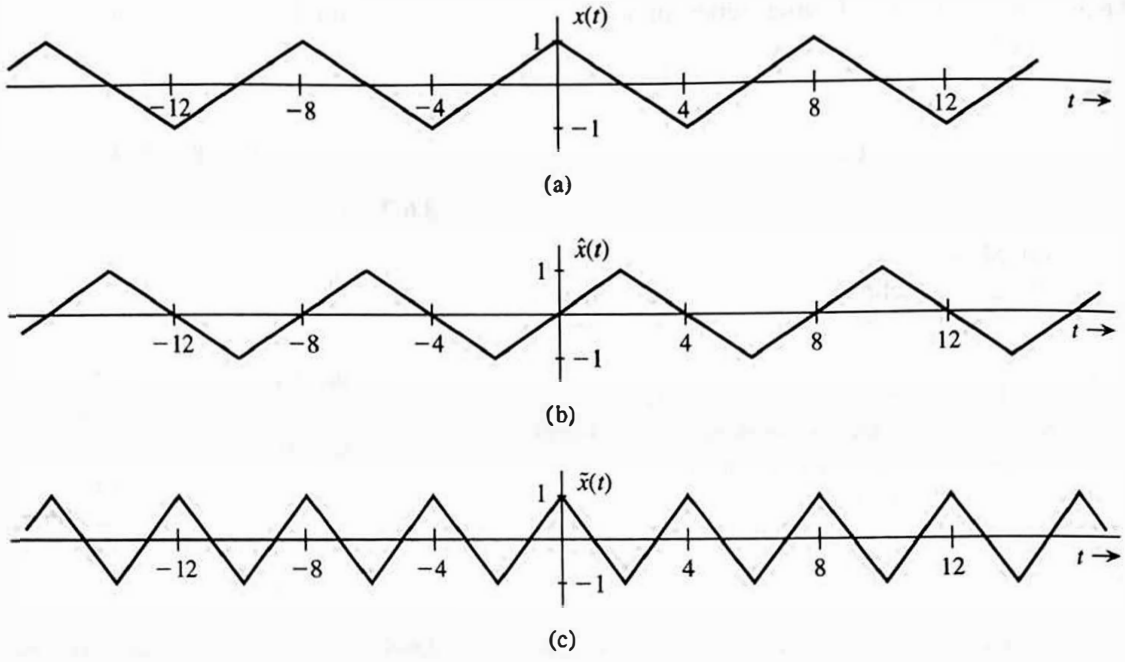

Figure P3.6-9

(b) If $x(t)$ has odd symmetry, then D_n also has odd symmetry.

(c) If $x(t)$ is real, then D_n is conjugate symmetric ($D_n = D^*_{-n}$).

(d) If $x(t)$ is imaginary, then D_n is conjugate antisymmetric ($D_n = -D^*_{-n}$).

3.6-9 (a) Find the exponential Fourier series for the signal in Fig. P3.6-9a.

(b) Using the results in part (a), find the Fourier series for the signal $\hat{x}(t)$ in Fig. P3.6-9b, which is a time-shifted version of the signal $x(t)$.

(c) Using the results in part (a), find the Fourier series for the signal $\tilde{x}(t)$ in Fig. P3.6-9c, which is a time-scaled version of the signal $x(t)$.

3.6-10 A periodic signal $x(t)$ is expressed as an exponential Fourier series

$$x(t) = \sum_{n=-\infty}^{\infty} D_n e^{jn\omega_0 t}$$

(a) Show that the exponential Fourier series for $\hat{x}(t) = x(t - T)$ is given by

$$\hat{x}(t) = \sum_{n=-\infty}^{\infty} \hat{D}_n e^{jn\omega_0 t}$$

in which

$$|\hat{D}_n| = |D_n| \quad \text{and} \quad \angle \hat{D}_n = \angle D_n - n\omega_0 T$$

This result shows that time shifting of a periodic signal by T seconds merely changes the phase spectrum by $n\omega_0 T$. The amplitude spectrum is unchanged.

(b) Show that the exponential Fourier series for $\tilde{x}(t) = x(at)$ is given by

$$\tilde{x}(t) = \sum_{n=-\infty}^{\infty} D_n e^{jn(a\omega_0)t}$$

This result shows that time compression of a periodic signal by a factor a expands its Fourier spectra along the ω axis by the same factor a. Similarly, time expansion of a periodic signal by a factor a compresses its Fourier spectra along the ω axis by the factor a. Intuitively explain this result.

3.6-11 (a) The Fourier series for the periodic signal in Fig. 3.15a is given in Drill 3.6. Verify Parseval's theorem for this series, given that

$$\sum_{n=1}^{\infty} \frac{1}{n^4} = \frac{\pi^4}{90}$$

(b) If $x(t)$ is approximated by the first N terms in this series, find N so that the power of the error signal is less than 1% of P_x.

3.6-12 (a) The Fourier series for the periodic signal in Fig. 3.15b is given in Drill 3.6. Verify Parseval's theorem for this series, given that

$$\sum_{n=1}^{\infty} \frac{1}{n^2} = \frac{\pi^2}{6}$$

(b) If $x(t)$ is approximated by the first N terms in this series, find N so that the power of the error signal is less than 10% of P_x.

3.6-13 The signal $x(t)$ in Fig. 3.25 is approximated by the first $2N+1$ terms (from $n=-N$ to N) in its exponential Fourier series given in Drill 3.10. Determine the value of N if this $(2N+1)$-term Fourier series power is to be no less than 99.75% of the power of $x(t)$.

3.6-14 (a) A 2 rad/s periodic signal $x_1(t)$ has Fourier series spectrum $X_1[n]$. Determine the Fourier series spectrum $X_2[n]$ of $x_2(t) = \frac{1}{3}x_1(-t-5)$ in terms of $X_1[n]$.

(b) A 2 rad/s periodic signal $x_1(t)$ has Fourier series spectrum $X_1[n]$. Determine the Fourier series spectrum $X_2[n]$ of $x_2(t) = \cos(10t)x_1(t)$ in terms of $X_1[n]$.

(c) A 3 rad/s periodic signal $x_1(t)$ has Fourier series spectrum $X_1[n]$. Determine the Fourier series spectrum $X_2[n]$ of $x_2(t) = x_1(-t) - 3x_1(t+2)$ in terms of $X_1[n]$.

3.6-15 A 2-periodic signal $x(t)$ is defined as

$$x(t) = \begin{cases} -t^2 - t + 0.25 & -1 \le t < 0 \\ t^2 - t + 0.25 & 0 \le t < 1 \\ x(t+2) & \forall t \end{cases}$$

(a) Plot $x(t)$ over $-2 \le t \le 2$.
(b) Determine D_0, the dc content of $x(t)$.
(c) Similar to Ex. 3.15, use properties and not integration to determine D_n for $n \neq 0$.
(d) Plot the magnitude spectrum $|D_n|$ over a suitable range of n.
(e) How does the magnitude spectrum $|D_n|$ compare to that of signal $y(t) = \cos(\pi t)$? Note similarities as well as major differences.

3.6-16 A 3-periodic signal $x(t)$ is defined as

$$x(t) = \begin{cases} |t| & -1 \le t \le 1 \\ 0 & 1 < |t| \le 1.5 \\ x(t+3) & \forall t \end{cases}$$

(a) Plot $x(t)$ over $-3 \le t \le 3$.
(b) Determine D_0, the dc content of $x(t)$.
(c) Similar to Ex. 3.15, use properties and not integration to determine D_n for $n \neq 0$.
(d) Plot the magnitude spectrum $|D_n|$ over a suitable range of n. What is the most dominant frequency component of this signal?

3.7-1 Find the response of an LTIC system with transfer function

$$H(s) = \frac{s}{s^2 + 2s + 3}$$

to the periodic input shown in Fig. 3.10b.

3.7-2 A periodic signal $x(t) = 1 + 2\cos(5\pi t) + 3\sin(14\pi t)$ is applied to an LTIC system to produce output $y(t)$.

(a) Determine ω_0, the fundamental radian frequency of $x(t)$.
(b) Determine D_n, the exponential Fourier series spectrum of $x(t)$.
(c) If the system is an ideal lowpass filter with cutoff frequency $f_c = 2$ Hz, what is the output $y(t)$?
(d) If the system is an ideal highpass filter with cutoff frequency $f_c = 2$ Hz, what is the output $y(t)$?
(e) If the system is an ideal bandpass filter with a 4 Hz passband centered at 4 Hz, what is the output $y(t)$?
(f) If the system is an ideal bandstop filter with a 5 Hz stopband centered at 10 Hz, what is the output $y(t)$?
(g) Describe the frequency response of a filter that, in response to $x(t)$, would produce the output $y(t) = 4\cos(5\pi t) - 9\sin(14\pi t)$.

3.7-3 Consider a $T_0 = 1$ periodic signal $x(t)$ defined as

$$x(t) = \begin{cases} 1 - t^2 & 0 < t \le 1 \\ x(t+1) & \forall t \end{cases}$$

(a) Sketch $x(t)$ for $-2 \le t \le 2$.
(b) Determine D_n, the exponential Fourier series spectrum of $x(t)$.

(c) If $x(t)$ is applied to an ideal bandpass filter with a 1 Hz passband centered at 3 Hz, determine the output $y(t)$.

3.7-4 (a) Find the exponential Fourier series for a signal $x(t) = \cos 5t \sin 3t$. You can do this without evaluating any integrals.

(b) Sketch the Fourier spectra.

(c) The signal $x(t)$ is applied at the input of an LTIC system with the frequency response shown in Fig. P3.7-4. Find the output $y(t)$.

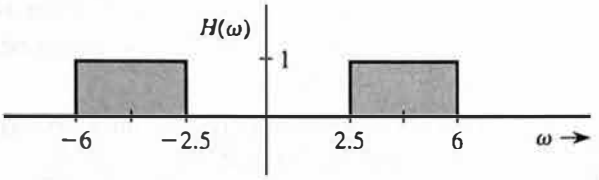

Figure P3.7-4

3.7-5 (a) Find the exponential Fourier series for the periodic signal $x(t)$ shown in Fig. P3.7-5a.

(b) The signal $x(t)$ is applied at the input of an LTIC system shown in Fig. P3.7-5b. Find the expression for the output $y(t)$.

3.7-6 A T-periodic τ/T duty-cycle square wave $p(t)$ is defined as

$$p(t) = \begin{cases} 1 & |t| < \frac{\tau}{2} \\ 0 & \frac{\tau}{2} < |t| < \frac{T}{2} \\ p(t+T) & \forall t \end{cases}$$

where $0 < \tau < T$. Also consider the frequency response $H(\omega)$ of a lowpass communications channel with 10 rad/s bandwidth (e.g., $|H(\omega)| \approx 0$ for $\omega > 10$). If T and τ are properly chosen, we can estimate $H(\omega)$ at points $\omega = n\omega_0$ as $\hat{H}(n\omega_0) = \frac{1}{P_0} Y_n$, where Y_n is the exponential FS spectrum of the channel output $y(t)$ in response to input $p(t)$ and P_0 is the dc component of $p(t)$.

(a) Using direct integration, determine the exponential Fourier series coefficients P_n of signal $p(t)$.

(b) Determine a suitable value T so that $p(t)$ applied to system $H(\omega)$ has 21 component frequencies over the system bandwidth $0 \leq \omega \leq 10$.

(c) Assuming T is properly chosen, determine a suitable duty cycle τ/T so that $H(n\omega_0) \approx Y_n$. Carefully justify your result.

(d) From the perspective of using $p(t)$ to help measure the system frequency response $H(\omega)$, what happens if T is properly chosen but τ/T is chosen too small?

(e) From the perspective of using $p(t)$ to help measure the system frequency response $H(\omega)$, what happens if T is properly chosen but τ/T is chosen too large?

3.9-1 A periodic signal has $\omega_0 = \frac{2}{3}\pi$ and exponential Fourier series spectrum $D_n = j\cos(\pi n/10)\,(u[n+10] - u[n-11])$. [*Hint:*

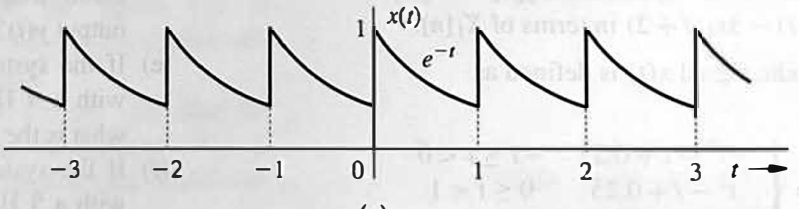

(a)

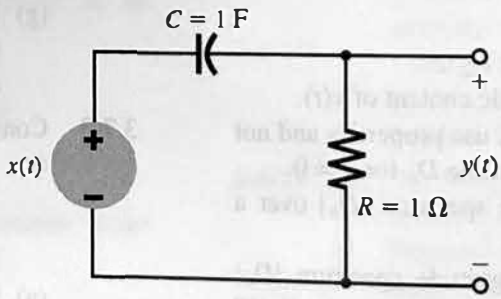

(b)

Figure P3.7-5

Refer to Prob. 3.6-8 for some useful properties.]

(a) Determine the period T_0 of the corresponding signal $x(t)$.

(b) Is the time-domain signal real, imaginary, or neither? Justify your answer.

(c) Is the time-domain signal even, odd, or neither? Justify your answer.

(d) Use MATLAB to synthesize the time-domain signal $x(t)$ and plot it over the interval $[-T_0, T_0]$.

3.9-2 Repeat Prob. 3.9-1 for a periodic signal with $\omega_0 = \frac{3}{2}\pi$ and $D_n = 2\sin(\pi n/10)(u[n+10] - u[n-11])$.

3.9-3 Consider the $(T_0 = 1)$-periodic signal $x(t)$:

$$x(t) = \begin{cases} 2t - t^2 & 0 < t \leq 1 \\ x(t+1) & \forall t \end{cases}$$

(a) Sketch $x(t)$ for $-2 \leq t \leq 2$.

(b) Using properties and minimal integration, determine D_n, the exponential Fourier spectrum of $x(t)$.

(c) Verify the correctness of D_n by using MATLAB to synthesize $x(t)$ with a suitable truncation of Eq. (3.46).

(d) Suppose $x(t)$ is applied to an ideal bandpass filter with a passband between 2.5 and 3.5 Hz. Determine the filter output $y(t)$. Simplify your answer.

[*Hint:* Refer to Ex. 3.15.]

3.9-4 Section 3.9 discusses the construction of a phase-optimized multitone test signal with linearly spaced frequency components. This problem investigates a similar signal with logarithmically spaced frequency components. A multitone test signal $m(t)$ is constructed by using a superposition of N real sinusoids:

$$m(t) = \sum_{n=1}^{N} \cos(\omega_n t + \theta_n)$$

where θ_n establishes the relative phase of each sinusoidal component.

(a) Determine a suitable set of $N = 10$ frequencies ω_n that logarithmically spans $[(2\pi) \leq \omega \leq 100(2\pi)]$ yet still results in a periodic test signal $m(t)$. Determine the period T_0 of your signal. Using $\theta_n = 0$, plot the resulting (T_0)-periodic signal over $-T_0/2 \leq t \leq T_0/2$.

(b) Determine a suitable set of phases θ_n that minimize the maximum magnitude of $m(t)$. Plot the resulting signal and identify the maximum magnitude that results.

(c) Many systems suffer from what is called one-over-f noise. The power of this undesirable noise is proportional to $1/f$. Thus, low-frequency noise is stronger than high-frequency noise. What modifications to $m(t)$ are appropriate for use in environments with $1/f$ noise? Justify your answer.

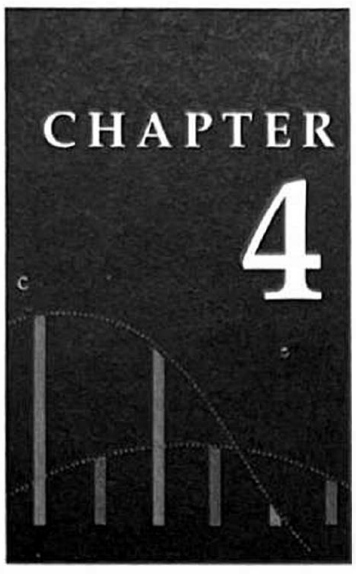

CHAPTER 4 CONTINUOUS-TIME SIGNAL ANALYSIS: THE FOURIER TRANSFORM

We can analyze linear systems in many different ways by taking advantage of the property of linearity, whereby the input is expressed as a sum of simpler components. The system response to any complex input can be found by summing the system's response to these simpler components of the input. In time-domain analysis, we separated the input into impulse components. In Ch. 3, we succeeded in representing periodic signals as a sum of (everlasting) sinusoids or exponentials of the form $e^{j\omega t}$. The Fourier integral developed in this chapter extends this spectral representation to aperiodic signals.

4.1 APERIODIC SIGNAL REPRESENTATION BY THE FOURIER INTEGRAL

Applying a limiting process, we now show that an aperiodic signal can be expressed as a continuous sum (integral) of everlasting exponentials. To represent an aperiodic signal $x(t)$ such as the one depicted in Fig. 4.1a by everlasting exponentials, let us construct a new periodic signal $x_{T_0}(t)$ formed by repeating the signal $x(t)$ at intervals of T_0 seconds, as illustrated in Fig. 4.1b. The period T_0 is made long enough to avoid overlap between the repeating pulses. The periodic signal $x_{T_0}(t)$ can be represented by an exponential Fourier series. If we let $T_0 \to \infty$, the pulses in the periodic signal repeat after an infinite interval and, therefore,

$$\lim_{T_0 \to \infty} x_{T_0}(t) = x(t)$$

Thus, the Fourier series representing $x_{T_0}(t)$ will also represent $x(t)$ in the limit $T_0 \to \infty$. The exponential Fourier series for $x_{T_0}(t)$ is given by

$$x_{T_0}(t) = \sum_{n=-\infty}^{\infty} D_n e^{jn\omega_0 t} \tag{4.1}$$

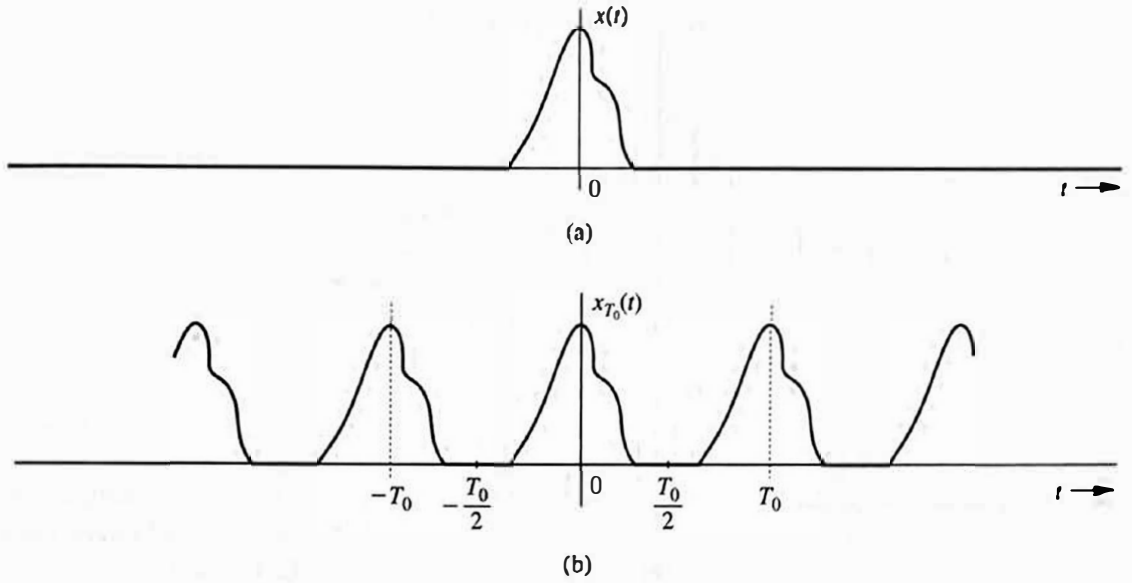

Figure 4.1 Construction of a periodic signal by periodic extension of $x(t)$.

where $\omega_0 = \frac{2\pi}{T_0}$ and

$$D_n = \frac{1}{T_0}\int_{-T_0/2}^{T_0/2} x_{T_0}(t)e^{-jn\omega_0 t}dt \tag{4.2}$$

Observe that integrating $x_{T_0}(t)$ over $(-T_0/2, T_0/2)$ is the same as integrating $x(t)$ over $(-\infty, \infty)$. Therefore, Eq. (4.2) can be expressed as

$$D_n = \frac{1}{T_0}\int_{-\infty}^{\infty} x(t)e^{-jn\omega_0 t}dt \tag{4.3}$$

It is interesting to see how the nature of the spectrum changes as T_0 increases. To understand this fascinating behavior, let us define $X(\omega)$, a continuous function of ω, as

$$X(\omega) = \int_{-\infty}^{\infty} x(t)e^{-j\omega t}dt \tag{4.4}$$

A glance at Eqs. (4.3) and (4.4) shows that

$$D_n = \frac{1}{T_0}X(n\omega_0) \tag{4.5}$$

This means that the Fourier coefficients D_n are $1/T_0$ times the samples of $X(\omega)$ uniformly spaced at intervals of ω_0, as depicted in Fig. 4.2a.† Therefore, $(1/T_0)X(\omega)$ is the envelope for the coefficients D_n. We now let $T_0 \to \infty$ by doubling T_0 repeatedly. Doubling T_0 halves the fundamental frequency ω_0 so that there are now twice as many components (samples) in the spectrum. However, by doubling T_0, the envelope $(1/T_0)X(\omega)$ is halved, as shown in Fig. 4.2b.

† For the sake of simplicity, we assume D_n, and therefore $X(\omega)$, in Fig. 4.2, to be real. The argument, however, is also valid for complex D_n [or $X(\omega)$].

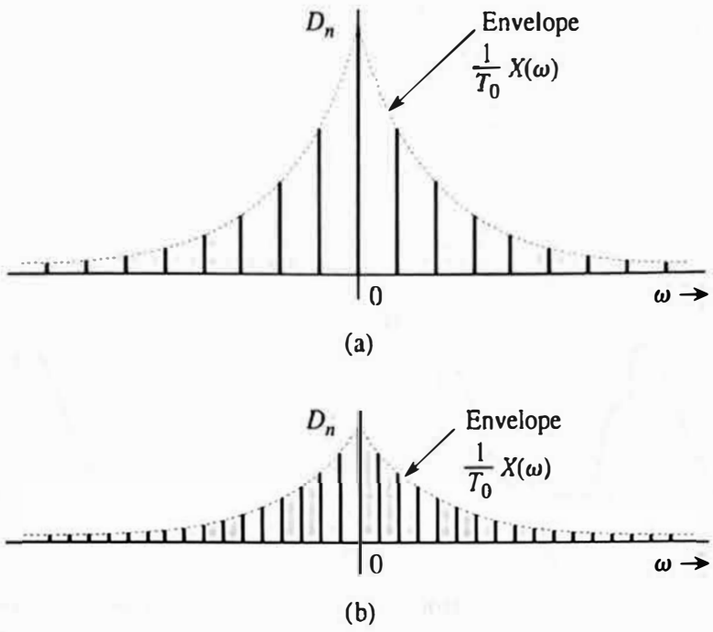

Figure 4.2 Change in the Fourier spectrum when the period T_0 in Fig. 4.1 is doubled.

If we continue this process of doubling T_0 repeatedly, the spectrum progressively becomes denser while its magnitude becomes smaller. Note, however, that the relative shape of the envelope remains the same [proportional to $X(\omega)$ in Eq. (4.4)]. In the limit as $T_0 \rightarrow \infty$, $\omega_0 \rightarrow 0$ and $D_n \rightarrow 0$. This result makes for a spectrum so dense that the spectral components are spaced at zero (infinitesimal) intervals. At the same time, the amplitude of each component is zero (infinitesimal). We have *nothing of everything, yet we have something!* This paradox sounds like *Alice in Wonderland,* but as we shall see, these are the classic characteristics of a very familiar phenomenon.[†]

Substitution of Eq. (4.5) in Eq. (4.1) yields

$$x_{T_0}(t) = \sum_{n=-\infty}^{\infty} \frac{X(n\omega_0)}{T_0} e^{jn\omega_0 t} \tag{4.6}$$

As $T_0 \rightarrow \infty$, ω_0 becomes infinitesimal ($\omega_0 \rightarrow 0$). Hence, we shall replace ω_0 by a more appropriate notation, $\Delta\omega$. In terms of this new notation, $\omega_0 = \frac{2\pi}{T_0}$ becomes

$$\Delta\omega = \frac{2\pi}{T_0}$$

and Eq. (4.6) becomes

$$x_{T_0}(t) = \sum_{n=-\infty}^{\infty} \left[\frac{X(n\Delta\omega)\Delta\omega}{2\pi}\right] e^{(jn\Delta\omega)t}$$

This equation shows that $x_{T_0}(t)$ can be expressed as a sum of everlasting exponentials of frequencies $0, \pm\Delta\omega, \pm 2\Delta\omega, \pm 3\Delta\omega, \ldots$ (the Fourier series). The amount of the component of

[†] If nothing else, the reader now has irrefutable proof of the proposition that 0% ownership of everything is better than 100% ownership of nothing.

frequency $n\Delta\omega$ is $[X(n\Delta\omega)\Delta\omega]/2\pi$. In the limit as $T_0 \to \infty$, $\Delta\omega \to 0$ and $x_{T_0}(t) \to x(t)$. Therefore,

$$x(t) = \lim_{T_0 \to \infty} x_{T_0}(t) = \lim_{\Delta\omega \to 0} \frac{1}{2\pi} \sum_{n=-\infty}^{\infty} X(n\Delta\omega) e^{(jn\Delta\omega)t} \Delta\omega \tag{4.7}$$

The sum on the right-hand side of Eq. (4.7) can be viewed as the area under the function $X(\omega)e^{j\omega t}$, as illustrated in Fig. 4.3. Therefore,

$$x(t) = \frac{1}{2\pi} \int_{-\infty}^{\infty} X(\omega) e^{j\omega t} d\omega \tag{4.8}$$

The integral on the right-hand side is called the *Fourier integral.* We have now succeeded in representing an aperiodic signal $x(t)$ by a Fourier integral (rather than a Fourier series).† This integral is basically a Fourier series (in the limit) with fundamental frequency $\Delta\omega \to 0$, as seen from Eq. (4.7). The amount of the exponential $e^{jn\Delta\omega t}$ is $X(n\Delta\omega)\Delta\omega/2\pi$. Thus, the function $X(\omega)$ given by Eq. (4.4) acts as a spectral function.

We call $X(\omega)$ the *direct* Fourier transform of $x(t)$, and $x(t)$ the *inverse* Fourier transform of $X(\omega)$. The same information is conveyed by the statement that $x(t)$ and $X(\omega)$ are a Fourier transform pair. Symbolically, this statement is expressed as

$$X(\omega) = \mathcal{F}[x(t)] \qquad \text{and} \qquad x(t) = \mathcal{F}^{-1}[X(\omega)]$$

or

$$x(t) \Longleftrightarrow X(\omega)$$

To recapitulate,

$$X(\omega) = \int_{-\infty}^{\infty} x(t) e^{-j\omega t} dt \tag{4.9}$$

and

$$x(t) = \frac{1}{2\pi} \int_{-\infty}^{\infty} X(\omega) e^{j\omega t} d\omega \tag{4.10}$$

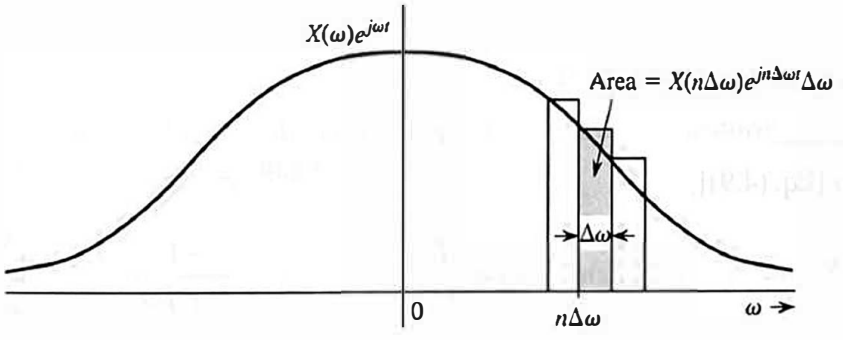

Figure 4.3 The Fourier series becomes the Fourier integral in the limit as $T_0 \to \infty$.

† This derivation should not be considered to be a rigorous proof of Eq. (4.8). The situation is not as simple as we have made it appear [1].

It is helpful to keep in mind that the Fourier integral in Eq. (4.10) is of the nature of a Fourier series with fundamental frequency $\Delta\omega$ approaching zero [Eq. (4.7)]. Therefore, most of the discussion and properties of Fourier series apply to the Fourier transform as well. *The transform $X(\omega)$ is the frequency-domain specification of $x(t)$.*

We can plot the spectrum $X(\omega)$ as a function of ω. Since $X(\omega)$ is complex, we have both amplitude and angle (or phase) spectra

$$X(\omega) = |X(\omega)|e^{j\angle X(\omega)}$$

in which $|X(\omega)|$ is the amplitude and $\angle X(\omega)$ is the angle (or phase) of $X(\omega)$. According to Eq. (4.9),

$$X(-\omega) = \int_{-\infty}^{\infty} x(t)e^{j\omega t}dt$$

Taking the conjugates of both sides yields

$$x^*(t) \Longleftrightarrow X^*(-\omega) \tag{4.11}$$

This property is known as the *conjugation property.* Now, if $x(t)$ is a real function of t, then $x(t) = x^*(t)$, and from the conjugation property, we find that

$$X(-\omega) = X^*(\omega)$$

This is the *conjugate symmetry* property of the Fourier transform, applicable to real $x(t)$. Therefore, for real $x(t)$,

$$|X(-\omega)| = |X(\omega)| \qquad \text{and} \qquad \angle X(-\omega) = -\angle X(\omega) \tag{4.12}$$

Thus, for real $x(t)$, the amplitude spectrum $|X(\omega)|$ is an even function, and the phase spectrum $\angle X(\omega)$ is an odd function of ω. These results were derived earlier for the Fourier spectrum of a periodic signal [Eq. (3.49)] and should come as no surprise.

EXAMPLE 4.1 Fourier Transform of a Causal Exponential

Find the Fourier transform of $e^{-at}u(t)$.

By definition [Eq. (4.9)],

$$X(\omega) = \int_{-\infty}^{\infty} e^{-at}u(t)e^{-j\omega t}dt = \int_{0}^{\infty} e^{-(a+j\omega)t}dt = \frac{-1}{a+j\omega}e^{-(a+j\omega)t}\Big|_0^{\infty}$$

But $|e^{-j\omega t}| = 1$. Therefore, as $t \to \infty$, $e^{-(a+j\omega)t} = e^{-at}e^{-j\omega t} = \infty$ if $a < 0$, but it is equal to 0 if $a > 0$. Therefore,

$$X(\omega) = \frac{1}{a+j\omega} \qquad a > 0$$

Expressing $a + j\omega$ in the polar form as $\sqrt{a^2+\omega^2}\,e^{j\tan^{-1}(\omega/a)}$, we obtain

$$X(\omega) = \frac{1}{\sqrt{a^2+\omega^2}}e^{-j\tan^{-1}(\omega/a)}$$

Therefore,

$$|X(\omega)| = \frac{1}{\sqrt{a^2+\omega^2}} \qquad \text{and} \qquad \angle X(\omega) = -\tan^{-1}\left(\frac{\omega}{a}\right)$$

The amplitude spectrum $|X(\omega)|$ and the phase spectrum $\angle X(\omega)$ are depicted in Fig. 4.4b. Observe that $|X(\omega)|$ is an even function of ω, and $\angle X(\omega)$ is an odd function of ω, as expected.

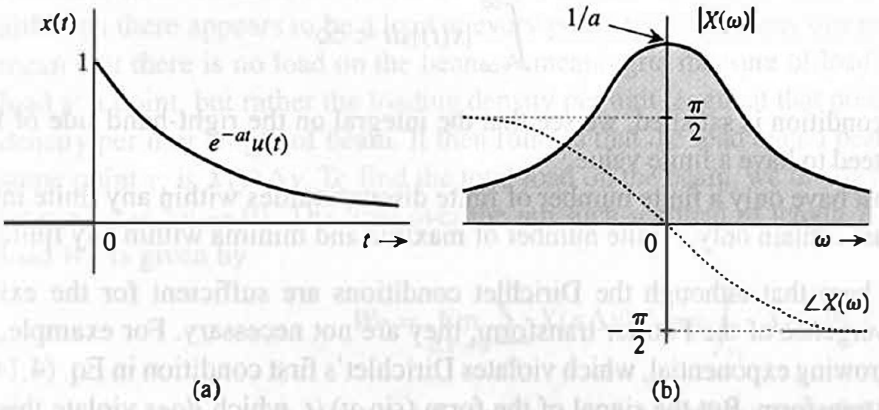

Figure 4.4 $e^{-at}u(t)$ and its Fourier spectra.

Existence of the Fourier Transform

In Ex. 4.1 we observed that when $a < 0$, the Fourier integral for $e^{-at}u(t)$ does not converge. Hence, the Fourier transform for $e^{-at}u(t)$ does not exist if $a < 0$ (growing exponential). Clearly, not all signals are Fourier transformable.

Because the Fourier transform is derived here as a limiting case of the Fourier series, it follows that the basic qualifications of the Fourier series, such as *equality in the mean* and convergence conditions in suitably modified form, apply to the Fourier transform as well. It can be shown that if $x(t)$ has a finite energy, that is, if

$$\int_{-\infty}^{\infty} |x(t)|^2\,dt < \infty$$

then the Fourier transform $X(\omega)$ is finite and converges to $x(t)$ in the mean. This means, if we let

$$\hat{x}(t) = \lim_{W\to\infty} \frac{1}{2\pi}\int_{-W}^{W} X(\omega)e^{j\omega t}\,d\omega$$

then Eq. (4.10) implies

$$\int_{-\infty}^{\infty} |x(t) - \hat{x}(t)|^2 \, dt = 0 \tag{4.13}$$

In other words, $x(t)$ and its Fourier integral [the right-hand side of Eq. (4.10)] can differ at some values of t without contradicting Eq. (4.13). We shall now discuss an alternate set of criteria due to Dirichlet for convergence of the Fourier transform.

As with the Fourier series, if $x(t)$ satisfies certain conditions (*Dirichlet conditions*), its Fourier transform is guaranteed to converge pointwise at all points where $x(t)$ is continuous. Moreover, at the points of discontinuity, $x(t)$ converges to the value midway between the two values of $x(t)$ on either side of the discontinuity. The Dirichlet conditions are as follows:

1. $x(t)$ should be absolutely integrable, that is,

$$\int_{-\infty}^{\infty} |x(t)| \, dt < \infty \tag{4.14}$$

   If this condition is satisfied, we see that the integral on the right-hand side of Eq. (4.9) is guaranteed to have a finite value.
2. $x(t)$ must have only a finite number of finite discontinuities within any finite interval.
3. $x(t)$ must contain only a finite number of maxima and minima within any finite interval.

We stress here that although the Dirichlet conditions are sufficient for the existence and pointwise convergence of the Fourier transform, they are not necessary. For example, we saw in Ex. 4.1 that a growing exponential, which violates Dirichlet's first condition in Eq. (4.14), does not have a Fourier transform. But the signal of the form $(\sin at)/t$, which *does* violate this condition, does have a Fourier transform.

Any signal that can be generated in practice satisfies the Dirichlet conditions and therefore has a Fourier transform. Thus, the physical existence of a signal is a sufficient condition for the existence of its transform.

Linearity of the Fourier Transform

The Fourier transform is linear; that is, if

$$x_1(t) \Longleftrightarrow X_1(\omega) \qquad \text{and} \qquad x_2(t) \Longleftrightarrow X_2(\omega)$$

then

$$a_1 x_1(t) + a_2 x_2(t) \Longleftrightarrow a_1 X_1(\omega) + a_2 X_2(\omega) \tag{4.15}$$

The proof is trivial and follows directly from Eq. (4.9). This result can be extended to any finite number of terms. It can be extended to an infinite number of terms only if the conditions required for interchangeability of the operations of summation and integration are satisfied.

4.1.1 Physical Appreciation of the Fourier Transform

In understanding any aspect of the Fourier transform, we should remember that Fourier representation is a way of expressing a signal in terms of everlasting sinusoids (or exponentials). The Fourier spectrum of a signal indicates the relative amplitudes and phases of sinusoids that

are required to synthesize that signal. A periodic signal Fourier spectrum has finite amplitudes and exists at discrete frequencies (ω_0 and its multiples). Such a spectrum is easy to visualize, but the spectrum of an aperiodic signal is not easy to visualize because it has a continuous spectrum. The continuous spectrum concept can be appreciated by considering an analogous, more tangible phenomenon. One familiar example of a continuous distribution is the loading of a beam. Consider a beam loaded with weights $D_1, D_2, D_3, \ldots, D_n$ units at the uniformly spaced points $y_1, y_2, \ldots, y_n$, as shown in Fig. 4.5a.

The total load W_T on the beam is given by the sum of these loads at each of the n points:

$$W_T = \sum_{i=1}^{n} D_i$$

Consider now the case of a continuously loaded beam, as depicted in Fig. 4.5b. In this case, although there appears to be a load at every point, the load at any one point is zero. This does not mean that there is no load on the beam. A meaningful measure of load in this situation is not the load at a point, but rather the loading density per unit length at that point. Let $X(y)$ be the loading density per unit length of beam. It then follows that the load over a beam length $\Delta y (\Delta y \to 0)$, at some point y, is $X(y)\Delta y$. To find the total load on the beam, we divide the beam into segments of interval $\Delta y (\Delta y \to 0)$. The load over the nth such segment of length Δy is $X(n\Delta y)\Delta y$. The total load W_T is given by

$$W_T = \lim_{\Delta y \to 0} \sum_{y_1}^{y_n} X(n\Delta y)\,\Delta y = \int_{y_1}^{y_n} X(y)\,dy$$

The load now exists at every point, and y is now a continuous variable. In the case of discrete loading (Fig. 4.5a), the load exists only at n discrete points. At other points, there is no load. On the other hand, in the continuously loaded case, the load exists at every point, but at any specific point y, the load is zero. The load over a small interval Δy, however, is $[X(n\Delta y)]\,\Delta y$ (Fig. 4.5b). Thus, even though the load at a point y is zero, the relative load at that point is $X(y)$.

An exactly analogous situation exists in the case of a signal spectrum. When $x(t)$ is periodic, the spectrum is discrete, and $x(t)$ can be expressed as a sum of discrete exponentials with finite amplitudes:

$$x(t) = \sum_{n} D_n e^{jn\omega_0 t}$$

For an aperiodic signal, the spectrum becomes continuous; that is, the spectrum exists for every value of ω, but the amplitude of each component in the spectrum is zero. The meaningful measure

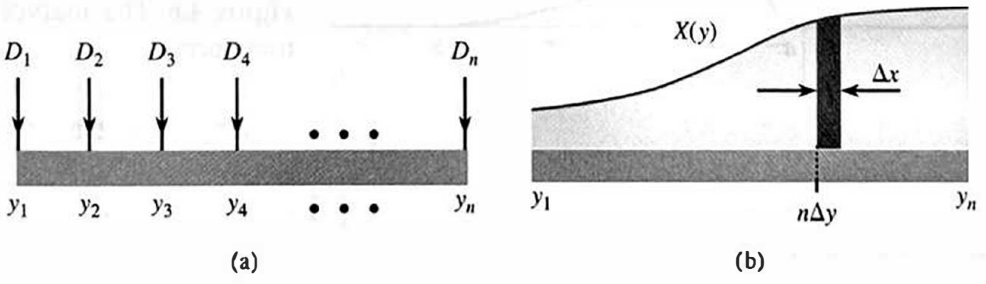

Figure 4.5 Weight-loading analogy for the Fourier transform.

here is not the amplitude of a component of some frequency but the spectral density per unit bandwidth. From Eq. (4.7), it is clear that $x(t)$ is synthesized by adding exponentials of the form $e^{jn\Delta\omega t}$, in which the contribution by any one exponential component is zero. But the contribution by exponentials in an infinitesimal band $\Delta\omega$ located at $\omega = n\Delta\omega$ is $(1/2\pi)X(n\Delta\omega)\Delta\omega$, and the addition of all these components yields $x(t)$ in the integral form:

$$x(t) = \lim_{\Delta\omega \to 0} \frac{1}{2\pi} \sum_{n=-\infty}^{\infty} X(n\Delta\omega) e^{(jn\Delta\omega)t} \Delta\omega = \frac{1}{2\pi} \int_{-\infty}^{\infty} X(\omega) e^{j\omega t} d\omega$$

Thus, $n\Delta\omega$ approaches a continuous variable ω. The spectrum now exists at every ω. The contribution by components within a band $d\omega$ is $(1/2\pi)X(\omega)\,d\omega = X(\omega)\,df$, where df is the bandwidth in hertz. Clearly, $X(\omega)$ is the *spectral density* per unit bandwidth (in hertz).[†] It also follows that even if the amplitude of any one component is infinitesimal, the relative amount of a component of frequency ω is $X(\omega)$. Although $X(\omega)$ is a spectral density, in practice, it is customarily called the *spectrum* of $x(t)$ rather than the spectral density of $x(t)$. Deferring to this convention, we shall call $X(\omega)$ the Fourier spectrum (or Fourier transform) of $x(t)$.

A Marvelous Balancing Act

An important point to remember here is that $x(t)$ is represented (or synthesized) by exponentials or sinusoids that are everlasting (not causal). Such conceptualization leads to a rather fascinating picture when we try to visualize the synthesis of a timelimited pulse signal $x(t)$ [Fig. 4.6] by the sinusoidal components in its Fourier spectrum. The signal $x(t)$ exists only over an interval (a,b) and is zero outside this interval. The spectrum of $x(t)$ contains an infinite number of exponentials (or sinusoids), which start at $t = -\infty$ and continue forever. The amplitudes and phases of these components add up exactly to $x(t)$ over the finite interval (a,b) and to zero everywhere outside this interval. Juggling the amplitudes and phases of an infinite number of components to achieve such a perfect and delicate balance boggles the human imagination. Yet the Fourier transform accomplishes it routinely, without much thinking on our part. Indeed, we become so involved in mathematical manipulations that we fail to notice this marvel.

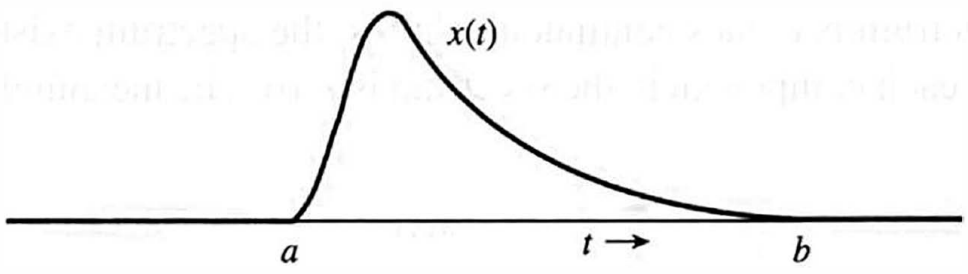

Figure 4.6 The marvel of the Fourier transform.

[†] To stress that the signal spectrum is a *density* function, we shall shade the plot of $|X(\omega)|$ (as in Fig. 4.4b). The representation of $\angle X(\omega)$, however, will be a line plot, primarily to avoid visual confusion.

A Word About Notation

In Ch. 2 [Eq. (2.39)], we defined the system transfer function $H(s)$ as

$$H(s) = \int_{-\infty}^{\infty} h(t)e^{-st}\,dt$$

Setting $s = j\omega$ in this equation yields

$$H(j\omega) = \int_{-\infty}^{\infty} h(t)e^{-j\omega t}\,dt$$

The right-hand side is the Fourier transform of $h(t)$, and according to our notation introduced in Eq. (4.4), this is $H(\omega)$, whereas the same entity is denoted by $H(j\omega)$ in the notation introduced in Ch. 2. Thus, to be consistent with the previous notation, we should have denoted the Fourier transform by $X(j\omega)$ rather than $X(\omega)$ in Eq. (4.4). In fact, the notation $X(j\omega)$ for the Fourier transform is often used in the literature. It is, however, a bit clumsy and does not lend itself so easily to manipulation as the notation $X(\omega)$. For this reason, we shall continue with the dual notation, while remembering that both $X(\omega)$ and $X(j\omega)$ represent the same entity. This fact is particularly important when we discuss the Laplace transform and filtering in the future, and should be kept in mind throughout the rest of the book. In the same way, we must remember that $H(\omega)$ and $H(j\omega)$ represent the same entity.

4.1.2 LTIC System Response Using the Fourier Transform

We wanted to represent a signal $x(t)$ as a sum of (everlasting) exponentials so that we could find a system response to $x(t)$ as a sum of the system's responses to the exponential components of $x(t)$. Consider an asymptotically stable LTIC system with transfer function $H(s)$. The response of this system to everlasting exponential $e^{j\omega t}$ is $H(\omega)e^{j\omega t}$. Such an input-output pair will be denoted by the directed arrow representation as

$$e^{j\omega t} \Longrightarrow H(\omega)e^{j\omega t}$$

Therefore,

$$e^{j(n\Delta\omega)t} \Longrightarrow H(n\Delta\omega)e^{j(n\Delta\omega)t}$$

and

$$\left[\frac{X(n\Delta\omega)\Delta\omega}{2\pi}\right]e^{(jn\Delta\omega)t} \Longrightarrow \left[\frac{X(n\Delta\omega)H(n\Delta\omega)\Delta\omega}{2\pi}\right]e^{j(n\Delta\omega)t}$$

Using the linearity property

$$\underbrace{\lim_{\Delta\omega\to 0}\sum_{n=-\infty}^{\infty}\left[\frac{X(n\Delta\omega)\Delta\omega}{2\pi}\right]e^{(jn\Delta\omega)t}}_{\text{input } x(t)} \Longrightarrow \underbrace{\lim_{\Delta\omega\to 0}\sum_{n=-\infty}^{\infty}\left[\frac{X(n\Delta\omega)H(n\Delta\omega)\Delta\omega}{2\pi}\right]e^{j(n\Delta\omega)t}}_{\text{output } y(t)}$$

The left-hand side is the input $x(t)$ [see Eq. (4.7)], and the right-hand side is the response $y(t)$. Thus,

$$\begin{aligned} y(t) &= \frac{1}{2\pi} \lim_{\Delta\omega \to 0} \sum_{n=-\infty}^{\infty} X(n\Delta\omega) H(n\Delta\omega) e^{j(n\Delta\omega)t} \Delta\omega \\ &= \frac{1}{2\pi} \int_{-\infty}^{\infty} X(\omega) H(\omega) e^{j\omega t} d\omega \\ &= \frac{1}{2\pi} \int_{-\infty}^{\infty} Y(\omega) e^{j\omega t} d\omega \end{aligned}$$

where $Y(\omega)$, the Fourier transform of $y(t)$, is given by[†]

$$Y(\omega) = X(\omega)H(\omega) \tag{4.16}$$

In conclusion, we have shown that for an LTIC system with transfer function $H(s)$, if the input and the output are $x(t)$ and $y(t)$, respectively, and if

$$x(t) \Longleftrightarrow X(\omega) \qquad \text{and} \qquad y(t) \Longleftrightarrow Y(\omega)$$

then for asymptotically stable systems

$$Y(\omega) = X(\omega)H(\omega)$$

We shall derive this result again later in a more formal way.

4.2 TRANSFORMS OF SOME USEFUL FUNCTIONS

For convenience, we now introduce a compact notation for the useful gate, triangle, and interpolation functions.

UNIT GATE FUNCTION

We define a unit gate function rect (x) as a gate pulse of unit height and unit width, centered at the origin, as illustrated in Fig. 4.7a[‡]:

[†] The result of Eq. (4.16) applies only to the asymptotically stable systems. The reason is that when $s = j\omega$, the integral on the right-hand side of Eq. (2.39) does not converge for unstable systems. Moreover, even for marginally stable systems, that integral does not converge in the ordinary sense, and $H(j\omega)$ [or $H(\omega)$] cannot be obtained by replacing s in $H(s)$ with $j\omega$. As shown later in Eq. (4.35), Eq. (4.16) can be applied to marginally stable systems, provided $H(\omega)$ is interpreted as the Fourier transform of $h(t)$ rather than as $H(s)$ with s replaced by $j\omega$.

[‡] At $|x| = 0.5$, we require rect $(x) = 0.5$ because the inverse Fourier transform of a discontinuous signal converges to the mean of its two values at the discontinuity.

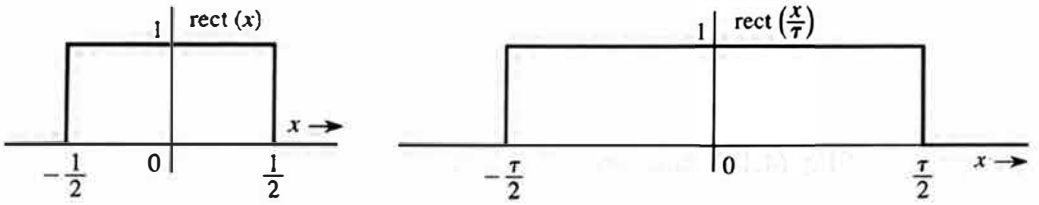

Figure 4.7 A gate pulse.

$$\text{rect}\,(x) = \begin{cases} 0 & |x| > \frac{1}{2} \\ \frac{1}{2} & |x| = \frac{1}{2} \\ 1 & |x| < \frac{1}{2} \end{cases} \tag{4.17}$$

The gate pulse in Fig. 4.7b is the unit gate pulse rect (x) expanded by a factor τ along the horizontal axis and therefore can be expressed as rect (x/τ) (see Sec. 1.2.2). Observe that τ, the denominator of the argument of rect (x/τ), indicates the width of the pulse.

Unit Triangle Function

We define a unit triangle function $\Delta(x)$ as a triangular pulse of unit height and unit width, centered at the origin, as shown in Fig. 4.8a

$$\Delta(x) = \begin{cases} 0 & |x| \geq \frac{1}{2} \\ 1 - 2|x| & |x| < \frac{1}{2} \end{cases} \tag{4.18}$$

The pulse in Fig. 4.8b is $\Delta(x/\tau)$. Observe that here, as for the gate pulse, the denominator τ of the argument of $\Delta(x/\tau)$ indicates the pulse width.

Interpolation Function sinc (x)

The function $\sin x/x$ is the "sine over argument" function denoted by sinc (x).[†] This function plays an important role in signal processing. It is also known as the *filtering* or *interpolating function*.

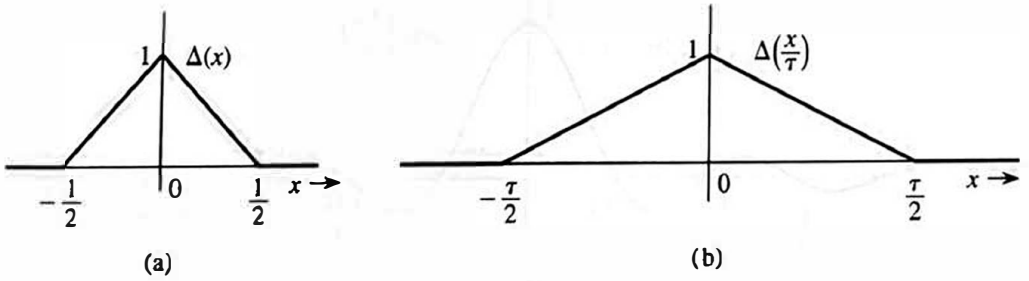

Figure 4.8 A triangle pulse.

[†] sinc(x) is also denoted by Sa (x) in the literature. Some authors define sinc (x) as

$$\text{sinc}\,(x) = \frac{\sin \pi x}{\pi x}$$

We define

$$\text{sinc}(x) = \frac{\sin x}{x} \tag{4.19}$$

Inspection of Eq. (4.19) shows the following:

1. $\text{sinc}(x)$ is an even function of x.
2. $\text{sinc}(x) = 0$ when $\sin x = 0$ except at $x = 0$, where it appears to be indeterminate. This means that $\text{sinc}\, x = 0$ for $x = \pm\pi, \pm 2\pi, \pm 3\pi, \ldots$.
3. Using L'Hôpital's rule, we find $\text{sinc}(0) = 1$.
4. $\text{sinc}(x)$ is the product of an oscillating signal $\sin x$ (of period 2π) and a monotonically decreasing function $1/x$. Therefore, $\text{sinc}(x)$ exhibits damped oscillations of period 2π, with the amplitude decreasing continuously as $1/x$.

Figure 4.9a shows $\text{sinc}(x)$. Observe that $\text{sinc}(x) = 0$ for values of x that are positive and negative integer multiples of π. Figure 4.9b shows $\text{sinc}(3\omega/7)$. The argument $3\omega/7 = \pi$ when $\omega = 7\pi/3$. Therefore, the first zero of this function occurs at $\omega = 7\pi/3$.

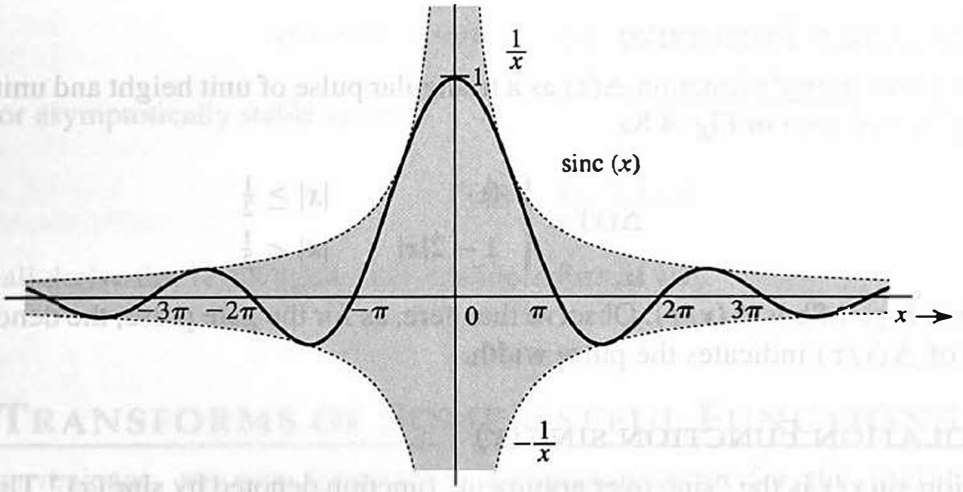

(a)

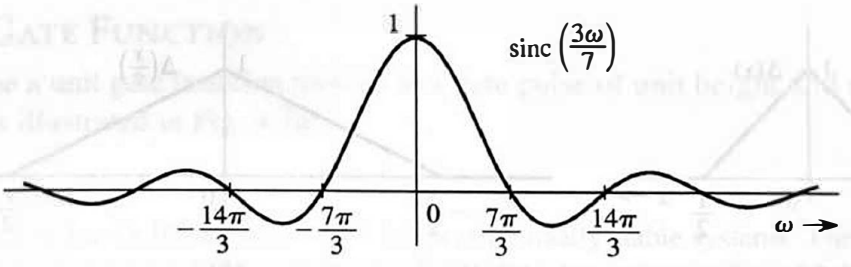

(b)

Figure 4.9 A sinc pulse.

DRILL 4.1 Sketching Basic Functions

Sketch: **(a)** rect $(x/8)$, **(b)** $\Delta(\omega/10)$, **(c)** sinc $(3\pi\omega/2)$, and **(d)** sinc (t) rect $(t/4\pi)$.

EXAMPLE 4.2 Fourier Transform of a Rectangular Pulse

Find the Fourier transform of $x(t) = \text{rect}(t/\tau)$ (Fig. 4.10a).

$$X(\omega) = \int_{-\infty}^{\infty} \text{rect}\left(\frac{t}{\tau}\right) e^{-j\omega t} dt$$

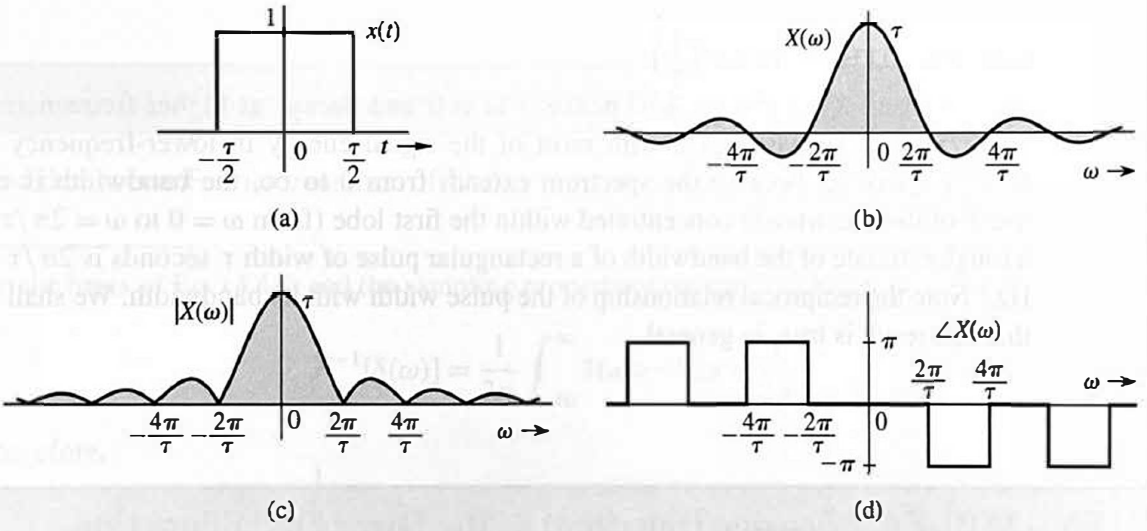

Figure 4.10 **(a)** A gate pulse $x(t)$, **(b)** its Fourier spectrum $X(\omega)$, **(c)** its amplitude spectrum $|X(\omega)|$, and **(d)** its phase spectrum $\angle X(\omega)$.

Since $\text{rect}(t/\tau) = 1$ for $|t| < \tau/2$, and since it is zero for $|t| > \tau/2$,

$$X(\omega) = \int_{-\tau/2}^{\tau/2} e^{-j\omega t} dt$$

$$= -\frac{1}{j\omega}(e^{-j\omega\tau/2} - e^{j\omega\tau/2}) = \frac{2\sin\left(\frac{\omega\tau}{2}\right)}{\omega}$$

$$= \tau \frac{\sin\left(\frac{\omega\tau}{2}\right)}{\left(\frac{\omega\tau}{2}\right)} = \tau\,\text{sinc}\left(\frac{\omega\tau}{2}\right)$$

Therefore,

$$\text{rect}\left(\frac{t}{\tau}\right) \Longleftrightarrow \tau\ \text{sinc}\left(\frac{\omega\tau}{2}\right) \tag{4.20}$$

Recall that $\text{sinc}(x) = 0$ when $x = \pm n\pi$. Hence, $\text{sinc}(\omega\tau/2) = 0$ when $\omega\tau/2 = \pm n\pi$; that is, when $\omega = \pm 2n\pi/\tau, (n = 1, 2, 3, \ldots)$, as depicted in Fig. 4.10b. The Fourier transform $X(\omega)$ shown in Fig. 4.10b exhibits positive and negative values. A negative amplitude can be considered to be a positive amplitude with a phase of $-\pi$ or π. We use this observation to plot the amplitude spectrum $|X(\omega)| = |\text{sinc}(\omega\tau/2)|$ (Fig. 4.10c) and the phase spectrum $\angle X(\omega)$ (Fig. 4.10d). The phase spectrum, which is required to be an odd function of ω, may be drawn in several other ways because a negative sign can be accounted for by a phase of $\pm n\pi$, where n is any odd integer. All such representations are equivalent.

Bandwidth of rect $\left(\frac{t}{\tau}\right)$

The spectrum $X(\omega)$ in Fig. 4.10 peaks at $\omega = 0$ and decays at higher frequencies. Therefore, $\text{rect}(t/\tau)$ is a lowpass signal with most of the signal energy in lower-frequency components. Strictly speaking, because the spectrum extends from 0 to ∞, the bandwidth is ∞. However, much of the spectrum is concentrated within the first lobe (from $\omega = 0$ to $\omega = 2\pi/\tau$). Therefore, a rough estimate of the bandwidth of a rectangular pulse of width τ seconds is $2\pi/\tau$ rad/s, or $1/\tau$ Hz.[†] Note the reciprocal relationship of the pulse width with its bandwidth. We shall observe later that this result is true, in general.

EXAMPLE 4.3 Fourier Transform of the Dirac Delta Function

Find the Fourier transform of the unit impulse $\delta(t)$.

Using the sampling property of the impulse [Eq. (1.11)], we obtain

$$\mathcal{F}[\delta(t)] = \int_{-\infty}^{\infty} \delta(t) e^{-j\omega t} dt = 1 \qquad \text{and} \qquad \delta(t) \Longleftrightarrow 1$$

[†] To compute bandwidth, we must consider the spectrum for positive values of ω only. See the discussion in Sec. 3.6.

Figure 4.11 shows $\delta(t)$ and its spectrum.

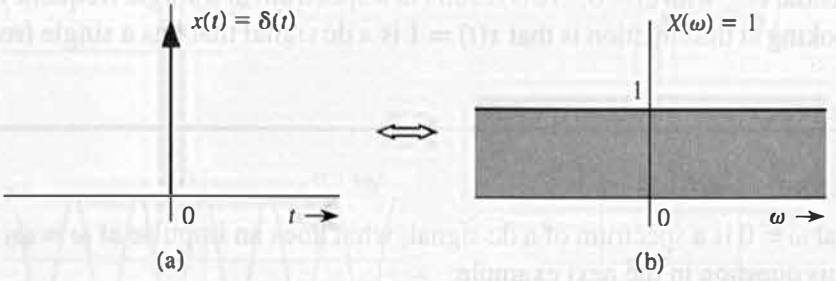

Figure 4.11 (**a**) Unit impulse and (**b**) its Fourier spectrum.

EXAMPLE 4.4 Inverse Fourier Transform of the Dirac Delta Function

Find the inverse Fourier transform of $\delta(\omega)$.

On the basis of Eq. (4.10) and the sampling property of the impulse function,

$$\mathcal{F}^{-1}[\delta(\omega)] = \frac{1}{2\pi}\int_{-\infty}^{\infty}\delta(\omega)e^{j\omega t}d\omega = \frac{1}{2\pi}$$

Therefore,

$$\frac{1}{2\pi} \Longleftrightarrow \delta(\omega) \qquad \text{and} \qquad 1 \Longleftrightarrow 2\pi\delta(\omega) \tag{4.21}$$

This result shows that the spectrum of a constant signal $x(t) = 1$ is an impulse $2\pi\delta(\omega)$, as illustrated in Fig. 4.12.

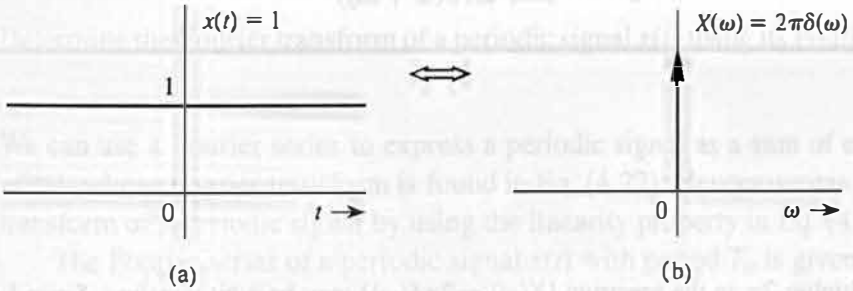

Figure 4.12 (**a**) A constant (dc) signal and (**b**) its Fourier spectrum.

The result [Eq. (4.21)] could have been anticipated on qualitative grounds. Recall that the Fourier transform of $x(t)$ is a spectral representation of $x(t)$ in terms of everlasting exponential components of the form $e^{j\omega t}$. Now, to represent a constant signal $x(t) = 1$, we need a single everlasting exponential $e^{j\omega t}$ with $\omega = 0$.[†] This results in a spectrum at a single frequency $\omega = 0$. Another way of looking at the situation is that $x(t) = 1$ is a dc signal that has a single frequency $\omega = 0$ (dc).

If an impulse at $\omega = 0$ is a spectrum of a dc signal, what does an impulse at $\omega = \omega_0$ represent? We shall answer this question in the next example.

EXAMPLE 4.5 Inverse Fourier Transform of a Shifted Dirac Delta Function

Find the inverse Fourier transform of $\delta(\omega - \omega_0)$.

Using the sampling property of the impulse function, we obtain

$$\mathcal{F}^{-1}[\delta(\omega - \omega_0)] = \frac{1}{2\pi}\int_{-\infty}^{\infty} \delta(\omega - \omega_0)e^{j\omega t}\,d\omega = \frac{1}{2\pi}e^{j\omega_0 t}$$

Therefore,

$$\frac{1}{2\pi}e^{j\omega_0 t} \Longleftrightarrow \delta(\omega - \omega_0) \qquad \text{and} \qquad e^{j\omega_0 t} \Longleftrightarrow 2\pi\delta(\omega - \omega_0) \tag{4.22}$$

This result shows that the spectrum of an everlasting exponential $e^{j\omega_0 t}$ is a single impulse at $\omega = \omega_0$. We reach the same conclusion by qualitative reasoning. To represent the everlasting exponential $e^{j\omega_0 t}$, we need a single everlasting exponential $e^{j\omega t}$ with $\omega = \omega_0$. Therefore, the spectrum consists of a single component at frequency $\omega = \omega_0$.

From Eq. (4.22), it follows that

$$e^{-j\omega_0 t} \Longleftrightarrow 2\pi\delta(\omega + \omega_0)$$

[†] The constant multiplier 2π in the spectrum $[X(\omega) = 2\pi\delta(\omega)]$ may be a bit puzzling. Since $1 = e^{j\omega t}$ with $\omega = 0$, it appears that the Fourier transform of $x(t) = 1$ should be an impulse of strength unity rather than 2π. Recall, however, that in the Fourier transform $x(t)$ is synthesized by exponentials, not of amplitude $X(n\Delta\omega)\Delta\omega$, but of amplitude $1/2\pi$ times $X(n\Delta\omega)\Delta\omega$, as seen from Eq. (4.7). Had we used variable f (hertz) instead of ω, the spectrum would have been the unit impulse.

EXAMPLE 4.6 Fourier Transform of a Sinusoid

Find the Fourier transform of the everlasting sinusoid $\cos \omega_0 t$ (Fig. 4.13a).

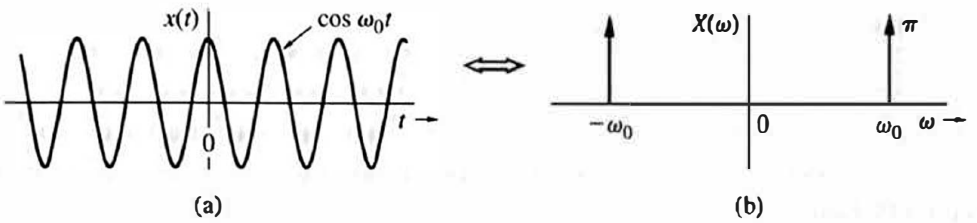

Figure 4.13 **(a)** A cosine signal and **(b)** its Fourier spectrum.

Recall Euler's formula

$$\cos \omega_0 t = \tfrac{1}{2}(e^{j\omega_0 t} + e^{-j\omega_0 t})$$

Applying Eq. (4.22), we obtain

$$\cos \omega_0 t \Longleftrightarrow \pi[\delta(\omega + \omega_0) + \delta(\omega - \omega_0)]$$

The spectrum of $\cos \omega_0 t$ consists of two impulses at ω_0 and $-\omega_0$, as shown in Fig. 4.13b. The result also follows from qualitative reasoning. An everlasting sinusoid $\cos \omega_0 t$ can be synthesized by two everlasting exponentials, $e^{j\omega_0 t}$ and $e^{-j\omega_0 t}$. Therefore, the Fourier spectrum consists of only two components of frequencies ω_0 and $-\omega_0$.

EXAMPLE 4.7 Fourier Transform of a Periodic Signal

Determine the Fourier transform of a periodic signal $x(t)$ using its Fourier series representation.

We can use a Fourier series to express a periodic signal as a sum of exponentials of the form $e^{jn\omega_0 t}$, whose Fourier transform is found in Eq. (4.22). Hence, we can readily find the Fourier transform of a periodic signal by using the linearity property in Eq. (4.15).

The Fourier series of a periodic signal $x(t)$ with period T_0 is given by

$$x(t) = \sum_{n=-\infty}^{\infty} D_n e^{jn\omega_0 t} \qquad \omega_0 = \frac{2\pi}{T_0}$$

Taking the Fourier transform of both sides, we obtain†

$$X(\omega) = 2\pi \sum_{n=-\infty}^{\infty} D_n \delta(\omega - n\omega_0) \tag{4.23}$$

EXAMPLE 4.8 Fourier Transform of a Dirac Delta Train

Determine the Fourier transform of a Dirac delta train $\delta_{T_0}(t)$ (Fig. 4.14a) using its Fourier series representation.

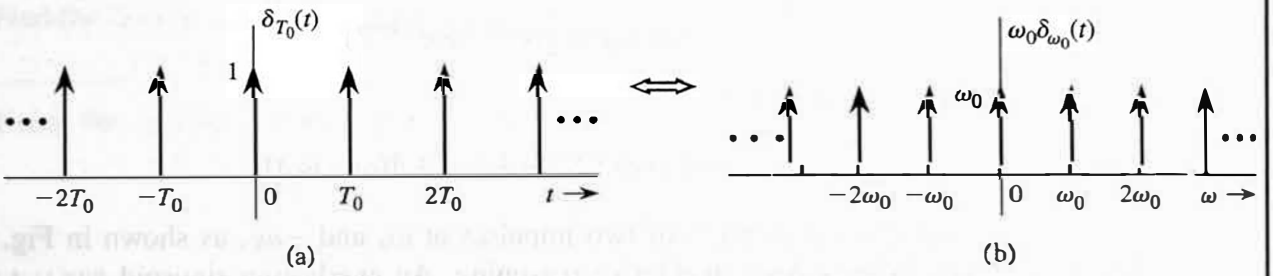

Figure 4.14 (a) The uniform impulse train and (b) its Fourier transform.

As shown in Eq. (3.51) from Ex. 3.13, the Fourier coefficients D_n for $\delta_{T_0}(t)$ are constant $D_n = 1/T_0$. From Eq. (4.23), the Fourier transform of $\delta_{T_0}(t)$ is therefore

$$X(\omega) = \frac{2\pi}{T_0} \sum_{n=-\infty}^{\infty} \delta(\omega - n\omega_0) = \omega_0 \delta_{\omega_0}(\omega), \qquad \text{where } \omega_0 = \frac{2\pi}{T_0}$$

The corresponding spectrum is shown in Fig. 4.14b.

† We assume here that the linearity property can be extended to an infinite sum.

EXAMPLE 4.9 Fourier Transform of the Unit Step Function

Find the Fourier transform of the unit step function $u(t)$.

Trying to find the Fourier transform of $u(t)$ by direct integration leads to an indeterminate result because

$$U(\omega) = \int_{-\infty}^{\infty} u(t)e^{-j\omega t}dt = \int_{0}^{\infty} e^{-j\omega t}dt = \frac{-1}{j\omega}e^{-j\omega t}\Big|_{0}^{\infty}$$

The upper limit of $e^{-j\omega t}$ as $t \to \infty$ yields an indeterminate answer. So we approach this problem by considering $u(t)$ to be a decaying exponential $e^{-at}u(t)$ in the limit as $a \to 0$ (Fig. 4.15a). Thus,

$$u(t) = \lim_{a\to 0} e^{-at}u(t)$$

and

$$U(\omega) = \lim_{a\to 0} \mathcal{F}\{e^{-at}u(t)\} = \lim_{a\to 0} \frac{1}{a + j\omega}$$

Expressing the right-hand side in terms of its real and imaginary parts yields

$$U(\omega) = \lim_{a\to 0}\left[\frac{a}{a^2+\omega^2} - j\frac{\omega}{a^2+\omega^2}\right] = \lim_{a\to 0}\left[\frac{a}{a^2+\omega^2}\right] + \frac{1}{j\omega}$$

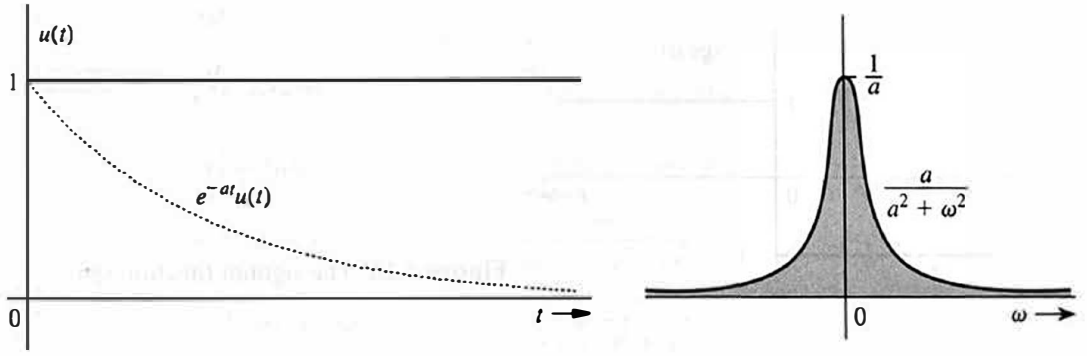

Figure 4.15 Derivation of the Fourier transform of the step function.

The function $a/(a^2 + \omega^2)$ has interesting properties. First, the area under this function (Fig. 4.15b) is π regardless of the value of a:

$$\int_{-\infty}^{\infty} \frac{a}{a^2+\omega^2}d\omega = \tan^{-1}\frac{\omega}{a}\Big|_{-\infty}^{\infty} = \pi$$

Second, when $a \to 0$, this function approaches zero for all $\omega \neq 0$, and all its area (π) is concentrated at a single point $\omega = 0$. Clearly, as $a \to 0$, this function approaches an impulse of strength π. Thus,

$$U(\omega) = \pi\delta(\omega) + \frac{1}{j\omega} \tag{4.24}$$

Note that $u(t)$ is not a "true" dc signal because it is not constant over the interval $-\infty$ to ∞. To synthesize "true" dc, we require only one everlasting exponential with $\omega = 0$ (impulse at $\omega = 0$). The signal $u(t)$ has a jump discontinuity at $t = 0$. It is impossible to synthesize such a signal with a single everlasting exponential $e^{j\omega t}$. To synthesize this signal from everlasting exponentials, we need, in addition to an impulse at $\omega = 0$, all the frequency components, as indicated by the term $1/j\omega$ in Eq. (4.24).

EXAMPLE 4.10 Fourier Transform of the Sign Function

Find the Fourier transform of the sign function sgn (t) [pronounced *signum* (t)], depicted in Fig. 4.16.

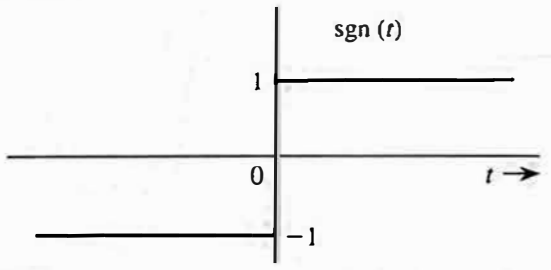

Figure 4.16 The signum function sgn(t).

Observe that

$$\text{sgn}\,(t) + 1 = 2u(t) \quad \Longrightarrow \quad \text{sgn}\,(t) = 2u(t) - 1$$

Using Eqs. (4.21) and (4.24) and the linearity property, we obtain

$$\text{sgn}\,(t) \Longleftrightarrow \frac{2}{j\omega}$$

Table 4.1 provides many common Fourier transform pairs.

TABLE 4.1 Select Fourier Transform Pairs

No.	$x(t)$	$X(\omega)$	
1	$e^{-at}u(t)$	$\dfrac{1}{a+j\omega}$	$a>0$
2	$e^{at}u(-t)$	$\dfrac{1}{a-j\omega}$	$a>0$
3	$e^{-a\lvert t\rvert}$	$\dfrac{2a}{a^2+\omega^2}$	$a>0$
4	$te^{-at}u(t)$	$\dfrac{1}{(a+j\omega)^2}$	$a>0$
5	$t^n e^{-at}u(t)$	$\dfrac{n!}{(a+j\omega)^{n+1}}$	$a>0$
6	$\delta(t)$	1	
7	1	$2\pi\delta(\omega)$	
8	$e^{j\omega_0 t}$	$2\pi\delta(\omega-\omega_0)$	
9	$\cos\omega_0 t$	$\pi[\delta(\omega-\omega_0)+\delta(\omega+\omega_0)]$	
10	$\sin\omega_0 t$	$j\pi[\delta(\omega+\omega_0)-\delta(\omega-\omega_0)]$	
11	$u(t)$	$\pi\delta(\omega)+\dfrac{1}{j\omega}$	
12	$\operatorname{sgn} t$	$\dfrac{2}{j\omega}$	
13	$\cos\omega_0 t\,u(t)$	$\dfrac{\pi}{2}[\delta(\omega-\omega_0)+\delta(\omega+\omega_0)]+\dfrac{j\omega}{\omega_0^2-\omega^2}$	
14	$\sin\omega_0 t\,u(t)$	$\dfrac{\pi}{2j}[\delta(\omega-\omega_0)-\delta(\omega+\omega_0)]+\dfrac{\omega_0}{\omega_0^2-\omega^2}$	
15	$e^{-at}\sin\omega_0 t\,u(t)$	$\dfrac{\omega_0}{(a+j\omega)^2+\omega_0^2}$	$a>0$
16	$e^{-at}\cos\omega_0 t\,u(t)$	$\dfrac{a+j\omega}{(a+j\omega)^2+\omega_0^2}$	$a>0$
17	$\operatorname{rect}\left(\dfrac{t}{\tau}\right)$	$\tau\operatorname{sinc}\left(\dfrac{\omega\tau}{2}\right)$	
18	$\dfrac{W}{\pi}\operatorname{sinc}(Wt)$	$\operatorname{rect}\left(\dfrac{\omega}{2W}\right)$	
19	$\Delta\left(\dfrac{t}{\tau}\right)$	$\dfrac{\tau}{2}\operatorname{sinc}^2\left(\dfrac{\omega\tau}{4}\right)$	
20	$\dfrac{W}{2\pi}\operatorname{sinc}^2\left(\dfrac{Wt}{2}\right)$	$\Delta\left(\dfrac{\omega}{2W}\right)$	
21	$\displaystyle\sum_{n=-\infty}^{\infty}\delta(t-nT)$	$\omega_0\displaystyle\sum_{n=-\infty}^{\infty}\delta(\omega-n\omega_0)$	$\omega_0=\dfrac{2\pi}{T}$
22	$e^{-t^2/2\sigma^2}$	$\sigma\sqrt{2\pi}e^{-\sigma^2\omega^2/2}$	

DRILL 4.2 Inverse Fourier Transform of a Rectangular Pulse

Show that the inverse Fourier transform of $X(\omega)$ illustrated in Fig. 4.17 is $x(t) = (\omega_0/\pi)$ sinc $(\omega_0 t)$. Sketch $x(t)$.

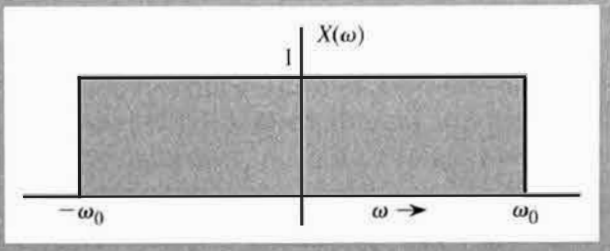

Figure 4.17 A frequency-domain rectangular pulse $X(\omega) = \text{rect}\left(\frac{\omega}{2\omega_0}\right)$.

DRILL 4.3 Fourier Transform of a General Sinusoid

Show that $\cos(\omega_0 t + \theta) \Longleftrightarrow \pi[\delta(\omega + \omega_0)e^{-j\theta} + \delta(\omega - \omega_0)e^{j\theta}]$.

4.3 SOME PROPERTIES OF THE FOURIER TRANSFORM

We now study some of the important properties of the Fourier transform and their implications as well as applications. We have already encountered two important properties, linearity [Eq. (4.15)] and the conjugation property [Eq. (4.11)].

Before embarking on this study, we shall explain an important and pervasive aspect of the Fourier transform: time-frequency duality.

TIME-FREQUENCY DUALITY IN THE TRANSFORM OPERATIONS

Equations (4.9) and (4.10) show an interesting fact: the direct and the inverse transform operations are remarkably similar. These operations, required to go from $x(t)$ to $X(\omega)$ and then from $X(\omega)$ to $x(t)$, are depicted graphically in Fig. 4.18. The inverse transform equation can be obtained from the direct transform equation by replacing $x(t)$ with $X(\omega)$, t with ω, and ω with t. In a similar way, we can obtain the direct from the inverse. There are only two minor differences in these operations: the factor 2π appears only in the inverse operator, and the exponential indices in the two operations have opposite signs. Otherwise, the two equations are duals of each other.[†]

[†] Of the two differences, the former can be eliminated by change of variable from ω to f (in hertz). In this case, $\omega = 2\pi f$ and $d\omega = 2\pi\, df$. Therefore, the direct and the inverse transforms are given by

$$X(2\pi f) = \int_{-\infty}^{\infty} x(t)e^{-j2\pi ft}\, dt \qquad \text{and} \qquad x(t) = \int_{-\infty}^{\infty} X(2\pi f)e^{j2\pi ft}\, df$$

This leaves only one significant difference, that of sign change in the exponential index.

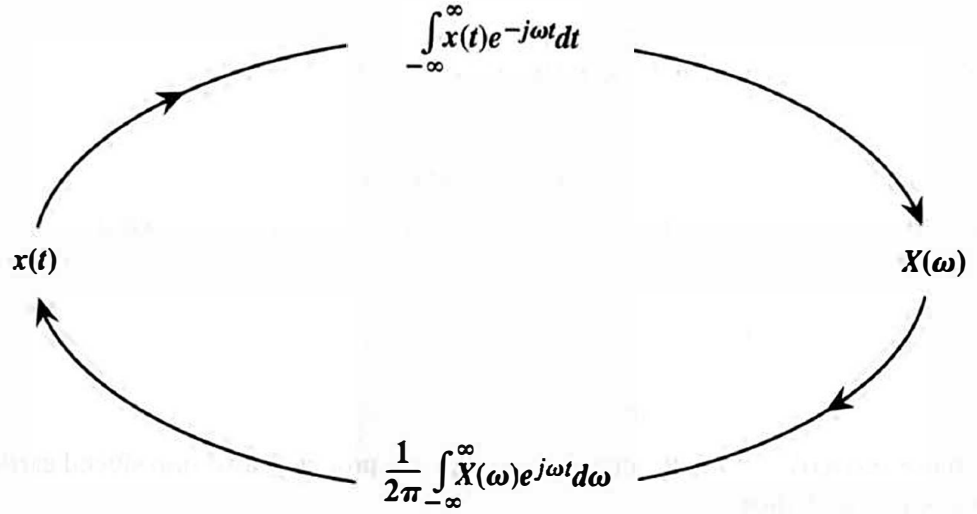

Figure 4.18 A near symmetry between the direct and the inverse Fourier transforms.

This observation has far-reaching consequences in the study of the Fourier transform. It is the basis of the so-called duality of time and frequency. *The duality principle may be compared with a photograph and its negative. A photograph can be obtained from its negative, and by using an identical procedure, a negative can be obtained from the photograph.* For any result or relationship between $x(t)$ and $X(\omega)$, there exists a dual result or relationship, obtained by interchanging the roles of $x(t)$ and $X(\omega)$ in the original result (along with some minor modifications arising because of the factor 2π and a sign change). For example, the time-shifting property, to be proved later, states that if $x(t) \Longleftrightarrow X(\omega)$, then

$$x(t - t_0) \Longleftrightarrow X(\omega)e^{-j\omega t_0}$$

The dual of this property (the frequency-shifting property) states that

$$x(t)e^{j\omega_0 t} \Longleftrightarrow X(\omega - \omega_0)$$

Observe the role reversal of time and frequency in these two equations (with the minor difference of the sign change in the exponential index). The value of this principle lies in the fact that *whenever we derive any result, we can be sure that it has a dual.* This possibility can give valuable insights about many unsuspected properties or results in signal processing.

The properties of the Fourier transform are useful not only in deriving the direct and inverse transforms of many functions, but also in obtaining several valuable results in signal processing. The reader should not fail to observe the ever-present duality in this discussion.

Linearity

The linearity property, already introduced as Eq. (4.15), states that if $x_1(t) \Longleftrightarrow X_1(\omega)$ and $x_2(t) \Longleftrightarrow X_2(\omega)$, then $a_1x_1(t) + a_2x_2(t) \Longleftrightarrow a_1X_1(\omega) + a_2X_2(\omega)$.

Conjugation and Conjugate Symmetry

The conjugation property, which has already been introduced, states that if $x(t) \Longleftrightarrow X(\omega)$, then

$$x^*(t) \Longleftrightarrow X^*(-\omega)$$

From this property follows the conjugate symmetry property, also introduced earlier, which states that if $x(t)$ is real, then

$$X(-\omega) = X^*(\omega)$$

Duality

The duality property states that if

$$x(t) \Longleftrightarrow X(\omega)$$

then

$$X(t) \Longleftrightarrow 2\pi x(-\omega) \tag{4.25}$$

Proof. From Eq. (4.10), we can write

$$x(t) = \frac{1}{2\pi} \int_{-\infty}^{\infty} X(u) e^{jut}\, du$$

Hence,

$$2\pi x(-t) = \int_{-\infty}^{\infty} X(u) e^{-jut}\, du$$

Changing t to ω yields Eq. (4.25).

EXAMPLE 4.11 Applying the Duality Property of the Fourier Transform

Apply the duality property [Eq. (4.25)] of the Fourier transform to the pair in Fig. 4.19a.

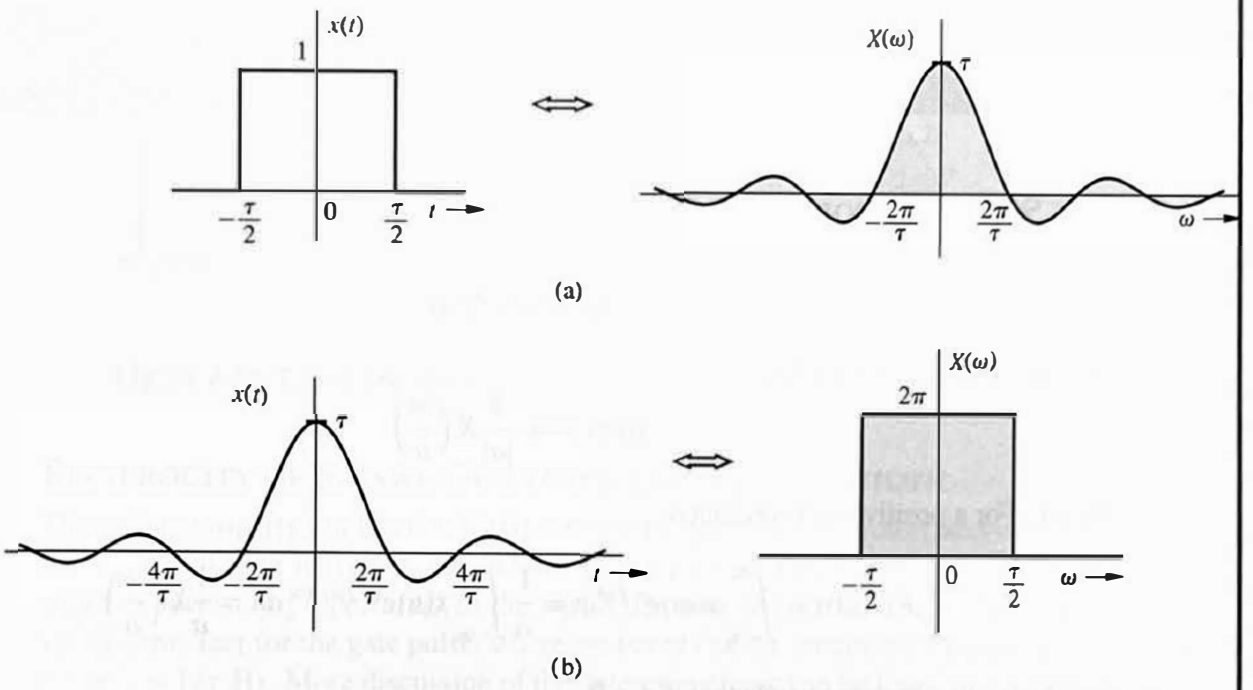

Figure 4.19 The duality property of the Fourier transform.

From Eq. (4.20), we have

$$\underbrace{\text{rect}\left(\frac{t}{\tau}\right)}_{x(t)} \Longleftrightarrow \underbrace{\tau\,\text{sinc}\left(\frac{\omega\tau}{2}\right)}_{X(\omega)}$$

Also, $X(t)$ is the same as $X(\omega)$ with ω replaced by t, and $x(-\omega)$ is the same as $x(t)$ with t replaced by $-\omega$. Therefore, the duality property of Eq. (4.25) yields

$$\underbrace{\tau\,\text{sinc}\left(\frac{\tau t}{2}\right)}_{X(t)} \Longleftrightarrow \underbrace{2\pi\,\text{rect}\left(\frac{-\omega}{\tau}\right)}_{2\pi x(-\omega)} = 2\pi\,\text{rect}\left(\frac{\omega}{\tau}\right)$$

In this result, we used the fact that $\text{rect}(-x) = \text{rect}(x)$ because rect is an even function. Figure 4.19b shows this pair graphically. Observe the interchange of the roles of t and ω (with the minor adjustment of the factor 2π). This result appears as pair 18 in Table 4.1 (with $\tau/2 = W$).

As an interesting exercise, the reader should generate the dual of every pair in Table 4.1 by applying the duality property.

DRILL 4.4 Applying the Duality Property of the Fourier Transform

Apply the duality property to pairs 1, 3, and 9 (Table 4.1) to show that

(a) $1/(jt+a) \Longleftrightarrow 2\pi e^{a\omega}u(-\omega)$

(b) $2a/(t^2+a^2) \Longleftrightarrow 2\pi e^{-a|\omega|}$

(c) $\delta(t+t_0)+\delta(t-t_0) \Longleftrightarrow 2\cos t_0\omega$

The Scaling Property

If

$$x(t) \Longleftrightarrow X(\omega)$$

then, for any real constant a,

$$x(at) \Longleftrightarrow \frac{1}{|a|}X\left(\frac{\omega}{a}\right) \tag{4.26}$$

Proof. For a positive real constant a,

$$\mathcal{F}[x(at)] = \int_{-\infty}^{\infty} x(at)e^{-j\omega t}dt = \frac{1}{a}\int_{-\infty}^{\infty} x(u)e^{(-j\omega/a)u}\,du = \frac{1}{a}X\left(\frac{\omega}{a}\right)$$

Similarly, we can demonstrate that if $a < 0$,

$$x(at) \Longleftrightarrow \frac{-1}{a}X\left(\frac{\omega}{a}\right)$$

Hence follows Eq. (4.26).

Significance of the Scaling Property

The function $x(at)$ represents the function $x(t)$ compressed in time by a factor a (see Sec. 1.2.2). Similarly, a function $X(\omega/a)$ represents the function $X(\omega)$ expanded in frequency by the same factor a. *The scaling property states that time compression of a signal results in its spectral expansion, and time expansion of the signal results in its spectral compression.* Intuitively, compression in time by factor a means that the signal is varying faster by factor a.[†] To synthesize such a signal, the frequencies of its sinusoidal components must be increased by the factor a, implying that its frequency spectrum is expanded by the factor a. Similarly, a signal expanded in time varies more slowly; hence, the frequencies of its components are lowered, implying that its frequency spectrum is compressed. For instance, the signal $\cos 2\omega_0 t$ is the same as the signal $\cos\omega_0 t$ time-compressed by a factor of 2. Clearly, the spectrum of the former (impulse at $\pm 2\omega_0$) is an expanded version of the spectrum of the latter (impulse at $\pm\omega_0$). The effect of this scaling is demonstrated in Fig. 4.20.

[†] We are assuming $a > 1$, although the argument still holds if $a < 1$. In the latter case, compression becomes expansion by factor $1/a$, and vice versa.

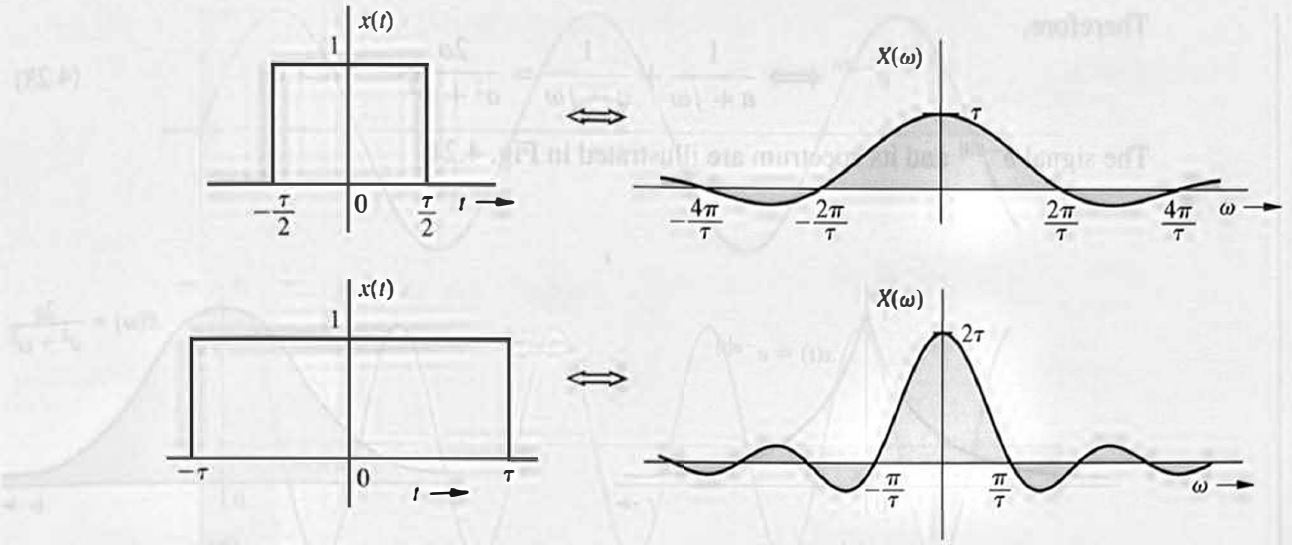

Figure 4.20 The scaling property of the Fourier transform.

Reciprocity of Signal Duration and Its Bandwidth

The scaling property implies that if $x(t)$ is wider, its spectrum is narrower, and vice versa. Doubling the signal duration halves its bandwidth, and vice versa. This suggests that the bandwidth of a signal is inversely proportional to the signal duration or width (in seconds).[†] We have already verified this fact for the gate pulse, where we found that the bandwidth of a gate pulse of width τ seconds is $1/\tau$ Hz. More discussion of this interesting topic can be found in the literature [2].

By letting $a = -1$ in Eq. (4.26), we obtain the *inversion (or reflection) property of time and frequency:*

$$x(-t) \Longleftrightarrow X(-\omega) \tag{4.27}$$

EXAMPLE 4.12 Fourier Transform Reflection Property

Using the reflection property of the Fourier transform and Table 4.1, find the Fourier transforms of $e^{at}u(-t)$ and $e^{-a|t|}$.

Application of Eq. (4.27) to pair 1 of Table 4.1 yields

$$e^{at}u(-t) \Longleftrightarrow \frac{1}{a - j\omega} \qquad a > 0$$

Also,

$$e^{-a|t|} = e^{-at}u(t) + e^{at}u(-t)$$

[†] When a signal has infinite duration, we must consider its effective or equivalent duration. There is no unique definition of effective signal duration. One possible definition is given in Eq. (2.47).

Therefore,

$$e^{-a|t|} \Longleftrightarrow \frac{1}{a+j\omega} + \frac{1}{a-j\omega} = \frac{2a}{a^2+\omega^2} \qquad a > 0 \tag{4.28}$$

The signal $e^{-a|t|}$ and its spectrum are illustrated in Fig. 4.21.

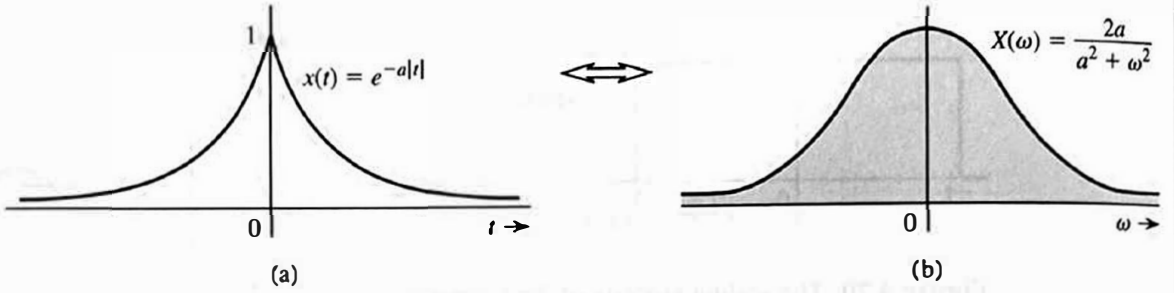

(a) (b)

Figure 4.21 (a) $e^{-a|t|}$ and (b) its Fourier spectrum.

The Time-Shifting Property

If

$$x(t) \Longleftrightarrow X(\omega)$$

then

$$x(t-t_0) \Longleftrightarrow X(\omega)e^{-j\omega t_0} \tag{4.29}$$

Proof. By definition,

$$\mathcal{F}[x(t-t_0)] = \int_{-\infty}^{\infty} x(t-t_0)e^{-j\omega t}\,dt$$

Letting $t - t_0 = u$, we have

$$\mathcal{F}[x(t-t_0)] = \int_{-\infty}^{\infty} x(u)e^{-j\omega(u+t_0)}\,du = e^{-j\omega t_0}\int_{-\infty}^{\infty} x(u)e^{-j\omega u}\,du = X(\omega)e^{-j\omega t_0}$$

This result shows that *delaying a signal by t_0 seconds does not change its amplitude spectrum. The phase spectrum, however, is changed by $-\omega t_0$.*

Physical Explanation of Linear Phase

Time delay in a signal causes a linear phase shift in its spectrum. This result can also be derived by heuristic reasoning. Imagine $x(t)$ being synthesized by its Fourier components, which are sinusoids of certain amplitudes and phases. The delayed signal $x(t - t_0)$ can be synthesized by the same sinusoidal components, each delayed by t_0 seconds. The amplitudes of the components remain unchanged. Therefore, the amplitude spectrum of $x(t - t_0)$ is identical to that of $x(t)$. The time delay of t_0 in each sinusoid, however, does change the phase of each component. Now, a sinusoid

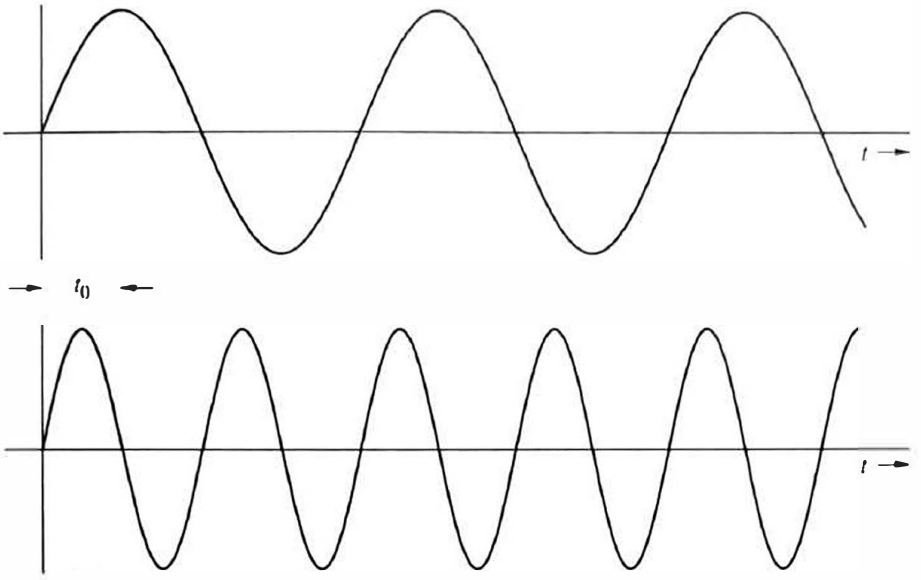

Figure 4.22 Physical explanation of the time-shifting property.

$\cos\omega t$ delayed by t_0 is given by

$$\cos\omega(t-t_0)=\cos(\omega t-\omega t_0)$$

Therefore, a time delay t_0 in a sinusoid of frequency ω manifests as a phase delay of ωt_0. This is a linear function of ω, meaning that higher-frequency components must undergo proportionately higher phase shifts to achieve the same time delay. This effect is depicted in Fig. 4.22 with two sinusoids, the frequency of the lower sinusoid being twice that of the upper. The same time delay t_0 amounts to a phase shift of $\pi/2$ in the upper sinusoid and a phase shift of π in the lower sinusoid. This verifies the fact that *to achieve the same time delay, higher-frequency sinusoids must undergo proportionately higher phase shifts.* The principle of linear phase shift is very important, and we shall encounter it again in distortionless signal transmission and filtering applications.

EXAMPLE 4.13 Fourier Transform Time-Shifting Property

Use the time-shifting property to find the Fourier transform of $e^{-a|t-t_0|}$.

This function, shown in Fig. 4.23a, is a time-shifted version of $e^{-a|t|}$ (depicted in Fig. 4.21a). From Eqs. (4.28) and (4.29), we have

$$e^{-a|t-t_0|}\Longleftrightarrow\frac{2a}{a^2+\omega^2}e^{-j\omega t_0}$$

The spectrum of $e^{-a|t-t_0|}$ (Fig. 4.23b) is the same as that of $e^{-a|t|}$ (Fig. 4.21b), except for an added phase shift of $-\omega t_0$.

Observe that the time delay t_0 causes a linear phase spectrum $-\omega t_0$. This example clearly demonstrates the effect of time shift.

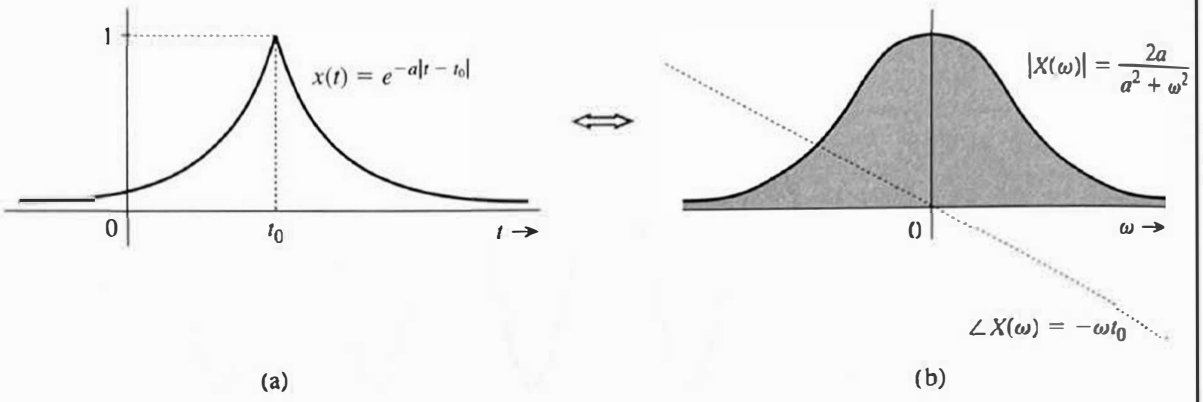

(a) (b)

Figure 4.23 Effect of time-shifting on the Fourier spectrum of a signal.

EXAMPLE 4.14 Fourier Transform of a Time-Shifted Rectangular Pulse

Find the Fourier transform of the time-shifted rectangular pulse $x(t)$ illustrated in Fig. 4.24a.

The pulse $x(t)$ is the gate pulse $\text{rect}(t/\tau)$ in Fig. 4.10a delayed by $3\tau/4$ seconds. Hence, according to Eq. (4.29), its Fourier transform is the Fourier transform of $\text{rect}(t/\tau)$ multiplied by $e^{-j\omega(3\tau/4)}$. Therefore,

$$X(\omega) = \tau \,\text{sinc}\left(\frac{\omega\tau}{2}\right) e^{-j\omega(3\tau/4)}$$

The amplitude spectrum $|X(\omega)|$ (depicted in Fig. 4.24b) of this pulse is the same as that indicated in Fig. 4.10c. But the phase spectrum has an added linear term $-3\omega\tau/4$. Hence, the phase spectrum of $x(t)$ (Fig. 4.24a) is identical to that in Fig. 4.10d plus a linear term $-3\omega\tau/4$, as shown in Fig. 4.24c.

Phase Spectrum Using Principal Values

There is an alternate way of spectral representation of $\angle X(\omega)$. The phase angle computed on a calculator or by using a computer subroutine is generally the principal value (modulo 2π value) of the phase angle, which always lies in the range $-\pi$ to π. For instance, the principal value of angle $3\pi/2$ is $-\pi/2$, and so on. The principal value differs from the actual value by $\pm 2\pi$ radians (and its integer multiples) in a way that ensures that the principal value remains within $-\pi$ to π. Thus, the principal value will show jump discontinuities of $\pm 2\pi$ whenever the actual

phase crosses $\pm\pi$. The phase plot in Fig. 4.24c is redrawn in Fig. 4.24d using the principal value for the phase. This phase pattern, which contains phase discontinuities of magnitudes 2π and π, becomes repetitive at intervals of $\omega = 8\pi/\tau$.

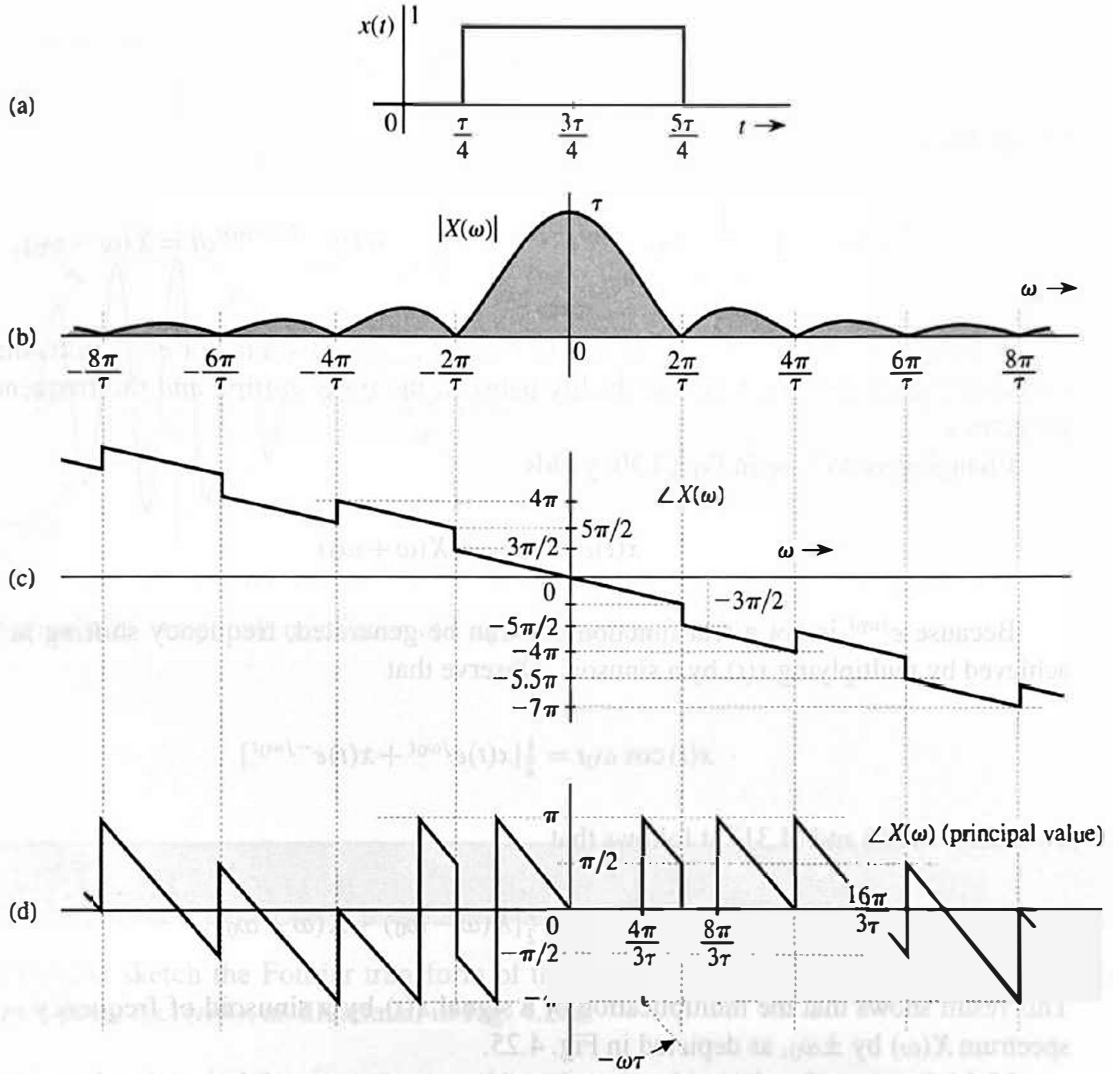

Figure 4.24 A time-shifted rectangular pulse and its Fourier spectrum.

DRILL 4.5 Fourier Transform Time-Shifting Property

Use pair 18 of Table 4.1 and the time-shifting property to show that the Fourier transform of $\text{sinc}[\omega_0(t-T)]$ is $(\pi/\omega_0)\,\text{rect}\,(\omega/2\omega_0)e^{-j\omega T}$. Sketch the amplitude and phase spectra of the Fourier transform.

The Frequency-Shifting Property

If

$$x(t) \Longleftrightarrow X(\omega)$$

then

$$x(t)e^{j\omega_0 t} \Longleftrightarrow X(\omega - \omega_0) \tag{4.30}$$

Proof. By definition,

$$\mathcal{F}[x(t)e^{j\omega_0 t}] = \int_{-\infty}^{\infty} x(t)e^{j\omega_0 t}e^{-j\omega t}\,dt = \int_{-\infty}^{\infty} x(t)e^{-j(\omega-\omega_0)t}dt = X(\omega - \omega_0)$$

According to this property, the multiplication of a signal by a factor $e^{j\omega_0 t}$ shifts the spectrum of that signal by $\omega = \omega_0$. Note the duality between the time-shifting and the frequency-shifting properties.

Changing ω_0 to $-\omega_0$ in Eq. (4.30) yields

$$x(t)e^{-j\omega_0 t} \Longleftrightarrow X(\omega + \omega_0) \tag{4.31}$$

Because $e^{j\omega_0 t}$ is not a real function that can be generated, frequency shifting in practice is achieved by multiplying $x(t)$ by a sinusoid. Observe that

$$x(t)\cos\omega_0 t = \tfrac{1}{2}[x(t)e^{j\omega_0 t} + x(t)e^{-j\omega_0 t}]$$

From Eqs. (4.30) and (4.31), it follows that

$$x(t)\cos\omega_0 t \Longleftrightarrow \tfrac{1}{2}[X(\omega - \omega_0) + X(\omega + \omega_0)] \tag{4.32}$$

This result shows that the multiplication of a signal $x(t)$ by a sinusoid of frequency ω_0 shifts the spectrum $X(\omega)$ by $\pm\omega_0$, as depicted in Fig. 4.25.

Multiplication of a sinusoid $\cos\omega_0 t$ by $x(t)$ amounts to modulating the sinusoid amplitude. This type of modulation is known as *amplitude modulation*. The sinusoid $\cos\omega_0 t$ is called the *carrier*, the signal $x(t)$ is the *modulating signal*, and the signal $x(t)\cos\omega_0 t$ is the *modulated signal*. Further discussion of modulation and demodulation appears in Secs. 4.7 and 4.8.

To sketch a signal $x(t)\cos\omega_0 t$, we observe that

$$x(t)\cos\omega_0 t = \begin{cases} x(t) & \text{when } \cos\omega_0 t = 1 \\ -x(t) & \text{when } \cos\omega_0 t = -1 \end{cases}$$

Therefore, $x(t)\cos\omega_0 t$ touches $x(t)$ when the sinusoid $\cos\omega_0 t$ is at its positive peaks and touches $-x(t)$ when $\cos\omega_0 t$ is at its negative peaks. This means that $x(t)$ and $-x(t)$ act as envelopes for the signal $x(t)\cos\omega_0 t$ (see Fig. 4.25). The signal $-x(t)$ is a mirror image of $x(t)$ about the horizontal axis. Figure 4.25 shows the signals $x(t)$ and $x(t)\cos\omega_0 t$ and their spectra.

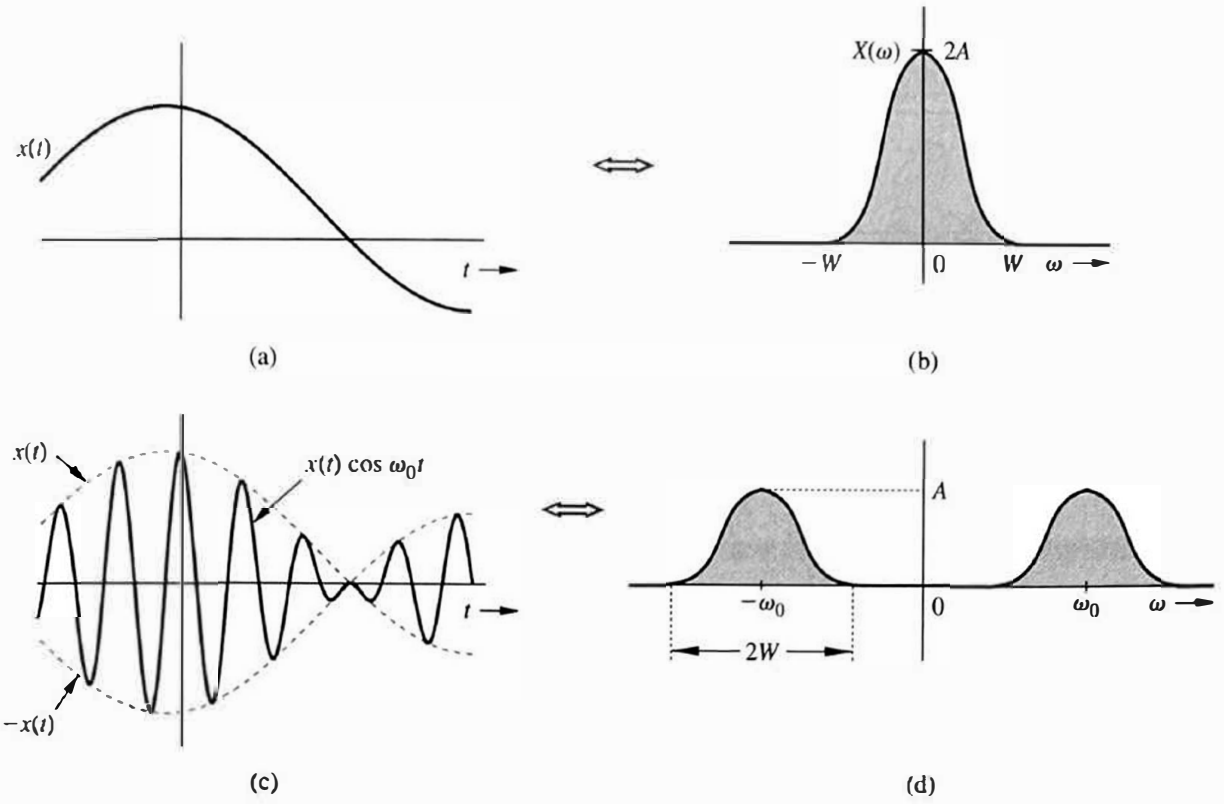

Figure 4.25 Amplitude modulation of a signal causes spectral shifting.

EXAMPLE 4.15 Spectral Shifting by Amplitude Modulation

Find and sketch the Fourier transform of the modulated signal $x(t)\cos 10t$ in which $x(t)$ is a gate pulse $\text{rect}\,(t/4)$, as illustrated in Fig. 4.26a.

From pair 17 of Table 4.1, we find $\text{rect}\,(t/4) \Longleftrightarrow 4\,\text{sinc}\,(2\omega)$, which is depicted in Fig. 4.26b. From Eq. (4.32), it follows that

$$x(t)\cos 10t \Longleftrightarrow \tfrac{1}{2}[X(\omega+10)+X(\omega-10)]$$

In this case, $X(\omega) = 4\,\text{sinc}\,(2\omega)$. Therefore,

$$x(t)\cos 10t \Longleftrightarrow 2\,\text{sinc}\,[2(\omega+10)]+2\,\text{sinc}\,[2(\omega-10)]$$

The spectrum of the Fig. 4.26c signal $x(t)\cos 10t$ is obtained by shifting $X(\omega)$ in Fig. 4.26b to the left by 10 and also to the right by 10, and then multiplying it by 0.5, as depicted in Fig. 4.26d.

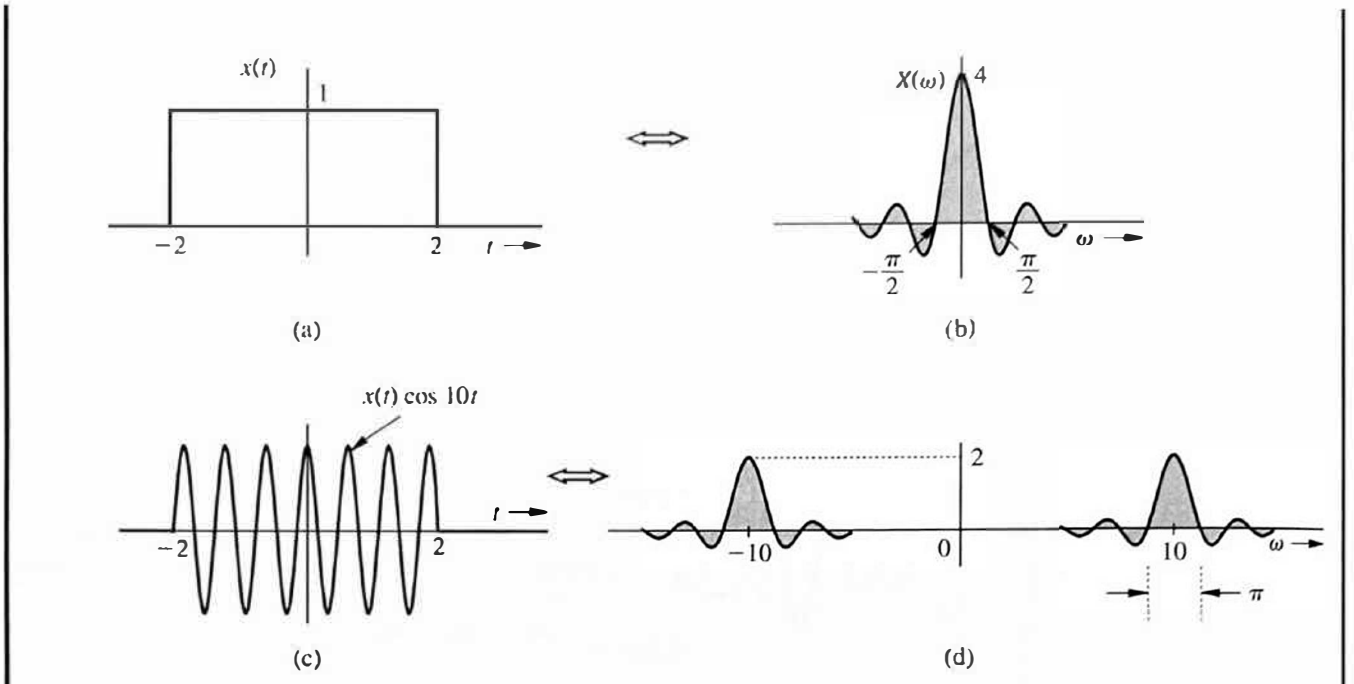

Figure 4.26 An example of spectral shifting by amplitude modulation.

DRILL 4.6 Fourier Transform of an Amplitude-Modulated Signal

Sketch signal $e^{-|t|}\cos 10t$. Find the Fourier transform of this signal and sketch its spectrum.

ANSWER

$X(\omega) = \frac{1}{(\omega-10)^2+1} + \frac{1}{(\omega+10)^2+1}$. See Fig. 4.21b for the spectrum of $e^{-a|t|}$.

DRILL 4.7 Amplitude Modulation using a Phase-Shifted Carrier

Show that

$$x(t)\cos(\omega_0 t+\theta) \Longleftrightarrow \tfrac{1}{2}\left[X(\omega-\omega_0)e^{j\theta} + X(\omega+\omega_0)e^{-j\theta}\right]$$

Applications of Modulation

Modulation is used to shift signal spectra. Some of the situations that call for spectrum shifting are presented next.

1. If several signals, all occupying the same frequency band, are transmitted simultaneously over the same transmission medium, they will all interfere; it will be impossible to separate or retrieve them at a receiver. For example, if all radio stations decide to broadcast audio signals simultaneously, a receiver will not be able to separate them. This problem is solved

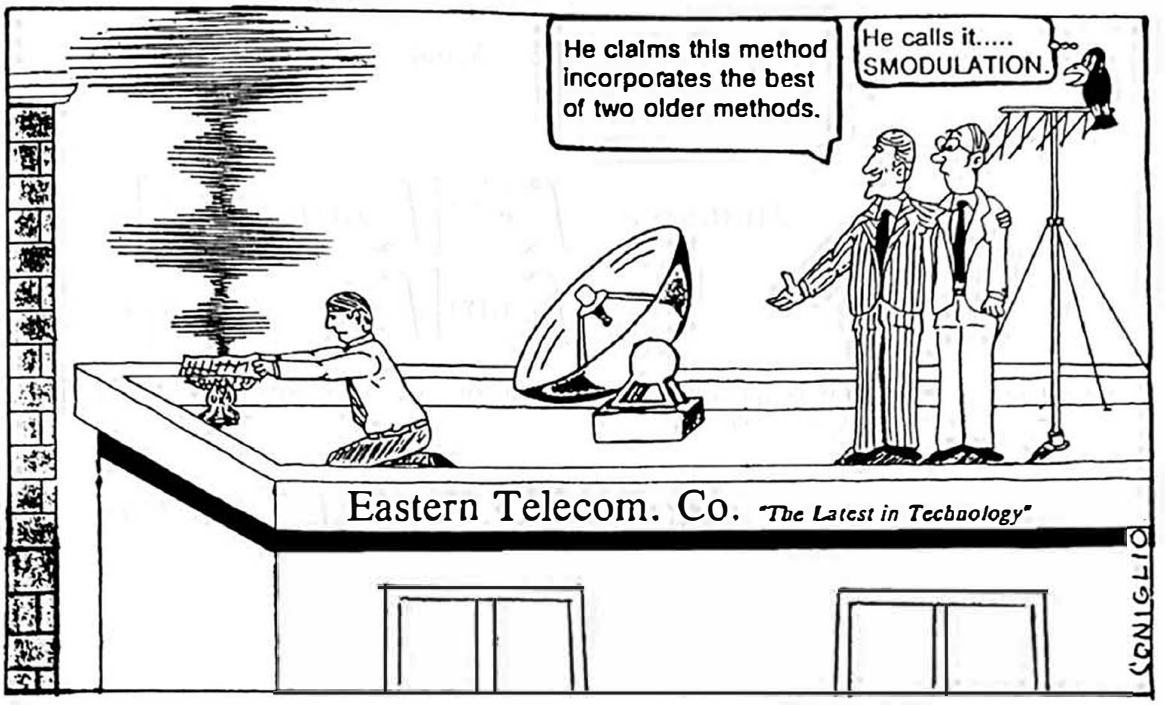

Old is gold, but sometimes it is fool's gold.

by using modulation, whereby each radio station is assigned a distinct carrier frequency. Each station transmits a modulated signal. This procedure shifts the signal spectrum to its allocated band, which is not occupied by any other station. A radio receiver can pick up any station by tuning to the band of the desired station. The receiver must now demodulate the received signal (undo the effect of modulation). Demodulation therefore consists of another spectral shift required to restore the signal to its original band. Note that both modulation and demodulation implement spectral shifting; consequently, demodulation operation is similar to modulation (see Sec. 4.7).

This method of transmitting several signals simultaneously over a channel by sharing its frequency band is known as *frequency-division multiplexing* (FDM).

2. For effective radiation of power over a radio link, the antenna size must be of the order of the wavelength of the signal to be radiated. Audio signal frequencies are so low (wavelengths are so large) that impracticably large antennas would be required for radiation. Here, shifting the spectrum to a higher frequency (a smaller wavelength) by modulation solves the problem.

Convolution

The time-convolution property and its dual, the frequency-convolution property, state that if

$$x_1(t) \Longleftrightarrow X_1(\omega) \qquad \text{and} \qquad x_2(t) \Longleftrightarrow X_2(\omega)$$

then

$$x_1(t) * x_2(t) \Longleftrightarrow X_1(\omega)X_2(\omega) \quad \text{(time convolution)} \tag{4.33}$$

and

$$x_1(t)x_2(t) \Longleftrightarrow \frac{1}{2\pi}X_1(\omega) * X_2(\omega) \quad \text{(frequency convolution)} \tag{4.34}$$

Proof. By definition,

$$\begin{aligned}\mathcal{F}|x_1(t) * x_2(t)| &= \int_{-\infty}^{\infty} e^{-j\omega t}\left[\int_{-\infty}^{\infty} x_1(\tau)x_2(t-\tau)\,d\tau\right]dt \\ &= \int_{-\infty}^{\infty} x_1(\tau)\left[\int_{-\infty}^{\infty} e^{-j\omega t}x_2(t-\tau)\,dt\right]d\tau\end{aligned}$$

The inner integral is the Fourier transform of $x_2(t-\tau)$, given by [time-shifting property in Eq. (4.29)] $X_2(\omega)e^{-j\omega\tau}$. Hence,

$$\mathcal{F}[x_1(t) * x_2(t)] = \int_{-\infty}^{\infty} x_1(\tau)e^{-j\omega\tau}X_2(\omega)\,d\tau = X_2(\omega)\int_{-\infty}^{\infty} x_1(\tau)e^{-j\omega\tau}\,d\tau = X_1(\omega)X_2(\omega)$$

Let $H(\omega)$ be the Fourier transform of the unit impulse response $h(t)$, that is,

$$h(t) \Longleftrightarrow H(\omega)$$

Application of the time-convolution property to $y(t) = x(t) * h(t)$ yields [assuming that both $x(t)$ and $h(t)$ are Fourier transformable]

$$Y(\omega) = X(\omega)H(\omega) \tag{4.35}$$

The frequency-convolution property of Eq. (4.34) can be proved in exactly the same way by reversing the roles of $x(t)$ and $X(\omega)$.

EXAMPLE 4.16 Time-Convolution Property to Show the Time-Integration Property

Use the time-convolution property to show that if

$$x(t) \Longleftrightarrow X(\omega)$$

then

$$\int_{-\infty}^{t} x(\tau)\,d\tau \Longleftrightarrow \frac{X(\omega)}{j\omega} + \pi X(0)\delta(\omega)$$

Because

$$u(t-\tau) = \begin{cases} 1 & \tau \le t \\ 0 & \tau > t \end{cases}$$

it follows that

$$x(t) * u(t) = \int_{-\infty}^{\infty} x(\tau)u(t-\tau)\,d\tau = \int_{-\infty}^{t} x(\tau)\,d\tau$$

Now, from the time-convolution property [Eq. (4.33)], it follows that

$$x(t)*u(t)=\int_{-\infty}^{t}x(\tau)\,d\tau \Longleftrightarrow X(\omega)\left[\frac{1}{j\omega}+\pi\delta(\omega)\right]$$
$$=\frac{X(\omega)}{j\omega}+\pi X(0)\delta(\omega)$$

In deriving the last result, we used Eq. (1.10).

DRILL 4.8 Fourier Transform Time-Convolution Property

Use the time-convolution property to show that:

(a) $x(t)*\delta(t)=x(t)$

(b) $e^{-at}u(t)*e^{-bt}u(t)=\frac{1}{b-a}[e^{-at}-e^{-bt}]u(t)$

Time Differentiation and Time Integration

If

$$x(t)\Longleftrightarrow X(\omega)$$

then†

$$\frac{dx(t)}{dt}\Longleftrightarrow j\omega X(\omega)\quad\text{(time differentiation)}\tag{4.36}$$

and

$$\int_{-\infty}^{t}x(\tau)\,d\tau\Longleftrightarrow\frac{X(\omega)}{j\omega}+\pi X(0)\delta(\omega)\quad\text{(time integration)}\tag{4.37}$$

† Valid only if the transform of dx/dt exists. In other words, dx/dt must satisfy the Dirichlet conditions. The first Dirichlet condition implies

$$\int_{-\infty}^{\infty}\left|\frac{dx(t)}{dt}\right|dt<\infty$$

We also require that $x(t)\to 0$ as $t\to\pm\infty$. Otherwise, $x(t)$ has a dc component, which gets lost in differentiation, and there is no one-to-one relationship between $x(t)$ and dx/dt.

TABLE 4.2 Fourier Transform Properties

Operation	$x(t)$	$X(\omega)$
Scalar multiplication	$kx(t)$	$kX(\omega)$
Addition	$x_1(t)+x_2(t)$	$X_1(\omega)+X_2(\omega)$
Conjugation	$x^*(t)$	$X^*(-\omega)$
Duality	$X(t)$	$2\pi x(-\omega)$
Scaling (a real)	$x(at)$	$\frac{1}{\lvert a\rvert}X\left(\frac{\omega}{a}\right)$
Time shifting	$x(t-t_0)$	$X(\omega)e^{-j\omega t_0}$
Frequency shifting (ω_0 real)	$x(t)e^{j\omega_0 t}$	$X(\omega-\omega_0)$
Time convolution	$x_1(t)*x_2(t)$	$X_1(\omega)X_2(\omega)$
Frequency convolution	$x_1(t)x_2(t)$	$\frac{1}{2\pi}X_1(\omega)*X_2(\omega)$
Time differentiation	$\frac{d^n x(t)}{dt^n}$	$(j\omega)^n X(\omega)$
Time integration	$\int_{-\infty}^{t} x(u)\,du$	$\frac{X(\omega)}{j\omega}+\pi X(0)\delta(\omega)$

Proof. Differentiation of both sides of Eq. (4.10) yields

$$\frac{dx(t)}{dt}=\frac{1}{2\pi}\int_{-\infty}^{\infty} j\omega X(\omega)e^{j\omega t}\,d\omega$$

This result shows that

$$\frac{dx(t)}{dt}\Longleftrightarrow j\omega X(\omega)$$

Repeated application of this property yields

$$\frac{d^n x(t)}{dt^n}\Longleftrightarrow (j\omega)^n X(\omega)$$

The time-integration property [Eq. (4.37)] has already been proved in Ex. 4.16.

Table 4.2 summarizes the most important properties of the Fourier transform.

EXAMPLE 4.17 Fourier Transform Time-Differentiation Property

Use the time-differentiation property to find the Fourier transform of the triangle pulse $\Delta(t/\tau)$ illustrated in Fig. 4.27a. Verify the correctness of the spectrum by using it to synthesize a periodic replication of the original time-domain signal with $\tau = 1$.

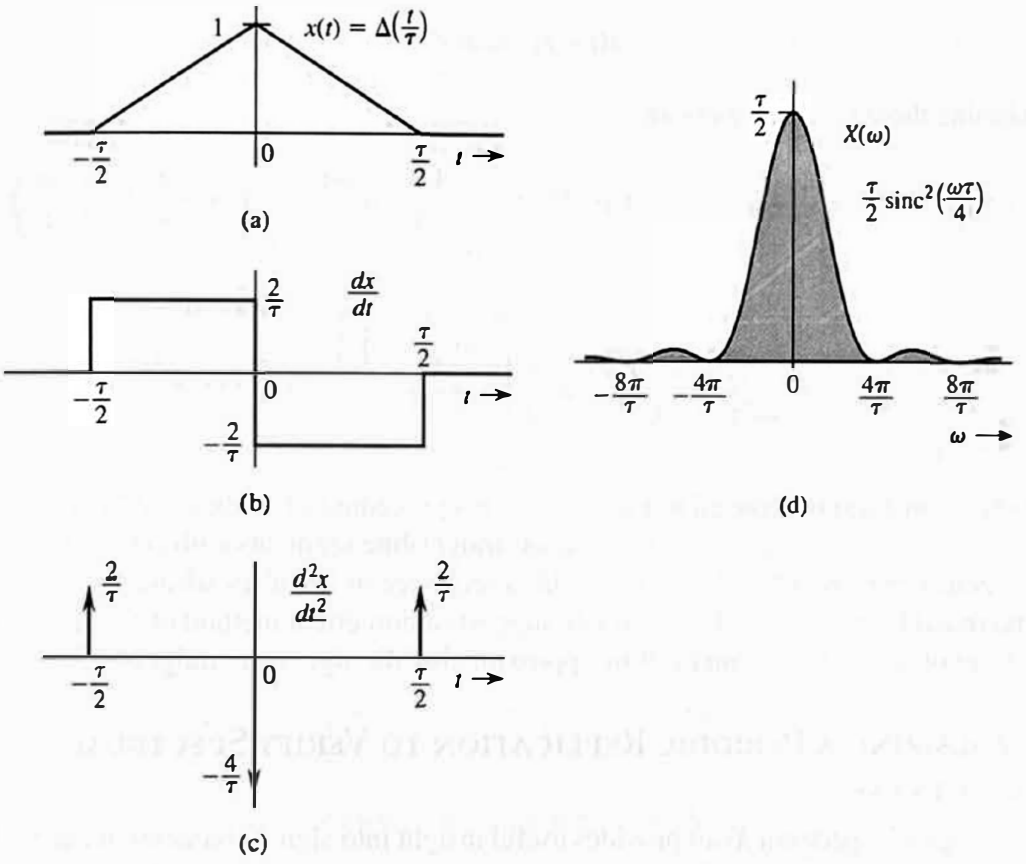

Figure 4.27 Finding the Fourier transform of a piecewise-linear signal using the time-differentiation property.

To find the Fourier transform of this pulse, we differentiate the pulse successively, as illustrated in Figs. 4.27b and 4.27c. Because dx/dt is constant everywhere, its derivative, d^2x/dt^2, is zero everywhere. But dx/dt has jump discontinuities with a positive jump of $2/\tau$ at $t = \pm\tau/2$, and a negative jump of $4/\tau$ at $t = 0$. Recall that the derivative of a signal at a jump discontinuity is an impulse at that point of strength equal to the amount of jump. Hence, d^2x/dt^2, the derivative of dx/dt, consists of a sequence of impulses, as depicted in Fig. 4.27c; that is,

$$\frac{d^2x(t)}{dt^2} = \frac{2}{\tau}\left[\delta\left(t+\frac{\tau}{2}\right) - 2\delta(t) + \delta\left(t-\frac{\tau}{2}\right)\right]$$

From the time-differentiation property [Eq. (4.36)],

$$\frac{d^2x(t)}{dt^2} \Longleftrightarrow (j\omega)^2X(\omega) = -\omega^2X(\omega)$$

Also, from the time-shifting property [Eq. (4.29)],

$$\delta(t-t_0) \Longleftrightarrow e^{-j\omega t_0}$$

Combining these results, we obtain

$$-\omega^2X(\omega) = \frac{2}{\tau}\left[e^{j(\omega\tau/2)} - 2 + e^{-j(\omega\tau/2)}\right] = \frac{4}{\tau}\left(\cos\frac{\omega\tau}{2} - 1\right) = -\frac{8}{\tau}\sin^2\left(\frac{\omega\tau}{4}\right)$$

and

$$X(\omega) = \frac{8}{\omega^2\tau}\sin^2\left(\frac{\omega\tau}{4}\right) = \frac{\tau}{2}\left[\frac{\sin\left(\frac{\omega\tau}{4}\right)}{\frac{\omega\tau}{4}}\right]^2 = \frac{\tau}{2}\text{sinc}^2\left(\frac{\omega\tau}{4}\right)$$

The spectrum $X(\omega)$ is depicted in Fig. 4.27d. This procedure of finding the Fourier transform can be applied to any function $x(t)$ made up of straight-line segments with $x(t) \to 0$ as $|t| \to \infty$. The second derivative of such a signal yields a sequence of impulses whose Fourier transform can be found by inspection. This example suggests a numerical method of finding the Fourier transform of an arbitrary signal $x(t)$ by approximating the signal by straight-line segments.

Synthesizing a Periodic Replication to Verify Spectrum Correctness

While a signal's spectrum $X(\omega)$ provides useful insight into signal character, it can be difficult to look at $X(\omega)$ and know that it is correct for a particular signal $x(t)$. Is it obvious, for example, that $X(\omega) = \frac{\tau}{2}\text{sinc}^2(\omega\tau/4)$ is really the spectrum of a τ-duration rectangle function? Or is it possible that a mathematical error was made in the determination of $X(\omega)$? It is difficult to be certain by simple inspection of the spectrum.

The same uncertainties exist when we are looking at a periodic signal's Fourier series spectrum. In the Fourier series case, we can verify the correctness of a signal's spectrum by synthesizing $x(t)$ with a truncated Fourier series; the synthesized signal will match the original only if the computed spectrum is correct. This is exactly the approach that was taken in Ex. 3.15. And since a truncated Fourier series involves a simple sum, tools like MATLAB make waveform synthesis relatively simple, at least in the case of the Fourier series.

In the case of the Fourier transform, however, synthesis of $x(t)$ using Eq. (4.10) requires integration, a task not well suited to numerical packages such as MATLAB. All is not lost, however. Consider Eq. (4.5). By scaling and sampling the spectrum $X(\omega)$ of an aperiodic signal $x(t)$, we obtain the Fourier series coefficient of a signal that is the periodic replication of $x(t)$.

Similar to Ex. 3.15, we can then synthesize a periodic replication of $x(t)$ with a truncated Fourier series to verify spectrum correctness. Let us demonstrate the idea for the current example with $\tau = 1$.

To begin, we represent $X(\omega) = \frac{\tau}{2}\text{sinc}^2(\omega\tau/4)$ using an anonymous function in MATLAB. Since MATLAB computes `sinc(x)` as $(\sin(\pi x))/\pi x$, we must scale the input by $1/\pi$ to match the notation of sinc in this book.

```
>> tau = 1; X = @(omega) tau/2*(sinc(omega*tau/(4*pi))).^2;
```

For our periodic replication, let us pick $T_0 = 2$, which is comfortably wide enough to accommodate our ($\tau = 1$)-width function without overlap. We use Eq. (4.5) to define the needed Fourier series coefficients D_n.

```
>> T0 = 2; omega0 = 2*pi/T0; D = @(n) X(n*omega0)/T0;
```

Let us use 25 harmonics to synthesize the periodic replication $x_{25}(t)$ of our triangular signal $x(t)$. To begin waveform synthesis, we set the dc portion of the signal.

```
>> t = (-T0:.001:T0); x25 = D(0)*ones(size(t));
```

To add the desired 25 harmonics, we enter a loop for $1 \leq n \leq 25$ and add in the D_n and D_{-n} terms. Although the result should be real, small round-off errors cause the reconstruction to be complex. These small imaginary parts are removed by using the `real` command.

```
>> for n = 1:25,
>>    x25 = x25+real(D(n)*exp(1j*omega0*n*t)+D(-n)*exp(-1j*omega0*n*t));
>> end
```

Lastly, we plot the resulting truncated Fourier series synthesis of $x(t)$.

```
>> plot(t,x25,'k'); xlabel('t'); ylabel('x_{25}(t)');
>> axis([-2 2 -.1 1.1]);
```

Since the synthesized waveform shown in Fig. 4.28 closely matches a 2-periodic replication of the triangle wave in Fig. 4.27a, we have high confidence that both the computed D_n and, by extension, the Fourier spectrum $X(\omega)$ are correct.

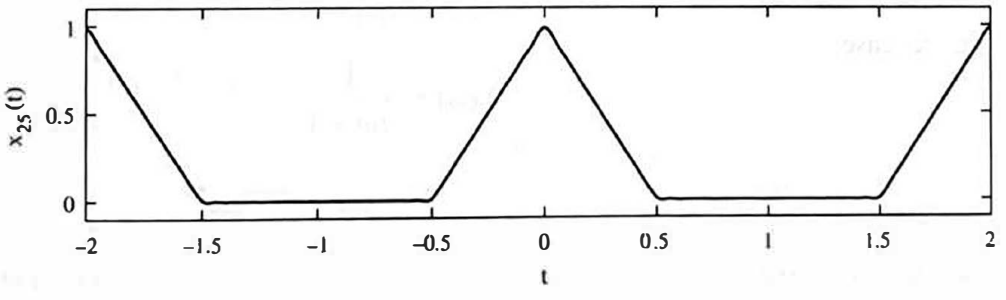

Figure 4.28 Synthesizing a 2-periodic replication of $x(t)$ using a truncated Fourier series.

DRILL 4.9 Fourier Transform Time-Differentiation Property

Use the time-differentiation property to find the Fourier transform of rect (t/τ).

4.4 SIGNAL TRANSMISSION THROUGH LTIC SYSTEMS

If $x(t)$ and $y(t)$ are the input and output of an LTIC system with impulse response $h(t)$, then, as demonstrated in Eq. (4.35),

$$Y(\omega) = H(\omega)X(\omega)$$

This equation does not apply to (asymptotically) unstable systems because $h(t)$ for such systems is not Fourier transformable. It applies to BIBO-stable as well as most of the marginally stable systems.[†] Similarly, this equation does not apply if $x(t)$ is not Fourier transformable.

In Ch. 6, we shall see that the Laplace transform, which is a generalized Fourier transform, is more versatile and capable of analyzing all kinds of LTIC systems whether stable, unstable, or marginally stable. The Laplace transform can also handle exponentially growing inputs. In comparison to the Laplace transform, the Fourier transform in system analysis is not just clumsier, but also very restrictive. Hence, the Laplace transform is preferable to the Fourier transform in LTIC system analysis. We shall not belabor the application of the Fourier transform to LTIC system analysis. We consider just one example here.

EXAMPLE 4.18 Fourier Transform to Determine the Zero-State Response

Use the Fourier transform to find the zero-state response of a stable LTIC system with frequency response

$$H(s) = \frac{1}{s+2}$$

and the input is $x(t) = e^{-t}u(t)$. Stability implies that the region of convergence of $H(s)$ includes the ω axis.

In this case,

$$X(\omega) = \frac{1}{j\omega+1}$$

[†] For marginally stable systems, if the input $x(t)$ contains a finite-amplitude sinusoid of the system's natural frequency, which leads to resonance, the output is not Fourier transformable. It does, however, apply to marginally stable systems if the input does not contain a finite-amplitude sinusoid of the system's natural frequency.

Moreover, because the system is stable, the frequency response $H(j\omega) = H(\omega)$. Hence,

$$H(\omega) = H(s)|_{s=j\omega} = \frac{1}{j\omega+2}$$

Therefore,

$$Y(\omega) = H(\omega)X(\omega) = \frac{1}{(j\omega+2)(j\omega+1)}$$

Expanding the right-hand side in partial fractions yields

$$Y(\omega) = \frac{1}{j\omega+1} - \frac{1}{j\omega+2}$$

and

$$y(t) = (e^{-t} - e^{-2t})u(t)$$

DRILL 4.10 Fourier Transform to Determine the Zero-State Response

For the system in Ex. 4.18, show that the zero-input response to the input $e^{t}u(-t)$ is $y(t) = \frac{1}{3}[e^{t}u(-t) + e^{-2t}u(t)]$. [*Hint:* Use pair 2 (Table 4.1) to find the Fourier transform of $e^{t}u(-t)$.]

Heuristic Understanding of Linear System Response

In finding the linear system response to arbitrary input, the time-domain method uses the convolution integral and the frequency-domain method uses the Fourier integral. Despite the apparent dissimilarities of the two methods, their philosophies are amazingly similar. In the time-domain case, we express the input $x(t)$ as a sum of its impulse components; in the frequency-domain case, the input is expressed as a sum of everlasting exponentials (or sinusoids). In the former case, the response $y(t)$ obtained by summing the system's responses to impulse components results in the convolution integral; in the latter case, the response obtained by summing the system's response to everlasting exponential components results in the Fourier integral. These ideas can be expressed mathematically as follows:

1. For the time-domain case,

$\delta(t) \Longrightarrow h(t)$	shows the system response to $\delta(t)$ is the impulse response $h(t)$
$x(t) = \int_{-\infty}^{\infty} x(\tau)\delta(t-\tau)\,d\tau$	expresses $x(t)$ as a sum of impulse components
$y(t) = \int_{-\infty}^{\infty} x(\tau)h(t-\tau)\,d\tau$	expresses $y(t)$ as a sum of responses to the impulse components of input $x(t)$

2. For the frequency-domain case,

$e^{j\omega t} \Longrightarrow H(\omega)e^{j\omega t}$	shows the system response to $e^{j\omega t}$ is $H(\omega)e^{j\omega t}$
$x(t) = \frac{1}{2\pi}\int_{-\infty}^{\infty} X(\omega)e^{j\omega t}d\omega$	expresses $x(t)$ as a sum of everlasting exponential components
$y(t) = \frac{1}{2\pi}\int_{-\infty}^{\infty} X(\omega)H(\omega)e^{j\omega t}d\omega$	expresses $y(t)$ as a sum of responses to the exponential components of input $x(t)$

The frequency-domain view sees a system in terms of its frequency response (system response to various sinusoidal components). It views a signal as a sum of various sinusoidal components. Transmission of an input signal through a (linear) system is viewed as transmission of various sinusoidal components of the input through the system.

It was not by coincidence that we used the impulse function in time-domain analysis and the exponential $e^{j\omega t}$ in studying the frequency domain. The two functions happen to be duals of each other. Thus, the Fourier transform of an impulse $\delta(t-\tau)$ is $e^{-j\omega\tau}$, and the Fourier transform of $e^{j\omega_0 t}$ is an impulse $2\pi\delta(\omega-\omega_0)$. This *time-frequency duality* is a constant theme in the Fourier transform and linear systems.

4.4.1 Signal Distortion During Transmission

For a system with frequency response $H(\omega)$, if $X(\omega)$ and $Y(\omega)$ are the spectra of the input and the output signals, respectively, then

$$Y(\omega) = X(\omega)H(\omega) \tag{4.38}$$

The transmission of the input signal $x(t)$ through the system changes it into the output signal $y(t)$. Equation (4.38) shows the nature of this change or modification. Here, $X(\omega)$ and $Y(\omega)$ are the spectra of the input and the output, respectively. Therefore, $H(\omega)$ is the spectral response of the system. The output spectrum is obtained by the input spectrum multiplied by the spectral response of the system. Equation (4.38), which clearly brings out the spectral shaping (or modification) of the signal by the system, can be expressed in polar form as

$$|Y(\omega)|e^{j\angle Y(\omega)} = |X(\omega)||H(\omega)|e^{j[\angle X(\omega)+\angle H(j\omega)]}$$

Therefore,

$$|Y(\omega)| = |X(\omega)|\,|H(\omega)| \quad \text{and} \quad \angle Y(\omega) = \angle X(\omega) + \angle H(\omega)$$

During transmission, the input signal amplitude spectrum $|X(\omega)|$ is changed to $|X(\omega)||H(\omega)|$. Similarly, the input signal phase spectrum $\angle X(\omega)$ is changed to $\angle X(\omega) + \angle H(\omega)$. An input signal spectral component of frequency ω is modified in amplitude by a factor $|H(\omega)|$ and is shifted in phase by an angle $\angle H(\omega)$. Clearly, $|H(\omega)|$ is the amplitude response, and $\angle H(\omega)$ is the phase response of the system. The plots of $|H(\omega)|$ and $\angle H(\omega)$ as functions of ω show at a glance how the system modifies the amplitudes and phases of various sinusoidal inputs. This is the reason why $H(\omega)$ is also called the *frequency response* of the system. During transmission through the system, some frequency components may be boosted in amplitude, while others may be attenuated.

The relative phases of the various components also change. In general, the output waveform will be different from the input waveform.

Distortionless Transmission

In several applications, such as signal amplification or message signal transmission over a communication channel, we require that the output waveform be a replica of the input waveform. In such cases, we need to minimize the distortion caused by the amplifier or the communication channel. It is, therefore, of practical interest to determine the characteristics of a system that allows a signal to pass without distortion (*distortionless transmission*).

Transmission is said to be distortionless if the input and the output have identical waveshapes within a multiplicative constant. A delayed output that retains the input waveform is also considered to be distortionless. Thus, in distortionless transmission, the input $x(t)$ and the output $y(t)$ satisfy the condition

$$y(t) = G_0 x(t - t_d)$$

The Fourier transform of this equation yields

$$Y(\omega) = G_0 X(\omega) e^{-j\omega t_d}$$

But

$$Y(\omega) = X(\omega) H(\omega)$$

Therefore,

$$H(\omega) = G_0 e^{-j\omega t_d}$$

This is the frequency response required of a system for distortionless transmission. From this equation, it follows that

$$|H(\omega)| = G_0 \quad \text{and} \quad \angle H(\omega) = -\omega t_d \tag{4.39}$$

This result shows that for distortionless transmission, the amplitude response $|H(\omega)|$ must be a constant, and the phase response $\angle H(\omega)$ must be a linear function of ω with slope $-t_d$, where t_d is the delay of the output with respect to input (Fig. 4.29).

Measure of Time-Delay Variation with Frequency

The gain $|H(\omega)| = G_0$ means that every spectral component is multiplied by a constant G_0. Also, as seen in connection with Fig. 4.22, a linear phase $\angle H(\omega) = -\omega t_d$ means that every spectral component is delayed by t_d seconds. This results in the output equal to G_0 times the input delayed

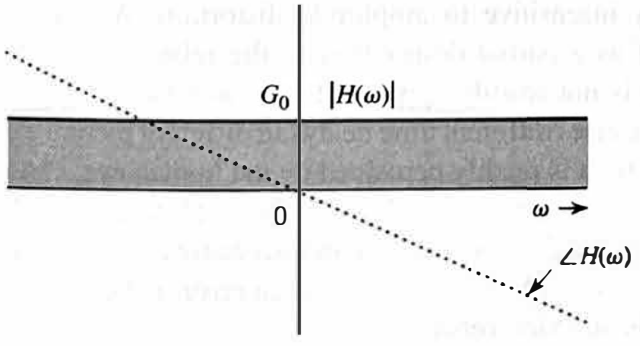

Figure 4.29 LTIC system frequency response for distortionless transmission.

by t_d seconds. Because each spectral component is attenuated by the same factor (G_0) and delayed by exactly the same amount (t_d), the output signal is an exact replica of the input (except for attenuating factor G_0 and delay t_d).

For distortionless transmission, we require a *linear phase* characteristic. The phase is not only a linear function of ω, it should also pass through the origin $\omega = 0$. In practice, many systems have a phase characteristic that may be only approximately linear. A convenient way of judging phase linearity is to plot the slope of $\angle H(\omega)$ as a function of frequency. This slope, which is constant for an ideal linear phase (ILP) system, is a function of ω in the general case and can be expressed as

$$t_g(\omega) = -\frac{d}{d\omega}\angle H(\omega) \tag{4.40}$$

If $t_g(\omega)$ is constant, all the components are delayed by the same time interval t_g. But if the slope is not constant, the time delay t_g varies with frequency. This variation means that different frequency components undergo different amounts of time delay, and consequently, the output waveform will not be a replica of the input waveform. As we shall see, $t_g(\omega)$ plays an important role in bandpass systems and is called the *group delay* or *envelope* delay. Observe that constant t_d [Eq. (4.39)] implies constant t_g. Note that $\angle H(\omega) = \phi_0 - \omega t_g$ also has a constant t_g. Thus, constant group delay is a more relaxed condition.

It is often thought (erroneously) that flatness of amplitude response $|H(\omega)|$ alone can guarantee signal quality. However, a system that has a flat amplitude response may yet distort a signal beyond recognition if the phase response is not linear (t_d not constant).

The Nature of Distortion in Audio and Video Signals

Generally speaking, the human ear can readily perceive amplitude distortion but is relatively insensitive to phase distortion. For the phase distortion to become noticeable, the variation in delay [variation in the slope of $\angle H(\omega)$] should be comparable to the signal duration (or the physically perceptible duration, in case the signal itself is long). In the case of audio signals, each spoken syllable can be considered to be an individual signal. The average duration of a spoken syllable is of a magnitude of the order of 0.01 to 0.1 second. Audio systems may have nonlinear phases, yet no noticeable signal distortion results because in practical audio systems, maximum variation in the slope of $\angle H(\omega)$ is only a small fraction of a millisecond. This is the real truth underlying the statement that "the human ear is relatively insensitive to phase distortion" [3]. As a result, the manufacturers of audio equipment make available only $|H(\omega)|$, the amplitude response characteristic of their systems.

For video signals, in contrast, the situation is exactly the opposite. The human eye is sensitive to phase distortion but is relatively insensitive to amplitude distortion. Amplitude distortion in television signals manifests itself as a partial destruction of the relative half-tone values of the resulting picture, but this effect is not readily apparent to the human eye. Phase distortion (nonlinear phase), on the other hand, causes different time delays in different picture elements. The result is a smeared picture, and this effect is readily perceived by the human eye. Phase distortion is also very important in digital communication systems because the nonlinear phase characteristic of a channel causes pulse dispersion (spreading out), which in turn causes pulses to interfere with neighboring pulses. Such interference between pulses can cause an error in the pulse amplitude at the receiver: a binary **1** may read as **0**, and vice versa.

4.4.2 Bandpass Systems and Group Delay

The distortionless transmission conditions [Eq. (4.39)] can be relaxed slightly for bandpass systems. For lowpass systems, the phase characteristics not only should be linear over the band of interest but also should pass through the origin. For bandpass systems, the phase characteristics must be linear over the band of interest but need not pass through the origin.

Consider an LTI system with amplitude and phase characteristics as shown in Fig. 4.30, where the amplitude spectrum is a constant G_0 and the phase is $\phi_0 - \omega t_g$ over a band $2W$ centered at frequency ω_c. Over this band, we can describe $H(\omega)$ as[†]

$$H(\omega) = G_0 e^{j(\phi_0 - \omega t_g)} \qquad \omega \geq 0 \tag{4.41}$$

The phase of $H(\omega)$ in Eq. (4.41), shown dotted in Fig. 4.30b, is linear but does not pass through the origin.

Consider a modulated input signal $z(t) = x(t)\cos\omega_c t$. This is a bandpass signal, whose spectrum is centered at $\omega = \omega_c$. The signal $\cos\omega_c t$ is the carrier, and the signal $x(t)$, which is a lowpass signal of bandwidth W (see Fig. 4.25), is the *envelope* of $z(t)$.[‡] We shall now show that the transmission of $z(t)$ through $H(\omega)$ results in distortionless transmission of the envelope $x(t)$. However, the carrier phase changes by ϕ_0. To show this, consider an input $\hat{z}(t) = x(t)e^{j\omega_c t}$ and the corresponding output $\hat{y}(t)$. From Eq. (4.30), $\hat{Z}(\omega) = X(\omega - \omega_c)$, and the corresponding output

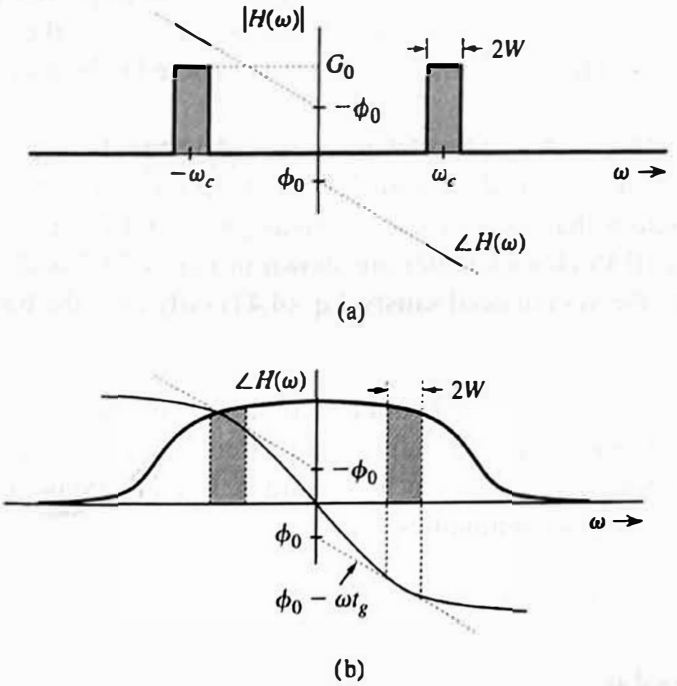

Figure 4.30 Generalized linear phase characteristics.

[†] Because the phase function is an odd function of ω, if $\angle H(\omega) = \phi_0 - \omega t_g$ for $\omega \geq 0$, over the band $2W$ (centered at ω_c), then $\angle H(\omega) = -\phi_0 - \omega t_g$ for $\omega < 0$ over the band $2W$ (centered at $-\omega_c$), as shown in Fig. 4.30a.

[‡] The envelope of a bandpass signal is well defined only when the bandwidth of the envelope is well below the carrier ω_c ($W \ll \omega_c$).

spectrum $\hat{Y}(\omega)$ is given by

$$\hat{Y}(\omega) = H(\omega)\hat{Z}(\omega) = H(\omega)X(\omega - \omega_c)$$

Recall that the bandwidth of $X(\omega)$ is W so that the bandwidth of $X(\omega - \omega_c)$ is $2W$, centered at ω_c. Over this range, $H(\omega)$ is given by Eq. (4.41). Hence,

$$\hat{Y}(\omega) = G_0X(\omega - \omega_c)e^{j(\phi_0 - \omega t_g)} = G_0e^{j\phi_0}X(\omega - \omega_c)e^{-\omega t_g}$$

Use of Eqs. (4.29) and (4.30) yields $\hat{y}(t)$ as

$$\hat{y}(t) = G_0e^{j\phi_0}x(t - t_g)e^{j\omega_c(t-t_g)} = G_0x(t - t_g)e^{j[\omega_c(t-t_g)+\phi_0]}$$

This is the system response to input $\hat{z}(t) = x(t)e^{j\omega_c t}$, which is a complex signal. We are really interested in finding the response to the input $z(t) = x(t)\cos\omega_c t$, which is the real part of $\hat{z}(t) = x(t)e^{j\omega_c t}$. Hence, we use Eq. (2.31) to obtain $y(t)$, the system response to the input $z(t) = x(t)\cos\omega_c t$, as

$$y(t) = G_0x(t - t_g)\cos[\omega_c(t - t_g) + \phi_0)] \tag{4.42}$$

where t_g, the *group* (or *envelope*) delay, is the negative slope of $\angle H(\omega)$ at ω_c.† The output $y(t)$ is basically the delayed input $z(t - t_g)$, except that the output carrier acquires an extra phase ϕ_0. The output envelope $x(t - t_g)$ is the delayed version of the input envelope $x(t)$ and is not affected by extra phase ϕ_0 of the carrier. In a modulated signal, such as $x(t)\cos\omega_c t$, the information generally resides in the envelope $x(t)$. Hence, the transmission is considered to be distortionless if the envelope $x(t)$ remains undistorted.

Most practical systems satisfy Eq. (4.41), at least over a very small band. Figure 4.30b shows a typical case in which this condition is satisfied for a small band W centered at frequency ω_c.

A system in Eq. (4.41) is said to have a *generalized linear phase* (GLP), as illustrated in Fig. 4.30. The ideal linear phase (ILP) characteristics are shown in Fig. 4.29. For distortionless transmission of bandpass signals, the system need satisfy Eq. (4.41) only over the bandwidth of the bandpass signal.

Caution. Recall that the phase response associated with the amplitude response may have jump discontinuities when the amplitude response goes negative. Jump discontinuities also arise because of the use of the principal value for phase. Under such conditions, to compute the group delay [Eq. (4.40)], we should ignore the jump discontinuities.

---

† Equation (4.42) can also be expressed as

$$y(t) = G_0x(t - t_g)\cos\omega_c(t - t_{ph})$$

where t_{ph}, called the *phase delay* at ω_c, is given by $t_{ph}(\omega_c) = (\omega_c t_g - \phi_0)/\omega_c$. Generally, t_{ph} varies with ω, and we can write

$$t_{ph}(\omega) = \frac{\omega t_g - \phi_0}{\omega}$$

Recall also that t_g itself may vary with ω.

EXAMPLE 4.19 Distortionless Bandpass Transmission

(a) A signal $z(t)$, shown in Fig. 4.31b, is given by

$$z(t) = x(t)\cos\omega_c t$$

where $\omega_c = 2000\pi$. The pulse $x(t)$ (Fig. 4.31a) is a lowpass pulse of duration 0.1 second and has a bandwidth of about 10 Hz. This signal is passed through a filter whose frequency response is shown in Fig. 4.31c (shown only for positive ω). Find and sketch the filter output $y(t)$.

(b) Find the filter response if $\omega_c = 4000\pi$.

(a) The spectrum $Z(\omega)$ is a narrow band of width 20 Hz, centered at frequency $f_0 = 1$ kHz. The gain at the center frequency (1 kHz) is 2. The group delay, which is the negative of the slope of the phase plot, can be found by drawing tangents at ω_c, as shown in Fig. 4.31c. The negative of the slope of the tangent represents t_g, and the intercept along the vertical axis by the tangent represents ϕ_0 at that frequency. From the tangents at ω_c, we find t_g, the group delay, as

$$t_g = \frac{2.4\pi - 0.4\pi}{2000\pi} = 10^{-3}$$

The vertical axis intercept is $\phi_0 = -0.4\pi$. Hence, by using Eq. (4.42) with gain $G_0 = 2$, we obtain

$$y(t) = 2x(t - t_g)\cos[\omega_c(t - t_g) - 0.4\pi] \qquad \omega_c = 2000\pi \quad t_g = 10^{-3}$$

Figure 4.31d shows the output $y(t)$, which consists of the modulated pulse envelope $x(t)$ delayed by 1 ms and the phase of the carrier changed by -0.4π. The output shows no distortion of the envelope $x(t)$, only the delay. The carrier phase change does not affect the shape of the envelope. Hence, the transmission is considered distortionless.

(b) Figure 4.31c shows that when $\omega_c = 4000\pi$, the slope of $\angle H(\omega)$ is zero so that $t_g = 0$. Also, the gain $G_0 = 1.5$, and the intercept of the tangent with the vertical axis is $\phi_0 = -3.1\pi$. Hence,

$$y(t) = 1.5x(t)\cos(\omega_c t - 3.1\pi)$$

This, too, is a distortionless transmission for the same reasons as for case (a).

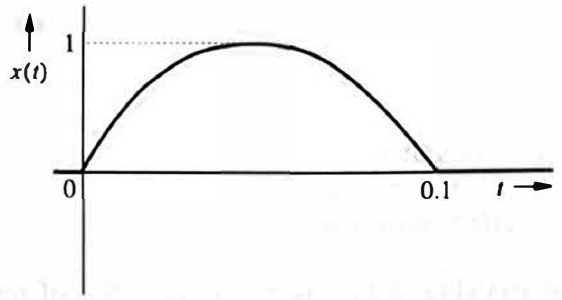

(a)

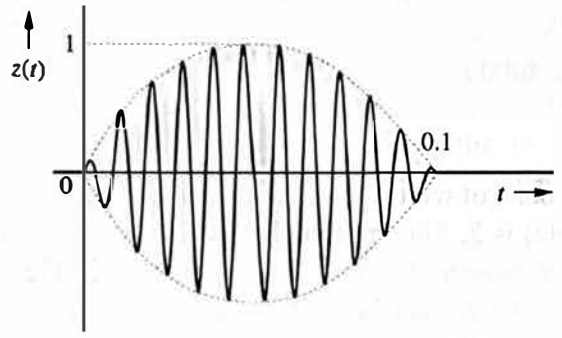

(b)

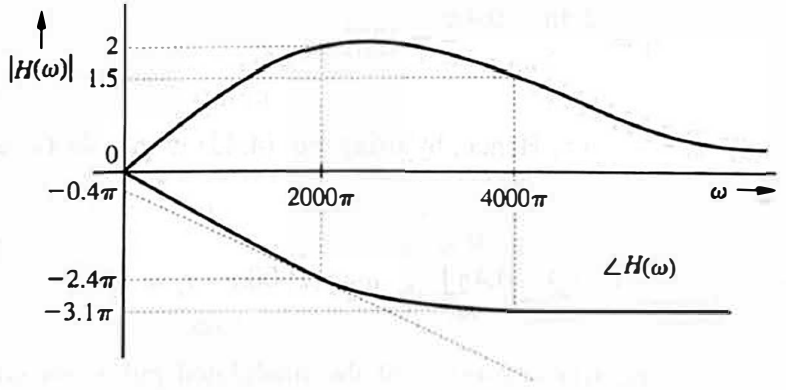

(c)

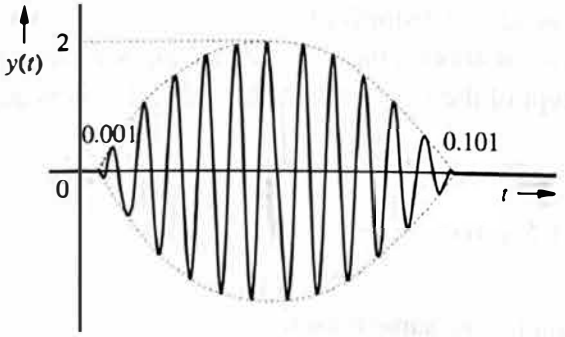

(d)

Figure 4.31 Plots for Ex. 4.19.

4.5 IDEAL AND PRACTICAL FILTERS

Ideal filters allow distortionless transmission of a certain band of frequencies and completely suppress the remaining frequencies. The ideal lowpass filter (Fig. 4.32), for example, allows all components below $\omega = W$ rad/s to pass without distortion and suppresses all components above $\omega = W$. Figure 4.33 illustrates ideal highpass and bandpass filter characteristics.

The ideal lowpass filter in Fig. 4.32a has a linear phase of slope $-t_d$, which results in a time delay of t_d seconds for all its input components of frequencies below W rad/s. Therefore, if the input is a signal $x(t)$ bandlimited to W rad/s, the output $y(t)$ is $x(t)$ delayed by t_d: that is,

$$y(t) = x(t - t_d)$$

The signal $x(t)$ is transmitted by this system without distortion, but with time delay t_d. For this filter, $|H(\omega)| = \text{rect}\,(\omega/2W)$ and $\angle H(\omega) = e^{-j\omega t_d}$ so that

$$H(\omega) = \text{rect}\left(\frac{\omega}{2W}\right) e^{-j\omega t_d}$$

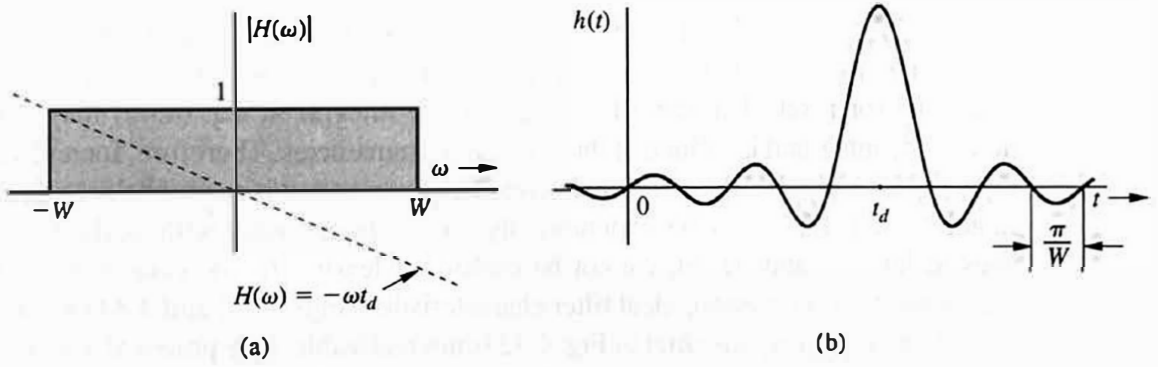

Figure 4.32 Ideal lowpass filter: (**a**) frequency response and (**b**) impulse response.

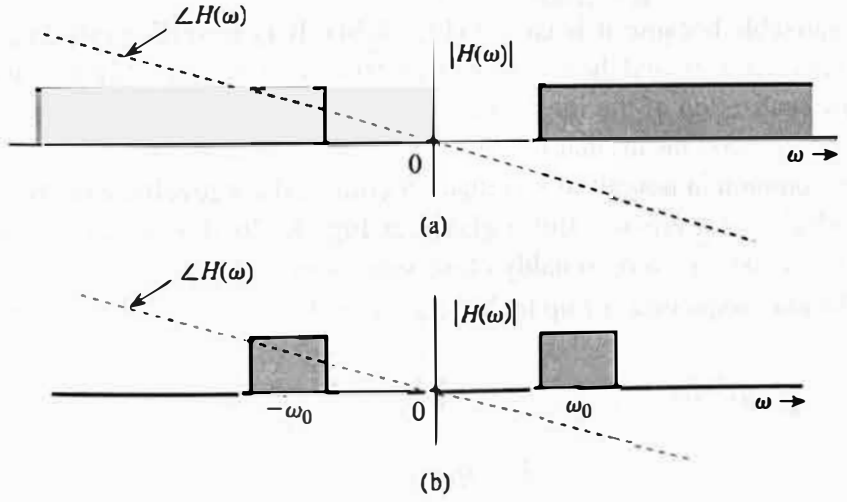

Figure 4.33 Ideal (**a**) highpass and (**b**) bandpass filter frequency responses.

The unit impulse response $h(t)$ of this filter is obtained from pair 18 (Table 4.1) and the time-shifting property

$$h(t) = \mathcal{F}^{-1}\left[\text{rect}\left(\frac{\omega}{2W}\right)e^{-j\omega t_d}\right] = \frac{W}{\pi}\,\text{sinc}[W(t-t_d)]$$

Recall that $h(t)$ is the system response to impulse input $\delta(t)$, which is applied at $t=0$. Figure 4.32b shows a curious fact: the response $h(t)$ begins even before the input is applied (at $t=0$). Clearly, the filter is noncausal and therefore physically unrealizable. Similarly, one can show that other ideal filters (such as the ideal highpass or ideal bandpass filters depicted in Fig. 4.33) are also physically unrealizable.

For a physically realizable system, $h(t)$ must be causal; that is,

$$h(t) = 0 \qquad \text{for } t < 0$$

In the frequency domain, this condition is equivalent to the well-known *Paley–Wiener criterion*, which states that the necessary and sufficient condition for the amplitude response $|H(\omega)|$ to be realizable is[†]

$$\int_{-\infty}^{\infty} \frac{|\ln|H(\omega)||}{1+\omega^2}\,d\omega < \infty \tag{4.43}$$

If $H(\omega)$ does not satisfy this condition, it is unrealizable. Note that if $|H(\omega)| = 0$ over any finite band, $|\ln|H(\omega)|| = \infty$ over that band, and Eq. (4.43) is violated. If, however, $H(\omega) = 0$ at a single frequency (or a set of discrete frequencies), the integral in Eq. (4.43) may still be finite even though the integrand is infinite at those discrete frequencies. Therefore, for a physically realizable system, $H(\omega)$ may be zero at some discrete frequencies, but it cannot be zero over any finite band. In addition, if $|H(\omega)|$ decays exponentially (or at a higher rate) with ω, the integral in Eq. (4.43) goes to infinity, and $|H(\omega)|$ cannot be realized. Clearly, $|H(\omega)|$ cannot decay too fast with ω. According to this criterion, ideal filter characteristics (Figs. 4.32 and 4.33) are unrealizable.

The impulse response $h(t)$ in Fig. 4.32 is not realizable. One practical approach to filter design is to cut off the tail of $h(t)$ for $t < 0$. The resulting causal impulse response $\widehat{h}(t)$, given by

$$\widehat{h}(t) = h(t)u(t)$$

is physically realizable because it is causal (Fig. 4.34). If t_d is sufficiently large, $\widehat{h}(t)$ will be a close approximation of $h(t)$, and the resulting filter $\widehat{H}(\omega)$ will be a good approximation of an ideal filter. This close realization of the ideal filter is achieved because of the increased value of time delay t_d. This observation means that the price of close realization is higher delay in the output; this situation is common in noncausal systems. Of course, theoretically, a delay $t_d = \infty$ is needed to realize the ideal characteristics. But a glance at Fig. 4.32b shows that a delay t_d of three or four times $\frac{\pi}{W}$ will make $\widehat{h}(t)$ a reasonably close version of $h(t-t_d)$. For instance, an audio filter is required to handle frequencies of up to 20 kHz ($W = 40{,}000\pi$). In this case, a t_d of about 10^{-4}

[†] We are assuming that $|H(\omega)|$ is square integrable, that is,

$$\int_{-\infty}^{\infty} |H(\omega)|^2\,d\omega < \infty$$

Note that the Paley–Wiener criterion is a criterion for the realizability of the amplitude response $|H(\omega)|$.

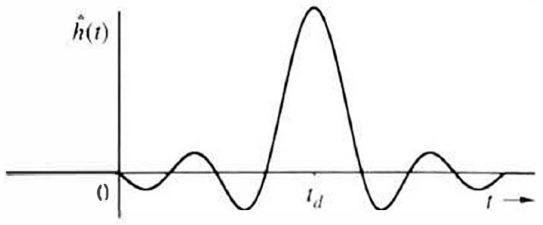

Figure 4.34 Approximate realization of an ideal lowpass filter by truncation of its impulse response.

(0.1 ms) would be a reasonable choice. The truncation operation [cutting the tail of $h(t)$ to make it causal], however, creates some unsuspected problems. We discuss these problems and their cure in Sec. 4.9.

In practice, we can realize a variety of filter characteristics that approach the ideal. Practical (realizable) filter characteristics are gradual, without jump discontinuities in amplitude response.

DRILL 4.11 The Unrealizable Gaussian Response

Show that a filter with Gaussian frequency response $H(\omega) = e^{-\alpha\omega^2}$ is unrealizable. Demonstrate this fact in two ways: first by showing that its impulse response is noncausal, and then by showing that $|H(\omega)|$ violates the Paley–Wiener criterion. [*Hint:* Use pair 22 in Table 4.1.]

Thinking in the Time and Frequency Domains: A Two-Dimensional View of Signals and Systems

Both signals and systems have dual personalities, the time domain and the frequency domain. For a deeper perspective, we should examine and understand both these identities because they offer complementary insights. An exponential signal, for instance, can be specified by its time-domain description such as $e^{-2t}u(t)$ or by its Fourier transform (its frequency-domain description) $1/(j\omega + 2)$. The time-domain description depicts the waveform of a signal. The frequency-domain description portrays its spectral composition [relative amplitudes of its sinusoidal (or exponential) components and their phases]. For the signal e^{-2t}, for instance, the time-domain description portrays the exponentially decaying signal with a time constant 0.5. The frequency-domain description characterizes it as a lowpass signal, which can be synthesized by sinusoids with amplitudes decaying with frequency roughly as $1/\omega$.

An LTIC system can also be described or specified in the time domain by its impulse response $h(t)$ or in the frequency domain by its frequency response $H(\omega)$. In Sec. 2.6, we studied intuitive insights in the system behavior offered by the impulse response, which consists of characteristic modes of the system. By purely qualitative reasoning, we saw that the system responds well to signals that are similar to the characteristic modes and responds poorly to signals that are very different from those modes. We also saw that the shape of the impulse response $h(t)$ determines the system time constant (speed of response), and pulse dispersion (spreading), which, in turn, determines the rate of pulse transmission.

The frequency response $H(\omega)$ specifies the system response to exponential or sinusoidal input of various frequencies. This is precisely the filtering characteristic of the system.

Experienced electrical engineers instinctively think in both domains (time and frequency) whenever possible. When they look at a signal, they consider its waveform, the signal width (duration), and the rate at which the waveform decays. This is basically a time-domain perspective. They also think of the signal in terms of its frequency spectrum, that is, in terms of its sinusoidal components and their relative amplitudes and phases, whether the spectrum is lowpass, bandpass, highpass, and so on. This is a frequency-domain perspective. Experienced electrical engineers think of a system in terms of its impulse response $h(t)$. The width of $h(t)$ indicates the time constant (response time): that is, how quickly the system is capable of responding to an input, and how much dispersion (spreading) it will cause. This is a time-domain perspective. From the frequency-domain perspective, these engineers view a system as a filter, which selectively transmits certain frequency components and suppresses the others [frequency response $H(\omega)$]. Knowing the input signal spectrum and the frequency response of the system, they create a mental image of the output signal spectrum. This concept is precisely expressed by $Y(\omega) = X(\omega)H(\omega)$.

We can analyze LTI systems by time-domain techniques or by frequency-domain techniques. Then why learn both? The reason is that the two domains offer complementary insights into system behavior. Some aspects are easily grasped in one domain; other aspects may be easier to see in the other domain. Both time-domain and frequency-domain methods are as essential for the study of signals and systems as two eyes are essential to a human being for correct visual perception of reality. A person can see with either eye, but for proper perception of three-dimensional reality, both eyes are essential.

It is important to keep the two domains separate, and not to mix the entities in the two domains. If we are using the frequency domain to determine the system response, we must deal with all signals in terms of their spectra (Fourier transforms) and all systems in terms of their frequency responses. For example, to determine the system response $y(t)$ to an input $x(t)$, we must first convert the input signal into its frequency-domain description $X(\omega)$. The system description also must be in the frequency domain, that is, the frequency response $H(\omega)$. The output signal spectrum $Y(\omega) = X(\omega)H(\omega)$. Thus, the result (output) is also in the frequency domain. To determine the final answer $y(t)$, we must take the inverse transform of $Y(\omega)$.

4.6 SIGNAL ENERGY

The signal energy E_x of a signal $x(t)$ was defined in Ch. 1 as

$$E_x = \int_{-\infty}^{\infty} |x(t)|^2 \, dt \tag{4.44}$$

Signal energy can be related to the signal spectrum $X(\omega)$ by substituting Eq. (4.10) in Eq. (4.44):

$$E_x = \int_{-\infty}^{\infty} x(t)x^*(t)\,dt = \int_{-\infty}^{\infty} x(t)\left[\frac{1}{2\pi}\int_{-\infty}^{\infty} X^*(\omega)e^{-j\omega t}\,d\omega\right] dt$$

Here, we used the fact that $x^*(t)$, being the conjugate of $x(t)$, can be expressed as the conjugate of the right-hand side of Eq. (4.10). Now, interchanging the order of integration yields

$$E_x = \frac{1}{2\pi}\int_{-\infty}^{\infty} X^*(\omega)\left[\int_{-\infty}^{\infty} x(t)e^{-j\omega t}\,dt\right]d\omega$$
$$= \frac{1}{2\pi}\int_{-\infty}^{\infty} X(\omega)X^*(\omega)\,d\omega = \frac{1}{2\pi}\int_{-\infty}^{\infty} |X(\omega)|^2\,d\omega$$

Consequently,

$$E_x = \int_{-\infty}^{\infty} |x(t)|^2\,dt = \frac{1}{2\pi}\int_{-\infty}^{\infty} |X(\omega)|^2 d\omega \tag{4.45}$$

This is *Parseval's theorem* (for the Fourier transform). A similar result was obtained in Eqs. (3.53) and (3.54) for a periodic signal and its Fourier series. This result allows us to determine the signal energy from either the time-domain specification $x(t)$ or the corresponding frequency-domain specification $X(\omega)$.

The right-hand side of Eq. (4.45) can be interpreted to mean that the energy of a signal $x(t)$ results from energies contributed by all the spectral components of the signal $x(t)$. The total signal energy is the area under $|X(\omega)^2|$ (divided by 2π). If we consider a small band $\Delta\omega$ ($\Delta\omega \to 0$), as illustrated in Fig. 4.35, the energy ΔE_x of the spectral components in this band is the area of $|X(\omega)|^2$ under this band (divided by 2π):

$$\Delta E_x = \frac{1}{2\pi}|X(\omega)|^2\,\Delta\omega = |X(\omega)|^2\,\Delta f \qquad \frac{\Delta\omega}{2\pi} = \Delta f \text{ Hz}$$

Therefore, the energy contributed by the components in this band of Δf (in hertz) is $|X(\omega)|^2\Delta f$. The total signal energy is the sum of energies of all such bands and is indicated by the area under $|X(\omega)|^2$ as in Eq. (4.45). Therefore, $|X(\omega)|^2$ is the *energy spectral density* (per unit bandwidth in hertz).

For real signals, $X(\omega)$ and $X(-\omega)$ are conjugates, and $|X(\omega)|^2$ is an even function of ω because

$$|X(\omega)|^2 = X(\omega)X^*(\omega) = X(\omega)X(-\omega)$$

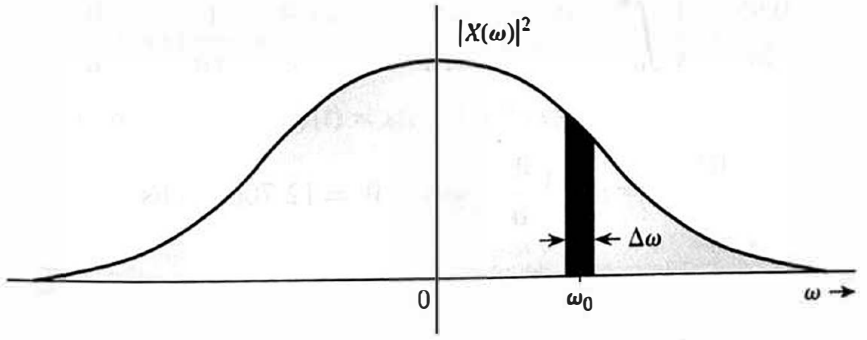

Figure 4.35 Interpretation of energy spectral density of a signal.

Therefore, the energy of real signal $x(t)$ can be expressed as†

$$E_x = \frac{1}{\pi}\int_0^\infty |X(\omega)|^2\, d\omega \tag{4.46}$$

The signal energy E_x, which results from contributions from all the frequency components from $\omega = 0$ to ∞, is given by ($1/\pi$ times) the area under $|X(\omega)|^2$ from $\omega = 0$ to ∞. It follows that the energy contributed by spectral components of frequencies between ω_1 and ω_2 is

$$\Delta E_x = \frac{1}{\pi}\int_{\omega_1}^{\omega_2} |X(\omega)|^2\, d\omega \tag{4.47}$$

EXAMPLE 4.20 Signal Energy and Parseval's Theorem

Find the energy of signal $x(t) = e^{-at}u(t)$. Determine the frequency W (rad/s) so that the energy contributed by the spectral components of all the frequencies below W is 95% of the signal energy E_x.

We have

$$E_x = \int_{-\infty}^{\infty} x^2(t)\, dt = \int_0^\infty e^{-2at}\, dt = \frac{1}{2a}$$

We can verify this result by Parseval's theorem. For this signal,

$$X(\omega) = \frac{1}{j\omega + a}$$

and

$$E_x = \frac{1}{\pi}\int_0^\infty |X(\omega)|^2\, d\omega = \frac{1}{\pi}\int_0^\infty \frac{1}{\omega^2 + a^2}\, d\omega = \frac{1}{\pi a}\tan^{-1}\frac{\omega}{a}\bigg|_0^\infty = \frac{1}{2a}$$

The band $\omega = 0$ to $\omega = W$ contains 95% of the signal energy, that is, $0.95/2a$. Therefore, from Eq. (4.47) with $\omega_1 = 0$ and $\omega_2 = W$, we obtain

$$\frac{0.95}{2a} = \frac{1}{\pi}\int_0^W \frac{d\omega}{\omega^2 + a^2} = \frac{1}{\pi a}\tan^{-1}\frac{\omega}{a}\bigg|_0^W = \frac{1}{\pi a}\tan^{-1}\frac{W}{a}$$

or

$$\frac{0.95\pi}{2} = \tan^{-1}\frac{W}{a} \quad \Longrightarrow \quad W = 12.706a \text{ rad/s}$$

---

† In Eq. (4.46), it is assumed that $X(\omega)$ does not contain an impulse at $\omega = 0$. If such an impulse exists, it should be integrated separately with a multiplying factor of $1/2\pi$ rather than $1/\pi$.

This result indicates that the spectral components of $x(t)$ in the band from 0 (dc) to $12.706a$ rad/s ($2.02a$ Hz) contribute 95% of the total signal energy; all the remaining spectral components (in the band from $12.706a$ rad/s to ∞) contribute only 5% of the signal energy.

DRILL 4.12 Signal Energy and Parseval's Theorem

Use Parseval's theorem to show that the energy of the signal $x(t) = 2a/(t^2 + a^2)$ is $2\pi/a$. [*Hint:* Find $X(\omega)$ using pair 3 of Table 4.1 and the duality property.]

The Essential Bandwidth of a Signal

The spectra of all practical signals extend to infinity. However, because the energy of any practical signal is finite, the signal spectrum must approach 0 as $\omega \to \infty$. Most of the signal energy is contained within a certain band of B Hz, and the energy contributed by the components beyond B Hz is negligible. We can therefore suppress the signal spectrum beyond B Hz with little effect on the signal shape and energy. The bandwidth B is called the *essential bandwidth* of the signal. The criterion for selecting B depends on the error tolerance in a particular application. We may, for example, select B to be that band that contains 95% of the signal energy.[†] This figure may be higher or lower than 95%, depending on the precision needed. Using such a criterion, we can determine the essential bandwidth of a signal. The essential bandwidth B for the signal $e^{-at}u(t)$, using 95% energy criterion, was determined in Ex. 4.20 to be $2.02a$ Hz.

Suppression of all the spectral components of $x(t)$ beyond the essential bandwidth results in a signal $\hat{x}(t)$, which is a close approximation of $x(t)$. If we use the 95% criterion for the essential bandwidth, the energy of the error (the difference) $x(t) - \hat{x}(t)$ is 5% of E_x.

Energy Spectral Density from the Autocorrelation Function

The correlation of a function $x(t)$ with itself is its *autocorrelation function* $\psi_x(t)$, which, for a real $x(t)$, is given by [see Eq. (3.11)]

$$\psi_x(t) \equiv \int_{-\infty}^{\infty} x(\tau)x^*(\tau - t)\,d\tau$$

Also, from Eq. (3.10) with $y(t) = x(t)$, it follows that

$$\psi_x(t) = x(t) * x(-t)$$

[†] For lowpass signals, the essential bandwidth may also be defined as a frequency at which the value of the amplitude spectrum is a small fraction (about 1%) of its peak value. In Ex. 4.20, for instance, the peak value, which occurs at $\omega = 0$, is $1/a$.

From this expression, it is clear that

$$\psi_x(-t) = x(-t) * x(t) = \psi_x(t)$$

Therefore, for real $x(t)$, the autocorrelation function $\psi_x(t)$ is an even function of t. Now, taking the Fourier transform yields

$$\psi_x(t) \Longleftrightarrow |X(\omega)|^2$$

Therefore, the Fourier transform of the autocorrelation function is its energy spectral density $|X(\omega)|^2$. It is clear that $\psi_x(t)$ provides the spectral information of $x(t)$ directly.

The direct link of the autocorrelation function to a signal's spectral information can be explained intuitively as follows. The autocorrelation function $\psi_x(t)$ is the correlation of a signal with itself delayed by t seconds. With a delay of zero, a signal $x(t)$ correlates perfectly with itself. But as delay increases, the similarity tends to decrease. Thus, the autocorrelation function $\psi_x(t)$ tends to decrease with t. If $x(t)$ is a slowly varying signal (low-frequency signal), it changes slowly with t. Consequently, such a signal will show considerable similarity or correlation with itself even for relatively large delay. The autocorrelation function $\psi_x(t)$ decays slowly with t and has a larger width. On the other hand, for a rapidly varying signal, the signal similarity will decrease rapidly with delay t and $\psi_x(t)$ has a smaller width. Thus, the shape of $\psi_x(t)$ has a direct link to spectral information of $x(t)$.

4.7 APPLICATION TO COMMUNICATIONS: AMPLITUDE MODULATION

Modulation causes a spectral shift in a signal and is used to gain certain advantages mentioned in our discussion of the frequency-shifting property. Broadly speaking, there are two classes of modulation: amplitude (linear) modulation and angle (nonlinear) modulation. In this section, we shall discuss some practical forms of amplitude modulation.

4.7.1 Double-Sideband, Suppressed-Carrier (DSB-SC) Modulation

In amplitude modulation, the amplitude A of the carrier $A\cos(\omega_c t + \theta_c)$ is varied in some manner with the *baseband* (message)† signal $m(t)$ (known as the *modulating signal*). The frequency ω_c and the phase θ_c are constant. We can assume $\theta_c = 0$ without loss of generality. If the carrier amplitude A is made directly proportional to the modulating signal $m(t)$, the modulated signal is $m(t)\cos\omega_c t$ (Fig. 4.36). As was indicated earlier [Eq. (4.32)], this type of modulation simply shifts the spectrum of $m(t)$ to the carrier frequency (Fig. 4.36c). Thus, if

$$m(t) \Longleftrightarrow M(\omega)$$

then

$$m(t)\cos\omega_c t \Longleftrightarrow \tfrac{1}{2}[M(\omega+\omega_c) + M(\omega-\omega_c)] \tag{4.48}$$

† The term *baseband* is used to designate the band of frequencies of the signal delivered by the source or the input transducer.

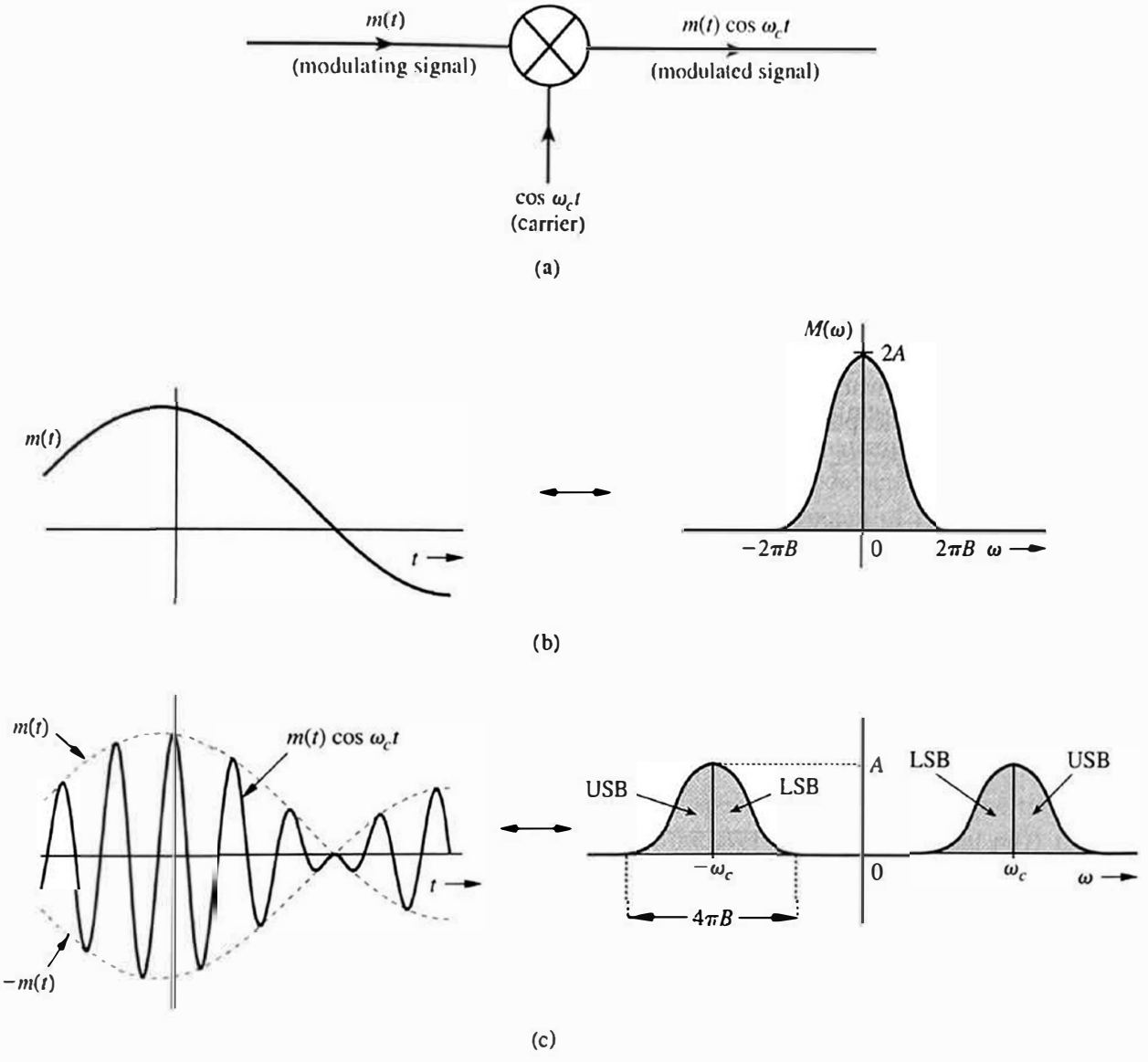

Figure 4.36 DSB-SC modulation.

Recall that $M(\omega - \omega_c)$ is $M(\omega)$-shifted to the right by ω_c and $M(\omega + \omega_c)$ is $M(\omega)$-shifted to the left by ω_c. Thus, the process of modulation shifts the spectrum of the modulating signal to the left and the right by ω_c. Note also that if the bandwidth of $m(t)$ is B Hz, then, as indicated in Fig. 4.36c, the bandwidth of the modulated signal is $2B$ Hz. We also observe that the modulated signal spectrum centered at ω_c is composed of two parts: a portion that lies above ω_c, known as the *upper sideband* (USB), and a portion that lies below ω_c, known as the *lower sideband* (LSB). Similarly, the spectrum centered at $-\omega_c$ has upper and lower sidebands. This form of modulation is called *double sideband* (DSB) modulation for the obvious reason.

The relationship of B to ω_c is of interest. Figure 4.36c shows that $\omega_c \geq 2\pi B$ to avoid the overlap of the spectra centered at $\pm\omega_c$. If $\omega_c < 2\pi B$, the spectra overlap and the information of

$m(t)$ are lost in the process of modulation, a loss that makes it impossible to get back $m(t)$ from the modulated signal $m(t)\cos\omega_c t$.[†]

EXAMPLE 4.21 Double-Sideband Suppressed-Carrier Modulation

For a baseband signal $m(t) = \cos\omega_m t$, find the DSB-SC signal and sketch its spectrum. Identify the upper and lower sidebands.

We shall work this problem in the frequency domain as well as the time domain to clarify the basic concepts of DSB-SC modulation. In the frequency-domain approach, we work with the signal spectra. The spectrum of the baseband signal $m(t) = \cos\omega_m t$ is given by

$$M(\omega) = \pi[\delta(\omega - \omega_m) + \delta(\omega + \omega_m)]$$

The spectrum consists of two impulses located at $\pm\omega_m$, as depicted in Fig. 4.37a.

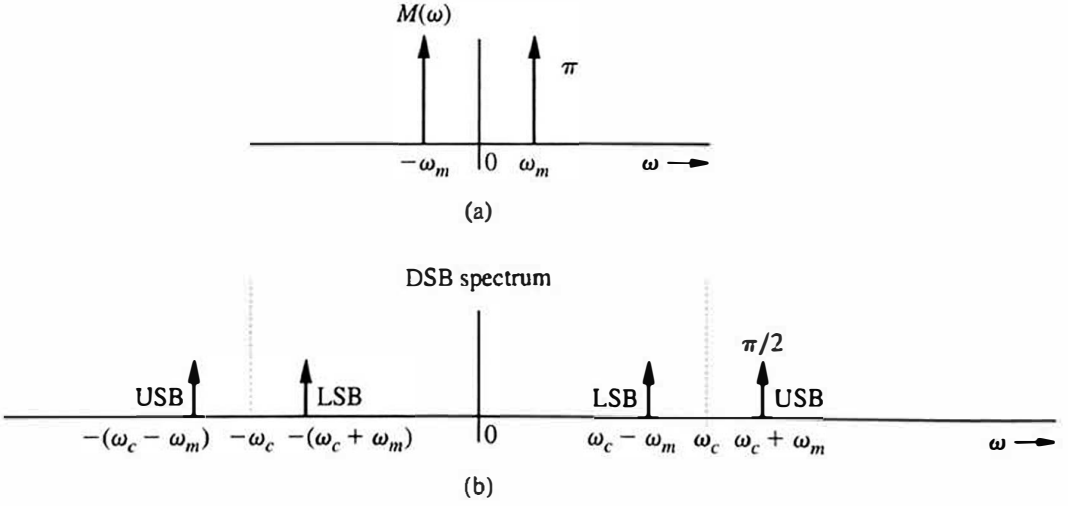

Figure 4.37 An example of DSB-SC modulation.

The DSB-SC (modulated) spectrum, as indicated by Eq. (4.48), is the baseband spectrum in Fig. 4.37a shifted to the right and the left by ω_c (times 0.5), as depicted in Fig. 4.37b.

[†] Practical factors may impose additional restrictions on ω_c. For instance, in broadcast applications, a radiating antenna can radiate only a narrow band without distortion. This restriction implies that avoiding distortion caused by the radiating antenna calls for $\omega_c/2\pi B \gg 1$. The broadcast band AM radio, for instance, with $B = 5$ kHz and the band of 550–1600 kHz for carrier frequency, gives a ratio of $\omega_c/2\pi B$ roughly in the range of 100–300.

This spectrum consists of impulses at $\pm(\omega_c - \omega_m)$ and $\pm(\omega_c + \omega_m)$. The spectrum beyond ω_c is the upper sideband (USB), and the one below ω_c is the lower sideband (LSB). Observe that the DSB-SC spectrum does not have as a component the carrier frequency ω_c. This is why the term *double-sideband, suppressed carrier* (DSB-SC) is used for this type of modulation.

In the time-domain approach, we work directly with signals in the time domain. For the baseband signal $m(t) = \cos \omega_m t$, the DSB-SC signal $\varphi_{\text{DSB-SC}}(t)$ is

$$\begin{aligned} \varphi_{\text{DSB-SC}}(t) &= m(t) \cos \omega_c t \\ &= \cos \omega_m t \cos \omega_c t \\ &= \tfrac{1}{2}[\cos(\omega_c + \omega_m)t + \cos(\omega_c - \omega_m)t] \end{aligned} \tag{4.49}$$

This result shows that when the baseband (message) signal is a single sinusoid of frequency ω_m, the modulated signal consists of two sinusoids: the component of frequency $\omega_c + \omega_m$ (the upper sideband), and the component of frequency $\omega_c - \omega_m$ (the lower sideband). Figure 4.37b illustrates precisely the spectrum of $\varphi_{\text{DSB-SC}}(t)$. Thus, each component of frequency ω_m in the modulating signal results in two components of frequencies $\omega_c + \omega_m$ and $\omega_c - \omega_m$ in the modulated signal. This being a DSB-SC (suppressed-carrier) modulation, there is no component of the carrier frequency ω_c on the right-hand side of Eq. (4.49).[†]

Demodulation of DSB-SC Signals

The DSB-SC modulation translates or shifts the frequency spectrum to the left and the right by ω_c (i.e., at $+\omega_c$ and $-\omega_c$), as seen from Eq. (4.48). To recover the original signal $m(t)$ from the modulated signal, we must retranslate the spectrum to its original position. The process of recovering the signal from the modulated signal (retranslating the spectrum to its original position) is referred to as *demodulation*, or *detection*. Observe that if the modulated signal spectrum in Fig. 4.36c is shifted to the left and to the right by ω_c (and halved), we obtain the spectrum illustrated in Fig. 4.38b, which contains the desired baseband spectrum in addition to an unwanted spectrum at $\pm 2\omega_c$. The latter can be suppressed by a lowpass filter. Thus, demodulation, which is almost identical to modulation, consists of multiplication of the incoming modulated signal $m(t)\cos \omega_c t$ by a carrier $\cos \omega_c t$ followed by a lowpass filter, as depicted in Fig. 4.38a. We can verify this conclusion directly in the time domain by observing that the signal $e(t)$ in Fig. 4.38a is

$$e(t) = m(t)\cos^2 \omega_c t = \tfrac{1}{2}[m(t) + m(t)\cos 2\omega_c t]$$

Therefore, the Fourier transform of the signal $e(t)$ is

$$E(\omega) = \tfrac{1}{2}M(\omega) + \tfrac{1}{4}[M(\omega + 2\omega_c) + M(\omega - 2\omega_c)]$$

[†] The term *suppressed carrier* does not necessarily mean absence of the spectrum at the carrier frequency. "Suppressed carrier" merely implies that there is no discrete component of the carrier frequency. Since no discrete component exists, the DSB-SC spectrum does not have impulses at $\pm\omega_c$, which further implies that the modulated signal $m(t)\cos \omega_c t$ does not contain a term of the form $k\cos \omega_c t$ [assuming that $m(t)$ has a zero mean value].

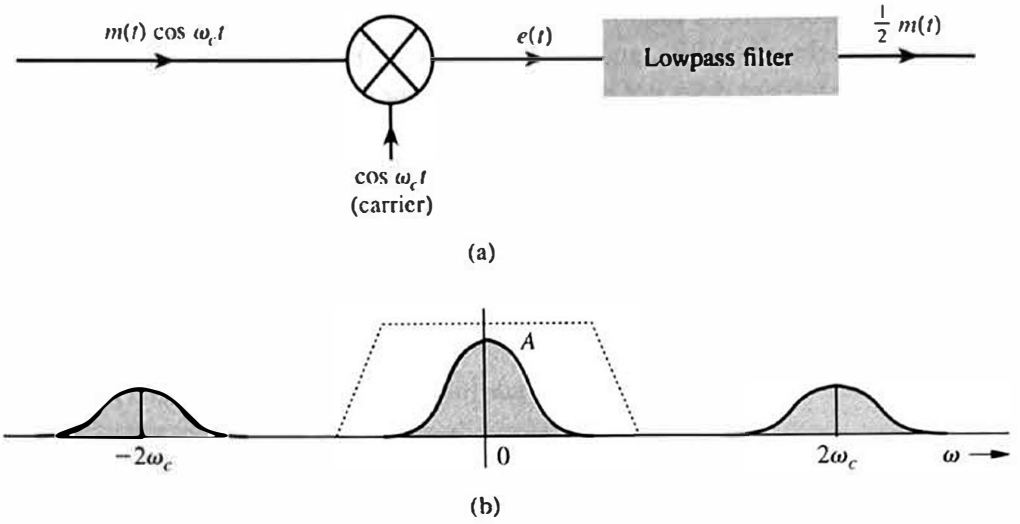

Figure 4.38 Demodulation of DSB-SC: (**a**) demodulator and (**b**) spectrum of $e(t)$.

Hence, $e(t)$ consists of two components $(1/2)m(t)$ and $(1/2)m(t)\cos 2\omega_c t$, with their spectra, as illustrated in Fig. 4.38b. The spectrum of the second component, being a modulated signal with carrier frequency $2\omega_c$, is centered at $\pm 2\omega_c$. Hence, this component is suppressed by the lowpass filter in Fig. 4.38a. The desired component $(1/2)M(\omega)$, being a lowpass spectrum (centered at $\omega = 0$), passes through the filter unharmed, resulting in the output $(1/2)m(t)$.

A possible form of lowpass filter characteristics is depicted (dotted) in Fig. 4.38b. In this method of recovering the baseband signal, called *synchronous detection*, or *coherent detection*, we use a carrier of exactly the same frequency (and phase) as the carrier used for modulation. Thus, for demodulation, we need to generate a local carrier at the receiver in frequency and phase coherence (synchronism) with the carrier used at the modulator. We shall demonstrate in Ex. 4.22 that both phase and frequency synchronism are extremely critical.

EXAMPLE 4.22 Frequency and Phase Incoherence in DSB-SC

Discuss the effect of lack of frequency and phase coherence (synchronism) between the carriers at the modulator (transmitter) and the demodulator (receiver) in DSB-SC.

Let the modulator carrier be $\cos\omega_c t$ (Fig. 4.36a). For the demodulator in Fig. 4.38a, we shall consider two cases: with carrier $\cos(\omega_c t + \theta)$ (phase error of θ) and with carrier $\cos(\omega_c + \Delta\omega)t$ (frequency error $\Delta\omega$).

(a) With the demodulator carrier $\cos(\omega_c t + \theta)$ (instead of $\cos\omega_c t$) in Fig. 4.38a, the multiplier output is $e(t) = m(t)\cos\omega_c t\cos(\omega_c t + \theta)$ instead of $m(t)\cos^2\omega_c t$. From the trigonometric identity, we obtain

$$e(t) = m(t)\cos\omega_c t\cos(\omega_c t+\theta)$$
$$= \tfrac{1}{2}m(t)[\cos\theta + \cos(2\omega_c t+\theta)]$$

The spectrum of the component $(1/2)m(t)\cos(2\omega_c t+\theta)$ is centered at $\pm 2\omega_c$. Consequently, it will be filtered out by the lowpass filter at the output. The component $(1/2)m(t)\cos\theta$ is the signal $m(t)$ multiplied by a constant $(1/2)\cos\theta$. The spectrum of this component is centered at $\omega = 0$ (lowpass spectrum) and will pass through the lowpass filter at the output, yielding the output $(1/2)m(t)\cos\theta$.

If θ is constant, the phase asynchronism merely yields an output that is attenuated (by a factor $\cos\theta$). Unfortunately, in practice, θ is often the phase difference between the carriers generated by two distant generators and varies randomly with time. This variation would result in an output whose gain varies randomly with time.

(b) In the case of frequency error, the demodulator carrier is $\cos(\omega_c + \Delta\omega)t$. This situation is very similar to the phase error case in part (a) with θ replaced by $(\Delta\omega)t$. Following the analysis in part (a), we can express the demodulator product $e(t)$ as

$$e(t) = m(t)\cos\omega_c t\cos(\omega_c+\Delta\omega)t$$
$$= \tfrac{1}{2}m(t)[\cos(\Delta\omega)t + \cos(2\omega_c+\Delta\omega)t]$$

The spectrum of the component $(1/2)m(t)\cos(2\omega_c + \Delta\omega)t$ is centered at $\pm(2\omega_c + \Delta\omega)$. Consequently, this component will be filtered out by the lowpass filter at the output. The component $(1/2)m(t)\cos(\Delta\omega)t$ is the signal $m(t)$ multiplied by a low-frequency carrier of frequency $\Delta\omega$. The spectrum of this component is centered at $\pm\Delta\omega$. In practice, the frequency error $(\Delta\omega)$ is usually very small. Hence, the signal $(1/2)m(t)\cos(\Delta\omega)t$ (whose spectrum is centered at $\pm\Delta\omega$) is a lowpass signal and passes through the lowpass filter at the output, resulting in the output $(1/2)m(t)\cos(\Delta\omega)t$. The output is the desired signal $m(t)$ multiplied by a very-low-frequency sinusoid $\cos(\Delta\omega)t$. The output in this case is not merely an attenuated replica of the desired signal $m(t)$, but represents $m(t)$ multiplied by a time-varying gain $\cos(\Delta\omega)t$. If, for instance, the transmitter and the receiver carrier frequencies differ just by 1 Hz, the output will be the desired signal $m(t)$ multiplied by a time-varying signal whose gain goes from the maximum to 0 every half-second. This is like a restless child fiddling with the volume control knob of a receiver, going from maximum volume to zero volume every half-second. This kind of distortion (called the *beat effect*) is beyond repair.

4.7.2 Amplitude Modulation (AM)

For the suppressed-carrier scheme just discussed, a receiver must generate a carrier in frequency and phase synchronism with the carrier at a transmitter that may be located hundreds or thousands of miles away. This situation calls for a sophisticated receiver, which could be quite costly. The other alternative is for the transmitter to transmit a carrier $A\cos\omega_c t$ [along with the modulated signal $m(t)\cos\omega_c t$] so that there is no need to generate a carrier at the receiver. In this case, the transmitter needs to transmit much larger power, a rather expensive procedure. In point-to-point communications, where there is one transmitter for each receiver, substantial complexity in the

receiver system can be justified, provided there is a large enough savings in expensive high-power transmitting equipment. On the other hand, for a broadcast system with a multitude of receivers for each transmitter, it is more economical to have one expensive high-power transmitter and simpler, less expensive receivers. The second option (transmitting a carrier along with the modulated signal) is the obvious choice in this case. This is amplitude modulation (AM), in which the transmitted signal $\varphi_{AM}(t)$ is given by

$$\varphi_{AM}(t) = A\cos\omega_c t + m(t)\cos\omega_c t = [A + m(t)]\cos\omega_c t \tag{4.50}$$

Recall that the DSB-SC signal is $m(t)\cos\omega_c t$. From Eq. (4.50), it follows that the AM signal is identical to the DSB-SC signal with $A + m(t)$ as the modulating signal [instead of $m(t)$]. Therefore, to sketch $\varphi_{AM}(t)$, we sketch $A + m(t)$ and $-[A + m(t)]$ as the envelopes and fill in between with the sinusoid of the carrier frequency. Two cases are considered in Fig. 4.39. In the first case, A is large enough so that $A + m(t) \geq 0$ (is nonnegative) for all values of t. In the second case, A is not large enough to satisfy this condition. In the first case, the envelope (Fig. 4.39d) has the same shape as $m(t)$ (although riding on a dc of magnitude A). In the second case, the envelope shape is not $m(t)$, for some parts get rectified (Fig. 4.39e). Thus, we can detect the desired signal $m(t)$ by detecting the envelope in the first case. In the second case, such a detection is not possible. We shall see that envelope detection is an extremely simple and inexpensive operation, which does not require generation of a local carrier for the demodulation. But as just noted, the envelope of AM has the information about $m(t)$ only if the AM signal $[A + m(t)]\cos\omega_c t$ satisfies the condition $A + m(t) > 0$ for all t. Thus, the condition for envelope detection of an AM signal is

$$A + m(t) \geq 0 \qquad \text{for all } t \tag{4.51}$$

If m_p is the peak amplitude (positive or negative) of $m(t)$, then Eq. (4.51) is equivalent to

$$A \geq m_p$$

Thus, the minimum carrier amplitude required for the viability of envelope detection is m_p. This point is clearly illustrated in Fig. 4.39.

We define the *modulation index* μ as

$$\mu = \frac{m_p}{A} \tag{4.52}$$

where A is the carrier amplitude. Note that m_p is a constant of the signal $m(t)$. Because $A \geq m_p$ and because there is no upper bound on A, it follows that

$$0 \leq \mu \leq 1$$

as the required condition for the viability of demodulation of AM by an envelope detector.

When $A < m_p$, Eq. (4.52) shows that $\mu > 1$ (overmodulation, shown in Fig. 4.39e). In this case, the option of envelope detection is no longer viable. We then need to use synchronous demodulation. Note that synchronous demodulation can be used for any value of μ (see Prob. 4.7-7). The envelope detector, which is considerably simpler and less expensive than the synchronous detector, can be used only when $\mu \leq 1$.

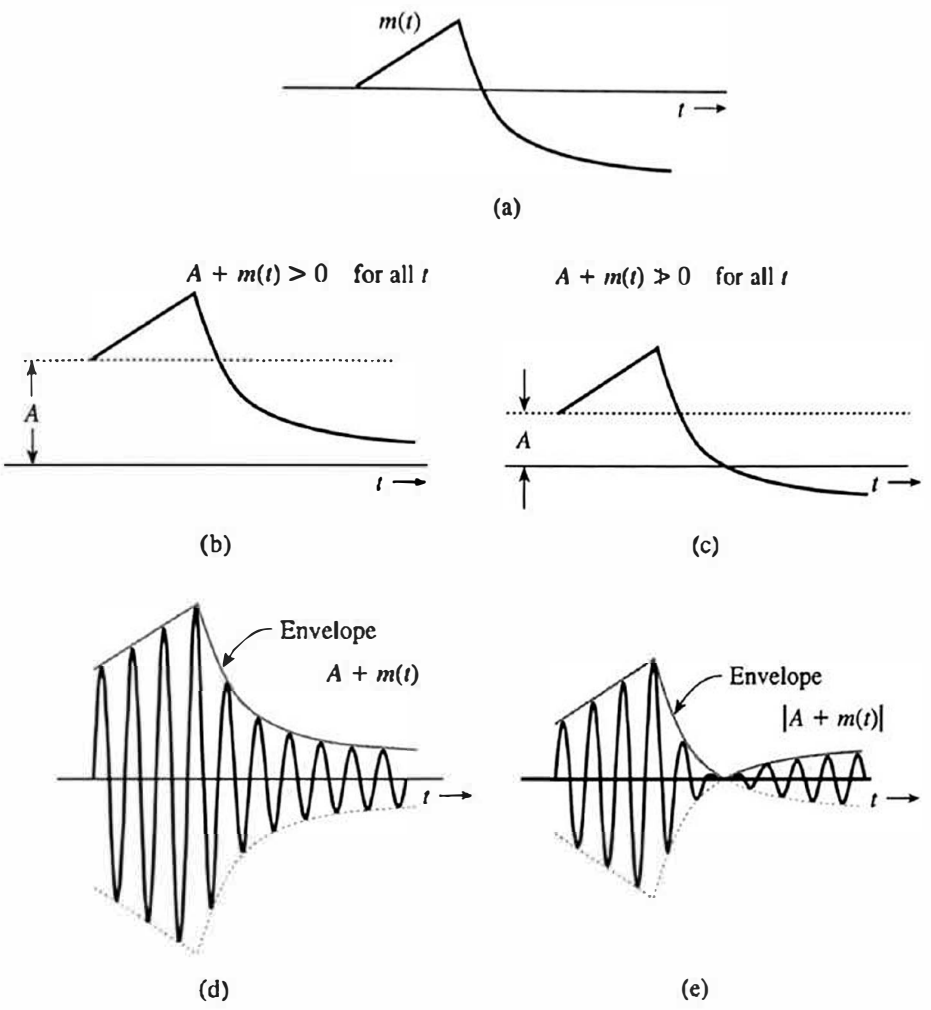

Figure 4.39 An AM signal **(a)** for two values of A **(b, c)** and the respective envelopes **(d, e)**.

EXAMPLE 4.23 Amplitude Modulation

Sketch $\varphi_{AM}(t)$ for modulation indices of $\mu = 0.5$ (50% modulation) and $\mu = 1$ (100% modulation), when $m(t) = B\cos\omega_m t$. This case is referred to as *tone modulation* because the modulating signal is a pure sinusoid (or tone).

In this case, $m_p = B$ and the modulation index according to Eq. (4.52) is

$$\mu = \frac{B}{A}$$

Hence, $B = \mu A$ and

$$m(t) = B\cos\omega_m t = \mu A\cos\omega_m t$$

Therefore,

$$\varphi_{AM}(t) = [A + m(t)]\cos\omega_c t = A[1 + \mu\cos\omega_m t]\cos\omega_c t$$

The modulated signals corresponding to $\mu = 0.5$ and $\mu = 1$ appear in Figs. 4.40a and 4.40b, respectively.

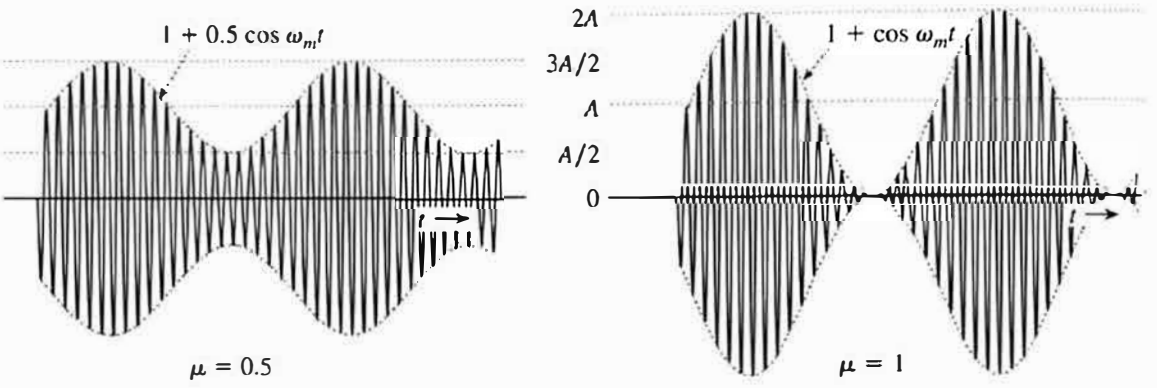

Figure 4.40 Tone-modulated AM: **(a)** $\mu = 0.5$ and **(b)** $\mu = 1$.

Demodulation of AM: The Envelope Detector

The AM signal can be demodulated coherently by a locally generated carrier (see Prob. 4.7-7). Since, however, coherent, or synchronous, demodulation of AM (with $\mu \leq 1$) will defeat the very purpose of AM, it is rarely used in practice. We shall consider here one of the noncoherent methods of AM demodulation, *envelope detection*.†

In an envelope detector, the output of the detector follows the envelope of the (modulated) input signal. The circuit illustrated in Fig. 4.41a functions as an envelope detector. During the positive cycle of the input signal, the diode conducts and the capacitor C charges up to the peak voltage of the input signal (Fig. 4.41b). As the input signal falls below this peak value, the diode is cut off, because the capacitor voltage (which is very nearly the peak voltage) is greater than the input signal voltage, a circumstance causing the diode to open. The capacitor now discharges through the resistor R at a slow rate (with a time constant RC). During the next positive cycle, the same drama repeats. When the input signal becomes greater than the capacitor voltage, the diode conducts again. The capacitor again charges to the peak value of this (new) cycle. As the input voltage falls below the new peak value, the diode cuts off again and the capacitor discharges slowly during the cutoff period, a process that changes the capacitor voltage very slightly.

In this manner, during each positive cycle, the capacitor charges up to the peak voltage of the input signal and then decays slowly until the next positive cycle. Thus, the output voltage $v_C(t)$ follows closely the envelope of the input. The capacitor discharge between positive peaks,

† There are also other methods of noncoherent detection. The rectifier detector consists of a rectifier followed by a lowpass filter. This method is also simple and almost as inexpensive as the envelope detector [4]. The nonlinear detector, although simple and inexpensive, results in a distorted output.

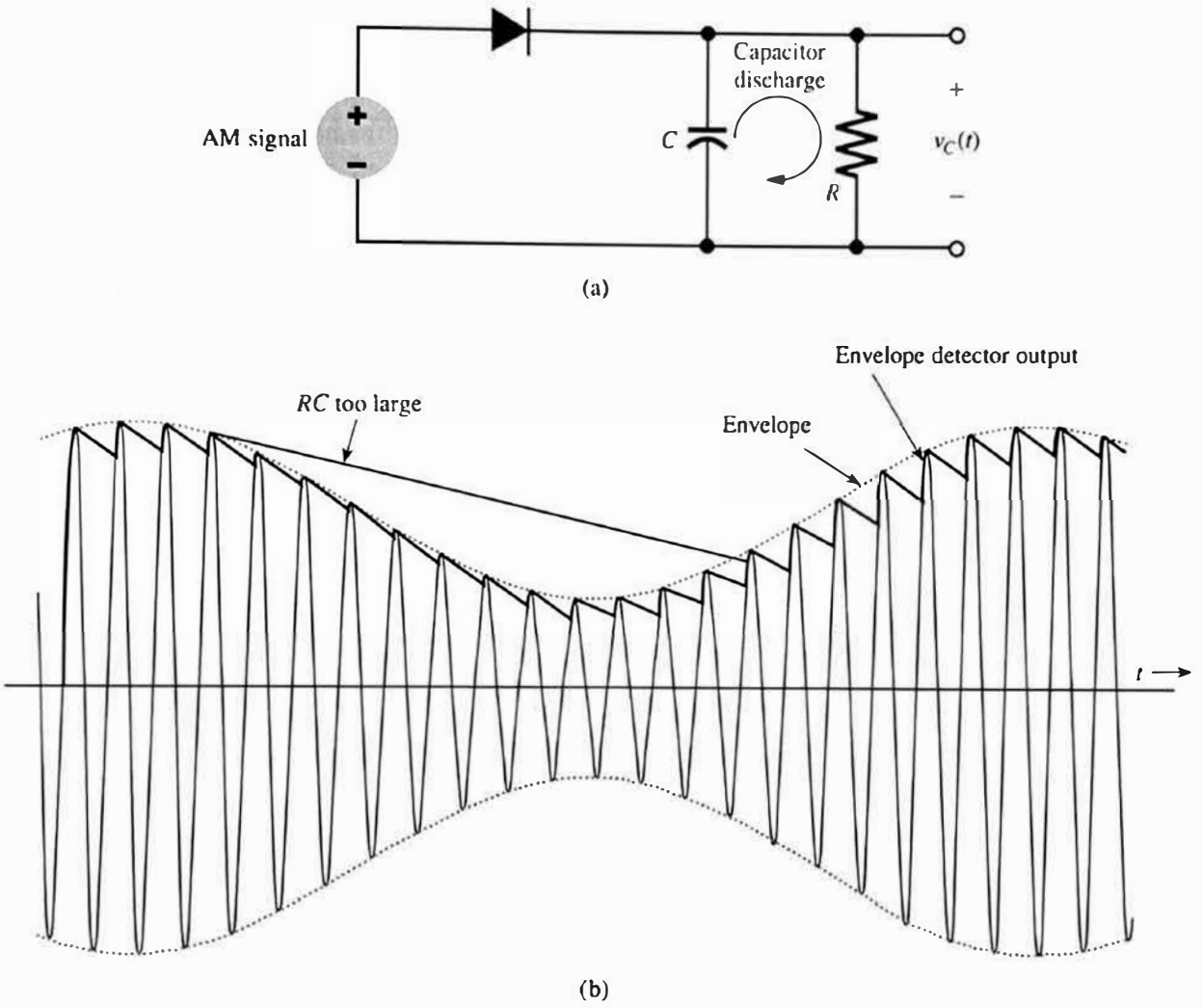

Figure 4.41 Demodulation by means of envelope detector.

however, causes a ripple signal of frequency ω_c in the output. This ripple can be reduced by increasing the time constant RC so that the capacitor discharges very little between the positive peaks ($RC \gg 1/\omega_c$). Making RC too large, however, would make it impossible for the capacitor voltage to follow the envelope (see Fig. 4.41b). Thus, RC should be large in comparison to $1/\omega_c$ but small in comparison to $1/2\pi B$, where B is the highest frequency in $m(t)$. Incidentally, these two conditions also require that $\omega_c \gg 2\pi B$, a condition necessary for a well-defined envelope.

The envelope-detector output $v_C(t)$ is $A + m(t)$ plus a ripple of frequency ω_c. The dc term A can be blocked out by a capacitor or a simple RC highpass filter. The ripple is reduced further by another (lowpass) RC filter. In the case of audio signals, the speakers also act as lowpass filters, which further enhances suppression of the high-frequency ripple.

4.7.3 Single-Sideband Modulation (SSB)

Now consider the baseband spectrum $M(\omega)$ (Fig. 4.42a) and the spectrum of the DSB-SC modulated signal $m(t)\cos \omega_c t$ (Fig. 4.42b). The DSB spectrum in Fig. 4.42b has two sidebands:

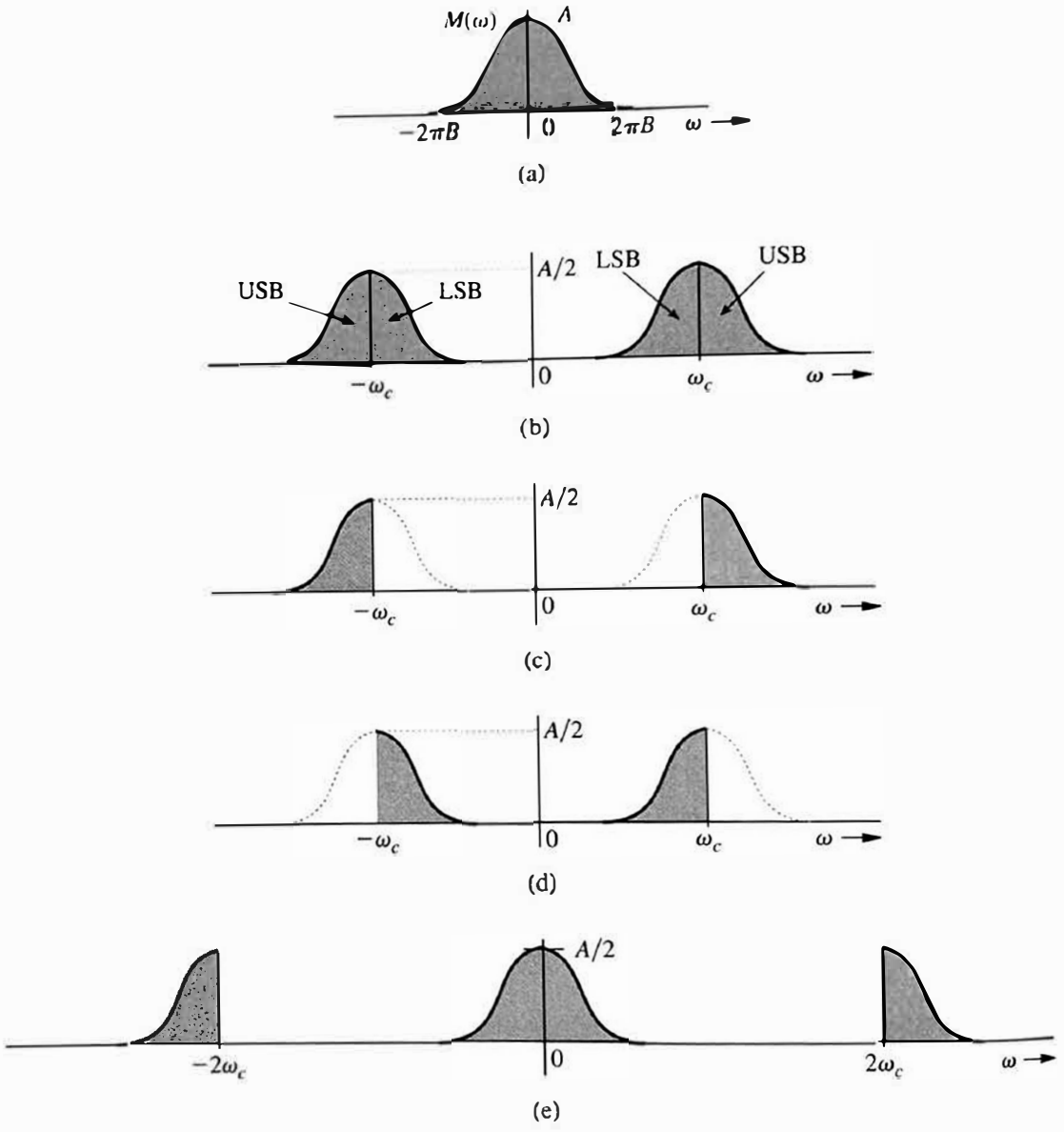

Figure 4.42 Spectra for single-sideband transmission: **(a)** baseband, **(b)** DSB, **(c)** USB, **(d)** LSB, and **(e)** synchronously demodulated signal.

the upper and the lower (USB and LSB), both containing complete information on $M(\omega)$ [see Eq. (4.12)]. Clearly, it is redundant to transmit both sidebands, a process that requires twice the bandwidth of the baseband signal. A scheme in which only one sideband is transmitted is known as *single-sideband* (SSB) *transmission,* which requires only half the bandwidth of the DSB signal. Thus, we transmit only the upper sidebands (Fig. 4.42c) or only the lower sidebands (Fig. 4.42d).

An SSB signal can be coherently (synchronously) demodulated. For example, multiplication of a USB signal (Fig. 4.42c) by $2\cos\omega_c t$ shifts its spectrum to the left and to the right by ω_c, yielding the spectrum in Fig. 4.42e. Lowpass filtering of this signal yields the desired baseband signal. The case is similar with an LSB signal. Hence, demodulation of SSB signals is identical to that of DSB-SC signals, and the synchronous demodulator in Fig. 4.38a can demodulate SSB signals. Note that we are talking of SSB signals without an additional carrier. Hence, they are suppressed-carrier signals (SSB-SC).

EXAMPLE 4.24 Single-Sideband Modulation

Find the USB (upper sideband) and LSB (lower sideband) signals when $m(t) = \cos\omega_m t$. Sketch their spectra, and show that these SSB signals can be demodulated using the synchronous demodulator in Fig. 4.38a.

The DSB-SC signal for this case is

$$\varphi_{\text{DSB-SC}}(t) = m(t)\cos\omega_c t = \cos\omega_m t\cos\omega_c t = \tfrac{1}{2}[\cos(\omega_c - \omega_m)t + \cos(\omega_c + \omega_m)t]$$

As pointed out in Ex. 4.21, the terms $(1/2)\cos(\omega_c + \omega_m)t$ and $(1/2)\cos(\omega_c - \omega_m)t$ represent the upper and lower sidebands, respectively. The spectra of the upper and lower sidebands are given in Figs. 4.43a and 4.43b. Observe that these spectra can be obtained from the DSB-SC spectrum in Fig. 4.37b by using a proper filter to suppress the undesired sidebands. For instance, the USB signal in Fig. 4.43a can be obtained by passing the DSB-SC signal (Fig. 4.37b) through a highpass filter of cutoff frequency ω_c. Similarly, the LSB signal in Fig. 4.43b can be obtained by passing the DSB-SC signal through a lowpass filter of cutoff frequency ω_c.

If we apply the LSB signal $(1/2)\cos(\omega_c - \omega_m)t$ to the synchronous demodulator in Fig. 4.38a, the multiplier output is

$$e(t) = \tfrac{1}{2}\cos(\omega_c - \omega_m)t\cos\omega_c t = \tfrac{1}{4}[\cos\omega_m t + \cos(2\omega_c - \omega_m)t]$$

The term $(1/4)\cos(2\omega_c - \omega_m)t$ is suppressed by the lowpass filter, producing the desired output $(1/4)\cos\omega_m t$ [which is $m(t)/4$]. The spectrum of this term is $\pi[\delta(\omega + \omega_m) + \delta(\omega - \omega_m)]/4$, as depicted in Fig. 4.43c. In the same way, we can show that the USB signal can be demodulated by the synchronous demodulator.

In the frequency domain, demodulation (multiplication by $\cos\omega_c t$) amounts to shifting the LSB spectrum (Fig. 4.43b) to the left and the right by ω_c (times 0.5) and then suppressing the high frequency, as illustrated in Fig. 4.43c. The resulting spectrum represents the desired signal $(1/4)m(t)$.

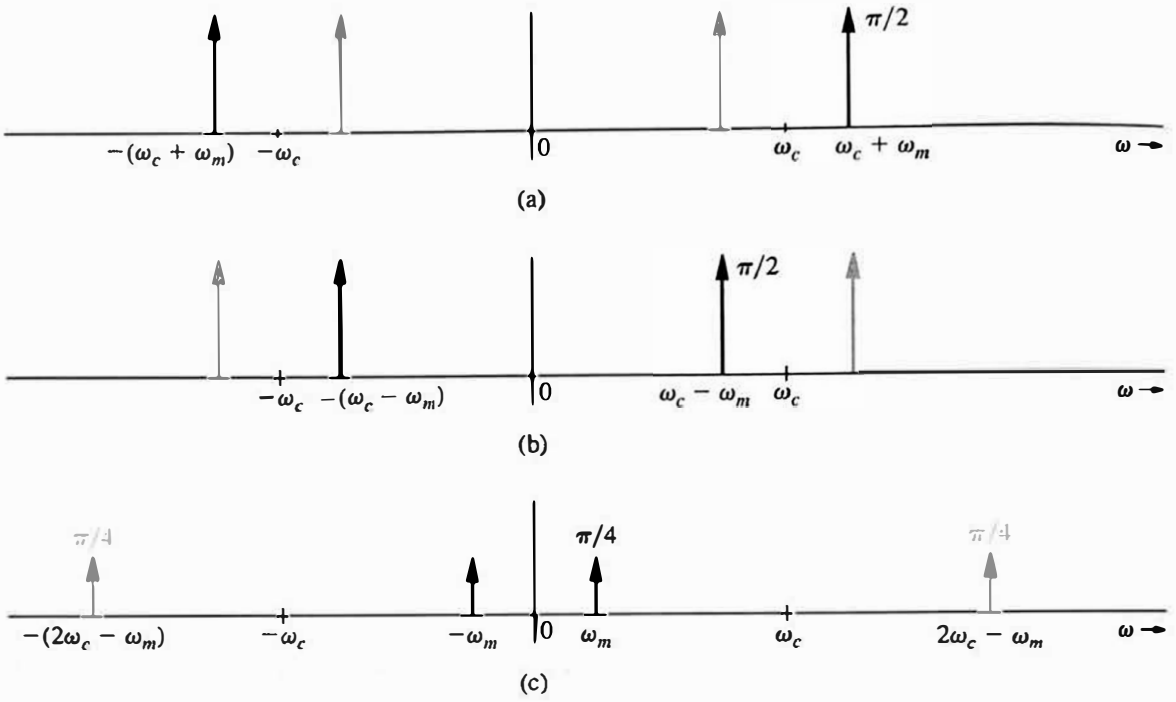

Figure 4.43 Single-sideband spectra for $m(t) = \cos \omega_m t$: **(a)** USB, **(b)** LSB, and **(c)** synchronously demodulated LSB signal.

Generation of SSB Signals

Two methods are commonly used to generate SSB signals. The *selective-filtering method* uses sharp cutoff filters to eliminate the undesired sideband, and the second method uses phase-shifting networks to achieve the same goal [4].† We shall consider here only the first method.

Selective filtering is the most commonly used method of generating SSB signals. In this method, a DSB-SC signal is passed through a sharp cutoff filter to eliminate the undesired sideband.

To obtain the USB, the filter should pass all components above ω_c unattenuated and completely suppress all components below ω_c. Such an operation requires an ideal filter, which is unrealizable. It can, however, be realized closely if there is some separation between the passband and the stopband. Fortunately, the voice signal provides this condition, because its spectrum shows little power content at the origin (Fig. 4.44). Moreover, articulation tests show that for speech signals, frequency components below 300 Hz are not important. In other words, we may suppress all speech components below 300 Hz without appreciably affecting intelligibility.‡ Thus, filtering of the unwanted sideband becomes relatively easy for speech signals because we have a 600 Hz transition region around the cutoff frequency ω_c. For some signals, which have considerable

† Yet another method, known as Weaver's method, is also used to generate SSB signals.

‡ Similarly, suppression of components of a speech signal above 3500 Hz causes no appreciable change in intelligibility.

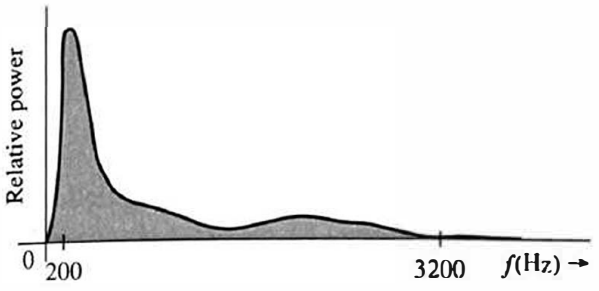

Figure 4.44 Voice spectrum.

power at low frequencies (around $\omega = 0$), SSB techniques cause considerable distortion. Such is the case with video signals. Consequently, for video signals, instead of SSB, we use another technique, the *vestigial sideband* (VSB), which is a compromise between SSB and DSB. It inherits the advantages of SSB and DSB but avoids their disadvantages at a cost of slightly increased bandwidth. VSB signals are relatively easy to generate, and their bandwidth is only slightly (typically 25%) greater than that of SSB signals. In VSB signals, instead of rejecting one sideband completely (as in SSB), we accept a gradual cutoff from one sideband [4].

4.8 ANGLE MODULATION

A sinusoid is characterized by its amplitude and angle (which includes its frequency and phase). In amplitude-modulated signals, the information content of the baseband (message) signal $m(t)$ appears in the amplitude variations of the carrier. In *angle modulation* discussed in this section, the information content of $m(t)$ is carried by the angle of the carrier. Angle modulation also goes by the name *exponential modulation*.

The generalized angle-modulated (or exponentially modulated) carrier can be described as

$$\varphi_{EM}(t) = A\cos[\omega_c t + k\psi(t)] \tag{4.53}$$

where k is an arbitrary constant and $\psi(t)$, which is a measure of $m(t)$, is obtained by an invertible linear operation on $m(t)$. In other words, $\psi(t)$ is the output of some linear system with a suitable transfer function $H(s)$ when the input is $m(t)$, as depicted in Fig. 4.45.†

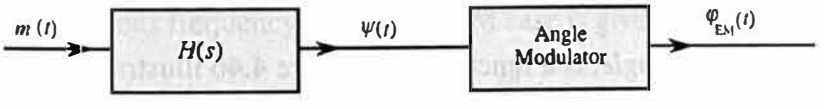

Figure 4.45 Generation of an angle-modulated signal.

† Because $H(s)$ is required to be invertible, we can obtain $m(t)$ by passing $\psi(t)$ through the inverse linear system, which has the transfer function $1/H(s)$.

If $h(t)$ is the unit impulse response of this system; that is, if $h(t) \Longleftrightarrow H(s)$, then

$$\psi(t) = \int_{-\infty}^{t} m(\alpha)h(t-\alpha)\,d\alpha \tag{4.54}$$

By selecting suitable $h(t)$, we can obtain a variety of subclasses of angle modulation. For instance, if we select $h(t) = u(t)$, the resulting form is the well-known case of *frequency modulation* (FM). In contrast, use of $h(t) = \delta(t)$ leads to *phase modulation* (PM). These are but two of the infinite possibilities. Although in digital communication the use of phase and frequency modulation is common, so-called broadcast FM is not FM in the classical sense, but is a generalized angle modulation because of the inclusion of a *preemphasis* filter used to improve its noise-suppressing abilities. It is called FM for the historical reason that angle modulation was first conceived and introduced in the form of frequency modulation. Broadcast FM, although originating as true FM during laboratory development, was modified in broadcasting for better performance. Yet, the term FM continues to be used to describe this scheme.

In amplitude modulation, the carrier frequency is constant, but the amplitude changes with $m(t)$. In contrast, in angle modulation, the carrier amplitude is always constant, but the carrier frequency varies continuously with the message $m(t)$. By definition, a sinusoidal signal is expected to have a constant frequency; hence, the variation of frequency with time appears to be contradictory to the conventional definition of a sinusoidal signal frequency. Therefore, we must generalize the notion of a sinusoid so as to make allowance for variation of frequency with time. This generalization leads us to a new concept of *instantaneous frequency*.

4.8.1 The Concept of Instantaneous Frequency

As just discussed, the carrier frequency is changing continuously every instant in FM. Prima facie, this does not make much sense because to define a frequency, we must have a sinusoidal signal at least over one cycle with the same frequency. We cannot imagine a sinusoid whose frequency is different at every instant. This problem is reminiscent of a first encounter with the concept of *instantaneous velocity* in a beginning mechanics course. Until that time, it is natural to think of velocity as being constant over a time interval and to resist imagining that velocity can vary at each instant. But after some mental struggle, the idea gradually sinks in. It is difficult to forget, however, the wonder and amazement that were caused by the idea when it was first introduced. A similar experience awaits the reader with the concept of instantaneous frequency.

Let us consider a generalized sinusoidal signal $\varphi(t)$ given by

$$\varphi(t) = A\cos\theta(t) \tag{4.55}$$

where $\theta(t)$, the *generalized angle*, is a function of t. Figure 4.46 illustrates a hypothetical case of $\theta(t)$. The generalized angle for a conventional sinusoid $A\cos(\omega_c t + \phi_0)$ is $\omega_c t + \phi_0$. This plot, a straight line with a slope ω_c and intercept ϕ_0, is also illustrated in Fig. 4.46. The plot shows a hypothetical case of $\theta(t)$ that happens to be tangential to the angle $(\omega_c t + \phi_0)$ at some instant t. The crucial point is that over a small interval $\Delta t \to 0$, the signal $\varphi(t) = A\cos\theta(t)$ and the sinusoid $A\cos(\omega_c t + \phi_0)$ are identical; that is,

$$\varphi(t) = A\cos(\omega_c t + \phi_0) \qquad t_1 < t < t_2$$

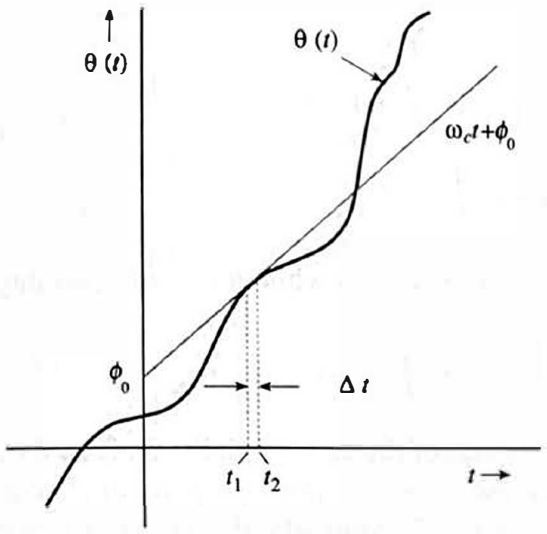

Figure 4.46 The concept of instantaneous frequency.

We are certainly justified in saying that over this small interval Δt, the frequency of $\varphi(t)$ is ω_c. Because $(\omega_c t + \phi_0)$ is tangential to $\theta(t)$, the frequency of $\varphi(t)$ is the slope of its angle $\theta(t)$ over this small interval. We can generalize this concept at every instant and say that the instantaneous frequency ω_i at any instant t is the slope of $\theta(t)$ at t. Thus, for $\varphi(t)$ in Eq. (4.55), instantaneous frequency $\omega_i(t)$ and generalized angle $\theta(t)$ are related according to

$$\omega_i(t) = \frac{d\theta}{dt} \qquad \text{and} \qquad \theta(t)4 = \int_{-\infty}^{t} \omega_i(\alpha)\, d\alpha \tag{4.56}$$

For a conventional sinusoid $A\cos(\omega_c t + \phi_0)$, we have $\theta(t) = \omega_c t + \phi_0$, and $\omega_i(t) = d\theta(t)/dt = \omega_c$, a constant, as desired. Clearly, the generalized definition of instantaneous frequency does not conflict with our old notion of frequency.

Now we can see the possibility of transmitting the information of $m(t)$ by varying the angle θ of a carrier. Two simple possibilities are *phase modulation* (PM) and *frequency modulation* (FM). In PM, the angle $\theta(t)$ varies linearly with $m(t)$ as

$$\theta(t) = \omega_c t + k_p m(t)$$

where k_p is a constant and ω_c is the carrier frequency. The resulting PM wave is

$$\varphi_{PM}(t) = A\cos[\omega_c t + k_p m(t)] \tag{4.57}$$

The instantaneous frequency $\omega_i(t)$ in the PM case is given by

$$\omega_i(t) = \frac{d\theta}{dt} = \omega_c + k_p \dot{m}(t) \tag{4.58}$$

Hence in phase modulation, the instantaneous frequency ω_i varies linearly with the derivative of the modulating signal. If the instantaneous frequency ω_i is varied linearly with the modulating signal, we have frequency modulation. Thus, in FM, the instantaneous frequency ω_i is

$$\omega_i(t) = \omega_c + k_f m(t) \tag{4.59}$$

where k_f is a constant. From Eq. (4.56), we find the angle $\theta(t)$ as

$$\theta(t) = \int_{-\infty}^{t} [\omega_c + k_f m(\alpha)]\, d\alpha$$
$$= \omega_c t + k_f \int_{-\infty}^{t} m(\alpha)\, d\alpha$$

Here, we have assumed the constant term in $\theta(t)$ to be zero without loss of generality. Thus, the FM wave is

$$\varphi_{\text{FM}}(t) = A\cos\left[\omega_c t + k_f \int_{-\infty}^{t} m(\alpha)\, d\alpha\right] \tag{4.60}$$

Observe that both PM and FM are special cases of the exponentially modulated signal $\varphi_{\text{EM}}(t)$ in Eq. (4.53). If $h(t) = \delta(t)$ in Eq. (4.54), then use of the sampling property of the impulse yields $\psi(t) = m(t)$, and Eq. (4.53) reduces to PM in Eq. (4.57). Similarly, if $h(t) = u(t)$, then the fact that $u(t-\alpha) = 1$ over $-\infty < \alpha \leq t$ yields $\int m(\alpha)h(t-\alpha)\, d\alpha = \int m(\alpha)\, d\alpha$, and Eq. (4.53) reduces to FM in Eq. (4.60).

ALL IN THE FAMILY

Equations (4.57) and (4.60) indicate that PM and FM are not only very similar but are also inseparable. Replacing $m(t)$ in Eq. (4.57) with $\int^t m(\alpha)\, d\alpha$ changes PM into FM. Thus, a signal that is an FM wave corresponding to $m(t)$ is also the PM wave corresponding to $\int^t m(\alpha)\, d\alpha$ (Fig. 4.47a). Similarly, a PM wave corresponding to $m(t)$ is the FM wave corresponding to $\dot{m}(t)$ (Fig. 4.47b).

We conclude that just by looking at an angle-modulated carrier, we cannot tell whether it is FM or PM. In fact, it is meaningless to inquire if a certain angle-modulated wave is FM or PM. An analogous situation would be to ask a person (who is married, with children) whether he is a father or a son. The person would be puzzled because he is both, a father (of his child) and a son (of his father).

We have seen that PM and FM are not different kinds of modulation, but two special cases of generalized angle modulation. Such a view is very fruitful because it shows the convertibility of

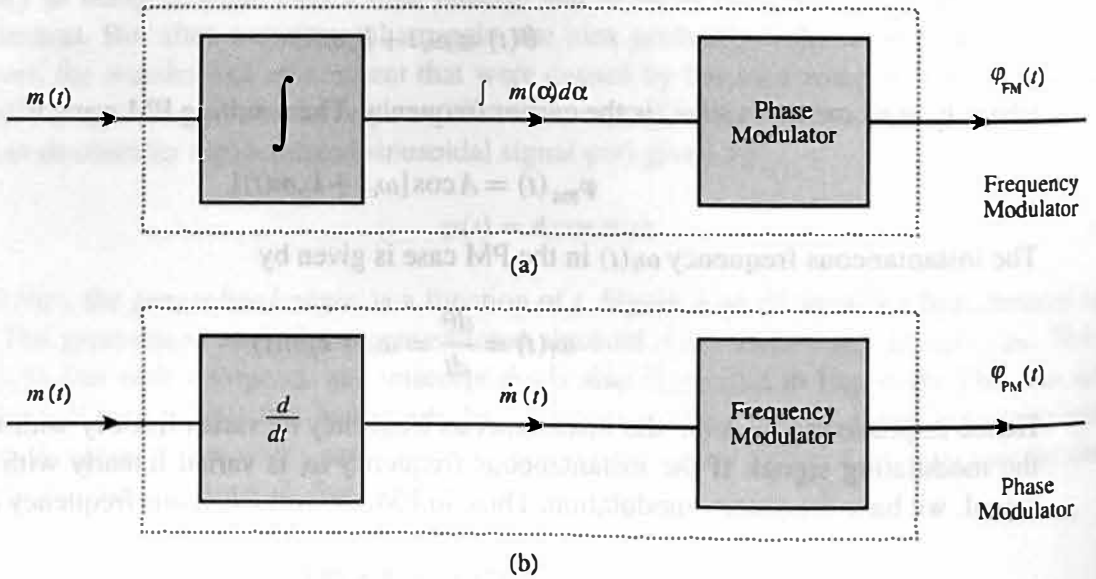

Figure 4.47 The concept of instantaneous frequency.

one type of angle modulation (such as PM) to another (such as FM). This convertibility is quite clear in Fig. 4.47. For instance, we show later that the bandwidth of FM is approximately $2k_f m_p$, where m_p is the peak amplitude of $m(t)$. We can derive the equivalent result for PM by referring to Fig. 4.47b, which shows that PM is actually FM when the modulating signal is $\dot{m}(t)$. Clearly, the bandwidth of PM is approximately $2k_p m_p'$, where m_p' is the peak amplitude of $\dot{m}(t)$. This argument shows that if we analyze one type of angle modulation (such as FM), we could readily extend those results to any other kind. Historically, the concept of angle modulation began with FM. Hence, it is customary to analyze FM and then modify those results for other forms, such as PM. But this does not imply that FM is superior to other kinds of angle modulation. On the contrary, PM is superior to FM for most analog signals such as audio and video. Actually, the optimum performance is realized neither by PM nor FM, but by some other form, depending on the nature of the baseband (message) signal.

This discussion also shows that we need not discuss methods of generation and demodulation of each type of modulation. Figure 4.47 clearly indicates that PM can be generated by an FM generator, and FM can be generated by a PM generator. One of the methods of generating FM in practice (the Armstrong indirect-FM system) actually integrates $m(t)$ and uses it to phase-modulate a carrier. Similar remarks apply to demodulation of FM and PM.

EXAMPLE 4.25 FM and PM for a Triangular Message Signal

Sketch FM and PM waves for the modulating signal $m(t)$ depicted in Fig. 4.48a. The constants k_f and k_p are $2\pi(10^5)$ and 10π, respectively, and the carrier frequency f_c is 100 MHz.

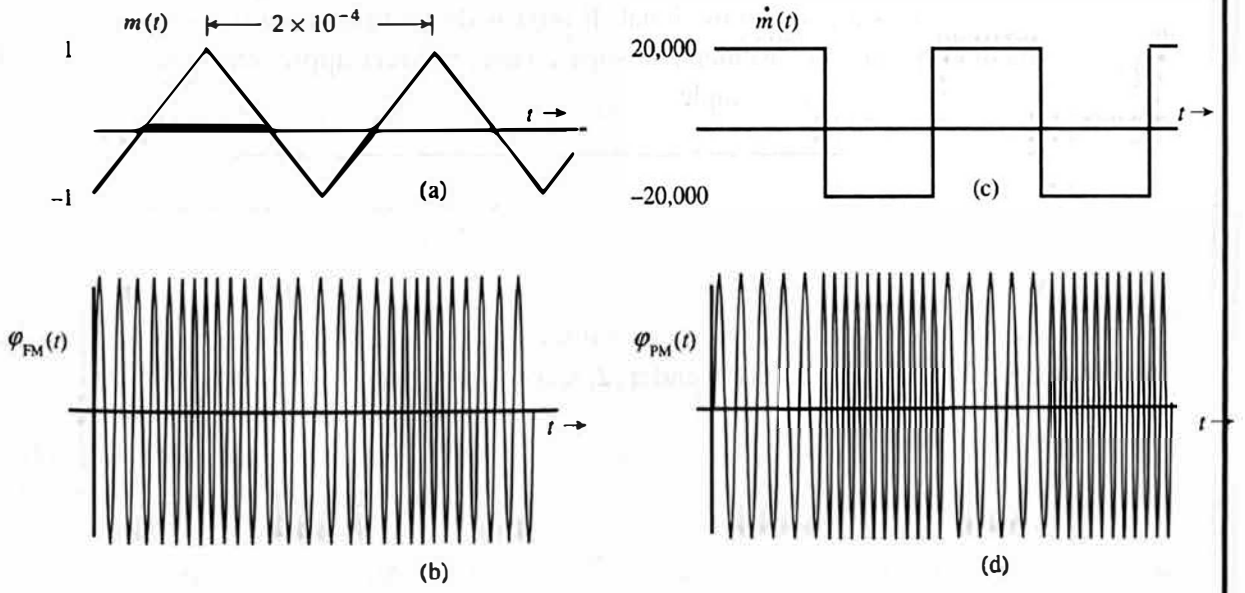

Figure 4.48 FM and PM waveforms for a triangular message signal.

FM Case

According to Eq. (4.59), the instantaneous frequency for FM is $\omega_i = \omega_c + k_f m(t)$. Dividing throughout by 2π, we obtain the equation in terms of Hertzian frequency f. The instantaneous frequency f_i is

$$f_i = f_c + \frac{k_f}{2\pi} m(t) = 10^8 + 10^5 m(t)$$

Further,

$$(f_i)_{\min} = 10^8 - 10^5 \left|[m(t)]_{\min}\right| = 99.9 \text{ MHz}$$

and

$$(f_i)_{\max} = 10^8 + 10^5 [m(t)]_{\max} = 100.1 \text{ MHz}$$

Because $m(t)$ increases and decreases linearly with time, the instantaneous frequency increases linearly from 99.9 to 100.1 MHz over a half-cycle and decreases linearly from 100.1 to 99.9 MHz over the remaining half-cycle of the modulating signal (Fig. 4.48b).

PM Case

PM for $m(t)$ is FM for $\dot{m}(t)$. This assertion also follows from Eq. (4.58) or Fig. 4.47b. In the PM case,

$$f_i = f_c + \frac{k_p}{2\pi} \dot{m}(t) = 10^8 + 5\,\dot{m}(t)$$

$$(f_i)_{\min} = 10^8 - 5\left|[\dot{m}(t)]_{\min}\right| = 10^8 - 10^5 = 99.9 \text{ MHz}$$

$$(f_i)_{\max} = 10^8 + 5[\dot{m}(t)]_{\max} = 100.1 \text{ MHz}$$

Because $\dot{m}(t)$ switches back and forth from a value of $-20{,}000$ to $20{,}000$, the carrier frequency switches back and forth from 99.9 to 100.1 MHz every half-cycle of $\dot{m}(t)$, as illustrated in Fig. 4.48d.

This indirect method of sketching PM (using $\dot{m}(t)$ to frequency-modulate a carrier) works as long as $m(t)$ is a continuous signal. If $m(t)$ is discontinuous, $\dot{m}(t)$ contains impulses, and this method is not so convenient. In such a case, a direct approach should be used. This is demonstrated in the next example.

EXAMPLE 4.26 FM and PM for a Square Message Signal

Sketch FM and PM waves for the digital modulating signal $m(t)$ depicted in Fig. 4.49a. The constants k_f and k_p are $2\pi(10^5)$ and $\pi/2$, respectively, and $f_c = 100$ MHz.

FM Case

For FM,

$$f_i = f_c + \frac{k_f}{2\pi} m(t) = 10^8 + 10^5 m(t)$$

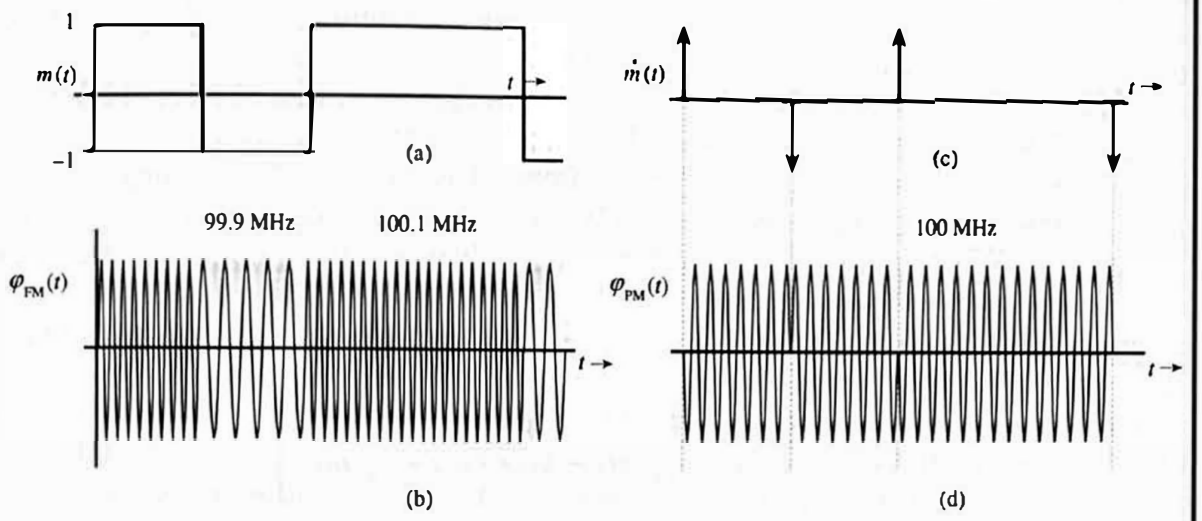

Figure 4.49 FM and PM waveforms for a square message signal.

Because $m(t)$ switches back and forth from 1 to -1 and vice versa, the FM wave frequency switches back and forth from 99.9 MHz to 100.1 MHz and vice versa, as shown in Fig. 4.49b. This scheme of carrier frequency modulation by a digital signal is known as *frequency-shift keying* (FSK), because the information digits are transmitted by shifting the carrier frequency.

PM Case

For PM,

$$f_i = f_c + \frac{k_f}{2\pi}\dot{m}(t) = 10^8 + \frac{1}{4}\dot{m}(t)$$

The derivative $\dot{m}(t) = 0$ everywhere except for impulses of strength ± 2 at the points of discontinuities of $m(t)$ (Fig. 4.49c). This fact means that the carrier frequency is $f_c = 100$ MHz everywhere except at the points of discontinuities, where it changes momentarily by an infinite amount. It is not immediately apparent how an instantaneous frequency can be changed by an infinite amount and then changed back to the original frequency in zero time. Let us consider the direct approach.

$$\begin{aligned}\varphi_{PM}(t) &= A\cos[\omega_c t + k_p m(t)] \\ &= A\cos\left[\omega_c t + \frac{\pi}{2}m(t)\right] \\ &= \begin{cases} A\sin\omega_c t & \text{when } m(t) = -1 \\ -A\sin\omega_c t & \text{when } m(t) = 1 \end{cases}\end{aligned}$$

This PM wave, illustrated in Fig. 4.49d, has the same frequency $f_c = 100$ MHz everywhere. However, there are phase discontinuities of π radians at the instants where impulses of $\dot{m}(t)$ are located. At these instants, the carrier phase shifts by π instantaneously. A finite phase shift in zero time implies infinite instantaneous frequency ($d\theta/dt = \infty$) at these instants. This conclusion agrees with our observation about $\dot{m}(t)$.

This scheme of carrier phase modulation by a digital signal is called *phase-shifting keying* (PSK), because information digits are transmitted by shifting the carrier phase. Note that PSK may also be viewed as a DSB-SC modulation by $m(t)$.

The amount of phase discontinuity in $\varphi_{PM}(t)$ at the instant where $m(t)$ is discontinuous is $k_p m_d$, where m_d is the amount of discontinuity in $m(t)$ at that instant. In the present example, the amplitude of $m(t)$ changes by 2 (from -1 to 1) at the discontinuity. Hence, the phase discontinuity in $\varphi_{PM}(t)$ is $k_p m_d = \frac{\pi}{2}(2) = \pi$ radians, which confirms our earlier result.

When $m(t)$ is a digital signal (as in Fig. 4.49a), $\varphi_{PM}(t)$ shows a phase discontinuity where $m(t)$ has a jump discontinuity. In such a case, the phase deviation $k_p m(t)$ must be restricted to a range $(-\pi, \pi)$ in order to avoid ambiguity in demodulation. For example, if k_p were $3\pi/2$ in the present example, then

$$\varphi_{PM}(t) = A\cos\left[\omega_c t + \frac{3\pi}{2}m(t)\right]$$

In this case, $\varphi_{PM}(t) = A\sin\omega_c t$ when $m(t) = 1$ or $-1/3$. This will certainly cause ambiguity at the receiver when $A\sin\omega_c t$ is received. Such ambiguity never arises if $k_p m(t)$ is restricted to the range $(-\pi, \pi)$.

The ambiguity arises only when $m(t)$ has jump discontinuities. In such a case, the phase of $\varphi_{PM}(t)$ changes instantaneously. Because a phase $\varphi_0 + 2n\pi$ is indistinguishable from the phase φ_0, ambiguities will be inherent in the demodulator unless the phase variations are limited to the range $(-\pi, \pi)$. For this reason, k_p should be small enough to restrict the phase change $k_p m(t)$ to the range $(-\pi, \pi)$.

No such restriction on k_p is required if $m(t)$ is continuous. In this case, the phase change is not instantaneous, but gradual over a time, and a phase $\varphi_0 + 2n\pi$ will exhibit n additional carrier cycles over the case of phase of only φ_0. This conclusion can also be verified from Ex. 4.25, where the maximum phase change $\Delta\varphi = 10\pi$.

Because a bandlimited signal cannot have jump discontinuities, we can say that when $m(t)$ is bandlimited, k_p has no restrictions.

4.8.2 Bandwidth of Angle-Modulated Signals

Unlike amplitude modulation, there is no simple relationship between the baseband signal waveform and the corresponding angle-modulated waveform. The same is true of their spectra. Because of the nonlinear nature of angle modulation, derivation of $\Phi_{EM}(\omega)$, the frequency spectrum of the modulated signal, is extremely complicated and can be obtained only for few special cases. Generally, the bandwidth of an angle-modulated signal is infinite even when the baseband signal bandwidth is finite. However, most of the signal power (or energy) resides in a finite band. We shall now try to estimate this essential bandwidth of an angle-modulated signal.

Let us start with the angle-modulated signal in Eq. (4.53), and consider first the case of small k ($k \to 0$).

$$\begin{aligned}\varphi_{EM}(t) &= A\cos[\omega_c t + k\psi(t)] \\ &= A\cos\omega_c t\cos[k\psi(t)] - A\sin\omega_c t\sin[k\psi(t)] \\ &\approx A\cos\omega_c t - Ak\psi(t)\sin\omega_c t \qquad k \to 0\end{aligned} \tag{4.61}$$

Comparison of the right-hand-side expression with $\varphi_{AM}(t)$ in Eq. (4.50) shows that the two expressions are very similar. The first term is the carrier, and the second term, representing the sidebands, has the same form as the DSB-SC signal corresponding to the baseband signal $Ak\psi(t)$. The only difference is that the carrier is sine instead of cosine. This is just a matter of a carrier phase difference of $\pi/2$. Hence, the bandwidth of the angle-modulated signal is the same as that of the AM signal corresponding to the baseband signal $\psi(t)$. If $m(t)$ is bandlimited to B Hz, then the bandwidth of $\psi(t)$ is also B Hz.† Hence, the bandwidth of $\varphi_{EM}(t)$ is $2B$ Hz, the same as that of AM. But this is true only when $k \to 0$. Let us now consider the general case.

In angle modulation, the carrier frequency is varied from its quiescent value ω_c. Let the maximum deviation of the carrier frequency be $\Delta\omega$. In other words, the carrier frequency varies in the range from $\omega_c - \Delta\omega$ to $\omega_c + \Delta\omega$. Because the carrier frequency always remains in this band of width $2\Delta\omega$ radians/s, could we say that the resulting spectrum also remains within this band and the bandwidth of the angle-modulated signal is $2\Delta\omega$? This assertion implies that if a sinusoid takes an instantaneous frequency ω_x, then the resulting spectrum is concentrated only at ω_x. This is true only if the carrier has infinite duration. For a finite duration sinusoid of frequency ω_x, the spectrum is not concentrated at ω_x, but spreads out on both sides of ω_x, as can be seen from Fig. 4.26d in Ex. 4.15. In a typical angle-modulated signal, the carrier frequency is directly proportional to $m(t)$, which changes with t. Hence, the instantaneous frequency will also change with t continuously. Such a continuous shift in frequency will cause spectral spread beyond the band $2\Delta\omega$. Clearly, the bandwidth of the angle-modulated signal is somewhat larger than $2\Delta\omega$ rads/s. How much larger? This missing link can be found by looking at the results derived earlier for the case of $k \to 0$. Let us first determine $\Delta\omega$.

From Eq. (4.53), it follows that

$$\omega_i(t) = \omega_c + k\dot{\psi}(t)$$

If the peak amplitude of $\dot{\psi}(t)$ is denoted by ψ_p', then the carrier frequency varies in the range from $\omega_c - k\psi_p'$ to $\omega_c + k\psi_p'$.‡ Therefore,

$$\Delta\omega = k\psi_p'$$

The carrier frequency deviation Δf in Hz is

$$\Delta f = \frac{\Delta\omega}{2\pi} = \frac{k}{2\pi}\psi_p'$$

As demonstrated earlier, because of spectral spreading, the angle-modulated signal bandwidth is somewhat larger than $2\Delta f$. Let the actual Hertzian bandwidth B_{EM} be

$$\begin{aligned} B_{EM} &= 2\Delta f + X \\ &= \frac{k}{\pi}\psi_p' + X \end{aligned} \tag{4.62}$$

† Because $\psi(t)$ is the output of a linear system when the input is $m(t)$, the bandwidth of $\psi(t)$ cannot be greater than B Hz. Moreover, the filter is invertible. Hence, the filter bandwidth cannot be less than B Hz, or some of the components of $m(t)$ will be lost. So, the bandwidth of $\psi(t)$ cannot be less than B Hz. Hence, it is exactly equal to B Hz.

‡ This assertion implies an assumption $\max(\dot{\psi}(t)) = |\min(\dot{\psi}(t))|$.

where X is unknown. To determine X, recall that for the case $k \to 0$, we found the bandwidth to be $2B$. But as Eq. (4.62) indicates, this bandwidth is X when $k \to 0$. Therefore, $X = 2B$, and

$$B_{EM} = 2(\Delta f + B) \text{ Hz}$$

A more rigorous derivation of this result appears in [4]. Note that when $k \to 0$, $\Delta f \to 0$ and $\Delta f \ll B$. On the other hand when k is very large, $\Delta f \gg B$. The former case is known as *narrowband* angle modulation and the latter is known as *wideband* angle modulation.

Recall that for FM, $\dot{\psi}(t) = m(t)$, and $\psi_p' = m_p$, where m_p is the peak amplitude of $m(t)$. Similarly, for PM, $\psi(t) = m(t)$. Hence, $\psi_p' = m_p'$, where m_p' is the peak amplitude of $\dot{m}(t)$. Thus,

$$(\Delta f)_{FM} = \frac{k_f}{\pi} m_p \qquad \text{and} \qquad (\Delta f)_{PM} = \frac{k_p}{\pi} m_p'$$

We observe an interesting fact in angle modulation. The bandwidth of the modulated signal is adjustable by choosing a suitable value of Δf or the constant k (k_f in FM or k_p in PM). Amplitude modulation lacks this feature. The bandwidth of each AM scheme is fixed. It is a general principle in communication theory that widening a signal bandwidth makes the signal more immune to noise during transmission. Thus, widening the transmission bandwidth makes angle-modulated signals more immune to noise. Moreover, this very property allows us to reduce the signal power required to achieve the same quality of transmission. Thus, angle modulation allows us to exchange signal power for bandwidth.

Also, because of its constant amplitude, angle modulation has a major advantage over amplitude modulation. This feature makes angle modulation less susceptible to nonlinear distortion. We shall see in the following section (Sec. 4.8.3) that no distortion results when we pass an angle-modulated signal through a nonlinear device whose output $y(t)$ and the input $x(t)$ are related by $y(t) = x^2(t)$ [in general, $y(t) = \sum a_n x^n(t)$]. Such a nonlinearity can be disastrous in amplitude-modulated systems. This is the primary reason why angle modulation is used in microwave relay systems, where nonlinear operation of amplifiers and other devices has thus far been unavoidable at the required high power levels. In addition, the constant amplitude of FM gives it a kind of immunity against rapid fading. The effect of amplitude variations caused by rapid fading can be eliminated by using automatic gain control and bandpass limiting. Angle modulation is also less vulnerable than amplitude modulation to small interference from adjacent channels. But the price for all these advantages is paid in terms of increased bandwidth. For the same bandwidth, we can demonstrate that pulse-code modulation (PCM), discussed in Ch. 5, is superior to angle modulation [4].

4.8.3 Generation and Demodulation of Angle-Modulated Signals

In Eq. (4.61), we see that a narrowband angle- (or exponential) modulated signal (NBEM) consists of a carrier term and a DSB-SC term whose carrier has a $\pi/2$ phase shift. Hence, we can readily generate this signal using the procedure discussed in Sec. 4.7. Wideband modulation (WBEM) can be obtained from NBEM by passing the NBEM signal through a nonlinear device. Consider, for example, a nonlinear device whose input $x(t)$ and output $y(t)$ are related by $y(t) = x^2(t)$. If the

input is an angle-modulated signal $\cos[\omega_c t + k\psi(t)]$, then the output $y(t)$ is given by

$$y(t) = \cos^2[\omega_c t + k\psi(t)] = \frac{1}{2} + \frac{1}{2}\cos[2\omega_c t + 2k\psi(t)]$$

If we pass this signal through a bandpass filter centered at $2\omega_c$, the output is

$$z(t) = \frac{1}{2}\cos[2\omega_c t + 2k\psi(t)]$$

Observe that the second order of nonlinearity has doubled the carrier frequency as well as the effective value of k without causing any distortion. In a similar way, we can show that an nth-order of nonlinearity increases n-fold the carrier frequency as well as the effective value of k. This fact allows us to convert an NBEM signal into a WBEM signal. This is the indirect method of generating an angle-modulated signal.

We can also generate an angle-modulated signal by a direct method, which uses a *voltage-controlled oscillator* (VCO). The output of a VCO is a constant amplitude sinusoid, whose instantaneous frequency is directly proportional to an input voltage $m(t)$. Clearly, a VCO is an FM generator. As demonstrated earlier, an FM generator, with minor modification, can be used to generate any other form of angle modulation.

Demodulation

We shall discuss here demodulation of FM waves. As explained earlier, an FM demodulator, with some minor modification, can be used for demodulation of any other form of angle modulation. Because the instantaneous frequency of an FM wave is proportional to the baseband signal $m(t)$, an FM demodulator is a device whose output is proportional to the frequency of the input signal. Thus, the gain $H(\omega)$ of an ideal FM demodulator is of the form $c_1\omega + c_2$. An ideal differentiator has this property. If the input to an ideal differentiator is an angle-modulated signal $x(t) = \cos[\omega_c t + k\psi(t)]$, then the output $y(t)$ is given by

$$\begin{aligned} y(t) = \frac{dx(t)}{dt} &= -[\omega_c + k\dot{\psi}(t)]\sin[\omega_c t + k\psi(t)] \\ &= [\omega_c + k\dot{\psi}(t)]\sin[\omega_c t + k\psi(t) + \pi] \end{aligned}$$

The output is also an angle-modulated signal, whose envelope is $\omega_c + k\dot{\psi}(t)$. Hence, an ideal differentiator followed by an envelope detector will result in the output $\omega_c + k\dot{\psi}(t)$. After blocking the dc, we obtain the desired output $k\dot{\psi}(t)$. Recall that for FM, $\psi(t) = \int^t m(\alpha)d\alpha$. Hence, $\dot{\psi}(t) = m(t)$. Another device that can be used as an FM demodulator is a tuned circuit, whose resonant frequency is selected either above or below the carrier frequency of the FM signal to be demodulated. The frequency response of a tuned circuit (below the resonant frequency) is approximately linear with the input frequency (at least over a small band). This method suffers from the fact that the slope of $H(\omega)$ of a tuned circuit is linear only over a small band, and therefore causes considerable distortion in the output. This fault can partially be corrected by a balanced discriminator that uses two resonant circuits, one tuned above and the other tuned below ω_c.

These days, a *phase-locked loop* (PLL), whose performance is superior to any of the methods discussed here (especially in the large noise environment), has become very popular as

a demodulator of angle-modulated signals because of its reasonable cost. More discussion about modulation and demodulation of angle-modulated signals appears in [4].

A Historical Note

In the 1920s, broadcasting was in its infancy. However, there was a constant search for techniques that would reduce noise (static). Since noise power is proportional to the modulated signal bandwidth (sidebands), attempts focused on finding a modulation scheme to reduce the bandwidth. It was rumored that a new method had been discovered for eliminating sidebands (no sidebands, no bandwidth!). The concept of FM, where the carrier frequency would be varied in proportion to the message $m(t)$, appeared quite intriguing. The carrier frequency $\omega(t)$ would be varied with time so that $\omega(t) = \omega_c + km(t)$, where k was an arbitrary constant. The carrier frequency would remain within the band from $\omega_c - km_p$ to $\omega_c + km_p$. The spectrum, centered at ω_c, would have a bandwidth $2km_p$, which was controlled by the arbitrary constant k. By using an arbitrarily small k, we could make the information bandwidth arbitrarily small. This was a passport to communication heaven. Unfortunately, the experimental results showed that something was seriously wrong somewhere. The FM bandwidth was found to be always greater than (at best equal to) the AM bandwidth. In some cases, its bandwidth was several times that of AM.

Careful analysis by Carson showed that the FM bandwidth could never be smaller than that of AM; at best, it was equal to that of AM. Unfortunately, Carson did not recognize the compensating advantage of FM in its ability to suppress noise. Without any justification, he stated, "Thus, FM introduces inherent distortion and has no compensating advantages whatsoever" [5]. In a later paper, he asserted, "In fact, as more and more schemes are analyzed and tested, and as the essential nature of the problem is clearly perceivable, we are unavoidably forced to the conclusion that static, like the poor, will always be with us" [6]. This opinion rendered by one of the ablest mathematicians of the day in the *communications* industry set back the development of FM. The noise-suppressing advantage of FM was later proved by Major Edwin H. Armstrong [7], a brilliant engineer whose contributions to the field of radio systems are comparable to those of Hertz and Marconi. It was largely the work of Armstrong that rekindled interest in FM. Lamentably, Armstrong, who became despondent over lengthy, acrimonious, and expensive court battles with some titans of the *communications* industry over his patent rights, committed suicide in 1954 by walking out of a window 13 stories above the street.

4.8.4 Frequency-Division Multiplexing

Signal multiplexing allows transmission of several signals on the same channel. Later, in Ch. 5 (Sec. 5.2.2), we shall discuss time-division multiplexing (TDM), where several signals time-share the same channel, such as a cable or an optical fiber. In frequency-division multiplexing (FDM), the use of modulation, as illustrated in Fig. 4.50, makes several signals share the band of the same channel. Each signal is modulated by a different carrier frequency. The various carriers are adequately separated to avoid overlap (or interference) between the spectra of various modulated signals. These carriers are referred to as *subcarriers*. Each signal may use a different kind of modulation, for example, DSB-SC, AM, SSB-SC, VSB-SC, or even other forms of modulation, not discussed here [such as FM (frequency modulation) or PM (phase modulation)]. The modulated-signal spectra may be separated by a small guard band to avoid interference and to facilitate signal separation at the receiver.

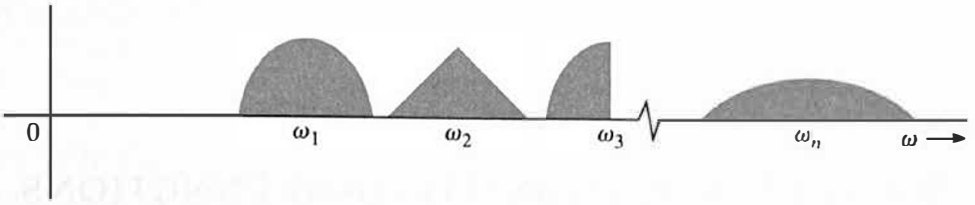

(a)

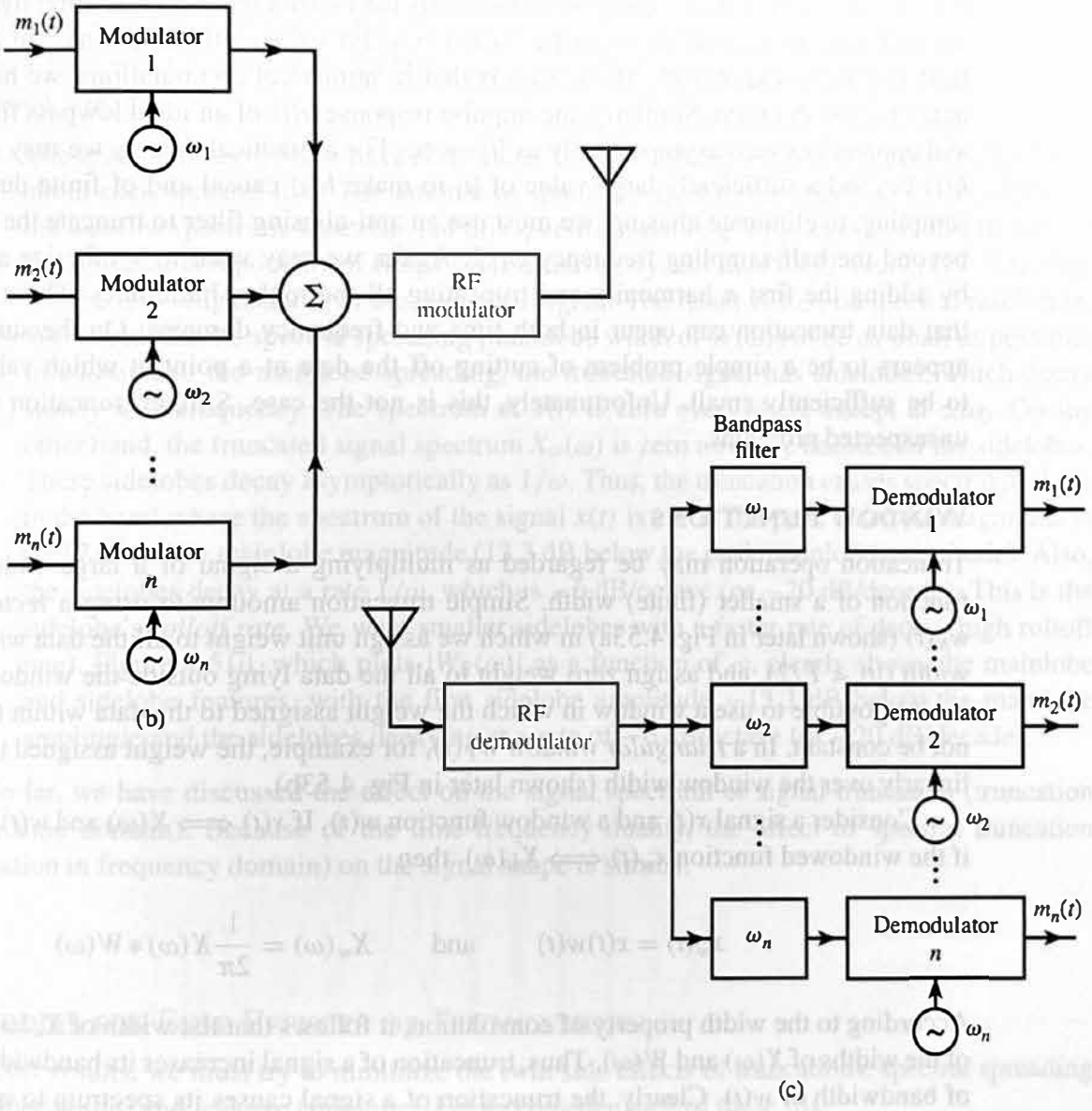

(b) (c)

Figure 4.50 Frequency-division multiplexing: **(a)** FDM spectrum **(b)** transmitter, and **(c)** receiver.

When all the modulated spectra are added, we have a composite signal that may be considered to be a new baseband signal. Sometimes, this composite baseband signal may be used to further modulate a high-frequency (radio frequency, or RF) carrier for the purpose of transmission.

At the receiver, the incoming signal is first demodulated by the RF carrier to retrieve the composite baseband, which is then bandpass-filtered to separate the modulated signals. Then each

modulated signal is individually demodulated by an appropriate subcarrier to obtain all the basic baseband signals.

4.9 DATA TRUNCATION: WINDOW FUNCTIONS

We often need to truncate data in diverse situations from numerical computations to filter design. For example, if we need to compute numerically the Fourier transform of some signal, say, $e^{-t}u(t)$, we will have to truncate the signal $e^{-t}u(t)$ beyond a sufficiently large value of t (typically, five time constants and above). The reason is that in numerical computations, we have to deal with data of finite duration. Similarly, the impulse response $h(t)$ of an ideal lowpass filter is noncausal and approaches zero asymptotically as $|t| \to \infty$. For a practical design, we may want to truncate $h(t)$ beyond a sufficiently large value of $|t|$ to make $h(t)$ causal and of finite duration. In signal sampling, to eliminate aliasing, we must use an anti-aliasing filter to truncate the signal spectrum beyond the half-sampling frequency $\omega_s/2$. Again, we may want to synthesize a periodic signal by adding the first n harmonics and truncating all the higher harmonics. These examples show that data truncation can occur in both time and frequency domains. On the surface, truncation appears to be a simple problem of cutting off the data at a point at which values are deemed to be sufficiently small. Unfortunately, this is not the case. Simple truncation can cause some unsuspected problems.

WINDOW FUNCTIONS

Truncation operation may be regarded as multiplying a signal of a large width by a window function of a smaller (finite) width. Simple truncation amounts to using a *rectangular window* $w_R(t)$ (shown later in Fig. 4.53a) in which we assign unit weight to all the data within the window width ($|t| < T/2$), and assign zero weight to all the data lying outside the window ($|t| > T/2$). It is also possible to use a window in which the weight assigned to the data within the window may not be constant. In a *triangular window* $w_T(t)$, for example, the weight assigned to data decreases linearly over the window width (shown later in Fig. 4.53b).

Consider a signal $x(t)$ and a window function $w(t)$. If $x(t) \Longleftrightarrow X(\omega)$ and $w(t) \Longleftrightarrow W(\omega)$, and if the windowed function $x_w(t) \Longleftrightarrow X_w(\omega)$, then

$$x_w(t) = x(t)w(t) \qquad \text{and} \qquad X_w(\omega) = \frac{1}{2\pi} X(\omega) * W(\omega)$$

According to the width property of convolution, it follows that the width of $X_w(\omega)$ equals the sum of the widths of $X(\omega)$ and $W(\omega)$. Thus, truncation of a signal increases its bandwidth by the amount of bandwidth of $w(t)$. Clearly, the truncation of a signal causes its spectrum to spread (or smear) by the amount of the bandwidth of $w(t)$. Recall that the signal bandwidth is inversely proportional to the signal duration (width). Hence, the wider the window, the smaller its bandwidth, and the smaller the *spectral spreading*. This result is predictable because a wider window means that we are accepting more data (closer approximation), which should cause smaller distortion (smaller spectral spreading). Smaller window width (poorer approximation) causes more spectral spreading (more distortion). In addition, since $W(\omega)$ is really not strictly bandlimited and its spectrum $\to 0$ only asymptotically, the spectrum of $X_w(\omega) \to 0$ asymptotically also at the same rate as that of $W(\omega)$, even if $X(\omega)$ is, in fact, strictly bandlimited. Thus, windowing causes the spectrum of $X(\omega)$

to spread into the band where it is supposed to be zero. This effect is called *leakage*. The following example clarifies these twin effects of spectral spreading and leakage.

Let us consider $x(t) = \cos \omega_0 t$ and a rectangular window $w_R(t) = \text{rect}(t/T)$, illustrated in Fig. 4.51b. The reason for selecting a sinusoid for $x(t)$ is that its spectrum consists of spectral lines of zero width (Fig. 4.51a). Hence, this choice will make the effect of spectral spreading and leakage easily discernible. The spectrum of the truncated signal $x_w(t)$ is the convolution of the two impulses of $X(\omega)$ with the sinc spectrum of the window function. Because the convolution of any function with an impulse is the function itself (shifted at the location of the impulse), the resulting spectrum of the truncated signal is $1/2\pi$ times the two sinc pulses at $\pm\omega_0$, as depicted in Fig. 4.51c (also see Fig. 4.26). Comparison of spectra $X(\omega)$ and $X_w(\omega)$ reveals the effects of truncation. These are:

1. The spectral lines of $X(\omega)$ have zero width. But the truncated signal is spread out by $2\pi/T$ about each spectral line. The amount of spread is equal to the width of the mainlobe of the window spectrum. One effect of this *spectral spreading* (or smearing) is that if $x(t)$ has two spectral components of frequencies differing by less than $4\pi/T$ rad/s ($2/T$ Hz), they will be indistinguishable in the truncated signal. The result is loss of spectral resolution. We would like the spectral spreading [mainlobe width of $W(\omega)$] to be as small as possible.
2. In addition to the mainlobe spreading, the truncated signal has sidelobes, which decay slowly with frequency. The spectrum of $x(t)$ is zero everywhere except at $\pm\omega_0$. On the other hand, the truncated signal spectrum $X_w(\omega)$ is zero nowhere because of the sidelobes. These sidelobes decay asymptotically as $1/\omega$. Thus, the truncation causes spectral *leakage* in the band where the spectrum of the signal $x(t)$ is zero. The peak *sidelobe* magnitude is 0.217 times the mainlobe magnitude (13.3 dB below the peak mainlobe magnitude). Also, the sidelobes decay at a rate $1/\omega$, which is -6 dB/octave (or -20 dB/decade). This is the sidelobe's *rolloff rate*. We want smaller sidelobes with a faster rate of decay (high rolloff rate). Figure 4.51d, which plots $|W_R(\omega)|$ as a function of ω, clearly shows the mainlobe and sidelobe features, with the first sidelobe amplitude -13.3 dB below the mainlobe amplitude and the sidelobes decaying at a rate of -6 dB/octave (or -20 dB/decade).

So far, we have discussed the effect on the signal spectrum of signal truncation (truncation in the time domain). Because of the time-frequency duality, the effect of spectral truncation (truncation in frequency domain) on the signal shape is similar.

Remedies for Side Effects of Truncation

For better results, we must try to minimize the twin side effects of truncations: spectral spreading (mainlobe width) and leakage (sidelobe). Let us consider each of these ills.

1. The spectral spread (mainlobe width) of the truncated signal is equal to the bandwidth of the window function $w(t)$. We know that the signal bandwidth is inversely proportional to the signal width (duration). Hence, to reduce the spectral spread (mainlobe width), we need to increase the window width.
2. To improve the leakage behavior, we must search for the cause of the slow decay of sidelobes. In Ch. 3, we saw that the Fourier spectrum decays as $1/\omega$ for a signal with jump discontinuity, decays as $1/\omega^2$ for a continuous signal whose first derivative is

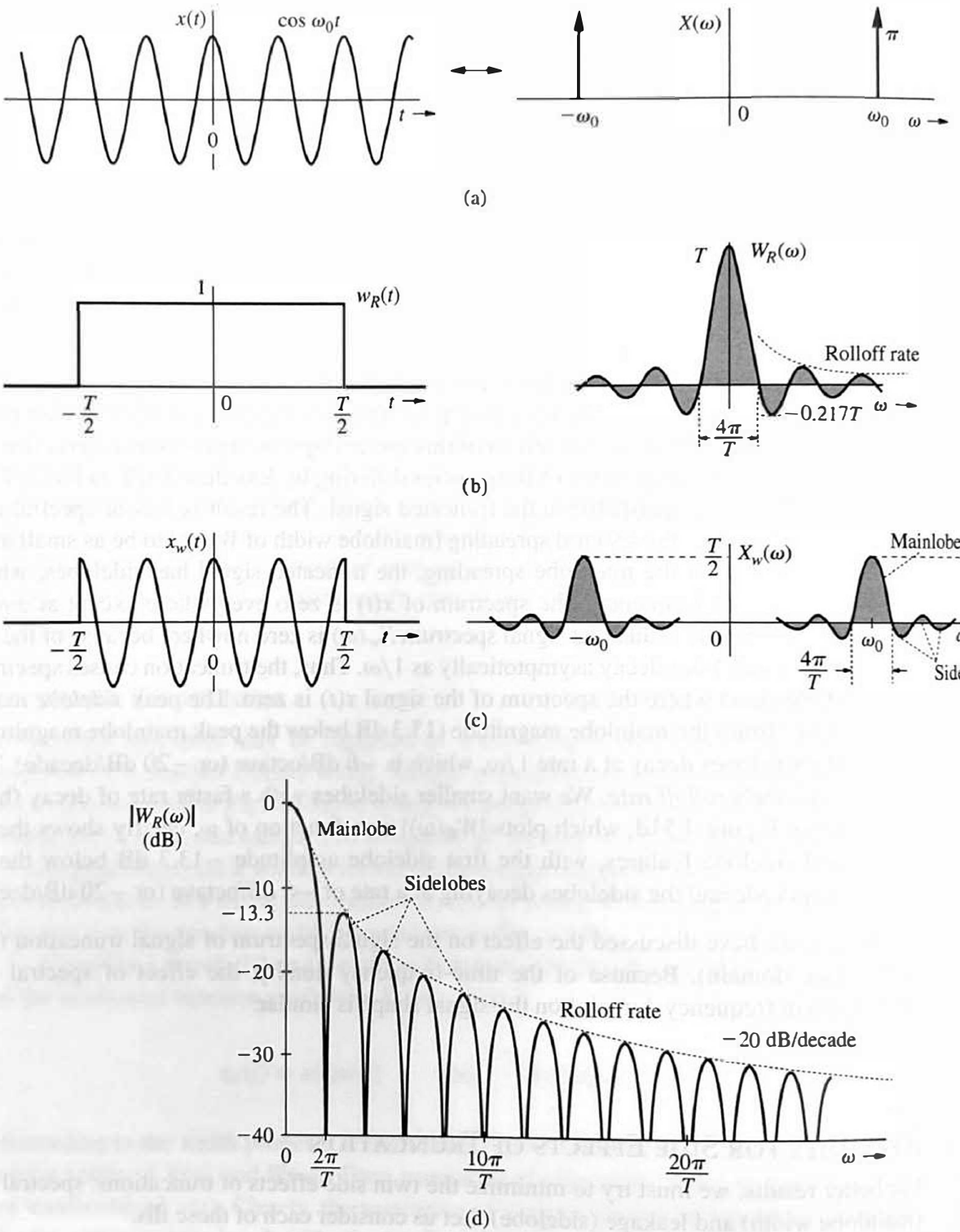

Figure 4.51 Windowing and its effects.

discontinuous, and so on.[†] Smoothness of a signal is measured by the number of continuous derivatives it possesses. The smoother the signal, the faster the decay of its spectrum. Thus, we can achieve a given leakage behavior by selecting a suitably smooth (tapered) window.

3. For a given window width, the remedies for the two effects are incompatible. If we try to improve one, the other deteriorates. For instance, among all the windows of a given width, the rectangular window has the smallest spectral spread (mainlobe width), but its sidelobes have high level and they decay slowly. A tapered (smooth) window of the same width has smaller and faster-decaying sidelobes, but it has a wider mainlobe.[‡] But we can compensate for the increased mainlobe width by widening the window. Thus, we can remedy both the side effects of truncation by selecting a suitably smooth window of sufficient width.

There are several well-known tapered-window functions, such as the Bartlett (triangular), Hanning (von Hann), Hamming, Blackman, and Kaiser windows, which truncate the data gradually. These windows offer different trade-offs with respect to spectral spread (mainlobe width), the peak sidelobe magnitude, and the leakage rolloff rate, as indicated in Table 4.3 [8,

TABLE 4.3 Some Window Functions and Their Characteristics

No.	Window $w(t)$	Mainlobe Width	Rolloff Rate Level (dB)	Peak Sidelobe
1	Rectangular: $\text{rect}\left(\frac{t}{T}\right)$	$\frac{4\pi}{T}$	-6	-13.3
2	Bartlett: $\Delta\left(\frac{t}{2T}\right)$	$\frac{8\pi}{T}$	-12	-26.5
3	Hanning: $0.5\left[1+\cos\left(\frac{2\pi t}{T}\right)\right]$	$\frac{8\pi}{T}$	-18	-31.5
4	Hamming: $0.54+0.46\cos\left(\frac{2\pi t}{T}\right)$	$\frac{8\pi}{T}$	-6	-42.7
5	Blackman: $0.42+0.5\cos\left(\frac{2\pi t}{T}\right)+0.08\cos\left(\frac{4\pi t}{T}\right)$	$\frac{12\pi}{T}$	-18	-58.1
6	Kaiser: $\frac{I_0\left[\alpha\sqrt{1-4\left(\frac{t}{T}\right)^2}\right]}{I_0(\alpha)}$ $0\le\alpha\le 10$	$\frac{11.2\pi}{T}$	-6 ($\alpha=8.168$)	-59.9

[†] This result was demonstrated for periodic signals. However, it applies to aperiodic signals also. This is because we showed in the beginning of this chapter that if $x_{T_0}(t)$ is a periodic signal formed by periodic extension of an aperiodic signal $x(t)$, then the spectrum of $x_{T_0}(t)$ is ($1/T_0$ times) the samples of $X(\omega)$. Thus, what is true of the decay rate of the spectrum of $x_{T_0}(t)$ is also true of the rate of decay of $X(\omega)$.

[‡] A tapered window yields a higher mainlobe width because the effective width of a tapered window is smaller than that of the rectangular window; see Sec. 2.6.2 [Eq. (2.47)] for the definition of effective width. Therefore, from the reciprocity of the signal width and its bandwidth, it follows that the rectangular window mainlobe is narrower than a tapered window.

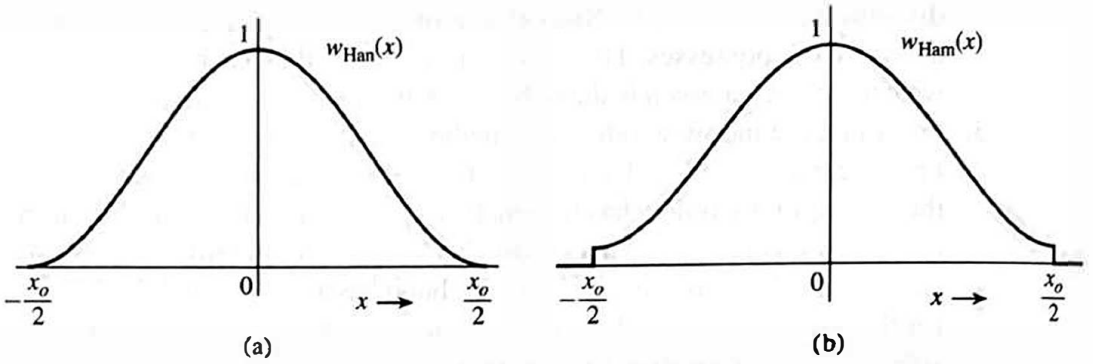

Figure 4.52 (**a**) Hanning and (**b**) Hamming windows.

9]. Observe that all windows are symmetrical about the origin (i.e., are even functions of t). Because of this feature, $W(\omega)$ is a real function of ω; that is, $\angle W(\omega)$ is either 0 or π. Hence, the phase function of the truncated signal has a minimal amount of distortion.

Figure 4.52 shows two well-known tapered-window functions, the von Hann (or Hanning) window $w_{\text{Han}}(x)$ and the Hamming window $w_{\text{Ham}}(x)$. We have intentionally used the independent variable x because windowing can be performed in the time domain as well as in the frequency domain, so x could be t or ω, depending on the application.

There are hundreds of windows, all with different characteristics. But the choice depends on a particular application. The rectangular window has the narrowest mainlobe. The Bartlett (triangle) window (also called the Fejer or Cesaro) is inferior in all respects to the Hanning window. For this reason, it is rarely used in practice. Hanning is preferred over Hamming in spectral analysis because it has faster sidelobe decay. For filtering applications, on the other hand, the Hamming window is chosen because it has the smallest sidelobe magnitude for a given mainlobe width. The Hamming window is the most widely used general-purpose window. The Kaiser window, which uses $I_0(\alpha)$, the modified zero-order Bessel function, is more versatile and adjustable. Selecting a proper value of α ($0 \leq \alpha \leq 10$) allows the designer to tailor the window to suit a particular application. The parameter α controls the mainlobe-sidelobe trade-off. When $\alpha = 0$, the Kaiser window is the rectangular window. For $\alpha = 5.4414$, it is the Hamming window, and when $\alpha = 8.885$, it is the Blackman window. As α increases, the mainlobe width increases and the sidelobe level decreases.

4.9.1 Using Windows in Filter Design

We shall design an ideal lowpass filter of bandwidth W rad/s, with frequency response $H(\omega)$, as shown in Fig. 4.53e or 4.53f. For this filter, the impulse response $h(t) = (W/\pi)\text{sinc}(Wt)$ (Fig. 4.53c) is noncausal and, therefore, unrealizable. Truncation of $h(t)$ by a suitable window (Fig. 4.53a) makes it realizable, although the resulting filter is now an approximation to the desired ideal filter.[†] We shall use a rectangular window $w_R(t)$ and a triangular (Bartlett) window $w_T(t)$ to truncate $h(t)$, and then examine the resulting filters. The truncated impulse responses

[†] In addition to truncation, we need to delay the truncated function by $T/2$ to render it causal. However, the time delay only adds a linear phase to the spectrum without changing the amplitude spectrum. Thus, to simplify our discussion, we shall ignore the delay.

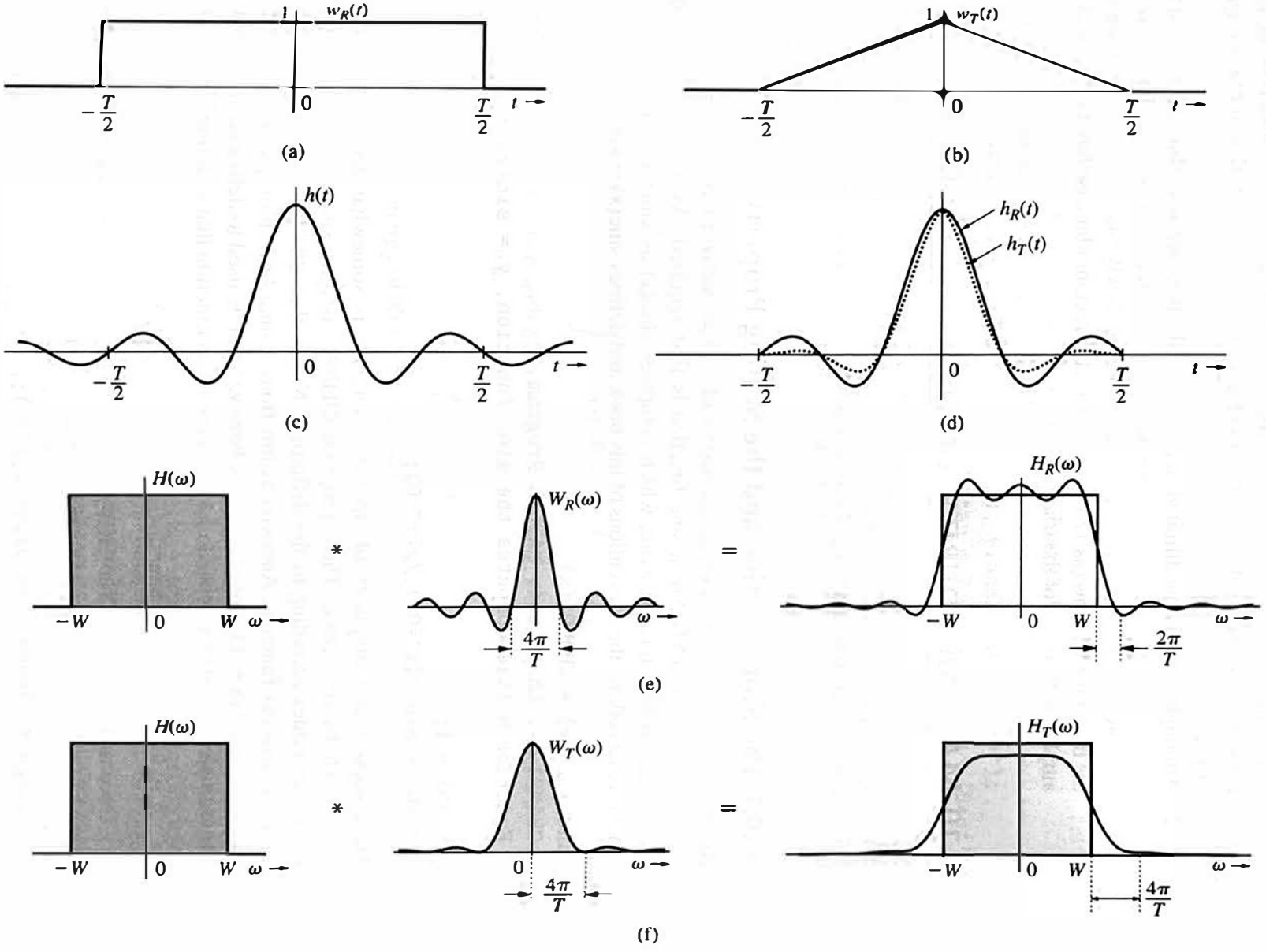

Figure 4.53 Window-based filter design.

$h_R(t) = h(t)w_R(t)$ and $h_T(t) = h(t)w_T(t)$ are depicted in Fig. 4.53d. Hence, the windowed filter frequency response is the convolution of $H(\omega)$ with the Fourier transform of the window, as illustrated in Figs. 4.53e and 4.53f. We make the following observations:

1. The windowed filter spectra show *spectral spreading* at the edges, and instead of a sudden switch there is a gradual transition from the passband to the stopband of the filter. The transition band is smaller ($2\pi/T$ rad/s) for the rectangular case than for the triangular case ($4\pi/T$ rad/s).
2. Although $H(\omega)$ is bandlimited, the windowed filters are not. But the stopband behavior of the triangular case is superior to that of the rectangular case. For the rectangular window, the leakage in the stopband decreases slowly (as $1/\omega$) in comparison to that of the triangular window (as $1/\omega^2$). Moreover, the rectangular case has a higher peak sidelobe amplitude than that of the triangular window.

4.10 MATLAB: FOURIER TRANSFORM TOPICS

MATLAB is useful for investigating a variety of Fourier transform topics. In this section, a rectangular pulse is used to investigate the scaling property, Parseval's theorem, essential bandwidth, and spectral sampling. Kaiser window functions are also investigated.

4.10.1 The Sinc Function and the Scaling Property

As shown in Ex. 4.2, the Fourier transform of $x(t) = \text{rect}(t/\tau)$ is $X(\omega) = \tau\,\text{sinc}(\omega\tau/2)$. To represent $X(\omega)$ in MATLAB, a sinc function is first required. As an alternative to the signal processing toolbox function `sinc`, which computes $\text{sinc}(x)$ as $\sin(\pi x)/\pi x$, we create our own function that follows the conventions of this book and defines $\text{sinc}(x) = \sin(x)/x$.

```
function [y] = CH4MP1(x)
% CH4MP1.m : Chapter 4, MATLAB Program 1
% Function M-file computes the sinc function, y = sin(x)/x.

y(x==0) = 1;
y(x~=0) = sin(x(x~=0))./x(x~=0);
```

The computational simplicity of $\text{sinc}(x) = \sin(x)/x$ is somewhat deceptive: $\sin(0)/0$ results in a divide-by-zero error. Thus, program `CH4MP1` assigns $\text{sinc}(0) = 1$ and computes the remaining values according to the definition. Notice that `CH4MP1` cannot be directly replaced by an anonymous function. Anonymous functions cannot have multiple lines or contain certain commands such as `=`, `if`, or `for`. M-files, however, can be used to define an anonymous function. For example, we can represent $X(\omega)$ as an anonymous function that is defined in terms of `CH4MP1`.

```
>> X = @(omega,tau) tau*CH4MP1(omega*tau/2);
```

Once we have defined $X(\omega)$, it is simple to investigate the effects of scaling the pulse width τ. Consider the three cases $\tau = 1.0$, $\tau = 0.5$, and $\tau = 2.0$.

```
>> omega = linspace(-4*pi,4*pi,1001);
```

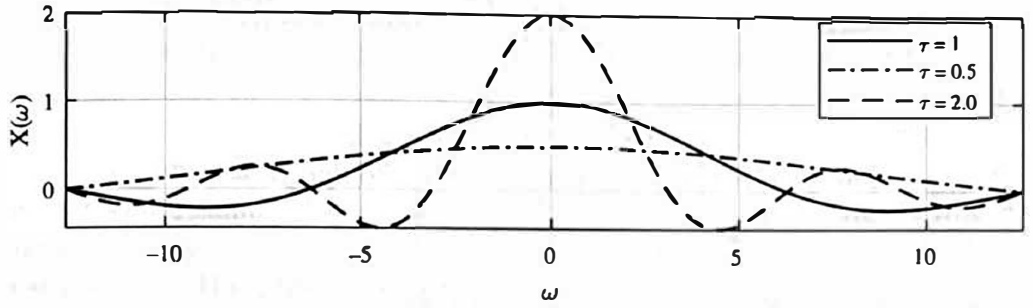

Figure 4.54 Spectra $X(\omega) = \tau \operatorname{sinc}(\omega\tau/2)$ for $\tau = 1.0$, $\tau = 0.5$, and $\tau = 2.0$.

```
>> plot(omega,X(omega,1),'k-',omega,X(omega,0.5),'k-.',...
>>     omega,X(omega,2),'k--');
>> grid; axis tight; xlabel('\omega'); ylabel('X(\omega)');
>> legend('\tau = 1','\tau = 0.5','\tau = 2.0','Location','Best');
```

Figure 4.54 confirms the reciprocal relationship between signal duration and spectral bandwidth: time compression causes spectral expansion, and time expansion causes spectral compression. Additionally, spectral amplitudes are directly related to signal energy. As a signal is compressed, signal energy and thus spectral magnitude decrease. The opposite effect occurs when the signal is expanded.

4.10.2 Parseval's Theorem and Essential Bandwidth

Parseval's theorem concisely relates energy between the time domain and the frequency domain:

$$\int_{-\infty}^{\infty} |x(t)|^2\, dt = \frac{1}{2\pi} \int_{-\infty}^{\infty} |X(\omega)|^2\, d\omega$$

This too is easily verified with MATLAB. For example, a unit amplitude pulse $x(t)$ with duration τ has energy $E_x = \tau$. Thus,

$$\int_{-\infty}^{\infty} |X(\omega)|^2\, d\omega = 2\pi\tau$$

Letting $\tau = 1$, the energy of $X(\omega)$ is computed by using the quad function.

```
>> X_squared = @(omega, tau) (tau*CH4MP1(omega*tau/2)).^2;
>> quad(X_squared,-1e6,1e6,[],[],1)
   ans = 6.2817
```

Although not perfect, the result of the numerical integration is consistent with the expected value of $2\pi \approx 6.2832$. For quad, the first argument is the function to be integrated, the next two arguments are the limits of integration, the empty square brackets indicate default values for special options, and the last argument is the secondary input τ for the anonymous function `X_squared`. Full format details for quad are available from MATLAB's help facilities.

A more interesting problem involves computing a signal's essential bandwidth. Consider, for example, finding the essential bandwidth W, in radians per second, that contains fraction β of the energy of the square pulse $x(t)$. That is, we want to find W such that

$$\frac{1}{2\pi}\int_{-W}^{W}|X(\omega)|^2 d\omega = \beta\tau$$

Program CH4MP2 uses a guess-and-check method to find W.

```
function [W,E_W] = CH4MP2(tau,beta,tol)
% CH4MP2.m : Chapter 4, MATLAB Program 2
% Function M-file computes essential bandwidth W for square pulse.
% INPUTS:   tau = pulse width
%           beta = fraction of signal energy desired in W
%           tol = tolerance of relative energy error
% OUTPUTS:  W = essential bandwidth [rad/s]
%           E_W = Energy contained in bandwidth W
W = 0; step = 2*pi/tau;     % Initial guess and step values
X_squared = @(omega,tau) (tau*CH4MP1(omega*tau/2)).^2;
E = beta*tau;               % Desired energy in W
relerr = (E-0)/E;           % Initial relative error is 100 percent
while(abs(relerr) > tol),
    if (relerr>0),          % W too small, so...
        W=W+step;           % ... increase W by step
    elseif (relerr<0),      % W too large, so...
        step = step/2;      % ... decrease step and then W
        W = W-step;
    end
    E_W = 1/(2*pi)*quad(X_squared,-W,W,[],[],tau);
    relerr = (E - E_W)/E;
end
```

Although this guess-and-check method is not the most efficient, it is relatively simple to understand: CH4MP2 sensibly adjusts W until the relative error is within tolerance. The number of iterations needed to converge to a solution depends on a variety of factors and is not known beforehand. The `while` command is ideal for such situations:

```
while expression,
      statements;
end
```

While the *expression* is true, the *statements* are continually repeated.

To demonstrate CH4MP2, consider the 90% essential bandwidth W for a pulse of 1 second duration. Typing `[W,E_W]=CH4MP2(1,0.9,0.001)` returns an essential bandwidth $W = 5.3014$ that contains 89.97% of the energy. Reducing the error tolerance improves the estimate. `CH4MP2(1,0.9,0.00005)` returns an essential bandwidth $W = 5.3321$ that contains 90.00% of the energy. These essential bandwidth calculations are consistent with estimates presented after Ex. 4.2.

4.10.3 Spectral Sampling

Consider a signal with finite duration τ. A periodic signal $x_{T_0}(t)$ is constructed by repeating $x(t)$ every T_0 seconds, where $T_0 \geq \tau$. From Eq. (4.5), we can write the Fourier series coefficients of $x_{T_0}(t)$ as $D_n = (1/T_0)X(n2\pi/T_0)$. Put another way, the Fourier series coefficients are obtained by sampling the spectrum $X(\omega)$.

By using spectral sampling, it is simple to determine the Fourier series coefficients for an arbitrary duty-cycle, square-pulse periodic signal. The square pulse $x(t) = \text{rect}(t/\tau)$ has spectrum $X(\omega) = \tau\,\text{sinc}(\omega\tau/2)$. Thus, the nth Fourier coefficient of the periodic extension $x_{T_0}(t)$ is $D_n = (\tau/T_0)\text{sinc}(n\pi\tau/T_0)$. As in Ex. 3.8, $\tau = \pi$ and $T_0 = 2\pi$ provide a square-pulse periodic signal. The Fourier coefficients are determined by

```
>> D = @(n,tau,T_0) tau/T_0*CH4MP1(n*pi*tau/T_0);
>> tau = pi; T_0 = 2*pi; n = [0:10];
>> stem(n,D(n,tau,T_0),'k.'); xlabel('n'); ylabel('D_n'); axis tight;
```

The results, shown in Fig. 4.55, agree with Fig. 3.14b. Doubling the period to $T_0 = 4\pi$ effectively doubles the density of spectral samples and halves the spectral amplitude, as shown in Fig. 4.56.

As T_0 increases, the spectral sampling becomes progressively finer while the amplitude becomes infinitesimal. An evolution of the Fourier series toward the Fourier integral is seen by allowing the period T_0 to become large. Figure 4.57 shows the result for $T_0 = 40\pi$.

If $T_0 = \tau$, the signal x_{T_0} is a constant and the spectrum should concentrate energy at dc. In this case, the sinc function is sampled at the zero crossings and $D_n = 0$ for all n not equal to 0.

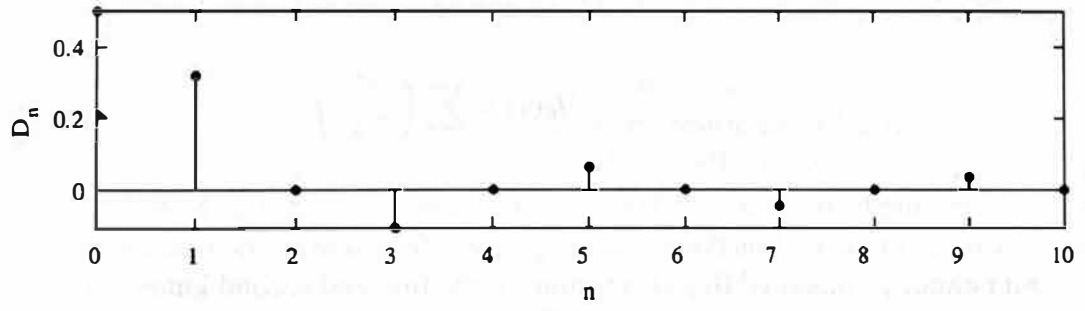

Figure 4.55 Fourier spectra for $\tau = \pi$ and $T_0 = 2\pi$.

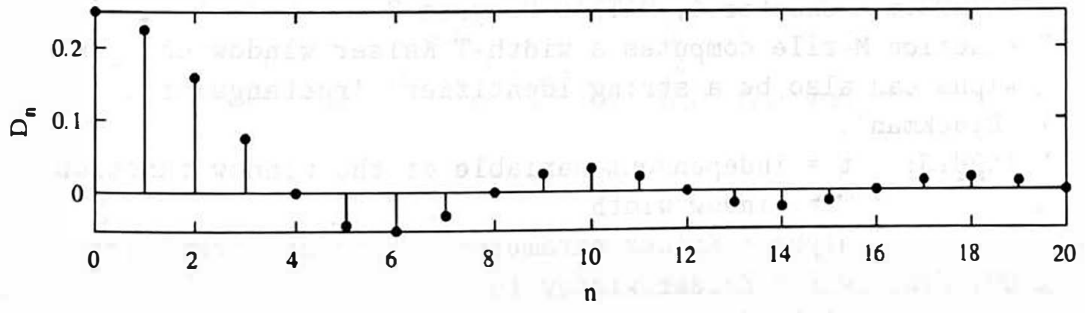

Figure 4.56 Fourier spectra for $\tau = \pi$ and $T_0 = 4\pi$.

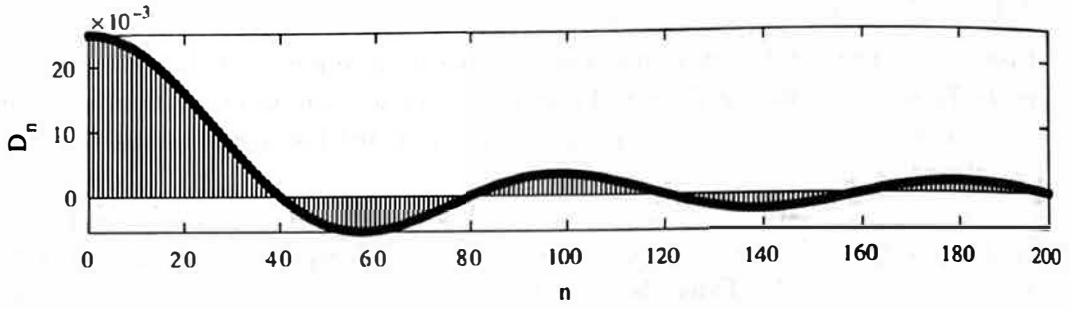

Figure 4.57 Fourier spectra for $\tau = \pi$ and $T_0 = 40\pi$.

Only the sample corresponding to $n = 0$ is nonzero, indicating a dc signal, as expected. It is a simple matter to modify the previous code to verify this case.

4.10.4 Kaiser Window Functions

A window function is useful only if it can be easily computed and applied to a signal. The Kaiser window, for example, is flexible but appears rather intimidating:

$$w_K(t) = \begin{cases} \dfrac{I_0\left(\alpha\sqrt{1-4(t/T)^2}\right)}{I_0(\alpha)} & |t| < T/2 \\ 0 & \text{otherwise} \end{cases}$$

Fortunately, the bark of a Kaiser window is worse than its bite! The function $I_0(x)$, a zero-order modified Bessel function of the first kind, can be computed according to

$$I_0(x) = \sum_{k=0}^{\infty} \left(\frac{x^k}{2^k k!}\right)^2$$

or, more simply, by using the MATLAB function `besseli(0,x)`. In fact, MATLAB supports a wide range of Bessel functions, including Bessel functions of the first and second kinds (`besselj` and `bessely`), modified Bessel functions of the first and second kinds (`besseli` and `besselk`), Hankel functions (`besselh`), and Airy functions (`airy`).

Program CH4MP3 computes Kaiser windows at times t by using parameters T and α.

```
function [w_K] = CH4MP3(t,T,alpha)
% CH4MP3.m : Chapter 4, MATLAB Program 3
% Function M-file computes a width-T Kaiser window using parameter alpha.
% Alpha can also be a string identifier: 'rectangular', 'Hamming', or
% 'Blackman'.
% INPUTS:   t = independent variable of the window function
%           T = window width
%           alpha = Kaiser parameter or string identifier
% OUTPUTS:  w_K = Kaiser window function
if strncmpi(alpha,'rectangular',1),
    alpha = 0;
```

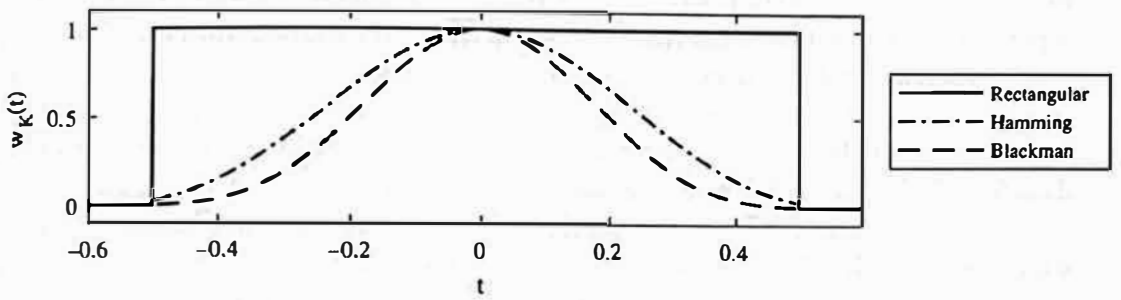

Figure 4.58 Special-case, unit duration Kaiser windows.

```
elseif strncmpi(alpha,'Hamming',3),
    alpha = 5.4414;
elseif strncmpi(alpha,'Blackman',1),
    alpha = 8.885;
elseif isa(alpha,'char')
    disp('Unrecognized string identifier.'); return
end
w_K = zeros(size(t)); i = find(abs(t)<T/2);
w_K(i) = besseli(0,alpha*sqrt(1-4*t(i).^2/(T^2)))/besseli(0,alpha);
```

Recall that $\alpha = 0$, $\alpha = 5.4414$, and $\alpha = 8.885$ correspond to rectangular, Hamming, and Blackman windows, respectively. `CH4MP3` is written to allow these special-case Kaiser windows to be identified by name rather than by α value. While unnecessary, this convenient feature is achieved with the help of the `strncmpi` command.

The `strncmpi(S1,S2,N)` command compares the first `N` characters of strings `S1` and `S2`, ignoring case. More completely, MATLAB has four variants of string comparison: `strcmp`, `strcmpi`, `strncmp`, and `strncmpi`. Comparisons are restricted to the first N characters when `n` is present; case is ignored when `i` is present. Thus, `CH4MP3` identifies any string `alpha` that starts with the letter `r` or `R` as a rectangular window. To prevent confusion with a Hanning window, the first three characters must match to identify a Hamming window. The `isa(alpha,'char')` command determines whether `alpha` is a character string. MATLAB help documents the many other classes that `isa` can identify. In `CH4MP3`, `isa` is used to terminate execution if a string identifier `alpha` has not been recognized as one of the three special cases.

Figure 4.58 shows the three special-case, unit duration Kaiser windows generated by

```
>> t = [-0.6:.001:0.6]; T = 1;
>> plot(t,CH4MP3(t,T,'r'),'k-',t,CH4MP3(t,T,'ham'),'k-.',t,CH4MP3(t,T,'b'),'k--');
>> axis([-0.6 0.6 -.1 1.1]); xlabel('t'); ylabel('w_K(t)');
>> legend('Rectangular','Hamming','Blackman','Location','EastOutside');
```

4.11 SUMMARY

In Ch. 3, we represented periodic signals as a sum of (everlasting) sinusoids or exponentials (Fourier series). In this chapter, we extended this result to aperiodic signals, which are represented

by the Fourier integral (instead of the Fourier series). An aperiodic signal $x(t)$ may be regarded as a periodic signal with period $T_0 \to \infty$ so that the Fourier integral is basically a Fourier series with a fundamental frequency approaching zero. Therefore, for aperiodic signals, the Fourier spectra are continuous. This continuity means that a signal is represented as a sum of sinusoids (or exponentials) of all frequencies over a continuous frequency interval. The Fourier transform $X(\omega)$, therefore, is the spectral density (per unit bandwidth in hertz).

An ever-present aspect of the Fourier transform is the duality between time and frequency, which also implies duality between the signal $x(t)$ and its transform $X(\omega)$. This duality arises because of near-symmetrical equations for direct and inverse Fourier transforms. The duality principle has far-reaching consequences and yields many valuable insights into signal analysis.

The scaling property of the Fourier transform leads to the conclusion that the signal bandwidth is inversely proportional to signal duration (signal width). Time shifting of a signal does not change its amplitude spectrum, but it does add a linear phase component to its spectrum. Multiplication of a signal by an exponential $e^{j\omega_0 t}$ shifts the spectrum to the right by ω_0. In practice, spectral shifting is achieved by multiplying a signal by a sinusoid such as $\cos\omega_0 t$ (rather than the exponential $e^{j\omega_0 t}$). This process is known as amplitude modulation. Multiplication of two signals results in convolution of their spectra, whereas convolution of two signals results in multiplication of their spectra.

For an LTIC system with the frequency response $H(\omega)$, the input and output spectra $X(\omega)$ and $Y(\omega)$ are related by the equation $Y(\omega) = X(\omega)H(\omega)$. This is valid only for asymptotically stable systems. It also applies to marginally stable systems if the input does not contain a finite-amplitude sinusoid of the natural frequency of the system. For asymptotically unstable systems, the frequency response $H(\omega)$ does not exist. For distortionless transmission of a signal through an LTIC system, the amplitude response $|H(\omega)|$ of the system must be constant, and the phase response $\angle H(\omega)$ should be a linear function of ω over a band of interest. Ideal filters, which allow distortionless transmission of a certain band of frequencies and suppress all the remaining frequencies, are physically unrealizable (noncausal). In fact, it is impossible to build a physical system with zero gain $[H(\omega) = 0]$ over a finite band of frequencies. Such systems (which include ideal filters) can be realized only with infinite time delay in the response.

The energy of a signal $x(t)$ is equal to $1/2\pi$ times the area under $|X(\omega)^2|$ (Parseval's theorem). The energy contributed by spectral components within a band Δf (in hertz) is given by $|X(\omega)|^2\Delta f$. Therefore, $|X(\omega)|^2$ is the energy spectral density per unit bandwidth (in hertz). The energy spectral density $|X(\omega)|^2$ of a signal $x(t)$ is the Fourier transform of the autocorrelation function $\psi_x(t)$ of the same signal $x(t)$. Thus, a signal autocorrelation function has a direct link to its spectral information.

The process of modulation shifts the signal spectrum to different frequencies. Modulation is used for many reasons: to transmit several messages simultaneously over the same channel for the sake of utilizing the channel's high bandwidth, to effectively radiate power over a radio link, to shift a signal spectrum at higher frequencies to overcome the difficulties associated with signal processing at lower frequencies, and to effect the exchange of transmission bandwidth and transmission power required to transmit data at a certain rate. Broadly speaking, there are two types of modulation, amplitude and angle modulation. Each class has several subclasses. Amplitude modulation bandwidth is generally fixed. The bandwidth in angle modulation, however, is controllable. The higher the bandwidth, the more immune is the scheme to noise.

In practice, we often need to truncate data. Truncating is like viewing data through a window, which permits only certain portions of the data to be seen and hides (suppresses) the remainder. Abrupt truncation of data amounts to a rectangular window, which assigns a unit weight to data

seen from the window and zero weight to the remaining data. Tapered windows, on the other hand, reduce the weight gradually from 1 to 0. Data truncation can cause some unsuspected problems. For example, in the computation of the Fourier transform, windowing (data truncation) causes spectral spreading (spectral smearing) that is characteristic of the window function used. A rectangular window results in the least spreading, but it does so at the cost of a high and oscillatory spectral leakage outside the signal band, which decays slowly as $1/\omega$. In comparison to a rectangular window, tapered windows, in general, have larger spectral spreading (smearing), but the spectral leakage is smaller and decays faster with frequency. If we try to reduce spectral leakage by using a smoother window, the spectral spreading increases. Fortunately, spectral spreading can be reduced by increasing the window width. Therefore, we can achieve a given combination of spectral spread (transition bandwidth) and leakage characteristics by choosing a suitable tapered window function of a sufficiently long width T.

REFERENCES

1. Churchill, R. V., and Brown, J. W., *Fourier Series and Boundary Value Problems,* 3rd ed., McGraw-Hill, New York, 1978.
2. Bracewell, R. N., *Fourier Transform and Its Applications,* rev. 2nd ed., McGraw-Hill, New York, 1986.
3. Guillemin, E. A., *Theory of Linear Physical Systems,* Wiley, New York, 1963.
4. Lathi, B. P. and Ding, Z., *Modern Digital and Analog Communication Systems,* 4th ed., Oxford University Press, New York, 2009.
5. Carson, J., "Notes on Theory of Modulation," *Proc. IRE,* vol. 10, pp. 57–64, February 1922.
6. Carson, J., "The Reduction of Atmospheric Disturbances," *Proc. IRE,* vol. 16, pp. 966–975, July 1928.
7. Armstrong, E. H., "A Method of Reducing Disturbances in Radio Signaling by a System of Frequency Modulation," *Proc. IRE,* vol. 24, pp. 689-740, May 1936.
8. Hamming, R. W., *Digital Filters,* 2nd ed., Prentice-Hall, Englewood Cliffs, NJ, 1983.
9. Harris, F. J., "On the Use of Windows for Harmonic Analysis with the Discrete Fourier Transform," *Proceedings of the IEEE,* vol. 66, no. 1, pp. 51–83, January 1978.

PROBLEMS

4.1-1 Suppose signal $x(t) = t^2[u(t) - u(t-2)]$ has Fourier transform $X(\omega)$. Define a 3-periodic replication of $x(t)$ as $y(t) = \sum_{n=-\infty}^{\infty} 2x(t-1-3n)$. Determine Y_k, the Fourier series of $y(t)$, in terms of the Fourier transform $X(\cdot)$.

4.1-2 Show that for a real $x(t)$, Eq. (4.10) can be expressed as

$$x(t) = \frac{1}{\pi}\int_0^{\infty} |X(\omega)| \cos[\omega t + \angle X(\omega)]\, d\omega$$

This is the trigonometric form of the Fourier integral. Compare this with the compact trigonometric Fourier series.

4.1-3 Show that if $x(t)$ is an even function of t, then

$$X(\omega) = 2\int_0^{\infty} x(t)\cos \omega t\, dt$$

and if $x(t)$ is an odd function of t, then

$$X(\omega) = -2j\int_0^{\infty} x(t)\sin \omega t\, dt$$

Hence, prove that if $x(t)$ is a real and even function of t, then $X(\omega)$ is a real and even function of ω. In addition, if $x(t)$ is a real and odd function of t, then $X(\omega)$ is an imaginary and odd function of ω.

4.1-4 A signal $x(t)$ can be expressed as the sum of even and odd components (see Sec. 1.5.2):

$$x(t) = x_e(t) + x_o(t)$$

(a) If $x(t) \Longleftrightarrow X(\omega)$, show that for real $x(t)$,

$$x_e(t) \Longleftrightarrow \text{Re}[X(\omega)]$$

and

$$x_o(t) \Longleftrightarrow j\,\text{Im}[X(\omega)]$$

(b) Verify these results by finding the Fourier transforms of the even and odd components of the following signals: (i) $u(t)$ and (ii) $e^{-at}u(t)$.

4.1-5 Using Eq. (4.9), find the Fourier transforms of the signals $x(t)$ in Fig. P4.1-5.

4.1-6 Using Eq. (4.9), find the Fourier transforms of the signals depicted in Fig. P4.1-6.

4.1-7 Use Eq. (4.10) to find the inverse Fourier transforms of the spectra in Fig. P4.1-7.

4.1-8 Use Eq. (4.10) to find the inverse Fourier transforms of the spectra in Fig. P4.1-8.

4.1-9 If $x(t) \Longleftrightarrow X(\omega)$, then show that

$$X(0) = \int_{-\infty}^{\infty} x(t)\,dt$$

and

$$x(0) = \frac{1}{2\pi}\int_{-\infty}^{\infty} X(\omega)\,d\omega$$

Also show that

$$\int_{-\infty}^{\infty} \text{sinc}\,(x)\,dx = \int_{-\infty}^{\infty} \text{sinc}^2\,(x)\,dx = \pi$$

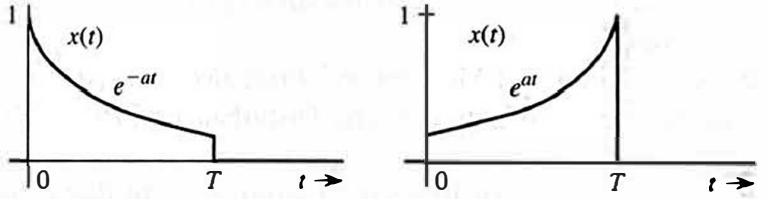

(a) (b)

Figure P4.1-5

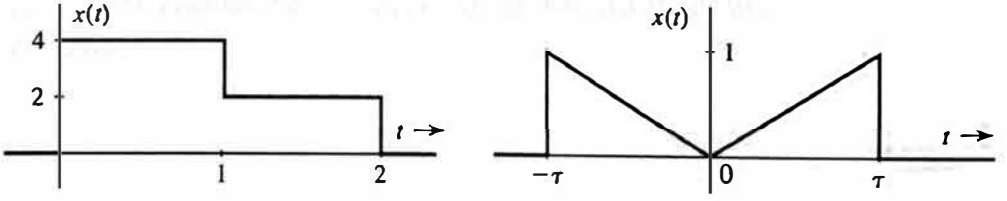

(a) (b)

Figure P4.1-6

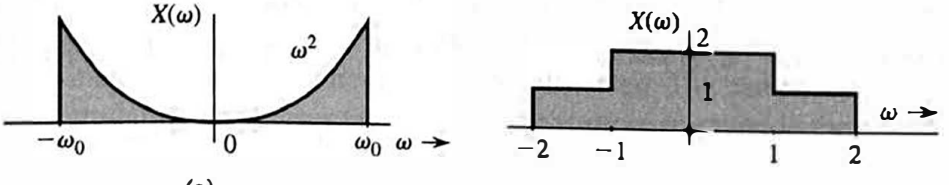

(a) (b)

Figure P4.1-7

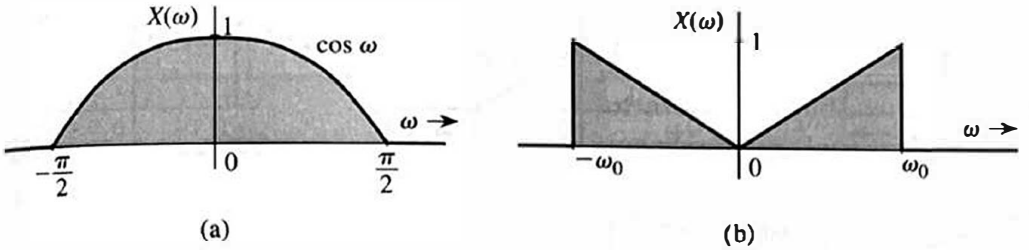

Figure P4.1-8

4.2-1 Sketch the following functions:
(a) rect $(t/2)$
(b) $\Delta(3\omega/100)$
(c) rect $((t-10)/8)$
(d) sinc $(\pi\omega/5)$
(e) sinc $((\omega/5)-2\pi)$
(f) sinc $(t/5)$ rect $(t/10\pi)$

4.2-2 Using Eq. (4.9), show that the Fourier transform of rect $(t-5)$ is sinc $(\omega/2)e^{-j5\omega}$. Sketch the resulting amplitude and phase spectra.

4.2-3 Using Eq. (4.10), show that the inverse Fourier transform of rect $((\omega-10)/2\pi)$ is sinc $(\pi t)\,e^{j10t}$.

4.2-4 Find the inverse Fourier transform of $X(\omega)$ for the spectra illustrated in Fig. P4.2-4. [*Hint*: $X(\omega) = |X(\omega)|e^{j\angle X(\omega)}$. This problem illustrates how different phase spectra (both with the same amplitude spectrum) represent entirely different signals.]

4.2-5 (a) Can you find the Fourier transform of $e^{at}u(t)$ when $a>1$ by setting $s = j\omega$ in the Laplace transform of $e^{at}u(t)$? Explain.
(b) Find the Laplace transform of $x(t)$ shown in Fig. P4.2-5. Can you find the Fourier transform of $x(t)$ by setting $s = j\omega$ in its Laplace transform? Explain. Verify your answer by finding the Fourier and the Laplace transforms of $x(t)$.

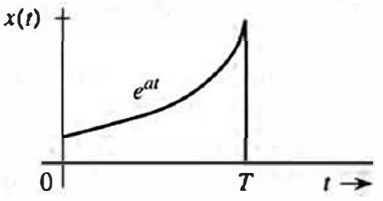

Figure P4.2-5

4.3-1 Apply the duality property to the appropriate pair in Table 4.1 to show that
(a) $\frac{1}{2}[\delta(t)+j/\pi t] \Longleftrightarrow u(\omega)$
(b) $\delta(t+T)+\delta(t-T) \Longleftrightarrow 2\cos T\omega$
(c) $\delta(t+T)-\delta(t-T) \Longleftrightarrow 2j\sin T\omega$

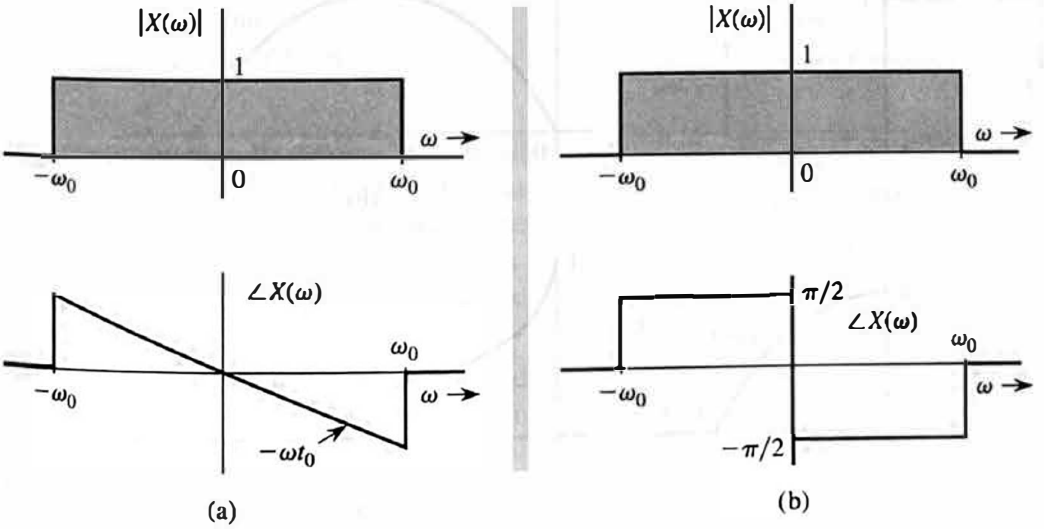

Figure P4.2-4

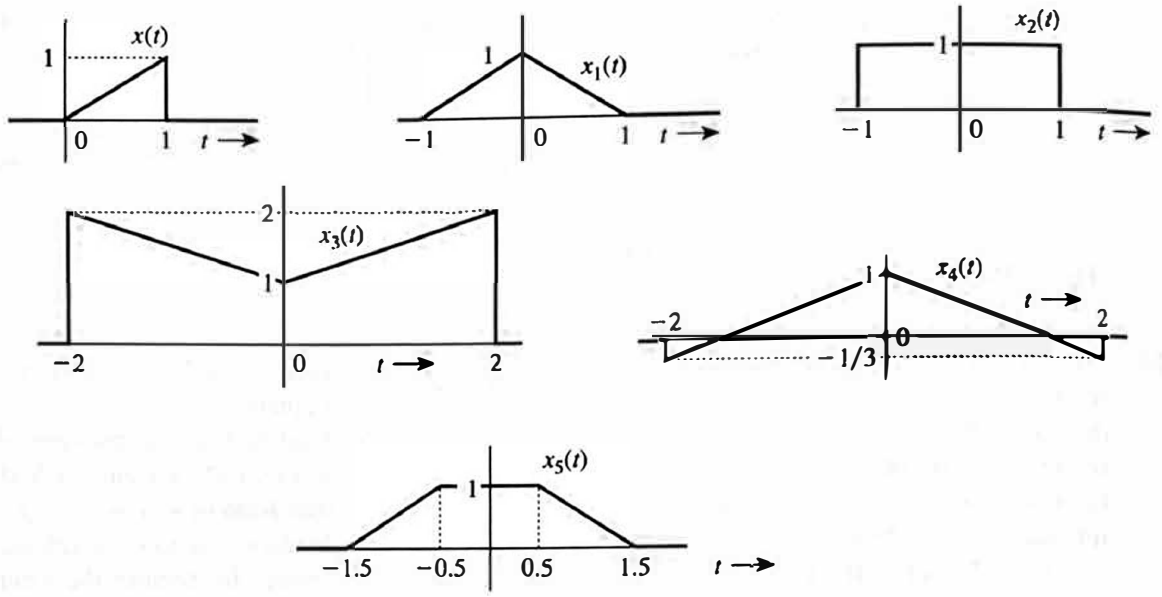

Figure P4.3-4

4.3-2 A signal $x(t)$ has Fourier transform $X(\omega)$. Determine the Fourier transform $Y(\omega)$ in terms of $X(\omega)$ for each of the following signals $y(t)$:

(a) $y(t) = \frac{1}{5}x(-2t+3)$

(b) $y(t) = e^{j2t}x^*(-3t-6)$

4.3-3 A signal $x(t)$ has Fourier transform $X(\omega)$. Determine the inverse Fourier transform $y(t)$ in terms of $x(t)$ for each of the following spectra $Y(\omega)$:

(a) $Y(\omega) = \frac{4}{3}e^{-j2\omega/3}X(-\omega/3)$

(b) $Y(\omega) = \frac{1}{3}e^{j2(\omega-2)}X^*\left(\frac{\omega-2}{3}\right)$

4.3-4 The Fourier transform of the triangular pulse $x(t)$ in Fig. P4.3-4 is expressed as

$$X(\omega) = \frac{1}{\omega^2}(e^{-j\omega} + j\omega e^{-j\omega} - 1)$$

Use this information, and the time-shifting and time-scaling properties, to find the Fourier transforms of the signals $x_i(t)(i = 1,2,3,4,5)$ shown in Fig. P4.3-4.

4.3-5 Using only the time-shifting property and Table 4.1, find the Fourier transforms of the signals depicted in Fig. P4.3-5.

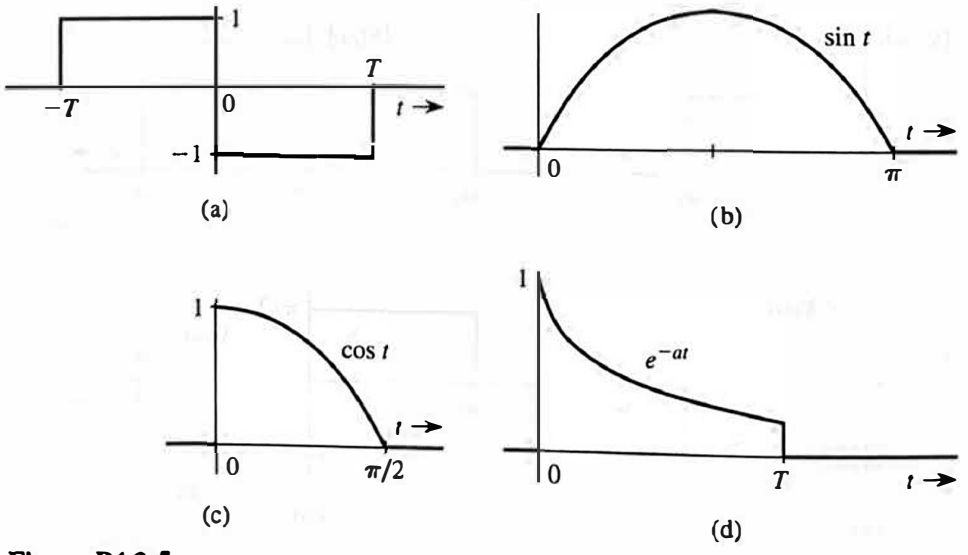

Figure P4.3-5

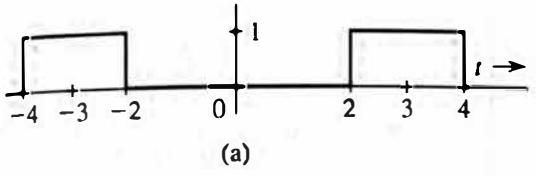

(a)

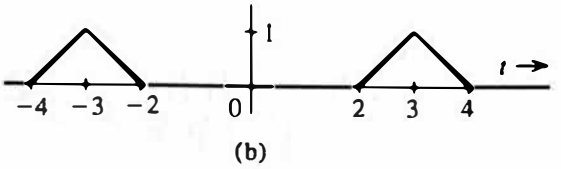

(b)

Figure P4.3-7

4.3-6 Consider the fact that the τ-duration triangle function $\Delta\left(\frac{\omega}{\tau}\right)$ has inverse Fourier transform $\frac{\tau}{4\pi}\text{sinc}^2\left(\frac{t\tau}{4}\right)$. Use the duality property to determine the Fourier transform $Y(\omega)$ of signal $y(t) = \Delta(t)$.

4.3-7 Use the time-shifting property to show that if $x(t) \Longleftrightarrow X(\omega)$, then

$$x(t+T) + x(t-T) \Longleftrightarrow 2X(\omega)\cos T\omega$$

This is the dual of Eq. (4.32). Use this result and Table 4.1 to find the Fourier transforms of the signals shown in Fig. P4.3-7.

4.3-8 Prove the following results, which are duals of each other:

$$x(t)\sin\omega_0 t \Longleftrightarrow \tfrac{1}{2j}[X(\omega-\omega_0) - X(\omega+\omega_0)]$$

$$\tfrac{1}{2j}[x(t+T) - x(t-T)] \Longleftrightarrow X(\omega)\sin T\omega$$

Use the latter result and Table 4.1 to find the Fourier transform of the signal in Fig. P4.3-8.

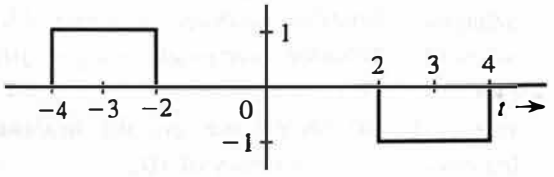

Figure P4.3-8

4.3-9 The signals in Fig. P4.3-9 are modulated signals with carrier $\cos 10t$. Find the Fourier transforms of these signals by using the appropriate properties of the Fourier transform and Table 4.1. Sketch the amplitude and phase spectra for Figs. P4.3-9a and P4.3-9b.

4.3-10 Use the frequency-shifting property and Table 4.1 to find the inverse Fourier transform of the spectra depicted in Fig. P4.3-10.

4.3-11 Let $X(\omega) = \text{rect}(\omega)$ be the Fourier transform of a signal $x(t)$.

(a) For $y_a(t) = x(t) * x(t)$, sketch $Y_a(\omega)$.

(b) For $y_b(t) = x(t) * x(t/2)$, sketch $Y_b(\omega)$.

(c) For $y_c(t) = 2x(t)$, sketch $Y_c(\omega)$.

(d) For $y_d(t) = x^2(t)$, sketch $Y_d(\omega)$.

(e) For $y_e(t) = 1 - x^2(t)$, sketch $Y_e(\omega)$.

4.3-12 Use the time-convolution property to prove pairs 2, 4, 13, and 14 in Table 2.1 (assume $\lambda < 0$ in pair 2, λ_1 and $\lambda_2 < 0$ in pair 4, $\lambda_1 < 0$ and $\lambda_2 > 0$ in pair 13, and λ_1 and $\lambda_2 > 0$ in pair 14). These restrictions are placed because of the Fourier transformability issue for the signals concerned. For pair 2, you need to apply the result in Eq. (1.10).

4.3-13 A signal $x(t)$ is bandlimited to B Hz. Show that the signal $x^n(t)$ is bandlimited to nB Hz.

4.3-14 Find the Fourier transform of the signal in Fig. P4.3-5a by three different methods:

(a) By direct integration using Eq. (4.9)

(b) Using only pair 17 (Table 4.1) and the time-shifting property

(c) Using the time-differentiation and time-shifting properties, along with the fact that $\delta(t) \Longleftrightarrow 1$

4.3-15 (a) Prove the frequency-differentiation property (dual of the time-differentiation property):

$$-jtx(t) \Longleftrightarrow \frac{d}{d\omega}X(\omega)$$

(b) Use this property and pair 1 (Table 4.1) to determine the Fourier transform of $te^{-at}u(t)$.

4.3-16 Adapt the method of Ex. 4.17 and use the frequency-differentiation (see Prob. 4.3-15) and other properties to find the inverse Fourier transform $x(t)$ of the triangular spectrum $X(\omega) = \Delta(\omega/2)$.

4.3-17 Adapt the method of Ex. 4.17 and use the frequency-differentiation (see Prob. 4.3-15) and other properties to find the inverse Fourier transform $x(t)$ of the spectrum $X(\omega) = \pi\left|\frac{\omega}{2}\right|\text{rect}\left(\frac{\omega}{4}\right)$.

4.4-1 For a stable LTIC system with transfer function

$$H(s) = \frac{1}{s+1}$$

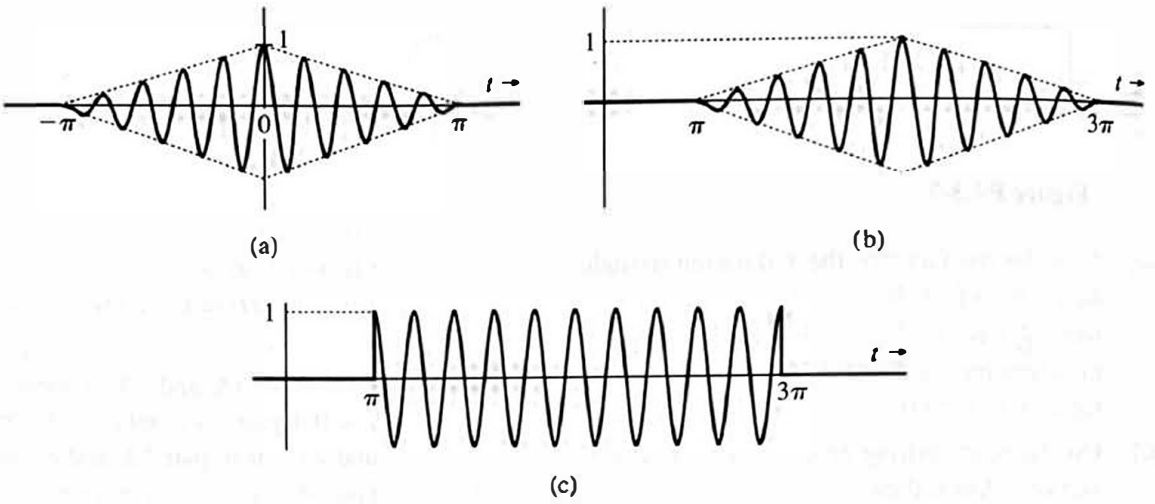

Figure P4.3-9

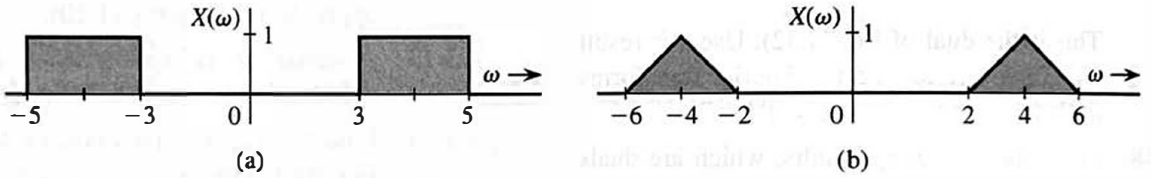

Figure P4.3-10

find the (zero-state) response if the input $x(t)$ is
(a) $e^{-2t}u(t)$
(b) $e^{-t}u(t)$
(c) $e^{t}u(-t)$
(d) $u(t)$

4.4-2 A stable LTIC system is specified by the frequency response

$$H(\omega) = \frac{-1}{j\omega - 2}$$

Find the impulse response of this system and show that this is a noncausal system. Find the (zero-state) response of this system if the input $x(t)$ is
(a) $e^{-t}u(t)$
(b) $e^{t}u(-t)$

4.4-3 A periodic signal $x(t) = 1 + 2\cos(5\pi t) + 3\sin(8\pi t)$ is applied to an LTIC system with impulse response $h(t) = 8\text{sinc}(4\pi t)\cos(2\pi t)$ to produce output $y(t) = x(t) * h(t)$.
(a) Determine ω_0, the fundamental radian frequency of $x(t)$.
(b) Determine $X(\omega)$, the Fourier transform of $x(t)$.
(c) Sketch the system's magnitude response $|H(\omega)|$ over $-10\pi \le \omega \le 10\pi$.
(d) Is the system $h(t)$ distortionless? Explain.
(e) Determine $y(t)$.

4.4-4 A periodic delta train $x(t) = \sum_{n=-\infty}^{\infty} \delta(t - \pi n)$ is applied to an LTIC system with impulse response $h(t) = \sin(3t)\text{sinc}^2(t)$ to produce zero-state output $y(t) = x(t) * h(t)$.
(a) Determine ω_0, the fundamental radian frequency of $x(t)$.
(b) Determine $X(\omega)$, the Fourier transform of $x(t)$.
(c) Sketch the system's magnitude response $|H(\omega)|$ over $-10 \le \omega \le 10$.
(d) Is the system $h(t)$ distortionless? Explain.
(e) Determine $y(t)$.

4.4-5 Signals $x_1(t) = 10^4\text{rect}(10^4 t)$ and $x_2(t) = \delta(t)$ are applied at the inputs of the ideal lowpass filters $H_1(\omega) = \text{rect}(\omega/40{,}000\pi)$ and $H_2(\omega) = \text{rect}(\omega/20{,}000\pi)$ (Fig. P4.4-5). The outputs $y_1(t)$ and $y_2(t)$ of these filters are multiplied to obtain the signal $y(t) = y_1(t)y_2(t)$.
(a) Sketch $X_1(\omega)$ and $X_2(\omega)$.

(b) Sketch $H_1(\omega)$ and $H_2(\omega)$.
(c) Sketch $Y_1(\omega)$ and $Y_2(\omega)$.
(d) Find the bandwidths of $y_1(t)$, $y_2(t)$, and $y(t)$.

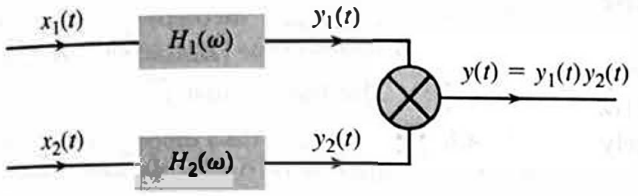

Figure P4.4-5

4.4-6 A lowpass system time constant is often defined as the width of its unit impulse response $h(t)$ (see Sec. 2.6.2). An input pulse $p(t)$ to this system acts like an impulse of strength equal to the area of $p(t)$ if the width of $p(t)$ is much smaller than the system time constant, and provided $p(t)$ is a lowpass pulse, implying that its spectrum is concentrated at low frequencies. Verify this behavior by considering a system whose unit impulse response is $h(t) = \text{rect}\,(t/10^{-3})$. The input pulse is a triangle pulse $p(t) = \Delta(t/10^{-6})$. Show that the system response to this pulse is very nearly the system response to the input $A\delta(t)$, where A is the area under the pulse $p(t)$.

4.4-7 A lowpass system time constant is often defined as the width of its unit impulse response $h(t)$ (see Sec. 2.6.2). An input pulse $p(t)$ to this system passes practically without distortion if the width of $p(t)$ is much greater than the system time constant, and provided $p(t)$ is a lowpass pulse, implying that its spectrum is concentrated at low frequencies. Verify this behavior by considering a system whose unit impulse response is $h(t) = \text{rect}\,(t/10^{-3})$. The input pulse is a triangle pulse $p(t) = \Delta(t)$. Show that the system output to this pulse is very nearly $kp(t)$, where k is the system gain to a dc signal, that is, $k = H(0)$.

4.4-8 A causal signal $h(t)$ has a Fourier transform $H(\omega)$. If $R(\omega)$ and $X(\omega)$ are the real and the imaginary parts of $H(\omega)$, that is, $H(\omega) = R(\omega) + jX(\omega)$, then show that

$$R(\omega) = \frac{1}{\pi}\int_{-\infty}^{\infty}\frac{X(\omega)}{\omega - y}\,d\omega$$

and

$$X(\omega) = -\frac{1}{\pi}\int_{-\infty}^{\infty}\frac{R(\omega)}{\omega - y}\,d\omega$$

assuming that $h(t)$ has no impulse at the origin. This pair of integrals defines the *Hilbert transform*. [*Hint:* Let $h_e(t)$ and $h_o(t)$ be the even and odd components of $h(t)$. Use the results in Prob. 4.1-4. See Fig. 1.24 for the relationship between $h_e(t)$ and $h_o(t)$.]
This problem states one of the important properties of causal systems: that the real and imaginary parts of the frequency response of a causal system are related. If one specifies the real part, the imaginary part cannot be specified independently. The imaginary part is predetermined by the real part, and vice versa. This result also leads to the conclusion that the magnitude and angle of $H(\omega)$ are related, provided all the poles and zeros of $H(\omega)$ lie in the LHP.

4.5-1 Consider a filter with the frequency response

$$H(\omega) = e^{-(k\omega^2 + j\omega t_0)}$$

Show that this filter is physically unrealizable by using the time-domain criterion [noncausal $h(t)$] and the frequency-domain (Paley–Wiener) criterion. Can this filter be made approximately realizable by choosing t_0 sufficiently large? Use your own (reasonable) criterion of approximate realizability to determine t_0. [*Hint:* Use pair 22 in Table 4.1.]

4.5-2 Show that a filter with frequency response

$$H(\omega) = \frac{2(10^5)}{\omega^2 + 10^{10}}e^{-j\omega t_0}$$

is unrealizable. Can this filter be made approximately realizable by choosing a sufficiently large t_0? Use your own (reasonable) criterion of approximate realizability to determine t_0.

4.5-3 Determine whether the filters with the following frequency response $H(\omega)$ are physically realizable. If they are not realizable, can they be realized approximately by allowing a finite time delay in the response?
(a) $10^{-6}\,\text{sinc}\,(10^{-6}\omega)$
(b) $10^{-4}\,\Delta\,(\omega/40{,}000\pi)$
(c) $2\pi\,\delta(\omega)$

4.5-4 Consider signal $x_1(t)$, its Fourier transform $X_1(f)$, and several other signals, as shown in

Fig. P4.5-4. Notice, spectra are drawn as a function of hertzian frequency f rather than radian frequency ω.

(a) Accurately sketch $X_2(f)$, the Fourier transform of $x_2(t)$.

(b) Accurately sketch $x_3(t)$, the inverse Fourier transform of $X_3(f)$.

(c) The signal $x_4(t) = x_1(t) + x_2(t)$ is passed through an ideal lowpass filter with 3 Hz cutoff to produce output $y_4(t)$. Accurately sketch $y_4(t)$.

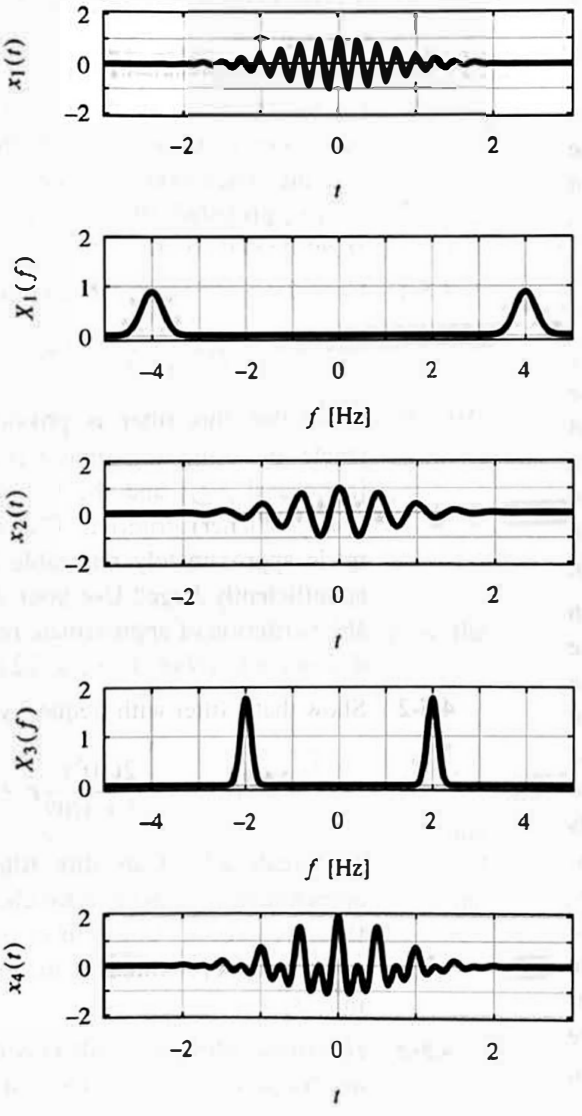

Figure P4.5-4

4.6-1 Define $x(t) = \frac{1}{2\pi}\text{sinc}(t/2)$ with Fourier transform $X(\omega) = \text{rect}(\omega)$. Use Parseval's theorem to determine $\int_{-\infty}^{\infty} \text{sinc}^2(t-2)\,dt$.

4.6-2 Show that the energy of a Gaussian pulse

$$x(t) = \frac{1}{\sigma\sqrt{2\pi}} e^{-t^2/2\sigma^2}$$

is $1/(2\sigma\sqrt{\pi})$. Verify this result by using Parseval's theorem to derive the energy E_x from $X(\omega)$. [*Hint:* See pair 22 in Table 4.1. Use the fact that $\int_{-\infty}^{\infty} e^{-x^2/2}\,dx = \sqrt{2\pi}$.]

4.6-3 Use Parseval's theorem of Eq. (4.45) to show that

$$\int_{-\infty}^{\infty} \text{sinc}^2(kx)\,dx = \frac{\pi}{k}$$

4.6-4 A lowpass signal $x(t)$ is applied to a squaring device. The squarer output $x^2(t)$ is applied to a lowpass filter of bandwidth Δf (in hertz) (Fig. P4.6-4). Show that if Δf is very small ($\Delta f \to 0$), then the filter output is a dc signal $y(t) \approx 2E_x\Delta f$. [*Hint:* If $x^2(t) \Longleftrightarrow A(\omega)$, then show that $Y(\omega) \approx [4\pi A(0)\Delta f]\delta(\omega)$ if $\Delta f \to 0$. Now, show that $A(0) = E_x$.]

4.6-5 Generalize Parseval's theorem to show that for real, Fourier-transformable signals $x_1(t)$ and $x_2(t)$:

$$\int_{-\infty}^{\infty} x_1(t)x_2(t)\,dt = \frac{1}{2\pi}\int_{-\infty}^{\infty} X_1(-\omega)X_2(\omega)\,d\omega = \frac{1}{2\pi}\int_{-\infty}^{\infty} X_1(\omega)X_2(-\omega)\,d\omega$$

4.6-6 Show that

$$\int_{-\infty}^{\infty} \text{sinc}(Wt - m\pi)\,\text{sinc}(Wt - n\pi)\,dt = \begin{cases} 0 & m \neq n \\ \dfrac{\pi}{W} & m = n \end{cases}$$

[*Hint:* Recognize that

$$\text{sinc}(Wt - k\pi) = \text{sinc}\left[W\left(t - \tfrac{k\pi}{W}\right)\right] \Longleftrightarrow \tfrac{\pi}{W}\,\text{rect}\left(\tfrac{\omega}{2W}\right)e^{-jk\pi\omega/W}$$

Use this fact and the result in Prob. 4.6-5.]

4.6-7 (a) What does it mean to compute the 95% essential bandwidth B of a signal $x(t)$ with Fourier transform $X(\omega)$?

(b) Determine the 95% essential bandwidth B of a signal with spectrum $X(\omega) = \text{rect}(\omega)$.

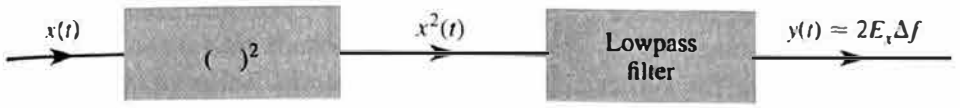

Figure P4.6-4

(c) Determine the 95% essential bandwidth B of a signal with spectrum $X(\omega) = \Delta(\omega)$.

4.6-8 Using a 95% energy criterion, determine the essential bandwidth B of a signal that has a Fourier transform given by $X(\omega) = e^{-|\omega|}$.

4.6-9 For the signal

$$x(t) = \frac{2a}{t^2 + a^2}$$

determine the essential bandwidth B (in hertz) of $x(t)$ such that the energy contained in the spectral components of $x(t)$ of frequencies below B Hz is 99% of the signal energy E_x.

4.7-1 For each of the following baseband signals **(i)** $m(t) = \cos 1000t$, **(ii)** $m(t) = 2\cos 1000t + \cos 2000t$, and **(iii)** $m(t) = \cos 1000t \cos 3000t$:

(a) Sketch the spectrum of $m(t)$.

(b) Sketch the spectrum of the DSB-SC signal $m(t)\cos 10{,}000t$.

(c) Identify the upper sideband (USB) and the lower sideband (LSB) spectra.

(d) Identify the frequencies in the baseband, and the corresponding frequencies in the DSB-SC, USB, and LSB spectra. Explain the nature of frequency shifting in each case.

4.7-2 A message signal $m(t)$ with spectrum $M(\omega) = \frac{1}{1000}\Delta\left(\frac{\omega}{2\pi 6000}\right)$ is to be transmitted using a communication system. Assume all single-sideband systems have suppressed carriers.

(a) What is the hertzian bandwidth of $m(t)$?

(b) Sketch the spectrum of the transmitted signal if the communication system is DSB-SC with $\omega_c = 2\pi\ 100{,}000$.

(c) Sketch the spectrum of the transmitted signal if the communication system is AM with $\omega_c = 2\pi\ 100{,}000$ and a modulation index of $\mu = 1$. What is the corresponding carrier amplitude A?

(d) Sketch the spectrum of the transmitted signal if the communication system is USB with $\omega_c = 2\pi\ 100{,}000$.

(e) Sketch the spectrum of the transmitted signal if the communication system is LSB with $\omega_c = 2\pi\ 100{,}000$.

(f) Suppose we want to transmit $m(t)$ on each of an FDM system's four channels: DSB-SC at carrier ω_1, AM ($\mu = 1$) at carrier ω_2, USB at carrier ω_3, and LSB at carrier ω_4. Determine carrier frequencies $\omega_1 < \omega_2 < \omega_3 < \omega_4$ so that the FDM spectrum begins at a frequency of 100,000 Hz with 5,000 Hz deadbands separating adjacent messages. What is the end hertzian frequency of the FDM signal?

4.7-3 You are asked to design a DSB-SC modulator to generate a modulated signal $km(t)\cos\omega_c t$, where $m(t)$ is a signal bandlimited to B Hz (Fig. P4.7-3a). Figure P4.7-3b shows a

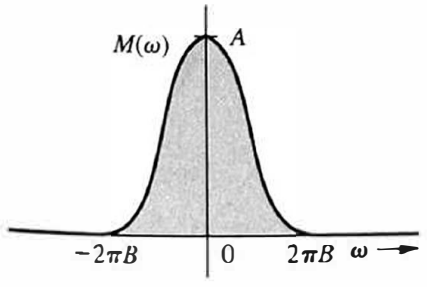

(a)

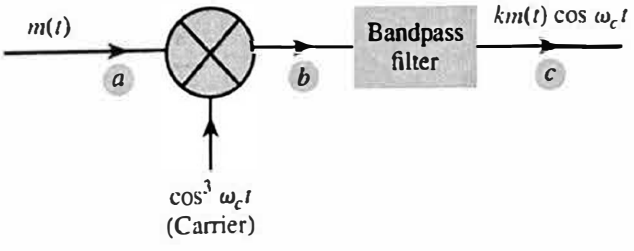

(b)

Figure P4.7-3

DSB-SC modulator available in the stockroom. The bandpass filter is tuned to ω_c and has a bandwidth of $2B$ Hz. The carrier generator available generates not $\cos \omega_c t$, but $\cos^3 \omega_c t$.

(a) Explain whether you would be able to generate the desired signal using only this equipment. If so, what is the value of k?

(b) Determine the signal spectra at points b and c, and indicate the frequency bands occupied by these spectra.

(c) What is the minimum usable value of ω_c?

(d) Would this scheme work if the carrier generator output were $\cos^2 \omega_c t$? Explain.

(e) Would this scheme work if the carrier generator output were $\cos^n \omega_c t$ for any integer $n \geq 2$?

4.7-4 In practice, the analog multiplication operation is difficult and expensive. For this reason, in amplitude modulators, it is necessary to find some alternative to multiplication of $m(t)$ with $\cos \omega_c t$. Fortunately, for this purpose, we can replace multiplication with a switching operation. A similar observation applies to demodulators. In the scheme depicted in Fig. P4.7-4a, the period of the rectangular periodic pulse $x(t)$ shown in Fig. P4.7-4b is $T_0 = 2\pi/\omega_c$. The bandpass filter is centered at $\pm\omega_c$ and has a bandwidth of $2B$ Hz. Note that multiplication by a square periodic pulse $x(t)$ in Fig. P4.7-4b amounts to periodic on–off switching of $m(t)$, which is bandlimited to B Hz. Such a switching operation is relatively simple and inexpensive. Show that this scheme can generate an amplitude-modulated signal $k \cos \omega_c t$. Determine the value of k. Show that the same scheme can also be used for demodulation, provided the bandpass filter in Fig. P4.7-4a is replaced by a lowpass (or baseband) filter.

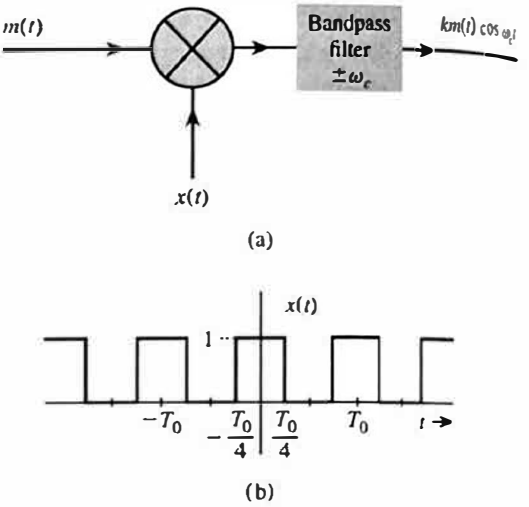

Figure P4.7-4

4.7-5 Figure P4.7-5a shows a scheme to transmit two signals $m_1(t)$ and $m_2(t)$ simultaneously on the same channel (without causing spectral interference). Such a scheme, which transmits more than one signal, is known as signal *multiplexing*. In this case, we transmit multiple signals by sharing an available spectral band on the channel; hence, this is an example of the *frequency-division* multiplexing. The signal at point b is the multiplexed signal, which now modulates a carrier of frequency

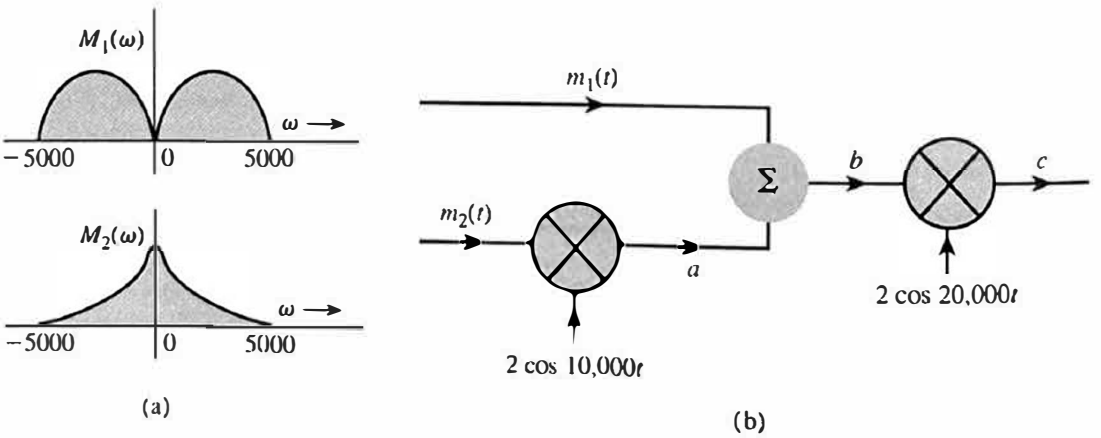

Figure P4.7-5

20,000 rad/s. The modulated signal at point c is now transmitted over the channel.

(a) Sketch the spectra at points a, b, and c.

(b) What must be the minimum bandwidth of the channel?

(c) Design a receiver to recover signals $m_1(t)$ and $m_2(t)$ from the modulated signal at point c.

4.7-6 The system shown in Fig. P4.7-6 is used for scrambling audio signals. The output $y(t)$ is the scrambled version of the input $m(t)$.

(a) Find the spectrum of the scrambled signal $y(t)$.

(b) Suggest a method of descrambling $y(t)$ to obtain $m(t)$.

A slightly modified version of this scrambler was first used commercially on the 25-mile radio-telephone circuit connecting Los Angeles and Santa Catalina Island.

4.7-7 Figure P4.7-7 presents a scheme for coherent (synchronous) demodulation. Show that this scheme can demodulate the AM signal $[A + m(t)]\cos \omega_c t$ regardless of the value of A.

4.7-8 Sketch the AM signal $[A + m(t)]\cos \omega_c t$ for the periodic triangle signal $m(t)$ illustrated in Fig. P4.7-8 corresponding to the following modulation indices:

(a) $\mu = 0.5$

(b) $\mu = 1$

(c) $\mu = 2$

(d) $\mu = \infty$

How do you interpret the case $\mu = \infty$?

4.8-1 Sketch $\varphi_{FM}(t)$ and $\varphi_{PM}(t)$ for the modulating signal $m(t)$ depicted in Fig. P4.8-1, given $\omega_c = 2\pi \times 10^7$, $k_f = 2\pi \times 10^5$, and $k_p = 50\pi$.

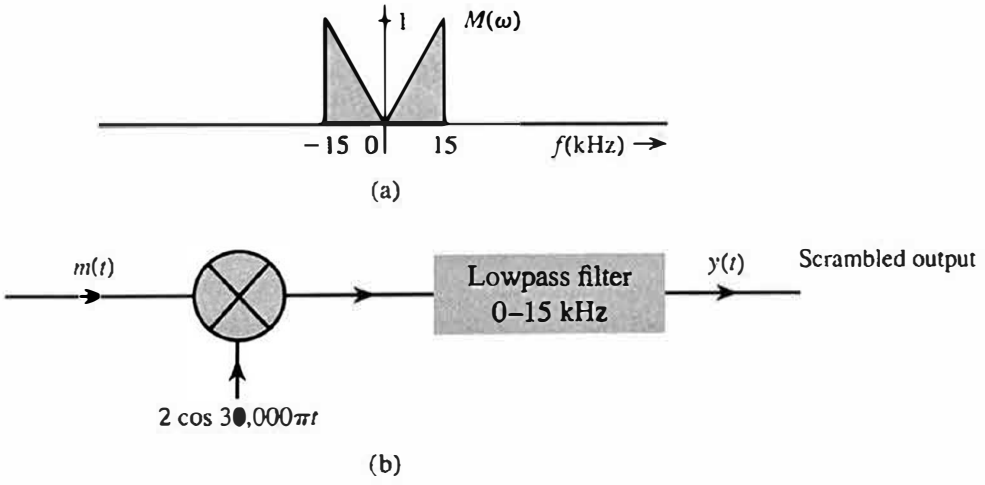

Figure P4.7-6

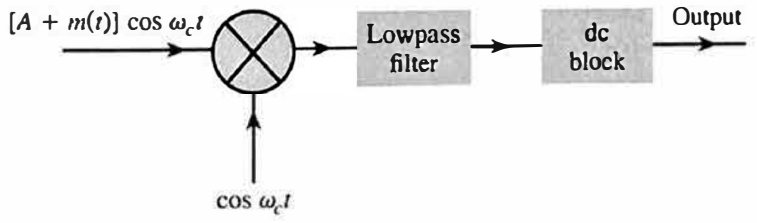

Figure P4.7-7

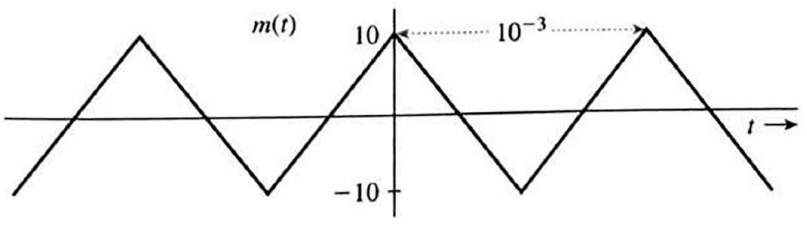

Figure P4.7-8

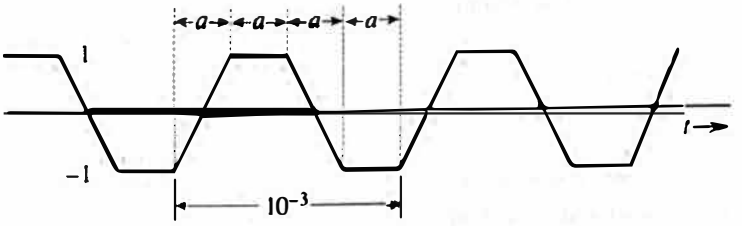

Figure P4.8-1

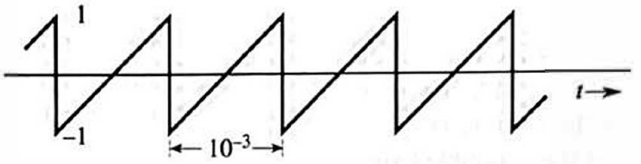

Figure P4.8-2

4.8-2 A baseband signal $m(t)$ is a periodic saw tooth signal shown in Fig. P4.8-2. Sketch $\varphi_{FM}(t)$ and $\varphi_{PM}(t)$ for this $m(t)$ if $\omega_c = 2\pi \times 10^6$, $k_f = 20{,}000\pi$, and $k_p = \pi/2$. Explain why it is necessary to use $k_p < \pi$ in this case.

4.8-3 Consider a modulating signal

$$m(t) = 2\cos 100t + 18\cos 2000\pi t$$

Determine the bandwidths of the corresponding $\varphi_{FM}(t)$ and $\varphi_{PM}(t)$ if $k_f = 1000\pi$ and $k_p = 1$.

4.8-4 An angle-modulated signal is described by the equation

$$\varphi_{EM}(t) = 10\cos(\omega_c t + 0.1\sin 2000\pi t)$$

(a) Find the frequency deviation Δf.
(b) Estimate the bandwidth of $\varphi_{EM}(t)$.

4.8-5 Repeat Prob. 4.8-4 if

$$\varphi_{EM}(t) = 5\cos(\omega_c t + 20\sin 1000\pi t + 10\sin 2000\pi t)$$

4.10-1 Consider the signal $x(t)$ defined as

$$x(t) = \begin{cases} 1-|t| & -\frac{1}{2} \le t \le \frac{1}{2} \\ 0 & \text{otherwise} \end{cases}$$

(a) Sketch the signal $x(t)$ over $-2 \le t \le 2$.
(b) Use time-differentiation and other Fourier transform properties to determine $X(\omega)$. The only integration you should use is to determine the dc component $X(0)$.
(c) Using MATLAB, verify the correctness of $X(\omega)$ by synthesizing a 3-periodic replication of the original time-domain signal $x(t)$.

[*Hint:* Follow the approach taken in Ex. 4.17.]

4.10-2 Consider the signal $x(t) = |t|\text{rect}\left(\frac{t-1}{3}\right)$.
(a) Sketch the signal $x(t)$ over $-5 \le t \le 5$.
(b) Use time-differentiation and other Fourier transform properties to determine $X(\omega)$. The only integration you should use is to determine the dc component $X(0)$.
(c) Use MATLAB to plot the magnitude spectrum $|X(\omega)|$ and the phase spectrum $\angle X(\omega)$ over suitable ranges of ω.
(d) Using MATLAB, verify the correctness of $X(\omega)$ by synthesizing a 10-periodic replication of the original time-domain signal $x(t)$.

[*Hint:* Follow the approach taken in Ex. 4.17.]

4.10-3 Consider the continuous-time aperiodic signal $x(t) = \text{rect}(t)$ with Fourier transform $X(\omega) = \text{sinc}(\omega/2)$. Furthermore, let $y(t) = (1 - |t-1|)(u(t) - u(t-2))$ with Fourier transform $Y(\omega)$.
(a) Express the Fourier transform $Y(\omega)$ in terms of $X(\omega)$.
(b) Suppose we create Fourier series coefficients V_k by sampling $Y(\omega)$ according

to $V_k = Y(2\pi k/3)$. Sketch the corresponding time-domain signal $v(t)$ over a suitable range of time t.

(c) Use MATLAB to synthesize and plot $v(t)$ using the Fourier series coefficients $V_k = Y(2\pi k/3)$. Verify that the synthesized waveform matches the result of part (b).

(d) Suppose we again create Fourier series coefficients V_k according to $V_k = Y(2\pi k/3)$. Next, we upsample V_k by factor 2 to create W_k. Sketch the time domain signal $p(t)$ that has Fourier series coefficients $P_k = V_k + W_k$.

(e) Use MATLAB to synthesize and plot $p(t)$ using the Fourier series coefficients $P_k = V_k + W_k$ defined in part (d). Verify that the synthesized waveform matches the result of part (d).

4.10-4 Consider the signal $x(t) = e^{-at}u(t)$. Modify CH4MP2 to compute the following essential bandwidths:

(a) Setting $a=1$, determine the essential bandwidth W_1 that contains 95% of the signal energy. Compare this value with the theoretical value presented in Ex. 4.20.

(b) Setting $a=2$, determine the essential bandwidth W_2 that contains 90% of the signal energy.

(c) Setting $a=3$, determine the essential bandwidth W_3 that contains 75% of the signal energy.

4.10-5 A unit amplitude pulse with duration τ is defined as

$$x(t) = \begin{cases} 1 & |t| \le \tau/2 \\ 0 & \text{otherwise} \end{cases}$$

(a) Determine the duration τ_1 that results in a 95% essential bandwidth of 5 Hz.

(b) Determine the duration τ_2 that results in a 90% essential bandwidth of 10 Hz.

(c) Determine the duration τ_3 that results in a 75% essential bandwidth 20 Hz.

4.10-6 Consider the signal $x(t) = e^{-at}u(t)$.

(a) Determine the decay parameter a_1 that results in a 95% essential bandwidth of 5 Hz.

(b) Determine the decay parameter a_2 that results in a 90% essential bandwidth of 10 Hz.

(c) Determine the decay parameter a_3 that results in a 75% essential bandwidth 20 Hz.

4.10-7 Use MATLAB to determine the 95, 90, and 75% essential bandwidths of a 1-second triangle function with a peak amplitude of 1. Recall that a triangle function can be constructed by the convolution of two rectangular pulses.

4.10-8 A 1/3 duty-cycle square-pulse T_0-periodic signal $x(t)$ is described as

$$x(t) = \begin{cases} 1 & -T_0/6 \le t \le T_0/6 \\ 0 & T_0/6 \le |t| \le T_0/2 \\ x(t+T_0) & \forall t \end{cases}$$

(a) Use spectral sampling to determine the Fourier series coefficients D_n of $x(t)$ for $T_0 = 2\pi$. Evaluate and plot D_n for $(0 \le n \le 10)$.

(b) Use spectral sampling to determine the Fourier series coefficients D_n of $x(t)$ for $T_0 = \pi$. Evaluate and plot D_n for $(0 \le n \le 10)$. How does this result compare with your answer to part (a)? What can be said about the relation of T_0 to D_n for signal $x(t)$, which has a fixed duty cycle of 1/3?

4.10-9 Determine the Fourier transform of a Gaussian pulse defined as $x(t) = e^{-t^2}$. Plot both $x(t)$ and $X(\omega)$. How do the two curves compare? [*Hint:*

$$\frac{1}{\sqrt{2\pi}} \int_{-\infty}^{\infty} e^{-(t-a)^2/2} dt = 1$$

for any real or imaginary a.]

CHAPTER 5

SAMPLING

A continuous-time signal can be processed by applying its samples through a discrete-time system. For this purpose, it is important to maintain the signal sampling rate high enough to permit the reconstruction of the original signal from these samples without error (or with an error within a given tolerance). The necessary quantitative framework for this purpose is provided by the sampling theorem derived in Sec. 5.1.

Sampling theory is the bridge between the continuous-time and discrete-time worlds. The information inherent in a sampled continuous-time signal is equivalent to that of a discrete-time signal. A sampled continuous-time signal is a sequence of impulses, while a discrete-time signal presents the same information as a sequence of numbers. These are basically two different ways of presenting the same data. Clearly, all the concepts in the analysis of sampled signals apply to discrete-time signals. We should not be surprised to see that the Fourier spectra of the two kinds of signal are also the same (within a multiplicative constant).

5.1 THE SAMPLING THEOREM

We now show that a real signal whose spectrum is bandlimited to B Hz [$X(\omega) = 0$ for $|\omega| > 2\pi B$] can be reconstructed exactly (without any error) from its samples taken uniformly at a rate $f_s > 2B$ samples per second. In other words, the minimum sampling frequency is $f_s = 2B$ Hz.[†]

To prove the sampling theorem, consider a signal $x(t)$ (Fig. 5.1a) whose spectrum is bandlimited to B Hz (Fig. 5.1b).[‡] For convenience, spectra are shown as functions of ω as well as of f (hertz). Sampling $x(t)$ at a rate of f_s Hz (f_s samples per second) can be accomplished by multiplying $x(t)$ by an impulse train $\delta_T(t)$ (Fig. 5.1c), consisting of unit impulses repeating periodically every T seconds, where $T = 1/f_s$. The schematic of a sampler is shown in Fig. 5.1d.

[†] The theorem stated here (and proved subsequently) applies to lowpass signals. A bandpass signal whose spectrum exists over a frequency band $f_c - (B/2) < |f| < f_c + (B/2)$ has a bandwidth of B Hz. Such a signal is uniquely determined by $2B$ samples per second. In general, the sampling scheme is a bit more complex in this case. It uses two interlaced sampling trains, each at a rate of B samples per second. See, for example, [1].

[‡] The spectrum $X(\omega)$ in Fig. 5.1b is shown as real, for convenience. However, our arguments are valid for complex $X(\omega)$ as well.

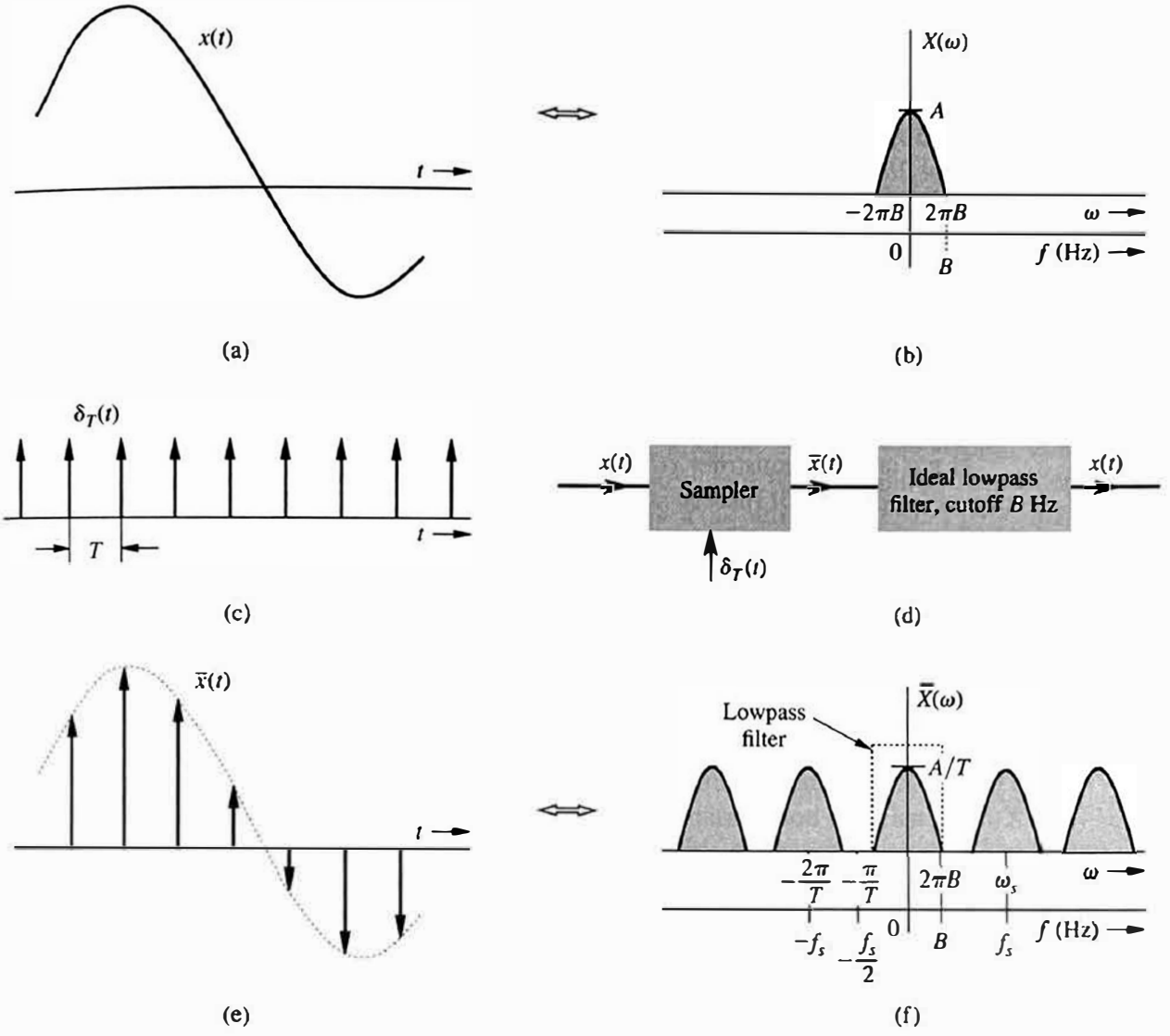

Figure 5.1 Sampled signal and its Fourier spectrum.

The resulting sampled signal $\bar{x}(t)$ is shown in Fig. 5.1e. The sampled signal consists of impulses spaced every T seconds (the sampling interval). The nth impulse, located at $t = nT$, has a strength $x(nT)$, the value of $x(t)$ at $t = nT$.

$$\bar{x}(t) = x(t)\delta_T(t) = \sum_n x(nT)\delta(t - nT)$$

Because the impulse train $\delta_T(t)$ is a periodic signal of period T, it can be expressed as a trigonometric Fourier series like that already obtained in Ex. 3.13 [Eq. (3.52)]:

$$\delta_T(t) = \frac{1}{T}[1 + 2\cos\omega_s t + 2\cos 2\omega_s t + 2\cos 3\omega_s t + \cdots] \qquad \omega_s = \frac{2\pi}{T} = 2\pi f_s$$

Therefore,

$$\bar{x}(t) = x(t)\delta_T(t) = \frac{1}{T}[x(t) + 2x(t)\cos\omega_s t + 2x(t)\cos 2\omega_s t + 2x(t)\cos 3\omega_s t + \cdots] \tag{5.1}$$

To find $\overline{X}(\omega)$, the Fourier transform of $\bar{x}(t)$, we take the Fourier transform of the right-hand side of Eq. (5.1), term by term. The transform of the first term in the brackets is $X(\omega)$. The transform of the second term $2x(t)\cos\omega_s t$ is $X(\omega-\omega_s)+X(\omega+\omega_s)$ [see Eq. (4.32)]. This represents spectrum $X(\omega)$ shifted to ω_s and $-\omega_s$. Similarly, the transform of the third term $2x(t)\cos 2\omega_s t$ is $X(\omega-2\omega_s)+X(\omega+2\omega_s)$, which represents the spectrum $X(\omega)$ shifted to $2\omega_s$ and $-2\omega_s$, and so on to infinity. This result means that the spectrum $\overline{X}(\omega)$ consists of $X(\omega)$ repeating periodically with period $\omega_s = 2\pi/T$ rad/s, or $f_s = 1/T$ Hz, as depicted in Fig. 5.1f. There is also a constant multiplier $1/T$ in Eq. (5.1). Therefore,

$$\overline{X}(\omega) = \frac{1}{T}\sum_{n=-\infty}^{\infty} X(\omega - n\omega_s) \tag{5.2}$$

If we are to reconstruct $x(t)$ from $\bar{x}(t)$, we should be able to recover $X(\omega)$ from $\overline{X}(\omega)$. This recovery is possible if there is no overlap between successive cycles of $\overline{X}(\omega)$. Figure 5.1f indicates that this requires

$$f_s > 2B \tag{5.3}$$

Also, the sampling interval $T = 1/f_s$. Therefore,

$$T < \frac{1}{2B}$$

Thus, as long as the sampling frequency f_s is greater than twice the signal bandwidth B (in hertz), $\overline{X}(\omega)$ consists of nonoverlapping repetitions of $X(\omega)$. Figure 5.1f shows that the gap between the two adjacent spectral repetitions is $f_s - 2B$ Hz, and $x(t)$ can be recovered from its samples $\bar{x}(t)$ by passing the sampled signal $\bar{x}(t)$ through an ideal lowpass filter having a bandwidth of any value between B and $f_s - B$ Hz. The minimum sampling rate $f_s = 2B$ required to recover $x(t)$ from its samples $\bar{x}(t)$ is called the *Nyquist rate* for $x(t)$, and the corresponding sampling interval $T = 1/2B$ is called the *Nyquist interval* for $x(t)$. Samples of a signal taken at its Nyquist rate are the *Nyquist samples* of that signal.

We are saying that the Nyquist rate $2B$ Hz is the minimum sampling rate required to preserve the information of $x(t)$. This contradicts Eq. (5.3), where we showed that to preserve the information of $x(t)$, the sampling rate f_s needs to be greater than $2B$ Hz. Strictly speaking, Eq. (5.3) is the correct statement. However, if the spectrum $X(\omega)$ contains no impulse or its derivatives at the highest frequency B Hz, then the minimum sampling rate $2B$ Hz is adequate. In practice, it is rare to observe $X(\omega)$ with an impulse or its derivatives at the highest frequency. If the contrary situation were to occur, we should use Eq. (5.3).[†]

[†] An interesting observation is that if the impulse is because of a cosine term, the sampling rate of $2B$ Hz is adequate. However, if the impulse is because of a sine term, then the rate must be greater than $2B$ Hz. This may be seen from the fact that samples of $\sin 2\pi Bt$ using $T = 1/2B$ are all zero because $\sin 2\pi BnT = \sin \pi n = 0$. But, samples of $\cos 2\pi Bt$ are $\cos 2\pi BnT = \cos \pi n = (-1)^n$. We can reconstruct $\cos 2\pi Bt$ from these samples. This peculiar behavior occurs because in the sampled signal spectrum corresponding to the signal $\cos 2\pi Bt$, the impulses, which occur at frequencies $(2n \pm 1)B$ Hz ($n = 0, \pm 1, \pm 2, \ldots$), interact constructively, whereas in the case of $\sin 2\pi Bt$, the impulses, because of their opposite phases ($e^{\pm j\pi/2}$), interact destructively and cancel out in the sampled signal spectrum. Hence, $\sin 2\pi Bt$ cannot be reconstructed from its samples at a rate $2B$ Hz. A similar situation exists for signal $\cos(2\pi Bt + \theta)$, which contains a component of the form $\sin 2\pi Bt$.

The sampling theorem proved here uses samples taken at uniform intervals. This condition is not necessary. Samples can be taken arbitrarily at any instants as long as the sampling instants are recorded and there are, on average, $2B$ samples per second [2]. The essence of the sampling theorem was known to mathematicians for a long time in the form of the *interpolation formula* [see later, Eq. (5.6)]. The origin of the sampling theorem was attributed by H. S. Black to Cauchy in 1841. The essential idea of the sampling theorem was rediscovered in the 1920s by Carson, Nyquist, and Hartley.

EXAMPLE 5.1 Sampling at, Below, and Above the Nyquist Rate

In this example, we examine the effects of sampling a signal at the Nyquist rate, below the Nyquist rate (undersampling), and above the Nyquist rate (oversampling). Consider a signal $x(t) = \text{sinc}^2(5\pi t)$ (Fig. 5.2a) whose spectrum is $X(\omega) = 0.2\,\Delta(\omega/20\pi)$ (Fig. 5.2b). The bandwidth of this signal is 5 Hz (10π rad/s). Consequently, the Nyquist rate is 10 Hz; that is, we must sample the signal at a rate no less than 10 samples/s. The Nyquist interval is $T = 1/2B = 0.1$ second.

Recall that the sampled signal spectrum consists of $(1/T)X(\omega) = (0.2/T)\,\Delta(\omega/20\pi)$ repeating periodically with a period equal to the sampling frequency f_s Hz. For the three sampling rates $f_s = 5$ Hz (undersampling), 10 Hz (Nyquist rate), and 20 Hz (oversampling), we see that

f_s (Hz)	$T = \frac{1}{f_s}$ (s)	$\frac{1}{T}X(\omega)$	Comments
5	0.2	$\Delta\left(\frac{\omega}{20\pi}\right)$	Undersampling
10	0.1	$2\Delta\left(\frac{\omega}{20\pi}\right)$	Nyquist rate
20	0.05	$4\Delta\left(\frac{\omega}{20\pi}\right)$	Oversampling

In the first case (undersampling), the sampling rate is 5 Hz (5 samples/s), and the spectrum $(1/T)X(\omega)$ repeats every 5 Hz (10π rad/s). The successive spectra overlap, as depicted in Fig. 5.2d, and the spectrum $X(\omega)$ is not recoverable from $\overline{X}(\omega)$; that is, $x(t)$ cannot be reconstructed from its samples $\bar{x}(t)$ in Fig. 5.2c. In the second case, we use the Nyquist sampling rate of 10 Hz (Fig. 5.2e). The spectrum $\overline{X}(\omega)$ consists of back-to-back, nonoverlapping repetitions of $(1/T)X(\omega)$ repeating every 10 Hz. Hence, $X(\omega)$ can be recovered from $\overline{X}(\omega)$ using an ideal lowpass filter of bandwidth 5 Hz (Fig. 5.2f). Finally, in the last case of

For this reason, it is advisable to maintain a sampling rate above $2B$ Hz if a finite-amplitude component of a sinusoid of frequency B Hz is present in the signal.

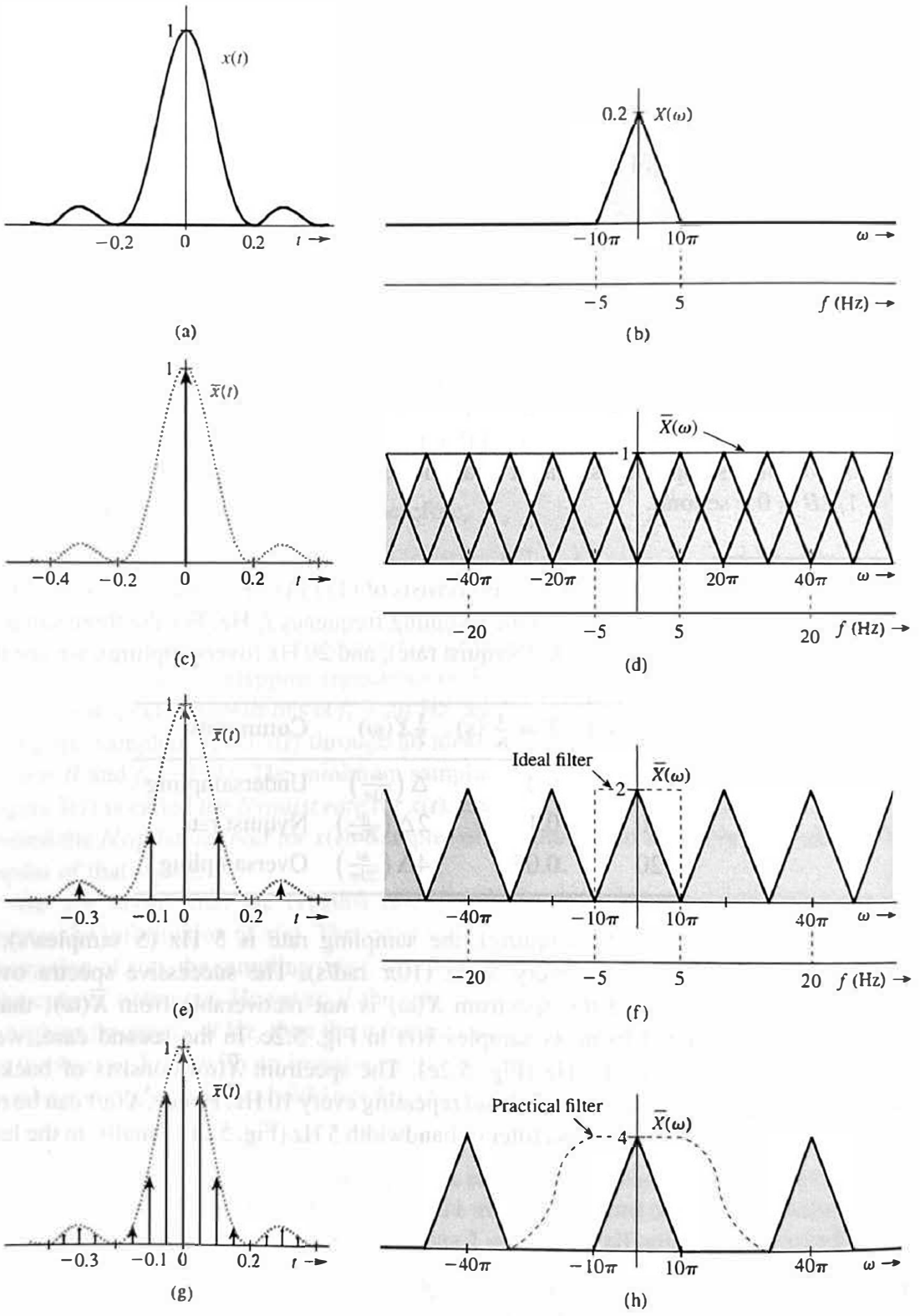

Figure 5.2 Effects of undersampling and oversampling.

oversampling (sampling rate 20 Hz), the spectrum $\overline{X}(\omega)$ consists of nonoverlapping repetitions of $(1/T)X(\omega)$ (repeating every 20 Hz) with empty bands between successive cycles (Fig. 5.2h). Hence, $X(\omega)$ can be recovered from $\overline{X}(\omega)$ by using an ideal lowpass filter or even a practical lowpass filter (shown dashed in Fig. 5.2h).[†]

DRILL 5.1 Nyquist Sampling

Find the Nyquist rate and the Nyquist sampling interval for the signals $\text{sinc}(100\pi t)$ and $\text{sinc}(100\pi t) + \text{sinc}(50\pi t)$.

ANSWER

The Nyquist sampling interval is 0.01 s and the Nyquist sampling rate is 100 Hz for both signals.

For Skeptics Only

Rare is the reader who, at first encounter, is not skeptical of the sampling theorem. It seems impossible that Nyquist samples can define the one and only signal that passes through those sample values. We can easily picture an infinite number of signals passing through a given set of samples. However, among all these (infinite number of) signals, only one has the minimum bandwidth $B \leq 1/2T$ Hz, where T is the sampling interval (see Prob. 5.2-15).

To summarize, for a given set of samples taken at a rate f_s Hz, there is only one signal of bandwidth $B \leq f_s/2$ that passes through those samples. All other signals that pass through those samples have bandwidths higher than $f_s/2$, and the samples are sub-Nyquist rate samples for those signals.

5.1.1 Practical Sampling

In proving the sampling theorem, we assumed ideal samples obtained by multiplying a signal $x(t)$ by an impulse train that is physically unrealizable. In practice, we multiply a signal $x(t)$ by a train of pulses of finite width, depicted in Fig. 5.3c. The sampler is shown in Fig. 5.3d. The sampled signal $\bar{x}(t)$ is illustrated in Fig. 5.3e. We wonder whether it is possible to recover or reconstruct $x(t)$ from this $\bar{x}(t)$. Surprisingly, the answer is affirmative, provided the sampling rate is not below the Nyquist rate. The signal $x(t)$ can be recovered by lowpass filtering $\bar{x}(t)$ as if it were sampled by impulse train.

The plausibility of this result becomes apparent when we consider the fact that reconstruction of $x(t)$ requires the knowledge of the Nyquist sample values. This information is available or built

[†] The filter should have a constant gain between 0 and 5 Hz and zero gain beyond 10 Hz. In practice, the gain beyond 10 Hz can be made negligibly small, but not zero.

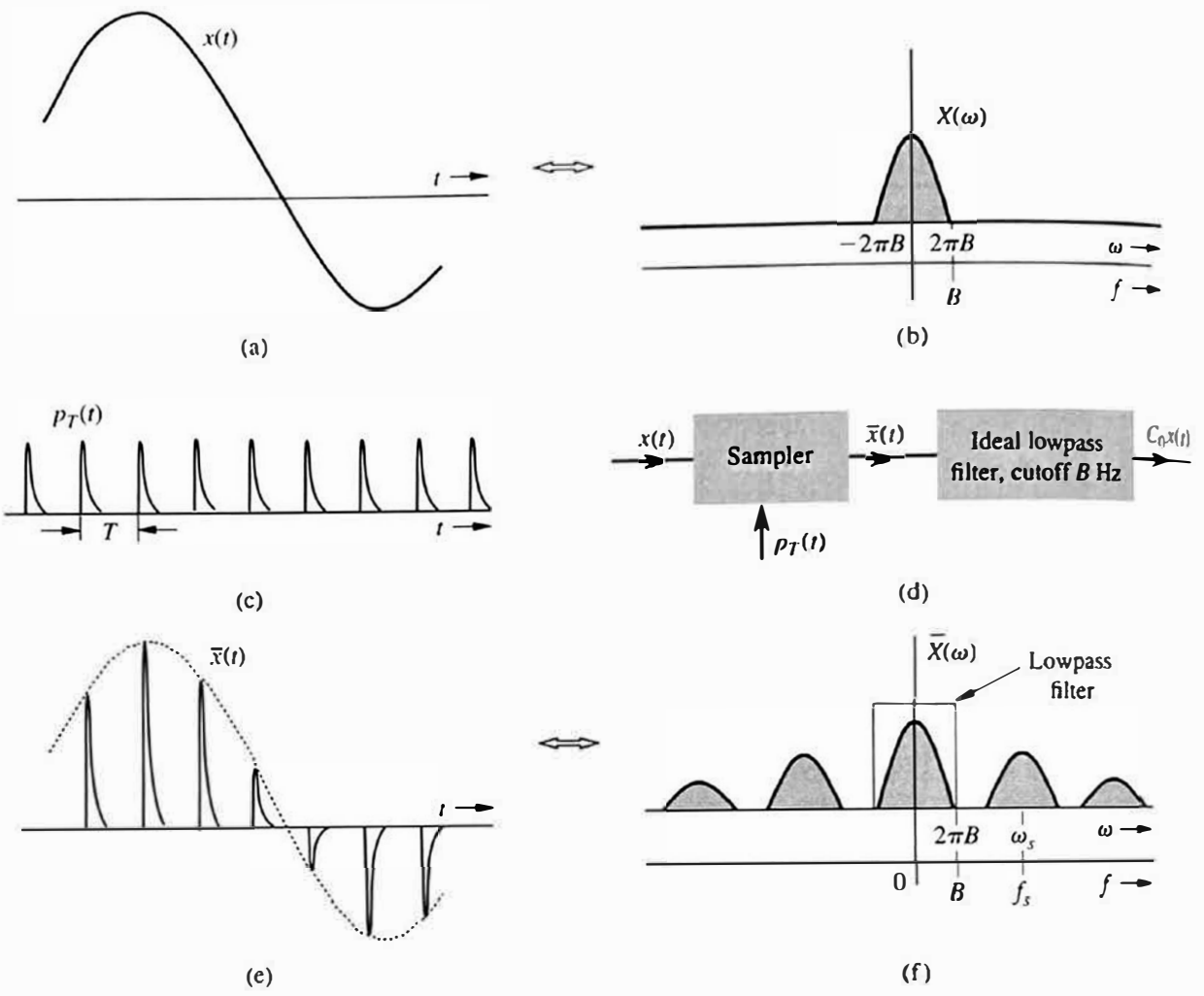

Figure 5.3 Effect of practical sampling.

into the sampled signal $\bar{x}(t)$ in Fig. 5.3e because the nth sampled pulse strength is $x(nT)$. To prove the result analytically, we observe that the sampling pulse train $p_T(t)$ depicted in Fig. 5.3c, being a periodic signal, can be expressed as a trigonometric Fourier series

$$p_T(t) = C_0 + \sum_{n=1}^{\infty} C_n \cos(n\omega_s t + \theta_n) \qquad \omega_s = \frac{2\pi}{T}$$

Thus,

$$\bar{x}(t) = x(t)p_T(t) = x(t)\left[C_0 + \sum_{n=1}^{\infty} C_n \cos(n\omega_s t + \theta_n)\right]$$

$$= C_0 x(t) + \sum_{n=1}^{\infty} C_n x(t) \cos(n\omega_s t + \theta_n)$$

The sampled signal $\bar{x}(t)$ consists of $C_0x(t)$, $C_1x(t)\cos(\omega_s t + \theta_1)$, $C_2x(t)\cos(2\omega_s t + \theta_2)$, ... Note that the first term $C_0x(t)$ is the desired signal and all the other terms are modulated signals with spectra centered at $\pm\omega_s, \pm 2\omega_s, \pm 3\omega_s, \ldots$, as illustrated in Fig. 5.3f. Clearly, the signal $x(t)$ can

be recovered by lowpass filtering of $\bar{x}(t)$, as shown in Fig. 5.3d. As before, it is necessary that $\omega_s > 4\pi B$ (or $f_s > 2B$).

EXAMPLE 5.2 Practical Sampling

Demonstrate practical sampling by sampling signal $x(t) = \text{sinc}^2(5\pi t)$ with the rectangular pulse sequence $p_T(t)$ illustrated in Fig. 5.4c. Sketch the original and sampled signals and their spectra, and discuss recovery of $x(t)$ from its samples.

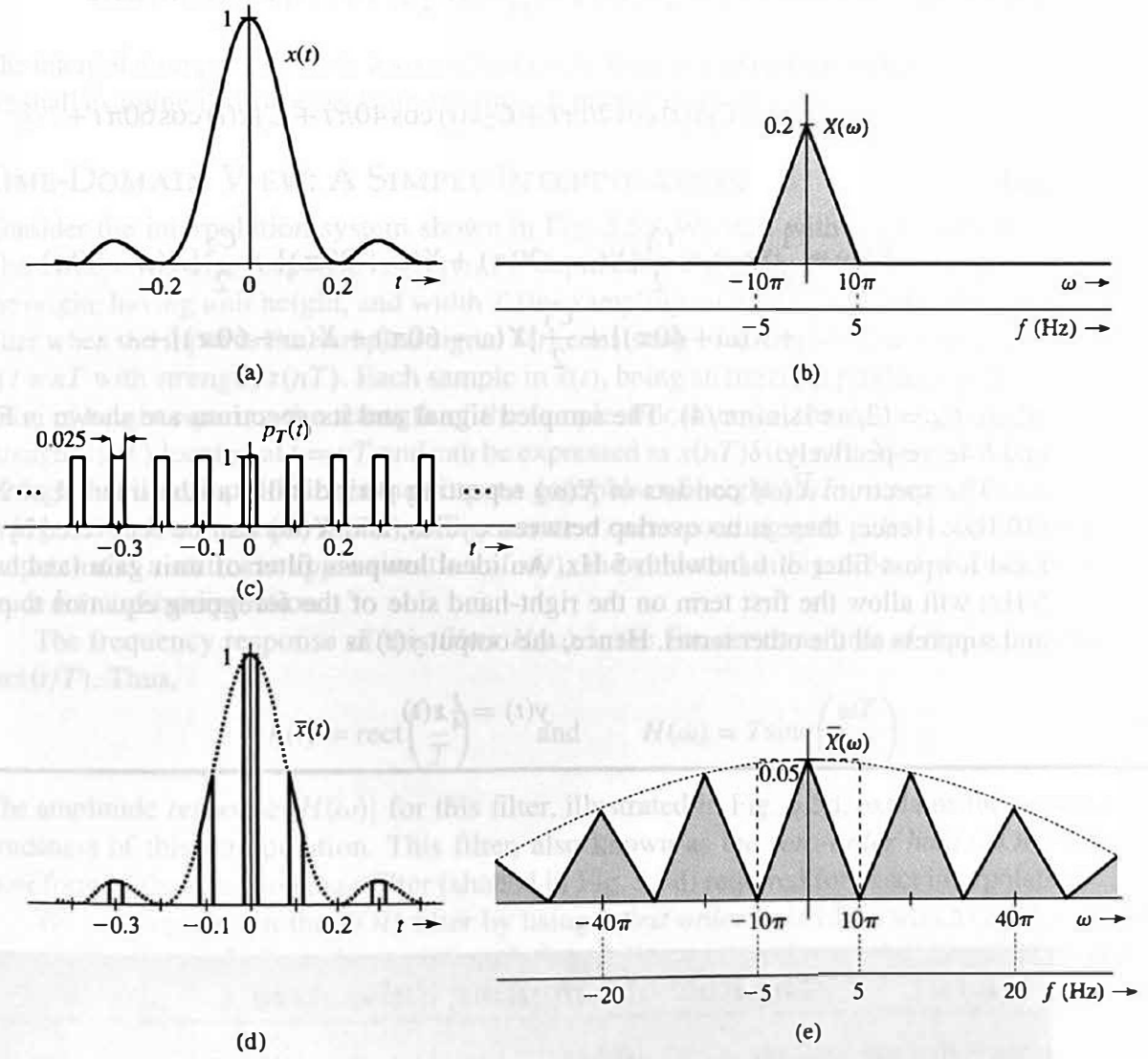

Figure 5.4 An example of practical sampling.

The signal $x(t)$ and its spectrum are shown in Figs. 5.4a and 5.4b, respectively.

The period of $p_T(t)$ is 0.1 second so that the fundamental frequency (which is the sampling frequency) is 10 Hz. Hence, $\omega_s = 20\pi$. The Fourier series for $p_T(t)$ can be expressed as

$$p_T(t) = C_0 + \sum_{n=1}^{\infty} C_n \cos n\omega_s t$$

Hence,

$$\begin{aligned}\bar{x}(t) &= x(t)p_T(t)\\ &= C_1x(t) + C_1x(t)\cos 20\pi t + C_2x(t)\cos 40\pi t + C_3x(t)\cos 60\pi t + \cdots\end{aligned}$$

Use of Eq. (3.41) yields $C_0 = \frac{1}{4}$ and $C_n = \frac{2}{n\pi}\sin\left(\frac{n\pi}{4}\right)$. Consequently, we have

$$\begin{aligned}\bar{x}(t) &= x(t)p_T(t)\\ &= \tfrac{1}{4}x(t) + C_1x(t)\cos 20\pi t + C_2x(t)\cos 40\pi t + C_3x(t)\cos 60\pi t + \cdots\end{aligned}$$

and

$$\begin{aligned}\overline{X}(\omega) = \frac{1}{4}X(\omega) + \frac{C_1}{2}[X(\omega - 20\pi) + X(\omega + 20\pi)] + \frac{C_2}{2}[X(\omega - 40\pi)\\ + X(\omega + 40\pi)] + \frac{C_3}{2}[X(\omega - 60\pi) + X(\omega + 60\pi)] + \cdots\end{aligned}$$

where $C_n = (2/n\pi)\sin(n\pi/4)$. The sampled signal and its spectrum are shown in Figs. 5.4d and 5.4e, respectively.

The spectrum $\overline{X}(\omega)$ consists of $X(\omega)$ repeating periodically at the interval of 20π rad/s (10 Hz). Hence, there is no overlap between cycles, and $X(\omega)$ can be recovered by using an ideal lowpass filter of bandwidth 5 Hz. An ideal lowpass filter of unit gain (and bandwidth 5 Hz) will allow the first term on the right-hand side of the foregoing equation to pass fully and suppress all the other terms. Hence, the output $y(t)$ is

$$y(t) = \tfrac{1}{4}x(t)$$

DRILL 5.2 The Role of Sampling Pulse Area

Show that the basic pulse $p(t)$ used in the sampling pulse train in Fig. 5.4c cannot have zero area if we wish to reconstruct $x(t)$ by lowpass-filtering the sampled signal.

5.2 SIGNAL RECONSTRUCTION

The process of reconstructing a continuous-time signal $x(t)$ from its samples is also known as *interpolation*. In Sec. 5.1, we saw that a signal $x(t)$ bandlimited to B Hz can be reconstructed (interpolated) exactly from its samples if the sampling frequency f_s exceeds $2B$ Hz or the sampling interval T is less than $1/2B$. This reconstruction is accomplished by passing the sampled signal through an ideal lowpass filter of gain T and having a bandwidth of any value between B and $f_s - B$ Hz. From a practical viewpoint, a good choice is the middle value $f_s/2 = 1/2T$ Hz or π/T rad/s. This value allows for small deviations in the ideal filter characteristics on either side of the cutoff frequency. With this choice of cutoff frequency and gain T, the ideal lowpass filter required for signal reconstruction (or interpolation) is

$$H(\omega) = T\,\text{rect}\left(\frac{\omega}{2\pi f_s}\right) = T\,\text{rect}\left(\frac{\omega T}{2\pi}\right) \tag{5.4}$$

The interpolation process here is expressed in the frequency domain as a filtering operation. Now we shall examine this process from the time-domain viewpoint.

TIME-DOMAIN VIEW: A SIMPLE INTERPOLATION

Consider the interpolation system shown in Fig. 5.5a. We start with a very simple interpolating filter, whose impulse response is $\text{rect}\,(t/T)$, depicted in Fig. 5.5b. This is a gate pulse centered at the origin, having unit height, and width T (the sampling interval). We shall find the output of this filter when the input is the sampled signal $\bar{x}(t)$ consisting of an impulse train with the nth impulse at $t = nT$ with strength $x(nT)$. Each sample in $\bar{x}(t)$, being an impulse, produces at the output a gate pulse of height equal to the strength of the sample. For instance, the nth sample is an impulse of strength $x(nT)$ located at $t = nT$ and can be expressed as $x(nT)\delta(t - nT)$. When this impulse passes through the filter, it produces at the output a gate pulse of height $x(nT)$, centered at $t = nT$ (shaded in Fig. 5.5c). Each sample in $\bar{x}(t)$ will generate a corresponding gate pulse, resulting in the filter output that is a staircase approximation of $x(t)$, shown dotted in Fig. 5.5c. This filter thus gives a crude form of interpolation.

The frequency response of this filter $H(\omega)$ is the Fourier transform of the impulse response $\text{rect}\,(t/T)$. Thus,

$$h(t) = \text{rect}\left(\frac{t}{T}\right) \quad \text{and} \quad H(\omega) = T\,\text{sinc}\left(\frac{\omega T}{2}\right) \tag{5.5}$$

The amplitude response $|H(\omega)|$ for this filter, illustrated in Fig. 5.5d, explains the reason for the crudeness of this interpolation. This filter, also known as the *zero-order hold* (ZOH) filter, is a poor form of the ideal lowpass filter (shaded in Fig. 5.5d) required for exact interpolation.[†]

We can improve on the ZOH filter by using a *first-order hold* filter, which results in a linear interpolation instead of a staircase interpolation. A linear interpolator, whose impulse response is a triangle pulse $\Delta(t/2T)$, results in an interpolation in which successive sample tops are connected by straight-line segments (see Prob. 5.2-3).

[†] Figure 5.5b shows that the impulse response of this filter is noncausal, and this filter is not realizable. In practice, we make it realizable by delaying the impulse response by $T/2$. This merely delays the output of the filter by $T/2$.

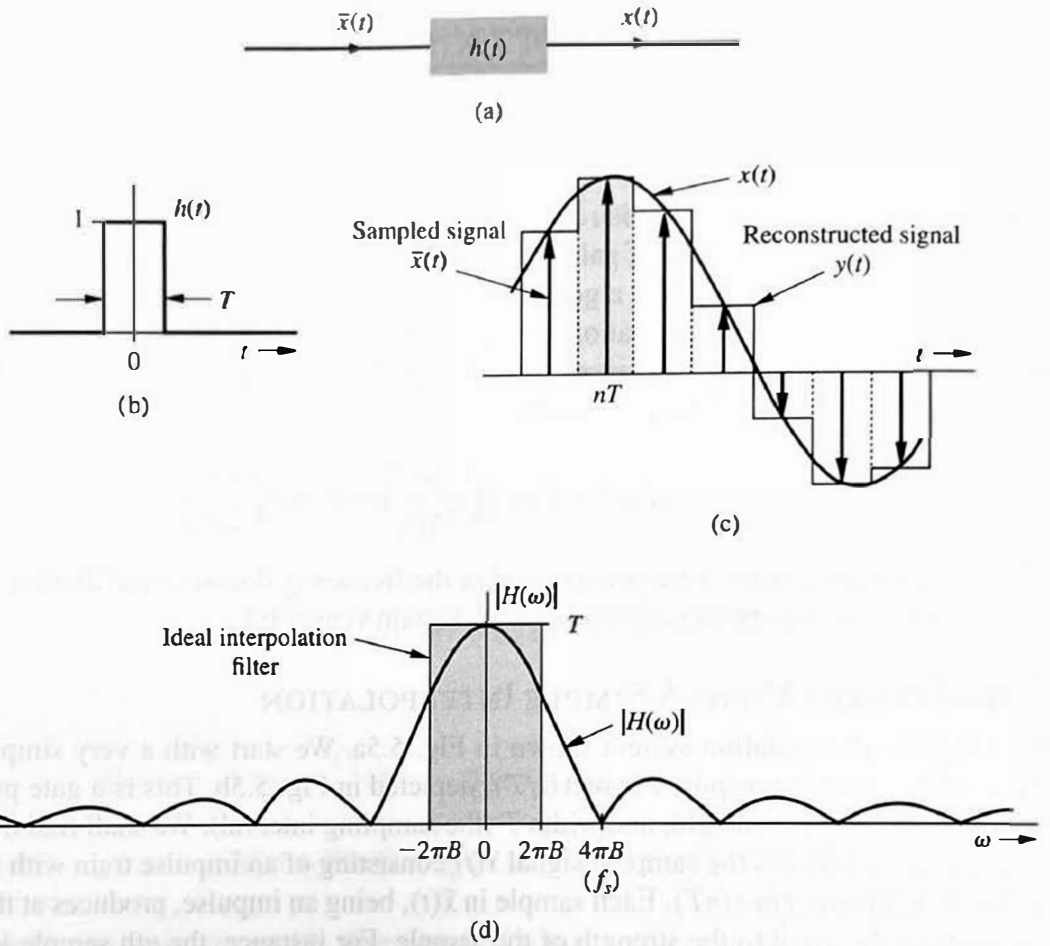

Figure 5.5 Simple interpolation by means of a zero-order hold (ZOH) circuit. (a) ZOH interpolator. **(b)** Impulse response of a ZOH circuit. **(c)** Signal reconstruction by ZOH, as viewed in the time domain. **(d)** Frequency response of a ZOH.

Time-Domain View: An Ideal Interpolation

The ideal interpolation filter frequency response obtained in Eq. (5.4) is illustrated in Fig. 5.6a. The impulse response of this filter, the inverse Fourier transform of $H(\omega)$, is

$$h(t) = \text{sinc}\left(\frac{\pi t}{T}\right)$$

For the Nyquist sampling rate, $T = 1/2B$, and

$$h(t) = \text{sinc}\,(2\pi Bt)$$

This $h(t)$ is depicted in Fig. 5.6b. Observe the interesting fact that $h(t) = 0$ at all Nyquist sampling instants ($t = \pm n/2B$) except at $t = 0$. When the sampled signal $\bar{x}(t)$ is applied at the input of this filter, the output is $x(t)$. Each sample in $\bar{x}(t)$, being an impulse, generates a sinc pulse of height equal to the strength of the sample, as illustrated in Fig. 5.6c. The process is identical to that depicted in Fig. 5.5c, except that $h(t)$ is a sinc pulse instead of a gate pulse. Addition of the sinc

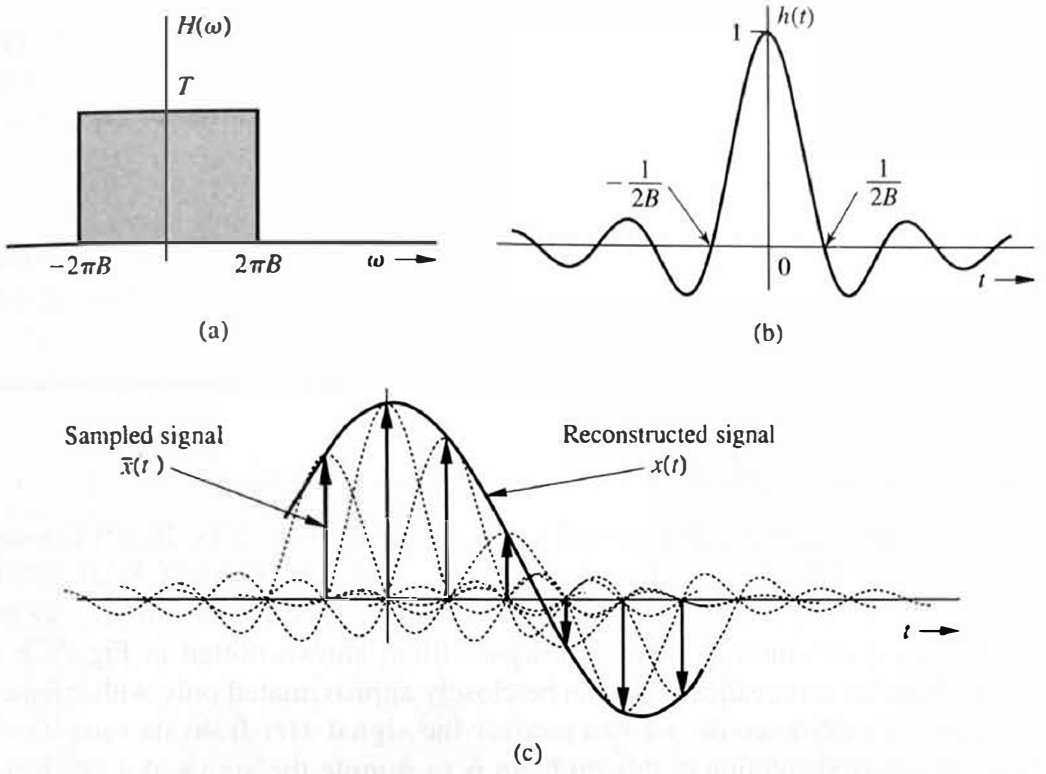

Figure 5.6 Ideal interpolation for Nyquist sampling rate.

pulses generated by all the samples results in $x(t)$. The nth sample of the input $\bar{x}(t)$ is the impulse $x(nT)\delta(t-nT)$; the filter output of this impulse is $x(nT)h(t-nT)$. Hence, the filter output to $\bar{x}(t)$, which is $x(t)$, can now be expressed as a sum

$$x(t) = \sum_n x(nT)h(t-nT) = \sum_n x(nT)\,\text{sinc}\left[\frac{\pi}{T}(t-nT)\right]$$

For the case of Nyquist sampling rate, $T = 1/2B$, this expression simplifies to

$$x(t) = \sum_n x(nT)\,\text{sinc}(2\pi Bt - n\pi) \tag{5.6}$$

Equation (5.6) is the *interpolation formula*, which yields values of $x(t)$ between samples as a weighted sum of all the sample values.

EXAMPLE 5.3 Bandlimited Interpolation of the Kronecker Delta Function

Find a signal $x(t)$ that is bandlimited to B Hz, and whose samples are

$$x(0) = 1 \qquad \text{and} \qquad x(\pm T) = x(\pm 2T) = x(\pm 3T) = \cdots = 0$$

where the sampling interval T is the Nyquist interval for $x(t)$, that is, $T = 1/2B$.

Because we are given the Nyquist sample values, we use the interpolation formula of Eq. (5.6) to construct $x(t)$ from its samples. Since all but one of the Nyquist samples are zero, only one term (corresponding to $n = 0$) in the summation on the right-hand side of Eq. (5.6) survives. Thus,

$$x(t) = \text{sinc}\,(2\pi Bt)$$

This signal is illustrated in Fig. 5.6b. Observe that this is the only signal that has a bandwidth B Hz and the sample values $x(0) = 1$ and $x(nT) = 0\,(n \neq 0)$. No other signal satisfies these conditions.

5.2.1 Practical Difficulties in Signal Reconstruction

Consider the signal reconstruction procedure illustrated in Fig. 5.7a. If $x(t)$ is sampled at the Nyquist rate $f_s = 2B$ Hz, the spectrum $\overline{X}(\omega)$ consists of repetitions of $X(\omega)$ without any gap between successive cycles, as depicted in Fig. 5.7b. To recover $x(t)$ from $\overline{x}(t)$, we need to pass the sampled signal $\overline{x}(t)$ through an ideal lowpass filter, shown dotted in Fig. 5.7b. As seen in Sec. 4.5, such a filter is unrealizable; it can be closely approximated only with infinite time delay in the response. In other words, we can recover the signal $x(t)$ from its samples with infinite time delay. A practical solution to this problem is to sample the signal at a rate higher than the Nyquist rate ($f_s > 2B$ or $\omega_s > 4\pi B$). The result is $\overline{X}(\omega)$, consisting of repetitions of $X(\omega)$ with a finite bandgap between successive cycles, as illustrated in Fig. 5.7c. Now, we can recover $X(\omega)$ from $\overline{X}(\omega)$ using a lowpass filter with a gradual cutoff characteristic, shown dotted in Fig. 5.7c. But even in this case, if the unwanted spectrum is to be suppressed, the filter gain must be zero beyond some frequency (see Fig. 5.7c). According to the Paley–Wiener criterion [Eq. (4.43)], it is impossible to realize even this filter. The only advantage in this case is that the required filter can be closely approximated with a smaller time delay. All this means that it is impossible in practice to recover a bandlimited signal $x(t)$ exactly from its samples, even if the sampling rate is higher than the Nyquist rate. However, as the sampling rate increases, the recovered signal approaches the desired signal more closely.

The Treachery of Aliasing

There is another fundamental practical difficulty in reconstructing a signal from its samples. The sampling theorem was proved on the assumption that the signal $x(t)$ is bandlimited. *All practical signals are timelimited*; that is, they are of finite duration or width. We can demonstrate (see Prob. 5.2-20) that a signal cannot be timelimited and bandlimited simultaneously. If a signal is timelimited, it cannot be bandlimited, and vice versa (but it can be simultaneously nontimelimited and nonbandlimited). Clearly, all practical signals, which are necessarily timelimited, are nonbandlimited, as shown in Fig. 5.8a; they have infinite bandwidth, and the spectrum $\overline{X}(\omega)$ consists of overlapping cycles of $X(\omega)$ repeating every f_s Hz (the sampling frequency), as illustrated in Fig. 5.8b.[†] Because of infinite bandwidth in this case, the spectral overlap is

[†] Figure 5.8b shows that from the infinite number of repeating cycles, only the neighboring spectral cycles overlap. This is a somewhat simplified picture. In reality, all the cycles overlap and interact with every other cycle because of the infinite width of all practical signal spectra. Fortunately, all practical spectra also must decay at higher frequencies. This results in an insignificant amount of interference from cycles other than the immediate neighbors. When such an assumption is not justified, aliasing computations become a little more involved.

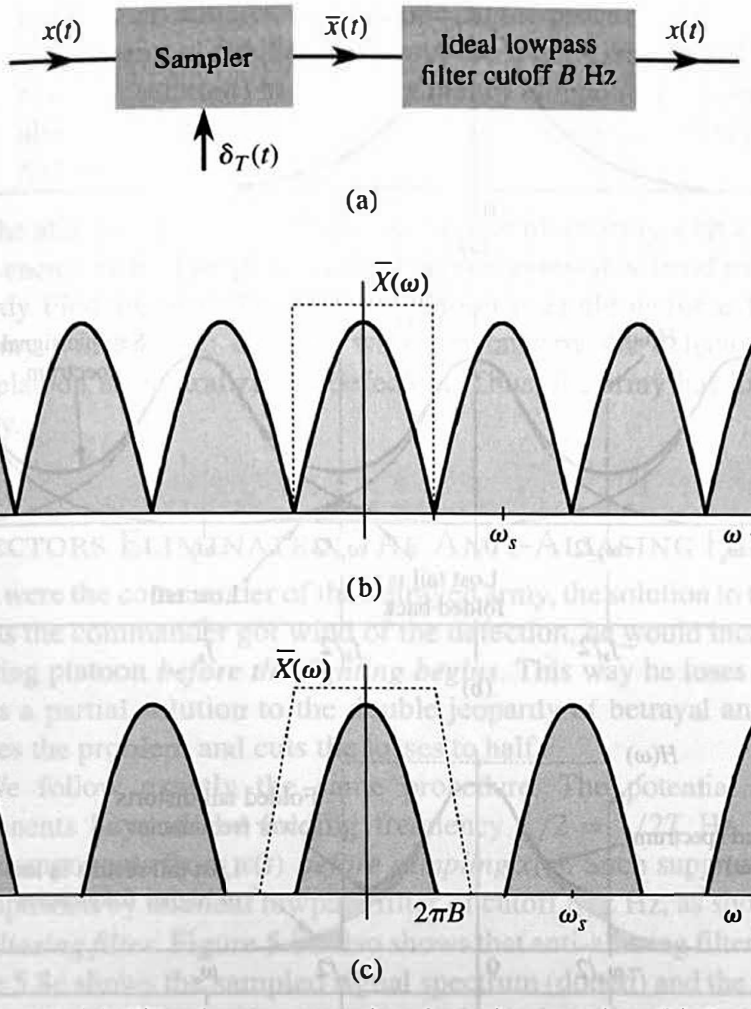

Figure 5.7 (**a**) Signal reconstruction from its samples. (**b**) Spectrum of a signal sampled at the Nyquist rate. (**c**) Spectrum of a signal sampled above the Nyquist rate.

unavoidable, regardless of the sampling rate. Sampling at a higher rate reduces but does not eliminate overlapping between repeating spectral cycles. Because of the overlapping tails, $\overline{X}(\omega)$ no longer has complete information about $X(\omega)$, and it is no longer possible, even theoretically, to recover $x(t)$ exactly from the sampled signal $\bar{x}(t)$. If the sampled signal is passed through an ideal lowpass filter of cutoff frequency $f_s/2$ Hz, the output is not $X(\omega)$ but $X_a(\omega)$ (Fig. 5.8c), which is a version of $X(\omega)$ distorted as a result of two separate causes:

1. The loss of the tail of $X(\omega)$ beyond $|f| > f_s/2$ Hz.
2. The reappearance of this tail inverted or folded onto the spectrum. Note that the spectra cross at frequency $f_s/2 = 1/2T$ Hz. This frequency is called the *folding* frequency. The spectrum may be viewed as if the lost tail is folding back onto itself at the folding frequency. For instance, a component of frequency $(f_s/2) + f_z$ shows up as or "impersonates" a component of lower frequency $(f_s/2) - f_z$ in the reconstructed signal. Thus, the components of frequencies above $f_s/2$ reappear as components of frequencies below $f_s/2$. This tail inversion, known as *spectral folding* or *aliasing,* is shown shaded

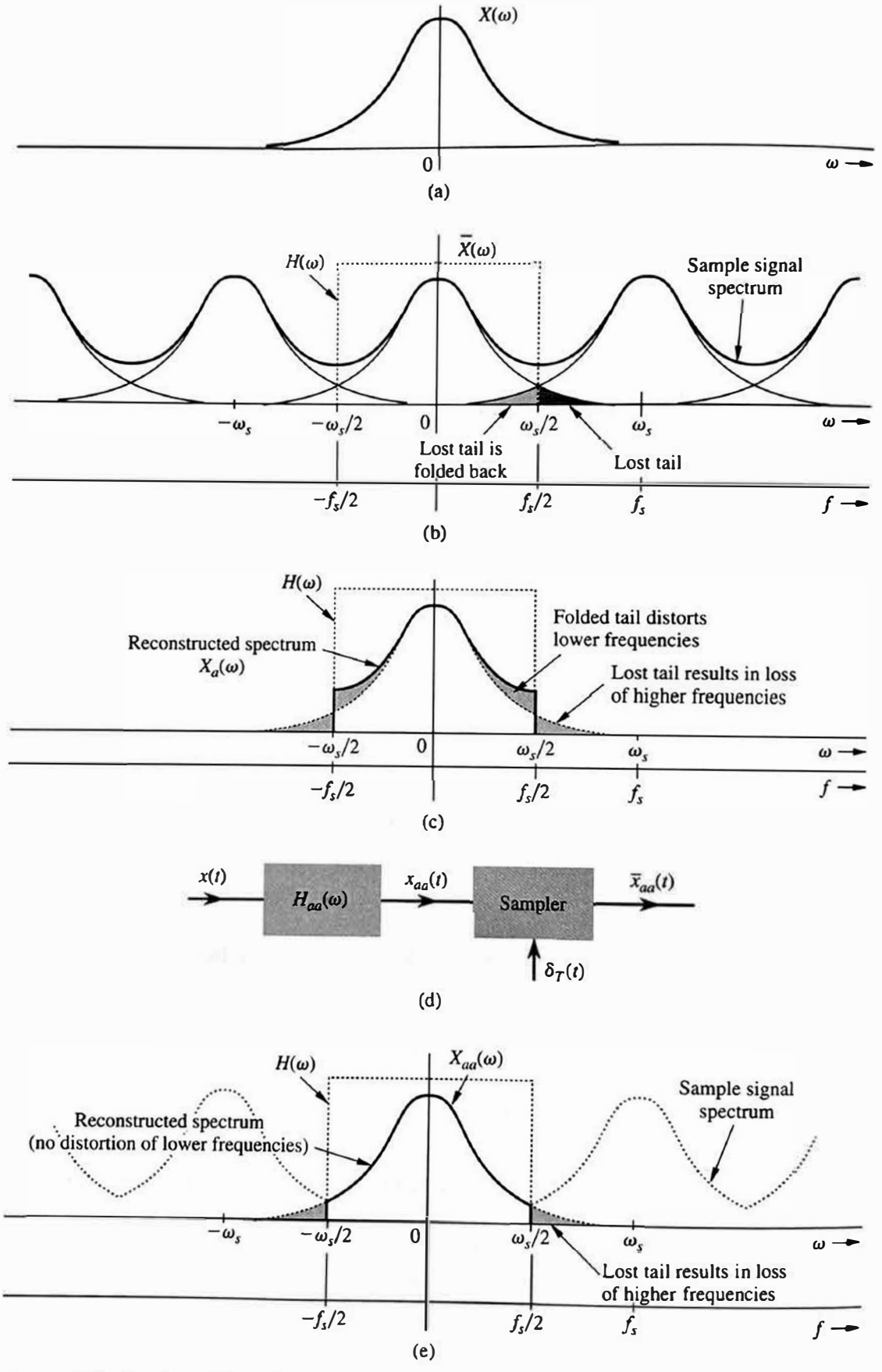

Figure 5.8 Aliasing effect. **(a)** Spectrum of a practical signal $x(t)$. **(b)** Spectrum of sampled $x(t)$. **(c)** Reconstructed signal spectrum. **(d)** Sampling scheme using anti-aliasing filter. **(e)** Sampled signal spectrum (dotted) and the reconstructed signal spectrum (solid) when anti-aliasing filter is used.

in Fig. 5.8b and also in Fig. 5.8c. In the process of aliasing, not only are we losing all the components of frequencies above the folding frequency $f_s/2$ Hz, but these very components reappear (aliased) as lower-frequency components, as shown in Figs. 5.8b and 5.8c. Such aliasing destroys the integrity of the frequency components below the folding frequency $f_s/2$, as depicted in Fig. 5.8c.

The aliasing problem is analogous to that of an army with a platoon that has secretly defected to the enemy side. The platoon is, however, ostensibly loyal to the army. The army is in double jeopardy. First, the army has lost this platoon as a fighting force. In addition, during actual fighting, the army will have to contend with sabotage by the defectors and will have to find another loyal platoon to neutralize the defectors. Thus, the army has lost two platoons in nonproductive activity.

Defectors Eliminated: The Anti-Aliasing Filter

If you were the commander of the betrayed army, the solution to the problem would be obvious. As soon as the commander got wind of the defection, he would incapacitate, by whatever means, the defecting platoon *before the fighting begins*. This way he loses only one (the defecting) platoon. This is a partial solution to the double jeopardy of betrayal and sabotage, a solution that partly rectifies the problem and cuts the losses to half.

We follow exactly the same procedure. The potential defectors are all the frequency components beyond the folding frequency $f_s/2 = 1/2T$ Hz. We should eliminate (suppress) these components from $x(t)$ *before sampling* $x(t)$. Such suppression of higher frequencies can be accomplished by an ideal lowpass filter of cutoff $f_s/2$ Hz, as shown in Fig. 5.8d. This is called the *anti-aliasing filter*. Figure 5.8d also shows that anti-aliasing filtering is performed before sampling. Figure 5.8e shows the sampled signal spectrum (dotted) and the reconstructed signal $X_{aa}(\omega)$ when an anti-aliasing scheme is used. An anti-aliasing filter essentially bandlimits the signal $x(t)$ to $f_s/2$ Hz. This way, we lose only the components beyond the folding frequency $f_s/2$ Hz. These suppressed components now cannot reappear to corrupt the components of frequencies below the folding frequency. Clearly, use of an anti-aliasing filter results in the reconstructed signal spectrum $X_{aa}(\omega) = X(\omega)$ for $|f| < f_s/2$. Thus, although we lost the spectrum beyond $f_s/2$ Hz, the spectrum for all the frequencies below $f_s/2$ remains intact. The effective aliasing distortion is cut in half owing to elimination of folding. We stress again that the anti-aliasing operation must be performed *before the signal is sampled.*

An anti-aliasing filter also helps to reduce noise. Noise, generally, has a wideband spectrum, and without anti-aliasing, the aliasing phenomenon itself will cause the noise lying outside the desired band to appear in the signal band. Anti-aliasing suppresses the entire noise spectrum beyond frequency $f_s/2$.

The anti-aliasing filter, being an ideal filter, is unrealizable. In practice, we use a steep cutoff filter, which leaves a sharply attenuated spectrum beyond the folding frequency $f_s/2$.

Sampling Forces Nonbandlimited Signals to Appear Bandlimited

Figure 5.8b shows that the spectrum of a signal $x(t)$ consists of overlapping cycles of $X(\omega)$. This means that $\bar{x}(t)$ are sub-Nyquist samples of $x(t)$. However, we may also view the spectrum in Fig. 5.8b as the spectrum $X_a(\omega)$ (Fig. 5.8c), repeating periodically every f_s Hz without overlap. The spectrum $X_a(\omega)$ is bandlimited to $f_s/2$ Hz. Hence, these (sub-Nyquist) samples of $x(t)$ are actually the Nyquist samples for signal $x_a(t)$. In conclusion, sampling a nonbandlimited signal $x(t)$ at a rate f_s Hz makes the samples appear to be the Nyquist samples of some signal $x_a(t)$, bandlimited to $f_s/2$ Hz. In other words, sampling makes a nonbandlimited signal appear to be a bandlimited signal $x_a(t)$ with bandwidth $f_s/2$ Hz. A similar conclusion applies if $x(t)$ is bandlimited but sampled at a sub-Nyquist rate.

Verification of Aliasing in Sinusoids

We showed in Fig. 5.8b how sampling a signal below the Nyquist rate causes aliasing, which makes a signal of higher frequency $(f_s/2)+f_z$ Hz masquerade as a signal of lower frequency $(f_s/2)-f_z$ Hz. Figure 5.8b demonstrates this result in the frequency domain. Let us now verify it in the time domain to gain a deeper appreciation of aliasing.

We can prove our proposition by showing that samples of sinusoids of frequencies $(\omega_s/2)+\omega_z$ and $(\omega_s/2)-\omega_z$ are identical when the sampling frequency is $f_s=\omega_s/2\pi$ Hz.

For a sinusoid $x(t)=\cos\omega t$, sampled at intervals of T seconds, $x(nT)$, its nth sample (at $t=nT$) is

$$x(nT)=\cos\omega nT \qquad n \text{ integer}$$

Hence, samples of sinusoids of frequency $\omega=(\omega_s/2)\pm\omega_z$ are[†]

$$x(nT)=\cos\left(\frac{\omega_s}{2}\pm\omega_z\right)nT=\cos\left(\frac{\omega_s}{2}\right)nT\cos\omega_z nT\mp\sin\left(\frac{\omega_s}{2}\right)nT\sin\omega_z nT$$

Recognizing that $\omega_s T=2\pi f_s T=2\pi$, and $\sin(\omega_s/2)nT=\sin\pi n=0$ for all integer n, we obtain

$$x(nT)=\cos\left(\frac{\omega_s}{2}\right)nT\cos\omega_z nT$$

Clearly, the samples of a sinusoid of frequency $(f_s/2)+f_z$ are identical to the samples of a sinusoid $(f_s/2)-f_z$.[‡] For instance, when a sinusoid of frequency 100 Hz is sampled at a rate of 120 Hz, the apparent frequency of the sinusoid that results from reconstruction of the samples is 20 Hz. This follows from the fact that here, $100=(f_s/2)+f_z=60+f_z$ so that $f_z=40$. Hence, $(f_s/2)-f_z=20$. Such would precisely be the conclusion arrived at from Fig. 5.8b.

[†] Here, we have ignored the phase aspect of the sinusoid. Sampled versions of a sinusoid $x(t)=\cos(\omega t+\theta)$ with two different frequencies $(\omega_s/2)\pm\omega_z$ have identical frequency, but the phase signs may be reversed depending on the value of ω_z.

[‡] The reader is encouraged to verify this result graphically by plotting the spectrum of a sinusoid of frequency $(\omega_s/2)+\omega_z$ (impulses at $\pm[(\omega_s/2)+\omega_z]$) and its periodic repetition at intervals ω_s. Although the result is valid for all values of ω_z, consider the case of $\omega_z<\omega_s/2$ to simplify the graphics.

This discussion again shows that sampling a sinusoid of frequency f aliasing can be avoided if the sampling rate $f_s > 2f$ Hz.

$$0 \le f < \frac{f_s}{2} \quad \text{or} \quad 0 \le \omega < \frac{\pi}{T}$$

Violating this condition leads to aliasing, implying that the samples appear to be those of a lower-frequency signal. Because of this loss of identity, it is impossible to reconstruct the signal faithfully from its samples.

General Condition for Aliasing in Sinusoids

We can generalize the foregoing result by showing that samples of a sinusoid of frequency f_0 are identical to those of a sinusoid of frequency $f_0 + mf_s$ Hz (integer m), where f_s is the sampling frequency. The samples of $\cos 2\pi(f_0 + mf_s)t$ are

$$\cos 2\pi(f_0 + mf_s)nT = \cos(2\pi f_0 nT + 2\pi mn) = \cos 2\pi f_0 nT$$

The result follows because mn is an integer and $f_s T = 1$. This result shows that sinusoids of frequencies that differ by an integer multiple of f_s result in an identical set of samples. In other words, samples of sinusoids separated by frequency f_s Hz are identical. This implies that samples of sinusoids in any frequency band of f_s Hz are unique; that is, no two sinusoids in that band have the same samples (when sampled at a rate f_s Hz). For instance, frequencies in the band from $-f_s/2$ to $f_s/2$ have unique samples (at the sampling rate f_s). This band is called the *fundamental band.* Recall also that $f_s/2$ is the folding frequency.

From the discussion thus far, we conclude that if a continuous-time sinusoid of frequency f Hz is sampled at a rate of f_s Hz (samples/s), the resulting samples would appear as samples of a continuous-time sinusoid of frequency f_a in the fundamental band, where

$$f_a = f - mf_s \qquad -\frac{f_s}{2} \le f_a < \frac{f_s}{2} \qquad m \text{ an integer} \tag{5.7}$$

The frequency f_a lies in the fundamental band from $-f_s/2$ to $f_s/2$. Figure 5.9a shows the plot of f_a versus f, where f is the actual frequency and f_a is the corresponding fundamental band frequency, whose samples are identical to those of the sinusoid of frequency f, when the sampling rate is f_s Hz.

Recall, however, that the sign change of a frequency does not alter the actual frequency of the waveform. This is because

$$\cos(-\omega_a t + \theta) = \cos(\omega_a t - \theta)$$

Clearly, the *apparent frequency* of a sinusoid of frequency $-f_a$ is also f_a. However, its phase undergoes a sign change. This means the apparent frequency of any sampled sinusoid lies in the range from 0 to $f_s/2$ Hz. To summarize, if a continuous-time sinusoid of frequency f Hz is sampled at a rate of f_s Hz (samples/second), the resulting samples would appear as samples of a continuous-time sinusoid of frequency $|f_a|$ that lies in the band from 0 to $f_s/2$. According to Eq. (5.7),

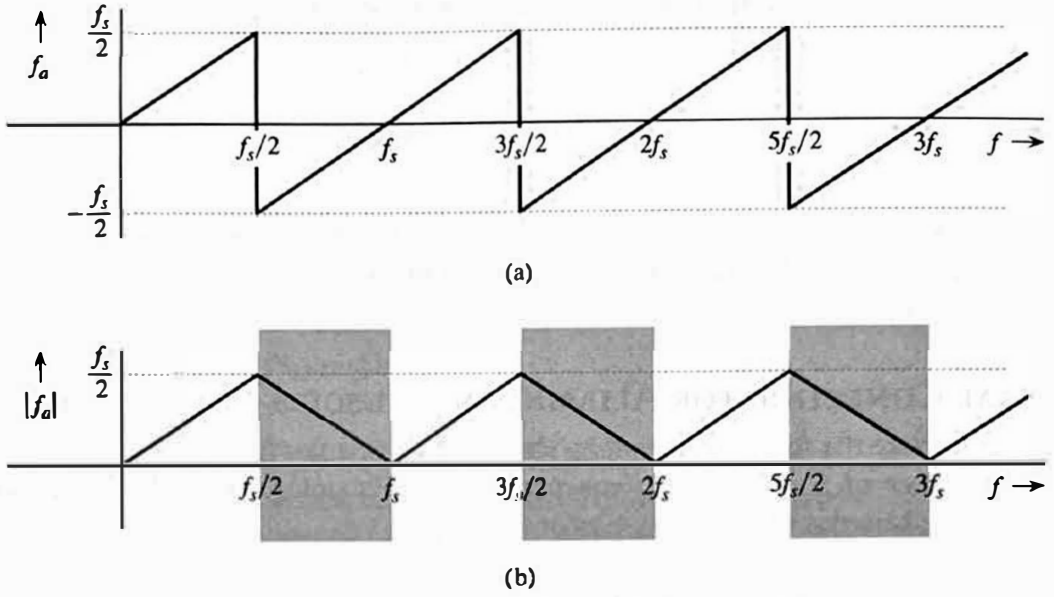

Figure 5.9 Apparent frequencies of a sampled sinusoid: **(a)** f_a versus f and **(b)** $|f_a|$ versus f.

$$|f_a| = |f - mf_s| \qquad |f_a| \leq \frac{f_s}{2} \qquad m \text{ an integer}$$

The plot of the apparent frequency $|f_a|$ versus f is shown in Fig. 5.9b. As expected, the apparent frequency $|f_a|$ of any sampled sinusoid, regardless of its frequency, is always in the range of 0 to $f_s/2$ Hz. However, when f_a is negative, the phase of the apparent sinusoid undergoes a sign change. The frequency belts in which such phase changes occur are shown shaded in Fig. 5.9b.

Consider, for example, a sinusoid $\cos(2\pi ft + \theta)$ with $f = 8000$ Hz sampled at a rate $f_s = 3000$ Hz. Using Eq. (5.7), we obtain $f_a = 8000 - 3 \times 3000 = -1000$. Hence, $|f_a| = 1000$. The samples would appear to have come from a sinusoid $\cos(2000\pi t - \theta)$. Observe the sign change of the phase because f_a is negative.[†]

In the light of the foregoing development, let us consider a sinusoid of frequency $f = (f_s/2) + f_z$, sampled at a rate of f_s Hz. According to Eq. (5.7),

$$f_a = \frac{f_s}{2} + f_z - (1 \times f_s) = -\frac{f_s}{2} + f_z$$

Hence, the apparent frequency is $|f_a| = (f_s/2) - f_z$, confirming our earlier result. However, the phase of the sinusoid will suffer a sign change because f_a is negative.

Figure 5.10 shows how samples of sinusoids of two different frequencies (sampled at the same rate) generate identical sets of samples. Both the sinusoids are sampled at a rate $f_s = 5$ Hz ($T = 0.2$ second). The frequencies of the two sinusoids, 1 Hz (period 1) and 6 Hz (period 1/6), differ by $f_s = 5$ Hz.

[†] For phase sign change, we are assuming that the signal has the form $\cos(2\pi ft + \theta)$. If the form is $\sin(2\pi ft + \theta)$, the rule changes slightly. It is left as an exercise for the reader to show that when $f_a < 0$, this sinusoid appears as $-\sin(2\pi |f_a| t - \theta)$. Thus, in addition to phase change, the amplitude also changes sign.

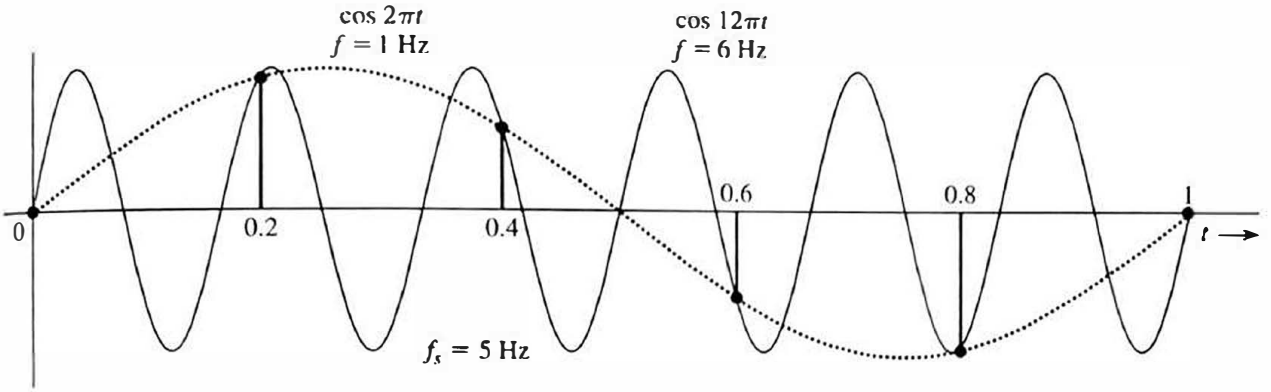

Figure 5.10 Demonstration of aliasing.

The reason for aliasing can be clearly seen in Fig. 5.10. The root of the problem is the sampling rate, which may be adequate for the lower-frequency sinusoid but is clearly inadequate for the higher-frequency sinusoid. The figure clearly shows that between the successive samples of the higher-frequency sinusoid, there are wiggles, which are bypassed or ignored, and are unrepresented in the samples, indicating a sub-Nyquist rate of sampling. The frequency of the apparent signal $x_a(t)$ is always the lowest possible frequency that lies within the band $|f| \leq f_s/2$. Thus, the apparent frequency of the samples in this example is 1 Hz. If these samples are chosen to reconstruct a signal using a lowpass filter of bandwidth $f_s/2$, we shall obtain a sinusoid of frequency 1 Hz.

EXAMPLE 5.4 Apparent Frequency of Sampled Sinusoids

A continuous-time sinusoid $\cos(2\pi ft + \theta)$ is sampled at a rate $f_s = 1000$ Hz. Determine the apparent (aliased) sinusoid of the resulting samples if the input signal frequency f is **(a)** 400 Hz, **(b)** 600 Hz, **(c)** 1000 Hz, and **(d)** 2400 Hz.

The folding frequency is $f_s/2 = 500$. Hence, sinusoids below 500 Hz (frequency within the fundamental band) will not be aliased and sinusoids of frequency above 500 Hz will be aliased.

(a) Since $f = 400$ Hz is less than 500 Hz, there is no aliasing. The apparent sinusoid is $\cos(2\pi ft + \theta)$ with $f = 400$.

(b) Since $f = 600$ Hz can be expressed as $600 = -400 + 1000$, we see that $f_a = -400$. Hence, the aliased frequency is 400 Hz and the phase changes sign. The apparent (aliased) sinusoid is $\cos(2\pi ft - \theta)$ with $f = 400$.

(c) Since $f = 1000$ Hz can be expressed as $1000 = 0 + 1000$, we see that $f_a = 0$. Hence, the aliased frequency is 0 Hz (dc), and there is no phase sign change. The apparent sinusoid is $y(t) = \cos(0\pi t \pm \theta) = \cos(\theta)$. This is a dc signal with constant sample values for all n.

(d) Here, $f = 2400$ Hz can be expressed as $2400 = 400 + (2 \times 1000)$ so that $f_a = 400$. Hence, the aliased frequency is 400 Hz and there is no sign change for the phase. The apparent sinusoid is $\cos(2\pi ft + \theta)$ with $f = 400$.

We could have found these answers directly from Fig. 5.9b. For example, for case (b), we read $|f_a| = 400$ corresponding to $f = 600$. Moreover, $f = 600$ lies in the shaded belt. Hence, there is a phase sign change.

DRILL 5.3 A Case When Sampled Sinusoids Are Identical

Show that samples of 90 Hz and 110 Hz sinusoids of the form $\cos \omega t$ are identical when sampled at a rate 200 Hz.

DRILL 5.4 Apparent Frequency of Sampled Sinusoids

A sinusoid of frequency f_0 Hz is sampled at a rate of 100 Hz. Determine the apparent frequency of the samples if f_0 is (a) 40 Hz, (b) 60 Hz, (c) 140 Hz, and (d) 160 Hz.

ANSWER

All four cases have an apparent frequency of 40 Hz.

5.2.2 Some Applications of the Sampling Theorem

The sampling theorem is very important in signal analysis, processing, and transmission because it allows us to replace a continuous-time signal with a discrete sequence of numbers. Processing a continuous-time signal is therefore equivalent to processing a discrete sequence of numbers. Such processing leads us directly into the area of digital filtering. In the field of communication, the transmission of a continuous-time message reduces to the transmission of a sequence of numbers by means of pulse trains. The continuous-time signal $x(t)$ is sampled, and sample values are used to modify certain parameters of a periodic pulse train. We may vary the amplitudes (Fig. 5.11b), widths (Fig. 5.11c), or positions (Fig. 5.11d) of the pulses in proportion to the sample values of the signal $x(t)$. Accordingly, we may have *pulse-amplitude modulation* (PAM), *pulse-width modulation* (PWM), or *pulse-position modulation* (PPM). The most important form of pulse modulation today is *pulse-code modulation* (PCM), discussed in Sec. 5.3 in connection with Fig. 5.14b. In all these cases, instead of transmitting $x(t)$, we transmit the corresponding pulse-modulated signal. At the receiver, we read the information of the pulse-modulated signal and reconstruct the analog signal $x(t)$.

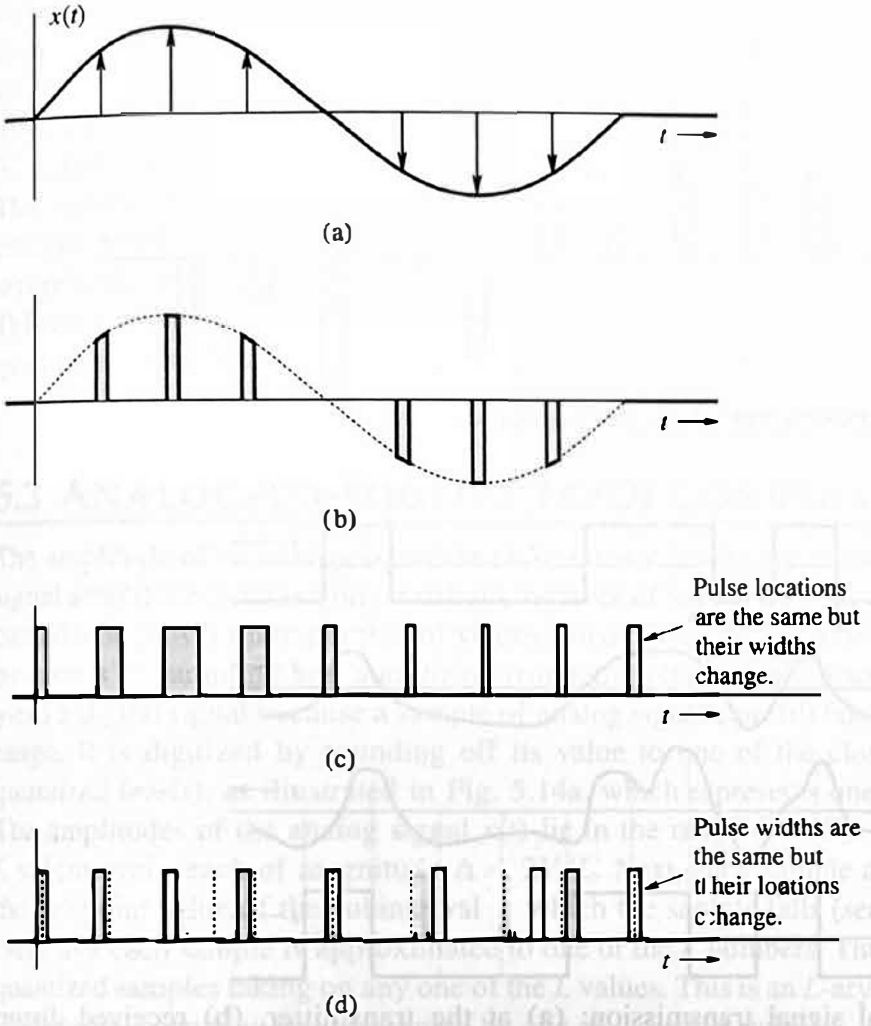

Figure 5.11 Pulse-modulated signals. **(a)** The signal. **(b)** The PAM signal. **(c)** The PWM (PDM) signal. **(d)** The PPM signal.

One advantage of using pulse modulation is that it permits the simultaneous transmission of several signals on a time-sharing basis—*time-division multiplexing* (TDM). Because a pulse-modulated signal occupies only a part of the channel time, we can transmit several pulse-modulated signals on the same channel by interweaving them. Figure 5.12 shows the TDM of two PAM signals. In this manner, we can multiplex several signals on the same channel by reducing pulse widths.[†]

Digital signals also offer an advantage in the area of communications, where signals must travel over distances. Transmission of digital signals is more rugged than that of analog signals because digital signals can withstand channel noise and distortion much better as long as the noise

[†] Another method of transmitting several baseband signals simultaneously is frequency-division multiplexing (FDM) discussed in Sec. 4.8.4. In FDM, various signals are multiplexed by sharing the channel bandwidth. The spectrum of each message is shifted to a specific band not occupied by any other signal. The information of various signals is located in nonoverlapping frequency bands of the channel (Fig. 4.50). In a way, TDM and FDM are duals of each other.

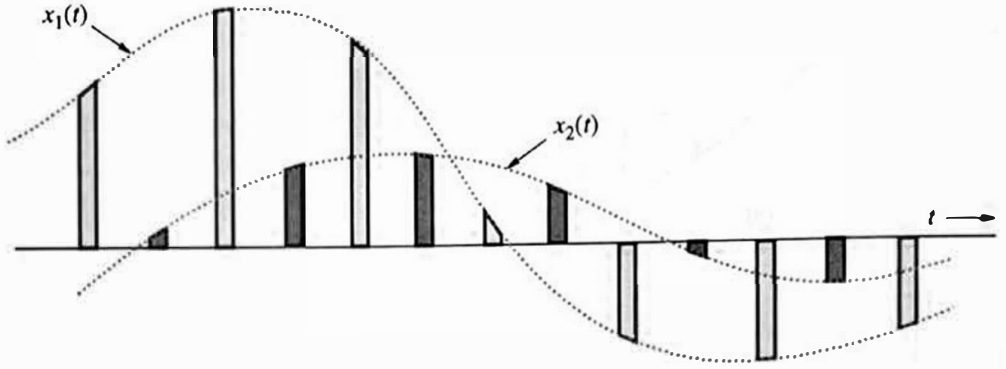

Figure 5.12 Time-division multiplexing of two signals.

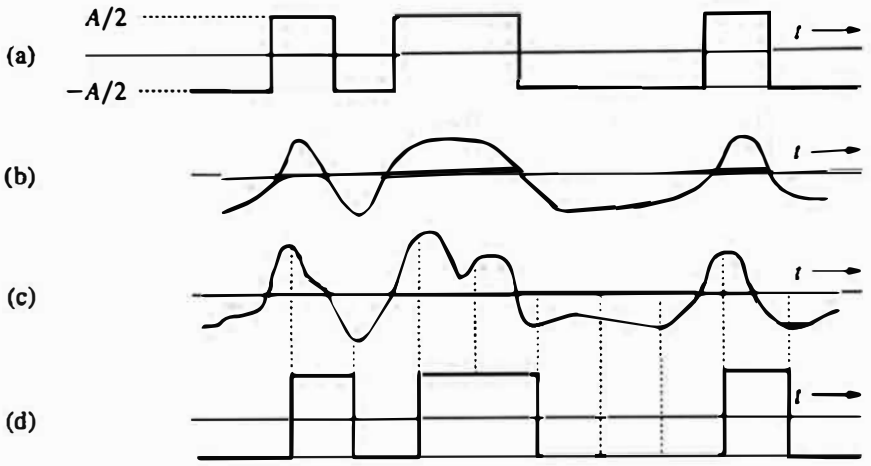

Figure 5.13 Digital signal transmission: **(a)** at the transmitter, **(b)** received distorted signal (without noise), **(c)** received distorted signal (with noise), and **(d)** regenerated signal at the receiver.

and the distortion are within limits. An analog signal can be converted to digital binary form through sampling and quantization (rounding off), as explained in the next section. The digital (binary) message in Fig. 5.13a is distorted by the channel, as illustrated in Fig. 5.13b. Yet if the distortion remains within a limit, we can recover the data without error because we need only make a simple binary decision: Is the received pulse positive or negative? Figure 5.13c shows the same data with channel distortion and noise. Here again, the data can be recovered correctly as long as the distortion and the noise are within limits. Such is not the case with analog messages. Any distortion or noise, no matter how small, will distort the received signal.

The greatest advantage of digital communication over the analog counterpart, however, is the viability of regenerative repeaters in the former. In an analog transmission system, a message signal grows progressively weaker as it travels along the channel (transmission path), whereas the channel noise and the signal distortion, being cumulative, become progressively stronger. Ultimately, the signal, overwhelmed by noise and distortion, is mutilated. Amplification is of little help because it enhances the signal and the noise in the same proportion. Consequently, the distance over which an analog message can be transmitted is limited by the transmitted power. If a transmission path is long enough, the channel distortion and noise will accumulate sufficiently to overwhelm even a

digital signal. The trick is to set up repeaters along the transmission path at distances short enough to permit detection of signal pulses before the noise and distortion have a chance to accumulate sufficiently. At each repeater, the pulses are detected, and new, clean pulses are transmitted to the next repeater, which, in turn, duplicates the same process. If the noise and distortion remain within limits (which is possible because of the closely spaced repeaters), pulses can be detected correctly.[†] This way the digital messages can be transmitted over longer distances with greater reliability. In contrast, analog messages cannot be cleaned up periodically, and their transmission is therefore less reliable. The most significant error in digitized signals comes from quantizing (rounding off). This error, discussed in Sec. 5.3, can be reduced as much as desired by increasing the number of quantization levels, at the cost of an increased bandwidth of the transmission medium (channel).

5.3 Analog-to-Digital (A/D) Conversion

The amplitude of an *analog* signal can take on any value over a continuous range. Hence, analog signal amplitude can take on an infinite number of values. In contrast, a *digital* signal amplitude can take on only a finite number of values. An analog signal can be converted into a digital signal by means of sampling and *quantizing* (rounding off). Sampling an analog signal alone will not yield a digital signal because a sample of analog signal can still take on any value in a continuous range. It is digitized by rounding off its value to one of the closest permissible numbers (or *quantized levels*), as illustrated in Fig. 5.14a, which represents one possible quantizing scheme. The amplitudes of the analog signal $x(t)$ lie in the range $(-V, V)$. This range is partitioned into L subintervals, each of magnitude $\Delta = 2V/L$. Next, each sample amplitude is approximated by the midpoint value of the subinterval in which the sample falls (see Fig. 5.14a for $L = 16$). It is clear that each sample is approximated to one of the L numbers. Thus, the signal is digitized with quantized samples taking on any one of the L values. This is an L-ary digital signal (see Sec. 1.3.2). Each sample can now be represented by one of L distinct pulses.

From a practical viewpoint, dealing with a large number of distinct pulses is difficult. We prefer to use the smallest possible number of distinct pulses, the very smallest number being 2. A digital signal using only two symbols or values is the binary signal. A binary digital signal (a signal that can take on only two values) is very desirable because of its simplicity, economy, and ease of engineering. We can convert an L-ary signal into a binary signal by using pulse coding. Figure 5.14b shows one such code for the case of $L = 16$. This code, formed by binary representation of the 16 decimal digits from 0 to 15, is known as the *natural binary code* (NBC). For L quantization levels, we need a minimum of b binary code digits, where $2^b = L$ or $b = \log_2 L$.

Each of the 16 levels is assigned one binary code word of four digits. Thus, each sample in this example is encoded by four binary digits. To transmit or digitally process the binary data, we need to assign a distinct electrical pulse to each of the two binary states. One possible way is to assign a negative pulse to a binary **0** and a positive pulse to a binary **1** so that each sample is now represented by a group of four binary pulses (pulse code), as depicted in Fig. 5.14b. The resulting binary signal is a digital signal obtained from the analog signal $x(t)$ through A/D conversion. In communications jargon, such a signal is known as a pulse-code-modulated (PCM) signal. The convenient contraction of "*bi*nary digi*t*" to *bit* has become an industry standard abbreviation.

[†] The error in pulse detection can be made negligible.

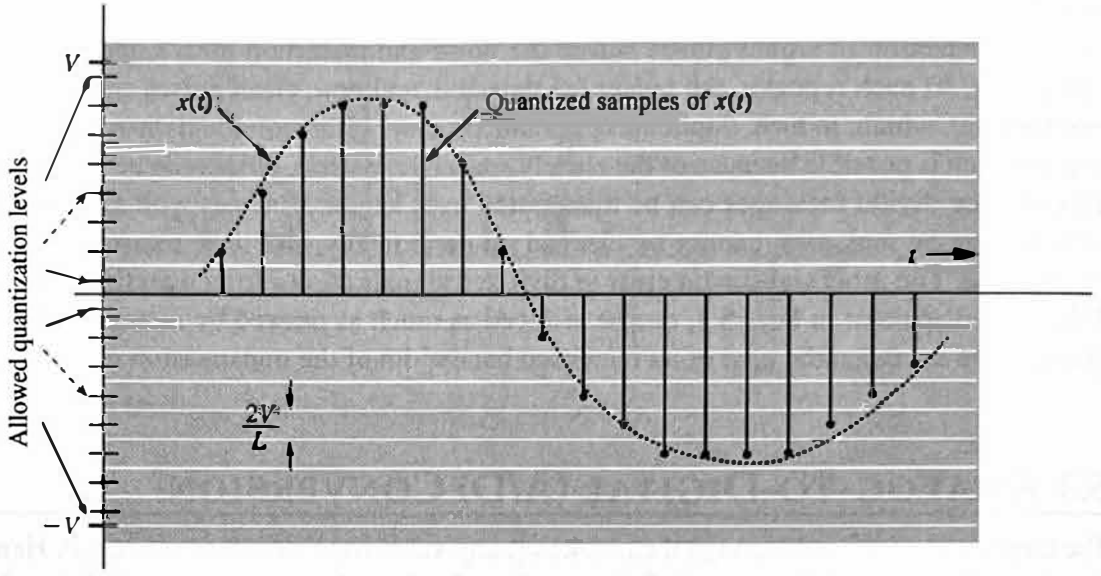

(a)

Digit	Binary equivalent	Pulse code waveform
0	0000	
1	0001	
2	0010	
3	0011	
4	0100	
5	0101	
6	0110	
7	0111	
8	1000	
9	1001	
10	1010	
11	1011	
12	1100	
13	1101	
14	1110	
15	1111	

(b)

Figure 5.14 Analog-to-digital (A/D) conversion of a signal: **(a)** quantizing and **(b)** pulse coding.

A typical audio signal's bandwidth is about 15 kHz, but subjective tests show that signal articulation (intelligibility) is not affected if all the components above 3400 Hz are suppressed [3]. Since the objective in telephone communication is intelligibility rather than high fidelity, the components above 3400 Hz are eliminated by a lowpass filter.† The resulting signal is then sampled at a rate of 8000 samples/s (8 kHz). This rate is intentionally kept higher than the Nyquist sampling rate of 6.8 kHz to avoid unrealizable filters required for signal reconstruction. Each sample is finally quantized into 256 levels ($L = 256$), which requires a group of eight binary pulses to encode each sample ($2^8 = 256$). Thus, a digitized telephone signal consists of data amounting to $8 \times 8000 = 64{,}000$ or 64 kbit/s, requiring 64,000 binary pulses per second for its transmission.

The compact disc (CD), a high-fidelity application of A/D conversion, requires the audio signal bandwidth of 20 kHz. Although the Nyquist sampling rate is only 40 kHz, an actual sampling rate of 44.1 kHz is used for the reason mentioned earlier. The signal is quantized into a rather large number of levels ($L = 65{,}536$) to reduce quantizing error. The binary-coded samples are now recorded on the CD.

A Historical Note

The binary system of representing any number by using **1**s and **0**s was invented in India by Pingala (ca. 200 BCE). It was again worked out independently in the West by Gottfried Wilhelm Leibniz (1646–1716). He felt a spiritual significance in this discovery, reasoning that **1** representing unity was clearly a symbol for God, while **0** represented the nothingness. He reasoned that if all numbers can be represented merely by the use of **1** and **0**, this surely proves that God created the universe out of nothing!

EXAMPLE 5.5 ADC Bit Number and Bit Rate

A signal $x(t)$ bandlimited to 3 kHz is sampled at a rate $33\frac{1}{3}\%$ higher than the Nyquist rate. The maximum acceptable error in the sample amplitude (the maximum error due to quantization) is 0.5% of the peak amplitude V. The quantized samples are binary-coded. Find the required sampling rate, the number of bits required to encode each sample, and the bit rate of the resulting PCM signal.

The Nyquist sampling rate is $f_{Nyq} = 2 \times 3000 = 6000$ Hz (samples/s). The actual sampling rate is $f_A = 6000 \times (1\frac{1}{3}) = 8000$ Hz.

The quantization step is Δ, and the maximum quantization error is $\pm\Delta/2$, where $\Delta = 2V/L$. The maximum error due to quantization, $\Delta/2$, should be no greater than 0.5% of the signal peak amplitude V. Therefore,

---

† Components below 300 Hz may also be suppressed without affecting the articulation.

$$\frac{\Delta}{2} = \frac{V}{L} = \frac{0.5}{100}V \quad \Longrightarrow \quad L = 200$$

For binary coding, L must be a power of 2. Hence, the next higher value of L that is a power of 2 is $L = 256$. Because $\log_2 256 = 8$, we need 8 bits to encode each sample. Therefore, the bit rate of the PCM signal is

$$8000 \times 8 = 64{,}000 \text{ bits/s}$$

DRILL 5.5 Bit Number and Bit Rate for ASCII

The American Standard Code for Information Interchange (ASCII) has 128 characters, which are binary-coded. A certain computer generates 100,000 characters per second. Show that

(a) 7 bits (binary digits) are required to encode each character.

(b) 700,000 bits/s are required to transmit the computer output.

5.4 DUAL OF TIME SAMPLING: SPECTRAL SAMPLING

As in other cases, the sampling theorem has its dual. In Sec. 5.1, we discussed the time-sampling theorem and showed that a signal bandlimited to B Hz can be reconstructed from the signal samples taken at a rate of $f_s > 2B$ samples/s. Note that the signal spectrum exists over the frequency range (in hertz) of $-B$ to B. Therefore, $2B$ is the spectral width (not the bandwidth, which is B) of the signal. This fact means that a signal $x(t)$ can be reconstructed from samples taken at a rate $f_s >$ the spectral width of $X(\omega)$ in hertz ($f_s > 2B$).

We now prove the dual of the time-sampling theorem. This is the *spectral sampling theorem*, which applies to timelimited signals (the dual of bandlimited signals). A timelimited signal $x(t)$ exists only over a finite interval of τ seconds, as shown in Fig. 5.15a. Generally, a timelimited signal is characterized by $x(t) = 0$ for $t < T_1$ and $t > T_2$ (assuming $T_2 > T_1$). The signal width or duration is $\tau = T_2 - T_1$ seconds.

The spectral sampling theorem states that the spectrum $X(\omega)$ of a signal $x(t)$ timelimited to a duration of τ seconds can be reconstructed from the samples of $X(\omega)$ taken at a rate R samples/Hz, where $R > \tau$ (the signal width or duration) in seconds.

Figure 5.15a shows a timelimited signal $x(t)$ and its Fourier transform $X(\omega)$. Although $X(\omega)$ is complex in general, it is adequate for our line of reasoning to show $X(\omega)$ as a real function.

$$X(\omega) = \int_{-\infty}^{\infty} x(t)e^{-j\omega t}dt = \int_{0}^{\tau} x(t)e^{-j\omega t}dt \tag{5.8}$$

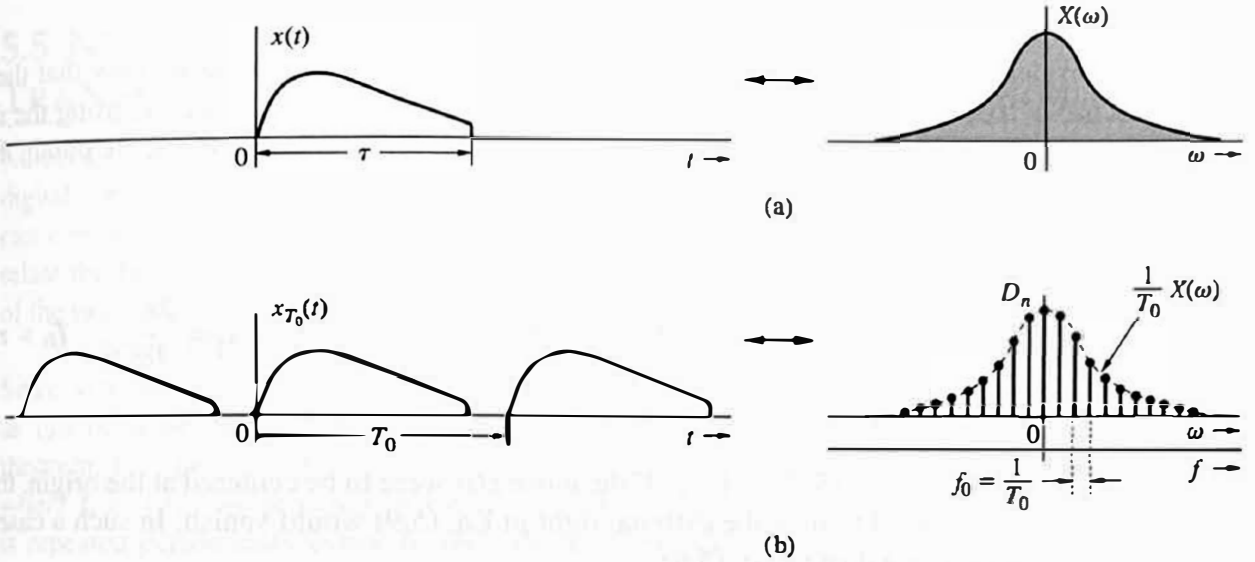

Figure 5.15 Periodic repetition of a signal amounts to sampling its spectrum.

We now construct $x_{T_0}(t)$, a periodic signal formed by repeating $x(t)$ every T_0 seconds ($T_0 > \tau$), as depicted in Fig. 5.15b. This periodic signal can be expressed by the exponential Fourier series

$$x_{T_0}(t) = \sum_{n=-\infty}^{\infty} D_n e^{jn\omega_0 t} \qquad \omega_0 = \frac{2\pi}{T_0}$$

where (assuming $T_0 > \tau$)

$$D_n = \frac{1}{T_0}\int_0^{T_0} x(t)e^{-jn\omega_0 t}dt = \frac{1}{T_0}\int_0^{\tau} x(t)e^{-jn\omega_0 t}dt$$

From Eq. (5.8), it follows that

$$D_n = \frac{1}{T_0}X(n\omega_0)$$

This result indicates that the coefficients of the Fourier series for $x_{T_0}(t)$ are $(1/T_0)$ times the sample values of the spectrum $X(\omega)$ taken at intervals of ω_0. This means that the spectrum of the periodic signal $x_{T_0}(t)$ is the sampled spectrum $X(\omega)$, as illustrated in Fig. 5.15b. Now as long as $T_0 > \tau$, the successive cycles of $x(t)$ appearing in $x_{T_0}(t)$ do not overlap, and $x(t)$ can be recovered from $x_{T_0}(t)$. Such recovery implies indirectly that $X(\omega)$ can be reconstructed from its samples. These samples are separated by the fundamental frequency $f_0 = 1/T_0$ Hz of the periodic signal $x_{T_0}(t)$. Hence, the condition for recovery is $T_0 > \tau$; that is,

$$f_0 < \frac{1}{\tau}\text{ Hz}$$

Therefore, to be able to reconstruct the spectrum $X(\omega)$ from the samples of $X(\omega)$, the samples should be taken at frequency intervals $f_0 < 1/\tau$ Hz. If R is the sampling rate (samples/Hz), then

$$R = \frac{1}{f_0} > \tau \text{ samples/Hz}$$

Spectral Interpolation

Consider a signal timelimited to τ seconds and centered at T_c. We now show that the spectrum $X(\omega)$ of $x(t)$ can be reconstructed from the samples of $X(\omega)$. For this case, using the dual of the approach employed to derive the signal interpolation formula in Eq. (5.6), we obtain the spectral interpolation formula[†]

$$X(\omega) = \sum_{n=-\infty}^{\infty} X(n\omega_0)\,\text{sinc}\left(\frac{\omega T_0}{2} - n\pi\right)e^{-j(\omega - n\omega_0)Tc} \qquad \omega_0 = \frac{2\pi}{T_0} \qquad T_0 > \tau \tag{5.9}$$

For the case in Fig. 5.15, $T_c = T_0/2$. If the pulse $x(t)$ were to be centered at the origin, then $T_c = 0$, and the exponential term at the extreme right in Eq. (5.9) would vanish. In such a case, Eq. (5.9) would be the exact dual of Eq. (5.6).

EXAMPLE 5.6 Spectral Sampling and Interpolation

The spectrum $X(\omega)$ of a unit-duration signal $x(t)$, centered at the origin, is sampled at the intervals of 1 Hz or 2π rad/s (the Nyquist rate). The samples are

$$X(0) = 1 \qquad \text{and} \qquad X(\pm 2\pi n) = 0 \qquad n = 1, 2, 3, \ldots$$

Find $x(t)$.

We use the interpolation formula Eq. (5.9) (with $T_c = 0$) to construct $X(\omega)$ from its samples. Since all but one of the Nyquist samples are zero, only one term (corresponding to $n = 0$) in the summation on the right-hand side of Eq. (5.9) survives. Thus, with $X(0) = 1$ and $\tau = T_0 = 1$, we obtain

$$X(\omega) = \text{sinc}\left(\frac{\omega}{2}\right) \qquad \text{and} \qquad x(t) = \text{rect}(t)$$

For a signal of unit duration, this is the only spectrum with the sample values $X(0) = 1$ and $X(2\pi n) = 0\,(n \neq 0)$. No other spectrum satisfies these conditions.

[†] This can be obtained by observing that the Fourier transform of $x_{T_0}(t)$ is $2\pi \sum_n D_n \delta(\omega - n\omega_0)$ [see Eq. (4.23)]. We can recover $x(t)$ from $x_{T_0}(t)$ by multiplying the latter with $\text{rect}(t - T_c)/T_0$, whose Fourier transform is $T_0\,\text{sinc}(\omega T_0/2)e^{-j\omega T_c}$. Hence, $X(\omega)$ is $1/2\pi$ times the convolution of these two Fourier transforms, which yields Eq. (5.9).

5.5 Numerical Computation of the Fourier Transform: The Discrete Fourier Transform

Numerical computation of the Fourier transform of $x(t)$ requires sample values of $x(t)$ because a digital computer can work only with discrete data (sequence of numbers). Moreover, a computer can compute $X(\omega)$ only at some discrete values of ω [samples of $X(\omega)$]. We therefore need to relate the samples of $X(\omega)$ to samples of $x(t)$. This task can be accomplished by using the results of the two sampling theorems developed in Secs. 5.1 and 5.4.

We begin with a timelimited signal $x(t)$ (Fig. 5.16a) and its spectrum $X(\omega)$ (Fig. 5.16b). Since $x(t)$ is timelimited, $X(\omega)$ is nonbandlimited. For convenience, we shall show all spectra as functions of the frequency variable f (in hertz) rather than ω. According to the sampling theorem, the spectrum $\overline{X}(\omega)$ of the sampled signal $\overline{x}(t)$ consists of $X(\omega)$ repeating every f_s Hz, where $f_s = 1/T$, as depicted in Fig. 5.16d.[†] In the next step, the sampled signal in Fig. 5.16c is repeated periodically every T_0 seconds, as illustrated in Fig. 5.16e. According to the spectral sampling theorem, such an operation results in sampling the spectrum at a rate of T_0 samples/Hz. This sampling rate means that the samples are spaced at $f_0 = 1/T_0$ Hz, as depicted in Fig. 5.16f.

The foregoing discussion shows that when a signal $x(t)$ is sampled and then periodically repeated, the corresponding spectrum is also sampled and periodically repeated. Our goal is to relate the samples of $x(t)$ to the samples of $X(\omega)$.

Number of Samples

One interesting observation from Figs. 5.16e and 5.16f is that N_0, the number of samples of the signal in Fig. 5.16e in one period T_0, is identical to N_0', the number of samples of the spectrum in Fig. 5.16f in one period f_s. To see this, we notice that

$$N_0 = \frac{T_0}{T} \quad N_0' = \frac{f_s}{f_0} \quad f_s = \frac{1}{T} \quad \text{and} \quad f_0 = \frac{1}{T_0} \tag{5.10}$$

Using these relations, we see that

$$N_0 = \frac{T_0}{T} = \frac{f_s}{f_0} = N_0'$$

Aliasing and Leakage in Numerical Computation

Figure 5.16f shows the presence of aliasing in the samples of the spectrum $X(\omega)$. This aliasing error can be reduced as much as desired by increasing the sampling frequency f_s (decreasing the sampling interval $T = 1/f_s$). The aliasing can never be eliminated for timelimited $x(t)$, however, because its spectrum $X(\omega)$ is nonbandlimited. Had we started with a signal having a bandlimited spectrum $X(\omega)$, there would be no aliasing in the spectrum in Fig. 5.16f. Unfortunately, such a signal is nontimelimited, and its repetition (in Fig. 5.16e) would result in signal overlapping (aliasing in the time domain). In this case, we shall have to contend with errors in signal samples. In other words, in computing the direct or inverse Fourier transform numerically, we can reduce the error as much as we wish, but the error can never be eliminated. This is true

[†] There is a multiplying constant $1/T$ for the spectrum in Fig. 5.16d [see Eq. (5.2)], but this is irrelevant to our discussion here.

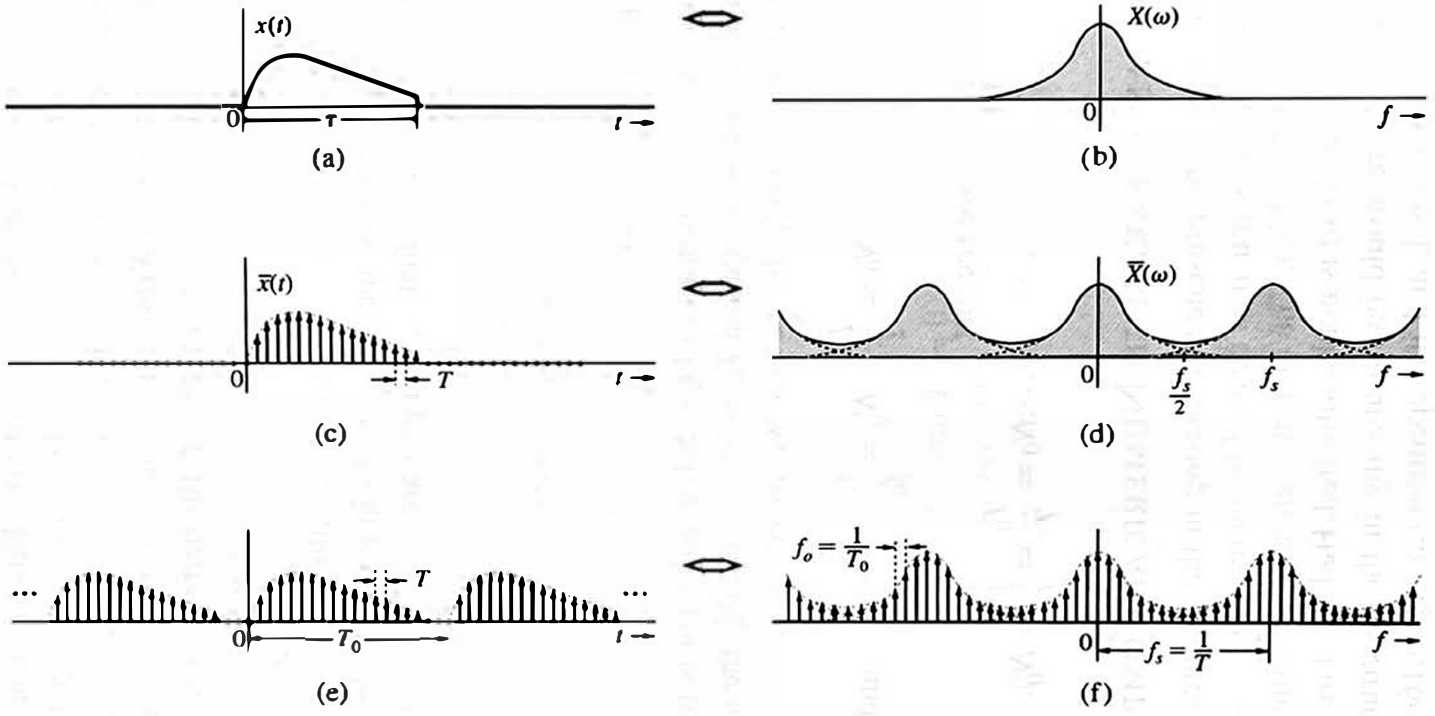

Figure 5.16 Relationship between samples of $x(t)$ and $X(\omega)$.

of numerical computation of the direct and inverse Fourier transforms, regardless of the method used. For example, if we determine the Fourier transform by direct integration numerically, by using Eq. (4.9), there will be an error because the interval of integration Δt can never be made zero. Similar remarks apply to numerical computation of the inverse transform. Therefore, we should always keep in mind the nature of this error in our results. In our discussion (Fig. 5.16), we assumed $x(t)$ to be a timelimited signal. If $x(t)$ were not timelimited, we would need to timelimit it because numerical computations can work only with finite data. Furthermore, this data truncation causes error because of spectral spreading (smearing) and leakage, as discussed in Sec. 4.9. The leakage also causes aliasing. Leakage can be reduced by using a tapered window for signal truncation. But this choice increases spectral spreading or smearing. Spectral spreading can be reduced by increasing the window width (i.e., more data), which increases T_0 and reduces f_0 (increases *spectral* or *frequency resolution*).

Picket Fence Effect

The numerical computation method yields only the uniform sample values of $X(\omega)$. The major peaks or valleys of $X(\omega)$ can lie between two samples and may remain hidden, giving a false picture of reality. Viewing samples is like viewing the signal and its spectrum through a "picket fence" with upright posts that are very wide and placed close together. What is hidden behind the pickets is much more than what we can see. Such misleading results can be avoided by using a sufficiently large N_0, the number of samples, to increase resolution. We can also use zero padding (discussed later) or the spectral interpolation formula [Eq. (5.9)] to determine the values of $X(\omega)$ between samples.

Points of Discontinuity

If $x(t)$ or $X(\omega)$ has a jump discontinuity at a sampling point, the sample value should be taken as the average of the values on the two sides of the discontinuity because the Fourier representation at a point of discontinuity converges to the average value.

Derivation of the Discrete Fourier Transform (DFT)

If $x(nT)$ and $X(r\omega_0)$ are the nth and rth samples of $x(t)$ and $X(\omega)$, respectively, then we define new variables x_n and X_r as

$$x_n = Tx(nT) = \frac{T_0}{N_0}x(nT) \tag{5.11}$$

and

$$X_r = X(r\omega_0)$$

where

$$\omega_0 = 2\pi f_0 = \frac{2\pi}{T_0}$$

We shall now show that x_n and X_r are related by the following equations[†]:

$$X_r = \sum_{n=0}^{N_0-1} x_n e^{-jr\Omega_0 n} \tag{5.12}$$

and

$$x_n = \frac{1}{N_0} \sum_{r=0}^{N_0-1} X_r e^{jr\Omega_0 n} \tag{5.13}$$

where

$$\Omega_0 = \omega_0 T = \frac{2\pi}{N_0}$$

These equations define the direct and the inverse *discrete Fourier transforms*, with X_r the direct discrete Fourier transform (DFT) of x_n, and x_n the inverse discrete Fourier transform (IDFT) of X_r. The notation

$$x_n \Longleftrightarrow X_r$$

is also used to indicate that x_n and X_r are a DFT pair. Remember that x_n is T_0/N_0 times the nth sample of $x(t)$ and X_r is the rth sample of $X(\omega)$. Knowing the sample values of $x(t)$, we can use the DFT to compute the sample values of $X(\omega)$—and vice versa. Note, however, that x_n is a function of n ($n = 0, 1, 2, \ldots, N_0 - 1$) rather than of t and that X_r is a function of r ($r = 0, 1, 2, \ldots, N_0 - 1$) rather than of ω. Moreover, both x_n and X_r are periodic sequences of period N_0 (Figs. 5.16e, 5.16f). Such sequences are called *N_0-periodic sequences*. The proof of the DFT relationships in Eqs. (5.12) and (5.13) follows directly from the results of the sampling theorem. The sampled signal $\bar{x}(t)$ (Fig. 5.16c) can be expressed as

$$\bar{x}(t) = \sum_{n=0}^{N_0-1} x(nT)\delta(t - nT)$$

Since $\delta(t - nT) \Longleftrightarrow e^{-jn\omega T}$, applying the Fourier transform yields

$$\overline{X}(\omega) = \sum_{n=0}^{N_0-1} x(nT)e^{-jn\omega T}$$

But from Fig. 5.1f [or Eq. (5.2)], it is clear that over the interval $|\omega| \leq \omega_s/2$, $\overline{X}(\omega)$, the Fourier transform of $\bar{x}(t)$ is $X(\omega)/T$, assuming negligible aliasing. Hence,

$$X(\omega) = T\overline{X}(\omega) = T \sum_{n=0}^{N_0-1} x(nT)e^{-jn\omega T} \qquad |\omega| \leq \frac{\omega_s}{2}$$

[†] In Eqs. (5.12) and (5.13), the summation is performed from 0 to $N_0 - 1$. It is shown in Sec. 10.1.1 [Eqs. (10.5) and (10.6)] that the summation may be performed over any successive N_0 values of n or r.

and

$$X_r = X(r\omega_0) = T\sum_{n=0}^{N_0-1} x(nT)e^{-nkr\omega_0 T} \tag{5.14}$$

If we let $\omega_0 T = \Omega_0$, then from Eq. (5.10),

$$\Omega_0 = \omega_0 T = 2\pi f_0 T = \frac{2\pi}{N_0}$$

Also, from Eq. (5.11),

$$Tx(nT) = x_n$$

Therefore, Eq. (5.14) becomes

$$X_r = \sum_{n=0}^{N_0-1} x_n e^{-jr\Omega_0 n} \qquad \Omega_0 = \frac{2\pi}{N_0}$$

This is Eq. (5.12), which we set to prove.

The inverse transform relationship of Eq. (5.13) can be derived by using a similar procedure with the roles of t and ω reversed, but here we shall use a more direct proof. To prove Eq. (5.13), we multiply both sides of Eq. (5.12) by $e^{jm\Omega_0 r}$ and sum over r as

$$\sum_{r=0}^{N_0-1} X_r e^{jm\Omega_0 r} = \sum_{r=0}^{N_0-1}\left[\sum_{n=0}^{N_0-1} x_n e^{-jr\Omega_0 n}\right] e^{jm\Omega_0 r}$$

By interchanging the order of summation on the right-hand side, we have

$$\sum_{r=0}^{N_0-1} X_r e^{jm\Omega_0 r} = \sum_{n=0}^{N_0-1} x_n\left[\sum_{r=0}^{N_0-1} e^{j(m-n)\Omega_0 r}\right]$$

As the footnote below readily shows, the inner sum on the right-hand side is zero for $n \neq m$ and is N_0 when $n = m$.† Thus, the outer sum will have only one nonzero term when $n = m$, and it is

† We show that

$$\sum_{n=0}^{N_0-1} e^{jk\Omega_0 n} = \begin{cases} N_0 & k = 0, \pm N_0, \pm 2N_0, \ldots \\ 0 & \text{otherwise} \end{cases} \tag{5.15}$$

Recall that $\Omega_0 N_0 = 2\pi$. So $e^{jk\Omega_0 n} = 1$ when $k = 0, \pm N_0, \pm 2N_0, \ldots$. Hence, the sum on the left-hand side of Eq. (5.15) is N_0. To compute the sum for other values of k, we note that the sum on the left-hand side of Eq. (5.15) is a geometric progression with common ratio $\alpha = e^{jk\Omega_0}$. Therefore (see Sec. B.8.3),

$$\sum_{n=0}^{N_0-1} e^{jk\Omega_0 n} = \frac{e^{jk\Omega_0 N_0} - 1}{e^{jk\Omega_0} - 1} = 0 \qquad (e^{jk\Omega_0 N_0} = e^{j2\pi m} = 1)$$

$N_0 x_n = N_0 x_m$. Therefore,

$$x_m = \frac{1}{N_0} \sum_{r=0}^{N_0-1} X_r e^{jm\Omega_0 r} \qquad \Omega_0 = \frac{2\pi}{N_0}$$

Because X_r is N_0 periodic, we need to determine the values of X_r over any one period. It is customary to determine X_r over the range $(0, N_0 - 1)$, rather than over the range $(-N_0/2, (N_0/2) - 1)$.†

Choice of T and T_0

In DFT computation, we first need to select suitable values for N_0 and T or T_0. For this purpose, we begin by deciding on B, the essential bandwidth (in hertz) of the signal. The sampling frequency f_s must be at least $2B$, that is,

$$\frac{f_s}{2} \geq B$$

Moreover, the sampling interval $T = 1/f_s$ [Eq. (5.10)], and

$$T \leq \frac{1}{2B} \tag{5.16}$$

Once we pick B, we can choose T according to Eq. (5.16). Also,

$$f_0 = \frac{1}{T_0} \tag{5.17}$$

where f_0 is the *frequency resolution* [separation between samples of $X(\omega)$]. Hence, if f_0 is given, we can pick T_0 according to Eq. (5.17). Knowing T_0 and T, we determine N_0 from

$$N_0 = \frac{T_0}{T}$$

Zero Padding

Recall that observing X_r is like observing the spectrum $X(\omega)$ through a picket fence. If the frequency sampling interval f_0 is not sufficiently small, we could miss out on some significant details and obtain a misleading picture. To obtain a higher number of samples, we need to reduce f_0. Because $f_0 = 1/T_0$, a higher number of samples requires us to increase the value of T_0, the period of repetition for $x(t)$. This option increases N_0, the number of samples of $x(t)$, by adding dummy samples of 0 value. This addition of dummy samples is known as *zero padding*. Thus, zero padding increases the number of samples and may help in getting a better idea of the spectrum $X(\omega)$ from its samples X_r. To continue with our picket fence analogy, zero padding is like using more, and narrower, pickets.

---

† The DFT of Eq. (5.12) and the IDFT of Eq. (5.13) represent a transform in their own right, and they are exact. There is no approximation. However, x_n and X_r, thus obtained, are only approximations to the actual samples of a signal $x(t)$ and of its Fourier transform $X(\omega)$.

Zero Padding Does Not Improve Accuracy or Resolution

Actually, we are not observing $X(\omega)$ through a picket fence. We are observing a distorted version of $X(\omega)$ resulting from the truncation of $x(t)$. Hence, we should keep in mind that even if the fence were transparent, we would see a reality distorted by aliasing. Seeing through the picket fence just gives us an imperfect view of the imperfectly represented reality. Zero padding only allows us to look at more samples of that imperfect reality. It can never reduce the imperfection in what is behind the fence. The imperfection, which is caused by aliasing, can be lessened only by reducing the sampling interval T. Observe that reducing T also increases N_0, the number of samples, and is like increasing the number of pickets while reducing their width. But in this case, the reality behind the fence is also better dressed and we see more of it.

EXAMPLE 5.7 Number of Samples and Frequency Resolution

A signal $x(t)$ has a duration of 2 ms and an essential bandwidth of 10 kHz. It is desirable to have a frequency resolution of 100 Hz in the DFT ($f_0 = 100$). Determine N_0.

To have $f_0 = 100$ Hz, the effective signal duration T_0 must be

$$T_0 = \frac{1}{f_0} = \frac{1}{100} = 10 \text{ ms}$$

Since the signal duration is only 2 ms, we need zero padding over 8 ms. Also, $B = 10{,}000$. Hence, $f_s = 2B = 20{,}000$ and $T = 1/f_s = 50$ μs. Furthermore,

$$N_0 = \frac{f_s}{f_0} = \frac{20{,}000}{100} = 200$$

The *fast Fourier transform* (FFT) algorithm (discussed later; see Sec. 5.6) is used to compute DFT, where it proves convenient (although not necessary) to select N_0 as a power of 2; that is, $N_0 = 2^n$ (n, integer). Let us choose $N_0 = 256$. Increasing N_0 from 200 to 256 can be used to reduce aliasing error (by reducing T), to improve resolution (by increasing T_0 using zero padding), or a combination of both.

Reducing Aliasing Error. We maintain the same T_0 so that $f_0 = 100$. Hence,

$$f_s = N_0 f_0 = 256 \times 100 = 25{,}600 \qquad \text{and} \qquad T = \frac{1}{f_s} = 39\,\mu\text{s}$$

Thus, increasing N_0 from 200 to 256 permits us to reduce the sampling interval T from 50 μs to 39 μs while maintaining the same frequency resolution ($f_0 = 100$).

Improving Resolution. Here, we maintain the same $T = 50$ μs, which yields

$$T_0 = N_0 T = 256(50 \times 10^{-6}) = 12.8 \text{ ms} \qquad \text{and} \qquad f_0 = \frac{1}{T_0} = 78.125 \text{ Hz}$$

Thus, increasing N_0 from 200 to 256 can improve the frequency resolution from 100 to 78.125 Hz while maintaining the same aliasing error ($T = 50$ μs).

Combination of Reducing Aliasing Error and Improving Resolution. To simultaneously reduce alias error and improve resolution, we could choose $T = 45$ μs and $T_0 = 11.5$ ms so that $f_0 = 86.96$ Hz. Many other combinations exist as well.

EXAMPLE 5.8 DFT to Compute the Fourier Transform of an Exponential

Use the DFT to compute (samples of) the Fourier transform of $e^{-2t}u(t)$. Plot the resulting Fourier spectra.

We first determine T and T_0. The Fourier transform of $e^{-2t}u(t)$ is $1/(j\omega + 2)$. This lowpass signal is not bandlimited. In Sec. 4.6, we used the energy criterion to compute the essential bandwidth of a signal. Here, we shall present a simpler, but workable alternative to the energy criterion. The essential bandwidth of a signal will be taken as the frequency at which $|X(\omega)|$ drops to 1% of its peak value (see the footnote on p. 387). In this case, the peak value occurs at $\omega = 0$, where $|X(0)| = 0.5$. Observe that

$$|X(\omega)| = \frac{1}{\sqrt{\omega^2 + 4}} \approx \frac{1}{\omega} \qquad \omega \gg 2$$

Also, 1% of the peak value is $0.01 \times 0.5 = 0.005$. Hence, the essential bandwidth B is at $\omega = 2\pi B$, where

$$|X(\omega)| \approx \frac{1}{2\pi B} = 0.005 \quad \Rightarrow \quad B = \frac{100}{\pi} \text{ Hz}$$

and from Eq. (5.16),

$$T \leq \frac{1}{2B} = \frac{\pi}{200} = 0.015708$$

Had we used 1% energy criterion to determine the essential bandwidth, following the procedure in Ex. 4.20, we would have obtained $B = 20.26$ Hz, which is somewhat smaller than the value just obtained by using the 1% amplitude criterion.

The second issue is to determine T_0. Because the signal is not timelimited, we have to truncate it at T_0 such that $x(T_0) \ll 1$. A reasonable choice would be $T_0 = 4$ because $x(4) = e^{-8} = 0.000335 \ll 1$. The result is $N_0 = T_0/T = 254.6$, which is not a power of 2. Hence, we choose $T_0 = 4$, and $T = 0.015625 = 1/64$, yielding $N_0 = 256$, which is a power of 2.

Note that there is a great deal of flexibility in determining T and T_0, depending on the accuracy desired and the computational capacity available. We could just as well have chosen $T = 0.03125$, yielding $N_0 = 128$, although this choice would have given a slightly higher aliasing error.

Because the signal has a jump discontinuity at $t = 0$, the first sample (at $t = 0$) is 0.5, the averages of the values on the two sides of the discontinuity. We compute X_r (the DFT) from the samples of $e^{-2t}u(t)$ according to Eq. (5.12). Note that X_r is the rth sample of $X(\omega)$, and these samples are spaced at $f_0 = 1/T_0 = 0.25$ Hz ($\omega_0 = \pi/2$ rad/s).

Because X_r is N_0 periodic, $X_r = X_{(r+256)}$ so that $X_{256} = X_0$. Hence, we need to plot X_r over the range $r = 0$ to 255 (not 256). Moreover, because of this periodicity, $X_{-r} = X_{(-r+256)}$, and the values of X_r over the range $r = -127$ to -1 are identical to those over the range $r = 129$ to 255. Thus, $X_{-127} = X_{129}, X_{-126} = X_{130}, \ldots, X_{-1} = X_{255}$. In addition, because of the property of conjugate symmetry of the Fourier transform, $X_{-r} = X_r^*$, it follows that $X_{-1} = X_1^*, X_{-2} = X_2^*, \ldots, X_{-128} = X_{128}^*$. Thus, we need X_r only over the range $r = 0$ to $N_0/2$ (128 in this case).

Figure 5.17 shows the computed plots of $|X_r|$ and $\angle X_r$. The exact spectra are depicted by continuous curves for comparison. Note the nearly perfect agreement between the two sets of spectra. We have depicted the plot of only the first 28 points rather than all 128 points, which would have made the figure very crowded, resulting in loss of clarity. The points are at the intervals of $1/T_0 = 1/4$ Hz or $\omega_0 = 1.5708$ rad/s. The 28 samples, therefore, exhibit the plots over the range $\omega = 0$ to $\omega = 28(1.5708) \approx 44$ rad/s or 7 Hz.

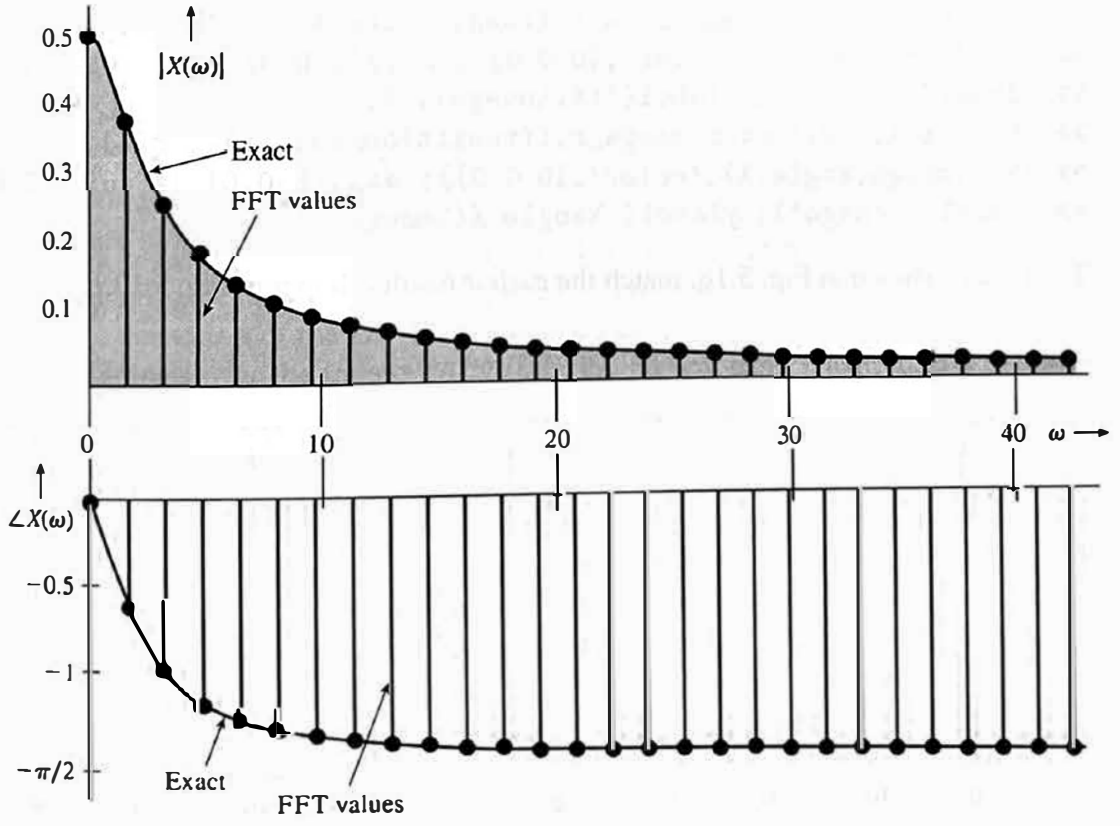

Figure 5.17 Discrete Fourier transform of an exponential signal $e^{-2t}u(t)$.

In this example, we knew $X(\omega)$ beforehand; hence, we could make intelligent choices for B (or the sampling frequency f_s). In practice, we generally do not know $X(\omega)$ beforehand. In fact, that is the very thing we are trying to determine. In such a case, we must make an intelligent guess for B or f_s from circumstantial evidence. We should then continue reducing the value of T and recomputing the transform until the result stabilizes within the desired number of significant digits.

Using MATLAB to Compute and Plot the Results

Let us now use MATLAB to confirm the results of this example. First, parameters are defined and MATLAB's `fft` command is used to compute the DFT.

```
>>  T_0 = 4; N_0 = 256; T = T_0/N_0; t = (0:T:T*(N_0-1))';
>>  x = T*exp(-2*t); x(1) = x(1)/2;
>>  X_r = fft(x); r = [-N_0/2:N_0/2-1]'; omega_r = r*2*pi/T_0;
```

The true Fourier transform is also computed for comparison.

```
>>  omega = linspace(-pi/T,pi/T,5001); X = 1./(j*omega+2);
```

For clarity, we display spectrum over a restricted frequency range.

```
>> subplot(1,2,1); stem(omega_r,fftshift(abs(X_r)),'k.');
>> line(omega,abs(X),'color',[0 0 0]); axis([-0.01 44 -0.01 0.51]);
>> xlabel('\omega'); ylabel('|X(\omega)|');
>> subplot(1,2,2); stem(omega_r,fftshift(angle(X_r)),'k.');
>> line(omega,angle(X),'color',[0 0 0]); axis([-0.01 44 -pi/2-0.01 0.01]);
>> xlabel('\omega'); ylabel('\angle X(\omega)');
```

The results, shown in Fig. 5.18, match the earlier results shown in Fig. 5.17.

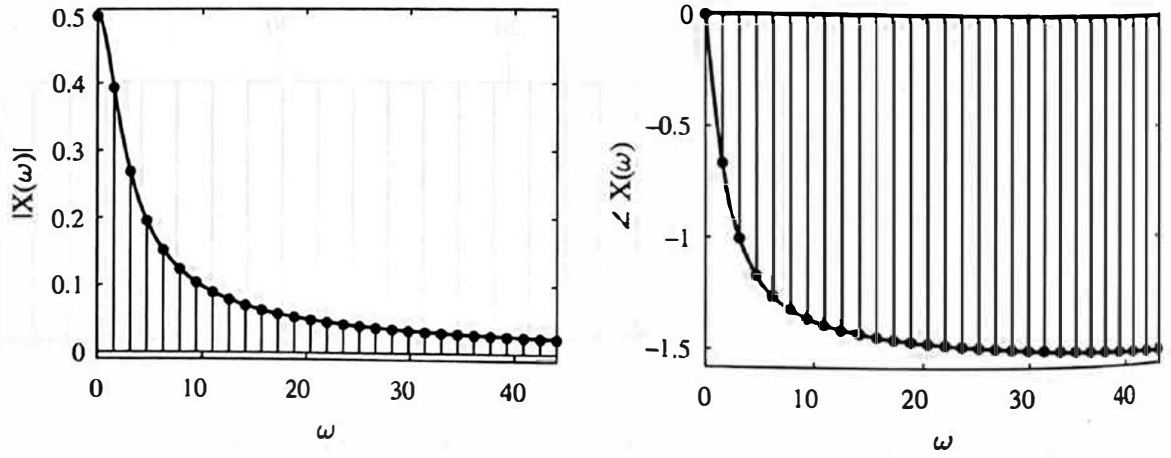

Figure 5.18 MATLAB-computed DFT of an exponential signal $e^{-2t}u(t)$.

EXAMPLE 5.9 DFT to Compute the Fourier Transform of a Rectangular Pulse

Use the DFT to compute the Fourier transform of 8 rect(t).

This gate function and its Fourier transform are illustrated in Figs. 5.19a and 5.19b. To determine the value of the sampling interval T, we must first decide on the essential bandwidth B. In Fig. 5.19b, we see that $X(\omega)$ decays rather slowly with ω. Hence, the essential bandwidth B is rather large. For instance, at $B = 15.5$ Hz (97.39 rad/s), $X(\omega) = -0.1643$, which is about 2% of the peak at $X(0)$. Hence, the essential bandwidth is well above 16 Hz if we use the 1% of the peak amplitude criterion for computing the essential bandwidth. However, we shall deliberately take $B = 4$ for two reasons: to show the effect of aliasing and because the use of $B > 4$ would give an enormous number of samples, which could not be conveniently displayed on the page without losing sight of the essentials. Thus, we shall intentionally accept approximation to graphically clarify the concepts of the DFT.

The choice of $B = 4$ results in the sampling interval $T = 1/2B = 1/8$. Looking again at the spectrum in Fig. 5.19b, we see that the choice of the frequency resolution $f_0 = 1/4$ Hz is reasonable. Such a choice gives us four samples in each lobe of $X(\omega)$. In this case, $T_0 = 1/f_0 = 4$ seconds and $N_0 = T_0/T = 32$. The duration of $x(t)$ is only 1 second. We must repeat it every 4 seconds ($T_0 = 4$), as depicted in Fig. 5.19c, and take samples every 1/8 second. This choice yields 32 samples ($N_0 = 32$). Also,

$$x_n = Tx(nT) = \tfrac{1}{8}x(nT)$$

Since $x(t) = 8\,\text{rect}\,(t)$, the values of x_n are 1, 0, or 0.5 (at the points of discontinuity), as illustrated in Fig. 5.19c, where x_n is depicted as a function of t as well as n, for convenience.

In the derivation of the DFT, we assumed that $x(t)$ begins at $t = 0$ (Fig. 5.16a), and then took N_0 samples over the interval $(0, T_0)$. In the present case, however, $x(t)$ begins at $-1/2$. This difficulty is easily resolved when we realize that the DFT obtained by this procedure is actually the DFT of x_n repeating periodically every T_0 seconds. Figure 5.19c clearly indicates that periodic repeating the segment of x_n over the interval from -2 to 2 seconds yields the same signal as the periodic repeating the segment of x_n over the interval from 0 to 4 seconds. Hence, the DFT of the samples taken from -2 to 2 seconds is the same as that of the samples taken from 0 to 4 seconds. Therefore, regardless of where $x(t)$ starts, we can always take the samples of $x(t)$ and its periodic extension over the interval from 0 to T_0. In the present example, the 32 sample values are

$$x_n = \begin{cases} 1 & 0 \le n \le 3 \quad \text{and} \quad 29 \le n \le 31 \\ 0 & 5 \le n \le 27 \\ 0.5 & n = 4, 28 \end{cases}$$

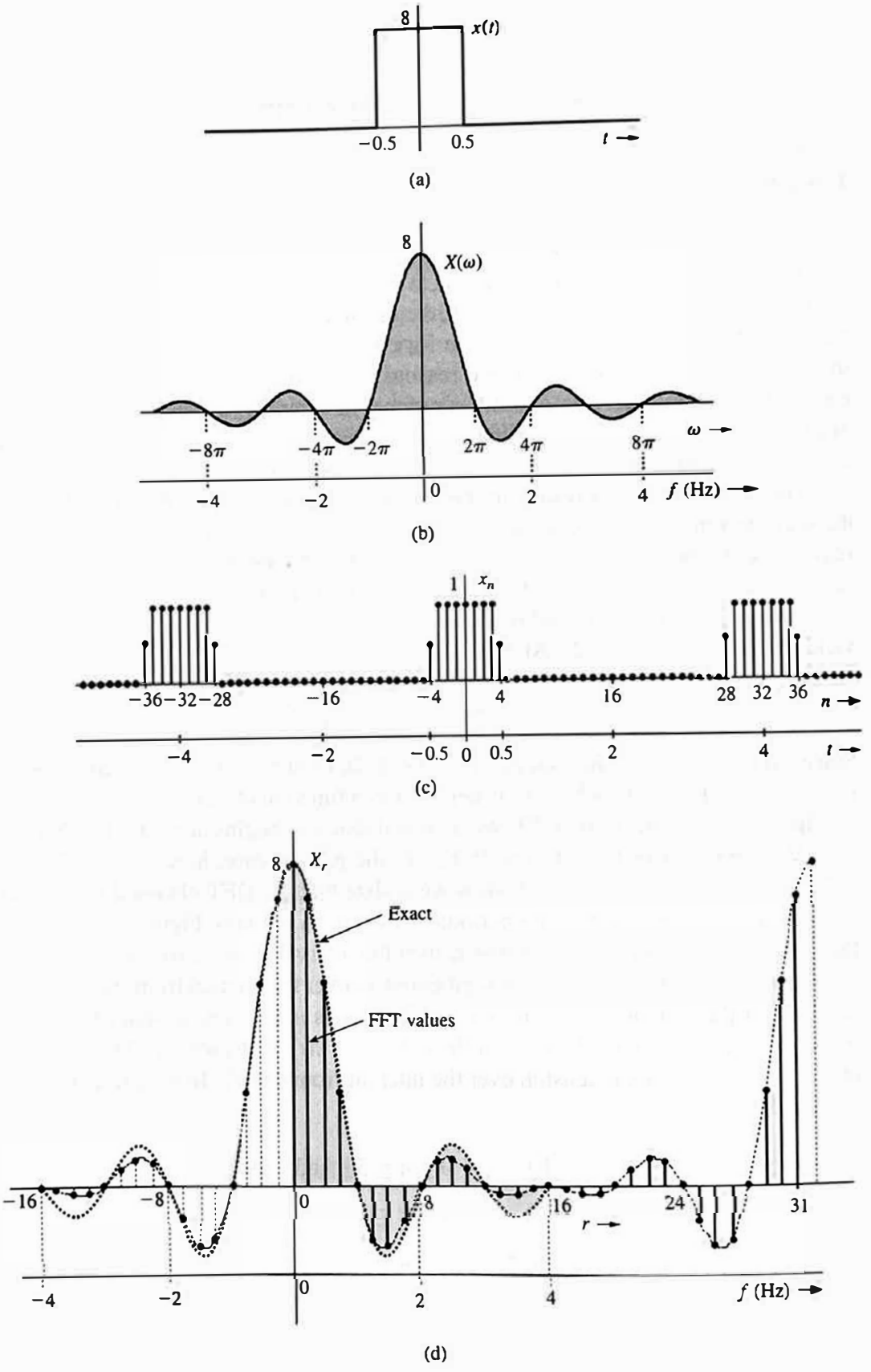

Figure 5.19 Discrete Fourier transform of a gate pulse.

Observe that the last sample is at $t = 31/8$, not at 4, because the signal repetition starts at $t = 4$, and the sample at $t = 4$ is the same as the sample at $t = 0$. Now, $N_0 = 32$ and $\Omega_0 = 2\pi/32 = \pi/16$. Therefore [see Eq. (5.12)],

$$X_r = \sum_{n=0}^{31} x_n e^{-jr(\pi/16)n}$$

Values of X_r are computed according to this equation and plotted in Fig. 5.19d.

The samples X_r are separated by $f_0 = 1/T_0$ Hz. In this case, $T_0 = 4$, so the frequency resolution f_0 is 1/4 Hz, as desired. The folding frequency $f_s/2 = B = 4$ Hz corresponds to $r = N_0/2 = 16$. Because X_r is N_0 periodic ($N_0 = 32$), the values of X_r for $r = -16$ to $n = -1$ are the same as those for $r = 16$ to $n = 31$. For instance, $X_{17} = X_{-15}$, $X_{18} = X_{-14}$, and so on. The DFT gives us the samples of the spectrum $X(\omega)$.

For the sake of comparison, Fig. 5.19d also shows the shaded curve $8\,\text{sinc}(\omega/2)$, which is the Fourier transform of $8\,\text{rect}(t)$. The values of X_r computed from the DFT equation show aliasing error, which is clearly seen by comparing the two superimposed plots. The error in X_2 is just about 1.3%. However, the aliasing error increases rapidly with r. For instance, the error in X_6 is about 12%, and the error in X_{10} is 33%. The error in X_{14} is a whopping 72%. The percent error increases rapidly near the folding frequency ($r = 16$) because $x(t)$ has a jump discontinuity, which makes $X(\omega)$ decay slowly as $1/\omega$. Hence, near the folding frequency, the inverted tail (due to aliasing) is very nearly equal to $X(\omega)$ itself. Moreover, the final values are the difference between the exact and the folded values (which are very close to the exact values). Hence, the percent error near the folding frequency ($r = 16$ in this case) is very high, although the absolute error is very small. Clearly, for signals with jump discontinuities, the aliasing error near the folding frequency will always be high (in percentage terms), regardless of the choice of N_0. To ensure a negligible aliasing error at any value r, we must make sure that $N_0 \gg r$. This observation is valid for all signals with jump discontinuities.

Using MATLAB to Compute and Plot the Results

Once again, MATLAB lets us easily confirm the results of this example. First, parameters are defined and MATLAB's `fft` command is used to compute the DFT.

```
>> T_0 = 4; N_0 = 32; T = T_0/N_0;
>> x_n = [ones(1,4) 0.5 zeros(1,23) 0.5 ones(1,3)]';
>> X_r = fft(x_n); r = [-N_0/2:N_0/2-1]'; omega_r = r*2*pi/T_0;
```

The true Fourier transform is also computed for comparison.

```
>> omega = linspace(-pi/T,pi/T,5001); X = 8*sinc(omega/(2*pi));
```

Since it is real, we can display the resulting spectrum using a single plot.

```
>> clf; stem(omega_r,fftshift(real(X_r)),'k.');
>> line(omega,X,'color',[0 0 0]);
>> xlabel('\omega'); ylabel('X(\omega)'); axis tight
```

The result, shown in Fig. 5.20, matches the earlier result shown in Fig. 5.19d. The DFT approximation does not perfectly follow the true Fourier transform, especially at high frequencies, because the parameter B is deliberately set too small.

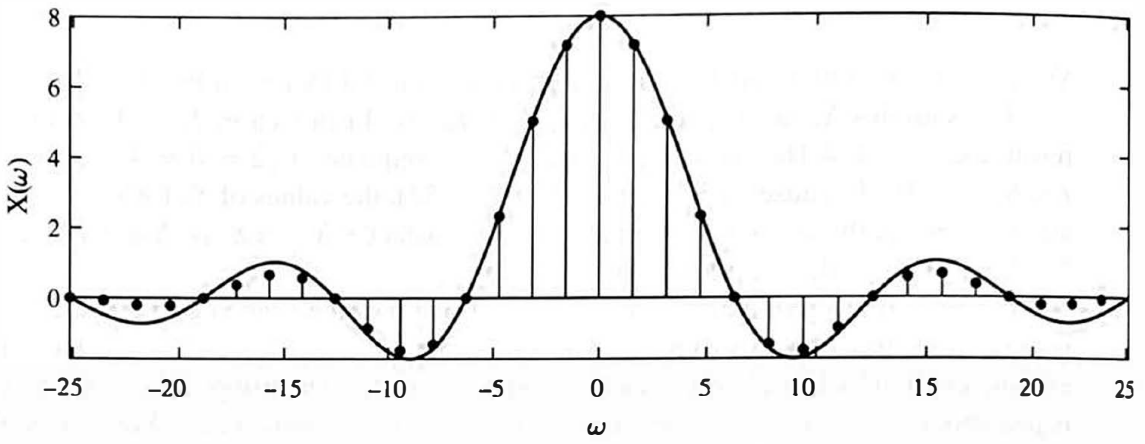

Figure 5.20 MATLAB-computed DFT of a gate pulse.

5.5.1 Some Properties of the DFT

The discrete Fourier transform is basically the Fourier transform of a sampled signal repeated periodically. Hence, the properties derived earlier for the Fourier transform apply to the DFT as well.

Linearity

If $x_n \Longleftrightarrow X_r$ and $g_n \Longleftrightarrow G_r$, then

$$a_1 x_n + a_2 g_n \Longleftrightarrow a_1 X_r + a_2 G_r$$

The proof is trivial.

Conjugate Symmetry

From the conjugation property $x^*(t) \Longleftrightarrow X^*(-\omega)$, we have

$$x_n^* \longleftrightarrow X_{-r}^*$$

From this equation and the time-reversal property, we obtain

$$x_{-n}^* \longleftrightarrow X_r^*$$

When $x(t)$ is real, then the conjugate-symmetry property states that $X^*(\omega) = X(-\omega)$. Hence, for real x_n,

$$X_r^* = X_{-r}$$

Moreover, X_r is N_0 periodic. Hence,

$$X_r^* = X_{N_0-r}$$

Because of this property, we need compute only half the DFTs for real x_n. The other half are the conjugates.

Time Shifting

The time-shifting (circular shifting) property states[†]

$$x_{n-k} \Longleftrightarrow X_r e^{-jr\Omega_0 k}$$

Proof. We use Eq. (5.13) to find the inverse DFT of $X_r e^{-jr\Omega_0 k}$ as

$$\frac{1}{N_0}\sum_{r=0}^{N_0-1} X_r e^{-jr\Omega_0 k} e^{jr\omega_0 n} = \frac{1}{N_0}\sum_{r=0}^{N_0-1} X_r e^{jr\Omega_0(n-k)} = x_{n-k}$$

Frequency Shifting

A dual of the time-shifting property, the frequency-shifting property states

$$x_n e^{jn\Omega_0 m} \Longleftrightarrow X_{r-m}$$

Proof. This proof is identical to that of the time-shifting property except that we start with Eq. (5.12).

Circular Convolution

The circular (or periodic) convolution property states

$$x_n \circledast g_n \Longleftrightarrow X_r G_r \tag{5.18}$$

and

$$x_n g_n \Longleftrightarrow \frac{1}{N_0} X_r \circledast G_r \tag{5.19}$$

For two N_0-periodic sequences x_n and g_n, circular (or periodic) convolution is defined by

$$x_n \circledast g_n = \sum_{k=0}^{N_0-1} x_k g_{n-k} = \sum_{k=0}^{N_0-1} g_k x_{n-k} \tag{5.20}$$

[†] Time shifting is also known as *circular shifting* because such a shift can be interpreted as a circular shift of the N_0 samples in the first cycle $0 \le n \le N_0 - 1$.

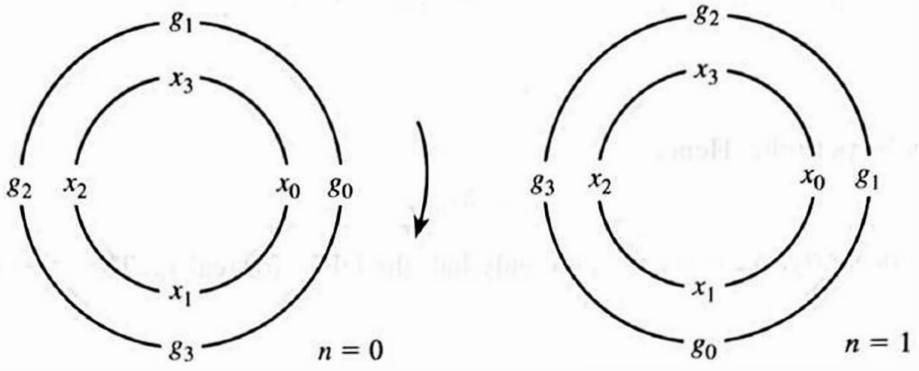

Figure 5.21 Graphical depictions of circular convolution.

To prove Eq. (5.18), we find the DFT of the circular convolution $x_n \circledast g_n$ as

$$\sum_{n=0}^{N_0-1}\left(\sum_{k=0}^{N_0-1} x_k g_{n-k}\right)e^{-jr\omega_0 n} = \sum_{k=0}^{N_0-1} x_k\left(\sum_{n=0}^{N_0-1} g_{n-k}e^{-jr\omega_0 n}\right)$$

$$= \sum_{k=0}^{N_0-1} x_k(G_r e^{-jr\Omega_0 k}) = X_r G_r$$

Equation (5.19) can be proved in the same way.

For periodic sequences, the convolution can be visualized in terms of two sequences, with one sequence fixed and the other inverted and moved past the fixed sequence, one digit at a time. If the two sequences are N_0 periodic, the same configuration will repeat after N_0 shifts of the sequence. Clearly, the convolution $x_n \circledast g_n$ becomes N_0 periodic. Such convolution can be conveniently visualized in terms of N_0 sequences, as illustrated in Fig. 5.21, for the case of $N_0 = 4$. The inner N_0-point sequence x_n is clockwise and fixed. The outer N_0-point sequence g_n is inverted so that it becomes counterclockwise. This sequence is now rotated clockwise 1 unit at a time. We multiply the overlapping numbers and add. For example, the value of $x_n \circledast g_n$ at $n = 0$ (Fig. 5.21) is

$$x_0 g_0 + x_1 g_3 + x_2 g_2 + x_3 g_1$$

and the value of $x_n \circledast g_n$ at $n = 1$ is (Fig. 5.21)

$$x_0 g_1 + x_1 g_0 + x_2 g_3 + x_3 g_2$$

and so on.

5.5.2 Some Applications of the DFT

The DFT is useful not only in the computation of direct and inverse Fourier transforms, but also in other applications such as convolution, correlation, and filtering. Use of the efficient FFT algorithm, discussed shortly (Sec. 5.6), makes it particularly appealing.

Linear Convolution

Let $x(t)$ and $g(t)$ be the two signals to be convolved. In general, these signals may have different time durations. To convolve them by using their samples, they must be sampled at the same rate (not below the Nyquist rate of either signal). Let x_n $(0 \le n \le N_1 - 1)$ and g_n $(0 \le n \le N_2 - 1)$ be the corresponding discrete sequences representing these samples. Now,

$$c(t) = x(t) * g(t)$$

and if we define three sequences as $x_n = Tx(nT)$, $g_n = Tg(nT)$, and $c_n = Tc(nT)$, then†

$$c_n = x_n * g_n$$

where we define the linear convolution sum of two discrete sequences x_n and g_n as

$$c_n = x_n * g_n = \sum_{k=-\infty}^{\infty} x_k g_{n-k}$$

Because of the width property of the convolution, c_n exists for $0 \le n \le N_1 + N_2 - 1$. To be able to use the DFT circular convolution technique, we must make sure that the circular convolution will yield the same result as does linear convolution. In other words, the signal resulting from the circular convolution must have the same length $(N_1 + N_2 - 1)$ as that of the signal resulting from linear convolution. This step can be accomplished by adding $N_2 - 1$ dummy samples of zero value to x_n and $N_1 - 1$ dummy samples of zero value to g_n (zero padding). This procedure changes the length of both x_n and g_n to $N_1 + N_2 - 1$. The circular convolution now is identical to the linear convolution except that it repeats periodically with period $N_1 + N_2 - 1$. A little reflection will show that in such a case the circular convolution procedure in Fig. 5.21 over one cycle $(0 \le n \le N_1 + N_2 - 1)$ is identical to the linear convolution of the two sequences x_n and g_n. We can use the DFT to find the convolution $x_n * g_n$ in three steps, as follows:

1. Find the DFTs X_r and G_r corresponding to suitably padded x_n and g_n.
2. Multiply X_r by G_r.
3. Find the IDFT of $X_r G_r$. This procedure of convolution, when implemented by the fast Fourier transform algorithm (discussed later), is known as *fast convolution*.

Filtering

We generally think of filtering in terms of a hardware-oriented solution (e.g., building a circuit with *RLC* components and operational amplifiers). However, filtering also has a software-oriented solution [a computer algorithm that yields the filtered output $y(t)$ for a given input $x(t)$]. This goal can be conveniently accomplished by using the DFT. If $x(t)$ is the signal to be filtered, then X_r, the DFT of x_n, is found. The spectrum X_r is then shaped (filtered) as desired by multiplying X_r by H_r, where H_r are the samples of $H(\omega)$ for the filter $[H_r = H(r\omega_0)]$. Finally, we take the IDFT of $X_r H_r$ to obtain the filtered output $y_n [y_n = Ty(nT)]$. This procedure is demonstrated in the following example.

† We can show that $c_n = \lim_{T \to 0} x_n * g_n$; [see 4]. Error is inherent in any numerical method used to compute convolution of continuous-time signals; since $T \neq 0$ in practice, there will be some error in this equation.

EXAMPLE 5.10 DFT to Determine Filter Output

The signal $x(t)$ in Fig. 5.22a is passed through an ideal lowpass filter of frequency response $H(\omega)$ depicted in Fig. 5.22b. Use the DFT to find the sampled version of the filter output.

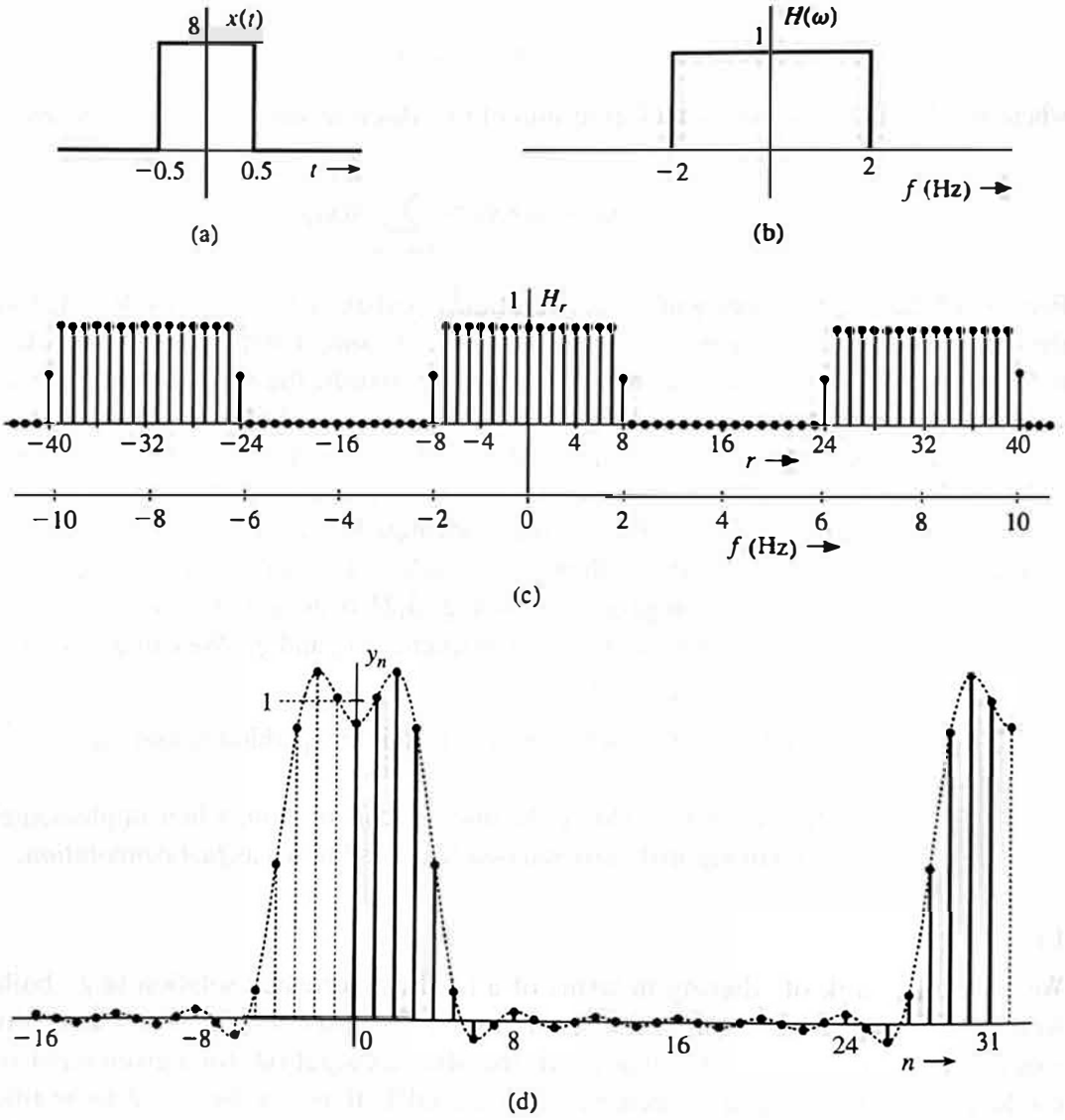

Figure 5.22 DFT solution for filtering $x(t)$ through $H(\omega)$.

We have already found the 32-point DFT of $x(t)$ (see Fig. 5.19d). Next we multiply X_r by H_r. To find H_r, we recall using $f_0 = 1/4$ in computing the 32-point DFT of $x(t)$. Because X_r is 32-periodic, H_r must also be 32-periodic with samples separated by 1/4 Hz. This fact means

that H_r must be repeated every 8 Hz or 16π rad/s (see Fig. 5.22c). The resulting 32 samples of H_r over $(0 \le \omega \le 16\pi)$ are as follows:

$$H_r = \begin{cases} 1 & 0 \le r \le 7 \quad \text{and} \quad 25 \le r \le 31 \\ 0 & 9 \le r \le 23 \\ 0.5 & r = 8, 24 \end{cases}$$

We multiply X_r with H_r. The desired output signal samples y_n are found by taking the inverse DFT of $X_r H_r$. The resulting output signal is illustrated in Fig. 5.22d.

It is quite simple to verify the results of this filtering example using MATLAB. First, parameters are defined, and MATLAB's `fft` command is used to compute the DFT of x_n.

```
>> T_0 = 4; N_0 = 32; T = T_0/N_0; n = (0:N_0-1); r = n;
>> x_n = [ones(1,4) 0.5 zeros(1,23) 0.5 ones(1,3)]';
>> X_r = fft(x_n);
```

The DFT of the filter's output is just the product of the filter response H_r and the input DFT X_r. The output y_n is obtained using the `ifft` command and then plotted.

```
>> H_r = [ones(1,8) 0.5 zeros(1,15) 0.5 ones(1,7)]';
>> Y_r = H_r.*X_r; y_n = ifft(Y_r);
>> clf; stem(n,real(y_n),'k.');
>> xlabel('n'); ylabel('y_n'); axis([0 31 -.1 1.1]);
```

The result, shown in Fig. 5.23, matches the earlier result shown in Fig. 5.22d. Recall, this DFT-based approach shows the samples y_n of the filter output $y(t)$ (sampled in this case at a rate $T = \frac{1}{8}$) over $0 \le n \le N_0 - 1 = 31$ when the input pulse $x(t)$ is periodically replicated to form samples x_n (see Fig. 5.19c).

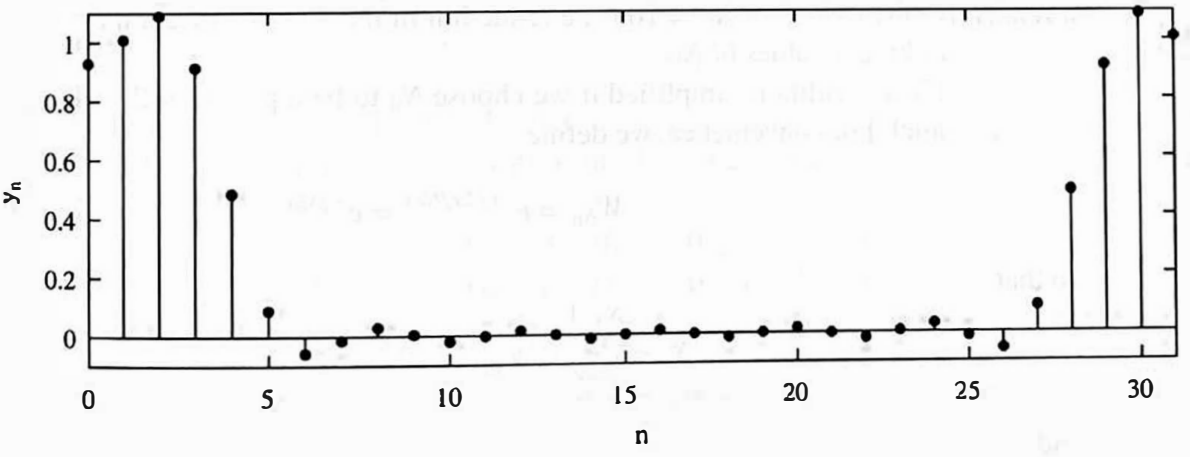

Figure 5.23 Using MATLAB and the DFT to determine filter output.

5.6 THE FAST FOURIER TRANSFORM (FFT)

The number of computations required in performing the DFT was dramatically reduced by an algorithm developed by Cooley and Tukey in 1965 [5]. This algorithm, known as the *fast Fourier transform* (FFT), reduces the number of computations from something on the order of N_0^2 to $N_0 \log N_0$. To compute one sample X_r from Eq. (5.12), we require N_0 complex multiplications and $N_0 - 1$ complex additions. To compute N_0 such values (X_r for $r = 0, 1, \ldots, N_0 - 1$), we require a total of N_0^2 complex multiplications and $N_0(N_0 - 1)$ complex additions. For a large N_0, these computations can be prohibitively time-consuming, even for a high-speed computer. The FFT algorithm is what made the use of the Fourier transform accessible for digital signal processing.

How Does the FFT Reduce the Number of Computations?

It is easy to understand the magic of the FFT. The secret is in the linearity of the Fourier transform and also of the DFT. Because of linearity, we can compute the Fourier transform of a signal $x(t)$ as a sum of the Fourier transforms of segments of $x(t)$ of shorter duration. The same principle applies to the computation of the DFT. Consider a signal of length $N_0 = 16$ samples. As seen earlier, DFT computation of this sequence requires $N_0^2 = 256$ multiplications and $N_0(N_0 - 1) = 240$ additions. We can split this sequence into two shorter sequences, each of length 8. To compute DFT of each of these segments, we need 64 multiplications and 56 additions. Thus, we need a total of 128 multiplications and 112 additions. Suppose, we split the original sequence in four segments of length 4 each. To compute the DFT of each segment, we require 16 multiplications and 12 additions. Hence, we need a total of 64 multiplications and 48 additions. If we split the sequence in eight segments of length 2 each, we need 4 multiplications and 2 additions for each segment, resulting in a total of 32 multiplications and 8 additions. Thus, we have been able to reduce the number of multiplications from 256 to 32 and the number of additions from 240 to 8. Moreover, some of these multiplications turn out to be multiplications by 1 or -1. All this fantastic economy in the number of computations is realized by the FFT without any approximation! The values obtained by the FFT are identical to those obtained by the DFT. In this example, we considered a relatively small value of $N_0 = 16$. The reduction in the number of computations is much more dramatic for higher values of N_0.

The FFT algorithm is simplified if we choose N_0 to be a power of 2, although such a choice is not essential. For convenience, we define

$$W_{N_0} = e^{-(j2\pi/N_0)} = e^{-j\Omega_0}$$

so that

$$X_r = \sum_{n=0}^{N_0-1} x_n W_{N_0}^{nr} \qquad 0 \le r \le N_0 - 1 \tag{5.21}$$

and

$$x_n = \frac{1}{N_0} \sum_{r=0}^{N_0-1} X_r W_{N_0}^{-nr} \qquad 0 \le n \le N_0 - 1 \tag{5.22}$$

Although there are many variations of the Tukey–Cooley algorithm, these can be grouped into two basic types: *decimation in time* and *decimation in frequency*.

The Decimation-in-Time Algorithm

Here, we divide the N_0-point data sequence x_n into two $(N_0/2)$-point sequences consisting of even- and odd-numbered samples, respectively, as follows:

$$\underbrace{x_0, x_2, x_4, \ldots, x_{N_0-2}}_{\text{sequence } g_n}, \underbrace{x_1, x_3, x_5, \ldots, x_{N_0-1}}_{\text{sequence } h_n}$$

Then, from Eq. (5.21),

$$X_r = \sum_{n=0}^{(N_0/2)-1} x_{2n} W_{N_0}^{2nr} + \sum_{n=0}^{(N_0/2)-1} x_{2n+1} W_{N_0}^{(2n+1)r}$$

Also, since

$$W_{N_0/2} = W_{N_0}^2$$

we have

$$\begin{aligned} X_r &= \sum_{n=0}^{(N_0/2)-1} x_{2n} W_{N_0/2}^{nr} + W_{N_0}^r \sum_{n=0}^{(N_0/2)-1} x_{2n+1} W_{N_0/2}^{nr} \\ &= G_r + W_{N_0}^r H_r \qquad 0 \le r \le N_0 - 1 \end{aligned} \tag{5.23}$$

where G_r and H_r are the $(N_0/2)$-point DFTs of the even- and odd-numbered sequences, g_n and h_n, respectively. Also, G_r and H_r, being the $(N_0/2)$-point DFTs, are $(N_0/2)$ periodic. Hence,

$$G_{r+(N_0/2)} = G_r \qquad \text{and} \qquad H_{r+(N_0/2)} = H_r \tag{5.24}$$

Moreover,

$$W_{N_0}^{r+(N_0/2)} = W_{N_0}^{N_0/2} W_{N_0}^r = e^{-j\pi} W_{N_0}^r = -W_{N_0}^r \tag{5.25}$$

From Eqs. (5.23), (5.24), and (5.25), we obtain

$$X_{r+(N_0/2)} = G_r - W_{N_0}^r H_r \tag{5.26}$$

This property can be used to reduce the number of computations. We can compute the first $N_0/2$ points $(0 \le n \le (N_0/2) - 1)$ of X_r by using Eq. (5.23) and the last $N_0/2$ points by using Eq. (5.26) as

$$\begin{aligned} X_r &= G_r + W_{N_0}^r H_r \qquad 0 \le r \le \tfrac{N_0}{2} - 1 \\ X_{r+(N_0/2)} &= G_r - W_{N_0}^r H_r \qquad 0 \le r \le \tfrac{N_0}{2} - 1 \end{aligned} \tag{5.27}$$

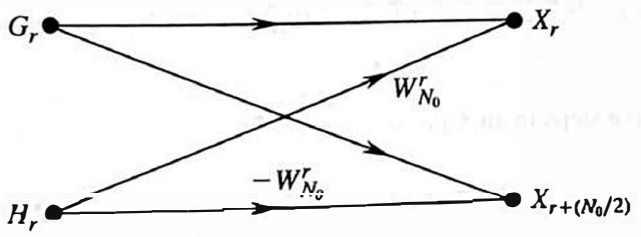

Figure 5.24 Butterfly signal flow graph.

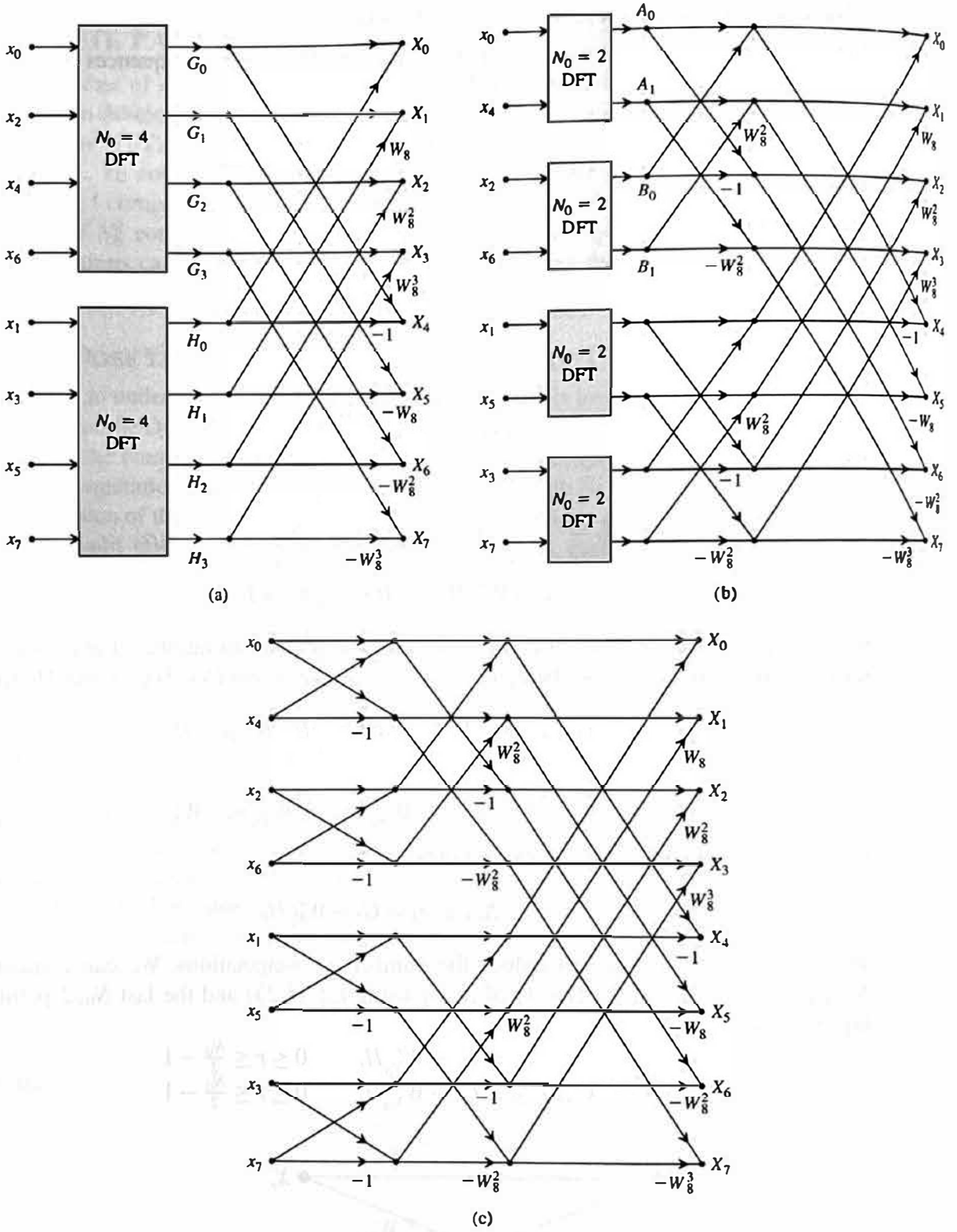

Figure 5.25 Successive steps in an 8-point FFT.

Thus, an N_0-point DFT can be computed by combining the two $(N_0/2)$-point DFTs, as in Eq. (5.27). These equations can be represented conveniently by the *signal flow* graph depicted in Fig. 5.24. This structure is known as a *butterfly*. Figure 5.25a shows the implementation of Eq. (5.24) for the case of $N_0 = 8$.

The next step is to compute the $(N_0/2)$-point DFTs G_r and H_r. We repeat the same procedure by dividing g_n and h_n into two $(N_0/4)$-point sequences corresponding to the even- and odd-numbered samples. Then we continue this process until we reach the one-point DFT. These steps for the case of $N_0 = 8$ are shown in Figs. 5.25a, 5.25b, and 5.25c. Figure 5.25c shows that the two-point DFTs require no multiplication.

To count the number of computations required in the first step, assume that G_r and H_r are known. Equation (5.27) clearly shows that to compute all the N_0 points of the X_r, we require N_0 complex additions and $N_0/2$ complex multiplications[†] (corresponding to $W_{N_0}^r H_r$).

In the second step, to compute the $(N_0/2)$-point DFT G_r from the $(N_0/4)$-point DFT, we require $N_0/2$ complex additions and $N_0/4$ complex multiplications. We require an equal number of computations for H_r. Hence, in the second step, there are N_0 complex additions and $N_0/2$ complex multiplications. The number of computations required remains the same in each step. Since a total of $\log_2 N_0$ steps is needed to arrive at a one-point DFT, we require, conservatively, a total of $N_0 \log_2 N_0$ complex additions and $(N_0/2)\log_2 N_0$ complex multiplications, to compute the N_0-point DFT. Actually, as Fig. 5.25c shows, many multiplications are multiplications by 1 or -1, which further reduces the number of computations.

The procedure for obtaining IDFT is identical to that used to obtain the DFT except that $W_{N_0} = e^{j(2\pi/N_0)}$ instead of $e^{-j(2\pi/N_0)}$ (in addition to the multiplier $1/N_0$). Another FFT algorithm, the *decimation-in-frequency* algorithm, is similar to the decimation-in-time algorithm. The only difference is that instead of dividing x_n into two sequences of even- and odd-numbered samples, we divide x_n into two sequences formed by the first $N_0/2$ and the last $N_0/2$ samples, proceeding in the same way until a single-point DFT is reached in $\log_2 N_0$ steps. The total number of computations in this algorithm is the same as that in the decimation-in-time algorithm.

5.7 MATLAB: The Discrete Fourier Transform

As an idea, the discrete Fourier transform (DFT) has been known for hundreds of years. Practical computing devices, however, are responsible for bringing the DFT into common use. MATLAB is capable of DFT computations that would have been impractical just a few decades ago.

5.7.1 Computing the Discrete Fourier Transform

The MATLAB command `fft(x)` computes the DFT of a vector x that is defined over $(0 \le n \le N_0 - 1)$ (Problem 5.7-1 considers how to scale the DFT to accommodate signals that do not begin at $n = 0$.) As its name suggests, the function `fft` uses the computationally more efficient fast Fourier transform algorithm when it is appropriate to do so. The inverse DFT is easily computed by using the `ifft` function.

[†] Actually, $N_0/2$ is a conservative figure because some multiplications corresponding to the cases of $W_{N_0}^r = 1, j$, and so on, are eliminated.

To illustrate MATLAB's DFT capabilities, consider 50 points of a 10 Hz sinusoid sampled at $f_s = 50$ Hz and scaled by $T = 1/f_s$.

```
>> T = 1/50; N_0 = 50; n = (0:N_0-1);
>> x = T*cos(2*pi*10*n*T);
```

In this case, the vector x contains exactly 10 cycles of the sinusoid. The `fft` command computes the DFT.

```
>> X = fft(x);
```

Since the DFT is both discrete and periodic, `fft` needs to return only the N_0 discrete values contained in the single period ($0 \leq f < f_s$).

While X_r can be plotted as a function of r, it is more convenient to plot the DFT as a function of frequency f. A frequency vector, in hertz, is created by using N_0 and T.

```
>> f = (0:N_0-1)/(T*N_0); stem(f,abs(X),'k.');
>> axis([0 50 -0.05 0.55]); xlabel('f [Hz]'); ylabel('|X(f)|');
```

As expected, Fig. 5.26 shows content at a frequency of 10 Hz. Since the time-domain signal is real, $X(f)$ is conjugate symmetric. Thus, content at 10 Hz implies equal content at -10 Hz. The content visible at 40 Hz is an alias of the -10 Hz content.

Often, it is preferred to plot a DFT over the principal frequency range ($-f_s/2 \leq f < f_s/2$). The MATLAB function `fftshift` properly rearranges the output of `fft` to accomplish this task.

```
>> stem(f-1/(T*2),fftshift(abs(X)),'k.');
>> axis([-25 25 -0.05 0.55]); xlabel('f [Hz]'); ylabel('|X(f)|');
```

When we use `fftshift`, the conjugate symmetry that accompanies the DFT of a real signal becomes apparent, as shown in Fig. 5.27.

Since DFTs are generally complex-valued, the magnitude plots of Figs. 5.26 and 5.27 offer only half the picture; the signal's phase spectrum, shown in Fig. 5.28, completes it.

```
>> stem(f-1/(T*2),fftshift(angle(X)),'k.');
>> axis([-25 25 -1.1*pi 1.1*pi]); xlabel('f [Hz]'); ylabel('\angle X(f)');
```

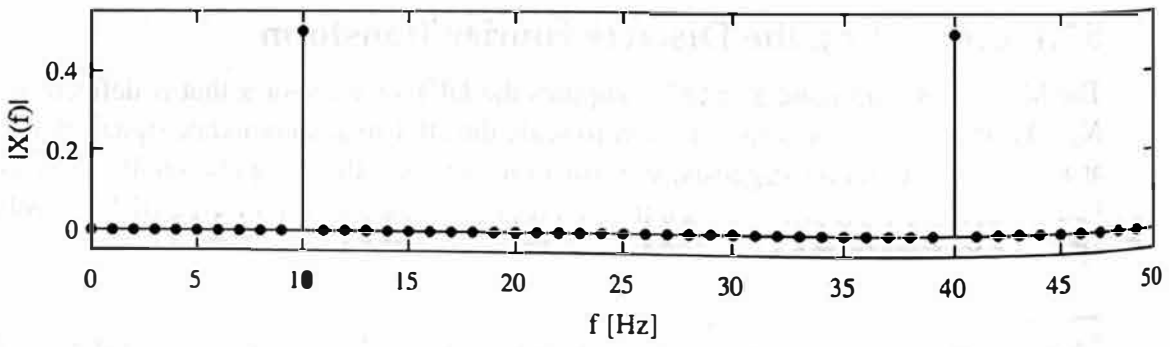

Figure 5.26 $|X(f)|$ computed over ($0 \leq f < 50$) by using `fft`.

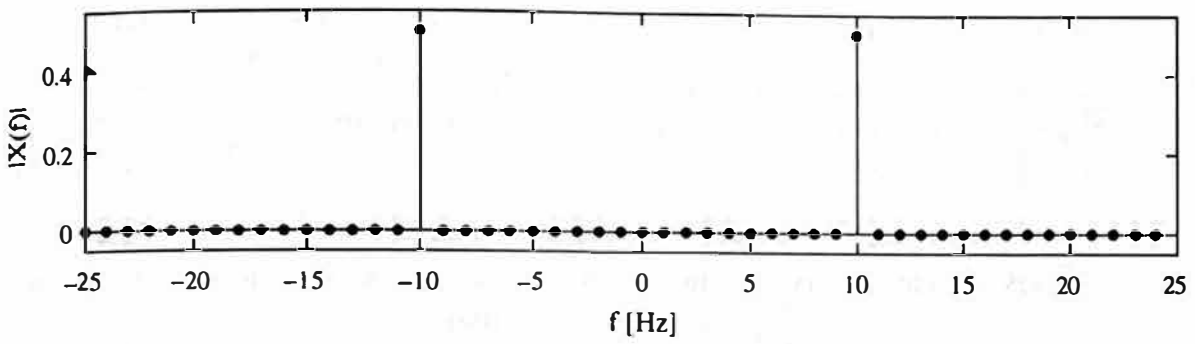

Figure 5.27 $|X(f)|$ displayed over $(-25 \leq f < 25)$ by using `fftshift`.

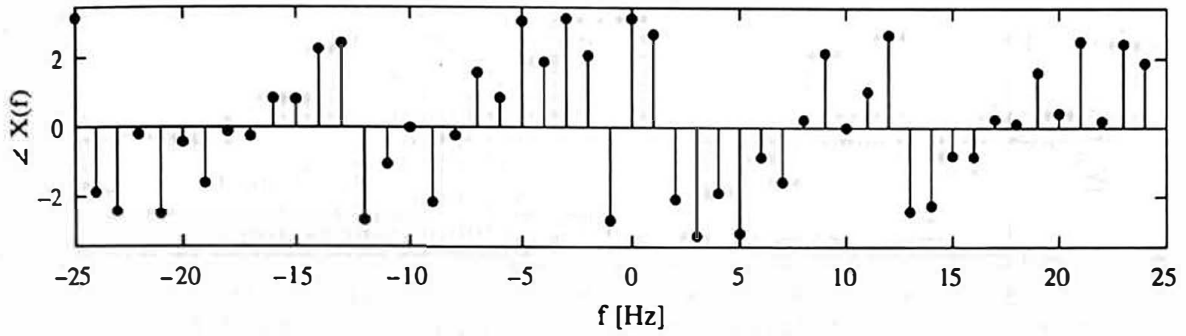

Figure 5.28 $\angle X(f)$ displayed over $(-25 \leq f < 25)$.

Since the signal is real, the phase spectrum necessarily has odd symmetry. Additionally, the phase at ± 10 Hz is zero, as expected for a zero-phase cosine function. More interesting, however, are the phase values found at the remaining frequencies. Does a simple cosine really have such complicated phase characteristics? The answer, of course, is no. The magnitude plot of Fig. 5.27 helps identify the problem: there is zero content at frequencies other than ± 10 Hz. Phase computations are not reliable at points where the magnitude response is zero. One way to remedy this problem is to assign a phase of zero when the magnitude response is near or at zero.

5.7.2 Improving the Picture with Zero Padding

DFT magnitude and phase plots paint a picture of a signal's spectrum. At times, however, the picture can be somewhat misleading. Given a sampling frequency $f_s = 50$ Hz and a sampling interval $T = 1/f_s$, consider the signal

$$y[n] = Te^{j2\pi\left(10\frac{1}{3}\right)nT}$$

This complex-valued, periodic signal contains a single positive frequency at $10\frac{1}{3}$ Hz. Let us compute the signal's DFT using 50 samples.

```
>> y = T*exp(j*2*pi*(10+1/3)*n*T); Y = fft(y);
>> stem(f-25,fftshift(abs(Y)),'k.');
>> axis([-25 25 -0.05 1.05]); xlabel('f [Hz]'); ylabel('|Y(f)|');
```

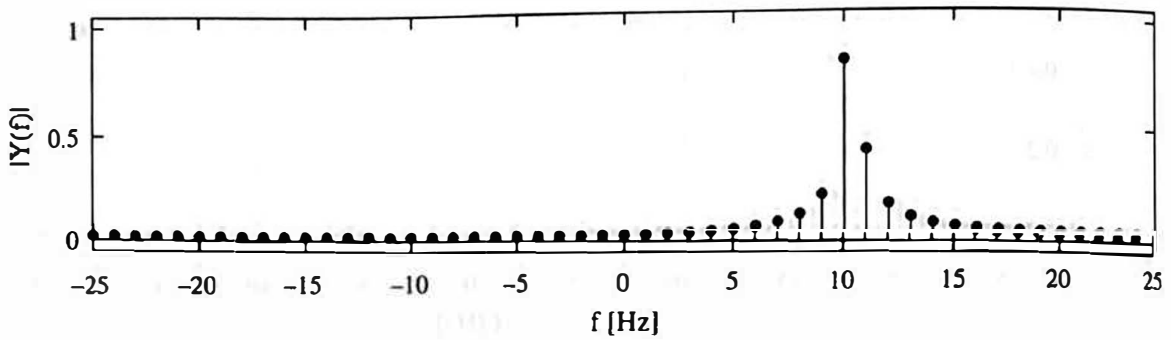

Figure 5.29 $|Y(f)|$ using 50 data points.

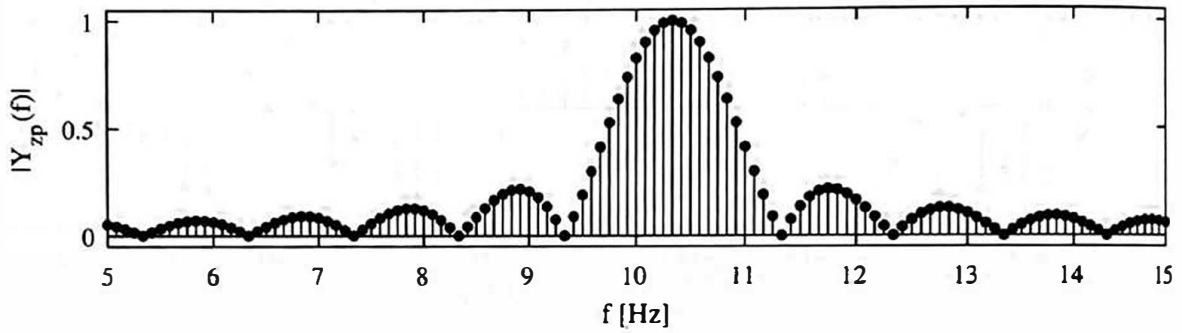

Figure 5.30 $|Y_{zp}(f)|$ over $5 \leq f \leq 15$ using 50 data points padded with 550 zeros.

In this case, the vector y contains a noninteger number of cycles. Figure 5.29 shows the significant frequency leakage that results. Also notice that since $y[n]$ is not real, the DFT is not conjugate symmetric.

In this example, the discrete DFT frequencies do not include the actual $10\frac{1}{3}$ Hz frequency of the signal. Thus, it is difficult to determine the signal's frequency from Fig. 5.29. To improve the picture, the signal is zero-padded to 12 times its original length.

```
>> y_zp = [y,zeros(1,11*length(y))]; Y_zp = fft(y_zp);
>> f_zp = (0:12*N_0-1)/(T*12*N_0);
>> stem(f_zp-25,fftshift(abs(Y_zp)),'k.');
>> axis([5 15 -0.05 1.05]); xlabel('f [Hz]'); ylabel('|Y_{zp}(f)|');
```

Figure 5.30, zoomed in to $5 \leq f \leq 15$, correctly shows the peak frequency at $10\frac{1}{3}$ Hz and better represents the signal's spectrum.

It is important to keep in mind that zero padding does not increase the resolution or accuracy of the DFT. To return to the picket fence analogy, zero padding increases the number of pickets in our fence but cannot change what is behind the fence. More formally, the characteristics of the sinc function, such as main beam width and sidelobe levels, depend on the fixed width of the pulse, not on the number of zeros that follow. Adding zeros cannot change the characteristics of the sinc function and thus cannot change the resolution or accuracy of the DFT. Adding zeros simply allows the sinc function to be sampled more finely.

5.7.3 Quantization

A B-bit analog-to-digital converter (ADC) samples an analog signal and quantizes amplitudes by using 2^B discrete levels. This quantization results in signal distortion that is particularly noticeable for small B. Typically, quantization is classified as symmetric or asymmetric and as either rounding or truncating. Let us investigate rounding-type quantizers.

The quantized output x_q of an asymmetric rounding converter is given as†

$$x_q = \frac{x_{max}}{2^{B-1}} \lfloor \frac{x}{x_{max}} 2^{B-1} + \frac{1}{2} \rfloor$$

The quantized output x_q of a symmetric rounding converter is given as

$$x_q = \frac{x_{max}}{2^{B-1}} \left(\lfloor \frac{x}{x_{max}} 2^{B-1} \rfloor + \frac{1}{2} \right)$$

Program CH5MP1 quantizes a signal using one of these two rounding quantizer rules and also ensures no more than 2^B output levels.

```
function [xq] = CH5MP1(x,xmax,B,method)
% CH5MP1.m : Chapter 5, MATLAB Program 1
% Function M-file quantizes x over (-xmax,xmax) using 2^b levels.
% Uses rounding rule, supports symmetric and asymmetric quantization
% INPUTS:   x = input signal
%           xmax = maximum magnitude of signal to be quantized
%           B = number of quantization bits
%           method = default 'sym' for symmetrical, 'asym' for asymmetrical
% OUTPUTS:  xq = quantized signal
if (nargin<3),
   disp('Insufficient number of inputs.'); return
elseif (nargin==3),
   method = 'sym';
elseif (nargin>4),
   disp('Too many inputs.'); return
end

x(abs(x)>xmax)=xmax*sign(x(abs(x)>xmax));   % Limit amplitude to xmax
switch lower(method)
   case 'asym'
      xq = xmax/(2^(B-1))*floor(x*2^(B-1)/xmax+1/2);
      xq(xq>=xmax)=xmax*(1-2^(1-B));        % Ensure only 2^B levels
   case 'sym'
      xq = xmax/(2^(B-1))*(floor(x*2^(B-1)/xmax)+1/2);
      xq(xq>=xmax)=xmax*(1-2^(1-B)/2);      % Ensure only 2^B levels
```

† Large values of x may return quantized values x_q outside the 2^B allowable levels. In such cases, x_q should be clamped to the nearest permitted level.

```
    otherwise
        disp('Unrecognized quantization method.'); return
end
```

Several MATLAB commands require discussion. First, the `nargin` function returns the number of input arguments. In this program, `nargin` is used to ensure that a correct number of inputs is supplied. If the number of inputs supplied is incorrect, an error message is displayed and the function terminates. If only three input arguments are detected, the quantization type is not explicitly specified and the program assigns the default symmetric method.

As with many high-level languages such as C, MATLAB supports general switch/case structures†:

```
switch  switch_expr,
case  case_expr,
      statements;
...
otherwise,
      statements;
end
```

`CH5MP1` switches among cases of the string `method`. In this way, method-specific parameters are easily set. The command `lower` is used to convert a string to all lowercase characters. In this way, strings such as SYM, Sym, and sym are all indistinguishable. Similar to `lower`, the MATLAB command `upper` converts a string to all uppercase.

The `floor` command rounds input values to the nearest integer toward minus infinity. Mathematically, it computes $\lfloor \cdot \rfloor$. To accommodate different types of rounding, MATLAB supplies three other rounding commands: `ceil`, `round`, and `fix`. The `ceil` command rounds input values to the nearest integers toward infinity, ($\lceil \cdot \rceil$); the `round` command rounds input values toward the nearest integer; the `fix` command rounds input values to the nearest integer toward zero. For example, if `x = [-0.5 0.5];`, `floor(x)` yields `[-1 0]`, `ceil(x)` yields `[0 1]`, `round(x)` yields `[-1 1]`, and `fix(x)` yields `[0 0]`. Finally, `CH5MP1` checks and, if necessary, corrects large values of x_q that may be outside the allowable 2^B levels.

To verify operation, `CH5MP1` is used to determine the transfer characteristics of a symmetric 3-bit quantizer operating over $(-10,10)$.

```
>>  x = (-10:.0001:10); xsq = CH5MP1(x,10,3,'sym');
>>  plot(x,xsq,'k'); axis([-10 10 -10.5 10.5]); grid on;
>>  xlabel('Quantizer input'); ylabel('Quantizer output');
```

Figure 5.31 shows the results. Clearly, the quantized output is limited to $2^B = 8$ levels. Zero is not a quantization level for symmetric quantizers, so half of the levels occur above zero and half of the levels occur below zero. In fact, *symmetric quantizers* get their name from the symmetry in quantization levels above and below zero.

By changing the method in `CH5MP1` from `'sym'` to `'asym'`, we obtain the transfer characteristics of an asymmetric 3-bit quantizer, as shown in Fig. 5.32. Again, the quantized output is limited to $2^B = 8$ levels, and zero is now one of the included levels. With zero as a quantization

† A functionally equivalent structure can be written by using `if`, `elseif`, and `else` statements.

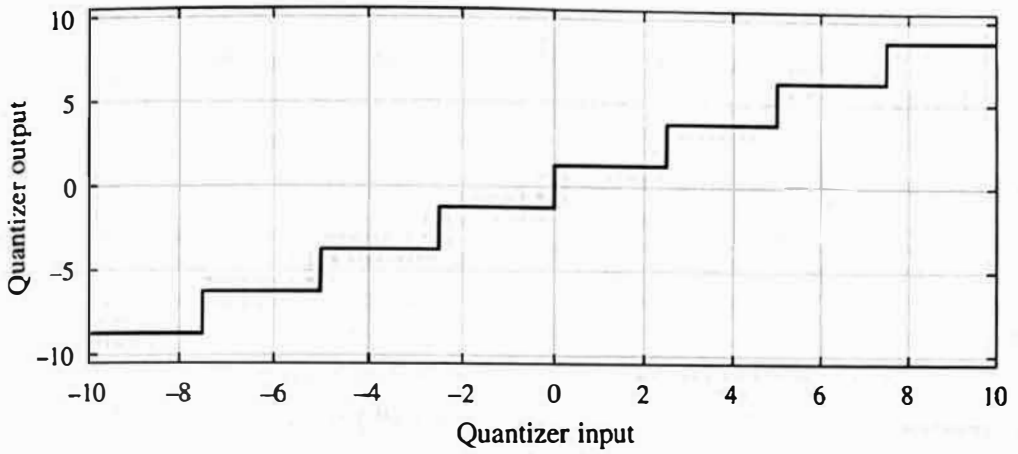

Figure 5.31 Transfer characteristics of a symmetric 3-bit quantizer.

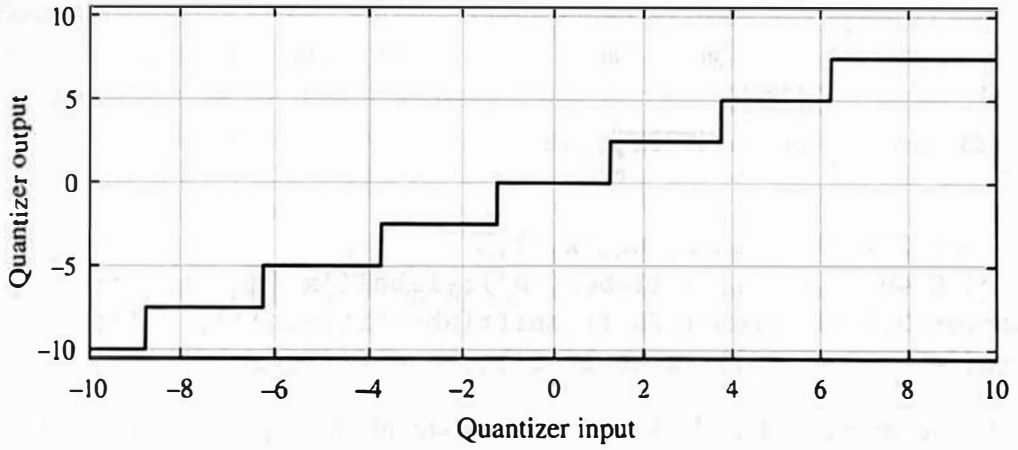

Figure 5.32 Transfer characteristics of an asymmetric 3-bit quantizer.

level, we need one fewer quantization level above zero than there are levels below. Not surprisingly, *asymmetric quantizers* get their name from the asymmetry in quantization levels above and below zero.

There is no doubt that quantization can change a signal. It follows that the spectrum of a quantized signal can also change. While these changes are difficult to characterize mathematically, they are easy to investigate by using MATLAB. Consider a 1 Hz cosine sampled at $f_s = 50$ Hz over 1 second.

```
>> T = 1/50; N_0 = 50; n = (0:N_0-1); f = (0:N_0-1)/(T*N_0);
>> x = cos(2*pi*n*T); X = fft(x);
```

Upon quantizing by means of a 2-bit asymmetric rounding quantizer, both the signal and spectrum are substantially changed.

```
>> xaq = CH5MP1(x,1,2,'asym'); Xaq = fft(xaq);
>> subplot(2,2,1); stem(n,x,'k.');
>> axis([0 49 -1.1 1.1]); xlabel('n');ylabel('x[n]');
>> subplot(2,2,2); stem(f-25,fftshift(abs(X)),'k.');
>> axis([-25,25 -1 26]); xlabel('f');ylabel('|X(f)|');
```

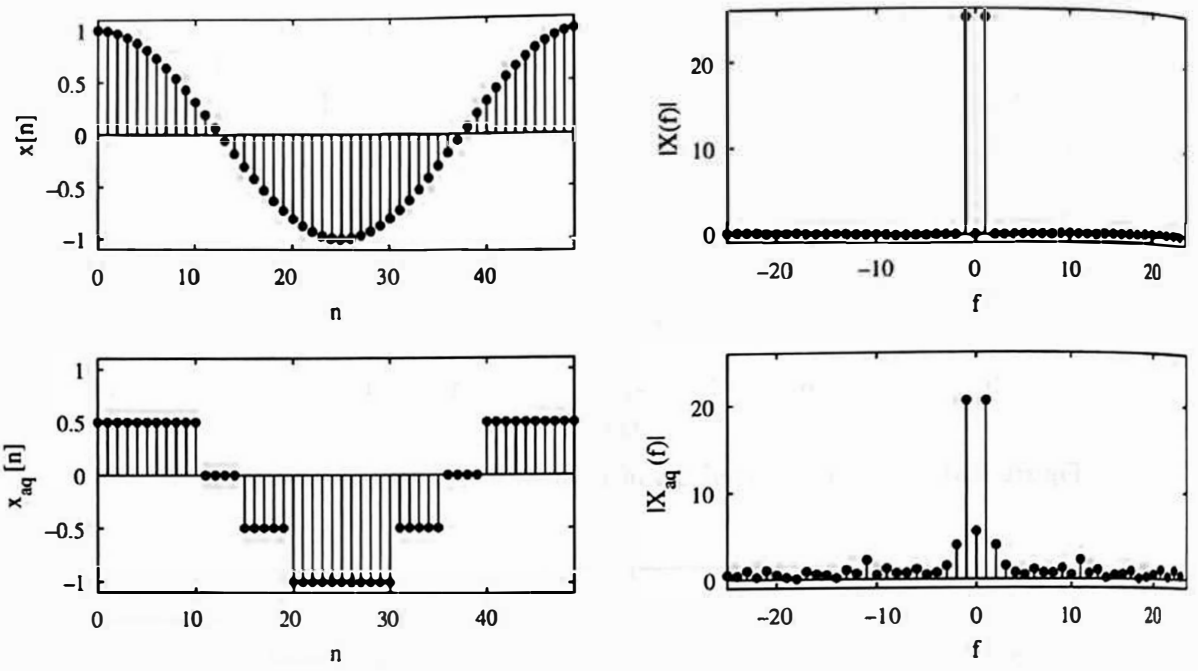

Figure 5.33 Signal and spectrum effects of quantization.

```
>> subplot(2,2,3); stem(n,xaq,'k.');
>> axis([0 49 -1.1 1.1]); xlabel('n');ylabel('x_{aq}[n]');
>> subplot(2,2,4); stem(f-25,fftshift(abs(fft(xaq))),'k.');
>> axis([-25,25 -1 26]); xlabel('f');ylabel('|X_{aq}(f)|');
```

The results are shown in Fig. 5.33. The original signal $x[n]$ appears sinusoidal and has pure spectral content at ± 1 Hz. The asymmetrically quantized signal $x_{aq}[n]$ is significantly distorted. The corresponding magnitude spectrum $|X_{aq}(f)|$ is spread over a broad range of frequencies.

5.8 SUMMARY

A signal bandlimited to B Hz can be reconstructed exactly from its samples if the sampling rate $f_s > 2B$ Hz (the sampling theorem). Such a reconstruction, although possible theoretically, poses practical problems such as the need for ideal filters, which are unrealizable or are realizable only with infinite delay. Therefore, in practice, there is always an error in reconstructing a signal from its samples. Moreover, practical signals are not bandlimited, which causes an additional error (aliasing error) in signal reconstruction from its samples. When a signal is sampled at a frequency f_s Hz, samples of a sinusoid of frequency $(f_s/2) + x$ Hz appear as samples of a lower frequency $(f_s/2) - x$ Hz. This phenomenon, in which higher frequencies appear as lower frequencies, is known as aliasing. Aliasing error can be reduced by bandlimiting a signal to $f_s/2$ Hz (half the sampling frequency). Such bandlimiting, done prior to sampling, is accomplished by an anti-aliasing filter that is an ideal lowpass filter of cutoff frequency $f_s/2$ Hz.

The sampling theorem is very important in signal analysis, processing, and transmission because it allows us to replace a continuous-time signal with a discrete sequence of numbers. Processing a continuous-time signal is therefore equivalent to processing a discrete sequence of numbers. This leads us directly into the area of digital filtering (discrete-time systems). In the field

of communication, the transmission of a continuous-time message reduces to the transmission of a sequence of numbers. This opens doors to many new techniques of communicating continuous-time signals by pulse trains.

The dual of the sampling theorem states that for a signal timelimited to τ seconds, its spectrum $X(\omega)$ can be reconstructed from the samples of $X(\omega)$ taken at uniform intervals not greater than $1/\tau$ Hz. In other words, the spectrum should be sampled at a rate not less than τ samples/Hz.

To compute the direct or the inverse Fourier transform numerically, we need a relationship between the samples of $x(t)$ and $X(\omega)$. The sampling theorem and its dual provide such a quantitative relationship in the form of a discrete Fourier transform (DFT). The DFT computations are greatly facilitated by a fast Fourier transform (FFT) algorithm, which reduces the number of computations from something on the order of N_0^2 to $N_0 \log N_0$.

References

1. Linden, D. A., "A Discussion of Sampling Theorems," *Proceedings of the IRE*, vol. 47, pp. 1219–1226, July 1959.
2. Siebert, W. M., *Circuits, Signals, and Systems*, MIT/McGraw-Hill, New York, 1986.
3. Bennett, W. R., *Introduction to Signal Transmission*, McGraw-Hill, New York, 1970.
4. Lathi, B. P. and Green, R., *Linear Systems and Signals*, 3rd ed., Oxford University Press, New York, 2018.
5. Cooley, J. W. and Tukey, J. W., "An Algorithm for the Machine Calculation of Complex Fourier Series," *Mathematics of Computation*, vol. 19, pp. 297–301, April 1965.

PROBLEMS

[*Note:* In many problems, the plots of spectra are shown as functions of frequency f Hz for convenience, although we have labeled them as functions of ω as $X(\omega)$, $Y(\omega)$, etc.]

5.1-1 If f_s is the Nyquist rate for signal $x(t)$, determine the Nyquist rate for each of the following signals:
(a) $y_a(t) = \frac{d}{dt}x(t)$
(b) $y_b(t) = x(t)\cos(2\pi f_0 t)$
(c) $y_c(t) = x(t+a) + x(t-b)$, for real constants a and b
(d) $y_d(t) = x(at)$, for real $a > 0$

5.1-2 Figure P5.1-2 shows Fourier spectra of signals $x_1(t)$ and $x_2(t)$. Determine the Nyquist sampling rates for signals $x_1(t), x_2(t), x_1^2(t), x_2^3(t)$, and $x_1(t)x_2(t)$.

5.1-3 A signal $x(t)$ has a bandwidth of $B = 1000$ Hz. For a positive integer N, what is the Nyquist rate for the signal $y(t) = x^N(t)$?

5.1-4 Determine the Nyquist sampling rate and the Nyquist sampling interval for the signals:
(a) $\text{sinc}^2(100\pi t)$
(b) $0.01\,\text{sinc}^2(100\pi t)$
(c) $\text{sinc}(100\pi t) + 3\text{sinc}^2(60\pi t)$
(d) $\text{sinc}(50\pi t)\text{sinc}(100\pi t)$

5.1-5 (a) Sketch $|X(\omega)|$, the amplitude spectrum of a signal $x(t) = 3\cos 6\pi t + \sin 18\pi t + 2\cos(28 - \epsilon)\pi t$, where ϵ is a very small number $\to 0$. Determine the minimum sampling rate required to be able to reconstruct $x(t)$ from these samples.
(b) Sketch the amplitude spectrum of the sampled signal when the sampling rate is 25% above the Nyquist rate (show the spectrum over the frequency range ± 50 Hz only). How would you reconstruct $x(t)$ from these samples?

5.1-6 (a) Derive the sampling theorem by considering the fact that the sample

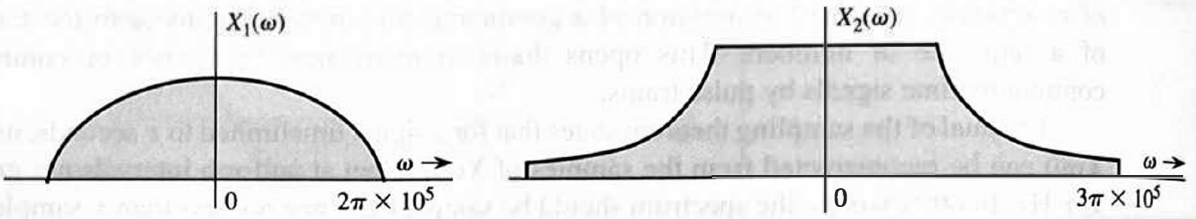

Figure P5.1-2

signal $\bar{x}(t) = x(t)\delta_T(t)$, and using the frequency-convolution property in Eq. (4.34).

(b) For a sampling train consisting of shifted unit impulses at instants $nT + \tau$ instead of at nT (for all positive and negative integer values of n), find the spectrum of the sampled signal.

5.1-7 A signal is bandlimited to 12 kHz. The band between 10 and 12 kHz has been so corrupted by excessive noise that the information in this band is nonrecoverable. Determine the minimum sampling rate for this signal so that the uncorrupted portion of the band can be recovered. If we were to filter out the corrupted spectrum prior to sampling, what would be the minimum sampling rate?

5.1-8 A continuous-time signal $x(t) = \Delta((t-1)/2)$ is sampled at three rates: 10, 2, and 1 Hz. Sketch the resulting sampled signals. Because $x(t)$ is timelimited, its bandwidth is infinite. However, most of its energy is concentrated in a small band. Determine a reasonable minimum sampling rate that will allow reconstruction of this signal with a small error. The answer is not unique. Make a reasonable assumption of what you define as a "negligible" or "small" error.

5.1-9 (a) A signal $x(t) = 5\text{sinc}^2(5\pi t) + \cos 20\pi t$ is sampled at a rate of 10 Hz. Find the spectrum of the sampled signal. Can $x(t)$ be reconstructed by lowpass filtering the sampled signal?

(b) Repeat part (a) for a sampling frequency of 20 Hz. Can you reconstruct the signal from this sampled signal? Explain.

(c) If $x(t) = 5\text{sinc}^2(5\pi t) + \sin 20\pi t$, can you reconstruct $x(t)$ from the samples of $x(t)$ at a rate of 20 Hz? Explain your answer with spectral representation(s).

(d) For $x(t) = 5\text{sinc}^2(5\pi t) + \sin 20\pi t$, can you reconstruct $x(t)$ from the samples of $x(t)$ at a rate of 21 Hz? Explain your answer with spectral representation(s). Comment on your results.

5.1-10 (a) The highest frequency in the spectrum $X(\omega)$ (Fig. P5.1-10a) of a bandpass signal $x(t)$ is 30 Hz. Hence, the minimum sampling frequency needed to sample $x(t)$ is 60 Hz. Show the spectrum of the signal sampled at a rate of 60 Hz. Can you reconstruct $x(t)$ from these samples? How?

(b) A certain busy student looks at $X(\omega)$, concludes that its bandwidth is really 10 Hz, and decides that the sampling rate 20 Hz is adequate for sampling $x(t)$. Sketch the spectrum of the signal sampled at a rate of 20 Hz. Can $x(t)$ be reconstructed from these samples?

(c) The same student, using the same reasoning, looks at $Y(\omega)$ in Fig. P5.1-10b, the spectrum of another bandpass signal $y(t)$, and concludes that the sampling rate of 20 Hz can be used to sample $y(t)$. Sketch the spectrum of the signal $y(t)$ sampled at a rate of 20 Hz. Can $y(t)$ be reconstructed from these samples?

5.1-11 A signal $x(t)$ whose spectrum $X(\omega)$, as shown in Fig. P5.1-11, is sampled at a frequency $f_s = f_1 + f_2$ Hz. Find all the sample values of $x(t)$ merely by inspection of $X(\omega)$.

5.1-12 As described in Sec. 5.1.1, practical sampling can be achieved by multiplying a signal $x(t)$ by a periodic train of pulses $p_T(t)$. The pulse train $p_T(t)$ can be created by the periodic replication of some pulse $p(t)$ as

$$p_T(t) = \sum_{k=-\infty}^{\infty} p(t - kT)$$

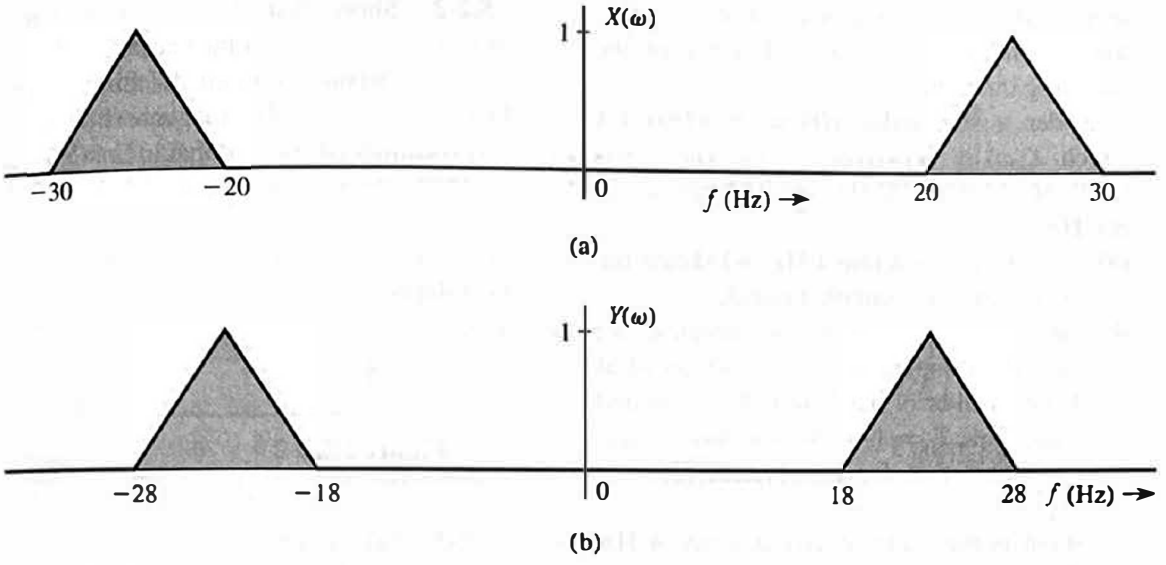

Figure P5.1-10

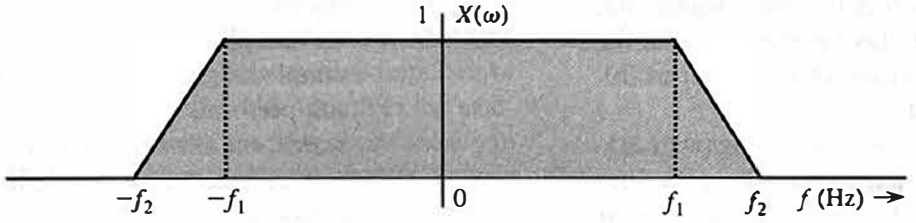

Figure P5.1-11

It is desired to sample a signal at a rate $f_s = 100$ Hz, and two pulses are under consideration:

$$p_a(t) = -\tfrac{1}{4}u(t) + \tfrac{5}{4}u(t - \tfrac{2T}{20}) + \\ -\tfrac{5}{4}u(t - \tfrac{3T}{20}) + \tfrac{1}{4}u(t - \tfrac{5T}{20})$$

and

$$p_b(t) = e^{-t/T}[u(t) - u(t - 1.5T)]$$

(a) Plot $p_T(t)$ using $p_a(t)$ over $0 \le t \le 4T$.
(b) Plot $p_T(t)$ using $p_b(t)$ over $0 \le t \le 4T$.
(c) Which pulse, $p_a(t)$ or $p_b(t)$, is more suitable as a sampling pulse? Carefully explain your answer.

5.1-13 In digital data transmission over a communication channel, it is important to know the upper theoretical limit on the rate of digital pulses that can be transmitted over a channel of bandwidth B Hz. In digital transmission, the relative shape of the pulse is not important. We are interested in knowing only the amplitude represented by the pulse. For instance, in binary communication, we are interested in knowing whether the received pulse amplitude is 1 or -1 (positive or negative). Thus, each pulse represents one piece of information. Consider one independent amplitude value (not necessarily binary) as one piece of information. Show that $2B$ independent pieces of information per second can be transmitted correctly (assuming no noise) over a channel of bandwidth B Hz. This important principle in communication theory states that 1 Hz of bandwidth can transmit two independent pieces of information per second. It represents the upper rate of pulse transmission over a channel without any error in reception in the absence of noise. [*Hint:* According to the interpolation formula [Eq. (5.6)], a continuous-time signal of bandwidth B Hz can be constructed from $2B$ pieces of information/second.]

5.1-14 This example is one of those interesting situations leading to a curious result in the category of defying gravity. The sinc function can be

recovered from its samples taken at extremely low frequencies in apparent defiance of the sampling theorem.

Consider a sinc pulse $x(t) = \text{sinc}(4\pi t)$ for which $X(\omega) = (1/4)\,\text{rect}(\omega/8\pi)$. The bandwidth of $x(t)$ is $B = 2$ Hz, and its Nyquist rate is 4 Hz.

(a) Sample $x(t)$ at a rate 4 Hz and sketch the spectrum of the sampled signal.

(b) To recover $x(t)$ from its samples, we pass the sampled signal through an ideal lowpass filter of bandwidth $B = 2$ Hz and gain $G = T = 1/4$. Sketch this system and show that for this system $H(\omega) = (1/4)\,\text{rect}(\omega/8\pi)$. Show also that when the input is the sampled $x(t)$ at a rate 4 Hz, the output of this system is indeed $x(t)$, as expected.

(c) Now sample $x(t)$ at half the Nyquist rate, at 2 Hz. Apply this sampled signal at the input of the lowpass filter used in part (b). Find the output.

(d) Repeat part (c) for the sampling rate 1 Hz.

(e) Show that the output of the lowpass filter in part (b) is $x(t)$ to the sampled $x(t)$ if the sampling rate is $4/N$, where N is any positive integer. This means that we can recover $x(t)$ from its samples taken at an arbitrarily small rate by letting $N \to \infty$.

(f) The mystery may be clarified a bit by examining the problem in the time domain. Find the samples of $x(t)$ when the sampling rate is $4/N$ (N integer).

5.2-1 A signal $x(t) = \text{sinc}\,(200\pi t)$ is sampled (multiplied) by a periodic pulse train $p_T(t)$ represented in Fig. P5.2-1. Find and sketch the spectrum of the sampled signal. Explain whether you will be able to reconstruct $x(t)$ from these samples. Find the filter output if the sampled signal is passed through an ideal lowpass filter of bandwidth 100 Hz and unit gain. What is the filter output if its bandwidth B Hz is between 100 and 150 Hz? What happens if the bandwidth exceeds 150 Hz?

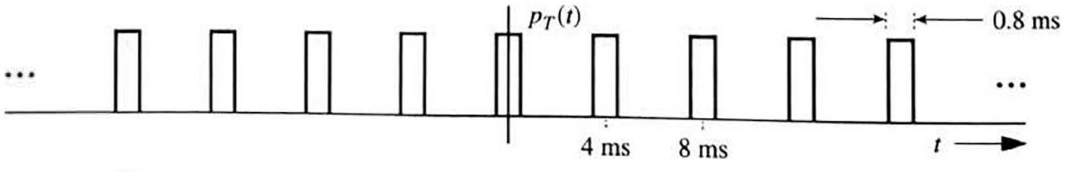

Figure P5.2-1

5.2-2 Show that the circuit in Fig. P5.2-2 is a realization of the causal ZOH (zero-order hold) circuit. You can do this by showing that the unit impulse response $h(t)$ of this circuit is indeed equal to that in Eq. (5.5) delayed by $T/2$ seconds to make it causal.

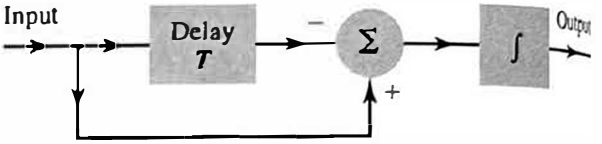

Figure P5.2-2

5.2-3 (a) A first-order hold circuit (FOH) can also be used to reconstruct a signal $x(t)$ from its samples. The impulse response of this circuit is $h(t) = \Delta(t/2T)$, where T is the sampling interval. Consider a typical sampled signal $\bar{x}(t)$ and show that this circuit performs linear interpolation. In other words, the filter output consists of sample tops connected by straight-line segments. Follow the procedure discussed in Sec. 5.2 (Fig. 5.5c).

(b) Determine the frequency response of this filter, and compare it with (i) the ideal filter required for signal reconstruction and (ii) a ZOH circuit.

(c) This filter, being noncausal, is unrealizable. By delaying its impulse response, the filter can be made realizable. What is the minimum delay required to make it realizable? How would this delay affect the reconstructed signal and the filter frequency response?

(d) Show that the causal FOH circuit in part (c) can be realized by the ZOH circuit depicted in Fig. P5.2-2 followed by an identical filter in cascade.

5.2-4 Suppose signal $x(t) = \sin(2\pi t/8)\,(u(t) - u(t-8))$ is sampled at a rate $f_s = 1$ Hz to generate signal $x[n]$.

(a) Sketch $x(t)$ and $x[n]$.
(b) Has aliasing occurred in sampling $x(t)$ to produce $x[n]$? Explain.
(c) Sketch the output $\hat{x}(t)$ produced when $x[n]$ is applied to the causal ZOH reconstructor of Prob. 5.2-2. How does $\hat{x}(t)$ compare with $x(t)$?
(d) Sketch the output $\hat{x}(t)$ produced when $x[n]$ is applied to the FOH reconstructor of Prob. 5.2-3. How does $\hat{x}(t)$ compare with $x(t)$?

5.2-5 Repeat Prob. 5.2-4 for the signal $x(t) = \cos(2\pi t/8)\,(u(t) - u(t-8))$.

5.2-6 Is it possible to sample a physically realizable (nonzero) signal $x(t)$ with a physically realizable system without aliasing? If possible, explain what conditions must be met. If not possible, explain why not.

5.2-7 In the text, for sampling purposes, we used timelimited narrow pulses such as impulses or rectangular pulses of width less than the sampling interval T. Show that it is not necessary to restrict the sampling pulse width. We can use sampling pulses of arbitrarily large duration and still be able to reconstruct the signal $x(t)$ as long as the pulse rate is no less than the Nyquist rate for $x(t)$.

Consider $x(t)$ to be bandlimited to B Hz. The sampling pulse to be used is an exponential $e^{-at}u(t)$. We multiply $x(t)$ by a periodic train of exponential pulses of the form $e^{-at}u(t)$ spaced T seconds apart. Find the spectrum of the sampled signal, and show that $x(t)$ can be reconstructed from this sampled signal provided the sampling rate is no less than $2B$ Hz or $T < 1/2B$. Explain how you would reconstruct $x(t)$ from the sampled signal.

5.2-8 In Ex. 5.2, the sampling of a signal $x(t)$ was accomplished by multiplying the signal by a pulse train $p_T(t)$, resulting in the sampled signal depicted in Fig. 5.4d. This procedure is known as the *natural sampling*. Figure P5.2-8 shows the so-called *flat-top sampling* of the same signal $x(t) = \text{sinc}^2(5\pi t)$.

(a) Show that the signal $x(t)$ can be recovered from flat-top samples if the sampling rate is no less than the Nyquist rate.
(b) Explain how you would recover $x(t)$ from the flat-top samples.
(c) Find the expression for the sampled signal spectrum $\overline{X}(\omega)$ and sketch it roughly.

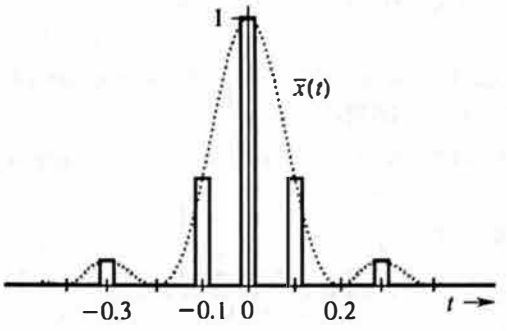

Figure P5.2-8

5.2-9 A sinusoid of frequency f_0 Hz is sampled at a rate $f_s = 20$ Hz. Find the apparent frequency of the sampled signal if f_0 is:
(a) 8 Hz
(b) 12 Hz
(c) 20 Hz
(d) 22 Hz
(e) 32 Hz

5.2-10 A sinusoid of unknown frequency f_0 is sampled at a rate 60 Hz. The apparent frequency of the samples is 20 Hz. Determine f_0 if it is known that f_0 lies in the range:
(a) 0–30 Hz
(b) 30–60 Hz
(c) 60–90 Hz
(d) 90–120 Hz

5.2-11 A signal $x(t) = 3\cos 6\pi t + \cos 16\pi t + 2\cos 20\pi t$ is sampled at a rate 25% above the Nyquist rate. Sketch the spectrum of the sampled signal. How would you reconstruct $x(t)$ from these samples? If the sampling frequency is 25% below the Nyquist rate, what are the frequencies of the sinusoids present in the output of the filter with a cutoff frequency equal to the folding frequency? Do not write the actual output; give just the frequencies of the sinusoids present in the output.

5.2-12 A complex signal $x(t)$ has a spectrum given as

$$X(\omega) = \begin{cases} \omega & 0 \le \omega \le 2\pi 10 \\ 0 & \text{otherwise} \end{cases}$$

Let $x(t)$ be sampled at rate $f_s = 24$ Hz to produce signal $\bar{x}(t)$ with spectrum $\overline{X}(\omega)$.
(a) Sketch $\overline{X}(\omega)$.

(b) Has aliasing occurred in sampling $x(t)$ to produce $\bar{x}(t)$? Explain.

(c) Can $x(t)$ be exactly recovered from $\bar{x}(t)$? Explain.

5.2-13 Repeat Prob. 5.2-12 for the sampling rate $f_s = 16$ Hz.

5.2-14 Repeat Prob. 5.2-12 for the sampling rate $f_s = 8$ Hz.

5.2-15 (a) Show that the signal $x(t)$, reconstructed from its samples $x(nT)$, using Eq. (5.6) has a bandwidth $B \leq 1/2T$ Hz.

(b) Show that $x(t)$ is the smallest bandwidth signal that passes through samples $x(nT)$. [*Hint:* Use the *reductio ad absurdum* method.]

5.2-16 In digital communication systems, the efficient use of channel bandwidth is ensured by transmitting digital data encoded by means of bandlimited pulses. Unfortunately, bandlimited pulses are non-timelimited; that is, they have infinite duration, which causes pulses representing successive digits to interfere and cause errors in the reading of true pulse values. This difficulty can be resolved by shaping a pulse $p(t)$ in such a way that it is bandlimited, yet causes zero interference at the sampling instants. To transmit R pulses per second, we require a minimum bandwidth $R/2$ Hz (see Prob. 5.1-13). The bandwidth of $p(t)$ should be $R/2$ Hz, and its samples, in order to cause no interference at all other sampling instants, must satisfy the condition

$$p(nT) = \begin{cases} 1 & n = 0 \\ 0 & n \neq 0 \end{cases} \qquad T = \frac{1}{R}$$

Because the pulse rate is R pulses per second, the sampling instants are located at intervals of $1/R$ seconds. Hence, the foregoing condition ensures that any given pulse will not interfere with the amplitude of any other pulse at its center. Find $p(t)$. Is $p(t)$ unique in the sense that no other pulse satisfies the given requirements?

5.2-17 The problem of pulse interference in digital data transmission was outlined in Prob. 5.2-16, where we found a pulse shape $p(t)$ to eliminate the interference. Unfortunately, the pulse found is not only noncausal (and unrealizable), but also has a serious drawback: because of its slow decay (as $1/t$), it is prone to severe interference due to small parameter deviation. To make the pulse decay rapidly, Nyquist proposed relaxing the bandwidth requirement from $R/2$ Hz to $kR/2$ Hz with $1 \leq k \leq 2$. The pulse must still have a property of noninterference with other pulses, for example,

$$p(nT) = \begin{cases} 1 & n = 0 \\ 0 & n \neq 0 \end{cases} \qquad T = \frac{1}{R}$$

Show that this condition is satisfied only if the pulse spectrum $P(\omega)$ has an odd symmetry about the set of dotted axes, as shown in Fig. P5.2-17. The bandwidth of $P(\omega)$ is $kR/2$ Hz ($1 \leq k \leq 2$).

5.2-18 The Nyquist samples of a signal $x(t)$ bandlimited to B Hz are

$$x(nT) = \begin{cases} 1 & n = 0, 1 \\ 0 & \text{all } n \neq 0, 1 \end{cases} \qquad T = \frac{1}{2B}$$

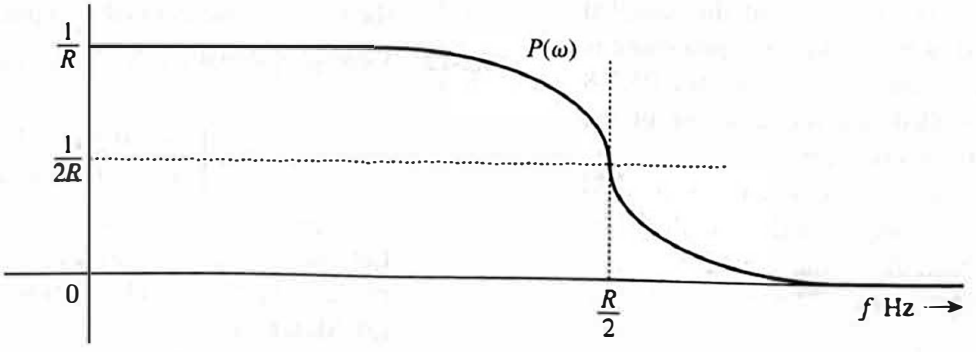

Figure P5.2-17

Show that

$$x(t) = \frac{\text{sinc}(2\pi Bt)}{1 - 2Bt}$$

This pulse, known as the *duobinary pulse*, is used in digital transmission applications.

5.2-19 A signal bandlimited to B Hz is sampled at a rate $f_s = 2B$ Hz. Show that

$$\int_{-\infty}^{\infty} x(t)\,dt = T\sum_{-\infty}^{\infty} x(nT)$$

$$\int_{-\infty}^{\infty} |x(t)|^2\,dt = T\sum_{-\infty}^{\infty} |x(nT)|^2$$

[*Hint:* Use the orthogonality property of the sinc function in Prob. 4.6-6.]

5.2-20 Prove that a signal cannot be simultaneously timelimited and bandlimited. [*Hint:* Show that a contrary assumption leads to contradiction. Assume a signal to be simultaneously timelimited and bandlimited so that $X(\omega) = 0$ for $|\omega| \geq 2\pi B$. In this case, $X(\omega) = X(\omega)\,\text{rect}(\omega/4\pi B')$ for $B' > B$. This fact means that $x(t)$ is equal to $x(t) * 2B'\,\text{sinc}\,(2\pi B't)$. The latter cannot be timelimited because the sinc function tail extends to infinity.]

5.3-1 Physically implementable digital systems, such as smartphones and computers, require that signals be both time-sampled and amplitude-quantized.

(a) Why is time sampling necessary? When does time sampling result in unrecoverable changes to the signal?

(b) Why is amplitude quantization necessary? When does amplitude quantization result in unrecoverable changes to the signal?

5.3-2 Typical analog-to-digital converters (ADCs) operate over a range of input amplitudes $[-V_{\text{ref}}, V_{\text{ref}}]$. Why is it desirable to condition the input $x(t)$ to an ADC so that its maximum magnitude is close to, but does not exceed, V_{ref}? What happens if the maximum magnitude of $x(t)$ is greater than V_{ref}? What happens if the maximum magnitude of $x(t)$ is much smaller than V_{ref}?

5.3-3 A compact disc (CD) records audio signals digitally by means of a binary code. Assume an audio signal bandwidth of 15 kHz.

(a) What is the Nyquist rate?

(b) If the Nyquist samples are quantized into 65,536 levels ($L = 65{,}536$) and then binary-coded, what number of binary digits is required to encode a sample?

(c) Determine the number of binary digits per second (bits/s) required to encode the audio signal.

(d) For practical reasons discussed in the text, signals are sampled at a rate well above the Nyquist rate. Practical CDs use 44,100 samples/s. If $L = 65{,}536$, determine the number of pulses per second required to encode the signal.

5.3-4 A TV signal (video and audio) has a bandwidth of 4.5 MHz. This signal is sampled, quantized, and binary-coded.

(a) Determine the sampling rate if the signal is to be sampled at a rate 20% above the Nyquist rate.

(b) If the samples are quantized into 1024 levels, what number of binary pulses is required to encode each sample?

(c) Determine the binary pulse rate (bits/s) of the binary-coded signal.

5.3-5 (a) In a certain A/D scheme, there are 16 quantization levels. Give one possible binary code and one possible quaternary (4-ary) code. For the quaternary code, use **0, 1, 2,** and **3** as the four symbols. Use the minimum number of digits in your code.

(b) To represent a given number of quantization levels L, we require a minimum of b_M digits for an M-ary code. Show that the ratio of the number of digits in a binary code to the number of digits in a quaternary (4-ary) code is 2, that is, $b_2/b_4 = 2$.

5.3-6 Five telemetry signals, each of bandwidth 1 kHz, are quantized and binary-coded. These signals are time-division multiplexed (signal bits interleaved). Choose the number of quantization levels so that the maximum error in sample amplitudes is no greater than 0.2% of the peak signal amplitude. The signals must be sampled at least 20% above the Nyquist rate. Determine the data rate (bits per second) of the multiplexed signal.

5.4-1 A triangle function $x(t) = \Delta(t/5)$ has spectrum $X(\omega)$. Sketch the corresponding time-domain signal $x_{T_0}(t)$ if $X(\omega)$ is sampled at the following rates:
(a) 10 samples/Hz
(b) 5 samples/Hz
(c) 4 samples/Hz
(d) 2.5 samples/Hz

5.4-2 The Fourier transform of a signal $x(t)$, bandlimited to B Hz, is $X(\omega)$. The signal $x(t)$ is repeated periodically at intervals T, where $T = 1.25/B$. The resulting signal $y(t)$ is

$$y(t) = \sum_{-\infty}^{\infty} x(t - nT)$$

Show that $y(t)$ can be expressed as

$$y(t) = C_0 + C_1 \cos(1.6\pi Bt + \theta_1)$$

where

$$C_0 = \frac{1}{T}X(0)$$

$$C_1 = \frac{2}{T}\left|X\left(\frac{2\pi}{T}\right)\right|$$

and

$$\theta_1 = \angle X\left(\frac{2\pi}{T}\right)$$

Recall that a bandlimited signal is not timelimited, and hence has infinite duration. The periodic repetitions are all overlapping.

5.5-1 For a signal $x(t)$ that is timelimited to 10 ms and has an essential bandwidth of 10 kHz, determine N_0, the number of signal samples necessary to compute a power-of-2 FFT with a frequency resolution f_0 of at least 50 Hz. Explain whether any zero padding is necessary.

5.5-2 To compute the DFT of signal $x(t)$ in Fig. P5.5-2, write the sequence x_n (for $n = 0$ to $N_0 - 1$) if the frequency resolution f_0 must be at least 0.25 Hz. Assume the essential bandwidth (the folding frequency) of $x(t)$ to be at least 3 Hz. Do not compute the DFT; just write the appropriate sequence x_n.

5.5-3 Suppose we want to sample a finite-duration signal $x(t)$ that occupies $0 \le t < T_0$.
(a) Devise a way to use the DFT to help select a suitable sampling rate f_s for signal $x(t)$. [*Hint:* Consider the characteristics of an oversampled signal's DFT spectrum.]
(b) Test the method you devised in part (a) using the signal $x(t) = \Delta(\frac{t-1}{2})$. Use MATLAB to compute any needed DFTs. What value f_s seems reasonable for this signal?

5.5-4 Choose appropriate values for N_0 and T and compute the DFT of the signal $e^{-t}u(t)$. Use two different criteria for determining the effective bandwidth of $e^{-t}u(t)$. As the bandwidth, use the frequency at which the amplitude response drops to 1% of its peak value (at $\omega = 0$). Next, use the 99% energy criterion for determining the bandwidth (see Ex. 4.20).

5.5-5 Repeat Prob. 5.5-4 for the signal

$$x(t) = \frac{2}{t^2 + 1}$$

5.5-6 For the signals $x(t)$ and $g(t)$ represented in Fig. P5.5-6, write the appropriate sequences x_n and g_n necessary for the computation of the convolution of $x(t)$ and $g(t)$ using DFT. Use $T = 1/8$.

5.5-7 For this problem, interpret the N-point DFT as an N-periodic function of r. To stress this fact, we shall change the notation X_r to $X(r)$. Are the following frequency-domain signals valid DFTs? Answer yes or no. For each valid DFT, determine the size N of the DFT and whether the time-domain signal is real.
(a) $X(r) = j - \pi$
(b) $X(r) = \sin(r/10)$
(c) $X(r) = \sin(\pi r/10)$

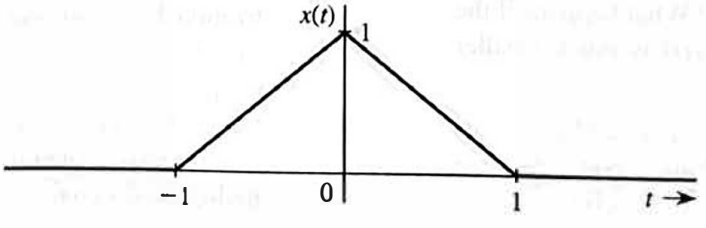

Figure P5.5-2

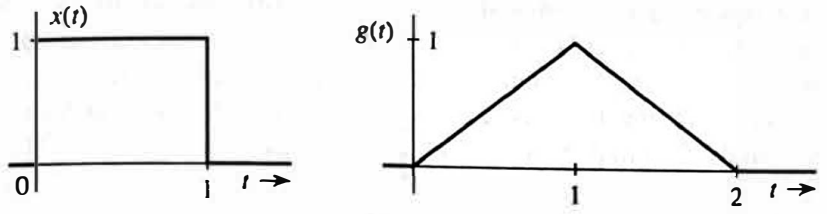

(a) (b)

Figure P5.5-6

(d) $X(r) = \left[(1+j)/\sqrt{2}\right]^r$

(e) $X(r) = \langle r + \pi \rangle_{10}$ where $\langle \cdot \rangle_{10}$ denotes the modulo-N operation

5.7-1 MATLAB's `fft` command computes the DFT of a vector `x` assuming the first sample occurs at time $n = 0$. Given that `X = fft(x)` has already been computed, derive a method to correct `X` to reflect an arbitrary starting time $n = n_0$.

5.7-2 Consider a complex signal composed of two closely spaced complex exponentials: $x_1[n] = e^{j2\pi n30/100} + e^{j2\pi n33/100}$. For each of the following cases, plot the length-N DFT magnitude as a function of frequency f_r, where $f_r = r/N$.

(a) Compute and plot the DFT of $x_1[n]$ using 10 samples ($0 \le n \le 9$). From the plot, can both exponentials be identified? Explain.

(b) Zero-pad the signal from part (a) with 490 zeros and then compute and plot the 500-point DFT. Does this improve the picture of the DFT? Explain.

(c) Compute and plot the DFT of $x_1[n]$ using 100 samples ($0 \le n \le 99$). From the plot, can both exponentials be identified? Explain.

(d) Zero-pad the signal from part (c) with 400 zeros and then compute and plot the 500-point DFT. Does this improve the picture of the DFT? Explain.

5.7-3 Repeat Prob. 5.7-2, using the complex signal $x_2[n] = e^{j2\pi n30/100} + e^{j2\pi n31.5/100}$.

5.7-4 Consider a complex signal composed of a dc term and two complex exponentials: $y_1[n] = 1 + e^{j2\pi n30/100} + 0.5 * e^{j2\pi n43/100}$. For each of the following cases, plot the length-N DFT magnitude as a function of frequency f_r, where $f_r = r/N$.

(a) Use MATLAB to compute and plot the DFT of $y_1[n]$ with 20 samples ($0 \le n \le 19$). From the plot, can the two non-dc exponentials be identified? Given the amplitude relation between the two, the lower-frequency peak should be twice as large as the higher-frequency peak. Is this the case? Explain.

(b) Zero-pad the signal from part (a) to a total length of 500. Does this improve locating the two non-dc exponential components? Is the lower-frequency peak twice as large as the higher-frequency peak? Explain.

(c) MATLAB's signal-processing toolbox function `window` allows window functions to be easily generated. Generate a length-20 Hanning window and apply it to $y_1[n]$. Using this windowed function, repeat parts (a) and (b). Comment on whether the window function helps or hinders the analysis.

5.7-5 Repeat Prob. 5.7-4, using the complex signal $y_2[n] = 1 + e^{j2\pi n30/100} + 0.5e^{j2\pi n38/100}$.

5.7-6 This problem investigates the idea of zero padding applied in the frequency domain. When asked, plot the length-N DFT magnitude as a function of frequency f_r, where $f_r = r/N$.

(a) In MATLAB, create a vector `x` that contains one period of the sinusoid $x[n] = \cos((\pi/2)n)$. Plot the result. How "sinusoidal" does the signal appear to be?

(b) Use the `fft` command to compute the DFT `X` of vector `x`. Plot the magnitude of the DFT coefficients. Do they make sense?

(c) Zero-pad the DFT vector to a total length of 100 by inserting the appropriate number of zeros in the middle of the vector `X`. Call this zero-padded DFT sequence `Y`. Why are zeros inserted in the middle rather than the end? Take the inverse DFT of `Y` and plot the result. What similarities exist

between the new signal y and the original signal x? What are the differences between x and y? What is the effect of zero padding in the frequency domain? How is this type of zero padding similar to zero padding in the time domain?

(d) Derive a general modification to the procedure of zero padding in the frequency domain to ensure that the amplitude of the resulting time-domain signal is left unchanged.

(e) Consider one period of a square wave described by the length-8 vector [1 1 1 1 −1 −1 −1 −1]. Zero-pad the DFT of this vector to a length of 100, and call the result S. Scale S according to part (d), take the inverse DFT, and plot the result. Does the new time-domain signal $s[n]$ look like a square wave? Explain.

5.7-7 The quantized output x_q of a truncating asymmetric converter is given as

$$x_q = \frac{x_{max}}{2^{B-1}} \left\lfloor \frac{x}{x_{max}} 2^{B-1} \right\rfloor$$

Any values outside the 2^B allowable levels should be clamped to the nearest level.

(a) Similar to Fig. 5.31, plot the transfer characteristics for a 3-bit version of this quantizer.

(b) Apply 3-bit truncating asymmetric quantization to a 1 Hz cosine sampled at f_s = 50 Hz over 1 second. Plot the original signal $x(t)$, the quantized signal $x_q(t)$, and the magnitude spectra of both. How does truncating asymmetric quantization compare to the results of asymmetric rounding quantization shown in Fig. 5.33?

5.7-8 The quantized output x_q of a symmetric truncating converter is given as

$$x_q = \frac{x_{max}}{2^{B-1}} \left(\left\lfloor \frac{x}{x_{max}} 2^{B-1} - \frac{1}{2} \right\rfloor + \frac{1}{2} \right)$$

Any values outside the 2^B allowable levels should be clamped to the nearest level.

(a) Similar to Fig. 5.31, plot the transfer characteristics for a 3-bit version of this quantizer.

(b) Apply 3-bit truncating symmetric quantization to a 1 Hz cosine sampled at f_s = 50 Hz over 1 second. Plot the original signal $x(t)$, the quantized signal $x_q(t)$, and the magnitude spectra of both. How does truncating symmetric quantization compare to the results of asymmetric rounding quantization shown in Fig. 5.33?

CHAPTER 6

CONTINUOUS-TIME SYSTEM ANALYSIS USING THE LAPLACE TRANSFORM

The Fourier transform is a tool that allows us to represent a signal $x(t)$ as a continuous sum of exponentials of the form $e^{j\omega t}$, whose frequencies are restricted to the imaginary axis in the complex plane ($s = j\omega$). As we saw in Chs. 4 and 5, such a representation is quite valuable in the analysis and processing of signals. In the area of system analysis, however, the use of Fourier transform leaves much to be desired. First, the Fourier transform exists only for a restricted class of signals and, therefore, cannot be used for such inputs as growing exponentials. Second, the Fourier transform cannot be used easily to analyze unstable or even marginally stable systems.

6.1 THE LAPLACE TRANSFORM

The basic reason for both these difficulties is that for some signals, such as $e^{at}u(t)$ ($a > 0$), the Fourier transform does not exist because ordinary sinusoids or exponentials of the form $e^{j\omega t}$ (on account of their constant amplitudes) are incapable of synthesizing exponentially growing signals. This problem could be resolved if it were possible to use basis signals of the form e^{st} (instead of $e^{j\omega t}$), where the complex frequency s is not restricted to just the imaginary axis (as in the Fourier transform). This is precisely what is done in the following extended transform known as the *bilateral Laplace transform,* where the frequency variable $s = j\omega$ is generalized to $s = \sigma + j\omega$. Such a generalization permits us to use exponentially growing sinusoids to synthesize a signal $x(t)$. Before developing the mathematical operations required for such an extension, it is illuminating to develop an intuitive understanding of such a generalization.

6.1.1 An Intuitive Understanding of the Laplace Transform

If a signal $x(t)$ shown in Fig. 6.1d is not Fourier transformable, we may be able to make it Fourier transformable by multiplying it with a decaying exponential such as $e^{-\sigma t}$.[†] For example, a signal

[†] This assumes that $|x(t)| < Me^{at}$ for some real, positive, and finite numbers M and a. Such signals are called *exponential-order* signals. Signals that do not satisfy this condition may not be Laplace transformable.

$e^{2t}u(t)$ can be made Fourier transformable by multiplying it with $e^{-\sigma t}$ with $\sigma > 2$. Let

$$\phi(t) = x(t)e^{-\sigma t}$$

as depicted in Fig. 6.1a. The signal $\phi(t)$ is now Fourier transformable, and its Fourier components are of the form $e^{j\omega t}$ with frequencies ω varying from $\omega = -\infty$ to ∞. The sum of the exponential components $e^{j\omega t}$ and $e^{-j\omega t}$ in the spectrum give a sinusoid of frequency ω. The spectrum contains an infinite number of such sinusoids, each having an infinitesimal amplitude. It would be very confusing to draw all these components; hence, in Fig. 6.1b, we show just two typical components. The addition of all such components (infinite in number) results in $\phi(t)$, illustrated in Fig. 6.1a. The exponential spectral components of $\phi(t)$ are of the form $e^{j\omega t}$ with complex frequencies $j\omega$ lying on the imaginary axis from $\omega = -\infty$ to ∞, as shown in Fig. 6.1c.

Figure 6.1a shows a signal $\phi(t) = x(t)e^{-\sigma t}$, Fig. 6.1b shows two of its infinite spectral components, and Fig. 6.1c shows the location in the complex plane of the frequencies of all the spectral components of $\phi(t)$. Now, the desired signal $x(t)$ can be obtained by multiplying $\phi(t)$ with $e^{\sigma t}$. This fact means that we can synthesize $x(t)$ by multiplying each spectral component of $\phi(t)$ with $e^{\sigma t}$ and adding them. But multiplying the spectral components of $\phi(t)$ (sinusoids in Fig. 6.1b) with $e^{\sigma t}$ results in the exponentially growing sinusoids as shown in Fig. 6.1e. Addition of all such exponentially growing sinusoids (infinite in number) results in $x(t)$ in Fig. 6.1d. The spectral components of $\phi(t)$ are of the form $e^{j\omega t}$. Multiplication of these components with $e^{\sigma t}$ results in the spectral components of the form $e^{\sigma t}e^{j\omega t} = e^{(\sigma + j\omega)t}$. Therefore, a component of frequency $j\omega$ in the spectrum of $\phi(t)$ is transformed into a component of frequency $\sigma + j\omega$ in the spectrum of $x(t)$. The location in the complex plane of the frequencies $\sigma + j\omega$ is along a vertical line, depicted in Fig. 6.1f.

It is clear that a signal $x(t)$ can be synthesized with growing everlasting exponentials lying along the path $\sigma + j\omega$, with ω varying from $-\infty$ to ∞. The value of σ is flexible. For example, if $x(t) = e^{2t}u(t)$, then $\phi(t) = x(t)e^{-\sigma t}$ can be made Fourier transformable if we choose $\sigma > 2$. Notice, there are infinite choices for σ. This means the spectrum of $x(t)$ is not unique, and there are infinite possible ways of synthesizing $x(t)$. Nevertheless, σ has a certain minimum value σ_0 for a given $x(t)$ [$\sigma_0 = 2$ for $x(t) = e^{2t}u(t)$]. The region in the complex plane where $\sigma > \sigma_0$ (Fig. 6.1g) is called the *region of convergence* (or *existence*) of the resulting transform of $x(t)$.

All of these conclusions reached here by pure heuristic reasoning will now be derived analytically. The frequency $j\omega$ in the Fourier transform will be generalized to $s = \sigma + j\omega$.

6.1.2 Analytical Development of the Bilateral Laplace Transform

Because we are unifying the Fourier and Laplace transforms, we need to use here the unified notation $X(j\omega)$ instead of $X(\omega)$ for the Fourier transform, which is given by

$$X(j\omega) = \int_{-\infty}^{\infty} x(t)e^{-j\omega t}\,dt \tag{6.1}$$

and

$$x(t) = \frac{1}{2\pi}\int_{-\infty}^{\infty} X(j\omega)e^{j\omega t}\,d\omega$$

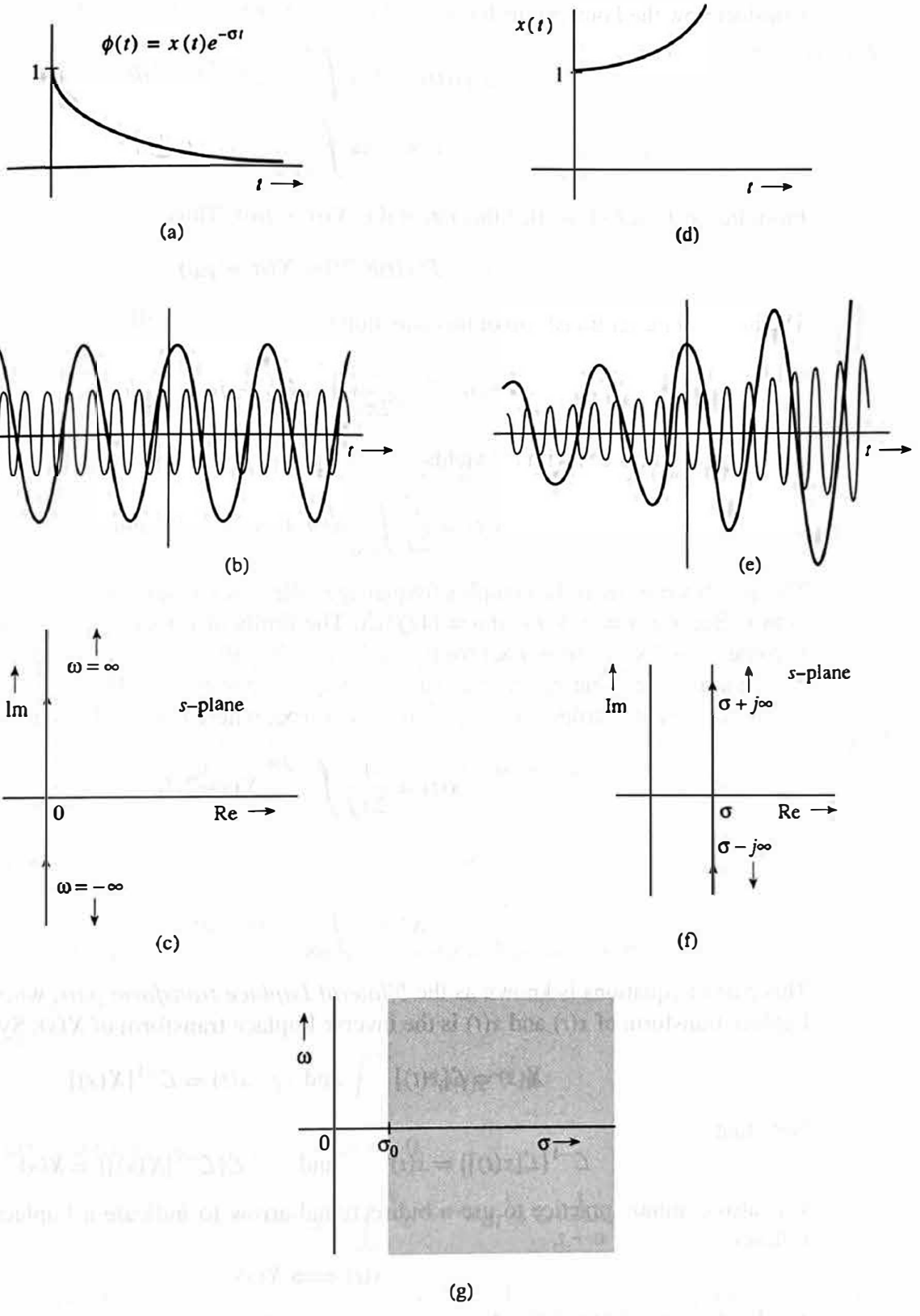

Figure 6.1 Heuristic explanation of the extension of the Fourier transform to the Laplace transform.

Consider now the Fourier transform of $x(t)e^{-\sigma t}$ (σ real)

$$\mathcal{F}[x(t)e^{-\sigma t}] = \int_{-\infty}^{\infty} x(t)e^{-\sigma t}e^{-j\omega t}\,dt$$
$$= \int_{-\infty}^{\infty} x(t)e^{-(\sigma+j\omega)t}\,dt \tag{6.2}$$

From Eq. (6.1), it follows that this integral is $X(\sigma + j\omega)$. Thus,

$$\mathcal{F}[x(t)e^{-\sigma t}] = X(\sigma + j\omega) \tag{6.3}$$

The inverse Fourier transform of this equation yields

$$x(t)e^{-\sigma t} = \frac{1}{2\pi}\int_{-\infty}^{\infty} X(\sigma + j\omega)e^{j\omega t}\,d\omega$$

Multiplying both sides with $e^{\sigma t}$ yields

$$x(t) = \frac{1}{2\pi}\int_{-\infty}^{\infty} X(\sigma + j\omega)e^{(\sigma+j\omega)t}\,d\omega \tag{6.4}$$

The quantity $\sigma + j\omega$ is the complex frequency s. We now change the variable in this integral from ω to s. Because $s = \sigma + j\omega$, $d\omega = (1/j)\,ds$. The limits of integration from $\omega = -\infty$ to ∞ now become $(\sigma - j\infty)$ to $(\sigma + j\infty)$ for the variable s. Recall, however, that for a given $x(t)$, σ has a certain minimum value σ_0, and we can select any value of $\sigma > \sigma_0$. In general, we can let the limits of integration range from $s = c - j\infty$ to $s = c + j\infty$, where $c > \sigma_0$. Thus, Eq. (6.4) becomes

$$x(t) = \frac{1}{2\pi j}\int_{c-j\infty}^{c+j\infty} X(s)e^{st}\,ds \tag{6.5}$$

From Eqs. (6.2) and (6.3), we obtain

$$X(s) = \int_{-\infty}^{\infty} x(t)e^{-st}\,dt \tag{6.6}$$

This pair of equations is known as the *bilateral Laplace transform pair*, where $X(s)$ is the direct Laplace transform of $x(t)$ and $x(t)$ is the inverse Laplace transform of $X(s)$. Symbolically,

$$X(s) = \mathcal{L}[x(t)] \qquad \text{and} \qquad x(t) = \mathcal{L}^{-1}[X(s)]$$

Note that

$$\mathcal{L}^{-1}\{\mathcal{L}[x(t)]\} = x(t) \qquad \text{and} \qquad \mathcal{L}\{\mathcal{L}^{-1}[X(s)]\} = X(s)$$

It is also common practice to use a bidirectional arrow to indicate a Laplace transform pair, as follows:

$$x(t) \Longleftrightarrow X(s)$$

The Laplace transform, defined in this way, can handle signals existing over the entire time interval from $-\infty$ to ∞ (causal and noncausal signals). For this reason, it is called the *bilateral* (or *two-sided*) Laplace transform. Later we shall consider a special case—the *unilateral* or *one-sided* Laplace transform—that can handle only causal signals.

Linearity of the Laplace Transform

We now prove that the Laplace transform is a linear operator by showing that the principle of superposition holds, implying that if

$$x_1(t) \Longleftrightarrow X_1(s) \qquad \text{and} \qquad x_2(t) \Longleftrightarrow X_2(s)$$

then

$$a_1x_1(t) + a_2x_2(t) \Longleftrightarrow a_1X_1(s) + a_2X_2(s)$$

The proof is simple. By definition,

$$\begin{aligned}\mathcal{L}[a_1x_1(t) + a_2x_2(t)] &= \int_{-\infty}^{\infty} [a_1x_1(t) + a_2x_2(t)]e^{-st}\,dt \\ &= a_1\int_{-\infty}^{\infty} x_1(t)e^{-st}\,dt + a_2\int_{-\infty}^{\infty} x_2(t)e^{-st}\,dt \\ &= a_1X_1(s) + a_2X_2(s) \end{aligned} \tag{6.7}$$

This result can be extended to any finite sum.

The Region of Convergence (ROC)

The *region of convergence* (ROC), also called the region of existence, for the Laplace transform, $X(s)$, is the set of values of s (the region in the complex plane) for which the integral in Eq. (6.6) converges. This concept will become clear in the following example.

EXAMPLE 6.1 Laplace Transform and ROC of a Causal Exponential

For a signal $x(t) = e^{-at}u(t)$, find the Laplace transform $X(s)$ and its ROC.

By definition,

$$X(s) = \int_{-\infty}^{\infty} e^{-at}u(t)e^{-st}\,dt$$

Because $u(t) = 0$ for $t < 0$ and $u(t) = 1$ for $t \geq 0$,

$$X(s) = \int_0^{\infty} e^{-at}e^{-st}\,dt = \int_0^{\infty} e^{-(s+a)t}\,dt = -\frac{1}{s+a}e^{-(s+a)t}\Big|_0^{\infty} \tag{6.8}$$

Note that s is complex and as $t \to \infty$, the term $e^{-(s+a)t}$ does not necessarily vanish. Here, we recall that for a complex number $z = \alpha + j\beta$,

$$e^{-zt} = e^{-(\alpha+j\beta)t} = e^{-\alpha t}e^{-j\beta t}$$

Now $|e^{-j\beta t}| = 1$ regardless of the value of βt. Therefore, as $t \to \infty$, $e^{-zt} \to 0$ only if $\alpha > 0$, and $e^{-zt} \to \infty$ if $\alpha < 0$. Thus,

$$\lim_{t\to\infty} e^{-zt} = \begin{cases} 0 & \text{Re } z > 0 \\ \infty & \text{Re } z < 0 \end{cases} \tag{6.9}$$

Clearly,

$$\lim_{t\to\infty} e^{-(s+a)t} = \begin{cases} 0 & \text{Re}(s+a) > 0 \\ \infty & \text{Re}(s+a) < 0 \end{cases}$$

Use of this result in Eq. (6.8) yields

$$X(s) = \frac{1}{s+a} \qquad \text{Re}(s+a) > 0$$

or

$$e^{-at}u(t) \Longleftrightarrow \frac{1}{s+a} \qquad \text{Re } s > -a \tag{6.10}$$

The ROC of $X(s)$ is Re $s > -a$, as shown in the shaded area in Fig. 6.2a. This fact means that the integral defining $X(s)$ in Eq. (6.8) exists only for the values of s in the shaded region in Fig. 6.2a. For other values of s, the integral in Eq. (6.8) does not converge. For this reason, the shaded region is called the *ROC* (or the *region of existence*) for $X(s)$.

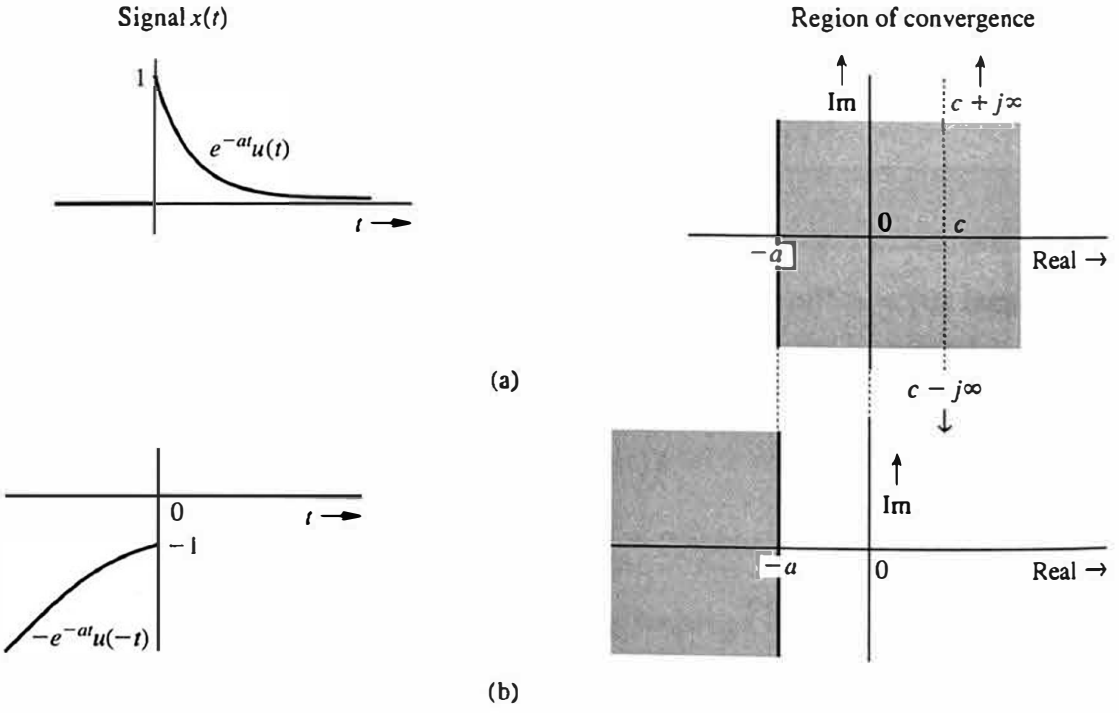

Figure 6.2 Signals **(a)** $e^{-at}u(t)$ and **(b)** $-e^{-at}u(-t)$ have the same Laplace transform but different regions of convergence.

Region of Convergence for Finite-Duration Signals

A finite-duration signal $x_f(t)$ is a signal that is nonzero only for $t_1 \leq t \leq t_2$, where both t_1 and t_2 are finite numbers and $t_2 > t_1$. For a finite-duration, absolutely integrable signal, the ROC is the entire s plane. This is clear from the fact that if $x_f(t)$ is absolutely integrable and a finite-duration signal, then $x(t)e^{-\sigma t}$ is also absolutely integrable for any value of σ because the integration is over the finite range of t only. Hence, the Laplace transform of such a signal converges for every value of s. This means that the ROC of a general signal $x(t)$ remains unaffected by the addition of any absolutely integrable, finite-duration signal $x_f(t)$ to $x(t)$. In other words, if $\mathcal{R}$ represents the ROC of a signal $x(t)$, then the ROC of a signal $x(t) + x_f(t)$ is also $\mathcal{R}$.

Role of the Region of Convergence

The ROC is required for evaluating the inverse Laplace transform $x(t)$ from $X(s)$, as defined by Eq. (6.5). The operation of finding the inverse transform requires an integration in the complex plane, which needs some explanation. The path of integration is along $c + j\omega$, with ω varying from $-\infty$ to ∞.† Moreover, the path of integration must lie in the ROC (or existence) for $X(s)$. For the signal $e^{-at}u(t)$, this is possible if $c > -a$. One possible path of integration is shown (dotted) in Fig. 6.2a. Thus, to obtain $x(t)$ from $X(s)$, the integration in Eq. (6.5) is performed along this path. When we integrate $[1/(s+a)]e^{st}$ along this path, the result is $e^{-at}u(t)$. Such integration in the complex plane requires a background in the theory of functions of complex variables. We can avoid this integration by compiling a table of Laplace transforms (Table 6.1), where the Laplace transform pairs are tabulated for a variety of signals. To find the inverse Laplace transform of, say, $1/(s+a)$, instead of using the complex integral of Eq. (6.5), we look up the table and find the inverse Laplace transform to be $e^{-at}u(t)$ (assuming that the ROC is Re $s > -a$). Although the table given here is rather short, it comprises the functions of most practical interest. A more comprehensive table appears in Doetsch [1].

The Unilateral Laplace Transform

To understand the need for defining unilateral transform, let us find the Laplace transform of signal $x(t)$ illustrated in Fig. 6.2b:

$$x(t) = -e^{-at}u(-t)$$

The Laplace transform of this signal is

$$X(s) = \int_{-\infty}^{\infty} -e^{-at}u(-t)e^{-st}\,dt$$

Because $u(-t) = 1$ for $t < 0$ and $u(-t) = 0$ for $t > 0$,

$$X(s) = \int_{-\infty}^{0} -e^{-at}e^{-st}\,dt = -\int_{-\infty}^{0} e^{-(s+a)t}\,dt = \frac{1}{s+a}e^{-(s+a)t}\Big|_{-\infty}^{0}$$

† The discussion about the path of convergence is rather complicated, requiring the concepts of contour integration and understanding of the theory of complex variables. For this reason, the discussion here is somewhat simplified.

TABLE 6.1 Select (Unilateral) Laplace Transform Pairs

No.	$x(t)$	$X(s)$
1	$\delta(t)$	1
2	$u(t)$	$\frac{1}{s}$
3	$tu(t)$	$\frac{1}{s^2}$
4	$t^n u(t)$	$\frac{n!}{s^{n+1}}$
5	$e^{\lambda t}u(t)$	$\frac{1}{s-\lambda}$
6	$te^{\lambda t}u(t)$	$\frac{1}{(s-\lambda)^2}$
7	$t^n e^{\lambda t}u(t)$	$\frac{n!}{(s-\lambda)^{n+1}}$
8a	$\cos bt\, u(t)$	$\frac{s}{s^2+b^2}$
8b	$\sin bt\, u(t)$	$\frac{b}{s^2+b^2}$
9a	$e^{-at}\cos bt\, u(t)$	$\frac{s+a}{(s+a)^2+b^2}$
9b	$e^{-at}\sin bt\, u(t)$	$\frac{b}{(s+a)^2+b^2}$
10a	$re^{-at}\cos(bt+\theta)u(t)$	$\frac{(r\cos\theta)s+(ar\cos\theta-br\sin\theta)}{s^2+2as+(a^2+b^2)}$
10b	$re^{-at}\cos(bt+\theta)u(t)$	$\frac{0.5re^{j\theta}}{s+a-jb}+\frac{0.5re^{-j\theta}}{s+a+jb}$
10c	$re^{-at}\cos(bt+\theta)u(t)$ $r=\sqrt{\frac{A^2c+B^2-2ABa}{c-a^2}}$ $\theta=\tan^{-1}\left(\frac{Aa-B}{A\sqrt{c-a^2}}\right)$ $b=\sqrt{c-a^2}$	$\frac{As+B}{s^2+2as+c}$
10d	$e^{-at}\left[A\cos bt+\frac{B-Aa}{b}\sin bt\right]u(t)$ $b=\sqrt{c-a^2}$	$\frac{As+B}{s^2+2as+c}$

Equation (6.9) shows that

$$\lim_{t\to-\infty} e^{-(s+a)t} = 0 \qquad \text{Re}\,(s+a) < 0$$

Hence,

$$X(s) = \frac{1}{s+a} \qquad \text{Re}\,s < -a$$

The signal $-e^{-at}u(-t)$ and its ROC (Re $s < -a$) are depicted in Fig. 6.2b. Note that the Laplace transforms for the signals $e^{-at}u(t)$ and $-e^{-at}u(-t)$ are identical except for their regions of convergence. Therefore, for a given $X(s)$, there may be more than one inverse transform, depending on the ROC. In other words, unless the ROC is specified, there is no one-to-one correspondence between $X(s)$ and $x(t)$. This fact increases the complexity in using the Laplace transform. The complexity is the result of trying to handle causal as well as noncausal signals. If we restrict all our signals to the causal type, such an ambiguity does not arise. There is only one inverse transform of $X(s) = 1/(s+a)$, namely, $e^{-at}u(t)$. To find $x(t)$ from $X(s)$, we need not even specify the ROC. In summary, if all signals are restricted to the causal type, then, for a given $X(s)$, there is only one inverse transform $x(t)$.[†]

The unilateral Laplace transform is a special case of the bilateral Laplace transform in which all signals are restricted to being causal; consequently, the limits of integration for the integral in Eq. (6.6) can be taken from 0 to ∞. Therefore, the unilateral Laplace transform $X(s)$ of a signal $x(t)$ is defined as

$$X(s) = \int_{0^-}^{\infty} x(t)e^{-st}\,dt \tag{6.11}$$

We choose 0^- (rather than 0^+ used in some texts) as the lower limit of integration. This convention not only ensures inclusion of an impulse function at $t = 0$, but also allows us to use initial conditions at 0^- (rather than at 0^+) in the solution of differential equations via the Laplace transform. In practice, we are likely to know the initial conditions before the input is applied (at 0^-), not after the input is applied (at 0^+). Indeed, the very meaning of the term "initial conditions" implies conditions at $t = 0^-$ (conditions before the input is applied). Detailed analysis of the desirability of using $t = 0^-$ appears in Sec. 6.3.

The unilateral Laplace transform simplifies the system analysis problem considerably because of its *uniqueness property*, which says that for a given $X(s)$, there is a unique inverse transform. But there is a price for this simplification: we cannot analyze noncausal systems or use noncausal inputs. However, in most practical problems, this restriction is of little consequence. For this reason, we shall first consider the unilateral Laplace transform and its application to system analysis. (The bilateral Laplace transform is discussed later, in Sec. 6.8.)

Basically, there is little difference between the unilateral and the bilateral Laplace transform. The unilateral transform is the bilateral transform that deals with a subclass of signals starting at $t = 0$ (causal signals). Therefore, the expression [Eq. (6.5)] for the inverse Laplace transform remains unchanged. In practice, the term *Laplace transform* means *the unilateral Laplace transform*.

[†] Actually, $X(s)$ specifies $x(t)$ within a null function $n(t)$, which has the property that the area under $|n(t)|^2$ is zero over any finite interval 0 to t ($t > 0$) (Lerch's theorem). For example, if two functions are identical everywhere except at a finite number of points, they differ by a null function.

Existence of the Laplace Transform

The variable s in the Laplace transform is complex in general, and it can be expressed as $s = \sigma + j\omega$. By definition,

$$X(s) = \int_{0^-}^{\infty} x(t)e^{-st}\,dt = \int_{0^-}^{\infty} [x(t)e^{-\sigma t}]e^{-j\omega t}\,dt$$

Because $|e^{j\omega t}| = 1$, the integral on the right-hand side of this equation converges if

$$\int_{0^-}^{\infty} |x(t)e^{-\sigma t}|\,dt < \infty \tag{6.12}$$

Hence, the existence of the Laplace transform is guaranteed if the integral in Eq. (6.12) is finite for some value of σ. Any signal that grows no faster than an exponential signal $Me^{\sigma_0 t}$ for some M and σ_0 satisfies the condition of Eq. (6.12). Thus, if for some M and σ_0,

$$|x(t)| \leq Me^{\sigma_0 t} \tag{6.13}$$

we can choose $\sigma > \sigma_0$ to satisfy Eq. (6.12).[†] The signal e^{t^2}, in contrast, grows at a rate faster than $e^{\sigma_0 t}$, and consequently is not Laplace transformable.[‡] Fortunately, such signals (which are not Laplace transformable) are of little consequence from either a practical or a theoretical viewpoint. If σ_0 is the smallest value of σ for which the integral in Eq. (6.12) is finite, σ_0 is called the *abscissa of convergence* and the ROC of $X(s)$ is Re $s > \sigma_0$. The abscissa of convergence for $e^{-at}u(t)$ is $-a$ (the ROC is Re $s > -a$).

EXAMPLE 6.2 Bilateral Laplace Transform of Common Causal Signals

Determine the Laplace transform of the following: **(a)** $\delta(t)$, **(b)** $u(t)$, and **(c)** $\cos \omega_0 t\, u(t)$.

(a)

$$\mathcal{L}[\delta(t)] = \int_{0^-}^{\infty} \delta(t)e^{-st}\,dt$$

Using the sampling property [Eq. (1.11) with $T = 0$], we obtain

$$\mathcal{L}[\delta(t)] = 1 \qquad \text{for all } s$$

that is,

$$\delta(t) \Longleftrightarrow 1 \qquad \text{for all } s$$

[†] The condition of Eq. (6.13) is sufficient but not necessary for the existence of the Laplace transform. For example, $x(t) = 1/\sqrt{t}$ is infinite at $t = 0$, and Eq. (6.13) cannot be satisfied; but the transform of $1/\sqrt{t}$ exists and is given by $\sqrt{\pi/s}$.

[‡] However, if we consider a truncated (finite-duration) signal e^{t^2}, the Laplace transform exists.

(b) To find the Laplace transform of $u(t)$, recall that $u(t) = 1$ for $t \geq 0$. Therefore,

$$\mathcal{L}[u(t)] = \int_{0^-}^{\infty} u(t)e^{-st}\,dt = \int_{0^-}^{\infty} e^{-st}\,dt = -\frac{1}{s}e^{-st}\Big|_{0^-}^{\infty}$$
$$= \frac{1}{s} \qquad \text{Re}\, s > 0$$

We also could have obtained this result from Eq. (6.10) by letting $a = 0$.

(c) Because $\cos \omega_0 t\, u(t) = \frac{1}{2}[e^{j\omega_0 t} + e^{-j\omega_0 t}]u(t)$, we know that

$$\mathcal{L}[\cos \omega_0 t\, u(t)] = \tfrac{1}{2}\mathcal{L}[e^{j\omega_0 t}u(t) + e^{-j\omega_0 t}u(t)]$$

From Eq. (6.10), it follows that

$$\mathcal{L}[\cos \omega_0 t\, u(t)] = \frac{1}{2}\left[\frac{1}{s - j\omega_0} + \frac{1}{s + j\omega_0}\right] \qquad \text{Re}(s \pm j\omega) = \text{Re}\, s > 0$$
$$= \frac{s}{s^2 + \omega_0^2} \qquad \text{Re}\, s > 0 \tag{6.14}$$

For the unilateral Laplace transform, there is a unique inverse transform of $X(s)$; consequently, there is no need to specify the ROC explicitly. For this reason, we shall generally ignore any mention of the ROC for unilateral transforms. Recall, also, that in the unilateral Laplace transform it is understood that every signal $x(t)$ is zero for $t < 0$, and it is appropriate to indicate this fact by multiplying the signal by $u(t)$.

DRILL 6.1 Bilateral Laplace Transform of Gate Functions

By direct integration, find the Laplace transform $X(s)$ and the region of convergence of $X(s)$ for the gate functions shown in Fig. 6.3.

ANSWERS

(a) $\frac{1}{s}(1 - e^{-2s})$ for all s

(b) $\frac{1}{s}(1 - e^{-2s})e^{-2s}$ for all s

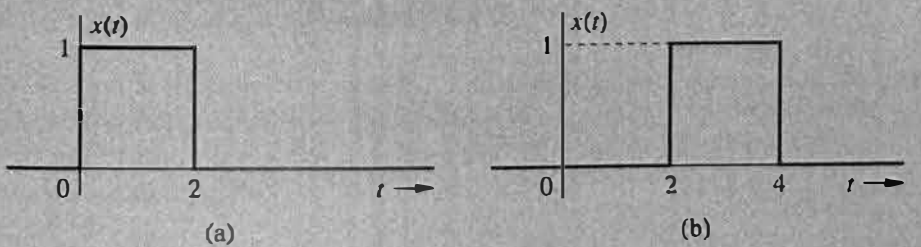

Figure 6.3 Gate functions for Drill 6.1.

Connection to the Fourier Transform

The definition of the Laplace transform is identical to that of the Fourier transform with $j\omega$ replaced by s. It is reasonable to expect $X(s)$, the Laplace transform of $x(t)$, to be the same as $X(\omega)$, the Fourier transform of $x(t)$ with $j\omega$ replaced by s. For example, we found the Fourier transform of $e^{-at}u(t)$ to be $1/(j\omega+a)$. Replacing $j\omega$ with s in the Fourier transform results in $1/(s+a)$, which is the Laplace transform as seen from Eq. (6.10). Unfortunately, this procedure is not valid for all $x(t)$. We may use it only if the region of convergence for $X(s)$ includes the imaginary ($j\omega$) axis. For instance, the Fourier transform of the unit step function is $\pi\delta(\omega)+(1/j\omega)$. The corresponding Laplace transform is $1/s$, and its region of convergence, which is $\text{Re}\, s > 0$, does not include the imaginary axis. In this case, the connection between the Fourier and Laplace transforms is not so simple. The reason for this complication is related to the convergence of the Fourier integral, where the path of integration is restricted to the imaginary axis. Because of this restriction, the Fourier integral for the step function does not converge in the ordinary sense as Ex. ?? demonstrates. We had to use a generalized function (impulse) for convergence. The Laplace integral for $u(t)$, in contrast, converges in the ordinary sense, but only for $\text{Re}\, s > 0$, a region forbidden to the Fourier transform. Another interesting fact is that although the Laplace transform is a generalization of the Fourier transform, there are signals (e.g., periodic signals) for which the Laplace transform does not exist, although the Fourier transform exists (but not in the ordinary sense).

6.1.3 Finding the Inverse Transform

Finding the inverse Laplace transform by using Eq. (6.5) requires integration in the complex plane, a subject beyond the scope of this book (but see, e.g., [2]). For our purpose, we can find the inverse transforms from Table 6.1. All we need is to express $X(s)$ as a sum of simpler functions of the forms listed in the table. Most of the transforms $X(s)$ of practical interest are *rational functions*, that is, ratios of polynomials in s. Such functions can be expressed as a sum of simpler functions by using partial fraction expansion (see Sec. B.5).

Values of s for which $X(s)=0$ are called the *zeros* of $X(s)$; the values of s for which $X(s)\to\infty$ are called the *poles* of $X(s)$. If $X(s)$ is a rational function of the form $P(s)/Q(s)$, the roots of $P(s)$ are the zeros and the roots of $Q(s)$ are the poles of $X(s)$.

EXAMPLE 6.3 Inverse Unilateral Laplace Transform

Find the inverse unilateral Laplace transforms of

(a) $\dfrac{7s-6}{s^2-s-6}$

(b) $\dfrac{2s^2+5}{s^2+3s+2}$

(c) $\dfrac{6(s+34)}{s(s^2+10s+34)}$

(d) $\dfrac{8s+10}{(s+1)(s+2)^3}$

In no case is the inverse transform of these functions directly available in Table 6.1. Rather, we need to expand these functions into partial fractions, as discussed in Sec. B.5.1. Today, it is very easy to find partial fractions via software such as MATLAB. However, just as the availability of a calculator does not obviate the need for learning the mechanics of arithmetical operations (addition, multiplication, etc.), the widespread availability of computers does not eliminate the need to learn the mechanics of partial fraction expansion.

(a)

$$X(s) = \frac{7s-6}{(s+2)(s-3)} = \frac{k_1}{s+2} + \frac{k_2}{s-3}$$

To determine k_1, corresponding to the term $(s+2)$, we cover up (conceal) the term $(s+2)$ in $X(s)$ and substitute $s=-2$ (the value of s that makes $s+2=0$) in the remaining expression (see Sec. B.5.2):

$$k_1 = \left.\frac{7s-6}{(s+2)(s-3)}\right|_{s=-2} = \frac{-14-6}{-2-3} = 4$$

Similarly, to determine k_2 corresponding to the term $(s-3)$, we cover up the term $(s-3)$ in $X(s)$ and substitute $s=3$ in the remaining expression

$$k_2 = \left.\frac{7s-6}{(s+2)(s-3)}\right|_{s=3} = \frac{21-6}{3+2} = 3$$

Therefore,

$$X(s) = \frac{7s-6}{(s+2)(s-3)} = \frac{4}{s+2} + \frac{3}{s-3} \tag{6.15}$$

Checking the Answer

It is easy to make a mistake in partial fraction computations. Fortunately, it is simple to check the answer by recognizing that $X(s)$ and its partial fractions must be equal for every value of s if the partial fractions are correct. Let us verify this assertion in Eq. (6.15) for some convenient value, say, $s=0$. Substitution of $s=0$ in Eq. (6.15) yields[†]

$$1 = 2 - 1 = 1$$

We can now be sure of our answer with a high margin of confidence. Using pair 5 of Table 6.1 in Eq. (6.15), we obtain

$$x(t) = \mathcal{L}^{-1}\left(\frac{4}{s+2} + \frac{3}{s-3}\right) = (4e^{-2t} + 3e^{3t})u(t)$$

[†] Because $X(s) = \infty$ at its poles, we should avoid the pole values (-2 and 3 in the present case) for checking. The answers may check even if partial fractions are wrong. This situation can occur when two or more errors cancel their effects. But the chances of this problem arising for randomly selected values of s are extremely small.

(b)

$$X(s) = \frac{2s^2+5}{s^2+3s+2} = \frac{2s^2+5}{(s+1)(s+2)}$$

Observe that $X(s)$ is an improper function with $M = N$. In such a case, we can express $X(s)$ as a sum of the coefficient of the highest power in the numerator plus partial fractions corresponding to the poles of $X(s)$ (see Sec. B.5.5). In the present case, the coefficient of the highest power in the numerator is 2. Therefore,

$$X(s) = 2 + \frac{k_1}{s+1} + \frac{k_2}{s+2}$$

where

$$k_1 = \left.\frac{2s^2+5}{(s+1)(s+2)}\right|_{s=-1} = \frac{2+5}{-1+2} = 7$$

and

$$k_2 = \left.\frac{2s^2+5}{(s+1)(s+2)}\right|_{s=-2} = \frac{8+5}{-2+1} = -13$$

Therefore,

$$X(s) = 2 + \frac{7}{s+1} - \frac{13}{s+2}$$

From Table 6.1, pairs 1 and 5, we obtain

$$x(t) = 2\delta(t) + (7e^{-t} - 13e^{-2t})u(t)$$

(c)

$$X(s) = \frac{6(s+34)}{s(s^2+10s+34)} = \frac{6(s+34)}{s(s+5-j3)(s+5+j3)}$$
$$= \frac{k_1}{s} + \frac{k_2}{s+5-j3} + \frac{k_2^*}{s+5+j3}$$

Note that the coefficients (k_2 and k_2^*) of the conjugate terms must also be conjugate (see Sec. B.5). Now

$$k_1 = \left.\frac{6(s+34)}{s(s^2+10s+34)}\right|_{s=0} = \frac{6 \times 34}{34} = 6$$

$$k_2 = \left.\frac{6(s+34)}{s(s+5-j3)(s+5+j3)}\right|_{s=-5+j3} = \frac{29+j3}{-3-j5} = -3+j4$$

Therefore,

$$k_2^* = -3-j4$$

To use pair 10b of Table 6.1, we need to express k_2 and k_2^* in polar form.

$$-3+j4 = \left(\sqrt{3^2+4^2}\right)e^{j\tan^{-1}(4/-3)} = 5e^{j\tan^{-1}(4/-3)}$$

Observe that $\tan^{-1}(4/-3) \neq \tan^{-1}(-4/3)$. This fact is evident in Fig. 6.4. For further discussion of this topic, see Ex. B.1.

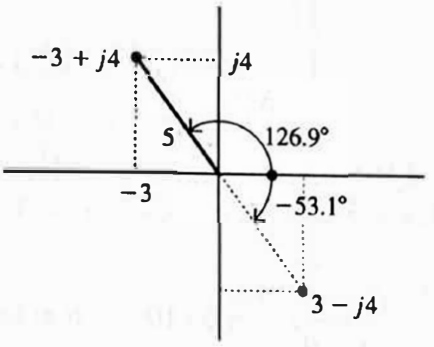

Figure 6.4 Visualizing $\tan^{-1}(-4/3) \neq \tan^{-1}(4/-3)$.

From Fig. 6.4, we observe that

$$k_2 = -3 + j4 = 5e^{j126.9°}$$

so

$$k_2^* = 5e^{-j126.9°}$$

Therefore,

$$X(s) = \frac{6}{s} + \frac{5e^{j126.9°}}{s+5-j3} + \frac{5e^{-j126.9°}}{s+5+j3}$$

From Table 6.1 (pairs 2 and 10b), we obtain

$$x(t) = [6 + 10e^{-5t}\cos(3t + 126.9°)]u(t)$$

Alternative Method Using Quadratic Factors

The foregoing procedure involves considerable manipulation of complex numbers. Pair 10c (Table 6.1) indicates that the inverse transform of quadratic terms (with complex conjugate poles) can be found directly without having to find first-order partial fractions. We discussed such a procedure in Sec. B.5.2. For this purpose, we shall express $X(s)$ as

$$X(s) = \frac{6(s+34)}{s(s^2+10s+34)} = \frac{k_1}{s} + \frac{As+B}{s^2+10s+34}$$

We have already determined that $k_1 = 6$ by the (Heaviside) "cover-up" method. Therefore,

$$\frac{6(s+34)}{s(s^2+10s+34)} = \frac{6}{s} + \frac{As+B}{s^2+10s+34}$$

Clearing the fractions by multiplying both sides by $s(s^2+10s+34)$ yields

$$6(s+34) = (6+A)s^2 + (60+B)s + 204$$

Now, equating the coefficients of s^2 and s on both sides yields

$$A = -6 \qquad \text{and} \qquad B = -54$$

and

$$X(s) = \frac{6}{s} + \frac{-6s - 54}{s^2 + 10s + 34}$$

We now use pairs 2 and 10c to find the inverse Laplace transform. The parameters for pair 10c are $A = -6$, $B = -54$, $a = 5$, $c = 34$, $b = \sqrt{c - a^2} = 3$, and

$$r = \sqrt{\frac{A^2c + B^2 - 2ABa}{c - a^2}} = 10 \qquad \theta = \tan^{-1} \frac{Aa - B}{A\sqrt{c - a^2}} = 126.9°$$

Therefore,

$$x(t) = [6 + 10e^{-5t} \cos(3t + 126.9°)]u(t)$$

which agrees with the earlier result.

SHORTCUTS

The partial fractions with quadratic terms also can be obtained by using shortcuts. We have

$$X(s) = \frac{6(s + 34)}{s(s^2 + 10s + 34)} = \frac{6}{s} + \frac{As + B}{s^2 + 10s + 34}$$

We can determine A by eliminating B on the right-hand side. This step can be accomplished by multiplying both sides of the equation for $X(s)$ by s and then letting $s \to \infty$. This procedure yields

$$0 = 6 + A \implies A = -6$$

Therefore,

$$\frac{6(s + 34)}{s(s^2 + 10s + 34)} = \frac{6}{s} + \frac{-6s + B}{s^2 + 10s + 34}$$

To find B, we let s take on any convenient value, say, $s = 1$, in this equation to obtain

$$\frac{210}{45} = 6 + \frac{B - 6}{45} \implies B = -54$$

a result that agrees with the answer found earlier.

(d)

$$X(s) = \frac{8s + 10}{(s + 1)(s + 2)^3} = \frac{k_1}{s + 1} + \frac{a_0}{(s + 2)^3} + \frac{a_1}{(s + 2)^2} + \frac{a_2}{s + 2}$$

where

$$k_1 = \left.\frac{8s + 10}{(s + 1)(s + 2)^3}\right|_{s=-1} = 2$$

$$a_0 = \left.\frac{8s+10}{(s+1)(s+2)^3}\right|_{s=-2} = 6$$

$$a_1 = \left\{\frac{d}{ds}\left[\frac{8s+10}{(s+1)(s+2)^3}\right]\right\}_{s=-2} = -2$$

$$a_2 = \frac{1}{2}\left\{\frac{d^2}{ds^2}\left[\frac{8s+10}{(s+1)(s+2)^3}\right]\right\}_{s=-2} = -2$$

Therefore,

$$X(s) = \frac{2}{s+1} + \frac{6}{(s+2)^3} - \frac{2}{(s+2)^2} - \frac{2}{s+2}$$

and

$$x(t) = [2e^{-t} + (3t^2 - 2t - 2)e^{-2t}]u(t)$$

Alternative Method: A Hybrid of Heaviside and Clearing Fractions

In this method, the simpler coefficients k_1 and a_0 are determined by the Heaviside "cover-up" procedure, as discussed earlier. To determine the remaining coefficients, we use the clearing-fraction method. Using the values $k_1 = 2$ and $a_0 = 6$ obtained earlier by the Heaviside "cover-up" method, we have

$$\frac{8s+10}{(s+1)(s+2)^3} = \frac{2}{s+1} + \frac{6}{(s+2)^3} + \frac{a_1}{(s+2)^2} + \frac{a_2}{s+2}$$

We now clear fractions by multiplying both sides of the equation by $(s+1)(s+2)^3$. This procedure yields[†]

$$\begin{aligned} 8s+10 &= 2(s+2)^3 + 6(s+1) + a_1(s+1)(s+2) + a_2(s+1)(s+2)^2 \\ &= (2+a_2)s^3 + (12+a_1+5a_2)s^2 + (30+3a_1+8a_2)s + (22+2a_1+4a_2) \end{aligned}$$

Equating coefficients of s^3 and s^2 on both sides, we obtain

$$0 = (2+a_2) \implies a_2 = -2$$

$$0 = 12+a_1+5a_2 = 2+a_1 \implies a_1 = -2$$

We can stop here if we wish, since the two desired coefficients a_1 and a_2 have already been found. However, equating the coefficients of s^1 and s^0 serves as a check on our answers. This step yields

[†] We could have cleared fractions without finding k_1 and a_0. This alternative, however, proves more laborious because it increases the number of unknowns to 4. By predetermining k_1 and a_0, we reduce the unknowns to 2. Moreover, this method provides a convenient check on the solution. This hybrid procedure achieves the best of both methods.

$$8 = 30 + 3a_1 + 8a_2$$
$$10 = 22 + 2a_1 + 4a_2$$

Substitution of $a_1 = a_2 = -2$, obtained earlier, satisfies these equations. This step confirms the correctness of our answers.

Another Alternative: A Hybrid of Heaviside and Shortcuts

In this method, the simpler coefficients k_1 and a_0 are determined by the Heaviside "cover-up" procedure, as discussed earlier. The usual shortcuts are then used to determine the remaining coefficients. Using the values $k_1 = 2$ and $a_0 = 6$, determined earlier by the Heaviside method, we have

$$\frac{8s+10}{(s+1)(s+2)^3} = \frac{2}{s+1} + \frac{6}{(s+2)^3} + \frac{a_1}{(s+2)^2} + \frac{a_2}{s+2}$$

There are two unknowns, a_1 and a_2. If we multiply both sides by s and then let $s \to \infty$, we eliminate a_1. This procedure yields

$$0 = 2 + a_2 \implies a_2 = -2$$

Therefore,

$$\frac{8s+10}{(s+1)(s+2)^3} = \frac{2}{s+1} + \frac{6}{(s+2)^3} + \frac{a_1}{(s+2)^2} - \frac{2}{s+2}$$

There is now only one unknown, a_1. This value can be determined readily by setting s equal to any convenient value, say, $s = 0$. This step yields

$$\frac{10}{8} = 2 + \frac{3}{4} + \frac{a_1}{4} - 1 \implies a_1 = -2$$

EXAMPLE 6.4 Inverse Laplace Transform with MATLAB

Using the MATLAB `residue` command, determine the inverse Laplace transform of each of the following functions:

(a) $X_a(s) = \dfrac{2s^2+5}{s^2+3s+2}$

(b) $X_b(s) = \dfrac{2s^2+7s+4}{(s+1)(s+2)^2}$

(c) $X_c(s) = \dfrac{8s^2+21s+19}{(s+2)(s^2+s+7)}$

In each case, we use the MATLAB `residue` command to perform the necessary partial fraction expansions. The inverse Laplace transform follows using Table 6.1.

(a)

```
>> num = [2 0 5]; den = [1 3 2];
>> [r, p, k] = residue(num,den)
   r = -13
         7
   p =  -2
        -1
   k =   2
```

Therefore, $X_a(s) = -13/(s+2) + 7/(s+1) + 2$ and $x_a(t) = (-13e^{-2t} + 7e^{-t})u(t) + 2\delta(t)$.

(b) Here, we use the `conv` command as a method to carry out polynomial multiplication and find the coefficients of the (expanded) denominator polynomial.

```
>> num = [2 7 4]; den = [conv([1 1],conv([1 2],[1 2]))];
>> [r, p, k] = residue(num,den)
   r =  3
        2
       -1
   p = -2
       -2
       -1
   k = []
```

Therefore, $X_b(s) = 3/(s+2) + 2/(s+2)^2 - 1/(s+1)$ and $x_b(t) = (3e^{-2t} + 2te^{-2t} - e^{-t})u(t)$.

(c) In this case, a few calculations are needed beyond the results of the `residue` command so that pair 10b of Table 6.1 can be utilized.

```
>> num = [8 21 19]; den = [conv([1 2],[1 1 7])];
>> [r, p, k]= residue(num,den)
   r =  3.5000-0.48113i
        3.5000+0.48113i
        1.0000
   p = -0.5000+2.5981i
       -0.5000-2.5981i
       -2.0000
   k = []
>> ang = angle(r), mag = abs(r)
   ang = -0.13661
          0.13661
          0
   mag =  3.5329
          3.5329
          1.0000
```

Thus,

$$X_c(s) = \frac{1}{s+2} + \frac{3.5329e^{-j0.13661}}{s+0.5-j2.5981} + \frac{3.5329e^{j0.13661}}{s+0.5+j2.5981}$$

and

$$x_c(t) = [e^{-2t} + 1.7665e^{-0.5t}\cos(2.5981t - 0.1366)]u(t).$$

EXAMPLE 6.5 Symbolic Laplace and Inverse Laplace Transforms with MATLAB

Using MATLAB's symbolic math toolbox, determine the following:

(a) the direct unilateral Laplace transform of $x_a(t) = \sin(at) + \cos(bt)$

(b) the inverse unilateral Laplace transform of $X_b(s) = as^2/(s^2 + b^2)$

(a) Here, we use the `sym` command to symbolically define our variables and expression for $x_a(t)$, and then we use the `laplace` command to compute the (unilateral) Laplace transform.

```
>> syms a b t; x_a = sin(a*t)+cos(b*t);
>> X_a = laplace(x_a);
   X_a = a/(a^2 + s^2) + s/(b^2 + s^2)
```

Therefore, $X_a(s) = \frac{a}{s^2+a^2} + \frac{s}{s^2+b^2}$. It is also easy to use MATLAB to determine $X_a(s)$ in standard rational form.

```
>> X_a = collect(X_a)
   X_a = (a^2*s + a*b^2 + a*s^2 + s^3)/(s^4 + (a^2 + b^2)*s^2 + a^2*b^2)
```

Thus, we also see that $X_a(s) = \frac{s^3+as^2+a^2s+ab^2}{s^4+(a^2+b^2)s^2+a^2b^2}$.

(b) A similar approach is taken for the inverse Laplace transform, except that the `ilaplace` command is used rather than the `laplace` command.

```
>> syms a b s; X_b = (a*s^2)/(s^2+b^2);
>> x_b = ilaplace(X_b)
   x_b = a*dirac(t) - a*b*sin(b*t)
```

Therefore, $x_b(t) = a\delta(t) - ab\sin(bt)u(t)$.

DRILL 6.2 Laplace Transform

Show that the Laplace transform of $10e^{-3t}\cos(4t+53.13°)$ is $(6s-14)/(s^2+6s+25)$. Use Table 6.1.

DRILL 6.3 Inverse Laplace Transform

Find the inverse Laplace transform of the following:

(a) $\dfrac{s+17}{s^2+4s-5}$

(b) $\dfrac{3s-5}{(s+1)(s^2+2s+5)}$

(c) $\dfrac{16s+43}{(s-2)(s+3)^2}$

ANSWERS

(a) $(3e^{t}-2e^{-5t})u(t)$

(b) $\left[-2e^{-t}+\frac{5}{2}e^{-t}\cos(2t-36.87°)\right]u(t)$

(c) $[3e^{2t}+(t-3)e^{-3t}]u(t)$

A Historical Note: Marquis Pierre-Simon de Laplace (1749–1827)

The Laplace transform is named after the great French mathematician and astronomer Laplace, who first presented the transform and its applications to differential equations in a paper published in 1779.

Laplace developed the foundations of potential theory and made important contributions to special functions, probability theory, astronomy, and celestial mechanics. In his *Exposition du système du monde* (1796), Laplace formulated a nebular hypothesis of cosmic origin and tried to explain the universe as a pure mechanism. In his *Traité de mécanique céleste* (celestial mechanics), which completed the work of Newton, Laplace used mathematics and physics to subject the solar system and all heavenly bodies to the laws of motion and the principle of gravitation. Newton had been unable to explain the irregularities of some heavenly bodies; in desperation, he concluded that God himself must intervene now and then to prevent such catastrophes as Jupiter eventually falling into the sun (and the moon into the earth), as predicted by Newton's calculations. Laplace proposed to show that these irregularities would correct themselves periodically and that a little patience—in Jupiter's case, 929 years—would see everything returning automatically to order; thus, there was no reason why the solar and the stellar systems could not continue to operate by the laws of Newton and Laplace to the end of time [3].

Laplace presented a copy of *Mécanique céleste* to Napoleon, who, after reading the book, took Laplace to task for not including God in his scheme: "You have written this huge book on the system of the world without once mentioning the author of the universe." "Sire," Laplace retorted, "I had no need of that hypothesis." Napoleon was not amused, and when he reported this reply to

Pierre-Simon de Laplace and Oliver Heaviside

another great mathematician-astronomer, Louis de Lagrange, the latter remarked, "Ah, but that is a fine hypothesis. It explains so many things" [4].

Napoleon, following his policy of honoring and promoting scientists, made Laplace the minister of the interior. To Napoleon's dismay, however, the new appointee attempted to bring "the spirit of infinitesimals" into administration, and so Laplace was transferred hastily to the Senate.

Oliver Heaviside (1850–1925)

Although Laplace published his transform method to solve differential equations in 1779, the method did not catch on until a century later. It was rediscovered independently in a rather awkward form by an eccentric British engineer, Oliver Heaviside (1850–1925), one of the tragic figures in the history of science and engineering. Despite his prolific contributions to electrical engineering, he was severely criticized during his lifetime and was neglected later to the point that hardly a textbook today mentions his name or credits him with contributions. Nevertheless, his studies had a major impact on many aspects of modern electrical engineering. It was Heaviside who made transatlantic communication possible by inventing cable loading, but few mention him as a pioneer or an innovator in telephony. It was Heaviside who suggested the use of inductive cable loading, but the credit is given to M. Pupin, who was not even responsible for building the first loading coil.[†] In addition, Heaviside was [5]:

- The first to find a solution to the distortionless transmission line.
- The innovator of lowpass filters.

[†] Heaviside developed the theory for cable loading, George Campbell built the first loading coil, and the telephone circuits using Campbell's coils were in operation before Pupin published his paper. In the legal fight over the patent, however, Pupin won the battle: he was a shrewd self-promoter, and Campbell had poor legal support.

- The first to write Maxwell's equations in modern form.
- The codiscoverer of rate energy transfer by an electromagnetic field.
- An early champion of the now-common phasor analysis.
- An important contributor to the development of vector analysis. In fact, he essentially created the subject independently of Gibbs [6].
- An originator of the use of operational mathematics used to solve linear integro-differential equations, which eventually led to rediscovery of the ignored Laplace transform.
- The first to theorize (along with Kennelly of Harvard) that a conducting layer (the Kennelly–Heaviside layer) of atmosphere exists, which allows radio waves to follow earth's curvature instead of traveling off into space in a straight line.
- The first to posit that an electrical charge would increase in mass as its velocity increases, an anticipation of an aspect of Einstein's special theory of relativity [7]. He also forecast the possibility of superconductivity.

Heaviside was a self-made, self-educated man. Although his formal education ended with elementary school, he eventually became a pragmatically successful mathematical physicist. He began his career as a telegrapher, but increasing deafness forced him to abandon this career at the age of 24. He then devoted himself to the study of electricity. His creative work was disdained by many professional mathematicians because of his lack of formal education and his unorthodox methods.

Heaviside had the misfortune to be criticized both by mathematicians, who faulted him for lack of rigor, and by men of practice, who faulted him for using too much mathematics and thereby confusing students. Many mathematicians, trying to find solutions to the distortionless transmission line, failed because no rigorous tools were available at the time. Heaviside succeeded because he used mathematics not with rigor, but with insight and intuition. Using his much maligned operational method, Heaviside successfully attacked problems that rigid mathematicians could not solve, problems such as the flow-of-heat in a body of spatially varying conductivity. Heaviside brilliantly used this method in 1895 to demonstrate a fatal flaw in Lord Kelvin's determination of the geological age of the earth by secular cooling; he used the same flow-of-heat theory as for his cable analysis. Yet the mathematicians of the Royal Society remained unmoved and were not the least impressed by the fact that Heaviside had found the answer to problems no one else could solve. Many mathematicians who examined his work dismissed it with contempt, asserting that his methods were either complete nonsense or a rehash of known ideas [5].

Sir William Preece, the chief engineer of the British Post Office, a savage critic of Heaviside, ridiculed Heaviside's work as too theoretical and, therefore, leading to faulty conclusions. Heaviside's work on transmission lines and loading was dismissed by the British Post Office and might have remained hidden, had not Lord Kelvin himself publicly expressed admiration for it [5].

Heaviside's operational calculus may be formally inaccurate, but, in fact, it anticipated the operational methods developed in more recent years [8]. Although his method was not fully understood, it provided correct results. When Heaviside was attacked for the vague meaning of his operational calculus, his pragmatic reply was, "Shall I refuse my dinner because I do not fully understand the process of digestion?"

Heaviside lived as a bachelor hermit, often in near-squalid conditions, and died largely unnoticed, in poverty. His life demonstrates the persistent arrogance and snobbishness of the intellectual establishment, which does not respect creativity unless it is presented in the strict language of the establishment.

6.2 SOME PROPERTIES OF THE LAPLACE TRANSFORM

Because it is a generalized form of the Fourier transform, we expect the Laplace transform to have properties similar to those of the Fourier transform. However, we are discussing here mainly the properties of the unilateral Laplace transform, and they differ somewhat from those of the Fourier transform (which is a bilateral transform).

Properties of the Laplace transform are useful not only in the derivation of the Laplace transform of functions but also in the solutions of linear integro-differential equations. A glance at Eqs. (6.5) and (6.6) shows that there is a certain measure of symmetry in going from $x(t)$ to $X(s)$, and vice versa. This symmetry or duality is also carried over to the properties of the Laplace transform. This fact will be evident in the following development.

We are already familiar with two properties: linearity [Eq. (6.7)] and the uniqueness property of the Laplace transform discussed earlier.

6.2.1 Time Shifting

The time-shifting property states that if

$$x(t) \Longleftrightarrow X(s)$$

then for $t_0 \geq 0$

$$x(t-t_0) \Longleftrightarrow X(s)e^{-st_0} \tag{6.16}$$

Observe that $x(t)$ starts at $t=0$, and, therefore, $x(t-t_0)$ starts at $t=t_0$. This fact is implicit, but is not explicitly indicated in Eq. (6.16). This often leads to inadvertent errors. To avoid such a pitfall, we should restate the property as follows. If

$$x(t)u(t) \Longleftrightarrow X(s)$$

then

$$x(t-t_0)u(t-t_0) \Longleftrightarrow X(s)e^{-st_0} \qquad t_0 \geq 0$$

Proof.

$$\mathcal{L}[x(t-t_0)u(t-t_0)] = \int_0^\infty x(t-t_0)u(t-t_0)e^{-st}\,dt$$

Setting $t-t_0=\tau$, we obtain

$$\mathcal{L}[x(t-t_0)u(t-t_0)] = \int_{-t_0}^\infty x(\tau)u(\tau)e^{-s(\tau+t_0)}\,d\tau$$

Because $u(\tau)=0$ for $\tau<0$ and $u(\tau)=1$ for $\tau\geq 0$, the limits of integration can be taken from 0 to ∞. Thus,

$$\begin{aligned}\mathcal{L}[x(t-t_0)u(t-t_0)] &= \int_0^\infty x(\tau)e^{-s(\tau+t_0)}\,d\tau \\ &= e^{-st_0}\int_0^\infty x(\tau)e^{-s\tau}\,d\tau \\ &= X(s)e^{-st_0}\end{aligned}$$

Note that $x(t-t_0)u(t-t_0)$ is the signal $x(t)u(t)$ delayed by t_0 seconds. The time-shifting property states that *delaying a signal by t_0 seconds amounts to multiplying its transform e^{-st_0}.*

This property of the unilateral Laplace transform holds only for positive t_0 because if t_0 were negative, the signal $x(t-t_0)u(t-t_0)$ may not be causal.

We can readily verify this property in Drill 6.1. If the signal in Fig. 6.3a is $x(t)u(t)$, then the signal in Fig. 6.3b is $x(t-2)u(t-2)$. The Laplace transform for the pulse in Fig. 6.3a is $(1/s)(1-e^{-2s})$. Therefore, the Laplace transform for the pulse in Fig. 6.3b is $(1/s)(1-e^{-2s})e^{-2s}$.

The time-shifting property proves very convenient in finding the Laplace transform of functions with different descriptions over different intervals, as the following example demonstrates.

EXAMPLE 6.6 Laplace Transform and the Time-Shifting Property

Find the Laplace transform of $x(t)$ depicted in Fig. 6.5a.

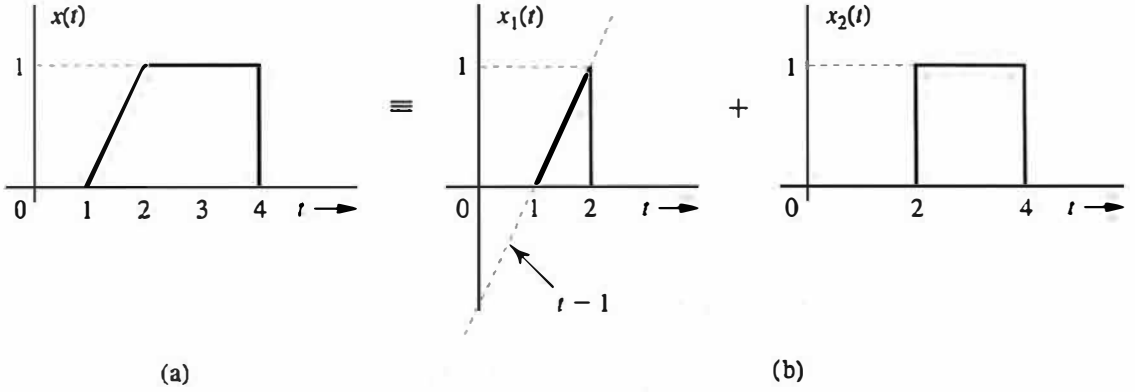

Figure 6.5 Finding a piecewise representation of a signal $x(t)$.

Describing mathematically a function such as the one in Fig. 6.5a is discussed in Sec. 1.4. The function $x(t)$ in Fig. 6.5a can be described as a sum of two components shown in Fig. 6.5b. The equation for the first component is $t-1$ over $1 \le t \le 2$ so that this component can be described by $(t-1)[u(t-1)-u(t-2)]$. The second component can be described by $u(t-2)-u(t-4)$. Therefore,

$$\begin{aligned} x(t) &= (t-1)[u(t-1)-u(t-2)]+[u(t-2)-u(t-4)] \\ &= (t-1)u(t-1)-(t-1)u(t-2)+u(t-2)-u(t-4) \end{aligned} \tag{6.17}$$

The first term on the right-hand side is the signal $tu(t)$ delayed by 1 second. Also, the third and fourth terms are the signal $u(t)$ delayed by 2 and 4 seconds, respectively. The second term, however, cannot be interpreted as a delayed version of any entry in Table 6.1. For this reason, we rearrange it as

$$(t-1)u(t-2) = (t-2+1)u(t-2) = (t-2)u(t-2) + u(t-2)$$

We have now expressed the second term in the desired form as $tu(t)$ delayed by 2 seconds plus $u(t)$ delayed by 2 seconds. With this result, Eq. (6.17) can be expressed as

$$x(t) = (t-1)u(t-1) - (t-2)u(t-2) - u(t-4)$$

Application of the time-shifting property to $tu(t) \Longleftrightarrow 1/s^2$ yields

$$(t-1)u(t-1) \Longleftrightarrow \frac{1}{s^2}e^{-s} \qquad \text{and} \qquad (t-2)u(t-2) \Longleftrightarrow \frac{1}{s^2}e^{-2s}$$

Also,

$$u(t) \Longleftrightarrow \frac{1}{s} \qquad \text{and} \qquad u(t-4) \Longleftrightarrow \frac{1}{s}e^{-4s}$$

Therefore,

$$X(s) = \frac{1}{s^2}e^{-s} - \frac{1}{s^2}e^{-2s} - \frac{1}{s}e^{-4s}$$

EXAMPLE 6.7 Inverse Laplace Transform and the Time-Shifting Property

Find the inverse Laplace transform of

$$X(s) = \frac{s+3+5e^{-2s}}{(s+1)(s+2)}$$

Observe the exponential term e^{-2s} in the numerator of $X(s)$, indicating time delay. In such a case, we should separate $X(s)$ into terms with and without a delay factor, as

$$X(s) = \underbrace{\frac{s+3}{(s+1)(s+2)}}_{X_1(s)} + \underbrace{\frac{5e^{-2s}}{(s+1)(s+2)}}_{X_2(s)e^{-2s}}$$

where

$$X_1(s) = \frac{s+3}{(s+1)(s+2)} = \frac{2}{s+1} - \frac{1}{s+2}$$

$$X_2(s) = \frac{5}{(s+1)(s+2)} = \frac{5}{s+1} - \frac{5}{s+2}$$

Therefore,

$$x_1(t) = (2e^{-t} - e^{-2t})u(t)$$
$$x_2(t) = 5(e^{-t} - e^{-2t})u(t)$$

Also, because

$$X(s) = X_1(s) + X_2(s)e^{-2s}$$

we can write

$$\begin{aligned} x(t) &= x_1(t) + x_2(t-2) \\ &= (2e^{-t} - e^{-2t})u(t) + 5\left[e^{-(t-2)} - e^{-2(t-2)}\right]u(t-2) \end{aligned}$$

DRILL 6.4 Laplace Transform and the Time-Shifting Property

Find the Laplace transform of the signal illustrated in Fig. 6.6.

ANSWER

$\frac{1}{s^2}(1 - 3e^{-2s} + 2e^{-3s})$

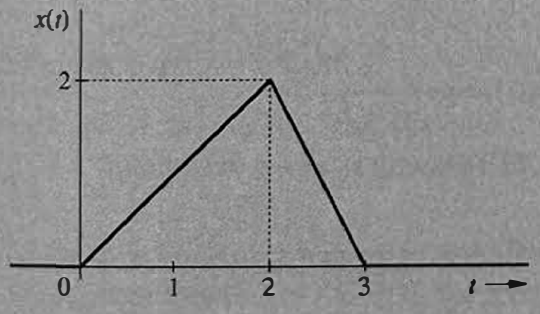

Figure 6.6 Signal for Drill 6.4.

DRILL 6.5 Inverse Laplace Transform and the Time-Shifting Property

Find the inverse Laplace transform of $X(s) = \dfrac{3e^{-2s}}{(s-1)(s+2)}$.

ANSWER

$\left[e^{t-2} - e^{-2(t-2)}\right]u(t-2)$

6.2.2 Frequency Shifting

The frequency-shifting property states that if

$$x(t) \Longleftrightarrow X(s)$$

then

$$x(t)e^{s_0 t} \Longleftrightarrow X(s - s_0) \tag{6.18}$$

Observe the symmetry (or duality) between this property and the time-shifting property of Eq. (6.16).

Proof.

$$\mathcal{L}[x(t)e^{s_0 t}] = \int_{0^-}^{\infty} x(t)e^{s_0 t}e^{-st}\,dt = \int_{0^-}^{\infty} x(t)e^{-(s-s_0)t}\,dt = X(s - s_0)$$

EXAMPLE 6.8 Frequency-Shifting Property

Derive pair 9a in Table 6.1 from pair 8a and the frequency-shifting property.

Pair 8a is

$$\cos bt\,u(t) \Longleftrightarrow \frac{s}{s^2 + b^2}$$

From the frequency-shifting property [Eq. (6.18)] with $s_0 = -a$, we obtain

$$e^{-at}\cos bt\,u(t) \Longleftrightarrow \frac{s + a}{(s + a)^2 + b^2}$$

DRILL 6.6 Frequency-Shifting Property

Derive pair 6 in Table 6.1 from pair 3 and the frequency-shifting property.

We are now ready to consider the two most important properties of the Laplace transform: time differentiation and time integration.

6.2.3 The Time-Differentiation Property

The time-differentiation property states that if†

$$x(t) \Longleftrightarrow X(s)$$

then

$$\frac{dx(t)}{dt} \Longleftrightarrow sX(s) - x(0^-)$$

Repeating this property a second time (differentiating twice) yields

$$\frac{d^2x(t)}{dt^2} \Longleftrightarrow s^2X(s) - sx(0^-) - \dot{x}(0^-)$$

Repeated differentiation yields

$$\begin{aligned}\frac{d^nx(t)}{dt^n} &\Longleftrightarrow s^nX(s) - s^{n-1}x(0^-) - s^{n-2}\dot{x}(0^-) - \cdots - x^{(n-1)}(0^-) \\ &= s^nX(s) - \sum_{k=1}^{n} s^{n-k}x^{(k-1)}(0^-)\end{aligned} \tag{6.19}$$

where $x^{(r)}(0^-)$ is d^rx/dt^r at $t = 0^-$.

Proof.

$$\mathcal{L}\left[\frac{dx(t)}{dt}\right] = \int_{0^-}^{\infty} \frac{dx(t)}{dt} e^{-st}\,dt$$

Integrating by parts, we obtain

$$\mathcal{L}\left[\frac{dx(t)}{dt}\right] = x(t)e^{-st}\Big|_{0^-}^{\infty} + s\int_{0^-}^{\infty} x(t)e^{-st}\,dt$$

For the Laplace integral to converge [i.e., for $X(s)$ to exist], it is necessary that $x(t)e^{-st} \to 0$ as $t \to \infty$ for the values of s in the ROC for $X(s)$. Thus,

$$\mathcal{L}\left[\frac{dx(t)}{dt}\right] = -x(0^-) + sX(s)$$

Repeated application of this procedure yields Eq. (6.19).

† The dual of the time-differentiation property is the frequency-differentiation property, which states that

$$tx(t) \Longleftrightarrow -\frac{d}{ds}X(s)$$

EXAMPLE 6.9 Laplace Transform and the Time-Differentiation Property

Find the Laplace transform of the signal $x(t)$ in Fig. 6.7a by using Table 6.1 and the time-differentiation and time-shifting properties of the Laplace transform.

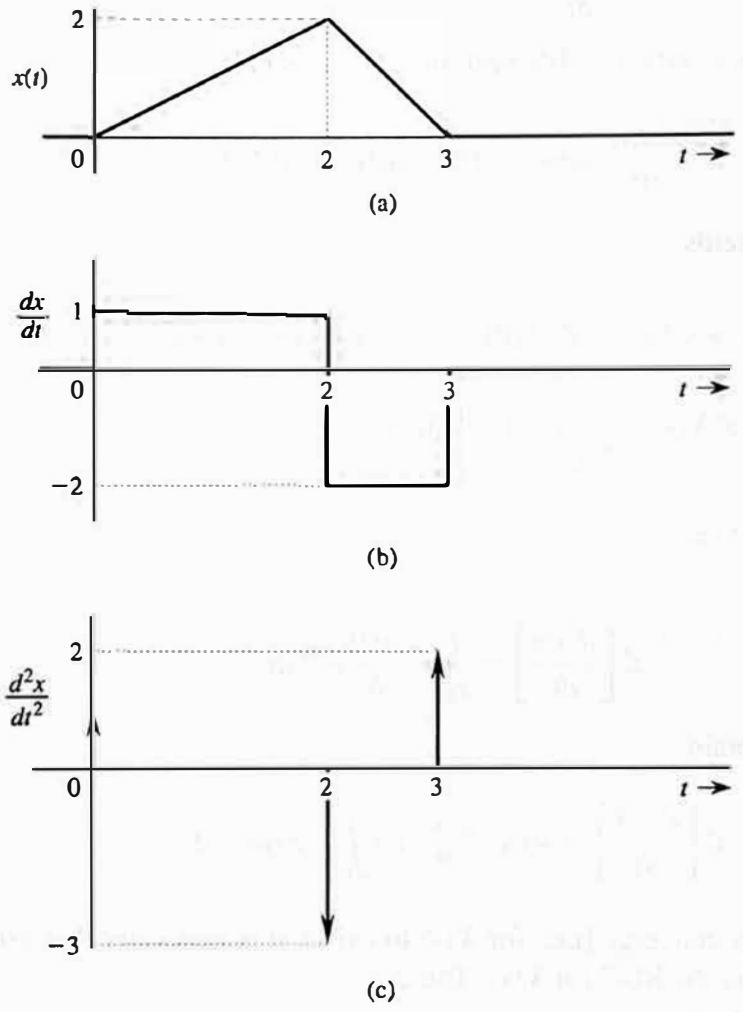

Figure 6.7 Finding the Laplace transform of a piecewise-linear function by using the time-differentiation property.

Figures 6.7b and 6.7c show the first two derivatives of $x(t)$. Recall that the derivative at a point of jump discontinuity is an impulse of strength equal to the amount of jump [see Eq. (1.12)]. Therefore,

$$\frac{d^2x(t)}{dt^2} = \delta(t) - 3\delta(t-2) + 2\delta(t-3)$$

The Laplace transform of this equation yields

$$\mathcal{L}\left(\frac{d^2x(t)}{dt^2}\right) = \mathcal{L}[\delta(t) - 3\delta(t-2) + 2\delta(t-3)]$$

Using the time-differentiation property of Eq. (6.19), the time-shifting property of Eq. (6.16), and the facts that $x(0^-) = \dot{x}(0^-) = 0$, and $\delta(t) \Longleftrightarrow 1$, we obtain

$$s^2X(s) - 0 - 0 = 1 - 3e^{-2s} + 2e^{-3s}$$

Therefore,

$$X(s) = \frac{1}{s^2}(1 - 3e^{-2s} + 2e^{-3s})$$

which confirms the earlier result in Drill 6.4.

6.2.4 The Time-Integration Property

The time-integration property states that if[†]

$$x(t) \Longleftrightarrow X(s)$$

then

$$\int_{0^-}^{t} x(\tau)\,d\tau \Longleftrightarrow \frac{X(s)}{s} \qquad \text{and} \qquad \int_{-\infty}^{t} x(\tau)\,d\tau \Longleftrightarrow \frac{X(s)}{s} + \frac{\int_{-\infty}^{0^-} x(\tau)\,d\tau}{s} \tag{6.20}$$

Proof. To prove the first part of Eq. (6.20), we define

$$g(t) = \int_{0^-}^{t} x(\tau)\,d\tau$$

so that

$$\frac{d}{dt}g(t) = x(t) \qquad \text{and} \qquad g(0^-) = 0$$

Now, if

$$g(t) \Longleftrightarrow G(s)$$

[†] The dual of the time-integration property is the frequency-integration property, which states that

$$\frac{x(t)}{t} \Longleftrightarrow \int_{s}^{\infty} X(z)\,dz$$

then

$$X(s) = \mathcal{L}\left[\frac{d}{dt}g(t)\right] = sG(s) - g(0^-) = sG(s)$$

Therefore,

$$G(s) = \frac{X(s)}{s}$$

or

$$\int_{0^-}^{t} x(\tau)\,d\tau \Longleftrightarrow \frac{X(s)}{s}$$

To prove the second part of Eq. (6.20), observe that

$$\int_{-\infty}^{t} x(\tau)\,d\tau = \int_{-\infty}^{0^-} x(\tau)\,d\tau + \int_{0^-}^{t} x(\tau)\,d\tau$$

Note that the first term on the right-hand side is a constant for $t \geq 0$. Taking the Laplace transform of the foregoing equation and using the first part of Eq. (6.20), we obtain

$$\int_{-\infty}^{t} x(\tau)\,d\tau \Longleftrightarrow \frac{\int_{-\infty}^{0^-} x(\tau)\,d\tau}{s} + \frac{X(s)}{s}$$

6.2.5 The Scaling Property

The scaling property states that if

$$x(t) \Longleftrightarrow X(s)$$

then for $a > 0$

$$x(at) \Longleftrightarrow \frac{1}{a}X\left(\frac{s}{a}\right)$$

The proof is identical to that of the scaling property of the Fourier transform derived in Ch. 4. Note that a is restricted to positive values because if $x(t)$ is causal, then $x(at)$ is anticausal (is zero for $t \geq 0$) for negative a, and anticausal signals are not permitted in the (unilateral) Laplace transform.

Recall that $x(at)$ is the signal $x(t)$ time-compressed by the factor a, and $X(\frac{s}{a})$ is $X(s)$ expanded along the s scale by the same factor a (see Sec. 1.2.2). The scaling property states that *time compression of a signal by a factor a causes expansion of its Laplace transform in the s scale by the same factor. Similarly, time expansion $x(t)$ causes compression of $X(s)$ in the s scale by the same factor.*

6.2.6 Time Convolution and Frequency Convolution

Another pair of properties states that if

$$x_1(t) \Longleftrightarrow X_1(s) \qquad \text{and} \qquad x_2(t) \Longleftrightarrow X_2(s)$$

then (*time-convolution property*)

$$x_1(t) * x_2(t) \Longleftrightarrow X_1(s)X_2(s) \tag{6.21}$$

and (*frequency-convolution property*)

$$x_1(t)x_2(t) \Longleftrightarrow \frac{1}{2\pi j}[X_1(s) * X_2(s)]$$

Observe the symmetry (or duality) between the two properties. Proofs of these properties are similar to the proofs in Ch. 4 for the Fourier transform.

Equation (2.39) indicates that $H(s)$, the transfer function of an LTIC system, is the Laplace transform of the system's impulse response $h(t)$; that is,

$$h(t) \Longleftrightarrow H(s)$$

If the system is causal, $h(t)$ is causal, and, according to Eq. (2.39), $H(s)$ is the unilateral Laplace transform of $h(t)$. Similarly, if the system is noncausal, $h(t)$ is noncausal, and $H(s)$ is the bilateral transform of $h(t)$.

We can apply the time-convolution property to the LTIC input–output relationship $y(t) = x(t) * h(t)$ to obtain

$$Y(s) = X(s)H(s) \tag{6.22}$$

The response $y(t)$ is the zero-state response of the LTIC system to the input $x(t)$. From Eq. (6.22), it follows that

$$H(s) = \frac{Y(s)}{X(s)} = \frac{\mathcal{L}[\text{zero-state response}]}{\mathcal{L}[\text{input}]} \tag{6.23}$$

This may be considered an alternate definition of the LTIC system transfer function $H(s)$. It is the *ratio of the transform of zero-state response to the transform of the input.*

EXAMPLE 6.10 Time-Convolution Property

Use the time-convolution property of the Laplace transform to determine $c(t) = e^{at}u(t) * e^{bt}u(t)$.

From Eq. (6.21), it follows that

$$C(s) = \frac{1}{(s-a)(s-b)} = \frac{1}{a-b}\left[\frac{1}{s-a} - \frac{1}{s-b}\right]$$

The inverse transform of this equation yields

$$c(t) = \frac{1}{a-b}(e^{at} - e^{bt})u(t)$$

Initial and Final Values

In certain applications, it is desirable to know the values of $x(t)$ as $t \to 0$ and $t \to \infty$ [initial and final values of $x(t)$] from the knowledge of its Laplace transform $X(s)$. Initial and final value theorems provide such information.

The initial value theorem states that if $x(t)$ and its derivative dx/dt are both Laplace transformable, then

$$x(0^+) = \lim_{s\to\infty} sX(s) \tag{6.24}$$

provided the limit on the right-hand side of Eq. (6.24) exists.

The final value theorem states that if both $x(t)$ and dx/dt are Laplace transformable, then

$$\lim_{t\to\infty} x(t) = \lim_{s\to 0} sX(s) \tag{6.25}$$

provided $sX(s)$ has no poles in the RHP or on the imaginary axis. To prove these theorems, we begin by setting $n = 1$ in Eq. (6.19). Using the definition of the Laplace transform, we see that

$$\begin{aligned} sX(s) - x(0^-) &= \int_{0^-}^{\infty} \frac{dx(t)}{dt} e^{-st}\,dt \\ &= \int_{0^-}^{0^+} \frac{dx(t)}{dt} e^{-st}\,dt + \int_{0^+}^{\infty} \frac{dx(t)}{dt} e^{-st}\,dt \\ &= x(t)\Big|_{0^-}^{0^+} + \int_{0^+}^{\infty} \frac{dx(t)}{dt} e^{-st}\,dt \\ &= x(0^+) - x(0^-) + \int_{0^+}^{\infty} \frac{dx(t)}{dt} e^{-st}\,dt \end{aligned}$$

Therefore,

$$sX(s) = x(0^+) + \int_{0^+}^{\infty} \frac{dx(t)}{dt} e^{-st}\,dt$$

and

$$\begin{aligned} \lim_{s\to\infty} sX(s) &= x(0^+) + \lim_{s\to\infty} \int_{0^+}^{\infty} \frac{dx(t)}{dt} e^{-st}\,dt \\ &= x(0^+) + \int_{0^+}^{\infty} \frac{dx(t)}{dt} \left(\lim_{s\to\infty} e^{-st}\right) dt \\ &= x(0^+) \end{aligned}$$

Comment. The initial value theorem applies only if $X(s)$ is strictly proper ($M < N$), because for $M \geq N$, $\lim_{s\to\infty} sX(s)$ does not exist, and the theorem does not apply. In such a case, we can still find the answer by using long division to express $X(s)$ as a polynomial in s plus a strictly proper fraction, where $M < N$. For example, by using long division, we can express

$$\frac{s^3 + 3s^2 + s + 1}{s^2 + 2s + 1} = (s + 1) - \frac{2s}{s^2 + 2s + 1}$$

The inverse transform of the polynomial in s is in terms of $\delta(t)$, and its derivatives, which are zero at $t = 0^+$. In the foregoing case, the inverse transform of $s + 1$ is $\dot{\delta}(t) + \delta(t)$. Hence, the desired $x(0^+)$ is the value of the remainder (strictly proper) fraction, for which the initial value theorem applies. In the present case,

$$x(0^+) = \lim_{s\to\infty} \frac{-2s^2}{s^2+2s+1} = -2$$

To prove the final value theorem, we let $n = 1$ and $s \to 0$ in Eq. (6.19) to obtain

$$\lim_{s\to 0}[sX(s) - x(0^-)] = \lim_{s\to 0} \int_{0^-}^{\infty} \frac{dx(t)}{dt} e^{-st}\, dt = \int_{0^-}^{\infty} \frac{dx(t)}{dt}\, dt$$
$$= x(t)\Big|_{0^-}^{\infty} = \lim_{t\to\infty} x(t) - x(0^-)$$

a deduction that leads to the desired result, Eq. (6.25).

Comment. The final value theorem applies only if the poles of $X(s)$ are in the LHP (including $s = 0$). If $X(s)$ has a pole in the RHP, $x(t)$ contains an exponentially growing term and $x(\infty)$ does not exist. If there is a pole on the imaginary axis, then $x(t)$ contains an oscillating term and $x(\infty)$ does not exist. However, if there is a pole at the origin, then $x(t)$ contains a constant term, and hence, $x(\infty)$ exists and is a constant.

EXAMPLE 6.11 Initial and Final Values

Determine the initial and final values of $y(t)$ if its Laplace transform $Y(s)$ is given by

$$Y(s) = \frac{10(2s+3)}{s(s^2+2s+5)}$$

Equations (6.24) and (6.25) yield

$$y(0^+) = \lim_{s\to\infty} sY(s) = \lim_{s\to\infty} \frac{10(2s+3)}{(s^2+2s+5)} = 0$$

$$y(\infty) = \lim_{s\to 0} sY(s) = \lim_{s\to 0} \frac{10(2s+3)}{(s^2+2s+5)} = 6$$

Table 6.2 summarizes the most important unilateral Laplace transform properties.

TABLE 6.2 Unilateral Laplace Transform Properties

Operation	$x(t)$	$X(s)$
Addition	$x_1(t)+x_2(t)$	$X_1(s)+X_2(s)$
Scalar multiplication	$kx(t)$	$kX(s)$
Time differentiation	$\frac{dx(t)}{dt}$	$sX(s)-x(0^-)$
	$\frac{d^2x(t)}{dt^2}$	$s^2X(s)-sx(0^-)-\dot{x}(0^-)$
	$\frac{d^3x(t)}{dt^3}$	$s^3X(s)-s^2x(0^-)-s\dot{x}(0^-)-\ddot{x}(0^-)$
	$\frac{d^nx(t)}{dt^n}$	$s^nX(s)-\sum_{k=1}^{n}s^{n-k}x^{(k-1)}(0^-)$
Time integration	$\int_{0^-}^{t}x(\tau)\,d\tau$	$\frac{1}{s}X(s)$
	$\int_{-\infty}^{t}x(\tau)\,d\tau$	$\frac{1}{s}X(s)+\frac{1}{s}\int_{-\infty}^{0^-}x(t)\,dt$
Time shifting	$x(t-t_0)u(t-t_0)$	$X(s)e^{-st_0}$ $t_0\geq 0$
Frequency shifting	$x(t)e^{s_0t}$	$X(s-s_0)$
Frequency differentiation	$-tx(t)$	$\frac{dX(s)}{ds}$
Frequency integration	$\frac{x(t)}{t}$	$\int_{s}^{\infty}X(z)\,dz$
Scaling	$x(at), a\geq 0$	$\frac{1}{a}X\left(\frac{s}{a}\right)$
Time convolution	$x_1(t)*x_2(t)$	$X_1(s)X_2(s)$
Frequency convolution	$x_1(t)x_2(t)$	$\frac{1}{2\pi j}X_1(s)*X_2(s)$
Initial value	$x(0^+)$	$\lim_{s\to\infty}sX(s)$ $(n>m)$
Final value	$x(\infty)$	$\lim_{s\to 0}sX(s)$ [poles of $sX(s)$ in LHP]

6.3 SOLUTION OF DIFFERENTIAL AND INTEGRO-DIFFERENTIAL EQUATIONS

The time-differentiation property of the Laplace transform has set the stage for solving linear differential (or integro-differential) equations with constant coefficients. Because $d^ky/dt^k \Longleftrightarrow s^kY(s)$, the Laplace transform of a differential equation is an algebraic equation that can be readily solved for $Y(s)$. Next we take the inverse Laplace transform of $Y(s)$ to find the desired solution $y(t)$. The following examples demonstrate the Laplace transform procedure for solving linear differential equations with constant coefficients.

EXAMPLE 6.12 Laplace Transform to Solve a Second-Order Linear Differential Equation

Solve the second-order linear differential equation

$$(D^2+5D+6)y(t)=(D+1)x(t)$$

for the initial conditions $y(0^-)=2$ and $\dot{y}(0^-)=1$ and the input $x(t)=e^{-4t}u(t)$.

The equation is

$$\frac{d^2y(t)}{dt^2}+5\frac{dy(t)}{dt}+6y(t)=\frac{dx(t)}{dt}+x(t) \tag{6.26}$$

Let

$$y(t)\Longleftrightarrow Y(s)$$

Then from Eq. (6.19),

$$\frac{dy(t)}{dt}\Longleftrightarrow sY(s)-y(0^-)=sY(s)-2$$

and

$$\frac{d^2y(t)}{dt^2}\Longleftrightarrow s^2Y(s)-sy(0^-)-\dot{y}(0^-)=s^2Y(s)-2s-1$$

Moreover, for $x(t)=e^{-4t}u(t)$,

$$X(s)=\frac{1}{s+4}\quad\text{and}\quad\frac{dx(t)}{dt}\Longleftrightarrow sX(s)-x(0^-)=\frac{s}{s+4}-0=\frac{s}{s+4}$$

Taking the Laplace transform of Eq. (6.26), we obtain

$$[s^2Y(s)-2s-1]+5[sY(s)-2]+6Y(s)=\frac{s}{s+4}+\frac{1}{s+4}$$

Collecting all the terms of $Y(s)$ and the remaining terms separately on the left-hand side, we obtain

$$(s^2+5s+6)Y(s)-(2s+11)=\frac{s+1}{s+4} \tag{6.27}$$

Therefore,

$$(s^2+5s+6)Y(s)=(2s+11)+\frac{s+1}{s+4}=\frac{2s^2+20s+45}{s+4}$$

and

$$Y(s)=\frac{2s^2+20s+45}{(s^2+5s+6)(s+4)}=\frac{2s^2+20s+45}{(s+2)(s+3)(s+4)}$$

Expanding the right-hand side into partial fractions yields

$$Y(s) = \frac{13/2}{s+2} - \frac{3}{s+3} - \frac{3/2}{s+4}$$

The inverse Laplace transform of this equation yields

$$y(t) = \left(\tfrac{13}{2}e^{-2t} - 3e^{-3t} - \tfrac{3}{2}e^{-4t}\right)u(t) \tag{6.28}$$

Example 6.12 demonstrates the ease with which the Laplace transform can solve linear differential equations with constant coefficients. The method is general and can solve a linear differential equation with constant coefficients of any order.

Zero-Input and Zero-State Components of Response

The Laplace transform method gives the total response, which includes zero-input and zero-state components. It is possible to separate the two components if we so desire. The initial condition terms in the response give rise to the zero-input response. For instance, in Ex. 6.12, the terms attributable to initial conditions $y(0^-) = 2$ and $\dot{y}(0^-) = 1$ in Eq. (6.27) generate the zero-input response. These initial condition terms are $-(2s + 11)$, as seen in Eq. (6.27). The terms on the right-hand side are exclusively due to the input. Equation (6.27) is reproduced below with the proper labeling of the terms:

$$(s^2 + 5s + 6)\,Y(s) - (2s + 11) = \frac{s+1}{s+4}$$

so that

$$(s^2 + 5s + 6)\,Y(s) = \underbrace{(2s + 11)}_{\text{initial condition terms}} + \underbrace{\frac{s+1}{s+4}}_{\text{input terms}}$$

Therefore,

$$Y(s) = \underbrace{\frac{2s+11}{s^2+5s+6}}_{\text{ZIR}} + \underbrace{\frac{s+1}{(s+4)(s^2+5s+6)}}_{\text{ZSR}}$$

$$= \left[\frac{7}{s+2} - \frac{5}{s+3}\right] + \left[\frac{-1/2}{s+2} + \frac{2}{s+3} - \frac{3/2}{s+4}\right]$$

Taking the inverse transform of this equation yields

$$y(t) = \underbrace{\left(7e^{-2t} - 5e^{-3t}\right)u(t)}_{\text{ZIR}} + \underbrace{\left(-\tfrac{1}{2}e^{-2t} + 2e^{-3t} - \tfrac{3}{2}e^{-4t}\right)u(t)}_{\text{ZSR}}$$

6.3.1 Comments on Initial Conditions at 0^- and at 0^+

The initial conditions in Ex. 6.12 are $y(0^-) = 2$ and $\dot{y}(0^-) = 1$. If we let $t = 0$ in the total response in Eq. (6.28), we find $y(0) = 2$ and $\dot{y}(0) = 2$, which is at odds with the given initial conditions. Why? Because the initial conditions are given at $t = 0^-$ (just before the input is applied), when only the zero-input response is present. The zero-state response is the result of the input $x(t)$ applied at $t = 0$. Hence, this component does not exist at $t = 0^-$. Consequently, the initial conditions at $t = 0^-$ are satisfied by the zero-input response, not by the total response. We can readily verify in this example that the zero-input response does indeed satisfy the given initial conditions at $t = 0^-$. It is the total response that satisfies the initial conditions at $t = 0^+$, which are generally different from the initial conditions at 0^-.

There also exists a $\mathcal{L}_+$ version of the Laplace transform, which uses the initial conditions at $t = 0^+$ rather than at 0^- (as in our present $\mathcal{L}_-$ version). The $\mathcal{L}_+$ version, which was in vogue until the early 1960s, is identical to the $\mathcal{L}_-$ version except the limits of the Laplace integral [Eq. (6.11)] are from 0^+ to ∞. Hence, by definition, the origin $t = 0$ is excluded from the domain. This version, still used in some math books, has some serious difficulties. For instance, the Laplace transform of $\delta(t)$ is zero because $\delta(t) = 0$ for $t \geq 0^+$. Moreover, this approach is rather clumsy in the theoretical study of linear systems because the response obtained cannot be separated into zero-input and zero-state components. As we know, the zero-state component represents the system response as an explicit function of the input, and without knowing this component, it is not possible to assess the effect of the input on the system response in a general way. The $\mathcal{L}_+$ version can separate the response in terms of the natural and the forced components, which are not as interesting as the zero-input and the zero-state components. Note that we can always determine the natural and the forced components from the zero-input and the zero-state components [e.g., Eq. (2.44) from Eq. (2.43)], but the converse is not true. Because of these and some other problems, electrical engineers (wisely) started discarding the $\mathcal{L}_+$ version in the early 1960s.

It is interesting to note the time-domain duals of these two Laplace versions. The classical method is the dual of the $\mathcal{L}_+$ method, and the convolution (zero-input/zero-state) method is the dual of the $\mathcal{L}_-$ method. The first pair uses the initial conditions at 0^+, and the second pair uses those at $t = 0^-$. The first pair (the classical method and the $\mathcal{L}_+$ version) is awkward in the theoretical study of linear system analysis. It was no coincidence that the $\mathcal{L}_-$ version was adopted immediately after the introduction to the electrical engineering community of state-space analysis (which uses zero-input/zero-state separation of the output).

DRILL 6.7 Laplace Transform to Solve a Second-Order Linear Differential Equation

Solve

$$\frac{d^2y(t)}{dt^2} + 4\frac{dy(t)}{dt} + 3y(t) = 2\frac{dx(t)}{dt} + x(t)$$

for the input $x(t) = u(t)$. The initial conditions are $y(0^-) = 1$ and $\dot{y}(0^-) = 2$.

ANSWER

$y(t) = \frac{1}{3}(1 + 9e^{-t} - 7e^{-3t})u(t)$

EXAMPLE 6.13 Laplace Transform to Solve an Electric Circuit

In the circuit of Fig. 6.8a, the switch is in the closed position for a long time before $t = 0$, when it is opened instantaneously. Find the inductor current $y(t)$ for $t \geq 0$.

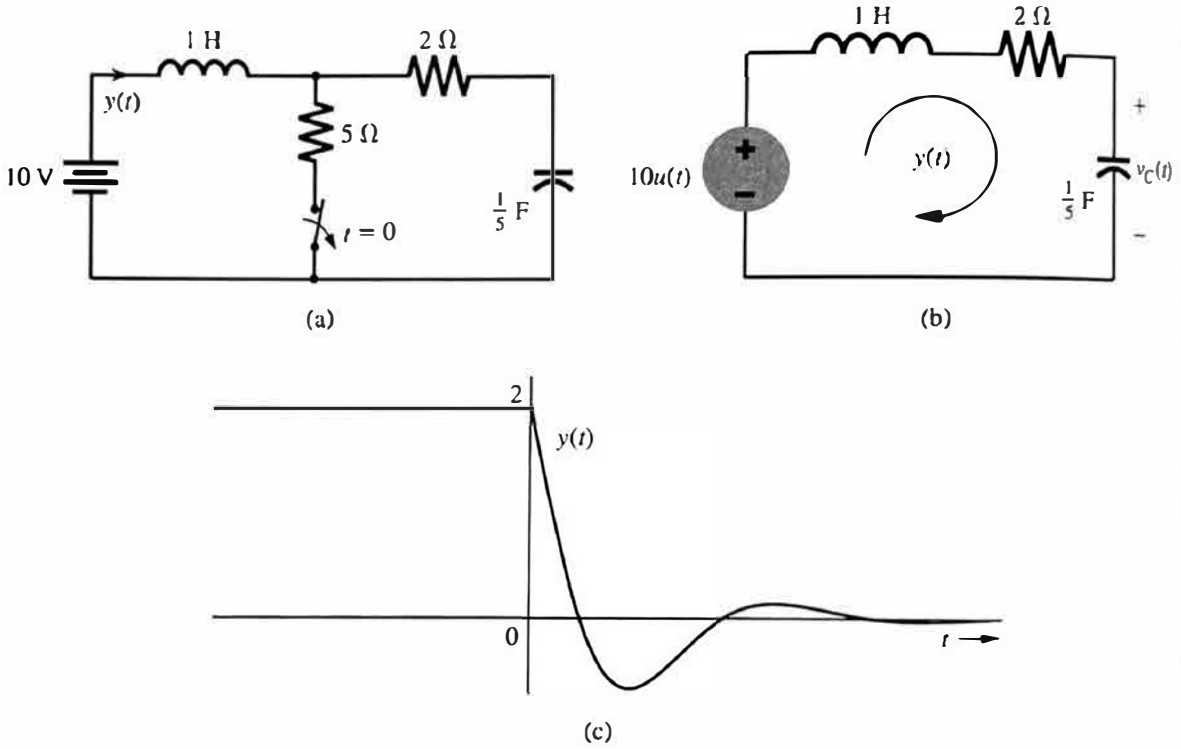

Figure 6.8 Analysis of a network with a switching action.

When the switch is in the closed position (for a long time), the inductor current is 2 amperes and the capacitor voltage is 10 volts. When the switch is opened, the circuit is equivalent to that depicted in Fig. 6.8b, with the initial inductor current $y(0^-) = 2$ and the initial capacitor voltage $v_C(0^-) = 10$. The input voltage is 10 volts, starting at $t = 0$, and, therefore, can be represented by $10u(t)$.

The loop equation of the circuit in Fig. 6.8b is

$$\frac{dy(t)}{dt} + 2y(t) + 5\int_{-\infty}^{t} y(\tau)\,d\tau = 10u(t) \tag{6.29}$$

If

$$y(t) \Longleftrightarrow Y(s)$$

then

$$\frac{dy(t)}{dt} \Longleftrightarrow sY(s) - y(0^-) = sY(s) - 2$$

and [see Eq. (6.20)]

$$\int_{-\infty}^{t} y(\tau)\,d\tau \Longleftrightarrow \frac{Y(s)}{s} + \frac{\int_{-\infty}^{0^-} y(\tau)\,d\tau}{s}$$

Because $y(t)$ is the capacitor current, the integral $\int_{-\infty}^{0^-} y(\tau)\,d\tau$ is $q_C(0^-)$, the capacitor charge at $t = 0^-$, which is given by C times the capacitor voltage at $t = 0^-$. Therefore,

$$\int_{-\infty}^{0^-} y(\tau)\,d\tau = q_C(0^-) = Cv_C(0^-) = \tfrac{1}{5}(10) = 2$$

and

$$\int_{-\infty}^{t} y(\tau)\,d\tau \Longleftrightarrow \frac{Y(s)}{s} + \frac{2}{s}$$

Using these results, the Laplace transform of Eq. (6.29) is

$$sY(s) - 2 + 2Y(s) + \frac{5Y(s)}{s} + \frac{10}{s} = \frac{10}{s}$$

or

$$\left[s + 2 + \frac{5}{s}\right] Y(s) = 2$$

and

$$Y(s) = \frac{2s}{s^2 + 2s + 5}$$

To find the inverse Laplace transform of $Y(s)$, we use pair 10c (Table 6.1) with values $A = 2$, $B = 0$, $a = 1$, and $c = 5$. This yields

$$r = \sqrt{\tfrac{20}{4}} = \sqrt{5}, \quad b = \sqrt{c - a^2} = 2, \quad \text{and} \quad \theta = \tan^{-1}\left(\tfrac{2}{4}\right) = 26.6^\circ$$

Therefore,

$$y(t) = \sqrt{5}e^{-t}\cos(2t + 26.6^\circ)u(t)$$

This response is shown in Fig. 6.8c.

Comment. In our discussion so far, we have multiplied input signals by $u(t)$, implying that the signals are zero prior to $t = 0$. This is needlessly restrictive. These signals can have any arbitrary value prior to $t = 0$. As long as the initial conditions at $t = 0$ are specified, we need only the knowledge of the input for $t \geq 0$ to compute the response for $t \geq 0$. Some authors use the notation $1(t)$ to denote a function that is equal to $u(t)$ for $t \geq 0$ and that has arbitrary value for negative t. We have abstained from this usage to avoid needless confusion caused by the introduction of a new function, which is very similar to $u(t)$.

6.3.2 Zero-State Response

Consider an Nth-order LTIC system specified by the equation

$$Q(D)y(t) = P(D)x(t)$$

or

$$(D^N + a_1 D^{N-1} + \cdots + a_{N-1}D + a_N)y(t) = (b_0 D^N + b_1 D^{N-1} + \cdots + b_{N-1}D + b_N)x(t) \quad (6.30)$$

We shall now find the general expression for the zero-state response of an LTIC system. Zero-state response $y(t)$, by definition, is the system response to an input when the system is initially relaxed (in zero state). Therefore, $y(t)$ satisfies Eq. (6.30) with zero initial conditions

$$y(0^-) = \dot{y}(0^-) = \ddot{y}(0^-) = \cdots = y^{(N-1)}(0^-) = 0$$

Moreover, the input $x(t)$ is causal so that

$$x(0^-) = \dot{x}(0^-) = \ddot{x}(0^-) = \cdots = x^{(N-1)}(0^-) = 0$$

Let

$$y(t) \Longleftrightarrow Y(s) \qquad \text{and} \qquad x(t) \Longleftrightarrow X(s)$$

Because of zero initial conditions,

$$D^r y(t) = \frac{d^r}{dt^r} y(t) \Longleftrightarrow s^r Y(s)$$
$$D^k x(t) = \frac{d^k}{dt^k} x(t) \Longleftrightarrow s^k X(s)$$

Therefore, the Laplace transform of Eq. (6.30) yields

$$(s^N + a_1 s^{N-1} + \cdots + a_{N-1}s + a_N)Y(s) = (b_0 s^N + b_1 s^{N-1} + \cdots + b_{N-1}s + b_N)X(s)$$

or

$$Y(s) = \frac{b_0 s^N + b_1 s^{N-1} + \cdots + b_{N-1}s + b_N}{s^N + a_1 s^{N-1} + \cdots + a_{N-1}s + a_N} X(s) = \frac{P(s)}{Q(s)} X(s)$$

But we have shown in Eq. (6.22) that $Y(s) = H(s)X(s)$. Consequently,

$$H(s) = \frac{P(s)}{Q(s)} \quad (6.31)$$

This is the transfer function of a linear differential system specified in Eq. (6.30). The same result has been derived earlier in Eq. (2.41) using an alternate (time-domain) approach.

We have shown that $Y(s)$, the Laplace transform of the zero-state response $y(t)$, is the product of $X(s)$ and $H(s)$, where $X(s)$ is the Laplace transform of the input $x(t)$ and $H(s)$ is the system transfer function [relating the particular output $y(t)$ to the input $x(t)$].

Intuitive Interpretation of the Laplace Transform

So far we have treated the Laplace transform as a machine that converts linear integro-differential equations into algebraic equations. There is no physical understanding of how this is accomplished or what it means. We now discuss a more intuitive interpretation and meaning of the Laplace transform.

In Ch. 2, Eq. (2.38), we showed that LTI system response to an everlasting exponential e^{st} is $H(s)e^{st}$. If we could express every signal as a linear combination of everlasting exponentials of the form e^{st}, we could readily obtain the system response to any input. For example, if

$$x(t) = \sum_{k=1}^{K} X(s_i)e^{s_i t}$$

the response of an LTIC system to such input $x(t)$ is given by

$$y(t) = \sum_{k=1}^{K} X(s_i)H(s_i)e^{s_i t}$$

Unfortunately, the class of signals that can be expressed in this form is very small. However, we can express almost all signals of practical utility as a sum of everlasting exponentials over a continuum of frequencies. This is precisely what the Laplace transform in Eq. (6.5) does.

$$x(t) = \frac{1}{2\pi j}\int_{c-j\infty}^{c+j\infty} X(s)e^{st}\,ds \tag{6.32}$$

Invoking the linearity property of the Laplace transform, we can find the system response $y(t)$ to input $x(t)$ in Eq. (6.32) as[†]

$$y(t) = \frac{1}{2\pi j}\int_{c'-j\infty}^{c'+j\infty} X(s)H(s)e^{st}\,ds = \mathcal{L}^{-1}X(s)H(s) \tag{6.33}$$

Clearly,

$$Y(s) = X(s)H(s)$$

We can now represent the transformed version of the system, as depicted in Fig. 6.9a. The input $X(s)$ is the Laplace transform of $x(t)$, and the output $Y(s)$ is the Laplace transform of (the zero-input response) $y(t)$. The system is described by the transfer function $H(s)$. The output $Y(s)$ is the product $X(s)H(s)$.

Recall that s is the complex frequency of e^{st}. This explains why the Laplace transform method is also called the *frequency-domain* method. Note that $X(s), Y(s)$, and $H(s)$ are the frequency-domain representations of $x(t), y(t)$, and $h(t)$, respectively. We may view the boxes marked $\mathcal{L}$ and $\mathcal{L}^{-1}$ in Fig. 6.9a as the interfaces that convert the time-domain entities into the corresponding frequency-domain entities, and vice versa. All real-life signals begin in the time domain, and the final answers must also be in the time domain. First, we convert the time-domain input(s) into the frequency-domain counterparts. The problem itself is solved in the frequency domain, resulting in the answer $Y(s)$, also in the frequency domain. Finally, we convert

[†] Recall that $H(s)$ has its own region of validity. Hence, the limits of integration for the integral in Eq. (6.32) are modified in Eq. (6.33) to accommodate the region of existence (validity) of $X(s)$ as well as $H(s)$.

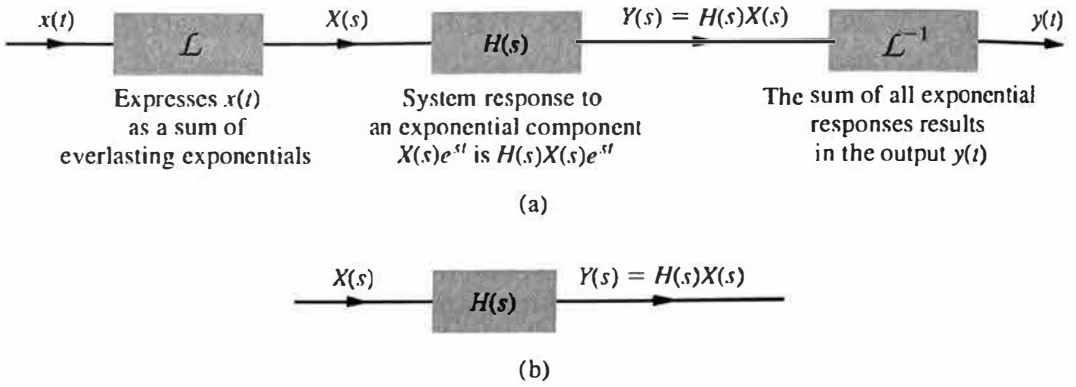

Figure 6.9 Alternate interpretation of the Laplace transform.

$Y(s)$ to $y(t)$. Solving the problem is relatively simpler in the frequency domain than in the time domain. Henceforth, we shall omit the explicit representation of the interface boxes $\mathcal{L}$ and $\mathcal{L}^{-1}$, representing signals and systems in the frequency domain, as shown in Fig. 6.9b.

EXAMPLE 6.14 Laplace Transform to Find the Zero-State Response

Find the response $y(t)$ of an LTIC system described by the equation

$$\frac{d^2y(t)}{dt^2}+5\frac{dy(t)}{dt}+6y(t)=\frac{dx(t)}{dt}+x(t)$$

if the input $x(t)=3e^{-5t}u(t)$ and all the initial conditions are zero; that is, the system is in the zero state.

The system equation is

$$\underbrace{(D^2+5D+6)\,y(t)}_{Q(D)}=\underbrace{(D+1)\,x(t)}_{P(D)}$$

Therefore,

$$H(s)=\frac{P(s)}{Q(s)}=\frac{s+1}{s^2+5s+6}$$

Also,

$$X(s)=\mathcal{L}[3e^{-5t}u(t)]=\frac{3}{s+5}$$

and

$$Y(s)=X(s)H(s)=\frac{3(s+1)}{(s+5)(s^2+5s+6)}$$

$$=\frac{3(s+1)}{(s+5)(s+2)(s+3)}=\frac{-2}{s+5}-\frac{1}{s+2}+\frac{3}{s+3}$$

The inverse Laplace transform of this equation is

$$y(t)=(-2e^{-5t}-e^{-2t}+3e^{-3t})u(t)$$

EXAMPLE 6.15 Laplace Transform to Find System Transfer Functions

Show that the transfer function of:

(a) an ideal delay of T seconds is e^{-sT}

(b) an ideal differentiator is s

(c) an ideal integrator is $1/s$

(a) Ideal Delay. For an ideal delay of T seconds, the input $x(t)$ and output $y(t)$ are related by

$$y(t) = x(t-T) \quad \text{and} \quad Y(s) = X(s)e^{-sT} \qquad \text{[see Eq. (6.16)]}$$

Therefore,

$$H(s) = \frac{Y(s)}{X(s)} = e^{-sT} \tag{6.34}$$

(b) Ideal Differentiator. For an ideal differentiator, the input $x(t)$ and the output $y(t)$ are related by

$$y(t) = \frac{dx(t)}{dt}$$

The Laplace transform of this equation yields

$$Y(s) = sX(s) \qquad [x(0^-) = 0 \text{ for a causal signal}]$$

and

$$H(s) = \frac{Y(s)}{X(s)} = s \tag{6.35}$$

(c) Ideal Integrator. For an ideal integrator with zero initial state, that is, $y(0^-) = 0$,

$$y(t) = \int_0^t x(\tau)\,d\tau \quad \text{and} \quad Y(s) = \frac{1}{s}X(s)$$

Therefore,

$$H(s) = \frac{1}{s} \tag{6.36}$$

DRILL 6.8 Differential Equation and Zero-State Response from a System Transfer Function

For an LTIC system with transfer function,

$$H(s) = \frac{s+5}{s^2+4s+3}$$

(a) Describe the differential equation relating the input $x(t)$ and output $y(t)$.

(b) Find the system response $y(t)$ to the input $x(t) = e^{-2t}u(t)$ if the system is initially in zero state.

ANSWERS

(a) $\dfrac{d^2y(t)}{dt^2} + 4\dfrac{dy(t)}{dt} + 3y(t) = \dfrac{dx(t)}{dt} + 5x(t)$

(b) $y(t) = (2e^{-t} - 3e^{-2t} + e^{-3t})u(t)$

6.3.3 Stability

Equation (6.31) shows that the denominator of $H(s)$ is $Q(s)$, which is apparently identical to the characteristic polynomial $Q(\lambda)$ defined in Ch. 2. Does this mean that the denominator of $H(s)$ is the characteristic polynomial of the system? This may or may not be the case, since if $P(s)$ and $Q(s)$ in Eq. (6.31) have any common factors, they cancel out, and the effective denominator of $H(s)$ is not necessarily equal to $Q(s)$. Recall also that the system transfer function $H(s)$, like $h(t)$, is defined in terms of measurements at the external terminals. Consequently, $H(s)$ and $h(t)$ are both external descriptions of the system. In contrast, the characteristic polynomial $Q(s)$ is an internal description. Clearly, we can determine only external stability, that is, BIBO stability, from $H(s)$. If all the poles of $H(s)$ are in the LHP, all the terms in $h(t)$ are decaying exponentials, and $h(t)$ is absolutely integrable [see Eq. (2.45)].† Consequently, the system is BIBO-stable. Otherwise, the system is BIBO-unstable.

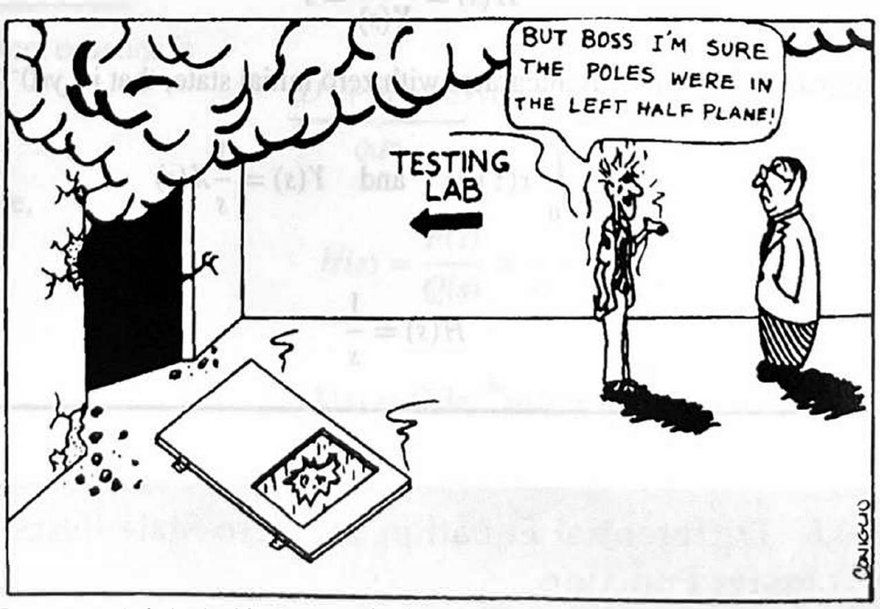

Beware of right half-plane poles!

† Values of s for which $H(s)$ is ∞ are the *poles* of $H(s)$. Thus, poles of $H(s)$ are the values of s for which the denominator of $H(s)$ is zero.

So far, we have assumed that $H(s)$ is a proper function, that is, $M \leq N$. We now show that if $H(s)$ is improper, that is, if $M > N$, the system is BIBO-unstable. In such a case, using long division, we obtain $H(s) = R(s) + H'(s)$, where $R(s)$ is an $(M-N)$th-order polynomial and $H'(s)$ is a proper transfer function. For example,

$$H(s) = \frac{s^3 + 4s^2 + 4s + 5}{s^2 + 3s + 2} = s + \frac{s^2 + 2s + 5}{s^2 + 3s + 2}$$

As shown in Eq. (6.35), the term s is the transfer function of an ideal differentiator. If we apply step function (bounded input) to this system, the output will contain an impulse (unbounded output). Clearly, the system is BIBO-unstable. Moreover, such a system greatly amplifies noise because differentiation enhances higher frequencies, which generally predominate in a noise signal. These are two good reasons to avoid improper systems ($M > N$). In our future discussion, we shall implicitly assume that the systems are proper, unless stated otherwise.

If $P(s)$ and $Q(s)$ do not have common factors, then the denominator of $H(s)$ is identical to $Q(s)$, the characteristic polynomial of the system. In this case, we can determine internal stability by using the criterion described in Sec. 2.5. Thus, if $P(s)$ and $Q(s)$ have no common factors, the asymptotic stability criterion in Sec. 2.5 can be restated in terms of the poles of the transfer function of a system, as follows:

1. An LTIC system is asymptotically stable if and only if all the poles of its transfer function $H(s)$ are in the LHP. The poles may be simple or repeated.
2. An LTIC system is unstable if and only if either one or both of the following conditions exist: (i) at least one pole of $H(s)$ is in the RHP; (ii) there are repeated poles of $H(s)$ on the imaginary axis.
3. An LTIC system is marginally stable if and only if there are no poles of $H(s)$ in the RHP and some unrepeated poles on the imaginary axis.

The locations of zeros of $H(s)$ have no role in determining the system stability.

EXAMPLE 6.16 BIBO and Asymptotic Stability

Figure 6.10a shows a cascade connection of two LTIC systems S_1 followed by S_2. The transfer functions of these systems are $H_1(s) = 1/(s-1)$ and $H_2(s) = (s-1)/(s+1)$, respectively. Determine the BIBO and asymptotic stability of the composite (cascade) system.

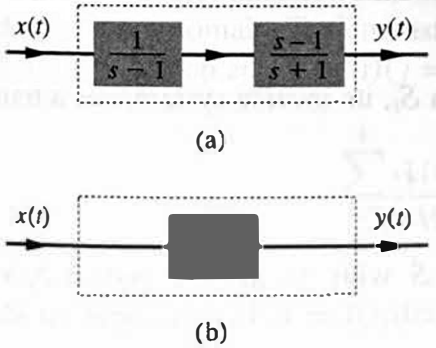

Figure 6.10 Distinction between BIBO and asymptotic stability.

If the impulse responses of $\mathcal{S}_1$ and $\mathcal{S}_2$ are $h_1(t)$ and $h_2(t)$, respectively, then the impulse response of the cascade system is $h(t) = h_1(t) * h_2(t)$. Hence, $H(s) = H_1(s)H_2(s)$. In the present case,

$$H(s) = \left(\frac{1}{s-1}\right)\left(\frac{s-1}{s+1}\right) = \frac{1}{s+1}$$

The pole of $\mathcal{S}_1$ at $s = 1$ cancels with the zero at $s = 1$ of $\mathcal{S}_2$. This results in a composite system having a single pole at $s = -1$. If the composite cascade system were to be enclosed inside a black box with only the input and the output terminals accessible, any measurement from these external terminals would show that the transfer function of the system is $1/(s+1)$, without any hint of the fact that the system is housing an unstable system (Fig. 6.10b).

The impulse response of the cascade system is $h(t) = e^{-t}u(t)$, which is absolutely integrable. Consequently, the system is BIBO-stable.

To determine the asymptotic stability, we note that $\mathcal{S}_1$ has one characteristic root at 1, and $\mathcal{S}_2$ also has one root at -1. Recall that the two systems are independent (one does not load the other), and the characteristic modes generated in each subsystem are independent of the other. Clearly, the mode e^t will not be eliminated by the presence of $\mathcal{S}_2$. Hence, the composite system has two characteristic roots, located at ± 1, and the system is asymptotically unstable, though BIBO-stable.

Interchanging the positions of $\mathcal{S}_1$ and $\mathcal{S}_2$ makes no difference in this conclusion. This example shows that BIBO stability can be misleading. If a system is asymptotically unstable, it will destroy itself (or, more likely, lead to a saturation condition) because of unchecked growth of the response due to intended or unintended stray initial conditions. BIBO stability is not going to save the system. Control systems are often compensated to realize certain desirable characteristics. One should never try to stabilize an unstable system by canceling its RHP pole(s) with RHP zero(s). Such a misguided attempt will fail, not because of the practical impossibility of exact cancellation but for the more fundamental reason, as just explained.

DRILL 6.9 BIBO and Asymptotic Stability

Show that an ideal integrator is marginally stable but BIBO-unstable.

6.3.4 Inverse Systems

If $H(s)$ is the transfer function of a system $\mathcal{S}$, then $\mathcal{S}_i$, its inverse system, has a transfer function $H_i(s)$ given by

$$H_i(s) = \frac{1}{H(s)}$$

This follows from the fact that the cascade of $\mathcal{S}$ with its inverse system $\mathcal{S}_i$ is an identity system, with impulse response $\delta(t)$, implying $H(s)H_i(s) = 1$. For example, an ideal integrator

and its inverse, an ideal differentiator, have transfer functions $1/s$ and s, respectively, leading to $H(s)H_i(s) = 1$.

6.4 Analysis of Electrical Networks: The Transformed Network

Example 6.12 shows how electrical networks may be analyzed by writing the integro-differential equation(s) of the system and then solving these equations by the Laplace transform. We now show that it is also possible to analyze electrical networks directly without having to write the integro-differential equations. This procedure is considerably simpler because it permits us to treat an electrical network as if it were a resistive network. For this purpose, we need to represent a network in the "frequency domain" where all the voltages and currents are represented by their Laplace transforms.

For the sake of simplicity, let us first discuss the case with zero initial conditions. If $v(t)$ and $i(t)$ are the voltage across and the current through an inductor of L henries, then

$$v(t) = L\frac{di(t)}{dt}$$

The Laplace transform of this equation (assuming zero initial current) is

$$V(s) = LsI(s)$$

Similarly, for a capacitor of C farads, the voltage-current relationship is $i(t) = C(dv/dt)$ and its Laplace transform, assuming zero initial capacitor voltage, yields $I(s) = CsV(s)$; that is,

$$V(s) = \frac{1}{Cs}I(s)$$

For a resistor of R ohms, the voltage-current relationship is $v(t) = Ri(t)$, and its Laplace transform is

$$V(s) = RI(s)$$

Thus, in the "frequency domain," the voltage-current relationships of an inductor and a capacitor are algebraic; these elements behave like resistors of "resistance" Ls and $1/Cs$, respectively. The generalized "resistance" of an element is called its *impedance* and is given by the ratio $V(s)/I(s)$ for the element (under zero initial conditions). The impedances of a resistor of R ohms, an inductor of L henries, and a capacitance of C farads are R, Ls, and $1/Cs$, respectively.

Also, the interconnection constraints (Kirchhoff's laws) remain valid for voltages and currents in the frequency domain. To demonstrate this point, let $v_j(t)$ $(j = 1, 2, \ldots, k)$ be the voltages across k elements in a loop and let $i_j(t)(j = 1, 2, \ldots, m)$ be the j currents entering a node. Then

$$\sum_{j=1}^{k} v_j(t) = 0 \quad \text{and} \quad \sum_{j=1}^{m} i_j(t) = 0$$

Now if

$$v_j(t) \Longleftrightarrow V_j(s) \quad \text{and} \quad i_j(t) \Longleftrightarrow I_j(s)$$

then

$$\sum_{j=1}^{k} V_j(s) = 0 \qquad \text{and} \qquad \sum_{j=1}^{m} I_j(s) = 0$$

This result shows that if we represent all the voltages and currents in an electrical network by their Laplace transforms, we can treat the network as if it consisted of the "resistances" R, Ls, and $1/Cs$ corresponding to a resistor R, an inductor L, and a capacitor C, respectively. The system equations (loop or node) are now algebraic. Moreover, the simplification techniques that have been developed for resistive circuits—equivalent series and parallel impedances, voltage and current divider rules, Thévenin and Norton theorems—can be applied to general electrical networks. The following examples demonstrate these concepts.

EXAMPLE 6.17 Transform Analysis of a Simple Circuit

Find the loop current $i(t)$ in the circuit shown in Fig. 6.11a if all the initial conditions are zero.

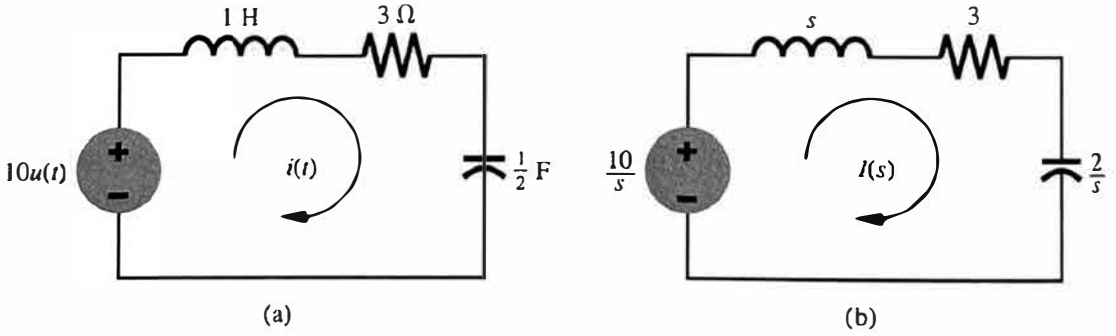

Figure 6.11 **(a)** A circuit and **(b)** its transformed version.

In the first step, we represent the circuit in the frequency domain, as illustrated in Fig. 6.11b. All the voltages and currents are represented by their Laplace transforms. The voltage $10u(t)$ is represented by $10/s$ and the (unknown) current $i(t)$ is represented by its Laplace transform $I(s)$. All the circuit elements are represented by their respective impedances. The inductor of 1 henry is represented by s, the capacitor of $1/2$ farad is represented by $2/s$, and the resistor of 3 ohms is represented by 3. We now consider the frequency-domain representation of voltages and currents. The voltage across any element is $I(s)$ times its impedance. Therefore, the total voltage drop in the loop is $I(s)$ times the total loop impedance, and it must be equal to $V(s)$, (transform of) the input voltage. The total impedance in the loop is

$$Z(s) = s + 3 + \frac{2}{s} = \frac{s^2 + 3s + 2}{s}$$

The input "voltage" is $V(s) = 10/s$. Therefore, the "loop current" $I(s)$ is

$$I(s) = \frac{V(s)}{Z(s)} = \frac{10/s}{(s^2+3s+2)/s} = \frac{10}{s^2+3s+2} = \frac{10}{(s+1)(s+2)} = \frac{10}{s+1} - \frac{10}{s+2}$$

The inverse transform of this equation yields the desired result:

$$i(t) = 10(e^{-t} - e^{-2t})u(t)$$

Initial Condition Generators

The discussion in which we assumed zero initial conditions can be readily extended to the case of nonzero initial conditions because the initial condition in a capacitor or an inductor can be represented by an equivalent source. We now show that a capacitor C with an initial voltage $v(0^-)$ (Fig. 6.12a) can be represented in the frequency domain by an uncharged capacitor of impedance $1/Cs$ in series with a voltage source of value $v(0^-)/s$ (Fig. 6.12b) or as the same uncharged capacitor in parallel with a current source of value $Cv(0^-)$ (Fig. 6.12c). Similarly, an inductor L with an initial current $i(0^-)$ (Fig. 6.12d) can be represented in the frequency domain by an inductor of impedance Ls in series with a voltage source of value $Li(0^-)$ (Fig. 6.12e) or by the same inductor in parallel with a current source of value $i(0^-)/s$ (Fig. 6.12f).

To prove this point, consider the terminal relationship of the capacitor in Fig. 6.12a:

$$i(t) = C\frac{dv(t)}{dt}$$

The Laplace transform of this equation yields

$$I(s) = C[sV(s) - v(0^-)]$$

This equation can be rearranged as

$$V(s) = \frac{1}{Cs}I(s) + \frac{v(0^-)}{s} \tag{6.37}$$

Observe that $V(s)$ is the voltage (in the frequency domain) across the charged capacitor and $I(s)/Cs$ is the voltage across the same capacitor without any charge. Therefore, the charged capacitor can be represented by the uncharged capacitor in series with a voltage source of value $v(0^-)/s$, as depicted in Fig. 6.12b. Equation (6.37) can also be rearranged as

$$V(s) = \frac{1}{Cs}[I(s) + Cv(0^-)]$$

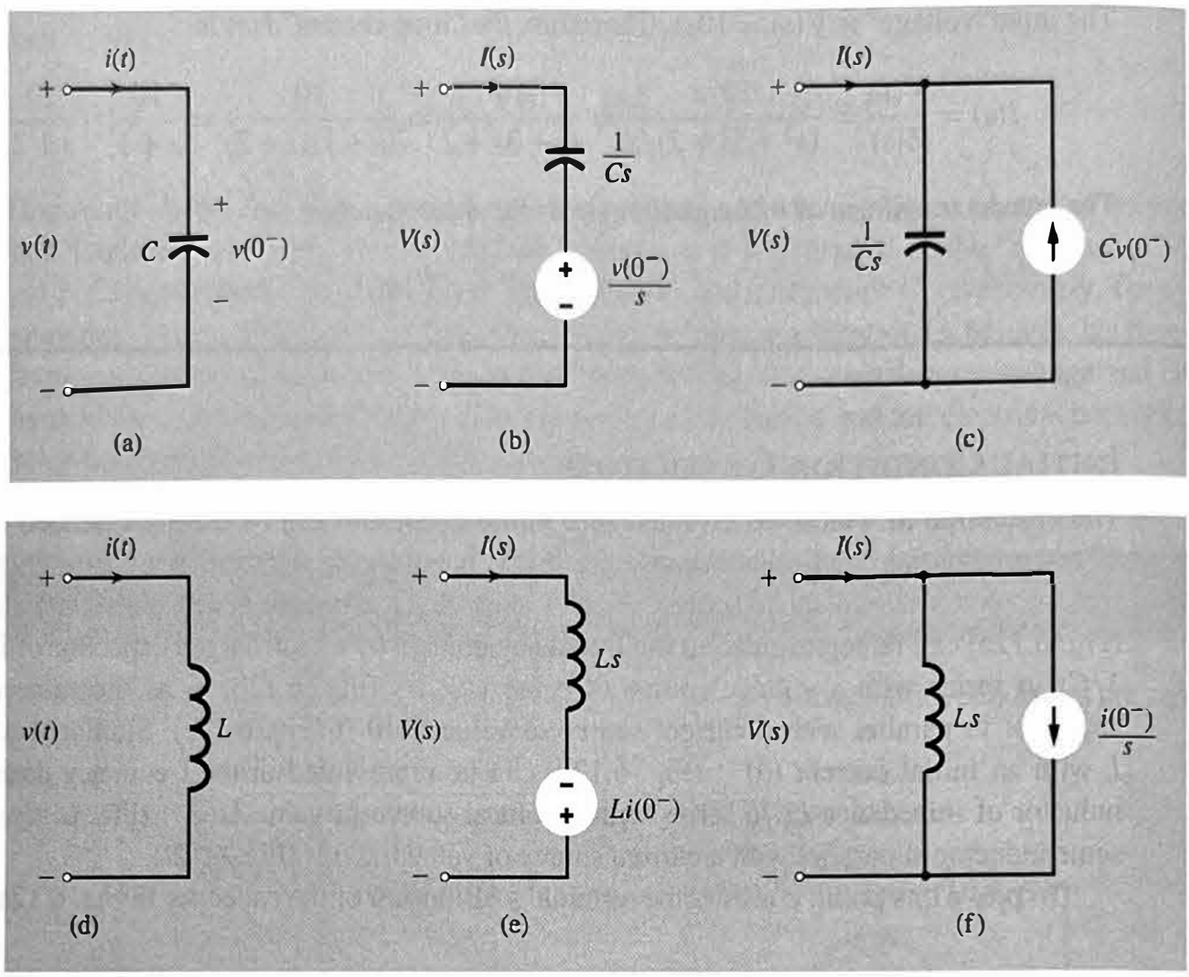

Figure 6.12 Initial condition generators for a capacitor and an inductor.

This equation shows that the charged capacitor voltage $V(s)$ is equal to the uncharged capacitor voltage caused by a current $I(s) + Cv(0^-)$. This result is reflected precisely in Fig. 6.12c, where the current through the uncharged capacitor is $I(s) + Cv(0^-)$.[†]

For the inductor in Fig. 6.12d, the terminal equation is

$$v(t) = L\frac{di(t)}{dt}$$

and

$$V(s) = L[sI(s) - i(0^-)] = LsI(s) - Li(0^-) \tag{6.38}$$

[†] In the time domain, a charged capacitor C with initial voltage $v(0^-)$ can be represented as the same capacitor uncharged in series with a voltage source $v(0^-)u(t)$, or in parallel with a current source $Cv(0^-)\delta(t)$. Similarly, an inductor L with initial current $i(0^-)$ can be represented by the same inductor with zero initial current in series with a voltage source $Li(0^-)\delta(t)$ or with a parallel current source $i(0^-)u(t)$.

This expression is consistent with Fig. 6.12e. We can rearrange Eq. (6.38) as

$$V(s) = Ls\left[I(s) - \frac{i(0^-)}{s}\right]$$

This expression is consistent with Fig. 6.12f.

Let us rework Ex. 6.13 using these concepts. Figure 6.13a shows the circuit in Fig. 6.8b with the initial conditions $y(0^-) = 2$ and $v_C(0^-) = 10$. Figure 6.13b shows the frequency-domain representation (transformed circuit) of the circuit in Fig. 6.13a. The resistor is represented by its impedance 2; the inductor with initial current of 2 amperes is represented according to the arrangement in Fig. 6.12e with a series voltage source $Ly(0^-) = 2$. The capacitor with an initial voltage of 10 volts is represented according to the arrangement in Fig. 6.12b with a series voltage source $v(0^-)/s = 10/s$. Note that the impedance of the inductor is s and that of the capacitor is $5/s$. The input of $10u(t)$ is represented by its Laplace transform $10/s$.

The total voltage in the loop is $(10/s) + 2 - (10/s) = 2$, and the loop impedance is $(s+2+(5/s))$. Therefore,

$$Y(s) = \frac{2}{s+2+5/s} = \frac{2s}{s^2+2s+5}$$

which confirms our earlier result in Ex. 6.13.

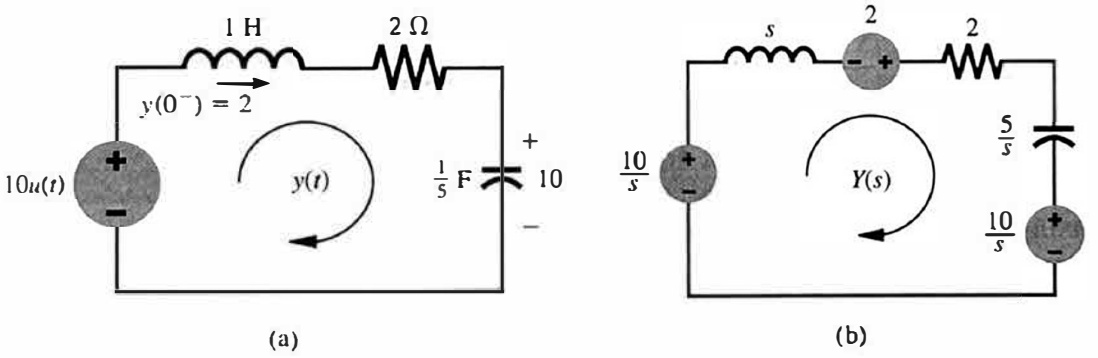

Figure 6.13 A circuit and its transformed version with initial condition generators.

EXAMPLE 6.18 Transformed Analysis of a Circuit with a Switch

The switch in the circuit of Fig. 6.14a is in the closed position for a long time before $t = 0$, when it is opened instantaneously. Find the currents $y_1(t)$ and $y_2(t)$ for $t \geq 0$.

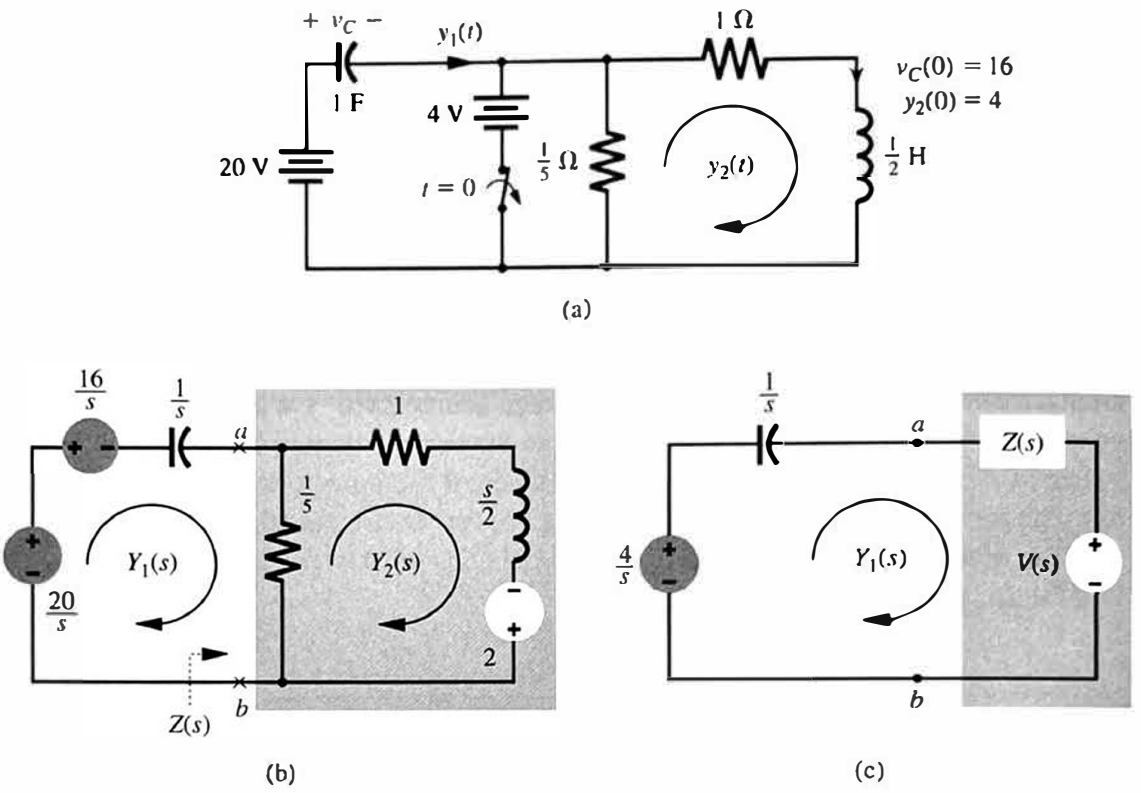

Figure 6.14 Using initial condition generators and Thévenin equivalent representation.

Inspection of this circuit shows that when the switch is closed and the steady-state conditions are reached, the capacitor voltage $v_C = 16$ volts, and the inductor current $y_2 = 4$ amperes. Therefore, when the switch is opened (at $t = 0$), the initial conditions are $v_C(0^-) = 16$ and $y_2(0^-) = 4$. Figure 6.14b shows the transformed version of the circuit in Fig. 6.14a. We have used equivalent sources to account for the initial conditions. The initial capacitor voltage of 16 volts is represented by a series voltage of $16/s$ and the initial inductor current of 4 amperes is represented by a source of value $Ly_2(0^-) = 2$.

From Fig. 6.14b, the loop equations can be written directly in the frequency domain as

$$\frac{Y_1(s)}{s} + \frac{1}{5}[Y_1(s) - Y_2(s)] = \frac{4}{s}$$

$$-\frac{1}{5}Y_1(s) + \frac{6}{5}Y_2(s) + \frac{s}{2}Y_2(s) = 2$$

$$\begin{bmatrix} \frac{1}{s} + \frac{1}{5} & -\frac{1}{5} \\ -\frac{1}{5} & \frac{6}{5} + \frac{s}{2} \end{bmatrix} \begin{bmatrix} Y_1(s) \\ Y_2(s) \end{bmatrix} = \begin{bmatrix} \frac{4}{s} \\ 2 \end{bmatrix}$$

Application of Cramer's rule to this equation yields

$$Y_1(s) = \frac{24(s+2)}{s^2 + 7s + 12} = \frac{24(s+2)}{(s+3)(s+4)} = \frac{-24}{s+3} + \frac{48}{s+4}$$

and

$$y_1(t) = (-24e^{-3t} + 48e^{-4t})u(t)$$

Similarly, we obtain

$$Y_2(s) = \frac{4(s+7)}{s^2+7s+12} = \frac{16}{s+3} - \frac{12}{s+4}$$

and

$$y_2(t) = (16e^{-3t} - 12e^{-4t})u(t)$$

We also could have used Thévenin's theorem to compute $Y_1(s)$ and $Y_2(s)$ by replacing the circuit to the right of the capacitor (right of terminals ab) with its Thévenin equivalent, as shown in Fig. 6.14c. Figure 6.14b shows that the Thévenin impedance $Z(s)$ and the Thévenin source $V(s)$ are

$$Z(s) = \frac{\frac{1}{5}\left(\frac{s}{2}+1\right)}{\frac{1}{5}+\frac{s}{2}+1} = \frac{s+2}{5s+12}$$

$$V(s) = \frac{-\frac{1}{5}}{\frac{1}{5}+\frac{s}{2}+1}2 = \frac{-4}{5s+12}$$

According to Fig. 6.14c, the current $Y_1(s)$ is given by

$$Y_1(s) = \frac{\frac{4}{s} - V(s)}{\frac{1}{s} + Z(s)} = \frac{24(s+2)}{s^2+7s+12}$$

which confirms the earlier result. We may determine $Y_2(s)$ in a similar manner.

EXAMPLE 6.19 Transformed Analysis of a Coupled Inductive Network

The switch in the circuit in Fig. 6.15a is at position a for a long time before $t = 0$, when it is moved instantaneously to position b. Determine the current $y_1(t)$ and the output voltage $v_0(t)$ for $t \geq 0$.

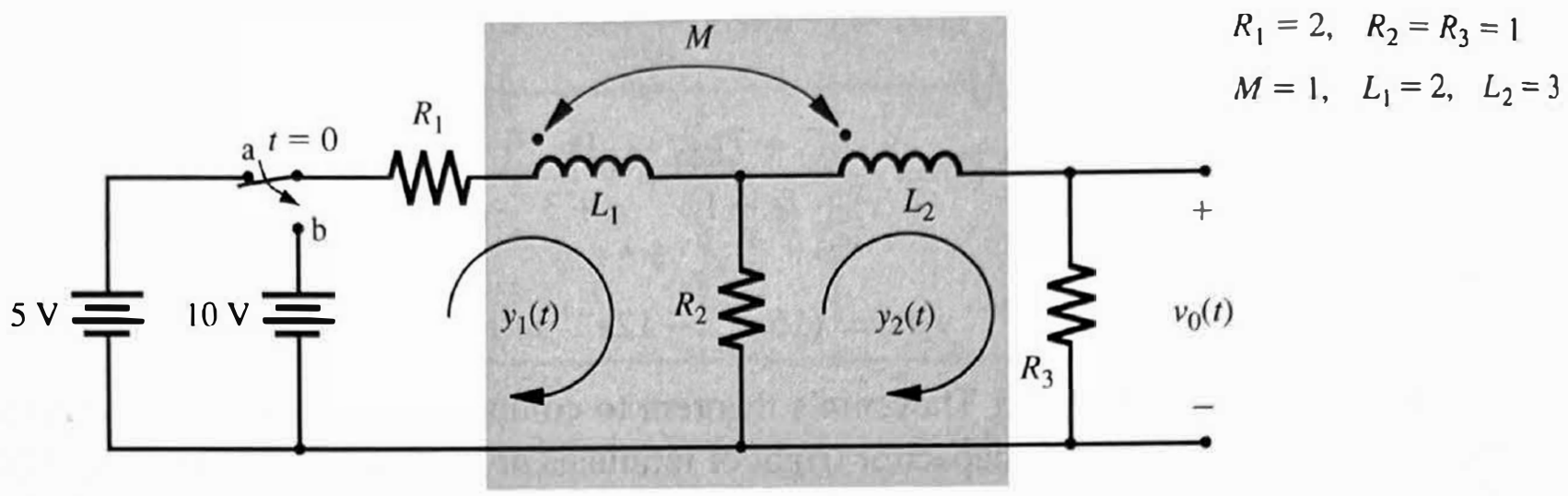

Figure 6.15 Solution of a coupled inductive network by the transformed circuit method.

Just before switching, the values of the loop currents are 2 and 1, respectively, that is, $y_1(0^-) = 2$ and $y_2(0^-) = 1$.

The equivalent circuits for two types of inductive coupling are illustrated in Figs. 6.15b and 6.15c. For our situation, the circuit in Fig. 6.15c applies. Figure 6.15d shows the transformed version of the circuit in Fig. 6.15a after switching. Note that the inductors $L_1 + M$, $L_2 + M$,

and $-M$ are 3, 4, and -1 henries with impedances $3s$, $4s$, and $-s$, respectively. The initial condition voltages in the three branches are $(L_1 + M)y_1(0^-) = 6$, $(L_2 + M)y_2(0^-) = 4$, and $-M[y_1(0^-) - y_2(0^-)] = -1$, respectively. The two loop equations of the circuit are

$$(2s+3)Y_1(s) + (s-1)Y_2(s) = \frac{10}{s} + 5$$
$$(s-1)Y_1(s) + (3s+2)Y_2(s) = 5$$

or

$$\begin{bmatrix} 2s+3 & s-1 \\ s-1 & 3s+2 \end{bmatrix} \begin{bmatrix} Y_1(s) \\ Y_2(s) \end{bmatrix} = \begin{bmatrix} \frac{5s+10}{s} \\ 5 \end{bmatrix}$$

Solving for $Y_1(s)$, we obtain

$$Y_1(s) = \frac{2s^2+9s+4}{s(s^2+3s+1)} = \frac{4}{s} - \frac{1}{s+0.382} - \frac{1}{s+2.618}$$

Therefore,

$$y_1(t) = (4 - e^{-0.382t} - e^{-2.618t})u(t)$$

Similarly,

$$Y_2(s) = \frac{s^2+2s+2}{s(s^2+3s+1)} = \frac{2}{s} - \frac{1.618}{s+0.382} + \frac{0.618}{s+2.618}$$

and

$$y_2(t) = (2 - 1.618e^{-0.382t} + 0.618e^{-2.618t})u(t)$$

The output voltage is therefore

$$v_0(t) = y_2(t) = (2 - 1.618e^{-0.382t} + 0.618e^{-2.618t})u(t)$$

DRILL 6.10 Transformed Analysis of an *RLC* Circuit with a Switch

For the *RLC* circuit in Fig. 6.16, the input is switched on at $t = 0$. The initial conditions are $y(0^-) = 2$ amperes and $v_C(0^-) = 50$ volts. Find the loop current $y(t)$ and the capacitor voltage $v_C(t)$ for $t \geq 0$.

ANSWER

$y(t) = 10\sqrt{2}e^{-t}\cos(2t + 81.8°)u(t)$ and $v_C(t) = [24 + 31.62e^{-t}\cos(2t - 34.7°)]u(t)$

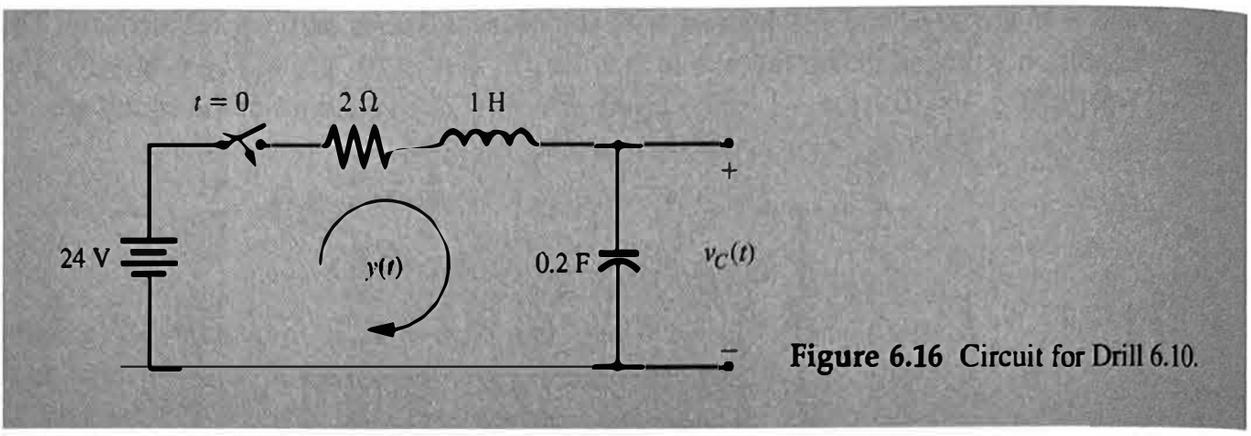

Figure 6.16 Circuit for Drill 6.10.

6.4.1 Analysis of Active Circuits

Although we have considered examples of only passive networks so far, the circuit analysis procedure using the Laplace transform is also applicable to active circuits. All that is needed is to replace the active elements with their mathematical models (or equivalent circuits) and proceed as before.

The operational amplifier (depicted by the triangular symbol in Fig. 6.17a) is a well-known element in modern electronic circuits. The terminals with the positive and the negative signs correspond to noninverting and inverting terminals, respectively. This means that the polarity of the output voltage v_2 is the same as that of the input voltage at the terminal marked by the positive sign (noninverting). The opposite is true for the inverting terminal, marked by the negative sign.

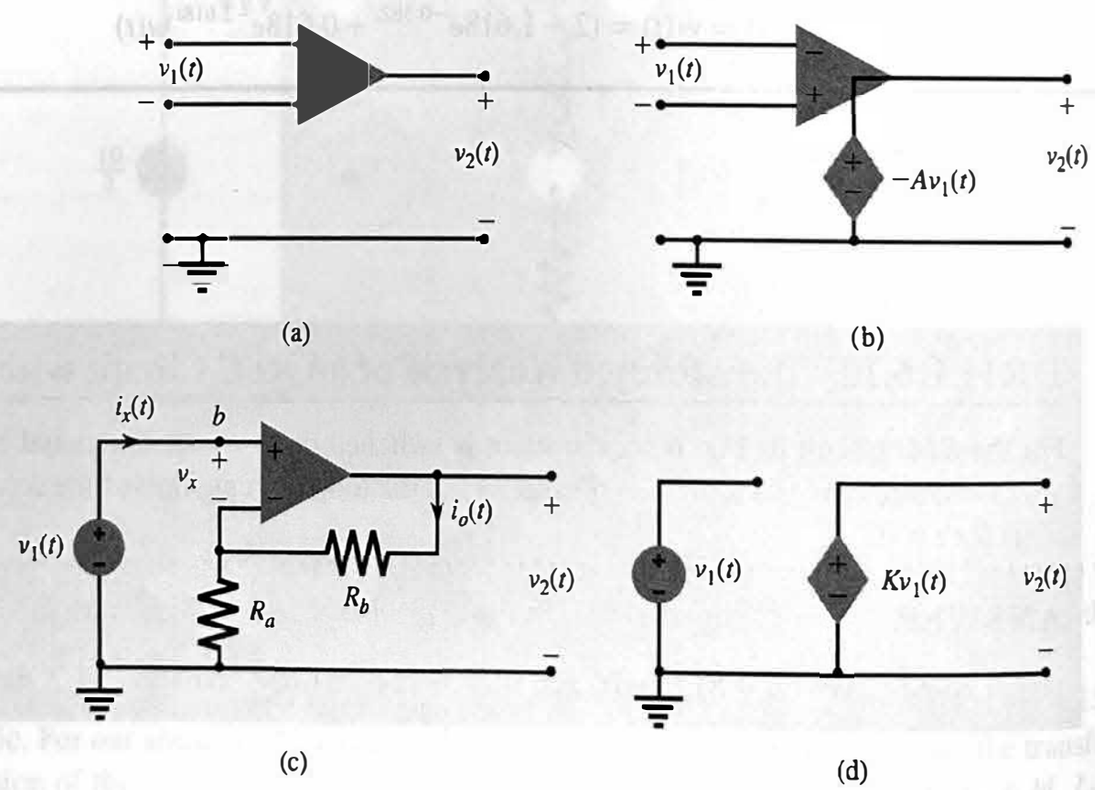

Figure 6.17 Operational amplifier and its equivalent circuit.

Figure 6.17b shows the model (equivalent circuit) of the operational amplifier (op amp) in Fig. 6.17a. A typical op amp has a very large gain. The output voltage $v_2 = -Av_1$, where A is typically 10^5 to 10^6. The input impedance is very high, on the order of 10^{12} ohms, and the output impedance is very low (50–100 ohms). For most applications, we are justified in assuming the gain A and the input impedance to be infinite and the output impedance to be zero. For this reason, we see an ideal voltage source at the output.

Consider now the operational amplifier with resistors R_a and R_b connected, as shown in Fig. 6.17c. This configuration is known as the *noninverting amplifier*. Observe that the input polarities in this configuration are inverted in comparison to those in Fig. 6.17a. We now show that the output voltage v_2 and the input voltage v_1 in this case are related by

$$v_2 = Kv_1, \qquad \text{where } K = 1 + \frac{R_b}{R_a}$$

First, we recognize that because the input impedance and the gain of the operational amplifier approach infinity, the input current i_x and the input voltage v_x in Fig. 6.17c are infinitesimal and may be taken as zero. The dependent source in this case is Av_x instead of $-Av_x$ because of the input polarity inversion. The dependent source Av_x (see Fig. 6.17b) at the output will generate current i_o, as illustrated in Fig. 6.17c. Now

$$v_2 = (R_b + R_a)i_o$$

and also

$$v_1 = v_x + R_a i_o = R_a i_o$$

Therefore,

$$\frac{v_2}{v_1} = \frac{R_b + R_a}{R_a} = 1 + \frac{R_b}{R_a} = K$$

or

$$v_2(t) = Kv_1(t)$$

The equivalent circuit of the noninverting amplifier is depicted in Fig. 6.17d.

EXAMPLE 6.20 Transform Analysis of a Sallen–Key Circuit

The circuit in Fig. 6.18a is called the *Sallen–Key* circuit, which is frequently used in filter design. Find the transfer function $H(s)$ relating the output voltage $v_o(t)$ to the input voltage $v_i(t)$.

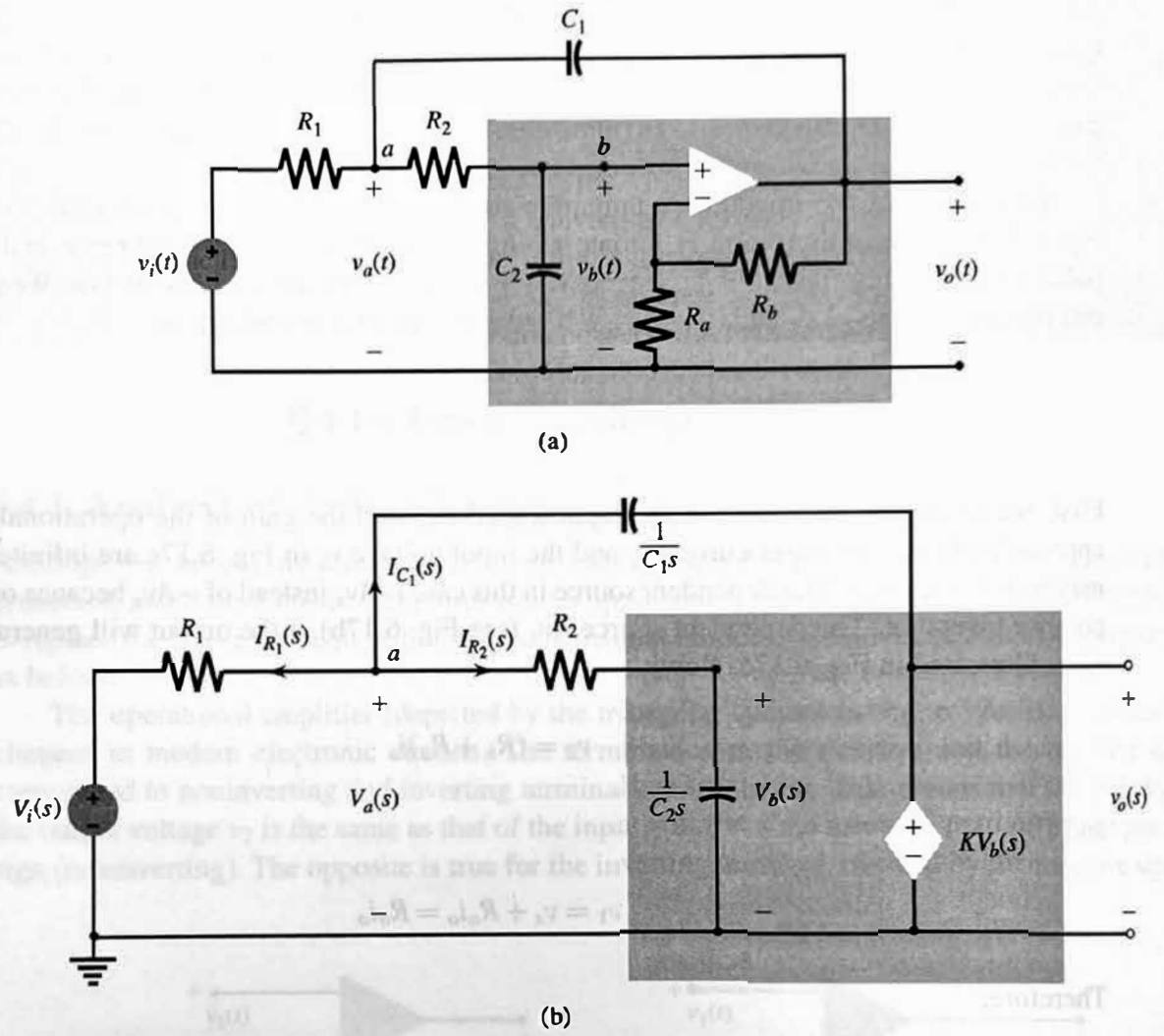

Figure 6.18 (a) Sallen–Key circuit and (b) its equivalent.

We are required to find

$$H(s) = \frac{V_o(s)}{V_i(s)}$$

assuming all initial conditions to be zero.

Figure 6.18b shows the transformed version of the circuit in Fig. 6.18a. The noninverting amplifier is replaced by its equivalent circuit. All the voltages are replaced by their Laplace transforms, and all the circuit elements are shown by their impedances. All the initial conditions are assumed to be zero, as required for determining $H(s)$.

We shall use node analysis to derive the result. There are two unknown node voltages, $V_a(s)$ and $V_b(s)$, requiring two node equations.

At node a, $I_{R_1}(s)$, the current in R_1 (leaving the node a), is $[V_a(s) - V_i(s)]/R_1$. Similarly, $I_{R_2}(s)$, the current in R_2 (leaving the node a), is $[V_a(s) - V_b(s)]/R_2$, and $I_{C_1}(s)$, the current in capacitor C_1 (leaving the node a), is $[V_a(s) - V_o(s)]C_1 s = [V_a(s) - KV_b(s)]C_1 s$.

The sum of all the three currents is zero. Therefore,

$$\frac{V_a(s) - V_i(s)}{R_1} + \frac{V_a(s) - V_b(s)}{R_2} + [V_a(s) - KV_b(s)]C_1 s = 0$$

or

$$\left(\frac{1}{R_1} + \frac{1}{R_2} + C_1 s\right) V_a(s) - \left(\frac{1}{R_2} + KC_1 s\right) V_b(s) = \frac{1}{R_1} V_i(s)$$

Similarly, the node equation at node b yields

$$\frac{V_b(s) - V_a(s)}{R_2} + C_2 s V_b(s) = 0$$

or

$$-\frac{1}{R_2} V_a(s) + \left(\frac{1}{R_2} + C_2 s\right) V_b(s) = 0$$

The two node equations in two unknown node voltages $V_a(s)$ and $V_b(s)$ can be expressed in matrix form as

$$\begin{bmatrix} G_1 + G_2 + C_1 s & -(G_2 + KC_1 s) \\ -G_2 & (G_2 + C_2 s) \end{bmatrix} \begin{bmatrix} V_a(s) \\ V_b(s) \end{bmatrix} = \begin{bmatrix} G_1 V_i(s) \\ 0 \end{bmatrix}$$

where

$$G_1 = \frac{1}{R_1} \quad \text{and} \quad G_2 = \frac{1}{R_2}$$

Application of Cramer's rule yields

$$\frac{V_b(s)}{V_i(s)} = \frac{G_1 G_2}{C_1 C_2 s^2 + [G_1 C_2 + G_2 C_2 + G_2 C_1 (1 - K)]s + G_1 G_2}$$

$$= \frac{{\omega_0}^2}{s^2 + 2\alpha s + {\omega_0}^2}$$

where

$$K = 1 + \frac{R_b}{R_a} \quad \text{and} \quad {\omega_0}^2 = \frac{G_1 G_2}{C_1 C_2} = \frac{1}{R_1 R_2 C_1 C_2}$$

$$2\alpha = \frac{G_1 C_2 + G_2 C_2 + G_2 C_1 (1 - K)}{C_1 C_2} = \frac{1}{R_1 C_1} + \frac{1}{R_2 C_1} + \frac{1}{R_2 C_2}(1 - K)$$

Now

$$V_o(s) = KV_b(s)$$

Therefore,

$$H(s) = \frac{V_o(s)}{V_i(s)} = K\frac{V_b(s)}{V_i(s)} = \frac{K{\omega_0}^2}{s^2 + 2\alpha s + {\omega_0}^2}$$

6.5 BLOCK DIAGRAMS

Large systems may consist of an enormous number of components or elements. As anyone who has seen the circuit diagram of a radio or a television receiver can appreciate, analyzing such systems all at once could be next to impossible. In such cases, it is convenient to represent a system by suitably interconnected subsystems, each of which can be readily analyzed. Each subsystem can be characterized in terms of its input–output relationships. A linear system can be characterized by its transfer function $H(s)$. Figure 6.19a shows a block diagram of a system with a transfer function $H(s)$ and its input and output $X(s)$ and $Y(s)$, respectively.

Subsystems may be interconnected by using cascade, parallel, and feedback interconnections (Figs. 6.19b, 6.19c, 6.19d), the three elementary types. When transfer functions appear in cascade, as depicted in Fig. 6.19b, then, as shown earlier, the transfer function of the overall system is the product of the two transfer functions. This result can also be proved by observing that in Fig. 6.19b

$$\frac{Y(s)}{X(s)} = \frac{W(s)}{X(s)}\,\frac{Y(s)}{W(s)} = H_1(s)H_2(s)$$

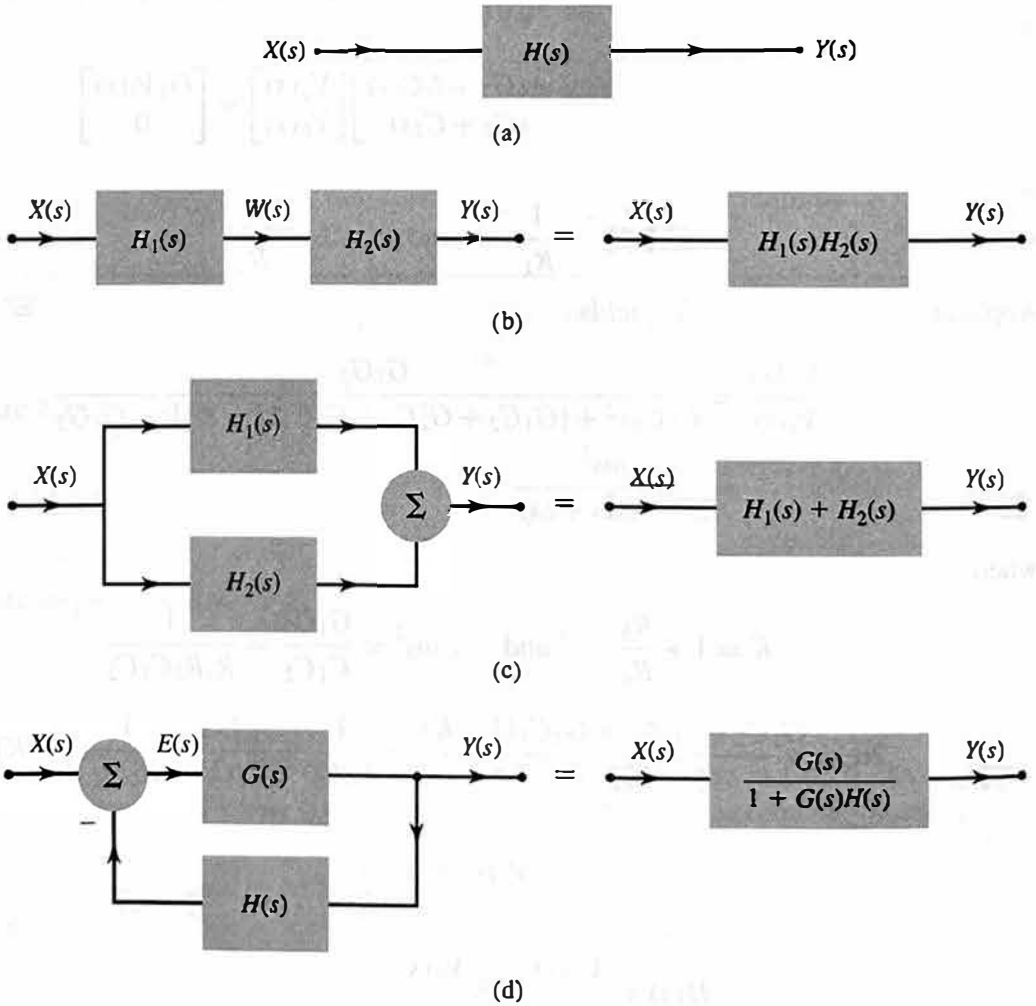

Figure 6.19 Elementary connections of blocks and their equivalents.

We can extend this result to any number of transfer functions in cascade. It follows from this discussion that the subsystems in cascade can be interchanged without affecting the overall transfer function. This commutation property of LTI systems follows directly from the commutative (and associative) property of convolution. We have already proved this property in Sec. 2.4.3. Every possible ordering of the subsystems yields the same overall transfer function. However, there may be practical consequences (such as sensitivity to parameter variation) affecting the behavior of different ordering.

Similarly, when two transfer functions, $H_1(s)$ and $H_2(s)$, appear in parallel, as illustrated in Fig. 6.19c, the overall transfer function is given by $H_1(s) + H_2(s)$, the sum of the two transfer functions. The proof is trivial. This result can be extended to any number of systems in parallel.

When the output is fed back to the input, as shown in Fig. 6.19d, the overall transfer function $Y(s)/X(s)$ can be computed as follows. The inputs to the adder are $X(s)$ and $-H(s)Y(s)$. Therefore, $E(s)$, the output of the adder, is

$$E(s) = X(s) - H(s)Y(s)$$

But

$$\begin{aligned} Y(s) &= G(s)E(s) \\ &= G(s)[X(s) - H(s)Y(s)] \end{aligned}$$

Therefore,

$$Y(s)[1 + G(s)H(s)] = G(s)X(s)$$

so that

$$\frac{Y(s)}{X(s)} = \frac{G(s)}{1 + G(s)H(s)} \tag{6.39}$$

Therefore, the feedback loop can be replaced by a single block with the transfer function shown in Eq. (6.39) (see Fig. 6.19d).

In deriving these equations, we implicitly assume that when the output of one subsystem is connected to the input of another subsystem, the latter does not load the former. For example, the transfer function $H_1(s)$ in Fig. 6.19b is computed by assuming that the second subsystem $H_2(s)$ was not connected. This is the same as assuming that $H_2(s)$ does not load $H_1(s)$. In other words, the input–output relationship of $H_1(s)$ will remain unchanged regardless of whether $H_2(s)$ is connected. Many modern circuits use op amps with high input impedances, so this assumption is justified. When such an assumption is not valid, $H_1(s)$ must be computed under operating conditions [i.e., with $H_2(s)$ connected].

EXAMPLE 6.21 Transfer Functions of Feedback Systems Using MATLAB

Consider the feedback system of Fig. 6.19d with $G(s) = K/(s(s+8))$ and $H(s) = 1$. Use MATLAB to determine the transfer function for each of the following cases: **(a)** $K = 7$, **(b)** $K = 16$, and **(c)** $K = 80$.

We solve these cases using the control system toolbox function `feedback`.

(a)

```
>> H = tf(1,1); K = 7; G = tf([0 0 K],[1 8 0]); TFa = feedback(G,H)
   Ha =
            7
     -------------
     s^2 + 8 s + 7
```

Thus, $H_a(s) = 7/(s^2+8s+7)$.

(b)

```
>> H = tf(1,1); K = 16; G = tf([0 0 K],[1 8 0]); TFb = feedback(G,H)
   Hb =
            16
     --------------
     s^2 + 8 s + 16
```

Thus, $H_b(s) = 16/(s^2+8s+16)$.

(c)

```
>> H = tf(1,1); K = 80; G = tf([0 0 K],[1 8 0]); TFc = feedback(G,H)
   Hc =
            80
     --------------
     s^2 + 8 s + 80
```

Thus, $H_c(s) = 80/(s^2+8s+80)$.

6.6 SYSTEM REALIZATION

We now develop a systematic method for realization (or implementation) of an arbitrary Nth-order transfer function. The most general transfer function with $M = N$ is given by

$$H(s) = \frac{b_0 s^N + b_1 s^{N-1} + \cdots + b_{N-1}s + b_N}{s^N + a_1 s^{N-1} + \cdots + a_{N-1}s + a_N} \tag{6.40}$$

Since realization is basically a synthesis problem, there is no unique way of realizing a system. A given transfer function can be realized in many different ways. A transfer function $H(s)$ can be realized by using integrators or differentiators along with adders and multipliers. We avoid use of differentiators for practical reasons discussed in Secs. 2.1 and 6.3.3. Hence, in our implementation, we shall use integrators along with scalar multipliers and adders. We are already familiar with representation of all these elements except the integrator. The integrator can be represented by a box with an integral sign (time-domain representation, Fig. 6.20a) or by a box with transfer function $1/s$ (frequency-domain representation, Fig. 6.20b).

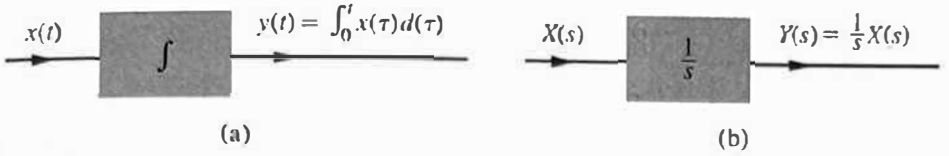

Figure 6.20 **(a)** Time-domain and **(b)** frequency-domain representations of an integrator.

6.6.1 Direct Form I Realization

Rather than realize the general Nth-order system described by Eq. (6.40), we begin with a specific case of the following third-order system and then extend the results to the Nth-order case:

$$H(s) = \frac{b_0 s^3 + b_1 s^2 + b_2 s + b_3}{s^3 + a_1 s^2 + a_2 s + a_3} = \frac{b_0 + \frac{b_1}{s} + \frac{b_2}{s^2} + \frac{b_3}{s^3}}{1 + \frac{a_1}{s} + \frac{a_2}{s^2} + \frac{a_3}{s^3}}$$

We can express $H(s)$ as

$$H(s) = \underbrace{\left(b_0 + \frac{b_1}{s} + \frac{b_2}{s^2} + \frac{b_3}{s^3}\right)}_{H_1(s)} \underbrace{\left(\frac{1}{1 + \frac{a_1}{s} + \frac{a_2}{s^2} + \frac{a_3}{s^3}}\right)}_{H_2(s)}$$

We can realize $H(s)$ as a cascade of transfer function $H_1(s)$ followed by $H_2(s)$, as depicted in Fig. 6.21a, where the output of $H_1(s)$ is denoted by $W(s)$. Because of the commutative property of LTI system transfer functions in cascade, we can also realize $H(s)$ as a cascade of $H_2(s)$ followed by $H_1(s)$, as illustrated in Fig. 6.21b, where the (intermediate) output of $H_2(s)$ is denoted by $V(s)$.

The output of $H_1(s)$ in Fig. 6.21a is given by $W(s) = H_1(s)X(s)$. Hence,

$$W(s) = \left(b_0 + \frac{b_1}{s} + \frac{b_2}{s^2} + \frac{b_3}{s^3}\right) X(s) \tag{6.41}$$

Also, the output $Y(s)$ and the input $W(s)$ of $H_2(s)$ in Fig. 6.21a are related by $Y(s) = H_2(s)W(s)$. Hence,

$$W(s) = \left(1 + \frac{a_1}{s} + \frac{a_2}{s^2} + \frac{a_3}{s^3}\right) Y(s) \tag{6.42}$$

We shall first realize $H_1(s)$. Equation (6.41) shows that the output $W(s)$ can be synthesized by adding the input $b_0X(s)$ to $b_1(X(s)/s), b_2(X(s)/s^2)$, and $b_3(X(s)/s^3)$. Because the transfer function

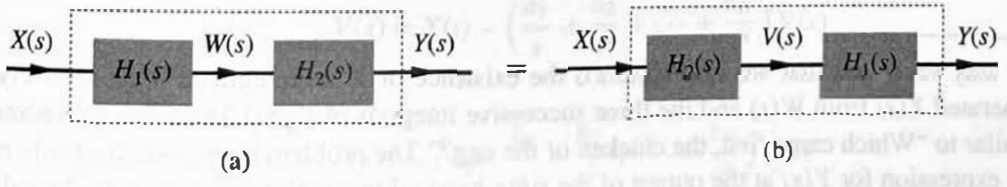

Figure 6.21 Realization of a transfer function in two steps.

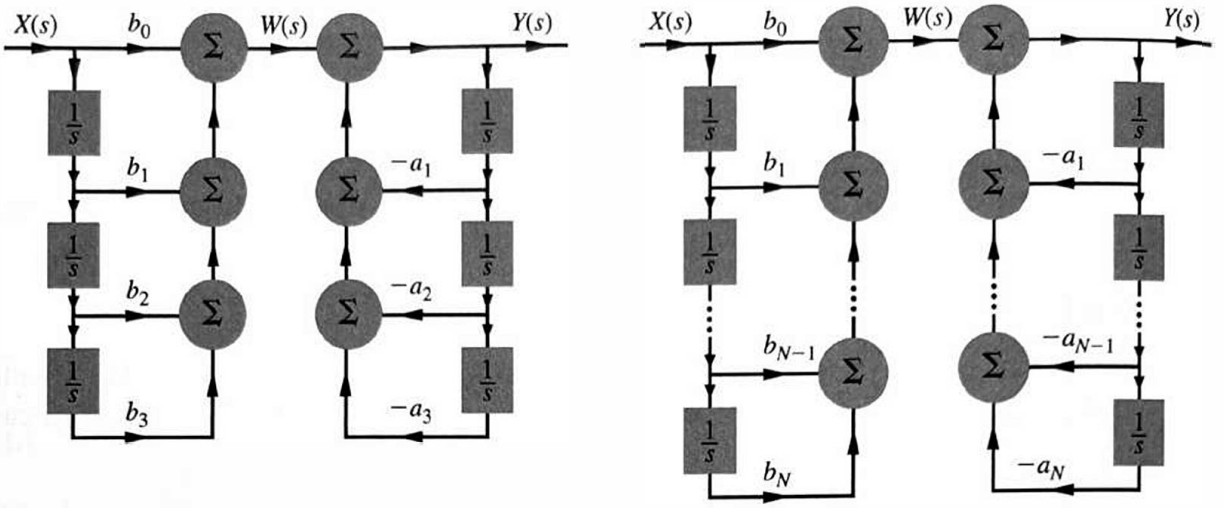

Figure 6.22 Direct form I realization of an LTIC system: **(a)** third-order and **(b)** Nth-order.

of an integrator is $1/s$, the signals $X(s)/s$, $X(s)/s^2$, and $X(s)/s^3$ can be obtained by successive integration of the input $x(t)$. The left-half section of Fig. 6.22a shows how $W(s)$ can be synthesized from $X(s)$, according to Eq. (6.41). Hence, this section represents a realization of $H_1(s)$.

To complete the picture, we shall realize $H_2(s)$, which is specified by Eq. (6.42). We can rearrange Eq. (6.42) as

$$Y(s) = W(s) - \left(\frac{a_1}{s} + \frac{a_2}{s^2} + \frac{a_3}{s^3}\right) Y(s) \tag{6.43}$$

Hence, to obtain $Y(s)$, we subtract $a_1 Y(s)/s$, $a_2 Y(s)/s^2$, and $a_3 Y(s)/s^3$ from $W(s)$. We have already obtained $W(s)$ from the first step [output of $H_1(s)$]. To obtain signals $Y(s)/s$, $Y(s)/s^2$, and $Y(s)/s^3$, we assume that we already have the desired output $Y(s)$. Successive integration of $Y(s)$ yields the needed signals $Y(s)/s$, $Y(s)/s^2$, and $Y(s)/s^3$. We now synthesize the final output $Y(s)$ according to Eq. (6.43), as seen in the right-half section of Fig. 6.22a.[†] The left-half section in Fig. 6.22a represents $H_1(s)$ and the right-half is $H_2(s)$. We can generalize this procedure, known as the *direct form I* (DFI) realization, for any value of N. This procedure requires $2N$ integrators to realize an Nth-order transfer function, as shown in Fig. 6.22b.

6.6.2 Direct Form II Realization

In the direct form I, we realize $H(s)$ by implementing $H_1(s)$ followed by $H_2(s)$, as shown in Fig. 6.21a. We can also realize $H(s)$, as shown in Fig. 6.21b, where $H_2(s)$ is followed by $H_1(s)$. This procedure is known as the *direct form II* realization. Figure 6.23a shows direct form II

[†] It may seem odd that we first assumed the existence of $Y(s)$, integrated it successively, and then in turn generated $Y(s)$ from $W(s)$ and the three successive integrals of signal $Y(s)$. This procedure poses a dilemma similar to "Which came first, the chicken or the egg?" The problem here is satisfactorily resolved by writing the expression for $Y(s)$ at the output of the right-hand adder (at the top) in Fig. 6.22a and verifying that this expression is indeed the same as Eq. (6.42).

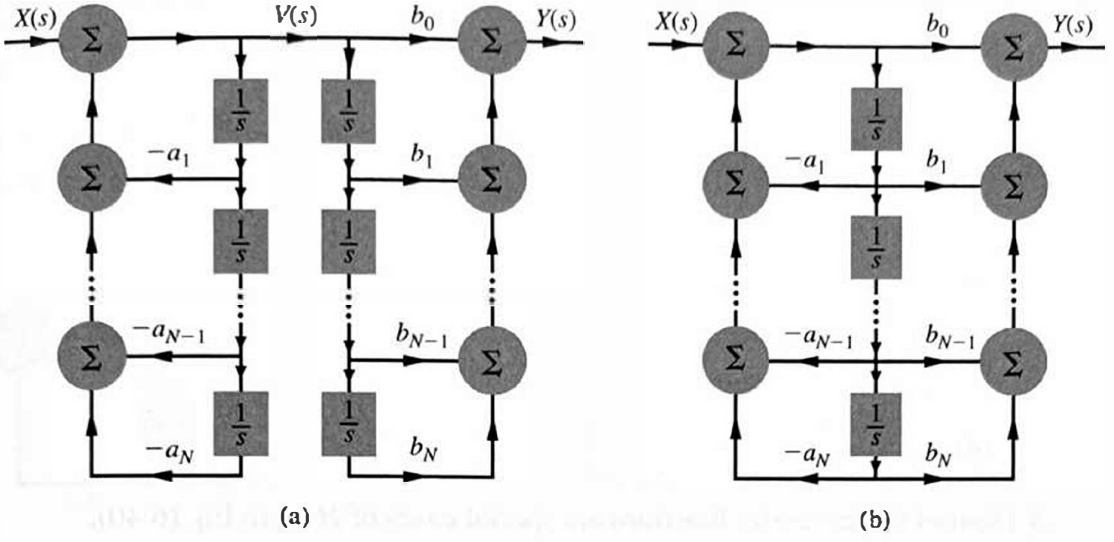

Figure 6.23 Direct form II realization of an Nth-order LTIC system.

realization, where we have interchanged sections representing $H_1(s)$ and $H_2(s)$ in Fig. 6.22b. The output of $H_2(s)$ in this case is denoted by $V(s)$.[†]

An interesting observation in Fig. 6.23a is that the input signal to both the chains of integrators is $V(s)$. Clearly, the outputs of integrators in the left-side chain are identical to the corresponding outputs of the right-side integrator chain, thus making the right-side chain redundant. We can eliminate this chain and obtain the required signals from the left-side chain, as shown in Fig. 6.23b. This implementation halves the number of integrators to N and, thus, is more efficient in hardware utilization than either Figs. 6.22b or 6.23a. This is the *direct form II* (DFII) realization.

An Nth-order differential equation with $N = M$ has a property that its implementation requires a minimum of N integrators. A realization is *canonic* if the number of integrators used in the realization is equal to the order of the transfer function realized. Thus, canonic realization has no redundant integrators. The DFII form in Fig. 6.23b is a canonic realization, and is also called the *direct canonic* form. Note that the DFI is noncanonic.

The direct form I realization (Fig. 6.23b) implements zeros first [the left-half section represented by $H_1(s)$] followed by realization of poles [the right-half section represented by $H_2(s)$] of $H(s)$. In contrast, canonic direct implements poles first followed by zeros. Although both these realizations result in the same transfer function, they generally behave differently from the viewpoint of sensitivity to parameter variations.

[†] The reader can show that the equations relating $X(s)$, $V(s)$, and $Y(s)$ in Fig. 6.23a are

$$V(s) = X(s) - \left(\frac{a_1}{s} + \frac{a_2}{s^2} + \cdots + \frac{a_N}{s^N}\right) V(s)$$

and

$$Y(s) = \left(b_0 + \frac{b_1}{s} + \frac{b_2}{s^2} + \cdots + \frac{b_N}{s^N}\right) V(s)$$

EXAMPLE 6.22 Canonic Direct Form Realizations

Find the canonic direct form realization of the following transfer functions:

(a) $\dfrac{5}{s+7}$

(b) $\dfrac{s}{s+7}$

(c) $\dfrac{s+5}{s+7}$

(d) $\dfrac{4s+28}{s^2+6s+5}$

All four of these transfer functions are special cases of $H(s)$ in Eq. (6.40).

(a) The transfer function $5/(s+7)$ is of the first order ($N=1$); therefore, we need only one integrator for its realization. The feedback and feedforward coefficients are

$$a_1 = 7 \qquad \text{and} \qquad b_0 = 0, \quad b_1 = 5$$

The realization is depicted in Fig. 6.24a. Because $N=1$, there is a single feedback connection from the output of the integrator to the input adder with coefficient $a_1 = 7$. For $N=1$, generally, there are $N+1=2$ feedforward connections. However, in this case, $b_0 = 0$, and there is only one feedforward connection with coefficient $b_1 = 5$ from the output of the integrator to the output adder. Because there is only one input signal to the output adder, we can do away with the adder, as shown in Fig. 6.24a.

(b)

$$H(s) = \frac{s}{s+7}$$

In this first-order transfer function, $b_1 = 0$. The realization is shown in Fig. 6.24b. Because there is only one signal to be added at the output adder, we can discard the adder.

(c)

$$H(s) = \frac{s+5}{s+7}$$

The realization appears in Fig. 6.24c. Here, $H(s)$ is a first-order transfer function with $a_1 = 7$ and $b_0 = 1$, $b_1 = 5$. There is a single feedback connection (with coefficient 7) from the integrator output to the input adder. There are two feedforward connections (Fig. 6.24c).†

---

† When $M = N$ (as in this case), $H(s)$ can also be realized in another way by recognizing that

$$H(s) = 1 - \frac{2}{s+7}$$

We now realize $H(s)$ as a parallel combination of two transfer functions, as indicated by this equation.

(d)

$$H(s) = \frac{4s + 28}{s^2 + 6s + 5}$$

This is a second-order system with $b_0 = 0$, $b_1 = 4$, $b_2 = 28$, $a_1 = 6$, and $a_2 = 5$. Figure 6.24d shows a realization with two feedback connections and two feedforward connections.

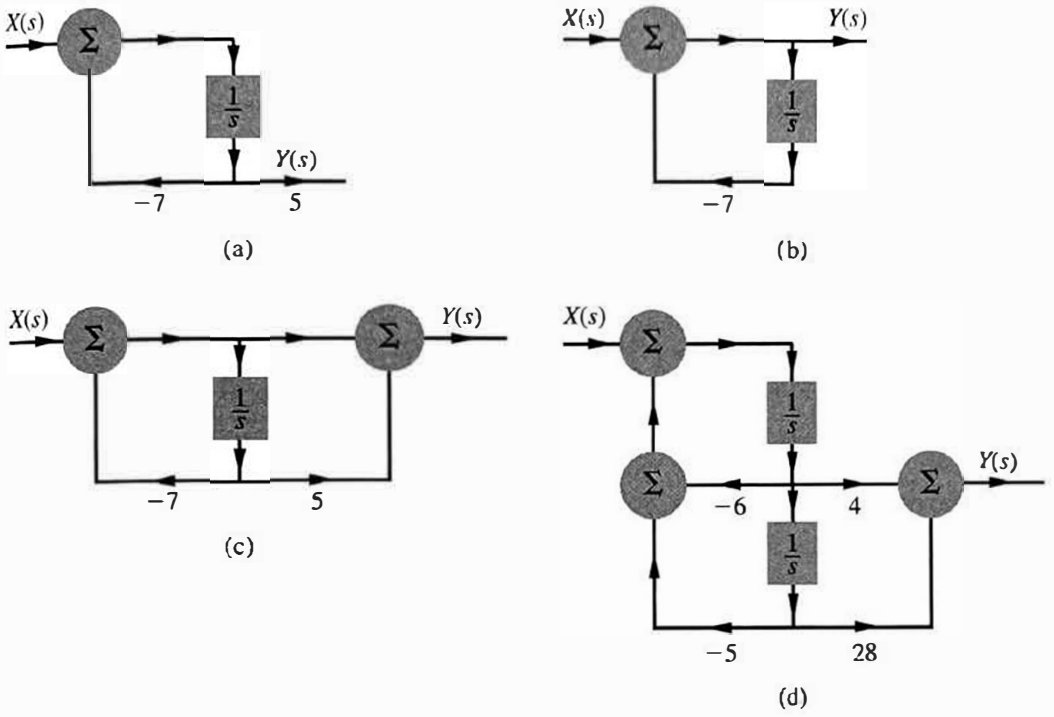

Figure 6.24 Realizations of $H(s)$ for Ex. 6.22.

DRILL 6.11 Canonic Direct Form Realization

Give the canonic direct realization of

$$H(s) = \frac{2s}{s^2 + 6s + 25}$$

6.6.3 Cascade and Parallel Realizations

An Nth-order transfer function $H(s)$ can be expressed as a product or a sum of N first-order transfer functions. Accordingly, we can also realize $H(s)$ as a cascade (series) or parallel form of these N

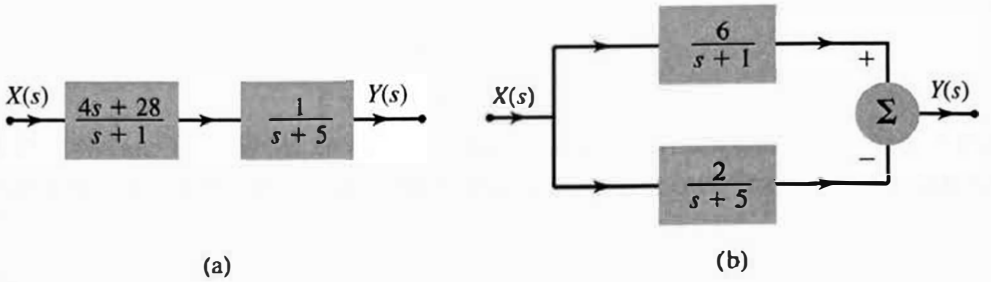

Figure 6.25 Realization of $(4s+28)/((s+1)(s+5))$: **(a)** cascade form and **(b)** parallel form.

first-order transfer functions. Consider, for instance, the transfer function in part (d) of Ex. 6.22.

$$H(s) = \frac{4s+28}{s^2+6s+5}$$

We can express $H(s)$ as

$$H(s) = \frac{4s+28}{(s+1)(s+5)} = \underbrace{\left(\frac{4s+28}{s+1}\right)}_{H_1(s)}\underbrace{\left(\frac{1}{s+5}\right)}_{H_2(s)}$$

We can also express $H(s)$ as a sum of partial fractions as

$$H(s) = \frac{4s+28}{(s+1)(s+5)} = \underbrace{\frac{6}{s+1}}_{H_3(s)} - \underbrace{\frac{2}{s+5}}_{H_4(s)}$$

These equations give us the option of realizing $H(s)$ as a cascade of $H_1(s)$ and $H_2(s)$, as shown in Fig. 6.25a, or a parallel of $H_3(s)$ and $H_4(s)$, as depicted in Fig. 6.25b. Each of the first-order transfer functions in Fig. 6.25 can be implemented by using canonic direct realizations, discussed earlier.

This discussion by no means exhausts all the possibilities. In the cascade form alone, there are different ways of grouping the factors in the numerator and the denominator of $H(s)$, and each grouping can be realized in DFI or canonic direct form. Accordingly, several cascade forms are possible. In Sec. 6.6.4, we shall discuss yet another form that essentially doubles the numbers of realizations discussed so far.

From a practical viewpoint, parallel and cascade forms are preferable because parallel and certain cascade forms are numerically less sensitive than canonic direct form to small parameter variations in the system. Qualitatively, this difference can be explained by the fact that in a canonic realization all the coefficients interact with each other, and a change in any coefficient will be magnified through its repeated influence from feedback and feedforward connections. In a parallel realization, in contrast, the change in a coefficient will affect only a localized segment; the case with a cascade realization is similar.

In the examples of cascade and parallel realization, we have separated $H(s)$ into first-order factors. For $H(s)$ of higher orders, we could group $H(s)$ into factors, not all of which are necessarily of the first order. For example, if $H(s)$ is a third-order transfer function, we could realize this function as a cascade (or a parallel) combination of a first-order and a second-order factor.

Realization of Complex Conjugate Poles

The complex poles in $H(s)$ should be realized as a second-order (quadratic) factor because we cannot implement multiplication by complex numbers. Consider, for example,

$$\begin{aligned} H(s) &= \frac{10s+50}{(s+3)(s^2+4s+13)} \\ &= \frac{10s+50}{(s+3)(s+2-j3)(s+2+j3)} \\ &= \frac{2}{s+3} - \frac{1+j2}{s+2-j3} \quad \frac{1-j2}{s+2+j3} \end{aligned}$$

We cannot realize first-order transfer functions individually with the poles $-2 \pm j3$ because they require multiplication by complex numbers in the feedback and the feedforward paths. Therefore, we need to combine the conjugate poles and realize them as a second-order transfer function.[†] In the present example, we can create a cascade realization from $H(s)$ expressed in product form as

$$H(s) = \left(\frac{10}{s+3}\right)\left(\frac{s+5}{s^2+4s+13}\right)$$

Similarly, we can create a parallel realization from $H(s)$ expressed in sum form as

$$H(s) = \frac{2}{s+3} - \frac{2s-8}{s^2+4s+13}$$

Realization of Repeated Poles

When repeated poles occur, the procedure for canonic and cascade realization is exactly the same as before. For a parallel realization, however, the procedure requires special handling, as explained in Ex. 6.23.

EXAMPLE 6.23 Parallel Realization

Determine the parallel realization of

$$H(s) = \frac{7s^2+37s+51}{(s+2)(s+3)^2} = \frac{5}{s+2} + \frac{2}{s+3} - \frac{3}{(s+3)^2}$$

This third-order transfer function should require no more than three integrators. But if we try to realize each of the three partial fractions separately, we require four integrators because of the one second-order term. This difficulty can be avoided by observing that the terms $1/(s+3)$ and

---

[†] It is possible to realize complex, conjugate poles indirectly by using a cascade of two first-order transfer functions and feedback. A transfer function with poles $-a \pm jb$ can be realized by using a cascade of two identical first-order transfer functions, each having a pole at $-a$ (see Prob. 6.6-15).

$1/(s+3)^2$ can be realized with a cascade of two subsystems, each having a transfer function $1/(s+3)$, as shown in Fig. 6.26. Each of the three first-order transfer functions in Fig. 6.26 may now be realized as in Fig. 6.24.

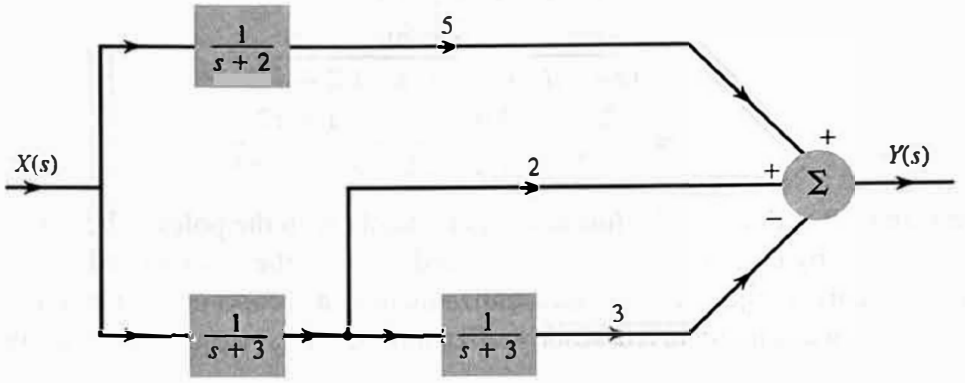

Figure 6.26 Parallel realization of $(7s^2+37s+51)/((s+2)(s+3)^2)$.

DRILL 6.12 Canonic, Cascade, and Parallel Realizations

Find the canonic, cascade, and parallel realization of

$$H(s)=\frac{s+3}{s^2+7s+10}=\left(\frac{s+3}{s+2}\right)\left(\frac{1}{s+5}\right)$$

6.6.4 Transposed Realization

Two realizations are said to be *equivalent* if they have the same transfer function. A simple way to generate an equivalent realization from a given realization is to use its *transpose*. To generate a transpose of any realization, we change the given realization as follows:

1. Reverse all the arrow directions without changing the scalar multiplier values.
2. Replace pickoff nodes by adders and vice versa.
3. Replace the input $X(s)$ with the output $Y(s)$ and vice versa.

Figure 6.27a shows the transposed version of the canonic direct form realization in Fig. 6.23b found according to the rules just listed. Figure 6.27b is Fig. 6.27a reoriented in the conventional form so that the input $X(s)$ appears at the left and the output $Y(s)$ appears at the right. Observe that this realization is also canonic.

Rather than prove the theorem on equivalence of the transposed realizations, we shall verify that the transfer function of the realization in Fig. 6.27b is identical to that in Eq. (6.40).

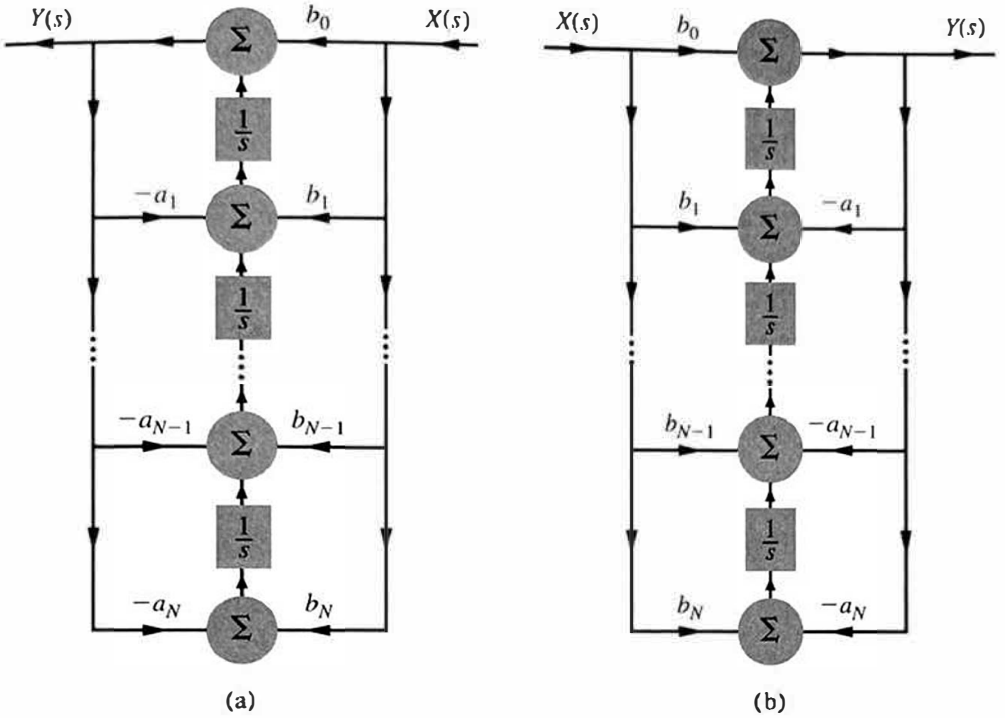

Figure 6.27 Realization of an Nth-order LTI transfer function in the transposed form.

Figure 6.27b shows that $Y(s)$ is being fed back through N paths. The fed-back signal appearing at the input of the top adder is

$$\left(\frac{-a_1}{s}+\frac{-a_2}{s^2}+\cdots+\frac{-a_{N-1}}{s^{N-1}}+\frac{-a_N}{s^N}\right)Y(s)$$

The signal $X(s)$, fed to the top adder through $N+1$ forward paths, contributes

$$\left(b_0+\frac{b_1}{s}+\cdots+\frac{b_{N-1}}{s^{N-1}}+\frac{b_N}{s^N}\right)X(s)$$

The output $Y(s)$ is equal to the sum of these two signals (feed forward and feed back). Hence,

$$\begin{aligned}Y(s)=&\left(\frac{-a_1}{s}+\frac{-a_2}{s^2}+\cdots+\frac{-a_{N-1}}{s^{N-1}}+\frac{-a_N}{s^N}\right)Y(s)\\&+\left(b_0+\frac{b_1}{s}+\cdots+\frac{b_{N-1}}{s^{N-1}}+\frac{b_N}{s^N}\right)X(s)\end{aligned}$$

Transporting all the $Y(s)$ terms to the left side and multiplying throughout by s^N, we obtain

$$(s^N+a_1s^{N-1}+\cdots+a_{N-1}s+a_N)Y(s)=(b_0s^N+b_1s^{N-1}+\cdots+b_{N-1}s+b_N)X(s)$$

Consequently,

$$H(s)=\frac{Y(s)}{X(s)}=\frac{b_0s^N+b_1s^{N-1}+\cdots+b_{N-1}s+b_N}{s^N+a_1s^{N-1}+\cdots+a_{N-1}s+a_N}$$

Hence, the transfer function $H(s)$ is identical to that in Eq. (6.40).

We have essentially doubled the number of possible realizations. Every realization that was found earlier has a transpose. Note that the transpose of a transpose results in the same realization.

EXAMPLE 6.24 Transposed Realizations

Find the transpose canonic direct realizations for parts (c) and (d) of Ex. 6.22 (Figs. 6.24c and 6.24d). The transfer functions are:

(a) $\dfrac{s+5}{s+7}$

(b) $\dfrac{4s+28}{s^2+6s+5}$

Both these realizations are special cases of the one in Fig. 6.27b.

(a) In this case, $N=1$ with $a_1=7, b_0=1, b_1=5$. The desired realization can be obtained by transposing Fig. 6.24c. However, we already have the general model of the transposed realization in Fig. 6.27b. The desired solution is a special case of Fig. 6.27b with $N=1$ and $a_1=7, b_0=1, b_1=5$, as shown in Fig. 6.28a.

(b) In this case, $N=2$ with $b_0=0$, $b_1=4$, $b_2=28$, $a_1=6$, $a_2=5$. Using the model of Fig. 6.27b, we obtain the desired realization, as shown in Fig. 6.28b.

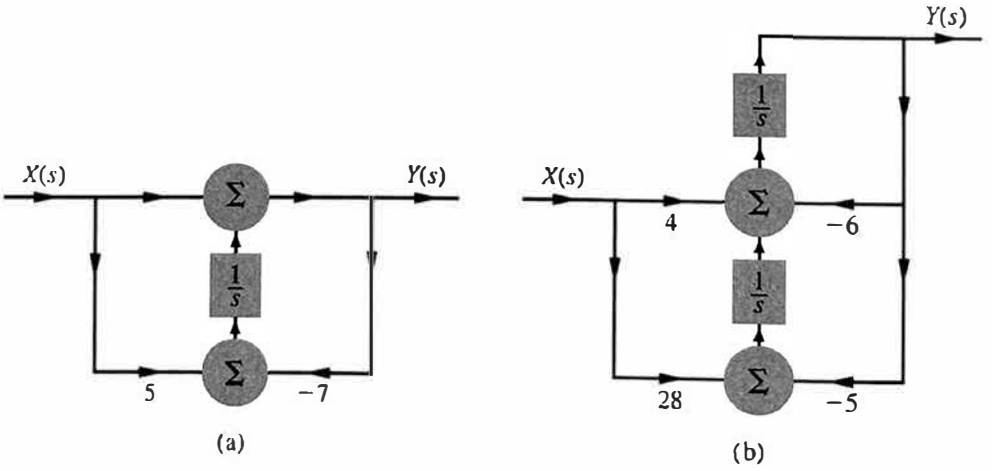

Figure 6.28 Transposed canonic direct form realizations of **(a)** $(s+5)/(s+7)$ and **(b)** $(4s+28)/(s^2+6s+5)$.

DRILL 6.13 Transposed Realizations

Find the transposed DFI and transposed canonic direct (TDFII) realizations of $H(s)$ in Drill 6.11.

6.6.5 Using Operational Amplifiers for System Realization

In this section, we discuss practical implementation of the realizations described in Sec. 6.6.4. Earlier we saw that the basic elements required for the synthesis of an LTIC system (or a given transfer function) are (scalar) multipliers, integrators, and adders. All these elements can be realized by operational amplifier (op-amp) circuits.

Operational Amplifier Circuits

Figure 6.29 shows an op-amp circuit in the frequency domain (the transformed circuit). Because the input impedance of the op amp is infinite (very high), all the current $I(s)$ flows in the feedback path, as illustrated. Moreover $V_x(s)$, the voltage at the input of the op amp, is zero (very small) because of the infinite (very large) gain of the op amp. Therefore, for all practical purposes,

$$Y(s) = -I(s)Z_f(s)$$

Moreover, because $v_x \approx 0$,

$$I(s) = \frac{X(s)}{Z(s)}$$

Substitution of the second equation in the first yields

$$Y(s) = -\frac{Z_f(s)}{Z(s)}X(s)$$

Therefore, the op-amp circuit in Fig. 6.29 has the transfer function

$$H(s) = -\frac{Z_f(s)}{Z(s)}$$

By properly choosing $Z(s)$ and $Z_f(s)$, we can obtain a variety of transfer functions, as the following development shows.

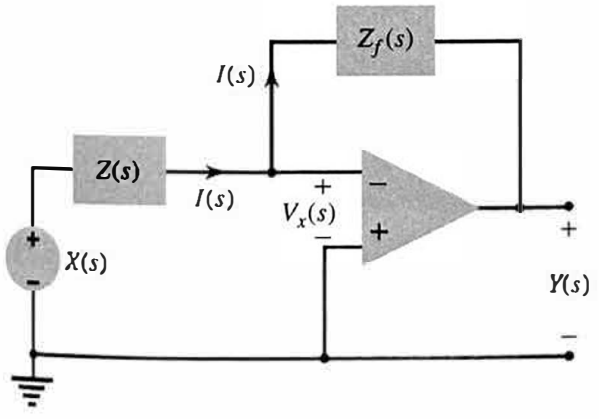

Figure 6.29 A basic inverting configuration op-amp circuit.

The Scalar Multiplier

If we use a resistor R_f in the feedback and a resistor R at the input (Fig. 6.30a), then $Z_f(s) = R_f$, $Z(s) = R$, and

$$H(s) = -\frac{R_f}{R}$$

The system acts as a scalar multiplier (or an amplifier) with a negative gain R_f/R. A positive gain can be obtained by using two such multipliers in cascade or by using a single noninverting amplifier, as depicted in Fig. 6.17c. Figure 6.30a also shows the compact symbol used in circuit diagrams for a scalar multiplier.

The Integrator

If we use a capacitor C in the feedback and a resistor R at the input (Fig. 6.30b), then $Z_f(s) = 1/Cs$, $Z(s) = R$, and

$$H(s) = \left(-\frac{1}{RC}\right)\frac{1}{s}$$

The system acts as an ideal integrator with a gain $-1/RC$. Figure 6.30b also shows the compact symbol used in circuit diagrams for an integrator.

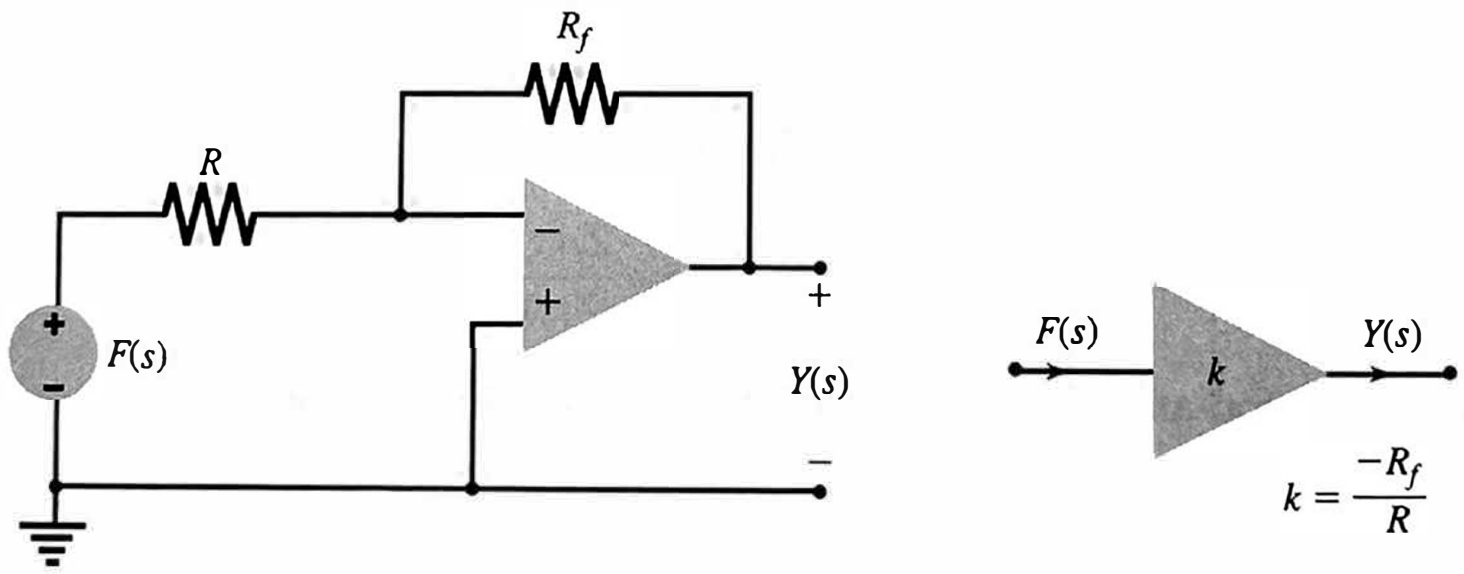

Figure 6.30 **(a)** Op-amp inverting amplifier. **(b)** Integrator.

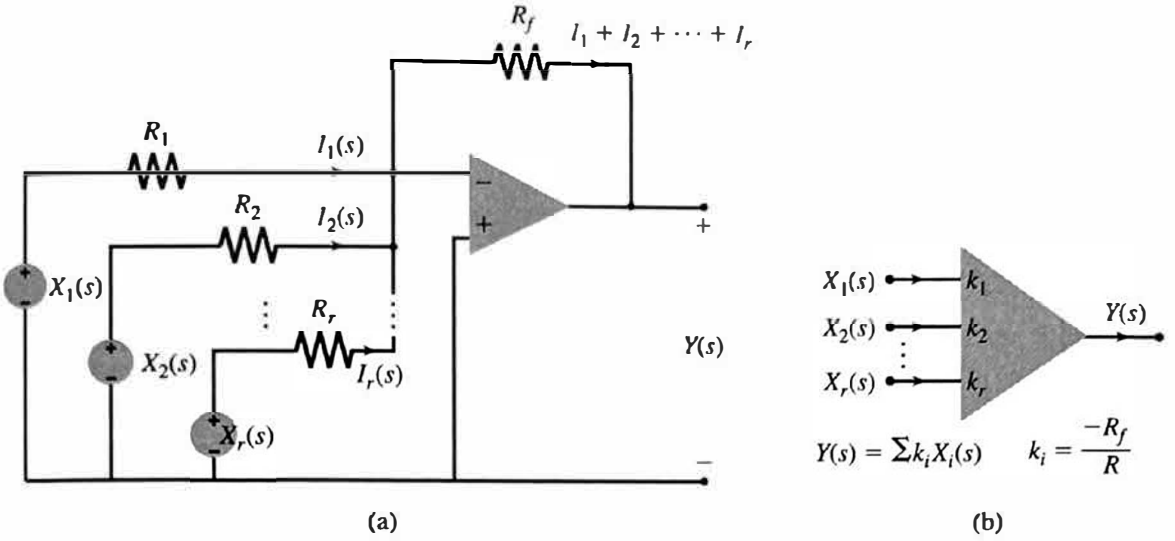

Figure 6.31 Op-amp summing and amplifying circuit.

The Adder

Consider now the circuit in Fig. 6.31a with r inputs $X_1(s), X_2(s), \ldots, X_r(s)$. As usual, the input voltage $V_x(s) \simeq 0$ because the op-amp gain $\to \infty$. Moreover, the current going into the op amp is very small ($\simeq 0$) because the input impedance $\to \infty$. Therefore, the total current in the feedback resistor R_f is $I_1(s) + I_2(s) + \cdots + I_r(s)$. Moreover, because $V_x(s) = 0$,

$$I_j(s) = \frac{X_j(s)}{R_j} \qquad j = 1, 2, \ldots, r$$

Also,

$$\begin{aligned} Y(s) &= -R_f[I_1(s) + I_2(s) + \cdots + I_r(s)] \\ &= -\left[\frac{R_f}{R_1}X_1(s) + \frac{R_f}{R_2}X_2(s) + \cdots + \frac{R_f}{R_r}X_r(s)\right] \\ &= k_1X_1(s) + k_2X_2(s) + \cdots + k_rX_r(s) \end{aligned}$$

where

$$k_i = \frac{-R_f}{R_i}$$

Clearly, the circuit in Fig. 6.31 serves an adder and an amplifier with any desired gain for each of the input signals. Figure 6.31b shows the compact symbol used in circuit diagrams for an adder with r inputs.

EXAMPLE 6.25 Op-Amp Realization

Use op-amp circuits to realize the canonic direct form of the transfer function

$$H(s) = \frac{2s + 5}{s^2 + 4s + 10}$$

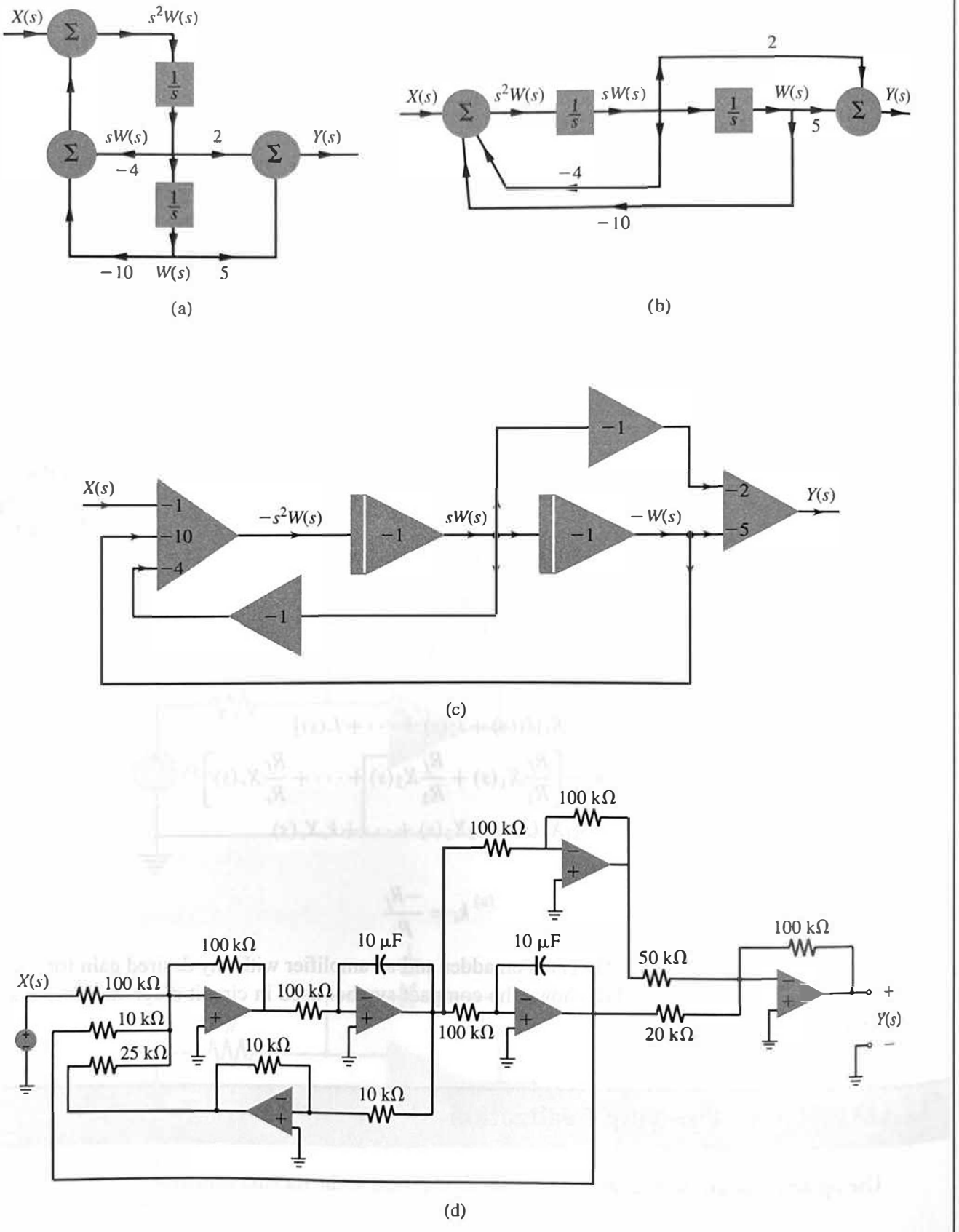

Figure 6.32 Op-amp realization of a second-order transfer function $(2s + 5)/(s^2 + 4s + 10)$.

The basic canonic realization is shown in Fig. 6.32a. The same realization with horizontal reorientation is shown in Fig. 6.32b. Signals at various points are also indicated in the realization. For convenience, we denote the output of the last integrator by $W(s)$. Consequently, the signals at the inputs of the two integrators are $sW(s)$ and $s^2W(s)$, as shown in Figs. 6.32a and 6.32b. Op-amp elements (multipliers, integrators, and adders) change the polarity of the output signals. To incorporate this fact, we modify the canonic realization in Fig. 6.32b to that depicted in Fig. 6.32c. In Fig. 6.32b, the successive outputs of the adder and the integrators are $s^2W(s), sW(s)$, and $W(s)$, respectively. Because of polarity reversals in op-amp circuits, these outputs are $-s^2W(s), sW(s)$, and $-W(s)$, respectively, in Fig. 6.32c. This polarity reversal requires corresponding modifications in the signs of feedback and feedforward gains. According to Fig. 6.32b,

$$s^2W(s) = X(s) - 4sW(s) - 10W(s)$$

Therefore,

$$-s^2W(s) = -X(s) + 4sW(s) + 10W(s)$$

Because the adder gains are always negative (see Fig. 6.31b), we rewrite the foregoing equation as

$$-s^2W(s) = -1[X(s)] - 4[-sW(s)] - 10[-W(s)]$$

Figure 6.32c shows the implementation of this equation. The hardware realization appears in Fig. 6.32d. Both integrators have a unity gain, which requires $RC = 1$. We have used $R = 100$ kΩ and $C = 10$ μF. The gain of 10 in the outer feedback path is obtained in the adder by choosing the feedback resistor of the adder to be 100 kΩ and an input resistor of 10 kΩ. Similarly, the gain of 4 in the inner feedback path is obtained by using the corresponding input resistor of 25 kΩ. The gains of 2 and 5, required in the feedforward connections, are obtained by using a feedback resistor of 100 kΩ and input resistors of 50 and 20 kΩ, respectively.[†]

The op-amp realization in Fig. 6.32 is not necessarily the one that uses the fewest op amps. This example is given just to illustrate a systematic procedure for designing an op-amp circuit of an arbitrary transfer function. There are more efficient circuits (such as Sallen–Key or biquad) that use fewer op amps to realize a second-order transfer function.

[†] It is possible to avoid the two inverting op amps (with gain −1) in Fig. 6.32d by adding signal $sW(s)$ to the input and output adders directly, using the noninverting amplifier configuration in Fig. 6.17d.

DRILL 6.14 Transfer Functions of Op-Amp Circuits

Show that the transfer functions of the op-amp circuits in Figs. 6.33a and 6.33b are $H_1(s)$ and $H_2(s)$, respectively, where

$$H_1(s) = \frac{-R_f}{R}\left(\frac{a}{s+a}\right) \qquad a = \frac{1}{R_fC_f}$$

$$H_2(s) = -\frac{C}{C_f}\left(\frac{s+b}{s+a}\right) \qquad a = \frac{1}{R_fC_f} \qquad b = \frac{1}{RC}$$

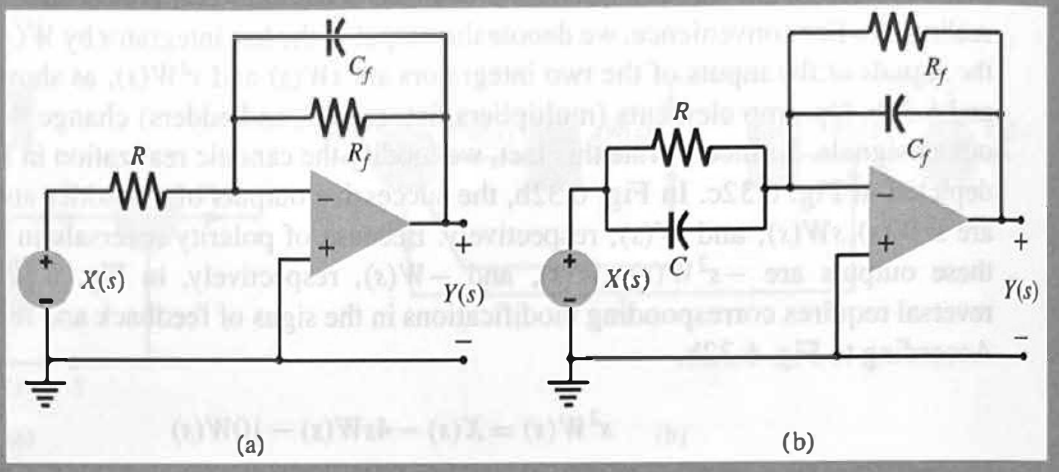

Figure 6.33 Op-amp circuits for Drill 6.14.

6.7 APPLICATION TO FEEDBACK AND CONTROLS

Generally, systems are designed to produce a desired output $y(t)$ for a given input $x(t)$. Using the given performance criteria, we can design a system, as shown in Fig. 6.34a. Ideally, such an open-loop system should yield the desired output. In practice, however, the system characteristics change with time, as a result of aging or replacement of some components, or because of changes in the operating environment. Such variations cause changes in the output for the same input. Clearly, this is undesirable in precision systems.

A possible solution to this problem is to add a signal component to the input that is not a predetermined function of time but will change to counteract the effects of changing system characteristics and the environment. In short, we must provide a correction at the system input to account for the undesired changes just mentioned. Yet since these changes are generally unpredictable, it is not clear how to preprogram appropriate corrections to the input. However, the difference between the actual output and the desired output gives an indication of the suitable correction to be applied to the system input. It may be possible to counteract the variations by feeding the output (or some function of output) back to the input.

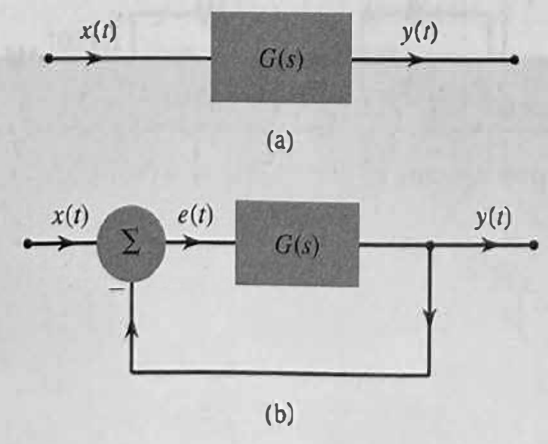

Figure 6.34 **(a)** Open-loop and **(b)** closed-loop (feedback) systems.

We unconsciously apply this principle in daily life. Consider an example of marketing a certain product. The optimum price of the product is the value that maximizes the profit of a merchant. The output in this case is the profit, and the input is the price of the item. The output (profit) can be controlled (within limits) by varying the input (price). The merchant may price the product too high initially, in which case, he will sell too few items, reducing the profit. Using feedback of the profit (output), he adjusts the price (input), to maximize his profit. If there is a sudden or unexpected change in the business environment, such as a strike-imposed shutdown of a large factory in town, the demand for the item goes down, thus reducing his output (profit). He adjusts his input (reduces price) using the feedback of the output (profit) in a way that will optimize his profit in the changed circumstances. If the town suddenly becomes more prosperous because a new factory opens, he will increase the price to maximize the profit. Thus, by continuous feedback of the output to the input, he realizes his goal of maximum profit (optimum output) in any given circumstances. We observe thousands of examples of feedback systems around us in everyday life. Most social, economical, educational, and political processes are, in fact, feedback processes. A block diagram of such a system, called the *feedback* or *closed-loop* system, is shown in Fig. 6.34b.

A feedback system can address the problems arising because of unwanted disturbances such as random-noise signals in electronic systems, a gust of wind affecting a tracking antenna, a meteorite hitting a spacecraft, and the rolling motion of anti-aircraft gun platforms mounted on ships or moving tanks. Feedback may also be used to reduce nonlinearities in a system or to control its rise time (or bandwidth). Feedback is used to achieve, with a given system, the desired objective within a given tolerance, despite partial ignorance of the system and the environment. A feedback system, thus, has an ability for supervision and self-correction in the face of changes in the system parameters and external disturbances (change in the environment).

Consider the feedback amplifier in Fig. 6.35. Let the forward amplifier gain $G = 10{,}000$. One-hundredth of the output is fed back to the input ($H = 0.01$). The gain T of the feedback amplifier is obtained by [see Eq. (6.39)]

$$T = \frac{G}{1+GH} = \frac{10{,}000}{1+100} = 99.01$$

Suppose that because of aging or replacement of some transistors, the gain G of the forward amplifier changes from 10,000 to 20,000. The new gain of the feedback amplifier is given by

$$T = \frac{G}{1+GH} = \frac{20{,}000}{1+200} = 99.5$$

Surprisingly, 100% variation in the forward gain G causes only 0.5% variation in the feedback amplifier gain T. Such reduced sensitivity to parameter variations is a must in precision amplifiers. In this example, we reduced the sensitivity of gain to parameter variations at the cost of forward gain, which is reduced from 10,000 to 99. There is no dearth of forward gain (obtained by cascading stages). But low sensitivity is extremely precious in precision systems.

Now, consider what happens when we add (instead of subtract) the signal fed back to the input. Such addition means the sign on the feedback connection is + instead of − (which is the same as changing the sign of H in Fig. 6.35). Consequently,

$$T = \frac{G}{1-GH}$$

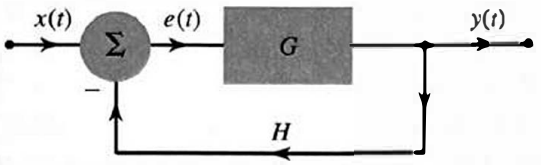

Figure 6.35 Effects of negative and positive feedback.

If we let $G = 10{,}000$ as before and $H = 0.9 \times 10^{-4}$, then

$$T = \frac{10{,}000}{1 - 0.9(10^4)(10^{-4})} = 100{,}000$$

Suppose that because of aging or replacement of some transistors, the gain of the forward amplifier changes to 11,000. The new gain of the feedback amplifier is

$$T = \frac{11{,}000}{1 - 0.9(11{,}000)(10^{-4})} = 1{,}100{,}000$$

Observe that in this case, a mere 10% increase in the forward gain G caused 1000% increase in the gain T (from 100,000 to 1,100,000). Clearly, the amplifier is very sensitive to parameter variations. This behavior is exactly the opposite of what was observed earlier, when the signal fed back was subtracted from the input.

What is the difference between the two situations? Crudely speaking, the former case is called the *negative feedback* and the latter is the *positive feedback*. The positive feedback increases system gain but tends to make the system more sensitive to parameter variations. It can also lead to instability. In our example, if G were to be 111,111, then $GH = 1$, $T = \infty$, and the system would become unstable because the signal fed back was exactly equal to the input signal itself, since $GH = 1$. Hence, once a signal has been applied, no matter how small and how short in duration, it comes back to reinforce the input undiminished, which further passes to the output, and is fed back again and again and again. In essence, the signal perpetuates itself forever. This perpetuation, even when the input ceases to exist, is precisely the symptom of instability.

Generally speaking, a feedback system cannot be described in black and white terms, such as positive or negative. Usually, H is a frequency-dependent component, more accurately represented by $H(s)$; hence, it varies with frequency. Consequently, what was negative feedback at lower frequencies can turn into positive feedback at higher frequencies and may give rise to instability. This is one of the serious aspects of feedback systems, which warrants a designer's careful attention.

6.7.1 Analysis of a Simple Control System

Figure 6.36a represents an automatic position control system, which can be used to control the angular position of a heavy object (e.g., a tracking antenna, an anti-aircraft gun mount, or the position of a ship). The input θ_i is the desired angular position of the object, which can be set at any given value. The actual angular position θ_o of the object (the output) is measured by a potentiometer whose wiper is mounted on the output shaft. The difference between the input θ_i (set at the desired output position) and the output θ_o (actual position) is amplified; the amplified output, which is proportional to $\theta_i - \theta_o$, is applied to the motor input. If $\theta_i - \theta_o = 0$ (the output

being equal to the desired angle), there is no input to the motor, and the motor stops. But if $\theta_o \neq \theta_i$, there will be a nonzero input to the motor, which will turn the shaft until $\theta_o = \theta_i$. It is evident that by setting the input potentiometer at a desired position in this system, we can control the angular position of a heavy remote object.

The block diagram of this system is shown in Fig. 6.36b. The amplifier gain is K, where K is adjustable. Let the motor (with load) transfer function that relates the output angle θ_o to the motor input voltage be $G(s)$ [for a starting point, see Eq. (1.32)]. This feedback arrangement is identical to that in Fig. 6.19d with $H(s) = 1$. Hence, $T(s)$, the (closed-loop) system transfer function relating the output θ_o to the input θ_i, is

$$\frac{\Theta_o(s)}{\Theta_i(s)} = T(s) = \frac{KG(s)}{1 + KG(s)}$$

From this equation, we shall investigate the behavior of the automatic position control system in Fig. 6.36a for a step and a ramp input.

Step Input

If we desire to change the angular position of the object instantaneously, we need to apply a step input. We may then want to know how long the system takes to position itself at the desired angle, whether it reaches the desired angle, and whether it reaches the desired position smoothly (monotonically) or oscillates about the final position. If the system oscillates, we may want to know how long it takes for the oscillations to settle down. All these questions can be readily answered by finding the output $\theta_o(t)$ when the input $\theta_i(t) = u(t)$. A step input implies instantaneous change in the angle. This input would be one of the most difficult to follow; if the system can perform well for this input, it is likely to give a good account of itself under most other expected situations. This is why we test control systems for a step input.

For the step input $\theta_i(t) = u(t)$, $\Theta_i(s) = 1/s$ and

$$\Theta_o(s) = \frac{1}{s} T(s) = \frac{KG(s)}{s[1 + KG(s)]}$$

Let the motor (with load) transfer function relating the load angle $\theta_o(t)$ to the motor input voltage be $G(s) = 1/(s(s+8))$. This yields

$$\Theta_o(s) = \frac{\dfrac{K}{s(s+8)}}{s\left[1 + \dfrac{K}{s(s+8)}\right]} = \frac{K}{s(s^2 + 8s + K)}$$

Let us investigate the system behavior for three different values of gain K.

For $K = 7$,

$$\Theta_o(s) = \frac{7}{s(s^2 + 8s + 7)} = \frac{7}{s(s+1)(s+7)} = \frac{1}{s} - \frac{\frac{7}{6}}{s+1} + \frac{\frac{1}{6}}{s+7}$$

and

$$\theta_o(t) = \left(1 - \tfrac{7}{6}e^{-t} + \tfrac{1}{6}e^{-7t}\right) u(t)$$

This response, illustrated in Fig. 6.36c, shows that the system reaches the desired angle, but at a rather leisurely pace. To speed up the response, let us increase the gain to, say, 80.

For $K = 80$,

$$\Theta_o(s) = \frac{80}{s(s^2+8s+80)} = \frac{80}{s(s+4-j8)(s+4+j8)}$$
$$= \frac{1}{s} + \frac{\frac{\sqrt{5}}{4}e^{j153^\circ}}{s+4-j8} + \frac{\frac{\sqrt{5}}{4}e^{-j153^\circ}}{s+4+j8}$$

and

$$\theta_o(t) = \left[1 + \tfrac{\sqrt{5}}{2}e^{-4t}\cos(8t+153^\circ)\right]u(t)$$

This response, also depicted in Fig. 6.36c, achieves the goal of reaching the final position at a faster rate than that in the earlier case ($K = 7$). Unfortunately, the improvement is achieved at the cost of ringing (oscillations) with high overshoot. In the present case, the *percent overshoot* (PO) is 21%. The response reaches its peak value at *peak time* $t_p = 0.393$ second. The *rise time*, defined as the time required for the response to rise from 10% to 90% of its steady-state value, indicates the speed of response.† In the present case, $t_r = 0.175$ second. The steady-state value of the response is unity so that the *steady-state error* is zero. Theoretically, it takes infinite time for the response to reach the desired value of unity. In practice, however, we may consider the response to have settled to the final value if it closely approaches the final value. A widely accepted measure of closeness is within 2% of the final value. The time required for the response to reach and stay within 2% of the final value is called the settling time t_s.‡ In Fig. 6.36c, we find $t_s \approx 1$ second (when $K = 80$). A good system has a small overshoot, small t_r and t_s, and a small steady-state error.

A large overshoot, as in the present case, may be unacceptable in many applications. Let us try to determine K (the gain) that yields the fastest response without oscillations. Complex characteristic roots lead to oscillations; to avoid oscillations, the characteristic roots should be real. In the present case, the characteristic polynomial is s^2+8s+K. For $K > 16$, the characteristic roots are complex; for $K < 16$, the roots are real. The fastest response without oscillations is obtained by choosing $K = 16$. We now consider this case.

For $K = 16$,

$$\Theta_o(s) = \frac{16}{s(s^2+8s+16)} = \frac{16}{s(s+4)^2} = \frac{1}{s} - \frac{1}{s+4} - \frac{4}{(s+4)^2}$$

and

$$\theta_o(t) = [1-(4t+1)e^{-4t}]u(t)$$

This response also appears in Fig. 6.36c. The system with $K > 16$ is said to be *underdamped* (oscillatory response), whereas the system with $K < 16$ is said to be *overdamped*. For $K = 16$, the system is said to be *critically damped*.

There is a trade-off between undesirable overshoot and rise time. Reducing overshoots leads to higher rise time (sluggish system). In practice, a small overshoot, which is still faster than

† *Delay time* t_d, defined as the time required for the response to reach 50% of its steady-state value, is another indication of speed. For the present case, $t_d = 0.141$ second.

‡ Typical percentage values used are 2 to 5% for t_s.

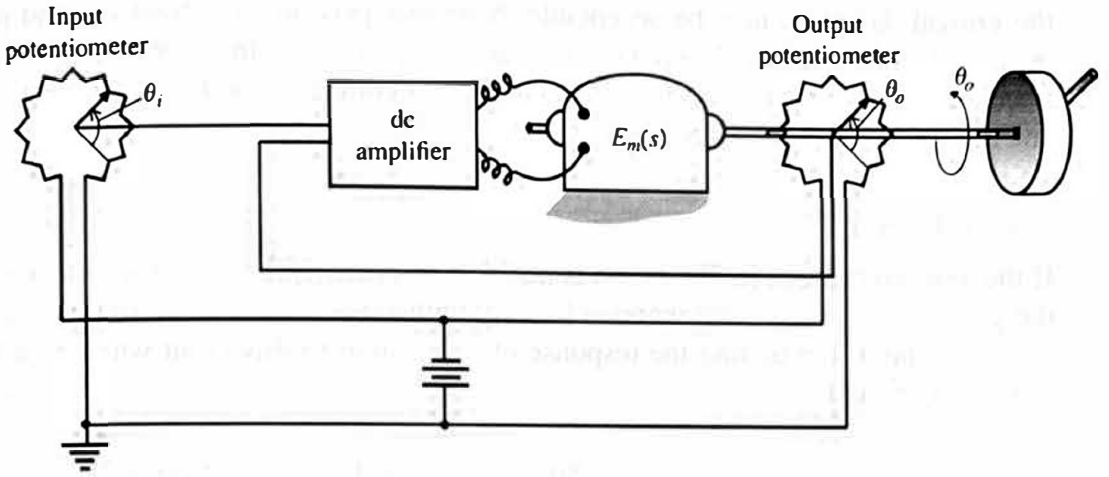

(a)

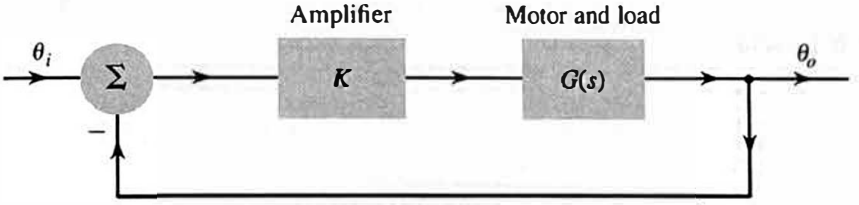

(b)

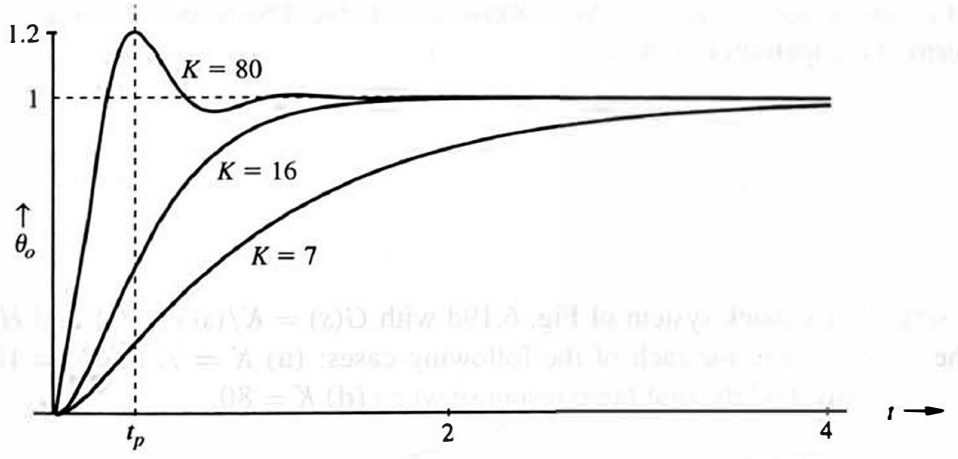

(c)

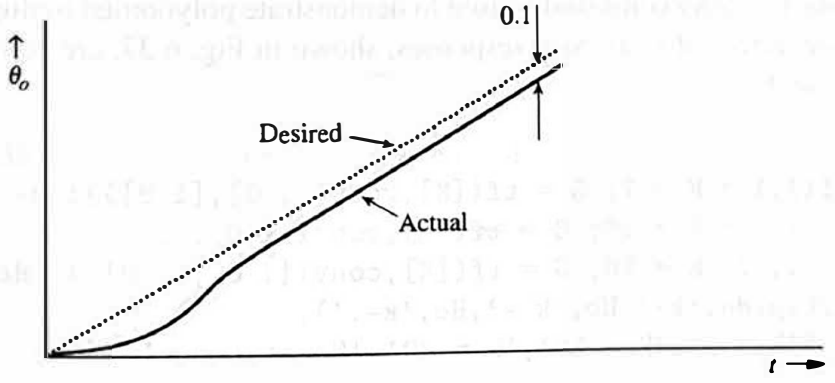

(d)

Figure 6.36 **(a)** An automatic position control system. **(b)** Its block diagram. **(c)** The unit step response. **(d)** The unit ramp response.

the critical damping, may be acceptable. Note that percent overshoot PO and peak time t_p are meaningless for the overdamped or critically damped cases. In addition to adjusting gain K, we may need to augment the system with some type of compensator if the specifications on overshoot and the speed of response are too stringent.

Ramp Input

If the anti-aircraft gun in Fig. 6.36a is tracking an enemy plane moving with a uniform velocity, the gun-position angle must increase linearly with t. Hence, the input in this case is a ramp; that is, $\theta_i(t) = tu(t)$. Let us find the response of the system to this input when $K = 80$. In this case, $\Theta_i(s) = 1/s^2$, and

$$\Theta_o(s) = \frac{80}{s^2(s^2+8s+80)} = -\frac{0.1}{s} + \frac{1}{s^2} + \frac{0.1(s-2)}{s^2+8s+80}$$

Use of Table 6.1 yields

$$\theta_o(t) = \left[-0.1 + t + \tfrac{1}{8}e^{-8t}\cos(8t + 36.87°)\right]u(t)$$

This response, sketched in Fig. 6.36d, shows that there is a steady-state error $e_r = 0.1$ radian. In many cases, such a small steady-state error may be tolerable. If, however, a zero steady-state error to a ramp input is required, this system in its present form is unsatisfactory. We must add some form of compensator to the system.

EXAMPLE 6.26 Step and Ramp Responses of Feedback Systems using MATLAB

Using the feedback system of Fig. 6.19d with $G(s) = K/(s(s+8))$ and $H(s) = 1$, determine the step response for each of the following cases: **(a)** $K = 7$, **(b)** $K = 16$, and **(c)** $K = 80$. Additionally, find the unit ramp response when **(d)** $K = 80$.

Example 6.21 computes the transfer functions of these feedback systems in a simple way. In this example, the conv command is used to demonstrate polynomial multiplication of the two denominator factors of $G(s)$. Step responses, shown in Fig. 6.37, are computed by using the `step` command.

(a–c)

```
>> H = tf(1,1); K = 7; G = tf([K],conv([1 0],[1 8])); Ha = feedback(G,H);
>> H = tf(1,1); K = 16; G = tf([K],conv([1 0],[1 8])); Hb = feedback(G,H);
>> H = tf(1,1); K = 80; G = tf([K],conv([1 0],[1 8])); Hc = feedback(G,H);
>> clf; step(Ha,'k-',Hb,'k--',Hc,'k-.');
>> legend('K = 7','K = 16','K = 80','Location','best');
```

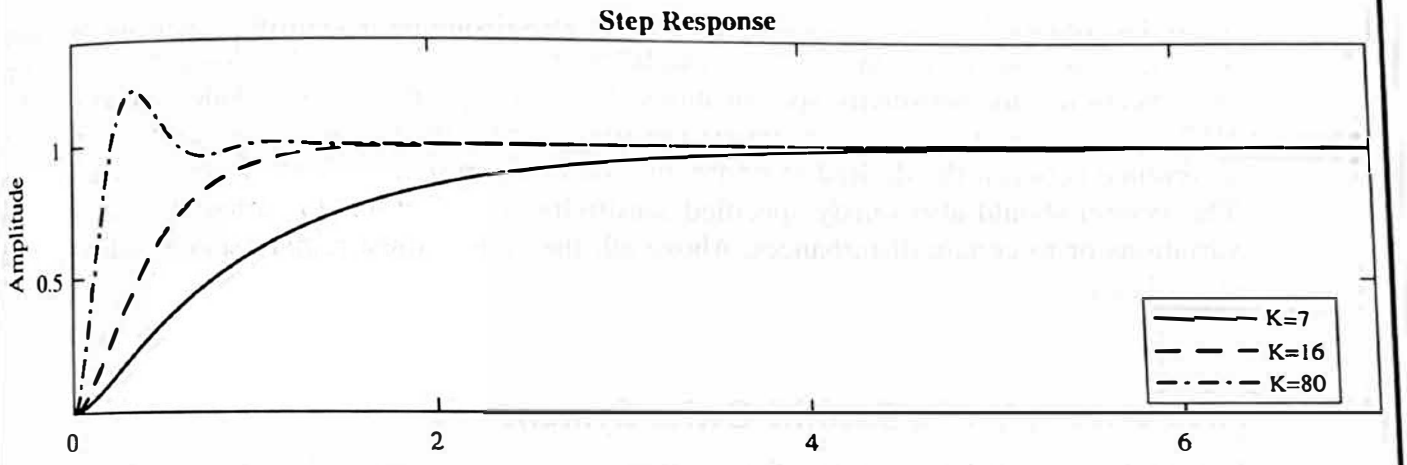

Figure 6.37 Step responses for Ex. 6.26.

(d) The unit ramp response is equivalent to the integral of the unit step response. We can obtain the ramp response by taking the step response of the system in cascade with an integrator. To help highlight waveform detail, we compute the ramp response over the short time interval of $0 \leq t \leq 1.5$ as shown in Fig. 6.38.

```
>> t = 0:.001:1.5; Hd = series(Hc,tf([1],[1 0]));
>> step(Hd,'k-',t); title('Unit Ramp Response');
```

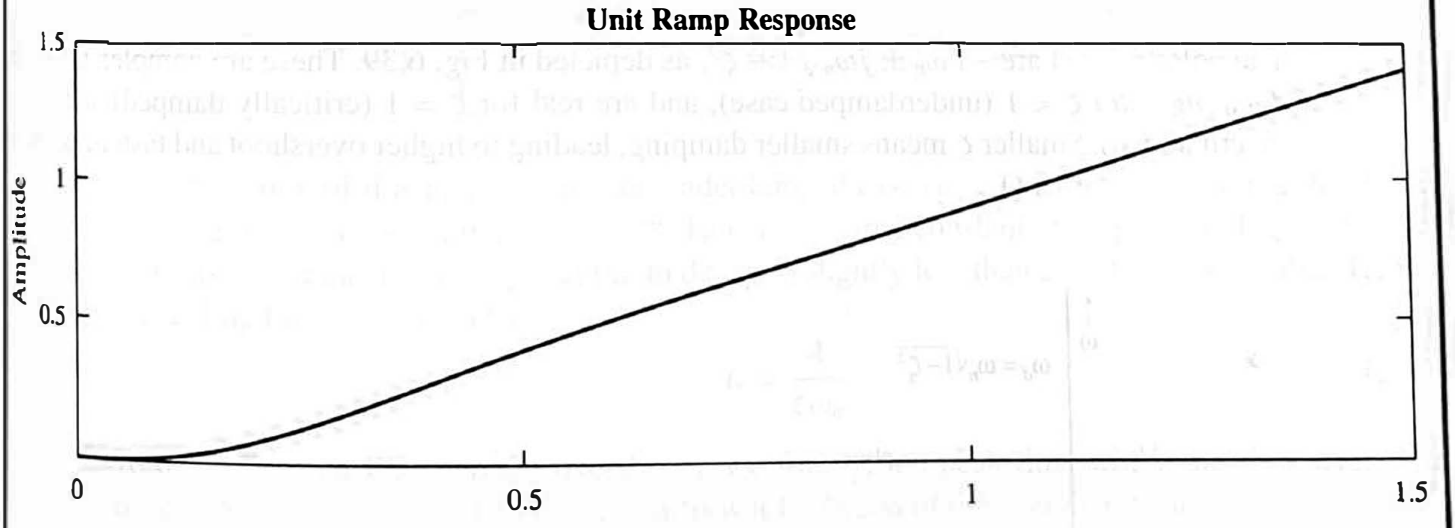

Figure 6.38 Ramp response for Ex. 6.26 with $K = 80$.

DESIGN SPECIFICATIONS

Now the reader has some idea of the various specifications a control system might require. Generally, a control system is designed to meet given transient specifications, steady-state error specifications, and sensitivity specifications. Transient specifications include percent overshoot (PO), rise time (t_r), and settling time (t_s) of the response to step input. Steady-state error is the difference between the desired response and the actual response to a test input in steady state. The system should also satisfy specified sensitivity specifications to various system parameter variations or to certain disturbances. Above all, the system must remain stable under operating conditions.

6.7.2 Analysis of a Second-Order System

Transient response depends upon the location of poles and zeros of the transfer function $T(s)$. In the general case, however, there is no quick way of predicting transient response parameters (PO, t_r, t_s) from the poles and zeros of $T(s)$. However, for a second-order system with no zeros, there is a direct relationship between the pole locations and the transient response. In such a case, the pole locations can be immediately determined from the knowledge of the transient parameter specifications. As we shall see, the study of the second-order system can be used to study many higher-order systems. For this reason, we shall now study the behavior of a second-order system in detail.

Let us consider a second-order transfer function $T(s)$, given by

$$T(s) = \frac{\omega_n^2}{s^2 + 2\zeta\omega_n s + \omega_n^2} \tag{6.44}$$

The poles of $T(s)$ are $-\zeta\omega_n \pm j\omega_n\sqrt{1-\zeta^2}$, as depicted in Fig. 6.39. These are complex when the *damping ratio* $\zeta < 1$ (underdamped case), and are real for $\zeta = 1$ (critically damped) and $\zeta > 1$ (overdamped). Smaller ζ means smaller damping, leading to higher overshoot and faster response.

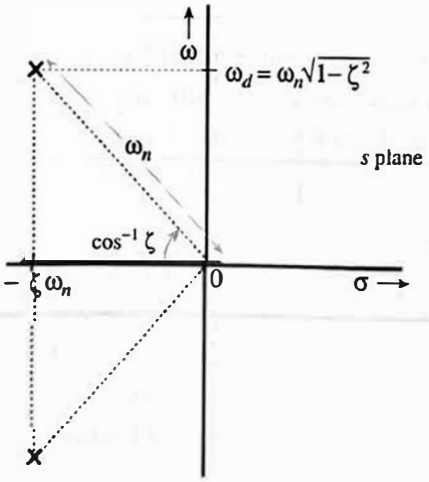

Figure 6.39 Pole locations of a second-order all-pole system.

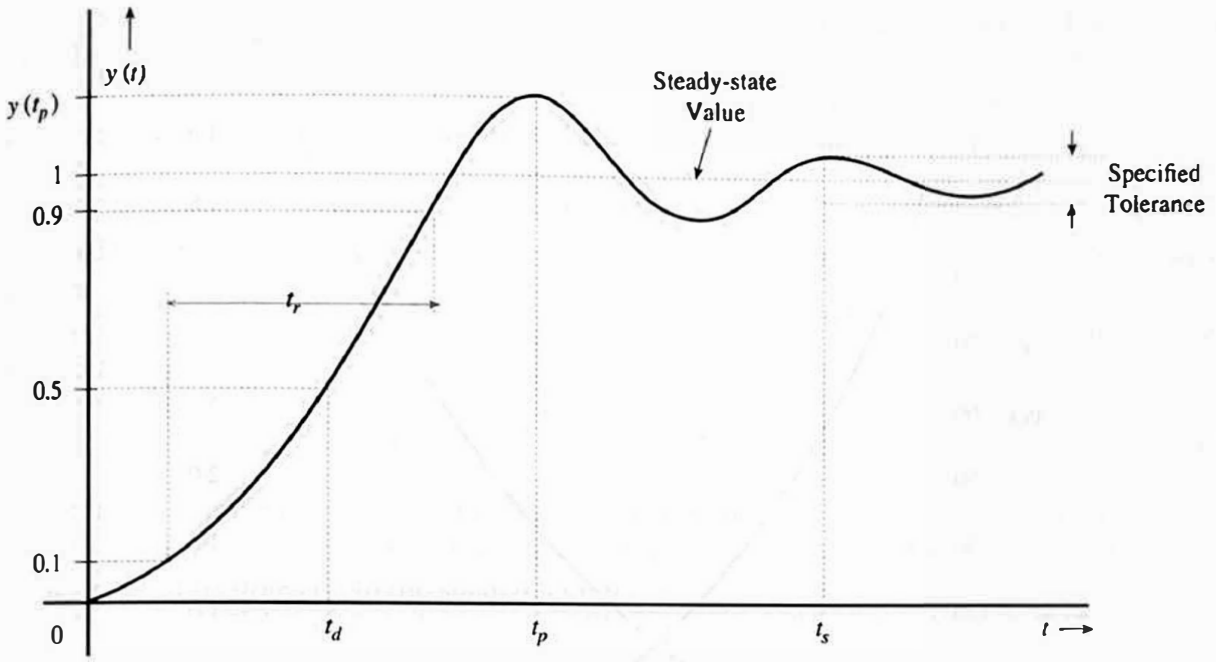

Figure 6.40 Unit step response of a second-order all-pole system.

For the unit step input $X(s) = 1/s$, we have output

$$Y(s) = \frac{\omega_n^2}{s(s^2 + 2\zeta\omega_n s + \omega_n^2)} = \frac{1}{s} - \frac{s + 2\zeta\omega_n}{s^2 + 2\zeta\omega_n s + \omega_n^2}$$

Use of Table 6.1 (pairs 1 and 10c) yields

$$y(t) = \left[1 - \frac{1}{\sqrt{1-\zeta^2}} e^{-\zeta\omega_n t} \sin(\omega_n\sqrt{1-\zeta^2}\, t + \cos^{-1}\zeta)\right] u(t)$$

The nature of this response for the underdamped case ($\zeta < 1$) is illustrated in Fig. 6.40. The response decays exponentially as $e^{-\zeta\omega_n t}$. Hence, the time constant of response is $1/\zeta\omega_n$. It takes four time constants for an exponential to decay to slightly less than 2% of its initial value. Hence, the settling time t_s is given by

$$t_s = \frac{4}{\zeta\omega_n} \tag{6.45}$$

To determine the PO (percent overshoot), we find t_p, the peak time where the peak overshoot occurs. At $t = t_p$, $dy/dt = 0$. The straightforward solution of this equation yields

$$t_p = \frac{\pi}{\omega_n\sqrt{1-\zeta^2}}$$

Moreover, PO is given by

$$\text{PO} = \frac{y(t_p) - 1}{1} \times 100\% = 100 e^{-\zeta\pi/\sqrt{1-\zeta^2}} \tag{6.46}$$

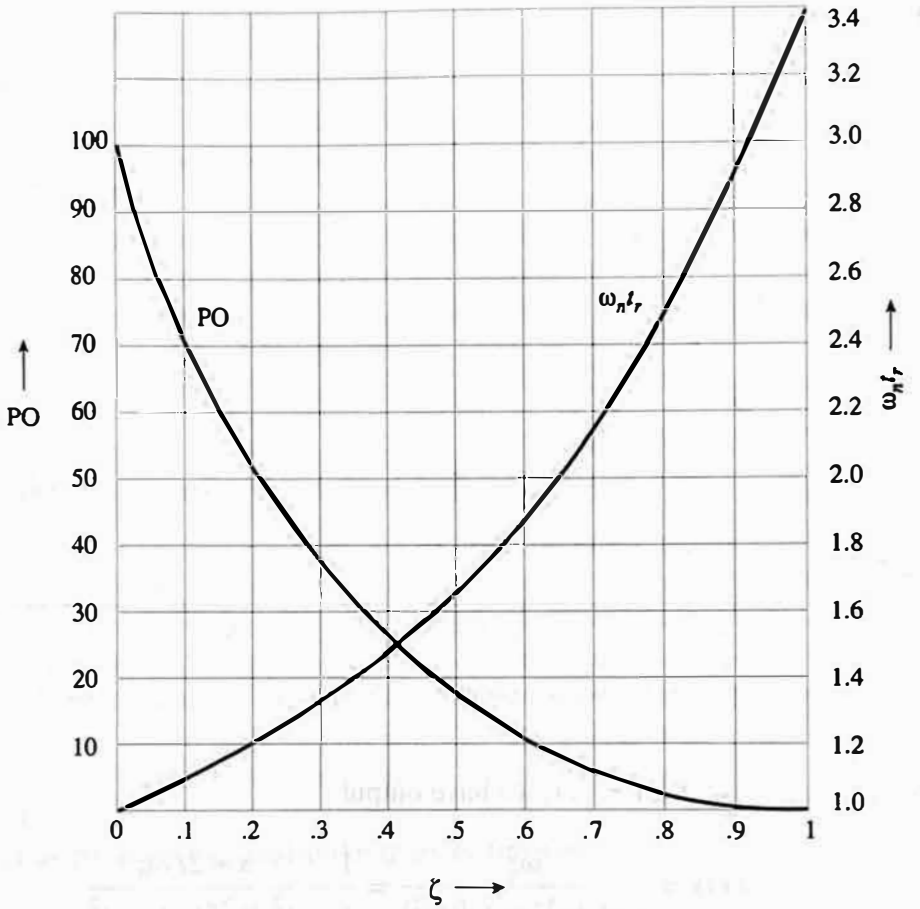

Figure 6.41 Plots of PO and $\omega_n t_r$ as functions of damping ratio ζ.

Figure 6.41 shows PO as a function of ζ. For a second-order system, the PO is directly related to the damping ratio ζ.

We may now proceed to determine similar expressions for t_r and t_d. Unfortunately, these turn out to be transcendental equations. However, these equations can be solved and plotted by computer, such as the curve of $\omega_n t_r$ in Fig. 6.41. Although precise expressions for t_r and t_d cannot be found, useful approximations are [9]

$$t_r \approx \frac{1-0.4167\zeta+2.917\zeta^2}{\omega_n} \quad \text{and} \quad t_d \approx \frac{1.1+0.125\zeta+0.469\zeta^2}{\omega_n} \tag{6.47}$$

Clearly, for a second-order system, the pole locations determine the transient behavior of the system. We observe that the closer the poles are to the ω axis, the smaller the value of ζ, and the larger the PO. Generally speaking, poles should not be too close to the ω axis, a positioning that leaves too small a safety margin for stability and makes the system sensitive to parameter variations. Hence, it is generally desirable to have a larger value for ζ (small PO). For a fast response, it is desirable to have small values for t_r, t_s, t_p, and t_d.

This discussion shows that for a second-order system in Eq. (6.44), all the transient parameters (PO, t_r, t_s, t_p and t_d) are related to the pole location of $T(s)$. From the point of view of the system design, it will be convenient to draw the contours representing different values of transient parameters in the s plane. For instance, each radial line drawn from the origin in the s plane

represents a constant ζ line (see Fig. 6.39). Since PO is directly related to ζ (Fig. 6.41), each radial line also represents a line of constant PO, as depicted in Fig. 6.42. Similarly, each vertical line represents constant $\zeta\omega_n$ (see Fig. 6.39). Because $t_s = 4/\zeta\omega_n$, the lines representing constant settling time are vertical lines, as shown in Fig. 6.42. This figure also shows the contours for constant t_r. These contours allow us to determine by inspection the important transient characteristics (PO, t_r, t_s) of a second-order system from the knowledge of its pole locations. Moreover, if we are required to synthesize a second-order system to meet some given transient specifications, we can find the desired $T(s)$ with the help of this figure.

As an example, consider the position control system in Fig. 6.36a. Let the transient specifications for this system be given as

$$\text{PO} \leq 16\%, \qquad t_r \leq 0.5 \text{ seconds}, \qquad t_s \leq 2 \text{ seconds} \tag{6.48}$$

We delineate appropriate contours in Fig. 6.42 to meet the given specifications. The shaded region defined by these contours in Fig. 6.43 meets all three requirements. Hence, $T(s)$ must be chosen so that both of its poles lie in the shaded region.

The transfer function $T(s)$ for the closed-loop system in Fig. 6.36a is given by

$$T(s) = \frac{KG(s)}{1 + KG(s)} = \frac{K}{s^2 + 8s + K}$$

This shows that locations of the poles of $T(s)$ can be adjusted by changing the gain K. We must choose the gain K so that the poles lie in the shaded region in Fig. 6.43. The poles of $T(s)$ are the roots of the characteristic equation

$$s^2 + 8s + K = 0$$

Hence, the poles are

$$s_{1,2} = -4 \pm \sqrt{16 - K}$$

The poles s_1 and s_2 (the roots of the characteristic equation) move along a certain path in the s plane as we vary K from 0 to ∞. When $K = 0$, the poles are -8, 0. For $K < 16$, the poles are real and both poles move toward a value -4 as K varies from 0 to 16 (overdamping). For $K = 16$, both poles coincide at -4 (critical damping). For $K > 16$, the poles become complex with values $-4 \pm j\sqrt{K - 16}$ (underdamping). Since the real part of the poles is -4 for all $K > 16$, the path of the poles is vertical, as illustrated in Fig. 6.43. One pole moves up and the other (its conjugate) moves down along the vertical line passing through -4. We can label the values of K for several points along these paths, as depicted in Fig. 6.43. Each of these paths represents the locus of a pole of $T(s)$ or the locus of a root of the characteristic equation of $T(s)$ as K is varied from 0 to ∞. For this reason, this set of paths is called the *root locus*. The root locus gives us information as to how the poles of the closed-loop transfer function $T(s)$ move as the gain K is varied from 0 to ∞. In our design problem, we must choose a value of K such that the poles of $T(s)$ lie in the shaded region illustrated in Fig. 6.43. This figure shows that the system will meet the given specifications [Eq. (6.48)] for $25 \leq K \leq 64$. For $K = 64$, for instance, we have

$$\text{PO} = 16\%, \qquad t_r = 0.2 \text{ seconds}, \qquad t_s = \frac{4}{4} = 1 \text{ seconds}$$

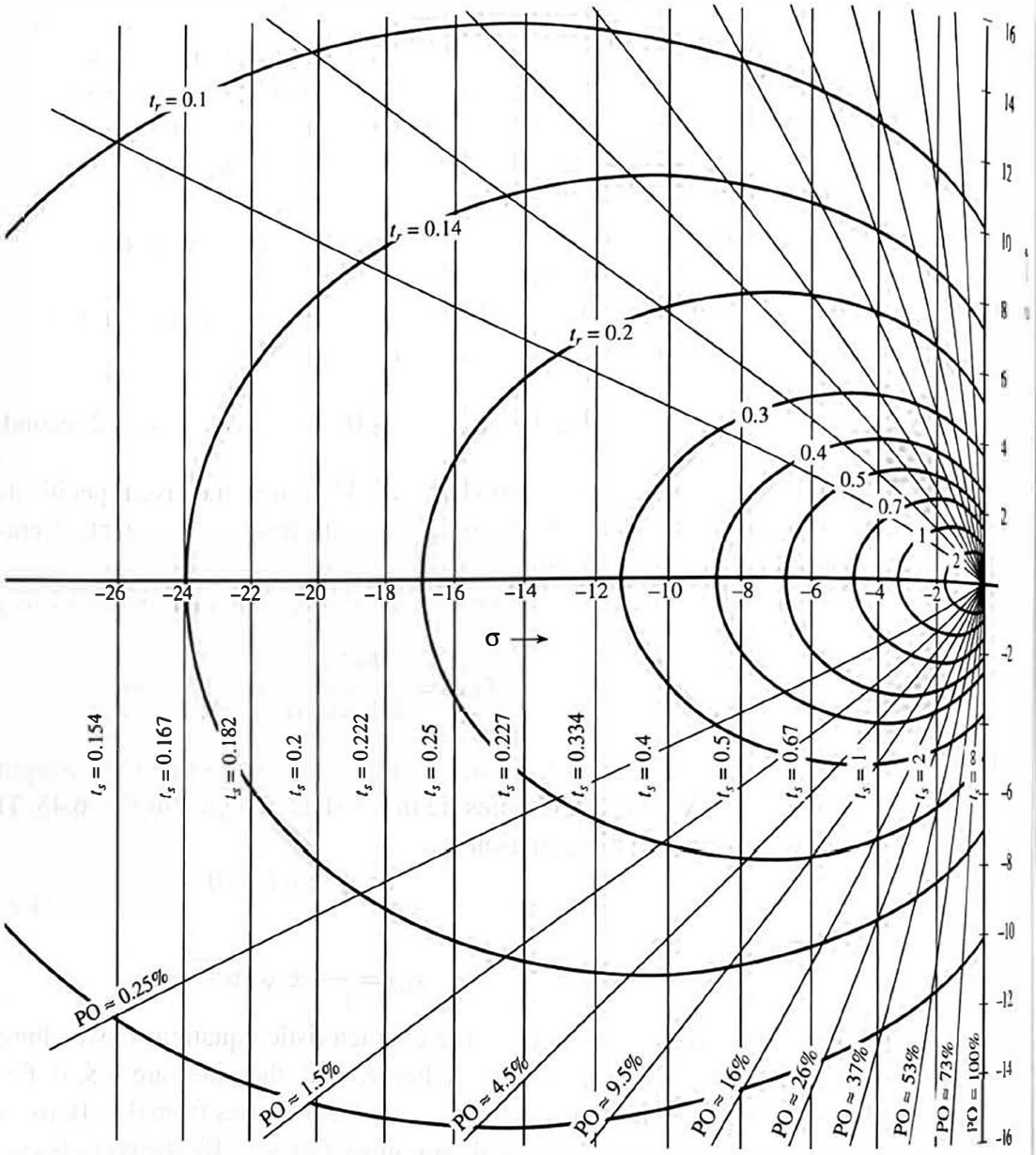

Figure 6.42 Contours of second-order system pole locations for constant PO, constant t_s, and constant t_r.

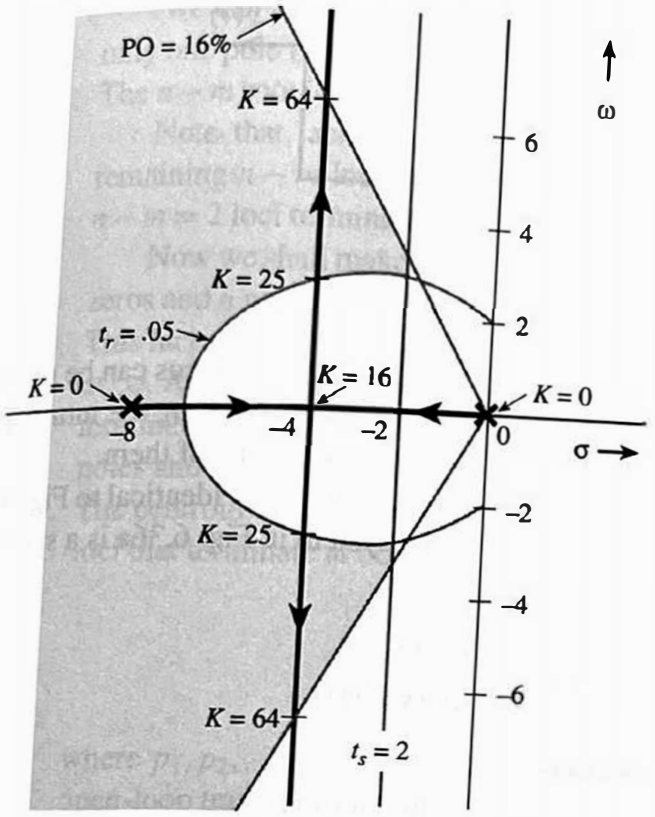

Figure 6.43 Designing a second-order system to meet a given set of transient specifications.

Higher-Order Systems

Our discussion, so far, has been limited to second-order $T(s)$ only. If $T(s)$ has additional poles that are far away to the left of the ω axis, they have only a negligible effect on the transient behavior of the system. The reason is that the time constants of such poles are considerably smaller when compared to the time constant of the complex conjugate poles near the ω axis. Consequently, the exponentials arising because of poles far away from the ω axis die quickly compared to those arising because of poles located near the ω axis. In addition, the coefficients of the former terms are much smaller than unity. Hence, they are also very small to begin with and decay rapidly. The poles near the ω axis are called the *dominant poles*. A criterion commonly used is that any pole that is five times as far from the ω axis as the dominant poles contributes negligibly to the step response, and the transient behavior of a higher-order system is often reduced to that of a second-order system. In addition, a closely placed pole-zero pair (called a *dipole*) contributes negligibly to transient behavior. For this reason, many of the pole-zero configurations, in practice, reduce to two or three poles with one or two zeros. Designers utilize computer-generated charts to track the transient behavior of these systems for several such pole-zero combinations, which may be used to design most higher-order systems.

6.7.3 Root Locus

The example in Sec. 6.7.2 gives a good idea of the utility of root locus in the design of control systems. Surprisingly, the root locus can be sketched quickly using certain basic rules provided by

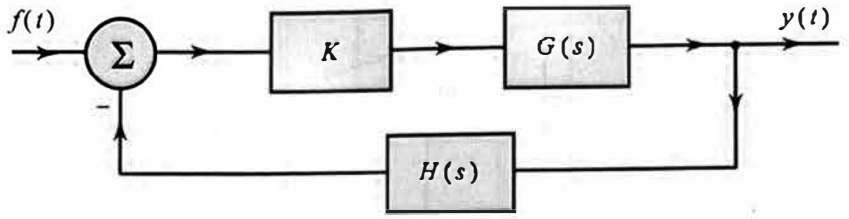

Figure 6.44 A feedback system with a variable gain K.

W. R. Evans in 1948.[†] With the ready availability of computers, root locus can be produced easily. Nevertheless, understanding these rules can be a great help in developing the intuition needed for design. Here, we shall present the rules, but omit the proofs for some of them.

We begin with a feedback system depicted in Fig. 6.44, which is identical to Fig. 6.19d, except for the explicit representation of a variable gain K. The system in Fig. 6.36a is a special case with $H(s) = 1$. For the system in Fig. 6.44,

$$T(s) = \frac{KG(s)}{1 + KG(s)H(s)} \tag{6.49}$$

The characteristic equation of this system is[‡]

$$1 + KG(s)H(s) = 0$$

We shall consider the paths of the roots of $1 + KG(s)H(s) = 0$ as K varies from 0 to ∞. In the parlance of control theory, $KG(s)H(s)$ is referred to as the *open-loop transfer function.*[§] The rules for sketching the root locus are as follows:

1. Root loci begin ($K = 0$) at the open-loop poles and terminate at the open-loop zeros ($K = \infty$). This fact means that the number of loci is exactly n, the order of the open-loop transfer function. Let $G(s)H(s) = N(s)/D(s)$, where $N(s)$ and $D(s)$ are polynomials of powers m and n, respectively. Hence, $1 + KG(s)H(s) = 0$ implies $D(s) + KN(s) = 0$. Therefore, $D(s) = 0$ when $K = 0$. In this case, the roots are poles of $G(s)H(s)$; that is, the open-loop poles. Similarly, when $K \to \infty$, $D(s) + KN(s) = 0$ implies $N(s) = 0$. Hence, the roots are the open-loop zeros. For the system in Fig. 6.36a, the open-loop transfer function is $K/s(s+8)$. The open-loop poles are 0 and -8 and the zeros [where $K/s(s+8) = 0$] are both ∞. We can verify from Fig. 6.43 that the root loci do begin at 0 and -8 and terminate at ∞.
2. A real axis segment is a part of the root locus if the sum of the real axis poles and zeros of $G(s)H(s)$ that lie to the right of the segment is odd. Moreover, the root loci are symmetric about the real axis.

[†] This procedure was developed as early as 1868 in Maxwell's paper "On Governors."

[‡] This characteristic equation is also valid when the gain K is in the feedback path [lumped with $H(s)$] rather than in the forward path. The equation applies as long as the gain K is in the loop at any point. Hence, the root locus rules discussed here apply to all such cases.

[§] This terminology is more clearly understandable viewed from another common feedback control configuration, where $H(s)$ is present in the feedforward loop rather than the feedback loop, as done in this text.

We can readily verify in Fig. 6.43 that the real axis segment to the right of -8 has only one pole (and no zeros). Hence, this segment is a part of the root locus.

3. The $n-m$ root loci terminate at ∞ at angles $k\pi/(n-m)$ for $k=1,3,5,\ldots$.

   Note that, according to rule 1, m loci terminate on the open-loop zeros, and the remaining $n-m$ loci terminate at ∞ according to this rule. In Fig. 6.43, we verify that $n-m=2$ loci terminate at ∞ at angles $k\pi/2$ for $k=1$ and 3.

   Now we shall make an interesting observation. If a transfer function $G(s)$ has m (finite) zeros and n poles, then $\lim_{s\to\infty} G(s)=s^m/s^n=1/s^{n-m}$. Hence, $G(s)$ has $n-m$ zeros at ∞. This fact shows that although $G(s)$ has only m finite zeros, there are additional $n-m$ zeros at ∞. According to rule 1, m loci terminate on m finite zeros and the remaining $n-m$ loci terminate at ∞, which are also zeros of $G(s)$. This result means all loci begin on open-loop poles and terminate on open-loop zeros.

4. The centroid of the asymptotes (the point where the asymptotes converge) of the $(n-m)$ loci that terminate at ∞ is

$$\sigma=\frac{(p_1+p_2+\cdots+p_n)-(z_1+z_2-\cdots+z_m)}{(n-m)}$$

   where $p_1,p_2,\ldots,p_n$ are the poles and $z_1,z_2,\ldots,z_m$ are the zeros, respectively, of the open-loop transfer function.

   Figure 6.43 verifies that the centroid of the loci is $[(-8+0)-0]/2=-4$.

5. There are additional rules that allow us to compute the points where the loci intersect and where they cross the ω axis to enter the right-half plane. These rules allow us to draw a quick and rough sketch of the root loci. But the ready availability of computers and programs makes it much easier to draw actual loci. The first four rules are still very helpful for a quick sketching of the root loci.

Understanding these rules can be helpful in the design of control systems, as demonstrated later. They aid in determining what modifications should be made (or what kind of compensator to add) to the open-loop transfer function in order to meet given design specifications.

EXAMPLE 6.27 Sketching the Root Locus of a Third-Order Feedback System

Using the four rules for root loci, sketch the root locus for a system with open-loop transfer function

$$KG(s)H(s)=\frac{K}{s(s+2)(s+4)}$$

Rule 1: For this $G(s)H(s)$, $n=3$. Hence, there are three root loci, which begin at the poles of $G(s)H(s)$; that is, at 0, -2, and -4.

Rule 2: There are odd numbers of poles to the right of the real axis segment $s < -4$, and $-2 < s < 0$. Hence, these segments are part of the root locus. In other words, the entire real axis in the left-half plane, except the segment between -2 and -4, is a part of the root locus.

Rule 3: In this case, $n - m = 3$. Hence, all three loci terminate at ∞ along asymptotes at angles $k\pi/3$ for $k = 1$, 3, and 5. Thus, the asymptote angles are 60°, 120°, and 180°.

Rule 4: The centroid (where all three asymptotes converge) is $(0 - 2 - 4)/3 = -2$.

We draw three asymptotes starting at -2 at angles 60°, 120° and 180°, as illustrated in Fig. 6.45. These three straight-line asymptotes suffice to give an idea about the root locus. The actual root loci are also shown as continuous curves in Fig. 6.45. Two of the asymptotes cross over to the RHP, behavior which shows that for some range of K, the system becomes unstable.

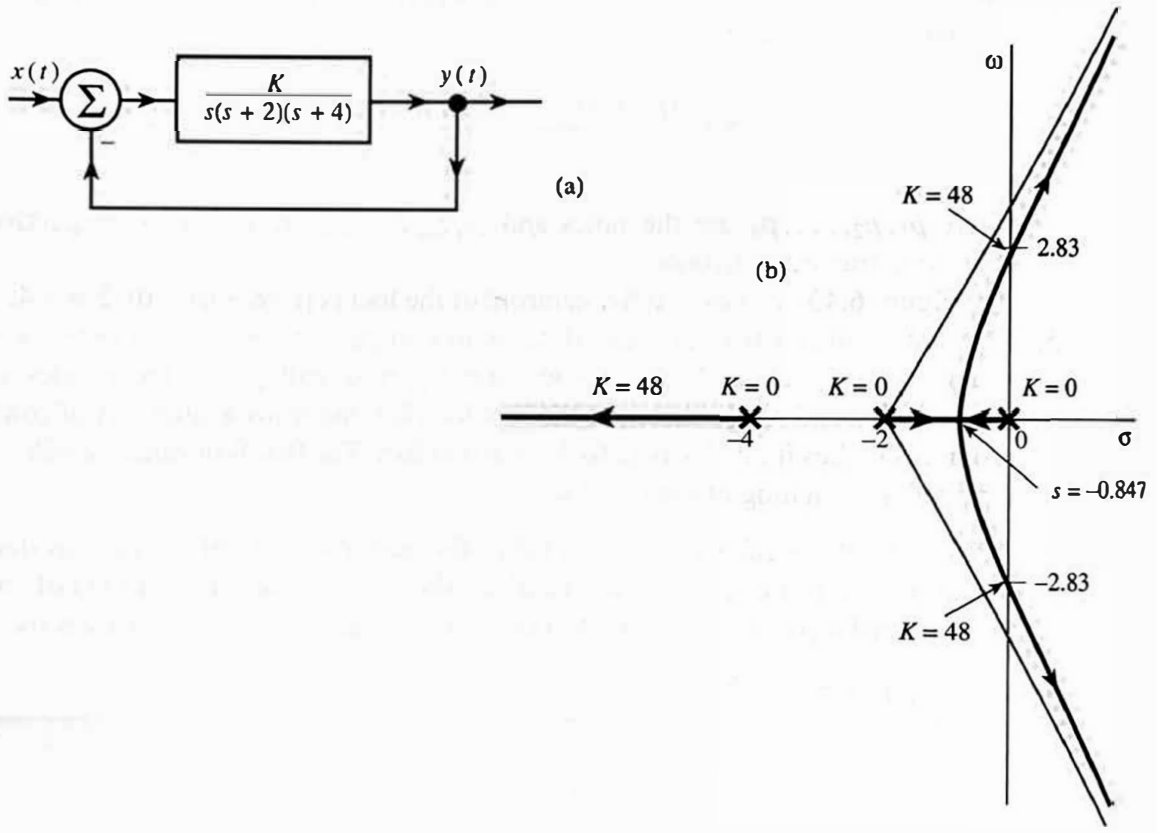

Figure 6.45 A third-order feedback system and its root locus.

MATLAB's control system toolbox provides a simple tool to generate a system's root locus plot. The result, shown in Fig. 6.46, matches our earlier result of Fig. 6.45b.

```
>> num = [0 0 0 1]; den = conv(conv([1 0],[1 2]),[1 4]);
>> H = tf(num,den); rlocusplot(H,'k-');
```

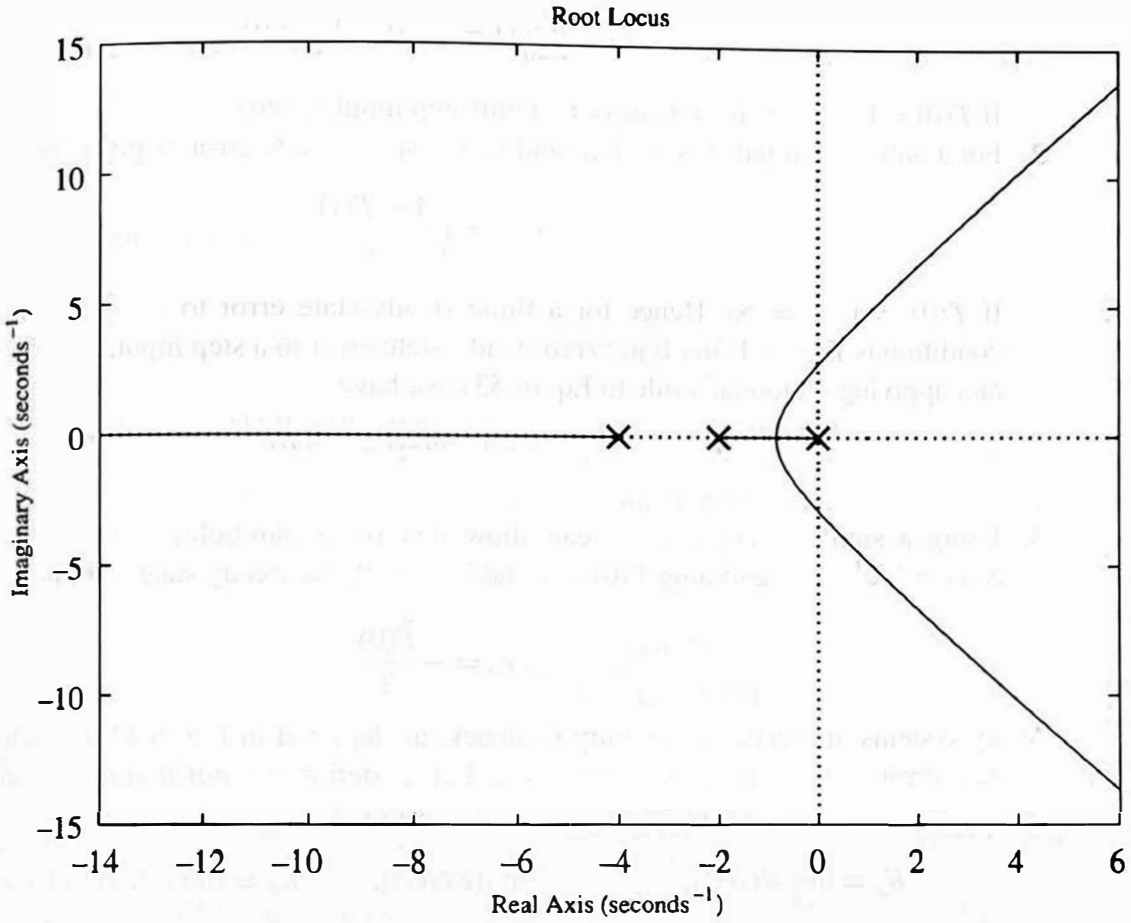

Figure 6.46 MATLAB root locus plot for Ex. 6.27.

6.7.4 Steady-State Errors

Steady-state specifications impose additional constraints on the closed-loop transfer function $T(s)$. We define the error as the difference between the desired output [reference $x(t)$] and the actual output $y(t)$. Thus, $e(t) = x(t) - y(t)$, and

$$E(s) = X(s) - Y(s) = X(s)\left[1 - \frac{Y(s)}{X(s)}\right] = X(s)[1 - T(s)] \tag{6.50}$$

The steady-state error e_{ss} is the value of $e(t)$ as $t \to \infty$. This value can be readily obtained from the final-value theorem [Eq. (6.25)] as

$$e_{ss} = \lim_{s \to 0} sE(s) = \lim_{s \to 0} sX(s)[1 - T(s)] \tag{6.51}$$

Let us look at steady-state error for a variety of inputs.

1. For the unit step input, the steady-state error e_s is given by

$$e_s = \lim_{s\to 0}[1 - T(s)] = 1 - T(0) \tag{6.52}$$

If $T(0) = 1$, the steady-state error to a unit step input is zero.

2. For a unit ramp input, $X(s) = 1/s^2$ and e_r, the steady-state error, is given by

$$e_r = \lim_{s\to 0}\frac{1 - T(s)}{s} \tag{6.53}$$

If $T(0) \neq 1$, $e_r = \infty$. Hence for a finite steady-state error to ramp input, a necessary condition is $T(0) = 1$, implying zero steady-state error to a step input. Assuming $T(0) = 1$ and applying L'Hopital's rule to Eq. (6.53), we have

$$e_r = \lim_{s\to 0}[-\dot{T}(s)] = -\dot{T}(0)$$

3. Using a similar argument, we can show that for a parabolic input $x(t) = (t^2/2)u(t)$, $X(s) = 1/s^3$, and, assuming $T(0) = 1$ and $\dot{T}(0) = 0$, the steady state error is

$$e_p = -\frac{\ddot{T}(0)}{2} \tag{6.54}$$

Many systems in practice have unity feedback, as depicted in Fig. 6.47. In such a case, the steady-state error analysis is greatly simplified. Let us define the *positional error constant* K_p, *velocity error constant* K_v, and *acceleration error constant* K_a as

$$K_p = \lim_{s\to 0}[KG(s)], \qquad K_v = \lim_{s\to 0} s[KG(s)], \qquad K_a = \lim_{s\to 0} s^2[KG(s)] \tag{6.55}$$

Because $T(s) = KG(s)/1 + KG(s)$, from Eq. (6.50), we obtain

$$E(s) = \frac{1}{1 + KG(s)}X(s)$$

The steady-state errors are given by

$$\begin{aligned} e_s &= \lim_{s\to 0} s\frac{1/s}{1 + KG(s)} = \frac{1}{1 + \lim_{s\to 0}[KG(s)]} = \frac{1}{1 + K_p} \\ e_r &= \lim_{s\to 0} s\frac{1/s^2}{1 + KG(s)} = \frac{1}{\lim_{s\to 0} s[KG(s)]} = \frac{1}{K_v} \\ e_p &= \lim_{s\to 0} s\frac{1/s^3}{1 + KG(s)} = \frac{1}{\lim_{s\to 0} s^2[KG(s)]} = \frac{1}{K_a} \end{aligned} \tag{6.56}$$

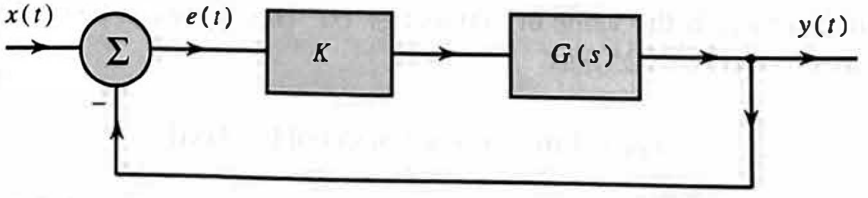

Figure 6.47 A unity feedback system with variable gain K.

For the system in Fig. 6.36a,

$$G(s) = \frac{1}{s(s+8)}$$

Hence, from Eq. (6.55),

$$K_p = \infty, \qquad K_v = \frac{K}{8}, \qquad K_a = 0 \tag{6.57}$$

Substitution of these values into Eq. (6.56) yields

$$e_s = 0, \qquad e_r = \frac{8}{K}, \qquad e_p = \infty$$

A system where $G(s)$ has one pole at the origin (as in the present case) is designated as a *type 1* system. Such a system can track the position of an object with zero (steady-state) error ($e_s = 0$), and yields a constant error in tracking an object moving with constant velocity (e_r = a constant). But the type 1 system is not suitable for tracking a constant acceleration object.

If $G(s)$ has no poles at the origin, then K_p is finite and $K_v = K_a = 0$. Thus, for

$$G(s) = \frac{(s+2)}{(s+1)(s+10)}$$

$K_p = K/5$ and $K_v = K_a = 0$. Hence, $e_s = 5/(5+K)$ and $e_r = e_p = \infty$. Such systems are designated as *type 0* systems. These systems have finite e_s, but infinite e_r and e_p. These systems may be acceptable for step inputs (position control), but not for ramp or parabolic inputs (tracking velocity or acceleration).

If $G(s)$ has two poles at the origin, the system is designated as a *type 2* system. In this case, $K_p = K_v = \infty$, and K_a is finite. Hence, $e_s = e_r = 0$ and e_p is finite.

In general, if $G(s)$ has q poles at the origin, it is a type q system. Clearly, for a unity feedback system, increasing the number of poles at the origin in $G(s)$ improves the steady-state performance. However, this procedure increases n and reduces the magnitude of σ, the centroid of the root locus asymptotes. This shifts the root locus toward the ω axis, with consequent deterioration in the transient performance and the system stability.

It should be remembered that the results in Eqs. (6.55) and (6.56) apply only to unity feedback systems (Fig. 6.47). Steady-state error specifications in this case are translated in terms of constraints on the open-loop transfer function $KG(s)$. In contrast, the results in Eqs. (6.52) through (6.54) apply to unity as well as nonunity feedback systems, and are more general. Steady-state-error specifications in this case are translated in terms of constraints on the closed-loop transfer function $T(s)$.

The unity feedback system in Fig. 6.36a is a type 1 system. We have designed this system earlier to meet the transient specifications of Eq. (6.48):

$$\text{PO} = 16\%, \qquad t_r \le 0.5, \qquad t_s \le 2$$

Let us further specify that the system meet the following steady-state specifications:

$$e_s = 0 \qquad \text{and} \qquad e_r \le 0.15 \tag{6.58}$$

For this case, we already found $e_s = 0$, $e_r = 8/K$, and $e_p = \infty$ [see Eq. (6.57)]. But we require $e_r \leq 0.15$. Therefore,

$$\frac{8}{K} \leq 0.15 \quad \Rightarrow K \geq 53.34$$

Turning to Fig. 6.43, we note that the poles of $T(s)$ lie in the acceptable region to meet transient specifications ($25 < K < 64$). Equation (6.58) shows that we must use $K \geq 53.34$ to meet steady-state performance. Therefore, to meet both the transient and the steady-state specifications, we must set the gain in the range $53.34 < K < 64$. The smallest steady-state error for a ramp input is obtained for $K = 64$. For this case,

$$e_r = \frac{8}{K} = \frac{8}{64} = 0.125$$

Thus if the system is to meet the transient performance [see Eq. (6.48)], the minimum $e_r = 0.125$. We can do no better. In case we are required to have $e_r < 0.125$ while maintaining the same transient performance, we will have to use some kind of compensation.

6.7.5 Compensation

The synthesis problem for the position control system in Fig. 6.36a is a very simple example where the transient and steady-state specifications could be met by a simple adjustment of gain K. In many cases, it may be impossible to meet both sets of specification (transient and steady state) by simple adjustment of the gain K. We may be able to satisfy one set of specifications or the other, but not both. Consider again the system in Fig. 6.36a, with the following specifications:

$$\text{PO} = 16\%, \qquad t_r \leq 0.5, \qquad t_s \leq 2, \qquad e_s = 0, \qquad \text{and} \qquad e_r \leq 0.05$$

To meet the steady-state specification, we must have

$$\frac{8}{K} \leq 0.05 \quad \Rightarrow \quad K \geq 160$$

But Fig. 6.43 indicates that for $K > 64$, the poles of $T(s)$ move out of the region acceptable for transient performance. Clearly, we can meet either the transient or the steady-state specification but not both. In such a case, we must add some kind of compensation, which will modify the root locus to meet all the specifications. A little familiarity with root locus techniques gives one the insight and judgment needed to choose a proper compensator transfer function. Figure 6.43 indicates that shifting the root locus to the left will accomplish the desired performance. We can place a compensator of transfer function $G_c(s)$ in series with $G(s)$ (Fig. 6.48a) and select the poles and zeros of $G_c(s)$ in such a way as to shift the centroid of the root locus to the left. If $G_c(s)$ has a single pole and a single zero, then choosing the pole farther to the left of the zero would shift the centroid to the left according to the fourth rule of the root locus. Thus, we use

$$G_c(s) = \frac{s+\alpha}{s+\beta} \qquad \beta > \alpha$$

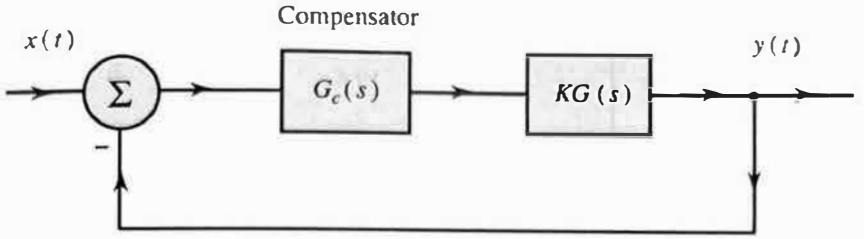

(a)

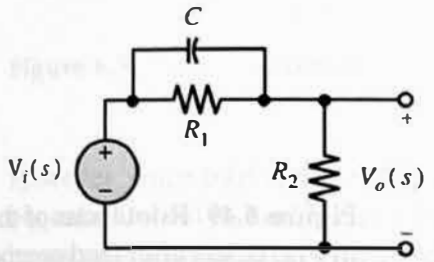

(b)

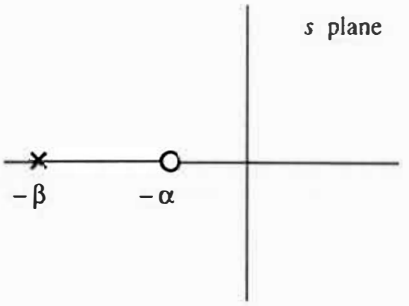

$$G_c(s) = \frac{V_o(s)}{V_i(s)} = \frac{s+\alpha}{s+\beta} \quad \text{where } \alpha = \frac{1}{R_1 C}, \ \beta = \frac{R_1+R_2}{R_1 R_2 C}$$

Figure 6.48 A lead compensator.

Such a compensator is called a *lead compensator*, which is readily realized using a simple *RC* circuit shown in Fig. 6.48b. We have a wide choice for values of α and β. To simplify the design, let us choose $\alpha = 8$ and $\beta = 30$. This choice yields

$$G_c(s)[KG(s)] = \left(\frac{s+8}{s+30}\right)\frac{K}{s(s+8)} = \frac{K}{s(s+30)}$$

To simplify our discussion, we deliberately chose $\alpha = 8$ to cancel the pole of $G(s)$. In practice, we do not necessarily have to cancel the pole of $G(s)$. In the present situation, $\sigma = (-30+0)/2 = -15$, and the new root locus appears as shown in Fig. 6.49.

With lead compensation, observe that the situation has improved considerably by shifting the centroid from -4 to -15. If we select $K = 600$, we have

$$T(s) = \frac{\frac{600}{s(s+30)}}{1+\frac{600}{s(s+30)}} = \frac{600}{s^2+30s+600}$$

In this case, $\omega_n = \sqrt{600} = 24.5$. Also, $\zeta\omega_n = 15$. Hence, $\zeta = 15/24.5 = 0.61$ and $t_s = 4/\zeta\omega_n = 4/15 = 0.266$. From Eq. (6.46), we find PO = 8.9%. Moreover, from Fig. 6.41 [or Eq. (6.47)], for $\zeta = 0.61$, we find $\omega_n t_r = 1.83$ so that $t_r = 1.83/24.5 = 0.0747$. We also have

$$K_p = \infty, \quad K_v = \frac{K}{30} = \frac{600}{30} = 20 \quad \Rightarrow \quad e_s = 0, \quad e_r = \frac{1}{20} = 0.05$$

The system meets all the specifications and more.

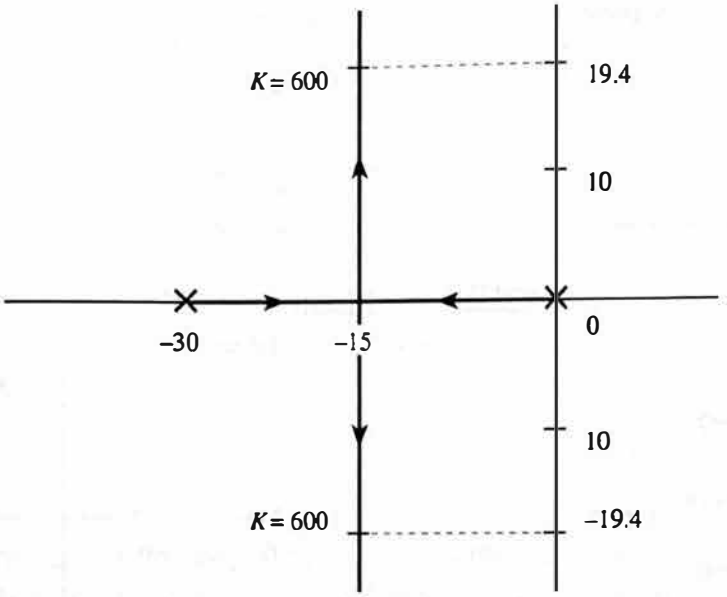

Figure 6.49 Root locus of the system in Fig. 6.36a after lead compensation.

We shall now discuss a compensation that is primarily used to improve steady-state performance. For unity feedback systems, the steady-state performance of a system is improved by placing an integrator in the forward path of $G(s)$. This procedure increases the system type, thus increasing K_p, K_v, K_a, and so on. The compensator in this case is $G_c(s) = 1/s$.

In this scheme, the compensator is an ideal integrator. Hence, this scheme is known as *integral control*. Design of an ideal integrator necessitates elaborate and expensive equipment. Hence, such a compensator is used where cost considerations are not very important. For example, integrating gyroscopes are used for this purpose in aircraft. In most cases, a *lag compensator* (described below), which closely approximates the behavior of an integrator, is used. A lag compensator transfer function is given by

$$G_c(s) = \frac{s+\alpha}{s+\beta} \qquad \alpha > \beta$$

so that

$$G_c(0) = \frac{\alpha}{\beta}$$

A lag compensator can be readily realized using a simple RC circuit, as depicted in Fig. 6.50. For a unity feedback system, the addition of a compensator $G_c(s)$ causes all the error constants K_p, K_v, K_a, and so on, to be multiplied by $G_c(0)$. Thus, the lag compensator increases K_p, K_v, K_a, and the like by a factor (α/β), thereby reducing steady-state errors.

A lag compensator improves steady-state performance, but, in general, degrades transient performance. Since $\alpha > \beta$, the magnitude of σ, the root locus centroid, is reduced. This reduction causes the root locus to shift toward the ω axis, with the consequent deterioration of the transient performance. This side effect of a lag compensator can be made negligible by choosing α and β such that $\alpha - \beta$ is very small, but the ratio α/β is high. Such a pair of pole and zero act like a dipole and have only a negligible effect on the transient behavior of the system. The root locus also changes very little. We can realize such a dipole by placing both the pole and the zero of $G_c(s)$ close to the origin (α and $\beta \to 0$). For instance, if we select $\alpha = 0.1$ and $\beta = 0.01$, the centroid will be shifted by only a negligible amount $(\alpha - \beta)/(n - m) = 0.09/(n - m)$.

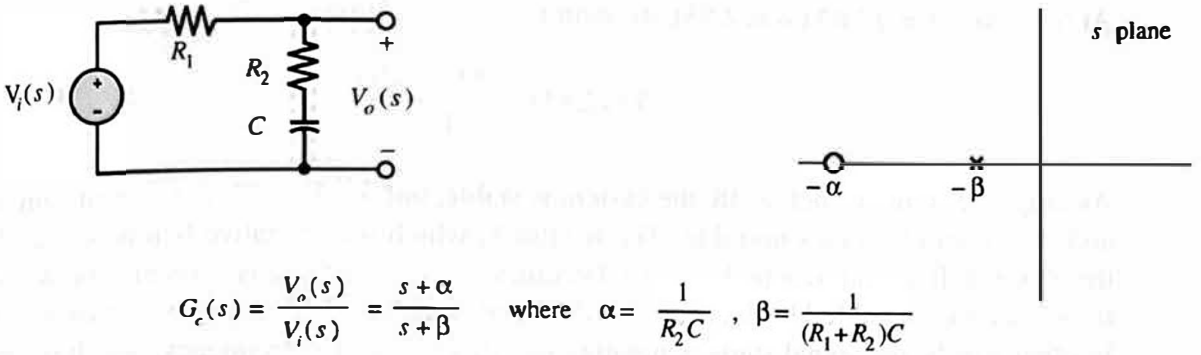

$$G_c(s) = \frac{V_o(s)}{V_i(s)} = \frac{s+\alpha}{s+\beta} \quad \text{where} \quad \alpha = \frac{1}{R_2 C}, \quad \beta = \frac{1}{(R_1+R_2)C}$$

Figure 6.50 A lag compensator.

However, since $\alpha/\beta = 10$, all the error constants are increased by a factor of 10. Thus, we can have our cake and eat it, too! We can improve the transient and steady-state performance simultaneously by using a combination of lead and lag networks.

6.7.6 Stability Considerations

In practice, we rarely use positive feedback because, as explained earlier, such systems are prone to instability and are very sensitive to changes in the system parameters or environment. Would negative feedback make a system stable and less sensitive to unwanted changes? Not necessarily! The reason is that if a feedback were truly negative, the system would be stable. But a system that has negative feedback at one frequency may have positive feedback at some other frequency because of phase shift in the transmission path. In other words, a feedback system generally cannot be described in black and white terms such as having positive or negative feedback. Let us clarify this statement by an example.

Consider the case $G(s)H(s) = 1/s(s+2)(s+4)$. The root locus of this system appears in Fig. 6.45b. This system shows negative feedback at lower frequencies. But because of phase shift at higher frequencies, the feedback becomes positive. Consider the loop gain $G(s)H(s)$ at a frequency $\omega = 2.83$ (at $s = j2.83$).

$$G(j\omega)H(j\omega) = \frac{1}{j\omega(j\omega+2)(j\omega+4)}$$

At $\omega = 2.83$,

$$G(j2.83)H(j2.83) = \frac{1}{j2.83(j2.83+2)(j2.83+4)}$$
$$= \frac{1}{48}e^{-j180^\circ} = -\frac{1}{48}$$

Recall that the overall gain (transfer function) $T(s)$ is

$$T(s) = \frac{KG(s)}{1+KG(s)H(s)}$$

At frequency $s = j2.83$ ($\omega = 2.83$), the gain is

$$T(j2.83) = \frac{KG(j2.83)}{1 - \frac{K}{48}}$$

As long as K remains below 48, the system is stable, but for $K = 48$, the system gain goes to ∞, and the system becomes unstable. The feedback, which was negative below $\omega = 2.83$ (because the phase shift has not reached $-180°$), becomes positive. If there is enough gain ($K = 48$) at this frequency, the signal fed back is equal to the input signal, and the signal perpetuates itself forever. In other words, the signal starts generating (oscillating) at this frequency, which is precisely the instability. Note that the system remains unstable for all values of $K > 48$. This is clear from the root locus in Fig. 6.45b, which shows that the two branches cross over to the RHP for $K > 48$. The crossing point is $s = j2.83$.

This discussion shows that the same system, which has negative feedback at lower frequency, may have positive feedback at higher frequency. For this reason, feedback systems are quite prone to instability, and the designer has to pay a great deal of attention to this aspect. Root locus does indicate the region of stability.

6.8 THE BILATERAL LAPLACE TRANSFORM

Situations involving noncausal signals and/or systems cannot be handled by the (unilateral) Laplace transform discussed so far. These cases can be analyzed by the *bilateral* (or *two-sided*) Laplace transform defined by

$$X(s) = \int_{-\infty}^{\infty} x(t)e^{-st}\,dt$$

and $x(t)$ can be obtained from $X(s)$ by the inverse transformation

$$x(t) = \frac{1}{2\pi j}\int_{c-j\infty}^{c+j\infty} X(s)e^{st}\,ds$$

Observe that the unilateral Laplace transform discussed so far is a special case of the bilateral Laplace transform, where the signals are restricted to the causal type. Basically, the two transforms are the same. For this reason, we use the same notation for the bilateral Laplace transform.

Earlier we showed that the Laplace transforms of $e^{-at}u(t)$ and of $-e^{-at}u(-t)$ are identical. The only difference is in their regions of convergence (ROC). The ROC for the former is $\text{Re}\,s > -a$; that for the latter is $\text{Re}\,s < -a$, as illustrated in Fig. 6.2. Clearly, the inverse Laplace transform of $X(s)$ is not unique unless the ROC is specified. If we restrict all our signals to the causal type, however, this ambiguity does not arise. The inverse transform of $1/(s+a)$ is $e^{-at}u(t)$. Thus, in the unilateral Laplace transform, we can ignore the ROC in determining the inverse transform of $X(s)$.

We now show that any bilateral transform can be expressed in terms of two unilateral transforms. It is, therefore, possible to evaluate bilateral transforms from a table of unilateral transforms.

Consider the function $x(t)$ appearing in Fig. 6.51a. We separate $x(t)$ into two components, $x_1(t)$ and $x_2(t)$, representing the positive time (*causal*) component and the negative time (*anticausal*) component of $x(t)$, respectively (Figs. 6.51b and 6.51c):

$$x_1(t) = x(t)u(t) \qquad \text{and} \qquad x_2(t) = x(t)u(-t)$$

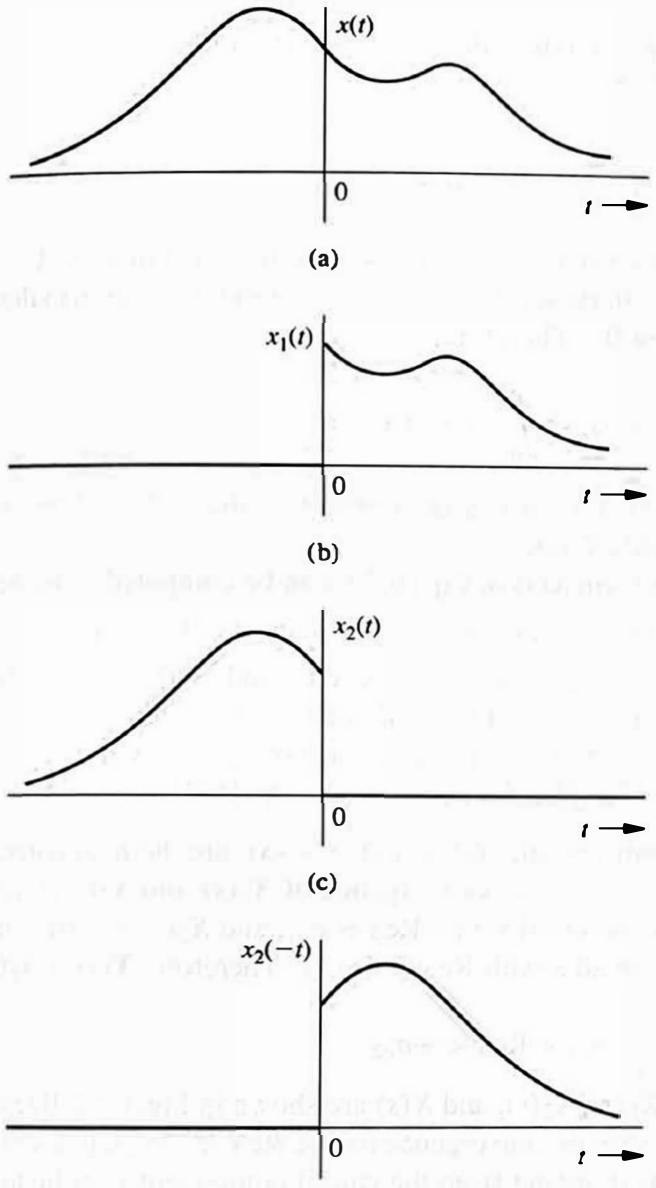

Figure 6.51 Expressing a signal as a sum of causal and anticausal components.

The bilateral Laplace transform of $x(t)$ is given by

$$\begin{aligned} X(s) &= \int_{-\infty}^{\infty} x(t)e^{-st}\,dt \\ &= \int_{-\infty}^{0^-} x_2(t)e^{-st}\,dt + \int_{0^-}^{\infty} x_1(t)e^{-st}\,dt \\ &= X_2(s) + X_1(s) \end{aligned} \tag{6.59}$$

where $X_1(s)$ is the Laplace transform of the causal component $x_1(t)$, and $X_2(s)$ is the Laplace transform of the anticausal component $x_2(t)$. Consider $X_2(s)$, given by

$$X_2(s) = \int_{-\infty}^{0^-} x_2(t)e^{-st}\,dt = \int_{0^+}^{\infty} x_2(-t)e^{st}\,dt$$

Therefore,

$$X_2(-s) = \int_{0^+}^{\infty} x_2(-t)e^{-st}\,dt$$

If $x(t)$ has any impulse or its derivative(s) at the origin, they are included in $x_1(t)$. Consequently, $x_2(t) = 0$ at the origin; that is, $x_2(0) = 0$. Hence, the lower limit on the integration in the preceding equation can be taken as 0^- instead of 0^+. Therefore,

$$X_2(-s) = \int_{0^-}^{\infty} x_2(-t)e^{-st}\,dt$$

Because $x_2(-t)$ is causal (Fig. 6.51d), $X_2(-s)$ can be found from the unilateral transform table. Changing the sign of s in $X_2(-s)$ yields $X_2(s)$.

To summarize, the bilateral transform $X(s)$ in Eq. (6.59) can be computed from the unilateral transforms in two steps:

1. Split $x(t)$ into its causal and anticausal components, $x_1(t)$ and $x_2(t)$, respectively.
2. Since the signals $x_1(t)$ and $x_2(-t)$ are both causal, take the (unilateral) Laplace transform of $x_1(t)$ and add to it the (unilateral) Laplace transform of $x_2(-t)$, with s replaced by $-s$. This procedure gives the (bilateral) Laplace transform of $x(t)$.

Since $x_1(t)$ and $x_2(-t)$ are both causal, $X_1(s)$ and $X_2(-s)$ are both unilateral Laplace transforms. Let σ_{c1} and σ_{c2} be the abscissas of convergence of $X_1(s)$ and $X_2(-s)$, respectively. This statement implies that $X_1(s)$ exists for all s with $\text{Re}\,s > \sigma_{c1}$, and $X_2(-s)$ exists for all s with $\text{Re}\,s > \sigma_{c2}$. Therefore, $X_2(s)$ exists for all s with $\text{Re}\,s < -\sigma_{c2}$.[†] Therefore, $X(s) = X_1(s) + X_2(s)$ exists for all s such that

$$\sigma_{c1} < \text{Re}\,s < -\sigma_{c2}$$

The regions of convergence of $X_1(s)$, $X_2(s)$, and $X(s)$ are shown in Fig. 6.52. Because $X(s)$ is finite for all values of s lying in the strip of convergence ($\sigma_{c1} < \text{Re}\,s < -\sigma_{c2}$), poles of $X(s)$ must lie outside this strip. The poles of $X(s)$ arising from the causal component $x_1(t)$ lie to the left of the *strip* (region) *of convergence*, and those arising from its anticausal component $x_2(t)$ lie to its right (see Fig. 6.52). This fact is of crucial importance in finding the inverse bilateral transform.

This result can be generalized to left-sided and right-sided signals. We define a signal $x(t)$ as a *right-sided* signal if $x(t) = 0$ for $t < T_1$ for some finite positive or negative number T_1. A causal signal is always a right-sided signal, but the converse is not necessarily true. A signal is said to be *left-sided* if it is zero for $t > T_2$ for some finite, positive, or negative number T_2. An anticausal signal is always a left-sided signal, but the converse is not necessarily true. A *two-sided* signal is of infinite duration on both positive and negative sides of t and is neither right-sided nor left-sided.

We can show that the conclusions for ROC for causal signals also hold for right-sided signals, and those for anticausal signals hold for left-sided signals. In other words, if $x(t)$ is causal or right-sided, the poles of $X(s)$ lie to the left of the ROC, and if $x(t)$ is anticausal or left-sided, the poles of $X(s)$ lie to the right of the ROC.

[†] For instance, if $x(t)$ exists for all $t > 10$, then $x(-t)$, its time-inverted form, exists for $t < -10$.

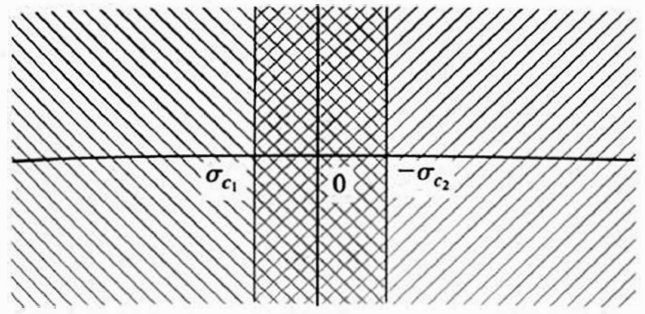

Figure 6.52 Regions of convergence for causal, anticausal, and combined signals.

To prove this generalization, we observe that a right-sided signal can be expressed as $x(t) + x_f(t)$, where $x(t)$ is a causal signal and $x_f(t)$ is some finite-duration signal. The ROC of any finite-duration signal is the entire s plane (no finite poles). Hence, the ROC of the right-sided signal $x(t) + x_f(t)$ is the region common to the ROCs of $x(t)$ and $x_f(t)$, which is the same as the ROC for $x(t)$. This proves the generalization for right-sided signals. We can use a similar argument to generalize the result for left-sided signals. Let us find the bilateral Laplace transform of

$$x(t) = e^{bt}u(-t) + e^{at}u(t) \tag{6.60}$$

We already know the Laplace transform of the causal component

$$e^{at}u(t) \Longleftrightarrow \frac{1}{s-a} \qquad \text{Re}s > a \tag{6.61}$$

For the anticausal component, $x_2(t) = e^{bt}u(-t)$, we have

$$x_2(-t) = e^{-bt}u(t) \Longleftrightarrow \frac{1}{s+b} \qquad \text{Re}s > -b$$

so that

$$X_2(s) = \frac{1}{-s+b} = \frac{-1}{s-b} \qquad \text{Re}s < b$$

Therefore,

$$e^{bt}u(-t) \Longleftrightarrow \frac{-1}{s-b} \qquad \text{Re}s < b \tag{6.62}$$

and the Laplace transform of $x(t)$ in Eq. (6.60) is

$$\begin{aligned} X(s) &= -\frac{1}{s-b} + \frac{1}{s-a} \qquad \text{Re}s > a \quad \text{and} \quad \text{Re}s < b \\ &= \frac{a-b}{(s-b)(s-a)} \qquad a < \text{Re}s < b \end{aligned} \tag{6.63}$$

Figure 6.53 shows $x(t)$ and the ROC of $X(s)$ for various values of a and b. Equation (6.63) indicates that the ROC of $X(s)$ does not exist if $a > b$, which is precisely the case in Fig. 6.53f.

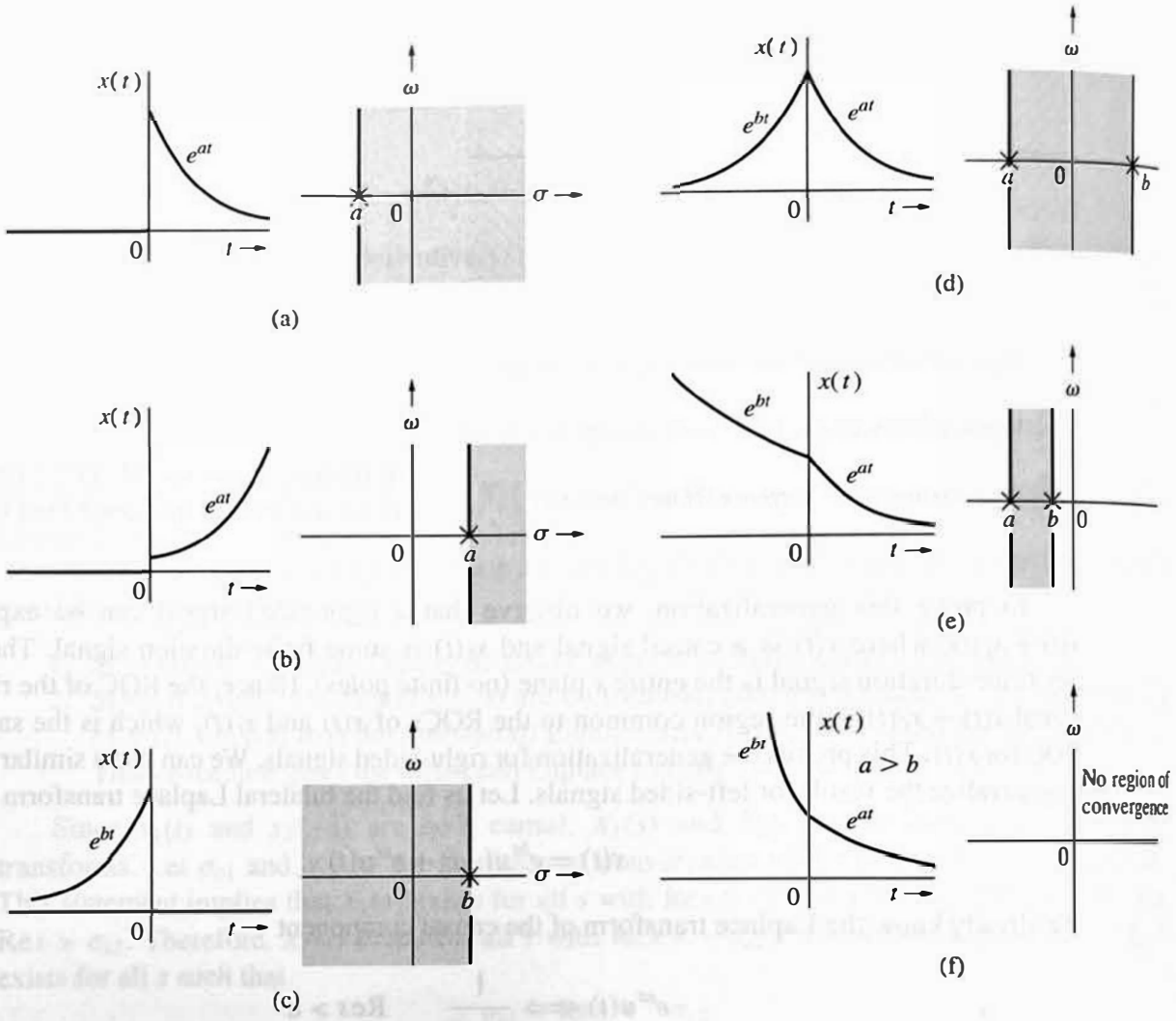

Figure 6.53 Various two exponential signals and their regions of convergence.

Observe that the poles of $X(s)$ are outside (on the edges) of the ROC. The poles of $X(s)$, because of the anticausal component of $x(t)$, lie to the right of the ROC, and those due to the causal component of $x(t)$ lie to its left.

When $X(s)$ is expressed as a sum of several terms, the ROC for $X(s)$ is the intersection of (region common to) the ROCs of all the terms. In general, if $x(t) = \sum_{i=1}^{k} x_i(t)$, then the ROC for $X(s)$ is the intersection of the ROCs (region common to all ROCs) for the transforms $X_1(s), X_2(s), \ldots, X_k(s)$.

EXAMPLE 6.28 Inverse Bilateral Laplace Transform

Find the inverse bilateral Laplace transform of

$$X(s) = \frac{-3}{(s+2)(s-1)}$$

if the ROC is **(a)** $-2 < \text{Re}\, s < 1$, **(b)** $\text{Re}\, s > 1$, and **(c)** $\text{Re}\, s < -2$.

(a)

$$X(s) = \frac{1}{s+2} - \frac{1}{s-1}$$

Now, $X(s)$ has poles at -2 and 1. The strip of convergence is $-2 < \text{Re}\, s < 1$. The pole at -2, being to the left of the strip of convergence, corresponds to a causal signal. The pole at 1, being to the right of the strip of convergence, corresponds to an anticausal signal. Equations (6.61) and (6.62) yield

$$x(t) = e^{-2t}u(t) + e^{t}u(-t)$$

(b) Both poles lie to the left of the ROC, so both poles correspond to causal signals. Therefore,

$$x(t) = (e^{-2t} - e^{t})u(t)$$

(c) Both poles lie to the right of the region of convergence, so both poles correspond to anticausal signals, and

$$x(t) = (-e^{-2t} + e^{t})u(-t)$$

Figure 6.54 shows the three inverse transforms corresponding to the same $X(s)$ but with different regions of convergence.

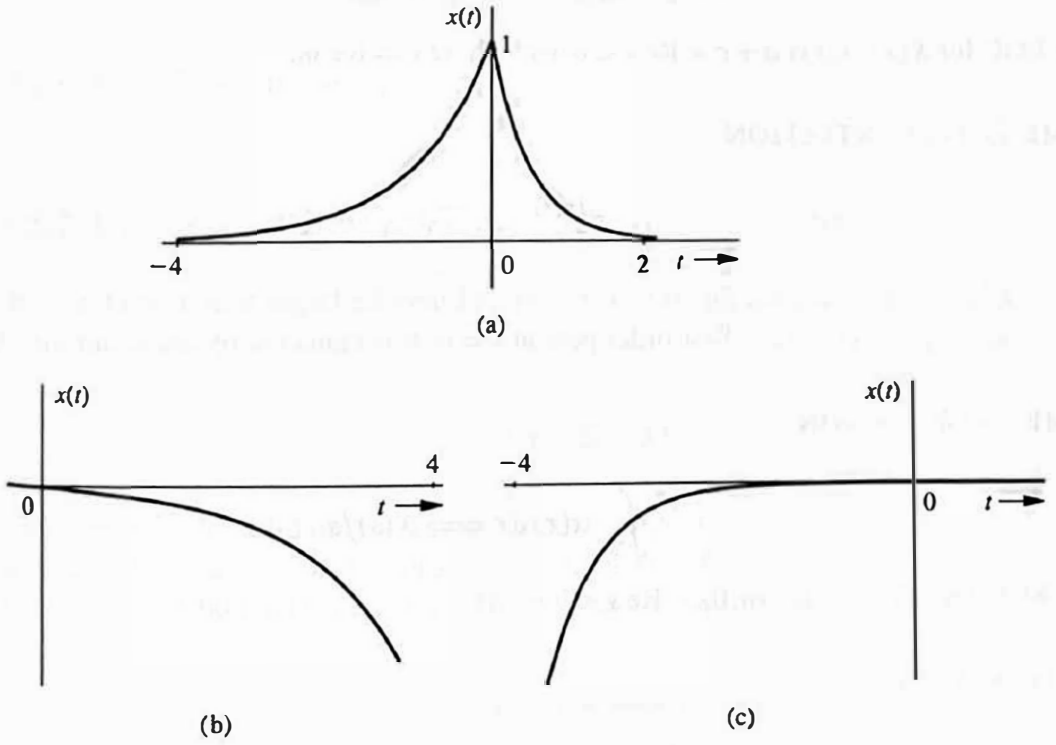

Figure 6.54 Three possible inverse transforms of $-3/((s+2)(s-1))$.

6.8.1 Properties of Bilateral Laplace Transform

Properties of the bilateral Laplace transform are similar to those of the unilateral transform. We shall merely state the properties here without proofs. Let the ROC of $X(s)$ be $a < \text{Re}\, s < b$. Similarly, let the ROC of $X_i(s)$ be $a_i < \text{Re}\, s < b_i$ for $(i = 1,2)$.

Linearity

$$a_1 x_1(t) + a_2 x_2(t) \Longleftrightarrow a_1 X_1(s) + a_2 X_2(s)$$

The ROC for $a_1 X_1(s) + a_2 X_2(s)$ is the region common to (intersection of) the ROCs for $X_1(s)$ and $X_2(s)$.

Time Shift

$$x(t-T) \Longleftrightarrow X(s)e^{-sT}$$

The ROC for $X(s)e^{-sT}$ is identical to the ROC for $X(s)$.

Frequency Shift

$$x(t)e^{s_0 t} \Longleftrightarrow X(s - s_0)$$

The ROC for $X(s - s_0)$ is $a + c < \text{Re}\, s < b + c$, where $c = \text{Re}\, s_0$.

Time Differentiation

$$\frac{dx(t)}{dt} \Longleftrightarrow sX(s)$$

The ROC for $sX(s)$ contains the ROC for $X(s)$ and may be larger than that of $X(s)$ under certain conditions [e.g., if $X(s)$ has a first-order pole at $s = 0$, it is canceled by the factor s in $sX(s)$].

Time Integration

$$\int_{-\infty}^{t} x(\tau)\, d\tau \Longleftrightarrow X(s)/s$$

The ROC for $sX(s)$ is $\max(a, 0) < \text{Re}\, s < b$.

Time Scaling

$$x(\beta t) \Longleftrightarrow \frac{1}{|\beta|} X\left(\frac{s}{\beta}\right)$$

The ROC for $X(s/\beta)$ is $\beta a < \text{Re}\, s < \beta b$. For $\beta > 1$, $x(\beta t)$ represents time compression and the corresponding ROC expands by factor β. For $0 > \beta > 1$, $x(\beta t)$ represents time expansion and the corresponding ROC is compressed by factor β.

Time Convolution

$$x_1(t) * x_2(t) \Longleftrightarrow X_1(s)X_2(s)$$

The ROC for $X_1(s)X_2(s)$ is the region common to (intersection of) the ROCs for $X_1(s)$ and $X_2(s)$.

Frequency Convolution

$$x_1(t)x_2(t) \Longleftrightarrow \frac{1}{2\pi j}\int_{c-j\infty}^{c+j\infty} X_1(w)X_2(s-w)\,dw$$

The ROC for $X_1(s) * X_2(s)$ is $a_1 + a_2 < \text{Re}\, s < b_1 + b_2$.

Time Reversal

$$x(-t) \Longleftrightarrow X(-s)$$

The ROC for $X(-s)$ is $-b < \text{Re}\, s < -a$.

6.8.2 Using the Bilateral Transform for Linear System Analysis

Since the bilateral Laplace transform can handle noncausal signals, we can analyze noncausal LTIC systems using the bilateral Laplace transform. We have shown that the (zero-state) output $y(t)$ is given by

$$y(t) = \mathcal{L}^{-1}[X(s)H(s)]$$

This expression is valid only if $X(s)H(s)$ exists. The ROC of $X(s)H(s)$ is the region in which both $X(s)$ and $H(s)$ exist. In other words, the ROC of $X(s)H(s)$ is the region common to the regions of convergence of both $X(s)$ and $H(s)$. These ideas are clarified in the following examples.

EXAMPLE 6.29 Circuit Response to a Noncausal Input

Find the current $y(t)$ for the RC circuit in Fig. 6.55a if the voltage $x(t)$ is

$$x(t) = e^{t}u(t) + e^{2t}u(-t)$$

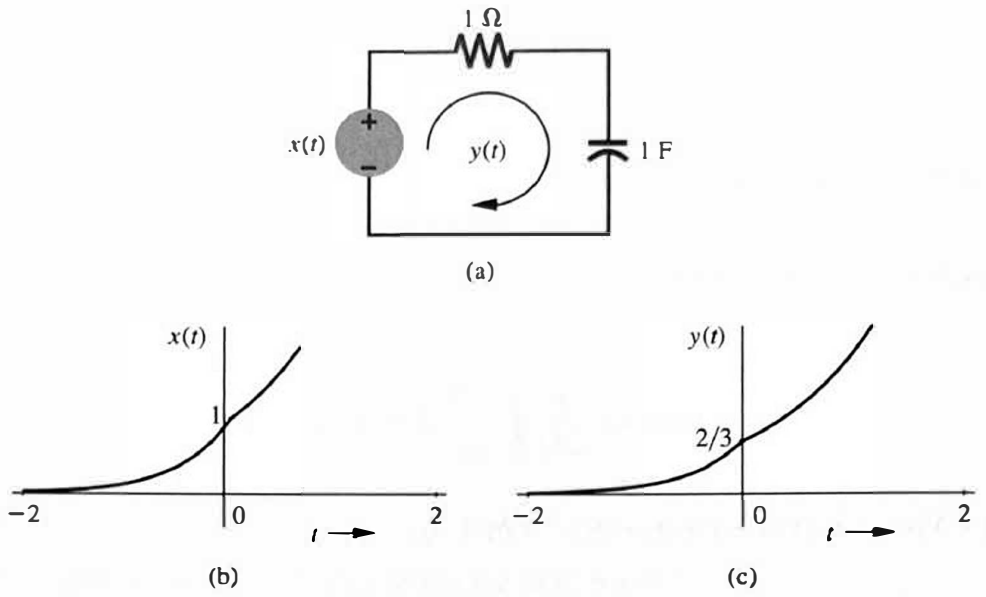

Figure 6.55 Response of a circuit to a noncausal input.

The transfer function $H(s)$ of the circuit is given by

$$H(s) = \frac{s}{s+1} \qquad \text{Re}\, s > -1$$

Because $h(t)$ is a causal function, the ROC of $H(s)$ is $\text{Re}\, s > -1$. Next, the bilateral Laplace transform of $x(t)$ is given by

$$X(s) = \frac{1}{s-1} - \frac{1}{s-2} = \frac{-1}{(s-1)(s-2)} \qquad 1 < \text{Re}\, s < 2$$

The response $y(t)$ is the inverse transform of $X(s)H(s)$:

$$y(t) = \mathcal{L}^{-1}\left[\frac{-s}{(s+1)(s-1)(s-2)}\right] = \mathcal{L}^{-1}\left[\frac{1}{6}\frac{1}{s+1} + \frac{1}{2}\frac{1}{s-1} - \frac{2}{3}\frac{1}{s-2}\right]$$

The ROC of $X(s)H(s)$ is that ROC common to both $X(s)$ and $H(s)$. This is $1 < \text{Re}\, s < 2$. The poles $s = \pm 1$ lie to the left of the ROC and, therefore, correspond to causal signals; the pole $s = 2$ lies to the right of the ROC and thus represents an anticausal signal. Hence,

$$y(t) = \tfrac{1}{6}e^{-t}u(t) + \tfrac{1}{2}e^{t}u(t) + \tfrac{2}{3}e^{2t}u(-t)$$

Figure 6.55c shows $y(t)$. Note that in this example, if

$$x(t) = e^{-4t}u(t) + e^{-2t}u(-t)$$

then the ROC of $X(s)$ is $-4 < \text{Re}\, s < -2$. Here, no region of convergence exists for $X(s)H(s)$. Hence, the response $y(t)$ goes to infinity.

EXAMPLE 6.30 Response of a Noncausal System

Find the response $y(t)$ of a noncausal system with the transfer function

$$H(s) = \frac{-1}{s-1} \qquad \text{Re}s < 1$$

to the input $x(t) = e^{-2t}u(t)$.

We have

$$X(s) = \frac{1}{s+2} \qquad \text{Re}s > -2$$

and

$$Y(s) = X(s)H(s) = \frac{-1}{(s-1)(s+2)}$$

The ROC of $X(s)H(s)$ is the region $-2 < \text{Re}s < 1$. By partial fraction expansion,

$$Y(s) = \frac{-1/3}{s-1} + \frac{1/3}{s+2} \qquad -2 < \text{Re}s < 1$$

and

$$y(t) = \tfrac{1}{3}[e^{t}u(-t) + e^{-2t}u(t)]$$

Note that the pole of $H(s)$ lies in the RHP at 1. Yet the system is not unstable. The pole(s) in the RHP may indicate instability or noncausality, depending on its location with respect to the region of convergence of $H(s)$. For example, if $H(s) = -1/(s-1)$ with $\text{Re}s > 1$, the system is causal and unstable, with $h(t) = -e^{t}u(t)$. In contrast, if $H(s) = -1/(s-1)$ with $\text{Re}s < 1$, the system is noncausal and stable, with $h(t) = e^{t}u(-t)$.

EXAMPLE 6.31 System Response to a Noncausal Input

Find the response $y(t)$ of a system with the transfer function

$$H(s) = \frac{1}{s+5} \qquad \text{Re}s > -5$$

and the input

$$x(t) = e^{-t}u(t) + e^{-2t}u(-t)$$

The input $x(t)$ is of the type depicted in Fig. 6.53f, and the region of convergence for $X(s)$ does not exist. In this case, we must determine separately the system response to each of the two input components, $x_1(t) = e^{-t}u(t)$ and $x_2(t) = e^{-2t}u(-t)$.

$$X_1(s) = \frac{1}{s+1} \qquad \text{Re}\, s > -1$$

$$X_2(s) = \frac{-1}{s+2} \qquad \text{Re}\, s < -2$$

If $y_1(t)$ and $y_2(t)$ are the system responses to $x_1(t)$ and $x_2(t)$, respectively, then

$$Y_1(s) = \frac{1}{(s+1)(s+5)} = \frac{1/4}{s+1} - \frac{1/4}{s+5} \qquad \text{Re}\, s > -1$$

so that

$$y_1(t) = \tfrac{1}{4}(e^{-t} - e^{-5t})u(t)$$

and

$$Y_2(s) = \frac{-1}{(s+2)(s+5)} = \frac{-1/3}{s+2} + \frac{1/3}{s+5} \qquad -5 < \text{Re}\, s < -2$$

so that

$$y_2(t) = \tfrac{1}{3}[e^{-2t}u(-t) + e^{-5t}u(t)]$$

Therefore,

$$y(t) = y_1(t) + y_2(t) = \tfrac{1}{3}e^{-2t}u(-t) + \left(\tfrac{1}{4}e^{-t} + \tfrac{1}{12}e^{-5t}\right)u(t)$$

6.9 SUMMARY

The Fourier transform cannot be used directly in the analysis of unstable or even marginally stable systems. Moreover, the inputs must also be restricted to Fourier transformable signals, which leaves out exponentially growing signals. Both these limitations are the result of the fact that the spectral components used in the Fourier transform to synthesize a signal $x(t)$ are ordinary sinusoids or exponentials of the form $e^{j\omega t}$, whose frequencies are restricted to the ω axis in the complex plane. These spectral components are incapable of synthesizing exponentially growing signals. We extend the Fourier transform by generalizing the frequency variable from $s = j\omega$ to $s = \sigma + j\omega$. The resulting transform is the Laplace transform, which can analyze all types of LTIC systems. The Laplace transform can also handle exponentially growing signals.

The system response to an everlasting exponential e^{st} is also an everlasting exponential $H(s)e^{st}$, where $H(s)$ is the system transfer function. We can view the Laplace transform as a tool by which a signal is expressed as a sum of everlasting exponentials e^{st}. The relative amount of a component e^{st} is $X(s)$. Therefore, $X(s)$, the Laplace transform of $x(t)$, represents the spectrum of exponential components of $x(t)$. Moreover, $H(s)$ is the system response (or gain) to a spectral component e^{st}, and the output signal spectrum is the input spectrum $X(s)$ times the spectral response (gain) $H(s)$ [$Y(s) = X(s)H(s)$].

The Laplace transform changes integro-differential equations of LTIC systems into algebraic equations. Therefore, solving these integro-differential equations reduces to solving algebraic equations. The Laplace transform method cannot generally be used for time-varying parameter systems or for nonlinear systems.

The transfer function $H(s)$ of an LTIC system is the Laplace transform of its impulse response. It may also be defined as a ratio of the Laplace transform of the output to the Laplace transform of the input when all initial conditions are zero (a system in zero state). If $X(s)$ is the Laplace transform of the input $x(t)$ and $Y(s)$ is the Laplace transform of the corresponding output $y(t)$ (when all initial conditions are zero), then $Y(s) = X(s)H(s)$. For an LTIC system described by an Nth-order differential equation $Q(D)y(t) = P(D)x(t)$, the transfer function $H(s) = P(s)/Q(s)$. Like the impulse response $h(t)$, the transfer function $H(s)$ is also an external description of the system.

Electrical circuit analysis can also be carried out by using a transformed circuit method, in which all signals (voltages and currents) are represented by their Laplace transforms, all elements by their impedances (or admittances), and initial conditions by their equivalent sources (initial condition generators). In this method, a network can be analyzed as if it were a resistive circuit.

Large systems can be depicted by suitably interconnected subsystems represented by blocks. Each subsystem, being a smaller system, can be readily analyzed and represented by its input–output relationship, such as its transfer function. Analysis of large systems can be carried out with the knowledge of input–output relationships of its subsystems and the nature of interconnection of various subsystems.

LTIC systems can be realized by scalar multipliers, adders, and integrators. A given transfer function can be synthesized in many different ways, such as canonic, cascade, and parallel. Moreover, every realization has a transpose, which also has the same transfer function. In practice, all the building blocks (scalar multipliers, adders, and integrators) can be obtained from operational amplifiers.

Feedback systems are closed-loop systems mainly used to counteract the effects of unpredictable variations in the system parameters, the load, and the environment. Such systems are designed for a specified speed and steady-state error. For speed, the useful transient parameters are rise time, peak time, and settling time. Percent overshoot indicates how smoothly the system output rises to its final value. We can relate steady-state error to system parameters. In many cases, adjusting the amplifier gain K can result in the desired performance. If the requirements cannot be satisfied by mere adjustment of gain, then some form of compensation must be used. The loci of the characteristic roots of the system are called the root locus, which proves extremely convenient in designing a feedback system.

Most of the input signals and practical systems are causal. Consequently, we are required most of the time to deal with causal signals. When all signals must be causal, the Laplace transform analysis is greatly simplified; the region of convergence of a signal becomes irrelevant to the analysis process. This special case of the Laplace transform (which is restricted to causal signals) is called the unilateral Laplace transform. Much of the chapter deals with this variety of Laplace transform. Section 6.8 discusses the general Laplace transform (the bilateral Laplace transform), which can handle causal and noncausal signals and systems. In the bilateral transform, the inverse transform of $X(s)$ is not unique but depends on the region of convergence of $X(s)$. Thus, the region of convergence plays a very crucial role in the bilateral Laplace transform.

REFERENCES

1. Doetsch, G., *Introduction to the Theory and Applications of the Laplace Transformation with a Table of Laplace Transformations,* Springer-Verlag, New York, 1974.
2. LePage, W. R., *Complex Variables and the Laplace Transforms for Engineers,* McGraw-Hill, New York, 1961.
3. Durant, W. and Durant, A., *The Age of Napoleon,* Part XI in *The Story of Civilization Series,* Simon & Schuster, New York, 1975.
4. Bell, E. T., *Men of Mathematics,* Simon & Schuster, New York, 1937.
5. Nahin, P. J., "Oliver Heaviside: Genius and Curmudgeon," *IEEE Spectrum,* vol. 20, pp. 63–69, July 1983.
6. Berkey, D., *Calculus*, 2nd ed., Saunders, Philadelphia, 1988.
7. Encyclopaedia Britannica, *Micropaedia IV,* 15th ed., p. 981, Chicago, 1982.
8. Churchill, R. V., *Operational Mathematics,* 2nd ed., McGraw-Hill, New York, 1958.
9. Yang, J. S. and Levine, W. S., ch. 10 of *The Control Handbook,* CRC Press, 1996.

PROBLEMS

6.1-1 By direct integration [Eq. (6.6)] find the Laplace transforms and the region of convergence of the following functions:

(a) $u(t)-u(t-1)$
(b) $te^{-t}u(t)$
(c) $t\cos\omega_0 t\,u(t)$
(d) $(e^{2t}-2e^{-t})u(t)$
(e) $\cos\omega_1 t\cos\omega_2 t\,u(t)$
(f) $\cosh(at)\,u(t)$
(g) $\sinh(at)\,u(t)$
(h) $e^{-2t}\cos(5t+\theta)\,u(t)$

6.1-2 By direct integration [Eq. (6.6)], find the Laplace transforms and the region of convergence of the following functions:

(a) $e^{-2t}u(t-5)+\delta(t-1)$
(b) $\pi e^{3t}u(t+5)-\delta(2t)$
(c) $\sum_{k=0}^{\infty}\delta(t-kT),\ T>0$

6.1-3 By direct integration, find the Laplace transforms of the signals shown in Fig. P6.1-3.

6.1-4 Find the inverse (unilateral) Laplace transforms of the following functions:

(a) $\dfrac{2s+5}{s^2+5s+6}$
(b) $\dfrac{3s+5}{s^2+4s+13}$
(c) $\dfrac{(s+1)^2}{s^2-s-6}$
(d) $\dfrac{5}{s^2(s+2)}$
(e) $\dfrac{2s+1}{(s+1)(s^2+2s+2)}$

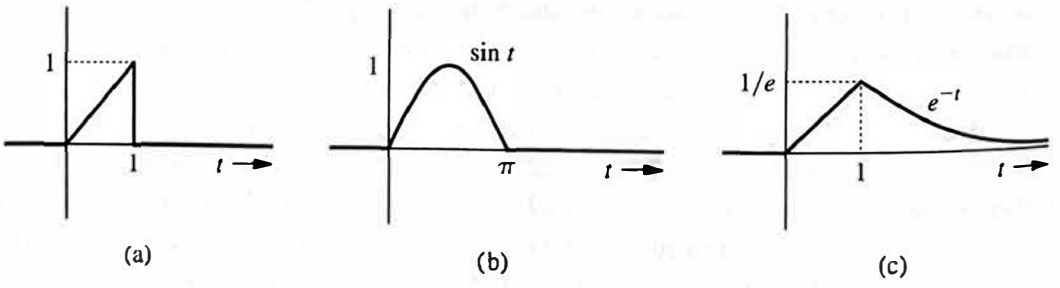

Figure P6.1-3

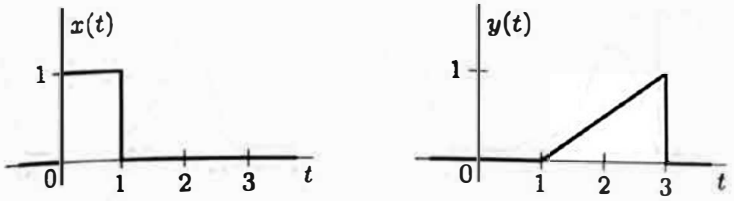

Figure P6.2-6

(f) $\dfrac{s+2}{s(s+1)^2}$

(g) $\dfrac{1}{(s+1)(s+2)^4}$

(h) $\dfrac{s+1}{s(s+2)^2(s^2+4s+5)}$

(i) $\dfrac{s^3}{(s+1)^2(s^2+2s+5)}$

6.2-1 Suppose a CT signal $x(t) = 2[u(t-2) - u(t+1)]$ has a transform $X(s)$.

(a) If $Y_a(s) = e^{-5s}sX\left(s+\frac{1}{2}\right)$, determine and sketch the corresponding signal $y_a(t)$.

(b) If $Y_b(s) = 2^{-s}sX(s-2)$, determine and sketch the corresponding signal $y_b(t)$.

6.2-2 Find the Laplace transforms of the following functions using only Table 6.1 and the time-shifting property (if needed) of the unilateral Laplace transform:

(a) $u(t) - u(t-1)$

(b) $e^{-(t-\tau)}u(t-\tau)$

(c) $e^{-(t-\tau)}u(t)$

(d) $e^{-t}u(t-\tau)$

(e) $te^{-t}u(t-\tau)$

(f) $\sin[\omega_0(t-\tau)]u(t-\tau)$

(g) $\sin[\omega_0(t-\tau)]u(t)$

(h) $\sin\omega_0 t\,u(t-\tau)$

(i) $t\sin(t)u(t)$

(j) $(1-t)\cos(t-1)u(t-1)$

6.2-3 Using only Table 6.1 and the time-shifting property, determine the Laplace transform of the signals in Fig. P6.1-3. [*Hint:* See Sec. 1.4 for a discussion of expressing such signals analytically.]

6.2-4 Prove the frequency-differentiation property, $-tx(t) \Longleftrightarrow \frac{d}{ds}X(s)$. This property holds for both the unilateral and bilateral Laplace transforms.

6.2-5 Consider the signal $x(t) = te^{-2(t-3)}u(t-2)$.

(a) Determine the *unilateral* Laplace transform $X_u(s) = \mathcal{L}_u\{x(t)\}$.

(b) Determine the *bilateral* Laplace transform $X(s) = \mathcal{L}\{x(t)\}$.

6.2-6 Consider the signals $x(t)$ and $y(t)$, as shown in Fig. P6.2-6.

(a) Using the definition, compute $X(s)$, the bilateral Laplace transform of $x(t)$.

(b) Using Laplace transform properties, express $Y(s)$, the bilateral Laplace transform of $y(t)$, as a function of $X(s)$, the bilateral Laplace transform of $x(t)$. Simplify as much as possible without substituting your answer from part (a).

6.2-7 Find the inverse Laplace transforms of the following functions:

(a) $\dfrac{(2s+5)e^{-2s}}{s^2+5s+6}$

(b) $\dfrac{se^{-3s}+2}{s^2+2s+2}$

(c) $\dfrac{e^{-(s-1)}+3}{s^2-2s+5}$

(d) $\dfrac{e^{-s}+e^{-2s}+1}{s^2+3s+2}$

6.2-8 Using ROC $\sigma > 0$, determine the inverse Laplace transform of $X(s) = s^{-1}\frac{d}{ds}\left(\frac{e^{-2s}}{s}\right)$.

6.2-9 The Laplace transform of a causal periodic signal can be determined from the knowledge of the Laplace transform of its first cycle (period).

(a) If the Laplace transform of $x(t)$ in Fig. P6.2-9a is $X(s)$, then show that $G(s)$, the Laplace transform of $g(t)$ (Fig. P6.2-9b), is

$$G(s) = \frac{X(s)}{1-e^{-sT_0}} \qquad \text{Re}s > 0$$

(b) Use this result to find the Laplace transform of the signal $p(t)$ illustrated in Fig. P6.2-9c.

6.2-10 Starting only with the fact that $\delta(t) \Longleftrightarrow 1$, build pairs 2 through 10b in Table 6.1, using various properties of the Laplace transform.

6.2-11 (a) Find the Laplace transform of the pulses in Fig. 6.3 by using only

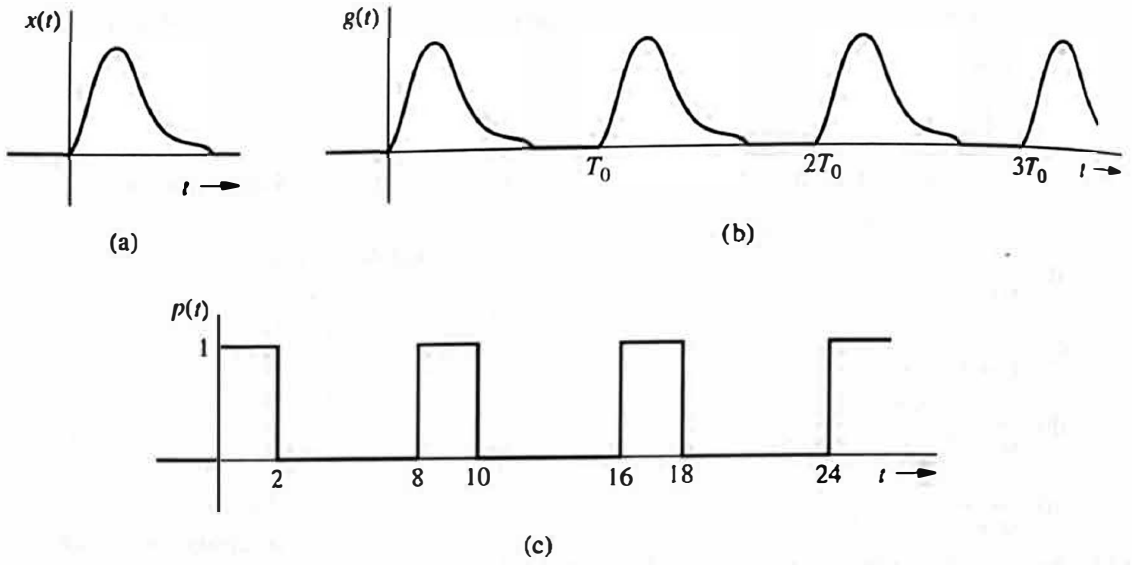

Figure P6.2-9

the time-differentiation property, the time-shifting property, and the fact that $\delta(t) \Longleftrightarrow 1$.

(b) In Ex. 6.9, the Laplace transform of $x(t)$ is found by finding the Laplace transform of d^2x/dt^2. Find the Laplace transform of $x(t)$ in that example by finding the Laplace transform of dx/dt and using Table 6.1, if necessary.

6.2-12 Determine the inverse unilateral Laplace transform of

$$X(s) = \frac{1}{e^{s+3}} \frac{s^2}{(s+1)(s+2)}$$

6.2-13 Since 13 is such a lucky number, determine the inverse Laplace transform of $X(s) = 1/(s+1)^{13}$ given the region of convergence $\sigma > -1$. [*Hint:* What is the nth derivative of $1/(s+a)$?]

6.2-14 It is difficult to compute the Laplace transform $X(s)$ of signal

$$x(t) = \frac{1}{t}u(t)$$

by using direct integration. Instead, properties provide a simpler method.

(a) Use Laplace transform properties to express the Laplace transform of $tx(t)$ in terms of the unknown quantity $X(s)$.

(b) Use the definition to determine the Laplace transform of $y(t) = tx(t)$.

(c) Solve for $X(s)$ by using the two pieces from (a) and (b). Simplify your answer.

6.3-1 Use the Laplace transform to solve the following differential equations:

(a) $(D^2 + 3D + 2)y(t) = Dx(t)$ if $y(0^-) = \dot{y}(0^-) = 0$ and $x(t) = u(t)$

(b) $(D^2 + 4D + 4)y(t) = (D+1)x(t)$ if $y(0^-) = 2$, $\dot{y}(0^-) = 1$ and $x(t) = e^{-t}u(t)$

(c) $(D^2 + 6D + 25)y(t) = (D+2)x(t)$ if $y(0^-) = \dot{y}(0^-) = 1$ and $x(t) = 25u(t)$

6.3-2 Solve the differential equations in Prob. 6.3-1 using the Laplace transform. In each case, determine the zero-input and zero-state components of the solution.

6.3-3 Consider a causal LTIC system described by the differential equation

$$2\dot{y}(t) + 6y(t) = \dot{x}(t) - 4x(t)$$

(a) Using transform-domain techniques, determine the ZIR $y_{zir}(t)$ if $y(0^-) = -3$.

(b) Using transform-domain techniques, determine the ZSR $y_{zsr}(t)$ to the input $x(t) = e\delta(t - \pi)$.

6.3-4 Consider a causal LTIC system described by the differential equation

$$\ddot{y}(t) + 3\dot{y}(t) + 2y(t) = 2\dot{x}(t) - x(t)$$

(a) Using transform-domain techniques, determine the ZIR $y_{zir}(t)$ if $\dot{y}(0^-) = 2$ and $y(0^-) = -3$.

(b) Using transform-domain techniques, determine the ZSR $y_{zsr}(t)$ to the input $x(t) = u(t)$.

6.3-5 Solve the following simultaneous differential equations using the Laplace transform, assuming all initial conditions to be zero and the input $x(t) = u(t)$:

(a) $(D+3)y_1(t) - 2y_2(t) = x(t)$
$-2y_1(t) + (2D+4)y_2(t) = 0$

(b) $(D+2)y_1(t) - (D+1)y_2(t) = 0$
$-(D+1)y_1(t) + (2D+1)y_2(t) = x(t)$

Determine the transfer functions relating outputs $y_1(t)$ and $y_2(t)$ to the input $x(t)$.

6.3-6 Consider a causal LTIC system described by $\dot{y}(t) + 2y(t) = \dot{x}(t)$.

(a) Determine the transfer function $H(s)$ for this system.

(b) Using your result from part (a), determine the impulse response $h(t)$ for this system.

(c) Using Laplace transform techniques, determine the output $y(t)$ if the input is $x(t) = e^{-t}u(t)$ and $y(0^-) = \sqrt{2}$.

6.3-7 Repeat Prob. 6.3-6 for a causal LTIC system described by $3y(t) + \dot{y}(t) + \dot{x}(t) = 0$.

6.3-8 For the circuit in Fig. P6.3-8, the switch is in the open position for a long time before $t = 0$, when it is closed instantaneously.

(a) Write loop equations (in time domain) for $t \geq 0$.

(b) Solve for $y_1(t)$ and $y_2(t)$ by taking the Laplace transform of loop equations found in part (a).

6.3-9 For each of the systems described by the following differential equations, find the system transfer function:

(a) $\dfrac{d^2y(t)}{dt^2} + 11\dfrac{dy(t)}{dt} + 24y(t) = 5\dfrac{dx(t)}{dt} + 3x(t)$

(b) $\dfrac{d^3y(t)}{dt^3} + 6\dfrac{d^2y(t)}{dt^2} - 11\dfrac{dy(t)}{dt} + 6y(t) = 3\dfrac{d^2x(t)}{dt^2} + 7\dfrac{dx(t)}{dt} + 5x(t)$

(c) $\dfrac{d^4y(t)}{dt^4} + 4\dfrac{dy(t)}{dt} = 3\dfrac{dx(t)}{dt} + 2x(t)$

(d) $\dfrac{d^2y(t)}{dt^2} - y(t) = \dfrac{dx(t)}{dt} - x(t)$

6.3-10 For each of the systems specified by the following transfer functions, find the differential equation relating the output $y(t)$ to the input $x(t)$, assuming that the systems are controllable and observable:

(a) $H(s) = \dfrac{s+5}{s^2+3s+8}$

(b) $H(s) = \dfrac{s^2+3s+5}{s^3+8s^2+5s+7}$

(c) $H(s) = \dfrac{5s^2+7s+2}{s^2-2s+5}$

6.3-11 For a system with transfer function

$$H(s) = \frac{2s+3}{s^2+2s+5}$$

(a) Find the (zero-state) response for inputs $x_1(t) = 10u(t)$ and $x_2(t) = u(t-5)$.

(b) For this system, write the differential equation relating the output $y(t)$ to the input $x(t)$, assuming that the systems are controllable and observable.

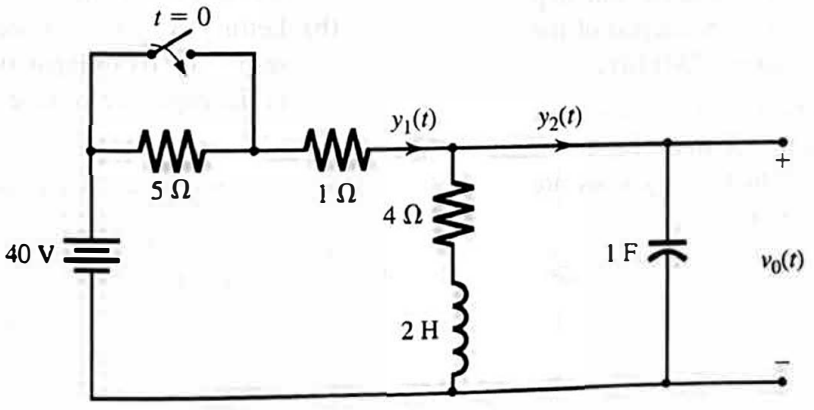

Figure P6.3-8

6.3-12 For a system with transfer function

$$H(s) = \frac{s}{s^2+9}$$

(a) Find the (zero-state) response if the input $x(t) = (1-e^{-t})u(t)$.

(b) For this system, write the differential equation relating the output $y(t)$ to the input $x(t)$, assuming that the systems are controllable and observable.

6.3-13 Consider a system with transfer function

$$H(s) = \frac{s+5}{s^2+5s+6}$$

Find the (zero-state) response for the following inputs:

(a) $x_a(t) = e^{-3t}u(t)$

(b) $x_b(t) = e^{-4t}u(t)$

(c) $x_c(t) = e^{-4(t-5)}u(t-5)$

(d) $x_d(t) = e^{-4(t-5)}u(t)$

(e) $x_e(t) = e^{-4t}u(t-5)$

Assuming that the system $H(s)$ is controllable and observable,

(f) write the differential equation relating the output $y(t)$ to the input $x(t)$.

6.3-14 An LTI system has a step response given by $s(t) = e^{-t}u(t) - e^{-2t}u(t)$. Determine the output of this system $y(t)$ given an input $x(t) = \delta(t-\pi) - \cos(\sqrt{3})u(t)$.

6.3-15 For an LTIC system with zero initial conditions (system initially in zero state), if an input $x(t)$ produces an output $y(t)$, then using the Laplace transform, show the following:

(a) The input dx/dt produces an output dy/dt.

(b) The input $\int_0^t x(\tau)\,d\tau$ produces an output $\int_0^t y(\tau)\,d\tau$. Hence, show that the unit step response of a system is an integral of the impulse response; that is, $\int_0^t h(\tau)\,d\tau$.

6.3-16 Discuss asymptotic and BIBO stabilities for the systems described by the following transfer functions, assuming that the systems are controllable and observable:

(a) $\dfrac{(s+5)}{s^2+3s+2}$

(b) $\dfrac{s+5}{s^2(s+2)}$

(c) $\dfrac{s(s+2)}{s+5}$

(d) $\dfrac{s+5}{s(s+2)}$

(e) $\dfrac{s+5}{s^2-2s+3}$

6.3-17 Repeat Prob. 6.3-16 for systems described by the following differential equations. Systems may be uncontrollable and/or unobservable.

(a) $(D^2+3D+2)y(t) = (D+3)x(t)$

(b) $(D^2+3D+2)y(t) = (D+1)x(t)$

(c) $(D^2+D-2)y(t) = (D-1)x(t)$

(d) $(D^2-3D+2)y(t) = (D-1)x(t)$

6.4-1 The circuit shown in Fig. P6.4-1 has system function given by $H(s) = \frac{1}{1+RCs}$. Let $R=2$ and $C=3$, and use Laplace transform techniques to solve the following:

(a) Find the output $y(t)$ given an initial capacitor voltage of $y(0^-) = 3$ and an input $x(t) = u(t)$.

(b) Given an input $x(t) = u(t-3)$, determine the initial capacitor voltage $y(0^-)$ so that the output $y(t)$ is 1 volt at $t = 6$ seconds.

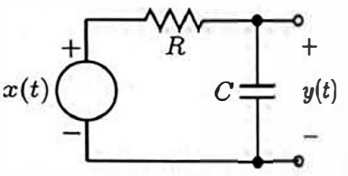

Figure P6.4-1

6.4-2 Consider the circuit shown in Fig. P6.4-2. Use Laplace transform techniques to solve the following:

(a) Determine the standard-form, constant-coefficient differential equation description of this circuit.

(b) Letting $R = C = 1$, determine the total response $y(t)$ to input $x(t) = 3e^{-t}u(t)$ and initial capacitor voltage of $v_C(0^-) = 5$.

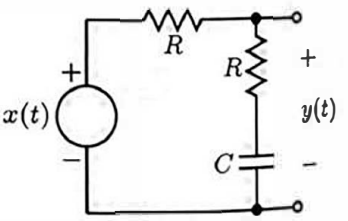

Figure P6.4-2

6.4-3 Find the zero-state response $y(t)$ of the network in Fig. P6.4-3 if the input voltage $x(t) = te^{-t}u(t)$. Find the transfer function relating the output $Y(s)$ to the input $X(s)$. From the transfer function, write the differential equation relating $y(t)$ to $x(t)$.

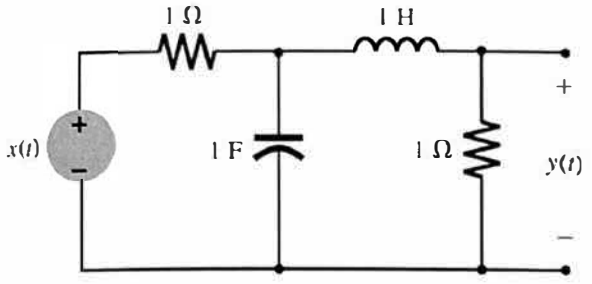

Figure P6.4-3

6.4-4 The switch in the circuit of Fig. P6.4-4 is closed for a long time and then opened instantaneously at $t = 0$. Find and sketch the current $y(t)$.

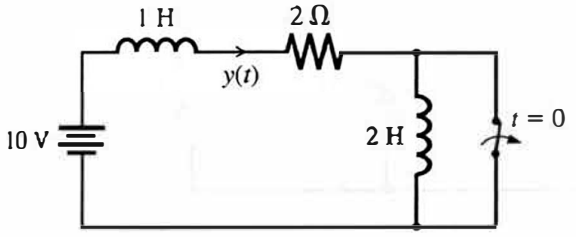

Figure P6.4-4

6.4-5 Find the current $y(t)$ for the parallel resonant circuit in Fig. P6.4-5 if the input is:
(a) $x(t) = A\cos \omega_0 t\, u(t)$
(b) $x(t) = A\sin \omega_0 t\, u(t)$

Assume all initial conditions to be zero and, in both cases, $\omega_0^2 = 1/LC$.

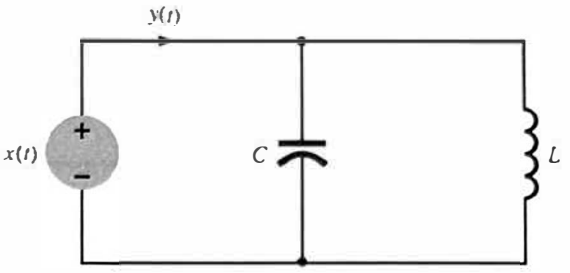

Figure P6.4-5

6.4-6 Find the loop currents $y_1(t)$ and $y_2(t)$ for $t \geq 0$ in the circuit of Fig. P6.4-6a for the input $x(t)$ in Fig. P6.4-6b.

6.4-7 For the network in Fig. P6.4-7, the switch is in a closed position for a long time before $t = 0$, when it is opened instantaneously. Find $y_1(t)$ and $v_s(t)$ for $t \geq 0$.

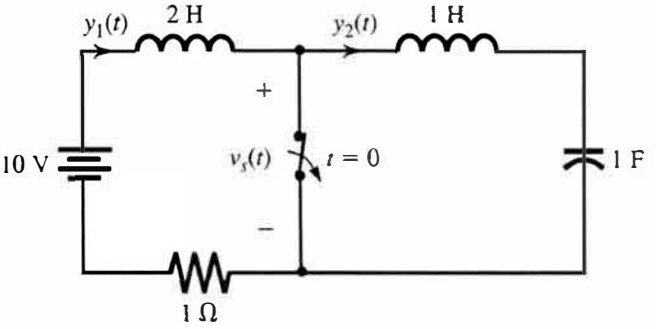

Figure P6.4-7

6.4-8 Find the output voltage $v_0(t)$ for $t \geq 0$ for the circuit in Fig. P6.4-8, if the input $x(t) = 100u(t)$. The system is in the zero state initially.

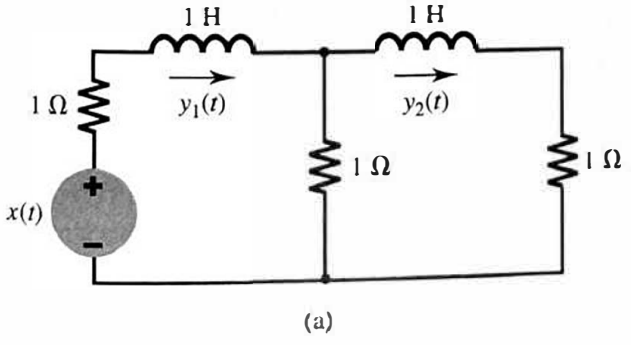

(a)

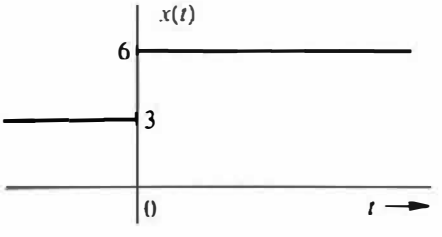

(b)

Figure P6.4-6

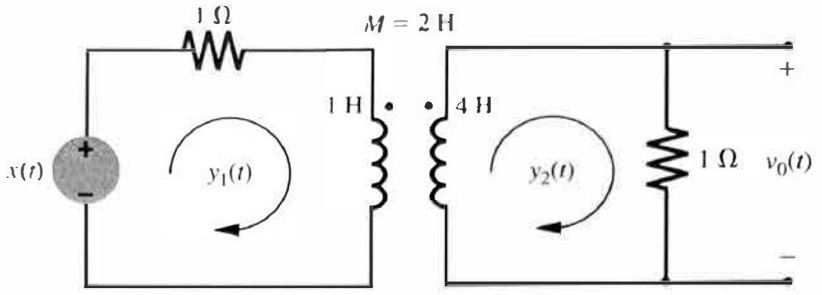

Figure P6.4-8

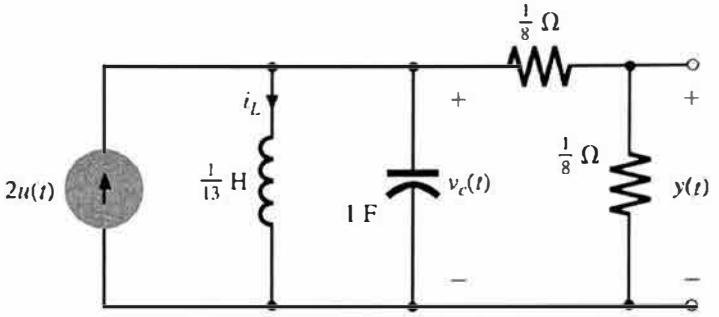

Figure P6.4-9

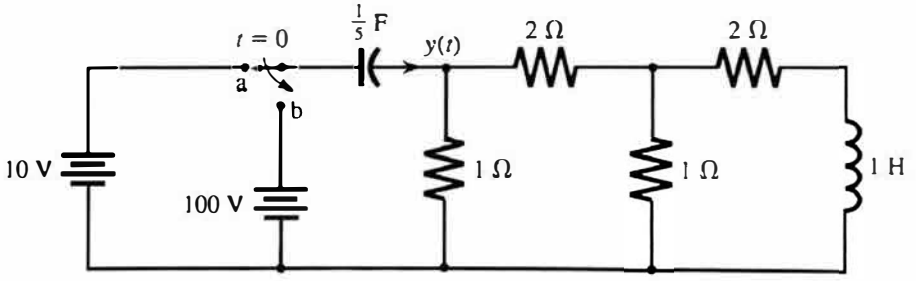

Figure P6.4-10

6.4-9 Find the output voltage $y(t)$ for the network in Fig. P6.4-9 for the initial conditions $i_L(0) =$ 1 A and $v_C(0) = 3$ V.

6.4-10 For the network in Fig. P6.4-10, the switch is in position a for a long time and then is moved to position b instantaneously at $t = 0$. Determine the current $y(t)$ for $t > 0$.

6.4-11 Consider the circuit of Fig. P6.4-11.

(a) Using transform-domain techniques, determine the system's standard-form transfer function $H(s)$.

(b) Using transform-domain techniques and letting $R = L = 1$, determine the circuit's zero-state response $y_{zsr}(t)$ to the input $x(t) = e^{-2t}u(t-1)$.

(c) Using transform-domain techniques and letting $R = 2L = 1$, determine the circuit's zero-state response $y_{zsr}(t)$ to the input $x(t) = e^{-2t}u(t-1)$.

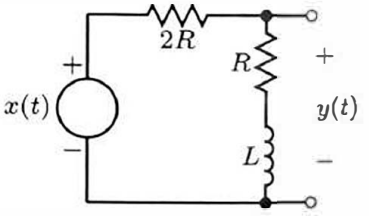

Figure P6.4-11

6.4-12 Show that the transfer function that relates the output voltage $y(t)$ to the input voltage $x(t)$ for the op-amp circuit in Fig. P6.4-12a is given by

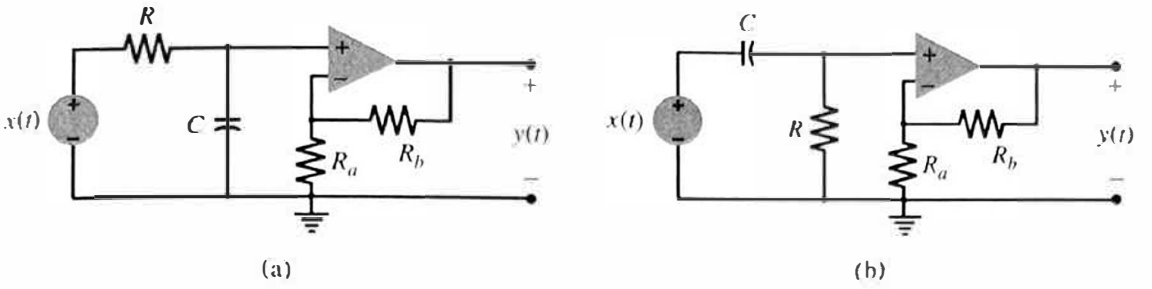

Figure P6.4-12

$$H(s) = \frac{Ka}{s+a}, \quad \text{where}$$

$$K = 1 + \frac{R_b}{R_a} \quad \text{and} \quad a = \frac{1}{RC}$$

and that the transfer function for the circuit in Fig. P6.4-12b is given by

$$H(s) = \frac{Ks}{s+a}$$

6.4-13 For the second-order op-amp circuit in Fig. P6.4-13, show that the transfer function $H(s)$ relating the output voltage $y(t)$ to the input voltage $x(t)$ is given by

$$H(s) = \frac{-s}{s^2 + 8s + 12}$$

6.4-14 Consider the op-amp circuit of Fig. P6.4-14.

(a) Determine the standard-form transfer function $H(s)$ of this system.

(b) Determine the standard-form constant coefficient linear differential equation description of this circuit.

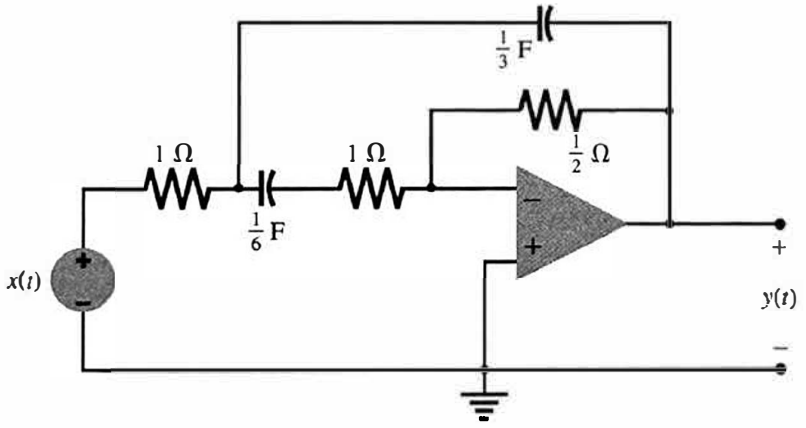

Figure P6.4-13

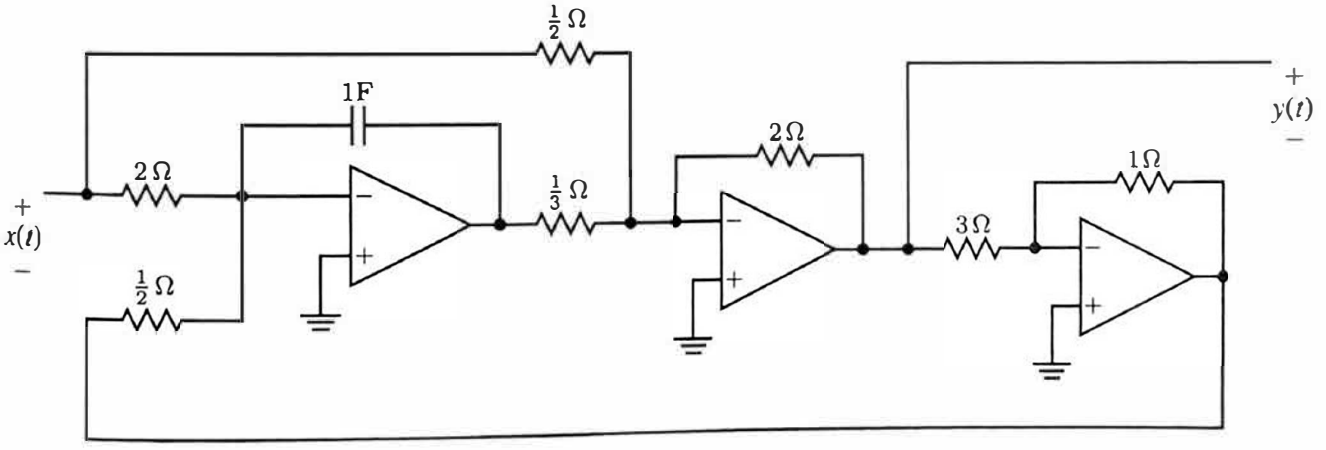

Figure P6.4-14

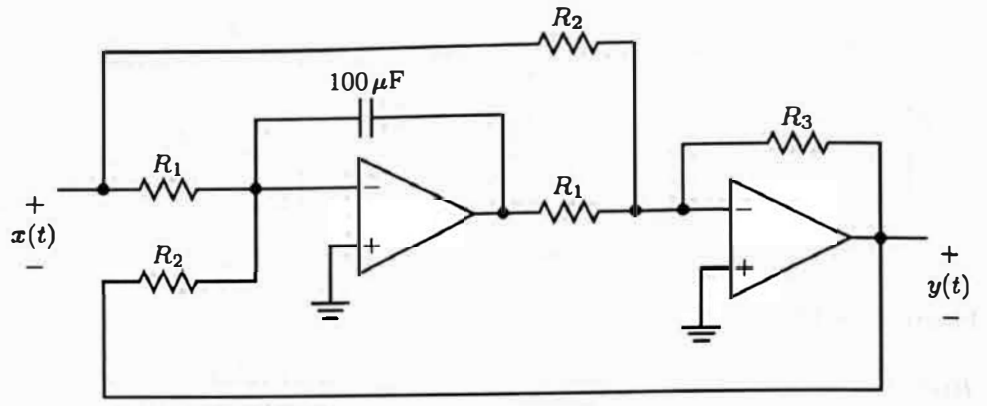

Figure P6.4-15

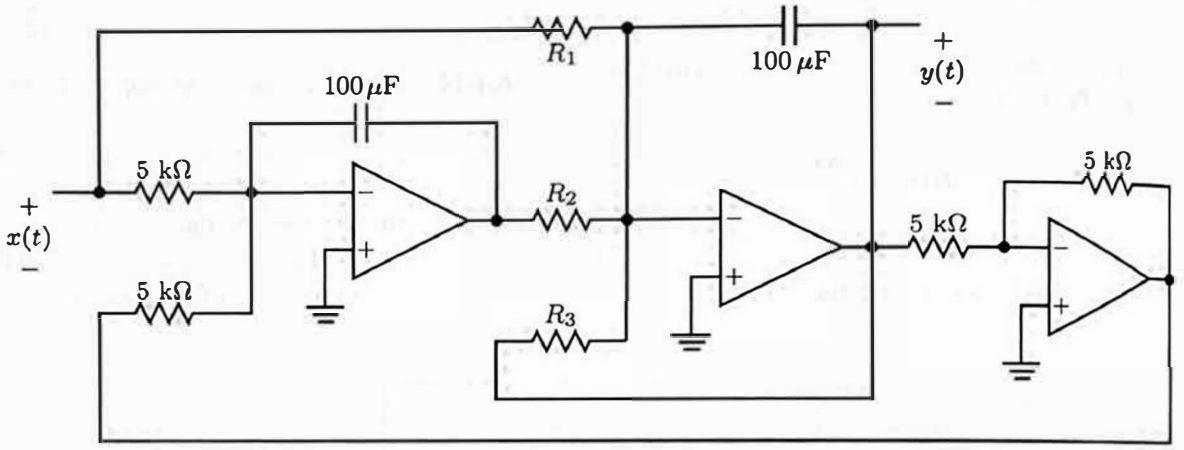

Figure P6.4-16

(c) Using transform-domain techniques, determine the circuit's zero-state response $y_{zsr}(t)$ to the input $x(t) = e^{2t}u(t+1)$.

(d) Using transform-domain techniques, determine the circuit's zero-input response $y_{zir}(t)$ if the $t = 0^-$ capacitor voltage (first op-amp output voltage) is 3 volts.

6.4-15 We desire the op-amp circuit of Fig. P6.4-15 to behave as $\dot{y}(t) - 1.5y(t) = -3\dot{x}(t) + 0.75x(t)$.

(a) Determine resistors R_1, R_2, and R_3 so that the circuit's input–output behavior follows the desired differential equation of $\dot{y}(t) - 1.5y(t) = -3\dot{x}(t) + 0.75x(t)$.

(b) Using transform-domain techniques, determine the circuit's zero-input response $y_{zir}(t)$ if the $t = 0$ capacitor voltage (first op-amp output voltage) is 2 volts.

(c) Using transform-domain techniques, determine the impulse response $h(t)$ of this circuit.

(d) Determine the circuit's zero-state response $y_{zsr}(t)$ to the input $x(t) = u(t-2)$.

6.4-16 We desire the op-amp circuit of Fig. P6.4-16 to behave as $\int\int y(t) + \frac{2}{5}\int y(t) + \frac{1}{5}y(t) = \int\int x(t) - \int x(t)$.

(a) Determine the resistors R_1, R_2, and R_3 to produce the desired behavior.

(b) Using transform-domain techniques, determine the circuit's zero-input response $y_{zir}(t)$ if the $t = 0$ capacitor voltages (first two op-amp outputs) are each 1 volt.

6.4-17 (a) Using the initial and final value theorems, find the initial and final values of the zero-state response of a system with the transfer function

$$H(s) = \frac{6s^2 + 3s + 10}{2s^2 + 6s + 5}$$

and input $x(t) = u(t)$.

(b) Repeat part (a) for the input $x(t) = e^{-t}u(t)$.

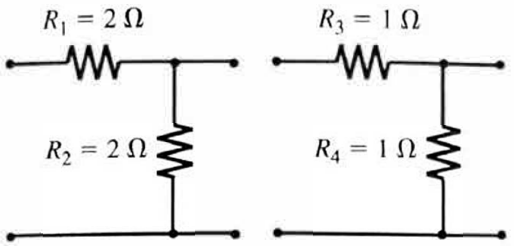

(a)

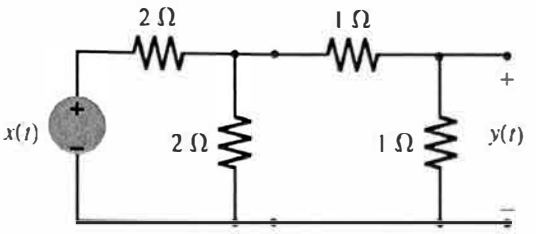

(b)

Figure P6.5-2

(c) Find $y(0^+)$ and $y(\infty)$ if $Y(s) = \dfrac{s^2+5s+6}{s^2+3s+2}$.

(d) Find $y(0^+)$ and $y(\infty)$ if $Y(s) = \dfrac{s^3+4s^2+10s+7}{s^2+2s+3}$.

6.5-1 Consider two LTIC systems. The first has transfer function $H_1(s) = \frac{2s}{s+1}$, and the second has transfer function $H_2(s) = \frac{1}{se^{3(s-1)}}$.

(a) Determine the overall impulse response $h_s(t)$ if the two systems are connected in series.

(b) Determine the overall impulse response $h_p(t)$ if the two systems are connected in parallel.

6.5-2 Figure P6.5-2a shows two resistive ladder segments. The transfer function of each segment (the ratio of output to input voltage) is 1/2. Figure P6.5-2b shows these two segments connected in cascade.

(a) Is the transfer function (the ratio of output to input voltage) of this cascaded network $(1/2)(1/2) = 1/4$?

(b) If your answer is affirmative, verify the answer by direct computation of the transfer function. Does this computation confirm the earlier value 1/4? If not, why?

(c) Repeat the problem with $R_3 = R_4 = 20\ \text{k}\Omega$. Does this result suggest the answer to the problem in part (b)?

6.5-3 In communication channels, a transmitted signal is propagated simultaneously by several paths of varying lengths. This causes the signal to reach the destination with varying time delays and varying gains. Such a system generally distorts the received signal. For error-free communication, it is necessary to undo this distortion as much as possible by using the system that is the inverse of the channel model. For simplicity, let us assume that a signal is propagated by two paths whose time delays differ by τ seconds. The channel over the intended path has a delay of T seconds and unity gain. The signal over the unintended path has a delay of $T + \tau$ seconds and gain a. Such a channel can be modeled, as shown in Fig. P6.5-3. Find the inverse system transfer function to correct the delay distortion and show that the inverse system can be realized by a feedback system. The inverse system should be causal to be realizable. [*Hint:* We want to correct only the distortion caused by the relative delay τ seconds. For distortionless transmission, the signal may be delayed. What is important is to maintain the shape of $x(t)$. Thus, a received signal of the form $cx(t-T)$ is considered to be distortionless.]

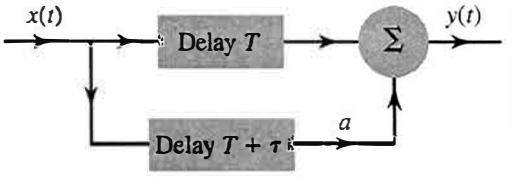

Figure P6.5-3

6.5-4 Discuss the BIBO stability of the feedback systems depicted in Fig. P6.5-4. For the system in Fig. P6.5-4b, consider three cases: **(a)** $K = 10$, **(b)** $K = 50$, and **(c)** $K = 48$.

6.6-1 Realize

$$H(s) = \frac{s(s+2)}{(s+1)(s+3)(s+4)}$$

by canonic direct, series, and parallel forms.

6.6-2 Realize the transfer function in Prob. 6.6-1 by using the transposed form of the realizations found in Prob. 6.6-1.

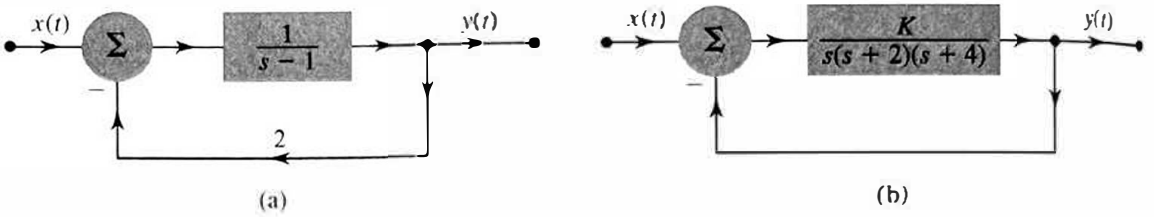

(a) (b)

Figure P6.5-4

6.6-3 Repeat Prob. 6.6-1 for

(a) $H(s) = \dfrac{3s(s+2)}{(s+1)(s^2+2s+2)}$

(b) $H(s) = \dfrac{2s-4}{(s+2)(s^2+4)}$

6.6-4 Realize the transfer functions in Prob. 6.6-3 by using the transposed form of the realizations found in Prob. 6.6-3.

6.6-5 Repeat Prob. 6.6-1 for

$$H(s) = \frac{2s+3}{5s(s+2)^2\,(s+3)}$$

6.6-6 Realize the transfer function in Prob. 6.6-5 by using the transposed form of the realizations found in Prob. 6.6-5.

6.6-7 Repeat Prob. 6.6-1 for

$$H(s) = \frac{s(s+1)(s+2)}{(s+5)(s+6)(s+8)}$$

6.6-8 Realize the transfer function in Prob. 6.6-7 by using the transposed form of the realizations found in Prob. 6.6-7.

6.6-9 Repeat Prob. 6.6-1 for

$$H(s) = \frac{s^3}{(s+1)^3(s+2)(s+3)}$$

6.6-10 Realize the transfer function in Prob. 6.6-9 by using the transposed form of the realizations found in Prob. 6.6-9.

6.6-11 Repeat Prob. 6.6-1 for

$$H(s) = \frac{s^3}{(s+1)(s^2+4s+13)}$$

6.6-12 Realize the transfer function in Prob. 6.6-11 by using the transposed form of the realizations found in Prob. 6.6-11.

6.6-13 Draw a TDFII block realization of a causal LTIC system with transfer function $H(s) = \frac{(s-2j)(s+2j)}{(s-j)(s+j)(s+2)}$. Give two reasons why TDFII tends to be a good structure.

6.6-14 Consider a causal LTIC system with transfer function $H(s) = \frac{(s-2j)(s+2j)(s-3j)(s+3j)}{9(s+1)(s+2)(s+1-j)(s+1+j)}$.

(a) Realize $H(s)$ using a single fourth-order real TDFII structure. Is this block realization unique? Explain.

(b) Realize $H(s)$ using a cascade of second-order real DFII structures. Is this block realization unique? Explain.

(c) Realize $H(s)$ using a parallel connection of second-order real DFI structures. Is this block realization unique? Explain.

6.6-15 In this problem, we show how a pair of complex conjugate poles may be realized by using a cascade of two first-order transfer functions and feedback. Show that the transfer functions of the block diagrams in Figs. P6.6-15a and P6.6-15b are:

(a)

$$H_a(s) = \frac{1}{(s+a)^2+b^2} = \frac{1}{s^2+2as+(a^2+b^2)}$$

(b)

$$H_b(s) = \frac{s+a}{(s+a)^2+b^2} = \frac{s+a}{s^2+2as+(a^2+b^2)}$$

Hence, show that the transfer function of the block diagram in Fig. P6.6-15c is

(c)

$$H_c(s) = \frac{As+B}{(s+a)^2+b^2} = \frac{As+B}{s^2+2as+(a^2+b^2)}$$

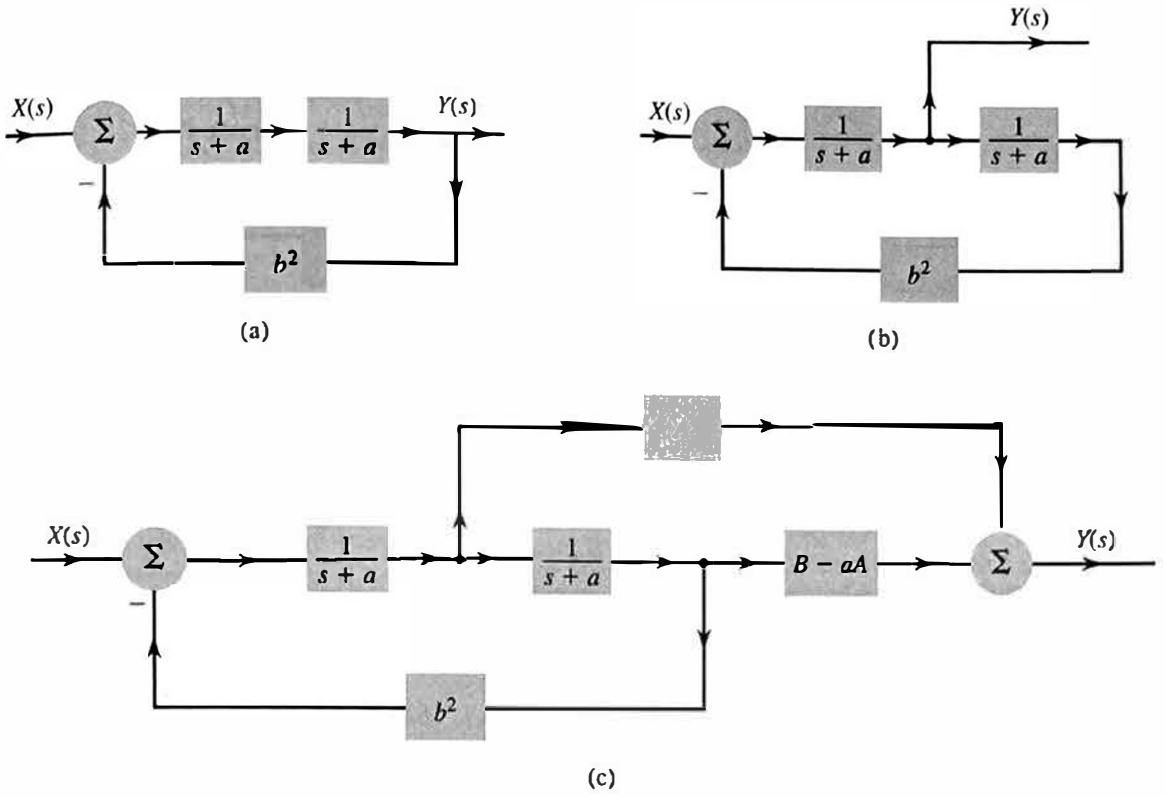

Figure P6.6-15

6.6-16 Show op-amp realizations of the following transfer functions:

(a) $\dfrac{-10}{s+5}$

(b) $\dfrac{10}{s+5}$

(c) $\dfrac{s+2}{s+5}$

6.6-17 Show two different op-amp circuit realizations of the transfer function

$$H(s) = \frac{s+2}{s+5} = 1 - \frac{3}{s+5}$$

6.6-18 Show an op-amp canonic direct realization of the transfer function

$$H(s) = \frac{3s+7}{s^2+4s+10}$$

6.6-19 Show an op-amp canonic direct realization of the transfer function

$$H(s) = \frac{s^2+5s+2}{s^2+4s+13}$$

6.6-20 Consider a system described by a constant-coefficient linear differential equation as $\frac{d}{dt}y(t) + 2y(t) = x(t) - 3\frac{d}{dt}x(t)$. Draw an op-amp realization of this system if resistors and inductors are available but not capacitors. Would using inductors rather than capacitors in this circuit pose any problem? Explain.

6.7-1 Determine the rise time t_r, the settling time t_s, the PO, and the steady-state errors e_s, e_r, and e_p for each of the following systems, whose transfer functions are:

(a) $H_a(s) = \frac{9}{s^2+3s+9}$

(b) $H_b(s) = \frac{4}{s^2+3s+4}$

(c) $H_c(s) = \frac{95}{s^2+10s+100}$

6.7-2 For the position control system depicted in Fig. P6.7-2, the unit step response shows a peak time $t_p = \pi/4$, a PO of $= 9\%$, and a steady-state response to the unit step input of $y_{ss} = 2$. Determine K_1, K_2, and a.

6.7-3 For the position control system depicted in Fig. P6.7-3 the following specifications are imposed: $t_r \leq 0.3$, $t_s \leq 1$, PO $\leq 30\%$, and $e_s = 0$. Which of these specifications cannot be met by the system for any value of K? Which

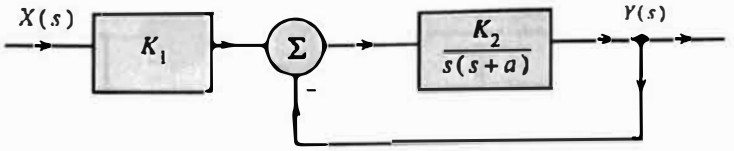

Figure P6.7-2

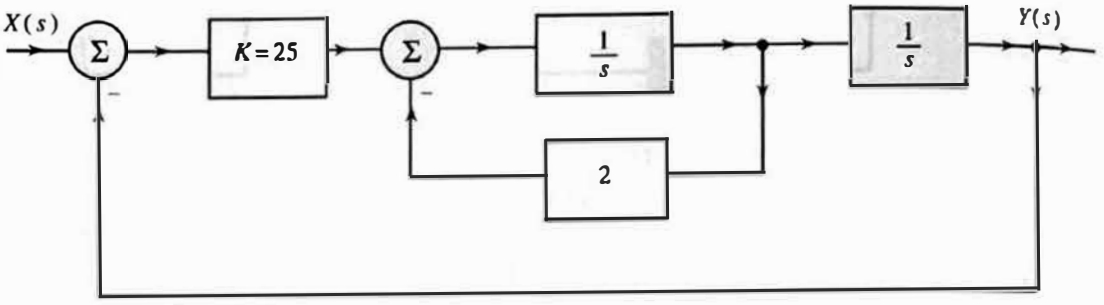

Figure P6.7-3

specifications can be met by simple adjustment of K?

6.7-4 The open-loop transfer functions of four closed-loop systems are given below. In each case, give a rough sketch of the root locus.

(a) $\frac{K(s+1)}{s(s+3)(s+5)}$

(b) $\frac{K(s+1)}{s(s+3)(s+5)(s+7)}$

(c) $\frac{K(s+5)}{s(s+3)}$

(d) $\frac{K(s+1)}{s(s+4)(s^2+2s+2)}$

6.7-5 The unity feedback system shown in Fig. P6.7-5 requires the following specifications: PO $\leq 16\%$, $t_r \leq 0.2$, $t_s \leq 0.5$, $e_s = 0$, and $e_r \leq 0.06$. Is it possible to meet these specifications just by adjusting K? If not, suggest a suitable form of compensator and find the resulting PO, t_s, t_r, e_s, and e_r.

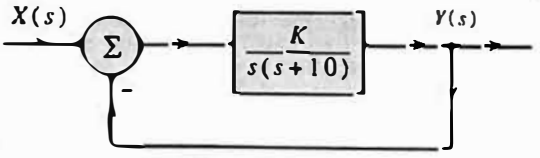

Figure P6.7-5

6.8-1 Find the ROC, if it exists, of the (bilateral) Laplace transform of the following signals:

(a) $e^{tu(t)}$

(b) $e^{-tu(t)}$

(c) $\frac{1}{1+t^2}$

(d) $\frac{1}{1+e^t}$

(e) e^{-kt^2}

6.8-2 Using the definition and direct integration, find the (bilateral) Laplace transform and the corresponding region of convergence for the following signals. If the Laplace transform does not exist, carefully explain why.

(a) $x_a(t) = e^{(-1-j)t}u(1-t)$

(b) $x_b(t) = j^{(t+1)}u(-t-1)$

(c) $x_c(t) = e^{j\pi/3}u(2-t) + j\delta(t-5)$

(d) $x_d(t) = 1 + 1 = 2$

(e) $x_e(t) = 3u(-t) + e^{-2t}[u(t) - u(t-10)]$

(f) $x_f(t) = e^{t-2}u(1-t) + e^{-2t}u(t+1)$

6.8-3 Determine the bilateral Laplace transform $X(s)$ of the signal

$$x(t) = \left[e^t u(-t)\right] * [t\cos(2t)u(t)]$$

6.8-4 A signal has bilateral Laplace transform $X(s) = \frac{(s+1)}{(s-2)(s-3)}$ but unknown region of convergence. What ROC results in the smallest maximum amplitude of $x(t)$? Justify your answer.

6.8-5 Find the (bilateral) Laplace transform and the corresponding region of convergence for the following signals:

(a) $e^{-|t|}$

(b) $e^{-|t|}\cos t$

(c) $e^t u(t) + e^{2t}u(-t)$

(d) $e^{-tu(t)}$

(e) $e^{tu(-t)}$

(f) $\cos\omega_0 t\, u(t) + e^t u(-t)$

6.8-6 Find the inverse (bilateral) Laplace transforms of the following functions:

(a) $\dfrac{2s+5}{(s+2)(s+3)}$ $\quad -3 < \sigma < -2$

(b) $\dfrac{2s-5}{(s-2)(s-3)}$ $\quad 2 < \sigma < 3$

(c) $\dfrac{2s+3}{(s+1)(s+2)}$ $\quad \sigma > -1$

(d) $\dfrac{2s+3}{(s+1)(s+2)}$ $\quad \sigma < -2$

(e) $\dfrac{3s^2-2s-17}{(s+1)(s+3)(s-5)}$ $\quad -1 < \sigma < 5$

6.8-7 Find

$$\mathcal{L}^{-1}\left[\frac{2s^2-2s-6}{(s+1)(s-1)(s+2)}\right]$$

if the ROC is

(a) $\text{Re}\, s > 1$

(b) $\text{Re}\, s < -2$

(c) $-1 < \text{Re}\, s < 1$

(d) $-2 < \text{Re}\, s < -1$

6.8-8 For a causal LTIC system having a transfer function $H(s) = 1/(s+1)$, find the output $y(t)$ if the input $x(t)$ is given by

(a) $e^{-|t|/2}$

(b) $e^{t}u(t) + e^{2t}u(-t)$

(c) $e^{-t/2}u(t) + e^{-t/4}u(-t)$

(d) $e^{2t}u(t) + e^{t}u(-t)$

(e) $e^{-t/4}u(t) + e^{-t/2}u(-t)$

(f) $e^{-3t}u(t) + e^{-2t}u(-t)$

6.8-9 The autocorrelation function $r_{xx}(t)$ of a signal $x(t)$ is given by

$$r_{xx}(t) = \int_{-\infty}^{\infty} x(\tau)x(\tau + t)\,d\tau$$

Derive an expression for $R_{xx}(s) = \mathcal{L}(r_{xx}(t))$ in terms of $X(s)$, where $X(s) = \mathcal{L}(x(t))$.

6.8-10 Determine the inverse Laplace transform of

$$X(s) = \frac{2}{s} + \frac{s}{2}$$

given that the region of convergence is $\sigma < 0$.

6.8-11 An absolutely integrable signal $x(t)$ has a pole at $s = \pi$. It is possible that other poles may be present. Recall that an absolutely integrable signal satisfies

$$\int_{-\infty}^{\infty} |x(t)|\,dt < \infty$$

(a) Can $x(t)$ be left-sided? Explain.

(b) Can $x(t)$ be right-sided? Explain.

(c) Can $x(t)$ be two-sided? Explain.

(d) Can $x(t)$ be of finite duration? Explain.

6.8-12 Using ROC $\sigma < 0$, determine the inverse Laplace transform of $X(s) = s\frac{d}{ds}\left(\frac{e^{-2s}}{s}\right)$. [*Hint:* Use Laplace transform properties to avoid tedious calculus.]

6.8-13 With the assistance of Laplace transform properties, determine the inverse bilateral Laplace transform $x(t)$ of signal

$$X(s) = \frac{2}{e^s} + \frac{1}{s}\left[e^s \frac{4}{\frac{s}{3}+2}\right]$$

where the ROC is $-6 < \text{Re}\{s\} < 0$.

6.8-14 With the assistance of Laplace transform properties, determine the inverse bilateral Laplace transform $x(t)$ of signal

$$X(s) = \frac{d^7}{ds^7}\left[\frac{e^{-4s}}{(s+2)(s+3)}\right]$$

where the ROC is $-3 < \text{Re}\{s\} < -2$.

6.8-15 Using the definition, compute the bilateral Laplace transform, including the region of convergence (ROC), of the following complex-valued functions:

(a) $x_a(t) = (j + e^{jt})u(t)$

(b) $x_b(t) = j\cosh(t)u(-t)$

(c) $x_c(t) = e^{j(\frac{\pi}{4})}u(-t+1) + j\delta(t-5)$

(d) $x_d(t) = j^t u(-t) + \delta(t-\pi)$

6.8-16 A bounded-amplitude signal $x(t)$ has bilateral Laplace transform $X(s)$ given by

$$X(s) = \frac{s2^s}{(s-1)(s+1)}$$

(a) Determine the corresponding region of convergence.

(b) Determine the time-domain signal $x(t)$.

CHAPTER 7

FREQUENCY RESPONSE AND ANALOG FILTERS

Filtering is an important area of signal processing. We have already discussed ideal filters in Ch. 4. In this chapter, we shall discuss the practical filter characteristics and their design. Filtering characteristics of a system are indicated by its response to sinusoids of various frequencies varying from 0 to ∞. Such characteristics are called the frequency response of the filter. Let us start with determining the frequency response of an LTIC system.

Recall that for $h(t)$, we use the notation $H(\omega)$ for its Fourier transform and $H(s)$ for its Laplace transform. Also, when the system is causal and asymptotically stable, all the poles of $H(s)$ lie in the LHP. Hence, the region of convergence for $H(s)$ includes the ω axis, and we can obtain the Fourier transform $H(\omega)$ by substituting $s = j\omega$ in the corresponding Laplace transform $H(s)$ (see p. 520). Therefore, $H(j\omega)$ and $H(\omega)$ represent the same entity when the system is asymptotically stable. In this and later chapters, we shall often find it convenient to use the notation $H(j\omega)$ instead of $H(\omega)$.

7.1 FREQUENCY RESPONSE OF AN LTIC SYSTEM

In this section, we find the system response to sinusoidal inputs. In Sec. 2.4.4, we showed that an LTIC system response to an everlasting exponential input $x(t) = e^{st}$ is also an everlasting exponential $H(s)e^{st}$. As before, we use an arrow directed from the input to the output to represent an input–output pair:

$$e^{st} \Longrightarrow H(s)e^{st} \tag{7.1}$$

Setting $s = j\omega$ in this relationship yields

$$e^{j\omega t} \Longrightarrow H(j\omega)e^{j\omega t} \tag{7.2}$$

Noting that $\cos\omega t$ is the real part of $e^{j\omega t}$, the use of Eq. (2.31) yields

$$\cos\omega t \Longrightarrow \mathrm{Re}[H(j\omega)e^{j\omega t}] \tag{7.3}$$

We can express $H(j\omega)$ in polar form as

$$H(j\omega) = |H(j\omega)|e^{j\angle H(j\omega)}$$

With this result, Eq. (7.3) becomes

$$\cos \omega t \Longrightarrow |H(j\omega)| \cos [\omega t + \angle H(j\omega)]$$

In other words, the system response $y(t)$ to a sinusoidal input $\cos \omega t$ is given by

$$y(t) = |H(j\omega)| \cos [\omega t + \angle H(j\omega)]$$

Using a similar argument, we can show that the system response to a sinusoid $\cos (\omega t + \theta)$ is

$$y(t) = |H(j\omega)| \cos [\omega t + \theta + \angle H(j\omega)] \tag{7.4}$$

This result is valid only for BIBO-stable systems. The frequency response is meaningless for BIBO-unstable systems. This follows from the fact that the frequency response in Eq. (7.2) is obtained by setting $s = j\omega$ in Eq. (7.1). But, as shown in Sec. 2.4.4 [Eqs. (2.38) and (2.39)], Eq. (7.1) applies only for the values of s for which $H(s)$ exists. For BIBO-unstable systems, the ROC for $H(s)$ does not include the ω axis, where $s = j\omega$ [see Eq. (6.14)]. This means that $H(s)$ when $s = j\omega$ is meaningless for BIBO-unstable systems.[†]

Equation (7.4) shows that for a sinusoidal input of radian frequency ω, the system response is also a sinusoid of the same frequency ω. *The amplitude of the output sinusoid is $|H(j\omega)|$ times the input amplitude, and the phase of the output sinusoid is shifted by $\angle H(j\omega)$ with respect to the input phase* (see later Fig. 7.1 in Ex. 7.1). For instance, a certain system with $|H(j10)| = 3$ and $\angle H(j10) = -30°$ amplifies a sinusoid of frequency $\omega = 10$ by a factor of 3 and delays its phase by 30°. The system response to an input $5\cos(10t + 50°)$ is $3 \times 5\cos(10t + 50° - 30°) = 15\cos(10t + 20°)$.

Clearly, $|H(j\omega)|$ is the amplitude *gain* of the system, and a plot of $|H(j\omega)|$ versus ω shows the amplitude gain as a function of frequency ω. We shall call $|H(j\omega)|$ the *amplitude response*. It also goes under the name *magnitude response*.[‡] Similarly, $\angle H(j\omega)$ is the *phase response*, and a plot of $\angle H(j\omega)$ versus ω shows how the system modifies or changes the phase of the input sinusoid. Plots of the magnitude response $|H(j\omega)|$ and phase response $\angle H(j\omega)$ show at a glance how a system responds to sinusoids of various frequencies. Observe that $H(j\omega)$ has the information of $|H(j\omega)|$ and $\angle H(j\omega)$ and is therefore termed the *frequency response* of the system. Clearly, the frequency response of a system represents its filtering characteristics.

[†] This may also be argued as follows. For BIBO-unstable systems, the zero-input response contains nondecaying natural mode terms of the form $\cos \omega_0 t$ or $e^{at} \cos \omega_0 t$ ($a > 0$). Hence, the response of such a system to a sinusoid $\cos \omega t$ will contain not just the sinusoid of frequency ω, but also nondecaying natural modes, rendering the concept of frequency response meaningless.

[‡] Strictly speaking, $|H(\omega)|$ is magnitude response. There is a fine distinction between amplitude and magnitude. Amplitude A can be positive and negative. In contrast, the magnitude $|A|$ is always nonnegative. We refrain from relying on this useful distinction between amplitude and magnitude in the interest of avoiding proliferation of essentially similar entities. This is also why we shall use the "amplitude" (instead of "magnitude") spectrum for $|H(\omega)|$.

EXAMPLE 7.1 Frequency Response

Find the frequency response (amplitude and phase responses) of a system whose transfer function is

$$H(s) = \frac{s+0.1}{s+5}$$

Also, find the system response $y(t)$ if the input $x(t)$ is

(a) $\cos 2t$

(b) $\cos(10t - 50°)$

In this case,

$$H(j\omega) = \frac{j\omega+0.1}{j\omega+5}$$

Therefore,

$$|H(j\omega)| = \frac{\sqrt{\omega^2+0.01}}{\sqrt{\omega^2+25}} \quad \text{and} \quad \angle H(j\omega) = \tan^{-1}\left(\frac{\omega}{0.1}\right) - \tan^{-1}\left(\frac{\omega}{5}\right)$$

Both the amplitude and the phase response are depicted in Fig. 7.1a as functions of ω. These plots furnish the complete information about the frequency response of the system to sinusoidal inputs.

(a) For the input $x(t) = \cos 2t$, $\omega = 2$ and

$$|H(j2)| = \frac{\sqrt{(2)^2+0.01}}{\sqrt{(2)^2+25}} = 0.372$$

$$\angle H(j2) = \tan^{-1}\left(\frac{2}{0.1}\right) - \tan^{-1}\left(\frac{2}{5}\right) = 87.1° - 21.8° = 65.3°$$

We also could have read these values directly from the frequency response plots in Fig. 7.1a corresponding to $\omega = 2$. This result means that for a sinusoidal input with frequency $\omega = 2$, the amplitude gain of the system is 0.372, and the phase shift is 65.3°. In other words, the output amplitude is 0.372 times the input amplitude, and the phase of the output is shifted with respect to that of the input by 65.3°. Therefore, the system response to the input $\cos 2t$ is

$$y(t) = 0.372\cos(2t + 65.3°)$$

The input $\cos 2t$ and the corresponding system response $0.372\cos(2t + 65.3°)$ are illustrated in Fig. 7.1b.

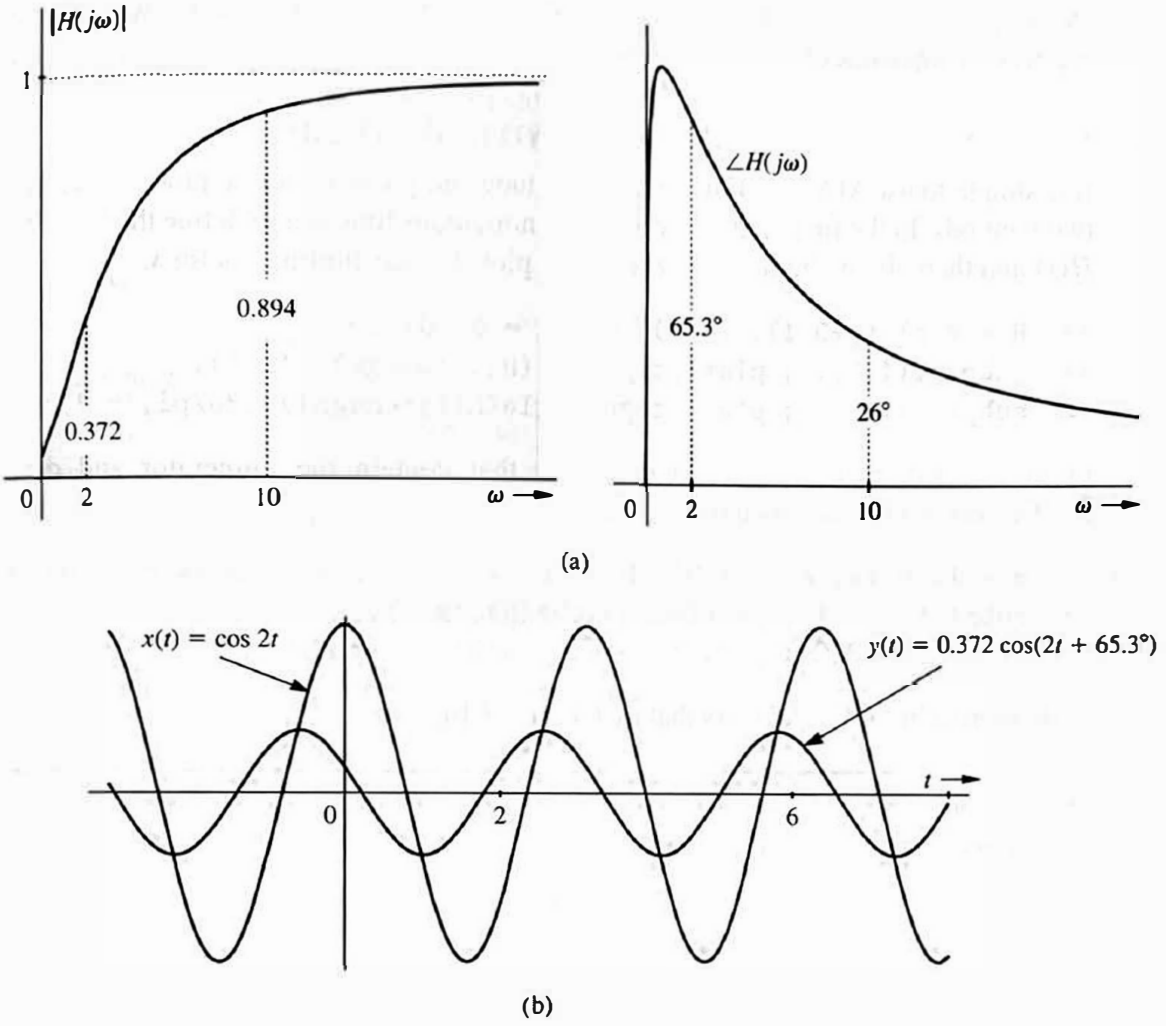

Figure 7.1 Responses for the system of Ex. 7.1.

(**b**) For the input $\cos(10t - 50°)$, instead of computing the values $|H(j\omega)|$ and $\angle H(j\omega)$ as in part (a), we shall read them directly from the frequency response plots in Fig. 7.1a corresponding to $\omega = 10$. These are

$$|H(j10)| = 0.894 \qquad \text{and} \qquad \angle H(j10) = 26°$$

Therefore, for a sinusoidal input of frequency $\omega = 10$, the output sinusoid amplitude is 0.894 times the input amplitude, and the output sinusoid is shifted with respect to the input sinusoid by 26°. Therefore, the system response $y(t)$ to an input $\cos(10t - 50°)$ is

$$y(t) = 0.894\cos(10t - 50° + 26°) = 0.894\cos(10t - 24°)$$

If the input were $\sin(10t - 50°)$, the response would be $0.894\sin(10t - 50° + 26°) = 0.894\sin(10t - 24°)$.

The frequency response plots in Fig. 7.1a show that the system has highpass filtering characteristics; it responds well to sinusoids of higher frequencies (ω well above 5), and suppresses sinusoids of lower frequencies (ω well below 5).

PLOTTING FREQUENCY RESPONSE WITH MATLAB

It is simple to use MATLAB to create magnitude and phase response plots. Here, we consider two methods. In the first method, we use an anonymous function to define the transfer function $H(s)$ and then obtain the frequency response plots by substituting $j\omega$ for s.

```
>> H = @(s) (s+0.1)./(s+5); omega = 0:.01:20;
>> subplot(1,2,1); plot(omega,abs(H(1j*omega)),'k-');
>> subplot(1,2,2); plot(omega,angle(H(1j*omega))*180/pi,'k-');
```

In the second method, we define vectors that contain the numerator and denominator coefficients of $H(s)$ and then use the `freqs` command to compute frequency response.

```
>> B = [1 0.1]; A = [1 5]; H = freqs(B,A,omega); omega = 0:.01:20;
>> subplot(1,2,1); plot(omega,abs(H),'k-');
>> subplot(1,2,2); plot(omega,angle(H)*180/pi,'k-');
```

Both approaches generate plots that match Fig. 7.1a.

EXAMPLE 7.2 Frequency Responses of Delay, Differentiator, and Integrator Systems

Find and sketch the frequency responses (magnitude and phase) for **(a)** an ideal delay of T seconds, **(b)** an ideal differentiator, and **(c)** an ideal integrator.

(a) Ideal delay of T seconds. The transfer function of an ideal delay is [see Eq. (6.34)]

$$H(s) = e^{-sT}$$

Therefore,

$$H(j\omega) = e^{-j\omega T}$$

Consequently,

$$|H(j\omega)| = 1 \qquad \text{and} \qquad \angle H(j\omega) = -\omega T$$

These amplitude and phase responses are shown in Fig. 7.2a. The amplitude response is constant (unity) for all frequencies. The phase shift increases linearly with frequency with a slope of $-T$. This result can be explained physically by recognizing that if a sinusoid $\cos\omega t$ is passed through an ideal delay of T seconds, the output is $\cos\omega(t-T)$. The output sinusoid

amplitude is the same as that of the input for all values of ω. Therefore, the amplitude response (gain) is unity for all frequencies. Moreover, the output $\cos\omega(t-T) = \cos(\omega t - \omega T)$ has a phase shift $-\omega T$ with respect to the input $\cos\omega t$. Therefore, the phase response is linearly proportional to the frequency ω with a slope $-T$.

(b) An ideal differentiator. The transfer function of an ideal differentiator is [see Eq. (6.35)]

$$H(s) = s$$

Therefore,

$$H(j\omega) = j\omega = \omega e^{j\pi/2}$$

Consequently,

$$|H(j\omega)| = \omega \qquad \text{and} \qquad \angle H(j\omega) = \frac{\pi}{2}$$

These amplitude and phase responses are depicted in Fig. 7.2b. The amplitude response increases linearly with frequency, and phase response is constant $(\pi/2)$ for all frequencies. This result can be explained physically by recognizing that if a sinusoid $\cos\omega t$ is passed through an ideal differentiator, the output is $-\omega\sin\omega t = \omega\cos[\omega t + (\pi/2)]$. Therefore, the output sinusoid amplitude is ω times the input amplitude; that is, the amplitude response (gain) increases linearly with frequency ω. Moreover, the output sinusoid undergoes a phase shift $\pi/2$ with respect to the input $\cos\omega t$. Therefore, the phase response is constant $(\pi/2)$ with frequency.

In an ideal differentiator, the amplitude response (gain) is proportional to frequency $[|H(j\omega)| = \omega]$ so that the higher-frequency components are enhanced (see Fig. 7.2b). All practical signals are contaminated with noise, which, by its nature, is a broadband (rapidly varying) signal containing components of very high frequencies. A differentiator can increase the noise disproportionately to the point of drowning out the desired signal. This is why ideal differentiators are avoided in practice.

(c) An ideal integrator. The transfer function of an ideal integrator is [see Eq. (6.36)]

$$H(s) = \frac{1}{s}$$

Therefore,

$$H(j\omega) = \frac{1}{j\omega} = \frac{-j}{\omega} = \frac{1}{\omega}e^{-j\pi/2}$$

Consequently,

$$|H(j\omega)| = \frac{1}{\omega} \qquad \text{and} \qquad \angle H(j\omega) = -\frac{\pi}{2}$$

These amplitude and phase responses are illustrated in Fig. 7.2c. The amplitude response is inversely proportional to frequency, and the phase shift is constant $(-\pi/2)$ with frequency. This result can be explained physically by recognizing that if a sinusoid $\cos\omega t$ is passed through an ideal integrator, the output is $(1/\omega)\sin\omega t = (1/\omega)\cos[\omega t - (\pi/2)]$. Therefore, the amplitude response is inversely proportional to ω, and the phase response is constant $(-\pi/2)$

with frequency.† Because its gain is $1/\omega$, the ideal integrator suppresses higher-frequency components but enhances lower-frequency components with $\omega < 1$. Consequently, noise signals (if they do not contain an appreciable amount of very-low-frequency components) are suppressed (smoothed out) by an integrator.

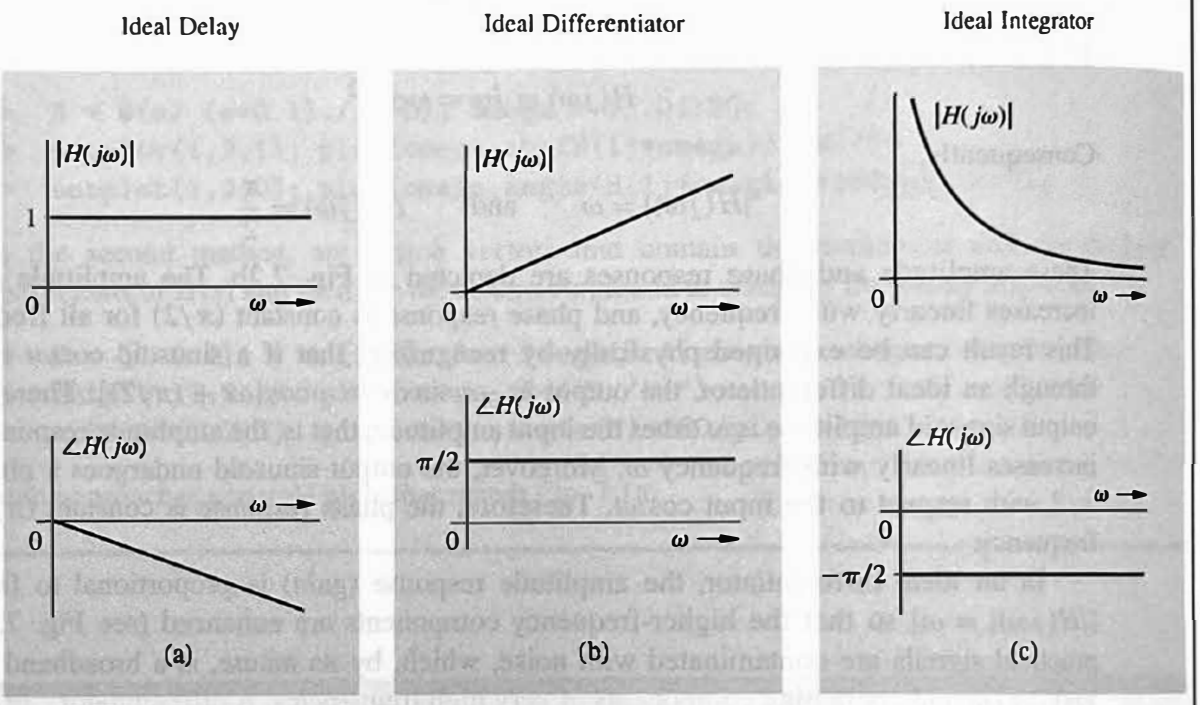

Figure 7.2 Frequency response of an ideal **(a)** delay, **(b)** differentiator, and **(c)** integrator.

† A puzzling aspect of this result is that in deriving the transfer function of the integrator in Eq. (6.36), we have assumed that the input starts at $t = 0$. In contrast, in deriving its frequency response, we assume that the everlasting exponential input $e^{j\omega t}$ starts at $t = -\infty$. There appears to be a fundamental contradiction between the everlasting input, which starts at $t = -\infty$, and the integrator, which opens its gates only at $t = 0$. Of what use is everlasting input, since the integrator starts integrating at $t = 0$? The answer is that the integrator gates are always open, and integration begins whenever the input starts. We restricted the input to start at $t = 0$ in deriving Eq. (6.36) because we were finding the transfer function using the unilateral transform, where the inputs begin at $t = 0$. So the integrator starting to integrate at $t = 0$ is restricted because of the limitations of the unilateral transform method, not because of the limitations of the integrator itself. If we were to find the integrator transfer function using Eq. (2.40), where there is no such restriction on the input, we would still find the transfer function of an integrator as $1/s$. Similarly, even if we were to use the bilateral Laplace transform, where t starts at $-\infty$, we would find the transfer function of an integrator to be $1/s$. The transfer function of a system is the property of the system and does not depend on the method used to find it.

DRILL 7.1 Sinusoidal Response of an LTIC System

Find the response of an LTIC system specified by

$$\frac{d^2y(t)}{dt^2}+3\frac{dy(t)}{dt}+2y(t)=\frac{dx(t)}{dt}+5x(t)$$

if the input is a sinusoid $20\sin(3t+35°)$.

ANSWER

$10.23\sin(3t-61.91°)$

7.1.1 Steady-State Response to Causal Sinusoidal Inputs

So far we have discussed the LTIC system response to everlasting sinusoidal inputs (starting at $t=-\infty$). In practice, we are more interested in causal sinusoidal inputs (sinusoids starting at $t=0$). Consider the input $e^{j\omega t}u(t)$, which starts at $t=0$ rather than at $t=-\infty$. In this case, $X(s)=1/(s-j\omega)$. Moreover, according to Eq. (6.31), $H(s)=P(s)/Q(s)$, where $Q(s)$ is the characteristic polynomial given by $Q(s)=(s-\lambda_1)(s-\lambda_2)\cdots(s-\lambda_N)$.[†] Hence,

$$Y(s)=X(s)H(s)=\frac{P(s)}{(s-\lambda_1)(s-\lambda_2)\cdots(s-\lambda_N)(s-j\omega)}$$

In the partial fraction expansion of the right-hand side, let the coefficients corresponding to the N terms $(s-\lambda_1)$, $(s-\lambda_2)$, $\ldots$, $(s-\lambda_N)$ be $k_1, k_2, \ldots, k_N$. The coefficient corresponding to the last term $(s-j\omega)$ is $P(s)/Q(s)|_{s=j\omega}=H(j\omega)$. Hence,

$$Y(s)=\sum_{i=1}^{n}\frac{k_i}{s-\lambda_i}+\frac{H(j\omega)}{s-j\omega}$$

and

$$y(t)=\underbrace{\sum_{i=1}^{n}k_ie^{\lambda_i t}u(t)}_{\text{transient component } y_{tr}(t)}+\underbrace{H(j\omega)e^{j\omega t}u(t)}_{\text{steady-state component } y_{ss}(t)}$$

For an asymptotically stable system, the characteristic mode terms $e^{\lambda_i t}$ decay with time and, therefore, constitute the so-called *transient* component of the response. The last term $H(j\omega)e^{j\omega t}$ persists forever, and is the *steady-state* component of the response given by

$$y_{ss}(t)=H(j\omega)e^{j\omega t}u(t)$$

This result also explains why an everlasting exponential input $e^{j\omega t}$ results in the total response $H(j\omega)e^{j\omega t}$ for BIBO systems. Because the input started at $t=-\infty$, at any finite time the decaying

[†] For simplicity, we have assumed nonrepeating characteristic roots. The procedure is readily modified for repeated roots, and the same conclusion results.

transient component has long vanished, leaving only the steady-state component. Hence, the total response appears to be $H(j\omega)e^{j\omega t}$.

From the argument that led to Eq. (7.4), it follows that for a causal sinusoidal input $\cos\omega t$, the steady-state response $y_{ss}(t)$ is given by

$$y_{ss}(t) = |H(j\omega)|\cos[\omega t + \angle H(j\omega)]u(t)$$

In summary, $|H(j\omega)|\cos[\omega t + \angle H(j\omega)]$ is the total response to everlasting sinusoid $\cos\omega t$. In contrast, it is the steady-state response to the same input applied at $t = 0$.

7.2 BODE PLOTS

Sketching frequency response plots ($|H(j\omega)|$ and $\angle H(j\omega)$ versus ω) is considerably facilitated by the use of logarithmic scales. The amplitude and phase response plots as a function of ω on a logarithmic scale are known as *Bode plots*. By using the asymptotic behavior of the amplitude and the phase responses, we can sketch these plots with remarkable ease, even for higher-order transfer functions.

Let us consider a system with the transfer function

$$H(s) = \frac{K(s+a_1)(s+a_2)}{s(s+b_1)(s^2+b_2s+b_3)} \tag{7.5}$$

where the second-order factor $(s^2+b_2s+b_3)$ is assumed to have complex conjugate roots.† We shall rearrange Eq. (7.5) in the form

$$H(s) = \frac{Ka_1a_2}{b_1b_3}\frac{\left(\frac{s}{a_1}+1\right)\left(\frac{s}{a_2}+1\right)}{s\left(\frac{s}{b_1}+1\right)\left(\frac{s^2}{b_3}+\frac{b_2}{b_3}s+1\right)}$$

and

$$H(j\omega) = \frac{Ka_1a_2}{b_1b_3}\frac{\left(1+\frac{j\omega}{a_1}\right)\left(1+\frac{j\omega}{a_2}\right)}{j\omega\left(1+\frac{j\omega}{b_1}\right)\left[1+j\frac{b_2\omega}{b_3}+\frac{(j\omega)^2}{b_3}\right]}$$

This equation shows that $H(j\omega)$ is a complex function of ω. The amplitude response $|H(j\omega)|$ and the phase response $\angle H(j\omega)$ are given by

$$|H(j\omega)| = \left|\frac{Ka_1a_2}{b_1b_3}\right|\frac{\left|1+\frac{j\omega}{a_1}\right|\left|1+\frac{j\omega}{a_2}\right|}{|j\omega|\left|1+\frac{j\omega}{b_1}\right|\left|1+j\frac{b_2\omega}{b_3}+\frac{(j\omega)^2}{b_3}\right|} \tag{7.6}$$

†Coefficients a_1, a_2 and b_1, b_2, b_3 used in this section are not to be confused with those used in the representation of Nth-order LTIC system equations given earlier [Eqs. (2.1) or (6.30)].

and

$$\angle H(j\omega) = \angle\left(\frac{Ka_1a_2}{b_1b_3}\right) + \angle\left(1 + \frac{j\omega}{a_1}\right) + \angle\left(1 + \frac{j\omega}{a_2}\right) - \angle j\omega - \angle\left(1 + \frac{j\omega}{b_1}\right) - \angle\left[1 + \frac{jb_2\omega}{b_3} + \frac{(j\omega)^2}{b_3}\right] \tag{7.7}$$

From Eq. (7.7), we see that the phase function consists of the addition of terms of four kinds: (i) the phase of a constant, (ii) the phase of $j\omega$, which is 90° for all values of ω, (iii) the phase for the first-order term of the form $1 + j\omega/a$, and (iv) the phase of the second-order term

$$\left[1 + \frac{jb_2\omega}{b_3} + \frac{(j\omega)^2}{b_3}\right]$$

We can plot these basic phase functions for ω in the range 0 to ∞ and then, using these plots, we can construct the phase function of any transfer function by properly adding these basic responses. Note that if a particular term is in the numerator, its phase is added, but if the term is in the denominator, its phase is subtracted. This makes it easy to plot the phase function $\angle H(j\omega)$ as a function of ω. Computation of $|H(j\omega)|$, unlike that of the phase function, however, involves the multiplication and division of various terms. This is a formidable task, especially when we have to plot this function for the entire range of ω (0 to ∞).

We know that a log operation converts multiplication and division to addition and subtraction. So, instead of plotting $|H(j\omega)|$, why not plot $\log |H(j\omega)|$ to simplify our task? We can take advantage of the fact that logarithmic units are desirable in several applications, where the variables considered have a very large range of variation. This is particularly true in frequency response plots, where we may have to plot frequency response over a range from a very low frequency, near 0, to a very high frequency, in the range of 10^{10} or higher. A plot on a linear scale of frequencies for such a large range will bury much of the useful information at lower frequencies. Also, the amplitude response may have a very large dynamic range from a low of 10^{-6} to a high of 10^6. A linear plot would be unsuitable for such a situation. Therefore, logarithmic plots not only simplify our task of plotting, but, fortunately, they are also desirable in this situation.

There is another important reason for using logarithmic scale. The Weber–Fechner law (first observed by Weber in 1834) states that human senses (sight, touch, hearing, etc.) generally respond in a logarithmic way. For instance, when we hear sound at two different power levels, we judge one sound to be twice as loud when the ratio of the two sound powers is 10. Human senses respond to equal ratios of power, not equal increments in power [1]. This is clearly a logarithmic response.[†]

The logarithmic unit is the *decibel* and is equal to 20 times the logarithm of the quantity (log to the base 10). Therefore, $20\log_{10} |H(j\omega)|$ is simply the log amplitude in decibels (dB).[‡] Thus, instead of plotting $|H(j\omega)|$, we shall plot $20\log_{10} |H(j\omega)|$ as a function of ω. These plots

[†] Observe that the frequencies of musical notes are spaced logarithmically (not linearly). The octave is a ratio of 2. The frequencies of the same note in the successive octaves have a ratio of 2. On the Western musical scale, there are 12 distinct notes in each octave. The frequency of each note is about 6% higher than the frequency of the preceding note. Thus, the successive notes are separated not by some constant frequency, but by a constant ratio of 1.06.

[‡] Originally, the unit *bel* (after the inventor of telephone, Alexander Graham Bell) was introduced to represent the power ratio as $\log_{10} P_2/P_1$ bels. A tenth of this unit is a decibel, as in $10 \log_{10} P_2/P_1$ decibels.

(log amplitude and phase) are called *Bode plots*. For the transfer function in Eq. (7.6), the *log amplitude* is

$$20\log|H(j\omega)| = 20\log\left|\frac{Ka_1a_2}{b_1b_3}\right| + 20\log\left|1+\frac{j\omega}{a_1}\right| + 20\log\left|1+\frac{j\omega}{a_2}\right| - 20\log|j\omega| - 20\log\left|1+\frac{j\omega}{b_1}\right| - 20\log\left|1+\frac{jb_2\omega}{b_3}+\frac{(j\omega)^2}{b_3}\right| \tag{7.8}$$

The term $20\log(Ka_1a_2/b_1b_3)$ is a constant. We observe that the log amplitude is a sum of four basic terms corresponding to a constant, a pole or zero at the origin ($20\log|j\omega|$), a first-order pole or zero ($20\log|1+j\omega/a|$), and complex-conjugate poles or zeros ($20\log|1+j\omega b_2/b_3+(j\omega)^2/b_3|$). We can sketch these four basic terms as functions of ω and use them to construct the log-amplitude plot of any desired transfer function. Let us discuss each of the terms.

7.2.1 Constant Ka_1a_2/b_1b_3

The log amplitude of the constant Ka_1a_2/b_1b_2 term is also a constant, $20\log|Ka_1a_2/b_1b_3|$. The phase contribution from this term is zero for a positive value and π for a negative value of the constant (complex constants can have different phases).

7.2.2 Pole (or Zero) at the Origin

Log Magnitude

A pole at the origin gives rise to the term $-20\log|j\omega|$, which can be expressed as

$$-20\log|j\omega| = -20\log\omega$$

This function can be plotted as a function of ω. However, we can effect further simplification by using the logarithmic scale for the variable ω itself. Let us define a new variable u such that

$$u = \log\omega$$

Hence,

$$-20\log\omega = -20u$$

The log-amplitude function $-20u$ is plotted as a function of u in Fig. 7.3a. This is a straight line with a slope of -20. It crosses the u axis at $u=0$. The ω-scale ($u=\log\omega$) also appears in Fig. 7.3a. Semilog graphs can be conveniently used for plotting, and we can directly plot ω on semilog paper. A ratio of 10 is a *decade*, and a ratio of 2 is known as an *octave*. Furthermore, a decade along the

---

Since the power ratio of two signals is proportional to the amplitude ratio squared, or $|H(j\omega)|^2$, we have $10\log_{10}P_2/P_1 = 10\log_{10}|H(j\omega)|^2 = 20\log_{10}|H(j\omega)|$ dB.

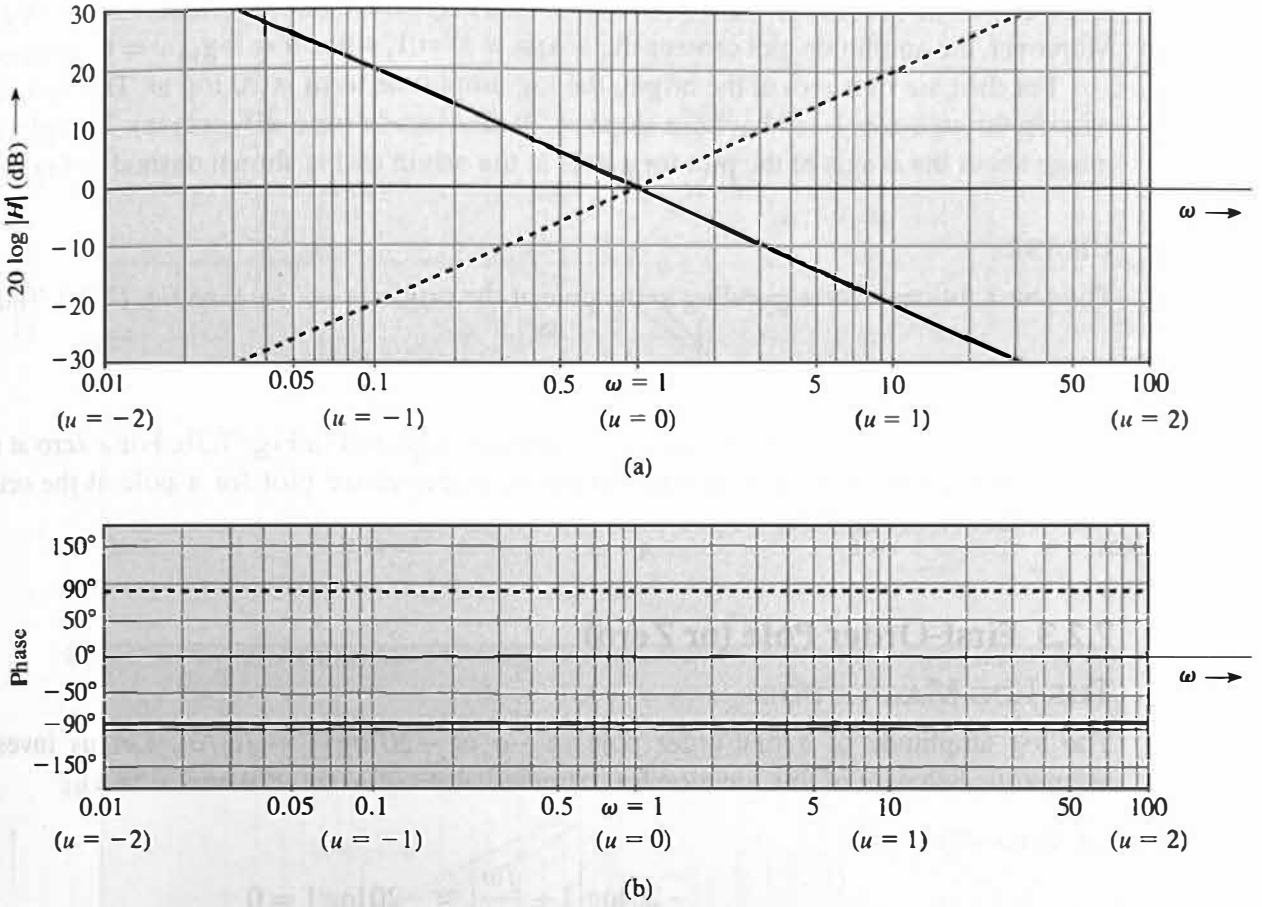

Figure 7.3 **(a)** Amplitude and **(b)** phase responses of a pole or a zero at the origin.

ω scale is equivalent to 1 unit along the u scale. We can also show that a ratio of 2 (an octave) along the ω scale equals 0.3010 (which is $\log_{10} 2$) along the u scale.†

Note that equal increments in u are equivalent to equal ratios on the ω scale. Thus, 1 unit along the u scale is the same as one decade along the ω scale. This means that the amplitude plot has a

† This point can be shown as follows. Let ω_1 and ω_2 along the ω scale correspond to u_1 and u_2 along the u scale so that $\log \omega_1 = u_1$ and $\log \omega_2 = u_2$. Then

$$u_2 - u_1 = \log_{10} \omega_2 - \log_{10} \omega_1 = \log_{10} (\omega_2/\omega_1)$$

Thus, if

$$(\omega_2/\omega_1) = 10 \qquad \text{(which is a decade)}$$

then

$$u_2 - u_1 = \log_{10} 10 = 1$$

and if

$$(\omega_2/\omega_1) = 2 \qquad \text{(which is an octave)}$$

then

$$u_2 - u_1 = \log_{10} 2 = 0.3010$$

slope of -20 dB/decade or $-20(0.3010) = -6.02$dB/octave (commonly stated as -6 dB/octave). Moreover, the amplitude plot crosses the ω axis at $\omega = 1$, since $u = \log_{10}\omega = 0$ when $\omega = 1$.

For the case of a zero at the origin, the log-amplitude term is $20 \log \omega$. This is a straight line passing through $\omega = 1$ and having a slope of 20 dB/decade (or 6 dB/octave). This plot is a mirror image about the ω axis of the plot for a pole at the origin and is shown dashed in Fig. 7.3a.

Phase

The phase function corresponding to the pole at the origin is $-\angle j\omega$ [see Eq. (7.7)]. Thus,

$$\angle H(j\omega) = -\angle j\omega = -90^\circ$$

The phase is constant (-90°) for all values of ω, as depicted in Fig. 7.3b. For a zero at the origin, the phase is $\angle j\omega = 90^\circ$. This is a mirror image of the phase plot for a pole at the origin and is shown dashed in Fig. 7.3b.

7.2.3 First-Order Pole (or Zero)

The Log Magnitude

The log amplitude of a first-order pole at $-a$ is $-20 \log |1 + j\omega/a|$. Let us investigate the asymptotic behavior of this function for extreme values of ω ($\omega \ll a$ and $\omega \gg a$).

(a) For $\omega \ll a$,

$$-20 \log \left|1 + \frac{j\omega}{a}\right| \approx -20 \log 1 = 0$$

Hence, the log-amplitude function $\to 0$ asymptotically for $\omega \ll a$ (Fig. 7.4a).

(a) For the other extreme case, where $\omega \gg a$,

$$-20 \log \left|1 + \frac{j\omega}{a}\right| \approx -20 \log \left(\frac{\omega}{a}\right) = -20 \log \omega + 20 \log a = -20u + 20 \log a$$

This represents a straight line (when plotted as a function of u, the log of ω) with a slope of -20 dB/decade (or -6 dB/octave). When $\omega = a$, the log amplitude is zero. Hence, this line crosses the ω axis at $\omega = a$, as illustrated in Fig. 7.4a. Note that the asymptotes in (a) and (b) meet at $\omega = a$.

The exact log amplitude for this pole is

$$-20 \log \left|1 + \frac{j\omega}{a}\right| = -20 \log \left(1 + \frac{\omega^2}{a^2}\right)^{1/2} = -10 \log \left(1 + \frac{\omega^2}{a^2}\right)$$

This exact log magnitude function also appears in Fig. 7.4a. Observe that the actual and the asymptotic plots are very close. A maximum error of 3 dB occurs at $\omega = a$. This frequency is known as the *corner frequency* or *break frequency*. The error everywhere else is less than 3 dB. A plot of the error as a function of ω is shown in Fig. 7.5a. This figure shows that the error at 1 octave above or below the corner frequency is 1 dB and the error at 2 octaves above or below the corner frequency is 0.3 dB. The actual plot can be obtained by adding the error to the asymptotic plot.

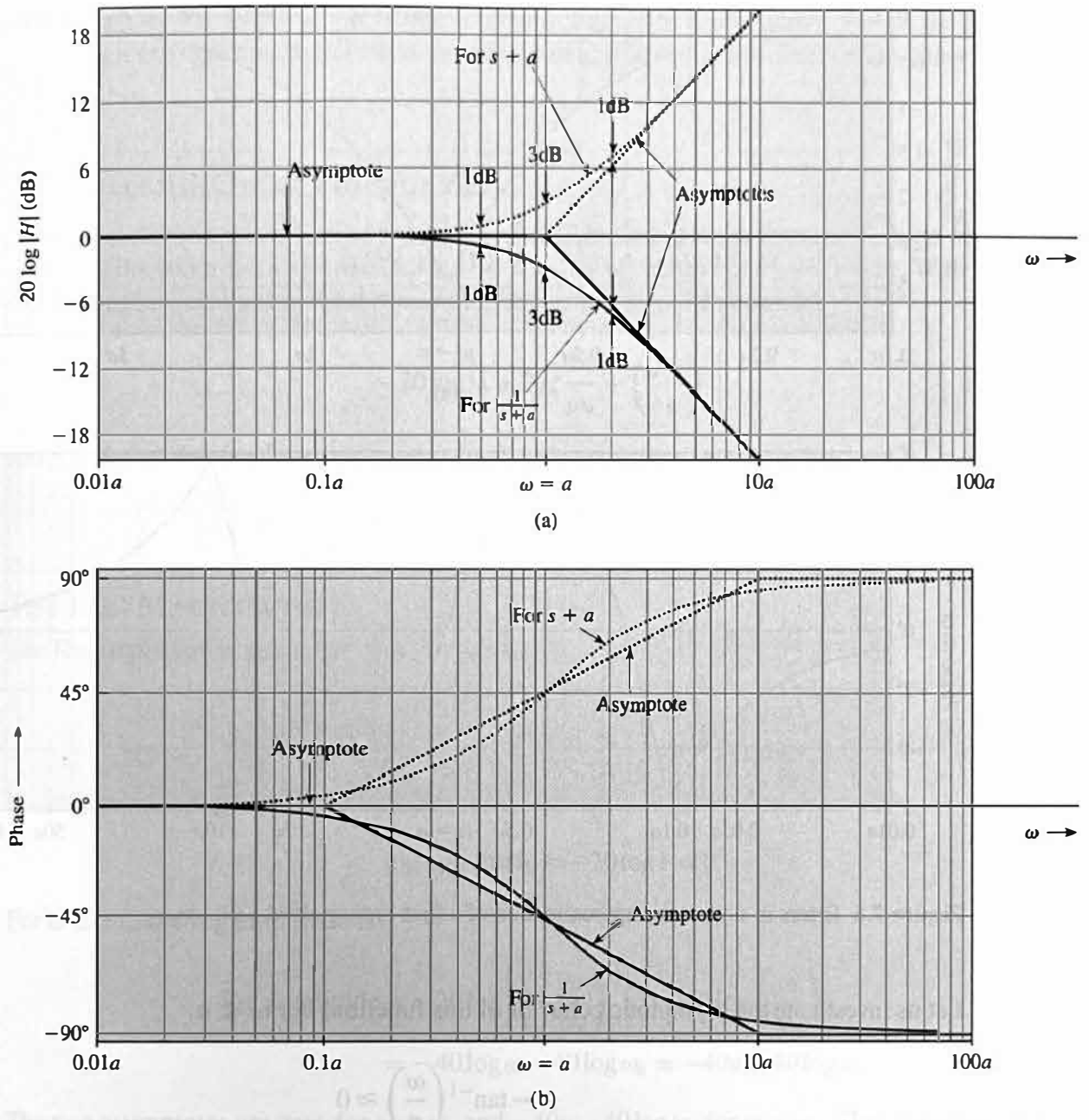

Figure 7.4 (a) Amplitude and (b) phase responses of a first-order pole or zero at $s = -a$.

The amplitude response for a zero at $-a$ (shown dotted in Fig. 7.4a) is identical to that of the pole at $-a$ with a sign change and therefore is the mirror image (about the 0 dB line) of the amplitude plot for a pole at $-a$.

PHASE

The phase for the first-order pole at $-a$ is

$$\angle H(j\omega) = -\angle\left(1 + \frac{j\omega}{a}\right) = -\tan^{-1}\left(\frac{\omega}{a}\right)$$

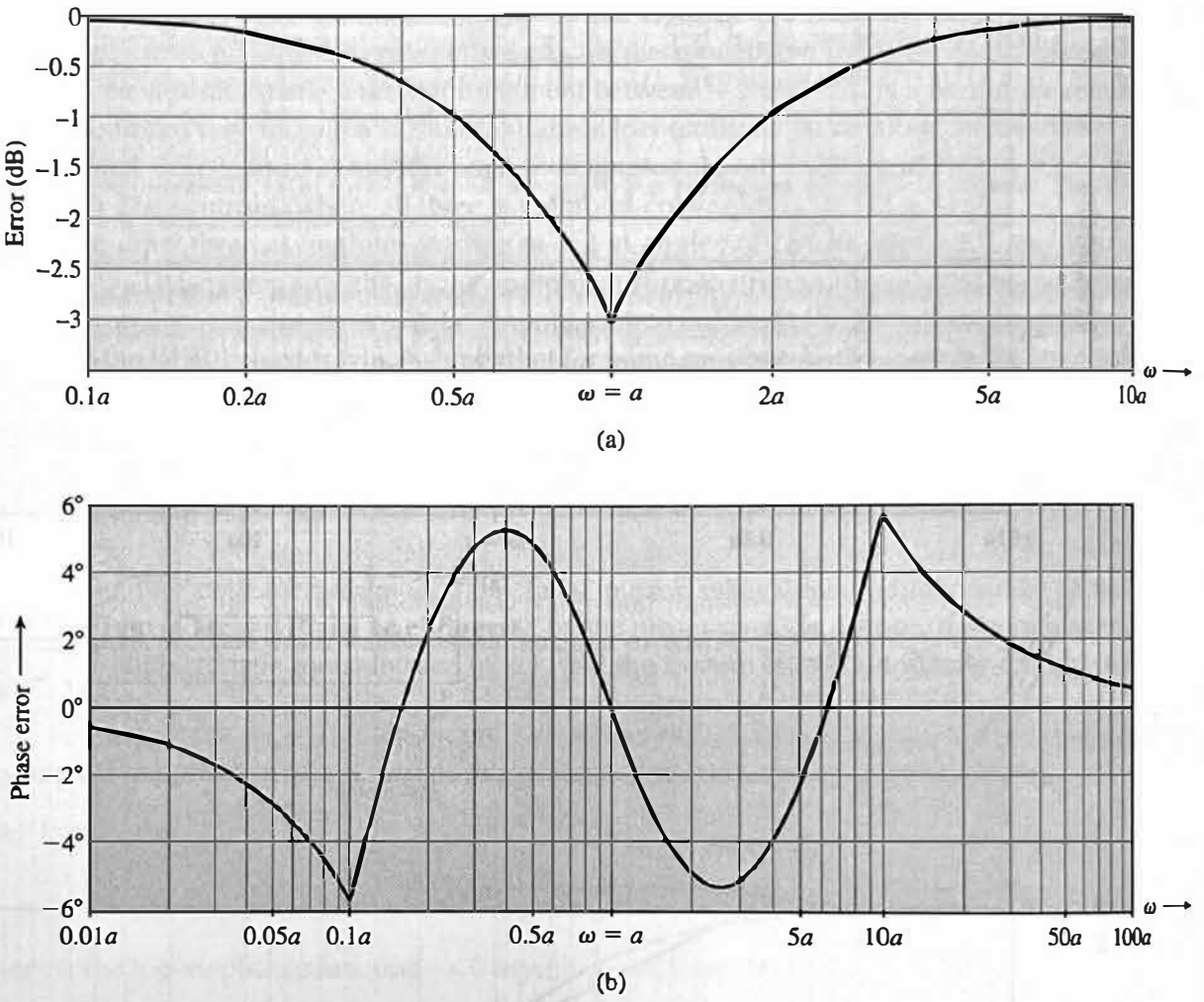

Figure 7.5 Errors in asymptotic approximation of a first-order pole at $s = -a$.

Let us investigate the asymptotic behavior of this function. For $\omega \ll a$,

$$-\tan^{-1}\left(\frac{\omega}{a}\right) \approx 0$$

and, for $\omega \gg a$,

$$-\tan^{-1}\left(\frac{\omega}{a}\right) \approx -90°$$

The actual plot along with the asymptotes is depicted in Fig. 7.4b. In this case, we use a three-line segment asymptotic plot for greater accuracy. The asymptotes are a phase angle of 0° for $\omega \leq a/10$, a phase angle of $-90°$ for $\omega \geq 10a$, and a straight line with a slope $-45°$/decade connecting these two asymptotes (from $\omega = a/10$ to $10a$) crossing the ω axis at $\omega = a/10$. It can be seen from Fig. 7.4b that the asymptotes are very close to the curve and the maximum error is 5.7°. Figure 7.5b plots the error as a function of ω; the actual plot can be obtained by adding the error to the asymptotic plot.

The phase for a zero at $-a$ (shown dotted in Fig. 7.4b) is identical to that of the pole at $-a$ with a sign change, and therefore is the mirror image (about the 0° line) of the phase plot for a pole at $-a$.

7.2.4 Second-Order Pole (or Zero)

Let us consider the second-order pole in Eq. (7.5). The denominator term is $s^2+b_2s+b_3$. We shall introduce the often-used standard form $s^2+2\zeta\omega_n s+\omega_n^2$ instead of $s^2+b_2s+b_3$. With this form, the log amplitude function for the second-order term in Eq. (7.8) becomes

$$-20\log\left|1+2j\zeta\frac{\omega}{\omega_n}+\left(\frac{j\omega}{\omega_n}\right)^2\right|$$

and the phase function is

$$-\angle\left[1+2j\zeta\frac{\omega}{\omega_n}+\left(\frac{j\omega}{\omega_n}\right)^2\right] \tag{7.9}$$

The Log Magnitude

The log amplitude is given by

$$\text{log amplitude}=-20\log\left|1+2j\zeta\left(\frac{\omega}{\omega_n}\right)+\left(\frac{j\omega}{\omega_n}\right)^2\right| \tag{7.10}$$

For $\omega\ll\omega_n$, the log amplitude becomes

$$\text{log amplitude}\approx -20\log 1=0$$

For $\omega\gg\omega_n$, the log amplitude is

$$\begin{aligned}\text{log amplitude}&\approx -20\log\left|\left(-\frac{\omega}{\omega_n}\right)^2\right|=-40\log\left(\frac{\omega}{\omega_n}\right)\\&=-40\log\omega-40\log\omega_n=-40u-40\log\omega_n\end{aligned} \tag{7.11}$$

The two asymptotes are zero for $\omega<\omega_n$ and $-40u-40\log\omega_n$ for $\omega>\omega_n$. The second asymptote is a straight line with a slope of -40 dB/decade (or -12 dB/octave) when plotted against the log ω scale. It begins at $\omega=\omega_n$ [see Eq. (7.11)]. The asymptotes are depicted in Fig. 7.6a. The exact log amplitude is given by [see Eq. (7.10)]

$$\text{log amplitude}=-20\log\left\{\left[1-\left(\frac{\omega}{\omega_n}\right)^2\right]^2+4\zeta^2\left(\frac{\omega}{\omega_n}\right)^2\right\}^{1/2} \tag{7.12}$$

The log amplitude in this case involves a parameter ζ, resulting in a different plot for each value of ζ. For complex-conjugate poles,[†] $\zeta<1$. Hence, we must sketch a family of curves for a number

[†] For $\zeta\geq 1$, the two poles in the second-order factor are no longer complex but real, and each of these two real poles can be dealt with as a separate first-order factor.

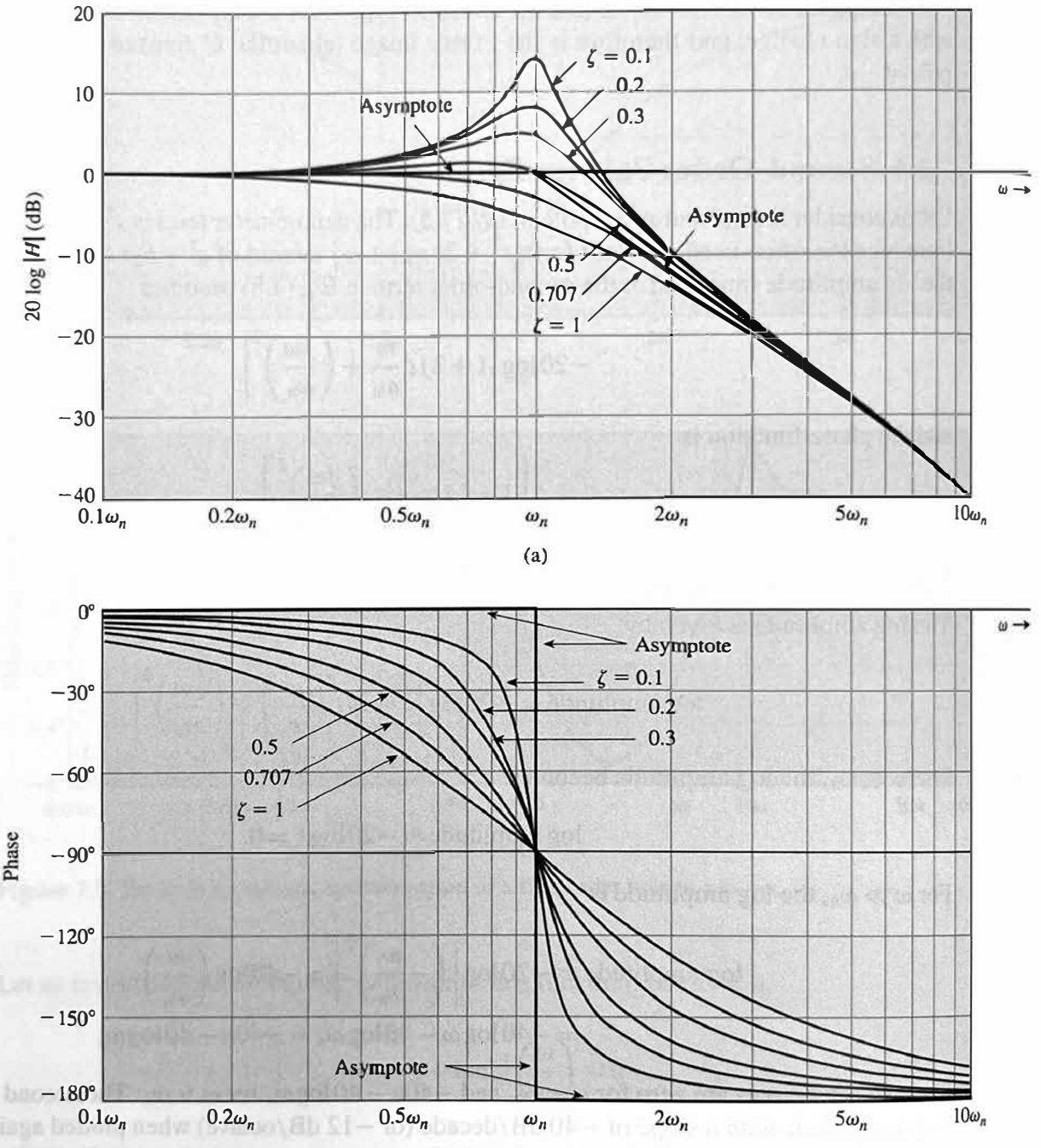

Figure 7.6 Amplitude and phase response of a second-order pole.

of values of ζ in the range 0 to 1. This is illustrated in Fig. 7.6a. The error between the actual plot and the asymptotes is shown in Fig. 7.7. The actual plot can be obtained by adding the error to the asymptotic plot.

For second-order zeros (complex-conjugate zeros), the plots are mirror images (about the 0 dB line) of the plots depicted in Fig. 7.6a. Note the resonance phenomenon of the complex-conjugate poles. This phenomenon is barely noticeable for $\zeta > 0.707$ but becomes pronounced as $\zeta \to 0$.

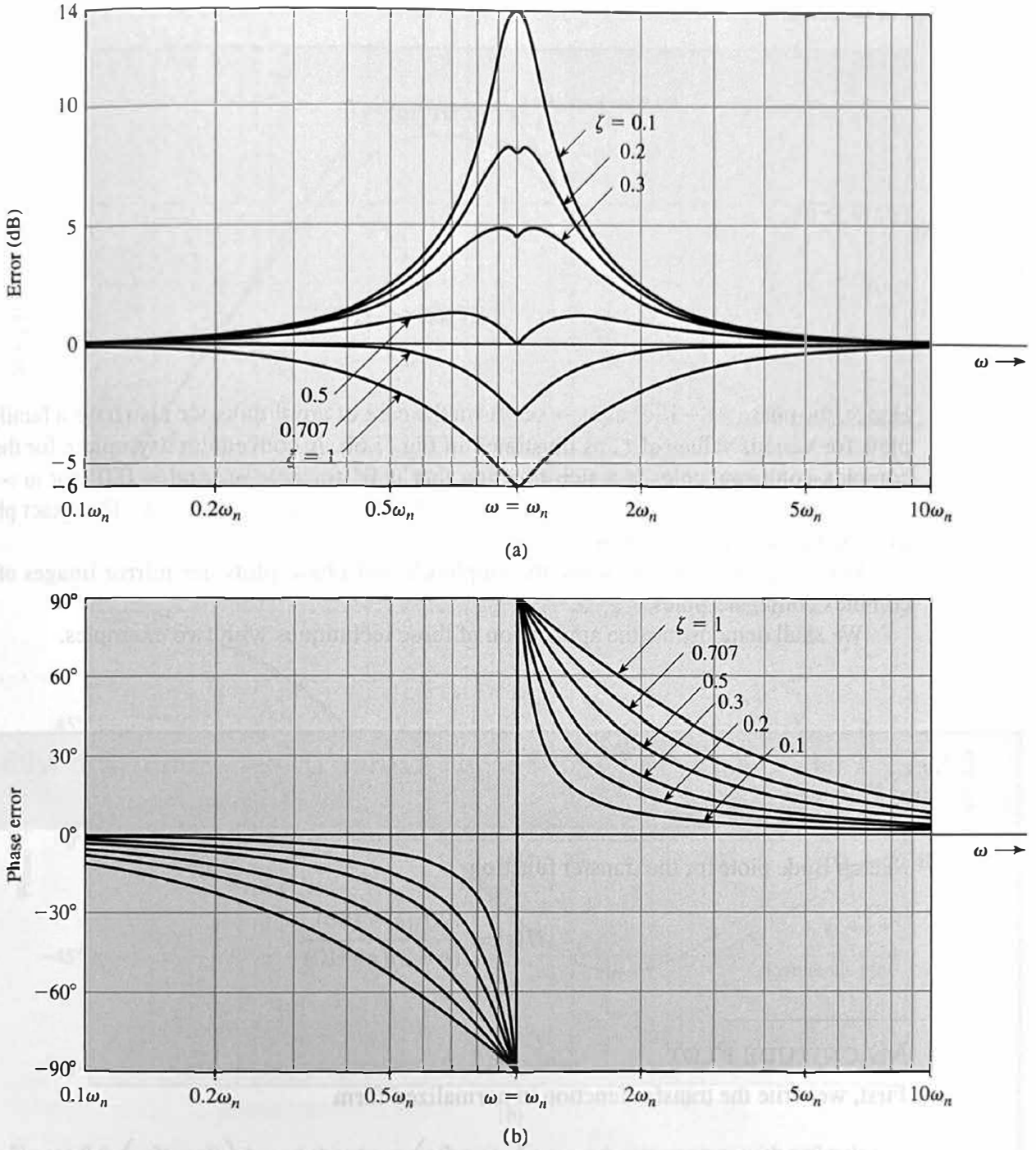

Figure 7.7 Errors in the asymptotic approximation of a second-order pole.

Phase

The phase function for second-order poles, as apparent in Eq. (7.9), is

$$\angle H(j\omega) = -\tan^{-1}\left[\frac{2\zeta\left(\frac{\omega}{\omega_n}\right)}{1-\left(\frac{\omega}{\omega_n}\right)^2}\right] \tag{7.13}$$

For $\omega \ll \omega_n$,

$$\angle H(j\omega) \approx 0$$

For $\omega \gg \omega_n$,

$$\angle H(j\omega) \simeq -180^\circ$$

Hence, the phase $\to -180^\circ$ as $\omega \to \infty$. As in the case of amplitude, we also have a family of phase plots for various values of ζ, as illustrated in Fig. 7.6b. A convenient asymptote for the phase of complex-conjugate poles is a step function that is 0° for $\omega < \omega_n$ and -180° for $\omega > \omega_n$. Error plots for such an asymptote are shown in Fig. 7.7 for various values of ζ. The exact phase is the asymptotic value plus the error.

For complex-conjugate zeros, the amplitude and phase plots are mirror images of those for complex conjugate-poles.

We shall demonstrate the application of these techniques with two examples.

EXAMPLE 7.3 Bode Plots for Second-Order Transfer Function with Real Roots

Sketch Bode plots for the transfer function

$$H(s) = \frac{20s(s+100)}{(s+2)(s+10)}$$

MAGNITUDE PLOT

First, we write the transfer function in normalized form

$$H(s) = \frac{20 \times 100}{2 \times 10} \frac{s\left(1+\frac{s}{100}\right)}{\left(1+\frac{s}{2}\right)\left(1+\frac{s}{10}\right)} = 100 \frac{s\left(1+\frac{s}{100}\right)}{\left(1+\frac{s}{2}\right)\left(1+\frac{s}{10}\right)}$$

Here, the constant term is 100; that is, 40 dB ($20 \log 100 = 40$). This term can be added to the plot by simply relabeling the horizontal axis (from which the asymptotes begin) as the 40 dB line (see Fig. 7.8a). Such a step implies shifting the horizontal axis upward by 40 dB. This is precisely what is desired.

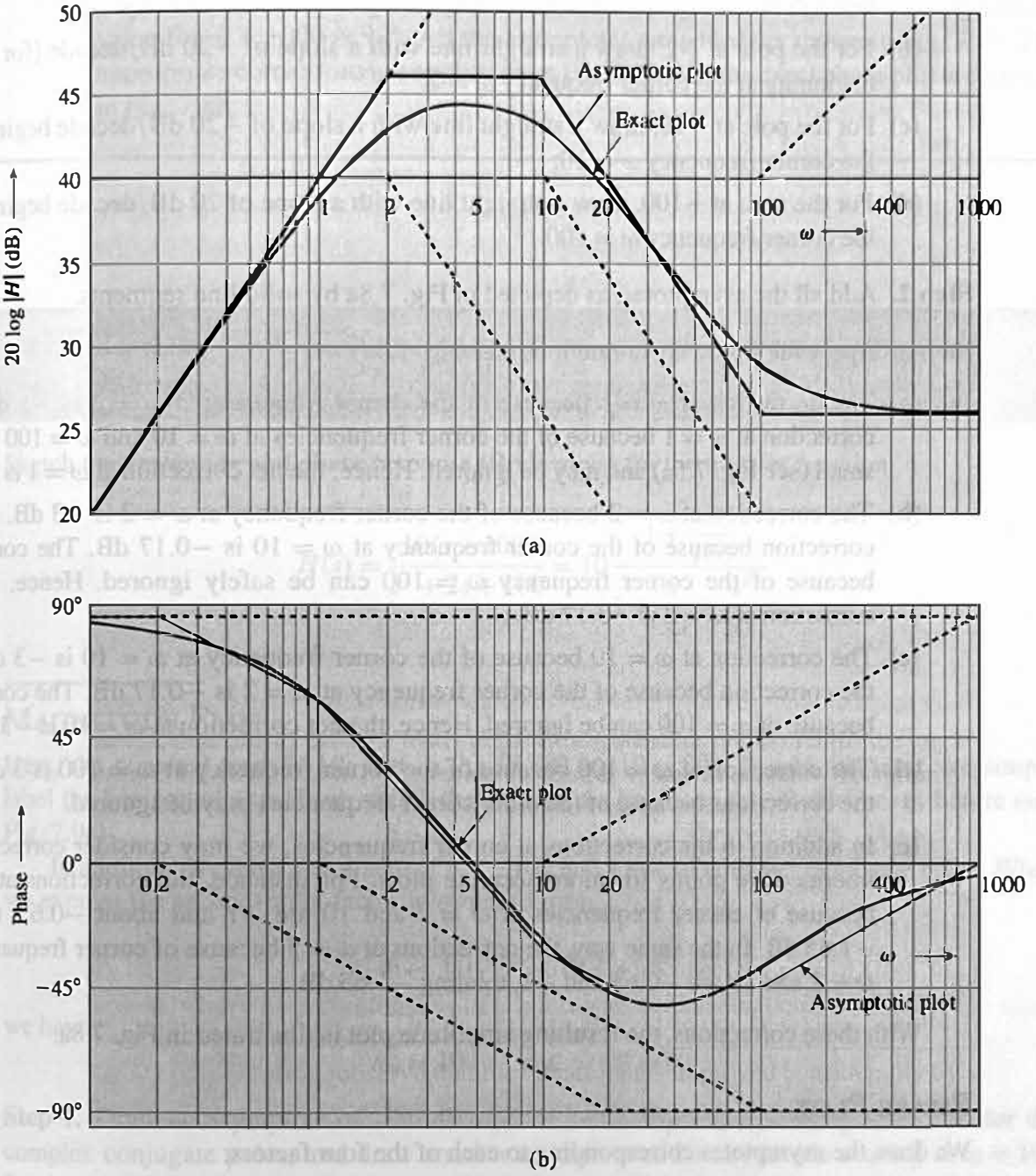

Figure 7.8 **(a)** Amplitude and **(b)** phase responses of a second-order system with real poles.

In addition, we have two first-order poles at -2 and -10, one zero at the origin, and one zero at -100.

Step 1. For each of these terms, we draw an asymptotic plot as follows (shown in Fig. 7.8a by dashed lines):

(a) For the zero at the origin, draw a straight line with a slope of 20 dB/decade passing through $\omega = 1$.

(b) For the pole at -2, draw a straight line with a slope of -20 dB/decade (for $\omega > 2$) beginning at the corner frequency $\omega = 2$.

(c) For the pole at -10, draw a straight line with a slope of -20 dB/decade beginning at the corner frequency $\omega = 10$.

(d) For the zero at -100, draw a straight line with a slope of 20 dB/decade beginning at the corner frequency $\omega = 100$.

Step 2. Add all the asymptotes, as depicted in Fig. 7.8a by solid line segments.

Step 3. Apply the following corrections (see Fig. 7.5a):

(a) The correction at $\omega = 1$ because of the corner frequency at $\omega = 2$ is -1 dB. The correction at $\omega = 1$ because of the corner frequencies at $\omega = 10$ and $\omega = 100$ is quite small (see Fig. 7.5a) and may be ignored. Hence, the net correction at $\omega = 1$ is -1 dB.

(b) The correction at $\omega = 2$ because of the corner frequency at $\omega = 2$ is -3 dB, and the correction because of the corner frequency at $\omega = 10$ is -0.17 dB. The correction because of the corner frequency $\omega = 100$ can be safely ignored. Hence, the net correction at $\omega = 2$ is -3.17 dB.

(c) The correction at $\omega = 10$ because of the corner frequency at $\omega = 10$ is -3 dB, and the correction because of the corner frequency at $\omega = 2$ is -0.17 dB. The correction because of $\omega = 100$ can be ignored. Hence, the net correction at $\omega = 10$ is -3.17 dB.

(d) The correction at $\omega = 100$ because of the corner frequency at $\omega = 100$ is 3 dB, and the corrections because of the other corner frequencies may be ignored.

(e) In addition to the corrections at corner frequencies, we may consider corrections at intermediate points for more accurate plots. For instance, the corrections at $\omega = 4$ because of corner frequencies at $\omega = 2$ and 10 are -1 and about -0.65, totaling -1.65 dB. In the same way, the corrections at $\omega = 5$ because of corner frequencies at $\omega = 2$ and 10 are -0.65 and -1, totaling -1.65 dB.

With these corrections, the resulting amplitude plot is illustrated in Fig. 7.8a.

Phase Plot

We draw the asymptotes corresponding to each of the four factors:

(a) The zero at the origin causes a 90° phase shift.

(b) The pole at $s = -2$ has an asymptote with a zero value for $-\infty < \omega < 0.2$ and a slope of $-45°$/decade beginning at $\omega = 0.2$ and going up to $\omega = 20$. The asymptotic value for $\omega > 20$ is $-90°$.

(c) The pole at $s = -10$ has an asymptote with a zero value for $-\infty < \omega < 1$ and a slope of $-45°$/decade beginning at $\omega = 1$ and going up to $\omega = 100$. The asymptotic value for $\omega > 100$ is $-90°$.

(d) The zero at $s = -100$ has an asymptote with a zero value for $-\infty < \omega < 10$ and a slope of 45°/decade beginning at $\omega = 10$ and going up to $\omega = 1000$. The asymptotic value for $\omega > 1000$ is 90°. All the asymptotes are added, as shown in Fig. 7.8b. The appropriate corrections are applied from Fig. 7.5b, and the exact phase plot is depicted in Fig. 7.8b.

EXAMPLE 7.4 Bode Plots for Second-Order Transfer Function with Complex Poles

Sketch the amplitude and phase response (Bode plots) for the transfer function

$$H(s) = \frac{10(s+100)}{s^2+2s+100} = 10\frac{1+\dfrac{s}{100}}{1+\dfrac{s}{50}+\dfrac{s^2}{100}}$$

Magnitude Plot

Here, the constant term is 10: that is, 20 dB (20 log 10 = 20). To add this term, we simply label the horizontal axis (from which the asymptotes begin) as the 20 dB line, as before (see Fig. 7.9a).

In addition, we have a real zero at $s = -100$ and a pair of complex conjugate poles. When we express the second-order factor in standard form,

$$s^2 + 2s + 100 = s^2 + 2\zeta\omega_n s + \omega_n^2$$

we have

$$\omega_n = 10 \qquad \text{and} \qquad \zeta = 0.1$$

Step 1. Draw an asymptote of −40 dB/decade (−12 dB/octave) starting at $\omega = 10$ for the complex conjugate poles, and draw another asymptote of 20 dB/decade starting at $\omega = 100$ for the (real) zero.

Step 2. Add both asymptotes.

Step 3. Apply the correction at $\omega = 100$, where the correction because of the corner frequency $\omega = 100$ is 3 dB. The correction because of the corner frequency $\omega = 10$, as seen from Fig. 7.7a for $\zeta = 0.1$, can be safely ignored. Next, the correction at $\omega = 10$ because of the corner frequency $\omega = 10$ is 13.90 dB (see Fig. 7.7a for $\zeta = 0.1$). The correction because of the real zero at −100 can be safely ignored at $\omega = 10$. We may find corrections at a few more points. The resulting plot is illustrated in Fig. 7.9a.

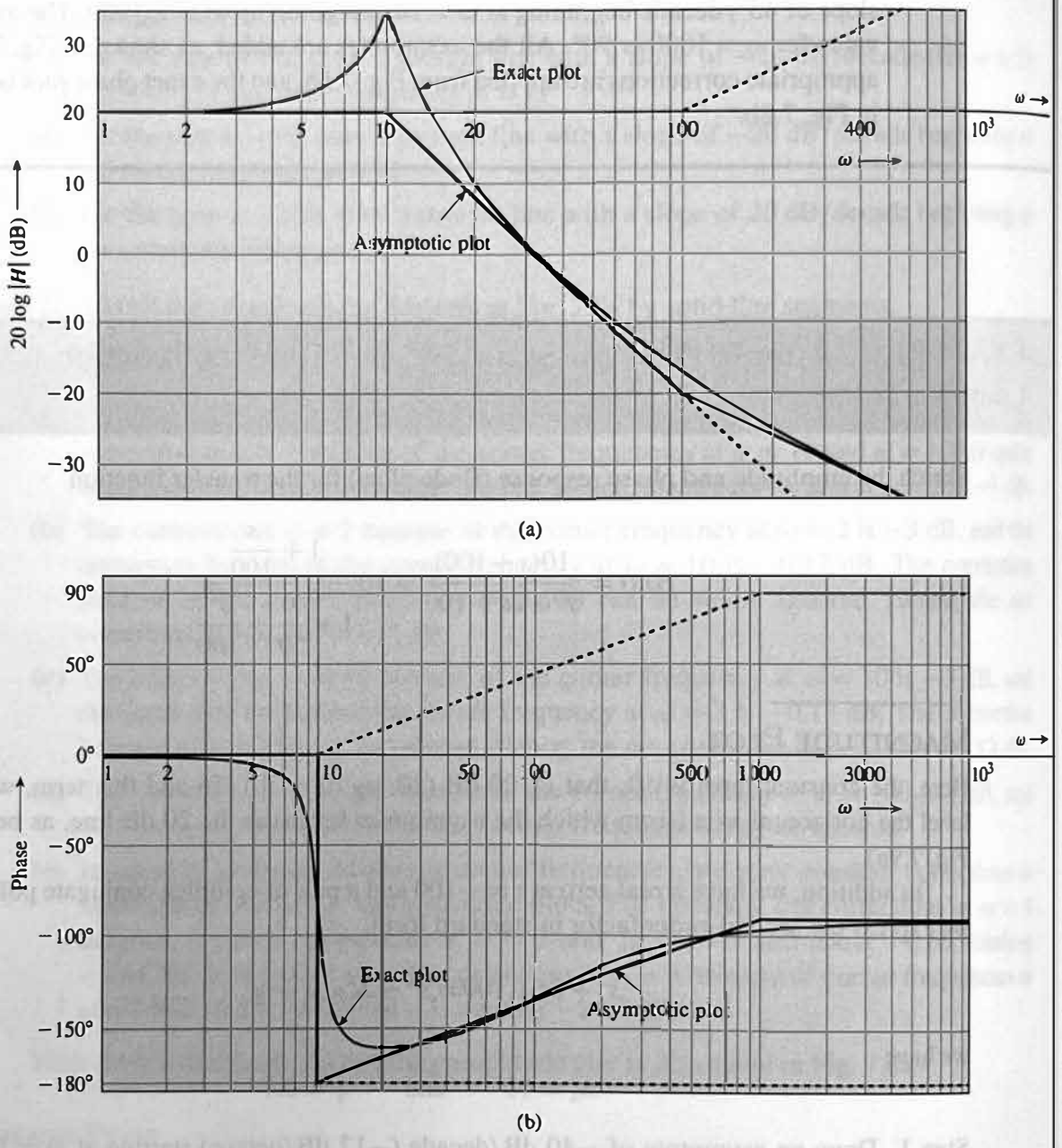

Figure 7.9 (a) Amplitude and **(b)** phase responses of a second-order system with complex-conjugate poles.

Phase Plot

The asymptote for the complex conjugate poles is a step function with a jump of $-180°$ at $\omega = 10$. The asymptote for the zero at $s = -100$ is zero for $\omega \leq 10$ and is a straight line with a slope of 45°/decade, starting at $\omega = 10$ and going to $\omega = 1000$. For $\omega \geq 1000$, the asymptote is 90°. The two asymptotes add to give the sawtooth shown in Fig. 7.9b. We now apply the corrections from Figs. 7.5b and 7.7b to obtain the exact plot.

Bode Plots with MATLAB

Bode plots make it relatively simple to hand-draw straight-line approximations to a system's magnitude and frequency responses. To produce exact Bode plots, we turn to MATLAB and its bode command.

```
>> bode(tf([10 1000],[1 2 100]),'k-');
```

The resulting MATLAB plots, shown in Fig. 7.10, match the plots shown in Fig. 7.9.

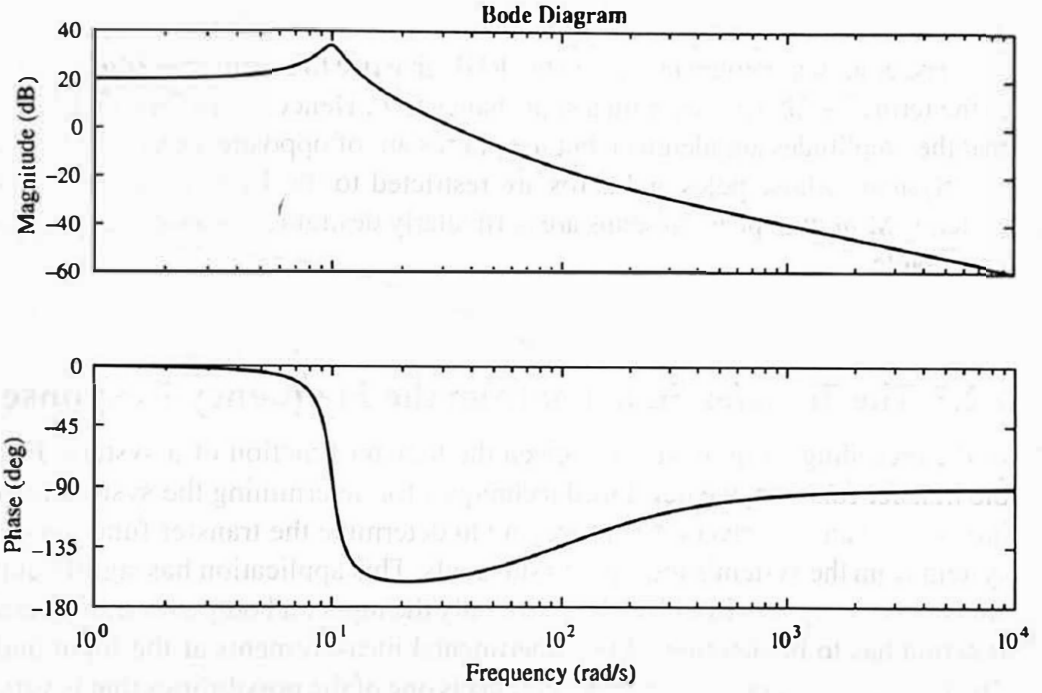

Figure 7.10 MATLAB-generated Bode plots for Ex. 7.4.

Comment. These two examples demonstrate that actual frequency response plots are very close to asymptotic plots, which are so easy to construct. Thus, by mere inspection of $H(s)$ and its poles and zeros, one can rapidly construct a mental image of the frequency response of a system. This is the principal virtue of Bode plots.

Poles and Zeros in the Right Half-Plane

In our discussion so far, we have assumed the poles and zeros of the transfer function to be in the left half-plane. What if some of the poles and/or zeros of $H(s)$ lie in the RHP? If there is a pole in the RHP, the system is unstable. Such systems are useless for any signal-processing application. For this reason, we shall consider only the case of the RHP zero. The term corresponding to RHP zero at $s = a$ is $(s/a) - 1$, and the corresponding frequency response is $(j\omega/a) - 1$. The amplitude response is

$$\left|\frac{j\omega}{a}-1\right|=\left(\frac{\omega^2}{a^2}+1\right)^{1/2}$$

This shows that the amplitude response of an RHP zero at $s=a$ is identical to that of an LHP zero or $s=-a$. Therefore, the log amplitude plots remain unchanged whether the zeros are in the LHP or the RHP. However, the phase corresponding to the RHP zero at $s=a$ is

$$\angle\left(\frac{j\omega}{a}-1\right)=\angle-\left(1-\frac{j\omega}{a}\right)=\pi+\tan^{-1}\left(\frac{-\omega}{a}\right)=\pi-\tan^{-1}\left(\frac{\omega}{a}\right)$$

whereas the phase corresponding to the LHP zero at $s=-a$ is $\tan^{-1}(\omega/a)$.

The complex-conjugate zeros in the RHP give rise to a term $s^2-2\zeta\omega_n s+\omega_n^2$, which is identical to the term $s^2+2\zeta\omega_n s+\omega_n^2$ with a sign change in ζ. Hence, from Eqs. (7.12) and (7.13), it follows that the amplitudes are identical, but the phases are of opposite signs for the two terms.

Systems whose poles and zeros are restricted to the LHP are classified as *minimum phase* systems. Minimum phase systems are particularly desirable because the system *and its inverse* are both stable.

7.2.5 The Transfer Function from the Frequency Response

In the preceding section, we were given the transfer function of a system. From a knowledge of the transfer function, we developed techniques for determining the system response to sinusoidal inputs. We can also reverse the procedure to determine the transfer function of a minimum phase system from the system's response to sinusoids. This application has significant practical utility. If we are given a system in a black box with only the input and output terminals available, the transfer function has to be determined by experimental measurements at the input and output terminals. The frequency response to sinusoidal inputs is one of the possibilities that is very attractive because the measurements involved are so simple. One needs only to apply a sinusoidal signal at the input and observe the output. We find the amplitude gain $|H(j\omega)|$ and the output phase shift $\angle H(j\omega)$ (with respect to the input sinusoid) for various values of ω over the entire range from 0 to ∞. This information yields the frequency response plots (Bode plots) when plotted against $\log\omega$. From these plots, we determine the appropriate asymptotes by taking advantage of the fact that the slopes of all asymptotes must be multiples of ± 20 dB/decade if the transfer function is a rational function (a function that is a ratio of two polynomials in s). From the asymptotes, the corner frequencies are obtained. Corner frequencies determine the poles and zeros of the transfer function. Because of the ambiguity about the location of zeros since LHP and RHP zeros (zeros at $s=\pm a$) have identical magnitudes, this procedure works only for minimum phase systems.

7.3 CONTROL SYSTEM DESIGN USING FREQUENCY RESPONSE

Figure 7.11a shows a basic closed-loop system, whose open-loop transfer function is $KG(s)H(s)$ (see Sec. 6.7.3). According to Eq. (6.49), the closed-loop transfer function is

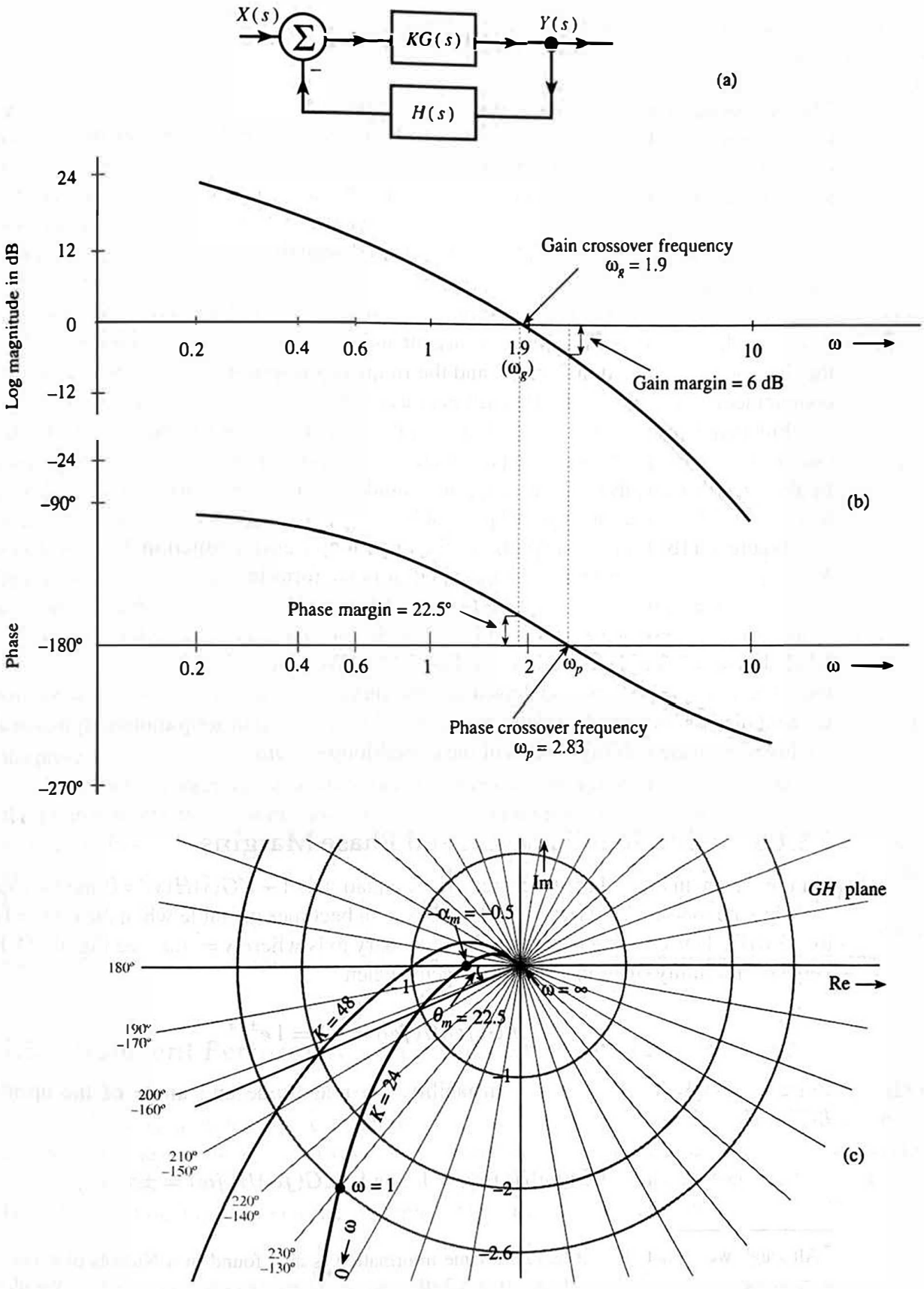

Figure 7.11 Gain and phase margins of a system with open-loop transfer function $\frac{24}{s(s+2)(s+4)}$.

$$T(s) = \frac{KG(s)}{1 + KG(s)H(s)}$$

The time-domain method of control system design discussed in Sec. 6.7 works only when the transfer function of the plant (the system to be controlled) is known and is a rational function (ratio of two polynomials in s). The input-output description of practical systems is often unknown and is more likely to be nonrational. A system containing an ideal time delay (dead time) is an example of a nonrational system. In such cases, we can determine the frequency response of the open-loop system empirically and use this data to design the (closed-loop) system. In this section, we shall discuss feedback system design procedure based on the frequency response description of a system. However, the frequency response design method is not as convenient as the time-domain design method from the viewpoint of transient and steady-state error specifications. Consequently, the time-domain method in Sec. 6.7 and the frequency response method should be considered as complementary rather than as alternatives or as rivals.

Frequency response information can be presented in various forms, of which the Bode plot is one. The same information can be presented by the *Nyquist plot* (also known as the *polar plot*) or by the *Nichols plot* (also known as log-magnitude versus angle plot). Here, we shall discuss the techniques using Bode and Nyquist plots only.

Figure 7.11b shows Bode plots for the open-loop transfer function $K/s(s+2)(s+4)$ when $K = 24$. The same information is presented in polar form in the corresponding Nyquist plot of Fig. 7.11c. For example, at $\omega = 1$, $|H(j\omega)| = 2.6$ and $\angle H(j\omega) = -130.6°$. For the polar plot, we plot a point at a distance 2.6 units and at an angle $-130.6°$ from the horizontal axis. This point is labeled as $\omega = 1$ for identification (see Fig. 7.11c). We plot such points for several frequencies in the range from $\omega = 0$ to ∞ and draw a smooth curve through them to obtain the Nyquist plot.[†] As we next discuss, Bode or Nyquist (or Nichols) plots of the open-loop transfer function allow us to readily investigate stability aspects of the closed-loop system.

7.3.1 Relative Stability: Gain and Phase Margins

For the system in Fig. 7.11a, the characteristic equation is $1 + KG(s)H(s) = 0$ and the characteristic roots are the roots of $KG(s)H(s) = -1$. The system becomes unstable when the root loci cross over to the RHP. This crossing occurs on the imaginary axis where $s = j\omega$ (see Fig. 6.45). Hence, the verge of instability (marginal stability) occurs when

$$KG(j\omega)H(j\omega) = -1 = 1e^{\pm j\pi}$$

Correspondingly, at the verge of instability, the magnitude and angle of the open loop gain $KG(j\omega)H(j\omega)$ are

$$|KG(j\omega)H(j\omega)| = 1 \quad \text{and} \quad \angle G(j\omega)H(j\omega) = \pm\pi$$

[†] Although we do not show it here, the same information is also found in a Nichols plot. For example, at $\omega = 1$, the log magnitude is $20\log 2.6 = 8.3$ dB, and the phase at $\omega = 1$ is $-130.6°$. We plot a point at coordinates $x = 8.3$, $y = -130.6°$ and label it as $\omega = 1$ for identification. We do this for several values of ω from 0 to ∞ and draw a curve through these points to obtain the Nichols plot.

Thus, on the verge of instability, the open-loop transfer function has unity gain and a phase of $\pm\pi$. In order to understand the significance of these conditions, let us consider the system in Fig. 7.11a, with open-loop transfer function $K/s(s+2)(s+4)$. The root locus for this system is illustrated in Fig. 6.45. The loci cross over to the RHP for $K > 48$. For $K < 48$, the system is stable. Let us consider the case $K = 24$. The Bode plot for the $K = 24$ case is depicted in Fig. 7.11b. Let the frequency where the angle plot crosses $-180°$ be ω_p (the *phase crossover frequency*). Observe that at ω_p, the gain is 0.5 or -6 dB. This shows that the gain K will have to double (to value 48) to have unity gain, which is the verge of instability. For this reason, we say that the system has a *gain margin* of 2 (6 dB). On the other hand, if ω_g is the frequency where the gain is unity or 0 dB (the *gain crossover frequency*), then the corresponding open-loop phase is $-157.5°$. The phase will have to decrease from this value to $-180°$ before the system becomes unstable. Thus, the system has a *phase margin* of 22.5°. Clearly, the gain and phase margins are measures of the relative stability of the system.

Figure 7.11c shows that the Nyquist plot of $KG(s)H(s)$ crosses the real axis at -0.5 for $K = 24$. If we double K to a value of 48, the magnitude of every point doubles (but the phase is unchanged). This step expands the Nyquist plot by a factor of 2. Hence, for $K = 48$, the Nyquist plot lies on the real axis at -1; that is, $KG(j\omega)H(j\omega) = -1$, and the system becomes unstable. For $K > 48$, the plot crosses and goes beyond the point -1. For unstable systems, the critical point -1 lies inside the curve; that is, the curve encircles the critical point -1. When the Nyquist plot of an open-loop transfer function encircles the critical point -1, the corresponding closed-loop system becomes unstable. This statement, roughly speaking, is the well-known *Nyquist criterion* in simplified form.[†] For the Nyquist plot in Fig. 7.11b (for $K = 24$), the gain will have to double before the system becomes unstable. Thus, the gain margin is 2 (6 dB) in this case. In general, if the Nyquist plot crosses the negative real axis at $-\alpha_m$, then the gain margin is $1/\alpha_m$. Similarly, if $-\pi + \theta_m$ is the angle at which the Nyquist plot crosses the unit circle, the phase margin is θ_m. In the present case, $\theta_m = 22.5°$.

In order to protect a system from instability because of variations in system parameters (or in the environment), the system should be designed with reasonable gain and phase margins. Small margins indicate that the poles of the closed-loop system are in the LHP but too close to the ω axis. The transient response of such systems will have a large percent overshoot (PO). On the other hand, very large (positive) gain and phase margins may indicate a sluggish system. Generally, a gain margin higher than 6 dB and a phase margin of about 30° to 60° are considered desirable. Design specifications for transient performance are often given in terms of gain and phase margins.

7.3.2 Transient Performance in Terms of Frequency Response

For a second-order system in Eq. (6.44), we saw the dependence of the transient response (PO, t_r, t_d, and t_s) on dominant pole locations. Using this knowledge, we developed in Sec. 6.7 a procedure for designing a control system for a specified transient performance. In order to develop a procedure based on the system's frequency response (rather than its transfer function), we must know the relationship between the frequency response and the transient response of the system

[†] The Nyquist criterion states as follows: a closed curve C_s in the s plane enclosing Z zeros and P poles of an open-loop transfer function $W(s)$ maps into a closed curve C_w in the W plane encircling the origin of the W plane $Z - P$ times, in the same direction as that of C_s.

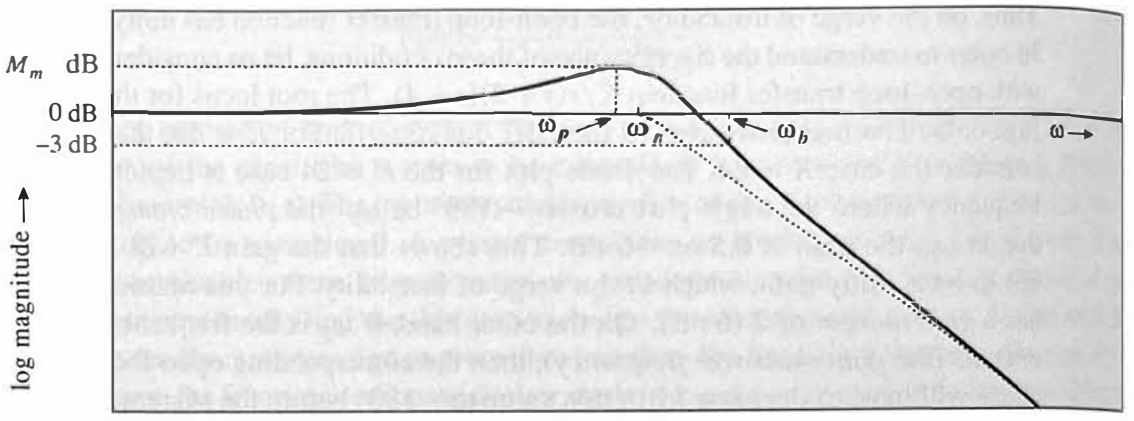

Figure 7.12 Frequency response of a second-order all-pole system.

in Eq. (6.44). Figure 7.12 shows the frequency response of a second-order system in Eq. (6.44). The peak frequency response M_p (the maximum value of the amplitude response), which occurs at frequency ω_p, indicates the relative stability of the system. A higher peak response generally indicates a smaller ζ (see Fig. 7.6a), which implies poles that are closer to the imaginary axis and have less relative stability. Higher M_p also means higher PO. Generally acceptable values of M_p, in practice, range from 1.1 to 1.5. The 3 dB bandwidth ω_b of the frequency response indicates the speed of the system. We can show that ω_b and t_r are inversely proportional. Hence, higher ω_b indicates smaller t_r (faster response).

For the second-oder system in Eq. (6.44), we have

$$T(j\omega) = \frac{\omega_n^2}{(j\omega)^2 + 2j\zeta\omega_n\omega + \omega_n^2}$$

To find M_p, we let $d|T(j\omega)|/d\omega = 0$. From the solution of this equation, we find

$$M_p = \frac{1}{2\zeta\sqrt{1-\zeta^2}} \qquad \zeta \le 0.707$$

$$\omega_p = \omega_n\sqrt{1-\zeta^2} \qquad \zeta \le 0.707$$

$$\omega_b = \omega_n\left[(1-2\zeta^2) + \sqrt{4\zeta^4 - 4\zeta^2 + 2}\right]^{1/2} \tag{7.14}$$

These equations show that we can determine ζ and ω_n from M_p and ω_p. Knowledge of ζ and ω_n allows us to determine the transient parameters, such as PO, t_r, and t_s, as seen from Eqs. (6.45), (6.46), and (6.47). Conversely, if we are given certain transient specifications PO, t_r, and t_s, we can determine the required M_p and ω_p. Thus, the problem now reduces to designing a system that has a certain M_p and ω_p for the closed-loop frequency response. In practice, we know the open-loop system frequency response. So, the ultimate problem reduces to relating the frequency response of the closed-loop system to that of the open-loop system. To do this, we shall consider the case of unity feedback system, where the feedback transfer function is $H(s) = 1$.[†] In this case, the closed-loop transfer function and frequency responses are

[†] The results for a unity feedback system can be extended to nonunity feedback systems.

$$T(s) = \frac{KG(s)}{1+KG(s)} \quad \text{and} \quad T(j\omega) = \frac{KG(j\omega)}{1+KG(j\omega)}$$

Let

$$T(j\omega) = Me^{j\alpha(\omega)} \quad \text{and} \quad KG(j\omega) = x(\omega) + jy(\omega)$$

Therefore,

$$Me^{j\alpha(\omega)} = \frac{x+jy}{1+x+jy}$$

Straightforward manipulation of this equation yields

$$\left(x + \frac{M^2}{M^2-1}\right)^2 + y^2 = \frac{M^2}{(M^2-1)^2}$$

This is an equation of a circle centered at $[-\frac{M^2}{M^2-1}, 0]$ and of radius $\frac{M}{M^2-1}$ in the $KG(j\omega)$ plane. Figure 7.13a shows circles for various values of M. Because M is the closed-loop system amplitude response, these circles are the contours of constant amplitude response of the closed-loop system. For example, the point $A = -2 - j1.85$ lies on the circle $M = 1.3$. This means, at a frequency where the open-loop transfer function is $G(j\omega) = -2 - j1.85$, the corresponding closed-loop transfer function amplitude response is 1.3.†

To obtain the closed-loop frequency response, we superimpose on these contours the Nyquist plot of the open-loop transfer function $KG(j\omega)$. For each point of $KG(j\omega)$, we can determine the corresponding value of M, the closed-loop amplitude response. From similar contours for constant α (the closed-loop phase response), we can determine the closed-loop phase response. Thus, the complete closed-loop frequency response can be obtained from this plot. We are primarily interested in finding M_p, the peak value of M, and ω_p, the frequency where it occurs. Figure 7.13b indicates how these values may be determined. The circle to which the Nyquist plot is tangent corresponds to M_p, and the frequency at which the Nyquist plot is tangential to this circle is ω_p. For the system, whose Nyquist plot appears in Fig. 7.13b, $M_p = 1.6$ and $\omega_p = 2$. From these values, we can estimate ζ and ω_n, and determine the transient parameters PO, t_r, and t_s.

In designing systems, we first determine the M_p and ω_p required to meet the given transient specifications. The Nyquist plot in conjunction with M circles suggests how these values of M_p and ω_p may be realized. In many cases, a mere change in gain K of the open-loop transfer function will suffice. Increasing K expands the Nyquist plot and changes the values M_p and ω_p correspondingly. If this is not enough, we should consider some form of compensation such as lag and/or lead networks. Using a computer, one can quickly observe the effect of a particular form of compensation on M_p and ω_p.

7.4 Filter Design by Placement of Poles and Zeros of $H(s)$

In this section, we explore the strong dependence of frequency response on the location of poles and zeros of $H(s)$. This dependence points to a simple intuitive procedure to filter design. Systematic filter design procedures to meet given specifications are discussed in later sections.

† We can find similar contours for constant α (the closed-loop phase response).

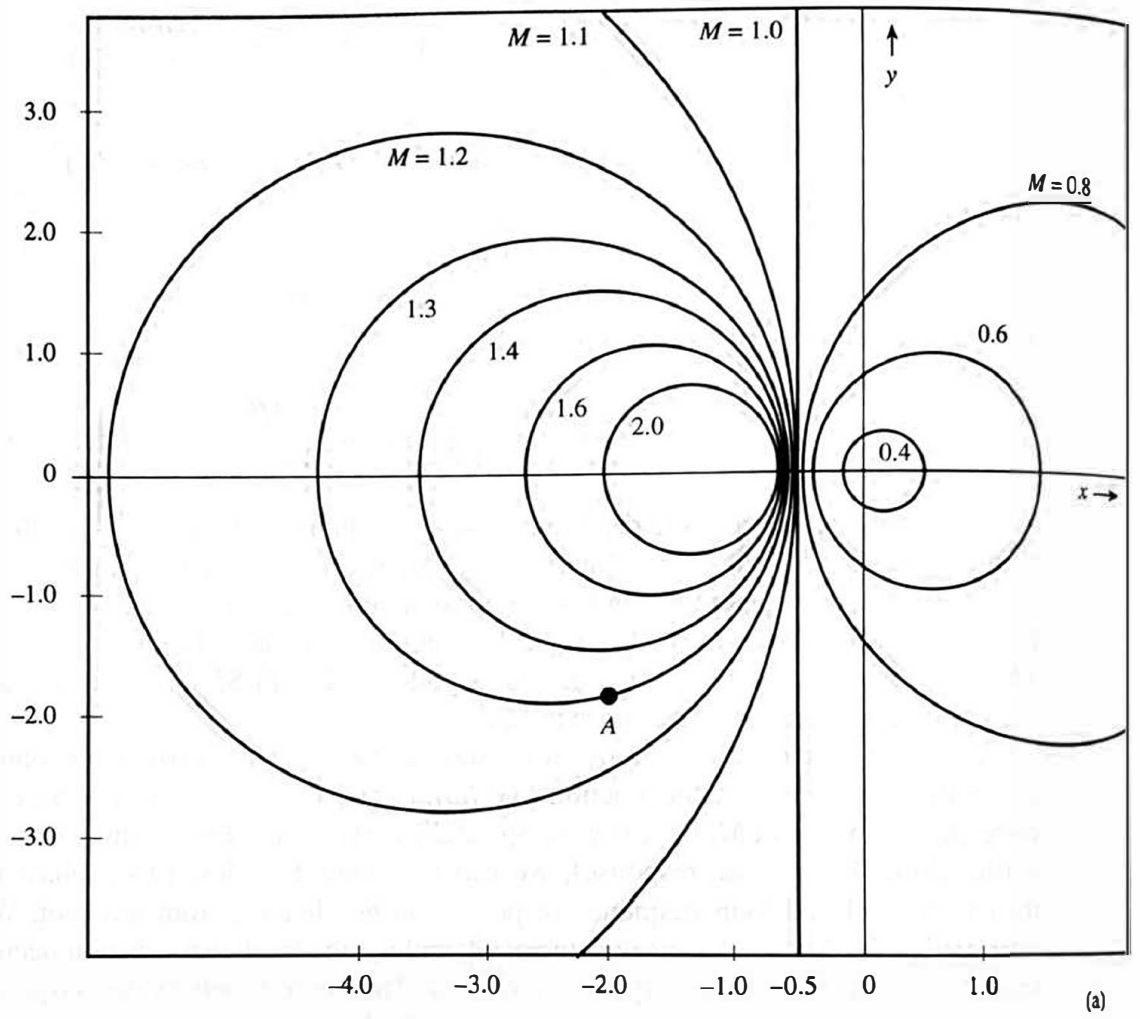

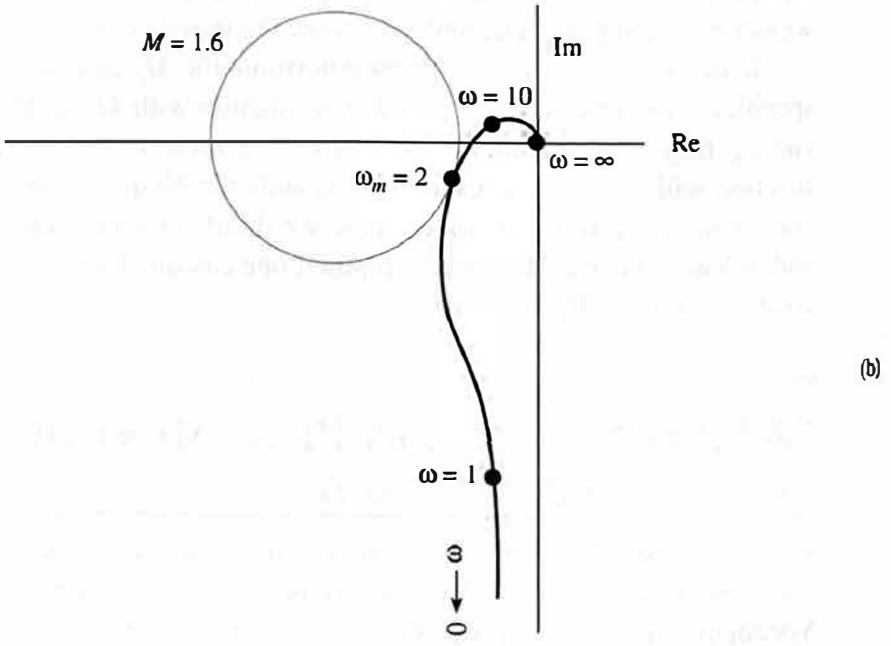

Figure 7.13 Relationship between open-loop and closed-loop frequency responses.

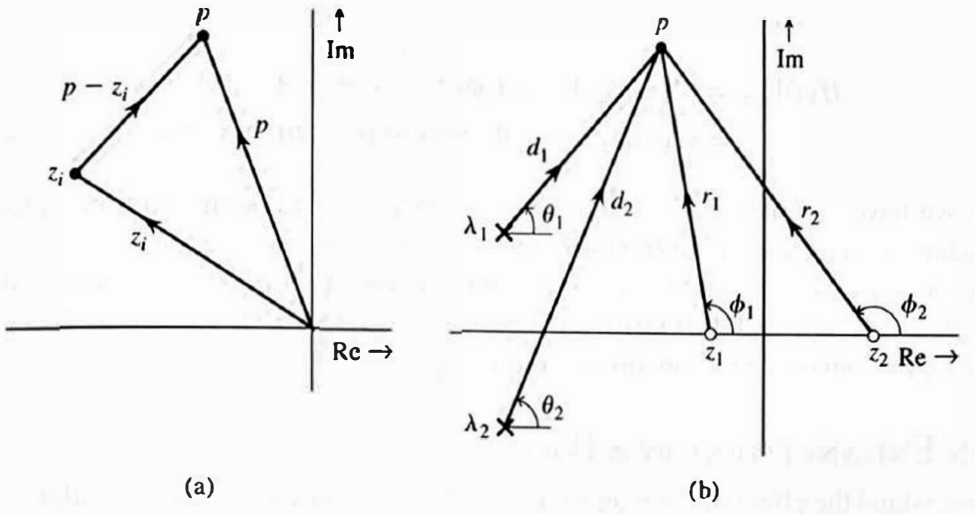

Figure 7.14 Vector representations of (a) complex numbers and (b) factors of $H(s)$.

7.4.1 Dependence of Frequency Response on Poles and Zeros of $H(s)$

Frequency response of a system is basically the information about the filtering capability of the system. A system transfer function can be expressed as

$$H(s) = \frac{P(s)}{Q(s)} = b_0 \frac{(s-z_1)(s-z_2)\cdots(s-z_N)}{(s-\lambda_1)(s-\lambda_2)\cdots(s-\lambda_N)}$$

where $z_1, z_2, \ldots, z_N$ and $\lambda_1, \lambda_2, \ldots, \lambda_N$ are the zeros and poles, respectively, of $H(s)$. Now the value of the transfer function $H(s)$ at some frequency $s = p$ is

$$H(s)|_{s=p} = b_0 \frac{(p-z_1)(p-z_2)\cdots(p-z_N)}{(p-\lambda_1)(p-\lambda_2)\cdots(p-\lambda_N)} \tag{7.15}$$

This equation consists of factors of the form $p - z_i$ and $p - \lambda_i$. The factor $p - z_i$ is a complex number represented by a vector drawn from point z to the point p in the complex plane, as illustrated in Fig. 7.14a. The length of this line segment is $|p - z_i|$, the magnitude of $p - z_i$. The angle of this directed line segment (with the horizontal axis) is $\angle(p - z_i)$. To compute $H(s)$ at $s = p$, we draw line segments from all poles and zeros of $H(s)$ to the point p, as shown in Fig. 7.14b. The vector connecting a zero z_i to the point p is $p - z_i$. Let the length of this vector be r_i, and let its angle with the horizontal axis be ϕ_i. Then $p - z_i = r_i e^{j\phi_i}$. Similarly, the vector connecting a pole λ_i to the point p is $p - \lambda_i = d_i e^{j\theta_i}$, where d_i and θ_i are the length and the angle (with the horizontal axis), respectively, of the vector $p - \lambda_i$. Now from Eq. (7.15) it follows that

$$\begin{aligned} H(s)|_{s=p} &= b_0 \frac{(r_1 e^{j\phi_1})(r_2 e^{j\phi_2})\cdots(r_N e^{j\phi_N})}{(d_1 e^{j\theta_1})(d_2 e^{j\theta_2})\cdots(d_N e^{j\theta_N})} \\ &= b_0 \frac{r_1 r_2 \cdots r_N}{d_1 d_2 \cdots d_N} e^{j[(\phi_1+\phi_2+\cdots+\phi_N)-(\theta_1+\theta_2+\cdots+\theta_N)]} \end{aligned}$$

Therefore,

$$|H(s)|_{s=p} = b_0 \frac{r_1 r_2 \cdots r_N}{d_1 d_2 \cdots d_N} = b_0 \frac{\text{product of distances of zeros to } p}{\text{product of distances of poles to } p} \tag{7.16}$$

and

$$\begin{aligned}\angle H(s)|_{s=p} &= (\phi_1 + \phi_2 + \cdots + \phi_N) - (\theta_1 + \theta_2 + \cdots + \theta_N) \\ &= \text{sum of angles of zeros to } p - \text{sum of angles of poles to } p\end{aligned} \tag{7.17}$$

Here, we have assumed positive b_0. If b_0 is negative, there is an additional phase π. Using this procedure, we can determine $H(s)$ for any value of s. To compute the frequency response $H(j\omega)$, we use $s = j\omega$ (a point on the imaginary axis), connect all poles and zeros to the point $j\omega$, and determine $|H(j\omega)|$ and $\angle H(j\omega)$ from Eqs. (7.16) and (7.17). We repeat this procedure for all values of ω from 0 to ∞ to obtain the frequency response.

Gain Enhancement by a Pole

To understand the effect of poles and zeros on the frequency response, consider a hypothetical case of a single pole $-\alpha + j\omega_0$, as depicted in Fig. 7.15a. To find the amplitude response $|H(j\omega)|$ for a certain value of ω, we connect the pole to the point $j\omega$ (Fig. 7.15a). If the length of this line is d, then $|H(j\omega)|$ is proportional to $1/d$:

$$|H(j\omega)| = \frac{K}{d} \tag{7.18}$$

where the exact value of constant K is not important at this point. As ω increases from zero, d decreases progressively until ω reaches the value ω_0. As ω increases beyond ω_0, d increases progressively. Therefore, according to Eq. (7.18), the amplitude response $|H(j\omega)|$ increases from $\omega = 0$ until $\omega = \omega_0$, and it decreases continuously as ω increases beyond ω_0, as illustrated in Fig. 7.15b. Therefore, a pole at $-\alpha + j\omega_0$ results in a frequency-selective behavior that enhances the gain at the frequency ω_0 (resonance). Moreover, as the pole moves closer to the imaginary axis (as α is reduced), this enhancement (resonance) becomes more pronounced. This is because α, the distance between the pole and $j\omega_0$ (d corresponding to $j\omega_0$), becomes smaller, which increases the gain K/d. In the extreme case, when $\alpha = 0$ (a pole on the imaginary axis), the gain at ω_0 goes to infinity. Repeated poles further enhance the frequency-selective effect. To summarize, we can enhance a gain at a frequency ω_0 by placing a pole opposite the point $j\omega_0$. The closer the pole is to $j\omega_0$, the higher is the gain at ω_0, and the gain variation is more rapid (more frequency selective) in the vicinity of frequency ω_0. Note that a pole must be placed in the LHP for stability.

Here, we have considered the effect of a single complex pole on the system gain. For a real system, a complex pole $-\alpha + j\omega_0$ must accompany its conjugate $-\alpha - j\omega_0$. We can readily show that the presence of the conjugate pole does not appreciably change the frequency-selective behavior in the vicinity of ω_0. This is because the gain in this case is K/dd', where d' is the distance of a point $j\omega$ from the conjugate pole $-\alpha - j\omega_0$. Because the conjugate pole is far from $j\omega_0$, there is no dramatic change in the length d' as ω varies in the vicinity of ω_0. There is a gradual increase in the value of d' as ω increases, which leaves the frequency-selective behavior as it was originally, with only minor changes.

Gain Suppression by a Zero

Using the same argument, we observe that zeros at $-\alpha \pm j\omega_0$ (Fig. 7.15d) will have exactly the opposite effect of suppressing the gain in the vicinity of ω_0, as shown in Fig. 7.15e. A zero on the imaginary axis at $j\omega_0$ will totally suppress the gain (zero gain) at frequency ω_0. Repeated zeros will further enhance the effect. Also, a closely placed pair of a pole and a zero (dipole) tend to

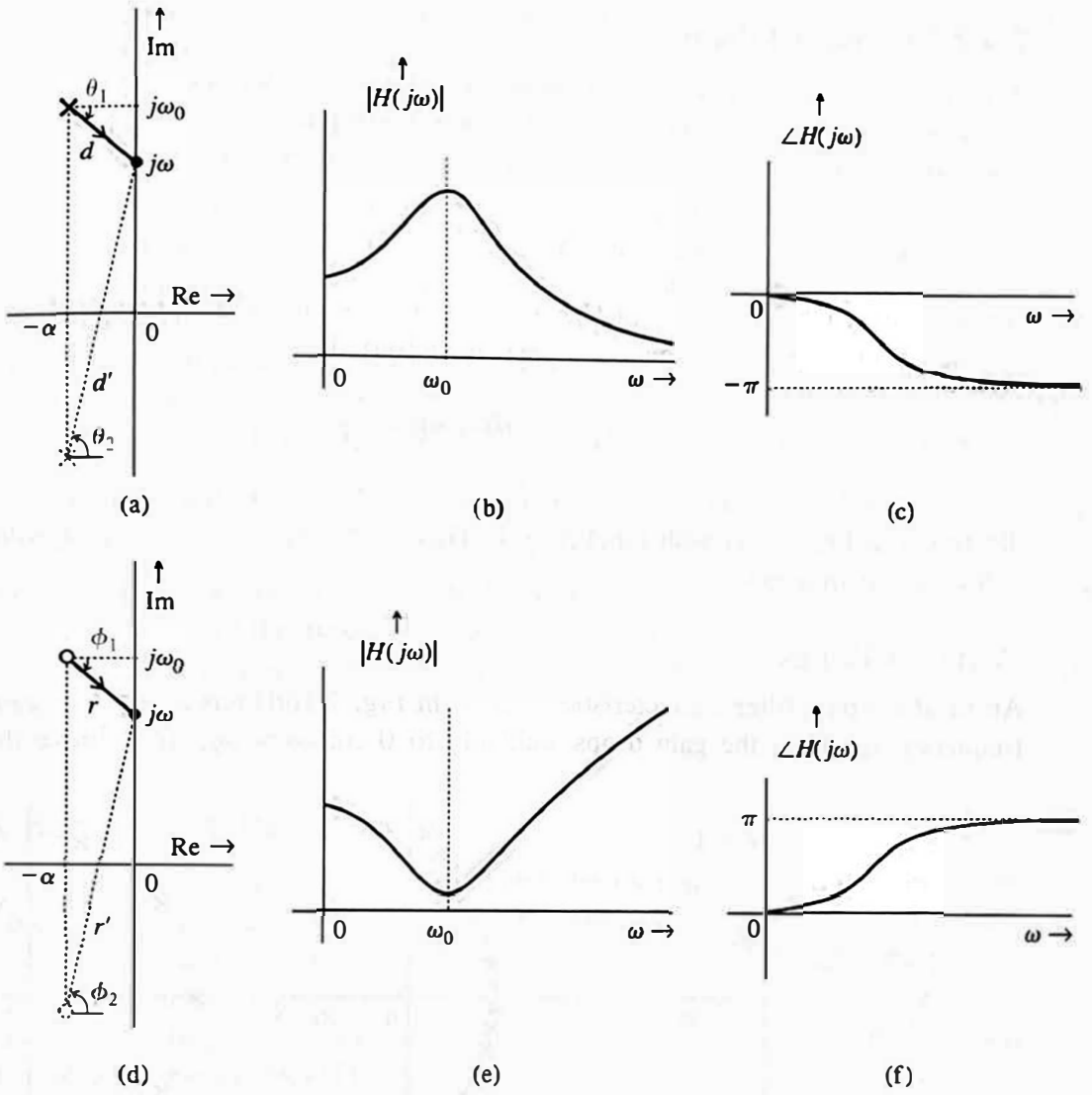

Figure 7.15 The role of poles and zeros in determining the frequency response of an LTIC system.

cancel out each other's influence on the frequency response. Clearly, a proper placement of poles and zeros can yield a variety of frequency-selective behavior. We can use these observations to design lowpass, highpass, bandpass, and bandstop (or notch) filters.

Phase response can also be computed graphically. In Fig. 7.15a, angles formed by the complex conjugate poles $-\alpha \pm j\omega_0$ at $\omega = 0$ (the origin) are equal and opposite. As ω increases from 0 up, the angle θ_1 (due to the pole $-\alpha + j\omega_0$), which has a negative value at $\omega = 0$, is reduced in magnitude; the angle θ_2 because of the pole $-\alpha - j\omega_0$, which has a positive value at $\omega = 0$, increases in magnitude. As a result, $\theta_1 + \theta_2$, the sum of the two angles, increases continuously, approaching a value π as $\omega \to \infty$. The resulting phase response $\angle H(j\omega) = -(\theta_1 + \theta_2)$ is illustrated in Fig. 7.15c. Similar arguments apply to zeros at $-\alpha \pm j\omega_0$. The resulting phase response $\angle H(j\omega) = (\phi_1 + \phi_2)$ is depicted in Fig. 7.15f.

We now focus on simple filters, using the intuitive insights gained in this discussion. The discussion is essentially qualitative.

7.4.2 Lowpass Filters

A typical lowpass filter has a maximum gain at $\omega = 0$. Because a pole enhances the gain at frequencies in its vicinity, we need to place a pole (or poles) on the real axis opposite the origin ($j\omega = 0$), as shown in Fig. 7.16a. The transfer function of this system is

$$H(s) = \frac{\omega_c}{s + \omega_c}$$

We have chosen the numerator of $H(s)$ to be ω_c to normalize the dc gain $H(0)$ to unity. If d is the distance from the pole $-\omega_c$ to a point $j\omega$ (Fig. 7.16a), then

$$|H(j\omega)| = \frac{\omega_c}{d}$$

with $H(0) = 1$. As ω increases, d increases and $|H(j\omega)|$ decreases monotonically with ω, as illustrated in Fig. 7.16d with label $N = 1$. This is clearly a lowpass filter with gain enhanced in the vicinity of $\omega = 0$.

Wall of Poles

An ideal lowpass filter characteristic (shaded in Fig. 7.16d) has a constant gain of unity up to frequency ω_c. Then the gain drops suddenly to 0 for $\omega > \omega_c$. To achieve the ideal lowpass

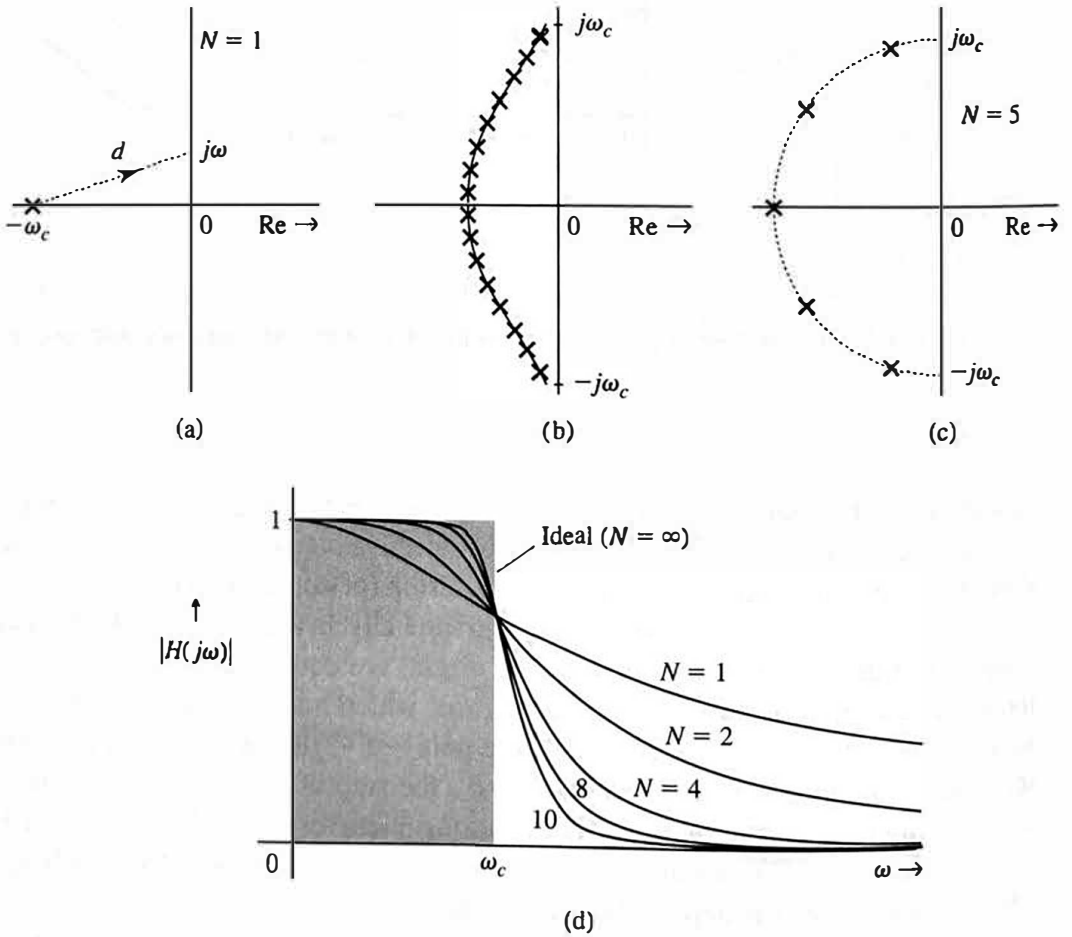

Figure 7.16 Pole-zero configuration and the amplitude response of a lowpass (Butterworth) filter.

characteristic, we need enhanced gain over the entire frequency band from 0 to ω_c. We know that to enhance a gain at any frequency ω, we need to place a pole opposite ω. To achieve an enhanced gain for all frequencies over the band (0 to ω_c), we need to place a pole opposite every frequency in this band. In other words, we need a *continuous wall of poles* facing the imaginary axis opposite the frequency band 0 to ω_c (and from 0 to $-\omega_c$ for conjugate poles), as depicted in Fig. 7.16b. At this point, the optimum shape of this wall is not obvious because our arguments are qualitative and intuitive. Yet, it is certain that to have enhanced gain (constant gain) at every frequency over this range, we need an infinite number of poles on this wall. We can show that for a maximally flat† response over the frequency range (0 to ω_c), the wall is a semicircle with an infinite number of poles uniformly distributed along the wall [2]. In practice, we compromise by using a finite number (N) of poles with less-than-ideal characteristics. Figure 7.16c shows the pole configuration for a fifth-order ($N = 5$) filter. The amplitude response for various values of N is illustrated in Fig. 7.16d. As $N \to \infty$, the filter response approaches the ideal. This family of filters is known as the *Butterworth* filters. There are also other families. In *Chebyshev* filters, the wall shape is a semiellipse rather than a semicircle. The characteristics of a Chebyshev filter are inferior to those of Butterworth over the passband $(0, \omega_c)$, where the characteristics show a rippling effect instead of the maximally flat response of Butterworth. But in the stopband ($\omega > \omega_c$), Chebyshev behavior is superior in the sense that Chebyshev filter gain drops faster than that of the Butterworth.

7.4.3 Bandpass Filters

The shaded characteristic in Fig. 7.17b shows the ideal bandpass filter gain. In the bandpass filter, the gain is enhanced over the entire passband. Our earlier discussion indicates that this can be realized by a wall of poles opposite the imaginary axis in front of the passband centered at ω_0. (There is also a wall of conjugate poles opposite $-\omega_0$.) Ideally, an infinite number of poles is required. In practice, we compromise by using a finite number of poles and accepting less-than-ideal characteristics (Fig. 7.17).

7.4.4 Notch (Bandstop) Filters

An ideal notch filter amplitude response (shaded in Fig. 7.18b) is a complement of the amplitude response of an ideal bandpass filter. Its gain is zero over a small band centered at some frequency ω_0 and is unity over the remaining frequencies. Realization of such a characteristic requires an infinite number of poles and zeros. Let us consider a practical second-order notch filter to obtain zero gain at a frequency $\omega = \omega_0$. For this purpose, we must have zeros at $\pm j\omega_0$. The requirement of unity gain at $\omega = \infty$ requires the number of poles to be equal to the number of zeros ($M = N$). This ensures that for very large values of ω, the product of the distances of poles from ω will be equal to the product of the distances of zeros from ω. Moreover, unity gain at $\omega = 0$ requires

† Maximally flat amplitude response means the first $2N - 1$ derivatives of $|H(j\omega)|$ with respect to ω are zero at $\omega = 0$.

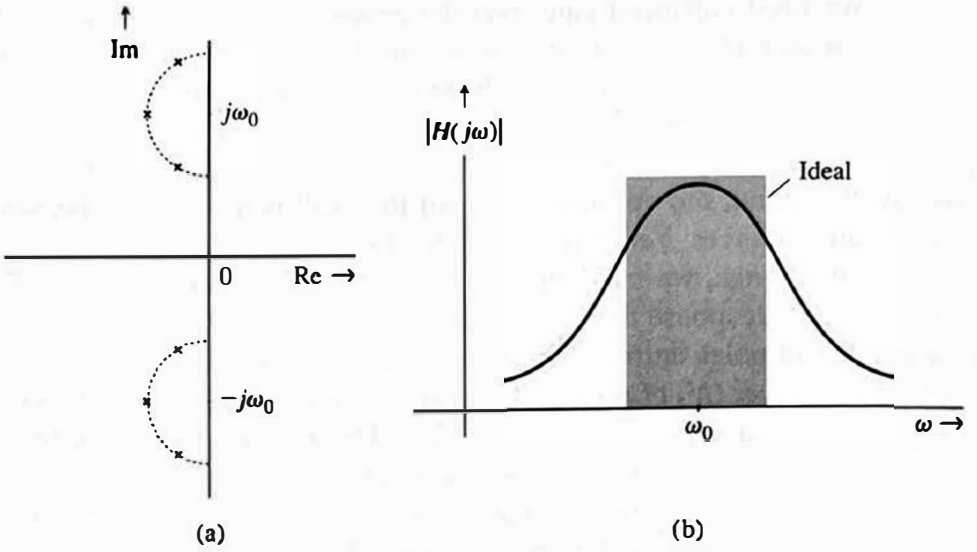

Figure 7.17 **(a)** Pole-zero configuration and **(b)** the amplitude response of a bandpass filter.

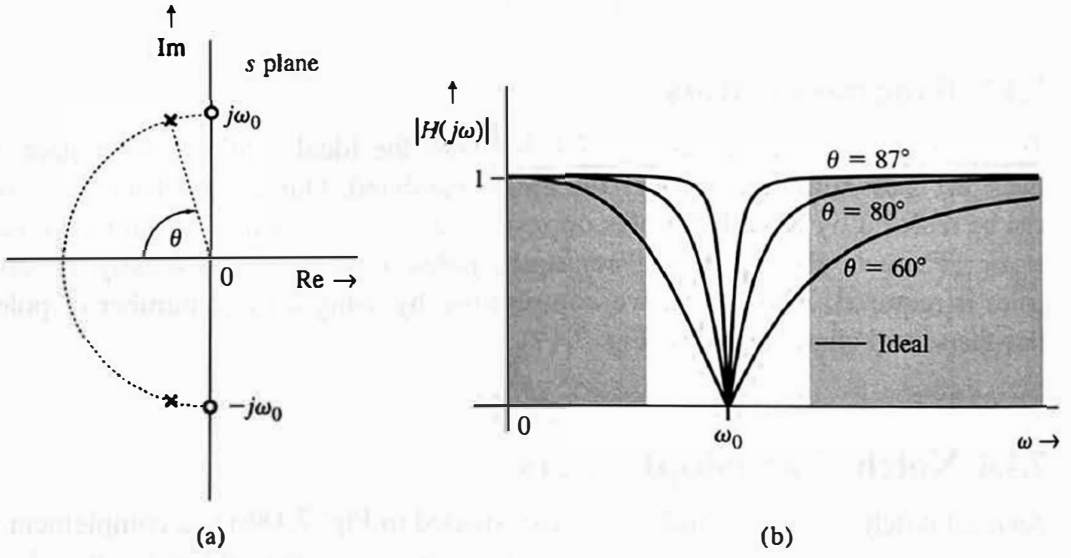

Figure 7.18 **(a)** Pole-zero configuration and **(b)** the amplitude response of a bandstop (notch) filter.

a pole and the corresponding zero to be equidistant from the origin. For example, if we use two (complex-conjugate) zeros, we must have two poles; the distance from the origin of the poles and of the zeros should be the same. This requirement can be met by placing the two conjugate poles on the semicircle of radius ω_0, as depicted in Fig. 7.18a. The poles can be anywhere on the semicircle to satisfy the equidistance condition. Let the two conjugate poles be at angles $\pm\theta$ with respect to the negative real axis. Recall that a pole and a zero in the same vicinity tend to cancel out each other's influences. Therefore, placing poles closer to zeros (selecting θ closer to $\pi/2$) results in a rapid recovery of the gain from value 0 to 1 as we move away from ω_0 in either direction. Figure 7.18b shows the gain $|H(j\omega)|$ for three different values of θ.

EXAMPLE 7.5 Notch Filter Design

Design a second-order notch filter to suppress 60 Hz hum in a radio receiver.

We use the poles and zeros in Fig. 7.18a with $\omega_0 = 120\pi$. The zeros are at $s = \pm j\omega_0$. The two poles are at $-\omega_0 \cos\theta \pm j\omega_0 \sin\theta$. The filter transfer function is (with $\omega_0 = 120\pi$)

$$H(s) = \frac{(s - j\omega_0)(s + j\omega_0)}{(s + \omega_0\cos\theta + j\omega_0\sin\theta)(s + \omega_0\cos\theta - j\omega_0\sin\theta)}$$
$$= \frac{s^2 + \omega_0^2}{s^2 + (2\omega_0\cos\theta)s + \omega_0^2} \quad \frac{s^2 + 142122.3}{s^2 + (753.98\cos\theta)s + 142122.3}$$

and

$$|H(j\omega)| = \frac{-\omega^2 + 142122.3}{\sqrt{(-\omega^2 + 142122.3)^2 + (753.98\omega\cos\theta)^2}}$$

The closer the poles are to the zeros (the closer θ is to $\pi/2$), the faster the gain recovery from 0 to 1 on either side of $\omega_0 = 120\pi$. Figure 7.18b shows the amplitude response for three different values of θ. This example is a case of very simple design. To achieve zero gain over a band, we need an infinite number of poles as well as an infinite number of zeros.

MATLAB easily computes and plots the magnitude response curves of Fig. 7.18b. To illustrate, let us plot the magnitude response using $\theta = 60°$ over a frequency range of $0 \le f \le 150$ Hz. The result, shown in Fig. 7.19, matches the $\theta = 60°$ case of Fig. 7.18b.

```
>> f = (0:.01:150); omega0 = 2*pi*60; theta = 60*pi/180;
>> H = @(s) (s.^2+omega0^2)./(s.^2+2*omega0*cos(theta)*s+omega0^2);
>> plot(f,abs(H(1j*2*pi*f)),'k-'); set(gca,'xtick',0:30:150);
>> xlabel('f [Hz]'); ylabel('|H(j2\pi f)|');
```

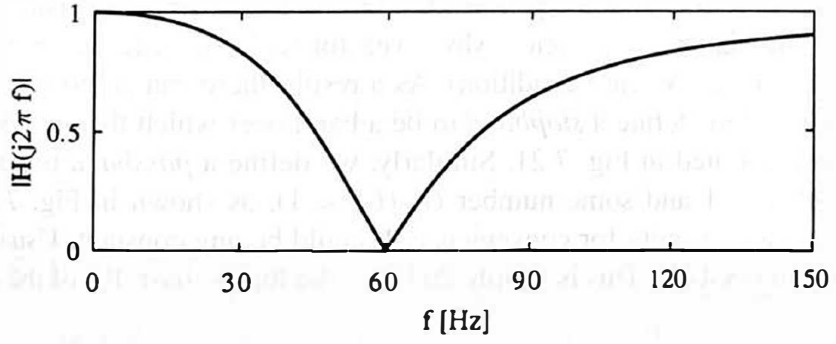

Figure 7.19 Magnitude response for notch filter with $\theta = 60°$.

DRILL 7.2 Magnitude Response from Pole-Zero Plots

Use the qualitative method of sketching the frequency response to show that the system with the pole-zero configuration in Fig. 7.20a is a highpass filter and the configuration in Fig. 7.20b is a bandpass filter.

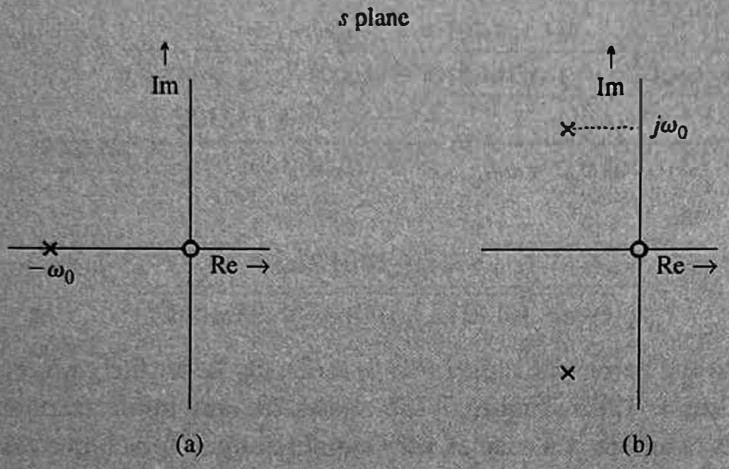

Figure 7.20 Pole-zero configuration of **(a)** a highpass filter and **(b)** a bandpass filter.

7.4.5 Practical Filters and Their Specifications

For ideal filters, everything is black and white; the gains are either zero or unity over certain bands. As we saw earlier, real life does not permit such a worldview. Things have to be gray or shades of gray. In practice, we can realize a variety of filter characteristics that can only approach ideal characteristics.

An ideal filter has a passband (unity gain) and a stopband (zero gain) with a sudden transition from the passband to the stopband. There is no transition band. For practical (or realizable) filters, on the other hand, the transition from the passband to the stopband (or vice versa) is gradual and takes place over a finite band of frequencies. Moreover, for realizable filters, the gain cannot be zero over a finite band (Paley–Wiener condition). As a result, there can be no true stopband for practical filters. We therefore define a *stopband* to be a band over which the gain is below some small number G_s, as illustrated in Fig. 7.21. Similarly, we define a *passband* to be a band over which the gain is between 1 and some number G_p ($G_p < 1$), as shown in Fig. 7.21. We have selected the passband gain of unity for convenience. It could be any constant. Usually, the gains are specified in terms of decibels. This is simply 20 times the log (to base 10) of the gain. Thus,

$$\hat{G}(\text{dB}) = 20\log_{10} G$$

A gain of unity is 0 dB and a gain of $\sqrt{2}$ is 3.01 dB, usually approximated by 3 dB. Sometimes the specification may be in terms of attenuation, which is the negative of the gain in dB. Thus, a gain of $1/\sqrt{2}$, that is, 0.707, is -3 dB, but is an attenuation of 3 dB.

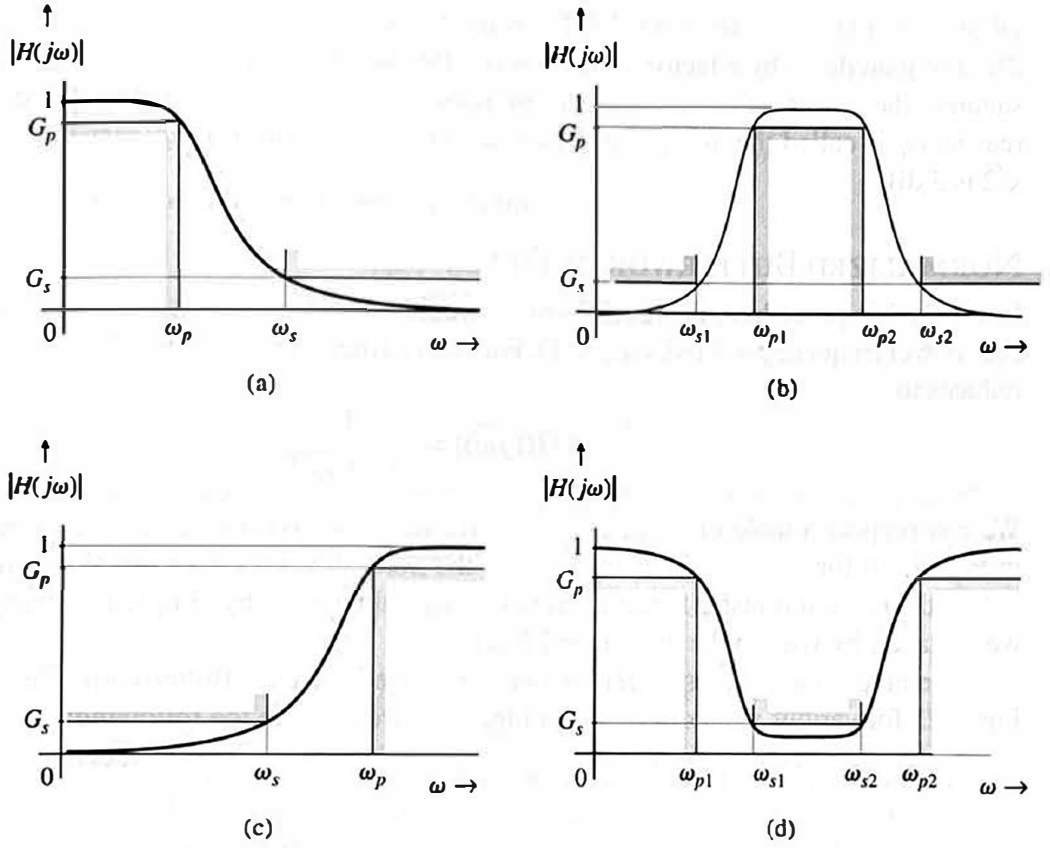

Figure 7.21 Passband, stopband, and transition band in filters of various types.

In a typical design procedure, G_p (*minimum passband gain*) and G_s (*maximum stopband gain*) are specified. Figure 7.21 shows the passband, the stopband, and the transition band for typical lowpass, bandpass, highpass, and bandstop filters. In this chapter, we shall discuss design procedures for these four types of filters. Fortunately, highpass, bandpass, and bandstop filters can be obtained from a basic lowpass filter by simple frequency transformations. For example, replacing s with ω_c/s in the lowpass filter transfer function results in a highpass filter. Similarly, other frequency transformations yield the bandpass and bandstop filters. Hence, it is necessary to develop a design procedure only for a basic lowpass filter. Then, by using appropriate transformations, we can design filters of other types. We shall consider here two well-known families of filters: Butterworth and Chebyshev filters.

7.5 BUTTERWORTH FILTERS

The amplitude response $|H(j\omega)|$ of an Nth-order Butterworth lowpass filter is given by

$$|H(j\omega)| = \frac{1}{\sqrt{1+\left(\frac{\omega}{\omega_c}\right)^{2N}}} \tag{7.19}$$

Observe that at $\omega = 0$, the gain $|H(j0)|$ is unity and at $\omega = \omega_c$, the gain $|H(j\omega_c)| = 1/\sqrt{2}$ or -3 dB. The gain drops by a factor $\sqrt{2}$ at $\omega = \omega_c$. Because the power is proportional to the amplitude squared, the power ratio (output power to input power) drops by a factor of 2 at $\omega = \omega_c$. For this reason, ω_c is called the *half-power frequency* or the *3 dB cutoff frequency* (an amplitude ratio of $\sqrt{2}$ is 3 dB).

Normalized Butterworth Filter

In the design procedure, it proves most convenient to consider a normalized filter $\mathcal{H}(s)$, whose half-power frequency is 1 rad/s ($\omega_c = 1$). For such a filter, the amplitude characteristic in Eq. (7.19) reduces to

$$|\mathcal{H}(j\omega)| = \frac{1}{\sqrt{1+\omega^{2N}}} \tag{7.20}$$

We can prepare a table of normalized transfer functions $\mathcal{H}(s)$ that yield the frequency response in Eq. (7.20) for various values of N. Once the normalized transfer function is obtained, we can obtain the desired transfer function $H(s)$ for any value of ω_c by simple frequency scaling, where we replace s by s/ω_c in the normalized $\mathcal{H}(s)$.

The amplitude responses $|\mathcal{H}(j\omega)|$ of normalized lowpass Butterworth filters are depicted in Fig. 7.22 for various values of N. From Fig. 7.22, we observe the following:

1. The Butterworth amplitude response decreases monotonically. Moreover, the first $2N-1$ derivatives of the amplitude response are zero at $\omega = 0$. This characteristic is why Butterworth filters are called *maximally flat* at $\omega = 0$. Observe that a constant characteristic (ideal) is maximally flat for all $\omega < 1$. In the Butterworth filter, we try to retain this property at least at the origin.†
2. The filter gain is 1 (0 dB) at $\omega = 0$ and 0.707 (-3 dB) at $\omega = 1$ for all N. Therefore, the 3 dB (or half power) bandwidth is 1 rad/s for all N.
3. For large N, the amplitude response approaches the ideal characteristic.

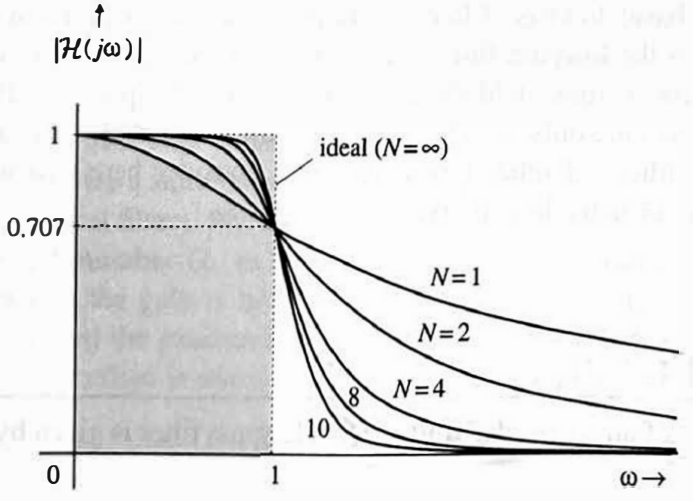

Figure 7.22 Amplitude responses of normalized lowpass Butterworth filters.

† A Butterworth filter exhibits a maximally flat characteristic also at $\omega = \infty$.

To determine the corresponding transfer function $\mathcal{H}(s)$, recall that $\mathcal{H}(-j\omega)$ is the complex conjugate of $\mathcal{H}(j\omega)$. Therefore,

$$\mathcal{H}(j\omega)\mathcal{H}(-j\omega) = |\mathcal{H}(j\omega)|^2 = \frac{1}{1+\omega^{2N}}$$

Substituting $s = j\omega$ in this equation, we obtain

$$\mathcal{H}(s)\mathcal{H}(-s) = \frac{1}{1+(s/j)^{2N}}$$

The poles of $\mathcal{H}(s)\mathcal{H}(-s)$ occur when

$$s^{2N} = -(j)^{2N}$$

In this result, we use the fact that $-1 = e^{j\pi(2k-1)}$ for integral values of k and $j = e^{j\pi/2}$ to obtain

$$s^{2N} = e^{j\pi(2k-1+N)} \qquad k \text{ integer}$$

This equation yields the poles of $\mathcal{H}(s)\mathcal{H}(-s)$ as

$$p_k = e^{\frac{j\pi}{2N}(2k+N-1)} \qquad k = 1, 2, 3, \ldots, 2N \tag{7.21}$$

Observe that all poles have a unit magnitude; that is, they are located on a unit circle in the s plane separated by angle π/N, as illustrated in Fig. 7.23 for odd and even N.

Since $\mathcal{H}(s)$ is stable and causal, its poles must lie in the LHP. The poles of $\mathcal{H}(-s)$ are the mirror images of the poles of $\mathcal{H}(s)$ about the vertical axis. Hence, the poles of $\mathcal{H}(s)$ are those in the LHP and the poles of $\mathcal{H}(-s)$ are those in the RHP in Fig. 7.23. The poles corresponding to $\mathcal{H}(s)$ are obtained by setting $k = 1, 2, 3, \ldots, N$ in Eq. (7.21); that is,

$$\begin{aligned} p_k &= e^{\frac{j\pi}{2N}(2k+N-1)} \\ &= \cos\frac{\pi}{2N}(2k+N-1) + j\sin\frac{\pi}{2N}(2k+N-1) \qquad k = 1, 2, 3, \ldots, N \end{aligned} \tag{7.22}$$

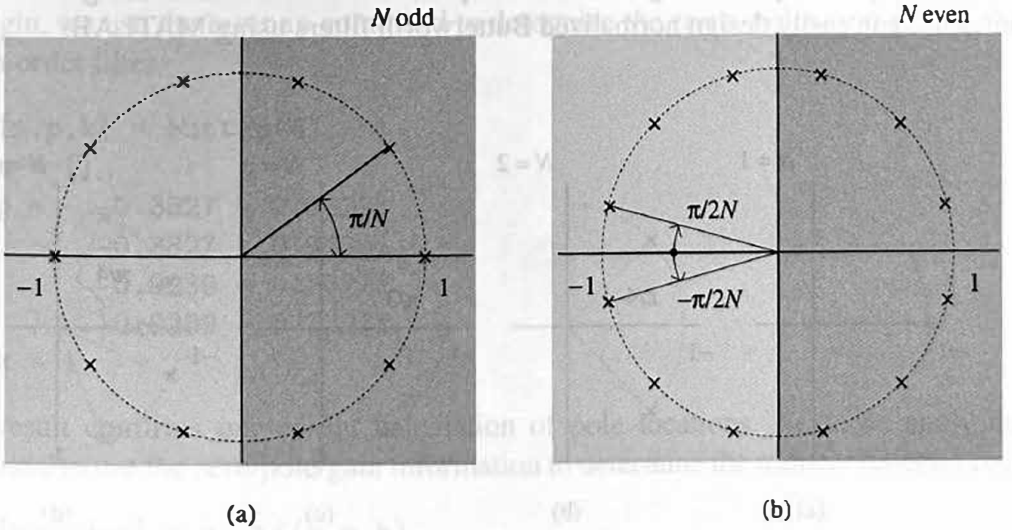

(a) (b)

Figure 7.23 Butterworth poles and mirrors: (a) odd order ($N = 5$) and (b) even order ($N = 6$).

and $\mathcal{H}(s)$ is given by

$$\mathcal{H}(s) = \frac{1}{(s-p_1)(s-p_2)\cdots(s-p_N)} \tag{7.23}$$

For instance, from Eq. (7.22), we find the poles of $\mathcal{H}(s)$ for $N = 4$ occur at angles $5\pi/8$, $7\pi/8$, $9\pi/8$, and $11\pi/8$. These lie on the unit circle, as shown in Fig. 7.24d, and are given by $-0.3827 \pm j0.9239$, $-0.9239 \pm j0.3827$. Hence, $\mathcal{H}(s)$ can be expressed as

$$\begin{aligned}\mathcal{H}(s) &= \frac{1}{(s+0.38-j0.92)(s+0.38+j0.92)(s+0.92-j0.38)(s+0.92+j0.38)} \\ &= \frac{1}{(s^2+0.7654s+1)(s^2+1.8478s+1)} \\ &= \frac{1}{s^4+2.6131s^3+3.4142s^2+2.6131s+1}\end{aligned}$$

We can proceed in this way to find $\mathcal{H}(s)$ for any value of N. In general,

$$\mathcal{H}(s) = \frac{1}{B_N(s)} = \frac{1}{s^N + a_{N-1}s^{N-1} + \cdots + a_1 s + 1} \tag{7.24}$$

where $B_N(s)$ is the Butterworth polynomial of the Nth order. Table 7.1 shows the coefficients a_1, a_2, . . ., a_{N-2}, a_{N-1} for various values of N; Table 7.2 shows $B_N(s)$ in factored form. Using these tables, we can simply write down our Butterworth filter's transfer function without calculation. For example, using these tables, we read for $N = 4$:

$$\begin{aligned}\mathcal{H}(s) &= \frac{1}{s^4+2.6131s^3+3.4142s^2+2.6131s+1} \\ &= \frac{1}{(s^2+0.7654s+1)(s^2+1.8478s+1)}\end{aligned} \tag{7.25}$$

This result confirms our earlier computations.

Nowadays, computer design has all but replaced table-based filter design. As the next example shows, we can easily design normalized Butterworth filters using MATLAB.

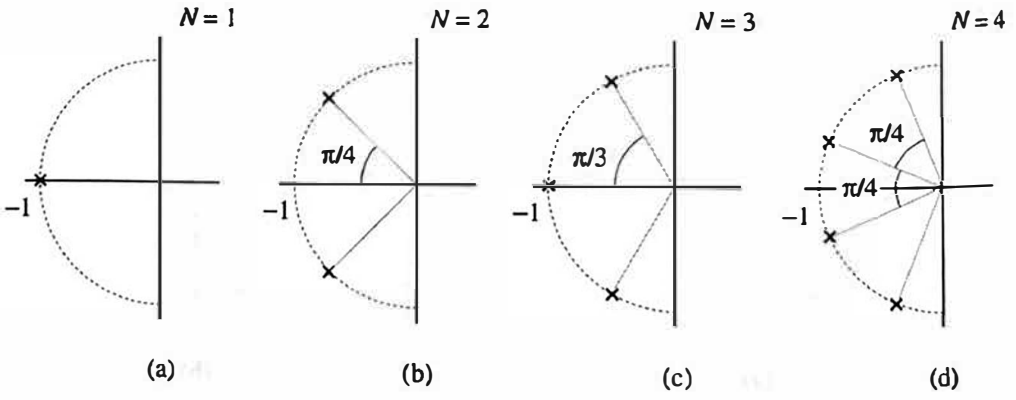

Figure 7.24 Poles of normalized lowpass Butterworth filters of various orders.

TABLE 7.1 Coefficients of Normalized Butterworth Polynomials $B_N(s) = s^N + a_{N-1}s^{N-1} + \cdots + a_1 s + 1$

N	a_7	a_6	a_5	a_4	a_3	a_2	a_1
2							1.414214
3						2.000000	2.000000
4					2.613126	3.414214	2.613126
5				3.236068	5.236068	5.236068	3.236068
6			3.863703	7.464102	9.141620	7.464102	3.863703
7		4.493959	10.097835	14.591794	14.591794	10.097835	4.493959
8	5.125831	13.137071	21.846151	25.688356	21.846151	13.137071	5.125831

TABLE 7.2 Normalized Butterworth Polynomials in Factored Form

N	Normalized Butterworth Polynomials $B_N(s)$, factored form
1	$s+1$
2	$s^2 + 1.414214s + 1$
3	$(s+1)(s^2+s+1)$
4	$(s^2 + 0.765367s + 1)(s^2 + 1.847759s + 1)$
5	$(s+1)(s^2 + 0.618034s + 1)(s^2 + 1.618034s + 1)$
6	$(s^2 + 0.517638s + 1)(s^2 + 1.414214s + 1)(s^2 + 1.931852s + 1)$
7	$(s+1)(s^2 + 0.445042s + 1)(s^2 + 1.246980s + 1)(s^2 + 1.801938s + 1)$
8	$(s^2 + 0.390181s + 1)(s^2 + 1.111140s + 1)(s^2 + 1.662939s + 1)(s^2 + 1.961571s + 1)$

EXAMPLE 7.6 Using MATLAB to Design Normalized Butterworth Filters

Use MATLAB to design a normalized fourth-order lowpass Butterworth filter.

To begin, we use the `buttap` command to determine the zeros, poles, and gain of the desired fourth-order filter.

```
>> [z,p,k] = buttap(4)
   z = []
   p =   -0.3827 + 0.9239i
         -0.3827 - 0.9239i
         -0.9239 + 0.3827i
         -0.9239 - 0.3827i
   k = 1
```

This result confirms our earlier calculation of pole locations. Next, we apply the `zp2tf` command to use the zero/pole/gain information to determine the transfer function coefficients.

```
>> [num,den] = zp2tf(z,p,k)
```

```
num = 0        0        0        0        1
den = 1.0000   2.6131   3.4142   2.6131   1.0000
```

This matches our previous result, given in Eq. (7.25).

Frequency Scaling

Although Tables 7.1 and 7.2 are for normalized Butterworth filters with 3 dB bandwidth $\omega_c = 1$, the results can be extended to any value of ω_c by simply replacing s by s/ω_c. This step implies replacing ω by ω/ω_c in Eq. (7.20). For example, a second-order Butterworth filter with $\omega_c = 100$ can be obtained from Table 7.1 by replacing s by $s/100$ as

$$H(s) = \frac{1}{\left(\frac{s}{100}\right)^2 + \sqrt{2}\left(\frac{s}{100}\right) + 1} = \frac{1}{s^2 + 100\sqrt{2}s + 10^4}$$

The amplitude response $|H(j\omega)|$ of this filter is identical to that of normalized $|\mathcal{H}(j\omega)|$ in Eq. (7.20), expanded by a factor of 100 along the horizontal (ω) axis (frequency scaling).

Determination of Butterworth Filter Order N

If $\hat{G}_x$ is the dB gain of a lowpass Butterworth filter at $\omega = \omega_x$, then according to Eq. (7.19),

$$\hat{G}_x = 20\log_{10}|H(j\omega_x)| = -10\log\left[1 + \left(\frac{\omega_x}{\omega_c}\right)^{2N}\right]$$

Substitution of the specifications in Fig. 7.21a (gains $\hat{G}_p$ at ω_p and $\hat{G}_s$ at ω_s) in this equation yields

$$\hat{G}_p = -10\log\left[1 + \left(\frac{\omega_p}{\omega_c}\right)^{2N}\right]$$

$$\hat{G}_s = -10\log\left[1 + \left(\frac{\omega_s}{\omega_c}\right)^{2N}\right]$$

or

$$\left(\frac{\omega_p}{\omega_c}\right)^{2N} = 10^{-\hat{G}_p/10} - 1 \tag{7.26}$$

$$\left(\frac{\omega_s}{\omega_c}\right)^{2N} = 10^{-\hat{G}_s/10} - 1 \tag{7.27}$$

Dividing Eq. (7.27) by Eq. (7.26), we obtain

$$\left(\frac{\omega_s}{\omega_p}\right)^{2N} = \left[\frac{10^{-\hat{G}_s/10} - 1}{10^{-\hat{G}_p/10} - 1}\right]$$

and

$$N = \frac{\log\left[\left(10^{-\hat{G}_s/10} - 1\right)/\left(10^{-\hat{G}_p/10} - 1\right)\right]}{2\log(\omega_s/\omega_p)} \tag{7.28}$$

Also from Eq. (7.26),

$$\omega_c = \frac{\omega_p}{\left[10^{-\hat{G}_p/10} - 1\right]^{1/2N}} \tag{7.29}$$

Alternatively, from Eq. (7.27),

$$\omega_c = \frac{\omega_s}{\left[10^{-\hat{G}_s/10} - 1\right]^{1/2N}} \tag{7.30}$$

Since N is rounded up to an integer value, Eqs. (7.26) and (7.27) do not generally return the same value of ω_c, as the next example shows.

EXAMPLE 7.7 Butterworth Lowpass Filter Design

Design a Butterworth lowpass filter to meet the specifications shown in Fig. 7.25. That is, passband gain must lie between 1 and $G_p = 0.794$ ($\hat{G}_p = -2\text{dB}$) for $0 \le \omega < 10$, and stopband gain must not exceed $G_s = 0.1$ ($\hat{G}_s = -20\text{dB}$) for $\omega \ge 20$.

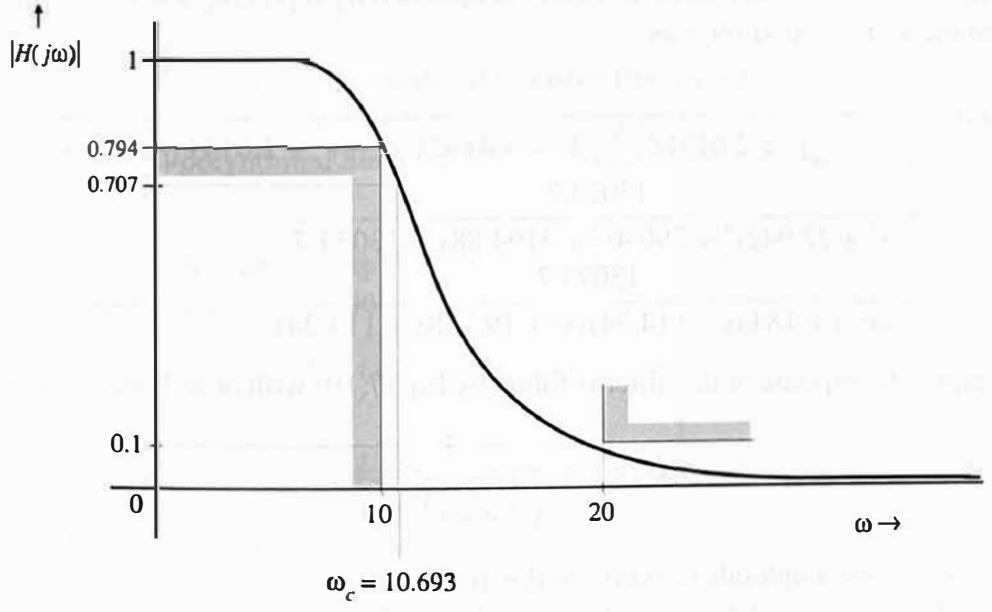

Figure 7.25 Amplitude response of the Butterworth lowpass filter for Ex. 7.7.

Step 1: Determine the order N
Here, $\omega_p = 10$, $\omega_s = 20$, $\hat{G}_p = -2$ dB, and $\hat{G}_s = -20$ dB. Substituting these values in Eq. (7.28) yields

$$N = 3.701$$

Since N can only be an integer, we round up to

$$N = 4$$

Step 2: Determine the half-power cutoff frequency ω_c
Substitution of $N = 4$, $\omega_p = 10$ in Eq. (7.29) yields

$$\omega_c = 10.693$$

Alternately, substitution of $N = 4$ in Eq. (7.30) yields

$$\omega_c = 11.261$$

Because we selected $N = 4$ rather than 3.701, we obtain two different values of ω_c. Choosing $\omega_c = 10.693$ will satisfy exactly the requirement $G_p = 0.794$ over the passband (0, 10), and will surpass the requirement $G_s = 0.1$ in the stopband $\omega \geq 20$. On the other hand, choosing $\omega_c = 11.261$ will exactly satisfy the requirement for G_s but will oversatisfy the requirement for G_p. Let us choose the first case, $\omega_c = 10.693$.

Step 3: Determine the normalized transfer function $\mathcal{H}(s)$
The normalized fourth-order transfer function $\mathcal{H}(s)$ is found from Table 7.1 as

$$\mathcal{H}(s) = \frac{1}{s^4 + 2.6131s^3 + 3.4142s^2 + 2.6131s + 1}$$

Step 4: Determine the final transfer function $H(s)$
The desired transfer function with $\omega_c = 10.693$ is obtained by replacing s with $s/10.693$ in the normalized transfer function $\mathcal{H}(s)$ as

$$\begin{aligned} H(s) &= \frac{1}{\left(\frac{s}{10.693}\right)^4 + 2.6131\left(\frac{s}{10.693}\right)^3 + 3.4142\left(\frac{s}{10.692}\right)^2 + 2.6131\left(\frac{s}{10.693}\right) + 1} \\ &= \frac{13073.7}{s^4 + 27.942s^3 + 390.4s^2 + 3194.88s + 13073.7} \\ &= \frac{13073.7}{(s^2 + 8.1844s + 114.34)(s^2 + 19.758s + 114.34)} \end{aligned}$$

The amplitude response of this filter is found by Eq. (7.19) with $N = 4$ and $\omega_c = 10.693$ as

$$|H(j\omega)| = \frac{1}{\sqrt{\left(\frac{\omega}{10.693}\right)^8 + 1}}$$

Figure 7.25 shows the amplitude response of this filter.

We could also have used the alternate value of $\omega_c = 11.261$. This choice would result in a slightly different design. Either of the two designs satisfies the specifications.

EXAMPLE 7.8 Butterworth Lowpass Filter Design Using MATLAB

Solve Ex. 7.7 using MATLAB, including generation of the filter's magnitude response plot.

Step 1: Determine the order N

Using $\omega_p = 10$ rad/s, $\hat{G}_p = -2$ dB, $\omega_s = 20$ rad/s, and $\hat{G}_s = -20$ dB, MATLAB evaluation of Eq. (7.28) yields the necessary order N.

```
>> omegap = 10; Ghatp = -2; omegas = 20; Ghats = -20;
>> N = ceil(log((10^(-Ghats/10)-1)/(10^(-Ghatp/10)-1))/...
>>     (2*log(omegas/omegap)))
   N = 4
```

Step 2: Determine the half-power cutoff frequency ω_c

Next, the range of possible ω_c is determined using Eqs. (7.29) and (7.30).

```
>> omegac = [omegap/(10^(-Ghatp/10)-1).^(1/(2*N)),...
>>     omegas/(10^(-Ghats/10)-1).^(1/(2*N))]
   omegac = 10.6934   11.2610
```

Choosing $\omega_c = 10.6934$ rad/s, which exactly meets passband specifications and exceeds stopband specifications, provides no margin for error on the passband side. Similarly, choosing $\omega_c = 11.2610$ rad/s, which just meets stopband requirements and surpasses passband requirements, provides no margin for error on the stopband side. As in Ex. 7.7, let us choose the first case, which exactly meets passband specifications.

```
>> omegac = omegac(1)
   omegac = 10.6934
```

Step 3: Determine the normalized transfer function $\mathcal{H}(s)$

By computing the Butterworth pole locations [see Eq. (7.22)] and then converting these polls to expanded polynomial form, MATLAB conveniently computes the desired transfer function coefficients.

```
>> k = 1:N; pk = exp(1j*pi/(2*N)*(2*k+N-1)); denHnorm = real(poly(pk))
   denHnorm = 1.0000   2.6131   3.4142   2.6131   1.0000
```

Using this result with Eq. (7.23) confirms the normalized transfer function as

$$\mathcal{H}(s) = \frac{1}{s^4 + 2.6131s^3 + 3.4142s^2 + 2.6131s + 1}$$

Step 4: Determine the final transfer function $H(s)$

The desired transfer function with $\omega_c = 10.693$ is obtained by replacing s with $s/10.693$ in the normalized transfer function $\mathcal{H}(s)$. This is equivalent to scaling the poles by ω_c and the numerator of $H(s)$ by ω_c^N.

```
>> numH = omegac^N, denH = real(poly(pk*omegac))
   numH = 13075.60
   denH = 1.00        27.94        390.41        3195.26        13075.60
```

This confirms the transfer function as

$$H(s) = \frac{13075.60}{s^4 + 27.94s^3 + 390.41s^2 + 3195.26s + 13075.60}$$

The corresponding magnitude response, plotted using MATLAB, is shown in Fig. 7.26. Following our design choice, notice that the filter exactly meets passband requirements and exceeds stopband requirements.

```
>> omega = linspace(0,25,1001);
>> H = (polyval(numH,1j*omega))./(polyval(denH,1j*omega));
>> plot(omega,abs(H),'k-'); grid on; set(gca,'xtick',[0 10 20])
>> set(gca,'ytick',[0 10^(Ghats/20) 10^(Ghatp/20) 1])
>> axis([0 25 0 1.05]); xlabel('\omega'); ylabel('|H(j\omega)|');
```

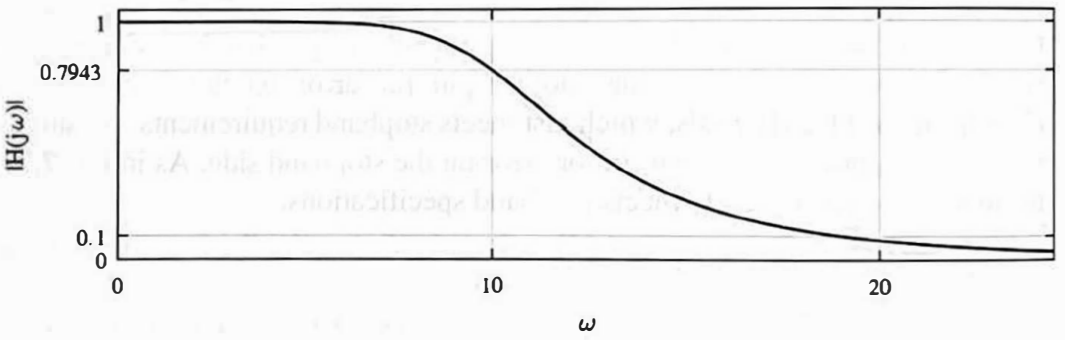

Figure 7.26 Magnitude response of the Butterworth lowpass filter for Ex. 7.8.

An Alternate Approach

We can also design this filter using the built-in MATLAB functions `buttord` and `butter`. We first use `buttord` to determine filter order and ω_c.

```
>> [N,omegac] = buttord(omegap,omegas,-Ghatp,-Ghats,'s')
   N = 4
   omegac = 11.26096
```

Notice, in using `buttord`, we cannot specify whether to exactly meet passband specifications, exactly meet stopband specifications, or something in between. Indeed, as we can tell from the value of ω_c computed, the `buttord` command automatically decides to design the filter to exactly meet stopband (rather than passband) requirements. This lack of choice is a limitation of using the canned function `buttord`.

Next, we use the `butter` command to determine the filter transfer function.

```
>> [numH,denH] = butter(N,omegac,'s')
numH =     0         0         0         0    16080.61
denH =  1.00     29.43    432.95   3731.53    16080.61
```

The corresponding transfer function is thus

$$H(s) = \frac{16080.61}{s^4 + 29.43s^3 + 432.95s^2 + 3731.53s + 16080.61}$$

As shown in Fig. 7.27, the corresponding magnitude response exactly meets stopband specifications and exceeds passband specifications, as expected.

```
>> omega = linspace(0,25,1001);
>> H = (polyval(numH,1j*omega))./(polyval(denH,1j*omega));
>> plot(omega,abs(H),'k-'); grid on; set(gca,'xtick',[0 10 20])
>> set(gca,'ytick',[0 10^(Ghats/20) 10^(Ghatp/20) 1])
>> axis([0 25 0 1.05]); xlabel('\omega'); ylabel('|H(j\omega)|');
```

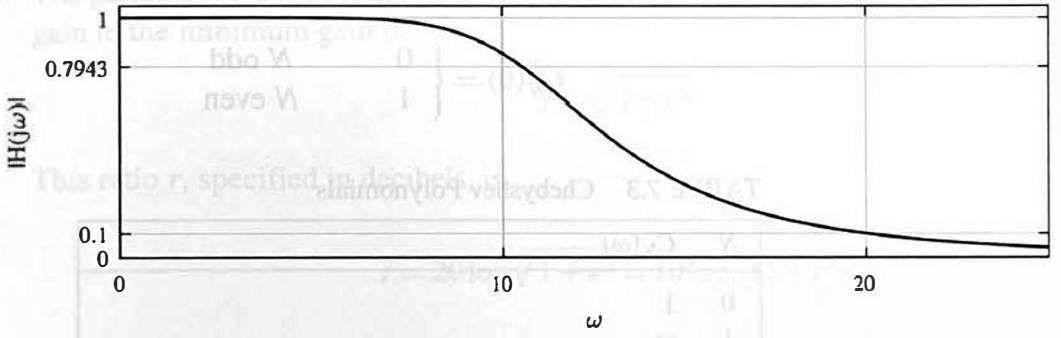

Figure 7.27 Alternate magnitude response for Ex. 7.8.

DRILL 7.3 Determining Butterworth Filter Order

Determine N, the order of a lowpass Butterworth filter, to meet the following specifications: $\hat{G}_p = -0.5$ dB, $\hat{G}_s = -20$ dB, $\omega_p = 100$, and $\omega_s = 200$.

ANSWER

5

7.6 CHEBYSHEV FILTERS

The amplitude response of a normalized Chebyshev lowpass filter is given by

$$|\mathcal{H}(j\omega)| = \frac{1}{\sqrt{1+\epsilon^2 C_N^2(\omega)}} \tag{7.31}$$

where $C_N(\omega)$, the Nth-order Chebyshev polynomial, is given by

$$C_N(\omega) = \cos(N\cos^{-1}\omega) \qquad \text{or} \qquad C_N(\omega) = \cosh(N\cosh^{-1}\omega) \tag{7.32}$$

The first form is most convenient to compute $C_N(\omega)$ for $|\omega| < 1$, while the second form is convenient for computing $C_N(\omega)$ for $|\omega| > 1$. We can show (see [3]) that $C_N(\omega)$ is also expressible in polynomial form, as shown in Table 7.3 for $N = 1$ to 10.†

The normalized Chebyshev lowpass amplitude response [Eq. (7.31)] is depicted in Fig. 7.28 for $N = 6$ and $N = 7$. We make the following general observations:

1. The Chebyshev amplitude response has ripples in the passband and is smooth (monotonic) in the stopband. The passband is $0 \le \omega \le 1$, and there is a total of N maxima and minima over the passband $0 \le \omega \le 1$.
2. From Table 7.3, we observe that

$$C_N^2(0) = \begin{cases} 0 & N \text{ odd} \\ 1 & N \text{ even} \end{cases}$$

TABLE 7.3 Chebyshev Polynomials

N	$C_N(\omega)$
0	1
1	ω
2	$2\omega^2 - 1$
3	$4\omega^3 - 3\omega$
4	$8\omega^4 - 8\omega^2 + 1$
5	$16\omega^5 - 20\omega^3 + 5\omega$
6	$32\omega^6 - 48\omega^4 + 18\omega^2 - 1$
7	$64\omega^7 - 112\omega^5 + 56\omega^3 - 7\omega$
8	$128\omega^8 - 256\omega^6 + 160\omega^4 - 32\omega^2 + 1$
9	$256\omega^9 - 576\omega^7 + 432\omega^5 - 120\omega^3 + 9\omega$
10	$512\omega^{10} - 1280\omega^8 + 1120\omega^6 - 400\omega^4 + 50\omega^2 - 1$

† The Chebyshev polynomial $C_N(\omega)$ has the property [3]

$$C_N(\omega) = 2\omega C_{N-1}(\omega) - C_{N-2}(\omega) \qquad N > 2$$

Thus, knowing that $C_0(\omega) = 1$ and $C_1(\omega) = \omega$, we can (recursively) construct $C_N(\omega)$ for any value of N. For example, $C_2(\omega) = 2\omega C_1(\omega) - C_0(\omega) = 2\omega^2 - 1$, and so on.

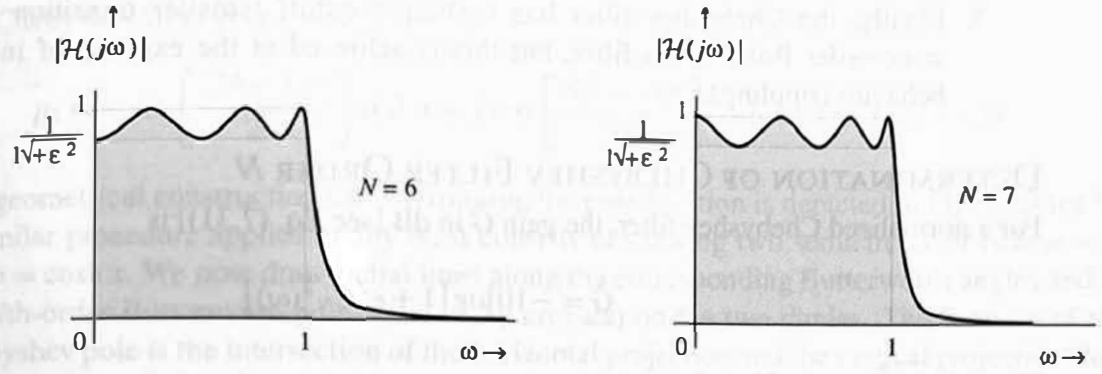

Figure 7.28 Amplitude responses of normalized sixth- and seventh-order lowpass Chebyshev filters.

Therefore, the dc gain is

$$|\mathcal{H}(0)| = \begin{cases} 1 & N \text{ odd} \\ \frac{1}{\sqrt{1+\epsilon^2}} & N \text{ even} \end{cases} \tag{7.33}$$

3. The parameter ϵ controls the passband ripple. In the passband, r, the ratio of the maximum gain to the minimum gain is

$$r = \sqrt{1+\epsilon^2}$$

This ratio r, specified in decibels, is

$$\hat{r} = 20\log\sqrt{1+\epsilon^2} = 10\log_{10}(1+\epsilon^2)$$

so that

$$\epsilon^2 = 10^{\hat{r}/10} - 1 \tag{7.34}$$

Because all the ripples in the passband are of equal height, Chebyshev polynomials $C_N(\omega)$ are known as *equal-ripple functions*.

4. Ripple is present only over the passband $0 \le \omega \le 1$. At $\omega = 1$, the amplitude response is $1/\sqrt{1+\epsilon^2} = 1/r$. For $\omega > 1$, the gain decreases monotonically.
5. For Chebyshev filters, the ripple parameter $\hat{r}$ [dB] takes the place of $\hat{G}_p$ (the minimum gain in the passband). For example, $\hat{r} \le 2$ dB specifies that gain variations of more than 2 dB cannot be tolerated in the passband. In a Butterworth filter, $\hat{G}_p = -2$ dB means the same thing.
6. If we reduce the ripple, the passband behavior improves, but it does so at the cost of stopband behavior. As r is decreased (ϵ is reduced), the gain in the stopband increases, and vice versa. Hence, there is a tradeoff between the allowable passband ripple and the desired attenuation in the stopband. Note that the extreme case $\epsilon = 0$ yields zero ripple, but the filter now becomes an allpass filter, as seen from Eq. (7.31) by letting $\epsilon = 0$.

7. Finally, the Chebyshev filter has a sharper cutoff (smaller transition band) than the same-order Butterworth filter, but this is achieved at the expense of inferior passband behavior (rippling).†

Determination of Chebyshev Filter Order N

For a normalized Chebyshev filter, the gain $\hat{G}$ in dB [see Eq. (7.31)] is

$$\hat{G} = -10\log\left[1+\epsilon^2 C_N{}^2(\omega)\right]$$

The gain is $\hat{G}_s$ at ω_s. Therefore,

$$\hat{G}_s = -10\log\left[1+\epsilon^2 C_N{}^2(\omega_s)\right]$$

or

$$\epsilon^2 C_N{}^2(\omega_s) = 10^{-\hat{G}_s/10} - 1$$

The use of Eqs. (7.32) and (7.34) in the above equation yields

$$\cosh\left[N\cosh^{-1}(\omega_s)\right] = \left[\frac{10^{-\hat{G}_s/10}-1}{10^{\hat{r}/10}-1}\right]^{1/2}$$

Hence,

$$N = \frac{1}{\cosh^{-1}(\omega_s)}\cosh^{-1}\left[\frac{10^{-\hat{G}_s/10}-1}{10^{\hat{r}/10}-1}\right]^{1/2}$$

Note that these equations are for normalized filters, where $\omega_p = 1$. For a general case, we replace ω_s with $\frac{\omega_s}{\omega_p}$ to obtain

$$N = \frac{1}{\cosh^{-1}(\omega_s/\omega_p)}\cosh^{-1}\left[\frac{10^{-\hat{G}_s/10}-1}{10^{\hat{r}/10}-1}\right]^{1/2} \tag{7.35}$$

Chebyshev Pole Locations and Normalized Transfer Function

We could follow the procedure of the Butterworth filter to obtain the pole locations of the Chebyshev filter. The procedure is straightforward but tedious and does not yield any special insight into our development. Butterworth filter poles lie on a semicircle. We can show that the poles of an Nth-order normalized Chebyshev filter lie on a semiellipse of the major and minor semiaxes $\cosh x$ and $\sinh x$, respectively, where (see [3])

$$x = \frac{1}{N}\sinh^{-1}\left(\frac{1}{\epsilon}\right) \tag{7.36}$$

† We can show (see [2]) that at higher (stopband) frequencies, the Chebyshev filter gain is smaller than the comparable Butterworth filter gain by about $6(n-1)$ dB.

The Chebyshev filter poles are

$$p_k = -\sin\left[\frac{(2k-1)\pi}{2N}\right]\sinh x + j\cos\left[\frac{(2k-1)\pi}{2N}\right]\cosh x \quad k = 1,2,\cdots,N \tag{7.37}$$

The geometrical construction for determining the pole location is depicted in Fig. 7.29 for $N = 3$. A similar procedure applies to any N; it consists of drawing two semicircles of radii $a = \sinh x$ and $b = \cosh x$. We now draw radial lines along the corresponding Butterworth angles and locate the Nth-order Butterworth poles (shown by crosses) on the two circles. The location of the kth Chebyshev pole is the intersection of the horizontal projection and the vertical projection from the corresponding kth Butterworth poles on the outer and inner circles, respectively.

The transfer function $\mathcal{H}(s)$ of a normalized Nth-order lowpass Chebyshev filter is

$$\begin{aligned}\mathcal{H}(s) &= \frac{K_N}{(s-p_1)(s-p_2)\cdots(s-p_N)} \\ &= \frac{K_N}{C'_N(s)} = \frac{K_N}{s^N + a_{N-1}s^{N-1} + \cdots + a_1 s + a_0}\end{aligned} \tag{7.38}$$

The constant K_N is selected following Eq. (7.33) to provide the proper dc gain:

$$K_N = \begin{cases} a_0 & N \text{ odd} \\ \dfrac{a_0}{\sqrt{1+\epsilon^2}} = \dfrac{a_0}{10^{\hat{r}/20}} & N \text{ even} \end{cases} \tag{7.39}$$

The design procedure is simplified by ready-made tables of the polynomial $C'_N(s)$ in Eq. (7.38). Table 7.4 lists the coefficients $a_0, a_1, a_2, \ldots, a_{N-1}$ of the polynomial $C'_N(s)$ in Eq. (7.38) for $\hat{r} = 0.5$, 1, 2, and 3 dB ripples corresponding to the values of $\epsilon = 0.3493$, 0.5088, 0.7648, and 0.9976, respectively. Computer tools, such as MATLAB, make Chebyshev filter design even more simple, as the next example demonstrates.

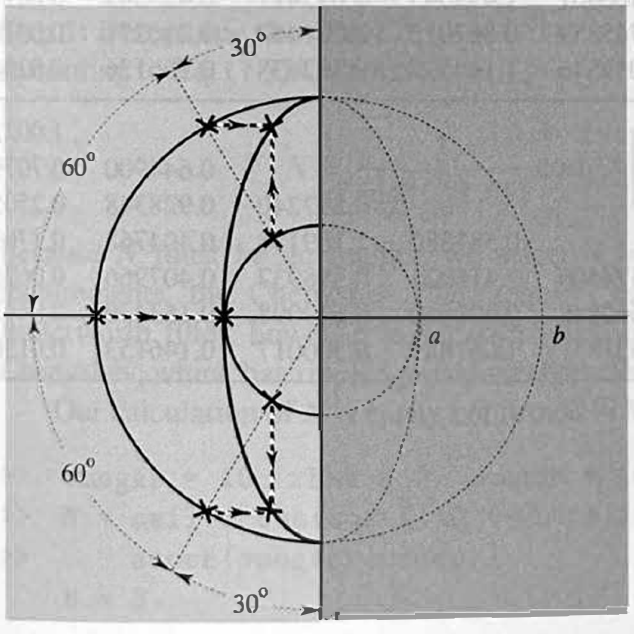

Figure 7.29 Poles of a normalized third-order lowpass Chebyshev filter and their connection to Butterworth pole locations.

TABLE 7.4 Coefficients of Normalized Chebyshev Denominator Polynomials $C'_N = s^N + a_{N-1}s^{N-1} + \cdots + a_1 s + a_0$

N	a_6	a_5	a_4	a_3	a_2	a_1	a_0
1	0.1 dB of ripple						6.552203
2	($\alpha_p = 0.1$)					2.372356	3.314037
3					1.938811	2.629495	1.638051
4				1.803773	2.626798	2.025501	0.828509
5			1.743963	2.770704	2.396959	1.435558	0.409513
6		1.712166	2.965756	2.779050	2.047841	0.901760	0.207127
7	1.693224	3.183504	3.169246	2.705144	1.482934	0.561786	0.102378
1	0.5 dB of ripple						2.862775
2	($\alpha_p = 0.5$)					1.425625	1.516203
3					1.252913	1.534895	0.715694
4				1.197386	1.716866	1.025455	0.379051
5			1.172491	1.937367	1.309575	0.752518	0.178923
6		1.159176	2.171845	1.589764	1.171861	0.432367	0.094763
7	1.151218	2.412651	1.869408	1.647903	0.755651	0.282072	0.044731
1	1 dB of ripple						1.965227
2	($\alpha_p = 1$)					1.097734	1.102510
3					0.988341	1.238409	0.491307
4				0.952811	1.453925	0.742619	0.275628
5			0.936820	1.688816	0.974396	0.580534	0.122827
6		0.928251	1.930825	1.202140	0.939346	0.307081	0.068907
7	0.923123	2.176078	1.428794	1.357545	0.548620	0.213671	0.030707
1	2 dB of ripple						1.307560
2	($\alpha_p = 2$)					0.803816	0.823060
3					0.737822	1.022190	0.326890
4				0.716215	1.256482	0.516798	0.205765
5			0.706461	1.499543	0.693477	0.459349	0.081723
6		0.701226	1.745859	0.867015	0.771462	0.210271	0.051441
7	0.698091	1.993665	1.039546	1.144597	0.382638	0.166126	0.020431
1	3 dB of ripple						1.002377
2	($\alpha_p = 3$)					0.644900	0.707948
3					0.597240	0.928348	0.250594
4				0.581580	1.169118	0.404768	0.176987
5			0.574500	1.415025	0.548937	0.407966	0.062649
6		0.570698	1.662848	0.690610	0.699098	0.163430	0.044247
7	0.568420	1.911551	0.831441	1.051845	0.300017	0.146153	0.015662

EXAMPLE 7.9 Chebyshev Lowpass Filter Design

Design a Chebyshev lowpass filter to satisfy the criteria shown in Fig. 7.30 and summarized as: $\hat{r} \leq 2$ dB over a passband $0 \leq \omega \leq 10$ ($\omega_p = 10$) and $\hat{G}_s \leq -20$ dB for $\omega > 16.5$ ($\omega_s = 16.5$).

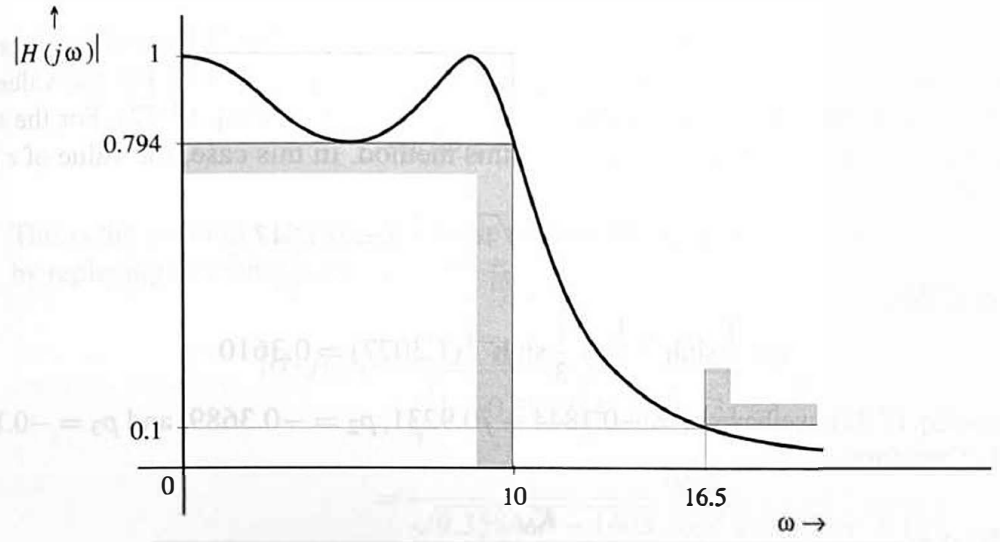

Figure 7.30 Amplitude response of the Chebyshev lowpass filter for Ex. 7.9.

Observe that the specifications are the same as those in Ex. 7.7, except for the transition band. Here, the transition band is from 10 to 16.5, whereas in Ex. 7.7 it is 10 to 20. Despite this more stringent requirement, we shall find that Chebyshev requires a lower-order filter than the Butterworth filter found in Ex. 7.7.

Step 1: Determine the order N

According to Eq. (7.35), we have

$$N = \frac{1}{\cosh^{-1}(1.65)} \cosh^{-1}\left[\frac{10^2 - 1}{10^{0.2} - 1}\right]^{1/2} = 2.999$$

Because N must be an integer, we select $N = 3$. Observe that even with more stringent requirements, the Chebyshev filter requires only $N = 3$. The passband behavior of the Butterworth filter, however, is superior (maximally flat at $\omega = 0$) compared to that of the Chebyshev, which has rippled passband characteristics.

Our calculation of N is easily confirmed in MATLAB.

```
>> omegap = 10; rhat = 2; omegas = 16.5; Ghats = -20;
>> N = ceil(acosh(sqrt((10^(-Ghats/10)-1)/(10^(rhat/10)-1)))/...
>>     acosh(omegas/omegap))
   N = 3
```

Step 2: Determine the normalized transfer function $\mathcal{H}(s)$

We may use Table 7.4 to determine $\mathcal{H}(s)$. For $N = 3$ and $\hat{r} = 2$ dB, we read the coefficients of the denominator polynomial of $\mathcal{H}(s)$ as $a_0 = 0.3269$, $a_1 = 1.0222$, and $a_2 = 0.7378$. Also in Eq. (07.39), for odd N, the numerator is given by a constant $K_N = a_0 = 0.3269$. Therefore,

$$\mathcal{H}(s) = \frac{0.3269}{s^3 + 0.7378s^2 + 1.0222s + 0.3269} \tag{7.40}$$

Because there are infinite possible combinations of N and $\hat{r}$, Table 7.4 can list values of the denominator coefficients for values of $\hat{r}$ in quantum increments only [3]. For the values of N and $\hat{r}$ not listed in the table, we can compute pole locations from Eq. (7.37). For the sake of demonstration, we now recompute $\mathcal{H}(s)$ using this method. In this case, the value of ϵ is [see Eq. (7.34)]

$$\epsilon = \sqrt{10^{\hat{r}/10} - 1} = \sqrt{10^{0.2} - 1} = 0.7647$$

From Eq. (7.36),

$$x = \frac{1}{n}\sinh^{-1}\frac{1}{\epsilon} = \frac{1}{3}\sinh^{-1}(1.3077) = 0.3610$$

Now from Eq. (7.37), we have $p_1 = -0.1844 + j0.9231$, $p_2 = -0.3689$, and $p_3 = -0.1844 - j0.9231$. Therefore,

$$\mathcal{H}(s) = \frac{K_N}{(s+0.3689)(s+0.1844+j0.9231)(s+0.1844-j0.9231)}$$
$$= \frac{K_N}{s^3+0.7378s^2+1.0222s+0.3269} = \frac{0.3269}{s^3+0.7378s^2+1.0222s+0.3269}$$

This confirms our earlier result of Eq. (7.40).

Of course, all of these calculations are easily performed in MATLAB as well.

```
>> epsilon = sqrt(10^(rhat/10)-1); x = asinh(1/epsilon)/N; k = 1:N;
>> pk = -sin((2*k-1)*pi/(2*N))*sinh(x)+1j*cos((2*k-1)*pi/(2*N))*cosh(x);
>> denHnorm = real(poly(pk));
   denHnorm = 1.0000    0.7378    1.0222    0.3269
```

Step 3: Determine the final transfer function $H(s)$

Recall that $\omega_p = 1$ for the normalized transfer function. For $\omega_p = 10$, the desired transfer function $H(s)$ can be obtained from the normalized transfer function $\mathcal{H}(s)$ by replacing s with $s/\omega_p = s/10$. Therefore,

$$H(s) = \frac{0.3269}{(\frac{s}{10}+0.3689)(\frac{s}{10}+0.1844+j0.9231)(\frac{s}{10}+0.1844-j0.9231)}$$
$$= \frac{326.9}{s^3+7.378s^2+102.22s+326.9}$$

These same coefficients for $H(s)$ are also easily computed using MATLAB.

```
>> numH = omegap^N*denHnorm(end), denH = real(poly(pk*omegap))
   numH = 326.8901
   denH = 1.0000    7.3782  102.2190  326.8901
```

Next, we turn our attention to the amplitude response of the filter. In the present case, $\hat{r} = 2$ dB means that [see Eq. (7.34)]

$$\epsilon^2 = 10^{0.2} - 1 = 0.5849$$

The frequency response is [see Eq. (7.31) and Table 7.3]

$$|\mathcal{H}(j\omega)| = \frac{1}{\sqrt{1 + 0.5849(4\omega^3 - 3\omega)^2}}$$

This is the normalized filter amplitude response. The actual filter response $|H(j\omega)|$ is obtained by replacing ω with $\frac{\omega}{\omega_p}$; that is, with $\frac{\omega}{10}$ in $\mathcal{H}(j\omega)$. Thus,

$$|H(j\omega)| = \frac{1}{\sqrt{1 + 0.5849\left[4\left(\frac{\omega}{10}\right)^3 - 3\left(\frac{\omega}{10}\right)^2\right]}}$$

$$= \frac{10^3}{\sqrt{9.3584\omega^6 - 1403.76\omega^4 + 52640\omega^2 + 10^6}}$$

Observe that despite more stringent specifications than those in Ex. 7.7, the Chebyshev filter requires $N = 3$ compared to the Butterworth filter in Ex. 7.7, which requires $N = 4$. Figure 7.30 shows the amplitude response.

We can easily generate the filter's magnitude response using MATLAB. The result, shown in Fig. 7.31, clearly confirms the response computed earlier and shown in Fig. 7.30.

```
>> omega = linspace(0,20,1001);
>> H = (polyval(numH,1j*omega))./(polyval(denH,1j*omega));
>> plot(omega,abs(H),'k-'); grid on; set(gca,'xtick',[0 omegap omegas])
>> set(gca,'ytick',[0 10^(Ghats/20) 10^(-rhat/20) 1])
>> axis([0 20 0 1.05]); xlabel('\omega'); ylabel('|H(j\omega)|');
```

An Alternate Approach

We can also design this filter using the built-in MATLAB functions `cheb1ord` and `cheby1`. We first use `cheb1ord` to determine filter order and ω_p.

```
>> [N,omegap] = cheb1ord(omegap,omegas,rhat,-Ghats,'s')
   N = 3
   omegap = 10
```

Next, we use the `cheby1` command to determine the filter transfer function.

```
>> [numH,denH] = cheby1(N,rhat,omegap,'s')
   numH =       0         0         0  326.8901
   denH = 1.0000    7.3782  102.2190  326.8901
```

This result agrees with our earlier calculations.

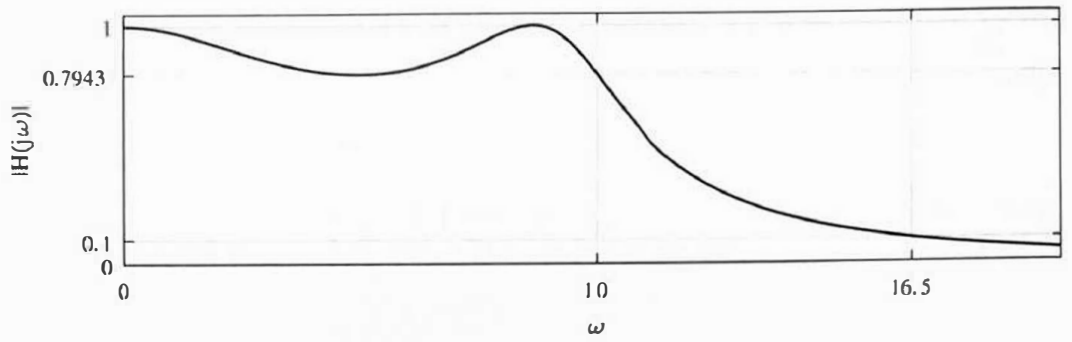

Figure 7.31 Magnitude response of the Chebyshev lowpass filter for Ex. 7.9.

DRILL 7.4 Chebyshev Lowpass Filter Design

Determine the order N and the transfer function $H(s)$ of a Chebyshev filter that meets the following specifications: $\hat{r} = 2$ dB, $\hat{G}_s = -20$ dB, $\omega_p = 10$ rad/s, and $\omega_s = 28$ rad/s.

ANSWER

$N = 2$ and $H(s) = 50.5823/(s^2 + 8.0381s + 63.6768)$

7.6.1 Inverse Chebyshev Filters

The passband behavior of Chebyshev filters exhibits ripples, and the stopband is smooth. Generally, passband behavior is more important, and we would prefer that the passband have a smooth response. However, ripples can be tolerated in the stopband as long as they meet given specifications. The *inverse Chebyshev* filter does exactly that. Both Butterworth and Chebyshev filters have finite poles and no finite zeros. An inverse Chebyshev filter has finite zeros and poles. It exhibits a maximally flat passband response and equal-ripple stopband response.

The inverse Chebyshev response can be obtained from the Chebyshev in two steps as follows. Let $\mathcal{H}_C(\omega)$ be the Chebyshev amplitude response given in Eq. (7.31). In the first step, we subtract $|\mathcal{H}_C(\omega)|^2$ from 1 to obtain a highpass filter characteristic where the stopband (from 0 to 1) has ripples and the passband (from 1 to ∞) is smooth. In the second step, we interchange the stopband and passband by a frequency transformation where ω is replaced by $1/\omega$. This step inverts the passband from the range 1 to ∞ to the range 0 to 1, and the stopband now goes from 1 to ∞. Moreover, the passband is now smooth and the stopband has ripples. This is precisely the inverse Chebyshev amplitude response, given as

$$|\mathcal{H}(\omega)|^2 = 1 - |\mathcal{H}_C(1/\omega)|^2 = \frac{\epsilon^2 C_N^2(1/\omega)}{1 + \epsilon^2 C_N^2(1/\omega)}$$

where $C_N(\omega)$ are the Nth-order Chebyshev polynomials listed in Table 7.3.

Inverse Chebyshev filters are preferable to Chebyshev filters in many ways. For example, the passband behavior, especially for small ω, is better for the inverse Chebyshev than for the Chebyshev or even for the Butterworth filter of the same order. An inverse Chebyshev filter also has the smallest transition band of the three filters. Moreover, the phase function (or time-delay) characteristic of an inverse Chebyshev filter is better than that of a Chebyshev filter [2]. Both Chebyshev and inverse Chebyshev filters require the same order N to meet a given set of specifications [3]. Although an inverse Chebyshev realization requires more elements, and thus is less economical, than a Chebyshev filter, it requires fewer elements than a comparable performance Butterworth filter. Rather than give the complete development of inverse Chebyshev filters, we shall demonstrate inverse Chebyshev filter design using functions from MATLAB's *Signal Processing Toolbox*.

EXAMPLE 7.10 Inverse Chebyshev Lowpass Filter Design

Design an inverse Chebyshev lowpass filter to satisfy the criteria of Ex. 7.9 and summarized as: $\hat{r} \leq 2$ dB over a passband $0 \leq \omega \leq 10$ ($\omega_p = 10$) and $\hat{G}_s \leq -20$ dB for $\omega > 16.5$ ($\omega_s = 16.5$).

We design this filter using the MATLAB functions `cheb2ord` and `cheby2`. We first use `cheb2ord` to determine filter order and stopband frequency ω_s.

```
>> omegap = 10; rhat = 2; omegas = 16.5; Ghats = -20;
>> [N,omegas] = cheb2ord(omegap,omegas,rhat,-Ghats,'s')
   N = 3
   omegas = 16.4972
```

Next, we use the `cheby2` command to determine the filter transfer function.

```
>> [numH,denH] = cheby2(N,-Ghats,omegas,'s')
   numH =    0       4.97          0       1804.97
   denH = 1.00      23.18        256.40     1804.97
```

The filter's transfer function is thus

$$H(s) = \frac{4.97s^2 + 1804.97}{s^3 + 23.18s^2 + 256.4s + 1804.97}$$

We next use MATLAB to plot the filter's magnitude response. As shown in Fig. 7.32, the filter displays the characteristics of an inverse Chebyshev filter (monotonic passband, equiripple stopband) and also meets design specifications.

```
>> omega = linspace(0,20,1001);
>> H = (polyval(numH,1j*omega))./(polyval(denH,1j*omega));
>> plot(omega,abs(H),'k-'); grid on; set(gca,'xtick',[0 omegap omegas])
>> set(gca,'ytick',[0 10^(Ghats/20) 10^(-rhat/20) 1])
>> axis([0 20 0 1.05]); xlabel('\omega'); ylabel('|H(j\omega)|');
```

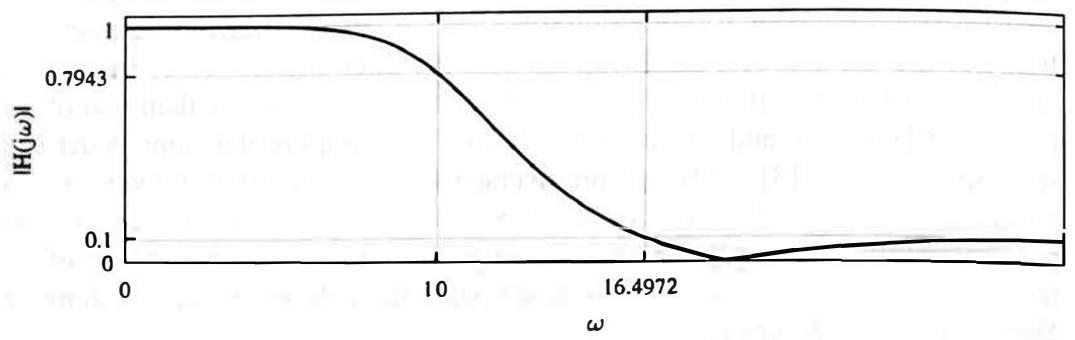

Figure 7.32 Magnitude response of the inverse Chebyshev lowpass filter for Ex. 7.10.

7.6.2 Elliptic Filters

Recall our discussion in Sec. 7.4 that placing a zero on the imaginary axis (at $s = j\omega$) causes the gain ($|H(j\omega)|$) to go to zero (infinite attenuation). We can realize a sharper cutoff characteristic by placing a zero (or zeros) near $\omega = \omega_s$. Butterworth and Chebyshev filters do not make use of zeros in $\mathcal{H}(s)$. Both inverse Chebyshev and elliptic filters do. This is part of the reason for their superior response characteristics.

A Chebyshev filter has a smaller transition band compared to that of a Butterworth filter because a Chebyshev filter allows rippling in the passband (or stopband). If we allow ripple in both the passband and the stopband, we can achieve further reduction in the transition band. Such is the case with elliptic (or Cauer) filters, whose normalized amplitude response is given by

$$|\mathcal{H}(j\omega)| = \frac{1}{\sqrt{1+\epsilon^2 R_N{}^2(\omega,\xi)}}$$

where $R_N(\omega,\xi)$ is an Nth-order *elliptic rational function* with discrimination factor ξ.[†] Using the properties of R_N (see [2]), we see that an elliptic filter's equiripple passband has magnitude limits of 1 and $1/\sqrt{1+\epsilon^2}$. The parameter ϵ controls the passband ripple, and the gain at the (normalized) passband frequency ($\omega_p = 1$) is $1/\sqrt{1+\epsilon^2}$. Similarly, the filter's equiripple stopband has magnitude limits of $1/\sqrt{1+\epsilon^2\xi^2}$ and 0. Thus, the discrimination factor ξ is directly related to the filter's maximum stopband gain. Like Chebyshev filters, elliptic filters are normalized in terms of the passband edge ω_p.

[†] Elliptic rational functions are sometimes referred to as *Chebyshev rational functions*, a name also given to an entirely different class of functions as well. We use the former convention to minimize potential confusion. Additionally, some sources express R_N in terms of a selectivity factor rather than the discrimination factor ξ; the discrimination factor provides more insight for filter design applications.

If we can tolerate both passband and stopband ripple, an elliptic filter is the most efficient type of filter. For a given transition band, it provides the largest ratio of the passband gain to stopband gain, or for a given ratio of passband to stopband gain, it requires the smallest transition band. In compensation, however, we must accept ripple in both the passband and the stopband. In addition, because of the zeros of $\mathcal{H}(s)$, an elliptic filter response decays at a slower rate at frequencies higher than ω_s. For instance, the amplitude response of a third-order elliptic filter decays at a rate of only -6 dB/octave at very high frequencies. This is because the filter has two zeros and three poles. The two zeros increase the amplitude response at a rate of 12 dB/octave, and the three poles reduce the amplitude response at a rate of -18 dB/octave, thus giving a net decay rate of -6 dB/octave. For Butterworth and Chebyshev filters, there are no zeros in $\mathcal{H}(s)$. Therefore, their amplitude response decays at a rate of -18 dB/octave. However, the rate of decay of the amplitude response is seldom important as long as we meet our specification of a given G_s at ω_s.

Calculation of pole-zero locations of elliptic filters is much more complicated than that in Butterworth or even Chebyshev filters. Fortunately, this task is greatly simplified by computer programs, such as MATLAB, as the next example demonstrates.[†]

EXAMPLE 7.11 Elliptic Lowpass Filter Design

Design an elliptic lowpass filter to satisfy the criteria of Ex. 7.9 and summarized as: $\hat{r} \leq 2$ dB over a passband $0 \leq \omega \leq 10$ ($\omega_p = 10$) and $\hat{G}_s \leq -20$ dB for $\omega > 16.5$ ($\omega_s = 16.5$).

We design this filter using the MATLAB functions `ellipord` and `ellip`. We first use `ellipord` to determine filter order and passband frequency ω_p.

```
>> omegap = 10; rhat = 2; omegas = 16.5; Ghats = -20;
>> [N,omegap] = ellipord(omegap,omegas,rhat,-Ghats,'s')
   N = 3
   omegap = 10
```

Next, we use the `ellip` command to determine the filter transfer function.

```
>> [numH,denH] = ellip(N,rhat,-Ghats,omegap,'s')
   numH =       0    2.7882         0  481.1613
   denH = 1.0000    7.2610  106.9988  481.1613
```

The filter's transfer function is thus

$$H(s) = \frac{2.7882s^2 + 481.1613}{s^3 + 7.2610s^2 + 106.9988s + 481.1613}$$

[†] Extensive ready-made design tables, available in resources such as [4], are still available for those with a sense of nostalgia and old-school determination.

We next use MATLAB to plot the filter's magnitude response. As shown in Fig. 7.33, the filter displays the characteristics of an elliptic filter (equiripple passband and stopband) and also meets design specifications.

```
>> omega = linspace(0,20,1001);
>> H = (polyval(numH,1j*omega))./(polyval(denH,1j*omega));
>> plot(omega,abs(H),'k-'); grid on; set(gca,'xtick',[0 omegap omegas])
>> set(gca,'ytick',[0 10^(Ghats/20) 10^(-rhat/20) 1])
>> axis([0 20 0 1.05]); xlabel('\omega'); ylabel('|H(j\omega)|');
```

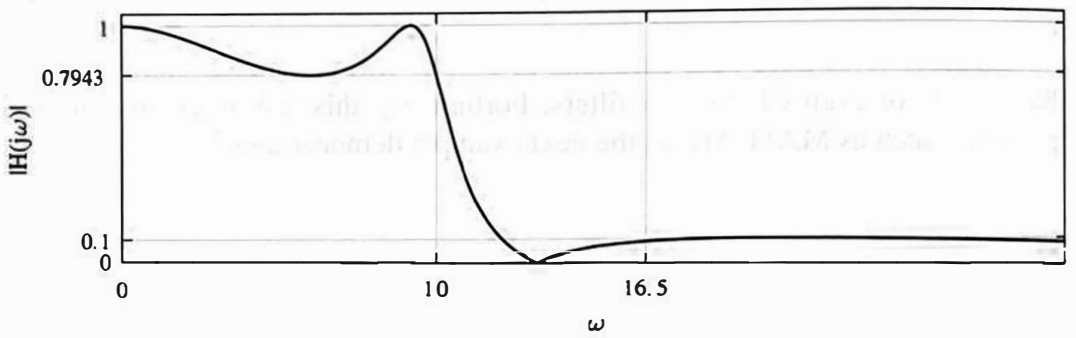

Figure 7.33 Magnitude response of the elliptic lowpass filter for Ex. 7.11.

7.7 FREQUENCY TRANSFORMATIONS

Earlier we saw how a lowpass filter transfer function of arbitrary specifications can be obtained from a normalized lowpass filter using frequency scaling. Using certain frequency transformations, we can obtain transfer functions of highpass, bandpass, and bandstop filters from a basic lowpass filter (the prototype filter) design. For example, a highpass filter transfer function can be obtained from a prototype lowpass filter transfer function (with normalized passband frequency) by replacing s with ω_p/s. Similar transformations allow us to design bandpass and bandstop filters from appropriate lowpass prototype filters.

The prototype filter may be of any kind, such as Butterworth, Chebyshev, elliptic, and so on. We first design a suitable prototype lowpass filter $\mathcal{H}_p(s)$. In the next step, we replace s with a proper transformation $T(s)$ to obtain the desired highpass, bandpass, or bandstop filter.

7.7.1 Highpass Filters

Figure 7.34a shows an amplitude response of a typical highpass filter. The appropriate lowpass prototype response required for the design of this highpass filter is depicted in Fig. 7.34b. We

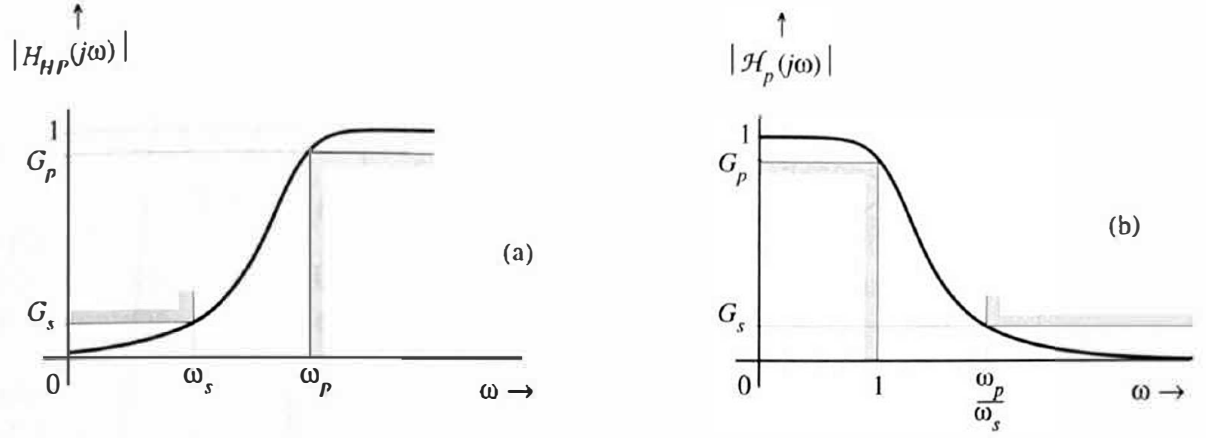

Figure 7.34 Frequency transformation for highpass filters.

must first determine this prototype filter transfer function $\mathcal{H}_p(s)$ with passband $0 \leq \omega \leq 1$ and stopband $\omega \geq \omega_p/\omega_s$. The desired transfer function of the highpass filter to satisfy specifications in Fig. 7.34a is then obtained by replacing s with $T(s)$ in $\mathcal{H}_p(s)$, where

$$T(s) = \frac{\omega_p}{s} \tag{7.41}$$

EXAMPLE 7.12 Chebyshev Highpass Filter Design

Design a Chebyshev highpass filter to satisfy the criteria shown in Fig. 7.35 and summarized as: $\omega_s = 100$, $\omega_p = 165$, $G_s = 0.1$ ($\hat{G}_s = -20$ dB), and $G_p = 0.794$ ($\hat{G}_p = -2$ dB).

Step 1: Determine the prototype lowpass filter $\mathcal{H}_p(s)$

The prototype lowpass filter has $\hat{\omega}_p = 1$ and $\hat{\omega}_s = 165/100 = 1.65$. This means the prototype filter in Fig. 7.34b has a passband $0 \leq \omega \leq 1$ and a stopband $\omega \geq 1.65$, as shown in Fig. 7.35b. Also, $G_p = 0.794$ ($\hat{G}_p = -2$ dB) and $G_s = 0.1$ ($\hat{G}_s = -20$ dB). We already designed a Chebyshev filter with these specifications in Ex. 7.9. The transfer function of this filter is [Eq. (7.40)]

$$\mathcal{H}_p(s) = \frac{0.3269}{s^3 + 0.7378s^2 + 1.0222s + 0.3269}$$

The amplitude response of this prototype filter is depicted in Fig. 7.35b.

Step 2: Determine the highpass filter $H(s)$

The desired highpass filter transfer function $H(s)$ is obtained from $\mathcal{H}_p(s)$ by replacing s with $T(s) = \omega_p/s = 165/s$. Therefore,

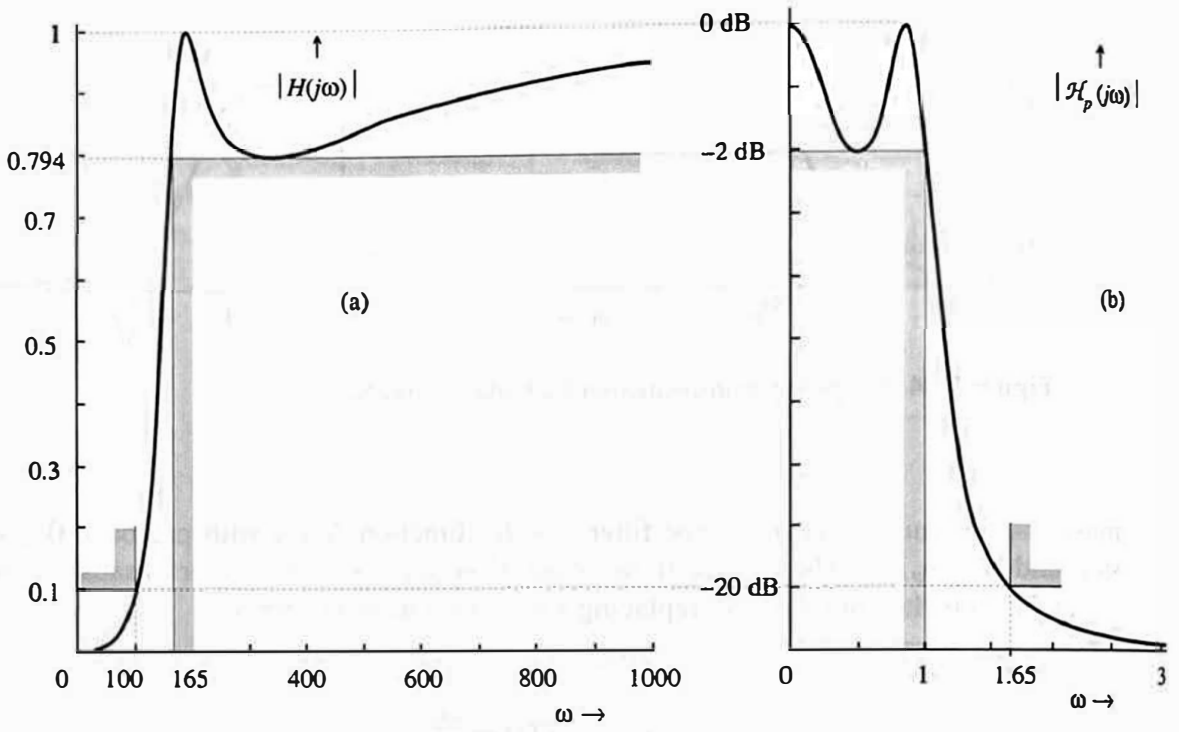

Figure 7.35 Chebyshev highpass filter design for Ex. 7.12.

$$H(s) = \frac{0.3269}{\left(\frac{165}{s}\right)^3 + 0.7378\left(\frac{165}{s}\right)^2 + 1.0222\left(\frac{165}{s}\right) + 0.3269}$$
$$= \frac{s^3}{s^3 + 515.94s^2 + 61445.75s + 13742005}$$

The amplitude response $|H(j\omega)|$ for this filter is illustrated in Fig. 7.35a.

HIGHPASS CHEBYSHEV FILTER DESIGN WITH MATLAB

We can also carry out this design using the MATLAB functions `cheb1ord` and `cheby1`. We first use `cheb1ord` to determine filter order and passband frequency ω_p.

```
>> omegap = 165; Ghatp = -2; omegas = 100; Ghats = -20;
>> [N,omegap] = cheb1ord(omegap,omegas,-Ghatp,-Ghats,'s')
   N = 3
   omegap = 165
```

Next, we use the `cheby1` command to determine the filter transfer function.

```
>> [numH,denH] = cheby1(N,-Ghatp,omegap,'high','s')
   numH = 1.00        0        0        0
   denH = 1.00   515.96  61449.38  13742005.16
```

The filter's transfer function is thus

$$H(s) = \frac{s^3}{s^3 + 515.96s^2 + 61449.38s + 13742005.16}$$

As expected, the MATLAB result matches our earlier hand calculations.

We next use MATLAB to plot the filter's magnitude response. The result, shown in Fig. 7.36, matches our earlier result of Fig. 7.35a.

```
>> omega = linspace(0,800,1001);
>> H = (polyval(numH,1j*omega))./(polyval(denH,1j*omega));
>> plot(omega,abs(H),'k-'); grid on;
>> set(gca,'xtick',[0 omegas omegap 300:200:800])
>> set(gca,'ytick',[0 10^(Ghats/20) 10^(Ghatp/20) 1])
>> axis([0 800 0 1.05]); xlabel('\omega'); ylabel('|H(j\omega)|');
```

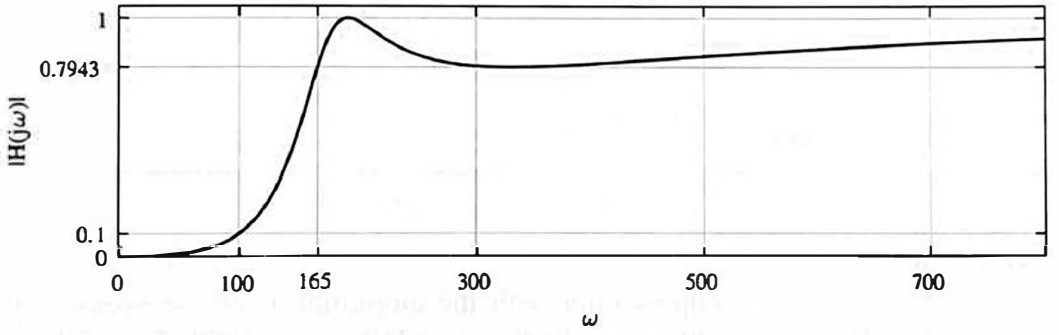

Figure 7.36 Magnitude response of the Chebyshev highpass filter for Ex. 7.12.

It is a simple matter to design different filter types for the same specifications in MATLAB. Rather than use `cheb1ord` and `cheby1`, we could use `buttord` and `butter` to design a Butterworth filter, `cheb2ord` and `cheby2` to design an inverse Chebyshev filter, and `ellipord` and `ellip` to design an elliptic filter.

7.7.2 Bandpass Filters

Figure 7.37a shows the amplitude response of a typical bandpass filter. To design such a filter, we first find $\mathcal{H}_p(s)$, the transfer function of a prototype lowpass filter (with normalized passband frequency), to meet the specifications in Fig. 7.37b, where ω_s is given by the smaller of

$$\frac{\omega_{p_1}\omega_{p_2} - {\omega_{s_1}}^2}{\omega_{s_1}(\omega_{p_2} - \omega_{p_1})} \quad \text{and} \quad \frac{{\omega_{s_2}}^2 - \omega_{p_1}\omega_{p_2}}{\omega_{s_2}(\omega_{p_2} - \omega_{p_1})} \tag{7.42}$$

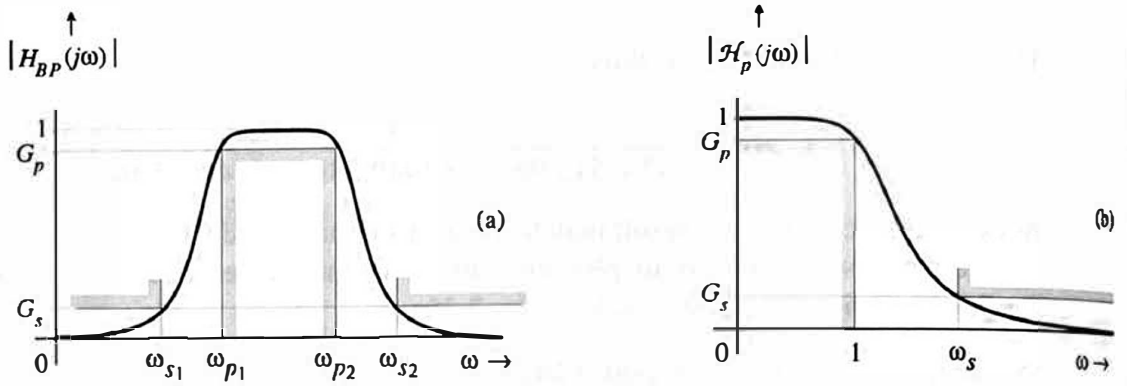

Figure 7.37 Frequency transformation for bandpass filters.

Now, the desired transfer function of the bandpass filter to satisfy the specifications in Fig. 7.37a is obtained from $\mathcal{H}_p(s)$ by replacing s with $T(s)$, where

$$T(s) = \frac{s^2 + \omega_{p_1}\omega_{p_2}}{(\omega_{p_2} - \omega_{p_1})s} \tag{7.43}$$

EXAMPLE 7.13 Chebyshev Bandpass Filter Design

Design a Chebyshev bandpass filter with the amplitude response specifications shown in Fig. 7.38a with $\omega_{p_1} = 1000$, $\omega_{p_2} = 2000$, $\omega_{s_1} = 450$, $\omega_{s_2} = 4000$, $G_s = 0.1$ ($\hat{G}_s = -20$ dB), and $G_p = 0.891$ ($\hat{G}_p = -1$ dB). Observe that for a Chebyshev filter, $\hat{G}_p = -1$ dB is equivalent to $\hat{r} = 1$ dB.

The solution is executed in two steps. In the first step, we determine the lowpass prototype filter transfer function $\mathcal{H}_p(s)$. In the second step, the desired bandpass filter transfer function is obtained from $\mathcal{H}_p(s)$ by substituting s with $T(s)$, the lowpass-to-bandpass transformation in Eq. (7.43).

Step 1: Determine the prototype lowpass filter $\mathcal{H}_p(s)$

To begin, we find the stopband frequency ω_s of the prototype. From Eq. (7.42), ω_s is the smaller of

$$\frac{(1000)(2000) - (450)^2}{450(2000 - 1000)} = 3.99 \quad \text{and} \quad \frac{(4000)^2 - (1000)(2000)}{4000(2000 - 1000)} = 3.5$$

Thus, $\omega_s = 3.5$.

We now need to design a prototype lowpass filter in Fig. 7.37b with $\hat{G}_p = -1$ dB, $\hat{G}_s = -20$ dB, $\omega_p = 1$, and $\omega_s = 3.5$, as illustrated in Fig. 7.38b. The Chebyshev filter order N required to meet these specifications is obtained from Eq. (7.35) as

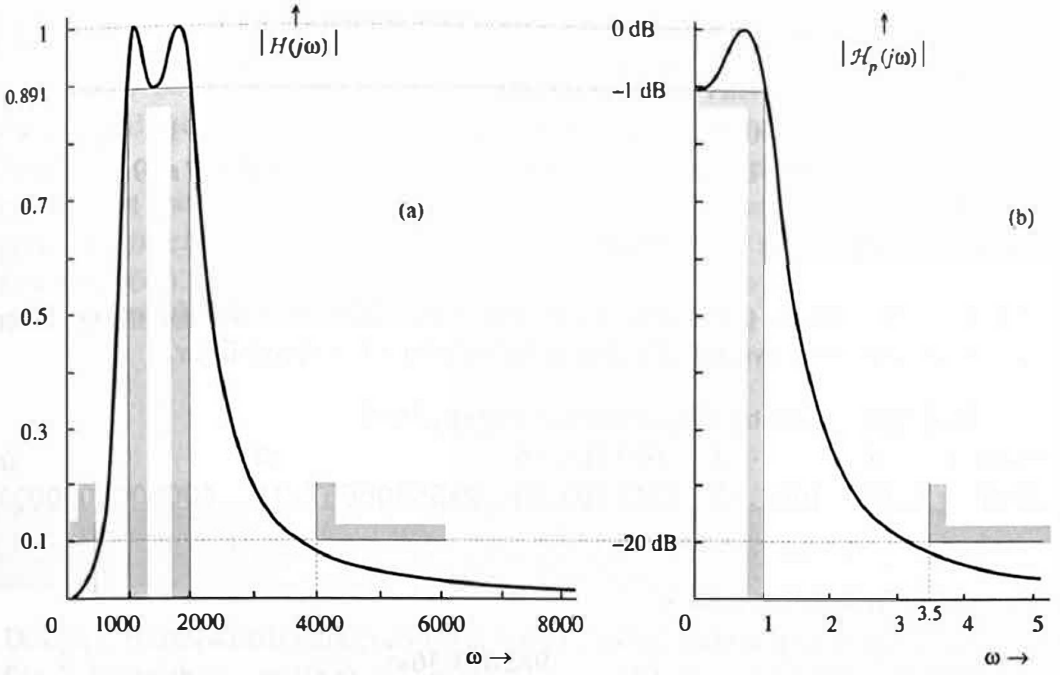

Figure 7.38 Chebyshev bandpass filter design for Ex. 7.13.

$$N = \frac{1}{\cosh^{-1}(3.5)} \cosh^{-1}\left[\frac{10^2-1}{10^{0.1}-1}\right]^{\frac{1}{2}} = 1.904$$

Rounding up to the nearest integer, we see that the required prototype order is $N = 2$.

We can obtain the prototype transfer function by computing its poles using Eq. (7.37) with $N = 2$ and $\hat{r} = 1$ ($\epsilon = 0.5088$). However, since Table 7.4 lists the denominator polynomial for $\hat{r} = 1$ and $N = 2$, we need not perform the computations and may use the ready-made transfer function directly as

$$\mathcal{H}_p(s) = \frac{0.9826}{s^2 + 1.0977s + 1.1025} \tag{7.44}$$

Here, we used Eq. (7.39) to find the numerator $K_N = \frac{a_0}{\sqrt{1+\epsilon^2}} = \frac{1.1025}{\sqrt{1.2589}} = 0.9826$. The amplitude response of this prototype filter is depicted in Fig. 7.38b.

Step 2: Determine the bandpass filter $H(s)$

Finally, the desired bandpass filter transfer function $H(s)$ is obtained from $\mathcal{H}_p(s)$ by replacing s with $T(s)$, where [see Eq. (7.43)]

$$T(s) = \frac{s^2 + 2(10)^6}{1000s}$$

Replacing s with $T(s)$ in the right-hand side of Eq. (7.44) yields the final bandpass transfer function

$$H(s) = \frac{9.826(10)^5 s^2}{s^4 + 1097.7s^3 + 5.1025(10)^6 s^2 + 2.195(10)^9 s + 4(10)^{12}}$$

The amplitude response $|H(j\omega)|$ of this filter is shown in Fig. 7.38a.

BANDPASS CHEBYSHEV FILTER DESIGN WITH MATLAB

We can readily verify this design using the MATLAB functions `cheb1ord` and `cheby1`. We first use `cheb1ord` to determine filter order and passband frequencies ω_p.

```
>> omegap = [1000,2000]; omegas= [450,4000]; Ghatp = -1; Ghats = -20;
>> [N,omegap] = cheb1ord(omegap,omegas,-Ghatp,-Ghats,'s')
   N = 2
   omegap = 1000.00        2000.00
```

Next, we use the `cheby1` command to determine the filter transfer function. Since ω_p is specified as a two-element vector, the design defaults to a bandpass filter.

```
>> [numH,denH] = cheby1(N,-Ghatp,omegap,'s')
   numH =     0         0   982613.36                0                0
   denH = 1.00   1097.73   5102510.33   2195468657.13   4000000000000
```

The filter's transfer function is thus

$$H(s) = \frac{982613.36s^2}{s^4 + 1097.73s^3 + 5102510.33s^2 + 2195468657.13s + 4000000000000}$$

This MATLAB result matches our earlier hand calculations.

We next use MATLAB to plot the filter's magnitude response. The result, shown in Fig. 7.39, matches our earlier result of Fig. 7.38a.

```
>> omega = linspace(0,8000,1001);
>> H = (polyval(numH,1j*omega))./(polyval(denH,1j*omega));
>> plot(omega,abs(H),'k-'); grid on;
>> set(gca,'xtick',[0 450 1000 2000 4000 6000 8000])
>> set(gca,'ytick',[0 10^(Ghats/20) 10^(Ghatp/20) 1])
>> axis([0 8000 0 1.05]); xlabel('\omega'); ylabel('|H(j\omega)|');
```

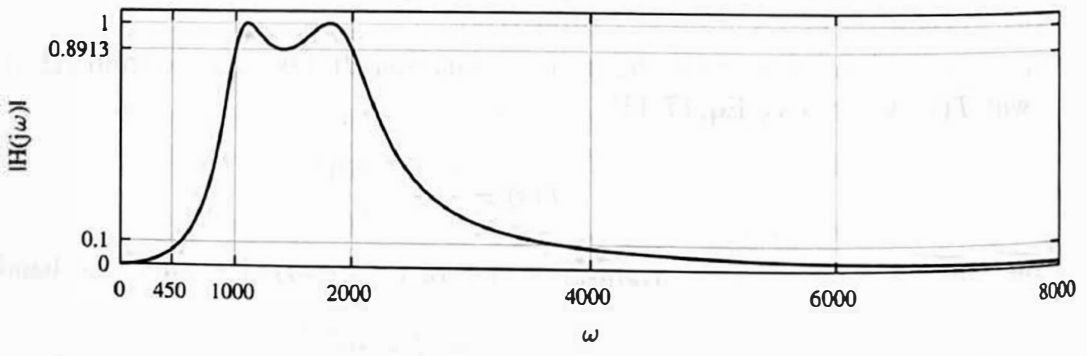

Figure 7.39 Magnitude response of the Chebyshev bandpass filter for Ex. 7.13.

We may use a similar procedure for Butterworth bandpass filters. Compared to the Chebyshev case, a Butterworth bandpass filter design involves two additional steps. First, we need to compute the cutoff frequency ω_c of the prototype filter. For a Chebyshev filter, the critical frequency happens to be the frequency where the gain is G_p. This frequency is $\omega = 1$ in the prototype filter. For Butterworth, on the other hand, the critical frequency is the half power (or 3 dB cutoff) frequency ω_c, which is not necessarily the frequency where the gain is G_p. To find the transfer function of the Butterworth prototype filter, it is essential to know ω_c. Once we know ω_c, the prototype filter transfer function is obtained by replacing s with s/ω_c in the normalized transfer function $\mathcal{H}(s)$. This step is also unnecessary in the Chebyshev filter design. Our next example demonstrates the procedure for Butterworth bandpass filter design.

EXAMPLE 7.14 Butterworth Bandpass Filter Design

Design a Butterworth bandpass filter with the amplitude response specifications illustrated in Fig. 7.40a with $\omega_{p_1} = 1000$, $\omega_{p_2} = 2000$, $\omega_{s_1} = 450$, $\omega_{s_2} = 4000$, $G_p = 0.7586$ ($\hat{G}_p = -2.4$ dB), and $G_s = 0.1$ ($\hat{G}_s = -20$ dB).

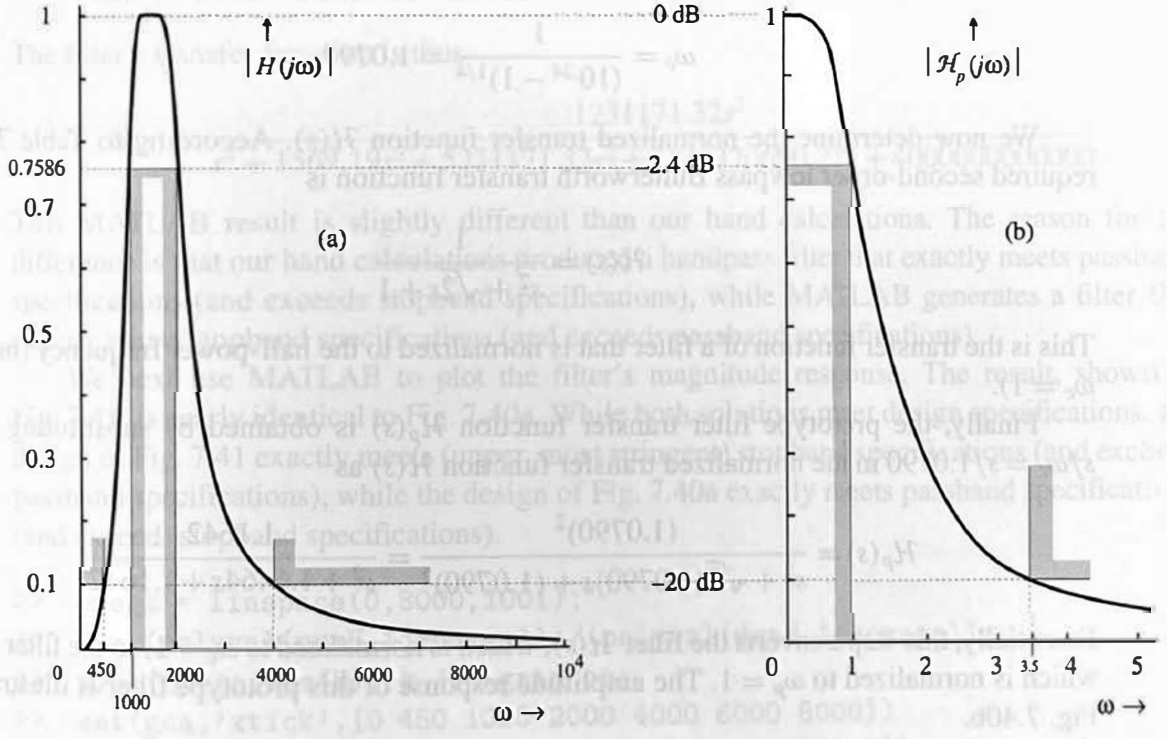

Figure 7.40 Butterworth bandpass filter design for Ex. 7.14.

As in Ex. 7.13, the solution is executed in two steps. In the first step, we determine the lowpass prototype filter transfer function $\mathcal{H}_p(s)$. In the second step, the desired bandpass filter transfer function is obtained from $\mathcal{H}_p(s)$ by substituting s with $T(s)$, the lowpass to bandpass transformation in Eq. (7.43).

Step 1: Determine the prototype lowpass filter $\mathcal{H}_p(s)$

Our goal here is the design of the prototype lowpass Butterworth filter (see Ex. 7.7). First, we find ω_s. For the prototype lowpass filter transfer function $\mathcal{H}_p(s)$ with the amplitude response shown in Fig. 7.40b, the frequency ω_s is found [using Eq. (7.42)] to be the smaller of

$$\frac{(1000)(2000)-(450)^2}{450(2000-1000)}=3.99 \quad \text{and} \quad \frac{(4000)^2-(1000)(2000)}{4000(2000-1000)}=3.5$$

Thus, $\omega_s = 3.5$, as depicted in Fig. 7.40b.

Next, we determine the filter order N. For a prototype lowpass filter in Fig. 7.37b, $\hat{G}_p = -2.4$ dB, $\hat{G}_s = -20$ dB, $\omega_p = 1$, and $\omega_s = 3.5$. Hence, according to Eq. (7.28), the Butterworth filter order N required to meet these specifications is

$$N=\frac{1}{2\log 3.5}\log\left[\frac{10^2-1}{10^{0.24}-1}\right]=1.955$$

Since filter order must be an integer, we round this result up to $N = 2$.

Next (which is not necessary for a Chebyshev design), we determine the half-power (3 dB) cutoff frequency ω_c for the prototype filter. Use of Eq. (7.29) yields

$$\omega_c=\frac{1}{(10^{.24}-1)^{1/4}}=1.0790$$

We now determine the normalized transfer function $\mathcal{H}(s)$. According to Table 7.1, the required second-order lowpass Butterworth transfer function is

$$\mathcal{H}(s)=\frac{1}{s^2+\sqrt{2}s+1}$$

This is the transfer function of a filter that is normalized to the half-power frequency (meaning $\omega_c = 1$).

Finally, the prototype filter transfer function $\mathcal{H}_p(s)$ is obtained by substituting s with $s/\omega_c = s/1.0790$ in the normalized transfer function $\mathcal{H}(s)$ as

$$\mathcal{H}_p(s)=\frac{(1.0790)^2}{s^2+\sqrt{2}(1.0790)s+(1.0790)^2}=\frac{1.1642}{s^2+1.6464s+1.1642} \tag{7.45}$$

Essentially, this step converts the filter $\mathcal{H}(s)$, which is normalized to $\omega_c = 1$, to the filter $\mathcal{H}_p(s)$, which is normalized to $\omega_p = 1$. The amplitude response of this prototype filter is illustrated in Fig. 7.40b.

Step 2: Determine the bandpass filter $H(s)$

Finally, the desired bandpass filter transfer function $H(s)$ is obtained from $\mathcal{H}_p(s)$ by replacing s with $T(s)$, where [see Eq. (7.43)]

$$T(s) = \frac{s^2 + 2(10)^6}{1000s}$$

Making this substitution in the right-hand side of Eq. (7.45) yields the final bandpass transfer function

$$H(s) = \frac{1.1642(10)^6 s^2}{s^4 + 1526s^3 + 5.1642(10)^6 s^2 + 3.0518(10)^9 s + 4(10)^{12}}$$

The amplitude response $|H(j\omega)|$ of this filter is shown in Fig. 7.40a.

Butterworth Bandpass Filter Design with MATLAB

Once again, we can easily use MATLAB to design a filter to meet the design specifications. We first use `buttord` to determine filter order and half-power frequencies ω_c.

```
>> omegap = [1000 2000]; omegas = [450 4000]; Ghatp = -2.4; Ghats = -20;
>> [N,omegac] = buttord(omegap,omegas,-Ghatp,-Ghats,'s')
   N = 2
   omegac = 964.35        2073.93
```

Next, we use the `butter` command to determine the filter transfer function. Since ω_c is specified as a two-element vector, the design defaults to a bandpass filter.

```
>> [numH,denH] = butter(N,omegac,'s')
   numH =    0         0  1231171.32              0              0
   denH = 1.00   1569.19  5231171.32  3138370690.27  4000000000000
```

The filter's transfer function is thus

$$H(s) = \frac{1231171.32s^2}{s^4 + 1569.19s^3 + 5231171.32s^2 + 3138370690.27s + 4000000000000}$$

This MATLAB result is slightly different than our hand calculations. The reason for the difference is that our hand calculations produced a bandpass filter that exactly meets passband specifications (and exceeds stopband specifications), while MATLAB generates a filter that exactly meets stopband specifications (and exceeds passband specifications).

We next use MATLAB to plot the filter's magnitude response. The result, shown in Fig. 7.41, is nearly identical to Fig. 7.40a. While both solutions meet design specifications, the design of Fig. 7.41 exactly meets (upper, most stringent) stopband specifications (and exceeds passband specifications), while the design of Fig. 7.40a exactly meets passband specifications (and exceeds stopband specifications).

```
>> omega = linspace(0,8000,1001);
>> H = (polyval(numH,1j*omega))./(polyval(denH,1j*omega));
>> plot(omega,abs(H),'k-'); grid on;
>> set(gca,'xtick',[0 450 1000 2000 4000 6000 8000])
>> set(gca,'ytick',[0 10^(Ghats/20) 10^(Ghatp/20) 1])
>> axis([0 8000 0 1.05]); xlabel('\omega'); ylabel('|H(j\omega)|');
```

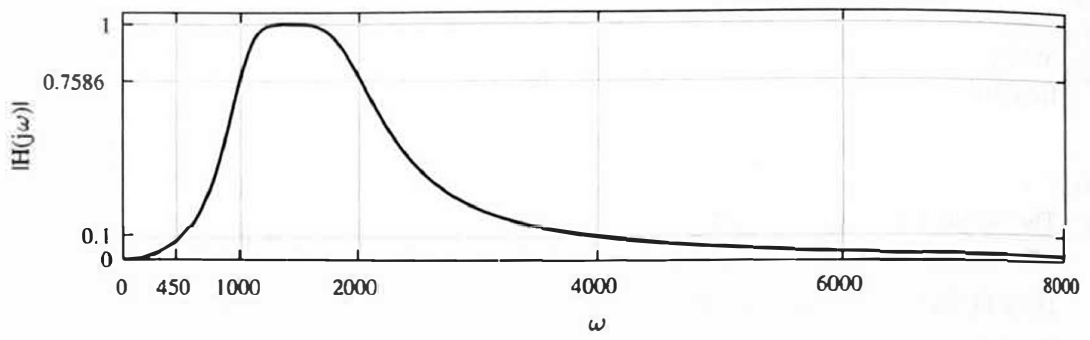

Figure 7.41 Magnitude response of the Butterworth bandpass filter for Ex. 7.15.

7.7.3 Bandstop Filters

Figure 7.42a shows an amplitude response of a typical bandstop filter. To design such a filter, we first find $\mathcal{H}_p(s)$, the transfer function of a prototype lowpass filter, to meet the specifications in Fig. 7.42b, where ω_s is given by the smaller of

$$\frac{(\omega_{p_2}-\omega_{p_1})\omega_{s_1}}{\omega_{p_1}\omega_{p_2}-{\omega_{s_1}}^2} \quad \text{and} \quad \frac{(\omega_{p_2}-\omega_{p_1})\omega_{s_2}}{{\omega_{s_2}}^2-\omega_{p_1}\omega_{p_2}} \tag{7.46}$$

The desired transfer function of the bandstop filter to satisfy the specifications in Fig. 7.42a is obtained from $\mathcal{H}_p(s)$ by replacing s with $T(s)$, where

$$T(s)=\frac{(\omega_{p_2}-\omega_{p_1})s}{s^2+\omega_{p_1}\omega_{p_2}} \tag{7.47}$$

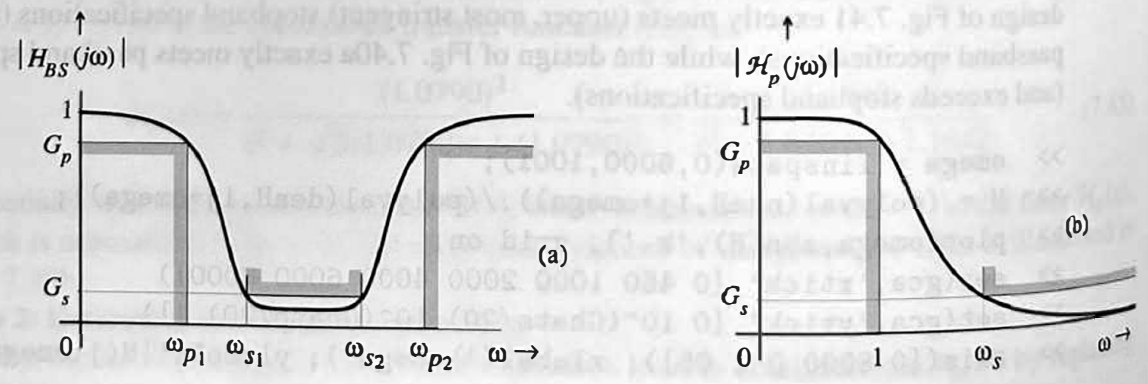

Figure 7.42 Frequency transformation for bandstop filters.

EXAMPLE 7.15 Butterworth Bandstop Filter Design

Design a Butterworth bandstop filter with the amplitude response specifications illustrated in Fig. 7.43a with $\omega_{p_1} = 60$, $\omega_{p_2} = 260$, $\omega_{s_1} = 100$, $\omega_{s_2} = 150$, $G_p = 0.7776$ ($\hat{G}_p = -2.2$ dB), and $G_s = 0.1$ ($\hat{G}_s = -20$ dB).

Here, our bandstop design solution follows a two-step procedure similar to that for the Butterworth bandpass filter design of Ex. 7.14. In the first step, we determine the lowpass prototype filter transfer function $\mathcal{H}_p(s)$. In the second step, we use the lowpass to bandstop transformation in Eq. (7.47) to obtain the desired bandstop filter transfer function $H(s)$.

Step 1: Determine the prototype lowpass filter $\mathcal{H}_p(s)$

Our goal here is the design of the prototype lowpass Butterworth filter (see Ex. 7.7). First, we find ω_s. For the prototype lowpass filter transfer function $\mathcal{H}_p(s)$ with the amplitude response shown in Fig. 7.43b, the frequency ω_s is found [using Eq. (7.46)] to be the smaller of

$$\frac{(100)(260-60)}{(260)(60)-100^2} = 3.57 \quad \text{and} \quad \frac{150(260-60)}{150^2-(260)(60)} = 4.347$$

Thus, $\omega_s = 3.57$, as depicted in Fig. 7.43b.

Next, we determine the filter order N. For the prototype lowpass filter in Fig. 7.43b, $\hat{G}_p = -2.2$ dB, $\hat{G}_s = -20$ dB, $\omega_p = 1$, and $\omega_s = 3.57$. According to Eq. (7.28), the Butterworth filter order N required to meet these specifications is

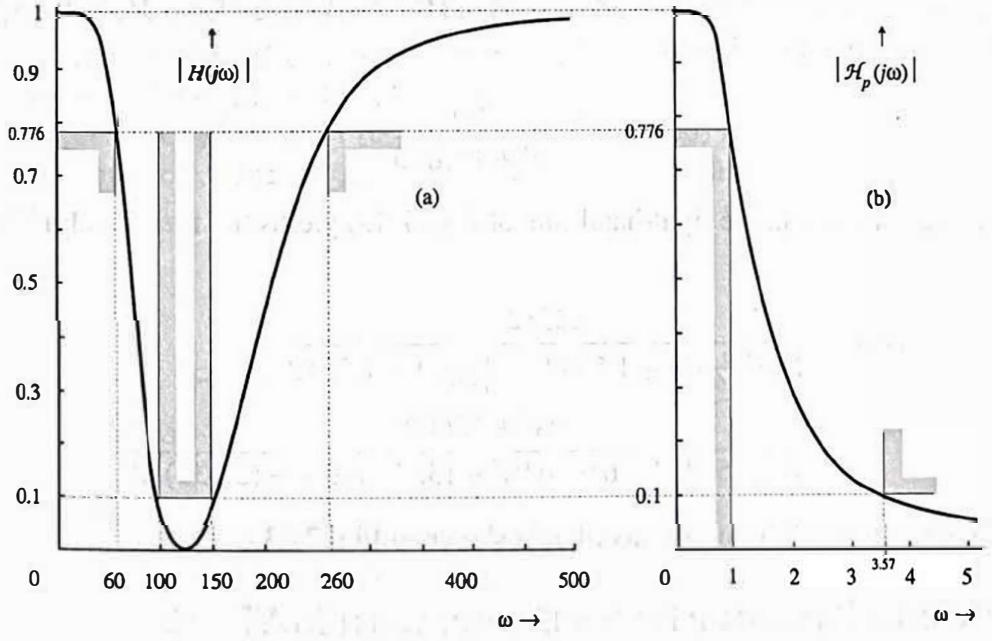

Figure 7.43 Butterworth bandstop filter design for Ex. 7.15.

$$N = \frac{1}{2\log(3.57)}\left[\frac{10^2 - 1}{10^{0.22} - 1}\right] = 1.9689$$

Since filter order must be an integer, we round this result up to $N = 2$.

The half-power frequency ω_c for the prototype Butterworth filter, using Eq. (7.29) with $\omega_p = 1$, is

$$\omega_c = \frac{\omega_p}{(10^{-\hat{G}_p/10} - 1)^{\frac{1}{4}}} = \frac{1}{(10^{0.22} - 1)^{\frac{1}{4}}} = 1.1096$$

We now determine the normalized transfer function $\mathcal{H}(s)$. According to Table 7.1, the required second-order lowpass Butterworth transfer function is

$$\mathcal{H}(s) = \frac{1}{s^2 + \sqrt{2}s + 1}$$

This is the transfer function of a filter that is normalized to the half-power frequency (meaning $\omega_c = 1$).

Finally, the prototype filter transfer function $\mathcal{H}_p(s)$ is obtained by substituting s with $s/\omega_c = s/1.1096$ in the normalized transfer function $\mathcal{H}(s)$ as

$$\mathcal{H}_p(s) = \frac{1}{(\frac{s}{\omega_c})^2 + \sqrt{2}\frac{s}{\omega_c} + 1} = \frac{1.2312}{s^2 + 1.5692s + 1.2312} \tag{7.48}$$

Essentially, this step converts the filter $\mathcal{H}(s)$, which is normalized to $\omega_c = 1$, to the filter $\mathcal{H}_p(s)$, which is normalized to $\omega_p = 1$. The amplitude response of this prototype filter is illustrated in Fig. 7.43b.

Step 2: Determine the bandstop filter $H(s)$

Finally, the desired bandstop filter transfer function $H(s)$ is obtained from $\mathcal{H}_p(s)$ by replacing s with $T(s)$, where [see Eq. (7.47)]

$$T(s) = \frac{200s}{s^2 + 15{,}600}$$

Making this substitution in the right-hand side of Eq. (7.48) yields the final bandpass transfer function

$$\begin{aligned} H(s) &= \frac{1.2312}{(\frac{200s}{s^2+15{,}600})^2 + 1.5692(\frac{200s}{s^2+15{,}600}) + 1.2312} \\ &= \frac{(s^2 + 15600)^2}{s^4 + 254.9s^3 + 63690.9s^2 + (3.977)10^6 s + (2.433)10^8} \end{aligned}$$

The amplitude response $|H(j\omega)|$ of this filter is shown in Fig. 7.43a.

Butterworth Bandstop Filter Design with MATLAB

We now use MATLAB to design a filter to meet the Butterworth bandstop design specifications. We first use `buttord` to determine filter order and half-power frequencies ω_c.

```
>> omegap = [60 260]; omegas = [100 150]; Ghatp = -2.2; Ghats = -20;
>> [N,omegac] = buttord(omegap,omegas,-Ghatp,-Ghats,'s')
   N = 2
   omegac = 66.8077  224.5249
```

Next, we use the `butter` command to determine the filter transfer function. In addition to ω_c being specified as a two-element vector, we must also specify that a bandstop (rather than bandpass) filter is desired.

```
>> [numH,denH] = butter(N,omegac,'stop','s')
   numH = 1.00            0      30000.00            0  225000022.66
   denH = 1.00       223.05      54874.69   3345685.76  225000022.66
```

The filter's transfer function is thus

$$H(s) = \frac{s^4 + 30000s^2 + 225000022.66}{s^4 + 223.05s^3 + 54874.69s^2 + 3345685.76s + 225000022.66}$$

As in Ex. 7.14, this MATLAB result is slightly different from our hand calculations. The reason for the difference is that our hand calculations produced a bandstop filter that exactly meets passband specifications (and exceeds stopband specifications), while MATLAB generates a filter that exactly meets stopband specifications (and exceeds passband specifications).

We next use MATLAB to plot the filter's magnitude response. The result, shown in Fig. 7.44, is nearly identical to Fig. 7.43a. While both solutions meet design specifications, the design of Fig. 7.44 exactly meets stopband specifications (and exceeds passband specifications), while the design of Fig. 7.43a exactly meets passband specifications (and exceeds stopband specifications).

```
>> omega = linspace(0,500,1001);
>> H = (polyval(numH,1j*omega))./(polyval(denH,1j*omega));
>> plot(omega,abs(H),'k-'); grid on;
>> set(gca,'xtick',[0 60 100 150 260 500])
>> set(gca,'ytick',[0 10^(Ghats/20) 10^(Ghatp/20) 1])
>> axis([0 500 0 1.05]); xlabel('\omega'); ylabel('|H(j\omega)|');
```

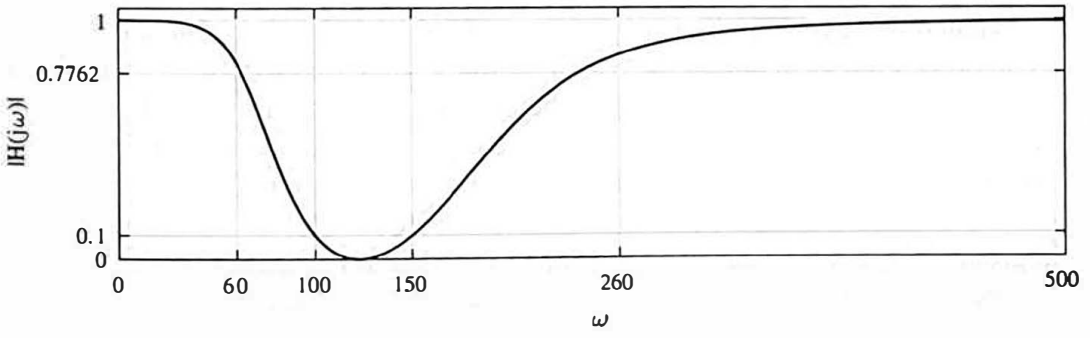

Figure 7.44 Magnitude response of the Butterworth bandpass filter for Ex. 7.15.

7.8 FILTERS TO SATISFY DISTORTIONLESS TRANSMISSION CONDITIONS

The purpose of a filter is to suppress unwanted frequency components and to transmit the desired frequency components without distortion. In Sec. 4.4, we saw that this requires the filter amplitude response to be constant and the phase response to be a linear function of ω over the passband.

The filters discussed so far have stressed the constancy of the amplitude response. The linearity of the phase response has been ignored. As we saw earlier, the human ear is sensitive to amplitude distortion but somewhat insensitive to phase distortion. For this reason, audio filters are designed primarily for constant amplitude response, and the phase response is only a secondary consideration.

We also saw earlier that the human eye is sensitive to phase distortion and relatively insensitive to amplitude distortion. Therefore, in video applications we cannot ignore phase distortion. In pulse communication, both amplitude and phase distortion are important for correct information transmission. Thus, in practice, we also need to design filters primarily for phase linearity in video applications. In pulse communication applications, it is important to have filters with a constant amplitude response and a linear phase response. We shall briefly discuss some aspects and approaches to the design of such filters. More discussion appears in the literature (see [2]).

We showed [see Eq. (4.40)] that the group delay t_g resulting from the transmission of a signal through a filter is the negative of the slope of the filter phase response $\angle H(j\omega)$; that is,

$$t_g(\omega) = -\frac{d}{d\omega}\angle H(j\omega)$$

If the slope of $\angle H(j\omega)$ is constant over the desired band (i.e., if $\angle H(j\omega)$ is linear with ω), all the components are delayed by the same time interval t_d (i.e., $t_g(\omega) = t_d$). In this case, the output is a replica of the input, assuming that all components are attenuated equally; that is, $|H(j\omega)|$ = constant over the passband.

If the slope of the phase response is not constant, group delay t_g varies with frequency. This variation means that different frequency components undergo different amounts of time delay, and consequently, the output waveform will not be a replica of the input waveform even if the amplitude response is constant over the passband. A good way of judging phase linearity is to plot t_g as a function of frequency. For a distortionless system, t_g (the negative slope of $\angle H(j\omega)$) should be constant over the band of interest. This is in addition to the requirement of constancy of the amplitude response.

Generally speaking, the two requirements of distortionless transmission conflict. The more we approach the ideal amplitude response, the further we deviate from the ideal phase response. The sharper the cutoff characteristic (the smaller the transition band), the more nonlinear is the phase response near the transition band. We can verify this fact from Fig. 7.45, which shows the group delay characteristics of various order Butterworth and Chebyshev filters. The Chebyshev filter, which has a sharper cutoff than that of the Butterworth, shows considerably more variation in group delay across frequency as compared to that of the Butterworth.

For applications where phase linearity is also important, there are two possible approaches:

1. If t_g = constant (phase linearity) is the primary requirement, we design a filter for which t_g is maximally flat around $\omega = 0$ and accept the resulting amplitude response, which may

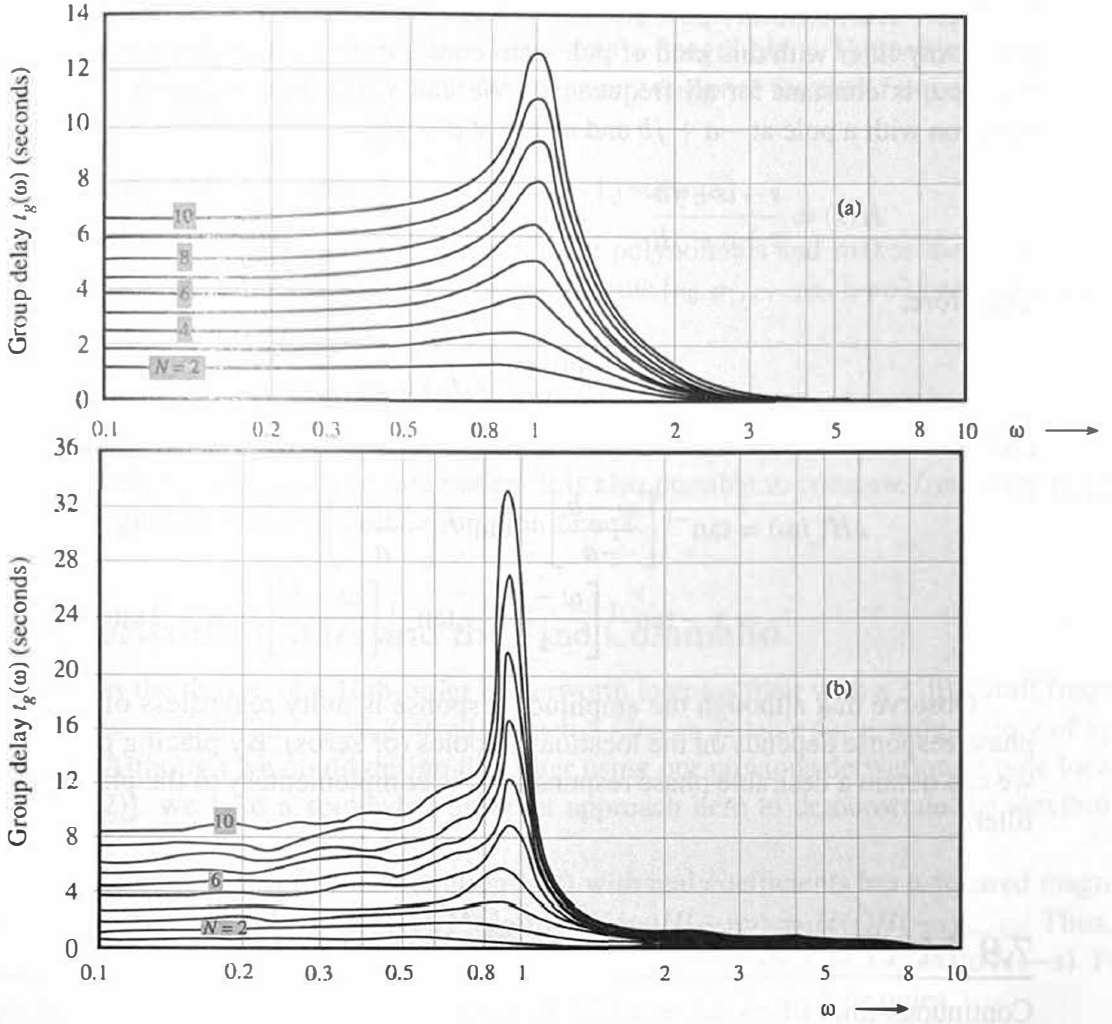

Figure 7.45 Group delay characteristics of Butterworth and Chebyshev filters.

not be so flat or have a sharp cutoff characteristic. Contrast this with the Butterworth filter, which is designed to yield the maximally flat amplitude response at $\omega = 0$ without any attention to the phase response. A family of filters that yields a maximally flat t_g goes under the name *Bessel–Thomson* filters, which use an Nth-order Bessel polynomial in the denominator of an Nth-order $H(s)$.

2. If both amplitude and phase response are important, we start with a filter to satisfy the amplitude response specifications, disregarding the phase response specifications. We cascade this filter with another filter, an *equalizer*, whose amplitude response is flat for all frequencies (*the allpass filter*) and whose t_g characteristic is complementary to that of the main filter in such a way that their composite phase characteristic is approximately linear. The cascade thus has a linear phase and the amplitude response of the main filter (as required).

Allpass Filters

An allpass filter has an equal number of poles and zeros. All the poles are in the LHP (left half-plane) for stability. All the zeros are mirror images of the poles about the imaginary axis.

In other words, for every pole at $-a+jb$, there is a zero at $a+jb$. Thus, all the zeros are in the RHP. Any filter with this kind of pole-zero configuration is an allpass filter; that is, its amplitude response is constant for all frequencies. We can verify this assertion by considering a transfer function with a pole at $-a+jb$ and a zero at $a+jb$:

$$H(s)=\frac{s-a-jb}{s+a-jb} \qquad \text{and} \qquad H(j\omega)=\frac{j\omega-a-jb}{j\omega+a-jb}=\frac{-a+j(\omega-b)}{a+j(\omega-b)}$$

Therefore,

$$|H(j\omega)|=\frac{\sqrt{(-a)^2+(\omega-b)^2}}{\sqrt{a^2+(\omega-b)^2}}=1$$

and

$$\begin{aligned}\angle H(j\omega)&=\tan^{-1}\left[\frac{\omega-b}{-a}\right]-\tan^{-1}\left[\frac{\omega-b}{a}\right]\\&=\pi-\tan^{-1}\left[\frac{\omega-b}{a}\right]-\tan^{-1}\left[\frac{\omega-b}{a}\right]=\pi-2\tan^{-1}\left[\frac{\omega-b}{a}\right]\end{aligned}$$

Observe that although the amplitude response is unity regardless of pole-zero locations, the phase response depends on the locations of poles (or zeros). By placing poles in proper locations, we can obtain a desirable phase response that is complementary to the phase response of the main filter.

7.9 MATLAB: CONTINUOUS-TIME FILTERS

Continuous-time filters are essential to many if not most engineering systems, and MATLAB is an excellent assistant for filter design and analysis. In this section, we build on previous examples to demonstrate MATLAB's ability to assist in the design and analysis of continuous-time filters, particularly those with relatively high order or complexity. To begin, we briefly review using MATLAB for frequency response and polynomial evaluation. Then, we investigate using MATLAB for a non-trivial Butterworth filter design.

7.9.1 Frequency Response and Polynomial Evaluation

Magnitude response plots help assess a filter's performance and quality, and MATLAB makes plotting such responses simple. A realizable LTIC system often has a rational transfer function [see Eq. (2.2)] that is represented in the s domain as

$$H(s)=\frac{Y(s)}{X(s)}=\frac{B(s)}{A(s)}=\frac{\sum_{k=0}^{M} b_{k+N-M}s^{M-k}}{\sum_{k=0}^{N} a_k s^{N-k}}$$

Frequency response $H(j\omega)$ is obtained by letting $s=j\omega$, where frequency ω is in radians per second.

MATLAB is ideally suited to evaluate frequency response functions. Defining a length-$(N+1)$ coefficient vector $\mathbf{A} = [a_0, a_1, \ldots, a_N]$ and a length-$(M+1)$ coefficient vector $\mathbf{B} = [b_{N-M}, b_{N-M+1}, \ldots, b_N]$, we can compute the frequency response for each frequency in the vector `omega` as

```
>> H = polyval(B,1j*omega)./polyval(A,1j*omega);
```

The function `polyval` efficiently evaluates simple polynomials and makes the program nearly trivial. For example, when `A` is the vector of coefficients $[a_0, a_1, \ldots, a_N]$, `polyval (A,j*omega)` computes

$$\sum_{k=0}^{N} a_k (j\omega)^{N-k}$$

for each value of the frequency vector `omega`. It is also possible to compute frequency responses by using the signal-processing toolbox function `freqs`.

7.9.2 Butterworth Filters and the `Find` Command

Let us consider the design of a 10th-order Butterworth lowpass filter with a 3 dB cutoff frequency of 3 kHz, or $\omega_c = 3000(2\pi) \approx 18{,}850$ rad/s. Such a filter is suitable for a wide variety of speech applications. Although we could design this filter using our previous derivation of pole locations [see Eq. (7.22)], we take a somewhat different approach here to demonstrate the flexibility of MATLAB.

To begin, notice that a transfer function $H(s)$ with real coefficients has a squared magnitude response given by $|H(j\omega)|^2 = H(j\omega)H^*(j\omega) = H(j\omega)H(-j\omega) = H(s)H(-s)|_{s=j\omega}$. Thus, half the poles of $|H(j\omega)|^2$ correspond to the filter $H(s)$, and the other half correspond to $H(-s)$. Filters that are both stable and causal require $H(s)$ to include only left-half-plane poles.

The squared magnitude response of a Butterworth filter is [see Eq. (7.19)]

$$|H(j\omega)| = \frac{1}{\sqrt{1 + \left(\frac{\omega}{\omega_c}\right)^{2N}}}$$

Notice that the denominator is a polynomial that describes the $2N$ roots of unity. As discussed in Sec. B.7, the roots of -1 must lie equally spaced on a circle centered at the origin. Thus, the $2N$ poles of $|H(j\omega)|^2$ naturally lie equally spaced on a circle of radius ω_c centered at the origin. Figure 7.46 displays the 20 poles corresponding to the case $N = 10$ and $\omega_c = 3000(2\pi)$ rad/s. An Nth-order Butterworth filter that is both causal and stable uses the N left-half-plane poles of $|H(j\omega)|^2$.

```
>> omegac = 3000*2*pi; N = 10;
>> denroots = roots([(1j*omegac)^(-2*N),zeros(1,2*N-1),1]);
>> plot(real(denroots),imag(denroots),'xk'); axis equal
>> xlabel('\sigma'); ylabel('\omega'); grid on
```

The `find` command is a powerful and useful function that returns the indices of a vector's nonzero elements. Combined with relational operators, the `find` command allows us to extract the 10 left-half-plane roots that correspond to the poles of our Butterworth filter.

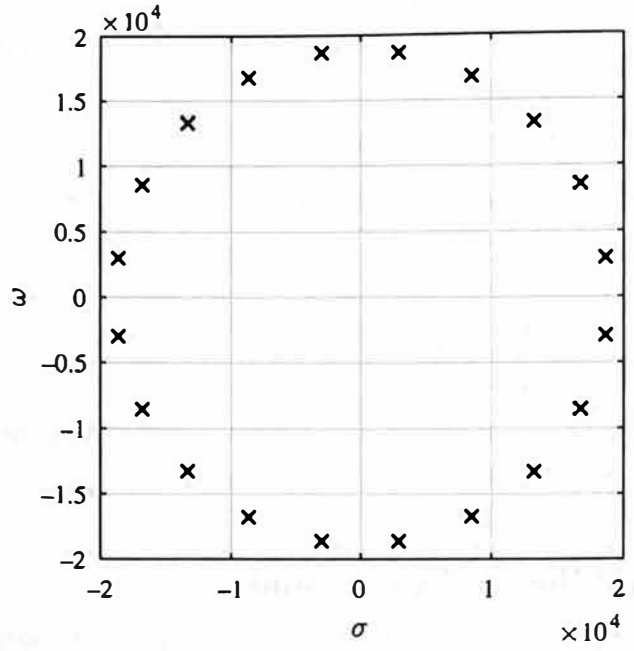

Figure 7.46 Roots of $|H(j\omega)|^2$ for $N = 10$ and $\omega_c = 3000(2\pi)$.

```
>> poles = poles(find(real(denroots)<0));
```

To compute the magnitude response, these roots are converted to coefficient vector A. Then, the `polyval` command is used. The resulting magnitude response plot is shown in Fig. 7.47. The Butterworth response closely approximates the brick-wall function and provides excellent filter characteristics: flat passband, rapid transition to the stopband, and excellent stopband attenuation (>40 dB at 5 kHz).

```
>> A = poly(poles); A = A/A(end); B = 1;
>> f = linspace(0,6000,501); omega = 2*pi*f;
>> Hmag = abs(polyval(B,1j*omega)./polyval(A,1j*omega));
>> plot(f,Hmag,'k-',f,abs(f*2*pi)<=omegac,'k--');
>> axis([0 6000 -0.05 1.05]); xlabel('f [Hz]'); ylabel('|H(j2\pi f)|');
```

7.9.3 Using Cascaded Second-Order Sections for Butterworth Filter Realization

For our Butterworth filter to be useful, we must be able to implement it. Since the transfer function $H(s)$ is known, the differential equation is also known. Therefore, it is possible to try to implement the design by using op-amp integrators, summers, and scalar multipliers. Unfortunately, this approach will not work well. To understand why, consider the denominator coefficients $a_0 = 1.766 \times 10^{-43}$ and $a_{10} = 1$. The smallest coefficient is 43 orders of magnitude smaller than the largest coefficient! It is practically impossible to accurately realize such a broad range in scale values. To understand this, skeptics should try to find realistic resistors such that

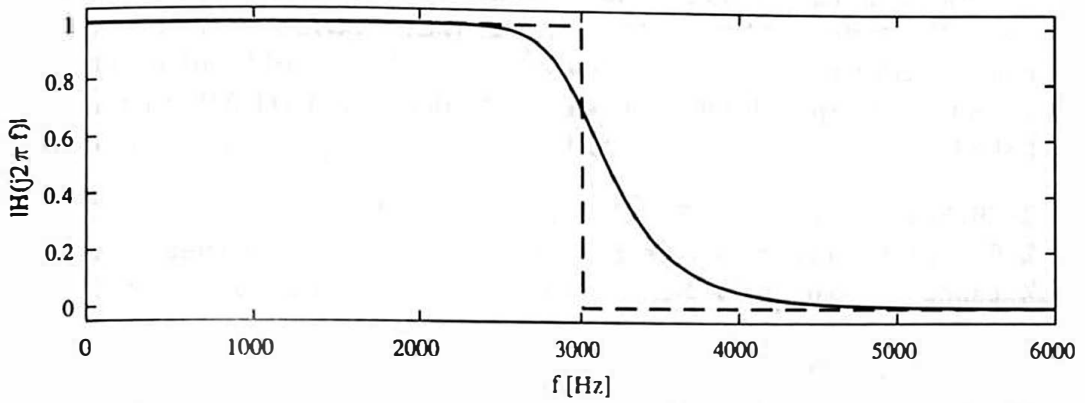

Figure 7.47 Magnitude response $|H(j2\pi f)|$ of a 10th-order Butterworth filter.

$R_f/R = 1.766 \times 10^{-43}$. Additionally, small component variations will cause large changes in actual pole location.

A better approach is to cascade five second-order sections, where each section implements one complex conjugate pair of poles. By pairing poles in complex conjugate pairs, each of the resulting second-order sections has real coefficients. With this approach, the smallest coefficients are only about nine orders of magnitude smaller than the largest coefficients. Furthermore, pole placement is typically less sensitive to component variations for cascaded structures.

The Sallen–Key circuit shown in Fig. 7.48 provides a good way to realize a pair of complex-conjugate poles.† The transfer function of this circuit is

$$H_{SK}(s) = \frac{\dfrac{1}{R_1R_2C_1C_2}}{s^2 + \left(\dfrac{1}{R_1C_1} + \dfrac{1}{R_2C_1}\right)s + \dfrac{1}{R_1R_2C_1C_2}} = \frac{\omega_0^2}{s^2 + \left(\dfrac{\omega_0}{Q}\right)s + \omega_0^2}$$

Geometrically, ω_0 is the distance from the origin to the poles and $Q = 1/2\cos\psi$, where ψ is the angle between the negative real axis and the pole. Termed the "quality factor" of a circuit, Q provides a measure of the peakedness of the response. High-Q filters have poles close to the ω axis, which boost the magnitude response near those frequencies.

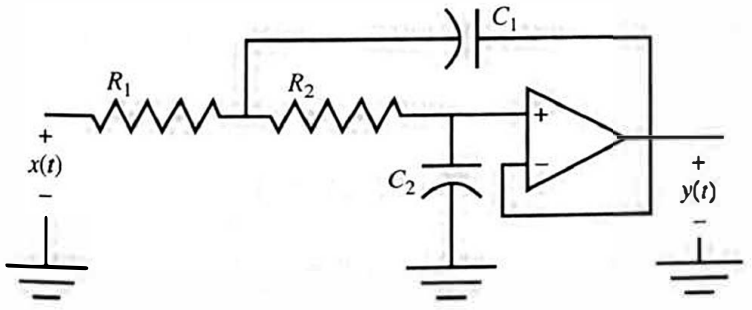

Figure 7.48 Sallen–Key filter stage.

† A more general version of the Sallen–Key circuit has a resistor R_a from the negative terminal to ground and a resistor R_b between the negative terminal and the output. In Fig. 7.48, $R_a = \infty$ and $R_b = 0$.

Although many ways exist to determine suitable component values, a simple method is to assign R_1 a realistic value and then let $R_2 = R_1$, $C_1 = 2Q/\omega_0 R_1$, and $C_2 = 1/2Q\omega_0 R_2$. Butterworth poles are a distance ω_c from the origin, so $\omega_0 = \omega_c$. For our 10th-order Butterworth filter, the angles ψ are regularly spaced at 9, 27, 45, 63, and 81 degrees. MATLAB program CH7MP1 automates the task of computing component values and magnitude responses for each stage.

```
% CH7MP1.m : Chapter 7, MATLAB Program 1
% Script M-file computes Sallen-Key component values and magnitude
% responses for each of the five cascaded second-order filter sections.

omega0 = 3000*2*pi; f = linspace(0,6000,501);
psi = [9 27 45 63 81]*pi/180; % Butterworth pole angles
Hmag_SK = zeros(5,501); % Pre-allocate array for magnitude responses
for stage = 1:5,
    Q = 1/(2*cos(psi(stage))); % Compute Q for current stage
    % Compute and display filter components to the screen:
    disp(['Stage ',num2str(stage),...
            ' (Q = ',num2str(Q),...
            '):  R1 = R2 = ',num2str(56000),...
            ', C1 = ',num2str(2*Q/(omega0*56000)),...
            ', C2 = ',num2str(1/(2*Q*omega0*56000))]);
    B = omega0^2; A = [1 omega0/Q omega0^2];
    Hmag_SK(stage,:) = abs(polyval(B,1j*2*pi*f)./polyval(A,1j*2*pi*f));
end
plot(f,Hmag_SK,'k',f,prod(Hmag_SK),'k:')
xlabel('f [Hz]'); ylabel('Magnitude Response')
```

The disp command displays a character string to the screen. Character strings must be enclosed in single quotation marks. The num2str command converts numbers to character strings and facilitates the formatted display of information. The prod command multiplies along the columns of a matrix; it computes the total magnitude response as the product of the magnitude responses of the five stages.

Executing the program produces the following output:

```
>>  CH7MP1
    Stage 1 (Q = 0.50623):  R1 = R2 = 56000, C1 = 9.5916e-10,
    C2 = 9.3569e-10
    Stage 2 (Q = 0.56116):  R1 = R2 = 56000, C1 = 1.0632e-09,
    C2 = 8.441e-10
    Stage 3 (Q = 0.70711):  R1 = R2 = 56000, C1 = 1.3398e-09,
    C2 = 6.6988e-10
    Stage 4 (Q = 1.1013):  R1 = R2 = 56000, C1 = 2.0867e-09,
    C2 = 4.3009e-10
    Stage 5 (Q = 3.1962):  R1 = R2 = 56000, C1 = 6.0559e-09, C2 = 1.482e-10
```

Since all the component values are practical, this filter is possible to implement. Figure 7.49 displays the magnitude responses for all five stages (solid lines). The total response (dotted line)

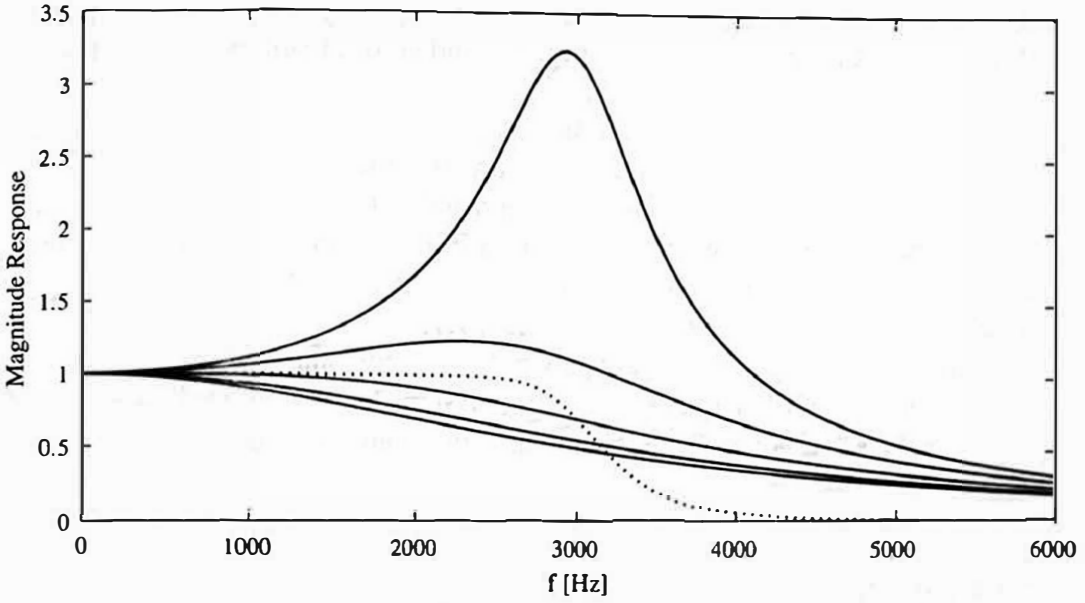

Figure 7.49 Magnitude responses for Sallen–Key filter stages.

confirms a 10th-order Butterworth response. Stage 5, which has the largest Q and implements the pair of conjugate poles nearest the ω axis, is the most peaked response. Stage 1, which has the smallest Q and implements the pair of conjugate poles furthest from the ω axis, is the least peaked response. In practice, it is best to order high-Q stages last; this reduces the risk that the high gains will saturate the filter hardware.

7.10 SUMMARY

The response of an LTIC system with transfer function $H(s)$ to an everlasting sinusoid of frequency ω is also an everlasting sinusoid of the same frequency. The output amplitude is $|H(j\omega)|$ times the input amplitude, and the output sinusoid is shifted in phase with respect to the input sinusoid by $\angle H(j\omega)$ radians. The plot of $|H(j\omega)|$ versus ω indicates the amplitude gain of sinusoids of various frequencies and is called the *amplitude response* of the system. The plot of $\angle H(j\omega)$ versus ω indicates the phase shift of sinusoids of various frequencies and is called the *phase response*.

Plotting of frequency response is remarkably simplified by using logarithmic units for amplitude as well as frequency. Such plots are known as Bode plots. The use of logarithmic units makes it possible to add (rather than multiply) the amplitude response of four basic types of factors that occur in transfer functions: (1) a constant, (2) a pole or a zero at the origin, (3) a first-order pole or zero, and (4) complex-conjugate poles or zeros. For phase plots, we use linear units for phase and logarithmic units for the frequency. Like the amplitude components, the phases corresponding to the basic types of factors mentioned above add. The asymptotic properties of the amplitude and phase responses allow their plotting with remarkable ease even for transfer functions of high orders.

The frequency response of a system is determined by the locations in the complex plane of the poles and zeros of its transfer function. We can design frequency selective filters by proper

placement of its transfer function poles and zeros. Placing a pole (a zero) near a frequency $j\omega_0$ in the complex plane enhances (suppresses) the frequency response at the frequency $\omega = \omega_0$. With this concept, a proper combination of poles and zeros at suitable locations can yield desired filter characteristics.

Two families of analog filters are considered: Butterworth and Chebyshev. A Butterworth filter has a maximally flat amplitude response over the passband. A Chebyshev amplitude response has ripples in the passband and is monotonic in the stopband. Further, the behavior of a Chebyshev filter in the stopband is superior to that of a Butterworth filter. The design procedure for lowpass filters can be readily applied to highpass, bandpass, and bandstop filters by using appropriate frequency transformations discussed in Sec. 7.7.

Allpass filters have a constant gain but a variable phase with respect to frequency. Therefore, placing an allpass filter in cascade with a system leaves its amplitude response unchanged, but alters its phase response. Thus, an allpass filter can be used to modify the phase response of a system.

REFERENCES

1. Truxal, J. G., *The Age of Electronic Messages,* McGraw-Hill, New York, 1990.
2. Van Valkenburg, M. E., *Analog Filter Design,* Holt, Rinehart, and Winston, New York, 1982.
3. Chen, Wai-Kai, *Passive and Active Filters,* Wiley, New York, 1986.
4. Christian E., and Eisenmann, E., *Filter Design Tables and Graphs,* Transmission Networks International, Inc., Knightdale, N.C., 1977.

PROBLEMS

7.1-1 Suppose an engineer builds a controllable, observable LTIC system with transfer function $H(s) = \frac{s^2+4}{2s^2+4s+4}$.

(a) By direct calculation, compute the magnitude response at frequencies $\omega = 0$, 1, 2, 3, 5, 10, and ∞. Use these calculations to roughly sketch the magnitude response over $0 \leq \omega \leq 10$.

(b) To test the system, the engineer connects a signal generator to the system in hopes to measure the magnitude response using a standard oscilloscope. What type of signal should the engineer input into the system to make the measurements? How should the engineer make the measurements? Provide sufficient detail to fully justify your answers.

(c) Suppose the engineer accidentally constructs the system $H^{-1}(s) = \frac{1}{H(s)} = \frac{2s^2+4s+4}{s^2+4}$. What impact will this mistake have on his or her tests?

7.1-2 For an LTIC system described by the transfer function

$$H(s) = \frac{s+2}{s^2+5s+4}$$

find the response to the following everlasting sinusoidal inputs:

(a) $5\cos(2t+30°)$

(b) $10\sin(2t+45°)$

(c) $10\cos(3t+40°)$

Observe that these are everlasting sinusoids.

7.1-3 For an LTIC system described by the transfer function

$$H(s) = \frac{s+3}{(s+2)^2}$$

find the steady-state system response to the following inputs:

(a) $10u(t)$
(b) $\cos(2t+60°)u(t)$
(c) $\sin(3t-45°)u(t)$
(d) $e^{j3t}u(t)$

7.1-4 For an allpass filter specified by the transfer function

$$H(s)=\frac{-(s-10)}{s+10}$$

find the system response to the following (everlasting) inputs:
(a) $e^{j\omega t}$
(b) $\cos(\omega t+\theta)$
(c) $\cos t$
(d) $\sin 2t$
(e) $\cos 10t$
(f) $\cos 100t$
Comment on the filter response.

7.1-5 The pole-zero plot of a second-order system $H(s)$ is shown in Fig. P7.1-5. The dc response of this system is -1, $H(j0)=-1$.
(a) Letting $H(s)=k(s^2+b_1s+b_2)/(s^2+a_1s+a_2)$, determine the constants k, b_1, b_2, a_1, and a_2.
(b) What is the output $y(t)$ of this system in response to the input $x(t)=4+\cos(t/2+\pi/3)$?

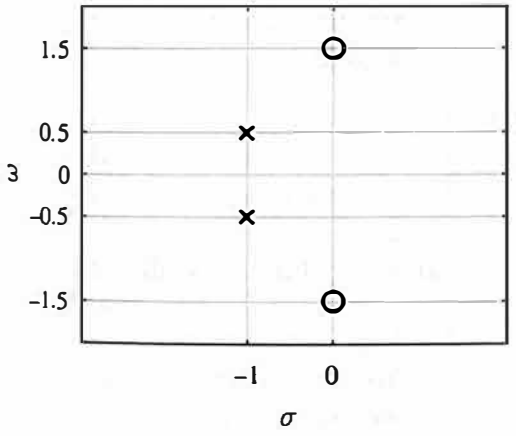

Figure P7.1-5

7.1-6 Consider a CT system described by $(D+1)(D+2)\{y(t)\}=x(t-1)$. Notice that this differential equation is in terms of $x(t-1)$, not $x(t)$!
(a) Determine the output $y(t)$ given input $x(t)=1$.
(b) Determine the output $y(t)$ given input $x(t)=\cos(t)$.

7.1-7 An LTIC system has transfer function $H(s)=\frac{4s}{s^2+2s+37}=\frac{4s}{(s+1+6j)(s+1-6j)}$. Determine the steady-state output in response to input $x(t)=\frac{1}{3}e^{j(6t+\pi/3)}u(6t+\pi/3)$.

7.2-1 Suppose a real first-order lowpass system $H(s)$ has unity gain in the passband, one finite pole at $s=-2$, and one finite zero at an unspecified location.
(a) Determine the location of the system zero so that the filter achieves 40 dB of stopband attenuation. Sketch the corresponding straight-line Bode approximation of the system magnitude response.
(b) Determine the location of the system zero so that the filter achieves 30 dB of stopband attenuation. Sketch the corresponding straight-line Bode approximation of the system magnitude response.

7.2-2 Repeat Prob. 7.2-1 for a highpass rather than a lowpass system.

7.2-3 Repeat Prob. 7.2-1 for a second-order system that has a pair of repeated poles and a pair of repeated zeros.

7.2-4 Sketch Bode plots for the following transfer functions:
(a) $\dfrac{s(s+100)}{(s+2)(s+20)}$
(b) $\dfrac{(s+10)(s+20)}{s^2(s+100)}$
(c) $\dfrac{(s+10)(s+200)}{(s+20)^2(s+1000)}$

7.2-5 Repeat Prob. 7.2-4 for
(a) $\dfrac{s^2}{(s+1)(s^2+4s+16)}$
(b) $\dfrac{s}{(s+1)(s^2+14.14s+100)}$
(c) $\dfrac{(s+10)}{s(s^2+14.14s+100)}$

7.2-6 Using the lowest order possible, determine a system function $H(s)$ with real-valued roots that matches the frequency response in Fig. P7.2-6. Verify your answer with MATLAB.

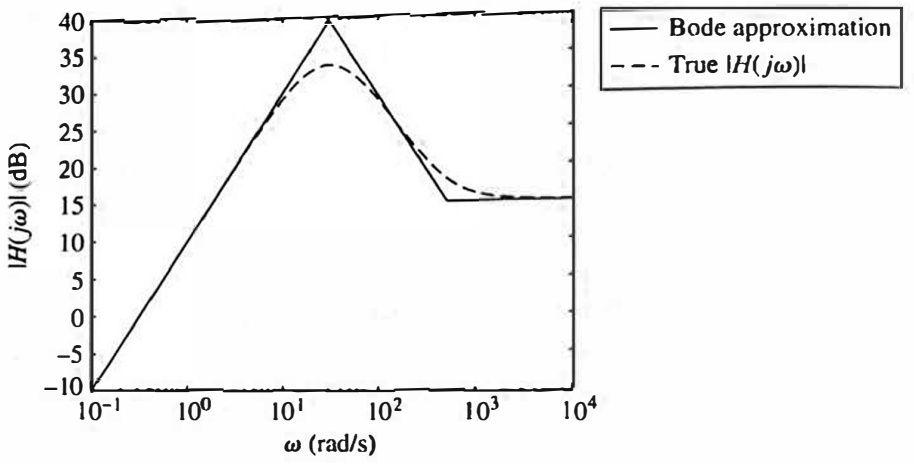

Figure P7.2-6

7.2-7 A graduate student recently implemented an analog phase lock loop (PLL) as part of his thesis. His PLL consists of four basic components: a phase/frequency detector, a charge pump, a loop filter, and a voltage-controlled oscillator. This problem considers only the loop filter, which is shown in Fig. P7.2-7a. The loop filter input is the current $x(t)$, and the output is the voltage $y(t)$.

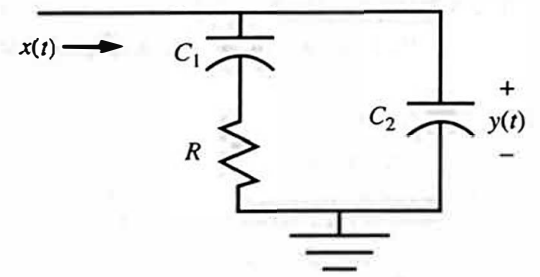

(a)

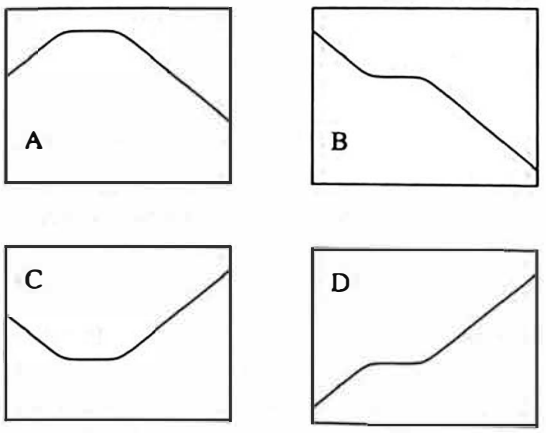

(b)

Figure P7.2-7

(a) Derive the loop filter's transfer function $H(s)$. Express $H(s)$ in standard form.

(b) Figure P7.2-7b provides four possible frequency response plots, labeled A through D. Each log-log plot is drawn to the same scale, and line slopes are either 20 dB/decade, 0 dB/decade, or −20 dB/decade. Clearly identify which plot(s), if any, could represent the loop filter.

(c) Holding the other components constant, what is the general effect of increasing the resistance R on the magnitude response for low-frequency inputs?

(d) Holding the other components constant, what is the general effect of increasing the resistance R on the magnitude response for high-frequency inputs?

7.3-1 Feedback can be used to increase (or decrease) the system bandwidth. Consider the system in Fig. P7.3-1a with transfer function $G(s) = \omega_c/(s+\omega_c)$.

(a) Show that the 3 dB bandwidth of this system is ω_c and the dc gain is unity; that is, $|H(j0)| = 1$.

(b) To increase the bandwidth of this system, we use negative feedback with $H(s) = 9$, as depicted in Fig. P7.3-1b. Show that the 3 dB bandwidth of this system is $10\omega_c$. What is the dc gain?

(c) To decrease the bandwidth of this system, we use positive feedback with $H(s) = -0.9$, as illustrated in Fig. P7.3-1c. Show that the 3 dB bandwidth of this system is $\omega_c/10$. What is the dc gain?

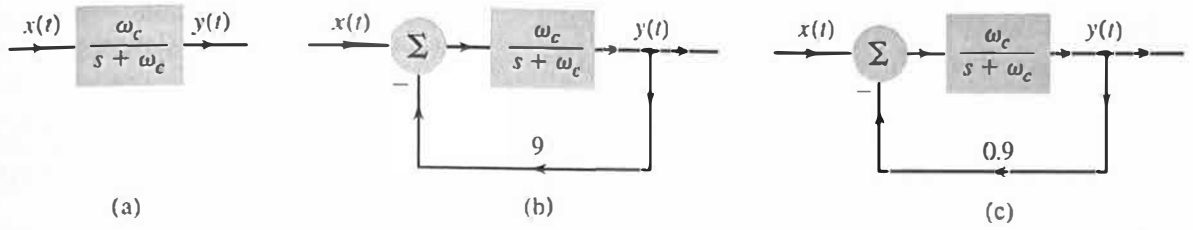

Figure P7.3-1

(d) The system gain at dc times its 3 dB bandwidth is the *gain-bandwidth product* of a system. Show that this product is the same for all three systems in Fig. P7.3-1. This result shows that if we increase the bandwidth, the gain decreases and vice versa.

7.4-1 A causal LTIC system $H(s) = \frac{2(s-4j)(s+4j)}{(s+1+2j)(s+1-2j)}$ has input $x(t) = -1 + 2\cos(2t) - 3\sin(4t + \pi/3) + 4\cos(10t)$. Below, perform accurate calculations at $\omega = 0, \pm 2, \pm 4$, and ± 10.

(a) Using the graphical method of Sec. 7.4.1, accurately sketch the magnitude response $|H(j\omega)|$ over $-10 \leq \omega \leq 10$.

(b) Using the graphical method of Sec. 7.4.1, accurately sketch the phase response $\angle H(j\omega)$ over $-10 \leq \omega \leq 10$.

(c) Approximate the system output $y(t)$ in response to the input $x(t)$.

7.4-2 The pole-zero plot of a second-order system $H(s)$ is shown in Fig. P7.4-2. The dc response of this system is -2, $H(j0) = -2$.

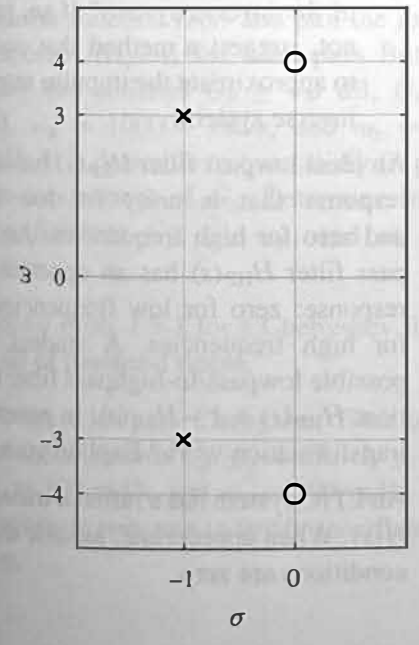

Figure P7.4-2

(a) Letting $H(s) = k\frac{s^2+b_1 s+b_2}{s^2+a_1 s+a_2}$, determine the constants k, b_1, b_2, a_1, and a_2.

(b) Using the graphical method of Sec. 7.4.1, hand-sketch the magnitude response $|H(j\omega)|$ over $-10 \leq \omega \leq 10$. Verify your sketch with MATLAB.

(c) Using the graphical method of Sec. 7.4.1, hand-sketch the phase response $\angle H(j\omega)$ over $-10 \leq \omega \leq 10$. Verify your sketch with MATLAB.

(d) What is the output $y(t)$ in response to input $x(t) = -3 + \cos(3t + \pi/3) - \sin(4t - \pi/8)$?

7.4-3 Using the graphical method of Sec. 7.4.1, draw a rough sketch of the amplitude and phase responses of an LTIC system described by the transfer function

$$H(s) = \frac{s^2 - 2s + 50}{s^2 + 2s + 50} = \frac{(s-1-j7)(s-1+j7)}{(s+1-j7)(s+1+j7)}$$

What kind of filter is this?

7.4-4 Using the graphical method of Sec. 7.4.1, draw a rough sketch of the amplitude and phase responses of LTIC systems whose pole-zero plots are shown in Fig. P7.4-4.

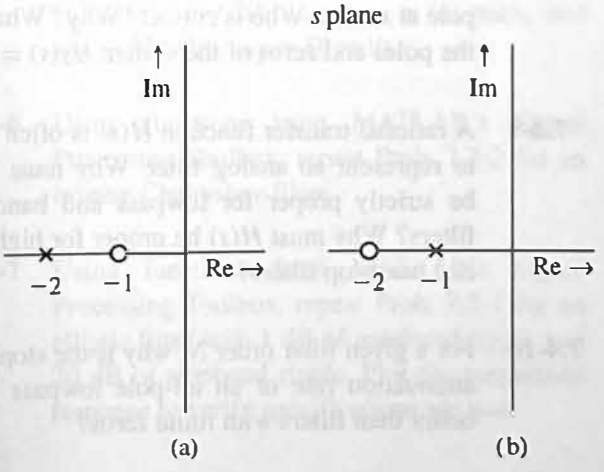

Figure P7.4-4

7.4-5 A causal LTIC system $H(s) = \frac{(s-3j)(s+3j)}{3(s+2+j)(s+2-j)}$ has input $x(t) = \cos(t) + \sin(3t + \pi/3) + \cos(100t)$.

(a) Using the graphical method of Sec. 7.4.1, sketch the magnitude response $|H(j\omega)|$ over $-10 \leq \omega \leq 10$.

(b) Determine the system output $y(t)$ in response to the input $x(t)$.

(c) Suppose we create a second causal system with transfer function $H_2(s) = H(-s)$. Sketch this system's pole/zero plot. What is the response $y_2(t)$ of system $H_2(s)$ to input $x(t)$?

7.4-6 Design a second-order bandpass filter with center frequency $\omega = 10$. The gain should be zero at $\omega = 0$ and at $\omega = \infty$. Select poles at $-a \pm j10$. Leave your answer in terms of a. Explain the influence of a on the frequency response.

7.4-7 The LTIC system described by $H(s) = (s-1)/(s+1)$ has unity magnitude response $|H(j\omega)| = 1$. Positive Pat claims that the output $y(t)$ of this system is equal to the input $x(t)$, since the system is allpass. Cynical Cynthia doesn't think so. "This is *signals and systems* class," she complains. "It *has* to be more complicated!" Who is correct, Pat or Cynthia? Justify your answer.

7.4-8 Two students Amy and Jeff disagree about an analog system function given by $H_1(s) = s$. Sensible Jeff claims the system has a zero at $s = 0$. Rebellious Amy, however, notes that the system function can be rewritten as $H_1(s) = 1/s^{-1}$ and claims that this implies a system pole at $s = \infty$. Who is correct? Why? What are the poles and zeros of the system $H_2(s) = 1/s$?

7.4-9 A rational transfer function $H(s)$ is often used to represent an analog filter. Why must $H(s)$ be strictly proper for lowpass and bandpass filters? Why must $H(s)$ be proper for highpass and bandstop filters?

7.4-10 For a given filter order N, why is the stopband attenuation rate of an all-pole lowpass filter better than filters with finite zeros?

7.4-11 Is it possible, with real coefficients $([k, b_1, b_2, a_1, a_2] \in \mathcal{R})$, for a system

$$H(s) = k\frac{s^2 + b_1 s + b_2}{s^2 + a_1 s + a_2}$$

to function as a lowpass filter? Explain your answer.

7.4-12 Nick recently built a simple second-order Butterworth lowpass filter for his home stereo. Although the system performs fairly well, Nick is an overachiever and hopes to improve the system performance. Unfortunately, Nick is lazy and doesn't want to design another filter. Thinking "Twice the filtering gives twice the performance," he suggests filtering the audio signal not once but twice with a cascade of two identical filters. His overworked, underpaid signals professor is skeptical and states, "If you are using *identical* filters, it makes no difference whether you filter once or twice!" Who is correct? Why?

7.4-13 An LTIC system impulse response is given by $h(t) = u(t) - u(t-1)$.

(a) Determine the transfer function $H(s)$. Using $H(s)$, determine and plot the magnitude response $|H(j\omega)|$. Which type of filter most accurately describes the behavior of this system: lowpass, highpass, bandpass, or bandstop?

(b) What are the poles and zeros of $H(s)$? Explain your answer.

(c) Can you determine the impulse response of the inverse system? If so, provide it. If not, suggest a method that could be used to approximate the impulse response of the inverse system.

7.4-14 An ideal lowpass filter $H_{LP}(s)$ has a magnitude response that is unity for low frequencies and zero for high frequencies. An ideal highpass filter $H_{HP}(s)$ has an opposite magnitude response: zero for low frequencies and unity for high frequencies. A student suggests a possible lowpass-to-highpass filter transformation: $H_{HP}(s) = 1 - H_{LP}(s)$. In general, will this transformation work? Explain your answer.

7.4-15 An LTIC system has a rational transfer function $H(s)$. When appropriate, assume that all initial conditions are zero.

(a) Is is possible for this system to output $y(t) = \sin(100\pi t)u(t)$ in response to an input $x(t) = \cos(100\pi t)u(t)$? Explain.
(b) Is is possible for this system to output $y(t) = \sin(100\pi t)u(t)$ in response to an input $x(t) = \sin(50\pi t)u(t)$? Explain.
(c) Is is possible for this system to output $y(t) = \sin(100\pi t)$ in response to an input $x(t) = \cos(100\pi t)$? Explain.
(d) Is is possible for this system to output $y(t) = \sin(100\pi t)$ in response to an input $x(t) = \sin(50\pi t)$? Explain.

7.5-1 Determine the transfer function $H(s)$ and plot the magnitude response $|H(j\omega)|$ for a third-order lowpass Butterworth filter if the 3 dB cutoff frequency $\omega_c = 100$.

7.5-2 Prove Eq. (7.28), the equation to determine Butterworth filter order.

7.5-3 Determine the lowest order N and the cutoff frequency ω_c of a lowpass Butterworth filter that satisfies the following specifications. Find both extreme values of ω_c, the one that oversatisfies the passband specifications and the one that oversatisfies the stopband specifications.
(a) $\hat{G}_p \geq -0.5$ dB, $\hat{G}_s \leq -20$ dB, $\omega_p = 100$ rad/s, and $\omega_s = 200$ rad/s.
(b) $G_p \geq 0.9885$, $G_s \leq 10^{-3}$, $\omega_p = 1000$ rad/s, and $\omega_s = 2000$ rad/s.
(c) The gain at $3\omega_c$ is required to be no greater than -50 dB.

7.5-4 Using the lowest order possible, find the transfer function $H(s)$ and plot the magnitude response $|H(j\omega)|$ for a lowpass Butterworth filter that satisfies $\hat{G}_p \geq -3$ dB, $\hat{G}_s \leq -14$ dB, $\omega_p = 100000$ rad/s, and $\omega_s = 150000$ rad/s. It is desirable to oversatisfy (if possible) the requirement of $\hat{G}_s$. Determine the actual specifications $\hat{G}_p$, $\hat{G}_s$, ω_p, and ω_s of your design.

7.6-1 Repeat Prob. 7.5-1 for a Chebyshev filter with 1 dB of passband ripple.

7.6-2 Design a lowpass Chebyshev filter to satisfy the specifications $\hat{G}_p \geq -1$ dB, $\hat{G}_s \leq -22$ dB, $\omega_p = 100$ rad/s, and $\omega_s = 200$ rad/s. Plot the magnitude response to verify specifications are met.

7.6-3 Design a lowpass Chebyshev filter to satisfy the specifications $\hat{G}_p \geq -2$ dB, $\hat{G}_s \leq -25$ dB, $\omega_p = 10$ rad/s, and $\omega_s = 15$ rad/s. Plot the magnitude response to verify specifications are met.

7.6-4 Design a lowpass Chebyshev filter with 1 dB of passband ripple whose gain drops to -50 dB at $3\omega_c$, where ω_c is the 3 dB cutoff frequency. Plot the magnitude response to verify specifications are met.

7.7-1 Find the transfer function $H(s)$ and plot the magnitude response for a highpass Butterworth filter that satisfies $\hat{G}_s \leq -20$ dB, $\hat{G}_p \geq -1$ dB, $\omega_s = 10$, and $\omega_p = 20$.

7.7-2 Find the transfer function $H(s)$ and plot the magnitude response for a highpass Chebyshev filter that satisfies $\hat{G}_s \leq -22$ dB, $\hat{G}_p \geq -1$ dB, $\omega_s = 10$, and $\omega_p = 20$.

7.7-3 Find the transfer function $H(s)$ and plot the magnitude response for a bandpass Butterworth filter that satisfies $\hat{G}_s \leq -17$ dB, $\hat{G}_p \geq -3$ dB, $\omega_{p_1} = 100$ rad/s, $\omega_{p_2} = 250$ rad/s, and $\omega_{s_1} = 40$ rad/s, $\omega_{s_2} = 500$ rad/s.

7.7-4 Find the transfer function $H(s)$ and plot the magnitude response for a bandpass Chebyshev filter that satisfies $\hat{G}_s \leq -17$ dB, $\hat{r} \leq 1$ dB, $\omega_{p_1} = 100$ rad/s, $\omega_{p_2} = 250$ rad/s, and $\omega_{s_1} = 40$ rad/s, $\omega_{s_2} = 500$ rad/s.

7.7-5 Find the transfer function $H(s)$ and plot the magnitude response for a bandstop Butterworth filter that satisfies $\hat{G}_s \leq -24$ dB, $\hat{G}_p \geq -3$ dB, $\omega_{p_1} = 20$ rad/s, $\omega_{p_2} = 60$ rad/s, and $\omega_{s_1} = 30$ rad/s, $\omega_{s_2} = 38$ rad/s.

7.7-6 Using functions from MATLAB's Signal Processing Toolbox, repeat Prob. 7.7-2 for an inverse Chebyshev filter.

7.7-7 Using functions from MATLAB's Signal Processing Toolbox, repeat Prob. 7.5-1 for an elliptic filter with 1 dB of passband ripple and 20 dB of stopband ripple. Plot the magnitude response to verify specifications are met.

7.9-1 Consider an LTIC system with

$$H(s) = \frac{1}{s^3 + 4s^2 + 8s + 8} = \frac{1}{(s^2 + 2s + 4)(s + 2)} = \frac{1}{(s - 2e^{j2\pi/3})(s - 2e^{-j2\pi/3})(s + 2)}$$

(a) Write MATLAB code that accurately plots the system magnitude response $|H(j\omega)|$ over $-10 \leq \omega \leq 10$.

(b) Write MATLAB code that accurately plots the system phase response over $-10 \leq \omega \leq 10$.

(c) Determine the max value y_{max} of output $y(t)$ in response to input $x(t) = 2 - \sin(2t + \pi/3)$.

(d) Draw a parallel representation of this system using real DFI structures of order 2 or less. [*Hint:* Use MATLAB to perform a partial fraction expansion of $H(s)$.]

7.9-2 Consider the op-amp circuit of Fig. P7.9-2. Further, let $RC = 1$.

(a) From Fig. P7.9-2, determine the (simplified, standard form, rational) transfer function $H(s)$.

(b) Use MATLAB to accurately plot $|H(j\omega)|$ over $-10 \leq \omega \leq 10$.

(c) Determine the output of this system in response to $x(t) = \cos(10t) - 1$.

(d) The circuit of Fig. P7.9-2 contains two capacitors. Suppose one capacitor must be a 25% tolerance part, while the other must be a 10% tolerance part. If the goal is to preserve the original magnitude response, should you use the 25% tolerance capacitor with the first op-amp or the second op-amp? Justify your answer with appropriate MATLAB simulations.

7.9-3 Design an order-12 Butterworth lowpass filter with a cutoff frequency of $\omega_c = 2\pi 5000$ by completing the following:

(a) Locate and plot the filter's poles and zeros in the complex plane. Plot the corresponding magnitude response $|H_{LP}(j\omega)|$ to verify proper design.

(b) Setting all resistor values to 100,000, determine the capacitor values to implement the filter using a cascade of six second-order Sallen–Key circuit sections. The form of a Sallen–Key stage is shown in Fig. 7.48. In a single figure, plot the magnitude response of each section as well as the overall magnitude response. Identify the poles that correspond to each section's magnitude response curve. Are the capacitor values realistic?

7.9-4 Rather than a Butterworth filter, repeat Prob. 7.9-3 for a Chebyshev LPF with 3 dB of passband ripple ($\hat{G}_p = -3$ dB). Since each Sallen–Key stage is constrained to have unity gain at dc, an overall gain error of $1/\sqrt{1+\epsilon^2}$ is acceptable.

7.9-5 An analog lowpass filter with cutoff frequency ω_c can be transformed into a highpass filter with cutoff frequency ω_c by using an *RC–CR* transformation rule: each resistor R_i is replaced

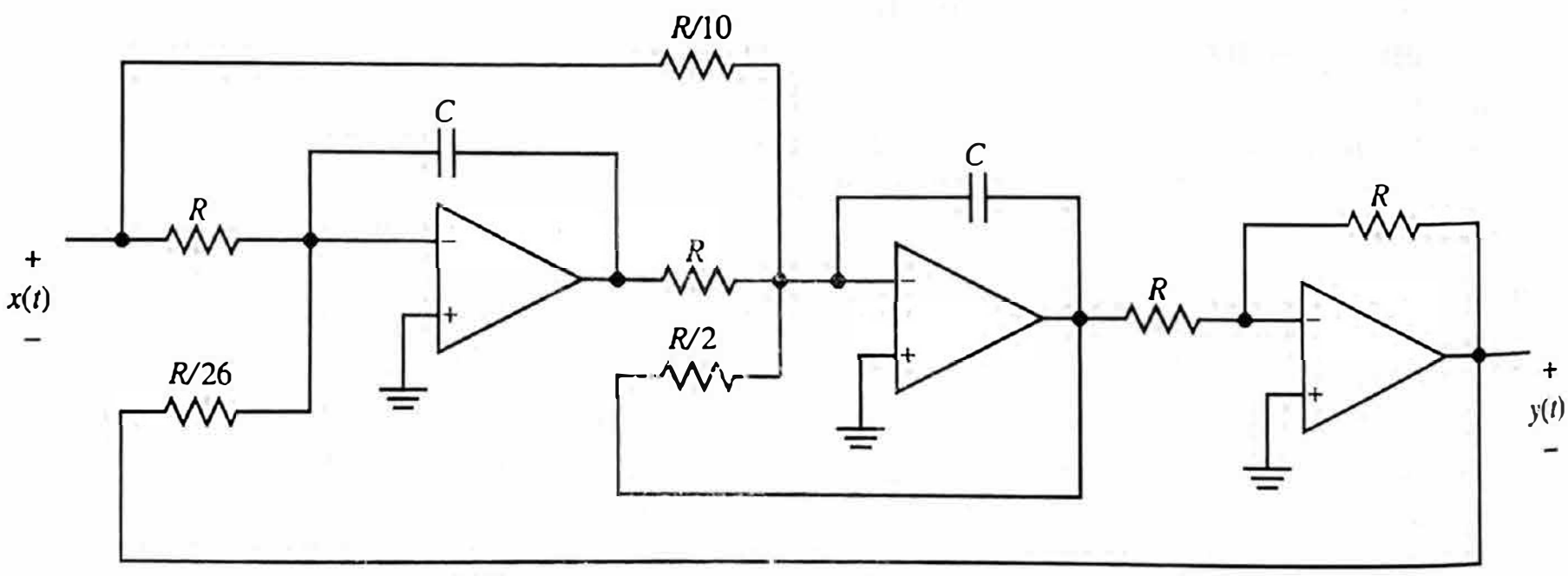

Figure P7.9-2

by a capacitor $C_i' = 1/R_i\omega_c$ and each capacitor C_i is replaced by a resistor $R_i' = 1/C_i\omega_c$.
Use this rule to design an order-8 Butterworth highpass filter with $\omega_c = 2\pi 4000$ by completing the following:

(a) Design an order-8 Butterworth lowpass filter with $\omega_c = 2\pi 4000$ by using four second-order Sallen–Key circuit stages, the form of which is shown in Fig. 7.48. Give resistor and capacitor values for each stage. Choose the resistors so that the *RC–CR* transformation will result in 1 nF capacitors. At this point, are the component values realistic?

(b) Draw an *RC–CR* transformed Sallen–Key circuit stage. Determine the transfer function $H(s)$ of the transformed stage in terms of the variables R_1', R_2', C_1', and C_2'.

(c) Transform the LPF designed in part (a) by using an *RC–CR* transformation. Give the resistor and capacitor values for each stage. Are the component values realistic? Using $H(s)$ derived in part (b), plot the magnitude response of each section as well as the overall magnitude response. Does the overall response look like a highpass Butterworth filter?
Plot the HPF system poles and zeros in the complex s plane. How do these locations compare with those of the Butterworth LPF?

7.9-6 Repeat Prob. 7.9-5, using $\omega_c = 2\pi 1500$ and an order-16 filter. That is, eight second-order stages need to be designed.

7.9-7 Rather than a Butterworth filter, repeat Prob. 7.9-5 for a Chebyshev LPF with 3 dB of passband ripple ($\hat{G}_p = -3$ dB). Since each transformed Sallen–Key stage is constrained to have unity gain at $\omega = \infty$, an overall gain error of $1/\sqrt{1+\epsilon^2}$ is acceptable.

7.9-8 The MATLAB signal-processing toolbox function `butter` helps design analog Butterworth filters. Use MATLAB help to learn how `butter` works. For each of the following cases, design the filter, plot the filter's poles and zeros in the complex s plane, and plot the decibel magnitude response $20\log_{10}|H(j\omega)|$.

(a) Design a sixth-order analog lowpass filter with $\omega_c = 2\pi 3500$.

(b) Design a sixth-order analog highpass filter with $\omega_c = 2\pi 3500$.

(c) Design a sixth-order analog bandpass filter with a passband between 2 and 4 kHz.

(d) Design a sixth-order analog bandstop filter with a stopband between 2 and 4 kHz.

7.9-9 The MATLAB signal-processing toolbox function `cheby1` helps design Chebyshev filters (also called Chebyshev type I filters). A Chebyshev filter has a passband ripple and smooth stopband. Setting the passband ripple to 3 dB ($\hat{G}_p = -3$ dB), repeat Prob. 7.9-8 using the `cheby1` command. With all other parameters held constant, what is the general effect of reducing the allowable passband ripple (making $|\hat{G}_p|$ smaller)?

7.9-10 The MATLAB signal-processing toolbox function `cheby2` helps design inverse Chebyshev filters (also called Chebyshev type II filters). An inverse Chebyshev filter has a smooth passband and ripple in the stopband. Setting the stopband ripple 20 dB down ($\hat{G}_s = -20$ dB), repeat Prob. 7.9-8 using the `cheby2` command. With all other parameters held constant, what is the general effect of increasing the minimum stopband attenuation (making $|\hat{G}_s|$ bigger)?

7.9-11 The MATLAB signal-processing toolbox function `ellip` helps design analog elliptic filters. An elliptic filter has a ripple in both the passband and stopband. Setting the passband ripple to 3 dB ($\hat{G}_p = -3$ dB) and the stopband ripple 20 dB down ($\hat{G}_s = -20$ dB), repeat Prob. 7.9-8 using the `ellip` command.

CHAPTER 8

DISCRETE-TIME SIGNALS AND SYSTEMS

In this chapter, we introduce the basic concepts of discrete-time signals and systems.

8.1 INTRODUCTION

A *discrete-time signal* is basically a sequence of numbers. Such signals arise naturally in inherently discrete-time situations such as population studies, amortization problems, national income models, and radar tracking. They may also arise as a result of sampling continuous-time signals in sampled data systems and digital filtering. Such signals can be denoted by $x[n]$, $y[n]$, and so on, where the variable n takes integer values, and $x[n]$ denotes the nth number in the sequence labeled x. In this notation, the discrete-time variable n is enclosed in square brackets instead of parentheses, which we have reserved for enclosing continuous-time variables, such as t.

Systems whose inputs and outputs are discrete-time signals are called *discrete-time systems*. A digital computer is a familiar example of this type of system. A discrete-time signal is a sequence of numbers, and a discrete-time system processes a sequence of numbers $x[n]$ to yield another sequence $y[n]$ as the output.†

A discrete-time signal, when obtained by uniform sampling of a continuous-time signal $x(t)$, can also be expressed as $x(nT)$, where T is the sampling interval and n the discrete variable taking on integer values. Thus, $x(nT)$ denotes the value of the signal $x(t)$ at $t = nT$. The signal $x(nT)$ is a sequence of numbers (sample values), and hence, by definition, is a discrete-time signal. Such a signal can also be denoted by the customary discrete-time notation $x[n]$, where $x[n] = x(nT)$. A typical discrete-time signal is depicted in Fig. 8.1, which shows both forms of notation. By way of an example, a continuous-time exponential $x(t) = e^{-t}$, when sampled every $T = 0.1$ seconds, results in a discrete-time signal $x(nT)$ given by

$$x(nT) = e^{-nT} = e^{-0.1n}$$

† There may be more than one input and more than one output.

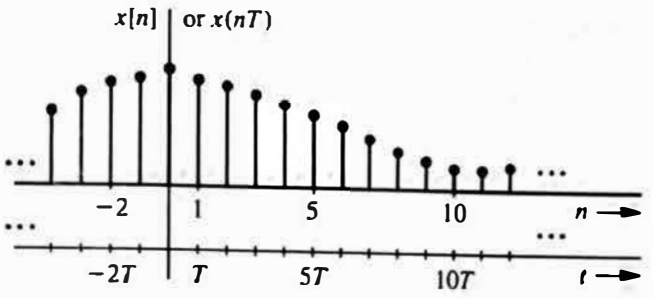

Figure 8.1 A discrete-time signal.

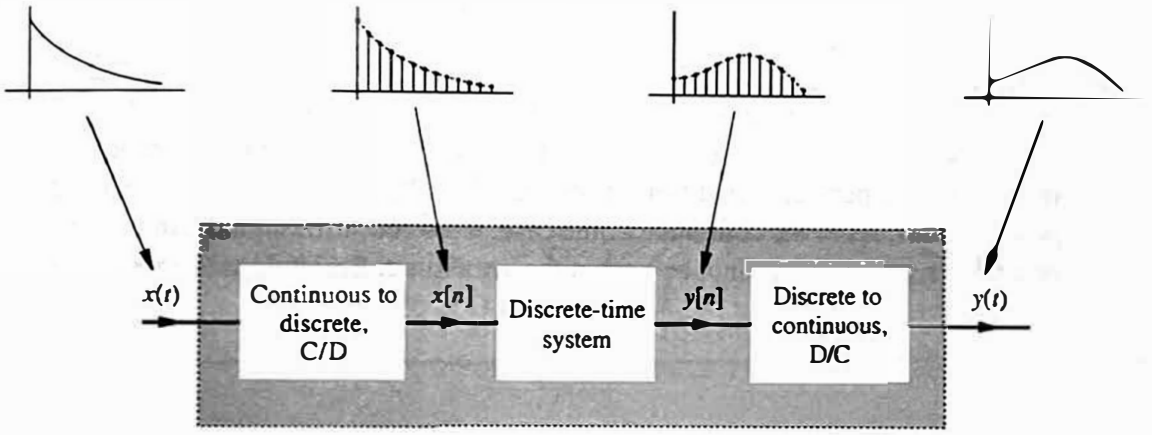

Figure 8.2 Processing a continuous-time signal by means of a discrete-time system.

Clearly, this signal is a function of n and may be expressed as $x[n]$. Such representation is more convenient and will be followed throughout this book, even for signals resulting from sampling continuous-time signals.

Digital filters can process continuous-time signals by discrete-time systems, using appropriate interfaces at the input and the output, as illustrated in Fig. 8.2. A continuous-time signal $x(t)$ is first sampled to convert it into a discrete-time signal $x[n]$, which is then processed by a discrete-time system to yield the output $y[n]$. A continuous-time signal $y(t)$ is finally constructed from $y[n]$. We shall use the notations C/D and D/C for conversion from continuous to discrete time and from discrete to continuous time. By using the interfaces in this manner, we can use an appropriate discrete-time system to process a continuous-time signal. As we shall see later in our discussion, discrete-time systems have several advantages over continuous-time systems. For this reason, there is an accelerating trend toward processing continuous-time signals with discrete-time systems.

8.1.1 Size of a Discrete-Time Signal

Arguing along the lines similar to those used for continuous-time signals, the size of a discrete-time signal $x[n]$ will be measured by its energy E_x, defined by

$$E_x = \sum_{n=-\infty}^{\infty} |x[n]|^2 \tag{8.1}$$

This definition is valid for real or complex $x[n]$. For this measure to be meaningful, the energy of a signal must be finite. A necessary condition for the energy to be finite is that the signal amplitude must $\to 0$ as $|n| \to \infty$. Otherwise, the sum in Eq. (8.1) will not converge. If E_x is finite, the signal is called an *energy signal*.

In some cases, for instance, when the amplitude of $x[n]$ does not $\to 0$ as $|n| \to \infty$, then the signal energy is infinite, and a more meaningful measure of the signal in such a case would be the time average of the energy (if it exists), which is the signal power P_x, defined by

$$P_x = \lim_{N\to\infty} \frac{1}{2N+1} \sum_{-N}^{N} |x[n]|^2$$

In this equation, the sum is divided by $2N + 1$ because there are $2N + 1$ samples in the interval from $-N$ to N. For periodic signals, the time averaging need be performed over only one period in view of the periodic repetition of the signal. If P_x is finite and nonzero, the signal is called a *power signal*. As in the continuous-time case, a discrete-time signal can either be an energy signal or a power signal, but cannot be both at the same time. Some signals are neither energy nor power signals.

EXAMPLE 8.1 Computing DT Energy and Power

Find the energy of the signal $x[n] = n(u[n] - u[n-6])$, shown in Fig. 8.3a, and the power for the periodic signal $y[n]$ in Fig. 8.3b.

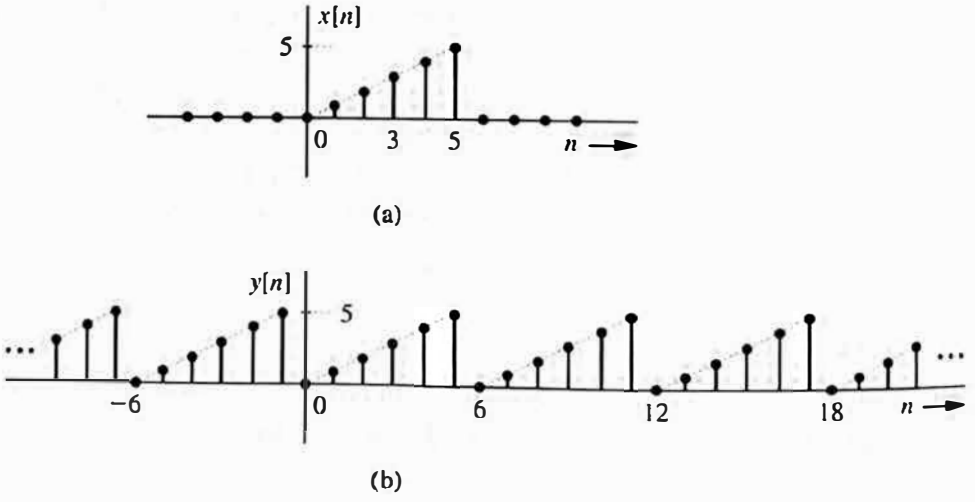

Figure 8.3 **(a)** Energy and **(b)** power computation for a signal.

By definition,

$$E_x = \sum_{n=0}^{5} n^2 = 55$$

A periodic signal $x[n]$ with period N_0 is characterized by the fact that

$$x[n] = x[n + N_0]$$

The smallest value of N_0 for which the preceding equation holds is the *fundamental period*. Such a signal is called N_0 *periodic*. Figure 8.3b shows an example of a periodic signal $y[n]$ of period $N_0 = 6$ because each period contains 6 samples. Note that if the first sample is taken at $n = 0$, the last sample occurs at $n = N_0 - 1 = 5$, not at $n = N_0 = 6$. Because the signal $y[n]$ is periodic, its power P_y can be found by averaging its energy over one period. Averaging the energy over one period, we obtain

$$P_y = \frac{1}{6}\sum_{n=0}^{5} n^2 = \frac{55}{6}$$

DRILL 8.1 DT Signal Classification: Energy, Power, and Neither

Let $x[n]$ be a^n for $n \geq 0$ and be 0 for $n < 0$ so that $x[n] = a^n u[n]$. Show that $x[n]$ is an energy signal of energy $E_x = 1/(1 - |a|^2)$ if $|a| < 1$, that it is a power signal of power $P_x = 0.5$ if $|a| = 1$, and that it is neither an energy signal nor a power signal if $|a| > 1$.

8.2 Useful Signal Operations

Signal operations for *shifting*, and *scaling*, as discussed for continuous-time signals also apply, with some modifications, to discrete-time signals.

Shifting

Consider a signal $x[n]$ (Fig. 8.4a) and the same signal delayed (right-shifted) by 5 units (Fig. 8.4b), which we shall denote by $x_s[n]$.[†] Using the argument employed for a similar operation in continuous-time signals (Sec. 1.2), we obtain

$$x_s[n] = x[n - 5]$$

[†] The terms "delay" and "advance" are meaningful only when the independent variable is time. For other independent variables, such as frequency or distance, it is more appropriate to refer to the "right shift" and "left shift" of a sequence.

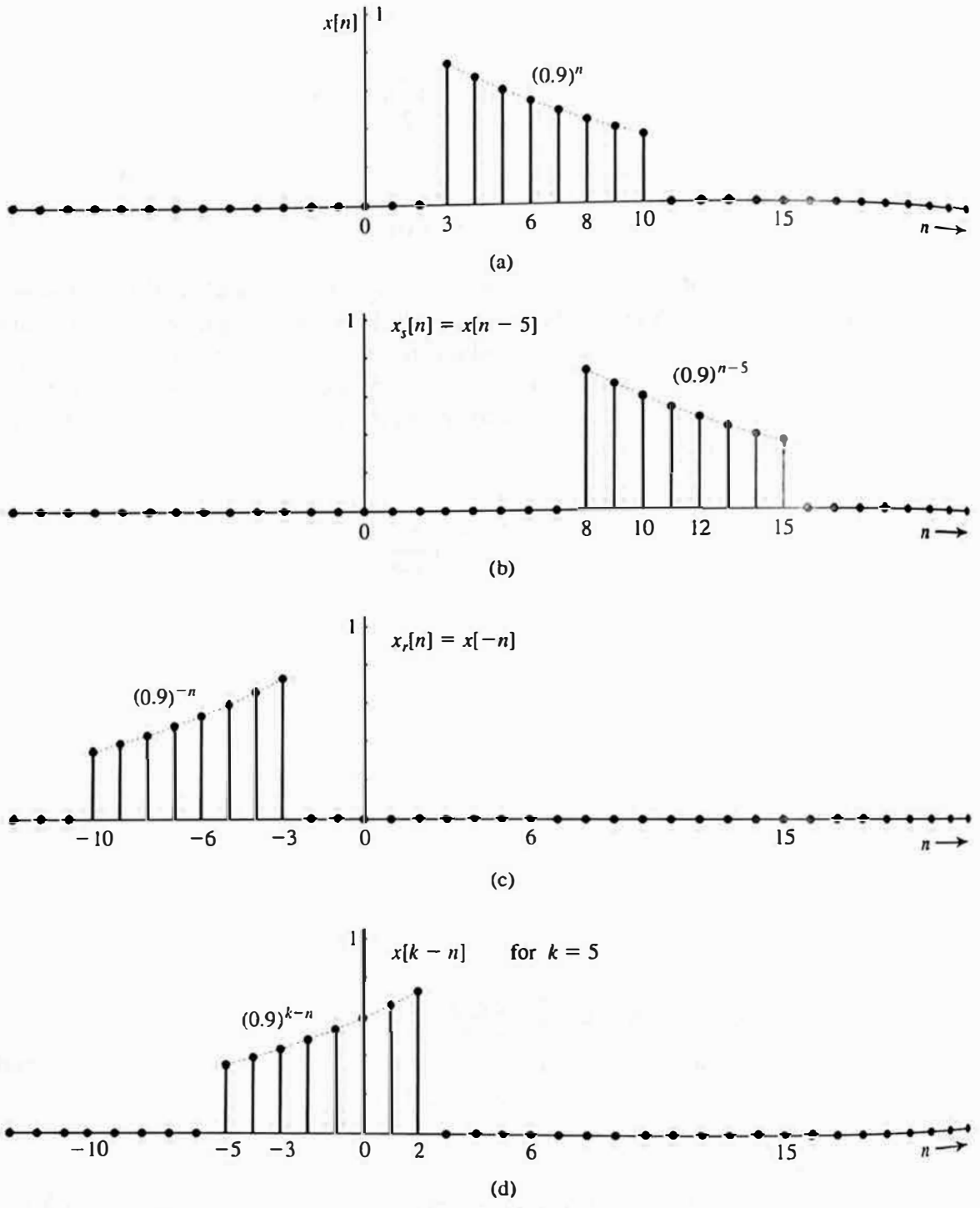

Figure 8.4 Shifting and time reversal of a signal.

Therefore, to shift a sequence by M units (M integer), we replace n with $n-M$. Thus, $x[n-M]$ represents $x[n]$ shifted by M units. If M is positive, the shift is to the right (delay). If M is negative, the shift is to the left (advance). Accordingly, $x[n-5]$ is $x[n]$ delayed (right-shifted) by 5 units, and $x[n+5]$ is $x[n]$ advanced (left-shifted) by 5 units.

DRILL 8.2 Left-Shift Operation

Show that $x[n]$ in Fig. 8.4a left-shifted by 3 units can be expressed as $0.729(0.9)^n$ for $0 \le n \le 7$, and zero otherwise. Sketch the shifted signal.

DRILL 8.3 Right-Shift Operation

Show that $x[-k-n]$ can be obtained from $x[n]$ by first right-shifting $x[n]$ by k units and then time-reversing this shifted signal.

Time Reversal

To time-reverse $x[n]$ in Fig. 8.4a, we rotate $x[n]$ about the vertical axis to obtain the time-reversed signal $x_r[n]$ shown in Fig. 8.4c. Using the argument employed for a similar operation in continuous-time signals (Sec. 1.2), we obtain

$$x_r[n] = x[-n]$$

Therefore, to time-reverse a signal, we replace n with $-n$ so that $x[-n]$ is the time-reversed $x[n]$. For example, if $x[n] = (0.9)^n$ for $3 \le n \le 10$, then $x_r[n] = (0.9)^{-n}$ for $3 \le -n \le 10$; that is, $-3 \ge n \ge -10$, as shown in Fig. 8.4c.

The origin $n = 0$ is the anchor point, which remains unchanged under time-reversal operation because at $n = 0$, $x[n] = x[-n] = x[0]$. Note that while the reversal of $x[n]$ about the vertical axis is $x[-n]$, the reversal of $x[n]$ about the horizontal axis is $-x[n]$.

EXAMPLE 8.2 Time Reversal and Shifting

In the convolution operation, discussed later, we need to find the function $x[k-n]$ from $x[n]$.

This can be done in two steps: (i) time-reverse the signal $x[n]$ to obtain $x[-n]$; (ii) now, right-shift $x[-n]$ by k. Recall that right-shifting is accomplished by replacing n with $n-k$. Hence, right-shifting $x[-n]$ by k units is $x[-(n-k)] = x[k-n]$. Figure 8.4d shows $x[5-n]$ obtained this way. We first time-reverse $x[n]$ to obtain $x[-n]$ in Fig. 8.4c. Next, we shift $x[-n]$ by $k = 5$ to obtain $x[k-n] = x[5-n]$, as shown in Fig. 8.4d.

In this particular example, the order of the two operations employed is interchangeable. We can first left-shift $x[k]$ to obtain $x[n+5]$. Next, we time-reverse $x[n+5]$ to obtain $x[-n+5] = x[5-n]$. The reader is encouraged to verify that this procedure yields the same result, as in Fig. 8.4d.

DRILL 8.4 Time Reversal

Sketch the signal $x[n] = e^{-0.5n}$ for $-3 \leq n \leq 2$, and zero otherwise. Sketch the corresponding time-reversed signal and show that it can be expressed as $x_r[n] = e^{0.5n}$ for $-2 \leq n \leq 3$.

Sampling Rate Alteration: Downsampling, Upsampling, and Interpolation

Alteration of the sampling rate is somewhat similar to time scaling in continuous-time signals. Consider a signal $x[n]$ compressed by factor M. Compressing a signal $x[n]$ by factor M yields $x_d[n]$ given by

$$x_d[n] = x[Mn]$$

Because of the restriction that discrete-time signals are defined only for integer values of the argument, we must restrict M to integer values. The values of $x[Mn]$ at $n = 0, 1, 2, 3, \ldots$ are $x[0]$, $x[M]$, $x[2M]$, $x[3M]$, $\ldots$. This means $x[Mn]$ selects every Mth sample of $x[n]$ and deletes all the samples in between. It reduces the number of samples by factor M. If $x[n]$ is obtained by sampling a continuous-time signal, this operation implies reducing the sampling rate by factor M. For this reason, this operation is commonly called *downsampling*. Figure 8.5a shows a signal $x[n]$ and Fig. 8.5b shows the signal $x[2n]$, which is obtained by deleting odd-numbered samples of $x[n]$.†

In the continuous-time case, time compression merely speeds up the signal without loss of any data. In contrast, downsampling $x[n]$ generally causes loss of data. Under certain conditions—for example, if $x[n]$ is the result of oversampling some continuous-time signal—then $x_d[n]$ may still retain the complete information about $x[n]$.

An *interpolated* signal is generated in two steps; first, we expand $x[n]$ by an integer factor L to obtain the expanded signal $x_e[n]$, as

$$x_e[n] = \begin{cases} x[n/L] & n = 0, \pm L, \pm 2L, \ldots, \\ 0 & \text{otherwise} \end{cases} \tag{8.2}$$

To understand this expression, consider a simple case of expanding $x[n]$ by a factor of 2 ($L = 2$). When n is odd, $n/2$ is a noninteger, and $x_e[n] = 0$. That is, $x_e[1] = x_e[3] = x_e[5], \ldots$ are all zero, as depicted in Fig. 8.5c. Moreover, $n/2$ is an integer for even n, and the values of $x_e[n] = x[n/2]$ for $n = 0, 2, 4, 6, \ldots$ are $x[0], x[1], x[2], x[3], \ldots$, as shown in Fig. 8.5c. In general, for $n = 0, 1, 2, \ldots$, $x_e[n]$ is given by the sequence

$$x[0], \underbrace{0, 0, \ldots, 0, 0}_{L-1 \text{ zeros}}, x[1], \underbrace{0, 0, \ldots, 0, 0}_{L-1 \text{ zeros}}, x[2], \underbrace{0, 0, \ldots, 0, 0}_{L-1 \text{ zeros}}, \ldots$$

Thus, the sampling rate of $x_e[n]$ is L times that of $x[n]$. Hence, this operation is commonly called *upsampling*. The upsampled signal $x_e[n]$ contains all the data of $x[n]$, although in an expanded form.

† Odd-numbered samples of $x[n]$ can be retained (and even-numbered samples deleted) by using the transformation $x_d[n] = x[2n + 1]$.

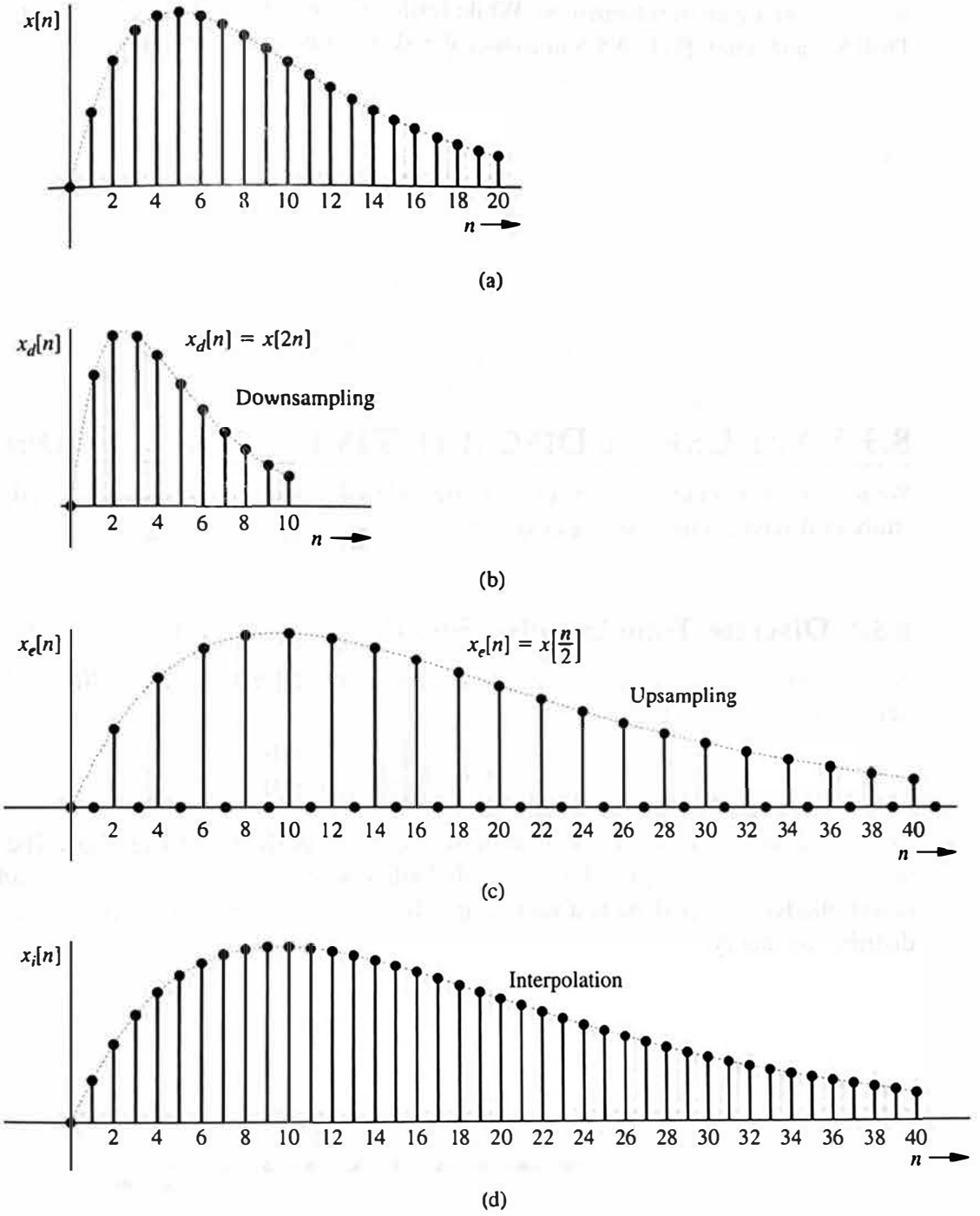

Figure 8.5 Compression (downsampling) and expansion (upsampling, interpolation) of a signal.

In the expanded signal in Fig. 8.5c, the missing (zero-valued) odd-numbered samples can be reconstructed from the non-zero-valued samples by using some suitable interpolation formula. Figure 8.5d shows such an interpolated signal $x_i[n]$, where the missing samples are constructed by using an interpolating filter. The optimum interpolating filter is usually an ideal lowpass filter, which is realizable only approximately. In practice, we may use an interpolation that is nonoptimum but realizable. The process of filtering to interpolate the zero-valued samples is called *interpolation*. Since the interpolated data are computed from the existing data, interpolation does

not result in a gain of information. While further discussion of interpolation is beyond our scope, Drill 8.5 and, later, Prob. 9.8-8 introduce the idea of linear interpolation.

DRILL 8.5 Expansion and Interpolation

A signal $x[n]$ is expanded by a factor of 2 to obtain signal $x[n/2]$. The odd-numbered samples (n odd) in this signal have zero value. Show that the linearly interpolated odd-numbered samples are given by $x_i[n] = (1/2)\{x[n-1] + x[n+1]\}$.

8.3 SOME USEFUL DISCRETE-TIME SIGNAL MODELS

We now discuss some important discrete-time signal models that are encountered frequently in the study of discrete-time signals and systems.

8.3.1 Discrete-Time Impulse Function $\delta[n]$

The discrete-time counterpart of the continuous-time impulse function $\delta(t)$ is $\delta[n]$, a Kronecker delta function, defined by

$$\delta[n] = \begin{cases} 1 & n = 0 \\ 0 & n \neq 0 \end{cases}$$

This function, also called the unit impulse sequence, is shown in Fig. 8.6a. The shifted impulse sequence $\delta[n-m]$ is depicted in Fig. 8.6b. Unlike its continuous-time counterpart $\delta(t)$ (the Dirac delta), the Kronecker delta is a very simple function, requiring no special esoteric knowledge of distribution theory.

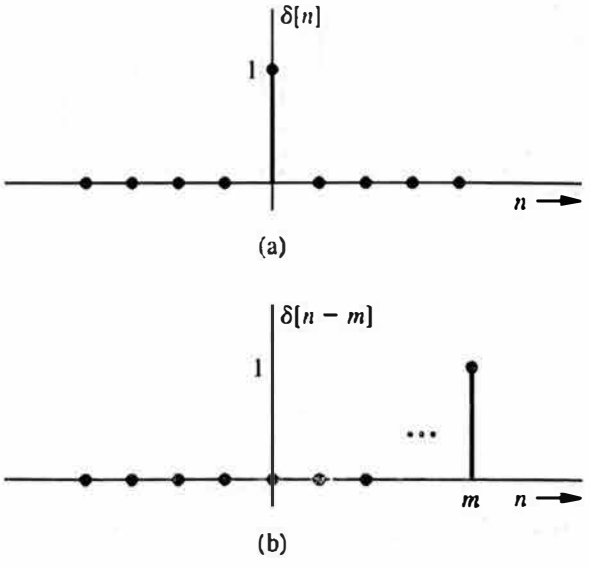

Figure 8.6 Discrete-time impulse function: (a) unit impulse sequence and (b) shifted impulse sequence.

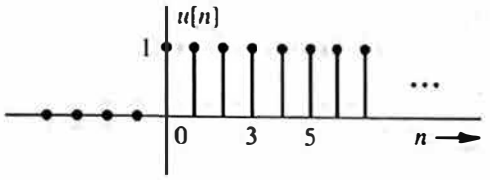

(a)

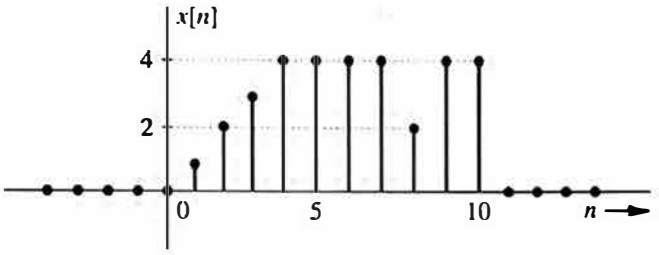

(b)

Figure 8.7 (**a**) A discrete-time unit step function $u[n]$ and (**b**) its application.

8.3.2 Discrete-Time Unit Step Function $u[n]$

The discrete-time counterpart of the unit step function $u(t)$ is $u[n]$ (Fig. 8.7a), defined by

$$u[n] = \begin{cases} 1 & \text{for } n \geq 0 \\ 0 & \text{for } n < 0 \end{cases}$$

If we want a signal to start at $n = 0$ (so that it has a zero value for all $n < 0$), we need only multiply the signal by $u[n]$.

EXAMPLE 8.3 Describing Signals with Unit Step and Unit Impulse Functions

Describe the signal $x[n]$ shown in Fig. 8.7b by a single expression valid for all n.

There are many different ways of viewing $x[n]$. Although each way of viewing yields a different expression, they are all equivalent. We shall consider here just one possible expression.

The signal $x[n]$ can be broken into three components: (1) a ramp component $x_1[n]$ from $n = 0$ to 4, (2) a scaled step component $x_2[n]$ from $n = 5$ to 10, and (3) an impulse component $x_3[n]$ represented by the negative spike at $n = 8$. Let us consider each one separately.

We express $x_1[n] = n(u[n] - u[n-5])$ to account for the signal from $n = 0$ to 4. Assuming that the spike at $n = 8$ does not exist, we can express $x_2[n] = 4(u[n-5] - u[n-11])$ to account for the signal from $n = 5$ to 10. Once these two components have been added, the only part that is unaccounted for is a spike of amplitude -2 at $n = 8$, which can be represented by

$x_3[n] = -2\delta[n-8]$. Hence,

$$\begin{aligned} x[n] &= x_1[n] + x_2[n] + x_3[n] \\ &= n(u[n] - u[n-5]) + 4(u[n-5] - u[n-11]) - 2\delta[n-8] \qquad \text{for all } n \end{aligned}$$

We stress again that the expression is valid for all values of n. The reader can find several other equivalent expressions for $x[n]$. For example, one may consider a scaled step function from $n = 0$ to 10, subtract a ramp over the range $n = 0$ to 3, and subtract the spike. You can also play with breaking n into different ranges for your expression.

8.3.3 Discrete-Time Exponential γ^n

A continuous-time exponential $e^{\lambda t}$ can be expressed in an alternate form as

$$e^{\lambda t} = \gamma^t \qquad (\gamma = e^{\lambda} \text{ or } \lambda = \ln \gamma)$$

For example, $e^{-0.3t} = (0.7408)^t$ because $e^{-0.3} = 0.7408$. Conversely, $4^t = e^{1.386t}$ because $e^{1.386} = 4$, that is, $\ln 4 = 1.386$. In the study of continuous-time signals and systems, we prefer the form $e^{\lambda t}$ rather than γ^t. In contrast, the exponential form γ^n is preferable in the study of discrete-time signals and systems, as will become apparent later. The discrete-time exponential γ^n can also be expressed by using a natural base, as

$$e^{\lambda n} = \gamma^n \qquad (\gamma = e^{\lambda} \text{ or } \lambda = \ln \gamma)$$

Because of unfamiliarity with exponentials with bases other than e, exponentials of the form γ^n may seem inconvenient and confusing at first. The reader is urged to plot some exponentials to acquire a sense of these functions. Also observe that $\gamma^{-n} = \left(\frac{1}{\gamma}\right)^n$.

DRILL 8.6 Equivalent Forms of DT Exponentials

(a) Show that (i) $(0.25)^{-n} = 4^n$, (ii) $4^{-n} = (0.25)^n$, (iii) $e^{2t} = (7.389)^t$, (iv) $e^{-2t} = (0.1353)^t = (7.389)^{-t}$, (v) $e^{3n} = (20.086)^n$, and (vi) $e^{-1.5n} = (0.2231)^n = (4.4817)^{-n}$.

(b) Show that (i) $2^n = e^{0.693n}$, (ii) $(0.5)^n = e^{-0.693n}$, and (iii) $(0.8)^{-n} = e^{0.2231n}$.

Nature of γ^n. The signal $e^{\lambda n}$ grows exponentially with n if $\text{Re}\,\lambda > 0$ (λ in the RHP), and decays exponentially if $\text{Re}\,\lambda < 0$ (λ in the LHP). It is constant or oscillates with constant amplitude if $\text{Re}\,\lambda = 0$ (λ on the imaginary axis). Clearly, the location of λ in the complex plane indicates whether the signal $e^{\lambda n}$ will grow exponentially, decay exponentially, or oscillate with constant amplitude (Fig. 8.8a). A constant signal ($\lambda = 0$) is also an oscillation with zero frequency. We now find a similar criterion for determining the nature of γ^n from the location of γ in the complex plane.

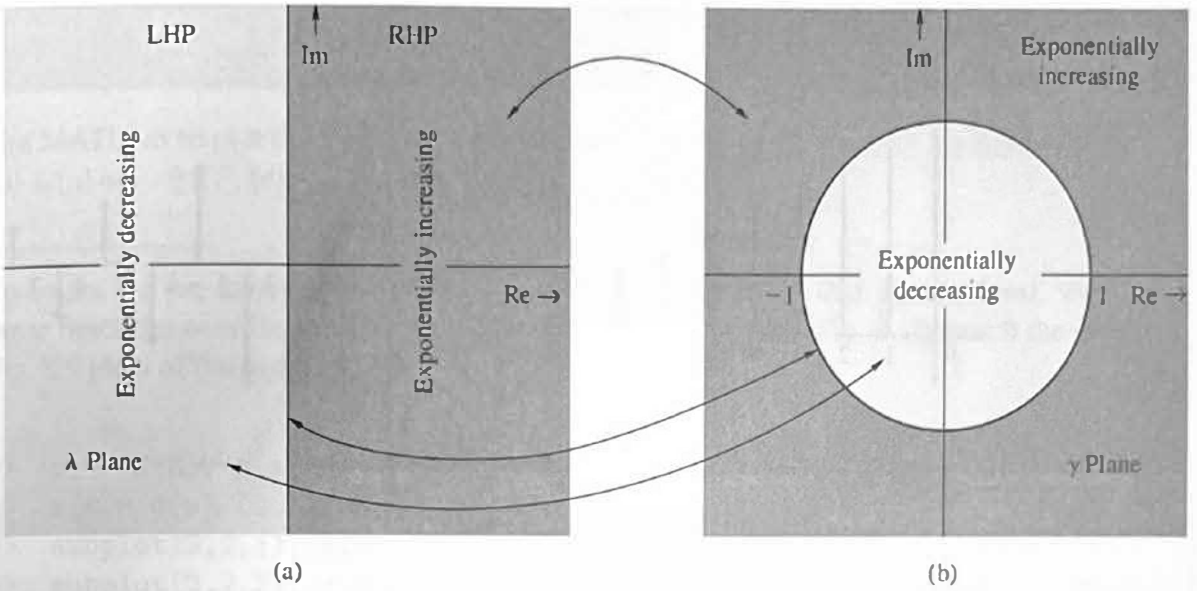

Figure 8.8 The λ plane, the γ plane, and their mapping.

Figure 8.8a shows a complex plane (λ plane). Consider a signal $e^{j\Omega n}$. In this case, $\lambda = j\Omega$ lies on the imaginary axis (Fig. 8.8a), and therefore is a constant-amplitude oscillating signal. This signal $e^{j\Omega n}$ can be expressed as γ^n, where $\gamma = e^{j\Omega}$. Because the magnitude of $e^{j\Omega}$ is unity, $|\gamma| = 1$. Hence, when λ lies on the imaginary axis, the corresponding γ lies on a circle of unit radius, centered at the origin (the *unit circle* illustrated in Fig. 8.8b). Therefore, a signal γ^n oscillates with constant amplitude if γ lies on the unit circle. Thus, the imaginary axis in the λ plane maps into the unit circle in the γ plane.

Next consider the signal $e^{\lambda n}$, where λ lies in the left half-plane in Fig. 8.8a. This means $\lambda = a + jb$, where a is negative ($a < 0$). In this case, the signal decays exponentially. This signal can be expressed as γ^n, where

$$\gamma = e^{\lambda} = e^{a+jb} = e^{a}\, e^{jb}$$

and

$$|\gamma| = |e^{a}||e^{jb}| = e^{a} \qquad \text{because } |e^{jb}| = 1$$

Also, a is negative ($a < 0$). Hence, $|\gamma| = e^{a} < 1$. This result means that the corresponding γ lies inside the unit circle. Therefore, a signal γ^n decays exponentially if γ lies within the unit circle (Fig. 8.8b). If, in the preceding case, we select a to be positive (λ in the right half-plane), then $|\gamma| > 1$, and γ lies outside the unit circle. Therefore, a signal γ^n grows exponentially if γ lies outside the unit circle (Fig. 8.8b).

To summarize, the imaginary axis in the λ plane maps into the unit circle in the γ plane. The left half-plane in the λ plane maps into the inside of the unit circle and the right half of the λ plane maps into the outside of the unit circle in the γ plane, as depicted in Fig. 8.8.

Plots of $(0.8)^n$ and $(-0.8)^n$ appear in Figs. 8.9a and 8.9b, respectively. Plots of $(0.5)^n$ and $(1.1)^n$ appear in Figs. 8.9c and 8.9d, respectively. These plots verify our earlier conclusions about the location of γ and the nature of signal growth. Observe that a signal $(-|\gamma|)^n$ alternates sign

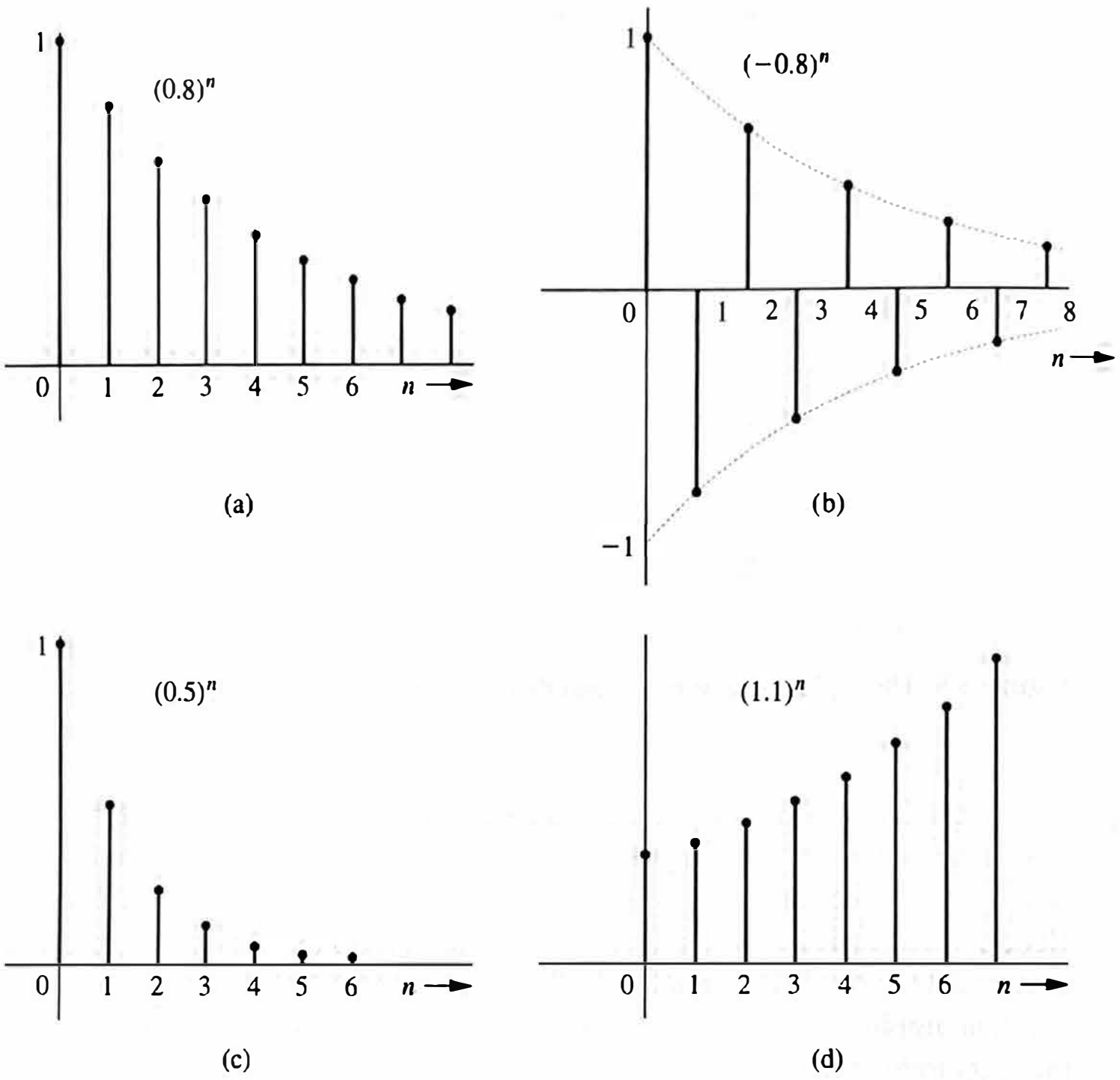

Figure 8.9 Discrete-time exponentials γ^n.

successively (is positive for even values of n and negative for odd values of n, as depicted in Fig. 8.9b). Also, the exponential $(0.5)^n$ decays faster than $(0.8)^n$ because 0.5 is closer to the origin than 0.8. The exponential $(0.5)^n$ can also be expressed as 2^{-n} because $(0.5)^{-1} = 2$.

DRILL 8.7 Sketching DT Exponentials

Sketch the following signals: **(a)** $(1)^n$, **(b)** $(-1)^n$, **(c)** $(0.5)^n$, **(d)** $(-0.5)^n$, **(e)** $(0.5)^{-n}$, **(f)** 2^{-n}, and **(g)** $(-2)^n$. Express these exponentials as γ^n, and plot γ in the complex plane for each case. Verify that γ^n decays exponentially with n if γ lies inside the unit circle and that γ^n grows with n if γ is outside the unit circle. If γ is on the unit circle, γ^n is constant or oscillates with a constant amplitude.

Accurately hand-sketching DT signals can be tedious and difficult. As the next example shows, MATLAB is particularly well suited to plot DT signals, including exponentials.

EXAMPLE 8.4 Plotting DT Exponentials with MATLAB

Use MATLAB to plot the following discrete-time signals over $(0 \leq n \leq 8)$: **(a)** $x_a[n] = (0.8)^n$, **(b)** $x_b[n] = (-0.8)^n$, **(c)** $x_c[n] = (0.5)^n$, and **(d)** $x_d[n] = (1.1)^n$.

To begin, we use anonymous functions to represent each of the four signals. Next, we plot these functions over the desired range of n. The results, shown in Fig. 8.10, match the earlier Fig. 8.9 plots of the same signals.

```
>> n = (0:8); x_a = @(n) (0.8).^n; x_b = @(n) (-0.8).^(n);
>> x_c = @(n) (0.5).^n; x_d = @(n) (1.1).^n;
>> subplot(2,2,1); stem(n,x_a(n),'k.'); ylabel('x_a[n]'); xlabel('n');
>> subplot(2,2,2); stem(n,x_b(n),'k.'); ylabel('x_b[n]'); xlabel('n');
>> subplot(2,2,3); stem(n,x_c(n),'k.'); ylabel('x_c[n]'); xlabel('n');
>> subplot(2,2,4); stem(n,x_d(n),'k.'); ylabel('x_d[n]'); xlabel('n');
```

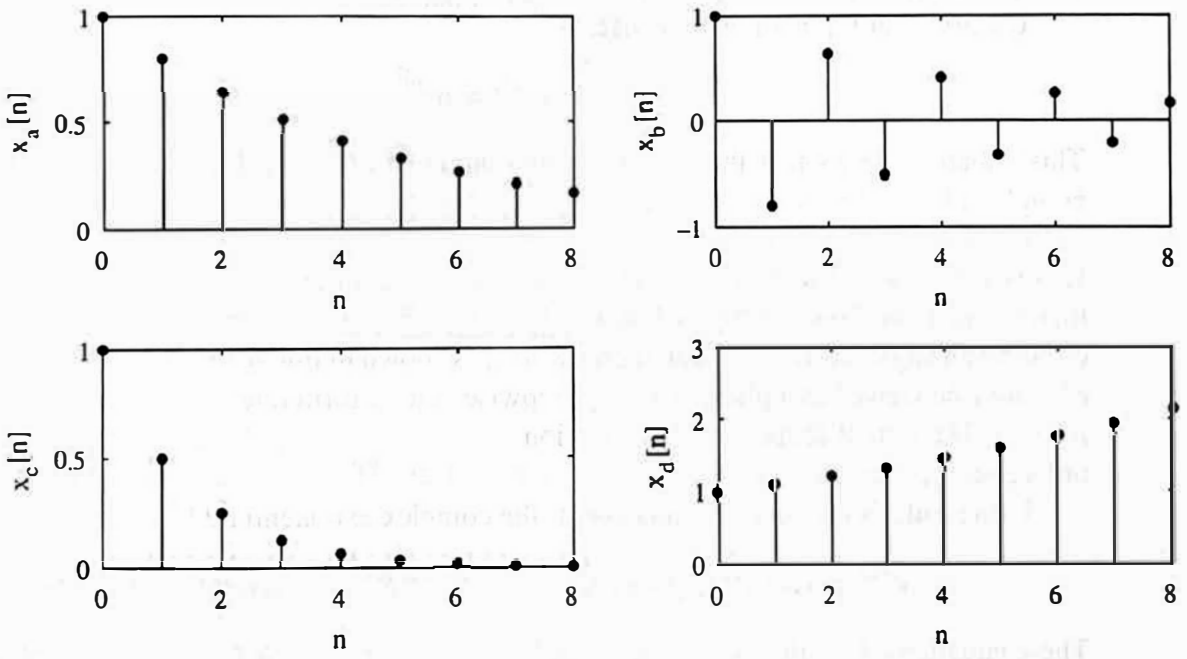

Figure 8.10 DT plots for Ex. 8.4.

8.3.4 Discrete-Time Complex Exponential $e^{j\Omega n}$

A general DT complex exponential $e^{j\Omega n}$ is a complex-valued function of n. Notice that Ωn is an angle in radians. The dimensions of the frequency Ω are *radians per sample*. At $n = 0, 1, 2, 3, \ldots$, the complex exponential $e^{j\Omega n}$ takes on values $e^{j0}, e^{j\Omega}, e^{j2\Omega}, e^{j3\Omega}, \ldots$, respectively. Rather than

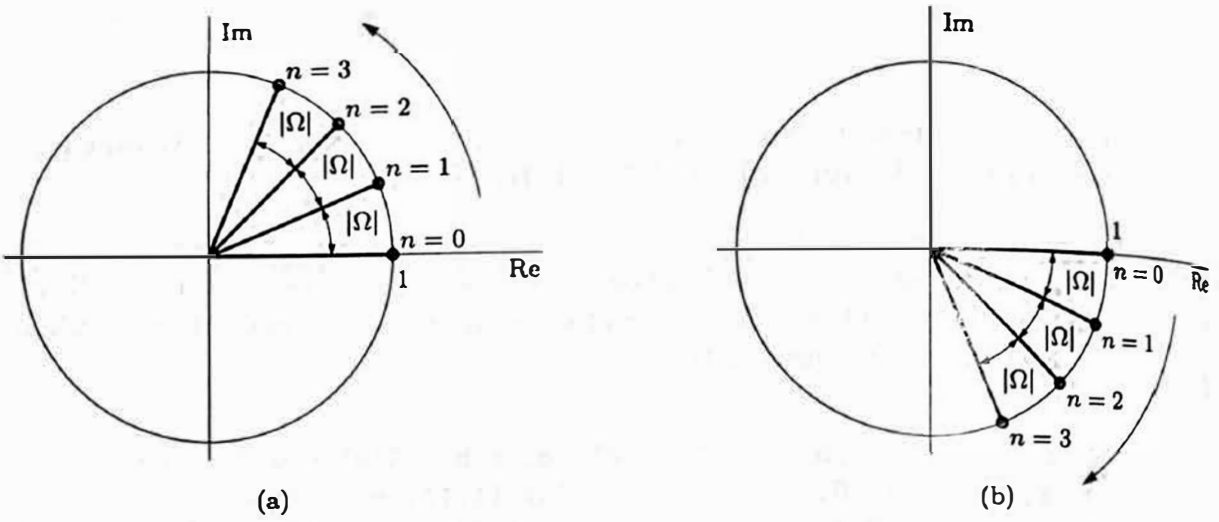

Figure 8.11 Loci of **(a)** $e^{j|\Omega|n}$ and **(b)** $e^{-j|\Omega|n}$.

use the typical dual plots of magnitude and phase (or real part and imaginary part), Fig. 8.11 plots $e^{j\Omega n}$ directly in the complex plane for various values of n.

Observe that for $r = 1$ and $\theta = n\Omega$,

$$e^{j\Omega n} = re^{j\theta}$$

This equation shows that the magnitude and angle of $e^{j\Omega n}$ are 1 and $n\Omega$, respectively. In the complex plane, $e^{j\Omega n}$ is a point on a unit circle at an angle $n\Omega$ (in radians). Therefore, the points $e^{j0}, e^{j\Omega}, e^{j2\Omega}, e^{j3\Omega}, \ldots$ lie on a circle of unit radius (unit circle) at angles $0, \Omega, 2\Omega, 3\Omega, \ldots$. For $\Omega > 0$, $e^{j\Omega n} = e^{j|\Omega|n}$ moves counterclockwise along the unit circle by an angle $|\Omega|$ for each unit increase in n, as shown in Fig. 8.11a. For $\Omega < 0$, $e^{j\Omega n} = e^{-j|\Omega|n}$ moves clockwise along the unit circle by an angle $|\Omega|$ for each unit increase in n, as shown in Fig. 8.11b. In either case, the locus of $e^{j\Omega n}$ may be viewed as a phasor rotating stepwise at a uniform rate of $|\Omega|$ radians per unit sample interval. The sign of Ω specifies the direction of rotation, while $|\Omega|$ establishes the rate of rotation, or frequency, of $e^{j\Omega n}$.

Using Euler's formula, we can express the complex exponential $e^{j\Omega n}$ in terms of sinusoids as

$$e^{j\Omega n} = (\cos\Omega n + j\sin\Omega n) \qquad \text{and} \qquad e^{-j\Omega n} = (\cos\Omega n - j\sin\Omega n) \tag{8.3}$$

These equations show that *the frequency of both* $e^{j\Omega n}$ *and* $e^{-j\Omega n}$ *is* Ω (radians/sample). Therefore, the frequency of $e^{j\Omega n}$ is $|\Omega|$. Because of Eq. (8.3), exponentials and sinusoids have similar properties and peculiarities. Discrete-time sinusoids will be considered next.

8.3.5 Discrete-Time Sinusoid $\cos(\Omega n + \theta)$

A general discrete-time sinusoid can be expressed as $C\cos(\Omega n + \theta)$, where C is the *amplitude*, and θ is the *phase* in radians. Also, Ωn is an angle in radians. Hence, the dimensions of the frequency Ω are *radians per sample*. This sinusoid may also be expressed as

$$C\cos(\Omega n + \theta) = C\cos(2\pi \mathcal{F} n + \theta)$$

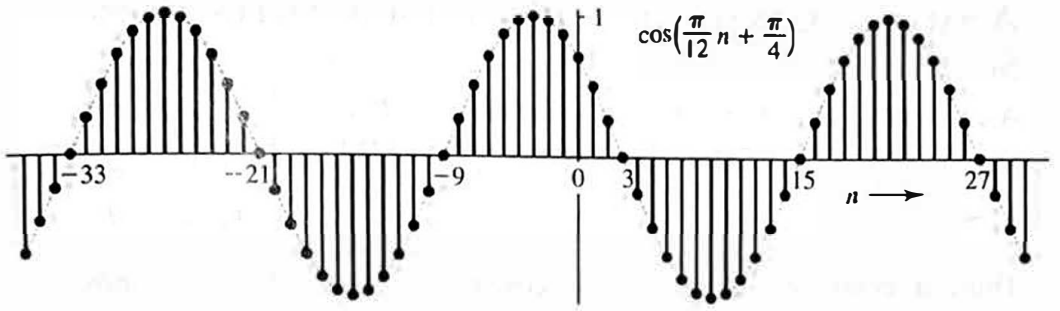

Figure 8.12 A discrete-time sinusoid $\cos\left(\frac{\pi}{12}n+\frac{\pi}{4}\right)$.

where $\mathcal{F}=\Omega/2\pi$. Therefore, the dimensions of the discrete-time frequency $\mathcal{F}$ are (radians/2π) per sample, which is equal to *cycles per sample*. This means if N_0 is the period (samples/cycle) of the sinusoid, then the frequency of the sinusoid $\mathcal{F}=1/N_0$ (samples/cycle).

Figure 8.12 shows a discrete-time sinusoid $\cos\left(\frac{\pi}{12}n+\frac{\pi}{4}\right)$. For this case, the frequency is $\Omega=\pi/12$ radians/sample. Alternately, the frequency is $\mathcal{F}=1/24$ cycles/sample. In other words, there are 24 samples in one cycle of the sinusoid.

Because $\cos(-x)=\cos(x)$,

$$\cos(-\Omega n+\theta)=\cos(\Omega n-\theta)$$

This shows that both $\cos(\Omega n+\theta)$ and $\cos(-\Omega n+\theta)$ have the same frequency (Ω). Therefore, *the frequency of* $\cos(\Omega n+\theta)$ *is* $|\Omega|$.

EXAMPLE 8.5 Plotting a DT Sinusoid with MATLAB

Using MATLAB, plot the discrete-time sinusoid $x[n]=\cos\left(\frac{\pi}{12}n+\frac{\pi}{4}\right)$.

We represent the desired sinusoid using an anonymous function. Next, we plot this function over the desired range of n. The result, shown in Fig. 8.13, matches the plot of the same signal shown in Fig. 8.12.

```
>> n = (-30:30); x = @(n) cos(n*pi/12+pi/4);
>> clf; stem(n,x(n),'k'); ylabel('x[n]'); xlabel('n');
```

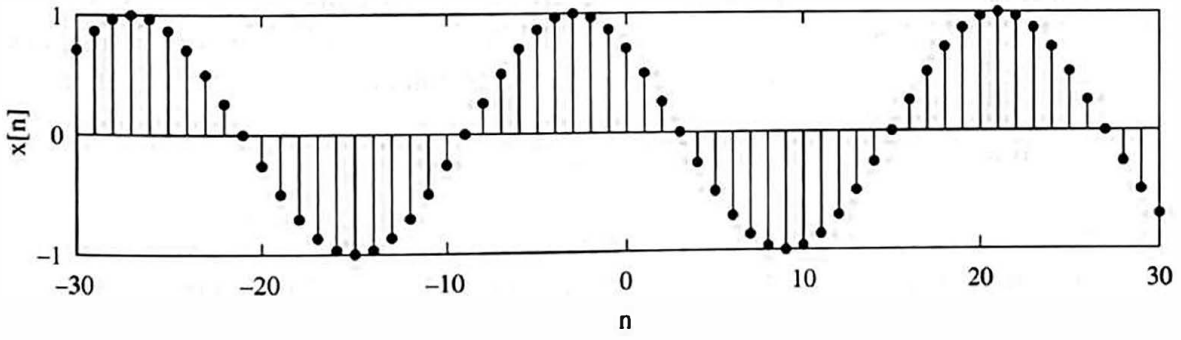

Figure 8.13 Sinusoid plot for Ex. 8.5.

A Sampled Continuous-Time Sinusoid Yields a Discrete-Time Sinusoid

A continuous-time sinusoid $\cos \omega t$ sampled every T seconds yields a discrete-time sequence whose nth element (at $t = nT$) is $\cos \omega nT$. Thus, the sampled signal $x[n]$ is given by

$$x[n] = \cos \omega nT = \cos \Omega n, \qquad \text{where } \Omega = \omega T$$

Thus, a continuous-time sinusoid $\cos \omega t$ sampled every T seconds yields a discrete-time sinusoid $\cos \Omega n$, where $\Omega = \omega T$. Superficially, it may appear that a discrete-time sinusoid is a continuous-time sinusoid's cousin in a striped suit. As we shall see, however, some of the properties of discrete-time sinusoids are very different from those of continuous-time sinusoids. In the continuous-time case, the period of a sinusoid can take on any value: integral, fractional, or even irrational. A discrete-time signal, in contrast, is specified only at integral values of n. Therefore, the period must be an integer (in terms of n) or an integral multiple of T (in terms of variable t).

Some Peculiarities of Discrete-Time Sinusoids

There are two unexpected properties of discrete-time sinusoids that distinguish them from their continuous-time relatives.

1. A continuous-time sinusoid is always periodic regardless of the value of its frequency ω. But a discrete-time sinusoid $\cos \Omega n$ is periodic only if Ω is 2π times some rational number ($\frac{\Omega}{2\pi}$ is a rational number).
2. A continuous-time sinusoid $\cos \omega t$ has a unique waveform for each value of ω. In contrast, a sinusoid $\cos \Omega n$ does not have a unique waveform for each value of Ω. In fact, discrete-time sinusoids with frequencies separated by multiples of 2π are identical. Thus, a sinusoid $\cos \Omega n = \cos (\Omega + 2\pi)n = \cos (\Omega + 4\pi)n = \cdots$.

We now examine each of these peculiarities.

Not All Discrete-Time Sinusoids Are Periodic

A discrete-time signal $x[n]$ is said to be N_0-periodic if

$$x[n] = x[n + N_0] \tag{8.4}$$

for some positive integer N_0. The smallest value of N_0 that satisfies Eq. (8.4) is the *period* of $x[n]$. Figure 8.14 shows an example of a periodic signal of period $N_0 = 6$. Observe that each period contains six samples (or values). If we consider the first cycle starts at $n = 0$, the last sample (or value) in this cycle occurs at $n = N_0 - 1 = 5$ (not at $n = N_0 = 6$). Note also that, by definition, a periodic signal must begin at $n = -\infty$ (an everlasting signal) for the reasons discussed in Sec. 1.3.3.

If a signal $\cos \Omega n$ is N_0-periodic, then

$$\cos \Omega n = \cos \Omega (n + N_0) = \cos (\Omega n + \Omega N_0)$$

This result is possible only if ΩN_0 is an integral multiple of 2π; that is,

$$\Omega N_0 = 2\pi m \qquad m \text{ integer}$$

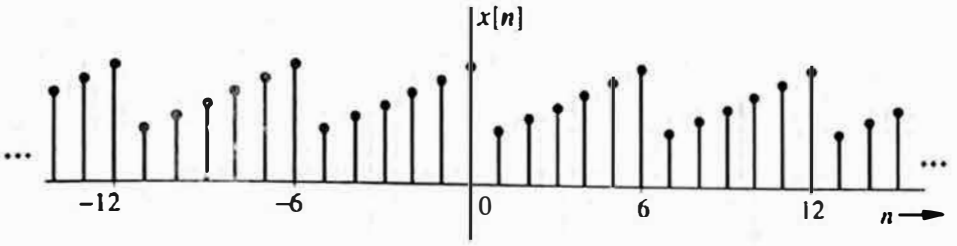

Figure 8.14 A discrete-time periodic signal.

or

$$\frac{\Omega}{2\pi} = \frac{m}{N_0}$$

Because both m and N_0 are integers, this equation implies that the sinusoid $\cos \Omega n$ is periodic only if $\frac{\Omega}{2\pi}$ is a rational number. In this case, the period N_0 is given by

$$N_0 = m\left(\frac{2\pi}{\Omega}\right) \tag{8.5}$$

To compute N_0, we must choose the smallest value of m that will make $m(\frac{2\pi}{\Omega})$ an integer. For example, if $\Omega = \frac{4\pi}{17}$, then the smallest value of m that will make $m\frac{2\pi}{\Omega} = m\frac{17}{2}$ an integer is 2. In this case, we therefore see that

$$N_0 = m\frac{2\pi}{\Omega} = 2\frac{17}{2} = 17$$

Using a similar argument, we can show that this discussion also applies to a discrete-time exponential $e^{j\Omega n}$. Thus, a discrete-time exponential $e^{j\Omega n}$ is periodic only if $\frac{\Omega}{2\pi}$ is a rational number.†

Physical Explanation of the Periodicity Relationship

Qualitatively, the periodicity relationship [see Eq. (8.5)] can be explained by recognizing that a discrete-time sinusoid $\cos \Omega n$ can be obtained by sampling a continuous-time sinusoid $\cos \Omega t$ at unit time interval $T = 1$; that is, $\cos \Omega t$ sampled at $t = 0, 1, 2, 3, \ldots$. This fact means $\cos \Omega t$ is the envelope of $\cos \Omega n$. Since the period of $\cos \Omega t$ is $2\pi/\Omega$, there are $2\pi/\Omega$ number of samples (elements) of $\cos \Omega n$ in one cycle of its envelope. This number may or may not be an integer.

Figure 8.15 shows three sinusoids: $\cos(\frac{\pi}{4}n)$, $\cos(\frac{4\pi}{17}n)$, and $\cos(0.8n)$. Figure 8.15a shows $\cos(\frac{\pi}{4}n)$, for which there are exactly eight samples in each cycle of its envelope ($\frac{2\pi}{\Omega} = 8$). Thus, $\cos(\frac{\pi}{4}n)$ repeats every cycle of its envelope. Clearly, $\cos(4n/\pi)$ is periodic with period 8. On the other hand, Fig. 8.15b, which shows $\cos(\frac{4\pi}{17}n)$, has an average of $\frac{2\pi}{\Omega} = 8.5$ samples (not an integral number) in one cycle of its envelope. Therefore, the second cycle of the envelope will not be identical to the first cycle. But there are 17 samples (an integral number) in two cycles of its envelope. Hence, the pattern becomes repetitive every two cycles of its envelope.

† We can also demonstrate this point by observing that if $e^{j\Omega n}$ is N_0-periodic, then

$$e^{j\Omega n} = e^{j\Omega(n+N_0)} = e^{j\Omega n}e^{j\Omega N_0}$$

This result is possible only if $\Omega N_0 = 2\pi m$ for some integer m. This conclusion leads to Eq. (8.5).

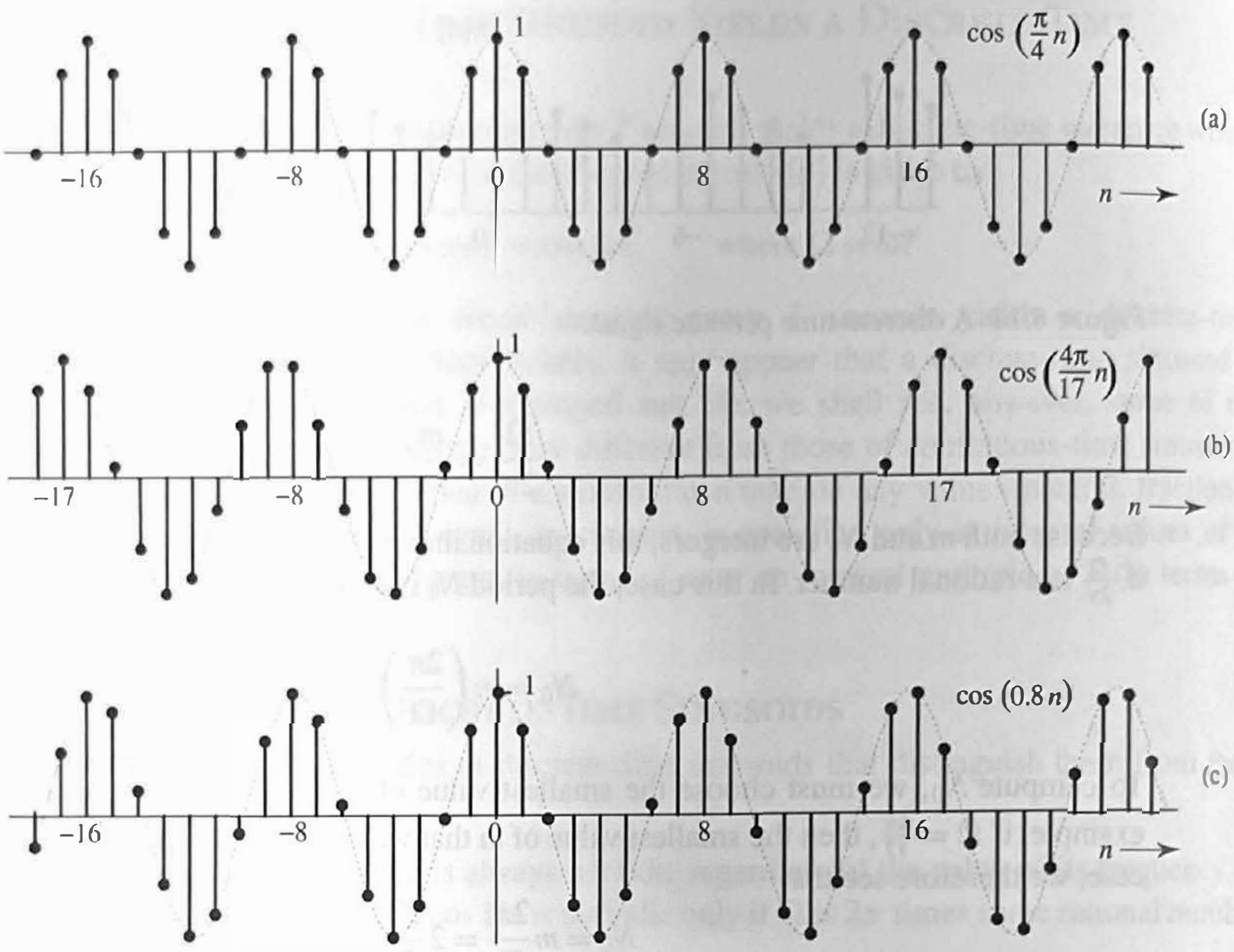

Figure 8.15 Physical explanation of the periodicity relationship.

Therefore, $\cos(\frac{4\pi}{17}n)$ is also repetitive but its period is 17 samples (two cycles of its envelope). This observation indicates that a signal $\cos \Omega n$ is periodic only if we can fit an integral number (N_0) of samples in m integral number of cycles of its envelope so that the pattern becomes repetitive every m cycles of its envelope. Because the period of the envelope is $\frac{2\pi}{\Omega}$, we conclude that

$$N_0 = m\left(\frac{2\pi}{\Omega}\right)$$

which is precisely the condition of periodicity in Eq. (8.5). If $\frac{\Omega}{2\pi}$ is irrational, it is impossible to fit an integral number (N_0) of samples in an integral number (m) of cycles of its envelope, and the pattern can never become repetitive. For instance, the sinusoid $\cos(0.8n)$ in Fig. 8.15c has an average of 2.5π samples (an irrational number) per envelope cycle, and the pattern can never be made repetitive over any integral number (m) of cycles of its envelope; so $\cos(0.8n)$ is not periodic.

DRILL 8.8 Assessing Periodicity

State with reasons if the following sinusoids are periodic. If periodic, find the period. **(a)** $\cos(\frac{3\pi}{7}n)$, **(b)** $\cos(\frac{10}{7}n)$, and **(c)** $\cos(\sqrt{\pi}n)$.

ANSWERS

(a) periodic with $N_0 = 14$; **(b)** and **(c)** are both aperiodic since $\Omega/2\pi$ is irrational.

Non-Uniqueness of Discrete-Time Sinusoid Waveforms

A continuous-time sinusoid $\cos \omega t$ has a unique waveform for every real value of ω in the range 0 to ∞. Increasing ω results in a sinusoid of ever-increasing frequency. Such is not the case for the discrete-time sinusoid $\cos \Omega n$ because

$$\cos[(\Omega \pm 2\pi m)n] = \cos \Omega n \qquad m \text{ integer}$$

and

$$e^{j(\Omega \pm 2\pi m)n} = e^{j\Omega n} \qquad m \text{ integer}$$

This shows that the discrete-time sinusoids $\cos \Omega n$ (and exponentials $e^{j\Omega n}$) separated by values of Ω in integral multiples of 2π are identical. The reason for the periodic nature of the frequency response of an LTID system is now clear. Since the sinusoids (or exponentials) with frequencies separated by interval 2π are identical, the system response to such sinusoids is also identical and, hence, is periodic with period 2π.

This discussion shows that the discrete-time sinusoid $\cos \Omega n$ has a unique waveform only for the values of Ω in the range $-\pi$ to π. This band is called the *fundamental band*. Every frequency Ω, no matter how large, is identical to some frequency, Ω_a, in the fundamental band $(-\pi \leq \Omega_a < \pi)$, where[†]

$$\Omega_a = \Omega - 2\pi m \qquad -\pi \leq \Omega_a < \pi \quad \text{and} \quad m \text{ integer} \tag{8.6}$$

The integer m can be positive or negative. We use Eq. (8.6) to plot the fundamental band frequency Ω_a versus the frequency Ω of a sinusoid (Fig. 8.16a). The frequency Ω_a is the modulo 2π value of Ω. All these conclusions are also valid for exponential $e^{j\Omega n}$.

All Discrete-Time Signals Are Inherently Bandlimited

This discussion leads to the surprising conclusion that all discrete-time signals are inherently bandlimited, with frequencies lying in the range $-\pi$ to π radians per sample. In terms of frequency $\mathcal{F} = \Omega/2\pi$, where $\mathcal{F}$ is in cycles per sample, all frequencies $\mathcal{F}$ separated by an integer number are identical. For instance, all discrete-time sinusoids of frequencies 0.3, 1.3, 2.3, . . . cycles per sample are identical. The fundamental range of frequencies is -0.5 to 0.5 cycles per sample.

Any discrete-time sinusoid of frequency beyond the fundamental band, when plotted, appears and behaves, in every way, like a sinusoid having its frequency in the fundamental band. It is impossible to distinguish between the two signals. Thus, in a basic sense, discrete-time frequencies beyond $|\Omega| = \pi$ or $|\mathcal{F}| = 1/2$ do not exist. Yet, in a "mathematical" sense, we must admit the existence of sinusoids of frequencies beyond $\Omega = \pi$. What does this mean?

A Man Named Robert

To give an analogy, consider a fictitious person Mr. Robert Thompson. His mother calls him Robby; his acquaintances call him Bob, his close friends call him by his nickname, Shorty. Yet, Robert, Robby, Bob, and Shorty are one and the same person. However, we cannot say that only

[†] More compactly, we can compute the apparent frequency of Eq. (8.6) as $\Omega_a = \langle \Omega + \pi \rangle_{2\pi} - \pi$, where $\langle \cdot \rangle_{2\pi}$ designates a modulo-2π operation.

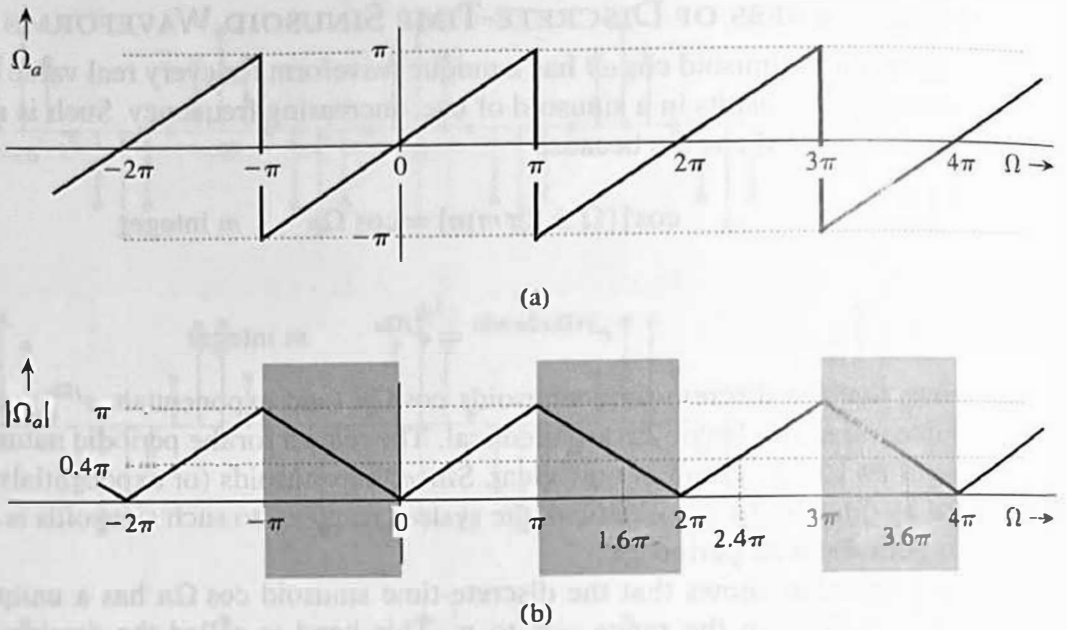

Figure 8.16 (a) Actual frequency versus (b) apparent frequency.

Mr. Robert Thompson exists, or only Robby exists, or only Shorty exists, or only Bob exists. All these four persons exist, although they are one and the same individual. In the same way, we cannot say that the frequency $\pi/2$ exists and frequency $5\pi/2$ does not exist; they are both the same entity, called by different names.

It is in this sense that we have to admit the existence of frequencies beyond the fundamental band. Indeed, mathematical expressions in the frequency domain automatically cater to this need by their built-in periodicity. As seen earlier, the very structure of the frequency response is 2π-periodic. We shall also see later, in Ch. 10, that discrete-time signal spectra are also 2π-periodic.

Admitting the existence of frequencies beyond π also serves mathematical and computational convenience in digital signal-processing applications. Values of frequencies beyond π may also originate naturally in the process of sampling continuous-time sinusoids. Because there is no upper limit on the value of ω, there is no upper limit on the value of the resulting discrete-time frequency $\Omega = \omega T$ either.[†]

The highest possible frequency is π and the lowest frequency is 0 (dc or constant). Clearly, the high frequencies are those in the vicinity of $\Omega = (2m+1)\pi$ and the low frequencies are those in the vicinity of $\Omega = 2\pi m$ for all positive or negative integer values of m.

Further Reduction in the Frequency Range

Because $\cos(-\Omega n + \theta) = \cos(\Omega n - \theta)$, a frequency in the range $-\pi$ to 0 is identical to the frequency (of the same magnitude) in the range 0 to π (but with a change in phase sign). Consequently, the *apparent frequency* for a discrete-time sinusoid of any frequency is equal to

[†] However, if Ω goes beyond π, the resulting aliasing reduces the apparent frequency to $\Omega_a < \pi$.

some value in the range 0 to π. Thus, $\cos(8.7\pi n + \theta) = \cos(0.7\pi n + \theta)$, and the apparent frequency is 0.7π. Similarly,

$$\cos(9.6\pi n + \theta) = \cos(-0.4\pi n + \theta) = \cos(0.4\pi n - \theta)$$

Hence, the frequency 9.6π is identical (in every respect) to frequency -0.4π, which, in turn, is equal (within the sign of its phase) to frequency 0.4π. In this case, the apparent frequency reduces to $|\Omega_a| = 0.4\pi$. We can generalize the result to say that the apparent frequency of a discrete-time sinusoid Ω is $|\Omega_a|$, as found from Eq. (8.6), and if $\Omega_a < 0$, there is a phase reversal. Figure 8.16b plots Ω versus the apparent frequency $|\Omega_a|$. The shaded bands represent the ranges of Ω for which there is a phase reversal, when represented in terms of $|\Omega_a|$. For example, the apparent frequency for both the sinusoids $\cos(2.4\pi + \theta)$ and $\cos(3.6\pi + \theta)$ is $|\Omega_a| = 0.4\pi$, as seen from Fig. 8.16b. But 2.4π is in a clear band and 3.6π is in a shaded band. Hence, these sinusoids appear as $\cos(0.4\pi + \theta)$ and $\cos(0.4\pi - \theta)$, respectively.

Although every discrete-time sinusoid can be expressed as having frequency in the range from 0 to π, we generally use the frequency range from $-\pi$ to π instead of 0 to π for two reasons. First, exponential representation of sinusoids with frequencies in the range 0 to π requires a frequency range $-\pi$ to π. Second, even when we are using a trigonometric representation, we generally need the frequency range $-\pi$ to π to have exact identity (without phase reversal) of a higher-frequency sinusoid.

For certain practical advantages, in place of the range $-\pi$ to π, we often use other contiguous ranges of width 2π. The range 0 to 2π, for instance, is used in many applications. It is left as an exercise for the reader to show that the frequencies in the range from π to 2π are identical to those in the range from $-\pi$ to 0.

The Apparent Laziness of DT Exponentials

To provide additional insight regarding apparent frequency, we next use a discrete-time exponential rather than a sinusoid. As shown in Fig. 8.11, a discrete-time complex exponential $e^{j\Omega n}$ can be viewed as a phasor rotating at a uniform angular speed of $|\Omega|$ rad/sample, where the direction of rotation depends on whether Ω is positive (counterclockwise rotation) or negative (clockwise rotation). For $|\Omega| < \pi$, angular speed increases with $|\Omega|$, as is natural. When $|\Omega|$ increases beyond π, however, something interesting happens. Let $\Omega = \pi + x$ and $x < \pi$. Figures 8.17a, 8.17b, and 8.17c show $e^{j\Omega n}$ as n progresses from $0 \rightarrow 1$, $1 \rightarrow 2$, and $2 \rightarrow 3$, respectively. Since $\Omega = \pi + x > 0$, we can rightly view this progression as angular steps of size $\pi + x$ rad/sample in the counterclockwise direction (solid arcs). However, we may also interpret the phasor motion as being clockwise at the lower speed of $\pi - x$ rad/sample (dotted arcs). Either of these interpretations describes the phasor motion correctly. If this motion is seen by a human eye, which is a lowpass filter, it will automatically interpret the speed as $\pi - x$, the lower of the two speeds. This interpretation is precisely $|\Omega_a|$, which equals $\pi - x$ in this case. This is the genesis of why, as Ω increases beyond π, the frequency displays a counterintuitive behavior and appears to slow down. Apparent frequency views all DT exponentials as incredibly lazy, only traveling the smallest possible angle to move from one sample to the next. This phenomenon is also commonly seen in movies, where at certain speeds wheels and other rotating objects such as helicopter blades appear to be stationary or move backward.

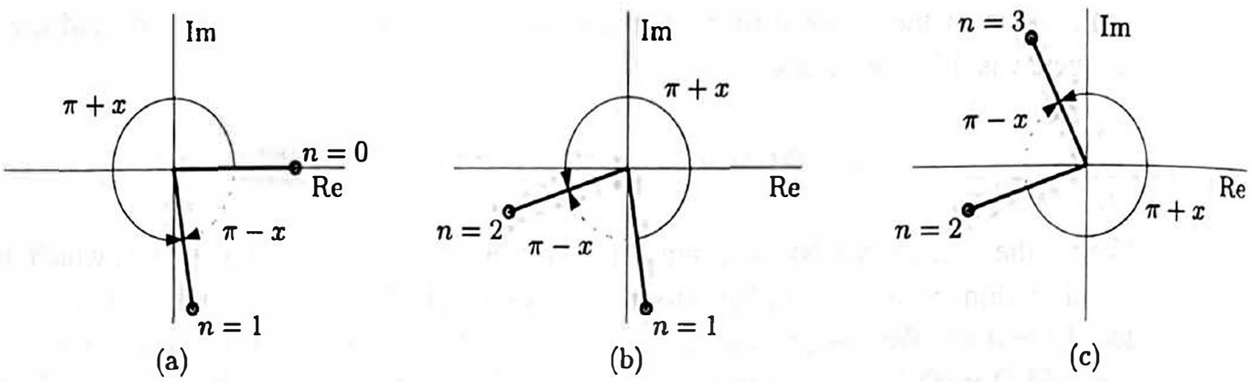

Figure 8.17 Progression of $e^{j(\pi+x)n}$ for n from **(a)** $0 \to 1$, **(b)** $1 \to 2$, and **(c)** $2 \to 3$.

EXAMPLE 8.6 Apparent Frequency

Express the following signals in terms of their apparent frequencies: **(a)** $\cos(0.5\pi n + \theta)$, **(b)** $\cos(1.6\pi n + \theta)$, **(c)** $\sin(1.6\pi n + \theta)$, **(d)** $\cos(2.3\pi n + \theta)$, and **(e)** $\cos(34.699n + \theta)$.

(a) $\Omega = 0.5\pi$ is in the reduced range already. This is also apparent from Fig. 8.16a or 8.16b. Because $\Omega_a = 0.5\pi$, there is no phase reversal, and the apparent sinusoid is $\cos(0.5\pi n + \theta)$.

(b) We express $1.6\pi = -0.4\pi + 2\pi$ so that $\Omega_a = -0.4\pi$ and $|\Omega_a| = 0.4\pi$. Also, Ω_a is negative, implying sign change for the phase. Hence, the apparent sinusoid is $\cos(0.4\pi n - \theta)$. This fact is also apparent from Fig. 8.16b.

(c) We first convert the sine form to cosine form as $\sin(1.6\pi n + \theta) = \cos(1.6\pi n - (\pi/2) + \theta)$. In part **(b)**, we found $\Omega_a = -0.4\pi$. Hence, the apparent sinusoid is $\cos(0.4\pi n + (\pi/2) - \theta) = -\sin(0.4\pi n - \theta)$. In this case, both the phase and the amplitude change signs.

(d) $2.3\pi = 0.3\pi + 2\pi$ so that $\Omega_a = 0.3\pi$. Hence, the apparent sinusoid is $\cos(0.3\pi n + \theta)$.

(e) We have $34.699 = -3 + 6(2\pi)$. Hence, $\Omega_a = -3$, and the apparent frequency $|\Omega_a| = 3$ rad/sample. Because Ω_a is negative, there is a sign change of the phase. Hence, the apparent sinusoid is $\cos(3n - \theta)$.

DRILL 8.9 Apparent Frequency

Show that the sinusoids having frequencies Ω of **(a)** 2π, **(b)** 3π, **(c)** 5π, **(d)** 3.2π, **(e)** 22.1327, and **(f)** $\pi + 2$ can be expressed, respectively, as sinusoids of frequencies **(a)** 0, **(b)** π, **(c)** π, **(d)** 0.8π, **(e)** 3, and **(f)** $\pi - 2$. Show that in cases (d), (e), and (f), the phase changes sign.

8.3.6 Exponentially Varying Discrete-Time Sinusoid $\gamma^n \cos(\Omega n + \theta)$

This is a sinusoid $\cos(\Omega n + \theta)$ with an exponentially varying amplitude γ^n. It is obtained by multiplying the sinusoid $\cos(\Omega n + \theta)$ by an exponential γ^n. Figure 8.18 shows signals

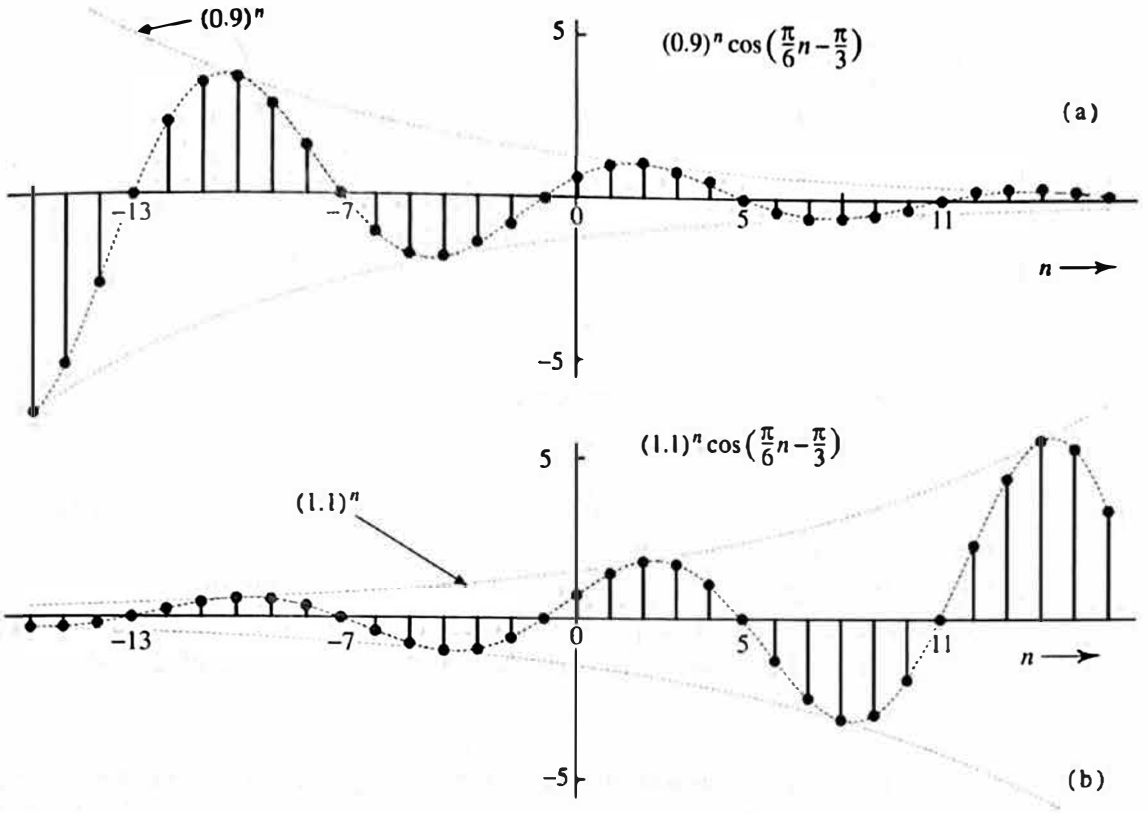

Figure 8.18 Examples of exponentially varying discrete-time sinusoids.

$(0.9)^n \cos(\frac{\pi}{6}n - \frac{\pi}{3})$ and $(1.1)^n \cos(\frac{\pi}{6}n - \frac{\pi}{3})$. Observe that if $|\gamma| < 1$, the amplitude decays, and if $|\gamma| > 1$, the amplitude grows exponentially.

8.4 Aliasing and Sampling Rate

The non-uniqueness of discrete-time sinusoids and the periodic repetition of the same waveforms at intervals of 2π may seem innocuous, but in reality it leads to a serious problem for processing continuous-time signals by digital filters. A continuous-time sinusoid $\cos\omega t$ sampled every T seconds ($t = nT$) results in a discrete-time sinusoid $\cos\omega nT$, which is $\cos\Omega n$ with $\Omega = \omega T$. The discrete-time sinusoids $\cos\Omega n$ have unique waveforms only for the values of frequencies in the range $\Omega < \pi$ or $\omega T < \pi$. Therefore, samples of continuous-time sinusoids of two (or more) different frequencies can generate the same discrete-time signal, as shown in Fig. 8.19. *This phenomenon is known as aliasing because through sampling, two entirely different analog sinusoids take on the same "discrete-time" identity.*[†]

[†] Figure 8.19 shows samples of two sinusoids $\cos 12\pi t$ and $\cos 2\pi t$ taken every 0.2 second. The corresponding discrete-time frequencies ($\Omega = \omega T = 0.2\omega$) are $\cos 2.4\pi$ and $\cos 0.4\pi$. The apparent frequency of 2.4π is 0.4π, identical to the discrete-time frequency corresponding to the lower sinusoid. This shows that the samples of both these continuous-time sinusoids at 0.2-second intervals are identical, as verified from Fig. 8.19.

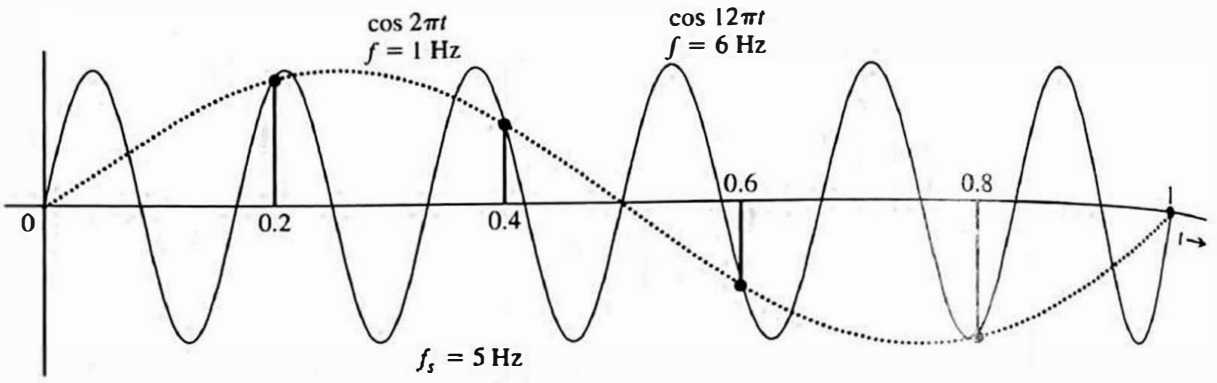

Figure 8.19 Demonstration of the aliasing effect.

Aliasing causes ambiguity in digital signal processing, which makes it impossible to determine the true frequency of the sampled signal. Consider, for instance, digitally processing a continuous-time signal that contains two distinct components of frequencies ω_1 and ω_2. The samples of these components appear as discrete-time sinusoids of frequencies $\Omega_1 = \omega_1 T$ and $\Omega_2 = \omega_2 T$. If Ω_1 and Ω_2 happen to differ by an integer multiple of 2π (if $\omega_2 - \omega_1 = 2k\pi/T$), the two frequencies will be read as the same (lower of the two) frequency by the digital processor.† As a result, the higher-frequency component ω_2 not only is lost for good (by losing its identity to ω_1), but also it reincarnates as a component of frequency ω_1, thus distorting the true amplitude of the original component of frequency ω_1. Hence, the resulting processed signal will be distorted. Clearly, aliasing is highly undesirable and should be avoided. To avoid aliasing, the frequencies of the continuous-time sinusoids to be processed should be kept within the fundamental band $\omega T \leq \pi$ or $\omega \leq \pi/T$. Under this condition, the question of ambiguity or aliasing does not arise because any continuous-time sinusoid of frequency in this range has a unique waveform when it is sampled. Therefore, if ω_h is the highest frequency to be processed, then, to avoid aliasing,

$$\omega_h < \frac{\pi}{T}$$

If f_h is the highest frequency in hertz, $f_h = \omega_h/2\pi$, and we avoid aliasing if

$$f_h < \frac{1}{2T} \quad \text{or} \quad T < \frac{1}{2f_h} \tag{8.7}$$

This shows that discrete-time signal processing places the limit on the highest frequency f_h that can be processed for a given value of the sampling interval T. Fortunately, we can process a signal of any frequency (without aliasing) by choosing a suitably small value of T. Since the sampling frequency f_s is the reciprocal of the sampling interval T, we can also express Eq. (8.7) as

† In the case shown in Fig. 8.19, $\omega_1 = 12\pi$, $\omega_2 = 2\pi$, and $T = 0.2$. Hence, $\omega_2 - \omega_1 = 10\pi T = 2\pi$, and the two frequencies are read as the same frequency $\Omega = 0.4\pi$ by the digital processor.

$$f_s = \frac{1}{T} > 2f_h \qquad \text{or} \qquad f_h < \frac{f_s}{2} \tag{8.8}$$

This result is a special case of the well-known *sampling theorem* (proof in Ch. 5). It states that for a discrete-time system to process a continuous-time sinusoid, the sampling rate must be greater than twice the frequency (in hertz) of the sinusoid. In short, *a sampled sinusoid must have a minimum of two samples per cycle*.† For sampling rates below this minimum value, the output signal will be aliased, which means it will be mistaken for a sinusoid of lower frequency.

Anti-Aliasing Filter

If the sampling rate fails to satisfy Eq. (8.8), aliasing occurs, causing the frequencies beyond $f_s/2$ Hz to masquerade as lower frequencies to corrupt the spectrum at frequencies below $f_s/2$. To avoid such a corruption, a signal to be sampled is passed through an *anti-aliasing* filter of bandwidth $f_s/2$ prior to sampling. This operation ensures the condition of Eq. (8.8). The drawback of such a filter is that we lose the spectral components of the signal beyond frequency $f_s/2$, which is preferable to the aliasing corruption of the signal at frequencies below $f_s/2$. Chapter 5 presents a detailed analysis of the aliasing problem.

EXAMPLE 8.7 Maximum Sampling Interval

Determine the maximum sampling interval T that can be used in a discrete-time oscillator that generates a sinusoid of 50 kHz.

Here, the highest significant frequency $f_h = 50$ kHz. Therefore from Eq. (8.7),

$$T < \frac{1}{2f_h} = 10\,\mu\text{s}$$

The sampling interval must be less than 10 μs. The sampling frequency is $f_s = 1/T > 100$ kHz.

EXAMPLE 8.8 Maximum Frequency Without Aliasing

A discrete-time amplifier uses a sampling interval $T = 25$ μs. What is the highest frequency of a signal that can be processed with this amplifier without aliasing?

From Eq. (8.7),

$$f_h < \frac{1}{2T} = 20\,\text{kHz}$$

† Strictly speaking, we must have more than two samples per cycle.

EXAMPLE 8.9 Determining Apparent Frequency in Hertz

A digital system with sampling interval $T = 0.001$ second samples continuous-time sinusoids of the following frequencies: **(a)** 400 Hz, **(b)** 1 kHz, **(c)** 1.4 kHz, **(d)** 1.5kHz, and **(e)** 3.622 kHz. Determine the apparent frequencies f_a (in Hz) of the resulting sampled signals.

The sampling frequency is $f_s = 1/T = 1000$ Hz. The folding frequency $f_s/2 = 500$ Hz. Hence, sinusoids below 500 Hz will not be aliased and sinusoids of frequency above 500 Hz will be aliased. To determine an expression for the hertzian apparent frequency, we substitute $\Omega = 2\pi f/f_s$ into Eq. (8.6) to obtain

$$f_a = f - mf_s \qquad -f_s/2 \le f_a < f_s/2 \quad \text{and} \quad m \text{ integer} \tag{8.9}$$

(a) Since 400 Hz is less than $f_s/2 = 500$ Hz, there is no aliasing and $f_a = 400$ Hz.

(b) Using Eq. (8.9), $f_a = 1000 - 1(f_s) = 0$ Hz. Thus, the sampled signal appears as samples of a dc signal.

(c) Using Eq. (8.9), $f_a = 1400 - 1(f_s) = 400$ Hz. Thus, the sampled signal appears as samples of a 400 Hz signal.

(d) Using Eq. (8.9), $f_a = 1600 - 2(f_s) = -400$ Hz. Thus, $|f_a| = 400$ Hz, and the sampled signal appears as samples of a 400 Hz signal.

(e) Using Eq. (8.9), $f_a = 3622 - 4(f_s) = -378$ Hz. Thus, $|f_a| = 378$ Hz, and the sampled signal appears as samples of a 378 Hz signal.

8.5 EXAMPLES OF DISCRETE-TIME SYSTEMS

We shall give here four examples of discrete-time systems. In the first two examples, the signals are inherently of the discrete-time variety. In the third and fourth examples, a continuous-time signal is processed by a discrete-time system, as illustrated in Fig. 8.2, by discretizing the signal through sampling.

EXAMPLE 8.10 Savings Account

A person makes a deposit (the input) in a bank regularly at an interval of T (say, 1 month). The bank pays a certain interest on the account balance during the period T and mails out a periodic statement of the account balance (the output) to the depositor. Find the equation relating the output $y[n]$ (the balance) to the input $x[n]$ (the deposit).

In this case, the signals are inherently discrete time. Let

$x[n]$ = deposit made at the nth discrete instant

$y[n]$ = account balance at the nth instant computed immediately after receipt of the nth deposit $x[n]$

r = interest per dollar per period T

The balance $y[n]$ is the sum of (i) the previous balance $y[n-1]$, (ii) the interest on $y[n-1]$ during the period T, and (iii) the deposit $x[n]$

$$\begin{aligned} y[n] &= y[n-1] + ry[n-1] + x[n] \\ &= (1+r)y[n-1] + x[n] \end{aligned}$$

or

$$y[n] - ay[n-1] = x[n] \qquad a = 1+r \tag{8.10}$$

In this example, the deposit $x[n]$ is the input (cause) and the balance $y[n]$ is the output (effect).

A withdrawal from the account is a negative deposit. Therefore, this formulation can handle deposits as well as withdrawals. It also applies to a loan payment problem with the initial value $y[0] = -M$, where M is the amount of the loan. A loan is an initial deposit with a negative value. Alternately, we may treat a loan of M dollars taken at $n = 0$ as an input of $-M$ at $n = 0$ (see Prob. 9.5-23).

We can express Eq. (8.10) in an alternate form. The choice of index n in Eq. (8.10) is completely arbitrary, so we can substitute $n+1$ for n to obtain

$$y[n+1] - ay[n] = x[n+1] \tag{8.11}$$

We also could have obtained Eq. (8.11) directly by realizing that $y[n+1]$, the balance at instant $(n+1)$, is the sum of $y[n]$ plus $ry[n]$ (the interest on $y[n]$) plus the deposit (input) $x[n+1]$ at instant $(n+1)$.

The difference equation in Eq. (8.10) uses delays, whereas the form in Eq. (8.11) uses advances. Thus, Eq. (8.10) is said to be in *delay form* and Eq. (8.11) is said to be in *advance form*. The delay form is more natural because operation of delay is causal, hence realizable. In contrast, advance operation, being noncausal, is unrealizable. We use the advance form primarily for its mathematical convenience over the delay form.†

We shall now represent this system in a block diagram form, which is basically a road map to a hardware (or software) realization of the system. For this purpose, the causal (realizable) delay form in Eq. (8.10) will be used. There are three basic operations in this equation: *addition, scalar multiplication,* and *delay*. Figure 8.20 shows their schematic representation. In addition, we also have a *pickoff* node (Fig. 8.20d), which is used to provide multiple copies of a signal at its input.

† Use of the advance form results in discrete-time system equations that are identical in form to those for continuous-time systems. This will become apparent later. In transform analysis, advance form leads to the more convenient variable z instead of the clumsy z^{-1} that arises from delay form.

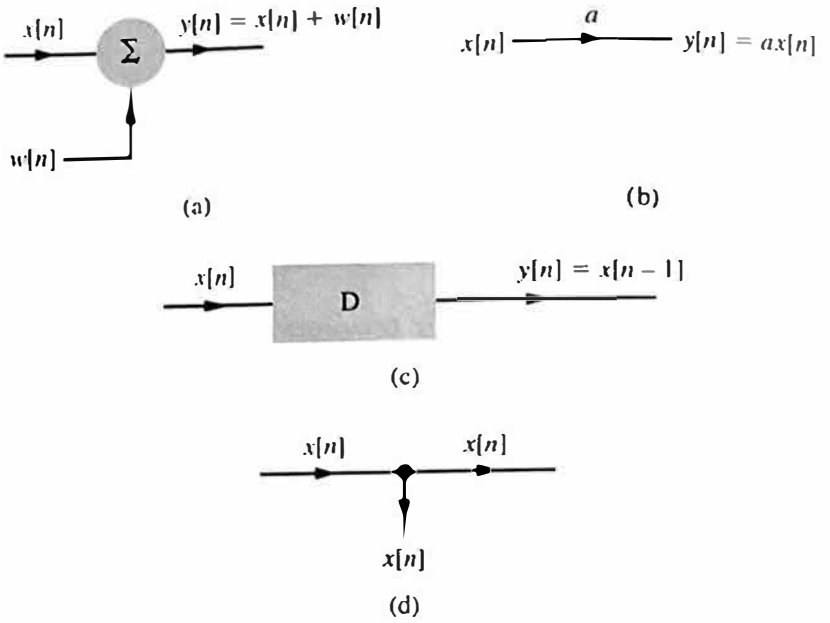

Figure 8.20 Schematic representations of basic operations on sequences.

Figure 8.21 shows in block diagram form a system represented by Eq. (8.10). To understand this realization, it is helpful to rewrite Eq. (8.10) as $y[n] = ay[n-1] + x[n]$ ($a = 1 + r$). Now, assume that the output $y[n]$ is available at the pickoff node N. A unit delay of $y[n]$ results in $y[n-1]$, which is multiplied by a scalar of value a to yield $ay[n-1]$. Next, we generate $y[n]$ by adding the input $x[n]$ and $ay[n-1]$.† Observe that node N is a pickoff node, from which two copies of the output signal flow out: one as the feedback signal and the other as the output signal.

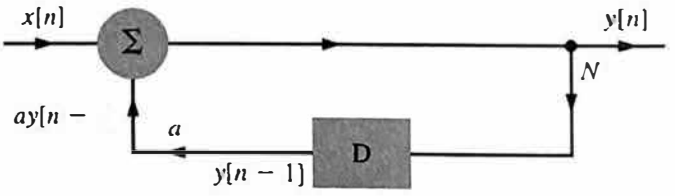

Figure 8.21 Realization of the savings account system.

† A unit delay represents one unit of time delay. In this example, one unit of delay in the output corresponds to period T for the actual output.

EXAMPLE 8.11 Sales Estimate

During semester n, $x[n]$ students enroll in a course requiring a certain textbook while the publisher sells $y[n]$ new copies of the same book. On average, one-quarter of students with books in salable condition resell the texts at the end of the semester, and the book life is three semesters. Write the equation relating $y[n]$, the new books sold by the publisher, to $x[n]$, the number of students enrolled in the nth semester, assuming that every student buys a book.

In the nth semester, the total books $x[n]$ sold to students must be equal to $y[n]$ (new books from the publisher) plus the used books from students enrolled in the preceding two semesters (because the book life is only three semesters). There are $y[n-1]$ new books sold in semester $(n-1)$, and one-quarter of these books, that is, $(1/4)y[n-1]$, will be resold in the nth semester. Also, $y[n-2]$ new books are sold in semester $n-2$, and one-quarter of these, that is, $(1/4)y[n-2]$, will be resold in semester $(n-1)$. Again, a quarter of these, that is, $(1/16)y[n-2]$, will be resold in the nth semester. Therefore, $x[n]$ must be equal to the sum of $y[n]$, $(1/4)y[n-1]$, and $(1/16)y[n-2]$.

$$y[n]+\tfrac{1}{4}y[n-1]+\tfrac{1}{16}y[n-2]=x[n] \tag{8.12}$$

Equation (8.12) can also be expressed in an alternative form by realizing that this equation is valid for any value of n. Therefore, replacing n by $n+2$, we obtain

$$y[n+2]+\tfrac{1}{4}y[n+1]+\tfrac{1}{16}y[n]=x[n+2] \tag{8.13}$$

This is the alternative form of Eq. (8.12).

To facilitate a realization of a system with this input–output equation, we rewrite the delay-form Eq. (8.12) as $y[n] = -\frac{1}{4}y[n-1] - \frac{1}{16}y[n-2] + x[n]$. Figure 8.22 shows a corresponding hardware realization using two unit delays in cascade.†

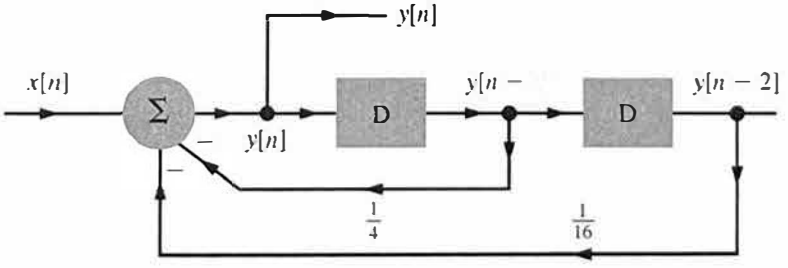

Figure 8.22 Realization of the system representing the sales estimate in Ex. 8.11.

---

† The comments in the preceding footnote apply here also. Although one unit of delay in this example is one semester, we need not use this value in the hardware realization. Any value other than one semester results in a time-scaled output.

EXAMPLE 8.12 Digital Differentiator

Design a discrete-time system, like the one in Fig. 8.2, to differentiate continuous-time signals. This differentiator is used in an audio system having an input signal bandwidth below 20 kHz.

In this case, the output $y(t)$ is required to be the derivative of the input $x(t)$. The discrete-time processor (system) G processes the samples of $x(t)$ to produce the discrete-time output $y[n]$. Let $x[n]$ and $y[n]$ represent the samples T seconds apart of the signals $x(t)$ and $y(t)$, respectively, that is,

$$x[n] = x(nT) \qquad \text{and} \qquad y[n] = y(nT) \tag{8.14}$$

The signals $x[n]$ and $y[n]$ are the input and the output for the discrete-time system G. Now, we require that

$$y(t) = \frac{dx(t)}{dt}$$

Therefore, at $t = nT$ (see Fig. 8.23a),

$$y(nT) = \left.\frac{dx(t)}{dt}\right|_{t=nT} = \lim_{T\to 0} \frac{1}{T}[x(nT) - x[(n-1)T]]$$

By using the notation in Eq. (8.14), the foregoing equation can be expressed as

$$y[n] = \lim_{T\to 0} \frac{1}{T}\{x[n] - x[n-1]\}$$

This is the input–output relationship for G required to achieve our objective. In practice, the sampling interval T cannot be zero. Assuming T to be sufficiently small, the equation just given can be expressed as

$$y[n] = \frac{1}{T}\{x[n] - x[n-1]\} \tag{8.15}$$

The approximation improves as T approaches 0. A discrete-time processor G to realize Eq. (8.15) is shown inside the shaded box in Fig. 8.23b. The system in Fig. 8.23b acts as a differentiator. This example shows how a continuous-time signal can be processed by a discrete-time system. From Eq. (8.8), we know the sampling interval must be chosen according to

$$T \le \frac{1}{2 \times \text{highest frequency}} = \frac{1}{40{,}000} = 25\ \mu\text{s}$$

To see how well this method works, let us consider the differentiator in Fig. 8.23b with a ramp input $x(t) = t$, depicted in Fig. 8.23c. If the system were to act as a differentiator, then the output $y(t)$ of the system should be the unit step function $u(t)$. Let us investigate how the system performs this particular operation and how well the system achieves the objective.

The samples of the input $x(t) = t$ at the interval of T seconds act as the input to the discrete-time system G. These samples, denoted by a compact notation $x[n]$, are, therefore,

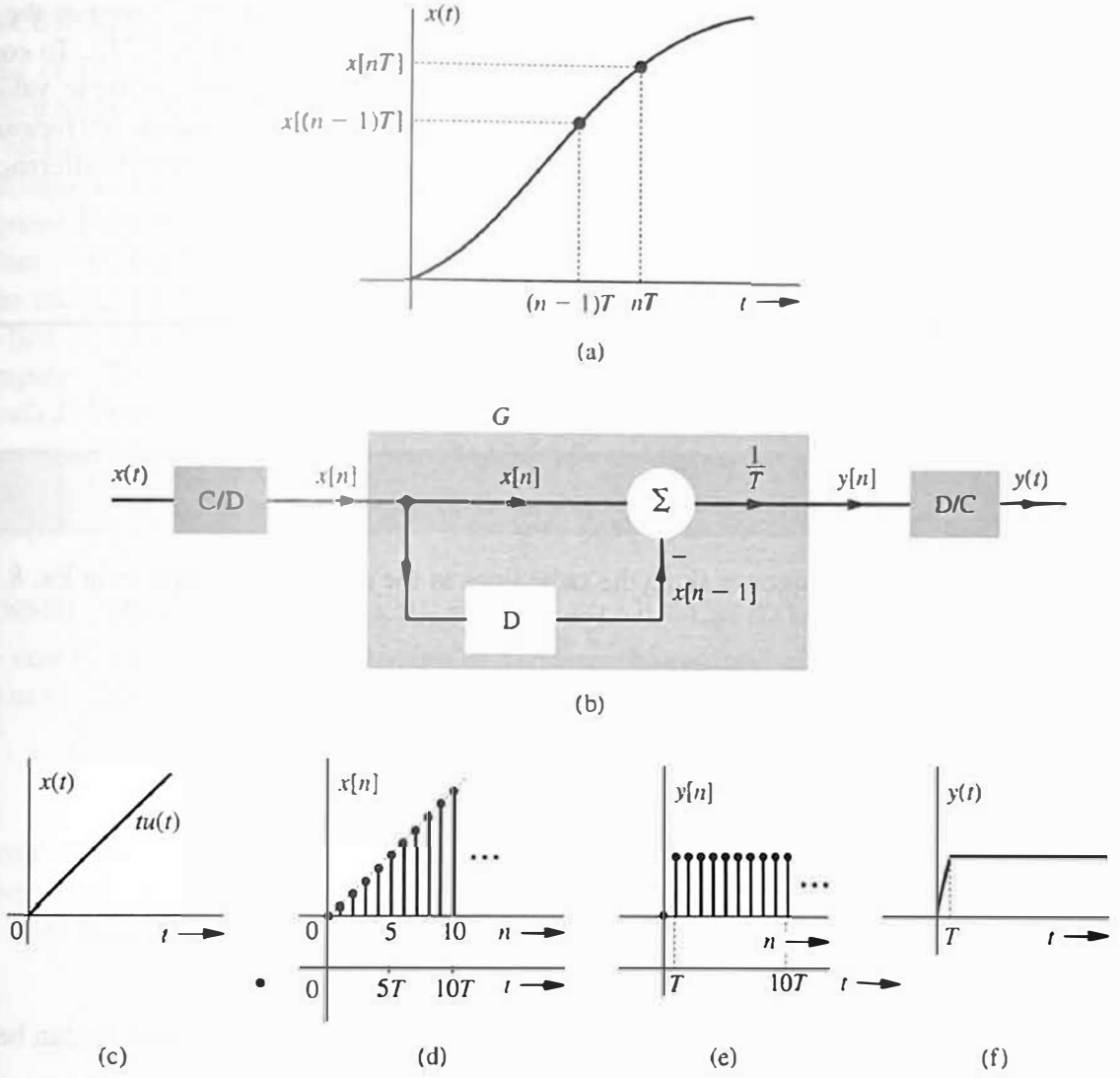

Figure 8.23 Digital differentiator and its realization.

$$x[n] = x(t)|_{t=nT} = t|_{t=nT} \qquad t \geq 0$$
$$= nT \qquad n \geq 0$$

Figure 8.23d shows the sampled signal $x[n]$. This signal acts as an input to the discrete-time system G. Figure 8.23b shows that the operation of G consists of subtracting a sample from the preceding (delayed) sample and then multiplying the difference with $1/T$. From Fig. 8.23d, it is clear that the difference between the successive samples is a constant $nT - (n-1)T = T$ for all samples, except for the sample at $n = 0$ (because there is no preceding sample at $n = 0$). The output of G is $1/T$ times the difference T, which is unity for all values of n, except $n = 0$, where it is zero. Therefore, the output $y[n]$ of G consists of samples of unit values for $n \geq 1$, as illustrated in Fig. 8.23e. The D/C (discrete-time to continuous-time) converter converts these samples into a continuous-time signal $y(t)$, as shown in Fig. 8.23f. Ideally, the output should have been $y(t) = u(t)$. This deviation from the ideal is due to our use of a nonzero sampling interval T. As T approaches zero, the output $y(t)$ approaches the desired output $u(t)$.

The digital differentiator in Eq. (8.15) is an example of what is known as the *backward difference* system. The reason for calling it so is obvious from Fig. 8.23a. To compute the derivative of $y(t)$, we are using the difference between the present sample value and the preceding (backward) sample value. If we use the difference between the next (forward) sample at $t = (n+1)T$ and the present sample at $t = nT$, we obtain a forward difference form of differentiator as

$$y[n] = \frac{1}{T}\{x[n+1] - x[n]\} \tag{8.16}$$

EXAMPLE 8.13 Digital Integrator

Design a digital integrator along the same lines as the digital differentiator in Ex. 8.12.

For an integrator, the input $x(t)$ and the output $y(t)$ are related by

$$y(t) = \int_{-\infty}^{t} x(\tau)\, d\tau$$

Therefore, at $t = nT$ (see Fig. 8.23a),

$$y(nT) = \lim_{T \to 0} \sum_{k=-\infty}^{n} x(kT)T$$

Using the usual notation $x(kT) = x[k], y(nT) = y[n]$, and so on, this equation can be expressed as

$$y[n] = \lim_{T \to 0} T \sum_{k=-\infty}^{n} x[k]$$

Assuming that T is small enough to justify the assumption $T \to 0$, we have

$$y[n] = T \sum_{k=-\infty}^{n} x[k] \tag{8.17}$$

This equation represents an example of an *accumulator* system. This digital integrator equation can be expressed in an alternate form. From Eq. (8.17), it follows that

$$y[n] - y[n-1] = Tx[n] \tag{8.18}$$

This is an altemate description for the digital integrator. Equations (8.17) and (8.18) are equivalent; the one can be derived from the other. Observe that the form of Eq. (8.18) is similar to that of Eq. (8.10). Hence, the block diagram representation of a digital integrator in the form of Eq. (8.18) is identical to that in Fig. 8.21 with $a = 1$ and the input multiplied by T.

Recursive and Nonrecursive Forms of Difference Equation

If Eq. (8.18) expresses Eq. (8.17) in another form, what is the difference between these two forms? Which form is preferable? To answer these questions, let us examine how the output is computed by each of these forms. In Eq. (8.17), the output $y[n]$ at any instant n is computed by adding all the past input values until n. This can mean a large number of additions. In contrast, Eq. (8.18) can be expressed as $y[n] = y[n-1] + Tx[n]$. Hence, computation of $y[n]$ involves the addition of only two values: the preceding output value $y[n-1]$ and the present input value $x[n]$. The computations are done recursively by using the preceding output values. For example, if the input starts at $n = 0$, we first compute $y[0]$. Then we use the computed value $y[0]$ to compute $y[1]$. Knowing $y[1]$, we compute $y[2]$, and so on. The computations are recursive. This is why the form of Eq. (8.18) is called the *recursive* form and the form of Eq. (8.17) is called the *nonrecursive* form. Clearly, "recursive" and "nonrecursive" describe two different ways of presenting the same information. Equations (8.10), (8.12), and (8.18) are examples of recursive form, and Eqs. (8.15) and (8.17) are examples of nonrecursive form.

Kinship of Difference Equations to Differential Equations

We now show that a digitized version of a differential equation results in a difference equation. Let us consider a simple first-order differential equation

$$\frac{dy(t)}{dt} + cy(t) = x(t) \tag{8.19}$$

Consider uniform samples of $x(t)$ at intervals of T seconds. As usual, we use the notation $x[n]$ to denote $x(nT)$, the nth sample of $x(t)$. Similarly, $y[n]$ denotes $y[nT]$, the nth sample of $y(t)$. From the basic definition of a derivative, we can express Eq. (8.19) at $t = nT$ as

$$\lim_{T \to 0} \frac{y[n] - y[n-1]}{T} + cy[n] = x[n]$$

Clearing the fractions and rearranging the terms yield (assuming nonzero, but very small T)

$$y[n] + \alpha y[n-1] = \beta x[n] \tag{8.20}$$

where

$$\alpha = \frac{-1}{1+cT} \quad \text{and} \quad \beta = \frac{T}{1+cT}$$

We can also express Eq. (8.20) in advance form as

$$y[n+1] + \alpha y[n] = \beta x[n+1]$$

It is clear that a differential equation can be approximated by a difference equation of the same order. In this way, we can approximate an nth-order differential equation by a difference equation of nth order. Indeed, a digital computer solves differential equations by using an equivalent difference equation, which can be solved by means of simple operations of addition, multiplication, and shifting. Recall that a computer can perform only these simple operations. It must necessarily approximate a complex operation like differentiation and integration in terms of such simple operations. The approximation can be made as close to the exact answer as possible by choosing a sufficiently small value for T.

Although we have developed some guidelines in this chapter as well as Ch. 5, we have not developed all the tools and knowledge required to choose a suitable value of the sampling interval T. This subject is discussed in Ch. 12, including Sec. 12.4 that discusses a systematic procedure (impulse invariance method) for finding a discrete-time system with which to realize an Nth-order LTIC system.

Order of a Difference Equation

Equations (8.10), (8.12), (8.16), (8.18), and (8.20) are examples of difference equations. The highest-order difference of the output signal or the input signal, whichever is higher, represents the *order* of the difference equation. Hence, Eqs. (8.10), (8.16), (8.18), and (8.20) are first-order difference equations, whereas Eq. (8.12) is of the second order.

DRILL 8.10 Digital Integrator Design

Design a digital integrator in Ex. 8.13 using the fact that for an integrator, the output $y(t)$ and the input $x(t)$ are related by $dy(t)/dt = x(t)$. Approximation (similar to that in Ex. 8.12) of this equation at $t = nT$ yields the recursive form in Eq. (8.18).

Analog, Digital, Continuous-Time, and Discrete-Time Systems

The basic difference between continuous-time systems and analog systems, as also between discrete-time and digital systems, is fully explained in Secs. 1.7.5 and 1.7.6.[†] Historically, discrete-time systems have been realized with digital computers, where continuous-time signals are processed through digitized samples rather than unquantized samples. Therefore, the terms *digital filters* and *discrete-time systems* are used synonymously in the literature. This distinction is irrelevant in the analysis of discrete-time systems. For this reason, we follow this loose convention in this book, where the term *digital filter* implies a *discrete-time system*, and *analog filter* means a *continuous-time system*. Moreover, the terms C/D (continuous-to-discrete-time) and D/C will occasionally be used interchangeably with the terms A/D (analog-to-digital) and D/A, respectively.

Advantages of Digital Signal Processing

1. Digital systems operation can tolerate considerable variation in signal values, and hence are less sensitive to changes in the component parameter values due to temperature variation, aging, and other factors. This results in a greater degree of precision and stability. Since digital systems are binary circuits, their accuracy can be increased by using more complex circuitry to increase word length, subject to cost limitations.
2. Digital systems do not require any factory adjustment and can be easily duplicated in volume without having to worry about precise component values. They can be fully integrated, and even highly complex systems can be placed on a single chip by using *VLSI* (very-large-scale integrated) circuits.

[†] The terms *discrete-time* and *continuous-time* qualify the nature of a signal along the time axis (horizontal axis). The terms *analog* and *digital*, in contrast, qualify the nature of the signal amplitude (vertical axis).

3. Digital filters are more flexible. Their characteristics can be easily altered simply by changing the program. Digital hardware implementation permits the use of microprocessors, miniprocessors, digital switching, and large-scale integrated circuits.
4. A greater variety of filters can be realized by digital systems.
5. Digital signals can be stored easily and inexpensively on various media (e.g., magnetic, optical, and solid state) without deterioration of signal quality. It is also possible (and increasingly popular) to search and select information from distant electronic storehouses, such as the cloud.
6. Digital signals can be coded to yield extremely low error rates and high fidelity, as well as privacy. Also, more sophisticated signal-processing algorithms can be used to process digital signals.
7. Digital filters can be easily time-shared and therefore can serve a number of inputs simultaneously. Moreover, it is easier and more efficient to multiplex several digital signals on the same channel.
8. Reproduction with digital messages is extremely reliable without deterioration. Analog messages such as photocopies and films, for example, lose quality at each successive stage of reproduction and have to be transported physically from one distant place to another, often at relatively high cost.

One must weigh these advantages against such disadvantages as increased system complexity due to use of A/D and D/A interfaces, limited range of frequencies available in practice (affordable rates are gigahertz or less), and use of more power than is needed for the passive analog circuits. Digital systems use power-consuming active devices.

8.6 MATLAB: Representing, Manipulating, and Plotting Discrete-Time Signals

MATLAB is naturally and ideally suited to discrete-time signals. Here, we overview using MATLAB to represent, manipulate, and plot discrete-time signals.

8.6.1 Discrete-Time Functions and Stem Plots

Consider the discrete-time function $x[n] = e^{-n/5}\cos(\pi n/5)u[n]$. In MATLAB, there are many ways to represent $x[n]$ including M-files or, for particular n, explicit command line evaluation. In this example, however, we use an anonymous function.

```
>> x = @(n) exp(-n/5).*cos(pi*n/5).*(n>=0);
```

A true discrete-time function is undefined (or zero) for noninteger n. Although anonymous function `x` is intended as a discrete-time function, its present construction does not restrict n to be integer, and it can therefore be misused. For example, MATLAB dutifully returns 0.8606 to `x(0.5)` when a NaN (not-a-number) or zero is more appropriate. The user is responsible for appropriate function use.

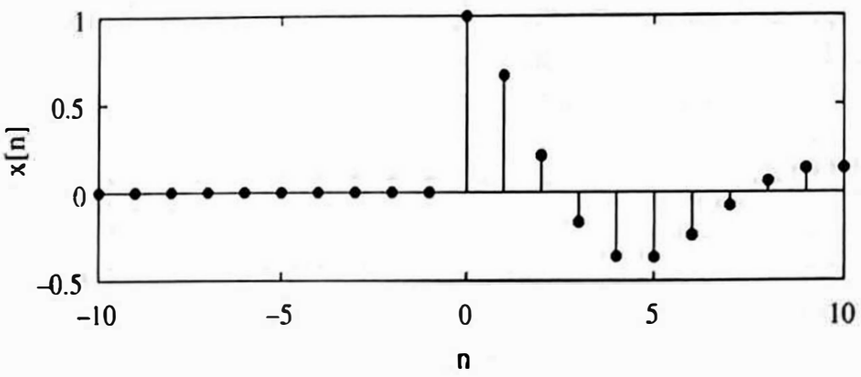

Figure 8.24 $x[n]$ over $(-10 \leq n \leq 10)$.

Next, consider plotting the discrete-time function $x[n]$ over $(-10 \leq n \leq 10)$. The `stem` command simplifies this task.

```
>> n = (-10:10)';
>> stem(n,x(n),'k.');
>> xlabel('n'); ylabel('x[n]');
```

Here, `stem` operates much like the `plot` command: dependent variable `x(n)` is plotted against independent variable `n` with black (because of the `k`) stem lines topped with solid dots (because of the `.`). The `stem` command emphasizes the discrete-time nature of the data, as Fig. 8.24 illustrates.

For discrete-time functions, the operations of shifting, inversion, and scaling can have surprising results. Compare $x[-2n]$ with $x[-2n+1]$. Contrary to the continuous case, the second is not a shifted version of the first. We can use separate subplots, each over $(-10 \leq n \leq 10)$, to help illustrate this fact. Notice that unlike the `plot` command, the `stem` command cannot simultaneously plot multiple functions on a single axis; overlapping stem lines would make such plots difficult to read anyway.

```
>> subplot(2,1,1); stem(n,x(-2*n),'k.'); ylabel('x[-2n]');
>> subplot(2,1,2); stem(n,x(-2*n+1),'k.'); ylabel('x[-2n+1]'); xlabel('n');
```

The results are shown in Fig. 8.25. Interestingly, the original function $x[n]$ can be recovered by interleaving samples of $x[-2n]$ and $x[-2n+1]$ and then time-reflecting the result.

Care must always be taken to ensure that MATLAB performs the desired computations. Our anonymous function `x` is a case in point: although it correctly downsamples, it does not properly upsample (see Prob. 8.6-1). MATLAB does what it is told, but it is not always told how to do everything correctly!

8.7 SUMMARY

Signals specified only at discrete instants such as $t = 0, T, 2T, 3T, \ldots, kT$ are discrete-time signals. Basically, a discrete-time signal is a sequence of numbers. Such a signal may be viewed as a function of time t, where the signal is defined or specified only at $t = nT$ with n any positive or negative integer. The signal therefore may be denoted as $x(nT)$. Alternately, such a signal may be viewed as a function of n, where n is any positive or negative integer. The latter approach results

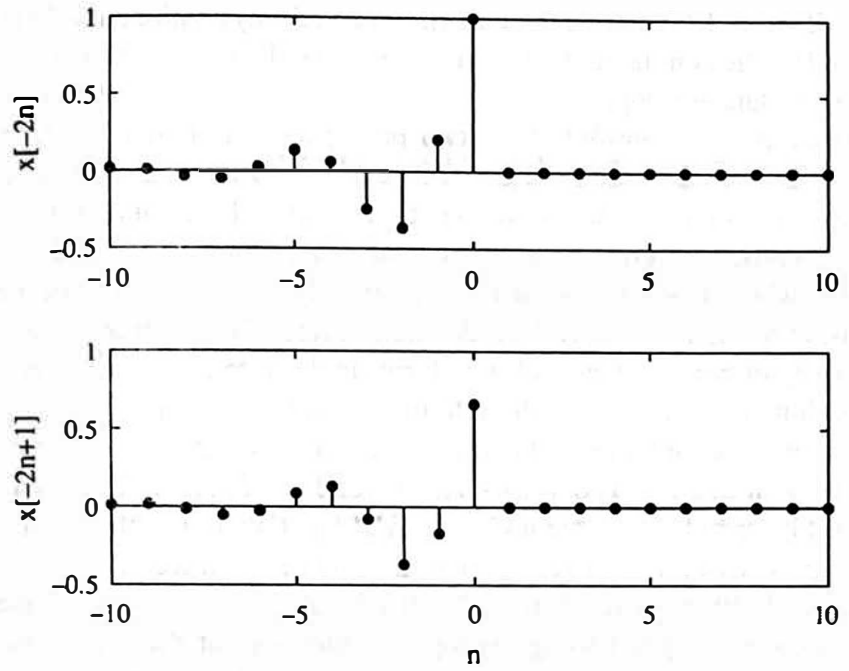

Figure 8.25 $x[-2n]$ and $x[-2n+1]$ over $(-10 \leq n \leq 10)$.

in a more compact notation such as $x[n]$, which is convenient and easier to manipulate. A system whose inputs and outputs are discrete-time signals is a discrete-time system.

One useful measure of the size of a discrete-time signal is its energy, defined by the sum $\sum_n |x[n]|^2$. If signal energy is infinite, the proper measure is its power. Signal power is the time average of its energy (averaged over the entire time interval from $n = -\infty$ to ∞). For periodic signals, the time averaging needs be performed only over one period in view of the periodic repetition of the signal. Signal power is also equal to the mean-squared value of the signal (averaged over the entire time interval from $n = -\infty$ to ∞).

Discrete-time signals classification is identical to that of continuous-time signals, discussed in Ch. 1. As with continuous-time signals, we can operate on a discrete-time signal's independent variable. A signal $x[n]$ delayed by M time units (right-shifted) is given by $x[n-M]$. On the other hand, $x[n]$ advanced (left-shifted) by M time units is given by $x[n+M]$. A signal $x[n]$, when time-inverted, is given by $x[-n]$. These operations are the same as those for the continuous-time case. The case of time scaling, however, is somewhat different because of the discrete nature of variable n. Unlike the continuous-time case, where time compression results in the same data at a higher speed, time compression in the discrete-time case eliminates part of the data and is called *downsampling*. A time-expansion operation of discrete-time signals results in time expanding the signal. Time expansion that inserts zeros between a signal's samples is called *upsampling*. A process of *interpolation* uses the signal's original samples to insert (generally nonzero) values that produce a smoother waveform.

In the study of continuous-time systems, exponentials with the natural base—that is, exponentials of the form $e^{\lambda t}$, where λ is complex in general—are more natural and convenient. In contrast, in the study of discrete-time systems, exponentials with a general base—that is, exponentials of the form γ^n, where γ is complex in general—are more convenient. One form of exponential can be readily converted to the other form by noting that $e^{\lambda n} = \gamma^n$, where $\gamma = e^{\lambda}$, or $\lambda = \ln \gamma$, and λ as well as γ are complex in general. The exponential γ^n grows exponentially

with n if $|\gamma| > 1$ (γ outside the unit circle) and decays exponentially if $|\gamma| < 1$ (γ within the unit circle). If γ lies on the unit circle (i.e., $|\gamma| = 1$), the exponential is either a constant or oscillates with a constant envelope.

Discrete-time sinusoids have two properties not shared by their continuous-time cousins. First, a discrete-time sinusoid $\cos \Omega n$ is periodic only if $\Omega/2\pi$ is a rational number. Second, discrete-time sinusoids whose frequencies Ω differ by an integral multiple of 2π are identical. Consequently, a discrete-time sinusoid of any frequency Ω is identical to some discrete-time sinusoid whose frequency (called the *apparent frequency* Ω_a) lies in the interval $-\pi$ to π. Notice, $|\Omega_a|$ is, at most, π, which reflects the highest rate of oscillation for a discrete-time sinusoid. This peculiarity of nonuniqueness of waveforms in discrete-time sinusoids of different frequencies has far-reaching consequences in discrete-time signal processing.

Sampling a continuous-time sinusoid $\cos(\omega t + \theta)$ at uniform intervals of T seconds results in a discrete-time sinusoid $\cos(\Omega n + \theta)$, where $\Omega = \omega T$. A continuous time sinusoid of frequency f Hz must be sampled at a rate no less than $2f$ Hz. Otherwise, the resulting sinusoid is aliased; that is, it appears as a sampled version of a sinusoid of lower frequency.

Discrete-time systems may be used to process discrete-time signals, or to process continuous-time signals using appropriate interfaces at the input and output. At the input, the continuous-time input signal is converted into a discrete-time signal through sampling. The resulting discrete-time signal is processed by a discrete-time system yielding a discrete-time output, which is then converted into a continuous-time output. Discrete-time systems are characterized by difference equations, and can be realized by using scalar multipliers, summers, and time delays. These operations can be readily performed by digital computers. As discussed in Sec. 8.5, discrete-time systems possess many advantages over continuous-time systems, which helps explain the ever-growing popularity of discrete-time systems.

PROBLEMS

8.1-1 Find the energy of the signals depicted in Fig. P8.1-1.

8.1-2 Find the power of the signals illustrated in Fig. P8.1-2.

8.1-3 Show that the power of a signal $\mathcal{D}e^{j(2\pi/N_0)n}$ is $|\mathcal{D}|^2$. Hence, show that the power of a signal $x[n] = \sum_{r=0}^{N_0-1} \mathcal{D}_r e^{jr(2\pi/N_0)n}$ is $P_x = \sum_{r=0}^{N_0-1} |\mathcal{D}_r|^2$. Use the fact that

$$\sum_{k=0}^{N_0-1} e^{j(r-m)2\pi k/N_0} = \begin{cases} N_0 & r = m \\ 0 & \text{otherwise} \end{cases}$$

8.1-4 The concepts of even and odd functions for discrete-time signals are identical to those of the continuous-time signals discussed in Sec. 1.5. Thus, a discrete-time signal can be decomposed into even and odd components as $x[n] = x_e[n] + x_o[n]$, where $x_e[n] = (x[n] + x[-n])/2$ and $x_o[n] = (x[n] - x[-n])/2$.

(a) Determine even and odd components of the signal $x[n] = (0.8)^n u[n]$.

(b) Show that the energy of $x[n]$ is the sum of energies of its odd and even components found in part (a).

(c) Generalize the result in part (b) for any finite energy signal.

8.1-5 Refer to Prob. 8.1-4 for an introduction to even and odd signal components.

(a) If $x_e[n]$ and $x_o[n]$ are the even and odd components of causal energy signal $x[n]$, then determine E_{x_e} and E_{x_o}, and show that $E_{x_e} + E_{x_o} = E_x$.

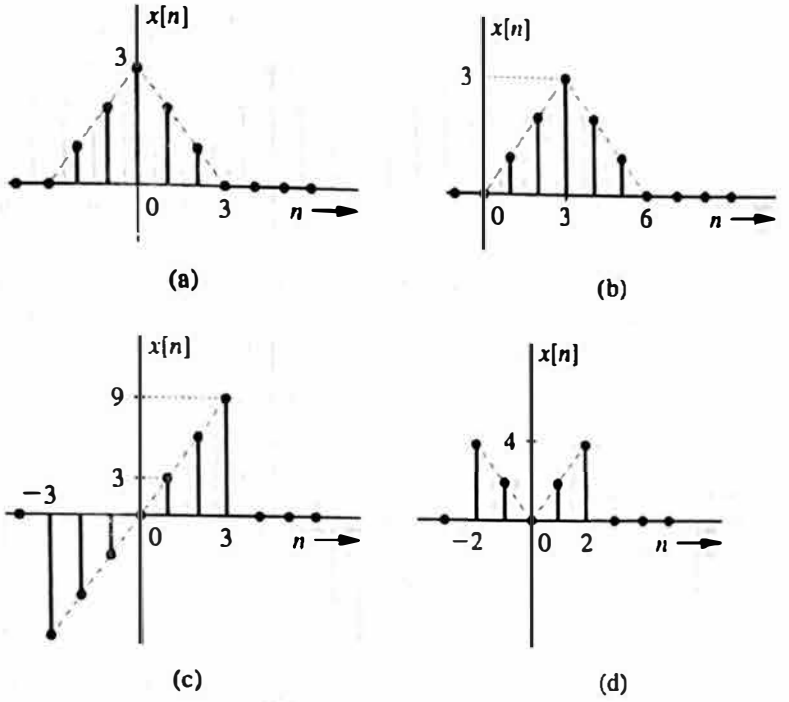

Figure P8.1-1

(b) Show that the cross-energy of x_e and x_o is zero, that is,

$$\sum_{n=-\infty}^{\infty} x_e[n]x_o[n] = 0$$

8.1-6 Define

$$x[n] = \begin{cases} \left(\frac{1}{3}\right)^n & n \geq 0 \\ A^n & n < 0 \end{cases}$$

(a) Determine the energy E_x and power P_x of $x[n]$ if $A = \frac{1}{2}$.
(b) Determine the energy E_x and power P_x of $x[n]$ if $A = 1$.
(c) Determine the energy E_x and power P_x of $x[n]$ if $A = 2$.

8.1-7 Determine the energy E_x and power P_x of the complex DT signal $x[n] = \text{Re}\left\{3(e^{j\pi/4})^n\right\}$.

8.2-1 If the energy of a signal $x[n]$ is E_x, then find the energy of the following:
(a) $x[-n]$
(b) $x[n-m]$ (m integer)
(c) $x[m-n]$ (m integer)
(d) $cx[n]$ (c constant)

8.2-2 If the power of a periodic signal $x[n]$ is P_x, find and comment on the powers and the rms values of the following:
(a) $-x[n]$
(b) $x[-n]$
(c) $x[n-m]$ (m integer)
(d) $cx[n]$ (c constant)
(e) $x[m-n]$ (m integer)

8.2-3 Letting $\downarrow$ identify $n = 0$, define the nonzero values of signal $x[n]$ as $[-1, 2, -3, 4, -5, 4, -3, \underset{\downarrow}{2}, -1]$.
(a) Using vector form, represent signal $y[n] = x[-3n + 2]$. Be sure to identify the $n = 0$ element.
(b) Using vector form, represent signal $z[n] = x[n/2 - 3]$. Be sure to identify the $n = 0$ element.

8.2-4 Letting $\downarrow$ identify $n = 0$, define the nonzero values of signal $x[n]$ as $[-1, \underset{\downarrow}{2}, -3, 4, -5, 4, -3, 2, -1]$.
(a) Determine the energy E_x and power P_x of the signal $x[n]$.
(b) Using vector form, represent signal $y[n] = x[2(n + 2)]$. Be sure to identify the $n = 0$ element.

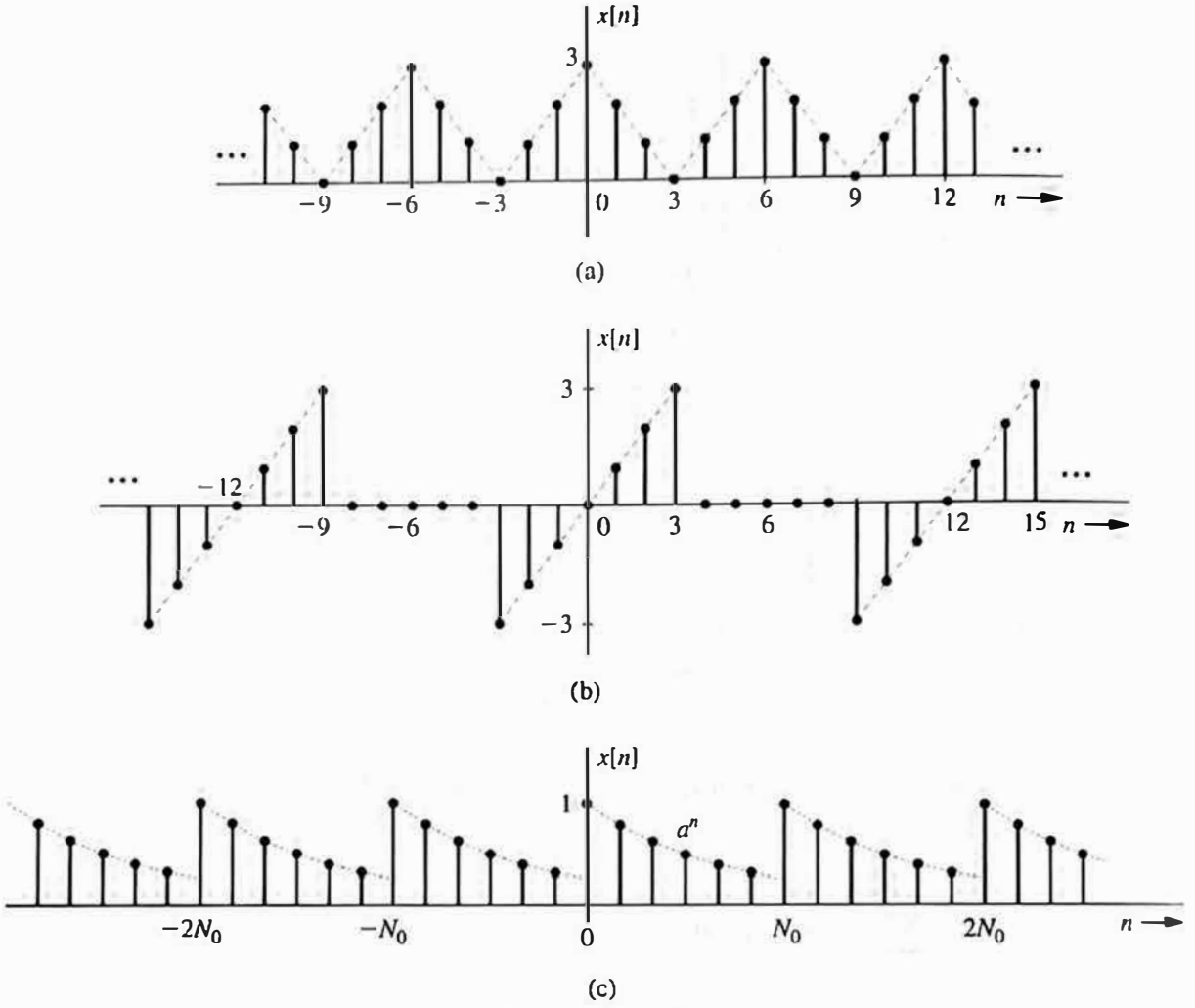

Figure P8.1-2

(c) Using vector form, represent signal $z[n] = x[-\frac{n-6}{3}]$. Be sure to identify the $n = 0$ element.

8.2-5 Letting $\downarrow$ identify the $n = 0$ value, describe a 4-periodic signal $w[n]$ using vector notation as $[\cdots, 1, 2, 3, 4, \underset{\downarrow}{1}, 2, 3, 4, 1, 2, 3, 4, \cdots]$.

(a) Determine the energy E_x and power P_x of signal $x[n] = w[2n]$.

(b) Determine the energy E_y and power P_y of signal $y[n] = w[2 - \frac{n}{3}]$.

8.2-6 Let DT signal $x[n]$ have values $[1, 2, 3, 4, 5, 6]$ for $0 \le n \le 5$ and let DT signal $y[n]$ have values $[5, 0, 0, 3, 0, 0, 1]$ for $0 \le n \le 6$. Both signals are zero outside the ranges given. Further, define a 6-periodic replication of $y[n]$ as $\tilde{y}[n] = \sum_{k=-\infty}^{\infty} y[n - 6k]$.

(a) Determine the energy E_x and power P_x of signal $x[n]$.

(b) Determine the smallest-magnitude integers N_1, N_2, and N_3 such that $y[n] = x[\frac{N_1 n}{N_2} + N_3]$.

(c) Determine the energy $E_{\tilde{y}}$ and power $P_{\tilde{y}}$ of $\tilde{y}[n]$.

8.2-7 For the signal shown in Fig. P8.1-1b, sketch the following signals:

(a) $x[-n]$

(b) $x[n + 6]$

(c) $x[n - 6]$

(d) $x[3n]$

(e) $x\left[\left\lceil \frac{n}{3} \right\rceil\right]$

(f) $x[3 - n]$

8.2-8 Repeat Prob. 8.2-7 for the signal depicted in Fig. P8.1-1c.

8.2-9 Letting $\downarrow$ identify $n = 0$, consider a DT signal $x[n]$ whose nonzero values are given

as $x[n] = [1, -3, 2, 2, 3, -2, -1, 1, 2, -3, \underset{\uparrow}{3}, 3, -2, 1, -3, 2, 3, -1]$. Accurately sketch $y[n] = x[-1 - 2n]$ and $z[n] = x[-2 + n/3]$ over $-5 \le n \le 4$.

8.2-10 Define

$$x[n] = \begin{cases} \left(\frac{1}{2}\right)^n & n \ge 0 \\ 0 & n < 0 \end{cases}$$

Determine and locate the two largest non-zero values of:

(a) $y_a[n] = x[2n]$
(b) $y_b[n] = x[n/3]$
(c) $y_c[n] = x[3n + 1]$
(d) $y_d[n] = x[-2n + 5]$
(e) $y_e[n] = x[-(n + 8)/2]$

8.3-1 Sketch, and find the power of, the following signals:

(a) $(1)^n$
(b) $(-1)^n$
(c) $u[n]$
(d) $(-1)^n u[n]$
(e) $\cos\left[\frac{\pi}{3}n + \frac{\pi}{6}\right]$

8.3-2 Show that

(a) $\delta[n] + \delta[n-1] = u[n] - u[n-2]$
(b) $2^{n-1}\sin\left(\frac{\pi n}{3}\right)u[n] = \frac{1}{2}2^n \sin\left(\frac{\pi n}{3}\right)u[n-1]$
(c) $n(n-1)\gamma^n u[n] = n(n-1)\gamma^n u[n-2]$
(d) $(u[n] + (-1)^n u[n])\sin\left(\frac{\pi n}{2}\right) = 0$ for all n
(e) $(u[n] + (-1)^{n+1}u[n])\cos\left(\frac{\pi n}{2}\right) = 0$ for all n

8.3-3 Sketch the following signals:

(a) $u[n-2] - u[n-6]$
(b) $n\{u[n] - u[n-7]\}$
(c) $(n-2)\{u[n-2] - u[n-6]\}$
(d) $(-n+8)\{u[n-6] - u[n-9]\}$
(e) $(n-2)\{u[n-2] - u[n-6]\} + (-n+8)\{u[n-6] - u[n-9]\}$

8.3-4 Describe each of the signals in Fig. P8.1-1 by a single expression valid for all n.

8.3-5 The following signals are in the form $e^{\lambda n}$. Express them in the form γ^n:

(a) $e^{-0.5n}$
(b) $e^{0.5n}$
(c) $e^{-j\pi n}$
(d) $e^{j\pi n}$

In each case, show the locations of λ and γ in the complex plane. Verify that an exponential is growing if γ lies outside the unit circle (or if λ lies in the RHP), is decaying if γ lies within the unit circle (or if λ lies in the LHP), and has a constant amplitude if γ lies on the unit circle (or if λ lies on the imaginary axis).

8.3-6 Express the following signals, which are in the form $e^{\lambda n}$, in the form γ^n:

(a) $e^{-(1+j\pi)n}$
(b) $e^{-(1-j\pi)n}$
(c) $e^{(1+j\pi)n}$
(d) $e^{(1-j\pi)n}$
(e) $e^{-[1+j(\pi/3)]n}$
(f) $e^{[1-j(\pi/3)]n}$

8.3-7 Referring to Prob. 8.1-4 for an introduction to even and odd signal components, find and sketch the odd and even components of the following:

(a) $u[n]$
(b) $nu[n]$
(c) $\sin\left(\frac{\pi n}{4}\right)$
(d) $\cos\left(\frac{\pi n}{4}\right)$

8.3-8 State with reason(s) whether the following signals are periodic:

(a) $\cos(0.5\pi n + 0.2)$ **(b)** $e^{j\frac{22}{7}n}$
(c) $\sin(0.5n + \frac{\pi}{3})$ **(d)** $e^{-(1+j\frac{\pi}{3})n}$
(e) $\cos(\sqrt{2}\pi n + 1.2)$ **(f)** $-6e^{j\frac{\pi}{7}n}$

If periodic, determine the period.

8.3-9 Repeat Prob. 8.3-8 for the signals

(a) $\cos(0.6\pi n + 0.3) + 3\sin(0.5\pi n + 0.4)$
(b) $\cos(1.6\pi n + 0.3) + 3\sin(1.5\pi n + 0.4) + 8\cos(1.8\pi n - \frac{\pi}{3})$
(c) $\cos(0.7\pi n + 0.3) + 3\sin(0.5n + 0.4)$

8.3-10 Express the following signals in terms of apparent frequencies:

(a) $\cos(0.8\pi n + \theta)$
(b) $\sin(1.2\pi n + \theta)$
(c) $\cos(6.9n + \theta)$
(d) $\cos(2.8\pi n + \theta) + 2\sin(3.7\pi n + \theta)$
(e) $\text{sinc}(\pi n/2)$
(f) $\text{sinc}(3\pi n/2)$
(g) $\text{sinc}(2\pi n)$

8.3-11 Show that $\cos(0.6\pi n + (\pi/6)) + \sqrt{3}\cos(1.4\pi n + (\pi/3)) = 2\cos(0.6\pi n - (\pi/6))$.

8.3-12 Express the following exponentials in the form $e^{j(\Omega n+\theta)}$, where $-\pi \le \Omega < \pi$:

(a) $e^{j(8.2\pi n+\theta)}$ (b) $e^{j4\pi n}$

(c) $e^{-j1.95n}$ (d) $e^{-j10.7\pi n}$

Repeat the problem if Ω is required to be in the range $0 \le \Omega < 2\pi$.

8.4-1 A continuous-time sinusoid $\cos(\omega_0 t)$ is sampled at a rate $f_s = 100$ Hz. The sampled signal is found to be $\cos(0.6\pi n)$. If there is more than one possible value for ω_0, find the general expression for ω_0, and determine the three smallest values of $|\omega_0|$.

8.4-2 Samples of a continuous-time sinusoid $\cos(100\pi t)$ are found to be $\cos(\pi n)$. Find the sampling frequency f_s. Explain whether there is only one possible value for f_s. If there is more than one possible value, find the general expression for the sampling frequency, and determine the three largest possible values.

8.4-3 A discrete-time processor uses a sampling interval $T = 0.5$ μs. What is the highest frequency of a signal that can be processed with this processor without aliasing? If a signal of frequency 2 MHz is sampled by this processor, what is the (aliased) frequency of the resulting sampled signal?

8.4-4 Continuous-time sinusoids $10\cos(11\pi t + \frac{\pi}{6})$ and $5\cos(29\pi t - \frac{\pi}{6})$ are sampled using a sampling interval of $T = 0.1$ s. Express the resulting discrete-time sinusoids in terms of their apparent frequencies.

8.4-5 Consider a signal $x(t) = 10\cos(2000\pi t) + \sqrt{2}\sin(3000\pi t) + 2\cos(5000\pi t + \frac{\pi}{4})$.

(a) Assuming that $x(t)$ is sampled at a rate of 4000 Hz, find the resulting sampled signal $x[n]$, expressed in terms of apparent frequencies. Does this sampling rate cause any aliasing? Explain.

(b) Determine the maximum sampling interval T that can be used to sample the signal $x(t)$ without aliasing.

8.4-6 A sampler with sampling interval $T = 0.1$ ms (10^{-4} s) samples continuous-time sinusoids of the following frequencies:

(a) $f = 12.5$ kHz (b) $f = 8500$ Hz

(c) $f = 10$ kHz (d) $f = 1500$ Hz

(e) $f = 32$ kHz (f) $f = 9600$ Hz

Determine the apparent frequency of the sampled signal in each case.

8.5-1 A cash register output $y[n]$ represents the total cost of n items rung up by a cashier. The input $x[n]$ is the cost of the nth item.

(a) Write the difference equation relating $y[n]$ to $x[n]$.

(b) Realize this system using a time-delay element.

8.5-2 Let $p[n]$ be the population of a certain country at the beginning of the nth year. The birth and death rates of the population during any year are 3.3 and 1.3%, respectively. If $i[n]$ is the total number of immigrants entering the country during the nth year, write the difference equation relating $p[n+1]$, $p[n]$, and $i[n]$. Assume that the immigrants enter the country throughout the year at a uniform rate.

8.5-3 A moving average is used to detect a trend of a rapidly fluctuating variable, such as the stock market average. A variable may fluctuate (up and down) daily, masking its long-term (secular) trend. We can discern the long-term trend by smoothing or averaging the past N values of the variable. For the stock market average, we may consider a 5-day moving average $y[n]$ to be the mean of the past 5 days' market closing values $x[n], x[n-1], \ldots, x[n-4]$.

(a) Write the difference equation relating $y[n]$ to the input $x[n]$.

(b) Use time-delay elements to realize the 5-day moving-average filter.

8.5-4 The digital integrator in Ex. 8.13 is specified by

$$y[n] - y[n-1] = Tx[n]$$

If an input $u[n]$ is applied to such an integrator, show that the output is $(n+1)Tu[n]$, which approaches the desired ramp $nTu[n]$ as $T \to 0$.

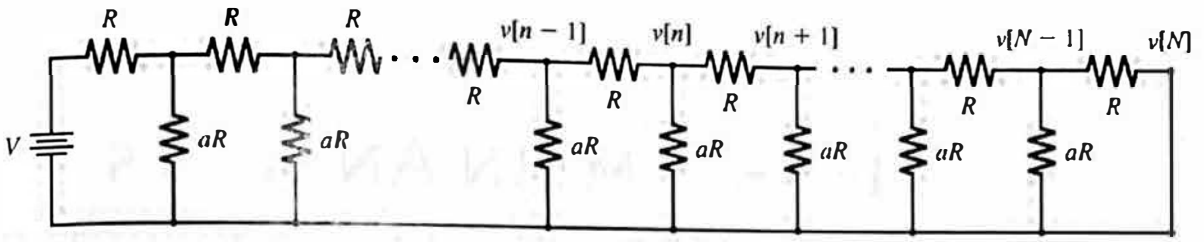

Figure P8.5-6

8.5-5 Approximate the following second-order differential equation with a difference equation:

$$\frac{d^2y(t)}{dt^2} + a_1\frac{dy(t)}{dt} + a_0y(t) = x(t)$$

8.5-6 The voltage at the nth node of a resistive ladder in Fig. P8.5-6 is $v[n]$, $(n = 0, 1, 2, \ldots, N)$. Show that $v[n]$ satisfies the second-order difference equation

$$v[n+2] - Av[n+1] + v[n] = 0 \quad A = 2 + \frac{1}{a}$$

[*Hint:* Consider the node equation at the nth node with voltage $v[n]$.]

8.5-7 Determine whether each of the following statements is true or false. If the statement is false, demonstrate by proof or example why the statement is false. If the statement is true, explain why.

(a) A discrete-time signal with finite power cannot be an energy signal.

(b) A discrete-time signal with infinite energy must be a power signal.

(c) If an energy signal $x[n]$ has energy E, then the energy of $x[an]$ is $E/|a|$.

8.6-1 Consider the discrete-time function $x[n] = e^{-n/5}\cos(\pi n/5)u[n]$. Section 8.6 uses anonymous functions in describing DT signals:

```
x = @(n) exp(-n/5).*cos(pi*n/5).*(n>=0);
```

While this anonymous function operates correctly for a downsampling operation such as `x[2n]`, it does not operate correctly for an upsampling operation such as `x[n/2]`. Modify the anonymous function `x` so that it also correctly accommodates upsampling operations. Test your code by computing and plotting `x(n/2)` over $(-10 \le n \le 10)$.

8.6-2 Suppose a vector `x` exists in the MATLAB workspace, corresponding to a finite-duration DT signal $x[n]$.

(a) Write a MATLAB function that, when passed vector `x`, computes and returns `Ex`, the energy of $x[n]$.

(b) Write a MATLAB function that, when passed vector `x`, computes and returns `Px`, the power of $x[n]$. Assume that $x[n]$ is periodic and that vector `x` contains data for an integer number of periods of $x[n]$.

CHAPTER 9

TIME-DOMAIN ANALYSIS OF DISCRETE-TIME SYSTEMS

In this chapter, we explore the time-domain analysis of linear, time-invariant, discrete-time (LTID) systems. We show how to compute the zero-input response, determine the unit impulse response, and use convolution to evaluate the zero-state response.. The procedure is parallel to that for continuous-time systems, with minor differences.

9.1 CLASSIFICATION OF DISCRETE-TIME SYSTEMS

Before examining the nature of discrete-time system equations, let us review the concepts of linearity, time invariance (or shift invariance), and causality, which apply to discrete-time systems much as they do to continuous-time systems.

LINEARITY AND TIME INVARIANCE

For discrete-time systems, the definition of *linearity* is identical to that for continuous-time systems, as given in Eq. (1.22). Referring to the examples from Sec. 8.5, we can show that the systems in Exs. 8.10, 8.11, 8.12, and 8.13 are all linear.

Time invariance (or *shift invariance*) for discrete-time systems is also defined in a way similar to that for continuous-time systems. Systems whose parameters do not change with time (with n) are *time-invariant* or shift-invariant (also *constant-parameter*) systems. For such a system, if the input is delayed by k units or samples, the output is the same as before but delayed by k samples (assuming the initial conditions also are delayed by k). The systems in Exs. 8.10, 8.11, 8.12, and 8.13 are time-invariant because the coefficients in the system equations are constants (independent of n). If these coefficients were functions of n (time), then the systems would be linear *time-varying* systems. Consider, for example, a system described by

$$y[n] = e^{-n}x[n]$$

For this system, let a signal $x_1[n]$ yield the output $y_1[n]$, and another input $x_2[n]$ yield the output $y_2[n]$. Then

$$y_1[n] = e^{-n}x_1[n] \qquad \text{and} \qquad y_2[n] = e^{-n}x_2[n]$$

If we let $x_2[n] = x_1[n - N_0]$, then

$$y_2[n] = e^{-n}x_2[n] = e^{-n}x_1[n - N_0] \neq y_1[n - N_0]$$

Clearly, this is a time-varying parameter system.

Causal and Noncausal Systems

A *causal* (also known as a *physical* or *nonanticipative*) system is one for which the output at any instant $n = k$ depends only on the value of the input $x[n]$ for $n \leq k$. In other words, the value of the output at the present instant depends only on the past and present values of the input $x[n]$, not on its future values. The systems in Exs. 8.10, 8.11, 8.12, and 8.13 are all causal. We shall soon introduce the unit impulse response $h[n]$ of a discrete-time system, and we shall see that causal systems require causal $h[n]$.

Invertible and Noninvertible Systems

A discrete-time system $\mathcal{S}$ is invertible if an inverse system $\mathcal{S}_i$ exists such that the cascade of $\mathcal{S}$ and $\mathcal{S}_i$ results in an *identity* system. An identity system is defined as one whose output is identical to the input. In other words, for an invertible system, the input can be uniquely determined from the corresponding output. For every input, there is a unique output. When a signal is processed through such a system, its input can be reconstructed from the corresponding output. There is no loss of information when a signal is processed through an invertible system.

A cascade of a unit delay with a unit advance results in an identity system because the output of such a cascaded system is identical to the input. Clearly, the inverse of an ideal unit delay is ideal unit advance, which is a noncausal (and unrealizable) system. In contrast, a compressor $y[n] = x[Mn]$ is not invertible because this operation loses all but every Mth sample of the input, and, generally, the input cannot be reconstructed. Similarly, operations, such as $y[n] = \cos x[n]$ or $y[n] = |x[n]|$, are not invertible.

DRILL 9.1 Invertibility

Show that a system specified by equation $y[n] = ax[n] + b$ is invertible but that the system $y[n] = |x[n]|^2$ is noninvertible.

Stable and Unstable Systems

The concept of stability is similar to that in continuous-time systems. Stability can be *internal* or *external*. If every *bounded input* applied at the input terminal results in a *bounded output*, the system is said to be stable *externally*. External stability can be ascertained by measurements at the external terminals of the system. This type of stability is also known as the stability in the BIBO (bounded-input/bounded-output) sense. Both internal and external stability are discussed in greater detail in Sec. 9.6.

Memoryless Systems and Systems with Memory

The concepts of memoryless (or instantaneous) systems and those with memory (or dynamic) are identical to the corresponding concepts of the continuous-time case. A system is memoryless if its response at any instant n depends at most on the input at the same instant n. The output at any instant of a system with memory generally depends on the past, present, and future values of the input. For example, $y[n] = \sin x[n]$ is an example of instantaneous system, and $y[n] - y[n-1] = x[n]$ is an example of a dynamic system or a system with memory.

EXAMPLE 9.1 Investigating DT System Properties

Consider a DT system described as $y[n+1] = x[n+1]x[n]$. Determine whether the system is **(a)** linear, **(b)** time-invariant, **(c)** causal, **(d)** invertible, **(e)** BIBO-stable, and **(f)** memoryless.

Let us delay the input–output equation by 1 to obtain the equivalent but more convenient representation of $y[n] = x[n]x[n-1]$.

(a) Linearity requires both homogeneity and additivity. Let us first investigate homogeneity. Assuming $x[n] \Longrightarrow y[n]$, we see that

$$ax[n] \Longrightarrow (ax[n])(ax[n-1]) = a^2 y[n] \neq ay[n]$$

Thus, the system does not satisfy the homogeneity property.

The system also does not satisfy the additivity property. Assuming $x_1[n] \Longrightarrow y_1[n]$ and $x_2[n] \Longrightarrow y_2[n]$, we see that input $x[n] = x_1[n] + x_2[n]$ produces output $y[n]$ as

$$\begin{aligned} y[n] &= (x_1[n] + x_2[n])(x_1[n-1] + x_2[n-1]) \\ &= x_1[n]x_1[n-1] + x_2[n]x_2[n-1] + x_1[n]x_2[n-1] + x_2[n]x_1[n-1] \\ &= y_1[n] + y_2[n] + x_1[n]x_2[n-1] + x_2[n]x_1[n-1] \\ &\neq y_1[n] + y_2[n] \end{aligned}$$

Clearly, additivity is not satisfied.

Since the system does not satisfy both the homogeneity and additivity properties, we conclude that the system is not linear.

(b) To be time-invariant, a shift in any input should cause a corresponding shift in respective output. Assume that $x[n] \Longrightarrow y[n]$. Applying a delay version of this input to the system yields

$$x[n-N] \Longrightarrow x[n-N]x[n-1-N] = x[(n-N)]x[(n-N)-1] = y[n-N]$$

Since shifting an input causes a corresponding shift in the output, we conclude that the system is time-invariant.

(c) To be causal, an output value cannot depend on any future input values. The output y at time n depends on the input x at present and past times n and $n-1$. Since the current output does not depend on future input values, the system is causal.

(d) For a system to be invertible, every input must generate a unique output, which allows exact recovery of the input from the output. Consider two inputs to this system: $x_1[n] = 1$ and $x_2[n] = -1$. Both inputs generate the same output: $y_1[n] = y_2[n] = 1$. Since unique inputs do not always generate unique outputs, we conclude that the system is not invertible.

(e) To be BIBO-stable, any bounded input must generate a bounded output. A bounded input satisfies $|x[n]| \leq M_x < \infty$ for all n. Given this condition, the system output magnitude behaves as

$$|y[n]| = |x[n]x[n-1]| = |x[n]|\,|x[n-1]| \leq M_x^2 < \infty$$

Since any bounded input is guaranteed to produce a bounded output, it follows that the system is BIBO-stable.

(f) To be memoryless, a system's output can only depend on the strength of the current input. Since the output y at time n depends on the input x not only at present time n but also on past time $n-1$, we see that the system is not memoryless.

9.2 Discrete-Time System Equations

In this section, we discuss time-domain analysis of LTID (linear, time-invariant, discrete-time systems). With minor differences, the procedure is parallel to that for continuous-time systems.

Difference Equations

Equations (8.10), (8.12), (8.15), and (8.20) are examples of difference equations. Equations (8.10), (8.15), and (8.20) are first-order difference equations, and Eq. (8.12) is a second-order difference equation. All these equations are linear, with constant (not time-varying) coefficients.[†] Before giving a general form of an Nth-order linear difference equation, we recall that a difference equation can be written in two forms: the first form uses delay terms such as $y[n-1]$, $y[n-2]$, $x[n-1]$, $x[n-2]$, and so on; and the alternate form uses advance terms such as $y[n+1]$, $y[n+2]$, and so on. Although the delay form is more natural, we shall often prefer the advance form, not just for the general notational convenience, but also for resulting notational uniformity with the operator form for differential equations. This facilitates the commonality of the solutions and concepts for continuous-time and discrete-time systems.

We start here with a general difference equation, written in advance form as

$$\begin{aligned} y[n+N] + a_1 y[n+N-1] + \cdots + a_{N-1} y[n+1] + a_N y[n] = \\ b_{N-M} x[n+M] + b_{N-M+1} x[n+M-1] + \cdots + b_{N-1} x[n+1] + b_N x[n] \end{aligned} \tag{9.1}$$

This is a linear difference equation whose order is $\max(N, M)$. We have assumed the coefficient of $y[n+N]$ to be unity ($a_0 = 1$) without loss of generality. If $a_0 \neq 1$, we can divide the equation throughout by a_0 to normalize the equation to have $a_0 = 1$.

[†] Equations such as (8.10), (8.12), (8.15), and (8.20) are considered to be linear according to the classical definition of linearity. Some authors label such equations as *incrementally linear*. We prefer the classical definition. It is just a matter of individual choice and makes no difference in the final results.

Causality Condition

For a causal system, the output cannot depend on future input values. This means that when the system equation is in the advance form of Eq. (9.1), causality requires $M \leq N$. If M were to be greater than N, then $y[n+N]$, the output at $n+N$ would depend on $x[n+M]$, which is the input at the later instant $n+M$. For a general causal case, $M=N$, and Eq. (9.1) can be expressed as

$$\begin{aligned} y[n+N]+a_1y[n+N-1]+\cdots+a_{N-1}y[n+1]+a_Ny[n]= \\ b_0x[n+N]+b_1x[n+N-1]+\cdots+b_{N-1}x[n+1]+b_Nx[n] \end{aligned} \tag{9.2}$$

where some of the coefficients on either side can be zero. In this Nth-order equation, a_0, the coefficient of $y[n+N]$, is normalized to unity. Equation (9.2) is valid for all values of n. Therefore, it is still valid if we replace n by $n-N$ throughout the equation [see Eqs. (8.10) and (8.11)]. Such replacement yields a delay-form alternative:

$$\begin{aligned} y[n]+a_1y[n-1]+\cdots+a_{N-1}y[n-N+1]+a_Ny[n-N]= \\ b_0x[n]+b_1x[n-1]+\cdots+b_{N-1}x[n-N+1]+b_Nx[n-N] \end{aligned} \tag{9.3}$$

9.2.1 Recursive (Iterative) Solution of Difference Equation

Equation (9.3) can be expressed as

$$\begin{aligned} y[n]= -a_1y[n-1]-a_2y[n-2]-\cdots-a_Ny[n-N] \\ +b_0x[n]+b_1x[n-1]+\cdots+b_Nx[n-N] \end{aligned} \tag{9.4}$$

In Eq. (9.4), $y[n]$ is computed from $2N+1$ pieces of information; the preceding N values of the output: $y[n-1], y[n-2], \ldots, y[n-N]$, and the preceding N values of the input: $x[n-1], x[n-2], \ldots, x[n-N]$, and the present value of the input $x[n]$. Initially, to compute $y[0]$, the N initial conditions $y[-1], y[-2], \ldots, y[-N]$ serve as the preceding N output values. Hence, knowing the N initial conditions and the input, we can determine recursively the entire output $y[0], y[1], y[2], y[3], \ldots$, one value at a time. For instance, to find $y[0]$, we set $n=0$ in Eq. (9.4). The left-hand side is $y[0]$, and the right-hand side is expressed in terms of N initial conditions $y[-1], y[-2], \ldots, y[-N]$ and the input $x[0]$ if $x[n]$ is causal (because of causality, other input terms $x[-n]=0$). Similarly, knowing $y[0]$ and the input, we can compute $y[1]$ by setting $n=1$ in Eq. (9.4). Knowing $y[0]$ and $y[1]$, we find $y[2]$, and so on. Thus, we can use this recursive procedure to find the complete response $y[0], y[1], y[2], \ldots$. For this reason, this equation is classed as a recursive form. This method basically reflects the manner in which a computer would solve a recursive difference equation, given the input and initial conditions. Equation (9.4) [or Eq. (9.3)] is nonrecursive if all the $N-1$ coefficients $a_i=0$ $(i=1,2,\ldots,N-1)$. In this case, it can be seen that $y[n]$ is computed only from the input values and without using any previous outputs. Generally speaking, the recursive procedure applies only to equations in the recursive form. The recursive (iterative) procedure is demonstrated by the following examples.

EXAMPLE 9.2 Iterative Solution to a First-Order Difference Equation

Solve iteratively

$$y[n] - 0.5y[n-1] = x[n]$$

with initial condition $y[-1] = 16$ and causal input $x[n] = n^2u[n]$. This equation can be expressed as

$$y[n] = 0.5y[n-1] + x[n] \tag{9.5}$$

If we set $n = 0$ in Eq. (9.5), we obtain

$$\begin{aligned} y[0] &= 0.5y[-1] + x[0] \\ &= 0.5(16) + 0 = 8 \end{aligned}$$

Now, setting $n = 1$ in Eq. (9.5) and using the value $y[0] = 8$ (computed in the first step) and $x[1] = (1)^2 = 1$, we obtain

$$y[1] = 0.5(8) + (1)^2 = 5$$

Next, setting $n = 2$ in Eq. (9.5) and using the value $y[1] = 5$ (computed in the previous step) and $x[2] = (2)^2$, we obtain

$$y[2] = 0.5(5) + (2)^2 = 6.5$$

Continuing in this way iteratively, we obtain

$$\begin{aligned} y[3] &= 0.5(6.5) + (3)^2 = 12.25 \\ y[4] &= 0.5(12.25) + (4)^2 = 22.125 \\ &\vdots \end{aligned}$$

The output $y[n]$ is depicted in Fig. 9.1.

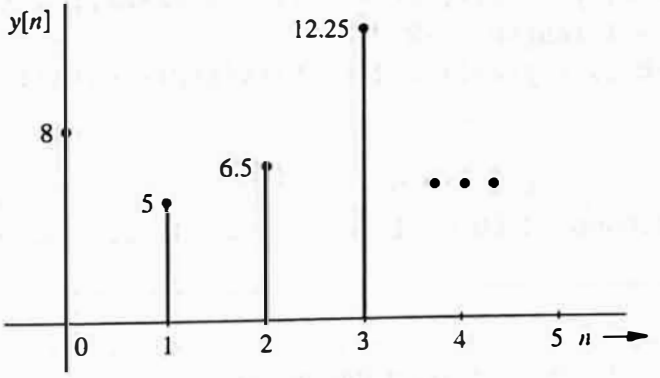

Figure 9.1 Iterative solution of a difference equation.

We now present one more example of iterative solution—this time for a second-order equation. The iterative method can be applied to a difference equation in delay form or advance form. In Ex. 9.2, we considered the former. Let us now apply the iterative method to the advance form.

EXAMPLE 9.3 Iterative Solution to a Second-Order Difference Equation

Solve iteratively

$$y[n+2]-y[n+1]+0.24y[n]=x[n+2]-2x[n+1]$$

with initial conditions $y[-1]=2$, $y[-2]=1$ and a causal input $x[n]=nu[n]$. The system equation can be expressed as

$$y[n+2]=y[n+1]-0.24y[n]+x[n+2]-2x[n+1] \tag{9.6}$$

Setting $n=-2$ in Eq. (9.6) and then substituting $y[-1]=2$, $y[-2]=1$, $x[0]=x[-1]=0$, we obtain

$$y[0]=2-0.24(1)+0-0=1.76$$

Setting $n=-1$ in Eq. (9.6) and then substituting $y[0]=1.76$, $y[-1]=2$, $x[1]=1$, $x[0]=0$, we obtain

$$y[1]=1.76-0.24(2)+1-0=2.28$$

Setting $n=0$ in Eq. (9.6) and then substituting $y[0]=1.76$, $y[1]=2.28$, $x[2]=2$, and $x[1]=1$ yield

$$y[2]=2.28-0.24(1.76)+2-2(1)=1.8576$$

and so on.

With MATLAB, we can readily verify and extend these recursive calculations.

```
>> n = -2:4; y = [1,2,zeros(1,length(n)-2)]; x = [0,0,n(3:end)];
>> for k = 1:length(n)-2,
>>     y(k+2) = y(k+1)-0.24*y(k)+x(k+2)-2*x(k+1);
>> end
>> n,y
    n = -2      -1       0       1       2       3       4
    y =  1.0000  2.0000  1.7600  2.2800  1.8576  0.3104 -2.1354
```

Note carefully the recursive nature of the computations. From the N initial conditions (and the input), we obtained $y[0]$ first. Then, using this value of $y[0]$ and the preceding $N-1$ initial conditions (along with the input), we find $y[1]$. Next, using $y[0]$, $y[1]$ along with the past $N-2$ initial conditions and input, we obtained $y[2]$, and so on. This method is general and can be applied to a recursive difference equation of any order. It is interesting that the hardware realization of

Eq. (9.5) depicted in Fig. 8.21 (with $a = 0.5$) generates the solution precisely in this (iterative) fashion.

DRILL 9.2 Iterative Solution to a Difference Equation

Using the iterative method, find the first three terms of $y[n]$ for

$$y[n+1] - 2y[n] = x[n]$$

The initial condition is $y[-1] = 10$ and the input $x[n] = 2$ starting at $n = 0$.

ANSWER

$y[0] = 20, y[1] = 42$, and $y[2] = 86$

We shall see in the future that the solution of a difference equation obtained in this direct (iterative) way is useful in many situations. Despite the many uses of this method, a closed-form solution of a difference equation is far more useful in the study of system behavior and its dependence on the input and various system parameters. For this reason, we shall develop a systematic procedure to analyze discrete-time systems along lines similar to those used for continuous-time systems.

Operator Notation

In difference equations, it is convenient to use operator notation similar to that used in differential equations for the sake of compactness. In continuous-time systems, we used the operator D to denote the operation of differentiation. For discrete-time systems, we shall use the operator E to denote the operation for advancing a sequence by one time unit. Thus,

$$Ex[n] \equiv x[n+1]$$
$$E^2x[n] \equiv x[n+2]$$
$$\vdots$$
$$E^Nx[n] \equiv x[n+N]$$

Let us use this advance operator notation to represent several systems investigated earlier. The first-order difference equation of a savings account is [see Eq. (8.11)]

$$y[n+1] - ay[n] = x[n+1]$$

Using the operator notation, we can express this equation as

$$Ey[n] - ay[n] = Ex[n] \qquad \text{or} \qquad (E-a)y[n] = Ex[n]$$

Similarly, the second-order book sales estimate described by Eq. (8.13) as

$$y[n+2] + \tfrac{1}{4}y[n+1] + \tfrac{1}{16}y[n] = x[n+2]$$

can be expressed in operator notation as

$$(E^2 + \tfrac{1}{4}E + \tfrac{1}{16})y[n] = E^2x[n]$$

The general Nth-order advance-form difference equation of Eq. (9.2) can be expressed as

$$(E^N + a_1E^{N-1} + \cdots + a_{N-1}E + a_N)y[n] = (b_0E^N + b_1E^{N-1} + \cdots + b_{N-1}E + b_N)x[n]$$

or

$$Q[E]y[n] = P[E]x[n] \tag{9.7}$$

where $Q[E]$ and $P[E]$ are Nth-order polynomial operators

$$Q[E] = E^N + a_1E^{N-1} + \cdots + a_{N-1}E + a_N$$
$$P[E] = b_0E^N + b_1E^{N-1} + \cdots + b_{N-1}E + b_N$$

Response of Linear Discrete-Time Systems

Following the procedure used for continuous-time systems, we can show that Eq. (9.7) is a linear equation (with constant coefficients). A system described by such an equation is a linear, time-invariant, discrete-time (LTID) system. We can verify, as in the case of LTIC systems (see the footnote on p. 151), that the general solution of Eq. (9.7) consists of zero-input and zero-state components.

9.3 System Response to Internal Conditions: The Zero-Input Response

The zero-input response $y_0[n]$ is the solution of Eq. (9.7) with $x[n] = 0$; that is,

$$Q[E]y_0[n] = 0$$

or

$$(E^N + a_1E^{N-1} + \cdots + a_{N-1}E + a_N)y_0[n] = 0 \tag{9.8}$$

Although we can solve this equation systematically, even a cursory examination points to the solution. This equation states that a linear combination of $y_0[n]$ and advanced $y_0[n]$ is zero, *not for some values of n, but for all n.* Such a situation is possible *if and only if* $y_0[n]$ and advanced $y_0[n]$ have the same form. Only an exponential function γ^n has this property, as the following equation indicates:

$$E^k\{\gamma^n\} = \gamma^{n+k} = \gamma^k\gamma^n$$

This expression shows that γ^n advanced by k units is a constant (γ^k) times γ^n. Therefore, the solution of Eq. (9.8) must be of the form[†]

$$y_0[n] = c\gamma^n \tag{9.9}$$

[†] A signal of the form $n^m\gamma^n$ also satisfies this requirement under certain conditions (repeated roots), discussed later.

To determine c and γ, we substitute this solution in Eq. (9.8). Since $E^k y_0[n] = y_0[n+k] = c\gamma^{n+k}$, this produces

$$c(\gamma^N + a_1\gamma^{N-1} + \cdots + a_{N-1}\gamma + a_N)\gamma^n = 0$$

For a nontrivial solution of this equation,

$$\gamma^N + a_1\gamma^{n-1} + \cdots + a_{N-1}\gamma + a_N = 0 \tag{9.10}$$

or

$$Q[\gamma] = 0$$

Our solution $c\gamma^n$ [Eq. (9.9)] is correct, provided γ satisfies Eq. (9.10). Now, $Q[\gamma]$ is an Nth-order polynomial and can be expressed in the factored form (assuming all distinct roots):

$$(\gamma - \gamma_1)(\gamma - \gamma_2)\cdots(\gamma - \gamma_N) = 0$$

Clearly, γ has N solutions $\gamma_1, \gamma_2, \ldots, \gamma_N$ and, therefore, Eq. (9.8) also has N solutions $c_1\gamma_1^n, c_2\gamma_2^n, \ldots, c_n\gamma_N^n$. In such a case, we have shown that the general solution is a linear combination of the N solutions (see the footnote on p. 153). Thus,

$$y_0[n] = c_1\gamma_1^n + c_2\gamma_2^n + \cdots + c_n\gamma_N^n$$

where $\gamma_1, \gamma_2, \ldots, \gamma_n$ are the roots of Eq. (9.10) and $c_1, c_2, \ldots, c_n$ are arbitrary constants determined from N auxiliary conditions, generally given in the form of initial conditions. The polynomial $Q[\gamma]$ is called the *characteristic polynomial* of the system, and $Q[\gamma] = 0$ [Eq. (9.10)] is the *characteristic equation* of the system. Moreover, $\gamma_1, \gamma_2, \ldots, \gamma_N$, the roots of the characteristic equation, are called *characteristic roots* or *characteristic values* (also *eigenvalues*) of the system. The exponentials γ_i^n $(i = 1, 2, \ldots, N)$ are the *characteristic modes* or *natural modes* of the system. A characteristic mode corresponds to each characteristic root of the system, and the *zero-input response is a linear combination of the characteristic modes of the system.*

EXAMPLE 9.4 Zero-Input Response of a Second-Order System with Real Roots

The LTID system described by the difference equation

$$y[n+2] - 0.6y[n+1] - 0.16y[n] = 5x[n+2]$$

has input $x[n] = 4^{-n}u[n]$ and initial conditions $y[-1] = 0$ and $y[-2] = 25/4$. Determine the zero-input response $y_0[n]$. The zero-state response of this system is considered later, in Ex. 9.13.

The system equation in operator notation is

$$(E^2 - 0.6E - 0.16)y[n] = 5E^2x[n]$$

The characteristic polynomial is

$$\gamma^2 - 0.6\gamma - 0.16 = (\gamma + 0.2)(\gamma - 0.8)$$

The characteristic equation is

$$(\gamma + 0.2)(\gamma - 0.8) = 0$$

The characteristic roots are $\gamma_1 = -0.2$ and $\gamma_2 = 0.8$. The zero-input response is

$$y_0[n] = c_1(-0.2)^n + c_2(0.8)^n \tag{9.11}$$

To determine arbitrary constants c_1 and c_2, we set $n = -1$ and -2 in Eq. (9.11), then substitute $y_0[-1] = 0$ and $y_0[-2] = 25/4$ to obtain†

$$\left.\begin{aligned} 0 &= -5c_1 + \tfrac{5}{4}c_2 \\ \tfrac{25}{4} &= 25c_1 + \tfrac{25}{16}c_2 \end{aligned}\right\} \implies \begin{aligned} c_1 &= \tfrac{1}{5} \\ c_2 &= \tfrac{4}{5} \end{aligned}$$

Therefore,

$$y_0[n] = \tfrac{1}{5}(-0.2)^n + \tfrac{4}{5}(0.8)^n \qquad n \geq 0$$

The reader can verify this solution by computing the first few terms using the iterative method (see Exs. 9.2 and 9.3).

† The initial conditions $y[-1]$ and $y[-2]$ are the conditions given on the total response. But because the input does not start until $n = 0$, the zero-state response is zero for $n < 0$. Hence, at $n = -1$ and -2, the total response consists of only the zero-input component so that $y[-1] = y_0[-1]$ and $y[-2] = y_0[-2]$.

DRILL 9.3 Zero-Input Response of First-Order Systems

Find and sketch the zero-input response for the systems described by the following equations:

(a) $y[n+1] - 0.8y[n] = 3x[n+1]$

(b) $y[n+1] + 0.8y[n] = 3x[n+1]$

In each case, the initial condition is $y[-1] = 10$. Verify the solutions by computing the first three terms using the iterative method.

ANSWERS

(a) $8(0.8)^n$

(b) $-8(-0.8)^n$

DRILL 9.4 Zero-Input Response of a Second-Order System with Real Roots

Find the zero-input response of a system described by the equation

$$y[n]+0.3y[n-1]-0.1y[n-2]=x[n]+2x[n-1]$$

The initial conditions are $y_0[-1]=1$ and $y_0[-2]=33$. Verify the solution by computing the first three terms iteratively.

ANSWER

$y_0[n]=(0.2)^n+2(-0.5)^n$

Section 9.2.1 introduced the method of recursion to solve difference equations. As the next example illustrates, the zero-input response can likewise be found through recursion. Since it does not provide a closed-form solution, recursion is generally not the preferred method of solving difference equations.

EXAMPLE 9.5 Iterative Solution to Zero-Input Response

Applying the initial conditions $y[-1]=2$ and $y[-2]=1$, use MATLAB to iteratively compute and then plot the zero-input response for the system described by $(E^2-1.56E+0.81)y[n]=(E+3)x[n]$.

```
>> n = (-2:20)'; y = [1;2;zeros(length(n)-2,1)];
>> for k = 1:length(n)-2,
>>     y(k+2) = 1.56*y(k+1)-0.81*y(k);
>> end;
>> stem(n,y,'k.'); xlabel('n'); ylabel('y[n]'); axis([-2 20 -1.5 2.5]);
```

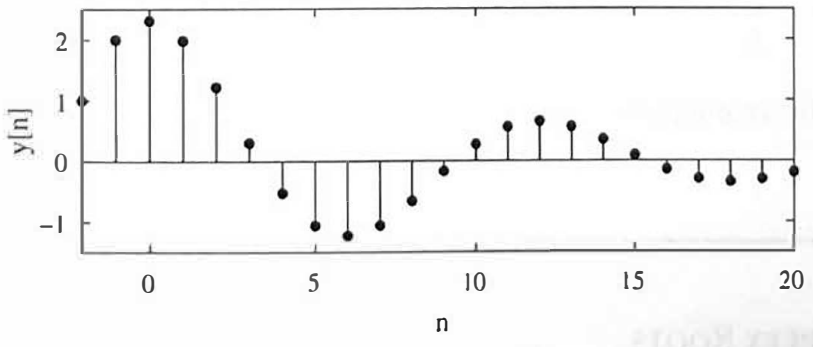

Figure 9.2 Zero-input response for Ex. 9.5.

Repeated Roots

So far we have assumed the system to have N distinct characteristic roots $\gamma_1, \gamma_2, \ldots, \gamma_N$ with corresponding characteristic modes $\gamma_1^n, \gamma_2^n, \ldots, \gamma_N^n$. If two or more roots coincide (repeated roots), the form of characteristic modes is modified. Direct substitution shows that if a root γ repeats r times (root of multiplicity r), the corresponding characteristic modes for this root are $\gamma^n, n\gamma^n, n^2\gamma^n, \ldots, n^{r-1}\gamma^n$. Thus, if the characteristic equation of a system is

$$Q[\gamma] = (\gamma - \gamma_1)^r(\gamma - \gamma_{r+1})(\gamma - \gamma_{r+2}) \cdots (\gamma - \gamma_N)$$

then the zero-input response of the system is

$$y_0[n] = (c_1 + c_2 n + c_3 n^2 + \cdots + c_r n^{r-1})\gamma_1^n + c_{r+1}\gamma_{r+1}^n + c_{r+2}\gamma_{r+2}^n + \cdots + c_n\gamma_N^n$$

EXAMPLE 9.6 Zero-Input Response of a Second-Order System with Repeated Roots

Consider a second-order difference equation with repeated roots:

$$(E^2 + 6E + 9)y[n] = (2E^2 + 6E)x[n]$$

Determine the zero-input response $y_0[n]$ if the initial conditions are $y_0[-1] = -1/3$ and $y_0[-2] = -2/9$.

The characteristic polynomial is $\gamma^2 + 6\gamma + 9 = (\gamma + 3)^2$, and we have a repeated characteristic root at $\gamma = -3$. The characteristic modes are $(-3)^n$ and $n(-3)^n$. Hence, the zero-input response is

$$y_0[n] = (c_1 + c_2 n)(-3)^n$$

Although we can determine the constants c_1 and c_2 from the initial conditions following a procedure similar to Ex. 9.4, we instead use MATLAB to perform the needed calculations.

```
>> c = inv([(-3)^(-1) -1*(-3)^(-1);(-3)^(-2) -2*(-3)^(-2)])*[-1/3;-2/9]
c = 4
    3
```

Thus, the zero-input response is

$$y_0[n] = (4 + 3n)(-3)^n \qquad n \geq 0$$

Complex Roots

As in the case of continuous-time systems, the complex roots of a discrete-time system will occur in pairs of conjugates if the system equation coefficients are real. Complex roots can be treated

exactly as we would treat real roots. However, just as in the case of continuous-time systems, we can also use the real form of solution as an alternative.

First we express the complex conjugate roots γ and γ^* in polar form. If $|\gamma|$ is the magnitude and β is the angle of γ, then

$$\gamma = |\gamma|e^{j\beta} \qquad \text{and} \qquad \gamma^* = |\gamma|e^{-j\beta}$$

The zero-input response is given by

$$y_0[n] = c_1\gamma^n + c_2(\gamma^*)^n = c_1|\gamma|^n e^{j\beta n} + c_2|\gamma|^n e^{-j\beta n}$$

For a real system, c_1 and c_2 must be conjugates so that $y_0[n]$ is a real function of n. Let

$$c_1 = \frac{c}{2}e^{j\theta} \qquad \text{and} \qquad c_2 = \frac{c}{2}e^{-j\theta}$$

Then

$$y_0[n] = \frac{c}{2}|\gamma|^n\left[e^{j(\beta n+\theta)} + e^{-j(\beta n+\theta)}\right] = c|\gamma|^n\cos(\beta n+\theta) \tag{9.12}$$

where c and θ are arbitrary constants determined from the auxiliary conditions. This is the solution in real form, which avoids dealing with complex numbers.

EXAMPLE 9.7 Zero-Input Response of a Second-Order System with Complex Roots

Consider a second-order difference equation with complex-conjugate roots:

$$(E^2 - 1.56E + 0.81)y[n] = (E+3)x[n]$$

Determine the zero-input response $y_0[n]$ if the initial conditions are $y_0[-1] = 2$ and $y_0[-2] = 1$.

The characteristic polynomial is $(\gamma^2 - 1.56\gamma + 0.81) = (\gamma - 0.78 - j0.45)(\gamma - 0.78 + j0.45)$. The characteristic roots are $0.78 \pm j0.45$; that is, $0.9e^{\pm j(\pi/6)}$. We could immediately write the solution as

$$y_0[n] = c(0.9)^n e^{j\pi n/6} + c^*(0.9)^n e^{-j\pi n/6}$$

Setting $n = -1$ and -2 and using the initial conditions $y_0[-1] = 2$ and $y_0[-2] = 1$, we find $c = 1.1550 - j0.2025 = 1.1726e^{-j0.1735}$ and $c^* = 1.1550 + j0.2025 = 1.1726e^{j0.1735}$.

```
>> gamma = roots([1 -1.56 0.81]);
>> c = inv([gamma(1)^(-1) gamma(2)^(-1);...
>>      gamma(1)^(-2) gamma(2)^(-2)])*[2;1]
   c = 1.1550 - 0.2025i
       1.1550 + 0.2025i
```

Alternately, we could also find the unknown coefficient by using the real form of the solution, as given in Eq. (9.12). In the present case, the roots are $0.9e^{\pm j(\pi/6)}$. Hence, $|\gamma| = 0.9$

and $\beta = \pi/6$, and the zero-input response, according to Eq. (9.12), is given by

$$y_0[n] = c(0.9)^n \cos\left(\frac{\pi}{6}n + \theta\right)$$

To determine the constants c and θ, we set $n = -1$ and -2 in this equation and substitute the initial conditions $y_0[-1] = 2$ and $y_0[-2] = 1$ to obtain

$$2 = \frac{c}{0.9}\cos\left(-\frac{\pi}{6} + \theta\right) = \frac{c}{0.9}\left[\frac{\sqrt{3}}{2}\cos\theta + \frac{1}{2}\sin\theta\right]$$

$$1 = \frac{c}{(0.9)^2}\cos\left(-\frac{\pi}{3} + \theta\right) = \frac{c}{0.81}\left[\frac{1}{2}\cos\theta + \frac{\sqrt{3}}{2}\sin\theta\right]$$

or

$$\frac{\sqrt{3}}{1.8}c\cos\theta + \frac{1}{1.8}c\sin\theta = 2$$

$$\frac{1}{1.62}c\cos\theta + \frac{\sqrt{3}}{1.62}c\sin\theta = 1$$

These are two simultaneous equations in two unknowns $c\cos\theta$ and $c\sin\theta$. Solution of these equations yields

$$c\cos\theta = 2.308$$

$$c\sin\theta = -0.397$$

Dividing $c\sin\theta$ by $c\cos\theta$ yields

$$\tan\theta = \frac{-0.397}{2.308} = \frac{-0.172}{1}$$

$$\theta = \tan^{-1}(-0.172) = -0.17 \text{ rad}$$

Substituting $\theta = -0.17$ radian in $c\cos\theta = 2.308$ yields $c = 2.34$ and

$$y_0[n] = 2.34(0.9)^n \cos\left(\frac{\pi}{6}n - 0.17\right) \quad n \geq 0$$

Observe that here we have used radian units for both β and θ. We also could have used the degree unit, although this practice is not recommended. The important consideration is to be consistent and to use the same units for both β and θ.

DRILL 9.5 Zero-Input Response of a Second-Order System with Complex Roots

Find the zero-input response of a system described by the equation

$$y[n]+4y[n-2]=2x[n]$$

The initial conditions are $y_0[-1]=-1/(2\sqrt{2})$ and $y_0[-2]=1/(4\sqrt{2})$. Verify the solution by computing the first three terms iteratively.

ANSWER

$y_0[n]=(2)^n\cos\left(\frac{\pi}{2}n-\frac{3\pi}{4}\right)$

9.4 THE UNIT IMPULSE RESPONSE $h[n]$

Consider an nth-order system specified by the equation

$$(E^N+a_1E^{N-1}+\cdots+a_{N-1}E+a_N)y[n]=(b_0E^N+b_1E^{N-1}+\cdots+b_{N-1}E+b_N)x[n]$$

or

$$Q[E]y[n]=P[E]x[n]$$

The unit impulse response $h[n]$ is the solution of this equation for the input $\delta[n]$ with all the initial conditions zero; that is,

$$Q[E]h[n]=P[E]\delta[n] \tag{9.13}$$

subject to initial conditions

$$h[-1]=h[-2]=\cdots=h[-N]=0$$

Equation (9.13) can be solved to determine $h[n]$ iteratively or in a closed form. The following example demonstrates the iterative solution.

EXAMPLE 9.8 Iterative Determination of the Impulse Response

Iteratively compute the first two values of the impulse response $h[n]$ of a system described by the equation

$$y[n]-0.6y[n-1]-0.16y[n-2]=5x[n]$$

To determine the unit impulse response, we substitute $\delta[n]$ for $x[n]$ and $h[n]$ for $y[n]$ in the system's difference equation to obtain

$$h[n]-0.6h[n-1]-0.16h[n-2]=5\delta[n]$$

subject to zero initial state; that is, $h[-1] = h[-2] = 0$.

Setting $n = 0$ in this equation yields

$$h[0] - 0.6(0) - 0.16(0) = 5(1) \implies h[0] = 5$$

Setting $n = 1$ in the same equation and using $h[0] = 5$, we obtain

$$h[1] - 0.6(5) - 0.16(0) = 5(0) \implies h[1] = 3$$

Continuing this way, we can determine any number of terms of $h[n]$. Unfortunately, such a solution does not yield a closed-form expression for $h[n]$. Nevertheless, determining a few values of $h[n]$ can be useful in determining the closed-form solution, as the following development shows.

9.4.1 The Closed-Form Solution of $h[n]$

Recall that $h[n]$ is the system response to input $\delta[n]$, which is zero for $n > 0$. We know that when the input is zero, only the characteristic modes can be sustained by the system. Therefore, $h[n]$ must be made up of characteristic modes for $n > 0$. At $n = 0$, it may have some nonzero value A_0 so that a general form of $h[n]$ can be expressed as[†]

$$h[n] = A_0\delta[n] + y_c[n]u[n] \tag{9.14}$$

where $y_c[n]$ is a linear combination of the characteristic modes. We now substitute Eq. (9.14) in Eq. (9.13) to obtain $Q[E]\,(A_0\delta[n] + y_c[n]u[n]) = P[E]\delta[n]$. Because $y_c[n]$ is made up of characteristic modes, $Q[E]y_c[n]u[n] = 0$, and we obtain $A_0Q[E]\delta[n] = P[E]\delta[n]$, that is,

$$A_0\,(\delta[n+N] + a_1\delta[n+N-1] + \cdots + a_N\delta[n]) = b_0\delta[n+N] + \cdots + b_N\delta[n]$$

Setting $n = 0$ in this equation and using the fact that $\delta[m] = 0$ for all $m \neq 0$, and $\delta[0] = 1$, we obtain

$$A_0a_N = b_N \implies A_0 = \frac{b_N}{a_N} \tag{9.15}$$

Hence,[‡]

$$h[n] = \frac{b_N}{a_N}\delta[n] + y_c[n]u[n] \tag{9.16}$$

The N unknown coefficients in $y_c[n]$ (on the right-hand side) can be determined from a knowledge of N values of $h[n]$. Fortunately, it is a straightforward task to determine values of $h[n]$ iteratively.

[†] We assume that the term $y_c[n]$ consists of characteristic modes for $n > 0$ only. To reflect this behavior, the characteristic terms should be expressed in the form $\gamma_j^n u[n-1]$. But because $u[n-1] = u[n] - \delta[n]$, $c_j\gamma_j^n u[n-1] = c_j\gamma_j^n u[n] - c_j\delta[n]$, and $y_c[n]$ can be expressed in terms of exponentials $\gamma_j^n u[n]$ (which start at $n = 0$), plus an impulse at $n = 0$.

[‡] If $a_N = 0$, then A_0 cannot be determined by Eq. (9.15). In such a case, we show in Sec. 9.9 that $h[n]$ is of the form $A_0\delta[n] + A_1\delta[n-1] + y_c[n]u[n]$. We have here $N+2$ unknowns, which can be determined from $N+2$ values $h[0], h[1], \ldots, h[N+1]$ found iteratively.

as demonstrated in Ex. 9.8. We compute N values $h[0], h[1], h[2], \ldots, h[N-1]$ iteratively. Now, setting $n = 0, 1, 2, \ldots, N-1$ in Eq. (9.16), we can determine the N unknowns in $y_c[n]$. This point will become clear in the following example.

EXAMPLE 9.9 Closed-Form Determination of the Impulse Response

Determine the unit impulse response $h[n]$ for a system in Ex. 9.8 specified by the equation

$$y[n] - 0.6y[n-1] - 0.16y[n-2] = 5x[n]$$

This equation can be expressed in the advance form as

$$y[n+2] - 0.6y[n+1] - 0.16y[n] = 5x[n+2]$$

or in advance operator form as

$$(E^2 - 0.6E - 0.16)y[n] = 5E^2x[n]$$

The characteristic polynomial is

$$\gamma^2 - 0.6\gamma - 0.16 = (\gamma + 0.2)(\gamma - 0.8)$$

The characteristic modes are $(-0.2)^n$ and $(0.8)^n$. Therefore,

$$y_c[n] = c_1(-0.2)^n + c_2(0.8)^n$$

Inspecting the system difference equation, we see that $a_N = -0.16$ and $b_N = 0$. Therefore, according to Eq. (9.16),

$$h[n] = [c_1(-0.2)^n + c_2(0.8)^n]u[n]$$

To determine c_1 and c_2, we need to find two values of $h[n]$ iteratively. From Ex. 9.8, we know that $h[0] = 5$ and $h[1] = 3$. Setting $n = 0$ and 1 in our expression for $h[n]$ and using the fact that $h[0] = 5$ and $h[1] = 3$, we obtain

$$\left.\begin{aligned} 5 &= c_1 + c_2 \\ 3 &= -0.2c_1 + 0.8c_2 \end{aligned}\right\} \implies \begin{aligned} c_1 &= 1 \\ c_2 &= 4 \end{aligned}$$

Therefore,

$$h[n] = \left[(-0.2)^n + 4(0.8)^n\right]u[n]$$

DRILL 9.6 Closed-Form Determination of the Impulse Response

Find $h[n]$, the unit impulse response of the LTID systems specified by the following equations:

(a) $y[n+1]-y[n]=x[n]$

(b) $y[n]-5y[n-1]+6y[n-2]=8x[n-1]-19x[n-2]$

(c) $y[n+2]-4y[n+1]+4y[n]=2x[n+2]-2x[n+1]$

(d) $y[n]=2x[n]-2x[n-1]$

ANSWERS

(a) $h[n]=u[n-1]$

(b) $h[n]=-\frac{19}{6}\delta[n]+\left[\frac{3}{2}(2)^n+\frac{5}{3}(3)^n\right]u[n]$

(c) $h[n]=(2+n)2^n u[n]$

(d) $h[n]=2\delta[n]-2\delta[n-1]$

EXAMPLE 9.10 Filtering Perspective of the Unit Impulse Response

Use the MATLAB `filter` command to solve Ex. 9.9.

There are several ways to find the impulse response using MATLAB. In this method, we first specify the unit impulse function, which will serve as our input. Vectors `a` and `b` are created to specify the system. The `filter` command is then used to determine the impulse response. In fact, this method can be used to determine the zero-state response for any input.

```
>> n = (0:19); delta = @(n) 1.0.*(n==0);
>> a = [1 -0.6 -0.16]; b = [5 0 0];
>> h = filter(b,a,delta(n));
>> stem(n,h,'k.'); xlabel('n'); ylabel('h[n]');
```

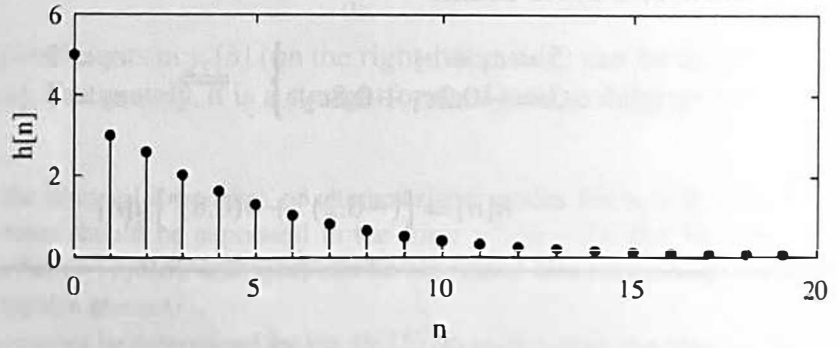

Figure 9.3 Impulse response for Ex. 9.10.

Comment. Although it is relatively simple to determine the impulse response $h[n]$ by using the procedure in this section, in Chs. 11 and 12, we shall discuss much simpler methods that utilize the z-transform.

9.5 System Response to External Input: The Zero-State Response

The zero-state response $y[n]$ is the system response to an input $x[n]$ when the system is in the zero state. In this section, we shall assume that systems are in the zero state unless mentioned otherwise so that the zero-state response will be the total response of the system. Here, we follow the procedure parallel to that used in the continuous-time case by expressing an arbitrary input $x[n]$ as a sum of impulse components. A signal $x[n]$ in Fig. 9.4a can be expressed as a sum of impulse components, such as those depicted in Figs. 9.4b–9.4f. The component of $x[n]$ at $n=m$ is $x[m]\delta[n-m]$, and $x[n]$ is the sum of all these components summed from $m=-\infty$ to ∞. Therefore,

$$\begin{aligned} x[n] &= x[0]\delta[n]+x[1]\delta[n-1]+x[2]\delta[n-2]+\cdots \\ &\quad +x[-1]\delta[n+1]+x[-2]\delta[n+2]+\cdots \\ &= \sum_{m=-\infty}^{\infty} x[m]\delta[n-m] \end{aligned} \tag{9.17}$$

For a linear system, if we know the system response to impulse $\delta[n]$, we can obtain the system response to any arbitrary input by summing the system response to various impulse components. Let $h[n]$ be the system response to impulse input $\delta[n]$. We shall use the notation

$$x[n] \Longrightarrow y[n]$$

to indicate the input and the corresponding response of the system. Thus, if

$$\delta[n] \Longrightarrow h[n]$$

then because of time invariance

$$\delta[n-m] \Longrightarrow h[n-m]$$

and because of linearity

$$x[m]\delta[n-m] \Longrightarrow x[m]h[n-m]$$

and again because of linearity

$$\underbrace{\sum_{m=-\infty}^{\infty} x[m]\delta[n-m]}_{x[n]} \Longrightarrow \underbrace{\sum_{m=-\infty}^{\infty} x[m]h[n-m]}_{y[n]}$$

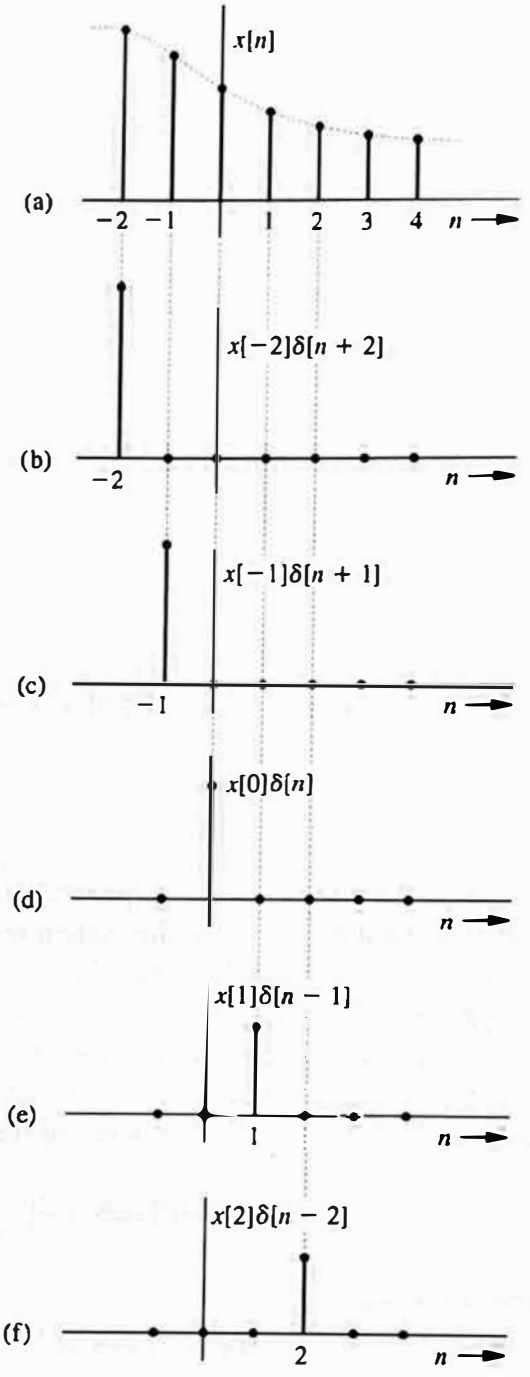

Figure 9.4 Representation of an arbitrary signal $x[n]$ in terms of impulse components.

The left-hand side is $x[n]$ [see Eq. (9.17)], and the right-hand side is the system response $y[n]$ to input $x[n]$. Therefore,†

† In deriving this result, we have assumed a time-invariant system. The system response to input $\delta[n-m]$ for a time-varying system cannot be expressed as $h[n-m]$; instead, it has the form $h[n, m]$. Using this form, Eq. (9.18) is modified as follows:

$$y[n] = \sum_{m=-\infty}^{\infty} x[m]h[n, m]$$

$$y[n] = \sum_{m=-\infty}^{\infty} x[m]h[n-m] \tag{9.18}$$

The summation on the right-hand side is known as the *convolution sum* of $x[n]$ and $h[n]$, and is represented symbolically by $x[n] * h[n]$:

$$x[n] * h[n] = \sum_{m=-\infty}^{\infty} x[m]h[n-m]$$

Properties of the Convolution Sum

The structure of the convolution sum is similar to that of the convolution integral. Moreover, the properties of the convolution sum are similar to those of the convolution integral. We shall enumerate these properties here without proof. The proofs are similar to those for the convolution integral and may be derived by the reader.

The Commutative Property.

$$x_1[n] * x_2[n] = x_2[n] * x_1[n]$$

The Distributive Property.

$$x_1[n] * (x_2[n] + x_3[n]) = x_1[n] * x_2[n] + x_1[n] * x_3[n]$$

The Associative Property.

$$x_1[n] * (x_2[n] * x_3[n]) = (x_1[n] * x_2[n]) * x_3[n]$$

The Shifting Property. If

$$x_1[n] * x_2[n] = c[n]$$

then

$$x_1[n-m] * x_2[n-p] = c[n-m-p] \tag{9.19}$$

Convolution with an Impulse.

$$x[n] * \delta[n] = x[n]$$

The Width Property. If $x_1[n]$ and $x_2[n]$ have finite widths of W_1 and W_2, respectively, then the width of $x_1[n] * x_2[n]$ is $W_1 + W_2$. The width of a signal is 1 less than the number of its elements (length). Thus, the signal in Fig. 9.6h has six elements (length of 6) but a width of only 5. Alternately, the property may be stated in terms of lengths as follows: if $x_1[n]$ and $x_2[n]$ have finite lengths of L_1 and L_2 elements, respectively, then the length of $x_1[n] * x_2[n]$ is $L_1 + L_2 - 1$ elements.

Causality and Zero-State Response

In deriving Eq. (9.18), we assumed the system to be linear and time-invariant. There were no other restrictions on either the input signal or the system. In our applications, almost all the input signals are causal, and a majority of the systems are also causal. These restrictions further simplify the limits of the sum in Eq. (9.18). If the input $x[n]$ is causal, $x[m] = 0$ for $m < 0$. Similarly, if the system is causal (i.e., if $h[n]$ is causal), then $h[x] = 0$ for negative x so that $h[n-m] = 0$ when $m > n$. Therefore, if $x[n]$ and $h[n]$ are both causal, the product $x[m]h[n-m] = 0$ for $m < 0$ and for $m > n$, and it is nonzero only for the range $0 \le m \le n$. Therefore, Eq. (9.18) in this case reduces to

$$y[n] = \sum_{m=0}^{n} x[m]h[n-m] \tag{9.20}$$

We shall evaluate the convolution sum first by an analytical method and later with graphical aid.

EXAMPLE 9.11 Convolution of Causal Signals

Determine $c[n] = x[n] * g[n]$ for

$$x[n] = (0.8)^n u[n] \qquad \text{and} \qquad g[n] = (0.3)^n u[n]$$

We have

$$c[n] = \sum_{m=-\infty}^{\infty} x[m]g[n-m]$$

Note that

$$x[m] = (0.8)^m u[m] \qquad \text{and} \qquad g[n-m] = (0.3)^{n-m} u[n-m]$$

Both $x[n]$ and $g[n]$ are causal. Therefore [see Eq. (9.20)],

$$c[n] = \sum_{m=0}^{n} x[m]g[n-m] = \sum_{m=0}^{n} (0.8)^m u[m]\,(0.3)^{n-m} u[n-m]$$

In this summation, m lies between 0 and n ($0 \le m \le n$). Therefore, if $n \ge 0$, then both m and $n-m \ge 0$ so that $u[m] = u[n-m] = 1$. If $n < 0$, m is negative because m lies between 0 and n, and $u[m] = 0$. Therefore,

$$c[n] = \begin{cases} \sum_{m=0}^{n} (0.8)^m\,(0.3)^{n-m} & n \ge 0 \\ 0 & n < 0 \end{cases}$$

or

$$c[n] = (0.3)^n \sum_{m=0}^{n} \left(\frac{0.8}{0.3}\right)^m u[n]$$

This is a geometric progression with common ratio (0.8/0.3). From Sec. B.8.3, we have

$$c[n] = (0.3)^n \frac{(0.8)^{n+1} - (0.3)^{n+1}}{(0.3)^n(0.8-0.3)} u[n]$$
$$= 2[(0.8)^{n+1} - (0.3)^{n+1}]u[n]$$

EXAMPLE 9.12 Filtering Perspective of the Zero-State Response

Use the MATLAB `filter` command to compute and sketch the zero-state response for the system described by $(E^2 + 0.5E - 1)y[n] = (2E^2 + 6E)x[n]$ and the input $x[n] = 4^{-n}u[n]$.

We solve this problem using the same approach as Ex. 9.10. Although the input is bounded and quickly decays to zero, the system itself is unstable and an unbounded output results.

```
>> n = (0:11); x = @(n) 4.^(-n).*(n>=0);
>> a = [1 0.5 -1]; b = [2 6 0]; y = filter(b,a,x(n));
>> clf; stem(n,y,'k.'); xlabel('n'); ylabel('y[n]');
>> axis([-0.5 11.5 -20 25]);
```

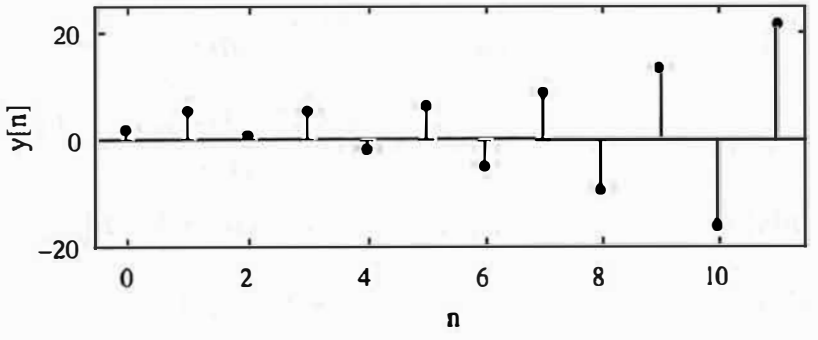

Figure 9.5 Zero-state response for Ex. 9.12.

DRILL 9.7 Convolution of Causal Signals

Show that $(0.8)^n u[n] * u[n] = 5[1 - (0.8)^{n+1}]u[n]$.

Convolution Sum from a Table

Just as in the continuous-time case, we have prepared a table (Table 9.1) from which convolution sums may be determined directly for a variety of signal pairs. For example, the convolution in

Ex. 9.11 can be read directly from this table (pair 4) as

$$(0.8)^n u[n] * (0.3)^n u[n] = \frac{(0.8)^{n+1} - (0.3)^{n+1}}{0.8 - 0.3} u[n] = 2[(0.8)^{n+1} - (0.3)^{n+1}]u[n]$$

We shall demonstrate the use of the convolution table in the following example.

TABLE 9.1 Select Convolution Sums

No.	$x_1[n]$	$x_2[n]$	$x_1[n] * x_2[n] = x_2[n] * x_1[n]$
1	$\delta[n-k]$	$x[n]$	$x[n-k]$
2	$\gamma^n u[n]$	$u[n]$	$\left[\frac{1-\gamma^{n+1}}{1-\gamma}\right]u[n]$
3	$u[n]$	$u[n]$	$(n+1)u[n]$
4	$\gamma_1^n u[n]$	$\gamma_2^n u[n]$	$\left[\frac{\gamma_1^{n+1} - \gamma_2^{n+1}}{\gamma_1 - \gamma_2}\right]u[n]$ $\quad \gamma_1 \neq \gamma_2$
5	$u[n]$	$nu[n]$	$\frac{n(n+1)}{2}u[n]$
6	$\gamma^n u[n]$	$nu[n]$	$\left[\frac{\gamma(\gamma^n - 1) + n(1-\gamma)}{(1-\gamma)^2}\right]u[n]$
7	$nu[n]$	$nu[n]$	$\frac{1}{6}n(n-1)(n+1)u[n]$
8	$\gamma^n u[n]$	$\gamma^n u[n]$	$(n+1)\gamma^n u[n]$
9	$n\gamma_1^n u[n]$	$\gamma_2^n u[n]$	$\frac{\gamma_1\gamma_2}{(\gamma_1-\gamma_2)^2}\left[\gamma_2^n - \gamma_1^n + \frac{\gamma_1-\gamma_2}{\gamma_2} n\gamma_1^n\right]u[n]$ $\quad \gamma_1 \neq \gamma_2$
10	$\lvert\gamma_1\rvert^n \cos(\beta n + \theta)u[n]$	$\lvert\gamma_2\rvert^n u[n]$	$\frac{1}{R}[\lvert\gamma_1\rvert^{n+1}\cos[\beta(n+1)+\theta-\phi] - \lvert\gamma_2\rvert^{n+1}\cos(\theta-\phi)]u[n]$ $R = [\lvert\gamma_1\rvert^2 + \lvert\gamma_2\rvert^2 - 2\lvert\gamma_1\rvert\lvert\gamma_2\rvert\cos\beta]^{1/2}$ $\phi = \tan^{-1}\left[\frac{(\lvert\gamma_1\rvert\sin\beta)}{(\lvert\gamma_1\rvert\cos\beta - \lvert\gamma_2\rvert)}\right]$
11	$\gamma_1^n u[-(n+1)]$	$\gamma_2^n u[n]$	$\frac{\gamma_2}{\gamma_1-\gamma_2}\gamma_2^n u[n] + \frac{\gamma_1}{\gamma_1-\gamma_2}\gamma_1^n u[-(n+1)]$ $\quad \lvert\gamma_1\rvert > \lvert\gamma_2\rvert$

EXAMPLE 9.13 Convolution by Tables

Using Table 9.1, find the (zero-state) response $y[n]$ of an LTID system described by the equation

$$y[n+2]-0.6y[n+1]-0.16y[n]=5x[n+2]$$

if the input $x[n]=4^{-n}u[n]$.

The input can be expressed as $x[n]=4^{-n}u[n]=(1/4)^n u[n]=(0.25)^n u[n]$. The unit impulse response of this system, obtained in Ex. 9.9, is

$$h[n]=[(-0.2)^n+4(0.8)^n]u[n]$$

Therefore,

$$\begin{aligned}y[n]&=x[n]*h[n]\\&=(0.25)^n u[n]*\left[(-0.2)^n u[n]+4(0.8)^n u[n]\right]\\&=(0.25)^n u[n]*(-0.2)^n u[n]+(0.25)^n u[n]*4(0.8)^n u[n]\end{aligned}$$

We use pair 4 (Table 9.1) to find the foregoing convolution sums.

$$\begin{aligned}y[n]&=\left[\frac{(0.25)^{n+1}-(-0.2)^{n+1}}{0.25-(-0.2)}+4\frac{(0.25)^{n+1}-(0.8)^{n+1}}{0.25-0.8}\right]u[n]\\&=(2.22[(0.25)^{n+1}-(-0.2)^{n+1}]-7.27[(0.25)^{n+1}-(0.8)^{n+1}])u[n]\\&=[-5.05(0.25)^{n+1}-2.22(-0.2)^{n+1}+7.27(0.8)^{n+1}]u[n]\end{aligned}$$

Recognizing that

$$\gamma^{n+1}=\gamma(\gamma)^n$$

we can express $y[n]$ as

$$\begin{aligned}y[n]&=[-1.26(0.25)^n+0.444(-0.2)^n+5.81(0.8)^n]u[n]\\&=[-1.26(4)^{-n}+0.444(-0.2)^n+5.81(0.8)^n]u[n]\end{aligned}$$

DRILL 9.8 Convolution by Tables

Use Table 9.1 to show that

(a) $(0.8)^{n+1}u[n]*u[n]=4[1-0.8(0.8)^n]u[n]$

(b) $n3^{-n}u[n]*(0.2)^n u[n]=\frac{15}{4}\left[(0.2)^n-\left(1-\frac{2}{3}n\right)3^{-n}\right]u[n]$

(c) $e^{-n}u[n]*2^{-n}u[n]=\frac{2}{2-e}\left[e^{-n}-\frac{e}{2}2^{-n}\right]u[n]$

Response to Complex Inputs

As in the case of real continuous-time systems, we can show that for an LTID system with real $h[n]$, if the input and the output are expressed in terms of their real and imaginary parts, then the real part of the input generates the real part of the response and the imaginary part of the input generates the imaginary part. Thus, if

$$x[n] = x_r[n] + jx_i[n] \qquad \text{and} \qquad y[n] = y_r[n] + jy_i[n]$$

using the right-directed arrow to indicate the input–output pair, we can show that

$$x_r[n] \Longrightarrow y_r[n] \qquad \text{and} \qquad x_i[n] \Longrightarrow y_i[n] \tag{9.21}$$

The proof is similar to that used to derive Eq. (2.31) for LTIC systems.

Multiple Inputs

Multiple inputs to LTI systems can be treated by applying the superposition principle. Each input is considered separately, with all other inputs assumed to be zero. The sum of all these individual system responses constitutes the total system output when all the inputs are applied simultaneously.

DRILL 9.9 Response to Multiple Inputs

Show that the system described by $y[n] - 0.6y[n-1] - 0.16y[n-2] = 5x[n]$ responds to input $x[n] = \delta[n] + 4^{-n}u[n]$ with output $y[n] = [-1.26(4)^{-n} + 1.444(-0.2)^n + 9.81(0.8)^n]u[n]$. [*Hint:* Use the results of Exs. 9.9 and 9.13.]

9.5.1 Graphical Procedure for the Convolution Sum

The steps in evaluating the convolution sum are parallel to those followed in evaluating the convolution integral. The convolution sum of causal signals $x[n]$ and $g[n]$ is given by

$$c[n] = \sum_{m=0}^{n} x[m]g[n-m]$$

We first plot $x[m]$ and $g[n-m]$ as functions of m (not n), because the summation is over m. Functions $x[m]$ and $g[m]$ are the same as $x[n]$ and $g[n]$, plotted, respectively, as functions of m (see Fig. 9.6). The convolution operation can be performed as follows:

1. Invert $g[m]$ about the vertical axis ($m = 0$) to obtain $g[-m]$ (Fig. 9.6d). Figure 9.6e shows both $x[m]$ and $g[-m]$.

2. Shift $g[-m]$ by n units to obtain $g[n-m]$. For $n > 0$, the shift is to the right (delay); for $n < 0$, the shift is to the left (advance). Figure 9.6f shows $g[n-m]$ for $n > 0$; for $n < 0$, see Fig. 9.6g.
3. Next we multiply $x[m]$ and $g[n-m]$ and add all the products to obtain $c[n]$. The procedure is repeated for each value of n over the range $-\infty$ to ∞.

We shall demonstrate by an example the graphical procedure for finding the convolution sum. Although both the functions in this example are causal, this procedure is applicable to the general case.

EXAMPLE 9.14 Graphical Procedure for the Convolution Sum

Find $c[n] = x[n] * g[n]$, where $x[n]$ and $g[n]$ are depicted in Figs. 9.6a and 9.6b, respectively.

We are given

$$x[n] = (0.8)^n \qquad \text{and} \qquad g[n] = (0.3)^n$$

Therefore,

$$x[m] = (0.8)^m \qquad \text{and} \qquad g[n-m] = (0.3)^{n-m}$$

Figure 9.6f shows the general situation for $n \geq 0$. The two functions $x[m]$ and $g[n-m]$ overlap over the interval $0 \leq m \leq n$. Therefore,

$$\begin{aligned} c[n] &= \sum_{m=0}^{n} x[m]g[n-m] \\ &= \sum_{m=0}^{n} (0.8)^m (0.3)^{n-m} \\ &= (0.3)^n \sum_{m=0}^{n} \left(\frac{0.8}{0.3}\right)^m \\ &= 2[(0.8)^{n+1} - (0.3)^{n+1}] \qquad n \geq 0 \qquad \text{(see Sec. B.8.3)} \end{aligned}$$

For $n < 0$, there is no overlap between $x[m]$ and $g[n-m]$, as shown in Fig. 9.6g, so that

$$c[n] = 0 \qquad n < 0$$

Combining pieces, we see that

$$c[n] = 2[(0.8)^{n+1} - (0.3)^{n+1}]u[n]$$

which agrees with the result found earlier in Ex. 9.11.

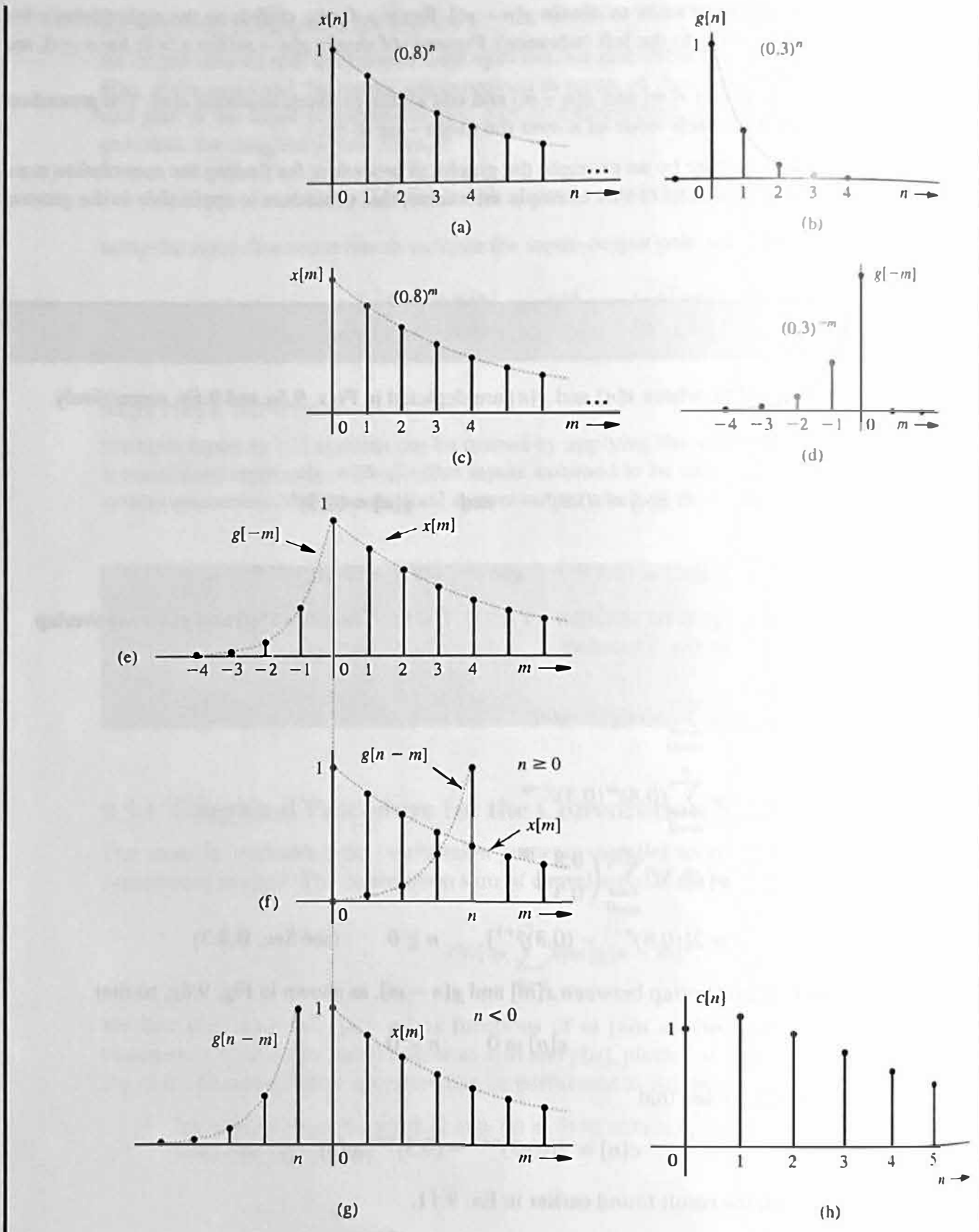

Figure 9.6 Graphical procedure to convolve $x[n]$ and $g[n]$.

DRILL 9.10 Graphical Procedure for the Convolution Sum

Find $(0.8)^n u[n] * u[n]$ graphically and sketch the result.

ANSWER

$5(1-(0.8)^{n+1})u[n]$

An Alternative Form of Graphical Procedure: The Sliding-Tape Method

This algorithm is convenient when the sequences $x[n]$ and $g[n]$ are short or when they are available only in graphical form. The algorithm is basically the same as the graphical procedure in Fig. 9.6. The only difference is that instead of presenting the data as graphical plots, we display it as a sequence of numbers on tapes. Otherwise, the procedure is the same, as will become clear in the following example.

EXAMPLE 9.15 Sliding-Tape Method for the Convolution Sum

Use the sliding-tape method to convolve the two sequences $x[n]$ and $g[n]$ depicted in Figs. 9.7a and 9.7b, respectively.

In this procedure, we write the sequences $x[n]$ and $g[n]$ in the slots of two tapes: x tape and g tape (Fig. 9.7c). Now leave the x tape stationary (to correspond to $x[m]$). The $g[-m]$ tape is obtained by inverting the $g[m]$ tape about the origin ($m=0$) so that the slots corresponding to $x[0]$ and $g[0]$ remain aligned (Fig. 9.7d). We now shift the inverted tape by n slots, multiply values on two tapes in adjacent slots, and add all the products to find $c[n]$. Figures 9.7d–9.7i show the cases for $n=0$–5. Figures 9.7j, 9.7k, and 9.7l show the cases for $n=-1$, -2, and -3, respectively.

For the case of $n=0$, for example (Fig. 9.7d),

$$c[0]=(-2\times 1)+(-1\times 1)+(0\times 1)=-3$$

For $n=1$ (Fig. 9.7e),

$$c[1]=(-2\times 1)+(-1\times 1)+(0\times 1)+(1\times 1)=-2$$

Similarly,

$$c[2]=(-2\times 1)+(-1\times 1)+(0\times 1)+(1\times 1)+(2\times 1)=0$$
$$c[3]=(-2\times 1)+(-1\times 1)+(0\times 1)+(1\times 1)+(2\times 1)+(3\times 1)=3$$
$$c[4]=(-2\times 1)+(-1\times 1)+(0\times 1)+(1\times 1)+(2\times 1)+(3\times 1)+(4\times 1)=7$$
$$c[5]=(-2\times 1)+(-1\times 1)+(0\times 1)+(1\times 1)+(2\times 1)+(3\times 1)+(4\times 1)=7$$

Figure 9.7i shows that $c[n]=7$ for $n\geq 4$.

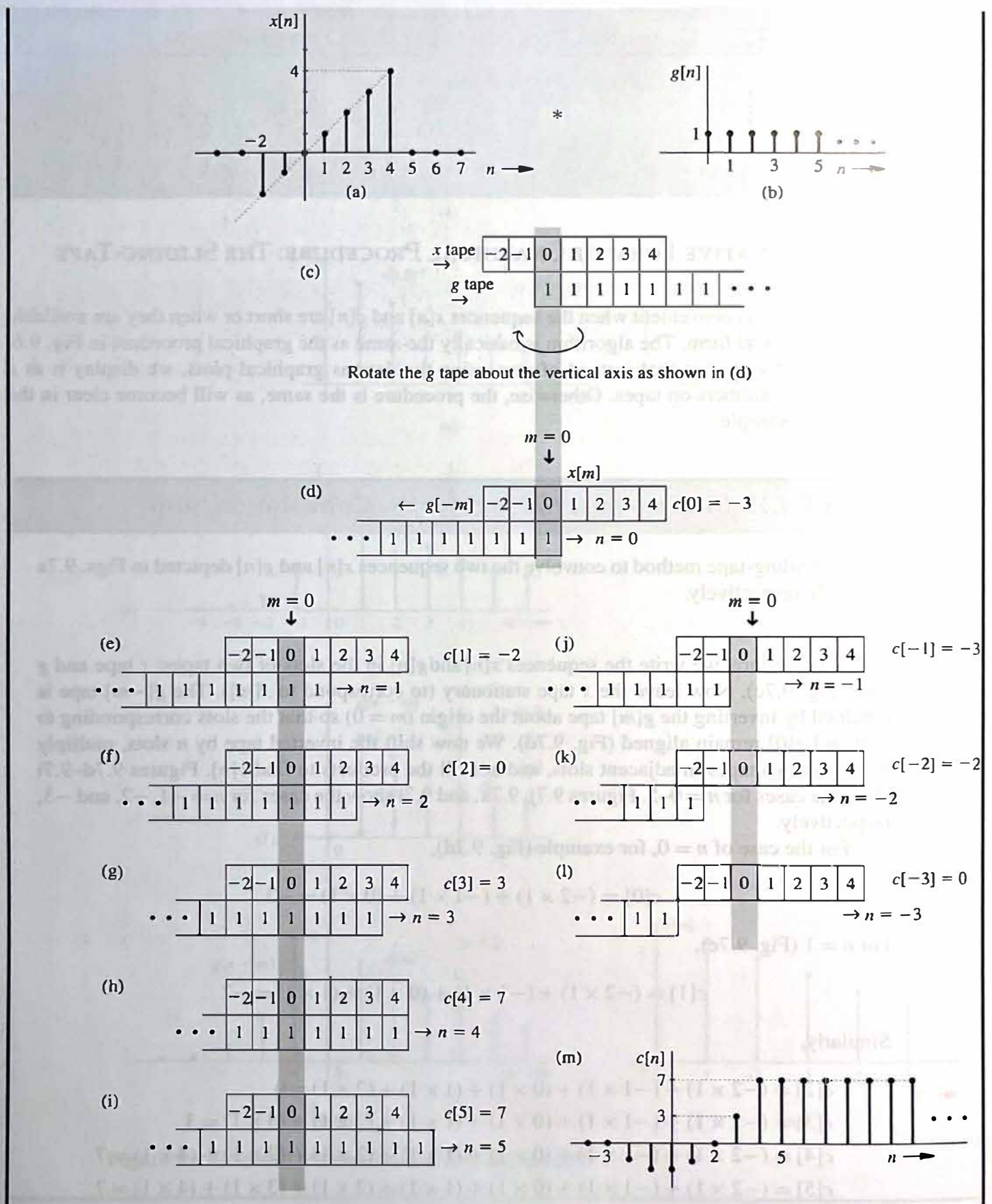

Figure 9.7 Sliding-tape algorithm for discrete-time convolution.

Similarly, we compute $c[n]$ for negative n by sliding the tape backward, one slot at a time, as shown in the plots corresponding to $n = -1, -2$, and -3, respectively (Figs. 9.7j, 9.7k, and 9.7l).

$$c[-1] = (-2 \times 1) + (-1 \times 1) = -3$$
$$c[-2] = (-2 \times 1) = -2$$
$$c[-3] = 0$$

Figure 9.7l shows that $c[n] = 0$ for $n \leq 3$. Figure 9.7m shows the plot of $c[n]$.

DRILL 9.11 Sliding Tape Method for the Convolution Sum

Use the graphical procedure of Ex. 9.15 (sliding-tape technique) to show that $x[n] * g[n] = c[n]$ in Fig. 9.8. Verify the width property of convolution.

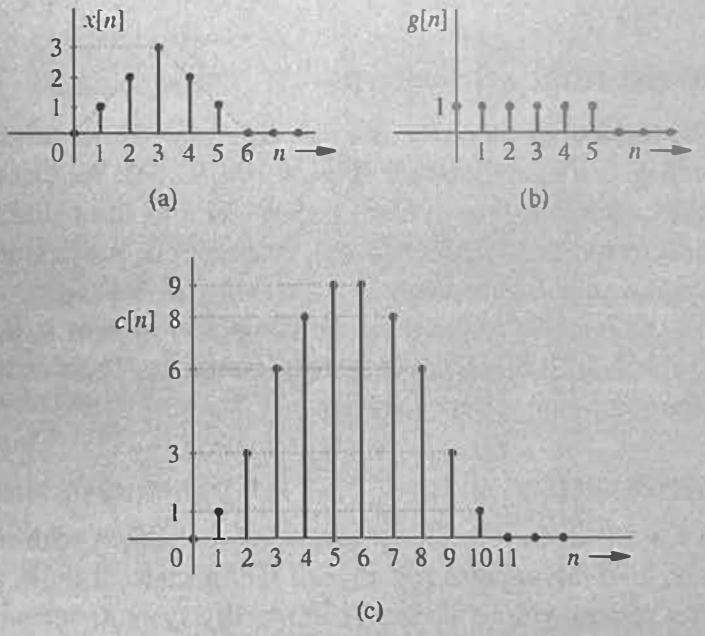

Figure 9.8 Signals for Drill 9.11.

EXAMPLE 9.16 Convolution of Two Finite-Duration Signals Using MATLAB

For the signals $x[n]$ and $g[n]$ depicted in Fig. 9.8, use MATLAB to compute and plot $c[n] = x[n] * g[n]$.

```
>> x = [0 1 2 3 2 1]; g = [1 1 1 1 1 1];
>> n = (0:1:length(x)+length(g)-2);
>> c = conv(x,g); stem(n,c,'k.');
>> xlabel('n'); ylabel('c[n]'); axis([-0.5 10.5 0 10]);
```

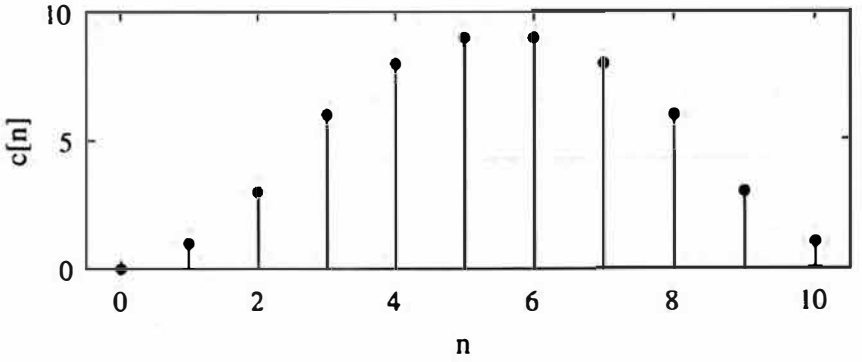

Figure 9.9 Convolution result for Ex. 9.16.

9.5.2 Interconnected Systems

As with the continuous-time case, we can determine the impulse response of systems connected in parallel (Fig. 9.10a) and cascade (Figs. 9.10b, 9.10c). We can use arguments identical to those used for the continuous-time systems in Sec. 2.4.3 to show that if two LTID systems S_1 and S_2 with impulse responses $h_1[n]$ and $h_2[n]$, respectively, are connected in parallel, the composite parallel system impulse response is $h_1[n] + h_2[n]$. Similarly, if these systems are connected in cascade, the impulse response of the composite system is $h_1[n] * h_2[n]$. Moreover, because $h_1[n] * h_2[n] = h_2[n] * h_1[n]$, linear systems commute. Their orders can be interchanged without affecting the composite system behavior.

Inverse Systems

If the two systems in cascade are the inverse of each other, with impulse responses $h[n]$ and $h_i[n]$, respectively, then the impulse response of the cascade of these systems is $h[n] * h_i[n]$. But, the cascade of a system with its inverse is an identity system, whose output is the same as the input. Hence, the unit impulse response of an identity system is $\delta[n]$. Consequently,

$$h[n] * h_i[n] = \delta[n]$$

As an example, we show that an accumulator system and a backward difference system are the inverse of each other. An accumulator system is specified by[†]

$$y[n] = \sum_{k=-\infty}^{n} x[k] \tag{9.22}$$

[†] Equations (9.22) and (9.23) are identical to Eqs. (8.17) and (8.15), respectively, with $T = 1$.

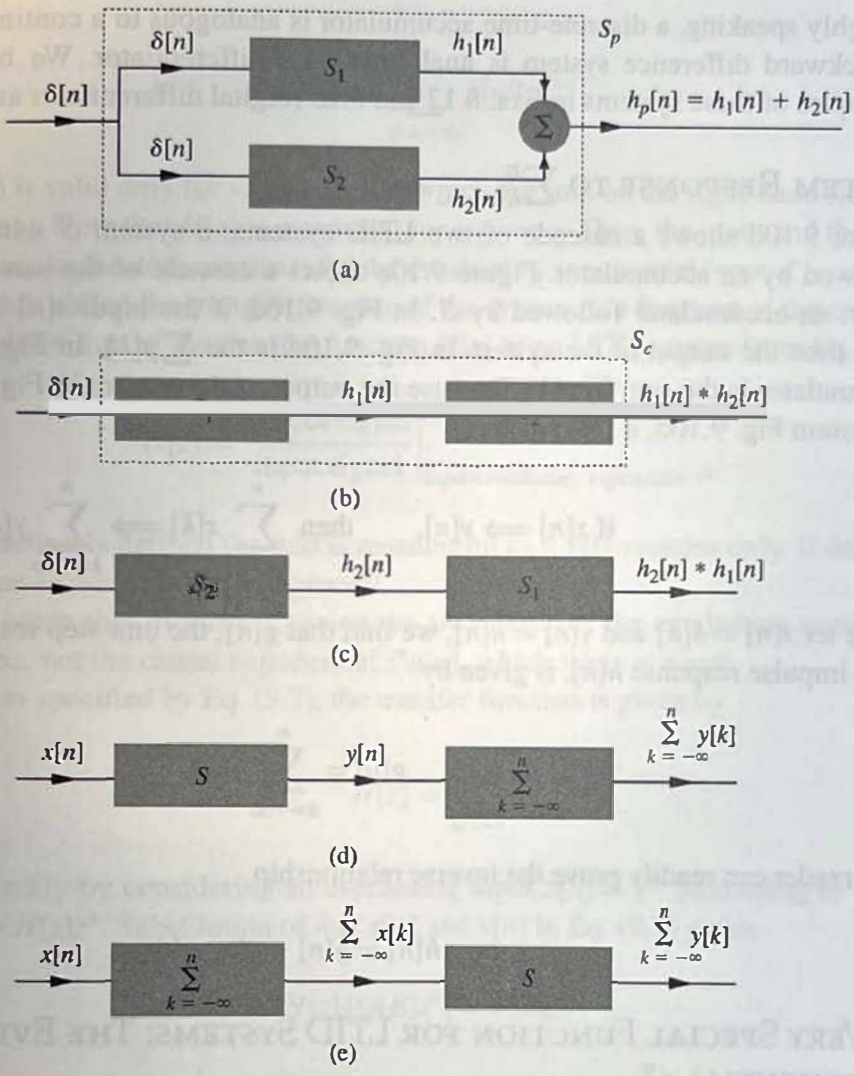

Figure 9.10 Interconnected systems.

The backward difference system is specified by

$$y[n] = x[n] - x[n-1] \tag{9.23}$$

From Eq. (9.22), we find $h_{\text{acc}}[n]$, the impulse response of the accumulator, as

$$h_{\text{acc}}[n] = \sum_{k=-\infty}^{n} \delta[k] = u[n]$$

Similarly, from Eq. (9.23), $h_{\text{bdf}}[n]$, the impulse response of the backward difference system is given by

$$h_{\text{bdf}}[n] = \delta[n] - \delta[n-1]$$

We can verify that

$$h_{\text{acc}} * h_{\text{bdf}} = u[n] * \{\delta[n] - \delta[n-1]\} = u[n] - u[n-1] = \delta[n]$$

Roughly speaking, a discrete-time accumulator is analogous to a continuous-time integrator, and a backward difference system is analogous to a differentiator. We have already encountered examples of these systems in Exs. 8.12 and 8.13 (digital differentiator and integrator).

System Response to $\sum_{k=-\infty}^{n} x[k]$

Figure 9.10d shows a cascade of two LTID systems: a system $\mathcal{S}$ with impulse response $h[n]$, followed by an accumulator. Figure 9.10e shows a cascade of the same two systems in reverse order: an accumulator followed by $\mathcal{S}$. In Fig. 9.10d, if the input $x[n]$ to $\mathcal{S}$ results in the output $y[n]$, then the output of the system in Fig. 9.10d is the $\sum y[k]$. In Fig. 9.10e, the output of the accumulator is the sum $\sum x[k]$. Because the output of the system in Fig. 9.10e is identical to that of system Fig. 9.10d, it follows that

$$\text{if } x[n] \Longrightarrow y[n], \qquad \text{then } \sum_{k=-\infty}^{n} x[k] \Longrightarrow \sum_{k=-\infty}^{n} y[k]$$

If we let $x[n] = \delta[n]$ and $y[n] = h[n]$, we find that $g[n]$, the unit step response of an LTID system with impulse response $h[n]$, is given by

$$g[n] = \sum_{k=-\infty}^{n} h[k] \tag{9.24}$$

The reader can readily prove the inverse relationship

$$h[n] = g[n] - g[n-1]$$

A Very Special Function for LTID Systems: The Everlasting Exponential z^n

In Sec. 2.4.4, we showed that there exists one signal for which the response of an LTIC system is the same as the input within a multiplicative constant. The response of an LTIC system to an everlasting exponential input e^{st} is $H(s)e^{st}$, where $H(s)$ is the system transfer function. We now show that for an LTID system, the same role is played by an everlasting exponential z^n. The system response $y[n]$ in this case is given by

$$\begin{aligned} y[n] &= h[n] * z^n \\ &= \sum_{m=-\infty}^{\infty} h[m] z^{n-m} \\ &= z^n \sum_{m=-\infty}^{\infty} h[m] z^{-m} \end{aligned}$$

For causal $h[n]$, the limits on the sum on the right-hand side would range from 0 to ∞. In any case, this sum is a function of z. Assuming that this sum converges, let us denote it by $H[z]$. Thus,

$$y[n] = H[z] z^n \tag{9.25}$$

where

$$H[z] = \sum_{m=-\infty}^{\infty} h[m]z^{-m} \tag{9.26}$$

Equation (9.25) is valid only for values of z for which the sum on the right-hand side of Eq. (9.26) exists (converges). Note that $H[z]$ is a constant for a given z. Thus, the input and the output are the same (within a multiplicative constant) for the everlasting exponential input z^n.

$H[z]$, which is called the *transfer function* of the system, is a function of the complex variable z. An alternate definition of the transfer function $H[z]$ of an LTID system from Eq. (9.25) is

$$H[z] = \left.\frac{\text{output signal}}{\text{input signal}}\right|_{\text{input=everlasting exponential } z^n} \tag{9.27}$$

The transfer function is defined for, and is meaningful to, LTID systems only. It does not exist for nonlinear or time-varying systems in general.

We repeat again that in this discussion we are talking of the everlasting exponential, which starts at $n = -\infty$, not the causal exponential $z^n u[n]$, which starts at $n = 0$.

For a system specified by Eq. (9.7), the transfer function is given by

$$H[z] = \frac{P[z]}{Q[z]} \tag{9.28}$$

This follows readily by considering an everlasting input $x[n] = z^n$. According to Eq. (9.27), the output is $y[n] = H[z]z^n$. Substitution of this $x[n]$ and $y[n]$ in Eq. (9.7) yields

$$H[z]\{Q[E]z^n\} = P[E]z^n$$

Moreover,

$$E^k z^n = z^{n+k} = z^k z^n$$

Hence,

$$P[E]z^n = P[z]z^n \qquad \text{and} \qquad Q[E]z^n = Q[z]z^n$$

Consequently,

$$H[z] = \frac{P[z]}{Q[z]}$$

DRILL 9.12 DT System Transfer Function

Show that the transfer function of the digital differentiator in Ex. 8.12 (big shaded block in Fig. 8.23b) is given by $H[z] = (z-1)/Tz$, and the transfer function of an unit delay, specified by $y[n] = x[n-1]$, is given by $1/z$.

9.5.3 Total Response

The total response of an LTID system can be expressed as a sum of the zero-input and zero-state responses:

$$\text{total response} = \underbrace{\sum_{j=1}^{N} c_j \gamma_j^n}_{\text{ZIR}} + \underbrace{x[n] * h[n]}_{\text{ZSR}}$$

In this expression, the zero-input response should be appropriately modified for the case of repeated roots. We have developed procedures to determine these two components. From the system equation, we find the characteristic roots and characteristic modes. The zero-input response is a linear combination of the characteristic modes. From the system equation, we also determine $h[n]$, the impulse response, as discussed in Sec. 9.4. Knowing $h[n]$ and the input $x[n]$, we find the zero-state response as the convolution of $x[n]$ and $h[n]$. The arbitrary constants $c_1, c_2, \ldots, c_n$ in the zero-input response are determined from the n initial conditions. For the system described by the equation

$$y[n+2] - 0.6y[n+1] - 0.16y[n] = 5x[n+2]$$

with initial conditions $y[-1] = 0, y[-2] = 25/4$ and input $x[n] = (4)^{-n}u[n]$, we have determined the two components of the response in Exs. 9.4 and 9.13, respectively. From the results in these examples, the total response for $n \geq 0$ is

$$\text{total response} = \underbrace{0.2(-0.2)^n + 0.8(0.8)^n}_{\text{ZIR}} + \underbrace{0.444(-0.2)^n + 5.81(0.8)^n - 1.26(4)^{-n}}_{\text{ZSR}} \qquad (9.29)$$

Natural and Forced Response

The characteristic modes of this system are $(-0.2)^n$ and $(0.8)^n$. The zero-input response is made up of characteristic modes exclusively, as expected, but the characteristic modes also appear in the zero-state response. When all the characteristic mode terms in the total response are lumped together, the resulting component is the *natural response*. The remaining part of the total response that is made up of noncharacteristic modes is the *forced response*. For the present case, Eq. (9.29) yields

$$\text{total response} = \underbrace{0.644(-0.2)^n + 6.61(0.8)^n}_{\text{natural response}} + \underbrace{-1.26(4)^{-n}}_{\text{forced response}} \qquad n \geq 0$$

Just like differential equations, the classical solution to difference equations includes the natural and forced responses, a decomposition that lacks the engineering intuition and utility afforded by the zero-input and zero-state responses. The classical approach cannot separate the responses arising from internal conditions and external input. While the natural and forced solutions can be obtained from the zero-input and zero-state responses, the converse is not true. Further, the classical method is unable to express the system response to an input $x[n]$ as an explicit function of $x[n]$. In fact, the classical method is restricted to a certain class of inputs and cannot handle arbitrary inputs, as can the method to determine the zero-state response. For these (and other) reasons, we do not further detail the classical approach and its direct calculation of the forced and natural responses.

9.6 System Stability

The concepts and criteria for the BIBO (external) stability and internal (asymptotic) stability for discrete-time systems are identical to those corresponding to continuous-time systems. The comments in Sec. 2.5 for LTIC systems concerning the distinction between external and internal stability are also valid for LTID systems. Let us begin with external (BIBO) stability.

9.6.1 External (BIBO) Stability

Recall that

$$y[n] = h[n] * x[n] = \sum_{m=-\infty}^{\infty} h[m]x[n-m]$$

and

$$|y[n]| = \left| \sum_{m=-\infty}^{\infty} h[m]x[n-m] \right| \leq \sum_{m=-\infty}^{\infty} |h[m]|\,|x[n-m]|$$

If $x[n]$ is bounded, then $|x[n-m]| < K_1 < \infty$, and

$$|y[n]| \leq K_1 \sum_{m=-\infty}^{\infty} |h[m]|$$

Clearly, the output is bounded if the summation on the right-hand side is bounded; that is, if

$$\sum_{n=-\infty}^{\infty} |h[n]| < K_2 < \infty \tag{9.30}$$

This is a sufficient condition for BIBO stability. We can show that this is also a necessary condition (see Prob. 9.6-1). Therefore, if the impulse response $h[n]$ of an LTID system is absolutely summable, the system is (BIBO) stable. Otherwise, it is unstable.

All the comments about the nature of external and internal stability in Ch. 2 apply to discrete-time case. We shall not elaborate them further.

9.6.2 Internal (Asymptotic) Stability

For LTID systems, as in the case of LTIC systems, internal stability, called asymptotical stability or stability in the sense of Lyapunov (also the zero-input stability), is defined in terms of the zero-input response of a system.

For an LTID system specified by a difference equation in the form of Eq. (9.2) [or Eq. (9.7)], the zero-input response consists of the characteristic modes of the system. The mode corresponding to a characteristic root γ is γ^n. To be more general, let γ be complex so that

$$\gamma = |\gamma| e^{j\beta} \qquad \text{and} \qquad \gamma^n = |\gamma|^n e^{j\beta n}$$

Since the magnitude of $e^{j\beta n}$ is always unity regardless of the value of n, the magnitude of γ^n is $|\gamma|^n$. Therefore,

$$\begin{aligned} &\text{if } |\gamma| < 1, && \text{then } \gamma^n \to 0 \text{ as } n \to \infty \\ &\text{if } |\gamma| > 1, && \text{then } \gamma^n \to \infty \text{ as } n \to \infty \\ &\text{and if } |\gamma| = 1, && \text{then } |\gamma|^n = 1 \text{ for all } n \end{aligned}$$

The characteristic modes corresponding to characteristic roots at various locations in the complex plane appear in Fig. 9.11.

These results can be grasped more effectively in terms of the location of characteristic roots in the complex plane. Figure 9.12 shows a circle of unit radius, centered at the origin in a complex plane. Our discussion shows that if all characteristic roots of the system lie inside the *unit circle*, $|\gamma_i| < 1$ for all i and the system is asymptotically stable. On the other hand, even if one characteristic root lies outside the unit circle, the system is unstable. If none of the characteristic roots lie outside the unit circle, but some simple (unrepeated) roots lie on the circle itself, the system is marginally stable. If two or more characteristic roots coincide on the unit circle (repeated roots), the system is unstable. The reason is that for repeated roots, the zero-input response is of the form $n^{r-1}\gamma^n$, and if $|\gamma| = 1$, then $|n^{r-1}\gamma^n| = n^{r-1} \to \infty$ as $n \to \infty$.[†] Note, however, that repeated roots inside the unit circle do not cause instability.

To summarize:

1. An LTID system is asymptotically stable if, and only if, all the characteristic roots are inside the unit circle. The roots may be simple or repeated.
2. An LTID system is unstable if, and only if, either one or both of the following conditions exist: (i) at least one root is outside the unit circle; (ii) there are repeated roots on the unit circle.
3. An LTID system is marginally stable if and only if there are no roots outside the unit circle and there are some unrepeated roots on the unit circle.

9.6.3 Relationship between BIBO and Asymptotic Stability

For LTID systems, the relation between the two types of stability is similar to those in LTIC systems. For a system specified by Eq. (9.2), we can readily show that if a characteristic root γ_k

[†] If the development of discrete-time systems is parallel to that of continuous-time systems, we wonder why the parallel breaks down here. Why, for instance, are LHP and RHP not the regions demarcating stability and instability? The reason lies in the form of the characteristic modes. In continuous-time systems, we chose the form of characteristic mode as $e^{\lambda_i t}$. In discrete-time systems, for computational convenience, we choose the form to be γ_i^n. Had we chosen this form to be $e^{\lambda_i n}$ where $\gamma_i = e^{\lambda_i}$, then the LHP and RHP (for the location of λ_i) again would demarcate stability and instability. The reason is that if $\gamma = e^{\lambda}$, $|\gamma| = 1$ implies $|e^{\lambda}| = 1$, and therefore $\lambda = j\omega$. This shows that the unit circle in γ plane maps into the imaginary axis in the λ plane.

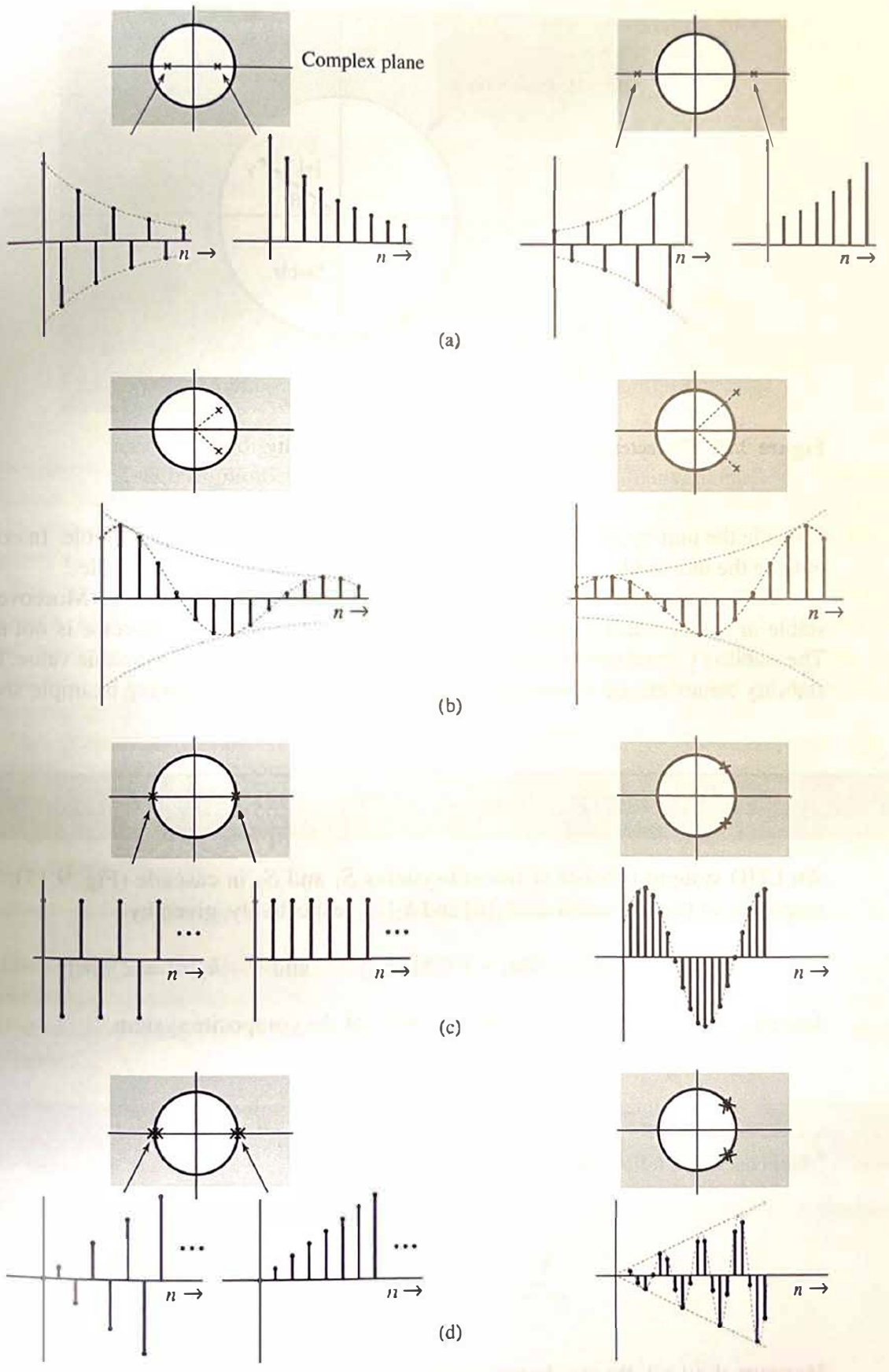

Figure 9.11 Characteristic roots locations and the corresponding characteristic modes.

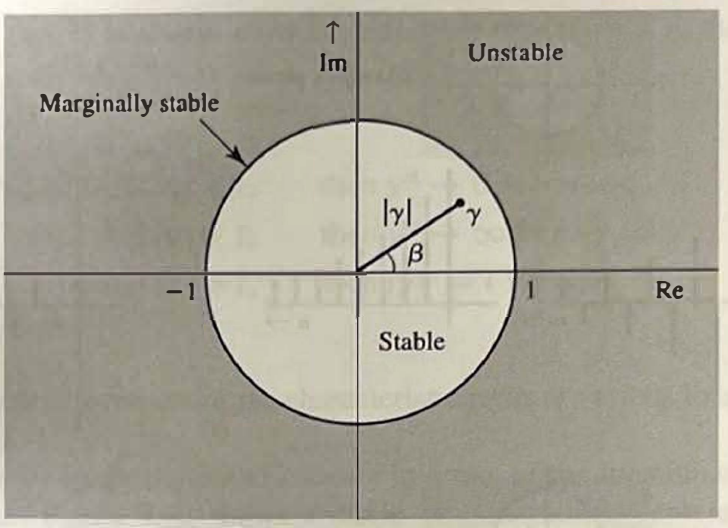

Figure 9.12 Characteristic root locations and system stability.

is inside the unit circle, the corresponding mode γ_k^n is absolutely summable. In contrast, if γ_k lies outside the unit circle, or on the unit circle, γ_k^n is not absolutely summable.†

This means that an asymptotically stable system is BIBO-stable. Moreover, a marginally stable or asymptotically unstable system is BIBO-unstable. The converse is not necessarily true. The stability picture portrayed by the external description is of questionable value. BIBO (external) stability cannot ensure internal (asymptotic) stability, as the following example shows.

EXAMPLE 9.17 A BIBO-Stable but Asymptotically Unstable System

An LTID systems consists of two subsystems $\mathcal{S}_1$ and $\mathcal{S}_2$ in cascade (Fig. 9.13). The impulse responses of these systems are $h_1[n]$ and $h_2[n]$, respectively, given by

$$h_1[n] = 4\delta[n] - 3(0.5)^n u[n] \qquad \text{and} \qquad h_2[n] = 2^n u[n]$$

Investigate the BIBO and asymptotic stability of the composite system.

---

† This conclusion follows from the fact that (see Sec. B.8.3)

$$\sum_{n=-\infty}^{\infty} |\gamma_k^n| u[n] = \sum_{n=0}^{\infty} |\gamma_k|^n = \frac{1}{1-|\gamma_k|} \qquad |\gamma_k| < 1$$

Moreover, if $|\gamma| \geq 1$, the sum diverges and goes to ∞. These conclusions are valid also for the modes of the form $n^r \gamma_k^n$.

Figure 9.13 Composite system for Ex. 9.17.

The composite system impulse response $h[n]$ is given by

$$h[n] = h_1[n] * h_2[n] = h_2[n] * h_1[n] = 2^n u[n] * (4\delta[n] - 3(0.5)^n u[n])$$
$$= 4(2)^n u[n] - 3\left[\frac{2^{n+1} - (0.5)^{n+1}}{2 - 0.5}\right] u[n]$$
$$= (0.5)^n u[n]$$

If the composite cascade system were to be enclosed in a black box with only the input and the output terminals accessible, any measurement from these external terminals would show that the impulse response of the system is $(0.5)^n u[n]$, without any hint of the unstable system sheltered inside the composite system.

The composite system is BIBO-stable because its impulse response $(0.5)^n u[n]$ is absolutely summable. However, the system $\mathcal{S}_2$ is asymptotically unstable because its characteristic root, 2, lies outside the unit circle. This system will eventually burn out (or saturate) because of the unbounded characteristic response generated by intended or unintended initial conditions, no matter how small.

The system is asymptotically unstable, though BIBO-stable. This example shows that BIBO stability does not necessarily ensure asymptotic stability when a system is uncontrollable, unobservable, or both. The internal and the external descriptions of a system are equivalent only when the system is controllable and observable. In such a case, BIBO stability means the system is asymptotically stable, and vice versa.

Fortunately, uncontrollable or unobservable systems are not common in practice. Henceforth, in determining system stability, we shall assume that unless otherwise mentioned, the internal and the external descriptions of the system are equivalent, implying that the system is controllable and observable.

EXAMPLE 9.18 Investigating Asymptotic and BIBO Stability

Determine the internal and external stability of systems specified by the following equations. In each case, plot the characteristic roots in the complex plane.

(a) $y[n+2] + 2.5y[n+1] + y[n] = x[n+1] - 2x[n]$

(b) $y[n] - y[n-1] + 0.21y[n-2] = 2x[n-1] + 3x[n-2]$

(c) $y[n+3] + 2y[n+2] + \frac{3}{2}y[n+1] + \frac{1}{2}y[n] = x[n+1]$

(d) $(E^2 - E + 1)^2 y[n] = (3E + 1)x[n]$

(a) The characteristic polynomial is

$$\gamma^2 + 2.5\gamma + 1 = (\gamma + 0.5)(\gamma + 2)$$

The characteristic roots are -0.5 and -2. Because $|-2| > 1$ (-2 lies outside the unit circle), the system is BIBO-unstable and also asymptotically unstable (Fig. 9.14a).

(b) The characteristic polynomial is

$$\gamma^2 - \gamma + 0.21 = (\gamma - 0.3)(\gamma - 0.7)$$

The characteristic roots are 0.3 and 0.7, both of which lie inside the unit circle. The system is BIBO-stable and asymptotically stable (Fig. 9.14b).

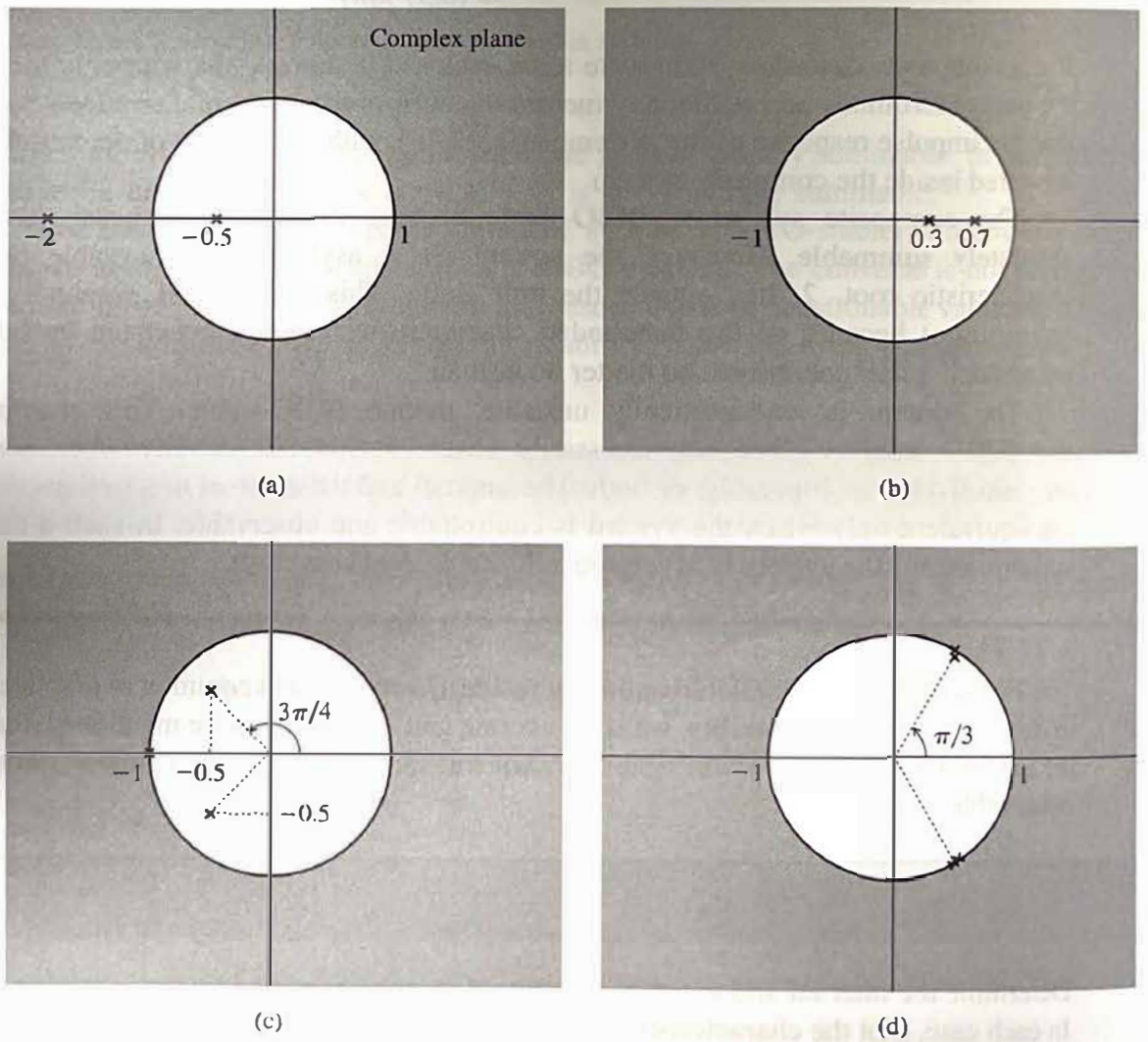

Figure 9.14 Characteristic root locations for the system of Ex. 9.18.

(c) The characteristic polynomial is

$$\gamma^3+2\gamma^2+\tfrac{3}{2}\gamma+\tfrac{1}{2}=(\gamma+1)\left(\gamma^2+\gamma+\tfrac{1}{2}\right)=(\gamma+1)(\gamma+0.5-j0.5)(\gamma+0.5+j0.5)$$

The characteristic roots are $-1, -0.5 \pm j0.5$ (Fig. 9.14c). One of the characteristic roots is on the unit circle and the remaining two roots are inside the unit circle. The system is BIBO-unstable but marginally stable.

(d) The characteristic polynomial is

$$(\gamma^2-\gamma+1)^2=\left(\gamma-\tfrac{1}{2}-j\tfrac{\sqrt{3}}{2}\right)^2\left(\gamma-\tfrac{1}{2}+j\tfrac{\sqrt{3}}{2}\right)^2$$

The characteristic roots are $(1/2)\pm j(\sqrt{3}/2)=1e^{\pm j(\pi/3)}$ repeated twice, and they lie on the unit circle (Fig. 9.14d). The system is BIBO-unstable and asymptotically unstable.

DRILL 9.13 Assessing Stability by Characteristic Roots

Using the complex plane, locate the characteristic roots of the following systems, and use the characteristic root locations to determine external and internal stability of each system.

(a) $(E+1)(E^2+6E+25)y[n]=3Ex[n]$

(b) $(E-1)^2(E+0.5)y[n]=(E^2+2E+3)x[n]$

ANSWER

Both systems are BIBO and asymptotically unstable.

9.7 Intuitive Insights into System Behavior

The intuitive insights into the behavior of continuous-time systems and their qualitative proofs, discussed in Sec. 2.6, also apply to discrete-time systems. For this reason, we shall merely mention here without discussion some of the insights presented in Sec. 2.6.

The system's entire (zero-input and zero-state) behavior is strongly influenced by the characteristic roots (or modes) of the system. The system responds strongly to input signals similar to its characteristic modes and poorly to inputs very different from its characteristic modes. In fact, when the input is a characteristic mode of the system, the response goes to infinity, provided the mode is a nondecaying signal. This is the resonance phenomenon. The width of an impulse response $h[n]$ indicates the response time (time required to respond fully to an input) of the system. It is the time constant of the system.[†] Discrete-time pulses are generally dispersed when passed through a discrete-time system. The amount of dispersion (or spreading out) is equal to the system

[†] This part of the discussion applies to systems with impulse response $h[n]$ that is a mostly positive (or mostly negative) pulse.

time constant (or width of $h[n]$). The system time constant also determines the rate at which the system can transmit information. A smaller time constant corresponds to a higher rate of information transmission, and vice versa. We keep in mind that concepts such as time constant and pulse dispersion only coarsely illustrate system behavior. Let us illustrate these ideas with an example.

EXAMPLE 9.19 Intuitive Insights into Lowpass DT System Behavior

Determine the time constant, rise time, pulse dispersion, and filter characteristics of a lowpass DT system with impulse response $h[n] = 2(0.6)^n u[n]$.

Since $h[n]$ resembles a single, mostly positive pulse, we know that the DT system is lowpass. Similar to the CT case shown in Sec. 2.6, we can determine the time constant T_h as the width of a rectangle that approximates $h[n]$. This rectangle possesses the same peak height and total sum (area), as does $h[n]$. The peak of $h[n]$ is 2, and the total sum (area) is

$$\sum_{n=0}^{\infty} 2(0.6)^n = 2\frac{1-0}{1-0.6} = 5$$

Since the width of a DT signal is 1 less than its length, we see that the time constant T_h (rectangle width) is

$$T_h = \text{rectangle width} = \frac{\text{area}}{\text{height}} - 1 = \frac{5}{2} - 1 = 1.5 \text{ samples}$$

Since time constant, rise time, pulse dispersion are all given by the same value, we see that

$$\text{time constant} = \text{rise time} = \text{pulse dispersion} = T_h = 1.5 \text{ samples}$$

The approximate cutoff frequency of our DT system can be determined as the frequency of a DT sinusoid whose period equals the length of the rectangle approximation to $h[n]$. That is,

$$\text{cutoff frequency} = \frac{1}{T_h + 1} = \frac{2}{5} \text{ cycles/sample}$$

Equivalently, we can express the cutoff frequency as $4\pi/5$ radians/sample.

Notice that T_h is not an integer and thus lacks a clear physical meaning for our DT system. How, for example, can it take 1.5 samples for our DT system to fully respond to an input? We can put our minds at ease by remembering the approximate nature of T_h, which is meant to provide only a rough understanding of system behavior.

9.8 MATLAB: DISCRETE-TIME SYSTEMS

Many special MATLAB functions are available to perform the operations of discrete-time systems, including the `filter` and `conv` commands. In this section, we investigate and apply these and other commands.

9.8.1 System Responses Through Filtering

MATLAB's `filter` command provides an efficient way to evaluate the system response of a constant coefficient linear difference equation represented in delay form as

$$\sum_{k=0}^{N} a_k y[n-k] = \sum_{k=0}^{N} b_k x[n-k] \tag{9.31}$$

In the simplest form, `filter` requires three input arguments: a length-$(N+1)$ vector of feedforward coefficients $[b_0, b_1, \ldots, b_N]$, a length-$(N+1)$ vector of feedback coefficients $[a_0, a_1, \ldots, a_N]$, and an input vector.[†] Since no initial conditions are specified, the output corresponds to the system's zero-state response.

To serve as an example, consider a system described by $y[n]-y[n-1]+y[n-2]=x[n]$. When $x[n]=\delta[n]$, the zero-state response is equal to the impulse response $h[n]$, which we compute over $(0 \le n \le 30)$.

```
>> b = [1 0 0]; a = [1 -1 1];
>> n = (0:30)'; delta = @(n) 1.0.*(n==0);
>> h = filter(b,a,delta(n)); stem(n,h,'k.');
>> axis([-.5 30.5 -1.1 1.1]); xlabel('n'); ylabel('h[n]');
```

As shown in Fig. 9.15, $h[n]$ appears to be $(N_0 = 6)$-periodic for $n \ge 0$. Since periodic signals are not absolutely summable, $\sum_{n=-\infty}^{\infty} |h[n]|$ is not finite and the system is not BIBO-stable.

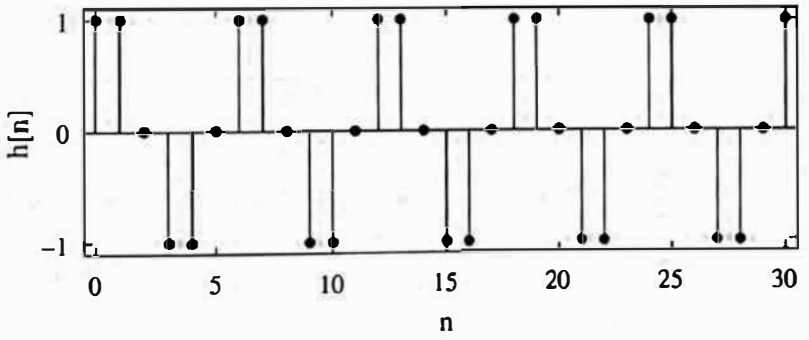

Figure 9.15 $h[n]$ for $y[n]-y[n-1]+y[n-2]=x[n]$.

[†] It is important to pay close attention to the inevitable notational differences found throughout engineering documents. In MATLAB help documents, coefficient subscripts begin at 1 rather than 0 to better conform with MATLAB indexing conventions. That is, MATLAB labels a_0 as `a(1)`, b_0 as `b(1)`, and so forth.

Furthermore, the sinusoidal input $x[n] = \cos(2\pi n/6)u[n]$, which is ($N_0 = 6$)-periodic for $n \geq 0$, should generate a resonant zero-state response.

```
>> x = @(n) cos(2*pi*n/6).*(n>=0);
>> y = filter(b,a,x(n));
>> stem(n,y,'k.'); xlabel('n'); ylabel('y[n]');
```

The response's linear envelope, shown in Fig. 9.16, confirms a resonant response. The characteristic equation of the system is $\gamma^2 - \gamma + 1$, which has roots $\gamma = e^{\pm j\pi/3}$. Since the input $x[n] = \cos(2\pi n/6)u[n] = (1/2)(e^{j\pi n/3} + e^{-j\pi n/3})u[n]$ coincides with the characteristic roots, a resonant response is guaranteed.

By adding initial conditions, the `filter` command can also compute a system's zero-input response and total response. Continuing the preceding example, consider finding the zero-input response for $y[-1] = 1$ and $y[-2] = 2$ over ($0 \leq n \leq 30$).

```
>> z_i = filtic(b,a,[1 2]);
>> y_0 = filter(b,a,zeros(size(n)),z_i);
>> stem(n,y_0,'k.'); xlabel('n'); ylabel('y_{0} [n]');
>> axis([-0.5 30.5 -2.1 2.1]);
```

There are many physical ways to implement a particular equation. MATLAB implements Eq. (9.31) by using the popular direct form II transposed structure.† Consequently, initial conditions must be compatible with this implementation structure. The signal-processing toolbox function `filtic` converts the traditional $y[-1], y[-2], \ldots, y[-N]$ initial conditions for use with the `filter` command. An input of zero is created with the `zeros` command. The dimensions of this zero input are made to match the vector `n` by using the `size` command. Finally, `_{ }` forces subscript text in the graphics window, and `^{ }` forces superscript text. The results are shown in Fig. 9.17.

Given $y[-1] = 1$ and $y[-2] = 2$ and an input $x[n] = \cos(2\pi n/6)u[n]$, the total response is easy to obtain with the `filter` command.

```
>> y_total = filter(b,a,x(n),z_i);
```

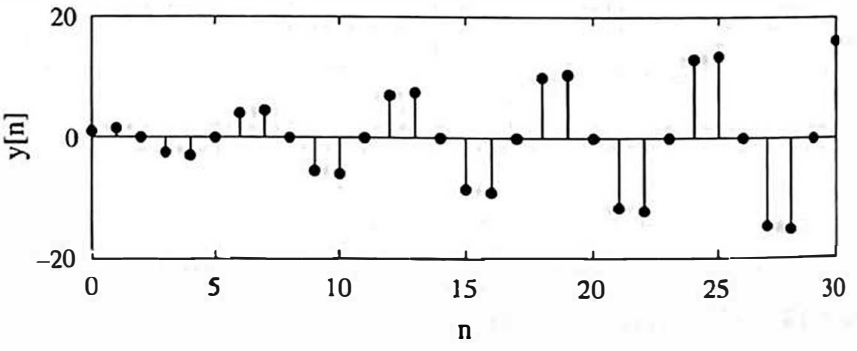

Figure 9.16 Resonant zero-state response $y[n]$ for $x[n] = \cos(2\pi n/6)u[n]$.

† Implementation structures, such as direct form II transposed, are discussed in Ch. 6.

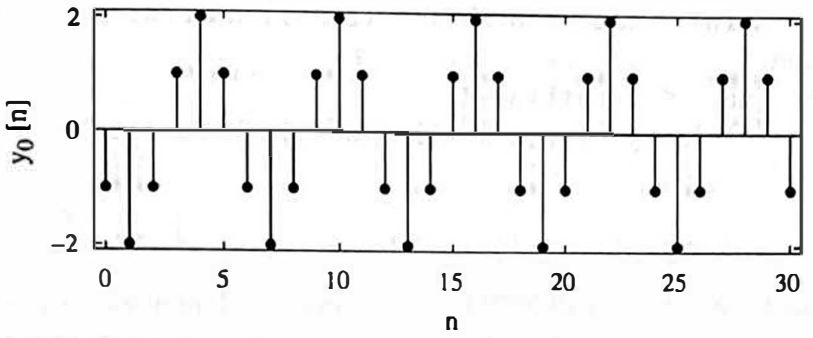

Figure 9.17 Zero-input response $y_0[n]$ for $y[-1] = 1$ and $y[-2] = 2$.

Summing the zero-state and zero-input response gives the same result. Computing the total absolute error provides a check.

```
>> sum(abs(y_total-(y + y_0)))
   ans = 1.8430e-014
```

Within computer round-off, both methods return the same sequence.

9.8.2 A Custom Filter Function

The `filtic` command is available only if the signal-processing toolbox is installed. To accommodate installations without the signal-processing toolbox and to help develop your MATLAB skills, consider writing a function similar in syntax to `filter` that directly uses the ICs $y[-1], y[-2], \ldots, y[-N]$. Normalizing $a_0 = 1$ and solving Eq. (9.31) for $y[n]$ yield

$$y[n] = \sum_{k=0}^{N} b_k x[n-k] - \sum_{k=1}^{N} a_k y[n-k]$$

This recursive form provides a good basis for our custom filter function.

```
function [y] = CH9MP1(b,a,x,yi);
% CH9MP1.m : Chapter 9, MATLAB Program 1
% Function M-file filters data x to create y
% INPUTS:   b = vector of feedforward coefficients
%           a = vector of feedback coefficients
%           x = input data vector
%           yi = vector of initial conditions [y[-1], y[-2], ...]
% OUTPUTS:  y = vector of filtered output data

yi = flipud(yi(:)); % Properly format IC's.
y = [yi;zeros(length(x),1)]; % Preinitialize y, beginning with IC's.
x = [zeros(length(yi),1);x(:)]; % Append x with zeros to match size of y.
b = b/a(1);a = a/a(1); % Normalize coefficients.
for n = length(yi)+1:length(y),
    for nb = 0:length(b)-1,
```

```
        y(n) = y(n) + b(nb+1)*x(n-nb); % Feedforward terms.
    end
    for na = 1:length(a)-1,
        y(n) = y(n) - a(na+1)*y(n-na); % Feedback terms.
    end
end
```

Most instructions in CH9MP1 have been discussed; now we turn to the `flipud` instruction. The flip up-down command `flipud` reverses the order of elements in a column vector. Although not used here, the flip left-right command `fliplr` reverses the order of elements in a row vector. Note that typing `help` *filename* displays the first contiguous set of comment lines in an M-file. Thus, it is good programming practice to document M-files, as in CH9MP1, with an initial block of clear comment lines.

As an exercise, the reader should verify that CH9MP1 correctly computes the impulse response $h[n]$, the zero-state response $y[n]$, the zero-input response $y_0[n]$, and the total response $y[n]+y_0[n]$. For example, the total response is computed by typing

```
>> y_total = CH9MP1(b,a,x(n),[1 2])
```

9.8.3 Discrete-Time Convolution

Convolution of two finite-duration discrete-time signals is accomplished by using the conv command. For example, the discrete-time convolution of two length-4 rectangular pulses, $g[n] = (u[n]-u[n-4])*(u[n]-u[n-4])$, is a length-$(4+4-1=7)$ triangle. Representing $u[n]-u[n-4]$ by the vector [1, 1, 1, 1], the convolution is computed by

```
>> conv([1 1 1 1],[1 1 1 1])
   ans = 1     2     3     4     3     2     1
```

Notice that $(u[n+4]-u[n])*(u[n]-u[n-4])$ is also computed by `conv([1 1 1 1],[1 1 1 1])` and obviously yields the same result. The difference between these two cases is the regions of support: $(0 \le n \le 6)$ for the first and $(-4 \le n \le 2)$ for the second. Although the conv command does not compute the region of support, it is relatively easy to obtain. If vector `w` begins at $n = n_w$ and vector `v` begins at $n = n_v$, then `conv(w,v)` begins at $n = n_w + n_v$.

In general, the conv command cannot properly convolve infinite-duration signals. This is not too surprising, since computers themselves cannot store an infinite-duration signal. For special cases, however, conv can correctly compute a portion of such convolution problems. Consider the common case of convolving two causal signals. By passing the first N samples of each, conv returns a length-$(2N-1)$ sequence. The first N samples of this sequence are valid; the remaining $N-1$ samples are not.

To illustrate this point, reconsider the zero-state response $y[n]$ over $(0 \le n \le 30)$ for system $y[n]-y[n-1]+y[n-2]=x[n]$ given input $x[n]=\cos(2\pi n/6)u[n]$. The results obtained by using a filtering approach are shown in Fig. 9.16.

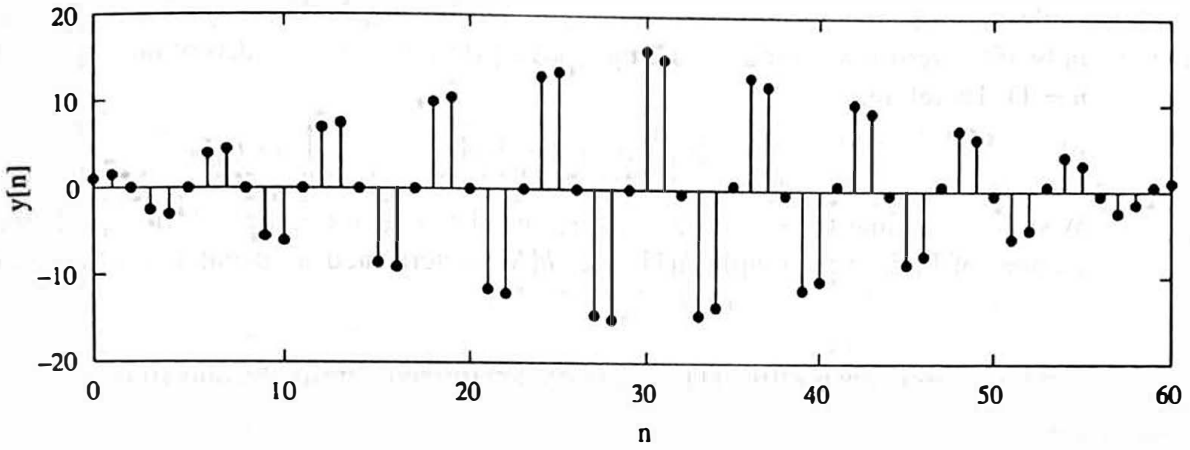

Figure 9.18 $y[n]$ for $x[n] = \cos(2\pi n/6)u[n]$ computed with conv.

The response can also be computed using convolution according to $y[n] = h[n] * x[n]$. The impulse response of this system is†

$$h[n] = \left\{\cos(\pi n/3) + \frac{1}{\sqrt{3}}\sin(\pi n/3)\right\} u[n]$$

Both $h[n]$ and $x[n]$ are causal and have infinite duration, so conv can be used to obtain a portion of the convolution.

```
>> u = @(n) 1.0.*(n>=0); h = @(n) (cos(pi*n/3)+sin(pi*n/3)/sqrt(3)).*u(n);
>> y = conv(h(n),x(n));
>> stem([0:60],y,'k.'); xlabel('n'); ylabel('y[n]');
```

The conv output is fully displayed in Fig. 9.18. As expected, the results are correct over $(0 \le n \le 30)$. The remaining values are clearly incorrect; the output envelope should continue to grow, not decay. Normally, these incorrect values are not displayed.

```
>> stem(n,y(1:31),'k.'); xlabel('n'); ylabel('y[n]');
```

The resulting plot is identical to Fig. 9.16.

9.9 Appendix: Impulse Response for a Special Case

When $a_N = 0$, $A_0 = b_N/a_N$ becomes indeterminate, and the procedure needs to be modified slightly. When $a_N = 0$, $Q[E]$ can be expressed as $E\hat{Q}[E]$, and Eq. (9.13) can be expressed as

$$E\hat{Q}[E]h[n] = P[E]\delta[n] = P[E]\{E\delta[n-1]\} = EP[E]\delta[n-1]$$

Hence,

$$\hat{Q}[E]h[n] = P[E]\delta[n-1]$$

† Techniques to analytically determine $h[n]$ are presented in Chs. 11 and 12.

In this case the input vanishes not for $n \geq 1$, but for $n \geq 2$. Therefore, the response consists not only of the zero-input term and an impulse $A_0\delta[n]$ (at $n = 0$), but also of an impulse $A_1\delta[n-1]$ (at $n = 1$). Therefore,

$$h[n] = A_0\delta[n] + A_1\delta[n-1] + y_c[n]u[n]$$

We can determine the unknowns A_0, A_1, and the $N-1$ coefficients in $y_c[n]$ from the $N+1$ number of initial values $h[0], h[1], \ldots, h[N]$, determined as usual from the iterative solution of the equation $Q[E]h[n] = P[E]\delta[n]$.† Similarly, if $a_N = a_{N-1} = 0$, we need to use the form $h[n] = A_0\delta[n] + A_1\delta[n-1] + A_2\delta[n-2] + y_c[n]u[n]$. The $N+1$ unknown constants are determined from the $N+1$ values $h[0], h[1], \ldots, h[N]$, determined iteratively, and so on.

9.10 SUMMARY

This chapter discusses time-domain analysis of LTID (linear, time-invariant, discrete-time) systems. The analysis is parallel to that of LTIC systems, with some minor differences. Discrete-time systems are described by difference equations. For an Nth-order system, N auxiliary conditions must be specified for a unique solution. Characteristic modes are discrete-time exponentials of the form γ^n corresponding to an unrepeated root γ, and the modes are of the form $n^i\gamma^n$ corresponding to a repeated root γ.

The unit impulse function $\delta[n]$ is a sequence of a single number of unit value at $n = 0$. The unit impulse response $h[n]$ of a discrete-time system is a linear combination of its characteristic modes.‡

The zero-state response (response due to external input) of a linear system is obtained by breaking the input into impulse components and then adding the system responses to all the impulse components. The sum of the system responses to the impulse components is in the form of a sum, known as the convolution sum, whose structure and properties are similar to the convolution integral. The system response is obtained as the convolution sum of the input $x[n]$ with the system's impulse response $h[n]$. Therefore, the knowledge of the system's impulse response allows us to determine the system response to any arbitrary input.

LTID systems have a very special relationship to the everlasting exponential signal z^n because the response of an LTID system to such an input signal is the same signal within a multiplicative constant. The response of an LTID system to the everlasting exponential input z^n is $H[z]z^n$, where $H[z]$ is the transfer function of the system.

The external stability criterion, the bounded-input/bounded-output (BIBO) stability criterion, states that a system is stable if and only if every bounded input produces a bounded output. Otherwise, the system is unstable.

The internal stability criterion can be stated in terms of the location of characteristic roots of the system as follows:

1. An LTID system is asymptotically stable if and only if all the characteristic roots are inside the unit circle. The roots may be repeated or unrepeated.

† $\hat{Q}[\gamma]$ is now an $(N-1)$-order polynomial. Hence, there are only $N-1$ unknowns in $y_c[n]$.

‡ There is a possibility of an impulse $\delta[n]$ in addition to characteristic modes.

2. An LTID system is unstable if and only if either one or both of the following conditions exist: (i) at least one root is outside the unit circle; (ii) there are repeated roots on the unit circle.
3. An LTID system is marginally stable if and only if there are no roots outside the unit circle and some unrepeated roots on the unit circle.

An asymptotically stable system is always BIBO-stable. The converse is not necessarily true.

PROBLEMS

9.1-1 Letting $\downarrow$ identify $n = 0$, define the nonzero values of signal $g[n]$ in vector form as $[1,2,3,4,5,4,3,\underset{\downarrow}{2},1]$. The impulse response of an LTID system is defined in terms of $g[n]$ as $h[n] = g[-2n-1]$.

(a) Express the nonzero values of $h[n]$ in vector form, taking care to identify the $n = 0$ point.
(b) Write a constant-coefficient linear difference equation (input $x[n]$ and output $y[n]$) that has impulse response $h[n]$.
(c) Show that the system is both linear and time-invariant.
(d) Determine, if possible, whether the system is BIBO-stable.
(e) Determine, if possible, whether the system is memoryless.
(f) Determine, if possible, whether the system is causal.

9.1-2 An LTID system has an impulse response function $h[n] = u[-(5-n)/3]$.

(a) Using an accurate sketch or vector representation, graphically depict $h[n]$.
(b) Determine, if possible, whether the system is BIBO-stable.
(c) Determine, if possible, whether the system is memoryless.
(d) Determine, if possible, whether the system is causal.

9.1-3 Determine whether each of the following statements is true or false. If the statement is false, demonstrate by proof or example why the statement is false. If the statement is true, explain why.

(a) The system described by $y[n] = (n+1)x[n]$ is causal.
(b) The system described by $y[n-1] = x[n]$ is causal.

9.1-4 A linear time-invariant system produces output $y_1[n]$ in response to input $x_1[n]$, as shown in Fig. P9.1-4. Determine and sketch the output $y_2[n]$ that results when input $x_2[n]$ is applied to the same system.

9.1-5 A system is described by

$$y[n] = \tfrac{1}{2} \sum_{k=-\infty}^{\infty} x[k](\delta[n-k] + \delta[n+k])$$

(a) Explain what this system does.
(b) Is the system BIBO-stable? Justify your answer.
(c) Is the system linear? Justify your answer.
(d) Is the system memoryless? Justify your answer.

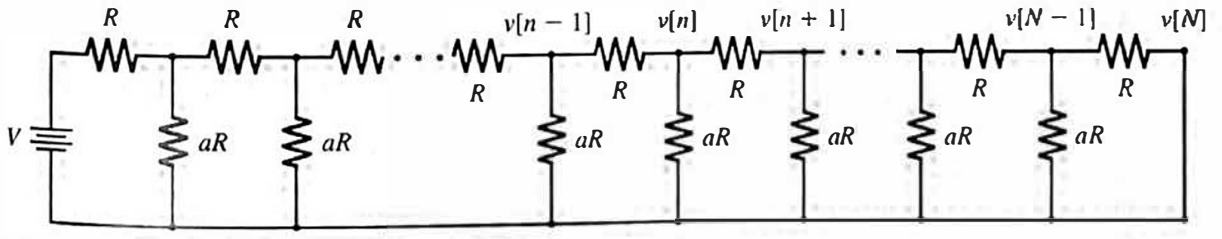

Figure P9.1–4

(e) Is the system causal? Justify your answer.
(f) Is the system time-invariant? Justify your answer.

9.1-6 A discrete-time system is given by

$$y[n+1] = \frac{x[n]}{x[n+1]}$$

(a) Is the system BIBO-stable? Justify your answer.
(b) Is the system memoryless? Justify your answer.
(c) Is the system causal? Justify your answer.

9.1-7 Explain why the continuous-time system $y(t) = x(2t)$ is always invertible, yet the corresponding discrete-time system $y[n] = x[2n]$ is not invertible.

9.1-8 Consider the input–output relationships of two similar discrete-time systems:

$$y_1[n] = \sin\left(\frac{\pi}{2}n + 1\right)x[n]$$

and

$$y_2[n] = \sin\left(\frac{\pi}{2}(n+1)\right)x[n]$$

Explain why $x[n]$ can be recovered from $y_1[n]$, yet $x[n]$ cannot be recovered from $y_2[n]$.

9.1-9 Consider a system that multiplies a given input by a ramp function, $r[n]$. That is, $y[n] = x[n]\,r[n]$.
(a) Is the system BIBO-stable? Justify your answer.
(b) Is the system linear? Justify your answer.
(c) Is the system memoryless? Justify your answer.
(d) Is the system causal? Justify your answer.
(e) Is the system time-invariant? Justify your answer.

9.1-10 A jet-powered car is filmed using a camera operating at 60 frames per second. Let variable n designate the film frame, where $n = 0$ corresponds to engine ignition (film before ignition is discarded). By analyzing each frame of the film, it is possible to determine the car position $x[n]$, measured in meters, from the original starting position $x[0] = 0$.

From physics, we know that velocity is the time derivative of position:

$$v(t) = \frac{d}{dt}x(t)$$

Furthermore, we know that acceleration is the time derivative of velocity:

$$a(t) = \frac{d}{dt}v(t)$$

We can estimate the car velocity from the film data by using a simple difference equation $v[n] = k(x[n] - x[n-1])$.
(a) Determine the appropriate constant k to ensure $v[n]$ has units of meters per second.
(b) Determine a standard-form constant coefficient difference equation that outputs an estimate of acceleration, $a[n]$, using an input of position, $x[n]$. Identify the advantages and shortcomings of estimating acceleration $a(t)$ with $a[n]$. What is the impulse response $h[n]$ for this system?

9.2-1 An LTID system is described by a constant coefficient linear difference equation $2y[n] + 2y[n-1] = x[n-1]$.
(a) Express this system in standard advance operator form.
(b) Using recursion, determine the first five values of the system impulse response $h[n]$.
(c) Using recursion, determine the first five values of the system zero-state response to input $x[n] = 2u[n]$.
(d) Using recursion, determine for $(0 \le n \le 4)$ the system zero-input response if $y[-1] = 1$.

9.2-2 Solve recursively (first three terms only):
(a) $y[n+1] - 0.5y[n] = 0$, with $y[-1] = 10$
(b) $y[n+1] + 2y[n] = x[n+1]$, with $x[n] = e^{-n}u[n]$ and $y[-1] = 0$

9.2-3 Solve the following equation recursively (first three terms only):

$$y[n] - 0.6y[n-1] - 0.16y[n-2] = 0$$

with

$$y[-1] = -25,\ y[-2] = 0.$$

9.2-4 Solve recursively the Ch. 8 second-order difference Eq. (8.13) for a sales estimate (first three

terms only), assuming $y[-1] = y[-2] = 0$ and $x[n] = 100u[n]$.

9.2-5 Solve the following equation recursively (first three terms only):

$$y[n+2] + 3y[n+1] + 2y[n] = x[n+2] + 3x[n+1] + 3x[n]$$

with $x[n] = (3)^n u[n]$, $y[-1] = 3$, and $y[-2] = 2$

9.2-6 Repeat Prob. 9.2-5 for

$$y[n] + 2y[n-1] + y[n-2] = 2x[n] - x[n-1]$$

with $x[n] = (3)^{-n} u[n]$, $y[-1] = 2$, and $y[-2] = 3$.

9.3-1 Given $y_0[-1] = 3$ and $y_0[-2] = -1$, determine the closed-form expression of the zero-input response $y_0[n]$ of an LTID system described by the equation

$$y[n] + \frac{1}{6}y[n-1] - \frac{1}{6}y[n-2] = \frac{1}{3}x[n] + \frac{2}{3}x[n-2]$$

9.3-2 Solve

$$y[n+2] + 3y[n+1] + 2y[n] = 0$$

if $y[-1] = 0$ and $y[-2] = 1$.

9.3-3 Solve

$$y[n+2] + 2y[n+1] + y[n] = 0$$

if $y[-1] = 1$ and $y[-2] = 1$.

9.3-4 Solve

$$y[n+2] - 2y[n+1] + 2y[n] = 0$$

if $y[-1] = 1$ and $y[-2] = 0$.

9.3-5 For the general Nth-order difference Eq. (9.3), letting

$$a_1 = a_2 = \cdots = a_N = 0$$

results in a general causal Nth-order LTI *nonrecursive* difference equation

$$y[n] = b_0 x[n] + b_1 x[n-1] + \cdots + b_N x[n-N]$$

Show that the characteristic roots for this system are zero—hence, that the zero-input response is zero. Consequently, the total response consists of the zero-state component only.

9.3-6 Leonardo Pisano Fibonacci, a famous thirteenth-century mathematician, generated the sequence of integers

$$\{0, 1, 1, 2, 3, 5, 8, 13, 21, 34, \ldots\}$$

while addressing, oddly enough, a problem involving rabbit reproduction. An element of the Fibonacci sequence is the sum of the previous two.

(a) Find the constant-coefficient difference equation whose zero-input response $f[n]$ with auxiliary conditions $f[1] = 0$ and $f[2] = 1$ is a Fibonacci sequence. Given $f[n]$ is the system output, what is the system input?

(b) What are the characteristic roots of this system? Is the system stable?

(c) Designating 0 and 1 as the first and second Fibonacci numbers, determine the 50th Fibonacci number. Determine the 1000th Fibonacci number.

9.3-7 Find $v[n]$, the voltage at the nth node of the Ch. 8 resistive ladder depicted in Fig. P8.5-6, if $V = 100$ volts and $a = 2$. [*Hint 1*: Consider the node equation at the nth node with voltage $v[n]$. *Hint 2*: See Prob. 8.5-6 for the equation for $v[n]$. The auxiliary conditions are $v[0] = 100$ and $v[N] = 0$.]

9.3-8 Consider the discrete-time system $y[n] + y[n-1] + 0.25y[n-2] = \sqrt{3}x[n-8]$. Find the zero input response, $y_0[n]$, if $y_0[-1] = 1$ and $y_0[1] = 1$.

9.3-9 Provide a standard-form polynomial $Q(X)$ such that $Q(E)\{y[n]\} = x[n]$ corresponds to a marginally stable third-order LTID system and $Q(D)\{y(t)\} = x(t)$ corresponds to a stable third-order LTIC system.

9.4-1 Find the unit impulse response $h[n]$ of systems specified by the following equations:

(a) $y[n+1] + 2y[n] = x[n]$

(b) $y[n] + 2y[n-1] = x[n]$

9.4-2 Determine the unit impulse response $h[n]$ of the following systems. In each case, use recursion to verify the $n = 3$ value of the closed-form expression of $h[n]$.

(a) $(E^2 + 1)\{y[n]\} = (E + 0.5)\{x[n]\}$

(b) $y[n] - y[n-1] + 0.25y[n-2] = x[n]$

(c) $y[n] - \frac{1}{6}y[n-1] - \frac{1}{6}y[n-2] = \frac{1}{3}x[n-2]$

(d) $y[n] + \frac{1}{6}y[n-1] - \frac{1}{6}y[n-2] = \frac{1}{3}x[n]$
(e) $y[n] + \frac{1}{4}y[n-2] = x[n]$
(f) $(E^2 - \frac{4}{9})\{y[n]\} = (E^2 + 1)\{x[n]\}$
(g) $(E^2 - \frac{1}{4})(E + \frac{1}{3})\{y[n]\} = E^3\{x[n]\}$
(h) $(E - \frac{1}{2})^2\{y[n]\} = x[n]$

9.4-3 Consider a DT system with input $x[n]$ and output $y[n]$ described by the difference equation

$$4y[n+1] + y[n-1] = 8x[n+1] + 8x[n]$$

(a) What is the order of this system?
(b) Determine the characteristic mode(s) of the system.
(c) Determine a closed-form expression for the system's impulse response $h[n]$.

9.4-4 Repeat Prob. 9.4-3 for a system described by the difference equation

$$y[n+3] - \frac{3}{10}y[n+2] - \frac{1}{10}y[n+1] = 2x[n+1]$$

9.4-5 Repeat Prob. 9.4-1 for

$$(E^2 - 6E + 9)y[n] = Ex[n]$$

9.4-6 Repeat Prob. 9.4-1 for

$$y[n] + 6y[n-1] + 25y[n-2] = 2x[n] - 4x[n-1]$$

9.4-7 (a) For the general Nth-order difference Eq. (9.3), letting

$$a_1 = a_2 = \cdots = a_N = 0$$

results in a general causal Nth-order LTI *nonrecursive* difference equation

$$y[n] = \sum_{i=0}^{N} b_i x[n-i]$$

Find the impulse response $h[n]$ for this system. [*Hint:* The characteristic equation for this case is $\gamma^n = 0$. Hence, all the characteristic roots are zero. In this case, $y_c[n] = 0$, and the approach in Sec. 9.4 does not work. Use a direct method to find $h[n]$ by realizing that $h[n]$ is the response to unit impulse input.]

(b) Find the impulse response of a nonrecursive LTID system described by the equation

$$y[n] = 3x[n] - 5x[n-1] - 2x[n-3]$$

Observe that the impulse response has only a finite (N) number of nonzero elements. For this reason, such systems are called *finite-impulse response* (FIR) systems. For a general recursive case [Eq. (9.7)], the impulse response has an infinite number of nonzero elements, and such systems are called *infinite-impulse response* (IIR) systems.

9.5-1 The convolution $y[n] = \left(\frac{5}{2^n}u[n+5]\right) * (3^n u[-n-2])$ can be represented as

$$y[n] = \begin{cases} C_1(\gamma_1)^n & n < N \\ C_2(\gamma_2)^n & n \geq N \end{cases}$$

Using the graphical convolution procedure, determine constants C_1, C_2, γ_1, γ_2, and N.

9.5-2 Use the graphical convolution procedure to determine the following:
(a) $y_a[n] = u[n] * (u[n-5] - u[n-9] + (0.5)^{(n-8)}u[n-9])$
(b) $y_b[n] = (\frac{1}{2})^{|n|} * u[-n+5]$

9.5-3 Let $x[n] = (0.5)^n(u[n+4] - u[n-4])$ be input into an LTID system with an impulse response given by

$$h[n] = \begin{cases} 2 & [(n \bmod 6) < 4] \text{ and } [n \geq 0] \\ 0 & \text{otherwise} \end{cases}$$

Recall, $(n \bmod p)$ is the remainder of the division n/p. The system is described according to the difference equation $y[n] - y[n-6] = 2x[n] + 2x[n-1] + 2x[n-2] + 2x[n-3]$.
(a) Determine the six characteristic roots (γ_1 through γ_6) of the system.
(b) Determine the value of $y[10]$, the zero-state output of system $h[n]$ in response to $x[n]$ at time $n = 10$. Express your result in decimal form to at least three decimal places (e.g., $y[10] = 3.142$).

9.5-4 An LTID system has impulse response $h[n] = (0.5)^{(n+3)}(u[n] - u[n+6])$. A 6-periodic DT

input signal $x[n]$ is given by

$$x[n] = \begin{cases} 1 & n = 0, \pm 3, \pm 6, \pm 9, \pm 12, \ldots \\ 2 & n = 1, 1 \pm 6, 1 \pm 12, \ldots \\ 3 & n = 2, 2 \pm 6, 2 \pm 12, \ldots \\ 0 & \text{otherwise} \end{cases}$$

(a) Is system $h[n]$ causal? Mathematically justify your answer.

(b) Determine the value of $y[12]$, the zero-state output of system $h[n]$ in response to $x[n]$ at time $n = 12$. Express your result in decimal form to at least three decimal places (e.g., $y[12] = 1.234$).

9.5-5 Find the (zero-state) response $y[n]$ of an LTID system whose unit impulse response is

$$h[n] = (-2)^n u[n-1]$$

and the input is $x[n] = e^{-n}u[n+1]$. Find your answer by computing the convolution sum and also by using Table 9.1.

9.5-6 Find the (zero-state) response $y[n]$ of an LTID system if the input is $x[n] = 3^{n-1}u[n+2]$, and

$$h[n] = \tfrac{1}{2}[\delta[n-2] - (-2)^{n+1}]u[n-3]$$

9.5-7 Find the (zero-state) response $y[n]$ of an LTID system if the input $x[n] = (3)^{n+2}u[n+1]$, and

$$h[n] = [(2)^{n-2} + 3(-5)^{n+2}]u[n-1]$$

9.5-8 Find the (zero-state) response $y[n]$ of an LTID system if the input $x[n] = (3)^{-n+2}u[n+3]$, and

$$h[n] = 3(n-2)(2)^{n-3}u[n-4]$$

9.5-9 Find the (zero-state) response $y[n]$ of an LTID system if its input $x[n] = (2)^n u[n-1]$, and

$$h[n] = (3)^n \cos\left(\frac{\pi}{3}n - 0.5\right)u[n]$$

Find your answer using only Table 9.1.

9.5-10 Consider an LTID system ("system 1") described by $(E - \frac{1}{2})\{y[n]\} = x[n]$.

(a) Determine the impulse response $h_1[n]$ for system 1. Simplify your answer.

(b) Determine the step response $s[n]$ for system 1 (the step response is the output in response to a unit step input). Simplify your answer.

(c) Determine the impulse response $h_{\text{cascade}}[n]$ of system 1 cascaded with an LTID system with impulse response $h_2[n] = -3u[n-13]$. Simplify your answer.

9.5-11 Derive the results in entries 1, 2, and 3 in Table 9.1. [*Hint:* You may need to use the information in Sec. B.8.3.]

9.5-12 Derive the results in entries 4, 5, and 6 in Table 9.1.

9.5-13 Derive the results in entries 7 and 8 in Table 9.1. [*Hint:* You may need to use the information in Sec. B.8.3.]

9.5-14 Derive the results in entries 9 and 11 in Table 9.1. [*Hint:* You may need to use the information in Sec. B.8.3.]

9.5-15 Find the total response of a system specified by the equation

$$y[n+1] + 2y[n] = x[n+1]$$

if $y[-1] = 10$, and the input $x[n] = e^{-n}u[n]$.

9.5-16 Find an LTID system (zero-state) response if its impulse response $h[n] = (0.5)^n u[n]$, and the input $x[n]$ is

(a) $2^n u[n]$

(b) $2^{n-3}u[n]$

(c) $2^n u[n-2]$

[*Hint:* You may need to use the convolution shift property of Eq. (9.19).]

9.5-17 For a system specified by equation

$$y[n] = x[n] - 2x[n-1]$$

find the system response to input $x[n] = u[n]$. What is the order of the system? What type of system (recursive or nonrecursive) is this? Is the knowledge of initial condition(s) necessary to find the system response? Explain.

9.5-18 (a) A discrete-time LTI system is shown in Fig. P9.5-18. Express the overall impulse response of the system, $h[n]$, in terms of $h_1[n]$, $h_2[n]$, $h_3[n]$, $h_4[n]$, and $h_5[n]$.

(b) Two LTID systems in cascade have impulse response $h_1[n]$ and $h_2[n]$, respectively. Show that if $h_1[n] = (0.9)^n u[n] - 0.5(0.9)^{n-1}u[n-1]$ and $h_2[n] = (0.5)^n u[n] - 0.9(0.5)^{n-1}u[n-1]$, the cascade system is an identity system.

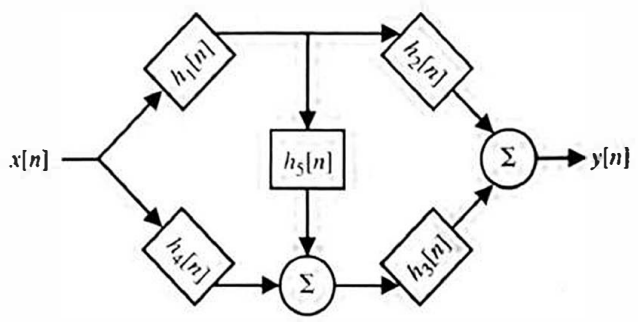

Figure P9.5-18

9.5-19 (a) Show that for a causal system, Eq. (9.24) can also be expressed as

$$g[n] = \sum_{k=0}^{n} h[n-k]$$

(b) How would the expressions in part (a) change if the system is not causal?

9.5-20 An LTID system with input $x[n]$ and output $y[n]$ has impulse response $h[n] = 2(u[n+2] - u[n-3])$.

(a) Write a constant-coefficient linear difference equation that has the given impulse response. [*Hint:* First express $h[n]$ in terms of delta functions $\delta[n]$.]

(b) Using graphical convolution, determine the zero-state output of this system in response to the anticausal input $x[n] = 2^n u[-n]$. A simplified closed-form solution is required.

9.5-21 Consider three LTID systems: system 1 has impulse response $h_1[n] = [\underset{\downarrow}{2}, -3, 4]$, system 2 has impulse response $h_2[n] = [\underset{\downarrow}{0}, 0, -6, -9, 3]$, and system 3 is an identity system (output equals input).

(a) Determine the overall impulse response $h[n]$ if system 1 is connected in cascade with a parallel connection of systems 2 and 3.

(b) For input $x[n] = u[-n]$, determine the zero-state response $y_{zsr}[n]$ of system 2.

9.5-22 In the Ch. 8 savings account problem described in Ex. 8.10, a woman deposits \$500 at the beginning of every month, starting at $n = 0$ with the exception at $n = 4$, when instead of depositing \$500, she withdraws \$1000. Find $y[n]$ if the interest rate is 1% per month ($r = 0.01$).

9.5-23 To pay off a loan of M dollars in N number of payments using a fixed monthly payment of P dollars, show that

$$P = \frac{rM}{1-(1+r)^{-N}}$$

where r is the interest rate per dollar per month. [*Hint:* This problem can be modeled by Ch. 8 Eq. (8.10) with the payments of P dollars starting at $n = 1$. The problem can be approached in two ways. First, consider the loan as the initial condition $y_0[0] = -M$, and the input $x[n] = Pu[n-1]$. The loan balance is the sum of the zero-input component (due to the initial condition) and the zero-state component $h[n] * x[n]$. Second, consider the loan as an input $-M$ at $n = 0$ along with the input due to payments. The loan balance is now exclusively a zero-state component $h[n] * x[n]$. Because the loan is paid off in N payments, set $y[N] = 0$.]

9.5-24 A man receives an automobile loan of \$10,000 from a bank at the interest rate of 1.5% per month. His monthly payment is \$500, with the first payment due one month after he receives the loan. Compute the number of payments required to pay off the loan. Note that the last payment may not be exactly \$500. [*Hint:* Follow the procedure in Prob. 9.5-23 to determine the balance $y[n]$. To determine N, the number of payments, set $y[N] = 0$. In general, N will not be an integer. The number of payments K is the largest integer $\leq N$. The residual payment is $|y[K]|$.]

9.5-25 Letting $\downarrow$ identify the $n = 0$ values, use the sliding-tape method to determine the following:

(a) $y_a = [\underset{\downarrow}{2}, 3, -2, -3] * [-10, \underset{\downarrow}{0}, -5]$

(b) $y_b = [2, \underset{\downarrow}{-1}, 3, -2] * [-1, -4, 1, \underset{\downarrow}{-2}]$

(c) $y_c = [\underset{\downarrow}{0}, 0, 3, 2, 1, 2, 3] * [2, 3, -2, \underset{\downarrow}{1}]$

(d) $y_d = [5, 0, 0, \underset{\downarrow}{-2}, 8] * [-1, 1, \underset{\downarrow}{3}, 3, -2, 3]$

(e) $y_e = ([1, \underset{\downarrow}{-1}] * [\underset{\downarrow}{1}, -1]) * ([\underset{\downarrow}{1}, -1] * [1, \underset{\downarrow}{-1}])$

(f) $y_f = ([2, \underset{\downarrow}{-1}] * [\underset{\downarrow}{1}, -2]) * ([\underset{\downarrow}{1}, -2] * [2, \underset{\downarrow}{-1}])$

Outside the values shown, assume all signals are zero.

9.5-26 Let $\downarrow$ identify the $n = 0$ and consider DT signals $x[n]$ and $h[n]$ whose nonzero values are given as $x[n] = [1, 2, 3, \underset{\downarrow}{4}, 5]$ and $h[n] = [-2, -1, 1, \underset{\downarrow}{2}]$. Use DT convolution (any method) to determine $y[n] = (2x[n - 30]) * \left(-\frac{3}{2}h[n - 10]\right)$. Express your result in vector notation, making sure to indicate the time index of the leftmost (nonzero) element.

9.5-27 Using the sliding-tape algorithm, show that

(a) $u[n] * u[n] = (n + 1)u[n]$

(b) $(u[n] - u[n - m]) * u[n] = (n + 1)u[n] - (n - m + 1)u[n - m]$

9.5-28 Using the sliding-tape algorithm, find $x[n] * g[n]$ for the signals shown in Fig. P9.5-28.

9.5-29 Repeat Prob. 9.5-28 for the signals shown in Fig. P9.5-29.

9.5-30 Repeat Prob. 9.5-28 for the signals shown in Fig. P9.5-30.

9.5-31 Letting $\downarrow$ identify $n = 0$, define the nonzero values of signal $x[n]$ as $[1, 2, \underset{\downarrow}{2}]$. Similarly, define the non-zero values of signal $y[n]$ as $[3, 4, 6, 6, 11, \underset{\downarrow}{2}, -2]$. Using the sliding-tape algorithm as the basis for your work, determine the signal $h[n]$ so that $y[n] = x[n] * h[n]$.

9.5-32 The convolution sum in Eq. (9.20) can be expressed in matrix form as $\boldsymbol{y} = \boldsymbol{H}\boldsymbol{x}$, where $\boldsymbol{y}$ is a column vector containing $y[0], y[1], \ldots y[n]$; $\boldsymbol{x}$ is a column vector containing $x[0], x[1], \ldots x[n]$; and $\boldsymbol{H}$ is a lower triangular matrix defined as

$$\boldsymbol{H} = \begin{bmatrix} h[0] & 0 & 0 & \cdots & 0 \\ h[1] & h[0] & 0 & \cdots & 0 \\ \vdots & \vdots & \vdots & \cdots & \vdots \\ h[n] & h[n-1] & \cdots & \cdots & h[0] \end{bmatrix}$$

Knowing $h[n]$ and the output $y[n]$, we can determine the input $x[n]$ according to $\boldsymbol{x} = \boldsymbol{H}^{-1}\boldsymbol{y}$. This operation is the reverse of convolution and is known as *deconvolution*. Moreover, knowing $x[n]$ and $y[n]$, we can determine $h[n]$. This can be done by expressing the foregoing matrix equation as $n + 1$ simultaneous equations in terms of $n + 1$ unknowns $h[0]$, $h[1]$, $\ldots$, $h[n]$. These equations can readily be solved iteratively. Thus, we can synthesize a system that yields a certain output $y[n]$ for a given input $x[n]$.

(a) Design a system (i.e., determine $h[n]$) that will yield the output sequence (8, 12, 14, 15, 15.5, 15.75, . . .) for the input sequence (1, 1, 1, 1, 1, 1, . . .).

(b) For a system with the impulse response sequence (1, 2, 4, . . .), the output sequence was (1, 7/3, 43/9, . . .). Determine the input sequence.

9.5-33 The sliding-tape method is conceptually quite valuable in understanding the convolution mechanism. With it, we can verify that DT convolution of Eq. (9.20) can be performed from an array using the sets $x[0]$, $x[1]$, $x[2]$, . . . and $h[0]$, $h[1]$, $h[2]$, . . ., as depicted in Fig. P9.5-33. The (i, j)th element (element in the ith row and jth column) is given by $x[i]h[j]$. We add the elements of the array along diagonals to produce $y[n] = x[n] * h[n]$. For example, if we sum the elements corresponding to the first diagonal of the array, we obtain $y[0]$. Similarly, if we sum along the second diagonal, we obtain $y[1]$, and so on. Draw the array for the signals $x[n]$ and $h[n]$ in Ex. 9.15, and find $x[n] * h[n]$.

9.5-34 Using Eq. (9.27), show that the transfer function of a unit delay is $H[z] = 1/z$.

9.5-35 A second-order LTID system has zero-input response

$$y_0[n] = \left[3, 2\tfrac{1}{3}, 2\tfrac{1}{9}, 2\tfrac{1}{27}, \ldots\right] = \sum_{k=0}^{\infty} \left\{2 + \left(\tfrac{1}{3}\right)^k\right\} \delta[n - k]$$

(a) Determine the characteristic equation of this system, $a_0\gamma^2 + a_1\gamma + a_2 = 0$.

(b) Find a bounded, causal input with infinite duration that would cause a strong response from this system. Justify your choice.

(c) Find a bounded, causal input with infinite duration that would cause a weak response from this system. Justify your choice.

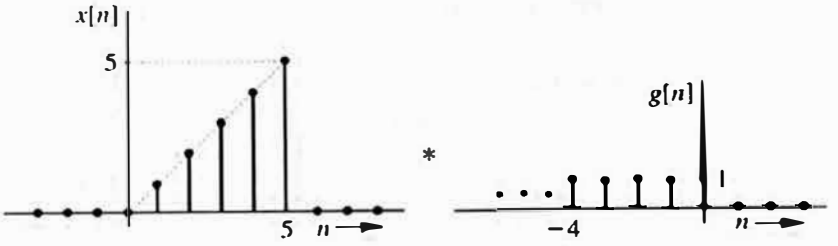

Figure P9.5-28

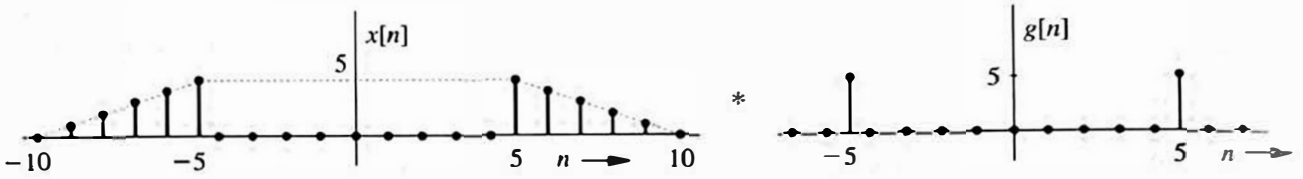

Figure P9.5-29

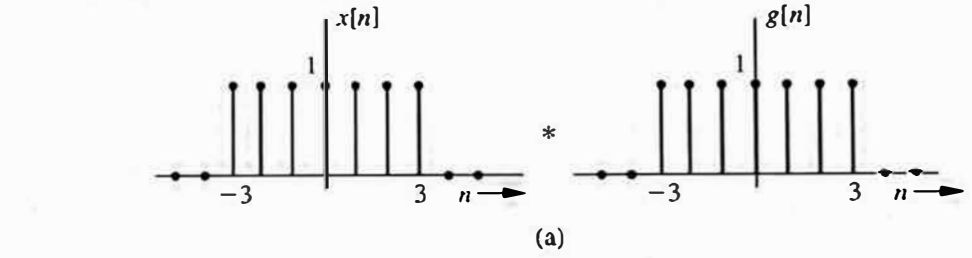

Figure P9.5-30

9.5-36 An LTID filter has an impulse response function given by $h_1[n] = \delta[n+2] - \delta[n-2]$. A second LTID system has an impulse response function given by $h_2[n] = n(u[n+4] - u[n-4])$.

(a) Carefully sketch the functions $h_1[n]$ and $h_2[n]$ over $(-10 \leq n \leq 10)$.

(b) Assume that the two systems are connected in parallel, as shown in Fig. P9.5-36a. Determine the impulse response $h_p[n]$ for the parallel system in terms of $h_1[n]$ and $h_2[n]$. Sketch $h_p[n]$ over $(-10 \leq n \leq 10)$.

(c) Assume that the two systems are connected in cascade, as shown in Fig. P9.5-36b. Determine the impulse response $h_s[n]$ for the cascade system in terms of $h_1[n]$ and $h_2[n]$. Sketch $h_s[n]$ over $(-10 \leq n \leq 10)$.

9.5-37 This problem investigates an interesting application of discrete-time convolution: the expansion of certain polynomial expressions.

(a) By hand, expand $(z^3 + z^2 + z + 1)^2$. Compare the coefficients to $[1,1,1,1] * [1,1,1,1]$.

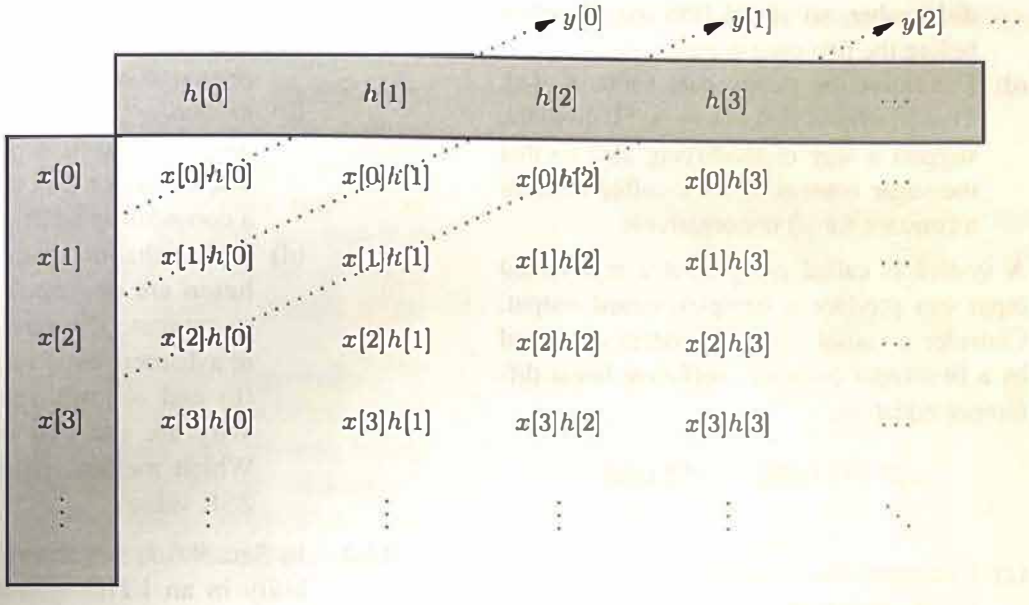

Figure P9.5-33

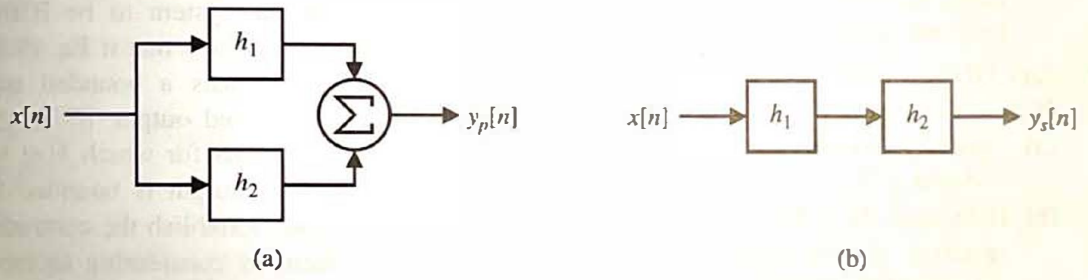

Figure P9.5-36

(b) Formulate a relationship between discrete-time convolution and the expansion of constant-coefficient polynomial expressions.

(c) Use convolution to expand $(z^{-4} - 2z^{-3} + 3z^{-2})^4$.

(d) Use convolution to expand $(z^5 + 2z^4 + 3z^2 + 5)^2(z^{-4} - 5z^{-2} + 13)$.

9.5-38 Joe likes coffee, and he drinks his coffee according to a very particular routine. He begins by adding 2 teaspoons of sugar to his mug, which he then fills to the brim with hot coffee. He drinks 2/3 of the mug's contents, adds another 2 teaspoons of sugar, and tops the mug off with steaming hot coffee. This refill procedure continues, sometimes for many, many cups of coffee. Joe has noted that his coffee tends to taste sweeter with the number of refills.

Let independent variable n designate the coffee refill number. In this way, $n = 0$ indicates the first cup of coffee, $n = 1$ is the first refill, and so forth. Let $x[n]$ represent the sugar (measured in teaspoons) added into the system (a coffee mug) on refill n. Let $y[n]$ designate the amount of sugar (again, teaspoons) contained in the mug on refill n.

(a) The sugar (teaspoons) in Joe's coffee can be represented using a standard second-order constant coefficient difference equation $y[n] + a_1 y[n-1] + a_2 y[n-2] = b_0 x[n] + b_1 x[n-1] + b_2 x[n-2]$. Determine the constants a_1, a_2, b_0, b_1, and b_2.

(b) Determine $x[n]$, the driving function to this system.

(c) Solve the difference equation for $y[n]$. This requires finding the total solution. Joe always starts with a clean mug from the

dishwasher, so $y[-1]$ (the sugar content before the first cup) is zero.

(d) Determine the steady-state value of $y[n]$. That is, what is $y[n]$ as $n \to \infty$? If possible, suggest a way of modifying $x[n]$ so that the sugar content of Joe's coffee remains a constant for all nonnegative n.

9.5-39 A system is called complex if a real-valued input can produce a complex-valued output. Consider a causal complex system described by a first-order constant coefficient linear difference equation:

$$(jE + 0.5)y[n] = (-5E)x[n]$$

(a) Determine the impulse response function $h[n]$ for this system.

(b) Given input $x[n] = u[n-5]$ and initial condition $y_0[-1] = j$, determine the system's total output $y[n]$ for $n \geq 0$.

9.5-40 An LTID system has impulse response function $h[n] = n(u[n-2] - u[n+2])$.

(a) Carefully sketch the function $h[n]$ over $(-5 \leq n \leq 5)$.

(b) Determine the difference equation representation of this system, using $y[n]$ to designate the output and $x[n]$ to designate the input.

9.5-41 Consider three discrete-time signals: $x[n]$, $y[n]$, and $z[n]$. Denoting convolution as $*$, identify the expression(s) that is(are) equivalent to $x[n](y[n] * z[n])$:

(a) $(x[n] * y[n])z[n]$

(b) $(x[n]y[n]) * (x[n]z[n])$

(c) $(x[n]y[n]) * z[n]$

(d) none of the above

Justify your answer!

9.5-42 A causal system with input $x[n]$ and output $y[n]$ is described by

$$y[n] - ny[n-1] = x[n]$$

(a) By recursion, determine the first six nonzero values of $h[n]$, the response to $x[n] = \delta[n]$. Do you think this system is BIBO-stable? Why?

(b) Compute $y_R[4]$ recursively from $y_R[n] - ny_R[n-1] = x[n]$, assuming all initial conditions are zero and $x[n] = u[n]$. The subscript R is only used to emphasize a recursive solution.

(c) Define $y_C[n] = x[n] * h[n]$. Using $x[n] = u[n]$ and $h[n]$ from part (a), compute $y_C[4]$. The subscript C is only used to emphasize a convolution solution.

(d) In this chapter, both recursion and convolution are presented as potential methods to compute the zero-state response (ZSR) of a discrete-time system. Comparing parts (b) and (c), we see that $y_R[4] \neq y_C[4]$. Why are the two results not the same? Which method, if any, yields the correct ZSR value?

9.6-1 In Sec. 9.6.1, we showed that for BIBO stability in an LTID system, it is sufficient for its impulse response $h[n]$ to satisfy Eq. (9.30). Show that this is also a necessary condition for the system to be BIBO-stable. In other words, show that if Eq. (9.30) is not satisfied, there exists a bounded input that produces unbounded output. [*Hint:* Assume that a system exists for which $h[n]$ violates Eq. (9.30), yet its output is bounded for every bounded input. Establish the contradiction in this statement by considering an input $x[n]$ defined by $x[n_1 - m] = 1$ when $h[m] > 0$ and $x[n_1 - m] = -1$ when $h[m] < 0$, where n_1 is some fixed integer.]

9.6-2 Each of the following equations specifies an LTID system. Determine whether each of these systems is BIBO-stable or -unstable. Determine also whether each is asymptotically stable, unstable, or marginally stable.

(a) $y[n+2] + 0.6y[n+1] - 0.16y[n] = x[n+1] - 2x[n]$

(b) $y[n] + 3y[n-1] + 2y[n-2] = x[n-1] + 2x[n-2]$

(c) $(E-1)^2(E+\frac{1}{2})y[n] = x[n]$

(d) $y[n] + 2y[n-1] + 0.96y[n-2] = x[n]$

(e) $y[n] + y[n-1] - 2y[n-2] = x[n] + 2x[n-1]$

(f) $(E^2 - 1)(E^2 + 1)y[n] = x[n]$

9.6-3 Consider two LTIC systems in cascade, as illustrated in Fig. 9.13. The impulse response of the system $\mathcal{S}_1$ is $h_1[n] = 2^n u[n]$ and the impulse response of the system $\mathcal{S}_2$ is $h_2[n] = \delta[n] - 2\delta[n-1]$. Is the cascaded system

asymptotically stable or unstable? Determine the BIBO stability of the composite system.

9.6-4 Figure P9.6-4 locates the characteristic roots of 10 causal, LTID systems, labeled A through J. Each system has only two roots and is described using operator notation as $Q(E)y[n] = P(E)x[n]$. All plots are drawn to scale, with the unit circle shown for reference. For each of the following parts, identify all the answers that are correct.

(a) Identify all systems that are unstable.

(b) Assuming all systems have $P(E) = E^2$, identify all systems that are real. Recall that a real system always generates a real-valued response to a real-valued input.

(c) Identify all systems that support oscillatory natural modes.

(d) Identify all systems that have at least one mode whose envelope decays at a rate of 2^{-n}.

(e) Identify all systems that have only one mode.

9.6-5 A discrete-time LTI system has an impulse response given by

$$h[n] = \delta[n] + \left(\tfrac{1}{3}\right)^n u[n-1]$$

(a) Is the system stable? Is the system causal? Justify your answers.

(b) Plot the signal $x[n] = u[n-3] - u[n+3]$.

(c) Determine the system's zero-state response $y[n]$ to the input $x[n] = u[n-3] - u[n+3]$. Plot $y[n]$ over $(-10 \le n \le 10)$.

9.6-6 An LTID system has an impulse response given by

$$h[n] = \left(\tfrac{1}{2}\right)^{|n|}$$

(a) Is the system causal? Justify your answer.

(b) Compute $\sum_{n=-\infty}^{\infty} |h[n]|$. Is this system BIBO-stable?

(c) Compute the energy and power of input signal $x[n] = 3u[n-5]$.

(d) Using input $x[n] = 3u[n-5]$, determine the zero-state response of this system at time $n = 10$. That is, determine $y_{zsr}[10]$.

9.6-7 Show that a marginally stable system is BIBO-unstable. Verify your result by considering a system with characteristic roots on the unit circle and show that for the input of the form of the natural mode (which is bounded), the response is unbounded.

9.7-1 Determine a constant coefficient linear difference equation that describes a system for which the input $x[n] = 2(\frac{1}{3})^n u[-n-4]$ causes resonance.

9.7-2 If one exists, determine a real input $x[n]$ that will cause resonance in the causal LTID system described by $(E^2 + 1)\{y[n]\} = (E + 0.5)\{x[n]\}$. If no such input exists, explain why not.

9.7-3 Consider two lowpass LTID systems, one with infinite-duration impulse response $h_1[n] = -(0.5)^n u[n]$ and the other with finite-duration impulse response $h_2[n] = 2(u[n] - u[n-4])$. Which system (1, 2, both, or neither) would more efficiently transmit a binary communication signal? Carefully justify your result.

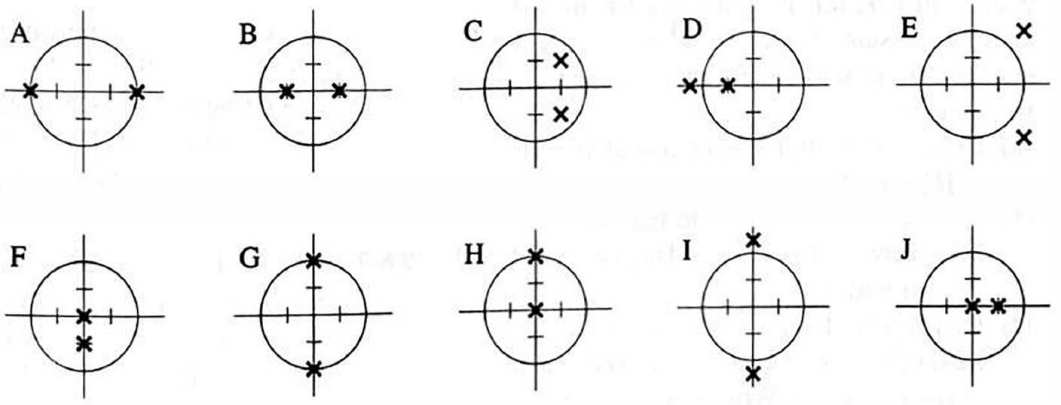

Figure P9.6-4

9.8-1 Write a MATLAB program that recursively computes and then plots the solution to $y[n] - \frac{1}{3}y[n-1] + \frac{1}{2}y[n-2] = x[n]$ for $(0 \le n \le 100)$ given $x[n] = \delta[n] + u[n-50]$ and $y[-2] = y[-1] = 2$.

9.8-2 Write MATLAB code to compute and plot the DT convolutions of Prob. 9.5-25.

9.8-3 An indecisive student contemplates whether he should stay home or take his final exam, which is being held 2 miles away. Starting at home, the student travels half the distance to the exam location before changing his mind. The student turns around and travels half the distance between his current location and his home before changing his mind again. This process of changing direction and traveling half the remaining distance continues until the student either reaches a destination or dies from exhaustion.

(a) Determine a suitable difference equation description of this system.

(b) Use MATLAB to simulate the difference equation in part (a). Where does the student end up as $n \to \infty$? How does your answer change if the student goes two-thirds the way each time, rather than halfway?

(c) Determine a closed-form solution to the equation in part (a). Use this solution to verify the results in part (b).

9.8-4 The cross-correlation function between $x[n]$ and $y[n]$ is given as

$$r_{xy}[k] = \sum_{n=-\infty}^{\infty} x[n]y[n-k]$$

Notice that $r_{xy}[k]$ is quite similar to the convolution sum. The independent variable k corresponds to the relative *shift* between the two inputs.

(a) Express $r_{xy}[k]$ in terms of convolution. Is $r_{xy}[k] = r_{yx}[k]$?

(b) Cross-correlation is said to indicate similarity between two signals. Do you agree? Why or why not?

(c) If $x[n]$ and $y[n]$ are both finite duration, MATLAB's `conv` command is well suited to compute $r_{xy}[k]$. Write a MATLAB function that computes the cross-correlation function using the `conv` command. Four vectors are passed to the function (`x`, `y`, `nx`, and `ny`) corresponding to the inputs $x[n]$, $y[n]$, and their respective time vectors. Notice that `x` and `y` are not necessarily the same length. Two outputs should be created (`rxy` and `k`) corresponding to $r_{xy}[k]$ and its shift vector.

(d) Test your code from part (c) using $x[n] = u[n-5] - u[n-10]$ over $(0 \le n = n_x \le 20)$ and $y[n] = u[-n-15] - u[-n-10] + \delta[n-2]$ over $(-20 \le n = n_y \le 10)$. Plot the result `rxy` as a function of the shift vector `k`. What shift k gives the largest magnitude of $r_{xy}[k]$? Does this make sense?

9.8-5 A causal N-point max filter assigns $y[n]$ to the maximum of $\{x[n], \ldots, x[n-(N-1)]\}$.

(a) Write a MATLAB function that performs N-point max filtering on a length-M input vector `x`. The two function inputs are vector `x` and scalar `N`. To create the length-M output vector `y`, initially pad the input vector with $N-1$ zeros. The MATLAB command `max` may be helpful.

(b) Test your filter and MATLAB code by filtering a length-45 input defined as $x[n] = \cos(\pi n/5) + \delta[n-30] - \delta[n-35]$. Separately plot the results for $N = 4$, $N = 8$, and $N = 12$. Comment on the filter behavior.

9.8-6 A causal N-point min filter assigns $y[n]$ to the minimum of $\{x[n], \ldots, x[n-(N-1)]\}$.

(a) Write a MATLAB function that performs N-point min filtering on a length-M input vector `x`. The two function inputs are vector `x` and scalar `N`. To create the length-M output vector `y`, initially pad the input vector with $N-1$ zeros. The MATLAB command `min` may be helpful.

(b) Test your filter and MATLAB code by filtering a length-45 input defined as $x[n] = \cos(\pi n/5) + \delta[n-30] - \delta[n-35]$. Separately plot the results for $N = 4$, $N = 8$, and $N = 12$. Comment on the filter behavior.

9.8-7 A causal N-point median filter assigns $y[n]$ to the median of $\{x[n], \ldots, x[n-(N-1)]\}$. The median is found by sorting sequence $\{x[n], \ldots, x[n-(N-1)]\}$ and choosing the middle value (odd N) or the average of the two middle values (even N).

(a) Write a MATLAB function that performs N-point median filtering on a length-M input vector `x`. The two function inputs are vector `x` and scalar `N`. To create the length-M output vector `y`, initially pad the input vector with $N-1$ zeros. The MATLAB command `sort` or `median` may be helpful.

(b) Test your filter and MATLAB code by filtering a length-45 input defined as $x[n] = \cos(\pi n/5) + \delta[n-30] - \delta[n-35]$. Separately plot the results for $N = 4$, $N = 8$, and $N = 12$. Comment on the filter behavior.

9.8-8 Recall that $y[n] = x[n/N]$ represents an upsample by N operation. An interpolation filter replaces the inserted zeros with more realistic values. A linear interpolation filter has impulse response

$$h[n] = \sum_{k=-(N-1)}^{N-1} \left(1 - \left|\frac{k}{N}\right|\right) \delta(n-k)$$

(a) Determine a constant coefficient difference equation that has impulse response $h[n]$.

(b) The impulse response $h[n]$ is noncausal. What is the smallest time shift necessary to make the filter causal? What is the effect of this shift on the behavior of the filter?

(c) Write a MATLAB function that will compute the parameters necessary to implement an interpolation filter using MATLAB's `filter` command. That is, your function should output filter vectors `b` and `a` given an input scalar N.

(d) Test your filter and MATLAB code. To do this, create $x[n] = \cos(n)$ for $(0 \leq n \leq 9)$. Upsample $x[n]$ by $N = 10$ to create a new signal $x_{up}[n]$. Design the corresponding $N = 10$ linear interpolation filter, filter $x_{up}[n]$ to produce $y[n]$, and plot the results.

9.8-9 A causal N-point moving-average filter has impulse response $h[n] = (u[n] - u[n-N])/N$.

(a) Determine a constant-coefficient difference equation that has impulse response $h[n]$.

(b) Write a MATLAB function that will compute the parameters necessary to implement an N-point moving-average filter using MATLAB's `filter` command. That is, your function should output filter vectors `b` and `a` given a scalar input N.

(c) Test your filter and MATLAB code by filtering a length-45 input defined as $x[n] = \cos(\pi n/5) + \delta[n-30] - \delta[n-35]$. Separately plot the results for $N = 4$, $N = 8$, and $N = 12$. Comment on the filter behavior.

(d) Problem 9.8-8 introduces linear interpolation filters, for use following an upsample by N operation. Within a scale factor, show that a cascade of two N-point moving-average filters is equivalent to the linear interpolation filter. What is the scale factor difference? Test this idea with MATLAB. Create $x[n] = \cos(n)$ for $(0 \leq n \leq 9)$. Upsample $x[n]$ by $N = 10$ to create a new signal $x_{up}[n]$. Design an $N = 10$ moving-average filter. Filter $x_{up}[n]$ twice and scale to produce $y[n]$. Plot the results. Does the output from the cascaded pair of moving-average filters linearly interpolate the upsampled data?

CHAPTER 10

FOURIER ANALYSIS OF DISCRETE-TIME SIGNALS

In Chs. 3, 4, and 6, we studied the ways of representing a continuous-time signal as a sum of sinusoids or exponentials. In this chapter, we shall discuss similar development for discrete-time signals. Our approach is parallel to that used for continuous-time signals. We first represent a periodic $x[n]$ as a Fourier series formed by a discrete-time exponential (or sinusoid) and its harmonics. Later we extend this representation to an aperiodic signal $x[n]$ by considering $x[n]$ as a limiting case of a periodic signal with the period approaching infinity.

10.1 PERIODIC SIGNAL REPRESENTATION BY DISCRETE-TIME FOURIER SERIES

A continuous-time periodic signal of period T_0 can be represented as a trigonometric Fourier series consisting of a sinusoid of the fundamental frequency $\omega_0 = 2\pi/T_0$, and all its harmonics. The exponential form of the Fourier series consists of exponentials e^{j0t}, $e^{\pm j\omega_0 t}$, $e^{\pm j2\omega_0 t}$, $e^{\pm j3\omega_0 t}$, ...

A discrete-time periodic signal can be represented by a discrete-time Fourier series using a parallel development. Recall that a periodic signal $x[n]$ with period N_0 is characterized by the fact that

$$x[n] = x[n + N_0]$$

The smallest value of N_0 for which this equation holds is the *fundamental period*. The *fundamental frequency* is $\Omega_0 = 2\pi/N_0$ rad/sample. An N_0-periodic signal $x[n]$ can be represented by a discrete-time Fourier series made up of sinusoids of fundamental frequency $\Omega_0 = 2\pi/N_0$ and its harmonics. As in the continuous-time case, we may use a trigonometric or an exponential form of the Fourier series. Because of its compactness and ease of mathematical manipulations, the exponential form is preferable to the trigonometric. For this reason, we shall bypass the trigonometric form and go directly to the exponential form of the discrete-time Fourier series.

The exponential Fourier series consists of the exponentials e^{j0n}, $e^{\pm j\Omega_0 n}$, $e^{\pm j2\Omega_0 n}$, ..., $e^{\pm jn\Omega_0 n}$, ..., and so on. There would be an infinite number of harmonics, except for the property proved in Sec. 8.3.5, that discrete-time exponentials whose frequencies are separated by 2π (or integer multiples of 2π) are identical because

$$e^{j(\Omega \pm 2\pi m)n} = e^{j\Omega n} e^{\pm 2\pi mn} = e^{j\Omega n} \qquad m \text{ integer}$$

The consequence of this result is that the rth harmonic is identical to the $(r+N_0)$th harmonic. To demonstrate this, let g_n denote the nth harmonic $e^{jn\Omega_0 n}$. Then

$$g_{r+N_0} = e^{j(r+N_0)\Omega_0 n} = e^{j(r\Omega_0 n + 2\pi n)} = e^{jr\Omega_0 n} = g_r$$

and

$$g_r = g_{r+N_0} = g_{r+2N_0} = \cdots = g_{r+mN_0} \qquad m \text{ integer}$$

Thus, the first harmonic is identical to the (N_0+1)th harmonic, the second harmonic is identical to the (N_0+2)th harmonic, and so on. In other words, there are only N_0 independent harmonics, and their frequencies range over an interval 2π (because the harmonics are separated by $\Omega_0 = 2\pi/N_0$). This means that, unlike the continuous-time counterpart, the discrete-time Fourier series has only a finite number (N_0) of terms. This result is consistent with our observation in Sec. 8.3.5 that all discrete-time signals are bandlimited to a band from $-\pi$ to π. Because the harmonics are separated by $\Omega_0 = 2\pi/N_0$, there can only be N_0 harmonics in this band. We also saw that this band can be taken from 0 to 2π or any other contiguous band of width 2π. This means we may choose the N_0 independent harmonics $e^{jr\Omega_0 n}$ over $0 \le r \le N_0 - 1$, or over $-1 \le r \le N_0 - 2$, or over $1 \le r \le N_0$, or over any other suitable choice for that matter. Every one of these sets will have the same harmonics, although in different order.

Let us consider the first choice, which corresponds to exponentials $e^{jr\Omega_0 n}$ for $r = 0, 1, 2, \ldots, N_0 - 1$. The Fourier series for an N_0-periodic signal $x[n]$ consists of only these N_0 harmonics, and can be expressed as

$$x[n] = \sum_{r=0}^{N_0-1} \mathcal{D}_r e^{jr\Omega_0 n} \qquad \Omega_0 = \frac{2\pi}{N_0}$$

To compute coefficients $\mathcal{D}_r$, we multiply both sides by $e^{-jm\Omega_0 n}$ and sum over n from $n = 0$ to $(N_0 - 1)$.

$$\sum_{n=0}^{N_0-1} x[n] e^{-jm\Omega_0 n} = \sum_{n=0}^{N_0-1} \sum_{r=0}^{N_0-1} \mathcal{D}_r e^{j(r-m)\Omega_0 n} \tag{10.1}$$

The right-hand sum, after interchanging the order of summation, results in

$$\sum_{r=0}^{N_0-1} \mathcal{D}_r \left[\sum_{n=0}^{N_0-1} e^{j(r-m)\Omega_0 n} \right]$$

The inner sum, according to Eq. (5.15) in Sec. 5.5, is zero for all values of $r \neq m$. It is nonzero with a value N_0 only when $r = m$. This fact means the outside sum has only one term $\mathcal{D}_m N_0$ (corresponding to $r = m$). Therefore, the right-hand side of Eq. (10.1) is equal to $\mathcal{D}_m N_0$, and

$$\sum_{n=0}^{N_0-1} x[n] e^{-jm\Omega_0 n} = \mathcal{D}_m N_0$$

and

$$\mathcal{D}_m = \frac{1}{N_0} \sum_{n=0}^{N_0-1} x[n] e^{-jm\Omega_0 n}$$

We now have a discrete-time Fourier series (DTFS) representation of an N_0-periodic signal $x[n]$ as

$$x[n] = \sum_{r=0}^{N_0-1} \mathcal{D}_r e^{jr\Omega_0 n} \tag{10.2}$$

where

$$\mathcal{D}_r = \frac{1}{N_0} \sum_{n=0}^{N_0-1} x[n] e^{-jr\Omega_0 n} \qquad \Omega_0 = \frac{2\pi}{N_0} \tag{10.3}$$

Observe that DTFS Eqs. (10.2) and (10.3) are identical (within a scaling constant) to the DFT Eqs. (5.13) and (5.12).[†] Therefore, we can use the efficient FFT algorithm to compute the DTFS coefficients.

10.1.1 Fourier Spectra of a Periodic Signal $x[n]$

The Fourier series consists of N_0 components

$$\mathcal{D}_0, \mathcal{D}_1 e^{j\Omega_0 n}, \mathcal{D}_2 e^{j2\Omega_0 n}, \ldots, \mathcal{D}_{N_0-1} e^{j(N_0-1)\Omega_0 n}$$

The frequencies of these components are 0, Ω_0, $2\Omega_0$, ..., $(N_0 - 1)\Omega_0$, where $\Omega_0 = 2\pi/N_0$. The amount of the rth harmonic is $\mathcal{D}_r$. We can plot this amount $\mathcal{D}_r$ (the Fourier coefficient) as a function of index r or frequency Ω. Such a plot, called the *Fourier spectrum* of $x[n]$, gives us, at a glance, the graphical picture of the amounts of various harmonics of $x[n]$.

In general, the Fourier coefficients $\mathcal{D}_r$ are complex, and they can be represented in the polar form as

$$\mathcal{D}_r = |\mathcal{D}_r| e^{j\angle \mathcal{D}_r}$$

The plot of $|\mathcal{D}_r|$ versus Ω is called the amplitude spectrum and that of $\angle \mathcal{D}_r$ versus Ω is called the angle (or phase) spectrum. These two plots together are the frequency spectra of $x[n]$. Knowing these spectra, we can reconstruct or synthesize $x[n]$ according to Eq. (10.2). Therefore, the Fourier (or frequency) spectra, which are an alternative way of describing a periodic signal $x[n]$, are in every way equivalent (in terms of the information) to the plot of $x[n]$ as a function of n. The Fourier spectra of a signal constitute the *frequency-domain* description of $x[n]$, in contrast to the time-domain description, where $x[n]$ is specified as a function of index n (representing time).

The results are very similar to the representation of a continuous-time periodic signal by an exponential Fourier series except that, generally, the continuous-time signal spectrum bandwidth is infinite and consists of an infinite number of exponential components (harmonics). The spectrum of the discrete-time periodic signal, in contrast, is bandlimited and has at most N_0 components.

[†] If we let $x[n] = N_0 x_k$ and $\mathcal{D}_r = X_r$, Eqs. (10.2) and (10.3) are identical to Eqs. (5.13) and (5.12), respectively.

Periodic Extension of Fourier Spectrum

We now show that if $\phi[r]$ is an N_0-periodic function of r, then

$$\sum_{r=0}^{N_0-1} \phi[r] = \sum_{r=\langle N_0 \rangle} \phi[r] \tag{10.4}$$

where $r = \langle N_0 \rangle$ indicates summation over any N_0 consecutive values of r. Because $\phi[r]$ is N_0-periodic, the same values repeat with period N_0. Hence, the sum of any set of N_0 consecutive values of $\phi[r]$ must be the same no matter the value of r at which we start summing. Basically, it represents the sum over one cycle.

To apply this result to the DTFS, we observe that $e^{-jr\Omega_0 n}$ is N_0-periodic because

$$e^{-jr\Omega_0(n+N_0)} = e^{-jr\Omega_0 n} e^{-j2\pi r} = e^{-jr\Omega_0 n}$$

Therefore, if $x[n]$ is N_0-periodic, $x[n]e^{-jr\Omega_0 n}$ is also N_0-periodic. Hence, from Eq. (10.3), it follows that $\mathcal{D}_r$ is also N_0-periodic, as is $\mathcal{D}_r e^{jr\Omega_0 n}$. Now, because of Eq. (10.4), we can express Eqs. (10.2) and (10.3) as

$$x[n] = \sum_{r=\langle N_0 \rangle} \mathcal{D}_r e^{jr\Omega_0 n} \tag{10.5}$$

and

$$\mathcal{D}_r = \frac{1}{N_0} \sum_{n=\langle N_0 \rangle} x[n] e^{-jr\Omega_0 n} \tag{10.6}$$

If we plot $\mathcal{D}_r$ for all values of r (rather than only $0 \le r \le N_0 - 1$), then the spectrum $\mathcal{D}_r$ is N_0-periodic. Moreover, Eq. (10.5) shows that $x[n]$ can be synthesized not only by the N_0 exponentials corresponding to $0 \le r \le N_0 - 1$, but also by any successive N_0 exponentials in this spectrum, starting at any value of r (positive or negative). For this reason, it is customary to show the spectrum $\mathcal{D}_r$ for all values of r (not just over the interval $0 \le r \le N_0 - 1$). *Yet we must remember that to synthesize $x[n]$ from this spectrum, we need to add only N_0 consecutive components.*

Along the Ω scale, $\mathcal{D}_r$ repeats every 2π intervals, and along the r scale, $\mathcal{D}_r$ repeats at intervals of N_0. Equations (10.5) and (10.6) show that both $x[n]$ and its spectrum $\mathcal{D}_r$ are N_0-periodic and both have exactly the same number of components (N_0) over one period.

Equation (10.6) shows that $\mathcal{D}_r$ is complex in general, and $\mathcal{D}_{-r}$ is the conjugate of $\mathcal{D}_r$ if $x[n]$ is real. Thus,

$$|\mathcal{D}_r| = |\mathcal{D}_{-r}| \qquad \text{and} \qquad \angle \mathcal{D}_r = -\angle \mathcal{D}_{-r}$$

so that the amplitude spectrum $|\mathcal{D}_r|$ is an even function, and $\angle \mathcal{D}_r$ is an odd function of r (or Ω). All these concepts will be clarified by the examples to follow. The first example is rather trivial and serves mainly to familiarize the reader with the basic concepts of DTFS.

EXAMPLE 10.1 Discrete-Time Fourier Series of a Sinusoid

Find the discrete-time Fourier series (DTFS) for $x[n] = \sin 0.1\pi n$ (Fig. 10.1a). Sketch the amplitude and phase spectra.

In this case, the sinusoid $\sin 0.1\pi n$ is periodic because $\Omega/2\pi = 1/20$ is a rational number and the period N_0 is [see Eq. (8.5)]

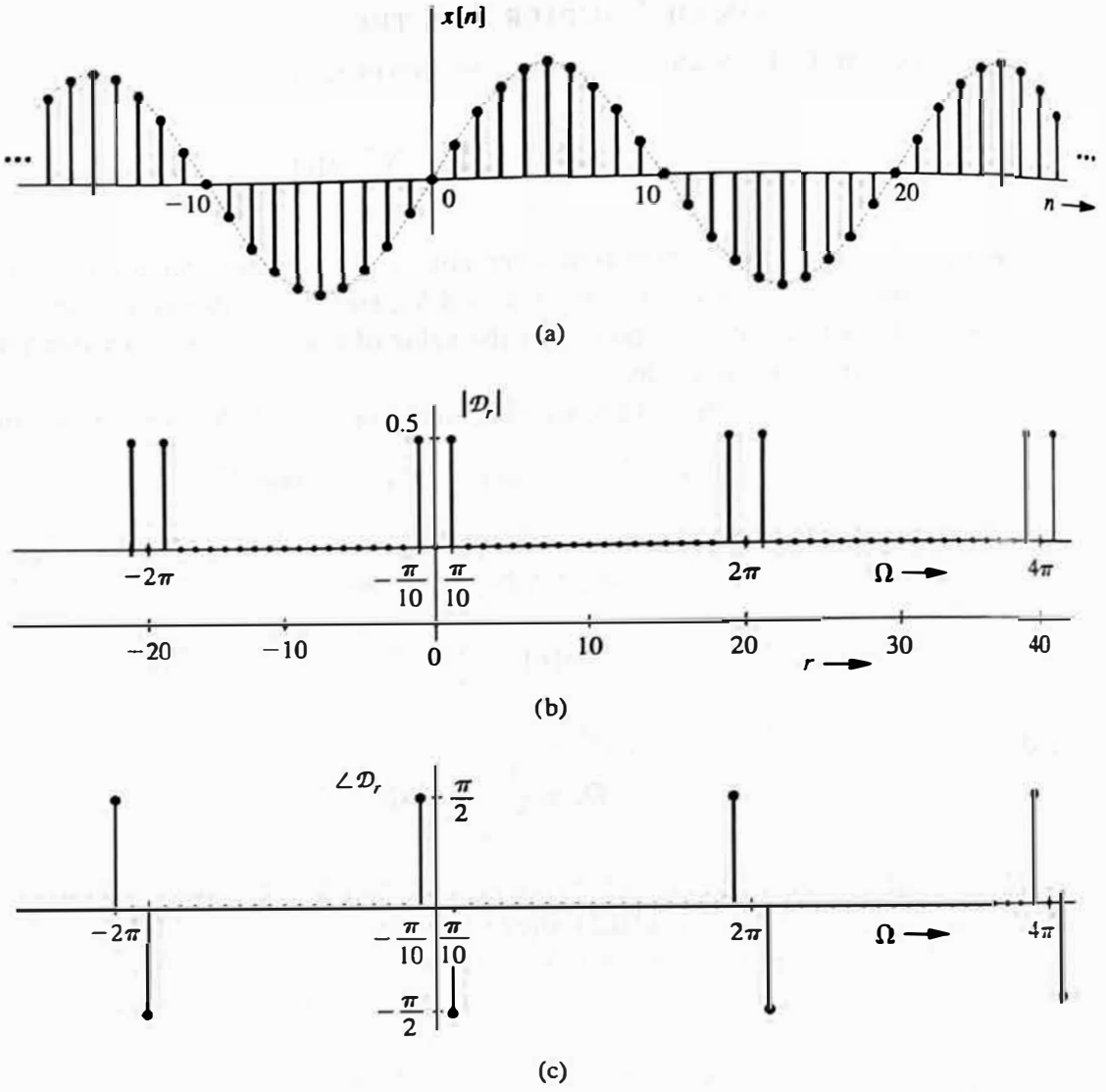

Figure 10.1 Discrete-time sinusoid $\sin 0.1\pi n$ and its Fourier spectra.

$$N_0 = m\left(\frac{2\pi}{\Omega}\right) = m\left(\frac{2\pi}{0.1\pi}\right) = 20m$$

The smallest value of m that makes $20m$ an integer is $m = 1$. Therefore, the period $N_0 = 20$ so that $\Omega_0 = 2\pi/N_0 = 0.1\pi$, and from Eq. (10.5),

$$x[n] = \sum_{r=\langle 20\rangle} \mathcal{D}_r e^{j0.1\pi rn}$$

where the sum is performed over any 20 consecutive values of r. We shall select the range $-10 \le r < 10$ (values of r from -10 to 9). This choice corresponds to synthesizing $x[n]$ using the spectral components in the fundamental frequency range ($-\pi \le \Omega < \pi$). Thus,

$$x[n] = \sum_{r=-10}^{9} \mathcal{D}_r e^{j0.1\pi rn}$$

where, according to Eq. (10.6),

$$\begin{aligned}\mathcal{D}_r &= \frac{1}{20}\sum_{n=-10}^{9} \sin 0.1\pi n\, e^{-j0.1\pi rn} \\ &= \frac{1}{20}\sum_{n=-10}^{9} \frac{1}{2j}(e^{j0.1\pi n} - e^{-j0.1\pi n})e^{-j0.1\pi rn} \\ &= \frac{1}{40j}\left[\sum_{n=-10}^{9} e^{j0.1\pi n(1-r)} - \sum_{n=-10}^{9} e^{-j0.1\pi n(1+r)}\right]\end{aligned}$$

In these sums, r takes on all values between -10 and 9. From Eq. (5.15), it follows that the first sum on the right-hand side is zero for all values of r except $r = 1$, when the sum is equal to $N_0 = 20$. Similarly, the second sum is zero for all values of r except $r = -1$, when it is equal to $N_0 = 20$. Therefore,

$$\mathcal{D}_1 = \frac{1}{2j} \quad \text{and} \quad \mathcal{D}_{-1} = -\frac{1}{2j}$$

and all other coefficients are zero. The corresponding Fourier series is given by

$$x[n] = \sin 0.1\pi n = \frac{1}{2j}(e^{j0.1\pi n} - e^{-j0.1\pi n}) \tag{10.7}$$

Here, the fundamental frequency $\Omega_0 = 0.1\pi$, and there are only two nonzero components:

$$\mathcal{D}_1 = \frac{1}{2j} = \frac{1}{2}e^{-j\pi/2} \quad \text{and} \quad \mathcal{D}_{-1} = -\frac{1}{2j} = \frac{1}{2}e^{j\pi/2}$$

Therefore,

$$|\mathcal{D}_1| = |\mathcal{D}_{-1}| = \frac{1}{2} \quad \text{and} \quad \angle\mathcal{D}_1 = -\frac{\pi}{2},\ \angle\mathcal{D}_{-1} = \frac{\pi}{2}$$

Sketches of $\mathcal{D}_r$ for the interval $(-10 \le r < 10)$ appear in Figs. 10.1b and 10.1c. According to Eq. (10.7), there are only two components corresponding to $r = 1$ and -1. The remaining 18 coefficients are zero. The rth component $\mathcal{D}_r$ is the amplitude of the frequency $r\Omega_0 = 0.1r\pi$. Therefore, the frequency interval corresponding to $-10 \le r < 10$ is $-\pi \le \Omega < \pi$, as depicted in Figs. 10.1b and 10.1c. This spectrum over the range $-10 \le r < 10$ (or $-\pi \le \Omega < \pi$) is sufficient to specify the frequency-domain description (Fourier series), and we can synthesize $x[n]$ by adding these spectral components. Because of the periodicity property discussed in this section, the spectrum $\mathcal{D}_r$ is a periodic function of r with period $N_0 = 20$. For this reason, we

repeat the spectrum with period $N_0 = 20$ (or $\Omega = 2\pi$), as illustrated in Figs. 10.1b and 10.1c, which are periodic extensions of the spectrum in the range $-10 \leq r < 10$. Observe that the amplitude spectrum is an even function and the angle or phase spectrum is an odd function of r (or Ω), as expected.

The result [Eq. (10.7)] is a trigonometric identity and could have been obtained immediately without the formality of finding the Fourier coefficients. We have intentionally chosen this trivial example to introduce the reader gently to the new concept of the discrete-time Fourier series and its periodic nature. The Fourier series is a way of expressing a periodic signal $x[n]$ in terms of exponentials of the form $e^{jr\Omega_0 n}$ and its harmonics. The result in Eq. (10.7) is merely a statement of the (obvious) fact that $\sin 0.1\pi n$ can be expressed as a sum of two exponentials $e^{j0.1\pi n}$ and $e^{-j0.1\pi n}$.

Because of the periodicity of the discrete-time exponentials $e^{jr\Omega_0 n}$, the Fourier series components can be selected in any range of length $N_0 = 20$ (or $\Omega = 2\pi$). For example, if we select the frequency range $0 \leq \Omega < 2\pi$ (or $0 \leq r < 20$), we obtain the Fourier series as

$$x[n] = \sin 0.1\pi n = \frac{1}{2j}(e^{j0.1\pi n} - e^{j1.9\pi n})$$

This series is equivalent to that in Eq. (10.7) because the two exponentials $e^{j1.9\pi n}$ and $e^{-j0.1\pi n}$ are equivalent. This follows from the fact that $e^{j1.9\pi n} = e^{j1.9\pi n} \times e^{-j2\pi n} = e^{-j0.1\pi n}$.

We could have selected the spectrum over any other range of width $\Omega = 2\pi$ in Figs. 10.1b and 10.1c as a valid discrete-time Fourier series. The reader may verify this by proving that such a spectrum starting anywhere (and of width $\Omega = 2\pi$) is equivalent to the same two components on the right-hand side of Eq. (10.7).

DRILL 10.1 DTFS Spectra on Alternate Intervals

From the spectra in Fig. 10.1, write the Fourier series corresponding to the interval $-10 \geq r > -30$ (or $-\pi \geq \Omega > -3\pi$). Show that this Fourier is equivalent to that in Eq. (10.7).

DRILL 10.2 Discrete-Time Fourier Series of a Sum of Sinusoids

Find the period and the DTFS for

$$x[n] = 4\cos 0.2\pi n + 6\sin 0.5\pi n$$

over the interval $0 \leq r \leq 19$. Use Eq. (10.3) to compute $\mathcal{D}_r$.

ANSWERS

$N_0 = 20$ and $x[n] = 2e^{j0.2\pi n} + (3e^{-j\pi/2})e^{j0.5\pi n} + (3e^{j\pi/2})e^{j1.5\pi n} + 2e^{j1.8\pi n}$

DRILL 10.3 Fundamental Period of Discrete-Time Sinusoids

Find the fundamental periods N_0, if any, for: **(a)** $\sin(301\pi n/4)$ and **(b)** $\cos 1.3n$.

ANSWERS

(a) $N_0 = 8$, **(b)** N_0 does not exist because the sinusoid is not periodic.

EXAMPLE 10.2 Discrete-Time Fourier Series of a Periodic Gate Function

Compute and plot the discrete-time Fourier series for the periodic sampled gate function shown in Fig. 10.2a.

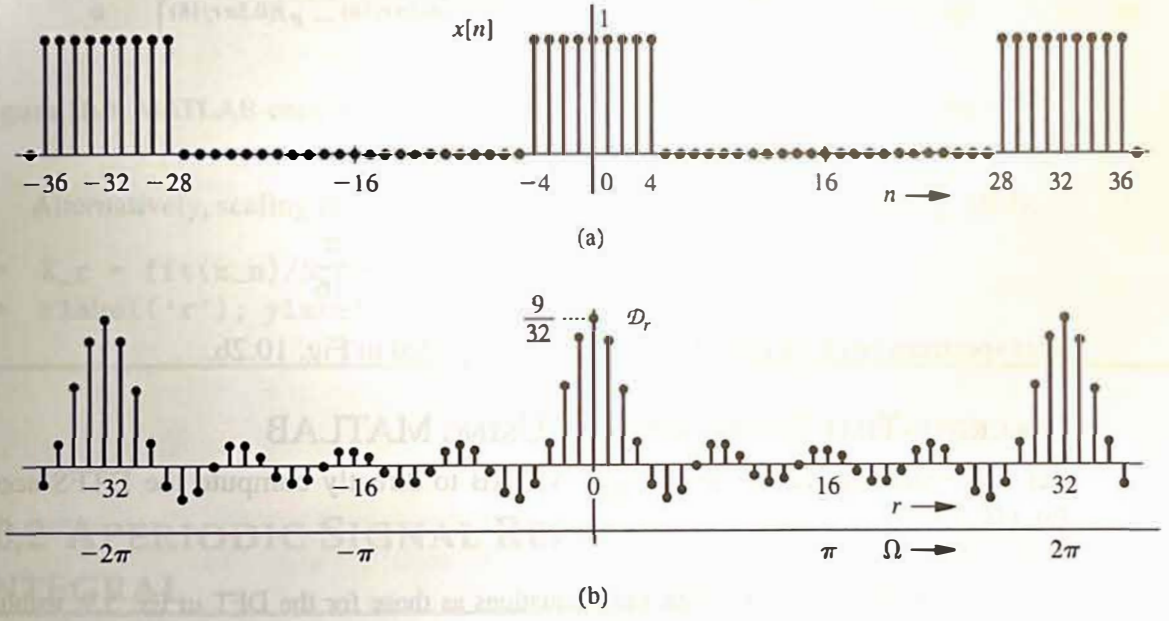

Figure 10.2 **(a)** Periodic sampled gate pulse and **(b)** its Fourier spectrum.

In this case, $N_0 = 32$ and $\Omega_0 = 2\pi/32 = \pi/16$. Therefore,

$$x[n] = \sum_{r=\langle 32\rangle} \mathcal{D}_r e^{jr(\pi/16)n}$$

where

$$\mathcal{D}_r = \frac{1}{32} \sum_{n=\langle 32\rangle} x[n] e^{-jr(\pi/16)n}$$

For our convenience, we shall choose the interval $-16 \le n \le 15$ for this summation, although any other interval of the same width (32 points) would give the same result.†

$$\mathcal{D}_r = \frac{1}{32} \sum_{n=-16}^{15} x[n] e^{-jr(\pi/16)n}$$

Now, $x[n] = 1$ for $-4 \le n \le 4$ and is zero for all other values of n. Therefore,

$$\mathcal{D}_r = \frac{1}{32} \sum_{n=-4}^{4} e^{-jr(\pi/16)n} \tag{10.8}$$

This is a geometric progression with a common ratio $e^{-j(\pi/16)r}$. Therefore (see Sec. B.8.3),‡

$$\begin{aligned}
\mathcal{D}_r &= \frac{1}{32}\left[\frac{e^{-j(5\pi r/16)} - e^{j(4\pi r/16)}}{e^{-j(\pi r/16)} - 1}\right] \\
&= \left(\frac{1}{32}\right) \frac{e^{-j(0.5\pi r/16)}\left[e^{-j(4.5\pi r/16)} - e^{j(4.5\pi r/16)}\right]}{e^{-j(0.5\pi r/16)}\left[e^{-j(0.5\pi r/16)} - e^{j(0.5\pi r/16)}\right]} \\
&= \left(\frac{1}{32}\right) \frac{\sin\left(\dfrac{4.5\pi r}{16}\right)}{\sin\left(\dfrac{0.5\pi r}{16}\right)} \\
&= \left(\frac{1}{32}\right) \frac{\sin(4.5r\Omega_0)}{\sin(0.5r\Omega_0)} \qquad \Omega_0 = \frac{\pi}{16}
\end{aligned} \tag{10.9}$$

This spectrum (with its periodic extension) is depicted in Fig. 10.2b.

Discrete-Time Fourier Series Using MATLAB

Let us confirm our results by using MATLAB to directly compute the DTFS according to Eq. (10.3).

---

† In this example, we have used the same equations as those for the DFT in Ex. 5.9, within a scaling constant. In the present example, the values of $x[n]$ at $n = 4$ and -4 are taken as 1 (full value), whereas in Ex. 5.9 these values are 0.5 (half the value). This is the reason for the slight difference in spectra in Figs. 10.2b and 5.19d. Unlike continuous-time signals, discontinuity is a meaningless concept in discrete-time signals.

‡ Strictly speaking, the geometric progression sum formula applies only if the common ratio $e^{-j(\pi/16)r} \neq 1$. When $r = 0$, this ratio is unity. Hence, Eq. (10.9) is valid for values of $r \neq 0$. For the case $r = 0$, the sum in Eq. (10.8) is given by

$$\tfrac{1}{32} \sum_{n=-4}^{4} x[n] = \tfrac{9}{32}$$

Fortunately, the value of $\mathcal{D}_0$, as computed from Eq. (10.9), also happens to be 9/32. Hence, Eq. (10.9) is valid for all r.

```
>> N_0 = 32; n = (0:N_0-1); Omega_0 = 2*pi/N_0;
>> x_n = [ones(1,5) zeros(1,23) ones(1,4)];
>> for r = 0:N_0-1,
>>     X_r(r+1) = sum(x_n.*exp(-j*r*Omega_0*n))/N_0;
>> end
>> r = n; stem(r,real(X_r),'k.');
>> xlabel('r'); ylabel('X_r'); axis([0 31 -.1 0.3]);
```

The MATLAB result, shown in Fig. 10.3, matches Fig. 10.2b.

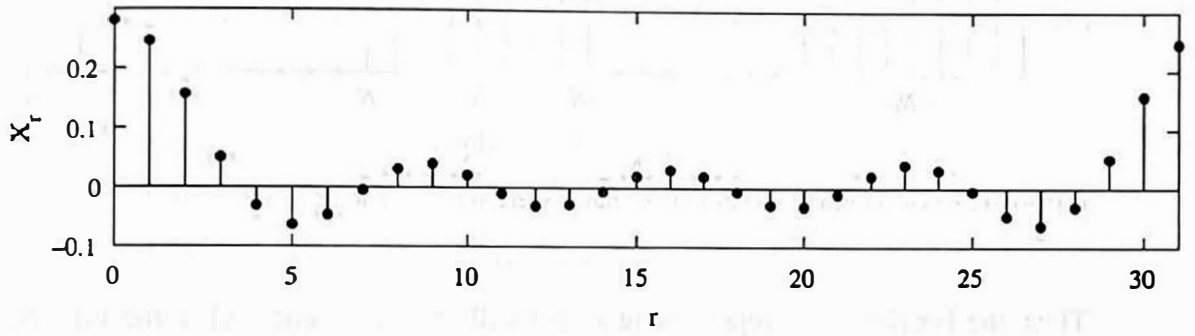

Figure 10.3 MATLAB-computed DTFS spectra for periodic sampled gate pulse of Ex. 10.2.

Alternatively, scaling the FFT by N_0 produces the exact same result (Fig. 10.3).

```
>> X_r = fft(x_n)/N_0; stem(r,real(X_r),'k.');
>> xlabel('r'); ylabel('X_r'); axis([0 31 -.1 0.3]);
```

10.2 Aperiodic Signal Representation by Fourier Integral

In Sec. 10.1, we succeeded in representing periodic signals as a sum of (everlasting) exponentials. In this section, we extend this representation to aperiodic signals. The procedure is identical conceptually to that used in Ch. 4 for continuous-time signals.

Applying a limiting process, we now show that an aperiodic signal $x[n]$ can be expressed as a continuous sum (integral) of everlasting exponentials. To represent an aperiodic signal $x[n]$ such as the one illustrated in Fig. 10.4a by everlasting exponential signals, let us construct a new periodic signal $x_{N_0}[n]$ formed by repeating the signal $x[n]$ every N_0 units, as shown in Fig. 10.4b. The period N_0 is made large enough to avoid overlap between the repeating cycles ($N_0 \geq 2N + 1$). The periodic signal $x_{N_0}[n]$ can be represented by an exponential Fourier series. If we let $N_0 \to \infty$, the signal $x[n]$ repeats after an infinite interval, and therefore,

$$\lim_{N_0 \to \infty} x_{N_0}[n] = x[n]$$

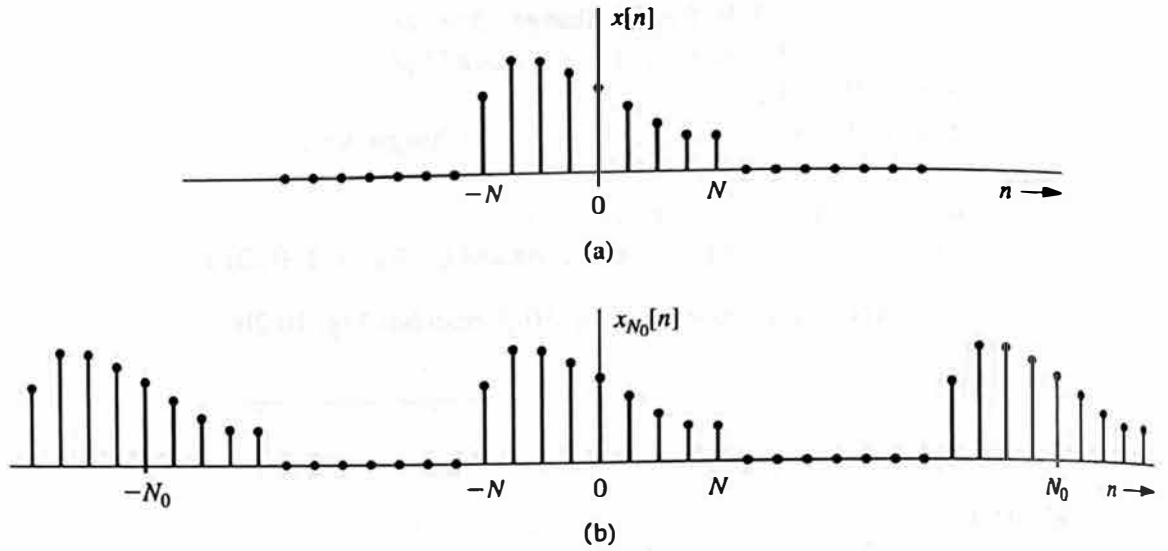

Figure 10.4 Generation of a periodic signal by periodic extension of a signal $x[n]$.

Thus, the Fourier series representing $x_{N_0}[n]$ will also represent $x[n]$ in the limit $N_0 \to \infty$. The exponential Fourier series for $x_{N_0}[n]$ is given by

$$x_{N_0}[n] = \sum_{r=\langle N_0 \rangle} \mathcal{D}_r e^{jr\Omega_0 n} \qquad \Omega_0 = \frac{2\pi}{N_0} \tag{10.10}$$

where

$$\mathcal{D}_r = \frac{1}{N_0} \sum_{n=-\infty}^{\infty} x[n] e^{-jr\Omega_0 n} \tag{10.11}$$

The limits for the sum on the right-hand side of Eq. (10.11) should be from $-N$ to N. But because $x[n] = 0$ for $|n| > N$, it does not matter if the limits are taken from $-\infty$ to ∞.

It is interesting to see how the nature of the spectrum changes as N_0 increases. To understand this behavior, let us define $X(\Omega)$, a continuous function of Ω, as

$$X(\Omega) = \sum_{n=-\infty}^{\infty} x[n] e^{-j\Omega n} \tag{10.12}$$

From this definition and Eq. (10.11), we have

$$\mathcal{D}_r = \frac{1}{N_0} X(r\Omega_0) \tag{10.13}$$

This result shows that the Fourier coefficients $\mathcal{D}_r$ are $1/N_0$ times the samples of $X(\Omega)$ taken every Ω_0 rad/s.† Therefore, $(1/N_0)X(\Omega)$ is the envelope for the coefficients $\mathcal{D}_r$. We now let $N_0 \to \infty$ by

† For the sake of simplicity, we assume $\mathcal{D}_r$ and therefore $X(\Omega)$ to be real. The argument, however, is also valid for complex $\mathcal{D}_r$ [or $X(\Omega)$].

doubling N_0 repeatedly. Doubling N_0 halves the fundamental frequency Ω_0, with the result that the spacing between successive spectral components (harmonics) is halved, and there are now twice as many components (samples) in the spectrum. At the same time, by doubling N_0, the envelope of the coefficients $\mathcal{D}_r$ is halved, as seen from Eq. (10.13). If we continue this process of doubling N_0 repeatedly, the number of components doubles in each step; the spectrum progressively becomes denser, while its magnitude $\mathcal{D}_r$ becomes smaller. Note, however, that the relative shape of the envelope remains the same [proportional to $X(\Omega)$ in Eq. (10.12)]. In the limit, as $N_0 \to \infty$, the fundamental frequency $\Omega_0 \to 0$, and $\mathcal{D}_r \to 0$. The separation between successive harmonics, which is Ω_0, is approaching zero (infinitesimal), and the spectrum becomes so dense that it appears to be continuous. But as the number of harmonics increases indefinitely, the harmonic amplitudes $\mathcal{D}_r$ become vanishingly small (infinitesimal). We discussed an identical situation in Sec. 4.1.

We follow the procedure in Sec. 4.1 and let $N_0 \to \infty$. According to Eq. (10.12),

$$X(r\Omega_0) = \sum_{n=-\infty}^{\infty} x[n]e^{-jr\Omega_0 n}$$

Using Eq. (10.13), we can express Eq. (10.10) as

$$x_{N_0}[n] = \frac{1}{N_0} \sum_{r=\langle N_0 \rangle} X(r\Omega_0)e^{jr\Omega_0 n} = \sum_{r=\langle N_0 \rangle} X(r\Omega_0)e^{jr\Omega_0 n}\left(\frac{\Omega_0}{2\pi}\right)$$

In the limit as $N_0 \to \infty$, $\Omega_0 \to 0$ and $x_{N_0}[n] \to x[n]$. Therefore,

$$x[n] = \lim_{\Omega_0 \to 0} \sum_{r=\langle N_0 \rangle} \left[\frac{X(r\Omega_0)\Omega_0}{2\pi}\right] e^{jr\Omega_0 n} \tag{10.14}$$

Because Ω_0 is infinitesimal, it will be appropriate to replace Ω_0 with an infinitesimal notation $\Delta\Omega$:

$$\Delta\Omega = \frac{2\pi}{N_0} \tag{10.15}$$

Equation (10.14) can be expressed as

$$x[n] = \lim_{\Delta\Omega \to 0} \frac{1}{2\pi} \sum_{r=\langle N_0 \rangle} X(r\Delta\Omega)e^{jr\Delta\Omega n}\Delta\Omega \tag{10.16}$$

The range $r = \langle N_0 \rangle$ implies the interval of N_0 number of harmonics, which is $N_0\Delta\Omega = 2\pi$ according to Eq. (10.15). In the limit, the right-hand side of Eq. (10.16) becomes the integral

$$x[n] = \frac{1}{2\pi} \int_{2\pi} X(\Omega)e^{jn\Omega}\, d\Omega \tag{10.17}$$

where $\int_{2\pi}$ indicates integration over any continuous interval of 2π. The spectrum $X(\Omega)$ is given by [Eq. (10.12)]

$$X(\Omega) = \sum_{n=-\infty}^{\infty} x[n]e^{-j\Omega n} \tag{10.18}$$

The integral on the right-hand side of Eq. (10.17) is called the *Fourier integral*. We have now succeeded in representing an aperiodic signal $x[n]$ by a Fourier integral (rather than a Fourier series). This integral is basically a Fourier series (in the limit) with fundamental frequency $\Delta\Omega \to 0$, as seen in Eq. (10.16). The amount of the exponential $e^{jr\Delta\Omega n}$ is $X(r\Delta\Omega)\Delta\Omega/2\pi$. Thus, the function $X(\Omega)$ given by Eq. (10.18) acts as a spectral function, which indicates the relative amounts of various exponential components of $x[n]$.

We call $X(\Omega)$ the (direct) discrete-time Fourier transform (DTFT) of $x[n]$, and $x[n]$ the inverse discrete-time Fourier transform (IDTFT) of $X(\Omega)$. This nomenclature can be represented as

$$X(\Omega) = \text{DTFT}\{x[n]\} \qquad \text{and} \qquad x[n] = \text{IDTFT}\{X(\Omega)\}$$

The same information is conveyed by the statement that $x[n]$ and $X(\Omega)$ are a (discrete-time) Fourier transform pair. Symbolically, this is expressed as

$$x[n] \Longleftrightarrow X(\Omega)$$

The Fourier transform $X(\Omega)$ is the frequency-domain description of $x[n]$.

10.2.1 Nature of Fourier Spectra

We now discuss several important features of the discrete-time Fourier transform and the spectra associated with it.

Fourier Spectra Are Continuous Functions of Ω

Although $x[n]$ is a discrete-time signal, $X(\Omega)$, its DTFT is a continuous function of Ω for the simple reason that Ω is a continuous variable, which can take any value over a continuous interval from $-\infty$ to ∞.

Fourier Spectra Are Periodic Functions of Ω with Period 2π

From Eq. (10.18), it follows that

$$X(\Omega + 2\pi) = \sum_{n=-\infty}^{\infty} x[n]e^{-j(\Omega+2\pi)n} = \sum_{n=-\infty}^{\infty} x[n]e^{-j\Omega n}e^{-j2\pi n} = X(\Omega)$$

Clearly, the spectrum $X(\Omega)$ is a continuous, periodic function of Ω with period 2π. We must remember, however, that to synthesize $x[n]$, we need to use the spectrum over a frequency interval of only 2π, starting at any value of Ω [see Eq. (10.17)]. As a matter of convenience, we shall choose this interval to be the fundamental frequency range $(-\pi, \pi)$. It is, therefore, not necessary to show discrete-time-signal spectra beyond the fundamental range, although we often do so.

The reason for the periodic behavior of $X(\Omega)$ was discussed in Sec. 8.3.5, where we showed that, in a basic sense, the discrete-time frequency Ω is bandlimited to $|\Omega| \leq \pi$. However, all discrete-time sinusoids with frequencies separated by an integer multiple of 2π are identical. This is why the spectrum is 2π periodic.

Conjugate Symmetry of $X(\Omega)$

From Eq. (10.18), we obtain the DTFT of $x^*[n]$ as

$$\text{DTFT}\{x^*[n]\} = \sum_{n=-\infty}^{\infty} x^*[n]e^{-j\Omega n} = X^*(-\Omega)$$

In other words,

$$x^*[n] \Longleftrightarrow X^*(-\Omega) \tag{10.19}$$

For real $x[n]$, Eq. (10.19) reduces to $x[n] \Longleftrightarrow X^*(-\Omega)$, which implies that for real $x[n]$

$$X(\Omega) = X^*(-\Omega)$$

Therefore, for real $x[n]$, $X(\Omega)$ and $X(-\Omega)$ are conjugates. Since $X(\Omega)$ is generally complex, we have both amplitude and angle (or phase) spectra

$$X(\Omega) = |X(\Omega)|e^{j\angle X(\Omega)}$$

Because of the conjugate symmetry of $X(\Omega)$, it follows that for real $x[n]$,

$$|X(\Omega)| = |X(-\Omega)| \qquad \text{and} \qquad \angle X(\Omega) = -\angle X(-\Omega)$$

Therefore, the amplitude spectrum $|X(\Omega)|$ is an even function of Ω and the phase spectrum $\angle X(\Omega)$ is an odd function of Ω for real $x[n]$.

Physical Appreciation of the Discrete-Time Fourier Transform

In understanding any aspect of the Fourier transform, we should remember that Fourier representation is a way of expressing a signal $x[n]$ as a sum of everlasting exponentials (or sinusoids). The Fourier spectrum of a signal indicates the relative amplitudes and phases of the exponentials (or sinusoids) required to synthesize $x[n]$.

A detailed explanation of the nature of such sums over a continuum of frequencies is provided in Sec. 4.1.1.

Existence of the DTFT

Because $|e^{-j\Omega n}| = 1$, from Eq. (10.18), it follows that the existence of $X(\Omega)$ is guaranteed if $x[n]$ is absolutely summable; that is,

$$\sum_{n=-\infty}^{\infty} |x[n]| < \infty \tag{10.20}$$

This shows that the condition of absolute summability is a sufficient condition for the existence of the DTFT representation. This condition also guarantees its uniform convergence. The inequality

$$\left[\sum_{n=-\infty}^{\infty} |x[n]|\right]^2 \geq \sum_{n=-\infty}^{\infty} |x[n]|^2$$

TABLE 10.1 Select Discrete-Time Fourier Transform Pairs

No.	$x[n]$	$X(\Omega)$	
1	$\delta[n-k]$	$e^{-jk\Omega}$	Integer k
2	$\gamma^n u[n]$	$\dfrac{e^{j\Omega}}{e^{j\Omega}-\gamma}$	$\lvert\gamma\rvert<1$
3	$-\gamma^n u[-(n+1)]$	$\dfrac{e^{j\Omega}}{e^{j\Omega}-\gamma}$	$\lvert\gamma\rvert>1$
4	$\gamma^{\lvert n\rvert}$	$\dfrac{1-\gamma^2}{1-2\gamma\cos\Omega+\gamma^2}$	$\lvert\gamma\rvert<1$
5	$n\gamma^n u[n]$	$\dfrac{\gamma e^{j\Omega}}{(e^{j\Omega}-\gamma)^2}$	$\lvert\gamma\rvert<1$
6	$\gamma^n\cos(\Omega_0 n+\theta)u[n]$	$\dfrac{e^{j\Omega}[e^{j\Omega}\cos\theta-\gamma\cos(\Omega_0-\theta)]}{e^{j2\Omega}-(2\gamma\cos\Omega_0)e^{j\Omega}+\gamma^2}$	$\lvert\gamma\rvert<1$
7	$u[n]-u[n-M]$	$\dfrac{\sin(M\Omega/2)}{\sin(\Omega/2)}e^{-j\Omega(M-1)/2}$	
8	$\dfrac{\Omega_c}{\pi}\operatorname{sinc}(\Omega_c n)$	$\displaystyle\sum_{k=-\infty}^{\infty}\operatorname{rect}\left(\frac{\Omega-2\pi k}{2\Omega_c}\right)$	$\Omega_c\le\pi$
9	$\dfrac{\Omega_c}{2\pi}\operatorname{sinc}^2\left(\dfrac{\Omega_c n}{2}\right)$	$\displaystyle\sum_{k=-\infty}^{\infty}\Delta\left(\frac{\Omega-2\pi k}{2\Omega_c}\right)$	$\Omega_c\le\pi$
10	$u[n]$	$\dfrac{e^{j\Omega}}{e^{j\Omega}-1}+\pi\displaystyle\sum_{k=-\infty}^{\infty}\delta(\Omega-2\pi k)$	
11	1 for all n	$2\pi\displaystyle\sum_{k=-\infty}^{\infty}\delta(\Omega-2\pi k)$	
12	$e^{j\Omega_0 n}$	$2\pi\displaystyle\sum_{k=-\infty}^{\infty}\delta(\Omega-\Omega_0-2\pi k)$	
13	$\cos\Omega_0 n$	$\pi\displaystyle\sum_{k=-\infty}^{\infty}\delta(\Omega-\Omega_0-2\pi k)+\delta(\Omega+\Omega_0-2\pi k)$	
14	$\sin\Omega_0 n$	$j\pi\displaystyle\sum_{k=-\infty}^{\infty}\delta(\Omega+\Omega_0-2\pi k)-\delta(\Omega-\Omega_0-2\pi k)$	
15	$(\cos\Omega_0 n)\,u[n]$	$\dfrac{e^{j2\Omega}-e^{j\Omega}\cos\Omega_0}{e^{j2\Omega}-2e^{j\Omega}\cos\Omega_0+1}+\dfrac{\pi}{2}\displaystyle\sum_{k=-\infty}^{\infty}\delta(\Omega-2\pi k-\Omega_0)+\delta(\Omega-2\pi k+\Omega_0)$	
16	$(\sin\Omega_0 n)\,u[n]$	$\dfrac{e^{j\Omega}\sin\Omega_0}{e^{j2\Omega}-2e^{j\Omega}\cos\Omega_0+1}+\dfrac{\pi}{2j}\displaystyle\sum_{k=-\infty}^{\infty}\delta(\Omega-2\pi k-\Omega_0)-\delta(\Omega-2\pi k+\Omega_0)$	

shows that the energy of an absolutely summable sequence is finite. However, not all finite-energy signals are absolutely summable. Signal $x[n] = \text{sinc}(n)$ is such an example. For such signals, the DTFT converges, not uniformly, but in the mean.†

To summarize, $X(\Omega)$ exists under a weaker condition

$$\sum_{n=-\infty}^{\infty} |x[n]|^2 < \infty \tag{10.21}$$

The DTFT under this condition is guaranteed to converge in the mean. Thus, the DTFT of the exponentially growing signal $\gamma^n u[n]$ does not exist when $|\gamma| > 1$ because the signal violates Eqs. (10.20) and (10.21). But the DTFT exists for the signal $\text{sinc}(n)$, which violates Eq. (10.20) but does satisfy Eq. (10.21) (see later, Ex. 10.6). In addition, if the use of $\delta(\Omega)$, the continuous-time impulse function, is permitted, we can even find the DTFT of some signals that violate both Eqs. (10.20) and (10.21). Such signals are not absolutely summable, nor do they have finite energy. For example, as seen from pairs 11 and 12 of Table 10.1, the DTFT of $x[n] = 1$ for all n and $x[n] = e^{j\Omega_0 n}$ exist, although they violate Eqs. (10.20) and (10.21).

EXAMPLE 10.3 DTFT of a Causal Exponential

Find the DTFT of $x[n] = \gamma^n u[n]$.

Using the definition, the DTFT is

$$X(\Omega) = \sum_{n=0}^{\infty} \gamma^n e^{-j\Omega n} = \sum_{n=0}^{\infty} (\gamma e^{-j\Omega})^n$$

This is an infinite geometric series with a common ratio $\gamma e^{-j\Omega}$. Therefore (see Sec. B.8.3),

$$X(\Omega) = \frac{1}{1 - \gamma e^{-j\Omega}}$$

provided $|\gamma e^{-j\Omega}| < 1$. But because $|e^{-j\Omega}| = 1$, this condition implies $|\gamma| < 1$. Therefore,

$$X(\Omega) = \frac{1}{1 - \gamma e^{-j\Omega}} \qquad |\gamma| < 1 \tag{10.22}$$

If $|\gamma| > 1$, $X(\Omega)$ does not converge. This result is in conformity with Eqs. (10.20) and (10.21). To determine magnitude and phase responses, we note that

---

† This means

$$\lim_{M\to\infty} \int_{-\pi}^{\pi} \left| X(\Omega) - \sum_{n=-M}^{M} x[n] e^{-j\Omega n} \right|^2 d\Omega = 0$$

$$X(\Omega) = \frac{1}{1 - \gamma \cos\Omega + j\gamma \sin\Omega} \tag{10.23}$$

so

$$|X(\Omega)| = \frac{1}{\sqrt{(1 - \gamma\cos\Omega)^2 + (\gamma \sin\Omega)^2}} = \frac{1}{\sqrt{1 + \gamma^2 - 2\gamma\cos\Omega}}$$

and

$$\angle X(\Omega) = -\tan^{-1}\left[\frac{\gamma \sin\Omega}{1 - \gamma\cos\Omega}\right]$$

Figure 10.5 shows $x[n] = \gamma^n u[n]$ and its spectra for $\gamma = 0.8$. Observe that the frequency spectra are continuous and periodic functions of Ω with the period 2π. As explained earlier, we need to use the spectrum only over the frequency interval of 2π. We often select this interval to be the fundamental frequency range $(-\pi, \pi)$.

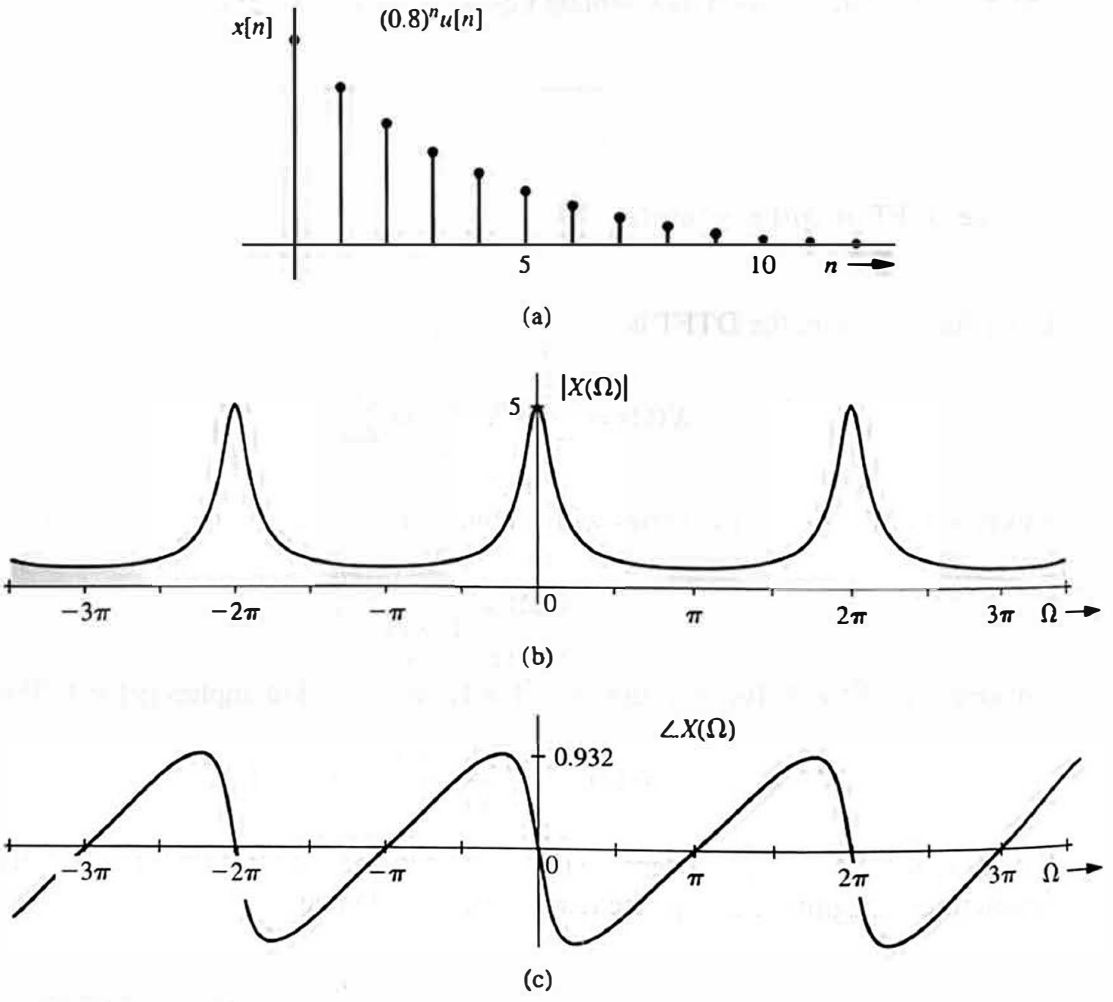

Figure 10.5 Exponential $\gamma^n u[n]$ and its frequency spectra.

The amplitude spectrum $|X(\Omega)|$ is an even function and the phase spectrum $\angle X(\Omega)$ is an odd function of Ω.

EXAMPLE 10.4 DTFT of an Anticausal Exponential

Find the DTFT of $\gamma^n u[-(n+1)]$ depicted in Fig. 10.6.

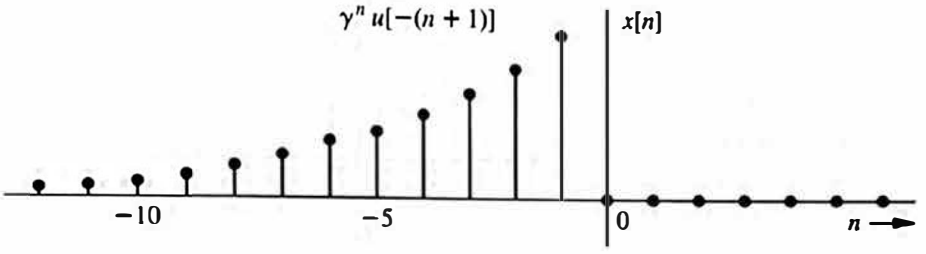

Figure 10.6 Exponential $\gamma^n u[-(n+1)]$.

Using the definition, the DTFT is

$$X(\Omega) = \sum_{n=-\infty}^{\infty} \gamma^n u[-(n+1)] e^{-j\Omega n} = \sum_{n=-1}^{-\infty} (\gamma e^{-j\Omega})^n = \sum_{n=-1}^{-\infty} \left(\frac{1}{\gamma} e^{j\Omega}\right)^{-n}$$

Setting $n = -m$ yields

$$x[n] = \sum_{m=1}^{\infty} \left(\frac{1}{\gamma} e^{j\Omega}\right)^m = \frac{1}{\gamma} e^{j\Omega} + \left(\frac{1}{\gamma} e^{j\Omega}\right)^2 + \left(\frac{1}{\gamma} e^{j\Omega}\right)^3 + \cdots$$

This is a geometric series with a common ratio $e^{j\Omega}/\gamma$. Therefore, from Sec. B.8.3,

$$X(\Omega) = \frac{1}{\gamma e^{-j\Omega} - 1} = \frac{1}{(\gamma \cos\Omega - 1) - j\gamma \sin\Omega}, \qquad |\gamma| > 1$$

Therefore,

$$|X(\Omega)| = \frac{1}{\sqrt{1 + \gamma^2 - 2\gamma \cos\Omega}} \qquad \text{and} \qquad \angle X(\Omega) = \tan^{-1}\left[\frac{\gamma \sin\Omega}{\gamma \cos\Omega - 1}\right]$$

Except for the change of sign, this Fourier transform (and the corresponding frequency spectra) is identical to that of $x[n] = \gamma^n u[n]$. Yet there is no ambiguity in determining the IDTFT of $X(\Omega) = 1/(\gamma e^{-j\Omega} - 1)$ because of the restrictions on the value of γ in each case. If $|\gamma| < 1$, then the inverse transform is $x[n] = -\gamma^n u[n]$. If $|\gamma| > 1$, it is $x[n] = \gamma^n[-(n+1)]$.

EXAMPLE 10.5 DTFT of a Rectangular Pulse

Find the DTFT of the discrete-time rectangular pulse illustrated in Fig. 10.7a. This pulse is also known as the 9-point rectangular window function.

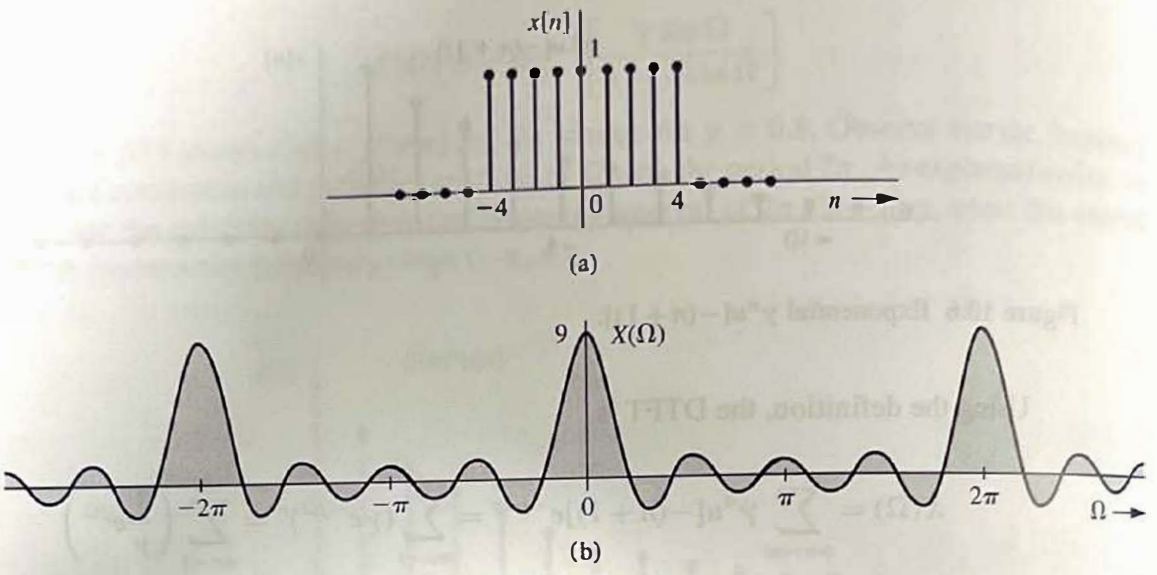

Figure 10.7 **(a)** Discrete-time gate pulse and **(b)** its Fourier spectrum.

$$X(\Omega) = \sum_{n=-\infty}^{\infty} x[n]e^{-j\Omega n} = \sum_{n=-(M-1)/2}^{(M-1)/2} (e^{-j\Omega})^n \qquad M = 9$$

This is a geometric progression with a common ratio $e^{-j\Omega}$ and (see Sec. B.8.3)

$$\begin{aligned} X(\Omega) &= \frac{e^{-j[(M+1)/2]\Omega} - e^{j[(M-1)/2]\Omega}}{e^{-j\Omega} - 1} \\ &= \frac{e^{-j\Omega/2}\left(e^{-j(M/2)\Omega} - e^{j(M/2)\Omega}\right)}{e^{-j\Omega/2}(e^{-j\Omega/2} - e^{j\Omega/2})} \\ &= \frac{\sin\left(\frac{M}{2}\Omega\right)}{\sin(0.5\Omega)} \\ &= \frac{\sin(4.5\Omega)}{\sin(0.5\Omega)} \qquad \text{for } M = 9 \end{aligned} \tag{10.24}$$

Figure 10.7b shows the spectrum $X(\Omega)$ for $M = 9$.

Discrete-Time Fourier Transform Using MATLAB

Within a scale factor, the DTFS is identical to the DFT and, therefore, the FFT. That is, the DTFS is just the FFT scaled by $\frac{1}{N_0}$. Combined with Eq. (10.13), we see that the DFT X_r of finite-duration signal $x[n]$ (repeated with period N_0 large enough to avoid overlap) is just samples of the DTFT $X(\Omega)$ taken at $\Omega = r\Omega_0$. That is, the length-N_0 DFT of signal $x[n]$ yields N_0 samples of its DTFT $X(\Omega)$ as

$$X_r = X(r\Omega_0), \qquad \text{where } \Omega_0 = \frac{2\pi}{N_0} \tag{10.25}$$

This relationship provides a way to use MATLAB's `fft` command to validate our DTFT calculations. By appropriately zero padding $x[n]$, we can obtain as many samples of $X(\Omega)$ as are desired. Let us demonstrate the process for the current example using $N_0 = 64$. Notice that in taking the DFT, we modulo-N_0 shift our rectangular pulse signal to occupy $0 \le n \le N_0 - 1$.

```
>> Omega = linspace(0,2*pi,1000);
>> X = sin(4.5*Omega)./sin(0.5*Omega);
>> X(mod(Omega,2*pi)==0) = 4.5/0.5; N_0 = 64; M = 9;
>> x = [ones(1,(M+1)/2) zeros(1,N_0-M) ones(1,(M-1)/2)];
>> Xr = fft(x); Omega_0 = 2*pi/N_0; r = 0:N_0-1;
>> plot(Omega,abs(X),'k-',Omega_0*r,abs(Xr),'k.'); axis([0 2*pi 0 9.5]);
>> xlabel('\Omega'); ylabel('|X(\Omega)|');
```

As shown in Fig. 10.8, the FFT samples align exactly with our analytical DTFT result.

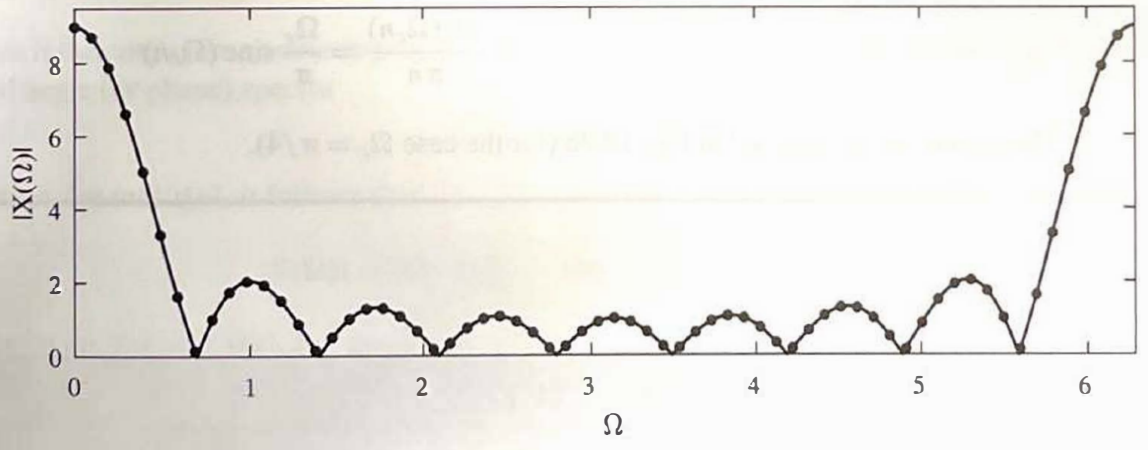

Figure 10.8 Using the FFT to verify the DTFT for Ex. 10.5.

EXAMPLE 10.6 Inverse DTFT of a Rectangular Spectrum

Find the inverse DTFT of the rectangular pulse spectrum described over the fundamental band ($|\Omega| \le \pi$) by $X(\Omega) = \text{rect}(\Omega/2\Omega_c)$ for $\Omega_c \le \pi$. Because of the periodicity property, $X(\Omega)$ repeats at the intervals of 2π, as shown in Fig. 10.9a.

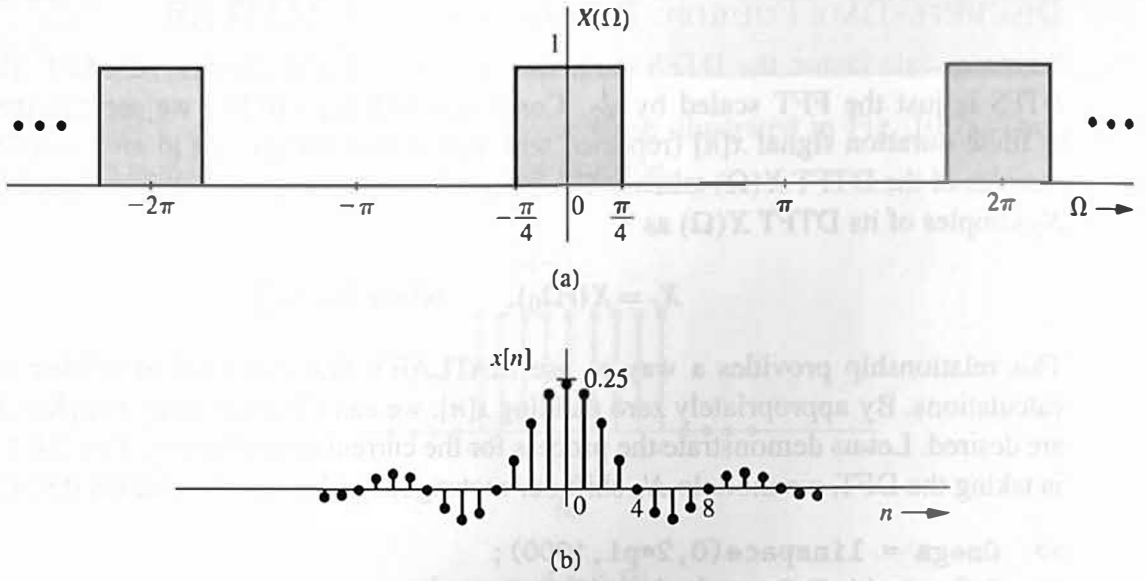

Figure 10.9 Periodic gate spectrum and its inverse discrete-time Fourier transform.

According to Eq. (10.17),

$$x[n] = \frac{1}{2\pi}\int_{-\pi}^{\pi} X(\Omega)e^{jn\Omega}\,d\Omega = \frac{1}{2\pi}\int_{-\Omega_c}^{\Omega_c} e^{jn\Omega}\,d\Omega$$

$$= \frac{1}{j2\pi n}e^{jn\Omega}\Big|_{-\Omega_c}^{\Omega_c} = \frac{\sin(\Omega_c n)}{\pi n} = \frac{\Omega_c}{\pi}\,\text{sinc}\,(\Omega_c n)$$

The signal $x[n]$ is depicted in Fig. 10.9b (for the case $\Omega_c = \pi/4$).

DRILL 10.4 Finding the DTFT

Find the DTFT and sketch the corresponding amplitude and phase spectra for

(a) $x[n] = \gamma^{|k|}$ with $|\gamma| < 1$

(b) $y[n] = \delta[n+1] - \delta[n-1]$

ANSWERS

(a) $X(\Omega) = \dfrac{1-\gamma^2}{1-2\gamma\cos\Omega+\gamma^2}$

(b) $|Y(\Omega)| = 2|\sin\Omega|$ and $\angle Y(\Omega) = (\pi/2)[1 - \text{sgn}(\sin\Omega)]$

10.3 PROPERTIES OF THE DTFT

A close connection exists between the DTFT and the CTFT (continuous-time Fourier transform). For this reason, which Sec. 10.4 discusses, the properties of the DTFT are very similar to those of the CTFT, as the following discussion shows.

LINEARITY OF THE DTFT

If

$$x_1[n] \Longleftrightarrow X_1(\Omega) \qquad \text{and} \qquad x_2[n] \Longleftrightarrow X_2(\Omega)$$

then

$$a_1x_1[n] + a_2x_2[n] \Longleftrightarrow a_1X_1(\Omega) + a_2X_2(\Omega)$$

The proof is trivial. The result can be extended to any finite sums.

CONJUGATE SYMMETRY OF $X(\Omega)$

In Eq. (10.19), we proved the *conjugation property*

$$x^*[n] \Longleftrightarrow X^*(-\Omega) \tag{10.26}$$

We also showed that as a consequence of this, when $x[n]$ is real, $X(\Omega)$ and $X(-\Omega)$ are conjugates, that is,

$$X(-\Omega) = X^*(\Omega)$$

This is the *conjugate symmetry* property. Since $X(\Omega)$ is generally complex, we have both amplitude and angle (or phase) spectra

$$X(\Omega) = |X(\Omega)|e^{j\angle X(\Omega)}$$

Hence, for real $x[n]$, it follows that

$$|X(\Omega)| = |X(-\Omega)| \qquad \text{and} \qquad \angle X(\Omega) = -\angle X(-\Omega)$$

Therefore, for real $x[n]$, the amplitude spectrum $|X(\Omega)|$ is an even function of Ω and the phase spectrum $\angle X(\Omega)$ is an odd function of Ω.

TIME AND FREQUENCY REVERSAL

Also called the reflection property, the time and frequency reversal property states that

$$x[-n] \Longleftrightarrow X(-\Omega) \tag{10.27}$$

Demonstration of this property is straightforward. From Eq. (10.18), the DTFT of $x[-n]$ is

$$\text{DTFT}\{x[-n]\} = \sum_{n=-\infty}^{\infty} x[-n]e^{-j\Omega n} = \sum_{m=-\infty}^{\infty} x[m]e^{j\Omega m} = X(-\Omega)$$

EXAMPLE 10.7 Using the Reflection Property

Use the time-frequency reversal property of Eq. (10.27) and pair 2 in Table 10.1 to derive pair 4 in Table 10.1.

Pair 2 states that

$$\gamma^n u[n] = \frac{e^{j\Omega}}{e^{j\Omega} - \gamma} \qquad |\gamma| < 1$$

Hence, from Eq. (10.27),

$$\gamma^{-n} u[-n] = \frac{e^{-j\Omega}}{e^{-j\Omega} - \gamma} \qquad |\gamma| < 1$$

Moreover, $\gamma^{|n|}$ could be expressed as a sum of $\gamma^n u[n]$ and $\gamma^{-n} u[-n]$, except that the impulse at $n = 0$ is counted twice (once from each of the two exponentials). Hence,

$$\gamma^{|n|} = \gamma^n u[n] + \gamma^{-n} u[-n] - \delta[n]$$

Combining these results and invoking the linearity property, we can write

$$\text{DTFT}\{\gamma^{|n|}\} = \frac{e^{j\Omega}}{e^{j\Omega} - \gamma} + \frac{e^{-j\Omega}}{e^{-j\Omega} - \gamma} - 1 = \frac{1 - \gamma^2}{1 - 2\gamma\cos\Omega + \gamma^2} \qquad |\gamma| < 1$$

which agrees with pair 4 in Table 10.1.

DRILL 10.5 Using the Reflection Property

In Table 10.1, derive pair 13 from pair 15 by using the time-reversal property of Eq. (10.27).

Multiplication by n: Frequency Differentiation

$$nx[n] \Longleftrightarrow j\frac{dX(\Omega)}{d\Omega} \tag{10.28}$$

The result follows immediately by differentiating both sides of Eq. (10.18) with respect to Ω.

EXAMPLE 10.8 Using the Frequency-Differentiation Property

Use the frequency-differentiation property of Eq. (10.28) and pair 2 in Table 10.1 to derive pair 5 in Table 10.1.

Pair 2 states that

$$\gamma^n u[n] = \frac{e^{j\Omega}}{e^{j\Omega} - \gamma} \qquad |\gamma| < 1$$

Hence, from Eq. (10.28),

$$n\gamma^n u[n] = j\frac{d}{d\Omega}\left\{\frac{e^{j\Omega}}{e^{j\Omega} - \gamma}\right\} = \frac{\gamma e^{j\Omega}}{(e^{j\Omega} - \gamma)^2} \qquad |\gamma| < 1$$

which agrees with pair 5 in Table 10.1.

Time-Shifting Property

If

$$x[n] \Longleftrightarrow X(\Omega)$$

then

$$x[n-k] \Longleftrightarrow X(\Omega)e^{-jk\Omega} \qquad \text{for integer } k \tag{10.29}$$

This property can be proved by direct substitution in the equation defining the direct transform. From Eq. (10.18), we obtain

$$x[n-k] \Longleftrightarrow \sum_{n=-\infty}^{\infty} x[n-k]e^{-j\Omega n} = \sum_{m=-\infty}^{\infty} x[m]e^{-j\Omega[m+k]}$$

$$= e^{-j\Omega k}\sum_{n=-\infty}^{\infty} x[m]e^{-j\Omega m} = e^{-jk\Omega}X(\Omega)$$

This result shows that *delaying a signal by k samples does not change its amplitude spectrum. The phase spectrum, however, is changed by* $-k\Omega$. This added phase is a linear function of Ω with slope $-k$.

Physical Explanation of Linear Phase

Time delay in a signal causes a linear phase shift in its spectrum. The heuristic explanation of this result is exactly parallel to that for continuous-time signals given in Sec. 4.3 (see Fig. 4.22).

EXAMPLE 10.9 Demonstrating Linear Phase

To demonstrate the linear phase associated with a time shift, find the DTFT of $x[n] = (1/4)\,\text{sinc}\,(\pi(n-2)/4)$, shown in Fig. 10.10a.

In Ex. 10.6, we found that

$$\frac{1}{4}\,\text{sinc}\left(\frac{\pi n}{4}\right) \Longleftrightarrow \sum_{m=-\infty}^{\infty} \text{rect}\left(\frac{\Omega - 2\pi m}{\pi/2}\right)$$

Use of the time-shifting property [Eq. (10.29)] yields (for integer k)

$$\frac{1}{4}\,\text{sinc}\left(\frac{\pi(n-2)}{4}\right) \Longleftrightarrow \sum_{m=-\infty}^{\infty} \text{rect}\left(\frac{\Omega - 2\pi m}{\pi/2}\right) e^{-j2\Omega}$$

The spectrum of the shifted signal is shown in Fig. 10.10b.

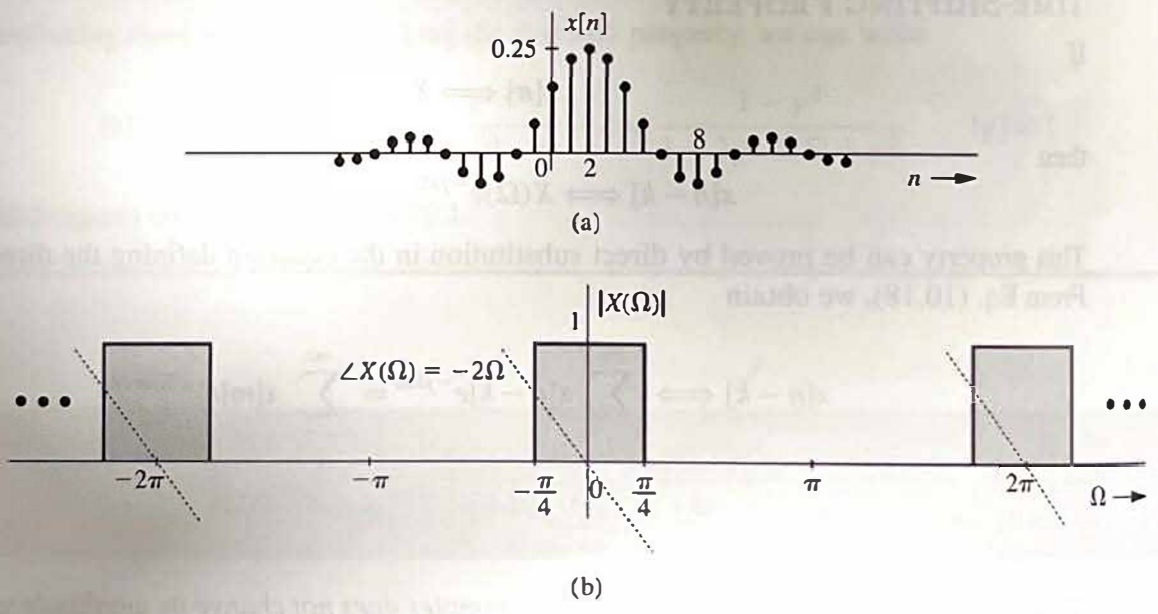

Figure 10.10 Shifted signal $x[n]$ possesses spectrum $X(\Omega)$ with linear phase component -2Ω.

DRILL 10.6 Using the Time-Shifting Property

Verify the result in Eq. (10.24) from pair 7 in Table 10.1 and the time-shifting property of the DTFT.

Frequency-Shifting Property

If

$$x[n] \Longleftrightarrow X(\Omega)$$

then

$$x[n]e^{j\Omega_c n} \Longleftrightarrow X(\Omega - \Omega_c) \tag{10.30}$$

This property is the dual of the time-shifting property. To prove the frequency-shifting property, we use Eq. (10.18) as

$$x[n]e^{j\Omega_c n} \Longleftrightarrow \sum_{n=-\infty}^{\infty} x[n]e^{j\Omega_c n}e^{-j\Omega n} = \sum_{n=-\infty}^{\infty} x[n]e^{-j(\Omega-\Omega_c)n} = X(\Omega - \Omega_c)$$

From this result, it follows that

$$x[n]e^{-j\Omega_c n} \Longleftrightarrow X(\Omega + \Omega_c)$$

Adding this pair to the pair in Eq. (10.30), we obtain

$$x[n]\cos(\Omega_c n) \Longleftrightarrow \tfrac{1}{2}\{X(\Omega - \Omega_c) + X(\Omega + \Omega_c)\} \tag{10.31}$$

This is the *modulation property*.

Multiplying both sides of pair (10.30) by $e^{j\theta}$, we obtain

$$x[n]e^{j(\Omega_c n+\theta)} \Longleftrightarrow X(\Omega - \Omega_c)e^{j\theta}$$

Using this pair, we can generalize the modulation property as

$$x[n]\cos(\Omega_c n + \theta) \Longleftrightarrow \tfrac{1}{2}\{X(\Omega - \Omega_c)e^{j\theta} + X(\Omega + \Omega_c)e^{-j\theta}\}$$

EXAMPLE 10.10 Modulation Property

A signal $x[n] = \text{sinc}(\pi n/4)$ modulates a carrier $\cos \Omega_c n$. Find and sketch the spectrum of the modulated signal $x[n]\cos \Omega_c n$ for

(a) $\Omega_c = \pi/2$

(b) $\Omega_c = 7\pi/8 = 0.875\pi$

(a) For $x[n] = \text{sinc}(\pi n/4)$, we find (Table 10.1, pair 8)

$$X(\Omega) = 4\sum_{m=-\infty}^{\infty} \text{rect}\left(\frac{\Omega - 2\pi m}{\pi/2}\right)$$

Figure 10.11a shows the DTFT $X(\Omega)$. From the modulation property of Eq. (10.31), we obtain

$$x[n]\cos(0.5\pi n) \Longleftrightarrow 2\sum_{m=-\infty}^{\infty} \text{rect}\left(\frac{\Omega - 0.5\pi - 2\pi m}{0.5\pi}\right) + \text{rect}\left(\frac{\Omega + 0.5\pi - 2\pi m}{0.5\pi}\right)$$

Figure 10.11b shows half the $X(\Omega)$ shifted by $\pi/2$, and Fig. 10.11c shows half the $X(\Omega)$ shifted by $-\pi/2$. The spectrum of the modulated signal is obtained by adding these two shifted spectra and multiplying by half, as shown in Fig. 10.11d.

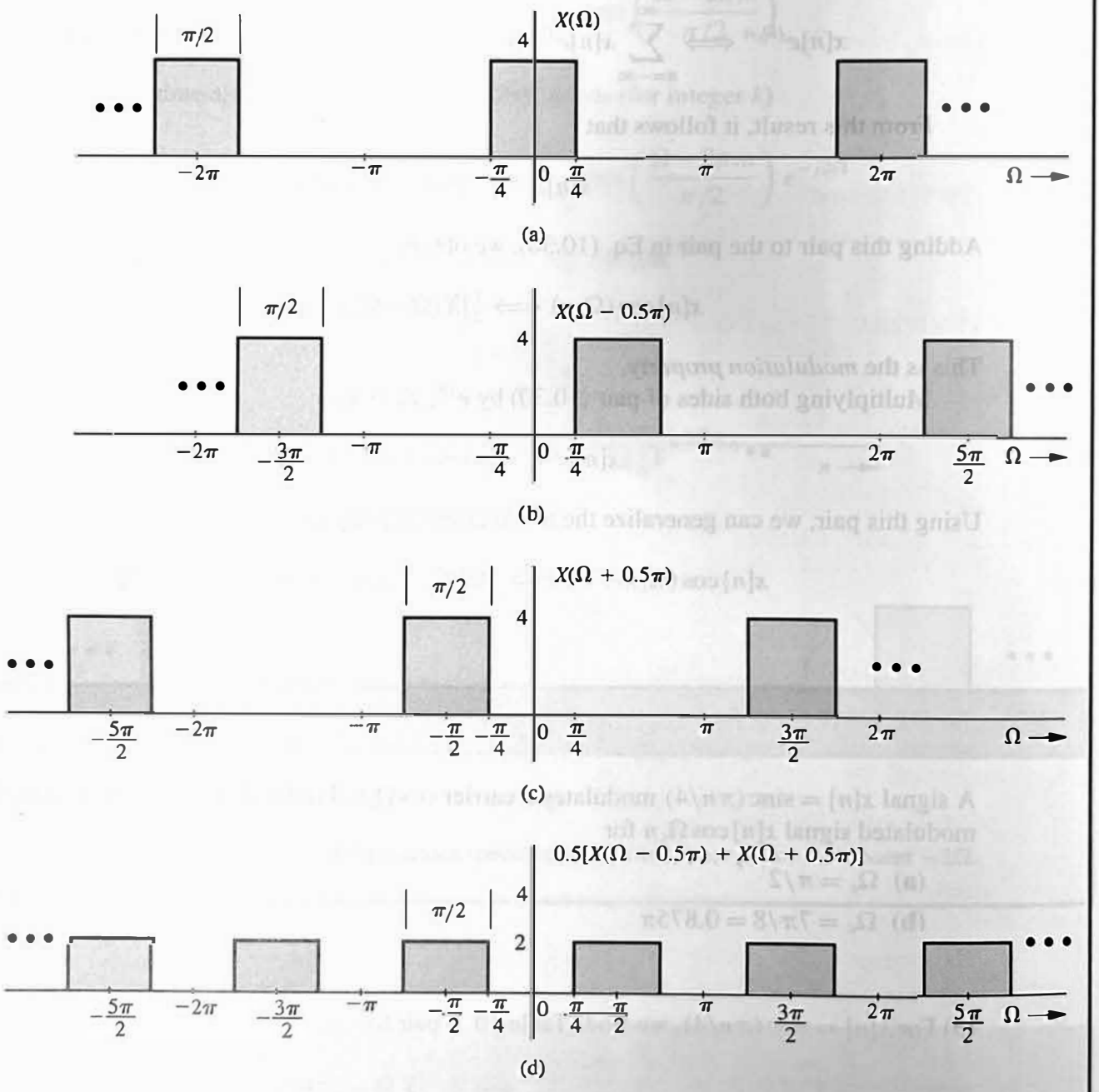

Figure 10.11 Instance of modulation for Ex. 10.10a.

(b) Figure 10.12a shows $X(\Omega)$, which is the same as that in part (a). For $\Omega_c = 7\pi/8 = 0.875\pi$, the modulation property of Eq. (10.31) yields

$$x[n]\cos(0.875\pi n) \Longleftrightarrow 2\sum_{m=-\infty}^{\infty} \text{rect}\left(\frac{\Omega - 0.875\pi - 2\pi m}{0.5\pi}\right) + \text{rect}\left(\frac{\Omega + 0.875\pi - 2\pi m}{0.5\pi}\right)$$

Figure 10.12b shows $X(\Omega)$ shifted by $7\pi/8$, and Fig. 10.12c shows $X(\Omega)$ shifted by $-7\pi/8$. The spectrum of the modulated signal is obtained by adding these two shifted spectra and multiplying by half, as shown in Fig. 10.12d. In this case, the two shifted spectra overlap. Since the operation of modulation thus causes aliasing, it does not achieve the desired effect of spectral shifting. In this example, to realize spectral shifting without aliasing requires $\Omega_c \leq 3\pi/4$.

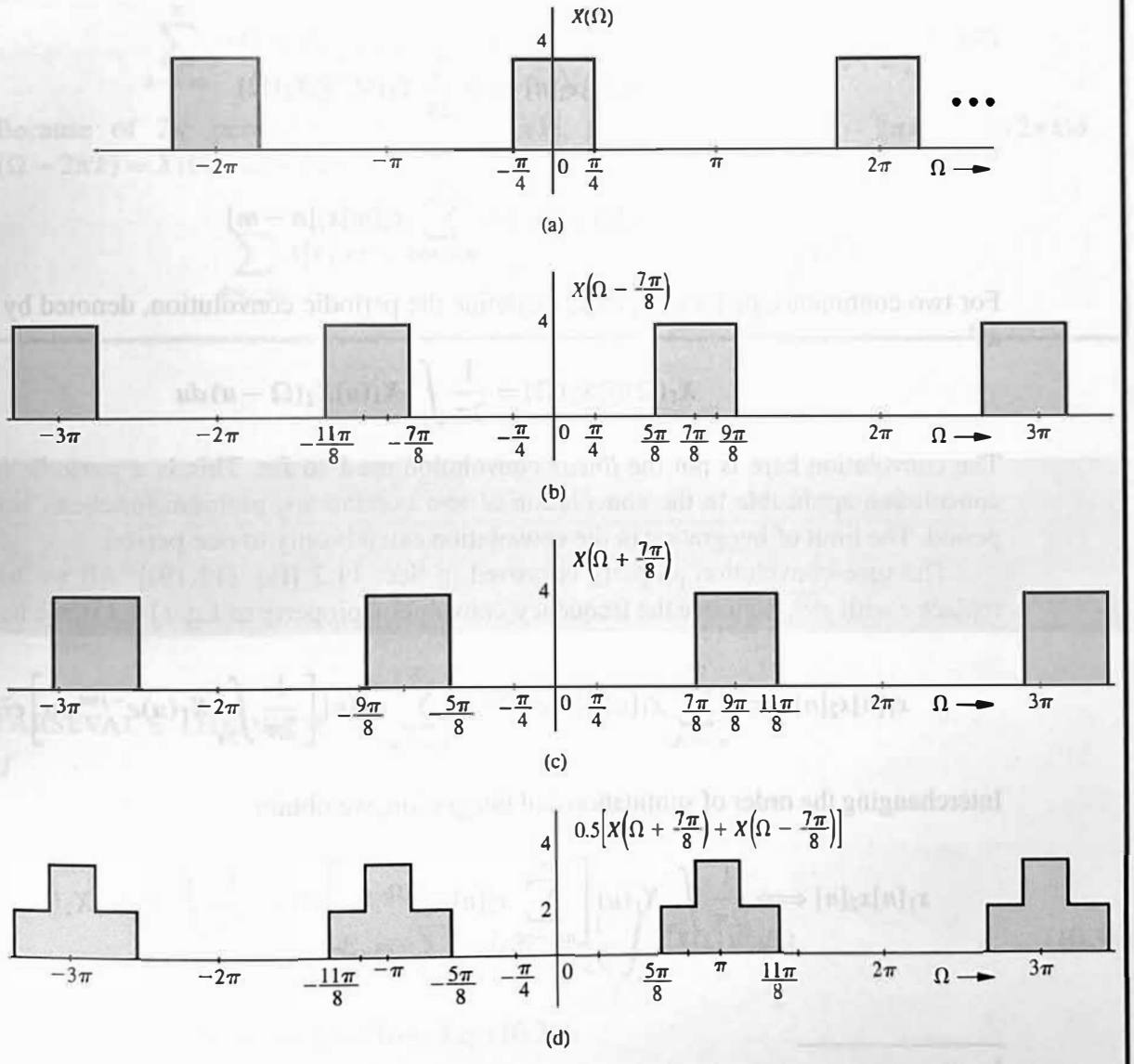

Figure 10.12 Instance of modulation for Ex. 10.10b.

DRILL 10.7 Using the Frequency-Shifting Property

In Table 10.1, derive pairs 12 and 13 from pair 11 and the frequency-shifting/modulation property.

Time- and Frequency-Convolution Property

If

$$x_1[n] \Longleftrightarrow X_1(\Omega) \qquad \text{and} \qquad x_2[n] \Longleftrightarrow X_2(\Omega)$$

then

$$x_1[n] * x_2[n] \Longleftrightarrow X_1(\Omega)X_2(\Omega) \tag{10.32}$$

and

$$x_1[n]x_2[n] \Longleftrightarrow \frac{1}{2\pi} X_1(\Omega) \circledast X_2(\Omega) \tag{10.33}$$

where

$$x_1[n] * x_2[n] = \sum_{m=-\infty}^{\infty} x_1[m]x_2[n-m]$$

For two continuous, periodic signals, we define the periodic convolution, denoted by symbol $\circledast$, as†

$$X_1(\Omega) \circledast X_2(\Omega) = \frac{1}{2\pi} \int_{2\pi} X_1(u)X_2(\Omega - u)\, du$$

The convolution here is not the *linear* convolution used so far. This is a *periodic* (or *circular*) convolution applicable to the convolution of two continuous, periodic functions with the same period. The limit of integration in the convolution extends only to one period.

The time-convolution property is proved in Sec. 11.2 [Eq. (11.19)]. All we have to do is replace z with $e^{j\Omega}$. To prove the frequency-convolution property of Eq. (10.33), we have

$$x_1[n]x_2[n] \Longleftrightarrow \sum_{n=-\infty}^{\infty} x_1[n]x_2[n]e^{-j\Omega n} = \sum_{n=-\infty}^{\infty} x_2[n] \left[\frac{1}{2\pi} \int_{2\pi} X_1(u)e^{-jnu}\, du \right] e^{-j\Omega n}$$

Interchanging the order of summation and integration, we obtain

$$x_1[n]x_2[n] \Longleftrightarrow \frac{1}{2\pi} \int_{2\pi} X_1(u) \left[\sum_{n=-\infty}^{\infty} x_2[n]e^{-j(\Omega-u)n} \right] du = \frac{1}{2\pi} \int_{2\pi} X_1(u)X_2(\Omega - u)\, du$$

† In Eq. (5.20), we defined periodic convolution for two discrete, periodic sequences in a different way. Although we are using the same symbol $\circledast$ for both discrete and continuous cases, the meaning will be clear from the context.

EXAMPLE 10.11 DTFT of an Accumulator System

If $x[n] \Longleftrightarrow X(\Omega)$, then show that $\sum_{k=-\infty}^{n} x[k] \Longleftrightarrow \pi X(0) \sum_{k=-\infty}^{\infty} \delta(\Omega - 2\pi k) + \frac{e^{j\Omega}}{e^{j\Omega} - 1} X(\Omega)$.

To begin, we notice that

$$x[n] * u[n] = \sum_{k=-\infty}^{\infty} x[k]u[n-k] = \sum_{k=-\infty}^{n} x[k]$$

Applying the time-convolution property of Eq. (10.32) and pair 10 in Table 10.1, it follows that

$$\sum_{k=-\infty}^{n} x[k] = x[n] * u[n] \Longleftrightarrow X(\Omega)\left(\pi \sum_{k=-\infty}^{\infty} \delta(\Omega - 2\pi k) + \frac{e^{j\Omega}}{e^{j\Omega} - 1}\right)$$

Because of 2π periodicity, $X(0) = X(2\pi k)$. Moreover, $X(\Omega)\delta(\Omega - 2\pi k) = X(2\pi k)\delta(\Omega - 2\pi k) = X(0)\delta(\Omega - 2\pi k)$. Hence,

$$\sum_{k=-\infty}^{n} x[k] \Longleftrightarrow \pi X(0) \sum_{k=-\infty}^{\infty} \delta(\Omega - 2\pi k) + \frac{e^{j\Omega}}{e^{j\Omega} - 1} X(\Omega)$$

DRILL 10.8 Using the Frequency-Convolution Property

In Table 10.1, derive pair 9 from pair 8, assuming $\Omega_c \leq \pi/2$. Use the frequency-convolution property.

Parseval's Theorem

If

$$x[n] \Longleftrightarrow X(\Omega)$$

then E_x, the energy of $x[n]$, is given by

$$E_x = \sum_{n=-\infty}^{\infty} |x[n]|^2 = \frac{1}{2\pi} \int_{2\pi} |X(\Omega)|^2 d\Omega \tag{10.34}$$

To prove this property, we have from Eq. (10.26):

$$X^*(\Omega) = \sum_{n=-\infty}^{\infty} x^*[n] e^{j\Omega n}$$

Now,

$$\sum_{n=-\infty}^{\infty} |x[n]|^2 = \sum_{n=-\infty}^{\infty} x^*[n]x[n] = \sum_{n=-\infty}^{\infty} x^*[n]\left[\frac{1}{2\pi}\int_{2\pi} X(\Omega)e^{j\Omega n}\,d\Omega\right]$$

$$= \frac{1}{2\pi}\int_{2\pi} X(\Omega)\left[\sum_{n=-\infty}^{\infty} x^*[n]e^{j\Omega n}\right]d\Omega$$

$$= \frac{1}{2\pi}\int_{2\pi} X(\Omega)X^*(\Omega)\,d\Omega = \frac{1}{2\pi}\int_{2\pi} |X(\Omega)|^2\,d\Omega$$

Table 10.2 summarizes Parseval's theorem and the other important properties of the DTFT.

TABLE 10.2 Properties of the DTFT

Operation	$x[n]$	$X(\Omega)$
Linearity	$a_1x_1[n] + a_2x_2[n]$	$a_1X_1(\Omega) + a_2X_2(\Omega)$
Conjugation	$x^*[n]$	$X^*(-\Omega)$
Scalar multiplication	$ax[n]$	$aX(\Omega)$
Multiplication by n	$nx[n]$	$j\dfrac{dX(\Omega)}{d\Omega}$
Time reversal	$x[-n]$	$X(-\Omega)$
Time shifting	$x[n-k]$	$X(\Omega)e^{-jk\Omega}$ k integer
Frequency shifting	$x[n]e^{j\Omega_c n}$	$X(\Omega-\Omega_c)$
Time convolution	$x_1[n] * x_2[n]$	$X_1(\Omega)X_2(\Omega)$
Frequency convolution	$x_1[n]x_2[n]$	$\dfrac{1}{2\pi}\displaystyle\int_{2\pi} X_1[u]X_2[\Omega-u]\,du$
Parseval's theorem	$E_x = \displaystyle\sum_{n=-\infty}^{\infty} \lvert x[n]\rvert^2$	$E_x = \dfrac{1}{2\pi}\displaystyle\int_{2\pi} \lvert X(\Omega)\rvert^2\,d\Omega$

EXAMPLE 10.12 Using Parseval's Theorem to Find Signal Energy

Find the energy of $x[n] = \text{sinc}\,(\Omega_c n)$, assuming $\Omega_c < \pi$.

From pair 8, Table 10.1, the fundamental band spectrum of $x[n]$ is

$$\text{sinc}(\Omega_c n) \Longleftrightarrow \frac{\pi}{\Omega_c}\,\text{rect}\left(\frac{\Omega}{2\Omega_c}\right) \qquad |\Omega| \le \pi$$

From Parseval's theorem [Eq. (10.34)], we have

$$E_x = \frac{1}{2\pi}\int_{-\pi}^{\pi} \frac{\pi^2}{\Omega_c^2}\left[\text{rect}\left(\frac{\Omega}{2\Omega_c}\right)\right]^2 d\Omega$$

Because $\text{rect}(\Omega/2\Omega_c) = 1$ over $|\Omega| \leq \Omega_c$ and is zero otherwise, the preceding integral yields

$$E_x = \frac{1}{2\pi}\left(\frac{\pi^2}{\Omega_c^2}\right)(2\Omega_c) = \frac{\pi}{\Omega_c}$$

10.4 DTFT Connection with the CTFT

Consider a continuous-time signal $x_c(t)$ (Fig. 10.13a) with the Fourier transform $X_c(\omega)$ bandlimited to B Hz (Fig. 10.13b). This signal is sampled with a sampling interval T. The sampling rate is at least equal to the Nyquist rate; that is, $T \leq 1/2B$. The sampled signal $\bar{x}_c(t)$ (Fig. 10.13c) can be expressed as

$$\bar{x}_c(t) = \sum_{n=-\infty}^{\infty} x_c(nT)\,\delta(t-nT)$$

The continuous-time Fourier transform of the foregoing equation yields

$$\bar{X}_c(\omega) = \sum_{n=-\infty}^{\infty} x_c(nT)\,e^{-jnT\omega} \tag{10.35}$$

In Sec. 5.1 (Fig. 5.1f), we showed that $\bar{X}_c(\omega)$ is $X_c(\omega)/T$ repeating periodically with a period $\omega_s = 2\pi/T$, as illustrated in Fig. 10.13d. Let us construct a discrete-time signal $x[n]$ such that its nth sample value is equal to the value of the nth sample of $x_c(t)$, as depicted in Fig. 10.13e, that is,

$$x[n] = x_c(nT) \tag{10.36}$$

Now, $X(\Omega)$, the DTFT of $x[n]$, is given by

$$X(\Omega) = \sum_{n=-\infty}^{\infty} x[n]\,e^{-jn\Omega} = \sum_{n=-\infty}^{\infty} x_c(nT)\,e^{-jn\Omega}$$

Comparison of this equation with Eq. (10.35) shows that letting $\omega T = \Omega$ in $\bar{X}_c(\omega)$ yields $X(\Omega)$, that is,

$$X(\Omega) = \bar{X}_c(\omega)|_{\omega T=\Omega}$$

Alternately, $X(\Omega)$ can be obtained from $\bar{X}_c(\omega)$ by replacing ω with Ω/T, that is,

$$X(\Omega) = \bar{X}_c\left(\frac{\Omega}{T}\right) \tag{10.37}$$

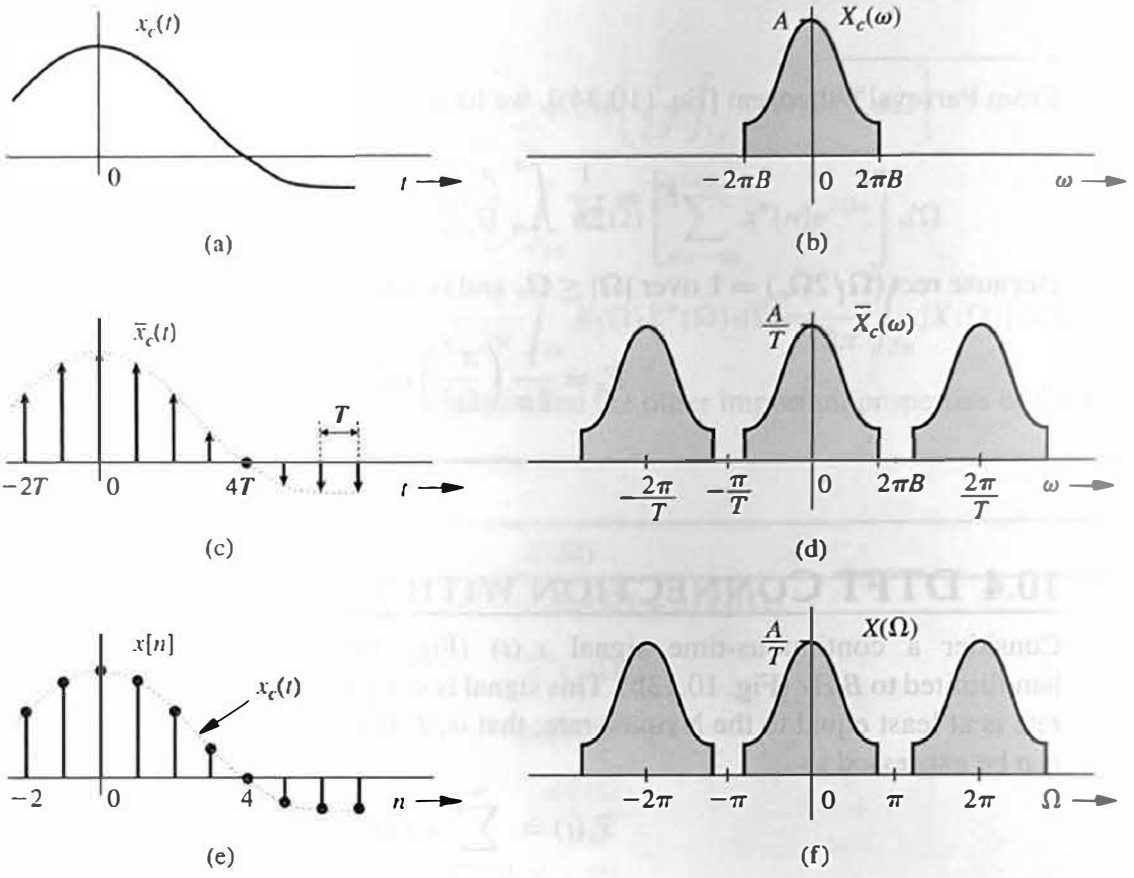

Figure 10.13 Connection between the DTFT and the Fourier transform.

Therefore, $X(\Omega)$ is identical to $\overline{X}_c(\omega)$, frequency-scaled by factor T, as shown in Fig. 10.13f. Thus, $\omega = 2\pi/T$ in Fig. 10.13d corresponds to $\Omega = 2\pi$ in Fig. 10.13f.

In the above derivation, we did not have to use the assumption that $x_c(t)$ is bandlimited or that $x_c(t)$ is sampled at a rate at least equal to its Nyquist rate. If the signal were not bandlimited, the only difference in our discussion would be in the sketches in Fig. 10.13. For instance, $X_c(\omega)$ in Fig. 10.13b would not be bandlimited. This fact would cause overlapping (aliasing) of repeating cycles of $X_c(\omega)$ in Figs. 10.13d and 10.13f. A similar thing happens when the signal $x_c(t)$ is sampled below the Nyquist rate.†

10.4.1 DTFT of Downsampled and Interpolated Signals

We can use Eq. (10.37) to find the DTFT of downsampled and interpolated signals, which are explained in Fig. 8.5. Consider a signal $x[n]$ and its DTFT $X(\Omega)$, as illustrated in Figs. 10.14a

† In case the signal is not bandlimited and/or the sampling rate is below its Nyquist rate, the samples $x_c(nT)$ can be interpreted as the Nyquist samples of the inverse Fourier transform of the first cycle (centered at $\omega = 0$) of $T\overline{X}_c(\omega)$.

and 10.14b. Figure 10.14c shows the downsampled signal $x[2n]$. If $x[n]$ is considered to be the sample sequence of a continuous-time signal $x_c(t)$, then $x[2n]$ is the sample sequence of $x_c(2t)$, whose Fourier transform is given by $\frac{1}{2}X_c(\omega/2)$ according to Eq. (4.26).† As seen in Eq. (10.37), $X(\Omega)$ is $X_c(\Omega/T)$ repeating periodically with period 2π, and the DTFT of $x[2n]$ is $\frac{1}{2}X_c(\Omega/2T)$ repeating periodically with period 2π. Note that $X(\Omega/2T)$ is $X(\Omega/T)$ time-expanded by a factor of 2, as shown in Figs. 10.14b and 10.14d. If we downsample by some factor M (i.e., we select every Mth element in the sequence), the resulting sequence is $x[Mn]$. Using the above argument, it follows that in the fundamental frequency range, the DTFT of $x[Mn]$ will be $1/M$ times $X(\Omega/M)$, and it repeats periodically with period 2π. If M is too large so that the first cycle of $X(\Omega/M)$ goes beyond π, the successive cycles of $X(\Omega/M)$ will overlap, as illustrated in Fig. 10.14d.

Now consider the interpolated signal $x_i[n]$ in Fig. 10.14c. This signal is $x[n/2]$ (obtained by upsampling $x[n]$ by a factor of 2), with the alternate (missing) points filled by interpolated values obtained by ideal lowpass filtering. If the envelope of $x[n]$ is $x_c(t)$, then the envelope of $x_i[n]$ is $x_c(t/2)$, whose Fourier transform is $2X_c(2\omega)$. Thus, in the fundamental frequency range, the spectrum of $x_i[n]$ is 2 times $X(\Omega)$ compressed by a factor of 2 along the frequency axis, and periodically repeating with period 2π as depicted in Fig. 10.14f. Using a similar argument, we can generalize this result for an upsampled signal $x[n/L]$ with missing values filled by ideal

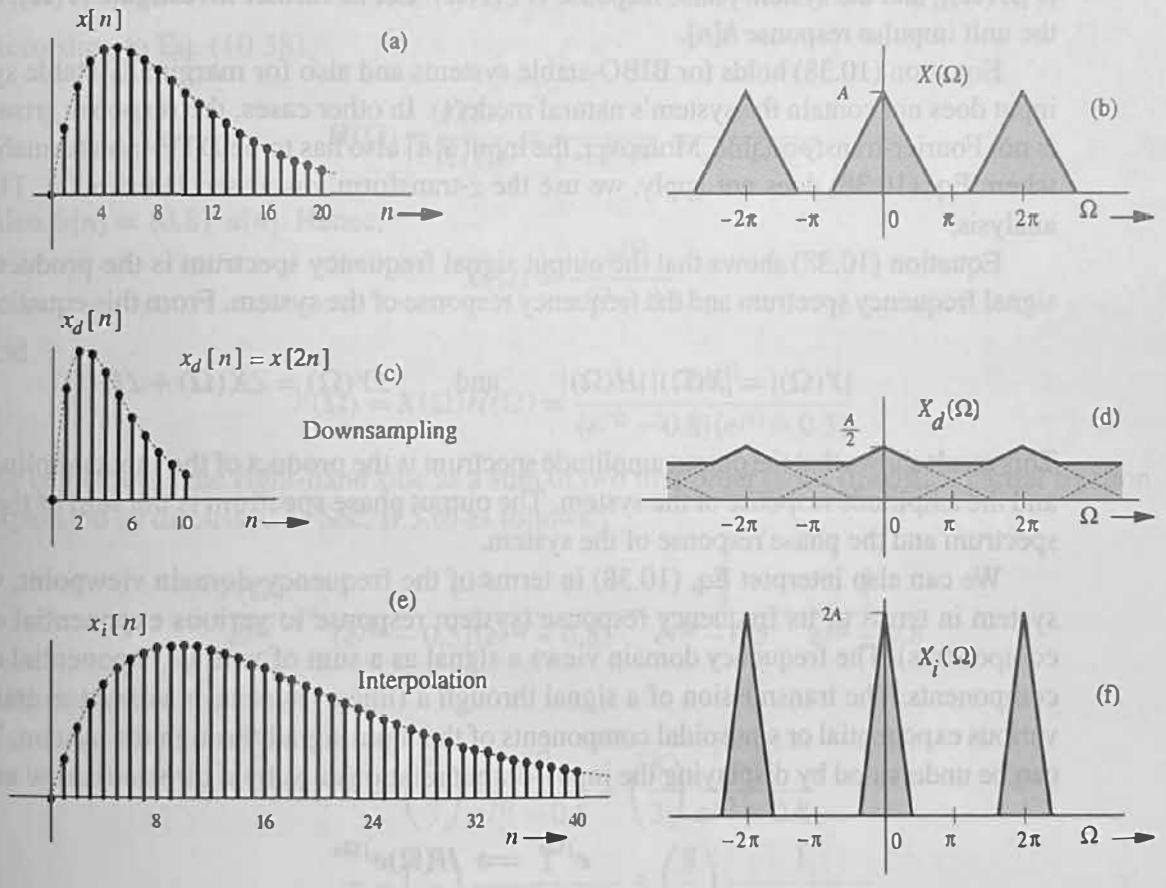

Figure 10.14 Spectra of downsampled and interpolated signals.

† Here, $X_c(\omega)$ should be interpreted as the first cycle (centered at $\omega = 0$) of $T\overline{X}_c(\omega)$.

interpolation. In this case, the spectrum in the fundamental frequency range will be L times $X(L\Omega)$ [$X(\Omega)$ frequency-compressed by factor L] repeating periodically with period 2π.

10.5 LTI DISCRETE-TIME SYSTEM ANALYSIS BY DTFT

Consider a linear, time-invariant, discrete-time system with the unit impulse response $h[n]$. We shall find the (zero-state) system response $y[n]$ for the input $x[n]$. Let

$$x[n] \Longleftrightarrow X(\Omega) \qquad y[n] \Longleftrightarrow Y(\Omega) \qquad \text{and} \qquad h[n] \Longleftrightarrow H(\Omega)$$

Because $y[n] = x[n] * h[n]$, it follows from Eq. (10.32) that

$$Y(\Omega) = X(\Omega)H(\Omega) \tag{10.38}$$

This result is similar to that obtained for continuous-time systems. Like the continuous-time case, $H(\Omega)$ is the system frequency response, a complex function of Ω. The system magnitude response is $|H(\Omega)|$, and the system phase response is $\angle H(\Omega)$. Let us further investigate $H(\Omega)$, the DTFT of the unit impulse response $h[n]$.

Equation (10.38) holds for BIBO-stable systems and also for marginally stable systems if the input does not contain the system's natural mode(s). In other cases, the response grows with n and is not Fourier-transformable. Moreover, the input $x[n]$ also has to be DTF-transformable. For cases where Eq. (10.38) does not apply, we use the z-transform, discussed later in Ch. 11, for system analysis.

Equation (10.38) shows that the output signal frequency spectrum is the product of the input signal frequency spectrum and the frequency response of the system. From this equation, we obtain

$$|Y(\Omega)| = |X(\Omega)|\,|H(\Omega)| \qquad \text{and} \qquad \angle Y(\Omega) = \angle X(\Omega) + \angle H(\Omega)$$

This result shows that the output amplitude spectrum is the product of the input amplitude spectrum and the amplitude response of the system. The output phase spectrum is the sum of the input phase spectrum and the phase response of the system.

We can also interpret Eq. (10.38) in terms of the frequency-domain viewpoint, which sees a system in terms of its frequency response (system response to various exponential or sinusoidal components). The frequency domain views a signal as a sum of various exponential or sinusoidal components. The transmission of a signal through a (linear) system is viewed as transmission of various exponential or sinusoidal components of the input signal through the system. This concept can be understood by displaying the input–output relationships by a directed arrow as follows:

$$e^{j\Omega n} \Longrightarrow H(\Omega)e^{j\Omega n}$$

which shows that the system response to $e^{j\Omega n}$ is $H(\Omega)e^{j\Omega n}$, and

$$x[n] = \frac{1}{2\pi}\int_{2\pi} X(\Omega)e^{j\Omega n}\,d\Omega$$

which shows $x[n]$ as a sum of everlasting exponential components. Invoking the linearity property, we obtain

$$y[n] = \frac{1}{2\pi}\int_{2\pi} X(\Omega)H(\Omega)e^{j\Omega n}\,d\Omega$$

which gives $y[n]$ as a sum of responses to all input components and is equivalent to Eq. (10.38). Thus, $X(\Omega)$ is the input spectrum and $Y(\Omega)$ is the output spectrum, given by $X(\Omega)H(\Omega)$.

EXAMPLE 10.13 LTID System Analysis by the DTFT

An LTID system is specified by the equation $y[n] - 0.5y[n-1] = x[n]$. Find $H(\Omega)$, the frequency response of this system. Determine the (zero-state) response $y[n]$ if the input $x[n] = (0.8)^n u[n]$.

Let $x[n] \Longleftrightarrow X(\Omega)$ and $y[n] \Longleftrightarrow Y(\Omega)$. Taking the DTFT of the system's difference equation yields

$$(1 - 0.5e^{-j\Omega})Y(\Omega) = X(\Omega)$$

According to Eq. (10.38),

$$H(\Omega) = \frac{Y(\Omega)}{X(\Omega)} = \frac{1}{1 - e^{-j\Omega}} = \frac{e^{j\Omega}}{e^{j\Omega} - 0.5}$$

Also, $x[n] = (0.8)^n u[n]$. Hence,

$$X(\Omega) = \frac{e^{j\Omega}}{e^{j\Omega} - 0.8}$$

and

$$Y(\Omega) = X(\Omega)H(\Omega) = \frac{2e^{j\Omega}}{(e^{j\Omega} - 0.8)(e^{j\Omega} - 0.5)}$$

We can express the right-hand side as a sum of two first-order terms (modified partial fraction expansion as discussed in Sec. B.5.6) as follows:[†]

$$\frac{Y(\Omega)}{e^{j\Omega}} = \frac{e^{j\Omega}}{(e^{j\Omega} - 0.5)(e^{j\Omega} - 0.8)} = \frac{-\frac{5}{3}}{e^{j\Omega} - 0.5} + \frac{\frac{8}{3}}{e^{j\Omega} - 0.8}$$

Consequently,

$$\begin{aligned} Y(\Omega) &= -\left(\frac{5}{3}\right)\frac{e^{j\Omega}}{e^{j\Omega} - 0.5} + \left(\frac{8}{3}\right)\frac{e^{j\Omega}}{e^{j\Omega} - 0.8} \\ &= -\left(\frac{5}{3}\right)\frac{1}{1 - 0.5e^{-j\Omega}} + \left(\frac{8}{3}\right)\frac{1}{1 - 0.8e^{-j\Omega}} \end{aligned}$$

[†] Here, $Y(\Omega)$ is a function of variable $e^{j\Omega}$. Hence, $x = e^{j\Omega}$ for the purpose of comparison with the expression in Sec. B.5.6.

From entry 2 of Table 10.1, the inverse DTFT of this equation is

$$y[n] = \left[-\tfrac{5}{3}(0.5)^n + \tfrac{8}{3}(0.8)^n\right] u[n]$$

This example demonstrates the procedure for using the DTFT to determine an LTID system response. It is similar to the Fourier transform method in the analysis of LTIC systems. As in the case of the Fourier transform, this method can be used only if the system is asymptotically or BIBO-stable and if the input signal is DTF-transformable.† We shall not belabor this method further because it is clumsier and more restrictive than the z-transform method discussed later in Ch. 11. In the z-transform, we generalize the frequency variable $j\Omega$ to $\sigma + j\Omega$ so that the resulting exponentials can grow or decay with n. This procedure is similar to what we did in the continuous-time case by generalizing the frequency variable $j\omega$ to $s = \sigma + j\omega$ (from a Fourier to Laplace transform).

10.5.1 Distortionless Transmission

In several applications, digital signals are passed through LTI systems, and we require that the output waveform be a replica of the input waveform. As in the continuous-time case, transmission is said to be distortionless if the input $x[n]$ and the output $y[n]$ satisfy the condition

$$y[n] = G_0 x[n - n_d]$$

Here, n_d, the delay (in samples), is assumed to be an integer. Taking the Fourier transform yields

$$Y(\Omega) = G_0 X(\Omega) e^{-j\Omega n_d}$$

But

$$Y(\Omega) = X(\Omega) H(\Omega)$$

Therefore,

$$H(\Omega) = G_0 e^{-j\Omega n_d}$$

This is the frequency response required for distortionless transmission. From this equation, it follows that

$$|H(\Omega)| = G_0 \qquad \text{and} \qquad \angle H(\Omega) = -\Omega n_d \tag{10.39}$$

Thus, for distortionless transmission, the amplitude response $|H(\Omega)|$ must be a constant, and the phase response $\angle H(\Omega)$ must be a linear function of Ω with slope $-n_d$, where n_d is the delay in the number of samples with respect to input (Fig. 10.15). These are precisely the characteristics of an ideal delay of n_d samples with a gain of G_0 [see Eq. (10.29)].

Measure of Delay Variation

For distortionless transmission, we require a *linear phase* characteristic. In practice, many systems have a phase characteristic that may be only approximately linear. A convenient way of judging

† It can also be applied to marginally stable systems if the input does not contain natural mode(s) of the system.

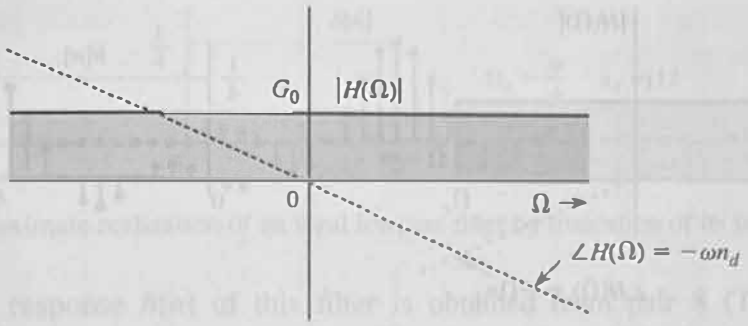

Figure 10.15 LTI system frequency response for distortionless transmission.

phase linearity is to plot the slope of $\angle H(\Omega)$ as a function of frequency. This slope is constant for the ideal linear phase (ILP) system, but it may vary with Ω in the general case. The slope can be expressed as

$$n_g(\Omega) = -\frac{d}{d\Omega}\angle H(\Omega) \tag{10.40}$$

If $n_g(\Omega)$ is constant, all the components are delayed by n_g samples. But if the slope is not constant, the delay n_g varies with frequency. This variation means that different frequency components undergo different amounts of delay, and consequently, the output waveform will not be a replica of the input waveform. As in the case of LTIC systems, $n_g(\Omega)$, as defined in Eq. (10.40), plays an important role in bandpass systems and is called the *group delay* or *envelope delay*. Observe that constant n_d implies constant n_g. Note that $\angle H(\Omega) = \phi_0 - \Omega n_d$ also has a constant n_g. Thus, constant group delay is a more relaxed condition.

Distortionless Transmission over Bandpass Systems

As in the case of continuous-time systems, the distortionless transmission conditions can be relaxed for discrete-time bandpass systems. For lowpass systems, the phase characteristic should not only be linear over the band of interest, it should also pass through the origin [Eq. (10.39)]. For bandpass systems, the phase characteristic should be linear over the band of interest, but it need not pass through the origin (n_g should be constant). The amplitude response is required to be constant over the passband. Thus, for distortionless transmission over a bandpass system, the frequency response for positive range of Ω is of the form[†]

$$H(\Omega) = G_0 e^{j(\phi_0 - \Omega n_g)} \qquad \Omega \geq 0$$

The proof is identical to that for the continuous-time case in Sec. 4.4.2 and will not be repeated. In using Eq. (10.40) to compute n_g, we should ignore jump discontinuities in the phase function.

10.5.2 Ideal and Practical Filters

Ideal filters allow distortionless transmission of a certain band of frequencies and suppress all the remaining frequencies. The general ideal lowpass filter shown in Fig. 10.16 for $|\Omega| \leq \pi$ allows

[†] Because the phase function is an odd function of Ω, if $\angle H(\Omega) = \phi_0 - \Omega n_g$ for $\Omega \geq 0$, over the band $2W$ (centered at Ω_c), then $\angle H(\Omega) = -\phi_0 - \Omega n_g$ for $\Omega < 0$ over the band $2W$ (centered at $-\Omega_c$).

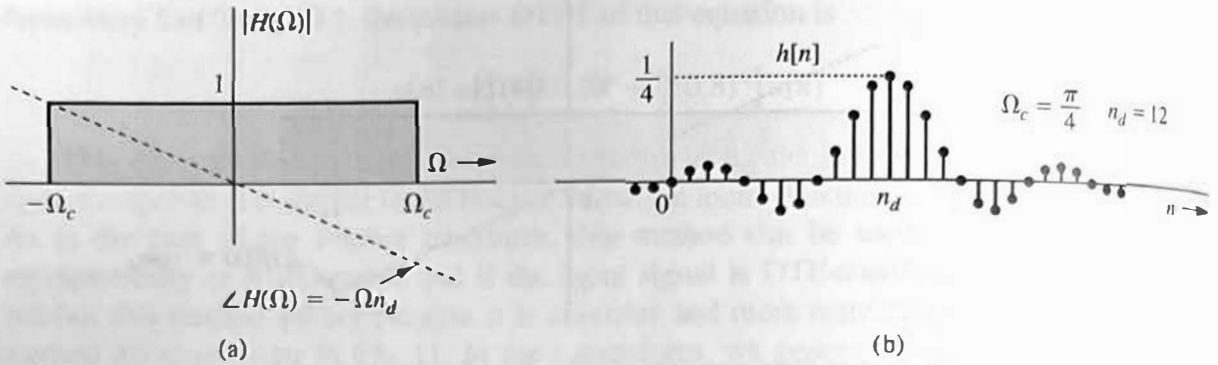

Figure 10.16 Ideal lowpass filter: its frequency response and impulse response.

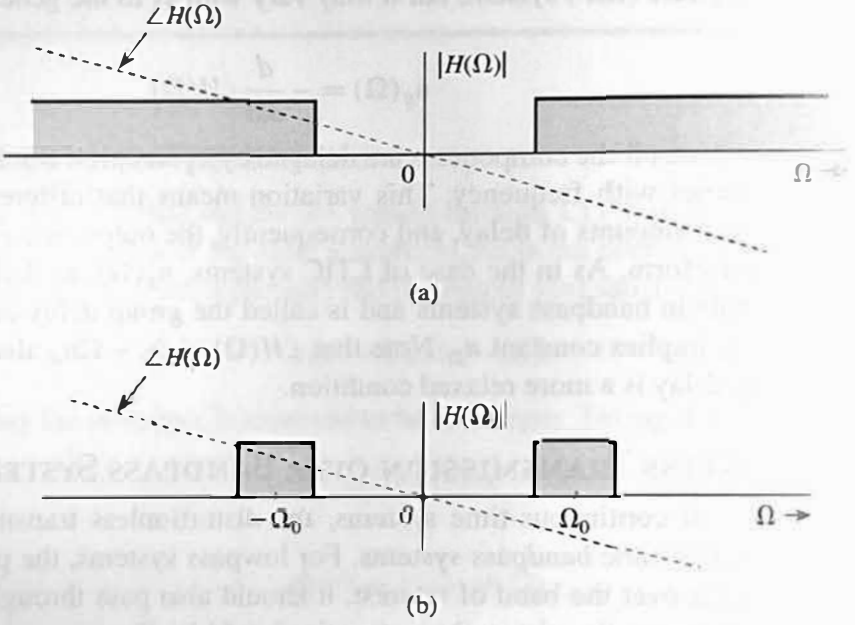

Figure 10.17 Ideal highpass and bandpass filter frequency response.

all components below the cutoff frequency $\Omega = \Omega_c$ to pass without distortion and suppresses all components above Ω_c. Figure 10.17 illustrates ideal highpass and bandpass filter characteristics.

The ideal lowpass filter in Fig. 10.16a has a linear phase of slope $-n_d$, which results in a delay of n_d samples for all its input components of frequencies below Ω_c rad/sample. Therefore, if the input is a signal $x[n]$ bandlimited to Ω_c, the output $y[n]$ is $x[n]$ delayed by n_d; that is,

$$y[n] = x[n - n_d]$$

The signal $x[n]$ is transmitted by this system without distortion, but with a delay of n_d samples. For this filter,

$$H(\Omega) = \sum_{m=-\infty}^{\infty} \text{rect}\left(\frac{\Omega - 2\pi m}{2\Omega_c}\right) e^{-j\Omega n_d}$$

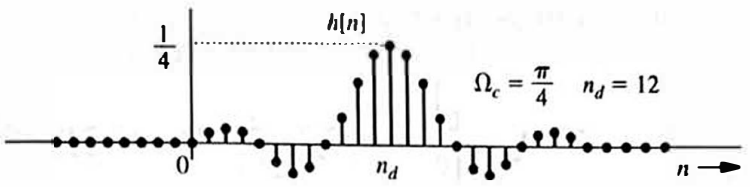

Figure 10.18 Approximate realization of an ideal lowpass filter by truncation of its impulse response.

The unit impulse response $h[n]$ of this filter is obtained from pair 8 (Table 10.1) and the time-shifting property

$$h[n] = \frac{\Omega_c}{\pi} \operatorname{sinc}[\Omega_c(n - n_d)]$$

Because $h[n]$ is the system response to impulse input $\delta[n]$, which is applied at $n = 0$, it must be causal (i.e., it must not start before $n = 0$) for a realizable system. Figure 10.16b shows $h[n]$ for $\Omega_c = \pi/4$ and $n_d = 12$. This figure also shows that $h[n]$ is noncausal, hence unrealizable. Similarly, one can show that other ideal filters (such as the ideal highpass and bandpass filters depicted in Fig. 10.17) are also noncausal and therefore physically unrealizable.

One practical approach to realize an ideal lowpass filter approximately is to truncate both tails (positive and negative) of $h[n]$ so that it has a finite length and then delay sufficiently to make it causal (Fig. 10.18). We now synthesize a system with this truncated (and delayed) impulse response. For closer approximation, the truncating window has to be correspondingly wider. The delay required also increases correspondingly. Thus, the price of closer realization is higher delay in the output; this situation is common in noncausal systems. We develop methods for practical DT filter design in Ch. 12.

10.6 Signal Processing by the DFT and FFT

In this section, we use the DFT (developed in Ch. 5) as a tool, which allows us to utilize a digital computer for digital signal processing. This signal processing includes spectral analysis of digital signals and LTID system analysis. By spectral analysis, we mean determining the discrete-time Fourier series of periodic signals and determining $X(\Omega)$ from $x[n]$ (and vice versa) for aperiodic signals. As a tool for LTID system analysis, the DFT can be used as a software-oriented solution to digital filtering. The DFT can be implemented on a digital computer by an efficient algorithm, the *fast Fourier transform* (FFT), which was also discussed in Ch. 5. The DFT, computed using the FFT, is truly the workhorse of modern digital signal processing.

10.6.1 Computation of the Discrete-Time Fourier Series (DTFS)

The discrete-time Fourier series (DTFS) equations [(10.2) and (10.3)] are identical to the DFT equations [(5.13) and (5.12)] within a scaling constant N_0. If we let $x[n] = N_0 x_n$ and $\mathcal{D}_r = X_r$ in Eqs. (10.3) and (10.2), we obtain

$$X_r = \sum_{n=0}^{N_0-1} x_n e^{-jr\Omega_0 n} \quad \text{and} \quad x_n = \frac{1}{N_0} \sum_{r=0}^{N_0-1} X_r e^{jr\Omega_0 n}, \quad \text{where} \quad \Omega_0 = \frac{2\pi}{N_0}$$

This is precisely the DFT and IDFT of Eqs. (5.12) and (5.13). For instance, to compute the DTFS for the periodic signal in Fig. 10.2a, we use the values of $x_n = x[n]/N_0$ as

$$x_n = \begin{cases} \frac{1}{32} & 0 \le n \le 4 \quad \text{and} \quad 28 \le n \le 31 \\ 0 & 5 \le n \le 27 \end{cases}$$

We use these values in the FFT algorithm discussed in Sec. 5.6 to obtain X_r.

10.6.2 Computation of the DTFT and Its Inverse

Spectral analysis of digital signals requires determination of the DTFT and IDTFT [determining $X(\Omega)$ from $x[n]$ and vice versa]. This determination could be accomplished by using the DTFT Eqs. (10.17) and (10.18) directly on a digital except for two difficulties.

1. Equation (10.18) involves summing an infinite number of terms, which is not possible because it requires infinite computer resources (time and memory).
2. Equation (10.17) requires integration, which is generally approximated as a sum on a computer.

The first problem can be surmounted either by restricting the analysis only to a finite-length $x[n]$ or by truncating $x[n]$ by a suitable window. The error due to windowing may be reduced by using wider, more tapered windows. We shall see that if $x[n]$ has a finite duration, the samples of $X(\Omega)$ can be computed using a finite sum (rather than an integral). This solves the second problem. Moreover, $x[n]$ is uniquely determined from these samples of $X(\Omega)$.

In order to derive appropriate relationships, consider the signal $x[n]$ starting at $n = 0$, and with a finite-length N_0, as shown in Fig. 10.19a. Let us construct a periodic signal $x_{N_0}[n]$ by repeating $x[n]$ periodically at intervals of N_0, as illustrated in Fig. 10.19b. We can represent the periodic signal $x_{N_0}[n]$ by the discrete-time Fourier series (DTFS) as [see Eqs. (10.2) and (10.3)]

$$x_{N_0}[n] = \sum_{r=0}^{N_0-1} \mathcal{D}_r e^{jr\Omega_0 n} \qquad \Omega_0 = \frac{2\pi}{N_0} \tag{10.41}$$

where

$$\mathcal{D}_r = \frac{1}{N_0} \sum_{n=0}^{N_0-1} x[n] e^{-jr\Omega_0 n} \tag{10.42}$$

In Eq. (10.42), we use the fact that $x_{N_0}[n] = x[n]$ for $n = 0, 1, 2, \ldots, N_0 - 1$.

By definition, the DTFT of $x[n]$ is

$$X(\Omega) = \sum_{n=0}^{N_0-1} x[n] e^{-j\Omega n}$$

Comparing this equation to Eq. (10.42), it follows that $N_0\mathcal{D}_r$ is $X(r\Omega_0)$, the rth sample of $X(\Omega)$. For convenience, we denote this sample by X_r. Thus,

$$N_0\mathcal{D}_r = X(r\Omega_0) = X_r \tag{10.43}$$

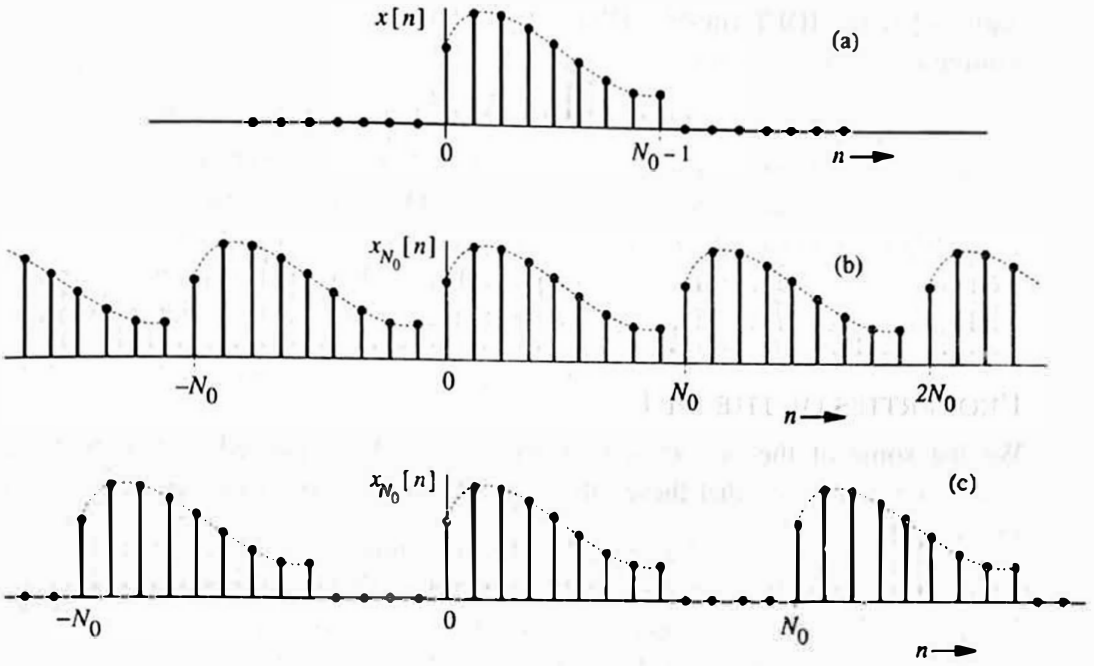

Figure 10.19 Periodic replication of a finite-length signal to compute the DTFT using the DFT.

Therefore, $N_0\mathcal{D}_r$ are the samples of $X(\Omega)$ taken uniformly at the frequency intervals of Ω_0. But because $\Omega_0 = 2\pi/N_0$, there are exactly N_0 number of these samples of $X(\Omega)$ over the fundamental frequency interval of 2π. According to Eqs. (10.41) and (10.43), it follows that

$$x_{N_0}[n] = \frac{1}{N_0}\sum_{r=0}^{N_0-1} X_r e^{jr\Omega_0 n} \tag{10.44}$$

where [from Eqs. (10.42) and (10.43)]

$$X_r = \sum_{n=0}^{N_0-1} x[n]e^{-jr\Omega_0 n} \tag{10.45}$$

Because $x_{N_0}[n] = x[n]$ for $n = 0, 1, 2, \ldots, (N_0 - 1)$, we can express Eq. (10.44) as

$$x[n] = \frac{1}{N_0}\sum_{r=0}^{N_0-1} X_r e^{jr\Omega_0 n} \qquad n = 0, 1, 2, \ldots, N_0 - 1 \tag{10.46}$$

Moreover, we need to determine X_r, the samples of the DTFT, only over the interval $0 \le \Omega < 2\pi$. Therefore, Eq. (10.45) can be expressed as

$$X_r = \sum_{n=0}^{N_0-1} x[n]e^{-jr\Omega_0 n} \qquad r = 0, 1, 2, \ldots, N_0 - 1 \tag{10.47}$$

Equations (10.46) and (10.47) are precisely the DFT pair derived in Eqs. (5.12) and (5.13). These equations relate X_r [the samples of $X(\Omega)$] to $x[n]$ and vice versa. Here, X_r is the DFT of $x[n]$,

and $x[n]$ is the IDFT (inverse DFT) of X_r. This transform relationship is also denoted by the bidirectional arrow notation as

$$x[n] \Longleftrightarrow X_r$$

To repeat, X_r, *the DFT of an* N_0*-point sequence* $x[n]$, *is a set of uniform samples of its DTFT* $X(\Omega)$ *taken at frequency intervals of* $\Omega_0 = \frac{2\pi}{N_0}$. The sequence $x[n]$ and its DFT X_r are related by Eqs. (10.46) and (10.47). Observe that there are N_0 elements in $x[n]$. Also, there are exactly N_0 elements in X_r (over the frequency range 2π). The DFT relationships are finite sums and can be readily computed on a digital computer using the efficient fast Fourier transform (FFT) algorithm.

PROPERTIES OF THE DFT

We list some of the important properties of the DFT proved in Ch. 5. From the preceding discussion, it follows that these DFT properties also apply to DTFT samples of a finite-length signal $x[n]$.

1. **Linearity:** If $x[n] \Longleftrightarrow X_r$ and $g[n] \Longleftrightarrow G_r$, then

$$a_1x[n] + a_2g[n] \Longleftrightarrow a_1X_r + a_2G_r$$

2. **Conjugate Symmetry:** For real $x[n]$,

$$X_{N_0-r} = X_r^*$$

When $x[n]$ is real, there is a conjugate symmetry about $N_0/2$, which enables us to determine roughly half the values of X_r from the other half of the values. For instance, in a 7-point DFT, $X_6 = X_1^*$, $X_5 = X_2^*$, and $X_4 = X_3^*$. In an 8-point DFT, $X_7 = X_1^*$, $X_6 = X_2^*$, $X_5 = X_3^*$, and so on.

3. **Time Shifting (Circular Shifting):**

$$x[n-k] \Longleftrightarrow X_re^{-jr\Omega_0k}$$

4. **Frequency Shifting:**

$$x[n]e^{jn\Omega_0m} \Longleftrightarrow X_{r-m}$$

5. **Circular (or Periodic) Convolution:**

$$x[n] \circledast g[n] \Longleftrightarrow X_rG_r$$

and

$$x[n]g[n] \Longleftrightarrow \frac{1}{N_0}X_r \circledast G_r \tag{10.48}$$

where the circular (or periodic) convolution of two N_0-point periodic sequences $x[n]$ and $g[n]$ is defined as

$$x[n] \circledast g[n] = \sum_{k=0}^{N_0-1} x[k]g[n-k] = \sum_{k=0}^{N_0-1} g[k]x[n-k]$$

Caution in Interpreting the DFT and IDFT

Equations (10.46) and (10.47) allow us to compute samples of the DTFT and IDTFT for a finite-length signal on a digital computer. To avoid certain pitfalls, we must understand clearly the nature of functions synthesized by the sums on the right-hand side of these equations. According to Eq. (10.44), it follows that the sum on the right-hand side of Eq. (10.46) is $x_{N_0}[n]$, which is a periodic signal of which $x[n]$ is the first cycle. Similarly, the sum on the right-hand side of Eq. (10.47) is periodic. This is because $X_r = N_0 \mathcal{D}_r$, which is periodic. Therefore, both of the DFT equations are periodic. We require only part of these results (over one cycle) to compute the samples of $X(\Omega)$ from $x[n]$ and vice versa. That is why we placed the restriction that n or $r = 0, 1, 2, \ldots, N_0 - 1$ in Eqs. (10.46) and (10.47).

Signal $x[n]$ Can Start at Any Value of n

In deriving the preceding results, we assumed that the signal $x[n]$ starts at $n = 0$. This restriction, fortunately, is not necessary. We now show that this procedure can be applied to $x[n]$ starting at any instant. Recall that the DFT found by this procedure is actually the DFT of $x_{N_0}[n]$, which is a periodic extension of $x[n]$ with period N_0. In other words, $x_{N_0}[n]$ can be generated from $x[n]$ by placing $x[n]$ and reproduction thereof end to end ad infinitum. Consider now the signal $x[n]$ in Fig. 10.7 in which $x[n]$ begins at $n = -4$. The periodic extension of this signal is depicted in Fig. 10.2a for $N_0 = 32$. A careful glance at this figure shows that this periodic signal can be constructed by any segment of length 32 and repeating it periodically by placing it end to end ad infinitum. We may choose a segment over the range $n = -16$ to 15 or a segment over the range $n = 0$ to 31, or any other segment of length 32. The reader should confirm that the periodic extension of any such segment yields the same periodic signal $x_{N_0}[n]$. Therefore, the DFT corresponding to the periodic signal $x_{N_0}[n]$ is the DFT of any of its segment of N_0 length starting at any point. So the signal $x[n]$ may start at any point. All we need is to construct a periodic signal $x_{N_0}[n]$ that is a periodic extension of $x[n]$, then compute the DFT according to Eq. (10.46) using the sample values in the range $n = 0$ to $N_0 - 1$. For instance, the signal $x[n]$ in Fig. 10.7 does not start at $k = 0$. But we can construct its periodic extension $x_{N_0}[n]$, as shown in Fig. 10.2a, and use the values for $n = 0, 1, 2, \ldots, 31$ in Eq. (10.47) to compute X_r. These values are

$$x[n] = \begin{cases} 1 & 0 \le n \le 4 \quad \text{and} \quad 28 \le n \le 31 \\ 0 & 5 \le n \le 27 \end{cases}$$

Hence, according to Eq. (10.47),

$$X_0 = \sum_{n=0}^{N_0-1} x[n] = 9$$

and

$$X_1 = e^{-j\Omega_0} + e^{-j2\Omega_0} + e^{-j3\Omega_0} + e^{-j4\Omega_0} + e^{-j28\Omega_0} + e^{-j29\Omega_0} + e^{-j30\Omega_0} + e^{-j31\Omega_0}$$

Because $\Omega_0 = \frac{\pi}{16}$, we recognize that $e^{-j31\Omega_0} = e^{j\Omega_0}$, $e^{-j30\Omega_0} = e^{j2\Omega_0}$, and so on. Hence,

$$X_1 = 1 + 2(\cos \Omega_0 + \cos 2\Omega_0 + \cos 3\Omega_0 + \cos 4\Omega_0) = 7.8865$$

Note that $X_0 = 9$ is the first sample of $X(\Omega)$, $X_1 = 7.8865$ is the second sample $X(\frac{\pi}{16})$, and so on. The samples are spaced $\pi/16$ radians apart, giving a total of 32 samples in the fundamental frequency range. The reader may confirm these values from Eq. (10.24).

EXAMPLE 10.14 3-Point DFT of a Length-3 Signal

Find the DFT of the length-3 signal $x[n] = 3\delta[n] + 2\delta[n-1] + 3\delta[n-2]$. Compare the DFT spectrum X_r with the corresponding DTFT spectrum $X(\Omega)$.

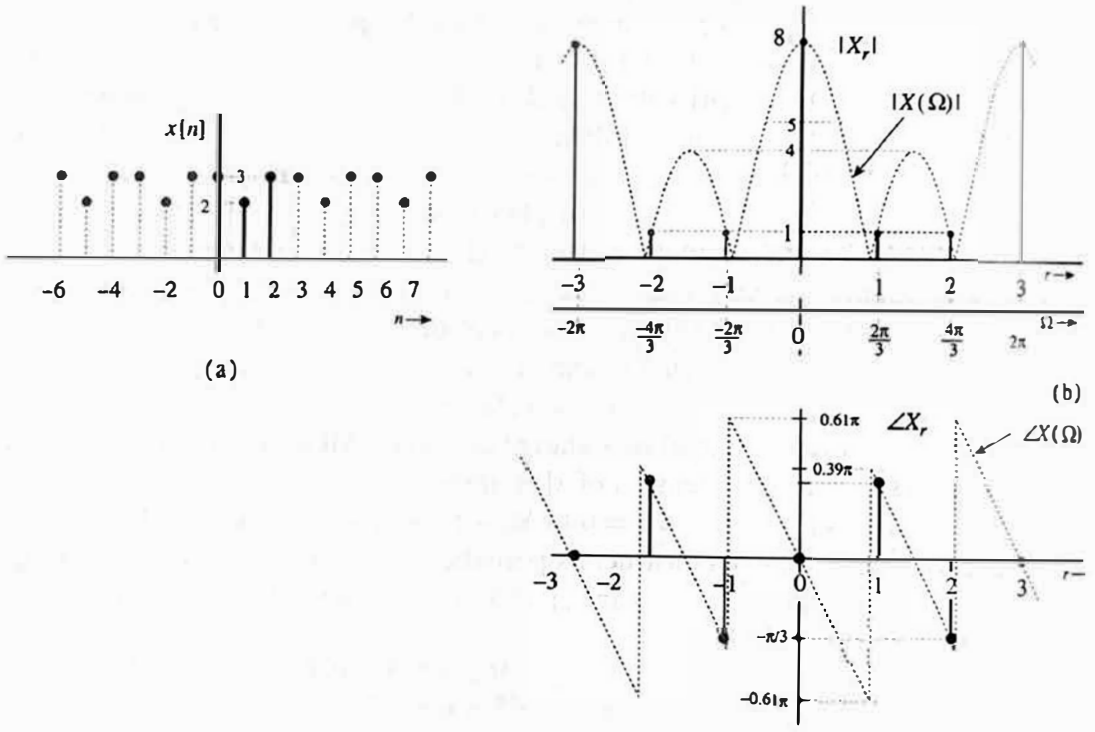

Figure 10.20 Computing the 3-point DFT of a length-3 signal.

Figure 10.20a shows $x[n]$ (solid stems) and $x_{N_0}[n]$ (dotted stems) obtained by periodic extension of $x[n]$. In this case, $N_0 = 3$ and $\Omega_0 = 2\pi/3$. From Eq. (10.47), we obtain

$$X_r = \sum_{n=0}^{2} x[n]e^{-jr\left(\frac{2\pi}{3}\right)n} = 3 + 2e^{-jr\frac{2\pi}{3}} + 3e^{-jr\frac{4\pi}{3}}$$

Therefore,

$$X_0 = 3+2+3 = 8$$

$$X_1 = 3+2e^{-j\frac{2\pi}{3}}+3e^{-j\frac{4\pi}{3}} = 3+\left(-1-j\sqrt{3}\right)+\left(-\frac{3}{2}+j\frac{3\sqrt{3}}{2}\right) = \left(\frac{1}{2}+j\frac{\sqrt{3}}{2}\right) = e^{j\frac{\pi}{3}}$$

$$X_2 = 3+2e^{-j\frac{4\pi}{3}}+3e^{-j\frac{8\pi}{3}} = 3+\left(-1+j\sqrt{3}\right)+\left(-\frac{3}{2}-j\frac{3\sqrt{3}}{2}\right) = \left(\frac{1}{2}-j\frac{\sqrt{3}}{2}\right) = e^{-j\frac{\pi}{3}}$$

In table form, the magnitudes and angles of X_r are thus

r	0	1	2
$\lvert X_r\rvert$	8	1	1
$\angle X_r$	0	$\frac{\pi}{3}$	$-\frac{\pi}{3}$

Observe that $X_2 = X_1^*$ (the conjugate symmetry property). Because $x[n]$ is a 3-point sequence, X_r (its DFT) is also a 3-point sequence, which repeats periodically. Figure 10.20b shows $|X_r|$ and $\angle X_r$. Recall that the DFT gives only samples of the DTFT $X(\Omega)$. We want to know if the current DFT has enough samples to give a reasonably good idea of the DTFT. The DTFT for $x[n]$ is given by Eq. (10.18) as

$$X(\Omega) = \sum_{n=0}^{2} x[n]e^{-j\Omega n} = 3+2e^{-j\Omega}+3e^{-j2\Omega} = e^{-j\Omega}[2+3e^{j\Omega}+3e^{-j\Omega}] = e^{-j\Omega}(2+6\cos\Omega)$$

The amplitude and phase spectra are given by

$$|X(\Omega)| = |2+6\cos(\Omega)| \quad \text{and} \quad \angle X(\Omega) = \begin{cases} -\Omega & 2+6\cos(\Omega) > 0 \\ -\Omega-\pi & 2+6\cos(\Omega) < 0 \end{cases}$$

Figure 10.20b shows $|X(\Omega)|$ and $\angle X(\Omega)$ (dotted). Observe that the DFT values exactly equal the DTFT at the sampled frequencies; there is no approximation. This is always true of the DFT of a finite-length signal $x[n]$. However, if $x[n]$ is obtained by truncating or windowing a longer sequence, we shall see that the DFT gives only approximate sample values of the DTFT.

The DFT in this example has too few points to give a reasonable picture of the DTFT. The peak of the DTFT appearing between the second and third samples (between $r = 1$ and 2), for instance, is missed by the DFT. The two valleys of the DTFT are also missed. We definitely need more points in the DFT for an acceptable resolution. This goal is accomplished by *zero padding*, explained next.

Zero Padding and the Picket Fence Effect

The DFT yields samples of the DTFT spaced at frequency intervals of $\Omega_0 = 2\pi/N_0$. In this way, the DFT size N_0 determines the frequency resolution Ω_0. Seeing the DTFT through the DFT is like viewing $X(\Omega)$ through a *picket fence*. Only the spectral components at the sampled frequencies

(which are integral multiples of Ω_0) are visible. All the remaining frequency components are hidden, as though behind the pickets of a fence. If the DFT has too few points, then peaks, valleys, and other details of $X(\Omega)$ that exist between the DFT points (sampled frequencies) will not be seen, thus giving an erroneous view of the spectrum $X(\Omega)$. This is precisely the case in Ex. 10.14. Actually, using the interpolation formula, it is possible to compute any number of values of the DTFT from the DFT. But having to use the interpolation formula really defeats the purpose of the DFT. We therefore seek to reduce Ω_0 so that the number of samples is increased for a better view of the DTFT.

Because $\Omega_0 = 2\pi/N_0$, we can reduce Ω_0 by increasing N_0, the length of $x[n]$. But how do we increase the length of a signal when its length is fixed? Simple! Just append a sufficient number of zero-valued samples to $x[n]$. This procedure, referred to as *zero padding*, is depicted in Fig. 10.19c. Recall that N_0 is the period of $x_{N_0}[n]$, which is formed by periodic repetition of $x[n]$. By appending a sufficient number of zeros to $x[n]$, as illustrated in Fig. 10.19c, we can increase the period N_0 as much as we wish, thereby increasing the number of points of the DFT. Zero padding allows us to obtain more samples of $X(\Omega)$ for clarity. Furthermore, this process does not change the underlying signal $x[n]$, which means that zero padding does not affect the underlying spectrum $X(\Omega)$. Returning to our picket fence analogy, zero padding increases the number of pickets in our fence (N_0), but it cannot change what is behind the fence ($X(\Omega)$). To demonstrate the idea, we next rework Ex. 10.14 using zero padding to double the number of samples of the DTFT.

EXAMPLE 10.15 6-Point DFT of a Length-3 Signal

Using zero padding, find the 6-point DFT of the length-3 signal of Ex. 10.14, $x[n] = 3\delta[n] + 2\delta[n-1] + 3\delta[n-2]$. Compare the 6-point DFT X_r with the corresponding DTFT spectrum $X(\Omega)$.

To compute a 6-point DFT from our length-3 signal, we must pad $x[n]$ with three zeros, as shown in Fig. 10.21a. In this way, we treat $x[n]$ as a 6-point signal with $x[0] = 3$, $x[1] = 2$, $x[2] = 3$, and $x[3] = x[4] = x[5] = 0$.

By padding $x[n]$ with three zeros, N_0 increases to 6, and Ω_0 decreases to $2\pi/6 = \pi/3$. From Eq. (10.47), we obtain

$$X_r = \sum_{n=0}^{5} x[n]e^{-jr(\frac{\pi}{3})n} = 3 + 2e^{-jr\frac{\pi}{3}} + 3e^{-jr\frac{2\pi}{3}}$$

Therefore,

$$X_0 = 3 + 2 + 3 = 8$$

$$X_1 = 3 + 2e^{-j\frac{\pi}{3}} + 3e^{-j\frac{2\pi}{3}} = 3 + \left(1 - j\sqrt{3}\right) + \left(-\frac{3}{2} - j\frac{3\sqrt{3}}{2}\right) = \left(\frac{5}{2} - j\frac{5\sqrt{3}}{2}\right) = 5e^{-j\frac{\pi}{3}}$$

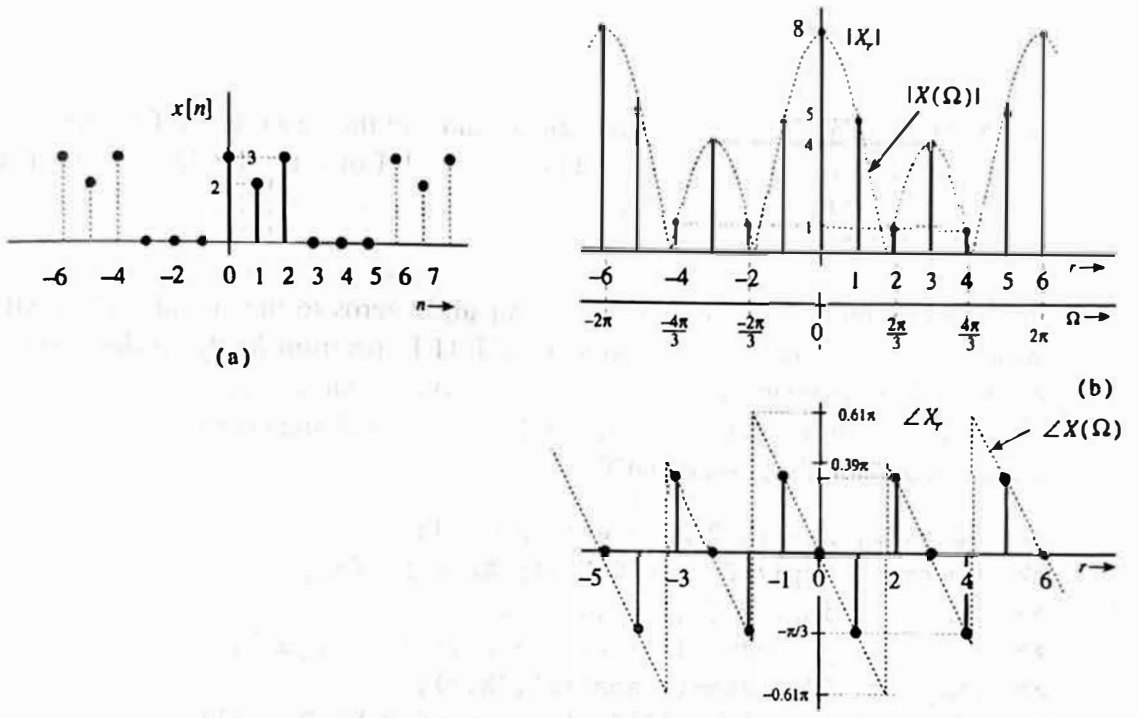

Figure 10.21 Computing the 6-point DFT of a zero-padded length-3 signal.

In the same way, we find

$$X_2 = 3 + 2e^{-j\frac{2\pi}{3}} + 3e^{-j\frac{4\pi}{3}} = e^{j\frac{\pi}{3}}$$
$$X_3 = 3 + 2e^{-j\pi} + 3e^{-j2\pi} = 4$$
$$X_4 = 3 + 2e^{-j\frac{4\pi}{3}} + 3e^{-j\frac{8\pi}{3}} = e^{-j\frac{\pi}{3}}$$
$$X_5 = 3 + 2e^{-j\frac{5\pi}{3}} + 3e^{-j\frac{10\pi}{3}} = 5e^{j\frac{\pi}{3}}$$

The magnitudes and angles of the resulting X_r are thus

r	0	1	2	3	4	5
$\lvert X_r\rvert$	8	5	1	4	1	5
$\angle X_r$	0	$-\frac{\pi}{3}$	$\frac{\pi}{3}$	0	$-\frac{\pi}{3}$	$\frac{\pi}{3}$

Observe that $X_5 = X_1^*$ and $X_4 = X_2^*$ as expected from the conjugate symmetry property. Figure 10.21b shows plots of $|X_r|$ and $\angle X_r$. Observe that we now have a 6-point DFT, which provides 6 samples of the DTFT spaced at a frequency interval of $\pi/3$ (in contrast to $2\pi/3$ spacing in Ex. 10.14). The samples corresponding to $r = 0$, 2, and 4 in Ex. 10.15 are identical to the samples corresponding to $r = 0$, 1, and 2 in Ex. 10.14. The DFT spectrum in Fig. 10.21b contains the three samples appearing in Fig. 10.20b plus 3 more samples in between. Clearly, zero padding allows us a better view of the DTFT. But even in this case, the valleys of $X(\Omega)$ are still largely missed by this 6-point DFT.

EXAMPLE 10.16 32-Point DFT of a Length-3 Signal Using MATLAB

Use MATLAB and zero padding to compute and plot the 32-point DFT of the length-3 signal of Ex. 10.14, $x[n] = 3\delta[n] + 2\delta[n-1] + 3\delta[n-2]$. Compare the 32-point DFT X_r with the corresponding DTFT spectrum $X(\Omega)$.

Because the signal length is 3, we need to pad 29 zeros to the signal. MATLAB is used to avoid tedious hand calculations. To plot the DTFT spectrum $X(\Omega)$ on the same plots as X_r, we normalize the frequency variable as Ω/Ω_0. As shown in Fig. 10.22, the plots of $|X_r|$ and $\angle X_r$ exactly follow the DTFT spectrum $X(\Omega)$. The underlying DTFT is clearly exposed by the dense sampling of the 32-point DFT.

```
>> N0 = 32; x = [3 2 3 zeros(1,N0-3)];
>> Omega0 = 2*pi/N0; r = 0:N0-1; Xr = fft(x);
>> Omega = linspace(0,2*pi,1001);
>> X = @(Omega) exp(-1j*Omega).*(2+6*cos(Omega));
>> subplot(121); stem(r,abs(Xr),'k.');
>> xlabel('r'); ylabel('|X_r|'); axis([0 N0 0 8.5]);
>> line(Omega/Omega0,abs(X(Omega)),'color',[0 0 0]);
>> subplot(122); stem(r,angle(Xr),'k.');
>> xlabel('r'); ylabel('\angle X_r'); axis([0 N0 -pi pi]);
>> line(Omega/Omega0,angle(X(Omega)),'color',[0 0 0]);
```

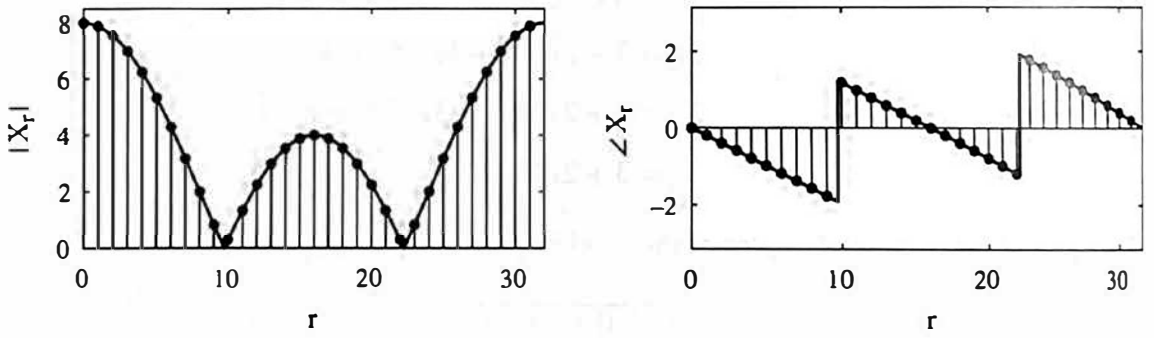

Figure 10.22 Computing the 32-point DFT of a zero-padded length-3 signal using MATLAB.

EXAMPLE 10.17 Choosing N_0 to Achieve Frequency Resolution

Determine the length N_0 to which signal $x[n]$ in Ex. 10.14 must be zero-padded to achieve a DFT frequency resolution of $\Omega_0 = \pi/6$. Write an expression for computing the DFT $X(\Omega)$.

For a resolution of $\Omega_0 = \pi/6$, the padded length N_0 of the signal is

$$N_0 = \frac{2\pi}{\Omega_0} = \frac{2\pi}{\pi/6} = 12$$

Since the signal in Ex. 10.14 has a length of 3, we need to pad 9 zeros to $x[n]$. The corresponding DFT is

$$X_r = \sum_{n=0}^{11} x[n]e^{-jr(\frac{\pi}{6})n}$$

However, the last 9 samples of $x[n]$ are zero. Therefore, the expression for X_r reduces to

$$X_r = \sum_{n=0}^{2} x[n]e^{-jr(\frac{\pi}{6})n}$$

DRILL 10.9 DFT and DTFT of a Length-3 Signal

A 3-point signal $x[n]$ is specified by $x[0] = 2$, $x[-1] = x[1] = 1$, and $x[n] = 0$ for all other n. Show that the DFT of this signal is $X_0 = 4$, $X_1 = 1$, and $X_2 = 1$. Find $X(\Omega)$, the DTFT of this signal, and verify that the DFT is equal to the samples of the DTFT at intervals of $\Omega_0 = 2\pi/N_0 = 2\pi/3$.

DRILL 10.10 DFT of a Length-8 Signal

Show that the 8-point DFT of the signal $x[n]$ in Drill 10.9 is

$$X_0 = 4,\ X_1 = 3.4142,\ X_2 = 2,\ X_3 = 0.5858,\ X_4 = 0,\ X_5 = 0.5858,\ X_6 = 2,\ X_7 = 3.4142$$

Observe the conjugate symmetry of X_r about $r = N_0/2 = 4$.

Practical Choice of N_0

The value of N_0 is determined by the desired resolution Ω_0. However, there is another consideration in selecting a value of N_0. If we are using the FFT algorithm to compute the DFT, then efficient computation requires that N_0 be a power of 2. Hence, we often pad sufficient numbers of zeros to ensure this requirement.

Effect of Signal Truncation

So far we have considered only finite-length sequences. For such sequences, we can readily find an N_0-point DFT, where N_0 is at least equal to the length of the sequence. How do we handle signals of infinite length? It is practically impossible to process infinite-length sequences because they generally require an infinite number of computations. Fortunately, every practical everlasting signal $x[n]$ must decay with n (because of a finite energy requirement), and such a signal becomes negligibly small beyond $n \geq N_0$ for some suitable value of N_0. For instance, the signal $x[n] = (0.6)^n$ has infinite length. However, $x[n] \leq 0.00028$ at $n \geq 16$. Hence, we may truncate this signal beyond $n = 16$ (or even a little earlier). Straightforward signal truncation in this manner amounts to using a rectangular window with a unit weight for the data in the range $0 \leq n \leq N_0$, and zero weight for the data beyond $n = N_0$. Such a truncation results in Gibbs phenomenon with consequent oscillations in the spectrum of the truncated signal as demonstrated in the following example.

EXAMPLE 10.18 DFT of a Truncated Signal

The signal $x[n] = (0.8)^n u[n]$ has infinite length. Truncate this signal using an 8-point rectangular window, plot its DFT magnitude spectrum, and compare it to the DTFT magnitude spectrum of the untruncated signal.

The DTFT of this signal obtained in Ex. 10.3 [see Eq. (10.22)] is

$$X(\Omega) = \frac{1}{1 - 0.8e^{-j\Omega}} \qquad \text{and} \qquad |X(\Omega)| = \frac{1}{\sqrt{1.64 - 1.6\cos\Omega}}$$

The 8-point rectangular window function is

$$w_R[n] = \begin{cases} 1 & 0 \leq n \leq 7 \\ 0 & \text{otherwise} \end{cases}$$

The windowed signal is

$$x_{w_R}[n] = \begin{cases} (0.8)^n & 0 \leq n \leq 7 \\ 0 & \text{otherwise} \end{cases}$$

The DFT of the windowed signal is obtained using the FFT algorithm. Figure 10.23a shows the windowed signal, and Fig. 10.23b shows the corresponding 8-point DFT. For comparison, Fig. 10.23b also shows the smooth DTFT magnitude $|X(\Omega)|$ (dotted line) of the original (untruncated) signal $(0.8)^n u[n]$ and the oscillating DTFT magnitude (solid line) of the 8-point truncation of $(0.8)^n u[n]$. As expected, the 8 DFT values computed from the truncated signal exactly intersect the DTFT of the truncated signal.

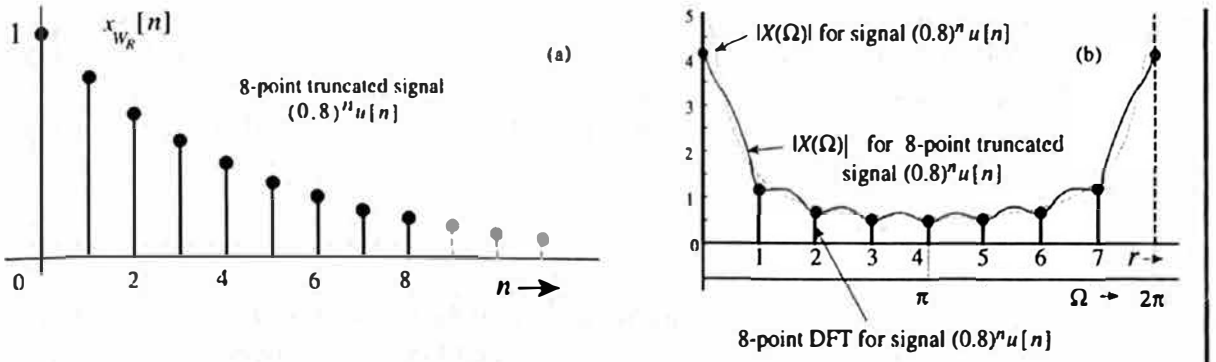

Figure 10.23 DFT computations for $x[n] = (0.8)^n u[n]$ using an 8-point rectangular window.

10.6.3 Discrete-Time Filtering (Convolution) Using the DFT

The DFT is useful not only in the computation of direct and inverse Fourier transforms, but also in other applications such as filtering, convolution, and correlation. Use of the efficient FFT algorithm makes a DFT-based approach particularly appealing. We generally think of filtering in terms of some hardware-oriented solution (using summers, multipliers, and delay elements). However, filtering also has a software-oriented solution (a computer algorithm that yields a filtered output $y[n]$ for a given input $x[n]$). Such filtering can be conveniently accomplished by using the DFT.

Filtering can be accomplished either in the frequency domain or in the time domain. In the frequency-domain approach, for a given input $x[n]$, we are required to find the output $y[n]$ of a filter with a given transfer function $H(\Omega)$. In the time-domain approach, for a given input $x[n]$, we are required to find the output $y[n]$ of a filter with a given impulse response $h[n]$. In the time domain, the output is obtained by the (linear) convolution of $x[n]$ with $h[n]$. In the frequency domain, the output is obtained as the IDFT of $X_r H_r$, where $X_r = X(r\Omega_0)$ and $H_r = H(r\Omega_0)$. Because the frequency-domain method appears as a substep of the time-domain method, we shall consider here only the time-domain (convolution) method.

We would like to perform linear convolution (filtering) using the DFT and computed via the FFT algorithm because of computational efficiency. However, the DFT most naturally aligns with computing circular convolution, not linear convolution. Fortunately, linear convolution can be made equivalent to circular convolution by suitably padding the two sequences with zeros. This statement, introduced in Ch. 5, will now be proved.

When Is Linear Convolution Equivalent to Circular Convolution?

Circular (or *periodic*) *convolution* is explained in Sec. 5.5.1. In circular convolution, both sequences to be convolved are N_0-periodic. If $x[n]$ and $g[n]$ are both N_0-periodic, their periodic (or circular) convolution $c[n]$ is defined as

$$c[n] = x[n] \circledast g[n] = \sum_{m=0}^{N_0-1} x[m]g[n-m]$$

Note that circular convolution differs from linear convolution by the fact that the summation is over one period (starting at any point). In linear convolution, the summation is from $-\infty$ to ∞. The result of a periodic convolution is also an N_0-periodic sequence.

Suppose we wish to convolve two finite-length sequences $x[n]$ and $h[n]$ of lengths N_x and N_h, respectively. Let $y[n]$ be the linear convolution of these sequences; that is,

$$y[n] = x[n] * h[n]$$

From the width property of convolution (Sec. 9.5), the length of $y[n]$ is $(N_x + N_h - 1)$. Let the DTFTs of $x[n]$, $h[n]$, and $y[n]$ be $X(\Omega)$, $H(\Omega)$, and $Y(\Omega)$, respectively. Then, from Eq. (10.32), we have

$$Y(\Omega) = X(\Omega)H(\Omega) \tag{10.49}$$

We know that the DFT of an N_0-point sequence is the set of uniform samples of its DTFT at frequency interval $\Omega_0 = 2\pi/N_0$. Therefore, if Y_r is the N_0-point DFT of $y[n]$, then

$$Y_r = Y(r\Omega_0) \qquad \Omega_0 = \frac{2\pi}{N_0}$$

According to Eq. (10.49) it follows that

$$Y_r = X_r H_r \tag{10.50}$$

where X_r and H_r are the rth samples of $X(\Omega)$ and $H(\Omega)$, respectively.

For Eq. (10.50) to be valid, X_r and H_r must be compatible for multiplication. In other words, both must be N_0-point sequences if Y_r is an N_0-point sequence. But we know that $x[n]$, $h[n]$, and $y[n]$ are N_x, N_h, and $N_0 = (N_x + N_h - 1)$-point sequences. Hence, we must pad $N_h - 1$ zeros to $x[n]$ and pad $N_x - 1$ zeros to $h[n]$ to ensure that X_r, H_r, and Y_r are all $N_0 = (N_x + N_h - 1)$-point sequences. Once we compute X_r and H_r (after suitably zero padding $x[n]$ and $h[n]$), we take the IDFT of $X_r H_r$ to obtain $y[n]$. However, we have shown in Ch. 5 [Eq. (5.18)] that $X_r H_r$ is the DFT of a circular convolution of $x[n]$ and $h[n]$; that is, $x[n] \circledast h[n] \Longleftrightarrow X_r H_r$. This result means $y[n]$ is equal to the circular convolution of (suitably padded) $x[n]$ and $h[n]$. Thus, $y[n]$ is a periodic sequence whose first period is the linear convolution of (unpadded) $x[n]$ and $h[n]$. To summarize, $y[n]$, which is the linear convolution of $x[n]$ and $h[n]$, is also equal to the circular convolution of suitably padded $x[n]$ and $h[n]$. This is an extremely important result. The system response is given by the linear convolution of $x[n]$ and $h[n]$. But the preceding result allows us to compute this convolution as if it were the circular convolution of (suitably padded) $x[n]$ and $h[n]$. This, in turn, allows us to use DFT to perform the computations.

The procedure to find the linear convolution of $x[n]$ and $h[n]$, whose lengths are N_x and N_h, respectively, can be summarized in four steps as follows:

1. Pad $N_h - 1$ zeros to $x[n]$ and $N_x - 1$ zeros to $h[n]$.
2. Find X_r and H_r, the DFTs of the zero-padded sequences $x[n]$ and $h[n]$.
3. Multiply X_r by H_r to obtain Y_r.
4. The desired convolution $y[n]$ is the IDFT of Y_r.

This procedure is known as *fast convolution* when the DFTs and IDFT are computed using the efficient FFT algorithm.

Filtering in the frequency domain: If we are given the filter transfer function $H(\Omega)$, we know H_r. We compute X_r, the DFT of $x[n]$. Then follow steps 3 and 4 to obtain the output $y[n]$.

EXAMPLE 10.19 Convolution of Finite-Length Signals Using the DFT

Using DFT-based convolution, determine the output $y[n]$ of an LTID filter with impulse response $h[n] = 2\delta[n] + 2\delta[n-1]$ to an input $x[n] = 3\delta[n] + 2\delta[n-1] + 3\delta[n-2]$.

The signals $x[n]$ and $h[n]$ are shown in Figs. 10.24a and 10.24b.

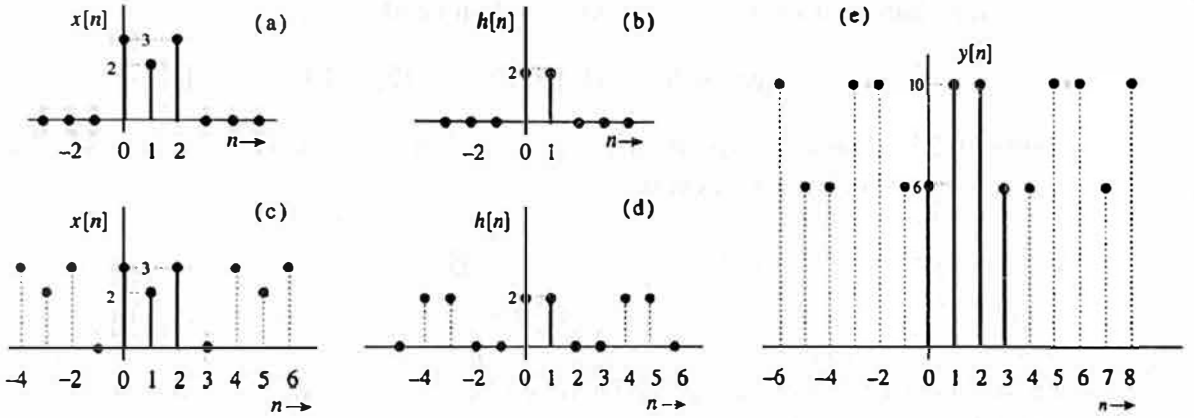

Figure 10.24 Convolution of finite-length signals $x[n]$ and $h[n]$ using the DFT.

The output $y[n]$ is the convolution $x[n] * h[n]$, which we compute using the outlined four-step procedure.

1. In this case $N_x = 3$ and $N_h = 2$. Therefore, we pad 1 zero to $x[n]$ and 2 zeros to $h[n]$, as depicted in Figs. 10.24c and 10.24d, respectively.
2. Now, $N_0 = 4$ and $\Omega_0 = \pi/2$. The DFTs X_r and H_r of the zero-padded sequences $x[n]$ and $h[n]$ are given by

$$X_r = \sum_{n=0}^{2} x[n]e^{-jr\Omega_0 n} = \sum_{n=0}^{2} x[n]e^{-jr\frac{\pi}{2}n} = 3 + 2e^{-j\frac{\pi}{2}r} + 3e^{-j\pi r}$$

and

$$H_r = \sum_{n=0}^{1} h[n]e^{-jr\Omega_0 n} = \sum_{n=0}^{1} h[n]e^{-jr\frac{\pi}{2}n} = 2 + 2e^{-j\frac{\pi}{2}r}$$

Substituting $r = 0, 1, 2, 3$, we obtain

$$X_0 = 8 \qquad X_1 = -2j \qquad X_2 = 4 \qquad X_3 = 2j$$

and

$$H_0 = 4 \qquad H_1 = 2\sqrt{2}e^{-j\frac{\pi}{4}} \qquad H_2 = 0 \qquad H_3 = 2\sqrt{2}e^{j\frac{\pi}{4}}$$

3. Multiply X_r by H_r to obtain Y_r. This step yields

$$Y_0 = 32 \qquad Y_1 = 4\sqrt{2}e^{-j\frac{3\pi}{4}} \qquad Y_2 = 0 \qquad Y_3 = 4\sqrt{2}e^{j\frac{3\pi}{4}}$$

4. The desired convolution is the IDFT of Y_r, given by

$$y[n] = \frac{1}{4}\sum_{r=0}^{3} Y_r e^{jr\Omega_0 n} = \frac{1}{4}\sum_{r=0}^{3} Y_r e^{jr\frac{\pi}{2}n}$$
$$= \frac{1}{4}\left(Y_0 + Y_1 e^{j\frac{\pi}{2}n} + Y_2 e^{j\pi n} + Y_3 e^{j\frac{3\pi}{2}n}\right)$$

Substitution of $r = 0, 1, 2, 3$ in this equation yields

$$y[0] = 6 \qquad y[1] = 10 \qquad y[2] = 10 \qquad y[3] = 6$$

Figure 10.24e shows $y[n]$ and its periodic extension (dotted). The IDFT yields the periodic signal. We need only the first cycle.

Verifying the Result with MATLAB

With MATLAB, we can readily confirm our hand-calculated DFT result (left side of Fig. 10.25) as well as the fact that our DFT result indeed matches the result of linear convolution (right side of Fig. 10.25). Notice that MATLAB's `fft` command supports simple zero padding by just adding the desired DFT length to the function argument.

```
>> x = [3 2 3]; h = [2 2]; N0 = length(x)+length(h)-1; n = 0:N0-1;
>> y = ifft(fft(x,N0).*fft(h,N0));
>> subplot(121); stem(n,y,'k.'); xlabel('n'); ylabel('y[n]');
>> axis([-.5 N0-.5 0 12]); set(gca,'ytick',[0,6,10]);
>> y = conv(x,h);
>> subplot(122); stem(n,y,'k.'); xlabel('n'); ylabel('y[n]');
>> axis([-.5 N0-.5 0 12]); set(gca,'ytick',[0,6,10]);
```

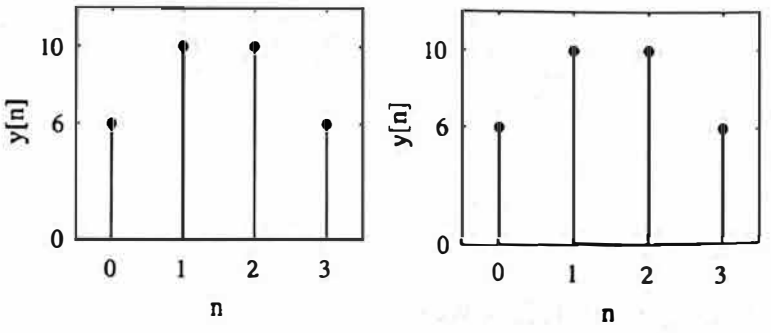

Figure 10.25 MATLAB convolution of finite-length signals $x[n]$ and $h[n]$ using the DFT and linear convolution.

Using the sliding-tape algorithm discussed in Ch. 9, we can perform the convolution in Ex. 10.19 with a mere 6 (real) multiplications and 2 additions. The DFT method discussed in this section appears much too laborious, and the use of the DFT for convolution may seem questionable. Recall, however, our discussion in Sec. 5.6, which showed that the use of the FFT algorithm to compute the DFT reduces the number of computations dramatically, especially for large N_0. For small-length sequences, direct convolution methods (such as the sliding-tape method) are faster than the DFT method. But for long sequences, the DFT method using the FFT algorithm is much faster and far more efficient.[†]

EXAMPLE 10.20 Convolution of Infinite-Length Signals Using the DFT

Use MATLAB and the DFT-based approach to approximate $y[n] = x[n] * h[n]$, where $x[n] = (0.8)^n u[n]$ and $h[n] = (0.5)^n u[n]$. Compare the DFT approximation to the true convolution result.

Since $x[n]$ and $h[n]$ are infinite duration, they must be truncated to employ the DFT-based approach, which will only be able to approximate the convolution result. Still, the approximation will be very good if we truncate the signals to a suitable-length N_0, beyond which both functions become negligible. For this purpose, $N_0 = 32$ is a reasonable choice. For comparison purposes, we use entry 4 of Table 9.1 to determine the actual convolution result as

$$y[n] = x[n] * h[n] = \left[\frac{(0.8)^{n+1} - (0.5)^{n+1}}{0.8 - 0.5}\right] u[n]$$

```
>> N0 = 32; n = 0:N0-1; x = (0.8).^(n); h = (0.5).^(n);
>> y = ifft(fft(x).*fft(h));
>> subplot(121); stem(n,y,'k.'); xlabel('n'); ylabel('y[n]');
>> axis([-.5 N0-.5 0 1.5]);
>> y = ((0.8).^(n+1)-(0.5).^(n+1))/(0.8-0.5);
>> subplot(122); stem(n,y,'k.'); xlabel('n'); ylabel('y[n]');
>> axis([-.5 N0-.5 0 1.5]);
```

The left side of Fig. 10.26 shows the DFT-based approximation of $y[n]$, while the right side shows the analytical (true) representation of $y[n]$. As the two graphs are visually indistinguishable, we know the DFT has produced a good approximation of the true result.

[†] It can be shown that in the convolution of two sequences, each of length N_0, the number of computations required is on the order of N_0^2, whereas for the DFT, computed using the FFT algorithm, the number of computations required is only on the order of $N_0 \log_2 N_0$.

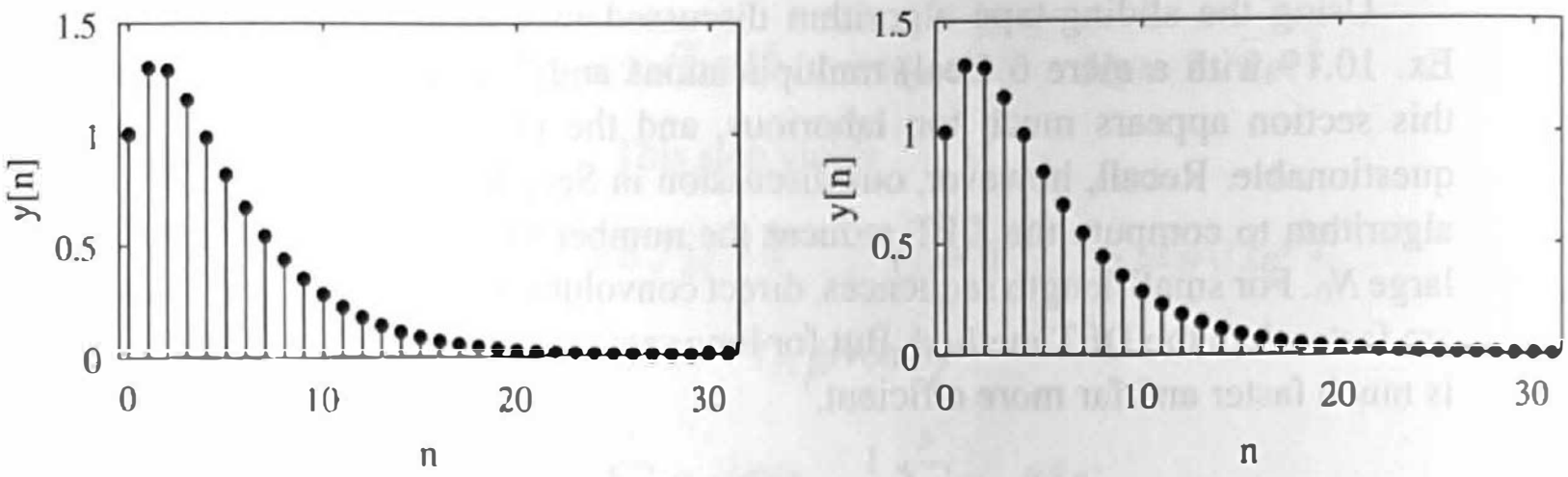

Figure 10.26 MATLAB convolution of infinite-length signals $x[n]$ and $h[n]$ using the DFT and linear convolution.

DRILL 10.11 Circular Convolution Using the DFT

Show that the circular convolution of the two 3-point sequences [3,2,3] and [1,2,3] (both starting at $n = 0$) is the 3-point sequence [15, 17, 16]. Find the answer by using the DFT, and verify your answer using the graphical method explained in Fig. 5.21. Using the sliding-tape method (Fig. 9.7), show that the linear convolution of these sequences is a 5-point sequence [3, 8, 16, 12, 9]. Indicate how you could obtain the linear convolution of these two sequences using circular convolution.

DRILL 10.12 LTID System Response Using the DFT

The input $x[n]$ of an LTID system is a 4-point sequence [1, 1, 1, 1], and the system impulse response $h[n]$ is a 3-point sequence [1, 2, 1]. Both sequences start at $n = 0$. Using the DFT, show that the output $y[n]$ is a 6-point sequence [1, 3, 4, 4, 3, 1] starting at $n = 0$. Verify your answer by deriving the output as a linear convolution of the two sequences using the sliding-tape method.

10.6.4 Block Convolution

In practice, the length of an input signal may be very large, whereas a computer processing such a signal may have limited memory. To process such long sequences, we can section the input signal into blocks of a length small enough to be processed by a given computer, and then add the outputs resulting from all the input blocks. This procedure can be used because the convolution operation is linear. Such a procedure would be desirable even if the processing computer had an unlimited memory. For longer inputs, we must wait a long time before the input is fed to the computer (before it even starts processing), and then an even longer time for processing the large amount

of data. Consequently, there is a long delay in the output. Sectioning the input allows the output to have a smaller processing delay. We shall now discuss two such methods of block processing: the *overlap and add* method and the *overlap and save* method. Either of these methods requires the same number of computations; hence, which method is used is largely a matter of preference.

Overlap and Add Method

Consider a filtering operation, where the output $y[n]$ is the convolution of the input $x[n]$ and a finite impulse response (FIR) filter $h[n]$ of length M. In practice, M is usually much smaller than the length of the input. Figure 10.27 illustrates a long input sequence sectioned into nonoverlapping blocks of a manageable length L. The number inside each block indicates its length. Let us assume that $L \gg M$. We now process each block of the input data in sequence. To be able to use circular convolution for performing linear convolution, we need to pad $M-1$ zeros at the end of each data block.† Figure 10.27 shows each data block augmented with $M-1$ zeros. The augmented portion of the block is shown shaded. Observe that the augmented (zero-padded) blocks of the input, each of length $L+M-1$, now overlap.

The output sequence corresponding to each block also has a length $L+M-1$ (recall that the length of the circular convolution of two sequences, each of length $L+M-1$, is also $L+M-1$). The output sequences, therefore, also overlap, as shown in Fig. 10.27. The total output is given by the sum of all these overlapping output blocks (each of length $L+M-1$). The contents of successive blocks are added wherever they overlap. This method is known as the *overlap and add* method.

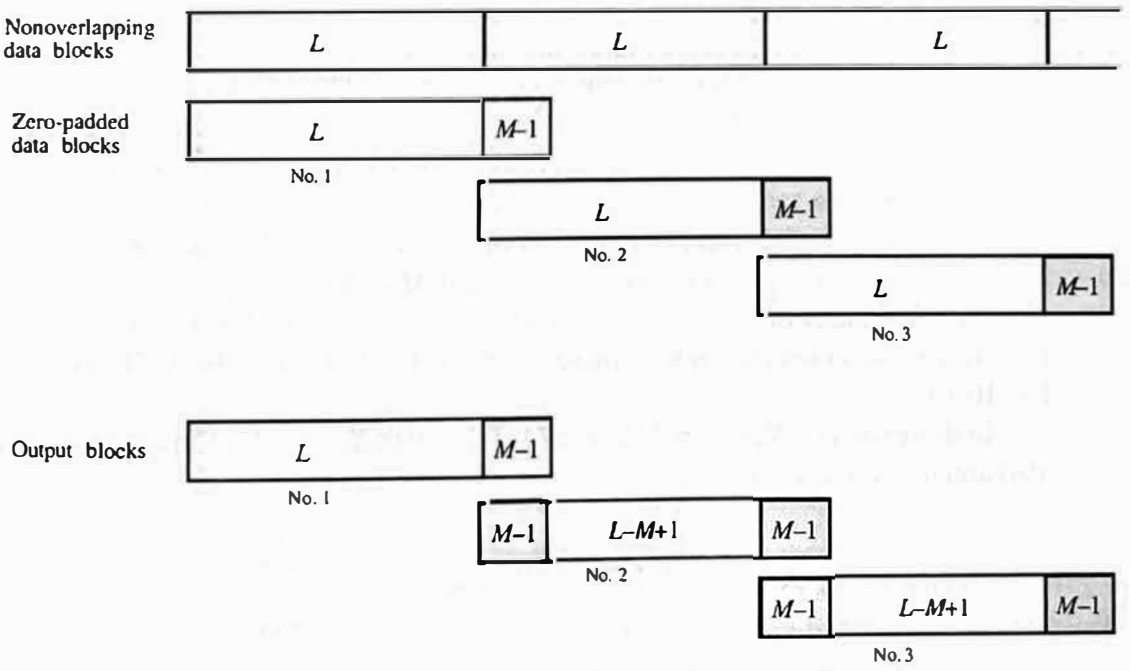

Figure 10.27 Overlap and add method of block convolution.

† We also pad $h[n]$ with $L-1$ zeros so that the length of the padded $h[n]$ is $L+M-1$.

EXAMPLE 10.21 Overlap and Add Method

Using the overlap and add method of block convolution, find the response $y[n]$ of an LTID system whose impulse response $h[n]$ and input $x[n]$ are shown in Fig. 10.28.

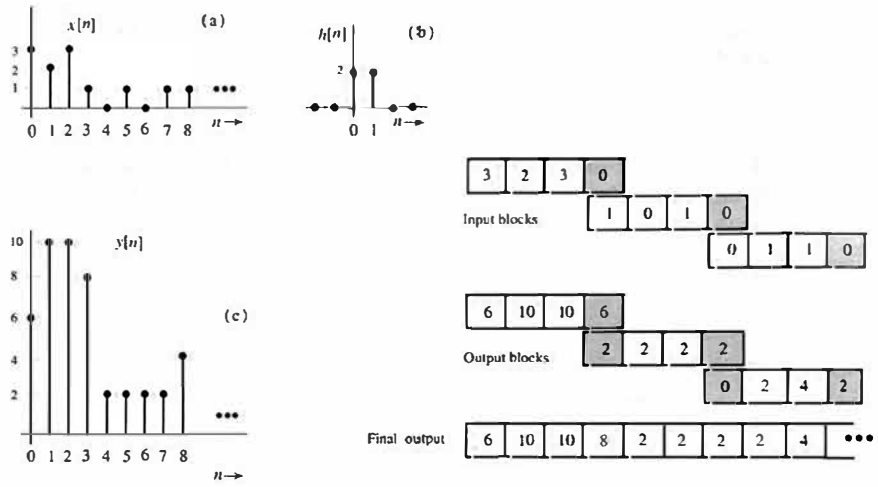

Figure 10.28 Demonstrating the overlap and add method of block convolution.

The output $y[n]$ is the linear convolution of $x[n]$ and $h[n]$. Let us use $L = 3$ for the block convolution. By inspection of $h[n]$, we see that $M = 2$. Hence, we need to break the input sequence in blocks of 3 samples and pad each block with $M - 1 = 1$ zero, as depicted in Fig. 10.28. We convolve each of these blocks with $h[n]$ using the DFT, as demonstrated in Ex. 10.19.

In this example, $N_0 = 4$ and $\Omega_0 = \pi/4$. The DFTs X_r and H_r of the zero-padded sequences $x[n]$ and $h[n]$ are given by

$$X_r = \sum_{n=0}^{2} x[n]e^{-jr\frac{\pi}{2}n} \qquad \text{and} \qquad H_r = \sum_{n=0}^{1} h[n]e^{-jr\frac{\pi}{2}n}$$

Also, $Y_r = X_r H_r$. We compute the values of X_r, H_r, and Y_r using these equations for each block.

For the first block,

$$X_r = 3 + 2e^{-j\frac{\pi}{2}r} + 3e^{-j\pi r}, \qquad H_r = 2 + 2e^{-j\frac{\pi}{2}r}, \qquad \text{and} \qquad Y_r = X_r H_r$$

Substituting $r = 0, 1, 2, 3$, we obtain

$$\begin{array}{llll} X_0 = 8 & X_1 = -2j & X_2 = 4 & X_3 = 2j \\ H_0 = 4 & H_1 = 2\sqrt{2}e^{-j\frac{\pi}{4}} & H_2 = 0 & H_3 = 2\sqrt{2}e^{j\frac{\pi}{4}} \\ Y_0 = 32 & Y_1 = 4\sqrt{2}e^{-j\frac{3\pi}{4}} & Y_2 = 0 & Y_3 = 4\sqrt{2}e^{j\frac{3\pi}{4}} \end{array}$$

Also

$$y[n] = \frac{1}{4}\sum_{r=0}^{3} Y_r e^{jr\frac{\pi}{2}n} = \frac{1}{4}\left(Y_0 + Y_1 e^{j\frac{\pi}{2}n} + Y_2 e^{j\pi n} + Y_3 e^{j\frac{3\pi}{2}n}\right)$$

Substituting the appropriate values, we obtain

$$y[0] = 6 \qquad y[1] = 10 \qquad y[2] = 10 \qquad y[3] = 6$$

Using the same procedure for the second block, we obtain

$$y[0] = 2 \qquad y[1] = 2 \qquad y[2] = 2 \qquad y[3] = 2$$

For the third block, we obtain

$$y[0] = 0 \qquad y[1] = 2 \qquad y[2] = 4 \qquad y[3] = 2$$

Figure 10.28 shows the overlapping input and output blocks, and the convolution sequence obtained by adding the output blocks.

In this example, DFT-based convolution is much more laborious than the direct convolution by the sliding-tape method (see Fig. 9.7). One reason is that we did not use the FFT algorithm to compute the DFTs. Furthermore, for the rather small N_0 of this example, even the FFT will have more computations than direct convolution. In practice, we generally deal with much larger values of N_0, and DFT-based methods that utilize the FFT really pay off.

Overlap and Save Method

In the *overlap and save* method, the input sequence is again sectioned into nonoverlapping blocks of a manageable length L. As before, each block is augmented with $M - 1$ data points. But unlike the previous method, this method places augmented points at the beginning of each block. The augmented $M - 1$ data points of a block are the same as the last $M - 1$ points of the previous block so that the last $M - 1$ data points of each block also appear as the first $M - 1$ data points of the succeeding block. The exception is the first block, where the first $M - 1$ data points are taken as zeros, as shown in Fig. 10.29. We now convolve each of these blocks with $h[n]$ (padded by $L - 1$ zeros). As before, DFT is used to perform convolution.

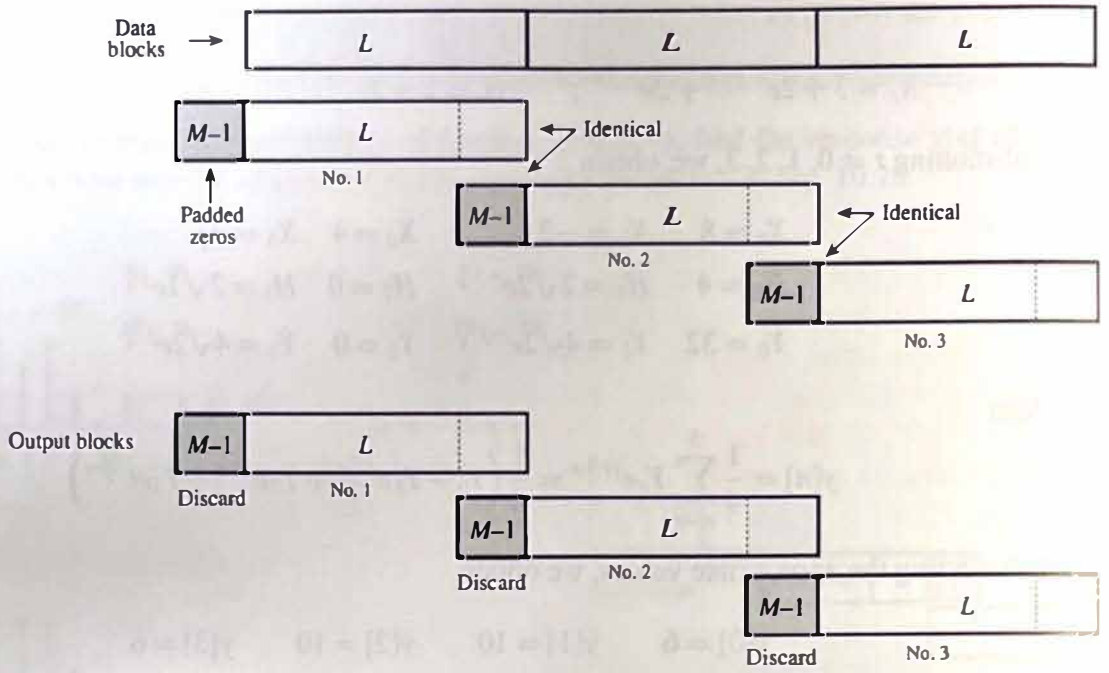

Figure 10.29 Overlap and save method of block convolution.

The output sequence corresponding to each block also has a length $L+M-1$. We discard the first $M-1$ data points and save the last L data points from each output block, as depicted in Fig. 10.29. The total output is given by combining all the saved blocks in sequence. This method is known as the *overlap and save* method. More details of this method can be found in the literature [1].

EXAMPLE 10.22 Overlap and Save Method

Using the overlap and save method of block convolution, find the response $y[n]$ of an LTID system whose impulse response $h[n]$ and input $x[n]$ are shown in Fig. 10.28.

We follow the procedure given in Fig. 10.29 to section the input data as shown in Fig. 10.30. Note that the first $M-1=1$ data point of the first block is padded (zero) and the last $M-1=1$ point of each block also appears as the first point of the next block. Each block of length $L-M+1=4$ is now convolved (using the DFT) with $h[n]$ (padded with two zeros). The DFT procedure is already explained in Ex. 10.21. We shall omit the details here. The resulting output blocks are depicted in Fig. 10.30. The first $M-1=1$ point of each output block is discarded. The total output is given by combining all the saved blocks in sequence.

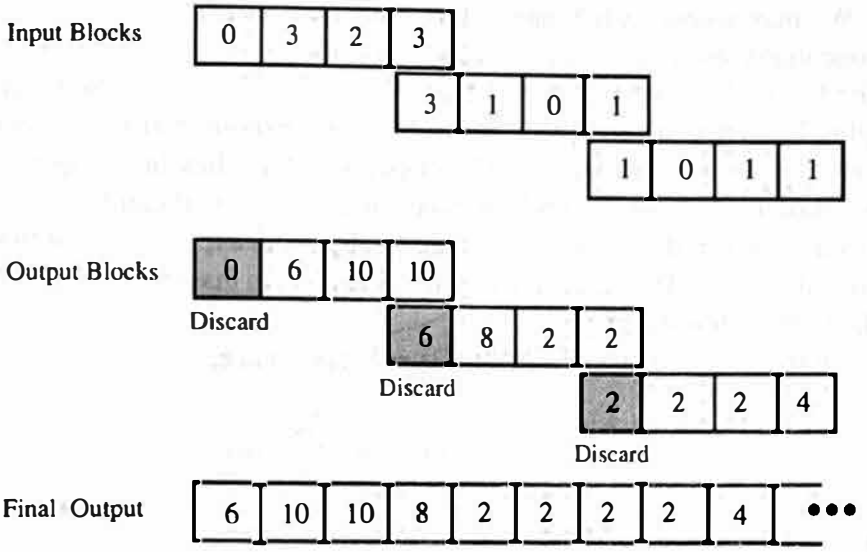

Figure 10.30 Demonstrating the overlap and save method of block convolution.

DRILL 10.13 Block Convolution

The input $x[n]$ of an LTID system is a sequence $[1,0,-1,2,\ldots]$, and the system impulse response $h[n]$ is a 3-point sequence $[3,2,3]$. Both sequences start at $n=0$. Using block convolution with $L=2$, show that the output is $[3,2,0,4,\ldots]$. Derive your answer using both methods of block convolution.

10.7 GENERALIZATION OF THE DTFT TO THE z-TRANSFORM

LTID systems can be analyzed by using the DTFT. This method, however, has the following limitations.

1. Existence of the DTFT is guaranteed only for absolutely summable signals. The DTFT does not exist for exponentially or even linearly growing signals. This means that the DTFT method is applicable only for a limited class of inputs.
2. Moreover, this method can be applied only to asymptotically or BIBO-stable systems; it cannot be used for unstable or even marginally stable systems.

These are serious limitations in the study of LTID system analysis. Actually, it is the first limitation that is also the cause of the second limitation. Because the DTFT is incapable of handling growing signals, it is incapable of handling unstable or marginally stable systems.[†] Our goal is, therefore, to extend the DTFT concept so that it can handle exponentially growing signals.

[†] Recall that the output of an unstable system grows exponentially. Also, the output of a marginally stable system to characteristic mode input grows with time.

We may wonder what causes this limitation on DTFT so that it is incapable of handling exponentially growing signals. Recall that in the DTFT, we are using sinusoids or exponentials of the form $e^{j\Omega n}$ to synthesize an arbitrary signal $x[n]$. These signals are sinusoids with constant amplitudes. They are incapable of synthesizing exponentially growing signals no matter how many such components we add. Our hope, therefore, lies in trying to synthesize $x[n]$ by using exponentially growing sinusoids or exponentials. This goal can be accomplished by generalizing the frequency variable $j\Omega$ to $\sigma + j\Omega$, that is, by using exponentials of the form $e^{(\sigma+j\Omega)n}$ instead of exponentials $e^{j\Omega n}$. The procedure is almost identical to that used in extending the Fourier transform to the Laplace transform.

Let us define a new variable $\hat{X}(j\Omega) = X(\Omega)$. Hence,

$$\hat{X}(j\Omega) = \sum_{n=-\infty}^{\infty} x[n]\, e^{-j\Omega n} \tag{10.51}$$

and

$$x[n] = \frac{1}{2\pi} \int_{-\pi}^{\pi} \hat{X}(j\Omega)\, e^{j\Omega n}\, d\Omega$$

Consider now the DTFT of $x[n]e^{-\sigma n}$ (σ real):

$$\text{DTFT}\{x[n]e^{-\sigma n}\} = \sum_{n=-\infty}^{\infty} x[n]\, e^{-\sigma n} e^{-j\Omega n} = \sum_{n=-\infty}^{\infty} x[n]\, e^{-(\sigma+j\Omega)n}$$

It follows from Eq. (10.51) that this sum is $\hat{X}(\sigma + j\Omega)$. Thus,

$$\text{DTFT}\{x[n]e^{-\sigma n}\} = \sum_{n=-\infty}^{\infty} x[n]\, e^{-(\sigma+j\Omega)n} = \hat{X}(\sigma + j\Omega) \tag{10.52}$$

Hence, the inverse DTFT of $\hat{X}(\sigma + j\Omega)$ is $x[n]e^{-\sigma n}$. Therefore,

$$x[n]e^{-\sigma n} = \frac{1}{2\pi} \int_{-\pi}^{\pi} \hat{X}(\sigma + j\Omega)\, e^{j\Omega n}\, d\Omega$$

Multiplying both sides by $e^{\sigma n}$ yields

$$x[n] = \frac{1}{2\pi} \int_{-\pi}^{\pi} \hat{X}(\sigma + j\Omega)\, e^{(\sigma+j\Omega)n}\, d\Omega \tag{10.53}$$

Let us define a new variable z as

$$z = e^{\sigma+j\Omega} \qquad \text{so that} \qquad \ln z = \sigma + j\Omega \qquad \text{and} \qquad \frac{1}{z}\, dz = j\, d\Omega$$

Because $z = e^{\sigma+j\Omega}$ is complex, we can express it as $z = re^{j\Omega}$, where $r = e^{\sigma}$. Thus, z lies on a circle of radius r, and as Ω varies from $-\pi$ to π, z circumambulates along this circle, completing exactly one counterclockwise rotation, as illustrated in Fig. 10.31. Changing to variable z in Eq. (10.53) yields

$$x[n] = \frac{1}{2\pi j} \oint \hat{X}(\ln z)\, z^{n-1}\, dz \tag{10.54}$$

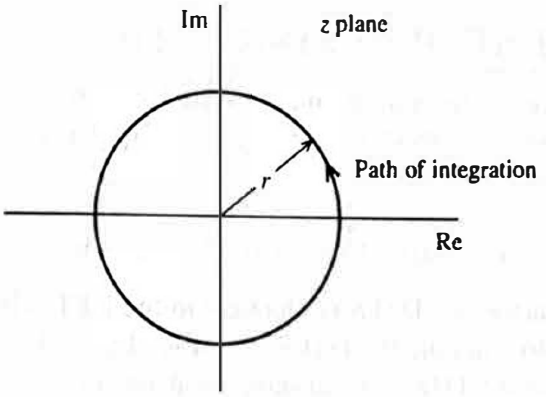

Figure 10.31 Contour of integration for the z-transform.

and from Eq. (10.52), we obtain

$$\hat{X}(\ln z) = \sum_{n=-\infty}^{\infty} x[n] z^{-n} \tag{10.55}$$

where the integral $\oint$ indicates a contour integral around a circle of radius r in the counterclockwise direction.

Equations (10.54) and (10.55) are the desired extensions. They are, however, in a clumsy form. For the sake of convenience, we make another notational change by observing that $\hat{X}(\ln z)$ is a function of z. Let us denote it by a simpler notation $X[z]$. Thus, Eq. (10.54) becomes

$$x[n] = \frac{1}{2\pi j} \oint X[z] z^{n-1} dz \tag{10.56}$$

and Eq. (10.55) becomes

$$X[z] = \sum_{n=-\infty}^{\infty} x[n] z^{-n} \tag{10.57}$$

This is the (bilateral) z-transform pair. Equation (10.56) expresses $x[n]$ as a continuous sum of exponentials of the form $z^n = e^{(\sigma + j\Omega)n} = r^n e^{j\Omega n}$. Thus, by selecting a proper value for r (or σ), we can make the exponential grow (or decay) at any exponential rate we desire.

If we let $\sigma = 0$, we have $z = e^{j\Omega}$ and

$$X[z]|_{z=e^{j\Omega}} = \hat{X}(\ln z)\Big|_{z=e^{j\Omega}} = \hat{X}(j\Omega) = X(\Omega) \tag{10.58}$$

Thus, the familiar DTFT is just a special case of the z-transform $X[z]$ obtained by letting $z = e^{j\Omega}$ and assuming that the sum on the right-hand side of Eq. (10.57) converges when $z = e^{j\Omega}$. This also implies that the ROC for $X[z]$ includes the unit circle.

10.8 MATLAB: WORKING WITH THE DTFS AND THE DTFT

This section investigates various methods to compute the discrete-time Fourier series (DTFS). Performance of these methods is assessed by using MATLAB's stopwatch and profiling functions.

10.8.1 Computing the Discrete-Time Fourier Series

Within a scale factor, the DTFS is identical to the DFT. Thus, methods to compute the DFT can be readily used to compute the DTFS. Specifically, the DTFS is the DFT scaled by $1/N_0$. As an example, consider a 50 Hz sinusoid sampled at 1000 Hz over one-tenth of a second.

```
>> T = 1/1000; N0 = 100; n = (0:N0-1)';
>> x = cos(2*pi*50*n*T);
```

The DTFS is obtained by scaling the DFT.

```
>> X = fft(x)/N0; f = (0:N0-1)/(T*N0);
>> stem(f-1/(2*T),fftshift(abs(X)),'k.');
>> axis([-500 500 -0.05 0.55]); xlabel('f [Hz]'); ylabel('|X(f)|');
```

Figure 10.32 shows a peak magnitude of 0.5 at ± 50 Hz. This result is consistent with Euler's representation

$$\cos(2\pi 50nT) = \frac{1}{2}e^{j2\pi 50nT} + \frac{1}{2}e^{-j2\pi 50nT}$$

Lacking the $1/N_0$ scale factor, the DFT would have a peak amplitude 100 times larger.

The inverse DTFS is obtained by scaling the inverse DFT by N_0.

```
>> x = real(ifft(X)*N0); stem(n,x,'k.');
>> axis([0 99 -1.1 1.1]); xlabel('n'); ylabel('x[n]');
```

Figure 10.33 confirms that the sinusoid $x[n]$ is properly recovered. Although the result is theoretically real, computer round-off errors produce a small imaginary component, which the `real` command removes.

Although MATLAB's `fft` command provides an efficient method to compute the DTFS, other important computational methods exist. A matrix-based approach is one popular way to implement Eq. (10.3). Although not as efficient as an FFT-based algorithm, matrix-based

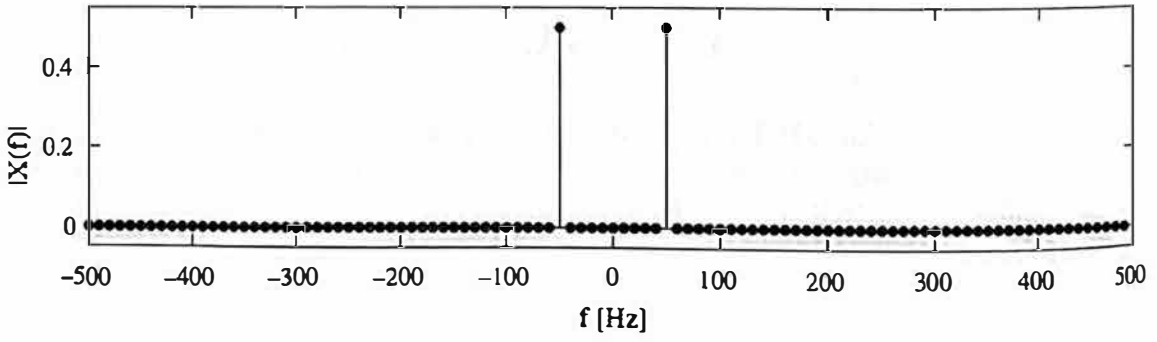

Figure 10.32 DTFS computed by scaling the DFT.

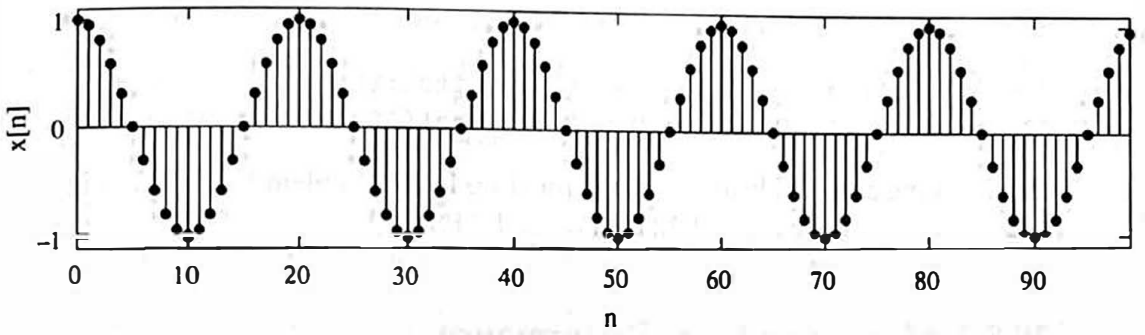

Figure 10.33 Inverse DTFS computed by scaling the inverse DFT.

approaches provide insight into the DTFS and serve as an excellent model for solving similarly structured problems.

To begin, define $W_{N_0} = e^{j\Omega_0}$, which is a constant for a given N_0. Substituting W_{N_0} into Eq. (10.3) yields

$$\mathcal{D}_r = \frac{1}{N_0} \sum_{n=0}^{N_0-1} x[n] W_{N_0}^{-nr}$$

An inner product of two vectors computes $\mathcal{D}_r$.

$$\mathcal{D}_r = \frac{1}{N_0} \begin{bmatrix} 1 & W_{N_0}^{-r} & W_{N_0}^{-2r} & \cdots & W_{N_0}^{-(N_0-1)r} \end{bmatrix} \begin{bmatrix} x[0] \\ x[1] \\ x[2] \\ \vdots \\ x[N_0-1] \end{bmatrix}$$

Stacking the results for all r yields

$$\begin{bmatrix} \mathcal{D}_0 \\ \mathcal{D}_1 \\ \mathcal{D}_2 \\ \vdots \\ \mathcal{D}_{N_0-1} \end{bmatrix} = \frac{1}{N_0} \begin{bmatrix} 1 & 1 & 1 & \cdots & 1 \\ 1 & W_{N_0}^{-1} & W_{N_0}^{-2} & \cdots & W_{N_0}^{-(N_0-1)} \\ 1 & W_{N_0}^{-2} & W_{N_0}^{-4} & \cdots & W_{N_0}^{-2(N_0-1)} \\ \vdots & \vdots & \vdots & \cdots & \vdots \\ 1 & W_{N_0}^{-(N_0-1)} & W_{N_0}^{-2(N_0-1)} & \cdots & W_{N_0}^{-(N_0-1)^2} \end{bmatrix} \begin{bmatrix} x[0] \\ x[1] \\ x[2] \\ \vdots \\ x[N_0-1] \end{bmatrix}$$

In matrix notation, this equation is compactly written as

$$\mathcal{D} = \frac{1}{N_0} \mathbf{W}_{N_0} \mathbf{x}$$

Since it is also used to compute the DFT, matrix $\mathbf{W}_{N_0}$ is often called a DFT matrix.

Let us create an anonymous function to compute the N_0-by-N_0 DFT matrix $\mathbf{W}_{N_0}$. Although not used here, the signal-processing toolbox function `dftmtx` computes the same DFT matrix, although in a less obvious but more efficient fashion.

```
>> W = @(N0) (exp(-j*2*pi/N0)).^((0:N0-1)'*(0:N0-1));
```

While less efficient than FFT-based methods, the matrix approach correctly computes the DTFS.

```
>> X = W(N0)*x/N0; stem(f-1/(2*T),fftshift(abs(X)),'k.');
>> axis([-500 500 -0.05 0.55]); xlabel('f [Hz]'); ylabel('|X(f)|');
```

The resulting plot is indistinguishable from Fig. 10.32. Problem 10.8-1 investigates a matrix-based approach to compute Eq. (10.2), the inverse DTFS.

10.8.2 Measuring Code Performance

Writing efficient code is important, particularly if the code is frequently used, requires complicated operations, involves large data sets, or operates in real time. MATLAB provides several tools for assessing code performance. When properly used, the `profile` function provides detailed statistics that help assess code performance. MATLAB help thoroughly describes the use of the sophisticated `profile` command.

A simpler method of assessing code efficiency is to measure execution time and compare it with a reference. The MATLAB command `tic` starts a stopwatch timer. The `toc` command reads the timer. Sandwiching instructions between `tic` and `toc` returns the elapsed time. For example, the execution time of the 100-point matrix-based DTFS computation is

```
>> tic; W(N0)*x/N0; toc
   Elapsed time is 0.002385 seconds.
```

Different machines operate at different speeds with different operating systems and with different background tasks. Therefore, elapsed-time measurements can vary considerably from machine to machine and from execution to execution. For relatively simple and short events like the present case, execution times can be so brief that MATLAB may report unreliable times or fail to register an elapsed time at all.

To increase the elapsed time and therefore the accuracy of the time measurement, a loop is used to repeat the calculation.

```
>> tic; for i=1:100, W(N0)*x/N0; end; toc
   Elapsed time is 0.179059 seconds.
```

This elapsed time suggests that each 100-point DTFS calculation takes a little under 2 milliseconds. What exactly does this mean, however? Elapsed time is only meaningful relative to some reference. Let us see what difference occurs by precomputing the DFT matrix, rather than repeatedly using our anonymous function.

```
>> W100 = W(100); tic; for i=1:100, W100*x/N0; end; toc
   Elapsed time is 0.001265 seconds.
```

Amazingly, this small change makes a hundredfold change in our computational efficiency! Clearly, it is much better to precompute the DFT matrix.

To provide another example, consider the time it takes to compute the same DTFS using the FFT-based approach.

```
>> tic; for i=1:100, fft(x)/N0; end; toc
   Elapsed time is 0.000419 seconds.
```

With this as a reference, our fastest matrix-based computations appear to be several times slower than the FFT-based computations. This difference becomes more dramatic as N_0 is increased. Since the two methods provide identical results, there is little incentive to use the slower matrix-based approach, and the FFT-based algorithm is generally preferred. Even so, the FFT can exhibit curious behavior: adding a few data points, even the artificial samples introduced by zero padding, can dramatically increase or decrease execution times. The `tic` and `toc` commands illustrate this strange result. Consider computing the DTFS of 1015 random data points 100 times.

```
>> x1 = rand(1015,1); tic; for i=1:100; fft(x1)/1015; end; T1 = toc
   T1 = 0.0038
```

Next, pad the sequence with four zeros.

```
>> x2 = [x1;zeros(4,1)]; tic; for i=1:100; fft(x2)/1019; end; T2 = toc
   T2 = 0.0087
```

The ratio of the two elapsed times indicates that adding four points to an already long sequence increases the computation time by a factor of 2. Next, the sequence is zero-padded to a length of $N_0 = 1024$.

```
>> x3 = [x2;zeros(5,1)]; tic; for i=1:100; fft(x3)/1024; end; T3 = toc
   T3 = 0.0017
```

In this case, the added data decrease the original execution time by a factor of 2 and the second execution time by a factor of 5! These results are particularly surprising when it is realized that the lengths of y1, y2, and y3 differ by less than 1%.

As it turns out, the efficiency of the `fft` command depends on the factorability of N_0. With the `factor` command, $1015 = (5)(7)(29)$, 1019 is prime, and $1024 = (2)^{10}$. The most factorable length, 1024, results in the fastest execution, while the least factorable length, 1019, results in the slowest execution. To ensure the greatest factorability and fastest operation, vector lengths are ideally a power of 2.

10.9 SUMMARY

This chapter deals with the analysis and processing of discrete-time signals. For analysis, our approach is parallel to that used in continuous-time signals. We first represent a periodic $x[n]$ as a Fourier series formed by a discrete-time exponential and its harmonics. Later we extend this representation to an aperiodic signal $x[n]$ by considering $x[n]$ to be a limiting case of a periodic signal with period approaching infinity.

Periodic signals are represented by discrete-time Fourier series (DTFS); aperiodic signals are represented by the discrete-time Fourier transform (DTFT). The development, although similar to that of continuous-time signals, also reveals some significant differences. The basic difference in the two cases arises because a continuous-time exponential $e^{j\omega t}$ has a unique waveform for every value of ω in the range $-\infty$ to ∞. In contrast, a discrete-time exponential $e^{j\Omega n}$ has a unique waveform only for values of Ω in a continuous interval of 2π. Therefore, if Ω_0 is the fundamental frequency, then at most $2\pi/\Omega_0$ exponentials in the Fourier series are independent. Consequently, the discrete-time exponential Fourier series has only $N_0 = 2\pi/\Omega_0$ terms.

The discrete-time Fourier transform (DTFT) of an aperiodic signal is a continuous function of Ω and is periodic with period 2π. We can synthesize $x[n]$ from spectral components of $X(\Omega)$ in any band of width 2π. In a basic sense, the DTFT has a finite spectral width of 2π, which makes it bandlimited to π radians.

Linear, time-invariant, discrete-time (LTID) systems can be analyzed by means of the DTFT if the input signals are DTF-transformable and if the system is stable. Analysis of unstable (or marginally stable) systems and/or exponentially growing inputs can be handled by the z-transform, which is a generalized DTFT. The relationship of the DTFT to the z-transform is similar to that of the Fourier transform to the Laplace transform. Whereas the z-transform is superior to the DTFT for analysis of LTID systems, the DTFT is preferable in signal analysis.

If $H(\Omega)$ is the DTFT of the system's impulse response $h[n]$, then $|H(\Omega)|$ is the amplitude response, and $\angle H(\Omega)$ is the phase response of the system. Moreover, if $X(\Omega)$ and $Y(\Omega)$ are the DTFTs of the input $x[n]$ and the corresponding output $y[n]$, then $Y(\Omega) = H(\Omega)X(\Omega)$. Therefore, the output spectrum is the product of the input spectrum and the system's frequency response.

Because of the similarity between the DFT and DTFT relationships, numerical computations of the DTFT of finite-length signals can be handled by using the DFT and the FFT, introduced in Secs. 5.5 and 5.6. For an N_0-point signal $x[n]$, its DFT yields exactly N_0 samples of $X(\Omega)$ at frequency intervals of $2\pi/N_0$. We can obtain a larger number of samples of $X(\Omega)$ by padding a sufficient number of zeros to $x[n]$. The N_0-point DFT of $x[n]$ gives exact values of the DTFT samples if $x[n]$ has a finite-length N_0. For signals of infinite length, we use a window of suitable length to truncate the signal so that the final results are within a given error tolerance.

Because of the convolution property, we can compute the convolution of two signals $x[n]$ and $h[n]$ using the DFT. For this purpose, we need to pad both signals by a suitable number of zeros so as to make the linear convolution of the two signals identical to the circular (or periodic) convolution of the padded signals. Large blocks of data may be processed by sectioning the data into smaller blocks and processing such smaller blocks in sequence. Such a procedure typically requires less memory and processing time.

Reference

1. Lathi, B. P. and Green, R. A., *Essentials of Digital Signal Processing*, Cambridge University Press, New York, 2014.

PROBLEMS

10.1-1 Find the discrete-time Fourier series (DTFS) and sketch their spectra $|\mathcal{D}_r|$ and $\angle\mathcal{D}_r$ for $0 \le r \le N_0 - 1$ for the following periodic signal:

$$x[n] = 4\cos 2.4\pi n + 2\sin 3.2\pi n$$

10.1-2 Repeat Prob. 10.1-1 for $x[n] = \cos 2.2\pi n \cos 3.3\pi n$.

10.1-3 Repeat Prob. 10.1-1 for $x[n] = 2\cos 3.2\pi(n-3)$.

10.1-4 Determine and sketch the DTFS spectrum $\mathcal{D}_r$ of a 7-periodic signal $x[n]$ that over $0 \le n \le 6$ is given by

$$[0, 1, -2, 3, -4, 5, -6]$$

How does the spectrum $\mathcal{D}_r$ change if $x[n]$ is time-reversed?

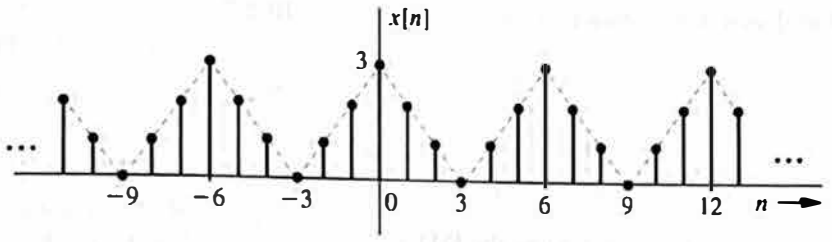

Figure P10.1-5

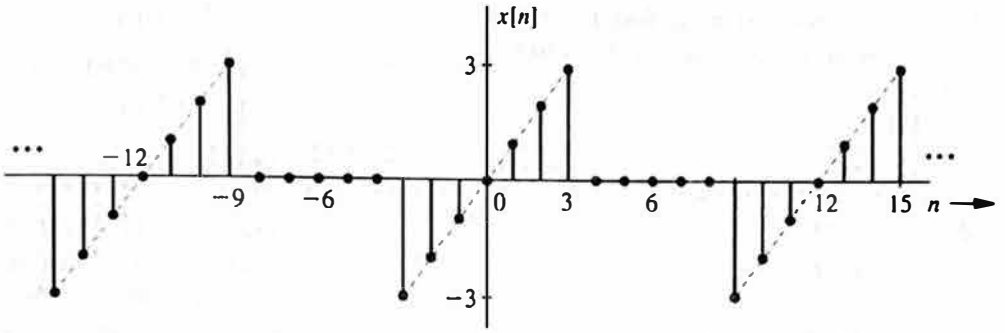

Figure P10.1-6

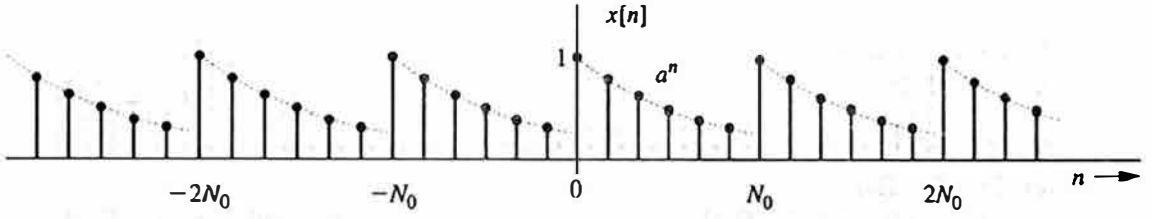

Figure P10.1-7

10.1-5 Find the discrete-time Fourier series and the corresponding amplitude and phase spectra for the $x[n]$ shown in Fig. P10.1-5.

10.1-6 Repeat Prob. 10.1-5 for the $x[n]$ depicted in Fig. P10.1-6.

10.1-7 Repeat Prob. 10.1-5 for the $x[n]$ illustrated in Fig. P10.1-7.

10.1-8 An N_0-periodic signal $x[n]$ is represented by its DTFS, as in Eq. (10.2). Prove Parseval's theorem (for the DTFS), which states that

$$\frac{1}{N_0}\sum_{n=\langle N_0\rangle}|x[n]|^2=\sum_{r=\langle N_0\rangle}|\mathcal{D}_r|^2$$

In the text [Eq. (10.34)], we obtain Parseval's theorem for the DTFT. [*Hint:* If w is complex, then $|w|^2=ww^*$ and use Eq. (5.15).]

10.1-9 Answer yes or no, and justify your answers with an appropriate example or proof.

(a) Is a sum of aperiodic discrete-time sequences ever periodic?

(b) Is a sum of periodic discrete-time sequences ever aperiodic?

10.2-1 Show that for a real $x[n]$, Eq. (10.17) can be expressed as

$$x[n]=\frac{1}{\pi}\int_0^{\pi}|X(\Omega)|\cos\left(\Omega n+\angle X(\Omega)\right)d\Omega$$

This is the trigonometric form of the DTFT.

10.2-2 A signal $x[n]$ can be expressed as the sum of even and odd components (Sec. 1.5.1):

$$x[n]=x_e[n]+x_o[n]$$

(a) If $x[n] \Longleftrightarrow X(\Omega)$, show that for real $x[n]$,

$$x_e[n] \Longleftrightarrow \text{Re}[X(\Omega)]$$

and

$$x_o[n] \Longleftrightarrow j\,\text{Im}[X(\Omega)]$$

(b) Verify these results by finding the DTFT of the even and odd components of the signal $(0.8)^n u[n]$.

10.2-3 For the following signals, find the DTFT directly, using the definition in Eq. (10.18). Assume $|\gamma| < 1$.

(a) $\delta[n]$
(b) $\delta[n-k]$
(c) $\gamma^n u[n-1]$
(d) $\gamma^n u[n+1]$
(e) $(-\gamma)^n u[n]$
(f) $\gamma^{|n|}$

10.2-4 Use Eq. (10.17) to find the inverse DTFT for the following spectra, given only over the interval $|\Omega| \le \pi$. Assume Ω_c and $\Omega_0 < \pi$.

(a) $e^{jk\Omega}$ integer k
(b) $\cos k\Omega$ integer k
(c) $\cos^2(\Omega/2)$
(d) $\Delta\left(\dfrac{\Omega}{2\Omega_c}\right)$
(e) $2\pi\delta(\Omega-\Omega_0)$
(f) $\pi[\delta(\Omega-\Omega_0)+\delta(\Omega+\Omega_0)]$

10.2-5 (a) Determine and plot the DTFT $X(\Omega)$ of the triangular signal $x[n]$ shown in Fig. P10.2-5.

(b) Using Ex. 10.5 as a guide, use MATLAB and the FFT to validate the DTFT calculations and plot of part (a).

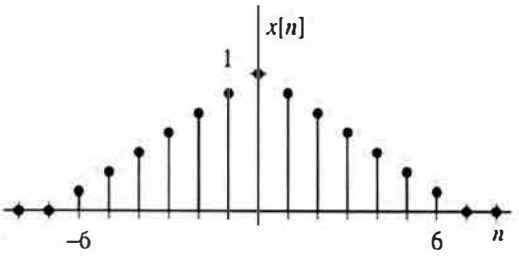

Figure P10.2-5

10.2-6 Using Eq. (10.17), show that the inverse DTFT of $\text{rect}((\Omega - \pi/4)/\pi)$ is $0.5\,\text{sinc}(\pi n/2)e^{j\pi n/4}$.

10.2-7 Using Eq. (10.18), find the DTFT of the signals $x[n]$ in Fig. P10.2-7.

10.2-8 Using Eq. (10.18), find the DTFT of the signals depicted in Fig. P10.2-8.

10.2-9 Use Eq. (10.17) to find the inverse DTFT of the spectra (shown only for $|\Omega| \le \pi$) in Fig. P10.2-9.

10.2-10 Use Eq. (10.17) to find the inverse DTFT of the spectra (shown only for $|\Omega| \le \pi$) in Fig. P10.2-10.

10.2-11 Find the DTFT for the signals shown in Fig. P10.2-11.

10.2-12 Find the inverse DTFT of $X(\Omega)$ (shown only for $|\Omega| \le \pi$) for the spectra illustrated in Fig. P10.2-12. [*Hint:* $X(\Omega) = |X(\Omega)|e^{j\angle X(\Omega)}$. This problem illustrates how different phase spectra (both with the same amplitude spectrum) represent entirely different signals.]

10.2-13 (a) Show that an upsampled signal $x[n/L]$ can be expressed as

$$x[n/L] = \sum_{k=-\infty}^{\infty} x[k]\delta[n-Lk]$$

(b) Find the DTFT of $x[n/L]$ by finding the DTFT of the right-hand side of the equation in part (a).

(c) Use the result in part (b) and Table 10.1 to find the DTFT of $z[n]$, shown in Fig. P10.2-13.

10.2-14 (a) A glance at Eq. (10.17) shows that the inverse DTFT equation is identical to the inverse (continuous-time) Fourier transform Eq. (4.10) for a signal $x(t)$ bandlimited to π rad/s. Hence, we should be able to use the continuous-time Fourier transform Table 4.1 to find DTFT pairs that correspond to continuous-time transform pairs for bandlimited signals. Use this fact to derive DTFT pairs 8, 9, 11, 12, 13, and 14 in Table 10.1 by means of the appropriate pairs in Table 4.1.

(b) Can this method be used to derive pairs 2, 3, 4, 5, 6, 7, 10, 15, and 16 in Table 10.1? Justify your answer with specific reason(s).

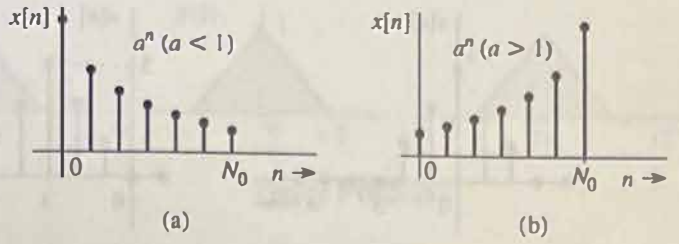

Figure P10.2-7

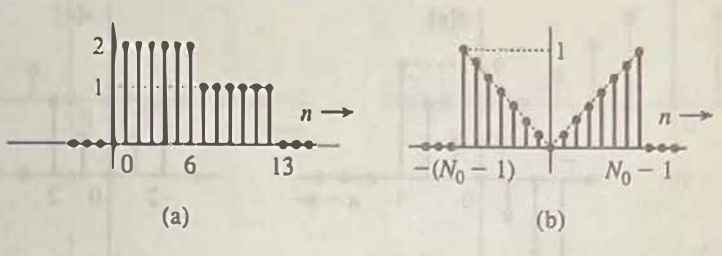

Figure P10.2-8

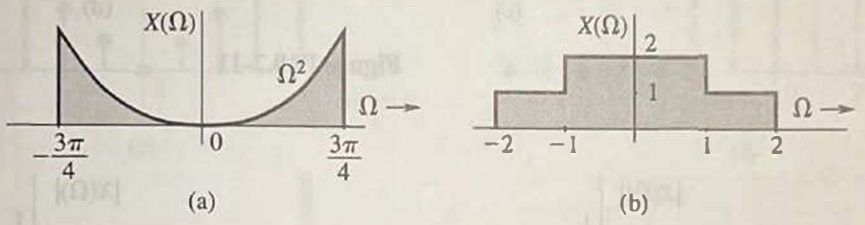

Figure P10.2-9

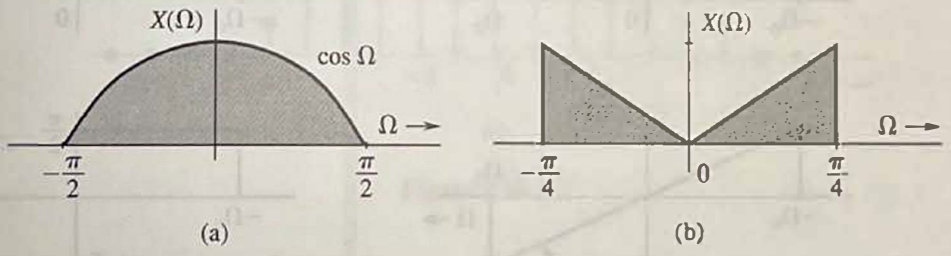

Figure P10.2-10

10.2-15 Are the following frequency-domain signals valid DTFTs? Answer yes or no, and justify your answers.

(a) $X(\Omega) = \Omega + \pi$
(b) $X(\Omega) = j + \pi$
(c) $X(\Omega) = \sin(10\Omega)$
(d) $X(\Omega) = \sin(\Omega/10)$
(e) $X(\Omega) = \delta(\Omega)$

10.2-16 Find the inverse DTFT for the spectrum depicted in Fig. P10.2-16.

10.3-1 Using only pairs 2 and 5 (Table 10.1) and the time-shifting property of Eq. (10.29), find the DTFT of the following signals, assuming $|a| < 1$:

(a) $u[n] - u[n-9]$
(b) $a^{n-m}u[n-m]$
(c) $a^{n-3}(u[n] - u[n-10])$
(d) $a^{n-m}u[n]$
(e) $a^n u[n-m]$
(f) $(n-m)a^{n-m}u[n-m]$
(g) $(n-m)a^n u[n]$
(h) $na^{n-m}u[n-m]$

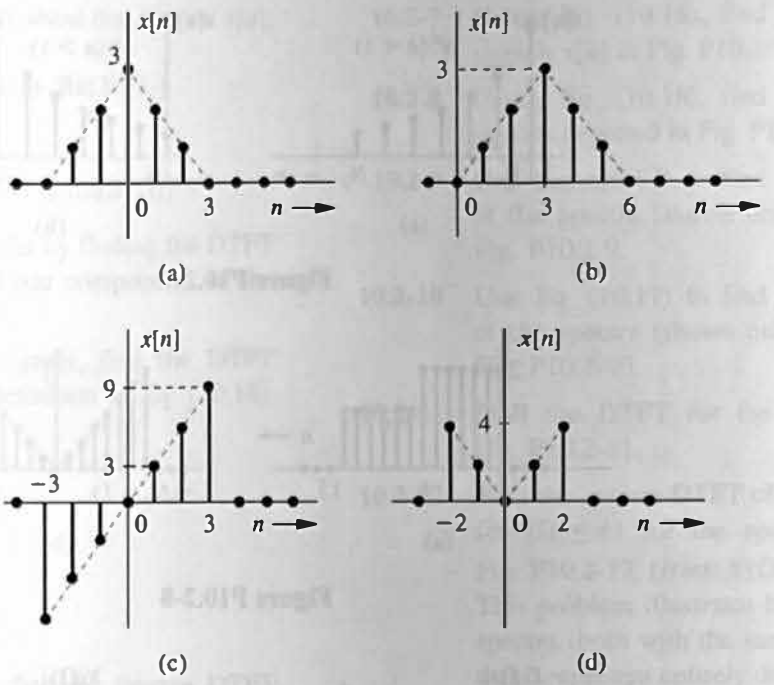

Figure P10.2-11

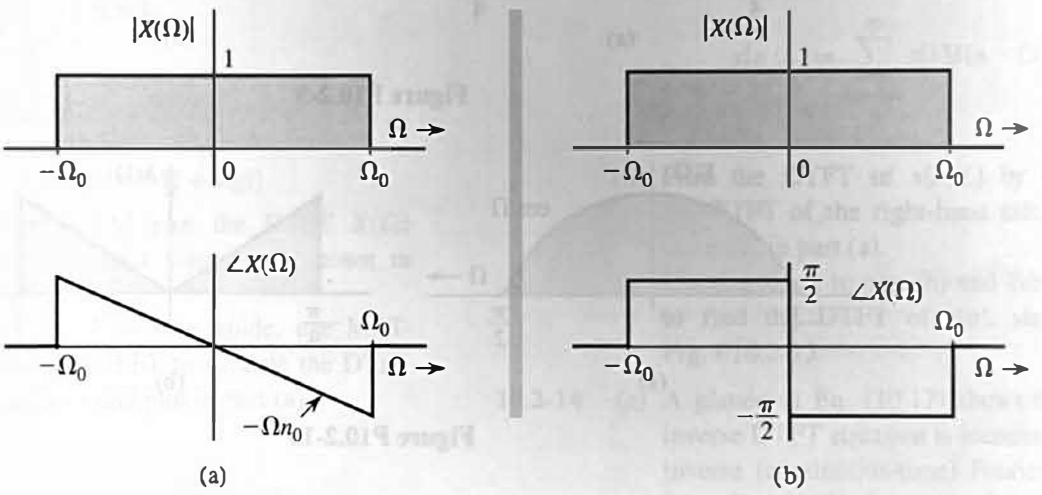

Figure P10.2-12

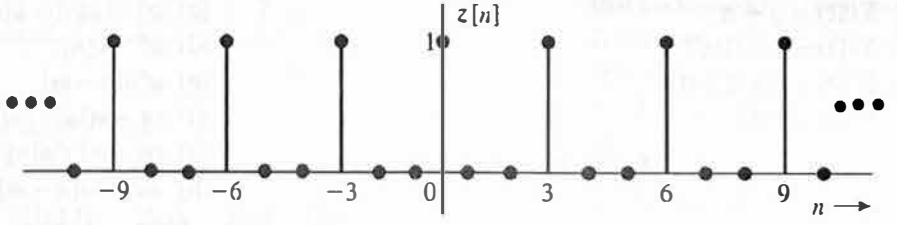

Figure P10.2-13

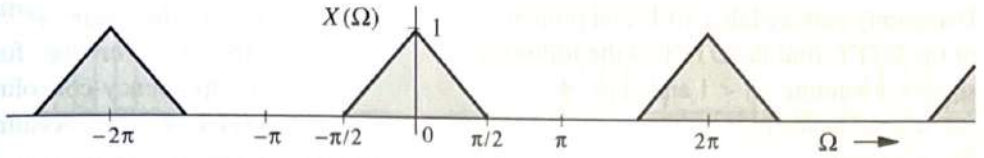

Figure P10.2-16

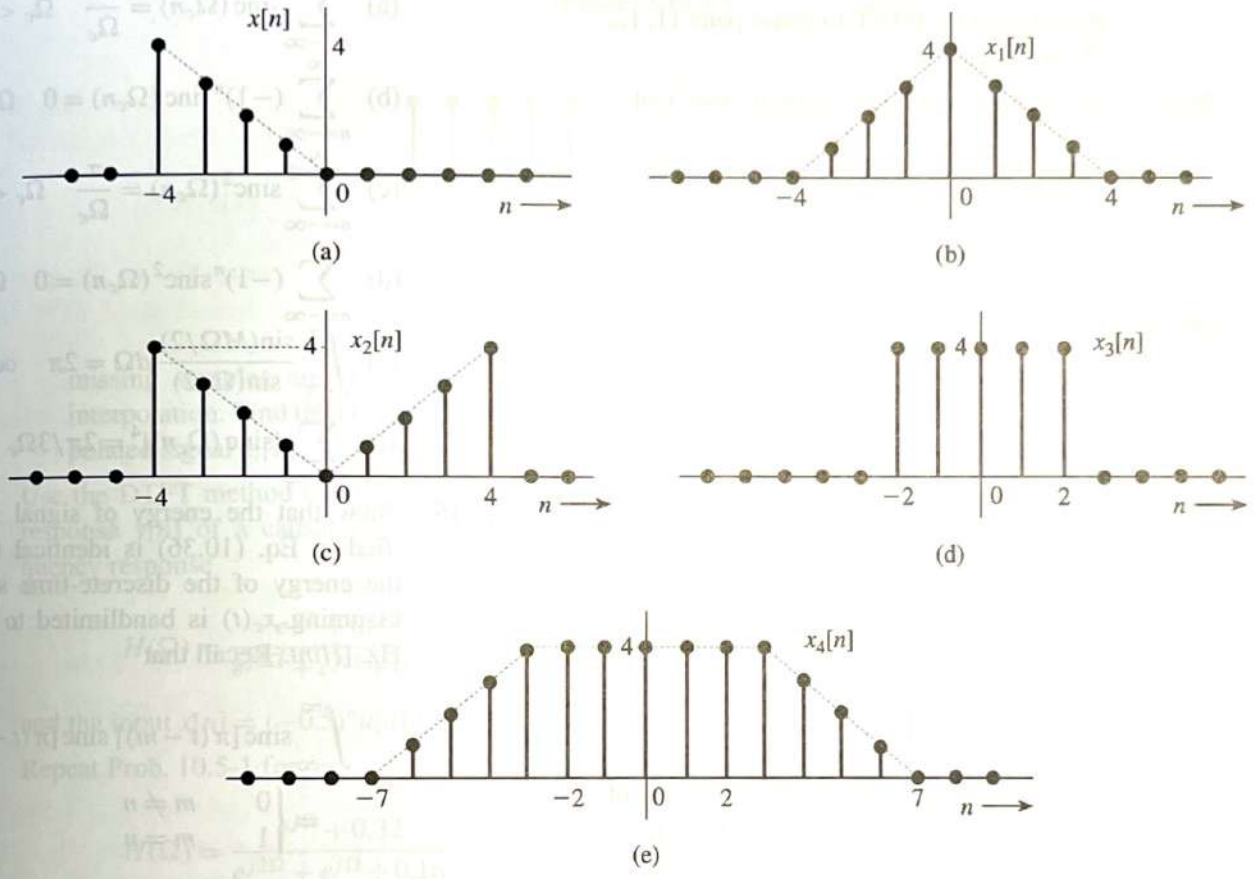

Figure P10.3-2

10.3-2 The triangular pulse $x[n]$ shown in Fig. P10.3-2a is given by

$$X(\Omega) = \frac{4e^{j6\Omega} - 5e^{j5\Omega} + e^{j\Omega}}{(e^{j\Omega} - 1)^2}$$

Use this information and the DTFT properties to find the DTFT of the signals $x_1[n]$, $x_2[n]$, $x_3[n]$, and $x_4[n]$ shown in Figs. P10.3-2b, P10.3-2c, P10.3-2d, and P10.3-2e, respectively.

10.3-3 Suppose signal $x[n] = \text{sinc}^2(\pi n/2)$ modulates a carrier $\cos(\Omega_c n)$ to produce signal $y[n] = x[n]\cos(\Omega_c n)$. Find and sketch the DTFT of:

(a) $x[n]$
(b) $y[n]$ for $\Omega_c = \pi/2$
(c) $y[n]$ for $\Omega_c = 3\pi/4$
(d) $y[n]$ for $\Omega_c = \pi$

10.3-4 Show that periodic convolution $X(\Omega) \circledast Y(\Omega) = 2\pi X(\Omega)$ if

$$X(\Omega) = \sum_{k=0}^{4} a_k e^{-jk\Omega}$$

and

$$Y(\Omega) = \frac{\sin(5\Omega/2)}{\sin(\Omega/2)} e^{-j2\Omega}$$

where a_k is a set of arbitrary constants.

10.3-5 Using only pair 2 (Table 10.1) and properties of the DTFT, find the DTFT of the following signals, assuming $|a| < 1$ and $\Omega_0 < \pi$:
(a) $a^n \cos \Omega_0 n u[n]$
(b) $n^2 a^n u[n]$
(c) $(n-k)a^{2n}u[n-m]$

10.3-6 Use pair 10 in Table 10.1, and suitable properties of the DTFT, to derive pairs 11, 12, 13, 14, 15, and 16.

10.3-7 Use the time-shifting property to show that

$$x[n+k]+x[n-k] \Longleftrightarrow 2X(\Omega)\cos k\Omega$$

Use this result to find the DTFT of the signals shown in Fig. P10.3-7.

10.3-8 Use the time-shifting property to show that

$$x[n+k]-x[n-k] \Longleftrightarrow 2jX(\Omega)\sin k\Omega$$

Use this result to find the DTFT of the signal shown in Fig. P10.3-8.

10.3-9 Suppose signal $x[n]$ has spectrum $X(\Omega)$ that is bandlimited to $\pi/2$ rad/sample. Next, define signal $y[n]$ as

$$y[n] = \begin{cases} x[n] & n \text{ even} \\ 0 & n \text{ odd} \end{cases}$$

Determine the spectrum of $Y(\Omega)$ in terms of $X(\Omega)$. Sketch $Y(\Omega)$ if, over $-\pi \le \Omega \le \pi$,

$$X(\Omega) = \begin{cases} |2\Omega/\pi| & -\pi/2 \le \Omega \le \pi/2 \\ 0 & \text{otherwise} \end{cases}$$

10.3-10 Repeat Prob. 10.3-9 if $y[n]$ is instead defined as

$$y[n] = \begin{cases} x[n] & n \text{ odd} \\ 0 & n \text{ even} \end{cases}$$

10.3-11 Using only pair 2 in Table 10.1 and the convolution property, find the inverse DTFT of $X(\Omega) = e^{2j\Omega}/(e^{j\Omega}-\gamma)^2$.

10.3-12 In Table 10.1, you are given pair 1. From this information and using suitable properties of the DTFT, derive pairs 2, 3, 4, 5, 6, and 7 of Table 10.1. For example, starting with pair 1, derive pair 2. From pair 2, use suitable properties of the DTFT to derive pair 3. From pairs 2 and 3, derive pair 4, and so on.

10.3-13 From the pair $e^{j(\Omega_0/2)n} \Longleftrightarrow 2\pi\delta(\Omega - (\Omega_0/2))$ over the fundamental band, and the frequency-convolution property, find the DTFT of $e^{j\Omega_0 n}$. Assume $|\Omega_0| < \pi$.

10.3-14 From the definition and properties of the DTFT, show that

(a) $\displaystyle\sum_{n=-\infty}^{\infty} \text{sinc}\,(\Omega_c n) = \frac{\pi}{\Omega_c} \quad \Omega_c < \pi$

(b) $\displaystyle\sum_{n=-\infty}^{\infty} (-1)^n \text{sinc}\,(\Omega_c n) = 0 \quad \Omega_c < \pi$

(c) $\displaystyle\sum_{n=-\infty}^{\infty} \text{sinc}^2(\Omega_c n) = \frac{\pi}{\Omega_c} \quad \Omega_c < \pi/2$

(d) $\displaystyle\sum_{n=-\infty}^{\infty} (-1)^n \text{sinc}^2(\Omega_c n) = 0 \quad \Omega_c < \pi/2$

(e) $\displaystyle\int_{-\pi}^{\pi} \frac{\sin(M\Omega/2)}{\sin(\Omega/2)}\,d\Omega = 2\pi \quad \text{odd}\, M$

(f) $\displaystyle\sum_{n=-\infty}^{\infty} |\text{sinc}\,(\Omega_c n)|^4 = 2\pi/3\Omega_c \quad \Omega_c < \pi/2$

10.3-15 Show that the energy of signal $x_c(t)$ specified in Eq. (10.36) is identical to T times the energy of the discrete-time signal $x[n]$, assuming $x_c(t)$ is bandlimited to $B \le 1/2T$ Hz. [*Hint:* Recall that

$$\int_{-\infty}^{\infty} \text{sinc}\,[\pi(t-m)]\,\text{sinc}\,[\pi(t-n)]\,dt = \begin{cases} 0 & m \ne n \\ 1 & m = n \end{cases}$$

That is, sinc functions are orthogonal.]

10.4-1 Determine the DTFT of $x[n] = \sin(\Omega_0 n)$ from the CTFT of $x_c(t) = \sin(\omega_0 t)$.

10.4-2 A CT signal $x(t)$, bandlimited to 25 kHz, is sampled at 50 kHz to produce

$$x[n] = \delta[n+4] - 2\delta[n+2] + \delta[n+1] - 3\delta[n] - \delta[n-1] - 2\delta[n-2] - \delta[n-4]$$

Determine the CTFT $X(\omega)$.

10.4-3 Consider the spectrum $X(\Omega)$ in Fig. P10.2-16.
(a) Find and sketch its IDTFT $x[n]$.
(b) Sketch $x[2n]$ and $x[4n]$, and find their DTFTs.
(c) Sketch $x[n/2]$ ($x[n]$ upsampled by 2). Sketch the interpolated signal $x_i[n]$ where

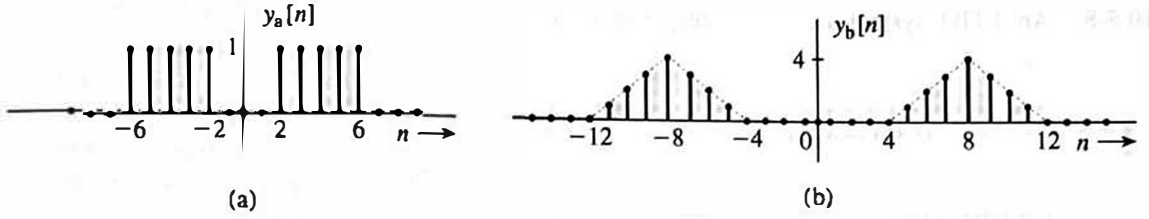

Figure P10.3-7

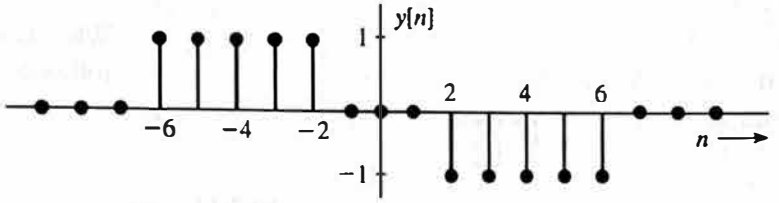

Figure P10.3-8

missing samples are filled using ideal interpolation. Find the DTFT of the interpolated signal $x_i[n]$.

10.5-1 Use the DTFT method to find the zero-state response $y[n]$ of a causal system with frequency response

$$H(\Omega) = \frac{e^{j\Omega} + 0.32}{e^{j2\Omega} + e^{j\Omega} + 0.16}$$

and the input $x[n] = (-0.5)^n u[n]$.

10.5-2 Repeat Prob. 10.5-1 for

$$H(\Omega) = \frac{e^{j\Omega} + 0.32}{e^{j2\Omega} + e^{j\Omega} + 0.16}$$

and input $x[n] = u[n]$.

10.5-3 Repeat Prob. 10.5-1 for

$$H(\Omega) = \frac{e^{j\Omega}}{e^{j\Omega} - 0.5}$$

and

$$x[n] = 0.8^n u[n] + 2(2)^n u[-(n+1)]$$

10.5-4 Determine and sketch the magnitude and phase response for an LTID system specified by the equation

$$y[n] + 0.5y[n-1] = x[n] - 0.9x[n-1]$$

Determine the system output $y[n]$ for the input $x[n] = \cos(\frac{\pi n}{3} + 0.5)$.

10.5-5 Repeat Prob. 10.5-4 if the LTID system is instead specified by the equation

$$y[n] - 0.5y[n-1] = x[n] + 0.9x[n-1]$$

10.5-6 An accumulator system has the property that an input $x[n]$ results in the output

$$y[n] = \sum_{k=-\infty}^{n} x[k]$$

(a) Find the unit impulse response $h[n]$ and the frequency response $H(\Omega)$ for the accumulator.

(b) Use the results of part (a) to find the DTFT of $u[n]$.

10.5-7 A noncausal 7-point moving average is described by the equation

$$y[n] = \frac{1}{7} \sum_{k=-3}^{3} x[n-k]$$

(a) Find and sketch the magnitude and phase responses of the system.

(b) How can this system be made causal? Plot the magnitude and phase responses of the causal system, and comment on any differences from part (a).

10.5-8 An LTID system frequency response over $|\Omega| \leq \pi$ is

$$H(\Omega) = \text{rect}\left(\frac{\Omega}{\pi}\right)e^{-j2\Omega}$$

Find the output $y[n]$ of this system, if the input $x[n]$ is given by
(a) $\text{sinc}(\pi n/2)$
(b) $\text{sinc}(\pi n)$
(c) $\text{sinc}^2(\pi n/4)$

10.5-9 (a) If $x[n] \Longleftrightarrow X(\Omega)$, then show that $(-1)^n x[n] \Longleftrightarrow X(\Omega - \pi)$.
(b) Sketch $\gamma^n u[n]$ and $(-\gamma)^n u[n]$ for $\gamma = 0.8$; see the spectra for $\gamma^n u[n]$ in Figs. 10.5b and 10.5c. From these spectra, sketch the spectra for $(-\gamma)^n u[n]$.
(c) An ideal lowpass filter of cutoff frequency Ω_c is specified by the frequency response $H(\Omega) = \text{rect}(\Omega/2\Omega_c)$. Find its impulse response $h[n]$. Find the frequency response of a filter whose impulse response is $(-1)^n h[n]$. Sketch the frequency response of this filter. What kind of filter is this?

10.5-10 An analog differentiator $y(t) = \frac{d}{dt}x(t)$ can be approximated using a backward difference system described as

$$y[n] = \frac{x[n] - x[n-1]}{T}$$

Find and sketch the magnitude and phase responses of this DT system. For what frequencies does the system most behave as a differentiator? For what frequencies does the system least behave as a differentiator?

10.5-11 A filter with impulse response $h[n]$ is modified as shown in Fig. P10.5-11. Determine the resulting filter impulse response $h_1[n]$. Find also the resulting filter frequency response $H_1(\Omega)$ in terms of the frequency response $H(\Omega)$. How are $H(\Omega)$ and $H_1(\Omega)$ related?

10.5-12 (a) Consider an LTID system $\mathcal{S}_1$, specified by a difference equation of the form of Eq. (9.3) in Ch. 9. We construct another system $\mathcal{S}_2$ by replacing coefficients a_i $(i = 0, 1, 2, \ldots, N)$ by coefficients $(-1)^i a_i$ and replacing all coefficients b_i $(i = 0, 1, 2, \ldots, N)$ with coefficients $(-1)^i b_i$. How are the frequency responses of the two systems related?
(b) If $\mathcal{S}_1$ represents a lowpass filter, what kind of filter is specified by $\mathcal{S}_2$?
(c) What type of filter (lowpass, highpass, etc.) is specified by the difference equation

$$y[n] - 0.8y[n-1] = x[n]$$

What kind of filter is specified by the following difference equation?

$$y[n] + 0.8y[n-1] = x[n]$$

10.5-13 (a) The system shown in Fig. P10.5-13 contains two identical LTID filters with frequency response $H_0(\Omega)$ and corresponding impulse response $h_0[n]$. It is easy to see that the system is linear. Show that this system is also time-invariant. Do this by finding the response of the system to input $\delta[n-k]$ in terms of $h_0[n]$.
(b) If $H_0(\Omega) = \text{rect}(\Omega/2W)$ over the fundamental band, and $\Omega_c + W \leq \pi$, find $H(\Omega)$, the frequency response of this system. What kind of filter is this?

10.6-1 Consider the 3-point signal $x[n]$ specified by $x[-1] = x[0] = 3$, $x[1] = 2$, and $x[n] = 0$ otherwise.
(a) Find the DFT X_r and DTFT $X(\Omega)$ of signal $x[n]$. Verify that the DFT values are samples of $X(\Omega)$.
(b) Show that the 3-point DFT of $x[n]$ is identical to that of the signal $x[n]$ in Fig. 10.20a. Explain why both DFTs are the same. Does equivalence of the DFTs mean that the DTFTs of the two signals are also identical? Support your answer mathematically.
(c) Using appropriate zero padding, find the 8-point DFT of $x[n]$.

10.6-2 Consider the 4-point signal $x[n]$ specified by the sequence $[1, 2, 2, 1]$ starting at $n = 0$.
(a) Find the 4-point DFT of $x[n]$.
(b) Using appropriate zero padding, find the 8-point DFT of $x[n]$.
(c) Find $X(\Omega)$, the DTFT of $x[n]$, and verify the DFTs from parts (a) and (b) are samples from $X(\Omega)$.

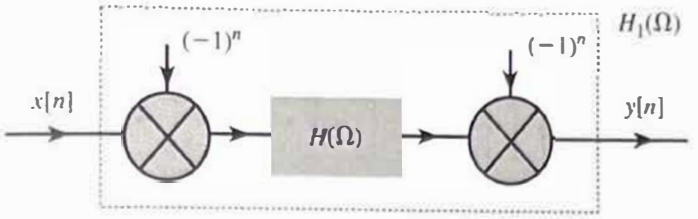

Figure P10.5-11

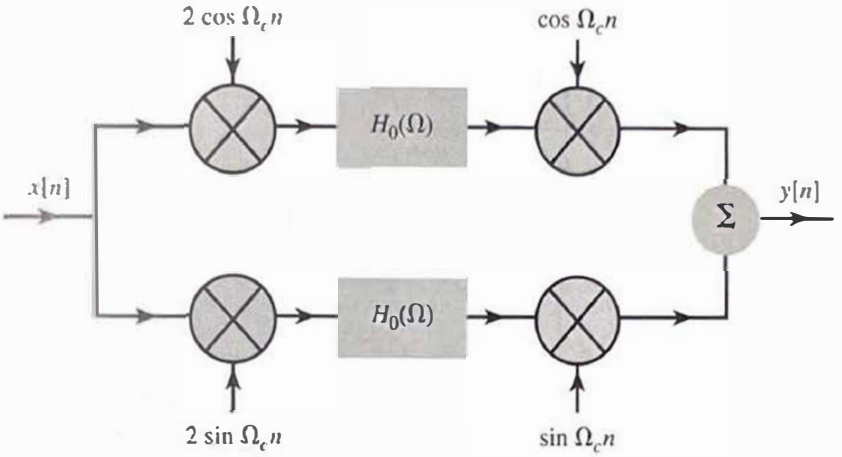

Figure P10.5-13

10.6-3 (a) Find the DFT of the signal $x[n] = \delta[n]$. Find also $X(\Omega)$, the DTFT of $\delta[n]$, and verify the DFT values are samples from $X(\Omega)$. Note that this is a 1-point signal ($N_0 = 1$).

(b) Show that the DFT of $y[n] = \delta[n - m]$ is the same as the DFT of $\delta[n]$ for any integral value of m. Explain this behavior.

(c) Repeat part (a) for the N_0-point DFT (found by padding $N_0 - 1$ zeros to $\delta[n]$). Explain this DFT from $X(\Omega)$ found in part (a).

10.6-4 (a) Find the DFT of the N_0-point signal $x[n] = u[n] - u[n - N_0]$. Find $X(\Omega)$, the DTFT of $x[n]$, and verify that the DFT values are uniform samples of the DTFT at frequency intervals of $\Omega_0 = 2\pi/N_0$.

(b) Is the DFT found in part (a) an adequate frequency-domain description of $x[n]$. If not, what needs to be done to obtain a reasonably adequate spectral picture using the DFT?

10.6-5 (a) Find the 5-point and 8-point DFTs of the signal $x[n]$ illustrated in Fig. P8.1-1d.

(b) Find $X(\Omega)$, the DTFT of $x[n]$, and verify the DFTs from part (a) are samples from $X(\Omega)$.

10.6-6 (a) Using the graphical method shown in Fig. 5.21, find the circular convolution of the sequences $x[n]$ and $h[n]$, depicted in Fig. P10.6-6.

(b) Using the sliding-tape method (Fig. 9.7), find the linear convolution of the first cycles (over the range $0 \le n \le 3$) of the sequences $x[n]$ and $h[n]$. Is the result the same as that found in part (a)?

(c) Circular convolution can be made equivalent to linear convolution by suitably padding (the first cycle of) the sequences $x[n]$ and $h[n]$ with zeros. How many zeros do you need to pad to $x[n]$ and $h[n]$? After suitably padding these sequences, perform the circular convolution using the graphical method illustrated in Fig. 5.21, and show that it is equivalent to the linear convolution found in part (b).

(d) Find the circular convolution of $x[n]$ and $h[n]$ obtained in part (a) using the DFT.

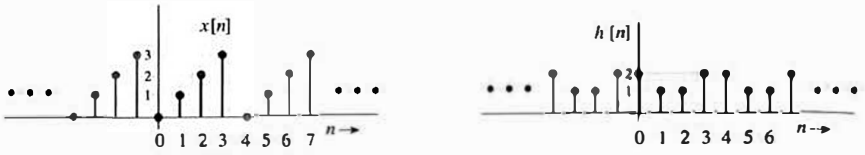

Figure P10.6-6

Figure P10.6-7

Figure P10.6-8

(e) Find the linear convolution of $x[n]$ and $h[n]$ obtained in part (b) using the DFT.

10.6-7 Find the output of a system with impulse response $h[n]$ and the input $x[n]$ shown in Fig. P10.6-7 by the following methods: (a) using the linear convolution of $x[n]$ and $h[n]$ by the sliding-tape method, (b) using circular convolution of suitably padded $x[n]$ and $h[n]$ using the graphical method depicted in Fig. 5.21, and (c) using the DFT.

10.6-8 Repeat Prob. 10.6-7 for the signals $x[n]$ and $h[n]$ illustrated in Fig. P10.6-8.

10.6-9 Using the overlap and add method of block convolution, find the output of a filter with impulse response $h[n]$ and the input $x[n]$ shown in Fig. P10.6-9. Take $L = 3$. Verify that the linear convolution of the input sequence $x[n] = [1, -2, 3, 0, -1, 2, \ldots]$ with $h[n] = [2, 2]$ gives the same output as that found by block convolution.

10.6-10 Repeat Prob. 10.6-9 using the overlap and save method of block convolution.

10.6-11 Find the 16-point IDFT of $X(\Omega)$ in Fig. 10.9a. Do the values of IDFT agree with the values of $x[n]$ found in Ex. 10.6? Explain.

10.8-1 This problem uses a matrix-based approach to investigate the computation of the inverse DTFS.

(a) Implement Eq. (10.2), the inverse DTFS, using a matrix-based approach.

(b) Compare the execution speed of the matrix-based approach to the IFFT-based approach for input vectors of sizes 10, 100, and 1000.

(c) What is the result of multiplying the DFT matrix $\mathbf{W}_{N_0}$ by the inverse DTFS matrix? Discuss your result.

10.8-2 A permutation matrix $\mathbf{P}$ has a single 1 in each row and column with the remaining elements all zero. Permutation matrices are useful for reordering the elements of a vector; the operation $\mathbf{Px}$ reorders the elements of a column vector $\mathbf{x}$ based on the form of $\mathbf{P}$.

(a) Fully describe an $N_0 \times N_0$ permutation matrix named $\mathbf{R}_{N_0}$ that reverses the order of the elements of a column vector $\mathbf{x}$.

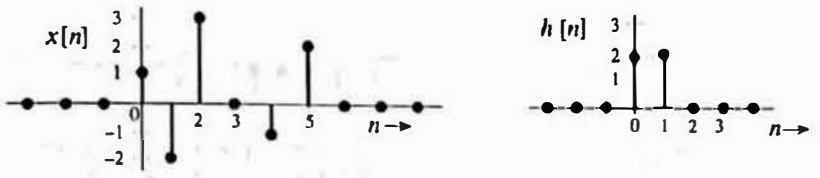

Figure P10.6-9

(b) Given DFT matrix $\mathbf{W}_{N_0}$, verify that $(\mathbf{W}_{N_0})(\mathbf{W}_{N_0}) = \mathbf{W}_{N_0}^2$ produces a scaled permutation matrix. How does $\mathbf{W}_{N_0}^2\mathbf{x}$ reorder the elements of $\mathbf{x}$?

(c) What is the result of $(\mathbf{W}_{N_0}^2)(\mathbf{W}_{N_0}^2)\mathbf{x} = \mathbf{W}_{N_0}^4\mathbf{x}$?

CHAPTER 11 DISCRETE-TIME SYSTEM ANALYSIS USING THE z-TRANSFORM

The counterpart of the Laplace transform for discrete-time systems is the z-transform. The Laplace transform converts integro-differential equations into algebraic equations. In the same way, the z-transform changes difference equations into algebraic equations, thereby simplifying the analysis of discrete-time systems. The z-transform method of analysis of discrete-time systems parallels the Laplace transform method of analysis of continuous-time systems, with some minor differences. In fact, we shall see that *the z-transform is the Laplace transform in disguise*.

The behavior of discrete-time systems is similar to that of continuous-time systems (with some differences). The frequency-domain analysis of discrete-time systems is based on the fact (proved in Sec. 9.5.2) that the response of a linear, time-invariant, discrete-time (LTID) system to an everlasting exponential z^n is the same exponential (within a multiplicative constant) given by $H[z]z^n$. We then express an input $x[n]$ as a sum of (everlasting) exponentials of the form z^n. The system response to $x[n]$ is then found as a sum of the system's responses to all these exponential components. The tool that allows us to represent an arbitrary input $x[n]$ as a sum of (everlasting) exponentials of the form z^n is the z-transform.

11.1 THE z-TRANSFORM

We define $X[z]$, the direct z-transform of $x[n]$, as

$$X[z] = \sum_{n=-\infty}^{\infty} x[n]z^{-n} \tag{11.1}$$

where z is a complex variable. The signal $x[n]$, which is the inverse z-transform of $X[z]$, can be obtained from $X[z]$ by using the following inverse z-transformation:

$$x[n] = \frac{1}{2\pi j} \oint X[z]z^{n-1}\,dz \tag{11.2}$$

The symbol $\oint$ indicates an integration in counterclockwise direction around a closed path in the complex plane (see Fig. 11.1). We derived this z-transform pair toward the end of Ch. 10, as an extension of the discrete-time Fourier transform pair.

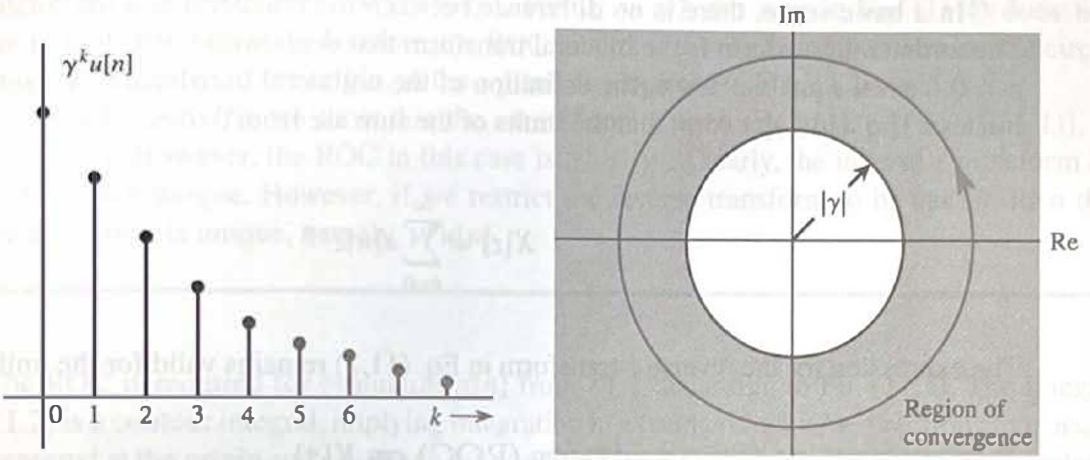

Figure 11.1 $\gamma^n u[n]$ and the region of convergence of its z-transform.

As in the case of the Laplace transform, we need not worry about this integral at this point because inverse z-transforms of many signals of engineering interest can be found in a z-transform table. The direct and inverse z-transforms can be expressed symbolically as

$$X[z] = \mathcal{Z}\{x[n]\} \qquad \text{and} \qquad x[n] = \mathcal{Z}^{-1}\{X[z]\}$$

or simply as

$$x[n] \Longleftrightarrow X[z]$$

Note that

$$\mathcal{Z}^{-1}[\mathcal{Z}\{x[n]\}] = x[n] \qquad \text{and} \qquad \mathcal{Z}[\mathcal{Z}^{-1}\{X[z]\}] = X[z]$$

Linearity of the z-Transform

Like the Laplace transform, the z-transform is a linear operator. If

$$x_1[n] \Longleftrightarrow X_1[z] \qquad \text{and} \qquad x_2[n] \Longleftrightarrow X_2[z]$$

then

$$a_1 x_1[n] + a_2 x_2[n] \Longleftrightarrow a_1 X_1[z] + a_2 X_2[z]$$

The proof is trivial and follows from the definition of the z-transform. This result can be extended to finite sums.

The Unilateral z-Transform

For the same reasons discussed in Ch. 6, we find it convenient to consider the unilateral z-transform. As seen for the Laplace case, the bilateral transform has some complications because of the non-uniqueness of the inverse transform. In contrast, the unilateral transform has a unique inverse. This fact simplifies the analysis problem considerably, but at a price: the unilateral version can handle only causal signals and systems. Fortunately, most of the practical cases are causal. The more general *bilateral z-transform* is discussed later, in Sec. 11.7. In practice, the term *z-transform* generally means the *unilateral z-transform*.

In a basic sense, there is no difference between the unilateral and the bilateral z-transform. The unilateral transform is the bilateral transform that deals with a subclass of signals starting at $n = 0$ (causal signals). Hence, the definition of the unilateral transform is the same as that of the bilateral [Eq. (11.1)], except that the limits of the sum are from 0 to ∞:

$$X[z] = \sum_{n=0}^{\infty} x[n]z^{-n} \tag{11.3}$$

The expression for the inverse z-transform in Eq. (11.2) remains valid for the unilateral case also.

The Region of Convergence (ROC) of $X[z]$

The sum in Eq. (11.1) [or Eq. (11.3)] defining the direct z-transform $X[z]$ may not converge (exist) for all values of z. The values of z (the region in the complex plane) for which the sum in Eq. (11.1) converges (or exists) are called the *region of existence*, or more commonly the *region of convergence* (ROC), for $X[z]$. This concept will become clear in the following example.

EXAMPLE 11.1 Bilateral z-Transform of a Causal Exponential

Find the z-transform and the corresponding ROC for the signal $\gamma^n u[n]$.

By definition,

$$X[z] = \sum_{n=0}^{\infty} \gamma^n u[n]z^{-n}$$

Since $u[n] = 1$ for all $n \geq 0$,

$$X[z] = \sum_{n=0}^{\infty} \left(\frac{\gamma}{z}\right)^n = 1 + \left(\frac{\gamma}{z}\right) + \left(\frac{\gamma}{z}\right)^2 + \left(\frac{\gamma}{z}\right)^3 + \cdots + \cdots \tag{11.4}$$

It is helpful to remember the geometric progression and its sum [see Sec. B.8.3]:

$$1 + x + x^2 + x^3 + \cdots = \frac{1}{1-x} \qquad \text{if} \quad |x| < 1$$

Applying this relationship to Eq. (11.4) yields

$$\begin{aligned} X[z] &= \frac{1}{1-\frac{\gamma}{z}} \qquad \left|\frac{\gamma}{z}\right| < 1 \\ &= \frac{z}{z-\gamma} \qquad |z| > |\gamma| \end{aligned} \tag{11.5}$$

Observe that $X[z]$ exists only for $|z| > |\gamma|$. For $|z| < |\gamma|$, the sum in Eq. (11.4) does not converge; it goes to infinity. Therefore, the ROC of $X[z]$ is the shaded region outside the circle of radius $|\gamma|$, centered at the origin, in the z plane, as depicted in Fig. 11.1b.

Later in Eq. (11.35), we show that the z-transform of another signal, $-\gamma^n u[-(n+1)]$, is also $z/(z-\gamma)$. However, the ROC in this case is $|z| < |\gamma|$. Clearly, the inverse z-transform of $z/(z-\gamma)$ is not unique. However, if we restrict the inverse transform to be causal, then the inverse transform is unique, namely, $\gamma^n u[n]$.

The ROC is required for evaluating $x[n]$ from $X[z]$, according to Eq. (11.2). The integral in Eq. (11.2) is a contour integral, implying integration in a counterclockwise direction along a closed path centered at the origin and satisfying the condition $|z| > |\gamma|$. Thus, any circular path centered at the origin and with a radius greater than $|\gamma|$ (Fig. 11.1b) will suffice. We can show that the integral in Eq. (11.2) along any such path (with a radius greater than $|\gamma|$) yields the same result, namely, $x[n]$.[†] Such integration in the complex plane requires a background in the theory of functions of complex variables. We can avoid this integration by compiling a table of z-transforms (Table 11.1), where z-transform pairs are tabulated for a variety of signals. To find the inverse z-transform of, say, $z/(z-\gamma)$, instead of using the complex integration in Eq. (11.2), we consult the table and find the inverse z-transform of $z/(z-\gamma)$ as $\gamma^n u[n]$. Because of the uniqueness property of the unilateral z-transform, there is only one inverse for each $X[z]$. Although the table given here is rather short, it comprises the functions of most practical interest.

The situation of the z-transform regarding the uniqueness of the inverse transform is parallel to that of the Laplace transform. For the bilateral case, the inverse z-transform is not unique unless the ROC is specified. For the unilateral case, the inverse transform is unique; the region of convergence need not be specified to determine the inverse z-transform. For this reason, we shall ignore the ROC in the unilateral z-transform Table 11.1.

Existence of the z-Transform

By definition,

$$X[z] = \sum_{n=0}^{\infty} x[n]z^{-n} = \sum_{n=0}^{\infty} \frac{x[n]}{z^n}$$

The existence of the z-transform is guaranteed if

$$|X[z]| \leq \sum_{n=0}^{\infty} \frac{|x[n]|}{|z|^n} < \infty$$

for some $|z|$. Any signal $x[n]$ that grows no faster than an exponential signal r_0^n, for some r_0, satisfies this condition. Thus, if

$$|x[n]| \leq r_0^n \qquad \text{for some } r_0 \tag{11.6}$$

[†] Indeed, the path need not even be circular. It can have any odd shape, as long as it encloses the pole(s) of $X[z]$ and the path of integration is counterclockwise.

TABLE 11.1 Select (Unilateral) z-Transform Pairs

No.	$x[n]$	$X[z]$
1	$\delta[n-k]$	z^{-k}
2	$u[n]$	$\dfrac{z}{z-1}$
3	$nu[n]$	$\dfrac{z}{(z-1)^2}$
4	$n^2u[n]$	$\dfrac{z(z+1)}{(z-1)^3}$
5	$n^3u[n]$	$\dfrac{z(z^2+4z+1)}{(z-1)^4}$
6	$\gamma^n u[n]$	$\dfrac{z}{z-\gamma}$
7	$\gamma^{n-1}u[n-1]$	$\dfrac{1}{z-\gamma}$
8	$n\gamma^n u[n]$	$\dfrac{\gamma z}{(z-\gamma)^2}$
9	$n^2\gamma^n u[n]$	$\dfrac{\gamma z(z+\gamma)}{(z-\gamma)^3}$
10	$\dfrac{n(n-1)(n-2)\cdots(n-m+1)}{\gamma^m m!}\gamma^n u[n]$	$\dfrac{z}{(z-\gamma)^{m+1}}$
11a	$\lvert\gamma\rvert^n \cos \beta n\, u[n]$	$\dfrac{z(z-\lvert\gamma\rvert\cos\beta)}{z^2-(2\lvert\gamma\rvert\cos\beta)z+\lvert\gamma\rvert^2}$
11b	$\lvert\gamma\rvert^n \sin \beta n\, u[n]$	$\dfrac{z\lvert\gamma\rvert\sin\beta}{z^2-(2\lvert\gamma\rvert\cos\beta)z+\lvert\gamma\rvert^2}$
12a	$r\lvert\gamma\rvert^n \cos(\beta n+\theta)u[n]$	$\dfrac{rz[z\cos\theta-\lvert\gamma\rvert\cos(\beta-\theta)]}{z^2-(2\lvert\gamma\rvert\cos\beta)z+\lvert\gamma\rvert^2}$
12b	$r\lvert\gamma\rvert^n \cos(\beta n+\theta)u[n] \qquad \gamma=\lvert\gamma\rvert e^{j\beta}$	$\dfrac{(0.5re^{j\theta})z}{z-\gamma}+\dfrac{(0.5re^{-j\theta})z}{z-\gamma^*}$
12c	$r\lvert\gamma\rvert^n \cos(\beta n+\theta)u[n]$	$\dfrac{z(Az+B)}{z^2+2az+\lvert\gamma\rvert^2}$

$$r=\sqrt{\frac{A^2|\gamma|^2+B^2-2AaB}{|\gamma|^2-a^2}}$$

$$\beta=\cos^{-1}\frac{-a}{|\gamma|}$$

$$\theta=\tan^{-1}\frac{Aa-B}{A\sqrt{|\gamma|^2-a^2}}$$

then

$$|X[z]| \le \sum_{n=0}^{\infty} \left(\frac{r_0}{|z|}\right)^n = \frac{1}{1-\dfrac{r_0}{|z|}} \qquad |z| > r_0$$

Therefore, $X[z]$ exists for $|z| > r_0$. Almost all practical signals satisfy Eq. (11.6) and are therefore z-transformable. Some signal models (e.g., γ^{n^2}) grow faster than the exponential signal r_0^n (for any r_0) and do not satisfy Eq. (11.6) and therefore are not z-transformable. Fortunately, such signals are of little practical or theoretical interest. Even such signals over a finite interval are z-transformable.

EXAMPLE 11.2 Bilateral z-Transform

Find the z-transforms of: **(a)** $\delta[n]$, **(b)** $u[n]$, **(c)** $\cos \beta n u[n]$, and **(d)** the signal shown in Fig. 11.2.

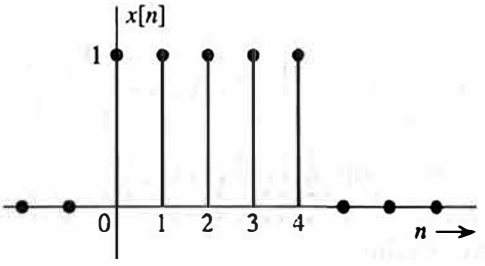

Figure 11.2 Signal for Ex. 11.2d.

Recall that by definition

$$X[z] = \sum_{n=0}^{\infty} x[n]z^{-n} = x[0] + \frac{x[1]}{z} + \frac{x[2]}{z^2} + \frac{x[3]}{z^3} + \cdots \tag{11.7}$$

(a) For $x[n] = \delta[n]$, $x[0] = 1$ and $x[2] = x[3] = x[4] = \cdots = 0$. Therefore,

$$\delta[n] \Longleftrightarrow 1 \qquad \text{for all } z$$

(b) For $x[n] = u[n]$, $x[0] = x[1] = x[3] = \cdots = 1$. Therefore,

$$X[z] = 1 + \frac{1}{z} + \frac{1}{z^2} + \frac{1}{z^3} + \cdots$$

This geometric sum simplifies [see Sec. B.8.3] to

$$X[z] = \frac{1}{1-\frac{1}{z}} \qquad \left|\frac{1}{z}\right| < 1$$
$$= \frac{z}{z-1} \qquad |z| > 1$$

Therefore,

$$u[n] \Longleftrightarrow \frac{z}{z-1} \qquad |z| > 1$$

(c) Recall that $\cos \beta n = (e^{j\beta n} + e^{-j\beta n})/2$. Moreover, according to Eq. (11.5),

$$e^{\pm j\beta n}u[n] \Longleftrightarrow \frac{z}{z-e^{\pm j\beta}} \qquad |z| > |e^{\pm j\beta}| = 1$$

Therefore,

$$X[z] = \frac{1}{2}\left[\frac{z}{z-e^{j\beta}} + \frac{z}{z-e^{-j\beta}}\right] = \frac{z(z-\cos\beta)}{z^2 - 2z\cos\beta + 1} \qquad |z| > 1$$

(d) Here, $x[0] = x[1] = x[2] = x[3] = x[4] = 1$ and $x[5] = x[6] = \cdots = 0$. Therefore, according to Eq. (11.7),

$$X[z] = 1 + \frac{1}{z} + \frac{1}{z^2} + \frac{1}{z^3} + \frac{1}{z^4} = \frac{z^4 + z^3 + z^2 + z + 1}{z^4} \qquad \text{for all } z \neq 0$$

We can also express this result in more compact form by summing the geometric progression on the right-hand side of the foregoing equation. From the result in Sec. B.8.3 with $r = 1/z$, $m = 0$, and $n = 4$, we obtain

$$X[z] = \frac{\left(\frac{1}{z}\right)^5 - \left(\frac{1}{z}\right)^0}{\frac{1}{z} - 1} = \frac{z}{z-1}(1 - z^{-5})$$

DRILL 11.1 Bilateral z-Transform

(a) Find the z-transform of a signal shown in Fig. 11.3.

(b) Use pair 12a (Table 11.1) to find the z-transform of $x[n] = 20.65(\sqrt{2})^n \cos[(\pi/4)n - 1.415]u[n]$.

ANSWERS

(a) $X[z] = \dfrac{z^5 + z^4 + +z^3 + z^2 + z + 1}{z^9}$ or $\dfrac{z}{z-1}(z^{-4} - z^{-10})$

(b) $\dfrac{z(3.2z + 17.2)}{z^2 - 2z + 2}$

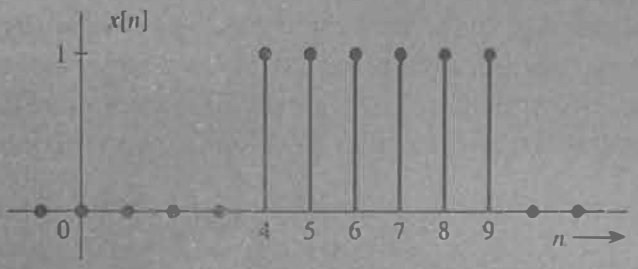

Figure 11.3 Signal for Drill 11.1a.

11.1.1 Inverse Transform by Partial Fraction Expansion and Tables

As in the Laplace transform, we shall avoid the integration in the complex plane required to find the inverse z-transform [Eq. (11.2)] by using the (unilateral) transform table (Table 11.1). Many of the transforms $X[z]$ of practical interest are rational functions (ratio of polynomials in z), which can be expressed as a sum of partial fractions, whose inverse transforms can be readily found in a transform table. The partial fraction method works because for every transformable $x[n]$ defined for $n \geq 0$, there is a corresponding unique $X[z]$ defined for $|z| > r_0$ (where r_0 is some constant), and vice versa.

EXAMPLE 11.3 Inverse z-Transform by Partial Fraction Expansion

Find the inverse z-transforms of

(a) $\dfrac{8z - 19}{(z-2)(z-3)}$

(b) $\dfrac{z(2z^2 - 11z + 12)}{(z-1)(z-2)^3}$

(c) $\dfrac{2z(3z + 17)}{(z-1)(z^2 - 6z + 25)}$

(a) Expanding $X[z]$ into partial fractions yields

$$X[z] = \frac{8z - 19}{(z-2)(z-3)} = \frac{3}{z-2} + \frac{5}{z-3}$$

From Table 11.1, pair 7, we obtain

$$x[n] = [3(2)^{n-1} + 5(3)^{n-1}]u[n-1] \tag{11.8}$$

If we expand rational $X[z]$ into partial fractions directly, we shall always obtain an answer that is multiplied by $u[n-1]$ because of the nature of pair 7 in Table 11.1. This form is rather awkward as well as inconvenient. We prefer the form that contains $u[n]$ rather than $u[n-1]$. A glance at Table 11.1 shows that the z-transform of every signal that is multiplied by $u[n]$ has a factor z in the numerator. This observation suggests that we expand $X[z]$ into *modified partial fractions*, where each term has a factor z in the numerator. This goal can be accomplished by expanding $X[z]/z$ into partial fractions and then multiplying both sides by z. We shall demonstrate this procedure by reworking part (a). For this case,

$$\frac{X[z]}{z} = \frac{8z-19}{z(z-2)(z-3)} = \frac{(-19/6)}{z} + \frac{(3/2)}{z-2} + \frac{(5/3)}{z-3}$$

Multiplying both sides by z yields

$$X[z] = -\frac{19}{6} + \frac{3}{2}\left(\frac{z}{z-2}\right) + \frac{5}{3}\left(\frac{z}{z-3}\right)$$

From pairs 1 and 6 in Table 11.1, it follows that

$$x[n] = -\tfrac{19}{6}\delta[n] + \left[\tfrac{3}{2}(2)^n + \tfrac{5}{3}(3)^n\right]u[n] \tag{11.9}$$

The reader can verify that this answer is equivalent to that in Eq. (11.8) by computing $x[n]$ in both cases for $n = 0, 1, 2, 3, \ldots$, and comparing the results. The form in Eq. (11.9) is more convenient than that in Eq. (11.8). For this reason, we shall always expand $X[z]/z$ rather than $X[z]$ into partial fractions and then multiply both sides by z to obtain modified partial fractions of $X[z]$, which have a factor z in the numerator.

(b)

$$X[z] = \frac{z(2z^2 - 11z + 12)}{(z-1)(z-2)^3}$$

and

$$\frac{X[z]}{z} = \frac{2z^2 - 11z + 12}{(z-1)(z-2)^3} = \frac{k}{z-1} + \frac{a_0}{(z-2)^3} + \frac{a_1}{(z-2)^2} + \frac{a_2}{(z-2)}$$

where

$$k = \left.\frac{2z^2 - 11z + 12}{(z-1)(z-2)^3}\right|_{z=1} = -3$$

$$a_0 = \left.\frac{2z^2 - 11z + 12}{(z-1)(z-2)^3}\right|_{z=2} = -2$$

Therefore,

$$\frac{X[z]}{z}=\frac{2z^2-11z+12}{(z-1)(z-2)^3}=\frac{-3}{z-1}-\frac{2}{(z-2)^3}+\frac{a_1}{(z-2)^2}+\frac{a_2}{(z-2)} \tag{11.10}$$

We can determine a_1 and a_2 by clearing fractions. Or we may use a shortcut. For example, to determine a_2, we multiply both sides of Eq. (11.10) by z and let $z\to\infty$. This yields

$$0=-3-0+0+a_2 \implies a_2=3$$

This result leaves only one unknown, a_1, which is readily determined by letting z take any convenient value, say, $z=0$, on both sides of Eq. (11.10). This produces

$$\frac{12}{8}=3+\frac{1}{4}+\frac{a_1}{4}-\frac{3}{2}$$

which yields $a_1=-1$. Therefore,

$$\frac{X[z]}{z}=\frac{-3}{z-1}-\frac{2}{(z-2)^3}-\frac{1}{(z-2)^2}+\frac{3}{z-2}$$

and

$$X[z]=-3\frac{z}{z-1}-2\frac{z}{(z-2)^3}-\frac{z}{(z-2)^2}+3\frac{z}{z-2}$$

Now the use of Table 11.1, pairs 6 and 10, yields

$$\begin{aligned}x[n]&=\left[-3-2\frac{n(n-1)}{8}(2)^n-\frac{n}{2}(2)^n+3(2)^n\right]u[n]\\&=-\left[3+\frac{1}{4}(n^2+n-12)2^n\right]u[n]\end{aligned}$$

(c) Complex Poles.

$$X[z]=\frac{2z(3z+17)}{(z-1)(z^2-6z+25)}=\frac{2z(3z+17)}{(z-1)(z-3-j4)(z-3+j4)}$$

The poles of $X[z]$ are 1, $3+j4$, and $3-j4$. Whenever there are complex-conjugate poles, the problem can be worked out in two ways. In the first method, we expand $X[z]$ into (modified) first-order partial fractions. In the second method, rather than obtain one factor corresponding to each complex-conjugate pole, we obtain quadratic factors corresponding to each pair of complex-conjugate poles. This procedure is explained next.

Method of First-Order Factors

$$\frac{X[z]}{z}=\frac{2(3z+17)}{(z-1)(z^2-6z+25)}=\frac{2(3z+17)}{(z-1)(z-3-j4)(z-3+j4)}$$

We find the partial fraction of $X[z]/z$ using the Heaviside "cover-up" method:

$$\frac{X[z]}{z} = \frac{2}{z-1} + \frac{1.6e^{-j2.246}}{z-3-j4} + \frac{1.6e^{j2.246}}{z-3+j4}$$

and

$$X[z] = 2\frac{z}{z-1} + (1.6e^{-j2.246})\frac{z}{z-3-j4} + (1.6e^{j2.246})\frac{z}{z-3+j4}$$

The inverse transform of the first term on the right-hand side is $2u[n]$. The inverse transform of the remaining two terms (complex-conjugate poles) can be obtained from pair 12b (Table 11.1) by identifying $r/2 = 1.6$, $\theta = -2.246$ rad, $\gamma = 3 + j4 = 5e^{j0.927}$, so that $|\gamma| = 5$, $\beta = 0.927$. Therefore,

$$x[n] = [2 + 3.2(5)^n \cos(0.927n - 2.246)]u[n]$$

Method of Quadratic Factors

$$\frac{X[z]}{z} = \frac{2(3z+17)}{(z-1)(z^2-6z+25)} = \frac{2}{z-1} + \frac{Az+B}{z^2-6z+25}$$

Multiplying both sides by z and letting $z \to \infty$, we find

$$0 = 2 + A \Longrightarrow A = -2$$

and

$$\frac{2(3z+17)}{(z-1)(z^2-6z+25)} = \frac{2}{z-1} + \frac{-2z+B}{z^2-6z+25}$$

To find B, we let z take any convenient value, say, $z = 0$. This step yields

$$\frac{-34}{25} = -2 + \frac{B}{25} \Longrightarrow B = 16$$

Therefore,

$$\frac{X[z]}{z} = \frac{2}{z-1} + \frac{-2z+16}{z^2-6z+25}$$

and

$$X[z] = \frac{2z}{z-1} + \frac{z(-2z+16)}{z^2-6z+25}$$

We now use pair 12c, where we identify $A = -2$, $B = 16$, $|\gamma| = 5$, and $a = -3$. Therefore,

$$r = \sqrt{\frac{100+256-192}{25-9}} = 3.2, \quad \beta = \cos^{-1}\left(\frac{3}{5}\right) = 0.927\,\text{rad}$$

and

$$\theta = \tan^{-1}\left(\tfrac{-10}{-8}\right) = -2.246\,\text{rad}$$

so that

$$x[n] = [2 + 3.2(5)^n \cos(0.927n - 2.246)]u[n]$$

Partial Fraction Expansion by MATLAB

Partial fraction expansions, including modified partial fraction expansions, are easily performed using MATLAB's `residue` command. To demonstrate, let us perform the modified partial fraction expansion for part (a). All that is required is to specify the numerator and denominator polynomial coefficients of $H[z]/z$. Notice that an extra root at $z = 0$ is added to the roots of $H[z]$ since this is a modified partial fraction expansion, where we expand $H[z]/z$ rather than $H[z]$. We use the `format rat` command so that MATLAB reports the results in rational form (ratios of integers rather than decimal numbers).

```
>> num = [8 -19]; den = poly([2,3,0]); format rat
>> [r,p,k] = residue(num,den)
    r = 5/3          3/2          -19/6
    p = 3            2              0
    k = []
```

The residues `r` provide the numerator coefficients for the roots `p`; thus,

$$\frac{H[z]}{z} = \frac{5/3}{z-3} + \frac{3/2}{z-2} + \frac{-19/6}{z}$$

This result matches our earlier hand calculations. Additional details on the `residue` command are available using MATLAB help facilities.

DRILL 11.2 Inverse z-Transform by Partial Fraction Expansion

Find the inverse z-transform of the following functions:

(a) $\dfrac{z(2z-1)}{(z-1)(z+0.5)}$

(b) $\dfrac{1}{(z-1)(z+0.5)}$

(c) $\dfrac{9}{(z+2)(z-0.5)^2}$

(d) $\dfrac{5z(z-1)}{z^2-1.6z+0.8}$

[*Hint:* $\sqrt{0.8} = 2/\sqrt{5}$.]

ANSWERS

(a) $\left[\frac{2}{3} + \frac{4}{3}(-0.5)^n\right]u[n]$

(b) $-2\delta[n] + \left[\frac{2}{3} + \frac{4}{3}(-0.5)^n\right]u[n]$

(c) $18\delta[n] - [0.72(-2)^n + 17.28(0.5)^n - 14.4n(0.5)^n]u[n]$

(d) $\frac{5\sqrt{5}}{2}\left(\frac{2}{\sqrt{5}}\right)^n \cos(0.464n + 0.464)u[n]$

11.1.2 Inverse z-Transform by Power Series Expansion

By definition,

$$\begin{aligned} X[z] &= \sum_{n=0}^{\infty} x[n]z^{-n} \\ &= x[0] + \frac{x[1]}{z} + \frac{x[2]}{z^2} + \frac{x[3]}{z^3} + \cdots \\ &= x[0]z^0 + x[1]z^{-1} + x[2]z^{-2} + x[3]z^{-3} + \cdots \end{aligned}$$

This result is a power series in z^{-1}. Therefore, if we can expand $X[z]$ into the power series in z^{-1}, the coefficients of this power series can be identified as $x[0], x[1], x[2], x[3], \ldots$. A rational $X[z]$ can be expanded into a power series of z^{-1} by dividing its numerator by the denominator. Consider, for example,

$$X[z] = \frac{z^2(7z-2)}{(z-0.2)(z-0.5)(z-1)} = \frac{7z^3 - 2z^2}{z^3 - 1.7z^2 + 0.8z - 0.1}$$

To obtain a series expansion in powers of z^{-1}, we divide the numerator by the denominator as follows:

$$\begin{array}{r} 7 + 9.9z^{-1} + 11.23z^{-2} + 11.87z^{-3} + \cdots \\ z^3 - 1.7z^2 + 0.8z - 0.1 \overline{)\,7z^3 - 2z^2} \\ \underline{7z^3 - 11.9z^2 + 5.60z - 0.7} \\ 9.9z^2 - 5.60z + 0.7 \\ \underline{9.9z^2 - 16.83z + 7.92 - 0.99z^{-1}} \\ 11.23z - 7.22 + 0.99z^{-1} \\ \underline{11.23z - 19.09 + 8.98z^{-1}} \\ 11.87 - 7.99z^{-1} \end{array}$$

Thus,

$$X[z] = \frac{z^2(7z-2)}{(z-0.2)(z-0.5)(z-1)} = 7 + 9.9z^{-1} + 11.23z^{-2} + 11.87z^{-3} + \cdots$$

Therefore,

$$x[0] = 7,\ x[1] = 9.9,\ x[2] = 11.23,\ x[3] = 11.87, \ldots$$

Although this procedure yields $x[n]$ directly, it does not provide a closed-form solution. For this reason, it is not very useful unless we want to know only the first few terms of the sequence $x[n]$.

DRILL 11.3 Inverse z-Transform by Long Division

Using long division to find the power series in z^{-1}, show that the inverse z-transform of $z/(z-0.5)$ is $(0.5)^n u[n]$ or $(2)^{-n} u[n]$.

Relationship Between $h[n]$ and $H[z]$

For an LTID system, if $h[n]$ is its unit impulse response, then from Eq. (9.26), where we defined $H[z]$, the system transfer function, we write

$$H[z] = \sum_{n=-\infty}^{\infty} h[n]z^{-n} \tag{11.11}$$

For causal systems, the limits on the sum are from $n = 0$ to ∞. This equation shows that the transfer function $H[z]$ is the z-transform of the impulse response $h[n]$ of an LTID system; that is,

$$h[n] \Longleftrightarrow H[z]$$

This important result relates the time-domain specification $h[n]$ of a system to $H[z]$, the frequency-domain specification of a system. The result is parallel to that for LTIC systems.

DRILL 11.4 Impulse Response by Inverse z-Transform

Redo Drill 9.6 by taking the inverse z-transform of $H[z]$, as given by Eq. (9.28).

11.2 Some Properties of the z-Transform

The z-transform properties are useful in the derivation of z-transforms of many functions and also in the solution of linear difference equations with constant coefficients. Here, we consider a few important properties of the z-transform.

In our discussion, the variable n appearing in signals, such as $x[n]$ and $y[n]$, may or may not stand for time. However, in most applications of interest, n is proportional to time. For this reason, we shall loosely refer to the variable n as time.

11.2.1 Time-Shifting Properties

In the following discussion of the shift property, we deal with shifted signals $x[n]u[n]$, $x[n-k]u[n-k]$, $x[n-k]u[n]$, and $x[n+k]u[n]$. Unless we physically understand the meaning of such shifts, our understanding of the shift property remains mechanical rather than intuitive or heuristic. For this reason, using a hypothetical signal $x[n]$, we have illustrated various shifted signals for $k = 1$ in Fig. 11.4.

Right Shift (Delay)

If

$$x[n]u[n] \Longleftrightarrow X[z]$$

then

$$x[n-1]u[n-1] \Longleftrightarrow \frac{1}{z}X[z] \tag{11.12}$$

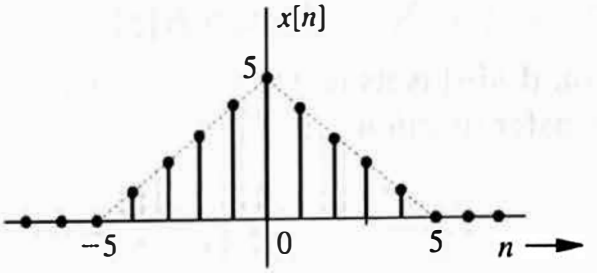

(a)

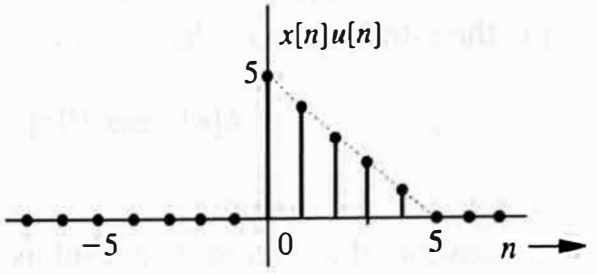

(b)

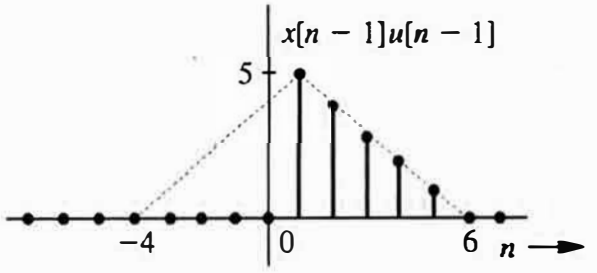

(c)

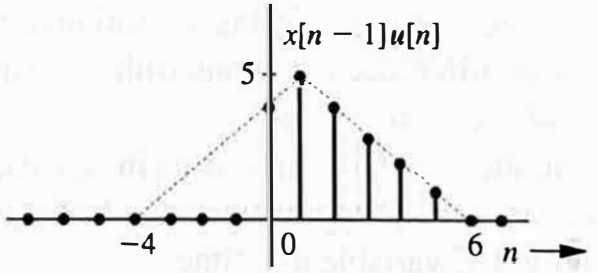

(d)

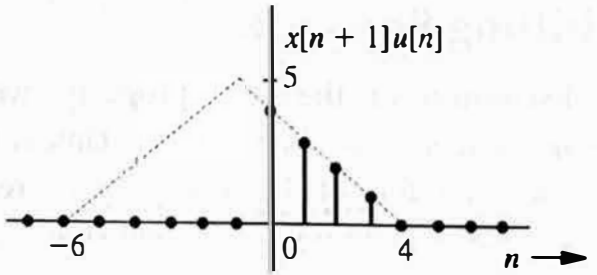

(e)

Figure 11.4 A signal $x[n]$ and its shifted versions.

In general,

$$x[n-m]u[n-m] \Longleftrightarrow \frac{1}{z^m}X[z] \tag{11.13}$$

Moreover,

$$x[n-1]u[n] \Longleftrightarrow \frac{1}{z}X[z]+x[-1] \tag{11.14}$$

Repeated application of this property yields

$$x[n-2]u[n] \Longleftrightarrow \frac{1}{z}\left[\frac{1}{z}X[z]+x[-1]\right]+x[-2]=\frac{1}{z^2}X[z]+\frac{1}{z}x[-1]+x[-2]$$

In general, for integer value of m,

$$x[n-m]u[n] \Longleftrightarrow z^{-m}X[z]+z^{-m}\sum_{n=1}^{m}x[-n]z^n \tag{11.15}$$

A look at Eqs. (11.12) and (11.14) shows that they are identical except for the extra term $x[-1]$ in Eq. (11.14). We see from Figs. 11.4c and 11.4d that $x[n-1]u[n]$ is the same as $x[n-1]u[n-1]$ plus $x[-1]\delta[n]$. Hence, the difference between their transforms is $x[-1]$.

Proof. For the integer value of m,

$$\mathcal{Z}\{x[n-m]u[n-m]\}=\sum_{n=0}^{\infty}x[n-m]u[n-m]z^{-n}$$

Recall that $x[n-m]u[n-m]=0$ for $n<m$ so that the limits on the summation on the right-hand side can be taken from $n=m$ to ∞. Therefore,

$$\begin{aligned}\mathcal{Z}\{x[n-m]u[n-m]\}&=\sum_{n=m}^{\infty}x[n-m]z^{-n}\\&=\sum_{r=0}^{\infty}x[r]z^{-(r+m)}\\&=\frac{1}{z^m}\sum_{r=0}^{\infty}x[r]z^{-r}=\frac{1}{z^m}X[z]\end{aligned}$$

To prove Eq. (11.15), we have

$$\begin{aligned}\mathcal{Z}\{x[n-m]u[n]\} &= \sum_{n=0}^{\infty} x[n-m]z^{-n} = \sum_{r=-m}^{\infty} x[r]z^{-(r+m)} \\ &= z^{-m}\left[\sum_{r=-m}^{-1} x[r]z^{-r} + \sum_{r=0}^{\infty} x[r]z^{-r}\right] \\ &= z^{-m}\sum_{n=1}^{m} x[-n]z^{n} + z^{-m}X[z]\end{aligned}$$

Left Shift (Advance)

If

$$x[n]u[n] \Longleftrightarrow X[z]$$

then

$$x[n+1]u[n] \Longleftrightarrow zX[z] - zx[0]$$

Repeated application of this property yields

$$x[n+2]u[n] \Longleftrightarrow z\{z(X[z] - zx[0]) - x[1]\} = z^2X[z] - z^2x[0] - zx[1]$$

and for the integer value of m,

$$x[n+m]u[n] \Longleftrightarrow z^mX[z] - z^m\sum_{n=0}^{m-1} x[n]z^{-n} \tag{11.16}$$

Proof. By definition,

$$\begin{aligned}\mathcal{Z}\{x[n+m]u[n]\} &= \sum_{n=0}^{\infty} x[n+m]z^{-n} \\ &= \sum_{r=m}^{\infty} x[r]z^{-(r-m)} \\ &= z^m\sum_{r=m}^{\infty} x[r]z^{-r} \\ &= z^m\left[\sum_{r=0}^{\infty} x[r]z^{-r} - \sum_{r=0}^{m-1} x[r]z^{-r}\right] \\ &= z^mX[z] - z^m\sum_{r=0}^{m-1} x[r]z^{-r}\end{aligned}$$

EXAMPLE 11.4 z-Transform Using the Right-Shift Property

Find the z-transform of the signal $x[n]$ depicted in Fig. 11.5.

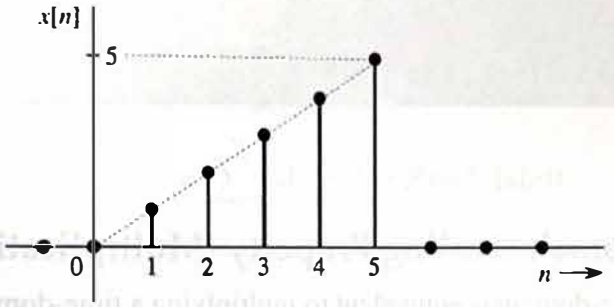

Figure 11.5 Signal for Ex. 11.4.

The signal $x[n]$ can be expressed as a product of n and a gate pulse $u[n]-u[n-6]$. Therefore,

$$x[n] = n\{u[n]-u[n-6]\} = nu[n]-nu[n-6]$$

We cannot find the z-transform of $nu[n-6]$ directly by using the right-shift property [Eq. (11.13)]. So we rearrange it in terms of $(n-6)u[n-6]$ as follows:

$$\begin{aligned} x[n] &= nu[n]-(n-6+6)u[n-6] \\ &= nu[n]-(n-6)u[n-6]-6u[n-6] \end{aligned}$$

We can now find the z-transform of the bracketed term by using the right-shift property [Eq. (11.13)]. Because $u[n] \Longleftrightarrow z/(z-1)$,

$$u[n-6] \Longleftrightarrow \frac{1}{z^6}\frac{z}{z-1} = \frac{1}{z^5(z-1)}$$

Also, because $nu[n] \Longleftrightarrow z/(z-1)^2$,

$$(n-6)u[n-6] \Longleftrightarrow \frac{1}{z^6}\frac{z}{(z-1)^2} = \frac{1}{z^5(z-1)^2}$$

Therefore,

$$X[z] = \frac{z}{(z-1)^2} - \frac{1}{z^5(z-1)^2} - \frac{6}{z^5(z-1)} = \frac{z^6-6z+5}{z^5(z-1)^2}$$

DRILL 11.5 z-Transform Using the Right-Shift Property

Using only the fact that $u[n] \Longleftrightarrow z/(z-1)$ and the right-shift property [Eq. (11.13)], find the z-transforms of the signals in Figs. 11.2 and 11.3.

ANSWERS

See Ex. 11.2d and Drill 11.1a.

11.2.2 z-Domain Scaling Property (Multiplication by γ^n)

Scaling in the z-domain is equivalent to multiplying a time-domain signal by an exponential. That is, if

$$x[n]u[n] \Longleftrightarrow X[z]$$

then

$$\gamma^n x[n]u[n] \Longleftrightarrow X\left[\frac{z}{\gamma}\right] \tag{11.17}$$

Proof.

$$\mathcal{Z}\{\gamma^n x[n]u[n]\} = \sum_{n=0}^{\infty} \gamma^n x[n] z^{-n} = \sum_{n=0}^{\infty} x[n]\left(\frac{z}{\gamma}\right)^{-n} = X\left[\frac{z}{\gamma}\right]$$

DRILL 11.6 Using the z-Domain Scaling Property

Use Eq. (11.17) to derive pairs 6 and 8 in Table 11.1 from pairs 2 and 3, respectively.

11.2.3 z-Domain Differentiation Property (Multiplication by n)

Multiplying a signal by n in the time domain produces differentiation in the z-domain. That is, if

$$x[n]u[n] \Longleftrightarrow X[z]$$

then

$$nx[n]u[n] \Longleftrightarrow -z\frac{d}{dz}X[z] \tag{11.18}$$

Proof.

$$\begin{aligned}-z\frac{d}{dz}X[z] &= -z\frac{d}{dz}\sum_{n=0}^{\infty}x[n]z^{-n}\\ &= -z\sum_{n=0}^{\infty}-nx[n]z^{-n-1}\\ &= \sum_{n=0}^{\infty}nx[n]z^{-n} = \mathcal{Z}\{nx[n]u[n]\}\end{aligned}$$

DRILL 11.7 Using the z-Domain Differentiation Property

Use Eq. (11.18) to derive pairs 3 and 4 in Table 11.1 from pair 2. Similarly, derive pairs 8 and 9 from pair 6.

11.2.4 Time-Reversal Property

If

$$x[n] \Longleftrightarrow X[z]$$

then†

$$x[-n] \Longleftrightarrow X[1/z]$$

Proof.

$$\mathcal{Z}\{x[-n]\} = \sum_{n=-\infty}^{\infty}x[-n]z^{-n}$$

Changing the sign of the dummy variable n yields

$$\begin{aligned}\mathcal{Z}\{x[-n]\} &= \sum_{n=-\infty}^{\infty}x[n]z^{n}\\ &= \sum_{n=-\infty}^{\infty}x[n](1/z)^{-n}\\ &= X[1/z]\end{aligned}$$

† For complex signal $x[n]$, the time-reversal property is modified as follows:

$$x^*[-n] \Longleftrightarrow X^*[1/z^*]$$

The region of convergence is also inverted; that is, if the ROC of $x[n]$ is $|z| > |\gamma|$, then the ROC of $x[-n]$ is $|z| < 1/|\gamma|$.

DRILL 11.8 Using the Time-Reversal Property

Use the time-reversal property and pair 2 in Table 11.1 to show that $u[-n] \Longleftrightarrow -1/(z-1)$ with the ROC $|z| < 1$.

11.2.5 Convolution Property

The time-convolution property states that if[†]

$$x_1[n] \Longleftrightarrow X_1[z] \qquad \text{and} \qquad x_2[n] \Longleftrightarrow X_2[z],$$

then (*time convolution*)

$$x_1[n] * x_2[n] \Longleftrightarrow X_1[z]X_2[z] \tag{11.19}$$

Proof. This property applies to causal as well as noncausal sequences. We shall prove it for the more general case of noncausal sequences, where the convolution sum ranges from $-\infty$ to ∞.

We have

$$\mathcal{Z}\{x_1[n] * x_2[n]\} = \mathcal{Z}\left[\sum_{m=-\infty}^{\infty} x_1[m]x_2[n-m]\right]$$

$$= \sum_{n=-\infty}^{\infty} z^{-n} \sum_{m=-\infty}^{\infty} x_1[m]x_2[n-m]$$

Interchanging the order of summation, we have

$$\mathcal{Z}[x_1[n] * x_2[n]] = \sum_{m=-\infty}^{\infty} x_1[m] \sum_{n=-\infty}^{\infty} x_2[n-m]z^{-n}$$

$$= \sum_{m=-\infty}^{\infty} x_1[m] \sum_{r=-\infty}^{\infty} x_2[r]z^{-(r+m)}$$

$$= \sum_{m=-\infty}^{\infty} x_1[m]z^{-m} \sum_{r=-\infty}^{\infty} x_2[r]z^{-r}$$

$$= X_1[z]X_2[z]$$

[†] There is also the frequency-convolution property, which states that

$$x_1[n]x_2[n] \Longleftrightarrow \frac{1}{2\pi j}\oint X_1[u]X_2\left[\frac{z}{u}\right]u^{-1}\,du$$

LTID System Response

It is interesting to apply the time-convolution property to the LTID input–output equation $y[n] = x[n] * h[n]$. Since $h[n] \Longleftrightarrow H[z]$, it follows from Eq. (11.19) that

$$Y[z] = X[z]H[z] \tag{11.20}$$

DRILL 11.9 Using the Convolution Property

Use the time-convolution property and appropriate pairs in Table 11.1 to show that $u[n] * u[n-1] = nu[n]$.

Initial and Final Values

For a causal $x[n]$, the initial value theorem states that

$$x[0] = \lim_{z\to\infty} X[z]$$

This result follows immediately from Eq. (11.7).

If $(z-1)X[z]$ has no poles outside the unit circle, then the final value theorem states that

$$\lim_{N\to\infty} x[N] = \lim_{z\to 1}(z-1)X[z]$$

This can be shown from the fact that

$$x[n] - x[n-1] \Longleftrightarrow \left\{1 - \frac{1}{z}\right\} X[z] = \frac{(z-1)X[z]}{z}$$

and

$$\frac{(z-1)X[z]}{z} = \sum_{n=-\infty}^{\infty} \{x[n] - x[n-1]\}z^{-n}$$

and

$$\lim_{z\to 1} \frac{(z-1)X[z]}{z} = \lim_{z\to 1}(z-1)X[z] = \lim_{z\to 1}\lim_{N\to\infty} \sum_{n=-\infty}^{N} \{x[n] - x[n-1]\}z^{-n} = \lim_{N\to\infty} x[N]$$

All these properties of the z-transform are listed in Table 11.2.

11.3 z-Transform Solution of Linear Difference Equations

The time-shifting (left-shift or right-shift) property has set the stage for solving linear difference equations with constant coefficients. As in the case of the Laplace transform with differential

TABLE 11.2 z-Transform Properties

Operation	$x[n]$	$X[z]$	
Addition	$x_1[n]+x_2[n]$	$X_1[z]+X_2[z]$	
Scalar multiplication	$ax[n]$	$aX[z]$	
Right shifting	$x[n-m]u[n-m]$	$\frac{1}{z^m}X[z]$	
	$x[n-m]u[n]$	$\frac{1}{z^m}X[z]+\frac{1}{z^m}\sum_{n=1}^{m}x[-n]z^n$	
	$x[n-1]u[n]$	$\frac{1}{z}X[z]+x[-1]$	
	$x[n-2]u[n]$	$\frac{1}{z^2}X[z]+\frac{1}{z}x[-1]+x[-2]$	
	$x[n-3]u[n]$	$\frac{1}{z^3}X[z]+\frac{1}{z^2}x[-1]+\frac{1}{z}x[-2]+x[-3]$	
Left shifting	$x[n+m]u[n]$	$z^mX[z]-z^m\sum_{n=0}^{m-1}x[n]z^{-n}$	
	$x[n+1]u[n]$	$zX[z]-zx[0]$	
	$x[n+2]u[n]$	$z^2X[z]-z^2x[0]-zx[1]$	
	$x[n+3]u[n]$	$z^3X[z]-z^3x[0]-z^2x[1]-zx[2]$	
Multiplication by γ^n	$\gamma^n x[n]u[n]$	$X\left[\frac{z}{\gamma}\right]$	
Multiplication by n	$nx[n]u[n]$	$-z\frac{d}{dz}X[z]$	
Time reversal	$x[-n]$	$X[1/z]$	
Time convolution	$x_1[n]*x_2[n]$	$X_1[z]X_2[z]$	
Initial value	$x[0]$	$\lim_{z\to\infty}X[z]$	
Final value	$\lim_{N\to\infty}x[N]$	$\lim_{z\to 1}(z-1)X[z]$	Poles of $(z-1)X[z]$ inside the unit circle

equations, the z-transform converts difference equations into algebraic equations that are readily solved to find the solution in the z domain. Taking the inverse z-transform of the z-domain solution yields the desired time-domain solution. The following examples demonstrate the procedure.

EXAMPLE 11.5 z-Transform Solution of a Linear Difference Equation

Solve

$$y[n+2]-5y[n+1]+6y[n]=3x[n+1]+5x[n]$$

if the initial conditions are $y[-1]=11/6$, $y[-2]=37/36$, and the input $x[n]=(2)^{-n}u[n]$.

As we shall see, difference equations can be solved by using the right-shift or the left-shift property. Because the difference equation here is in advance form, the use of the left-shift property in Eq. (11.16) may seem appropriate for its solution. Unfortunately, this left-shift property requires a knowledge of auxiliary conditions $y[0], y[1], \ldots, y[N-1]$ rather than of the initial conditions $y[-1], y[-2], \ldots, y[-n]$, which are generally given. This difficulty can be overcome by expressing the difference equation in delay form (obtained by replacing n with $n-2$) and then using the right-shift property.† The resulting delay-form difference equation is

$$y[n]-5y[n-1]+6y[n-2]=3x[n-1]+5x[n-2] \tag{11.21}$$

We now use the right-shift property to take the z-transform of this equation. But before proceeding, we must be clear about the meaning of a term like $y[n-1]$ here. Does it mean $y[n-1]u[n-1]$ or $y[n-1]u[n]$? In any equation, we must have some time reference $n=0$, and every term is referenced from this instant. Hence, $y[n-k]$ means $y[n-k]u[n]$. Remember also that although we are considering the situation for $n\geq 0$, $y[n]$ is present even before $n=0$ (in the form of initial conditions). Now

$$y[n]u[n] \Longleftrightarrow Y[z]$$

$$y[n-1]u[n] \Longleftrightarrow \frac{1}{z}Y[z]+y[-1]=\frac{1}{z}Y[z]+\frac{11}{6}$$

$$y[n-2]u[n] \Longleftrightarrow \frac{1}{z^2}Y[z]+\frac{1}{z}y[-1]+y[-2]=\frac{1}{z^2}Y[z]+\frac{11}{6z}+\frac{37}{36}$$

Noting that for causal input $x[n]$,

$$x[-1]=x[-2]=\cdots=x[-n]=0$$

We obtain

$$x[n]=(2)^{-n}u[n]=(2^{-1})^n u[n]=(0.5)^n u[n] \Longleftrightarrow \frac{z}{z-0.5}$$

$$x[n-1]u[n] \Longleftrightarrow \frac{1}{z}X[z]+x[-1]=\frac{1}{z}\frac{z}{z-0.5}+0=\frac{1}{z-0.5}$$

$$x[n-2]u[n] \Longleftrightarrow \frac{1}{z^2}X[z]+\frac{1}{z}x[-1]+x[-2]=\frac{1}{z^2}X[z]+0+0=\frac{1}{z(z-0.5)}$$

---

† Another approach is to find $y[0], y[1], y[2], \ldots, y[N-1]$ from $y[-1], y[-2], \ldots, y[-n]$ iteratively, as in Sec. 9.2.1, and then apply the left-shift property to the advance-form difference equation.

In general,

$$x[n-r]u[n] \Longleftrightarrow \frac{1}{z^r}X[z]$$

Taking the z-transform of Eq. (11.21) and substituting the foregoing results, we obtain

$$Y[z]-5\left[\frac{1}{z}Y[z]+\frac{11}{6}\right]+6\left[\frac{1}{z^2}Y[z]+\frac{11}{6z}+\frac{37}{36}\right]=\frac{3}{z-0.5}+\frac{5}{z(z-0.5)}$$

or

$$\left(1-\frac{5}{z}+\frac{6}{z^2}\right)Y[z]-\left(3-\frac{11}{z}\right)=\frac{3}{z-0.5}+\frac{5}{z(z-0.5)} \tag{11.22}$$

from which we obtain

$$(z^2-5z+6)Y[z]=\frac{z(3z^2-9.5z+10.5)}{(z-0.5)}$$

so that

$$Y[z]=\frac{z(3z^2-9.5z+10.5)}{(z-05)(z^2-5z+6)}$$

and

$$\frac{Y[z]}{z}=\frac{3z^2-9.5z+10.5}{(z-0.5)(z-2)(z-3)}=\frac{(26/15)}{z-0.5}-\frac{(7/3)}{z-2}+\frac{(18/5)}{z-3}$$

Therefore,

$$Y[z]=\frac{26}{15}\left(\frac{z}{z-0.5}\right)-\frac{7}{3}\left(\frac{z}{z-2}\right)+\frac{18}{5}\left(\frac{z}{z-3}\right)$$

and

$$y[n]=\left[\tfrac{26}{15}(0.5)^n-\tfrac{7}{3}(2)^n+\tfrac{18}{5}(3)^n\right]u[n] \tag{11.23}$$

This example demonstrates the ease with which linear difference equations with constant coefficients can be solved by the z-transform. This method is general: it can be used to solve a single difference equation or a set of simultaneous difference equations of any order as long as the equations are linear with constant coefficients.

Comment. Sometimes, instead of initial conditions $y[-1]$, $y[-2]$, ..., $y[-n]$, auxiliary conditions $y[0]$, $y[1]$, ..., $y[N-1]$ are given to solve a difference equation. In this case, the equation can be solved by expressing it in the advance form and then using the left-shift property (see Drill 11.11).

DRILL 11.10 z-Transform Solution of a Linear Difference Equation

Solve the following equation if the initial conditions $y[-1]=2$, $y[-2]=0$, and the input $x[n]=u[n]$:

$$y[n+2]-\tfrac{5}{6}y[n+1]+\tfrac{1}{6}y[n]=5x[n+1]-x[n]$$

ANSWER

$y[n]=\left[12-15\left(\frac{1}{2}\right)^n+\frac{14}{3}\left(\frac{1}{3}\right)^n\right]u[n]$

DRILL 11.11 Difference Equation Solution Using $y[0], y[1], \ldots, y[N-1]$

Solve the following equation if the auxiliary conditions are $y[0]=1$, $y[1]=2$, and the input $x[n]=u[n]$:

$$y[n]+3y[n-1]+2y[n-2]=x[n-1]+3x[n-2]$$

ANSWER

$y[n]=\left[\frac{2}{3}+2(-1)^n-\frac{5}{3}(-2)^n\right]u[n]$

Zero-Input and Zero-State Components

In Ex. 11.5, we found the total solution of the difference equation. It is relatively easy to separate the solution into zero-input and zero-state components. All we have to do is to separate the response into terms arising from the input and terms arising from initial conditions (IC). We can separate the response in Eq. (11.22) as follows:

$$\left(1-\frac{5}{z}+\frac{6}{z^2}\right)Y[z]-\underbrace{\left(3-\frac{11}{z}\right)}_{\text{IC terms}}=\underbrace{\frac{3}{z-0.5}+\frac{5}{z(z-0.5)}}_{\text{input terms}}$$

Therefore,

$$\left(1-\frac{5}{z}+\frac{6}{z^2}\right)Y[z]=\underbrace{\left(3-\frac{11}{z}\right)}_{\text{IC terms}}+\underbrace{\frac{(3z+5)}{z(z-0.5)}}_{\text{input terms}}$$

Multiplying both sides by z^2 yields

$$(z^2-5z+6)Y[z]=\underbrace{z(3z-11)}_{\text{IC terms}}+\underbrace{\frac{z(3z+5)}{z-0.5}}_{\text{input terms}}$$

and

$$Y[z]=\underbrace{\frac{z(3z-11)}{z^2-5z+6}}_{\text{zero-input response}}+\underbrace{\frac{z(3z+5)}{(z-0.5)(z^2-5z+6)}}_{\text{zero-state response}}$$

We expand both terms on the right-hand side into modified partial fractions to yield

$$Y[z] = \underbrace{\left[5\left(\frac{z}{z-2}\right) - 2\left(\frac{z}{z-3}\right)\right]}_{\text{zero-input response}} + \underbrace{\left[\frac{26}{15}\left(\frac{z}{z-0.5}\right) - \frac{22}{3}\left(\frac{z}{z-2}\right) + \frac{28}{5}\left(\frac{z}{z-3}\right)\right]}_{\text{zero-state response}}$$

and

$$y[n] = \underbrace{(5(2)^n - 2(3)^n)u[n]}_{\text{zero-input response}} + \underbrace{\left(\tfrac{26}{15}(0.5)^n - \tfrac{22}{3}(2)^n + \tfrac{28}{5}(3)^n\right)u[n]}_{\text{zero-state response}}$$
$$= \left[-\tfrac{7}{3}(2)^n + \tfrac{18}{5}(3)^n + \tfrac{26}{15}(0.5)^n\right]u[n]$$

which agrees with the result in Eq. (11.23).

DRILL 11.12 Separating Zero-Input and Zero-State Responses

Solve

$$y[n+2] - \tfrac{5}{6}y[n+1] + \tfrac{1}{6}y[n] = 5x[n+1] - x[n]$$

if the initial conditions are $y[-1] = 2$, $y[-2] = 0$, and the input $x[n] = u[n]$. Separate the response into zero-input and zero-state responses.

ANSWER

$$y[n] = \underbrace{\left(3\left(\tfrac{1}{2}\right)^n - \tfrac{4}{3}\left(\tfrac{1}{3}\right)^n\right)u[n]}_{\text{zero-input response}} + \underbrace{\left(12 - 18\left(\tfrac{1}{2}\right)^n + 6\left(\tfrac{1}{3}\right)^n\right)u[n]}_{\text{zero-state response}}$$
$$= \left[12 - 15\left(\tfrac{1}{2}\right)^n + \tfrac{14}{3}\left(\tfrac{1}{3}\right)^n\right]u[n]$$

11.3.1 Zero-State Response of LTID Systems: The Transfer Function

Consider an Nth-order LTID system specified by the difference equation

$$Q[E]y[n] = P[E]x[n]$$

or

$$(E^N + a_1E^{N-1} + \cdots + a_{N-1}E + a_N)y[n]$$
$$= (b_0E^N + b_1E^{N-1} + \cdots + b_{N-1}E + b_N)x[n]$$

or

$$y[n+N]+a_1y[n+N-1]+\cdots+a_{N-1}y[n+1]+a_Ny[n]$$
$$=b_0x[n+N]+\cdots+b_{N-1}x[n+1]+b_Nx[n] \tag{11.24}$$

We now derive the general expression for the zero-state response: that is, the system response to input $x[n]$ when all the initial conditions $y[-1]=y[-2]=\cdots=y[-N]=0$ (zero state). The input $x[n]$ is assumed to be causal so that $x[-1]=x[-2]=\cdots=x[-N]=0$.

Equation (11.24) can be expressed in delay form as

$$y[n]+a_1y[n-1]+\cdots+a_Ny[n-N]$$
$$=b_0x[n]+b_1x[n-1]+\cdots+b_Nx[n-N] \tag{11.25}$$

Because $y[-r]=x[-r]=0$ for $r=1,2,\ldots,N$,

$$y[n-m]u[n]\Longleftrightarrow\frac{1}{z^m}Y[z]$$
$$x[n-m]u[n]\Longleftrightarrow\frac{1}{z^m}X[z]\qquad m=1,2,\ldots,N$$

Now the z-transform of Eq. (11.25) is given by

$$\left(1+\frac{a_1}{z}+\frac{a_2}{z^2}+\cdots+\frac{a_N}{z^N}\right)Y[z]=\left(b_0+\frac{b_1}{z}+\frac{b_2}{z^2}+\cdots+\frac{b_N}{z^N}\right)X[z]$$

Multiplication of both sides by z^N yields

$$(z^N+a_1z^{N-1}+\cdots+a_{N-1}z+a_N)Y[z]$$
$$=(b_0z^N+b_1z^{N-1}+\cdots+b_{N-1}z+b_N)X[z]$$

Therefore,

$$Y[z]=\left(\frac{b_0z^N+b_1z^{N-1}+\cdots+b_{N-1}z+b_N}{z^N+a_1z^{N-1}+\cdots+a_{N-1}z+a_N}\right)X[z]$$
$$=\frac{P[z]}{Q[z]}X[z]$$

We have shown in Eq. (11.20) that $Y[z]=X[z]H[z]$. Hence, it follows that

$$H[z]=\frac{P[z]}{Q[z]}=\frac{b_0z^N+b_1z^{N-1}+\cdots+b_{N-1}z+b_N}{z^N+a_1z^{N-1}+\cdots+a_{N-1}z+a_N} \tag{11.26}$$

As in the case of LTIC systems, this result leads to an alternative definition of the LTID system transfer function as the ratio of $Y[z]$ to $X[z]$ (assuming all initial conditions are zero).

$$H[z]\equiv\frac{Y[z]}{X[z]}=\frac{\mathcal{Z}[\text{zero-state response}]}{\mathcal{Z}[\text{input}]}$$

Alternate Interpretation of the z-Transform

So far we have treated the z-transform as a machine that converts linear difference equations into algebraic equations. There is no physical understanding of how this is accomplished or what it means. We now discuss more intuitive interpretation and meaning of the z-transform.

In Ch. 9, Eq. (9.25), we showed that the LTID system response to an everlasting exponential z^n is $H[z]z^n$. If we could express every discrete-time signal as a linear combination of everlasting exponentials of the form z^n, we could readily obtain the system response to any input. For example, if

$$x[n] = \sum_{k=1}^{K} X[z_k] z_k^n \tag{11.27}$$

the response of an LTID system to this input is given by

$$y[n] = \sum_{k=1}^{K} X[z_k] H[z_k] z_k^n$$

Unfortunately, a very small class of signals can be expressed in the form of Eq. (11.27). However, we can express almost all signals of practical utility as a sum of everlasting exponentials over a continuum of values of z. This is precisely what the z-transform in Eq. (11.2) does.

$$x[n] = \frac{1}{2\pi j} \oint X[z] z^{n-1}\, dz \tag{11.28}$$

Invoking the linearity property of the z-transform, we can find the system response $y[n]$ to input $x[n]$ in Eq. (11.28) as[†]

$$y[n] = \frac{1}{2\pi j} \oint X[z]H[z] z^{n-1}\, dz = \mathcal{Z}^{-1}\{X[z]H[z]\}$$

Clearly,

$$Y[z] = X[z]H[z]$$

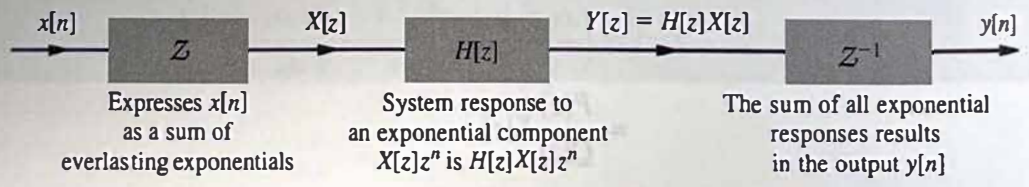

(a)

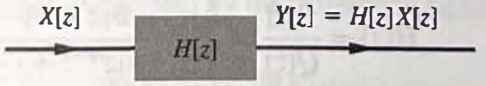

(b)

Figure 11.6 The transformed representation of an LTID system.

[†] In computing $y[n]$, the contour along which the integration is performed is modified to consider the ROC of $X[z]$ as well as $H[z]$. We ignore this consideration in this intuitive discussion.

This viewpoint of finding the response of an LTID system is illustrated in Fig. 11.6a. Just as in continuous-time systems, we can model discrete-time systems in the transformed manner by representing all signals by their z-transforms and all system components (or elements) by their transfer functions, as shown in Fig. 11.6b.

The result $Y[z] = H[z]X[z]$ greatly facilitates derivation of the system response to a given input. We shall demonstrate this assertion by an example.

EXAMPLE 11.6 Transfer Function to Find the Zero-State Response

Find the response $y[n]$ of an LTID system described by the difference equation

$$y[n+2]+y[n+1]+0.16y[n]=x[n+1]+0.32x[n]$$

or

$$(E^2+E+0.16)y[n]=(E+0.32)x[n]$$

for the input $x[n] = (-2)^{-n}u[n]$ and with all the initial conditions zero (system in the zero state).

From the difference equation, we find

$$H[z]=\frac{P[z]}{Q[z]}=\frac{z+0.32}{z^2+z+0.16}$$

For the input $x[n]=(-2)^{-n}u[n]=[(-2)^{-1}]^n u(n)=(-0.5)^n u[n]$,

$$X[z]=\frac{z}{z+0.5}$$

and

$$Y[z]=X[z]H[z]=\frac{z(z+0.32)}{(z^2+z+0.16)(z+0.5)}$$

Therefore,

$$\frac{Y[z]}{z}=\frac{(z+0.32)}{(z^2+z+0.16)(z+0.5)}=\frac{(z+0.32)}{(z+0.2)(z+0.8)(z+0.5)}$$
$$=\frac{2/3}{z+0.2}-\frac{8/3}{z+0.8}+\frac{2}{z+0.5}$$

so that

$$Y[z]=\frac{2}{3}\left(\frac{z}{z+0.2}\right)-\frac{8}{3}\left(\frac{z}{z+0.8}\right)+2\left(\frac{z}{z+0.5}\right)$$

and

$$y[n]=\left[\tfrac{2}{3}(-0.2)^n-\tfrac{8}{3}(-0.8)^n+2(-0.5)^n\right]u[n]$$

EXAMPLE 11.7 Transfer Function of a Unit Delay

Show that the transfer function of a unit delay is $1/z$.

If the input to the unit delay is $x[n]u[n]$, then its output (Fig. 11.7) is given by

$$y[n] = x[n-1]u[n-1]$$

The z-transform of this equation yields [see Eq. (11.12)]

$$Y[z] = \frac{1}{z}X[z] = H[z]X[z]$$

It follows that the transfer function of the unit delay is

$$H[z] = \frac{1}{z}$$

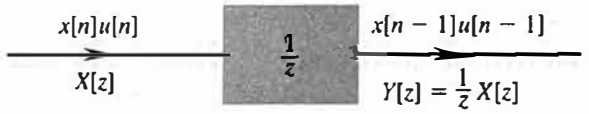

Figure 11.7 Ideal unit delay and its transfer function.

DRILL 11.13 Transfer Function to Find Zero-State Response and Difference Equation

A discrete-time system is described by the following transfer function:

$$H[z] = \frac{z-0.5}{(z+0.5)(z-1)}$$

(a) Find the system response to input $x[n] = 3^{-(n+1)}u[n]$ if all initial conditions are zero.

(b) Write the difference equation relating the output $y[n]$ to input $x[n]$ for this system.

ANSWERS

(a) $y[n] = \frac{1}{3}\left[\frac{1}{2} - 0.8(-0.5)^n + 0.3\left(\frac{1}{3}\right)^n\right]u[n]$

(b) $y[n+2] - 0.5y[n+1] - 0.5y[n] = x[n+1] - 0.5x[n]$

11.3.2 Stability

Equation (11.26) shows that the denominator of $H[z]$ is $Q[z]$, which is apparently identical to the characteristic polynomial $Q[\gamma]$ defined in Ch. 9. Does this mean that the denominator of $H[z]$ is the characteristic polynomial of the system? This may or may not be the case: if $P[z]$ and $Q[z]$ in Eq. (11.26) have any common factors, they cancel out, and the effective denominator of $H[z]$ is not necessarily equal to $Q[z]$. Recall also that the system transfer function $H[z]$, like $h[n]$, is defined in terms of measurements at the external terminals. Consequently, $H[z]$ and $h[n]$ are both external descriptions of the system. In contrast, the characteristic polynomial $Q[z]$ is an internal description. Clearly, we can determine only external stability, that is, BIBO stability, from $H[z]$. If all the poles of $H[z]$ are within the unit circle, all the terms in $h[n]$ are decaying exponentials, and as shown in Sec. 9.6, $h[n]$ is absolutely summable. Consequently, the system is BIBO-stable. Otherwise, the system is BIBO-unstable.

If $P[z]$ and $Q[z]$ do not have common factors, then the denominator of $H[z]$ is identical to $Q[z]$.[†] The poles of $H[z]$ are the characteristic roots of the system. We can now determine internal stability. The internal stability criterion in Sec. 9.6.2 can be restated in terms of the poles of $H[z]$, as follows.

1. An LTID system is asymptotically stable if and only if all the poles of its transfer function $H[z]$ are within the unit circle. The poles may be repeated or simple.
2. An LTID system is unstable if and only if either one or both of the following conditions exist: (i) at least one pole of $H[z]$ is outside the unit circle; (ii) there are repeated poles of $H[z]$ on the unit circle.
3. An LTID system is marginally stable if and only if there are no poles of $H[z]$ outside the unit circle, and there are some simple poles on the unit circle.

DRILL 11.14 Transfer Function to Determine Stability

Show that an *accumulator* whose impulse response is $h[n] = u[n]$ is marginally stable but BIBO-unstable.

11.3.3 Inverse Systems

If $H[z]$ is the transfer function of a system $\mathcal{S}$, then $\mathcal{S}_i$, its inverse system, has a transfer function $H_i[z]$ given by

$$H_i[z] = \frac{1}{H[z]}$$

[†] There is no way of determining whether any common factors in $P[z]$ and $Q[z]$ were canceled out. This is because in our derivation of $H[z]$, we generally get the final result after the cancellations have been effected. When we use internal description of the system to derive $Q[z]$, however, we find pure $Q[z]$ unaffected by any common factor in $P[z]$.

This follows from the fact that the inverse system S_i undoes the operation of S. Hence, if $H[z]$ is placed in cascade with $H_i[z]$, the transfer function of the composite system (identity system) is unity. For example, an *accumulator* whose transfer function is $H[z] = z/(z-1)$ and a *backward difference system* whose transfer function is $H_i[z] = (z-1)/z$ are inverses of each other. Similarly, if

$$H[z] = \frac{z-0.4}{z-0.7}$$

its inverse system transfer function is

$$H_i[z] = \frac{z-0.7}{z-0.4}$$

as required by the property $H[z]H_i[z] = 1$. Hence, it follows that

$$h[n] * h_i[n] = \delta[n]$$

DRILL 11.15 Inverse Systems

Find the impulse responses of an accumulator and a first-order backward difference system. Show that the convolution of the two impulse responses yields $\delta[n]$.

11.4 SYSTEM REALIZATION

Because of the similarity between LTIC and LTID systems, conventions for block diagrams and rules of interconnection for LTID are identical to those for continuous-time (LTIC) systems. It is not necessary to rederive these relationships. We shall merely restate them to refresh the reader's memory.

The block diagram representations of the basic operations, such as an adder, a scalar multiplier, unit delay, and pickoff points, are shown in Fig. 8.20. In our development, the unit delay, which is represented by a box marked D in Fig. 8.20, will be represented by its transfer function $1/z$. All the signals will also be represented in terms of their z-transforms. Thus, the input and the output will be labeled $X[z]$ and $Y[z]$, respectively.

When two systems with transfer functions $H_1[z]$ and $H_2[z]$ are connected in cascade (as in Fig. 6.19b), the transfer function of the composite system is $H_1[z]H_2[z]$. If the same two systems are connected in parallel (as in Fig. 6.19c), the transfer function of the composite system is $H_1[z] + H_2[z]$. For a feedback system (as in Fig. 6.19d), the transfer function is $G[z]/(1 + G[z]H[z])$.

We now consider a systematic method for realization (or simulation) of an arbitrary Nth-order LTID transfer function. Since realization is basically a synthesis problem, there is no unique way of realizing a system. A given transfer function can be realized in many different ways. We present here the two forms of *direct realization*. Each of these forms can be executed in several other ways, such as cascade and parallel. Furthermore, a system can be realized by the transposed version of

any known realization of that system. This artifice doubles the number of system realizations. A transfer function $H[z]$ can be realized by using time delays along with adders and multipliers.

We shall consider a realization of a general Nth-order causal LTID system, whose transfer function is given by

$$H[z] = \frac{b_0 z^N + b_1 z^{N-1} + \cdots + b_{N-1} z + b_N}{z^N + a_1 z^{N-1} + \cdots + a_{N-1} z + a_N} \tag{11.29}$$

This equation is identical to the transfer function of a general Nth-order proper LTIC system given in Eq. (6.40). The only difference is that the variable z in the former is replaced by the variable s in the latter. Hence, the procedure for realizing an LTID transfer function is identical to that for

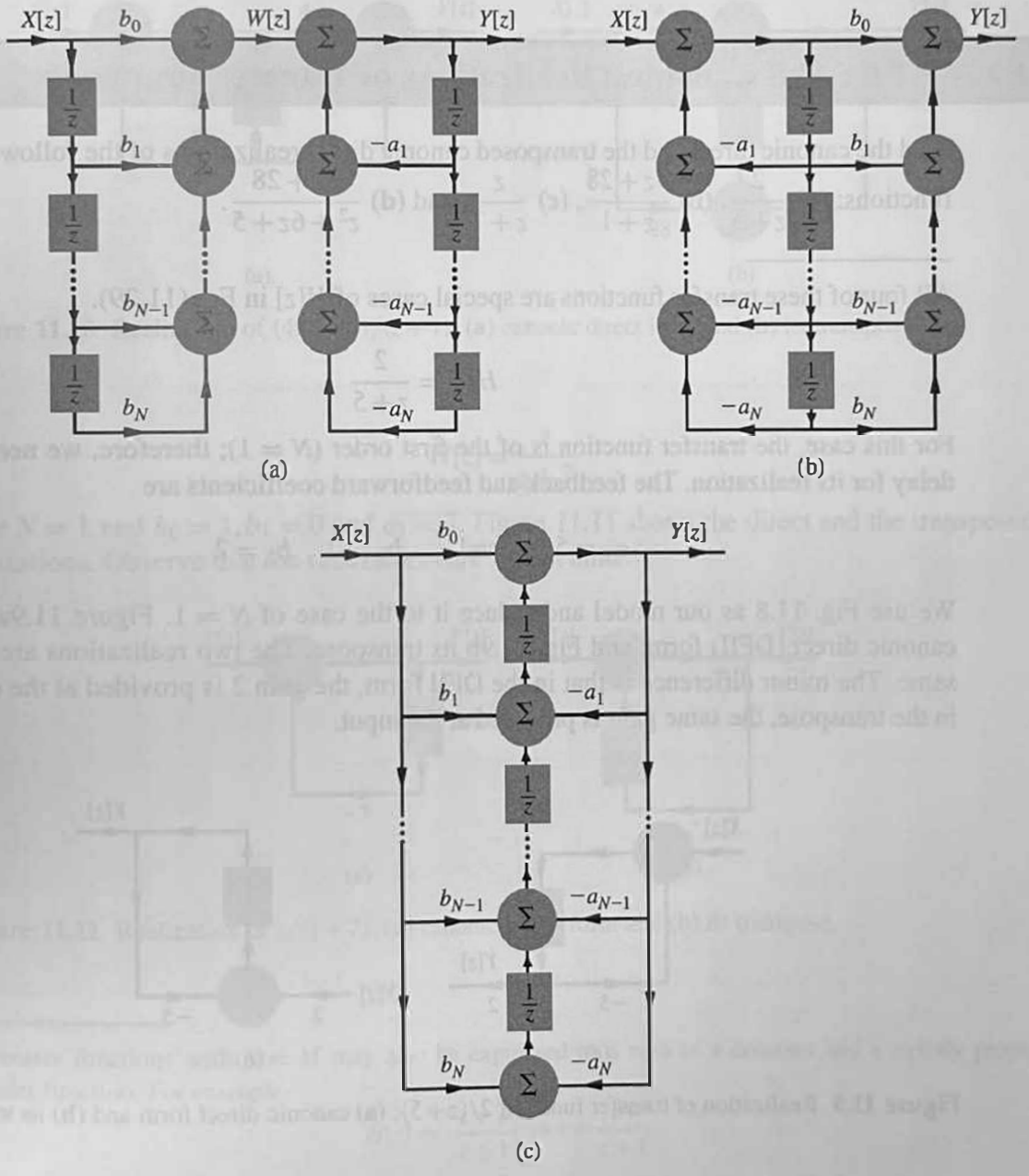

Figure 11.8 Realization of an Nth-order causal LTID system transfer function by using **(a)** DFI, **(b)** canonic direct (DFII), and **(c)** the transpose form of DFII.

the LTIC transfer function with the basic element $1/s$ (integrator) replaced by the element $1/z$ (unit delay). The reader is encouraged to follow the steps in Sec. 6.6 and rederive the results for the LTID transfer function in Eq. (11.29). Here, we shall merely reproduce the realizations from Sec. 6.6 with integrators $(1/s)$ replaced by unit delays $(1/z)$.

The direct form I (DFI) is shown in Fig. 11.8a, the canonic direct form (DFII) is shown in Fig. 11.8b, and the transpose of canonic direct is shown in Fig. 11.8c. The DFII and its transpose are canonic because they require N delays, which is the minimum number needed to implement the Nth-order LTID transfer function in Eq. (11.29). In contrast, the form DFI is noncanonic because it generally requires $2N$ delays. The DFII realization in Fig. 11.8b is also called a *canonic direct* form.

EXAMPLE 11.8 Canonical Realizations of Transfer Functions

Find the canonic direct and the transposed canonic direct realizations of the following transfer functions: **(a)** $\frac{2}{z+5}$, **(b)** $\frac{4z+28}{z+1}$, **(c)** $\frac{z}{z+7}$, and **(d)** $\frac{4z+28}{z^2+6z+5}$.

All four of these transfer functions are special cases of $H[z]$ in Eq. (11.29).

(a)

$$H[z]=\frac{2}{z+5}$$

For this case, the transfer function is of the first order ($N=1$); therefore, we need only one delay for its realization. The feedback and feedforward coefficients are

$$a_1=5 \quad \text{and} \quad b_0=0, \quad b_1=2$$

We use Fig. 11.8 as our model and reduce it to the case of $N=1$. Figure 11.9a shows the canonic direct (DFII) form, and Fig. 11.9b its transpose. The two realizations are almost the same. The minor difference is that in the DFII form, the gain 2 is provided at the output, and in the transpose, the same gain is provided at the input.

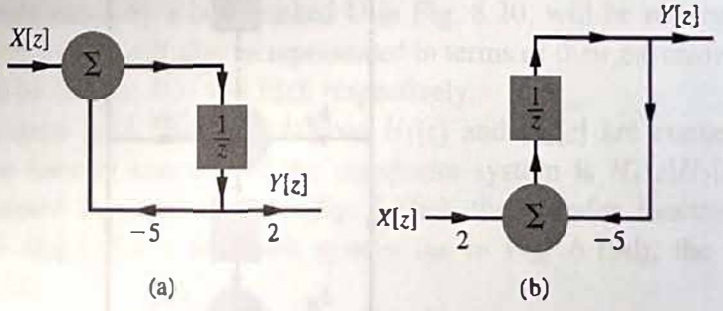

Figure 11.9 Realization of transfer function $2/(z+5)$: **(a)** canonic direct form and **(b)** its transpose.

In a similar way, we realize the remaining transfer functions.

(b)

$$H[z] = \frac{4z+28}{z+1}$$

In this case also, the transfer function is of the first order ($N = 1$); therefore, we need only one delay for its realization. The feedback and feedforward coefficients are

$$a_1 = 1 \qquad \text{and} \qquad b_0 = 4, \quad b_1 = 28$$

Figure 11.10 illustrates the canonic direct and its transpose for this case.†

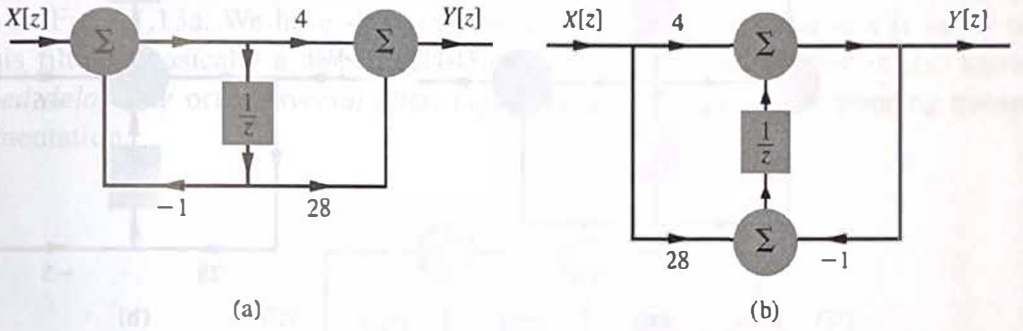

Figure 11.10 Realization of $(4z+28)/(z+1)$: **(a)** canonic direct form and **(b)** its transpose.

(c)

$$H[z] = \frac{z}{z+7}$$

Here $N = 1$ and $b_0 = 1, b_1 = 0$ and $a_1 = 7$. Figure 11.11 shows the direct and the transposed realizations. Observe that the realizations are almost alike.

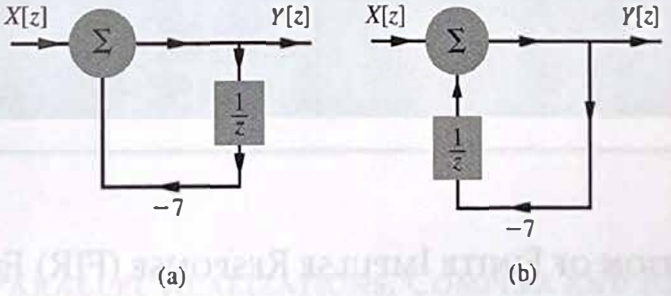

Figure 11.11 Realization of $z/(z+7)$: **(a)** canonic direct form and **(b)** its transpose.

† Transfer functions with $N = M$ may also be expressed as a sum of a constant and a strictly proper transfer function. For example,

$$H[z] = \frac{4z+28}{z+1} = 4 + \frac{24}{z+1}$$

Hence, this transfer function can also be realized as two transfer functions in parallel.

(d)

$$H[z]=\frac{4z+28}{z^2+6z+5}$$

This is a second-order system ($N=2$) with $b_0=0, b_1=4, b_2=28, a_1=6, a_2=5$. Figure 11.12 shows the canonic direct and transposed canonic direct realizations.

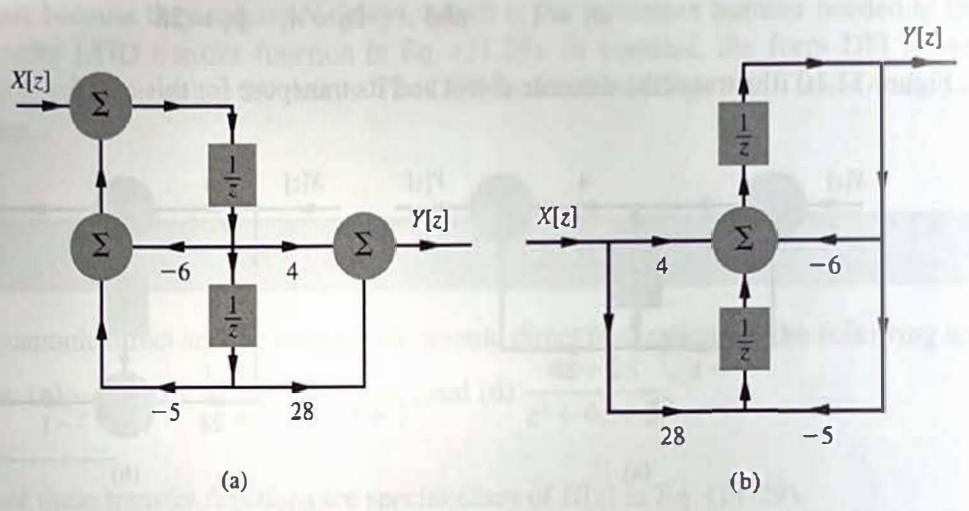

Figure 11.12 Realization of $(4z+28)/(z^2+6z+5)$: **(a)** canonic direct form and **(b)** its transpose.

DRILL 11.16 Realization of a Second-Order Transfer Function

Realize the transfer function

$$H[z]=\frac{2z}{z^2+6z+25}$$

Realization of Finite Impulse Response (FIR) Filters

So far we have been quite general in our development of realization techniques. They can be applied to infinite impulse response (IIR) or FIR filters. For FIR filters, the coefficients $a_i=0$ for all $i\neq 0$.[†] Hence, FIR filters can be readily implemented by means of the schemes developed so far by eliminating all branches with a_i coefficients. The condition $a_i=0$ implies that all the poles of a FIR filter are at $z=0$.

[†] This statement is true for all $i\neq 0$ because a_0 is assumed to be unity.

EXAMPLE 11.9 Realization of an FIR Filter

Realize $H[z] = (z^3 + 4z^2 + 5z + 2)/z^3$ using canonic direct and transposed forms.

We can express $H[z]$ as

$$H[z] = \frac{z^3 + 4z^2 + 5z + 2}{z^3}$$

For $H[z]$, $b_0 = 1$, $b_1 = 4$, $b_2 = 5$, and $b_3 = 2$. Hence, we obtain the canonic direct realization, shown in Fig. 11.13a. We have shown the horizontal orientation because it is easier to see that this filter is basically a tapped delay line. That is why this structure is also known as a *tapped delay line* or *transversal filter*. Figure 11.13b shows the corresponding transposed implementation.

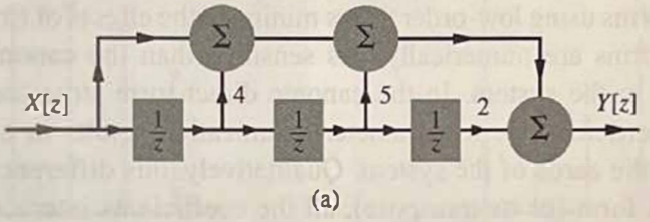

(a)

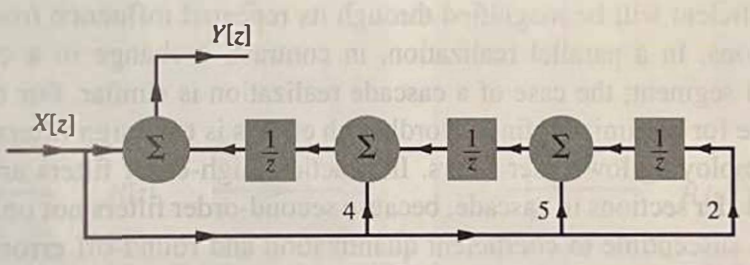

(b)

Figure 11.13 Realization of $(z^3 + 4z^2 + 5z + 2)/z^3$.

Cascade and Parallel Realizations, Complex and Repeated Poles

The considerations and observations for cascade and parallel realizations as well as complex and multiple poles are identical to those discussed for LTIC systems in Sec. 6.6.3.

DRILL 11.17 Cascade and Parallel Realizations of a Transfer Function

Find canonic direct realizations of the following transfer function by using the cascade and parallel forms. The specific cascade decomposition is as follows:

$$H[z] = \frac{z+3}{z^2+7z+10} = \left(\frac{z+3}{z+2}\right)\left(\frac{1}{z+5}\right)$$

Do All Realizations Lead to the Same Performance?

For a given transfer function, we have presented here several possible different realizations (DFI, canonic form DFII, and its transpose). There are also cascade and parallel versions, and there are many possible groupings of the factors in the numerator and the denominator of $H[z]$, leading to different realizations. We can also use various combinations of these forms in implementing different subsections of a system. Moreover, the transpose of each version doubles the number. However, this discussion by no means exhausts all the possibilities. Transforming variables affords limitless potential realizations of the same transfer function.

Theoretically, all these realizations are equivalent; that is, they lead to the same transfer function. This, however, is true only when we implement them with infinite precision. In practice, finite wordlength restriction causes each realization to behave differently in terms of sensitivity to parameter variation, stability, frequency response distortion error, and so on. These effects are serious for higher-order transfer functions, which require correspondingly higher numbers of delay elements. The finite wordlength errors that plague these implementations are coefficient quantization, overflow errors, and round-off errors. From a practical viewpoint, parallel and cascade forms using low-order filters minimize the effects of finite wordlength. Parallel and certain cascade forms are numerically less sensitive than the canonic direct form to small parameter variations in the system. In the canonic direct-form structure with large N, a small change in a filter coefficient due to parameter quantization results in a big change in the location of the poles and the zeros of the system. Qualitatively, this difference can be explained by the fact that in a direct form (or its transpose), all the coefficients interact with each other, and a change in any coefficient will be magnified through its repeated influence from feedback and feedforward connections. In a parallel realization, in contrast, a change in a coefficient will affect only a localized segment; the case of a cascade realization is similar. For this reason, the most popular technique for minimizing finite wordlength effects is to design filters by using cascade or parallel forms employing low-order filters. In practice, high-order filters are realized by using multiple second-order sections in cascade, because second-order filters not only are easier to design but are also less susceptible to coefficient quantization and round-off errors, and their implementations allow easier data word scaling to reduce the potential overflow effects of data word-size growth. A cascaded system using second-order building blocks usually requires fewer multiplications for a given filter frequency response [1].

There are several ways to pair the poles and zeros of an Nth-order $H[z]$ into a cascade of second-order sections, and several ways to order the resulting sections. Quantizing error will be different for each combination. Although several papers published provide guidelines in predicting and minimizing finite wordlength errors, it is advisable to resort to computer simulation of the filter design. This way, one can vary filter hardware characteristics, such as coefficient wordlengths, accumulator register sizes, sequencing of cascaded sections, and input signal sets. Such an approach is both reliable and economical [1].

11.5 Connecting the Laplace and z-Transforms

We now show that discrete-time systems also can be analyzed by means of the Laplace transform. In fact, we shall see that *the z-transform is the Laplace transform in disguise* and that discrete-time systems can be analyzed as if they were continuous-time systems.

So far we have considered the discrete-time signal as a sequence of numbers and not as an electrical signal (voltage or current). Similarly, we considered a discrete-time system as a mechanism that processes a sequence of numbers (input) to yield another sequence of numbers (output). The system was built by using delays (along with adders and multipliers) that delay sequences of numbers. A digital computer is a perfect example: every signal is a sequence of numbers, and the processing involves delaying sequences of numbers (along with addition and multiplication).

Now suppose we have a discrete-time system with transfer function $H[z]$ and input $x[n]$. Consider a continuous-time signal $x(t)$ such that its nth sample value is $x[n]$, as shown in Fig. 11.14.† Let the sampled signal be $\bar{x}(t)$, consisting of impulses spaced T seconds apart with the

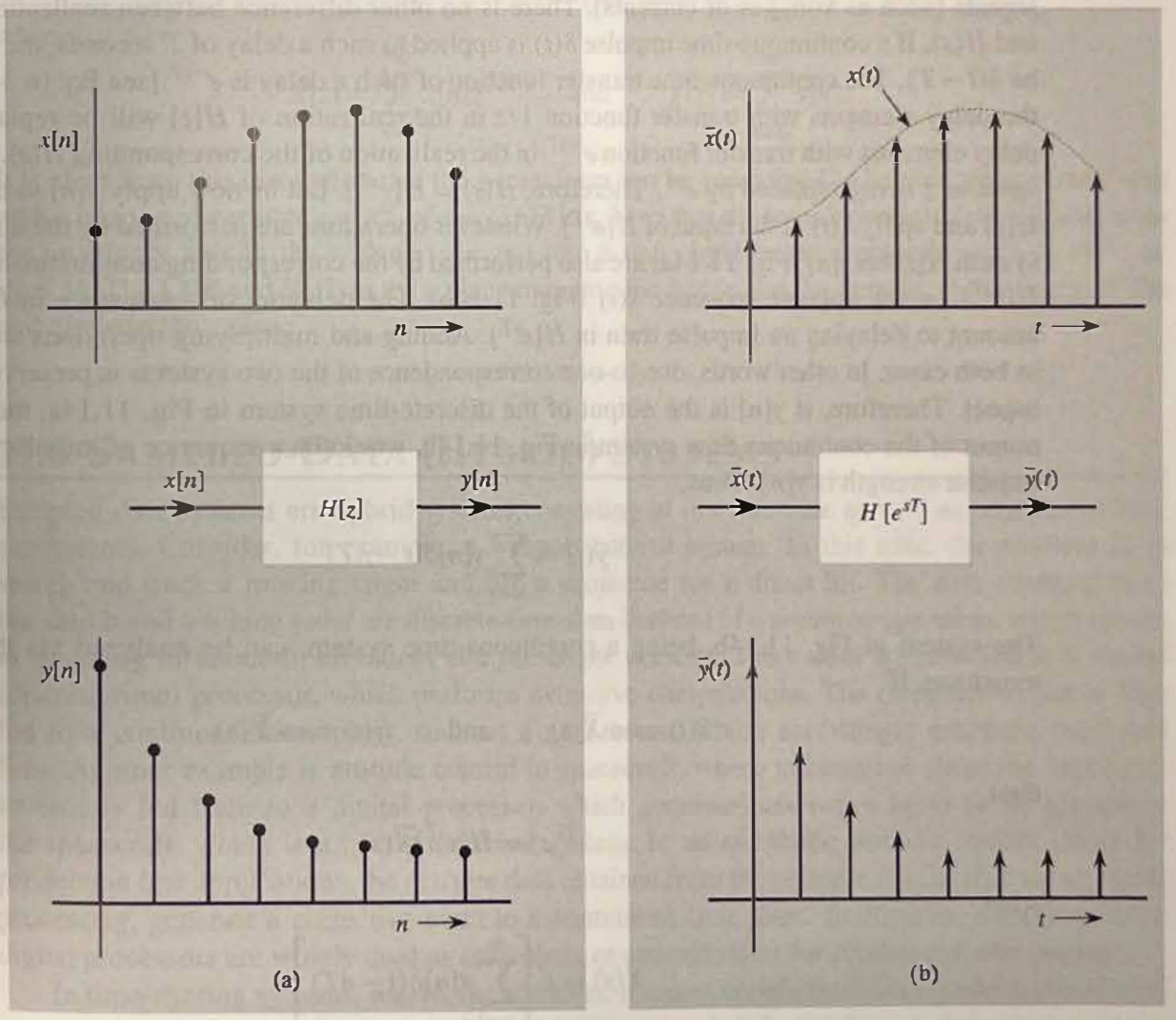

Figure 11.14 Connection between the Laplace transform and the z-transform.

† We can construct such $x(t)$ from the sample values, as explained in Ch. 5.

nth impulse of strength $x[n]$. Thus,

$$\bar{x}(t) = \sum_{n=0}^{\infty} x[n]\delta(t - nT)$$

Figure 11.14 shows $x[n]$ and the corresponding $\bar{x}(t)$. The signal $x[n]$ is applied to the input of a discrete-time system with transfer function $H[z]$, which is generally made up of delays, adders, and scalar multipliers. Hence, processing $x[n]$ through $H[z]$ amounts to operating on the sequence $x[n]$ by means of delays, adders, and scalar multipliers. Suppose for $\bar{x}(t)$ samples, we perform operations identical to those performed on the samples of $x[n]$ by $H[z]$. For this purpose, we need a continuous-time system with transfer function $H(s)$ that is identical in structure to the discrete-time system $H[z]$ except that the delays in $H[z]$ are replaced by elements that delay continuous-time signals (such as voltages or currents). There is no other difference between realizations of $H[z]$ and $H(s)$. If a continuous-time impulse $\delta(t)$ is applied to such a delay of T seconds, the output will be $\delta(t - T)$. The continuous-time transfer function of such a delay is e^{-sT} [see Eq. (6.34)]. Hence, the delay elements with transfer function $1/z$ in the realization of $H[z]$ will be replaced by the delay elements with transfer function e^{-sT} in the realization of the corresponding $H(s)$. This is the same as z being replaced by e^{sT}. Therefore, $H(s) = H[e^{sT}]$. Let us now apply $x[n]$ to the input of $H[z]$ and apply $\bar{x}(t)$ at the input of $H[e^{sT}]$. Whatever operations are performed by the discrete-time system $H[z]$ on $x[n]$ (Fig. 11.14a) are also performed by the corresponding continuous-time system $H[e^{sT}]$ on the impulse sequence $\bar{x}(t)$ (Fig. 11.14b). The delaying of a sequence in $H[z]$ would amount to delaying an impulse train in $H[e^{sT}]$. Adding and multiplying operations are the same in both cases. In other words, one-to-one correspondence of the two systems is preserved in every aspect. Therefore, if $y[n]$ is the output of the discrete-time system in Fig. 11.14a, then $\bar{y}(t)$, the output of the continuous-time system in Fig. 11.14b, would be a sequence of impulse whose nth impulse strength is $y[n]$. Thus,

$$\bar{y}(t) = \sum_{n=0}^{\infty} y[n]\delta(t - nT)$$

The system in Fig. 11.14b, being a continuous-time system, can be analyzed via the Laplace transform. If

$$\bar{x}(t) \Longleftrightarrow \bar{X}(s) \qquad \text{and} \qquad \bar{y}(t) \Longleftrightarrow \bar{Y}(s)$$

then

$$\bar{Y}(s) = H[e^{sT}]\bar{X}(s) \tag{11.30}$$

Also,

$$\bar{X}(s) = \mathcal{L}\left[\sum_{n=0}^{\infty} x[n]\delta(t - nT)\right]$$

Now because the Laplace transform of $\delta(t - nT)$ is e^{-snT},

$$\bar{X}(s) = \sum_{n=0}^{\infty} x[n]e^{-snT} \qquad \text{and} \qquad \bar{Y}(s) = \sum_{n=0}^{\infty} y[n]e^{-snT}$$

Substitution of these expressions into Eq. (11.30) yields

$$\sum_{n=0}^{\infty} y[n]e^{-snT} = H[e^{sT}]\left[\sum_{n=0}^{\infty} x[n]e^{-snT}\right]$$

By introducing a new variable $z = e^{sT}$, this equation can be expressed as

$$\sum_{n=0}^{\infty} y[n]z^{-n} = H[z]\sum_{n=0}^{\infty} x[n]z^{-n}$$

or

$$Y[z] = H[z]X[z]$$

where

$$X[z] = \sum_{n=0}^{\infty} x[n]z^{-n} \qquad \text{and} \qquad Y[z] = \sum_{n=0}^{\infty} y[n]z^{-n}$$

It is clear from this discussion that the z-transform can be considered to be the Laplace transform with a change of variable $z = e^{sT}$ or $s = (1/T)\ln z$. Note that the transformation $z = e^{sT}$ transforms the imaginary axis in the s plane ($s = j\omega$) into a unit circle in the z plane ($z = e^{sT} = e^{j\omega T}$, or $|z| = 1$). The LHP and RHP in the s plane map into the inside and the outside, respectively, of the unit circle in the z plane.

11.6 Sampled-Data (Hybrid) Systems

Sampled-data systems are hybrid systems consisting of discrete-time as well as continuous-time subsystems. Consider, for example, a weapon control system. In this case, the problem is to search and track a moving target and fire a projectile for a direct hit. The data obtained from the search and tracking radar are discrete-time data because of a scanning operation, which results in sampling of azimuth, elevation, and the target velocity. These data are now fed to a digital (discrete-time) processor, which performs extensive computations. The computer output is then fed to a continuous-time plant, such as a gun mount, which accordingly positions itself and fires. Another example is attitude control in spacecraft, where information about the spacecraft attitude is fed back to a digital processor, which generates corrective input to be applied to the spacecraft, which is a continuous-time system. In an automatic periodic quality check for production line applications, the discrete data obtained from the periodic check, after some digital processing, generate a corrective input to a continuous-time plant. In complex control systems, digital processors are widely used as controllers or compensators for continuous-time plants.

In time-sharing systems, where, for economic reasons, certain facilities are shared by several systems, the signals are, by nature, discrete-time or sampled. In regulator-type control systems, where an output variable must be maintained at a constant value, the external disturbance and plant parameter variations are usually so slow that continuous monitoring (or feedback) is unnecessary. It is adequate to sample the output periodically and then feed back these discrete data. In such cases, feedback transducers, data-processing facilities, and possibly long and expensive feedback communication facilities can be shared among several control systems.

Figure 11.15 shows some typical sampled-data systems. Figure 11.15a contains a digital processor, whereas in Fig. 11.15b, the sampled signal is directly applied to a D/A converter (the hold circuit) without further digital processing. Figure 11.15c shows a practical system where the input signal itself is a discrete-time signal $x[n]$, and the sampler is in the feedback path. This system is equivalent to that in Fig. 11.15b. How do we analyze such hybrid systems, where continuous-time and discrete-time signals intermingle? An effective strategy in such a situation is to relate the samples of the output to those of the input. But this procedure yields information about the output only at sampling instants. We can overcome this difficulty by taking the samples at instants in between samples using the *modified z-transform* as explained later.

In sampled-data systems, the discrete-time signals are often obtained as a result of sampling continuous-time signals. These samples are narrow pulses, which may be considered as impulses, provided the pulse width is small compared to the system time constant. Thus, in the following discussion, a discrete-time signal, when it appears in conjunction with a continuous-time system, is a sequence of impulses rather than a sequence of numbers. Hence, a discrete-time signal $x[n]$ can also be considered as a continuous-time signal $x(t)$, where

$$x(t) = \sum_n x[n]\delta(t - nT)$$

Observe an interesting fact: in this representation, a discrete-time unit impulse $\delta[n]$ *is* the continuous-time unit impulse $\delta(t)$. Thus, at the input of a discrete-time processor, a discrete-time signal $x[n]$ is just a sequence of numbers. But at the input of a continuous-time system, $x[n]$ is a sequence of impulses. There are appropriate converters at the interface of discrete-time and continuous-time systems to carry out signal conversion to appropriate forms.

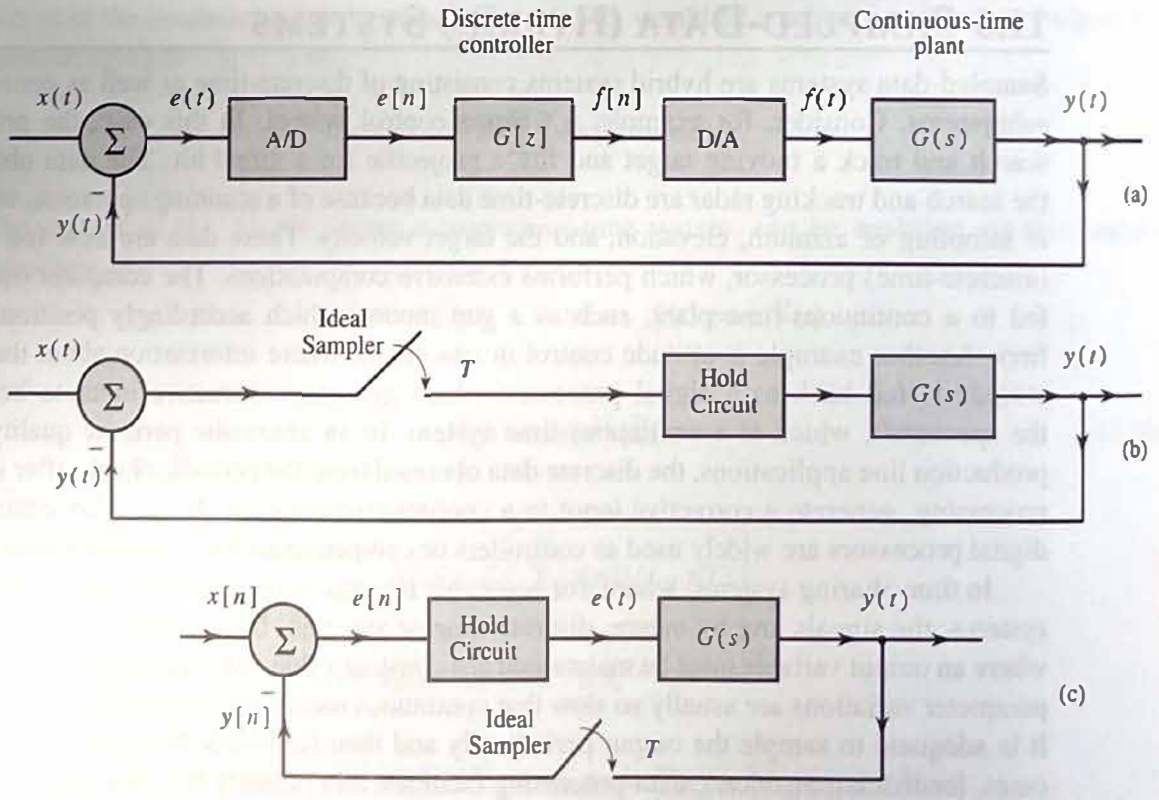

Figure 11.15 Typical sampled-data systems.

To begin with, consider a basic continuous-time system (Fig. 11.16a) with transfer function $H(s)$. The input $x(t)$ is sampled, and the sampled signal $x[n]$ is applied to the input of $H(s)$. Although $y(t)$, the output of this system, is continuous, we shall endeavor to find the values of $y(t)$ only at the discrete instants $t = nT$. Such an analysis is relatively simple using z-transforms. For this purpose, we consider what would happen if the output is sampled by a hypothetical sampler, shown dotted in Fig. 11.16a. Now, we shall relate the input samples $x[n]$ and the output samples $y[n]$. Let $h[n]$ be the unit impulse response relating the output samples to the input samples. In other words, $y[n] = h[n] * x[n]$. Recall also that a unit impulse $\delta[n]$ is $\delta(t)$ when considered in conjunction with a continuous-time system. Hence, $h[n]$, the unit impulse response, is the sampled version of the system's unit impulse response $h(t)$. Thus,

$$h[n] = h(nT)$$

where T is the sampling interval. For instance, if $H(s) = \frac{1}{s-\lambda}$, then $h(t) = e^{\lambda t}$ and

$$h[n] = e^{\lambda nT}$$

Therefore, the equivalent discrete-time transfer function $H[z]$ of this system is given by

$$H[z] = \mathcal{Z}\{h[n]\} = \mathcal{Z}\{e^{\lambda nT}\} = \frac{z}{z - e^{\lambda T}} \tag{11.31}$$

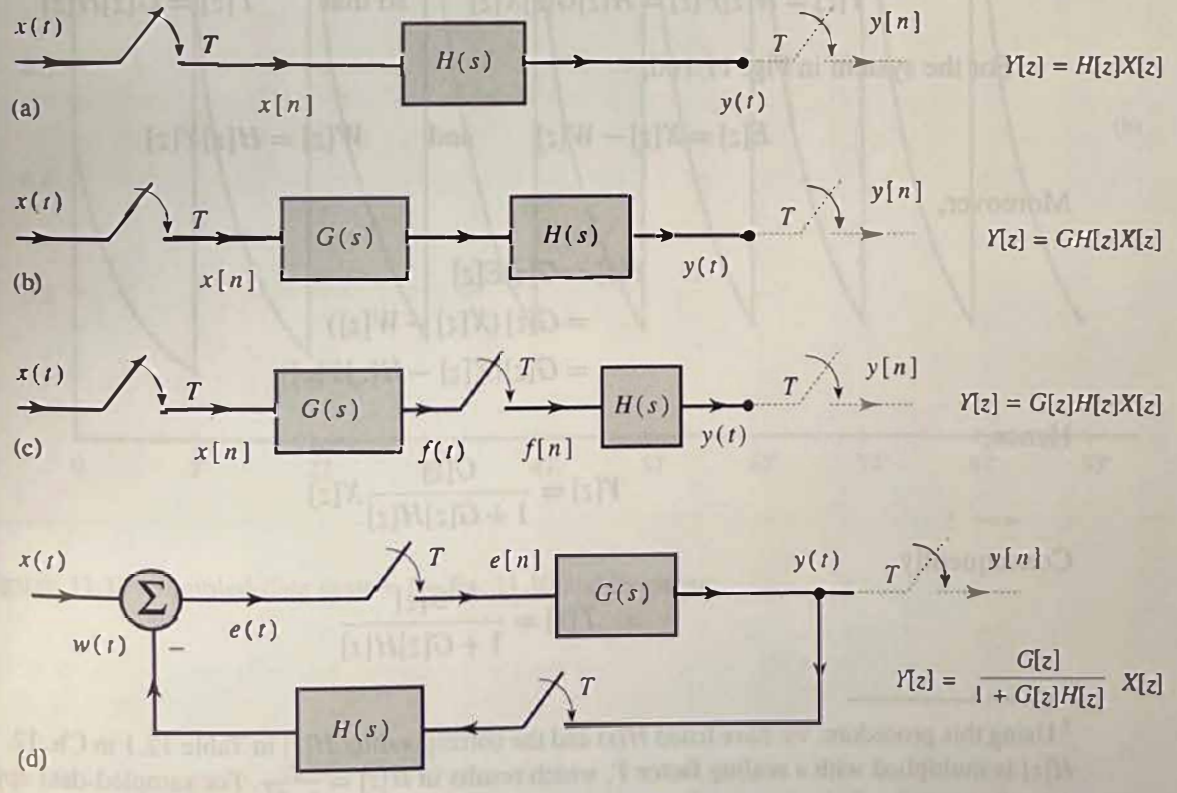

Figure 11.16 Computing the outputs of various sampled-data systems.

Thus, $H[z]$ is the discrete-time transfer function of $H(s) = \frac{1}{s+\lambda}$ that relates $y[n]$ (the output samples) to the discrete-time input $x[n]$.†

If we have two systems with transfer functions $G(s)$ and $H(s)$ in cascade (Fig. 11.16b), the equivalent transfer function $T[z] \neq G[z]H[z]$, but is $GH[z]$, where $G[z]$, $H[z]$, and $GH[z]$ correspond to discrete-time transfer functions of $G(s)$, $H(s)$, and $G(s)H(s)$, respectively. For instance, if

$$G(s) = \frac{1}{s+2} \qquad \text{and} \qquad H(s) = \frac{1}{s}$$

Then, according to Eq. (11.31),

$$G[z] = \frac{z}{z-e^{-2T}} \qquad \text{and} \qquad H[z] = \frac{z}{z-1}$$

However, the continuous-time system transfer function is $G(s)H(s)$, where

$$G(s)H(s) = \frac{1}{s(s+2)} = \frac{1}{2}\left[\frac{1}{s} - \frac{1}{s+2}\right]$$

From Eq. (11.31),

$$T[z] = \frac{1}{2}\left(\frac{z}{z-1} - \frac{z}{z-e^{-2T}}\right) \neq G[z]H[z]$$

In this case, we use the notation $GH[z]$ for $T[z]$. Thus, $GH[z] \neq G[z]H[z]$, but it is the discrete-time transfer function that corresponds to $G(s)H(s)$.

For the system in Fig. 11.16c,

$$Y[z] = H[z]F[z] = H[z]G[z]X[z] \qquad \text{so that} \qquad T[z] = G[z]H[z]$$

For the system in Fig. 11.16d,

$$E[z] = X[z] - W[z] \qquad \text{and} \qquad W[z] = H[z]Y[z]$$

Moreover,

$$\begin{aligned} Y[z] &= G[z]E[z] \\ &= G[z]\,(X[z] - W[z]) \\ &= G[z](X[z] - H[z]Y[z]) \end{aligned}$$

Hence,

$$Y[z] = \frac{G[z]}{1+G[z]H[z]}X[z]$$

Consequently,

$$T[z] = \frac{G[z]}{1+G[z]H[z]}$$

---

† Using this procedure, we have listed $H(s)$ and the corresponding $H[z]$ in Table 12.1 in Ch. 12. In Table 12.1, $H[z]$ is multiplied with a scaling factor T, which results in $H[z] = \frac{Tz}{z-e^{\lambda T}}$. For sampled-data applications, the extra factor T should be ignored throughout Table 12.1.

EXAMPLE 11.10 Discrete-Time Output of a Sampled-Data System

Find the output samples $y[n]$ for the sampled-data system illustrated in Fig. 11.17a when the input is a unit step function $u(t)$, the sampling interval $T = 0.5$ second, and

$$G_c[z] = \frac{z}{z-1} \quad \text{and} \quad G(s) = \frac{1}{s+4}$$

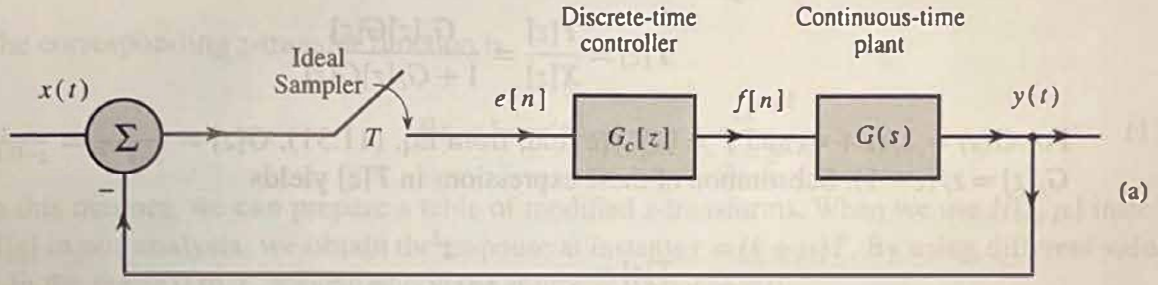

(a)

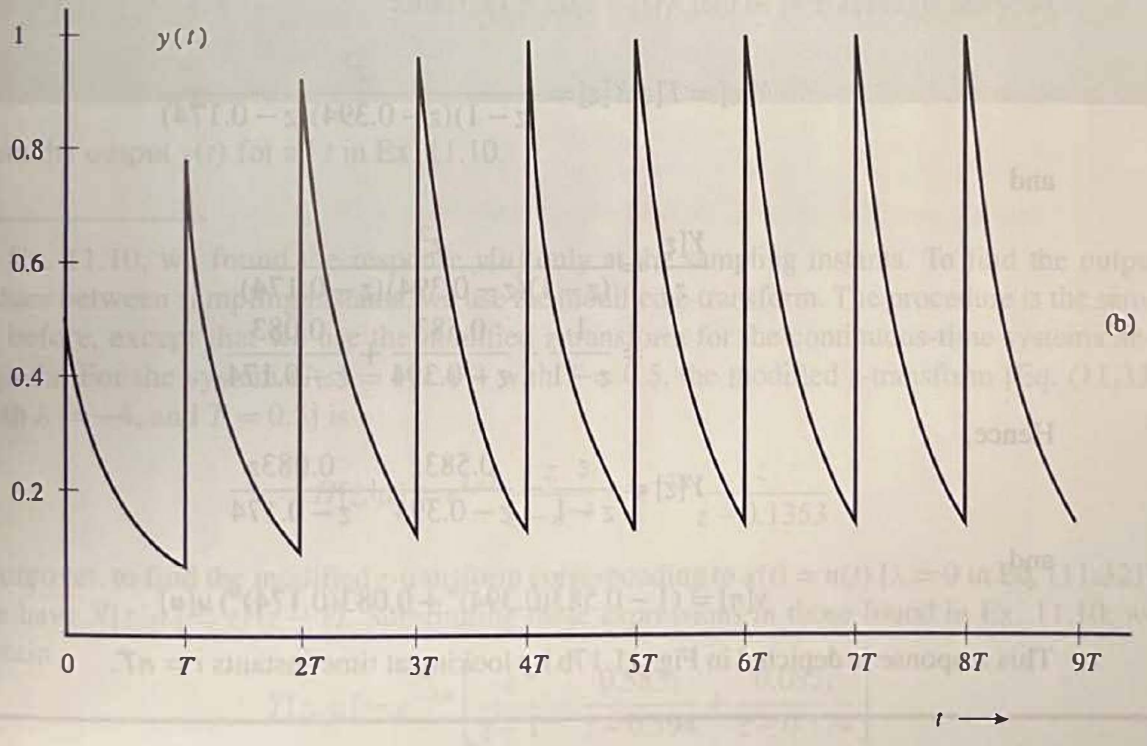

(b)

Figure 11.17 Sampled-data system for Ex. 11.10 and its output.

This system has a discrete-time controller and a continuous-time plant.† To find the transfer function of this system, we observe that

$$Y[z] = G[z]F[z], \qquad F[z] = G_c[z]E[z], \qquad \text{and} \qquad E[z] = X[z] - Y[z]$$

Hence,

$$Y[z] = G_c[z]G[z](X[z] - Y[z])$$

and the system transfer function $T[z]$ is

$$T[z] = \frac{Y[z]}{X[z]} = \frac{G_c[z]G[z]}{1 + G_c[z]G[z]}$$

For $G(s) = 1/(s+4)$ and $T = 0.5$, we find, from Eq. (11.31), $G[z] = \frac{z}{z-e^{-2}} = \frac{z}{z-0.1353}$. Also $G_c[z] = z/(z-1)$. Substitution of these expressions in $T[z]$ yields

$$T[z] = \frac{z^2}{(z-0.894)(z-0.174)}$$

The output $Y[z]$ is given by $Y[z] = T[z]X[z]$. For the step input $x(t) = u(t)$, the corresponding sampled signal is $u[n]$ so that $X[z] = z/(z-1)$. Hence,

$$Y[z] = T[z]X[z] = \frac{z^3}{(z-1)(z-0.394)(z-0.174)}$$

and

$$\frac{Y[z]}{z} = \frac{z^2}{(z-1)(z-0.394)(z-0.174)} = \frac{1}{z-1} - \frac{0.583}{z-0.394} + \frac{0.083}{z-0.174}$$

Hence,

$$Y[z] = \frac{z}{z-1} - \frac{0.583z}{z-0.394} + \frac{0.083z}{z-0.174}$$

and

$$y[n] = (1 - 0.583(0.394)^n + 0.083(0.174)^n)\,u[n]$$

This response is depicted in Fig. 11.17b by looking at time instants $t = nT$.

†The block diagram in Fig. 11.17a does not show the appropriate converters required at the interface of discrete-time and continuous-time systems; these are implied. Thus, the output of the sampler, which consists of an impulse sequence, is converted into a sequence of numbers to act as the input to the discrete-time controller. Similarly, the output of a discrete-time controller, which is a sequence of numbers, is converted to a sequence of impulses to act as an input to the plant.

11.6.1 Response Between Sampling Instants: The Modified z-Transform

The preceding analysis yields the output only at sampling instants. We can readily find the response between successive sampling instants by using the *modified z-transform.* This goal can be accomplished by considering the response at another set of sampling instants $t = (k + \mu)T$, where $0 < \mu < 1$.

Consider the system in Fig. 11.16a with $H(s) = 1/(s - \lambda)$. The impulse response is $h(t) = e^{\lambda t}$, and its samples at instants $t = (k + \mu)T$ are

$$h(t, \mu) = e^{\lambda(k+\mu)T} = e^{\lambda\mu T}\left[e^{\lambda kT}\right] \tag{11.32}$$

The corresponding z-transfer function is

$$H[z, \mu] = e^{\lambda\mu T}\frac{z}{z - e^{\lambda T}} = \frac{ze^{\lambda\mu T}}{z - e^{\lambda T}} \tag{11.33}$$

In this manner, we can prepare a table of modified z-transforms. When we use $H[z, \mu]$ instead of $H[z]$ in our analysis, we obtain the response at instants $t = (k + \mu)T$. By using different values of μ in the range 0 to T, we can obtain the complete response $y(t)$.

EXAMPLE 11.11 Modified z-Transform to Compute Sampled-Data System Output

Find the output $y(t)$ for all t in Ex. 11.10.

In Ex. 11.10, we found the response $y[n]$ only at the sampling instants. To find the output values between sampling instants, we use the modified z-transform. The procedure is the same as before, except that we use the modified z-transform for the continuous-time systems and signals. For the system $G(s) = 1/s + 4$ with $T = 0.5$, the modified z-transform [Eq. (11.33) with $\lambda = -4$, and $T = 0.5$] is

$$H[z, \mu] = e^{\lambda\mu T}\frac{z}{z - e^{-2}} = e^{-2\mu}\frac{z}{z - 0.1353}$$

Moreover, to find the modified z-transform corresponding to $x(t) = u(t)$ [$\lambda = 0$ in Eq. (11.32)], we have $X[z, \mu] = z/(z - 1)$. Substituting these expressions in those found in Ex. 11.10, we obtain

$$Y[z, \mu] = e^{-2\mu}\left[\frac{z}{z - 1} - \frac{0.583z}{z - 0.394} + \frac{0.083z}{z - 0.174}\right]$$

The inverse (modified) z-transform of this equation, determined using Eqs. (11.32) and (11.33), rs

$$y[(n + \mu)T] = e^{-2\mu}\left[1 - 0.583(0.394)^n + 0.083(-0.174)^n\right]u[n] \qquad 0 < \mu < 1$$

The complete response is shown in Fig. 11.17.

Design of Sampled-Data Systems

As with continuous-time control systems, sampled-data systems are designed to meet certain transient (PO, t_r, t_s, etc.) and steady-state specifications. The design procedure follows along the lines similar to those used for continuous-time systems. We begin with a general second-order system. The relationship between closed-loop pole locations and the corresponding transient parameters PO, t_r, t_s, . . . are determined. Hence, for given transient specifications, an acceptable region in the z plane, where the dominant poles of the closed-loop transfer function $T[z]$ should lie, is determined. Next, we sketch the root locus for the system. The rules for sketching the root locus are the same as those for continuous-time systems. If the root locus passes through the acceptable region, the transient specifications can be met by simple adjustment of the gain K. If not, we must use a compensator, which will steer the root locus in the acceptable region.

11.7 The Bilateral z-Transform

Situations involving noncausal signals or systems cannot be handled by the (unilateral) z-transform discussed so far. Such cases can be analyzed by the *bilateral* (or two-sided) z-transform defined in Eq. (11.1) as

$$X[z] = \sum_{n=-\infty}^{\infty} x[n]z^{-n}$$

As in Eq. (11.2), the inverse z-transform is given by

$$x[n] = \frac{1}{2\pi j}\oint X[z]z^{n-1}\,dz$$

These equations define the bilateral z-transform. Earlier, we showed that

$$\gamma^n u[n] \Longleftrightarrow \frac{z}{z-\gamma} \qquad |z| > |\gamma| \tag{11.34}$$

In contrast, the z-transform of the signal $-\gamma^n u[-(n+1)]$, illustrated in Fig. 11.18a, is

$$\begin{aligned}
\mathcal{Z}\{-\gamma^n u[-(n+1)]\} &= \sum_{-\infty}^{-1} -\gamma^n z^{-n} = \sum_{-\infty}^{-1} -\left(\frac{\gamma}{z}\right)^n \\
&= -\left[\frac{z}{\gamma} + \left(\frac{z}{\gamma}\right)^2 + \left(\frac{z}{\gamma}\right)^3 + \cdots\right] \\
&= 1 - \left[1 + \frac{z}{\gamma} + \left(\frac{z}{\gamma}\right)^2 + \left(\frac{z}{\gamma}\right)^3 + \cdots\right] \\
&= 1 - \frac{1}{1-\frac{z}{\gamma}} \qquad \left|\frac{z}{\gamma}\right| < 1 \\
&= \frac{z}{z-\gamma} \qquad |z| < |\gamma|
\end{aligned}$$

Therefore,

$$\mathcal{Z}\{-\gamma^n u[-(n+1)]\} = \frac{z}{z-\gamma} \qquad |z| < |\gamma| \tag{11.35}$$

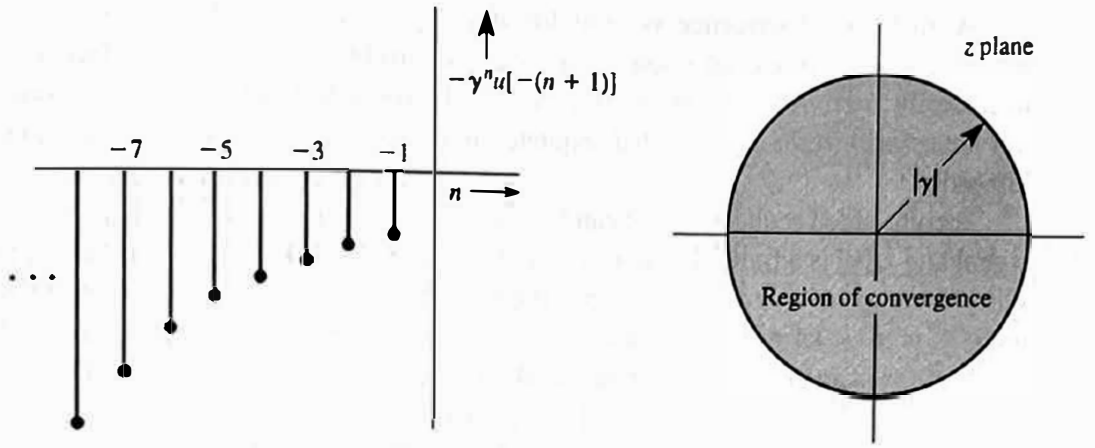

Figure 11.18 (a) $-\gamma^n u[-(n+1)]$ and (b) the region of convergence (ROC) of its z-transform.

A comparison of Eqs. (11.34) and (11.35) shows that the z-transform of $\gamma^n u[n]$ is identical to that of $-\gamma^n u[-(n+1)]$. The regions of convergence, however, are different. In the former case, $X[z]$ converges for $|z| > |\gamma|$; in the latter, $X[z]$ converges for $|z| < |\gamma|$ (see Fig. 11.18b). Clearly, the inverse transform of $X[z]$ is not unique unless the region of convergence is specified. If we add the restriction that all our signals be causal, however, this ambiguity does not arise. The inverse transform of $z/(z-\gamma)$ is $\gamma^n u[n]$ even without specifying the ROC. Thus, in the unilateral transform, we can ignore the ROC in determining the inverse z-transform of $X[z]$.

As in the case of the bilateral Laplace transform, if $x[n] = \sum_{i=1}^{k} x_i[n]$, then the ROC for $X[z]$ is the intersection of the ROCs (region common to all ROCs) for the transforms $X_1[z], X_2[z], \ldots, X_k[z]$.

The preceding results lead to the conclusion (similar to that for the Laplace transform) that if $z = \beta$ is the largest magnitude pole for a causal sequence, its ROC is $|z| > |\beta|$. If $z = \alpha$ is the smallest magnitude nonzero pole for an anticausal sequence, its ROC is $|z| < |\alpha|$.

Region of Convergence for Left-Sided and Right-Sided Sequences

Let us first consider a finite-duration sequence $x_f[n]$, defined as a sequence that is nonzero for $N_1 \le n \le N_2$, where both N_1 and N_2 are finite numbers and $N_2 > N_1$. Also,

$$X_f[z] = \sum_{n=N_1}^{N_2} x_f[n] z^{-n}$$

For example, if $N_1 = -2$ and $N_2 = 1$, then

$$X_f[z] = x_f[-2]z^2 + x_f[-1]z + x_f[0] + \frac{x_f[1]}{z}$$

Assuming all the elements in $x_f[n]$ are finite, we observe that $X_f[z]$ has two poles at $z = \infty$ because of terms $x_f[-2]z^2 + x_f[-1]z$ and one pole at $z = 0$ because of term $x_f[1]/z$. Thus, a finite-duration sequence could have poles at $z = 0$ and $z = \infty$. Observe that $X_f[z]$ converges for all values of z except possibly $z = 0$ and $z = \infty$.

This means that the ROC of a general signal $x[n] + x_f[n]$ is the same as the ROC of $x[n]$ with the possible exception of $z = 0$ and $z = \infty$.

A *right-sided* sequence is zero for $n < N_2 < \infty$ and a left-sided sequence is zero for $n > N_1 > -\infty$. A causal sequence is always a right-sided sequence, but the converse is not necessarily true. An anticausal sequence is always a left-sided sequence, but the converse is not necessarily true. A *two-sided* sequence is of infinite duration and is neither right-sided nor left-sided.

A right-sided sequence $x_r[n]$ can be expressed as $x_r[n] = x_c[n] + x_f[n]$, where $x_c[n]$ is a causal signal and $x_f[n]$ is a finite-duration signal. Therefore, the ROC for $x_r[n]$ is the same as the ROC for $x_c[n]$ except possibly $z = \infty$. If $z = \beta$ is the largest magnitude pole for a right-sided sequence $x_r[n]$, its ROC is $|\beta| < |z| \leq \infty$. Similarly, a left-sided sequence can be expressed as $x_l[n] = x_a[n] + x_f[n]$, where $x_a[n]$ is an anticausal sequence and $x_f[n]$ is a finite-duration signal. Therefore, the ROC for $x_l[n]$ is the same as the ROC for $x_a[n]$ except possibly $z = 0$. Thus, if $z = \alpha$ is the smallest magnitude nonzero pole for a left-sided sequence, its ROC is $0 \leq |z| < |\alpha|$.

EXAMPLE 11.12 Bilateral z-Transform

Determine the bilateral z-transform of

$$x[n] = \underbrace{(0.9)^n u[n]}_{x_1[n]} + \underbrace{(1.2)^n u[-(n+1)]}_{x_2[n]}$$

From the results in Eqs. (11.34) and (11.35), we have

$$X_1[z] = \frac{z}{z-0.9} \qquad |z| > 0.9$$

$$X_2[z] = \frac{-z}{z-1.2} \qquad |z| < 1.2$$

The common region where both $X_1[z]$ and $X_2[z]$ converge is $0.9 < |z| < 1.2$ (Fig. 11.19b). Hence,

$$\begin{aligned} X[z] &= X_1[z] + X_2[z] \\ &= \frac{z}{z-0.9} - \frac{z}{z-1.2} \\ &= \frac{-0.3z}{(z-0.9)(z-1.2)} \qquad 0.9 < |z| < 1.2 \end{aligned}$$

The sequence $x[n]$ and the ROC of $X[z]$ are depicted in Fig. 11.19.

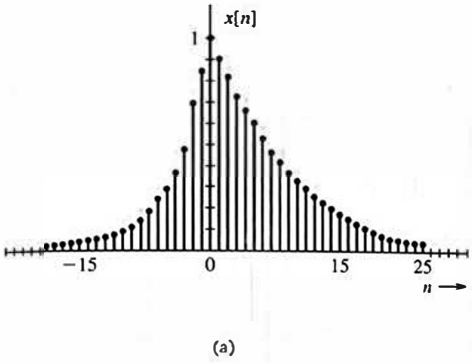

Figure 11.19 (a) Signal $x[n]$ and (b) ROC of $X[z]$.

EXAMPLE 11.13 Inverse Bilateral z-Transform

Find the inverse bilateral z-transform of

$$X[z] = \frac{-z(z+0.4)}{(z-0.8)(z-2)}$$

if the ROC is (a) $|z| > 2$, (b) $|z| < 0.8$, and (c) $0.8 < |z| < 2$.

(a)

$$\frac{X[z]}{z} = \frac{-(z+0.4)}{(z-0.8)(z-2)} = \frac{1}{z-0.8} - \frac{2}{z-2}$$

and

$$X[z] = \frac{z}{z-0.8} - 2\frac{z}{z-2}$$

Since the ROC is $|z| > 2$, both terms correspond to causal sequences and

$$x[n] = [(0.8)^n - 2(2)^n]u[n]$$

This sequence appears in Fig. 11.20a.

(b) In this case, $|z| < 0.8$, which is less than the magnitudes of both poles. Hence, both terms correspond to anticausal sequences, and

$$x[n] = [-(0.8)^n + 2(2)^n]u[-(n+1)]$$

This sequence appears in Fig. 11.20b.

(c) In this case, $0.8 < |z| < 2$; the part of $X[z]$ corresponding to the pole at 0.8 is a causal sequence, and the part corresponding to the pole at 2 is an anticausal sequence:

$$x[n] = (0.8)^n u[n] + 2(2)^n u[-(n+1)]$$

This sequence appears in Fig. 11.20c.

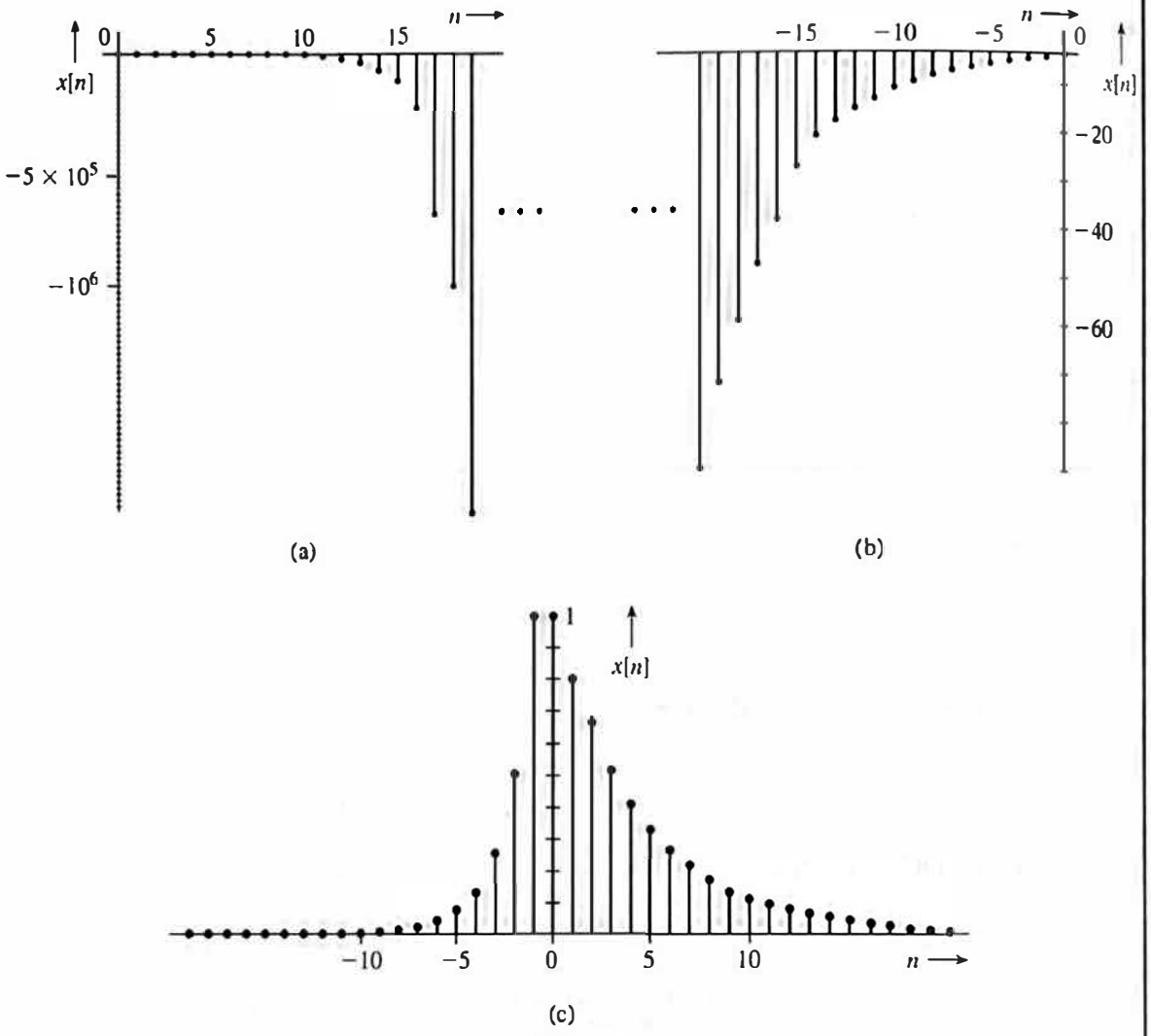

Figure 11.20 Three possible inverse transforms of $X[z]$.

DRILL 11.18 Inverse Bilateral z-Transform

Find the inverse bilateral z-transform of

$$X[z] = \frac{z}{z^2 + \frac{5}{6}z + \frac{1}{6}} \qquad \tfrac{1}{2} > |z| > \tfrac{1}{3}$$

ANSWER

$\left(-\frac{1}{3}\right)^n u[n] + 6\left(-\frac{1}{2}\right)^n u[-(n+1)]$

Inverse Transform by Expansion of $X[z]$ in Power Series of z

We have

$$X[z] = \sum_n x[n]z^{-n}$$

For an anticausal sequence, which exists only for $n \leq -1$, this equation becomes

$$X[z] = x[-1]z + x[-2]z^2 + x[-3]z^3 + \cdots$$

We can find the inverse z-transform of $X[z]$ by dividing the numerator polynomial by the denominator polynomial, both in ascending powers of z, to obtain a polynomial in ascending powers of z. Thus, to find the inverse transform of $z/(z-0.5)$ (when the ROC is $|z| < 0.5$), we divide z by $-0.5+z$ to obtain $-2z-4z^2-8z^3-\cdots$. Hence, $x[-1]=-2, x[-2]=-4, x[-3]=-8$, and so on.

11.7.1 Properties of the Bilateral z-Transform

The properties of the bilateral z-transform are similar to those of the unilateral transform. We shall merely state the properties here, without proofs, for $x_i[n] \Longleftrightarrow X_i[z]$.

Linearity

$$a_1x_1[n] + a_2x_2[n] \Longleftrightarrow a_1X_1[z] + a_2X_2[z]$$

The ROC for $a_1X_1[z] + a_2X_2[z]$ is the region common to (the intersection of) the ROCs for $X_1[z]$ and $X_2[z]$.

Shift

$$x[n-m] \Longleftrightarrow \frac{1}{z^m}X[z] \qquad m \text{ is positive or negative integer}$$

The ROC for $X[z]/z^m$ is the ROC for $X[z]$ except for the addition or deletion of $z=0$ or $z=\infty$ caused by the factor $1/z^m$.

Convolution

$$x_1[n] * x_2[n] \Longleftrightarrow X_1[z]X_2[z]$$

The ROC for $X_1[z]X_2[z]$ is the region common to (the intersection of) the ROCs for $X_1[z]$ and $X_2[z]$.

MULTIPLICATION BY γ^n

$$\gamma^n x[n] \Longleftrightarrow X\left[\frac{z}{\gamma}\right]$$

If the ROC for $X[z]$ is $|\gamma_1| < |z| < |\gamma_2|$, then the ROC for $X[z/\gamma]$ is $|\gamma\gamma_1| < |z| < |\gamma\gamma_2|$, indicating that the ROC is scaled by the factor $|\gamma|$.

MULTIPLICATION BY n

$$nx[n]u[n] \Longleftrightarrow -z\frac{d}{dz}X[z]$$

The ROC for $-z(dX/dz)$ is the same as the ROC for $X[z]$.

TIME REVERSAL

$$x[-n] \Longleftrightarrow X[1/z]$$

If the ROC for $X[z]$ is $|\gamma_1| < |z| < |\gamma_2|$, then the ROC for $X[1/z]$ is $1/|\gamma_1| > |z| > |1/\gamma_2|$.

COMPLEX CONJUGATION

$$x^*[n] \Longleftrightarrow X^*[z^*]$$

The ROC for $X^*[z^*]$ is the same as the ROC for $X[z]$.

11.7.2 Using the Bilateral z-Transform for Analysis of LTID Systems

Because the bilateral z-transform can handle noncausal signals, we can use this transform to analyze noncausal linear systems. The zero-state response $y[n]$ is given by

$$y[n] = \mathcal{Z}^{-1}\{X[z]H[z]\}$$

provided $X[z]H[z]$ exists. The ROC of $X[z]H[z]$ is the region in which both $X[z]$ and $H[z]$ exist, which means that the region is the common part of the ROC of both $X[z]$ and $H[z]$.

EXAMPLE 11.14 Zero-State Response by Bilateral z-Transform

For a causal system specified by the transfer function

$$H[z] = \frac{z}{z-0.5}$$

find the zero-state response to input

$$x[n] = (0.8)^n u[n] + 2(2)^n u[-(n+1)]$$

$$X[z] = \frac{z}{z-0.8} - \frac{2z}{z-2} = \frac{-z(z+0.4)}{(z-0.8)(z-2)}$$

The ROC corresponding to the causal term is $|z| > 0.8$, and that corresponding to the anticausal term is $|z| < 2$. Hence, the ROC for $X[z]$ is the common region, given by $0.8 < |z| < 2$. Hence,

$$X[z] = \frac{-z(z+0.4)}{(z-0.8)(z-2)} \qquad 0.8 < |z| < 2$$

Therefore,

$$Y[z] = X[z]H[z] = \frac{-z^2(z+0.4)}{(z-0.5)(z-0.8)(z-2)}$$

Since the system is causal, the ROC of $H[z]$ is $|z| > 0.5$. The ROC of $X[z]$ is $0.8 < |z| < 2$. The common region of convergence for $X[z]$ and $H[z]$ is $0.8 < |z| < 2$. Therefore,

$$Y[z] = \frac{-z^2(z+0.4)}{(z-0.5)(z-0.8)(z-2)} \qquad 0.8 < |z| < 2$$

Expanding $Y[z]$ into modified partial fractions yields

$$Y[z] = -\frac{z}{z-0.5} + \frac{8}{3}\left(\frac{z}{z-0.8}\right) - \frac{8}{3}\left(\frac{z}{z-2}\right) \qquad 0.8 < |z| < 2$$

Since the ROC extends outward from the pole at 0.8, both poles at 0.5 and 0.8 correspond to causal sequence. The ROC extends inward from the pole at 2. Hence, the pole at 2 corresponds to anticausal sequence. Therefore,

$$y[n] = \left[-(0.5)^n + \tfrac{8}{3}(0.8)^n\right]u[n] + \tfrac{8}{3}(2)^n u[-(n+1)]$$

EXAMPLE 11.15 Zero-State Response for an Input with No z-Transform

For the system in Ex. 11.14, find the zero-state response to input

$$x[n] = \underbrace{(0.8)^n u[n]}_{x_1[n]} + \underbrace{(0.6)^n u[-(n+1)]}_{x_2[n]}$$

The z-transforms of the causal and anticausal components $x_1[n]$ and $x_2[n]$ of the output are

$$X_1[z] = \frac{z}{z-0.8} \qquad |z| > 0.8$$
$$X_2[z] = \frac{-z}{z-0.6} \qquad |z| < 0.6$$

Observe that a common ROC for $X_1[z]$ and $X_2[z]$ does not exist. Therefore, $X[z]$ does not exist. In such a case, we take advantage of the superposition principle and find $y_1[n]$ and $y_2[n]$, the system responses to $x_1[n]$ and $x_2[n]$, separately. The desired response $y[n]$ is the sum of $y_1[n]$ and $y_2[n]$. Now

$$H[z] = \frac{z}{z-0.5} \qquad |z| > 0.5$$
$$Y_1[z] = X_1[z]H[z] = \frac{z^2}{(z-0.5)(z-0.8)} \qquad |z| > 0.8$$
$$Y_2[z] = X_2[z]H[z] = \frac{-z^2}{(z-0.5)(z-0.6)} \qquad 0.5 < |z| < 0.6$$

Expanding $Y_1[z]$ and $Y_2[z]$ into modified partial fractions yields

$$Y_1[z] = -\frac{5}{3}\left(\frac{z}{z-0.5}\right) + \frac{8}{3}\left(\frac{z}{z-0.8}\right) \qquad |z| > 0.8$$
$$Y_2[z] = 5\left(\frac{z}{z-0.5}\right) - 6\left(\frac{z}{z-0.6}\right) \qquad 0.5 < |z| < 0.6$$

Therefore,

$$y_1[n] = \left[-\tfrac{5}{3}(0.5)^n + \tfrac{8}{3}(0.8)^n\right]u[n]$$
$$y_2[n] = 5(0.5)^n u[n] + 6(0.6)^n u[-(n+1)]$$

and

$$y[n] = y_1[n] + y_2[n] = \left[\tfrac{10}{3}(0.5)^n + \tfrac{8}{3}(0.8)^n\right]u[n] + 6(0.6)^n u[-(n+1)]$$

DRILL 11.19 Zero State Response by Bilateral z-Transform

For the causal system in Ex. 11.14, find the zero-state response to input

$$x[n] = \left(\tfrac{1}{4}\right)^n u[n] + 5(3)^n u[-(n+1)]$$

ANSWER

$$\left[-\left(\tfrac{1}{4}\right)^n + 3\left(\tfrac{1}{2}\right)^n\right]u[n] + 6(3)^n u[-(n+1)]$$

11.8 SUMMARY

In this chapter, we discussed the analysis of linear, time-invariant, discrete-time (LTID) systems by means of the z-transform. The z-transform is an extension of the DTFT with the frequency variable $j\Omega$ generalized to $\sigma + j\Omega$. Such an extension allows us to synthesize discrete-time signals by using exponentially growing (discrete-time) sinusoids. The relationship of the z-transform to the DTFT is identical to that of the Laplace transform to the Fourier transform. Because of the generalization of the frequency variable, we can analyze all kinds of LTID systems and also handle exponentially growing inputs.

The z-transform changes the difference equations of LTID systems into algebraic equations. Therefore, solving these difference equations reduces to solving algebraic equations.

The transfer function $H[z]$ of an LTID system is equal to the ratio of the z-transform of the output to the z-transform of the input when all initial conditions are zero. Therefore, if $X[z]$ is the z-transform of the input $x[n]$ and $Y[z]$ is the z-transform of the corresponding output $y[n]$ (when all initial conditions are zero), then $Y[z] = H[z]X[z]$. For an LTID system specified by the difference equation $Q[E]y[n] = P[E]x[n]$, the transfer function $H[z] = P[z]/Q[z]$. Moreover, $H[z]$ is the z-transform of the system impulse response $h[n]$. We showed in Ch. 9 that the system response to an everlasting exponential z^n is $H[z]z^n$.

LTID systems can be realized by scalar multipliers, adders, and time delays. A given transfer function can be synthesized in many different ways. We discussed canonical, transposed canonical, cascade, and parallel forms of realization. The realization procedure is identical to that for continuous-time systems with $1/s$ (integrator) replaced by $1/z$ (unit delay).

In Sec. 11.5, we showed that discrete-time systems can be analyzed by the Laplace transform as if they were continuous-time systems. In fact, we showed that the z-transform is the Laplace transform with a change in variable.

In practice, we often have to deal with hybrid systems consisting of discrete-time and continuous-time subsystems. Feedback hybrid systems are also called sampled-data systems. In such systems, we can relate the samples of the output to those of the input. However, the output is generally a continuous-time signal. The output values during the successive sampling intervals can be found by using the modified z-transform.

The majority of the input signals and practical systems are causal. Consequently, we are required to deal with causal signals most of the time. Restricting all signals to the causal type greatly simplifies z-transform analysis; the ROC of a signal becomes irrelevant to the analysis process. This special case of z-transform (which is restricted to causal signals) is called the unilateral z-transform. Much of the chapter deals with this transform. Section 11.7 discusses the general variety of the z-transform (bilateral z-transform), that can handle causal and noncausal signals and systems. In the bilateral transform, the inverse transform of $X[z]$ is not unique, but depends on the ROC of $X[z]$. Thus, the ROC plays a crucial role in the bilateral z-transform.

Reference

1. Lyons, R. G., *Understanding Digital Signal Processing*, Addison-Wesley, Reading, MA, 1997.

PROBLEMS

11.1-1 Using the definition, compute the z-transform of $x[n] = (-1)^n(u[n] - u[n-8])$. Sketch the poles and zeros of $X[z]$ in the z plane. No calculator is needed to do this problem!

11.1-2 Determine the unilateral z-transform $X[z]$ of the signal $x[n]$ shown in Fig. P11.1-2. As the picture suggests, $x[n] = -3$ for all $n \geq 9$ and $x[n] = 0$ for all $n < 3$.

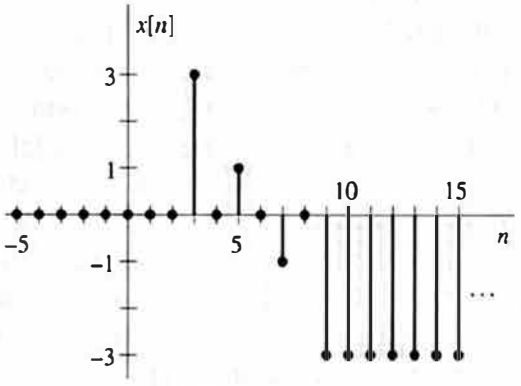

Figure P11.1-2

11.1-3 (a) A causal signal has a z-transform given by $X[z] = \frac{z^2}{z^3-1}$. Determine the time-domain signal $x[n]$ and sketch $x[n]$ over $-4 \leq n \leq 11$. [*Hint:* No complex arithmetic is needed to solve this problem!]

(b) Consider the causal semiperiodic signal $y[n]$ shown in Fig. P11.1-3. Notice, $y[n]$ continually repeats the sequence $[1,2,3]$ for $n \geq 0$. Determine the unilateral z-transform $Y[z]$ of this signal. If possible, express your result as a rational function in standard form.

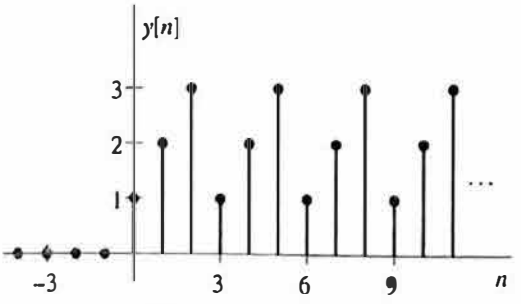

Figure P11.1-3

11.1-4 Using the definition of the z-transform, find the z-transform and the ROC for each of the following signals:

(a) $u[n-m]$

(b) $\gamma^n \sin \pi n\, u[n]$

(c) $\gamma^n \cos \pi n\, u[n]$

(d) $\gamma^n \sin \frac{\pi n}{2} u[n]$

(e) $\gamma^n \cos \frac{\pi n}{2} u[n]$

(f) $\sum_{k=0}^{\infty} 2^{2k} \delta[n-2k]$

(g) $\gamma^{n-1} u[n-1]$

(h) $n\gamma^n u[n]$

(i) $nu[n]$

(j) $\frac{\gamma^n}{n!} u[n]$

(k) $[2^{n-1} - (-2)^{n-1}]u[n]$

(l) $\frac{(\ln \alpha)^n}{n!} u[n]$

11.1-5 Showing all work, evaluate $\sum_{n=0}^{\infty} n(-3/2)^{-n}$.

11.1-6 Using only the z-transforms of Table 11.1, determine the z-transform of each of the following signals:

(a) $u[n] - u[n-2]$

(b) $\gamma^{n-2} u[n-2]$

(c) $2^{n+1} u[n-1] + e^{n-1} u[n]$

(d) $\left[2^{-n} \cos\left(\frac{\pi}{3} n\right)\right] u[n-1]$

(e) $n\gamma^n u[n-1]$

(f) $n(n-1)(n-2)2^{n-3} u[n-m]$ for $m = 0, 1, 2, 3$

(g) $(-1)^n nu[n]$

(h) $\sum_{k=0}^{\infty} k\delta(n-2k+1)$

11.1-7 Find the inverse unilateral z-transform of each of the following:

(a) $\frac{z(z-4)}{z^2-5z+6}$

(b) $\frac{z-4}{z^2-5z+6}$

(c) $\frac{(e^{-2}-2)z}{(z-e^{-2})(z-2)}$

(d) $\dfrac{(z-1)^2}{z^3}$

(e) $\dfrac{z(2z+3)}{(z-1)(z^2-5z+6)}$

(f) $\dfrac{z(-5z+22)}{(z+1)(z-2)^2}$

(g) $\dfrac{z(1.4z+0.08)}{(z-0.2)(z-0.8)^2}$

(h) $\dfrac{z(z-2)}{z^2-z+1}$

(i) $\dfrac{2z^2-0.3z+0.25}{z^2+0.6z+0.25}$

(j) $\dfrac{2z(3z-23)}{(z-1)(z^2-6z+25)}$

(k) $\dfrac{z(3.83z+11.34)}{(z-2)(z^2-5z+25)}$

(l) $\dfrac{z^2(-2z^2+8z-7)}{(z-1)(z-2)^3}$

11.1-8 (a) Expanding $X[z]$ as a power series in z^{-1}, find the first three terms of $x[n]$ if

$$X[z]=\frac{2z^3+13z^2+z}{z^3+7z^2+2z+1}$$

(b) Extend the procedure used in part (a) to find the first four terms of $x[n]$ if

$$X[z]=\frac{2z^4+16z^3+17z^2+3z}{z^3+7z^2+2z+1}$$

11.1-9 A right-sided signal $x[n]$ has z-transform given by $X[z]=\frac{z^6+2z^5+3z^4+4z^3}{z^4-1}$. Using a power series expansion of $X[z]$, determine $x[n]$ over $-5\le n\le 5$.

11.1-10 Find $x[n]$ by expanding

$$X[z]=\frac{\gamma z}{(z-\gamma)^2}$$

as a power series in z^{-1}.

11.1-11 (a) In Table 11.1, if the numerator and the denominator powers of $X[z]$ are M and N, respectively, explain why in some cases $N-M=0$, while in others $N-M=1$ or $N-M=m$ (m any positive integer).

(b) Without actually finding the z-transform, state what $N-M$ is for $X[z]$ corresponding to $x[n]=\gamma^n u[n-4]$.

11.2-1 For a discrete-time signal shown in Fig. P11.2-1, show that

$$X[z]=\frac{1-z^{-m}}{1-z^{-1}}$$

Find your answer by using the definition in Eq. (11.1) and by using Table 11.1 and an appropriate property of the z-transform.

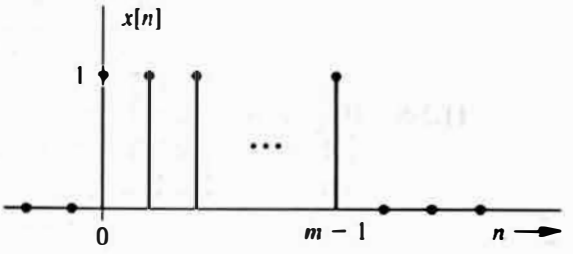

Figure P11.2-1

11.2-2 Determine the unilateral z-transform of signal $x[n]=(1-n)\cos\left(\frac{\pi}{2}(n-1)\right)u[n-1]$.

11.2-3 Suppose a DT signal $x[n]=2(u[n-10]-u[n-6])$ has a transform $X(z)$. Define $Y(z)=\frac{1}{2z^{-3}}\frac{d}{dz}X(2z)$. Using graphic plot or vector notation, determine the corresponding signal $y[n]$.

11.2-4 Suppose a DT signal $x[n]=3(u[n]-u[n-5])$ has a transform $X(z)$. Define $Y(z)=2z^{-4}\frac{d}{dz}X\left(\frac{z}{2}\right)$. Using graphic plot or vector notation, determine the corresponding signal $y[n]$.

11.2-5 Find the z-transform of the signal illustrated in Fig. P11.2-5. Solve this problem in two ways, as in Exs. 11.2d and 11.4. Verify that the two answers are equivalent.

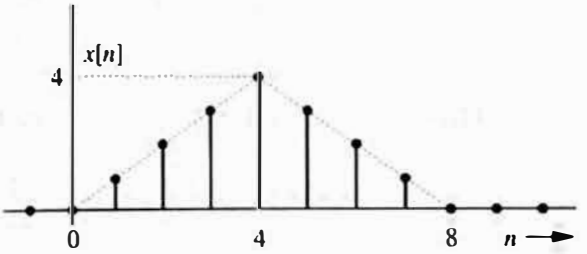

Figure P11.2-5

11.2-6 Using z-transform techniques and properties (no time-domain convolution sum!),

determine the convolution $y[n] = (\frac{1}{2})^n u[n-3] * (\frac{1}{3})^{n-6} u[n-4]$. Express your answer in the form $y[n] = c_1\gamma_1^{n-N_1}u[n-N_1] + c_2\gamma_2^{n-N_2}u[n-N_2]$, making sure to clearly identify the constants c_1, c_2, γ_1, γ_2, N_1, and N_2.

11.2-7 Determine the inverse unilateral z-transform $x[n]$ of the signal

$$X[z] = \frac{d^7}{dz^7}\left[\frac{z^{-4}}{(z-\frac{1}{2})(z+3)}\right]$$

11.2-8 Using only the fact that $\gamma^n u[n] \Longleftrightarrow z/(z-\gamma)$ and properties of the z-transform, find the z-transform of each of the following:

(a) $n^2u[n]$
(b) $n^2\gamma^n u[n]$
(c) $n^3u[n]$
(d) $a^n[u[n]-u[n-m]]$
(e) $ne^{-2n}u[n-m]$
(f) $(n-2)(0.5)^{n-3}u[n-4]$

11.2-9 Using only pair 1 in Table 11.1 and appropriate properties of the z-transform, derive iteratively pairs 2 through 9. In other words, first derive pair 2. Then use pair 2 (and pair 1, if needed) to derive pair 3, and so on.

11.2-10 Find the z-transform of $\cos(\pi n/4)u[n]$ using only pairs 1 and 11b in Table 11.1 and a suitable property of the z-transform.

11.2-11 Apply the time-reversal property to pair 6 of Table 11.1 to show that $\gamma^n u[-(n+1)] \Longleftrightarrow -z/(z-\gamma)$ and the ROC is given by $|z| < |\gamma|$.

11.2-12 (a) If $x[n] \Longleftrightarrow X[z]$, then show that $(-1)^n x[n] \Longleftrightarrow X[-z]$.

(b) Use this result to show that $(-\gamma)^n u[n] \Longleftrightarrow z/(z+\gamma)$.

(c) Use these results to find the z-transforms of $x_i[n] = [2^{n-1} - (-2)^{n-1}]u[n]$ and $x_{ii}[n] = \gamma^n \cos \pi n u[n]$.

11.2-13 (a) If $x[n] \Longleftrightarrow X[z]$, then show that

$$\sum_{k=0}^{n} x[k] \Longleftrightarrow \frac{zX[z]}{z-1}$$

(b) Use this result to derive pair 2 from pair 1 in Table 11.1.

11.2-14 A number of causal time-domain functions are shown in Fig. P11.2-14. List the function of time that corresponds to each of the following functions of z. Few or no calculations are necessary! Be careful, the graphs may be scaled differently.

(a) $\dfrac{z^2}{(z-0.75)^2}$

(b) $\dfrac{z^2 - 0.9z/\sqrt{2}}{z^2 - 0.9\sqrt{2}z + 0.81}$

(c) $\displaystyle\sum_{k=0}^{4} z^{-2k}$

(d) $\dfrac{z^{-5}}{1-z^{-1}}$

(e) $\dfrac{z^2}{z^4-1}$

(f) $\dfrac{0.75z}{(z-0.75)^2}$

(g) $\dfrac{z^2 - z/\sqrt{2}}{z^2 - \sqrt{2}z + 1}$

(h) $\dfrac{z^{-1} - 5z^{-5} + 4z^{-6}}{5(1-z^{-1})^2}$

(i) $\dfrac{z}{z-1.1}$

(j) $\dfrac{0.25z^{-1}}{(1-z^{-1})(1-0.75z^{-1})}$

11.2-15 Suppose we upsample a causal signal $x[n]$ by factor N to produce signal $y[n]$. Express $Y(z)$ in terms of $X(z)$, taking care to mathematically justify your result.

11.3-1 Using z-transform techniques, find the output $y[n]$ of an LTID system specified by the equation $y[n] - \frac{1}{3}y[n-1] = x[n-1]$ if the initial condition is $y[-1] = 2$ and the input is $x[n] = -u[n]$.

11.3-2 Consider an LTID system $y[n] - y[n-2] = x[n]$ with $y[-1] = 0$, $y[-2] = 1$, and $x[n] = u[n]$.

(a) Determine $Y[z]$, expressed as a rational function in standard factored form.

(b) Use $Y[z]$ from part (a) to solve for the system output $y[n]$.

11.3-3 Solve Prob. 9.5-23 by the z-transform method.

11.3-4 Consider a DT system with transfer function $H[z] = \frac{2z-2}{z-0.5}$. Assuming the system is both

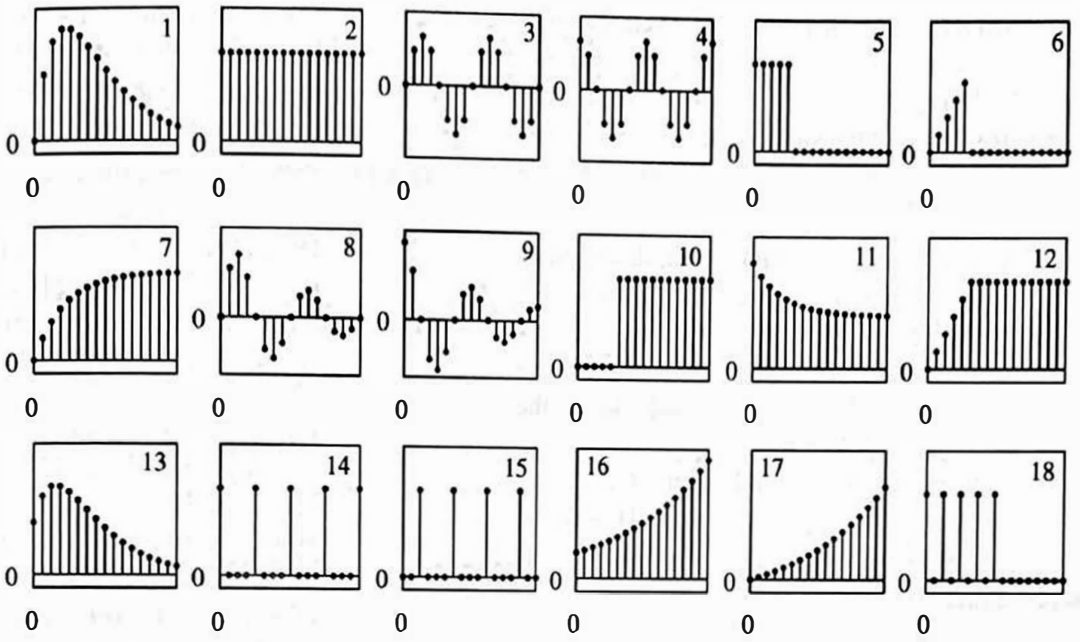

Figure P11.2-14

controllable and observable, determine the ZIR $y_{zir}[n]$ given $y[-1] = 1$.

11.3-5 (a) Solve

$$y[n+1] + 2y[n] = x[n+1]$$

when $y[0] = 1$ and $x[n] = e^{-(n-1)}u[n]$.

(b) Find the zero-input and the zero-state components of the response.

11.3-6 Consider a LTID system that is described by the difference equation $y[n] - \frac{1}{4}y[n-2] = x[n-1]$.

(a) Use transform-domain techniques to determine the zero-state response $y_{zsr}[n]$ to input $x[n] = 3u[n-5]$.

(b) Use transform-domain techniques to determine the zero-input response $y_{zir}[n]$ given $y_{zir}[-2] = y_{zir}[-1] = 1$.

11.3-7 (a) Find the output $y[n]$ of an LTID system specified by the equation

$$2y[n+2] - 3y[n+1] + y[n] = 4x[n+2] - 3x[n+1]$$

for input $x[n] = (4)^{-n}u[n]$ and initial conditions $y[-1] = 0$ and $y[-2] = 1$.

(b) Find the zero-input and the zero-state components of the response.

(c) Find the transient and the steady-state components of the response.

11.3-8 Solve Prob. 11.3-7 if initial conditions $y[-1]$ and $y[-2]$ are instead replaced with auxiliary conditions $y[0] = 3/2$ and $y[1] = 35/4$.

11.3-9 (a) Solve

$$4y[n+2] + 4y[n+1] + y[n] = x[n+1]$$

with $y[-1] = 0$, $y[-2] = 1$, and $x[n] = u[n]$.

(b) Find the zero-input and the zero-state components of the response.

(c) Find the transient and the steady-state components of the response.

11.3-10 Solve

$$y[n+2] - 3y[n+1] + 2y[n] = x[n+1]$$

if $y[-1] = 2$, $y[-2] = 3$, and $x[n] = (3)^n u[n]$.

11.3-11 Solve

$$y[n+2] - 2y[n+1] + 2y[n] = x[n]$$

with $y[-1] = 1$, $y[-2] = 0$, and $x[n] = u[n]$.

11.3-12 Consider a causal LTID system described as $H(z) = \frac{21(z^2+1)}{16(z^2+\frac{1}{4}z-\frac{3}{8})}$.

(a) Determine the standard delay-form difference equation description of this system.

(b) Using transform-domain techniques, determine the system impulse response $h[n]$.

(c) Using transform-domain techniques, determine $y_{zir}[n]$ given $y[-1] = 16$ and $y[-2] = 8$.

11.3-13 Consider a causal LTID system described as $y[n] - \frac{5}{6}y[n-1] + \frac{1}{6}y[n-2] = \frac{3}{2}x[n-1] + \frac{3}{2}x[n-2]$.

(a) Determine the (standard-form) system transfer function $H(z)$ and sketch the system pole-zero plot.

(b) Using transform-domain techniques, determine $y_{zir}[n]$ given $y[-1] = 2$ and $y[-2] = -2$.

11.3-14 Solve

$$y[n] + 2y[n-1] + 2y[n-2] = x[n-1] + 2x[n-2]$$

with $y[0] = 0$, $y[1] = 1$, and $x[n] = e^n u[n]$.

11.3-15 A system with impulse response $h[n] = 2(1/3)^n u[n-1]$ produces an output $y[n] = (-2)^n u[n-1]$. Determine the corresponding input $x[n]$.

11.3-16 A professor recently received an unexpected \$10 (a futile bribe attached to a test). Being the savvy investor that she is, the professor decides to invest the \$10 in a savings account that earns 0.5% interest compounded monthly (6.17% APY). Furthermore, she decides to supplement this initial investment with an additional \$5 deposit made every month, beginning the month immediately following her initial investment.

(a) Model the professor's savings account as a constant coefficient linear difference equation. Designate $y[n]$ as the account balance at month n, where $n = 0$ corresponds to the first month that interest is awarded (and that her \$5 deposits begin).

(b) Determine a closed-form solution for $y[n]$. That is, you should express $y[n]$ as a function only of n.

(c) If we consider the professor's bank account as a system, what is the system impulse response $h[n]$? What is the system transfer function $H[z]$?

(d) Explain this fact: if the input to the professor's bank account is the everlasting exponential $x[n] = 1^n = 1$, then the output is **not** $y[n] = 1^n H[1] = H[1]$.

11.3-17 Sally deposits \$100 into her savings account on the first day of every month except for each December, when she uses her money to buy holiday gifts. Define $b[m]$ as the balance in Sally's account on the first day of month m. Assume Sally opens her account in January ($m = 0$), continues making monthly payments forever (except each December!), and that her monthly interest rate is 1%. Sally's account balance satisfies a simple difference equation $b[m] = (1.01)b[m-1] + p[m]$, where $p[m]$ designates Sally's monthly deposits. Determine a closed-form expression for $b[m]$ that is only a function of the month m.

11.3-18 For each impulse response, determine the number of system poles, whether the poles are real or complex, and whether the system is BIBO-stable.

(a) $h_1[n] = (-1 + (0.5)^n)u[n]$

(b) $h_2[n] = (j)^n(u[n] - u[n-10])$

11.3-19 Find the following sums:

(a) $\sum_{k=0}^{n} k$

(b) $\sum_{k=0}^{n} k^2$

[*Hint:* Consider a system whose output $y[n]$ is the desired sum. Examine the relationship between $y[n]$ and $y[n-1]$. Note also that $y[0] = 0$.]

11.3-20 Find the following sum:

$$\sum_{k=0}^{n} k^3$$

[*Hint:* See the hint for Prob. 11.3-19.]

11.3-21 Find the following sum:

$$\sum_{k=0}^{n} ka^k \qquad a \neq 1$$

[*Hint:* See the hint for Prob. 11.3-19.]

11.3-22 Redo Prob. 11.3-19 using the result in Prob. 11.2-13a.

11.3-23 Redo Prob. 11.3-20 using the result in Prob. 11.2-13a.

11.3-24 Redo Prob. 11.3-21 using the result in Prob. 11.2-13a.

11.3-25 (a) Find the zero-state response of an LTID system with transfer function

$$H[z] = \frac{z}{(z+0.2)(z-0.8)}$$

and the input $x[n] = e^{(n+1)}u[n]$.

(b) Write the difference equation relating the output $y[n]$ to input $x[n]$.

11.3-26 Repeat Prob. 11.3-25 for $x[n] = u[n]$ and

$$H[z] = \frac{2z+3}{(z-2)(z-3)}$$

11.3-27 Repeat Prob. 11.3-25 for

$$H[z] = \frac{6(5z-1)}{6z^2-5z+1}$$

and the input $x[n]$ is

(a) $(4)^{-n}u[n]$

(b) $(4)^{-(n-2)}u[n-2]$

(c) $(4)^{-(n-2)}u[n]$

(d) $(4)^{-n}u[n-2]$

11.3-28 Repeat Prob. 11.3-25 for $x[n] = u[n]$ and

$$H[z] = \frac{2z-1}{z^2-1.6z+0.8}$$

11.3-29 Find the transfer functions corresponding to each of the systems specified by difference equations in Probs. 11.3-5, 11.3-7, 11.3-9, and 11.3-14.

11.3-30 Find $h[n]$, the unit impulse response of the systems described by the following equations:

(a) $y[n] + 3y[n-1] + 2y[n-2] = x[n] + 3x[n-1] + 3x[n-2]$

(b) $y[n+2] + 2y[n+1] + y[n] = 2x[n+2] - x[n+1]$

(c) $y[n] - y[n-1] + 0.5y[n-2] = x[n] + 2x[n-1]$

11.3-31 Find $h[n]$, the unit impulse response of the systems in Probs. 11.3-25, 11.3-26, and 11.3-28.

11.3-32 A system has impulse response $h[n] = u[n-3]$.

(a) Determine the impulse response of the inverse system $h^{-1}[n]$.

(b) Is the inverse stable? Is the inverse causal?

(c) Your boss asks you to implement $h^{-1}[n]$ to the best of your ability. Describe your realizable design, taking care to identify any deficiencies.

11.4-1 A system has an impulse response given by

$$h[n] = \left[\left(\frac{1+j}{\sqrt{8}}\right)^n + \left(\frac{1-j}{\sqrt{8}}\right)^n\right]u[n]$$

This system can be implemented according to Fig. P11.4-1.

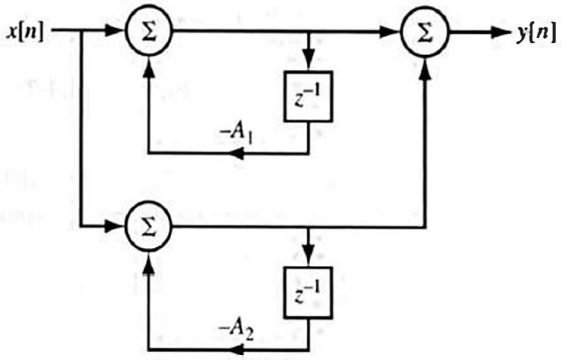

Figure P11.4-1

(a) Determine the coefficients A_1 and A_2 to implement $h[n]$ using the structure shown in Fig. P11.4-1.

(b) What is the zero-state response $y_0[n]$ of this system, given a shifted unit step input $x[n] = u[n+3]$?

11.4-2 (a) Show the canonic direct form, a cascade, and a parallel realization of

$$H[z] = \frac{z(3z-1.8)}{z^2-z+0.16}$$

(b) Find the transpose of the realizations obtained in part (a).

11.4-3 Repeat Prob. 11.4-2 for

$$H[z] = \frac{5z+2.2}{z^2+z+0.16}$$

11.4-4 Repeat Prob. 11.4-2 for

$$H[z] = \frac{3.8z - 1.1}{(z - 0.2)(z^2 - 0.6z + 0.25)}$$

11.4-5 Repeat Prob. 11.4-2 for

$$H[z] = \frac{z(1.6z - 1.8)}{(z - 0.2)(z^2 + z + 0.5)}$$

11.4-6 Repeat Prob. 11.4-2 for

$$H[z] = \frac{z(2z^2 + 1.3z + 0.96)}{(z + 0.5)(z - 0.4)^2}$$

11.4-7 Consider the LTID system shown in Fig. P11.4-7.

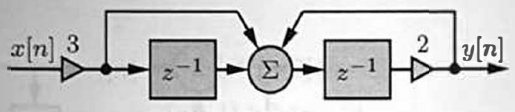

Figure P11.4-7

(a) Determine the standard delay-form difference equation description of this system.
(b) Determine the impulse response $h[n]$ of this system.
(c) Is this realization canonical? Explain.
(d) Is this system stable? Explain.
(e) Is this system causal? Explain.

11.4-8 Realize a system whose transfer function is

$$H[z] = \frac{2z^4 + z^3 + 0.8z^2 + 2z + 8}{z^4}$$

11.4-9 Realize a system whose transfer function is

$$H[z] = \sum_{n=0}^{6} nz^{-n}$$

11.4-10 Consider the LTID system shown in Fig. P11.4-10, where parameter c is an arbitrary, real constant.

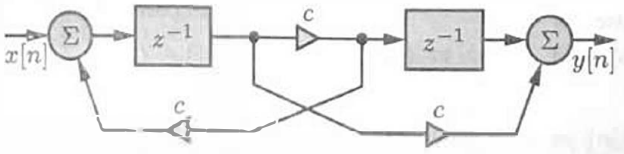

Figure P11.4-10

(a) Determine the system transfer function $H[z]$, expressed in standard rational form.
(b) Determine all system poles and all system zeros.
(c) Is the system of Fig. P11.4-10 canonical? Explain.
(d) What constraints, if any, exist on parameter c to ensure that the system is stable?

11.4-11 This problem demonstrates the enormous number of ways of implementing even a relatively low-order transfer function. A second-order transfer function has two real zeros and two real poles. Discuss various ways of realizing such a transfer function. Consider canonic direct, cascade, parallel, and the corresponding transposed forms. Note also that the interchange of cascaded sections yields a different realization.

11.4-12 Consider a digital audio system: an input analog-to-digital converter (ADC) is used to collect input samples at a CD-quality rate $f_s = 44$ kHz. Input samples are processed with a digital filter to generate output samples, which are sent to a digital-to-analog converter (DAC) at the same rate f_s. Every sample interval $T = 1/f_s$, the digital processor executes the following MATLAB-compatible code:

```
% Read input sample from the ADC
x = read_ADC;
% Process input and...
mem(1) = x - mem(3)*9/16;
% ...compute output sample
y = mem(1)*7/16 - mem(3)*7/16;
% Send output sample to the DAC
write_DAC = y;
% Update memory for next iteration
mem(3) = mem(2);
mem(2) = mem(1);
```

(a) Does the code implement DFI, DFII, TDFI, or TDFII? Support your answer by drawing the appropriate block diagram labeled in a manner that is consistent with the code.
(b) Determine the transfer function $H[z]$ of this system.
(c) What is the basic filtering function of this system: LP, HP, BP, or BS? Justify your answer.

(d) Determine the transfer function $H^{-1}[z]$ of the inverse system to $H[z]$ and draw its DFI block implementation. How well will the inverse system operate?

11.4-13 Repeat Prob. 11.4-12 but instead use the code:

```
% Read input sample from the ADC
x = read_ADC;
% Compute output sample
y = x*7/32+mem(1);
% Send output sample to the DAC
write_DAC = y;
% Update memory for next iteration
mem(1) = mem(2);
mem(2) = x*7/32 + y*9/16;
```

11.6-1 Determine $y[n]$, the output samples for the system depicted in Fig. P11.6-1 if the input $x(t) = e^{-2t}u(t)$.

11.6-2 For the sampled-data system in Fig. P11.6-2, show that the transfer function is

$$T[z] = \frac{G[z]}{1 + GH[z]}$$

where the transfer function $GH[z]$ corresponds to $G(s)H(s)$ in Table 12.1.

11.6-3 For the sampled-data system in Fig. P11.6-3, show that the output $Y[z]$ is given by

$$Y[z] = \frac{XG[z]}{1 + GH[z]}$$

Note that $XG[z]$ corresponds to the entry for $X(s)G(s)$ in Table 12.1. It is not the same as $X[z]G[z]$. In this case, it is not possible to express the output as $Y[z] = T[z]X[z]$. Consequently, the z-transfer function of such systems does not exist, and their analysis is a little more complicated.

11.7-1 Find the bilateral z-transform (if it exists) and the corresponding ROC for each of the following signals:

(a) $(0.8)^n u[n] + 2^n u[-(n+1)]$
(b) $2^n u[n] - 3^n u[-(n+1)]$
(c) $(-2)^{n+3}u[-n] + \sum_{k=0}^{\infty}(0.5)^{k-1}\delta(n-2k)$
(d) $(0.8)^n u[n] + (0.9)^n u[-(n+1)]$
(e) $[(0.8)^n + 3(0.4)^n]u[-(n+1)]$
(f) $[(0.8)^n + 3(0.4)^n]u[n]$
(g) $(0.8)^n u[n] + 3(0.4)^n u[-(n+1)]$
(h) $(0.5)^{|n|}$
(i) $n\,u[-(n+1)]$

11.7-2 Using the definition, compute the bilateral z-transform $X(z)$ of

(a) $x[n] = 3^{nu[-n]}$
(b) $x[n] = (\frac{1}{3})^{nu[n]}$

Express your answers in standard rational form.

11.7-3 Determine the inverse z-transform $x[n]$ of $X[z] = \frac{z^2 - \frac{1}{3}z}{(z-1)(z+2)}$ with ROC $1 < |z| < 2$.

11.7-4 Find the inverse z-transform of

$$X[z] = \frac{(e^{-2} - 2)z}{(z - e^{-2})(z - 2)}$$

when the ROC is

(a) $|z| > 2$
(b) $e^{-2} < |z| < 2$
(c) $|z| < e^{-2}$

11.7-5 Use partial fraction expansions, z-transform tables, and a region of convergence ($|z| < 1/2$) to determine the inverse z-transform of

$$X(z) = \frac{1}{(2z+1)(z+1)\left(z+\frac{1}{2}\right)}$$

11.7-6 Using z-transform techniques and properties (no time-domain convolution sum!), determine the convolution $y[n] = (\frac{1}{3})^{n-3}u[n-2] * (2)^n u[-n]$. Express your answer in the form $y[n] = c_1\gamma_1^n u[n+N_1] + c_2\gamma_2^n u[-n+N_2]$, making sure to clearly identify the constants c_1, c_2, γ_1, γ_2, N_1, and N_2.

11.7-7 Using partial fraction expansions, z-transform tables, and the fact that $h[n]$ is stable, determine the inverse z-transform of

$$H[z] = \frac{z^4 + z^3}{(z-2)(z+\frac{1}{2})}$$

11.7-8 Consider the system

$$H[z] = \frac{z\left(z - \frac{1}{2}\right)}{\left(z^3 - \frac{27}{8}\right)}$$

(a) Draw the pole-zero diagram for $H[z]$ and identify all possible regions of convergence.
(b) Draw the pole-zero diagram for $H^{-1}[z]$ and identify all possible regions of convergence.

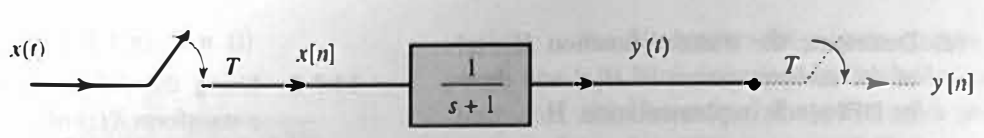

Figure P11.6-1

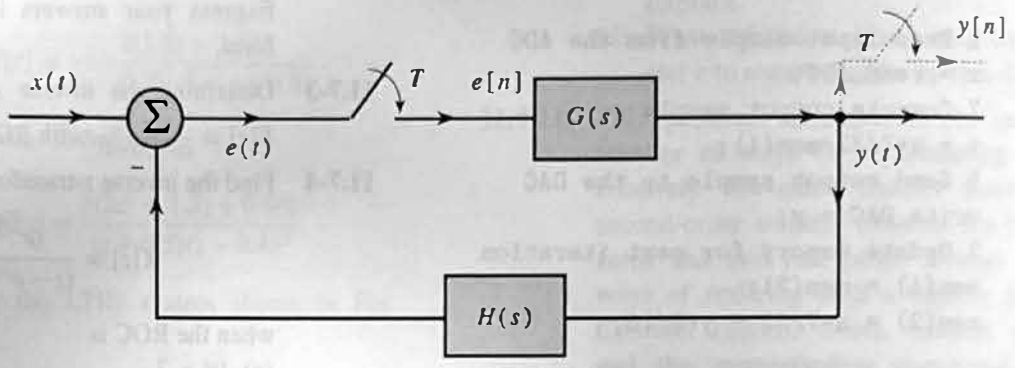

Figure P11.6-2

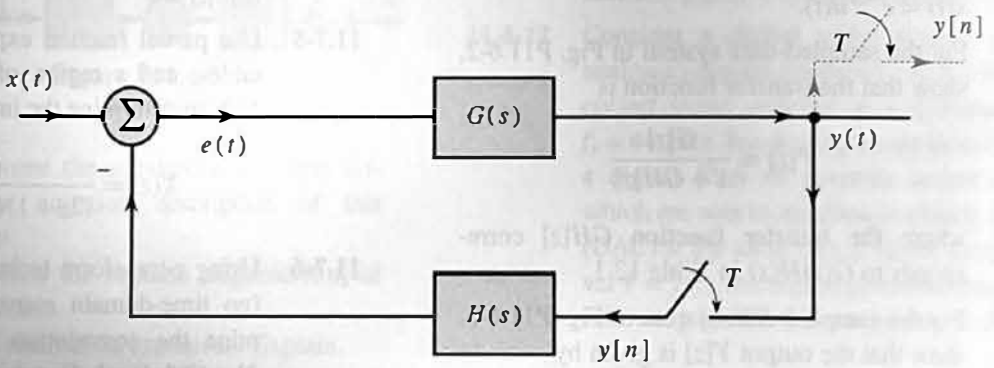

Figure P11.6-3

11.7-9 A discrete-time signal $x[n]$ has a rational z-transform that contains a pole at $z = 0.5$. Given that $x_1[n] = (1/3)^n x[n]$ is absolutely summable and $x_2[n] = (1/4)^n x[n]$ is **not** absolutely summable, determine whether $x[n]$ is left-sided, right-sided, or two-sided. Justify your answer!

11.7-10 Let $x[n]$ be an absolutely summable signal with rational z-transform $X[z]$. $X[z]$ is known to have a pole at $z = (0.75 + 0.75j)$, and other poles may be present. Recall that an absolutely summable signal satisfies $\sum_{-\infty}^{\infty} |x[n]| < \infty$.

(a) Can $x[n]$ be left-sided? Explain.
(b) Can $x[n]$ be right-sided? Explain.
(c) Can $x[n]$ be two-sided? Explain.
(d) Can $x[n]$ be of finite duration? Explain.

11.7-11 Consider a causal system that has transfer function

$$H[z] = \frac{z - 0.5}{z + 0.5}$$

When appropriate, assume initial conditions of zero.

(a) Determine the output $y_1[n]$ of this system in response to $x_1[n] = (3/4)^n u[n]$.
(b) Determine the output $y_2[n]$ of this system in response to $x_2[n] = (3/4)^n$.
(c) Determine the output $y_3[n]$ of this system in response to $x_3[n] = (3/4)^n u[-n-1]$.

11.7-12 Let $x[n] = (-1)^n u[n - n_0] + \alpha^n u[-n]$. Determine the constraints on the complex number α and the integer n_0 so that the z-transfonn $X[z]$ exists with region of convergence $1 < |z| < 2$.

11.7-13 Using the definition, compute the bilateral z-transform, including the region of convergence (ROC), of the following complex-valued functions:

(a) $x_1[n] = (-j)^{-n}u[-n] + \delta[-n]$

(b) $x_2[n] = (j)^n \cos(n+1)u[n]$

(c) $x_3[n] = j \sinh(n)u[-n+1]$

(d) $x_4[n] = \sum_{k=-\infty}^{0} (2j)^n \delta[n-2k]$

11.7-14 Use partial fraction expansions, z-transform tables, and a region of convergence ($0.5 < |z| < 2$) to determine the inverse z-transform of

(a) $X_1[z] = \dfrac{1}{1 + \frac{13}{6}z^{-1} + \frac{1}{6}z^{-2} - \frac{1}{3}z^{-3}}$

(b) $X_2[z] = \dfrac{1}{z^{-3}(2 - z^{-1})(1 + 2z^{-1})}$

11.7-15 Use partial fraction expansions, z-transform tables, and the fact that the systems are stable to determine the inverse z-transform of

(a) $H_1[z] = \dfrac{z^{-1}}{(z - \frac{1}{2})(1 + \frac{1}{2}z^{-1})}$

(b) $H_2[z] = \dfrac{z+1}{z^3(z-2)(z+\frac{1}{2})}$

11.7-16 By inserting $N-1$ zeros between every sample of a unit step, we obtain a signal

$$h[n] = \sum_{k=0}^{\infty} \delta[n - Nk]$$

Determine $H[z]$, the bilateral z-transform of $h[n]$. Identify the number and location(s) of the poles of $H[z]$.

11.7-17 Using transform-domain techniques, determine the zero-state response $y_{zsr}[n]$ of LTID system $y[n] - \frac{1}{4}y[n-2] = x[n]$ to the non-causal input $x[n] = 2^n u[2-n]$.

11.7-18 Determine the zero-state response of a system having a transfer function

$$H[z] = \frac{z}{(z+0.2)(z-0.8)} \qquad |z| > 0.8$$

and an input $x[n]$ given by

(a) $x[n] = e^n u[n]$

(b) $x[n] = 2^n u[-(n+1)]$

(c) $x[n] = e^n u[n] + 2^n u[-(n+1)]$

(d) $x[n] = 2^n u[n] + u[-(n+1)]$

(e) $x[n] = e^{-2n} u[-(n+1)]$

11.7-19 The discrete cross-correlation between real signal $x[n]$ and real signal $y[n]$ is

$$c_{xy}[n] = \sum_{k=-\infty}^{\infty} x[k]y[k-n]$$

Let signal $x[n]$ have z-transform $X[z]$ with ROC R_x, and let signal $y[n]$ have z-transform $Y[z]$ with ROC R_y. Determine $C_{XY}[z]$ (the bilateral z-transform of $c_{xy}[n]$) in terms of the z-transforms of $x[n]$ and $y[n]$.

11.7-20 Transform properties can be very useful. The accumulation property states

$$\sum_{k=-\infty}^{n} x[k] \Longleftrightarrow \frac{z}{z-1}X[z]$$

This property is the DT version of the Laplace transform "integration in time" property. Given $x[n] \Longleftrightarrow X[z]$, prove the accumulation property. [*Hint:* Polynomial long division can be helpful.]

CHAPTER 12

FREQUENCY RESPONSE AND DIGITAL FILTERS

Filtering characteristics of a system are specified by its frequency response. For this reason, it is important to study frequency response of discrete-time systems, which is very similar to the frequency response of continuous-time systems with some significant differences.

12.1 FREQUENCY RESPONSE OF DISCRETE-TIME SYSTEMS

For (asymptotically or BIBO-stable) continuous-time systems, we showed that the system response to an input $e^{j\omega t}$ is $H(j\omega)e^{j\omega t}$ and that the response to an input $\cos \omega t$ is $|H(j\omega)|\cos[\omega t + \angle H(j\omega)]$. Similar results hold for discrete-time systems. We now show that for an (asymptotically or BIBO-stable) LTID system, the system response to an input $e^{j\Omega n}$ is $H[e^{j\Omega}]e^{j\Omega n}$ and the response to an input $\cos \Omega n$ is $|H[e^{j\Omega}]|\cos(\Omega n + \angle H[e^{j\Omega}])$.

The proof is similar to the one used for continuous-time systems. In Sec. 9.5.2, we showed that an LTID system response to an (everlasting) exponential z^n is also an (everlasting) exponential $H[z]z^n$. This result is valid only for values of z for which $H[z]$, as defined in Eq. (11.11), exists (converges). As usual, we represent this input–output relationship by a directed arrow notation as

$$z^n \Longrightarrow H[z]z^n \tag{12.1}$$

Setting $z = e^{j\Omega}$ in this relationship yields

$$e^{j\Omega n} \Longrightarrow H[e^{j\Omega}]e^{j\Omega n} \tag{12.2}$$

Noting that $\cos \Omega n$ is the real part of $e^{j\Omega n}$, the use of Eq. (9.21) yields

$$\cos \Omega n \Longrightarrow \text{Re}\{H[e^{j\Omega}]e^{j\Omega n}\} \tag{12.3}$$

Expressing $H[e^{j\Omega}]$ in the polar form

$$H[e^{j\Omega}] = |H[e^{j\Omega}]|e^{j\angle H[e^{j\Omega}]}$$

Eq. (12.3) can be expressed as

$$\cos \Omega n \Longrightarrow |H[e^{j\Omega}]|\cos(\Omega n + \angle H[e^{j\Omega}])$$

In other words, the system response $y[n]$ to a sinusoidal input $\cos \Omega n$ is given by

$$y[n] = |H[e^{j\Omega}]| \cos (\Omega n + \angle H[e^{j\Omega}])$$

Following the same argument, the system response to a sinusoid $\cos(\Omega n + \theta)$ is

$$y[n] = |H[e^{j\Omega}]| \cos (\Omega n + \theta + \angle H[e^{j\Omega}]) \tag{12.4}$$

This result is valid only for BIBO-stable or asymptotically stable systems. The frequency response is meaningless for BIBO-unstable systems (which include marginally stable and asymptotically unstable systems). This follows from the fact that the frequency response in Eq. (12.2) is obtained by setting $z = e^{j\Omega}$ in Eq. (12.1). But, as shown in Sec. 9.5.2 [Eqs. (9.25) and (9.26)], the relationship of Eq. (12.1) applies only for values of z for which $H[z]$ exists. For BIBO-unstable systems, the ROC for $H[z]$ does not include the unit circle where $z = e^{j\Omega}$. This means, for BIBO-unstable systems, that $H[z]$ is meaningless when $z = e^{j\Omega}$.†

This important result shows that the response of an asymptotically or BIBO-stable LTID system to a discrete-time sinusoidal input of frequency Ω is also a discrete-time sinusoid of the same frequency. *The amplitude of the output sinusoid is $|H[e^{j\Omega}]|$ times the input amplitude, and the phase of the output sinusoid is shifted by $\angle H[e^{j\Omega}]$ with respect to the input phase.* Clearly, $|H[e^{j\Omega}]|$ is the amplitude gain, and a plot of $|H[e^{j\Omega}]|$ versus Ω is the amplitude response of the discrete-time system. Similarly, $\angle H[e^{j\Omega}]$ is the phase response of the system, and a plot of $\angle H[e^{j\Omega}]$ versus Ω shows how the system modifies or shifts the phase of the input sinusoid. Note that $H[e^{j\Omega}]$ incorporates the information of both amplitude and phase responses and therefore is called the *frequency responses* of the system.

Steady-State Response to Causal Sinusoidal Input

As in the case of continuous-time systems, we can show that the response of an LTID system to a causal sinusoidal input $\cos \Omega n\, u[n]$ is $y[n]$ in Eq. (12.4), plus a natural component consisting of the characteristic modes (see Prob. 12.1-9). For a stable system, all the modes decay exponentially, and only the sinusoidal component in Eq. (12.4) persists. For this reason, this component is called the sinusoidal *steady-state* response of the system. Thus, $y_{ss}[n]$, the steady-state response of a system to a causal sinusoidal input $\cos \Omega n\, u[n]$, is

$$y_{ss}[n] = |H[e^{j\Omega}]| \cos (\Omega n + \angle H[e^{j\Omega}])u[n]$$

System Response to Sampled Continuous-Time Sinusoids

So far we have considered the response of a discrete-time system to a discrete-time sinusoid $\cos \Omega n$ (or exponential $e^{j\Omega n}$). In practice, the input may be a sampled continuous-time sinusoid $\cos \omega t$ (or an exponential $e^{j\omega t}$). When a sinusoid $\cos \omega t$ is sampled with sampling interval T, the resulting

† This may also be argued as follows. For BIBO-unstable systems, the zero-input response contains nondecaying natural mode terms of the form $\cos \Omega_0 n$ or $\gamma^n \cos \Omega_0 n$ ($\gamma > 1$). Hence, the response of such a system to a sinusoid $\cos \Omega n$ will contain not just the sinusoid of frequency Ω but also nondecaying natural modes, rendering the concept of frequency response meaningless. Alternately, we can argue that when $z = e^{j\Omega}$, a BIBO-unstable system violates the dominance condition $|\gamma_i| < |e^{j\Omega}|$ for all i, where γ_i represents the ith characteristic root of the system.

signal is a discrete-time sinusoid $\cos \omega nT$, obtained by setting $t = nT$ in $\cos \omega t$. Therefore, all the results developed in this section apply if we substitute ωT for Ω:

$$\Omega = \omega T \tag{12.5}$$

EXAMPLE 12.1 Sinusoidal Response of a Difference Equation System

For a system specified by the equation

$$y[n+1] - 0.8y[n] = x[n+1]$$

find the system response to the inputs

(a) $1^n = 1$

(b) $\cos\left[\frac{\pi}{6}n - 0.2\right]$

(c) a sampled sinusoid $\cos 1500t$ with sampling interval $T = 0.001$

The system equation can be expressed as

$$(E - 0.8)y[n] = Ex[n]$$

Therefore, the transfer function of the system is

$$H[z] = \frac{z}{z - 0.8} = \frac{1}{1 - 0.8z^{-1}}$$

The frequency response is

$$H[e^{j\Omega}] = \frac{1}{1 - 0.8e^{-j\Omega}} = \frac{1}{(1 - 0.8\cos\Omega) + j0.8\sin\Omega}$$

Therefore,

$$|H[e^{j\Omega}]| = \frac{1}{\sqrt{(1 - 0.8\cos\Omega)^2 + (0.8\sin\Omega)^2}} = \frac{1}{\sqrt{1.64 - 1.6\cos\Omega}} \tag{12.6}$$

and

$$\angle H[e^{j\Omega}] = -\tan^{-1}\left[\frac{0.8\sin\Omega}{1 - 0.8\cos\Omega}\right] \tag{12.7}$$

The amplitude response $|H[e^{j\Omega}]|$ can also be obtained by observing that $|H|^2 = HH^*$. Since our system is real, we therefore see that

$$|H[e^{j\Omega}]|^2 = H[e^{j\Omega}]H^*[e^{j\Omega}] = H[e^{j\Omega}]H[e^{-j\Omega}] \tag{12.8}$$

Substituting for $H[e^{j\Omega}]$, it follows that

$$|H[e^{j\Omega}]|^2 = \left(\frac{1}{1-0.8e^{-j\Omega}}\right)\left(\frac{1}{1-0.8e^{j\Omega}}\right) = \frac{1}{1.64-1.6\cos\Omega}$$

which matches the result found earlier.

Figure 12.1 shows plots of amplitude and phase response as functions of Ω. We now compute the amplitude and the phase response for the various inputs.

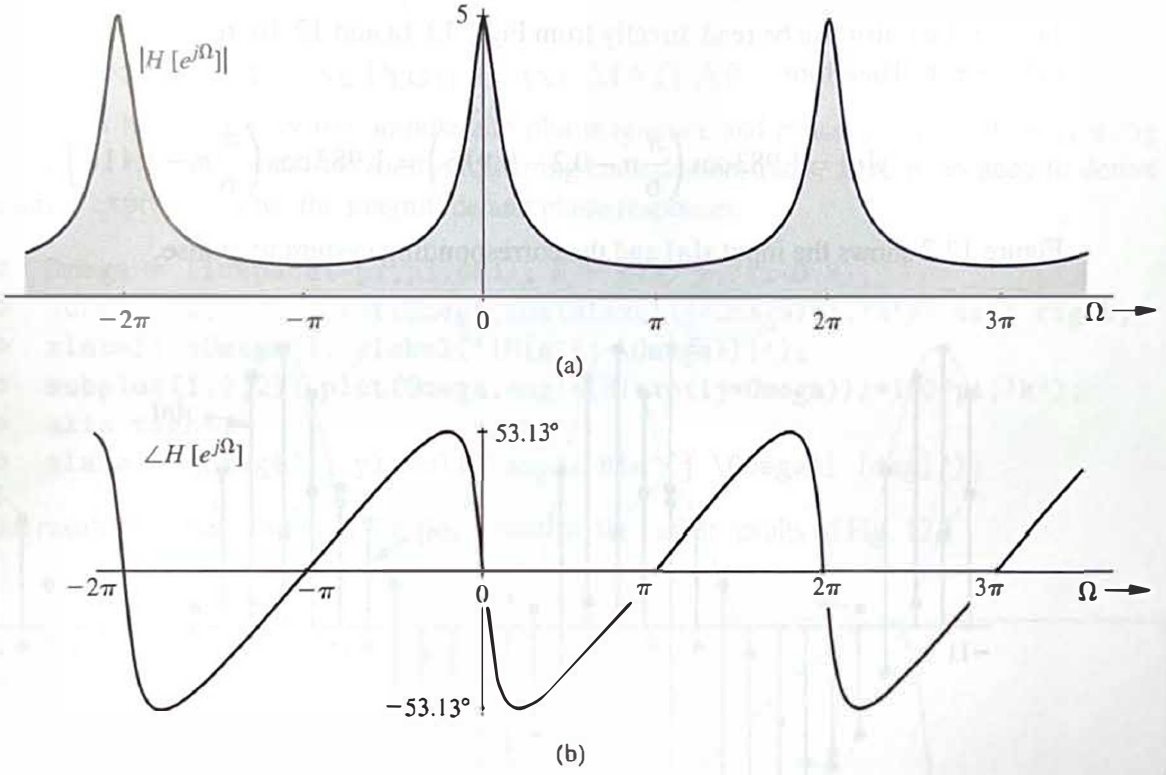

Figure 12.1 Frequency response of the LTID system of Ex. 12.1.

(a) Since $1^n = (e^{j\Omega})^n$ with $\Omega = 0$, the amplitude response is $H[e^{j0}]$. From Eq. (12.6), we obtain

$$H[e^{j0}] = \frac{1}{\sqrt{1.64-1.6\cos(0)}} = \frac{1}{\sqrt{0.04}} = 5 = 5\angle 0$$

Therefore,

$$|H[e^{j0}]| = 5 \qquad \text{and} \qquad \angle H[e^{j0}] = 0$$

These values also can be read directly from Figs. 12.1a and 12.1b, respectively, corresponding to $\Omega = 0$. Therefore, the system response to input 1 is

$$y[n] = 5(1^n) = 5 \qquad \text{for all } n$$

(b) For $x[n] = \cos[(\pi/6)n - 0.2]$, $\Omega = \pi/6$. According to Eqs. (12.6) and (12.7),

$$|H[e^{j\pi/6}]| = \frac{1}{\sqrt{1.64 - 1.6\cos\frac{\pi}{6}}} = 1.983$$

$$\angle H[e^{j\pi/6}] = -\tan^{-1}\left[\frac{0.8\sin\frac{\pi}{6}}{1 - 0.8\cos\frac{\pi}{6}}\right] = -0.916 \text{ rad}$$

These values also can be read directly from Figs. 12.1a and 12.1b, respectively, corresponding to $\Omega = \pi/6$. Therefore,

$$y[n] = 1.983\cos\left(\frac{\pi}{6}n - 0.2 - 0.916\right) = 1.983\cos\left(\frac{\pi}{6}n - 1.116\right)$$

Figure 12.2 shows the input $x[n]$ and the corresponding system response.

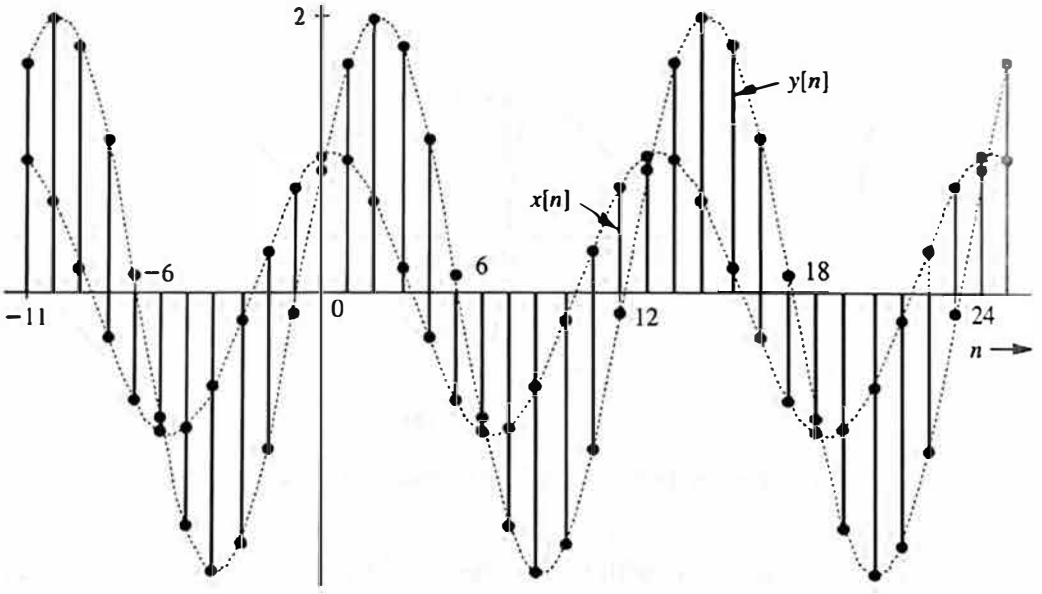

Figure 12.2 Sinusoidal input and the corresponding output of the LTID system of Ex. 12.1.

(c) A sinusoid $\cos 1500t$ sampled every T seconds ($t = nT$) results in a discrete-time sinusoid

$$x[n] = \cos 1500nT$$

For $T = 0.001$, the input is

$$x[n] = \cos(1.5n)$$

In this case, $\Omega = 1.5$. According to Eqs. (12.6) and (12.7),

$$|H[e^{j1.5}]| = \frac{1}{\sqrt{1.64 - 1.6\cos(1.5)}} = 0.809$$

$$\angle H[e^{j1.5}] = -\tan^{-1}\left[\frac{0.8\sin(1.5)}{1 - 0.8\cos(1.5)}\right] = -0.702\,\text{rad}$$

These values also could be read directly from Fig. 12.1 corresponding to $\Omega = 1.5$. Therefore,

$$y[n] = 0.809\cos(1.5n - 0.702)$$

Frequency Response Plots Using MATLAB

MATLAB makes it easy to compute and plot magnitude and phase responses directly using a system's transfer function. As the following code demonstrates, there is no need to derive separate expressions for the magnitude and phase responses.

```
>> Omega = linspace(-pi,pi,401); H = @(z) z./(z-0.8);
>> subplot(1,2,1); plot(Omega,abs(H(exp(1j*Omega))),'k'); axis tight;
>> xlabel('\Omega'); ylabel('|H[e^{j \Omega}]|');
>> subplot(1,2,2); plot(Omega,angle(H(exp(1j*Omega)))*180/pi,'k');
>> axis tight;
>> xlabel('\Omega'); ylabel('\angle H[e^{j \Omega}] [deg]');
```

The resulting plots, shown in Fig. 12.3, confirm the earlier results of Fig. 12.1.

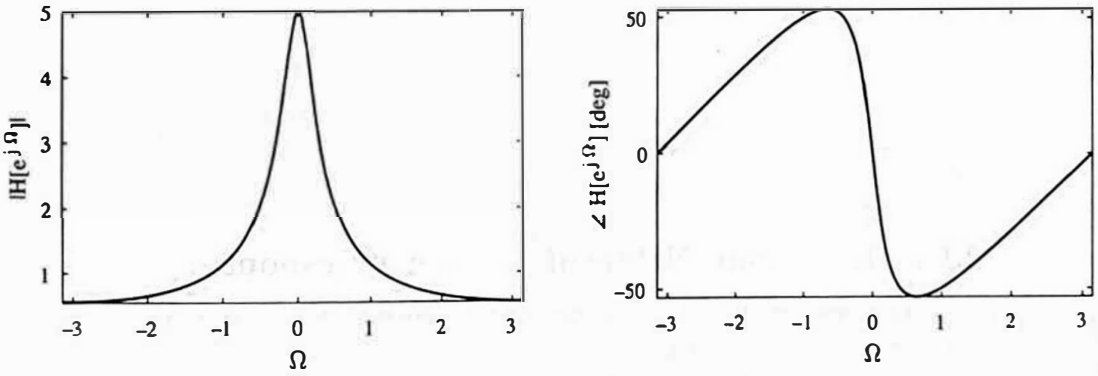

Figure 12.3 MATLAB-generated magnitude and phase responses for Ex. 12.1.

Comment: Figures 12.1 and 12.3 show amplitude and phase response plots as functions of Ω. These plots as well as Eqs. (12.6) and (12.7) indicate that the frequency response of a discrete-time system is a continuous (rather than discrete) function of frequency Ω. There is no contradiction here. This behavior is merely an indication of the fact that the frequency variable Ω is continuous (takes on all possible values) and therefore the system response exists at every value of Ω.

DRILL 12.1 Frequency Response of Difference Equation

For a system specified by the equation

$$y[n+1]-0.5y[n]=x[n]$$

find the amplitude and the phase response. Find the system response to sinusoidal input $\cos[1000t-(\pi/3)]$ sampled every $T=0.5$ ms.

ANSWER

$$|H[e^{j\Omega}]|=\frac{1}{\sqrt{1.25-\cos\Omega}}$$

$$\angle H[e^{j\Omega}]=-\tan^{-1}\left[\frac{\sin\Omega}{\cos\Omega-0.5}\right]$$

$$y[n]=1.639\cos\left(0.5n-\frac{\pi}{3}-0.904\right)=1.639\cos(0.5n-1.951)$$

DRILL 12.2 Frequency Response of an Ideal Delay System

Show that for an ideal delay ($H[z]=1/z$), the amplitude response $|H[e^{j\Omega}]|=1$, and the phase response $\angle H[e^{j\Omega}]=-\Omega$. Thus, a pure time delay does not affect the amplitude gain of sinusoidal input, but it causes a phase shift (delay) of Ω radians in a discrete sinusoid of frequency Ω. Thus, for an ideal delay, the phase shift of the output sinusoid is proportional to the frequency of the input sinusoid (linear-phase shift).

12.1.1 The Periodic Nature of Frequency Response

In Ex. 12.1 and Fig. 12.1, we saw that the frequency response $H[e^{j\Omega}]$ is a periodic function of Ω. This is not a coincidence. Unlike continuous-time systems, all LTID systems have periodic frequency response. This is seen clearly from the nature of the expression of the frequency response of an LTID system. Because $e^{\pm j2\pi m}=1$ for all integer values of m [see Eq. (B.10)],

$$H[e^{j\Omega}]=H\left[e^{j(\Omega+2\pi m)}\right] \qquad m \text{ integer}$$

Therefore, the frequency response $H[e^{j\Omega}]$ is a periodic function of Ω with a period 2π. This is the mathematical explanation of the periodic behavior. A more physical and intuitive explanation is provided in the discussion of discrete-time sinusoids, found in the latter part of Sec. 8.3.5. Because the frequency response of discrete-time systems is necessarily 2π-periodic, we need to plot a discrete-time system's frequency response only over the frequency range from $-\pi$ to π (or from 0 to 2π).

12.2 Frequency Response from Pole-Zero Locations

The frequency responses (amplitude and phase responses) of a system are determined by pole-zero locations of the transfer function $H[z]$. Just as in continuous-time systems, it is possible to determine quickly the amplitude and the phase response and to obtain physical insight into the filter characteristics of a discrete-time system by using a graphical technique. The general Nth-order transfer function $H[z]$ in Eq. (11.26) can be expressed in factored form as

$$H[z] = b_0 \frac{(z-z_1)(z-z_2)\cdots(z-z_N)}{(z-\gamma_1)(z-\gamma_2)\cdots(z-\gamma_N)}$$

We can compute $H[z]$ graphically by using the concepts discussed in Sec. 7.4. The directed line segment from z_i to z in the complex plane (Fig. 12.4a) represents the complex number $z - z_i$. The length of this segment is $|z - z_i|$ and its angle with the horizontal axis is $\angle(z - z_i)$.

To compute the frequency response $H[e^{j\Omega}]$, we evaluate $H[z]$ at $z = e^{j\Omega}$. But for $z = e^{j\Omega}$, $|z| = 1$ and $\angle z = \Omega$ so that $z = e^{j\Omega}$ represents a point on the unit circle at an angle Ω with the horizontal. We now connect all zeros $(z_1, z_2, \ldots, z_N)$ and all poles $(\gamma_1, \gamma_2, \ldots, \gamma_N)$ to the point $e^{j\Omega}$, as indicated in Fig. 12.4b. Let $r_1, r_2, \ldots, r_N$ be the lengths and $\phi_1, \phi_2, \ldots, \phi_N$ be the angles, respectively, of the straight lines connecting $z_1, z_2, \ldots, z_N$ to the point $e^{j\Omega}$. Similarly, let $d_1, d_2, \ldots, d_N$ be the lengths and $\theta_1, \theta_2, \ldots, \theta_N$ be the angles, respectively, of the lines connecting $\gamma_1, \gamma_2, \ldots, \gamma_N$ to $e^{j\Omega}$. Then

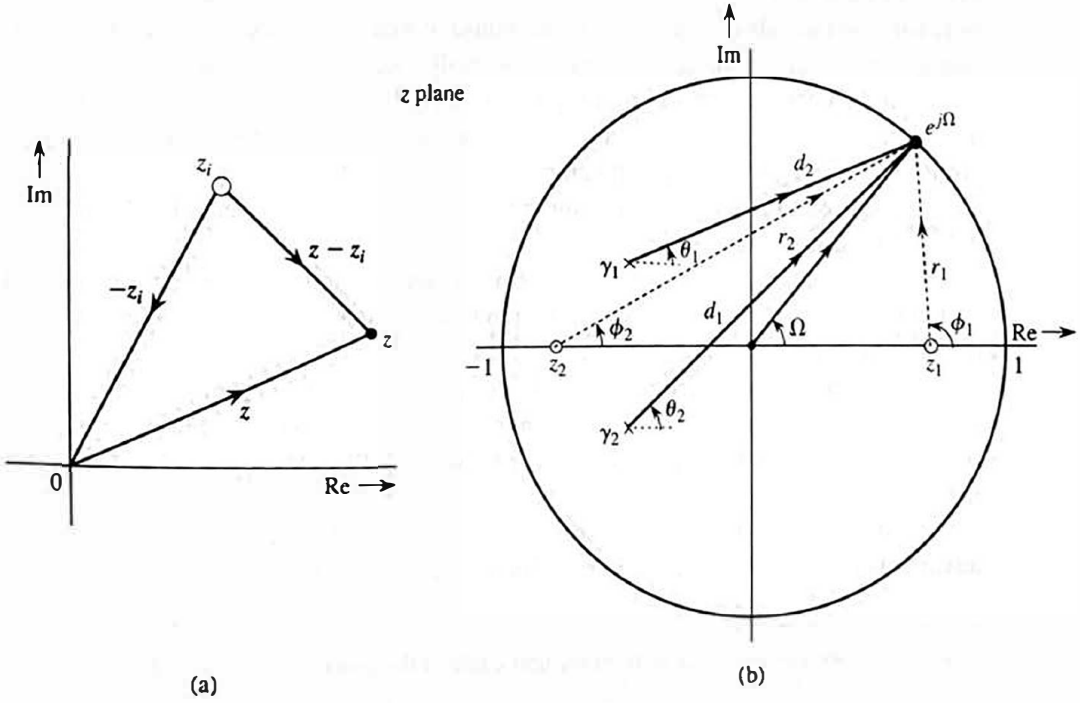

Figure 12.4 Vector representations of (a) complex numbers and (b) factors of $H[z]$.

$$H[e^{j\Omega}] = H[z]|_{z=e^{j\Omega}} = b_0 \frac{(r_1 e^{j\phi_1})(r_2 e^{j\phi_2}) \cdots (r_N e^{j\phi_N})}{(d_1 e^{j\theta_1})(d_2 e^{j\theta_2}) \cdots (d_N e^{j\theta_N})}$$
$$= b_0 \frac{r_1 r_2 \cdots r_N}{d_1 d_2 \cdots d_N} e^{j[(\phi_1+\phi_2+\cdots+\phi_N)-(\theta_1+\theta_2+\cdots+\theta_N)]}$$

Therefore (assuming $b_0 > 0$),

$$|H[e^{j\Omega}]| = b_0 \frac{r_1 r_2 \cdots r_N}{d_1 d_2 \cdots d_N} = b_0 \frac{\text{product of the distances of zeros to } e^{j\Omega}}{\text{product of distances of poles to } e^{j\Omega}} \tag{12.9}$$

and

$$\angle H[e^{j\Omega}] = (\phi_1 + \phi_2 + \cdots + \phi_N) - (\theta_1 + \theta_2 + \cdots + \theta_N)$$
$$= \text{sum of zero angles to } e^{j\Omega} - \text{sum of pole angles to } e^{j\Omega}$$

In this manner, we can compute the frequency response $H[e^{j\Omega}]$ for any value of Ω by selecting the point on the unit circle at an angle Ω. This point is $e^{j\Omega}$. To compute the frequency response $H[e^{j\Omega}]$, we connect all poles and zeros to this point and use the foregoing equations to determine $|H[e^{j\Omega}]|$ and $\angle H[e^{j\Omega}]$. We repeat this procedure for all values of Ω from 0 to π to obtain the frequency response.

Controlling Gain by Placement of Poles and Zeros

The nature of the influence of pole and zero locations on the frequency response is similar to that observed in continuous-time systems, with minor differences. In place of the imaginary axis of the continuous-time systems, we have the unit circle in the discrete-time case. The nearer the pole (or zero) is to a point $e^{j\Omega}$ (on the unit circle) representing some frequency Ω, the more influence that pole (or zero) wields on the amplitude response at that frequency because the length of the vector joining that pole (or zero) to the point $e^{j\Omega}$ is small. The proximity of a pole (or a zero) has a similar effect on the phase response. From Eq. (12.9), it is clear that to enhance the amplitude response at a frequency Ω, we should place a pole as close as possible to the point $e^{j\Omega}$ (which is on the unit circle).[†] Similarly, to suppress the amplitude response at a frequency Ω, we should place a zero as close as possible to the point $e^{j\Omega}$ on the unit circle. Placing repeated poles or zeros will further enhance their influence.

Total suppression of signal transmission at any frequency can be achieved by placing a zero on the unit circle at a point corresponding to that frequency. This observation is used in the notch (bandstop) filter design.

Placing a pole or a zero at the origin does not influence the amplitude response because the length of the vector connecting the origin to any point on the unit circle is unity. However, a pole (or a zero) at the origin adds angle $-\Omega$ (or Ω) to $\angle H[e^{j\Omega}]$. Hence, the phase spectrum $-\Omega$ (or Ω) is a linear function of frequency and therefore represents a pure time delay (or time advance) of T seconds (see Drill 12.2). Therefore, a pole (a zero) at the origin causes a time delay (or a time advance) of T seconds in the response. There is no change in the amplitude response.

[†] The closest we can place a pole is on the unit circle at the point representing Ω. This choice would lead to infinite gain, but should be avoided because it will render the system marginally stable (BIBO-unstable). The closer the point to the unit circle, the more sensitive the system gain to parameter variations.

For a stable system, all the poles must be located inside the unit circle. The zeros may lie anywhere. Also, for a physically realizable system, $H[z]$ must be a proper fraction, that is, $N \geq M$. If, to achieve a certain amplitude response, we require $M > N$, we can still make the system realizable by placing a sufficient number of poles at the origin to make $N = M$. This will not change the amplitude response, but it will increase the time delay of the response.

In general, a pole at a point has the opposite effect of a zero at that point. Placing a zero closer to a pole tends to cancel the effect of that pole on the frequency response.

Lowpass Filters

A lowpass filter generally has a maximum gain at or near $\Omega = 0$, which corresponds to point $e^{j0} = 1$ on the unit circle. Clearly, placing a pole inside the unit circle near the point $z = 1$ (Fig. 12.5a) would result in a lowpass response.† The corresponding amplitude and phase response appear in Fig. 12.5a. For smaller values of Ω, the point $e^{j\Omega}$ (a point on the unit circle at an angle Ω) is closer to the pole, and consequently the gain is higher. As Ω increases, the distance of the point $e^{j\Omega}$ from the pole increases. Consequently the gain decreases, resulting in a lowpass characteristic. Placing a zero at the origin does not change the amplitude response but it does modify the phase response, as illustrated in Fig. 12.5b. Placing a zero at $z = -1$, however, changes both the amplitude and the phase response (Fig. 12.5c). The point $z = -1$ corresponds to frequency $\Omega = \pi$ ($z = e^{j\Omega} = e^{j\pi} = -1$). Consequently, the amplitude response now becomes more attenuated at higher frequencies, with a zero gain at $\Omega = \pi$. We can approach ideal lowpass characteristics by using more poles staggered near $z = 1$ (but within the unit circle). Figure 12.5d shows a third-order lowpass filter with three poles near $z = 1$ and a third-order zero at $z = -1$, with corresponding amplitude and phase response. For an ideal lowpass filter, we need an enhanced gain at every frequency in the band $(0, \Omega_c)$. This can be achieved by placing a continuous wall of poles (requiring an infinite number of poles) opposite this band.

Highpass Filters

A highpass filter has a small gain at lower frequencies and a high gain at higher frequencies. Such a characteristic can be realized by placing a pole or poles near $z = -1$ because we want the gain at $\Omega = \pi$ to be the highest. Placing a zero at $z = 1$ further enhances suppression of gain at lower frequencies. Figure 12.5e shows a possible pole-zero configuration of the third-order highpass filter with corresponding amplitude and phase responses.

In the following two examples, we shall realize analog filters by using digital processors and suitable interface devices (C/D and D/C), as shown in Fig. 8.2. In these two examples, we shall examine the design of a digital processor with the transfer function $H[z]$ for the purpose of realizing bandpass and bandstop filters.

As Fig. 8.2 shows, the C/D device samples the continuous-time input $x(t)$ to yield a discrete-time signal $x[n]$, which serves as the input to $H[z]$. The output $y[n]$ of $H[z]$ is converted to a continuous-time signal $y(t)$ by a D/C device. We also saw in Eq. (12.5) that a continuous-time sinusoid of frequency ω, when sampled, results in a discrete-time sinusoid $\Omega = \omega T$.

† Placing the pole at $z = 1$ results in maximum (infinite) gain but renders the system BIBO-unstable; hence, it should be avoided.

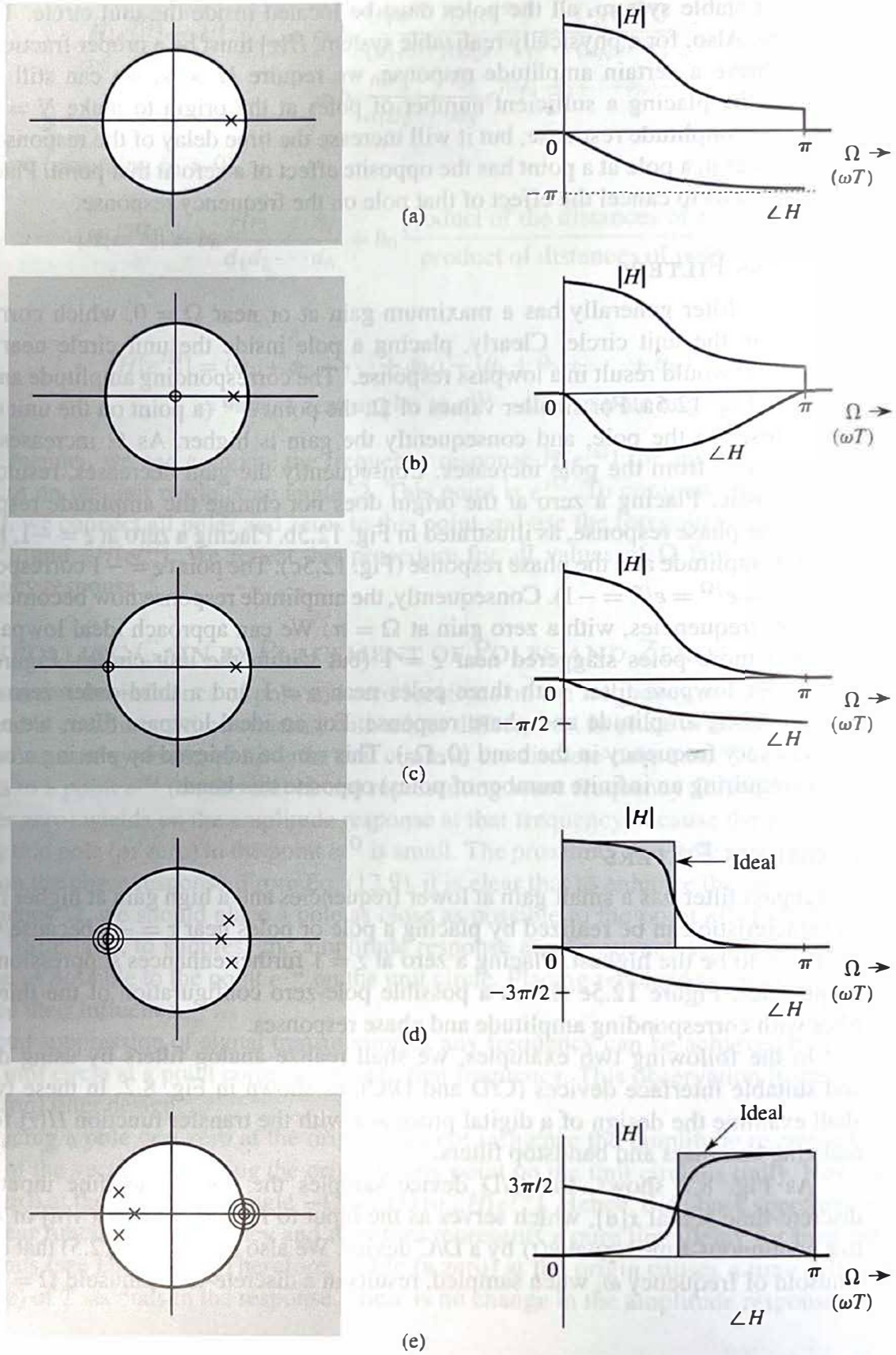

Figure 12.5 Various pole-zero configurations and the corresponding frequency responses.

EXAMPLE 12.2 Bandpass Filter by Pole-Zero Placement

By trial and error, design a tuned (bandpass) analog filter with zero transmission at 0 Hz and also at the highest frequency $f_h = 500$ Hz. The resonant frequency is required to be 125 Hz.

Because $f_h = 500$, we require $T < 1/1000$ [see Eq. (8.7)]. Let us select $T = 10^{-3}$.† Recall that the analog frequencies ω correspond to digital frequencies $\Omega = \omega T$. Hence, analog frequencies $\omega = 0$ and 1000π correspond to $\Omega = 0$ and π, respectively. The gain is required to be zero at these frequencies. Hence, we need to place zeros at $e^{j\Omega}$ corresponding to $\Omega = 0$ and $\Omega = \pi$. For $\Omega = 0$, $z = e^{j\Omega} = 1$; for $\Omega = \pi$, $e^{j\Omega} = -1$. Hence, there must be zeros at $z = \pm 1$. Moreover, we need enhanced response at the resonant frequency $\omega = 250\pi$, which corresponds to $\Omega = \pi/4$, which, in turn, corresponds to $z = e^{j\Omega} = e^{j\pi/4}$. Therefore, to enhance the frequency response at $\omega = 250\pi$, we place a pole in the vicinity of $e^{j\pi/4}$. Because this is a complex pole, we also need its conjugate near $e^{-j\pi/4}$, as indicated in Fig. 12.6a. Let us choose these poles γ_1 and γ_2 as

$$\gamma_1 = |\gamma| e^{j\pi/4} \qquad \text{and} \qquad \gamma_2 = |\gamma| e^{-j\pi/4}$$

where $|\gamma| < 1$ for stability. The closer γ is to the unit circle, the more sharply peaked is the response around $\omega = 250\pi$. We also have zeros at ± 1. Hence,

$$H[z] = K\frac{(z-1)(z+1)}{(z-|\gamma|e^{j\pi/4})(z-|\gamma|e^{-j\pi/4})} = K\frac{z^2-1}{z^2-\sqrt{2}|\gamma|z+|\gamma|^2}$$

For convenience, we shall choose $K = 1$. The amplitude response is given by

$$|H[e^{j\Omega}]| = \frac{|e^{j2\Omega}-1|}{|e^{j\Omega}-|\gamma|e^{j\pi/4}||e^{j\Omega}-|\gamma|e^{-j\pi/4}|}$$

Now, by using Eq. (12.8), we obtain

$$|H[e^{j\Omega}]|^2 = \frac{2(1-\cos 2\Omega)}{\left[1+|\gamma|^2-2|\gamma|\cos\left(\Omega-\frac{\pi}{4}\right)\right]\left[1+|\gamma|^2-2|\gamma|\cos\left(\Omega+\frac{\pi}{4}\right)\right]}$$

Figure 12.6b shows the amplitude response as a function of ω, as well as $\Omega = \omega T = 10^{-3}\omega$ for values of $|\gamma| = 0.83$, 0.96, and 1. As expected, the gain is zero at $\omega = 0$ and at 500 Hz ($\omega = 1000\pi$). The gain peaks at about 125 Hz ($\omega = 250\pi$). The resonance (peaking) becomes pronounced as $|\gamma|$ approaches 1. Figure 12.6c shows a canonical realization of this filter, which follows from the transfer function $H[z]$.

---

† Strictly speaking, we need $T < 0.001$. Recall from Ch. 5 that if the input does not contain a finite amplitude component of 500 Hz, $T = 0.001$ is adequate. Generally, practical signals satisfy this condition.

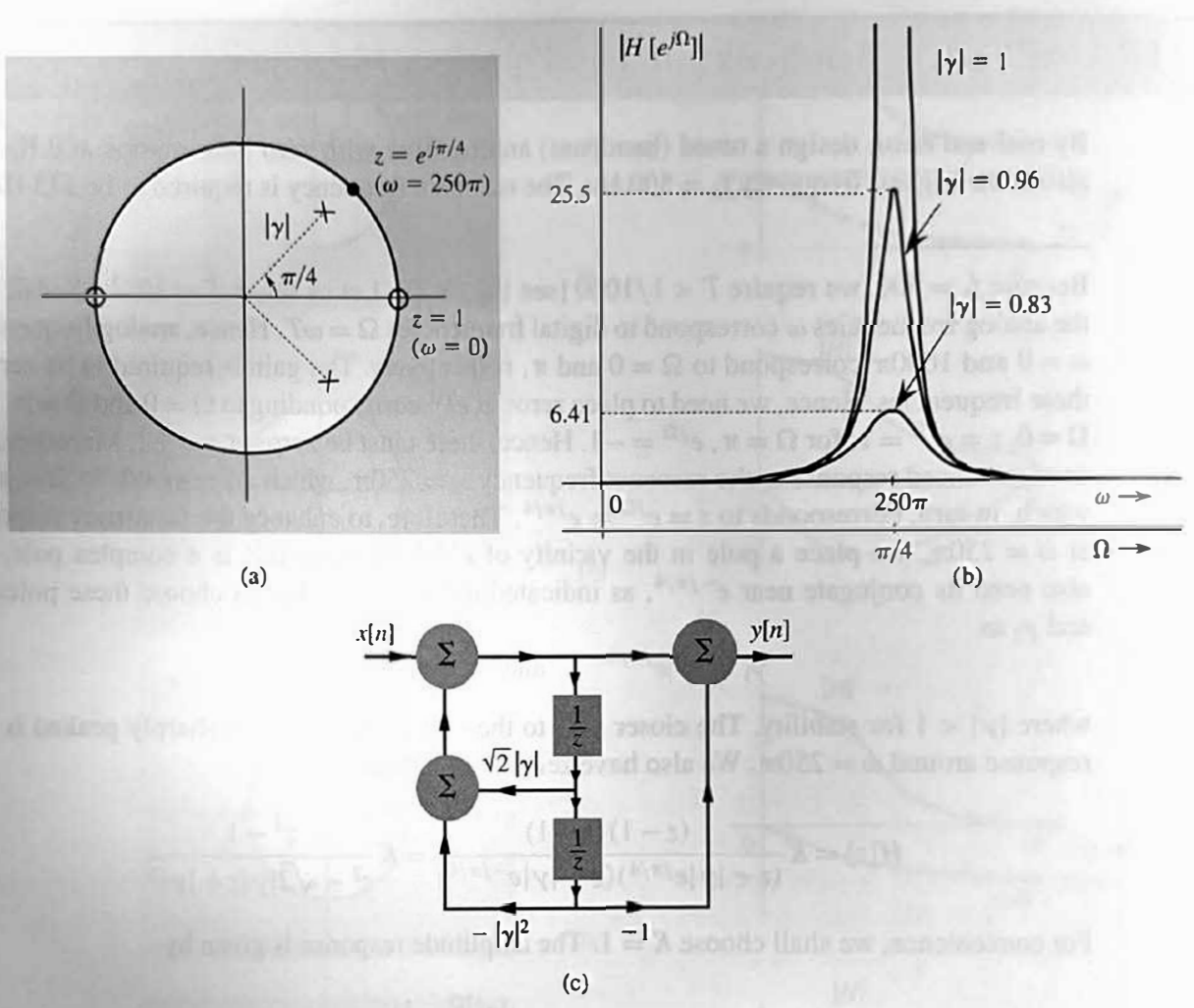

Figure 12.6 Designing a bandpass filter.

MULTIPLE MAGNITUDE RESPONSE CURVES USING MATLAB

By defining an anonymous function of the two variables z and γ in MATLAB, it is straightforward to duplicate the three magnitude response curves in Fig. 12.6b, corresponding to the cases $\gamma = 0.83$, 0.96, and 1.

```
>> Omega = linspace(0,pi,400);
>> H = @(z,gamma_m) (z.^2-1)./(z.^2-sqrt(2)*gamma_m*z+gamma_m^2);
>> plot(Omega,abs(H(exp(1j*Omega),0.83)),...
>>     Omega,abs(H(exp(1j*Omega),0.96)),...
>>     Omega,abs(H(exp(1j*Omega),0.99)));
>> text(.27*pi,35,'|\gamma|=1');
>> text(.28*pi,25.5,'|\gamma|=0.96');
>> text(.35*pi,6.41,'|\gamma|=0.83');
>> set(gca,'xtick',0:pi/4:pi,'ytick',[0 6.41,25.5]);
>> axis([0 pi 0 40]); xlabel('\Omega'); ylabel('|H[e^{j \Omega}]|');
```

The result, shown in Fig. 12.7, confirms the earlier result of Fig. 12.6b. Phase response curves can be generated with minor modification to the MATLAB code.

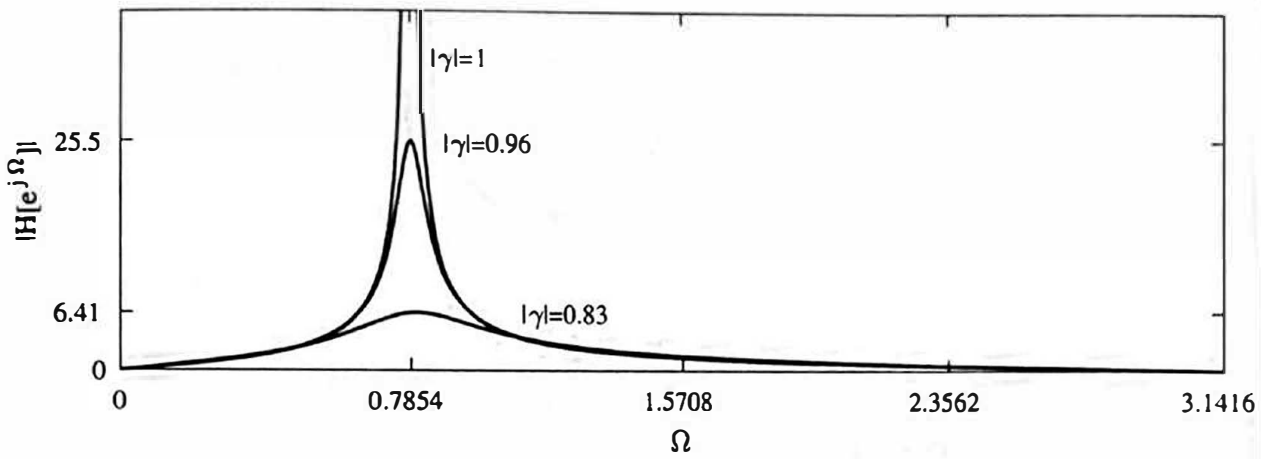

Figure 12.7 MATLAB-generated magnitude response curves for Ex. 12.2.

EXAMPLE 12.3 Bandstop Filter by Pole-Zero Placement

Design a second-order notch filter to have zero transmission at 250 Hz and a sharp recovery of gain to unity on both sides of 250 Hz. The highest significant frequency to be processed is $f_h = 400$ Hz.

In this case, $T < 1/2f_h = 1.25 \times 10^{-3}$. Let us choose $T = 10^{-3}$. For the frequency 250 Hz, $\Omega = 2\pi(250)T = \pi/2$. Thus, the frequency 250 Hz is represented by a point $e^{j\Omega} = e^{j\pi/2} = j$ on the unit circle, as depicted in Fig. 12.8a. Since we need zero transmission at this frequency, we must place a zero at $z = e^{j\pi/2} = j$ and its conjugate at $z = e^{-j\pi/2} = -j$. We also require a sharp recovery of gain on both sides of frequency 250 Hz. To accomplish this goal, we place two poles close to the two zeros, to cancel out the effect of the two zeros as we move away from the point j (corresponding to frequency 250 Hz). For this reason, let us use poles at $\pm ja$ with $a < 1$ for stability. The closer the poles are to zeros (the closer the a to 1), the faster is the gain recovery on either side of 250 Hz. The resulting transfer function is

$$H[z] = K\frac{(z-j)(z+j)}{(z-ja)(z+ja)} = K\frac{z^2+1}{z^2+a^2}$$

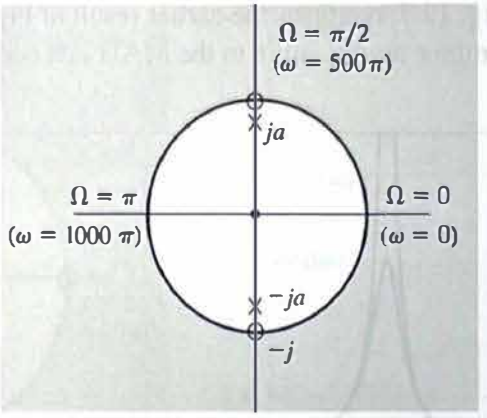

(a)

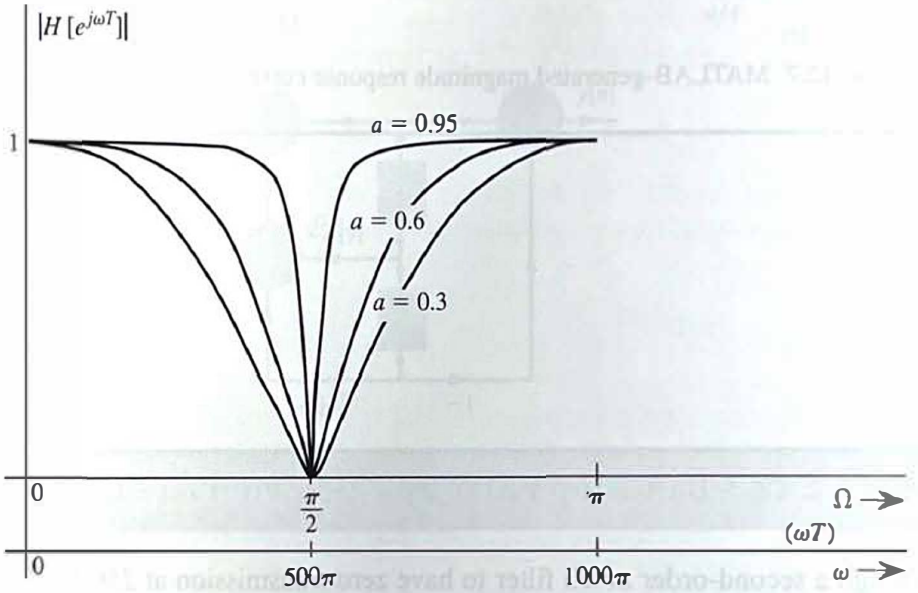

(b)

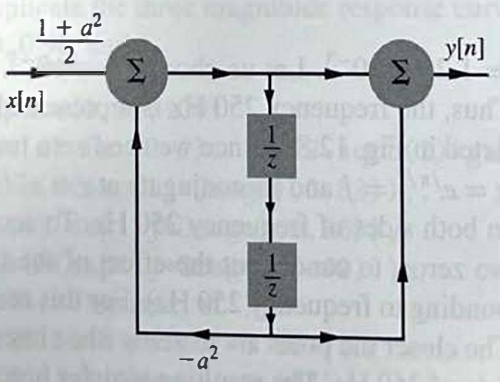

(c)

Figure 12.8 Designing a notch (bandstop) filter.

The dc gain (gain at $\Omega = 0$, or $z = 1$) of this filter is

$$H[1] = K\frac{2}{1+a^2}$$

Because we require a dc gain of unity, we must select $K = (1+a^2)/2$. The transfer function is therefore

$$H[z] = \frac{(1+a^2)(z^2+1)}{2(z^2+a^2)}$$

and according to Eq. (12.8),

$$|H[e^{j\Omega}]|^2 = \frac{(1+a^2)^2}{4}\frac{(e^{j2\Omega}+1)(e^{-j2\Omega}+1)}{(e^{j2\Omega}+a^2)(e^{-j2\Omega}+a^2)}$$
$$= \frac{(1+a^2)^2(1+\cos 2\Omega)}{2(1+a^4+2a^2\cos 2\Omega)}$$

Figure 12.8b shows $|H[e^{j\Omega}]|$ for values of $a = 0.3$, 0.6, and 0.95. Figure 12.8c shows a realization of this filter.

DRILL 12.3 Highpass Filter by Pole-Zero Placement

Use the graphical argument to show that a filter with transfer function

$$H[z] = \frac{z-0.9}{z}$$

acts like a highpass filter. Make a rough sketch of the amplitude response.

12.3 DIGITAL FILTERS

Digital filters and some of their advantages were discussed in Sec. 8.5. Digital filters can be classified as either *recursive* or *nonrecursive*.

RECURSIVE FILTERS

The terms *recursive* and *nonrecursive* are easily understood in terms of a specific example. Consider a third-order system with the transfer function

$$H[z] = \frac{b_0z^3+b_1z^2+b_2z+b_3}{z^3+a_1z^2+a_2z+a_3} \tag{12.10}$$

The input $x[n]$ and the corresponding output $y[n]$ of this system are related by the difference equation

$$y[n] + a_1 y[n-1] + a_2 y[n-2] + a_3 y[n-3] = b_0 x[n] + b_1 x[n-1] + b_2 x[n-2] + b_3 x[n-3]$$

or

$$y[n] = \underbrace{-a_1 y[n-1] - a_2 y[n-2] - a_3 y[n-3]}_{\text{output terms}} + \underbrace{b_0 x[n] + b_1 x[n-1] + b_2 x[n-2] + b_3 x[n-3]}_{\text{input terms}}$$

Here, $y[n]$, the output at instant n, is determined by the input values $x[n]$, $x[n-1]$, $x[n-2]$, and $x[n-3]$ as well as by the past output values $y[n-1]$, $y[n-2]$, and $y[n-3]$. The output is therefore determined iteratively or recursively from its past values. To compute the present output of this third-order system, we use the past three values of the output. In general, for an Nth-order system we use the past N values of the output. Such a system is called a *recursive system*.

An interesting feature of a recursive system is that once an output exists, it tends to propagate itself forever because of its recursive nature. This is also seen from the realizations of $H[z]$ shown in Fig. 11.8. Once an input (any input) is applied, the feedback connections loop the output continuously back into the system, and the output continues forever. This propagation of the output in perpetuity occurs because of the nonzero values of coefficients $a_1, a_2, \ldots, a_N$. These coefficients [appearing in the denominator of $H[z]$ in Eq. (12.10)] are the *recursive coefficients*. The coefficients $b_0, b_1, \ldots, b_N$ (appearing in the numerator of $H[z]$) are the *nonrecursive coefficients*. If an input $\delta[n]$ is applied at the input of a recursive filter, the response $h[n]$ will continue forever up to $n = \infty$. For this reason, recursive filters are also known as *infinite impulse response* (IIR) filters.

Nonrecursive Filters

If the recursive coefficients a_1, a_2, and a_3 are zero, $H[z]$ in Eq. (12.10)) reduces to

$$H[z] = \frac{b_0 z^3 + b_1 z^2 b_2 z + b_3}{z^3} = b_0 + \frac{b_1}{z} + \frac{b_2}{z^2} + \frac{b_3}{z^3}$$

The difference equation corresponding to this system now reduces to

$$y[n] = b_0 x[n] + b_1 x[n-1] + b_2 x[n-2] + b_3 x[n-3]$$

Note that $y[n]$ is now computed from the present and three past values of the input $x[n]$. Such filters are called *nonrecursive filters*. The realizations of nonrecursive filters are identical to the realizations of recursive filters (see Fig. 11.8) except that all feedback paths are eliminated (since the recursive coefficients are zero). If we apply an input $x[n] = \delta[n]$ to this system, the input will pass through the system and will be completely out of the system by $n = 4$. There are no feedback connections to perpetuate the output. Therefore, $h[n]$ will be nonzero only for $n = 0, 1, 2$, and 3. For an Nth-order nonrecursive filter, $h[n]$ is zero for $n > N$. Therefore, the duration of $h[n]$ is

finite for a nonrecursive filter. For this reason, nonrecursive filters are also known as *finite impulse response* (FIR) filters. Nonrecursive filters are a special case of recursive filters, in which all the recursive coefficients $a_1, a_2, \ldots, a_N$ are zero.

An Nth-order nonrecursive filter transfer function is given by ($a_1 = a_2 = \cdots = a_N = 0$)

$$H[z] = \frac{b_0 z^N + b_1 z^{N-1} + \cdots + b_{N-1} z + b_N}{z^n}$$
$$= b_0 + \frac{b_1}{z} + \frac{b_2}{z^2} + \cdots + \frac{b_{N-1}}{z^{N-1}} + \frac{b_N}{z^N}$$

The inverse z-transform of this equation yields

$$h[n] = b_0\delta[n] + b_1\delta[n-1] + \cdots + b_{N-1}\delta[n-N+1] + b_N\delta[n-N]$$

Observe that $h[n] = 0$ for $n > N$.

Because nonrecursive filters are a special case of recursive filters, we expect the performance of recursive filters to be superior. This expectation is true in the sense that a given amplitude response can be achieved by a recursive filter of an order smaller than that required for the corresponding nonrecursive filter. However, nonrecursive filters have the advantage that they can be designed to have linear-phase characteristics. Recursive filters can realize linear phase only approximately.

12.4 Filter Design Criteria

A digital filter processes discrete-time signals to yield a discrete-time output. Digital filters can also process analog signals by converting them into discrete-time signals. If the input is a continuous-time signal $x(t)$, it is converted into a discrete-time signal $x[n] = x(nT)$ by a C/D (continuous-time to discrete-time) converter. The signal $x[n]$ is now processed by a "digital" (meaning discrete-time) system with transfer function $H[z]$. The output $y[n]$ of $H[z]$ is then converted into an "analog" (meaning continuous-time) signal $y(t)$. The system in Fig. 12.9a, therefore, acts as a continuous-time (or "analog") system. Our objective is to determine the "digital" (discrete-time) processor $H[z]$ that will make the system in Fig. 12.9a equivalent to a desired "analog" (continuous-time) system with transfer function $H_a(s)$, shown in Fig. 12.9b.

We may strive to make the two systems behave similarly in the time domain or in the frequency domain. Accordingly, we have two different design procedures. Let us now determine the equivalence criterion of the two systems in the time domain and in the frequency domain.

12.4.1 Time-Domain Equivalence Criterion

By time-domain equivalence, we mean that for the same input $x(t)$, the output $y(t)$ of the system in Fig. 12.9a is equal to the output $y(t)$ of the system in Fig. 12.9b. Therefore, $y(nT)$, the samples of the output in Fig. 12.9b, are identical to $y[n]$, the output of $H[z]$ in Fig. 12.9a.

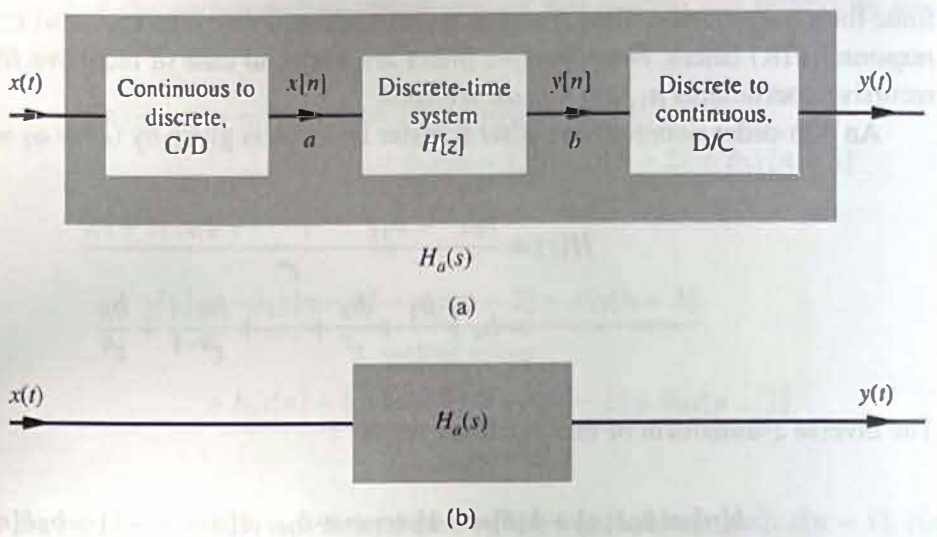

Figure 12.9 Analog filter realization with a digital filter.

The output $y(t)$ of the system in Fig. 12.9b is

$$y(t) = \int_{-\infty}^{\infty} x(\tau)h_a(t-\tau)\,d\tau = \lim_{\Delta\tau\to 0} \sum_{m=-\infty}^{\infty} x(m\Delta\tau)h_a(t-m\Delta\tau)\Delta\tau$$

For our purpose, it is convenient to use the notation T for $\Delta\tau$. Assuming T (the sampling interval) to be small enough, such a change of notation yields

$$y(t) = T\sum_{m=-\infty}^{\infty} x(mT)h_a(t-mT)$$

The response at the nth sampling instant is $y(nT)$ obtained by setting $t = nT$ in the equation as

$$y(nT) = T\sum_{m=-\infty}^{\infty} x(mT)h_a[(n-m)T] \tag{12.11}$$

In Fig. 12.9a, the input to $H[z]$ is $x(nT) = x[n]$. If $h[n]$ is the unit impulse response of $H[z]$, then $y[n]$, the output of $H[z]$, is given by

$$y[n] = \sum_{m=-\infty}^{\infty} x[m]h[n-m] \tag{12.12}$$

If the two systems are to be equivalent, $y(nT)$ in Eq. (12.11) must be equal to $y[n]$ in Eq. (12.12). Therefore,

$$h[n] = Th_a(nT) \tag{12.13}$$

This is the time-domain criterion for equivalence of the two systems.† According to this criterion, $h[n]$, the unit impulse response of $H[z]$ in Fig. 12.9a should be T times the samples of $h_a(t)$, the unit impulse response of the system in Fig. 12.9b. This is known as the *impulse invariance criterion* of filter design.

12.4.2 Frequency-Domain Equivalence Criterion

In Sec. 2.4.4 [Eq. (2.38)], we proved that for an analog system with transfer function $H_a(s)$, the system response $y(t)$ to the everlasting exponential input $x(t) = e^{st}$ is also an everlasting exponential

$$y(t) = H_a(s)e^{st} \tag{12.14}$$

Similarly, in Eq. (9.25), we showed that for a discrete-time system with transfer function $H[z]$, the system response $y[n]$ to an everlasting exponential input $x[n] = z^n$ is also an everlasting exponential $H[z]z^n$; that is,

$$y[n] = H[z]z^n$$

If the systems in Figs. 12.9a and 12.9b are equivalent, then the response of both systems to an everlasting exponential input $x(t) = e^{st}$ should be the same. A continuous-time signal $x(t) = e^{st}$ sampled every T seconds results in a discrete-time signal

$$x[n] = e^{snT} = z^n \qquad \text{with } z = e^{sT}$$

This discrete-time exponential z^n is applied at the input of $H[z]$ in Fig. 12.9a, whose response is

$$y[n] = H[z]z^n|_{z=e^{sT}} = H[e^{sT}]e^{snT} \tag{12.15}$$

Now, for the system in Fig. 12.9b, $y(nT)$, the nth sample of the output $y(t)$ in Eq. (12.14), is

$$y(nT) = H_a(s)e^{snT} \tag{12.16}$$

If the two systems are to be equivalent, a necessary condition is that $y[n]$ in Eq. (12.15) must be equal to $y(nT)$ in Eq. (12.16). This condition means that

$$H[e^{sT}] = H_a(s) \tag{12.17}$$

This is the frequency-domain criterion for equivalence of the two systems. It should be remembered, however, that with this criterion we are ensuring only that the digital filter's response matches exactly that of the desired analog filter at sampling instants. If we want the two responses to match at every value of t, we must have $T \to 0$. Therefore,

$$\lim_{T\to 0} H[e^{sT}] = H_a(s) \tag{12.18}$$

† Because T is a constant, some authors ignore the factor T, which yields a simplified criterion $h[n] = h_a(nT)$. Ignoring T merely scales the amplitude response of the resulting filter.

A Practical Difficulty

Both of these criteria for filter design require the condition $T \to 0$ for realizing a digital filter equivalent to a given analog filter. However, this condition is impossible in practice because it necessitates an infinite sampling rate, resulting in an infinite data rate. In practice, we must choose a small but nonzero T to achieve a compromise between the two conflicting requirements, namely, closeness of approximation and system cost.

This approximation, however, does not mean that the system in Fig. 12.9a is inferior to that in Fig. 12.9b, because often $H_a(s)$ itself is an approximation to what we are seeking. For example, in lowpass filter design we strive to design a system with ideal lowpass characteristics. Failing that, however, we settle for some approximation such as Butterworth lowpass transfer functions. In fact, it is entirely possible that $H[z]$, which is an approximation of $H_a(s)$, may be a better approximation of the desired characteristics than is $H_a(s)$ itself.

12.5 Recursive Filter Design by the Time-Domain Criterion: The Impulse Invariance Method

The time-domain design criterion for the equivalence of the systems in Figs. 12.9a and 12.9b is [see Eq. (12.13)]

$$h[n] = \lim_{T \to 0} Th_a(nT) \tag{12.19}$$

where $h[n]$ is the unit impulse response of $H[z]$, $h_a(t)$ is the unit impulse response of $H_a(s)$, and T is the sampling interval in Fig. 12.9a.

As indicated earlier, it is impractical to let $T \to 0$. In practice, T is chosen to be small but nonzero. We have already discussed the effect of aliasing and the consequent distortion in the frequency response caused by nonzero T. Assuming that we have selected a suitable value of T, we can ignore the condition $T \to 0$, and Eq. (12.19) can be expressed as

$$h[n] = Th_a(nT) \tag{12.20}$$

The z-transform of this equation yields

$$H[z] = T\mathcal{Z}\{h_a(nT)\} \tag{12.21}$$

This result yields the desired transfer function $H[z]$.

Let us consider a first-order transfer function

$$H_a(s) = \frac{c}{s - \lambda}$$

Taking the inverse Laplace transform of $H_a(s)$, the impulse response of this filter is

$$h_a(t) = ce^{\lambda t}u(t)$$

The corresponding digital filter unit impulse response is given by Eq. (12.20) as

$$h[n] = Th_a(nT) = Tce^{n\lambda T}$$

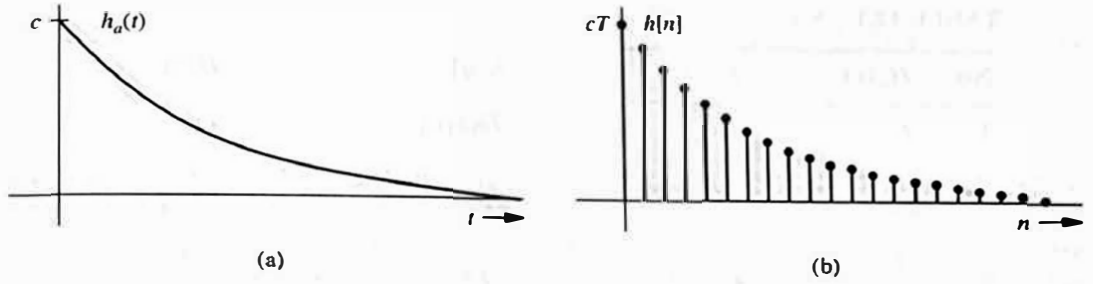

Figure 12.10 Impulse responses for analog and digital systems in the impulse invariance method of filter design.

Figures 12.10a and 12.10b show $h_a(t)$ and $h[n]$.

According to Eq. (12.21), $H[z]$ is T times the z-transform of $h[n]$. Thus,

$$H[z] = \frac{Tcz}{z - e^{\lambda T}} \tag{12.22}$$

The procedure of finding $H[z]$ can be systematized for any Nth-order system. First we express an Nth-order analog transfer function $H_a(s)$ as a sum of partial fractions as†

$$H_a(s) = \sum_{i=1}^{N} \frac{c_i}{s - \lambda_i}$$

Then the corresponding $H[z]$ is given by

$$H[z] = T \sum_{i=1}^{N} \frac{c_i z}{z - e^{\lambda_i T}}$$

This transfer function can be readily realized, as explained in Sec. 11.4. Table 12.1 lists several pairs of $H_a(s)$ and their corresponding $H[z]$. For instance, to realize a digital integrator, we examine its $H_a(s) = 1/s$. From Table 12.1, corresponding to $H_a(s) = 1/s$ (pair 2), we find $H[z] = Tz/(z-1)$. This is exactly the result we obtained in Ex. 8.13 using another approach. Note that the frequency response $H_a(j\omega)$ of a practical analog filter cannot be bandlimited. Consequently, all these realizations are approximate.

Choosing the Sampling Interval T

The impulse-invariance criterion (12.13) was derived under the assumption that $T \to 0$. Such an assumption is neither practical nor necessary for satisfactory design. The avoidance of aliasing is the most important consideration for the choice of T. In Eq. (8.7), we showed that for a sampling interval T seconds, the highest frequency that can be sampled without aliasing is $1/2T$ Hz or π/T radians per second. This implies that $H_a(j\omega)$, the frequency response of the analog filter in

† Assuming $H_a(s)$ has simple poles. For repeated poles, the form changes accordingly. Entry 6 in Table 12.1 is suitable for repeated poles.

TABLE 12.1 Select Impulse Invariance Pairs

No.	$H_a(s)$	$h_a(t)$	$h[n]$	$H[z]$
1	K	$K\delta(t)$	$TK\delta[n]$	TK
2	$\frac{1}{s}$	$u(t)$	$Tu[n]$	$\frac{Tz}{z-1}$
3	$\frac{1}{s^2}$	t	nT^2	$\frac{T^2z}{(z-1)^2}$
4	$\frac{1}{s^3}$	$\frac{t^2}{2}$	$\frac{k^2T^3}{2}$	$\frac{T^3z(z+1)}{2(z-1)^3}$
5	$\frac{1}{s-\lambda}$	$e^{\lambda t}$	$Te^{\lambda nT}$	$\frac{Tz}{z-e^{\lambda T}}$
6	$\frac{1}{(s-\lambda)^2}$	$te^{\lambda t}$	$nT^2e^{\lambda nT}$	$\frac{T^2ze^{\lambda T}}{(z-e^{\lambda T})^2}$
7	$\frac{As+B}{s^2+2as+c}$	$Tre^{-at}\cos(bt+\theta)$	$Tre^{-anT}\cos(bnT+\theta)$	$\frac{Trz[z\cos\theta - e^{-aT}\cos(bT-\theta)]}{z^2-(2e^{-aT}\cos bT)z+e^{-2aT}}$
	$r=\sqrt{\frac{A^2c+B^2-2ABa}{c-a^2}}$,	$b=\sqrt{c-a^2}$,	$\theta=\tan^{-1}\left(\frac{Aa-B}{A\sqrt{c-a^2}}\right)$	

Fig. 12.9b, should not have spectral components beyond frequency π/T radians per second. In other words, to avoid aliasing, the frequency response of the system $H_a(s)$ must be bandlimited to π/T radians per second. As shown in Ch. 4, the frequency response of a realizable LTIC system cannot be bandlimited; that is, the response generally exists for all frequencies up to ∞. Therefore, it is impossible to digitally realize an LTIC system exactly without aliasing. The saving grace is that the frequency response of every realizable LTIC system decays with frequency. This allows for a compromise in digitally realizing an LTIC system with an acceptable level of aliasing. The smaller the value of T, the smaller the aliasing, and the better the approximation. Since it is impossible to make $|H_a(j\omega)|$ zero, we are satisfied with making it negligible beyond the frequency π/T. As a rule of thumb [1], we choose T such that $|H_a(j\omega)|$ at the frequency $\omega=\pi/T$ is less than a certain fraction (often taken as 1%) of the peak value of $|H_a(j\omega)|$. This ensures that aliasing is negligible. The peak $|H_a(j\omega)|$ usually occurs at $\omega=0$ for lowpass filters and at the band center frequency ω_c for bandpass filters.

EXAMPLE 12.4 Butterworth Filter Design by the Impulse-Invariance Method

Design a digital filter to realize a first-order lowpass Butterworth filter with the transfer function

$$H_a(s)=\frac{\omega_c}{s+\omega_c} \qquad \omega_c=10^5 \tag{12.23}$$

For this filter, we find the corresponding $H[z]$ according to Eq. (12.22) (or pair 5 in Table 12.1) as

$$H[z] = \frac{\omega_c T z}{z - e^{-\omega_c T}} \tag{12.24}$$

Next, we select the value of T by means of the criterion according to which the gain at $\omega = \pi/T$ drops to 1% of the maximum filter gain. However, this choice results in such a good design that aliasing is imperceptible. The resulting amplitude response is so close to the desired response that we can hardly notice the aliasing effect in our plot. For the sake of demonstrating the aliasing effect, we shall deliberately select a 10% criterion (instead of 1%). We have

$$|H_a(j\omega)| = \left| \frac{\omega_c}{\sqrt{\omega^2 + \omega_c^2}} \right|$$

In this case, $|H_a(j\omega)|_{\text{max}} = 1$, which occurs at $\omega = 0$. Use of 10% criterion leads to $|H_a(\pi/T)| = 0.1$. Observe that

$$|H_a(j\omega)| \approx \frac{\omega_c}{\omega} \qquad \omega \gg \omega_c$$

Hence,

$$|H_a(\pi/T)| \approx \frac{\omega_c}{\pi/T} = 0.1 \quad \Longrightarrow \quad \pi/T = 10\omega_c = 10^6$$

Thus, the 10% criterion yields $T = 10^{-6}\pi$. The 1% criterion would have given $T = 10^{-7}\pi$. Substitution of $T = 10^{-6}\pi$ in Eq. (12.24) yields

$$H[z] = \frac{0.3142z}{z - 0.7304} \tag{12.25}$$

A canonical realization of this filter is shown in Fig. 12.11a.

To find the frequency response of this digital filter, we rewrite $H[z]$ as

$$H[z] = \frac{0.3142}{1 - 0.7304z^{-1}}$$

Therefore,

$$H[e^{j\omega T}] = \frac{0.3142}{1 - 0.7304e^{-j\omega T}} = \frac{0.3142}{(1 - 0.7304\cos\omega T) + j0.7304\sin\omega T}$$

The corresponding magnitude response is

$$\begin{aligned} |H[e^{j\omega T}]| &= \frac{0.3142}{\sqrt{(1 - 0.7304\cos\omega T)^2 + (0.7304\sin\omega T)^2}} \\ &= \frac{0.3142}{\sqrt{1.533 - 1.4608\cos\omega T}} \end{aligned} \tag{12.26}$$

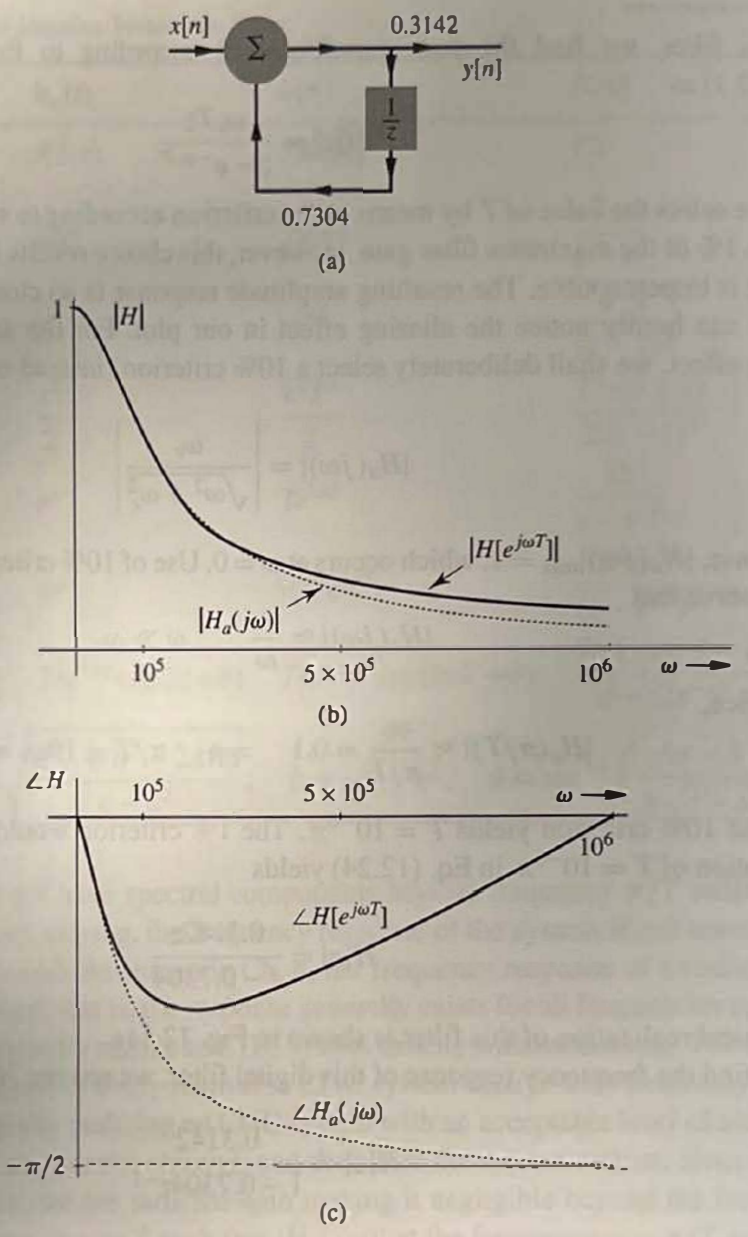

Figure 12.11 An example of filter design by the impulse invariance method: (a) filter realization, (b) amplitude response, and (c) phase response.

and the phase response is

$$\angle H[e^{j\omega T}] = -\tan^{-1}\left(\frac{0.7304\sin\omega T}{1-0.7304\cos\omega T}\right) \tag{12.27}$$

This frequency response differs from the desired response $H_a(j\omega)$ because aliasing causes frequencies above π/T to appear as frequencies below π/T. This generally results in increased gain for frequencies below π/T. For instance, the realized filter gain at $\omega = 0$ is $H[e^{j0}] = H[1]$. This value, as obtained from Eq. (12.25), is 1.1654 instead of the desired value 1. We can partly compensate for this distortion by multiplying $H[z]$ or $H[e^{j\omega T}]$ by a normalizing constant

$K = H_a(0)/H[1] = 1/1.1654 = 0.858$. This forces the resulting gain of $H[e^{j\omega T}]$ to be equal to 1 at $\omega = 0$. The normalized $H_n[z] = 0.858H[z] = 0.858(0.1\pi z/(z - 0.7304))$. The amplitude response in Eq. (12.26) is multiplied by $K = 0.858$ and plotted in Fig. 12.11b over the frequency range $0 \le \omega \le \pi/T = 10^6$. The multiplying constant K has no effect on the phase response in Eq. (12.27), which is shown in Fig. 12.11c.

Also, the desired frequency response, according to Eq. (12.23) with $\omega_c = 10^5$, is

$$H_a(j\omega) = \frac{\omega_c}{j\omega + \omega_c} = \frac{10^5}{j\omega + 10^5}$$

Therefore,

$$|H_a(j\omega)| = \frac{10^5}{\sqrt{\omega^2 + 10^{10}}} \quad \text{and} \quad \angle H_a(j\omega) = -\tan^{-1}\frac{\omega}{10^5}$$

This desired amplitude and phase response are plotted (dotted) in Figs. 12.11b and 12.11c for comparison with the realized digital filter response. Observe that the amplitude response behavior of the analog and the digital filter is very close over the range $\omega \le \omega_c = 10^5$. However, for higher frequencies, there is considerable aliasing, especially in the phase spectrum. Had we used the 1% rule, the realized frequency response would have been closer over another decade of the frequency range.

Impulse Invariance by MATLAB

We can readily use the MATLAB `impinvar` command to confirm our digital filter designed by the impulse-invariance method.

```
>> omegac = 10^5; Ba = [omegac]; Aa = [1 omegac]; Fs = 10^6/pi;
>> [B,A] = impinvar(Ba,Aa,Fs)
   B = 0.3142
   A = 1.0000  -0.7304
```

This confirms our earlier result of Eq. (12.25) that the digital filter transfer function is

$$H[z] = \frac{0.3142z}{z - 0.7304}$$

DRILL 12.4 Filter Design by the Impulse-Invariance Method

Design a digital filter to realize an analog transfer function

$$H_a(s) = \frac{20}{s + 20}$$

ANSWER

$$H[z] = \frac{20Tz}{z - e^{-20T}} \text{ with } T = \frac{\pi}{2000}$$

Limitations of the Impulse Invariance Method

The impulse invariance method is handicapped by aliasing. Consequently, this method can be used to design filters where $H_a(j\omega)$ becomes negligible beyond some frequency B Hz. This condition restricts the procedure to lowpass and bandpass filters. The impulse invariance method cannot be used for true highpass or bandstop filters. Moreover, to reduce aliasing effects, the sampling rate has to be very high, which makes its implementation costly. In general, the frequency-domain method discussed in the next section is superior to the impulse invariance method.

12.6 Recursive Filter Design by the Frequency-Domain Criterion: The Bilinear Transformation Method

The bilinear transformation method discussed in this section is preferable to the impulse invariance method in filtering problems where the gains are constant over certain bands (piecewise constant amplitude response). This condition exists in lowpass, bandpass, highpass, and bandstop filters. Moreover, this method requires a lower sampling rate compared to the impulse invariance method because of the absence of aliasing errors in the filter design process. In addition, the filter rolloff characteristics are sharper with this method compared to those obtained using the impulse invariance method. The absence of aliasing is the result of one-to-one mapping from the s plane to the z plane inherent in this method.

The frequency-domain design criterion is [see Eq. (12.18)]

$$\lim_{T\to 0} H[e^{sT}] = H_a(s) \tag{12.28}$$

Let us consider the following power series for the hyperbolic tangent (see Sec. B.8.5):

$$\tanh\left(\frac{sT}{2}\right) \equiv \frac{e^{sT/2}-e^{-sT/2}}{e^{sT/2}+e^{-sT/2}} = \left[\frac{sT}{2} - \frac{1}{3}\left(\frac{sT}{2}\right)^3 + \frac{2}{15}\left(\frac{sT}{2}\right)^5 + \cdots\right]$$

For small T ($T \to 0$), we can ignore the higher-order terms in the infinite series on the right-hand side to yield

$$\lim_{T\to 0}\left(\frac{e^{sT/2}-e^{-sT/2}}{e^{sT/2}+e^{-sT/2}}\right) = \frac{sT}{2}$$

Therefore, as $T \to 0$,

$$s = \left(\frac{2}{T}\right)\frac{e^{sT/2}-e^{-sT/2}}{e^{sT/2}+e^{-sT/2}} = \left(\frac{2}{T}\right)\frac{e^{sT}-1}{e^{sT}+1}$$

Equation (12.28) now can be expressed as

$$H[e^{sT}] = H_a\left(\frac{2}{T}\,\frac{e^{sT}-1}{e^{sT}+1}\right) \tag{12.29}$$

From this result, it follows that

$$H[z] = H_a\left(\frac{2}{T}\frac{z-1}{z+1}\right) = H_a(s)|_{s=\frac{2}{T}\frac{z-1}{z+1}}$$

Therefore, we can obtain $H[z]$ from $H_a(s)$ by using the transformation†

$$s = \left(\frac{2}{T}\right)\frac{z-1}{z+1} \tag{12.30}$$

This transformation is known as the *bilinear transformation*.

Choice of T in the Bilinear Transformation

Because of the absence of aliasing in the bilinear transformation method, the value of the sampling interval T can be much smaller compared to the impulse invariance method. By the absence of aliasing, we mean only an absence of aliasing in transforming the analog filter into the digital filter. Signal aliasing, which limits the highest usable frequency, is still present. Thus if the highest frequency to be processed is f_h Hz, then to avoid signal aliasing, we must still follow [see Eq. (8.7)]

$$T < \frac{1}{2f_h} \tag{12.31}$$

EXAMPLE 12.5 Butterworth Filter Design by the Bilinear Transformation Method

Using the bilinear transformation, synthesize

$$H_a(s) = \frac{\omega_c}{s+\omega_c} \qquad \omega_c = 10^5$$

From Eq. (12.30), we obtain

$$H[z] = \frac{\omega_c}{\left(\frac{2}{T}\frac{z-1}{z+1}\right)+\omega_c} = \frac{\omega_c T\,(z+1)}{(2+\omega_c T)z-(2-\omega_c T)}$$

Ordinarily, we should use Eq. (12.31) to select a suitable value for T. However, to facilitate comparison with the impulse invariance method, we choose here the same value $T = \frac{\pi}{10\omega_c}$ as that in Ex. 12.4. The substitution of $\omega_c T = \pi/10$ in the above equation yields

---

† There exist other transformations that can be used to derive $H[z]$ from $H_a(s)$. Taking the first two terms of the power series $e^{-sT} = 1 - sT + \frac{1}{2}(sT)^2 - \frac{1}{3}(sT)^3 + \cdots$ results in $s = \frac{1}{T}(1 - e^{-sT})$ from which we obtain the transformation $s = \frac{1}{T}(1 - \frac{1}{z}) = \frac{z-1}{Tz}$. Similarly, a power series for e^{sT} yields $s = \frac{1}{T}(z - 1)$. Although these simple transformations work reasonably well for lowpass and bandpass filters, they cannot be used for highpass and bandstop filters and are, in any case, inferior to the bilinear transformation.

$$H[z] = 0.1358\left(\frac{z+1}{z-0.7285}\right)$$

Hence,

$$H[e^{j\omega T}] = \frac{0.1358(e^{j\omega T}+1)}{e^{j\omega T}-0.7285}$$
$$= \frac{0.1358(\cos\omega T + 1 + j\sin\omega T)}{\cos\omega T - 0.7285 + j\sin\omega T} \qquad T = \pi \times 10^{-6}$$

From this, we obtain

$$|H[e^{j\omega T}]| = \left[\frac{0.024(1+\cos\omega T)}{1-0.9518\cos\omega T}\right]^{1/2} \qquad T = \pi \times 10^{-6}$$

and

$$\angle H[e^{j\omega T}] = \tan^{-1}\frac{\sin\omega T}{1+\cos\omega T} - \tan^{-1}\frac{\sin\omega T}{\cos\omega T - 0.7285}$$

Figure 12.12 shows the resulting magnitude response $|H|$ and phase response $\angle H$. Comparing these curves with the filter characteristics shown in Fig. 12.11, we see that the bilinear transformation produces superior results to the impulse invariance method.

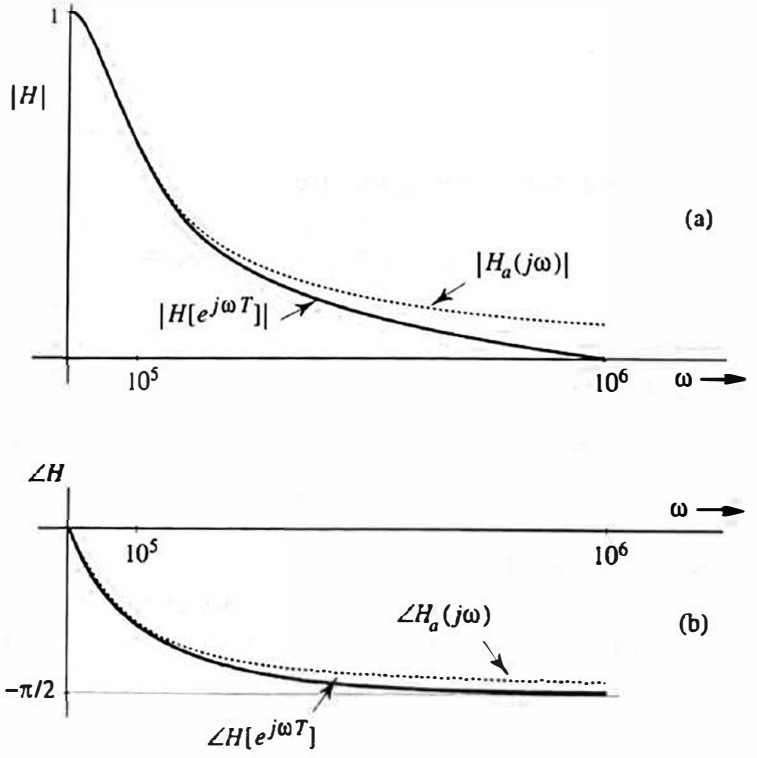

Figure 12.12 Bilinear transformation method of design: (**a**) amplitude response and (**b**) phase response.

Bilinear Transformation by MATLAB

We can readily use the MATLAB `bilinear` command to confirm our digital filter designed by the bilinear transformation method. Since $T = 10^{-6}\pi$ in this case, the sampling frequency is $f_s = 10^6/\pi$.

```
>> omegac = 10^5; Ba = [omegac]; Aa = [1 omegac]; Fs = 10^6/pi;
>> [B,A] = impinvar(Ba,Aa,Fs)
   B = 0.1358    0.1358
   A = 1.0000   -0.7285
```

This confirms our earlier result that the digital filter transfer function is

$$H[z] = 0.1358\left(\frac{z+1}{z-0.7285}\right)$$

Frequency Warping Inherent in the Bilinear Transformation

Figure 12.12 shows that $|H[e^{j\omega T}]| \simeq |H_a(j\omega)|$ for small ω. For large values of ω, the error increases. Moreover, $|H[e^{j\omega T}]| = 0$ at $\omega = \pi/T$. In fact, it appears as if the entire frequency band (0 to ∞) in $|H_a(j\omega)|$ is compressed within the range $(0, \frac{\pi}{T})$ in $H[e^{j\omega T}]$. Such warping of the frequency scale is peculiar to this transformation. To understand this behavior, consider Eq. (12.29) with $s = j\omega$:

$$H[e^{j\omega T}] = H_a\left(\frac{2}{T}\frac{e^{j\omega T}-1}{e^{j\omega T}+1}\right) = H_a\left(\frac{2}{T}\frac{e^{\frac{j\omega T}{2}}-e^{\frac{-j\omega T}{2}}}{e^{\frac{j\omega T}{2}}+e^{\frac{-j\omega T}{2}}}\right) = H_a\left(j\tfrac{2}{T}\tan\tfrac{\omega T}{2}\right)$$

Therefore, the response of the resulting digital filter at some frequency ω_d is

$$H[e^{j\omega_d T}] = H_a\left(j\tfrac{2}{T}\tan\tfrac{\omega_d T}{2}\right) = H_a(j\omega_a)$$

where

$$\omega_a = \frac{2}{T}\tan\frac{\omega_d T}{2} \tag{12.32}$$

Thus, in the resulting digital filter, the behavior of the desired response $H_a(j\omega)$ at some frequency ω_a appears not at ω_a but at frequency ω_d, where [from Eq. (12.32)]

$$\omega_d = \frac{2}{T}\tan^{-1}\frac{\omega_a T}{2}$$

Figure 12.13a shows the plot of ω_d as a function of ω_a. For small ω_a, the curve in Fig. 12.13a is practically linear, so $\omega_d \simeq \omega_a$. At higher values of ω_a, there is considerable diversion in the values of ω_a and ω_d. Thus, the digital filter imitates the desired analog filter at low frequencies, but at higher frequencies there is considerable distortion. Using this method, if we are trying to synthesize a filter to realize $H_a(j\omega)$ depicted in Fig. 12.13b, the resulting digital filter frequency response will be warped, as illustrated in Fig. 12.13c. The analog filter behavior in the entire range

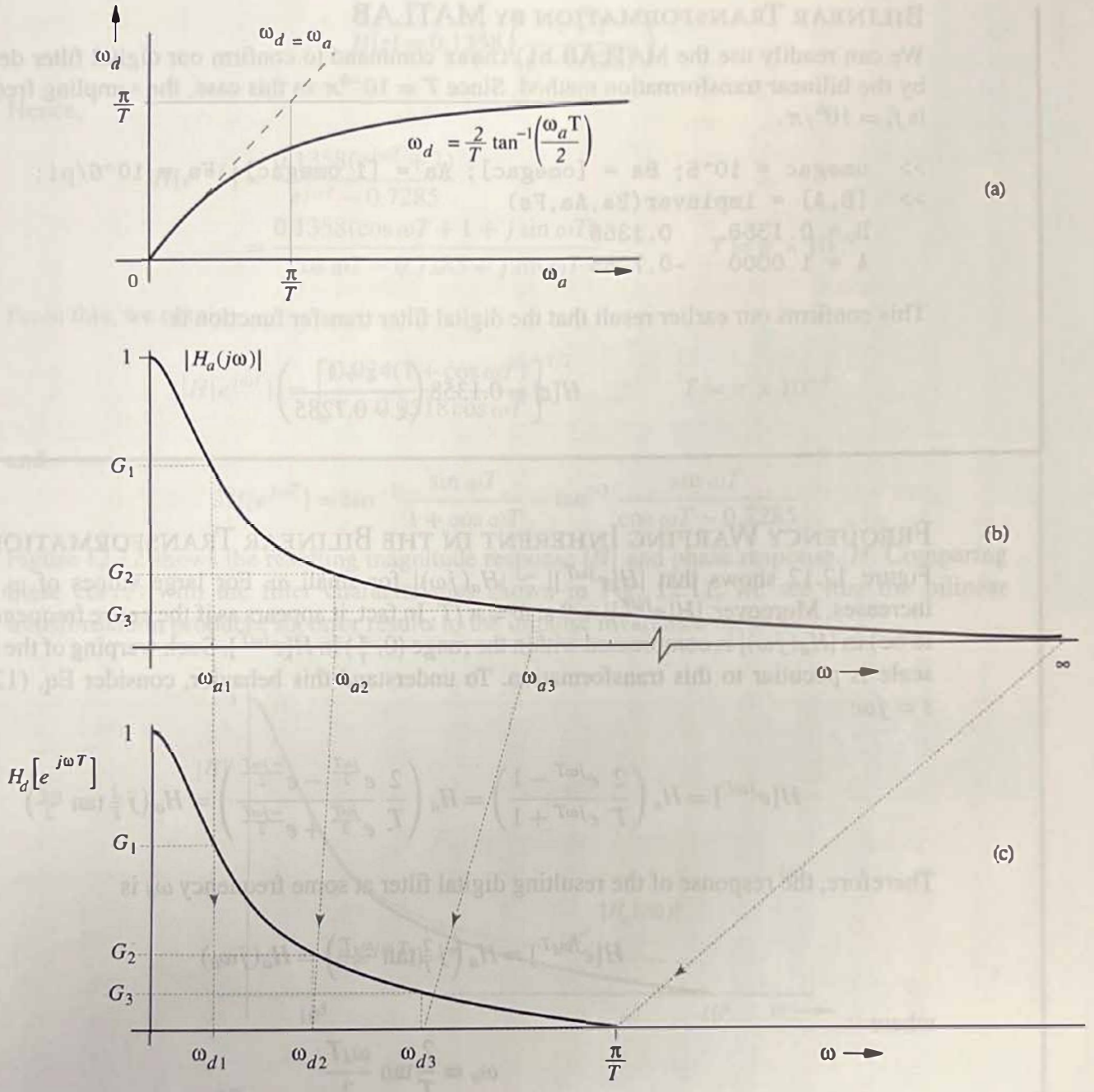

Figure 12.13 Frequency warping in the bilinear transformation: (**a**) mapping relationship of analog and digital frequencies, (**b**) analog response, and (**c**) corresponding digital response.

of ω_a from 0 to ∞ is compressed in the digital filter in the range of ω_d from 0 to π/T. This is as if a promising 20-year-old man, who, after learning that he has only a year to live, tries to crowd his last year with every possible adventure, passion, and sensation that a normal human being would have experienced in an entire lifetime. This compression and frequency warping effect is a peculiarity of the bilinear transformation.

There are two ways of overcoming frequency warping. The first is to reduce T (increase the sampling rate) so that the signal bandwidth is kept well below $\frac{\pi}{T}$ and $\omega_a \simeq \omega_d$ over the desired frequency band. This step is easy to execute, but it requires a higher sampling rate (lower T)

than necessary. The second approach, known as *prewarping*, solves the problem without unduly reducing T.

12.6.1 Bilinear Transformation Method with Prewarping

In prewarping, we start not with the desired $H_a(j\omega)$ but with a prewarped $H_a(j\omega)$ in such a way that the warping of the bilinear transformation will compensate for the prewarping exactly. The idea here is to begin with a distorted analog filter (prewarping) so that the distortion caused by bilinear transformation will be canceled by the built-in (prewarping) distortion. The idea is similar to the one used in prestressed concrete, in which a concrete beam is precompressed initially. When loaded, the beam experiences tension, which is canceled by the built-in compression.

Usually, prewarping is done at certain critical frequencies rather than over the entire band. The final filter behavior is exactly equal to the desired behavior at these selected frequencies. Such a filter is adequate for most filtering problems if we choose the critical frequencies properly.

If we require a filter to have gains $G_1, G_2, \ldots, G_m$ at frequencies (critical frequencies) $\omega_1, \omega_2, \ldots, \omega_m$ respectively, then we must start with an analog filter $H'(j\omega)$ that has gains $G_1, G_2, \ldots, G_m$ at frequencies $\omega_1', \omega_2', \ldots, \omega_m'$ respectively, where

$$\omega_i' = \frac{2}{T}\tan\frac{\omega_i T}{2} \qquad i = 1,2,\cdots,m \tag{12.33}$$

This results in prewarped filter $H'(j\omega)$. Application of the bilinear transformation of Eq. (12.30) to this filter yields the desired digital filter that has gains $G_1, G_2, \ldots, G_m$ at frequencies $\omega_1, \omega_2, \ldots, \omega_m$, respectively. This is because, according to Eq. (12.32), the behavior of the analog filter at a frequency ω_i' appears in the digital filter at frequency

$$\frac{2}{T}\tan^{-1}\left(\frac{\omega_i' T}{2}\right) = \frac{2}{T}\tan^{-1}\left[\tan\left(\frac{\omega_i T}{2}\right)\right] = \omega_i$$

We clarify these ideas with an example of a lowpass Butterworth filter.

EXAMPLE 12.6 Bilinear Transformation with Prewarping: Butterworth Lowpass Filter

Design a Butterworth lowpass filter with the following specifications: a gain of unity at $\omega = 0$, a gain no less than -2 dB ($G_p = 0.785$) over the passband $0 \le \omega \le 10$, and a gain no greater than -11 dB ($G_s = 0.2818$) over the stopband $\omega \ge 15$. The highest frequency to be processed is $\omega_h = 35$ rad/s, which yields $T \le \pi/35$. Let us use $T = \pi/35$.

For this design, the Butterworth specifications are $\omega_p = 8$, $\omega_s = 15$, $\hat{G}_p = -2$ dB, and $\hat{G}_s = -11$ dB. In the first step, we prewarp the critical frequencies ω_p and ω_s. According to Eq. (12.33), we obtain

$$\omega_p' = \frac{2}{T}\tan\frac{\omega_p T}{2} = \frac{70}{\pi}\tan\left(\frac{4\pi}{35}\right) = 8.3623$$

and

$$\omega_s' = \frac{2}{T}\tan\frac{\omega_s T}{2} = \frac{70}{\pi}\tan\left(\frac{15\pi}{70}\right) = 17.7696$$

In the second step, we design a Butterworth filter with critical frequencies $\omega_p' = 8.3623$ and $\omega_s' = 17.7696$ with $\hat{G}_p = -2$ dB and $\hat{G}_s = -11$ dB. The filter order N is obtained from Eq. (7.28) as

$$N = \frac{\log[(10^{1.1}-1)/(10^{0.2}-1)]}{2\log(17.7696/8.3623)} = 1.9405$$

We round up the value of N to 2. There are two possible values of ω'_c. We shall choose the one given by Eq. (7.30), which satisfies the stopband specifications exactly but oversatisfies the passband. This choice yields a 3 dB cutoff frequency ω_c' as

$$\omega_c' = \frac{17.7696}{(10^{1.1}-1)^{\frac{1}{4}}} = 9.6308$$

From Table 7.1, we find the prewarped filter transfer function $H_a(s)$ for $N = 2$ and $\omega_c' = 9.6308$ as

$$H_a(s) = \frac{1}{\left(\frac{s}{9.6308}\right)^2 + \sqrt{2}\left(\frac{s}{9.6308}\right) + 1} = \frac{92.7529}{s^2 + 13.62s + 92.7529}$$

Finally, we obtain $H[z]$ from $H_a(s)$ using the bilinear transformation

$$s = \left(\frac{2}{T}\right)\frac{z-1}{z+1} = \left(\frac{70}{\pi}\right)\frac{z-1}{z+1}$$

This substitution yields

$$\begin{aligned} H[z] &= H_a(s)\big|_{s=\left(\frac{70}{\pi}\right)\frac{z-1}{z+1}} \\ &= \frac{92.7529}{s^2 + 13.62s + 92.7529}\bigg|_{s=\left(\frac{70}{\pi}\right)\frac{z-1}{z+1}} \\ &= \frac{0.1039(z+1)^2}{z^2 - 0.9045z + 0.3201} \end{aligned}$$

The frequency response of this filter is given by

$$H\left[e^{j\omega T}\right] = \frac{0.1039(e^{j\omega T}+1)^2}{e^{j2\omega T} - 0.9045e^{j\omega T} + 0.3201}$$

The magnitude response $|H[e^{j\omega T}]|$, with $T = 70/\pi$, is depicted in Fig. 12.14.

It is also relatively straightforward to complete this design using the MATLAB functions `buttord` and `butter`.† The `buttord` function requires frequencies normalized to a radian

† For Chebyshev filters, there are the `cheb1ord` and `cheby1` commands; for inverse Chebyshev filters, there are the `cheb2ord` and `cheby2` commands; and for elliptic filters, there are the `ellipord` and `ellip` commands.

sampling frequency of 2. This requirement means the sampling radian frequency, which is $2\pi/T$, must be normalized to 2. Therefore, all the radian frequencies can be normalized by multiplying each of them by T/π. In the present case, $T = \pi/35$ so that $T/\pi = 1/35$. Thus, to normalize any radian frequency, we just divide it by 35. The normalized passband and stopband frequencies are therefore 8/35 and 15/35, respectively.

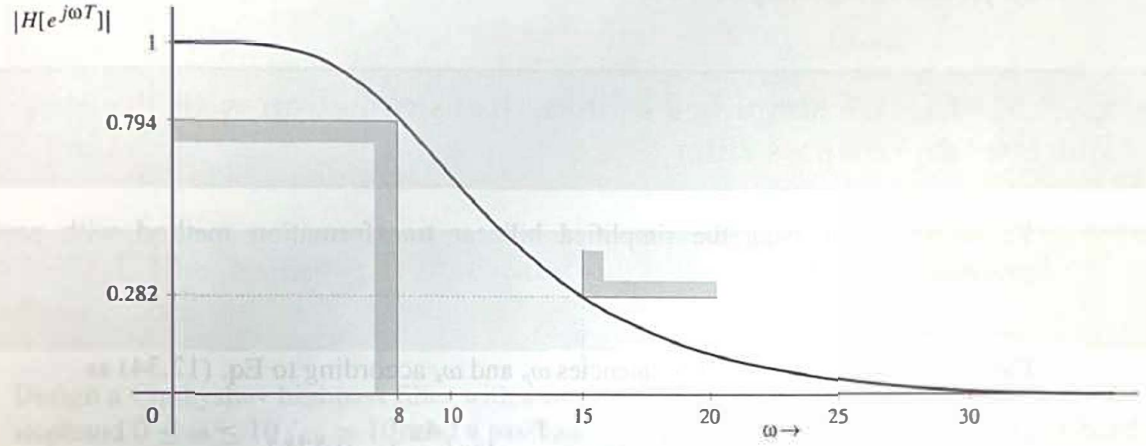

Figure 12.14 Magnitude response of the Butterworth filter in Ex. 12.6.

```
>> omegap = 8/35; omegas = 15/35;
>> Ghatp = -2; Ghats = -11; T = pi/35;
>> [N,omegac] = buttord(omegap,omegas,-Ghatp,-Ghats);
>> [B,A] = butter(N,omegac)
   B = 0.1039    0.2078    0.1039
   A = 1.0000   -0.9045    0.3201
```

Thus,

$$H[z] = \frac{0.1039(z^2 + 2z + 1)}{z^2 - 0.9045z + 0.3201}$$

This result exactly matches our earlier design. One disadvantage of using the `buttord` command is that it results in a design that exactly meets the stopband requirements; the function does not provide the option to instead exactly meet the passband requirements.

A Simplified Procedure

In the bilinear transform with prewarping, all the critical frequencies ω_i are transformed (prewarped) by the equation $\omega_i' = \frac{2}{T}\tan\left(\frac{\omega_i T}{2}\right)$ [Eq. (12.33)]. These prewarped frequencies are used to find the prewarped CT filter transfer function $H_a(s)$. Finally, we substitute $s = \frac{2}{T}\left(\frac{z-1}{z+1}\right)$ [Eq. (12.30)] in $H_a(s)$ to obtain the desired digital filter transfer function $H(z)$.

This procedure can be simplified by observing that the scaling factor $\frac{2}{T}$ is irrelevant to the combination of Eqs. (12.33) and (12.30). Instead of using these two equations, we can ignore the scaling factor $\frac{2}{T}$ and use the simplified equations

$$\omega_i' = \tan\left(\frac{\omega_i T}{2}\right) \qquad \text{and} \qquad s = \frac{z-1}{z+1}. \tag{12.34}$$

This simplification works because the factor $2/T$ in Eq. (12.33) is a frequency-scaling factor, and ignoring it, as in Eq. (12.34), results in the pretransformed filter that is frequency-scaled by a factor $2/T$. This scaling is undone by using $s = \frac{z-1}{z+1}$ instead of Eq. (12.30). Next, we demonstrate the process by repeating Ex. 12.6.

EXAMPLE 12.7 Simplified Bilinear Transformation with Prewarping: Butterworth Lowpass Filter

Repeat Ex. 12.6 using the simplified bilinear transformation method with prewarping procedure [Eq. (12.34)].

First, we prewarp the critical frequencies ω_p and ω_s according to Eq. (12.34) as

$$\omega_p' = \tan\frac{\omega_p T}{2} = \tan\left(\frac{4\pi}{35}\right) = 0.3753$$

$$\omega_s' = \tan\frac{\omega_s T}{2} = \tan\left(\frac{15\pi}{70}\right) = 0.7975$$

Next, we design a Butterworth filter with critical frequencies $\omega_p' = 0.3753$ and $\omega_s' = 0.7975$ with $\hat{G}_p = -2$ dB and $\hat{G}_s = -11$ dB. The filter order N is found from Eq. (7.28) as

$$N = \frac{\log[(10^{1.1}-1)/(10^{0.2}-1)]}{2\log(0.7975/0.3753)} = 1.9405$$

We round up the value of N to 2. Also from Eq. (7.30), we find the 3 dB cutoff frequency ω_c' as

$$\omega_c' = \frac{0.7975}{(10^{1.1}-1)^{\frac{1}{4}}} = 0.4322$$

From Table 7.1, we find the prewarped filter transfer function $H_a(s)$ for $N = 2$ and $\omega_c' = 0.4322$ as

$$H_a(s) = \frac{1}{\left(\frac{s}{0.4322}\right)^2 + \sqrt{2}\left(\frac{s}{0.4322}\right) + 1} = \frac{0.1868}{s^2 + 0.6112s + 0.1868}$$

Using the simplified bilinear transformation $s = \frac{z-1}{z+1}$ [see Eq. (12.34)], we determine $H[z]$ from $H_a(s)$ as

$$H[z] = H_a(s)\big|_{s=\frac{z-1}{z+1}} = \left.\frac{0.1868}{s^2 + 0.6112s + 0.1868}\right|_{s=\frac{z-1}{z+1}} = \frac{0.1039(z+1)^2}{z^2 + 0.904z + 0.3201}$$

This result is identical to the result obtained in Ex. 12.6.

DRILL 12.5 Bilinear Transformation with Prewarping

Using the bilinear transformation method with prewarping (regular and/or simplified procedure), design a first-order Butterworth lowpass filter where the analog and digital gains are identical at $\omega = 0$ and at the 3 dB cutoff frequency ω_c. Use $T = \pi/4\omega_c$.

ANSWER

$$H[z] = \frac{0.8284(z+1)}{2.8284z - 1.1716} = \frac{0.2929(z+1)}{z - 0.4142}$$

EXAMPLE 12.8 Bilinear Transformation with Prewarping: Chebyshev Highpass Filter

Design a Chebyshev highpass filter with a stopband gain $\hat{G}_s \leq -6.3$ dB ($G_s \leq 0.484$) over the stopband $0 \leq \omega \leq 10$ ($\omega_s = 10$) and a passband ripple $\hat{r} \leq 1$ dB ($G_p \geq 0.891$) over a passband $\omega \geq 15$ ($\omega_p = 15$). The highest frequency to be processed is $\omega_h = 80$ radians/s.

In order to avoid signal aliasing, Eq. (12.31) requires that $T \leq \frac{\pi}{\omega_h} = \frac{\pi}{80}$. Let us choose $T = \frac{\pi}{100}$. The critical frequencies are $\omega_s = 10$ and $\omega_p = 15$. According to Eq. (12.34), the prewarped critical frequencies are

$$\omega_s' = \tan\frac{\omega_s T}{2} = \tan\left(\frac{\pi}{20}\right) = 0.1584$$

and

$$\omega_p' = \tan\frac{\omega_p T}{2} = \tan\left(\frac{3\pi}{40}\right) = 0.24$$

Next, we design a prewarped Chebyshev highpass filter with critical frequencies $\omega_s' = 0.1584$ and $\omega_p' = 0.24$ and with $\hat{r} = -1$ dB and $\hat{G}_s = -6.3$ dB (Fig. 12.15b). Following the procedure in Sec. 7.6, we first design a prototype lowpass filter with specifications as shown in Fig. 12.15b. Observe that the critical frequencies of the prototype filter are 1 (passband) and $\omega_p'/\omega_s' = 1.515$ (stopband) as explained in Sec. 7.6.

The value of N needed to satisfy these specifications is given by Eq. (7.35) as

$$N = \frac{1}{\cosh^{-1}\left(\frac{1.515}{1}\right)} \cosh^{-1}\left[\frac{(10^{0.63} - 1}{10^{0.1} - 1}\right]^{1/2} = 1.988$$

We round up the value of N to 2. From Eq. (7.39) and Table 7.4 (Chebyshev filter with $\hat{r} = 1$ and $N = 2$), the prototype transfer function is

$$\mathcal{H}_p(s) = \frac{0.982614}{s^2 + 1.0978s + 1.1025} \tag{12.35}$$

To obtain the desired highpass transfer function, we replace s with ω_p'/s in the above prototype transfer function [see Eq. (7.41)]. To obtain the desired digital transfer function $H[z]$, we then replace s with $\frac{z-1}{z+1}$ [the bilinear transformation in Eq. (12.34)]. This two-step operation may be combined in a single-step transformation as

$$s \Longrightarrow \frac{\omega_p'}{\left(\frac{z-1}{z+1}\right)} = \frac{\omega_p'(z+1)}{(z-1)}$$

In this case, $\omega_p' = 0.24$ so that we replace s with $\frac{0.24(z+1)}{z-1}$ in the prototype transfer function in Eq. (12.35) to obtain the desired digital transfer function

$$H[z] = \frac{0.6902(z-1)^2}{z^2 - 1.4678z + 0.6298}$$

The curve in Fig. 12.15a shows the magnitude response of this filter.

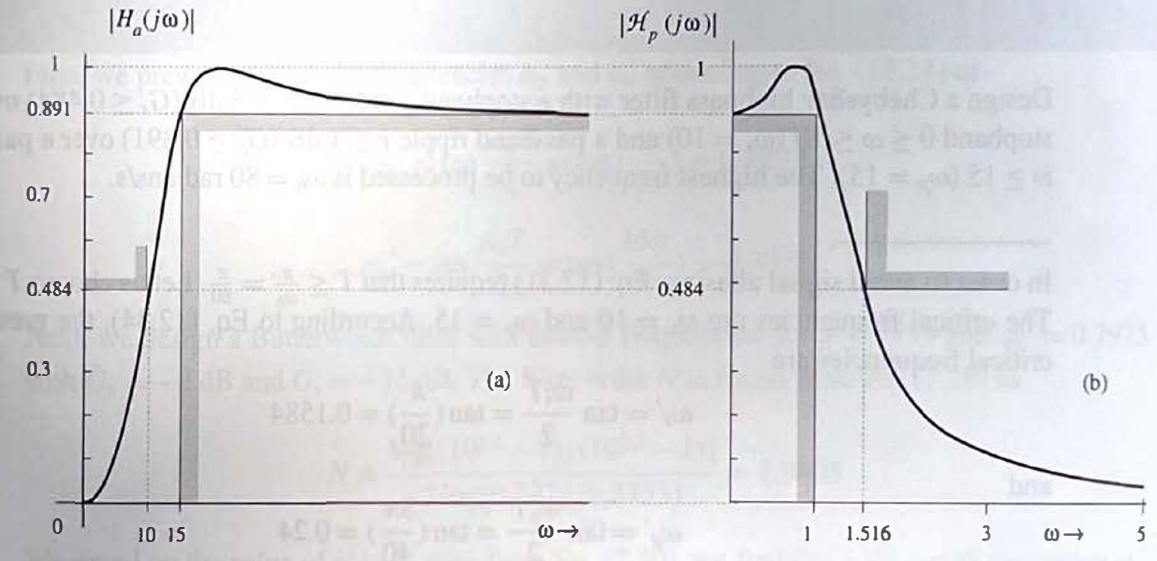

Figure 12.15 Chebyshev highpass filter design using the bilinear transformation method with prewarping.

As in Ex. 12.6, it is also relatively straightforward to complete this design using the MATLAB functions `cheb1ord` and `cheby1`. The `cheb1ord` function requires frequencies normalized to a radian sampling frequency of 2. As explained in Ex. 12.6, all the radian frequencies can be normalized by multiplying each of them by T/π. In the present case, $T = \pi/100$ so that $T/\pi = 1/100$. Thus, to normalize any radian frequency, we just divide it by 100. The normalized passband and stopband frequencies are therefore 15/100 and 10/100, respectively.

```
>> omegap = 15/100; omegas = 10/100;
>> Ghatp = -1; Ghats = -6.3; T = pi/100;
>> [N,omegap] = cheb1ord(omegap,omegas,-Ghatp,-Ghats);
>> [B,A] = cheby1(N,-Ghatp,omegap,'high')
```

```
B = 0.6902    -1.3804    0.6902
A = 1.0000    -1.4678    0.6298
```

Thus,

$$H[z] = \frac{0.6902(z^2 - 2z + 1)}{z^2 - 1.4678z + 0.6298}$$

This result exactly matches our earlier design.

Bandpass and Bandstop Filters

For bandpass and bandstop filters, we follow a similar procedure. All the critical frequencies are first prewarped using the simplified form in Eq. (12.34). Next, we determine a prototype lowpass filter, which is then converted to the desired analog filter using appropriate transformations discussed in Sec. 7.7. Finally, we use the bilinear transformation in Eq. (12.34) to obtain the desired digital filter. As in the case of the highpass filter (discussed in Ex. 12.8), we can combine the two transformations into a single transformation. For a bandpass filter, we first use the transformation

$$T(s) = \frac{s^2 + \omega_{p_1}'\omega_{p_2}'}{(\omega_{p_2}' - \omega_{p_1}')s}$$

and then use the bilinear transformation in Eq. (12.34). Thus, in the first step, we replace s in the prototype transfer function $\mathcal{H}_p(s)$ with $T(s)$ (the frequency transformation). In the second step, we replace s with $\frac{z-1}{z+1}$ (the simplified bilinear transformation). Thus, the final transformation is equivalent to replacing s with $T_{bp}[z]$ in the prototype filter transfer function $\mathcal{H}_p(s)$, where

$$\begin{aligned} T_{bp}[z] = T(s)|_{s=\frac{z-1}{z+1}} &= \frac{s^2 + \omega_{p_1}'\omega_{p_2}'}{(\omega_{p_2}' - \omega_{p_1}')s}\Big|_{s=\frac{z-1}{z+1}} \\ &= \frac{(z-1)^2 + \omega_{p_1}'\omega_{p_2}'(z+1)^2}{(\omega_{p_2}' - \omega_{p_1}')(z^2-1)} \\ &= \frac{(\omega_{p_1}'\omega_{p_2}' + 1)z^2 + 2(\omega_{p_1}'\omega_{p_2}' - 1)z + (\omega_{p_1}'\omega_{p_2}' + 1)}{(\omega_{p_2}' - \omega_{p_1}')(z^2-1)} \end{aligned}$$

Using the same argument, we can show that for the bandstop filter, the desired digital filter transfer function $H[z]$ can be obtained from the corresponding bandstop prototype filter $\mathcal{H}_p(s)$ by replacing s with $T_{bs}[z]$, which is the reciprocal of $T_{bp}[z]$. Both these transformations can be expressed in more compact form as

$$T_{bp}[z] = \frac{z^2 + 2az + 1}{b(z^2 - 1)} \quad \text{and} \quad T_{bs}[z] = \frac{b(z^2 - 1)}{z^2 + 2az + 1} \tag{12.36}$$

where

$$a = \frac{\omega_{p_1}'\omega_{p_2}' - 1}{\omega_{p_1}'\omega_{p_2}' + 1} \quad \text{and} \quad b = \frac{\omega_{p_2}' - \omega_{p_1}'}{\omega_{p_1}'\omega_{p_2}' + 1} \tag{12.37}$$

Thus, a digital filter transfer function $H[z]$ can be obtained from $\mathcal{H}_p(s)$ by replacing s with $T_{bp}[z]$ for a bandpass filter, and replacing s with $T_{bs}[z]$ for a bandstop filter.

EXAMPLE 12.9 Bilinear Transformation with Prewarping: Butterworth Bandpass Filter

Design a digital Butterworth bandpass filter with $\omega_{p_1} = 1000$, $\omega_{p_2} = 2000$, $\omega_{s_1} = 450$, $\omega_{s_2} = 4000$, $G_p = 0.7852$ (−2.1 dB), and $G_s = 0.1$ (−20 dB). Take $T = \pi/10{,}000$.

The solution is executed in three steps. In the first step, we determine the prewarped critical frequencies. In the second step, the lowpass prototype filter transfer function $\mathcal{H}_p(s)$ is found from the prewarped critical frequencies. Finally, the desired $H[z]$ is found using the lowpass analog to bandpass digital transformation by replacing s in $\mathcal{H}_p(s)$ with $T_{bp}[z]$.

Step 1: Find the prewarped critical frequencies.
Using Eq. (12.34), the prewarped frequencies ω_{p_1}', ω_{p_2}', ω_{s_1}', and ω_{s_2}' (corresponding to the four critical frequencies ω_{p_1}, ω_{p_2}, ω_{s_1}, and ω_{s_2}) are

$$\omega_{s_1}' = \tan\frac{\omega_{s_1}T}{2} = \tan\left(\frac{450\pi}{20{,}000}\right) = 0.0708$$

$$\omega_{p_1}' = \tan\frac{\omega_{p_1}T}{2} = \tan\left(\frac{1000\pi}{20{,}000}\right) = 0.1584$$

$$\omega_{p_2}' = \tan\frac{\omega_{p_2}T}{2} = \tan\left(\frac{2000\pi}{20{,}000}\right) = 0.3249$$

$$\omega_{s_2}' = \tan\frac{\omega_{s_2}T}{2} = \tan\left(\frac{4000\pi}{20{,}000}\right) = 0.7265$$

Step 2: Find $\mathcal{H}_p(s)$, the prewarped lowpass prototype analog filter.
This step identically follows step 1 in the analog bandpass filter design of Ex. 7.14.

First, we find ω_s'. For the prototype lowpass filter transfer function $\mathcal{H}_p(s)$ with the amplitude response shown in Fig. 12.16b, the frequency ω_s' is found [using Eq. (7.42)] to be the smaller of

$$\frac{(0.1584)(0.3249) - (0.0708)^2}{0.0708(0.3249 - 0.1584)} = 3.939 \quad \text{and} \quad \frac{(0.7265)^2 - (0.1584)(0.3249)}{0.7265(0.3249 - 0.1584)} = 3.937$$

Thus, $\omega_s = 3.937$. We now require a prototype lowpass filter, depicted in Fig. 12.16b, with $\hat{G}_p = -2.1$ dB, $\hat{G}_s = -20$ dB, $\omega_p' = 1$, and $\omega_s' = 3.937$.

Next, we determine the filter order N. According to Eq. (7.28), the required N is

$$N = \frac{1}{2\log 3.937}\log\left[\frac{10^2 - 1}{10^{0.21} - 1}\right] = 1.8498$$

Since filter order must be an integer, we round this result up to $N = 2$.

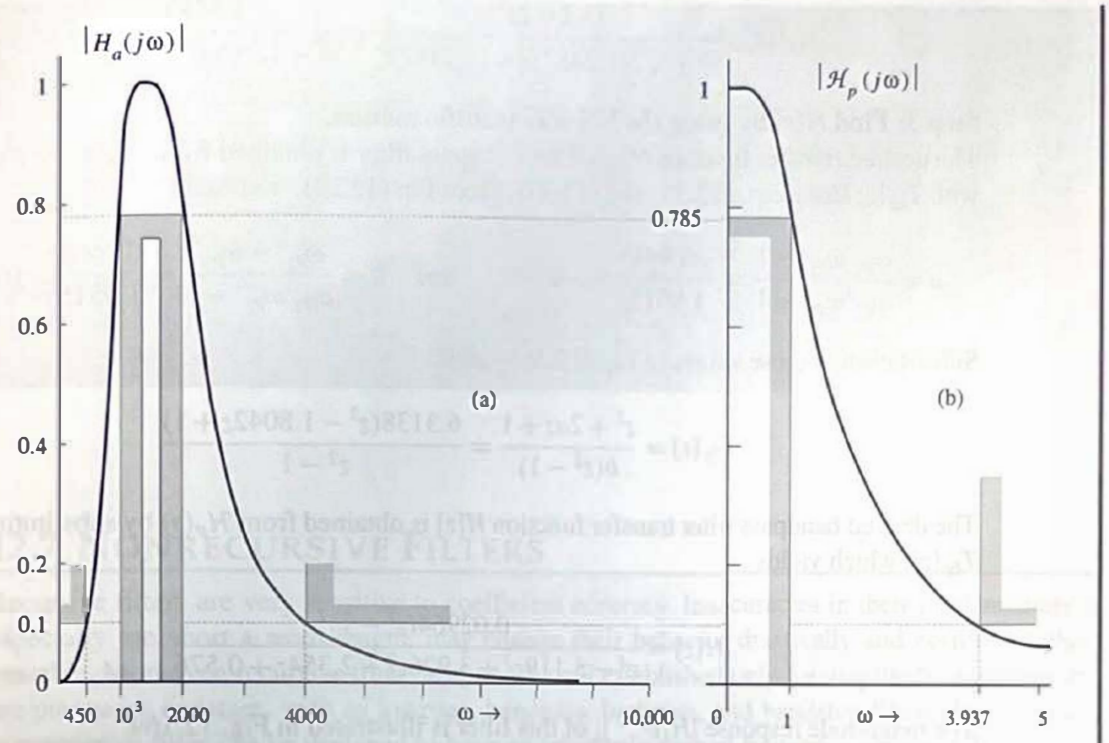

Figure 12.16 Butterworth bandpass filter design using the bilinear transformation method with prewarping.

Next, we determine the half-power (3 dB) cutoff frequency ω_c for the prototype filter. The use of Eq. (7.29) yields

$$\omega_c' = \frac{\omega_s'}{(10^2 - 1)^{1/4}} = 1.2482$$

We now determine the normalized transfer function $\mathcal{H}(s)$. According to Table 7.1, the required second-order lowpass Butterworth transfer function is

$$\mathcal{H}(s) = \frac{1}{s^2 + \sqrt{2}s + 1}$$

This is the transfer function of a filter that is normalized to the half-power frequency (meaning $\omega_c = 1$).

Finally, the prototype filter transfer function $\mathcal{H}_p(s)$ is obtained by substituting s with $s/\omega_c = s/1.2482$ in the normalized transfer function $\mathcal{H}(s)$ as

$$\mathcal{H}_p(s) = \frac{(1.2482)^2}{s^2 + \sqrt{2}(1.2482)s + (1.2482)^2} = \frac{1.5581}{s^2 + 1.7653s + 1.5581}$$

Step 3: Find $H[z]$ by using the bilinear transformation.
The desired transfer function $H[z]$ of the bandpass filter is obtained from $\mathcal{H}_p(s)$ by replacing s with $T_{bp}[z]$ from Eqs. (12.36) and (12.37). From Eq. (12.37), we obtain

$$a = \frac{\omega_{p_1}'\omega_{p_2}' - 1}{\omega_{p_1}'\omega_{p_2}' + 1} = \frac{-0.9485}{1.0515} = -0.9021 \quad \text{and} \quad b = \frac{\omega_{p_2}' - \omega_{p_1}'}{\omega_{p_1}'\omega_{p_2}' + 1} = \frac{0.1665}{1.0515} = 0.1584$$

Substitution of these values in Eq. (12.36) yields

$$T_{bp}[z] = \frac{z^2 + 2az + 1}{b(z^2 - 1)} = \frac{6.3138(z^2 - 1.8042z + 1)}{z^2 - 1}$$

The desired bandpass filter transfer function $H[z]$ is obtained from $\mathcal{H}_p(s)$ by substituting s with $T_{bp}[z]$, which yields

$$H[z] = \frac{0.02964(z^2 - 1)^2}{z^4 - 3.119z^3 + 3.926z^2 - 2.354z + 0.576}$$

The magnitude response $|H[e^{j\omega T}]|$ of this filter is illustrated in Fig. 12.16a.

As in Ex. 12.6, it is also relatively straightforward to complete this design using the MATLAB functions `buttord` and `butter`. The `buttord` function requires frequencies normalized to a radian sampling frequency of 2. As explained in Ex. 12.6, all the radian frequencies can be normalized by multiplying each of them by T/π. In the present case, $T = \pi/10^4$ so that $T/\pi = 1/10^4$. Thus, to normalize any radian frequency, we just divide it by 10^4. Since this is a bandpass filter, there are two critical frequencies for both the passband and the stopband.

```
>> omegap = [1000 2000]/10^4; omegas = [450 4000]/10^4;
>> Ghatp = -2.1; Ghats = -20; T = pi/10000;
>> [N,omegac] = buttord(omegap,omegas,-Ghatp,-Ghats);
>> [B,A] = butter(N,omegac)
   B = 0.0296         0   -0.0593         0    0.0296
   A = 1.0000   -3.1190    3.9259   -2.3539    0.5760
```

Thus,

$$H[z] = \frac{0.0296z^4 - 0.0593a^2 + 0.0296}{z^4 - 3.119z^3 + 3.9259z^2 - 2.3539z + 0.576}$$

As expected, this result exactly matches our earlier design.

DRILL 12.6 Bilinear Transformation with Prewarping: Chebyshev Bandstop Filter

Using the bilinear transformation with prewarping, design a Chebyshev bandstop digital filter with $\omega_{s_1} = 1000$, $\omega_{s_2} = 2000$, $\omega_{p_1} = 450$, $\omega_{p_2} = 4000$, $G_p = 0.7852$ (−2.1 dB), and $G_s = 0.1$ (−20 dB). Use $T = \pi/10^4$.

ANSWER

$$H[z] = \frac{0.3762(z^4 - 3.6086z^3 + 5.2555z^2 - 3.6086z + 1)}{z^4 - 2.2523z^3 + 2.0563z^2 - 1.2053z + 0.4197}$$

12.7 NONRECURSIVE FILTERS

Recursive filters are very sensitive to coefficient accuracy. Inaccuracies in their implementation, especially too short a word length, may change their behavior drastically and even make them unstable. Moreover, recursive filter designs are well established only for amplitude responses that are piecewise constant, such as lowpass, bandpass, highpass, and bandstop filters. In contrast, a nonrecursive filter can be designed to have an arbitrarily shaped frequency response. In addition, nonrecursive filters can be designed to have linear-phase response. On the other hand, if a recursive filter can be found to do the job of a nonrecursive filter, the recursive filter is of lower order; that is, it is faster (with less processing delay) and requires less memory. If processing delay is not critical, a nonrecursive filter is the obvious choice. Recursive filters also have an important place in non-audio applications where a linear-phase response is desirable. We shall review the concept of nonrecursive systems briefly.

As discussed in Sec. 12.3, nonrecursive filters may be viewed as recursive filters where all the feedback or recursive coefficients are zero; that is, when

$$a_1 = a_2 = \cdots = a_N = 0$$

The transfer function of the resulting Nth-order nonrecursive filter is

$$\begin{aligned} H[z] &= \frac{b_0 z^N + b_1 z^{N-1} + \cdots + b_{N-1} z + b_N}{z^N} \\ &= b_0 + b_1 z^{-1} + b_2 z^{-2} + \cdots + b_{N-1} z^{-(N-1)} + b_N z^{-N} \end{aligned} \tag{12.38}$$

Now, by definition, $H[z]$ is the z-transform of $h[n]$:

$$H[z] = \sum_{n=0}^{\infty} h[n] z^{-n} = h[0] + h[1] z^{-1} + h[2] z^{-2} + \cdots + h[N] z^{-N} + h[N+1] z^{-(N+1)} + \cdots \tag{12.39}$$

Comparison of this equation with Eq. (12.38) shows that $h[n] = 0$ for $n > N$, and Eq. (12.39) becomes

$$\begin{aligned} H[z] &= h[0] + h[1]z^{-1} + h[2]z^{-2} + \cdots + h[N-1]z^{-(N-1)} + h[N]z^{-N} \\ &= \frac{h[0]z^N + h[1]z^{N-1} + \cdots + h[N-1]z + h[N]}{z^N} \end{aligned} \tag{12.40}$$

where

$$h[n] = \begin{cases} b_n & 0 \le n \le N \\ 0 & \text{otherwise} \end{cases} \tag{12.41}$$

The impulse response $h[n]$ has a finite length of $(N+1)$ elements. Hence, these filters are *finite impulse response* (FIR) filters. We shall use the terms nonrecursive and FIR interchangeably. Similarly, the terms recursive and IIR (infinite impulse response) will be used interchangeably in our future discussion.

The impulse response $h[n]$ of an FIR filter can be expressed as

$$h[n] = h[0]\delta[n] + h[1]\delta[n-1] + \cdots + h[N]\delta[n-N] \tag{12.42}$$

The frequency response of this filter is obtained using Eq. (12.40) as

$$H[e^{j\omega T}] = h[0] + h[1]e^{-j\omega T} + \cdots + h[N]e^{-jN\omega T} = \sum_{n=0}^{N} h[n]e^{-jn\omega T} \tag{12.43}$$

FIR Filter Realization

The nonrecursive (FIR) filter in Eq. (12.38) is a special case of a general filter with all feedback (or recursive) coefficients zero. Therefore, the realization of this filter is the same as that of the Nth-order recursive filter with all the feedback connections omitted. The typical canonical FIR filter realization is easily obtained by setting $a_1 = \cdots = a_N = 0$ in Fig. 11.8c. It is easy to verify from this figure that for the input $\delta[n]$, the output is $h[n]$ given in Eq. (12.42).

An FIR filter realization, such as obtained by setting $a_1 = \cdots = a_N = 0$ in Fig. 11.8c, is a tapped delay line with successive taps at unit delay (T seconds) intervals. Such a filter is known as a *transversal* filter. Tapped analog delays are available commercially in integrated circuit form. In these circuits, the time delay is implemented by using charge transfer devices, which sample the input signal every T seconds (unit delay) and transfer the successive values of the samples to N storage cells. The stored signal at the kth tap is the input signal delayed by k time units (kT seconds). The sampling interval can be varied electronically over a wide range. Time delay can also be obtained by using shift registers.

12.7.1 Symmetry Conditions for Linear-Phase Response

Consider an Nth-order recursive (FIR) filter described by the transfer function $H[z]$ [Eq. (12.38) or Eq. (12.40)] and the corresponding impulse response $h[n]$ [Eq. (12.42)]. We now show that if $h[n]$ is either symmetric (Fig. 12.17a) or antisymmetric (Fig. 12.17b) about its center point, the filter's phase response is a linear function of ω (or, equivalently, a linear function of Ω). We consider a case where N is even. To avoid too much abstractness, we choose some convenient value for N,

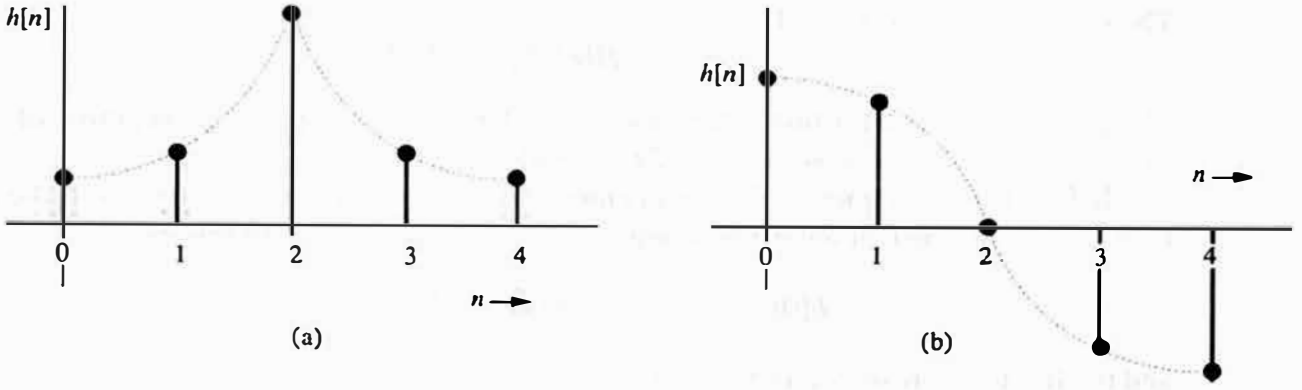

Figure 12.17 Symmetry conditions for linear-phase frequency response in nonrecursive filters.

say, $N = 4$, to demonstrate our point. It will then be easier to understand the generalization to the Nth-order case.

For $N = 4$, the impulse response in Eq. (12.42) reduces to

$$h[n] = h[0]\delta[n] + h[1]\delta[n-1] + h[2]\delta[n-2] + h[3]\delta[n-3] + h[4]\delta[n-4]$$

The transfer function $H[z]$ in Eq. (12.40) reduces to

$$\begin{aligned} H[z] &= h[0] + h[1]z^{-1} + h[2]z^{-2} + h[3]z^{-3} + h[4]z^{-4} \\ &= z^{-2}\left(h[0]z^2 + h[1]z + h[2] + h[3]z^{-1} + h[4]z^{-2}\right) \end{aligned}$$

Therefore, the frequency response is

$$H[e^{j\omega T}] = e^{-j2\omega T}\left(h[0]e^{j2\omega T} + h[1]e^{j\omega T} + h[2] + h[3]e^{-j\omega T} + h[4]e^{-j2\omega T}\right)$$

If $h[n]$ is symmetric about its center point ($n = 2$ in this case), then

$$h[0] = h[4], \qquad h[1] = h[3]$$

and the frequency response reduces to

$$\begin{aligned} H[e^{j\omega T}] &= e^{-j2\omega T}\left(h[0]\left[e^{j2\omega T} + e^{-j2\omega T}\right] + h[2] + h[1]\left[e^{j\omega T} + e^{-j\omega T}\right]\right) \\ &= e^{-j2\omega T}\left(h[2] + 2h[1]\cos\omega T + 2h[0]\cos 2\omega T\right) \end{aligned}$$

The quantity inside the parenthesis is real; it may be positive over some bands of frequencies and negative over other bands. This quantity represents the amplitude response $|H[e^{j\omega T}]|$.†

† Strictly speaking, $|H[e^{j\omega T}]|$ cannot be negative. Recall, however, that the only restriction on amplitude is that it cannot be complex. It has to be real; it can be positive or negative. We could have used some other notation such as $A(\omega)$ to denote the amplitude response. But this would create too many related functions causing possible confusion. Another alternative is to incorporate the negative sign of the amplitude in the phase response, which will be increased (or decreased) by π over the band where the amplitude response is negative. This alternative will still maintain the phase linearity.

The phase response is given by

$$\angle H[e^{j\omega T}] = -2\omega T$$

The phase response is a linear function of ω. The group delay is the negative of the slope of $\angle H[e^{j\omega T}]$ with respect to ω, which is $2T$ seconds in this case [see Eq. (4.40)].

If $h[n]$ is antisymmetric about its center point, then the antisymmetry about the center point requires that $h[n] = 0$ at the center point (see Fig. 12.17b).† Thus, in this case

$$h[0] = -h[4], \qquad h[1] = -h[3], \qquad h[2] = 0$$

and the frequency response reduces to

$$\begin{aligned} H[e^{j\omega T}] &= e^{-j2\omega T}\left(h[0](e^{j2\omega T} - e^{-j2\omega T}) + h[1](e^{j\omega T} - e^{-j\omega T})\right) \\ &= 2je^{-j2\omega T}\left(h[1]\sin\omega T + h[0]\sin 2\omega T\right) \\ &= 2e^{j(\frac{\pi}{2} - 2\omega T)}\left(h[1]\sin\omega T + h[0]\sin 2\omega T\right) \end{aligned}$$

Thus, the phase response in this case is

$$\angle H[e^{j\omega T}] = \frac{\pi}{2} - 2\omega T$$

The phase response in this case is also a linear function of ω. The system has a group delay (the negative slope of $\angle H[e^{j\omega T}]$ with respect to ω) of $2T$ seconds (2 units), the same as in the symmetric case. The only difference is that the phase response has a constant term $\pi/2$.

We can obtain similar results for odd values of N (see Prob. 12.7-1). This result can be generalized for an Nth-order case to show that the phase response is linear, and the group delay is $\frac{NT}{2}$ seconds (or $\frac{N}{2}$ units).

EXAMPLE 12.10 Transfer Function of FIR Comb Filter

Determine the transfer function and the frequency response of a sixth-order FIR comb filter whose impulse response is given by

$$h[n] = \delta[n] - \delta[n-6]$$

This impulse response is illustrated in Fig. 12.18a. Its canonical realization is depicted in Fig. 12.18b.

† Antisymmetry requires that $h[n] = -h[-n]$ at the center point also. This condition is possible only if $h[n] = 0$ at this point.

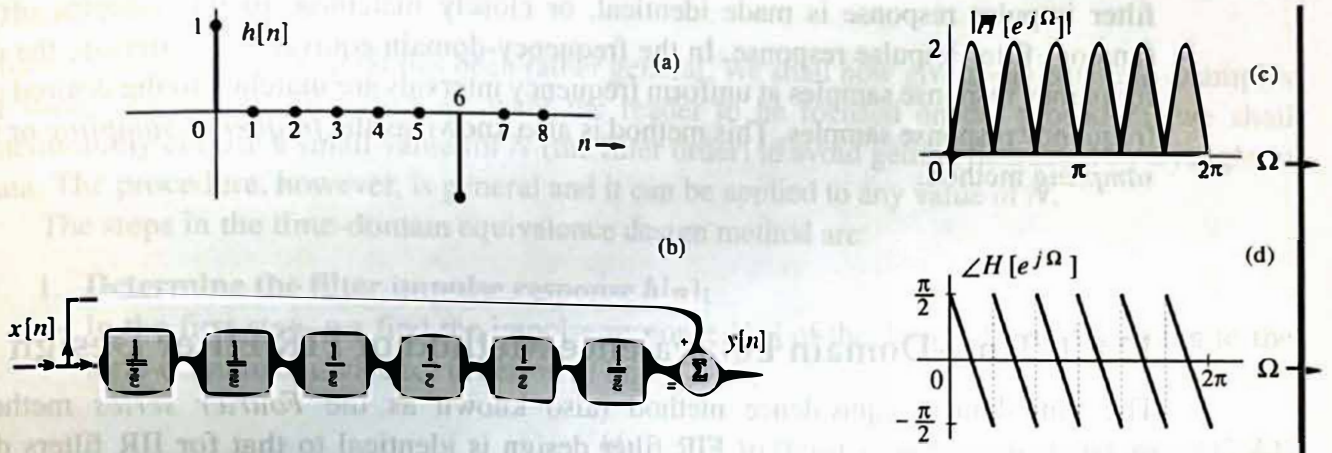

Figure 12.18 Impulse response, realization, and frequency response of an FIR comb filter.

Observe that $h[n]$ is antisymmetric about $n = 3$. Also

$$H[z] = \sum_{n=-\infty}^{\infty} h[n]z^{-n} = 1 - z^{-6} = \frac{z^6 - 1}{z^6}$$

The frequency response is given by

$$H[e^{j\Omega}] = 1 - e^{-j6\Omega} = e^{-j3\Omega}(e^{j3\Omega} - e^{-j3\Omega})$$

$$= 2je^{-j3\Omega} \sin 3\Omega = 2e^{j\left(\frac{\pi}{2} - 3\Omega\right)} \sin 3\Omega$$

The term $\sin 3\Omega$ can be positive as well as negative. Therefore,

$$|H[e^{j\Omega}]| = 2|\sin 3\Omega|$$

and $\angle H[e^{j\Omega}]$ is as indicated in Fig. 12.18d. The amplitude response, illustrated in Fig. 12.18c, is shaped like a comb with periodic nulls.

Using the same argument, the reader can show that an Nth-order comb filter transfer function is

$$H[z] = \frac{z^n - 1}{z^n}$$

The corresponding Nth-order comb filter frequency response is

$$H[e^{j\Omega}] = 2e^{j\left(\frac{\pi}{2} - j\frac{n\Omega}{2}\right)} \sin \frac{n\Omega}{2}$$

12.8 NONRECURSIVE FILTER DESIGN

As in the case of recursive (IIR) filters, nonrecursive filters can be designed by using time-domain and frequency-domain equivalence criteria. In the time-domain equivalence criterion, the digital

filter impulse response is made identical, or closely matching, to the samples of the desired (analog) filter impulse response. In the frequency-domain equivalence criterion, the digital filter frequency response samples at uniform frequency intervals are matched to the desired analog filter frequency response samples. This method is also known as the *frequency sampling* or the *spectral sampling* method.

12.8.1 Time-Domain Equivalence Method of FIR Filter Design

The time-domain equivalence method (also known as the *Fourier series* method when a rectangular window is used) of FIR filter design is identical to that for IIR filters discussed in Sec. 12.5, except that the FIR filter impulse response must be causal and of finite duration. Therefore, the desired impulse response must be shifted and truncated. Truncating the impulse response abruptly will result in an oscillatory frequency response because of the Gibbs phenomenon discussed in Sec. 3.5.2. In some filtering applications, the oscillatory frequency response (which decays slowly as $1/\omega$ for a rectangular window) in the stopband may not be acceptable. By using a tapered window function for truncation, the oscillatory behavior can be reduced or even eliminated at the cost of increasing the transition band as discussed in Sec. 4.9. Note that the impulse response of an Nth-order FIR filter has $N+1$ samples. Hence, for truncating $h[n]$ for an Nth-order filter, we must use an $(N+1)$-point window. Several window functions and their tradeoffs appear in Table 12.2.

TABLE 12.2 Common Discrete-Time Window Functions and Their Approximate Characteristics

	Window $w[n]$ for $0 \le n \le N$, 0 otherwise	Main Lobe Width	Rolloff Rate [dB/dec]	Peak Side Lobe Level [dB]
1.	Rectangular: 1	$\frac{4\pi}{L_w}$	-20	-13.3
2.	Triangular (Bartlett): $1-\frac{\lvert 2n-N\rvert}{N}$	$\frac{8\pi}{N+1}$	-40	-26.5
3.	Hann: $\frac{1}{2}\left[1-\cos\left(\frac{2\pi n}{N}\right)\right]$	$\frac{8\pi}{N+1}$	-60	-31.5
4.	Hamming: $0.54-0.46\cos\left(\frac{2\pi n}{N}\right)$	$\frac{8\pi}{N+1}$	-20	-42.7
5.	Blackman: $0.42-0.5\cos\left(\frac{2\pi n}{N}\right)+0.08\cos\left(\frac{4\pi n}{N}\right)$	$\frac{12\pi}{N+1}$	-60	-58.1
6.	Kaiser: $\frac{I_0\left(\alpha\sqrt{1-\left(\frac{2n-(N)}{N}\right)^2}\right)}{I_0(\alpha)}$	varies with α	-20	varies with α

Design Procedure

Much of the discussion so far has been rather general. We shall now give some concrete examples of such filter design. Because we want the reader to be focused on the procedure, we shall intentionally choose a small value for N (the filter order) to avoid getting distracted by a jungle of data. The procedure, however, is general and it can be applied to any value of N.

The steps in the time-domain equivalence design method are:

1. **Determine the filter impulse response $h[n]$:**
   In the first step, we find the impulse response $h[n]$ of the desired filter. According to the time-domain equivalence criterion in Eq. (12.13),

$$h[n] = Th_a(nT) \tag{12.44}$$

   Here, $h_a(t)$ is the impulse response of the analog filter $H_a(s)$. Therefore, $h_a(t)$ is the inverse Laplace transform of $H_a(s)$ or the inverse Fourier transform of $H_a(j\omega)$. Thus,

$$h_a(t) = \frac{1}{2\pi}\int_{-\pi/T}^{\pi/T} H_a(j\omega)e^{j\omega t}\,d\omega \tag{12.45}$$

   Recall that a digital filter frequency response is periodic with the first period in the frequency range $-\frac{\pi}{T} \le \omega < \frac{\pi}{T}$. Hence, the best we could hope is to realize the equivalence of $H_a(j\omega)$ within this range. For this reason, the limits of integration are taken from $-\pi/T$ to π/T. Therefore, according to Eq. (12.44),

$$h[n] = Th_a(nT) = \frac{T}{2\pi}\int_{-\pi/T}^{\pi/T} H_a(j\omega)e^{j\omega nT}\,d\omega \tag{12.46}$$

2. **Delay and window:**
   For linear-phase filters, we generally start with zero-phase filters for which $H_a(j\omega)$ is either real or imaginary. The impulse response $h_a(t)$ is either an even or odd function of t (see Prob. 4.1-3). In either case, $h_a(t)$ is centered at $t = 0$ and has infinite duration in general. But $h[n]$ must have only a finite duration and it must start at $n = 0$ (causal) for filter realizability. Consequently, the $h[n]$ found in step 1 needs to come from a shifted and truncated version of $h_a(t)$. Specifically, we require

$$h[n] = Th_a([n - \tfrac{N}{2}]T)w[n]$$

   where $w[n]$ is a finite duration symmetric window function over $0 \le n \le N$. Combined with Eq. (12.46), we see that

$$h[n] = Th_a([n - \tfrac{N}{2}]T)w[n] = \left(\frac{T}{2\pi}\int_{-\pi/T}^{\pi/T} H_a(j\omega)e^{j\omega(n-\frac{N}{2})T}\,d\omega\right)w[n] \tag{12.47}$$

   This produces an $h[n]$ that is finite in duration as well as causal. The delay necessary to ensure a causal (realizable) system is what also produces the desired linear-phase frequency response.

   Straight truncation of data amounts to using a rectangular window, which has a unit weight over the window width, and zero weight for all other n. We saw that although such

a window gives the smallest transition band, it results in a slowly decaying oscillatory frequency response in the stopband. This behavior can be corrected by using a tapered window of a suitable width.

3. **Filter frequency response and realization:**
   Knowing $h[0], h[1], h[2], \ldots, h[N]$, we determine $H[z]$ using Eq. (12.40) and the frequency response $H[e^{j\omega T}]$ using Eq. (12.43). We now realize the truncated $h[n]$ using the structure in Fig. 11.8c with $a_1 = \cdots = a_N = 0$.

Optimality of the Rectangular Window

If the truncating window is rectangular, the procedure outlined here is optimum in the sense that the energy of the error (difference) between the desired frequency response $H_a(j\omega)$ and the realized frequency response $H[e^{j\omega T}]$ is the minimum for a given N. This conclusion follows from the fact that the resulting filter frequency response $H[e^{j\omega T}]$ is given by

$$H[e^{j\omega T}] = \sum_n h[n]e^{-j\omega nT}$$

This frequency response is an approximation of the desired frequency response $H_a(j\omega)$ because of the finite length of $h[n]$. Thus,

$$H_a(j\omega) \approx \sum_n h[n]e^{-j\omega nT} \tag{12.48}$$

How do we select $h[n]$ for the best approximation in the sense of minimizing the energy of the error $H_a(j\omega) - H[e^{j\omega T}]$? We have already solved this problem in Sec. 3.3.2. The preceding equation shows that the right-hand side is the finite-term exponential Fourier series for $H_a(j\omega)$ with period $2\pi/T$. As seen from Eq. (12.46), $h[n]$ are the Fourier coefficients, which explains why the rectangular window method is also called the *Fourier series method*. According to the *finality property* (see p. 252), a finite Fourier series is the optimum (in the sense of minimizing the error energy) for a given N. In other words, for a given number of terms $(N + 1)$, any choice for $h[n]$ other than the Fourier coefficients in Eq. (12.48) will lead to higher error energy. For windows other than rectangular, this minimum mean square error optimality deteriorates, and the filter is somewhat suboptimal.

EXAMPLE 12.11 Window Method Lowpass Filter Design

Using rectangular and Hamming windows, design $N = 6$ FIR filters to approximate an audio lowpass filter with cutoff frequency $f_c = 20$ kHz. Plot the magnitude response of each filter. Set the sampling frequency f_s equal to four times the cutoff frequency f_c.

In this case, the impulse response length (and thus the window length) is $N+1=7$, and the sampling interval T is computed as

$$f_s = \frac{1}{T} = 4f_c = 80000 \quad \Longrightarrow \quad T = 12.5 \times 10^{-6}$$

Recall that a continuous-time frequency ω appears as a discrete-time frequency $\Omega = \omega T$. Thus, the desired CT cutoff frequency $\omega_c = 2\pi f_c = \frac{\pi f_s}{2} = \frac{\pi}{2T}$ appears at $\Omega_c = \frac{\pi}{2}$, which is halfway to the highest (non-aliased) digital frequency $\Omega = \pi$.

Although we could now use Eq. (12.47) to find the desired impulse responses, we shall derive the results in steps. This approach, although more lengthy, will help clarify the basic design concepts. Let us consider the rectangular window (Fourier series method) first.

Using pair 18 of Table 4.1, the impulse response of the desired ideal (zero-phase) lowpass filter is

$$h_a(t) = \frac{1}{2T}\text{sinc}\left(\frac{\pi t}{2T}\right)$$

Next, we delay $h_a(t)$ by $\frac{NT}{2} = 3T$ to obtain

$$h_a(t-3T) = \frac{1}{2T}\text{sinc}\left(\frac{\pi(t-3T)}{2T}\right)$$

This response is now scaled by T, truncated (windowed), and sampled by setting $t = nT$ to obtain the desired FIR impulse response

$$h_{\text{rec}}[n] = Th_a(nT-3T)w_{\text{rec}}[n] = \frac{1}{2}\text{sinc}\left(\frac{\pi(n-3)}{2}\right)w_{\text{rec}}[n]$$

This result also follows directly from Eq. (12.47).

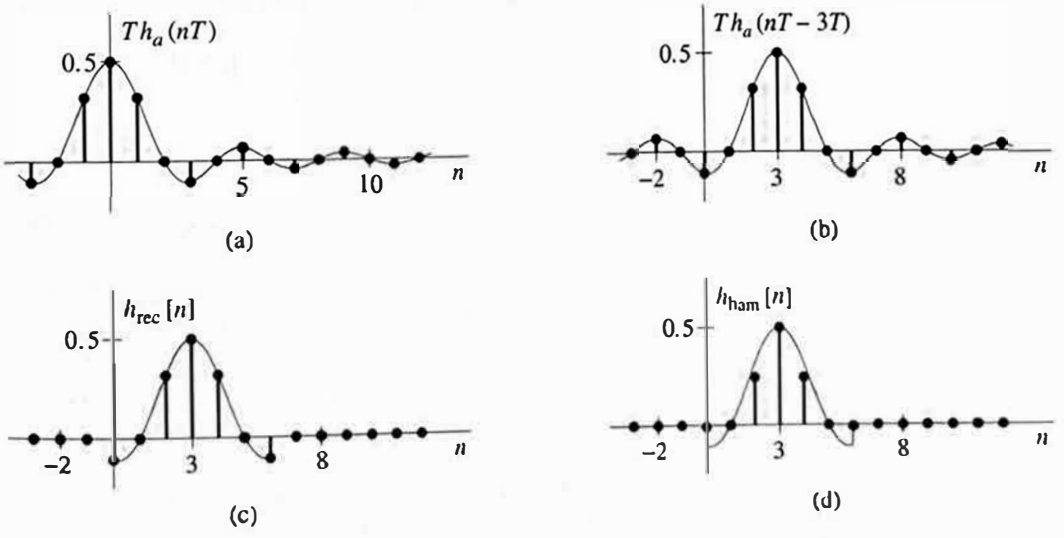

Figure 12.19 Discrete-time LPF impulse responses: (a) ideal, (b) shifted ideal, (c) rectangular windowed, and (d) Hamming windowed.

To visualize these three steps, consider Fig. 12.19. Using the impulse invariance method, the ideal but noncausal DT impulse response is $Th_a(nT) = 0.5\,\mathrm{sinc}(\pi n/2)$ (Fig. 12.19a). To obtain a causal and finite-duration solution, we first delay the CT response by $NT/2 = 3T$ (Fig. 12.19b) and then truncate it with a length-7 rectangular window (Fig. 12.19c). In this case, the noncausal filter is made realizable at a cost of a $3T$-second delay. Over the window duration $0 \le n \le 6$, the samples $h_{\mathrm{rec}}[n]$ exactly match the underlying CT impulse response. Notice, too, that $h_{\mathrm{rec}}[n]$ is also midpoint symmetric and will thus have a linear-phase response.

Using Eq. (12.40) and computing each value of $h_{\mathrm{rec}}[n]$, the transfer function is

$$H_{\mathrm{rec}}(z) = \sum_{n=0}^{6} h_{\mathrm{rec}}[n]z^{-n} = -\frac{1}{3\pi} + \frac{1}{\pi}z^{-2} + \frac{1}{2}z^{-3} + \frac{1}{\pi}z^{-4} - \frac{1}{3\pi}z^{-6}$$

Setting $z = e^{j\Omega}$, the frequency response is

$$H_{\mathrm{rec}}[e^{j\Omega}] = \sum_{n=0}^{6} h_{\mathrm{rec}}[n]e^{-j\Omega n} = -\frac{1}{3\pi} + \frac{1}{\pi}e^{-j2\Omega} + \frac{1}{2}e^{-j3\Omega} + \frac{1}{\pi}e^{-j4\Omega} - \frac{1}{3\pi}e^{-j6\Omega}$$

Factoring out $e^{-j3\Omega}$ and simplifying using trigonometric functions yield

$$H_{\mathrm{rec}}[e^{j\Omega}] = \left[\frac{1}{2} + \frac{2}{\pi}\cos(\Omega) - \frac{2}{3\pi}\cos(3\Omega)\right]e^{-j3\Omega}$$

The right-hand term $e^{-j3\Omega}$ confirms the filter's linear-phase characteristics and represents three samples ($3T$ seconds) of delay. Computed using MATLAB, Fig. 12.20 shows the resulting magnitude response $|H_{\mathrm{rec}}[e^{j\Omega}]|$ as well as the ideal lowpass response (shaded) for reference. The magnitude response exhibits oscillatory behavior that decays rather slowly over the stopband. Although increasing N improves the frequency response, the oscillatory nature persists due to the Gibbs phenomenon.

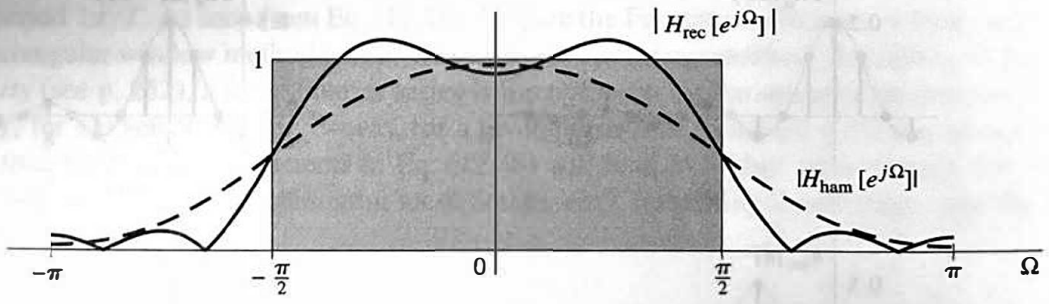

Figure 12.20 Window method LPF magnitude responses: rectangular (solid) and Hamming (dashed).

We can readily confirm this example's calculations and plots using MATLAB. Since MATLAB computes `sinc(x)` as $(\sin(\pi x))/\pi x$, we create a function `mysinc` that scales the MATLAB `sinc` input by $1/\pi$ to match the notation of the sinc function in this book. To produce the filter designed using the rectangular window, we execute the following code:

```
>> mysinc = @(x) sinc(x/pi); Omega = linspace(-pi,pi,1001);
>> N = 6; fc = 20000; T = 1/(4*fc); n = [0:N];
>> ha = @(t) 1/(2*T)*mysinc(pi*t/(2*T));
>> wrec = @(n) 1.0*((n>=0)&(n<=N));
>> hrec = T*ha(n*T-N/2*T).*wrec(n)
   hrec = -0.1061  -0.0000  0.3183  0.5000  0.3183  0.0000  -0.1061
>> Hrec = polyval(hrec,exp(1j*Omega)).*exp(-1j*N*Omega);
>> plot(Omega,abs(Hrec),'.k');
```

The resulting calculations and plots match the results shown in Figs. 12.19 and 12.20.

The side lobes in the rectangular window are rather large (−13 dB), which results in a filter with poor stopband attenuation. The Hamming window, which has smaller side lobes (−43 dB), produces a filter with better stopband attenuation but wider transition band. Using a Hamming window rather than a rectangular window, the desired impulse response is

$$h_{\text{ham}}[n] = Th_a(nT - 3T)w_{\text{ham}}[n] = \frac{1}{2}\text{sinc}\left(\frac{\pi(n-3)}{2}\right)w_{\text{ham}}[n]$$

Using Table 12.2 to define $w_{\text{ham}}[n]$, MATLAB readily computes $h_{\text{ham}}[n]$, which is shown in Fig. 12.19d.

```
>> wham = @(n) (0.54-0.46*cos(2*pi*n/N)).*((n>=0)&(n<=N));
>> hham = T*ha(n*T-N/2*T).*wham(n)
   hham = -0.0085  -0.0000  0.2451  0.5000  0.2451  0.0000  -0.0085
```

Unlike the result obtained using the rectangular window, $h_{\text{ham}}[n]$ does not exactly match the underlying CT impulse response. The largest differences occur at the edges, where the taper of the Hamming window is greatest.

Using Eq. (12.43) and the computed values of $h_{\text{ham}}[n]$, the frequency response is

$$H_{\text{ham}}[e^{j\Omega}] = -0.0085 + 0.2451e^{-j2\Omega} + 0.5e^{-j3\Omega} + 0.2451e^{-j4\Omega} - 0.0085e^{-j6\Omega}$$

The magnitude response $|H_{\text{ham}}[e^{j\Omega}]|$ is shown dashed in Fig. 12.20.

```
>> Hham = polyval(hham,exp(1j*Omega)).*exp(-1j*N*Omega);
>> plot(Omega,abs(Hham),'.k');
```

Observe that the transition band corresponding to the Hamming window is wider than that corresponding to the rectangular window. Both $h_{\text{rec}}[n]$ and $h_{\text{ham}}[n]$ are symmetric about $n = 3$ and, hence, have linear phase responses.

Comments:

Referring to Fig. 12.20, the ideal (unwindowed) filter transitions from passband to stopband abruptly, resulting in a zero-width transition band. In the windowed filters, on the other hand, the spectrum spreads out, which results in a gradual transition from the passband to the stopband. For the rectangular window case, the distance (spectral spread) between the two peaks on either side of the transition region approximately equals $\frac{4\pi}{N+1}$, the main lobe width of the rectangular window spectrum. Clearly, increasing the window width decreases the

transition width. This result is intuitive because a wider window means that we are accepting more data (closer approximation), which should cause smaller distortion (smaller spectral spreading). Smaller window length (poorer approximation) causes more spectral spreading (more distortion).

The windowed filters also possess passband and stopband ripple. These characteristics are a result of the side lobes of the window spectra. When the ideal impulse response is windowed, its spectrum is convolved with the window's spectrum, and the window's side lobes leak into the passband and stopband. To keep this spectral leakage small, the window side lobes must also be small and decay rapidly with Ω. It is the type of window, not its length, that largely determines side lobe levels and decay rates.

DRILL 12.7 Triangular Window Lowpass Filter Design

Using the window method and an $N = 8$ triangular (Bartlett) window, show that the transfer function of a lowpass FIR filter with $\Omega_c = \pi/2$ is

$$H(z) = -0.0265z^{-1} + 0.2387z^{-3} + 0.5z^{-4} + 0.2387z^{-5} - 0.0265z^{-7}$$

EXAMPLE 12.12 Window Method Differentiator Design

Using rectangular and Hamming windows, design $N = 10$ FIR filters to realize a digital differentiator. Plot the magnitude response of each filter.

The transfer function of an ideal continuous-time differentiator is $H_a(s) = s$, and its frequency response is $H_a(j\omega) = j\omega$. Restricting our attention to the frequencies of interest to our digital differentiator, the desired impulse response is found from Eq. (12.47) as

$$h[n] = \left(\frac{T}{2\pi}\int_{-\pi/T}^{\pi/T} j\omega e^{j\omega(n-\frac{N}{2})T}\,d\omega\right) w[n]$$

Letting $x = (n - \frac{N}{2})T$, we have

$$h[n] = \left(\frac{T}{2\pi}\int_{-\pi/T}^{\pi/T} j\omega e^{j\omega x}\,d\omega\right) w[n]$$

$$= \begin{cases} \frac{T}{2\pi}\left(\frac{\frac{2\pi x}{T}\cos(\pi x/T) - 2\sin(\pi x/T)}{x^2}\right) w[n] & x \neq 0 \\ 0 & x = 0 \end{cases}$$

For integer n, observe that $\sin(\pi x/T) = \sin\left(\pi[n - \frac{N}{2}]\right) = 0$ when N is even. Similarly, $\cos(\pi x/T) = \cos\left(\pi[n - \frac{N}{2}]\right) = 0$ when N is odd. Hence, for $n \neq N/2$,

$$h[n] = \begin{cases} \dfrac{\cos\left(\pi[n-\frac{N}{2}]\right)}{[n-\frac{N}{2}]T} w[n] & N \text{ even} \\ \dfrac{-\sin\left(\pi[n-\frac{N}{2}]\right)}{\pi[n-\frac{N}{2}]^2 T} w[n] & N \text{ odd} \end{cases} \tag{12.49}$$

When N is even, $h[n] = 0$ at the midpoint $n = N/2$.

For this problem, we have $N = 10$, which is an even order. We use MATLAB to compute $Th[n]$ using Eq. (12.49).

```
>> N = 10; n = 0:N; Omega = linspace(-pi,pi,1001);
>> wrec = @(n) 1.0*((n>=0)&(n<=N));
>> wham = @(n) (0.54-0.46*cos(2*pi*n/N)).*((n>=0)&(n<=N));
>> Threc = cos(pi*(n-N/2))./(n-N/2).*wrec(n)
   Threc = 0.200  -0.250  0.333  -0.500  1.000  Inf  -1.000  0.500
          -0.333  0.250  -0.200
>> Thham = cos(pi*(n-N/2))./(n-N/2).*wham(n)
>> Threc(n==N/2) = 0; Thham(n==N/2) = 0;
   Thham = 0.016  -0.042  0.133  -0.341  0.912  Inf  -0.912  0.341
          -0.133  0.042  -0.016
>> Threc(n==(Lh-1)/2) = 0; Thham(n==(Lh-1)/2) = 0;
```

In each of the two cases, the $n = N/2 = 5$ point is initially computed incorrectly as ∞. It is a simple matter to adjust this point to the correct value of 0 (final line of code).

Figures 12.21a and 12.21b show the (scaled) impulse responses $Th_{\text{rec}}[n]$ and $Th_{\text{ham}}[n]$, and Fig. 12.21c compares their corresponding magnitude responses (rectangular solid, Hamming dashed) to an ideal differentiator (shaded). Notice once again that the rectangular window produces oscillatory behavior (the Gibbs phenomenon). The tapered Hamming window produces a much smoother response.

```
>> subplot(221); stem(n,Threc,'k.'); subplot(222); stem(n,Thham,'k.');
>> THrec = polyval(Threc,exp(1j*Omega)).*exp(-1j*N*Omega);
>> THham = polyval(Thham,exp(1j*Omega)).*exp(-1j*N*Omega);
>> subplot(212); plot(Omega,abs(THrec),Omega,abs(THham),'--k');
```

Although we do not here display the phase responses of these filters, since the impulse responses are odd length and antisymmetric, both possess linear-phase characteristics. Except for occasional jumps of $\pm\pi$ and a linear-phase component of -5Ω (corresponding to a time delay of $5T$ seconds), both filters exactly match the phase response of an ideal differentiator. Notice that the Hamming-windowed filter is more accurate for low frequencies, but the rectangular-windowed filter operates over a broader frequency range. The taper of the Hamming window effectively shrinks the passband of the differentiator. This is generally true for all tapered windows. To compensate for this shrinkage, we usually start with a passband somewhat larger (typically, 25% larger) than the design passband. For example, to ensure that

our Hamming-windowed differentiator works in the 20-kHz audio range, we might select T such that

$$2\pi \times 20000 \leq \frac{2\pi}{3T} \quad \Longrightarrow \quad T \leq 16.67\ \mu s$$

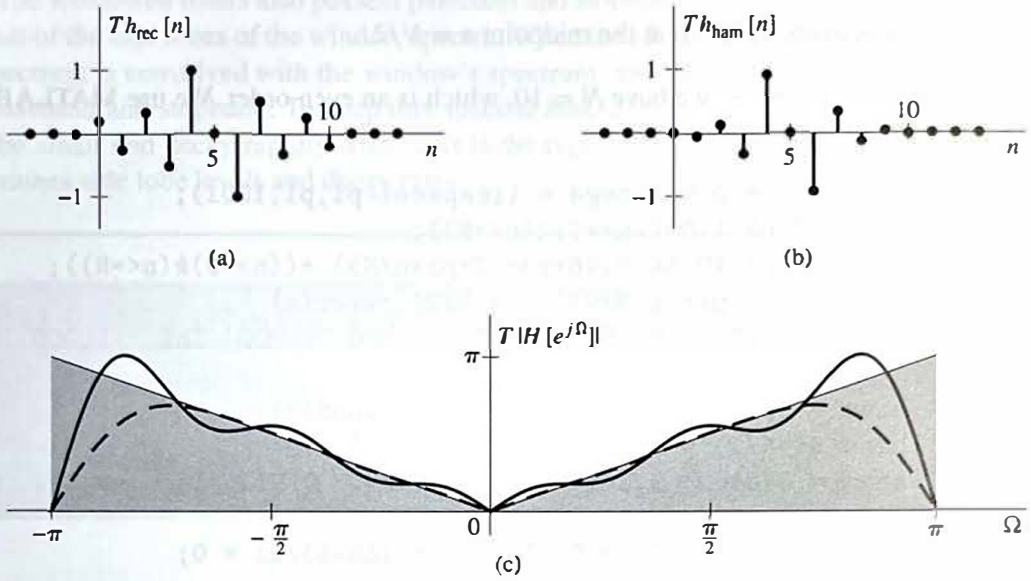

Figure 12.21 $N = 10$ digital differentiators: (a) $Th_{\text{rec}}[n]$, (b) $Th_{\text{ham}}[n]$, and (c) $T|H_{\text{rec}}[e^{j\Omega}]|$ (solid) and $T|H_{\text{ham}}[e^{j\Omega}]|$ (dashed).

DRILL 12.8 Window Method Differentiator Design with Odd Order

Although the technical reasons are outside the scope of this book, odd-order digital differentiators have superior performance, particularly at high frequencies, than do digital differentiators of similar complexity but even order. Repeat Ex. 12.12 for $N = 7$ and verify that, despite being lower order (lower complexity), the resulting digital differentiators have superior performance to the $N = 10$ digital differentiators.

DRILL 12.9 Another Window Method Design

Using a rectangular window, design an $N = 6$ FIR filter to realize the triangular response $H_a(j\omega) = \Delta(\omega T/\pi)$. Determine the transfer function $H[z]$ and plot the filter's magnitude response.

ANSWER

$$H(z) = 0.0225 + 0.1023z^{-1} + 0.2026z^{-2} + 0.25z^{-3} + 0.2026z^{-4} + 0.1013z^{-5} + 0.0225z^{-6}$$

12.8.2 Nonrecursive Filter Design by the Frequency-Domain Criterion: The Frequency Sampling Method

The frequency-domain criterion is [see Eq. (12.17)]

$$H_a(s) = H[e^{sT}]$$

In this case, we shall realize this equality for purely sinusoidal frequencies; that is, for $s = j\omega$:

$$H_a(j\omega) = H[e^{j\omega T}] \tag{12.50}$$

For an Nth-order FIR filter, there are $N_0 = N + 1$ elements in $h[n]$, and we can hope to force the two frequency spectra in Eq. (12.50) to be equal only at N_0 points. Because the spectral width is $\frac{2\pi}{T}$, we choose these frequencies $\omega_0 = \frac{2\pi}{N_0 T}$ rad/s apart; that is,

$$\omega_0 = \frac{2\pi}{N_0 T}$$

We require that

$$H_a(jr\omega_0) = H[e^{jr\omega_0 T}] \qquad r = 0, 1, 2, , \ldots, N_0 - 1 \tag{12.51}$$

Note that these are the samples of the periodic extension of $H_a(j\omega)$ (or $H[e^{j\omega T}]$). Because we force the frequency response of the filter to be equal to the desired frequency response at N_0 equidistant frequencies in the spectrum, this method is known as the *frequency sampling* or the *spectral sampling* method.

In order to find the filter transfer function, we first determine the filter impulse response $h[n]$. Thus, our problem is to determine the filter impulse response from the knowledge of the N_0 uniform samples of the periodic extension of the filter frequency response $H[e^{j\omega T}]$. But $H[e^{j\omega T}]$ is the DTFT of $h[n]$ [see Eq. (10.58)]. Hence, as shown in Sec. 10.6 [Eqs. (10.46) and (10.47)], $h[n]$ and $H[e^{jr\omega_0 T}]$ (the N_0 uniform samples of $H[e^{j\omega T}]$) are a DFT pair with $\Omega_0 = \omega_0 T$. Hence, the desired $h[n]$ is the IDFT of $H[e^{j\omega T}]$, given by

$$\begin{aligned} h[n] &= \frac{1}{N_0} \sum_{r=0}^{N_0-1} H[e^{jr\omega_0 T}] e^{jrn\omega_0 T} \\ &= \frac{1}{N_0} \sum_{r=0}^{N_0-1} H[e^{jr\omega_0 T}] e^{j\frac{2\pi rn}{N_0}} \qquad n = 0, 1, 2, , \ldots, N_0 - 1 \end{aligned} \tag{12.52}$$

Note that $H[e^{jr\omega_0 T}] = H_a(jr\omega_0)$ are known [Eq. (12.51)]. We can use the IFFT to compute the N_0 values of $h[n]$. From these values of $h[n]$, we can determine the filter transfer function $H[z]$ as

$$H[z] = \sum_{n=0}^{N_0-1} h[n] z^{-n} \tag{12.53}$$

Linear Phase (Constant Delay) Filters

We desire that $H_a(j\omega) = H[e^{j\omega T}]$. The filter featured in Eqs. (12.52) and (12.53) satisfies this condition only at N_0 values of ω. If we specify ideal filter characteristics (brick wall, zero phase) at these points, the filter frequency response between samples can deviate considerably. As we shall see in later examples, a filter delay of $(N_0 - 1)/2$ generally produces superior results, including the desirable filter characteristic of linear phase. It is a sensible adjustment. It is not reasonable to assume a realizable (causal) filter with zero delay (zero phase); rather, we expect practical filters to have a delay that increases with filter complexity (order). To achieve this delay and consequent improvement in overall filter performance, we modify our filter design procedure slightly.

First, we start with a zero phase (or a constant phase $\pm\frac{\pi}{2}$) response (usually by specifying the desired response using ideal filter characteristics). To produce a delay of $(N_0 - 1)/2$ units in $h[n]$, we multiply $H[e^{j\omega T}]$ with $e^{-j\frac{N_0-1}{2}\omega T}$. Notice, the added filter delay does not alter the filter amplitude response, but the phase response changes by $-(N_0 - 1)\omega T/2$, which is a linear function of ω. In our modified procedure to realize a frequency response $H[e^{j\omega T}]$, we thus begin with $H[e^{j\omega T}]e^{-j\frac{N_0-1}{2}\omega T}$ and find the IDFT of its N_0 samples. The resulting IDFT at $n = 0, 1, 2, 3, \ldots, N_0 - 1$ is the desired (and improved) impulse response.

Note that $\omega_0 T = \frac{2\pi}{N_0}$, and the N_0 uniform samples of $H[e^{j\omega T}]e^{-j\frac{N_0-1}{2}\omega T}$ are

$$H_r = H[e^{jr\omega_0 T}]e^{-jr\frac{N_0-1}{2}\omega_0 T} = H\left[e^{j\frac{2\pi r}{N_0 T}}\right]e^{-jr\pi\frac{N_0-1}{N_0}} \tag{12.54}$$

Recall that the N_0 samples H_r are the uniform samples of a periodic extension of $H[e^{j\omega T}]e^{-j\frac{N_0-1}{2}\omega T}$. Hence, Eq. (12.54) applies to samples of the frequency range from $0 \le \omega \le \frac{\pi}{T}$. The remaining samples are obtained by using the conjugate symmetry property $H_r = H^*_{N_0-r}$. The desired $h[n]$ is the IDFT of H_r; that is,

$$h[n] = \frac{1}{N_0}\sum_{r=0}^{N_0-1} H_r e^{j\frac{2\pi rn}{N_0}} \qquad n = 0, 1, 2, \ldots, N_0 - 1 \tag{12.55}$$

As before, the filter transfer function $H[z]$ is determined using Eq. (12.53). Let us now demonstrate the procedure through an example.

EXAMPLE 12.13 Lowpass FIR Filter Design by Frequency Sampling

Using the frequency sampling method, design a sixth-order linear-phase FIR lowpass filter of cutoff frequency $\frac{\pi}{2T}$ rad/s.

The frequency response $H[e^{j\omega T}]$ of an ideal lowpass filter is shown (shaded) in Fig. 12.22.

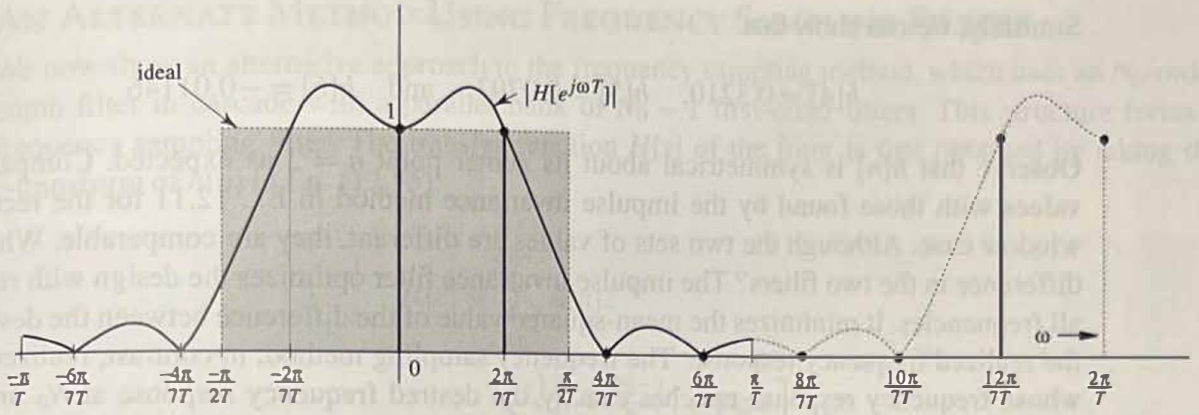

Figure 12.22 Lowpass filter design using the frequency sampling method.

For this design,

$$N_0 = 7, \quad \frac{N_0 - 1}{N_0} = \frac{6}{7}, \quad \omega_0 = \frac{2\pi}{N_0 T} = \frac{2\pi}{7T}$$

Using Eq. (12.54), the seven samples of H_r are

$$H_r = H\left[e^{j\frac{2\pi r}{7T}}\right] e^{-j\frac{6\pi r}{7}}$$

Thus,

$$H_0 = 1, H_1 = e^{-j\frac{6\pi}{7}}, H_2 = H_3 = 0$$

The remaining three samples are determined using the conjugation property of the DFT, $H_r = H^*_{N_0 - r}$. Thus,

$$H_4 = H_3^* = 0, H_5 = H_2^* = 0, H_6 = H_1^* = e^{j\frac{6\pi}{7}}$$

According to Eq. (12.55), the desired $h[n]$ is the IDFT of H_r; that is,

$$h[n] = \sum_{r=0}^{6} H_r e^{j\frac{2\pi rn}{7}} \qquad n = 0, 1, 2, 3, \ldots, 6$$

We may compute this IDFT by using the IFFT algorithm or by straightforward substitution of values of H_r in the above equation as

$$h[0] = \frac{1}{7}\sum_{r=0}^{6} H_r = \frac{1}{7}[1 + e^{-j6\pi/7} + e^{j6\pi/7}] = \frac{1}{7}\left(1 + 2\cos\frac{6\pi}{7}\right) = -0.1146$$

$$h[1] = \frac{1}{7}\sum_{r=0}^{6} H_r e^{j\frac{2\pi r}{7}} = \frac{1}{7}[1 + e^{-j4\pi/7} + e^{j4\pi/7}] = \frac{1}{7}\left(1 + 2\cos\frac{4\pi}{7}\right) = 0.0793$$

$$h[2] = \frac{1}{7}\sum_{r=0}^{6} H_r e^{jr\frac{4\pi r}{7}} = \frac{1}{7}[1 + e^{-j2\pi/7} + e^{j2\pi/7}] = \frac{1}{7}\left(1 + 2\cos\frac{2\pi}{7}\right) = 0.3210$$

$$h[3] = \frac{1}{7}\sum_{r=0}^{6} H_r e^{j\frac{6\pi r}{7}} = \frac{1}{7}[1 + 1 + 1] = 0.4286$$

Similarly, we can show that

$$h[4] = 0.3210, \quad h[5] = 0.0793, \quad \text{and} \quad h[6] = -0.01146$$

Observe that $h[n]$ is symmetrical about its center point $n = 3$ as expected. Compare these values with those found by the impulse invariance method in Ex. 12.11 for the rectangular window case. Although the two sets of values are different, they are comparable. What is the difference in the two filters? The impulse invariance filter optimizes the design with respect to all frequencies. It minimizes the mean-squared value of the difference between the desired and the realized frequency response. The frequency sampling method, in contrast, realizes a filter whose frequency response matches exactly the desired frequency response at N_0 uniformly spaced frequencies. The mean-squared error in this design will generally be higher than that in the impulse invariance method.

The filter transfer function is

$$\begin{aligned} H[z] &= -0.1146 + \frac{0.0793}{z} + \frac{0.3210}{z^2} + \frac{0.4286}{z^3} + \frac{0.3210}{z^4} + \frac{0.0793}{z^5} - \frac{0.1146}{z^6} \\ &= \frac{-0.1146z^6 + 0.0793z^5 + 0.3210z^4 + 0.4286z^3 + 0.3210z^2 + 0.0793z - 0.1146}{z^6} \end{aligned}$$

The filter frequency response is

$$\begin{aligned} H[e^{j\omega T}] &= -0.1146 + 0.0793e^{-j\omega T} + 0.3210e^{-j2\omega T} + 0.4286e^{-j3\omega T} \\ &\quad + 0.3210e^{-j4\omega T} + 0.0793e^{-j5\omega T} - 0.1146e^{-j6\omega T} \\ &= e^{-j3\omega T}[0.4286 + 0.6420\cos\omega T + 0.1586\cos 2\omega T - 0.2291\cos 3\omega T] \end{aligned}$$

Figure 12.22 shows that the realized filter's magnitude response exactly matches the desired response at the N_0 sample points. The time delay adds a linear phase $-3T\omega$ to the filter characteristic.

We can also use MATLAB to readily compute the desired impulse response $h[n]$.

```
>> N = 6; N0 = N+1; r = 0:N; Omega0 = 2*pi/N0;
>> Hr = 1.0*(r*Omega0<=pi/2).*exp(-1j*r*pi*(N0-1)/N0);
>> Hr(1,fix(N0/2)+2:end) = conj(Hr(1,round(N0/2):-1:2));
>> h = ifft(Hr)
   h = -0.1146   0.0793   0.3210   0.4286   0.3210   0.0793   -0.1146
```

It is likewise simple to compute and plot the magnitude response.

```
>> Omega = linspace(0,2*pi,201);
>> H = polyval(h,exp(1j*Omega)).*exp(-1j*N*Omega)
>> stem(r*Omega0,abs(Hr),'k.');
>> line(Omega,abs(H),'color',[0 0 0]);
>> xlabel('\Omega'); ylabel('|H[e^{j\Omega}]|');
```

This resulting MATLAB plot confirms the magnitude response in Fig. 12.22.

An Alternate Method Using Frequency Sampling Filters

We now show an alternative approach to the frequency sampling method, which uses an N_0-order comb filter in cascade with a parallel bank of $N_0 - 1$ first-order filters. This structure forms a frequency sampling filter. The transfer function $H[z]$ of the filter is first obtained by taking the z-transform of $h[n]$ in Eq. (12.55):

$$\begin{aligned} H[z] &= \sum_{n=0}^{N_0-1} h[n]z^{-n} \\ &= \sum_{n=0}^{N_0-1} \left[\frac{1}{N_0} \sum_{r=0}^{N_0-1} H_r e^{j\frac{2\pi nr}{N_0}} \right] z^{-n} \\ &= \frac{1}{N_0} \sum_{r=0}^{N_0-1} H_r \sum_{n=0}^{N_0-1} (e^{j\frac{2\pi r}{N_0}} z^{-1})^n \end{aligned}$$

The second sum on the right-hand side is a geometric series. From Sec. B.8.3, we therefore have

$$\begin{aligned} H[z] &= \frac{1}{N_0} \sum_{r=0}^{N_0-1} H_r \left[\frac{1 - z^{-N_0} e^{j2\pi r}}{1 - e^{j\frac{2\pi r}{N_0}} z^{-1}} \right] \\ &= \frac{1}{N_0} \sum_{r=0}^{N_0-1} H_r \left[\frac{z^{-N_0}(z^{N_0} - 1)}{z^{-1}(z - e^{j\frac{2\pi r}{N_0}})} \right] \end{aligned}$$

Hence,

$$H[z] = \underbrace{\frac{z^{N_0} - 1}{N_0 z^{N_0}}}_{H_1[z]} \underbrace{\sum_{r=0}^{N_0-1} \frac{zH_r}{z - e^{j\frac{2\pi r}{N_0}}}}_{H_2[z]} \tag{12.56}$$

Observe that we do not need to perform IDFT (or IFFT) computations to obtain the desired filter transfer function. All we need are the values of the frequency samples H_r, which are given. Equation (12.56) shows that the desired filter is realized as a cascade of two filters with transfer functions $H_1[z]$ and $H_2[z]$. The first filter with transfer function $H_1[z]$ is an N_0-order comb filter (see Ex. 12.10). The second filter with transfer function $H_2[z]$ is a parallel combination of N_0 first-order filters whose poles lie on the unit circle at $e^{j\frac{2\pi r}{N_0}}$ $(r = 0, 1, 2, \ldots, N_0 - 1)$. Especially for lowpass and bandpass filters, notice that many coefficients H_r appearing in $H_2[z]$ are zero. For example, the lowpass filter of Ex. 12.13 has four out of seven coefficients that are zero. Thus, in practice the final filter is usually much simpler than it appears in Eq. (12.56). As a result, this method may require a fewer computations (multiplications and additions) than a filter obtained by the direct method (using the IDFT).

The poles of the frequency sampling filter are complex in general because they lie on the unit circle. Therefore, the realization of $H_2[z]$ should combine conjugate poles to form a parallel connection of quadratic transfer functions. All these points will be clarified by designing the filter in Ex. 12.13 by this method.

EXAMPLE 12.14 Lowpass FIR Filter Design by a Frequency Sampling Filter

Redo Ex. 12.13 using a frequency sampling filter.

In this case, $N = 6$, $N_0 = N + 1 = 7$. Also,

$$H_2 = H_3 = H_4 = H_5 = 0$$

and

$$H_0 = 1,\ H_1 = e^{-j6\pi/7},\ H_6 = e^{j6\pi/7}$$

Substituting these values in the transfer function $H[z]$ of the desired filter in Eq. (12.56), we obtain

$$H[z] = \underbrace{\frac{z^7 - 1}{7z^7}}_{H_1[z]} \underbrace{\left[\frac{z}{z-1} + \frac{ze^{-j6\pi/7}}{z - e^{j2\pi/7}} + \frac{ze^{j6\pi/7}}{z - e^{-j2\pi/7}}\right]}_{H_2[z]}$$

We combine the last two complex-conjugate pole terms on the right-hand side to obtain

$$\begin{aligned} H[z] &= \frac{z^7 - 1}{7z^7}\left[\frac{z}{z-1} + \frac{z(2z\cos\frac{6\pi}{7} - 2\cos\frac{8\pi}{7})}{z^2 - (2\cos\frac{2\pi}{7}z + 1)}\right] \\ &= \underbrace{\frac{z^7 - 1}{7z^7}}_{H_1[z]} \underbrace{\left[\frac{z}{z-1} - \frac{1.802z(z-1)}{z^2 - 1.247z + 1}\right]}_{H_2[z]} \end{aligned}$$

We can realize this filter by placing the comb filter $H_1[z]$ in cascade with $H_2[z]$, which consists of a first-order filter and a second-order filter in parallel.

Pole-Zero Cancellation in Frequency Sampling Filters

With frequency sampling filters, we make an intriguing observation that a nonrecursive (FIR) filter is realized by a cascade of $H_1[z]$ and $H_2[z]$. However, $H_2[z]$ is recursive (IIR). This strange fact should alert us to the possibility of something interesting going on in this filter. For a nonrecursive filter, there can be no poles other than those at the origin [see Eq. (12.38)]. In the frequency sampling filter of Eq. (12.56), however, $H_2[z]$ has N_0 poles at $e^{jr\Omega_0}$ ($r = 0, 1, 2, \ldots, N_0 - 1$). All these poles lie on the unit circle at equally spaced points. These poles simply *cannot be* in a truly

nonrecursive filter. They must somehow get canceled along the way somewhere. This is precisely what happens. The zeros of $H_1[z]$ are exactly where the poles of $H_2[z]$ are because

$$z^{N_0} - 1 = (z - e^{j0\frac{2\pi}{N_0}})(z - e^{j\frac{2\pi}{N_0}})(z - e^{j2\frac{2\pi}{N_0}}) \cdots (z - e^{jn\frac{2\pi}{N_0}})$$

Thus, the poles of $H_2[z]$ are canceled by the zeros of $H_1[z]$, rendering the final filter nonrecursive.

Pole-zero cancellation in this filter is a potential cause for mischief because such a perfect cancellation assumes exact realization of both $H_1[z]$ and $H_2[z]$. Such a realization requires the use of infinite precision arithmetic, which is a practical impossibility because of quantization effects (finite word lengths). Imperfect cancellation of poles and zeros means there will still be poles on the unit circle, and the filter will not have a finite impulse response. More serious, however, is the fact that the resulting system will be marginally stable. Such a system provides no damping of the round-off noise that is introduced in filter computations. In fact, such noise tends to increase with time and may render the filter useless.

We can partially mitigate this problem by moving both the poles (of $H_2[z]$) and zeros (of $H_1[z]$) to a circle of radius $r = 1 - \epsilon$, where ϵ is a small positive number $\rightarrow$ 0. This artifice will make the overall system asymptotically stable.

Spectral Sampling with Windowing

The frequency sampling method can be modified to take advantage of windowing. We first design a frequency sampling filter using a value N_0' that is much higher than the design value N_0. The result is a filter that matches with the desired frequency response at a very large number (N_0') of points. Then we use a suitable N_0-point window to truncate the N_0'-point impulse response. This procedure yields the final design of a desired order.

12.9 MATLAB: Designing High-Order Filters

Continued hardware advancements have only solidified the popularity of discrete-time filters. Unlike their continuous-time counterparts, the performance of discrete-time filters is not affected by component variations, temperature, humidity, or age. Furthermore, digital hardware is easily reprogrammed, which allows convenient change of device function. For example, certain digital hearing aids are individually programmed to match the required response of a user.

Digital filters also allow for the implementation of high-order designs that are simply not practical using analog filters. Programs such as MATLAB greatly facilitate the design of high-order digital filters. In this section, we use MATLAB to design higher-order digital filters. We start with an IIR filter design using the bilinear transform and conclude with several examples of FIR design using the frequency sampling method.

12.9.1 IIR Filter Design Using the Bilinear Transform

Transformation of a continuous-time filter to a discrete-time filter begins with the desired continuous-time transfer function

$$H_a(s) = \frac{Y(s)}{X(s)} = \frac{B(s)}{A(s)} = \frac{\sum_{k=0}^{M} b_{k+N-M} s^{M-k}}{\sum_{k=0}^{N} a_k s^{N-k}}$$

As a matter of convenience, $H_a(s)$ is represented in factored form as

$$H_a(s) = \frac{b_{N-M}}{a_0} \frac{\prod_{k=1}^{M}(s - z_k)}{\prod_{k=1}^{N}(s - p_k)} \tag{12.57}$$

where z_k and p_k are the system poles and zeros, respectively.

A mapping rule converts the rational function $H_a(s)$ to a rational function $H[z]$. Section 12.6 introduced the bilinear transform, which maps s to z according to $s = 2(1 - z^{-1})/T(1 + z^{-1})$. Making this substitution into Eq. (12.57) yields

$$H[z] = \left(\frac{b_{N-M} \prod_{k=1}^{M}(2/T - z_k)}{a_0 \prod_{k=1}^{N}(2/T - p_k)} \right) \frac{\prod_{k=1}^{M} \left(1 - \frac{1+z_k T/2}{1-z_k T/2} z^{-1}\right)}{\prod_{k=1}^{N} \left(1 - \frac{1+p_k T/2}{1-p_k T/2} z^{-1}\right)} (1 + z^{-1})^{N-M} \tag{12.58}$$

In addition to the M zeros at $(1 + z_k T/2)/(1 - z_k T/2)$ and N poles at $(1 + p_k T/2)/(1 - p_k T/2)$, there are $N - M$ zeros at -1. Since practical continuous-time filters require $M \leq N$ for stability, the number of added zeros is thankfully always nonnegative.

If the continuous-time filter $H_a(s)$ does not prewarp critical frequencies, it is still possible to prewarp one critical CT frequency ω_c to match a desired digital frequency Ω_c by setting the parameter T used in Eq. (12.58) according to

$$T = \frac{2}{\omega_c} \tan\left(\frac{\Omega_c}{2}\right) \tag{12.59}$$

Let us illustrate the process with an example.

EXAMPLE 12.15 High-Order Butterworth LPF Design via MATLAB

Applying the bilinear transform to a normalized ($\omega_c = 1$) analog prototype, use MATLAB to design a 20th-order Butterworth lowpass filter with cutoff frequency $\Omega_c = \pi/3$. Create the filter's pole-zero and magnitude response plots.

To begin, we establish a few design variables and use Eq. (7.22) to compute the poles of the analog Butterworth prototype, which is an all-pole filter ($M = 0$).

```
>> omegac = 1; Omegac = pi/3; N = 20; M = 0;
>> k = 1:N; pk = exp(1j*pi*(2*k+N-1)/(2*N));
```

Next, we adjust T so the normalized cutoff frequency $\omega_c = 1$ transforms to the desired digital cutoff frequency $\Omega_c = \pi/3$.

```
>> T = 2/omegac*tan(Omegac/2);
```

Using Eq. (12.58), we determine the gain, zeros, and poles of our digital filter $H[z]$.

```
>> gain = 1/prod(2/T-pk); zeros = -1*ones(1,N);
>> poles = (1+pk*T/2)./(1-pk*T/2);
```

Next, we determine the polynomial coefficients of $H[z]$ and compute the digital filter's frequency response $H[e^{j\Omega}]$.

```
>> B = gain*poly(zeros); A = poly(poles);
>> Omega = linspace(0,pi,1001);
>> H = polyval(B,exp(1j*Omega))./polyval(A,exp(1j*Omega));
```

Due to the large order of the filter, we do not print out the coefficient vectors `B` and `A`; instead, we rely on pole-zero and magnitude response plots to verify the filter design.

```
>> subplot(121); circle = exp(1j*(0:.01:2*pi));
>> plot(real(zeros),imag(zeros),'ko',real(poles),imag(poles),'kx');
>> line(real(circle),imag(circle),'color',[0 0 0],'linestyle',':');
>> axis equal; axis([-1.1 1.1 -1.1 1.1]);
>> subplot(122);
>> plot(Omega,abs(H),'k-'); axis([0 pi 0 1.1]);
>> xlabel('\Omega'); ylabel('|H[e^{j\Omega}]|');
>> set(gca,'xtick',0:pi/3:pi); grid on;
```

As Fig. 12.23 shows, the resulting pole-zero and magnitude response plots confirm the final design is correct.

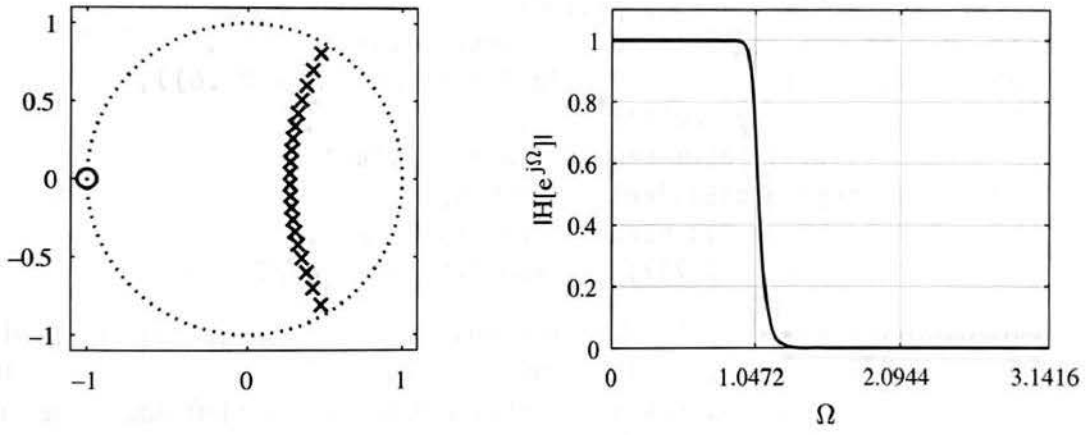

Figure 12.23 Pole-zero and magnitude response plots of a 20th-order Butterworth lowpass filter.

12.9.2 FIR Filter Design Using Frequency Sampling

Next, let us design several high-order FIR filters using the frequency sampling method described in Sec. 12.8.2. We shall look at the difference between a lowpass filter designed in an attempt to have no delay (zero phase) compared to one that allows a delay of half the filter length (linear phase). We also consider a design example of a filter that does not conform to the standard classification of lowpass, highpass, bandpass, or bandstop.

EXAMPLE 12.16 Effect of Delay on FIR LPF Performance

Repeat Ex. 12.13 using $N = 30$ for two cases: specifying frequency samples with zero phase (attempting a filter with no delay) and specifying frequency samples that allow a delay of half the filter length (linear phase). Plot the impulse response and magnitude response of each filter.

We can easily achieve this design with minor modification of the code in Ex. 12.13. In the first case, we change the order to $N = 30$, remove the linear-phase component, and add plotting routines for the impulse response.

```
>> N = 30; N0 = N+1; r = 0:N; Omega0 = 2*pi/N0;
>> Hr = 1.0*(r*Omega0<=pi/2);
>> Hr(1,fix(N0/2)+2:end) = conj(Hr(1,round(N0/2):-1:2));
>> h = ifft(Hr);
>> Omega = linspace(0,2*pi,1001);
>> H = polyval(h,exp(1j*Omega)).*exp(-1j*N*Omega);
>> subplot(211); stem(0:N,h,'k.'); axis([0 N -.2 .6]);
>> xlabel('n'); ylabel('h[n]');
>> subplot(212); stem(r*Omega0,abs(Hr),'k.');
>> line(Omega,abs(H),'color',[0 0 0]);
>> xlabel('\Omega'); ylabel('|H[e^{j\Omega}]|');
>> axis([0 2*pi 0 1.7]); set(gca,'xtick',0:pi/2:2*pi);
```

As shown in Fig. 12.24, although the magnitude response intersects the specified samples, it varies wildly between samples. The impulse response doesn't look very sinc-like. It has a peak at $n = 0$, but there is a big jump at the end as well. It is as if the left side of the sinc was split apart and wrapped to the end of $h[n]$.

Next, we reinsert the linear-phase component by changing the second line of code to

```
>> Hr = 1.0*(r*Omega0<=pi/2).*exp(-1j*r*pi*(N0-1)/N0);
```

Re-executing the code produces Fig. 12.25. Again, the magnitude response intersects the specified samples, but it is dramatically smoother (improved) between samples. This response looks like a lowpass filter. Correspondingly, the impulse response looks like the expected sinc function, albeit a delayed sinc function.

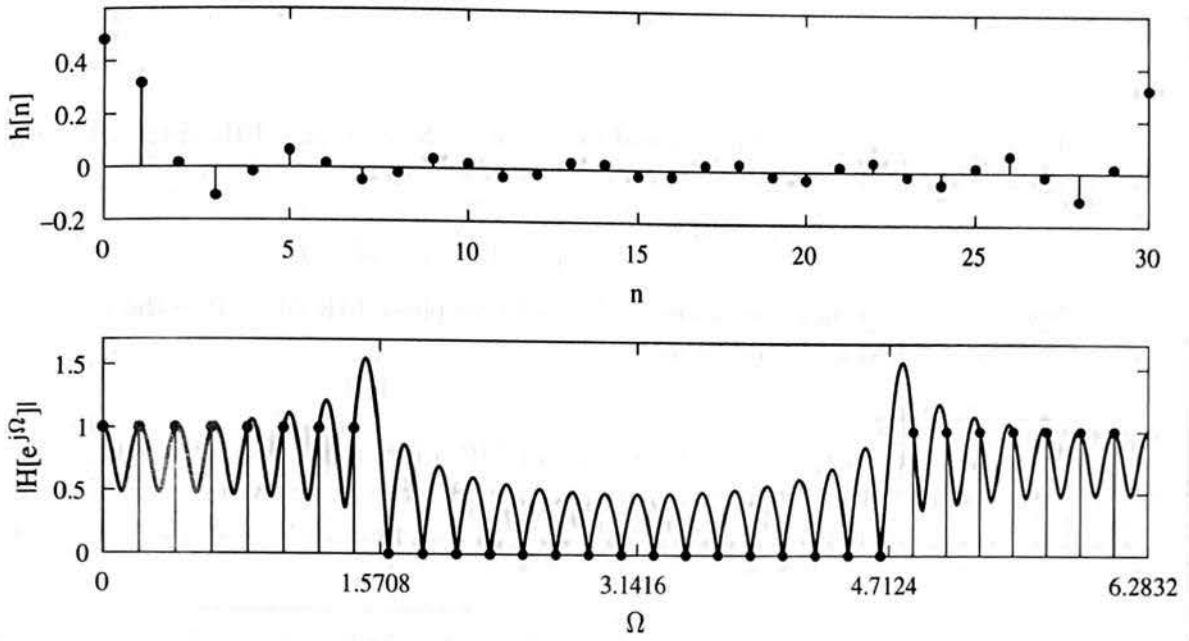

Figure 12.24 Impulse response and magnitude response plots of a 30th-order FIR LPF attempting zero delay.

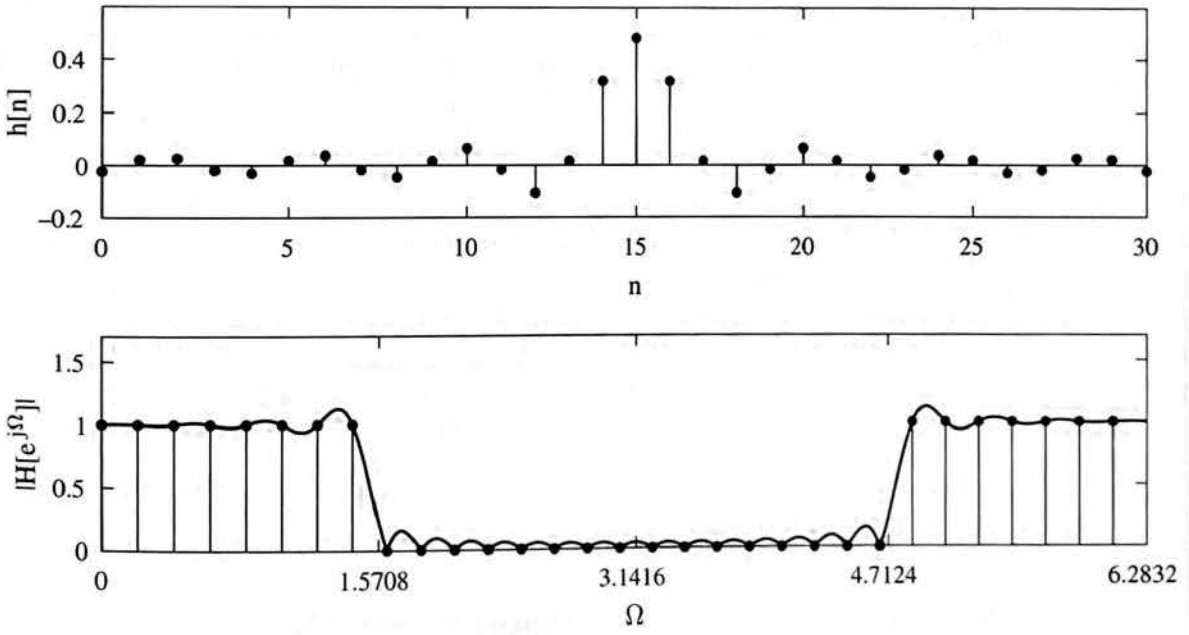

Figure 12.25 Impulse response and magnitude response plots of a 30th-order FIR LPF with linear phase.

EXAMPLE 12.17 FIR Filter with Arbitrary Magnitude Response

Use the frequency-sampling method to design an $N = 50$ real FIR filter whose magnitude response follows

$$|H[e^{j\Omega}]| = \begin{cases} 2-\Omega & 0 \le \Omega \le 2 \\ 0 & 2 < \Omega \le \pi \end{cases}$$

Specify the frequency samples to produce a linear-phase FIR filter. Plot the impulse response and magnitude response of the filter.

What we are trying to design here is an FIR filter that has a triangular response for low frequencies and rejects high frequencies. This is an easy filter to design with the frequency-sampling method, and requires only minor modification to the code in Ex. 12.13.

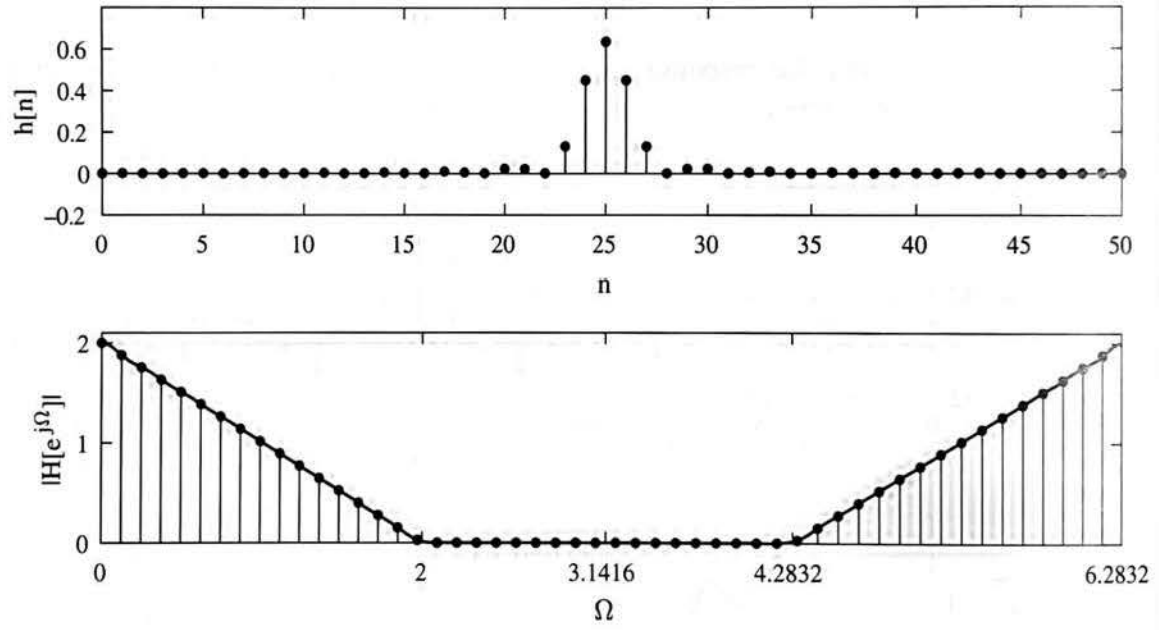

Figure 12.26 Impulse response and magnitude response plots of a 50th-order FIR filter with triangular magnitude response.

```
>> N = 50; N0 = N+1; r = 0:N; Omega0 = 2*pi/N0;
>> Hr = (2-r*Omega0).*(r*Omega0<=2).*exp(-1j*r*pi*(N0-1)/N0);
>> Hr(1,fix(N0/2)+2:end) = conj(Hr(1,round(N0/2):-1:2));
>> h = ifft(Hr);
>> Omega = linspace(0,2*pi,1001);
>> H = polyval(h,exp(1j*Omega)).*exp(-1j*N*Omega);
>> subplot(211); stem(0:N,h,'k.'); axis([0 N -.2 .8]);
>> xlabel('n'); ylabel('h[n]');
>> subplot(212); stem(r*Omega0,abs(Hr),'k.');
```

```
>> line(Omega,abs(H),'color',[0 0 0]);
>> xlabel('\Omega'); ylabel('|H[e^{j\Omega}]|');
>> axis([0 2*pi 0 2.1]); set(gca,'xtick',[0 2 pi 2*pi-2 2*pi]);
```

As shown in Fig. 12.26, the magnitude response closely follows the desired triangular shape. Since the impulse response is symmetric about its midpoint, we know that the filter has a linear-phase response. Since the edges of $h[n]$ are very close to zero, it is reasonable to expect that a lower-order filter would also produce acceptable results.

12.10 SUMMARY

The response of an LTID system with transfer function $H[z]$ to an everlasting sinusoid of frequency Ω is also an everlasting sinusoid of the same frequency. The output amplitude is $|H[e^{j\Omega}]|$ times the input amplitude, and the output sinusoid is shifted in phase with respect to the input sinusoid by $\angle H[e^{j\Omega}]$ radians. A plot of $|H[e^{j\Omega}]|$ versus Ω indicates the amplitude gain of sinusoids of various frequencies and is called the *amplitude response* of the system. A plot of $\angle H[e^{j\Omega}]$ versus Ω indicates the phase shift of sinusoids of various frequencies and is called the *phase response*. The frequency response of an LTID system is a periodic function of Ω with period 2π. This periodicity is the result of the fact that discrete-time sinusoids with frequencies differing by an integral multiple of 2π are identical.

The frequency response of a system is determined by locations in the complex plane of poles and zeros of its transfer function. We can design frequency-selective filters by proper placement of its transfer function poles and zeros. Placing a pole (or a zero) near the point $e^{j\Omega_0}$ in the complex plane enhances (or suppresses) the frequency response at the frequency $\Omega = \Omega_0$. Using this concept, a proper combination of poles and zeros at suitable locations can yield desired filter characteristics.

Digital filters are classified into recursive and nonrecursive filters. The duration of the impulse response of a recursive filter is infinite; that of the nonrecursive filter is finite. For this reason, recursive filters are also called infinite impulse response (IIR) filters, and nonrecursive filters are called finite impulse response (FIR) filters.

Using A/D and D/A interfaces, digital filters can process analog signals. Procedures for designing a digital filter that behaves like a given analog filter are discussed. A digital filter can approximate the behavior of a given analog filter in either the time domain or the frequency domain. This leads to two different design procedures, one using a time-domain equivalence criterion and the other a frequency-domain equivalence criterion.

For recursive or IIR filters, the time-domain equivalence criterion yields the impulse invariance method, and the frequency-domain equivalence criterion yields the bilinear transformation method. The impulse invariance method is handicapped by aliasing and cannot be used for highpass and bandstop filters. The bilinear transformation method, which is generally superior to the impulse invariance method, suffers from a frequency warping effect. However, this effect can be neutralized by prewarping.

For nonrecursive or FIR filters, the time-domain equivalence criterion leads to the method of windowing (Fourier series method), and the frequency-domain equivalence criterion leads to the method of frequency sampling. Because nonrecursive filters are a special case of recursive

filters, we expect the performance of recursive filters to be superior. This statement is true in the sense that a given amplitude response can be achieved by a recursive filter of an order smaller than that required for the corresponding nonrecursive filter. However, nonrecursive filters have the advantage that they can realize arbitrarily shaped amplitude responses and can possess linear-phase characteristics. Recursive filters are good for piecewise constant amplitude responses, and they can realize linear phase only approximately. A linear-phase characteristic in nonrecursive filters requires that the impulse response $h[n]$ be either symmetric or antisymmetric about its center point.

Reference

1. Mitra, S. K. *Digital Signal Processing: A Computer-Based Approach*, 2nd ed. McGraw-Hill, New York, 2001.

PROBLEMS

12.1-1 A CT sinusoid $x(t) = \cos(\omega t)$ is sampled at a greater-than-Nyquist rate $f_s = 1000$ Hz to produce a DT sinusoid $x(t) = \cos(\Omega n)$. Determine the analog frequency ω if

(a) $\Omega = \frac{\pi}{4}$

(b) $\Omega = \frac{2\pi}{3}$

(c) $\Omega = \frac{7}{8}$

12.1-2 Find the amplitude and phase response of the digital filters depicted in Fig. P12.1-2.

12.1-3 A causal LTID system $H[z] = \frac{21(z-j)(z+j)}{16(z-\frac{1}{2})(z+\frac{3}{4})}$ has a periodic input $x[n]$ that toggles between the values 1 and 2. That is, $x[n] = [\ldots, 1, 2, 1, \underset{\downarrow}{2}, 1, 2, 1, \ldots]$, where $x[0] = 2$.

(a) Plot the magnitude response $|H[e^{j\Omega}]|$ over $-2\pi \le \Omega \le 2\pi$.

(b) Plot the phase response $\angle H[e^{j\Omega}]$ over $-2\pi \le \Omega \le 2\pi$.

(c) Determine the system output $y[n]$ in response to the periodic input $x[n]$.

12.1-4 A causal LTID system $H[z] = \frac{-7(z+1)}{32(z-j\frac{3}{4})(z+j\frac{3}{4})}$ has a periodic input $x[n]$ that cycles through the four values 3, 2, 1, and 2. That is, $x[n] = [\ldots, 3, 2, 1, 2, \underset{\downarrow}{3}, 2, 1, 2, \ldots]$, where $x[0] = 3$.

(a) Plot the magnitude response $|H[e^{j\Omega}]|$ over $-2\pi \le \Omega \le 2\pi$.

(b) Plot the phase response $\angle H[e^{j\Omega}]$ over $-2\pi \le \Omega \le 2\pi$.

(c) Determine the system output $y[n]$ in response to the periodic input $x[n]$.

12.1-5 Find the amplitude and the phase response of the filters shown in Fig. P12.1-5. [*Hint:* Express $H[e^{j\Omega}]$ as $e^{-j2.5\Omega}H_a[e^{j\Omega}]$.]

12.1-6 Find the frequency response for the moving-average system in Prob. 8.5-3. The input–output equation of this system is given by

$$y[n] = \frac{1}{5}\sum_{k=0}^{4} x[n-k]$$

12.1-7 (a) Input–output relationships of two filters are described by

(i) $y[n] = -0.9y[n-1] + x[n]$

(ii) $y[n] = 0.9y[n-1] + x[n]$

For each case, find the transfer function, the amplitude response, and the phase response. Sketch the amplitude response, and state the type (highpass, lowpass, etc.) of each filter.

(b) Find the response of each of these filters to a sinusoid $x[n] = \cos\Omega n$ for $\Omega = 0.01\pi$ and 0.99π. In general, show that

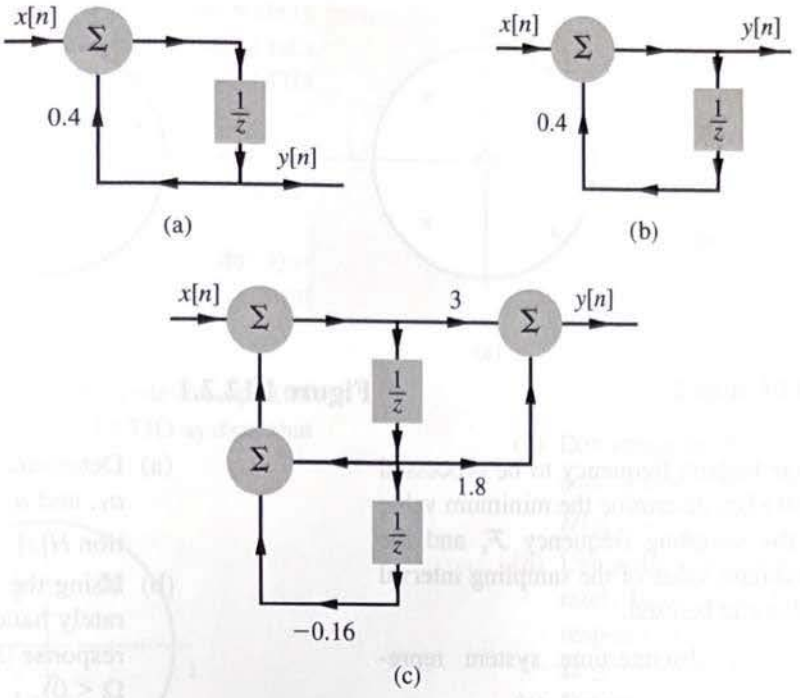

Figure P12.1-2

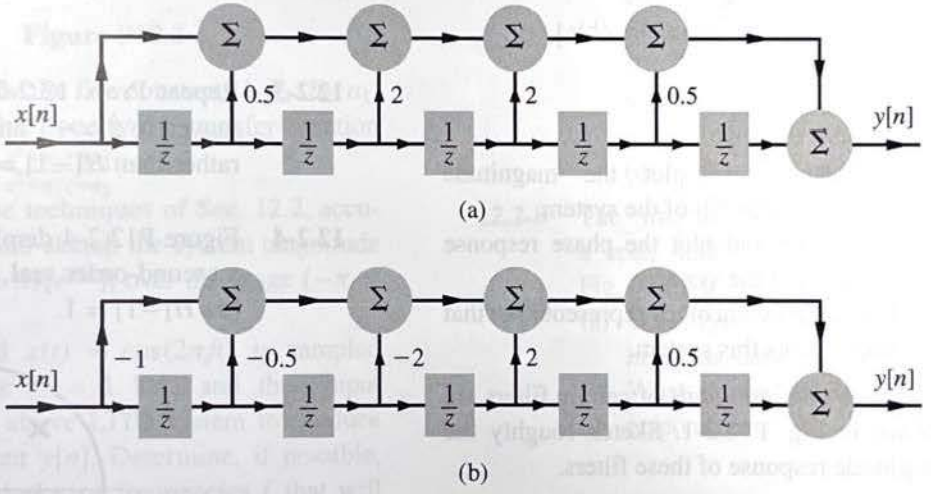

Figure P12.1-5

the gain (amplitude response) of filter (i) at frequency Ω_0 is the same as the gain of filter (ii) at frequency $\pi - \Omega_0$.

12.1-8 For an LTID system specified by the equation

$$y[n+1] - 0.5y[n] = x[n+1] + 0.8x[n]$$

(a) Find the amplitude and the phase response.

(b) Find the system response $y[n]$ for the input $x[n] = \cos(0.5k - (\pi/3))$.

12.1-9 For an asymptotically stable LTID system, show that the steady-state response to input $e^{j\Omega n}u[n]$ is $H[e^{j\Omega}]e^{j\Omega n}u[n]$. The steady-state response is that part of the response that does not decay with time and persists forever.

12.1-10 (a) A digital filter has the sampling interval $T = 50\,\mu s$. Determine the highest frequency that can be processed by this filter without aliasing.

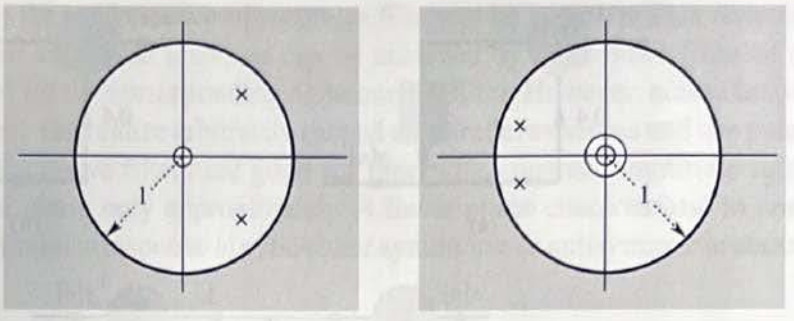

(a) (b)

Figure P12.2.1

(b) If the highest frequency to be processed is 50 kHz, determine the minimum value of the sampling frequency $\mathcal{F}_s$ and the maximum value of the sampling interval T that can be used.

12.1-11 Consider the discrete-time system represented by

$$y[n] = \sum_{k=0}^{\infty} (0.5)^k x[n-k]$$

(a) Determine and plot the magnitude response $|H[e^{j\Omega}]|$ of the system.
(b) Determine and plot the phase response $\angle H[e^{j\Omega}]$ of the system.
(c) Find an efficient block representation that implements this system.

12.2-1 Pole-zero configurations of certain filters are shown in Fig. P12.2-1. Sketch roughly the amplitude response of these filters.

12.2-2 Figure P12.2-2 displays the pole-zero plot of a second-order real, causal LTID system that has $H[-1] = -1$.

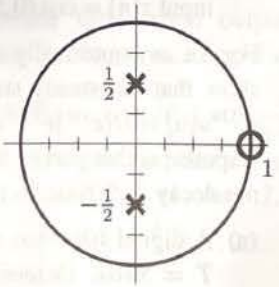

Figure P12.2-2

(a) Determine the five constants b_0, b_1, b_2, a_1, and a_2 that specify the transfer function $H[z] = \frac{b_0 z^2 + b_1 z + b_2}{z^2 + a_1 z + a_2}$.
(b) Using the techniques of Sec. 12.2, accurately hand-sketch the system magnitude response $|H[e^{j\Omega}]|$ over the range $(-2\pi \leq \Omega \leq 0)$.
(c) Determine the output $y[n]$ of this system if the input is $x[n] = \sin\left(\frac{\pi n}{2}\right)$.

12.2-3 Repeat Prob. 12.2-2 if the zero at $z = 1$ is moved to $z = -1$ and $H[1] = -1$ is specified rather than $H[-1] = -1$.

12.2-4 Figure P12.2-4 displays the pole-zero plot of a second-order real, causal LTID system that has $H[-1] = 1$.

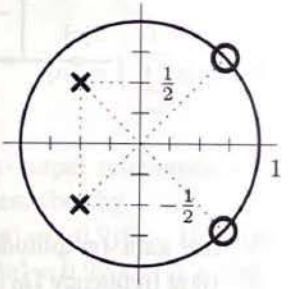

Figure P12.2-4

(a) Determine the five constants k, b_1, b_2, a_1, and a_2 that specify the transfer function $H[z] = k\frac{z^2 + b_1 z + b_2}{z^2 + a_1 z + a_2}$.
(b) Using the techniques of Sec. 12.2, accurately hand-sketch the system magnitude response $|H[e^{j\Omega}]|$ over the range $(-\pi \leq \Omega \leq \pi)$.

(c) A signal $x(t) = \cos(100\pi t) + \cos(500\pi t)$ is sampled at a greater than Nyquist rate f_s Hz and then input into the above LTID system to produce DT output $y[n] = \beta\cos(\Omega_0 n + \theta)$. Determine f_s and Ω_0. You do not need to find constants β and θ.

(d) Is the impulse response $h[n]$ of this system absolutely summable? Justify your answer.

12.2-5 Figure P12.2-5 displays the pole-zero plot of a second-order real, causal LTID system that has $H[1] = -1$.

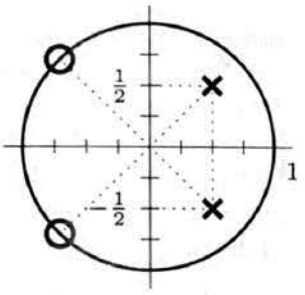

Figure P12.2-5

(a) Determine the five constants k, b_1, b_2, a_1, and a_2 that specify the transfer function $H[z] = k\frac{z^2+b_1z+b_2}{z^2+a_1z+a_2}$.

(b) Using the techniques of Sec. 12.2, accurately hand-sketch the system magnitude response $|H[e^{j\Omega}]|$ over the range $(-\pi \leq \Omega \leq \pi)$.

(c) A signal $x(t) = \cos(2\pi ft)$ is sampled at a rate $f_s = 1$ kHz and then input into the above LTID system to produce DT output $y[n]$. Determine, if possible, the frequency or frequencies f that will produce zero output, $y[n] = 0$.

12.2-6 The system $y[n] - y[n-1] = x[n] - x[n-1]$ is an all-pass system that has zero phase response. Is there any difference between this system and the system $y[n] = x[n]$? Justify your answer.

12.2-7 Figure P12.2-7 displays the pole-zero plot of a second-order real, causal LTID system that has a repeated zero and $H[1] = 4$. The solid circle is the unit circle.

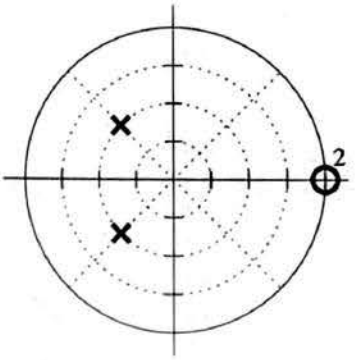

Figure P12.2-7

(a) Determine the five constants k, b_1, b_2, a_1, and a_2 that specify the transfer function $H[z] = k\frac{z^2+b_1z+b_2}{z^2+a_1z+a_2}$.

(b) Using the techniques of Sec. 12.2, accurately hand-sketch the system magnitude response $|H[e^{j\Omega}]|$ over the range $(-\pi \leq \Omega \leq \pi)$.

(c) Determine the steady-state output $y_{ss}[n]$ of this system if the input is $x[n] = \cos(\frac{3\pi n}{4})u[n]$.

(d) State whether this system is LP, HP, BP, BS, or something else. If the digital system operates at $f_s = 8$ kHz, what is the approximate Hertzian cutoff frequency (or frequencies) of this system?

12.2-8 The magnitude and phase responses of a real, stable, LTI system are shown in Fig. P12.2-8.

(a) What type of system is this: lowpass, highpass, bandpass, or bandstop?

(b) What is the output of this system in response to

$$x_1[n] = 2\sin\left(\frac{\pi}{2}n + \frac{\pi}{4}\right)$$

(c) What is the output of this system in response to

$$x_2[n] = \cos\left(\frac{7\pi}{4}n\right)$$

12.2-9 Consider an LTID system with system function $H[z] = b_0\frac{z^2+1}{z^2-9/16}$.

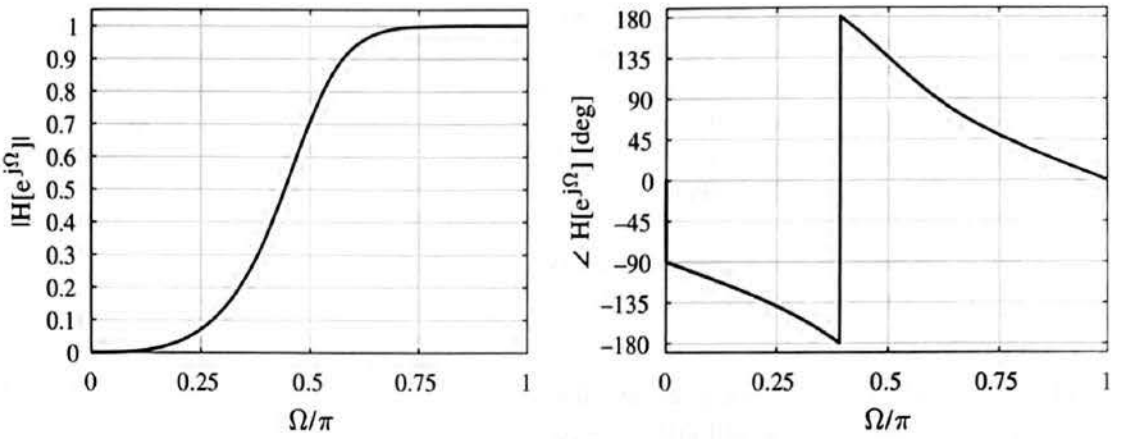

Figure P12.2-8

(a) Determine the constant b_0 so that the system frequency response at $\Omega = -\pi$ is -1.

(b) Accurately sketch the system poles and zeros.

(c) Using the locations of the system poles and zeros, sketch $|H[e^{j\Omega}]|$ over $0 \leq \Omega \leq 2\pi$.

(d) Determine the response $y[n]$ to the input $x[n] = (-1 + j) + j^n + (1 - j)\sin(\pi n + 1)$.

(e) Draw an appropriate block diagram representation of this system.

12.2-10 Do Prob. 12.9-3 by graphical procedure. Make the sketches approximately, without using MATLAB.

12.2-11 (a) Realize a digital filter whose transfer function is given by

$$H[z] = K\frac{z+1}{z-a}$$

(b) Sketch the amplitude response of this filter, assuming $|a| < 1$.

(c) The amplitude response of this lowpass filter is maximum at $\Omega = 0$. The 3 dB bandwidth is the frequency at which the amplitude response drops to 0.707 (or $1/\sqrt{2}$) times its maximum value. Determine the 3 dB bandwidth of this filter when $a = 0.2$.

12.2-12 Design a digital notch filter to reject frequency 5000 Hz completely and to have a sharp recovery on either side of 5000 Hz to a gain of unity. The highest frequency to be processed is 20 kHz ($\mathcal{F}_h = 20{,}000$). [*Hint:* See Ex. 12.3. The zeros should be at $e^{\pm j\omega T}$ for ω corresponding to 5000 Hz, and the poles are at $ae^{\pm j\omega T}$ with $a < 1$. Leave your answer in terms of a. Realize this filter using the canonical form. Find the amplitude response of the filter.]

12.2-13 Consider the desired DT system magnitude response $|H[e^{j\Omega}]|$ in Fig. P12.2-13.

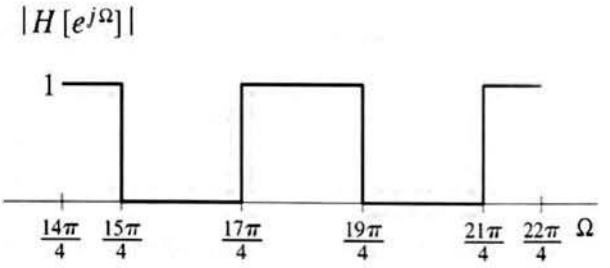

Figure P12.2-13

(a) Is the filter LP, HP, BP, BS, or something else? Explain.

(b) Sketch the pole-zero plot of a second-order system that behaves as a reasonable approximation of Fig. P12.2-13. What is the coefficient b_0?

12.2-14 Show that a first-order LTID system with a pole at $z = r$ and a zero at $z = 1/r$ ($r \leq 1$) is an allpass filter. In other words, show that the amplitude response $|H[e^{j\Omega}]|$ of a system with the transfer function

$$H[z] = \frac{z - \frac{1}{r}}{z - r} \qquad r \leq 1$$

is constant with frequency. This is a first-order allpass filter. [*Hint:* Show that the ratio of the distances of any point on the unit circle from the zero (at $z = 1/r$) and the pole (at $z = r$) is a constant $1/r$.]

Generalize this result to show that an LTID system with two poles at $z = re^{\pm j\theta}$ and two zeros at $z = (1/r)e^{\pm j\theta}$ $(r \leq 1)$ is an allpass filter. In other words, show that the amplitude response of a system with the transfer function

$$H[z] = \frac{\left(z - \frac{1}{r}e^{j\theta}\right)\left(z - \frac{1}{r}e^{-j\theta}\right)}{(z - re^{j\theta})(z - re^{-j\theta})} = \frac{z^2 - \left(\frac{2}{r}\cos\theta\right)z + \frac{1}{r^2}}{z^2 - (2r\cos\theta)z + r^2} \qquad r \leq 1$$

is constant with frequency.

12.2-15 (a) If $h_1[n]$ and $h_2[n]$, the impulse responses of two LTID systems, are related by $h_2[n] = (-1)^n h_1[n]$, then show that

$$H_2[e^{j\Omega}] = H_1[e^{j(\Omega \pm \pi)}]$$

How is the frequency response spectrum $H_2[e^{j\Omega}]$ related to $H_1[e^{j\Omega}]$?

(b) If $H_1[z]$ represents an ideal lowpass filter with cutoff frequency Ω_c, sketch $H_2[e^{j\Omega}]$. What type of filter is $H_2[e^{j\Omega}]$?

12.2-16 Mappings such as the bilinear transformation are useful in the conversion of continuous-time filters to discrete-time filters. Another useful type of transformation is one that converts a discrete-time filter into a different type of discrete-time filter. Consider a transformation that replaces z with $-z$.

(a) Show that this transformation converts lowpass filters into highpass filters and highpass filters into lowpass filters.

(b) If the original filter is an FIR filter with impulse response $h[n]$, what is the impulse response of the transformed filter?

12.4-1 A lowpass digital filter with a sampling interval $T = 50$ μs has a cutoff frequency of $f_c = 10$ kHz.

(a) What is the corresponding digital cutoff frequency Ω_c?

(b) If the system running the filter now operates at $T = 25$ μs, determine the cutoff frequencies f_c and Ω_c.

(c) If the system running the filter now operates at $T = 100$ μs, determine the cutoff frequencies f_c and Ω_c.

12.5-1 In Ch. 8, we used another approximation to find a digital system to realize an analog system. We showed that an analog system specified by Eq. (8.19) can be realized by using the digital system specified by Eq. (8.20). Compare that solution with the one resulting from the impulse-invariance method. Show that one result is a close approximation of the other and that the approximation improves as $T \to 0$.

12.5-2 A CT system has impulse response $h_{ct}(t) = e^{-t}u(t)$. Draw the DFI realization of the corresponding DT system designed by the impulse-invariance method with $T = 0.1$.

12.5-3 (a) Using the impulse-invariance criterion, design a digital filter to realize an analog filter with transfer function

$$H_a(s) = \frac{7s + 20}{2(s^2 + 7s + 10)}$$

(b) Show a canonical and a parallel realization of the filter. Use a 1% criterion for the choice of T.

12.5-4 Use the impulse-invariance criterion to design a digital filter to realize the second-order analog Butterworth filter with transfer function

$$H_a(s) = \frac{1}{s^2 + \sqrt{2}s + 1}$$

Use a 1% criterion for the choice of T.

12.5-5 Design a digital integrator using the impulse-invariance method. Find and give a rough sketch of the amplitude response, and compare it with that of the ideal integrator. If this integrator is used primarily for integrating audio signals (whose bandwidth is 20 kHz), determine a suitable value for T.

12.5-6 An oscillator by definition is a source (no input) that generates a sinusoid of a certain frequency ω_0. Therefore, an oscillator is a system whose zero-input response is a sinusoid of the desired frequency. Find the

transfer function of a digital oscillator to oscillate at 10 kHz by the methods described in parts (a) and (b). In both methods, select T so that there are 10 samples in each cycle of the sinusoid.

(a) Choose $H[z]$ directly so that its zero-input response is a discrete-time sinusoid of frequency $\Omega = \omega T$ corresponding to 10 kHz.

(b) Choose $H_a(s)$ whose zero-input response is an analog sinusoid of 10 kHz. Now use the impulse invariance method to determine $H[z]$.

(c) Show a canonical realization of the oscillator.

12.5-7 A variant of the impulse invariance method is the *step-invariance* method of digital filter synthesis. In this method, for a given $H_a(s)$, we design $H[z]$ in Fig. 12.9a such that $y(nT)$ in Fig. 12.9b is identical to $y[n]$ in Fig. 12.9a when $x(t) = u(t)$.

(a) Show that, in general,

$$H[z] = \frac{z-1}{z}\mathcal{Z}\left[\left(\mathcal{L}^{-1}\frac{H_a(s)}{s}\right)_{t=kT}\right]$$

(b) Use this method to design $H[z]$ for

$$H_a(s) = \frac{\omega_c}{s+\omega_c}$$

(c) Use the step-invariance method to synthesize a discrete-time integrator and compare its amplitude response with that of the ideal integrator.

12.5-8 Use the *ramp-invariance* method to synthesize a discrete-time differentiator and integrator. In this method, for a given $H_a(s)$, we design $H[z]$ such that $y(nT)$ in Fig. 12.9b is identical to $y[n]$ in Fig. 12.9a when $x(t) = tu(t)$.

12.5-9 In an impulse-invariance design, show that if $H_a(s)$ is a transfer function of a stable system, the corresponding $H[z]$ is also a transfer function of a stable system.

12.6-1 The bilinear transformation is defined by the rule $s = 2(1-z^{-1})/T(1+z^{-1})$.

(a) Show that this transformation maps the ω axis in the s plane to the unit circle $z = e^{j\Omega}$ in the z plane.

(b) Show that this transformation maps Ω to $2\arctan(\omega T/2)$.

12.6-2 Consider the design of a digital differentiator $H[z]$.

(a) Determine $H[z]$ using the bilinear transform.

(b) Show a realization of this filter.

(c) Find and sketch the magnitude response of this filter, and compare it with that of an ideal differentiator.

(d) If this filter is used primarily for processing audio signals (voice and music) up to 20 kHz, determine a suitable value for T.

12.6-3 Repeat Prob. 12.6-2 for a digital integrator.

12.6-4 Using the bilinear transform with prewarping, design a digital lowpass Butterworth filter that satisfies $\hat{G}_p = -2$ dB, $\hat{G}_s = -11$ dB, $\omega_p = 100\pi$ rad/s, and $\omega_s = 200\pi$ rad/s. The highest significant frequency is 250 Hz. If possible, it is desirable to oversatisfy the requirement of $\hat{G}_s$.

12.6-5 Repeat Prob. 12.6-4 for a Chebyshev filter.

12.6-6 Using the bilinear transform with prewarping, design a digital highpass Butterworth filter that satisfies $\hat{G}_p = -2$ dB, $\hat{G}_s = -10$ dB, $\omega_p = 150\pi$ rad/s, and $\omega_s = 100\pi$ rad/s. The highest significant frequency is 200 Hz.

12.6-7 Repeat Prob. 12.6-6 using an inverse Chebyshev filter.

12.6-8 Using the bilinear transform with prewarping, design a digital bandpass Butterworth filter that satisfies $\hat{G}_p = -2$ dB, $\hat{G}_s = -12$ dB, $\omega_{p_1} = 120$ rad/s, $\omega_{p_2} = 300$ rad/s, $\omega_{s_1} = 45$ rad/s, and $\omega_{s_2} = 450$ rad/s. The highest significant frequency is 500 Hz.

12.6-9 Repeat Prob. 12.6-8 for a Chebyshev filter.

12.6-10 Using the bilinear transform with prewarping, design a digital bandstop Butterworth filter that satisfies $\hat{G}_p = -1$ dB, $\hat{G}_s = -22$ dB, $\omega_{p_1} = 40$ rad/s, $\omega_{p_2} = 195$ rad/s, $\omega_{s_1} = 80$ rad/s, and $\omega_{s_2} = 120$ rad/s. The highest significant frequency is 200 Hz.

12.6-11 Repeat Prob. 12.6-10 for a Chebyshev filter.

12.6-12 The bilinear transform, given by Eq. (12.30), is actually a one-to-one mapping relationship between the s plane and the z plane.

(a) Show that the bilinear transform maps the ω axis in the s plane to the unit circle in the z plane.

(b) Show that the bilinear transform maps the LHP and the RHP of the s plane map to the interior and the exterior, respectively, of the unit circle in the z plane.

(c) Show that the bilinear transform maps a stable continuous-time system $H_a(s)$ to a stable discrete-time system $H[z]$.

12.7-1 (a) Show that the frequency response of a third-order ($N = 3$) FIR filter with a midpoint symmetric impulse response $h[n]$ is given by

$$H[e^{j\Omega}] = 2e^{-j1.5\Omega} \times (h[0]\cos(3\Omega/2) + h[1]\cos(\Omega/2))$$

(b) Show that the frequency response of a third-order ($N = 3$) FIR filter with a midpoint antisymmetric impulse response $h[n]$ is given by

$$H[e^{j\Omega}] = 2e^{j(\frac{\pi}{2}-1.5\Omega)} \times (h[0]\sin(3\Omega/2) + h[1]\sin(\Omega/2))$$

12.7-2 Another form of comb filter is given by the transfer function

$$H[z] = 1 + z^{-N}$$

For this problem, let $N = 6$.

(a) Find the filter's impulse response $h[n]$.

(b) Determine a canonical realization of this filter.

(c) Find and plot the magnitude and phase responses of this filter.

12.8-1 Using the Fourier series method, design an $N = 14$ FIR filter to approximate an ideal lowpass filter with a cutoff frequency of 20 kHz. Let the sampling frequency be $f_s = 200$ kHz.

12.8-2 Repeat Prob. 12.8-1 using the window design method and a Hamming window.

12.8-3 Using the Fourier series method, design an $N = 10$ FIR filter to approximate the ideal bandpass filter shown in Fig. P12.8-3. Let $T = 2 \times 10^{-3}$.

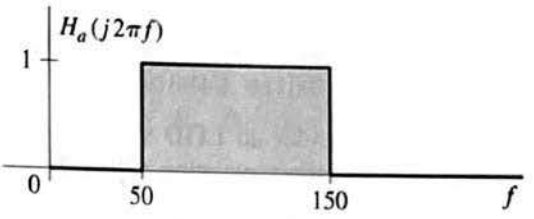

Figure P12.8-3

12.8-4 Consider the length-7 ($N = 6$) lowpass FIR filter of Ex. 12.11. Redesign this filter using a Hann window, and plot the resulting magnitude response $|H[e^{j\Omega}]|$. How does this filter compare with those of Ex. 12.11?

12.8-5 Consider the $N = 10$ FIR differentiators of Ex. 12.12. Redesign this filter using a Blackman window, and plot the resulting magnitude response. How does this solution compare with those of Ex. 12.12?

12.8-6 An ideal (bandlimited) $\pi/2$ phase shifter (Hilbert transformer) is given by

$$H_a(j\omega) = -j\,\mathrm{sgn}(\omega)\Pi\left(\frac{\omega}{2\pi/T}\right)$$

(a) Sketch $|H_a(j\omega)|$ and $\angle H_a(j\omega)$.

(b) Using rectangular and Hamming windows, apply the window method to design $N = 14$ FIR filters to approximate $H_a(j\omega)$. Plot the resulting magnitude and phase responses, and compare them with the ideal.

12.8-7 Using the frequency sampling method (with linear phase), design an $N = 10$ digital differentiator. Compare both $h[n]$ and $H[e^{j\Omega}]$ of the resulting design with the $N = 10$ designs of Ex. 12.12.

12.9-1 Use MATLAB to generate pole-zero plots for the causal systems with the following transfer functions:

(a) $H_a[z] = \frac{z^4 - \sqrt{2}z^2 + 1}{z^4 + 0.4096}$

(b) $H_b[z] = \frac{-3z^{-1} + \frac{3}{4}z^{-3}}{3 + \frac{3}{2}z^{-2} + 2z^{-4}}$

In each case, determine whether the system is stable.

12.9-2 For each of the following stable LTID systems, use MATLAB to generate magnitude and phase response plots over $-\pi \leq \Omega < \pi$.

(a) $H_a[z] = \frac{\cos(z)}{z-0.5}$

(b) $H_b[z] = z^3 \sin(z^{-1})$

12.9-3 Consider an LTID system described by the difference equation $4y[n+2] - y[n] = x[n+2] + x[n]$.

(a) Plot the pole-zero diagram for this system.

(b) Plot the system's magnitude response $|H[e^{j\Omega}]|$ over $-\pi \leq \Omega \leq \pi$.

(c) What type of system is this: lowpass, highpass, bandpass, or bandstop?

(d) Is this system stable? Justify your answer.

(e) Is this system real? Justify your answer.

(f) If the system input is of the form $x[n] = \cos(\Omega n)$, what is the greatest possible amplitude of the output? Justify your answer.

(g) Draw an efficient, causal implementation of this system using only add, scale, and delay blocks.

12.9-4 Consider an LTID system with system function $H(z) = b_0 \frac{z^2+1}{z^2-4/9}$.

(a) Determine the constant b_0 so that the system frequency response at $\Omega = -\pi$ is -1.

(b) Plot the pole-zero diagram for this system.

(c) Plot the system's magnitude response $|H[e^{j\Omega}]|$ over $-\pi \leq \Omega \leq \pi$.

(d) Plot the system's phase response $\angle H[e^{j\Omega}]$ over $-\pi \leq \Omega \leq \pi$.

(e) What type of system is this: lowpass, highpass, bandpass, or bandstop?

(f) Determine the response $y[n]$ to the input $x[n] = (-1-j) + (-j)^n + (1-j)\cos(\pi n + \frac{1}{3})$.

(g) Draw a TDFII block diagram representation of this system.

12.9-5 Consider the LTID system shown in Fig. P12.9-5, where parameters c_1 and c_2 are arbitrary constants.

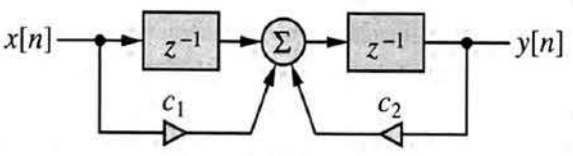

Figure P12.9-5

(a) Determine the system function $H[z]$, expressed in standard rational form.

(b) What is the order N of this system?

(c) Determine the N poles and N zeros of this system. Use MATLAB to create the corresponding pole-zero plot.

(d) What constraints, if any, exist on parameters c_1 and c_2 to ensure that the system is stable?

(e) Determine c_1 and c_2 so that this system functions as an LPF with narrow passband. Use MATLAB to generate the corresponding magnitude response $|H[e^{j\Omega}]|$ over $-\pi \leq \Omega \leq \pi$.

(f) Ms. Zeroine, the heroine of DT systems, believes that if $x[n] = 0$, then $y[n] = 0$ also. Is Ms. Zeroine correct? Fully justify your answer.

(g) Dr. Strange suggests that by setting $c_1 = -1$ and $c_2 = -2$, the system will act as a highpass filter. Is Dr. Strange right? Fully justify your answer.

12.9-6 One interesting and useful application of discrete systems is the implementation of complex (rather than real) systems. A complex system is one in which a real-valued input can produce a complex-valued output. Complex systems that are described by constant coefficient difference equations require at least one complex-valued coefficient, and they are capable of operating on complex-valued inputs.

Consider the complex discrete-time system

$$H[z] = \frac{z^2 - j}{z - 0.9e^{j3\pi/4}}$$

(a) Determine and plot the system zeros and poles.

(b) Sketch the magnitude response $|H[e^{j\omega}]|$ of this system over $-2\pi \leq \omega \leq 2\pi$. Comment on the system's behavior.

12.9-7 Consider the complex system

$$H[z] = \frac{z^4 - 1}{2(z^2 + 0.81j)}$$

Refer to Prob. 12.9-6 for an introduction to complex systems.

(a) Plot the pole-zero diagram for $H[z]$.

(b) Plot the system's magnitude response $|H[e^{j\Omega}]|$ over $-\pi \leq \Omega \leq \pi$.

(c) Explain why $H[z]$ is a noncausal system. Do not give a general definition of causality; specifically identify what makes this system noncausal.

(d) One way to make this system causal is to add two poles to $H[z]$. That is,

$$H_{\text{causal}}[z] = H[z]\frac{1}{(z-a)(z-b)}$$

Find poles a and b such that $|H_{\text{causal}}[e^{j\Omega}]| = |H[e^{j\Omega}]|$.

(e) Draw an efficient block implementation of $H_{\text{causal}}[z]$.

12.9-8 The MATLAB signal-processing toolbox function `butter` helps design digital Butterworth filters. Use MATLAB help to learn how `butter` works. For each of the following cases, design the filter, plot the filter's poles and zeros in the complex z plane, and plot the decibel magnitude response $20\log_{10}|H[e^{j\Omega}]|$.

(a) Design an eighth-order digital lowpass filter with $\Omega_c = \pi/3$.

(b) Design an eighth-order digital highpass filter with $\Omega_c = \pi/3$.

(c) Design an eighth-order digital bandpass filter with a passband between $5\pi/24$ and $11\pi/24$.

(d) Design an eighth-order digital bandstop filter with a stopband between $5\pi/24$ and $11\pi/24$.

12.9-9 The MATLAB signal-processing toolbox function `cheby1` helps design digital Chebyshev type I filters. A Chebyshev type I filter has passband ripple and smooth stopband. Setting the passband ripple to $R_p = 3$ dB, repeat Prob. 12.9-8 using the `cheby1` command. With all other parameters held constant, what is the general effect of reducing R_p, the allowable passband ripple?

12.9-10 The MATLAB signal-processing toolbox function `cheby2` helps design digital inverse Chebyshev filters. An inverse Chebyshev filter has a smooth passband and ripple in the stopband. Setting the stopband ripple $R_s =$ 20 dB down, repeat Prob. 12.9-8 using the `cheby2` command. With all other parameters held constant, what is the general effect of increasing R_s, the minimum stopband attenuation?

12.9-11 The MATLAB signal-processing toolbox function `ellip` helps design digital elliptic filters. An elliptic filter has ripple in both the passband and the stopband. Setting the passband ripple to $R_p = 3$ dB and the stopband ripple $R_s = 20$ dB down, repeat Prob. 12.9-8 using the `ellip` command.

12.9-12 Using the frequency sampling method, design an $N = 34$ linear-phase FIR highstop filter that has cutoff frequency $\Omega_c = 2\pi/3$. Plot the resulting filter's impulse response $h[n]$ and magnitude response $|H[e^{j\Omega}]|$.

12.9-13 Using the frequency sampling method, design an $N = 70$ linear-phase FIR bandstop filter that has stopband $(\pi/3 < |\Omega| < \pi/2)$. Plot the resulting filter's impulse response $h[n]$ and magnitude response $|H[e^{j\Omega}]|$.

12.9-14 A real FIR filter is desired whose magnitude response follows

$$|H[e^{j\Omega}]| = \begin{cases} \frac{4\Omega}{\pi} & 0 \leq \Omega < \frac{\pi}{4} \\ 2 - \frac{4\Omega}{\pi} & \frac{\pi}{4} \leq \Omega < \frac{\pi}{2} \\ 0 & \frac{\pi}{2} \leq \Omega \leq \pi \end{cases}$$

Since the digital filter is real, $|H[e^{j\Omega}]| = |H[e^{-j\Omega}]|$ and $|H[e^{j\Omega}]| = |H[e^{j(\Omega+2\pi)}]|$ for all Ω.

(a) Can a realizable filter have this exact magnitude response? Explain your answer.

(b) Use the frequency sampling method to design an FIR filter with this magnitude response (or a reasonable approximation). Use MATLAB to plot the magnitude response of your filter.

12.9-15 A real FIR comb filter is needed that has magnitude response $|H[e^{j\Omega}]| = [0,3,0,3,0,3,0,3]$ for $\Omega = [0,\pi/4,\pi/2,3\pi/4,\pi,5\pi/4,3\pi/2,7\pi/4]$, respectively. Provide the impulse response $h[n]$ of a filter that accomplishes these specifications.

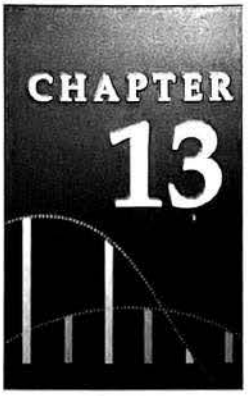

STATE-SPACE ANALYSIS

In Sec. 1.10, basic notions of *state variables* were introduced. In this chapter, we shall discuss state variables in more depth.

Most of this book deals with an external (input–output) description of systems. As noted in Ch. 1, such a description may be inadequate in some cases, and we need a systematic way of finding a system's *internal description*. State-space analysis of systems meets this need. In this method, we first select a set of key variables, called the *state variables*, in the system. Every possible signal or variable in the system at any instant t can be expressed in terms of the state variables and the input(s) at that instant t. If we know all the state variables as a function of t, we can determine every possible signal or variable in the system at any instant with a relatively simple relationship. The system description in this method consists of two parts:

1. A set of equations relating the state variables to the inputs (*the state equation*)
2. A set of equations relating outputs to the state variables and the inputs (*the output equation*)

The analysis procedure, therefore, consists of solving the state equation first, and then solving the output equation. The state-space description is capable of determining every possible system variable (or output) from knowledge of the input and the initial state (conditions) of the system. For this reason, it is an *internal description* of the system.

By its nature, state variable analysis is eminently suited for multiple-input, multiple-output (MIMO) systems. A single-input, single output (SISO) system is a special case of MIMO systems. In addition, the state-space techniques are useful for several other reasons, mentioned in Sec. 1.10, and repeated here.

1. The state equations of a system provide a mathematical model of great generality that can describe not just linear systems, but also nonlinear systems; not just time-invariant systems, but also time-varying parameter systems; not just SISO systems, but also MIMO systems. Indeed, state equations are ideally suited for analysis, synthesis, and optimization of MIMO systems.
2. Compact matrix notation along with powerful techniques of linear algebra greatly facilitates complex manipulations. Without such features, many important results of modern system theory would have been difficult to obtain. State equations can yield a great deal of information about a system even when they are not solved explicitly.

3. State equations lend themselves readily to digital computer simulation of complex systems of high order, with or without nonlinearities, and with multiple inputs and outputs.
4. For second-order systems ($N = 2$), a graphical method called *phase-plane analysis* can be used on state equations, whether they are linear or nonlinear.

13.1 MATHEMATICAL PRELIMINARIES

This chapter requires some understanding of matrix algebra. Section B.6 introduces basic concepts of matrix algebra, but misses a few needed mathematical concepts, which we present next.

13.1.1 Derivatives and Integrals of a Matrix

Elements of a matrix need not be constants; they may be functions of a variable. For example, if

$$\mathbf{A} = \begin{bmatrix} e^{-2t} & \sin t \\ e^{t} & e^{-t} + e^{-2t} \end{bmatrix} \tag{13.1}$$

then the matrix elements are functions of t. Here, it is helpful to denote $\mathbf{A}$ by $\mathbf{A}(t)$. Next, we define the derivative and integral of $\mathbf{A}(t)$.

The derivative of a matrix $\mathbf{A}(t)$ (with respect to t) is defined as a matrix whose ijth element is the derivative (with respect to t) of the ijth element of the matrix $\mathbf{A}$. Thus, if

$$\mathbf{A}(t) = [a_{ij}(t)]_{m\times n}$$

then

$$\frac{d}{dt}[\mathbf{A}(t)] = \left[\frac{d}{dt}a_{ij}(t)\right]_{m\times n} \quad \text{or} \quad \dot{\mathbf{A}}(t) = [\dot{a}_{ij}(t)]_{m\times n}$$

Thus, the derivative of the matrix in Eq. (13.1) is given by

$$\dot{\mathbf{A}}(t) = \begin{bmatrix} -2e^{-2t} & \cos t \\ e^{t} & -e^{-t} - 2e^{-2t} \end{bmatrix}$$

Similarly, we define the integral of $\mathbf{A}(t)$ (with respect to t) as a matrix whose ijth element is the integral (with respect to t) of the ijth element of the matrix $\mathbf{A}$:

$$\int \mathbf{A}(t)\,dt = \left(\int a_{ij}(t)\,dt\right)_{m\times n}$$

Thus, for the matrix $\mathbf{A}$ in Eq. (13.1), we have

$$\int \mathbf{A}(t)\,dt = \begin{bmatrix} \int e^{-2t}\,dt & \int \sin dt \\ \int e^{t}\,dt & \int (e^{-t} + 2e^{-2t})\,dt \end{bmatrix}$$

Since differentiation is a linear operation, it is easy to show that

$$\frac{d}{dt}(\mathbf{A}+\mathbf{B}) = \frac{d\mathbf{A}}{dt} + \frac{d\mathbf{B}}{dt} \quad \text{and} \quad \frac{d}{dt}(c\mathbf{A}) = c\frac{d\mathbf{A}}{dt}$$

The derivative of a matrix product is given as

$$\frac{d}{dt}(\mathbf{AB}) = \frac{d\mathbf{A}}{dt}\mathbf{B} + \mathbf{A}\frac{d\mathbf{B}}{dt} = \dot{\mathbf{A}}\mathbf{B} + \mathbf{A}\dot{\mathbf{B}} \tag{13.2}$$

We can prove Eq. (13.2) as follows. Let $\mathbf{A}$ be an $m \times n$ matrix and $\mathbf{B}$ an $n \times p$ matrix. Then, if

$$\mathbf{C} = \mathbf{AB}$$

from Eq. (B.33), we have

$$c_{ik} = \sum_{j=1}^{n} a_{ij} b_{jk}$$

and

$$\dot{c}_{ik} = \underbrace{\sum_{j=1}^{n} \dot{a}_{ij} b_{jk}}_{d_{ik}} + \underbrace{\sum_{j=1}^{n} a_{ij} \dot{b}_{jk}}_{e_{ik}} \qquad \text{or} \qquad \dot{c}_{ik} = d_{ik} + e_{ik} \tag{13.3}$$

Equation (13.3) along with the multiplication rule clearly indicates that d_{ik} is the ikth element of matrix $\dot{\mathbf{A}}\mathbf{B}$ and e_{ik} is the ikth element of matrix $\mathbf{A}\dot{\mathbf{B}}$. Equation (13.2) then follows.

If we let $\mathbf{B} = \mathbf{A}^{-1}$ in Eq. (13.2), we obtain

$$\frac{d}{dt}(\mathbf{A}\mathbf{A}^{-1}) = \frac{d\mathbf{A}}{dt}\mathbf{A}^{-1} + \mathbf{A}\frac{d}{dt}\mathbf{A}^{-1}$$

But since

$$\frac{d}{dt}(\mathbf{A}\mathbf{A}^{-1}) = \frac{d}{dt}\mathbf{I} = 0$$

we have

$$\frac{d}{dt}(\mathbf{A}^{-1}) = -\mathbf{A}^{-1}\frac{d\mathbf{A}}{dt}\mathbf{A}^{-1}$$

13.1.2 The Characteristic Equation of a Matrix: The Cayley–Hamilton Theorem

For an $(n \times n)$ square matrix $\mathbf{A}$, any vector $\mathbf{x}$ $(\mathbf{x} \neq 0)$ that satisfies the equation

$$\mathbf{Ax} = \lambda\mathbf{x} \tag{13.4}$$

is an *eigenvector* (or *characteristic vector*), and λ is the corresponding *eigenvalue* (or *characteristic value*) of $\mathbf{A}$. Equation (13.4) can be expressed as

$$(\mathbf{A} - \lambda\mathbf{I})\mathbf{x} = 0 \qquad \text{or} \qquad (\lambda\mathbf{I} - \mathbf{A})\mathbf{x} = 0$$

The solution for this set of homogeneous equations exists if and only if

$$|\lambda\mathbf{I}-\mathbf{A}| = \begin{vmatrix} \lambda-a_{11} & -a_{12} & \cdots & -a_{1n} \\ -a_{21} & \lambda-a_{22} & \cdots & -a_{2n} \\ \vdots & \vdots & \cdots & \vdots \\ -a_{n1} & -a_{n2} & \cdots & \lambda-a_{nn} \end{vmatrix} = 0 \tag{13.5}$$

Equation (13.5) is known as the *characteristic equation* of matrix **A** and can be expressed as

$$Q(\lambda) = |\lambda\mathbf{I}-\mathbf{A}| = \lambda^n + a_{n-1}\lambda^{n-1} + \cdots + a_1\lambda + a_0\lambda^0 = 0 \tag{13.6}$$

Here, $Q(\lambda)$ is called the *characteristic polynomial* of matrix **A**. The n zeros of the characteristic polynomial are the eigenvalues of **A** and, corresponding to each eigenvalue, there is an eigenvector that satisfies Eq. (13.4).

The *Cayley–Hamilton theorem* states that every $n \times n$ matrix **A** satisfies its own characteristic equation. In other words, Eq. (13.6) is valid if λ is replaced by **A**:

$$\mathbf{Q}(\mathbf{A}) = \mathbf{A}^n + a_{n-1}\mathbf{A}^{n-1} + \cdots + a_1\mathbf{A} + a_0\mathbf{A}^0 = 0 \tag{13.7}$$

Functions of a Matrix

We now demonstrate the use of the Cayley–Hamilton theorem [Eq. (13.7)] to evaluate functions of an $n \times n$ square matrix **A**.

Consider a function $f(\lambda)$ in the form of an infinite power series:

$$f(\lambda) = \alpha_0 + \alpha_1\lambda + \alpha_2\lambda_2^2 + \cdots = \sum_{i=0}^{\infty} \alpha_i\lambda^i \tag{13.8}$$

Since λ, being an eigenvalue (characteristic root) of **A**, satisfies the characteristic equation [Eq. (13.6)], we can write

$$\lambda^n = -a_{n-1}\lambda^{n-1} - a_{n-2}\lambda^{n-2} - \cdots - a_1\lambda - a_0 \tag{13.9}$$

If we multiply both sides by λ, the left-hand side is λ^{n+1}, and the right-hand side contains the terms $\lambda^n, \lambda^{n-1}, \ldots, \lambda$. Using Eq. (13.9), we substitute λ^n in terms of $\lambda^{n-1}, \lambda^{n-2}, \ldots, \lambda$ so that the highest power on the right-hand side is reduced to $n-1$. Continuing in this way, we see that λ^{n+k} can be expressed in terms of $\lambda^{n-1}, \lambda^{n-2}, \ldots, \lambda$ for any k. Hence, the infinite series on the right-hand side of Eq. (13.8) can always be expressed in terms of $\lambda^{n-1}, \lambda^{n-2}, \ldots, \lambda$ and a constant as

$$f(\lambda) = \beta_0 + \beta_1\lambda + \beta_2\lambda^2 + \cdots + \beta_{n-1}\lambda^{n-1} \tag{13.10}$$

If we assume that there are n distinct eigenvalues $\lambda_1, \lambda_2, \ldots, \lambda_n$, then Eq. (13.10) holds for these n values of λ. The substitution of these values in Eq. (13.10) yields n simultaneous equations

$$\begin{bmatrix} f(\lambda_1) \\ f(\lambda_2) \\ \vdots \\ f(\lambda_n) \end{bmatrix} = \begin{bmatrix} 1 & \lambda_1 & \lambda_1^2 & \cdots & \lambda_1^{n-1} \\ 1 & \lambda_2 & \lambda_2^2 & \cdots & \lambda_2^{n-1} \\ \vdots & \vdots & \vdots & \cdots & \vdots \\ 1 & \lambda_n & \lambda_n^2 & \cdots & \lambda_n^{n-1} \end{bmatrix} \begin{bmatrix} \beta_0 \\ \beta_1 \\ \vdots \\ \beta_{n-1} \end{bmatrix}$$

Solving for the β coefficients yields

$$\begin{bmatrix} \beta_0 \\ \beta_1 \\ \vdots \\ \beta_{n-1} \end{bmatrix} = \begin{bmatrix} 1 & \lambda_1 & \lambda_1^2 & \cdots & \lambda_1^{n-1} \\ 1 & \lambda_2 & \lambda_2^2 & \cdots & \lambda_2^{n-1} \\ \vdots & \vdots & \vdots & \cdots & \vdots \\ 1 & \lambda_n & \lambda_n^2 & \cdots & \lambda_n^{n-1} \end{bmatrix}^{-1} \begin{bmatrix} f(\lambda_1) \\ f(\lambda_2) \\ \vdots \\ f(\lambda_n) \end{bmatrix} \tag{13.11}$$

Since $\mathbf{A}$ also satisfies Eq. (13.9), we may advance a similar argument to show that if $f(\mathbf{A})$ is a function of a square matrix $\mathbf{A}$ expressed as an infinite power series in $\mathbf{A}$, then

$$f(\mathbf{A}) = \alpha_0\mathbf{I} + \alpha_1\mathbf{A} + \alpha_2\mathbf{A}^2 + \cdots = \sum_{i=0}^{\infty} \alpha_i \mathbf{A}^i$$

and, as argued earlier, the right-hand side can be expressed by using terms of power less than or equal to $n-1$,

$$f(\mathbf{A}) = \beta_0\mathbf{I} + \beta_1\mathbf{A} + \beta_2\mathbf{A}^2 + \cdots + \beta_{n-1}\mathbf{A}^{n-1} = \sum_{i=0}^{n-1} \beta_i \mathbf{A}^i \tag{13.12}$$

in which the coefficients β_is are found from Eq. (13.11). If some of the eigenvalues are repeated (multiple roots), the results are somewhat modified.

We shall demonstrate the utility of this result with the following two examples.

13.1.3 Computation of an Exponential and a Power of a Matrix

Let us compute $e^{\mathbf{A}t}$ defined by

$$e^{\mathbf{A}t} = \mathbf{I} + \mathbf{A}t + \frac{\mathbf{A}^2t^2}{2!} + \cdots + \frac{\mathbf{A}^n t^n}{n!} + \cdots = \sum_{k=0}^{\infty} \frac{\mathbf{A}^k t^k}{k!}$$

From Eq. (13.12), we can express

$$e^{\mathbf{A}t} = \sum_{i=1}^{n-1} \beta_i (\mathbf{A})^i$$

in which the β_is are given by Eq. (13.11), with $f(\lambda_i) = e^{\lambda_i t}$.

EXAMPLE 13.1 Computing the Exponential of a Matrix

Compute $e^{\mathbf{A}t}$ for the case

$$\mathbf{A} = \begin{bmatrix} 0 & 1 \\ -2 & -3 \end{bmatrix}$$

The characteristic equation is

$$|\lambda\mathbf{I}-\mathbf{A}| = \begin{vmatrix} \lambda & -1 \\ 2 & \lambda+3 \end{vmatrix} = \lambda^2+3\lambda+2 = (\lambda+1)(\lambda+2) = 0$$

Hence, the eigenvalues are $\lambda_1 = -1$, $\lambda_2 = -2$, and

$$e^{\mathbf{A}t} = \beta_0\mathbf{I}+\beta_1\mathbf{A}$$

in which

$$\begin{bmatrix} \beta_0 \\ \beta_1 \end{bmatrix} = \begin{bmatrix} 1 & -1 \\ 1 & -2 \end{bmatrix}^{-1} \begin{bmatrix} e^{-t} \\ e^{-2t} \end{bmatrix} = \begin{bmatrix} 2 & -1 \\ 1 & -1 \end{bmatrix} \begin{bmatrix} e^{-t} \\ e^{-2t} \end{bmatrix} = \begin{bmatrix} 2e^{-t}-e^{-2t} \\ e^{-t}-e^{-2t} \end{bmatrix}$$

and

$$\begin{aligned} e^{\mathbf{A}t} &= (2e^{-t}-e^{-2t}) \begin{bmatrix} 1 & 0 \\ 0 & 1 \end{bmatrix} + (e^{-t}-e^{-2t}) \begin{bmatrix} 0 & 1 \\ -2 & -3 \end{bmatrix} \\ &= \begin{bmatrix} 2e^{-t}-e^{-2t} & e^{-t}-e^{-2t} \\ -2e^{-t}+2e^{-2t} & -e^{-t}+2e^{-2t} \end{bmatrix} \end{aligned} \tag{13.13}$$

Computation of $\mathbf{A}^k$

As Eq. (13.12) indicates, we can express $\mathbf{A}^k$ as

$$\mathbf{A}^k = \beta_0\mathbf{I}+\beta_1\mathbf{A}+\cdots+\beta_{n-1}\mathbf{A}^{n-1}$$

in which the β_is are given by Eq. (13.11) with $f(\lambda_i) = \lambda_i^k$. For a completed example of the computation of $\mathbf{A}^k$ by this method, see Ex. 13.13.

13.2 Introduction to State Space

From the discussion in Ch. 1, we know that to determine a system's response(s) at any instant t, we need to know the system's inputs during its entire past, from $-\infty$ to t. If the inputs are known only for $t > t_0$, we can still determine the system output(s) for any $t > t_0$, provided we know certain initial conditions in the system at $t = t_0$. These initial conditions collectively are called the *initial state* of the system (at $t = t_0$).

The *state variables* $q_1(t), q_2(t), \ldots, q_N(t)$ are the minimum number of system variables such that their initial values at any instant t_0 are sufficient to determine the behavior of the system for all time $t \geq t_0$ when the input(s) to the system is known for $t \geq t_0$. This statement implies that an output of a system at any instant is determined completely from a knowledge of the values of the system state and the input at that instant.

Initial conditions of a system can be specified in many different ways. Consequently, the system state can also be specified in many different ways. This means that state variables are not unique.

This discussion is also valid for multiple-input, multiple-output (MIMO) systems, where every possible system output at any instant t is determined completely from knowledge of the system state and the input(s) at the instant t. These ideas should become clear from the following example of an *RLC* circuit.

EXAMPLE 13.2 State-Space Description and Output Equations of an *RLC* Circuit

Find a state-space description of the *RLC* circuit shown in Fig. 13.1. Verify that all possible system outputs at some instant t can be determined from knowledge of the system state and the input at that instant t.

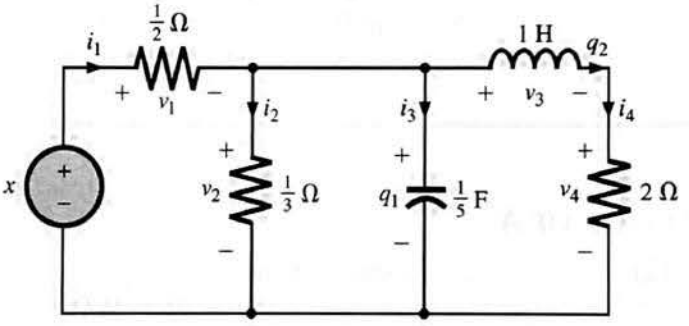

Figure 13.1 Circuit for Ex. 13.2.

It is known that inductor currents and capacitor voltages in an *RLC* circuit can be used as one possible choice of state variables. For this reason, we shall choose q_1 (the capacitor voltage) and q_2 (the inductor current) as our state variables.

The node equation at the intermediate node is

$$i_3 = i_1 - i_2 - q_2$$

but $i_3 = 0.2\dot{q}_1$, $i_1 = 2(x - q_1)$, and $i_2 = 3q_1$. Hence,

$$0.2\dot{q}_1 = 2(x - q_1) - 3q_1 - q_2$$

or

$$\dot{q}_1 = -25q_1 - 5q_2 + 10x$$

This is the first state equation. To obtain the second state equation, we sum the voltages in the extreme right loop formed by C, L, and the 2 Ω resistor so that they are equal to zero:

$$-q_1 + \dot{q}_2 + 2q_2 = 0$$

or

$$\dot{q}_2 = q_1 - 2q_2$$

Thus, the two state equations are

$$\dot{q}_1 = -25q_1 - 5q_2 + 10x$$
$$\dot{q}_2 = q_1 - 2q_2$$

Every possible output can now be expressed as a linear combination of q_1, q_2, and x. From Fig. 13.1, we have

$$v_1 = x - q_1$$
$$i_1 = 2(x - q_1)$$
$$v_2 = q_1$$
$$i_2 = 3q_1$$
$$i_3 = i_1 - i_2 - q_2 = 2(x - q_1) - 3q_1 - q_2 = -5q_1 - q_2 + 2x$$
$$i_4 = q_2$$
$$v_4 = 2i_4 = 2q_2$$
$$v_3 = q_1 - v_4 = q_1 - 2q_2$$

This set of equations is known as the *output equation* of the system. It is clear from this set that every possible output at some instant t can be determined from knowledge of $q_1(t)$, $q_2(t)$, and $x(t)$, the system state, and the input at the instant t. Once we have solved the state equations to obtain $q_1(t)$ and $q_2(t)$, we can determine every possible output for any given input $x(t)$.

For continuous-time systems, the state equations are N simultaneous first-order differential equations in N state variables $q_1, q_2, \ldots, q_N$ of the form

$$\dot{q}_i = g_i(q_1, q_2, \ldots, q_N, x_1, x_2, \ldots, x_j) \qquad i = 1, 2, \ldots, N$$

where $x_1, x_2, \ldots, x_j$ are the j system inputs. For a linear system, these equations reduce to a simpler linear form

$$\dot{q}_i = a_{i1}q_1 + a_{i2}q_2 + \cdots + a_{iN}q_N + b_{i1}x_1 + b_{i2}x_2 + \cdots + b_{ij}x_j \qquad i = 1, 2, \ldots, N \tag{13.14}$$

If there are k outputs $y_1, y_2, \ldots, y_k$, the k output equations are of the form

$$y_m = c_{m1}q_1 + c_{m2}q_2 + \cdots + c_{mN}q_N + d_{m1}x_1 + d_{m2}x_2 + \cdots + d_{mj}x_j \qquad m = 1, 2, \ldots, k \tag{13.15}$$

The N simultaneous first-order state equations are also known as the *normal-form* equations.

These equations can be written more conveniently in matrix form:

$$\underbrace{\begin{bmatrix} \dot{q}_1 \\ \dot{q}_2 \\ \vdots \\ \dot{q}_N \end{bmatrix}}_{\dot{\mathbf{q}}} = \underbrace{\begin{bmatrix} a_{11} & a_{12} & \cdots & a_{1N} \\ a_{21} & a_{22} & \cdots & a_{2N} \\ \vdots & \vdots & \cdots & \vdots \\ a_{N1} & a_{N2} & \cdots & a_{NN} \end{bmatrix}}_{\mathbf{A}} \underbrace{\begin{bmatrix} q_1 \\ q_2 \\ \vdots \\ q_N \end{bmatrix}}_{\mathbf{q}} + \underbrace{\begin{bmatrix} b_{11} & b_{12} & \cdots & b_{1j} \\ b_{21} & b_{22} & \cdots & b_{2j} \\ \vdots & \vdots & \cdots & \vdots \\ b_{N1} & b_{N2} & \cdots & b_{Nj} \end{bmatrix}}_{\mathbf{B}} \underbrace{\begin{bmatrix} x_1 \\ x_2 \\ \vdots \\ x_j \end{bmatrix}}_{\mathbf{x}}$$

and

$$\underbrace{\begin{bmatrix} y_1 \\ y_2 \\ \vdots \\ y_k \end{bmatrix}}_{\mathbf{y}} = \underbrace{\begin{bmatrix} c_{11} & c_{12} & \cdots & c_{1N} \\ c_{21} & c_{22} & \cdots & c_{2N} \\ \vdots & \vdots & \cdots & \vdots \\ c_{k1} & c_{k2} & \cdots & c_{kN} \end{bmatrix}}_{\mathbf{C}} \underbrace{\begin{bmatrix} q_1 \\ q_2 \\ \vdots \\ q_N \end{bmatrix}}_{\mathbf{q}} + \underbrace{\begin{bmatrix} d_{11} & d_{12} & \cdots & d_{1j} \\ d_{21} & d_{22} & \cdots & d_{2j} \\ \vdots & \vdots & \cdots & \vdots \\ d_{k1} & d_{k2} & \cdots & d_{kj} \end{bmatrix}}_{\mathbf{D}} \underbrace{\begin{bmatrix} x_1 \\ x_2 \\ \vdots \\ x_j \end{bmatrix}}_{\mathbf{x}}$$

or

$$\dot{\mathbf{q}} = \mathbf{A}\mathbf{q} + \mathbf{B}\mathbf{x} \tag{13.16}$$

and

$$\mathbf{y} = \mathbf{C}\mathbf{q} + \mathbf{D}\mathbf{x} \tag{13.17}$$

Equation (13.16) is the state equation and Eq. (13.17) is the output equation; **q**, **y**, and **x** are the state vector, the output vector, and the input vector, respectively.

For discrete-time systems, the state equations are N simultaneous first-order difference equations. Discrete-time systems are discussed in Sec. 13.7.

13.3 A Systematic Procedure to Determine State Equations

We shall discuss here a systematic procedure to determine the state-space description of linear time-invariant systems. In particular, we shall consider systems of two types: (1) *RLC* networks and (2) systems specified by block diagrams or Nth-order transfer functions.

13.3.1 Electrical Circuits

The method used in Ex. 13.2 proves effective in most of the simple cases. The steps are as follows:

1. Choose all independent capacitor voltages and inductor currents to be the state variables.
2. Choose a set of loop currents; express the state variables and their first derivatives in terms of these loop currents.
3. Write loop equations, and eliminate all variables other than state variables (and their first derivatives) from the equations derived in steps 2 and 3.

EXAMPLE 13.3 State Equations of an *RLC* Circuit

Write the state equations for the network shown in Fig. 13.2.

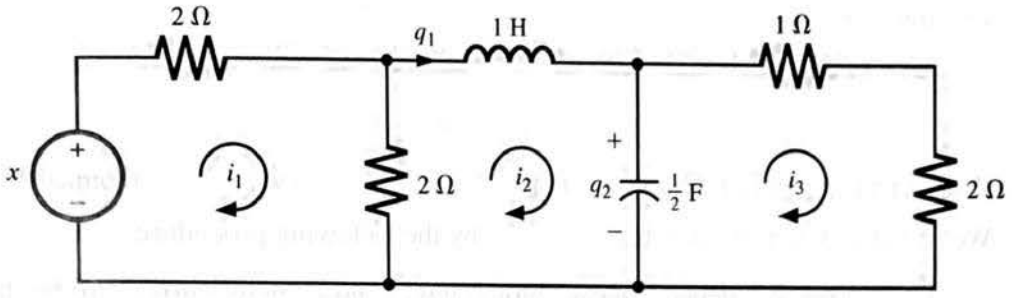

Figure 13.2 Circuit for Ex. 13.3.

Step 1. There is one inductor and one capacitor in the network. Therefore, we shall choose the inductor current q_1 and the capacitor voltage q_2 as the state variables.

Step 2. The relationship between the loop currents and the state variables can be written by inspection:

$$q_1 = i_2 \tag{13.18}$$

$$\tfrac{1}{2}\dot{q}_2 = i_2 - i_3 \tag{13.19}$$

Step 3. The loop equations are

$$4i_1 - 2i_2 = x \tag{13.20}$$

$$2(i_2 - i_1) + \dot{q}_1 + q_2 = 0 \tag{13.21}$$

$$-q_2 + 3i_3 = 0 \tag{13.22}$$

Now we eliminate i_1, i_2, and i_3 from the state and loop equations as follows. From Eq. (13.21), we have

$$\dot{q}_1 = 2(i_1 - i_2) - q_2$$

We can eliminate i_1 and i_2 from this equation by using Eqs. (13.18) and (13.20) to obtain

$$\dot{q}_1 = -q_1 - q_2 + \tfrac{1}{2}x$$

The substitution of Eqs. (13.18) and (13.22) in Eq. (13.19) yields

$$\dot{q}_2 = 2q_1 - \tfrac{2}{3}q_2$$

These are the desired state equations. We can express them in matrix form as

$$\begin{bmatrix} \dot{q}_1 \\ \dot{q}_2 \end{bmatrix} = \begin{bmatrix} -1 & -1 \\ 2 & -\frac{2}{3} \end{bmatrix} \begin{bmatrix} q_1 \\ q_2 \end{bmatrix} + \begin{bmatrix} \frac{1}{2} \\ 0 \end{bmatrix} x \tag{13.23}$$

The derivation of state equations from loop equations is facilitated considerably by choosing loops in such a way that only one loop current passes through each of the inductors or capacitors.

An Alternative Procedure

We can also determine the state equations by the following procedure:

1. Choose all independent capacitor voltages and inductor currents to be the state variables.
2. Replace each capacitor by a voltage source equal to the capacitor voltage, and replace each inductor by a current source equal to the inductor current. This step will transform the *RLC* network into a network consisting only of resistors, current sources, and voltage sources.
3. Find the current through each capacitor and equate it to $C\dot{q}_i$, where q_i is the capacitor voltage. Similarly, find the voltage across each inductor and equate it to $L\dot{q}_j$, where q_j is the inductor current.

EXAMPLE 13.4 Alternate Procedure to Determine State Equations

Use the three-step alternative procedure just outlined to write the state equations for the network in Fig. 13.2.

In the network in Fig. 13.2, we replace the inductor by a current source of current q_1 and the capacitor by a voltage source of voltage q_2, as shown in Fig. 13.3. The resulting network consists of four resistors, two voltage sources, and one current source.

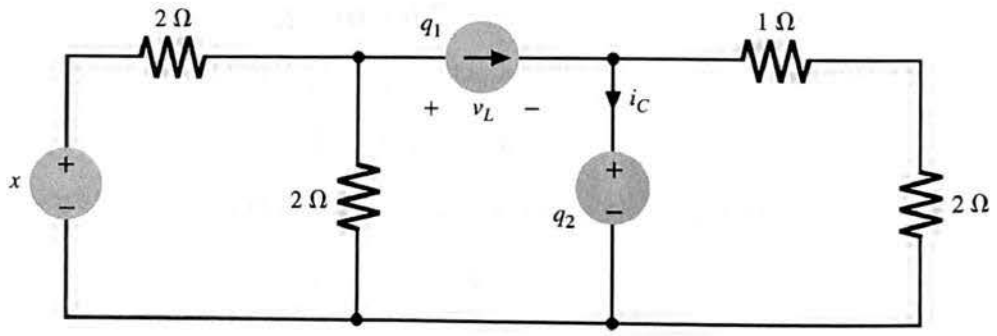

Figure 13.3 Equivalent circuit of the network in Fig. 13.2.

We can determine the voltage v_L across the inductor and the current i_c through the capacitor by using the principle of superposition. This step can be accomplished by inspection. For example, v_L has three components arising from three sources. To compute the component due to x, we assume that $q_1 = 0$ (open circuit) and $q_2 = 0$ (short circuit). Under these conditions, the entire network to the right of the 2 Ω resistor is opened, and the component of v_L due to x is the voltage across the 2 Ω resistor. This voltage is clearly $(1/2)x$. Similarly, to find the component of v_L due to q_1, we short x and q_2. The source q_1 sees an equivalent resistor of 1 Ω across it, and hence $v_L = -q_1$. Continuing the process, we find that the component of v_L due to q_2 is $-q_2$. Hence,

$$v_L = \dot{q}_1 = \tfrac{1}{2}x - q_1 - q_2$$

Using the same procedure, we find

$$i_c = \tfrac{1}{2}\dot{q}_2 = q_1 - \tfrac{1}{3}q_2$$

These equations are identical to the state equations [Eq. (13.23)] obtained earlier.†

13.3.2 State Equations from a Transfer Function

It is relatively easy to determine the state equations of a system specified by its transfer function.‡ Consider, for example, a first-order system with the transfer function

$$H(s) = \frac{1}{s+a}$$

The system realization appears in Fig. 13.4. The integrator output q serves as a natural state variable since, in practical realization, initial conditions are placed on the integrator output. The integrator input is naturally $\dot{q}$. From Fig. 13.4, we have

† This procedure requires modification if the system contains all-capacitor and voltage-source tie sets or all-inductor and current-source cut sets. In the case of all-capacitor and voltage-source tie sets, all capacitor voltages cannot be independent. One capacitor voltage can be expressed in terms of the remaining capacitor voltages and the voltage source(s) in that tie set. Consequently, one of the capacitor voltages should not be used as a state variable, and that capacitor should not be replaced by a voltage source. Similarly, in all-inductor and current-source tie sets, one inductor should not be replaced by a current source. If there are all-capacitor tie sets or all-inductor cut sets only, no further complications occur. In all-capacitor voltage-source tie sets and/or all-inductor current-source cut sets, we have additional difficulties in that the terms involving derivatives of the input may occur. This problem can be solved by redefining the state variables. The final state variables will not be capacitor voltages and inductor currents.

‡ We implicitly assume that the system is controllable and observable. This implies that there are no pole-zero cancellations in the transfer function. If such cancellations are present, the state variable description represents only the part of the system that is controllable and observable (the part of the system that is coupled to the input and the output). In other words, the internal description represented by the state equations is no better than the external description represented by the input–output equation.

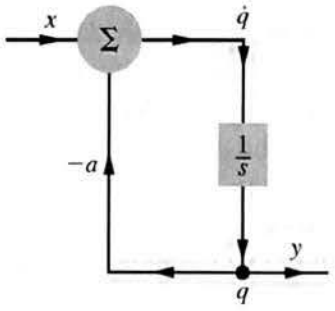

Figure 13.4 Block realization of $H(s) = \frac{1}{s+a}$.

$$\dot{q} = -aq + x \qquad \text{and} \qquad y = q$$

In Sec. 6.6, we saw that a given transfer function can be realized in several ways. Consequently, we should be able to obtain different state-space descriptions of the same system by using different realizations. This assertion will be clarified by the following example.

EXAMPLE 13.5 State-Space Description from a Transfer Function

Consider a system specified by the transfer function

$$H(s) = \underbrace{\frac{2s+10}{s^3+8s^2+19s+12}}_{\text{direct form}} = \underbrace{\left(\frac{2}{s+1}\right)\left(\frac{s+5}{s+3}\right)\left(\frac{1}{s+4}\right)}_{\text{cascade}} = \underbrace{\frac{\frac{4}{3}}{s+1} - \frac{2}{s+3} + \frac{\frac{2}{3}}{s+4}}_{\text{parallel}}$$

The procedure developed in Sec. 6.6 allows us to realize $H(s)$ as, among others, direct form II (DFII), transpose DFII (TDFII), cascade, and parallel. These realizations are depicted in Fig. 13.5. Determine state-space descriptions for each of these realizations. As mentioned earlier, the output of each integrator serves as a natural state variable.

Direct Form II and Its Transpose

Here, we shall realize the system using the canonical form (direct form II and its transpose) discussed in Sec. 6.6. If we choose the state variables to be the three integrator outputs q_1, q_2, and q_3, then, according to Fig. 13.5a,

$$\dot{q}_1 = q_2$$
$$\dot{q}_2 = q_3$$
$$\dot{q}_3 = -12q_1 - 19q_2 - 8q_3 + x$$

Also, the output y is given by

$$y = 10q_1 + 2q_2$$

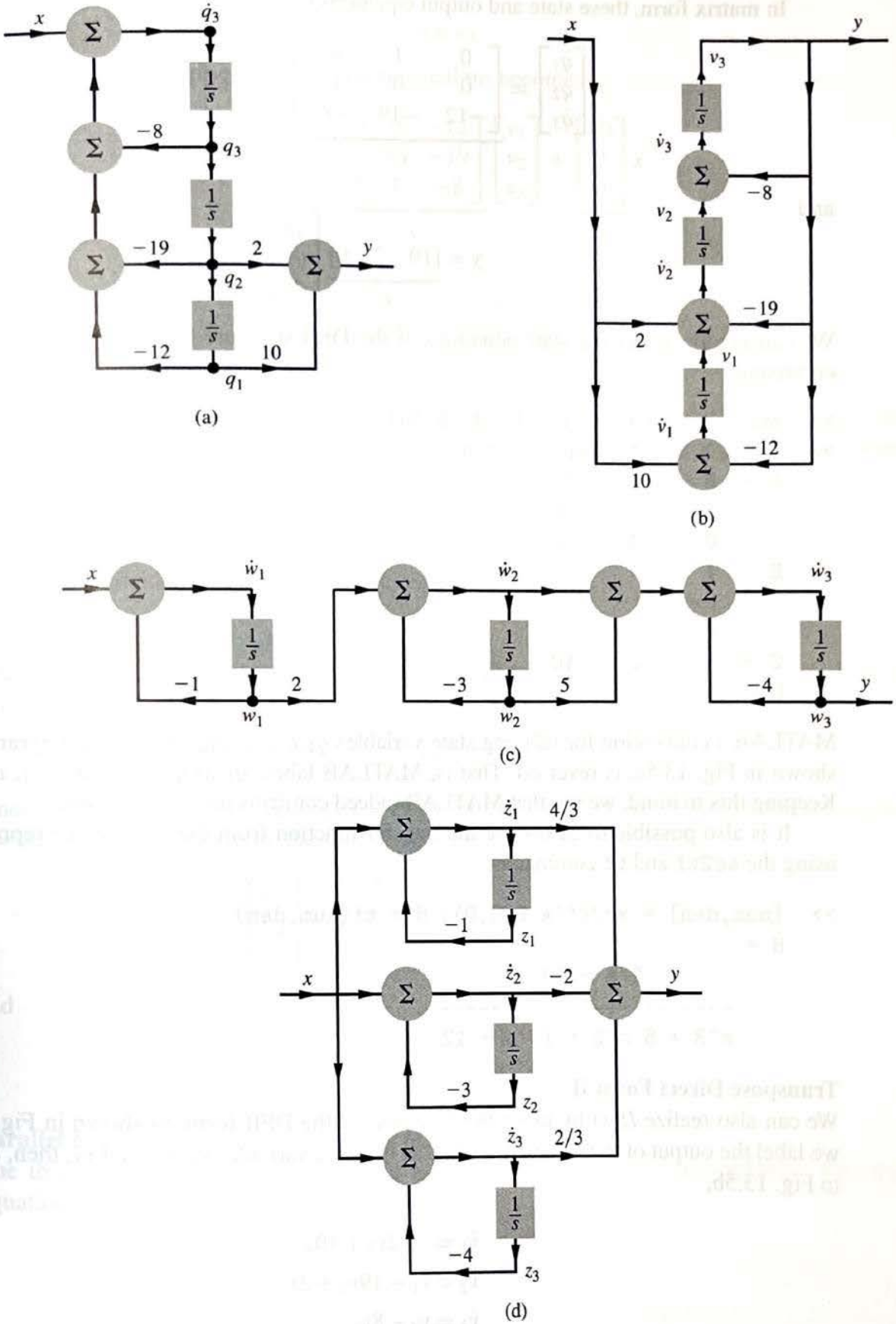

Figure 13.5 **(a)** DFII, **(b)** TDFII, **(c)** cascade, and **(d)** parallel realizations of $H(s)$.

In matrix form, these state and output equations become

$$\begin{bmatrix} \dot{q}_1 \\ \dot{q}_2 \\ \dot{q}_3 \end{bmatrix} = \underbrace{\begin{bmatrix} 0 & 1 & 0 \\ 0 & 0 & 1 \\ -12 & -19 & -8 \end{bmatrix}}_{\mathbf{A}} \begin{bmatrix} q_1 \\ q_2 \\ q_3 \end{bmatrix} + \underbrace{\begin{bmatrix} 0 \\ 0 \\ 1 \end{bmatrix}}_{\mathbf{B}} x$$

and

$$\mathbf{y} = \underbrace{[10 \quad 2 \quad 0]}_{\mathbf{C}} \begin{bmatrix} q_1 \\ q_2 \\ q_3 \end{bmatrix}$$

We can readily verify the state equations of the DFII structure by using MATLAB's `tf2ss` command:

```
>> num = [2 10]; den = [1 8 19 12];
>> [A,B,C,D] = tf2ss(num,den)
   A = -8   -19   -12
        1     0     0
        0     1     0
   B =  1
        0
        0
   C =  0     2    10
   D =  0
```

MATLAB's convention for labeling state variables $q_1, q_2, \ldots, q_n$ in a block diagram, such as shown in Fig. 13.5a, is reversed. That is, MATLAB labels q_1 as q_n, q_2 and q_{n-1}, and so on. Keeping this in mind, we see that MATLAB indeed confirms our earlier results.

It is also possible to determine the transfer function from the state-space representation using the `ss2tf` and `tf` commands:

```
>> [num,den] = ss2tf(A,B,C,D); H = tf(num,den)
   H =
              2 s + 10
     ----------------------
     s^3 + 8 s^2 + 19 s + 12
```

Transpose Direct Form II

We can also realize $H(s)$ by using the transpose of the DFII form, as shown in Fig. 13.5b. If we label the output of the three integrators as the state variables v_1, v_2, and v_3, then, according to Fig. 13.5b,

$$\begin{aligned} \dot{v}_1 &= -12v_3 + 10x \\ \dot{v}_2 &= v_1 - 19v_3 + 2x \\ \dot{v}_3 &= v_2 - 8v_3 \end{aligned}$$

and the output y is given by

$$y = v_3$$

The matrix form of these state and output equations becomes

$$\begin{bmatrix} \dot{v}_1 \\ \dot{v}_2 \\ \dot{v}_3 \end{bmatrix} = \underbrace{\begin{bmatrix} 0 & 0 & -12 \\ 1 & 0 & -19 \\ 0 & 1 & -8 \end{bmatrix}}_{\hat{\mathbf{A}}} \begin{bmatrix} v_1 \\ v_2 \\ v_3 \end{bmatrix} + \underbrace{\begin{bmatrix} 10 \\ 2 \\ 0 \end{bmatrix}}_{\hat{\mathbf{B}}} x$$

and

$$\mathbf{y} = \underbrace{[0 \quad 0 \quad 1]}_{\hat{\mathbf{C}}} \begin{bmatrix} v_1 \\ v_2 \\ v_3 \end{bmatrix}$$

Observe closely the relationship between the state-space descriptions of $H(s)$ by means of the DFII and TDFII realizations. The $\mathbf{A}$ matrices in these two cases are the transpose of each other; also, the $\mathbf{B}$ of one is the transpose of $\mathbf{C}$ in the other, and vice versa. Hence,

$$(\mathbf{A})^T = \hat{\mathbf{A}}, \qquad (\mathbf{B})^T = \hat{\mathbf{C}}, \qquad \text{and} \qquad (\mathbf{C})^T = \hat{\mathbf{B}}$$

This is no coincidence. This duality relation is generally true [1].

Cascade Realization

The three integrator outputs w_1, w_2, and w_3 in Fig. 13.5c are the state variables. Writing equations for the summer outputs yields

$$\dot{w}_1 = -w_1 + x, \qquad \dot{w}_2 = 2w_1 - 3w_2, \qquad \text{and} \qquad \dot{w}_3 = 5w_2 + \dot{w}_2 - 4w_3$$

Since $\dot{w}_2 = 2w_1 - 3w_2$, we see that $\dot{w}_3 = 2w_1 + 2w_2 - 4w_3$. From Fig. 13.5c, we further see that $y = w_3$. Put into matrix form, the state and output equations are therefore

$$\begin{bmatrix} \dot{w}_1 \\ \dot{w}_2 \\ \dot{w}_3 \end{bmatrix} = \begin{bmatrix} -1 & 0 & 0 \\ 2 & -3 & 0 \\ 2 & 2 & -4 \end{bmatrix} \begin{bmatrix} w_1 \\ w_2 \\ w_3 \end{bmatrix} + \begin{bmatrix} 1 \\ 0 \\ 0 \end{bmatrix} x$$

and

$$y = [0 \quad 0 \quad 1] \begin{bmatrix} w_1 \\ w_2 \\ w_3 \end{bmatrix}$$

Parallel Realization (Diagonal Representation)

The three integrator outputs z_1, z_2, and z_3 in Fig. 13.5d are the state variables. The state equations are

$$\dot{z}_1 = -z_1 + x$$
$$\dot{z}_2 = -3z_2 + x$$
$$\dot{z}_3 = -4z_3 + x$$

and the output equation is

$$y = \tfrac{4}{3}z_1 - 2z_2 + \tfrac{2}{3}z_3$$

In matrix form, these equations are

$$\begin{bmatrix} \dot{z}_1 \\ \dot{z}_2 \\ \dot{z}_3 \end{bmatrix} = \begin{bmatrix} -1 & 0 & 0 \\ 0 & -3 & 0 \\ 0 & 0 & -4 \end{bmatrix} \begin{bmatrix} z_1 \\ z_2 \\ z_3 \end{bmatrix} + \begin{bmatrix} 1 \\ 1 \\ 1 \end{bmatrix} x$$

$$y = \begin{bmatrix} \frac{4}{3} & -2 & \frac{2}{3} \end{bmatrix} \begin{bmatrix} z_1 \\ z_2 \\ z_3 \end{bmatrix}$$

A General Case

It is clear that a system has several state-space descriptions. Notable among these are the variables obtained from the DFII, its transpose, and the diagonalized variables (in the parallel realization). State equations in these forms can be written immediately by inspection of the transfer function. Consider the general Nth-order transfer function

$$H(s) = \frac{b_0 s^N + b_1 s^{N-1} + \cdots + b_{N-1}s + b_N}{s^N + a_1 s^{N-1} + \cdots + a_{N-1}s + a_N} \tag{13.24}$$

$$= \frac{b_0 s^N + b_1 s^{N-1} + \cdots + b_{N-1}s + b_N}{(s-\lambda_1)(s-\lambda_2)\cdots(s-\lambda_N)}$$

$$= b_0 + \frac{k_1}{s-\lambda_1} + \frac{k_2}{s-\lambda_2} + \cdots + \frac{k_N}{s-\lambda_N} \tag{13.25}$$

The realizations of $H(s)$ found by using direct form II [Eq. (13.24)] and the parallel form [Eq. (13.25)] appear in Figs. 13.6a and 13.6b, respectively.

The N integrator outputs $q_1, q_2, \ldots, q_N$ in Fig. 13.6a are the state variables. By inspection of this figure, we obtain

$$\begin{aligned} \dot{q}_1 &= q_2 \\ \dot{q}_2 &= q_3 \\ &\vdots \\ \dot{q}_{N-1} &= q_N \\ \dot{q}_N &= -a_N q_1 - a_{N-1} q_2 - \cdots - a_2 q_{N-1} - a_1 q_N + x \end{aligned}$$

and output y is

$$y = b_N q_1 + b_{N-1} q_2 + \cdots + b_1 q_N + b_0 \dot{q}_N$$

We can eliminate $\dot{q}_N$ in this output equation by using the last state equation to yield

$$\begin{aligned} y &= (b_N - b_0 a_N) q_1 + (b_{N-1} - b_0 a_{N-1}) q_2 + \cdots + (b_1 - b_0 a_1) q_N + b_0 x \\ &= \hat{b}_N q_1 + \hat{b}_{N-1} q_2 + \cdots + \hat{b}_1 q_N + b_0 x \end{aligned}$$

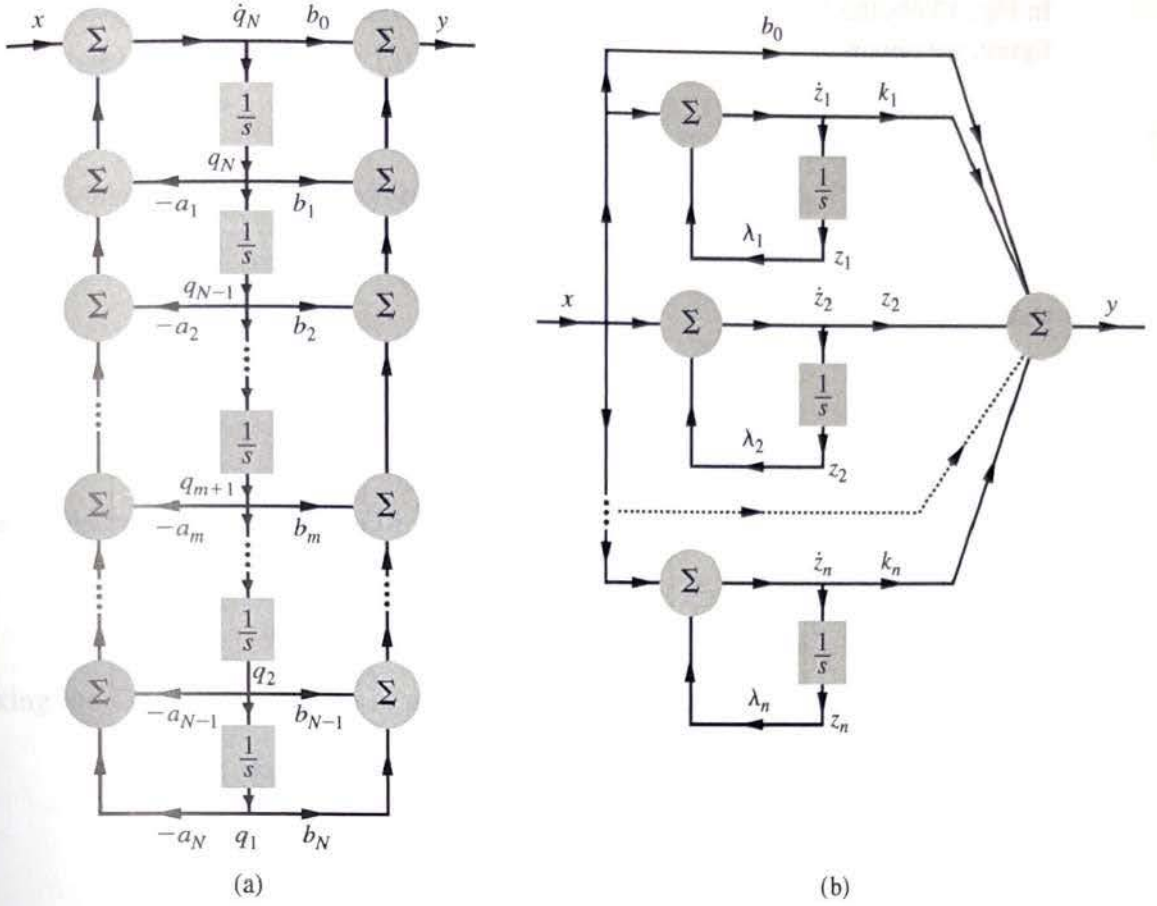

Figure 13.6 (**a**) Direct form II and (**b**) parallel realizations for an Nth-order LTIC system.

where $\hat{b}_i = b_i - b_0 a_i$. In matrix form, we obtain

$$\begin{bmatrix} \dot{q}_1 \\ \dot{q}_2 \\ \vdots \\ \dot{q}_{N-1} \\ \dot{q}_N \end{bmatrix} = \begin{bmatrix} 0 & 1 & 0 & \cdots & 0 & 0 \\ 0 & 0 & 1 & \cdots & 0 & 0 \\ \vdots & \vdots & \vdots & \cdots & \vdots & \vdots \\ 0 & 0 & 0 & \cdots & 0 & 1 \\ -a_N & -a_{N-1} & -a_{N-2} & \cdots & -a_2 & -a_1 \end{bmatrix} \begin{bmatrix} q_1 \\ q_2 \\ \vdots \\ q_{N-1} \\ q_N \end{bmatrix} + \begin{bmatrix} 0 \\ 0 \\ \vdots \\ 0 \\ 1 \end{bmatrix} x$$

and

$$y = [\hat{b}_N \quad \hat{b}_{N-1} \quad \cdots \quad \hat{b}_1] \begin{bmatrix} q_1 \\ q_2 \\ \vdots \\ q_N \end{bmatrix} + b_0 x$$

In Fig. 13.6b, the N integrator outputs $z_1, z_2, \ldots, z_N$ are the state variables. By inspection of this figure, we obtain

$$\begin{aligned}\dot{z}_1 &= \lambda_1 z_1 + x\\ \dot{z}_2 &= \lambda_2 z_2 + x\\ &\vdots\\ \dot{z}_N &= \lambda_N z_N + x\end{aligned}$$

and

$$y = k_1 z_1 + k_2 z_2 + \cdots + k_N z_N + b_0 x$$

or

$$\begin{bmatrix}\dot{z}_1\\ \dot{z}_2\\ \vdots\\ \dot{z}_{N-1}\\ \dot{z}_N\end{bmatrix} = \begin{bmatrix}\lambda_1 & 0 & \cdots & 0 & 0\\ 0 & \lambda_2 & \cdots & 0 & 0\\ \vdots & \vdots & \cdots & \vdots & \vdots\\ 0 & 0 & \cdots & \lambda_{N-1} & 0\\ 0 & 0 & \cdots & 0 & \lambda_N\end{bmatrix}\begin{bmatrix}z_1\\ z_2\\ \vdots\\ z_{N-1}\\ z_N\end{bmatrix} + \begin{bmatrix}1\\ 1\\ \vdots\\ 1\\ 1\end{bmatrix} x \tag{13.26}$$

and

$$y = \begin{bmatrix}k_1 & k_2 & \cdots & k_{N-1} & k_N\end{bmatrix}\begin{bmatrix}z_1\\ z_2\\ \vdots\\ z_{N-1}\\ z_N\end{bmatrix} + b_0 x$$

Observe that the diagonalized form of the state matrix [Eq. (13.26)] has the transfer function poles as its diagonal elements. The presence of repeated poles in $H(s)$ will modify the procedure slightly. The handling of these cases is discussed in Sec. 6.6.

It is clear from the foregoing discussion that a state-space description is not unique. For any realization of $H(s)$ obtained from integrators, scalar multipliers, and adders, a corresponding state-space description exists. Since there are uncountable possible realizations of $H(s)$, there are uncountable possible state-space descriptions.

The advantages and drawbacks of various types of realization were discussed in Sec. 6.6.

13.4 SOLUTION OF STATE EQUATIONS

The state equations of a linear system are N simultaneous linear differential equations of the first order. We studied the techniques of solving linear differential equations in Chs. 2 and 6. The same techniques can be applied to state equations without any modification. However, it is more convenient to carry out the solution in the framework of matrix notation.

These equations can be solved in both the time and frequency domains (Laplace transform). The latter is relatively easier to deal with than the time-domain solution. For this reason, we shall first consider the Laplace transform solution.

13.4.1 Laplace Transform Solution of State Equations

The ith state equation [Eq. (13.14)] is of the form

$$\dot{q}_i = a_{i1}q_1 + a_{i2}q_2 + \cdots + a_{iN}q_N + b_{i1}x_1 + b_{i2}x_2 + \cdots + b_{ij}x_j \tag{13.27}$$

We shall take the Laplace transform of this equation. Let

$$q_i(t) \Longleftrightarrow Q_i(s)$$

so that

$$\dot{q}_i(t) \Longleftrightarrow sQ_i(s) - q_i(0)$$

Also, let

$$x_i(t) \Longleftrightarrow X_i(s)$$

The Laplace transform of Eq. (13.27) yields

$$\begin{aligned} sQ_i(s) - q_i(0) = a_{i1}Q_1(s) + a_{i2}Q_2(s) + \cdots + a_{iN}Q_N(s) + b_{i1}X_1(s) \\ + b_{i2}X_2(s) + \cdots + b_{ij}X_j(s) \end{aligned}$$

Taking the Laplace transforms of all N state equations, we obtain

$$s\underbrace{\begin{bmatrix} Q_1(s) \\ Q_2(s) \\ \vdots \\ Q_N(s) \end{bmatrix}}_{\mathbf{Q}(s)} - \underbrace{\begin{bmatrix} q_1(0) \\ q_2(0) \\ \vdots \\ q_N(0) \end{bmatrix}}_{\mathbf{q}(0)} = \underbrace{\begin{bmatrix} a_{11} & a_{12} & \cdots & a_{1N} \\ a_{21} & a_{22} & \cdots & a_{2N} \\ \vdots & \vdots & \cdots & \vdots \\ a_{N1} & a_{N2} & \cdots & a_{NN} \end{bmatrix}}_{\mathbf{A}} \underbrace{\begin{bmatrix} Q_1(s) \\ Q_2(s) \\ \vdots \\ Q_N(s) \end{bmatrix}}_{\mathbf{Q}(s)}$$

$$+ \underbrace{\begin{bmatrix} b_{11} & b_{12} & \cdots & b_{1j} \\ b_{21} & b_{22} & \cdots & b_{2j} \\ \vdots & \vdots & \cdots & \vdots \\ b_{N1} & b_{N2} & \cdots & b_{Nj} \end{bmatrix}}_{\mathbf{B}} \underbrace{\begin{bmatrix} X_1(s) \\ X_2(s) \\ \vdots \\ X_j(s) \end{bmatrix}}_{\mathbf{X}(s)}$$

Defining the vectors, as indicated, we have

$$s\mathbf{Q}(s) - \mathbf{q}(0) = \mathbf{A}\mathbf{Q}(s) + \mathbf{B}\mathbf{X}(s)$$

or

$$s\mathbf{Q}(s) - \mathbf{A}\mathbf{Q}(s) = \mathbf{q}(0) + \mathbf{B}\mathbf{X}(s)$$

and

$$(s\mathbf{I} - \mathbf{A})\mathbf{Q}(s) = \mathbf{x}(0) + \mathbf{B}\mathbf{X}(s)$$

where $\mathbf{I}$ is the $N \times N$ identity matrix. Solving for $\mathbf{Q}(s)$, we have

$$\begin{aligned} \mathbf{Q}(s) &= (s\mathbf{I} - \mathbf{A})^{-1}[\mathbf{q}(0) + \mathbf{B}\mathbf{X}(s)] \\ &= \mathbf{\Phi}(s)[\mathbf{q}(0) + \mathbf{B}\mathbf{X}(s)] \end{aligned} \tag{13.28}$$

where

$$\mathbf{\Phi}(s) = (s\mathbf{I} - \mathbf{A})^{-1}$$

Thus, from Eq. (13.28),

$$\mathbf{Q}(s) = \mathbf{\Phi}(s)\mathbf{q}(0) + \mathbf{\Phi}(s)\mathbf{B}\mathbf{X}(s)$$

and

$$\mathbf{q}(t) = \underbrace{\mathcal{L}^{-1}[\mathbf{\Phi}(s)]\mathbf{q}(0)}_{\text{zero-input response}} + \underbrace{\mathcal{L}^{-1}[\mathbf{\Phi}(s)\mathbf{B}\mathbf{X}(s)]}_{\text{zero-state response}} \tag{13.29}$$

Equation (13.29) gives the desired solution. Observe the two components of the solution. The first component yields $\mathbf{q}(t)$ when the input $x(t) = 0$. Hence, the first component is the zero-input response. In a similar manner, we see that the second component is the zero-state response.

EXAMPLE 13.6 Laplace Transform Solution to State Equations

Using the Laplace transform, find the state vector $\mathbf{q}(t)$ for the system whose state equation is given by

$$\dot{\mathbf{q}} = \mathbf{A}\mathbf{q} + \mathbf{B}\mathbf{x}$$

where

$$\mathbf{A} = \begin{bmatrix} -12 & \frac{2}{3} \\ -36 & -1 \end{bmatrix} \qquad \mathbf{B} = \begin{bmatrix} \frac{1}{3} \\ 1 \end{bmatrix} \qquad \mathbf{x}(t) = u(t)$$

and the initial conditions are $q_1(0) = 2$, $q_2(0) = 1$.

From Eq. (13.28), we have

$$\mathbf{Q}(s) = \mathbf{\Phi}(s)[\mathbf{q}(0) + \mathbf{B}\mathbf{X}(s)]$$

Let us first find $\mathbf{\Phi}(s)$. We have

$$(s\mathbf{I} - \mathbf{A}) = s\begin{bmatrix} 1 & 0 \\ 0 & 1 \end{bmatrix} - \begin{bmatrix} -12 & \frac{2}{3} \\ -36 & -1 \end{bmatrix} = \begin{bmatrix} s+12 & -\frac{2}{3} \\ 36 & s+1 \end{bmatrix}$$

and

$$\mathbf{\Phi}(s) = (s\mathbf{I} - \mathbf{A})^{-1} = \begin{bmatrix} \frac{s+1}{(s+4)(s+9)} & \frac{2/3}{(s+4)(s+9)} \\ \frac{-36}{(s+4)(s+9)} & \frac{s+12}{(s+4)(s+9)} \end{bmatrix}$$

Now, $\mathbf{q}(0)$ is given as

$$\mathbf{q}(0) = \begin{bmatrix} 2 \\ 1 \end{bmatrix}$$

Also, $X(s) = 1/s$, and

$$\mathbf{B}\mathbf{X}(s) = \begin{bmatrix} \frac{1}{3} \\ 1 \end{bmatrix}\frac{1}{s} = \begin{bmatrix} \frac{1}{3s} \\ \frac{1}{s} \end{bmatrix}$$

Therefore,

$$\mathbf{q}(0) + \mathbf{B}\mathbf{X}(s) = \begin{bmatrix} 2 + \frac{1}{3s} \\ 1 + \frac{1}{s} \end{bmatrix} = \begin{bmatrix} \frac{6s+1}{3s} \\ \frac{s+1}{s} \end{bmatrix}$$

and

$$\begin{aligned}\mathbf{Q}(s) &= \mathbf{\Phi}(s)[\mathbf{q}(0) + \mathbf{B}\mathbf{X}(s)] \\ &= \begin{bmatrix} \frac{s+1}{(s+4)(s+9)} & \frac{2/3}{(s+4)(s+9)} \\ \frac{-36}{(s+4)(s+9)} & \frac{s+12}{(s+4)(s+9)} \end{bmatrix} \begin{bmatrix} \frac{6s+1}{3s} \\ \frac{s+1}{s} \end{bmatrix} \\ &= \begin{bmatrix} \frac{2s^2+3s+1}{s(s+4)(s+9)} \\ \frac{s-59}{(s+4)(s+9)} \end{bmatrix} \\ &= \begin{bmatrix} \frac{1/36}{s} - \frac{21/20}{s+4} + \frac{136/45}{s+9} \\ \frac{-63/5}{s+4} + \frac{68/5}{s+9} \end{bmatrix}\end{aligned}$$

The inverse Laplace transform of this equation yields

$$\begin{bmatrix} q_1(t) \\ q_2(t) \end{bmatrix} = \begin{bmatrix} \left(\frac{1}{36} - \frac{21}{20}e^{-4t} + \frac{136}{45}e^{-9t}\right)u(t) \\ \left(-\frac{63}{5}e^{-4t} + \frac{68}{5}e^{-9t}\right)u(t) \end{bmatrix}$$

This result is readily confirmed using MATLAB and its symbolic toolbox.

```
>> syms s
>> A = [-12 2/3;-36 -1]; B = [1/3; 1]; q0 = [2;1]; X = 1/s;
>> q = ilaplace(inv(s*eye(2)-A)*(q0+B*X))
   q = (136*exp(-9*t))/45 - (21*exp(-4*t))/20 + 1/36
            (68*exp(-9*t))/5 - (63*exp(-4*t))/5
```

To create a plot of the state vector, we use MATLAB's subs command to substitute the symbolic variable t with a vector of desired values.

```
>> t = (0:.01:2); q = subs(q); q1 = q(1,:); q2 = q(2,:);
>> plot(t,q1,'k',t,q2,'k--'); xlabel('t'); ylabel('Amplitude');
>> legend('q_1(t)','q_2(t)','Location','SE');
```

The resulting plot is shown in Fig. 13.7.

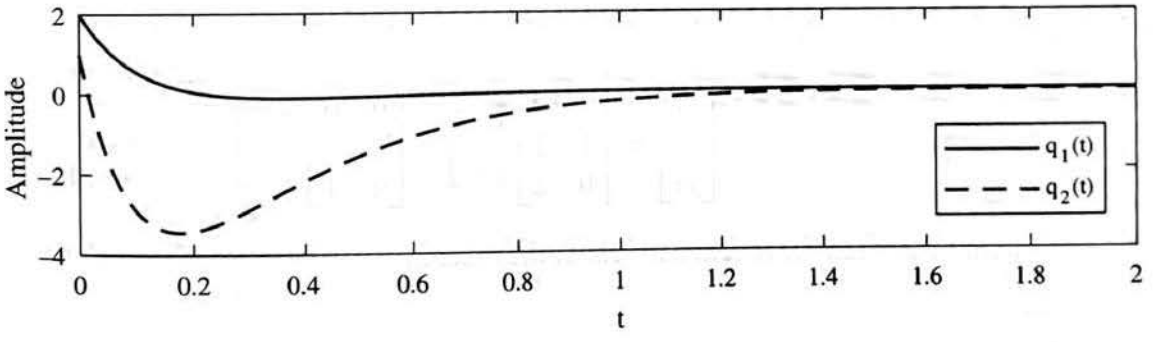

Figure 13.7 State vector plot for Ex. 13.6.

THE OUTPUT

The output equation is given by

$$\mathbf{y} = \mathbf{Cq} + \mathbf{Dx}$$

and

$$\mathbf{Y}(s) = \mathbf{CQ}(s) + \mathbf{DX}(s)$$

Upon substituting Eq. (13.28) into this equation, we have

$$\begin{aligned}\mathbf{Y}(s) &= \mathbf{C}\{\mathbf{\Phi}(s)[\mathbf{q}(0) + \mathbf{Bx}\,\mathbf{X}(s)]\} + \mathbf{DX}(s) \\ &= \underbrace{\mathbf{C\Phi}(s)\mathbf{q}(0)}_{\text{zero-input response}} + \underbrace{[\mathbf{C\Phi}(s)\mathbf{B} + \mathbf{D}]\mathbf{X}(s)}_{\text{zero-state response}}\end{aligned} \tag{13.30}$$

The zero-state response [i.e., the response $\mathbf{Y}(s)$ when $\mathbf{q}(0) = \mathbf{0}$] is given by

$$\mathbf{Y}(s) = [\mathbf{C\Phi}(s)\mathbf{B} + \mathbf{D}]\mathbf{X}(s)$$

Note that the transfer function of a system is defined under the zero-state condition [see Eq. (6.23)]. The matrix $\mathbf{C\Phi}(s)\mathbf{B} + \mathbf{D}$ is the *transfer function matrix* $\mathbf{H}(s)$ of the system, which relates the responses $y_1, y_2, \ldots, y_k$ to the inputs $x_1, x_2, \ldots, x_j$:

$$\mathbf{H}(s) = \mathbf{C\Phi}(s)\mathbf{B} + \mathbf{D} \tag{13.31}$$

and the zero-state response is

$$\mathbf{Y}(s) = \mathbf{H}(s)\mathbf{X}(s)$$

The matrix $\mathbf{H}(s)$ is a $k \times j$ matrix (k is the number of outputs and j is the number of inputs). The ijth element $H_{ij}(s)$ of $H(s)$ is the transfer function that relates the output $y_i(t)$ to the input $x_j(t)$.

EXAMPLE 13.7 Transfer Function Matrix from State-Space Description

Let us consider a system with a state equation

$$\begin{bmatrix}\dot{q}_1 \\ \dot{q}_2\end{bmatrix} = \begin{bmatrix}0 & 1 \\ -2 & -3\end{bmatrix}\begin{bmatrix}q_1 \\ q_2\end{bmatrix} + \begin{bmatrix}1 & 0 \\ 1 & 1\end{bmatrix}\begin{bmatrix}x_1 \\ x_2\end{bmatrix}$$

and an output equation

$$\begin{bmatrix}y_1 \\ y_2 \\ y_3\end{bmatrix} = \begin{bmatrix}1 & 0 \\ 1 & 1 \\ 0 & 2\end{bmatrix}\begin{bmatrix}q_1 \\ q_2\end{bmatrix} + \begin{bmatrix}0 & 0 \\ 1 & 0 \\ 0 & 1\end{bmatrix}\begin{bmatrix}x_1 \\ x_2\end{bmatrix}$$

Determine the transfer function matrix of the system.

In this case,

$$\mathbf{A} = \begin{bmatrix}0 & 1 \\ -2 & -3\end{bmatrix} \quad \mathbf{B} = \begin{bmatrix}1 & 0 \\ 1 & 1\end{bmatrix} \quad \mathbf{C} = \begin{bmatrix}1 & 0 \\ 1 & 1 \\ 0 & 2\end{bmatrix} \quad \mathbf{D} = \begin{bmatrix}0 & 0 \\ 1 & 0 \\ 0 & 1\end{bmatrix} \tag{13.32}$$

and

$$\mathbf{\Phi}(s) = (s\mathbf{I} - \mathbf{A})^{-1} = \begin{bmatrix} s & -1 \\ 2 & s+3 \end{bmatrix}^{-1} = \begin{bmatrix} \frac{s+3}{(s+1)(s+2)} & \frac{1}{(s+1)(s+2)} \\ \frac{-2}{(s+1)(s+2)} & \frac{s}{(s+1)(s+2)} \end{bmatrix} \tag{13.33}$$

Hence, the transfer function matrix $\mathbf{H}(s)$ is given by

$$\begin{aligned} \mathbf{H}(s) &= \mathbf{C}\mathbf{\Phi}(s)\mathbf{B} + \mathbf{D} \\ &= \begin{bmatrix} 1 & 0 \\ 1 & 1 \\ 0 & 2 \end{bmatrix} \begin{bmatrix} \frac{s+3}{(s+1)(s+2)} & \frac{1}{(s+1)(s+2)} \\ \frac{-2}{(s+1)(s+2)} & \frac{s}{(s+1)(s+2)} \end{bmatrix} \begin{bmatrix} 1 & 0 \\ 1 & 1 \end{bmatrix} + \begin{bmatrix} 0 & 0 \\ 1 & 0 \\ 0 & 1 \end{bmatrix} \\ &= \begin{bmatrix} \frac{s+4}{(s+1)(s+2)} & \frac{1}{(s+1)(s+2)} \\ \frac{s+4}{s+2} & \frac{1}{s+2} \\ \frac{2(s-2)}{(s+1)(s+2)} & \frac{s^2+5s+2}{(s+1)(s+2)} \end{bmatrix} \end{aligned} \tag{13.34}$$

and the zero-state response is

$$\mathbf{Y}(s) = \mathbf{H}(s)\mathbf{X}(s)$$

Remember that the ijth element of the transfer function matrix in Eq. (13.34) represents the transfer function that relates the output $y_i(t)$ to the input $x_j(t)$. For instance, the transfer function that relates the output y_3 to the input x_2 is $H_{32}(s)$, where

$$H_{32}(s) = \frac{s^2+5s+2}{(s+1)(s+2)}$$

We can readily verify the transfer function matrix using MATLAB and its symbolic toolbox functions.

```
>> A = [0 1;-2 -3]; B = [1 0;1 1];
>> C = [1 0;1 1;0 2]; D = [0 0;1 0;0 1];
>> syms s; H = collect(simplify(C*inv(s*eye(2)-A)*B+D))
   H =
       [   (s + 4)/(s^2 + 3*s + 2),                1/(s^2 + 3*s + 2)]
       [            (s + 4)/(s + 2),                        1/(s + 2)]
       [ (2*s - 4)/(s^2 + 3*s + 2), (s^2 + 5*s + 2)/(s^2 + 3*s + 2)]
```

Transfer functions relating particular inputs to particular outputs, such as $H_{32}(s)$, can be obtained using the `ss2tf` and `tf` functions.

```
>> [num,den] = ss2tf(A,B,C,D,2); H_32 = tf(num(3,:),den)
   H_32 =
          s^2 + 5 s + 2
          -------------
          s^2 + 3 s + 2
```

Characteristic Roots (Eigenvalues) of a Matrix

It is interesting to observe that the denominator of every transfer function in Eq. (13.34) is $(s+1)(s+2)$ except for $H_{21}(s)$ and $H_{22}(s)$, where the factor $(s+1)$ is canceled. This is no coincidence. We see that the denominator of every element of $\mathbf{\Phi}(s)$ is $|s\mathbf{I}-\mathbf{A}|$ because $\mathbf{\Phi}(s) = (s\mathbf{I}-\mathbf{A})^{-1}$, and the inverse of a matrix has its determinant in the denominator. Since $\mathbf{C}$, $\mathbf{B}$, and $\mathbf{D}$ are matrices with constant elements, we see from Eq. (13.31) that the denominator of $\mathbf{\Phi}(s)$ will also be the denominator of $\mathbf{H}(s)$. Hence, the denominator of every element of $\mathbf{H}(s)$ is $|s\mathbf{I}-\mathbf{A}|$, except for the possible cancellation of the common factors mentioned earlier. In other words, the zeros of the polynomial $|s\mathbf{I}-\mathbf{A}|$ are also the poles of all transfer functions of the system. *Therefore, the zeros of the polynomial $|s\mathbf{I}-\mathbf{A}|$ are the characteristic roots of the system.* Hence, the characteristic roots of the system are the roots of the equation

$$|s\mathbf{I}-\mathbf{A}| = 0 \tag{13.35}$$

Since $|s\mathbf{I}-\mathbf{A}|$ is an Nth-order polynomial in s with N zeros $\lambda_1, \lambda_2, \ldots, \lambda_N$, we can write Eq. (13.35) as

$$|s\mathbf{I}-\mathbf{A}| = s^N + a_1 s^{N-1} + \cdots + a_{N-1}s + a_N = (s-\lambda_1)(s-\lambda_2)\cdots(s-\lambda_N) = 0$$

For the system in Ex. 13.7,

$$|s\mathbf{I}-\mathbf{A}| = \begin{vmatrix} s & 0 \\ 0 & s \end{vmatrix} - \begin{vmatrix} 0 & 1 \\ -2 & -3 \end{vmatrix} = \begin{vmatrix} s & -1 \\ 2 & s+3 \end{vmatrix}$$
$$= s^2 + 3s + 2 = (s+1)(s+2)$$

Hence,

$$\lambda_1 = -1 \qquad \text{and} \qquad \lambda_2 = -2$$

Equation (13.35) is known as the *characteristic equation of the matrix* $\mathbf{A}$, and $\lambda_1, \lambda_2, \ldots, \lambda_N$ are the characteristic roots of $\mathbf{A}$. The term *eigenvalue,* meaning "characteristic value" in German, is also commonly used in the literature. Thus, we have shown that the characteristic roots of a system are the eigenvalues (characteristic values) of the matrix $\mathbf{A}$.

At this point, the reader will recall that if $\lambda_1, \lambda_2, \ldots, \lambda_N$ are the poles of the transfer function, then the zero-input response is of the form

$$y_0(t) = c_1 e^{\lambda_1 t} + c_2 e^{\lambda_2 t} + \cdots + c_N e^{\lambda_N t} \tag{13.36}$$

This fact is also obvious from Eq. (13.30). The denominator of every element of the zero-input response matrix $\mathbf{C\Phi}(s)\mathbf{q}(0)$ is $|s\mathbf{I}-\mathbf{A}| = (s-\lambda_1)(s-\lambda_2)\cdots(s-\lambda_N)$. Therefore, the partial fraction expansion and the subsequent inverse Laplace transform will yield a zero-input component of the form in Eq. (13.36).

13.4.2 Time-Domain Solution of State Equations

The state equation is

$$\dot{\mathbf{q}} = \mathbf{A}\mathbf{q} + \mathbf{B}\mathbf{x} \tag{13.37}$$

We now show that the solution of the vector differential Eq. (13.37) is

$$\mathbf{q}(t) = e^{\mathbf{A}t}\mathbf{q}(0) + \int_0^t e^{\mathbf{A}(t-\tau)}\mathbf{B}\mathbf{x}(\tau)\,d\tau$$

Before proceeding further, we must define the matrix exponential $e^{\mathbf{A}t}$. An exponential of a matrix is defined by an infinite series identical to that used in defining an exponential of a scalar. We shall define

$$e^{\mathbf{A}t} = \mathbf{I} + \mathbf{A}t + \frac{\mathbf{A}^2t^2}{2!} + \frac{\mathbf{A}^3t^3}{3!} + \cdots + \frac{\mathbf{A}^nt^n}{n!} + \cdots = \sum_{k=0}^{\infty} \frac{\mathbf{A}^kt^k}{k!} \tag{13.38}$$

For example, if

$$\mathbf{A} = \begin{bmatrix} 0 & 1 \\ 2 & 1 \end{bmatrix}$$

then

$$\mathbf{A}t = \begin{bmatrix} 0 & 1 \\ 2 & 1 \end{bmatrix} t = \begin{bmatrix} 0 & t \\ 2t & t \end{bmatrix}$$

and

$$\frac{\mathbf{A}^2t^2}{2!} = \begin{bmatrix} 0 & 1 \\ 2 & 1 \end{bmatrix}\begin{bmatrix} 0 & 1 \\ 2 & 1 \end{bmatrix}\frac{t^2}{2} = \begin{bmatrix} 2 & 1 \\ 2 & 3 \end{bmatrix}\frac{t^2}{2} = \begin{bmatrix} t^2 & \frac{t^2}{2} \\ t^2 & \frac{3t^2}{2} \end{bmatrix}$$

and so on.

We can show that the infinite series in Eq. (13.38) is absolutely and uniformly convergent for all values of t. Consequently, it can be differentiated or integrated term by term. Thus, to find $(d/dt)e^{\mathbf{A}t}$, we differentiate the series on the right-hand side of Eq. (13.38) term by term:

$$\begin{aligned} \frac{d}{dt}e^{\mathbf{A}t} &= \mathbf{A} + \mathbf{A}^2t + \frac{\mathbf{A}^3t^2}{2!} + \frac{\mathbf{A}^4t^3}{3!} + \cdots \\ &= \mathbf{A}\left[\mathbf{I} + \mathbf{A}t + \frac{\mathbf{A}^2t^2}{2!} + \frac{\mathbf{A}^3t^3}{3!} + \cdots\right] = \mathbf{A}e^{\mathbf{A}t} \\ &= \left[\mathbf{I} + \mathbf{A}t + \frac{\mathbf{A}^2t^2}{2!} + \frac{\mathbf{A}^3t^3}{3!} + \cdots + \cdots\right]\mathbf{A} = e^{\mathbf{A}t}\mathbf{A} \end{aligned}$$

Hence,

$$\frac{d}{dt}e^{\mathbf{A}t} = \mathbf{A}e^{\mathbf{A}t} = e^{\mathbf{A}t}\mathbf{A}$$

Also note that from Eq. (13.38), it follows that

$$e^{\mathbf{0}} = \mathbf{I}$$

where $\mathbf{I}$ is just the identity matrix. If we premultiply or postmultiply the infinite series for $e^{\mathbf{A}t}$ [Eq. (13.38)] by an infinite series for $e^{-\mathbf{A}t}$, we find that

$$(e^{-\mathbf{A}t})(e^{\mathbf{A}t}) = (e^{\mathbf{A}t})(e^{-\mathbf{A}t}) = \mathbf{I} \tag{13.39}$$

In Sec. 13.1.1, we showed that

$$\frac{d}{dt}(\mathbf{UV}) = \frac{d\mathbf{U}}{dt}\mathbf{V} + \mathbf{U}\frac{d\mathbf{V}}{dt}$$

Using this relationship, we observe that

$$\begin{aligned}\frac{d}{dt}[e^{-\mathbf{A}t}\mathbf{q}] &= \left(\frac{d}{dt}e^{-\mathbf{A}t}\right)\mathbf{q} + e^{-\mathbf{A}t}\dot{\mathbf{q}} \\ &= -e^{-\mathbf{A}t}\mathbf{A}\mathbf{q} + e^{-\mathbf{A}t}\dot{\mathbf{q}}\end{aligned} \tag{13.40}$$

We now premultiply both sides of Eq. (13.37) by $e^{-\mathbf{A}t}$ to yield

$$e^{-\mathbf{A}t}\dot{\mathbf{q}} = e^{-\mathbf{A}t}\mathbf{A}\mathbf{q} + e^{-\mathbf{A}t}\mathbf{B}\mathbf{x}$$

or

$$-e^{-\mathbf{A}t}\mathbf{A}\mathbf{q} + e^{-\mathbf{A}t}\dot{\mathbf{q}} = e^{-\mathbf{A}t}\mathbf{B}\mathbf{x}$$

Substituting this result into Eq. (13.40) yields

$$\frac{d}{dt}[e^{-\mathbf{A}t}\mathbf{q}] = e^{-\mathbf{A}t}\mathbf{B}\mathbf{x}$$

The integration of both sides of this equation from 0 to t yields

$$e^{-\mathbf{A}t}\mathbf{q}\Big|_0^t = \int_0^t e^{-\mathbf{A}\tau}\mathbf{B}\mathbf{x}(\tau)\,d\tau$$

or

$$e^{-\mathbf{A}t}\mathbf{q}(t) - \mathbf{q}(0) = \int_0^t e^{-\mathbf{A}\tau}\mathbf{B}\mathbf{x}(\tau)\,d\tau$$

Hence,

$$e^{-\mathbf{A}t}\mathbf{q} = \mathbf{q}(0) + \int_0^t e^{-\mathbf{A}\tau}\mathbf{B}\mathbf{x}(\tau)\,d\tau$$

Premultiplying this result by $e^{\mathbf{A}t}$ and using Eq. (13.39), we have

$$\mathbf{q}(t) = \underbrace{e^{\mathbf{A}t}\mathbf{q}(0)}_{\text{ZIR}} + \underbrace{\int_0^t e^{\mathbf{A}(t-\tau)}\mathbf{B}\mathbf{x}(\tau)\,d\tau}_{\text{ZSR}} \tag{13.41}$$

This is the desired solution. The first term on the right-hand side represents $q(t)$ when the input $x(t) = 0$. Hence, it is the zero-input component. The second term, by a similar argument, is seen to be the zero-state component.

The results of Eq. (13.41) can be expressed more conveniently in terms of the matrix convolution. We can define the convolution of two matrices in a manner similar to the multiplication of two matrices, except that the multiplication of two elements is replaced by their convolution. For example,

$$\begin{bmatrix} x_1 & x_2 \\ x_3 & x_4 \end{bmatrix} * \begin{bmatrix} g_1 & g_2 \\ g_3 & g_4 \end{bmatrix} = \begin{bmatrix} (x_1 * g_1 + x_2 * g_3) & (x_1 * g_2 + x_2 * g_4) \\ (x_3 * g_1 + x_4 * g_3) & (x_3 * g_2 + x_4 * g_4) \end{bmatrix}$$

By using this definition of matrix convolution, we can express Eq. (13.41) as

$$\mathbf{q}(t) = e^{\mathbf{A}t}\mathbf{q}(0) + e^{\mathbf{A}t} * \mathbf{B}\mathbf{x}(t) \tag{13.42}$$

Note that the limits of the convolution integral [Eq. (13.41)] are from 0 to t. Hence, all the elements of $e^{\mathbf{A}t}$ in the convolution term of Eq. (13.42) are implicitly assumed to be multiplied by $u(t)$.

The result of Eqs. (13.41) and (13.42) can be easily generalized for any initial value of t. It is left as an exercise for the reader to show that the solution of the state equation can be expressed as

$$\mathbf{q}(t) = e^{\mathbf{A}(t-t_0)}\mathbf{q}(t_0) + \int_{t_0}^{t} e^{\mathbf{A}(t-\tau)}\mathbf{B}\mathbf{x}(\tau)\,d\tau$$

Determining $e^{\mathbf{A}t}$

The exponential $e^{\mathbf{A}t}$ required in Eqs. (13.41) and (13.42) can be computed from the definition in Eq. (13.38). Unfortunately, this is an infinite series, and its computation can be quite laborious. Moreover, we may not be able to recognize the closed-form expression for the answer. There are several efficient methods of determining $e^{\mathbf{A}t}$ in closed form. It was shown in Sec. 13.1.3 that for an $N \times N$ matrix $\mathbf{A}$,

$$e^{\mathbf{A}t} = \beta_0\mathbf{I} + \beta_1\mathbf{A} + \beta_2\mathbf{A}^2 + \cdots + \beta_{N-1}\mathbf{A}^{N-1} \tag{13.43}$$

where

$$\begin{bmatrix} \beta_0 \\ \beta_1 \\ \vdots \\ \beta_{N-1} \end{bmatrix} = \begin{bmatrix} 1 & \lambda_1 & \lambda_1^2 & \cdots & \lambda_1^{N-1} \\ 1 & \lambda_2 & \lambda_2^2 & \cdots & \lambda_2^{N-1} \\ \vdots & \vdots & \vdots & \cdots & \vdots \\ 1 & \lambda_N & \lambda_N^2 & \cdots & \lambda_N^{N-1} \end{bmatrix}^{-1} \begin{bmatrix} e^{\lambda_1 t} \\ e^{\lambda_2 t} \\ \vdots \\ e^{\lambda_N t} \end{bmatrix}$$

and $\lambda_1, \lambda_2, \ldots, \lambda_N$ are the N characteristic values (eigenvalues) of $\mathbf{A}$.

We can also determine $e^{\mathbf{A}t}$ by comparing Eqs. (13.41) and (13.29). It is clear that

$$e^{\mathbf{A}t} = \mathcal{L}^{-1}[\mathbf{\Phi}(s)] = \mathcal{L}^{-1}[(s\mathbf{I} - \mathbf{A})^{-1}] \tag{13.44}$$

Thus, $e^{\mathbf{A}t}$ and $\mathbf{\Phi}(s)$ are a Laplace transform pair. To be consistent with Laplace transform notation, $e^{\mathbf{A}t}$ is often denoted by $\boldsymbol{\phi}(t)$, the *state transition matrix* (STM):

$$e^{\mathbf{A}t} = \boldsymbol{\phi}(t)$$

EXAMPLE 13.8 Time-Domain Method to Solve State Equations

Use the time-domain method to solve Ex. 13.6.

For this case, the characteristic roots are given by

$$|s\mathbf{I} - \mathbf{A}| = \begin{vmatrix} s+12 & -\frac{2}{3} \\ 36 & s+1 \end{vmatrix} = s^2 + 13s + 36 = (s+4)(s+9) = 0$$

The roots are $\lambda_1 = -4$ and $\lambda_2 = -9$, so

$$\begin{bmatrix}\beta_0\\ \beta_1\end{bmatrix} = \begin{bmatrix}1 & -4\\ 1 & -9\end{bmatrix}^{-1}\begin{bmatrix}e^{-4t}\\ e^{-9t}\end{bmatrix} = \frac{1}{5}\begin{bmatrix}9e^{-4t} - 4e^{-9t}\\ e^{-4t} - e^{-9t}\end{bmatrix}$$

and

$$\begin{aligned} e^{\mathbf{A}t} &= \beta_0\mathbf{I} + \beta_1\mathbf{A}\\ &= \left(\tfrac{9}{5}e^{-4t} - \tfrac{4}{5}e^{-9t}\right)\begin{bmatrix}1 & 0\\ 0 & 1\end{bmatrix} + \left(\tfrac{1}{5}e^{-4t} - \tfrac{1}{5}e^{-9t}\right)\begin{bmatrix}-12 & \frac{2}{3}\\ -36 & -1\end{bmatrix}\\ &= \begin{bmatrix}\left(\frac{-3}{5}e^{-4t} + \frac{8}{5}e^{-9t}\right) & \frac{2}{15}(e^{-4t} - e^{-9t})\\ \frac{36}{5}(-e^{-4t} + e^{-9t}) & \left(\frac{8}{5}e^{-4t} - \frac{3}{5}e^{-9t}\right)\end{bmatrix} \end{aligned}$$

The zero-input response is given by [see Eq. (13.41)]

$$\begin{aligned} e^{\mathbf{A}t}\mathbf{q}(0) &= \begin{bmatrix}\left(-\frac{3}{5}e^{-4t} + \frac{8}{5}e^{-9t}\right) & \frac{2}{15}(e^{-4t} - e^{-9t})\\ \frac{36}{5}(-e^{-4t} + e^{-9t}) & \left(\frac{8}{5}e^{-4t} - \frac{3}{5}e^{-9t}\right)\end{bmatrix}\begin{bmatrix}2\\ 1\end{bmatrix}\\ &= \begin{bmatrix}\left(\frac{-16}{15}e^{-4t} + \frac{46}{15}e^{-9t}\right)u(t)\\ \left(\frac{-64}{5}e^{-4t} + \frac{69}{5}e^{-9t}\right)u(t)\end{bmatrix} \end{aligned}$$

Note here the presence of $u(t)$, indicating that the response begins at $t = 0$.

The zero-state component is $e^{\mathbf{A}t} * \mathbf{Bx}$ [see Eq. (13.42)], where

$$\mathbf{Bx} = \begin{bmatrix}\frac{1}{3}\\ 1\end{bmatrix}u(t) = \begin{bmatrix}\frac{1}{3}u(t)\\ u(t)\end{bmatrix}$$

and

$$e^{\mathbf{A}t} * \mathbf{Bx}(t) = \begin{bmatrix}\left(\frac{-3}{5}e^{-4t} + \frac{8}{5}e^{-9t}\right)u(t) & \frac{2}{15}(e^{-4t} - e^{-9t})u(t)\\ \frac{36}{5}(-e^{-4t} + e^{-9t}u(t)) & \left(\frac{8}{5}e^{-4t} - \frac{3}{5}e^{-9t}\right)u(t)\end{bmatrix} * \begin{bmatrix}\frac{1}{3}u(t)\\ u(t)\end{bmatrix}$$

Note again the presence of the term $u(t)$ in every element of $e^{\mathbf{A}t}$. This is the case because the limits of the convolution integral run from 0 to t [Eq. (13.41)]. Thus,

$$\begin{aligned} e^{\mathbf{A}t} * \mathbf{Bx}(t) &= \begin{bmatrix}\left(-\frac{3}{5}e^{-4t} + \frac{8}{5}e^{-9t}\right)u(t) * \frac{1}{3}u(t) & \frac{2}{15}(e^{-4t} - e^{-9t})u(t) * u(t)\\ \frac{36}{5}(-e^{-4t} + e^{-9t})u(t) * \frac{1}{3}u(t) & \left(\frac{8}{5}e^{-4t} - \frac{3}{5}e^{-9t}\right)u(t) * u(t)\end{bmatrix}\\ &= \begin{bmatrix}-\frac{1}{15}e^{-4t}u(t) * u(t) + \frac{2}{5}e^{-9t}u(t) * u(t)\\ -\frac{4}{5}e^{-4t}u(t) * u(t) + \frac{9}{5}e^{-9t}u(t) * u(t)\end{bmatrix} \end{aligned}$$

Substitution for the preceding convolution integrals from the convolution table (Table 2.1) yields

$$e^{\mathbf{A}t} * \mathbf{B}\mathbf{x}(t) = \begin{bmatrix} -\frac{1}{60}(1-e^{-4t})u(t) + \frac{2}{45}(1-e^{-9t})u(t) \\ -\frac{1}{5}(1-e^{-4t})u(t) + \frac{1}{5}(1-e^{-9t})u(t) \end{bmatrix}$$
$$= \begin{bmatrix} \left(\frac{1}{36} + \frac{1}{60}e^{-4t} - \frac{2}{45}e^{-9t}\right)u(t) \\ \frac{1}{5}(e^{-4t} - e^{-9t})u(t) \end{bmatrix}$$

The sum of the two components now gives the desired solution for $\mathbf{q}(t)$:

$$\mathbf{q}(t) = \begin{bmatrix} q_1(t) \\ q_2(t) \end{bmatrix} = \begin{bmatrix} \left(\frac{1}{36} - \frac{21}{20}e^{-4t} + \frac{136}{45}e^{-9t}\right)u(t) \\ \left(\frac{-63}{5}e^{-4t} + \frac{68}{5}e^{-9t}\right)u(t) \end{bmatrix}$$

This result confirms the solution obtained by using the frequency-domain method [see Ex. 13.6]. Once the state variables q_1 and q_2 have been found for $t \geq 0$, all the remaining variables can be determined from the output equation.

The Output

The output equation is given by

$$\mathbf{y}(t) = \mathbf{C}\mathbf{q}(t) + \mathbf{D}\mathbf{x}(t)$$

The substitution of the solution for $\mathbf{q}$ [Eq. (13.42)] in this equation yields

$$\mathbf{y}(t) = \mathbf{C}[e^{\mathbf{A}t}\mathbf{q}(0) + e^{\mathbf{A}t} * \mathbf{B}\mathbf{x}(t)] + \mathbf{D}\mathbf{x}(t)$$

Since the elements of $\mathbf{B}$ are constants,

$$e^{\mathbf{A}t} * \mathbf{B}\mathbf{x}(t) = e^{\mathbf{A}t}\mathbf{B} * \mathbf{x}(t)$$

With this result, the output equation becomes

$$\mathbf{y}(t) = \mathbf{C}[e^{\mathbf{A}t}\mathbf{q}(0) + e^{\mathbf{A}t}\mathbf{B} * \mathbf{x}(t)] + \mathbf{D}\mathbf{x}(t)$$

Now recall that the convolution of $x(t)$ with the unit impulse $\delta(t)$ yields $x(t)$. Let us define a $j \times j$ diagonal matrix $\boldsymbol{\delta}(t)$ such that all its diagonal terms are unit impulse functions. It is then obvious that

$$\boldsymbol{\delta}(t) * \mathbf{x}(t) = \mathbf{x}(t)$$

and the output equation can be expressed as

$$\mathbf{y}(t) = \mathbf{C}[e^{\mathbf{A}t}\mathbf{q}(0) + e^{\mathbf{A}t}\mathbf{B} * \mathbf{x}(t)] + \mathbf{D}\boldsymbol{\delta}(t) * \mathbf{x}(t)$$
$$= \mathbf{C}e^{\mathbf{A}t}\mathbf{q}(0) + [\mathbf{C}e^{\mathbf{A}t}\mathbf{B} + \mathbf{D}\boldsymbol{\delta}(t)] * \mathbf{x}(t)$$

With the notation $\boldsymbol{\phi}(t)$ for $e^{\mathbf{A}t}$, the output equation may be expressed as

$$\mathbf{y}(t) = \underbrace{\mathbf{C}\boldsymbol{\phi}(t)\mathbf{q}(0)}_{\text{zero-input response}} + \underbrace{[\mathbf{C}\boldsymbol{\phi}(t)\mathbf{B} + \mathbf{D}\delta(t)] * \mathbf{x}(t)}_{\text{zero-state response}}$$

The zero-state response, that is, the response when $\mathbf{q}(0) = \mathbf{0}$, is

$$\mathbf{y}(t) = [\mathbf{C}\boldsymbol{\phi}(t)\mathbf{B} + \mathbf{D}\delta(t)] * \mathbf{x}(t) = \mathbf{h}(t) * \mathbf{x}(t)$$

where

$$\mathbf{h}(t) = \mathbf{C}\boldsymbol{\phi}(t)\mathbf{B} + \mathbf{D}\delta(t) \tag{13.45}$$

The matrix $\mathbf{h}(t)$ is a $k \times j$ matrix known as the *impulse response matrix*. The reason for this designation is obvious. The ijth element of $\mathbf{h}(t)$ is $h_{ij}(t)$, which represents the zero-state response y_i when the input $x_j(t) = \delta(t)$ and when all other inputs (and all the initial conditions) are zero. Not surprisingly, vectors $\mathbf{h}(t)$ and $\mathbf{H}(s)$ form a Laplace transform pair:

$$\mathcal{L}[\mathbf{h}(t)] = \mathbf{H}(s)$$

EXAMPLE 13.9 State Transition Matrix by Inverse Laplace Transform

For the system described in Ex. 13.7, use Eq. (13.44) to determine $e^{\mathbf{A}t}$:

$$\boldsymbol{\phi}(t) = e^{\mathbf{A}t} = \mathcal{L}^{-1}\boldsymbol{\Phi}(s)$$

This problem was solved earlier with frequency-domain techniques. From Eq. (13.33), we have

$$\begin{aligned}
\boldsymbol{\phi}(t) &= \mathcal{L}^{-1}\begin{bmatrix} \frac{s+3}{(s+1)(s+2)} & \frac{1}{(s+1)(s+2)} \\ \frac{-2}{(s+1)(s+2)} & \frac{s}{(s+1)(s+2)} \end{bmatrix} \\
&= \mathcal{L}^{-1}\begin{bmatrix} \frac{2}{s+1} - \frac{1}{s+2} & \frac{1}{s+1} - \frac{1}{s+2} \\ \frac{-2}{s+1} + \frac{2}{s+2} & \frac{-1}{s+1} + \frac{2}{s+2} \end{bmatrix} \\
&= \begin{bmatrix} 2e^{-t} - e^{-2t} & e^{-t} - e^{-2t} \\ -2e^{-t} + 2e^{-2t} & -e^{-t} + 2e^{-2t} \end{bmatrix}
\end{aligned}$$

The same result is obtained in Ex. 13.1 (Sec. 13.1.3) by using Eq. (13.43) [see Eq. (13.13)].

Also, $\delta(t)$ is a diagonal $j \times j$ or 2×2 matrix:

$$\delta(t) = \begin{bmatrix} \delta(t) & 0 \\ 0 & \delta(t) \end{bmatrix}$$

Substituting the matrices $\boldsymbol{\phi}(t)$, $\delta(t)$, $\mathbf{C}$, $\mathbf{D}$, and $\mathbf{B}$ [Eq. (13.32)] into Eq. (13.45), we have

$$\mathbf{h}(t) = \begin{bmatrix} 1 & 0 \\ 1 & 1 \\ 0 & 2 \end{bmatrix} \begin{bmatrix} 2e^{-t} - e^{-2t} & e^{-t} - e^{-2t} \\ -2e^{-t} + 2e^{-2t} & -e^{-t} + 2e^{-2t} \end{bmatrix} \begin{bmatrix} 1 & 0 \\ 1 & 1 \end{bmatrix} + \begin{bmatrix} 0 & 0 \\ 1 & 0 \\ 0 & 1 \end{bmatrix} \begin{bmatrix} \delta(t) & 0 \\ 0 & \delta(t) \end{bmatrix}$$

$$= \begin{bmatrix} 3e^{-t} - 2e^{-2t} & e^{-t} - e^{-2t} \\ \delta(t) + 2e^{-2t} & e^{-2t} \\ -6e^{-t} + 8e^{-2t} & \delta(t) - 2e^{-2t} + 4e^{-2t} \end{bmatrix}$$

As the reader can verify, the Laplace transform of this equation yields the transfer function matrix $\mathbf{H}(s)$ in Eq. (13.34).

13.5 Linear Transformation of a State Vector

In Sec. 13.2, we saw that the state of a system can be specified in several ways. The sets of all possible state variables are related—in other words, if we are given one set of state variables, we should be able to relate it to any other set. We are particularly interested in a linear type of relationship. Let $q_1, q_2, \ldots, q_N$ and $w_1, w_2, \ldots, w_N$ be two different sets of state variables specifying the same system. Let these sets be related by linear equations as

$$\begin{aligned} w_1 &= p_{11}q_1 + p_{12}q_2 + \cdots + p_{1N}q_N \\ w_2 &= p_{21}q_1 + p_{22}q_2 + \cdots + p_{2N}q_N \\ &\vdots \\ w_N &= p_{N1}q_1 + p_{N2}q_2 + \cdots + p_{NN}q_N \end{aligned}$$

or

$$\underbrace{\begin{bmatrix} w_1 \\ w_2 \\ \vdots \\ w_N \end{bmatrix}}_{\mathbf{w}} = \underbrace{\begin{bmatrix} p_{11} & p_{12} & \cdots & p_{1N} \\ p_{21} & p_{22} & \cdots & p_{2N} \\ \vdots & \vdots & \cdots & \vdots \\ p_{N1} & p_{N2} & \cdots & p_{NN} \end{bmatrix}}_{\mathbf{P}} \underbrace{\begin{bmatrix} q_1 \\ q_2 \\ \vdots \\ q_N \end{bmatrix}}_{\mathbf{q}}$$

Defining the vector $\mathbf{w}$ and matrix $\mathbf{P}$ as just shown, we obtain the compact matrix representation

$$\mathbf{w} = \mathbf{P}\mathbf{q} \tag{13.46}$$

and

$$\mathbf{q} = \mathbf{P}^{-1}\mathbf{w}$$

Thus, the state vector $\mathbf{q}$ is transformed into another state vector $\mathbf{w}$ through the linear transformation in Eq. (13.46).

If we know $\mathbf{w}$, we can determine $\mathbf{q}$ from $\mathbf{q} = \mathbf{P}^{-1}\mathbf{w}$, provided $\mathbf{P}^{-1}$ exists. This is equivalent to saying that $\mathbf{P}$ is a nonsingular matrix[†] ($|\mathbf{P}| \neq 0$). Thus, if $\mathbf{P}$ is a nonsingular matrix, the vector $\mathbf{w}$ defined by Eq. (13.46) is also a state vector. Consider the state equation of a system

$$\dot{\mathbf{q}} = \mathbf{A}\mathbf{q} + \mathbf{B}\mathbf{x}$$

If

$$\mathbf{w} = \mathbf{P}\mathbf{q}$$

then

$$\mathbf{q} = \mathbf{P}^{-1}\mathbf{w}$$

and

$$\dot{\mathbf{q}} = \mathbf{P}^{-1}\dot{\mathbf{w}}$$

Hence, the state equation now becomes

$$\mathbf{P}^{-1}\dot{\mathbf{w}} = \mathbf{A}\mathbf{P}^{-1}\mathbf{w} + \mathbf{B}\mathbf{x}$$

or

$$\begin{aligned}\dot{\mathbf{w}} &= \mathbf{P}\mathbf{A}\mathbf{P}^{-1}\mathbf{w} + \mathbf{P}\mathbf{B}\mathbf{x} \\ &= \hat{\mathbf{A}}\mathbf{w} + \hat{\mathbf{B}}\mathbf{x}\end{aligned} \tag{13.47}$$

where

$$\hat{\mathbf{A}} = \mathbf{P}\mathbf{A}\mathbf{P}^{-1} \quad \text{and} \quad \hat{\mathbf{B}} = \mathbf{P}\mathbf{B} \tag{13.48}$$

Equation (13.47) is a state equation for the same system, but now it is expressed in terms of the state vector $\mathbf{w}$.

The output equation is also modified. Let the original output equation be

$$\mathbf{y} = \mathbf{C}\mathbf{q} + \mathbf{D}\mathbf{x}$$

In terms of the new state variable $\mathbf{w}$, this equation becomes

$$\begin{aligned}\mathbf{y} &= \mathbf{C}(\mathbf{P}^{-1}\mathbf{w}) + \mathbf{D}\mathbf{x} \\ &= \hat{\mathbf{C}}\mathbf{w} + \mathbf{D}\mathbf{x}\end{aligned}$$

where

$$\hat{\mathbf{C}} = \mathbf{C}\mathbf{P}^{-1} \tag{13.49}$$

[†] This condition is equivalent to saying that all N equations in Eq. (13.46) are linearly independent; that is, none of the N equations can be expressed as a linear combination of the remaining equations.

EXAMPLE 13.10 Linear Transformation of the State Vector

The state equations of a certain system are given by

$$\begin{bmatrix}\dot{q}_1\\ \dot{q}_2\end{bmatrix}=\begin{bmatrix}0 & 1\\ -2 & -3\end{bmatrix}\begin{bmatrix}q_1\\ q_2\end{bmatrix}+\begin{bmatrix}1\\ 2\end{bmatrix}x(t)$$

Find the state equations for this system when the new state variables w_1 and w_2 are given as

$$\begin{bmatrix}w_1\\ w_2\end{bmatrix}=\begin{bmatrix}1 & 1\\ 1 & -1\end{bmatrix}\begin{bmatrix}q_1\\ q_2\end{bmatrix} \tag{13.50}$$

According to Eq. (13.47), the state equation for the state variable $\mathbf{w}$ is given by

$$\dot{\mathbf{w}}=\hat{\mathbf{A}}\mathbf{w}+\hat{\mathbf{B}}\mathbf{x}$$

where [see Eqs. (13.48) and (13.49)]

$$\begin{aligned}\hat{\mathbf{A}}=\mathbf{PAP}^{-1}&=\begin{bmatrix}1 & 1\\ 1 & -1\end{bmatrix}\begin{bmatrix}0 & 1\\ -2 & -3\end{bmatrix}\begin{bmatrix}1 & 1\\ 1 & -1\end{bmatrix}^{-1}\\ &=\begin{bmatrix}1 & 1\\ 1 & -1\end{bmatrix}\begin{bmatrix}0 & 1\\ -2 & -3\end{bmatrix}\begin{bmatrix}\frac{1}{2} & \frac{1}{2}\\ \frac{1}{2} & -\frac{1}{2}\end{bmatrix}\\ &=\begin{bmatrix}-2 & 0\\ 3 & -1\end{bmatrix}\end{aligned}$$

and

$$\hat{\mathbf{B}}=\mathbf{PB}=\begin{bmatrix}1 & 1\\ 1 & -1\end{bmatrix}\begin{bmatrix}1\\ 2\end{bmatrix}=\begin{bmatrix}3\\ -1\end{bmatrix}$$

Therefore,

$$\begin{bmatrix}\dot{w}_1\\ \dot{w}_2\end{bmatrix}=\begin{bmatrix}-2 & 0\\ 3 & -1\end{bmatrix}\begin{bmatrix}w_1\\ w_2\end{bmatrix}+\begin{bmatrix}3\\ -1\end{bmatrix}x(t)$$

This is the desired state equation for the state vector $\mathbf{w}$. The solution of this equation requires knowledge of the initial state $\mathbf{w}(0)$. This can be obtained from the given initial state $\mathbf{q}(0)$ by using Eq. (13.50).

We can obtain the same result with less effort using MATLAB.

```
>> A = [0 1;-2 -3]; B = [1; 2];
>> P = [1 1;1 -1];
>> Ahat = P*A*inv(P), Bhat = P*B
   Ahat =    -2     0
              3    -1

   Bhat =     3
             -1
```

Invariance of Eigenvalues

We have seen that the poles of all possible transfer functions of a system are the eigenvalues of the matrix **A**. If we transform a state vector from **q** to **w**, the variables $w_1, w_2, \ldots, w_N$ are linear combinations of $q_1, q_2, \ldots, q_N$ and therefore may be considered to be outputs. Hence, the poles of the transfer functions relating $w_1, w_2, \ldots, w_N$ to the various inputs must also be the eigenvalues of matrix **A**. On the other hand, the system is also specified by Eq. (13.47). This means that the poles of the transfer functions must be the eigenvalues of $\hat{\mathbf{A}}$. Therefore, the eigenvalues of matrix **A** remain unchanged for the linear transformation of variables represented by Eq. (13.46), and the eigenvalues of matrix **A** and matrix $\hat{\mathbf{A}}(\hat{\mathbf{A}} = \mathbf{PAP}^{-1})$ are identical, implying that the characteristic equations of **A** and $\hat{\mathbf{A}}$ are also identical. This result also can be proved alternately as follows.

Consider the matrix $\mathbf{P}(s\mathbf{I} - \mathbf{A})\mathbf{P}^{-1}$. We have

$$\mathbf{P}(s\mathbf{I} - \mathbf{A})\mathbf{P}^{-1} = \mathbf{P}s\mathbf{I}\mathbf{P}^{-1} - \mathbf{PAP}^{-1} = s\mathbf{PIP}^{-1} - \hat{\mathbf{A}} = s\mathbf{I} - \hat{\mathbf{A}}$$

Taking the determinants of both sides, we obtain

$$|\mathbf{P}||s\mathbf{I} - \mathbf{A}||\mathbf{P}^{-1}| = |s\mathbf{I} - \hat{\mathbf{A}}|$$

The determinants $|\mathbf{P}|$ and $|\mathbf{P}^{-1}|$ are reciprocals of each other. Hence,

$$|s\mathbf{I} - \mathbf{A}| = |s\mathbf{I} - \hat{\mathbf{A}}|$$

This is the desired result. We have shown that the characteristic equations of **A** and $\hat{\mathbf{A}}$ are identical. Hence, the eigenvalues of **A** and $\hat{\mathbf{A}}$ are identical.

In Ex. 13.10, matrix **A** is given as

$$\mathbf{A} = \begin{bmatrix} 0 & 1 \\ -2 & -3 \end{bmatrix}$$

The characteristic equation is

$$|s\mathbf{I} - \mathbf{A}| = \begin{vmatrix} s & -1 \\ 2 & s+3 \end{vmatrix} = s^2 + 3s + 2 = 0$$

Also,

$$\hat{\mathbf{A}} = \begin{bmatrix} -2 & 0 \\ 3 & -1 \end{bmatrix}$$

and

$$|s\mathbf{I} - \hat{\mathbf{A}}| = \begin{bmatrix} s+2 & 0 \\ -3 & s+1 \end{bmatrix} = s^2 + 3s + 2 = 0$$

This result verifies that the characteristic equations of **A** and $\hat{\mathbf{A}}$ are identical.

13.5.1 Diagonalization of Matrix A

For several reasons, it is desirable to make matrix $\mathbf{A}$ diagonal. If $\mathbf{A}$ is not diagonal, we can transform the state variables such that the resulting matrix $\hat{\mathbf{A}}$ is diagonal.† One can show that for any diagonal matrix $\mathbf{A}$, the diagonal elements of this matrix must necessarily be $\lambda_1, \lambda_2, \ldots, \lambda_N$ (the eigenvalues) of the matrix. Consider the diagonal matrix $\mathbf{A}$:

$$\mathbf{A} = \begin{bmatrix} a_1 & 0 & 0 & \cdots & 0 \\ 0 & a_2 & 0 & \cdots & 0 \\ \vdots & \vdots & \vdots & \cdots & \vdots \\ 0 & 0 & 0 & \cdots & a_N \end{bmatrix}$$

The characteristic equation is given by

$$|s\mathbf{I} - \mathbf{A}| = \begin{bmatrix} (s-a_1) & 0 & 0 & \cdots & 0 \\ 0 & (s-a_2) & 0 & \cdots & 0 \\ \vdots & \vdots & \vdots & \cdots & \vdots \\ 0 & 0 & 0 & \cdots & (s-a_N) \end{bmatrix} = 0$$

or

$$(s-a_1)(s-a_2)\cdots(s-a_N) = 0$$

The nonzero (diagonal) elements of a diagonal matrix are therefore its eigenvalues $\lambda_1, \lambda_2, \ldots, \lambda_N$. We shall denote the diagonal matrix by a special symbol, $\mathbf{\Lambda}$:

$$\mathbf{\Lambda} = \begin{bmatrix} \lambda_1 & 0 & 0 & \cdots & 0 \\ 0 & \lambda_2 & 0 & \cdots & 0 \\ \vdots & \vdots & \vdots & \cdots & \vdots \\ 0 & 0 & 0 & \cdots & \lambda_N \end{bmatrix} \tag{13.51}$$

Let us now consider the transformation of the state vector $\mathbf{A}$ such that the resulting matrix $\hat{\mathbf{A}}$ is a diagonal matrix $\mathbf{\Lambda}$.

Consider the system

$$\dot{\mathbf{q}} = \mathbf{A}\mathbf{q} + \mathbf{B}\mathbf{x}$$

We shall assume that $\lambda_1, \lambda_2, \ldots, \lambda_N$, the eigenvalues of $\mathbf{A}$, are distinct (no repeated roots). Let us transform the state vector $\mathbf{q}$ into the new state vector $\mathbf{z}$, using the transformation

$$\mathbf{z} = \mathbf{P}\mathbf{q} \tag{13.52}$$

Then, after the development of Eq. (13.47), we have

$$\dot{\mathbf{z}} = \mathbf{P}\mathbf{A}\mathbf{P}^{-1}\mathbf{z} + \mathbf{P}\mathbf{B}\mathbf{x}$$

We desire the transformation to be such that $\mathbf{P}\mathbf{A}\mathbf{P}^{-1}$ is a diagonal matrix $\mathbf{\Lambda}$ given by Eq. (13.51), or

$$\dot{\mathbf{z}} = \mathbf{\Lambda}\mathbf{z} + \hat{\mathbf{B}}\mathbf{x} \tag{13.53}$$

† In this discussion, we assume distinct eigenvalues. If the eigenvalues are not distinct, we can reduce the matrix to a modified diagonalized (Jordan) form.

Hence,

$$\mathbf{\Lambda} = \mathbf{PAP}^{-1}$$

or

$$\mathbf{\Lambda P} = \mathbf{PA} \tag{13.54}$$

We know $\mathbf{\Lambda}$ and $\mathbf{A}$. Equation (13.54) therefore can be solved to determine $\mathbf{P}$.

EXAMPLE 13.11 Diagonal Form of the State Equations

Find the diagonalized form of the state equations for the system in Ex. 13.10.

In this case,

$$\mathbf{A} = \begin{bmatrix} 0 & 1 \\ -2 & -3 \end{bmatrix}$$

We found $\lambda_1 = -1$ and $\lambda_2 = -2$. Hence,

$$\mathbf{\Lambda} = \begin{bmatrix} -1 & 0 \\ 0 & -2 \end{bmatrix}$$

and Eq. (13.54) becomes

$$\begin{bmatrix} -1 & 0 \\ 0 & -2 \end{bmatrix} \begin{bmatrix} p_{11} & p_{12} \\ p_{21} & p_{22} \end{bmatrix} = \begin{bmatrix} p_{11} & p_{12} \\ p_{21} & p_{22} \end{bmatrix} \begin{bmatrix} 0 & 1 \\ -2 & -3 \end{bmatrix}$$

Equating the four elements on two sides, we obtain

$$\begin{aligned} -p_{11} &= -2p_{12} \\ -p_{12} &= p_{11} - 3p_{12} \\ -2p_{21} &= -2p_{22} \\ -2p_{22} &= p_{21} - 3p_{22} \end{aligned}$$

The reader will immediately recognize that the first two equations are identical and that the last two equations are identical. Hence, two equations may be discarded, leaving us with only two equations [$p_{11} = 2p_{12}$ and $p_{21} = p_{22}$] and four unknowns. This observation means that there is no unique solution. There is, in fact, an infinite number of solutions. We can assign any value to p_{11} and p_{21} to yield one possible solution.[†] If $p_{11} = k_1$ and $p_{21} = k_2$, then we have $p_{12} = k_1/2$ and $p_{22} = k_2$:

$$\mathbf{P} = \begin{bmatrix} k_1 & \frac{k_1}{2} \\ k_2 & k_2 \end{bmatrix}$$

[†] If, however, we want the state equations in diagonalized form, as in Eq. (13.26), where all the elements of $\hat{\mathbf{B}}$ matrix are unity, there is a unique solution. The reason is that the equation $\hat{\mathbf{B}} = \mathbf{PB}$, where all the elements of $\hat{\mathbf{B}}$ are unity, imposes additional constraints. In the present example, this condition will yield $p_{11} = 1/2$, $p_{12} = 1/4$, $p_{21} = 1/3$, and $p_{22} = 1/3$. The relationship between $\mathbf{z}$ and $\mathbf{q}$ is then

$$z_1 = \tfrac{1}{2}q_1 + \tfrac{1}{4}q_2 \quad \text{and} \quad z_2 = \tfrac{1}{3}q_1 + \tfrac{1}{3}q_2$$

We may assign any values to k_1 and k_2. For convenience, let $k_1 = 2$ and $k_2 = 1$. This substitution yields

$$\mathbf{P} = \begin{bmatrix} 2 & 1 \\ 1 & 1 \end{bmatrix}$$

The transformed variables [Eq. (13.52)] are

$$\begin{bmatrix} z_1 \\ z_2 \end{bmatrix} = \begin{bmatrix} 2 & 1 \\ 1 & 1 \end{bmatrix} \begin{bmatrix} q_1 \\ q_2 \end{bmatrix} = \begin{bmatrix} 2q_1 + q_2 \\ q_1 + q_2 \end{bmatrix}$$

This expression relates the new state variables z_1 and z_2 to the original state variables q_1 and q_2. The system equation with $\mathbf{z}$ as the state vector is given by [see Eq. (13.53)]

$$\dot{\mathbf{z}} = \mathbf{\Lambda z} + \hat{\mathbf{B}}\mathbf{x}$$

where

$$\hat{\mathbf{B}} = \mathbf{PB} = \begin{bmatrix} 2 & 1 \\ 1 & 1 \end{bmatrix} \begin{bmatrix} 1 \\ 2 \end{bmatrix} = \begin{bmatrix} 4 \\ 3 \end{bmatrix}$$

Hence,

$$\begin{bmatrix} \dot{z}_1 \\ \dot{z}_2 \end{bmatrix} = \begin{bmatrix} -1 & 0 \\ 0 & -2 \end{bmatrix} \begin{bmatrix} z_1 \\ z_2 \end{bmatrix} + \begin{bmatrix} 4 \\ 3 \end{bmatrix} x \tag{13.55}$$

or

$$\dot{z}_1 = -z_1 + 4x$$
$$\dot{z}_2 = -2z_2 + 3x$$

Note the distinctive nature of these state equations. Each state equation involves only one variable and therefore can be solved by itself. A general state equation has the derivative of one state variable equal to a linear combination of all state variables. Such is not the case with the diagonalized matrix $\mathbf{\Lambda}$. Each state variable z_i is chosen so that it is uncoupled from the rest of the variables; hence, a system with N eigenvalues is split into N decoupled systems, each with an equation of the form

$$\dot{z}_i = \lambda_i z_i + (\text{input terms})$$

This fact also can be readily seen from Fig. 13.8a, which is a realization of the system represented by Eq. (13.55). In contrast, consider the original state equations [see Ex. 13.10]

$$\dot{q}_1 = q_2 + x(t)$$
$$\dot{q}_2 = -2q_1 - 3q_2 + 2x(t)$$

A realization for these equations is shown in Fig. 13.8b. It can be seen from Fig. 13.8a that the states z_1 and z_2 are decoupled, whereas the states q_1 and q_2 (Fig. 13.8b) are coupled. It should be remembered that Figs. 13.8a and 13.8b are realizations of the same system.†

† Here, we only have a simulated state equation; the outputs are not shown. The outputs are linear combinations of state variables (and inputs). Hence, the output equation can be easily incorporated into these diagrams.

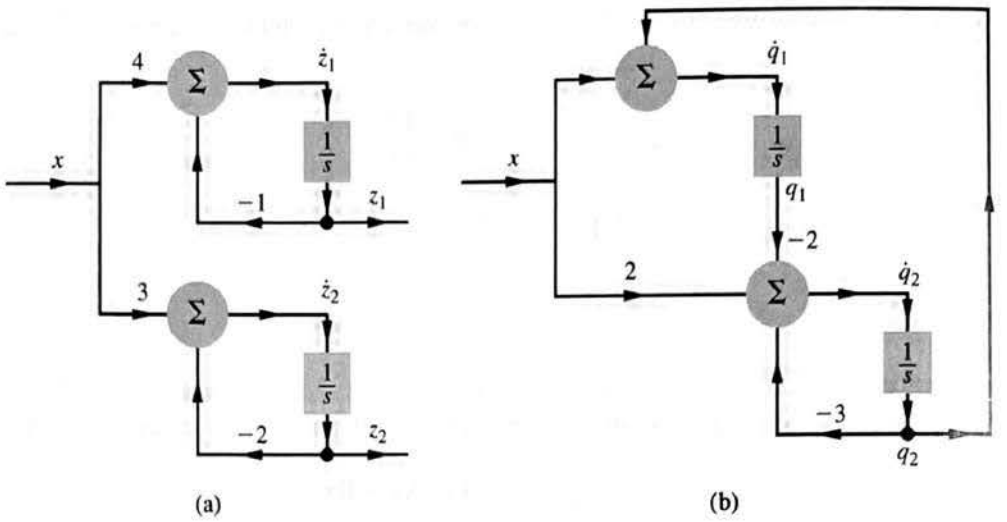

Figure 13.8 Two realizations of the second-order system.

MATRIX DIAGONALIZATION VIA MATLAB

The key to diagonalizing matrix **A** is to determine a matrix **P** that satisfies $\mathbf{\Lambda P} = \mathbf{PA}$ [Eq. (13.54)], where $\mathbf{\Lambda}$ is a diagonal matrix of the eigenvalues of **A**. This problem is directly related to the classic eigenvalue problem, stated as

$$\mathbf{AV} = \mathbf{V\Lambda}$$

where **V** is a matrix of eigenvectors for **A**. If we can find **V**, we can take its inverse to determine **P**. That is, $\mathbf{P} = \mathbf{V}^{-1}$. This relationship is more fully developed in Sec. 13.8.

MATLAB's built-in function `eig` can determine the eigenvectors of a matrix and, therefore, can help us determine a suitable matrix **P**. Let us demonstrate this approach for the current case.

```
>> A = [0 1;-2 -3]; B = [1; 2];
>> [V, Lambda] = eig(A);
>> P = inv(V), Lambda, Bhat = P*B
   P =    2.8284    1.4142
          2.2361    2.2361
   Lambda =    -1     0
                0    -2
   Bhat =    5.6569
             6.7082
```

Therefore,

$$\mathbf{z} = \begin{bmatrix} z_1 \\ z_2 \end{bmatrix} = \begin{bmatrix} 2.8284 & 1.4142 \\ 2.2361 & 2.2361 \end{bmatrix} \begin{bmatrix} q_1 \\ q_2 \end{bmatrix} = \mathbf{Pq}$$

and

$$\dot{\mathbf{z}} = \begin{bmatrix} \dot{z}_1 \\ \dot{z}_2 \end{bmatrix} = \begin{bmatrix} -1 & 0 \\ 0 & -2 \end{bmatrix} \begin{bmatrix} z_1 \\ z_2 \end{bmatrix} + \begin{bmatrix} 5.6569 \\ 6.7082 \end{bmatrix} x(t) = \mathbf{\Lambda z} + \hat{\mathbf{B}}\mathbf{x}$$

Recall that neither $\mathbf{P}$ nor $\hat{\mathbf{B}}$ are unique, which explains why the MATLAB output does not need to match our previous solution. Still, the MATLAB results do their job and successfully diagonalize matrix $\mathbf{A}$.

13.6 Controllability and Observability

Consider a diagonalized state-space description of a system

$$\dot{\mathbf{z}} = \mathbf{\Lambda z} + \hat{\mathbf{B}}\mathbf{x} \qquad \text{and} \qquad \mathbf{Y} = \hat{\mathbf{C}}\mathbf{z} + \mathbf{D}\mathbf{x} \tag{13.56}$$

We shall assume that all N eigenvalues $\lambda_1, \lambda_2, \ldots, \lambda_N$ are distinct. The state equations in Eq. (13.56) are of the form

$$\dot{z}_m = \lambda_m z_m + \hat{b}_{m1}x_1 + \hat{b}_{m2}x_2 + \cdots + \hat{b}_{mj}x_j \qquad m = 1,2,\ldots,N$$

If $\hat{b}_{m1}, \hat{b}_{m2}, \ldots, \hat{b}_{mj}$ (the mth row in matrix $\hat{\mathbf{B}}$) are all zero, then

$$\dot{z}_m = \lambda_m z_m$$

and the variable z_m is uncontrollable because z_m is not coupled to any of the inputs. Moreover, z_m is decoupled from all the remaining $(N-1)$ state variables because of the diagonalized nature of the variables. Hence, there is no direct or indirect coupling of z_m with any of the inputs, and the system is uncontrollable. In contrast, if at least one element in the mth row of $\hat{\mathbf{B}}$ is nonzero, z_m is coupled to at least one input and is therefore controllable. *Thus, a system with a diagonalized state [Eq. (13.56)] is completely controllable if and only if the matrix $\hat{\mathbf{B}}$ has no row of zero elements.*

The outputs [see Eq. (13.56)] are of the form

$$y_i = \hat{c}_{i1}z_1 + \hat{c}_{i2}z_2 + \cdots + \hat{c}_{iN}z_N + \sum_{m=1}^{j} d_{im}x_m \qquad i = 1,2,\ldots,k$$

If $\hat{c}_{im} = 0$, then the state z_m will not appear in the expression for y_i. Since all the states are decoupled because of the diagonalized nature of the equations, the state z_m cannot be observed directly or indirectly (through other states) at the output y_i. Hence, the mth mode $e^{\lambda_m t}$ will not be observed at the output y_i. If $\hat{c}_{1m}, \hat{c}_{2m}, \ldots, \hat{c}_{km}$ (the mth column in matrix $\hat{\mathbf{C}}$) are all zero, the state z_m will not

be observable at any of the k outputs, and the state z_m is unobservable. In contrast, if at least one element in the mth column of $\hat{\mathbf{C}}$ is nonzero, z_m is observable at least at one output. *Thus, a system with diagonalized equations of the form in Eq. (13.56) is completely observable if and only if the matrix $\hat{\mathbf{C}}$ has no column of zero elements.* In this discussion, we assumed distinct eigenvalues; for repeated eigenvalues, the modified criteria can be found in the literature [1, 2].

If the state-space description is not in diagonalized form, it may be converted into diagonalized form using the procedure in Ex. 13.11. It is also possible to test for controllability and observability even if the state-space description is in undiagonalized form [1, 2].

EXAMPLE 13.12 Controllability and Observability

Investigate the controllability and observability of the systems in Fig. 13.9.

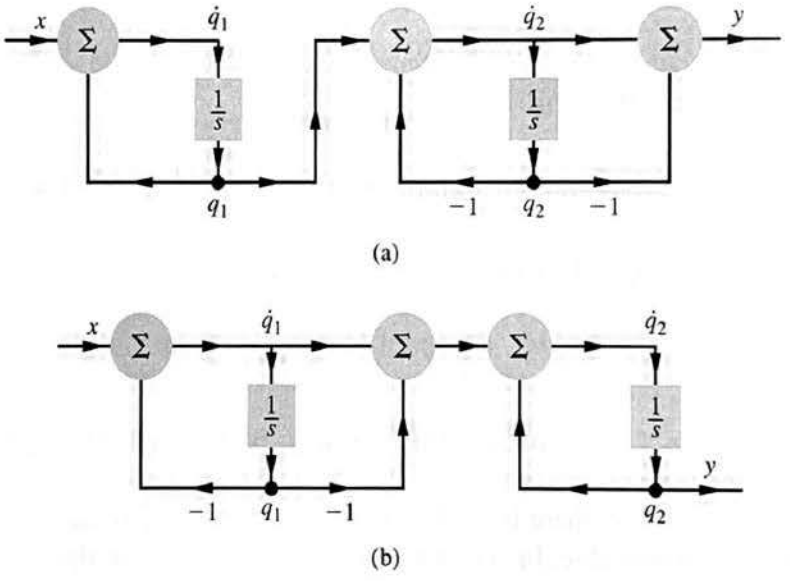

Figure 13.9 Systems for Ex. 13.12.

In both cases, the state variables are identified as the two integrator outputs, q_1 and q_2. The state equations for the system in Fig. 13.9a are

$$\begin{aligned} \dot{q}_1 &= q_1 + x \\ \dot{q}_2 &= q_1 - q_2 \end{aligned} \tag{13.57}$$

and

$$y = \dot{q}_2 - q_2 = q_1 - 2q_2$$

Hence,

$$\mathbf{A}=\begin{bmatrix}1 & 0\\ 1 & -1\end{bmatrix} \qquad \mathbf{B}=\begin{bmatrix}1\\ 0\end{bmatrix} \qquad \mathbf{C}=[1 \quad -2] \qquad \mathbf{D}=0$$

$$|s\mathbf{I}-\mathbf{A}|=\begin{vmatrix}s-1 & 0\\ -1 & s+1\end{vmatrix}=(s-1)(s+1)$$

Therefore,

$$\lambda_1=1 \qquad \text{and} \qquad \lambda_2=-1$$

and

$$\mathbf{\Lambda}=\begin{bmatrix}1 & 0\\ 0 & -1\end{bmatrix}$$

We shall now use the procedure in Sec. 13.5.1 to diagonalize this system. According to Eq. (13.54), we have

$$\begin{bmatrix}1 & 0\\ 0 & -1\end{bmatrix}\begin{bmatrix}p_{11} & p_{12}\\ p_{21} & p_{22}\end{bmatrix}=\begin{bmatrix}p_{11} & p_{12}\\ p_{21} & p_{22}\end{bmatrix}\begin{bmatrix}1 & 0\\ 1 & -1\end{bmatrix}$$

The solution of this equation yields

$$p_{12}=0 \qquad \text{and} \qquad -2p_{21}=p_{22}$$

Choosing $p_{11}=1$ and $p_{21}=1$, we have

$$\mathbf{P}=\begin{bmatrix}1 & 0\\ 1 & -2\end{bmatrix}$$

and

$$\hat{\mathbf{B}}=\mathbf{PB}=\begin{bmatrix}1 & 0\\ 1 & -2\end{bmatrix}\begin{bmatrix}1\\ 0\end{bmatrix}=\begin{bmatrix}1\\ 1\end{bmatrix}$$

All the rows of $\hat{\mathbf{B}}$ are nonzero. Hence, the system is controllable. Also,

$$\mathbf{Y}=\mathbf{Cq}=\mathbf{CP}^{-1}\mathbf{z}=\hat{\mathbf{C}}\mathbf{z}$$

and

$$\hat{\mathbf{C}}=\mathbf{CP}^{-1}=[1 \quad -2]\begin{bmatrix}1 & 0\\ 1 & -2\end{bmatrix}^{-1}=[1 \quad -2]\begin{bmatrix}1 & 0\\ \frac{1}{2} & -\frac{1}{2}\end{bmatrix}=[0 \quad 1]$$

The first column of $\hat{\mathbf{C}}$ is zero. Hence, the mode z_1 (corresponding to $\lambda_1=1$) is unobservable. The system is therefore controllable but not observable. We come to the same conclusion by realizing the system with the diagonalized state variables z_1 and z_2, whose state equations are

$$\dot{\mathbf{z}}=\mathbf{\Lambda}\mathbf{z}+\hat{\mathbf{B}}x$$

$$y=\hat{\mathbf{C}}\mathbf{z}$$

Using our previous calculations, we have

$$\dot{z}_1 = z_1 + x$$
$$\dot{z}_2 = -z_2 + x$$

and

$$y = z_2$$

Figure 13.10a shows a realization of these equations. It is clear that each of the two modes is controllable, but the first mode (corresponding to $\lambda = 1$) is not observable at the output.

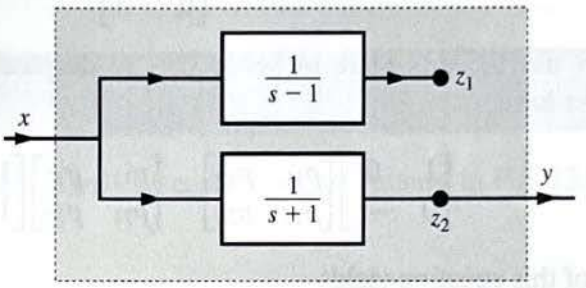

(a)

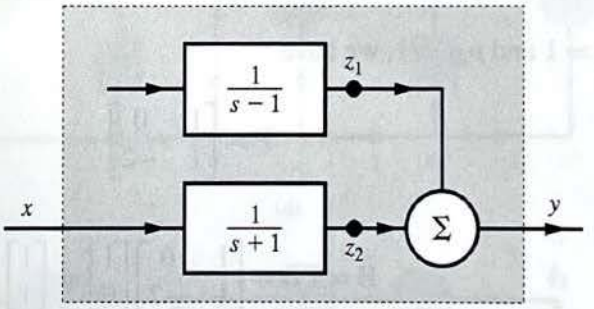

(b)

Figure 13.10 Equivalents of the systems in Fig. 13.9.

The state equations for the system in Fig. 13.9b are

$$\dot{q}_1 = -q_1 + x$$
$$\dot{q}_2 = \dot{q}_1 - q_1 + q_2 = -2q_1 + q_2 + x \tag{13.58}$$

and

$$y = q_2$$

Hence,

$$\mathbf{A} = \begin{bmatrix} -1 & 0 \\ -2 & 1 \end{bmatrix} \qquad \mathbf{B} = \begin{bmatrix} 1 \\ 1 \end{bmatrix} \qquad \mathbf{C} = \begin{bmatrix} 0 & 1 \end{bmatrix} \qquad \mathbf{D} = 0$$

$$|s\mathbf{I}-\mathbf{A}| = \begin{vmatrix} s+1 & 0 \\ -1 & s-1 \end{vmatrix} = (s+1)(s-1)$$

so that $\lambda_1 = -1$, $\lambda_2 = 1$, and

$$\mathbf{\Lambda} = \begin{bmatrix} -1 & 0 \\ 0 & 1 \end{bmatrix}$$

Diagonalizing the matrix, we have

$$\begin{bmatrix} 1 & 0 \\ 0 & -1 \end{bmatrix}\begin{bmatrix} p_{11} & p_{12} \\ p_{21} & p_{22} \end{bmatrix} = \begin{bmatrix} p_{11} & p_{12} \\ p_{21} & p_{22} \end{bmatrix}\begin{bmatrix} -1 & 0 \\ -2 & 1 \end{bmatrix}$$

The solution of this equation yields $p_{11} = -p_{12}$ and $p_{22} = 0$. Choosing $p_{11} = -1$ and $p_{21} = 1$, we obtain

$$\mathbf{P} = \begin{bmatrix} -1 & 1 \\ 1 & 0 \end{bmatrix}$$

and

$$\hat{\mathbf{B}} = \mathbf{PB} = \begin{bmatrix} -1 & 1 \\ 1 & 0 \end{bmatrix}\begin{bmatrix} 1 \\ 1 \end{bmatrix} = \begin{bmatrix} 0 \\ 1 \end{bmatrix}$$

$$\hat{\mathbf{C}} = \mathbf{CP}^{-1} = \begin{bmatrix} 0 & 1 \end{bmatrix}\begin{bmatrix} 0 & 1 \\ 1 & 1 \end{bmatrix} = \begin{bmatrix} 1 & 1 \end{bmatrix}$$

The first row of $\hat{\mathbf{B}}$ is zero. Hence, the mode corresponding to $\lambda_1 = 1$ is not controllable. However, since none of the columns of $\hat{\mathbf{C}}$ vanish, both modes are observable at the output. Hence, the system is observable but not controllable.

We reach the same conclusion by realizing the system with the diagonalized state variables z_1 and z_2. The two state equations are

$$\dot{\mathbf{z}} = \mathbf{\Lambda z} + \hat{\mathbf{B}}x$$

$$y = \hat{\mathbf{C}}\mathbf{z}$$

Using our previous calculations, we have

$$\dot{z}_1 = z_1$$

$$\dot{z}_2 = -z_2 + x$$

and thus,

$$y = z_1 + z_2$$

Figure 13.10b shows a realization of these equations. Clearly, each of the two modes is observable at the output, but the mode corresponding to $\lambda_1 = 1$ is not controllable.

USING MATLAB TO DETERMINE CONTROLLABILITY AND OBSERVABILITY

As demonstrated in Ex. 13.11, we can use MATLAB's `eig` function to determine the matrix $\mathbf{P}$ that will diagonalize $\mathbf{A}$. We can then use $\mathbf{P}$ to determine $\hat{\mathbf{B}}$ and $\hat{\mathbf{C}}$, from which we can determine the controllability and observability of a system. Let us demonstrate the process for the two present systems.

First, let us use MATLAB to compute $\hat{\mathbf{B}}$ and $\hat{\mathbf{C}}$ for the system in Fig. 13.9a.

```
>> A = [1 0;1 -1]; B = [1; 0]; C = [1 -2];
>> [V, Lambda] = eig(A); P=inv(V); Bhat = P*B, Chat = C*inv(P)
   Bhat =   -0.5000
             1.1180
   Chat =   -2     0
```

Since all the rows of $\hat{\mathbf{B}}$ are nonzero, the system is controllable. However, one column of $\hat{\mathbf{C}}$ is zero, so one mode is unobservable.

Next, let us use MATLAB to compute $\hat{\mathbf{B}}$ and $\hat{\mathbf{C}}$ for the system in Fig. 13.9b.

```
>> A = [-1 0;-2 1]; B = [1; 1]; C = [0 1];
>> [V, Lambda] = eig(A); P=inv(V); Bhat = P*B, Chat = C*inv(P)
   Bhat =         0
            1.4142
   Chat =   1.0000    0.7071
```

One of the rows of $\hat{\mathbf{B}}$ is zero, so one mode is uncontrollable. Since all of the columns of $\hat{\mathbf{C}}$ are nonzero, the system is observable.

As expected, the MATLAB results confirm our earlier conclusions regarding the controllability and observability of the systems of Fig. 13.9.

13.6.1 Inadequacy of the Transfer Function Description of a System

Example 13.12 demonstrates the inadequacy of the transfer function to describe an LTI system in general. The systems in Figs. 13.9a and 13.9b both have the same transfer function

$$H(s) = \frac{1}{s+1}$$

Yet the two systems are very different. Their true nature is revealed in Figs. 13.10a and 13.10b, respectively. Both the systems are unstable, but their transfer function $H(s) = 1/(s+1)$ does not give any hint of it. Moreover, the systems are very different from the viewpoint of controllability and observability. The system in Fig. 13.9a is controllable but not observable, whereas the system in Fig. 13.9b is observable but not controllable.

The transfer function description of a system looks at a system only from the input and output terminals. Consequently, the transfer function description can specify only the part of the system that is coupled to the input and the output terminals. From Figs. 13.10a and 13.10b, we see that in both cases only a part of the system that has a transfer function $H(s) = 1/(s+1)$ is coupled

to the input and the output terminals. This is why both systems have the same transfer function $H(s) = 1/(s+1)$.

The state variable description [Eqs. (13.57) and (13.58)], on the other hand, contains all the information about these systems to describe them completely. The reason is that the state variable description is an internal description, not the external description obtained from the system behavior at external terminals.

Apparently, the transfer function fails to describe these systems completely because the transfer functions of these systems have a common factor $s-1$ in the numerator and denominator; this common factor is canceled out in the systems in Fig. 13.9, with a consequent loss of the information. Such a situation occurs when a system is uncontrollable and/or unobservable. If a system is both controllable and observable (which is the case with most of the practical systems), the transfer function describes the system completely. In such a case, the internal and external descriptions are equivalent.

13.7 State-Space Analysis of Discrete-Time Systems

We have shown that an Nth-order differential equation can be expressed in terms of N first-order differential equations. In the following analogous procedure, we show that a general Nth-order difference equation can be expressed in terms of N first-order difference equations.

Consider the z-transfer function

$$H[z] = \frac{b_0 z^N + b_1 z^{N-1} + \cdots + b_{N-1} z + b_N}{z^N + a_1 z^{N-1} + \cdots + a_{N-1} z + a_N}$$

The input $x[n]$ and the output $y[n]$ of this system are related by the difference equation

$$(E^N + a_1 E^{N-1} + \cdots + a_{N-1} E + a_N) y[n] = (b_0 E^N + b_1 E^{N-1} + \cdots + b_{N-1} E + b_N) x[n]$$

The DFII realization of this equation is illustrated in Fig. 13.11.

Signals appearing at the outputs of N delay elements are denoted by $q_1[n], q_2[n], \ldots, q_N[n]$. The input of the first delay is $q_N[n+1]$. We can now write N equations, one at the input of each delay:

$$\begin{aligned} q_1[n+1] &= q_2[n] \\ q_2[n+1] &= q_3[n] \\ &\vdots \\ q_{N-1}[n+1] &= q_N[n] \\ q_N[n+1] &= -a_N q_1[n] - a_{N-1} q_2[n] - \cdots - a_1 q_N[n] + x[n] \end{aligned} \tag{13.59}$$

and

$$y[n] = b_N q_1[n] + b_{N-1} q_2[n] + \cdots + b_1 q_N[n] + b_0 q_{N+1}[n]$$

We can eliminate $q_{N+1}[n]$ from this equation by using the last equation in Eq. (13.59) to yield

$$\begin{aligned} y[n] &= (b_N - b_0 a_N) q_1[n] + (b_{N-1} - b_0 a_{N-1}) q_2[n] + \cdots + (b_1 - b_0 a_1) q_N[n] + b_0 x[n] \\ &= \hat{b}_N q_1[n] + \hat{b}_{N-1} q_2[n] + \cdots + \hat{b}_1 q_N[n] + b_0 x[n] \end{aligned} \tag{13.60}$$

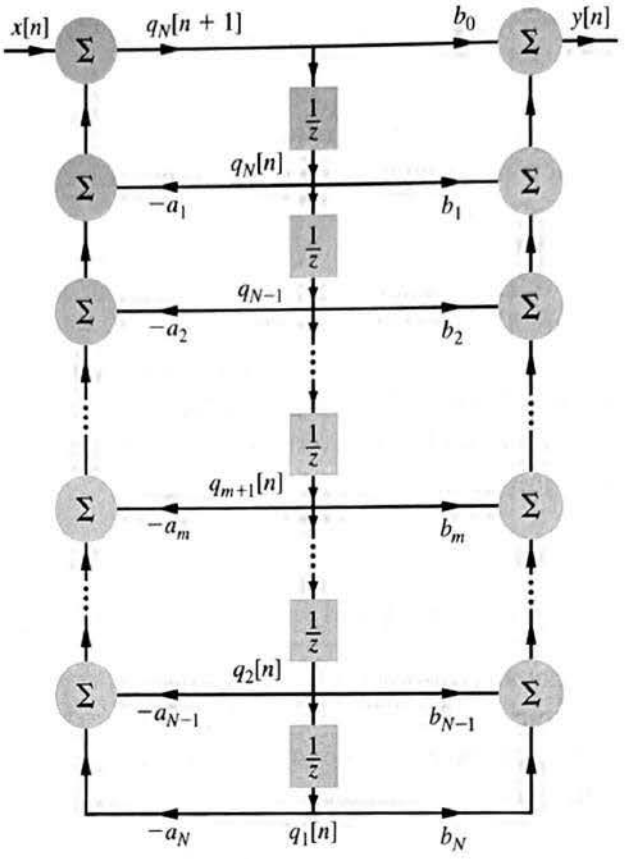

Figure 13.11 Direct form II realization of an Nth-order, discrete-time system.

where $\hat{b}_i = b_i - b_0 a_i$.

Equation (13.59) shows N first-order difference equations in N variables $q_1[n]$, $q_2[n]$, ..., $q_N[n]$. These variables should immediately be recognized as state variables, since the specification of the initial values of these variables in Fig. 13.11 will uniquely determine the response $y[n]$ for a given $x[n]$. Thus, Eq. (13.59) represents the state equations, and Eq. (13.60) is the output equation. In matrix form, we can write these equations as

$$\underbrace{\begin{bmatrix} q_1[n+1] \\ q_2[n+1] \\ \vdots \\ q_{N-1}[n+1] \\ q_N[n+1] \end{bmatrix}}_{\mathbf{q}[n+1]} = \underbrace{\begin{bmatrix} 0 & 1 & 0 & \cdots & 0 & 0 \\ 0 & 0 & 1 & \cdots & 0 & 0 \\ \vdots & \vdots & \vdots & \cdots & \vdots & \vdots \\ 0 & 0 & 0 & \cdots & 0 & 1 \\ -a_N & -a_{N-1} & -a_{N-2} & \cdots & -a_2 & -a_1 \end{bmatrix}}_{\mathbf{A}} \underbrace{\begin{bmatrix} q_1[n] \\ q_2[n] \\ \vdots \\ q_{N-1}[n] \\ q_N[n] \end{bmatrix}}_{\mathbf{q}[n]} + \underbrace{\begin{bmatrix} 0 \\ 0 \\ \vdots \\ 0 \\ 1 \end{bmatrix}}_{\mathbf{B}} x[n] \quad (13.61)$$

and

$$\mathbf{y}[n] = \underbrace{\begin{bmatrix} \hat{b}_N & \hat{b}_{N-1} & \cdots & \hat{b}_1 \end{bmatrix}}_{\mathbf{C}} \begin{bmatrix} q_1[n] \\ q_2[n] \\ \vdots \\ q_N[n] \end{bmatrix} + \underbrace{b_0}_{\mathbf{D}} x[n] \quad (13.62)$$

In general,

$$\mathbf{q}[n+1] = \mathbf{A}\mathbf{q}[n] + \mathbf{B}\mathbf{x}[n]$$
$$\mathbf{y}[n] = \mathbf{C}\mathbf{q}[n] + \mathbf{D}\mathbf{x}[n]$$

Here, we have represented a discrete-time system with state equations for DFII form. There are several other possible representations, as discussed in Sec. 13.3. We may, for example, use the cascade, parallel, or transpose of DFII forms to realize the system, or we may use some linear transformation of the state vector to realize other forms. In all cases, the output of each delay element qualifies as a state variable. We then write the equation at the input of each delay element. The N equations thus obtained are the N state equations.

13.7.1 Solution in State Space

Consider the state equation

$$\mathbf{q}[n+1] = \mathbf{A}\mathbf{q}[n] + \mathbf{B}\mathbf{x}[n]$$

From this equation, it follows that

$$\mathbf{q}[n] = \mathbf{A}\mathbf{q}[n-1] + \mathbf{B}\mathbf{x}[n-1]$$

and

$$\mathbf{q}[n-1] = \mathbf{A}\mathbf{q}[n-2] + \mathbf{B}\mathbf{x}[n-2]$$
$$\mathbf{q}[n-2] = \mathbf{A}\mathbf{q}[n-3] + \mathbf{B}\mathbf{x}[n-3]$$
$$\vdots$$
$$\mathbf{q}[1] = \mathbf{A}\mathbf{q}[0] + \mathbf{B}\mathbf{x}[0]$$

Substituting the expression for $\mathbf{q}[n-1]$ into that for $\mathbf{q}[n]$, we obtain

$$\mathbf{q}[n] = \mathbf{A}^2\mathbf{q}[n-2] + \mathbf{A}\mathbf{B}\mathbf{x}[n-2] + \mathbf{B}\mathbf{x}[n-1]$$

Substituting the expression for $\mathbf{q}[n-2]$ in this equation, we obtain

$$\mathbf{q}[n] = \mathbf{A}^3\mathbf{q}[n-3] + \mathbf{A}^2\mathbf{B}\mathbf{x}[n-3] + \mathbf{A}\mathbf{B}\mathbf{x}[n-2] + \mathbf{B}\mathbf{x}[n-1]$$

Continuing in this way, we obtain

$$\mathbf{q}[n] = \mathbf{A}^n\mathbf{q}[0] + \mathbf{A}^{n-1}\mathbf{B}\mathbf{x}[0] + \mathbf{A}^{n-2}\mathbf{B}\mathbf{x}[1] + \cdots + \mathbf{B}\mathbf{x}[n-1]$$
$$= \mathbf{A}^n\mathbf{q}[0] + \sum_{m=0}^{n-1} \mathbf{A}^{n-1-m}\mathbf{B}\mathbf{x}[m]$$

The upper limit of this summation is nonnegative. Hence, $n \geq 1$, and the summation is recognized as the convolution sum

$$\mathbf{A}^{n-1}u[n-1] * \mathbf{B}\mathbf{x}[n]$$

Consequently,

$$\mathbf{q}[n] = \underbrace{\mathbf{A}^n\mathbf{q}[0]}_{\text{zero input}} + \underbrace{\mathbf{A}^{n-1}u[n-1] * \mathbf{Bx}[n]}_{\text{zero state}} \tag{13.63}$$

and

$$\begin{aligned}\mathbf{y}[n] &= \mathbf{Cq} + \mathbf{Dx} \\ &= \mathbf{CA}^n\mathbf{q}[0] + \sum_{m=0}^{n-1} \mathbf{CA}^{n-1-m}\mathbf{Bx}[m] + \mathbf{Dx} \\ &= \mathbf{CA}^n\mathbf{q}[0] + \mathbf{CA}^{n-1}u[n-1] * \mathbf{Bx}[n] + \mathbf{Dx}\end{aligned} \tag{13.64}$$

In Sec. 13.1.3, we showed that

$$\mathbf{A}^n = \beta_0\mathbf{I} + \beta_1\mathbf{A} + \beta_2\mathbf{A}^2 + \cdots + \beta_{N-1}\mathbf{A}^{N-1} \tag{13.65}$$

where (assuming N distinct eigenvalues of $\mathbf{A}$)

$$\begin{bmatrix} \beta_0 \\ \beta_1 \\ \vdots \\ \beta_{N-1} \end{bmatrix} = \begin{bmatrix} 1 & \lambda_1 & \lambda_1^2 & \cdots & \lambda_1^{N-1} \\ 1 & \lambda_2 & \lambda_2^2 & \cdots & \lambda_2^{N-1} \\ \vdots & \vdots & \vdots & \cdots & \vdots \\ 1 & \lambda_N & \lambda_N^2 & \cdots & \lambda_N^{N-1} \end{bmatrix}^{-1} \begin{bmatrix} \lambda_1^n \\ \lambda_2^n \\ \vdots \\ \lambda_N^n \end{bmatrix} \tag{13.66}$$

and $\lambda_1, \lambda_2, \ldots, \lambda_N$ are the N eigenvalues of $\mathbf{A}$.

We can also determine $\mathbf{A}^n$ from the z-transform formula, which will be derived later, in Eq. (13.70):

$$\mathbf{A}^n = \mathcal{Z}^{-1}[(\mathbf{I} - z^{-1}\mathbf{A})^{-1}]$$

EXAMPLE 13.13 State-Space Analysis of a Discrete-Time System

Give a state-space description of the system in Fig. 13.12. Find the output $y[n]$ if the input $x[n] = u[n]$ and the initial conditions are $q_1[0] = 2$ and $q_2[0] = 3$.

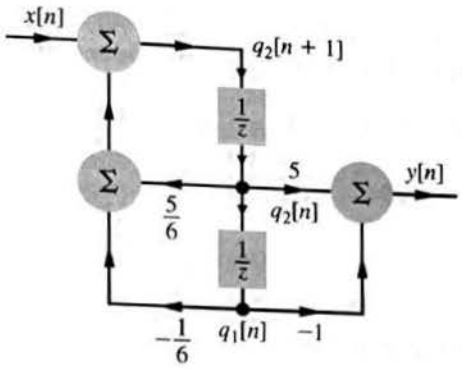

Figure 13.12 System for Ex. 13.13.

Recognizing that $q_2[n] = q_1[n+1]$, the state equations are [see Eqs. (13.61) and (13.62)]

$$\begin{bmatrix} q_1[n+1] \\ q_2[n+1] \end{bmatrix} = \begin{bmatrix} 0 & 1 \\ -\frac{1}{6} & \frac{5}{6} \end{bmatrix} \begin{bmatrix} q_1[n] \\ q_2[n] \end{bmatrix} + \begin{bmatrix} 0 \\ 1 \end{bmatrix} x$$

and

$$y[n] = \begin{bmatrix} -1 & 5 \end{bmatrix} \begin{bmatrix} q_1[n] \\ q_2[n] \end{bmatrix}$$

To find the solution [Eq. (13.64)], we must first determine $\mathbf{A}^n$. The characteristic equation of $\mathbf{A}$ is

$$|\lambda \mathbf{I} - \mathbf{A}| = \begin{vmatrix} \lambda & -1 \\ \frac{1}{6} & \lambda - \frac{5}{6} \end{vmatrix} = \lambda^2 - \frac{5}{6}\lambda + \frac{1}{6} = \left(\lambda - \frac{1}{3}\right)\left(\lambda - \frac{1}{2}\right) = 0$$

Hence, $\lambda_1 = 1/3$ and $\lambda_2 = 1/2$ are the eigenvalues of $\mathbf{A}$ and [see Eq. (13.65)]

$$\mathbf{A}^n = \beta_0 \mathbf{I} + \beta_1 \mathbf{A}$$

where [see Eq. (13.66)]

$$\begin{bmatrix} \beta_0 \\ \beta_1 \end{bmatrix} = \begin{bmatrix} 1 & \frac{1}{3} \\ 1 & \frac{1}{2} \end{bmatrix}^{-1} \begin{bmatrix} \left(\frac{1}{3}\right)^n \\ \left(\frac{1}{2}\right)^n \end{bmatrix} = \begin{bmatrix} 3 & -2 \\ -6 & 6 \end{bmatrix} \begin{bmatrix} (3)^{-n} \\ (2)^{-n} \end{bmatrix} = \begin{bmatrix} 3(3)^{-n} - 2(2)^{-n} \\ -6(3)^{-n} + 6(2)^{-n} \end{bmatrix}$$

and

$$\begin{aligned} \mathbf{A}^n &= [3(3)^{-n} - 2(2)^{-n}] \begin{bmatrix} 1 & 0 \\ 0 & 1 \end{bmatrix} + [-6(3)^{-n} + 6(2)^{-n}] \begin{bmatrix} 0 & 1 \\ -\frac{1}{6} & \frac{5}{6} \end{bmatrix} \\ &= \begin{bmatrix} 3(3)^{-n} - 2(2)^{-n} & -6(3)^{-n} + 6(2)^{-n} \\ (3)^{-n} - (2)^{-n} & -2(3)^{-n} + 3(2)^{-n} \end{bmatrix} \end{aligned} \tag{13.67}$$

We can now determine the state vector $\mathbf{q}[n]$ from Eq. (13.63). Since we are interested in the output $y[n]$, we shall use Eq. (13.64) directly. Note that

$$\mathbf{CA}^n = [-1 \quad 5]\mathbf{A}^n = [2(3)^{-n} - 3(2)^{-n} \quad -4(3)^{-n} + 9(2)^{-n}]$$

and the zero-input response is $\mathbf{CA}^n\mathbf{q}[0]$, with

$$\mathbf{q}[0] = \begin{bmatrix} 2 \\ 3 \end{bmatrix}$$

Hence, the zero-input response is

$$\mathbf{CA}^n\mathbf{q}[0] = -8(3)^{-n} + 21(2)^{-n}$$

The zero-state component is given by the convolution sum of $\mathbf{CA}^{n-1}u[n-1]$ and $\mathbf{Bx}[n]$. We can use the shifting property of the convolution sum [Eq. (9.19)] to obtain the zero-state component by finding the convolution sum of $\mathbf{CA}^n u[n]$ and $\mathbf{Bx}[n]$ and then replacing n with $n-1$ in the result. We use this procedure because the convolution sums are listed in Table 9.1 for functions of the type $x[n]u[n]$, rather than $x[n]u[n-1]$.

$$\begin{aligned} \mathbf{CA}^n u[n] * \mathbf{B}x[n] &= [2(3)^{-n} - 3(2)^{-n} - 4(3)^{-n} + 9(2)^{-n}] * \begin{bmatrix} 0 \\ u[n] \end{bmatrix} \\ &= -4(3)^{-n} * u[n] + 9(2)^{-n} * u[n] \end{aligned}$$

Using Table 9.1 (pair 4), we obtain

$$\begin{aligned} \mathbf{CA}^n u[n] * \mathbf{B}x[n] &= -4\left[\frac{1-3^{-(n+1)}}{1-\frac{1}{3}}\right]u[n] + 9\left[\frac{1-2^{-(n+1)}}{1-\frac{1}{2}}\right]u[n] \\ &= \left[12 + 6\left(3^{-(n+1)}\right) - 18\left(2^{-(n+1)}\right)\right]u[n] \end{aligned}$$

Now the desired (zero-state) response is obtained by replacing n by $n-1$. Hence,

$$\mathbf{CA}^n u[n] * \mathbf{B}x[n-1] = [12 + 6(3)^{-n} - 18(2)^{-n}]u[n-1]$$

It follows that

$$y[n] = [-8(3)^{-n} + 21(2)^{-n}u[n] + [12 + 6(3)^{-n} - 18(2)^{-n}]u[n-1]$$

This is the desired answer. We can simplify this answer by observing that $12 + 6(3)^{-n} - 18(2)^{-n} = 0$ for $n = 0$. Hence, $u[n-1]$ may be replaced by $u[n]$, and

$$y[n] = [12 - 2(3)^{-n} + 3(2)^{-n}]u[n] \tag{13.68}$$

Using MATLAB to Obtain a Graphical Solution

MATLAB is equipped with tools to simulate digital systems, which makes it easy to obtain a graphical solution to the system. Let us use MATLAB simulation to determine the total system output over $0 \le n \le 25$.

```
>> A = [0 1;-1/6 5/6]; B = [0; 1]; C = [-1 5]; D = 0;
>> N = 25; n = (0:N); x = ones(1,N+1); q0 = [2;3];
>> sys = ss(A,B,C,D,-1); % Discrete-time state space model
>> [y,q] = lsim(sys,x,n,q0); % Simulate output and state vector
>> clf; stem(n,y,'k.'); xlabel('n'); ylabel('y[n]');
>> axis([-.5 25.5 11.5 13.5]);
```

The MATLAB results, shown in Fig. 13.13, exactly align with the analytical solution derived earlier. Also notice that the zero-input and zero-state responses can be separately obtained using the same code and respectively setting either x or q0 to zero.

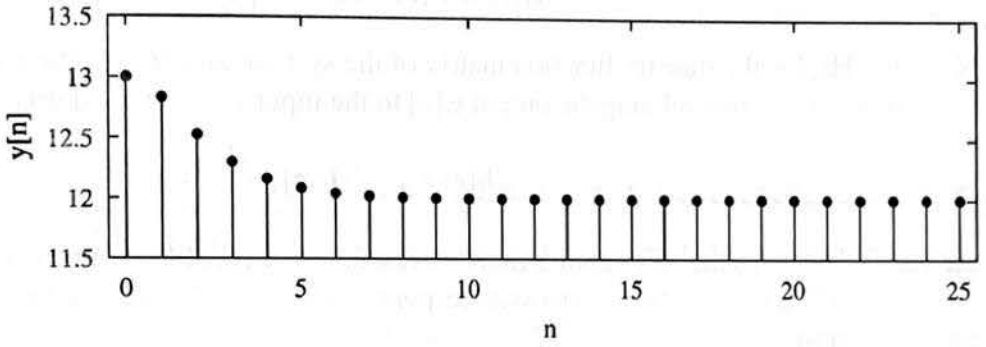

Figure 13.13 Graphical solution to Ex. 13.13 by MATLAB simulation.

13.7.2 The z-Transform Solution

The z-transform of Eq. (13.61) is given by

$$z\mathbf{Q}[z] - z\mathbf{q}[0] = \mathbf{A}\mathbf{Q}[z] + \mathbf{B}\mathbf{X}[z]$$

Therefore,

$$(z\mathbf{I} - \mathbf{A})\mathbf{Q}[z] = z\mathbf{q}[0] + \mathbf{B}\mathbf{X}[z]$$

and

$$\begin{aligned}\mathbf{Q}[z] &= (z\mathbf{I} - \mathbf{A})^{-1}z\mathbf{q}[0] + (z\mathbf{I} - \mathbf{A})^{-1}\mathbf{B}\mathbf{X}[z] \\ &= (\mathbf{I} - z^{-1}\mathbf{A})^{-1}\mathbf{q}[0] + (z\mathbf{I} - \mathbf{A})^{-1}\mathbf{B}\mathbf{X}[z]\end{aligned}$$

Hence,

$$\mathbf{q}[n] = \underbrace{\mathcal{Z}^{-1}[(\mathbf{I} - z^{-1}\mathbf{A})^{-1}]\mathbf{q}[0]}_{\text{zero-input response}} + \underbrace{\mathcal{Z}^{-1}[(z\mathbf{I} - \mathbf{A})^{-1}\mathbf{B}\mathbf{X}[z]]}_{\text{zero-state response}} \tag{13.69}$$

A comparison of Eq. (13.69) with Eq. (13.63) shows that

$$\mathbf{A}^n = \mathcal{Z}^{-1}[(\mathbf{I} - z^{-1}\mathbf{A})^{-1}] \tag{13.70}$$

The output equation is given by

$$\begin{aligned}\mathbf{Y}[z] &= \mathbf{C}\mathbf{Q}[z] + \mathbf{D}\mathbf{X}[z] \\ &= \mathbf{C}[(\mathbf{I} - z^{-1}\mathbf{A})^{-1}\mathbf{q}[0] + (z\mathbf{I} - \mathbf{A})^{-1}\mathbf{B}\mathbf{X}[z]] + \mathbf{D}\mathbf{X}[z] \\ &= \mathbf{C}(\mathbf{I} - z^{-1}\mathbf{A})^{-1}\mathbf{q}[0] + [\mathbf{C}(z\mathbf{I} - \mathbf{A})^{-1}\mathbf{B} + \mathbf{D}]\mathbf{X}[z] \\ &= \underbrace{\mathbf{C}(\mathbf{I} - z^{-1}\mathbf{A})^{-1}\mathbf{q}[0]}_{\text{zero-input response}} + \underbrace{\mathbf{H}[z]\mathbf{X}[z]}_{\text{zero-state response}}\end{aligned} \tag{13.71}$$

where

$$\mathbf{H}[z] = \mathbf{C}(z\mathbf{I} - \mathbf{A})^{-1}\mathbf{B} + \mathbf{D} \tag{13.72}$$

Note that $\mathbf{H}[z]$ is the transfer function matrix of the system, and $H_{ij}[z]$, the ijth element of $\mathbf{H}[z]$, is the transfer function relating the output $y_i[n]$ to the input $x_j[n]$. If we define $\mathbf{h}[n]$ as

$$\mathbf{h}[n] = \mathcal{Z}^{-1}[\mathbf{H}[z]]$$

then $\mathbf{h}[n]$ represents the unit impulse function response matrix of the system. Thus, $h_{ij}[n]$, the ijth element of $\mathbf{h}[n]$, represents the zero-state response $y_i[n]$ when the input $x_j[n] = \delta[n]$ and all other inputs are zero.

EXAMPLE 13.14 z-Transform Solution to State Equations

Use the z-transform to find the response $y[n]$ for the system in Ex. 13.13.

According to Eq. (13.71),

$$\begin{aligned}\mathbf{Y}[z] &= \begin{bmatrix}-1 & 5\end{bmatrix}\begin{bmatrix}1 & -\frac{1}{z} \\ \frac{1}{6z} & 1-\frac{5}{6z}\end{bmatrix}^{-1}\begin{bmatrix}2 \\ 3\end{bmatrix} + \begin{bmatrix}-1 & 5\end{bmatrix}\begin{bmatrix}z & -1 \\ \frac{1}{6} & z-\frac{5}{6}\end{bmatrix}^{-1}\begin{bmatrix}0 \\ \frac{z}{z-1}\end{bmatrix} \\ &= \begin{bmatrix}-1 & 5\end{bmatrix}\begin{bmatrix}\frac{z(6z-5)}{6z^2-5z+1} & \frac{6z}{6z^2-5z+1} \\ \frac{-z}{6z^2-5z+1} & \frac{6z^2}{6z^2-5z+1}\end{bmatrix}\begin{bmatrix}2 \\ 3\end{bmatrix} + \begin{bmatrix}-1 & 5\end{bmatrix}\begin{bmatrix}\frac{z}{(z-1)\left(z^2-\frac{5}{6}z+\frac{1}{6}\right)} \\ \frac{z^2}{(z-1)\left(z^2-\frac{5}{6}z+\frac{1}{6}\right)}\end{bmatrix} \\ &= \frac{13z^2-3z}{z^2-\frac{5}{6}z+\frac{1}{6}} + \frac{(5z-1)z}{(z-1)\left(z^2-\frac{5}{6}z+\frac{1}{6}\right)} \\ &= \frac{-8z}{z-\frac{1}{3}} + \frac{21z}{z-\frac{1}{2}} + \frac{12z}{z-1} + \frac{12z}{z-1} + \frac{6z}{z-\frac{1}{3}} - \frac{18z}{z-\frac{1}{2}}\end{aligned}$$

Therefore,

$$y[n] = \underbrace{[-8(3)^{-n} + 21(2)^{-n}}_{\text{zero-input response}} + \underbrace{12 + 6(3)^{-n} - 18(2)^{-n}]}_{\text{zero-state response}}u[n]$$

Linear Transformation, Controllability, and Observability

The procedure for linear transformation is parallel to that in the continuous-time case (Sec. 13.5). If $\mathbf{w}$ is the transformed-state vector given by

$$\mathbf{w} = \mathbf{P}\mathbf{q}$$

then

$$\mathbf{w}[n+1] = \mathbf{P}\mathbf{A}\mathbf{P}^{-1}\mathbf{w}[n] + \mathbf{P}\mathbf{B}\mathbf{x}$$

and

$$\mathbf{y}[n] = (\mathbf{C}\mathbf{P}^{-1})\mathbf{w} + \mathbf{D}\mathbf{x}$$

Controllability and observability may be investigated by diagonalizing the matrix, as explained in Sec. 13.5.1.

13.8 MATLAB: Toolboxes and State-Space Analysis

The preceding MATLAB sections provide a comprehensive introduction to the basic MATLAB environment. However, MATLAB also offers a wide range of toolboxes that perform specialized tasks. Once installed, toolbox functions operate no differently from ordinary MATLAB functions. Although toolboxes are purchased at extra cost, they save time and offer the convenience of predefined functions. It would take significant effort to duplicate a toolbox's functionality by using custom user-defined programs.

Three toolboxes are particularly appropriate in the study of signals and systems: the control system toolbox, the signal-processing toolbox, and the symbolic math toolbox. Functions from these toolboxes have been utilized throughout the text in the MATLAB examples as well as certain end-of-chapter problems. This section provides a more formal introduction to a selection of functions, both standard and toolbox, that are appropriate for state-space problems.

13.8.1 z-Transform Solutions to Discrete-Time, State-Space Systems

As with continuous-time systems, it is often more convenient to solve discrete-time systems in the transform domain rather than in the time domain. As given in Ex. 13.13, consider the state-space description of the system shown in Fig. 13.12.

$$\begin{bmatrix} q_1[n+1] \\ q_2[n+1] \end{bmatrix} = \begin{bmatrix} 0 & 1 \\ -\frac{1}{6} & \frac{5}{6} \end{bmatrix} \begin{bmatrix} q_1[n] \\ q_2[n] \end{bmatrix} + \begin{bmatrix} 0 \\ 1 \end{bmatrix} x[n]$$

and

$$y[n] = \begin{bmatrix} -1 & 5 \end{bmatrix} \begin{bmatrix} q_1[n] \\ q_2[n] \end{bmatrix}$$

We are interested in the output $y[n]$ in response to the input $x[n] = u[n]$ with initial conditions $q_1[0] = 2$ and $q_2[0] = 3$.

To describe this system, the state matrices $\mathbf{A}$, $\mathbf{B}$, $\mathbf{C}$, and $\mathbf{D}$ are first defined.

```
>> A = [0 1;-1/6 5/6]; B = [0; 1]; C = [-1 5]; D = 0;
```

Additionally, the vector of initial conditions is defined.

```
>> q_0 = [2;3];
```

In the transform domain, the solution to the state equation is

$$\mathbf{Q}[z] = (\mathbf{I} - z^{-1}\mathbf{A})^{-1}\mathbf{q}[0] + (z\mathbf{I} - \mathbf{A})^{-1}\mathbf{B}\mathbf{X}[z] \tag{13.73}$$

The solution is separated into two parts: the zero-input response and the zero-state response.

MATLAB's symbolic toolbox makes possible a symbolic representation of Eq. (13.73). First, a symbolic variable z needs to be defined.

```
>> z = sym('z');
```

The `sym` command is used to construct symbolic variables, objects, and numbers. Typing `whos` confirms that `z` is indeed a symbolic object. The `syms` command is a shorthand command for constructing symbolic objects. For example, `syms z s` is equivalent to the two instructions `z = sym('z');` and `s = sym('s');`.

Next, a symbolic expression for $X[z]$ needs to be constructed for the unit step input, $x[n] = u[n]$. The z-transform is computed by means of the `ztrans` command.

```
>> X = ztrans(sym('1'))
   X = z/(z-1)
```

Several comments are in order. First, the `ztrans` command assumes a causal signal. For $n \geq 0$, $u[n]$ has a constant value of 1. Second, the argument of `ztrans` needs to be a symbolic expression, even if the expression is a constant. Thus, a symbolic one `sym('1')` is required. Also note that continuous-time systems use Laplace transforms rather than z-transforms. In such cases, the `laplace` command replaces the `ztrans` command.

Construction of $\mathbf{Q}[z]$ is now trivial.

```
>> Q = inv(eye(2)-z^(-1)*A)*q_0 + inv(z*eye(2)-A)*B*X
   Q =
    (18*z)/(6*z^2-5*z+1) + (2*z*(6*z-5))/(6*z^2-5*z+1) + (6*z)/((z-1)*(6*z^2-5*z+1))
          (18*z^2)/(6*z^2-5*z+1) - (2*z)/(6*z^2-5*z+1) + (6*z^2)/((z-1)*(6*z^2-5*z+1))
```

Unfortunately, not all MATLAB functions work with symbolic objects. Still, the symbolic toolbox overloads many standard MATLAB functions, such as `inv`, to work with symbolic objects. Recall that overloaded functions have identical names but different behavior; proper function selection is typically determined by context.

The expression `Q` is somewhat unwieldy. The `simplify` command uses various algebraic techniques to simplify the result.

```
>> Q = simplify(Q)
   Q = -(2*z*(- 6*z^2 + 2*z + 1))/(6*z^3 - 11*z^2 + 6*z - 1)
          (2*z*(9*z^2 - 7*z + 1))/(6*z^3 - 11*z^2 + 6*z - 1)
```

The resulting expression is mathematically equivalent to the original but notationally more compact.

Since $\mathbf{D} = 0$, the output $Y[z]$ is given by $Y[z] = \mathbf{C}\mathbf{Q}[z]$.

```
>> Y = simplify(C*Q)
   Y = (6*z*(13*z^2 - 11*z + 2))/(6*z^3 - 11*z^2 + 6*z - 1)
```

The corresponding time-domain expression is obtained by using the inverse z-transform command `iztrans`.

```
>> y = iztrans(Y)
   y = 3*(1/2)^n - 2*(1/3)^n + 12
```

Like `ztrans`, the `iztrans` command assumes a causal signal, so the result implies multiplication by a unit step. That is, the system output is $y[n] = (3(1/2)^n - 2(1/3)^n + 12)u[n]$, which is equivalent to Eq. (13.68) derived in Ex. 13.13. Continuous-time systems use inverse Laplace transforms rather than inverse z-transforms. In such cases, the `ilaplace` command therefore replaces the `iztrans` command.

Following a similar procedure, it is a simple matter to compute the zero-input response $y_{zir}[n]$:

```
>> y_zir = iztrans(simplify(C*inv(eye(2)-z^(-1)*A)*q_0))
   y_zir = 21*(1/2)^n - 8*(1/3)^n
```

The zero-state response is given by

```
>> y_zsr = y - y_zir
   y_zsr = 6*(1/3)^n - 18*(1/2)^n + 12
```

Typing `iztrans(simplify(C*inv(z*eye(2)-A)*B*X))` produces the same result.

MATLAB plotting functions, such as `plot` and `stem`, do not directly support symbolic expressions. By using the `subs` command, however, it is easy to replace a symbolic variable with a vector of desired values.

```
>> n = [0:25]; stem(n,subs(y,n),'k.');
>> xlabel('n'); ylabel('y[n]'); axis([-.5 25.5 11.5 13.5]);
```

Figure 13.14 shows the results, which are equivalent to the results obtained in Ex. 13.13. Although there are plotting commands in the symbolic math toolbox such as `ezplot` that plot symbolic expressions, these plotting routines lack the flexibility needed to satisfactorily plot discrete-time functions.

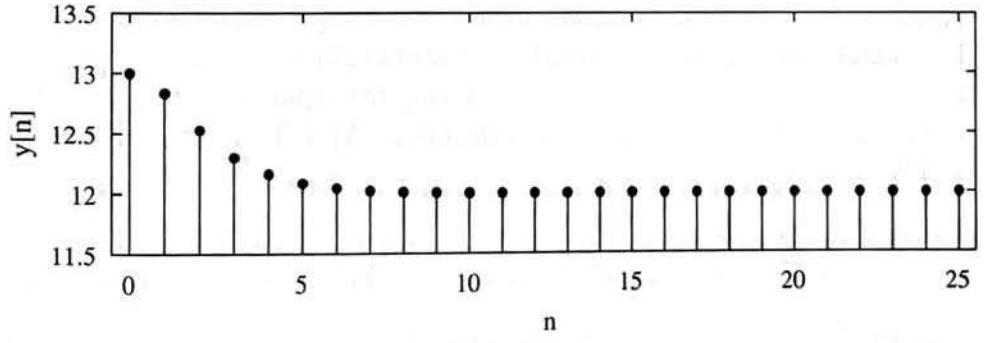

Figure 13.14 Output $y[n]$ computed by using the symbolic math toolbox.

13.8.2 Transfer Functions from State-Space Representations

A system's transfer function provides a wealth of useful information. From Eq. (13.72), the transfer function for the system described in Ex. 13.13 is

```
>> H = collect(simplify(C*inv(z*eye(2)-A)*B+D))
   H = (30*z - 6)/(6*z^2 - 5*z + 1)
```

It is also possible to determine the numerator and denominator transfer function coefficients from a state-space model by using the signal-processing toolbox function `ss2tf`.

```
>> [num,den] = ss2tf(A,B,C,D)
   num =      0    5.0000   -1.0000
   den = 1.0000   -0.8333    0.1667
```

The denominator of $H[z]$ provides the characteristic polynomial

$$\gamma^2 - \tfrac{5}{6}\gamma + \tfrac{1}{6}$$

Equivalently, the characteristic polynomial is the determinant of $(z\mathbf{I} - \mathbf{A})$.

```
>> syms gamma; char_poly = subs(det(z*eye(2)-A),z,gamma)
   char_poly = gamma^2 - (5*gamma)/6 + 1/6
```

Here, the `subs` command replaces the symbolic variable `z` with the desired symbolic variable `gamma`.

The `roots` command does not accommodate symbolic expressions. Thus, the `sym2poly` command converts the symbolic expression into a polynomial coefficient vector suitable for the `roots` command.

```
>> roots(sym2poly(char_poly))
   ans = 0.5000
         0.3333
```

Taking the inverse z-transform of $H[z]$ yields the impulse response $h[n]$.

```
>> h = iztrans(H)
   h = 18*(1/2)^n - 12*(1/3)^n - 6*kroneckerDelta(n, 0)
```

As suggested by the characteristic roots, the characteristic modes of the system are $(1/2)^n$ and $(1/3)^n$. Notice that the symbolic math toolbox represents $\delta[n]$ as `kroneckerDelta(n, 0)`. In general, $\delta[n-a]$ is represented as `kroneckerDelta(n-a, 0)`. This notation is frequently encountered. Consider, for example, delaying the input $x[n] = u[n]$ by 2, $x[n-2] = u[n-2]$. In the transform domain, this is equivalent to $z^{-2}X[z]$. Taking the inverse z-transform of $z^{-2}X[z]$ yields

```
>> iztrans(z^(-2)*X)
   ans = 1 - kroneckerDelta(n, 0) - kroneckerDelta(n - 1, 0)
```

That is, MATLAB represents the delayed unit step $u[n-2]$ as $(-\delta[n-1] - \delta[n-0] + 1)u[n]$.

The transfer function also permits convenient calculation of the zero-state response.

```
>>  y_zsr = iztrans(H*X)
    y_zsr = 6*(1/3)^n - 18*(1/2)^n + 12
```

The result agrees with previous calculations.

13.8.3 Controllability and Observability of Discrete-Time Systems

In their controllability and observability, discrete-time systems are analogous to continuous-time systems. For example, consider the LTID system described by the constant coefficient difference equation

$$y[n]+\tfrac{5}{6}y[n-1]+\tfrac{1}{6}y[n-2]=x[n]+\tfrac{1}{2}x[n-1]$$

Figure 13.15 illustrates the direct form II (DFII) realization of this system. The system input is $x[n]$, the system output is $y[n]$, and the outputs of the delay blocks are designated as state variables $q_1[n]$ and $q_2[n]$.

The corresponding state and output equations (see Prob. 13.8-1) are

$$\mathbf{Q}[n+1]=\begin{bmatrix}q_1[n+1]\\q_2[n+1]\end{bmatrix}=\begin{bmatrix}0 & 1\\ -\frac{1}{6} & -\frac{5}{6}\end{bmatrix}\begin{bmatrix}q_1[n]\\q_2[n]\end{bmatrix}+\begin{bmatrix}0\\1\end{bmatrix}x[n]=\mathbf{A}\mathbf{Q}[n]+\mathbf{B}x[n]$$

and

$$y[n]=\begin{bmatrix}-\frac{1}{6} & -\frac{1}{3}\end{bmatrix}\begin{bmatrix}q_1[n]\\q_2[n]\end{bmatrix}+1x[n]=\mathbf{C}\mathbf{Q}[n]+\mathbf{D}x[n]$$

To describe this system in MATLAB, the state matrices **A**, **B**, **C**, and **D** are first defined.

```
>>  A = [0 1;-1/6 -5/6]; B = [0; 1]; C = [-1/6 -1/3]; D = 1;
```

To assess the controllability and observability of this system, the state matrix **A** needs to be diagonalized.† As shown in Eq. (13.54), this requires a transformation matrix **P** such that

$$\mathbf{PA}=\mathbf{\Lambda P} \tag{13.74}$$

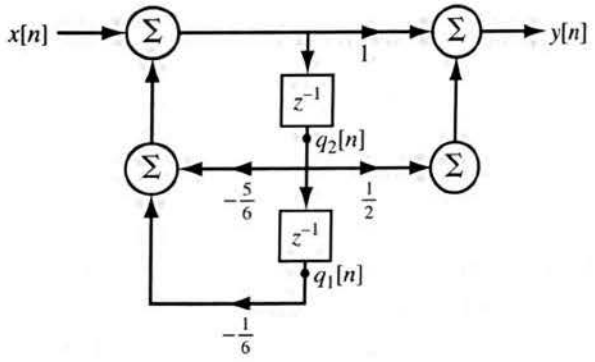

Figure 13.15 Direct form II realization of $y[n]+(5/6)y[n-1]+(1/6)y[n-2]=x[n]+(1/2)x[n-1]$.

† This approach requires that the state matrix **A** have unique eigenvalues. Systems with repeated roots require that state matrix **A** be transformed into a modified diagonal form, also called the Jordan form. The MATLAB function `jordan` is used in these cases.

where $\mathbf{\Lambda}$ is a diagonal matrix containing the unique eigenvalues of $\mathbf{A}$. Recall, the transformation matrix $\mathbf{P}$ is not unique.

To determine a matrix $\mathbf{P}$, it is helpful to review the eigenvalue problem. Mathematically, an eigendecomposition of $\mathbf{A}$ is expressed as

$$\mathbf{AV} = \mathbf{V\Lambda}$$

where $\mathbf{V}$ is a matrix of eigenvectors and $\mathbf{\Lambda}$ is a diagonal matrix of eigenvalues. Pre- and post-multiplying both sides of this equation by $\mathbf{V}^{-1}$ yields

$$\mathbf{V}^{-1}\mathbf{AVV}^{-1} = \mathbf{V}^{-1}\mathbf{V\Lambda V}^{-1}$$

Simplification yields

$$\mathbf{V}^{-1}\mathbf{A} = \mathbf{\Lambda V}^{-1} \tag{13.75}$$

Comparing Eqs. (13.74) and (13.75), we see that a suitable transformation matrix $\mathbf{P}$ is given by an inverse eigenvector matrix $\mathbf{V}^{-1}$.

The `eig` command is used to verify that $\mathbf{A}$ has the required distinct eigenvalues as well as compute the needed eigenvector matrix $\mathbf{V}$.

```
>> [V,Lambda] = eig(A)
   V =
       0.9487   -0.8944
      -0.3162    0.4472
   Lambda =
      -0.3333         0
            0   -0.5000
```

Since the diagonal elements of `Lambda` are all unique, a transformation matrix $\mathbf{P}$ is given by

```
>> P = inv(V);
```

The transformed state matrices $\hat{\mathbf{A}} = \mathbf{PAP}^{-1}$, $\hat{\mathbf{B}} = \mathbf{PB}$, and $\hat{\mathbf{C}} = \mathbf{CP}^{-1}$ are easily computed by using transformation matrix $\mathbf{P}$. Notice that matrix $\mathbf{D}$ is unaffected by state variable transformations.

```
>> Ahat = P*A*inv(P), Bhat = P*B, Chat = C*inv(P)
   Ahat =
      -0.3333   -0.0000
       0.0000   -0.5000
   Bhat =
       6.3246
       6.7082
   Chat =
      -0.0527   -0.0000
```

The proper operation of $\mathbf{P}$ is verified by the correct diagonalization of $\mathbf{A}$, $\hat{\mathbf{A}} = \mathbf{\Lambda}$. Since no row of $\hat{\mathbf{B}}$ is zero, the system is controllable. Since, however, at least one column of $\hat{\mathbf{C}}$ is zero, the system is not observable. These characteristics are no coincidence. The DFII realization, which is more descriptively called the controller canonical form, is always controllable but not always observable.

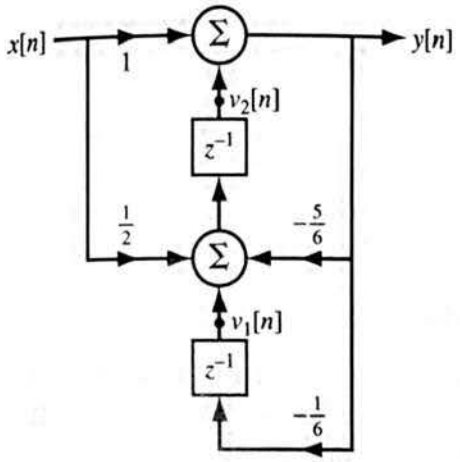

Figure 13.16 Transposed direct form II realization of $y[n]+(5/6)y[n-1]+(1/6)y[n-2]=x[n]+(1/2)x[n-1]$.

As a second example, consider the same system realized using the transposed direct form II structure (TDFII), as shown in Fig. 13.16. The system input is $x[n]$, the system output is $y[n]$, and the outputs of the delay blocks are designated as state variables $v_1[n]$ and $v_2[n]$.

The corresponding state and output equations (see Prob. 13.8-2) are

$$\mathbf{V}[n+1]=\begin{bmatrix}v_1[n+1]\\v_2[n+1]\end{bmatrix}=\begin{bmatrix}0 & -\frac{1}{6}\\1 & -\frac{5}{6}\end{bmatrix}\begin{bmatrix}v_1[n]\\v_2[n]\end{bmatrix}+\begin{bmatrix}-\frac{1}{6}\\-\frac{1}{3}\end{bmatrix}x[n]=\mathbf{A}\mathbf{V}[n]+\mathbf{B}x[n]$$

and

$$y[n]=\begin{bmatrix}0 & 1\end{bmatrix}\begin{bmatrix}v_1[n]\\v_2[n]\end{bmatrix}+1x[n]=\mathbf{C}\mathbf{V}[n]+\mathbf{D}x[n]$$

To describe this system in MATLAB, the state matrices **A**, **B**, **C**, and **D** are defined.

```
>> A = [0 -1/6;1 -5/6]; B = [-1/6; -1/3]; C = [0 1]; D = 1;
```

To diagonalize **A**, a transformation matrix **P** is created.

```
>> [V,Lambda] = eig(A)
V =
    0.4472    0.3162
    0.8944    0.9487
Lambda =
   -0.3333         0
         0   -0.5000
```

The characteristic modes of a system do not depend on implementation, so the eigenvalues of the DFII and TDFII realizations are the same. However, the eigenvectors of the two realizations are quite different. Since the transformation matrix **P** depends on the eigenvectors, different realizations can possess different observability and controllability characteristics.

Using transformation matrix **P**, the transformed state matrices $\hat{\mathbf{A}}=\mathbf{P}\mathbf{A}\mathbf{P}^{-1}$, $\hat{\mathbf{B}}=\mathbf{P}\mathbf{B}$, and $\hat{\mathbf{C}}=\mathbf{C}\mathbf{P}^{-1}$ are computed.

```
>> P = inv(V);
>> Ahat = P*A*inv(P), Bhat = P*B, Chat = C*inv(P)
```

```
Ahat =
   -0.3333         0
    0.0000   -0.5000
Bhat =
   -0.3727
   -0.0000
Chat =
    0.8944    0.9487
```

Again, the proper operation of $\mathbf{P}$ is verified by the correct diagonalization of $\mathbf{A}$, $\hat{\mathbf{A}} = \mathbf{\Lambda}$. Since no column of $\hat{\mathbf{C}}$ is zero, the system is observable. However, at least one row of $\hat{\mathbf{B}}$ is zero, and therefore the system is not controllable. The TDFII realization, which is more descriptively called the observer canonical form, is always observable but not always controllable. It is interesting to note that the properties of controllability and observability are influenced by the particular realization of a system.

13.8.4 Matrix Exponentiation and the Matrix Exponential

Matrix exponentiation is important to many problems, including the solution of discrete-time state-space equations. Equation (13.63), for example, shows that the state response requires matrix exponentiation, $\mathbf{A}^n$. For a square $\mathbf{A}$ and specific n, MATLAB happily returns $\mathbf{A}^n$ by using the ^ operator. From the system in Ex. 13.13 and $n = 3$, we have

```
>> A = [0 1;-1/6 5/6]; n = 3; A^n
   ans =
      -0.1389    0.5278
      -0.0880    0.3009
```

The same result is also obtained by typing `A*A*A`.

Often, it is useful to solve $\mathbf{A}^n$ symbolically. Noting $\mathbf{A}^n = \mathcal{Z}^{-1}[(\mathbf{I} - z^{-1}\mathbf{A})^{-1}]$, the symbolic toolbox can produce a symbolic expression for $\mathbf{A}^n$.

```
>> syms z n; An = simplify(iztrans(inv(eye(2)-z^(-1)*A)))
   An =
   [ 3*(1/3)^n - 2*(1/2)^n, 6*(1/2)^n - 6*(1/3)^n]
   [         1/3^n - 1/2^n,         3/2^n - 2/3^n]
```

Notice that this result is identical to Eq. (13.67), derived earlier. Substituting the case $n = 3$ into `An` provides a result that is identical to the one elicited by the previous `A^n` command.

```
>> double(subs(An,n,3))
   ans =
      -0.1389    0.5278
      -0.0880    0.3009
```

For continuous-time systems, the matrix exponential e^{At} is commonly encountered. The `expm` command can compute the matrix exponential symbolically. Using the system from Ex. 13.8 yields

```
>> syms t; A = [-12 2/3;-36 -1]; eAt = simplify(expm(A*t))
   eAt =
   [  -(exp(-9*t)*(3*exp(5*t) - 8))/5, (2*exp(-9*t)*(exp(5*t) - 1))/15]
   [ -(36*exp(-9*t)*(exp(5*t) - 1))/5,  (exp(-9*t)*(8*exp(5*t) - 3))/5]
```

This result is identical to the result computed in Ex. 13.8. Similar to the discrete-time case, an identical result is obtained by typing `syms s; simplify(ilaplace(inv(s*eye(2)-A)))`.

For a specific t, the matrix exponential is also easy to compute, either through substitution or direct computation. Consider the case $t = 3$.

```
>> double(subs(eAt,t,3))
   ans = 1.0e-004 *
      -0.0369    0.0082
      -0.4424    0.0983
```

The command `expm(A*3)` produces the same result.

13.9 SUMMARY

An Nth-order system can be described in terms of N key variables—the state variables of the system. The state variables are not unique; rather, they can be selected in a variety of ways. Every possible system output can be expressed as a linear combination of the state variables and the inputs. Therefore, the state variables describe the entire system, not merely the relationship between certain input(s) and output(s). For this reason, the state variable description is an internal description of the system. Such a description is therefore the most general system description, and it contains the information of the external descriptions, such as the impulse response and the transfer function. The state variable description can also be extended to time-varying parameter systems and nonlinear systems. An external description of a system may not characterize the system completely.

The state equations of a system can be written directly from knowledge of the system structure, from the system equations, or from the block diagram representation of the system. State equations consist of a set of N first-order differential equations and can be solved by time-domain or frequency-domain (transform) methods. Suitable procedures exist to transform one given set of state variables into another. Because a set of state variables is not unique, we can have an infinite variety of state-space descriptions of the same system. The use of an appropriate transformation allows us to see clearly which of the system states are controllable and which are observable.

References

1. Kailath, T., *Linear Systems,* Prentice-Hall, Englewood Cliffs, NJ, 1980.
2. Zadeh, L. and Desoer, C., *Linear System Theory,* McGraw-Hill, New York, 1963.

PROBLEMS

13.2-1 Convert each of the following second-order differential equations into a set of two first-order differential equations (state equations). State which of the sets represent nonlinear equations.

(a) $\ddot{y} + 10\dot{y} + 2y = x$

(b) $\ddot{y} + 2e^{y}\dot{y} + \log y = x$

(c) $\ddot{y} + \phi_1(y)\dot{y} + \phi_2(y)y = x$

13.3-1 Write the state equations for the *RLC* network in Fig. P13.3-1.

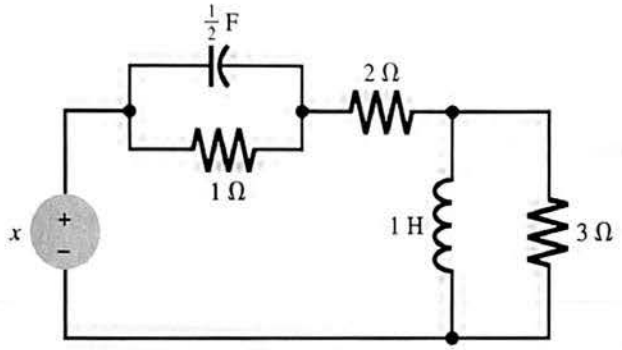

Figure P13.3-1

13.3-2 Write the state and output equations for the network in Fig. P13.3-2.

13.3-3 Write the state and output equations for the network in Fig. P13.3-3.

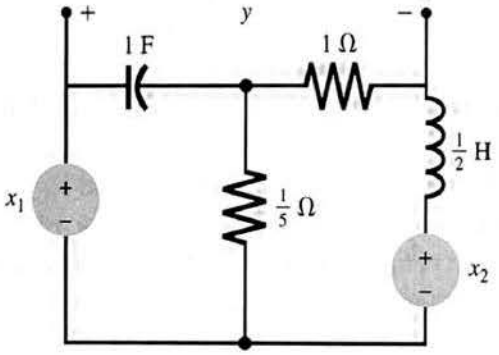

Figure P13.3-3

13.3-4 Write the state and output equations for the electrical network in Fig. P13.3-4.

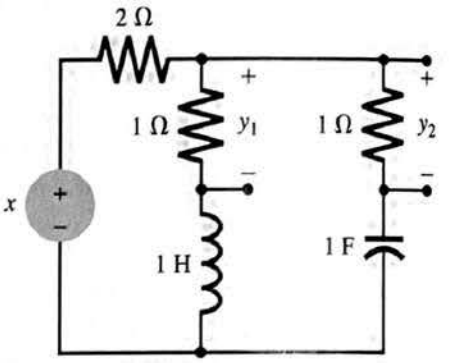

Figure P13.3-4

13.3-5 Write the state and output equations for the network in Fig. P13.3-5.

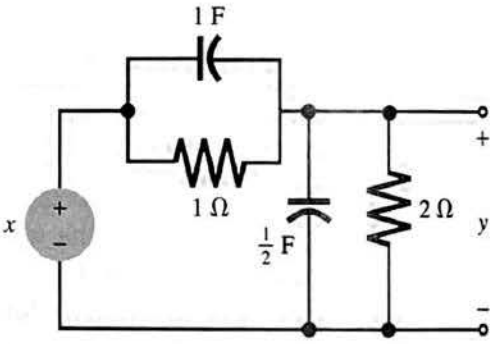

Figure P13.3-5

13.3-6 Write the state and output equations of the system shown in Fig. P13.3-6.

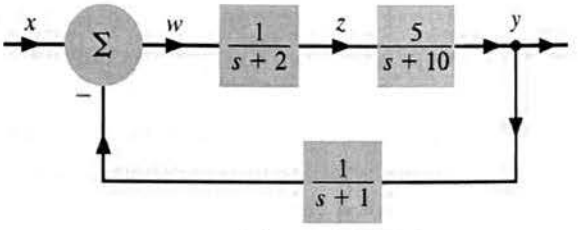

Figure P13.3-6

13.3-7 Write the state and output equations of the system shown in Fig. P13.3-7.

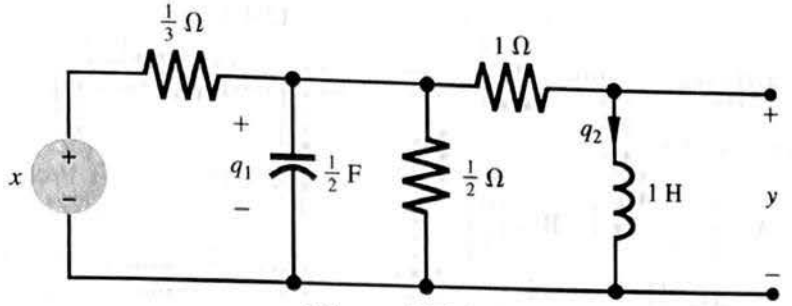

Figure P13.3-2

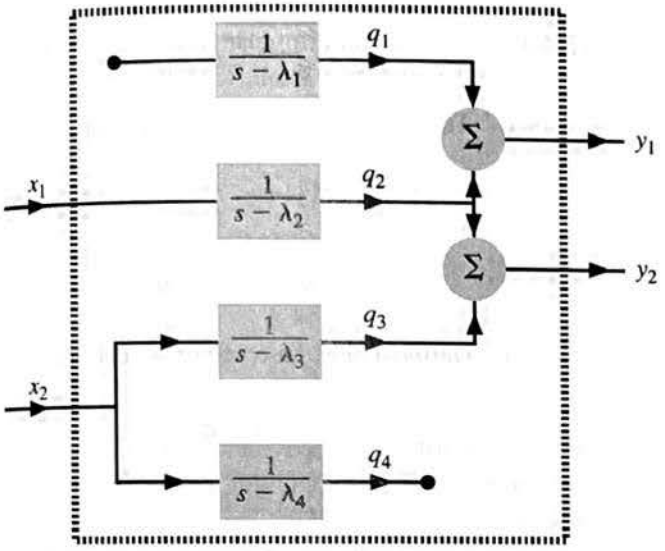

Figure P13.3-7

13.3-8 For a system specified by the transfer function

$$H(s) = \frac{3s+10}{s^2+7s+12}$$

write sets of state equations for DFII and its transpose, cascade, and parallel forms. Also write the corresponding output equations.

13.3-9 Repeat Prob. 13.3-8 for

(a)

$$H(s) = \frac{4s}{(s+1)(s+2)^2}$$

(b)

$$H(s) = \frac{s^3+7s^2+12s}{(s+1)^3(s+2)}$$

13.4-1 Find the state vector $\mathbf{q}(t)$ by using the Laplace transform method if

$$\dot{\mathbf{q}} = \mathbf{A}\mathbf{q} + \mathbf{B}\mathbf{x}$$

where

$$\mathbf{A} = \begin{bmatrix} 0 & 2 \\ -1 & -3 \end{bmatrix} \qquad \mathbf{B} = \begin{bmatrix} 0 \\ 1 \end{bmatrix}$$

$$\mathbf{q}(0) = \begin{bmatrix} 2 \\ 1 \end{bmatrix} \qquad x(t) = 0$$

13.4-2 Repeat Prob. 13.4-1 for

$$\mathbf{A} = \begin{bmatrix} -5 & -6 \\ 1 & 0 \end{bmatrix} \qquad \mathbf{B} = \begin{bmatrix} 1 \\ 0 \end{bmatrix}$$

$$\mathbf{q}(0) = \begin{bmatrix} 5 \\ 4 \end{bmatrix} \qquad x(t) = \sin(100t)u(t)$$

13.4-3 Repeat Prob. 13.4-1 for

$$\mathbf{A} = \begin{bmatrix} -2 & 0 \\ 1 & -1 \end{bmatrix} \qquad \mathbf{B} = \begin{bmatrix} 1 \\ 0 \end{bmatrix}$$

$$\mathbf{q}(0) = \begin{bmatrix} 0 \\ -1 \end{bmatrix} \qquad x(t) = u(t)$$

13.4-4 Repeat Prob. 13.4-1 for

$$\mathbf{A} = \begin{bmatrix} -1 & 1 \\ 0 & -2 \end{bmatrix} \qquad \mathbf{B} = \begin{bmatrix} 1 & 1 \\ 0 & 1 \end{bmatrix}$$

$$\mathbf{q}(0) = \begin{bmatrix} 1 \\ 2 \end{bmatrix} \qquad \mathbf{x} = \begin{bmatrix} u(t) \\ \delta(t) \end{bmatrix}$$

13.4-5 Use the Laplace transform method to find the response y for

$$\dot{\mathbf{q}} = \mathbf{A}\mathbf{q} + \mathbf{B}\mathbf{x}(t)$$
$$y = \mathbf{C}\mathbf{q} + \mathbf{D}\mathbf{x}(t)$$

where

$$\mathbf{A} = \begin{bmatrix} -3 & 1 \\ -2 & 0 \end{bmatrix} \qquad \mathbf{B} = \begin{bmatrix} 1 \\ 0 \end{bmatrix}$$

$$\mathbf{C} = [0 \quad 1] \qquad \mathbf{D} = 0$$

and

$$x(t) = u(t) \qquad \mathbf{q}(0) = \begin{bmatrix} 2 \\ 0 \end{bmatrix}$$

13.4-6 Repeat Prob. 13.4-5 for

$$\mathbf{A} = \begin{bmatrix} -1 & 1 \\ -1 & -1 \end{bmatrix} \quad \mathbf{B} = \begin{bmatrix} 0 \\ 1 \end{bmatrix}$$

$$\mathbf{C} = [1 \quad 1] \qquad \mathbf{D} = 1$$

$$x(t) = u(t) \qquad \mathbf{q}(0) = \begin{bmatrix} 2 \\ 1 \end{bmatrix}$$

13.4-7 The transfer function $H(s)$ in Prob. 13.3-8 is realized as a cascade of $H_1(s)$ followed by $H_2(s)$, where

$$H_1(s) = \frac{1}{s+3}$$

$$H_2(s) = \frac{3s+10}{s+4}$$

Let the outputs of these subsystems be state variables q_1 and q_2, respectively. Write the state equations and the output equation for this system and verify that $\mathbf{H}(s) = \mathbf{C}\boldsymbol{\phi}(s)\mathbf{B} + \mathbf{D}$.

13.4-8 Find the transfer function matrix $\mathbf{H}(s)$ for the system in Prob. 13.4-5.

13.4-9 Find the transfer function matrix $\mathbf{H}(s)$ for the system in Prob. 13.4-6.

13.4-10 Find the transfer function matrix $\mathbf{H}(s)$ for the system

$$\dot{\mathbf{q}} = \mathbf{A}\mathbf{q} + \mathbf{B}\mathbf{x}$$

$$y = \mathbf{C}\mathbf{q} + \mathbf{D}\mathbf{x}$$

where

$$\mathbf{A} = \begin{bmatrix} 0 & 1 \\ -1 & -2 \end{bmatrix} \quad \mathbf{B} = \begin{bmatrix} 0 & 1 \\ 1 & 0 \end{bmatrix} \quad \mathbf{x} = \begin{bmatrix} x_1(t) \\ x_2(t) \end{bmatrix}$$

$$\mathbf{C} = \begin{bmatrix} 1 & 2 \\ 4 & 1 \\ 1 & 1 \end{bmatrix} \qquad \mathbf{D} = \begin{bmatrix} 0 & 0 \\ 0 & 0 \\ 1 & 0 \end{bmatrix}$$

13.4-11 Repeat Prob. 13.4-1 using the time-domain method.

13.4-12 Repeat Prob. 13.4-2 using the time-domain method.

13.4-13 Repeat Prob. 13.4-3 using the time-domain method.

13.4-14 Repeat Prob. 13.4-4 using the time-domain method.

13.4-15 Repeat Prob. 13.4-5 using the time-domain method.

13.4-16 Repeat Prob. 13.4-6 using the time-domain method.

13.4-17 Find the unit impulse response matrix $\mathbf{h}(t)$ for the system in Prob. 13.4-7 using Eq. (13.45).

13.4-18 Find the unit impulse response matrix $\mathbf{h}(t)$ for the system in Prob. 13.4-6.

13.4-19 Find the unit impulse response matrix $\mathbf{h}(t)$ for the system in Prob. 13.4-10.

13.5-1 The state equations of a certain system are given as

$$\dot{q}_1 = q_2 + 2x$$

$$\dot{q}_2 = -q_1 - q_2 + x$$

Define a new state vector $\mathbf{w}$ such that

$$w_1 = q_2$$

$$w_2 = q_2 - q_1$$

Find the state equations of the system with $\mathbf{w}$ as the state vector. Determine the characteristic roots (eigenvalues) of the matrix $\mathbf{A}$ in the original and the transformed state equations.

13.5-2 The state equations of a certain system are

$$\dot{q}_1 = q_2$$

$$\dot{q}_2 = -2q_1 - 3q_2 + 2x$$

(a) Determine a new state vector $\mathbf{w}$ (in terms of vector $\mathbf{q}$) such that the resulting state equations are in diagonalized form.

(b) For output $\mathbf{y}$ given by

$$\mathbf{y} = \mathbf{C}\mathbf{q} + \mathbf{D}\mathbf{x}$$

where

$$\mathbf{C} = \begin{bmatrix} 1 & 1 \\ -1 & 2 \end{bmatrix} \qquad \mathbf{D} = 0$$

determine the output $\mathbf{y}$ in terms of the new state vector $\mathbf{w}$.

13.5-3 Given a system

$$\dot{\mathbf{q}} = \begin{bmatrix} 0 & 1 & 0 \\ 0 & 0 & 1 \\ 0 & -2 & -3 \end{bmatrix} \mathbf{q} + \begin{bmatrix} 0 \\ 0 \\ 1 \end{bmatrix} x$$

determine a new state vector $\mathbf{w}$ such that the state equations are diagonalized.

13.5-4 The state equations of a certain system are given in diagonalized form as

$$\dot{\mathbf{q}} = \begin{bmatrix} -1 & 0 & 0 \\ 0 & -3 & 0 \\ 0 & 0 & -2 \end{bmatrix} \mathbf{q} + \begin{bmatrix} 1 \\ 1 \\ 1 \end{bmatrix} x$$

The output equation is given by

$$y = [1 \quad 3 \quad 1]\mathbf{q}$$

Determine the output y for

$$\mathbf{q}(0) = \begin{bmatrix} 1 \\ 2 \\ 1 \end{bmatrix} \qquad x(t) = u(t)$$

13.6-1 Write the state equations for the systems depicted in Fig. P13.6-1. Determine a new state vector $\mathbf{w}$ such that the resulting state equations are in diagonalized form. Write the output $\mathbf{y}$ in terms of $\mathbf{w}$. Determine in each case whether the system is controllable and observable.

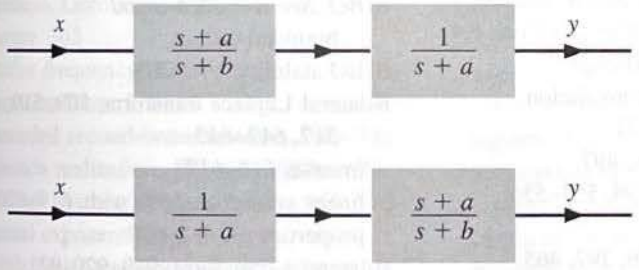

Figure P13.6-1

13.7-1 An LTI discrete-time system is specified by

$$\mathbf{A} = \begin{bmatrix} 2 & 0 \\ 1 & 1 \end{bmatrix} \qquad \mathbf{B} = \begin{bmatrix} 0 \\ 1 \end{bmatrix}$$
$$\mathbf{C} = [0 \quad 1] \qquad \mathbf{D} = [1]$$

and

$$\mathbf{q}(0) = \begin{bmatrix} 2 \\ 1 \end{bmatrix} \qquad x[n] = u[n]$$

(a) Find the output $y[n]$ using the time-domain method.
(b) Find the output $y[n]$ using the frequency-domain method.

13.7-2 An LTI discrete-time system is specified by the difference equation

$$y[n+2] + y[n+1] + 0.16y[n] = x[n+1] + 0.32x[n]$$

(a) Show the DFII, its transpose, cascade, and parallel realizations of this system.
(b) Write the state and the output equations from these realizations, using the output of each delay element as a state variable.

13.7-3 Repeat Prob. 13.7-2 for

$$y[n+2] + y[n+1] - 6y[n] = 2x[n+2] + x[n+1]$$

13.8-1 Verify the state and output equations for the LTID system shown in Fig. 13.15.

13.8-2 Verify the state and output equations for the LTID system shown in Fig. 13.16.

INDEX

The page numbers in italic refers to both Figures and Tables

Abscissa of convergence, 518
Absolute value, 6
Acceleration error constant, 606
Acceleration error constant K_a, 606
Accumulator system, 762, 949, 950
Active circuits, Laplace transform and analysis of, 566–569
A/D conversion. *See* Analog-to-digital conversion
Adders, 585
Additive property, 97
Advance form, 757
Algebra
  of complex numbers, 5–15
  matrix, 37–42, 1065–1069
Aliasing, 452–453, *454*, 455
  general condition for, in sinusoids, 457–459
  leakage in numerical computation and, 469, 471
  sampling rate and, 753–756
  verification of, in sinusoids, 456–457
Aliasing error, 307
Allpass filter, 715–716
AM. *See* Amplitude modulation
American Standard Code for Information Interchange (ASCII), 466
Amplitude, 16
  in discrete-time sinusoids, 744
  waveshaping role of, 279–284
Amplitude modulation (AM), 362–365, 393–397, 412
Amplitude response, 639
Amplitude spectrum, 264, 358
Analog filters. *See* Continuous-time system analysis
Analog signals, 78, 80
Analog systems, 109
Analog-to-digital conversion (A/D conversion), 463–466, *464*, 495
Angle modulation, 401–414
Angles
  computing with electronic calculators, 8–11
  generalized, 402
  principal value of, 9
Angular acceleration, 116
Angular position, 116
Angular velocity, 116
Anonymous functions, 126–128
Anti-aliasing filter, 455, 755
Anti-causal exponential, DTFT of, 855
Anti-causal signal, 81
Antipodal scheme, 247
Aperiodic signals, 79–81, 330–340, 847–858
Apparent frequency, 457–460, 750–752, 756
Armstrong, Edwin H., 412
Ars Magna (The Great Art) (Cardano), 2
ASCII. *See* American Standard Code for Information Interchange
Associative property, convolution integration and, 171
Asymmetric quantizers, 497
Asymptotic stability, 198, 555–556, 811–812
Audio signals, 365, 376, 397, 465
Autocorrelation, 249, 387–388
Automatic position control system, 590–596
Auxiliary conditions, 161

Backward difference system, 762, 806–808, 950
Bandlimited interpolation, 451–452
Bandlimited signals, 408, 440, 449, 451–452, 465, 466
Bandpass filters, 673, 703, 997–999, 1023
  Butterworth, 707–710, 1024–1026
  Chebyshev, 704–706
Bandpass systems, 377–380, 875
Bandstop filters, 673–675, 710–713, 999–1001, 1023–1026
Bandwidth
  of angle-modulated signals, 408–410
  essential, 387, 421–422
  of rectangular pulse, 344
  signal duration reciprocity with, 357
  of signals, 293, 408–410
Bartlett (triangle) window, 417–418
Baseband signal, 388, 390–392, 398–399, 401, 408–409, 411, 413–414
Basis functions, 253
Basis signals, 253, 257, 306, 509
Basis vectors, 251
Beat effect, 393
Bessel-Thomson filters, 715
Bhaskar, 2
BIBO. *See* Bounded-input/bounded-output
BIBO stability, 196–203
Bilateral Laplace transform, 509, 510, 512, 612–615
  inverse, 616–617
  linear system analysis with, 619–620
  properties of, 618–619
Bilateral z-transform, 919, 920–921, 923–924, 966–974
Bilinear transformation method, 1012–1026, 1047–1049
Binary communication, 247
Black, H. S., 443
Black box, 95, 119, 120, 201, 556, 662, 815
Blackman window, 417–418, 425
Block convolution, 894–899
Block diagrams, *570*, 570–572
Bode plots, 646–647
  first-order pole, 650–653

with MATLAB, 661
pole at origin, 648–650
second-order pole, 653–656, 661–662
for second-order transfer functions, 656–661
transfer function from frequency response, 662
Bombelli, Raphael, 3–4
Bonaparte, Napoleon, 259–260, 529–530
Bounded input, 110, 775
Bounded-input/bounded-output (BIBO), 110, 555–556, 775, 811–812, 814–817, 986–987
Bounded output, 110, 775
Break frequency, 650
Butterfly structure, 489, 491
Butterworth filters, 673, 677–687
bandpass, 707–710, 1024–1026
bandstop, 711–713
bilinear transformation method for designing, 1013–1015
cascaded second-order sections for, 718–721
higher-order lowpass, 1048–1049
impulse-invariance method for designing, 1008–1011
in MATLAB, 717–718
Butterworth lowpass filters, 683–687, 1006, 1017–1020

Canonical realizations, of transfer function, 952–954
Canonic direct form, 952
Cardano, Gerolamo, 2–3, *4*
Carrier, 362
Carrier frequency, 402, 403
Cartesian form, 5, 8–14
Cascaded second-order sections, 718–721
Cascade realization, 577–579, 955, 1079
Cascade systems, 190–192, 201, 555–556
Causal exponential
bilateral z-transform of, 920–921
DTFT of, 852, 854
Fourier transform of, 334–335
Laplace transform and ROC of, 513–514
Causality condition, 778
Causal signal, 81, 172
Causal systems, 104–107, 172, 775
Cayley-Hamilton theorem, 1066–1068
Champollion, Jean-François, 260
Characteristic equation, 153, 783, 1066–1068, 1088, 1099
Characteristic function, 193
Characteristic modes, 162, 163, 203–205, 783
Characteristic polynomial, 153–156, 164, 166, 202–203, 220, 554–555, 592, 645, 783–784, 786–787, 791
Characteristic roots, 153, 783, 812, *813*, 1088
Characteristic value, 1066, 1088
Chebyshev filters, 673, 677, 688–700, 704–706
Chebyshev highpass filters, 701–703, 1021–1023
Chebyshev lowpass filters, 693–696
Circular convolution, 483–484, 866, 889–890
Circular shifting property, 483
Clearing fractions, 26–27, 32–33, 525–526
Clipped sinusoids, 298–299
Closed-loop feedback, *588*, 589
Closed-loop frequency response, 667
Coherent detection, 392
Column vector, 35
Communications industry, 412
Commutation, of matrices, 39
Commutative property, convolution integration and, 170
Compact trigonometric Fourier series, 263–267, 269–274, *288*
Compensation, 608–611
Complete set, 251, 253
Complex conjugate poles, 653–654, 927
phase of, 656
realization of, 579
Complex-conjugate zeros, 654, 656
Complex factors of $Q(x)$, 28–29
Complex frequency plane, 90
Complex numbers
algebra of, 5–15
arithmetical operations, powers, and roots of, 11–15
conjugate of, 6–7
defining, 1
historical background for, 1–4
logarithms of, 15
mathematical formulas for, 54
standard forms of, 14–15
Complex roots, 154, 786–788
Complex signals, 95, 242–243
Conformable, 39
Conjugate of complex numbers, 6–7
Conjugate symmetry, 95, 334, 354
DFT and, 482–483
of $X(\Omega)$, 851, 859
Conjugation property, 334, 354, 859
Constant Ka_1a_2/b_1b_3, 648
Constant-parameter systems, 101, 774
Continuous-time Fourier transform (CTFT), 859, 869–872
Continuous-time signals, 78, *79*, 107
Continuous-time sinusoids, sampled, 746
Continuous-time system analysis
block diagrams and, 570–571
differential and integro-differential equation solutions, 544–556
of electrical networks, 557–569
feedback and controls applications of, 588–611
sampled-data systems and, 959–966
system realization, 572–587
Continuous-time systems, 107–108, 764. *See also* Linear, time-invariant, continuous-time systems
Continuous wall of poles, 673
Controllability/observability, 123–124, 1103–1109, 1117, 1121–1124
Control systems
design specifications, 596
frequency response and design of, 662–667
higher-order, 601
second-order, 596–599
simple, 590–596
Converge in the mean, 278
Convergence, of Fourier series, 277–286, 335
Convolution, 189–190
block, 894–899
of causal signals, 796–797
circular, 483–484, 889–890
correlation and, 249
discrete-time, 822–823, 889–894
fast, 890
Fourier transform and, 365–367
graphical understanding of, 178, *179*, 180–187, 217–219
linear, 485, 889–890
by tables, 175, 177, 797–799
z-transform and, 938–939
Convolution integral, 170–177, *176*
Convolution sum, 795, 797, 798, *798*, 800–805
Convolved functions, width of, 187
Corner frequency, 650
Correlation
convolution and, 249
functions, 248–249
signal comparison, 243–249
signal detection and, 246–248
Correlation coefficient, 244–246

Coupled inductive networks, transformed analysis of, 563–565
Cramer's rule, 22–25, 569
Critically damped, 592
Crosscorrelation function, 248
CTFT. *See* Continuous-time Fourier transform
Cubic equations, 58
Custom filter functions, 821–822
Cutoff filter, 455
Cutoff frequency, 208, 678
Cycles per sample, 745

Damping coefficient, 115, 162
Damping ratio, 596
Dashpots
  linear, 115
  torsional, 116
Data truncation, 414–420
Decade, 648
Decibels, 647
Decimation-in-frequency algorithm, 491
Decimation-in-time algorithm, 489, 491
Decomposition property, 99, 100
Delayed impulse, 168
Delay form, 757
Demodulation, 391–392, 396–397, 411–412
Depressed cubic equation, 3
Derivative formulas, 56
Design specifications, 596
Detection, 391. *See also* Demodulation
  correlation and, 246–248
  envelope, 396–397
  synchronous or coherent, 392
  threshold, 247
Deterministic signals, 82
DFII realization. *See* Direct form II realization
DFI realization. *See* Direct form I realization
DFT. *See* Discrete Fourier transform
Diagonalization, 1099–1103
Diagonal matrix, 37
Difference equations, 777
  differential equations and, 763–764
  of linear, 939–950
  order of, 764
  recursive and nonrecursive forms of, 763
  recursive (iterative) solution of, 778–781
  sinusoidal response of system of, 988–991
Differential equations
  auxiliary conditions and solutions of, 161
  difference equations and, 763–764
  Laplace transform and solutions of, 544–546
  natural and forced solutions, 196
Differentiation property, z-transform and, 936–937
Differentiators
  digital, 760–762
  ideal, 643
  window method for design of, 1038–1039
Digital computers, 730, 880
Digital differentiators, 760–762
Digital filters, 731, 764, 1001–1003. *See also* Discrete-time systems; Recursive filters
Digital integrators, 762
Digital signal processing, 764–765, 877
Digital signals, 78, 80, 461, *462*
Digital systems, 109
Dirac delta function, 344–346
Dirac delta train, 348
Direct canonic form, 575–577
Direct form II realization (DFII realization), 574–577, 952, 1076–1080, *1081*, 1109, *1110*
Direct form I realization (DFI realization), 573–574, *574*, 952
Direct realization, 950
Dirichlet conditions, 261, 279
Discontinuous functions, Fourier synthesis of, 283–284
Discrete Fourier transform (DFT), 307, 469–487
  applications of, 484–487
  derivation of, 471–474
  interpreting, 881
  in MATLAB, 491–498, 886
  N_0 for, 886–887
  properties of, 482–484, 880
  signal processing by, 877–899
  6-point, 884–885
  3-point, 882–883
  truncated signals and, 888–889
Discrete-time complex exponential $e^{j\Omega n}$, 743–744
Discrete-time convolution or filtering, 822–823, 889–894
Discrete-time exponential γ^n, 740–743
Discrete-time Fourier series (DTFS), 838–847, 877–878, 899–905
Discrete-time Fourier transform (DTFT), 850, *853*, 878–880
  CTFT connection with, 869–872
  of decimated and interpolated signals, 870–872
  interpreting, 881
  LTI discrete-time system analysis by, 872–877
  in MATLAB, 857, 902–905
  properties of, 859–869, *868*
Discrete-time functions, 765–766
Discrete-time impulse function $\delta(t)$, 738, 739–740
Discrete-time signals, 78, *79*, 107, 730
  energy and power of, 732–733
  in MATLAB, 765–766
  models of, 738–753
  operations for, 733–738
  size of, 731–732
Discrete-time sinusoid $\cos(\Omega n + 0)$, 744–751
Discrete-time systems, 107–108, 730, 756–765
  classification of, 774–777
  equations for, 777–782
  frequency response of, 986–992
  in MATLAB, 819–823
  properties of, 776–777
  sampled-data systems and, 959–966
  state-space analysis of, 1109–1117
  unit impulse response, 789–793
  ZIR, 782–788
  ZSR, 793–810
Discrete-time unit step function $u[n]$, 739–740
Discrete-time window functions, *1032*
Distortion, 374–376
Distortionless transmission, 375, 376
  bandpass, 379–380
  DTFT and, 874–875
  filters for, 714–716
Distributive property, convolution integration and, 171
D_n, numerical computation of, 307
Dominant poles, 601
Double-sideband, suppressed-carrier modulation (DSB-SC), 388–393, *389*
Downsampling, 736–738
DSB-SC. *See* Double-sideband, suppressed-carrier modulation
DTFS. *See* Discrete-time Fourier series
DTFT. *See* Discrete-time Fourier transform

Duality property, of Fourier transform, 354–355, 374
Dual of time sampling, 466–468

Eigenfunction, 193, 305
Eigenvalue, 153, 1066, 1067, 1088, 1098, 1103
Eigenvector, 1066
Electrical circuits, state equations for, 1072–1075
Electrical networks, analysis of, 557–569
Electrical systems, input-output description, 111–114
Electromechanical systems, input-output description, 118
Elliptic filters, 698–700
Elliptic rational function, 698
Energy
  of discrete-time signals, 732–733
  error, 253
  of error signal, 253–254
  estimating in MATLAB, 131–133
  signal, 384–388, 868–869
  sum of orthogonal signals, 243
Energy signals, 81–82, 732
Energy spectral density, 385, 387–388
Envelope, 377
Envelope delay, 376, 378, 875
Envelope detector, 396–397
Equality in the mean, 335
Equalizer, 715
Equal-ripple functions, 689
Equilibrium states, 196, 198
Equivalent realizations, 580
Error energy, 253
Errors
  aliasing, 307
  steady-state, 605–608
Error signal, energy of, 253–254
Error vector, 238
Essential bandwidth, 387, 421–422
Euler, Leonhard, 2
Euler's equality, 286
Euler's formula, 6, 90
Even and odd functions, 92–95
Everlasting exponential function e^{st}, 189, 193–195
Everlasting exponential function z^n, 808–809
Everlasting signals, 81
Exponential Fourier series, 286–302, *288*, 838
Exponential Fourier spectra, 289–297
Exponential function e^{st}, 89–91
Exponentially varying discrete-time sinusoid $\gamma^n \cos(\Omega n + \theta)$, 752–753
Exponentially varying sinusoids, 22
Exponential modulation. *See* Angle modulation
Exponential-order signals, 509
Exponentials
  Fourier transform of, 476–478
  matrix, 1124–1125
  monotonic, 20–21
  sinusoids in terms of, 20
  time constants of, 20
Exponential signals, 305–306
External description, 119–120
External input, system response to, 168–196
External (BIBO) stability, 196–197, 775

Fast convolution, 890
Fast Fourier transform (FFT), 307, 475, 488–491, 877–899
FDM. *See* Frequency-division multiplexing
Feedback and controls, 588–612
  compensation, 608–611
  root locus, 601–605
  stability and, 611–612
  steady-state errors, 605–608
FFT. *See* Fast Fourier transform
Filter design, pole and zeros of $H(s)$ and design of, 667–677
Filtering
  DFT and, 485–487
  discrete-time, using DFT, 889–894
  discrete-time system response through, 819–821
  ideal and practical filters, 381–384
  interpolation function sinc (x) and, 341–342
  time constant and, 207–208
  using windows in, 418, *419*, 420
  ZSR and, 799
Filtering function, 341
Filters. *See also specific filters*
  anti-aliasing, 455, 755
  design criteria for, 1003–1006
  for distortionless transmission, 714–716
  higher-order, 1047–1052
  ideal, 381–384, 875–877
  nonrecursive, 1002–1003
  practical, 381–384, 676–677, 875–877
  recursive, 1001–1002
Finality property, 252, 1034
Final value theorem, 542–543
Finite impulse response filters (FIR filters), 954–955, 1003, 1028
  with arbitrary magnitude response, 1051–1052
  comb, 1030–1031
  delay and, 1049–1051
  frequency sampling method in design of, 1040–1047
  lowpass, 1042–1046
  time-domain equivalence method for design of, 1032–1039
Finite-memory systems, 104
First-order factors, inverse z-transform and, 927–928
First-order hold filter, 449
FM. *See* Frequency modulation
Folding frequency, 453
Forced response, 196, 810
Forced solution, 196
Fourier, Jean-Baptiste-Joseph, 259–261
Fourier integral, 850
  aperiodic signal representation by, 330–340
Fourier series, 261, 277–286, 1032, 1034. *See also* Trigonometric Fourier series
  exponential, 286–302
  Legendre, 257–259
  limitations of method of analysis, 306–307
  MATLAB applications, 309–315
  properties, *300*, 300–302
  square wave synthesis by truncated, 281–282
Fourier spectra, 264
  exponential, 289–297
  of impulse train, 293–295
  MATLAB plotting of, 267, 290
  nature of, 850–858
  numerical computation of, 308
  periodic extension of, 841
  of periodic signal $x[n]$, 840–841
  sampled signal and, 440–441, *441*
Fourier transform, 334–339. *See also* Continuous-time Fourier transform; Discrete-time Fourier transform
  determining ZSR with, 372–373
  of Dirac delta function, 344–345
  duality property of, 354–355
  frequency-shifting property of, 362–365
  Laplace transform and, 520
  linearity of, 336
  LTIC system response using, 339–340
  in MATLAB, 420–425, 478
  numerical computation of, 469–487

Fourier transform (*continued*)
of periodic signals, 347–348
properties of, 352–372, *368*
of rectangular pulse, 343–344, 479–482
scaling property of, 356, *357*
of sign function, 350
of sinusoids, 347
time differentiation and integration and, 367–371
time-frequency duality in operations of, 352–353
time-shifting property of, 358–361
of unit step function $u(t)$, 349–350
Frequency, 16
apparent, 750, 752, 756
break, 650
carrier, 402, 403
corner, 650
cutoff, 208
fundamental, 838–847
gain crossover, 665
half-power, 678
Hertzian, 16
instantaneous, 402–405
phase crossover, 665
radian, 16
Frequency convolution
bilateral Laplace transform and, 619
DTFT and, 866–867
Laplace transform and, 540–541
Frequency differentiation, 860, 861
Frequency-division multiplexing (FDM), 365, 412–414
Frequency-domain analysis, 383–384
Frequency-domain description, 264, 840
Frequency-domain equivalence criterion, 1005, 1012–1026, 1040–1047
Frequency-domain method, 551
Frequency modulation (FM), 402–408, 412
Frequency resolution, 474, 886–887
Frequency response, 374
Bode plots, 646–662
control system design using, 662–667
of discrete-time systems, 986–992
of LTIC systems, 638–646
in MATLAB, 716–717, 991
periodic nature of, 992
pole and zeros of $H(s)$ and, 669–671
from pole-zero locations, 993–1001
transfer function from, 662
transient performance in terms of, 665–667
Frequency reversal, 859
Frequency sampling method, 1032, 1040–1047, 1049
Frequency scaling, 682
Frequency shifting, 362–365, 482–483, 536, 618, 863–865
Frequency spectra, 264
Frequency warping, 1015–1017
Full-wave rectifier, 303–305
Function M-files, 214–215
Fundamental, 261, 276–277
Fundamental band, 457, 749
Fundamental frequency, 838–847
Fundamental period, 733, 838–847

Gain, controlling with pole and zero placement, 994–995
Gain crossover frequency, 665
Gain enhancement, by pole, 670
Gain margin, 665
Gain suppression, by zero, 670–671
Gauss, Karl Friedrich, 4
GCF. *See* Greatest common factor
Generalized angle, 402
Generalized Fourier series, 257
Generalized function, 88
Generalized linear phase (GLP), 378
Gibbs, Josiah Willard, 283, 285–286
Gibbs phenomenon, 283–286, 309–311, 1032, 1039
GLP. *See* Generalized linear phase
Greatest common factor (GCF), 276
Group delay, 376, 377–378, 875

Half-power frequency, 678
Half-wave symmetry, 275
Hamming window, 417–418, 1037–1039
Hanning window, 417–418
Harmonically related frequencies, 276
Harmonic distortion, 298–299
Heaviside, Oliver, 261, 530–531
Heaviside "cover-up" method, 27–30, 32–33, 525–526
Hertzian bandwidth, 409
Hertzian frequency, 16
Higher-order filters, 1047–1052
Higher-order systems, poles and, 601
Highpass filters, 700–703, 995
Homogeneity property, 97

Ideal delay, 642–643
Ideal differentiator, 643
Ideal filters, 381–384, 676, 875–877
Ideal integrator, 643–644
Ideal interpolation, 450–451, *451*
Ideal linear phase (ILP), 378
Identity matrix, 37
Identity systems, 109, 775
IDTFT. *See* Inverse discrete-time Fourier transform
IIR filters. *See* Infinite impulse response filters
ILP. *See* Ideal linear phase
Imaginary numbers, 1, 2
Impedance, 557
Improper functions, 25, 33–34
Impulse invariance criterion, 1005
Impulse invariance method, 1006–1012
Impulse matching, 164–167
Impulse response, 163–168, 205, 220–221, 791–792, 823–824, 1033
Impulse response matrix, 1094
Impulses, 171, 189
Impulse train, Fourier series spectra of, 293–295
Incrementally linear equations, 777
Indefinite integrals, 57
Inductive cable loading, 530
Inertia, moment of, 116
Infinite impulse response filters (IIR filters), 1002, 1047–1049
Information transmission rate, time constants and, 209–210
Initial conditions, 158–159, 161, 547, 559–561, 1069
Initial state, 1069
Initial value theorem, 542–543
Inner product, 240
Input. *See also* External input; Multiple-input, multiple-output; Single-input, single-output
bounded, 110, 775
noncausal, 619–622
ramp, *593*, 594–595
step, 591–592, *593*, 594–595
Input-output description, 111–118
Inputs, 64
Instantaneous frequency, 402–405
Instantaneous systems, 103–104
Instantaneous velocity, 402
Integral control, 610
Integrator, in operational amplifier circuits, 584
Integro-differential equations, Laplace transform and solutions of, 544–546
Interconnected systems, 806–809
Internal conditions
continuous-time system response to, 151–163

discrete-time system response to, 782–788
Internal description, 119–125, 1064
Internal stability, 198, 775, 811–812
Internal (asymptotic) stability, 198, 811–812, 814–817
Interpolation, 449, *450*, 450–451, *451*, 468, 736–738
Interpolation formula, 443, 451
Interpolation function sinc(x), 341–342
Inverse bilateral z-transform, 969–970
Inverse Chebyshev filters, 696–698
Inverse discrete-time Fourier transform (IDTFT), 472, 878–881
Inverse Fourier transform, 333
of Dirac delta function, 345–346
Inverse Laplace transform, 520–529, 1006, 1094–1095
Inverse systems, 556–557, 806–808, 949–950
Inverse z-transform, 921, 925–930
Inversion, of matrices, 40–42
Inversion property of time and frequency, 357
Invertible systems, 109–110, 775
Irrational numbers, 2

Jump discontinuities, 268, 281, 282, 378, 471

Kaiser window functions, 417–418, 424–425
Key variables, 120
Kirchhoff laws, 111, 213, 557
Kronecker delta function, 451–452

Lag compensator, 610, *611*
Lagrange, Louis de, 530
Laplace, Pierre-Simon de (Marquis), 529–530
Laplace transform, 509–531, *511*. *See also* Bilateral Laplace transform
active circuit analysis with, 566–569
differential and integro-differential equation solutions and, 544–546
electrical network analysis and, 557–569
electric circuit solutions and, 548–549
Fourier transform and, 520
frequency convolution and, 540–541
frequency shifting and, 536
initial and final values and, 542–543
initial conditions and, 547
intuitive interpretation of, 551–552
inverse, 520–529, 1006, 1094–1095
properties of, 532–544, *544*
stability and, 554–556
state equation solutions with, 1083–1088
system transfer functions and, 553
zero-input and zero-state components of response, 546
ZSR and, 541, 546, 551–552
z-transform and, 918, 956–959
Lead compensator, 609, *609*, *610*
Left half-plane (LHP), 91
Left shift, 71, 130, 134, 178, 181, 733–735, 934, 939–942
Left-sided sequence, 968
Left-sided signal, 614
Legendre Fourier series, 257–259
Leibniz, Gottfried Wilhelm, 465
L'Hôpital's rule, 58
LHP. *See* Left half-plane
Linear, time-invariant, continuous-time systems (LTIC systems), 150
everlasting exponential function e^{st} and, 193–195
Fourier transform for response of, 339–340
frequency response of, 638–646
impulse response determination for, 220–221
periodic input response of, 303–307
signal transmission through, 372–380
Linear, time-invariant, discrete-time systems (LTID systems), 774
DTFT analysis of, 872–877
equations for, 777–782
external input response, 793–810
interconnected, 806–809
internal conditions responses, 782–788
stability, 811–817
system realization, 950–956, *951*
unit impulse response, 788–793
ZSR of, 944–948
Linear convolution, 485, 889–890
Linear dashpot, 115
Linear difference equations, z-transform solution of, 939–950
Linear differential systems, 150
Linear discrete-time systems, 782
Linearity, 97–98
bilateral Laplace transform and, 618
DFT and, 482
of discrete-time systems, 774–775
DTFT and, 859
Fourier transform and, 354
Laplace transform and, 513
z-transform and, 919
Linear phase, 358–359, 376, 861–862, 874
Linear phase filters, 1041–1042
Linear-phase response, symmetry conditions for, 1028–1030
Linear springs, 114
Linear systems, 97–101
bilateral Laplace transform in analysis of, 619–620
heuristic understanding of response of, 373–374
total response of, 195–196
Linear time-invariant systems (LTI systems), 150, 305–306
Linear time-varying systems, 102
Linear transformation, 36, 1095–1103, 1117
Log amplitude, 648, 650, 653
Logarithms, of complex numbers, 15
Log magnitude, 648–650, 653–654
Louis SVIII (King), 260
Lower sideband (LSB), 389
Lowpass DT systems, 818
Lowpass filters, 672–673
Butterworth, 683–687, 1006, 1048–1049
Chebyshev, 693–696
elliptic, 698–700
FIR, 1042–1046
frequency response of, 995
window method for design of, 1034–1037
LSB. *See* Lower sideband
LTIC systems. *See* Linear, time-invariant, continuous-time systems
LTID systems. *See* Linear, time-invariant, discrete-time systems
LTI systems. *See* Linear time-invariant systems
Lyapunov sense, 198, 222, 811

Maclaurin series, 55
Magnitude, 6
Magnitude response, 639, 1036
Marginal stability, 198
Mass, 114
rotational, 116
MATLAB
anonymous functions, 126–128
bilinear transformation in, 1015, 1047–1049
Bode plots with, 661

MATLAB (*continued*)
Butterworth bandpass filters with, 709–710
Butterworth bandstop filters, 712–713
Butterworth filters in, 717–721
Butterworth lowpass filters with, 685–687
calculator operations, 43–45
cascaded second-order sections, 718–721
Chebyshev bandpass filters with, 704–706
code performance measurement, 904–905
continuous-time filters, 716–721
controllability and observability with, 1108, 1121–1124
control system toolbox, 604–605
convolution of two finite-duration signals with, 805–806
custom filter functions, 821–822
DFT in, 491–498, 886
discrete-time convolution, 822–823
discrete-time exponentials with, 743
discrete-time signals in, 765–766
discrete-time sinusoids with, 745
discrete-time systems in, 819–823
DTFS with, 846–847, 902–905
DTFT with, 857, 902–905
element-by-element operations, 48–49
Find command, 717–718
for-loops, 215–217
Fourier series applications, 309–315
Fourier series spectra plotting with, 267, 290
Fourier transform, 420–425, 478
frequency response in, 642, 716–717, 991
graphical understanding of convolution and, 217–219
higher-order filter design in, 1047–1052
highpass Chebyshev filters with, 702–703
impulse invariance in, 1011
impulse response, 167
inverse Chebyshev filters with, 697–698
inverse Laplace transform with, 526–528
Kaiser window functions, 424–425
magnitude response with, 1036
matrix diagonalization in, 1102–1103
matrix exponentiation and matrix exponential, 1124–1125
matrix operations, 49–53
M-files, 212–220
multiple magnitude response curves in, 998–999
normalized Butterworth filters, 681–682
numerical computation of Fourier spectra, 308
numerical integration and signal energy estimation, 131–133
overview of, 42–43
Parseval's theorem and, 421–422
partial fraction expansion in, 53, 929
polynomial evaluation in, 716–717
polynomial roots, 157
relational operators and unit step function, 128–130
simple plotting, 46–48
Sinc function, 420–421
spectral sampling in, 423–424
square wave synthesis by truncated Fourier series, 281–282
state-space analysis with, 1117–1125
symbolic Laplace transform with, 528
synthesizing periodic replication, 370–371
transfer functions from state-space representations, 1120–1121
transfer functions of feedback systems with, 571–572
unit impulse response in, 792
vector operations, 45–46
visualizing operations on independent variable, 130–131
working with functions, 126–133
ZIR, 157–158
Matrices, 35–36
Cayley-Hamilton theorem and, 1066–1068
characteristic equation of, 1066–1068
characteristic roots of, 1088
computing exponential and power of, 1068–1069
derivatives and integrals of, 1065–1066
impulse response, 1094
inversion of, 40–42
MATLAB operations, 49–53
state transition, 1091, 1095
transfer function, 1086–1087
vector multiplication of, 40
Matrix algebra, 37–42, 1065–1069
Matrix exponentiation, 1124–1125
Maximum stopband gain, 677
Mean-square value, 65
Mechanical systems, input-output description, 114–118
Memoryless systems, 103, 776
Method of residues. *See* Heaviside "cover-up" method
M-files, 212–215
Michelson, Albert, 285
MIMO. *See* Multiple-input, multiple-output
Minimum passband gain, 677
Modes, 153
Modified partial fractions, 35, 926
Modified z-transform, 959, 960, 965
Modulating signal, 362
Modulation. *See also specific types*
defining, 388
Modulation index, 394
Modulation property, 863–865
Moment of inertia, 116
Monotonic exponentials, 20–21
Multiple-input, multiple-output (MIMO), 98, 125, 1064, 1070

N_0 periodic, 733
N_0-periodic sequences, 472
Narrowband angle-modulated signal (NBEM), 410–411
Natural binary code (NBC), 463
Natural frequencies, 153
Natural modes, 153
Natural response, 196, 810
Natural solution, 196
NBC. *See* Natural binary code
NBEM. *See* Narrowband angle-modulated signal
Negative feedback, 590
Negative frequencies, 291
Negative numbers, 2
Neper frequency, 90
Neutral equilibrium, 196, 198
Nichols plot, 664
Nonanticipative systems, 775
Noncausal input, 619–622
Noncausal signal, 81
Noncausal systems, 104–107, 621, 775
Noninvertible systems, 109–110, 775
Noninverting amplifier, 567
Nonlinear systems, 97–101
Nonrecursive filters, 1002–1003, 1027–1047
Nonrecursive form, of difference equation, 763
Normalized Butterworth filter, 678–682
Normalized set, 251
Notch (bandstop) filters, 673–675
Numerical computation, leakage in, 469, 471

Nyquist criterion, 665
Nyquist interval, 442
Nyquist plot, 664, 665, 667
Nyquist rate, 442, 456, 869
Nyquist samples, 442, 456

Octave, 648
Open-loop feedback, *588*
Open-loop transfer function, 667
Operational amplifier, *566*, 566–567, 583–587, *584*, *585*
Operator notation, 781–782
Orthogonal signal set, signal representation by, 250–261
Orthogonal signal space, 251–259
Orthogonal vector space, 250–251
Orthonormal set, 251
Output equation, 122, 1064, 1070–1071, 1093–1094
Outputs, 64
Overdamped, 592
Overlap and add method, *895*, 895–897
Overlap and save method, *888*, 897–899

Paley-Wiener criterion, 382, 452
PAM. *See* Pulse-amplitude modulation
Parallel realization, 577–580, 955, 1079–1080
Parseval's theorem, 254, 297, 385, 386–387, 421–422, 867–869
Partial fraction expansion, 25
  combination of Heaviside "cover-up" and clearing fractions, 32–33
  Heaviside "cover-up" method, 27–30
  improper $F(x)$, 33–34
  inverse z-transform by, 925–929
  MATLAB operations, 53, 929
  method of clearing fractions, 26–27
  modified partial fractions, 35
  repeated factors of $Q(x)$, 30–32
Passband, 676
PCM. *See* Pulse-code modulation
Percent overshoot (PO), 592, 665
Periodic convolution, 866
Periodic extension of Fourier spectrum, 841
Periodic functions, 309–311
Periodic gate function, DTFS of, 845–847
Periodic inputs, LTIC system response to, 303–307
Periodicity, 276–277, 747–748, 992
Periodic replication, synthesizing, 370–371
Periodic signals, 79–81, *80*, *81*
  discrete-time Fourier series representation of, 838–847
  Fourier spectra of, 840–841
  Fourier transform of, 347–348
Phase angle, 360
Phase crossover frequency, 665
Phase-locked loop (PLL), 411
Phase margin, 665
Phase modulation (PM), 402–408
Phase-plane analysis, 125, 1065
Phase response, 639, 671
Phase shifts, 359
Phase spectra, 264, 279–284, 311–315, 358, 360–361
Phasors, 18, 19
Physical systems, 775
Picket fence effect, 471, 883–884
Pickoff node, 757–758
Piecewise function, 85
Piecewise polynomial periodic functions, 301
Pingala, 465
PLL. *See* Phase-locked loop
PM. *See* Phase modulation
PO. *See* Percent overshoot
Pointwise convergent series, 278
Polar form, 8–11
Pole zero cancellation, 1046, 1075
Pole zero placement, 993–1001
Polynomial evaluation, in MATLAB, 716–717
Positional error constant, 606
Positional error constant K_p, 606
Positive feedback, 590
Postmultiplied matrices, 39
Power series, 55, 930
Power signals, 81–82, 732
PPM. *See* Pulse-position modulation
Practical filters, 381–384, 676–677, 875–877
Practical sampling, 445–448, *446*
Preece, William, 531
Preemphasis filter, 402
Premultiplied matrices, 39
Prewarping, 1017–1026
Principal value of angles, 9, 12, 14, 15, 360–361
Proper functions, 25, 27
Pulse-amplitude modulation (PAM), 460, *461*
Pulse-code modulation (PCM), 460
Pulse dispersion or spreading, time constants and, 209
Pulse-position modulation (PPM), 460
Pulse-width modulation (PWM), 460, *461*
Pythagoras, 2

Quadratic equations, 58
Quadratic factors, 29, 523–524, 928
Quantization, 463, 495–498

Radian frequency, 16, 90
Radians per sample, 743, 744
Ramp functions, 241
Ramp input, *593*, 594–595
Ramp signal, 257
Random signals, 82
Rational functions, 25, 26, 520
RC circuit, 113–114, 161, 162
Real time, 105
Rectangular pulse
  DTFT of, 856–857
  Fourier transform of, 343–344, 479–482
Rectangular spectrum, inverse DTFT of, 857–858
Rectangular window, 1033, 1034, 1038
Recursive filters, 1001–1002, 1006–1026
Recursive form, of difference equation, 763
Recursive system, 1002
Reflected unit step functions, 85–86
Reflection property, 357–358, 859–860
Region of convergence (ROC), 193, 510, 513–515, 517, 614, 920–921, 967–968
Region of existence, 514, 920
Relational operators, 128–130
Relative stability, 664–665
Repeated factors of $Q(x)$, 30–32
Repeated poles, realization of, 579
Repeated roots, 153–154, 786
Resonance phenomenon, 163, 210–212
Right half-plane (RHP), 91
Right shift, 71–72, 131, 134, 178, 181, 733–735, 931–936, 939–942
Right-sided sequence, 968
Right-sided signal, 614
Rise time, 206, 592
RLC circuit, 111–112, 114, 125, 1070–1071, 1073–1074
RMS. *See* Root-mean-square
ROC. *See* Region of convergence
Rolloff rate, 415
Root locus, 599, 601–605
Root-mean-square (RMS), 65, 68–70
Rotational mass, 116

Rotational systems, 116–118
Row vector, 35

Sallen-Key circuit, 567–569
Sampled-data systems, 959–966
Samples, 469, *470*, 475–476
  cycles per, 745
  radians per, 743, 744
Sampling, 445–448, *446*, 456
Sampling instants, 965
Sampling intervals, 755, 1007–1008
Sampling property of unit impulse, 87
Sampling rate
  aliasing and, 753–756
  altering, 736–738
Sampling theorem, 440–448, 460–463, 472, 755
Scalar multiplier, 584
Scaling property, 97, 733
  of Fourier transform, 356, *357*
  of Laplace transform, 540
  MATLAB Sinc function and, 420–421
  z-transform and, 936
Schwarz inequality, 244
Script M-files, 213–214
Second-order control systems, analysis of, 596–599
Second-order poles, 653–662
Second-order zeros, 654
Shifting, 733–735
Shift invariance, 774
Shift property, convolution integration and, 171
Sidelobes, 415
Sifting property of unit impulse, 87
Signal comparison, correlation, 243–249
Signal detection, correlation and, 246–248
Signal distortion, during transmission, 374–376
Signal duration, bandwidth reciprocity with, 357
Signal energy, 65–70, 384–388, 868–869
Signal flow graph, 489, 491
Signal power, 65–70
Signal reconstruction, 449–460
Signal representation, by orthogonal signal set, 250–261
Signals
  bandwidth of, 293, 408–410
  classification of, 78–82
  combined operations on, 77–78
  components of, 239–241
  defining, 64
  dual personality of, 306
  estimating energy in MATLAB, 131–133
  even and odd components, 93–95
  size of, 64–70
  time reversal, 76–77
  time scaling, 73–75
  time shifting, 71–73
  useful models for, 82–91
  as vectors, 237–243
Signal transmission, through LTIC systems, 372–380
Signal truncation, 888–889
Sign function, Fourier transform of, 350
Simple interpolation, 449, *450*
Simplified impulse matching, 165–167
sinc(x), 341
Sine waves, approximation of, 240–241, 254–256
Single-input, single-output (SISO), 98, 125, 1064
Single-sideband modulation (SSB), 397–401
Singularity functions, 89
Sinusoids, 16–17
  addition of, 18–20
  aliasing general condition for aliasing in, 457–459
  aliasing verification in, 456–457
  clipped, 298–299
  compression and expansion of, 76
  discrete-time, 744–751
  DTFS of, 841–844
  exponentially varying, 22
  Fourier transform of, 347
  harmonic distortion of clipped, 298–299
  in terms of exponentials, 20
SISO. *See* Single-input, single-output
Sliding-tape method, 803–805
Space, 64
Spectral compression, 356
Spectral decay, 284
Spectral density, 338
Spectral folding, 453
Spectral interpolation, 468
Spectral leakage, 415
Spectral sampling, 423–424, 466–468, 1032, 1041, 1047
Spectral shifting, 363–364
Spectral spreading, 414, 415, 420, 471
Spectrum of $x(t)$, 335
Square matrix, 36
Square waves
  compact trigonometric Fourier series of, 272–274
  complex exponential approximation of, 243
  set of harmonic sine wave approximation of, 254–256
  sine-wave approximation of, 240–241
SSB. *See* Single-sideband modulation
Stability
  feedback and control and, 611–612
  transfer function and, 949
  z-transform and, 949
Stable equilibrium, 196
Stable systems, 110, 775
Standard forms of complex numbers, 14–15
State equation, 122, 1064
  determining, 1072–1082
  diagonalization, 1099–1103
  Laplace transform solution of, 1083–1088
  solutions to, 1082–1095
  time-domain solution of, 1088–1095
State equations, from transfer function, 1075–1082
State space, 1069–1072
  controllability and observability and, 1103–1109
  discrete-time system analysis with, 1109–1117
  MATLAB for analysis with, 1117–1125
  transfer function and description in, 1076–1080
State-space description, 121–125
State transition matrix (STM), 1091, 1094–1095
State variables, 121, 1064, 1069
State vectors, linear transformation of, 1095–1103
Steady-state component, 645
Steady-state errors, 592, 605–608
Steady-state response, to causal sinusoidal inputs, 645–646, 987
Stem plots, 765–766
Step input, 591–592, *593*, 594–595
Stiffness, 114
STM. *See* State transition matrix
Stopband, 676
Strip of convergence. *See* Region of convergence
Subcarriers, 412
Superposition, 98, 100
Suppressed carrier, 391, 399
Symbolic Laplace transform, 528
Symmetric matrix, 37
Symmetric quantizers, 496

Symmetry
conjugate, 354
in exponential Fourier series, 295
half-wave, 275
linear-phase response conditions, 1028–1030
trigonometric Fourier series and, 274–275
Synchronous demodulation, 394
Synchronous detection, 392
System behavior
characteristic modes and, 203–205
filtering, 207–208
intuitive insights into, 817–818
pulse dispersion or spreading, 209
rate of information transmission, 209–210
resonance phenomenon and, 210–212
response time, 205–206
rise time, 206
System memory, 104, 776
System realization, 572–587, 950–956, *951*, 954–956, 1079–1080. *See also* Direct form II realization; Direct form I realization
System responses
to external inputs, 168–196
to internal conditions, 161–163
to sampled continuous-time sinusoids, 987–988
unit impulse response, 163–168
Systems, 95
classification of, 97–110
data for computing response of, 96–97
defining, 64
input-output description of, 111–118
internal and external descriptions of, 119–125, 1064
with memory, 776
memory in, 104
System stability
external (BIBO), 196–197
implications of, 203
internal (asymptotic), 198
of LTID systems, 811–817
relationship between BIBO and asymptotic, 198–203
System time constant, 205–206
System transfer functions
inverse systems and, 556–557
Laplace transform for finding, 553

Tables, convolution by, 175, 177, 797–799
Tapered-window functions, 417–418
Taylor series, 55
TDM. *See* Time-division multiplexing
Third-order feedback systems, 603–605
Threshold detector, 247
Time, 64
Time advance, 73
Time compression, 76, 356, 540, 736
Time constants
of exponentials, 20
filtering and, 207–208
information transmission rate and, 209–210
pulse dispersion or spreading and, 209
rise time and, 206
system, 205–206
Time convolution
bilateral Laplace transform and, 619
DTFT and, 866
Laplace transform and, 540–541
Time delay, 73
Time differentiation
bilateral Laplace transform and, 618
Fourier transform and, 367–371
Laplace transform and, 537–539
Time-division multiplexing (TDM), 412, 461
Time-domain analysis, 150, 383–384
Time-domain description, 264
Time-domain equivalence criterion, 1003–1012, 1032–1039
Time-domain solution of state equations, 1088–1095
Time expansion, 540
Time-frequency duality, in Fourier transform operations, 352–353, 374
Time integration
bilateral Laplace transform and, 618
Fourier transform and, 367–371
Laplace transform and, 539–540
Time invariance, of discrete-time systems, 774–775
Time-invariant systems, 101–103, 774
Time reversal, 76–77, 735, 859
bilateral Laplace transform and, 619
z-transform and, 937–938
Time scaling, 73–75, 618
Time shifting, 71–73, 735
DFT and, 482–483
DTFT and, 861
Fourier transform and, 358–361
Laplace transform and, 532–535
z-transform and, 931–935
Time-varying systems, 101–103
Torque, 116–117
Torsional dashpots, 116
Torsional springs, 116
Total response, 195–196
Transfer function, 193
equivalent realizations and, 580
of FIR comb filter, 1030–1031
from frequency response, 662
inadequacy of description with, 1108–1109
of LTID systems, 809
in MATLAB, 571–572, 1120–1121
realization of, *573*, 573–574, 952–954, 956
second order, 656–661
stability and, 949
state equations from, 1075–1082
state-space description from, 1076–1080, 1086–1087
of unit delay, 948
z-transform and, 944–945
Transfer function matrix, 1086–1087
Transient component, 645
Transient performance, in frequency response terms, 665–667
Translational systems, 114–116
Transmission
distortionless, 375, 376, 379–380, 714–716, 874–875
signal distortion during, 374–376
time constants and rate of, 209–210
Transpose, 37
Transposed realization, 580–582
Transversal filter, 1028
Triangle function, 84–85
Triangle wave, compact trigonometric Fourier series of, 269–270
Trigonometric Fourier series, 261–277, *288*, 838
amplitude and phase spectra role in waveshaping, 279–284
compact, 263–267, 269–274
convergence at jump discontinuities, 268
exponential Fourier series and, 291–293
Fourier spectrum, 264
fundamental frequency and period, 276–277
periodicity of, 267–268
symmetry and, 274–275
Trigonometric identities, 55–56
Trigonometric set, 262
Truncated signals, 888–889
Tukey-Cooley algorithm, 488
Two-sided sequence, 968
Two-sided signal, 614

Uncontrollable systems, 120
Underdamped, 592
Uniformly convergent series, 278
Unilateral Laplace transform, 515, *516*, 517
Unilateral z-transform, 919–920
Uniqueness property, of unilateral Laplace transform, 517
Unit circle, 741
Unit delay, transfer function of, 948
Unit gate function, 340–341
Unit impulse function $\delta(t)$, 86–89
Unit impulse response $h(n)$, of discrete-time systems, 789–793
Unit impulse response $h(t)$, 163–168, 172
  of filters, 382
Unit matrix, 37
Unit step function $u(t)$, 82–86, *83*, 128–130, 349–350
Unit triangle function, 341
Unobservable systems, 120
Unstable equilibrium, 196
Unstable systems, 110, 775
Upper sideband (USB), 389
Upsampling, 736–738
USB. *See* Upper sideband

VCO. *See* Voltage-controlled oscillator
Vectors, 35–36
  components of, 237–239
  error, 238
  MATLAB operations, 45–46
  matrix multiplication by, 40
  signals as, 237–243
  state, 1095–1103
Velocity error constant, 606
Velocity error constant K_v, 606
Vestigial sideband (VSB), 401
Voltage-controlled oscillator (VCO), 411
VSB. *See* Vestigial sideband

Wall of poles, 672–673
Weber-Fechner law, 647
Wideband angle-modulated signal (WBEM), 410–411
Wideband angle modulation, 410
Width property
  convolution integration and, 172
  of convolved functions, 187
Window functions, 414–420, *417*
  discrete-time, *1032*
Windowing, 1047
Window method
  for differentiator design, 1038–1039
  for lowpass filter design, 1034–1037

Young, Thomas, 260

z-Domain differentiation property, 936–937
z-Domain scaling property, 936
Zero-input response (ZIR), 98, 151–163, 203
  complex roots, 154
  of discrete-time systems, 782–788
  Laplace transform and, 546
  repeated roots, 153–154
  total response and, 195–196
Zero-input stability, 199
Zero matrix, 37
Zero-order hold filter (ZOH filter), 449
Zero padding, 474, 475, 493–494, 883–884
Zero-state response (ZSR), 98, 168–196
  bilateral z-transform and, 972–974
  causality and, 172–173
  convolution integral for, 170–177, *176*
  of discrete-time systems, 793–810
  filtering and, 799
  Fourier transform for determining, 372–373
  interconnected systems and, 190–193, 806–809
  Laplace transform and, 541, 546, 550–553
  of LTID systems, 944–948
  total response and, 195–196
  z-transform and, 944–948
Zero-state stability, 199
ZIR. *See* Zero-input response
ZOH filter. *See* Zero-order hold filter
ZSR. *See* Zero-state response
Z-transform, 899–901, 918–925, 922, 1006
  bilateral, 920–921, 923–924, 966–974
  existence of, 921, 923
  inverse, 925–929
  inverse systems, 949–950
  Laplace transform and, 918, 956–959
  linear difference equation solutions with, 939–950
  MATLAB state-space analysis and, 1117–1119
  modified, 959, 965
  properties of, 931–939, *940*
  stability and, 949
  state-space analysis of discrete-time systems and, 1115–1116
  transfer function and, 944–945

A comprehensive introductory treatment of signals and linear systems with material on discrete-time systems that can be used in both a traditional course in Signals and Systems and in an introductory course in Digital Signal Processing.

Praise from the Experts:

"This is an excellent textbook for a junior-level course in System Analysis."
— Eshan Sheybani, *Virginia State University*

"This book has strong continuous signals and systems related content."
— Mohammed Yeasin, *University of Memphis*

"The book's greatest strength is the experience and insight that the author obviously has in continuous time systems and the subtleties and history of the methods that are used to analyze and design them."
— Peter Mathys, *University of Colorado*

New to This Edition

- Updated MATLAB material
- Improved navigation/titling of examples and drills
- Approximately half of the problems are new or revised

For additional information see also: www.oup.com/us/he

About the Author

B.P. Lathi is Professor Emeritus of Electrical Engineering at California State University, Sacramento. Dr. Lathi is renowned for his excellent writing across the upper-level electrical engineering curriculum.

Roger Green is an Associate Professor of Electrical Engineering at North Dakota State University. He has published numerous scholarly articles and given presentations on MATLAB, Signal Processing, and Fourier Analysis as a member of both the IEEE and ASEE. Along with four colleagues, he is the proud owner of a patent for a Vector Calibration System, designed to identify vector mismatch between a plurality of signal paths and frequencies.

OXFORD
UNIVERSITY PRESS
www.oup.com/us/he

ISBN 978-0-19-029904-0

Cover Photo: Slot entrance into the Wave, Pariah Canyon, Utah, Vermillion Cliffs NM, by Oksana Perkins, courtesy of Shutterstock.
Cover Design: OUP Design